Mobile Information Systems

Intelligent Decision Support Systems for Mobile Communications: Opportunities and Challenges

Lead Guest Editor: Shadi Aljawarneh
Guest Editors: Absalom Ezugwu and Juan Alfonso Lara

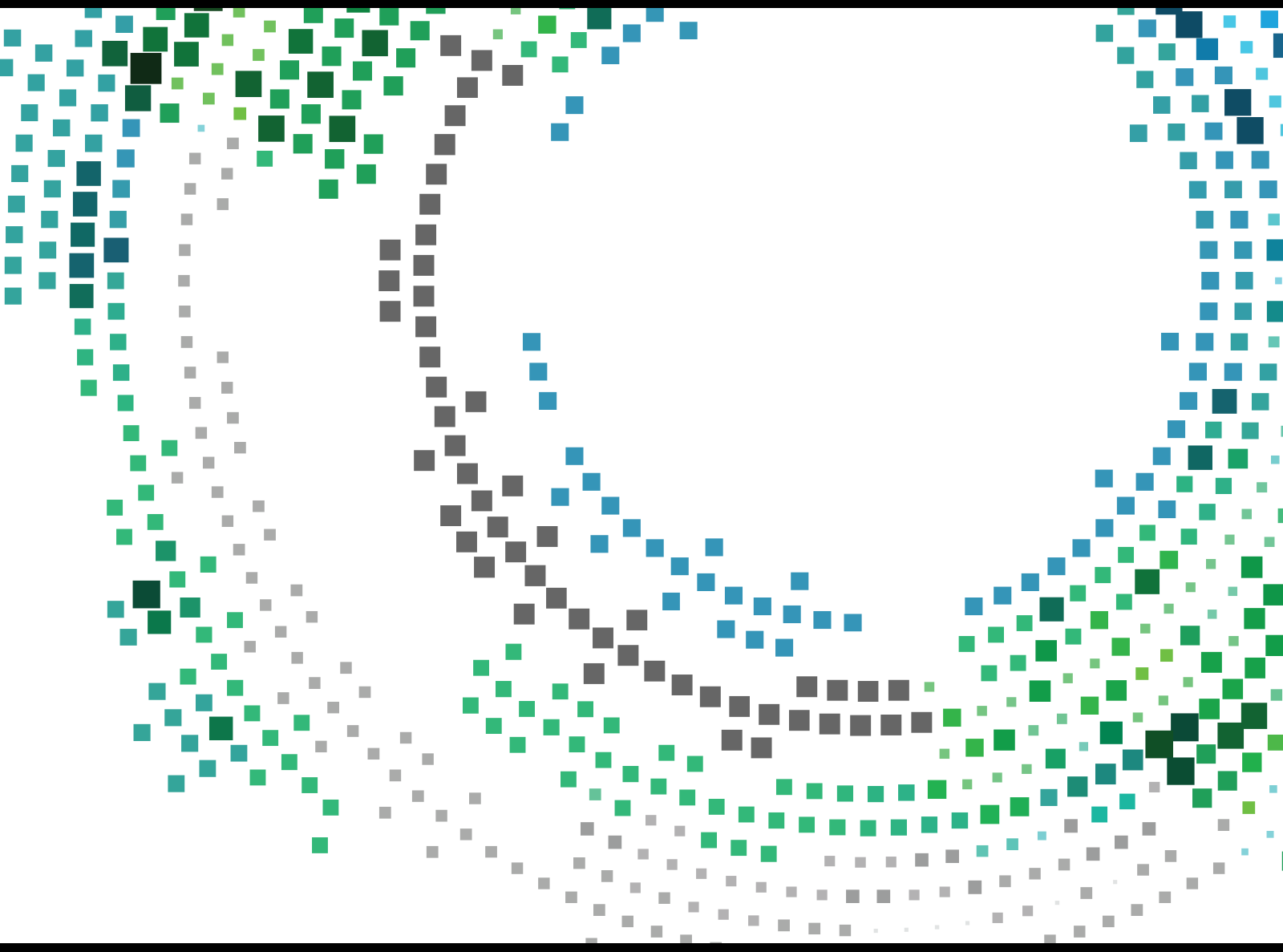

Intelligent Decision Support Systems for Mobile Communications: Opportunities and Challenges

Mobile Information Systems

Intelligent Decision Support Systems for Mobile Communications: Opportunities and Challenges

Lead Guest Editor: Shadi Aljawarneh
Guest Editors: Absalom Ezugwu and Juan Alfonso Lara

Chief Editor

Academic Editors

Contents

Contents

Contents

Contents

Contents

Hindawi
Mobile Information Systems
Volume 2023, Article ID 9761629, 1 page
https://doi.org/10.1155/2023/9761629

Retraction

Retracted: Recommendation of Knowledge Graph Convolutional Networks Based on Multilayer BiLSTM and Self-Attention

Mobile Information Systems

Received 13 September 2023; Accepted 13 September 2023; Published 14 September 2023

This article has been retracted by Hindawi following an investigation undertaken by the publisher [1]. This investigation has uncovered evidence of one or more of the following indicators of systematic manipulation of the publication process:

(1) Discrepancies in scope

(2) Discrepancies in the description of the research reported

(3) Discrepancies between the availability of data and the research described

(4) Inappropriate citations

(5) Incoherent, meaningless and/or irrelevant content included in the article

(6) Peer-review manipulation

The presence of these indicators undermines our confidence in the integrity of the article's content and we cannot, therefore, vouch for its reliability. Please note that this notice is intended solely to alert readers that the content of this article is unreliable. We have not investigated whether authors were aware of or involved in the systematic manipulation of the publication process.

Wiley and Hindawi regrets that the usual quality checks did not identify these issues before publication and have since put additional measures in place to safeguard research integrity.

We wish to credit our own Research Integrity and Research Publishing teams and anonymous and named external researchers and research integrity experts for contributing to this investigation.

The corresponding author, as the representative of all authors, has been given the opportunity to register their agreement or disagreement to this retraction. We have kept a record of any response received.

References

[1] Y. Qiu, Y. Liu, Y. Tong, and X. Xiang, "Recommendation of Knowledge Graph Convolutional Networks Based on Multilayer BiLSTM and Self-Attention," *Mobile Information Systems*, vol. 2022, Article ID 8247846, 9 pages, 2022.

Hindawi
Mobile Information Systems
Volume 2023, Article ID 9842536, 1 page
https://doi.org/10.1155/2023/9842536

Retraction

Retracted: Data Mining and Video Target Detection-Based Analysis of Martial Arts Cultural Communication and Martial Arts Athletes' Posture

Mobile Information Systems

Received 1 August 2023; Accepted 1 August 2023; Published 2 August 2023

This article has been retracted by Hindawi following an investigation undertaken by the publisher [1]. This investigation has uncovered evidence of one or more of the following indicators of systematic manipulation of the publication process:

(1) Discrepancies in scope
(2) Discrepancies in the description of the research reported
(3) Discrepancies between the availability of data and the research described
(4) Inappropriate citations
(5) Incoherent, meaningless and/or irrelevant content included in the article
(6) Peer-review manipulation

The presence of these indicators undermines our confidence in the integrity of the article's content and we cannot, therefore, vouch for its reliability. Please note that this notice is intended solely to alert readers that the content of this article is unreliable. We have not investigated whether authors were aware of or involved in the systematic manipulation of the publication process.

Wiley and Hindawi regrets that the usual quality checks did not identify these issues before publication and have since put additional measures in place to safeguard research integrity.

We wish to credit our own Research Integrity and Research Publishing teams and anonymous and named external researchers and research integrity experts for contributing to this investigation.

The corresponding author, as the representative of all authors, has been given the opportunity to register their agreement or disagreement to this retraction. We have kept a record of any response received.

References

[1] Z. Ma and Y. Ma, "Data Mining and Video Target Detection-Based Analysis of Martial Arts Cultural Communication and Martial Arts Athletes' Posture," *Mobile Information Systems*, vol. 2022, Article ID 2214724, 8 pages, 2022.

Hindawi
Mobile Information Systems
Volume 2023, Article ID 9840459, 1 page
https://doi.org/10.1155/2023/9840459

Retraction

Retracted: Case Study on Berthing and Disembarking of Ships and Traffic Organization in Rugao Port of Nantong

Mobile Information Systems

Received 1 August 2023; Accepted 1 August 2023; Published 2 August 2023

This article has been retracted by Hindawi following an investigation undertaken by the publisher [1]. This investigation has uncovered evidence of one or more of the following indicators of systematic manipulation of the publication process:

(1) Discrepancies in scope
(2) Discrepancies in the description of the research reported
(3) Discrepancies between the availability of data and the research described
(4) Inappropriate citations
(5) Incoherent, meaningless and/or irrelevant content included in the article
(6) Peer-review manipulation

The presence of these indicators undermines our confidence in the integrity of the article's content and we cannot, therefore, vouch for its reliability. Please note that this notice is intended solely to alert readers that the content of this article is unreliable. We have not investigated whether authors were aware of or involved in the systematic manipulation of the publication process.

Wiley and Hindawi regrets that the usual quality checks did not identify these issues before publication and have since put additional measures in place to safeguard research integrity.

We wish to credit our own Research Integrity and Research Publishing teams and anonymous and named external researchers and research integrity experts for contributing to this investigation.

The corresponding author, as the representative of all authors, has been given the opportunity to register their agreement or disagreement to this retraction. We have kept a record of any response received.

References

[1] P. Lu, "Case Study on Berthing and Disembarking of Ships and Traffic Organization in Rugao Port of Nantong," *Mobile Information Systems*, vol. 2022, Article ID 4261240, 9 pages, 2022.

Hindawi
Mobile Information Systems
Volume 2023, Article ID 9803761, 1 page
https://doi.org/10.1155/2023/9803761

Retraction

Retracted: The Implementation Measures of Environmental Accounting in Heavy Pollution Industry in the Context of Sustainable Development

Mobile Information Systems

Received 1 August 2023; Accepted 1 August 2023; Published 2 August 2023

This article has been retracted by Hindawi following an investigation undertaken by the publisher [1]. This investigation has uncovered evidence of one or more of the following indicators of systematic manipulation of the publication process:

(1) Discrepancies in scope

(2) Discrepancies in the description of the research reported

(3) Discrepancies between the availability of data and the research described

(4) Inappropriate citations

(5) Incoherent, meaningless and/or irrelevant content included in the article

(6) Peer-review manipulation

The presence of these indicators undermines our confidence in the integrity of the article's content and we cannot, therefore, vouch for its reliability. Please note that this notice is intended solely to alert readers that the content of this article is unreliable. We have not investigated whether authors were aware of or involved in the systematic manipulation of the publication process.

Wiley and Hindawi regrets that the usual quality checks did not identify these issues before publication and have since put additional measures in place to safeguard research integrity.

We wish to credit our own Research Integrity and Research Publishing teams and anonymous and named external researchers and research integrity experts for contributing to this investigation.

The corresponding author, as the representative of all authors, has been given the opportunity to register their agreement or disagreement to this retraction. We have kept a record of any response received.

References

[1] C. Cui and D. Chen, "The Implementation Measures of Environmental Accounting in Heavy Pollution Industry in the Context of Sustainable Development," *Mobile Information Systems*, vol. 2022, Article ID 3614435, 11 pages, 2022.

Hindawi
Mobile Information Systems
Volume 2023, Article ID 9790269, 1 page
https://doi.org/10.1155/2023/9790269

Retraction

Retracted: The Impact of Rural Labor Force Feminizing Fluctuation on Grain Production and its Regional Differences: Evidence from China

Mobile Information Systems

Received 1 August 2023; Accepted 1 August 2023; Published 2 August 2023

This article has been retracted by Hindawi following an investigation undertaken by the publisher [1]. This investigation has uncovered evidence of one or more of the following indicators of systematic manipulation of the publication process:

(1) Discrepancies in scope

(2) Discrepancies in the description of the research reported

(3) Discrepancies between the availability of data and the research described

(4) Inappropriate citations

(5) Incoherent, meaningless and/or irrelevant content included in the article

(6) Peer-review manipulation

The presence of these indicators undermines our confidence in the integrity of the article's content and we cannot, therefore, vouch for its reliability. Please note that this notice is intended solely to alert readers that the content of this article is unreliable. We have not investigated whether authors were aware of or involved in the systematic manipulation of the publication process.

Wiley and Hindawi regrets that the usual quality checks did not identify these issues before publication and have since put additional measures in place to safeguard research integrity.

We wish to credit our own Research Integrity and Research Publishing teams and anonymous and named external researchers and research integrity experts for contributing to this investigation.

The corresponding author, as the representative of all authors, has been given the opportunity to register their agreement or disagreement to this retraction. We have kept a record of any response received.

References

[1] H. Wang, G. Li, and Y. Hu, "The Impact of Rural Labor Force Feminizing Fluctuation on Grain Production and its Regional Differences: Evidence from China," *Mobile Information Systems*, vol. 2022, Article ID 2004465, 9 pages, 2022.

Hindawi
Mobile Information Systems
Volume 2023, Article ID 9786865, 1 page
https://doi.org/10.1155/2023/9786865

Retraction

Retracted: Adaptive Feature Analysis in Target Detection and Image Forensics Based on the Dual-Flow Layer CNN Model

Mobile Information Systems

Received 1 August 2023; Accepted 1 August 2023; Published 2 August 2023

This article has been retracted by Hindawi following an investigation undertaken by the publisher [1]. This investigation has uncovered evidence of one or more of the following indicators of systematic manipulation of the publication process:

(1) Discrepancies in scope
(2) Discrepancies in the description of the research reported
(3) Discrepancies between the availability of data and the research described
(4) Inappropriate citations
(5) Incoherent, meaningless and/or irrelevant content included in the article
(6) Peer-review manipulation

The presence of these indicators undermines our confidence in the integrity of the article's content and we cannot, therefore, vouch for its reliability. Please note that this notice is intended solely to alert readers that the content of this article is unreliable. We have not investigated whether authors were aware of or involved in the systematic manipulation of the publication process.

Wiley and Hindawi regrets that the usual quality checks did not identify these issues before publication and have since put additional measures in place to safeguard research integrity.

We wish to credit our own Research Integrity and Research Publishing teams and anonymous and named external researchers and research integrity experts for contributing to this investigation.

The corresponding author, as the representative of all authors, has been given the opportunity to register their agreement or disagreement to this retraction. We have kept a record of any response received.

References

[1] N. Liang, H. Xu, W. Zhang, and L. Cui, "Adaptive Feature Analysis in Target Detection and Image Forensics Based on the Dual-Flow Layer CNN Model," *Mobile Information Systems*, vol. 2022, Article ID 7140594, 14 pages, 2022.

Hindawi
Mobile Information Systems
Volume 2023, Article ID 9785954, 1 page
https://doi.org/10.1155/2023/9785954

Retraction

Retracted: The Application of AI-Based Technology in Computer Network Operation and Maintenance

Mobile Information Systems

Received 1 August 2023; Accepted 1 August 2023; Published 2 August 2023

This article has been retracted by Hindawi following an investigation undertaken by the publisher [1]. This investigation has uncovered evidence of one or more of the following indicators of systematic manipulation of the publication process:

(1) Discrepancies in scope
(2) Discrepancies in the description of the research reported
(3) Discrepancies between the availability of data and the research described
(4) Inappropriate citations
(5) Incoherent, meaningless and/or irrelevant content included in the article
(6) Peer-review manipulation

The presence of these indicators undermines our confidence in the integrity of the article's content and we cannot, therefore, vouch for its reliability. Please note that this notice is intended solely to alert readers that the content of this article is unreliable. We have not investigated whether authors were aware of or involved in the systematic manipulation of the publication process.

Wiley and Hindawi regrets that the usual quality checks did not identify these issues before publication and have since put additional measures in place to safeguard research integrity.

We wish to credit our own Research Integrity and Research Publishing teams and anonymous and named external researchers and research integrity experts for contributing to this investigation.

The corresponding author, as the representative of all authors, has been given the opportunity to register their agreement or disagreement to this retraction. We have kept a record of any response received.

References

[1] L. Li, "The Application of AI-Based Technology in Computer Network Operation and Maintenance," *Mobile Information Systems*, vol. 2022, Article ID 2971393, 10 pages, 2022.

Hindawi
Mobile Information Systems
Volume 2022, Article ID 1778469, 10 pages
https://doi.org/10.1155/2022/1778469

Research Article

Big Data e-Commerce Economic Development by Using IoT and Support Vector Machine

Jie Zheng[1] **and Guohua Yang**[2]

[1]*Business Administration Department, Zhanjiang University of Science and Technology, Zhanjiang 524255, China*
[2]*Shipping Management Department, Guangdong Ocean University, Zhanjiang 524088, China*

Correspondence should be addressed to Guohua Yang; yghua@gdou.edu.cn

Received 18 August 2022; Revised 20 September 2022; Accepted 3 October 2022; Published 13 October 2022

Academic Editor: Shadi Aljawarneh

The development of e-commerce economy is closely related to the progress of computer technology, which provides an effective data basis for the development of e-commerce economy. Support vector machines are not only used to analyze and solve the second-class classification problems but also can analyze and solve the first-class classification problems. The rise of the e-commerce economy is not only conducive to increasing people's income but also conducive to the realization of income increase in some economically backward areas and the improvement of various infrastructures, thus breaking the characteristics of inconvenient transportation in some areas and promoting the development of regional economy. Therefore, this study introduces the concept of Internet of Things and robust support vector machine technology, which are more advanced in computer technology, into the e-commerce system to optimize the existing e-commerce platform and knowledge mode. From the regression results of the fixed effect model, the e-commerce economy will have a certain positive impact on the regional economic gap, although the magnitude of the impact is not large. From the overidentification test and the regression results of the dynamic panel, the sign of the variable regression coefficient has been relatively stable, which means that the dynamic panel model described in this study not only does not have the problem of overidentification but also has stability.

1. Introduction

Support vector machine is a kind of machine learning method. Because it can realize the optimization problem, it has not only made major breakthroughs in theory but also advanced in algorithms. Especially, in these years, the research and analysis in this field have been paid attention to worldwide [1]. The use of support vector machines can obtain more accurate classification results because this method obtains the optimal partition hyperplane through the maximum interval method. However, the traditional support vector machine has certain drawbacks. In the original problem, the noise will have a great influence on the regularization term based on the L2 norm, which will cause the robustness of the support vector machine to decrease [2]. The higher the robustness of the support vector machine, the better the effect can be achieved in pattern recognition and machine learning, so it is necessary to strengthen the research on robustness [3]. The basic network architecture of the Internet of Things is as follows: perception layer, which generally collects and processes information, network layer, whose task is to transmit information, and application layer, which first analyzes and processes information and then makes control and decision-making [4]. The three layers are arranged in the order of the perception layer, the network layer, and the application layer. The network layer in the middle has the role of a bridge between uploads and releases and is the information exchange center between the first and third layers. The application layer can not only process the transmitted information but also realize information sharing, which can provide better support for the business processing of the e-commerce economy and can also promote the informatization and intelligence of various industries to a large extent [5]. The e-commerce economy has

injected new vitality into China's overall economy, which is conducive to the adjustment of China's industrial structure and the transformation of economic development, but it also has the same problem as all industries [6]. We can see from the development model of the e-commerce economy in the current era that this is a broader economic model than the traditional economy, which can realize the participation of all people. So, this economic form has a great effect on increasing the personal income of residents [7]. Literature analysises and discusses on regional economic development and differences, as well as the role of e-commerce in the middle [8].

2. Related Work

Since the support vector machine method began to appear, it has shown very good performance in pattern recognition and machine learning, and the research on support vector machine has become more and more mature in recent years. Standard support vector machines are good at handling two-class classification problems, but in people's production and life, in addition to two-class classifications, there are also single-class classifications [9]. Therefore, to solve this problem, a smooth support vector machine method is proposed. This new method is correct. The standard support vector machine has been improved. By expanding the smooth strategy, the unsolvable constrained optimization problem in the standard support vector machine has been turned into a smooth unconstrained optimization [10]. The literature describes the training process of the SVM algorithm as follows: first solve the convex quadratic programming problem (with linear constraints) and then continue to solve the dual problem through this result. Generally speaking, the calculation method of smooth support vector machine is used most of the time because this algorithm can solve the optimization problem with strong convexity and differentiability [11]. Looking at the research conclusions of various countries around the world, it can be seen that if the parameters in the sliding support vector machine model tend to be infinite, the unconstrained optimal solution it solves is more convergent [12]. The literature points out that OC-SVM, a type of support vector machine, are also a special form of SVM. In training, it is generally only necessary to carry out training operations on normal data, which are mostly used in anomaly detection. However, based on many experimental results, it can be seen that this algorithm has the disadvantage of being very sensitive to the reflection of abnormal points [13]. Therefore, in order to overcome the influence of noise on it, a more robust type of support has been studied and analyzed. The literature points out that the main areas of the Internet of Things can not only be balanced through relevant research and analysis but also use an extended general model. So, it can be concluded that it is very important to use the extended ecosystem to improve the analysis capabilities of the device itself [6]. The literature shows that there have been many relatively large changes in the e-commerce economy in recent years, and these changes may have a very large impact on the development of the service industry in the future. For example, the functions of the e-commerce economy in all aspects are becoming more and more independent, and their division of labor is becoming more and more precise and efficient [14]. Independence and precise division of labor are more obvious in the logistics industry and electronic payment. The scale of development in these two fields has grown rapidly, and the competition has become more and more fierce, which provides a strong support for the better and faster development of the electronic economy. The e-commerce economy has become an indispensable part of the current overall economic development [15]. In recent years, various relevant departments have formulated some policies that are conducive to the sound and sustainable development of the e-commerce economy according to their different functions. This has made China's e-commerce economy more effective [16].

3. Robust Support Vector Machine

3.1. Support Vector Machine, First-Class Support Vector Machine, and Smooth Support Vector Machine. We have studied and analyzed nonlinearities in these situations. When the sample set can be accurately divided by a straight line, there will be an optimal dividing hyperplane under the condition of the largest interval. This hyperplane will divide the two different samples on two sides:

$$(w \cdot x) + b = 0. \tag{1}$$

The original problem is solved first, and then, the dual problem is obtained as

$$\begin{aligned} &\min_{\alpha} \frac{1}{2}\sum_{i=1}^{l}\sum_{j=1}^{l} y_i y_j \alpha_i \alpha_j \left(x_i, x_j\right) - \sum_{j=1}^{l} \alpha_j \\ &s.t. \sum_{i=1}^{l} y_i \alpha_i = 0 \\ &\alpha_i \geq 0, i = 1, l. \end{aligned} \tag{2}$$

In $\alpha^* = (\alpha_1^*, \alpha_l^*)^T, w^* = \sum_{i=1}^{l} \alpha_i^* y_i x_i$, the corresponding component α_j^* of α^* is selected:

$$b^* = y_j - \sum_{i=1}^{l} y_i \alpha_i^* \left(x_i, x_j\right). \tag{3}$$

The training sample points are mapped from the original low-dimensional space to the high-dimensional space to obtain a new convex quadratic programming problem:

$$\begin{aligned} &\min_{\alpha} \frac{1}{2}\sum_{i=1}^{l}\sum_{j=1}^{l} y_i y_j \alpha_i \alpha_j \left(\varphi\left(x_i\right) \cdot \varphi\left(x_j\right)\right) - \sum_{j=1}^{l} \alpha_j \\ &s.t. \sum_{i=1}^{l} y_i \alpha_i = 0 \\ &0 \leq \alpha_i \leq C, i = 1, l. \end{aligned} \tag{4}$$

Using this method, we can solve some nonlinear classification problems in real life, but, at the same time, there are difficulties in determining the mapping function. There are many types of kernel functions, and we also have a lot of basis in the selection process. In the actual use process, the following are more commonly used. The linear kernel function is shown as

$$K(x, y) = x \cdot y. \tag{5}$$

The radial basis function kernel function is shown as

$$K(x, y) = \exp\left(-\frac{\|x - y\|^2}{2\sigma^2}\right). \tag{6}$$

The sigmoid kernel function is shown as

$$K(x, y) = \tanh[v(x \cdot y)+c]. \tag{7}$$

The effect of the radial basis function among these kinds of kernel functions is better and relatively ideal. Therefore, this study selects the radial basis function as the kernel function. A type of support vector machine generally only needs to perform training operations on normal data during training and is generally used in anomaly detection. This algorithm is based on the establishment of the optimal partition hyperplane to achieve classification. The decision function is shown as

$$f(x) = sign((w \cdot \varphi(x)) - \rho). \tag{8}$$

The sample point with a value of 1 represents a normal sample, and the sample point with a value of −1 represents an abnormal point.

The optimization problem is solved first, and then, the dual problem is obtained as

$$\min_{\alpha} \frac{1}{2} \sum_{ij} \alpha_i \alpha_j K(x_i, x)$$
$$s.t. 0 \le \alpha_i \le \frac{1}{vl}, \sum_i \alpha_i = 1. \tag{9}$$

Finally, the decision function can be expressed as

$$f(x) = sign\left(\sum_i \alpha_i K(x_i, x) - \rho\right). \tag{10}$$

It can be seen from formula (13) that if you want to solve the decision function of a type of support vector machine, you do not need a very accurate mapping function, but only need to use a kernel function.

The smooth support vector machine is improved on the basis of a class of support vector machines. It can solve the constrained optimization problems that cannot be solved in the traditional class of support vector machines through smooth technology and can obtain smooth unconstrained optimization problems.

If α and ξ are the normal vector and the slack variable and $C > 0$ is the compromise parameter, then the nonlinear classification hyperplane is shown as

$$K(x', A')D\alpha = b. \tag{11}$$

ξ can be rewritten as

$$\xi = (e - D(K(A, A')D\alpha - eb))_+. \tag{12}$$

The result of the optimization problem obtained by the smoothing strategy is unique.

The function $p(\Delta, \lambda)$ is introduced to replace Δ_+ approximately. When $\lambda \longrightarrow \infty$, it converges to Δ_+. The expression of $p(\Delta, \lambda)$ is shown as

$$p(\Delta, \lambda) = \Delta + \frac{1}{\lambda} 1n\left(1 + e^{-\Delta\lambda}\right), \lambda > 0. \tag{13}$$

(16) can be expressed as

$$\min_u \frac{c}{2}\left\|p(e - DKD_1 u, \lambda)\right\|_2^2 + \frac{1}{2}\|u\|_2^2. \tag{14}$$

Among them, $K = (K(A, A'), -1), D1 = \begin{pmatrix} 1, 0 \\ 0, D \end{pmatrix}$, and $u = (b, \alpha)$.

3.2. Robust Support Vector Machine. M-estimators can be expressed by the potential function Φ, and instead of the regularization term based on the L2 norm in formula (14) and (15),we can obtain

$$L(u) = \min_u \frac{c}{2}\left\|p(e - DKD_1 u, \lambda)\right\|_2^2 + \frac{1}{2}\Phi(u). \tag{15}$$

Proposition 1. *Based on the theory of conjugate convex function, potential function* Φ *will get a conjugate convex function* ϕ*:*

$$\Phi(u) = \min_v \left\{(u - v)^2 - \phi(v)\right\}, \tag{16}$$

where $v = (v_0, v_1, v_m)^T$ *is an auxiliary variable.*

When different Φ functions are selected, the minimum value function v obtained by formula (16) is also different. According to Proposition 1, it can be concluded that the optimization problem (18) can be rewritten as

$$L(u, v) = \min_{u,v} \frac{c}{2}\left\|p(e - DKD_1 u, \lambda)\right\|_2^2 + \frac{1}{2}\left[(u - v)^2 - \phi(v)\right]. \tag{17}$$

We solve the optimization problem (20), make the derivative equal to 0, and combine with equation (16) to get

$$\frac{\partial L}{\partial u_j} = c\sum_{i=0}^{l} (\Delta_i)_+ \times \frac{\partial \Delta_i}{\partial u_j} \times \frac{e^{\lambda\Delta_i}}{1 + e^{\lambda\Delta_i}} + \left(u_j - v_j\right). \tag{18}$$

Let the derivative be equal to 0, and the expression for u is $u = v - h$. Therefore, the optimization problem (20) can be solved through the following iterative process as

$$v^\tau = u^{\tau-1} - \frac{u^{\tau-1}}{\sqrt{\theta + \left(u^{\tau-1}\right)^2}}$$
$$u^\tau = v^\tau - h, \tag{19}$$

Table 1: Parameter settings of SSVM and RSSVM on two artificial datasets.

Dataset	SSVM		RSSVM		
	c	σ	C	θ	σ
Two-Moon	0.001	0.005	0.001	10^{-3}	0.25
Ripley	0.02	0.01	0.003	10^{-2}	0.25

Note. C is the penalty parameter, θ is the parameter greater than 0, and σ is the width parameter.

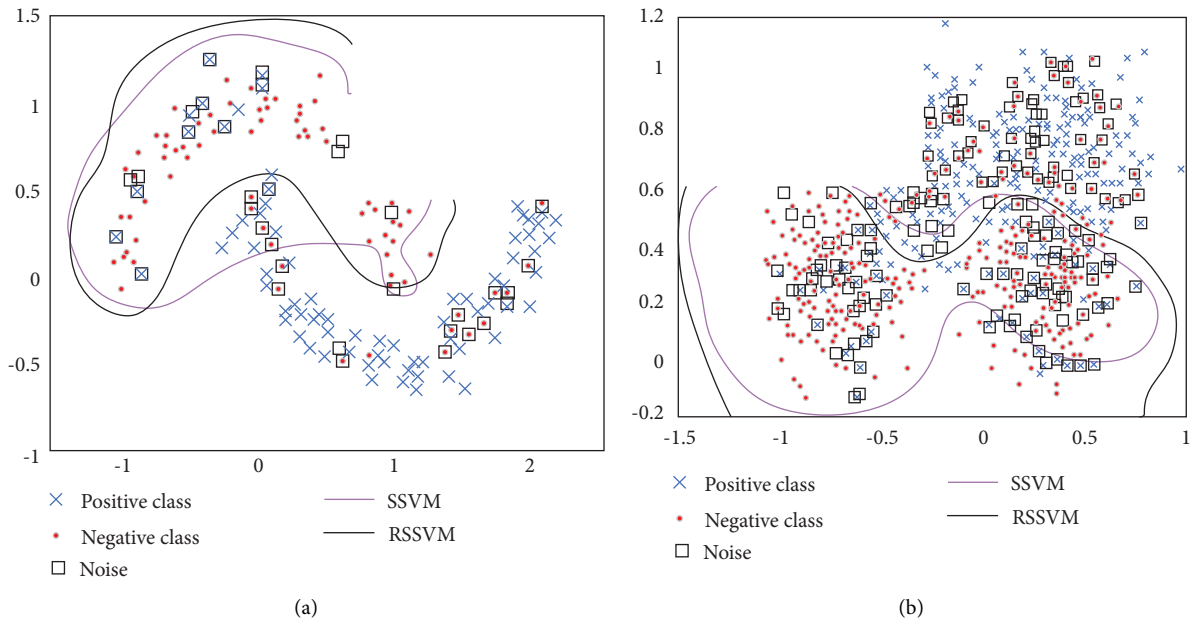

Figure 1: Classification effect of SSVM and RSSVM on two artificial datasets. (a) Two-Moon. (b) Ripley.

where τ represents the τth iteration and $h = (h_0, h_1, \ldots h_m)^T$, v is determined by the potential function Φ; this study selects $\Phi(u) = \sqrt{\theta + u^2}$ so that the potential function Φ obtains the minimum value of $v(u) = u - u/\sqrt{\theta + u^2}.u$, which is obtained by deriving formula (19).

Both the SSVM and RSSVM methods use Gaussian kernel functions. The parameters of the two algorithms in the two artificial datasets are shown in Table 1.

50% of the sample dataset is randomly selected as the training sample, and the other 50% as the test sample. SSVM and RSSVM, respectively, conduct 100 experiments in two types of samples, analyze 100 experimental results, and obtain the average accuracy of training samples and test samples. Take this average value as the accuracy of the final training sample and test sample, as shown in Figure 1.

In this study, the two algorithms are tested on the standard dataset. The detailed description of the standard dataset is shown in Table 2.

3.3. A Robust Support Vector Machine. A robust support vector machine introduces the function $p(\Delta, \lambda)$ to replace Δ_+ approximately. When $\lambda \longrightarrow \infty$, $p(\Delta, \lambda)$ converges to Δ_+. The expression of $p(\Delta, \lambda)$ is shown as

$$p(\Delta, \lambda) = \Delta + \frac{1}{\lambda} 1n\left(1 + e^{-\Delta\lambda}\right), \lambda > 0. \tag{20}$$

The optimization problem of a smooth type of support vector machine SOC-SVM is shown as

$$\min_{\alpha,\rho} \frac{1}{2vl} \sum_{i=1}^{l} \left\| p\left(\left(\rho - \sum_{j=1}^{l} \alpha_j K(x_i, x_j)\right), \lambda\right)\right\|_2^2 + \frac{1}{2}\alpha'\alpha - \rho. \tag{21}$$

M-estimators can be expressed by the potential function Φ, and then, replacing the regularization term based on the L2 norm in Equation (21), we can obtain

$$L(\alpha) = \min_{\alpha,\rho} \frac{1}{2vl} \sum_{i=1}^{l} \left\| p\left(\left(\rho - \sum_{j=1}^{l} \alpha_j K(x_i, x_j)\right), \lambda\right)\right\|_2^2 + \frac{1}{2}\Phi(\alpha) - \rho. \tag{22}$$

The optimization problem (22) is solved by the semi-quadratic minimization optimization method.

According to Proposition 1, the optimization problem (22) can be rewritten as

$$L(\alpha, v) = \min_{\alpha,v,\rho} \frac{1}{2vl} \sum_{i=1}^{l} \left\| p\left(\left(\rho - \sum_{j=1}^{l} \alpha_j K(x_i, x_j)\right), \lambda\right)\right\|_2^2 - \rho + \frac{1}{2}\left[(\alpha - v)^2 - \phi(v)\right]. \tag{23}$$

Table 2: Information about the standard dataset.

Dataset	Number of samples	Feature number
Banana	5300	2
Banknote authentication	1372	4
Breast cancer	263	9
Checkdata	345	7
Curie 1 data	35	25
Fertility	100	9
Titanic	24	3
Transfusion	748	4
Planning relax	182	12
Wpbc	194	33

Two sets of artificial datasets are selected to carry out comparative experiments. The two sets of data are defined as Line_noise and Square_noise. The experimental comparison of OC-SVM and RSOC-SVM on the Line_noise dataset is shown in Figure 2.

The experimental comparison between OC-SVM and RSOC-SVM on the Square_noise dataset is shown in Figure 3. We can see from it that, on the two artificial datasets of Line_noise and Square_noise, the generalization performance of RSOC-SVM is better than that of OC-SVM Better.

4. The Internet of Things in the Economic Application of Big Data e-Commerce

4.1. Big Data Technology Framework in the Internet of Things. An agreement is a set of standard regulations and requirements, which allows two electronic products to connect and exchange information with each other. The protocol makes corresponding specifications for the data transmission of different devices in a network connection and then realizes the corresponding functions. They stipulate not only how to carry out error checking but also how to carry out other specifications such as compressing data. The main task of the Internet of Things is to process some problematic network signals, such as frequently interrupted network signals and slower network signals. This study introduces a more appropriate protocol that has been used in the IoT world.

The AMQP model includes producer, exchange, binding, and queue. The producer creates the message and then transmits it to the exchange. If the exchange determines that the received information meets the binding standards after analysis, it is transmitted to the queue. The message queue saves the information and transmits the message to the consumer queue that has completed the subscription. The specific principle diagram of the AMQP protocol is shown in Figure 4.

Before transmitting the established message, the producer in the model can set the attributes of the message, such as the persistence of the message. MRG is an open standard application message with both high-speed and low-latency characteristics. MRG also has lasting properties, which means that even if the broker's hardware fails, the message will not disappear and can be restored.

Generally, edge devices are used for data collection in the Internet of Things. Edge devices refer to devices that often reside at the edge of the network. Radio frequency identification is a mechanism that has been used to collect data relatively early. At the same time, there are more and more devices that use other mechanisms, including some devices that use sensors, such as MEMS and mobile phones. The Internet of Things will be driven by the economic value. At the same time, the development of the Internet of Things will not only promote the improvement of social and economic benefits but also reduce production costs. M2M, or machine-to-machine technology, refers to the communication between devices of the same type, which can be wired or wireless, and then uses applications to capture and transmits sensor data. M2M generally cannot achieve complex communication and can often only meet the communication requirements between an enterprise's own devices. In the current Internet of Things, M2M technology is widely used and almost everywhere. It is an important part of the Internet of Things. The M2M terminal bears the responsibility of connecting the sensing extension layer and the network layer in the Internet of Things structure. The basic task is to collect data and process data. The system architecture of the Internet of Things is shown in Figure 5.

The terminal of M2M technology generally has two forms: one is a single-node terminal, which is a terminal device that can not only be directly connected to the telecommunication network but also has a sensing function; the other is a sensor gateway, which generally needs to be integrated transfer data, then process, and store it.

If you want a more suitable method to obtain data on edge devices, you must have a consistent protocol to achieve it. However, currently, there is no fully consistent protocol in the entire field, and only a part of the special field is implemented. However, at the same time, more and more IoT standardization organizations have begun to appear and contribute to the standardization of the Internet of Things, such as OIC and AllSeen Alliance. Some related standardization organizations and the main research areas of these organizations are shown in Figure 6

The data of the Internet of Things are obtained from multiple directions and channels. The versatility of this data source is also a significant feature of the Internet of Things. It is precisely because of this universality that the task of data quality and management becomes more onerous, and processing heterogeneous data is a very important task.

To achieve the increase in the number of data collections, it is necessary to have a basic technical framework that matches it. A powerful framework can not only provide support in storage and query but also increase the percentage of effective data obtained. Because the data are not necessarily in the same network or the same machine, it is very complicated to collect and process the data in different networks and machines. Therefore, we must pay attention to the research and analysis of distributed data analysis, including how to conduct high-speed and efficient search and indexing.

4.2. Current Status and Characteristics of e-Commerce Economic Development. The beginning of China's e-commerce development can be said to be in 1997. Both China's

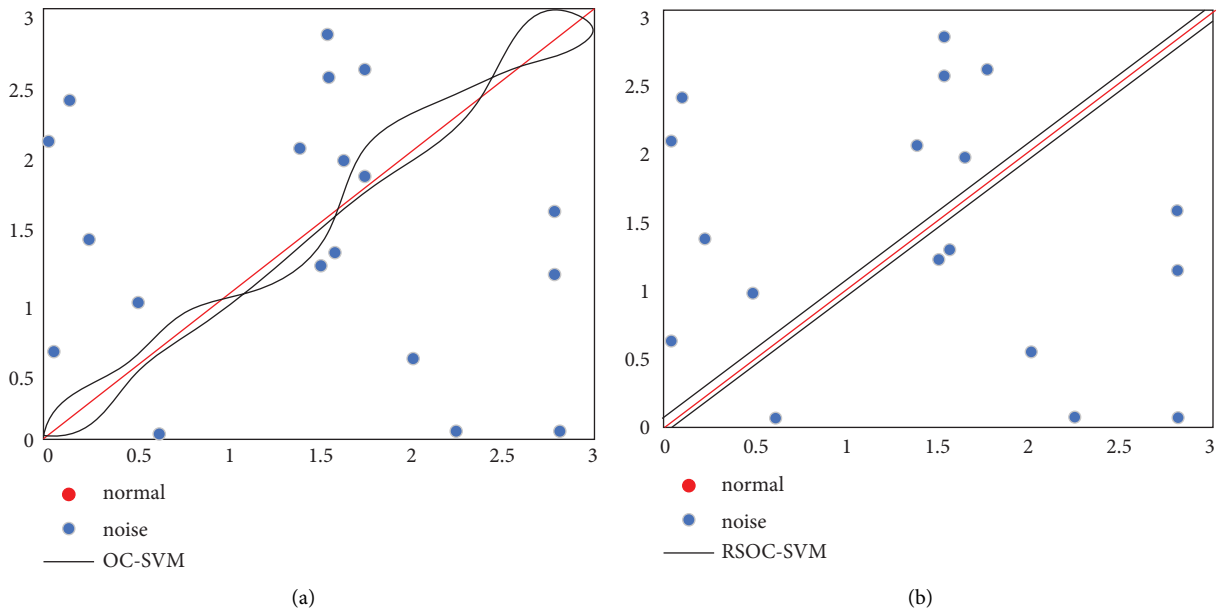

Figure 2: The classification effect of OC-SVM and RSOC-SVM on the line_noise dataset.

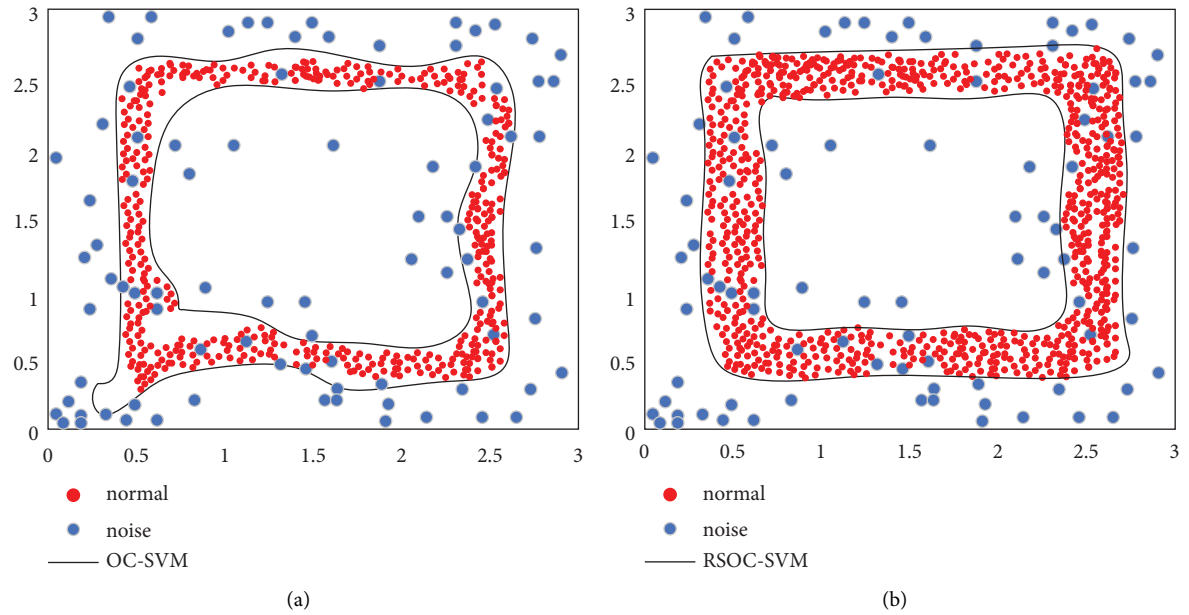

Figure 3: The classification effect of OC-SVM and RSOC-SVM on the square_noise dataset.

e-commerce and China's overall economic development are very fast. The development of e-commerce economy has injected new vitality into the overall economy, and the sound development of the overall economy has also given electronics. Business provides a good development environment. China's e-commerce transaction volume ranked second in the world as early as 2012. Not only the volume of transactions is large but also the compound growth rate of e-commerce is even more impressive. As early as 2003, it achieved a growth of 120%. Although the Internet was developed by learning from other countries, it is very important in people's hearts, especially for the younger generation. Many e-commerce websites in China are developing rapidly, such as China Chemical Network, Alibaba, and Dangdang. Compared with other countries, it has also achieved better growth. Basically, it can achieve a growth of more than 30% in all years. From the economic development in recent years, it can be seen that e-commerce occupies a high proportion in the economic development of some relatively backward areas. This paper conducts a study on it, using the static panel effect model and the dynamic panel model to carry out a comparative analysis, and found that

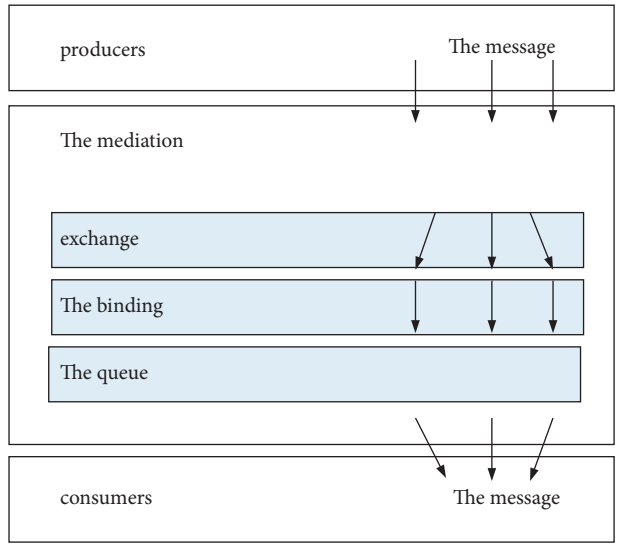

Figure 4: Schematic diagram of AMQP protocol.

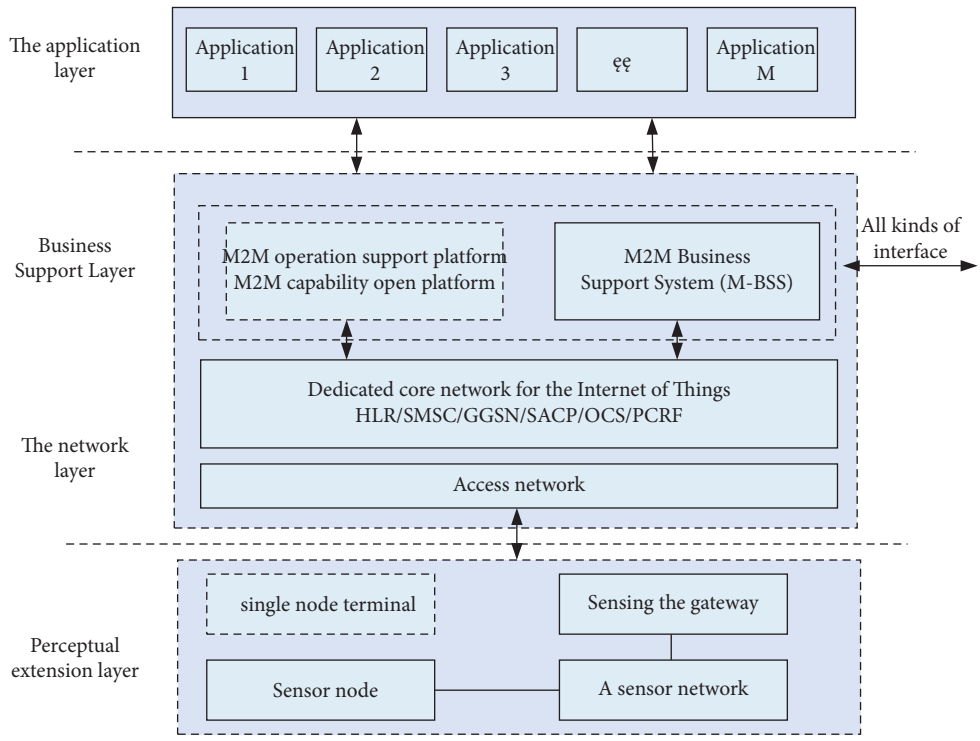

Figure 5: IoT system architecture.

the regional economic gap is not static, but dynamic. The economic development of e-commerce also has a very positive effect on the improvement of infrastructure in relatively backward areas. This way can indirectly enable some regions with relatively late economic development to get more development opportunities and narrow the gap between them and economically developed regions. This also requires the government to pay attention to the industrial cluster development of e-commerce economy, focus on establishing and cultivating some advantageous enterprises, and continue to strengthen regional construction. The cooperation between them will strengthen investment in various facilities, logistics, and distribution in the agglomeration area and continuously improve the competitiveness of the agglomeration area.

In recent years, China's e-commerce has developed very fast, and the growth rate of transaction volume has continued to increase. Especially, in the online retail market, it has achieved even more gratifying results. In 2012, it has already achieved a transaction volume of 1,311 billion yuan in the online retail market. According to the exchange rate at the time, it was equivalent to 206.8 billion U.S. dollars, and it

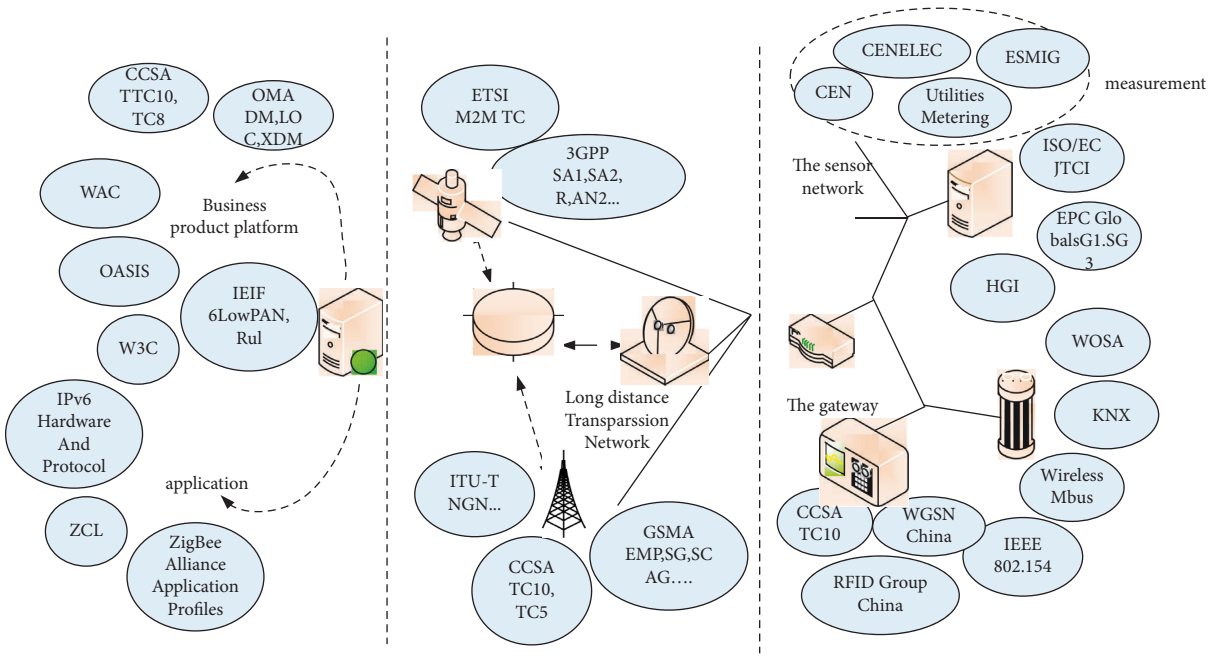

Figure 6: Standardization organizations related to the Internet of Things and their general research scope.

became the country with the largest transaction volume in the online retail market in 2013. In the online retail market, Alibaba is an e-commerce website with a relatively large market share. There will be large-scale promotions on November 11 every year, and consumers rush to buy. On the day of the "Double Eleven" event in 2018, the transaction volume was 19.1 billion yuan, and it increased every year for the next two years. This allowed people to see the rapid development of the online retail market. E-commerce is a new economic situation generated in accordance with the development requirements of the times. It provides an important guarantee for the rapid and sustainable growth of the overall economy and is an indispensable part of the overall economy. Researching and analyzing the survey results of the National Bureau of Statistics, we can see that, in 2011, it has reached the level of 0.67 websites on average for an enterprise. Many traditional retail companies in China have seen the huge potential of e-commerce and have begun to vigorously develop e-commerce. Since 2012, 60% of China's top 100 chain companies have begun to enter online retail. Research and analysis of the development of e-commerce transactions over the years shows that e-commerce has some new development models. However, from the perspective of the retail market, although C2C is still the main part, the market share of B2C is also gradually increasing.

4.3. The Influence of e-Commerce Economy on Regional Economic Development. Before the operation of regression analysis, the stationarity verification of each variable must be performed first, so as to ensure that the model will not have the problem of pseudoregression. Because of the use of panel data, it is not possible to simply use only one test method. Therefore, the LLC and PP methods are used to test the stationarity of the variables, respectively. The test results are shown in Table 3.

From the stationarity test in Table 4, under the two test methods, all variables are stable in the 5% significance test. Therefore, this study determines that there is no false regression problem based on the test results, so the data can be processed.

According to the analysis of the results of the Hausmann test, the model test value is 8.23, which means that the 1% significance test can be passed, so the fixed effects' model should not be used. From the regression results of the fixed effects' model, the e-commerce economy will have a certain positive impact on the regional economic gap, although the impact is not large. At present, there is still a certain economic gap between different regions in China, which has a lot to do with the previous inter-regional economic gap, which means that the economic gap can be self-adjusted. So, this study will conduct a dynamic panel model regression analysis. To obtain more accurate experimental data, this study conducts regression analysis on the two models. From the overidentification test and the regression results of the dynamic panel, the sign of the variable regression coefficient has been relatively stable, which means that the dynamic panel model described in this study not only has no overidentification problem but also has stability. From Table 4, we can see that different regional economic gaps have the function of self-regulation. It also shows from another angle that there is no problem using the dynamic panel model for analysis. From the regression results of the variables in the dynamic panel model in Table 4, it can be seen that the development of the e-commerce economy has a significant effect on reducing the regional economic gap. According to the analysis of the relevant regression results of the control variables, there are many factors that can have a positive impact on the regional economic gap, such as the level of economic development and the rate of urbanization. Table 4 shows regression result.

Table 3: Variable stationarity test.

Variable	LLC	Is it stable"	PP	Is it stable?
lntheil	−7.9602***	Yes	169.8863***	Yes
lndian	−8.2476***	Yes	168.6589***	Yes
lnurban	−11.7795***	Yes	416.0828***	Yes
lngdp	−6.5019***	Yes	87.5478**	Yes
lnroad	−8.3762***	Yes	72.4722**	Yes

Note. ***, **, and * indicate that they have passed the 1%, 5%, and 10% significance test, respectively.

Table 4: Regression result.

Variable	Static panel effect		Dynamic panel GMM	
	Random	Fixed	Difference	System
$Lntheil_{i,t-1}$	—	—	0.43*** (8.25)	0.37*** (9.12)
lndian	−0.23*** (−3.62)	0.20 (0.28)	−0.16** (−1.98)	−0.13*** (−4.14)
lnurban	0.12*** (5.20)	0.07*** (4.36)	0.08** (2.21)	0.04* (1.82)
lngdp	0.48*** (6.83)	0.52*** (8.20)	0.23*** (4.92)	0.35*** (8.45)
lnroad	0.07** (2.46)	0.04** (2.38)	0.03*** (4.08)	0.04*** (6.30)
Constant term	1.04* (1.87)	1.02* (1.92)	2.53*** (15.94)	2.51*** (20.06)
Hausman	8.23***	—	—	
Sargan test	—	—	268.29***	424.34***

Note. The values in parentheses in the table represent the *t* statistic, and ***, **, and * represent passing the 1%, 5%, and 10% significance test.

5. Conclusion

The current Internet can be said to have changed people's life, and people have enjoyed the convenience of the Internet in all aspects. In the field of electronic commerce, the existing pattern has been relatively mature; people can use e-commerce software to buy products for free. However, from the perspective of economic development, the existing model pays more attention to services. Therefore, it is necessary to systematically analyze the data of economic development and electric power Daqu and also to take certain technical optimization. In terms of technology optimization, this study puts forward the idea of Internet of Things and the technology of robust support vector machine. In recent years, the support vector machine method has not only been widely used and promoted in machine learning but also often used in pattern recognition. The application of these two fields and their related research are hotspots in the academic world. However, the traditional support vector machine has certain drawbacks. The noise in the original problem will have a great influence on the regularization term based on the L2 norm, which will cause the robustness of the support vector machine to decrease. The higher the robustness of the support vector machine, the better the effect will be achieved in pattern recognition and machine learning. Therefore, the research on robustness has been strengthened, and the new method proposed has obtained a type of support through some experiments. The robustness of vector machines has been improved to a certain extent. In recent years, China's e-commerce has developed very fast, with the growth rate of transaction volume. It keeps getting bigger, especially in the online retail market, and has achieved more gratifying results.

Data Availability

The data used to support the findings of this study can be obtained from the corresponding author upon request.

Conflicts of Interest

All the authors do not have any conflicts of interest.

Acknowledgments

This work was supported by Scientific research start-up project of Guangdong Ocean University: The Study on the Development Path of Shipping Financial Derivatives in Guangdong Province (Grant no. R19096).

References

[1] W. S. Noble, "What is a support vector machine?" *Nature Biotechnology*, vol. 24, no. 12, pp. 1565–1567, 2006.

[2] A. Widodo and B. S. Yang, "Support vector machine in machine condition monitoring and fault diagnosis," *Mechanical Systems and Signal Processing*, vol. 21, no. 6, pp. 2560–2574, 2007.

[3] X. Wang, N. Fan, and P. M. Pardalos, "Robust chance-constrained support vector machines with second-order moment information," *Annals of Operations Research*, vol. 263, no. 1-2, pp. 45–68, 2018.

[4] V. Aleksandrovičs, E. Filičevs, and J. Kampars, "Internet of things: structure, features and management," *Information Technology and Management Science*, vol. 19, no. 1, pp. 78–84, 2016.

[5] B. W. Jo, R. M. A. Khan, and Y. S. Lee, "Hybrid blockchain and internet-of-things network for underground structure health monitoring," *Sensors*, vol. 18, no. 12, p. 4268, 2018.

[6] H. Yu and L. Cui, "China's e-commerce: empowering rural women?" *The China Quarterly*, vol. 238, pp. 418–437, 2019.

[7] S. Geng, T. Z. Ren, and M. H. Wang, "Technology and infrastructure considerations for e-commerce in Chinese agriculture," *Agricultural Sciences in China*, vol. 6, no. 1, pp. 1–10, 2007.

[8] H. Zhang and J. Dong, "Prediction of repeat customers on e-commerce platform based on blockchain," *Wireless Communications and Mobile Computing*, vol. 2020, no. 12, Article ID 8841437, 15 pages, 2020.

[9] R. Zhang and J. Ma, "An improved SVM method P-SVM for classification of remotely sensed data," *International Journal of Remote Sensing*, vol. 29, no. 20, pp. 6029–6036, 2008.

[10] T. Xiong and V. Cherkassky, "A combined SVM and LDA approach for classification," *Proceedings. 2005 IEEE International Joint Conference on Neural Networks*, vol. 3, pp. 1455–1459, 2005.

[11] A. Sun, E. P. Lim, and Y. Liu, "On strategies for imbalanced text classification using SVM: a comparative study," *Decision Support Systems*, vol. 48, no. 1, pp. 191–201, 2009.

[12] M. Hu, Y. Chen, and J. T. Y. Kwok, "Building sparse multiple-kernel SVM classifiers," *IEEE Transactions on Neural Networks*, vol. 20, no. 5, pp. 827–839, 2009.

[13] R. Velazquez-Pupo, A. Sierra-Romero, D. Torres-Roman et al., "Vehicle detection with occlusion handling, tracking, and OC-SVM classification: a high performance vision-based system," *Sensors*, vol. 18, no. 2, p. 374, 2018.

[14] A. M. Purnamasari, "E-commerce product recommendations using xgboost with user clusters and clickstream," *International Journal of Advanced Trends in Computer Science and Engineering*, vol. 9, no. 4, pp. 5942–5948, 2020.

[15] M. G. Martinsons, "Relationship-based e-commerce: theory and evidence from China," *Information Systems Journal*, vol. 18, no. 4, pp. 331–356, 2008.

[16] S. Ma, Y. Chai, and H. Zhang, "Rise of cross-border E-commerce exports in China," *China and World Economy*, vol. 26, no. 3, pp. 63–87, 2018.

Hindawi
Mobile Information Systems
Volume 2022, Article ID 8615251, 11 pages
https://doi.org/10.1155/2022/8615251

Research Article

Social Work Management Intelligent System Based on Improved Genetic Algorithm

Xiaojian Guo [1] **and Ye Ma** [2]

[1]*School of Civil Affairs and Social Governance, Chongqing City Management College, Gaoxinqu, Chongqing 401331, China*
[2]*Department of Public Administration, Beijing City University, Haidian District, Beijing 100083, China*

Correspondence should be addressed to Xiaojian Guo; guoxiaojian@cqc.edu.cn

Received 11 August 2022; Revised 16 September 2022; Accepted 26 September 2022; Published 12 October 2022

Academic Editor: Shadi Aljawarneh

With the continuous development of society, social work is gradually professionalized, and relevant service fields are also growing. However, the limited resources of social work activities and the different needs of service projects are also more prominent. The intelligent management concept can assist social work services, thus providing fresh vitality for the field. How to effectively apply this vitality to the actual work process and form a unique intelligent management mode of social work service has always been the core issue of the sustainable development of social work specialization. Intelligent social work management is a new development trend. Based on this background, in this paper, a class of the intelligent social work management system is designed. The core technology of this system is an improved genetic algorithm. The system design is generally divided into four modules, and each module has different functions, including user-level acquisition module, intermediate acquisition module, load balancing module, and platform-level data storage and analysis module. Through the design and test, after the design simulation experiment test, it can be known that the system can effectively complete the design objectives, solve practical application problems, reasonably complete the work tasks, and meet the needs of users. In addition, the application of the system can improve the efficiency and management of social work services. Finally, this paper makes an in-depth analysis of the problems existing in the field of actual social work management and proposes corresponding solutions on this basis. In this study, an improved genetic algorithm is combined with social work management, and an effective intelligent management system is designed to realize work assistance.

1. Introduction

At present, the social work environment in China is changing faster and faster. With the continuous professional development of social work, the actual demands of its service objects for social work services are constantly improving [1]. Therefore, the traditional concepts and related technologies cannot meet the increasing actual demands and service needs of customers under the new situation [2]. Social work organizations need to strengthen the full integration of resources, carry out activities with characteristics, timeliness, and innovation so that services can move from the grassroots level to a higher level, achieve qualitative change, and provide support for the rapid and healthy development process of social work organizations [3]. Based on this background, the paper created the research topic of social work service intelligent management. For a long time, the development of social work has been affected by professional and administrative issues. Professional and administrative issues are only two one-sided focuses of social work services [4]. The use of social service intelligent management can provide an effective solution to this problem. First, the application of intelligent technology in social work management will have an impact on the management of social work organizations. Through intelligent management, resources can be effectively integrated to achieve effective management of working organizations [5]. Second, the use of intelligent management of social work services can win more room for progress in the development of social work. Applying intelligent management techniques and concepts

in the actual social work service process can have a significant impact on social work practice [6]. Therefore, this study will systematically explain the knowledge of social work service and intelligent management and try to prove the positive role that intelligent management theory can play in the practical work application process and the inevitable trend of using this technology. Therefore, this study builds a kind of the intelligent social work management system. The core technology of the system is the improved genetic algorithm. The system completes a three-layer system design by applying the concept of the improved genetic algorithm. They are user interaction layer, application service layer, and infrastructure floor. By introducing the concept of intelligent management and relevant methods, this system helps to improve the actual impact of social work services and is committed to improving the management efficiency of social work services and improving its development environment, assisting social work services to develop in a better direction. Through the research on the intelligent management of social work, this study is expected to promote the intelligent management technology to be widely recognized and applied in social work services, so as to promote the good and healthy development of social work specialization.

2. Relevant Work

A kind of the multiobjective genetic algorithm is designed for the identification of noninferior files in the literature. This algorithm can deal with the practical problems of multiobjective optimization that cannot be handled by traditional algorithms and avoid falling into the local optimal value in the calculation process, so that the global optimal solution can be obtained by further calculation [7, 8].The literature uses the abovementioned algorithm to solve the multiobjective optimization problem in the weight distribution process and obtains the global optimal solution, which is input as the initial value of the population and completes further calculation processing, including population mutation, selection, and crossover [9]. In the literature, a class of optimized multiobjective genetic algorithms was designed, and the idea of information entropy was added in the design process. Based on the comprehensive information entropy in the literature, this algorithm is based on nsga-2. After improvement, it can obtain the technical value and cluster value of the population based on the specific target, so as to obtain the information entropy value of the overall population, and input it into the calculation as a factor that changes the probability of crossover and mutation, so that it can control the convergence of the population and obtain the optimal value [10, 11]. The main objectives of the business system domain model are formulated in the literature, and the logic of the business system domain model and the main business system domain model and the relationship and media between the business system domain model and other data are designed [12]. Then, the information processing model and main domain model of the domain model are designed, and the relationship between this domain model and other domain models is explained. This literature has designed a collaborative management platform with Microsoft products, completed tool configuration by integrating relevant technologies, and completed the construction of the business process management system platform by combining SQL server database network-related technologies, web service technologies, network technologies, and so on [13]. Through simulation experiments, its effectiveness is tested. From the results, it can be seen that the system can safely transmit the business information generated in each link, realize the "coordination bridge" of data-related businesses, and promote the resource sharing and interaction between related businesses [14].

3. Improved Genetic Algorithm

3.1. Principle of Genetic Algorithm. The genetic algorithm (GA) was first proposed in 1975. It is a search method derived from the thinking and research type of "natural selection and survival of the fittest," which is the law of reproduction and evolution in the biological world. The genetic algorithm simulates gene crossover and gene mutation in biological reproduction. Evolution starts from a predetermined initial population according to the strategy.

Optimization problems are usually divided into two categories, namely, finding the minimum value of a function in a specific target domain; the maximum value of the function was found in the specified target domain. There are two basic methods to convert the target value of a point in the problem feasible solution space into the fitness corresponding to that point as follows:

(1) Select F(x) to represent the objective function value, and its fitness value can be represented by the following:

$$\text{Fitness}_x = \begin{cases} F(x) & "\text{Find the maximum value of the objective function}", \\ -F(x) & "\text{Find the minimum value of the objective function}". \end{cases} \tag{1}$$

(2) Let $C_{\max}$ be the maximum value of $F(x)$ and $C_{\min}$ be the minimum estimate of $F(x)$.

$$\text{Fitness}_x = \begin{cases} C_{\max} - F(x) & F(x) < C_{\max}, \\ 0 & \text{other}, \end{cases}$$
$$\text{Fitness}_x = \begin{cases} C_{\min} + F(x) & F(x) > C_{\min}, \\ 0 & \text{other}. \end{cases} \quad (2)$$

"Find the maximum value of the objective function"

Design the penalty function method as follows:

$$F'(X) = \begin{cases} F(X) & \text{When X satisfies the constraints}, \\ F(X) - P(X) & \text{When X does not satisfy the constraints}. \end{cases} \quad (3)$$

In Equation (3), $F(X)$ is the initial fitness value of the quasi-feasible solution, $F'(X)$ is the fitness value after considering constraints, and $P(X)$ is the penalty function under the strategy.

Let the training point set L be the training set as follows:

$$T = \{(x_1, y_1), \cdots, (x_L, y_L)\},$$
$$y = \text{sgn}(x). \quad (4)$$

Suppose there are two different types of data objects and their distribution is shown in Figure 1. All particles in the thick black line between the endpoints a and b of the horizontal axis are considered to be of the positive class, and the particles are on either side of the thin black line of the negative class. In this case, it is obviously impossible to meet the conditions, but we can find a quadratic curve similar to Figure 1 (find a random point on the horizontal axis, calculate the function value of this point, and it can be seen that the function in the positive category points must have values greater than 0 and negative category points must be less than 0).

This curve is a quadratic curve, and its function expression can be written as follows:

$$g(x) = c_0 + c_1 x + c_2 x^2. \quad (5)$$

Figure 2 shows two kinds of data demarcated by quadratic curve.

The most widely used kernel function Gaussian radial basis function kernel (RBF kernel) in SVM classification is defined as follows:

$$K(x, x') = \exp\left(-\frac{\|x - x'\|_2^2}{2\sigma^2}\right). \quad (6)$$

Real polynomial kernel function is as follows:

$$K(x, x') = \frac{\left(1 - (x \cdot x')^q\right)}{\left(1 - (x \cdot x')\right)}. \quad (7)$$

Among them, $(x \cdot x')$ satisfies $1 < (x \cdot x') < 1$.

Complete polynomial kernel function is as follows:

$$K(x, x') = \left(\frac{(x, x')}{a} + b\right)^q. \quad (8)$$

3.2. Model Establishment. Let the chromosome be expressed as $X = (X_1, X_2, \ldots, X_m)$, where m is the length of the chromosome, that is, the number of decision variables in the target problem and $F(x)$ is the target function. According to the knowledge of mathematical theory, we know that the extreme point has some characteristics as follows: (1) for a general smooth continuous function, the closer it is to the region where the extreme point is located, the derivative of the point tends to 0; (2) the function value of the extreme point is usually larger or smaller than the function value of the surrounding points. For an m-dimensional objective function, the fitness component i and the total fitness can be calculated by the following:

$$\text{Fitness}_i = e^{-|\overrightarrow{x_i}|}$$
$$\text{Fitness} = \sum_{i=1}^{m} \text{Fitness}_i. \quad (9)$$

According to the knowledge of mathematical theory, we know that the extreme point is the stagnation point of the multimodal function, and the derivative of the stagnation point is zero.

In the t generation, the ith gene locus of the mother is defined as $x_i(t)$, and the ith gene locus of the father is defined as $y_i(t)$, and the relationship between the children's genes and the parents' genes is as follows:

$$x_i(t+1) = \alpha x_i(t) + (1 - \alpha) y_i(t),$$
$$y_i(t+1) = \alpha x_i(t) - (1 - \alpha) y_i(t). \quad (10)$$

The individual chromosome in the multimodal function is represented as $X = (X_1, X_2, \ldots, X_i \ldots, X_n)$; when the ith locus moves, the current individual chromosome is

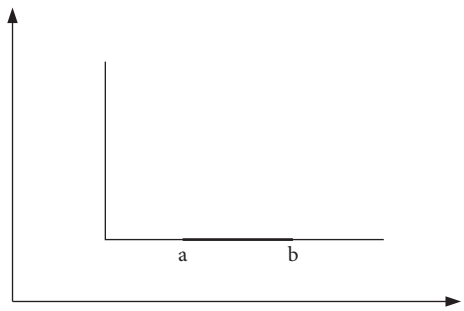

Figure 1: Complex nonlinear separable case.

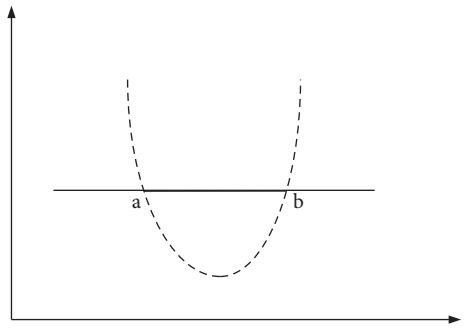

Figure 2: Two kinds of data with quadratic curve as the boundary.

represented as $X = (X_1, X_2, \ldots, X_i \ldots, X_n)$; the relationship between x_i' and x_i is determined by equation as follows:

$$x_i' = \begin{cases} x_i + \Delta(\text{Fitness}_i) & "\text{In the same direction}", \\ x_i - \Delta(\text{Fitness}_i) & "\text{Otherwise}". \end{cases} \quad (11)$$

3.3. Algorithm Improvement. In multiobjective problems, each objective may have different units, such as the problem of maximizing the revenue in the shortest time, the revenue unit is yuan, and the time unit is hours. Therefore, these target values need to be combined into a similar normalized form. For each target, there is a certain range of values. The maximum value of the target k is denoted as max fk, and the minimum value is denoted as min fk. Let the normalized interval be $[a, b]$, then the normalized function becomes

$$\varphi_k(X) = a + \frac{f_k(X) - \min f_k}{\max f_k - \min f_k} \cdot (b - a) k = 1, 2 \ldots, r. \quad (12)$$

It can be proved that the optimal solution set of the normal function corresponds to the optimal solution set of the original problem.

In the weighted sum method, each objective of the multiobjective function is multiplied by a coefficient i, $i \in [0,1]$, and the sum of all coefficients is 1, that is,

$$w_1 + w_2 + \cdots + w_r = 1. \quad (13)$$

Adding all the objective functions with coefficients to make it a single-objective function, the model of the transformed problem becomes

$$\text{Minimize} F(X) = \sum_{i=1}^{r} w_i f_i(X). \quad (14)$$

The optimal point of the modified single-objective optimization problem is the noninferior optimal front-end point. The verification process is as follows.

Each objective of the optimization function has a maximum value and a minimum value, that is, if the multiobjective problem requires the subobjectives to be as small as possible, each objective has a minimum value within the feasible solution range, that is, similar to the maximum value. As mentioned above, the multiobjective problem can be decomposed into multiple single-objective problems, and then the minimum value of the single-objective function can be calculated to obtain $(X', (X'))$, which satisfies the following:

$$\text{Minimize} F(X) = w_1 f_1(X') + w_2 f_2(X') + \cdots + w_r f_r(X'). \quad (15)$$

There are inequalities as follows:

$$w_1 f_1(Y) + w_2 f_2(Y) + \cdots + w_r f_r(Y) < w_1 f_1(X') + w_2 f_2(X') + \cdots + w_r f_r(X'). \quad (16)$$

For the same kernel function parameter value, the classification hyperplane corresponding to the penalty factor in an interval has the same classification accuracy, and a step-by-step evolution strategy can be used.

The entire evolution process of the improved genetic algorithm for the SVM parameter optimization problem is carried out in two steps. First, it is necessary to find the variable combination corresponding to the highest classification accuracy, which is expressed as the combination of penalty factor and kernel function parameter. There are many combinations of these combinations, and these combinations can be migrated to other locations to form new breeding populations. The second stage of work is to cultivate excellent breeding populations. The task is to achieve the evolution of the penalty factor while keeping the classification accuracy constant. This is done by using the lower bound of the penalty factor and the current value of the penalty factor to create a small floating random mutation based on the range of change. Due to the particularity of the genetic strategy of the improved genetic algorithm proposed in this study, some filtering operations are performed on the individuals saved in the last evolution of the elite population, and the final individual is the optimal solution.

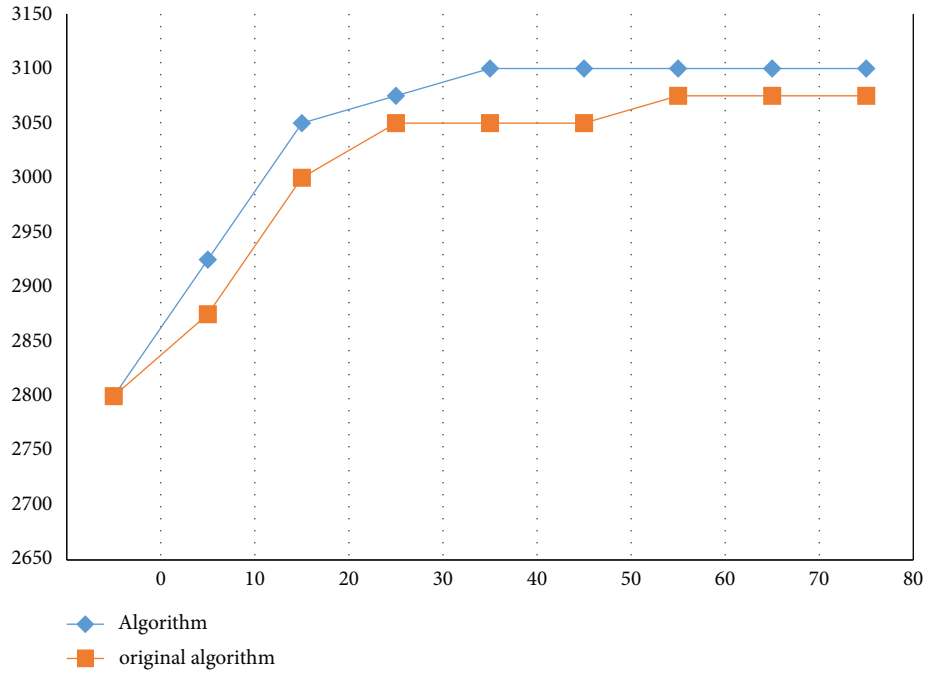

Figure 3: The comparison between this algorithm and the existing algorithms on the knapsack problem.

3.4. Simulation Results. This study proves that the improved coarse-grained genetic algorithm may be more suitable for cloud task scheduling by researching and improving the traditional genetic algorithm for two types of similar experimental data.

First, we conducted experiments on the knapsack problem between the algorithm in this study and the original algorithm. As shown in Figure 3, under the same problem environment, the optimization algorithm designed in this study has faster convergence speed and can obtain better solutions.

The second experiment is the comparison result of the task completion time between the algorithm in this study and the original algorithm, as shown in Figure 4.

It can be seen from the above experimental results that the algorithm in this study is superior to the traditional genetic algorithm in terms of task quality and task completion time.

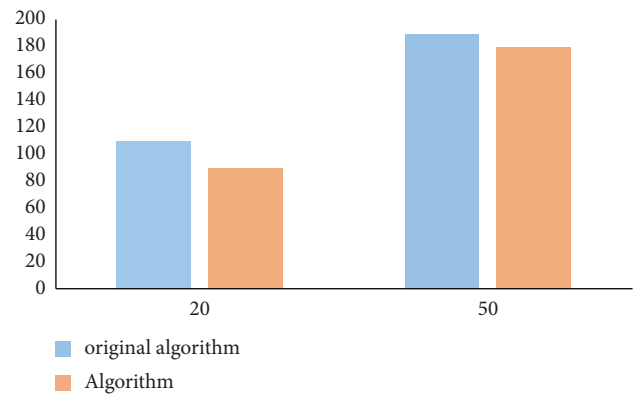

Figure 4: Comparison of the task completion time between the algorithm in this study and the original algorithm.

4. Design and Implementation of Intelligent System for Social Work Management

4.1. System Requirements. With the continuous development of society and the continuous increase of the scale of cities, in urban management, event management, security management, and population information management have become more prominent problems. The information age puts forward higher requirements for urban management, so it is urgent to build a modern management system [15]. To this end, the government decided to build an urban management information system to solve the actual problems of current urban management, gradually realize the refinement of urban management, meet the needs of data sharing, resource optimization, case evaluation, delivery, approval, verification, and so on, promote the informatization of urban management and efficiency, and promote the refined development of urban management [16].

(1) Resident information management: establish grid areas in the city and buildings (buildings) in each grid area, divide the grid responsibility areas of each city, and designate appropriate grid leaders; grid leaders collect responsible areas, houses, organizations, and so on.

(2) Urban civil administration functions: the grass-roots staff can provide processing and reporting of incident problems found during daily visits. In daily information collection and visits, grass-roots personnel can report residents' calls, neighbor disputes, city appearance and environment, and city management to the system platform through

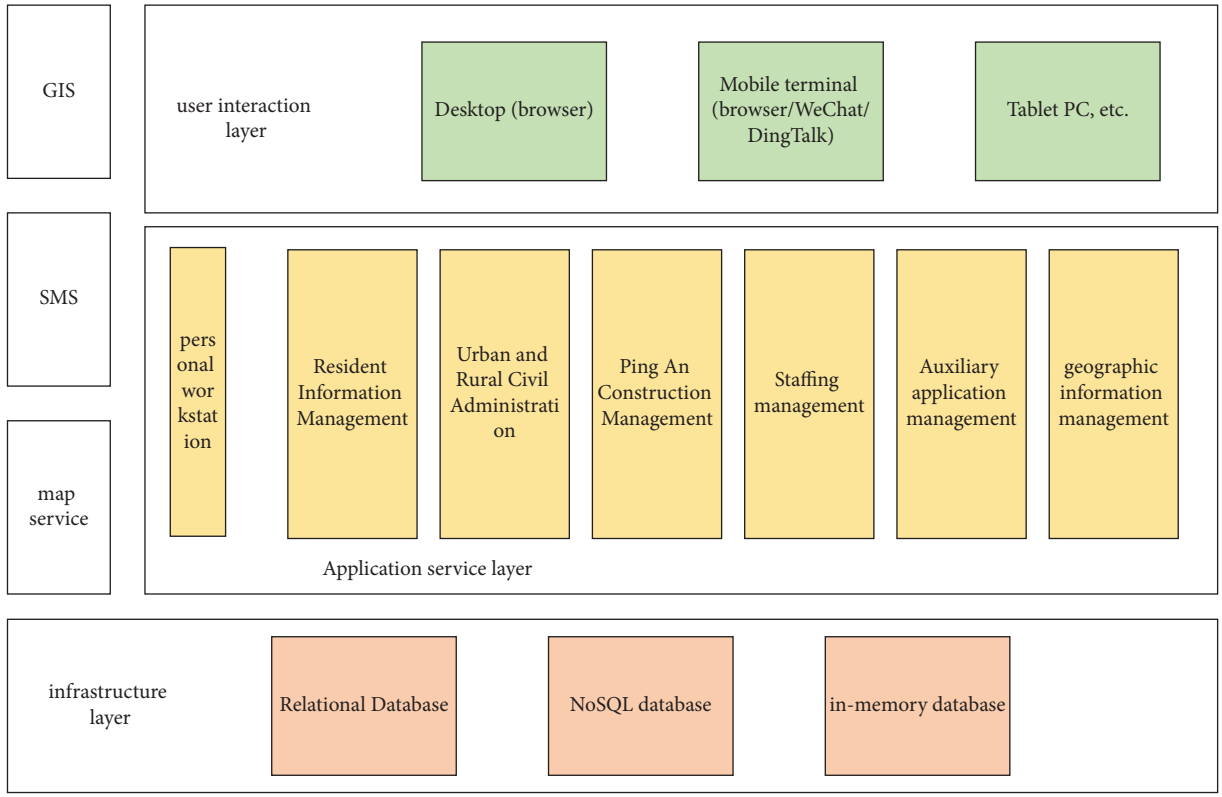

Figure 5: Architecture diagram of the social work management intelligent system.

mobile phones or computers. Special handling for other events occurs within the jurisdiction [17] whereas self-management issues are reported as being managed on a level-based basis. At the same time, for incidents reported and managed by grass-roots staff, such staff are required to review the results before closing the case [18].

(3) Ping a construction management obligations: report and inform the daily work of the grass-roots, city, town, street staff, and the political and legal committee. City and grass-roots staff register information on cases affecting social security in the network, so that the community political and legal committee can inquire about the situation at any time and record and report daily review data. This type of information is classified according to special groups and is divided into the following: released persons, urban correctional personnel, persons prone to mental accidents, drug-related persons, AIDS persons, cult organization personnel, key petitioners, key youth personnel, and persons carrying out dangerous goods and other activities.

(4) Personnel management activities: record the information of comprehensive management agencies and agency members at all levels. The comprehensive management facilities are divided into the following: the comprehensive management committee, the comprehensive management office, the comprehensive management work center, and the comprehensive management studio. Record information on members of mass prevention and mass governance bodies at all levels. Group defense management agencies are divided into the following: full-time patrols, volunteer patrols, security companies, volunteer teams, and so on.

(5) Auxiliary executive function: grass-roots personnel report the activities of the previous day to the system platform in the form of the next day's log. Cities, towns, streets, and blocks can be sorted by the number of logs reported by city and grass-roots workers. Users in cities, towns, streets, and blocks can view the log content of each grass-roots employee. The work logs of grass-roots employees will be used as one of the indicators for evaluating grass-roots employees.

(6) Geographic information management function: display information about people, places, organizations, and so on. Through the three-dimensional virtual map, the district grid, buildings, population, and other information are displayed through the district GIS map (2D).

For a system to achieve long-term success, on the one hand, it must provide complete functions and simple and elegant interactive pages, and on the other hand, it must ensure stable performance and simple operation. Only by combining the advantages of all aspects, the system can have

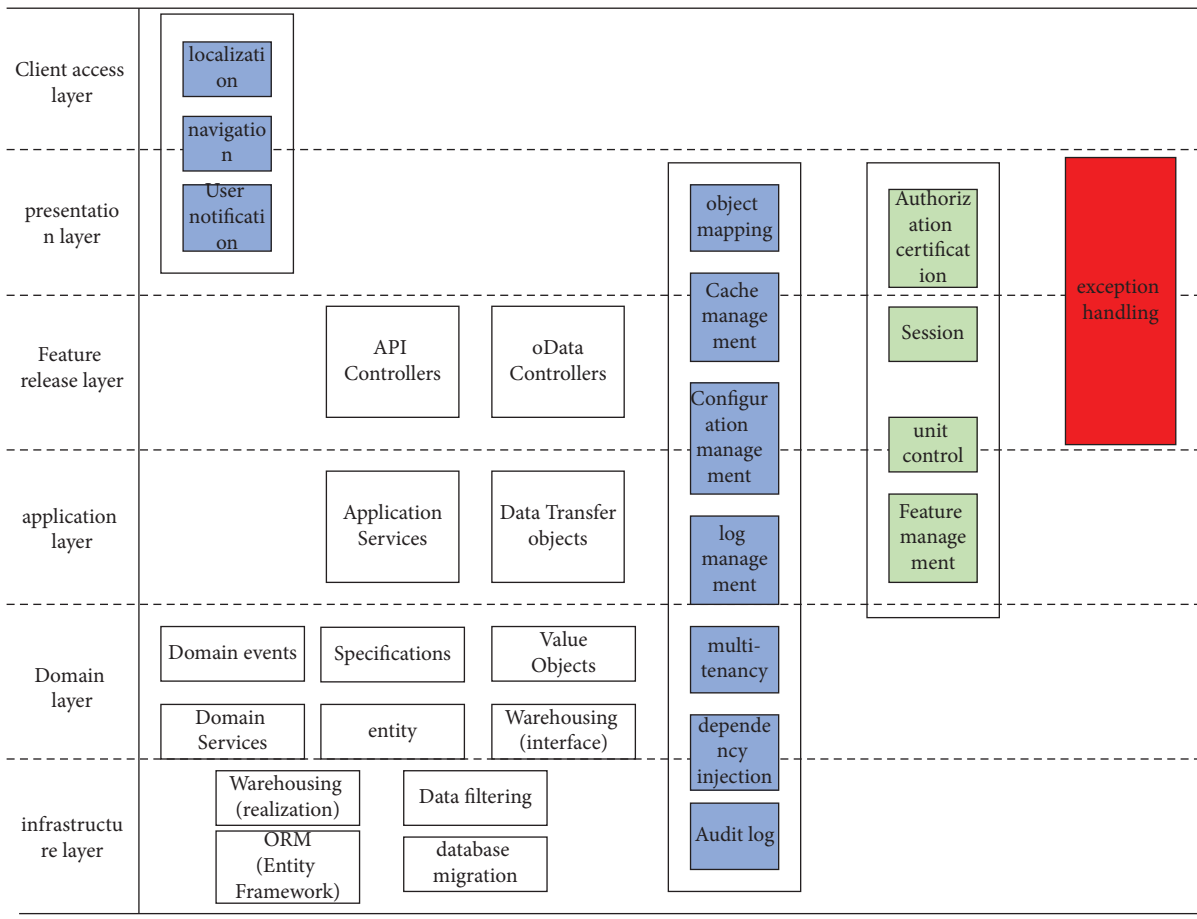

Figure 6: Technical architecture diagram.

a broad space for development and be welcomed and promoted by users. The following is a comprehensive description of the performance analysis of the urban management refinement system.

4.1.1. Scalability. To make the system have good scalability and extensibility, it is very important to develop the system framework. In the creation of the refined city management system, the overall development is mainly carried out with the help of the B/S architecture, which effectively ensures the "high integration and low coupling" of the system, making the system hierarchical and useable on many platforms. At the same time, it also allows the system to be connected with the outside through the interface, which promotes the development and expansion of the system.

4.1.2. Reliability. System reliability manifests itself in many different ways. On the one hand, it is reflected in the stability, maturity, and fault tolerance of the system. Generally speaking, maturity means that the system can maintain stable operation without frequent failures and provide users with stable and sustainable services; fault tolerance means that the system can automatically repair itself when minor errors occur, improving the stability of the operating system. Recovery refers to the ability of a system to store, retrieve, and back up data and information. Achieving this performance guarantee has a large impact on user operations, reduces the occurrence of data and information loss, and reduces negative impacts.

4.1.3. Security. Security is a mandatory requirement for all systems. For a refined urban management system, its business activities and development will involve a large amount of resident data and city data, and data leakage will bring many adverse effects to residents and the city, so data security needs to be ensured. Under normal circumstances, when researchers build a system, they will perform system operations such as encryption, setting firewalls, permissions, and backup and implement a number of protection measures to defend against external attacks and illegal operations, maintain the security and stability of the system, and provide users with the most optimal simple operation guarantee.

4.2. System Architecture Design. First, the architecture diagram of the social work management intelligent system will be displayed through Figure 5.

The overall technical architecture of the intelligent social work management system follows the DDD method

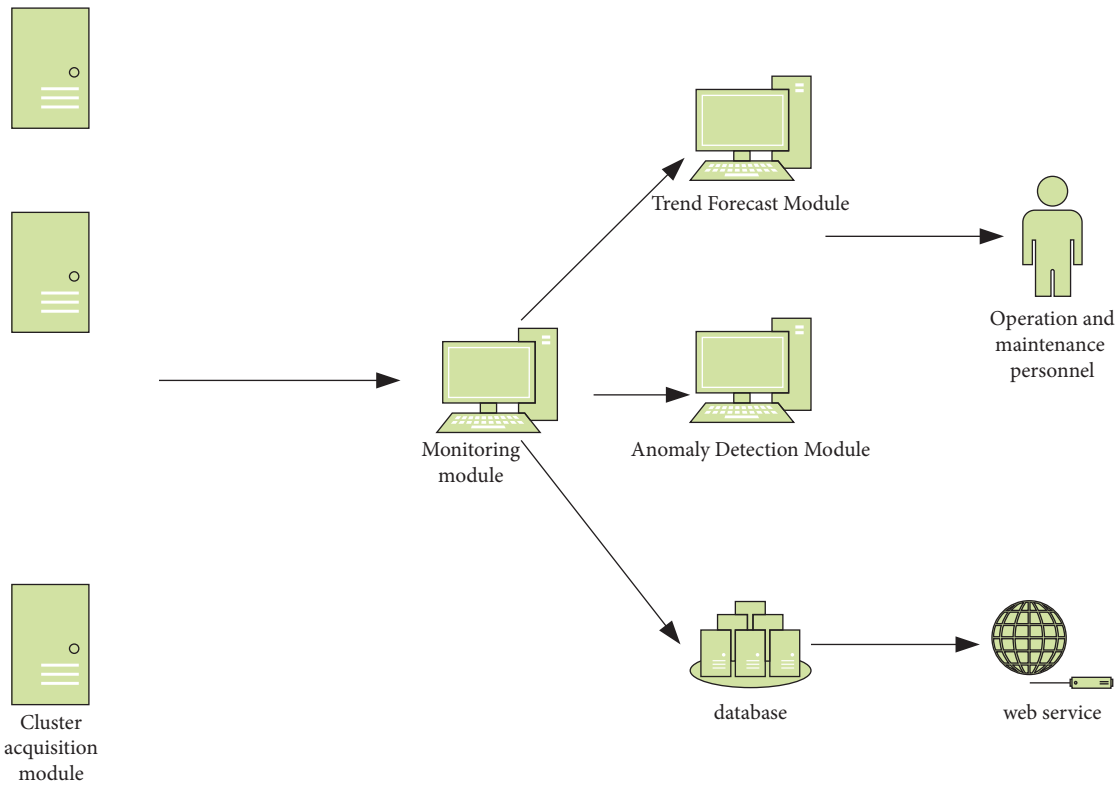

Figure 7: Framework diagram of monitoring system of social work management intelligent platform.

and adopts a 6-layer architecture design, as shown in Figure 6.

4.3. Functional Module Design. At present, the collection system of the intelligent social work management system can be divided into three modules, namely, the user-side collection module, the intermediate collection module, and the platform data storage and analysis module.

4.3.1. User Side Acquisition Module. This module is the original data entry module of the platform. It has tens of thousands of network devices installed on the user side and is responsible for collecting the actual daily network traffic of service network users. Every time a user accesses traffic, the device will report log information to the data platform, including timestamps, device IDs, visited websites, and other information.

4.3.2. Intermediate Acquisition Module. This module corresponds to an information transfer station, which is responsible for processing the information from the user side and then transmitting it to the platform side. The collection servers are distributed in computer rooms in different cities.

4.3.3. Platform Data Storage and Analysis Module. This module is responsible for further processing the online log information of the user equipment collected by the collection server and storing it in the nonrelational HBase database. Finally, log files are analyzed and further processed by MapReduce and Spark jobs to meet business needs.

There are two flaws in the current network traffic collection system. First, there is no user-side monitoring and analysis of individual network devices. Currently, the system passively accepts information reported by users but does not actively analyze traffic types and device health. Second, user-side network devices in the same area will upload all log information to the same collection server, which may cause some problems. If all devices are in the same mode, they will be peaking at the same time, i.e., each device's traffic will be peaking at the same time. If all devices are in peak state, the acquisition server may encounter performance bottlenecks or even crash; on the contrary, if all devices are in a trough state, the acquisition server is in a low utilization state, wasting resources.

4.3.4. Load Balancing Mode. For common user network devices, by summarizing recent historical data, each device can obtain a corresponding time series curve, the time interval is 1 hour, and this value is the current Internet traffic of the device. K-means clustering is performed on all-time series, Manhattan distance is selected for similarity distance, 3 is selected for the number of cluster centers, and the model is updated every week.

The frame diagram of the monitoring system of the intelligent social work management platform is shown in Figure 7.

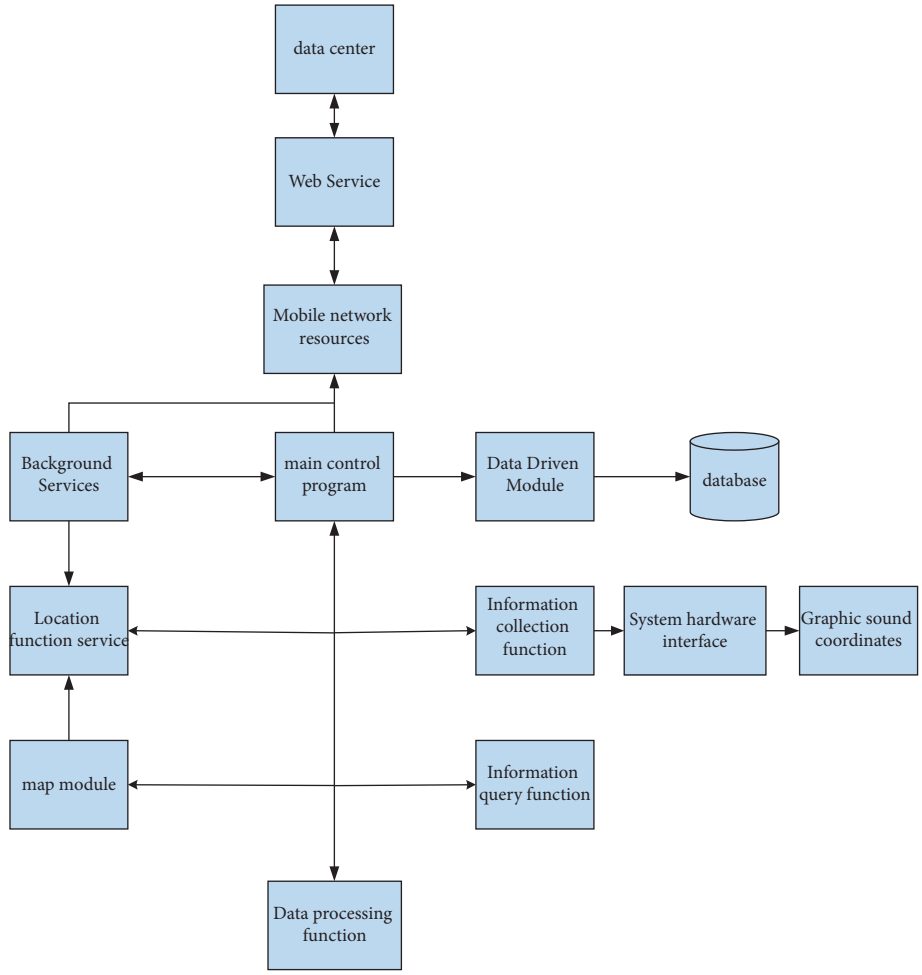

Figure 8: Overall design process of the wireless data acquisition subsystem.

The wireless data acquisition system mainly exchanges the collected valid information with the data center through Web services and audits and processes the information. The overall design flow of the wireless data acquisition subsystem is shown in Figure 8.

4.4. System Test. According to the system model, to provide effective information for urban management and related law enforcement, this study uses a certain proportion of data information as a test case to test whether the system meets the use standard, as shown in Table 1.

4.4.1. Pressure Test. By using the program testing tool that comes with Visual Studio.NET and by using the negative pressure testing tool to test the system website, you can record detailed program execution parameters and display the running status with icons, which is an ideal testing tool. According to the analysis of the test results, the system can judge the high-load operation and carrying capacity of the system, as well as the stability and reliability of the system. The system in this study has been tested with valid data for many times, and it has effectively realized the needs of users, completed the daily work flow, and met the relevant standards of system users.

Table 1: Analysis of test results.

	Numbers	Proportion (%)
Number of test cases	100	100
Exact execution quantity	98	98
Inaccurate execution quantity	2	2

5. Social Work Management Development Strategies

5.1. Problems. It is not allowed for social workers to provide professional services to clients. Due to the nonprofit nature of social work, the development process cannot be without the support of the government. Social work services in China are largely paid for by the government. The government's financial support has greatly promoted the rapid development of social work, but it has also made social work services subject to government orders. The development of "nanny-style" social work suffers from insufficient funding. The normal functioning of social work organizations and the development of social work services face some difficulties.

Social work services cover a wide range, including children, adolescents, the elderly, women, families, and the disabled. The positions of social workers are basically divided by field, which can provide services to the service objects more easily and directly, but this positioning method also increases management measures. In addition, some positions have obvious "administrative" characteristics, that is, social workers assigned to designated positions are affected by the working environment and cultural characteristics of the employer during the work process, thus weakening the professionalism of social work services.

Social work provides services in the form of individual counseling, group counseling, and targeted activities, generally providing professional and effective services to those in need. However, the services provided by the existing service methods are relatively independent. As social work-related concepts spread, people become more familiar with social work, and the corresponding needs for the services it provides are gradually changing from a targeted gradual transition to an ongoing systemic one. Social workers focus on the client's needs, and the services they provide are no longer a simple supplement to many services but carry out continuous and systematic service activities according to the client's classification.

5.2. Development Strategy. In the traditional multicenter governance model, the intelligent social work management system is only used as a government management tool and still cannot eliminate the unfavorable situation that the government completely dominates other subjects. Judging from the operation of a city's intelligent social work management system, the system is still under the high control of the government. The public will only participate in individual activities directly related to their vital interests and have no interest in changing the urban governance environment. The effective operation of the system itself can only depend on the government's attention and has little to do with businesses and the public. Therefore, in order to achieve true multicenter management, the participation of the public and enterprises must be increased. This study designs a multicenter social work management system by introducing intelligent technology.

First, improve the treatment and conditions of urban management practitioners and attract unique talents with stronger professional skills, richer service knowledge, and more advanced concepts to participate in the construction of the system. In particular, professional information collectors must have the corresponding capabilities to ensure the quality of the source system, and equipped with the second is to increase training efforts, improve the work quality of existing employees, strengthen the knowledge of serving the people and the enterprise, and build a disciplined, skilled, and good at solving complex problems. The third is to strengthen personnel management, adjust the staffing ratio, focus on multiangle start and multiparty coordination, continuously strengthen the construction of the intelligent system of social work management, and improve the operation efficiency of the intelligent system of social work management.

In the traditional bureaucratic and block management system, when dealing with urban management issues, the responsibilities of each responsible department are unclear, and they will shirk their responsibilities, thereby further affecting the service and disposal of cases. Professors in the professional field analyzed the role of the government in the multicenter governance model and believed that the government should not play an "intermediary" role, but they mainly established a macroframework and code of conduct to maintain the smooth operation of the multicenter system. Through the intelligent management system of social work, the traditional management system with high internal cost has been broken, and the pattern of urban management has been changed.

An intelligent social work management system must meet the urgent needs of real-time urban management. By combining video surveillance with intelligent image recognition technology, a new way of information collection is provided. The integration of the Internet of things and 5G technology will change the shortcomings of the lack of authenticity and professionalism of manual collection of information in the past activity areas; by changing the form of human subjective experience and judgment of likes and dislikes, data can be used to assist decision-making.

6. Conclusion

The main theme of the current era is efficiency and responsibility, and the theory of intelligent management technology perfectly fits this theme and can effectively assist social workers in related work. Due to the particularity of social management work itself, it is impossible to rely on theoretical knowledge alone. Therefore, management methods must be combined in the actual application process to improve work efficiency and work income, so as to provide more professional and efficient services for target users. Based on this point, this study combines intelligent technology with social work management technology and introduces the improved genetic algorithm to build a social work intelligent management system, which is expected to assist social work service management to move towards a new development route.

Data Availability

The data used to support the findings of this study are available from the corresponding authors upon request.

Conflicts of Interest

The authors declare that they do not have any possible conflicts of interest.

Acknowledgments

This study was supported by 2022 humanities and social sciences research project of Chongqing Municipal Commission of Education: Research on the mode and

optimization of the three-level service system of social work in Chongqing, 22SKGH568.

References

[1] W. Wu, S. Ma, Y. Su, and C. H. Wu, "Double-layer learning, leaders' forgetting, and knowledge performance in online work community organizations," *Journal of Organizational and End User Computing*, vol. 33, no. 1, pp. 92–117, 2021.

[2] M. Chung and K. W. Cheung, "The politics of indigenization: a case study of development of social work in China," *Journal of Sociology & Social Welfare*, vol. 33, p. 63, 2006.

[3] Y. Xiong and S. Wang, "Development of social work education in China in the context of new policy initiatives: issues and challenges," *Social Work Education*, vol. 26, no. 6, pp. 560–572, 2007.

[4] N. T. Moulding, "Intelligent design: student perceptions of teaching and learning in large social work classes," *Higher Education Research and Development*, vol. 29, no. 2, pp. 151–165, 2010.

[5] D. Schoech, D. Fitch, R. Macfadden, and L. L. Schkade, "From data to intelligence," *Administration in Social Work*, vol. 26, no. 1, pp. 1–21, 2002.

[6] C. Coombs, D. Hislop, S. K. Taneva, and S. Barnard, "The strategic impacts of Intelligent Automation for knowledge and service work: an interdisciplinary review," *The Journal of Strategic Information Systems*, vol. 29, no. 4, Article ID 101600, 2020.

[7] Y. Gao, L. Shi, and P. Yao, "Study on multi-objective genetic algorithm," in *Proceedings of the 3rd World Congress on Intelligent Control and Automation (Cat. No. 00EX393)*, pp. 646–650, Beijing China, July 2000.

[8] M. Jain, V. Singh, and A. Rani, "A novel nature-inspired algorithm for optimization: squirrel search algorithm," *Swarm and Evolutionary Computation*, vol. 44, pp. 148–175, 2019.

[9] W. Yu, B. Li, H. Jia, M. Zhang, and D. Wang, "Application of multi-objective genetic algorithm to optimize energy efficiency and thermal comfort in building design," *Energy and Buildings*, vol. 88, pp. 135–143, 2015.

[10] W. Wang, R. Zmeureanu, and H. Rivard, "Applying multi-objective genetic algorithms in green building design optimization," *Building and Environment*, vol. 40, no. 11, pp. 1512–1525, 2005.

[11] W. C. Yeh and M. C. Chuang, "Using multi-objective genetic algorithm for partner selection in green supply chain problems," *Expert Systems with Applications*, vol. 38, no. 4, pp. 4244–4253, 2011.

[12] F. Gonzalez-Lopez, G. Bustos, J. Munoz-Gama, and M. Sepúlveda, "Domain model based design of business process architectures," *Applied Sciences*, vol. 12, no. 5, p. 2563, 2022.

[13] M. Wu, X. Hao, Y. Lv, and Z. Hu, "Design of intelligent management platform for industry-education cooperation of vocational education by data mining," *Applied Sciences*, vol. 12, no. 14, p. 6836, 2022.

[14] Y. Hasegawa and H. Yamamoto, "Reliable IoT data management platform based on real-world cooperation through blockchain," *IEEE Consumer Electronics Magazine*, vol. 10, no. 1, pp. 82–92, 2021.

[15] W. Jichuan and W. Shengjin, "Research on architecture design of urban comprehensive management service platform," *E3S Web of Conferences*, vol. 236, Article ID 03023, 2021.

[16] H. Zhang, S. A. Padua, and Y. Li, "Research on the design of preschool education management information system based on computer technology," *Journal of Physics: Conference Series*, vol. 1915, no. 2, Article ID 022003, 1915.

[17] Z. Gao, W. Luan, W. Lin, J. Zhang, and R. Chang, "Research on integrated management platform of smart park based on CIM," *IOP Conference Series: Earth and Environmental Science*, vol. 768, no. 1, Article ID 012128, 2021.

[18] M. A. Hossain, "Community participation in disaster management: role of social work to enhance participation," *Sociology*, vol. 159, p. 171, 2012.

Hindawi
Mobile Information Systems
Volume 2022, Article ID 1518258, 10 pages
https://doi.org/10.1155/2022/1518258

Research Article

Monitoring Simulation of Athlete Dynamic Injury Based on NoSQL Database and Localization Algorithm

Yin Cheng,[1] **Hongmei Lu**,[1] **Yani Qian**,[1] **Quanfeng Li**,[2] **Bing He**,[1] **and Chengnong Guan**[1]

[1]*The Second Clinical Medical College, Guangdong Medical University, Dongguan, Guangdong 523808, China*
[2]*Department of Physical Education, Guangdong Medical University, Zhanjiang, Guangdong 524002, China*

Correspondence should be addressed to Yin Cheng; chengyin@gdmu.edu.cn

Received 12 August 2022; Revised 22 September 2022; Accepted 3 October 2022; Published 11 October 2022

Academic Editor: Shadi Aljawarneh

This article analyzes NoSQL databases, including three NoSQL data models, and analyzes the principles of two NoSQL representative products, Redis and MongoDB. Secondly, dynamic damage monitoring was introduced into the development of a Redis-based question-and-answer system. After proper improvement, certain noise and reverberation can also have relatively good positioning accuracy, which can be widely used in the system. The identification and classification of damage are based on the corresponding standards of the sports federation's damage monitoring system. Through expert interviews and investigations, the effectiveness and adequacy of physiological and biochemical indicator monitoring are understood to ensure a better evaluation of athletes' performance indicators. The method of experimental observation was used to monitor the physical function of athletes. During winter training, indicators were monitored, data were recorded, test conditions were recorded, and dynamic injury monitoring mathematical statistics were used for experimental analysis to objectively evaluate the physiological and biochemical indicators of athletes. This article mainly introduces the NoSQL database and sound source localization to dynamic damage monitoring so as to promote its continuous development.

1. Introduction

The purpose of this paper is to design and implement a set of visual image recognition systems for a big data environment based on the NoSQL database and design concept [1]. According to the current status of the Internet video and image inventory and the essential requirements of the business system for the high throughput, high stability, and low-cost deployment of the video image recognition, this system is realized through a pipelined information transmission mode and a highly independent module design for data processing. It is a visual image recognition system with low module coupling, high functional robustness, and support for distributed redundant deployment [2]. When studying the selection of adjustment factors, this paper uses algorithms to estimate the number of sound sources under the condition of known sound source positioning and studies the distribution law of multilevel adjustment factors $D(n)$ to obtain the optimal value. Simulation experiments show that the optimal adjustment factor selected by this method can be adapted to the identification of the number of multiple sound sources. At the same time, the system fully considers the difficulty of current Internet data acquisition. Most video resources are sourced from a NoSQL database, which is difficult to download explicitly, bringing a lot of trouble to the business system [3]. Therefore, the data collection function is integrated into the system design, and the web crawler is used [4]. The module collects Internet data by itself, which improves the business competitiveness of the system. In addition, in terms of identification costs, through research on a large amount of Internet data, the innovative use of continuous self-maintaining of the black-and-white list library avoids the waste of computing resources for repeated data and greatly reduces the cost of system deployment. The MSGDE algorithm is actually similar to the multiple operations of the traditional GDE algorithm [5]. Based on the assumptions, it performs multiple classification operations on the same data, which greatly reduces the

estimation error caused by a single operation and improves the number of sound source localization recognition. Compared with traditional GDE, in the range of −20 dB~10 dB signal-to-noise ratio given in the experiment, the recognition accuracy is generally improved by 10%~80% [6]. Based on the research method and the proposed algorithm in this paper, the subsequent use of more efficient calculation methods will greatly improve the performance of sound source identification and location. Through experiments, monitoring training is very important for monitoring the training of five athletes [7]. The five indicators selected by the dynamic injury monitor reflect the function of the player's material and energy metabolism system, showing the athlete's exercise volume and exercise intensity to ensure they successfully complete the team training tasks and reflect the physical condition of the athletes during the rest period [8]. As a whole, the physical function status of athletes has been maintained in a stable state, and the appearance of excessive fatigue and difficulty in recovery provides a theoretical basis for scientific training.

2. Related Work

The literature introduces the technical principles of the NoSQL database, analyzes the current popular products according to the technical characteristics of NoSQL, and provides a theoretical basis for the design and development of the following question-and-answer system [9]. The literature introduces the requirements of system construction and puts forward the deployment environment and basic design requirements that the system needs to meet; secondly, it explains the requirements analysis of the system and discusses the overall system from several aspects such as user scope, functional scope, business composition, and functional module description [10]. The design requirements of the system: finally, the nonfunctional requirements of the system are clarified, and the design requirements and reasons for the general system are explained. The literature introduces the deployment method of the system. This system adopts the docker virtualization deployment method [11]. Therefore, a set of deployment strategies that use shell scripts and configuration files to achieve a one-click deployment system for multiple servers have been designed, which greatly reduces the difficulty of deployment; secondly, after the deployment is completed, we test the system performance indicator and export the final test data. The literature introduces the sound pressure sensor array. The sound pressure sensor array is a sound collection system that uses multiple sound pressure sensors to collect sound information [12]. Through interaction, it is widely used in other fields. The array structure is in the position of the point source and plays an important role. Compared with line arrays and neutral arrays, three-dimensional arrays have higher positioning accuracy because of the directionality of their sensors. They are suitable for the spatial location of additional rotating systems. The literature introduces the influence of sound pressure sensors on the hard disk system, the audio source frequency, and the setting of the sampling speed in system A/D conversion [13]. Because the array element spacing is too small, the distance between the audio source and the receiving system will not be too large, and the narrow area model is no longer applicable.

3. Sound Source Localization Method for the NoSQL Database

3.1. NoSQL Data Model Design. The data model represents the model used when storing users. It is a logical model that describes how users interact with data in the database [14]. Different from describing the database storage model on the actual physical computer, the user does not need to manage this part, and we need to understand the system performance requirements. The data model can be viewed from the above definition. When saving data, we can select the data model to understand how it plays an important role in maximizing database performance.

In a relational database, each form in the data model represents a set of relationships. Each table contains multiple rows. These entities have fixed values between rows and columns [15]. This table is used to set up links between tables (related columns are called foreign keys) to form tables with associations. Compared with traditional relational databases, the most important function of NoSQL technology is to abandon the relational model, which is also the attraction of NoSQL [16]. Abandoned models can make it easier for us to achieve high performance and expand storage in the system. It does not provide value operations, and the key-value database is mainly used for primary key access operations [17, 18].

3.2. Structural Design of Point Sound Source Positioning System. The virtual instrument positioning system mainly includes a sound pressure sensor data acquisition array, 20-channel sound pressure sensor array signal preprocessing module, STM32 single chip microcomputer acquisition signal preprocessing module, power supply module, wireless transmission module, USB transmission module, and computer LabVIEW software platform.

As a front-end data acquisition module, the sensor array is mainly responsible for collecting spatial acoustic signals in the environment and converting the acoustic signals into analog voltage or current signals through the piezoelectric effect. The array consists of 20 omnidirectional sound pressure sensors, which are distributed on a hemisphere with a radius of 10 cm according to the C60 structure designed in this paper.

The array signal preprocessing module is mainly responsible for preprocessing the signals collected by the sound pressure sensor. The collected analog signals are processed to facilitate subsequent analysis.

STM32 is responsible for converting the preprocessed analog signal into a digital signal, which is transmitted to the host computer LabVIEW data analysis and processing platform in real time via USB cable or wireless transmission. STM32 is used as a lower computer and front-end data preprocessing module. In order to prevent crashes during the front-end data acquisition and processing, a reset circuit

is added to the circuit module. When the acquisition fails, the upper front-end acquisition system can be reset by one key to restore the original status and continue to work.

LabVIEW data processing analysis module is mainly completed on the computer by independently designing a data processing and display platform, using the powerful cross-platform interaction capabilities of LabVIEW, calling MATLAB software, locating the location of the spatial sound source through the MUSIC algorithm, and combining the multistage separation GDE algorithm proposed in this paper to identify the number of sound sources. The two algorithms analyze data together to achieve the purpose of complementarity and mutual verification and improve the accuracy of the system's calculation results. The LabVIEW visualization panel displays the location (elevation angle and azimuth angle) and the number of sound sources of the localized spatial sound source in real time, which is convenient for users to observe the experimental results intuitively.

This system has a high multisound source localization accuracy rate and certain portability. The system adopts the front end of the lower computer signal acquisition and the upper computer data analysis and processing, and the result displays terminal design. Since the number of channels of the C60 structure of the hemispherical conformal sound pressure sensor array designed in this paper is 20, according to the limitation of the algorithm, the theoretical upper limit of the number of sound source recognition in this system is 19, that is, the number of sound sources in the recognition and localization space is less than that of the array. The overall design structure of the system is shown in Figure 1.

3.3. Point Sound Source Localization Algorithm Design. High-resolution spectrum estimation techniques, such as regression models and minimum variance spectrum estimation, come from several of the latest high-resolution spectrum estimation techniques. The MUSIC algorithm first decomposes the data output by the covariance matrix in the array to find the signal subspace and the noise subspace related to the signal components. Finally, the orthogonality of the two spaces is used to estimate the angle of incidence, polarization information, signal strength, signal amplitude, phase, and other information.

The data covariance matrix can be decomposed into two parts: the signal covariance matrix and the noise covariance matrix. The data covariance matrix of the array is

$$R_X = AR_S A + \sigma^2 I. \tag{1}$$

Feature decomposition of R_X:

$$\mathbf{R}_X = \mathbf{U}\Lambda\mathbf{U} = \sum_{k=1}^{M} \lambda_k u_k \mathbf{u}_k^T. \tag{2}$$

By the relationship between eigenvalues and eigenvectors,

$$\mathbf{R}_X \mathbf{u}_k = \lambda_k \mathbf{u}_k (k = 1, 2, \ldots, M). \tag{3}$$

The signal direction vector is orthogonal to the noise subspace, namely,

$$\mathbf{A}^H \mathbf{U}_N = \mathbf{A}^H \mathbf{u}_j = \mathbf{a}_i^H \mathbf{U}_N = \mathbf{0}\,(j = L+1, L+2, \ldots, M; i = 1, 2, \ldots, L). \tag{4}$$

In practice, the data collected by the array is time-limited, so the data covariance matrix is replaced by limited sampling as

$$\mathbf{R}_X = \frac{1}{L} \sum_{l=1}^{L} \mathbf{X}\mathbf{X}^H. \tag{5}$$

The eigen decomposition of the data covariance matrix is composed of unique values, which can calculate the signal subspace, the noise subspace, and the diagonal matrix and use the smallest optimization to search for the direction of arrival of the position signal.

$$(\theta, \varphi)_{\text{MUSIC}} = \arg\left[\min\left(a^H(\theta, \varphi) U_N U_N^H a(\theta, \varphi)\right)\right]. \tag{6}$$

The MUSIC algorithm has a high resolution, high accuracy, and robustness under certain conditions. Based on the MUSIC algorithm, scholars continue to propose a series of improvements to the MUSIC and MUSIC algorithms, such as weighted MUSIC.

Based on the formation of a controllable beam, the basic principle of the method for mastering the sound source position is to filter the signal received from the sound pressure sensor, add weights to form a beam, search for possible sound source positions and execute the beam. The point that will cause the maximum output power of the beam is the location of the sound source. The algorithm can be divided into delayed storage beam algorithm and adaptive beam algorithm. The delayed storage beam algorithm is relatively simple and can restore the signal more accurately, but it can only be better when it is very sensitive to noise, and there are more elements in the array. The adaptive beam algorithm is more complex, the signal distortion is greater, and it can use fewer array elements to obtain better results.

The controllable beamforming technology based on the sound pressure sensor array has been widely used in the field of controlling the position of the sound source, but it is still difficult to obtain the position of the real-time sound source. The main reason is that this method requires a lot of calculations and requires a global search, making it difficult to perform real-time operations. The position of the sound source of the sound pressure sensor array is not too firm, and it is susceptible to interference from reverberation and environmental noise. Using a certain iterative method requires a small amount of calculation, but it is difficult to obtain an effective global peak value. And it is very sensitive to the initial value of the search. It is mainly used to further limit the scope of the algorithm and higher computational complexity and to locate long-range narrowband signals.

The signal model received by the kth element is shown in the formula:

$$x_k(t) = s(t - \tau_k) + n_k(t) (k = 1, 2, \cdots, M). \tag{7}$$

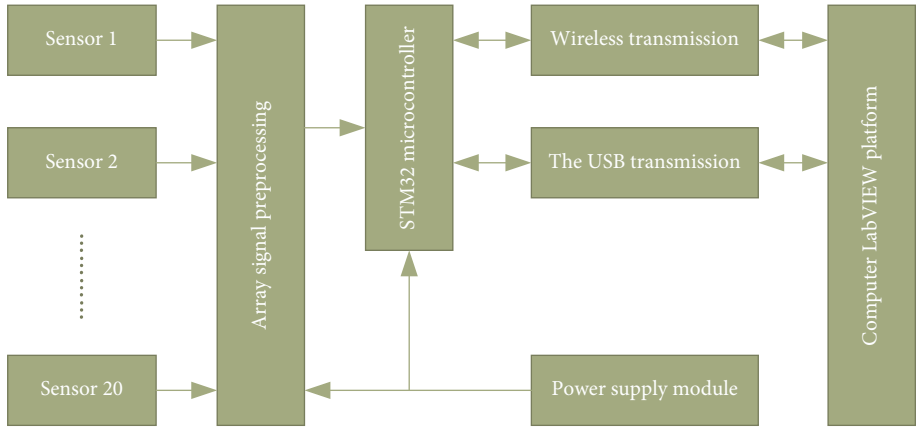

Figure 1: The overall framework of the point source positioning system.

We find the Fourier transform on both sides of formula (7) to get

$$X_k(\omega) = e^{-j\omega\tau_k(\theta,\varphi)}S(\omega) + N_k(\omega)(k = 1, 2, \cdots, M). \tag{8}$$

For an array system with M sound pressure sensors, the vector form of the formula can be expressed as

$$X(\omega_1) = A(\omega_l)S(\omega_l) + N(\omega_l). \tag{9}$$

Since the Gaussian stochastic process is extensive and stable, the conditional probability distribution is

$$p(X \mid (\theta, \varphi)) = \left(\frac{1}{\pi^M \det P}\right)\exp\left(-X^H P^{-1} X\right). \tag{10}$$

The input signal of the array is a cross-spectral density matrix.

$$P(\omega_l) = E\left[X(\omega_l)X^H(\omega_l)\right]. \tag{11}$$

Putting formula (10) into formula (11), we can get

$$P(\omega_l) = R_S(\omega_l)A(\omega_l)A^H(\omega_l) + R_N(\omega_l). \tag{12}$$

We calculate both sides of formula (12) to get

$$\ln\left(p(X \mid (\theta, \varphi))\right) = -\ln\left(\pi^M \det P\right) - X^H P^{-1} X. \tag{13}$$

Finding the maximum value of formula (13) is equivalent to finding the maximum value of formula (14).

$$P(\omega_l) = \left|H(\omega_l)\right|^2 \left|Z(\omega_l)\right|^2. \tag{14}$$

In fact, the power of all frequency bands should be added, but the sound source position estimation at this time can only be obtained by the following:

$$(\widehat{\theta}, \widehat{\varphi}) = \arg\max_{(\theta,\varphi)}\left\{\int \mathbf{P}(\omega)\mathrm{d}\omega\right\}. \tag{15}$$

The method of grasping the sound source position based on time delay estimation is to grasp the position in two stages. This method first estimates the time difference between the sound sources of different sound pressure sensors and then finds the position of the sound source through the geometric relationship caused by multiple time differences.

The sound source location algorithm based on time delay estimation requires less computational complexity, better real-time performance, and lower hardware requirements. However, this algorithm is not suitable for capturing the positions of multiple sound sources. In an environment with strong reverberation and noise, it is difficult to obtain an accurate delay time, and larger errors may occur in subsequent position capturing. However, the positioning algorithm based on time delay estimation is easy to apply to real-time systems. After proper improvement, certain noise and reverberation can also have relatively good positioning accuracy, which can be widely used in the system.

Assuming that the correlated noise is weak and the influence of reverberation is not considered, the data model of the signal received by the array can be expressed as the following equation:

$$x_k(n) = \alpha_k s(n - \tau_k) + v_k(n), \tag{16}$$

$$R_{x_k x_j}(\tau) = E\left[x_k(n)x_j(n - \tau)\right], \tag{17}$$

$$R_{x_k x_j}(\tau) = E\{\alpha_k s(n - \tau_k) + v_k(n)\left[\alpha_j s\left(n - \tau_j - \tau\right) + v_f(n - \tau)\right]. \tag{18}$$

Noise and sound sources are independent of each other. The middle binary of (17) is 0, and (18) can be simplified as follows:

$$R_{x_i x_j}(\tau) = \alpha_i \alpha_j R_{ss}\left(\tau - \tau_{ij}\right) + R_{v_i v_j}(\tau). \tag{19}$$

If the noise is uncorrelated or the signal-to-noise ratio is large enough, the following equation can be further simplified:

$$R_{x_i x_j}(\tau) = \alpha_i \alpha_j R_{ss}\left(\tau - \tau_{ij}\right). \tag{20}$$

However, in practical applications, due to the interference of some unfavorable factors, it is difficult to observe the maximum peak of the correlation function. There may be multiple correlations, especially when the noise and reverberation are quite high, which will cause the peak to cause a large estimation error, so it is difficult to find the actual peak.

For narrowband signals, under certain conditions, the number of larger eigenvalues in the covariance matrix corresponds to the number of spatial sources, while other smaller eigenvalues are the same. Therefore, in the calculation process, the number of spatial signal sources can be directly determined according to the eigenvalues of the data covariance matrix, but in actual experiments, the obtained data covariance matrix is unique, and the value is obvious. A sequence of eigenvalues with obvious numerical limits is obtained. The focus of scholars' research is how to determine the number of spatial sources to distinguish them from unknown unique values.

Wax and Kailath proposed the AIC method and MDL (minimum length description standard) to deal with the problems caused by the subjective threshold setting. These two methods circumvent the research; that is, setting a subjective threshold can more accurately estimate the number of spatial sources.

The number of spatial sources estimated by AIC and MDL standards is expressed as follows:

$$\begin{aligned} \mathrm{AIC}\ (k) &= -\ln\left[\frac{\prod_{i=k+1}^{M}\lambda_i^{1/M-k}}{(1/M-k)\sum_{i=k+1}^{M}\lambda_i}\right]^{(M-k)K} + k(2M-k), \\ \mathrm{MDL}\ (k) &= -\ln\left[\frac{\prod_{i=k+1}^{M}\lambda_i^{1/M-k}}{(1/M-k)\sum_{i=k+1}^{M}\lambda_i}\right]^{(M-k)R} + \frac{1}{2}k(2M-k)\ln K. \end{aligned} \tag{21}$$

When AIC (k) or MDL (k) takes the minimum value, the estimated number of spatial signal sources, P is the value of k.

$$\widehat{P} = \arg\left\{\min_k \ \mathrm{AIC}(k)\right\} = \arg\left\{\min_k \ \mathrm{MDL}(k)\right\}. \tag{22}$$

The estimated value of the AIC standard is inconsistent, which means that even for the AIC with a high signal-to-noise ratio, the estimated result of the AIC standard still has a higher probability of error. The standard also has a high probability of error, while the MDL standard is a consistent estimate. The standard with a high signal-to-noise ratio has better estimation performance. If the signal-to-noise ratio is small, the error probability is higher than the AIC standard. Therefore, the MDL criterion is better than the AIC criterion in terms of estimating the number of spatial sources.

The information theory standard method of estimating the number of signal sources is to use the eigenvalues of the data covariance matrix received from the array and signals based on the difference between the signal and the eigenvalues and the number of spatial sources. Eigenvalues of noise: the GDE-based source number estimation algorithm does not use the eigenvalues of the data covariance matrix to classify the signal and noise but uses the Geyswon radius of the data covariance matrix to estimate the number of sources. However, there is no obvious difference between the signal Gai source and the noise Gai source of the covariance matrix, and it cannot be directly used to effectively estimate the number of spatial sources.

Under the assumption that the eigenvalues of the data covariance matrix are unchanged, the data covariance matrix of the original array undergoes a transformation first, so the Geys corresponding to the signal and the noise can distinguish the number of signal sources.

Assuming that the array data covariance matrix is R, the actual received data matrix has a time limit, so the data covariance matrix can be replaced by limited sampling.

$$\mathbf{R} = \frac{1}{N}\sum_{i=1}^{N}\mathbf{X}\mathbf{X}^H. \tag{23}$$

First, the data covariance matrix is divided into blocks, namely,

$$\mathbf{R} = \begin{pmatrix} \mathbf{R}_0 & \mathbf{r} \\ \mathbf{r}^H & \mathbf{r}_{MM} \end{pmatrix}. \tag{24}$$

The corresponding eigenvector matrix U is separated by dividing the matrix R_0 by the matrix R and performing a transformation.

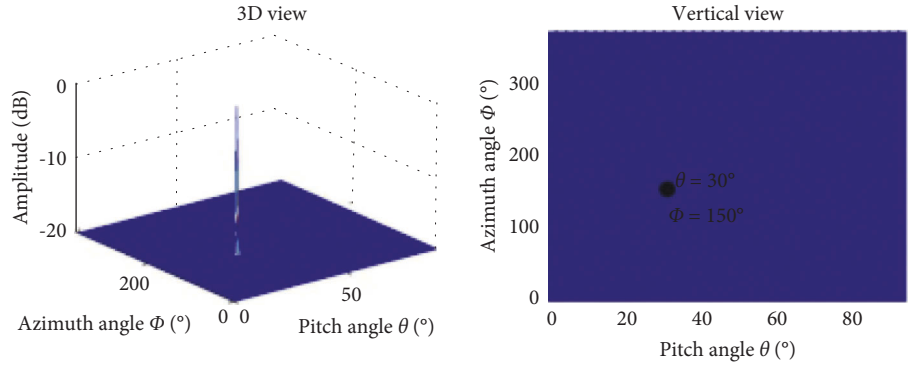

Figure 2: Sound field distribution of the single sound source.

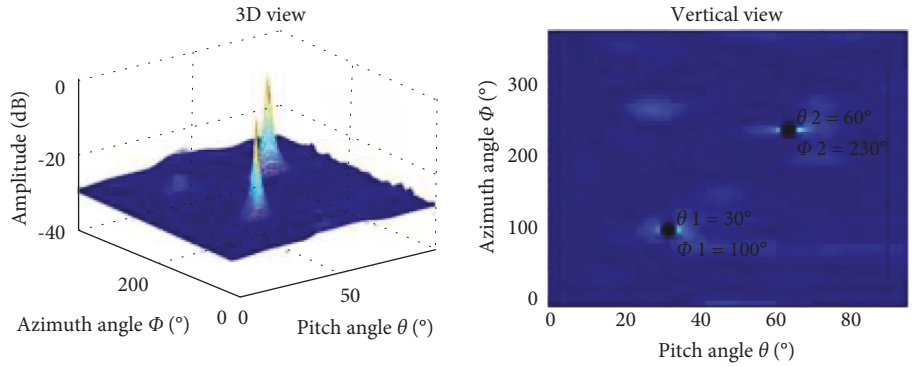

Figure 3: Composite sound field distribution of two sound sources.

$$\mathbf{S} = \mathbf{U}^H \mathbf{R}_0 \mathbf{U} = \mathrm{diag}\{\lambda_1, \lambda_2, \cdots, \lambda_{M-1}\}. \tag{25}$$

In the free sound field of space, the point sound source propagates outward in the form of a square wave. Among them, the sound wave propagation distance is inversely proportional to the sound pressure. If the transmission distance of the sound wave is much larger than the geometric size of the sound source itself, and the direction of the sound wave is not very directional, the square wave can be regarded as a plane wave, and the sound source can be regarded as a spatial point source. In terms of noise, if the distance between the geometric center of the sound source and the detection position is twice the geometric size of the sound source itself, the noise can be regarded as the noise of a point sound source.

$$L_p(r) = L_p(r_0) - 20\lg(r/r_0). \tag{26}$$

In actual sound source localization, there are often multiple sound sources. When the sound source is complicated, coherence, attenuation, and superposition will occur. The collected sound source information is not the original sound source signal information, and different conclusions can be drawn when the same multiple sound sources are studied individually and comprehensively. For example, when measuring two-point sound sources in space, there are two situations: one- or two-point sound sources are kept unchanged, such as the position and sound intensity, and the two-point sound sources are separately sounded and measured; two-point sound sources sound at the same time and then measure. They are all the same sound source, and there is a big difference in the distribution of the sound field when sounding separately and simultaneously. When measuring a single sound source, the sound field distribution of the single sound source is almost in the form of pulses, and there is no obvious attenuation amplitude around it, as shown in Figure 2.

However, when the measured sound source is a two-point sound source simultaneously, the distribution of two sound sources in the same measured sound field is obviously different, and an obvious amplitude attenuation trend appears around each sound source, as shown in Figure 3, which is caused by the superposition of two sound sources. When the number of sound sources continues to increase, the attenuation amplitude around the sound source will become smaller and smaller with the increase of the number of sound sources. Finally, the amplitude of each sound source is submerged, so it is impossible to distinguish each sound source point. Of course, this is also related to the structure of the detection array and the number of sensors. Therefore, it is particularly important to study the distribution of multipoint sound sources in the three-dimensional sound field. In the section of sound source identification and location, the distribution law of multipoint sound sources will be further analyzed.

We introduce the application of one-dimensional linear array, two-dimensional planar array, three-dimensional array, and virtual array in detail and expound the specific

Table 1: Single source localization result.

Positioning	1	2	3	4	5
(60°, 150°)	(61.7°, 151°)	(59.1°, 151.0°)	(61.0°, 148.5°)	(60.5°, 151°)	(58.9.2°, 150.9°)

Table 2: Two sound source localization results.

Positioning	1	2	3	4	5
(30°, 100°)	(32.3°, 101.4°)	(30.5°, 99.1°)	(31.0°, 100.9°)	(28.3°, 100°)	(31°, 103.0°)
(40°, 0°)	(39.7°, 0°)	(41.1°, 0.9°)	(40.2°, 1.5°)	(39.1°, 0.5°)	(40.3°, 2.1°)

Table 3: Three sound source localization results.

Positioning	1	2	3	4	5
(70°, 300°)	(73°, 302°)	(70.9°, 298°)	(71.0°, 302°)	(69°, 300.8°)	(72.7°, 301.9°)
(10°, 50°)	(9.2°, 52.3°)	(11.6°, 48.9°)	(8.9°, 50.7°)	(12.2°, 49.4°)	(13.1°, 50.5°)
(25°, 105°)	(26°, 103.5°)	(27.1°, 107.6°)	(23°, 105.7°)	(26°, 104.4°)	(23°, 107.1°)

Table 4: Subject's basic information sheet.

Number	Height (cm)	Body weight (kg)	Age (years)
1	1.65	55	25
2	1.68	50	26
3	1.63	54	25
4	1.61	48	25
5	1.70	53	24
6	1.60	452	25

operation process of various array direction vectors. In the array signal receiving data model, the wideband signal model is analyzed and compared with the narrowband signal model. We will study the classical source location and source number recognition algorithms in detail, compare the advantages and disadvantages of different algorithms, and briefly analyze the distribution of the three-dimensional composite sound field between spatial and multipoint sources, which provides a theoretical basis for the subsequent simulation experiments.

3.4. Experimental Results and Error Analysis. When the sound is in the air, the error between the actual sound source information and the sound source information is received by the array; when the sound factor propagates in the air, its intensity, amplitude, and phase will change randomly. The main factors causing these changes are the attenuation of air resistance to sound, the reflection, reverberation of sound, and the interference of environmental noise caused by rigidly confined space.

In the sound source location system, there are corresponding requirements for the selection of sound pressure sensors, which need to be selected according to different situations. After selecting sensors, because of the sensitivity difference between sensors, each sensor needs to be calibrated. The best way is to calibrate the array, which can reduce the secondary error caused by disassembly.

The measurement error of the sound source positioning system can be reduced or even eliminated by simulation calibration and physical calibration. In this paper, we mainly discuss the influence of the time delay error among the elements of the array on positioning accuracy. The error formula of sound source position estimation is as follows:

$$\sigma_{(\theta,\varphi)} = \frac{\sqrt{2}c}{2d\sin\theta\cos\varphi}\sigma_{\tau}. \tag{27}$$

We test in the laboratory, sound velocity $c = 344$ m/s. The indoor noise is very small, but due to a large number of instruments and equipment in the laboratory and the complicated space environment, there is a certain degree of reverberation problems. In this experiment, the spatial single sound source, two sound sources, and three sound sources were located, respectively. The results of the single sound source localization experiment are shown in Table 1.

The experimental results of two sound source localization are shown in Table 2.

The experimental results of three sound source localization are shown in Table 3.

Table 5: Test sample size table.

Pant-like part	Waist line valley	Hipline	Pant length	Width of trousers
Size (cm)	65	840	90	123

4. Athlete Dynamic Injury Monitoring and Result Analysis

4.1. Athlete Dynamic Injury Monitoring Method. The research objects of this thesis selected 6 young women with an average age of 24 ± 2 years old, with similar physical fitness, body shape, and leg shape. Before the experiment, let the subjects understand the design of the experimental plan, be familiar with the test methods and procedures, and clarify the test indicators and tasks to be completed (Table 4.

One of them has a flexible sensor in the knee joint, which is easy to remove during cleaning. Table 5 shows the specific size.

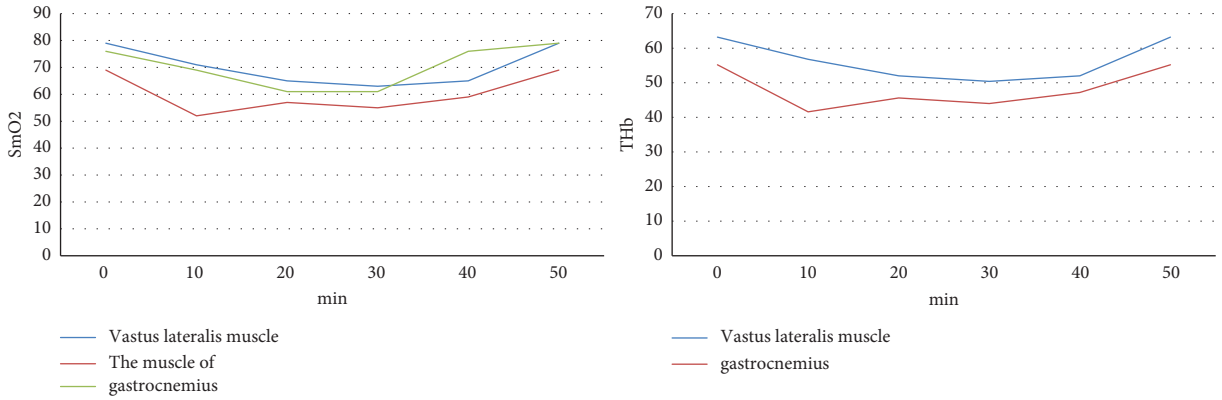

Figure 4: Map of muscle oxygen test results.

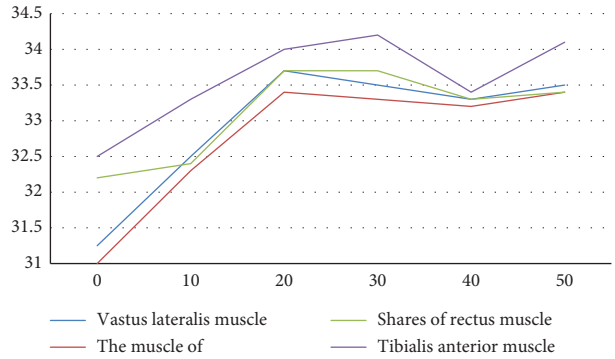

Figure 5: Figure of mean body surface temperature.

4.2. Objective Experiment Results and Analysis. The SHT10 temperature and humidity sensor are mainly used to measure the temperature and humidity environment between the innermost clothing and the human skin. The measured data is closest to the surface temperature of the human body, which is very useful for determining the heat and humidity comfort of the human body. According to the difference in the heat of vaporization of various parts of the human body, the human body can be divided into four parts, namely the strong sweat part, the medium sweat part, the weak sweat part, and the minimum sweat part. Based on this research, four regions were selected for research.

During the real-time monitoring experiment, the specific muscle total hemoglobin (THb) of 6 subjects was monitored with muscle oxygen saturation (SmO_2), and the oxygen saturation (SmO_2) of these muscles was monitored in real time, mainly total hemoglobin (THb) changes with muscle oxygen saturation (SmO_2). The proportion of hemoglobin oxygen concentration in a part of muscle tissue can reflect the oxygen concentration of muscle, and the change can reflect the balance of oxygen supply. Changes in muscle oxygen can be used to increase training intensity, a measure to reduce fatigue and improve training effects. Finally, the data was calculated and sorted, and the final result was obtained, as shown in Figure 4.

It can be seen from Figure 5 that during the whole exercise, the muscle surface temperature of the four parts changes smoothly, and the temperature value is better for warmth retention and comfort without sudden overheating or supercooling. In the early running process, with the gradual increase of exercise load, the body's metabolic activities begin to increase, the heart rate gradually increases, the heat production increases, the capillary dilation, and the temperature rises. After a period of time, due to the increase of sweat and humidity, when the humidity increases rapidly, the evaporation of sweat, the absorption of fabric, and sweat are deprived of part of the pipeline, and the temperature value begins to decline. The heart rate at the end of the run will not recover slowly, but it will produce continuous heat, and the body surface temperature has a tendency to increase. Figure 5 shows that the temperature of sweating in the second half of exercise is significantly lower, and a lot of heat is released into the air.

4.3. Subjective Evaluation Test. The subjective indexes of this experiment are the sense of bondage, sense of heat, sense of sticky body, sense of moisture, sense of softness, sense of pressure, the convenience of movement, and comprehensive comfort of wearing.

In this experiment, the 5-scale method was used. On the scale, the numbers −2 to 2 were used to indicate −2 to indicate poor subjective feeling, −1 to indicate poor subjective feeling, 0 to indicate general subjective feeling, 1 to indicate good subjective feeling, and 2 to indicate good subjective feeling, as shown in Figure 6.

As can be seen from Figure 7, the comprehensive wearing comfort of the sample pants is good. At first, when standing still, the score was the highest; due to the stretch of the fabric caused by the action, the sense of restraint and pressure decreased, and the comfort was more obvious in the acceleration process of the third stage; Because of the sweat discharge during running, the comfort of stuffy heat, moist feeling, and sticky body feeling will decrease, especially in the third stage of incremental load running, and in the fourth stage, with the continuous running time, the comfort will decrease.

Through the complete sample pants evaluation system test, it is found that in the process of the pressure test experiment, the pressure value of the knee joint of the subjects is measured by the airbag pressure sensor

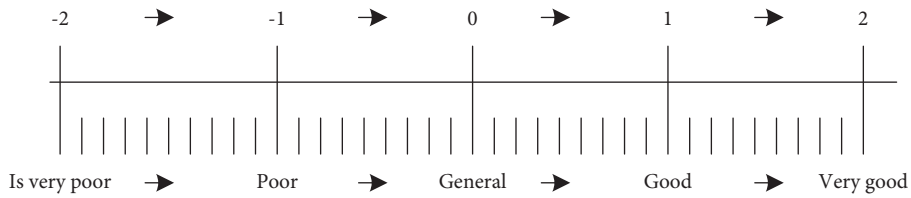

Figure 6: Psychological scale of quintuple.

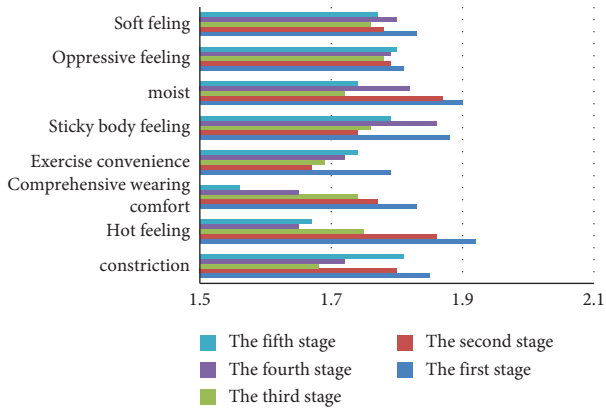

Figure 7: Subjective evaluation result chart.

simultaneously. After testing, the oxygen content and total hemoglobin concentration will decrease with the increase in running speed but after a certain degree, they will not continue to decline, but gradually rise and will return to a relatively stable state. Muscle oxygen saturation and total hemoglobin concentration after exercise were higher than those before exercise. It can be seen from the body surface temperature test that the thermal comfort is good, and there is no sudden overheating or supercooling phenomenon. In the subjective test of wearing comfort, the psychological scale of five equal points is used. Through taking the average score of six subjects to get the results of each index, it is found that the comprehensive wearing comfort of sample pants is good.

4.4. Analysis of Changes of Main Physiological and Biochemical Indexes of Athletes. Before training, the hemoglobin content of athletes is in the normal range (120–160 g/L). With the beginning of training, the hemoglobin content of athletes decreases significantly. This phenomenon is that the decrease of hemoglobin stimulates the athletes' training and body. In this training stage, combined with the training plan, the athletes gradually adapt to the training stimulation, mainly in aerobic training, the content of red egg shows a normal upward trend. As winter training continues, the intensity of the training program increases gradually, which indicates that the hemoglobin content monitored in the later stage of training continues to increase, which indicates that the athletes are well adapted to the training.

Research shows that the activity of creatine kinase increases after exercise. The general rule is that with the increase in exercise intensity, the level of creatine kinase in the human body will also increase, and the exercise ability will also increase. The increase of CK level is more frequent in athletes with higher training levels. If the athletes cannot recover, they will have a sports injury.

In the process of monitoring, the characteristics of the concentration changes of each element in athletes' blood were statistically analyzed. The content first decreased and then increased, then adjusted, and then decreased to a more stable state, indicating that the adaptability of athletes has been improved. In the pretraining period, there is no significant difference in the test results, but in the intermediate training period compared with the pretraining period, there is no significant difference. In order to make a more intuitive and detailed analysis of the changes in athletes, we made a detailed analysis of the changes in athletes' blood components.

5. Conclusion

With the emergence of Internet Web 2.0 sites, in terms of high concurrency and large-scale data processing, existing relational databases have become more and more difficult to handle. NoSQL databases are designed to focus on distribution and high-level aspects and are favored by researchers. First, we will study the theoretical basis of NoSQL databases, including the two aspects of CAP and BASE theory. Essentially, data storage revolves around three main areas: consistency, availability, and partition tolerance. Because these three cannot be used at the same time and cannot satisfy both aspects, the traditional relational database is not a distributed application. NoSQL can easily handle large amounts of data, which makes up for the lack of scalability of relational databases. These relational databases focus on the final result but also focus on partitioning and availability. But for business scenarios that emphasize the strong consistency of relational storage, relational databases are much better. This topic mainly focuses on the research of knee joints and mainly introduces the fragility of knee joints and the changes in appearance and extension when not running. Based on the two backgrounds of wearable technology and changes in health monitoring methods, combined with the special application environment in which it is located, the technical path and system structure of the research on monitoring knee joint pressure intelligent movement are deduced.

Data Availability

The data used to support the findings of this study are available from the corresponding author upon request.

Conflicts of Interest

The authors declare that they do not have any possible conflicts of interest.

References

[1] S. Divya and N. Shivaprasad, "Bigdata: a survey on rdbms and various nosql databases on storing medical images," *International Journal for Advance Research and Development*, vol. 2, no. 5, 2017.

[2] A. V. Savchenko, "Adaptive video image recognition system using a committee machine," *Optical Memory & Neural Networks*, vol. 21, no. 4, pp. 219–226, 2012.

[3] I. Kotenko, A. Krasov, I. Ushakov, and K. Izrailov, "An approach for stego-insider detection based on a hybrid NoSQL database," *Journal of Sensor and Actuator Networks*, vol. 10, no. 2, p. 25, 2021.

[4] V. Abramova, J. Bernardino, and P. Furtado, "Which nosql database? a performance overview," *Open Journal of Databases (OJDB)*, vol. 1, no. 2, pp. 17–24, 2014.

[5] S. Fadıl and B. Urazel, "A security constrained environmental/economic power dispatch technique using F-MSG algorithm for a power system area including limited energy supply thermal units," *International Journal of Electrical Power & Energy Systems*, vol. 56, pp. 185–197, 2014.

[6] Q. Liu, A. Pruteanu, and S. Dulman, "GDE: a distributed gradient-based algorithm for distance estimation in large-scale networks," in *Proceedings of the 14th ACM International Conference on Modeling, Analysis and Simulation of Wireless and mobile Systems*, pp. 151–158, Miami Beach, FL, USA, 2011.

[7] M. Abdolmaleky, M. Naseri, J. Batle, A. Farouk, and L. H. Gong, "Red-Green-Blue multi-channel quantum representation of digital images," *Optik*, vol. 128, pp. 121–132, 2017.

[8] W. A. Yost and X. Zhong, "Sound source localization identification accuracy: bandwidth dependencies," *Journal of the Acoustical Society of America*, vol. 136, no. 5, pp. 2737–2746, 2014.

[9] J. Keenahan, E. J. Obrien, P. J. McGetrick, and A. Gonzalez, "The use of a dynamic truck-trailer drive-by system to monitor bridge damping," *Structural Health Monitoring*, vol. 13, no. 2, pp. 143–157, 2014.

[10] N. Višnjevac, R. Mihajlović, M. Šoškić, Ž. Cvijetinović, and B. Bajat, "Prototype of the 3D cadastral system based on a NoSQL database and a Javascript visualization application," *ISPRS International Journal of Geo-Information*, vol. 8, no. 5, p. 227, 2019.

[11] S. K. Dwivedi and V. Singh, "Research and reviews in question answering system," *Procedia Technology*, vol. 10, pp. 417–424, 2013.

[12] B. L. Cairns, R. D. Nielsen, J. J. Masanz et al., "The MiPACQ clinical question answering system," in *AMIA annual symposium proceedings*vol. 171, 2011.

[13] S. Kumar, T. Kolekar, S. Patil et al., "A low-cost multi-sensor data acquisition system for fault detection in fused deposition modelling," *Sensors*, vol. 22, no. 2, p. 517, 2022.

[14] S. Swamy and R. K.V, "An efficient speech recognition system," *Computer Science and Engineering: International Journal*, vol. 3, no. 4, pp. 21–27, 2013.

[15] K. Choudhary, U. Pandey, M. K. Nayak, and D. K. Mishra, "Electronic data interchange: a review," in *2011 Proceedings of the Third International Conference on Computational Intelligence, Communication Systems and Networks*, pp. 323–327, Bali, Indonesia, 2011.

[16] S. Wang, I. Pandis, C. Wu et al., "High dimensional biological data retrieval optimization with NoSQL technology," *BMC Genomics*, vol. 15, no. S8, pp. S3–S8, 2014.

[17] V. Abramova, J. Bernardino, and P. Furtado, "Experimental evaluation of NoSQL databases," *International Journal of Database Management Systems*, vol. 6, no. 3, pp. 01–16, 2014.

[18] Q. Liu and H. Yuan, "A high performance memory key-value database based on Redis," *Journal of Computers*, vol. 14, no. 3, pp. 170–183, 2019.

Hindawi
Mobile Information Systems
Volume 2022, Article ID 6176675, 10 pages
https://doi.org/10.1155/2022/6176675

Research Article

Internet Plus Innovation and Entrepreneurship Education Model Based on Machine Learning Algorithms

Xiaoxia Chen

Yiwu Industrial & Commercial College, Yiwu 322000, Zhejiang, China

Correspondence should be addressed to Xiaoxia Chen; chenxx321@ywicc.edu.cn

Received 9 August 2022; Revised 17 September 2022; Accepted 27 September 2022; Published 11 October 2022

Academic Editor: Shadi Aljawarneh

Innovation and entrepreneurship is a spiritual attitude. With the dissemination and wide application of the concept and technology of "Internet Plus," Internet Plus innovative thinking has had a strong impact on innovation and entrepreneurship education, such as teaching concepts, changes in teaching methods, optimization of teaching staff and curriculum systems, and resource sharing. Therefore, according to the actual needs of innovation and entrepreneurship teaching in colleges and universities, this paper combines the concept of Internet and college education with the help of machine learning algorithms to build a new education system. First, the article designs the overall platform architecture and core business processes and develops and implements front-end and various platform functions. The system includes different modules such as preschool skill diagnosis, online learning, stage testing and evaluation, information and resource sharing, team building and project implementation management, and so on. Then, the experiment shows that the precision rate, recall rate, and F1 value of the system are all high, indicating that the system is stable and efficient. Finally, it briefly expounds the development strategies of the Internet Plus education model under the influence of relevant systems, which will help students and teachers develop innovation and entrepreneurship theories and improve students' knowledge quality. The combination of Internet technology and innovation and entrepreneurship teaching can make innovation education more in line with the current learning needs and promote the improvement of entrepreneurship ability.

1. Introduction

Due to the vigorous promotion of national policies, colleges and universities are gradually promoting the "Internet +" Innovation and Entrepreneurship Competition launched by the Ministry of Education in 2015 through reform demonstrations, competition incubation, and industry-university-research cooperation [1, 2]. In 2018, the country launched a series of activities such as "College Student Maker Show," "Red Youth Dreaming Journey," and "Maritime Silk Road." Through innovation and entrepreneurship, education and rural revitalization strategies, and the concerted efforts of the government, enterprises, and schools, the influence and motivation of the reform have been greatly enhanced, and the relevant innovation and entrepreneurship teaching models and supporting teaching platforms have been gradually improved [3, 4]. At present, the globalized economy has become an unchangeable reality, and the Internet has become inseparable from people's lives. The scale of mobile Internet users reached 8.47%. The innovation and development of integrating "Internet +" 2.0 has entered the life of people in society. In every respect, it is imperative. In the context of the development of education informatization 2.0, guided by the "Internet +" strategy, China has re-deconstructed education, established smart teaching activities, balanced resource allocation, and designed various organizational forms to achieve a new ecosystem and talent training [5, 6]. The goal of smart campus construction in the context of the new form has greatly changed the contemporary education model, fundamentally changed the object, environment, model, and resources of higher education, and brought new opportunities and platforms [7]. Therefore, by introducing machine learning algorithms, this paper builds an

Internet + innovation and entrepreneurship education system and strives to produce good practical results for college students to form innovative spirit, cultivate entrepreneurial awareness, pioneer and cultivate innovative and entrepreneurial spirit, and collaborate to enhance the value of independent learning. Also, to a certain extent, it improves the theory and practice of college students' innovation and entrepreneurship education. Entrepreneurship is realized with specific guidance and charter arrangements to guide students to go further on the road of innovation and entrepreneurship. It also provides a specific reference for the learning, course organization, and operation of other platforms of the same type, thereby promoting the development of educational model informatization results and providing a certain information basis for other project designs in related fields.

2. Related Work

Through the visits and investigations of the functional departments of teaching management, the literature studies the curriculum evaluation model. It covers the dimension of the teaching team, obtains sufficient teaching content and teaching resources, and establishes a curriculum evaluation index system for teachers' behavior, teaching level, and other dimensions [8]. A system for observing the results of research activities and subsequently determining the data structure for multi-dimensional assessments, including students, teachers, peer experts, and instructional supervisors is developed. The literature designs a prototype teaching management system running under Windows 10 environment [9]. In terms of data collection and management, the data warehouse model is designed using SQL Server 2012 tools; the data sources are determined to include undergraduate course platform, teaching operation management, questionnaire survey platform, and so on [10]. The literature adopts MVC model design, AJAX, ASP, NET, and other technologies, and adopts BP neural network and fuzzy comprehensive evaluation methods to build a comprehensive evaluation analysis model of comprehensive evaluation factor set and multifactor and related factor index set. And based on this data background, they designed and improved student education [11, 12]. Through the analysis of the management evaluation system and evaluation results, it can be seen that colleges and universities pay more attention to intelligence education, less attention to moral education, more attention to performance, less attention to ability, more attention to the number of posts, and less attention to personality development [13]. From the analysis of student management, it can be seen that many college students have lack of values, which is inconsistent with the talent demand structure needed by the current society [14]. The literature puts forward coping strategies based on multi-factor analysis, including changing educational concepts, deepening education reform, changing student education management methods, strengthening college self-education evaluation, and further improving college student management assessment system for student work [15]. The literature designs architectures that separate computing and storage to help businesses properly rent the appropriate computing resources. By combining containerization technology with Docker and Kubernetes, it helps to dynamically scale services and reduce operational costs [16].

3. Internet + Innovation and Entrepreneurship Education System Design

3.1. System Architecture. In this paper, the system adopts a three-layer structure: data access layer, business logic layer, and presentation layer, as shown in Figure 1.

Presentation Layer. The user interface has a strong self-adaptive expansion function, and multi-terminal access input such as portal website, mobile phone application, WeChat application, and WeChat public account is designed.

Business Logic Layer. It is the core of the platform, providing functions such as user registration and authority management, information release and push, online learning, online submission and coaching of new projects and businesses, teamwork requirements and release management, project incubation and release, and so on. It also includes learning behaviors analysis, intelligent group analysis, skill learning direction assessment, and so on.

Data Access Layer. Database design mainly includes user database, course learning resource database, text information database, project management database, skill model database, and so on, which are used to judge the appropriate courses based on students' learning ability.

3.2. System Function Analysis. In order to sort out the system requirements more accurately, this paper uses the questionnaire survey, including Internet + information module; Internet + teaching module; Internet + sharing module; Internet + team module; Internet + project module; Internet + incubation module. The specific business function modules are as follows:

3.2.1. Front-End Design. Page design: front-end website; mobile phone page design; information resources: relevant information policy announcements and resource sharing; online courses: introduction to innovation and entrepreneurship theory courses, Internet technology courses and practice courses; sharing: display of past case results and excellent experience, creative library, and resource library; Q&A: The interactive community part of the platform can answer questions and communicate with each other.

3.2.2. Student User Management. Personal center: basic personal information management; preschool skills diagnosis: online assessment of preschool skills, preliminary personal learning plan; course progress: course status record, course question and answer; team management: release, review, and supervise individual work in the team; project

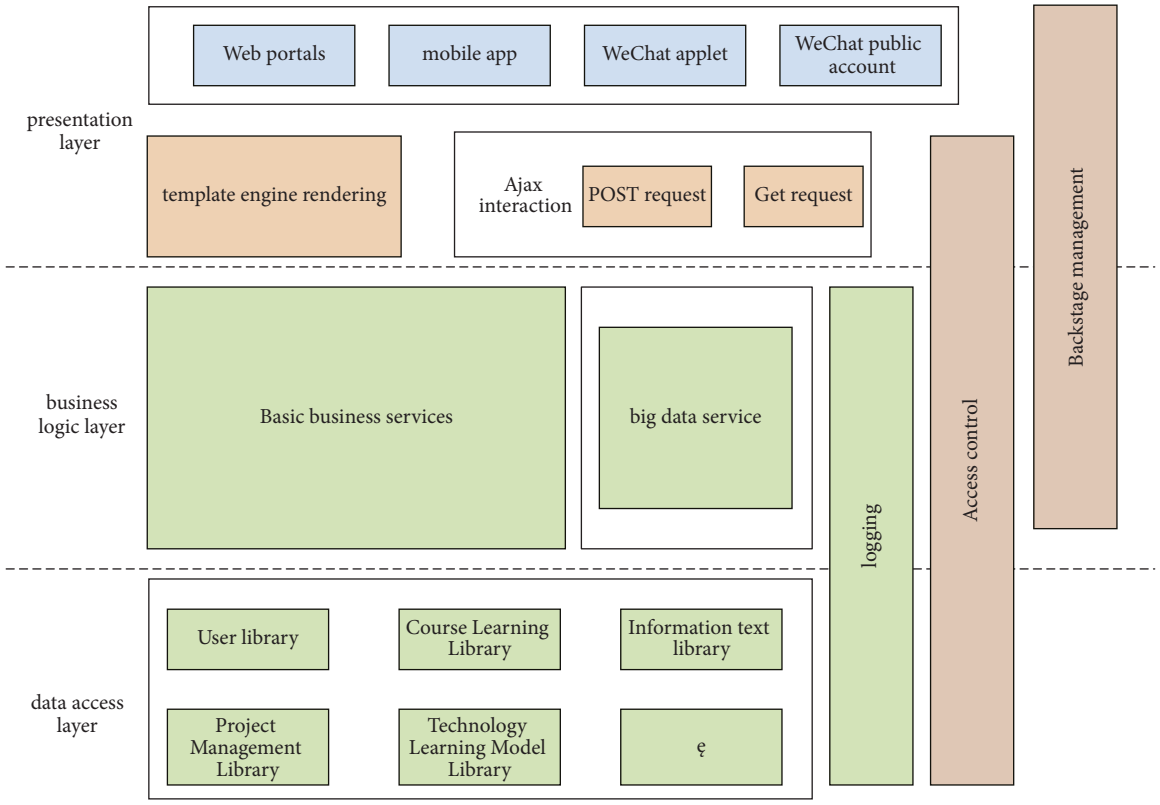

Figure 1: Internet + innovation and entrepreneurship education system architecture.

management: personal release, publicity, question, and answer, etc. of project work; online examination: comprehensive evaluation of innovation and entrepreneurship education.

3.2.3. Comprehensive Management Mode. Permission management: user role permission, password, and other management permissions; information management: information release, modification, deletion, etc., and upload files; course management: release and manage courses; team management: view and edit team information; project management: view and edit project information; examination management: entrance examination paper and score statistics management; learning ability management: build a learning ability evaluation model and manage the ability evaluation test questionnaire.

3.3. System Environment Configuration. This section establishes the system test environment from the software and hardware configuration of the system, as shown in Table 1. The hardware configuration includes the real-time concurrent calculation of the algorithm model, so the GPU server is selected. The server where the system is located has been installed, and it is located on the server with 6-core CPU, which is used to build the hardware environment; the development environment is divided into algorithm environment and system development environment; in terms of software settings, this paper applies basic tool software.

4. Design of Functional Modules Based on Machine Learning Algorithms

4.1. Innovation and Entrepreneurship Education Achievement Prediction Module Based on SVM Algorithm. The SVM algorithm first forms a hyperplane according to a specific function in a two-dimensional space. A hyperplane separates the two data types to the greatest extent possible. For multi-classification problems, the SVM algorithm must map it to a high-dimensional data space, forming a hyperplane to divide the data.

Suppose a training set $D = \{(x_1,y_1), (x_2,y_2), \ldots, (x_n,y_n)\}$ is given in the feature space where $x_i \in R_n, y_i \in \{+1,-1\}, i = 1,2, \ldots, n$, y_i is the class sign of x_i, and (x_i,y_i) is called the sample point. The sample data can be classified into the hyperplane shown in equation (1), and the standard shape constraints are shown in equation (2).

$$wx + b = 0, \tag{1}$$

$$y_i(wx + b) \geq 1, i = 1, 2, \ldots, l. \tag{2}$$

Among them, b is the classification threshold, which can be represented by any support vector. The distance from the data sample point x to the hyperplane is calculated as shown in the following formula:

$$d = \frac{|wx + b|}{\| w \|}. \tag{3}$$

Table 1: System environment configuration.

Classification	Name	System configuration
Hardware	CPU	Intel i5-12490f
	GPU	Nvidia GTX 3080 Ti
Development environment	CPU server operating system	Ubuntu 20.04
	GPU server operating system	Ubuntu 20.04
Development tool software	Algorithm IDEA	PyCharm
	System IDEA	IntelliJ IDEA
	TensorFlow	1.12.0
	OpenCV	3.5
	Python	3.10
	Java	1.7

This distance is the classification distance. If the classification interval is required to reach the maximum value, the maximum classification interval is equivalent to reaching the minimum value of $1/2||w||^{2}$. Support vector machines can be solved by quadratic programming problems, namely, (4) and (5).

$$\min \frac{1}{2}\|w\|^{2} + C\sum_{i=1}^{l}\xi_i, \tag{4}$$

$$\text{st.}\, y_i\left(x_i w + b\right) \geq 1 - \xi_i, \tag{5}$$

where ξ_i is greater than 0 and C is the penalty factor. Adding α to the conditional constraints contained in the objective function results in the Lagrangian norm.

$$L(w, b, \alpha) = \frac{1}{2}\|w\|^{2} - \sum_{i}^{l}\alpha_i\left[y_i\left(wx_i + b\right) - 1\right], \tag{6}$$

where αi is the Lagrangian factor, and formula (7) can be obtained from formula (6).

$$\frac{\partial L}{\partial b} = 0 \longrightarrow \sum_{i=0}^{l}\alpha_i y_i = 0. \tag{7}$$

Similarly, formula (8) can be obtained from formula (6).

$$\frac{\partial L}{\partial w} = 0 \longrightarrow \sum_{i=0}^{l}\alpha_i x_i y_i = 0. \tag{8}$$

The dual optimization problem obtained from equations (5)–(7) is shown in the following equation:

$$Q(\alpha) = \sum_{i=0}^{l}\alpha_i - \frac{1}{2}\sum_{i,j=1}^{l}\alpha_i\alpha_j x_i y_j\left(x_i x_j\right). \tag{9}$$

Solving (8), α_i can be obtained, and then the optimal classification function can be obtained.

$$f(x) = \operatorname{sgn}(wx + b) = \operatorname{sgn}\left[\sum_{i=0}^{l}\alpha_i y_i\left(x_i x\right) + b\right]. \tag{10}$$

4.2. Teaching Evaluation Module of Innovation and Entrepreneurship Education Based on BP Neural Network. The BP neural network first obtains the network error by feeding forward the input signal, then feeds the network error back to each layer, and finally updates the network according to the error. The structure diagram of the three-layer network is shown in Figure 2.

The propagation algorithm of BP neural network is as follows:

$$h_j = f_1\left(\sum_{i=1}^{n} w_{ij}x_i - \theta_j\right). \tag{11}$$

Similarly, the output value y_k of the neurons in the output layer can be obtained.

$$y_k = f_2\left(\sum_{i=1}^{m} w_{jk}h_j - \varphi_k\right). \tag{12}$$

The loss function is shown in the following equation:

$$E = \frac{1}{2}\sum_{i=1}^{m}\left(y_k - o_k\right)^{2}. \tag{13}$$

In the forward expansion process of the BP algorithm, the input information is sent to the hidden layer after passing through the input layer and finally reaches the output end after being processed by the next network layer to obtain the error result network, which is fed back to the neurons of each layer. The BP neural network will modify the connection weights and thresholds of neurons through equations (14)–(16).

$$w_{jk} = w_{jk} + \Delta w_{jk}, \tag{14}$$

$$\varphi_k = \varphi_k + \Delta\varphi_k, \tag{15}$$

$$\Delta w_{jk} = -\eta\frac{\partial E}{\partial w_{jk}} = -\eta\frac{\partial E}{\partial y_k}\cdot\frac{\partial y_k}{\partial y_{jk}} = -\eta\left(o_k - y_k\right)y_k\left(1 - y_k\right)h_j. \tag{16}$$

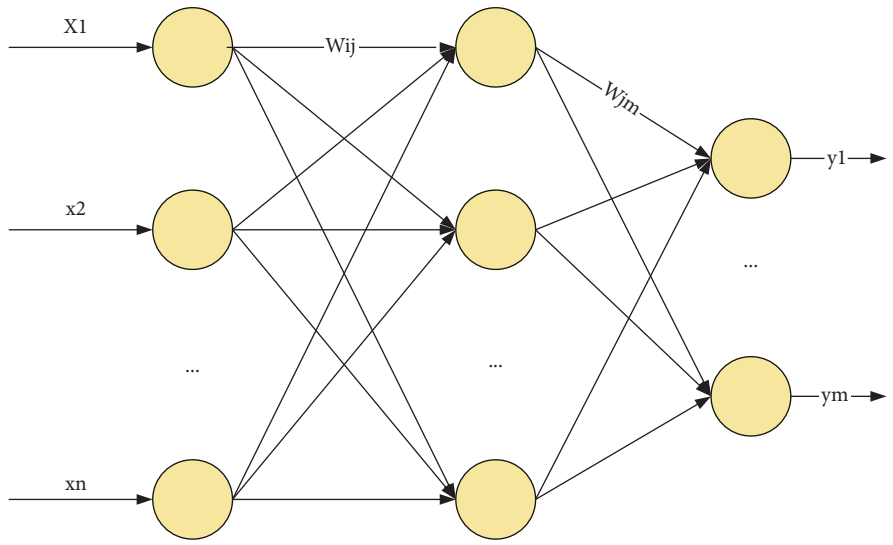

Figure 2: Structure diagram of three-layer BP neural network.

Define d_k as the correction error of the output layer.

$$d_k = (o_k - y_k) y_k (1 - y_k). \tag{17}$$

The correction error *ej* of the hidden layer is expressed as

$$e_j = \left(\sum_{k=1}^{m} w_{jk} \cdot d_k \right) h_j (1 - h_j). \tag{18}$$

Then, the following relationships can be derived:

$$\Delta w_{ij} = \eta \cdot e_j \cdot x_i, \tag{19}$$

$$\Delta \theta_j = \eta \cdot e_j, \tag{20}$$

$$\Delta w_{jk} = \eta \cdot d_k \cdot h_j, \tag{21}$$

$$\Delta \varphi_k = \eta \cdot d_k, \tag{22}$$

where η is the learning coefficient $(0 < \eta < 1)$.

When the set of comments V and the set of indices U are determined, we can create a fuzzy mapping from U to $F(V)$:

$$f: U \longrightarrow F(V), \forall u_i \in U,$$
$$u_i \longrightarrow f(u_i) = \frac{r_{i1}}{v_1} + \frac{r_{i2}}{v_2} + \ldots + \frac{r_{im}}{v_{m0 \le r \le 1, 1 \le i \le n, 1 \le j \le m}}. \tag{23}$$

A fuzzy matrix R can be obtained from f, which is called a single-factor evaluation matrix or a single-factor membership degree matrix. So, (U, V, R) constitute a comprehensive evaluation model.

If the target is a first-level model, then the membership matrix is expressed as

$$R = \begin{bmatrix} r_{11} & r_{12} & \cdots & r_{1m} \\ r_{21} & r_{22} & \cdots & r_{2m} \\ \cdots & \cdots & \cdots & \cdots \\ r_{n1} & r_{n2} & \cdots & r_{nm} \end{bmatrix}. \tag{24}$$

Among them, $rij (i = 1, 2, \ldots, n, j = 1, 2, \ldots, m)$ represents the membership degree of the i-th evaluation index *ui* of the j-th related evaluation object.

If it is a multi-level model, the membership matrix of the k-th sub-factor contained in the main factor is expressed as

$$R = \begin{bmatrix} r_{11} & r_{12} & \cdots & r_{1m} \\ r_{21} & r_{22} & \cdots & r_{2m} \\ \cdots & \cdots & \cdots & \cdots \\ r_{n1} & r_{n2} & \cdots & r_{nm} \end{bmatrix}. \tag{25}$$

Among them, $rij (i = 1, 2, \ldots, n, j = 1, 2, \ldots, m)$ represents the membership degree of the k-th sub-factor of the i-th evaluation index *uki* related to the j-th level comment.

According to different evaluation models, different formulas are used to calculate the score matrix. The formula for calculating the result matrix for the first-level model is

$$B = \mathrm{AOR} = (b_1, b_2, \ldots, b_m). \tag{26}$$

Among them, A is the weight set, R is the single-factor evaluation matrix, $B = (b1, b2, \ldots, bm)$ is the result matrix, and the number of elements in B is the same as that in the review set.

If using a multi-level model, first compute the evaluation outcome matrix for each sub-factor:

$$B_k = A_k o R_k = (b_{k1}, b_{k2}, \ldots, b_{km}). \quad (27)$$

Among them, AK is the set of k-th sub-factor weights, Rk is the k-th sub-factor single-factor evaluation matrix, and $Bk = (bk1, bk2, \ldots, bkm)$ is the k-th result matrix sub-factor. Next, calculate the result of the principal factor rating matrix using the following formula:

$$B = \mathrm{AOR} = (b_1, b_2, \ldots, b_m). \quad (28)$$

Calculate the result matrix of the main factor, where A is the weight set of the main factor, b isthe normalized result matrix of the$i$-th sub-factor, and m is the number of elements in the review set.

$$R = \begin{bmatrix} b_{11} & b_{12} & \ldots & b_{1m} \\ b_{21} & b_{22} & \cdots & b_{2m} \\ \ldots & \cdots & \cdots & \ldots \\ b_{n1} & b_{n2} & \ldots & b_{nm} \end{bmatrix}, (b_{i1}, b_{i2}, \cdots, b_{im})(i = 1, 2, \cdots, n). \quad (29)$$

After obtaining the result matrix, normalize the result matrix using the following method:

$$b_i' = \frac{b_i}{\sum_{j=1}^{n} b_j}, \quad (30)$$

where bi represents element i of the resulting matrix and $b1$' is the corresponding normalized value.

In the system development process, the system framework design and detailed design are completed using the popular Visual Studio 2020 and SQL Server 2020 and other system and database development tools. Finally, the system can realize information management, education management evaluation, and so on. The main functional modules of the system are shown in Figure 3.

5. Internet + Innovation and Entrepreneurship Education System Test

5.1. System Performance Analysis. Assuming that the content of the compressed data records is repeated but the data IDs are different, this paper compares the MySQL database based on the compression algorithm storage engine with the MySQL database based on the original algorithm storage engine. After the test, the uncompressed MySQL database occupies 1500 GB, the MySQL database based on the original compression algorithm occupies more than 900 GB, and the database based on the algorithm engine occupies about 400 GB of data, which saves more than 70% storage space compared to the original data. Figure 4 shows the compression trends in capacity usage.

As shown in Table 2, the data inserted into the RocksDB engine and the QPS in the general environment and the system environment of this article are compared and analyzed. Through comparative analysis, it can be seen that the performance of the system designed around this paper is better than QPS in the overall pattern, and the performance system bottleneck of distributed storage can be seen.

5.2. Analysis of Performance Prediction Results. SVMs perform better on linear problems, but problems often encountered in real life are not linear. When the SVM algorithm solves nonlinear data, it must transform the nonlinearity into another linear problem in a high-dimensional space to solve it. The ratio transformation through the kernel function $K(x_i,x_j) = < f(x_i), f(x_j) >$ is a high-dimensional linear problem. The kernel functions mainly include polynomial kernel functions and Gaussian kernel functions. This experiment uses the third-party library sklearn of the Python language for experiments. The kernel function uses a Gaussian kernel, and the model undergoes ten-fold cross-validation. Model evaluation is also performed using precision, recall, F1 value (score), and confusion matrix. The evaluation results are shown in Table 3.

From the evaluation results in Table 3, the SVM algorithm classifies a total of 54 samples, including 10 excellent samples, 7 correctly classified samples, accounting for 70%, and 18 good samples. The sample classification is average, 10 samples are correctly classified, accounting for 71%, 12 samples are classified as poor, and 8 samples are correctly classified, accounting for 67%.

5.3. Analysis of Education Evaluation Results

Accuracy. It is the proportion of the total number of correct predictions. However, the good or bad classification effect is sometimes not explained by high accuracy. The calculation formula is

$$\mathrm{accuracy} = \frac{TP + TN}{TP + TN + FP + FN}. \quad (31)$$

Accuracy: 99.5753%.

$$F_1 = 2 \cdot \frac{\mathrm{precision} \cdot \mathrm{recall}}{\mathrm{precision} + \mathrm{recall}}. \quad (32)$$

F1 value: 82.96%.

Kappa. The main function is to check the degree of agreement between two individuals, usually using experience to judge, but if the data distribution is irregular, using the accuracy rate may not be a good measure. The specific formula is as follows: p_o is the ratio of the overall observed number, and p_c is the ratio of the overall expected number.

$$k = \frac{p_o - p_c}{1 - p_c}. \quad (33)$$

Kappa coefficient: 88.01%.

6. Development Strategies of Internet + Innovation and Entrepreneurship Education Model under the Influence of Related Systems

6.1. Reform of the Traditional Education Model. In the context of the "Internet +" era, the cultivation of students' innovative and entrepreneurial ability must continue to rely

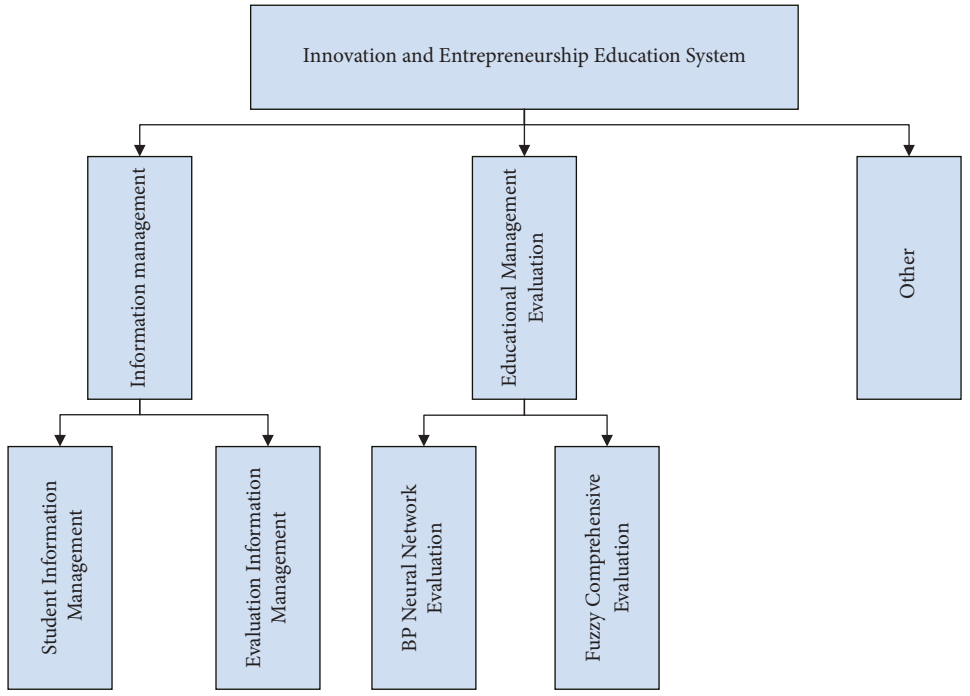

Figure 3: System function block diagram.

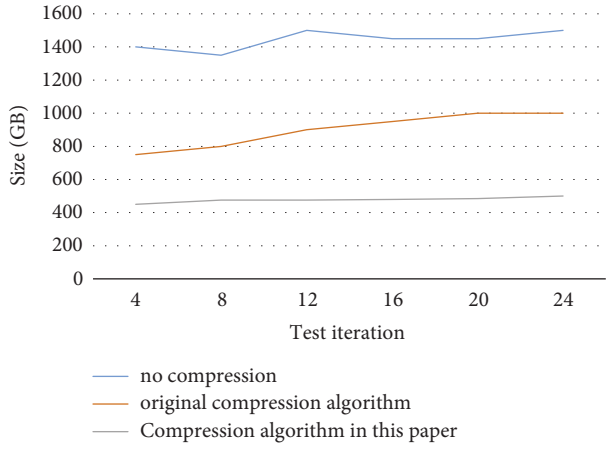

Figure 4: Compression capacity usage trend.

Table 2: Test experimental data with RocksDB engine in the general environment and the system environment of this article.

Number of concurrent requests	Universal environment-QPS	This article system environment-QPS
1	4343	10302
10	15150	21210
20	25210	34752
30	38784	46680
40	46420	58492
50	57419	69698
60	67569	82222
70	71266	93332
80	83386	105452
90	84901	119069
100	85860	131532

Table 3: Experimental results of SVM algorithm.

Evaluation	Precision	Recall	F1 score	Support
1 (excellent)	0.65	0.71	0.68	0.18
2 (good)	0.72	0.68	0.70	0.32
3 (middle)	0.63	0.72	0.68	0.25
4 (poor)	0.81	0.68	0.74	0.21

on a series of education and learning methods. At present, the main way to carry out innovation and entrepreneurship education for students in various courses in China is still the teaching method of transmitting materials and information through language, such as lectures, dialogues, and so on. The main teaching methods are experimental method, discovery method, and so on. Teachers of different majors engaged in innovation and entrepreneurship should fully consider the dominant position of students in different majors in colleges and universities, widely implement different methods such as group discussion, classroom inspiration, practical participation, project design, and so on, and conduct project-based research and other forms of teaching. In addition, for students participating in various courses, the latest professional knowledge of cutting-edge, innovation and entrepreneurship, and its analysis and research results are incorporated into the school classroom to fully stimulate the innovation and entrepreneurship inspiration of students of various majors under the background of the "Internet +" era.

In addition, it is necessary to deeply analyze the learning needs and laws of contemporary students in various sports disciplines and actively rely on information analysis technology. It is necessary to encourage and support the innovation and entrepreneurship path chosen by college students of various majors. Secondly, it is necessary to deeply

explore and reform the content and methods of comprehensive evaluation of students' quality in different schools, actively explore and create nonstandard evaluation methods, and try to transform from evaluation methods. Different assessment methods are used for evaluation, such as choosing knowledge-based skills assessment.

6.2. Construction of the Guarantee System. College students' experience comes partly from teachers' teaching and partly from their own practice. Therefore, schools need to carry out innovation and entrepreneurship education and impart more effective experience, and there must be certain standards and guidelines. This paper believes that the scope of entrepreneurship education is quite large, and the construction of the system itself must be thoughtful, detailed, and time-consuming. Therefore, the institutional construction system of entrepreneurship education should be considered from the three aspects of government, school, and society, and at the same time, it should follow the principle of overall construction, clear hierarchy, and gradual implementation. The first is the government. The focus of government system construction is the combination of entrepreneurial guidance and pressure, but it should not interfere directly. It is necessary to use laws and policies as the main means to formulate systematic, targeted, and enforceable policies and build systems on this basis to ensure that the system can play a role in educating students to improve entrepreneurship. Second is the school. When establishing entrepreneurship education-related systems, schools should comprehensively consider social needs, student needs, and their own circumstances. At the macrolevel, we must attach importance to the formation of business opinions, requirements, and rules and regulations and organically combine systems such as teaching, scientific research, academic activities, and work. We will also provide the same opportunities and resources to implement and play the integrated role of the college, such as the entrepreneurship education department. To design sufficient teaching objectives, each system and department should take corresponding measures according to the general opinions of colleges and universities and their own actual conditions to ensure that courses, platforms, teaching methods, and time can provide sufficient support for entrepreneurship education. In addition, colleges and universities can also formulate policies to encourage and promote entrepreneurship among college students. The last is society. Student entrepreneurship has a very close relationship with society, so we must also attach importance to the construction of social entrepreneurship education system. Compared with the government and universities, the guarantees and services that the society can provide for students' entrepreneurship mainly include policy guidance, project development, risk assessment, incubation support, and entrepreneurial consultation. Corresponding system construction should also start from these aspects.

Improve the knowledge and literacy of teachers in entrepreneurship education. Invite entrepreneurship and innovation experts to the school regularly or irregularly to communicate or arrange knowledge lectures and other activities, gradually introduce the concept of entrepreneurship into all courses of the school, subtly influence teachers and students, and realize the development of knowledge structure in teachers' entrepreneurship education. The second is to attach importance to carrying out relevant training activities. For entrepreneurship education, create a characteristic training system. At the same time, organize some teachers who have done a good job in entrepreneurship education to participate in relevant seminars at home and abroad and organize all teachers to exchange experience and lessons in entrepreneurship education on a regular or irregular basis, so as to better conduct entrepreneurship education. The third is to build a dedicated entrepreneurial practice team. As mentioned above, most colleges and universities currently lack practical experience and knowledge of entrepreneurship education. In this regard, colleges and universities can first hire some experts who have studied entrepreneurship education and have achieved certain results or can directly hire successful entrepreneurs, engineering and technical experts, venture capitalists, and other personnel as mentors for corporate practice activities. The existing teachers will learn the teaching contents and methods of these tutors and actively participate in various practical activities, so as to gradually form professional and high-level education, entrepreneurship training and teacher training institutions. In addition, we must also attach importance to the cultivation of talents with high research potential to ensure that the development of entrepreneurship education for students is guided at a higher level.

Special intermediary agencies should also be established to provide students with commercial loan guarantees, business tax consulting, guidance, and other services. The second is information services. It is necessary to establish a special information platform to timely push the market information, policies, and other information of college students' entrepreneurship to students, so as to provide extensive and multi-faceted support for entrepreneurship.

6.3. Optimization of Education Management. To some extent, innovation and entrepreneurship education in colleges and universities is closely related to the achievements of student talent training. Therefore, colleges and universities need to attach importance to innovation and entrepreneurship education, not only to set up special departments for teaching research and development, but also to provide help for the development of innovation and entrepreneurship teaching from multiple levels, or establish a special management group for innovation and entrepreneurship to achieve education, which needs to be independent of secondary colleges and departments. In addition, assign job responsibilities, be responsible for work-related innovation and entrepreneurship education, and work with other departments to achieve a synergistic effect of $1 + 1 > 2$. Responsibilities include elaborating and

implementing relevant innovation and entrepreneurship education policies issued by government departments and universities; guiding teachers and students to carry out innovation and entrepreneurship activities according to the policies; cooperating with other departments, especially the Academic Affairs Office, to optimize innovation and entrepreneurship courses and standardize teacher training; formulating talent training plan; find appropriate practice opportunities for students and do a good job in school enterprise cooperation; tracking students' innovation and entrepreneurship projects, providing students with professional innovation and entrepreneurship projects and implement teacher guidance, and improving the implementation of project results as soon as possible.

Different from the common employment counseling in the society, the school pays more attention to the comprehensive education, resulting in information asymmetry, and teachers and students receive relevant information late or do not know, hindering the effective development of innovation and entrepreneurship activities. Therefore, the comprehensive service platform for innovation and entrepreneurship must set up two sites: online and offline, mainly collecting online innovation and entrepreneurship related information, and promoting innovation and entrepreneurship policies, knowledge information, competition information, etc. In addition, we can also choose some forms that are easy for students to accept, such as we-media short videos, Douyin Live, and so on, to provide students with more comprehensive and innovative innovation and entrepreneurship education services. The content provided can also be more diverse, such as interpretation of relevant policies, dissemination of recruitment information, dissemination of competition information, and so on. It is necessary to keep track of the progress of students' innovation and entrepreneurship projects, provide students with professional and technical guidance in a timely manner, create quality projects, improve project implementation, help students avoid entrepreneurial risks, and improve the survival rate of students' entrepreneurship.

Faced with the complexity of the social environment and the high standards of employers, the creation of innovative and entrepreneurial activities requires the support of a multi-disciplinary environment and rich interdisciplinary knowledge, and the deep integration of disciplines and industries can improve the effectiveness of innovation. The construction of the innovation and entrepreneurship education system cannot only rely on the unilateral efforts of the school but must be combined with the enterprise. The school can take the lead in introducing students, promote school enterprise cooperation, build a one-stop teaching platform, provide more practical opportunities for students, campus cooperation, domestic and international cooperation, expand and deepen government participation, strengthen the connection with social forces, carry out reform and entrepreneurship education with connotation development, and meet the practical application needs of social innovation and entrepreneurship.

7. Conclusion

The current economic situation and the development of Internet technology give innovation and entrepreneurship education more options. At present, the entrepreneurship education of college students is far from being in place. Many students are confused when they graduate. Therefore, it is necessary to carry out effective innovation and entrepreneurship education guidance for students. Therefore, this paper builds an Internet + innovation and entrepreneurship education system based on machine learning algorithms, aiming to develop entrepreneurship education and guide the correct direction of entrepreneurship education for college students, and it can also enhance students' ability to adapt to the society, cultivate good innovation quality, and promote students' development in the society.

Data Availability

The data used to support the findings of this study are available from the corresponding author upon request.

Conflicts of Interest

The author declares that there are no conflicts of interest.

References

[1] X. Zhang, "Research on innovation mode of quality education of higher vocational college students based on the integration of enterprise and campus culture," in *Proceedings of the 2016 5th International Conference on Social Science*, Education and Humanities Research, Tianjin, China, June 2016.

[2] S. J. Harkema and H. Schout, "Incorporating student-centred learning in innovation and entrepreneurship education," *European Journal of Education*, vol. 43, no. 4, pp. 513–526, 2008.

[3] H. Li and L. Jiao, "Research on innovation and entrepreneurship education and practice in shandong province based on the Internet," *Journal of Physics: Conference Series*, vol. 1744, no. 3, Article ID 032092, 2021.

[4] D. F. Kuratko, "The emergence of entrepreneurship education: development, trends, and challenges," *Entrepreneurship: Theory and Practice*, vol. 29, no. 5, pp. 577–597, 2005.

[5] C. Meng-yue, L. Dan, and W. Jun, "A study of college English culture intelligence-aided teaching system and teaching pattern," *English Language Teaching*, vol. 13, no. 3, pp. 77–83, 2020.

[6] C. Wei and L. Yuan, "Reflection on college informationized teaching model under the background of educational informationization," in *Proceedings of the 2019 IEEE International Conference on Computer Science and Educational Informatization (CSEI)*, pp. 81–83, Kunming, China, August 2019.

[7] L. Pittaway and J. Cope, "Entrepreneurship education: a systematic review of the evidence," *International Small Business Journal*, vol. 25, no. 5, pp. 479–510, 2007.

[8] J. Zhang, "Research on classroom teaching evaluation and instruction system based on gis mobile terminal," *Mobile Information Systems*, vol. 2021, no. 11, p. 1, Article ID 9790766, 2021.

[9] N. A. Alias and A. M. Zainuddin, "Innovation for better teaching and learning: adopting the learning management system," *Malaysian online journal of instructional technology*, vol. 2, no. 2, pp. 27–40, 2005.

[10] Q. Wang, H. L. Woo, C. L. Quek, Y. Yang, and M. Liu, "Using the Facebook group as a learning management system: an exploratory study," *British Journal of Educational Technology*, vol. 43, no. 3, pp. 428–438, 2012.

[11] X. F. Zheng, "Research on the Whole Teaching of Vocal Music Course in University Music Performance Major Based on Multimedia Technology," *Scientific Programming*, vol. 2022, Article ID 7599969, 2022.

[12] H. P. Yueh and S. Hsu, "Designing a learning management system to support instruction," *Communications of the ACM*, vol. 51, no. 4, pp. 59–63, 2008.

[13] T. J. McGill and J. E. Klobas, "A task–technology fit view of learning management system impact," *Computers & Education*, vol. 52, no. 2, pp. 496–508, 2009.

[14] F. Zhu, C. Zhang, Z. Zheng, and A. Farouk, "Practical network coding technologies and softwarization in wireless networks," *IEEE Internet of Things Journal*, vol. 8, no. 7, pp. 5211–5218, 2021.

[15] J. Rhode, S. Richter, P. Gowen, T. Miller, and C. Wills, "Understanding faculty use of the learning management system," *Online Learning*, vol. 21, no. 3, pp. 68–86, 2017.

[16] A. Horvat, M. Dobrota, M. Krsmanovic, and M. Cudanov, "Student perception of Moodle learning management system: a satisfaction and significance analysis," *Interactive Learning Environments*, vol. 23, no. 4, pp. 515–527, 2015.

Hindawi
Mobile Information Systems
Volume 2022, Article ID 3615958, 9 pages
https://doi.org/10.1155/2022/3615958

Research Article

Smart System Design for College Physical Education Class Based on Abnormal Audio Detection Algorithm

Yonghui Bai

School of Physical Education and Health, Wenzhou University, Wenzhou, Zhejiang 325035, China

Correspondence should be addressed to Yonghui Bai; tyxybyh@wzu.edu.cn

Received 16 August 2022; Revised 20 September 2022; Accepted 29 September 2022; Published 10 October 2022

Academic Editor: Shadi Aljawarneh

Based on dual-core technology and the theory of nontransmission and noninterference of information flow, this paper conducts a detailed system trust environment investigation on key issues such as trust routing design and reliability analysis in the embedded structure. At the same time, we will study the method of extracting features from speech data. When dealing with abnormal audio detection, firstly, the preprocessed valid audio clips are framed and windowed and have stable short-term characteristics; after the feature is stable, the frequency feature and time domain feature of audio data are analyzed and compared. And then combined with specific applications, a detailed demand analysis is carried out, and the development plan and implementation method of the college physical education network auxiliary system are proposed. The teaching system follows a three-tier system structure. In order to expand the existing functions, this paper uses the principle of modularity, starting from the following four aspects: educational resources, online question and answer, coursework, and test-related modules. We choose object-oriented and easy-to-expandable modules, such as the development and implementation of programming language environments and database systems. By applying the abnormal audio detection technology to the embedded system of college P.E. classroom, it can effectively optimize the traditional P.E. teaching mode and promote the teaching efficiency and the new development of P.E. teaching in the information age.

1. Introduction

This article explains how to use a bootloader and a stable kernel to create a root of trust for embedded systems. The article starts the FLASH accelerator program and test, verifies the trusted kernel, and protects the FLASH boot program by preventing users and advanced software from writing [1]. Through the combination of the two, the reliable root of trust security function can be guaranteed; the trusted kernel is integrated in the trusted platform in the component (vTPM), and a unified system interface is provided for users to realize the easy configuration and compatible storage of different FLASH domain installation platforms and regions [2]. Compared with a reliable computing organization structure, this method does not require additional equipment and can avoid cost overruns, power consumption, and volume, and make it more versatile [3]. In this article, a prototype system has been built to implement this method. Experimental results show that this method can provide the trusted platform module (TPM) cryptographic service-related functions and effectively improve system security. Then, we will study the classification method of abnormal audio detection [4, 5]. This article uses deep feedforward neural network as the classifier to analyze the basic unit and architecture of deep feedforward neural network and compares the advantages and disadvantages of various activation, loss, and optimization algorithms [6]. In this article, we will design two deep feedforward model architectures for neural networks, all of which are suitable for high-performance servers with powerful computing power and energy-saving embedded devices [7]. Comparison experiments with traditional algorithms show that the algorithm has good performance classification effect. Taking the development of online sports as the theme and the establishment of a sports network auxiliary system as the content, the research on the auxiliary role of network technology in physical education is

studied [8]. In the designed college sports system, physical education teachers can learn the online environment through the Internet, and they can prepare courses and PPT and use online technology to upload videos, post homework, and post test standards and results [9, 10]. Students can access the course materials on the server at any time, avoiding the problem of lack of knowledge due to the difficulty of certain technical movements in physical education [11]. The teaching system breaks the time and space boundaries of the traditional physical education model and realizes online learning and answering students' questions, and uploading and downloading data and other functions. The system interface is simple, easy to use, and easy for teachers and students to use, realizes the educational resource information management and educational resource sharing between teachers, and helps contemporary students to better study physical education, not to just focus on the knowledge of books, and let its morality, intelligence, physical, beauty, and labor get all-round development [12, 13].

2. Related Work

The literature introduces deep feedforward neural networks, analyzes the basic units and architecture of deep feedforward neural networks in detail, compares and analyzes the advantages and disadvantages of different activation functions, loss functions, and optimization algorithms, and uses Adam optimization algorithms for deep learning training the optimizer in the process, and two deep feedforward neural network model architectures are designed [14]. The literature introduces the audio event detection algorithm, introduces the framework and process of the audio event detection algorithm, and specifically states the audio preprocessing process (framing, windowing, etc.) and some classic features commonly used in audio; the basic knowledge of deep learning is related to event detection, including some commonly used networks, such as convolutional neural networks [15]. The literature introduces the CRNN abnormal audio event detection algorithm of spectrogram, extracts the spectrogram of abnormal audio event, and converts the abnormal audio into the form of spectrogram. This time-frequency representation of audio is very suitable and can be effectively input into the deep learning audio recognition model to perform further feature learning and classification; select a hybrid CRNN model as the basic recognition model, learn the features in the spectrogram, and finally give the classification results; conduct experimental training of the model, and test the accuracy of the model. With generalization ability, verify the performance of the algorithm. The literature introduces the neural network abnormal audio event CRDNN, which exists as an enhancement module of audio data [16]. The CRDNN performs a series of data enhancement calculations on the input abnormal audio data such as encoding, translation, and decoding [17]. It is experimentally proved that the CRDNN data enhancement module makes the model have stronger anti-noise performance, which proves that the addition of the module effectively suppresses environmental noise and improves the accuracy of abnormal audio event detection in different situations and real environments with different signal-to-noise ratios [18]. The literature introduces the related technologies used to construct the physical education network auxiliary system, such as the three-tier model, database access technology, and programming technology [19, 20].

3. Embedded System and Abnormal Audio Detection

3.1. Embedded System. The original purpose of trusted computing is to solve the hidden dangers of computer systems, and most of the existing researches are also carried out on computer systems. Embedded systems and computer systems are very different in their technical roots and application fields. Therefore, research results applicable to computer systems cannot be directly transferred to the embedded field. Building an integrated trusted computing environment faces many new scientific problems.

Embedded computer, as a computer designed for specific applications, not only has some common characteristics of computers, but also has its own obvious characteristics. Embedded devices have a special technical environment, such as significant differences between different architectures and systems. These attributes prevent embedded devices from using the security protection that was originally applicable to traditional IT devices. The reliability research of embedded computing environment can learn from the results of computer reliability collaborative research, but the unique attributes and requirements of embedded systems must also be considered.

The main body of embedded system computing is the application software running on it. Building a reliable embedded computer environment includes providing reliable operating media and related technical mechanisms for the application software, such as computer hardware and software environments.

Establish a comprehensive trust route, that is, how to design a trusted route according to the requirements of the embedded system. The core concept of DRTM dynamic trust routing technology is to introduce new CPU commands and use the commands and related mechanisms provided by the processor to achieve a dynamic structured and reliable measurement environment. We can use new instructions to create a controllable and verifiable execution environment that is not affected by the components loaded by the system, ensuring that the program is loaded under the instructions and not manipulated by other components, forming reliable dynamic execution surroundings.

3.2. Abnormal Audio Feature Extraction. For different short-term analysis methods, in order to obtain different audio data characteristic parameters, different window functions need to be selected according to the analysis method. The process of framing and windowing audio data requires multiplying the audio waveform by the time domain window function. This process should make the gradient at both ends

of the time frame as small as possible to avoid sudden changes at both ends of the time frame. The intercepted audio waveform is slowly reduced to zero, which weakens the interception effect of the audio frame. The window function should increase the bandwidth of 3 dB in the frequency range, and the maximum sideband should be small.

The formula for the rectangular window is

$$h(n) = \begin{cases} 1, 0 \le n \le (N-1), \\ 0, n = other. \end{cases} \tag{1}$$

The frequency response of the digital filter is

$$H\left(e^{j\omega T}\right) = \sum_{n=0}^{N-1} e^{-j\omega T} = \frac{\sin(N\omega T/2)}{\sin(\omega T/2)} e^{-\frac{j\omega T(N-1)}{2}}. \tag{2}$$

The rectangular window has a linear frequency response, and the frequency corresponding to the first zero value of the frequency response is

$$f_{01} = \frac{f_s}{N} = \frac{1}{NT_s}. \tag{3}$$

The Hamming window function is as follows:

$$h(n) = \begin{cases} 0.54 - 0.46\cos\left[\frac{2\pi n}{N-1}\right], 0 \le n \le N-1, \\ 0, \qquad n = ft. \end{cases} \tag{4}$$

The rectangular window has better spectral smoothness, but it damages high-frequency information greatly, causing loss of waveform details. The Hamming window protects high-frequency information better and preserves the details of audio signal data. Therefore, the Hamming window is in the audio; the performance in classification is better than rectangular windows.

The choice of window shape is very important in audio signal data analysis. The choice of different window functions will affect the short-term characteristics of time domain analysis parameters. Choosing a suitable window function is the basis of audio signal analysis.

If the sampling period is T_s, the window length is N, and the frequency resolution is $\triangle f$, that is,

$$\Delta f = \frac{1}{NT_s}. \tag{5}$$

It can be seen from the above formula that the time resolution decreases as the frequency resolution increases, and the frequency resolution also decreases as the window length decreases, which improves the time resolution. In the time domain analysis of audio data, if the window length N is large, the window function corresponds to a low-pass filter, which shields the high-frequency part of the audio signal, the waveform of the high-frequency part of the audio is lost, short-term energy fluctuations occur, and the change with time is too small to accurately reproduce the change of the audio signal amplitude; if the window length N is too small, the passband of the filter becomes wider, the short-term energy changes greatly, and the energy function oscillates greatly. Generally speaking, the window length is usually 80–160 points when the sampling rate is 8000 Hz.

The time domain analysis of the audio signal refers to the separation and analysis of the time domain parameters of the audio signal. The best understood audio visualization model is the delay time line waveform. The audio signal is in the time domain because the essence of the audio signal is time. Domain signal and time domain analysis is one of the most widely used audio analysis methods. Time domain analysis is usually applied to the most basic parameter analysis and feature extraction. The time domain analysis method has several notable characteristics. The time domain signal of the speech signal is relatively intuitive, and the physical meaning is relatively clear. The time domain signal analysis algorithm is easier to implement, and the calculation is complicated. Degree is low. The characteristic parameters of the audio signal in the time domain include short-term energy, short-term zero crossing, etc., which will be further analyzed below.

Assuming that the audio signal in the time domain is $x(l)$, and the n-th frame audio signal obtained after frame and window processing is $x_n(m)$, then $x_n(m)$ has the following relationship:

$$x_n(m) = \omega(m)x(n+m) n \le m \le N-1, \tag{6}$$

$$\omega(m) = \begin{cases} 1, & m = 0 \sim (N-1), \\ 0, & m = others. \end{cases} \tag{7}$$

Use E_n to represent the short-term energy of the n-th frame audio signal, namely,

$$E_n = \sum_{m=0}^{N-1} x_n^2(m). \tag{8}$$

Since E_n is the square sum of the amplitude of the audio signal, the high-level audio signal with larger amplitude has a great influence on the function value. It can be improved to the short-term average amplitude function M_n, which can weaken its effect on high voltage; the sensitivity of the flat signal is defined as follows:

$$M_n = \sum_{m=0}^{N-1} \left|x_n(m)\right|. \tag{9}$$

If the short-time zero-crossing rate of the n-th frame audio signal $x_n(m)$ is Z, that is,

$$Z_n = \frac{1}{2}\sum_{m=0}^{N-1} \left|sgn\left[x_n(m)\right] - sgn\left[x_n(m-1)\right]\right|. \tag{10}$$

When calculating short-term over-limit parameters, if the input audio signal passes through the converter, its operating point is shifted, or it contains 50 Hz mains frequency interference, the calculation process will cause larger errors. In the audio signal input process, the cut-off frequency of the anti-aliasing bandpass filter is usually set higher than 50 Hz to prevent influence. Therefore, it does not work for the operating point of the cheap converter, and the

DC component of each frame is usually calculated and excluded.

In the field of speech classification, Mel frequency cepstral coefficient (MFCC) is a commonly used speech function. The Mel scale is the frequency scale corresponding to the characteristics of the human ear, which roughly corresponds to the log-normal distribution of the actual frequency. The specific corresponding relationship is given by the following formula:

$$Mel\ (f) = 2595lg\left(1 + \frac{f}{700}\right). \tag{11}$$

If the critical frequency bandwidth is less than 1000 Hz, the bandwidth is about 100 Hz, which is almost linearly distributed. If the critical frequency bandwidth is higher than 1000 Hz, the critical frequency bandwidth is log-normal.

The lower, center, and upper limit frequency of adjacent triangular bandpass filters has the following relationship:

$$C(l) = h(1-1) = l(l+1). \tag{12}$$

According to the amplitude spectrum of the audio signal, the output of each triangular bandpass filter is

$$m(\mathrm{l}) = \sum_{k=l(l)}^{h(l)} W_l(k)\left|X_n(k)\right| l = 1, 2, 3, \ldots, L. \tag{13}$$

Calculate the logarithm of all filter outputs obtained by the above formula, and perform the discrete cosine transform shown in the following formula to obtain the Mel frequency cepstral coefficient.

$$c_{mfcc}(i) = \sqrt{\frac{2}{N}}\sum_{l=1}^{l} lgm\ (l)\cos\ \left\{\left(l - \frac{1}{2}\right)\frac{i\pi}{L}\right\}. \tag{14}$$

The process of calculating the frequency coefficients of the Mel cepstrum requires fast Fourier transform, but the fast Fourier transform has a great impact on the system. If the number of fast, there are too few Fourier transform points, and the frequency resolution is too low, which will cause large errors and reduce the accuracy; if the number of fast Fourier transform points is too small, the calculation of the system will be complicated and cannot meet the requirements of real-time processing. For hardware with different processing capabilities, the parameters of the MFCC calculation process need to be adjusted to find a balance between accuracy and efficiency.

3.3. Abnormal Audio Detection Algorithm. Due to the strong feature self-learning ability of deep learning and the continuous development of the strong classifier of neural network, it has successfully been widely used in various audio-related tasks. This paper conducts research on the abnormal audio event detection algorithm related to deep learning. Two different features are used as the input data of the deep learning model: the first is the original sampling point of the abnormal audio signal; that is, the original sampling point of the audio is directly used without any feature engineering, and they are arranged in chronological order into two dimensions. The graph structure is used as the input of the deep learning model to form an end-to-end algorithm mode; the second is to extract the spectrogram of the abnormal audio signal as the input of the deep learning model. Both features are graph structures, and the same hybrid neural network model of convolutional neural network and cyclic neural network is used to calculate and fit them; finally, the abnormal sound classification and results are obtained through the Softmax function.

The above two abnormal sound recognition algorithms use the same neural network model. The difference is the input features, which are the folded map of the original audio sampling points and the audio spectrogram. The flowchart of the abnormal sound recognition algorithm based on deep learning is shown in Figure 1.

Since this article studies an abnormal audio event detection algorithm based on deep learning, and the CNN part of the CRNN model used next is a two-dimensional convolutional layer, the input features must be data with a two-dimensional structure. The audio original sampling point folded map refers to the original waveform; sampling point of the audio signal is expanded by frames, and each frame is arranged in a row. All the frames are arranged in chronological order to form a two-dimensional data structure, which is called folded image of the original audio sampling points.

Figure 2 shows the conversion of an abnormal sound into a spectrogram. The time-frequency representation of this audio is very suitable and can be efficiently input into the subsequent deep learning audio recognition model for further feature learning and classification, and the specific transformation details are as follows.

First, each independent abnormal audio is divided into frames to obtain L frame audio, where i is the frame number, sequence number, and n is the sequence mark of the data point in a frame of audio. The specific calculation formula is

$$S_i(k) = \left|\sum_{n=0}^{N-1} s_i(n)\cdot w(n)\cdot e^{-j2\pi nk/N}\right|. \tag{15}$$

After stacking all the frames after FFT transformation, the audio spectrogram is obtained. Because the dimensionality of FFT is too high, and audio monitoring requires strong real-time performance, it needs to be reduced in dimensionality. Studies have shown that human hearing is not linear. It is logarithmic at high frequencies and more linear at low frequencies. Therefore, the Mel scale is designed as a method of bending the linear frequency domain to make it more in line with natural perception:

$$mel\ (f) = 1125\cdot \ln\left(\frac{1+f}{700}\right). \tag{16}$$

The core of the CNN is convolution and max pooling (Max Pooling), and the other network layers are just some nonlinear components. When CNN is working, the convolution window (convolution kernel) is used as a local feature classifier to learn high-level features. By obtaining

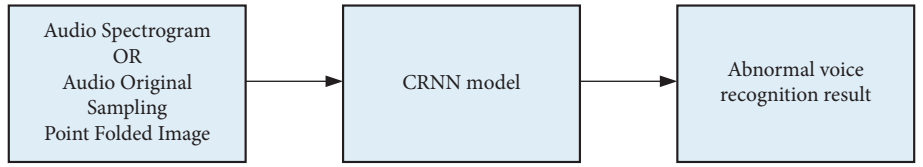

Figure 1: General block diagram of abnormal sound recognition algorithm based on deep learning.

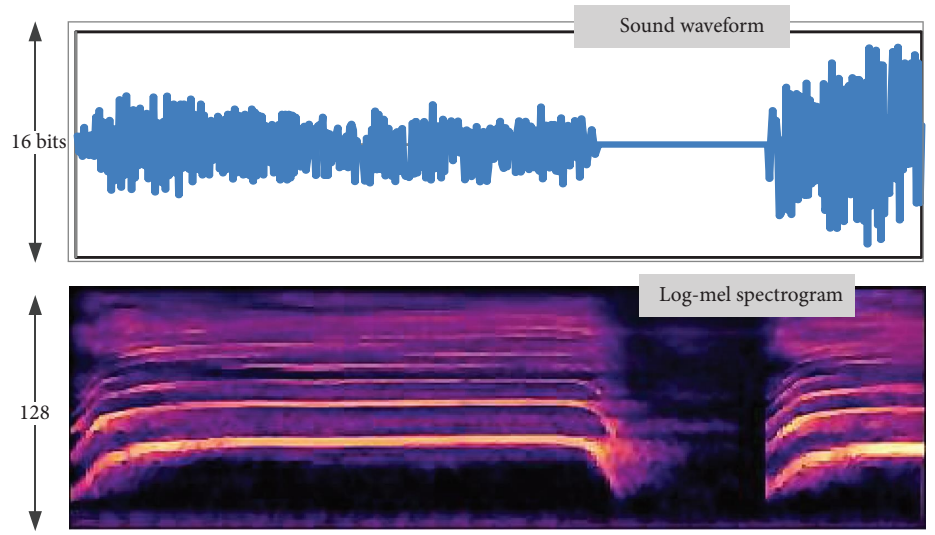

Figure 2: Spectrogram of abnormal sound.

these weights, the product combination between the two is obtained, and a relatively high-level value and corresponding feature map are given, so first-order local features are obtained from the original image, and then higher-order features are obtained. When putting all of this into GPUs, CNN can be optimized very fast. The specific formula is as follows:

$$a_j^l = f\left(\sum_{i=1}^{M_j} a_j^{l-1} \cdot k_{ij}^l + b_j^l\right). \tag{17}$$

Excluding some discrete points and noise, the data provided for the same problem all have the same distribution and characteristics. The model learns this distribution characteristic of the data in the training data and is applied in the test data. However, in deep learning, with the deepening of the network layer and the superposition of nonlinear transformations, the data distribution often faces the problem of internal changes in sample points and gradually becomes unstable. The role of the batch normalization layer is to maintain this data distribution and the stability of the characteristics, after the data of each layer are passed through the batch normalization layer, and the original distribution that is about to be deformed is fixed back, so as to avoid the problem, as shown in Figure 3.

BN can reduce this negative impact. Through the normalized calculation method, the output value of each intermediate layer is pulled back to a standard normal distribution with a mean of 0 and a variance of 1. When this standard after the distributed data enters the activation layer, the activation value gradually stabilizes, the gradient back propagation becomes larger, and the convergence speed becomes faster, thereby avoiding the problem of gradient disappearance. The specific operating formulas of BN are shown in formulas (18)–(20):

$$\mu_B \leftarrow \frac{1}{m}\sum_{i=1}^{m} x_i, \tag{18}$$

$$\sigma_B^2 \leftarrow \frac{1}{m}\sum_{i=1}^{m} (x_i - \mu_B)^2, \tag{19}$$

$$\widehat{x}_i \leftarrow \frac{x_i - \mu_B}{\sqrt{\sigma_B^2 + \varepsilon}}, \tag{20}$$

$$y_i \leftarrow \gamma \widehat{x}_i + \beta \equiv BN_{\gamma,\beta}(x_i). \tag{21}$$

Since the algorithm in this article uses maximum pooling, we will mainly introduce the schematic diagram of the maximum pooling layer and the maximum pooling. The specific formula is shown

$$T_j^1 = f\left(down\left(T_j^{l-1}\right) + b_j^l\right). \tag{22}$$

The parameters of the maximum pooling are the pooling area and stride. The pooling area is a matrix that represents the range involved in the pooling operation. The stride is the amplitude of the matrix moving up and down. Once the

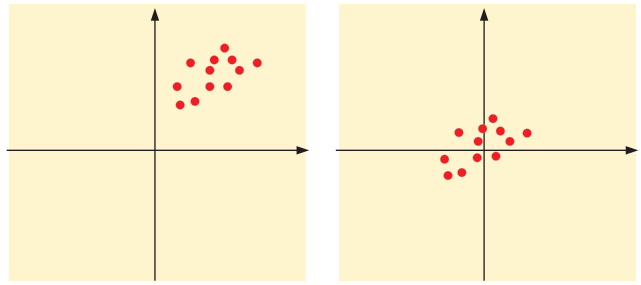

Figure 3: Batch normalization effect diagram. (a) Before batch normalization. (b) After batch normalization.

maximum pooling area and stride are determined, the maximum pooling operation is also fixed, there are no parameters that need to be iteratively optimized, and gradient descent does not need to change any values. The idea of maximum pooling is based on the consideration of the redundancy of the extracted features. It is simple to think that when the maximum feature of a certain adjacent region is extracted, it is often enough to represent all the characteristics of the region; that is, the maximum value is retained. The maximum value often means that certain specific features may have been detected.

3.4. Analysis of Simulation Results. In the GRU part of the cyclic network in the CRNN model, setting different time steps affects the performance of abnormal sound recognition. The abnormal sound data set used in the experiment is the pure data set A, and the test recognition rate is shown in Figure 4.

The CRNN model convolves the input Log-Mel spectrogram in the frequency domain and the time domain, and then performs Max Pooling. Max Pooling achieves the purpose of data dimensionality reduction by selecting the local maximum eigenvalues and pooling in the frequency domain. For audio, it is clear that the class task is effective. The only controversy is that the frequency domain pooling will discard some pitch changes, but all these depend on the data type and are not important for abnormal sound recognition. The key question is whether pooling in the time domain is a good idea, and whether the time domain pooling operation will lose the timing information that is important for the sound. This is still open.

Whether the time domain pooling affects the feature size input to the recurring layer after the CNN is over, a rigorous understanding, time domain pooling will reduce the time scale of the features extracted from the spectrogram. The number of cycles in the final cycle layer decreases; that is, the number of time steps decreases. Of course, the feature dimension of each time step remains unchanged, which is still the number of convolution kernels in the last convolution layer. In order to test the impact of time domain pooling on network performance, by not adding pooling in the time domain and gradually adding large pooling, the characteristics of different time scale dimensions are input to the loop layer and the recognition effect is obtained. From the

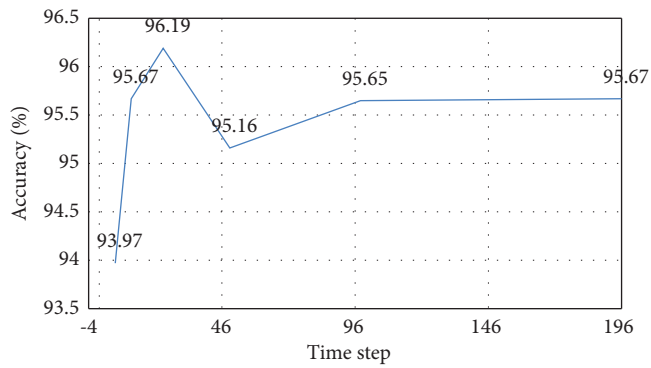

Figure 4: The accuracy rate changes with the number of time steps.

experimental result graph, it can be seen that pooling in the time domain does not significantly reduce the recognition effect, but the performance is better at 24 steps. Secondly, the fewer time steps represent the faster running speed.

4. Application of College Physical Education System Based on Related Technology

4.1. System Requirement Analysis. As the basis of online sports teaching support, the business needs of the system are mainly analyzed from the perspective of education design. When designing online education, we must adhere to the following teaching design principles: focus on the analysis of educational objectives and content, focus on the creation of situations in the design of educational activities, and emphasize and value the important role of educational activities. At the same time of learning, it pays attention to the design of information resources to assist "learning," emphasizes the use of various information resources, and emphasizes student-centered autonomous learning design and "collaboration," and collaborative learning environment design and network design are the main educational strategies.

First of all, we need to clarify the goal of network technology to support physical education. When deciding educational goals, we must carefully consider the technical characteristics of computers and networks, and combine them with the characteristics of sports itself. In actual physical education courses, network technology can only play an auxiliary role, because only through actual

operations and practical exercises can the expected effects of the courses be achieved.

The educational goal of the system is to enable students to use the network-supported education system for physical education, which will greatly increase students' interest in learning, help understand and master the curriculum, teaching points and difficulties of this article, and give students enough room for maneuver. Promote students' learning initiative. The exchange and communication between students and teachers can strengthen teachers' understanding of students' learning through online question and answer, and quickly and accurately understand students' learning and knowledge. Through video and multimedia, it is possible to reproduce the content of the physical education class, learn the difficult content repeatedly, and put it into practice in theory.

Due to the diversity of student groups, a single classroom teaching is far from meeting the diverse learning needs of students. Establish a sports network auxiliary system to create an environment for students to learn knowledge outside of sports. Through this system, students can make up for their shortcomings in physical education. At the same time, teachers can also use the teaching assistant system to organize and control their courses to guide them in learning.

We hope that we can use the interactive network education model to design sports network auxiliary systems, use the networked education environment to support physical education, and achieve the following goals:

(1) The system design must fully demonstrate the benefits of online education: give full play to the leading role of students, consciously carry out independent learning, teacher-student interaction is no longer restricted by the time and place of traditional education, and the networked education environment becomes teachers and elective students. The communication channels between each other provide space for information exchange between each other.

(2) Fully demonstrate the benefits of physical education in the classroom: fully demonstrate the leadership role of teachers, guide students to set learning goals according to the curriculum requirements, and understand the main points and difficulties of education.

(3) Utilize the network education environment to give full play to the advantages of multimedia education: if information media such as symbols, sounds, graphics, animations, and videos are integrated to create a human-computer with a graphical interactive interface and interactive window controls, the interactive capabilities will be greatly improved.

(4) Convenient for teachers and students: physical education teachers prepare online lessons in a networked learning environment, upload PPT and technical videos, publish assignments and grade exams, and announce final evaluation standards and results through the Internet. In physical education, to avoid performance problems such as technical difficulty, you can refer to the teaching materials on the server at any time to listen to the lessons more carefully.

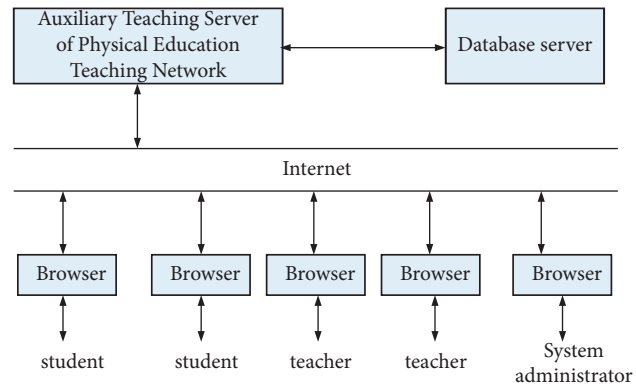

Figure 5: A brief description of the physical education network auxiliary system.

4.2. System Structure Design. Online education mainly chooses Internet-based application systems, and all functions are completed through the interaction between the application server and the user's browser. System-related data are maintained and organized by the database server. Figure 5 shows brief description of the system.

The educational resource module contains five submodules. This module is an open module. Students only need to enter the system URL in the address bar of the browser to directly access the educational resource module. Therefore, when designing this module, the response speed of students' questions should be considered, making the entire page as simple and generous as possible, making each sub-module easy to access, and complying with the design rules of today's major Web applications.

Links in the system navigation bar point to each submodule and other modules. The structure of each submodule corresponds to this figure, and two methods are needed to achieve this effect: one is how to use the framework, how to customize the framework, and how to insert different parts into the framework; the other is to call the ASP statement and use table methods where appropriate to complete this operation. This system uses a table format, which makes the entire system more uniform and the overall effect more coordinated.

4.3. System Function Module Design. There are three tables in the database of the online Q&A subsystem: teachers, students, and teaching management. Table 1 shows the main structure of the teacher table.

Table 2 shows the main structure of the student table.

The name and message content are required, and others are optional. When students input message content, the system supports HTML editing functions, such as bolding the message content and setting it as a hyperlink. In this way,

Table 1: The main structure of the teacher table.

Data item	Field name	Significance
Teacher ID	int, IDENTITY(1.1), not null	Teacher ID number automatically assigned by the system
Name	nshedbsjr(21), not null	The name of the teacher in the system
Pwd	Varchar(10), not null	Teacher's password in the system
Name	nvarchar(20), not null	Teacher's real name
Trouble	bhsdbhb(50), not null	Problems when looking for a password
Firstanswer	nvarchar(50), not null	The answer
Status	Int	Status, currently reserved
Regstatus	smallint, not null	Status at the time of registration
Code	nvarchar(10), not null	Teacher's ID number
E-mail	bxndk(50)	Teacher's e-mail

Table 2: The main structure of the student table.

Data item	Type of data	Significance
Student ID	int, IDENTIT Y(1,1), not null	Student ID number automatically assigned by the system
Name	nvarchar(20), not null	Student's real name
Username	nvarchar(20), not null	Username in the student system
Pwd	Varchar(10), not null	Student's password in the system
Trouble	bhsdbhb(50), not null	Problems when looking for a password
Answer	hbhghsnr(50), not null	The answer
E-mail	bxndk(30)	Student's e-mail address

Table 3: Database structure table.

Table name	Field name	Description
Examine	Type, test questions, A, B, C, D, answer	Type: select
Exercise	Type, test questions, A, B, C, D, answer, analysis	Same as above
Account	Grade D, B, C, A	Analyze the use of statistics
Score	User, grades, multiple-choice questions, fill-in-the-blank questions, test date	User: exam ID
Admin	Username password	Administrator profile
User	Student ID, name, last reference date, application ID	Candidate form
News	Title, content, time	Related notice
Manage	Exam time, number of choices, score, number of fill-in-the-blanks, score	Score: select each
Request	Name, gender, class, contact information, e-mail	The score of the question

Table 4: Class table.

Data item	Type of data	Significance
Class ID	int, IDENTITY(1.1), not null	Class ID number automatically assigned by the system
Class name	nvarchar(20), not null	Class name
Teacher ID	int, not null	The ID of the teacher who created the class
Pwd	varchar(10), not null	Class password

you can enrich the information content and insert symbols and pictures.

The coursework module contains two sub-modules. This module is an open module with a physical education resource module. Students only need to enter the system URL in the browser address bar to directly enter the course module. The two sub-modules of this module are modified according to the difference in the curriculum. Therefore, in the same educational resource module, the design and implementation of these two sub-modules are electronic resources provided by these two sub-modules mainly used for the educational process. This part of the content is managed by the administrator, including adding resources and deleting resources.

The tables and related fields in the database are shown in Table 3.

4.4. Database Design. The teacher ID number is the unique identification of the teacher. The system administrator is a special teacher (user name: admin), and the basic information is stored here. Regstatus is used to view teacher status information during the registration process: 0—users who can use the system; 1—the teacher is registered but not confirmed by the system administrator.

Class table structure is shown in Table 4.

Student-class table is shown in Table 5.

Table 5: Student-class table.

Data item	Type of data	Significance
Student ID	int, not null	Student ID number
Class ID	int, not null	Class ID number
Student #	Varchar(20), not null	Student ID

Table 6: Teacher-class table.

Data item	Type of data	Significance
Teacher ID	int, not null	Teacher ID number
Class ID	int, not null	Class ID number
Pwd	Varchar(10), not null	Class password

The table shows that students belong to different classes and can have their own student IDs in different classes. Both the student ID number and the class ID number together identify a student in a unique class.

Teacher-class table is shown in Table 6.

This table shows that teachers can teach multiple classes, and each class has its own class password. The teacher ID number and the class ID number uniquely identify the class owned by the teacher.

5. Conclusion

This paper adopts theories and methods such as dual-core technology and uninterrupted information flow model to design trust path, trust transfer chain, reliability analysis, construction of remote authentication, and other technical methods, and apply them in the embedded trusted computing environment. Appropriate trust routing construction methods, reliability analysis models, and remote authentication methods have been experimented with, and good results have also been achieved. The network-based complementary education system is a new application field, which can overcome the limitations of time and space and provide a better educational environment for students. In this article, based on the status quo of physical education, we examine the application of network technology in sports support network systems in sports auxiliary network systems.

Data Availability

The data used to support the findings of this study can be obtained from the author upon request.

Conflicts of Interest

The author declares that there are no conflicts of interest.

References

[1] K. Janczak and D. Janczak, "Nonlinear signal processing with minimization of spectral distortion for embedded systems," *IFAC-PapersOnLine*, vol. 51, no. 6, pp. 450–455, 2018.

[2] P. H. Coppock, M. K. Yacoub, B. L. Qin, A. J. Daftardar, Z. Tolaymat, and V. J. Mooney III, "Hardware Root-of-Trust-based integrity for shared library function pointers in embedded systems," *Microprocessors and Microsystems*, vol. 79, Article ID 103270, 2020.

[3] C. C. Duru, A. C. O. Azubogu, and A. N. Aniedu, "Review of embedded systems security," *Journal of Engineering and Applied Sciences*, vol. 17, no. 2, pp. 196–206, 2020.

[4] S. Bajikar, "Trusted platform module (tpm) based security on notebook pcs-white paper," *Mobile Platforms Group Intel Corporation*, vol. 1, p. 20, 2002.

[5] Z. Shen and Q. Tong, "The security of cloud computing system enabled by trusted computing technology," in *Proceedings of the 2010 2nd International Conference on Signal Processing Systems*, vol. 2, pp. V2–V11, IEEE, Dalian, China, July 2010.

[6] T. K. Gupta and K. Raza, "Optimizing deep feedforward neural network architecture: a tabu search based approach," *Neural Processing Letters*, vol. 51, no. 3, pp. 2855–2870, 2020.

[7] X. J. Luo, L. O. Oyedele, A. O. Ajayi et al., "Genetic algorithm-determined deep feedforward neural network architecture for predicting electricity consumption in real buildings," *Energy and AI*, vol. 2, Article ID 100015, 2020.

[8] M. Da'i, O. D. Cahyani, and S. S, "Motivation in physical education (PE) learning through online system," *Kinestetik: Jurnal Ilmiah Pendidikan Jasmani*, vol. 5, no. 1, pp. 102–110, 2021.

[9] J. Zhou, "Virtual reality sports auxiliary training system based on embedded system and computer technology," *Microprocessors and Microsystems*, vol. 82, Article ID 103944, 2021.

[10] H. J. Wu, X. K. Li, and H. Y. Zhao, "A research on sports training auxiliary system based on cloud computing," *Applied Mechanics and Materials*, vol. 397-400, pp. 2495–2498, 2013.

[11] X. Liu, Z. Lin, and Z. Lin, "An auxiliary system for rehabilitation training," *Journal of Physics: Conference Series*, vol. 1920, no. 1, Article ID 012078, 2021.

[12] M. McClelland, "Standards - metadata standards for educational resources," *Computer*, vol. 36, no. 11, pp. 107–109, 2003.

[13] J. Atenas, L. Havemann, and E. Priego, "Open data as open educational resources: towards transversal skills and global citizenship," *Open Praxis*, vol. 7, no. 4, pp. 377–389, 2015.

[14] I. K. M. Jais, A. R. Ismail, and S. Q. Nisa, "Adam optimization algorithm for wide and deep neural network," *Knowledge Engineering and Data Science*, vol. 2, no. 1, pp. 41–46, 2019.

[15] C. J. C. Bravo, R. Á. Berríos, and T. M. Aide, "Species-specific audio detection: a comparison of three template-based detection algorithms using random forests," *PeerJ Computer Science*, vol. 3, p. e113, 2017.

[16] H. Abulkasim, H. N. Alsuqaih, W. F. Hamdan et al., "Improved dynamic multi-party quantum private comparison for next-generation mobile network," *IEEE Access*, vol. 7, pp. 17917–17926, 2019.

[17] P. Plantinga, D. Bagchi, and E. Fosler-Lussier, "Perceptual loss with recognition model for single-channel enhancement and robust ASR," 2021, http://arXiv.org/abs/2112.06068.

[18] Y. Xiang, T. Tang, T. Su et al., "Fast crdnn: towards on site training of mobile construction machines," *IEEE Access*, vol. 9, pp. 124253–124267, 2021.

[19] C. Zheng, X. Peng, Y. Zhang, S. Srinivasan, and Y. Lu, "Interactive speech and noise modeling for speech enhancement," in *Proceedings of the AAAI Conference on Artificial Intelligence*, vol. 35, no. 16, pp. 14549–14557, March 2021.

[20] P. López Matencio, J. V. Alonso, F. J. González Castano, J. L. Sieiro, and J. J. Alcaraz, "Ambient intelligence assistant for running sports based on k-NN classifiers," in *Proceedings of the 3rd International Conference on Human System Interaction*, pp. 605–611, IEEE, Melbourne, Australia, May 2010.

Hindawi
Mobile Information Systems
Volume 2022, Article ID 7438159, 11 pages
https://doi.org/10.1155/2022/7438159

Research Article

Artificial Intelligence Aerobics Action Image Simulation Based on the Image Segmentation Algorithm

Tao Jiang

School of Physical Education, Hebei Normal University, Shijiazhuang 050000, Hebei, China

Correspondence should be addressed to Tao Jiang; jiangtao0727@hebtu.edu.cn

Received 2 August 2022; Revised 17 September 2022; Accepted 26 September 2022; Published 10 October 2022

Academic Editor: Shadi Aljawarneh

At present, aerobics is becoming a popular fashion with the continuous development of cultural needs. Because aerobics has the characteristics of many movements, rapid changes, strong complexity, and difficult performance of difficult movements, the current aerobics teaching still presents shortcomings such as low teaching level, limited teachers' resources, and energy. Therefore, it is difficult to effectively meet the actual learning needs of students. Based on this point, artificial intelligence can be used to simulate and guide the technical movements of aerobics to effectively teach students. In this paper, an artificial intelligence aerobics image simulation system is researched and developed and the GrabCut image segmentation algorithm is mainly used. After analyzing some shortcomings of the algorithm, the GrabCut algorithm cascade and graph-based are selected to complete the optimization, so as to lay a good system foundation and then build the aerobics artificial intelligence image simulation system according to the algorithm foundation. Finally, it analyzes and researches the actual problems of aerobics teaching activities in colleges and universities and focuses on the problems, achievements, and personal satisfaction of students who use the system in actual learning, which proves that the system can effectively assist aerobics teaching activities. By studying the image segmentation algorithm and artificial intelligence technology, this paper applies it to the field of aerobics action image simulation, so as to promote its technological development.

1. Introduction

In the early 1980s, aerobics became popular all over the world with the global fitness boom because of its strong vitality. The success of Beijing's bid for the Olympic Games in 2008 greatly affected national fitness awareness, and more and more people participated in sports activities [1]. Aerobics is one of the ten most popular "national fitness" sports in China. It not only has the unique charm of sports but also can help people maintain themselves and pursue the spirit of the times. It is a fashionable sport and is favored by people [2]. In modern society, due to environmental reasons and various other factors, people's living standards are improving day by day. Aerobics is widely valued by people due to its many advantages and practicability and attracts enthusiasts of all ages to participate, forming a certain large-scale loyal consumer group [3]. Various media took the opportunity to produce and promote aerobics-themed TV programs, thus earning enough ratings. Aerobics can be performed in a variety of environments, and its use of venues has a certain collective nature, so it provides a variety of opportunities for corporate advertising. Aerobics is favored by many companies [4, 5]. However, due to the complexity and professionalism of the technical movements of aerobics, ordinary people often face different situations in the learning process. Therefore, it is important to perform image simulation for the aerobics exercise process, which can be realized using artificial intelligence and image segmentation algorithm. Image simulation based on computer technology has completely changed the camera imaging process. It can study the influence of each imaging link on the imaging results and qualitatively or quantitatively describe the comprehensive performance of the measurement system. This helps us understand many factors that affect system performance. It also provides data support for the parameter optimization and design of the system modules. In addition,

this paper also designs a kind of virtual experimental platform, which can save a lot of costs compared with the field test, and provides an analysis method for forming related strategies to further improve the actual imaging system. This paper studies the artificial intelligence aerobics action image simulation system, introduces the principle and optimization of the image segmentation algorithm, the artificial intelligence aerobics action image simulation design, and the aerobics exercise action image, and introduces the effect of the simulation application. Finally, the system is evaluated, and it is found that the system can effectively assist teachers in aerobics teaching.

2. Related Work

tThe literature proposes an image-oriented object detection algorithm, which is based on YOLO's traditional convolutional neural network Gaussian model. The article first analyzes the target image detection algorithm, explains in detail the YOLO convolutional neural network, summarizes the advantages and disadvantages of such algorithms, and solves problems such as the defect of candidate frame accuracy, based on this algorithm optimization [6, 7]. The literature proposes a target tracking algorithm for video, which has the characteristics of multifeature fusion and can filter the target video to identify its target features. The literature proposes a fusion target tracking algorithm, which can be simulated based on CN features. The HOG and LBP features are simulated, experiments are designed to prove the superiority of the fusion algorithm, and then the optimal parameters are selected [8]. The simulation results show that the optimization of the target detection algorithm can effectively improve its tracking accuracy. However, due to the increase in segment size, the complexity of the algorithm increases slightly, which can achieve a certain optimization effect [9]. The literature uses the transfer function method to explain the basic theory of image simulation, and then based on the analysis of the principle of the physical image of the camera, from the perspective of the modulation transfer function, the mathematical model of the spatial filtering effect is established [10]. Each sublink is studied from the camera imaging link, focusing on analyzing the influence of the changes in the model parameters on the imaging results. The literature establishes the corresponding calculation simulation model of each model, realizes the graphical modeling of each module under the Simulink platform, and completes the design and parameter setting of the input and output ports [11]. Based on the establishment of the model library, the imaging system of the target space measurement camera and the space measurement camera imaging system based on the Earth's atmosphere background were developed, respectively, and then the imaging correctness of the simulation model was verified [12].

3. The Principle and Optimization of the Image Segmentation Algorithm

3.1. Principle of the Traditional Image Segmentation Algorithm. The pixel value vector of an image consisting of N pixels is Z ($Z1$, $Z2$, $Z3$,. . ., ZN), and the pixel values can be grayscale values or RGB values. The segmentation of this image is represented by a mask vector. In general, determining the value of the mask vector is the solution to an optimization problem, i.e., x is the solution of the following optimization problem:

$$\begin{aligned} &\min_{r} \ f(\alpha) \\ &s.t. \\ &\alpha_i \in \{0,1\}, i = 1, \ldots, N. \end{aligned} \tag{1}$$

In general, the objective function $f(a)$ is the cost function of the segmentation.

The objective function $f(a)$ of the GrabCut segmentation algorithm is an energy function, which consists of two parts: one is the energy of the data element, and the other is the energy of the smoothing term.

In order to give the specific mathematical expression of the energy function, the s-t network diagram corresponding to the image is first introduced, as shown in Figure 1:

Figure 1 shows a schematic diagram of an s-t network graph. The sum of all t-links edge weights is called the energy smoothing term, denoted by V; the sum of all "n-link" edge weights is called the energy data term, denoted by U. The weighted average of the energy data term and the energy smoothing term is called the graph energy.

Define the matrix:

$\Phi_i = (\varphi(\alpha_i, k_i))_{2\sim K'}, i = 1, \ldots, N; \quad \Phi = (\Phi_1; \Phi_2; \ldots; \Phi_N)_2 < NK, \Omega_i = (\mu(\alpha_i, k_i))_{2\sim K}, i = 1, \ldots, N; \ \Omega = (\Omega_1; \Omega_2; \ldots; \Omega_N)_{2\times NK}, \Sigma_i = (\Sigma_i(\alpha_i, k_i))_{2K}, \ i = 1, \ldots, N; \Sigma = (\Sigma_1; \Sigma_2; \ldots; \Sigma_N)_{2\sim NK}.$ (2)

Then, define the GMM model parameter set matrix Θ as follows:

$$\theta = (\Phi; \Omega; \Sigma)_{2\cdot 3NK} \triangleq \theta(\alpha, \mathbf{K}). \tag{3}$$

Let U be the data object energy, i.e., the edge weight between the pixel and the source and sink points of the s-t grid; then, U can be expressed as follows:

$$U(\alpha, \mathbf{K}, \theta, \mathbf{Z}) = \sum_{i-0}^{N} D(\alpha_i, k_i, \theta_i). \tag{4}$$

The expression of D (a_i,k_i, θ_i) is as follows:

$$D(\alpha_i, k_i, \theta, z_i) = \log \ \varphi(\alpha_i, k_i) p z_i \mid \alpha_i, k_i \theta, \tag{5}$$

where p ( ) is the probability density function of the Gaussian model function. Further calculation can be obtained as follows:

$$\begin{aligned} D(\alpha_i, k_i, \theta_{z_i}) = -\log \ \varphi(\alpha_i, k_i) + \frac{1}{2} \log \ \det \Sigma(\alpha_i, k_i), \\ + \frac{1}{2}[z_n - \mu(\alpha_i, k_i)]^T \Sigma(\alpha_i, k_i)^1 [z_n - \mu(\alpha_i, k_i)]. \end{aligned} \tag{6}$$

Let C be the neighborhood of a pixel (usually four neighborhoods or eight neighborhoods), and let V be the energy of the smooth term, that is, the weight of the edge between each pixel in the s-t network, then V can be expressed as follows:

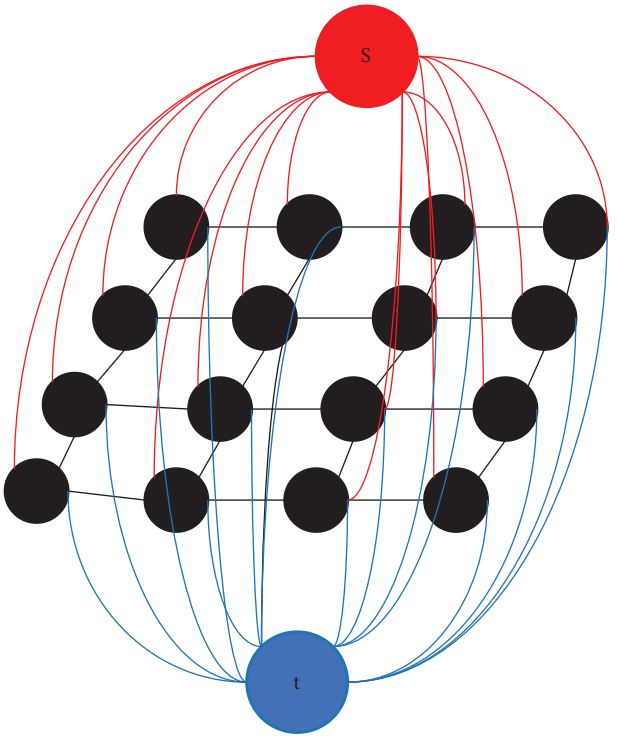

Figure 1: s-t network structure diagram.

$$V(\alpha, \mathbf{Z}) = \sum_{(m,n)iC} \left(1 - \delta_{a_m{}^a}\right) \| m - n\|^1 \exp\ -\beta 3 z_m - z_n \|, \tag{7}$$

where m *and* n are the positions of the pixels and δ_{aman} is the discrete δ function:

$$\delta_{\alpha_m \alpha_n} = \begin{cases} 1, & \alpha_m = \alpha_n, \\ 0, & \alpha_m \neq \alpha_n. \end{cases} \tag{8}$$

The parameter β has the following representation:

$$\beta = \left(2\langle \| z_m - z_n \|^2 \rangle\right)^1. \tag{9}$$

The Gibbs energy E of an image is defined as follows:

$$E(\alpha, K, 0, Z) = U(\alpha, K, 0, Z) + \gamma V(\alpha, Z), \tag{10}$$

where Υ is a coefficient greater than 0, representing the weight of the smoothing term.

3.2. Improvement of the Image Segmentation Algorithm. Aiming at the segmentation defect of GrabCut, this paper proposes a segmentation algorithm based on graph-based + GrabCut, which improves the segmentation performance. The specific flow of the algorithm is shown in Figure 2.

The specific steps to optimize the GrabCut algorithm are as follows:

(1) Perform graph-based region segmentation on the input image, maintain segmentation labels, and calculate segmentation results.

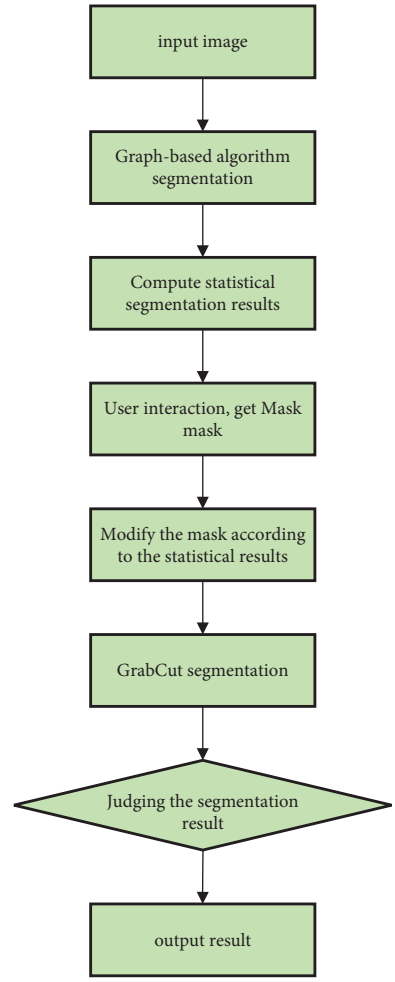

Figure 2: The improved GrabCut algorithm.

(2) Foruser interaction, start the mask graph and modify the mask according to the result of step 1. The scale of each label in the graph-based section that defines the user's rectangular area is L_i; then,

$$L_i - \frac{R_i}{S_i} i - 1, 2, \ldots, n, \tag{11}$$

where R_i is the number of labeled pixels i in the rectangle, S_i is the number of labeled pixels i in the entire image, and n is the number of all annotations in the rectangle. If L_i is less than a certain threshold, then it means that most of the pixels in this area are distributed outside the rectangular box, so changing the mask map of this area can be easily segmented.

(3) GrabCut segmentation is performed on the image to judge the segmentation effect.

3.3. Analysis of Image Segmentation Results. In the data point competition algorithm, the data point aggregation can be defined as the sum of the first r maximum similarities of the data points and the aggregation energy can be used to determine the result of the data point competition. The smaller the relative energy, the more likely it is to become a member

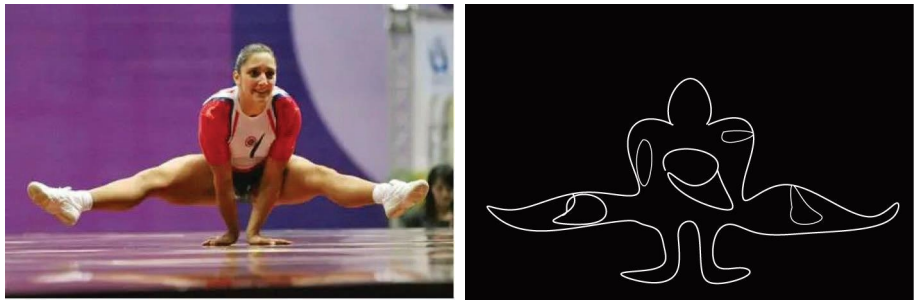

Figure 3: Image segmentation of aerobics movements.

of the class. The data point competition clustering algorithm performs clustering according to the aggregation energy defined by the data similarity matrix to obtain the final image segmentation result. The image segmentation result of aerobics is shown in Figure 3.

The optimized Jetson Nano model is deployed for testing. The accuracy and real-time performance of PR_Yolact before and after using TensorRT are compared. At the same time, TensorRT-based model inference accelerates and compares low-precision operations with different optimization precisions in the test set and test video. The experimental results of the inference acceleration control are shown in Table 1.

As can be seen from Table 1, the initial Yolact network model is not very good in terms of recognition time and accuracy. In terms of accuracy, the mAP changes on both the device side and the PC side are the same, but the delay speed is very different. At the same time, the influence of data types between different FPS models is also obvious. It can be seen that compared to the PR_Yolact model, the fp32-optimized half-precision TensorRT model increases the FPS by 2.65 times. Compared with the Yolact model, the FPS of the half-precision network hybrid fp32 model is improved to 2.70. Compared to the unoptimized Yolact model in the table, TensorRT fp16 loses 4% mAP when accelerated with TensorRT inference but improves the frame rate by 3.3x. Compared with TensorRT fp32, TensorRT fp16 has the highest optimization structure loss, reaching 56.74 and 34.38, respectively, while the FPS is increased to 2.70, and the converted model parameters are the lowest, which basically meet the expected design indicators.

Table 1: Inference effect on Jetson Nano.

Model	mAPBbox	mAPMask	FPS
Yolact	56.12	36.03	0.79
PR-Yolact	61.40	38.00	0.82
TensorRT fp32	58.33	35.76	2.17
TensorRT fpl6	56.74	34.38	2.70

4. Artificial Intelligence Aerobics Action Image Simulation Design

4.1. Image Simulation Process. The simulation calculation must use the input conditions, calculate, and output the correct simulated image according to the pixel equation. To achieve the goal of fast frame-by-frame computing, it is necessary to rely on GPU (Graphics Processing Unit) programming technology.

According to the calculation order and logical structure, GPU programming units are divided into vertex processors and fragment processors. Among them, the vertex processor first converts the 3D model: converts the top-level mesh data of the 3D model from the model coordinate system to the world coordinate system, and then converts it to the observation coordinate system by position. This process is based on the direction of the camera view surface and finally passes steps such as frustum clipping being mapped to the screen coordinate system; the fragment processor first calculates the pixel equation: first rasterizes the output data of the vertex processor to obtain two-dimensional data in the screen space, and then inputs the coordinates of the texture unit and simulation input. The data is substituted into the pixel equation for calculation, and finally, the simulated image is output pixel by pixel. In the GPU programming language, Cg can be used to write node and fragment handlers that perform grayscale calculations on the target background image. Synthesizer techniques are required for backscatter, noise, and MTF effects where pattern grid peaks are difficult to pinpoint. In essence, the synthesizer technology still uses the Cg language, but it belongs to the image postprocessing operation, that is, after the rendering is completed and before the image is output, the fragment processor is used again to perform operations such as grayscale superposition and convolution.

As shown in Figure 4, in the simulation calculation of aerobics motion, firstly, the vertex processor sends the vertex coordinates of the aerobics motion image grid to the fragment processor, such as factors and grid vertex positions, to calculate the aerobics motion image and the ambient light BRDF of the fragment processor; then, according to the pixel equation of the aerobics action image, the grayscale of the image is calculated pixel by pixel on the GPU; finally, according to the backscatter pixel equation, the noise is equal to the energy and the MTF convolution kernel and the post adds a synthesizer to the scattering, noise, and MTF effects to get a graphic simulation of aerobics movements and output.

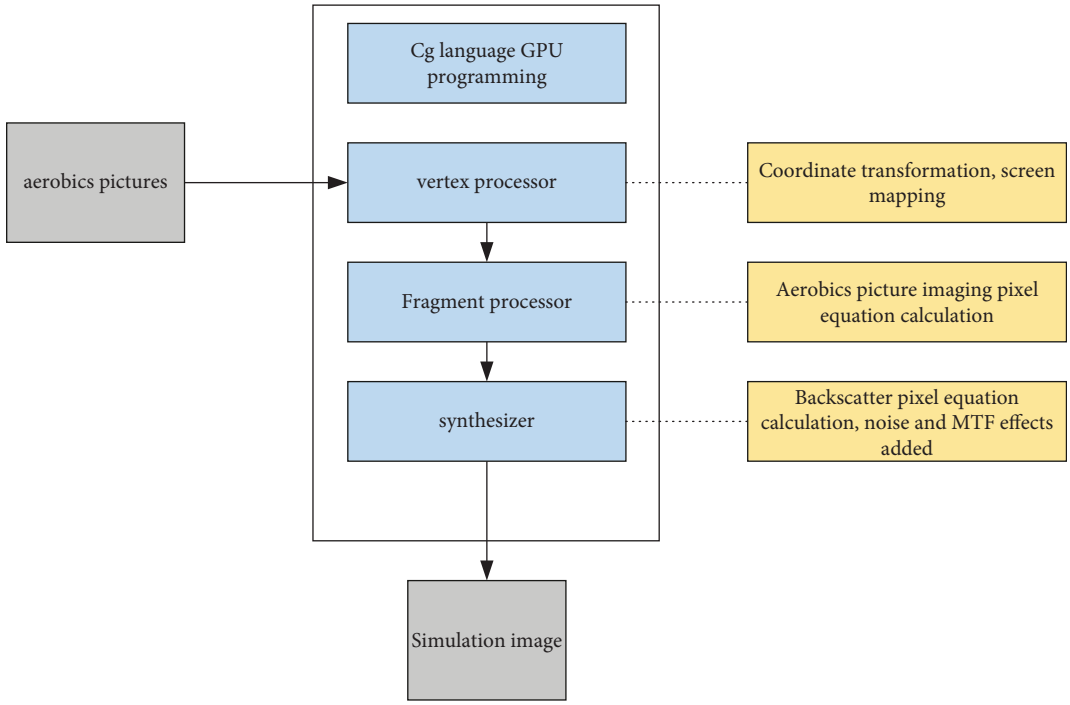

Figure 4: Schematic diagram of simulation calculation flow.

4.2. Design of Aerobics Action Image Simulation Module Library. A more powerful module is built based on Simulink's own module, which is equivalent to a subsystem of the simulation system. By encapsulating this subsystem, a user-defined function module can be obtained. The module library developed in this paper is mainly based on the existing Simulink module library and a small number of user-defined function modules built with function *S*. The current module library is as follows:

(1) Analyze the module to be created according to user needs and usage, and determine the module's function, name, input and output interfaces, and internal parameters.

(2) According to the function of the module, establish a mathematical model, analyze the data flow of the model, and establish a calculation model corresponding to the mathematical model.

(3) Convert the computational model to a Simulink model according to the data flow direction. The specific operation is as follows: open Simulink, first create an mdl file, then drag the required modules into the mdl file, connect the modules with connecting lines, and obtain the Simulink model corresponding to the mathematical model.

(4) Perform standard module encapsulation, and sett parameters, names, display icons, background colors, and so on.

The coordinate change module group is usually divided into the basic coordinate change module group of aerobics action shots and the common coordinate change module group. When the coordinate system is transformed, the main function of this group of modules is to translate and rotate the point or space vector according to the transformed value, as shown in Figure 5.

This group of electronic circuit filter modules consists of the CCD charge transfer module, low-pass filter module, high-pass filter module, and high-frequency lift module, which are used to simulate the effect of spatial signal modulation. It is established based on the mathematical model of the formula, as shown in Table 2. Parameter settings for all electronic circuit filter modules are listed.

The platform motion module group is composed of the linear motion module, high-frequency axial motion module, vertical axis high-frequency motion module, low-frequency axial motion module, vertical axis low frequency, and random module. They are used to simulate blurring of images due to platform movement. It is mainly based on the mathematical model acquisition of formulas. Table 3 lists the parameter settings of all platform motion filtering modules.

4.3. Experimental Environment Construction. The purpose of the scene management layer is to create and manage dynamic 3D scenes that can be rendered in real time. The scene should include the target background element and the camera element. By integrating the target background, controlling the camera window, and calculating the simulated image, the simulation results of any spatial position can be dynamically output.

This section mainly depends on the environment configuration of OGRE 3D image rendering engine and image simulation platform. Among them, OGRE is an open-source multi-GUI 3D rendering engine, which implements the core encapsulation of Direct3D and

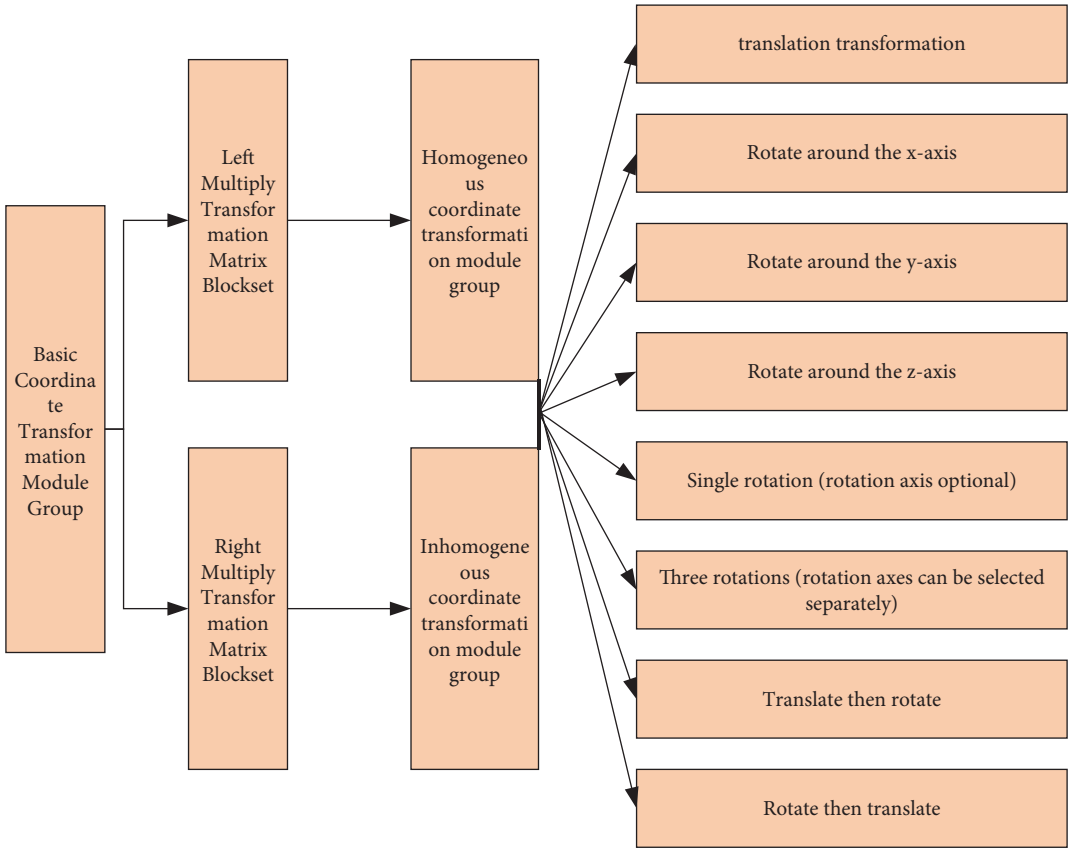

Figure 5: Basic coordinate transformation module group.

Table 2: Electronic circuit filtering Simulink block parameter settings.

Electronic circuit filter module	Parameter settings
High lift	Maximum lift frequency, lift multiple and order
High-pass filter	High-frequency cut-off frequency, filter order
Low-pass filtering	Photosensitive element center distance, low-frequency cut-off frequency, clock frequency of transfer output area, filter order
CCD charge transfer	Total number of charges transferred, charge transfer efficiency, pixel size

Table 3: Simulink block parameter settings for platform motion filtering.

Platform motion filter module	Parameter settings
Random jitter	RMS displacement
Nonaxial low frequency vibration	The equivalent image movement in the x-direction during the integration time and the equivalent image movement in the y-direction during the integration time
Axial low frequency vibration	Equivalent defocus amount during integration time
Nonaxial high frequency vibration	Amplitude in the x-direction, amplitude in the y-direction
Axial high frequency vibration	Amplitude, F-number of optical systems
Linear motion	Exposure time, image movement speed

OpenGL, supports Cg language and synthesizer technology, and only exposes an easy-to-use API (application programming interface). Using the C++ programming language to call the API, real-time interaction and data calculation can be realized, and simulated images can be dynamically generated in the screen space. In addition, the operation of the simulation platform depends on the reasonable configuration of the environment. The configuration used for development is shown in Table 4. At about 120 frames, the measured frequency can be stable and the output is smooth.

4.4. Quality Evaluation of Aerobics Action Image Simulation. Evaluating the quality of the simulated images can directly identify the imaging performance of the current system and

Table 4: Environment configuration of the image simulation platform.

Hardware Configuration	Central processing unit (CPU)	Intel(R) core(™) i5-12400 CPU @ 3.00 Hz
	Memory and hard disk capacity	16.00 GB RAM + 256 GB HDD
	Graphics card model	NVIDIA GeForce GTX 2080s
	Monitor	1920 × 1080 resolution
Software configuration	Operating system	Windows 10 64 bit
	Dependency library	Microsoft DirectX SDK (August 2021) vcredist x86
	Rendering engine	OGRE SDK 1.6.4

can also provide direction for further system design and optimization. In this section, the physical effect model and simulated images are comprehensively applied. By controlling the detection conditions and image effects, the degree of image blurring is studied, the target and background, signal-to-noise ratio, and action distance and influence are compared, and the influencing factors and system performance evaluation charts under each index are obtained. Due to the large number of parameters, the default input data selected in this section is only explained when data is replaced.

There are many factors that affect the degree of image blur, which can be quantified by entering fidelity. If the image size is $N \times M$, $f_s(I, j)$ is the grayscale of the simulated image pixel, and $f(i, j)$ is the grayscale of the image pixel after deblurring; the fidelity formula is as follows:

$$\text{fidelity} = 1 - \frac{\sum_{i=0}^{N-1} \sum_{j=0}^{M-1} \left(f(i,j) - f_s(i,j)\right)^2}{\sum_{i=0}^{N-1} \sum_{j=0}^{M-1} f^2(i,j)}. \tag{12}$$

The closer fidelity is to 1, the greater the image similarity and the clearer the simulated image.

The background contrast of the target mainly affects the detection and recognition of the target in the background. The higher the contrast, the sharper the target segment. For the aerobics action image imaging system, the background can be divided into the ground object background and the sky background. When taking the grayscale of the image as a parameter and referring to the concept of relative contrast, this paper defines the target background contrast as follows:

$$C = \frac{\left| \text{Gray}_t - \text{Gray}_b \right|}{\max\left(\text{Gray}_t, \text{Gray}_b\right)}. \tag{13}$$

In the formula, Grayt is the average gray level of the target area, and Grayb is the average gray level of the background in a smaller area outside the target contour.

5. Effect of Aerobics Action Image Simulation

5.1. Analysis of the Current Situation of Aerobics Teaching. From the results in Table 5, it can be seen from the students' point of view that the most obvious disadvantage of traditional aerobics teaching is that the teaching is too mechanical, and it is difficult to enhance students' interest in learning, accounting for 54.8%. 39.1% of people have different understandings of technical movements due to different angles. Because they know themselves better than others, students have little understanding of the influence of teachers on aerobics teaching and the same principle applies to teachers. From the teacher's point of view, 58.9% of the teachers believed that in the traditional teaching method, the nonstandard teacher's demonstration actions affected the teaching quality. 52.6% of teachers believe that teachers' performance in the classroom affects the quality of teaching. With the increase of age, their physical quality gradually declines. In teaching, there are many movements that may not be perfectly realized and the demonstration is not in place, thus affecting students' learning of skill movements; 31.6% of teachers mentioned that teachers' professional skills affect the teaching quality. In the aerobics teaching process there are multiple aerobics teachers at the same time. However, due to the different styles of aerobics, teachers are good at different styles. In teaching, they prefer their own teaching style. Some teachers may not change their teaching style for many years. The main disadvantage of the traditional teaching mode is that the method of acquiring information and knowledge is relatively conservative, and it is not easy for students to learn. Statistical table of problems in the auxiliary teaching of aerobics system in a university is as shown in Table 6.

Comparing Table 5 with Table 6, it can be seen that aerobics teachers and students in a certain college clearly feel the advantages of multimedia-assisted teaching and the ratio of teachers is higher than that of students. Teachers need to pay attention to the learning situation of students and the use of multimedia equipment in actual teaching. There are many tasks that should be held responsible. Therefore, they feel that controlling the classroom is no easier than traditional teaching methods. 37.9% of the teachers believed that the teachers could not use the aerobics auxiliary teaching system skillfully, which affected the teaching level; 29.5% of the teachers believed that the teachers failed to adapt to the current teaching mode, which led to the disorder of the teaching order. Similarly, when students see that teachers do not use or are not proficient in using equipment, they will think that teachers have poor teaching ability; 41.1% of students think that the effect of action image simulation is slightly lower than that of real-life demonstrations, which affects students' learning and understanding ability. This is because students learn by themselves based on the aerobics system. If the video effect is not good, such as failure to play, blur, irregular movements, and wrong teaching methods, it is easy to cause misunderstanding or direct learning of wrong actions, which will lead to the learning of teaching content. The progress is slowed down, which affects the teaching progress; teachers not only teach students knowledge but also take the responsibility of educating students' mental health. Therefore, some teachers (46.3%)

Table 5: Statistical table of problems in the traditional teaching mode of aerobics in a university.

Problems in the traditional teaching mode of aerobics	Teacher ratio (%)	Student ratio (%)
Teaching is too mechanical; it is difficult to enhance students' interest in learning	16.9	54.8
Teachers' professional skills affect the quality of teaching	31.6	18.2
Teachers' performance in the classroom affects the quality of teaching	52.6	26.8
Teachers' nonstandard demonstration actions affect the quality of teaching	58.9	23.0
Students from different positions and angles have different observation effects and different teaching results	40.0	39.1
Other	0.0	10.9

Table 6: Statistical table of problems in the auxiliary teaching of aerobics system in a university.

Problems in assisted teaching of aerobics system	Teacher ratio (%)	Student ratio (%)
Teachers fail to adapt to the current teaching model, leading to disordered teaching	29.5	16.0
Teachers are not proficient in using the aerobics auxiliary teaching system, which affects the teaching level	37.9	10.6
Compared with the real-life demonstration, the action image simulation is slightly less effective, which affects the students' learning and comprehension ability	23.1	41.1
Facing the camera and image collection may affect the sports confidence of some students	46.3	24.5
Other	8.4	8.6

still think that video feedback is useful for students to discover mistakes and correct themselves, but they are worried that doing so would affect their psychological level and students' self-confidence, so they did not use video feedback for teaching. But if the students cannot face the facts correctly, is this a good form of education? Therefore, it is unscientific to refuse to use video feedback for teaching. Instead, students should understand what it means before using it and should have a good attitude to get more benefit from it. In addition, some students resist the aerobics system-assisted teaching because of poor teaching quality and their ability to learn and understand cannot keep up with most of their peers. Therefore, different levels of teaching are carried out according to their needs.

5.2. Problems Existing in the Teaching of Aerobics in Colleges and Universities

5.2.1. Some Teachers Have Too Deep Traditional Teaching Concepts. Many teachers still feel that multimedia teaching is far removed from the teaching methods they usually use. Modern teaching emphasizes taking students as the main body, allowing students to be independent, innovative, and individualized. The teaching method of teachers is important, but more important is the education of students [13]. If the learning method becomes monotonous, it will burden the students' subtle thinking, which will reduce the students' future development space, which is an unsustainable teaching method. Without the aid of computerization, teaching will soon become out of date. Outdated concepts of teachers are a potential large-scale risk [14].

5.2.2. The Level of Production and Use of Aerobics System Courseware in Aerobics Theory Class Are Relatively Low. The problems existing in the production of aerobics theory courses are mainly that the courses come from a wide range of sources, the courses lack a unified orientation and systematization, and the courses designed by teachers themselves are of low quality and lack of focus. There are difficulties in the content, the content is too much, the teaching method is single, and there is a lack of characteristic image. The advantages of the aerobics system have not been fully utilized, the content of the teaching materials is simply copied in the course, and the aerobics system is like a projector [15]. In use, because the lecture speed is too fast and the content is too large, it is difficult for students to understand the key points and it is inconvenient to take notes, which affects the learning effect and has a specific impact on the review effect and after-class exams. Some teachers' teaching process is as rigid and mechanical as chanting scriptures [16]. Combined with the dim lighting in the classroom, it is easy to make students feel bored and sleepy. Over time, students get bored and lose their initial interest and enthusiasm [17].

5.2.3. Teachers Rely Too Much on the Aerobics System in Teaching. Due to the many advantages of the aerobics system teaching, it has become an important part of the physical education teaching method, but in the process of using it, some teachers have a wrong understanding of the aerobics system teaching and think that a good class should use the aerobics system. Many teachers blindly rely on the aerobics system technology, continue to use the aerobics system technology, but do not focus on improving their own teaching quality, so that if the equipment fails during the class, the teaching will not continue.

5.3. Analysis of Aerobics Action Image Simulation. The comparative analysis of the accuracy, proficiency, coordination, and expressiveness of aerobics movements in the experimental class and the control class is shown in Table 7:

Table 7: Comparative analysis of the accuracy, proficiency, coordination, and expressiveness of aerobics movements between the experimental class and the control class.

Accuracy	Very accurate (%)	More accurate (%)	Precise (%)	Inaccurate (%)
Experimental class	34	56	8.4	1.6
Control class	20	57	16.4	6.6
Proficiency	Very skilled (%)	More proficient (%)	Proficiency (%)	Unskilled (%)
Experimental class	36.2	50	8.8	5
Control class	33.1	51	10.9	5
Coordination	Very coordinated (%)	More coordinated (%)	Coordination (%)	Dissonance (%)
Experimental class	40	40	15	5
Control class	35.4	51	4.6	10
Expressiveness	Very good (%)	Good (%)	Fair (%)	Poor (%)
Experimental class	21	55.5	16	6.5
Control class	8.4	62	13	16.6

Table 8: Comparative analysis of the experimental class and the control class.

Group	Mean	SD	T value	P value
Experimental class	72.28	4.577	0.198	0.355
Control class	73.47	4.866		
—	Girls class		Boys class	
	Number	Percentage	Number	Percentage
Excellent	16	80.00%	10	50%
Good	4	20.00%	8	40%
Pass	0	0	2	10%
Failed	0	0	0	0
Total	20	100%	20	100%
The average score	83.2	81.4		
P value		0.0136		
—	Boys control class		Girls experimental class	
	Number	Percentage	Number	Percentage
Excellent	3	15.00%	16	80.00%
Good	10	50.00%	4	20.00%
Pass	7	35.00%	0	0
Failed	0	0	0	0
Total	20	100%	20	100%
The average score	78.6		83.2	
P value		0.0746		

From the data analysis in Table 7, it can be seen that there is a certain gap between the motion accuracy design of the experimental class and the control class, and the score of the experimental group is higher than that of the control group. Therefore, adding a video feedback mode during the teaching process can effectively improve the accuracy of students' movements. There is only a small gap between the technical ability of the students in the experimental group and the control group. The former has a higher coordination score than the latter, and most of the latter's data are in a relatively coordinated stage. Multimedia assistance for the actual teaching of aerobics can effectively promote the development of students' coordinated physical quality.

As shown in Table 8, the results of the girls' experimental class are higher than that of the boys' experimental class, but there is no significant difference.

As shown in Table 9, 15% of aerobics teachers are very satisfied with using the aerobics system to teach aerobics practice classes, 25% of teachers are relatively satisfied, 35% of aerobics teachers are basically satisfied, 15% of teachers are not satisfied, and only 10% of teachers expressed dissatisfaction. From the data in the table, we can draw the following conclusions: most aerobics teachers believe that it is necessary to use the aerobics system for auxiliary teaching in aerobics classes, which can give full play to the advantages of the aerobics system and make up for the shortcomings of traditional aerobics teaching. Some aerobics teachers with backward educational concepts feel that it is meaningless, and they are not satisfied with the use of aerobics system to assist teaching.

The survey results in Table 10 show that 40% of the students are very satisfied with the use of the aerobics system for auxiliary teaching in aerobics teaching, 30% of the students are relatively satisfied, and only 5% of the students are dissatisfied with the aerobics system for auxiliary teaching.

5.4. Application Strategy of Aerobics Action Image Simulation

(1) According to different teaching stages and different teaching tasks, we grasp the time and frequency of using the intelligent aerobics action simulation system.

Table 9: Statistical table of satisfaction of teachers using the aerobics system in practice class of aerobics teaching in a university ($n = 20$).

Teacher satisfaction	Frequency	(%)
Very satisfied	3	15.0
Quite satisfied	5	25.0
Basically satisfied	7	35.0
Not so satisfied	3	15.0
Not satisfied	2	10.0

Table 10: Statistical table of students' satisfaction with the use of aerobics system in practice classes of aerobics teaching in a university ($n = 100$).

Student satisfaction	Frequency	%
Very satisfied	40	40.0
Quite satisfied	30	30.0
Basically satisfied	15	15.0
Not so satisfied	10	10.0
Not satisfied	5	5.0

(2) People should summarize various experimental research results and create a comprehensive and complete theoretical system of the intelligent aerobics exercise simulation system.

(3) Teachers should adjust the teaching plan in time, update the teaching method in time, and find the most suitable teaching method according to the teaching effect of each class and the feedback of students.

(4) The teaching method of intelligent aerobics action simulation system not only cultivates students' action imitation thinking but also helps teachers to improve their own teaching level. Teachers should not only operate the software system proficiently but also use it freely in the classroom, which is a test of teachers' ability to accept new things. Therefore, teachers should always learn and improve their abilities according to the requirements of the times.

6. Conclusion

Aerobics is an emerging sport that combines gymnastics, dance, and music. It has unique creativity and unique sense of rhythm and is an organic combination of art and sports, fitness, and beauty. There are many movements in aerobics, which help to improve the coordination and flexibility of the movement, but its own technical movements are more complicated. Based on this point, this paper studies an artificial intelligence aerobics action image simulation system using artificial intelligence technology and the image segmentation algorithm and uses image simulation feedback as a new method of aerobics teaching, which can be used to improve and adjust the movement requirements of aerobics teaching. This paper mainly introduces the image simulation and system design in detail and analyzes and improves the image segmentation algorithm, which is superior to the traditional GrabCut algorithm in segmentation accuracy and can be well divided. In terms of movement teaching, the system can help students who are exposed to aerobics to effectively reduce the injury rate of aerobics.

Data Availability

The data used to support the findings of this study are available from the author upon request.

Conflicts of Interest

The author declares that he has no conflicts of interest.

References

[1] L. Fuxiang, "Adaptive recognition method of aerobics decomposition action image based on feature extraction," *Science Technology and Engineering*, vol. 19, no. 7, pp. 148–153, 2019.

[2] P. Zaletel, G. Gabrilo, and M. Perić, "The training effects of dance aerobics: a review with an emphasis on the perspectives of investigations," *Collegium Antropologicum*, vol. 37, no. Suppl 2, pp. 125–130, 2013.

[3] A. Vitartaite, A. Vainoras, V. Sedekerskiene, and J. Poderys, "The influence of aerobics exercise to cardiovascular functional parameters of 30-40 year old women," *Medicina*, vol. 40, no. 5, pp. 451–458, 2004.

[4] M. Said, N. Lamya, N. Olfa, and M. Hamda, "Effects of high-impact aerobics vs. low-impact aerobics and strength training in overweight and obese women," *The Journal of Sports Medicine and Physical Fitness*, vol. 57, no. 3, pp. 278–288, 2017.

[5] M. MacKay-Lyons, S. A. Billinger, J. J. Eng et al., "Aerobic exercise recommendations to optimize best practices in care after stroke: AEROBICS 2019 update," *Physical Therapy*, vol. 100, no. 1, pp. 149–156, 2020.

[6] L. Yang, Z. Wang, and S. Gao, "Pipeline magnetic flux leakage image detection algorithm based on multiscale SSD network," *IEEE Transactions on Industrial Informatics*, vol. 16, no. 1, pp. 501–509, 2020.

[7] L. Qi, B. Li, L. Chen et al., "Ship target detection algorithm based on improved faster R-CNN," *Electronics*, vol. 8, no. 9, p. 959, 2019.

[8] D. Smith and S. Singh, "Approaches to multisensor data fusion in target tracking: a survey," *IEEE Transactions on Knowledge and Data Engineering*, vol. 18, no. 12, pp. 1696–1710, 2006.

[9] É. L. Souza, E. F. Nakamura, and R. W. Pazzi, "Target tracking for sensor networks: a survey," *ACM Computing Surveys*, vol. 49, no. 2, pp. 1–31, 2016.

[10] Z. Wang, Z. Zhou, H. Zhang, G. Zhang, H. Ding, and A. Farouk, "AI-based cloud-edge-device collaboration in 6G space-air-ground integrated power IoT," *IEEE Wireless Communications*, vol. 29, no. 1, pp. 16–23, 2022.

[11] L. Zhou, W. Min, D. Lin, Q. Han, and R. Liu, "Detecting motion blurred vehicle logo in IoV using Filter-DeblurGAN and VL-YOLO," *IEEE Transactions on Vehicular Technology*, vol. 69, no. 4, pp. 3604–3614, 2020.

[12] B. Y. Lee, K. M. Bacon, M. E. Bottazzi, and P. J. Hotez, "Global economic burden of Chagas disease: a computational simulation model," *The Lancet Infectious Diseases*, vol. 13, no. 4, pp. 342–348, 2013.

[13] J. Peng, W. Xu, and H. Yuan, "An efficient pose measurement method of a space non-cooperative target based on stereo vision," *IEEE Access*, vol. 5, pp. 22344–22362, 2017.
[14] L. Huang, "Research on the application of the function of computer management system in college aerobics teaching," *Journal of Physics: Conference Series*, vol. 1744, no. 3, Article ID 032148, 2021.
[15] C. Deng, "Optimization of college physical education curriculum system based on sports literacy theory," *Leisure*, vol. 21, no. 2, p. 155+158, 2019.
[16] B. A. Sibley and S. M. Bergman, "Relationships among goal contents, exercise motivations, physical activity, and aerobic fitness in university physical education courses," *Perceptual & Motor Skills*, vol. 122, no. 2, pp. 678–700, 2016.
[17] Z. Liu and Y. Wu, "Design of a university aerobics teaching network information platform (ATNIP)," *World Trans. on Engng. and Technol. Educ*, vol. 13, no. 1, pp. 34–37, 2015.

Hindawi
Mobile Information Systems
Volume 2022, Article ID 2958176, 12 pages
https://doi.org/10.1155/2022/2958176

Research Article

Simulation Analysis of Artificial Intelligence in Enterprise Financial Management Based on Parallel Computing

Zhu Feng

School of Accounting, Zhongnan University of Economics and Law, Hubei, Wuhan 430073, China

Correspondence should be addressed to Zhu Feng; z0003893@zuel.edu.cn

Received 15 August 2022; Revised 18 September 2022; Accepted 30 September 2022; Published 10 October 2022

Academic Editor: Shadi Aljawarneh

Under the background of today's society, people's daily life and production are inseparable from the use of information technology. With the rapid development of Internet technology and national information industry, more and more small and medium-sized enterprises choose to apply AI financial information management system. Based on this background, this paper introduces the principle of parallel computing and applies it to the financial management of enterprises together with artificial intelligence technology. Firstly, the paper discusses the model and form of the basic technology, then optimizes it, studies the actual financial management needs of small and medium-sized enterprises, completes the design and implementation of the system structure, and conducts simulation experiments to test the effectiveness of the system's functional performance. It can be seen from the test results that the system meets the design goals and has basic functions, but some details and contents need to be improved and supplemented. Therefore, we must strive to ensure the accuracy, preciseness, and reliability of financial management data. When more data are needed, faster and better data processing based on user needs and feedback is required. This paper delves into artificial intelligence technology and the idea of parallel computing. This paper applies it to the field of enterprise financial management to create an effective management system.

1. Introduction

The development of Chinese enterprises has ushered in a new era. First of all, China has become the fastest growing region in the world today. China's optical fiber data transmission and update volume is at the forefront of the world, and Chinese enterprises have entered the information age. Secondly, China's logistics technology has developed rapidly. Today's logistics and transportation volume is at the forefront of the world, and the logistics supply chain of enterprises has undergone great changes. Finally, China's mobile payment is in a leading position. Globally, China has become the most convenient mobile payment country for online and offline transactions in the world. Therefore, in order to take advantage of China's rapidly developing technologies, Chinese enterprise management will also face many pressures and challenges. In today's more important modern financial management field, the role of financial management is self-evident, and the quality of financial management system affects the overall quality of enterprise management [1]. Accordingly, optimizing the financial management system is the main goal of development in this field [2]. The traditional form of manual bookkeeping has been unable to meet the actual needs under the background of the gradual development of the enterprise business, and the main function of the financial management system is to use excellent computerized bookkeeping to replace the traditional inefficient manual bookkeeping [3]. The Chinese finance department emphasized that computerization of accounting is the main direction for the development of accounting activities in various fields in China in the future [4]. Institutions and state-owned enterprises need to realize the transformation of computer accounting and bookkeeping as soon as possible and follow the principle of step by step in the process [5]. However, due to the large number of small and medium-sized enterprises in China, the fields and business contents involved are different. Small and medium-sized enterprises conform to the trend of information technology development and realize optimization and reform for traditional operation methods. It hopes to

use network technology to realize the transformation of information management, so as to make itself develop better and faster. For businesses, the first step in managing information is financial management. Through information-based financial management, managers can plan, control, and further manage financial activities. Therefore, we need to use information technology to design a better and more practical financial management system to promote the healthy development of the enterprise and the entire enterprise financial system. In view of the current needs and development direction of small and medium-sized enterprises, this paper combines parallel computing and artificial intelligence to design a financial management system that can effectively meet the actual needs of small and medium-sized enterprises, so as to help small and medium-sized enterprises carry out more effective financial supervision and management, thus improving the development speed of enterprises and strengthening management [6].

2. Related Work

The literature believes that the ultimate goal of enterprise development is not only to pursue short-term profit maximization but also to achieve the goal of enterprise value maximization and wealth appreciation. At present, many countries are committed to improving the efficiency and level of the use of enterprise funds and improving the business activities of enterprises as much as possible, so as to maximize the output of enterprise investment [7]. After a lot of investigation and practice by scientific researchers, the modern financial management system is different from the previous accounting-based accounting management system and expands other business operations on the basis of the traditional financial management system [8]. In order to effectively combine the actual business process and operation, the management and interaction of data resources can be completed. In the context of the in-depth development of information technology, the financial management system and the business information systems of other industries are more coordinated and integrated [9]. The literature studies the relevant market and shows that computer management software usually consists of financial system, distribution system, production system, and decision support system, which is a highly integrated system. Each subsystem can work in coordination or independently [10]. When the subsystems are in cooperative operation mode, only a small amount of data needs to be input, and the entire system can exchange information. In this way, a complete scheme can be provided for the implementation of enterprise decision making [11]. The enterprise management information system is an organic combination of enterprise management, production management, accounting, and financial management [12]. The literature studies and analyzes the operation of the enterprise financial management system, discusses the problems and reasons that affect the normal operation of the financial management system, and, on this premise, designs an effective management control for the financial management system [13]. The business risk system adjusts the system operation mechanism, realizes business process reengineering, strengthens the effectiveness of the original system, and establishes a dynamic management platform for financial management that supports sustainable business development [14]. The literature shows that traditional financial processes have been unable to keep pace with the evolution of AI-powered financial management system capabilities. In response to this problem, the article conducts a preliminary study on the financial operation of artificial intelligence in business and summarizes some suggestions for guiding the reform of business financial processes [15, 16].

3. Algorithm Design of Parallel Computing

3.1. Basic Model of Existing Parallel Algorithms

3.1.1. DOT Model. The DOT model describes the implementation behavior of big data workloads in the form of arrays. The DOT model includes basic DOT blocks, combined DOT blocks, and DOT expressions. It can be described as

$$\begin{aligned}\overrightarrow{\mathrm{DJOT}} &= [D_1 \cdots D_n]\begin{bmatrix} o_1 \\ \vdots \\ o_n \end{bmatrix}[t] = \left[\bigcup_{i=1}^{n}\left(o_i\left(D_i\right)\right)\right][t], \\ &= [t\left(o_1\left(D_1\right), \cdots, o_n\left(D_n\right)\right)].\end{aligned} \tag{1}$$

Since the translation layer of the basic DOT block has only one node, the data it can handle are very limited. Therefore, several independent basic DOT blocks are combined into a unified DOT block. The formal description is

$$\begin{aligned}\overrightarrow{\mathrm{DOT}} &= [D_1 \cdots D_n] \\ &\quad \begin{bmatrix} o_{1,1} & o_{1,2} & \cdots & o_{1,m} \\ o_{2,1} & o_{2,2} & \cdots & o_{2,m} \\ \vdots & \vdots & \ddots & \vdots \\ o_{n,1} & o_{n,2} & \cdots & o_{n,m} \end{bmatrix}\begin{bmatrix} t_1 & 0 & \cdots & 0 \\ 0 & t_2 & \cdots & 0 \\ \vdots & \vdots & \ddots & \vdots \\ 0 & 0 & \cdots & t_m \end{bmatrix}, \\ &= \left[\bigcup_{i=1}^{n}\left(o_{i,1}\left(D_i\right)\right) \cdots \bigcup_{i=1}^{n}\left(o_{i,m}\left(D_i\right)\right)\right]\begin{bmatrix} t_1 & 0 & \cdots & 0 \\ 0 & t_2 & \cdots & 0 \\ \vdots & \vdots & \ddots & \vdots \\ 0 & 0 & \cdots & t_m \end{bmatrix}, \\ &= \left[t_1\left(o_{1,1}\left(D_1\right) \cdots o_{n,1}\left(D_n\right)\right)\right. \\ &\qquad \left. \cdots t_m\left(o_{1,m}\left(D_1\right) \cdots o_{n,m}\left(D_n\right)\right)\right].\end{aligned} \tag{2}$$

A DOT expression composed of multiple basic DOT blocks or combined DOT blocks can be used to describe the data flow of a large data payload.

It can be seen from the formal definition and description of the four layers: the operation layer and the aggregation layer only contain computing tasks, and their corresponding

0 and A matrices are both diagonal matrices, indicating that separate calculations can be performed. Independent concurrency: The communication task completed by the transport layer, the corresponding matrix T is a regular matrix, indicating that the communication must interact with each other.

In a concurrent storage system, a single miss does not necessarily cause a CPU hang, only pure errors do. C-AMAT is characterized by five parameters: C_H represents storage request access concurrency, Cm represents storage request pure miss concurrency, H represents storage request access time, pMR (PureMissRate) represents storage request pure miss rate, and pAMP (PureAverageMissPenalty) represents Pure average loss for storage requests. Through the derivation of a series of formulas, its formal description is as follows:

$$C - \mathrm{AMAT} = \frac{H}{C_H} + \mathrm{pMR} \times \frac{\mathrm{pAMP}}{C_M}. \tag{3}$$

Hit Concurrency Detector (HitConcurrency Detector, HCD) counts all hit cycles and records the status of each hit stage, calculates the CH hit concurrency of storage requests, and informs Miss. Concurrency Detector (MCD) of the current cycle if it occurs A hit occurs; MCD records the state of the pAMP cost of each pure loss cycle by counting the number of pure loss cycles, and calculates the pure loss concurrent Cm, the pure loss rate pMR, and the pure average loss storage requirement.

3.2. Parallel Computing Model Design. The p-DOT model consists of a series of iterations, the "p-phase DOT model." In each stage q, the p-DOT model consists of three layers, as shown in Figure 1.

D layer (data layer): in a distributed system, datasets (D1 to Dn) are distributed and stored in n data nodes.

O layer (computing layer): in phase q, nodes (01 to ong) perform independent simultaneous computations, and each O node only processes the corresponding data (including input data or intermediate data) and stores intermediate results.

T layer (communication layer): in phase q ($q \neq p$), each communication operator $t_{i,j}$ performs point-to-point message transmission, and the working node $o_i (i \in [1,\ n_q])$ of connection phase q is generated as an intermediary. The result is sent to the worker node o_j ($j \in [1, n_q + 1]$) in step $(q + 1)$. Note that if $t_{i,\ j} = 0$, there is no communication between nodes o_{i} and o_{j}.

Figure 1 shows the general data flow of the p-DOT model. For any stage q, if $q \neq p$, the output of this stage is the input of the next stage; otherwise, its result will be stored as the final result.

For a given big data load and a given environmental load that can be represented by the p-DOT model, the time cost of the load is

$$\Phi = \mathrm{O}\left(\frac{w}{n} + n\right) \times \mathrm{p}. \tag{4}$$

For a given big data load that can be represented by the p-DOT model, the computational complexity of the q-phase load is $\mathrm{O}(k_{\mathrm{q}})$.

Consider the computational behavior of phase q, which is described in the following form:

$$\begin{aligned}\vec{D}_q O_q &= \left[D_1 \cdots D_{n_q}\right] \begin{bmatrix} 0_1 & 0 & \cdots & 0 \\ 0 & 0_2 & \cdots & 0 \\ \vdots & \vdots & \ddots & \vdots \\ 0 & 0 & \cdots & o_{n_q} \end{bmatrix}, \\ &= \begin{bmatrix} d_{1,1} & d_{1,2} & \cdots & d_{1,n_q} \\ d_{2,1} & d_{2,2} & \cdots & d_{2,n_q} \\ \vdots & \vdots & \ddots & \vdots \\ d_{k_q,1} & d_{k_q,2} & \cdots & d_{k_q,n_q} \end{bmatrix} \begin{bmatrix} \mathrm{o}_1 & 0 & \cdots & 0 \\ 0 & \mathrm{o}_2 & \cdots & 0 \\ \vdots & \vdots & \ddots & \vdots \\ 0 & 0 & \cdots & o_{n_q} \end{bmatrix}, \\ &\left(\vec{D}_q = \vec{D}_{q-1} O_{q-1} T_{q-1}, D_i\right. \\ &= \left(d_{1,i}\ \ d_{2,i}\ \cdots\ d_{k_q,i}\right)^T, i \in \left[1, n_q\right]). \end{aligned} \tag{5}$$

Considering the communication behavior in phase q ($q \neq p$), its formal description is as follows:

$$\left(\vec{D}_q O_q\right) T_q = \left(\left[D_1 \cdots D_{n_q}\right] \begin{bmatrix} o_1 & 0 & \cdots & 0 \\ 0 & o_2 & \cdots & 0 \\ \vdots & \vdots & \ddots & \vdots \\ 0 & 0 & \cdots & o_{n_q} \end{bmatrix} \right),$$

$$\begin{bmatrix} t_{1,1} & t_{1,2} & \cdots & t_{1,n_{q+1}} \\ t_{2,1} & t_{2,2} & \cdots & t_{2,n_{q+1}} \\ \vdots & \vdots & \ddots & \vdots \\ t_{n_q,1} & t_{n_q,2} & \cdots & t_{n_q,n_{q+1}} \end{bmatrix} = \left[o_1(D_1) \cdots o_1\left(D_{n_q}\right)\right], \tag{6}$$

$$\begin{bmatrix} t_{1,1} & t_{1,2} & \cdots & t_{1,n_{q+1}} \\ t_{2,1} & t_{2,2} & \cdots & t_{2,n_{q+1}} \\ \vdots & \vdots & \ddots & \vdots \\ t_{n_q,1} & t_{n_q,2} & \cdots & t_{n_q,n_{q+1}} \end{bmatrix}.$$

Calculation result; each communication operator $t_{i,\ j}$ distributes the intermediate result $o_{\mathrm{i}}(D_{\mathrm{i}})$ generated by the worker node O_{i} in step q to the step by means of point-to-point message passing (including file transfer, TCP protocol and shared memory FIFO strategy, etc.) Worker nodes in $(q + 1)$.

According to formula (6), the total complexity of the computing task is

$$\Phi_{\sum \mathrm{comp}} = \sum_{q=1}^{p} \Phi_{\mathrm{comp}} = \sum_{q=1}^{p} O\left(k_q\right), \tag{7}$$

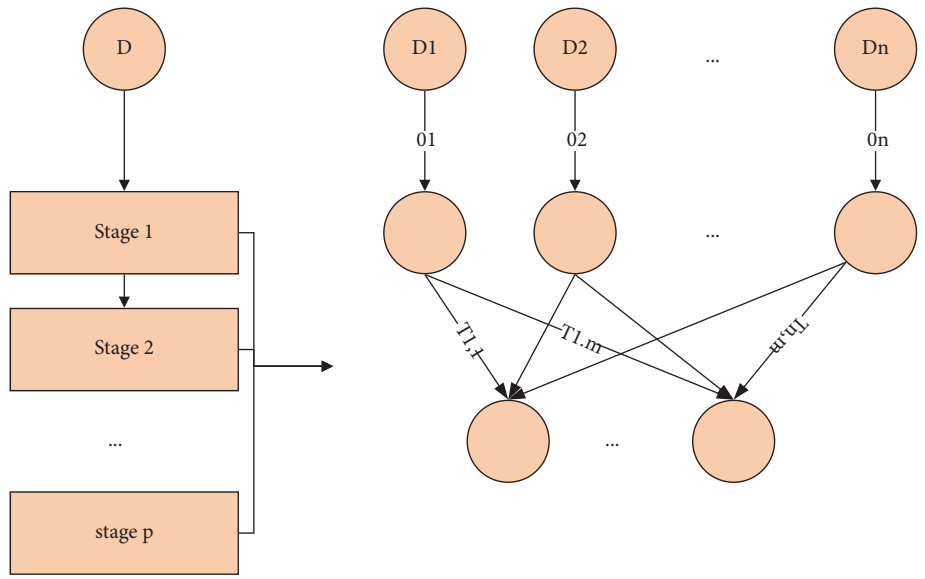

Figure 1: Data flow of the p-DOT model.

because

$$k_q = \left[\frac{w_q}{(n_q \times m)}\right] + 1. \tag{8}$$

Also, m is constant for a given ambient load. But,

$$O(k_q) = O\left(\frac{w_q}{n_q}\right) \Rightarrow \Phi_{\sum \text{comp}} = \sum_{q=1}^{p} O\left(\frac{w_q}{n_q}\right). \tag{9}$$

It can be seen from the foregoing that

$$O\left(\frac{w_q}{n_q}\right) = O\left(\frac{w_{q-1}}{n_{q-1}}\right)(\forall q \in [2, p]),$$
$$O(n_1) = O(n), w_1 = w, \tag{10}$$

but

$$\Phi_{\sum \text{comp}} = O\left(\frac{w_1}{n_1}\right) \times p = O\left(\frac{w}{n}\right) \times p. \tag{11}$$

According to formula (5), the total computational complexity of the task is

$$\Phi_{\sum \text{comm}} = \sum_{q=1}^{p} \Phi_{\text{comm}} = \sum_{q=1}^{p} O\left(\max\left(n_q, n_{q+1}\right)\right), \tag{12}$$

because

$$n = \max\left(n_q\right), \tag{13}$$

but

$$O\left(\max\left(n_q, n_{q+1}\right)\right) = O(n),$$
$$\Phi_{\sum \text{comm}} = \sum_{q=1}^{p} O(n) \times p = O(n) \times p. \tag{14}$$

To sum up, for a given big data load that can be represented by the p-DOT model and a given environmental load, the overall complexity of load communication is $O(n) \times p$ and the proof is completed.

3.3. Parallel Computing Algorithm Optimization. The p-DOT model can be selected to represent the data load and environmental load, where $O(w/(cn) + n + c)xp$ is the time cost function of the load, and based on the period p, its form is further described as the following formula.

Consider the period q, whose form is described as follows:

$$\vec{D}_q O_q T_q = \vec{D}_q O_q T_{\text{thread}} T_{\text{process}}$$
$$= \left[(d_1' \cdots d_c') \cdots \left(d_{c\times(n_q-1)+1}' \cdots d_{c\times n_q}'\right)\right],$$
$$\begin{bmatrix} o_1 & 0 & \cdots & 0 \\ 0 & 0_2 & \cdots & 0 \\ \vdots & \vdots & \ddots & \vdots \\ 0 & 0 & \cdots & o_{c\times n_q} \end{bmatrix},$$
$$\begin{bmatrix} t_{1,1}' & \cdots & t_{1,c}' & 0 & \cdots & 0 & 0 & 0 & \cdots & 0 \\ 0 & \cdots & 0 & t_{2,1}' & \cdots & t_{2,c}' & 0 & 0 & \cdots & 0 \\ \vdots & \ddots & \vdots & \vdots & \ddots & \vdots & \ddots & \vdots & \ddots & \vdots \\ 0 & \cdots & 0 & 0 & \cdots & 0 & 0 & t_{n_q,1}' & \cdots & t_{n_q,c}' \end{bmatrix},$$

$$\begin{bmatrix} t_{1,1}'' & t_{1,2}'' & \cdots & t_{1,n_{q+1}}'' \\ t_{2,1}'' & t_{2,2}'' & \cdots & t_{2,n_{q+1}}'' \\ \vdots & \vdots & \ddots & \vdots \\ t_{n_q,1}'' & t_{n_q,2}'' & \cdots & t_{n_q,n_{q+1}}'' \end{bmatrix},$$

$$\left(D_i = \left(d_{c\times(i-1)+1}' \cdots d_{c\times i}'\right), i \in \left[1, n_q\right]\right)$$

$$\left[\sum_{j=1}^{c} t_{1,j}'\left(o_j\left(d_j'\right)\right) \cdots \sum_{j=1}^{c} t_{n_q,j}'\left(o_{c\times\left(n_q-1\right)+j}\left(d_{c\times\left(n_q-1\right)+j}'\right)\right)\right],$$

$$\begin{bmatrix} t_{1,1}'' & t_{1,2}'' & \cdots & t_{1,n_{q+1}}'' \\ t_{2,1}'' & t_{2,2}'' & \cdots & t_{2,n_{q+1}}'' \\ \vdots & \vdots & \ddots & \vdots \\ t_{n_q,1}'' & t_{n_q,2}'' & \cdots & t_{n_q,n_{q+1}}'' \end{bmatrix}. \tag{15}$$

From a computational perspective, consider computational complexity

$$\Phi_{\sum}\text{comp} = O\left(\frac{w}{n}\right) \times p. \tag{16}$$

Since the computing layer 0 of DOT_{top} is expanded by a factor of c, then

$$\Phi_{\sum}\text{comp}'\left(p - \text{DOT}_{\text{top}}\right) = O\left(\frac{w}{(cn)}\right) \times p. \tag{17}$$

From a communication perspective, consider communication complexity

$$\Phi_{\sum}\text{comm} = O(n) \times p. \tag{18}$$

Since the communication layer T of DOT_{top} is divided into process-level communication $\text{T}_{\text{process}}$ and thread-level communication T_{thread},

$$\begin{aligned}\Phi_{\sum}\text{comm}'\left(p - \text{DOT}_{\text{top}}\right) &= \Phi_{\sum}\text{process} + \Phi_{\sum}\text{thread} \\ &= O(n) \times p + O(c) \times p = O(n+c) \times p.\end{aligned} \tag{19}$$

It can be known by derivation that

$$\begin{aligned}\Phi'\left(p - \text{DOT}_{\text{top}}\right) &= \Phi_{\sum}'\text{comp} + \Phi_{\sum}'\text{comm} \\ &= O\left(\frac{w}{(cn)} + n + c\right) \times p.\end{aligned} \tag{20}$$

To sum up, for a given big data load that can be represented by the p-DOT model and a given environmental load, when using multi-core technology, the time cost of the load is $\varphi' = O\ (w/(cn) + n + c)xp$, and the proof is complete.

If the task has partial synchronization conditions, the time cost function of its partial synchronization is $\varphi = 0\ (w/n + s)\ xp$, where S is the number of machines where the communication behavior occurs, and p is the number of stages.

Consider period q. Assuming the first sq machine ($s_q < n_g$) where the communication behavior occurs, the formal description of the normal task execution process is as follows:

$$\begin{aligned}&\vec{\text{D}}_q\left(O_q T_q^s\right)_{\text{exec}} \\ &= \begin{bmatrix} D_1 & \cdots & D_{n_q} \end{bmatrix} \begin{bmatrix} o_1 & 0 & \cdots & 0 \\ 0 & 0_2 & \cdots & 0 \\ \vdots & \vdots & \ddots & \vdots \\ 0 & 0 & \cdots & o_{n_q} \end{bmatrix} \\ &\quad \begin{bmatrix} t_{1,1} & \cdots & t_{1,s_{q+1}} & 0 & \cdots & 0 \\ \vdots & \ddots & \vdots & \vdots & \ddots & \vdots \\ t_{s_q,1} & \cdots & t_{s_q,s_{q+1}} & 0 & \cdots & 0 \\ 0 & \cdots & 0 & 0 & \cdots & 0 \\ \vdots & \ddots & \vdots & \vdots & \ddots & \vdots \\ 0 & \cdots & 0 & 0 & \cdots & 0 \end{bmatrix}.\end{aligned} \tag{21}$$

From a computing point of view, considering the computational complexity, then the computing layer O of $D\ (OT^S)_{\text{exec}}$ remains unchanged, and then

$$\Phi_{\sum}\text{comp}''\left(p - D\left(OT^s\right)_{\text{exec}}\right) = O\left(\frac{w}{n}\right) \times p. \tag{22}$$

From the communication point of view, considering the communication complexity, the number of machines that have communication behaviors in the communication layer T of $D\ (OT^S)_{\text{exec}}$ is

$$s = \max\left\{s_q \mid q \in [1, p]\right\}, \tag{23}$$

and

$$\Phi_{\sum}\text{comm}''\left(p - D\left(OT^s\right)_{\text{exec}}\right) = O(s) \times p. \tag{24}$$

It can be known by derivation that

$$\begin{aligned}\Phi''\left(p - D\left(O^s\right)_{\text{exec}}\right) &= \Phi_{\sum}\text{comp}'' + \Phi_{\sum}\text{comm} \\ &= O\left(\frac{w}{n+s}\right) \times p.\end{aligned} \tag{25}$$

Under normal circumstances, the time complexity of judging whether the task currently meets the convergence conditions will not exceed the normal task execution process, that is,

$$\Phi''\left(p - D(OT)_{\text{judge}}\right) < \Phi''\left(p - D\left(O^s\right)_{\text{exec}}\right), \tag{26}$$

and therefore

$$\begin{aligned}&\Phi''\left(p - D\left(OT^s\right)_{\text{exec}}(OT)_{\text{judge}}\right), \\ &= \Phi''\left(p - D\left(O^s\right)_{\text{exec}}\right) = O\left(\frac{w}{n+s}\right) \times p.\end{aligned} \tag{27}$$

To sum up, for a big data iterative task that can be represented by the p-DOT model and a given environmental load, if the task has partial synchronization conditions, then the time cost function of its partial synchronization is $\varphi'' = O(w/n + s)v$, and the proof is complete.

3.4. Algorithm Detection. This paper tests the optimal number of machines n^* corresponding to the input data w of different scales and verifies the correctness of the time cost function of the p-DOT model and its inference. When testing the first 4 datasets, in order to avoid I/O acquisition conflicts between processes, only one process is running on each machine, but when testing the 5th dataset, due to the number of machines in the MPI cluster Limited, so run two processes on each machine. The number of machines in the experiment is the number of processes actually participating in the work, as shown in Table 1.

As can be seen from Figures 2 and 3, although there is a certain deviation, $\sqrt{e}(w)$ and $e(n^*)$ are obviously linearly related, that is, $e(n^*) = O(\sqrt{e}(w))$. Therefore, it can be seen that the optimal machine n^* is proportional to the square root of the data size w.

Combining the curves in Figures 2 and 3, we can see that for a given big data load that can be represented by the p-DOT model and a given environmental load, the time cost of the load is $\varphi = O(w/n + n)\, xp$ which is also correct.

The reasons for the deviation are as follows. (1) There are many factors that affect the performance of big data applications. The p-DOT model only selects the scale w of the input data and the number of machines n as the first two parameters, which makes the model parameters imperfect in terms of accuracy. (2) The experimental platform has interference from other network loads, resulting in the above communication measurement errors.

4. Enterprise Financial Management System Design

4.1. System Requirement Analysis. With the continuous development of economy and technology, people's life is more and more inseparable from computers and the Internet, which promote people's modern life with convenient, fast, and intelligent systems. But to realize good network management, it must have the support of powerful computer system. This paper designs a kind of special financial management system after actually investigating the financial management needs of small and medium-sized enterprises to meet their business operations. Based on the principle of practicality, the system uses information technology to manage financial information and data and inputs data and financial information into standard computers in actual work, giving full play to the computer's rapid processing capabilities and standardized management. Through the analysis and investigation of the actual situation, the functions of master data management, voucher management, and data security problems such as user authentication and user authority in system management have been solved.

Table 1: Input data scale w and corresponding optimal number of machines n^*.

w/n^*	0.5 GB	7.5 GB	50 GB	500 GB	1 TB
Wordcount (MPI)	128	320	1280	4000	8000
Terasort (MPI)	128	640	1600	5000	10000
Wordcount (Hadoop)	64	256	800	4096	—
Terasort (Hadoop)	64	128	640	2048	—

The main system requirements are as follows.

Simple Operation and Friendly Interface. It adopts Windows operating habits, which is beautiful and elegant. After simple training, administrators can easily operate the interface.

Permission Control, Safe and Reliable. Different permissions are assigned to different categories of administrators. Users can change the permissions of each operator. After the operator logs in to the system and enters a password, the system will automatically grant permissions to prevent unauthorized operations, which is safe and reliable and can prevent the unclear division of responsibilities.

Data Query, Fast and Convenient. According to the basic information system, it provides a powerful daily processing query function, which can realize simple query and fuzzy query, and users can also print reports.

The report is reasonable and easy to use. According to the system requirements, the system can meet the statistical requirements of financial managers.

System performance requirements refer to the requirements for system reliability and functional scalability in addition to system functional requirements, which have a greater impact on the use environment and business specifications of the system.

4.1.1. Quick Response Capability. Although the management system designed in this paper involves a small range of management, it also includes a large number of commodity types. When multiple users access the system, higher requirements are placed on the database system and server that can quickly respond to query requests sent to users' needs. In addition, the frequent exchange of system business data requires the system to control the response time within an acceptable range.

4.1.2. Load Capacity. The system load depends on the number of users used and the frequency of services. After running for a period of time, the number of users will stabilize at a certain number, and the system load requirements can be set at this time. In addition, although the system-related data storage is relatively large, the storage capacity of the database is not a problem.

4.1.3. Security. System security is achieved through user authentication. The user enters the correct user name and password to log in to the system. If the input is incorrect, you

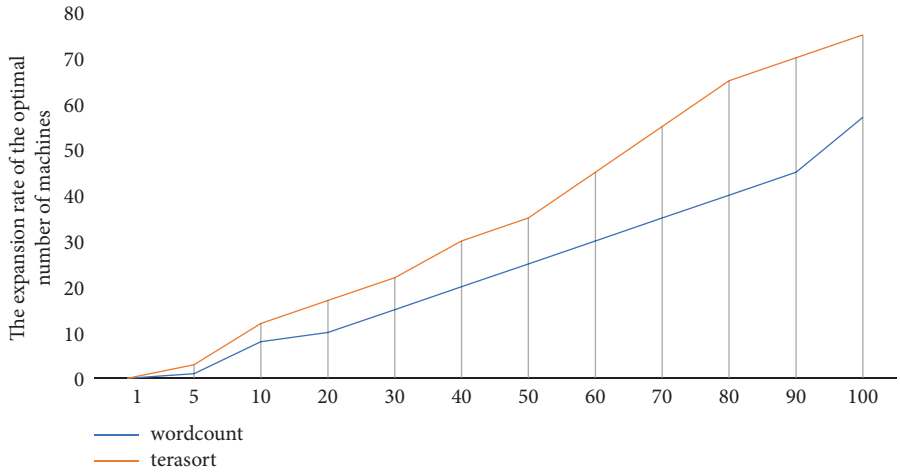

Figure 2: The square root of the expansion rate of the input data size in the MPI test.

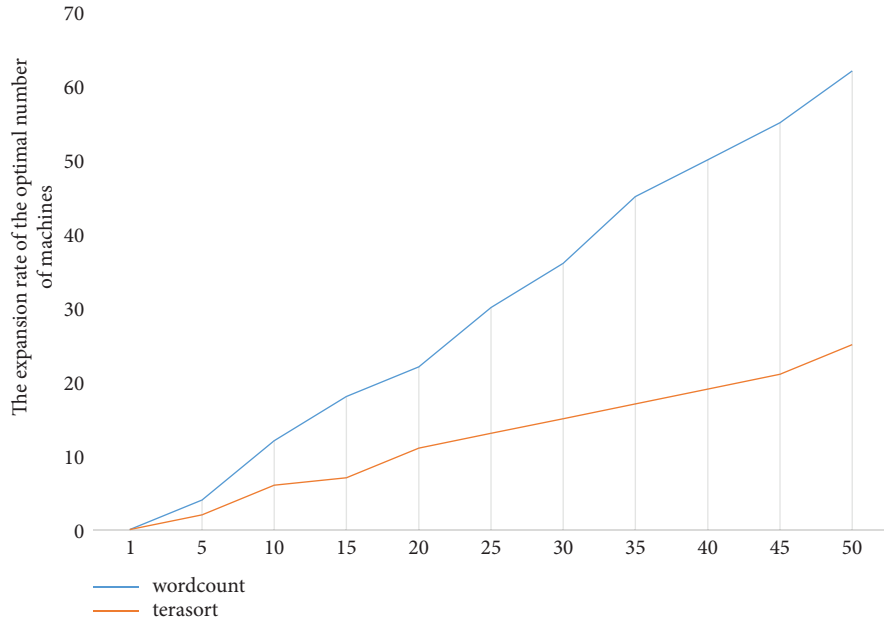

Figure 3: The square root of the expansion rate of the input data size in the Hadoop test.

will be returned to the login window. Also, the system needs to be equipped with data recovery and backup functions to avoid the risk of data loss due to crashes.

4.1.4. Reliability. System reliability refers to the ability of management system software to maintain its own performance after practical application, involving hardware environment, network environment, system platform characteristics, system development platform, and so on. System reliability is a global, system-specific requirement that includes fault tolerance, fault resilience, and system maturity. Fault tolerance refers to the ability of system software to withstand and prevent such errors when the management system fails. Failure is unavoidable, but if the system can avoid the collapse of the whole system, it also meets the design conditions. System stability refers to whether the normal state of the system can be restored by re-entering the system if there is a serious failure that affects the normal operation of the system during the operation of the system, such as the protection mechanism during data input.

4.1.5. Ease of Use. Ease of use is a system feature demanded by every customer. After completing the development of the management system, in addition to ensuring complete functions and normal use, it is also essential for the company's existing operators to quickly use the system. Operators can fully understand the functional use and maintenance operations of the system in a short time or after simple training, indicating that the system is easy to use. Enterprise software users need little logical thinking to understand the full capabilities of the software. Users can master the use of the software according to the instructions

contained in the software, which greatly shortens the software training process. The navigation of the software interface is concise and clear, and the user can achieve the desired operation function through fewer pages during the operation.

4.1.6. Maintainability. According to the principle of software development, a software should be handed over to the customer for testing and actual use after the design is completed. No matter how much manpower and material resources are spent, there must be various defects in software design, which can be reflected in the failure of operation. The complexity of the maintenance process and the level of maintenance costs in the event of a failure indicate the sustainability of the system. After a software failure occurs, the system needs to provide a log-like function, so that maintenance personnel can find the cause of the failure in a short period of time based on the log and experience. Once software administrators have discovered the cause of the failure, they can fix the failure with minimal cost and time.

4.2. System Architecture Design. Based on actual needs, after opening the browser software of the operating system and entering a fixed domain name, the user can enter the system login page under the condition of networking. After the user completes the login and authentication, he can access various functions provided by the system.

MVC is usually divided into view presentation layer, model layer, control layer, and other components. Indicates the interaction with the user interface and is responsible for the realization of the system UI functions. The model layer mainly processes the data entering the business. The control layer receives and processes all the user's requests and calls the processing interface of the system model layer to respond to the user's request.

The main functional structure of the business financial management system developed in this paper is shown in Figure 4.

As shown in Figure 4, in the system architecture design, Spring is used to coordinate various processing operations and business logic layers. The Struts presentation layer describes the technical details of the implementation of the functional modules related to the system and then separates the modules through Spring. Hibernate architecture uses session factory for integrated database operations. Hibernate's transaction processing mechanism is used to handle complex data interactions and data manipulations.

Based on the analysis of system requirements, this paper develops and designs a financial management system that meets the needs of enterprises. The system function structure is shown in Figure 5.

4.3. System Interface Design. According to the principle of object-oriented design and the relevant guiding ideology of SOA framework, it is planned to execute and complete various operations of the financial management system of small and medium-sized enterprises through the services in web services. The service is defined as follows:

```
public interface SourceManage {
@Profiled (tag = "SourceManage")
public int uploadSource (String sourcePath);
@Profiled (tag = "SourceManage")
public int updateSource (int sourceId, SourceInfo sourceInfo);
@Profiled (tag = "SourceManage")
public SourceInfo downloadSource (int sourceId);
@Profiled (tag = "SourceManage")
public SourceInfo getSourceById (int sourceId);
@Profiled (tag = "SourceManage")
public List<SourceInfo> getSourceBySourceName (String sourceName);
@Profiled (tag = "SourceManage")
public int deleteSource (int sourceId);
@Profiled (tag = "SourceManage")
public int isSourceExit (int sourceId);
}
```

As shown in the code snippet above, the SourceManage interface of financial management mainly includes operations such as uploading (uploadSource), downloading (downloadSource), querying (getBySourceId, getBySourceName), deleting (deleteSource), querying whether the financial resource file exists (isSourceExit) information data, and so on to fully realize the full authority management of access to related resources.

4.4. Analysis of System Test Results. The test environment of the client is shown in Table 2. The test process is similar to the development process, and it is also carried out in stages and steps. It is impossible to test the entire system as a separate entity from the beginning. To test this system, start with each functional module.

First, start with each functional module of the system and test it as a unit. Jump from one form to another, examine different situations, and use single-step tracing, set breakpoints, and output intermediate variables in between. Finally, the different processes are combined and tested in a relatively complete compilation part. Because it is not clear whether the results obtained are correct, we first output the results to the file, then evaluate the accuracy of the results according to different situations, and gradually follow up to determine the aspects that need to be changed or improved.

Second, while making sure the main part is working properly, try to change other non-main parts of the module and make improvements with reference to the related functions of WordPad and Notepad in Windows.

Finally, the system as a whole has been fully tested in many aspects, and many errors and imperfections have been modified to ensure that the system functions meet the design requirements and can work normally. Test each module of the system. After testing each module, assemble all the

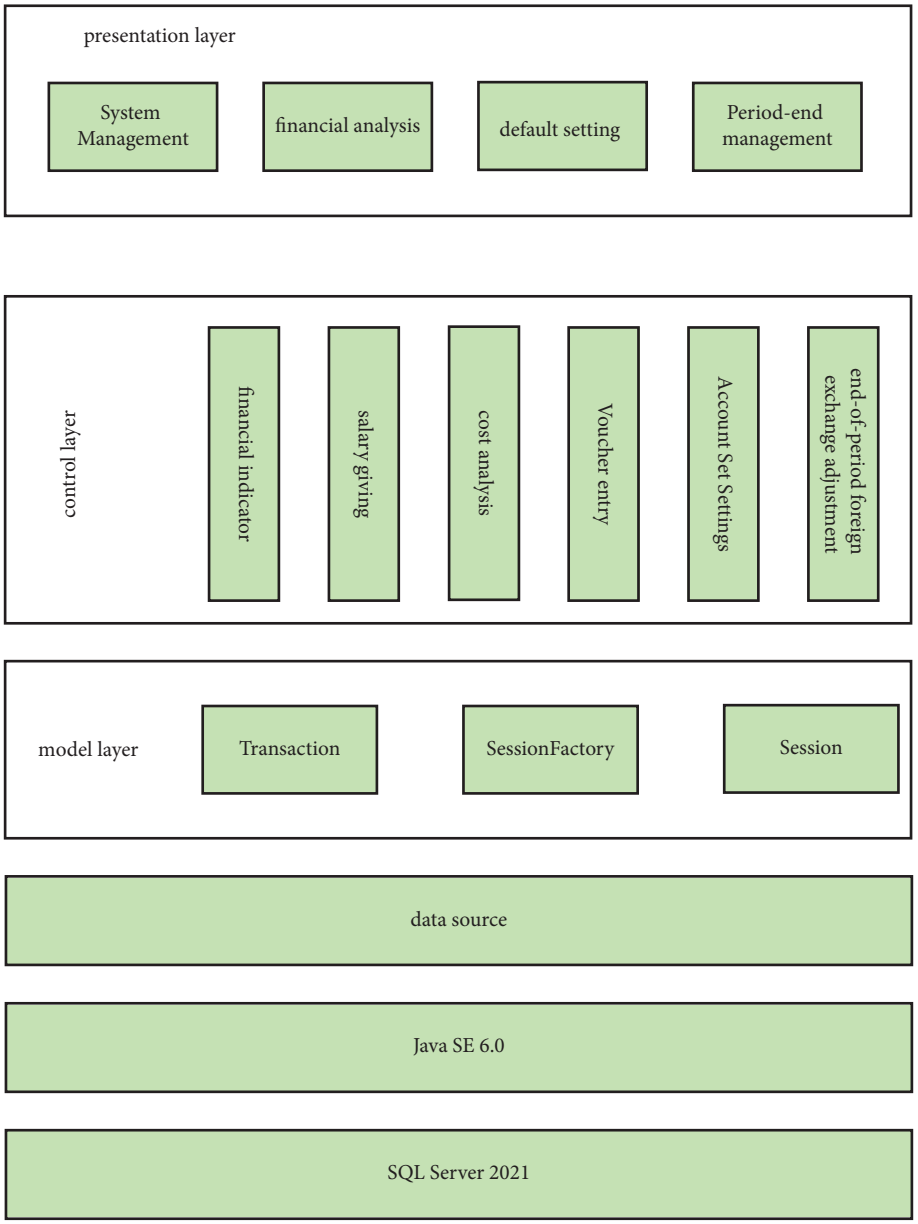

Figure 4: Architecture diagram of enterprise financial management system.

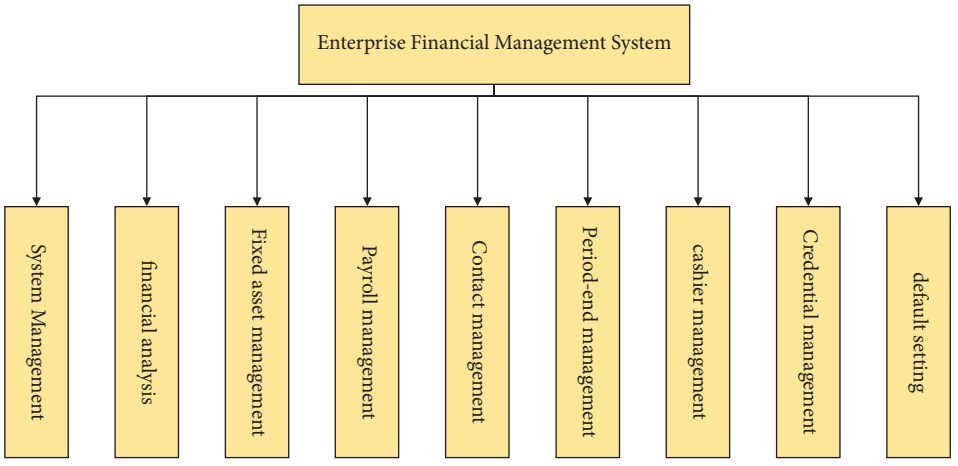

Figure 5: Functional structure diagram of enterprise financial management system.

Table 2: Client test environment.

-	OS type		Browser tools	Hardware information
Client environment 1		Windows XP	IE10	—
			Chrome	—
			Firefox	—
			Opera V24	—
Client environment 2	Windows	Win 7	IE10	CPU intel (R) i5-12400f@ 2.4 GHz
			Chrome	Memory: 12 GB
			Firefox	
			Opera	Screen resolution: 1920*1080
			V24	
Client environment 3		Win 10	IE10	—
			Chrome	—
			Firefox	—
			Opera V24	—

Table 3: System test.

No.	Test content	Testing method	Test results
1	Security system	Software deployment based on design criteria	System can be successfully installed
2	Uninstall the system	Software deployment based on design criteria	Can successfully uninstall the system
3	Basic data	System, administrator, and user	The system automatically updates the data within 24 hours and accurately enters the data
4	Manage business	Different administrators can perform corresponding business management operations	Accurately manage system data
5	Inquiry business	Corresponding information can be released, and data query can be performed after entering the operation module	Complete target data query based on conditions
6	Business functions	Statistics, management, analysis of input data	Display target data and analysis results
7	Maintenance system	Perform system data operations and user rights management	Set for user role permissions
8	Software fault tolerance	Judgment at test time	When the system fails, report an error and recover

Table 4: Financial management system performance test results.

Test indicators	Test results
Delay test	The delay time is 1.34 seconds
	The delay time is 2.11 seconds
	The delay time is 3.46 seconds
Reliability test	Success rate: 98.32%
Concurrency testing	The number of concurrent users is greater than or equal to 250

modules, and then test the interface as a whole. The operation stability of this system is tested through the following aspects, as shown in Table 3.

The main goals of the test are system reliability, system page latency, and system performance. Set system uptime to 48 hours. During the test, we observe the operation of various system indicators within 48 hours and calculate the average value of the test through multiple tests, as shown in Table 4. The test results show that the software design can meet the expected performance requirements.

Through the test of the system, the results show that the system is simple, easy to operate, and practical, and each interface meets the requirements of system safety.

5. Application Directions of Artificial Intelligence in Enterprise Financial Management

5.1. Reducing Process Time and Facilitating Real-Time Management. In terms of financial analysis, it is gradually shifting from traditional financial analysis to analysis supported by real-time system data. With the popularization and implementation of enterprise financial management systems, financial activities are becoming more and more concise, which can give enterprises more time and space to optimize and operate financial function management. In the later stage of financial system optimization, procurement projects can consider further developing the functions of the

financial statement module to facilitate the acquisition of data and ultimately provide financial evaluation, analysis, and decision making for enterprises.

5.2. Information Disclosure and Sharing to Improve Management Efficiency. With the development of society and technology, in order to optimize the financial management process, promote the centralization of decentralized financial management, and improve the efficiency of financial activities, enterprises must establish a center that can be used for internal information exchange and communication. Financial information sharing can effectively improve the efficiency of enterprise system information interaction, thereby promoting information sharing among various departments, and sharing with other departments, and clearly establish a special financial information platform within the enterprise. The system includes customer information, business information, decision-making information, and so on. This will shape the future of business management.

5.3. Strengthening Risk Management and Improving Decision-Making Ability. Financial risk management is one of the core contents of an enterprise's financial management system, and its main function is that the decision-making system acts directly through risk monitoring and feedback. However, because the company lacks a risk management system, the lack of financial risk management directly leads to a negative impact on business operations. Therefore, it is necessary to improve the risk management and control system.

In terms of effectively building a financial risk monitoring system, enterprises can start from the following three aspects. First, enterprises can form relevant standardized data indicators according to their own conditions through comparative analysis of other enterprises. Second, use real-time relevant data analysis to obtain suitable data and compare it with real-time indicators and standardized risk indicators. Furthermore, link processing is performed for the appropriate business. For example, taking the changes in the company's accounts receivable recovery rate and budget cost allocation as an example, we combine these indicators with the company's initial alert threshold for real-time monitoring and adjustment.

6. Conclusion

By using the financial management system, enterprises can improve the efficiency of financial management and achieve twice the result with half the effort, especially in the fierce market competition, which can give enterprises a development advantage. In the case of relatively low production level and production efficiency of small and medium-sized enterprises, their market share is very low. At this time, the financial management system is not only a simple application software system but also an important part of production and operation. Practice shows that the system has the following advantages: friendly interface and simple operation. Operators with limited computer access can also operate the menu item prompts; detailed information management, including adding, deleting, and other specific operations, provides powerful navigation, query, and statistical functions; the system supports multi-identity user operations. Users are effectively connected to facilitate the comprehensive operation and management of basic financial information and enterprise information; the business process is arranged reasonably, and the division of labor in the voucher verification stage and the posting stage is clear, which is in line with expectations; the report statistics are detailed, and users can print statistical reports based on their needs. The data are accurate and clear, which is convenient for data analysis. Due to the limited level, the system is not perfect in some aspects, and more research is needed. (1) The security and reliability of the financial management system need to be improved and optimized. (2) The functional module design is not detailed enough, and the data analysis integration function still needs to be perfected.

Data Availability

The data used to support the findings of this study are available from the corresponding author upon request.

Conflicts of Interest

The author declares that there are no conflicts of interest.

References

[1] L. Wang and Y. Wang, "Supply chain financial service management system based on block chain IoT data sharing and edge computing," *Alexandria Engineering Journal*, vol. 61, no. 1, pp. 147–158, 2022.

[2] C. Pollitt, "Integrating financial management and performance management," *OECD Journal on Budgeting*, vol. 1, no. 2, pp. 7–37, 2001.

[3] H. Karadag, "Financial management challenges in small and medium-sized enterprises: a strategic management approach," *Emerging Markets Journal*, vol. 5, no. 1, pp. 26–40, 2015.

[4] K. Lu, Y. Fu, C. Gu, and L. Zhang, "Problems and solutions of popularization of accounting computerization," *Physics Procedia*, vol. 33, pp. 1155–1159, 2012.

[5] L. Zhou, "The research on issue and countermeasures of accounting information of SMEs," *International Journal of Business and Management*, vol. 5, no. 3, p. 223, 2010.

[6] S. Murungi and C. Kayigamba, "The impact of computerized accounting system on financial reporting in the ministry of local government of Rwanda," *Journal of Emerging Trends in Economics and Management Sciences*, vol. 6, no. 4, pp. 261–265, 2015.

[7] M. M. Gadzhiev and Y. G. Buchaev, "Efficiency assessment of enterprise innovation activities," *Life Science Journal*, vol. 11, no. 10, pp. 581–586, 2014.

[8] A. Chornovol, J. Tabenska, T. Tomniuk, and L. Prostebi, "Public finance management system in modern conditions," *Investment Management and Financial Innovations*, vol. 17, no. 4, pp. 402–410, 2020.

[9] H. He, Y. Hong, W. Liu, and S. A. Kim, "Data mining model for multimedia financial time series using information

entropy," *Journal of Intelligent and Fuzzy Systems*, vol. 39, no. 4, pp. 5339–5345, 2020.

[10] O. Bulkot, "Modern system of international financial management in multinational companies," Економічний часоПис-ЧЧІ, vol. 1-2, no. 2, pp. 8–11, 2015.

[11] S. Selvanayaki, S. D. Sivakumar, A. Rohini, and K. Mani, "Financial management practices and profitability of modern rice milling firms in Kangayam Cluster, Tamil Nadu," *Agricultural Economics Research Review*, vol. 29, no. 2, pp. 297–306, Article ID 17251, 2016.

[12] R. P. Dameri, "Improving the benefits of IT compliance using enterprise management information systems," *Electronic Journal of Information Systems Evaluation*, vol. 12, no. 1, pp. 27–38, 2009.

[13] Z. Zhang, Y. Liu, J. Zhang, and X. Song, "Research on the influence of new generation of information technology on contemporary enterprise logistics management information system," *Journal of Physics: Conference Series*, vol. 1648, no. 4, Article ID 042039, 2020.

[14] X. Huang and F. Guo, "A kernel fuzzy twin SVM model for early warning systems of extreme financial risks," *International Journal of Finance & Economics*, vol. 26, no. 1, pp. 1459–1468, 2021.

[15] D. Mhlanga, "Industry 4.0 in finance: the impact of artificial intelligence (ai) on digital financial inclusion," *International Journal of Financial Studies*, vol. 8, no. 3, p. 45, 2020.

[16] J. De Weerdt, A. Schupp, A. Vanderloock, and B. Baesens, "Process Mining for the multi-faceted analysis of business processes—a case study in a financial services organization," *Computers in Industry*, vol. 64, no. 1, pp. 57–67, 2013.

Hindawi
Mobile Information Systems
Volume 2022, Article ID 5465340, 10 pages
https://doi.org/10.1155/2022/5465340

Research Article

Design and Implementation of Continuing Education Online Training System Based on Artificial Intelligence Algorithm

Shihua Zheng

Jinhua Polytechnic, Jinhua 321007, Zhejiang, China

Correspondence should be addressed to Shihua Zheng; 20151011315@stu.qhnu.edu.cn

Received 11 August 2022; Revised 18 September 2022; Accepted 28 September 2022; Published 9 October 2022

Academic Editor: Shadi Aljawarneh

With the continuous development and maturity of artificial intelligence algorithms, there are more cross-concepts in continuing education, so continuing education has begun to develop on the Internet. The continuing education online training system realizes nonreal-time teaching methods, breaks the limitations of time and space, solves the conflict between continuing education engineering and learning, and promotes the sharing of high-quality teaching resources. However, the current continuing education online training system has many defects and imperfections. For example, many continuing education colleges only consider building resources and teaching forms to design online learning systems, and these high-quality resources and teaching forms are difficult to be effectively utilized. Based on this background, this paper establishes a continuing education online training system combined with artificial intelligence algorithms, which is divided into course management, question bank management, learning management, homework management, question-and-answer management, online learning process monitoring management, basic data management, system management, etc. Then, by matching the relevance of the above courses, individual courses are recommended for students to complete the continuing online training education. The system has been highly appraised by the majority of students. The user said that the system can effectively solve practical problems, which is known for the effectiveness of the system design in this paper, thus providing reasonable help for improving the teaching quality. In this paper, we deeply study artificial intelligence algorithms and apply them to the field of continuing education to design a new type of online education system.

1. Introduction

With the continuous development of society, the demand in the field of education is growing, and the application of artificial intelligence technology to the field of education has become the mainstream trend. The combination of artificial intelligence technology and information technology can effectively improve the efficiency of education, and it is also the main way to complete online continuing education. How to obtain information? [1]. The development and application of such technologies will gradually change the characteristics and forms of continuing education teaching itself, and guide the transformation of adult students' concept of knowledge acquisition, thereby changing the learning style of adult students [2]. Continuing teaching can effectively meet the needs of educational development and reform. It is a teaching method with a new teaching concept, and its main target is adult students [3]. Judging from the current development outline of China's long-term education reform, the country has vigorously developed adult online learning under the mass education model and established a flexible and open education system [4]. Only by conducting relevant research on the online continuing education system can some practical problems in the field of continuing education be solved. This point is also in line with the educational reform concept formulated by the state and can improve the rate of students in class [5]. In the information age, with the rapid development of Internet technology, the research on continuing education in the online training system will become the center and primary task of continuing education reform research [6]. Special research on this technology can effectively improve and comprehensively enhance the theoretical and practical application levels of continuing education. In recent years, the enrollment scale of continuing

education in continuing education colleges in major universities has doubled, and the distribution of students has become more dispersed, resulting in continuous growth of teaching sites, increased teaching load, and serious shortage of teaching resources, especially teacher resources [7]. In order to solve these practical problems, further ensure the quality of education and teaching in continuing education, improve the learning conditions of students participating in continuing education, cultivate students' self-learning awareness and interest in learning, realize a nonreal-time online learning system, provide learners with knowledge, and it is very important to promote the exchange of high-quality resources among universities and realize resource sharing. The development of an online continuing learning system can promote the continuous, stable, and efficient operation of continuing education, and can meet the actual needs of learners. Based on this background, this paper develops an online training system for continuing education by combining artificial intelligence technology and is committed to improving the learning experience of learners, stimulating their learning initiative and enthusiasm, and further reforming continuing education based on the teaching quality evaluation system. Through testing, it is found that the design of the system can effectively help the reform of continuing education and promote its further development.

2. Related Work

The literature proposes a personalized course recommendation method for online learning platforms based on multi-features. First analyze online course learning records by using student extraction data, and then add course information using an XMMC model [8]. Through the students' historical learning records, cluster analysis is performed on students with similar learning styles to analyze their learning interests and preferences [9, 10]. The literature proposes a unified extraction model (XMMC) for knowledge entities and relations in the educational domain based on deep learning [11]. By using this model, the knowledge points of the course can be captured at the same time through entities and relationships, then the knowledge structure of the course can be dynamically displayed, then the correlation of knowledge points between different other courses can be explored, and the knowledge chain can be traced back to the source through the implicit relationship, so as to improve the recommendation effect of personalized courses [12]. The literature establishes a prediction model based on an improved decision tree algorithm (FGDT) and a prediction model based on an improved support vector machine (FGSM) algorithm [13]. The literature is based on the theory of S–O–R model and the correlation analysis of user perceived value on contextual factors [14]. The literature examines the potential impact of contextual factors on users' continued use intentions based on existing research results [15]. The article first proposes a set of curriculum index system, that is, a new index system for evaluating online courses based on course content [16]. First, three algorithms are used to extract the features of the index: the improved FastText algorithm is used to classify the course introduction text, and three features related to the difficulty of the course are extracted; that is, the SVM algorithm is used to analyze the course-related sentiment and extract the relevant field features of the course evaluation; Jaccard similarity is applied to fine-grained clustering of similar courses to calculate the knowledge point coverage of each course [17, 18].

3. Design of Online Training System for Continuing Education

3.1. System Architecture Design. Analyze the business requirements of the continuing education online training system, further decompose the data flow of the continuing education online training system layer by layer, and obtain the functional structure diagram of the continuing education online training system. The block diagram of the online continuous training system is shown in Figure 1.

The continuing education online training system is divided into 8 modules. Among them, the course management module is mainly responsible for the construction and management of various educational resources of the course, as well as the management of teacher declaration courses, such as the management of teacher class declaration information and teacher management, construction course information, teaching progress management, and video and PPT document information; question bank management mainly manages subject information; learning management module mainly manages a series of learning records of students who have completed online courses, such as the time when students start learning, the time when learning ends, and student identity verification information records; homework management mainly completes students' homework project management, which can record the audio of the teacher explaining the homework. And it can be used to fully understand the students' learning results; the Q&A management module is a function set up for students who encounter difficult problems, which can help students put forward solutions to difficult problems and communicate with them. Through the teaching process of education administrators, we can understand the dynamic summary of students in real time, understand the status of students' learning courses in the online learning system, and manage teaching teachers in real time; the main data management is to manage the main information of teachers, the main information of students themselves, the planned courses for this semester and implementation of semester information, student master information and course information of selected student courses, as well as additions, deletions, revisions, and checking of basic information of students and teachers; the main function of system management is to monitor continuing education managers, online training system log information, and dissertation information and ongoing access information for backup management and maintenance.

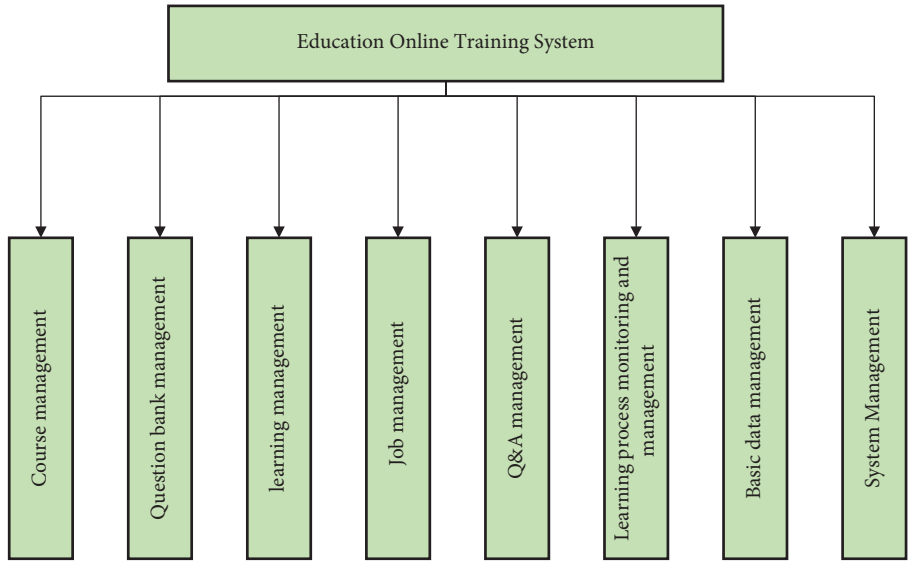

Figure 1: Overall functional structure diagram of continuing education online learning system.

3.2. System Function Analysis. The course management business process is described. Curriculum is the most important element in the online continuing education and training system and runs through the online continuing education and training system. The first is the teacher's course declaration. The teaching staff prepares the course plan according to the teaching plan and announces the course plan to the platform. The teacher applies for the course according to the course plan, completes the teacher's personal basic information and class filling requirements, and sends the summary to the system. At the beginning of the lesson plan, teachers need to summarize the course and apply to become a teacher, and then review the qualifications of teachers, set teachers and class time, etc. Secondly, for curriculum development, teaching staff prepare syllabus according to the curriculum plan and release the syllabus to teachers and students. Teachers arrange teaching materials according to the curriculum. For example, teachers write syllabuses based on selected textbooks and report to the teacher review system. According to the arrangement of the syllabus and the content of the books, prepare teaching materials such as PPT, and submit them to the provost for review. After the review is passed, the business is archived. Teachers teach according to a timetable.

Describe business processes related to system administration. Question bank is a standard for testing students' learning status, and it is an indispensable data in students' learning process. The first is the preparation stage. The registrar requires teachers to complete the question bank construction according to the selected courses and books, and the registrar forms the question bank template. The second is the query phase. Teachers select topics according to the content of the textbook and the syllabus, and according to the question bank model. The test information includes the title, option 1, option 2, option 3, option 4, standard answers, and information analysis, followed by the review stage. After the teacher completes the information in the question bank, it is submitted to the teaching staff for review. After the review, the question bank is archived, and the question bank is grouped by the question bank group, which is made into this test or homework, and distributed to the students to complete.

Learn to manage business process descriptions. Students are the helmsman of learning, and teachers are the vitality of learning. Only by working together can the course continue. The first is to organize courses. Teachers and staff organize teachers and students to attend classes according to the timetable, and teachers and students attend classes on time according to the information in the timetable; the second step is the learning stage. Teachers explain the course content to students according to the syllabus, PPT documents, textbooks, and other teaching materials. Students listen carefully and take notes in class. And record student attendance through roll call and recording in class. In the classroom, teachers organize students to discuss and complete homework to test students' academic performance, etc., and record these classroom performances in the scorebook as the students' regular performance scores to provide the basis for the final results of the comprehensive assessment; third for learning outcomes, students create learning records such as study notes, homework, and attendance through learning. College administrators can view these learning records and manage the learning process.

Job management business process description: First, after the students listen to the course explanation, the teacher assigns the homework, and the students record the homework and complete it; secondly, the students send the completed homework to the teacher for review, and the teacher reviews the students' homework, marks the wrong places, and grades the students' homework, so as to complete the entire homework review process; at the end, students review the homework and the teacher explains the homework.

Q&A management business process description: Answering questions is an important part of student learning.

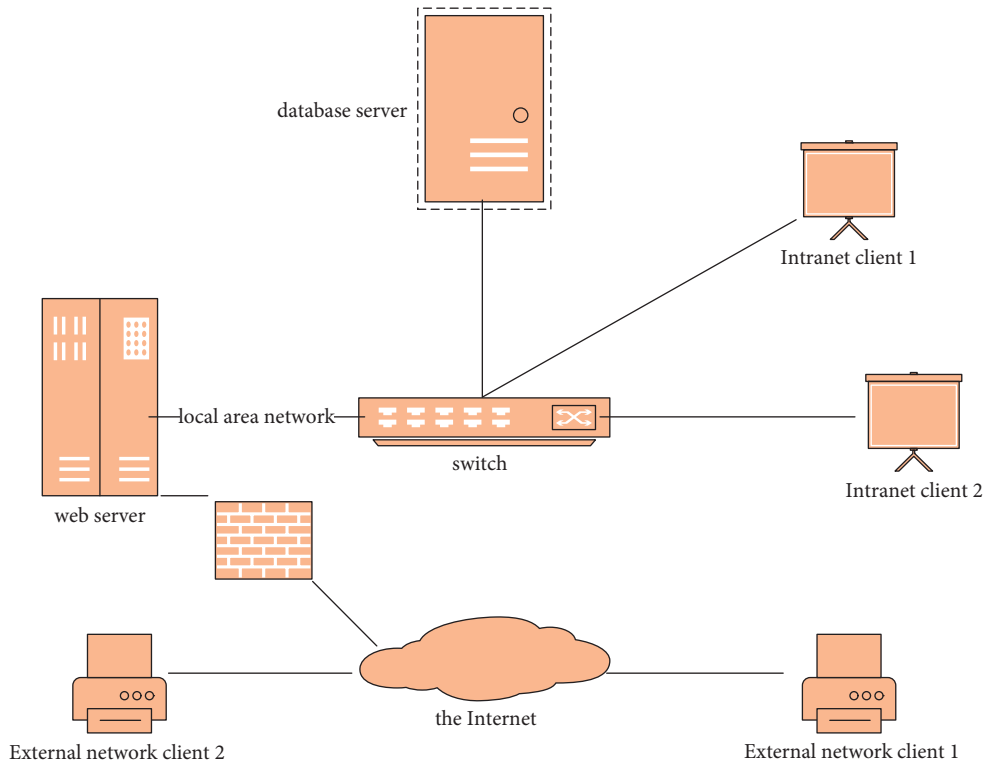

Figure 2: Network structure diagram.

Learning itself is to solve puzzles, so students will encounter doubts in the learning process and need the help of teachers to solve them. The first step is for students to participate in the course study, complete the homework, and look for problems; the second step is for students to choose a method to solve the problem, such as searching for relevant answers on the Internet to solve the problem, or to solve the problem by themselves; the third step is that teachers listen to students' questions and answer their puzzles with their own knowledge; in the fourth step, students record the teacher's answer.

Learning to monitor business processes describes management processes. The main purpose of monitoring the learning process is to ensure that students complete the tasks specified in the course on time and in quantity. First, the registrar analyzes the student's learning by recording the student's learning, and warns or encourages the student to study; second, the clerk monitors the student's learning by collecting and checking the student's work; finally, the clerk takes classes according to the course schedule and monitors students' learning status by showing them in class.

3.3. System Network Architecture Design. The network structure of the continuing education online training system designed and implemented in this paper is consistent with other popular websites in the market. The network structure diagram is shown in Figure 2.

In the continuing education online training system designed in this paper, there must be two PCs in the computer room as system servers. Database servers can be networked in a clustered system. Using the network, one database server and two application servers can be connected to the storage array using SαN switches. In this way, a server system integrating storage resources can be formed.

3.4. System Test Environment Construction. Software testing refers to testing whether software works normally under certain conditions, and is an important way to ensure software quality. This article will examine multiple aspects of online learning recommendation platforms. It mainly includes platform function test, platform security and compatibility test, platform performance test, etc.

Once the platform is developed and implemented, it must be deployed and tested. The general details of the platform test environment are shown in Table 1.

4. Continuing Education Functional Modules Based on Artificial Intelligence Algorithms

4.1. Theoretical Basis of Support Vector Machine Algorithm. Before calculating the optimal classification surface, the range must be calculated first. In the sample space, the segmentation hyperplane can be described by the following linear equation:

$$\omega x + b = 0. \tag{1}$$

The general form is

$$f(x) = \omega \cdot x + b. \tag{2}$$

The training samples (x_i, y_i) must satisfy the following conditions: where $\alpha_i \geq 0$ is the Lagrange multiplier. According to Lagrangian duality, the optimization problem

Table 1: System environment.

Test environment	Hardware	Software
Service terminal	Database version: MySQL 10.0 Running memory: 32 G Storage memory: 1T	Operating system: CentOS 7.9 JDK version: JDK 1.8 Server: Tomcat
Client	Handling Intel i7-12700 Storage memory: 256 G Running memory: 32 G	Operating system: Windows 11 — Browser: Google Chrome, Microsoft Edge

can be transformed into an equivalent dual problem to solve, and the steps are as follows:

To find the minimum first, you need to differentiate w, $\underline{b}$, α:

$$\begin{cases} \dfrac{\partial L}{\partial \omega} = 0 \Rightarrow \omega = \sum_{i-1}^{n} \alpha_i y_i x_i, \\ \dfrac{\partial L}{\partial \alpha} = 0 \Rightarrow \alpha_i \left[y_i (\omega \cdot x_i + b) - 1 \right] = 0, \\ \dfrac{\partial L}{\partial b} = 0 \Rightarrow \sum_{i-1}^{n} \alpha_i y_i = 0. \end{cases} \tag{3}$$

The formula obtained after optimizing the above formula is as follows:

$$\max = \sum_{i=1}^{n} \alpha_i - \frac{1}{2} \sum_{i=1,j=1}^{n} \alpha_i \alpha_j y_i y_j \left(x_i \cdot x_j \right). \tag{4}$$

Its constraints are

$$\begin{cases} \sum_{i=1}^{n} \alpha_i y_i = 0, \\ \alpha_i \geq 0. \end{cases} \tag{5}$$

In the solution process, if $\alpha_i \neq 0$, it corresponds to the support vector. The final optimal classification function is

$$f(x) = \operatorname{sgn}\left(\sum_{i=1}^{n} \alpha_i y_i \left(x \cdot x_j \right) + b \right). \tag{6}$$

In this case, there is also a special case; that is, the small number of samples will affect the performance of the classifier when the original linearly separable problem becomes nonlinearly separable.

4.2. Course Recommendation Module. Traditional learning and online learning differ in many ways. For example, students in a traditional learning environment may have preferences for classroom sound conduction, lighting, and temperature, factors that are not suitable for an online learning environment, where the main element of an online learning environment is an interactive web page. Students who study online can publish and exchange comments online anytime, anywhere, and study without time constraints, which is not available in traditional learning.

In the process of calculating similarity, the contributions of user behavior variables (study hours, discussions, visits, activity points completed, and lessons learned) are not the same, so we have to give these five variables the nature of the referral process.

In this paper, the Euclidean distance is calculated in ascending order. The Euclidean distance algorithm is calculated as shown in formula :

$$\operatorname{sim}_{ktglo}\left(S_j, S_j\right) = \frac{1}{1 + d\left(S_i, S_j\right)} = \frac{1}{1 + \sqrt{\sum_{k=1}^{5} \left(E_{jk} - E_{jk} \right)^2}}. \tag{7}$$

After calculating the user's learning style similarity, we can get the N most similar UN learning peers of user u through TOP-N sorting. Finally, a preference weight is created according to the user's behavioral characteristics, and the weight calculation is shown in formula :

$$\text{weight } t_{ue\varepsilon}(u, c) = \frac{1}{N} \operatorname{sim}_{syle}(u, u') \sum_{N' e U_N} I_{C' \cdot (c)}. \tag{8}$$

To understand courses closely related to students' interests in historical access logs, we use the XMMC information extraction model to extract entity and relation features from course text description information. If the knowledge entity information is obtained from the text description information of the two courses, the similarity of the two courses will be greater.

After the vector representation of each course, we can use Euclidean distance to calculate the similarity between any two courses. For example, for course c and course c', the Euclidean distance algorithm is calculated as

$$\operatorname{sim}_{\text{cotso}}(c, c') = \frac{1}{1 + d(c, c')} = \frac{1}{1 + \sqrt{\sum_{k=1}^{d} \left(E_{kc} - E_{kc} \right)^2}}. \tag{9}$$

After calculating the course similarity, for any course c, we can get the K courses that are most similar to the course through the TOP-N ranking. Finally, the preference weight is generated according to the characteristics of the course content, and the weight calculation is shown in formula:

$$\text{weight}_{\text{course}}(u, c) = \frac{1}{K} \text{sim course}(c, c') \sum_{c' e C'_{C,K}} I_{U_e(w)}. \tag{10}$$

The actual requirements of the course are practical education and online education. For example, "Data Structures I" and "Data Structures II" courses or "Advanced Mathematics" and "Advanced Mathematics II" courses have a clear required course relationship (the former is more

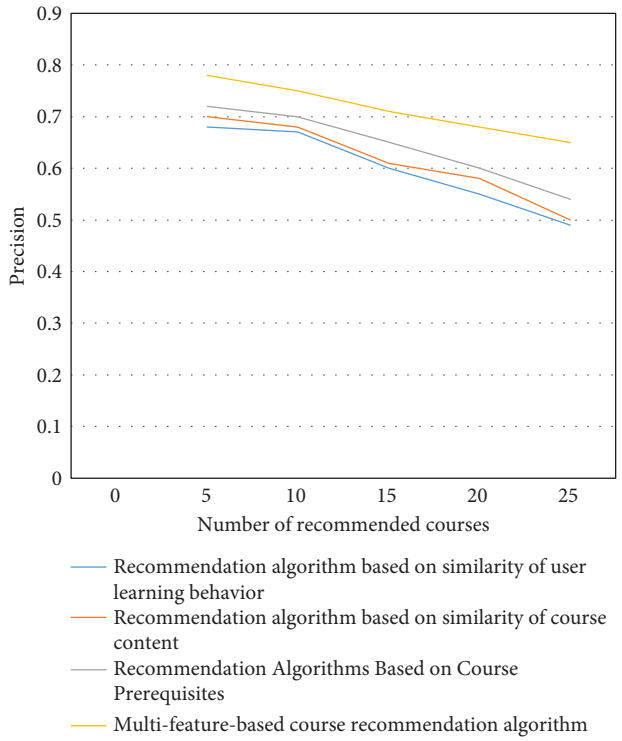

Figure 3: Recommended courses on the accuracy of different algorithms.

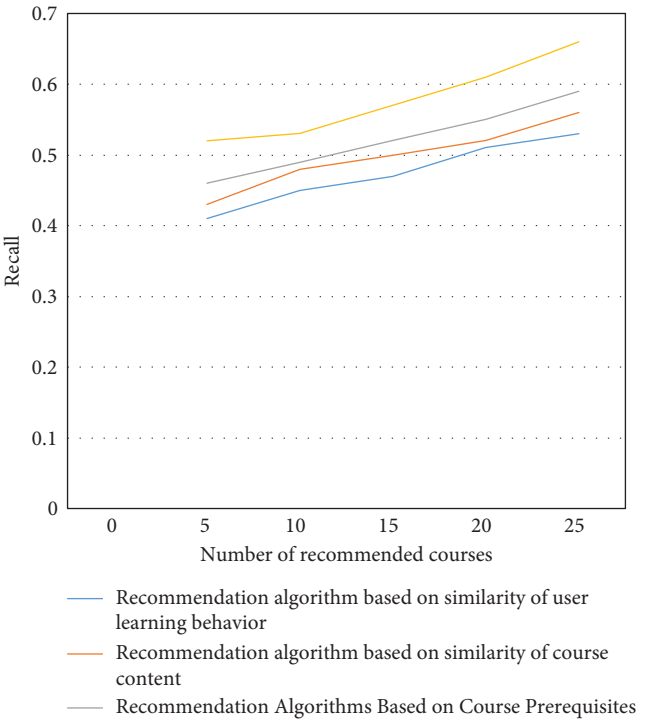

Figure 4: The effect of the number of recommended courses on the recall rate of different algorithms.

basic). To measure the relationship between different courses, for the set Uc of users who study course c, after calculating the percentage of users who study course c', we define the transition probability p for each ordered course pair (c, c') (c, c'). For example, tp ("Data Structure I," "Data Structure II") is higher than tp ("Data Structure II," "Data Structure I"), indicating that the transition trend from the former to the latter may be higher. This transition probability is shown in

$$p(c,c') = \frac{\left|\left\{u \mid u \in U_c \cap U_{c'}, t_{u,c} \le t_{u,c'}\right\}\right|}{\left|U_c\right|}. \tag{11}$$

After calculating the course transfer probability, we use the above transfer probability to finally generate the preference weight according to the required courses. The calculation formula is

$$\text{weight}_{tp}(u,c) = \sum_{c' \in C_n} tp(c',c). \tag{12}$$

After calculating preference weights according to different features, the total preference weights of users in course c can be written as

$$\begin{aligned}\text{weight}(u,c) = {} & \alpha \times \text{weight}_1(u,c) + \beta \times \text{weight}_2(u,c) \\ & + \gamma \times \text{weight}_3(u,c),\end{aligned} \tag{13}$$

where α, β, γ are parameters that control the proportion of weights from different sources.

The effect of the number of recommended courses on the accuracy of different algorithms is shown in Figure 3.

The effect of the number of recommended courses on the recall rate of different algorithms is shown in Figure 4.

In terms of the effectiveness of algorithm implementation, due to the personalized course recommendation algorithm based on multiple characteristics of our online learning platform, compared with the traditional user-based collaborative filtering, the grouping of students is first realized when calculating the similarity of students. For the recommendation algorithm, the algorithm has a shorter response time when calculating the same user set among target users, which improves the efficiency to a certain extent.

4.3. Course Quality Evaluation. Course quality is a key factor in measuring course excellence. In this paper, CQ is used to represent the course quality (Course Quality), and the index to measure the course quality is

$$\begin{aligned}\text{CQ} = \{ & \text{TeamQuality}, \text{VideoQuality}, \\ & \text{PopularQuality}, \text{TeacherInput}\}.\end{aligned} \tag{14}$$

Among them, Team Quality refers to the quality of the teaching team, Video Quality refers to the quality of the course video, Popular Quality refers to the popularity of the course, and Teacher Input refers to the teaching interaction. The literature shows the main factors that affect the success of MOOCs, and finds the value of teacher input (teacher-student interaction, teacher feedback, etc.), student interaction (question-and-answer behavior, etc.), and course

content (homework and exercise content) in online courses. The learning process has a positive impact.

4.3.1. Quality of Teaching Team.

$$\begin{aligned} 0 \leqslant & f_t\ (''\text{Teachers and Others}'') \\ & < f_t(''\text{Associate Professor}'') \\ & < f_t\ (''\text{professor}'') \leqslant 1. \end{aligned} \tag{15}$$

Considering that the number of teachers in different courses is different, it is necessary to add up the scores of all teachers' titles to obtain the average value. The calculation formula is

$$\text{teachers score} = \frac{\sum_{i=1}^{n} \text{teacherscore}_i}{n}, \tag{16}$$

where n is the number of teachers.

4.3.2. Video Lesson Quality. After analysis, it was found that many students watched the video for less than 60 seconds in total. They might just browse the video or open it accidently. After removing these invalid behavior records, calculate the average video watch time. Let w_j be the average viewing time of the jth video, and the calculation process is as follows:

$$w_j = \text{Average}\left\{d_{ij} \mid d_{ij} \geq 60,\ \ i = 1,2,\ldots,m\right\}, j = 1,2,3,\ldots,n. \tag{17}$$

Among them, m is the number of students watching the video, n is the number of course videos, and d_{ij} is the viewing time of the jth video of the ith student. Let v_j represent the length of the jth video, then the R value of the jth video is defined as

$$R_j = \frac{w_j}{v_j}, \quad j = 1, 2, \ldots, n. \tag{18}$$

Finally, take the mode of R_j to represent the R value of the course; then, the value of R is

$$R = \text{Mode}\left\{R_j, \quad j = 1, 2 \ldots, n\right\}. \tag{19}$$

Teaching interaction refers to the amount of interaction between teachers and students in a course, and it is also one of the factors that determine the quality of a course. In this study, teaching interaction was defined as teacher activity in the discussion area, and teacher activity was the ratio of the sum of the number of posts and responses by teachers in the discussion area to the total number of posts in the discussion area representing the course. The calculation process is shown in formula (20). The data required to calculate the above features come from the course teaching behavior data.

$$\text{active ratio} = \frac{\text{post} + \text{reply}}{\text{total}}. \tag{20}$$

This experiment uses k-fold cross-validation to determine optimal hyperparameters to check model performance and avoid model overfitting. The F1 value comparison of the two is shown in Figure 5.

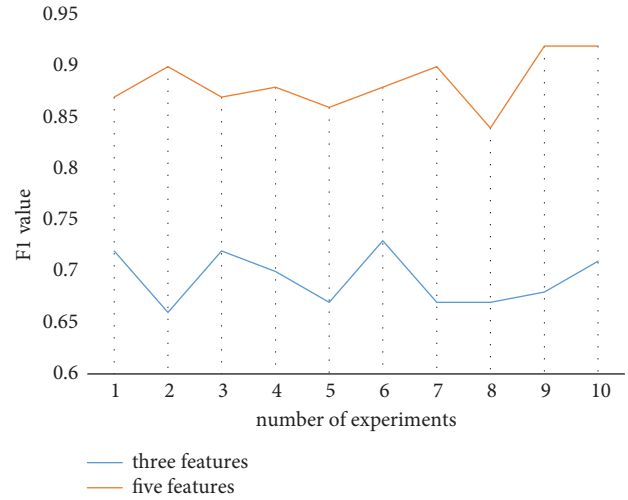

Figure 5: Comparison of F1 values of a 10-fold crossover experiment.

Table 2: The main purpose of users using the continuing education online training system.

Main purpose	Proportion (%)
Other	5.74
Hobby	33.28
Improve professional skills	58.53
Assisting on-campus study	47.06
Vocational qualification exam	46.48

Table 3: The duration of users using the continuing education online training system.

Duration	Proportion (%)
Less than 3 months	24
3–6 months	26.53
6 months–1 year	22.90
1–3 years	16.89
Over 3 years	9.68

It can be seen from Figure 5 that the average F1 value is increased by 19%, which proves that the online training system in this paper is effective.

5. Realization Effect of Continuing Education Online Training System

5.1. Market Development of Continuing Education. As can be seen from Table 2, among the main purposes of continuing education for online training system users, the highest proportion is to improve professional skills, accounting for 58.53%, followed by assisting campus course study and conducting vocational qualification examinations, entertainment and others, accounting for 47.06%, 46.48%, 33.28%, and 5.74%, respectively. Among them, the development of professional skills is particularly prominent, indicating that users have a strong willingness to use online education platforms, which is consistent with the distribution data of classroom statistical variables.

Table 4: Analysis of user satisfaction with continuing education online training system.

Satisfaction	Proportion (%)
Very satisfied	50
Satisfied	24
General	11
Dissatisfied	11
Very dissatisfied	4

The time intervals for using the CET online training system (see Table 3) are 3–6 months, less than 3 months, and 6 months–1 year, respectively, and the proportions are relatively close, 26.53%, 24%, and 22.90%, respectively. The proportion of more than one year is the lowest at 9.68%, indicating that the purpose of most users is to achieve a specific short-term learning effect, which is also consistent with the distribution variables of statistical data.

5.2. Satisfaction Analysis of Continuing Education Online Training System. It can be seen from Table 4 the online continuing education training system designed in this paper has been recognized by most users, 50% of users are very satisfied, and 24% of users are satisfied.

6. Application Directions of Continuing Education Online Training System

6.1. Standardization of System Design. The first step in the reform of continuing education is the standardization and institutionalization of the information management of the continuing education system. Implementing the information management construction under institutional standards and realizing that the teaching management process conforms to institutional standards have an important impact on the quality and stability of the entire educational reform process.

Since colleges and universities can independently construct online course resources in the process of actual teaching reform and management, this freedom will hinder the construction of "artificial intelligence + education" network teaching platform. Increase the complexity of college database construction and increase the workload. Curriculum resources can negatively impact the effectiveness of information management applications and cause unnecessary problems with information maintenance. Therefore, in the management of continuing education, system standards need to be built to promote the further development of artificial intelligence technology in the field of continuing education. Judging from the response speed of the national emergency response system to online teaching, teaching at all levels basically has the basic conditions for online teaching. As far as the convenience of online teaching platforms is concerned, the reason why such rapid and large-scale online teaching can be implemented is because of the implementation of the system standards for online teaching.

Therefore, in order to expand the teaching network standard of continuing education, a standardized system can be developed to promote the reform of teaching network. The "Internet +" era provides a good platform for standardized and institutionalized school-level regional cooperation network teaching management. First, by using the regional characteristics of colleges and universities, it can promote regional continuing education cooperation, realize inter-school resource sharing, establish a good teaching cooperation system, and promote good cooperation and reform and development of inter-school teaching networks; it can form a network teaching park, strengthen the resource sharing of regional colleges and universities, build a continuing education network teaching platform, promote a more unified teaching standard construction, and improve the management and delivery quality evaluation process. The above projects have a strong role in promoting the development of continuing education.

6.2. The Quality of Curriculum Design. Continuing education is an integral part of higher education, a part of the process of creating a learning society, and a new way of education. In the process of realizing lifelong education, more emphasis is placed on mass education and education, and its audience is wider than ordinary higher education. However, there are differences between the two in terms of training objectives and details, social adaptation, etc., and there are naturally differences in educational management and teaching quality. At present, continuing education management implements both "online + offline," focusing on face-to-face teaching and online teaching. However, the use efficiency of online teaching platform is obviously low, which hinders the improvement of teaching management quality. At present, in the process of continuous education online teaching quality reform and improvement, it is necessary to formulate corresponding teaching management quality standards, gradually improve the information-based teaching management model, and realize the full integration of public resources, and teaching and public management with various platforms.

(1) Promote the construction and use of networked teaching platforms in colleges and universities. At present, colleges and universities cannot fully realize the full implementation of online teaching. Therefore, while ensuring the quality of current centralized face-to-face teaching, it is necessary to speed up the construction of their own online teaching platform quality management standards to ensure teaching quality and teaching process progress.

(2) Establish a continuous learning system on the education network platform. In view of the outbreak of the epidemic all over the country and in response to the call for "suspending classes without stopping learning," we can notice the country's investment in online teaching and know that all levels of education have implemented a check-in system for online teaching courses. Of course, for primary and secondary school students and full-time college students, the daily punch-in system can actually play a good role in teaching management, but for online

teaching in continuing education, it is necessary to adapt to local conditions. It is necessary to form targeted teaching management quality standards according to the fragmentation of the adult learning process, rather than having to be online every day, so it is necessary to implement flexible system introduction. The first step is that teachers and teaching administrators formulate teaching plans according to the characteristics of the courses, complete the standards, and reasonably quantify the learning progress of students. The second step is to use social software groups such as network platforms managed by QQ groups and WeChat groups to teach professionally. Publish the teaching plan management regulations corresponding to uploading online courses.

6.3. Sharing of Platform Resources. At present, there are still some difficulties in realizing the joint reform of continuing education in colleges and universities and building a large-scale "artificial intelligence + education" continuing education network platform. If we want to break this independence, we need to continue the educational network, realize the joint sharing of teaching resources, realize the development of regional inter-school teaching cooperation, and gradually expand and develop into an "artificial intelligence + education" network teaching platform.

The continuing education network construction of the teaching management platform carried out by various colleges and universities is currently decentralized, and there is a certain gap in the implementation of resource sharing. When implementing online teaching, continuing education colleges have their own systems to build online teaching platforms. In fact, in the process of continuing education, there is a certain degree of overlap between majors and courses, and although colleges and universities have developed other aspects of the learning management platform, the training resources are not. If there is no effective resource sharing, it will cause waste and uneven quality of online education resources, which will seriously affect the quality of continuing education.

Therefore, in the process of developing continuing education management informatization, we can consider creating a resource sharing platform, establishing unified standards and designing compatible public interfaces, so that educational resources can be attached to the platform. At present, a province in China has built a continuing education network park, integrating continuing education resources supported by colleges and universities in the province to build an online education management platform.

7. Conclusion

The online continuing teaching system can effectively meet the actual needs of students. The core application technologies of the system are multimedia technology and artificial intelligence technology. The continuous education online training system can be used to discuss and exchange learning problems in real time, thus becoming a paradise for learning lovers. The continuing education online training system is composed of various educational materials such as text, images, and animations, which can effectively realize online classroom education. Through the rational use of continuing education online training system can bring more knowledge to people. The online education and training system can learn the required knowledge anytime and anywhere, so this system is recognized by most people.

Data Availability

The data used to support the findings of this study can be obtained from the author upon request.

Conflicts of Interest

The author declares that there are no conflicts of interest.

Acknowledgments

This work was supported by Research on the design and implementation of continuing education online training system based on artificial intelligence algorithm.

References

[1] H. Luan, P. Geczy, H. Lai et al., "Challenges and future directions of big data and artificial intelligence in education," *Frontiers in Psychology*, vol. 11, Article ID 580820, 2020.

[2] K. Paranjape, M. Schinkel, R. Nannan Panday, J. Car, and P. Nanayakkara, "Introducing artificial intelligence training in medical education," *JMIR medical education*, vol. 5, no. 2, Article ID e16048, 2019.

[3] Y. C. Wu, L. F. Hsieh, and J. J. Lu, "What's the relationship between learning satisfaction and continuing learning intention?" *Procedia-Social and Behavioral Sciences*, vol. 191, pp. 2849–2854, 2015.

[4] A. Syakur, L. Musyarofah, S. Sulistiyaningsih, and W. Wike, "The effect of project-based learning (PjBL) continuing learning innovation on learning outcomes of English in higher education," *Budapest International Research and Critics in Linguistics and Education (BirLE) Journal*, vol. 3, no. 1, pp. 625–630, 2020.

[5] J. M. Phillips, "Strategies for active learning in online continuing education," *The Journal of Continuing Education in Nursing*, vol. 36, no. 2, pp. 77–83, 2005.

[6] Y. L. Chiu and C. C. Tsai, "The roles of social factor and internet self-efficacy in nurses' web-based continuing learning," *Nurse Education Today*, vol. 34, no. 3, pp. 446–450, 2014.

[7] P. Zhang, F. D. Liu, and Z. Shan, "Thinking and practice of online teaching under COVID-19 epidemic," in *Proceedings of the 2nd International Conference on Computer Science and Educational Informatization*, pp. 165–167, Xinxiang, China, June 2020.

[8] M. E. Ibrahim, Y. Yang, D. L. Ndzi, G. Yang, and M. Al-Maliki, "Ontology-based personalized course recommendation framework," *IEEE Access*, vol. 7, pp. 5180–5199, 2019.

[9] F. H. Wang and H. M. Shao, "Effective personalized recommendation based on time-framed navigation clustering and association mining," *Expert Systems with Applications*, vol. 27, no. 3, pp. 365–377, 2004.

[10] M. Adil, M. K. Khan, M. Jamjoom, and A. Farouk, "MHADBOR: AI-enabled administrative distance based opportunistic load balancing scheme for an agriculture internet of things network," *IEEE Micro*, vol. 42, 2021.
[11] X. Chen and H. Deng, "Research on personalized recommendation methods for online video learning resources," *Applied Sciences*, vol. 11, no. 2, p. 804, 2021.
[12] X. Li, L. Bing, P. Li, and W. Lam, "A unified model for opinion target extraction and target sentiment prediction," in *Proceedings of the AAAI Conference on Artificial Intelligence*, vol. 33, pp. 6714–6721, Honolulu, HL, USA, February 2019.
[13] Z. Gulzar, A. A. Leema, and G. Deepak, "Pcrs: personalized course recommender system based on hybrid approach," *Procedia Computer Science*, vol. 125, pp. 518–524, 2018.
[14] B. Charbuty and A. Abdulazeez, "Classification based on decision tree algorithm for machine learning," *Journal of Applied Science and Technology Trends*, vol. 2, no. 01, pp. 20–28, 2021.
[15] Y. Freund and L. Mason, "The alternating decision tree learning algorithm," in *Proceedings of the Sixteenth International Conference on Machine Learning ICML*, pp. 124–133, San Francisco, CA, USA, June 1999.
[16] F. Guder and M. Malliaris, "Online and paper course evaluations," *American Journal of Business Education*, vol. 3, no. 2, pp. 131–138, 2010.
[17] W. S. Noble, "What is a support vector machine?" *Nature Biotechnology*, vol. 24, no. 12, pp. 1565–1567, 2006.
[18] J. Zhao, X. Yang, Q. Qiao, and L. Chen, "Sentiment analysis of course evaluation data based on SVM model," in *Proceedings of the 2020 IEEE International Conference on Progress in Informatics and Computing (PIC)*, pp. 375–379, Shanghai, China, December 2020.

Hindawi
Mobile Information Systems
Volume 2022, Article ID 8169753, 9 pages
https://doi.org/10.1155/2022/8169753

Research Article

Cloud Data System Design for Mental Crisis State Recognition of College Students Based on Machine Learning

Huimin Zhang[1] **and Sidong Guo**[2]

[1]*Student Office Mental Health Center, Harbin Institute of Finance, Harbin 150010, China*
[2]*Faculty of Educational Sciences, Harbin Normal University, Harbin 150010, China*

Correspondence should be addressed to Huimin Zhang; 2009129@hrbfu.edu.cn

Received 29 July 2022; Revised 17 September 2022; Accepted 27 September 2022; Published 7 October 2022

Academic Editor: Shadi Aljawarneh

At present, Chinese college students are facing a lot of psychological pressure; whether it is teaching pressure or life pressure, it will have a certain adverse impact on college students' psychological state, and if timely guidance is not provided, it will result in some adverse consequences. Therefore, it is necessary to timely identify the psychological crisis situation of college students, but the existing form of manual identification has high limitations, which cannot obtain the psychological state of students more accurately and efficiently, so it is necessary to optimize and improve with the help of network technology. Cloud computing data system is one of the mature big data systems at present. The combination of cloud computing system and machine learning technology is effectively applied to the field of psychological crisis analysis, which can quickly screen the psychological status of college students and report abnormal data in a timely manner, so as to help college psychological teachers identify the state of college students' psychological crisis and intervene in a timely manner to promote the physical and mental health of students. By applying machine learning technology for the establishment of a cloud computing data system and putting the system into the field of psychological crisis identification of Chinese college students, this study lays a theoretical and practical foundation for preventing students from the psychological crisis.

1. Introduction

The development of cloud computing technology has changed the operation mode of computers, and it can easily meet the needs of the industry and academia for computing and storage. Cloud computing can easily expand the service scope and infrastructure according to user needs and can adapt to the management of the services provided [1]. Therefore, high-performance cloud computing services can not only improve the quality of cloud application services but can also bring more benefits to cloud providers [2]. In addition, the progress of machine learning technology can not only provide good solutions for the needs of multiuser shared hardware resources but can also provide reliable technical support for the realization of many computer technologies [3]. Because cloud computing has innovative resource management, excellent performance isolation services, and low-cost use sources, it has become the best choice for large-scale data-intensive computing applications [4]. At present, many applications need to use special internal servers to run, so it is turning to a cloud computing environment for processing and storing a large amount of data generated by users every day. Data system cloud storage plays an important role in the cloud computing environment, such as healthcare systems, smart homes, or environmental monitors. Therefore, this study applies this technology to the field of psychological crisis analysis of Chinese college students [5]. At present, the psychological crisis of college students has become one of the main problems affecting college teaching, so effective early intervention means for psychological crisis is very important. However, at present, the means of warning students' psychological crisis are relatively single. In most cases, SCL is only used to test the students who have just entered the

freshman stage [6]. Therefore, the effective use of new technologies to extract and analyze students' behavior data to determine the realization of early psychological warning is very important to manage students' mental health. This study proposes a student psychological crisis early warning method based on a cloud computing data system [7]. We identify the status of students according to different values of behavior characteristics, so as to judge whether the subject may have a psychological crisis [8]. In the process of selecting personality traits, this study consulted the opinions of student management experts and conducted a binary logistic regression analysis on some traits [9]. Finally, six personality traits, such as family composition, family economy, family relations, class leave, personality characteristics, and failing grades were selected and applied to the modeling decision tree, and the model was qualitatively analyzed according to relevant data by confirming its credibility and reference value [10]. Comparing the test results of several different datasets in the model, it can be seen that the overall prediction accuracy of the model reaches more than 95%, the average recall rate can reach more than 60%, and the F value is stable at more than 70%, which proves that the model has good generalization ability.

2. Related Work

The literature implements a kind of application system architecture focusing on early warning models. The system is based on the Web-based B/S system, the back-end adopts Spring MVC framework, the front-end adopts JSP language, and the database adopts MySQL development [11]. It has key functions such as collecting students' basic information, managing grades, and application approval, and these functions can be used to generate corresponding data so as to finally realize the early warning function for students' psychological crisis and to complete students' management tasks. The literature introduces the multitenant characteristics of the cloud computing environment, optimizes the overall architecture of traditional cloud storage, and then optimizes and improves each component in terms of high performance and high reliability [12]. It mainly includes data index organization, data storage method, data replication mechanism, data confidentiality mechanism, and data positioning mechanism optimization design form. As a part of the early warning of psychological crisis, the discussion was launched, and finally, the internal structure, technical route, and organizational structure of the system were introduced [13]. The literature explains the purpose and background of the system research and construction, combines the real needs of users to analyze the actual application scenarios, and carries out the overall design and detailed system design of the system, including system management module, information collection module, scoring management module, and leave approval module [14]. Compared with the related existing research results, the experimental results prove that the dynamic sample entropy model proposed in this study performs better in identifying individual emotions, has excellent universality and generalization ability, and can establish cognition for cross-individual state recognition [15]. The calculation method realizes the optimization and innovation of emotional EEG pattern recognition and can effectively predict human emotions based on EEG signals [16]. The literature collected the cognitive EEG data of 21 subjects for experimental research. Experimental data show that the proposed method can recognize the target speech through selective auditory attention to the subject and can obtain the highest recognition accuracy [17]. The research results found that the selective auditory attention decoding method based on the LSTM model can achieve high-precision decoding of the auditory attention selected from EEG signals [18].

3. Data System Design Based on Cloud Computing

3.1. Cloud Computing Data Placement Model Design. In the process of selecting the data storage location, we need to consider factors such as the intensity of user data, the indexing time of the data, and the correct loading on the storage node. Based on this point, we first carried out mathematical modeling, which fully considered the abovementioned data factors and described the placement of data in a mathematical form. Subsequently, the placement algorithm is selected to solve the above problems in a targeted manner. The algorithm first considers some factors and then makes the best choice for other factors. Since the load balancing of storage nodes has an impact on cluster strength and data strength, we choose to provide an implementation solution that meets the minimum data retrieval time while satisfying the stability of the storage nodes to load and store data.

We use (S_1, S_2, . . .,and S_M) to represent the strategy of placing the main data block in cloud storage, and we use $Si \neq 0$ to represent a data block of size Si to be stored on node i, indicating that if $Si = 0$, it means that the node cannot be used to store data blocks.

Subsequently, the retrieval time required to recover the data in the read data request is calculated. Let node p instruct the user to send the required reading to the access point. We assume that the same user always uses the same access point to store and read data. If the data block Si stored in node i is brought to the access point of user p, there may be several different transmission paths. We can calculate the shortest transmission path between access point p and node i. Therefore, the time to transmit a data block of size Si from node i to access point p is as follows:

$$T_{S_i} = \sum_{l \in P_{i,p}} \frac{S_i}{B_{l_s,l_e}}, \tag{1}$$

where l represents the path of P_i and p in the shortest path, B_{ls}, l_e is the bandwidth of path l, and l_s and l_e are the source and destination of link l, respectively. If M different data blocks are sent from M different storage nodes at the access point p, where the total size of the data block M is D, then the total transmission time required is as follows:

$$T_D = \sum_{i=1}^{M} \sum_{l \in P_{i,p}} \frac{S_i}{B_{l_s,l_e}}. \quad (2)$$

The mathematical model is as follows:
Minimize

$$T_D = \sum_{i=1}^{M} \sum_{l \in P_{i,p}} \frac{S_i}{B_{l_s,l_e}}. \quad (3)$$

Subject to

$$\begin{aligned} \sum_{i=1}^{M} S_i &= D, \\ S_i &\geq 0, i = 1, \ldots, M, \\ S_i &\leq S^{\max}, i = 1, \ldots, M, \\ S_i &\leq C_i, i = 1, \ldots, M, \\ V_i &\geq L, i = 1, \ldots, M. \end{aligned} \quad (4)$$

We use V_i to represent the remaining storage load of storage node i, then V_i can be expressed as follows:

$$V_i = \frac{C_i}{A_i}. \quad (5)$$

In formula (5), C_i represents the remaining storage space of node i, A_i represents the total storage space of node i. and L is expressed as follows:

$$L = \max\left\{\frac{C_i - S_i}{A_i}\right\}, i = 1, \ldots M. \quad (6)$$

3.2. Cloud Computing Data Positioning Scheme Design. We set server performance indicators including CPU, memory, IO, and network. Then, we calculate the CPU utilization of node iP^i_{cpu}, as shown in formula (7).

$$P^i_{cpu} = \frac{U^i_{cpu}}{T^i_{cpu}}. \quad (7)$$

Similarly, we calculate the resource utilization of memory and IO separately, and the formula can be expressed as follows:

$$\begin{aligned} P^i_m &= \frac{U^i_m}{T^i_m}, \\ P^i_{io} &= \frac{U^i_{io}}{T^i_m}. \end{aligned} \quad (8)$$

Since the storage node group to be accessed has already been determined, there is no need to compare the creation of the storage node with all storage nodes in the entire system. It is only necessary to compare the creation of storage nodes that store data block S at the same time. Here, we first calculate the average utilization of each collection indicator in the data storage block S of the storage node K_s. The utilization rate of the processor source in this set P_{cpus} is expressed by the following formula, where P_{cpu} is the average utilization rate of the processor resources in the entire system and n is the number of points at the summary point.

$$P^s_{cpu} = \frac{1}{n} \sum_{i \in K_s} P^i_{cpu}. \quad (9)$$

Similarly, the average resource utilization of memory and IO is as follows.

$$\begin{aligned} P^s_m &= \frac{1}{n} \sum_{i \in K_S} P^i_m, \\ P^s_{io} &= \frac{1}{n} \sum_{i \in K_S} P^i_{io}. \end{aligned} \quad (10)$$

Among them, P^s_m is the average usage of the storage node memory in the storage data block S and P^s_{io} is the average usage of the IO in the storage node set in the storage data block S. Since we use the network hop count to measure the quality of the network, for different copies of the same data, we can calculate the average hop count L_{net}, and the formula is as follows.

$$P^s_{net} = \frac{1}{n} \sum_{i \in K_S} P_{i,p}. \quad (11)$$

We then calculate the usage rate of each index on each server and the average usage rate of the source code. Then, we classify the set of servers storing S data blocks according to their original storage. It can be divided into five categories, namely, A, B, C, D, and E. Class A indicates that the current server's CPU, memory, and IO resource usage which is lower than that of the average system source usage, and the corresponding indicators and network hop counts are also lower than the average. Type B indicates that one of the indicators such as processor usage, memory usage, IO usage, and network hops is higher than that of the corresponding system value, and C, D, and E can be deduced by analogy.

3.3. Encrypted Storage Design of Cloud Computing Data. With the addition of encrypted storage mechanisms, it will inevitably affect the overall performance of the system. Therefore, we need to implement a secure encryption mechanism as soon as possible when the system performance is affected.

Key stream management involves generating and accessing the key stream. The user key stream generation can be generated in the secure storage module or can be independently set by the user. To prevent encrypted data from being erased due to unintentional changes in the user's key stream, two key streams with the same security level can only be set once. In order to prevent the key stream from leaking, we use a pair of asymmetric key pairs to encrypt and store the key stream. If the user automatically specifies the key stream, then the public key of the nonpeer key pair of the security module must be used to encrypt the key, and then we send them to the security module for storage.

The second module is the data encryption and decryption module, which is mainly used to receive user requests and provide encryption and decryption services. If the receiver of the security module receives the request, the external interface (API) of the data encryption module sends the requested encryption operation to the server, and the encryption operation is responsible for using encryption algorithms to process user data. The data encryption module requests the user's key stream from the key management module through the key manager. The key manager retrieves the database key based on the user information and security level information to verify whether there is an appropriate key stream. If not, it checks whether there is a user-defined secret key. If it is customized, it then saves the ciphertext and decrypt it and return the plaintext. If it is not specified, the key management module will automatically generate the key of the corresponding level, encrypt it, save it, and return it to plain text. After the data encryption and decryption module receive the key stream, it performs data encryption and decryption services.

In addition, we provide optional levels of security encryption for users who use the default key stream. Users can set their own security level according to the characteristics of their own data or can use the default security level of the security module. For users who provide their own key streams, they can provide key streams of different lengths of security modules according to different data to meet changes in security levels. Because the stream user key must be stored in the security module, we use the ID that specifically identifies the user information and the security level that uniquely identifies the user key information to identify the stream that will be streamed to the user. Therefore, the database table must contain internal information such as <key_id, level, key.string>, and the structure of the data table is shown in Table 1.

In Table 1, Key_id represents the current key id, User_id is the user id, and level is the encryption level. Key_length represents the length of the user-defined key. Only one of the two fields, level and Key_length, is valid. If a custom key stream is used, Key_length is valid, otherwise Level is valid. Key_string is a specific key value. We can apply the user id and encryption level according to the key and the value is unique.

3.4. Analysis of Test Results of Cloud Computing Data System Storage Node Balancing Load. In this test, we conducted the same test to realize the design of the cloud storage system and the creation of the MooseFS system in this article. Among them, we use the dd command to periodically write data to the storage system for 2 minutes. Multiple group experiments are conducted, and the stored data after each test are deleted to ensure a consistent test environment. Finally, we use the multiple average results as the final experimental result. Due to a large amount of data, the results are not intuitive enough, so we tested the values for some time and extracted several datasets, that is, the resource utilization of each storage node at a certain time. The loading results of each node of the MooseFS storage system are shown in Figure 1.

Table 1: Key database table structure.

Filed	Type
Key_id	Integer
User_id	Integer
Level	Character
Key_length	Integer
Key_string	String

We use the same test environment and methods to test the load balancing of storage nodes in the cloud storage system designed and implemented in this article and capture the resource usage of each storage node, as shown in Figure 2. It can be seen from the figure that as time goes by, the amount of data in the storage system continues to increase, and the resource usage of each storage node gradually tends to balance.

4. Recognition of Psychological Crisis State Based on Machine Learning

4.1. Theoretical Basis and Model Design of Machine Learning. Through the evaluation and display of the performance of the two models, the four indicators of accuracy, precision, recall, and F value are analyzed, and the most suitable algorithm for this research is selected, as shown in Table 2.

Category information entropy: for example, S is a training instruction sample set, S is composed of s data samples, then S is considered to have a different sample category m, which is defined as $C_i (i = 1,2, \ldots, m)$. If Si is calculated as the number of samples in the category C_i; then, for a given sample dataset, the entropy of category information, that is, the amount of information required for classification can be calculated as follows:

$$I(S_1, S_2, \ldots, S_m) = -\sum_{i=1}^{m} p_i \log_2 p_i. \tag{12}$$

Conditional information entropy: assuming that attribute A has different values, a total of $v\{a_1, a_2, \cdots, av\}$, attribute A can be used to divide S into v subsets $\{S_1, S_2, \ldots, S_V\}$, suppose S_j has the same value $a_j (j = 1, 2, \ldots, v)$ in all samples of A.

Information gain: according to formulas 22 and 23, the information gain obtained by branching on attribute A is as follows:

$$\text{Gain}(A) = I(S_1, S_2, \ldots, S_m) - E(A). \tag{13}$$

Split information entropy: in the training sample set S, the samples are classified based on the attribute A value, then the split information entropy calculation formula of A is as follows:

$$SplitI(A) = -\sum_{j=1}^{v} p_j \log_2 p_j. \tag{14}$$

4.2. The Design of the Recognition System for the Psychological Crisis State of College Students. The overall design of the

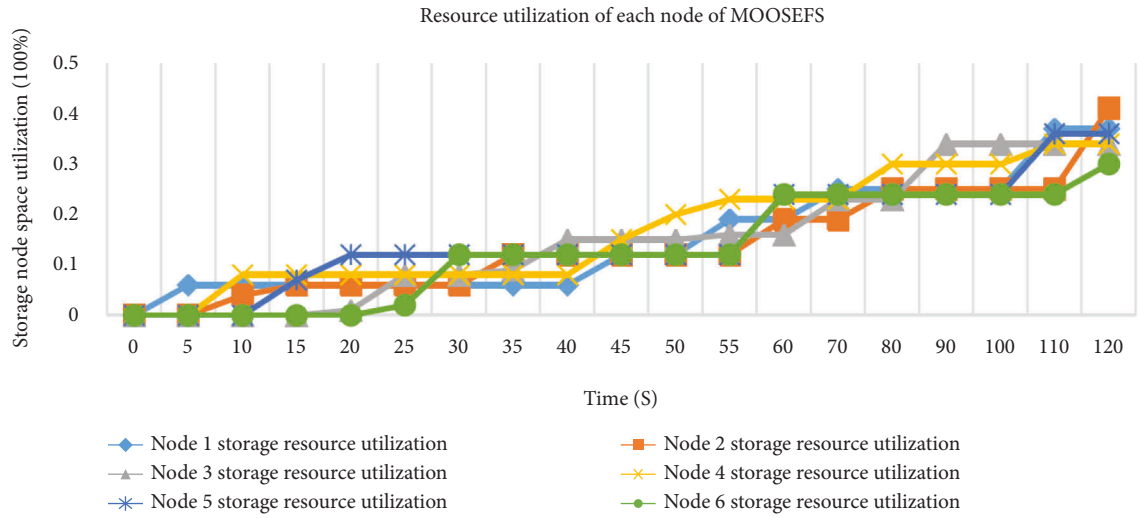

Figure 1: MooseFS resource utilization of each node.

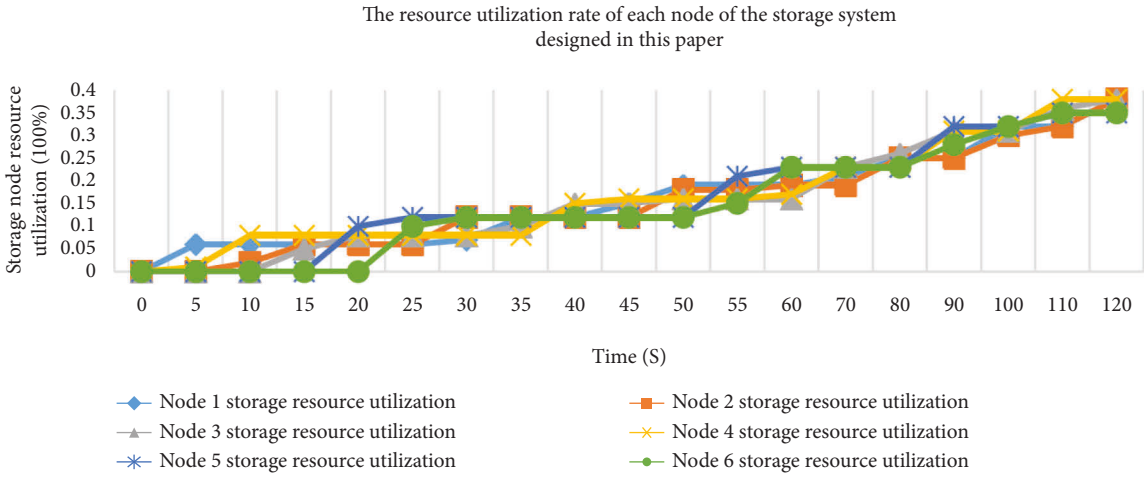

Figure 2: The resource utilization rate of each node of the storage system designed in this study.

Table 2: Algorithm performance evaluation.

Evaluation index	C4.5 (%)	CART (%)
Accuracy	97.3	95.7
Accuracy rate	81.9	66.6
Recall rate	64.7	42.8
F value	72.1	52.3

system follows the principles of code reuse. In the development process of the system, not only the performance of basic functions should be paid attention to, but also the function improvement of the system should be considered, and the fast interface of the node should be kept as much as possible. In places that can be extended, such as placing trigger points in the early update of alert rules, if the model is optimized in the future, the rules set by the system can be updated at the same time to facilitate the update and improvement of the next system.

Principle of intuitive interface. the system is suitable for three different types of users and has a wide range. The purpose of research and development is to promote student management by student managers and classroom teachers. The system is easy to understand and easy to use.

The application system architecture takes the early warning model as the core, adopts the Web-based B/S architecture, and uses the Apache Tomcat server. Database applications can more efficiently separate and store data and can access MySQL databases. The back-end adopts the Spring MVC deployment framework and the main components adopt JSP technology. The overall system architecture is divided into five layers from top to bottom, namely the visual view layer, the control layer, the business logic layer, the data access layer and the data storage layer. The general architecture of the system is shown in Figure 3.

4.3. Analysis of the Recognition Results of the Psychological Crisis State of College Students. In order to test the design of the ETR model learning method based on dynamic entropy to determine the recognition of emotional valence, first, the sliding method is used to obtain dynamic entropy

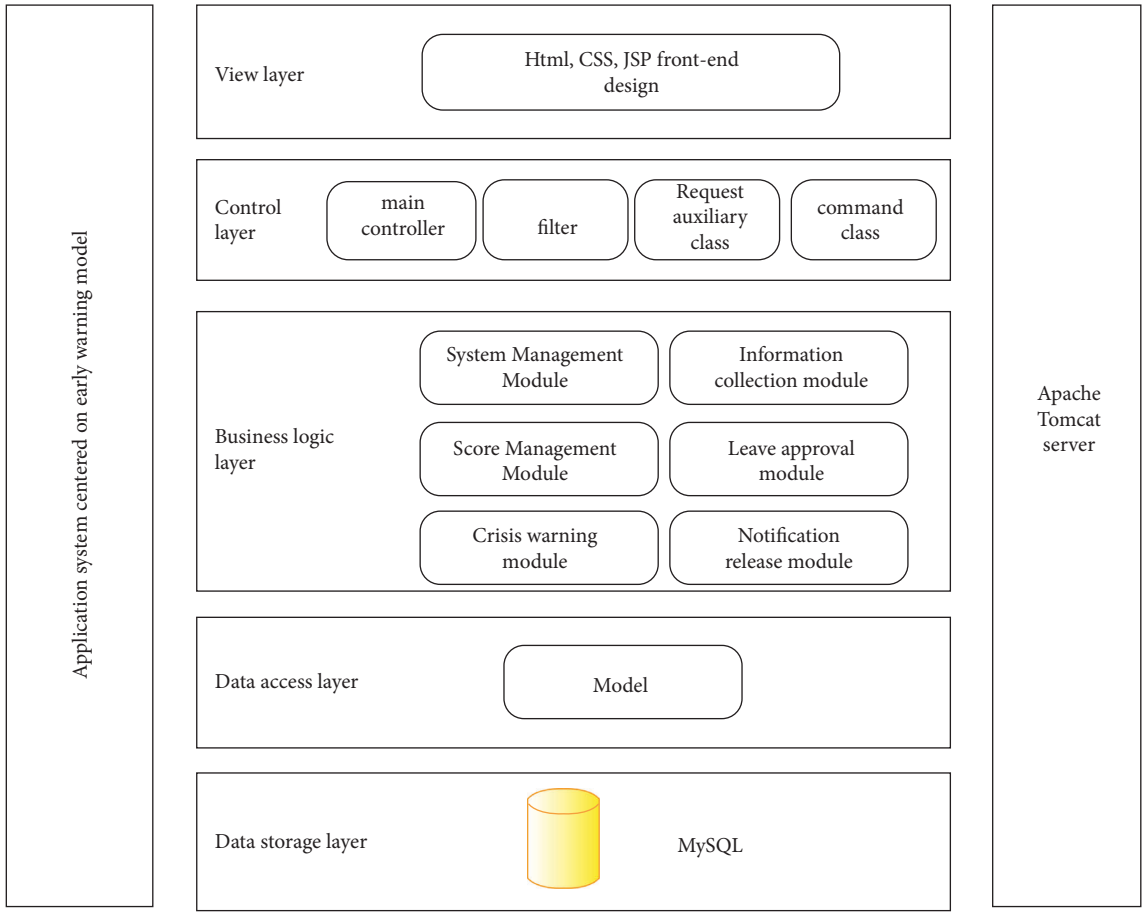

Figure 3: System overall architecture diagram.

component samples from the EEG signal. The EEG data used in the experiment lasted 60 seconds. We use a time window with a duration of 4 seconds, and the duration of each movement of the window is 2 seconds. Therefore, each channel in the EEG time series can capture the entropy patterns in 29 consecutive EEG samples. Figure 4 shows the statistical results of dynamic samples of the EEG signal entropy components of all channels in the 29-hour window, and the subjects are in a negative emotional state.

Subsequently, the correlation t-test was used to test the significance of the EEG entropy characteristics of positive and negative emotions. Figure 5 shows the p value of the entropy result of the dynamic EEG samples of all channels in the 29-hour window of positive and negative emotional states. As shown in Figure 5, the horizontal axis represents the 29-hour window arranged in chronological order, and the vertical axis represents approximately 62 EEG channels. The redder the area, the more significant is the variability of the entropy characteristics of the brain electrical channels corresponding to the time window of the positive and negative sensory states.

Table 3 lists the EEG model learning method based on dynamic entropy to determine the consequences of positive and negative emotion recognition. The experimental result data include the test result standard and definition deviation of 15 subjects. The experimental stage (session order, SesOrd) is the corresponding data of 1, 2, and 3 EEG emotions and the EEG model learning method based on dynamic entropy to obtain the accuracy of individual positive and negative emotion recognition are 82.01% ± 13.21% and 82.68, respectively. % ± 16.21% and 82.68% ± 19.08%. For the EEG data samples collected in these three experiments, the overall accuracy of identifying cross-individual negative and positive emotions is very close. The experimental results show that the EEG model learning method based on dynamic entropy can identify cross individual emotional valence and has good stability.

Table 4 shows the comparison of methods for detecting emotional valence based on EEG signals. Experimental comparison results show that the proposed EEG emotion recognition method based on the dynamic entropy input model shows a better overall recognition rate and generalization performance.

4.4. Work Strategies Based on the Psychological Status of College Students. This study confirms the intermediary role of College Students' basic literacy and personality development in the psychological crisis caused by college students' life pressure and also confirms that college students' core literacy and students' personality advantages should be paid more attention. The university stage is not only an

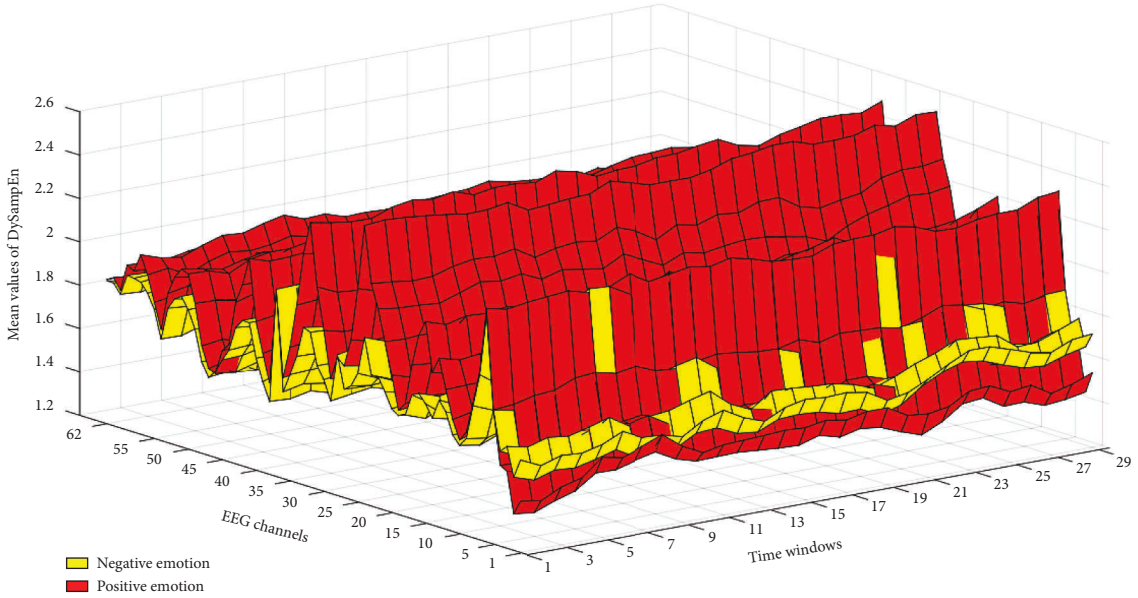

Figure 4: The average entropy of the EEG dynamic sample entropy corresponding to each channel in each time window under positive and negative emotional states.

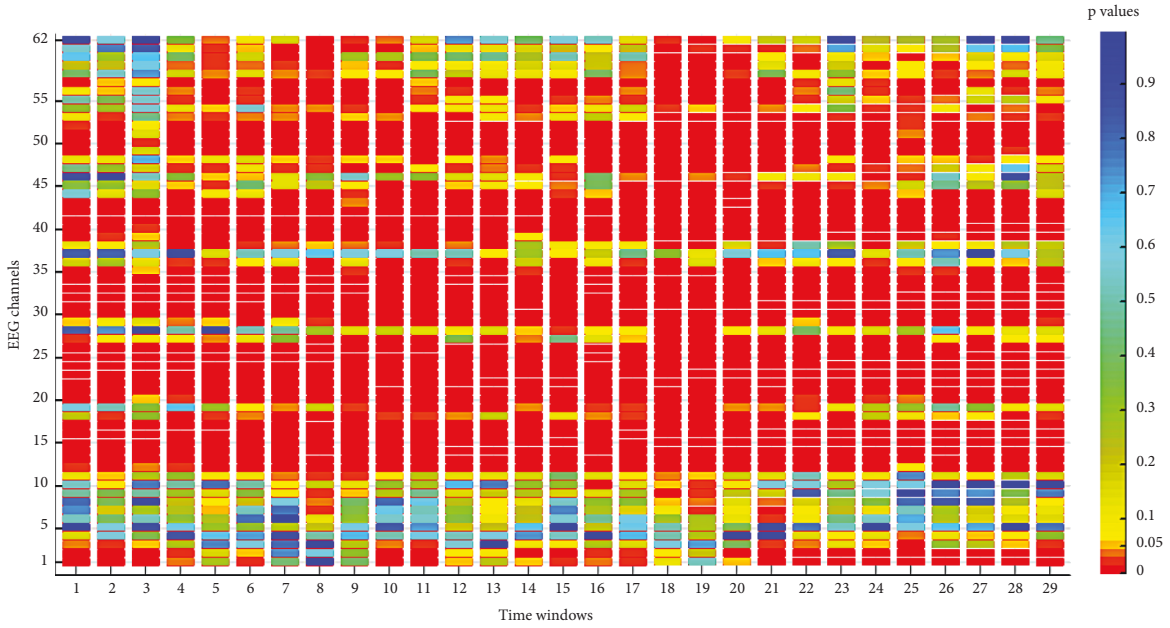

Figure 5: The entropy of the EEG dynamic samples corresponding to each channel in each time window is the p value result of the paired sample t-test in the positive and negative emotional states.

Table 3: EEG emotion pattern learning method based on dynamic entropy realizes cross individual positive and negative emotion recognition results.

Experimental rounds	Accuracy (%)	Sensitivity (%)	Specificity (%)	Error rate (%)	Number of samples
1	82.01 ± 13.21	82.68 ± 24.93	81.34 ± 20.67	18.00 ± 13.21	150
2	82.68 ± 16.21	86.68 ± 24.68	78.68 ± 31.58	17.34 ± 16.25	150
3	82.68 ± 19.08	80.01 ± 34.65	85.34 ± 27.75	17.34 ± 19.08	150
1, 2, 3	84.65 ± 12.02	85.34 ± 18.88	84.01 ± 23.08	15.34 ± 12.02	450

Table 4: Performance comparison between the research work in this article and existing related emotion recognition research.

Method	Cross individual verification	Result
QTFD and SVM	NO	85.9% (valences, 2 classes)
Statistical, power spectral and HOC features, and SVM	NO	58.9% (valences, 3 classes)
Entropy, PS features, LSP, KNN, SVM, and MLP	NO	63.48% (valences, 3 classes)
DE, DASM, RASM, and SVM	NO	83.98% (3 classes)
DE and SVM	Yes	60.94% (3 classes)
ApEn, PerEn, ShEn, and SVM	Yes	83.34% (2 classes)
DySampEns and SVM	Yes	85.12% (2 classes) 64.16% (3 classes)

important moment for teenagers' physical and mental development but also a key moment for cultivating the characteristics and advantages of basic values and health care quality. Based on the theory of students' basic core quality and personality advantages, this study puts forward the following suggestions by studying the relationship between them and students' psychological crisis

First, we cultivate students' positive psychological quality and improve their psychological pressure resistance. While improving students' core literacy and culture, we strive to improve their own core competitiveness from all angles and fields, especially focusing on cultivating psychological literacy, so as to make them have excellent psychological quality, and to prevent the occurrence of psychological crisis.

Second, we carry forward the character advantages and enhance the students' individual judgment and will quality. The development and cultivation of personality advantage is not only an important factor in forming a good personality but it also an important factor for the premise of cultivating faith quality and strong will. College students' activity areas are mainly dormitories and classrooms. Therefore, it is necessary for college educators to create a positive educational environment on campus, promote students' all-round progress, shape students' behavior and moral standards, and affect students to establish good psychological quality.

Third, due to the differences between colleges and universities, different students have different growth environments and life experiences, so their psychological states and learning level are different, and the psychological attitudes of students at different training levels are also slightly different. Based on the analysis results, in view of the differences in the psychological crisis of students in provincial colleges, vocational colleges, and private colleges, individualized education for students' basic literacy and personality advantages should be implemented. Colleges and universities in the province should pay attention to promoting students' cultural accumulation and improving students' aesthetic quality. In the field of students' technical training, provincial colleges and universities need to pay attention to professional knowledge, skills, and innovative consciousness. According to the characteristics of colleges and universities, such as literature and history, science and technology, electronics, architecture, petroleum, and other fields, it aims to cultivate students with unique skills in this field.

Fourth, various power systems need to be fully developed and improved. If an individual encounters pressure, makes psychological actions and falls into a psychological crisis, then the individual cannot respond to thinking, reasoning and decision-making in time. Therefore, it is necessary to deal with the psychological crisis with the help of external forces. Nowadays, most students of crisis prevention and psychological intervention tend to work in the school system, thus ignoring the impact on the social environment and family growth environment. The intervention of students' psychological crisis not only needs to improve the system but also needs to have various support and defense. In a psychological crisis, school intervention is necessary, and the family environment must be effectively used. The positive synergy between school education and social culture interferes with the four levels of individual family school society in terms of a psychological crisis. At the same time, social networks should have a sense of social responsibility when reporting students' psychological crisis events, avoid exaggerating and using negative public opinion, and enable the public to pay attention, respect, and accept individuals or groups.

5. Conclusion

The purpose of this study is to analyze the student data that student managers often come into contact with in their daily work, so as to explore the hidden laws behind the data, so as to better identify the psychological dynamics of students and provide early warning for possible psychological crisis problems. First of all, this study sorted out and studied the research materials in related fields in recent years, and carried out a special study on the identification of psychological crisis states. The results show that the cloud computing system based on the data decision tree algorithm is most suitable for this research and it fully meets the requirements. Based on this point, this article has determined the scope of studying student data through field surveys, collected available data using questionnaire surveys, and established a basic dataset of students. Based on the basic common sense, relevant work experience and suggestions of the student management experts, the attributes of nonobvious research importance are screened, and the binary logistic regression analysis is performed on the whitened data matrix of the remaining quality attributes, and 6 attributes obtained retrospectively are highly related to psychological crisis. The characteristic attributes of sex are personality characteristics, family composition, family economics, family relations, leave type, and status of school

leave. The abovementioned six characteristic attributes are used to construct the main psychological crisis early warning system. Through experiments to test the performance of the two classic judgment tree algorithms C4.5 and CART in decision-making, comprehensively considering the precision, accuracy, and recall rate, this study finally chooses to use C4.5 psychological crisis as the early warning decision tree model application. Through experiments, 14 rules with positive warning results are obtained to describe the model. Through effective scientific explanation and quantitative analysis of the measured results, the reference value and comprehensive ability of the model can be scientifically demonstrated and proved.

Data Availability

The data supporting the current study are available from the corresponding author upon request.

Conflicts of Interest

The authors declare that they have no conflicts of interest.

References

[1] M. Attaran and J. Woods, "Cloud computing technology: improving small business performance using the Internet," *Journal of Small Business and Entrepreneurship*, vol. 31, no. 6, pp. 495–519, 2019.

[2] H. ru Zhang, "Application of cloud computing technology in the university's information construction and development," *Software Engineering and Applications*, vol. 08, no. 02, pp. 32–37, 2019.

[3] Z. Shen and Q. Tong, "The security of cloud computing system enabled by trusted computing technology," in *Proceedings of the 2010 2nd International Conference on Signal Processing Systems*vol. 2, pp. 2–11, IEEE, Dalian, China, July 2010.

[4] M. Masrom and A. Rahimli, "A review of cloud computing technology solution for healthcare system," *Research Journal of Applied Sciences, Engineering and Technology*, vol. 8, no. 20, pp. 2150–2153, 2014.

[5] K. Liu and L. J. Dong, "Research on cloud data storage technology and its architecture implementation," *Procedia Engineering*, vol. 29, pp. 133–137, 2012.

[6] F. Yao and A. Zhang, "Integration of education management and mental health in psychological crisis intervention in colleges and universities," *ASP Transactions on Psychology and Education*, vol. 1, no. 1, pp. 31–38, 2021.

[7] Q. Liu and X. Liao, "Research on university mental health education based on computer big data statistical analysis," in *Proceedings of the 2021 2nd International Conference on Big Data and Informatization Education (ICBDIE)*, pp. 29–34, IEEE, Hangzhou, China, April 2021.

[8] B. Inkster, "Early warning signs of a mental health tsunami: a coordinated response to gather initial data insights from multiple digital services providers," *Front. Digit," Health*, vol. 2, Article ID 578902, 2020.

[9] H. Ying, "Problems and countermeasures of mental health education for college students under the background of the epidemic," *Quality and Market*, vol. 263, no. 12, pp. 32–34, 2020.

[10] Q. Shi, N. Cai, and W. Jiao, "Monitoring and evaluating college students' mental health based on big data analysis," *American Journal of Health Behavior*, vol. 46, no. 2, pp. 164–176, 2022.

[11] J. Wang, Z. Zhang, H. Luo, Y. Liu, W. Chen, and G. Wei, "Research on early warning model of college Students' psychological crisis based on genetic BP neural network," *American Journal of Applied Psychology*, vol. 8, no. 6, pp. 112–120, 2019.

[12] M. Su, L. Zhang, Y. Wu, K. Chen, and K. Li, "Systematic data placement optimization in multi-cloud storage for complex requirements," *IEEE Transactions on Computers*, vol. 65, no. 6, pp. 1964–1977, 2016.

[13] K. P. Dwyer, D. Osher, and C. C. Hoffman, "Creating responsive schools: contextualizing early warning, timely response," *Exceptional Children*, vol. 66, no. 3, pp. 347–365, 2000.

[14] W. Zheng, Y. Zong, X. Zhou, and M. Xin, "Cross-domain color facial expression recognition using transductive transfer subspace learning," *IEEE transactions on Affective Computing*, vol. 9, no. 1, pp. 21–37, 2018.

[15] X. Chai, Q. Wang, Y. Zhao et al., "A fast, efficient domain adaptation technique for cross-domain electroencephalography (EEG)-based emotion recognition," *Sensors*, vol. 17, no. 5, p. 1014, 2017.

[16] Z. He, Y. Zhong, and J. Pan, "An adversarial discriminative temporal convolutional network for EEG-based cross-domain emotion recognition," *Computers in Biology and Medicine*, vol. 141, Article ID 105048, 2022.

[17] G. Sn and H. Meena, "Socio-demographic factors and locus of control on mental health among college students," *International Journal of Scientific Research*, vol. 15, no. 1, pp. 53–55, 2021.

[18] H. Soltau, H. Liao, and H. Sak, "Neural speech recognizer: acoustic-to-word LSTM model for large vocabulary speech recognition," 2016, https://arxiv.org/abs/1610.09975.

Hindawi
Mobile Information Systems
Volume 2022, Article ID 8152991, 11 pages
https://doi.org/10.1155/2022/8152991

Research Article

Development of Interactive English Teaching Online Platform Based on Collaborative Filtering Algorithm

Cao Hao

Xuzhou University of Technology, Xuzhou 221018, Jiangsu, China

Correspondence should be addressed to Cao Hao; caohao@xzit.edu.cn

Received 2 August 2022; Revised 18 August 2022; Accepted 19 September 2022; Published 7 October 2022

Academic Editor: Shadi Aljawarneh

In order to better promote the development of Interactive English teaching, we develop the existing online teaching platform on the basis of an improved collaborative filtering recommendation algorithm and construct an online English teaching platform that can meet the needs of teaching interaction. With the help of the "hierarchical learning" mode, an interactive teaching model in the form of self-study is constructed to provide users with the most suitable English learning resources. A new method is used to search the nearest neighbor set intelligently for the target user as a supplement to its similarity. This algorithm can be used well in interactive English teaching mode. On this basis, the system module of this study mainly includes a communication page, course evaluation, collaborative editing, and resource sharing. This study also investigates the actual use of students. The results show that the interactive English online teaching platform can meet most of the students' needs. In this study, the interactive English online teaching platform developed based on a collaborative filtering algorithm has a significant effect, which enhances the interactivity of teaching, improves the quality of English teaching, and increases the breadth of teaching.

1. Introduction

The new English Curriculum Standards mention that the overall goal of English teaching is to cultivate students' comprehensive language ability. Therefore, in the actual situation of English teaching, it is necessary to reasonably control the form and content of classroom teaching scientifically and effectively [1]. The cultivation of English learning interests can cultivate students' self-confidence. Therefore, teachers should not only pay attention to knowledge supplement, but also guide their interest intention, study, and explore their interest points in English, so that students can gain more [2]. This study argues that language interaction is a joint activity that involves senders and receivers of information based on paragraph context and article, and establishes a triangular relationship between the three. The interactive process not only receives information, but also publishes information. It must be a collaborative process [3]. The premise of interaction is that the subjects on both sides of the communication must have certain interests and communication tendencies. This study argues that language interaction (often translated as "interaction") refers to the process in which two or more people can transmit information and interact with each other in a specific environment, and can influence each other [4]. For English learning, language is used for communication and interaction, so as the basis of communication, English is also the core of language teaching, so it is particularly important to improve language skills [5]. English classroom teaching as a kind of learning from each other communication modes, as well as between students and students, between teachers and students is given by the teacher material to understand and learn knowledge, so as the communication in the teaching process and teaching content, is a kind of to understand each other, mutual exchange and communication of dynamic interaction [6]. Therefore, it is necessary to let students participate in the classroom teaching process, always take students as the center, and earnestly carry out this teaching concept. Teachers need to understand, analyze, and master the individual differences of different students, design the most appropriate and effective

teaching content teaching methods according to their different learning abilities and interest points, and enhance the communication and communication with students in the course on the basis of satisfying students' knowledge learning, so as to improve classroom interaction [7, 8]. In this context, this study develops an interactive online English teaching platform based on the collaborative filtering algorithm. The application process of an online teaching platform is a process of continuous machine learning. Students search for the learning content and learning focus that they are interested in on the platform. After obtaining the user's permission, these data are recorded and used in the machine learning of collaborative filtering algorithm. Collaborative filtering algorithm is used to search historical behavior data mining and analyze students' interest in learning and learning situation, so as to interact with students in the learning process and recommend content related to their search. This can expand students' vision, expand the scope of learning, and improve learning efficiency. In the application process of the whole system, the main purpose of the collaborative filtering algorithm is to better recommend interactive English teaching to students on the online platform, so that they are interested in interactive English teaching methods. Interactive teaching and related content can bring a better learning experience to the students who use it. Teachers can also recommend students who are more suitable for this type of learning, so as to increase the convenience and comfort of each other's classrooms, and realize equal and frank classroom interaction based on the online platform and emotional communication between teachers and students. Through the collision of sparks of wisdom, it fully provides students with a space for personal expression, which can explore students' learning autonomy and improve the quality of teaching to a certain extent.

2. Related Work

According to the collaborative filtering algorithm, an improved version of the personalized recommendation algorithm is proposed in the literature. According to the basic attributes of the collaborative filtering algorithm, various thoughts of users are enhanced, such as the thought of trust, the thought of changing over time, and the related structuring thought, so as to optimize and improve the prediction and evaluation strategy of collaborative filtering algorithm [9]. On the original basis, the algorithm proposed for user interest changes can calculate the similarity according to the user's evaluation, optimization, and improvement strategies, which can distinguish user interest changes. It can be divided into historical changes and current changes and improve the accuracy of similarity between user application purposes [10, 11]. This study designs and implements a recommendation subsystem based on the collaborative filtering recommendation model, which mainly includes the design and implementation of the system logic function module, data acquisition module, collaborative filtering recommendation engine function, and other modules, and comprehensively realizes the construction of recommendation subsystem

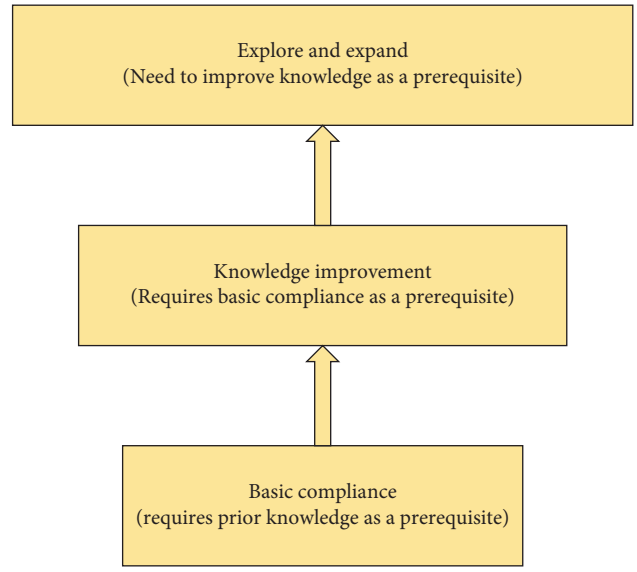

Figure 1: Three levels of learning model (student section).

[12]. The literature establishes a personalized recommendation model based on collaborative filtering technology, analyzes the requirements and functions of the personalized recommendation system, and designs simulation experiments to test the system functions and algorithms [13]. Based on collaborative filtering technology, the personalized recommendation system can solve a series of complex technical application problems. For example, it can make a targeted personalized recommendation to users in the digital campus platform, comprehensively grasp the course learning progress, and improve the accuracy and effectiveness of learning resource push. The learning efficiency of each user is improved at an exponential level [14]. The literature designs a linear model for the fusion of a variety of collaborative filtering algorithms and uses the least square method to solve the weight [15, 16]. According to the importance of data automatic training of each algorithm, the fusion model can reduce the prediction error of fixed scores. In order to improve the accuracy of recommendation in terms of learning resources, based on the trust model of users' rating of courses and recommendation times, this study organically combines the model with a collaborative filtering algorithm to improve the accuracy of the collaborative filtering algorithm to a new height [17, 18].

3. Development and Design of Interactive English Teaching Online Platform

3.1. Interactive Teaching Needs. The basic core layer, the knowledge and skill development layer and the exploration and expansion layer are the three structural levels of the learning model, which are conducive to improving students' basic and higher-order abilities and realizing the purpose of hierarchical teaching. In the process of self-directed learning in class, students need to conduct hierarchical English learning according to the logical sequence shown in Figure 1. Only after mastering the knowledge content of developing

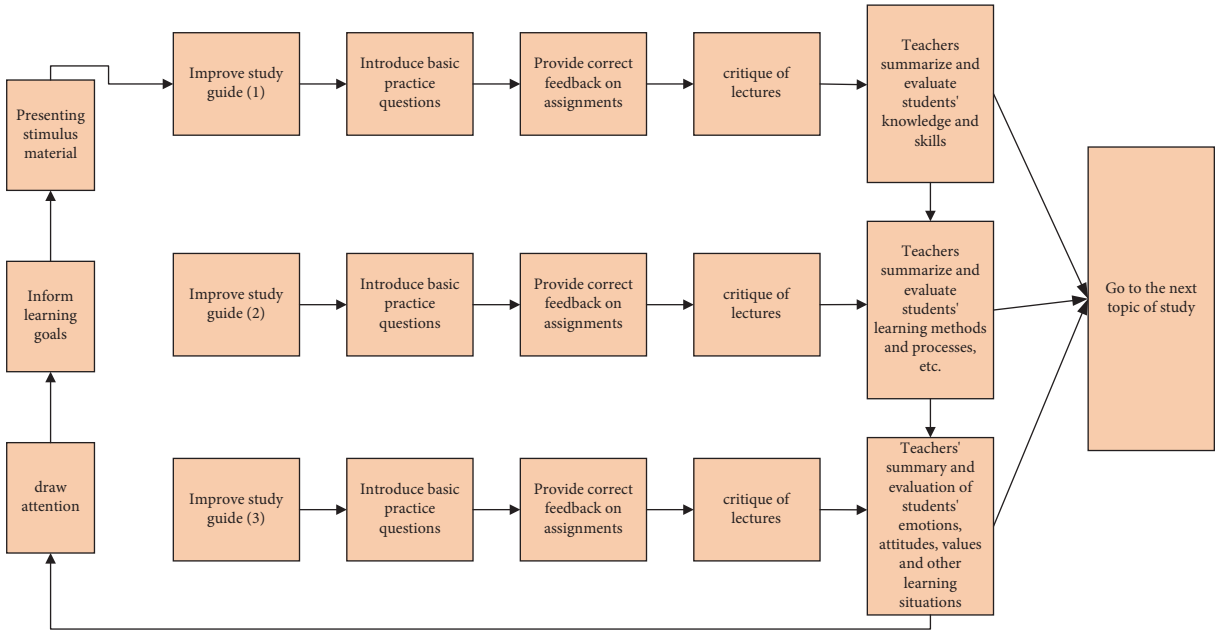

Figure 2: Interactive teaching model based on autonomous learning (teacher section).

basic knowledge and skills we can further reach the highest level of exploration and expansion of the learning stage. That is, students should learn to recognize and strictly understand the meaning of each specific concept, rule, and concept. Figure 1 shows three levels of the learning model (student section).

The online English teaching platform designed in this study is mainly divided into three closed-loop structures which are independent but logically connected internally. First of all, the first major learning cycle consists of many major learning items. According to the general order of learning, its structure is: determining learning objectives, stimulating students' enthusiasm for learning, reviewing knowledge, self-learning textbooks, strengthening basic exercises, etc. It also includes the final stage of students' self-summary and self-evaluation. This cycle is designed for all students in the whole class, in order to lay a solid knowledge foundation at the beginning of learning and prepare for further learning. Therefore, I mainly learn objective declarative knowledge, such as basic concepts, laws, theories, consensus, and so on. The second main learning cycle consists of seven parts: first, determining learning objectives, then stimulating learning motivation, second, memorizing knowledge, then self-learning textbooks, expanding knowledge, consolidating knowledge and practice, and finally, self-learning summary and students' self-assessment. This cycle is designed for middle and advanced students who have the ability to study on the basis of previous studies. The third learning cycle is specifically designed to expand students' advanced level, so its audience is mainly students with excellent academic performance, quick thinking, and hard work. It mainly includes the determination of learning objectives, the activation of learning motivation, the recall of existing knowledge, the self-study of teaching materials, exploration and expansion, strengthening and expanding exercises, and the self-evaluation of students. This system can expand students' horizons, cultivate their problem-solving ability, and achieve the goal of solving real-life problems through learning.

As shown in Figure 2, according to the three-level structure of students' learning model, the teaching method of teachers is extended, which is divided into three levels of auxiliary teaching cycle. The first cycle is lead to students' learning interest, inform the students learning goals, provide incentives and material, the basic knowledge of learning guidance, the design of exercises, provide feedback, evaluate the operation and the suggestion, the teachers' self-summary, to student's knowledge and skills for accurate summary and evaluation. The second cycle is to guide students' interest in learning, inform students of their learning objectives, and provide incentive conditions, materials, and learning guidance. In addition, it can also provide appropriate task feedback, guidance, and job evaluation. Teachers can summarize and evaluate students' learning processes and methods. The third cycle is lead to students' learning interest, inform the students learning objective, provides the incentive conditions and materials, provide students with learning method guidance, provide further exploration and extension exercises, provide the appropriate expansion operation feedback, homework evaluation, teachers' self-summary, as well as to the students' emotional attitudes/values for evaluation.

3.2. System Architecture Design. The hierarchical structure of the English online teaching platform and the overall logical layout of teaching are shown in Figure 3.

3.3. Network Topology Design. The interactive online English teaching platform mainly serves campus teachers and students, so each subsystem of the interactive online English teaching platform is implemented in the school network.

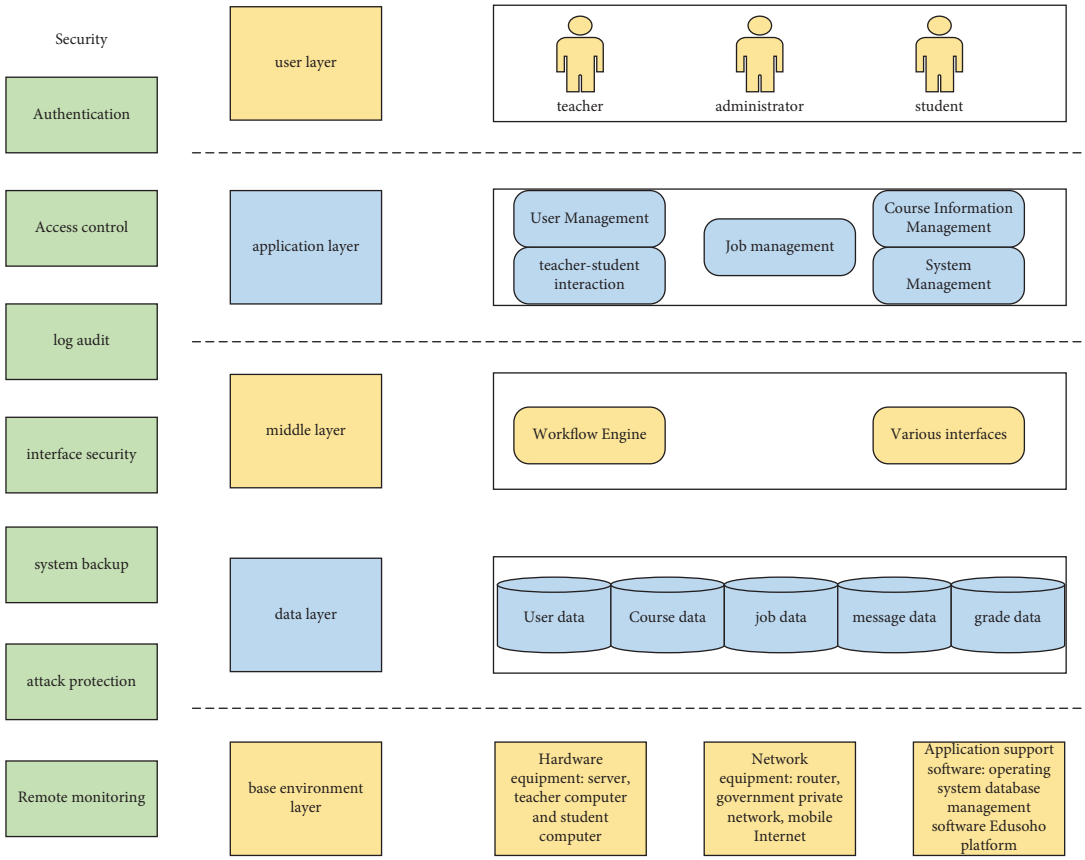

Figure 3: Overall architecture of the system.

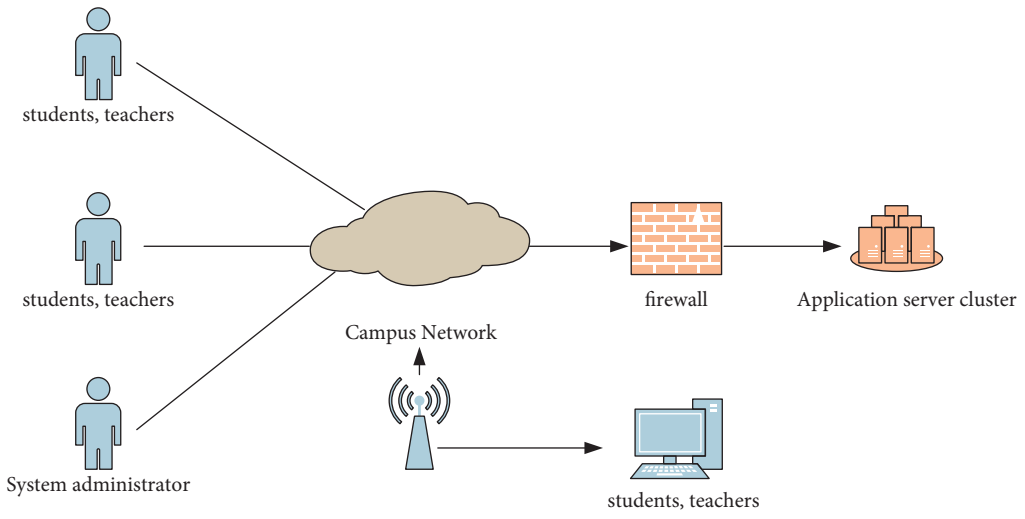

Figure 4: Network topology.

Students, teachers, and other users can access the campus digital platform through the campus network environment, and set up firewalls in the computer room where the interactive online teaching English platform server and internal network are implemented. The network topology is shown in Figure 4.

3.4. Interactive Teaching Module Design. The analysis of interface elements shows that the interaction between teachers and students usually occurs in four functional interaction modules: communication window, lecture comments, collaborative editing, and shared documents. The distribution of these modules on three typical platforms

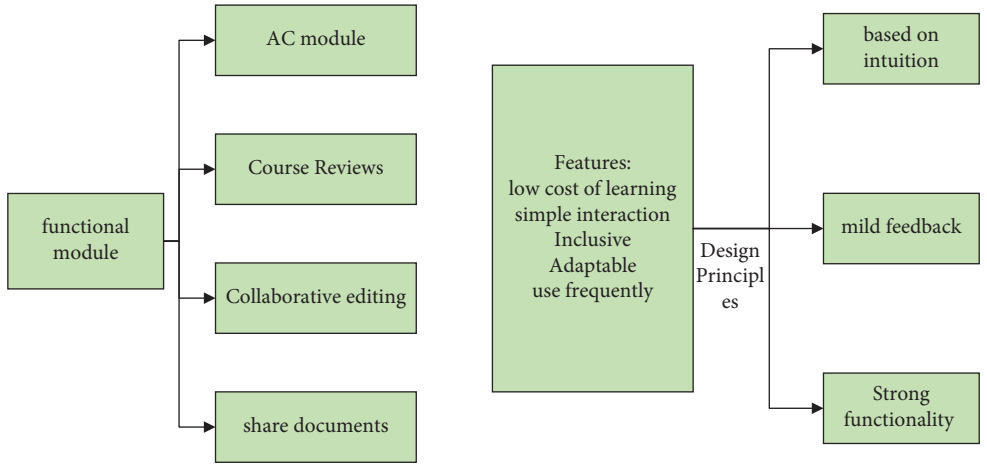

Figure 5: Design principles of functional modules.

has the characteristics of low learning cost, simple interaction, strong inclusiveness, and strong adaptability. Functional interaction modules are often used as interaction units in online teaching interactions. So, the design of interaction modules should satisfy the design principles based on intuition, gentle feedback, and powerful functions (see Figure 5).

4. Model Construction of Collaborative Filtering Algorithm

4.1. User-Based Collaborative Filtering Algorithm. The user-based collaborative filtering algorithm has three main steps:

(1) Let M be the number of users in the system, N be the number of statistics of projects, Rui be the matrix element, and its value represents the evaluation score of user U on project I. The value range of the matrix element Rui does not change much. It is usually an integer value from 1 to 5. If there is no user rating, it is replaced by the number 0. The lower the Rui, the lower the evaluation score of user U on element I, and the worse satisfaction.

(2) Realize the function of searching for the nearest group of neighboring users. The core is to find the most matching recommendation for target users according to the nearest neighbor principle, that is, to find the nearest neighbor set for target users, so as to guarantee the accuracy of the recommended content. The first step to realize this function is to compare the similarity between the target user and other users. The second step is to introduce some metric rules to select the most recent set of users that are most similar to the target users and then pick them out.

In this collaborative filtering algorithm, the basic data of similarity calculation are usually obtained by calculating the rating based on users. In the data model, the vector in the N-dimensional space refers to the user rating, and the similarity between users is measured by the cosine Angle between their respective vectors. The higher the number, the more similar the two users are. Assuming two vectors, they are respectively expressed as vectors $\hat{u}$ and $\hat{V}$, which represent the score of user U and user V in the N-dimensional item space, formula (1) can be obtained, so as to realize the calculation of SIM (u, v) similarity of user U and user V:

$$\text{sim}\ (u,v) = \cos\ (\vec{u},\vec{v}) = \frac{\vec{u}\bullet\vec{V}}{\|\vec{u}\|\bullet\|\vec{V}\|} = \frac{\sum_{i=1}^{n} R_{ui} * R_{vi}}{\sqrt{\sum_{i=1}^{n} R_{ui}^2}\sqrt{\sum_{i=1}^{n} R_{vi}^2}}. \tag{1}$$

To calculate the Pearson correlation coefficient, we first need to find a set of items rated by two users and then calculate the correlation coefficient of the two user vectors based on this set. The formula for calculating the similarity between user u and user v is defined as follows:

$$\text{sim}(u,V) = \frac{\sum_{i\in I_{uv}}\left(R_{ui}-\overline{R}_u\right)\left(R_{vi}-\overline{R}_v\right)}{\sqrt{\sum_{i\in I_{uv}}\left(R_{ui}-\overline{R}_u\right)^2}\sqrt{\sum_{i\in I_{uv}}\left(R_{vi}-\overline{R}_v\right)^2}}, \tag{2}$$

where luv represents the set of items jointly rated by user u and user v.

The formula for predicting the target user's rating for item i is defined as follows:

$$P_{u_u} = \overline{R}_u + \frac{\sum_{(v\in I_u(i))}\text{sim}\ (u,v) * \left(R_{vi}-\overline{R}_v\right)}{\sum_{(v\in I_u(i))}|\text{sim}\ (u,v)|},$$
$$\overline{R}_u = \frac{1}{|I_u|}\sum_{j\in I_u} R_{uj}, I_u = \left\{j \in I \text{ and } R_{uj} \neq \Phi\right\}. \tag{3}$$

After scoring the target user and predicting all recommendable items, this group of items can be recommended to the target user according to certain rules. One method is to select the top N items with the highest test scores as the results to recommend to users (usually N is between 1–20, $N = 10$ is the most common); the other is to select items with predicted scores and more than be sure to specify a value. The results are determined by the user, and both recommendation methods depend on application-specific requirements, with the top-N recommendation being more widely used.

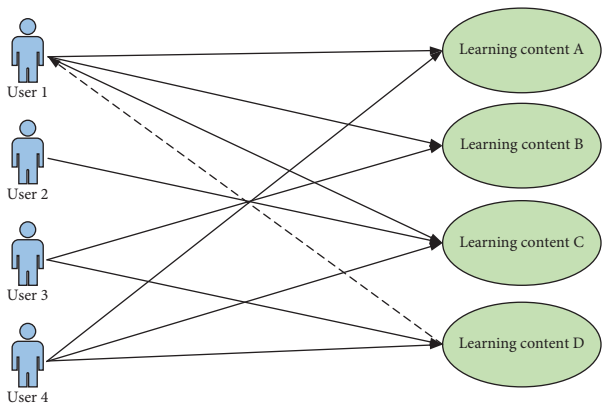

Figure 6: Schematic diagram of user-based collaborative filtering.

The main idea of user-based collaborative filtering is based on the above assumption that users who rate some articles will also rate other articles similarly. Figure 6 shows a schematic diagram of the recommended algorithm.

Among users 2, 3, and 4, compared to user 1, user 4 has the closest preference to user 1. User 4 learns content D in addition to content A, B, and C that user 1 likes. So we recommend D to user 1.

4.2. Item-Based Collaborative Filtering Algorithm. Rui and Ruj represent user us rating values for item i and item j, respectively, and $\overline{R}_i$ and $\overline{R}_j$ represent the average rating of item i and item j in Uij, respectively, namely,

$$R_i = \frac{1}{\left|U_{ij}\right|} \sum_{u \in U_{ij}} R_{ui}, \quad R_j = \frac{1}{\left|U_{ij}\right|} \sum_{u \in U_{ij}} R_{uj}. \tag{4}$$

The number of item sets selected affects the quality of subsequent recommendations. In order to judge this effect, two methods can be adopted: one is to set the threshold value, then among all items to be selected, the item whose similarity with the target object is greater than the threshold value will select the relatively recent item set. The other method also sets a threshold value, K is the number of recent items, and the maximum K objects with the highest similarity to the target object are used as the set of recent items.

According to the score of the target user u in the K-nearest neighbors of the target item i, we predict the score of the user u of the item i, and then select the item with the highest predicted score value to recommend to the user, and get the score from all the possible recommended items.

Pui's scoring formula for target user u of item i is defined as follows:

$$P_{ui} = \overline{R}_i + \frac{\sum_{j \in I_u(u)} \text{sim}\ (i, j) * \left(R_{uj} - \overline{R}_j\right)}{\sum_{j \in I_e(u)} |\text{sim}\ (i, j)|}. \tag{5}$$

$\overline{R}_j$ in the above formula represents all the ratings of item j in all user spaces U, namely,

$$\overline{R}_j = \frac{1}{\left|U_j\right|} \sum_{u \in U,} R_{uj}, U_j = \left\{u \in U, R_{uj} \neq \Phi\right\}. \tag{6}$$

After scoring the target user and predicting all recommendable items, this group of items can be recommended to the target user according to certain rules. One method is to select the top N items with the highest test scores as the results to recommend to the user (usually N is between 1–20, $N = 10$ is the most common); the other is to select the estimated score greater than a certain score value. Project. Results are recommended by users. Both recommended methods depend on the specific application requirements.

4.3. Collaborative Filtering Algorithm Model Construction. There are many ways to integrate recommendation algorithms, but starting from the algorithm itself, the most suitable method is the weighted combination of recommendation algorithms. The weighted fusion method assigns different weights to the results generated by the current algorithm and synthesizes new results, so as to achieve a lower prediction error than the original algorithm. Assuming that we have established two score prediction models r(1) and r(2) based on the recommendation algorithm, an original weighted fusion method is to set different weights according to the effects of the two models to balance the contributions of the two algorithms, and then make the recommended end result. The form of the model is shown in (12):

$$\hat{r} = \alpha \cdot r^{(1)} + (1 - \alpha) \cdot r^{(2)}. \tag{7}$$

Such a weighted fusion method cannot be modified to handle and adapt to different usage scenarios, because different algorithms can achieve different effects for different scenarios and different data, and a fixed weight system cannot adapt to changes from the environment in real time.

Suppose there are N rating predictors defined as $\{r^{(1)}, r^{(2)}, \ldots, r^{(N)}\}$, ε is the error constant used to fit the N predictors to the final model, and θ is the prediction variable weight, the final regression model is shown in

$$\hat{r} = \varepsilon + \sum_{n=1}^{N} \theta_n r^{(n)}. \tag{8}$$

In order to adapt the weighted parameters of the model to different scenarios and automatically assign the best parameters for different application environments, machine learning methods can be used to train the model to obtain better parameters. In order for the model to finally better match the actual results, we construct the loss function using the least squares difference and then learn the parameters by minimizing the loss function. For the convenience of writing, we take the error constant as one of the weights and use it as the weight coefficient of r(0). We assume that r(0) is always equal to 1, then the regression model (13) becomes simplified (14):

$$\hat{r} = \sum_{n=0}^{N} \theta_n r^{(n)}. \tag{9}$$

Formula (9) represents the loss function of the regression model, where M represents the number of samples in the training set, y represents the specific value of the actual score, {{r(0),r(1),r(2). The meaning of r(N)} is the output item of each score variable, which is taken as the input of the model, where the coefficients 1/2m are set coefficients to simplify the calculation of the derived coefficients.

$$J(\theta) = \frac{1}{2m} \sum_{i=1}^{m} \left(\hat{r}^{(i)} - y^{(i)}\right)^2. \tag{10}$$

The parameters are solved by the above loss function, which can be solved using the gradient descent method or the normal equation (Normal Equation). Both have their own advantages and disadvantages. The gradient descent method requires multiple iterations, and the normal equation requires matrix operations. This study adopts the same normal equation as the previous alternating least squares method. According to the loss function 17, the steps to solve the normal equation are defined as follows:

$$J(\theta) = \frac{1}{2m} \|R \cdot \theta - Y\|^2, \tag{11}$$

$$\Rightarrow J(\theta) = \frac{1}{2m} (R \cdot \theta - Y)^T (R \cdot \theta - Y), \tag{12}$$

$$\Rightarrow J(\theta) = \frac{1}{2m} \left(\theta^T R^T R\theta - Y^T R\theta - \theta^T R^T Y + Y^T Y\right), \tag{13}$$

$$\Rightarrow J(\theta) = \frac{1}{2m} \left(\theta^T R^T R\theta - 2\theta^T R^T Y + Y^T Y\right). \tag{14}$$

Taking the derivative of θ according to Equation (20) and setting the derivative to zero, the solution for the weight θ is shown in Equation (22):

$$\theta = \left(R^T R\right)^{-1} R^T Y. \tag{15}$$

5. Testing and Application of Interactive English Teaching Online Platform

5.1. Test Results of the System. Figure 7 shows the test topology used for this test.

All users can access through the domain name of the interactive online English teaching platform, but users who are not logged in can only access some open resources. To obtain additional resources, users must register and log in to the online learning platform, and apply for corresponding permissions. Administrators can set user registration-related functions, set registration information fields, customize the field information that must be provided during user registration, and drag and drop to adjust fields. After students log in to the system, they have functions such as managing personal information, submitting assignments, and interactive discussions. After logging in to the system, teachers can manage personal information, manage courses, upload resources, download assignments, and reply to messages.

5.2. Users' Willingness to Use the Interactive English Teaching Online Platform. The main reasons why learners use the interactive English teaching online platform are shown in Figure 8.

Figure 8 investigates the main reasons why students use interactive online English teaching platforms. The results showed that submitting assignments was the main reason for most students to use the interactive English teaching platform (44.7%), followed by viewing course materials (39.4%). However, at the request of teachers (11.2%), the number of people who expanded their knowledge and communicated with teachers and classmates was very small, less than 5% of the total. The above data show that students passively use the interactive English teaching platform to complete classroom teaching tasks. As for taking the initiative to expand knowledge outside the classroom and communicate with teachers and classmates after class, students do not like to use online platforms for interactive English teaching.

The frequency of students using the interactive online English teaching platform is shown in Figure 9.

From Figure 9, we can see that course notifications and downloading materials are the most used functions by learners.

5.3. The Teaching Effect of the Interactive English Teaching Online Platform. As can be seen from Table 1, the students' English scores in this semester are better than those in the previous semester. Judging from the test scores of the excellent rate in the second semester, there are 20 outstanding students with a score of 85 or above in this semester, accounting for 22.22% of the total, while only 11 outstanding students with a score of 85 or above in the last semester, accounting for 8.9% of the total number; There are 45 students with excellent grades this semester, accounting for 43.53% of the total number of students, while only 26 students in this grade range last semester, accounting for 21.0% of the total number of students; from the point of view of the failure rate, there are 8 students this semester, 6.48% of the total, while 37 students failed last semester, accounting for 29.8% of the total.

It can be seen from Table 2 that at least 67.37% of the students are satisfied with the interactive English teaching online platform.

5.4. Application Strategies of Interactive English Teaching Online Platform. Whether multiple interactions can be effectively realized in the network environment is not only affected by objective factors such as the network environment, but also by the subjective factors of students. Students' learning motivation, learning needs, and current cognitive level directly affect their participation in many interactive network activities. In order to provide students with all support for learning, teachers must create a good network teaching environment, carefully design the content

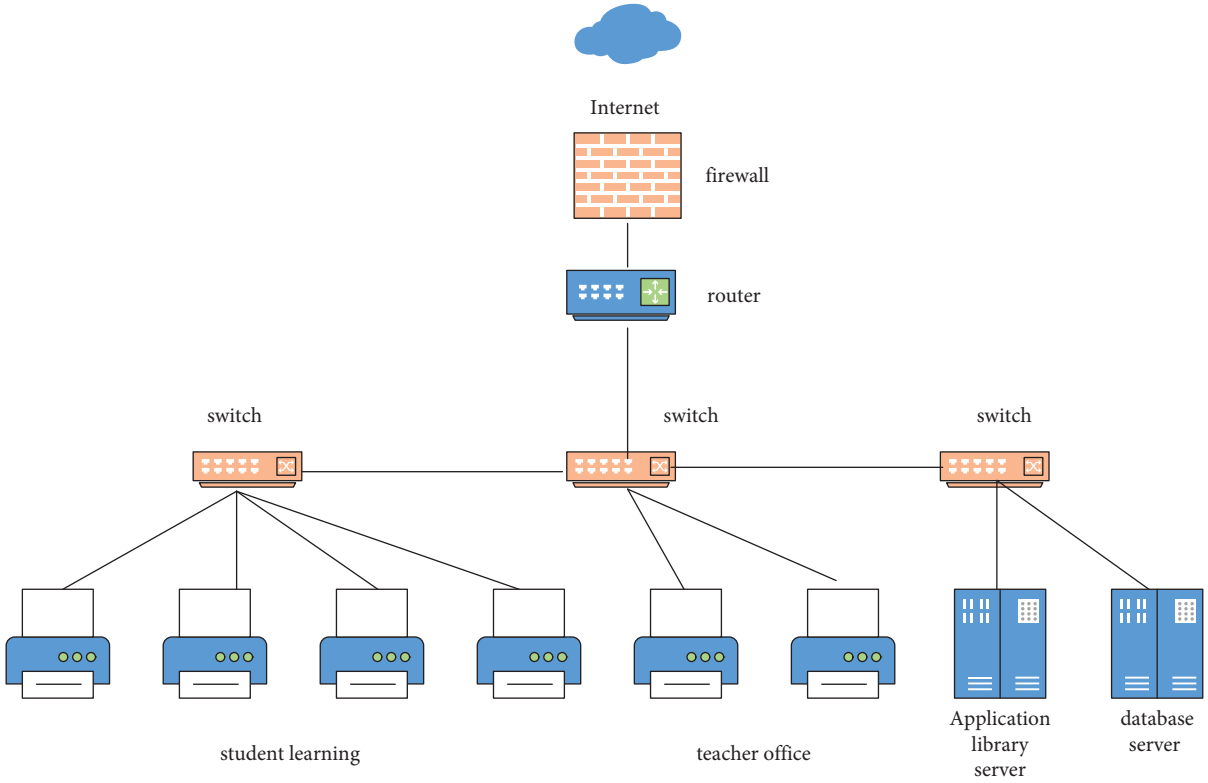

Figure 7: Test topology diagram.

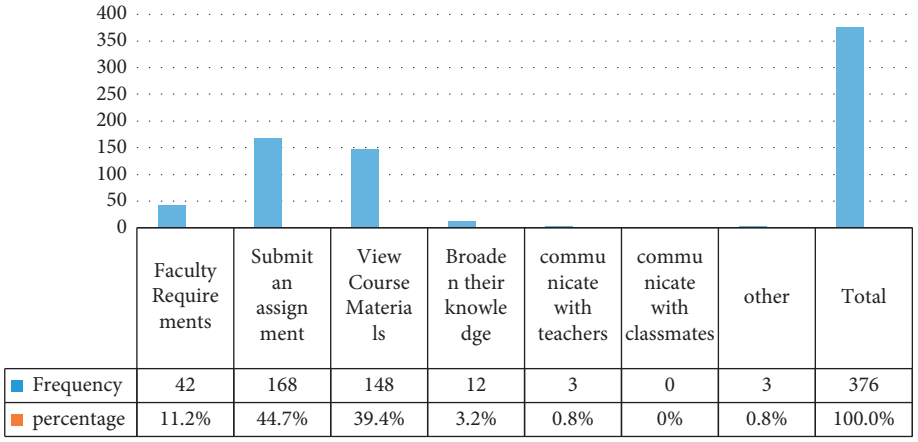

	Faculty Requirements	Submit an assignment	View Course Materials	Broaden their knowledge	communicate with teachers	communicate with classmates	other	Total
Frequency	42	168	148	12	3	0	3	376
percentage	11.2%	44.7%	39.4%	3.2%	0.8%	0%	0.8%	100.0%

Figure 8: Main reasons for using interactive English teaching online platforms.

environment of each teaching unit, and improve the configuration of network resources. When designing learning tasks, attention should be paid to relevance and moderate difficulty. Providing students with novel and interesting learning content that meets their cognitive needs is a necessary factor to help students learn effectively.

In addition to ensuring the level of teaching content, teachers should try their best to design rich and diverse learning and teaching situations, and provide a guarantee for students' self-study effect on the Internet through innovative means based on the platform., so that students can obtain emotional satisfaction in the learning process. They can be motivated and supported in their motivation to learn, stimulating their enthusiasm for learning. In face-to-face tutoring courses, in order to give students more opportunities to demonstrate their learning achievements, teachers need to create a relaxed, free, and democratic atmosphere in the classroom, and through demonstrations, students' learning achievements can be recognized by teachers and other students. Therefore, students are more willing to communicate with teachers and other classmates. In the interactive process, with the improvement of the network quality, students can maintain a more stable and active learning state, and have a stronger learning motivation for the learning content, so as to participate in the multi-interactive teaching process. In face-to-face classes, teachers

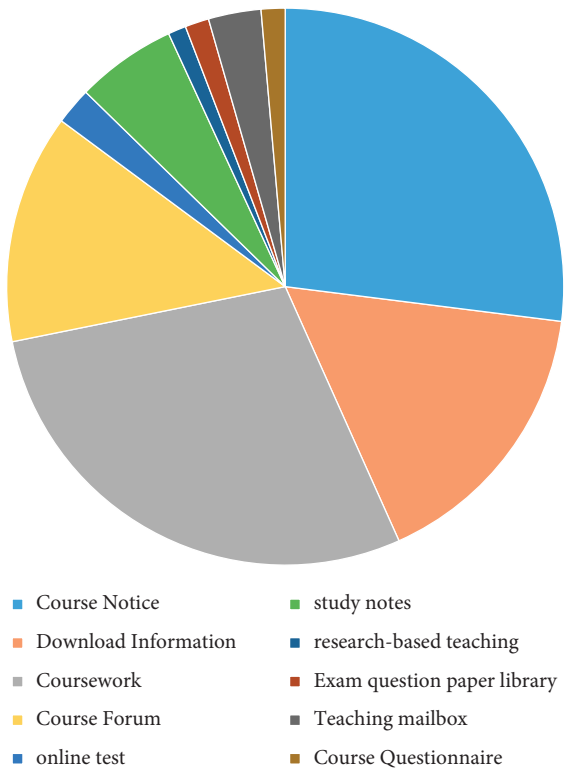

Figure 9: Frequency of learners using online platforms for interactive English teaching.

Table 1: Comparison of scores of interactive English teaching online platforms.

Each fraction	Exam results this semester (109 people)		Last semester's test scores (124 people)	
	Frequency	Percent	Frequency	Percent
Above 85	20	22.22	11	8.9
75–84	45	43.53	26	21.0
60–74	36	31.51	50	40.3
Below 60	8	6.48	37	29.8

need to respect every student, pay attention to every student at all times, help students with different learning backgrounds to participate in every learning activity, encourage them to talk with their classmates, discuss with teachers, and boldly put forward their own views and their own ideas and existing learning problems, strengthen their courage and stimulate their interest in learning. When teachers step off the podium and become helpers, guides, and advocates of student learning, it can broaden the communication channels between teachers and students, meet more diverse communication needs, and provide teachers and students with a good teacher–student interaction effect and teaching efficiency. The traditional way of English teaching is mainly one-way input, that is, the way that the teacher imparts knowledge to the students one way. Closed teaching is not conducive to students' active learning. As we all know, it is quite common to copy textbooks, and it is not uncommon for teachers to become "language teachers". According to relevant statistics, more than 80% of the problems in the classroom are closed ended. With such a form of teaching, there is little chance of effective interaction. In this study, we boldly designed an open classroom, where students are the "protagonists" of the classroom, and teachers act as "behind the scenes" to guide students to participate in interaction and achieve better results.

In the actual online teaching situation, teachers can complete the interaction between teachers and students through QQ groups, WeChat, online platform discussion boards, and other channels, through the above ways to provide targeted and constructive guidance to students in learning. The survey shows that more than 90% of the students are unwilling to listen to the teacher's lectures, and 70% of the students are more willing to acquire knowledge from books through independent exploration, communication and cooperation, and practical operation. In terms of teaching, the online learning platform, with its rich teaching resources, comprehensive teaching functions, and convenient operation interface, allows students to freely study, communicate, interact with their peers and teachers, and acquire knowledge at any time; and through WeChat, QQ groups and other networks, the interactive platform creates more convenient opportunities for teacher–student interaction and student–student interaction, and brings a new perspective to the study of the effective interaction between teachers and students, students and human–computer. Classroom teaching evaluation will be more diversified, and students need to participate in the evaluation. Teachers' comprehensive evaluation, group member evaluation, student self-evaluation, and other multi-faceted evaluation systems can be used to enable students to more clearly discover their own shortcomings, discover the advantages of classmates, and correctly evaluate themselves and others. Whether the classroom teaching evaluation mechanism can be used well is the key to the effectiveness of students' cooperative learning, student leadership, and classroom teaching.

In terms of evaluation strategy, it is necessary to abandon the traditional "discriminatory evaluation" model and establish a more reasonable "incentive evaluation" mechanism to give each student, especially those with poor performance, sufficient respect and consideration for their learning achievements. We must strive to stimulate the enthusiasm for learning in our diverse students and help them build confidence and focus on their growth and development. To this end, the method of group assessment can be used to divide students into several groups and guide learning and discussion in groups. When grouping, teachers should pay attention to introverted and extroverted students, and pair students with good and bad foundations with each other, which will help them achieve mutual benefit and win–win results in group cooperation, and increase their sense of cooperation and competition. In the classroom, teachers make positive comments on reading, dialogue, answering, debating, etc. Students are praised for their outstanding performance and therefore more motivated to learn.

For most students, English class has only one chance to show themselves. It is difficult to fully satisfy their desire for performance, and it is not conducive to cultivating students'

Table 2: Satisfaction survey of interactive English teaching online platform ($n = 78$).

Survey questions	Satisfied	Percent	Common	Percent	Dissatisfied	Percent
More able to use their own methods to solve problems in learning	53	67.37	26	32.37	11	12.95
A certain degree of freedom to choose their own learning tasks	59	75.14	33	41.44	14	16.84
It can improve my English self-learning ability	57	72.52	24	29.78	8	9.06
More freedom to control their own learning progress	66	84.13	29	36.26	11	12.95
The overall level of English has improved significantly	60	75.45	21	25.90	11	12.95
More direct and accurate understanding of their own learning	64	81.61	22	27.19	9	10.36
It enables me to have access to more authentic English materials, and I have more confidence in English learning	58	73.83	25	31.08	7	7.77
It can improve my interest in learning English, and I can learn English more consciously	62	78.98	28	34.97	13	15.53
Increased willingness to invest more time in English language learning, English language skills improved	53	66.46	32	40.14	12	14.24
More preparation in extra-curricular time, and more efficient learning in face-to-face tutoring classes	67	84.34	23	28.49	9	10.36

active learning and participation attitude. Therefore, when designing teaching activities, teachers should try to expand students' participation and increase the opportunities for students to participate. Each student in the class has their own specialties, some can perform, some are good at communication, and some can sing and dance. For this reason, teachers should fully consider the personality characteristics and ability level of each student in the process of designing the teaching content and lecture sequence, and guide each student to experience the continuous and effective learning process. At the same time, it provides more opportunities for students to participate in activities and evaluate results and forms a good communication situation with the outside world, so that the majority of students' learning has a good experience and effect.

6. Conclusion

In the traditional English classroom teaching mode, teachers often adopt a one-way teaching method to teach students the knowledge that teachers think is important, which is not conducive to the interaction and knowledge communication between teachers and students, ignores students' own feelings, and is not conducive to the personalized development of students. At present, the development of online interactive teaching mode is gradually deepening. At the same time, with the increasing promotion of curriculum and textbooks in the new era, as well as the reform of college entrance examination, teachers' teaching concepts should also be changed. Based on this, this article studies a collaborative filtering algorithm and develops an online interactive English online teaching platform. The development and application of an interactive English system can promote students' active learning, realize all-round and multifaceted personalized education, and improve their comprehensive ability to acquire and absorb knowledge points, which has positive significance for ensuring students' better participation in the teaching process; the change of teachers' concept has also followed. The advantages of implementing interactive teaching in the classroom can be confirmed by many teachers, thus providing a new type of English teaching.

Data Availability

The data used to support the findings of this study are available from the corresponding author upon request.

Conflicts of Interest

All the authors declare no conflicts of interest.

References

[1] L. Susanty, Z. Hartati, R. Sholihin, A. Syahid, and F. Y. Liriwati, "Why English teaching truth on digital trends as an effort for effective learning and evaluation: opportunities and challenges: analysis of teaching English," *Linguistics and Culture Review*, vol. 5, no. S1, pp. 303–316, 2021.

[2] A. Wiriyachitra, "English language teaching and learning in Thailand in this decade," *Thai TESOL focus*, vol. 15, no. 1, pp. 4–9, 2002.

[3] A. Shook and V. Marian, "The bilingual language interaction network for comprehension of speech," *Bilingualism: Language and Cognition*, vol. 16, no. 2, pp. 304–324, 2013.

[4] R. O'Dowd, "Online foreign language interaction: moving from the periphery to the core of foreign language education?" *Language Teaching*, vol. 44, no. 3, pp. 368–380, 2011.

[5] M. A. Saydaliyeva, E. B. Atamirzayeva, and F. X. Dadaboyeva, "Modern methods of teaching English in Namangan state university," *International Journal on Integrated Education*, vol. 3, no. 1, pp. 8-9, 2020.

[6] J. Gilkerson, J. A. Richards, and K. J. Topping, "The impact of book reading in the early years on parent–child language interaction," *Journal of Early Childhood Literacy*, vol. 17, no. 1, pp. 92–110, 2017.

[7] M. Van Dijk, P. van Geert, K. Korecky-Kröll et al., "Dynamic adaptation in child–adult language interaction," *Language Learning*, vol. 63, no. 2, pp. 243–270, 2013.

[8] E. Chan and L. Unsworth, "Image–language interaction in online reading environments: challenges for students' reading comprehension," *Australian Educational Researcher*, vol. 38, no. 2, pp. 181–202, 2011.

[9] D. Kluver, M. D. Ekstrand, and J. A. Konstan, "Rating-based collaborative filtering: algorithms and evaluation," pp. 344–390, Social Information Access, 2018.

[10] J. S. Breese, D. Heckerman, and C. Kadie, "Empirical analysis of predictive algorithms for collaborative filtering," 2013, https://arxiv.org/ftp/arxiv/papers/1301/1301.7363.pdf.

[11] H. Abulkasim, A. Farouk, H. Alsuqaih, W. Hamdan, S. Hamad, and S. Ghose, "Improving the security of quantum key agreement protocols with single photon in both polarization and spatial-mode degrees of freedom," *Quantum Information Processing*, vol. 17, no. 11, pp. 316–411, 2018.

[12] J. Zhang, Y. Lin, M. Lin, and J. Liu, "An effective collaborative filtering algorithm based on user preference clustering," *Applied Intelligence*, vol. 45, no. 2, pp. 230–240, 2016.

[13] D. Bokde, S. Girase, and D. Mukhopadhyay, "Matrix factorization model in collaborative filtering algorithms: a survey," *Procedia Computer Science*, vol. 49, pp. 136–146, 2015.

[14] Q. Wu, "Application of user collaborative filtering algorithm in class suspension management system," *Electronic technology and software engineering*, vol. 19, pp. 196-197, 2021.

[15] Y. Shi, M. Larson, and A. Hanjalic, "Collaborative filtering beyond the user-item matrix: a survey of the state of the art and future challenges," *ACM Computing Surveys*, vol. 47, no. 1, pp. 1–45, 2014.

[16] Z. Huang, D. Zeng, and H. Chen, "A comparison of collaborative-filtering recommendation algorithms for e-commerce," *IEEE Intelligent Systems*, vol. 22, no. 5, pp. 68–78, 2007.

[17] M. D. Ekstrand, J. T. Riedl, and J. A. Konstan, "Collaborative filtering recommender systems," *Foundations and Trends® in Human–Computer Interaction*, vol. 4, no. 2, pp. 81–173, 2011.

[18] F. Cacheda, V. Carneiro, D. Fernández, and V. Formoso, "Comparison of collaborative filtering algorithms: limitations of current techniques and proposals for scalable, high-performance recommender systems," *ACM Transactions on the Web*, vol. 5, no. 1, pp. 1–33, 2011.

Hindawi
Mobile Information Systems
Volume 2022, Article ID 7964391, 9 pages
https://doi.org/10.1155/2022/7964391

Research Article

Big Data Analysis Application in News Service Mode Based on Genetic Algorithm

Jie Li[1] **and Qiuli Wu**[2]

[1]*Propaganda Department, Cangzhou Normal University, Cangzhou, Hebei 061001, China*
[2]*International Exchange Center, Cangzhou Normal University, Cangzhou, Hebei 061001, China*

Correspondence should be addressed to Jie Li; lijie1989@caztc.edu.cn

Received 2 August 2022; Revised 13 September 2022; Accepted 23 September 2022; Published 6 October 2022

Academic Editor: Shadi Aljawarneh

Due to the development and popularization of technologies such as the Internet, traditional forms of media have been greatly affected. Therefore, the way people receive news has also undergone certain changes. Due to the dramatic increase in the amount of information data and the variety of sources that are very rich, the complexity of the rational use of data information is also increasing. In order to improve the speed and accuracy of text classification, for the problems of classification efficiency and classification accuracy, this study adopts a large-scale text classification method based on genetic algorithm optimization. After designing the experimental analysis, the optimized genetic algorithm can be used to classify effectively, thus providing a new processing idea and method for the news application in the context of big data. First, we analyze and review excellent data work at home and abroad, emphatically analyze the impact of new news models on traditional news production, and propose that in the current news service model, big data can be combined to realize informatization applications. To predict information in the context of current data results, the application and sharing of data information can be realized by designing an open-source news database. The finished design of the media database can be used as the basis for the development of self-news and can take the lead in the news competition. This work analyzes and studies big data technology and genetic algorithms and introduces them into the field of news service model design, thus promoting the development of new news models.

1. Introduction

At the quantitative level, information data are constantly expanding with the rapid development of computer technology. As such information data enriches people's lives, its own complexity is gradually increasing, making it more difficult for information data to be used by people, causing people to spend a lot of money, time, and energy, resulting in a huge waste of human and material resources [1, 2]. In addition, there are a lot of useless and harmful information in the information data, which have great negative influence and adverse events on the information processing process. Therefore, how to use information data efficiently and effectively has become a hot research topic in all walks of life and fields [3]. The resources created by big data technology have made an impact on the traditional news media industry, making it undergo revolutionary changes and transformations and leaving a deep imprint, changing the information reporting form of the traditional media industry to a certain extent [4]. One of the core resources of mass media is the data foundation, and the application of big data solves the problem of information scarcity in the traditional media industry. Today, the basic problem of mass media providing information services is how to extract complex original data to obtain target-deep information [5]. Mining and presenting information to the public through searching and filtering has become a major challenge in the field of news applications. In the era of big data, data journalism is a new way of reporting news [6]. In the context of big data, mobile news clients have gradually become the preferred way for mobile netizens to obtain information due to their rich resources and convenient information acquisition methods, which can provide high-quality information content. One of the key factors for the success of today's

mobile news service clients is big data technology [7]. Current news clients have their own characteristics, but there are also many similarities. Today, the commonly used news clients can be roughly divided into three categories: one is the news client created by portal websites such as NetEase, Sohu, and Tencent; the other is the news client managed by traditional media such as People's Daily, Southern Weekly, and other news clients The other type is the personalized recommendation news client produced by emerging Internet companies such as Toutiao and Yidian News. This study takes the era of big data as the research background, conducts user surveys and in-depth interviews based on the optimization process of genetic algorithms, and predicts the future development trend of data news by analyzing user experience, hoping to provide a data foundation for the development and transformation of news service models [8].

2. Related Work

Research on the current news service model: the literature believes that compared with traditional media and traditional media methods, mobile media has three unique characteristics: first, the terminal is the medium, and second, the medium is the terminal; it relies more on mobile platform operations; third, mobile media in a broad sense is not only omnimedia but also a multifunctional personal center, and its finished products have different forms and are constantly changing [9]. It can be seen from the literature that the amount of data in the world is currently in a state of exponential growth. Through big data analysis, the growing competition for new productivity can be realized and provide a data foundation for it. [10] In the era of big data, there are many challenges that can impact traditional industries, and such challenges are also opportunities, which can promote the development of the industry if grasped properly. Therefore, for the news media, how to reasonably apply related technologies is a topic worthy of further study [11, 12]. Literature shows that new-age news sites have rich news resources from journalists, editors, designers, and developers who use news data. By browsing the website, users can get the information behind the data news from all over the world, learn new techniques and new methods of effective data analysis, and find out about the latest achievements in the field by searching for training and job opportunities in user-related fields [13]. The literature assumes that the integration of news customer information is presented through various media forms such as text, video, Atlas, and sound, and the news content is presented in a multiangle and multilevel stereoscopic manner, which enriches the user's audio-visual enjoyment [14]. This article takes Sohu News Client, The Paper, and Today's Toutiao as examples, analyzes the main role and influence of big data in news clients, and discusses the growth and evolution of mobile news clients in the era of big data [15]. In the research of big data based on genetic algorithms, the literature believes that the creation and consumption of technologies, products, economies, and cultures that rely on the production, dissemination, use, and absorption of relevant information make the world an organically connected whole [16, 17].

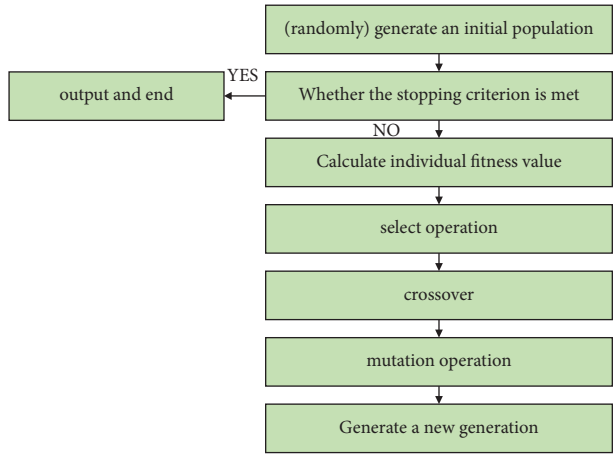

Figure 1: The calculation process of the genetic algorithm.

3. Principles of Genetic Algorithms

3.1. Theoretical Basis of Genetic Algorithm. The calculation process of the genetic algorithm is shown in Figure 1.

(1) Encode different decodings of a practical problem into bit strings, i.e., individuals (xi)

(2) Define the adaptation function f

(3) Determine the genetic strategy, crossover probability, and mutation probability

(4) Initial population

(5) Calculate the fitness $f(xi)$ of xi and then select the individual according to the individual fitness according to a certain proportion $Ps[xi]$ (the general selection strategy is the roulette algorithm)

(6) If the maximum genetic algebra is reached or the fitness requirements are met, continue to execute; otherwise, go to (5);

(7) Display the result and output

Finally, the decoding operation is performed, and the obtained solution is the optimal solution.

3.2. Design of Genetic Operators. Crossover probability is another important aspect of crossover operator design. A high crossover probability may lead to sufficient crossover in each generation, but it may also destroy a good population pattern; a lower crossover probability makes it possible to find the global optimal solution, but the speed of genetic search slows down or even stops.

In this project,

$$P_c = \begin{cases} \dfrac{P_{cmax} - P_{cmin}}{1 + \exp\left(2\left(f' - \overline{f}\right)/f_{\max} - \overline{f}\right)} + P_{cmin}, & f' \geq \overline{f}, \\ P_{cmax}, & f' < \overline{f}. \end{cases} \quad (1)$$

As evolution progresses, individuals tend to be more adaptable and more closely linked, resulting in individual structures becoming more and more monolithic. If evolution does not occur over many consecutive generations, it may not be possible to find an optimal solution based on the current population. At this time, the mutation rate can be increased to expand the search range. The formula is as follows:

$$P_m = \begin{cases} P_{\min} + \dfrac{t}{T_{\max}}, 0 \le \dfrac{t}{T_{\max}} \le (P_{\max} - P_{mmin}), \\ \dfrac{P_{mmax}}{P_{mmax} - P_{\min} - 1} \times \dfrac{t}{T_{\max}} + \dfrac{P_{\max}}{P_{mmin} + 1 - P_{mmax}}, (P_{mmax} - P_{\min}) \le \dfrac{t}{T_{\max}} \le 1. \end{cases} \tag{2}$$

The individuals in the genetic algorithm have no memory function, each individual can only reflect the current situation, and the scope and direction of evolution are blind, which will lead to the destruction of the stability of the population; at the same time, all individuals share information with each other in competition, so that the entire population is divided. To this end, this project introduces particle swarm optimization. Individuals in particle swarm optimization have memory functions and can control the order and direction of evolution based on historical information and current conditions. In most cases, they converge to the optimal solution faster; swarm algorithms find the optimal solution through cooperation among individuals. Only the best position in the group sends information to other particles in one direction, and individuals do not share information directly, so the entire search and update process always follows the current optimal solution, which helps maintain the diversity of the population.

3.3. Crossover and Mutation of Genetic Operators. Crossover is also called genetic recombination, and its basic principle is to recombine parts of the genes of two parental individuals to generate new individuals. Genetic recombination or crossover operation plays an important role in the genetic algorithm, which can obtain excellent new individuals. Some of the most commonly used crossover operators are selected.

3.3.1. Point Cross. The basic process of point intersection is to randomly generate one or more intersection positions and then exchange the corresponding strings of the parent individual. The basic point intersection process is shown in the following formula:

$$\begin{matrix} [01110 \mid 110] \\ [10101 \mid 001] \end{matrix} \Rightarrow \begin{matrix} [01110 \mid 001^{\text{or}} [01|110|]110] \\ [10101 \mid 110] \quad [10|101|001] \end{matrix} \Rightarrow \begin{matrix} [01|101|110] \\ [10|110|001] \end{matrix}. \tag{3}$$

3.3.2. Evenly Cross. The basic process of uniform intersection is to change each segment of two separate parent strings according to the probability. The specific process is to first randomly generate a control template with the same length as the parent's respective strings, 1 means exchange and 0 means no exchange, and then cross-process the parent and child strings according to the control template. For example, the generated control pattern is [10011100], and the basic process of uniform crossing is shown in the following equation:

$$\begin{matrix} [01110110] \\ [10101001] \end{matrix} \longrightarrow [10011100] \Rightarrow \begin{matrix} [11101010] \\ [00110101] \end{matrix}. \tag{4}$$

From the perspective of crossover patterns, uniform crossover and point crossover have the following characteristics: the point crossover pattern does not change much, but the search pattern is small, and the uniform crossover pattern has a high probability of changing, but the searched pattern does not change much. Therefore, in practical problems, uniform intersection is usually used when the group size is small, and point intersection is usually used when the group size is large.

The following two types of differences are usually identified:

① Basic variation

The basic process of basic mutation is as follows: randomly generate a mutation position or multiple mutation positions, and reverse the corresponding code value. The basic process of basic mutation is shown in the following formula.

$$[10101010] \Rightarrow [10001110]. \tag{5}$$

② Reverse mutation:

$$[10101010] \Rightarrow [10010110]. \tag{6}$$

4. News Big Data Processing Method Based on Genetic Algorithm

4.1. Data Sources. According to the statistical analysis of various data sources, combined with the sources of media, this study divides news data sources into the following categories:

Table 1: News distribution.

Classification category	Training text	Test text
Society	387	40
Healthy	417	47
Internationality	302	35
Finance	0	56
Film and television	0	59
Physical education	0	30
Total	1106	267

(1) Government: mainly official data released by the government and other organizations, such as government departments such as the National Bureau of Statistics of China and large organizations such as the European Union and OCED

(2) Enterprises or nongovernmental organizations: the survey data released by enterprises such as Alibaba and British Airways, as well as nongovernmental organizations such as the International Committee of the Red Cross (ICRC) and the International Accreditation Association (IPA)

(3) Universities, research institutions or individuals: universities and professional research institutions, as well as survey data or research reports published by scholars, researchers, and enthusiasts' data news

(4) Social networks: data obtained from social networks at home and abroad such as Twitter, Facebook, Weibo, and WeChat

In terms of news, excluding some repeated news, this study collects 1373 news and divides them into 6 categories, of which 1106 texts are used as training texts, and the remaining 267 texts are used as sample tests, as given in Table 1.

4.2. Acquisition of News Text Data. A sentence contains several pairs of entities and several semantic descriptions of the entities, and these semantic descriptions contain entity relationships. The correct extraction of entity pairs and their semantic descriptions from sentences is the main research goal of this section. In order to facilitate the subsequent analysis, we first define the entity pair.

An entity pair refers to two entities in a sentence that have direct dependencies. We formally define it as pair (e_i, e_j) = {<e_i, type (e_i) >, <e_j, type (e_j) >}, where e_j refers to an entity and type (e_j) represents the entity type, such as location, organization, and personnel.

An entity pair describes a sequence of segments and refers to a set of words that can describe the semantic relationship between two entities, which can be entity context. In this study, a set of gerunds in the shortest dependency path of two entity-dependent syntax trees are used as the order to describe the entities. We denote the feature sequence description of the combined entity pair as fs (e_i, e_j), and its definition is formally expressed as

$$fs\left(e_i, e_j\right) = \{w_i \mid pos\ (w_i) \in \{v, n\}, 1 \le i \le K\}. \tag{7}$$

Among them, $pos\ (w_i)$ represents the part of speech in the vocabulary of W_i; v, n represent that the part of speech is a verb or a noun; K is the length of the segment sequence.

Heuristic rules extract sequence descriptions. According to Chinese expression habits, the closer the edit distance between words in a sentence, the stronger the semantic correlation between two words. Therefore, when taking the sequence part of an entity pair, the following rules exist:

(1) Since the dependence between words weakens with the increase of the length of the dependence distance, the words in the feature sequence of the entity pair must be words directly connected to the entity words with dependent edges

(2) If the sentence has three entities, e_1, e_2, e_3, it is determined that there are two entity pairs, pair (e_1, e_3), pair (e_2, e_3), and the dependency path dependency Path (e_1, e_3) contains dependency Path (e_2, e_3); then, the shortest dependency path between these two entities is as follows:

$$\text{shortPath}\left(\text{pair}\left(e_2, e_3\right)\right) = \text{dependencePath}\left(e_2, e_3\right), \tag{8}$$

$$\begin{aligned}\text{shortPath}\left(\text{pair}\left(e_1, e_3\right)\right) = {} & \text{dependencePath}\left(e_1, e_3\right) \\ & - \text{dependencePath}\left(e_2, e_3\right).\end{aligned} \tag{9}$$

According to the semantic localization rules, we extract entity pairs with semantic dependencies from sentences and then extract the descriptive feature sequences of entity pairs that determine the relationship through partial descriptive sequence extraction rules. It should be emphasized that if an entity pair has multiple dependency paths, each entity pair and triplet consisting of segment description sequences are considered to be different individuals, that is, multiple relationships are allowed for the same entity pair.

Since this study extracts entity pairs based on syntactic dependencies and uses the shortest dependency path as the feature sequence of entity pairs, therefore, the number of feature words contained in the feature sequence of the entity pair cannot be determined, and the similarity cannot be obtained by using a conventional calculation method. Based on this background, this study decides to use the sequence kernel function to measure the entity similarity. The calculation formula is

$$K(X, Y) = \frac{1}{Z(X, Y)} \sum_{n=1}^{K} K_n(X, Y). \tag{10}$$

Among them, X and Y represent the feature description intervals of two pairs of entities, and the lengths of the two intervals are not necessarily the same; Z (X, Y) is the normalization factor, which is defined as follows:

$$Z(X, Y) = \sqrt{\sum_{n=1}^{|X|} K_n(X, X) \times \sum_{n=1}^{|Y|} K_n(Y, Y)}. \tag{11}$$

The calculation formula of the semantic kernel function is as follows:

$$K_n(X,Y) = \sum_{u \in \sum_n^*} \sum_{i:u=X[i]} \sum_{j:u=Y[j]} \lambda^{l(i)+l(j)} \times \prod_{k=1}^{n} SIM\left(X_{i_k}.\text{word}, Y_k.\text{word}\right). \tag{12}$$

Among them, u represents the common sequence of two entities in the feature sequence; λ is the decay factor starting from (0, 1), using the entire text of the encyclopedia to train the word vector, and calculating the difference between the two words by the similarity of the word vector, the semantic similarity between the two is calculated as follows:

$$SIM\ (W_A, W_B) = \frac{\overrightarrow{W}_A \cdot \overrightarrow{W}_B}{\| \overrightarrow{W}_A \| \cdot \overrightarrow{W_B} \|}. \tag{13}$$

In summary, we use (13) to calculate the similarity of two sets of features. The disadvantage of this method is the high computational complexity, but this complexity is usually affected by the length of the feature sequence. In this study, the shortest reliable path is used as the segment description sequence, and the length itself can be well controlled, so that the operation cost will not be too high.

First, we create a similarity matrix of entity pairs by calculating the similarity between entity pairs, which is represented as follows:

$$\begin{pmatrix} \text{k}(\text{entityPair}_1, \text{entityPair}_1) & \cdots & \text{k}(\text{entityPair r}_1, \text{entityPair r}_n) \\ \vdots & \ddots & \vdots \\ \text{k}(\text{entityPair}_n, \text{entityPai r}_1) & \cdots & \text{k}(\text{entityPair r}_n, \text{entityPair}_n) \end{pmatrix}. \tag{14}$$

The general process of the spectral clustering algorithm is shown in Figure 2.

According to the description of Figure 2, combined with the requirements of this section, we summarize the detailed steps of the entity pair set spectral clustering algorithm as follows:

Step 1: Construct the similarity matrix of the sample set, measure the correlation between samples according to formula (10), construct the similarity matrix W shown in formula (12), and construct the degree matrix D at the same time

Step 2: Calculate the Laplace matrix $L = D - W$ and standardize the D matrix

Step 3: Perform feature synthesis on the matrix and select the eigenvector f corresponding to the minimum k eigenvalues

Step 4: Normalize the matrix composed of the corresponding eigenvectors f in the row and finally obtain the $n \times k1$ eigenmatrix F

Step 5 Each row of the $k1$-dimensional vector of F is a sample, a total of n samples input the clustering algorithm, cluster the samples, and finally output the clustering result.

Whether to divide the cluster centers in the X-means algorithm is determined by the division criterion. We pick a cluster center, then create a center next to it, and evaluate whether both centers perform better, if so, split the class, and if not, go back to the previous step. The algorithm judges performance by the BIC score. The BIC calculation formula is as follows:

$$BIC\left(M_j\right) = \widehat{l}_j(D) - \frac{p_j}{2} \cdot \log\ R, \tag{15}$$

where D represents the dataset, M_j represents the model, and different models represent different K values.

Relation label extraction refers to extracting the corresponding words from the same category entity as the category relation label for the feature set description sequence. This method aims to obtain the most discriminative word from the feature sequence category of the entity pair as the label of the category, which is based only on the word frequency, ignoring the semantic features of each word. However, the idea of this method is simple and easy to implement, and the accuracy rate is high. In this study, DCM is used for label extraction. The plan is divided into the following two phases:

First, we determine the importance of the feature word fi in the class; we define it as $WC_{i,k}$, and the calculation formula is as follows:

$$WC_{i,k} = \frac{\log_2\left(df_{i,k} + 1\right)}{\log_2\left(N_k + 1\right)}, \tag{16}$$

where $\text{d}f_{i,k}$ represents the number of entity pairs with a certain word fi in category k; N_k represents the total number of entity pairs in the dataset. The formula for calculating the importance between categories is as follows:

$$CC_i = \log\ \frac{N \cdot \max_{k \in C_i}\left\{WC_{i,k}\right\}}{\sum_{k=1}^{N} WC_{i,k}} \cdot \frac{1}{\log N}. \tag{17}$$

Among them, C_i is the set of all the classes with the feature word f_i, and we take the feature word with the highest weight in each class as the label of the class relationship.

$$\text{Weight}\left(f_i\right) = \frac{W_{i,k}^2 \times CC_i^2}{\sqrt{W_{i,k}^2 \times CC_i^2}}. \tag{18}$$

The words of the relationship label between the entity pairs are usually arranged in the order of the entity pair features, so after obtaining the category label, we use the formula (19) to select the feature description sequence in the word label with the highest matching degree of the category vocabulary, and put it as a specific label for entity pairs.

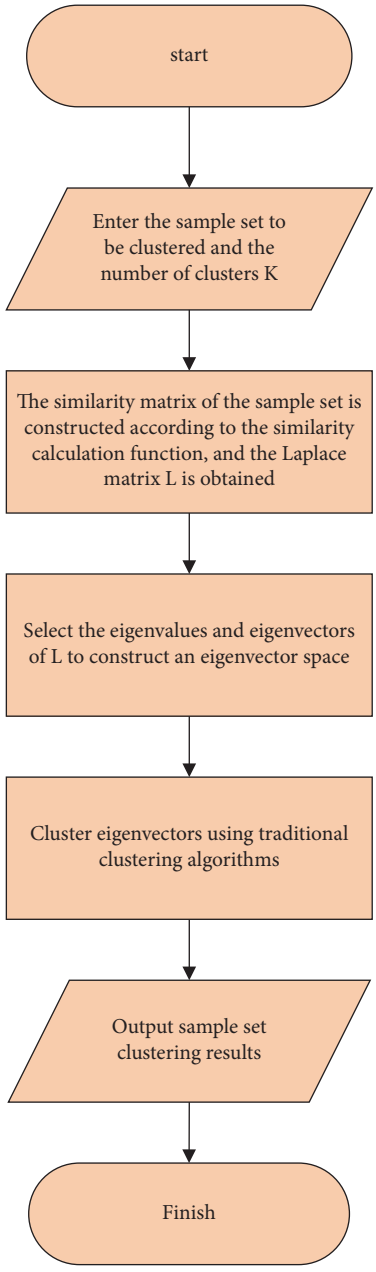

Figure 2: Flowchart of the spectral clustering algorithm for similar relationship entities.

$$\underset{f_i}{\operatorname{argmax}} \operatorname{sim}\left(f_i, f_i^C\right). \tag{19}$$

Among them, $f_i \in f_s$ (e_i, e_j), that is, the label word is generated from the feature sequence of the entity pair pair (e_i, e_j).

4.3. Evaluation Indicators. Evaluation metrics usually include text classification complexity and text classification effectiveness. The classification types of text classification are generally divided into 4 categories, namely, c_i classification categories. One is the amount of text information that belongs to the c_i classification category and is correctly classified into the c_i classification category, which is recorded as TP; the other category belongs to the c_i classification category, but is wrongly classified. Classification. The amount of text information assigned to other classification categories is denoted as FP; one category is the amount of information in the text that does not belong to the c_i classification category, but is wrongly placed in the c_i classification category, denoted as FN; other categories do not belong to the classification category. The amount of textual information is not classified in a categorical category, but is represented as TN. The performance evaluation indicators are recall rate, precision rate, and F measurement, and the specific content is defined as follows.

4.3.1. Accuracy (P). The specific calculation formula of the accuracy rate is as follows:

$$P = \frac{TP}{TP + FP} \times 100\%. \tag{20}$$

4.3.2. Recall Rate (R). The specific calculation formula of recall rate is as follows:

$$R = \frac{TP}{TP + FN} \times 100\%. \tag{21}$$

4.3.3. F Measurement. As can be seen from the above, precision and recall are two opposite standard evaluation metrics. F measurement is a measurement method that combines the characteristics of the two. The specific calculation formula is as follows:

$$F_\beta(P, R) = \frac{\left(\beta^2 + 1\right)\mathrm{PR}}{\beta^2 P + R}, \tag{22}$$

where β is a constant. By varying different values of the beta constant, we can control and modify the effects of precision and recall. If β is 1, then F_β is equal to the value of F_1, which is the average of recall and precision. The specific calculation formula is as follows:

$$F_1 = \frac{2\mathrm{PR}}{P + R}. \tag{23}$$

4.3.4. Macroaverage and Microaverage. Through the analysis of the above three methods, these methods analyze the classification results of a classification category. When we need to evaluate a classification method, we usually average the text classification results, such as macroaverage and microaverage. However, if there are many differences in the classification categories of text information, then the values of the two are also very different.

Table 2: Comparison of text classification effects based on genetic algorithms.

	Optimization algorithms			Traditional algorithms		
Number of clusters	Recall	Precision	*F*-measure	Recall	Precision	*F*-measure
2	0.593	0.483	0.532	0.558	0.365	0.440
3	0.849	0.861	0.855	0.696	0.688	0.692
4	0.587	0.812	0.681	0.390	0.500	0.438
5	0.466	0.622	0.532	0.455	0.737	0.563
6	0.376	0.673	0.482	0.370	0.712	0.487
7	0.356	0.860	0.503	0.311	0.674	0.426
8	0.198	0.740	0.313	0.306	0.194	0.237
Mean	0.487	0.719	0.554	0.438	0.550	0.467

4.4. Analysis of News Big Data Processing Results. It can be seen from Table 2 that the precision, recall, and F-measure are greatly improved after text classification is combined with the genetic algorithm. It can also be seen in the analysis of the number of clusters that the number of clusters is defined as 3 clusters. The group effect has the largest measure *F* in groups 2–8. Therefore, we can clearly see that after grouping the text information that cannot be classified into existing categories, the grouped categories of the text information can be effectively identified. Grouping categories can be added to existing categories through an optimization algorithm. Textual information that may not be classified into existing categories is processed in the future.

This study also compares some commonly used methods for clustering similar textual information, aiming to divide the groups into 3 groups. As can be seen from Figure 3, in the case of similar text information, the recognition effect of the method in this study is much greater than that of other algorithms.

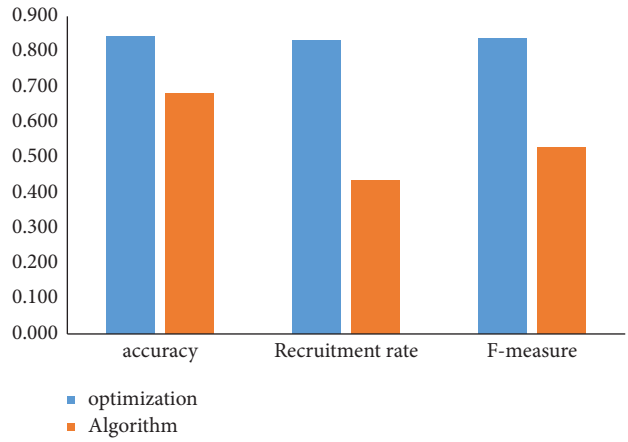

Figure 3: Comparison of the effect of the algorithm in this study and some existing algorithms.

5. The Changing Trend of the Current News Service Model

5.1. Changes in News Service Content. Compared with film and television, sports, and financial news, social news and international news are more inclined to hard news. Choosing this topic reflects setting the mobile news client's agenda to focus on news content coverage. At the same time, public use of mobile news media is often limited to a fraction of the time. Users expect short, timely, and rich news content and high-quality news coverage in a very short period of time. The data show that during the morning peak hours of 08: 00 to 10: 00 am, viewers tend to get high-quality hard news.

As can be seen from Figure 4, the selection of different types of news topics is uneven in the sampling time series of the mobile news client: on the one hand, in the reporting of social news, political news, and military news, the three show similar situations. On the other hand, the other three types of news are quite different, showing an irregular state. The reason is that some news topics have their own "soft" attributes, that is, movies, sports, and finance, and other news types with soft news characteristics have relatively low timeliness requirements, and client-side publishers will "prioritize" to browse high-frequency news. Hard news with a large amount of information and a high degree of topicality are chosen to deliver. We should take advantage of the number of reports, complete

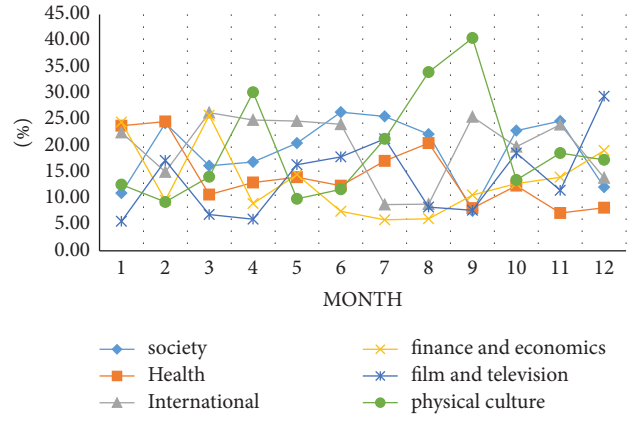

Figure 4: Changes in different types of news.

the agenda setting, and guide the audience to pay attention to the news content with a large proportion of reports. On the other hand, in the morning peak hours of mobile news browsing, the audience's tendency to choose news types also affects and determines the market and value of hard news, thus diluting the existence of soft news.

5.2. Analysis of News Service Demand and Satisfaction. As shown in Figure 5, in the mobile news accuracy market survey, it can be seen that only 1.89% of people are

dissatisfied with mobile news; in addition, 53.56% of users are satisfied with the accuracy of mobile news, the highest proportion. This shows that, as the core competitive push service of mobile news, it can generally better meet the needs of users.

As shown in Figure 6, according to the market survey questionnaire, when 50% of users were asked "what makes you most satisfied with the news model in the new era," they said that mobile news is most satisfied with "abundant information," some in-depth interviewees indicated that mobile news is rich and comprehensive, and the ability to refresh new news at any time is its most satisfying advantage. This indicates that users have specific needs for the quantity and richness of news content.

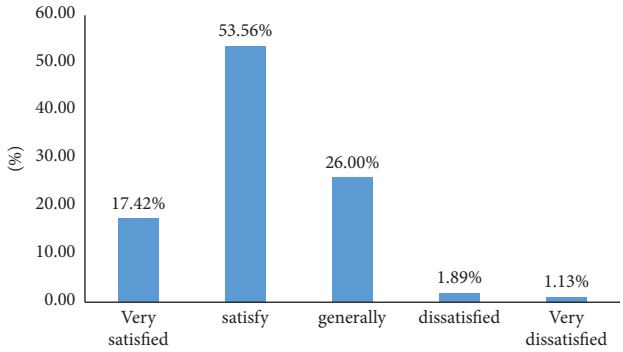

Figure 5: User satisfaction of news mode in the new era.

5.3. Development Trend of Current News Service Mode

5.3.1. Predict Information Based on Existing Data Results. Predictive journalism is forward-looking reporting of events that are about to happen but have not yet happened. It focuses on the scientific prediction of the development process or news viewpoints. Traditional predictive news reports emphasize the subjective perception of reporters, but due to factors such as insufficient personal experience and limited knowledge, predictions often lack scientificity and accuracy. The lack of scientific and quantifiable forecasting methods and technical analysis methods hinders the accuracy and objectivity of forecasting reports to a certain extent.

5.3.2. Design of Open-Source News Database, Application, and Sharing of Data Information. As data technology continues to mature, more databases appear. These databases are diverse and include not only publicly available government information but also databases created by third parties, as well as the work of media organizations. These databases have various forms, some are for profit and require users to pay for use and some are open source and free. The raw data used in data journalism are open and free.

5.3.3. Design of the Media Database as a Competitive Advantage for Its Own News Development. Since the rapid development of Internet technology, many media have created their own information databases to adapt to the changing environment. According to new communication technologies, in the era of big data, different environments have different applications for big data. Enterprises form the foundation of big data by establishing their own databases. However, newspaper big data are not the same as news data. It is only a small part of the application, including the source product.

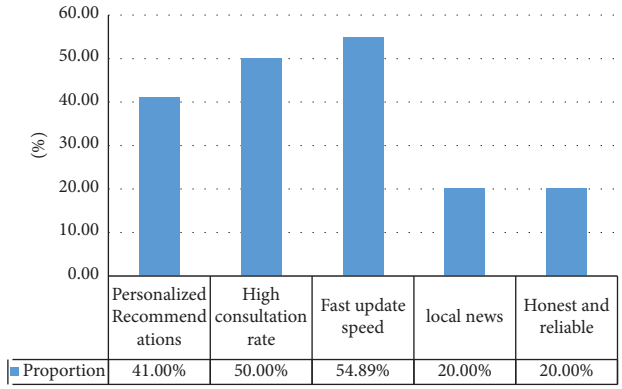

Figure 6: User satisfaction points of the new era news model.

6. Conclusion

With the continuous development of the information age, the amount of data is increasing day by day, which has brought a profound imprint on the news industry, and even changed the news reporting methods and ecology of traditional media. With the development of the times, the types of news data will continue to improve, and the demand will continue to grow. The news industry needs to push news according to the needs of the audience and improve the news service model for optimization and development. According to the above data, media products can be targeted, accurately analyze the characteristics of each user, and push on-demand content in a targeted manner, thereby winning clicks and user satisfaction. Although the use of new technology can make up for the shortcomings of traditional news production and is an innovative technology, it does not mean blindly following technological progress. News services must still follow industry rules and maintain the original intention of the media.

Data Availability

The data used to support the findings of this study are available from the corresponding author upon request.

Conflicts of Interest

The authors declare that they have no conflicts of interest.

References

[1] C. Elmer, F. Badenschier, and H. Wormer, "Science for everybody? How the coverage of research issues in German newspapers has increased dramatically," *Journalism & Mass Communication Quarterly*, vol. 85, no. 4, pp. 878–893, 2008.

[2] X. Liu and Z. Li, "False data attacks against AC state estimation with incomplete network information," *IEEE Transactions on Smart Grid*, vol. 8, no. 5, pp. 2239–2248, 2017.

[3] X. Liao, Y. Li, and B. Lu, "A model for selecting an ERP system based on linguistic information processing," *Information Systems*, vol. 32, no. 7, pp. 1005–1017, 2007.

[4] M. T. Odenkirk, D. M. Reif, and E. S. Baker, "Multiomic big data analysis challenges: increasing confidence in the interpretation of artificial intelligence assessments," *Analytical Chemistry*, vol. 93, no. 22, pp. 7763–7773, 2021.

[5] S. Koike, S. Yamaguchi, Y. Ojio, K. Ohta, and S. Ando, "Effect of name change of schizophrenia on mass media between 1985 and 2013 in Japan: a text data mining analysis," *Schizophrenia Bulletin*, vol. 42, no. 3, pp. 552–559, 2016.

[6] E. Borges-Rey, "Unravelling data journalism: a study of data journalism practice in British newsrooms," *Journalism Practice*, vol. 10, no. 7, pp. 833–843, 2016.

[7] C. Pentzold, C. Brantner, and L. Fölsche, "Imagining big data: illustrations of "big data" in US news articles," *New Media & Society*, vol. 21, no. 1, pp. 139–167, 2019.

[8] R. G. Picard, "Twilight or new dawn of journalism? Evidence from the changing news ecosystem," *Journalism Practice*, vol. 8, no. 5, pp. 488–498, 2014.

[9] Y. Aoudni, C. Donald, A. Farouk et al., "Cloud security based attack detection using transductive learning integrated with Hidden Markov Model," *Pattern Recognition Letters*, vol. 157, pp. 16–26, 2022.

[10] T. He, C. Huang, M. Li, Y. Zhou, and S. Li, "Social participation of the elderly in China: the roles of conventional media, digital access and social media engagement," *Telematics and Informatics*, vol. 48, Article ID 101347, 2020.

[11] A. Kamilaris, A. Kartakoullis, and F. X. Prenafeta-Boldú, "A review on the practice of big data analysis in agriculture," *Computers and Electronics in Agriculture*, vol. 143, pp. 23–37, 2017.

[12] F. Arena and G. Pau, "An overview of big data analysis," *Bulletin of Electrical Engineering and Informatics*, vol. 9, no. 4, pp. 1646–1653, 2020.

[13] C. K. S. Leung, "Big data analysis and mining," in *Advanced Methodologies and Technologies in Network Architecture, mobile Computing, and Data Analytics*, D. B. A. Mehdi Khosrow, Ed., pp. 15–27, IGI Global, 2019.

[14] J. Zhang, X. Yang, and D. Appelbaum, "Toward effective big data analysis in continuous auditing," *Accounting Horizons*, vol. 29, no. 2, pp. 469–476, 2015.

[15] A. Kim and A. R. Dennis, "Says who? The effects of presentation format and source rating on fake news in social media," *MIS Quarterly*, vol. 43, no. 3, pp. 1025–1039, 2019.

[16] D. Vazquez, C. Dennis, and Y. Zhang, "Understanding the effect of smart retail brand—consumer communications via mobile instant messaging (MIM)—an empirical study in the Chinese context," *Computers in Human Behavior*, vol. 77, pp. 425–436, 2017.

[17] T. A. Mohammed, O. Bayat, O. N. Uçan, and S. Alhayali, "Hybrid efficient genetic algorithm for big data feature selection problems," *Foundations of Science*, vol. 25, no. 4, pp. 1009–1025, 2020.

Hindawi
Mobile Information Systems
Volume 2022, Article ID 7202172, 10 pages
https://doi.org/10.1155/2022/7202172

Research Article

Application of Data Mining System in User Network Environment Based on SVM Optimization Algorithm

Yang Yanying

Nanjing Forest Police College, Nanjing, Jiangsu 210023, China

Correspondence should be addressed to Yang Yanying; yhq@lcu.edu.cn

Received 18 August 2022; Revised 13 September 2022; Accepted 21 September 2022; Published 6 October 2022

Academic Editor: Shadi Aljawarneh

Nowadays, different types of data and information combine and interact with each other, forming a complex and huge information network. Using data mining technology, one can effectively obtain the hidden data contained in the data bureau. This technology is the most commonly used way to obtain network target data at present. In this paper, we try to practically apply related algorithms by studying the theory of multi-information fusion. Aiming at the diversity and practicality of the network, the multi-information fusion method was optimized and improved on the basis of the traditional multi-information fusion method. Secondly, a data mining system based on the concept and algorithm of association rules is established, which simplifies the working mode of frequent mining and then improves the data mining model. Finally, an empirical analysis is designed. A group of data samples are selected from the network for preliminary processing, and the data set is brought into the system for testing. From the test results, it can be seen that the algorithm designed in this paper can effectively obtain the target data and works well in a complex network environment, can analyze meaningful data association using user network rules, and provides important guidance for optimizing network information and improving extraction efficiency. This paper combines data mining technology and multi-information fusion technology to conduct in-depth research and further complete the algorithm design by combining the two technologies, which proves the accuracy and processing efficiency of the algorithm.

1. Introduction

With the continuous development of society and technology, new scientific and technological achievements have sprung up like mushrooms after a spring rain. Among them, the most vigorous development is the emerging technology represented by big data and the Internet [1]. The Internet as the carrier of global big data has entered a period of rapid development, and the speed of data growth and the amount of data are also expanding. At present, emerging information technology has been developed by leaps and bounds and has been fully applied by the majority of people [2]. Through the influence of information technology, there are closer interaction channels between major systems. Data and information act as the bridge of system connection, which can fully connect all systems with the network as the carrier, so as to promote the interaction and communication of the system. But in this process, there are also many redundant data points [3]. Therefore, how to effectively deal with useless data in the process of applying information technology has become a key research project. After in-depth research, it was found that the use of data mining technology can effectively deal with redundant data and further convert it into practical data. The reduced data in the application has received widespread attention [4]. The main purpose of data mining is to process and manage multistructured data for large databases. Its scope is quite wide, involving many applications in various fields such as statistical analysis, pattern recognition, social networks, algorithm design, and machine learning. This technology has many applications in machine learning and other fields. It is precisely because of the emergence of data mining technology that the information age has become more computerized, modern society has become more intelligent, and people's lives have become easier. Based on this point, experts from various fields try to combine this technology to create value. Data mining

technology is the most commonly used data processing technology at present, and it is one of the popular application branches based on database technology. It meets the needs of people to acquire useful knowledge and make decisions while working in the context of the current era. Therefore, the use of associated user network rules in a social network can better optimize the process and results of information mining, which is also the goal of this paper [5]. This paper designs and conducts an analysis experiment for user behavior, and the data source is the network data of the target user. Firstly, the original data set is preprocessed, and then the data mining algorithm is applied to complete the processing of the sequence problem. By introducing a multi-information fusion algorithm, the advantages of the algorithm are used to realize the data mining of association rules and the acquisition of user behavior rules, which can provide an information basis for the effective and reasonable application of big data technology [6].

2. Related Work

Fusion is a process of combining, analyzing, and comprehensively processing multisource data or multisensor information to draw new, reliable, and effective conclusions. The applications of multisensor information fusion include multisensor recognition, detection, data association, target tracking, situation assessment, early warning, and so on [7]. The literature shows that more accurate information can be obtained through fusion than from a single input of data, which is also the basic purpose of information fusion technology and the result of synergy. That is, due to the joint action of multiple sensors, the effectiveness of the system has been improved [8]. The literature shows that information fusion is the collection and integration of information from different formats, different sources, and different media with a comprehensive analysis to create more complete, accurate, timely, and effective information, so as to achieve the best consistent estimation of the subject and its attributes [9]. According to the literature, military applications are the source of the birth of multi-sensor data fusion technology, which is mainly used in multistatic radar early warning systems and combat systems, including military target detection, positioning, tracking, and identification (ships), fighters, missiles, etc. The literature shows that not only military but also civil information fusion technology has also made great progress [10]. It is generally used in industrial fields such as robots, smart home manufacturing, transportation, and medical convenience services. It can be used for detection, fault repair, etc. The literature uses a variety of methods to fuse signal change and reconstruction to achieve target signal processing and can realize the feature extraction of the target signal through various domains. The methods used include spectrum analysis, time-domain technology, and so on [11]. A new kind of clustering self-organizing network is designed in the literature, which has many advantages. Compared with traditional networks, it does not need prior information and has a strong anti-interference ability. It can apply relatively simple neurodynamics technology to achieve clustering. Because this is a new technology, it has fewer practical applications, but it has sufficient potential. Data mining is an interdisciplinary technology that includes a large number of other application technologies [12]. It can mine and express hidden data and predict the future trend of data so as to achieve the user's goal by exploring the internal hidden rules of data. The literature shows that data mining algorithms are widely used in many fields, which can promote marketing and industrial production, assist in financial investment, deal with e-government, etc., and they also shine in medicine, biology, and other fields [13]. Such commonly used techniques include envelope anomaly analysis, classification, correlation analysis, clustering, summary regression, time series analysis, etc [14, 15]. The literature discusses the practical problems in the process of sequence analysis. People can sort the original transaction information database, merge the sorted results into the transaction database for operation, and return the results [16]. The literature shows that the average value can be replaced by N adjacent values in the process of trend analysis, followed by simple averaging or weighting, so as to effectively reduce the impact of specific points [17]. If special points are found in the processing process, a smoother and more stable curve can be obtained [18]. This algorithm will obtain uneven curves without obvious specificity [19]. Based on relevant knowledge, the literature divides sequential pattern mining into the following: (1) sorting. In this stage, the transaction subject in the transaction information database is sorted with the primary key and the transaction time as the secondary key, and the sorted data is sorted into the database, and its pattern is transformed into the sorted pattern; (2) big data project processing: at this stage, find all big data sets L, map them to sets of adjacent integers, and each big data set can correspond to an integer; (3) data conversion: at this stage, each entity of the entity sequence value in the database can be replaced with the corresponding big data set object; (4) in the process of sequence processing, large data sets are used to process sequence patterns; (5) maximize the sequence step to obtain the maximum sequence set [20, 21].

3. Theoretical Study of Multi-Information Fusion

3.1. Principle of Multi-Information Fusion. Multi-information fusion is actually an imitation of the process of the human brain processing information, which is similar to other information processing methods. More information about the detected target and environment can be obtained through the information fusion system. At present, there is no unified structure classification form and standard for the information fusion system, but it can be roughly divided into three categories: centralized structure, distributed structure, and hierarchical structure, according to the actual usage habits. All fusion processes are carried out at one fusion center. Each subsystem sends the acquired information and data to the fusion center, and the fusion center conducts a comprehensive analysis and processing of these data and finally obtains the decision-making results. This method has good real-time performance, complete

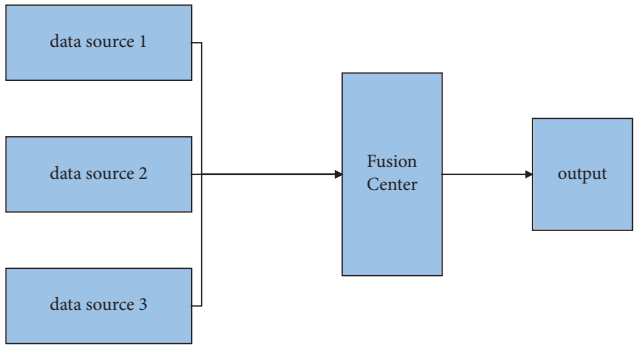

Figure 1: Centralized structure of information fusion.

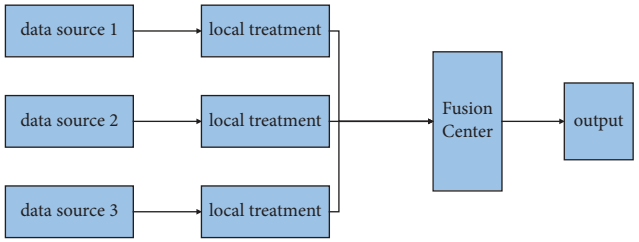

Figure 2: Distributed structure of information fusion.

information processing, and high accuracy. However, it also has certain disadvantages. For example, the processing background of all data is located in the fusion center, which will lead to its complexity. In a certain period of time, due to a large amount of data transmission, it may lead to system collapse and low stability. In this structure, due to the lack of necessary linkages between core sensors, the information and data of each sensor must be sent on time. Therefore, a bus must be provided in the high-speed transmission system and fusion center to achieve a wider range of data transmission. It must also have a more powerful central processing unit to process data, which increases the cost of the project implementation. The structure of the centralized system is shown in Figure 1.

In the distributed structure, the sensor will establish a decision-making system independently and carry out decision-making processing according to the information it receives. After processing, the data will be returned to the fusion center and combined. After the local decision is generated, all decision-making systems jointly estimate and evaluate. This structure does not need the original information, so it greatly reduces the required channel capacity and has a certain fault tolerance. Compared with the actual project, it is easy to realize. This structure has the following disadvantages: the fusion center cannot obtain the target information first. If the decision-making system of a sensor in the system is wrong, the whole system will produce the wrong final results. This means that the uncertainty of integration and the increase of processing projects. Its structure is shown in Figure 2.

The hierarchical structure is to establish a limited connection between each sensor. Some sensors correspond to a fusion node. There can be multiple fusion nodes in the entire system. There are two forms of hierarchy, one without feedback and the other with feedback.

3.2. Overview of Traditional Information Fusion Methods. When using the Bayesian method for multisensor information fusion, the possible decisions of the system must be independent of each other. The Bayesian conditional probability formula is as follows:

$$P\left(\frac{A_i}{B}\right) = \frac{P\left(B/A_i\right)/P\left(A_i\right)}{\sum_{j=1}^{m} P\left(B/A_j\right)/P\left(A_j\right)} \quad i = 1, 2, \ldots, m. \tag{1}$$

If the system has n sensors, the total posterior probability of each decision can be obtained as follows:

$$P\left(\frac{A_i}{B_1 \wedge B_2 \wedge \ldots \wedge B_n}\right) = \frac{\prod_{k=1}^{n} P\left(B_k/A_i\right)P\left(A_i\right)}{\sum_{j}^{m} \prod_{k=1}^{n} P\left(B_k/A_j\right)P\left(A_j\right) \;\; i=1,2,\ldots,m.} \tag{2}$$

Multisensors capture specific features of the target and then simulate and estimate the environment composed of these features to obtain the final synthetic information.

3.3. SVM Optimization Algorithm Design. The SVM training problem can be transformed into a hyperplane optimal classification problem, as shown in the following equation:

$$Q(\alpha) = \sum_{i=1}^{n} \alpha_i - \frac{1}{2} \sum_{i,j=1}^{n} \alpha_i \alpha_j y_i y_j K\left(x_i, x_j\right), \tag{3}$$

$$\sum_{i=1}^{n} y_i a_i = 0, \alpha_i \geq 0, i = 1, 2, \cdots, n.$$

For binary classification problems, the SVM classification discriminant function has the following form:

$$f(x) = \operatorname{sgn}\left(\sum_{i=1}^{n} \alpha_i^* y_i K\left(x_i, x\right) + b^*\right). \tag{4}$$

Through training, the SVM obtains the corresponding o vector w of the optimal classification hyperplane. This can be represented as a linear combination containing all vectors in the following feature space:

$$w = \sum_{i=1}^{n} a_i y_i \left(x_i\right). \tag{5}$$

We simplify the SVM and replace the initial vector set with a reduced vector set; the equation is as follows:

$$\tilde{w} = \sum_{i=1}^{m} \beta_i \left(x_i\right). \tag{6}$$

The decision function of SVM is shown in formula (7), m is the number of vectors included in the simplified vector set, and $m < n$:

$$f(x) = \operatorname{sgn}\left(\sum_{i=1}^{m} \beta_i K\left(x_i', x\right) + b^*\right). \tag{7}$$

The processing speed of the classifier can be effectively improved by collecting the simplified vector set with the smallest $m << n$, thereby simplifying the SVM classifier. This process needs to be carried out on the premise of reducing the loss of classification accuracy as much as possible.

There are currently four algorithms:

1.Create a new parsimonious vector and the corresponding weights ($z1$, $\beta 1$) to approximate the following equation:

$$\phi = \sum_{i=1}^{N_x} \alpha_i \varphi(x_i). \tag{8}$$

Then, an iterative construction of the (z_{m+1}, β_{m+1}) approximation vector is performed as follows:

$$\phi_m = \sum_{i=1}^{N_x} \alpha_i y_i \varphi(x_i) - \sum_{i=1}^{m} \beta_i \varphi(z_i). \tag{9}$$

It can be seen from the following equation (10) that this kind of problem can be transformed into a nonlinear multiparameter class optimization problem:

$$\delta = \| \phi_{m-1} - \beta_m \varphi(z_m) \|^2. \tag{10}$$

2. Let the support vector (x_k, y_k) depend linearly on other support vectors in the feature space, namely as follows:

$$k(x, x_k) = \sum_{i=1, i \neq k}^{N_s} c_i k(x, x_i). \tag{11}$$

Then, the corresponding SVM classification discriminant function can be rewritten as follows:

$$f(x) = \operatorname{sgn}\left(\sum_{i=1, i \neq k}^{N_x} \alpha_i y_i k(x, x_i) + \alpha_k y_k \sum_{i=1, i \neq k}^{N_x} c_i k(x, x_i) + b \right). \tag{12}$$

Defining $\alpha_k y_k \gamma_i = \alpha_i y_i \gamma_i$, the classification discriminant function can be rewritten as follows:

$$\begin{aligned} f(x) &= \operatorname{sgn}\left(\sum_{i=1, i \neq k}^{N_x} \alpha_i y_i (1 + \lambda_i) k(x, x_i) + b \right) \\ &= \operatorname{sgn}\left(\sum_{i=1, i \neq k}^{N_x} \overline{\alpha}_i y_i k(x, x_i) \right). \end{aligned} \tag{13}$$

3. A kernel function matrix is given as follows:

$$K = \begin{bmatrix} k_{11} & k_{21} & \dots & k_{l1} \\ k_{12} & k_{22} & \dots & k_{l2} \\ .. & .. & .. & .. \\ k_{1N} & k_{2N} & \dots & k_{\mathrm{lN}} \end{bmatrix} = \begin{bmatrix} \varphi(x_1) \cdot \varphi(s_1) & \varphi(x_2) \cdot \varphi(s_1) & \dots & \varphi(x_l) \cdot \varphi(s_1) \\ \varphi(x_1) \cdot \varphi(s_2) & \varphi(x_2) \cdot \varphi(s_2) & \dots & \varphi(x_l) \cdot \varphi(s_2) \\ .. & .. & .. & .. \\ \varphi(x_1) \cdot \varphi(s_N) & \varphi(x_2) \cdot \varphi(s_N) & \dots & \varphi(x_l) \cdot \varphi(s_N) \end{bmatrix}. \tag{14}$$

Decomposing the kernel function matrix into Km and Kn,

$$\begin{aligned} K_m &= \begin{bmatrix} k_{11} & k_{21} & \dots & k_{l1} \\ k_{12} & k_{22} & \dots & k_{l2} \\ .. & .. & .. & .. \\ k_{1m} & k_{2m} & \dots & k_{lm} \end{bmatrix} = \begin{bmatrix} \varphi(x_1) \cdot \varphi(s_1) & \varphi(x_2) \cdot \varphi(s_1) & \dots & \varphi(x_l) \cdot \varphi(s_1) \\ \varphi(x_1) \cdot \varphi(s_2) & \varphi(x_2) \cdot \varphi(s_2) & \dots & \varphi(x_l) \cdot \varphi(s_2) \\ \dots & \dots & \dots & \dots \\ \varphi(x_1) \cdot \varphi(s_m) & \varphi(x_2) \cdot \varphi(s_m) & \dots & \varphi(x_l) \cdot \varphi(s_m) \end{bmatrix} \\ K_n &= \begin{bmatrix} k_{1m+1} & k_{2m+1} & \dots & k_{lm+1} \\ k_{1m+2} & k_{2m+2} & \dots & k_{lm+2} \\ .. & .. & .. & .. \\ k_{1N-m} & k_{2N-m} & \dots & k_{\mathrm{lN}-m} \end{bmatrix} = \begin{bmatrix} \varphi(x_1) \cdot \varphi(s_{m+1}) & \varphi(x_2) \cdot \varphi(s_{m+1}) & \dots & \varphi(x_l) \cdot \varphi(s_{m+1}) \\ \varphi(x_1) \cdot \varphi(s_{m+2}) & \varphi(x_2) \cdot \varphi(s_{m+2}) & \dots & \varphi(x_l) \cdot \varphi(s_{m+2}) \\ \dots & \dots & \dots & \dots \\ \varphi(x_1) \cdot \varphi(s_{N-m}) & \varphi(x_2) \cdot \varphi(s_{N-m}) & \dots & \varphi(x_l) \cdot \varphi(s_{N-m}) \end{bmatrix}. \end{aligned} \tag{15}$$

The classification discriminant function is given as follow:

$$\begin{aligned} f(x) &= \operatorname{sgn}\left[\sum_{j=1}^{N} \alpha_j y_j k(x, s_j) + b \right] \\ &= \operatorname{sgn}\left[\sum_{j=1}^{m} \alpha_j y_j k(x, s_j) + \sum_{j=m+1}^{N} \alpha_j y_j k(x, s_j) + b \right]. \end{aligned} \tag{16}$$

Make,

$$W^T = \begin{bmatrix} w_{11} & w_{12} & \cdots & w_{1m} \\ w_{21} & w_{22} & \cdots & w_{2m} \\ \cdots & \cdots & \cdots & \cdot \\ w_{n1} & w_{n2} & \cdots & w_{nm} \end{bmatrix}. \tag{17}$$

Also, with $K_n = W^T K_m$, the discriminant function can be transformed into the following:

$$f(x_t) = \operatorname{sgn}\left(\left(A_m^T + A_n^T W^T\right)K_t + b\right). \tag{18}$$

Only W and m are required. The problem turns into a request,

$$\begin{aligned} &\min\{\varepsilon = \| \Theta' - \Theta \|\} \\ &\text{s.t. } K_n = W^T K_m. \end{aligned} \tag{19}$$

4. Obtain the support vector centroid O_k by kernel clustering.

$$O_k = \sum_{i=1}^{nk} b_{ki}\varphi(x_{ki}) i = 1, 2 \ldots nk = 1, \ldots, \text{cluster num}'. \tag{20}$$

In which,

$$b_{ki} = \frac{\alpha_{ki}}{\sum_{i=1}^{nk} \alpha_{ki} i} = 1, 2 \ldots n, k = 1, \ldots, \text{cluster num}. \tag{21}$$

Calculate the distance from any sample point x_i to the centroid O_k in the feature space.

$$\begin{aligned} \tilde{d}_i^2(O_k, \varphi(x_i)) = K(x_i, x_i) - 2\sum_{p=1}^{nk} b_{kp} K\left(x_{kp}, x_i\right) \\ + \sum_{p,q=1}^{nk} b_{kq} b_{kp} K\left(x_{kp}, x_{kq}\right) k = 1, \ldots, \text{cluster}_{\text{num}}. \end{aligned} \tag{22}$$

For the Gaussian kernel function, there is the following relationship:

$$d_i(z_k, x_i) = -2\sigma^2 \ln\left(1 - \frac{1}{2}\tilde{d}_i^2(\varphi(z_k), \varphi(x_i))\right). \tag{23}$$

An approximation of zk is calculated from this relationship, as a parsimony vector, defined

$$d(\beta_k) = \| \beta_k \varphi(z_k) - \sum_{i=1}^{nk} \alpha_{ki} y_{ki} \varphi(x_{ki}) \|^2, \tag{24}$$

make it the smallest, get the best

$$\beta_k = \frac{\sum_{i=1}^{nk} \alpha_{ki} y_{ki} k(z_k, x_{ki})}{k(z_k, z_k)}, \tag{25}$$

thereby, simplifying is realized.

3.4. Optimal Design of Multi-Information Fusion Method. Generally speaking, the structure of the multisensor information fusion mode is as follows:

Multiple sensors together form a multisensor system, which can provide environmental information and object information about the target. This system is equipped with m fusion nodes, which can fuse the multitarget information. Each fusion node can fuse information according to specific requirements and finally integrate the resulting information Y. In the actual usage process, the choice of fusion method is not fixed and needs to be analyzed in detail. The multi-information fusion node problem based on SVM technology can be expressed as: for an n-dimensional input parameter x, design I independent distributed observation samples are as follows:

$$\begin{aligned} T = \{(x_1, y_1), \cdots (x_l, y_l)\} \in (X \times Y)^l x_i \in X = R^n, \\ y_i \in Y = \{1, 2, \cdots k\}, i = 1, 2, \cdots l. \end{aligned} \tag{26}$$

Find an optimal function f(x) to express the dependency between x and y. In the original space, the resulting decision function is as follows:

$$f(x) = \operatorname{sgn}\left[\sum_{i=1}^{1} a_i^* y_i K(x \cdot x_i) + b^*\right]. \tag{27}$$

To sum up, the multi-information sensor fusion model based on SVM technology can be summarized, and it is found that it has many advantages compared to the traditional multisensor information fusion model: firstly, the model can completely correspond to the general information integration process of output and input nodes. It can convert the nonlinear relationship between the measured parameters and other related parameters, so as to change the fusion form of related information into a mapping relationship and be able to explain part of the content; secondly, the system can convert each parameter into a model function f(x) and transform the problem into a quadratic optimization problem to solve. The value solved in this way can determine the extreme value as the global optimal solution so that the model is consistent; during the test, the accuracy of the system fusion test can be improved by adjusting the kernel function K (x, x) and its related parameters; in addition, this model can effectively solve the nonlinear and high-dimensional problems between related parameters and measurement parameters. In the overall process, since the nonlinear transformation cannot be performed in the input space, it needs to be solved in the feature space. After the solution is obtained, the input of the space vector is compared, so that the nonlinear results are exchanged. In this way, more target work can be done in high-dimensional space, and it can effectively solve the "curse of dimensionality" problem that may occur in other algorithms.

4. Design of Associated User Network Data Mining Algorithm

4.1. Design of Data Mining System. Target knowledge can be obtained by using data mining technology, and data mining can also be carried out in the context of big data. By analyzing the main application process of this technology, we can know that the data mining system can be divided into five main modules, namely preprocessing, data extraction and mining, model evaluation, and output. The structure of the data mining system depends on its organic composition, including the above five functional modules. The architecture diagram of the data mining system is shown in Figure 3.

The key steps of data mining are as follows:

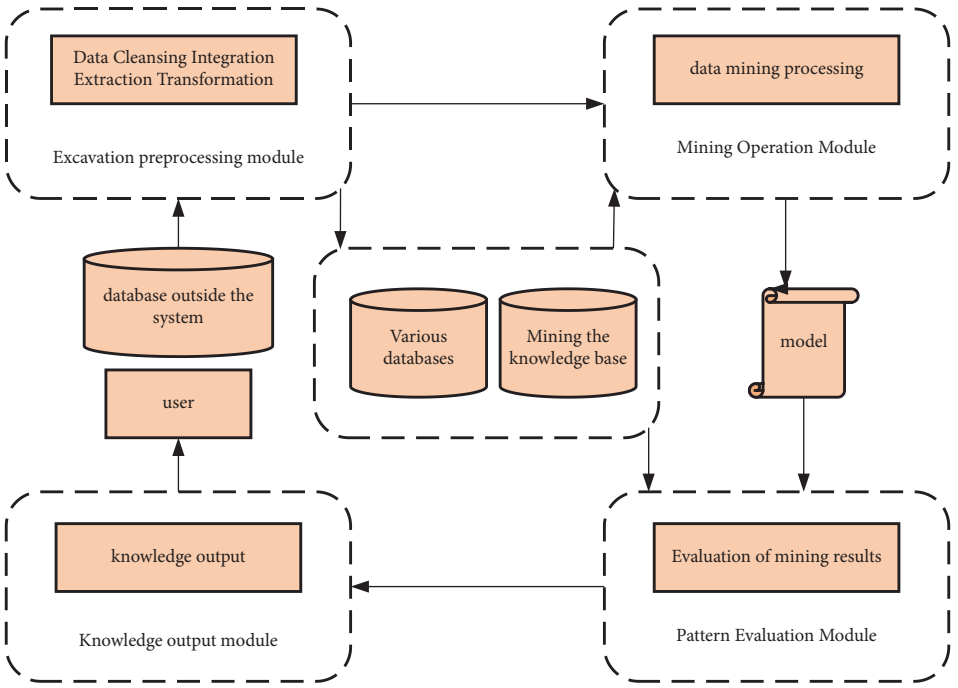

Figure 3: Architecture diagram of a data mining system.

(1) Data preprocessing.

This involves the process of sorting, combining, transforming, and filtering different types of data. Data preprocessing can maintain the database and knowledge base of the system and conduct targeted management. Such databases need to transform, clean, and purify the original data before management and maintenance. The essence of data sorting is data cleaning, which is the basis of data mining preprocessing, including removing redundant data, combining different similar data items, thereby removing data noise, and removing nonidentical data. Data integration is a process of summarizing and combining data, and a database can be used to manage data resources from different sources and databases in real-time to complete the data integration process. The process of data filtering is the act of separating and extracting data from aggregated data and filtering out valuable data that meets the requirements. Data transformation is the secondary integration and data adjustment of the filtered data to integrate the original data elements into a specific form and format more suitable for data mining operations.

(2) Data mining.

The purpose of data mining is to obtain hidden target data and knowledge . This is the most basic content and goal of data-mining technology. This module is mainly composed of a set of fixed functional modules, whose purpose is to perform different types of analysis, including association analysis, characterization, and cluster classification.

(3) Evaluation of the model.

The model evaluation mainly evaluates the results of data mining. Multiple patterns may have been discovered in the previous step, and it is necessary to analyze and compare the user interest points of these standards, and then to evaluate the value of the extracted standards and analyze the reasons for their deficiencies. If the output method is very different from the user's interest, you need to return to the previous process to adjust the parameters and execute it again.

(4) Knowledge output.

In this module, the excavated target data is mainly explained, so as to provide it to the demander in a reasonable and commonly used form. Special data display and interpretation method are used here, which can visualize the result data obtained by mining and provide it to decision-makers for decision-making.

(5) Functional model of data mining system.

Although data mining methods are different, after collecting the application methods of different data mining models, we can develop data mining models by analyzing the needs of users. The development process is based on the summary and analysis of various user problem descriptions and then creates corresponding data models to complete the analysis process and user problem solving process. This process is usually divided into six steps: (1) collect user requirements and complete the definition of various problems; (2) prepare various problems and related basic materials; (3) view and analyze various

data; (4) develop different approaches to solve the problem; (5) validate these generated models to obtain the best model; (6) implement the model.

4.2. The Concept of Association Rules. Based on association rules, the association between item sets in large data sets can be obtained. This process occupies an important position in data mining technology and belongs to an important technical branch.

Unknown associations between unknown relationships and attributes of target objects in the database can be obtained through the study of association rules, and they are hidden in advance, which means that they cannot be obtained through logical database operations (such as table joins) or statistical methods. The inherent attributes of data itself (such as functional dependency) are realized through the symbiotic characteristics between data. Decision making behavior can be assisted by the processing of association rules to facilitate scheme design, website design, business processing, market operation, and decision processing.

In the current era, the use of association rule processing can optimize decision-making, which has attracted the attention of researchers and research institutions in various fields, including big data, artificial intelligence, statistics, and visualization. Through relevant research, relatively fruitful results have been obtained. Because of its easy understanding and simple structure, visualization rules are widely used and become a research hotspot in the field of data mining in recent years, which can effectively analyze the relationship between data.

The confidence level of an association rule is defined as follows:

$$\text{Conf}(\mathbf{R}) = \frac{\text{Sup}(X \cup Y)}{\text{Sup}(X)}. \tag{28}$$

The basic model of association rule mining is shown in Figure 4:

When building the model, the association rule mining algorithm has the following two steps: the first step is to determine all constant datasets in set D according to the minimum support criterion; the second step is to create all association rules based on the constant dataset and minimum confidence threshold.

4.3. Association Rule Algorithm Design. In the process of putting the association rule algorithm into practice, however, since signal level, signal-to-noise ratio, and block error rate are continuous signals, they must be discretized, and the following rules exist for their ternary relationship. The constants set are signal level, signal-to-noise ratio, and block error rate.

As shown in Figure 5, first extract the interference data from the test data, then discretize the data according to the data interval and set the analysis topics of signal level, signal-to-noise ratio and block error rate, realize the analysis algorithm, and obtain the confidence table. Set the appropriate confidence level to obtain the participation relationships of

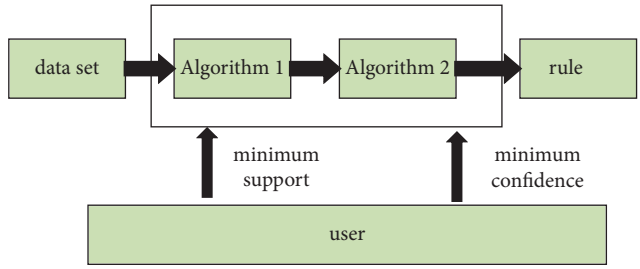

Figure 4: Basic model of association rule mining.

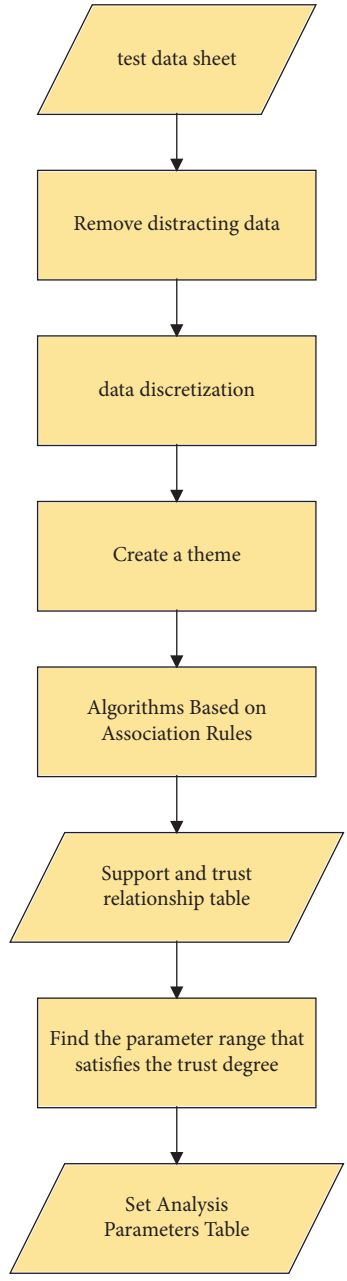

Figure 5: Schematic diagram of association rule module.

signal level, signal-to-noise ratio and block error rate. Relational table values are stored in the database.

4.4. Data Mining Model Construction. Probabilistic knowledge can be used to express the ratio of the support (s) of the association rule X⇒Y to the ratio of tuples with X∪Y in the database, expressed in probability theory as follows:

$$s(X \Rightarrow Y) = \Pr(X \cup Y). \tag{29}$$

The confidence or concentration (α) of an association rule X⇒Y is the ratio of the number of tuples with X∪Y to the number of tuples with X in the database, expressed in probability theory as follows:

$$\alpha(X \Rightarrow Y) = \Pr(Y \mid X). \tag{30}$$

In addition to the two features described above, a third feature can be used to characterize the correlation (σ) between X and Y, which is defined as follows:

$$\sigma_{X,Y} = \frac{\Pr(X \cup Y)}{\Pr(X)P(Y)}. \tag{31}$$

According to probability theory, if $\Pr(X \cup Y) = \Pr(X)\Pr(Y)$ holds, it means that pattern X occurs independently of pattern Y. Therefore, if the correlation is greater than 1, it proves that modes X and Y are positively correlated.

Based on the above three characteristics, the following rules can be defined,

An X⇒Y association rule is said to be valid if the following three conditions are met:

$$\begin{aligned} s(X \Rightarrow Y) &\geq s_{\min}, \\ \alpha(X \Rightarrow Y) &\geq \alpha_{\min}, \\ \sigma_{X,Y} &\geq \sigma_{\min}. \end{aligned} \tag{32}$$

Here, $s_{\min}$, $_{\min}$a>0,$\sigma_{\min}$>1 are all custom data mining thresholds.

5. Implementation and Detection of Associated User Network Data Mining Algorithm

5.1. Sample Processing

5.1.1. Data Cleaning. Because the experimental data is relatively large and these data have some impurities, it may lead to deviations in future data analysis. Some data are not very complete, some even have noise, some have obvious deviations from the real data, and some data is repeated. So, the content of this section is to discuss how to perform data cleaning, smoothing, and denoising. Since the main body of the data is the user, data cleaning is also based on the user. The main principles are as follows:

(1) Delete user data with incomplete information. Such user registration information is incomplete and does not contain explicit personal information.

(2) Remove inactive users who have been inactive for a long time. Although such users may have complete information, they have been silent for a long time and are useless users.

(3) Remove vest users. A vest user is a situation where a user registers multiple IDs on the same website or forum. These vest accounts only serve the user's main account and have no other operations, so these account data will be deleted.

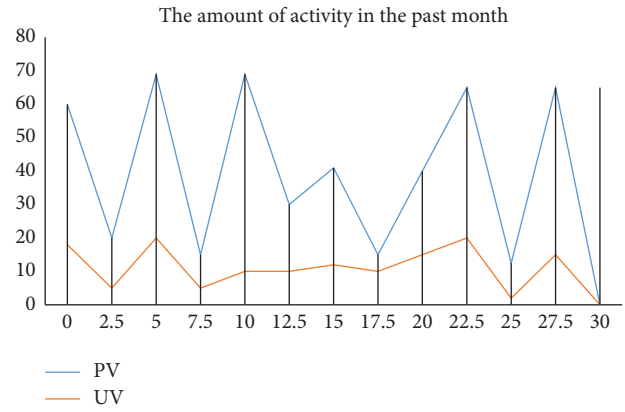

Figure 6: The K-line chart of users' visit data in the past month.

5.1.2. Data Sampling. Although the database size is reduced to 1/5 after the basic database is removed, the database analysis still lacks certain validity and operability because the entire database is still large and there are often hidden data points in the analysis process. Therefore, we use the principles of statistics and use the method of sampling analysis to conduct a sampling analysis of the data.

Advantages of sampling analysis: this is an important statistical research method that shows the relationship and related information of the entire parent group through random sampling of the parent group sample analysis. Its advantage is that it can accurately predict the characteristics of the parent group while reducing the workload, so it takes less time and requires less hardware, greatly improving work efficiency and increasing economic benefits.

Determination of data sampling method and sample size: in the sampling process, three sampling principles must be followed: the principle of validity, the principle of measurement, and the principle of identification and reproducibility; because real comprehensive analysis research must be guided by scientific accuracy. In this study on data sampling, we will choose the principle of stratified sampling. The stratified sampling method divides the population into several layers according to one or more attributes or characteristics, and then draws several samples from each layer and integrates the extracted subsamples into the total sample. Specific operation steps: first, stratify the samples according to specific characteristics or several attributes; second, determine the number of samples that should be drawn from each layer; and finally combine all the obtained samples into the overall sample.

As shown in Figure 6, after statistical analysis, the K-line chart of the user's access data in the last month is obtained. The specific distribution is shown in Figure 6.

Table 1: Test dataset features.

Dataset	Number of transactions	Number of items	Average transaction length
Date 1	3325	65	42
Date 2	8735	116	28

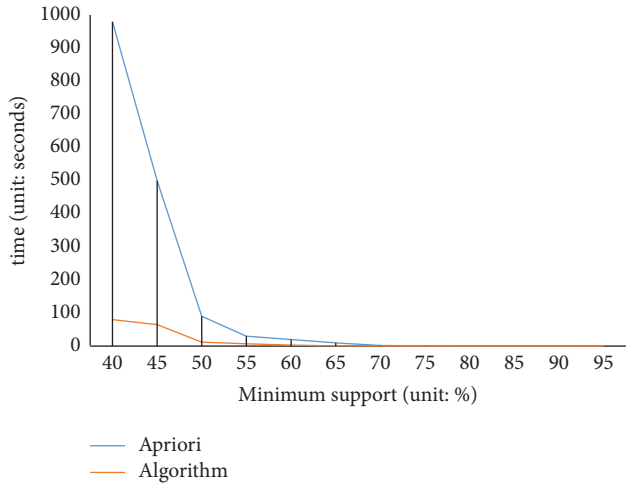

Figure 7: Date1 dataset experiment.

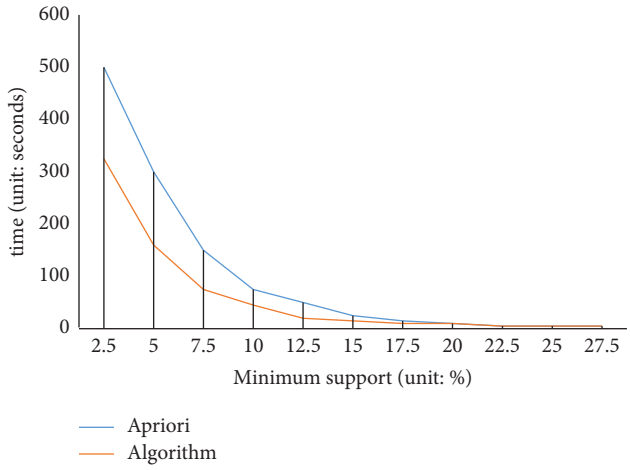

Figure 8: Date2 dataset experiment.

Table 1 lists the eigenvalues of the test dataset.

5.2. Setting up the Experimental Environment. Hardware experimental environment: the hardware requirements of this system are general, and only a few common dual-core machines are needed. Select a computer with better performance as a data mining server to analyze the behavior of network users. Other computers are used by users, and users can generate test access data, access web pages on the network through this data, and store them in the system.

5.3. Experiment Design and Result Analysis. The experimental results of the algorithm running on Date1 and Date2 are shown in Figures 7 and 8.

It can be seen from Figure 8 that the algorithm is better than Apriori in performance, especially in the case of low support.

Experiments show that the algorithm designed in this paper is better than Apriori in terms of time efficiency and has better performance when the minimum support is small.

6. Conclusion

Today, with the rapid development of emerging technologies and society, data mining technology has been fully applied and researched, and it is an emerging branch based on this technology to associate it with multi-information fusion. It contains knowledge in multiple fields and can effectively discover hidden target data and analyze the relationships contained in it. By using the related technologies of extracting network data from associated users, it can better discover valuable information from big data for users, which is a topic worthy of further study. This paper comprehensively analyzes the multi-information fusion algorithm, association rule algorithm, and other related data mining algorithms and then establishes the algorithm as the core algorithm of the user behavior data mining system. Its advantages can better solve related problems. At the same time, because the association rule extraction algorithm is an undirected algorithm, even if the data is preprocessed, some unreasonable rules will be generated. Therefore, effective rules need to be formulated at the same time, so the algorithm still has room for improvement.

Data Availability

The data used to support the findings of this study are available from the corresponding author upon request.

Conflicts of Interest

The authors declare that there are no conflicts of interest.

Acknowledgments

The study was supported by the Jiangsu University philosophy and social science research project "Research on the practice of identifying and tracking epidemic related personnel based on epidemic prediction model"(Grant no.2020SJA0592) and by the Fundamental Research Funds for the Central Universities "Research on named entity depth recognition based on Neural Network"(Grant no. LGYB201703).

References

[1] E. Ahmed, I. Yaqoob, I. A. T. Hashem et al., "The role of big data analytics in Internet of Things," *Computer Networks*, vol. 129, pp. 459–471, 2017.

[2] Y. Sun, H. Song, A. J. Jara, and R. Bie, "Internet of things and big data analytics for smart and connected communities," *IEEE Access*, vol. 4, pp. 766–773, 2016.

[3] A. Sestino, M. I. Prete, L. Piper, and G. Guido, "Internet of Things and Big Data as enablers for business digitalization strategies," *Technovation*, vol. 98, Article ID 102173, 2020.

[4] C. Zhang, "Classification rule mining algorithm combining intuitionistic fuzzy rough sets and genetic algorithm," *International Journal of Fuzzy Systems*, vol. 22, no. 5, pp. 1694–1715, 2020.

[5] M. Atzmueller, "Data mining on social interaction networks," *Journal of Data Mining & Digital Humanities*, 2014.

[6] X. Zhou and T. Peng, "Application of multi-sensor fuzzy information fusion algorithm in industrial safety monitoring system," *Safety Science*, vol. 122, Article ID 104531, 2020.

[7] S. Chen, L. Huang, J. Bai, H. Jiang, and L. Chang, *Multi-sensor Information Fusion Algorithm with central Level Architecture for Intelligent Vehicle Environmental Perception System*, SAE Technical Paper, Beijing China, 2016.

[8] Z. Zhenxing Li, X. Xianggen Yin, Z. Zhe Zhang, and Z. Zhiqin He, "Wide-area protection fault identification algorithm based on multi-information fusion," *IEEE Transactions on Power Delivery*, vol. 28, no. 3, pp. 1348–1355, 2013.

[9] E. Varol Altay and B. Alatas, "Performance analysis of multi-objective artificial intelligence optimization algorithms in numerical association rule mining," *Journal of Ambient Intelligence and Humanized Computing*, vol. 11, no. 8, pp. 3449–3469, 2020.

[10] M. Li, H. Chen, X. Shi, S. Liu, M. Zhang, and S. Lu, "A multi-information fusion "triple variables with iteration" inertia weight PSO algorithm and its application," *Applied Soft Computing*, vol. 84, Article ID 105677, 2019.

[11] M. Zhou, Y. Li, M. J. Tahir, X. Geng, Y. Wang, and W. He, "Integrated statistical test of signal distributions and access point contributions for Wi-Fi indoor localization," *IEEE Transactions on Vehicular Technology*, vol. 70, no. 5, pp. 5057–5070, 2021.

[12] A. Noore, R. Singh, and M. Vatsa, "Robust memory-efficient data level information fusion of multi-modal biometric images," *Information Fusion*, vol. 8, no. 4, pp. 337–346, 2007.

[13] G. Liu and H. Yang, "Self-organizing network for variable clustering," *Annals of Operations Research*, vol. 263, no. 1-2, pp. 119–140, 2018.

[14] A. Bhattacharya, R. T. Goswami, and K. Mukherjee, "A feature selection technique based on rough set and improvised pso algorithm (psors-fs) for permission based detection of android malwares," *International journal of machine learning and cybernetics*, vol. 10, no. 7, pp. 1893–1907, 2019.

[15] T. L. Lai, "Sequential analysis: some classical problems and new challenges," *Statistica Sinica*, vol. 7, pp. 303–351, 2001.

[16] O. Lindwall, G. Lymer, and C. Greiffenhagen, "The sequential analysis of instruction," *The Handbook of Classroom Discourse and Interaction*, vol. 23, pp. 142–157, 2015.

[17] E. V. Altay and B. Alatas, "Chaos numbers based a new representation scheme for evolutionary computation: applications in evolutionary association rule mining," *Concurrency and Computation: Practice and Experience*, vol. 34, no. 5, Article ID e6744, 2022.

[18] R. Bakeman and J. R. Brownlee, "The strategic use of parallel play: a sequential analysis," *Child Development*, vol. 51, no. 3, pp. 873–878, 1980.

[19] E. V. Altay and B. Alatas, "Differential evolution and sine cosine algorithm based novel hybrid multi-objective approaches for numerical association rule mining," *Information Sciences*, vol. 554, pp. 198–221, 2021.

[20] A. Farouk, A. Alahmadi, S. Ghose, and A. Mashatan, "Blockchain platform for industrial healthcare: vision and future opportunities," *Computer Communications*, vol. 154, pp. 223–235, 2020.

[21] B. S. Maitner, B. Boyle, N. Casler, R. Condit, J. Donoghue, and S. M. Durán, "The bien r package: a tool to access the Botanical Information and Ecology Network (BIEN) database," *Methods in Ecology and Evolution*, vol. 9, no. 2, pp. 373–379, 2018.

Hindawi
Mobile Information Systems
Volume 2022, Article ID 3725657, 13 pages
https://doi.org/10.1155/2022/3725657

Research Article

Towards SLA-Driven Autoscaling of Cloud Distributed Services for Mobile Communications

Carlos Miguel,[1] **Víctor Rampérez**,[1] **Javier Soriano**,[1] **and Shadi Aljawarneh**[2]

[1]*Department of Computer Languages and Systems and Software Engineering, Universidad Politecnica de Madrid (UPM), Madrid, Spain*
[2]*Department of Software Engineering, Jordan University of Science and Technology (JUST), Irbid, Jordan*

Correspondence should be addressed to Carlos Miguel; carlos.miguel.alonso@alumnos.upm.es

Received 21 June 2022; Revised 14 September 2022; Accepted 19 September 2022; Published 3 October 2022

Academic Editor: Claudio Agostino Ardagna

In recent years cloud computing has established itself as the computing paradigm that supports most distributed systems, which are essential in mobile communications, such as publish-subscribe (pub/sub) systems or complex event processing (CEP). The cornerstone of cloud computing is elasticity, and today's autoscaling systems leverage that property by making scaling decisions based on estimates of future workload to satisfy service level agreements (SLAs). However, these autoscaling systems are not generic enough, as the workload definition is application-based. On the other hand, the workload prediction needs to be mapped in terms of SLA parameters, which introduces a double prediction problem. This work presents an empirical study on the relationship between different types of workloads in the literature and their relationship in terms of SLA parameters in the context of mobile communications. In addition, more than 30 prediction models have been trained using different techniques (time series analysis, regression, random forests) to test which ones offer better prediction results of the SLA parameters based on the type of workload and the prediction horizon. Finally, a series of conclusions on the predictive models to be used as a first step towards an autonomous decision system are presented.

1. Introduction

In recent years, cloud computing has become an essential technology in our daily lives due to the constant connection we maintain with the Internet through mobile systems and the elastic capabilities of this computing technique. These capabilities allow users to use and pay for the resources needed by acquiring and releasing them on-demand (pay-per-use or pay-as-you-go model), decreasing the cost of using this infrastructure [1]. Despite these model benefits, the service level agreements (SLAs), an agreement between the cloud customer and the cloud service provider, composed of service level objectives (SLOs) (we will use "SLA parameters" in the rest of this document), that meeting certain application performance levels [2, 3] must. The service must find the point at which the applications/services use the minimum amount of resources to fulfil the established obligations, which, in turn, minimizes both cost and energy consumption [4, 5]. This leads to a double-edged problem since both under- and over-provisioning (either does not have enough resources to process all tasks/requests on time, which is essential for mobile communications, or it has more resources than required to process the current load, respectively) could lead to saturation of the system or waste of resources, respectively [1, 6]. Both of these situations lead to the system operating outside the agreed SLA parameters, which constitutes an SLA violation.

Predictive autoscaling systems can use one or more variables to predict the system behavior and use this prediction to decide if it needs more resources, is using too many, or requires no changes in resource allocation. This decision triggers the appropriate scaling action.

In the literature, the workload itself is used to predict the system behavior by identifying different parameters (e.g., its trend to check how much the load is changing) and using them to predict the system load in the immediate future.

Despite this, the system could use other variables to predict its behavior, e.g., its level of saturation (e.g., CPU and RAM consumption) or its current performance and efficiency (e.g., the mean response time of the events received), resulting in a prediction based on results that might reflect the system status more accurately.

One of the major problems of using the workload as the predictor is the need for a precise definition due to the ambiguity of the term itself [7]. The definition of workload varies between systems, and so do its contents and structure. The workload of a publish/subscribe (pub/sub) system (e.g., a sensors system [8], a messaging service, etc.) workload is composed of publications, subscriptions, and unsubscriptions; a batch application workload is composed of processing orders; and a complex event processing system (CEP) workload that contains different events to be processed (e.g., text messages, weather reports, monetary transactions). This problem has a direct impact on any predictive autoscaling system not tuned to the expected workload pattern, for example, a system adjusted to receive a periodic workload will underperform if it changes to an unpredictable workload. Creating a sufficiently generic predictive autoscaling system capable of using any workload on any cloud service is a very complex task [9] due to the limited capabilities of this type of system caused by this ambiguity.

Furthermore, workload prediction might not produce direct information about the possibility of an SLA violation of the predicted workload, which is essential for the decision-making process of triggering a scaling action and the number of resources this action will manage. Also, this prediction might not reflect the number of resources used by the system, which does not provide a snapshot of its performance based on its SLA parameters (high-level metrics).

The autoscaling system will benefit from having additional information related to the SLA parameters (i.e., throughput and response time) to decide about said scaling action.

To get this extra information the autoscaling system must predict its SLA parameters to check if any will not be met with the forecasted workload it will receive, which creates a "double-prediction" problem (predicting the workload and SLA violations) that could lead to problems, mainly related to the dependence of the SLA prediction on the workload prediction. For example, the decision made by the SLA prediction might be incorrect due to an incorrect workload prediction, triggering a scaling action that might waste resources or produce an SLA violation since an imprecise workload prediction might lead to an unreliable prediction of the SLA parameters.

A solution to these problems might be a system that manages this "double-prediction" which might make it less efficient than a system that does not use the workload as the predictor and hence, does not have these problems. Furthermore, the complexity of implementing a system that treats these problems might be an obstacle to its development in comparison with a generic autoscaling system that does not have them.

To summarise, the main disadvantages of workload prediction-based predictive autoscaling systems are the following:

> Problem 1: the definition of workload is strongly coupled to the type of system (a workload is not defined in the same way for a pub/sub system as for a batch processing system), therefore, autoscaling systems that rely on workload prediction suffer from this same limitation, and therefore cannot be generic as they are system-dependent.
>
> Problem 2: autoscaling systems based on workload prediction need to map these workload predictions to the SLA parameters, which is not trivial and generates a double prediction problem in many cases.

To solve these limitations, we propose an autoscaling strategy to predict SLA parameters (e.g., throughput and response time), avoiding the "double-prediction" problem and making the system sufficiently generic to handle any workload on any cloud platform. This approach will use the most accurate prediction model for the three main workload patterns to forecast the system SLA parameters and produce a well-informed answer that will trigger any required scaling action. We have used 30 trained prediction models to measure their accuracy with each workload type and choose the most accurate one for further research.

This approach results in the following hypothesis:

Hypothesis: the accuracy of predictive autoscaling systems can be improved by choosing the appropriate prediction model to forecast the most relevant SLA parameters.

Due to the great relevance of event-driven architectures in current technologies, solving these problems is this research next natural step, to reduce the aforementioned cost while increasing the quality of service for end-users. In order to achieve this, this paper aims to empirically prove these limitations and find a prediction model that fits the requirements of the proposed autoscaling strategy which allows the further development of this autoscaling system.

We have conducted several experiments to gather information and empirically prove this information and its effects on the system related to its performance metrics and behavior to prove this hypothesis. (i) a study on the effects of different workload patterns (i.e., growing, periodic, unpredictable) have on different systems in terms of SLA parameters and SLA violations; (ii) an experiment to empirically prove the behavior and effects (i.e., changes in its performance metrics, saturation point) of different workload patterns on different systems, to solve the first problem previously mentioned; (iii) an empirical evaluation of the results of predicting the system SLA parameters using different predictive models and workload patterns on a cloud platform to find the best predictive model for each case.

Based on the results obtained from these experiments and evaluations, we elaborate a conclusion on which model is the best predictive model depending on some system parameters, such as environment, configuration, and workload pattern.

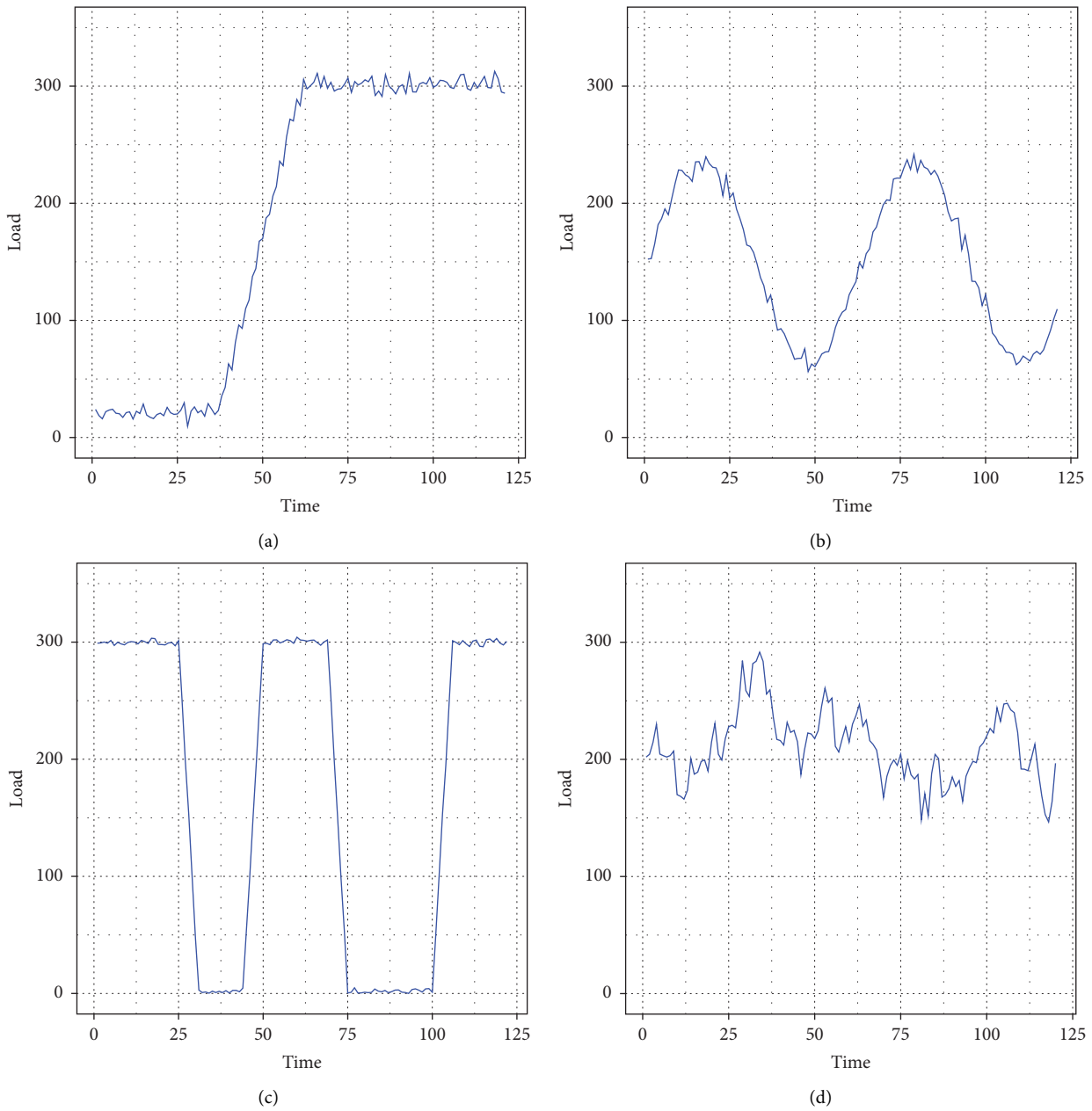

Figure 1: Workload patterns, left to right: growing, on-and-off, periodic, static, unpredictable.

The main contributions of this work are as follows.

(i) An empirical study on the relationship between different types of workloads in the literature and their relationship in terms of SLA parameters in the context of mobile communications.

(ii) An empirical study composed of more than 30 prediction models has been trained using different techniques (time series analysis, regression, random forests, etc.) to test which ones offer better prediction results of the SLA parameters based on the type of workload and the prediction horizon.

(iii) A set of conclusions on the predictive models to be used as the first step toward an autonomous autoscaling decision system is presented.

The remainder of this paper is organised as follows: Section 2 background and related work, introduces essential information about workloads and predictive autoscaling systems; Section 3 SLA parameters prediction approach, explains the relevant concepts of SLA parameters, our approach to predicting them and the experiments we have used to prove out hypothesis; Section 4 introduces the experiment environment and its results with a brief analysis of them;

Section 5 conclusions, presents the knowledge obtained from these experiments and the overview of this work; and Section 6 future work, explains what is ahead of this project and what are our next steps on this subject.

2. Background and Related Work

This section briefly introduces the essential concepts and related work used in this paper. Section 2.1 workload presents an overview of the concepts of workload and its different patterns present in the literature. Section 2.2 autoscaling systems introduces and explains the main principles of these systems and the types there are. Section 2.3 predictive autoscaling approaches presents the different autoscaling techniques and brief analysis of the available predictive models.

2.1. Workload. A generic yet inaccurate definition of the term workload is a series of events sent to a system of some sort that processes them or does something with them. Each type of system has a specific and well-defined workload which can be defined with great precision. According to [6, 7, 10], there are five major workload patterns in cloud computing environments.

(i) Growing workload is characterised by a rapid and constant load increase (Figure 1(a)).

(ii) Periodic workload is characterised by changes in the load spaced at regular time intervals (Figure 1(b)).

(iii) Unpredictable workload represents the load that cloud service will face once deployed, with constant fluctuations without a recognizable pattern or seasonal changes (Figure 1(d)).

(iv) Static workload is characterised by a load with no (or very small) changes or fluctuations (i.e., constant number of events).

(v) On-and-off workload represents a load with regular or occasional intervals without load (i.e., no user is interacting with the cloud service) (Figure 1(c)).

In this paper, we focus on growing, periodic, and unpredictable workloads, since they represent environments in which an autoscaling action might be required. Both static and on-and-off (batch application) workloads fall outside the scope of our work since applications with this type of workload do not require any autoscaling actions.

2.2. Autoscaling Systems. Autoscaling systems take advantage of cloud computing's key feature, elasticity, to automatically balance the resource allocation, complying with the SLA obligations by adapting the system resources to the demand at all times. The SLA parameters are the cornerstone of autoscaling systems since they are the reason these systems are necessary in the first place. In previous works [11], the authors used the system's high-level metrics (SLA parameters) together with its low-level metrics to build a model that maps these two metrics, which makes predictions and eventually generates a scaling decision. In [12], the authors use response time and throughput to make a more robust decision about the scaling actions.

According to [13], there are three main autoscaling systems based on the technique used to perform the scaling actions: reactive, proactive, and predictive. Reactive autoscaling systems are the most popular ones used on cloud computing and scale in/out according to the current system performance. Despite this, when they detect an SLA violation is occurring (or is about to occur), it might be too late for a scale action to avoid this SLA violation since his action takes some time, and during that time, the violation is well-underway [6, 10]. Proactive autoscaling systems allow the user to pre-define a scaling system schedule, which could solve some SLA violations but requires a predictable environment. That is not the case with predictive autoscaling systems that solve this problem by predicting its behavior and adjusting its resources to comply with SLA obligations [14].

2.3. Predictive Autoscaling Approaches. A predictive autoscaling system predicts future system behavior to adjust the application resources allocated in advance of changes in the environment (i.e., an increase in the workload) to meet its SLA obligations and minimise the hosting cost of the cloud application.

As shown in Figure 2, a predictive autoscaling system is composed of monitor, predictor, and decision maker components, which measure the chosen variable, such as the workload, predicts future values of it, and makes decisions based on the predicted values, respectively [14].

Autoscaling systems use different resource allocation techniques to manage the computing resources assigned to the system based on the decisions made by the decision maker component.

Resource allocation techniques can be classified into horizontal scaling (that is, adding new operator instances) and vertical scaling (that is, increasing the resources assigned to an already running system instance, such as memory or CPU). According to [10], since most of the cloud service providers do not support changing the resources allocated to an already running instance without rebooting it and the operating systems (OS) do not support this action, the most used resource allocation technique (and the one we will focus on) is horizontal scaling.

Lorido-Botran et al. [10] state that classifying this technique is also a difficult task due to the wide diversity of approaches found in the literature and because some techniques are a combination of two or more methods. The main techniques are (i) static threshold-based policies, (ii) reinforcement learning, (iii) queuing theory, (iv) control theory, (v) time-series analysis.

The static threshold-based policies are based on a set of rules, usually two, one for scaling out and one for scaling in, that use one or more performance metrics, involving several user-defined parameters: an upper and lower threshold, thUp and thDown, respectively, and two time-values, vUp and vDown, which denote the time interval in which the

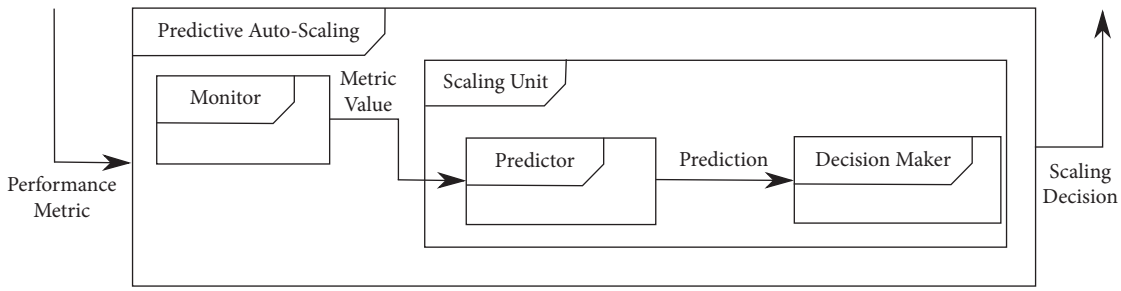

Figure 2: Architectural overview of a predictive autoscaling system. Extracted from [14].

condition must be met to trigger a scaling action. The user must define a fixed amount of resources (i.e., VMs or operators) to be allocated or deallocated once the corresponding scaling action is triggered. If a scaling action is performed, another will not be triggered for tUp/tDown seconds, respectively.

To perform a scale in action and allocate s resources, the performance metric must be greater than thUp for vUp seconds. Another scale-in action will not be triggered for tUp seconds, as shown in equation.

$$\begin{aligned} &\text{if } s > th \text{ Up for } v \text{ Up then} \\ &\qquad \text{allocates} \\ &\qquad \text{wait } t\text{Up} \end{aligned} \tag{1}$$

On the other hand, to perform a scale-out action to relocate s resources, the performance metric must be less than *thDown* for *vDown* seconds. If triggered, another next scale-out action will not occur for *tDown* seconds, as shown in equation.

$$\begin{aligned} &\text{if } s < th\text{Down for } v \text{ Down then} \\ &\qquad \text{de allocate s} \\ &\qquad \text{wait } t\text{Down} \end{aligned} \tag{2}$$

For example, the autoscaling system will allocate 2 new instances if the CPU and RAM consumption of it is above 75% for more than 2 minutes.

Reinforcement learning techniques are based on learning through interaction between an agent, in this case, the autoscaler, and its environment, to automate the goal-directed learning and decision-making process. *Queuing theory* uses the mathematical study of queues to estimate the main system performance metrics, i.e., the response time or the average waiting time for requests. *Control theory* techniques aim to automate the management of systems such as data centres or storage systems to reduce the need for human input. These control systems are mainly reactive, but there are also some proactive approaches. *Time-series analysis* is mainly used to find a (repeating) pattern in the input or to forecast future values. This input (the time-series) is a sequence of values measured at sequential and evenly spaced time instants.

In [7], Masdari and Khoshnevis performed an in-depth analysis of the cloud computing workload prediction methods used in the literature, showcasing mathematical, data mining, and machine learning methods. Despite using different algorithms and techniques, these methods face the problems showcased in this work, such as detailed knowledge of the system to predict system variables (e.g., CPU, memory, and disk) using workload prediction. Furthermore, historical data are required to train models, and some methods take long periods to train and tune to the specific environment the system will face (e.g., twin support vector machine for regression (TSVR) [15]).

In [16], Nikravesh et al. proposed a new self-adaptive prediction technique focused on improving the accuracy of predictive autoscaling systems by choosing the appropriate prediction algorithm according to the incoming workload pattern. To this end, the workload pattern is identified by decomposing it into its *seasonal*, *trend*, and *remainder* components, using the LOESS [17] *R* package. Each workload pattern marks the usage of a different algorithm to predict its respective time series. To perform this prediction, the authors have used three different artificial neural network (ANN) algorithms; multilayer perceptron (MLP), multilayer perceptron with weight decay (MLPWD), and support vector machine (SVM). The system will identify the pattern of the received workload and automatically chooses the most accurate model to perform the workload prediction. The test metrics show that using the appropriate prediction algorithm for the incoming workload improved the prediction accuracy of the autoscaling system. Despite dealing with some problems mentioned previously, this solution still uses the workload as the predictor.

Predicting SLA violations is another method found in the literature that avoids the problems inherited by using the workload as the predictor. In [18], Leitner et al. proposed a predictive system that monitors and predicts SLA violations through machine learning and prevents them by triggering scaling actions when needed, called prevent. Through the regression used on the monitored data, the system can generate values that can be used to trigger the appropriate scaling action. These values are adjusted with *mean prediction error* (arithmetic average of the differences between predicted and monitored values for a given number of instances) and *prediction error standard deviation* (variability of the prediction error). Low predictive precision is expected until the system has enough data to make the necessary corrections. Despite this, the results of the experiments show that between 12% and 40% SLA violations could not be prevented, depending on the method and strategy used.

Table 1: Comparison of related works key characteristics.

References	Prediction algorithm	Technique	Performance Metric	Advantages	Disadvantages
[16]	Workload prediction	MLP, MLPWD, SVM	MAE, RMSE, PRED, R2PA	Uses best prediction algorithm automatically	Uses the workload as predictor
[18]	SLA violation prediction	Regression and MPE	Number of violations	Reduced impact of SLA violations	Low violation prevention rate (78% maximum)
[12]	Predict resource demand	SVM, NN, LR	MAPE, RMSE, PRED	Resources need prediction without workload as predictor	Complex system with 11 input parameters
[19]	Resource usage prediction	Bayesian information	MAE, RMSE, MAPE	Prediction based on resource usage history	Only applied to CPU load
[21]	Workload clustering, resource usage prediction	*K*-means, Bayesian learning	Delay, cost, SLA-violation rate, energy consumption	Considers SLA cost on the decision-making process	The prediction only takes one performance metric (response time)
[22]	Resource usage prediction	Fuzzy C-means, gray wolf	Energy consumption, execution time and cost, SLA violation and failure rates	Does not use the workload as the predictor	Two-stage prediction algorithm (clustering and GWO)
[20]	Resource need prediction	MVA	*Unknown* ([20] does not give enough information about performance metrics and evaluation)	Does not use workload as predictor	The prediction only takes one performance metric (response time)

A more direct approach to dealing with an unpredictable environment is by predicting the SLA parameters, also found in the literature, giving clear answers if a scale action is required. In [12], Bakole and Ajila developed and evaluated cloud client prediction models using support vector machine (SVM), neural networks (NN), and linear regression (LR), using 11 input parameters to predict CPU utilisation, response time and throughput of the system. For CPU utilisation and throughput, SVM shows the best results, and for response time, LR is the best prediction model. The resulting system can manage and predict the three key parameters correctly but results in a complex system that handles and monitors 11 input parameters, making it difficult to integrate them into a real system. In [19], Tofighy et al. proposed an ensemble CPU load prediction model that chooses the best prediction model using a Bayesian information criterion based on the resource usage history which, with the proposed framework for cloud resource management, achieved greater prediction accuracy that similar algorithms. In [20], Kouki and Ledoux proposed an SLA-driven autoscaling model that uses response time, service abandon rate, and service financial cost, combined with the SLA requirements, workload, and infrastructure information to compute the required scale actions using mean value analysis to achieve the required system configuration to meet the SLA requirements and expected QoS.

In [21], Ghobaei-Arani proposed a workload clustering-based resource provisioning mechanism that uses biogeography optimization with *K*-means clustering to classify the workload according to the system quality of service requirements. Additionally, the system uses a Bayesian learning technique to make the scaling decisions to fulfil the requirements. The test results show a reduced cost (due to using the SLA cost on the decision-making process), energy consumption, and SLA violations. Following a similar procedure, in [22], Ghobaei-Arani and Shahidinejad proposed a metaheuristic-based clustering mechanism used in combination with fuzzy *C*-means technique to find the clusters according to the quality-of-service requirements. These clusters are later used by a gray wolf optimizer to produce the appropriate scaling decision. The tests and simulations show that CPU utilisation efficiency, elasticity, and response time improved compared to other solutions.

To conclude this section, Table 1 contains a summary of the most relevant works mentioned previously comparing their key characteristics: (1) utilized prediction algorithm, (2) utilized technique, (3) performance metrics, (4) advantages of the model, and (5) disadvantages of the model.

3. SLA Parameters Prediction Approach

This section introduces the concepts related to SLA parameters and their prediction, along with a detailed overview of the empirical analysis that proves the statements about the SLA parameter-related effects of workload patterns on predictive autoscaling systems.

3.1. SLA Parameters. Sufficient prediction accuracy is necessary so the system SLA parameters (high-level metrics), for example, the response time and throughput, are within the constraints specified in the SLA throughout its execution. These values are agreed upon between the cloud customer and the cloud service provider and must be met to max the quality of service (QoS) offered to the end-users while minimising the cost of running the cloud application.

Following our experience from previous works [11], we have focused our efforts on the three most common high-level metrics, that are also the most relevant to our work; (i) response time, which is the time to process a message, which depends on the occupation of the system, since if the system

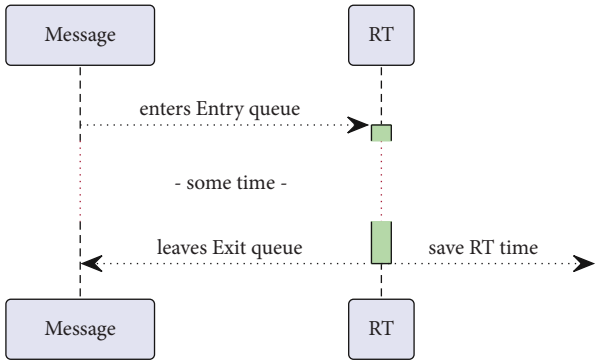

Figure 3: Measurement of response time.

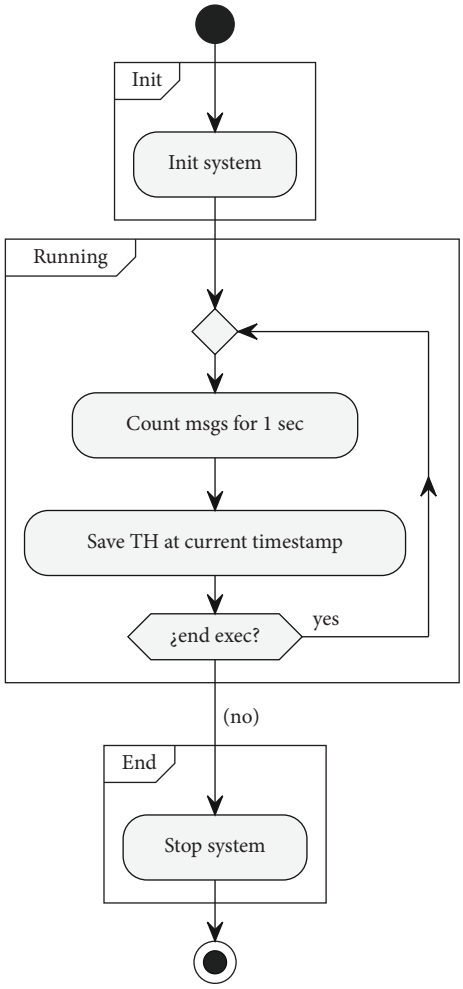

Figure 4: Measurement of throughput.

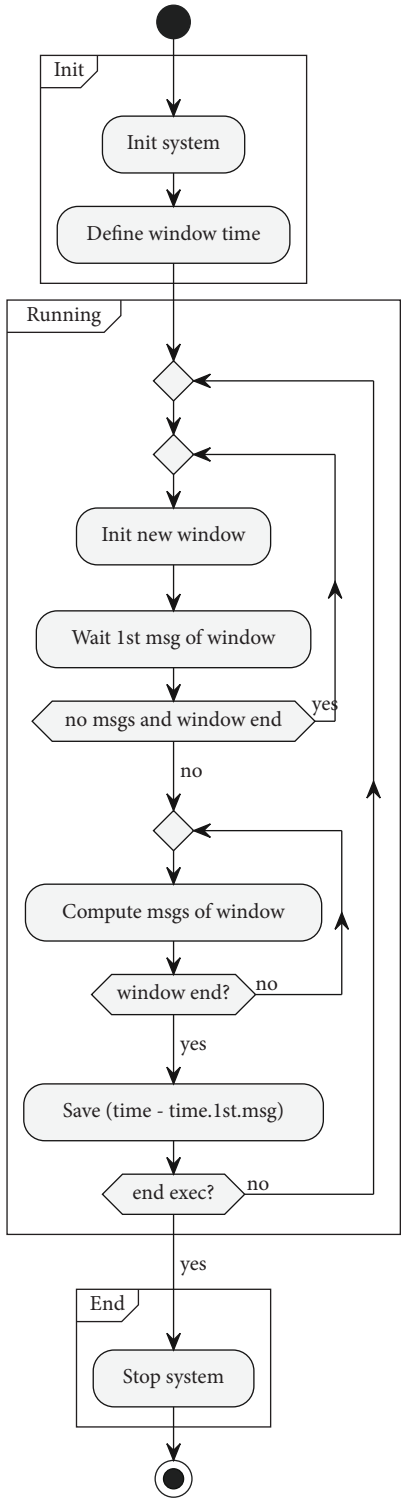

Figure 5: Measurement of window processing time.

is saturated, the response time will be higher because it has, in addition to the processing time (PT, the time required to process a single message), to wait for some time in the queue before being processed; (ii) throughput, the number of messages that the system can process per unit of time, also affected by system saturation, since a saturated system will output fewer messages per unit of time due to the higher processing time; and (iii) the window processing time (WPT), the time from the first message of the window to the moment the system closes the window and produces a result, over a defined window of time, which is also affected by system saturation.

Despite the diverse ecosystem of this type of system and its prediction methods and techniques, the type (pattern) of the workload it receives is also a key factor in its behavior since the same workload affects the SLA parameters of

different systems in various ways. If a system adjusted to a workload pattern receives a different one, it will behave erratically and may trigger out-of-the-ordinary scaling actions, which may cause SLA violations and affect the QoS of the end-users. Choosing a prediction algorithm that fits the expected workload pattern and produces the best results is imperative to obtain the best prediction accuracy, as proven in [7, 10, 16].

3.2. Prediction of SLA Parameters. As mentioned above, the method for predicting the SLA parameters of the system are different in each predictive autoscaling system [11, 12, 14], despite this, the use of a monitor component is essential to measure the chosen prediction parameter(s), which, in our case, are the window processing time (WPT) [23], the response time (RT), and the throughput (TH). Together, these measurements represent a high-fidelity snapshot of the system status.

Each measurement is implemented with a different technique since they occur and start at different times and places. We attach a sequence number to each message so that each measurement can be used by the prediction algorithm later: (i) the response time (RT) measurement starts once the message enters the entry queue and stops when it exits the exit queue (see Figure 3); (ii) the throughput (TH) is measured each second, counting the number of messages output since the last measurement (see Figure 4); and (iii) the window processing time (WPT) is measured every N seconds, N being the time defined for the window, processing the messages on each window (see Figure 5).

The prediction algorithm will use these measured values to estimate future values and cross this knowledge with previous knowledge of the system behaviour using machine learning (ML) and deep learning (DL) methods, through which the autoscaling system will decide on the necessity of a scaling action.

3.3. Empirical Analysis. To prove our hypothesis, we studied the relation of the workload pattern of a system with its SLA parameters using different workload patterns in a single system, and each workload pattern in different systems. Through this technique, we have collected data on the SLA parameters of the system throughout this test execution to compare their results and to prove that workloads affect both SLA parameters and low-level metrics.

Furthermore, we have also conducted an empirical analysis with various workload patterns and predictive models, using multiple ML and DL methods to predict the SLA parameters and compare the results of each model to find which predictive model suits each environment in terms of system SLA parameters and behaviour.

For these tests, we have used three of the previously mentioned workloads (growing, periodic, and unpredictable) since they represent situations the system might face in a real environment. Each pattern helps measure the changes of the SLA parameters being the unpredictable workload closer to a real environment due to the sudden changes in the load, testing the prediction models and their ability to keep the SLA parameters on the constraints defined by the SLA. Growing workloads stress the system to find its limits, whereas periodic workloads oscillate the system load to test if it can keep up with the constant changes.

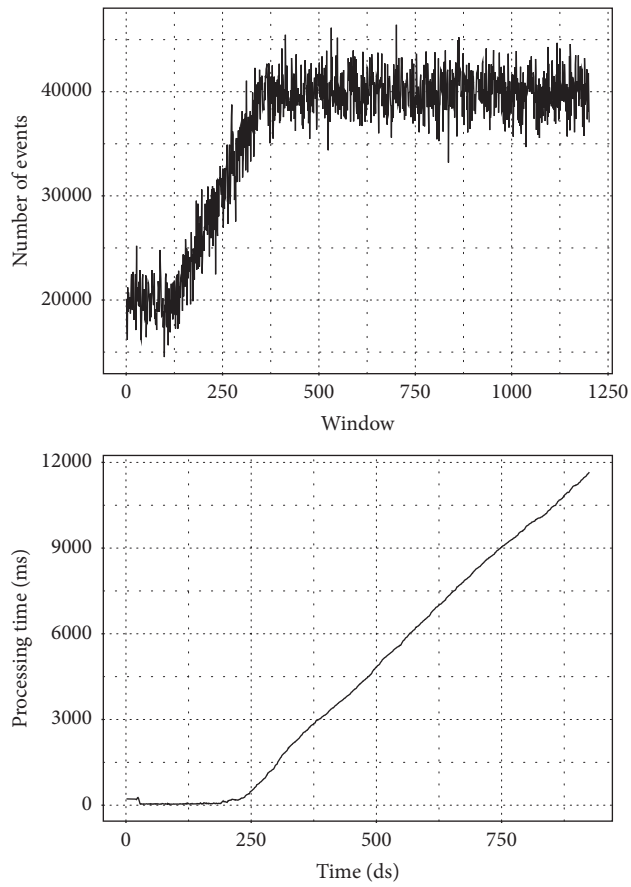

Figure 6: Growing workload and system WPT.

The study results (see Section 4.2) have been gathered by measuring the system throughput and response time in the same configuration while applying different workload patterns and comparing their effects on these values to prove that they do affect them. We have used an analogous technique to measure the results of a workload pattern on different systems.

For the empirical analysis, based on the positive results observed in some previous and similar works [6, 11, 14, 16], we used time series (e.g., roller forecasting origin, ARIMA, and STL + ETS models) and machine learning and deep learning methods (e.g., linear regression, linear congruential generators, random forest, and neural network models). To evaluate each method's root mean squared error (RMSE) and mean absolute error (MAE) metrics and prove which predictive model is the most accurate, we have performed a k-fold cross-validation (https://otexts.com/fpp2/accuracy.html) ($k = 10$) comparing the deviation of predicted values from the actual values. Once trained, these models should predict the SLA parameters with the highest possible prediction based on the model and training data.

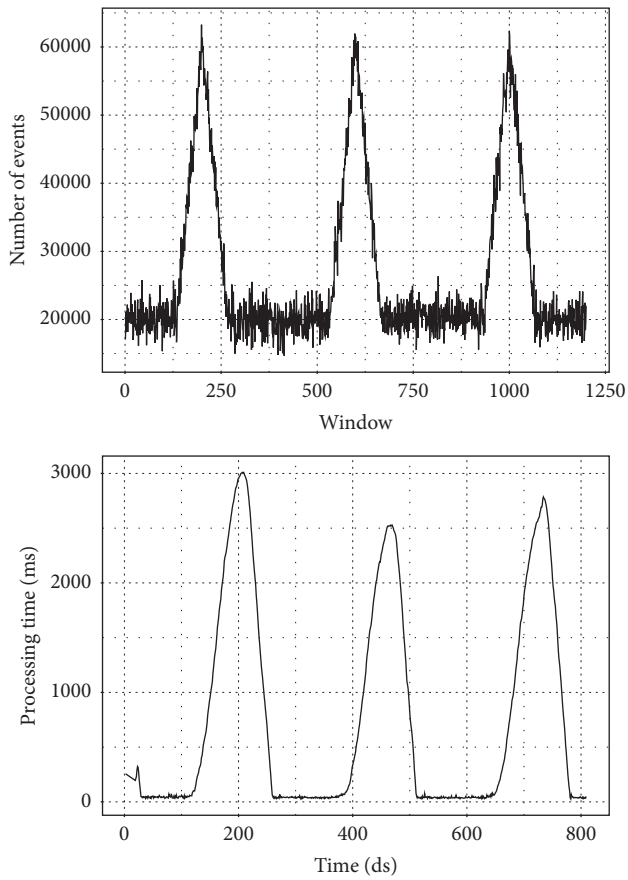

Figure 7: Periodic workload and system WPT.

Table 2: RMSE and MAE of prediction models with growing workload.

model	meanRMSE	meanMAE
Cubist	18.96	17.19
Gam	25.64	24.17
Bam	25.65	24.18
Qrf	61.41	56.99
gamLoess	65.96	64.74
parRF	67.97	63.96
Rf	67.98	63.97
Cforest	129.2	126.8
M5	134.2	131.5
M5Rules	134.2	131.5
svmRadialSigma	194.6	193.8
svmPoly	207.5	206.9
Nnet	292.4	291.3
svmRadialCost	313.1	305.2
svmRadial	317	309.1

A trade-off between training time and energy consumed is required to achieve the desired accuracy. The training phase may take more time than similar algorithms but reduces the energy consumed and time taken for each prediction while working in a live environment, which helps reduce the cost of running this system.

For each predictive model, we have used the SLA parameters measured from our system, running each of the chosen workload patterns, and applied these results to each predictive algorithm, measuring its RMSE and MAE and saving these measurements for later comparison and analysis.

Table 3: RMSE and MAE of prediction models with periodic workload.

model	meanRMSE	meanMAE
Cubist	32.42	28.46
Qrf	102.7	95.51
M5	104.8	97.69
M5Rules	105.4	98.23
parRF	114.3	107.7
Rf	114.3	107.7
svmRadialSigma	174.3	167.9
svmRadialCost	177	170.3
svmRadial	178	171.1
Gam	321.2	316.8
Bam	323.3	318.9
Cforest	369.1	365.3
gamLoess	648.1	644.1
Nnet	663.7	659.9
svmPoly	709.6	706.3

Table 4: RMSE and MAE of prediction models with unpredictable workload.

model	meanRMSE	meanMAE
Cubist	24.56	22.29
Qrf	27.09	24.47
parRF	29.1	26.59
Rf	29.11	26.6
M5	30.81	28.41
M5Rules	31.81	29.44
Bam	48.02	46.03
Gam	48.02	46.03
Cforest	81.52	79.77
svmRadialCost	88.72	84.74
svmRadial	90.79	86.79
svmRadialSigma	93.83	89.66
gamLoess	155	152.5
svmPoly	222.1	220.8
Nnet	233.2	231.8

4. Experimental Evaluation

This section presents information related to the experimental environment, relevant concepts, and the experiment results as well as their analysis.

4.1. Experimental Environment. The system we have used for the experiments, a complex event processing (CEP) distributed system, that calculates the topk using the MinTopK + N algorithm developed in [23] has been deployed using Apache Kafka and Zoopeker. For these experiments, we have used two T2 EC2 instances of Amazon Web Services cloud, each with 16 GB of RAM, 4 vCPUs running the 4.14 Amazon Linux kernel and Java OpenJDK 11.0.7 2020-04-14 LTS.

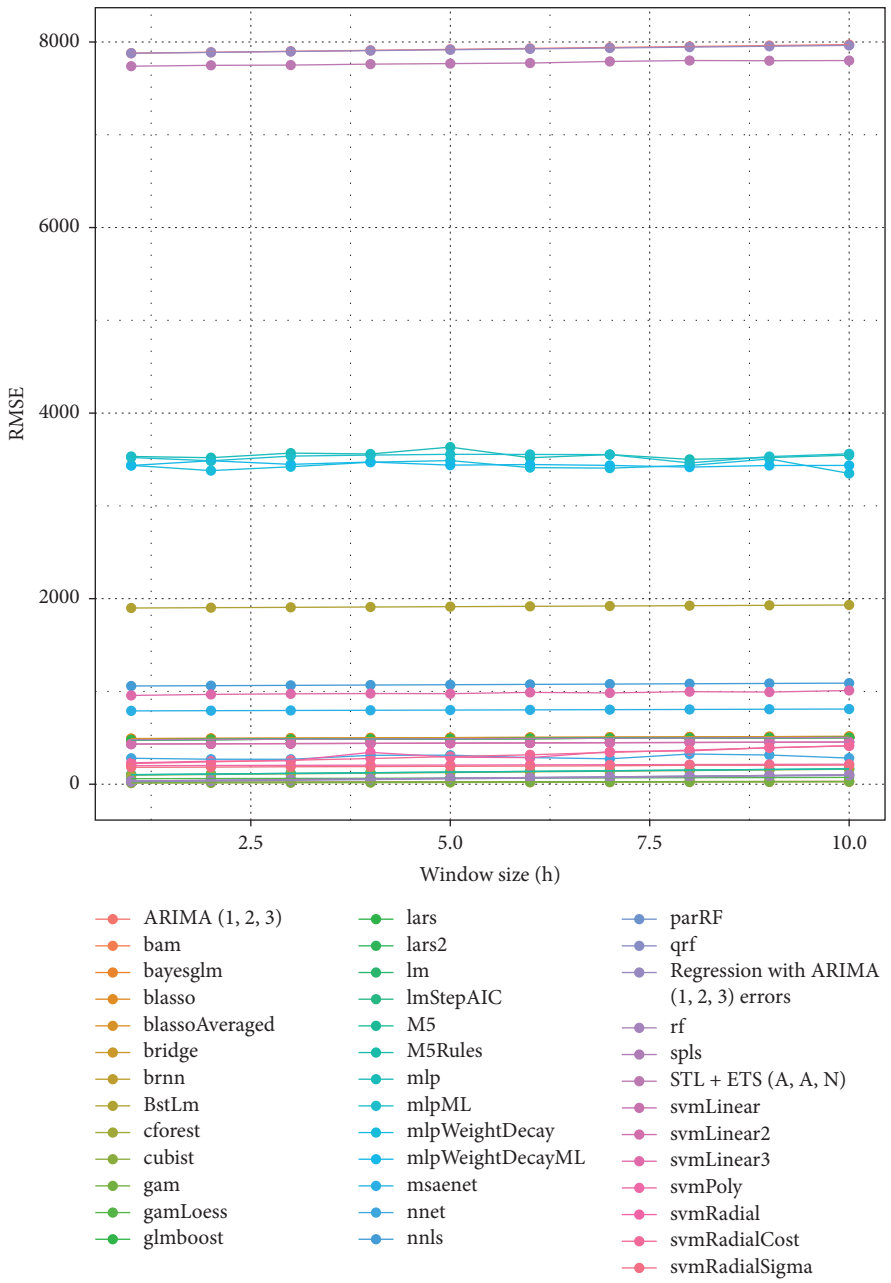

(a)

Figure 8: Continued.

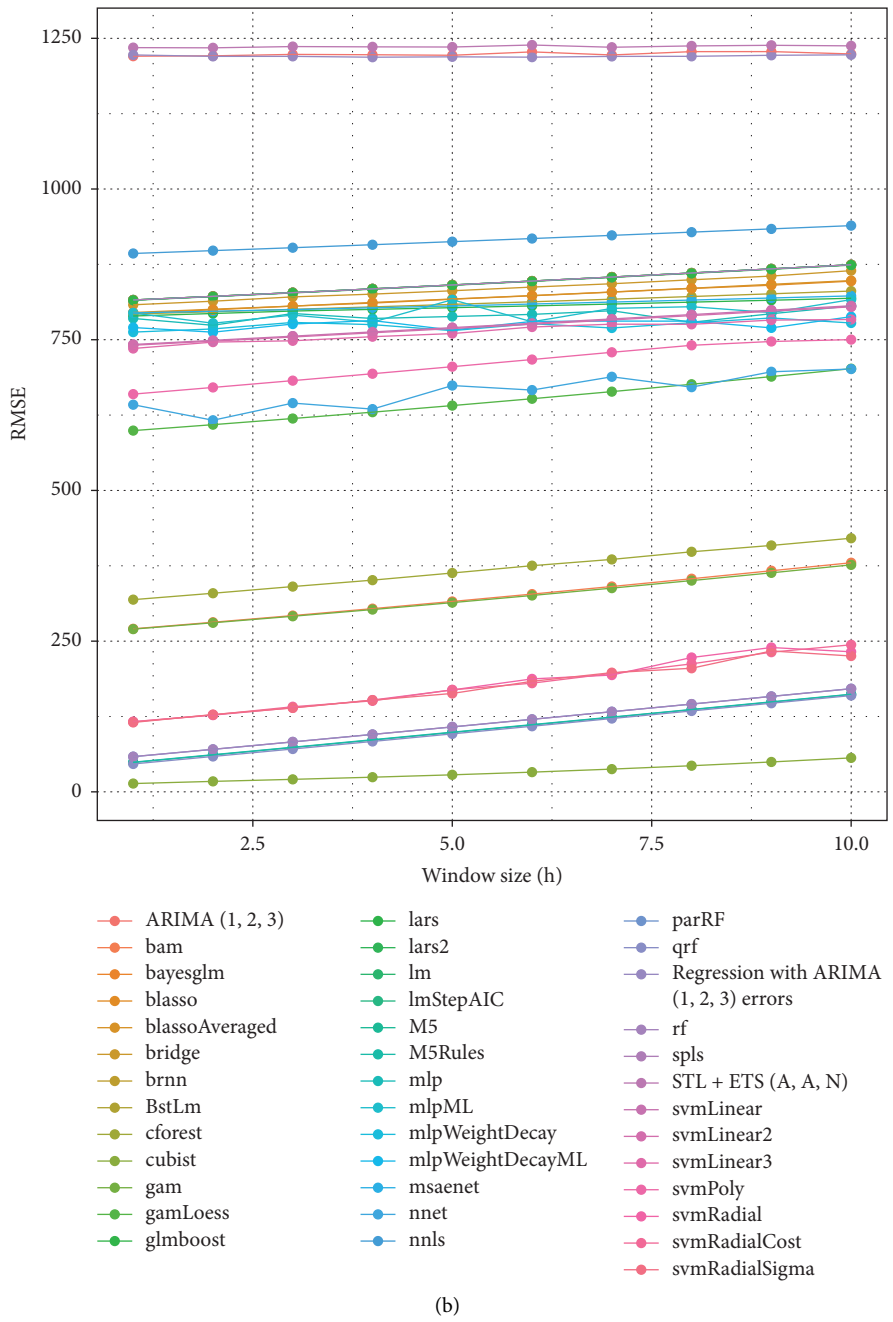

(b)

Figure 8: Comparison of RMSE of prediction models with growing workload based on window size (h).

As a workload, we have used an over-sampled real dataset that contains tweets mentioning 400 verified users of Twitter, collected using the Twitter streaming API. We increased the number of users to 200 k, randomized the number of followers of each user, and added more user interactions to include some saturation points while keeping the load true to the original. For more information, see [23].

4.2. Experimental Results. Figures 6 and 7 show the effects of a workload on the SLA parameters, in this case, the window processing time. We have used growing, periodic, and unpredictable workload patterns, that, as figures show, affect SLA parameters.

In Figure 6, when the load increases (top graph), the window processing time increases constantly, even when the load stops increasing. This is due to the number of messages queued waiting to be processed since the system is saturated and cannot process messages fast enough to return to normal operations. Furthermore, in Figure 7, the spikes of the periodic load cause the window processing time to increase drastically in a very small window of time since the messages are queued very rapidly. Once the load spike ends, the system can process all those queued messages and return

to its normal state. These spikes may cause SLA violations, since the system saturates and is unable to process the messages fast enough, which decreases the QoS for the end-users.

Tables 2–4 show the results of the empirical analysis that represent the root mean squared error (RMSE) and mean absolute error (MAE), which are the deviation of the predicted values from the expected ones of each model. Out of the 30 models we have tested, these tables show the 15 models with the least mean RMSE and MAE.

As shown in Table 2, the most accurate prediction model, with the least RMSE and MAE, is the cubists model, a rule-based regression model, followed by the gam and bam generalised additive models and quantile random forest, M5, and M5 rules random forest models. In contrast, in Table 3, all models show worse accuracy, with much higher RMSE and MAE. While being the most accurate, the cubist model shows worse accuracy than the previous, and the same happens with the gam and bam, and M5, and M5 rules. These random forest models are now more accurate than the previous quantile random forest model, using a periodic workload. We have also measured the RMSE and MAE of the predictive models using an unpredictable workload (Table 4) with similar results to the ones obtained with a periodic workload. The cubist model is still the most accurate, followed by the M5 and M5 rules models, also followed closely by the bam and gam models.

With these results, we see that the random forest cubist model is the most accurate predictive model regardless of the workload pattern, and the one to be used for a generic autoscaling system since our system will be workload-independent.

Furthermore, we have analyzed the effects of changing the prediction window on each predictive model. This window represents how far in the future the prediction is made. For example, a prediction window of 1 means that the predicted values correspond to the immediate next value; but if the prediction window is 5, the predicted values will correspond to the fifth next value. In Figure 8(a), we have measured the prediction accuracy for each predictive model using a growing workload, and as can be observed, the prediction error remains stable despite the increase of the prediction window. This means that the prediction window does not affect the prediction results significantly. Therefore, the forecasting models are robust enough to predict values over a distant forecast horizon with the same accuracy as the more immediate forecasts.

On the other hand, Figure 8(b) shows that the prediction models are not as robust for periodic workloads, as the prediction error increases slightly as the prediction horizon gets further away. This decrease in prediction accuracy is not the same for all models. For example, the cubist model has worse accuracy when the higher the prediction window, but this change is not significant enough.

To conclude this analysis, we have repeated this comparison with an unpredictable workload with the same results as the predictions with the previous workloads (Figure 8).

The results obtained from these experiments show that the workload does have a direct influence on the system SLA parameters, with the risk of SLA violations if the load spikes are not managed correctly; and the most suitable and accurate model for a generic predictive autoscaling system is the cubist random forest model, disregarding the received workload.

5. Conclusions

In this work, we have raised some problems with the predictive autoscaling approach based on workload prediction. In addition, we have proposed an alternative approach based on the prediction of the SLA parameters, thus avoiding double prediction problems and offering a solution less coupled to the type of system to be scaled and, therefore, more generic.

For this purpose, this work has developed an empirical experiment that has allowed us to analyze the impact of different workload patterns on the SLA parameters, demonstrating the problems of the classical approaches of autoscaling based on workload prediction. In addition, we have presented an experiment in which more than 30 predictive models were trained to predict the window processing time with different workloads of a CEP used in mobile communications. Finally, we have analyzed the results of this experiment to offer a set of conclusions and recommendations for the development of autonomous predictive autoscaling systems.

6. Future Work

One feature that would add great value would be to extend the study of prediction models. To this end, we consider several lines of action: testing whether using low-level metrics as predictors improves model predictions and predicting not only SLA parameters but their first derivative as well, to take into account the trend. Furthermore, we want to extend the study and experimentation shown in this work to other distributed cloud-based systems relevant to mobile communications, such as pub/sub systems. We also want to extend our evaluation to other workloads to study our findings in different environments.

Moreover, it would be of a great value to create an autonomous system capable of deciding which prediction model to use based on the conclusions of this work. In this way, the autoscaling system would choose the best prediction model for the SLA parameters based on the type of workload, system, and similar parameters. This autonomous system will be designed and implemented using the knowledge obtained from this and previous works to further improve our research.

Data Availability

The data used to support the findings of this study can be obtained from the corresponding author upon request.

Conflicts of Interest

The authors declare that they have no conflicts of interest.

References

[1] S. Mustafa, K. Sattar, J. Shuja et al., "Sla-aware best fit decreasing techniques for workload consolidation in clouds," *IEEE Access*, vol. 7, pp. 135256–135267, 2019.

[2] J. Gao, H. Wang, and H. Shen, "Machine learning based workload prediction in cloud computing," in *Proceedings of the 2020 29th International Conference on Computer Communications and Networks (ICCCN)*, pp. 1–9, Honolulu, HI, USA, September 2020.

[3] M. R. Raza and A. Varol, "Qos parameters for viable sla in cloud," in *Proceedings of the 2020 8th International Symposium on Digital Forensics and Security (ISDFS)*, pp. 1–5, Beirut, Lebanon, June 2020.

[4] M. Shaukat, W. Alasmary, E. Alanazi, J. Shuja, S. A. Madani, and C.-H. Hsu, "Balanced energy-aware and fault-tolerant data center scheduling," *Sensors*, vol. 22, no. 4, p. 1482, 2022.

[5] M. Ghobaei-Arani, M. Shamsi, and A. A. Rahmanian, "An efficient approach for improving virtual machine placement in cloud computing environment," *Journal of Experimental & Theoretical Artificial Intelligence*, vol. 29, no. 6, pp. 1149–1171, 2017.

[6] A. Y. Nikravesh, S. A. Ajila, and C.-H. Lung, "Measuring prediction sensitivity of a cloud auto-scaling system," in *Proceedings of the 2014 IEEE 38th International Computer Software and Applications Conference Workshops*, pp. 690–695, Vasteras, Sweden, July 2014.

[7] M. Masdari and A. Khoshnevis, "A survey and classification of the workload forecasting methods in cloud computing," *Cluster Computing*, vol. 23, no. 4, pp. 2399–2424, 2020.

[8] R. M. A. Haseeb-Ur-Rehman, M. Liaqat, A. H. M. Aman et al., "Sensor cloud frameworks: state-of-the-art, taxonomy, and research issues," *IEEE Sensors Journal*, vol. 21, no. 20, pp. 22347–22370, 2021.

[9] A. Bahga and V. K. Madisetti, "Synthetic workload generation for cloud computing applications," *Journal of Software Engineering and Applications*, vol. 4, no. 7, pp. 396–410, 2011.

[10] T. Lorido-Botran, J. Miguel-Alonso, and J. A. Lozano, "A review of auto-scaling techniques for elastic applications in cloud environments," *Journal of Grid Computing*, vol. 12, no. 4, pp. 559–592, 2014.

[11] V. Rampérez, J. Soriano, D. Lizcano, J. A. Lara, and Flas, "FLAS: a combination of proactive and reactive auto-scaling architecture for distributed services," *Future Generation Computer Systems*, vol. 118, pp. 56–72, 2021.

[12] A. A. Bankole and S. A. Ajila, "Cloud client prediction models for cloud resource provisioning in a multitier Web application environment," in *Proceedings of the 2013 IEEE Seventh International Symposium on Service-Oriented System Engineering*, pp. 156–161, San Francisco, CA, USA, March 2013.

[13] V. Ramperez, J. Soriano, D. Lizcano, and C. Miguel, "Automatic Evaluation and Comparison of Pub/sub Systems Performance Improvements," *Journal of Web Engineering*, vol. 16, 2022.

[14] A. Y. Nikravesh, S. A. Ajila, and C. H. Lung, "Towards an autonomic auto-scaling prediction system for cloud resource provisioning," in *Proceedings of the 2015 IEEE/ACM 10th International Symposium on Software Engineering for Adaptive and Self-Managing Systems*, pp. 35–45, Florence, Italy, May 2015.

[15] X. Peng, "Tsvr: an efficient twin support vector machine for regression," *Neural Networks*, vol. 23, no. 3, pp. 365–372, 2010.

[16] A. Y. Nikravesh, S. A. Ajila, and C.-H. Lung, "An autonomic prediction suite for cloud resource provisioning," *Journal of Cloud Computing*, vol. 6, no. 1, p. 3, 2017.

[17] Statsmodels Org, "Seasonal-trend decomposition using loess (Stl)," 2022, https://bit.ly/3lykgJf.

[18] P. Leitner, A. Michlmayr, F. Rosenberg, and S. Dustdar, "Monitoring, prediction and prevention of sla violations in composite services," in *Proceedings of the 2010 IEEE International Conference on Web Services*, pp. 369–376, IEEE, Miami, FL, USA, July 2010.

[19] S. Tofighy, A. A. Rahmanian, and M. Ghobaei-Arani, "An ensemble cpu load prediction algorithm using a bayesian information criterion and smooth filters in a cloud computing environment," *Software: Practice and Experience*, vol. 48, no. 12, pp. 2257–2277, 2018.

[20] Y. Kouki and T. Ledoux, "Scaling: sla-driven cloud auto-scaling," in *Proceedings of the 28th Annual ACM Symposium on Applied Computing, SAC'13*, pp. 411–414, Association for Computing Machinery, New York, NY, USA, June 2013.

[21] M. Ghobaei-Arani, "A workload clustering based resource provisioning mechanism using biogeography based optimization technique in the cloud based systems," *Soft Computing*, vol. 25, no. 5, pp. 3813–3830, 2021.

[22] M. Ghobaei-Arani and A. Shahidinejad, "An efficient resource provisioning approach for analyzing cloud workloads: a metaheuristic-based clustering approach," *The Journal of Supercomputing*, vol. 77, no. 1, pp. 711–750, 2021.

[23] V. Ramperez, S. Zahmatkesh, and E. D. Valle, "Scaling the monitoring of approximate top-K queries in streaming windows," in *Proceedings of the 2021 IEEE International Conference on Big Data (Big Data)*, pp. 181–189, IEEE, Orlando, FL, USA, December 2021.

Hindawi
Mobile Information Systems
Volume 2022, Article ID 1919707, 9 pages
https://doi.org/10.1155/2022/1919707

Research Article

Mobile App News English Communication Based on Machine Learning Algorithm

Jun Zhang

Department of Culture Education, Henan Institute of Economics and Trade, Zhengzhou, Henan 450000, China

Correspondence should be addressed to Jun Zhang; 183103009@xzyz.edu.cn

Received 8 July 2022; Revised 9 August 2022; Accepted 4 September 2022; Published 3 October 2022

Academic Editor: Shadi Aljawarneh

With the rapid development of information technology, especially wireless Internet, the application of mobile terminals has gradually become an indispensable part of people's life and provides new opportunities for higher education. At present, with the rise of the Internet, Chinese English online media have mushroomed and are facing fierce competition. In order to further test the current communication strategies of mobile app News English, this paper uses machine learning algorithms to capture the superficial and deep semantic features of words and sentences in English news and comprehensively uses existing methods to express semantic features. The surface and deep parts of English news are analyzed and classified by regression calculation. Then, in order to analyze the communication of mobile app English news, this paper uses random questionnaires and interviews to investigate students, combined with machine learning algorithm knowledge, analyzes the communication effect of Chinese English news mobile program on college students, and analyzes its influencing factors on the communication effect of news. It is hoped that the results of this study can clearly identify the advantages and disadvantages of English News Mobile Applications in the development of the current era and timely adjust strategic decisions. By studying machine learning algorithm and introducing it into the field of English news communication, this paper tests an English news communication mobile app and analyzes its effect on English news communication.

1. Introduction

With the implementation of the reform and opening-up policy, China has gradually developed into a global media power in all aspects in the past three decades. In terms of television, radio, Internet, newspapers, and other media, both the development scale and the number of media are in the forefront of the world. But this does not mean that China has become a communication power. As the largest developing country in the world, China has less media and less influence than developed countries. China's national image is still mostly depicted by Western media, and the export volume of media products is far lower than the import volume of Western media products. According to the data, the number of Chinese Internet users reached 989 million in December 2021. At this stage of development, any Internet user can connect to the Internet through various ways, such as mobile phones and tablets. Mobile terminals play a very important role in every aspect of people's life. Mobile phones and other mobile devices have had a huge impact on public life. In order to meet the needs of the current mobile device Internet era, user sharing environment and competing for public attention, major media institutions continue to improve the attractiveness of media information to users. The development of smart mobile devices such as mobile phones and tablets makes it easier for users to retrieve information, and the introduction of machine learning algorithms makes the information acquisition scene smaller and fragmented.

The progress of media technology, the popularity of intelligent devices, and the development of mobile applications are changing the mode of modern communication [1]. English online media in China has sprung up and joined the fierce competition in the English media industry. Due to the development trend of economic globalization and informatization of social life, English has become the main way of communication for international talents [2]. As we all

know, college students are a powerful reserve force in China. They are in the stage of constantly improving their English learning level, and English news applications provide a convenient platform for their autonomous learning and also stimulate the development of Internet English education in China [3]. The communication power of English news mobile app can provide effective information to distance vocational education institutions, thus paving the way for the win-win cooperation between English news app and English learning app [4]. At the same time, carrying out such research is also an exploration and attempt of the development of English journalism and communication in China, which can provide good reference and data support for the teaching and development of international journalism in colleges and universities [5].

2. Related Work

Based on empirical investigation, the literature analyzes the communication effect and influencing factors of English media in China from both positive and negative aspects. The results show that the development role of English media in China is irreplaceable, and great progress has been made, but there are still some problems, such as convergence of positioning [6]. According to the literature, the single media management means, poor management ability, great cultural differences between the east and the west, and low media credibility are the main factors affecting the communication effect of Chinese English media [7]. The literature shows that the media literacy of news publishers in the 5G era mainly focuses on the overall analysis of the current media environment. People mainly focus on improving the symbiotic environment of the Internet, changing the communication mode, and changing the requirements of media literacy, and less on the specific editing process [8]. Literature interprets the essence of news from the perspective of technology intermediary. In addition to the two dimensions determined in objective academic facts (ontology) and text expression facts (epistemology or news practice theory), in the new technological environment, the presentation of technology intermediary law (intermediary facts) has had an unprecedented impact on the way news is reported [9]. From the perspective of communication, the communication report is indirect, which is manifested in some facts recorded by means of information technology or the real picture, real situation, or state of affairs processed by technology [10]. According to the literature, the contradictions of current news algorithms mainly focus on human subjectivity and algorithm objectivity, the public interest of the media and the profitability of the algorithm, as well as the diversity and closeness of society [11, 12]. Taking people's network as an example, the literature discusses the system of people's network push information from information collection to information processing to information storage and transmission, and then points out that mobile phone manufacturers actually have great influence in news publicity [13]. According to the literature, stereotype is a form of subjective prejudice that people have toward things. Based on this point, it is manifested as an independent consciousness. Although it can quickly establish a reference for people to recognize things, it will also prevent the public from receiving new information and updating old ideas to a certain extent. The literature emphasizes that the public has the freedom of consciousness, and the dissemination of information needs to respect the freedom of consciousness of the public; otherwise, it will be resisted and excluded [14]. This view overemphasizes the self-consciousness of the media information audience and ignores the psychological variability of the audience, thus ignoring the adjustment and guidance for the information carrier.

According to the literature, mass communication may not be a necessary and sufficient factor to produce audience effect in general, but it is more likely to interact in different factors and play a role through these constraints and influences. The literature believes that the impact of news communication is two-fold [15]. The first is the impact of news reports on the audience and the consistency with the expected goal of communication. Generally speaking, the higher the degree of coincidence, the better the transmission effect. This kind of communication effect is the standard to measure the level of news business, indicating whether app has correctly used the way of news communication. Based on the general environment, the literature analyzes the challenges of the international situation and the development of international media to China's English news media in the new century. It also analyzes the problems existing in Chinese English media at present and then describes the development trend since the 21st century—more diversified media forms, updated communication concepts, more advanced reporting methods, and more reasonable talent structure [16].

This paper expounds the three major trends of the future development of the media: the central government is the main, and the local government is the auxiliary; integrate external communication with the market; English media will return to journalistic standards. The literature takes online forums as the research object, analyzes the communication impact of various types of posts, and predicts the development trend of topics [17]. In the discussion of the impact of forum communication, the impact of communication is specifically divided into meeting the public's right to know and spiritual and emotional needs; publicity hot spots to attract the attention of traditional media; carry out reasonable opinion expression and exchange, as well as timely interactive feedback; and realize group behavior to discuss the micro-effect [18, 19].

3. Theoretical Basis and Application of Machine Learning Algorithm

3.1. Support Vector Machine. Support vector machine is a classification algorithm using supervised learning training. SVM is determined by important training samples, such as support vector. Therefore, if all classifications are correct, the SVM classification problem can be described as a finite problem of optimizing linear classification, as shown in

$$\min_{\omega,b} \frac{1}{2}|\omega|^2 \tag{1}$$

$$\text{s.t. } y_i(\omega \cdot x_i + b) - 1 \geq 0. \tag{2}$$

For each inequality constraint, Lagrange multipliers $\text{AI} \geq 0$, $i = 1, 2, N$; the Lagrangian function is constructed as follows:

$$\text{L}(\omega, \text{b}, \alpha) = \frac{1}{2}|\omega|^2 - \sum_{i=1}^{N} a_i[y_i(\omega \cdot \text{x}_i + \text{b}) - 1]. \tag{3}$$

According to Lagrange duality, the original finite optimization problem can be equivalent to the dipole minimax problem, as shown in

$$\max_{\alpha} \min_{\omega,b} L(\omega, b, \alpha). \tag{4}$$

Next, $l(\omega, b, A)$ after deriving, we get

$$\begin{aligned} \frac{\partial L}{\partial \omega} &= \omega - \sum_{i-1}^{N} \alpha_i y_i x_i, \\ \frac{\partial L}{\partial b} &= \sum_{i-1}^{N} \alpha_i y_i. \end{aligned} \tag{5}$$

After it is brought into the Lagrange function, the solution of the SVM problem can be equivalent to the problem of optimizing the following functions, and the solution learning algorithm can be completed by the following operations:

$$\begin{aligned} \min_{\alpha} \frac{1}{2}\sum_{i=1}^{N}\sum_{j=1}^{N} \alpha_i\alpha_j y_i y_j(x_i \cdot x_j) - \sum_{i=1}^{N} \alpha_i, \\ \text{s.t. } \sum_{i=1}^{N} a_i y_i = 0, \\ \alpha_i \geq 0, i = 1, 2 \ldots, N. \end{aligned} \tag{6}$$

3.2. Bayes Theorem. The concept of conditional probability is particularly important in Bayesian theorem. Conditional probability means that there are two events A and B, and the probability of event B is greater than 0. Then, in the case of event B, the probability of event A is called the conditional probability of A when B occurs, that is, $P(a|b)$. For event B, there are

$$\text{P}(\text{B}) = \sum_{i-1}^{\infty} P(A_i)P(A \mid B_i). \tag{7}$$

Naive Bayes formula is shown in

$$P(B_i \mid A) = \frac{P(B_i)P(A \mid B_i)}{\sum_{j=1}^{n} P(B_j)P(A \mid B_j)}. \tag{8}$$

Bayesian formula is used to classify the dimensional components of the data set, assuming that the components of the training set are independent of each other. But in real life, this assumption is almost impossible. There may be an inseparable relationship between any features. If there is a strong potential relationship between features, the effect of naive Bayesian classification will be affected.

3.3. Text Classification of English News. Firstly, the English news text data are encoded into the template, and the granularity text data are obtained by using the template. Then, the semantic vectorization of news text topic is carried out.

The sentence coding method uses the average value of Bert layer coding from 9 to 12 to represent the word w_i, and the formulas are shown in

$$w_i = BERT^{\text{represent}}(t_i), \tag{9}$$

$$\text{represent} = \frac{1}{3}\sum_{k} \text{layer}_k. \tag{10}$$

The superscript of t_i represents the specific coding method of the current word t_i, and layer k represents the Bert coding of layer K $(9 \leq K \leq 11)$. Based on the sequence of input data, the text decision model uses the structure of BiLSTM attention model to determine the pairs of input sentences. In order to let the model learn the influence of keywords on connectivity, the granularity of words is taken as the input of the model, and the attention mechanism is used to give weight to the input. The main decision-making model is shown in Figure 1.

Specifically, suppose that the input data sentence I, sentence $i+1$, sentence I, sentence $i+1 = [w_1, w_2, \ldots, w_m]$, and BiLSTM first encode the input at each time, as shown in

$$o_t = \text{BiLSTM}(w_t). \tag{11}$$

Use the attention mechanism to calculate the weight of the output of BiLSTM model at each time point, and the formulas are shown in

$$u_t = \tanh\ (W_w \cdot O_t + b_w), \tag{12}$$

$$a_t = \frac{\exp\left(u_t^T \cdot u_w\right)}{\sum_t \exp\ \left(u_t^T \cdot u_w\right)}. \tag{13}$$

UT, WW, and BW are the parameters of the layer where the attention mechanism is located, and at is the weight of the input sequence in the total input at the t-th time point. Therefore, after the attention mechanism layer, the calculation formula of the input vector expression VT and the weighting expression obtained is as follows:

$$v_t = a_t \cdot O_t. \tag{14}$$

After using the attention mechanism to calculate the vector representation with lexical weight, attach it to a full connection layer to reduce the size, and then use the softmax function to classify. Let it be the combined vector V', and the calculation formula is shown in equations (17) to (19).

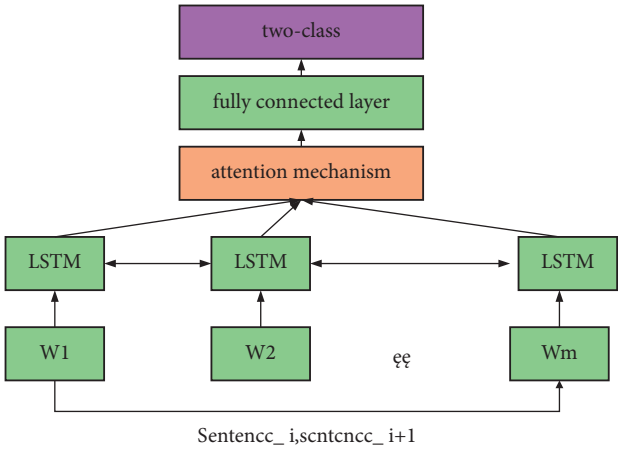

Figure 1: Topic decision model.

$$\begin{aligned} v &= \text{con}\ (v_1, v_2, \cdots, v_m) \\ v' &= f_c(v) \\ y &= \text{softmax}\ (v' \cdot W_s + b_s). \end{aligned} \tag{15}$$

Taking a training group as an example, suppose that the current training group $e = \{e_1, e_2, ..., e_n\}$ in N training samples, the mean square error function is expressed as shown in

$$\%\ \text{loss}\left(Y_E, Y_{\widetilde{E}}\right) = -\frac{1}{n}\sum_{i=1}^{n}\left(y_i \cdot \log\left(\widetilde{y}_i\right) + \left(1 - y_i\right) \cdot \log\left(1 - \widetilde{y}_i\right)\right). \tag{16}$$

YE is the current batch data category. The semantic vectorization of composition subject and topic is the key to accurately capture the similarities between them and verify the methodology of this paper. Once the topic and subject are semantically vectorized, they are projected into the same semantic space, and the distance between them reflects the semantic similarity between them. By calculating the distance between two vectors, we can get the similarity between them.

4. Analysis of the Mobile App Propagation Model

4.1. System Architecture Design. According to the characteristics of mobile application development, in the overall architecture design, the whole software mainly includes two parts: mobile end and server end. The main functions and levels of each part are shown in Table 1.

In order to cope with high concurrency, applications are separated from static resources by grouping, such as placing static resources and service programs on static resource servers and application servers, and using Nginx as the reverse proxy server, as the front-end server, to process server integration requests and send various requests, such as static resource requests and application requests. Load balancing is created between clustered servers. The specific physical topology of the network is shown in Figure 2.

Table 1: System architecture.

Server	Mobile terminal
Data layer (DB, DAO, DTO)	Integrated app
Business logic layer (service)	UI interface
Service (resource) layer (resource)	Offline service
Control layer (web api)	Remote service (http)

4.2. Relevant Machine Learning Models and Parameter Design

4.2.1. Learning Process of AdaBoost Algorithm. First, extract the first weak classifier by learning n training samples. The initial learning samples of weak classification with other new data are established in the new N training samples, and a weak classifier is obtained by relearning; combine the first and second error samples with other new sample data to form a new N training relearning samples and relearn; cycle until the end of the algorithm, and finally a strong classifier is formed.

4.2.2. Algorithm Flow of AdaBoost. Initialize training data weight distribution:

$$D_1 = (w_{11}, \ldots, w_{1i}, \ldots, w_{1N}), w_{1i} = \frac{1}{N}, \mathbf{i} = 1, 2, \ldots, \mathrm{N}, \tag{17}$$

$m = 1, 2, ..., M$.

The basic classifier is obtained by learning the training data set of weight distribution DM:

$$G_m(x): X \longrightarrow \{-1, 1\}. \tag{18}$$

Calculate the classification error rate of the basic classifier GM (x) on the training data set:

$$e_m = P\left(G_m(x_1) \neq y_1\right) = \sum_{i=1}^{N} w_{mi} I\left(G_m(x_1) \neq y_1\right). \tag{19}$$

Calculate the coefficients of the basic classifier GM (x):

$$\alpha_m = \frac{1}{2}\log\ \frac{1 - e_m}{e_m}. \tag{20}$$

Update the weight distribution of the training database:

$$\begin{aligned} D_{m+1} &= \left(w_{m+1,1}, \ldots, w_{m+1,i}, \ldots, w_{m+1,N}\right) \\ w_{m+1,i} &= \frac{w_{mi}}{z_m}\exp\ \left(-\alpha_m y_i G_m(x_i)\right), i = 1, 2, \ldots, N \\ Z_m &= \sum_{i=1}^{N} w_{mi}\exp\ \left(-\alpha_m y_i G_m(x_i)\right). \end{aligned} \tag{21}$$

Z_m is the normalization factor, which makes D_{m+1} a probability distribution.

Construct linear combination of basic classifiers:

$$f(x) = \sum_{m=1}^{M} \alpha_m G_m(x). \tag{22}$$

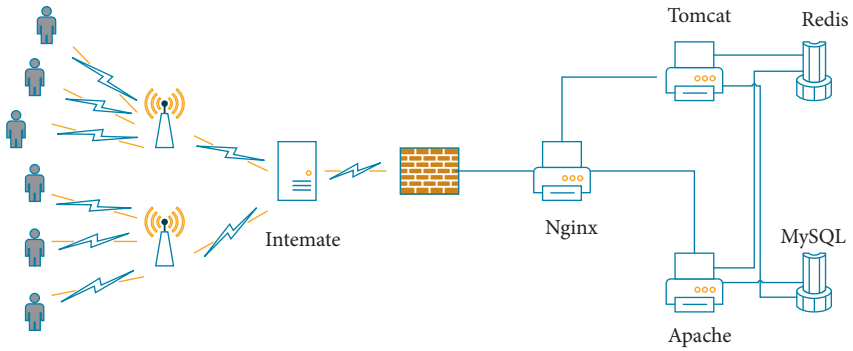

Figure 2: Physical network topology of the system.

Finally, the final classifier is obtained:

$$G(x) = \operatorname{sign}(f(x)) = \operatorname{sign}\left(\sum_{m=1}^{M} \alpha_m G_m(x)\right). \quad (23)$$

4.2.3. AdaBoost Framework Parameters

Base estimator: the decision tree is used here as the weak classification learner.

N estimators: number of weak learners (maximum iterations), default_50.

Learning rate: the weight reduction coefficient of each weak learner, which is 1 by default. In the process of effectively adjusting parameters, n estimators and learning are often considered at the same time_Rate parameter to determine the algorithm fitting that performs properly.

Algorithm: this parameter represents two AdaBoost classification algorithms implemented in scikit-learn. The default value of AdaBoost classifier algorithm is also SAMME.R.

4.2.4. AdaBoost Decision Tree Parameters

Max features: the largest feature part, which means that all features are considered in the division. This parameter can take several different values, and the default is "None."

Max depth is the maximum depth of the decision tree, and the normally used value is between 10 and 100.

Min sample split: the minimum number of samples required for internal node subdivision.

Min leaf samples: the minimum number of leaf samples. The default is 1.

Min weight fraction leaf: the minimum weight of the leaf node sample, that is, the weight problem is not considered.

Max leaf nodes: the maximum number of leaf nodes, which is "None" by default. In general, this parameter is limited to avoid overfitting.

Table 2: Comparison of prediction effects of various models.

Model	Log-loss	AUC
LIBFFM	0.12211911457	0.698978541173
Light GBM	0.117594174587	0.748343536724
Vowpal Wabbit	0.142824534763	0.697595468316
XGBoost	0.122167834152	0.775976543747
Random forest	0.12453878976	0.775674287815
AdaBoost	0.112341876876	0.78748377195

4.3. Analysis of Experimental Results. Here, five machine learning models, LIBFFM, light GBM, Vowpal Wabbit, XGBoost, and random forest, are used to train the data, and AdaBoost model is used to train and compare the generated data set. The final prediction results of the five models are shown in Table 2.

As shown in Table 3, the prediction effect of AdaBoost model is enhanced in both indicators, indicating that AdaBoost model has advantages over other models. In addition, we calculate the cumulative distribution of positive samples in the prediction results, divide the prediction probability of positive samples into 10 levels, and calculate the cumulative distribution of positive samples at each level. The calculation results show that the cumulative distribution of the sixth-level positive samples is higher than the normal value, which also shows that the prediction method used in this paper is correct and can be used to solve the model of CTR prediction problem.

5. Investigation on the Spread of Mobile App News English

5.1. Investigation Objects and Methods. In order to make the survey more orderly and the results more systematic, this paper aims to limit the survey objects to freshmen to seniors in colleges and universities according to the principle of demography and the age difference and education level. From the perspective of college students' media literacy, they are loyal users of various media. In addition, they have rich basic knowledge, fast acceptance of new things, strong understanding, high initiative, strong thirst for knowledge, and a spirit of inquiry. Such qualities determine their higher

Table 3: AdaBoost model positive sample accumulation distribution.

Grade	Number of positive samples	Number of negative samples	Total number of samples	Cumulative distribution of positive samples
1	1154	7375	8529	0.478
2	307	8220	8527	0.605
3	228	8300	8528	0.700
4	187	8341	8527	0.777
5	166	8363	8528	0.845
6	142	8385	8527	0.905
7	102	8425	8527	0.946
8	89	8440	8528	0.984
9	45	8482	8527	1.002
10	17	8509	8526	1.010

requirements for the media. From the perspective of college students' influence on the media, no matter what kind of media, college students will be an important group to use this kind of media in the future. These habits will inevitably affect and further determine their tendency to use media in the future. In the highly competitive media industry, there is now a comprehensive discussion from lifestyle to ideology. The transformation of audience-centered communication relationship is particularly valued in the media. Therefore, when this group grows into the social backbone or the main user group of the media, it is the main audience of the major media. This study adopts a combination of random questionnaires and interviews.

A total of 600 samples were collected in this survey, and 586 samples were recovered, with a recovery rate of 97.67%. After screening, 12 nonconformities were eliminated, and 574 questionnaires were collected, with an effective rate of 95.67%.

5.2. Analysis of English News Reading Preference of Mobile App. As shown in Figure 3, in terms of the frequency of use of the mobile app, college students do not often use the mobile app. About 81.9% of students use it at most twice a week, about 15.5% of students use it 3-4 times a week, and only 2.6% of students use it more than 5 times a week. The low frequency of use proves, to a certain extent, that college students are less dependent on mobile app.

As shown in Figure 4, in terms of the average time spent, about half of the students usually spend between 30 minutes and 1 hour, nearly 40% of the students spend less than half an hour, and only a few students spend more than 1 hour. From the use time, it can be seen that most students' use of mobile applications is only in the stage of "quick browsing" or "light reading"; that is, they prefer to choose content that can quickly attract attention to browse the web, such as titles, images, and keywords. This kind of reading method is difficult to give students the opportunity to have in-depth communication and interaction with app, thus reducing dependence and weakening influence.

Figure 5 shows the reading preferences of mobile app English news. By analyzing English mobile applications, we find that these applications significantly increase the coverage of international news events, which meets the needs of students. In addition, in the report of app news, we also pay attention to this problem: with the development of China, more and more people are eager to understand the human rights, legal system, and economic situation of today's Chinese society.

As shown in Figure 6, from the perspective of the purpose of using the app, the original intention of the respondents to use the mobile app from top to bottom is learning English (49.0%), obtaining news information (25.1%), collecting data (15.0%), and only 9% of the students are curious or for other purposes. Although this survey shows that the purpose of students' use of app is relatively clear and targeted, it is not all the same, which also means that there is still much room for improvement in the attractiveness of English app to college students.

5.3. Enlightenment of Mobile App News English Communication. Communication power, as the name suggests, refers to "the ability of media communication, including the amount of information, the speed of information transmission, and the coverage and influence of information. The influence effect is the main feature of communication effect. In media communication, technical means are the decisive factor affecting communication." "Communication power" exists as a power, there must be different indicators to measure this power, and these indicators naturally become a part of "communication power." Generally, indicators can be divided into two categories. One is hard indicators, including quantifiable indicators such as media audience coverage, infrastructure, income funds, and the number of employees; the other is the soft index, which is mainly determined by the quality of communicators and the credibility of the media. The two are complementary and necessary systems. High-quality communicators help to improve the credibility of the media, and high credibility media can cultivate and absorb high-quality communication practitioners. At present, 5G and artificial intelligence technology are being initially applied and gradually popularized. The mobile bandwidth will be effectively improved, the connection delay will be shorter, and everything can be interconnected. These application technologies create conditions for media to enhance sensory forms and optimize interactive experience. As an integrated media platform, app is partly based on the credibility of CCTV and has the advantages of fast speed, multimedia support, fast

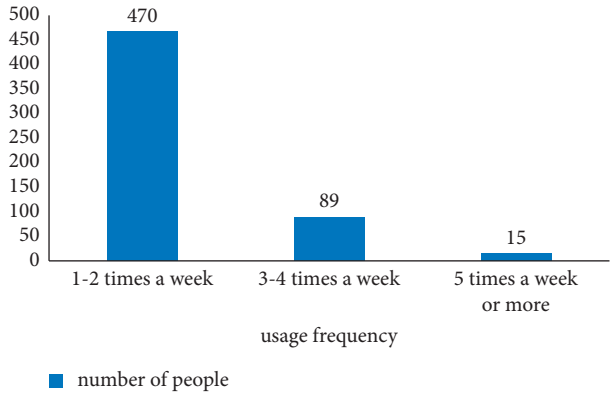

Figure 3: Reading frequency of English news on mobile app.

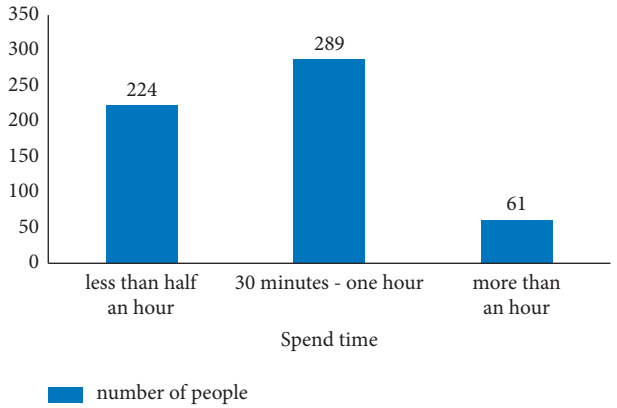

Figure 4: Reading duration of English news on mobile app.

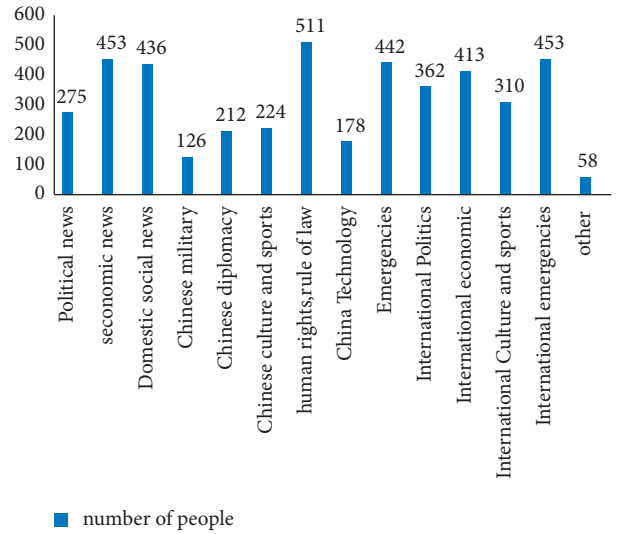

Figure 5: Reading preferences of mobile app English news.

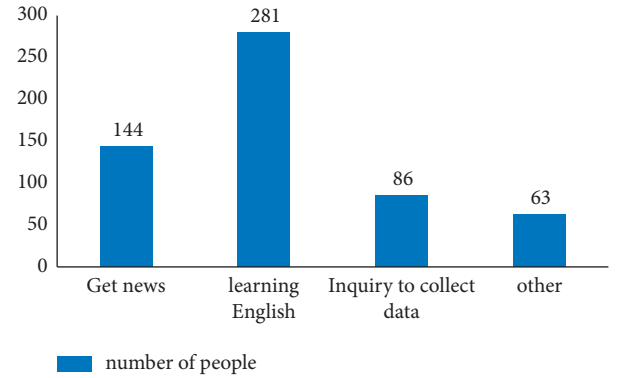

Figure 6: Reading purpose of mobile app English news.

interaction, and other new media communication. Combining the two to build a short video media system can create a more intuitive English cultural experience for users. The platform can not only launch the production and release function of English short videos, but also experience and big data analysis of the target audience, discover the interests, preferences, and attention trends of short video users, and build a short video service model. Considering the communication needs of the audience, videos can be shared to other social platforms such as circle of friends, Weibo, and QQ space, which are favored by a large number of young people. In this way, by designing and promoting short video services, app can solve the fragmented reading needs of the audience from the perspective of the current task, promote communication and interaction within the platform, and enable the media to achieve the creation of high-quality online services and the sustainable development of English news applications.

The intelligent design of app integrating media experience can use artificial intelligence technology, combined with QR code scanning, to optimize user interaction through robot news, image recognition, language recognition, audio reading, machine translation, and other technologies. Provide users with simpler and more convenient English cultural service resources, and stimulate users' active participation. On the one hand, with the support of AI technology, app can use face recognition system to make it easier for users to identify themselves, such as registration, login, and authentication. On the other hand, AI applets can also be developed. For example, unique symbols such as the applet logo can be drawn into humanized images for dialogue and interaction with users. It can also complete commands such as automatic playback, screen projection playback, and live video streaming through voice interaction, which can realize voice reading news and bring users a multi-sensory experience of audio-visual integration. These functions are more interactive and interesting, optimize the user experience, and help improve user participation. In addition to the reporter function, AI applications can also be used as robot customer service to provide better services to the public through more knowledge base reserves, application scenario-based scheme adjustment, intelligent guidance and related problems, automatic service effect evaluation, and other functions, and to collect problems and highlight weaknesses according to platform changes.

Hypertext and hyperlink technology broke through the past linear and single media communication mode, not only spread information through the network in multiple dimensions, but also strengthened the function of collecting and network communication. App disseminators organize information according to specific connections, which makes the form of online news display emerge one after another, and relevant news, news rankings, news recommendations, and other forms of expression emerge in a timely manner, which undoubtedly helps to improve network utilization. However, the convergence of the Internet puts forward higher requirements for reporters and editors to organize information in English news applications. They need to carefully study the psychological characteristics of the audience, constantly create intensive columns, and regularly create live and intensive columns to effectively organize information. It will make it easier for the public to find, obtain more, and understand the event more deeply.

Even if the communication effect is only a manifestation of the final result, any element in the communication process will change this result. If the founder of app is proficient in news, English, Internet, brand, and other aspects, even in all fields, that is, "one specialty and many abilities," or even "many specialties and many abilities," then the efficiency of editing manuscripts, page layout web, app maintenance, and other work will be greatly improved, and the spread of app will be smoother. At present, there are three main ways to cultivate English Media Talents in China: one is the on-the-job training organized by the media itself, the other is the short-term training of local propagandists through a variety of ways, and the third is the joint training of the college of journalism and the college of foreign languages as a reserve force for the cause of news media communication. These three ways have a strong guiding role in building and training Chinese English news application talents.

In addition to the continuous improvement of professional ability, news communicators must also strengthen the construction of professional ethics. From the very beginning, the English media in China have been shouldering the task of national propaganda. Every subtle point of view, such as what pictures are used in the daily app to make question maps and how English words are expressed, will have a great or small impact on society. Therefore, the professional ethics of English news app workers is very important in practical work. Staff engaged in English news online broadcasting must carry out professional ethics quality training under the joint action of heteronomy and self-discipline. Heteronomy means to strengthen the training of laws and regulations of online media, attach great importance to the establishment of Internet laws and regulations, strictly abide by laws and regulations, and clarify the rights and obligations of English online news practitioners to run websites in a civilized manner. Self-discipline refers to the fact that the most direct driving force of English online news self-discipline comes from the communication topic. Professional ethics must be transformed into self-journalistic ethics, forming professional conscience, professional honor, and basic professional ethics, so as to dominate their own journalistic communication activities and provide strong spiritual support for objective communication.

6. Conclusion

At present, there are some problems in Chinese English news apps, such as the convergence of content settings, the rigidity of news reporting style, the prominent phenomenon of Chinglish, the low level of marketing, and the insufficient popularity of applications. And most of the news reports are translated directly from Chinese manuscripts, lacking characteristics, and innovation. At present, many apps rely on the government and large media groups and regard them as the parents of food and clothing, thus ignoring the basic needs of the public. These problems have more or less affected the dissemination effect of apps. In the context of information globalization and increasingly frequent information exchange between countries, English media should play an important role in shaping a positive national image. In a longer period of time, China English news app has great development potential. Therefore, this paper mainly focuses on the problems reflected in the questionnaire and the factors affecting communication, combined with the characteristics of network communication, especially the communication power and the public reliability of app, the progressiveness of communication technology, environmental comfort, the professional ethics of communicators, and other aspects to improve the brand construction of app, trying to improve the communication influence construction effect of English news app.

Data Availability

The data used to support the findings of this study are available from the author upon request.

Conflicts of Interest

The author declares no conflicts of interest.

References

[1] F. B. Saghezchi, A. Radwan, J. Rodriguez, and T. Dagiuklas, "Coalition formation game toward green mobile terminals in heterogeneous wireless networks," *IEEE Wireless Communications*, vol. 20, no. 5, pp. 85–91, 2013.

[2] F. Deng, "The optimization research on college English classroom teaching under the network environment—based on the feedback report of college English stratified teaching in SASU," *Teaching English in China and America*, vol. 17, no. 10, pp. 4–19, 2020.

[3] H. E. Yi, "Research and building of optimization measures of college English teaching," *International Technology Management*, vol. 2, pp. 13–25, 2015.

[4] D. U. Yan-Fei, "Exploration of college English teaching model in mobile Internet time," *DEStech Transactions on Environment Energy and Earth Science*, vol. 4, pp. 789–299, 2017.

[5] X. U. Jingting and H. Liu, "Research on the teaching strategy optimization of architectural English course under the double orientation of EAP+EOP," *The Guide of Science & Education*, vol. 13, no. 2, pp. 5467–5478, 2019.

[6] A. H. Arsenault, "The datafication of media: big data and the media industries," *International Journal of Media and Cultural Politics*, vol. 13, no. 1, pp. 7–24, 2017.
[7] C. A. C. McMellon, "Book review: the daily you: how the new advertising industry is defining your identity and your worth," *Journal of Advertising Education*, vol. 17, no. 1, pp. 55-56, 2013.
[8] A. I. Naimi and D. J. Westreich, "Big data: a revolution that will transform how we live, work, and think," *American Journal of Epidemiology*, vol. 179, no. 9, pp. 1143-1144, 2014.
[9] C. H. E. N. Xiaohong, "Trend analysis of technology fusion and application innovation in the digital economy era," *Journal of Central South University*, vol. 5, pp. 1–8, 2018.
[10] M. Jiang and K. W. Fu, "Chinese social media and big data: big data, big brother, big profit?" *Policy & Internet*, vol. 10, no. 4, pp. 372–392, 2018.
[11] J. Li, H. Shi, and K.-S. Hwang, "An explainable ensemble feedforward method with Gaussian convolutional filter," *Knowledge-Based Systems*, vol. 225, Article ID 107103, 2021.
[12] G. Wang, F. Fang, and Q. Chen, "The spreading of network rumors: procedure, motivation and causes————a case study of earthquake rumors," *Journal of Beijing Institute of Technology (Social Sciences Edition)*, vol. 2, pp. 112–116, 2011.
[13] H. Shi, J. Li, J. Mao, and K. S. Hwang, "Lateral transfer learning for multiagent reinforcement learning," *IEEE Transactions on Cybernetics*, vol. 10, pp. 1–13, 2021.
[14] G. Tesfom and C. H. M. Lutz, "Consumers' advertising media use: a cross-cultural study," *Services Marketing Quarterly*, vol. 43, no. 1, pp. 32–47, 2022.
[15] B. Urrutikoetxea Arrieta, A. I. Polo Peña, and C. Martínez Medina, "The moderating effect of blogger social influence and the reader's experience on loyalty toward the blogger," *Online Information Review*, vol. 43, no. 3, pp. 326–349, 2019.
[16] M. Adil, H. Alshahrani, A. Rajab, A. Shaikh, H. Song, and A. Farouk, "QoS review: smart sensing in wake of COVID-19, current trends and specifications with future research directions," *IEEE Sensors Journal*, vol. 8, p. 1, 2022.
[17] R. Asmara, W. R. Kusumaningrum, A. Wulansari, M. Munirah, and H. Hersulastuti, "Measuring the effect of a flipped classroom model on critical thinking skills," *Proceedings of the 2nd workshop on language literature and society for education Wol2SED*, Indonesia, December 2018.
[18] D. Zhang, "The Analysis of Evidentiality from the Perspective of Interpersonal Function in English News Discourse," *Proceedings of the 2020 International Conference on Big Data and Social Sciences (ICBDSS)*, Xi'an, China, August 2020.
[19] A. M. Kaplan and M. Haenlein, "Users of the world, unite! the challenges and opportunities of Social Media," *Business Horizons*, vol. 53, no. 1, pp. 59–68, 2010.

Hindawi
Mobile Information Systems
Volume 2022, Article ID 4807395, 10 pages
https://doi.org/10.1155/2022/4807395

Research Article

A Decision Support System Model for Middle School Education Management Based on Sparse Clustering Algorithm

Bin Peng [1,2] **and Xinhua Pei** [3]

[1]*Shaanxi Institute of Teacher Development, Shaanxi Normal University, Xi'an 710062, Shaanxi, China*
[2]*Faculty of Education, Xi'an Siyuan University, Xi'an 710038, Shaanxi, China*
[3]*Faculty of Art, Shaanxi Normal University, Xi'an 710062, Shaanxi, China*

Correspondence should be addressed to Bin Peng; pengshaohui@snnu.edu.cn

Received 11 August 2022; Revised 30 August 2022; Accepted 19 September 2022; Published 30 September 2022

Academic Editor: Shadi Aljawarneh

With the development of China's economy, education has also been greatly improved, and the enrollment scale has been continuously expanded. It has become increasingly difficult to manage student performance. The traditional manual management of student grades has shortcomings such as low efficiency, poor privacy, difficulty to find and maintain, and incomplete knowledge mining of student grade data resources, so it is impossible to fully test and utilize related technologies. Based on this background, this paper designs and develops a set of decision support systems for middle school education management combined with a sparse clustering algorithm according to the actual needs of middle school education. The article first introduces the concept of sparse clustering algorithm and the four levels of the decision support system for middle school education management, data layer, model layer, application layer, and display layer, and then introduces based on five system models, namely, database design, online analysis process module design, data mining design, model library design, function design, and finally, the system model of educational decision management support is constructed, and the model test is completed. The practice shows that the system proposed in this paper can manage the current educational information of students scientifically, extract the information from the changes in students' achievements in time, and make certain assistance for teachers' educational decisions. This paper designs an effective decision support system by studying the sparse clustering algorithm and introducing it into the field of middle school education management.

1. Introduction

"Using educational informatization to drive educational modernization" is a common trend in the world's educational reform and development, and it is also an important criterion for the rapid development of China's education [1]. In view of the problems in traditional education, China is making great efforts to build educational informatization, collect students' data information, and establish an educational data analysis system [2]. Compared with universities, higher vocational colleges and primary schools, the informatization construction of middle schools started relatively late. At the same time, due to factors such as region, economy, and teaching resources, the development of middle schools in the country is uneven. At present, most schools do not have information management standards. School leaders do not have real-time visibility into what is going on at the school [3]. The education administrative department has learned that there is a delay in the teaching data of each school, and some data are incompletely processed. Such phenomena do not help leaders to understand the actual situation of school teaching, so they cannot analyze and solve problems in a timely manner, and there is no objective database to make management decisions and formulate strategies [4]. In the actual development process, how to effectively solve these problems in middle school education management is a difficult problem faced by education authorities and school leaders [5]. On the basis of

certain environmental conditions and equipment, people can make certain decisions according to their current conditions and their own purpose needs [6]. The educational decision-making system is also like this. It analyzes the existing situation, combines with the changes in students' information, makes corresponding predictions on students' information, and carries out simulation according to the current environmental information, so as to obtain a possibility of optimal results, and then feeds back this possibility to managers as information recommendation [7]. In the aspect of traditional school management, the method of manual recording and summarizing is often adopted. Although it can be easy to judge and make everything handled in a better way, it undoubtedly brings huge administrative pressure, and the management is not comprehensive enough and the timeliness is insufficient; therefore, to the introduction of the computer technology and integrated systems to the relevant system, through the effectiveness of computer technology for large data processing, machine learning related-databases, to encode some daily transaction summary, so that you can through the integrated system faster processing everyday things, and some important things to feedback, so as to improve the efficiency of information processing. Under such circumstances, the educational management decision aid system proposed in this paper is very necessary. It can help teachers timely grasp the learning and living conditions of students, make correct decisions, and promote the scientific and standardized management of schools. The model of this paper can also provide a large number of data basis for the information construction of schools and improve the management efficiency of schools.

2. Related Work

Based on Oracle data warehouse, SSH framework, Lucene full-text search engine, OLAP data statistics, front-end JS visualization plug-ins, and other related technologies, the literature studies common data mining algorithms in the open-source machine learning main framework and data mining Mahout platform [8]. On this basis, a basic decision support framework is created and applied to the middle school management process. The literature proposes an improved algorithm, the structural weighted subspace clustering (SwSsc) algorithm, which makes up for the lack of local constraints [9]. The improved algorithm can be demonstrated in synthetic data clustering experiments and applied to color image classification due to its effectiveness. The literature proposes an improved algorithm, structure adaptive subspace clustering (ASSC), which improves intra-class density and inter-class dispersion [10]. The effectiveness of the improved algorithm has been verified in synthetic data clustering experiments, and it can be used to process image clustering, color image classification, and color image segmentation. The literature makes a detailed analysis and design of the middle school management decision support system [11, 12]. Among them, the general requirements analysis combines the current situation of requirements with scientific research data, the real requirements of middle school management, and the technical concept of a decision support system; the overall architecture design includes system structure design, technical architecture, and functional architecture; the basic design of the structure includes data warehouse design, analysis, and online processing design, data mining design and pattern library design; application module design includes function design and interface design [13, 14]. The literature introduces the theoretical overview and research stage of the decision support system; secondly, it understands the modern management technology of student information, teacher information, course information, and grade information, and starts to collect student grades; finally, it uses Microsoft SQL Server2008 to create a data warehouse based on student grades, uses Microsoft Visual Studio 2010 as a development tool to implement a decision support system for student achievement management, and uses data mining algorithms to discover effective rules hidden behind the data [15, 16].

3. Sparse Clustering Algorithms

3.1. Basic Principles. Sparse model optimization is to establish a sparse representation optimization model through sparse data constraints, use alternating direction multiplication (ADMM) to solve sparse coefficients, and then use the obtained sparse coefficients to build an association matrix. The spectral clustering of the correlation matrix can cluster high-dimensional data into low-dimensional latent subspaces, and at the same time, the number of subspaces and their corresponding dimensions can be obtained.

Currently, in the same subspace, each data can refer to the other through a certain correlation with other data, which is the self-representation of data. The specific algorithm is as follows:

$$x_i = Xc_i, c_{ii} = 0. \tag{1}$$

In the earlier literature, methods such as norm-constrained least squares regression or low-rank representations using nuclear norm constraints were often used to find the best representation for a correctly classified dataset. After the sparsity theory is proposed, sparse subspace clustering uses $l1$ norm regularization to find the sparse representation coefficient ci so that its nonempty elements and the data corresponding to x_i come from the same subspace. Therefore, for each $i = 1,\ldots,n$, there is an optimized model:

$$\min \| c_i \|_1 s.t.\ x_i = Xc_i, c_{ij} = 0. \tag{2}$$

There is an optimized model for the data matrix X:

$$\min \| C \|_1 s.t.\ X = XC, \mathrm{diag}\ (C) = 0. \tag{3}$$

The sparse subspace clustering optimization model is written in the following ADMM form:

$$\min_{C} \| C \|_1 + \frac{\mu_1}{2} \| XZ - X \|_2^2 s.t.\ Z - C = 0, \tag{4}$$

Where U1 is the equilibrium parameter. According to the multiplier method, the augmented Lagrangian equation can be obtained:

$$L_{\mu_2}(Z,C,\lambda_2) = \frac{\mu_1}{2} \| XZ - X\|_2^2 + \| C \|_1 + tr\left(\lambda_2^T (Z-C)\right) + \frac{\mu_2}{2} \| Z - C\|_2^2. \tag{5}$$

The dual variable is abbreviated as

$$u_2 = \frac{\lambda_2}{\mu_2}. \tag{6}$$

This results in a shorthand form:

$$L_{\mu_2}(Z,C,u_2) = \frac{\mu_1}{2} \| XZ - X\|_2^2 + \| C \|_1 + \frac{\mu_2}{2} \| Z - C + u_2 \|_2^2 - \frac{\mu_2}{2} \| u_2 \|_2^2. \tag{7}$$

When the other variables no longer change, the Z value is updated.

$$Z^{k+1} = \text{argmin } \frac{\mu_1}{2} \| XZ^k - X \|_2^2 + \frac{\mu_2}{2} \| Z^k - C^k + u_2^k \|_2^2. \tag{8}$$

According to the derivation formula, the solution can be obtained as

$$Z^{k+1} = \left(\mu_1 X^T X + \mu_2\right)^{-1} \left[\mu_1 X^T X + \mu_2 \left(C^k - u_2^k\right)\right]. \tag{9}$$

Similarly, the updated form of C is

$$C^{k+1} = \text{argmin} \| C^k \|_1 + \frac{\mu_2}{2} \| Z^{k+1} - C^k + u_2^k \|_2^2. \tag{10}$$

Since the soft threshold is an optimal approximation of the $l1$ norm, the solution of the above equation can be expressed as

$$C^{k+1} = S_{1/\mu_2}\left(Z^{k+1} + u_2^k\right), \tag{11}$$

where $S\eta(a)$ is the soft threshold shrinking operation for each element in the given matrix, which is defined as

$$S_\eta(a) = \max(|a| - \eta, 0) \cdot \text{sgn}(a). \tag{12}$$

When Z and C are updated, update the Lagrangian multipliers with gradient ascent with step size u_2:

$$\lambda_2^{k+1} = \lambda_2^k + \mu_2\left(Z^{k+1} - C^{k+1}\right). \tag{13}$$

The first step in spectral clustering is to compute the Laplace matrix from the correlation matrix:

$$L_W = I - D^{-\frac{1}{2}} U D^{-\frac{1}{2}}. \tag{14}$$

3.2. Algorithm Improvement. In order to consider the local and global dataset structure in the algorithm model, so that the resulting correlation matrix has a block-diagonal structure in the case of being as small as possible, the LSGS algorithm proposed in this section incorporates the log determinant function of F. Combining these rules, the following mathematical model is created:

$$\min_C \log\det\left(I + C^T C\right) + \lambda_1 \| C \|_F + \lambda_2 \| E\|_F \; s.t.\; X = XC + E. \tag{15}$$

Since the Logdet (I + CTC) function is non-convex, the objective function of the model (15) is in non-convex form. To solve this problem, we can add a matrix Z, let $Z = C$, so model (15) can be rewritten as

$$\min_C \log\det\left(I + Z^T Z\right) + \lambda_1 \| Z\|_F + \lambda_2 \| E\|_h \quad s.t.\; X = XC + E, C = Z. \tag{16}$$

ALM algorithm is used to solve the above formula to expand the calculation scale, suitable for processing a large number of data.

$$L(E,Z,Y_1,Y_2,C,\mu) = \log\ det\left(I + Z^T Z\right) + \lambda_1 \| Z\|_F + \lambda_2 \| E\|_1 + tr\left(Y_1^T (Z-C)\right) + tr\left(Y_2^T (X - XC - E)\right) + \frac{\mu}{2}\left(\| Z - C\|_F^2 + \| X - XC - E\|_F^2\right), \tag{17}$$

where Y is the Lagrange multiplier and $u > 0$ is the penalty parameter, the variable can be updated using alternative minimization ideas. The plan is

$$C^{t+1} = \underset{C}{\text{argmin}}\, \text{tr}\left(\left(Y_1^t\right)^T \left(Z^t - C\right)\right) + \text{tr}\left(\left(Y_2^t\right)^T \left(X - XC - E^t\right)\right) + \frac{\mu^t}{2} \| Z^t - C \|_F^2 + \frac{\mu^t}{2} \| X - XC - E\|_F^2, \tag{18}$$

$$Z^{t+1} = \underset{Z}{\text{argmin}} \log\ \det\left(I + Z^T Z\right) + \lambda_1 \| Z\|_F + \frac{\mu^t}{2}\left(\| Z - \left(C^{t+1} - \frac{Y_1^t}{\mu^t}\right) \|_F^2\right). \tag{19}$$

Update C: After derivation of (18), the solution of matrix C can be easily obtained:

$$C^{t+1} = \left(I + X^T X\right)^{-1} \left[X^T \left(X - E^t\right) + J^t + \frac{Y_1^t + X^T Y_2^t}{\mu^t}\right]. \tag{20}$$

Update Z: The last step is to update the matrix Z. For the minimization problem,

$$\min_z F(Z) + \frac{\beta}{2} \| Z - A\|_F^2. \tag{21}$$

Rearranging this equation yields a cubic equation with three roots. If you want to solve it, you can set the parameter $\beta = 5.7$ in the experiment, and then get the update method of the Z variable:

$$Z^{t+1} = U\, \text{diag}\left(\sigma_1^{t+1}, \ldots, \sigma_n^{t+1}\right) V^T. \tag{22}$$

After updating E: The solution of E can be obtained by a similar method.

$$E^{t+1} = \frac{Y_2^t + \mu^t\left(X - XC^{t+1}\right)}{\mu^t + 2\lambda}, \tag{23}$$

$$E_{ij}^{t+1} = \begin{cases} Q_{ij} - \dfrac{\lambda}{\mu^t}\operatorname{sgn}\left(Q_{ij}\right) \text{if} \left|Q_{ij}\right| < \dfrac{\lambda}{\mu^t}, \\ 0, \text{otherwise} \end{cases} \tag{24}$$

$$\left[E^{t+1}\right]_{:i} = \begin{cases} \dfrac{\| Q_{i,i} \|_2 - \lambda/\mu^t}{\| Q_{i,i} \|_2} Q_{:i} \text{ if } \| Q_{:i} \|_2 < \dfrac{\lambda}{\mu^t} \\ 0, \text{otherwise.} \end{cases} \tag{25}$$

The remaining multipliers are easily obtained:

$$\begin{aligned} Y_1^{t+1} &= Y_1^t + \mu^t\left(Z^{t+1} - C^{t+1}\right), \\ Y_2^{t+1} &= Y_2^t + \mu^t\left(X - XC^{t+1} - E^{t+1}\right). \end{aligned} \tag{26}$$

3.3. Simulation Experiment. The synthetic data for this experiment consists of three linear subspaces, two of which intersect at a point. By increasing the number of data points, the model in this paper is known to perform better on big data, so the experimental results listed in the table below are based on 300 data points per subspace. The clustering errors of the four experimental datasets are shown in Table 1. By comparison, it is not difficult to find that the performance of the LSGS algorithm proposed in this paper is better than other clustering methods.

To achieve a good clustering effect, the core idea is that the relationship between subspaces should be sparse, and the relationship between data in the same subspace should be close. This phenomenon can be displayed using an association matrix structure. Figure 1 is the correlation matrix image of each algorithm in the above experiment. It can be seen that the diagonal part of the correlation matrix block of the LSGS algorithm is clearer.

4. Research on the Model of Decision Support System for Middle School Education Management

4.1. System Requirements Analysis. There are a large number of secondary schools in China and they are widely distributed. Due to the unbalanced economic development in the regions, the ruling leaders place different emphasis on secondary education, schools, and building information. Some schools in more economically developed areas have realized the general computerization of school construction and information-based teaching, while some schools in less developed areas have not realized office computerization, or even have no campus network.

Due to the current situation of building informatization in middle schools and the above problems, the design of data collection methods will also be different.

Table 1: Average clustering error rates for synthetic data.

Algorithms	SSC	LRR	CLAR	LSGS
Errors	38.71	41.41	31.75	19.76

In order to realize the original collection and dynamic collection of data collection activities, it is necessary to establish a standard, unique, real-time dynamic data center, so that the school-wide data can serve various applications and information systems and avoid repeated construction and information islands within the school. It is necessary to integrate and connect the general information data platform with other application systems, realize the intercommunication of the whole school data between different business subsystems, and realize the real-time sharing and exchange of data. The data center architecture of the secondary education management decision support system is shown in Figure 2:

There is a default timeline within the data center that can perform operations such as data aggregation, drill-through, and year-over-year and month-over-month comparisons. Through the data center, multi-party data exchange can be achieved to maintain data consistency. Each module of the system can realize information exchange and interconnection, and the establishment of a data center is independent of application programs. A data center can be equated with many software applications. It is beneficial for schools to make full use of various programs (including legacy software) for information exchange, information push, and business reorganization between application software. Integrate digital campus software systems to completely eliminate information silos.

4.2. System Architecture Design. The overall design architecture diagram is shown in Figure 3. We can understand the structure of the existing decision support system for middle school education management.

The middle school education management decision support system is implemented on the middle school management platform, and its development framework is mainly based on the three-level structure of the B/S model. Users can access it directly through different browsers without installing any applications, which is the biggest advantage of the C/S architecture. The overall technical architecture of the secondary education management decision support system is shown in Figure 4.

4.3. System Module Design

4.3.1. Data Warehouse Design. A data warehouse is a highly integrated set of data that can create a single point of data management by pulling data from other production databases and integrating them with similar themes and schemas. Building a data warehouse often relies on ETL tools to perform data processing. Since the data warehouse and production database are relatively isolated, incremental data needs to be extracted from time to time.

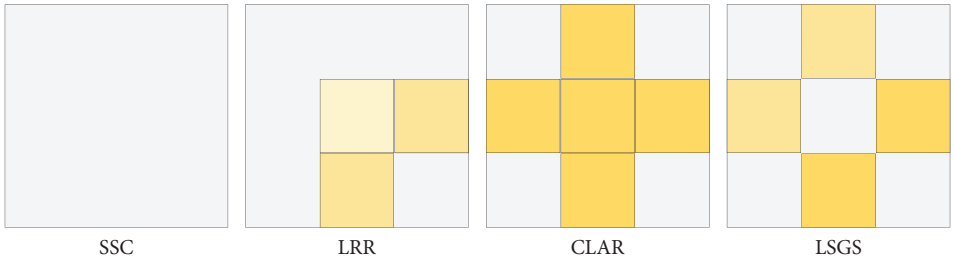

Figure 1: Coefficient structure matrix of the four algorithms.

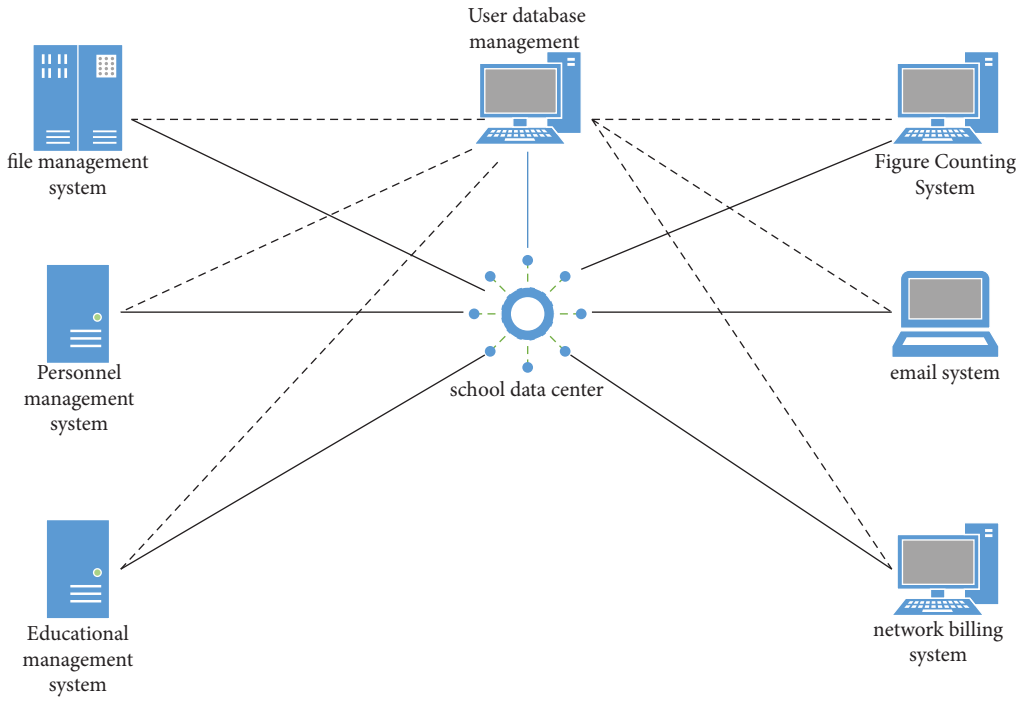

Figure 2: Data center architecture of secondary education management decision support system.

4.3.2. Online Analytical Processing Design. OLAP, online analysis and processing, is an important part of the decision support system for middle school education management, and its commonly used operations include drilling and segmentation. Online Analytical Processing for this topic is implemented based on Mondrian and MDX. Through the open source OLAP server Mondrian, MDX multi-dimensional query statements are parsed into SQL statements, and finally, the results are obtained through SQL query operations in the data warehouse.

4.3.3. Data Mining Design. This topic covers four algorithmic applications in data mining. The design idea of using these four algorithms is as follows.

The association algorithm analyzes the correlation from the interdependence of historical data, the clustering algorithm analyzes the similarity under a certain attribute, and project prediction based on the classification algorithm is usually used to predict the closure of open projects. The personalized recommendation is a recommendation algorithm based on collaborative filtering.

4.3.4. Design Pattern Libraries. There are three business functions in the middle school education management decision support system; that is, the same algorithm is suitable for three models, so all algorithm models must be managed based on the model library. Considering the scalability and easy accessibility of other components of the algorithm, the author designs a hierarchy with the Instrument layer and Data layer as the core. Among them, a tool corresponds to the application of the algorithm, and data corresponds to the training model of a specific business function. That is to say, in this system, since there are three major business functions, one Tool is equal to three corresponding Data.

4.3.5. Functional Design Part. The secondary education management decision support system is used to analyze the overall situation of secondary school subject development and program development and to provide assistance to managers so that they can easily establish a macro understanding of secondary school development. Users can freely choose the content section of the final analysis decision

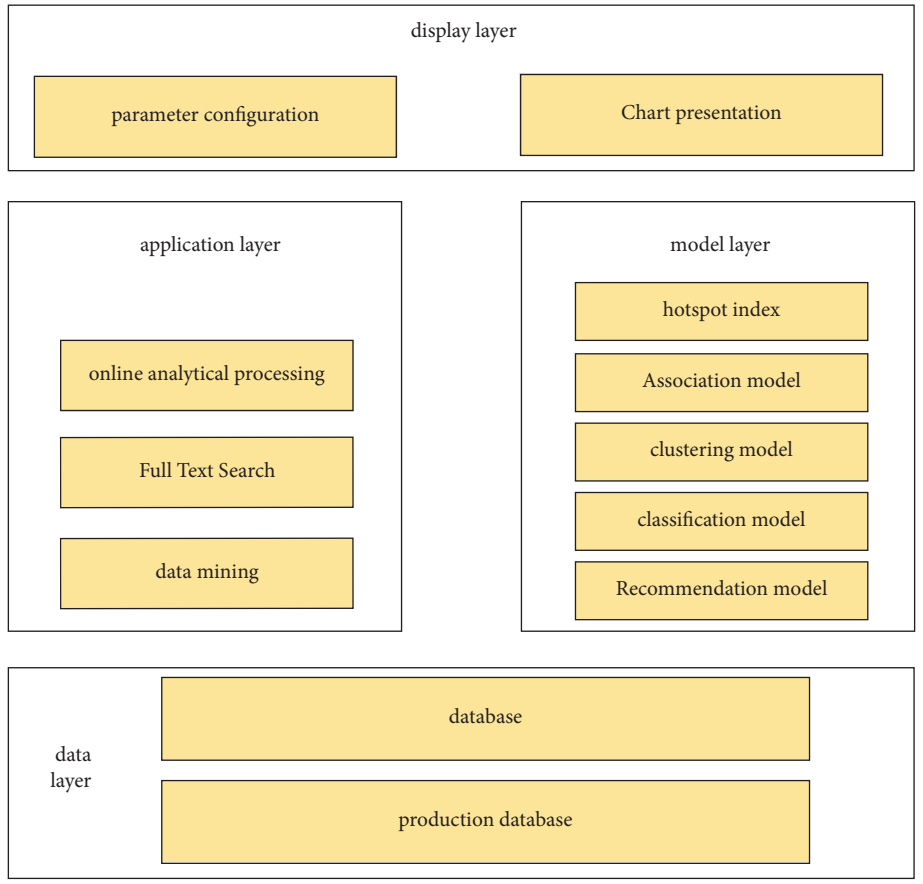

Figure 3: Overall design architecture diagram.

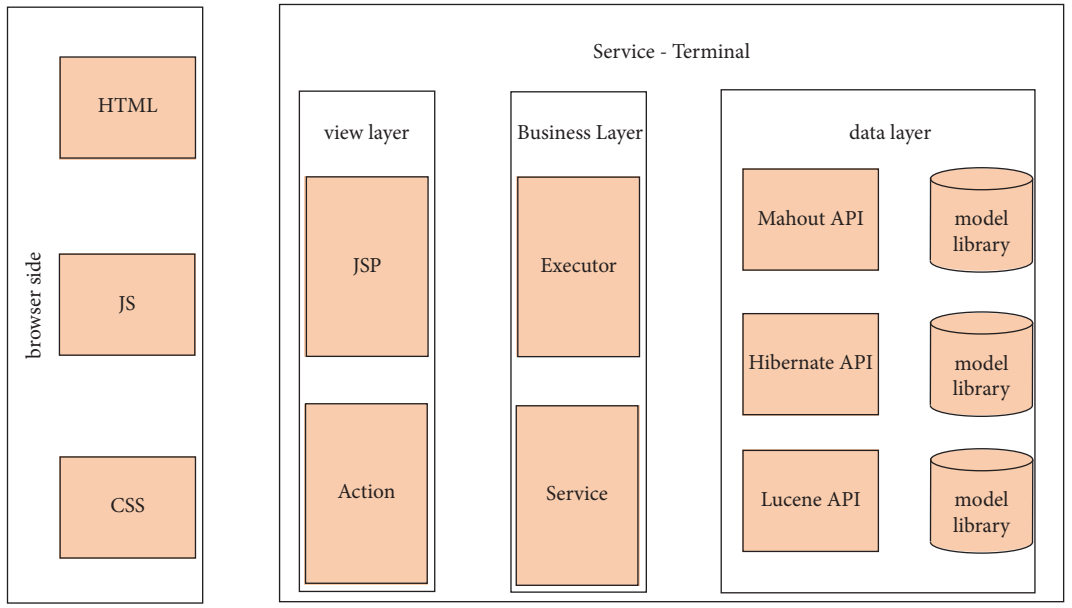

Figure 4: Overall technical architecture diagram.

report and customize the final result through the parameter configuration function provided by the submission interface. If necessary, you can also configure specific model updates to get the latest analysis results. Finally, users can freely export the corresponding PDF documents. The functions corresponding to this part are briefly described as follows: secondary school selection, model update, analysis decision, and document export.

In the KPI data collection and decision support system, we combine core management modules such as user management, authority management, and application management with system functions to achieve unified management and services for each business system.

User management can provide a unified way to determine user information and personnel relations, personnel relations, and system organization. Implementing personnel and organizational management, it provides unified views and services for different business systems, facilitating the definition and control of business flows between business system personnel.

Authorization management mainly provides access control functions for application systems and is an important part of application security. Simplify the development and maintenance of specific application systems.

System security requires a reliable authorization management system to limit the access and operation of each user's connection resources so that it is controlled by the content provided by the system, so authorization management plays an important role in the entire security application.

The secondary education management decision support system for data collection is usually used for each school to complete and report various data related to school teaching, support data aggregation and export, and report data to the superior. The main function of the module is to manage the configuration of the school data collection report, the management of the data collection process, and the management of the collection results. Figure 5 shows the functional structure of data collection in the decision support system for secondary education management.

4.4. System Test. System testing is the process of running a program using a manual method to determine system operation. The purpose is to verify that the system meets the system requirements and achieves the expected results. The importance of system testing and how it affects the reliability of software needs to be emphasized. During the software development process, we face many complex problems. The designer's understanding is not completely consistent with the objective facts, and everyone's operating habits are also different. Therefore, system testing is very important. Before running, it is necessary to find and correct software errors as much as possible to minimize losses. The fundamental goal of software engineering is to complete high-quality software that meets user needs.

In the system test summary, this work constitutes the core of the test. The final test results are obtained according to the functional modules analyzed by the requirements, and detailed data operation tests are carried out for each functional module to test whether the functional operation of each module is normal. The design of the examination system includes students' examination information management, score management, invigilator teacher management, and examination related information consultation. Then combined with the students' results, the design of the results of the statistical analysis chart, to discuss the changes in class results, as well as the students' individual behavior combined with the results of correlation analysis, the situation of learning statistics, and put forward some optimization suggestions. The detailed design is shown in Table 2.

In the user login test, mainly for the consideration of system security, the system will not log in to the system with different roles, and the test results are shown in Table 3.

5. Research on the Development of Middle School Education Management Decision-Making

5.1. Problems Faced by Decision Support Systems. Since the 1960s, with the development of data management requirements and the development of information technology, the construction of databases has experienced a process of developing from traditional databases to advanced databases. Different data models emerge one after another, and new technologies such as data mining continue to emerge. The continuous updating of data storage and presentation methods makes data occupy a very important position in the decision-making process and public management, and the database has become indispensable technical support for public decision-making.

In the field of education, with the development of China's education, especially the use of information management, such as the establishment of information systems for student status management and education funding management, the establishment of education databases has entered a period of rapid development. Assessing student quality, allocating educational resources, and evaluating satisfaction with public education services have become popular topics in database construction. At the same time, in order to overcome the functional limitations of the database, the construction of various indicators, especially the construction of comprehensive indicators such as student academic indicators, satisfaction indicators, and poverty alleviation indicators, is also constantly developing. It is undeniable that the construction of these indicators and the comprehensive database supported by the back-end are more reflective of the current state or future expectations of technological development than individual indicators or database types.

However, the development of database technology and even the model cannot completely overcome the limitations of the database itself. In the decision-making process, what supports the decision is evidence, not data. Data is a source of evidence, but not a substitute for evidence. Its function is to present the material and method of the problem, not the argument itself. Having a database does not mean having evidence. As far as decision analysts are concerned, databases are of great value and are the source of decision analysis. However, when the database is handed over to decision-makers, they may not necessarily attach importance to these data sets, nor may they have the will and ability to make decisions based on these data sets.

A database can only play a role in supporting decision-making when it is associated with a problem. Sometimes the

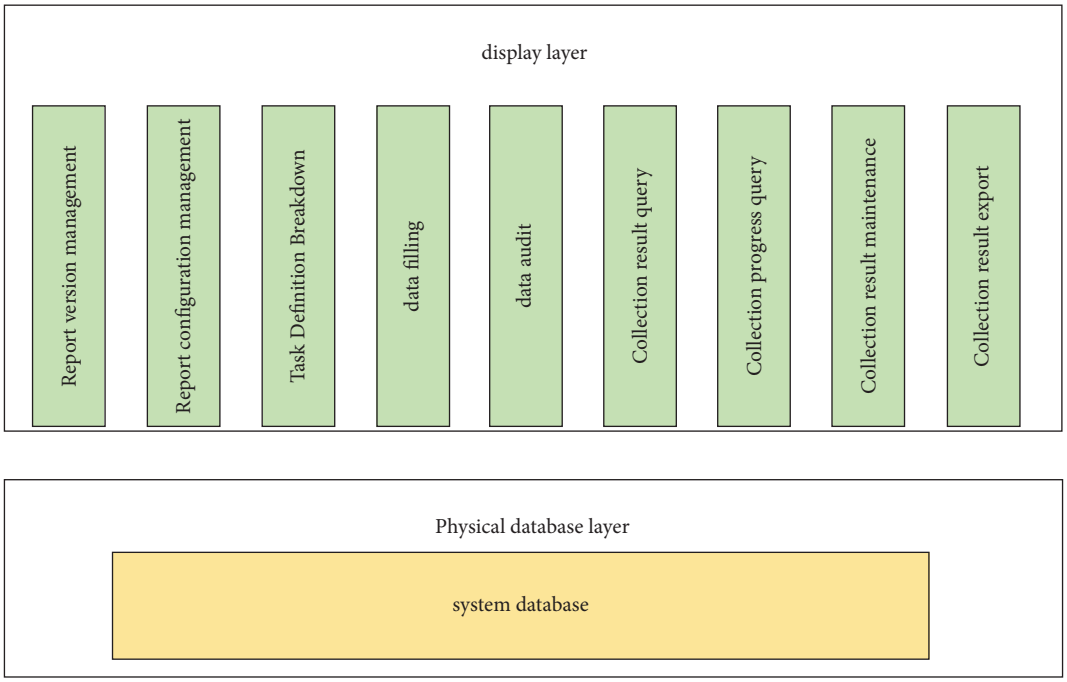

Figure 5: Structure diagram of school data collection function.

Table 2: Function item distribution and test results.

Test requirements	Test focus and results	Test results
System help	Whether the system help class file is available	Qualified
Develop and analyze lesson plans	Provide policy for the development of teaching plans and test whether certain subjects need to be adjusted for quality according to the set conditions	Qualified
Correlate and analyze subject grades	Ability to obtain hidden relationships between disciplines by setting conditions	Qualified
Graphs that count the grades of failing students	Whether the score records of failing students can be obtained through the corresponding statistical conditions and the corresponding charts can be generated by using the software	Qualified
Statistics on student grades	Whether the student's grade information data can be counted through the corresponding statistical conditions	Qualified
Query student grade information	Whether the student's grade information data can be queried through the corresponding query conditions	Qualified
Query course information	Whether the target course information data can be retrieved through the corresponding query conditions	Qualified
Inquire about teacher information	Whether the target teacher information data can be retrieved through the corresponding query conditions	Qualified
Inquire about student information	Whether the target student information data can be retrieved through the corresponding query conditions	Qualified
Manage student grade information	Whether the management module of student grade information is normal, including whether to modify, add, or delete student grade information and prompts for corresponding messages, etc.	Qualified
Manage course information	Whether the management module of the overall course information is normal, including whether to modify, add, or delete the overall course information and the corresponding message prompts, etc.	Qualified
Manage teacher information	Whether the management module of teacher information is normal, including whether to modify, add, or delete teacher information and prompts for corresponding messages, etc.	Qualified
Manage student information	Whether the management module of student information is normal, including whether to modify, add, or delete student information and prompts for corresponding messages, etc	Qualified
Management operator	Whether the management module of operator information is normal, including whether to modify, add, or delete operator information and corresponding message prompts, etc.	Qualified
Log in	Log in to the system, this operation requires the correct user name and password	Qualified

Table 3: User login test.

Project	Use case type	Test data	Desired result
User account	Whether to complete the entry verification	Null	Username required
	Perform length range validation	zhanghexuan2009400127	The username length does not match, too long
	Whether the user has completed the verification	123	This username does not exist
	Enter correct verification	Admin	Success
User Password	Whether to enter the verification	Null character	Password required
	Length range validation	zhanghexuanl234567890	Password length does not match, too long
	Validity verification	1112444585845	Wrong password
	Security check	Enter the wrong password 3 times	Exit system
	Correct input validation	admin1983	Success

importance of the data can obscure the real concerns of the decision maker, and sometimes a small difference in the statistics does not mean there are no problems. Due to the risky social focus on "Leviathan" data, individual characteristics may be overlooked if the general characteristics of the group are presented as "mechanized and faceted." From the perspective of policy or decision-making, paying attention to minority groups or special groups is the best embodiment of public welfare and public spirit. The database argument is based on an understanding of the problem, the legality of data use, and a focus on people. From this perspective, providing concrete cases around decision-making issues can also constitute support for educational decision-making.

At the same time, with the increase in the amount of data and the expansion of the database, the abuse of data selection and use rights will lead to data abuse, misuse, and even data violence, thus endangering the democratic process. The data itself is emotionless, fair, and objective, but after human understanding and use, it has a subjective color. The same data can be used for two different decision-making scenarios. Differences in data usage are determined by the purpose of use and the personality of the user. As a result, there is a fatal misunderstanding of the database as one that can automatically support decision-making. Databases seem to help achieve functional goals for those hungry for quick profits, at the expense of some, and a high cost. Therefore, it is necessary to maintain a high degree of vigilance against the traps of databases and big data, soberly recognize that data and databases are "embedded in a specific personality subject," and strive to achieve the transcendence of databases.

5.2. Educational Management Development Strategies

(1) Decision-making needs to adopt different decision-making concepts so that as many people as possible can participate in decision-making. When making decisions, many aspects should be considered, not only the quality of department management but also the benefits. With the development of the economy and society, any unit that does not consider interests may be eliminated by society. Also, listen to as many students as possible.

(2) According to different decision-making content, determine the personnel involved in decision-making and conduct systematic analysis on different decision-making issues. In this way, sufficient attention will be paid to recruitment and employment, purchase and maintenance of equipment and facilities, site construction, and fund allocation, so as to avoid losing content in the decision-making process.

(3) In view of the traditional decision-making mode dominated by leaders, this paper believes that we should build a new evaluation system to evaluate the form of scoring, so as to make the evaluation more open and fairer.

(4) In view of the traditional annual and quarterly summary, this paper believes that a real-time evaluation system should be established to provide timely information exchange and feedback and better grasp the situation.

The key to making good decisions is "90% intelligence plus 10% intuition (hunch)," which shows the important role of information in the decision-making process. Therefore, only by mastering a large amount of effective information before making a decision, the information can be comprehensively and systematically summarized, compared, and screened, and then the false and the true can be removed, various information materials can be analyzed, and then decision-making can be provided. That is, we need to provide service information for our decision-making tasks. In terms of management information systems, the physical education department is still very backward, displaying inaccurate and incomplete information, low reliability, slow transmission and feedback speed, and backward technology.

Decision-making is an important activity for human society to determine action goals, determine action policies and strategies, propose action plans and programs, and formulate different policies. It is an action that plans and affects the future. Whether the formulated policy or action plan is correct and feasible must be tested in practice. The principle of future forecasting must be based on accurate information because only accurate and reliable information can make correct predictions about future developments. To make the right decision, you also need to make the right

judgment about the possible consequences of the decision, and if you make a hasty decision without knowing the consequences of the action, you may make the wrong decision. The effects of many decisions are often invisible in the short term. If you find that corrections are needed, it will be too late and cause losses. Therefore, applying technical theories and methods to future research, making scientific predictions, and providing a scientific basis for decision-making are important principles for scientific decision-making.

6. Conclusion

With the continuous development of education and the continuous construction of public and private schools, education management has become a very important point in school competition. Therefore, the management of students' scores, the management of teaching situation, the management of teachers, and so on are the current school leaders pay more attention to the content. The middle school education management decision support system developed in this paper can effectively help the school management to grasp the implementation situation more comprehensively and put forward some rectification suggestions. The system uses a sparse clustering algorithm to find potentially useful information about students, provide relevant decision-making for education administrators, better serve the school education process and improve teaching quality.

Data Availability

The data used to support the findings of this study are available from the corresponding author upon request.

Conflicts of Interest

The authors declare that they have no conflicts of interest.

Acknowledgments

No funding was used in this paper.

References

[1] B. Cumbo and N. Selwyn, "Using participatory design approaches in educational research," *International Journal of Research and Method in Education*, vol. 45, no. 1, pp. 60–72, 2022.

[2] Ø. Hammer, D. A. Harper, and P. D. Ryan, "PAST: paleontological statistics software package for education and data analysis," *Palaeontologia Electronica*, vol. 4, no. 1, p. 9, 2001.

[3] B. J. Hicks, "Lean information management: understanding and eliminating waste," *International Journal of Information Management*, vol. 27, no. 4, pp. 233–249, 2007.

[4] M. Franklin, A. Halevy, and D. Maier, "From databases to dataspaces: a new abstraction for information management," *ACM Sigmod Record*, vol. 34, no. 4, pp. 27–33, 2005.

[5] J. Xue and Y. Mao, "Research on the impact of 5G technology on teaching behavior," *Journal of Physics: Conference Series*, 012117, vol. 1955, 2021.

[6] J. Mysiak, C. Giupponi, and P. Rosato, "Towards the development of a decision support system for water resource management," *Environmental Modelling & Software*, vol. 20, no. 2, pp. 203–214, 2005.

[7] R. Shibl, M. Lawley, and J. Debuse, "Factors influencing decision support system acceptance," *Decision Support Systems*, vol. 54, no. 2, pp. 953–961, 2013.

[8] E. F. Malik, K. W. Khaw, B. Belaton, W. P. Wong, and X. Chew, "Credit card fraud detection using a new hybrid machine learning architecture," *Mathematics*, vol. 10, no. 9, p. 1480, 2022.

[9] Z. Deng, K. S. Choi, Y. Jiang, J. Wang, and S. Wang, "A survey on soft subspace clustering," *Information Sciences*, vol. 348, pp. 84–106, 2016.

[10] S. F. Tonellato, "Bayesian nonparametric clustering as a community detection problem," *Computational Statistics & Data Analysis*, vol. 152, Article ID 107044, 2020.

[11] J. Xu and L. Corno, "Family help and homework management reported by middle school student," *The Elementary School Journal*, vol. 103, no. 5, pp. 503–517, 2003.

[12] J. McCarthy and J. Benally, "Classroom management in a Navajo middle school," *Theory Into Practice*, vol. 42, no. 4, pp. 296–304, 2003.

[13] M. Adil, J. Ali, M. Attique et al., "Three byte-based mutual authentication scheme for autonomous internet of vehicles," *IEEE Transactions on Intelligent Transportation Systems*, vol. 23, no. 7, pp. 9358–9369, 2021.

[14] Y. Wang and J. Talim, "Online mobile teaching methods based on Android in the 5G environment," *International Journal of Continuing Engineering Education and Life Long Learning*, vol. 30, no. 2, pp. 133–147, 2020.

[15] R. Moodley, F. Chiclana, J. Carter, and F. Caraffini, "Using data mining in educational administration: a case study on improving school attendance," *Applied Sciences*, vol. 10, no. 9, p. 3116, 2020.

[16] W. I. D. Mining, "Data mining: concepts and techniques," *Morgan Kaufinann*, vol. 10, pp. 559–569, 2006.

Hindawi
Mobile Information Systems
Volume 2022, Article ID 7221157, 9 pages
https://doi.org/10.1155/2022/7221157

Research Article

Air Quality Prediction Model Using Deep Learning in Internet of Things Environmental Monitoring System

Yongliang Feng

College of Information Engineering, Xi'an University, Xi'an, Shaanxi 710065, China

Correspondence should be addressed to Yongliang Feng; fengyongliangwlxy@126.com

Received 14 June 2022; Revised 10 August 2022; Accepted 1 September 2022; Published 29 September 2022

Academic Editor: Shadi Aljawarneh

In order to realize the accurate prediction of spatial-temporal air quality index, this paper constructs a STAQI prediction model based on deep learning, including data processing, spatial feature acquisition, temporal feature acquisition, and STAQI prediction. Firstly, the spatial interpolation method is used to optimize the sample data set to provide reliable data; the improved graph convolutional network and the improved long short-term memory are used to effectively extract the spatial and temporal distribution characteristics of AQI data; and then, the extreme learning machine model is used to accurately predict and analyze AQI data. Simulation results show that the evaluation indexes RMSE and MAE of the constructed prediction model are 4.51 and 3.92, respectively, showing excellent curve fitting ability and AQI prediction ability.

1. Introduction

With the rapid development of the world economy and the acceleration of industrialization and urbanization, energy consumption has increased sharply, and the problem of air pollution is particularly prominent [1, 2]. In recent years, the concentration of air pollutants exceeds the standard frequently [3, 4]. Air pollution not only leads to a significant decline in atmospheric visibility in some areas but also poses a great threat to human health [5].

Research shows that suspended particulate matter is one of the most deadly air pollutants, containing a large number of harmful substances. Long-term exposure to the suspended particulate matter will increase the risk of the respiratory system, cardiovascular system, lung cancer, and other diseases, and even increase mortality [6, 7]. Therefore, air quality index (AQI) is the fundamental point to achieve comprehensive environmental governance, which is of great significance to people's healthy life and government decision-making [8].

Traditional air quality prediction can be divided into numerical prediction method and regression statistical prediction method. The principle of the numerical prediction model is to simulate the pollutant movement process by using the monitoring data of a fixed number of air quality monitoring stations. It depends on a large number of empirical assumptions and parameters, which is not enough to accurately reflect the real atmospheric environment, and its prediction performance is subject to certain constraints [9]. The regression statistical method focuses on analyzing the internal laws of the data, does not involve the complex physical and chemical reactions between air pollutants, and uses the statistical modeling method to obtain the predicted value, which depends on the stationary hypothesis, which limits the fitting ability of the model to a certain extent [10].

To solve the above problems, this paper analyzes the time and spatial aspects, and constructs a spatial-temporal air quality index (STAQI) prediction model based on deep learning. The model mainly optimizes the Graph Convolutional Network (GCN) and gated recurrent unit (GRU) models to realize the deep extraction of spatial features of the STAQI. At the same time, the F-LSTM prediction network can also quickly obtain the time characteristics of data, so as to improve the fitting ability of the prediction model. Simulation results show that the proposed model has excellent curve fitting ability and prediction ability.

2. Air Quality Monitoring and Data Preprocessing

2.1. Air Quality Monitoring. Air quality prediction mainly faces the following four challenges:

(1) Air quality will be affected by many factors, such as traffic. These influencing factors are difficult to obtain or model in advance.

(2) Air quality shows high uncertainty in the time dimension [20, 21]. As shown in Figure 1, taking the PM2.5 mass concentration parameter, one of the main pollutants characterizing air quality, as an example, the mass concentration at each time in a given 2d varies greatly, and the PM2.5 mass concentration shows significant changes at different times in 1d, and the difference between the highest and lowest mass concentrations can reach 100 mg/m3.

(3) There are significant differences in air quality data in different geographical locations [22]. As shown in Figure 2, the PM2.5 mass concentration change curves of three monitoring stations in Beijing were different within 1d. The two monitoring points A and B are close, while the monitoring point C is located in the suburbs and far away from monitoring points A and B. It can be seen from Figure 2 that in most periods, the PM2.5 mass concentration monitored by the three stations is quite different, and the PM2.5 mass concentration of monitoring point C is relatively low.

(4) Due to the limitation of practical conditions, there will be a certain amount of missing basic data obtained for prediction, such as the lack of timestamp attribute value in the data entry or the lack of specific monitoring data.

Table 1 lists the missing data of the real data set used in the study. PM10 lacks tens of thousands of data, and other data are also missing to varying degrees, which has a great impact on the work efficiency of the model. Therefore, it is necessary to design and construct corresponding data preprocessing schemes to reduce data noise.

2.2. Data Preprocessing. According to the analysis of regional division results, an air quality monitoring station is affected by multiple surrounding affected subareas. The number of stations contained in each subarea is different, and there may be zero, one, or more stations. Therefore, for different division results, corresponding methods are adopted for area filling, and finally, the air quality value of each affected subarea can be obtained.

For the affected subarea with one monitoring station, the monitoring value can be directly used as the air pollution degree of the current area. During prediction, the monitoring value is directly used as the input parameter for model training. The relationship between regional air quality and monitoring station air quality can be expressed as

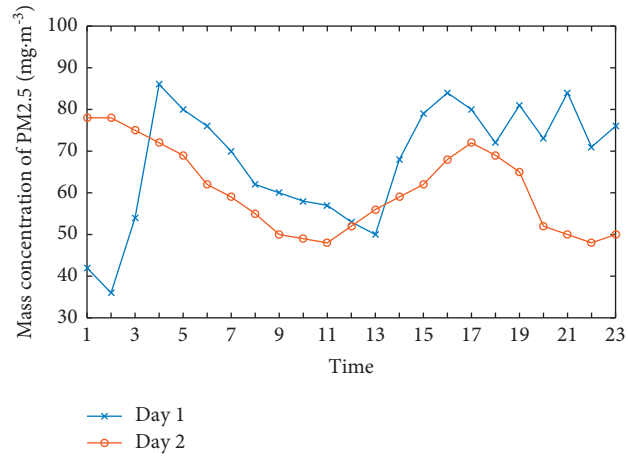

Figure 1: Change in mass concentration during different monitoring periods.

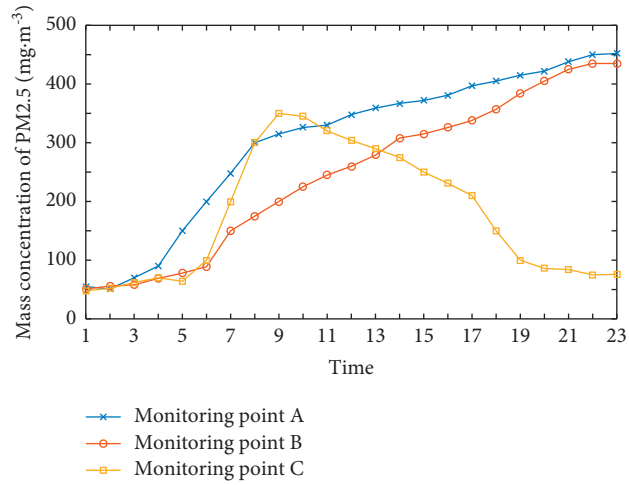

Figure 2: Changes in mass concentration at different monitoring stations.

Table 1: Sample characteristics of real data set.

Parameter	Amount of missing data	Proportion of missing data (%)
CO	549918	5.152
O_3	454912	3.219
NO_2	494861	4.594
SO_2	554842	5.184
PM2.5	611845	7.157
PM10	724489	9.154

$a_i^{AQI} = s^{AQI}(s \in a_i)$, where $s \in a_i$ means that the monitoring station s is in the affected subarea a_i, i means the number of the affected subarea, and AQI is the air quality collection, including PM2.5, PM10, SO2, NO2, CO, and O_3.

The situation that there are no monitoring stations and multiple monitoring stations in the affected subregion needs to be considered separately. When there are multiple monitoring stations in the affected subarea, different weights are set according to the distance from each monitoring station to the monitoring station to be predicted. The

monitoring values of each monitoring station in the area are multiplied by the weights and accumulated. The result is the average air quality of the area and reflects the average air pollution degree of the affected subarea. The calculation method when there are multiple monitoring stations in the affected subarea is shown in (1):

$$a_i^{AQI} = \sum_{j=1}^{k} s_j^{AQI} W_j, \quad (1)$$

where k is the number of monitoring stations in the area, and its value range is $(1 - k)$; j refers to the number of monitoring stations in the area; and W_j is the influence weight of the j monitoring station.

If there are no monitoring stations in the affected subarea and there are missing values, the spatial interpolation method is used for spatial interpolation. As shown in Figure 3, the left side of the figure shows the air quality distribution around the monitoring station without filling the null area, and the right side of the figure shows the air quality distribution around the monitoring station after filling the null area with the spatial interpolation method.

In order to better realize the quantitative analysis of data, the air quality index is numerically transformed according to the division of air quality grade. The specific replacement method is shown in Table 2. If the air quality index is in the range of 0 ~ 50, replace it with the number 1 in the original data set; if it is in the range of 51 ~ 100, replace it with the number 2; if it is in the range of 101 ~ 150, replace it with the number 3; if it is in the range of 151 ~ 200, replace it with the number 4; if it is in the range of 201 ~ 300, replace it with the number 5; if it is greater than 300, replace it with the number 6.

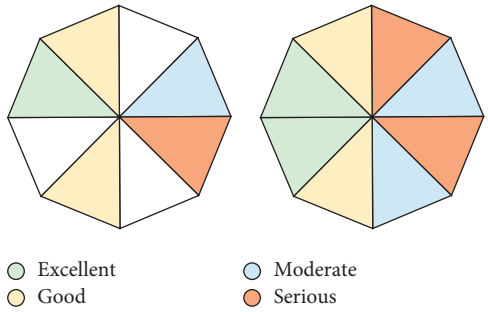

Figure 3: Air quality distribution map.

Table 2: Air quality index classification.

Air quality grade	AQI	Classification level
Excellent	0~50	1
Good	51~100	2
Light pollution	101~150	3
Moderate pollution	151~200	4
Severe pollution	201~300	5
Serious pollution	>300	6

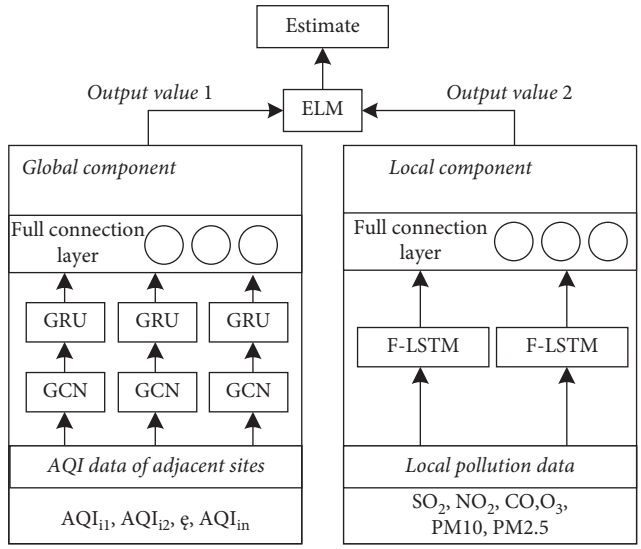

Figure 4: STAQI prediction model.

3. Short-Term Single Step Prediction Model of Air Quality

3.1. Model Building. There is a strong spatial-temporal correlation between air quality data sets [23]. In the prediction process, only considering the temporal correlation and ignoring the analysis of spatial features will inevitably reduce the prediction performance of the model.

Considering the special spatial-temporal data such as air quality, this study applies a STAQI prediction model based on deep learning to the short-term one-step prediction of AQI at target stations. As shown in Figure 4, the STAQI prediction model can be structurally divided into global components and local components, which respectively model and analyze the air quality (spatial correlation) in the adjacent area and the concentration (temporal correlation) of multiple air pollutants at the target site. Finally, the temporal and spatial features extracted from local components and global components are fused to obtain the AQI single-step prediction value of the target site. The specific implementation process is as follows.

3.2. Global Component. The distribution of monitoring stations in the city is not established with a certain law and equal spacing, and the topology between monitoring stations is a typical graph structure. Therefore, the data composed of air quality information monitored by multiple stations is a special kind of graph data. The core idea of graph convolution neural network is to learn a function mapping so that the nodes in the graph can aggregate the characteristics of their own nodes and neighbor nodes to obtain a new representation of nodes. The emergence of GCN makes it possible for deep learning to effectively extract spatial features from graph data.

Definition 1. Topology graph G: $G = (V, E)$ can be used to describe the topology between multiple environmental monitoring sites. The graph is composed of nodes and edges. Each node in the figure represents an environmental monitoring station; V represents the collection of multiple

monitoring stations, i.e., $V = \{V_1, V_2, \ldots, V_N\}$, where N is the total number of monitoring stations and E represents the collection of edges between monitoring stations.

According to the first law of geography, everything has different degrees of influence, and the closer things are, the more obvious the relevance is. The spatial correlation of air quality among multistations also obviously conforms to the law. Therefore, the distance between every two stations in the city is calculated according to (2). The greater the distance is, the weaker the correlation is, and on the contrary, the stronger the correlation is. The strong and weak correlation degree between the two STAQI is expressed by calculating the reciprocal of the distance between the two stations and is stored in the adjacency matrix A as the edge weight value of the corresponding station, $A \in R^{N \times N}$.

$$L = 2r * \arcsin \cdot \left(\sqrt{\left(\sin\left(\frac{a-c}{2}\right)\right)^2 + \cos(a) * \cos(c) * \left(\sin\left(\frac{b-d}{2}\right)\right)^2} \right), \tag{2}$$

where $X(a, b)$ and $Y(c, d)$ are the geographical locations of the two stations; a and c are the respective latitude information of the station; b and d are the longitude information of each point; and r is the radius of the ball.

Definition 2. Characteristic matrix $X^{N \times r}$: The characteristic matrix is used to store the attribute characteristics of each node in the graph, that is, the STAQI data of each monitoring station, expressed as $X \in R^{N \times r}$; P represents the quantitative characteristics of the node in the graph, corresponding to the historical time window size of model input; $X_t \in R^{N \times i}$ represents the STAQI value of each monitoring station at time i.

The implementation process of GCN is as follows:

(1) According to the geographical location information of each station, the topology G of the urban environmental monitoring station where the target station is located is constructed, and the correlation degree between the two stations is calculated and stored in the adjacency matrix A.

(2) The characteristic matrix X is constructed based on the STAQI observations of the target urban environmental monitoring station at different times.

(3) The adjacency matrix A generates matrix $\widehat{A}$ ($\widehat{A} = \widetilde{D}^{12}\widetilde{A}\widetilde{D}^{12}$) through Laplace transform, where $\widehat{A} = A + I_N$ is the self-connected adjacency matrix, I_N is the identity matrix, and $\widetilde{D}$ is the degree matrix.

(4) Use (3) to aggregate and transform the characteristics of associated nodes to calculate the new characteristics of target nodes:

$$H^{(i+1)} = \sigma\left(\widehat{A}H^{(i)}W^{(i)}\right), \tag{3}$$

where σ is the nonlinear activation function; $W^{(i)}$ is the weight matrix of layer i; $H^{(i)}$ is the activation value of layer i; and $H^{(0)} = X$.

According to the geographical location information of environmental monitoring stations in different corners of the city, the geographical distance between different stations is calculated. The inverse distance value is taken as the edge weight of the corresponding edge between two stations and stored in the adjacency matrix. At the same time, the air quality of multiple historical moments at all monitoring stations in the city is used as the input matrix. By multiplying the information of the column of the target site in the Laplace matrix with the input matrix to dynamically aggregate the impact of the air quality status of different environmental monitoring sites on the air quality status of the target site at the same time, a new expression of the air quality of the target site can be obtained. The data of spatial features extracted by the graph convolution network is input into the GRU, the temporal features are dynamically obtained through the information transmission between units, and the network output is transformed by the fully connected layers.

Figure 5 visually shows the internal structure of the global component. The left area represents the overall structure of the global component. Each basic cycle unit block is GG (GCN-GRU). The right area is the specific structure of GG unit cells. Among them, GCN represents the graph convolution operation on the current data, and the input data x_t generates x_t' after extracting spatial features through GCN. u_t represents the update gate, r_t represents the reset gate, c_t represents the cell state at time t, and h_t represents the output at time t. GCN extracts the spatial features in the multistation air quality feature data by relying on the topology G of multiple monitoring stations and the corresponding air quality feature matrix X, so that the nodes in the graph have the ability to deeply extract the features of their own nodes and adjacent nodes.

The global component calculation process is as follows:

$$\begin{aligned} u_t &= \sigma\left(W_u\left[f\left(A, X_t\right), h_{t-1}\right] + b_u\right), \\ r_t &= \sigma\left(W_r\left[f\left(A, X_t\right), h_{t-1}\right] + b_r\right), \\ c_t &= \tanh\left(W_c\left[f\left(A, X_t\right), \left(r_t * h_{t-1}\right)\right] + b_c\right), \\ h_t &= u_t * h_{t-1} + \left(1 - u_t\right) * c_t, \end{aligned} \tag{4}$$

where $f(A, X_t)$ is the graph convolution process; W is the weight in the training process; and b represents the bias during training.

3.3. Local Component. The local components are composed of LSTM network, which is characterized by multivariate historical time series composed of predicting the concentration of main air pollutants and air quality at the station.

This paper improves the cell structure of LSTM, eliminates the dependence of the current cell state and hidden layer state on the last hidden layer state, realizes faster state update, and obtains the F-LSTM (fast long short-term

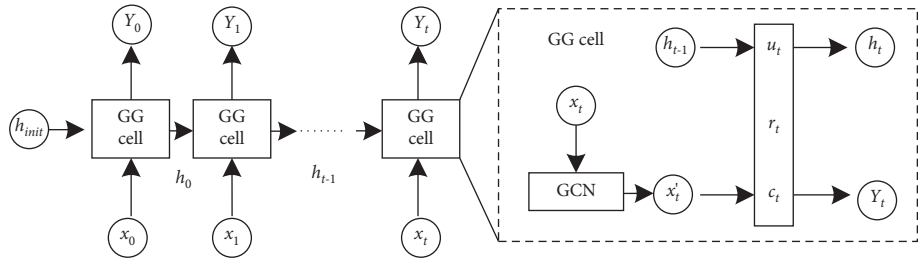

Figure 5: Internal structure of global components.

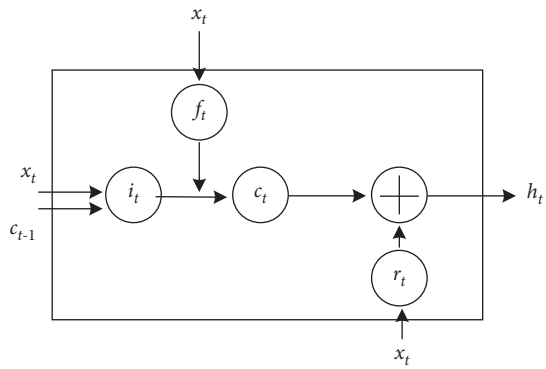

Figure 6: F-LSTM structure.

memory) cell structure. The F-LSTM structure is shown in Figure 6.

F-LSTM includes an input gate i_t, a forgetting gate f_t, and a reset gate r_t. First, calculate the intermediate state $\tilde{x}_t$ according to the input, and then calculate the state of other doors. The calculation formula is as follows:

$$\begin{aligned} \tilde{x}_t &= Wx_t, \\ f_t &= \sigma\left(W_f x_t + b_f\right), \\ r_t &= \sigma\left(W_r x_t + b_r\right). \end{aligned} \tag{5}$$

The above operation only depends on x_t, which makes this part of the operation in the F-LSTM unit can be expanded in parallel. The forgetting gate is used to control the internal state c_t, c_t and the reset gate is used to calculate the output state C. The calculation formula is as follows:

$$\begin{aligned} c_t &= f_t \odot c_{t-1} + \left(1 - f_t\right) \odot \tilde{x}_t, \\ h_t &= r_t \odot g\left(c_t\right) + \left(1 - r_t\right) \odot x_t, \end{aligned} \tag{6}$$

where g is the activation function used to calculate the output state.

3.4. ELM Prediction. After multilayer hidden layer feature learning, the learned data features are input into the extreme learning machine (ELM) model for training and prediction [24, 25]. Let the eigenvector x of the air quality data and the corresponding STAQI prediction vector be t. For a set of samples $[x_i, t_i]\,(i = 1, 2, 3, \ldots, k)$, the neural network with L hidden layer nodes can be expressed as follows:

$$o_L(x) = \sum_{i=1}^{L} \beta_q\left(w_i x_i + c_i\right), x_i \in R^k, w_i \in R^k, \beta_i \in R^m, \tag{7}$$

where $x_i = [x_{i1}, x_{i2}, x_{i3}, \ldots, x_{in}]^T \in R^k$, $t_i = [t_{i1}, t_{i2}, t_{i3}, \ldots, t_{in}]^T \in R^m$, β_i is the output weight matrix connecting the i hidden layer and the output layer, w_i is the connection weight between the feature vector layer and the hidden layer, c_i is the offset vector of the hidden layer, and q is the activation function.

The purpose of single hidden layer neural network training is to minimize the output error, that is, there are w,β, and c, so that o and t are approximately equal.

$$\sum_{i=1}^{L} \beta_g\left(w_i x_i + c_i\right) = t_i. \tag{8}$$

3.5. Loss Function. Loss function plays a key role in the process of model training. Minimizing the value of loss function is the ultimate goal of model training. The smaller the loss value, the higher the learning ability of the model to the input data and the better the performance of the model. Compared with shallow neural network, the number of model parameters w of deep neural network increases gradually due to the increase in the number of network layers. The overfitting phenomenon is prevented by adding the L2 regularization term to the original loss function $L_o(w)$. The loss function $L(w)$ can be expressed as follows:

$$L(w) = L_o(w) + \frac{\lambda}{2n} \sum_{i=1}^{n} w_i^2. \tag{9}$$

Derivative $L(w)$:

$$\frac{\partial L(w)}{\partial w} = \frac{\partial L_0(w)}{\partial w} + \lambda w. \tag{10}$$

Update parameter w as follows:

$$\begin{aligned} w' &= w - \eta \frac{\partial L(w)}{\partial w} \\ &= w - \frac{\eta \lambda w}{n} - \frac{\partial L_0(w)}{\partial w} \\ &= \left(1 - \frac{\eta \lambda}{n}\right) w - \frac{\partial L_0(w)}{\partial w}. \end{aligned} \tag{11}$$

It can be seen that when w approaches 0, adding the L2 regularized loss function can restrict the model parameters to a small range, reduce the computational complexity of the model, and improve the training speed of the model. The loss function used in the STAQI model is as follows:

$$loss = \left\| Y_i - \widehat{Y}_i \right\| + \lambda L_{reg}, \tag{12}$$

where Y_i is the actual STAQI value of the target site; $\widehat{Y}_i$ is the predicted STAQI value of the target station; L_{reg} is the L2 regularization term; and λ is a super parameter.

3.6. Model Algorithm Flow. The process of the proposed model is shown in Algorithm 1:

4. Example Verification

This paper develops an air quality prediction system based on multisource data fusion. The main functions of the system include data import, data preprocessing, model training, model prediction, prediction result display, etc. By importing the data set of the city and selecting the training parameters of the model, the system conducts training. After the model training is completed, different models and different time spans can be selected for analysis and prediction, and the prediction and analysis results can be conveniently presented.

The hardware environment of the experimental simulation is NVIDIA GeForce MX450 graphics card and Intel Core i7 1165g7 processor; the software environment is Python 3.6 and the machine learning framework is Keras. Keras is a high-level neural network API, which can encapsulate Theano and TensorFlow again and omit the underlying development details. Therefore, it has good scalability and thus it is easy to build a network.

In this paper, a total of 1520 groups of air quality data from January 2019 to January 2021 in Beijing, China, are obtained. The sample database is constructed after preprocessing the original data. 80% of the data in the sample database are randomly selected as the training set, and the remaining sample datasets are used as the test set for model training and testing.

4.1. Evaluating Indicator. The purpose of this study is to predict the changing trend of air quality and pollutant concentration in the air of small and micromonitoring stations in grid monitoring. Therefore, in order to better measure the prediction effect, this paper adopts two evaluation indexes: mean absolute error (MAE) and root mean squared error (RMSE). This paper uses these two evaluation indexes to analyze the deviation between the predicted results and the real measured values.

Generally speaking, the smaller the deviation between the predicted value and the real value, the smaller the values of MAE and RMSE, that is, the smaller the values of MAE and RMSE, the better the prediction effect.

$$\begin{aligned} MAE &= \frac{1}{N}\sum_{i=1}^{N}\left|y_i - \widehat{y}_i\right|, \\ RMSE &= \sqrt{\frac{1}{N}\sum_{i=1}^{N}\left(y_i - \widehat{y}_i\right)^2}, \end{aligned} \tag{13}$$

where y_i is the true STAQI measurement and B is the predicted value of STAQI.

4.2. Parameter Sensitivity Analysis. For the prediction model proposed in this paper, the number of hidden layer units is very important for the prediction accuracy of the model. Therefore, the number of hidden layer elements is discussed in this paper. Table 3 shows the results of network under different number of hidden layer units.

As shown in Table 3, with the gradual increase of the number of hidden layer units, the evaluation index of the STAQI prediction model decreases first and then increases. When it exceeds a certain critical value, the model loses the ability to effectively learn the data, resulting in an increase in the prediction deviation of the model. When the number of hidden layer units in the STAQI prediction model is 64, the minimum value of RMSE is 4.51 and the value of MAE is 3.92. Therefore, it can be explained that when the number of hidden layer units of the prediction model is 64, its prediction performance is the best.

4.3. Model Prediction Analysis. In this paper, the simulation results of the model are analyzed by using the fitting curve of STAQI predicted value and real value, the MAE curve of STAQI, and the RMSE curve of STAQI.

Figure 7 shows the prediction and analysis results of the STAQI prediction model proposed in this paper in Beijing.

As can be seen from Figure 7, the prediction results of the STAQI prediction model proposed in this paper are basically consistent with the actual measured values. Based on the temporal and spatial characteristics of STAQI data, it provides reliable and complete data support for elm network model. Therefore, the proposed model can show good fitting ability.

In order to intuitively evaluate the tracking analysis ability of the proposed prediction model, this paper also uses RMSE and MAE to realize mathematical quantitative evaluation and analysis. Figure 8 shows the evaluation index analysis of the proposed model.

As shown in Figure 8(a), the RMSE of the predicted value of most test samples is less than 6, and the RMSE of a few samples is between 6 and 8; at the same time, it can be seen from Figure 8(b) that most of the MAE prediction indicators are within 5, and only a few samples have MAE between 5 and 7. From the above results, it can be seen that the air quality evaluation and prediction model has high

Input: test data
Output: predicted value
Steps:
(1) Assign values to multiple groups of super parameters of the model.
(2) Obtain the constructed adjacency matrix A and model sample data set from external files.
(3) The min-max method is used to normalize the data to eliminate the impact of different dimensions among multiple influencing factors on the model prediction.
(4) According to the size of the specific time window, the supervised data set is constructed and divided into training set and test set.
(5) Calculate the total training batch according to the batch size and the total number of training samples.
(6) Build global components. By inheriting the RNN cell class and overriding _init_ and _call_ Methods, the cell structure of the GG unit was realized. In _init_, the activation function, the number of nodes, the number of hidden cells, and other parameters need to be specified, and the Laplace matrix calculated by the adjacency matrix is loaded. The _ call_ Function to extract the spatial features of the input data and calculate the cell state of GRU unit. Call the user-defined GG cell class that can extract spatial-temporal features, and take the output value of the last cell state as the input of the fully connected layer.
(7) Build local components. The output value of the last unit time obtained by the forward propagation of the F-LSTM network is used as the input of the fully connected layer.
(8) The temporal and spatial features extracted by global and local components are weighted and fused to obtain the prediction results.
(9) Specify the loss function used in model training and the error evaluation index used in model testing.
(10) Adam optimizer is used to minimize the loss value.
(11) Train the model and repeat the following steps within a specific number of training times: first, the input data in the training set is divided into global component and local component. Second, call the model. Thirdly, the local component input, global component input, and label data of the current batch are used as filling data to dynamically perform the calculation of optimizer, loss function value, and prediction value.
(12) Test the trained model and obtain the model output value.
(13) Carry out inverse normalization processing of the output value to obtain the actual prediction value.
(14) The error between the predicted value and the real value is evaluated by a variety of evaluation indexes.

Algorithm 1: Model algorithm flow.

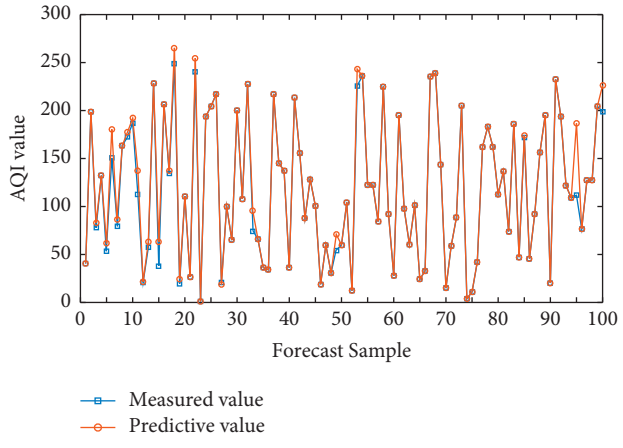

Figure 7: STAQI prediction fitting curve.

prediction accuracy. Based on the spatial distribution characteristics of AQI data, the effective spatial feature extraction of sample data is realized by using the depth network combined with GCN and GRU.

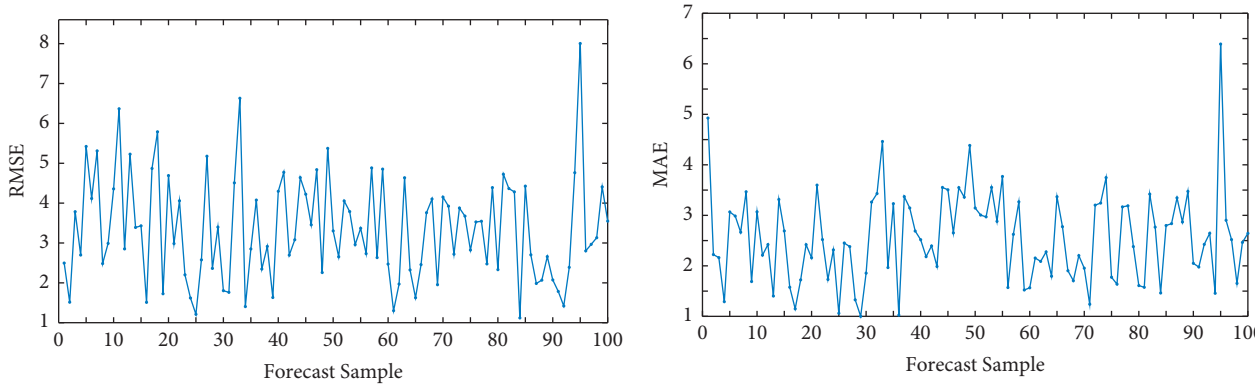

(a) (b)

Figure 8: Evaluation index of the proposed model: (a) RMSE; (b) MAE.

Table 3: Evaluation indexes under different number of hidden layer units.

Number of hidden layer cells	RMSE	MAE
8	7.89	6.54
16	7.01	5.14
32	5.64	5.06
64	4.51	3.92
128	4.82	4.24
256	4.99	4.69

In order to more comprehensively evaluate the performance of the spatial-temporal air quality prediction model in this paper, the MAE and RMSE are used to compare the algorithm in this paper with References [16, 19]. The results are shown in Table 4.

In conclusion, it can be confirmed that the STAQI model constructed in this paper has excellent tracking and fitting ability, and can achieve accurate and efficient STAQI prediction.

5. Conclusion

The accurate prediction of air quality index (AQI) has important practical significance and social value. However, the current method ignores the temporal and spatial distribution characteristics of AQI data, which is difficult to extract the characteristics of sample data effectively. To solve this problem, this paper constructs an air quality prediction model based on deep learning. Based on the spatial distribution characteristics of AQI data, the effective spatial feature extraction of sample data is realized by using the depth network combined with GCN and GRU. Based on the time distribution characteristics of AQI data, the improved LSTM network model is used to realize faster state update and effectively extract the time distribution characteristics of sample data.

Air quality analysis is actually affected by many complex factors. This paper only takes the air pollutant concentration data as the model input, which has a certain one-sidedness. The modeling and analysis of meteorological conditions, human activities, and other influencing factors will be added to future research work, so as to more accurately predict the change trend of air quality in the future.

Table 4: Analysis of prediction results under prediction models.

Method	RMSE	MAE
The proposed model	4.51	3.92
Reference [16]	6.57	5.99
Reference [19]	5.83	5.82

Data Availability

The data used to support the findings of this study are included within the article.

Conflicts of Interest

The author declares that there are no conflicts of interest.

Acknowledgments

This article is supported by Xi'an Science and Technology Planning Project (No. GXYD16.1): Internet of Things Application Engineering Laboratory of Xi'an.

References

[1] C. Jiang, X. He, Y. Le, Y. Ban, and D. Wang, "Spatiotemporal patterns and driving forces of air quality in Jiangsu Province, China, 2014," *Fresenius Environmental Bulletin*, vol. 27, no. 6, pp. 4076–4083, 2018.

[2] P. Morovati, A. Valipour, S. Geravandi, A. Karimyan, and M. J. Mohammadi, "Association of air quality index related to criteria air pollutants in Abadan, Iran," *Fresenius Environmental Bulletin*, vol. 27, no. 6, pp. 4023–4028, 2018.

[3] W. Xu, Y. Tian, Y. Liu, B. Zhao, Y. Liu, and X. Zhang, "Understanding the spatial-temporal patterns and influential factors on air quality index: The case of North China," *International Journal of Environmental Research and Public Health*, vol. 16, no. 16, pp. 2820–2823, 2019.

[4] Y. Li, Y. Tang, Z. Fan, H. Zhou, and Z. Yang, "Assessment and comparison of three different air quality indices in China," *Environmental Engineering Research*, vol. 23, no. 1, pp. 21–27, 2017.

[5] J. Xue, Y. Xu, L. Zhao et al., "Air pollution option pricing model based on AQI," *Atmospheric Pollution Research*, vol. 10, no. 3, pp. 665–674, 2019.

[6] S. F. Jin, Z. Q. Han, X. L. Liao et al., "Reduced spring festival effects on the air quality in beijing: Evidence from 2014 to 2019," *Fresenius Environmental Bulletin*, vol. 28, no. 12A, pp. 10242–10246, 2019.

[7] K. Dimitriou, E. Liakakou, M. Lianou et al., "Implementation of an aggregate index to elucidate the influence of atmospheric synoptic conditions on air quality in Athens, Greece," *Air Quality, Atmosphere & Health*, vol. 13, no. 4, pp. 447–458, 2020.

[8] B. Chen, "Air quality index forecasting via deep dictionary learning," *IEICE - Transactions on Info and Systems*, vol. E103.D, no. 5, pp. 1118–1125, 2020.

[9] J. Chen, K. Chen, C. Ding, G. Wang, Q. Liu, and X. Liu, "An adaptive Kalman filtering approach to sensing and predicting air quality index values," *IEEE Access*, vol. 8, no. 1, pp. 4265–4272, 2020.

[10] A. Shishegaran, M. Saeedi, A. Kumar, and H. Ghiasinejad, "Prediction of air quality in Tehran by developing the nonlinear ensemble model," *Journal of Cleaner Production*, vol. 259, no. 1, pp. 120825–120915, 2020.

[11] K. Yang, Y. N. Gou, W. Xu, and P. Yang, "Prediction of pollutant diffusion trend using CNN-GRU hybrid network in IoT air monitoring system," *Fresenius Environmental Bulletin*, vol. 30, no. 2, pp. 1095–1104, 2021.

[12] Q. Wu and H. Lin, "A novel optimal-hybrid model for daily air quality index prediction considering air pollutant factors," *Science of the Total Environment*, vol. 683, no. 1, pp. 808–821, 2019.

[13] T. J. Chang, Z. Y. Guo, and L. L. Xu, "Prediction of air quality index scale based on Prophet Stochastic Forest optimization model," *Environmental pollution and prevention*, vol. 41, no. 7, pp. 758–761, 2019.

[14] J. H. Zhao, T. Dong, and B. Cai, "AQI prediction based on long short-term memory model with spatial-temporal optimizations and fireworks algorithm," *Journal of Wuhan University (Natural Science Edition)*, vol. 65, no. 3, pp. 250–262, 2019.

[15] Z. C. Wang, H. Y. Chen, J. M. Zhu, and Z. Ding, "Multi-scale deep learning and optimal combination ensemble approach for AQI forecasting using big data with meteorological conditions," *Journal of Intelligent and Fuzzy Systems*, vol. 40, no. 3, pp. 5483–5500, 2021.

[16] L. Zhang, Z. Fang, and T. F. Ma, "Study on BP neural network AQI prediction based on wavelet decomposition of time series," *Journal of Xuzhou Institute of Engineering (Natural Science Edition)*, vol. 35, no. 1, pp. 45–52, 2020.

[17] L. J. Guo, H. M. Jing, Y. X. Nan, and C. B. Xiu, "Prediction of air quality index based on Kalman filter fusion algorithm," *Environmental pollution and prevention*, vol. 39, no. 4, pp. 388–391, 2017.

[18] C. L. Zhang and Y. P. Bai, "Application of LSTM model based on Tensorflow in prediction of air quality AQI in Taiyuan," *Journal of Chongqing University of Technology (NATURAL SCIENCE)*, vol. 32, no. 8, pp. 137–141, 2018.

[19] M. M. Wu, J. X. Xu, and Q. Wang, "Research on CEEMD-Elman neural network prediction of AQI based on data decomposition," *China Environmental Science*, vol. 39, no. 11, pp. 4580–4588, 2019.

[20] Y. L. Wu, C. M. Li, Z. X. Dai, and Z. Wu, "Analysis on temporal and spatial distribution characteristics and impact mechanism of urban air quality index," *Surveying and mapping bulletin*, vol. 1, no. 4, pp. 81–86, 2020.

[21] L. Perlmutt, D. Stieb, and K. Cromar, "Accuracy of quantification of risk using a single-pollutant air quality index," *Journal of Exposure Science and Environmental Epidemiology*, vol. 27, no. 1, pp. 24–32, 2017.

[22] H. Pu, K. Luo, P. Wang, S. Wang, and S. Kang, "Spatial variation of air quality index and urban driving factors linkages: evidence from Chinese cities," *Environmental Science and Pollution Research*, vol. 24, no. 5, pp. 4457–4468, 2017.

[23] H. X. Xue, Y. P. Bai, H. P. Hu, T. Xu, and H. Liang, "A novel hybrid model based on TVIW-PSO-GSA algorithm and support vector machine for classification problems," *IEEE Access*, vol. 7, no. 1, pp. 27789–27801, 2019.

[24] D. Y. Wang, S. Wei, H. Y. Luo, C. Q. Yue, and O. Grunder, "A novel hybrid model for air quality index forecasting based on two-phase decomposition technique and modified extreme learning machine," *Science of the Total Environment*, vol. 580, no. 15, pp. 719–733, 2017.

[25] F. Jiang, J. He, and T. Tian, "A clustering-based ensemble approach with improved pigeon-inspired optimization and extreme learning machine for air quality prediction," *Applied Soft Computing*, vol. 85, no. 1, pp. 105827–105914, 2019.

Hindawi
Mobile Information Systems
Volume 2022, Article ID 1351399, 10 pages
https://doi.org/10.1155/2022/1351399

Research Article

IOT-Based Injection-Locked Microwave Photonic Frequency Division Signal Processing

Lin Wang,[1] **Guangying Wang**,[2] **and Jingxu Chen**[2]

[1]*School of Electronic and Electrical Engineering, Zhaoqing University, Zhaoqing 526061, China*
[2]*Institute of Photonics Technology, Jinan University, Guangzhou 510632, China*

Correspondence should be addressed to Lin Wang; 1910300328@mail.sit.edu.cn

Received 9 August 2022; Revised 25 August 2022; Accepted 19 September 2022; Published 27 September 2022

Academic Editor: Shadi Aljawarneh

When building an injection-locked microwave photonic frequency division signal processing model for the Internet of Things, the waveform and frequency of the microwave have an important impact on its performance. How to optimize and adjust the injection-locked microwave photonic frequency division signal processing effect needs more research and exploration. Taking the traditional mode architecture as a reference, this paper constructs an injection-locked microwave photonic frequency division signal processing model based on the Internet of Things. In this paper, the popular deep analysis method is used to optimize the model, and the photonic technology is matched with the microwave analysis. The purpose of this construction is to weaken the microwave integration error and improve the calculation accuracy to a higher level. In addition, aiming at the difficult problem of microwave signal generation, this paper uses the optical injection method to lock the microwave photons and generate waveform signals, which makes the model data more representative, so as to solve the problems of unstable microwave signals and high transmission costs. This paper also discusses the possibility of microwave photon filtering and frequency division signal processing of microwaves. The optimal solution is determined by analyzing the experimental results of various technical means, thus proving that the injection-locked microwave photonic frequency division signal processing means has better stability and a higher fitting degree.

1. Introduction

Traditional microwave technology has solved many scientific and technological problems due to its unique microwave conduction mode. However, with the innovation of technology, the problem of technological bottlenecks has become increasingly prominent. In the field of optics, technologies such as semiconductor lasers and photodetectors are led. Scientific and technological means have shown a thriving development trend, which provides excellent means and ideas for solving the bottleneck problem of microwave technology. In view of this, microwave photonics, which combines microwave and optics, came into being. The application principle of microwave photonics is mainly reflected in the use of optical principles to replace the original processing methods in the electrical field, reducing energy loss, improving broadband speed, and reducing electromagnetic interference from many aspects. Because of its stable and efficient characteristics, it is not only used in military communication and civil communication but also has a wide range of applications in home communication, such as civil network switching, microwave communication, and optical fiber conduction.

Optical injection technology mainly improves the applicability of processing information and feedback information by optimizing the application performance of distributed feedback semiconductor lasers [1]. Through the optical injection locking mode, the semiconductor laser can expand the broadband amplitude, strengthen the resonance peak, reduce signal interference, and reduce noise and other functions [2]. The booming development of the Internet of Things has led to the continuous application of low-power RF transceiver components to wireless networks, which has also made it a new research hotspot. Low-power RF

transceiver components can reduce power consumption to a watt level, which is achieved by optimizing the circuit structure and directly supplying power to wireless network nodes after energy collection, thus eliminating the trouble of replacing the power supply [3]. This low-cost and high-efficiency IoT network can be used in many aspects of social life, for example, urban construction detection, biological tracking and control, experimental process monitoring, social security, and citizen health management [4]. On the other hand, in the microwave field, power, frequency, and phase are three important parameters to measure the strength of microwave signals. Among them, the signal amplitude of microwave power is extremely important. In a series of transmission and transformation processes of microwave signals, the measurement of microwave power is electromagnetic measurement [5].. Taking communication as an example, microwave power measurement not only undertakes monitoring, circuit maintenance, and efficiency control but also realizes the supervision of various microwave power detectors [6, 7]. The principle of microwave technology is to convert light wave signals into low-frequency electrical energy or thermal energy. Therefore, this paper is guided by the application of microwave photonics, explores the characteristics of optical injection-locked semiconductor lasers, and proposes a new microwave photonic filter and frequency division signal processing scheme [8].

2. Related Work

At present, the common microwave power detectors in life mainly include the following types, such as diode type, thermal resistance type, and capacitive type. The literature considers that the first two are active devices [9]. The diode microwave power detector uses the rectification principle of diodes to convert microwave signals into low-frequency signals for acquisition and processing. The advantages of this method are fast response and wide capture range [10]. It converts the signal into heat energy and indirectly obtains the microwave power data according to the influence of temperature on the resistance value; while the rest are passive devices [11]. The capacitive microwave power detector completes the microwave power measurement through the conversion of electricity and force. The advantages of this method are mainly reflected in the accurate numerical value, high linearity, and high measurement mean square [12]. The literature suggests that with the advancement of MEMS technology, thermoelectric microwave power detectors based on this technology have attracted more and more attention. This is mainly because of its lighter volume and mass, and higher processing costs compared with traditional detectors [13]. It has low output and larger output, so it has a broader prospect in the application of portable equipment. The literature points out that microwave photonics can be studied through the following aspects: such as optical generation of microwave/millimeter-wave signals, optical domain processing of microwave/millimeter-wave signals, and optical carrier microwave/millimeter-wave signal transmission technology [14]. The literature studies various aspects including microwave technology and optical communication technology according to its arguments and also proposes some targeted solutions. The experiment believes that the total microwave photonic technology in practice is far more complex and changeable than expected. According to the literature, a microwave photonics system should not only be used as a functional module, such as a microwave photonic filter and signal source in optical fiber communication but also be responsible for amplifying microwave signals [15]. The literature points out that the current research focus on microwave photonic technology is still focused on improving the quality of microwave signals and microwave processing. The literature also admits that the microwave photonics field generally uses the abovementioned methods to achieve microwave signal regeneration [16]. However, with the exploration of the field of microwave photonics, people's attempts at some interdisciplinary subjects are also common, such as optically controlled phased arrays and optical-borne wireless communication technology. The literature summarizes the scope of application of these technologies, of which applications in radar, wireless communication, measurement, etc., are the most common. The literature points out that the waveform signals involved in these systems and the study of high-quality frequency arbitrary waveform regeneration technology are particularly important.

Several kinds of measurement systems using microwave photonic technology have been reported in the literature [17]. One of the principles is that the feedback signal is frequency-converted and then processed and measured. Based on this idea, the literature measures the DFS by obtaining the frequency difference between the unknown and the feedback signal through photon mixing. Although this method is a breakthrough, some kinds of literature believe that the measurement of DFS requires not only the photon frequency offset but also the photon frequency offset [18]. Considering its direction, therefore, it is possible to change the thinking to combine the optical frequency shift with the frequency mixing, and use the reference signal and the echo signal frequency to compare the frequency of the Doppler frequency shift to determine the direction of the Doppler frequency shift. This method has higher accuracy [19]. The literature uses two series-connected EOMs to perform DFS measurements, which mainly measure the DFS of plus or minus 90 kHz at 10, 15, and 30 GHz, using a laser light source, a photodetector (PD), and an electrical modulator (EOM) to measure the DFS. The low-frequency electrical signal is processed to obtain the Doppler frequency shift [20].

3. IoT Technologies and Applications

3.1. IoT Structure. The vigorous development of the Internet of Things reflects the power of science and technology, and it is not limited to the assistance of science and technology and has its own unique advantages. The definition of the Internet of Things varies according to different application conditions. The more general point of view is the network that

connects objects. The conventional Internet of Things not only has a primary perception layer but also has a core network layer and a final application layer structure. Among them, the basic perception layer is at the forefront, covering a variety of sensors, representative spectral sensors, spectral sensors, humidity sensors, etc.; the network layer, as the link between the upper and lower layers of the Internet of Things, is mainly responsible for the transmission and processing of information data; and the application layer. It is an intelligent application formulated according to the actual needs of life. The structure division of the Internet of Things is shown in Figure 1.

3.2. Technology Application. In order to solve the problems of harmonic distortion and heat loss in microwave photons, a low-power sensor scheme using self-powered RF transceiver components for the Internet of Things is proposed. As shown in Figure 2(a), one of the main structural elements of this scheme is thermoelectric. The microwave signal detector is matched with a thermoelectric-optical integrated microenergy harvester. The former uses a microwave coupler for frequency detection; the latter is composed of photovoltaic cells and hybrid thermoelectric generators, which are also the main components to reduce energy consumption.

The demonstration of a self-powered low-power thermoelectric-optical integrated micro-sensor is shown in Figures 2(b) and 2(c). Based on the positive correlation between the temperature of the transceiver or load and the transmit power, the MEMS micro thermocouple can be used as a sensor. The microwave detector of the temperature element further monitors the degree of harmonic distortion by analyzing the correlation, so it can realize power overload protection, avoid damage to the component machine, and detect aging components in time. In addition, the MEMS miniature thermocouple is used as a thermoelectric generator, which can realize secondary energy recovery, and store electric energy through DC-DC conversion to avoid energy loss. It can supply power to the microwave system to achieve self-powering of the microwave system. The current single thermoelectric power supply capacity is obviously insufficient, so the use of photovoltaic energy collectors and thermal energy collectors to supply power together will be a good solution. The advantage of this approach is that both are solid-state converters, with components that have a longer life, lower maintenance costs, and less ambient noise.

4. Optical Injection Locked Microwave Photonic Signal Generation

4.1. Principle of Optical Injection Locking. At present, in the research on the combination of optical injection locking technology and microwave technology, the most common one is for the generation of microwave signals, that is, frequency doubling of microwave signals. Using optical injection locking technology, the lasing field of the master and slave lasers can be easily made through phase synchronization and correlation. The content of this paper includes the use of optical injection locking technology to complete the photonic microwave signal frequency doubling. Similar to the output light field of a semiconductor laser, if the energy loss during the injection process is ignored, the output light field after injection locking can be expressed as follows:

$$\frac{dE(t)}{dt} = \frac{1}{2}g[N(t) - N_{th}](1 + j\delta)E(t) + \kappa E_{inj}(t) - j\Delta\omega_{inj}E(t). \tag{1}$$

The last two terms on the right side of the equation are the injection terms, that is, the output light field and the injected light field of the slave laser, which are respectively defined as follows:

$$\begin{aligned} E(t) &= \sqrt{S(t)}\exp\ [j\psi(t)], \\ E_{inj}(t) &= \sqrt{S_{inj}(t)}\exp\ \left[j\psi_{inj}(t)\right]. \end{aligned} \tag{2}$$

The abovementioned Equation (1) can also be split into the form of the semiconductor laser rate equation:

$$\begin{aligned} \frac{dS(t)}{dt} &= g[N(t) - N_{th}]S(t) \\ &\quad + 2\kappa\sqrt{S(t)S_{inj}(t)}\cos\ \left[\psi(t) - \psi_{inj}(t)\right], \\ \frac{d\psi(t)}{dt} &= \frac{\delta}{2}g[N(t) - N_{th}] \\ &\quad - \kappa\sqrt{\frac{S_{inj}(t)}{S(t)}}\sin\left[\psi(t) - \psi_{inj}(t)\right] - \Delta\omega_{inj}, \\ \frac{dN(t)}{dt} &= J(t) - \gamma_N N(t) \\ &\quad - \left\{\gamma_p + g[N(t) - N_{th}]\right\}S(t). \end{aligned} \tag{3}$$

When the modulated signal light is injected into the slave laser and locked, the number of photons, optical field phase, and carrier number of the slave laser will reach a relatively stable state, namely:

$$\begin{aligned} \frac{dS(t)}{dt} &= 0, \\ \frac{d\psi(t)}{dt} &= 0, \\ \frac{dN(t)}{dt} &= 0. \end{aligned} \tag{4}$$

It can be concluded that:

$$\%\ \Delta\omega_{inj} = -\kappa\sqrt{1 + \delta^2}\sqrt{\frac{S_{inj}(t)}{S(t)}}\sin\left[\psi(t) - \psi_{inj}(t) + \tan^{-1}\delta\right]. \tag{5}$$

In the locked state, the detuning frequency is a fixed value. According to the formula, it can be known that the slow-varying envelope of the laser output light field and the

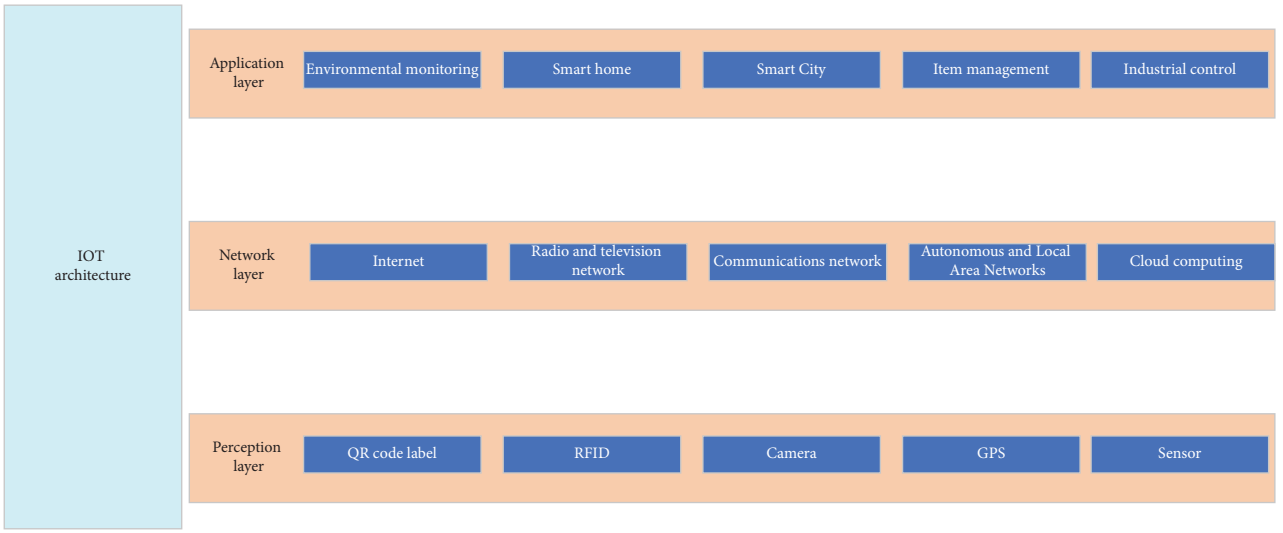

Figure 1: The structure of the internet of things.

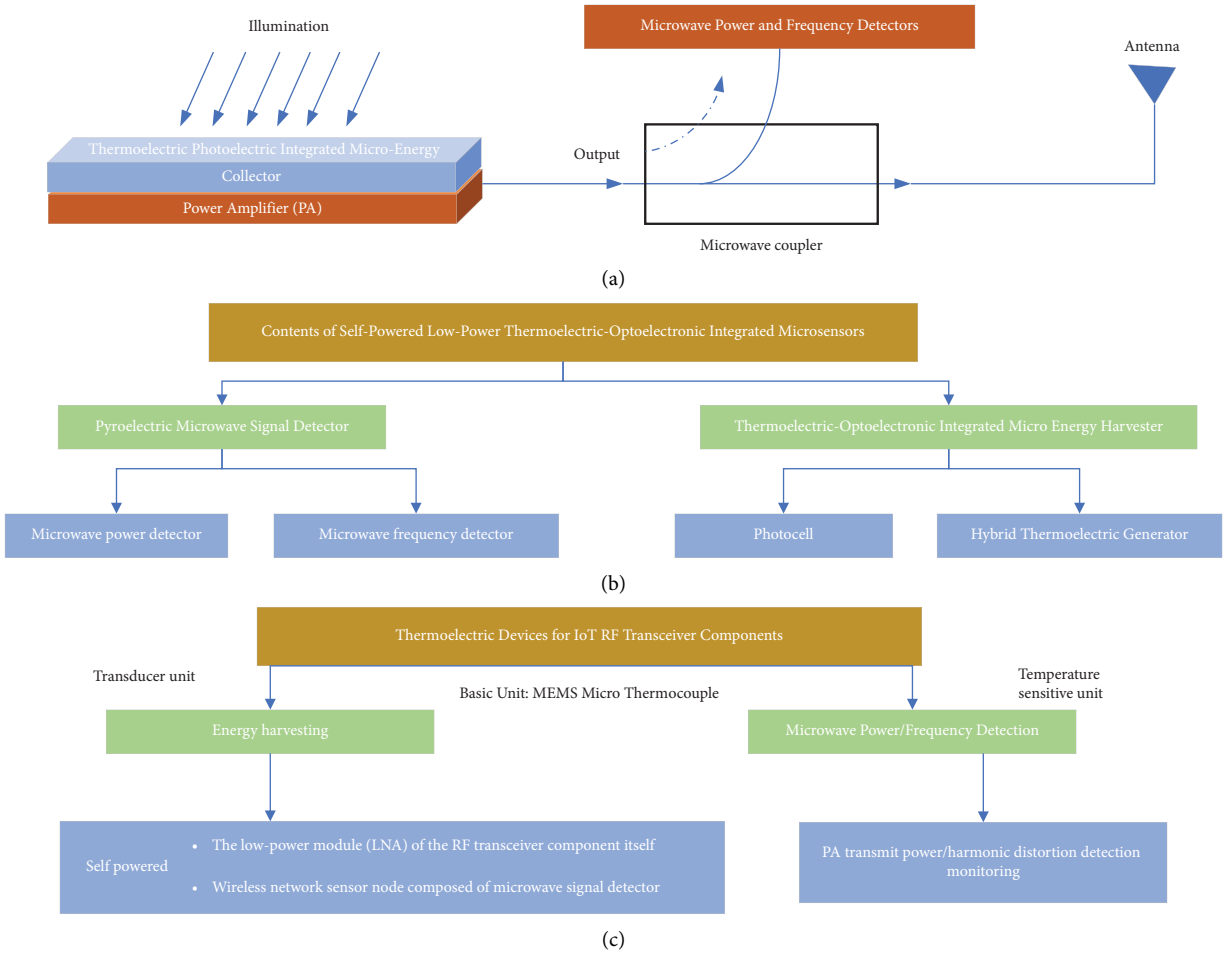

Figure 2: (a). Microwave power detector, microwave frequency detector, and thermoelectric-optical integrated microenergy harvester for IoT RF transceiver components; (b). Contents of self-powered low-power thermoelectric-optical integrated microsensor; (c). The role of thermoelectric devices in the scheme.

carrier phase are related to the injected light field. If the injected light is a phase modulation signal, the output light field phase is locked. And the envelope phase of the output signal is locked when an intensity-modulated signal is injected. The research in this paper mainly utilizes the injection locking technique to lock-in amplification of weak power high-order modulation sidebands. Injecting an external continuous light source can more effectively generate an amplified frequency-doubled optical microwave signal. This is because the low-frequency modulated signal light has a certain amplification effect when injected into the slave laser, and further amplification of the high-order sideband can be obtained. High-frequency optical microwave signal with a frequency of about 20 times.

4.2. Microwave Photons. The practicality of microwave photonics is higher, and how to generate high-purity, low-phase noise microwave signals and how to process and transmit the microwave signals is a hot topic at present. Microwave signals with high purity and low phase noise can be generated through optical principles and methods.

The advantage of processing optical signals by optical methods is that it can break through the thinking mode of traditional circuit design and improve the degree of signal control and sampling range. Optical fiber radio mainly uses optical fiber for long-distance transmission of signals, so it has the advantages of low cost, low loss, and resistance to external signal interference. In addition, microwave signals generated by optical methods have the characteristics of high frequency and low phase noise, so they are widely used in radar, wireless communication, and modern network instruments. Aiming at the source of wave signals in microwave communication, the old method is to use frequency doubling to generate microwave/millimeter wave signals, but the cost is high, and the loss of wave signals in coaxial cables is greater due to the long transmission distance. The applicability of this method is not high. But it still has certain advantages. For example, optical fiber can better replace cables for signal transmission, and electrical signals can be better converted into optical signals for long-distance transmission.

According to the current research results, the generation of millimeter waves mainly depends on the generation of high-frequency low-noise microwave signals, which are specifically explained as follows:

4.2.1. Generate Microwave Signal Based on Optical Heterodyne Method. This method mainly uses a photodetector (PD) to capture the optical frequency difference of different illumination wavelengths. Suppose there are two light waves:

$$\begin{aligned} E_1(t) &= E_{01}\cos\left(\omega_1 t + \phi_1\right), \\ E_2(t) &= E_{02}\cos\left(\omega_2 t + \phi_2\right). \end{aligned} \tag{6}$$

Considering the bandwidth limitation of the PD, the output current of the PD is given as follows:

$$I_{RF} = A\cos\left[\left(\omega_1 - \omega_2\right) + \left(\phi_1 - \phi_2\right)\right. . \tag{7}$$

It can be found from this that the electrical signal generated by the PD is equal to the frequency difference between the two input optical signals. If the bandwidth of the photodetector is unlimited, this method can generate an electrical signal of the order of THz, but due to the fact that the light wave of the free oscillator has no phase correlation, the phase noise of the microwave signal will increase accordingly. In response to this problem, some kinds of literature have proposed many solutions, which can be summarized into the following categories: (1) optical injection locking method, (2) optical phase-locked loop method, (3) external modulation method, and (4) dual wavelength laser method.

4.2.2. Generate Microwave Signal Based on Photoelectric Oscillator. In order to enhance the detection capability of the airborne radar, the phase noise of the microwave signal obtained by the radar is required to be lower than a certain threshold. Therefore, a large number of experiments and types of research on how to enhance the performance of OEO have been put on the agenda, such as: how to reduce the phase noise, while enhancing the stability of the microwave signal and increasing the microwave output frequency. At present, the latest research shows that the lowest phase noise is the OEO structure using 16 km single-mode fiber, and the phase noise can reach as low as -163dBc/Hz@ 10 kHz, but its tunable frequency range is only 4 GHz, which greatly limits its use in social life. application. In order to solve this problem, some kinds of literature propose a construction method based on MPF, which makes the highest tunable threshold reach 38.38 GHz. In view of the fact that the energy storage element of OEO is an optical fiber delay line, the influence of environmental factors such as temperature and humidity on the performance of optical fiber is more prominent, resulting in poor stability of OEO.

4.3. Signal Generation. How to realize the RF arbitrary waveform signal with ultrahigh repetition frequency is a major photonic microwave problem that scientific researchers have always wanted to solve. In terms of current research technology, converting a low-frequency local oscillator signal (electrically modulated signal) into a high-rate waveform signal is the main research idea to solve this problem. As one of the simplest and most efficient methods, optical injection locking technology is also widely used. This paper first introduces the scheme of using injection locking technology to generate the triangular wave. Secondly, according to this scheme, the generation of frequency-doubling triangular waves is realized. The principle of the scheme based on the DFB-LD injection locking process and time domain synthesis is as follows: the tunable laser emits continuous light and is modulated by the MZM to obtain a sinusoidal signal. And then the sinusoidal signal is divided into two channels, one of which is injected into the DFB-LD for locking modulation. The high-order sideband of the signal, and then the envelope signal of the modulation

frequency amplified by three times can be obtained. Finally, the required triangular wave can be synthesized by the phase and power superposition of the two signals.

Here, the power of the two signals is controlled by the polarization controller and the beam combiner to form a triangular wave with a corresponding proportional relationship. Figure 3 simulates the process of synthesizing the triangular wave. The triangular wave signal of the red solid line is formed by the superposition of the other two sinusoidal envelope signals.

Although the method provided in this paper generates triangular waves, the modulation frequency of triangular waves still has some problems. When a higher repetition frequency is required, the actual cost value increases. By comprehensively considering the modulation characteristics of MZM, when MZM is at matb and MITB points, the frequency doubling signal can be directly output. Therefore, this modulation characteristic of MZM can be combined with the injection locking process to generate triangular waves. This process can be roughly as follows: the continuous light emitted by ECL is captured and modulated by MZM, amplified by fiber amplifier (EDFA), and then divided into two channels by the coupler. The low-power channel signal is injected into DFB-LD to generate a signal of six times the frequency. Finally, the frequency-doubled triangular wave is output through PD detection. By the abovementioned operation, the problem that the actual cost increasing due to the higher repetition frequency can be solved.

According to the Fourier analysis method in analysis, the Fourier expansion of a periodic triangular wave can be expressed as follows:

$$T_{tr}(t) = DC + \sum_{N=1,3,5,\ldots}^{\infty} \frac{1}{N^2} \cos\ (N\omega_m t). \tag{8}$$

It can be seen from the abovementioned formula that a periodic triangular wave is composed of an infinite number of cosine signals in phase and with a frequency interval of 2. Moreover, the order of the harmonic is negatively correlated with the amplitude coefficient, and the influence of the harmonic component after the third order on the waveform envelope can be ignored. Therefore, a triangular wave signal can be expressed as follows:

$$T_{tr}(t) = DC + \cos\ (\omega_m t) + \frac{1}{9} \cos\ (3\omega_m t). \tag{9}$$

Converted into relative power ratio:

$$L_p = 10lg\frac{P_1}{P_3} = 10lg\frac{1}{(1/9)^2}\, 10lg81 \approx 19.08\ \text{dB}. \tag{10}$$

It can be seen from the formula that the first and third harmonic power ratio of the synthesized triangular wave envelope signal should reach about 19.08 dB. In this scheme, the carrier suppression modulation method is used to obtain the second harmonic optical microwave signal as the initial fundamental frequency signal, and the optical field output after the carrier suppression modulation can be expressed as follows:

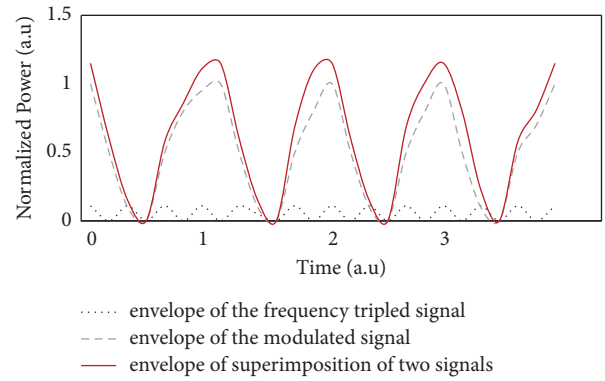

Figure 3: Simulation results of triangular wave synthesized by modulation signal and injection locking signal.

$$\%\ E_{out}(t) \approx E_{in}(t) J_1(\beta)\{\cos\left[(\omega_0 - \omega_m)t\right] + \cos\left[(\omega_0 + \omega_m)t\right]\}. \tag{11}$$

In the study, the continuous light emitted by ECL is modulated by carrier suppression using a 3 GHz sinusoidal drive signal to obtain a more accurate double frequency envelope signal. When the modulated signal is injected into the DFB-LD after splitting, the 5th order sideband of the modulated light falls into the stable locking region of the slave laser by adjusting the wavelengths in front of the master and slave lasers and is locked and amplified. Figure 4 shows the signal locking spectrum. It can be found that the 6th harmonic signal is the strongest and the suppression ratio of high and low harmonics exceeds 9 dB. At this time, multiple harmonic components are included, resulting in the waveform is not completely standard. In addition, by comparing the graph in Figure 4, it can be found that after injection locking, a partial red shift occurs from the wavelength of the laser.

Finally, adjust the ODL to match the phases of the two signals, and then use PC3, PC4, and PBC to control the optical power ratio of the two signals, and then the frequency-doubling triangular wave can be detected.

5. Microwave Photon Filtering and Frequency Division Signal Processing

5.1. Light Injection Microwave Photonic Filters. The integration degree of MPF has a high correlation with the algorithm completion degree. Therefore, according to its characteristics, this paper attempts to use the optical injection locking technology as a breakthrough to combine the F-P cavity semiconductor laser into the MPF. This method changes the injection ratio and detuning frequency by changing the wavelength amplification during optical injection locking, thereby realizing a tunable single-passband MPF. This scheme has the advantages of simple structure, low noise and high frequency, and tunable wide-narrow rejection ratio. Its tunable threshold is 32 GHz, which greatly improves the tuning range and provides a new idea for the conversion of optical and microwave signals. By adjusting the bias current injected into the laser, the power

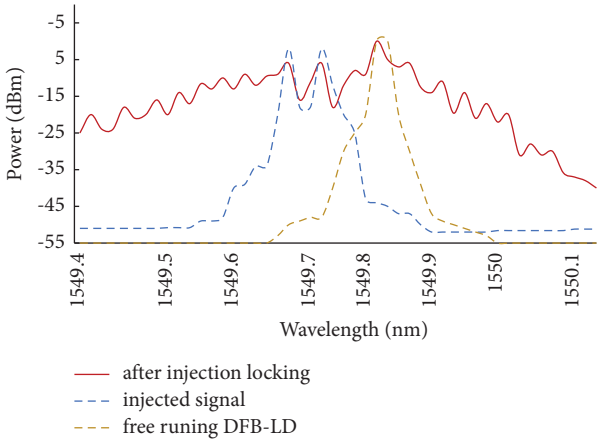

Figure 4: Spectrum.

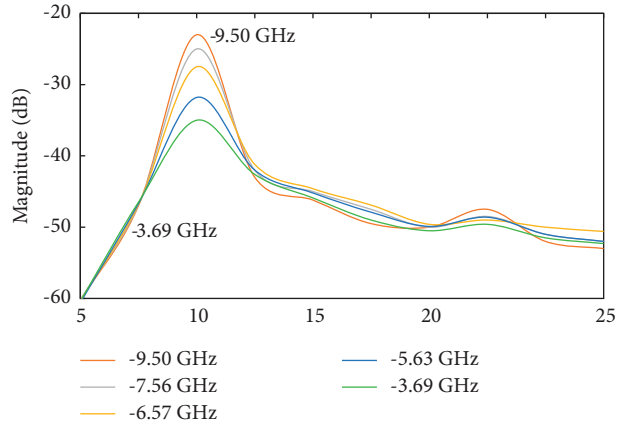

Figure 5: Frequency response curve of MPF under different detuning frequency conditions.

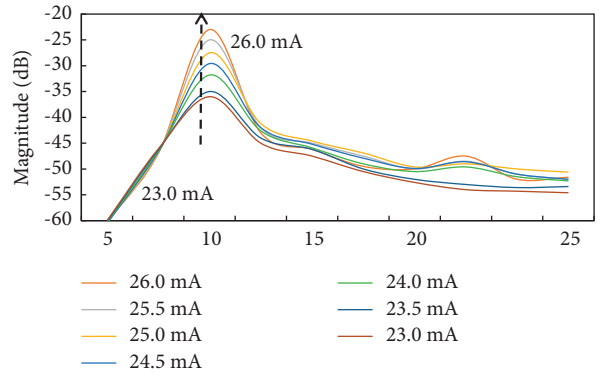

Figure 6: Frequency response curve of MPF under different bias current conditions.

distribution of the four longitudinal modes of the FP laser can be realized, thereby realizing the power redistribution of the longitudinal modes. When continuous light is injected into the FP, the longitudinal mode can be locked by changing the injection ratio and detuning frequency, resulting in the red-shift effect of the cavity mode. In the MPF scheme of the optical injection locking F-P cavity semiconductor laser proposed in this paper, the rate equation of the FP cavity laser can be expressed as follows:

$$\begin{aligned}
\frac{dE_m t}{dt} &= \frac{1}{2}(1+i\alpha)[G_m(N)-\gamma]E_m t, \\
\frac{dN(t)}{dt} &= \gamma_e[C_0 N_{th}-N]-\sum_{m=-M-1/2}^{M-1/2} G_m(N)|E_m(t)|^2, \\
f_m &= f_0 + m\Delta f_L = f_0 + \frac{m}{\tau_L}, \\
G_m(N) &= \frac{g_C(N-N_0)}{1+s\sum_{m=-M-1/2}^{M-1/2}|E_m(t)|^2}\left[1-\left(\frac{f_m-f_0}{\Delta f_g}\right)^2\right].
\end{aligned} \tag{12}$$

In this paper, the stability of MPF was tested. The frequency response amplitude of the MPF is measured every 5 minutes, the center frequency variation amplitude is 57 MHz, and the fluctuation range is less than 0.288 dB, so it has higher stability. And let R and I be fixed, the spectral response curve of the measured MPF is shown in Figure 5. Δf has a negative correlation with MPF. It also appears that the 3 dB bandwidth of the spectral response decreases as Δf decreases, and at high frequencies, another peak appears. Analysis of Figure 5 shows that with the decrease of Δf, the out-of-band rejection ratio of MPF increases.

Finally, the frequency response curve of the MPF as a function of I is shown in Figure 6, and changing I result in a change in the parameters of the FP laser. It can be seen from Figure 6 that as I increase, the center frequency of the MPF increases, and the insertion loss of the MPF increases. When the value of I increases, the bandwidth of the spectral response curve and the insertion loss of the MPF both decrease.

5.2. Principle of Microwave Photonic Photoelectric Oscillator. Once the photoelectric oscillator was proposed, it became the research focus of scientific researchers. After the continuous research and development of scientific researchers, the function of the photoelectric oscillator has become more and more perfect. The basic working principle of the photoelectric oscillator is that after the laser is emitted from the pump laser, it is first modulated by the electro-optical modulator, and then the light is output, and then passes through a certain distance of optical fiber, and finally, enters the photodetector. After the photodetector captures the laser, it amplifies and filters the electrical signal of the laser, and finally, outputs the laser to the RF port of the modulator. The laser processing of the photoelectric oscillator is a positive feedback system. When the gain of the loop is greater than the threshold gain, the photoelectric oscillator can work, the photoelectric oscillator starts to vibrate, and then outputs a microwave input signal of a certain frequency.

The threshold gain of the optoelectronic oscillator can be understood as, in this loop, after the optical power of the laser is output from the electro-optical modulator, the value is related to the voltage $V(t)$:

$$\mathrm{P}(t) = (\alpha P_0/2)\{1 - \eta \sin \pi[V_{in}(t)/V_\pi + V_R(t)/V_\pi]\}. \quad (13)$$

When the optical signal is processed by the photodetector, it becomes an electrical signal that is easier to capture, and then amplified by the amplifier to complete the expansion of the electrical signal. The signal is given as follows:

$$\begin{aligned} V_{\text{out}}(t) &= \rho \mathrm{P}(t) R G_A, \\ &= V_{ph}\{1 - \eta \sin \pi[V_{in}(t)/V_\pi + V_B(t)/V_\pi]\}. \end{aligned} \quad (14)$$

This paper defines the photovoltage:

$$V_{ph} = (\alpha P_0 \rho/2) R G_A. \quad (15)$$

The open-loop small-signal gain of the optoelectronic oscillator is given as follows:

$$\begin{aligned} G_S &= \left.\frac{\mathrm{d}V_{\text{out}}}{\mathrm{d}V_{\text{in}}}\right|_{V_{in}=0}, \\ &= -\frac{\eta \pi V_{ph}}{V_\pi} \cos\left(\frac{\pi V_B}{V_\pi}\right). \end{aligned} \quad (16)$$

According to the abovementioned analysis and research, it can be concluded that when the modulator is biased at the quadrature point, we can obtain the maximum small signal gain. Through the analysis of the formula, it can be obtained that the small signal gain value can be positive or negative, and its value is determined by the bias voltage. We can set the forward bias value to be greater than 0, so if the bias voltage is equal to 0, the modulator is biased at the negative quadrature point, and if the bias voltage is equal to the half-wave voltage, then the modulation bias is in quadrature point. According to relevant research, it can be known that in most photonic links, if an external modulator is used, the bias of the electro-optic modulator, whether at the quadrature point or the negative quadrature point, will not affect the performance of the modulator. But in order to start the photoelectric oscillator, the small-signal open-loop gain of the system must be higher than the loss of the system.

Through the abovementioned formula, we can obtain that the threshold value of the optoelectronic oscillator is given as follows:

$$V_{ph} = \frac{V_\pi}{\left[\pi \eta \left|\cos\left(\pi V_B/V_\pi\right)\right|\right]}. \quad (17)$$

Ideally:

$$V_{ph} = \frac{V_\pi}{\pi}. \quad (18)$$

Through the abovementioned analysis, it can be seen that the amplifier cannot determine whether the photoelectric oscillator can start to oscillate. Under certain conditions, the photoelectric oscillator can also start to oscillate without the amplifier. This is because the light source can provide energy for the photoelectric oscillator. This property of the photoelectric oscillator has high practical value. In actual production and life, the optical fiber can be used to provide energy for the photoelectric oscillator under the condition of long distances. At the same time, the use of the amplifier will also produce certain side effects, such as noise. If the amplifier is not used in the loop, the hidden danger of noise will be eliminated naturally. This operation can further improve the stability of the photoelectric oscillator. In this paper, the responsivity of the photodetector can be set to 0.8 A/W, the optical power value is 25 mW, the half-wave voltage of the modulator is 3.14 V, the impedance is 50 ohms, and the photocurrent is 20 mA, then the photoelectric oscillator system can operate normal vibration, no need to use an amplifier.

5.3. Simulation of Microwave Photonic Signal Measurement. It can be seen from the laser principle that the measurement range of the frequency point needs to be controlled in order to ensure the effect, that is, the measurement range cannot be larger than the fundamental frequency of a cavity. It can be seen from Figure 7 that when the cavity length value increases, the measurement frequency range decreases, and the variation trend of the measurement range is quite different before and after the inflection point; when the cavity length value decreases, the measurement frequency range increases and the change will be flattened. It can also be seen from the Atlas that if the cavity length exceeds a certain length, the measurement sensitivity will be affected, and when the cavity length is short, the measurement range will be affected. Therefore, in actual use, it can be designed according to the needs. If the range of the measurement frequency is required to be relatively small and high sensitivity is required, then the long cavity length structure should be used.

It can be seen from the abovementioned discussion that if the structure of the measurement system remains unchanged, the fundamental frequency of the cavity will not change. It can be seen from Figure 8 that the larger the harmonic mode-locking order, the smaller the measurement sensitivity, and when the harmonic mode-locking order increases to a certain value, the changing trend will be significantly different.

5.4. Frequency Division Signal Processing. Experiments are carried out on the microwave photon signal, and the measurement effect of the system is judged by the frequency measurement error. The frequency measurement error value of the system for the unknown microwave photon signal can be obtained from Figure 9. It can be seen from the analysis of the values in the figure that the measurement range of this experiment is between 10 and 39 GHz, and the error value of the system is ±1 MHz. The unknown microwave photon signals in 13 different frequency bands.

The data are used as the main basis to measure the measurement effect of the existing system and the experimental system, and the results reflect the fitness of the system model in this paper. The measurement system proposed in this paper combines two instantaneous frequency

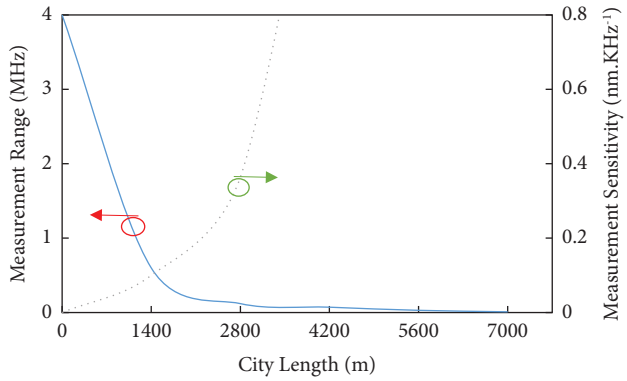

Figure 7: Variation of measurement frequency range and measurement sensitivity with laser cavity length L.

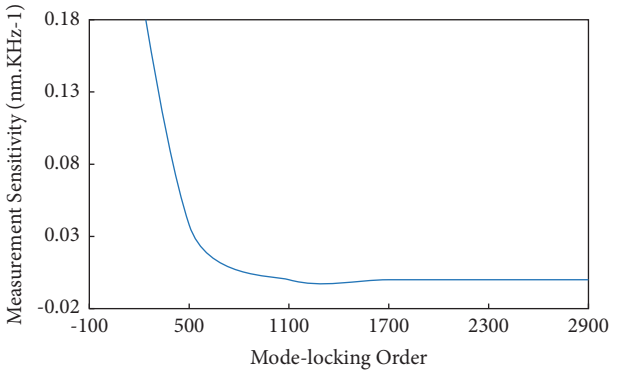

Figure 8: Relationship between measurement sensitivity and harmonic mode-locking order.

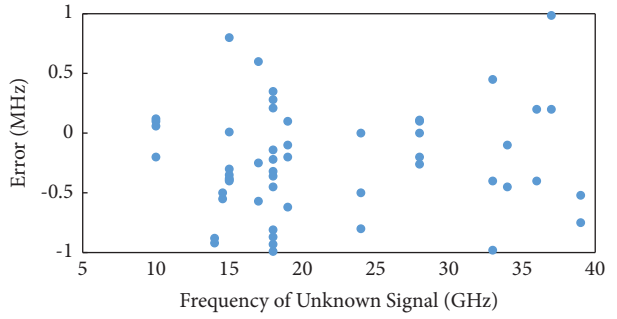

Figure 9: Frequency measurement error: measurement range is 9–38 GHz, error <±1 MHz.

measurement techniques to process the optical signal. The system can reflect the performance of the two techniques. The advantage is that it adopts the wide measurement range characteristics of the swept frequency receiving system and the characteristics of allowing simultaneous measurement of multiple frequencies, and also combines the high measurement accuracy characteristics of the ACF system. The advantages of the above two systems are reflected in the proposed method. The analysis method based on the experimental results can analyze the problem from an objective point of view, and measure the advantages and disadvantages of the conventional system, it is necessary to combine the measurement range and measurement accuracy of the system to make scientific judgments. This paper uses the ratio of measurement range and measurement accuracy to measure the measurement effect of the system.

6. Conclusion

The combination of IoT and microwave photonic signals is still in its infancy, and similar studies are rarely reported. This paper expounds on the structure level of the Internet of Things through multi-channel search and extends to its corresponding functions at specific levels. At the same time, it analyzes and summarizes the functional characteristics, thereby spreading the related characteristics of the Internet of Things. Then, the application of transceiver components for microwave photonic signals in the field of the Internet of Things is explained, and the detection and energy collection of microwave photonic signals are demonstrated. In this paper, the microwave photonic signal generation of optical injection locking is introduced, the mathematical model of optical injection locking is proposed, and the characteristics of optical injection locking are analyzed. The manifestations of microwave photon signals are classified and introduced, and the generation of microwave photon signals is simulated. The data simulation and experiment are carried out for the light injection microwave photonic filter, and the principle of the microwave photonic oscillator is introduced. The measurement frequency range of microwave photonic signals needs to be determined according to the actual work needs. If the range is small and high sensitivity is required, a long cavity and a long structure should be used. When measuring high-frequency signals, a short cavity structure should be used to ensure measurement sensitivity. Finally, the experimental comparison of frequency division signal processing is carried out in this paper, and the measurement range and measurement accuracy are combined. It can be seen that the system proposed in this paper has a higher measurement effect.

Data Availability

The data used to support the findings of this study can be obtained from the corresponding author upon request.

Conflicts of Interest

The authors have no conflicts of interest.

References

[1] B. Gainey, D. Hariharan, Z. Yan, S. Zilg, M. Rahimi Boldaji, and B. Lawler, "A split injection of wet ethanol to enable thermally stratified compression ignition," *International Journal of Engine Research*, vol. 21, no. 8, pp. 1441–1453, 2020.

[2] T. Numai, "Fundamentals of semiconductor lasers," *Fundamentals of Semiconductor Lasers*, pp. 89–186, 2015.

[3] D. Jiang, "The construction of smart city information system based on the Internet of Things and cloud computing," *Computer Communications*, vol. 150, pp. 158–166, 2020.

[4] C. Liu and T. Ma, "Green logistics management and supply chain system construction based on internet of things technology," *Sustainable Computing: Informatics and Systems*, vol. 35, Article ID 100773, 2022.
[5] S. H. Gold and G. S. Nusinovich, "Review of high-power microwave source research," *Review of Scientific Instruments*, vol. 68, no. 11, pp. 3945–3974, 1997.
[6] W. Lu, H. Huang, Z. Qian, N. Gong, and Y. Gong, "SWIPT cooperative spectrum sharing for 6G-enabled cognitive IoT network," *IEEE Internet of Things Journal*, vol. 8, no. 20, pp. 15070–15080, 2021.
[7] J. M. Osepchuk, "Microwave power applications," *IEEE Transactions on Microwave Theory and Techniques*, vol. 50, no. 3, pp. 975–985, 2002.
[8] M. K. Thumm and W. Kasparek, "Passive high-power microwave components," *IEEE Transactions on Plasma Science*, vol. 30, no. 3, pp. 755–786, 2002.
[9] K. Pitchai, S. L. Birla, J. Subbiah, D. Jones, and H. Thippareddi, "Coupled electromagnetic and heat transfer model for microwave heating in domestic ovens," *Journal of Food Engineering*, vol. 112, no. 1-2, pp. 100–111, 2012.
[10] R. A. Ginley, "Traceability for microwave power measurements: past, present, and future," in *Proceedings of the 2015 IEEE 16th Annual Wireless and Microwave Technology Conference (WAMICON)*, pp. 1–5, Cocoa Beach, FL, USA, April, 2015.
[11] Y. H. Suh and K. Chang, "A novel low-cost high-conversion-efficiency microwave power detector using GaAs FET," *Microwave and Optical Technology Letters*, vol. 44, no. 1, pp. 29–31, 2005.
[12] F. Ö. Alkurt, O. Altıntaş, M. Bakır et al., "Microwave power imaging detector based on metamaterial absorber," *Optical Engineering*, vol. 59, no. 08, Article ID 087104, 2020.
[13] T. Zhang, W. R. Eisenstadt, R. M. Fox, and Q. Yin, "Bipolar microwave RMS power detectors," *IEEE Journal of Solid-State Circuits*, vol. 41, no. 9, pp. 2188–2192, 2006.
[14] X. Fan, R. Cao, T. Moriyama, W. Wang, H. W. Zhang, and J. Q. Xiao, "Magnetic tunnel junction based microwave detector," *Applied Physics Letters*, vol. 95, no. 12, Article ID 122501, 2009.
[15] J. Capmany and D. Novak, "Microwave photonics combines two worlds," *Nature Photonics*, vol. 1, no. 6, pp. 319–330, 2007.
[16] D. Marpaung, C. Roeloffzen, R. Heideman, A. Leinse, S. Sales, and J. Capmany, "Integrated microwave photonics," *Laser & Photonics Reviews*, vol. 7, no. 4, pp. 506–538, 2013.
[17] W. Lu, S. Hu, X. Liu, C. He, and Y. Gong, "Incentive mechanism based cooperative spectrum sharing for OFDM cognitive IoT network," *IEEE Transactions on Network Science and Engineering*, vol. 7, no. 2, pp. 662–672, 2020.
[18] T. Berceli and P. R. Herczfeld, "Microwave photonics-A historical perspective," *IEEE Transactions on Microwave Theory and Techniques*, vol. 58, no. 11, pp. 2992–3000, 2010.
[19] D. Marpaung, J. Yao, and J. Capmany, "Integrated microwave photonics," *Nature Photonics*, vol. 13, no. 2, pp. 80–90, 2019.
[20] H. Memarzadeh-Tehran, J. J. Laurin, and R. Kashyap, "Optically modulated probe for precision near-field measurements," *IEEE Transactions on Instrumentation and Measurement*, vol. 59, no. 10, pp. 2755–2762, 2010.

Hindawi
Mobile Information Systems
Volume 2022, Article ID 7473614, 10 pages
https://doi.org/10.1155/2022/7473614

Research Article

Design of the Physical Education Teaching System by Using Edge Calculation and the Fuzzy Clustering Algorithm

Han Ning

School of Sports and Health Engineering, Hebei University of Engineering, Handan 056038, Hebei, China

Correspondence should be addressed to Han Ning; 2007059@muc.edu.cn

Received 7 July 2022; Revised 10 August 2022; Accepted 17 September 2022; Published 27 September 2022

Academic Editor: Shadi Aljawarneh

With the increasing number and types of terminal access, real-time processing of increasingly complex Internet of things applications has become increasingly difficult. On the one hand, cloud computing environment in virtual reality, ultrahigh definition live video, intelligent manufacturing, and other application fields put forward complex, diverse, real-time, and other new business requirements. On the other hand, modern IOT terminals have shortcomings such as insufficient computing power and limited battery capacity, which make it difficult to provide real-time processing for Internet applications. The emergence of edge computing services provides effective solutions for these applications, which can improve the local data processing capacity, shorten the data transmission delay, and reduce the hardware cost to a certain extent. Since computing offload, resource allocation, cache content placement, and edge server deployment are the basis of localized data processing and resource allocation, their performance is closely related to the efficiency and accuracy of data processing in the whole system. In the application of the current system, online learning resources and cutting-edge software and hardware teaching environment continue to emerge, shaping a unique smart classroom. The system proposed in this paper not only has the traditional physical education knowledge but also the advanced visualization principle. The combination of them can promote the practice of the new concept of physical education. Through research on edge computing and resource allocation, this paper applies it to the development of cloud computing environment and sports teaching visualization system so that the cloud computing environment and sports teaching visualization system can flourish.

1. Introduction

There are many definitions of cloud computing. At present, the most widely accepted definition is the new computing mode that cloud computing charges through cumulative usage. This computing mode provides customers with more convenient and efficient computing services [1]. As long as they are allowed to enter the resource sharing pool, cloud computing environment resources such as servers can be provided immediately, and customers do not need to invest too much management work on the cloud platform [2]. Due to the limited service capacity of a single server and the need to wait for task execution, the efficiency is very low. Therefore, this paper collects data through sensors, cameras, smartphones, and other devices, provides computing and storage capabilities at the edge of the network close to the user end, and processes IOT applications in real time [3, 4]. When the edge computing resources are not allocated enough, user terminals can be allowed to use cloud computing resources. We can clearly see from edge computing applications that remote network communication is required between user devices such as sensors and smartphones and cloud computing [5]. In order to reduce data traffic and provide low latency services, edge servers are deployed at the edge of the network close to terminal devices to take over part of computing, caching, and communication with cloud data centers. The closer the edge server is to user devices, the faster the response speed is. However, the more nodes it is needed to be deployed, the higher the cost [6]. Then this paper also studies physical education. Education is the development direction of improving productivity and culture, representing the interests of the people. Vigorously giving priority to the development of education can meet the growing cultural needs of the people [7]. Traditional physical

teaching pattern, although in the past time is proved on the promotion of students to have a good effect, is not consistent with the current development of science and technology level. As the development and demand of science and technology also promote the improvement of teaching technology, sports teaching has carried out diversified reforms to adapt to the existing scientific and technological environment [8]. In order to promote the scientific construction of physical education, it is necessary to build an effective sports science and technology teaching platform. Only when relevant knowledge is perfected can scientific and technological means be combined with traditional physical education and a new mode of physical education be developed [9]. Physical education can significantly improve the physical quality of the people, which is a major livelihood project benefiting the people. It is also an important carrier for the implementation of the strategy of strengthening the country with science and technology, strengthening the country with talents and modernizing education [10].

2. Related Work

The relevant concepts of cloud computing are sorted out in the literature, including the way of its generation and the development status at home and abroad, which provides the basic concept analysis for this paper [11]. The literature introduces the concept of cloud computing and specifically defines the characteristics of cloud computing from three aspects: the basic characteristics of cloud computing, cloud computing architecture, and cloud computing service mode [12]. Then it summarizes the problems encountered in the current resource allocation and lists the existing improvement methods. At the same time, the most commonly used resource allocation algorithm is also obtained. Finally, the related resource allocation technologies are introduced, including parallel programming technology, virtualization technology, and load balancing technology [13]. A resource allocation model based on time energy consumption is proposed in the literature, and the specific implementation of ant colony algorithm and genetic algorithm is introduced later. Three improvements of the ant colony algorithm are also mentioned, which improve the transfer probability, improve the pheromone volatilization coefficient, and introduce the load balancing adjustment factor [14]. Then the combination of ant colony algorithm and genetic algorithm is introduced in detail. The literature introduces the competitive model of multiple service providers in the edge computing environment. This paper considers the competition and cooperation among multiple service providers and believes that the resources provided by the servers of multiple service providers have a certain substitution relationship, so it is difficult for service providers to know the resource prices of other competitors [15]. Based on the vision of service providers to improve benefits, this paper determines the game model as Bayesian game and estimates the server location to meet the server resource requirements of terminal devices. The literature explains the benefits of service providers, resource utilization, user satisfaction, etc., and uses user information to make decisions on the layout of servers to maximize the benefits of service providers under the constraints of meeting the delay requirements to the greatest extent [16].

3. Research on Edge Computing Resource Allocation in Cloud Computing Environment

3.1. Relevant Calculation Model Design. In order to enable enterprises to work efficiently, cloud computing usually uses three service models: infrastructure as a service (IaaS), platform as a service (PaaS), and software as a service (SaaS), as shown in Figure 1:

At the bottom of the cloud computing service model is IaaS, which means that enterprises and individuals can use cloud computing technology to achieve the goal of efficient use of various computing resources in the cloud environment. Hosts, storage centers, and communication networks work together to create IaaS infrastructure. The unique cloud computing virtualization technology enables IaaS to provide customers with exclusive personalized services such as data storage, big data computing, load balancing control, and key data backup. IT companies such as Microsoft, Google, and HP can now rely on virtualization technology to combine different computing resources to form a resource pool. Customers can choose appropriate services from the resource pool according to their actual needs. In addition to providing ultrahigh computing power, IaaS can also rearrange and arrange cloud computing resources on demand, and dynamically deploy applications installed in IaaS. With IaaS, users can quickly acquire DevOps capabilities. According to the actual business needs, people choose IT resources and middleware models. Through customization, packaging, and other operations, new IT products can be delivered quickly in a very short time. IaaS provides the most advanced operation functions for IT companies. IT enterprises are not only an operation and maintenance platform but also an operation platform and a platform that can constantly exchange services for different customers.

$T_{\text{exe}}(i, j)$ indicates that if task I is given to calculate the expected execution completion time of node j. $X_{\text{lon}}(i)$ represents the task data length I, and $Y_{\text{cal}}(j)$ represents the execution rate J of the computing node, then $T_{\text{exe}}(i, i)$ can be expressed as

$$\mathrm{T}_{\text{exe}}(\mathrm{i},\mathrm{j}) = \frac{\mathrm{X}_{\text{lon}}(\mathrm{i})}{\mathrm{Y}_{\text{cal}}(\mathrm{j})}. \tag{1}$$

$T_{\text{dur}}(i, j)$ represents the expected time required to transfer task I to computing node j. $X_{\text{siz}}(i)$ represents the amount of data to be transmitted by task I, and $Y_{\text{del}}(j)$ represents the data transmission speed of computing node j, then $T_{\text{dur}}(i, j)$ can be expressed as

$$\mathrm{T}_{\text{dur}}(\mathrm{i},\mathrm{j}) = \frac{\mathrm{X}_{\text{siz}}(\mathrm{i})}{\mathrm{Y}_{\text{del}}(\mathrm{j})}. \tag{2}$$

$T_{\text{sum}}(i, j)$ refers to the expected time taken to calculate the target J to complete all tasks in task I, and its value can be expressed as

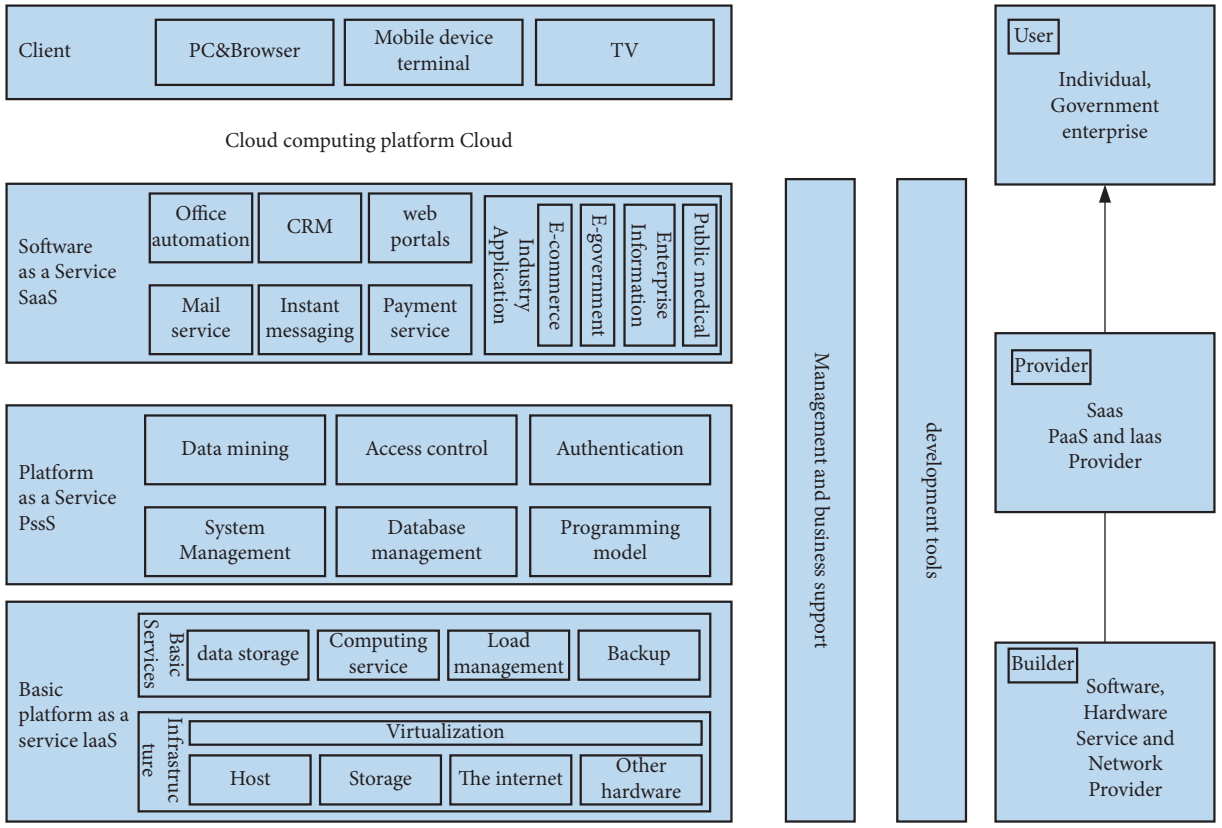

Figure 1: Cloud computing service model.

$$T_{sum}(i,j) = T_{exe}(i,j) + T_{dur}(i,j). \tag{3}$$

Since the allocation of cloud computing resources is parallel, and each computing node completes its own work independently, the expected time for the system to process all tasks higher than T_{cos} can be expressed as

$$T_{cos} = \max\left(\sum_{i=1}^{m} T_{sum}(i,j)\right). \tag{4}$$

The energy consumption cost of C_{cos} to complete resource allocation can be expressed as

$$C_{cos} = \sum_{j=1}^{n}\sum_{i=1}^{m}\left(T_{exe}(i,j) * C_{exe} + T_{dur}(i,j) * C_{dur}\right). \tag{5}$$

3.2. Unloading Strategy of Edge Computing. Component clustering should collect data about component behavior to express its characteristic attributes. According to the characteristics of Internet of things applications, this search selects the behavior of components for classification. The behavior of components includes relevant information, performance information, and basic information. The information describing component behavior can be obtained from the component document, and the CBD matrix using component behavior description can be defined as

$$CBD = \begin{bmatrix} \{c_d, c_{re}, c_r, \ldots\}_T \\ \{c_d, c_{trme}, c_m, \ldots\}_P \\ \{c_k, c_s, \ldots\}_B \end{bmatrix}. \tag{6}$$

The topological information between components (i, j) includes the amount of data transmission, the amount of data feedback, and the proximity between components. When there is an adjacency relationship, the t_{ij} value of the topological information index is defined as equation (7), and a is the influence factor of attribute $0 \le a \le 1$:

$$t_{ij} = a \times c_{tz} + (1 - a) \times c_{re}. \tag{7}$$

Component performance information includes CPU call C_d, delay c_{time}, and memory requirement c_m. The p_{ij} value of the performance information index is defined as (8). b1, b2, and b3 are the factors that affect the attribute $0 \le bi \le 1$.

$$p_{j}^{\cdot} = b_1 \times c_d + b_2 \times c_{time} + b_3 \times c_m. \tag{8}$$

Basic component information includes c_k component type and security level c_s. When the component can be unloaded, the value f_{ij} of the component basic information index is defined as formula (9). d is the influence factor of attribute, $0 \le d \le 1$, which can be given as

$$f_{ij} = d \times c_k + (1 - d) \times c_s. \tag{9}$$

Therefore, the w_{ij} weight of the directed arc on the component dependency graph is the dependency between v_i

and v_j components, which can be quantified by weighted summation as

$$w_{ij} = k_1 \times t_{\dot{\eta}} + k_2 \times p_{ij} + k_3 \times f_{\dot{i}}. \tag{10}$$

Among them, k_1, k_2, and k_3 represent the weights of topology information, function information, and basic component information, respectively. $k_1 + k_2 + k_3 = 1$. Map the weighted digraph to the dependency matrix W, and the dependency matrix between n components is

$$W = \begin{bmatrix} w_{11} & w_{12} & \cdots & w_{1n} \\ w_{21} & w_{22} & \cdots & w_{2n} \\ \vdots & \vdots & \ddots & \vdots \\ w_{n1} & w_{n2} & \cdots & w_{nn} \end{bmatrix}. \tag{11}$$

Specific components have different degrees of membership, which belong to multiple sets. The classification matrix corresponding to the component classification result is fuzzy matrix R. Because the diagonal element of fuzzy matrix is 0, fuzzy clustering cannot be carried out directly, and it must be transformed into fuzzy similarity matrix. The transfer function $h_{ij} = (w_{ij} + w_{ji})/2$ is used to determine the component dependency, and then the included angle cosine method is used to calculate the similarity coefficient r_{ij} between components in the application as

$$r_y = \frac{\sum_{k=1}^{n} \left(h_{ik} h_{jk}\right)}{\sqrt{\sum_{k=1}^{n} h_{ik}^2} \cdot \sqrt{\sum_{k=1}^{n} h_{jk}^2}}. \tag{12}$$

Then, the component fuzzy similarity matrix R composed of r_{ij} is

$$R = \begin{bmatrix} r_{11} & r_{12} & \cdots & r_{1n} \\ r_{21} & r_{22} & \cdots & r_{2n} \\ \vdots & \vdots & \ddots & \vdots \\ r_{n1} & r_{n2} & \cdots & r_{nn} \end{bmatrix} \tag{13}$$

$$\lambda r_j' = \begin{cases} 1, r_j' \geq \lambda \\ 0, \text{others} \end{cases}$$

3.3. Edge Computing Resource Allocation Based on Energy Consumption Perception. The definition of indication variable is

$$x_{i,m}^{p,q} = \begin{cases} 1 \\ or. \\ 0 \end{cases} \tag{14}$$

Therefore, the completion time of DAG workflow job j_i with dependency is

$$\begin{aligned} ET_{j_i} &= \max_{x_{t,*}^{'-}} \left\{ FT\left(j_i^p, s_m^q\right) \times x_{i,m}^{p,q} \right\}, \\ FT\left(j_i^\rho, s_m^q\right) &= ET\left(j_i^p, s_m^q\right) + EST\left(j_i^r, s_n^q\right). \end{aligned} \tag{15}$$

In the project executed by the application, EST is recursively defined, as

$$\begin{aligned} EST\ \left(j_i^p, s_m^q\right) = \max \Bigg\{ & t_{enbble}\left(s_m^q\right) \\ & \max\left(x_{i,m}^{p,q} \times \left(FT\left(j_i^{pre}\right) + TM\left(j_i^{pre}, j_i^p\right)\right)\right), j_i^{pre} \in j_i \\ TM\left(j_i^{pre}, j_i^p\right) &= d_i^{pre,p} \cdot delay_{loc\left(j_i^{pc}\right), loc\left(j_i^p\right)}. \end{aligned} \tag{16}$$

When online jobs are constantly submitted to the system, each server node in the cluster is in a specific state, such as running, idle, conversion, and shutdown. It is assumed that the host server consumes power when running, idle, and switching states. Let p_i be the power of each node in the indicated state, which has four constant values as

$$p_i = \begin{cases} 0, \\ e_1, \\ e_2, \\ e_3. \end{cases} \tag{17}$$

Therefore, the definition of total energy consumption of the system is

$$E_{cluster} = \sum_{i=1}^{m} \left(\int_{t_a}^{t_b} p_i dt \right). \tag{18}$$

Each subtask can be sent to each resource for execution. The resource is an abstract unit. Different resource management systems have different number and performance of resources such as CPU and memory, and the execution time of each task allocated to resources is also different. When a user submits a job request, the resource scheduler must provide specific resources and allocate resources to the corresponding job. Due to the limited resource capacity (processor, memory, storage space, and network resources) of the edge MDC data center, the job request tasks that can be performed are also limited; At the same time, some tasks require a lot of resources, and the processing of the resources they depend on cannot be carried out. Multiple resources are needed to manage it. The more resources invested in the same time period, the larger the scale of parallel processing, and the shorter the completion time; Otherwise, it will either queue in the edge environment for processing, or send it to other data centers for collaborative processing, which will increase computing time and energy consumption. Then the energy aware multilevel resource allocation problem is expressed as the multidimensional knapsack problem (MKP) as

$$\begin{aligned} & \min \sum_m \sum_q \sum_i \sum_p x_{i,m}^{p,q} \cdot t_{i,m}^{p,q} \cdot p_m^q \\ & \text{C1: } \sum_i \sum_p x_{i,m}^{p,q} \cdot o_i^p \leq c_m^q \forall m, q \\ & \text{C2: } \sum_i \sum_p \sum_m \sum_q x_{i,m}^{p,q} \leq 1 \\ & \text{C3: } \max ET_{i_{level}} \leq D_{i_{level}} \\ & \text{C4: } \sum_i \sum_p x_{i,m}^{p,a} \cdot x_{i,m}^{p,b} \cdot d_i^p \leq B_{a,b}, \forall m, a, b. \end{aligned} \tag{19}$$

According to the weighted vino diagram, the terminal set provided by the ESM edge server is

Table 1: Values of three performance indicators when the starting time is 30 seconds.

Idle node delay	Sampling interval (5 s)				Sampling interval (10 s)				Sampling interval (20 s)			
	$N_{t>\text{deadline}}$	E_{total}	$T_{1,\text{exe}}$	$T_{2,\text{exe}}$	$N_{t>\text{deadline}}$	E_{total}	$T_{1,\text{exe}}$	$T_{2,\text{exe}}$	$N_{t>\text{deadline}}$	E_{total}	$T_{1,\text{exe}}$	$T_{2,\text{exe}}$
60	9.2	27135.4	15.5	45.4	12.44	27036.7	15.5	45.8	9.8	26484.2	15.8	46.2
100	8.2	28381.4	15.2	42.2	6.2	28384.3	11.6	42.7	9.3	28346.3	12.5	43.3
120	10.8	29020.3	15.3	42.3	7.8	28844.6	11.3	42.5	5.5	29103.5	10.2	40.4

Table 2: Values of three performance indicators when the starting time is 60 seconds.

Idle node delay	Sampling interval (5 s)				Sampling interval (10 s)				Sampling interval (20 s)			
	$N_{t>\text{deadline}}$	E_{total}	$T_{1,\text{exe}}$	$T_{2,\text{exe}}$	$N_{t>\text{deadline}}$	E_{total}	$T_{1,\text{exe}}$	$T_{2,\text{exe}}$	$N_{t>\text{deadline}}$	E_{total}	$T_{1,\text{exe}}$	$T_{2,\text{exe}}$
60	25.4	28041.2	17.3	46.4	34.3	27669.5	18.7	46.8	34.3	27619.3	18.8	47.1
100	17.6	28718.1	16.2	45.2	21.1	28516.3	16.6	45.9	12.7	28654.5	15.3	44.3
120	12.8	28962.4	15.8	43.3	12.7	28974	14.3	42.8	13.9	29134.6	14.3	43.2

$$\mathrm{V}\left(\mathrm{ec}_{\mathrm{m}}, \mathrm{t}_{\mathrm{m}}^{\mathrm{exe}}\right) = \underset{\mathrm{m}\neq\neq'}{\cap}\left(\mathrm{ue} \mid \mathrm{d}\left(\mathrm{ue}, \mathrm{ec}_{\mathrm{m}}\right) \times \mathrm{t}_{\mathrm{me}}^{\mathrm{exe}} \leq \mathrm{d}\left(\mathrm{ue}, \mathrm{ec}_{\mathrm{m}'}\right) \times \mathrm{t}_{\mathrm{m}'}^{\mathrm{exe}}\right), \left(\mathrm{m}, \mathrm{m}' = 1, 2, \ldots, \mathrm{N}_{\mathrm{ec}}\right). \tag{20}$$

The terminal equipment collection of all edge MDC service areas is

$$\mathrm{V}_{\mathrm{EC}} = \underset{\mathrm{ec}_{\mathrm{m}}\in\mathrm{EC}}{\cup} \mathrm{V}\left(\mathrm{ec}_{\mathrm{m}}, \mathrm{t}_{\mathrm{m}}^{\mathrm{exe}}\right), \mathrm{m} = 1, 2, 3, \ldots, \mathrm{N}_{\mathrm{ec}}. \tag{21}$$

For the time series load at i edges of the service area, the autocorrelation model AR (P) can be expressed as

$$\mathrm{x}_{\mathrm{t}}^{\mathrm{j}} = \theta_1 \mathrm{x}_{\mathrm{t-1}}^{\mathrm{i}} + \theta_2 \mathrm{x}_{\mathrm{t.2}}^{\mathrm{i}} + \ldots + \theta_{\mathrm{p}} \mathrm{x}_{\mathrm{t-p}}^{\mathrm{i}} + \varepsilon_{\mathrm{t}}, \varepsilon_{\mathrm{t}} \sim \mathrm{NID}\left(0, \sigma_{\varepsilon}^2\right). \tag{22}$$

The $p+1$ parameter is estimated using the least square method θ_1, θ_2, …, θ_3 and σ_ε^2:

$$\varepsilon_{\mathrm{t}} = \mathrm{x}_{\mathrm{t}}^{\mathrm{i}} - \theta_1 \mathrm{x}_{\mathrm{t-1}}^{\mathrm{i}} - \theta_2 \mathrm{x}_{\mathrm{t-2}}^{\mathrm{i}} - \ldots - \theta_{\mathrm{p}} \mathrm{x}_{\mathrm{t-p}}^{\mathrm{i}}, \tag{23}$$

$$\sigma_{\varepsilon}^2 = \frac{1}{\mathrm{P}-\mathrm{p}} \sum_{\mathrm{t=p+1}}^{\mathrm{P}} \left(\mathrm{x}_{\mathrm{i}} - \theta_{\mathrm{i}} \mathrm{x}_{\mathrm{t-i}}\right)^2. \tag{24}$$

3.4. Analysis of Simulation Results. Table 1 shows that when the sampling interval is 5S and the delay interval of idle nodes changes from 60 s to 100 s and 120 s, respectively, the corresponding energy consumption value of "cloud edge" resources is 27135.4 kJ, 28381.4 kJ increases to 29020.3 kJ, and the execution time of the two tasks begins to decrease, and finally remains stable.

As can be seen from Table 2, when the node startup time is 60 s and 120 s, the number of violations increases compared with the startup time of 30 seconds.

As the result of parameter sensitivity evaluation, the best setting of parameter node startup time is 30 s, idle duration delay interval is 100 s, and sampling interval is 10 s, as shown in Table 3.

Figure 2 starts from the time taken by the system to process data. It can be seen from the figure that the efficiency of several algorithms is similar when dealing with low-volume tasks. The algorithm presented in this paper shows obvious superiority when dealing with high-capacity tasks. The reason is that both PSO-GA and PSI-ACO algorithms adopt the random path selection strategy, which affects the search speed to a certain extent. The LBGACO algorithm proposed in this paper first uses GA algorithm for global search at the beginning of the algorithm and then converts the better solution obtained from the search into the initial pheromone distribution of ACO algorithm. This makes the convergence speed of LBGAACO algorithm faster than PSO-GA and PSO-ACO algorithm. In addition, by changing the transition probability and the pheromone volatilization coefficient, the globality of the algorithm search is improved.

In Figure 3, the power of the system is analyzed based on Figure 2, which also proves the superiority of the system in this paper. With the increase in the number of tasks, this phenomenon will become more obvious. This further proves that the power optimization model in LBGAACO algorithm proposed in this paper can track the power consumption of each node of computing resources in real time and effectively prevent a large number of tasks from being concentrated on specific nodes of computing resources, resulting in the increase of energy consumption of the whole system.

In this set of experiments, we compared the performance of the four strategies by installing different number of servers on each edge MDC. The number of servers per MDC increased from 2 to 12. As shown in Figure 4, the x-axis represents the number of servers in each MDC, and the y-axis represents the number of job violations, system power consumption, and average job completion time. As the number of servers in edge MDC increases, the ability of edge servers to share resources will also increase. In the figure, we can see that the number of task violations decreases with the increase of the number of MDC edge servers. When the size of the edge resource is 12, the number of violations of the task is the smallest. This figure shows the energy consumption of EAGA compared with that of auto scale. Even if the number of servers is small, the energy-saving effect of EAGA is good. With the increase of server resources, the load of the system decreases. The energy-saving effect of EAGA is better than auto scale and is close to opt strategy.

The estimated time to complete the job is shown in Figure 5. Under heavy load, the job execution time is better than autoscale. When resources are sufficient, this strategy

Table 3: Values of three performance indicators when the starting time is 120 seconds.

Idle node delay	Sampling interval (5 s)				Sampling interval (10 s)				Sampling interval (20 s)			
	$N_{t>\text{deadline}}$	E_{total}	$T_{1,\text{exe}}$	$T_{2,\text{exe}}$	$N_{t>\text{deadline}}$	E_{total}	$T_{1,\text{exe}}$	$T_{2,\text{exe}}$	$N_{t>\text{deadline}}$	E_{total}	$T_{1,\text{exe}}$	$T_{2,\text{exe}}$
60	61.3	30118.5	18.8	48.2	51.4	30545.9	18.8	48.2	56.7	30063.7	19.8	48.7
100	37	29445.7	17.2	47.6	31.8	29527.5	16.9	45.8	31.2	29634.5	17.5	46.3
120	21.8	29555	16.8	46.3	19.2	295257	16.6	45.5	26.5	29595	17.4	46.2

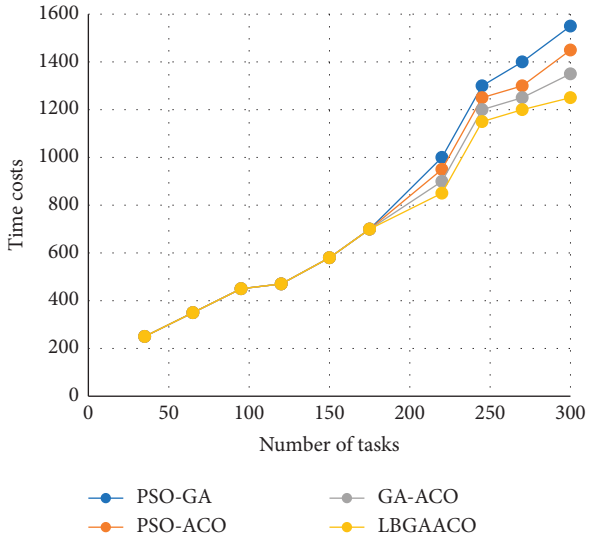

Figure 2: Time cost comparison chart.

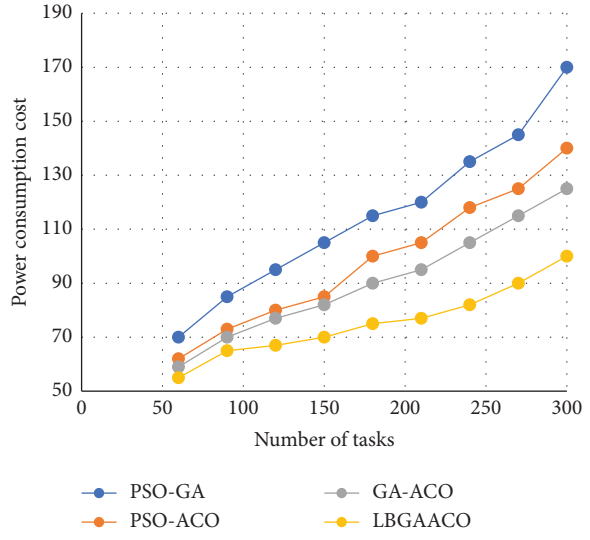

Figure 3: Power consumption cost comparison chart.

carries out energy-saving scheduling and energy-efficient allocation of resources on the premise of deadline driven. Although when the number of nodes is greater than or equal to 8, the job completion time is higher than AlwaysOn and autoscale, making it close to opt, but the number of job violations is relatively small. From experiments, it can be seen that the performance of Eaga in power consumption and the number of job violations is significantly better than the autoscale dynamic resource allocation strategy, close to opt, and while ensuring the lowest power consumption, it meets the low latency requirements of users.

4. Requirements and Application of the Physical Education Visualization System

4.1. Development and Demand of Physical Education Teaching Concept. The historical experience of Chinese school physical education concept research is mainly reflected in China which attaches great importance to the development of school sports. Through the promulgation and implementation of China's major policies and policies, we need to promote physical education in the contemporary new development.

The essence and core of Chinese school sports ideological trend is the law of internal development of school sports. After 40 years of reform and opening up, its development has become irreversible. The formation and changes of the ideological trend of school physical education in China can reflect the connotation and extension of school physical education and will change with the passage of time and evolution. The concept of school physical education belongs to the category of educational concept, and its reform and development are consistent with the overall direction of the development of educational concept. With the implementation of quality education and health in school sports and the implementation of the healthy China strategy, the concept of school sports has also changed, showing the characteristics of "richer connotation and broader extension."

Adhering to educational ideas is as important as innovation. In the new era, under the guidance of the core connotation, Chinese school physical education must assume responsibility, fulfill its mission, think and explore new development paths. The renewal and development of the concept of school sports in China must comply with the trend of social development, actively integrate with the world's advanced school sports in China, actively participate in global competition, cultivate more talents, strive to occupy an active position in the competition, and grasp the initiative of competition.

We should adhere to the values and concepts of traditional school sports with Chinese characteristics, critically learn from the essence of foreign higher education concepts when introducing and learning foreign culture, not stick to foreign models, innovate implementation methods, and adhere to Chinese characteristics as the starting point and foothold.

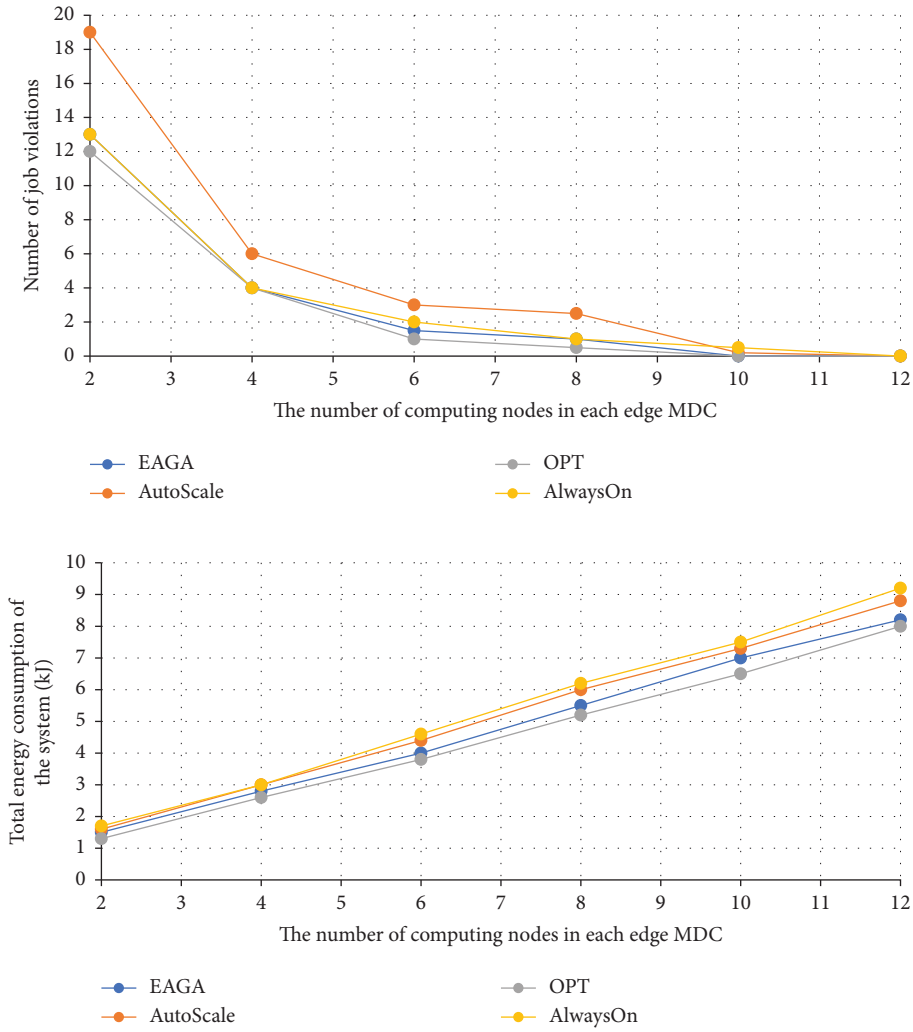

Figure 4: Number of job violations and total energy consumption of the system.

4.2. Construction of the Visual Teaching Model for Indoor Sports Teaching. Visual teaching design in smart classroom must fully combine the "wisdom" of smart classroom with the educational advantages of visualization. The advantage of visualization in teaching lies in the use of various visualization technologies to express tacit knowledge by different visual representation means, which directly affects people's visual senses, so as to promote the dissemination and innovation of knowledge. "Intelligence" includes five aspects such as the presentation of learning content, the management of classroom environment, the acquisition of learning resources, in-depth and timely interaction, and the perception of learning situations. It is a high-quality form of traditional multimedia and online classroom.

Due to the shortcomings of Addie model, a visual teaching model suitable for intelligent classroom is constructed on this basis, as shown in Figure 6. In this visual teaching model, students can fully participate in the learning process. From preclass preparation to active classroom interaction, and finally after class evaluation and feedback, students actively participate so that students can change from traditional simple knowledge reception to active participation in classroom interaction and improve classroom performance and students' interest in learning. Teachers led the whole teaching process and are mainly responsible for guiding students to learn, tapping and developing learners' potential, and conducting curriculum evaluation. The visual teaching model in the whole smart classroom is divided into preparation stage, design stage, learning stage, evaluation stage, and feedback stage.

4.3. Analysis of Visual Teaching Design Concept. Visual representation is the theoretical basis for the development and application of visual education. Only a reasonable concept of visual representation can play the greatest role. Visual teaching takes visual representation as the main teaching method, which requires learners to compile the characteristics, color, depth, and other information of the object image and then to simplify and organize this information to understand how the image is transformed into knowledge. Its characteristics are the visualization of text knowledge, the simulation of abstract knowledge, and the virtualization of complex knowledge, and make full use of

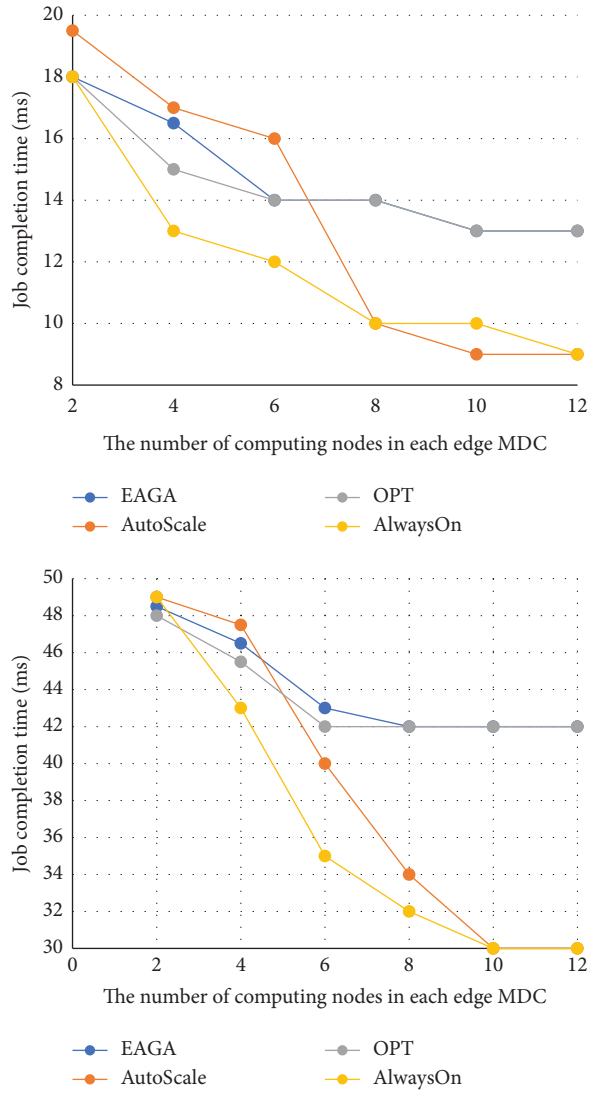

Figure 5: Operation completion time.

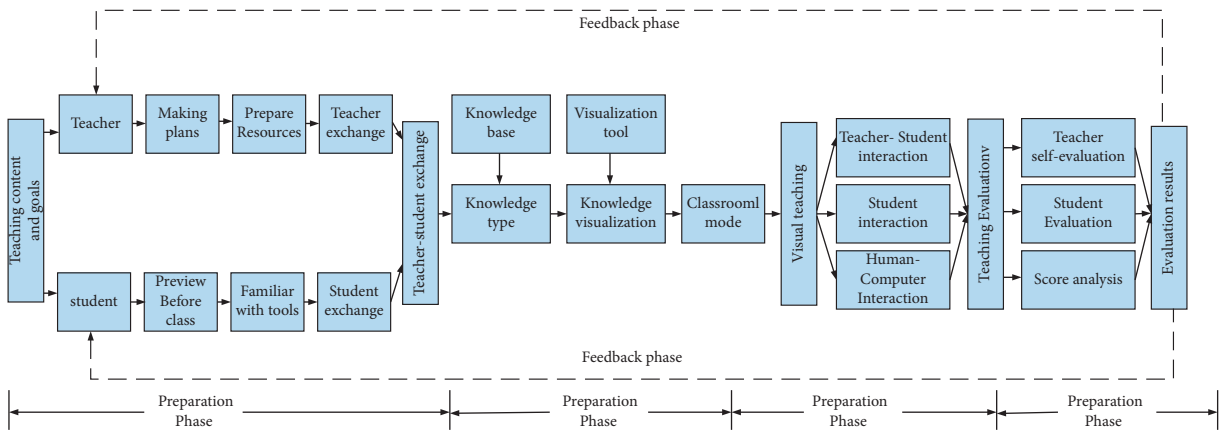

Figure 6: Visual teaching model in smart classroom.

Table 4: Visual teaching design of a typical classroom in the smart classroom.

Classroom mode	Teaching characteristics	Visual representation	Interactive form	Dual-track teaching
Teaching classroom	Teachers teach and students accept	Concept map and mind map	Focus on teacher-student interaction	Mind map + knowledge content
Inquiry class	Teacher guidance and student inquiry	Animation and simulation tools	Focus on the interaction between teachers and students and vitality	Simulation animation + difficult and difficult tips
Collaborative classroom	Teacher assistance and student collaboration	Interactive visual science tools	Focus on the interaction between teachers and students and vitality	Interactive visualization + operation skills

various visual elements (image, text, color, etc.) to express some information or relationships that are difficult to understand by text and data alone. Using the communication advantages of visual language to promote effective knowledge dissemination and communication innovation can also reduce the cognitive load of text knowledge and encourage learners to explore deep meaning. External things need our subjective choice and participation in order to enter visual thinking and be perceived and understood.

The teaching method of combining words with visual knowledge helps to improve the effectiveness of learning and improve students' understanding and memory of knowledge. According to the dual coding theory, there are two independent and interdependent cognitive systems in the representation and semantics of human cognitive system. They process information through representation code and semantic code and are activated by corresponding stimuli, which refers to an important principle; that is, knowledge presented together with language and visual information can get better recognition and memory effects. With the help of the teaching method of double electronic whiteboards, we can not only realize the joint display of visual images and words but also create conditions for the interaction between students and the media. This can not only adapt to different learners' learning styles but also provide learners with sufficient opportunities to participate in learning activities.

4.4. Visual Teaching Design Based on the Classroom Mode. Multiterminal interaction gives students more opportunities to interact with multimedia and teachers and students, which is one of the keys to create an active, efficient, and harmonious classroom. In the traditional multimedia environment, teaching methods are mainly based on teachers who impart knowledge to students. There is little or no interaction between teachers and students, and students are in a state of passive acceptance of knowledge. In the multiterminal teaching method, learners can more naturally integrate into teachers' teaching, question and answer, classroom homework, and other learning activities. The classroom gradually changes from knowledge instigator and lecturer to the guide and organizer of classroom activities, and students also complete the role transformation from the knowledge receiver to active participant in the classroom. Through multiterminal interactive learning, students can use various touch terminals for collaborative learning, synchronous exercises, student competitions, and other activities to improve students' learning experience, help improve students' practical ability, and cultivate students' team spirit. Teachers can change the overall learning state of teaching strategies and classroom interactive participation through the resource organization technology of mind mapping and resources, synchronous visual multiterminal teaching methods, real-time data analysis homework and other activities, and help create interactive classes and inquiry learning, which lays a solid foundation for improving teaching efficiency and implementing effective learning.

Based on the self-built smart classroom, this paper summarizes three typical teaching modes of smart classroom. As shown in Table 4, according to the teaching characteristics of various classroom operation modes, combined with the concept of intelligent classroom visual teaching design, different classroom visual teaching designs are carried out from three perspectives such as visual presentation, interactive form, and dual-track teaching.

5. Conclusion

Firstly, this paper combs the concept and logic of the system applied in this paper, and on this basis, it emphasizes the importance of resource allocation selection for research. At the same time, it introduces the research results of using the metaheuristic algorithm to solve the resource allocation problem of cloud computing at home and abroad. Then, introduce the relevant background of cloud computing in more detail and explain the concept of cloud computing from three different perspectives. Then, it launches the related technologies of resource allocation, introduces the specific workflow and allocation idea of parallel programming of resource allocation, explains the virtualization technology and load balancing technology, and finally makes a brief summary of the concepts of four commonly used metaheuristic resource allocation algorithms. Then people apply it to the physical education teaching environment. Generally speaking, the emergence and development of the traditional school physical education concept with Chinese characteristics are closely related to the general policy. At the government level, China has continuously promoted the reform of school physical education, vertically from the central to the local, and horizontally from the sports department to the major systems. School physical education policies, opinions, revision opinions, notices, and other

policies have been issued and implemented, promoting the continuous development of Chinese School Physical Education to the visual system teaching mode so that physical education and the development of science and technology truly combined to promote the progress of physical education cause.

Data Availability

The data used to support the findings of this study are available from the corresponding author upon request.

Conflicts of Interest

All the authors do not have any possible conflicts of interest.

References

[1] P. K. Senyo, J. Effah, and E. Addae, "Preliminary insight into cloud computing adoption in a developing country," *Journal of Enterprise Information Management*, vol. 29, no. 4, pp. 505–524, 2016.

[2] C. He, X. Fan, and Y. Li, "Toward ubiquitous healthcare services with a novel efficient cloud platform," *IEEE Transactions on Biomedical Engineering*, vol. 60, no. 1, pp. 230–234, 2013.

[3] S. Chen, H. Xu, D. Liu, B. Hu, and H. Wang, "A vision of IoT: applications, challenges, and opportunities with China perspective," *IEEE Internet of Things Journal*, vol. 1, no. 4, pp. 349–359, 2014.

[4] X. Zeng, S. K. Garg, P. Strazdins, P. P. Jayaraman, D. Georgakopoulos, and R. Ranjan, "IOTSim: a simulator for analysing IoT applications," *Journal of Systems Architecture*, vol. 72, pp. 93–107, 2017.

[5] J. Nieplocha, V. Tipparaju, M. Krishnan, and D. K. Panda, "High performance remote memory access communication: the ARMCI approach," *International Journal of High Performance Computing Applications*, vol. 20, no. 2, pp. 233–253, 2006.

[6] G. Zhang, Y. Chen, and G. Li, "The evolution and emerging trends of cloud computing adoption research: visual analysis of CiteSpace based on WOS papers," in *Proceedings of the 2020 3rd International Conference on Signal Processing and Machine Learning*, pp. 40–47, Beijing, China, October 2020.

[7] R. Bailey, K. Armour, D. Kirk et al., "The educational benefits claimed for physical education and school sport: an academic review," *Research Papers in Education*, vol. 24, no. 1, pp. 1–27, 2009.

[8] D. Penney and T. Chandler, "Physical education: what future (s)?" Sport," *Sport, Education and Society*, vol. 5, no. 1, pp. 71–87, 2000.

[9] B. Dyson, "Cooperative learning in an elementary physical education program," *Journal of Teaching in Physical Education*, vol. 20, no. 3, pp. 264–281, 2001.

[10] T. L. Wallhead, A. C. Garn, and C. Vidoni, "Effect of a sport education program on motivation for physical education and leisure-time physical activity," *Research Quarterly for Exercise & Sport*, vol. 85, no. 4, pp. 478–487, 2014.

[11] L. Wang, G. Von Laszewski, A. Younge et al., "Cloud computing: a perspective study," *New Generation Computing*, vol. 28, no. 2, pp. 137–146, 2010.

[12] Y. Wang, I. R. Chen, and D. C. Wang, "A survey of mobile cloud computing applications: perspectives and challenges," *Wireless Personal Communications*, vol. 80, no. 4, pp. 1607–1623, 2015.

[13] M. Ismail and W. Zhuang, "A distributed multi-service resource allocation algorithm in heterogeneous wireless access medium," *IEEE Journal on Selected Areas in Communications*, vol. 30, no. 2, pp. 425–432, 2012.

[14] R. Putha, L. Quadrifoglio, and E. Zechman, "Comparing ant colony optimization and genetic algorithm approaches for solving traffic signal coordination under oversaturation conditions," *Computer-Aided Civil and Infrastructure Engineering*, vol. 27, no. 1, pp. 14–28, 2012.

[15] U. Schroeders, O. Wilhelm, and G. Olaru, "Meta-heuristics in short scale construction: ant colony optimization and genetic algorithm," *PLoS One*, vol. 11, no. 11, p. e0167110, 2016.

[16] R. Yu, C. Wu, B. Yan et al., "Analysis of the impact of big data on E-commerce in cloud computing environment," *Complexity*, vol. 2021, no. 2, pp. 1–12, Article ID 5613599, 2021.

Hindawi
Mobile Information Systems
Volume 2022, Article ID 4155732, 8 pages
https://doi.org/10.1155/2022/4155732

Research Article

Experimental Study of Constant-Amplitude Fatigue Performance of *M*39 High-Strength Bolts in Grid Structures with Bolt-Sphere Joints

Zichun Zhou, Honggang Lei, Xu Yang, and Bin Qiu

College of Civil Engineering, Taiyuan University of Technology, Taiyuan 030000, Shanxi, China

Correspondence should be addressed to Honggang Lei; 20151255222@mail.sdufe.edu.cn

Received 4 August 2022; Revised 5 September 2022; Accepted 15 September 2022; Published 26 September 2022

Academic Editor: Shadi Aljawarneh

Grid structures with bolt-sphere joints are widely used in industrial plants. With the installation of suspension cranes, high-strength bolts are subjected to repeated alternating loads and cause fatigue problems. Due to their dispersive nature, the degree of difficulty and cost of fatigue tests are extremely high. Due to the lack of a recognized fatigue design method, engineering designers have encountered great difficulties, and the promotion and application of such methods are severely restricted. In this paper, we successfully implemented a constant-amplitude fatigue test of M39 high-strength bolt specimens on an American MTS Landmark 370.50 fatigue testing machine and obtained the corresponding *S-N* curve from the statistical analysis of the test data. Using the nominal stress amplitude $\Delta\sigma$ and the hot point stress amplitude $\Delta\sigma_k$ as the design parameters, we established a corresponding constant-amplitude fatigue design method. We performed a microscopic analysis of the fracture surface using a TESCAN Mira3 LMH scanning electron microscope and revealed the fatigue failure mechanism of the high-strength bolts.

1. Introduction

Grid structures with bolt-sphere joints are space structures with a high degree of statical indeterminacy [1]. Due to their suitable stress ranges, factory prefabrication, on-site assembly, and broad scope of applicability, they are widely used for industrial building construction. To meet production needs, the bolt-sphere grid structures in industrial buildings are usually installed with suspension cranes for lifting and transporting equipment. The installation of suspension cranes takes full advantage of the statically indeterminate structure of the grid to quickly spread the concentrated force, and the grid can also be flexibly laid out to change the industrial flow processes. Grid structures have been used for a broad range of applications in construction, aerospace, metallurgy, machinery, and light industries [2].

In the reciprocating loading process of the suspension crane on the bolt-sphere grid structure, fatigue will occur at the bolt-sphere joint of the grid and result in fatigue failure [3]. Fatigue failure is a type of brittle failure that usually occurs suddenly, and the failure is complete. The goal of studying fatigue is to establish a fatigue calculation method or a fatigue life estimation method. Although the fatigue problem of the grid structure under the action of a suspended crane has gained attention, to date, there has not been an explicit stipulation on how to carry out the fatigue design. In China's national standard grid structure design and construction procedures (JGJ7-91) [4], article 1.0.4 stipulates that "The fatigue strength and construction of grid structures directly subjected to medium or heavy class loads of suspension cranes should be determined through special tests." This is an evasive statement. In the classification of components and joints that require fatigue calculations in Appendix E of design code for steel structures [5], connecting structures related to grid structures were not included. With no standards to rely on, designers can only act based on experience. This can not only put engineering design at risk but has also greatly restricted the large-scale application of suspension cranes in the grid structures of industrial plants. In this regard, the experimental and theoretical research on the fatigue of bolt-sphere joints in

grid structures has important scientific value and practical engineering significance.

Nam et al. investigated a novel method to construct a unified stress-life (S-N) curve that was proposed for the three different bolts with different sizes and lengths subjected to various external axial loading conditions and preloads, ranging from 44% to 88% of the ultimate tensile stress [6]. Maljaars and Euler drew on a large number of fatigue tests to assess bolts and bolted connections, which revealed the possibility to improve current design specifications [7]. Bartsch and Feldmann analyzed the fatigue test data and concluded that bolts should be designed with possibly large diameters and be placed as close as possible to the tension flanges, while end plates should be dimensioned thick enough, at least as thick as the bolt diameter [8]. Ding et al. investigated the reliability of the high-strength bolts' fake tightened-up phenomena of the bolted spherical joints and developed a group of calculation formulas for predicting the tensile strength of bolted spherical joints with different bolt screwing depths [9]. Yuan et al. studied the bearing performance of the bolt-sphere joint portion of the bolted spherical node with stochastic pitting corrosion damage [10].

The key to the fatigue problem of the grid structure is at the joints. Researchers have performed theoretical and experimental studies on the fatigue performances of the welded hollow sphere joints and the bolt-sphere joints commonly used in grid structures. These results are summarized as follows. In 1994, researchers carried out uniaxial tensile constant-amplitude fatigue tests on twelve *M*24 and three *M*33 high-strength bolts, and they obtained 15 effective fracture points and the corresponding *S-N* curves [11]. In addition, microscopic analysis of the fracture surface was performed using a PSEM-500X scanning electron microscope and EDA *X*-711 spectrometer. In 1995, researchers carried out uniaxial tensile constant-amplitude fatigue tests on four *M*14, eight *M*24, and eight *M*33 high-strength bolts and obtained 20 effective fracture points [2]. They obtained the corresponding *S-N* curves and established an empirical formula using the stress amplitude as the design parameter. Additionally, they found that the tensile fatigue strength of the high-strength bolts was related to the stress ratio ρ.

In 2016 and 2017, researchers conducted constant amplitude fatigue tests on *M*20 and *M*27 high-strength bolts and fitted the corresponding *S-N* curves to the data [12, 13]. A preliminary constant amplitude fatigue calculation method was established based on a design expression of the allowed stress amplitude. In 2019, researchers conducted a variable-amplitude fatigue test on *M*30 high-strength bolts and revealed the variable-amplitude fatigue performance of the *M*30 high-strength bolts [14].

The above-cited studies on fatigue problems and the research methods adopted, without exception, were fatigue tests. Based on this research trend, fatigue tests will remain the most reliable research tool for investigating fatigue performance for the foreseeable future. This article presents the first systematic investigation of the constant-amplitude fatigue performances of *M*39 high-strength bolts in grid structures with bolt-sphere joints, aimed at establishing a fatigue calculation method.

2. Materials and Methods

2.1. Design of Fatigue Specimen. The fatigue test procedures for grid structures with bolt-sphere joints were created according to the specifications in the technical specification for space frame structures (JGJ7-2010) [15], the bolted spherical nodes of steel grid structures (JGT10-2009) [16], and the high-strength bolts for joints of space grid structures (GBT 16939-2016) [17].

*M*39 high-strength bolts: the *M*39 thread specifications were as follows: the nominal length $L = 128$ mm, the performance class was 9.8 s, the effective cross-sectional area was 976 mm^2, the ultimate tensile load was 878–1074 kN, and the material was 40 Cr. Since the wedge grip on the fatigue testing machine can accommodate a maximum diameter of 55 mm but the nut diameter of the *M*39 high-strength bolt was 60 mm, it was necessary to modify the nut of the *M*39 high-strength bolt and cut it down to a diameter less than 55 mm.

Bolt-sphere BS200: the outer diameter of the No. 45 steel bolt-sphere was 200 mm. The bolt-sphere was machined from a blank forged steel sphere. The material met the specifications of the high-quality carbon structural steel (GB/T 699) [18]. Three pairs of threaded holes were machined on each sphere. When one thread failed, the sphere could be rotated to use the threads in another direction for fatigue testing. Thus, a bolt-sphere could be efficiently used three times.

2.2. Test Program

2.2.1. Static Failure Test. To understand the mechanical properties of the high-strength bolts used in the tests and determine the magnitude of the applied load in the subsequent constant-amplitude fatigue tests, the high-strength bolts were first subjected to a tensile test before the fatigue test. Randomly select three *M*39 high-strength bolts, prepare test samples according to relevant provisions of ISO 6892-1: 2009 [19], as shown in Figure 1, and conduct static performance tensile tests on high-strength bolt materials with a WAW-1000 kN microcomputer-controlled electro-hydraulic servo universal testing machine. See Table 1 for the mechanical property test results of the obtained materials and the stress-strain curve. All mechanical property indexes of the high-strength bolts meet the requirements.

2.2.2. Constant-Amplitude Fatigue Test. In order to obtain a complete *S-N* curve, we will set several stress ranges, each of which contains more than 2 specimens. The stress ratio is set to 0.1 and 0.6, respectively, and the values of the maximum stress and the minimum stress in this range can be calculated according to formulas (1) and (2).

$$R = \frac{\sigma_{\min}}{\sigma_{\max}}, \tag{1}$$

$$\Delta\sigma = \sigma_{\max} - \sigma_{\min}. \tag{2}$$

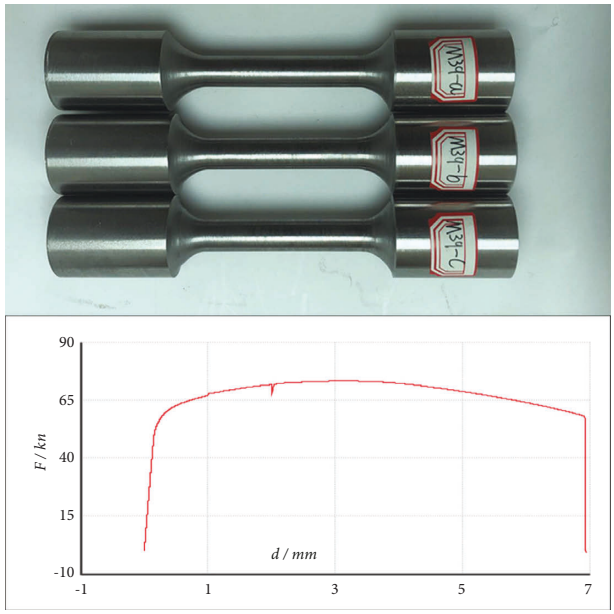

Figure 1: . The s force—displacement curve of the *M*39 high-strength bolt.

Table 1: Static test results of high-strength bolts.

Bolt number	$\sigma_{0.2}$	$\overline{\sigma_{0.2}}$	σ_b	$\overline{\sigma_b}$	$\overline{\delta}$ (%)	$\overline{\Psi}$ (%)
M39-a	783.6		964.4			
M39-b	757.9	781.6	951.1	969.7	11.2	44
M39-c	803.4		993.6			

$\sigma_{0.2}$—Conditional yield strength (MPa); $\overline{\sigma_{0.2}}$—average value of conditional yield strength (MPa); σ_b—ultimate tensile strength (MPa); $\overline{\sigma_b}$—average value of ultimate tensile strength (MPa); $\overline{\delta}$—rate of extension; $\overline{\Psi}$—rate of contraction.

According to the loading capacity of the fatigue testing machine, the loading system shown in Table 2 is formulated.

All the constant-amplitude fatigue tests of the high-strength bolts were completed on the MTS Landmark 370.50 hydraulic servo fatigue testing machine. The maximum applied load of the testing machine was 500 kN, the minimum load was 15 kN, and the frequency of the loading cycles could reach 60 Hz. Under a hydraulic cycle, the actuator at the bottom of the fatigue testing machine produced a vertical displacement and applied an axial tension to the bolt held in the fixture. The applied stress load was exactly the same as the load experienced by the bolt in actual engineering applications, as shown in Figure 2.

Using the test setup described above, fatigue tests were conducted on 34 high-strength bolts under constant-amplitude alternating loads. The stress ratio ρ of this test was set to the range of 0.1 to 0.6, and the loads were applied in a specified order.

2.2.3. Experimental Procedure

(1) Using the MTS Landmark 370.50 fatigue tester (Figure 3), constant-amplitude fatigue tests were performed on two high-strength bolts at a time. The load was applied according to the desired stress amplitude on the bolt.

(2) The test stopped automatically, and the MTS Landmark 370.50 fatigue testing machine was shut down when the bolt fractured and failed under fatigue.

(3) The number of final cycles at which the bolt broke was recorded, the fractured surface was photographed, and the test information was analyzed (Figure 3).

(4) The failed bolt was replaced with a new bolt, and the next round of constant-amplitude fatigue loading was conducted with a new stress amplitude. The undamaged bolt then became the test specimen for the variable-amplitude fatigue tests, and so forth, until all the high-strength bolts were tested.

3. Results and Discussion

3.1. Analysis of Fatigue Test Results. At present, the most commonly used fatigue curve expression is the log-log expression, given as follows:

$$\lg(\Delta\sigma) = A + BlgN \pm 2s, \tag{3}$$

where s is the statistical deviation of the test points.

Using the MTS Landmark 370.50 fatigue tester, we carried out constant-amplitude fatigue tests on 34 *M*39 high-strength bolts. Ten of the specimens had a stress ratio of $\sigma = 0.1$, 24 of the specimens had a stress ratio of $\sigma = 0.6$, and only one specimen, *M*39-23, did not fail after 2×10^6 cycles. Thus, there were 33 effective data points available for the regression analysis.

Perform regression analysis on 10 constant amplitude fatigue test data with a stress ratio of 0.1 to obtain the corresponding *S-N* curve (Figure 3). The corresponding equation is as follows. Correlation coefficient $R^2 = 0.958$, $[\Delta\sigma]2 \times 10^6 = 76.97$ MPa.

$$lg(\Delta\sigma) = -0.2924lgN + 3.7153 \pm 0.1109. \tag{4}$$

The regression analysis is conducted on 23 constant amplitude fatigue test data with a stress ratio of 0.6 to obtain the corresponding S-N curve (Figure 3). The corresponding equation is as follows. Correlation coefficient $R^2 = 0.697$, $[\Delta\sigma]2 \times 10^6 = 42.48$ MPa.

$$lg(\Delta\sigma) = -0.3229lgN + 3.9568 \pm 0.2319. \tag{5}$$

It can be concluded that the fatigue test data obtained under different stress ratios have a good correlation through the regression analysis, but the correlation between the constant amplitude fatigue test data of the *M*39 high-strength bolts with a stress ratio of $R = 0.1$ is better than that of *M*39 high-strength bolts with a stress ratio of $R = 0.6$, and the fatigue strength is higher.

Now, the 10 constant amplitude fatigue test data points of *M*39 high-strength bolts with a stress ratio of $R = 0.1$ and the 23 constant amplitude fatigue test data points of *M*39 high-strength bolts with a stress ratio of $R = 0.6$ are analyzed

Table 2: Results of constant-amplitude fatigue tests for M39 high-strength bolts.

Specimen	Maximum stress σ_{max} (MPa)	Minimum stress σ_{min} (MPa)	Stress range $\Delta\ \sigma$ (MPa)	Fatigue life N ($\times 10^4$)	Stress ratio R
*M*39-31	385	38.5	346.5	2.97	0.1
*M*39-32	385	38.5	346.5	2.72	0.1
*M*39-33	315	31.5	283.5	3.46	0.1
*M*39-34	315	31.5	283.5	4.35	0.1
*M*39-37	280	28	252	8.42	0.1
*M*39-38	280	28	252	6.11	0.1
*M*39-39	210	21	189	13.50	0.1
*M*39-40	210	21	189	15.17	0.1
*M*39-35	175	17.5	157.5	34.45	0.1
*M*39-36	175	17.5	157.5	24.39	0.1
*M*39-1	385	231	154	20.62	0.6
*M*39-2	385	231	154	20.13	0.6
*M*39-4	385	231	154	19.02	0.6
*M*39-5	350	210	140	48.31	0.6
*M*39-6	350	210	140	41.89	0.6
*M*39-7	350	210	140	28.69	0.6
*M*39-9	315	189	126	43.51	0.6
*M*39-10	315	189	126	57.24	0.6
*M*39-11	315	189	126	39.52	0.6
*M*39-13	280	168	112	38.41	0.6
*M*39-14	280	168	112	29.84	0.6
*M*39-16	280	168	112	40.02	0.6
*M*39-26	280	168	112	39.52	0.6
*M*39-27	280	168	112	49.79	0.6
*M*39-17	245	147	98	42.30	0.6
*M*39-18	245	147	98	102.70	0.6
*M*39-19	245	147	98	48.36	0.6
*M*39-28	245	147	98	61.79	0.6
*M*39-29	245	147	98	47.08	0.6
*M*39-21	210	126	84	159.15	0.6
*M*39-22	210	126	84	143.96	0.6
*M*39-23	210	126	84	272.37	0.6
*M*39-24	210	126	84	125.49	0.6
*M*39-25	210	126	84	85.70	0.6

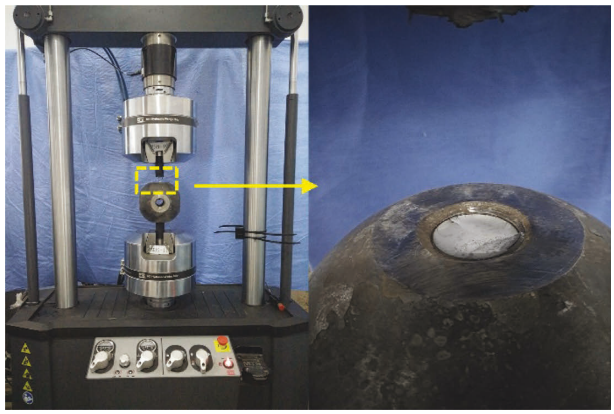

Figure 2: . Fatigue test machine and loading device.

together, and the constant amplitude fatigue *S*-*N* curve of the *M*39 high-strength bolt connection is shown in Figure 4. The correlation coefficient $R^2 = 0.914$, $[\Delta\ \sigma]2 \times 10^6 = 40.82$ MPa. The power *S*-*N* curve of *M*39 high-strength bolts with the stress amplitude $\Delta\ \sigma$ as the parameter is shown in Figure 5.

$$lg(\Delta\sigma) = -0.3229lgN + 3.9568 \pm 0.1065. \quad (6)$$

It can be seen from Figures 4 and 5 that when the regression analysis is performed with the stress amplitude $\Delta\sigma$ as the parameter, the correlation of the regular fatigue test data is good, indicating that the stress comparison has no effect on the fatigue intensity.

3.2. Analysis of Fatigue and Fracture. In this experiment, the failure mode of the *M*39 high-strength bolts was consistently fractured at the first thread below the surface of the bolt-sphere on the shank of the bolt damage, as shown in Figure 1. To study the fatigue failure mechanism, the surfaces of the fatigue fracture on the high-strength bolt were examined systematically under an EVOMA15 scanning electron microscope (Zeiss, Germany). In this experiment, the failure mode of the *M*39 high-strength bolts was consistently fractured at the first thread below the surface of the bolt-sphere on the shank of the bolt damage. A representative fracture failure, designated as *M*39-10, was chosen for macroscopic and microscopic analysis.

In the macroscopic photograph in Figure 6(a), the failure was brittle, in nature and there were no evident signs of plastic deformation near the fracture. There were three characteristic zones: a fatigue source zone, a fatigue

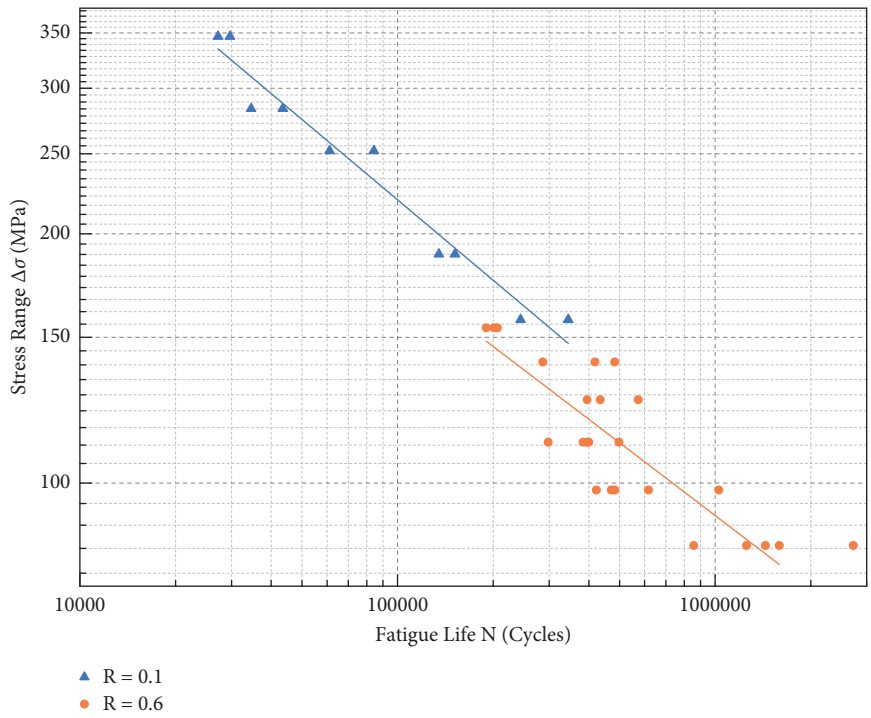

Figure 3: . The *S-N* curve of the *M*39 high-strength bolt ($R = 0.1$ and $R = 0.6$).

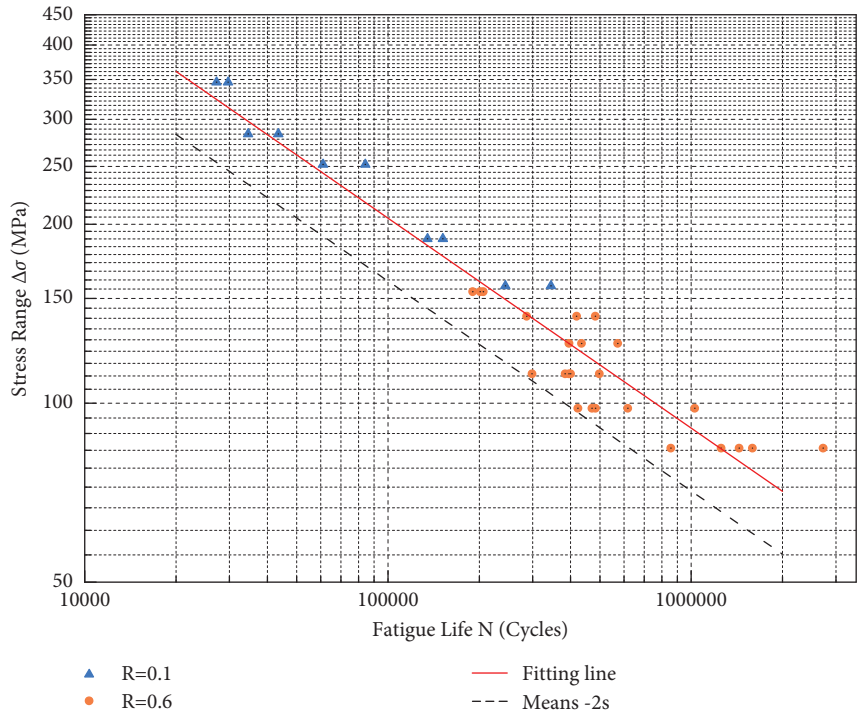

Figure 4: . The *S-N* curve of the *M*39 high-strength bolt (33data).

crack steady-propagation zone, and an instantaneous failure zone. The fatigue source zone was the earliest failure that occurred for the *M*39-10 high-strength bolts. In this region, the crack growth rate was slow, and the repeated opening and closing of the cracks caused friction on the mating surfaces of the fracture. The fatigue source zone was therefore macroscopically flat and smooth. There were multiple fatigue source zones at the notch around the circumference of the bolt fracture. Microscopically, the thread of a high-strength bolt had a notch where there was large residual stress. Being constructed from industrial materials, high-strength bolts often

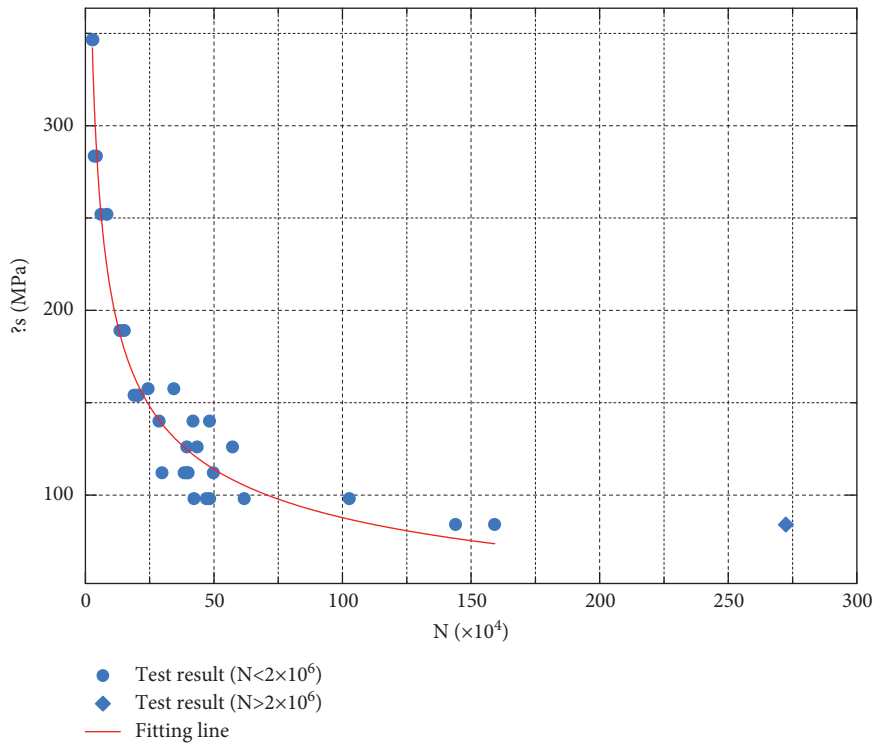

Figure 5: . The power *S-N* curve of the *M*39 high-strength bolts with the stress amplitude $\Delta\sigma$ as the parameter.

contain slag, voids, inclusions, indentations, bruises, and regions of inhomogeneous and discontinuous microstructures and chemical compositions. Fatigue cracks often occurred int these positions. Figure 6(b) shows the stress concentration regions where fatigue cracks occurred at the surface notch.

The second stage of fatigue failure was steady crack propagation, with the path of propagation perpendicular to the principal stress direction. On the macrophotographs of this region, the macroscopic characteristics of the fracture surface were relatively smooth and occupied more than half of the fracture. The fatigue bands could be clearly observed on the microphotograph. Figure 6(c) shows the fatigue bands that appeared at this stage. The key characteristic is that they were basically parallel to each other, and the direction of the band was perpendicular to the local crack propagation direction. The bands produced by brittle fatigue failure were uneven and irregular, but overall, the region could still be recognized.

The rough and protruding areas in the lower parts of Figure 6(d)show the instantaneous failure zone. This was a region formed by the unstable propagation after the fatigue crack had grown to a critical size. The microscopic morphology of this region mostly manifested as static-load transient characteristics, with more dimples, as shown in Figure 6.

3.3. Establishing a Calculation Method for Constant-Amplitude Fatigue. Based on the results of the constant-amplitude fatigue tests of high-strength bolts described above, we established the following calculation method for the constant-amplitude fatigue of the high-strength bolts in grid structures with bolt-sphere joints using the nominal stress amplitude $\Delta\sigma$ as the design parameter.

3.3.1. Nominal Stress Amplitude Method

This method uses $\Delta\sigma$ as the design parameter and the following equations:

$$\Delta\sigma \le [\Delta\sigma],$$
$$[\Delta\sigma] = \left(\frac{C}{N}\right)^{1/\beta}, \tag{7}$$

where $\Delta\sigma$ is the nominal stress amplitude (MPa) at the joint of the high-strength bolt, N is the number of cycles, and C and β are parameters. Article 6.2.1 of the standard GB50017-2003 design specification for steel structures stipulates that the converted stress amplitude of the non-welded part is $\Delta\sigma = \sigma\text{max}—0.7\ \sigma\text{min}$. In this study, it was concluded that 0.7 should be changed to 1.0, or $\Delta\sigma = \sigma\text{max}—\sigma\text{min}$. σmax and σmin are the maximum and minimum stresses (MPa) at the joint of the high-strength bolt, respectively, and $[\Delta\sigma]$ is the allowable stress amplitude (MPa) of the high-strength bolt joint.

Taking $N = 2 \times 10^6$ as the base period, it follows from (7) that the allowable stress amplitude of *M*39 high-strength bolts should be $[\Delta\sigma]_{2\times10}{}^6 = 40.82$ MPa. The values of C and β were 2.23×10^{10} and 2.5131, respectively, based on (7).

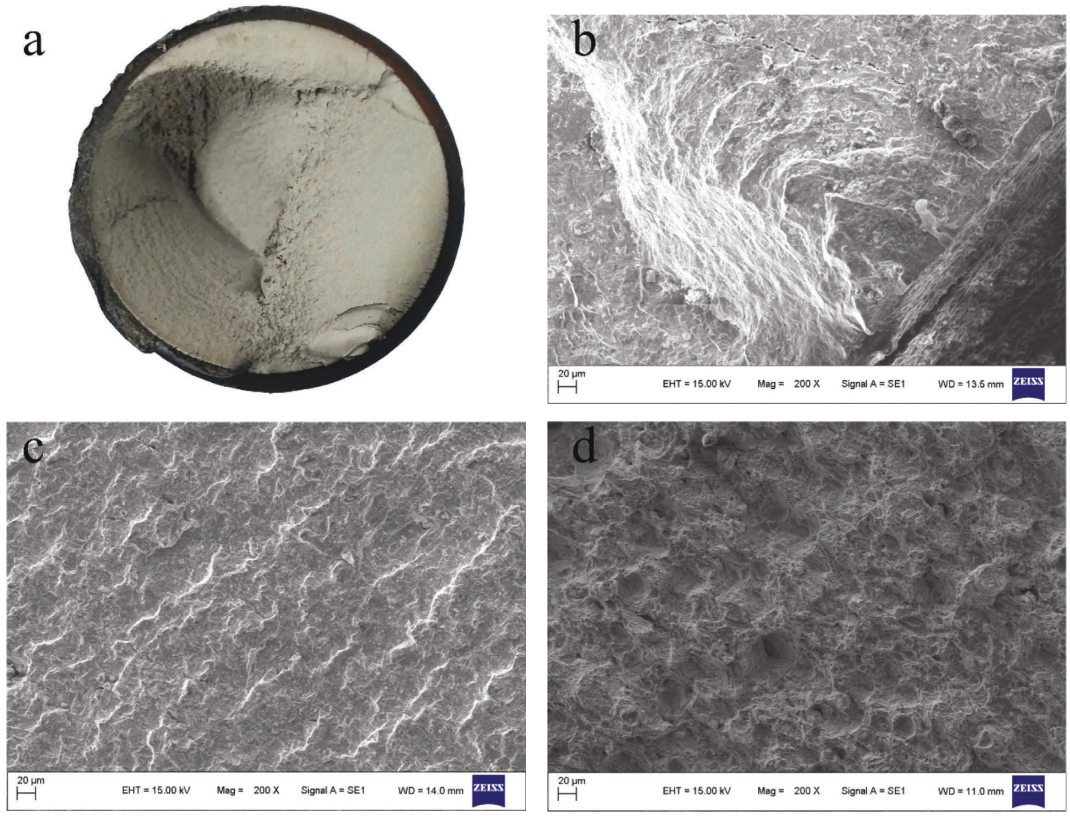

Figure 6: Fracture morphology of a bolt.

3.3.2. Allowable Hot-Spot Stress Amplitude Method. This article uses the hot stress amplitude $\Delta\sigma$h as the design parameter, which can better reflect the real stress state of the destructive position, which is more scientific.

In this method, the hot-spot stress amplitude $\Delta\sigma$h was used as a design parameter, and both sides of (8) were multiplied by the fatigue notch coefficient Kf, which was in the range of 4.35–4.89. For safety reasons, the minimum value of 4.35 was taken on the right-hand side of the equation. Using $N = 2 \times 10^6$ as the base period, the allowable hot-spot stress amplitude of the *M*39 high-strength bolts was $[\Delta\sigma h] = 177.57$ MPa

$$\Delta\sigma\_(h) = K\_(f)\Delta\sigma \leq [\Delta\sigma\_(h)]. \quad (8)$$

4. Conclusions

By conducting constant-amplitude fatigue tests of *M*39 high-strength bolts on an MTS fatigue testing machine, we obtained the *S-N* curve of the *M*39 high-strength bolts and established a design method for the constant-amplitude fatigue tests of the *M*39 high-strength bolts in grid structures with bolt-sphere joints. Taking $N = 2 \times 10^6$ as the base period, we obtained the allowable stress amplitude of *M*39 high-strength bolts as $[\Delta\sigma]2 \times 10^6 = 40.82$ MPa and the allowable hot-spot stress amplitude of M39 high-strength bolts as $[\Delta\sigma h] = 177.57$ Mpa. In the calculation of the constant-amplitude fatigue, it is reasonable to take the stress amplitude $\Delta\sigma$ as the design parameter. In calculating the fatigue strengths of high-strength bolts in grid structures with bolt-sphere joints, using the hot-spot stress amplitude as a design parameter yielded better agreement with the actual stress state of the high-strength bolts.

By analyzing the constant-amplitude fatigue test data of the *M*39 high-strength bolts with two different stress ratios, we found a good correlation in the experimental data, indicating that the stress ratio had no effect on the fatigue strength. Observations of the fatigue source zone revealed that there may be one or more fatigue sources for the fracture of high-strength bolts. By observing the fatigue propagation zone, we found distinct fatigue bands in the fracture propagation zone of the high-strength bolts. Near the fatigue source zone, the fatigue bands were denser, and the fracture surface propagated slowly. Far from the fatigue source zone, the bands were far apart, and the fracture surface propagated faster.

In summary, fatigue fracture is a very complex process, affected by a variety of internal and external factors. The internal cause of the failure fracture in this study mostly stress concentration at the thread of the high-strength bolt and the incomplete quenching during the manufacturing process. Under the action of a constant-amplitude alternating load, cracks were initiated and, under the tensile–tensile stress, the crack tip became blunted due to double slip, followed by further blunting by subsequent stretching action. Thus, the crack propagated forward by a certain

distance, forming a steady propagation zone of the fatigue crack and resulting in a band. This was the earliest occurrence of fatigue failure.

Data Availability

The data used to support the findings of this study are available from the corresponding author upon request.

Conflicts of Interest

The authors declare that they have no conflicts of interest.

References

[1] J. Chilton, *Space Grid Structures*, Routledge, London, UK, 2007.

[2] X. Feng and X. Lin, "Fatigue performance under suspension crane action of bolt ball grid nodes," *Journal of Building Structures*, vol. 16, pp. 3–12, 1995, in Chinese.

[3] J. Lin and H. G. Lei, "Analysis on the causes of fatigue accidents of a bolt-ball structure plant in shanxi," *Applied Mechanics and Materials*, vol. 851, pp. 864–869, 2016.

[4] C. Standard, "Technical Specification for Space Frame Structures," Chinese Standard, Beijing, China, JGJ7-2010, 2010.

[5] Z. Wayne, "Code for Design of Steel Structures," Ministry of Housing and Urban-Rural Development of the People's Republic of China, General Administration of Quality Supervision, Inspection and Quarantine of the People's Republic of China, Beijing, China, GB50017-2017, 2017.

[6] J. Nam, D. Kim, K. Kim, S. Choi, and J. H. Oh, "Unified fatigue life prediction of bolts with different sizes and lengths under various axial loading conditions," *Engineering Failure Analysis*, vol. 131, Article ID 105841, 2022.

[7] J. Maljaars and M. Euler, "Fatigue S-N curves of bolts and bolted connections for application in civil engineering structures," *International Journal of Fatigue*, vol. 151, Article ID 106355, 2021.

[8] H. Bartsch and M. Feldmann, "Reassessment of fatigue detail categories of bolts and rods according to EC 3-1-9," *Journal of Constructional Steel Research*, vol. 180, Article ID 106588, 2021.

[9] B. Ding, Y. Zhao, Z. Huang, L. Cai, and N. Wang, "Tensile bearing capacity for bolted spherical joints with different screwing depths of high-strength bolts," *Engineering Structures*, vol. 225, Article ID 111255, 2020.

[10] H. Yuan, H. Liu, X. Ren, X. Zhang, D. Ai, and Y. Luo, "The bearing performance of the bolt-sphere joints with stochastic pitting corrosion damage," *Journal of Constructional Steel Research*, vol. 160, pp. 359–373, 2019.

[11] G. Xu and J. Cui, "Grid structure fatigue and fatigue life calculation," *Journal of Building Structures*, vol. 15, pp. 25–34, 1994.

[12] X. Yang and L. Honggang, "Constant Amplitude Fatigue Test of High Strength Bolts in Grid Structures with Bolt-Sphere Joints," *Steel and Composite Structures*, vol. 25, 2017.

[13] C. Zhang, G. L. Hong, S. J. Tian, and Y. Xu, "The Fatigue Properties of the M27 Higher Strength Bolt in the Grid Structure with Bolted Spherical Joints," *Applied Mechanics and Materials*, vol. 851, 2016.

[14] B. Qiu, H. Lei, X. Yang, Z. Zhou, and W. Guoqing, "Variable amplitude fatigue test of M30 high-strength bolt in bolt-sphere joint grid structures," *Steel and Composite Structures*, vol. 3, 2019.

[15] Z. Wayne, "Technical Specification for Space Frame Structures," General Administration of Quality Supervision, Inspection and Quarantine of the People's Republic of China, Beijing, China, JGJ7:2010, 2010.

[16] Z. Wayne, "Bolted Spherical Node of Space Grid Structures," General Administration of Quality Supervision, Inspection and Quarantine of the People's Republic of China, Beijing, China, JG/T 10-2009, 2009.

[17] Z. Wayne, "High Strength Bolts For Joints Of Space Grid Structures," General Administration of Quality Supervision, Inspection and Quarantine of the People's Republic of China, Beijing, China, GB/T 16939-2016, 2016.

[18] Z. Wayne, "Quality Carbon Structure Steels," General Administration of Quality Supervision, Inspection and Quarantine of the People's Republic of China, Beijing, China, GB/T 699-2015, 2015.

[19] E. Iso, "Metallic materials–tensile testing–Part 1: method of test at room temperature," ISO, Switzerland, Eroupe, ISO 6892-1:2009, 2009.

Hindawi
Mobile Information Systems
Volume 2022, Article ID 3849079, 9 pages
https://doi.org/10.1155/2022/3849079

Research Article

Evaluation System of Mobile English Learning Platform by Using Deep Learning Algorithm

Yu Cui [1] **and Hao Li** [2]

[1]*International Education College, Hebei Finance University, Baoding, Hebei, China*
[2]*College of Mechanical and Electrical Engineering, Hebei Agricultural University, Baoding, Hebei, China*

Correspondence should be addressed to Hao Li; lihao2016@hebau.edu.cn

Received 24 July 2022; Revised 30 August 2022; Accepted 12 September 2022; Published 24 September 2022

Academic Editor: Shadi Aljawarneh

At present, China's economic development continues to progress and foreign exchanges are also increasingly frequent. Learning to master the world's universal pronunciation, English, has become a more important link. However, people's living habits make it difficult to carry heavy desktop devices for a long time, so mobile English learning platform meets the development needs of people's English teaching. Based on the existing English mobile learning platform, this paper puts forward the concept of integrating artificial intelligence and deep learning technology into it. Through deep learning, the learning status and learning situation of students in the process of English learning are extracted, so as to analyze the needs and learning interests of each student in English learning and then push corresponding English materials to each student, which improves the efficiency of English learning. In addition, deep learning can also model the data of students' behaviors and build a language vector feature extraction mechanism and translation quality evaluation model, so as to carry out certain intelligent auxiliary correction and correction on students' English grammatical expressions and spoken English. The research in this paper has achieved good results through practice. The practice results show that the integration of deep learning into the existing mobile English teaching platform can optimize the functions of the existing platform, provide more ideas for the development of online English learning, and has good theoretical and practical value.

1. Introduction

The term "deep learning" comes from the machine learning industry, which means a form of neural network that builds and simulates the human brain for analysis and interpretation, which is called deep learning. This deep learning network is extremely prominent in some complex problems. In the final analysis, it can strongly simulate the neural sensor system in the human brain for data analysis. This way of deep learning algorithm has been tested in many industries. In particular, the development and technological progress of image computer industry and computer industry promote the innovation of deep learning algorithm at the same time, and the complexity of which is no longer a problem. Therefore, the research and application of deep learning algorithm in the study of English learning methods can also greatly improve the data and information processing ability of English, improve the information processing efficiency of learners, and improve the overall user experience of learners. In English learning, many people will use repeaters, MP3, MP4, and other players, as well as mobile phone software, to achieve the purpose of learning English at any time, but most of the facilities cannot fully achieve the purpose of learning. They can closely realize the functions of search and follow-up, and there is no way to intuitively give English learners some guidance and advice, as well as follow-up learning and other ways. Moreover, due to the limitations of technical conditions, many network systems focus on the spelling of words and the English of grammar. Only one or two learning indicators are tested, which is not perfect in function, making English learners unable to intuitively feel the progress of learning. However, due to the differences in English learners' English level, it is difficult to correct themselves and correct them in time

through the errors prompted on the client. On the other hand, the final test of English is also subjective, and manual scoring is dominant for pronunciation standards and grammatical errors. In terms of manual scoring, because experts have different levels and experiences, the same expert may give multiple scores, so there are also many deviations. Experts like this also spend a lot of human and material resources, so it is not suitable for English learners.

In order to avoid the above shortcomings, we apply deep learning to the construction of English learning methods and establish a learning method model based on deep learning algorithm, so as to improve the accuracy and speed of English learners' learning English [1]. In addition, the traditional English learning methods have been improved, and a reasonable and objective English learning method model has been established considering the pronunciation, grammar, composition, and other parameters involved in learning English [2, 3]. This research will obtain a number of original research results, such as English learning methods. In the future, the research results can be used in many applications, such as human-computer interactive English learning training and evaluation [4]. Giving corresponding guidance methods for error information in English teaching mode can effectively enable learners to learn English well. In addition, the research results can effectively solve the problems formed in teaching and improve the current situation of learners' learning English [5].

2. Related Work

Aiming at the problem that some English songs may have melody changes, leading to difficulty in recognition, the literature designed melody factors, constructed prosody model, and added melody recognition to the original monotonic one-tone and three-tone models, thus improving the accuracy of speech recognition [6, 7]. In view of the current situation that speech quality is difficult to be guaranteed in noisy environments, the literature puts forward the improvement of target speech acoustic model confusion [8]. In view of the details of phoneme pronunciation, the literature introduced the GMM model to model and sort out the feature distribution of sonic speed in a more detailed way, so as to solve the details in English pronunciation recognition more pertinently and improve the efficiency and accuracy of English pronunciation recognition [9]. In the literature, a new computational strategy is introduced in the grading of English speech, so as to further narrow the gap between the grading proposed by the machine-assisted correction and that proposed by the teacher's manual modification, so that the machine can learn the grading rules more accurately and improve the performance of the computer-aided learning system [10]. In terms of the design of English mobile teaching platform, the literature has proposed that the current English mobile teaching platform is more in the form of database [11]. The course is sorted out in advance by teachers and platform staff, and the materials are collected in the online platform for students to use [12]. According to the literature, the current mobile English teaching platform is the use of social software in the field of learning, and learning is essentially completed through interpersonal communication [13]. The literature summarizes the previous research experiences and puts forward that the current mobile English teaching platform is actually a new application of the traditional social network carried by the Internet in the field of education [14]. The existence of the Internet provides teachers and students with more technical support, which is essentially a new media [15]. According to the literature, under the current development status of artificial intelligence, traditional social networks have made new progress, and artificial intelligence technology should also be introduced into the design of English mobile teaching platform [16]. However, there is still a lack of application of relevant technologies in this direction, so it is necessary to learn and master relevant artificial intelligence technologies as much as possible and optimize the existing mobile English teaching platform through machine learning [17, 18].

3. Design of Mobile English Learning Platform

3.1. System Architecture Design. At present, the system architecture of mobile English learning platform is still a common three-tier application service structure.

The overall block diagram of the system structure is shown in Figure 1. The intelligent control layer includes commonly used mobile phones or laptops. The mobile smart client controls the service management layer through the built-in fixed access system and application server and manages the entire system server by logging in to the browser.

The focus of this system research is to realize the functions of the whole mobile intelligent client. After the installation of the mobile intelligent device system, the client preinstalls the logic functions of the whole client business. This application is only one end of the server. The focus of the system is on the request function of the mobile smart client to send business logic. The design requirements of the whole server system should be combined with the interaction of the data server to interact and transfer data between the system client and the data server. All data should be processed and transferred by the unified server, that is, after receiving the data request from the client, the server should transmit and send the data of the application operation. The data information processed in the database should also be transmitted to the server terminal for system processing and unified transmission. Finally, the system should be screened and displayed in the mobile intelligent data terminal.

3.2. System Function Analysis. The mobile client of this system is simply like a smart phone or tablet computer using 5G mobile network. This kind of smart device has the characteristics of convenient carrying and light use. Through the whole mobile intelligent client platform, the system client can use its spare time every day to learn interesting knowledge. If the English learning materials and services provided by the system are not satisfied, you can go to the

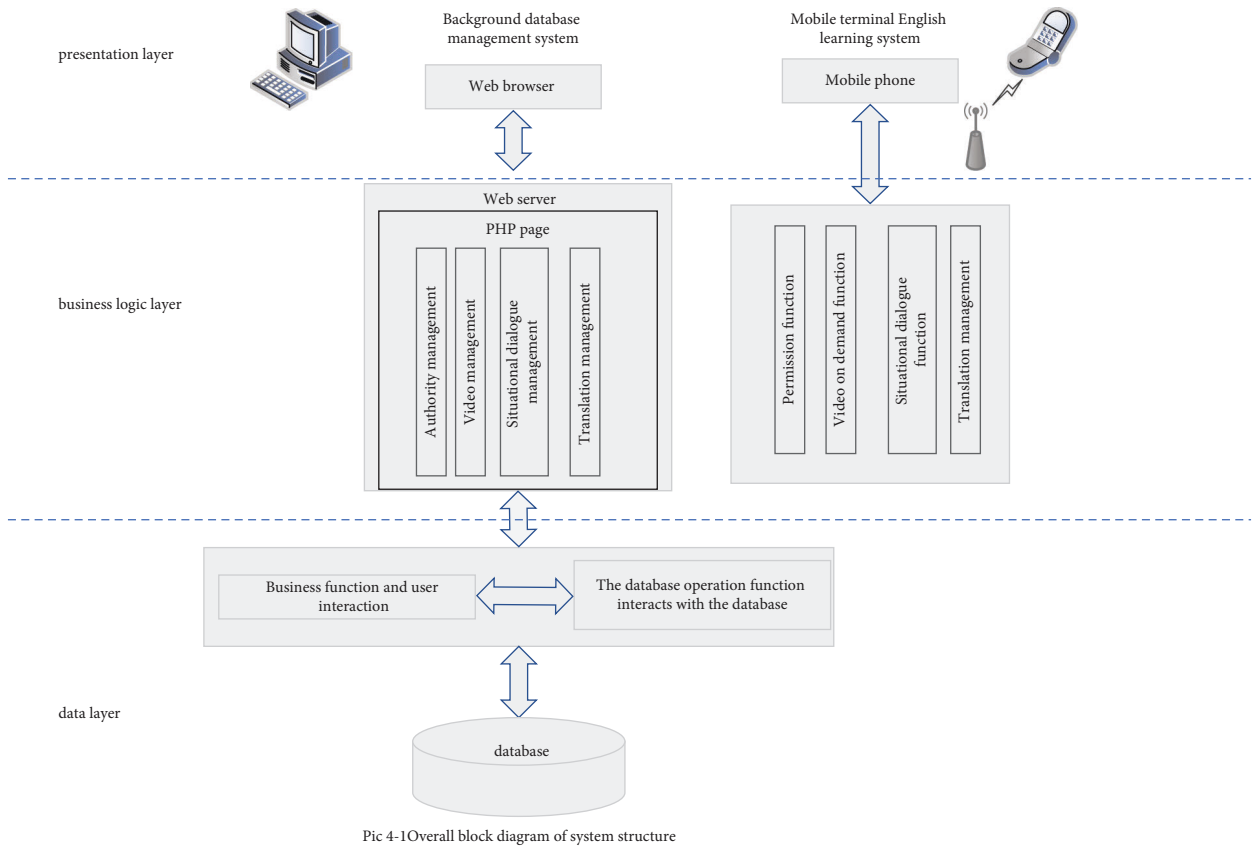

FIGURE 1: Overall block diagram of system structure.

customer service terminal for demand analysis and push more qualified learning materials.

In terms of technology, under the current network technology environment in China, 5G network has been widely spread to medium and large cities and regions. Moreover, 3G network technology has a fast Internet speed, which is unmatched by ordinary broadband networks. Therefore, it is convenient and effective to use 5G network to transmit data. This system also has additional online video on demand function, which is not a small breakthrough for English learning software in 4G environment. This is because the users of English learning system have greatly improved the efficiency of English learning. Video media can be seen in the whole English learning system, which makes the whole English learning more intuitive. The addition of audition function is more conducive to the learning and practice of English knowledge.

However, in terms of other business functions and service requirements, this system also covers the functional requirements of most users for learning English, so that the English learning system can more meet the needs of potential customers. After analyzing and comparing many users of professional English learning, several aspects are added to the English learning system.

3.2.1. Online Simulated English Test Function. Under the English level test function, the client of this English learning system can screen several popular English level tests at home and abroad and simulate the learning process under the test environment. The popular English tests at home and abroad include CET-4 and CET-6, public English level test, Cambridge Business English test, IELTS, and TOEFL. The background of the English system will push the real questions over the years and conduct online simulation tests according to the test content selected by the candidate, judge and analyze the test results, give standard answers, and uniformly explain the wrong answers. Of course, this system design only provides the option of objective questions, which is not open for subjective classes such as composition questions.

3.2.2. English Short Plays, Movies, and Other Videos on Demand Functions. For potential client users who need to strengthen the practice of listening and speaking, this system also provides English film series for oral material practice. In the video content push, the system pushes different materials for users at different levels, including educational films, cartoons, English films, and other materials with slow pronunciation standard sentences, which lays a solid foundation for practitioners in English listening and speaking. For some basic system clients, it provides some high-end English film classics to learn.

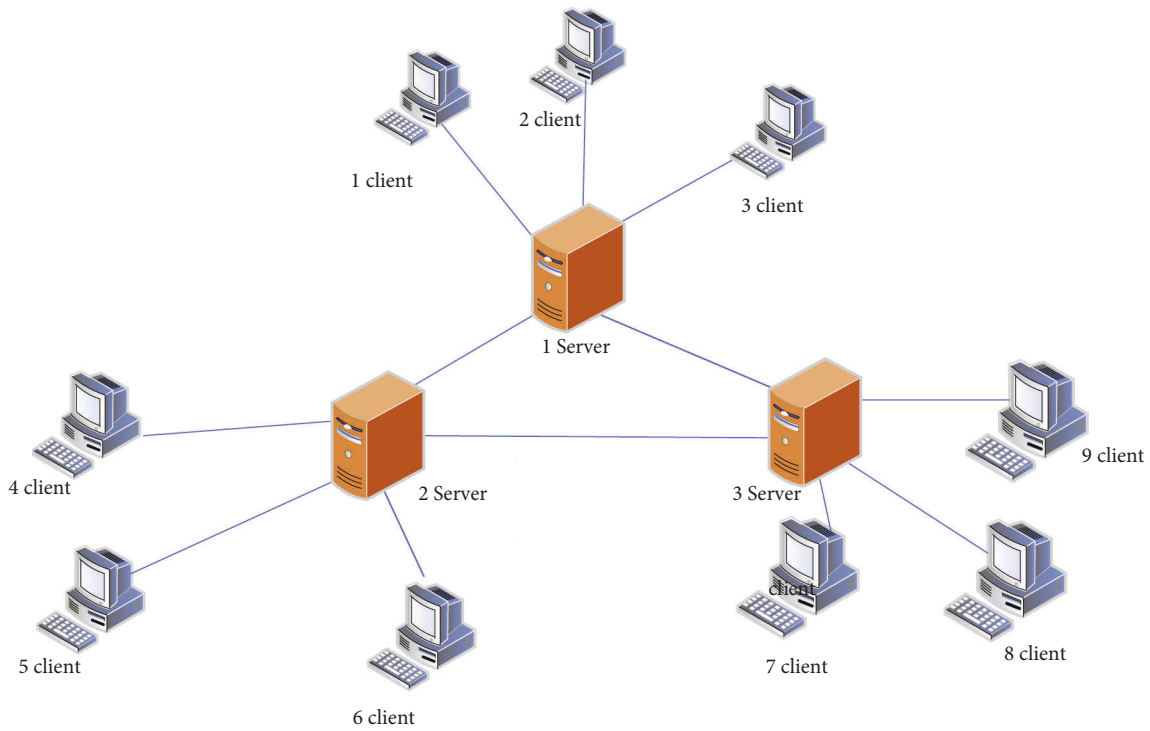

Figure 2: Simple mobile terminal architecture protocol system architecture.

3.2.3. Life and Work Situation Simulation Dialog Function. For some English system learners who need to go abroad, it will provide some daily functional scene simulation environments, so that learners have an immersive sense of dialog and always cultivate the ability of emergency dialog. These scenes usually include restaurants, hotels, banks, stations, supermarkets, and airports and even provide common sentences such as alarm, inquiry, and thank you to learn and use.

3.2.4. Online Translation Function. This function is aimed at some English fresh users to translate and carry out certain online translation according to the provided words and sentences. This translation function is not only implemented in the third-party translation function but also to facilitate the use of English client users to solve the troubles of jump software.

3.3. Mobile Terminal Architecture Protocol Design. Mobile end architecture protocol is an open chat technology, which can be used to customize any chat software. Although the agreement can provide many customized functions, many expanded functions need users to realize and experience by themselves. Among them, the basic function is to realize single person or multiperson chat, as well as personal data display function. This paper starts from the specific content of the mobile terminal architecture protocol and describes its functions, internal implementation principles, and the way of network data transmission.

3.3.1. Protocol Architecture. The architecture used by the mobile end architecture protocol is based on the form of client server cluster, which has multiple forms of interaction with each other. The following figure shows a simple system architecture. The corresponding background is the open-source server that runs the whole server and completes the writing. It dominates a huge amount of information and has powerful functions. The amount of background data contained in this system is huge, so the amount of relevant client software is also increasing. If these data can be subject to the mobile end architecture protocol, the responsibility separation mode between the client and the server can be realized. In this way, system development researchers do not need to install complex processing logic, but only need to pay attention to how to write the operating system of the client to make it run at high speed. Openfire server needs very professional logic processing ability and receives and processes data requests transmitted from different clients at the same time. Many clients will customize different personality modules according to their own service providers. Therefore, the mobile client protocol has strong scalability requirements and is deeply loved by customers, as shown in Figure 2.

3.3.2. Network Communication Mode. On the basis of mobile Internet communication, if one party wants to receive the information of the other party, it will generate a specific address as its identity mark. The selfsymbol in the mobile architecture protocol is called JID, which is a kind of running code. JID is a kind of entity and unique sign, just

like everyone's ID number is different. JID format code and e-mail address format are very similar. Like e-mail address example@Jabber.org, similarly, the example in this refers to the user's name, and the address after the @ symbol is the server address information. In the common mobile end architecture protocol, the transmission format between the two mainly uses the idea of layering to split information. It is divided into three information elements, and the content labeled by each element is a file message, including the sender's information, the discoverer's Avatar, and the sending content. The presence tab is mainly used to obtain whether the user is online, as well as the list of relevant friends and other information. After we get the network communication and analyze it, we can get the useful information we want.

3.4. Mobile Software Development Environment. Before the preliminary design, we must first build a stable development environment. From the perspective of the overall system architecture, the system should be divided into two modules: server and mobile client. The development and configuration environment is usually background management server: 64 bit cent OS 7.0; Openfire server: Apache 2.0; background database: my SQL 5.5 is configured on the background management server; client development environment: Mac OS X 10.10 Yosemite + I Phone7 mobile phone.

At this stage, the background service manager uses Alibaba cloud virtual server to transfer the corresponding Apache server and my SQL database to the cloud server. The corresponding website of the cloud server is www.bigtree com. Download the latest Openfire server and configure it in the background. Local services can be provided in the whole test phase. On this basis, database information needs to be selected and connected with my SQL database.

The program development voice form of the mobile client is operated on the Apple system, but because the Apple system and Android system are not interconnected, the commercial operating system developed by Apple is adopted instead of Android system. IOS software development kit, known as iPhone SDK, is a software development kit specially established and developed by Apple to develop IOS applications. The first development was in early 2008. After its release, the software development package can only host IOS or Mac OS operating systems, and other operating systems cannot host and run. This system is not open to the public and must be operated on an Apple system. When developers develop software, they can only download and use it for other users on the application manager where they are located. Developers need to pay a certain fee to release the application. Therefore, developers can freely customize their own system price in the application software. The tool for developing IOS programs uses Xcode, which is the only software for developing IOS programs. The software can not only develop IOS applications but also develop computer applications. Apple generally releases two versions at the same time when it releases the system, one is a stable version that has been tested many times, and the other is a beta version for developers. The advantage of the two versions is to let everyone debug the vulnerabilities under this version and increase the stability of the system.

4. Application of Deep Learning Algorithm in the System

4.1. Foundation of Deep Learning Algorithm. A deep learning adjustment algorithm means that the learning adjustment parameters are $\theta = \{w, a, b\}$, assuming a given training sample, even if the distribution probability of the corresponding deep learning calculation algorithm matches it under this condition. The sample set satisfying the distribution conditions given: $S = v_{(1)}, v_{(2)}, \ldots, v_{(N)}$, which maximizes the goal of training the deep learning algorithm, as shown in formula (1):

$$L_\theta = \prod_{i=1}^{N} P\left(v^i\right). \tag{1}$$

Due to the relatively cumbersome processing of concatenation in the formula, the strict monotonicity of function Ln_x can be known, maximizing L_θ is equivalent to maximizing LN_{l}.

4.2. English Learning Level Evaluation Algorithm. English learning level usually tests the speed of oral pronunciation, which is reflected in the speed of speaking intonation when learning English. It can also be calculated by calculating the change of syllable length in unit time by computer, or by the length of pause between two English words. Due to the differences of individual speaking, different people have certain differences in the pronunciation of different sentences. Moreover, the different emotional states of speaking also affect the effect of sentences. For example, in the state of anger and happiness, the sentences expressed are slightly gentle, while in the state of sadness, the sentences are slightly slow.

This paper studies the change of English sentence length by calculating the duration ratio φ, as shown in formula (2):

$$\varphi = \frac{\text{Len}_{\text{Std}}}{\text{Len}_{\text{Test}}}. \tag{2}$$

Among them, Len_{std} is the standardized parameter duration and Len_{test} is the duration of the test statement. For further setting and comparison of data, see Figure 3.

The pronunciation speed displayed by sentences can be followed by rules and cycles. For speaking rhythm, it can be divided into stress type, incomplete stress type, and stress type. In English, learning, reading, and talking, rhythm combination patterns in different states alternate, and language rhythm has different itineraries. Therefore, the English Sentence Rhythm evaluation mechanism is shown in Figure 4, and the specific steps are as follows:

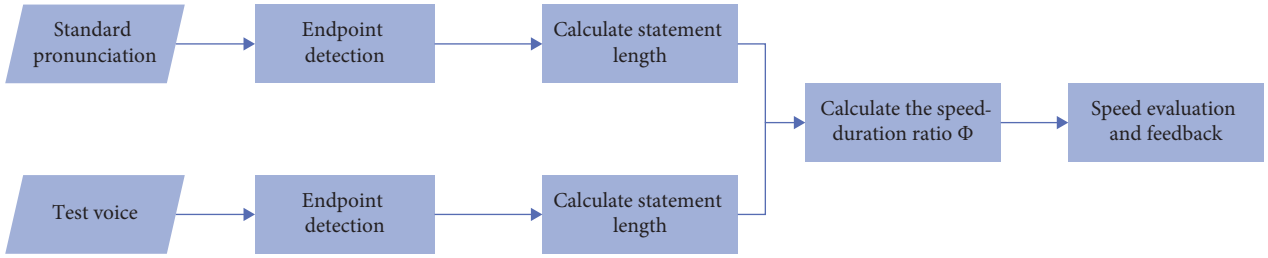

Figure 3: Speech speed evaluation.

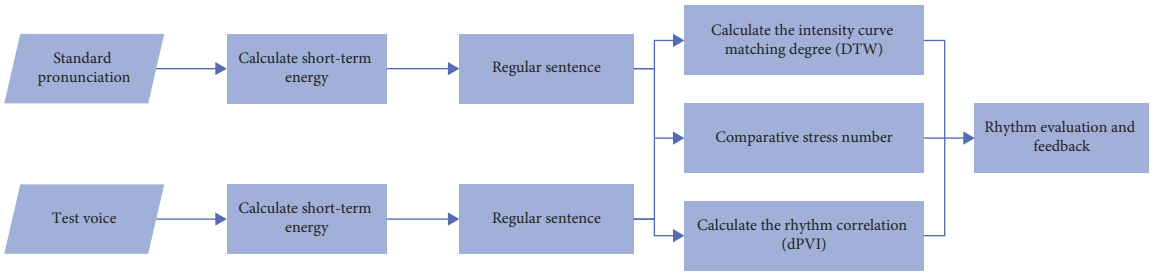

Figure 4: Rhythm evaluation.

4.2.1. Extract English Short-Term Energy Values to Form an English Intensity Curve. The poisoned scale characteristics in the sentence reflect the change of energy intensity. The greater the change of English intensity of stressed sections, the definition of short-term energy of English signal $s(n)$ formed in this state is shown in formula (3):

$$E_n = \sum_{m=-\infty}^{\infty} [s(n)\omega(n-m)]^2. \tag{3}$$

For short English sentences, the corresponding calculation mode can be formed. Each frame on the X-axis matches the frame between $[y_{\min}, y_{\max}]$ on the Y-axis. The calculation of $y_{\min}$ and $y_{\max}$ is as follows:

$$y_{\min} = \begin{cases} \frac{1}{2}x, & x \in [0, X_b], \\ 2x + (M - 2N), & x \in (X_b, N], \end{cases} \tag{4}$$

$$y_{\max} = \begin{cases} 2x, x \in [0, X_a], \\ \frac{1}{2}x + \left(M - \frac{1}{2}N\right), x \in (X_a, N], \end{cases}$$

where D and d represent cumulative distance and frame matching distance, respectively. This paper uses the double threshold comparison method to detect the accent endpoint and sets the threshold after data comparison, such as formulas (5) and (6):

$$T_u = \frac{(\max(sig\_in) + \min(sig\_in))}{2.5}, \tag{5}$$

$$T_j = \frac{(\max(sig\_in) + \min(sig\_in))}{10}. \tag{6}$$

According to the time length analysis of English learning, the improved dPvi parameter calculation formula is adopted to compare the length of fragments of complete English sentences and test sentences, and the converted parameters are processed systematically, as shown in formula (7):

$$\mathrm{dPVI} = 100 \times \frac{\left(\sum_{k=1}^{m-1} |\mathrm{dl}_k - \mathrm{d2}_k| + |\mathrm{dl}_t - \mathrm{d2}_t|\right)}{\mathrm{Len}}. \tag{7}$$

For the correlation function between the correlation function algorithms, calculate the similarity between the sound frame $s(i)$, $\{i = 0, 1, 2, \ldots, n-1\}$ and itself, as shown in formula (9):

$$acf(\tau) = \sum_{i=0}^{n-1-\tau} s(i)s(i+\tau). \tag{8}$$

4.3. English Writing Level Evaluation Algorithm. The level of English writing under this system is very different from the situation of English texts. It is the main purpose of the establishment of English learning system. It is to process the text data transmitted from the front end, remove the classification under complex English texts, and select English words and sentences with low correlation. The corresponding English words and sentences are transformed into vector data in the computer processing mode, so that the classification of the English original text is one-to-one corresponding.

The constructed co-occurrence matrix is expressed as equations (10) to (11):

$$\begin{aligned} M_{to,human} &+= 1, \\ M_{to,instinct} &+= 1, \\ M_{to,get} &+= 1, \\ M_{to,promoted} &+= 1. \end{aligned} \tag{9}$$

The formula of GloVe model is as follows (10):

$$J = \sum_{i,j}^{N} f\left(X_{i,j}\right)\left(v_i^T v_j + b_i + b_j - \log\left(X_{i,j}\right)\right)^2, \tag{10}$$

v_i and v_j represent the word vector of words i and j, respectively, b_i and b_j represent deviation, f represents weight, and the number of words is represented by N. it can be seen that this model does not involve any derivation and exercise in the form of neural network.

$$M_i = \sum_{j=1}^{N} M_{i,j}. \tag{11}$$

The frequency of word i and other words in the sentence can be expressed as formula (12):

$$r_{i,j,a} = \frac{P_{i,a}}{P_{j,a}}. \tag{12}$$

Therefore, the generated vector words have to go through the derivation exercise of some function. The text related information contained in this word vector is expressed as formula (13):

$$f\left(v_i, v_j, v_a\right) = r_{i,j,a} = \frac{P_{i,a}}{P_{j,a}}. \tag{13}$$

The three variables are infinitely close. The variance between the two can be used as a function.

$$J = \sum_{i,j,a}^{N} \left(\frac{P_{i,a}}{P_{j,a}} - f\left(v_i, v_j, v_a\right)\right). \tag{14}$$

Considering the linear relationship between the two words and the constancy of the result, let

$$\begin{aligned} f\left(v_i, v_j, v_a\right) &= \exp\left(\left(v_i - v_j\right)^T v_a\right), \\ \frac{P_{i,k}}{P_{j,k}} &= \frac{\exp\left(v_i^T v_a\right)}{\exp\left(v_j^T v_a\right)}, \\ P_{i,k} &= \exp\left(v_i^T v_a\right). \end{aligned} \tag{15}$$

The brought in function can be expressed as follows:

$$J = \sum_{i,j}^{N} \left(\log\left(P_{i,j}\right) - v^T v_j\right)^2. \tag{16}$$

The expanded formula is as follows:

$$\log\left(X_{i,j}\right) - \log\left(X_i\right) = v_i^T v_j. \tag{17}$$

Let b_i and b_j be deviation values, then J satisfies the following formula:

$$J = \sum_{i,j}^{N} f\left(X_{i,j}\right)\left(v_i^T v_j + b_i + b_j - \log\left(X_{i,j}\right)\right)^2. \tag{18}$$

It can be seen that GloVe model can well show the relevance between the two words, and its actual expression effect is also higher than other models. The quantitative expression of English text words and sentences is transformed into text sequences, and hash search is carried out.

5. Application of Mobile English Learning Platform

5.1. Platform Test Results. For the delay effect of the English learning platform test system, when English learners enter the interface, click the function key to request to send data, and the time interval between data sending and receiving can be calculated under the test module of mobile data terminal. By testing the increase of users one by one, the curve formed by the delay time under multiple modules is shown in Figure 5.

The results of the reaction on the graph show that the functions realized by the system affect the effect of delay. According to the data analysis, the unit of delay is seconds. Therefore, there is almost no so-called lag and hysteresis. With the increasing number of users, the response time did not increase significantly and gradually became a flat trend. The test results show the stability of the mobile platform system and achieve the effect of user satisfaction.

5.2. Application Effect Analysis. In terms of specific experimental classification, in addition to the distinction between single group and multiple groups of experimental objects, there are also differences between pretest and post-test. In order to further study the application effect of this system, the paper chooses the way of controlled experiment. The experimental group adopted the online mobile English teaching platform based on deep learning proposed in this paper, while the control group adopted the traditional online English learning platform. After one semester of online course learning, the final scores of the two groups of students were compared, as shown in Table 1.

In this group of satisfaction tests, a data analysis form of four options is designed to test the difference between English and learners' overall satisfaction with setting up an English learning platform. The satisfaction test results are shown in Table 2 below:

The test results show that in the comparison of pretest and post-test, English learners analyze the difference data from the mean value and standardization, and the data results formed by the post-test are more prominent than the pretest. For the establishment effect of the teaching mode of mobile English learning platform, the degree of satisfaction formed is more distinct. This means that in this

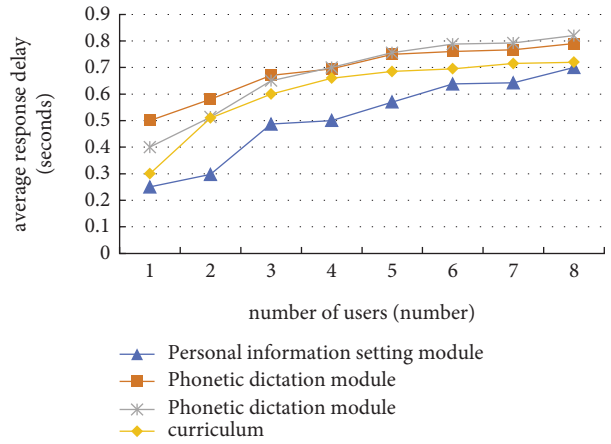

Figure 5: Comparison of response delay.

Table 1: Comparison of final grades between the experimental group and the control group.

	Lowest score	Highest score	Average score
Test group	65.363	97.578	84.462
Control group	62.535	91.562	75.635

Table 2: Overall satisfaction test of mobile English learning platform.

Satisfaction	Mean		Difference test P-value
	Before	After	
I Like the teaching mode of mobile English learning platform	1.651	3.216	0.000
Satisfied with the mobile English learning platform process	3.834	4.066	0.207
Like to incorporate a variety of new media technologies into learning	2.884	3.082	0.172
Very satisfied with the effect of the mobile English learning platform	3.466	4.434	0.000

environment, English learners from the beginning of the unfamiliar attitude, after learning for a period of time into love and identity. The changes in this period are significant in many aspects, such as cognition, emotion, ability, and behavior effect. Among them, there is no obvious change in the satisfaction of English learning process. The main reason is the dependence on traditional learning methods. Individual English learners believe that although the establishment effect of mobile English learning platform is very obvious, due to individual differences and differences in learning concepts, it is difficult to achieve long-term persistence learning effect, and there is a certain sense of laziness. From the perspective of this theoretical concept, we have more realized the responsibilities and obligations of educators. As long as English learners are educated in ideas and theoretical concepts, they should also form quality-oriented training in the face of many individualized student development. Only by constantly updating the educational concept and innovating the teaching mode we can change the current English teaching quality and make students develop in an all-round way.

6. Conclusion

The core of building mobile English learning platform is the research and evaluation technology of English learning system, and the technology of English learning system is the key. As learning English becomes more and more complex, English learners have a huge amount of data and information, and there are more characteristic parameters in the English learning industry. Therefore, the English learning system and evaluative calculation involved are also huge, which makes the processing of information under the English learning system have higher hardware requirements and algorithm requirements. Traditional English learning system algorithm and artificial algorithm have their own advantages and disadvantages and have different bottlenecks for their development, so it is difficult to judge their accuracy. In recent years, with the development and

accumulation of deep learning algorithm definition and deep learning achievements, the technology of establishing English learning system has developed rapidly. Deep learning algorithm is a nonlinear network structure form, characterized by the distribution of information and data processing, and rationalized the ability to show multiple features sorted out by the sample set. It is more excellent in learning algorithms that simulate human brain and has played a prominent role in the development of mobile English learning platform.

Data Availability

The data used to support the findings of this study are available from the corresponding author upon request.

Conflicts of Interest

The authors declare that they have no conflicts of interest.

References

[1] Y. Bin and D. Mandal, "English teaching practice based on artificial intelligence technology," *Journal of Intelligent & Fuzzy Systems*, vol. 37, no. 3, pp. 3381–3391, 2019.

[2] J. C. Yang, C. H. Chen, and M. Chang Jeng, "Integrating video-capture virtual reality technology into a physically interactive learning environment for English learning," *Computers & Education*, vol. 55, no. 3, pp. 1346–1356, 2010.

[3] B. Akhmedov and K. Shuhkrat, "Cluster methods of learning English using information technology," *Scientific Progress*, vol. 1, no. 2, pp. 40–43, 2020.

[4] M. Duan, K. Li, X. Liao, and K. Li, "A parallel multiclassification algorithm for big data using an extreme learning machine," *IEEE Transactions on Neural Networks and Learning Systems*, vol. 29, no. 6, pp. 2337–2351, 2018.

[5] B. Klimova and M. Pikhart, "Cognitive and applied linguistics aspects of using social media: the impact of the use of facebook on developing writing skills in learning English as a foreign language," *European Journal of Investigation in Health, Psychology and Education*, vol. 10, no. 1, pp. 110–118, 2019.

[6] L. Schillingmann, J. Ernst, V. Keite, B. Wrede, A. S. Meyer, and E. Belke, "AlignTool: the automatic temporal alignment of spoken utterances in German, Dutch, and British English for psycholinguistic purposes," *Behavior Research Methods*, vol. 50, no. 2, pp. 466–489, 2018.

[7] J. Zheng, C. Huang, M. Chu, F. K. Soong, and W. P. Ye, "Generalized segment posterior probability for automatic Mandarin pronunciation evaluation," in *Proceedings of the IEEE International Conference on Acoustics, Speech and Signal Processing-ICASSP'07*, vol. 4, pp. IV–201, HI, USA, April 2007.

[8] H. Abulkasim, A. Farouk, H. Alsuqaih, W. Hamdan, S. Hamad, and S. Ghose, "Improving the security of quantum key agreement protocols with single photon in both polarization and spatial-mode degrees of freedom," *Quantum Information Processing*, vol. 17, no. 11, p. 411, 2018.

[9] J. Chen, K. Li, K. Bilal, X. Zhou, K. Li, and P. S. Yu, "A Bi-layered parallel training architecture for large-scale convolutional neural networks," *IEEE Transactions on Parallel and Distributed Systems*, vol. 30, no. 5, pp. 965–976, 2019.

[10] J. Wang, Y. Zou, and P. Lei, "Research on recurrent neural network based crack opening prediction of concrete dam," *Journal of Internet Technology*, vol. 21, no. 4, pp. 1151–1160, 2020.

[11] C. H. Kuo, D. Wible, M. C. Chen, L. C. Sung, N. L. Tsao, and C. L. Chio, "The design of an intelligent web-based interactive language learning system," *Journal of Educational Computing Research*, vol. 27, no. 3, pp. 229–248, 2002.

[12] M. Sarma, P. Ghahremani, D. Povey, N. K. Goel, K. K. Sarma, and N. Dehak, "Emotion identification from raw speech signals using DNNs," in *Proceedings of the Interspeech*, pp. 3097–3101, Hyderabad, India, September 2018.

[13] S. A. Nossier, J. Wall, M. Moniri, C. Glackin, and N. Cannings, "An experimental analysis of deep learning architectures for supervised speech enhancement," *Electronics*, vol. 10, no. 1, p. 17, 2020.

[14] M. Naseri, M. Abdolmaleky, F. Parandin, N. Fatahi, A. Farouk, and R. Nazari, "A new quantum gray-scale image encoding scheme," *Communications in Theoretical Physics*, vol. 69, no. 2, p. 215, 2018.

[15] J. Wang, Y. Yang, T. Wang, R. Sherratt, and J. Zhang, "Big data service architecture: a survey," *Journal of Internet Technology*, vol. 21, no. 2, pp. 393–405, 2020.

[16] C. Chen, K. Li, S. G. Teo, X. Zou, K. Li, and Z. Zeng, "Citywide traffic flow prediction based on multiple gated spatio-temporal convolutional neural networks," *ACM Trans. Knowl. Discov. Data*, vol. 14, no. 4, pp. 1–23, 2020.

[17] N. P. Nguyen, T. N. Dinh, Y. Xuan, and M. T. Thai, "Adaptive algorithms for detecting community structure in dynamic social networks," in *Proceedings of the IEEE Conference on Computer Communications (INFOCOM '11)*, pp. 2282–2290, Shanghai, China, April 2011.

[18] S. Hurlburt, "Defining tools for a new learning space: writing and reading class blogs," *MERLOT Journal of Online Learning and Teaching*, vol. 4, no. 2, pp. 182–189, 2008.

Hindawi
Mobile Information Systems
Volume 2022, Article ID 6732861, 10 pages
https://doi.org/10.1155/2022/6732861

Research Article

Visual Simulation for Numerical Solution of Fourth-Order Partial Differential Equations Based on the Improved Neural Network Algorithm

Jing Zhang, Yongyan Fan, and Zhixiao Li

College of Mathematics and Statistics, Cangzhou Normal University, Cangzhou, Hebei 061001, China

Correspondence should be addressed to Jing Zhang; 1733271192@xzyz.edu.cn

Received 18 June 2022; Revised 12 August 2022; Accepted 7 September 2022; Published 16 September 2022

Academic Editor: Shadi Aljawarneh

The topic of this paper is to study the numerical solution of the fourth-order partial differential equation and analyze its visual application in software simulation. Therefore, for the initial circular domain, the expansion should be transformed into a fourth-order problem in the plane dimension. Then, we introduced appropriate-weighted Sobolev space based on the improved neural network algorithm and established a weak form and the corresponding discrete form for each one-dimensional fourth-order problem. The approximation properties of the cubic Hermite interpolation operator are used to verify the error value of the approximation solution. After obtaining the relevant algorithms, numerical empirical analysis is carried out to prove that the proposed algorithm is effective. Therefore, this article applies it to the visualization simulation technology, and the visualization module mainly completes two tasks: collecting geometric data and drawing models. At present, the application of the visualization module in the program mainly has two aspects: on the one hand, the boundary information of geometry can be obtained by screening the existing database so that the boundary model can be displayed in the visualization; on the other hand, from the calculation result file. Read the geometric information of particles and boundaries and perform dynamic simulation playback of the calculated results.

1. Introduction

There are many numerical methods for solving fourth-order equations, such as spectral methods and finite difference methods. As far as we know, although the solution domain of the finite element method is flexible, it is cumbersome to deal with some areas with curved boundaries, especially the high-dimensional fourth-order equations on the boundary areas of some curved surfaces [1]. Although classical finite element methods have been widely used in fourth-order equations, they are solved directly in two- or three-dimensional regions. Since the basis function of the approximation space generally needs to be continuously differentiable at the unit boundary, solving the fourth-order equation directly in these special regions will consume a lot of calculation time and memory capacity [2]. Therefore, the objective of this paper is to solve the fourth-order partial differential equations numerically, with the help of the improved neural network algorithm in the sphere domain and the circle domain. For the spherical domain, in order to overcome the pole singularity introduced by the spherical coordinate transformation, we first obtain the essential pole condition of the pole [3]. Based on the intersecting feature of sphere domain and plane, the existing sphere domain problem is transformed into a plane dimension solution method, and then weighted Sobolve space is introduced, and the weak form and the corresponding discrete form of each one-dimensional fourth-order problem are derived [4]. From the Lax–Milgram theorem and from the approximation properties of the cubic Hermite interpolation operator, the unique existence and error estimation of weak solutions and numerical solutions are proved. Finally, we give some numerical examples, using the numerical solutions presented in this article, the numerical results also

illustrate the effectiveness of our algorithm [5]. Then this article applies it to the visualization simulation technology. Although the visualization module of the fourth-order partial differential equation simulation analysis software can already be used for particle modeling, boundary modeling, and dynamic playback of calculation result files, better simulation results are obtained, but with the continuous improvement and optimization of the software proposed in this article, the continuous expansion of simulation analysis functions, more information needs to be displayed on the screen in a visual manner, and more and more complex visual effects and the function of the extended program display module need to be displayed [6]. This article uses methods such as color, light processing, color mixing, and stylization to add functions to the visualization module of the simulation analysis software and a global display of the deflection direction of the boundary. Display the OXYZ coordinate system. When playing the calculation result file, it has the function of displaying the simulation time and the actual playing time, which makes the software display module more user-friendly [7]; the simulation particle color setting function is added, and more particle attributes can be obtained in a visual form displayed in the visualization window, and it enriches the effect of particle simulation display; the new border model color and transparency setting function makes the simulation border display effect more realistic, beautiful, and changeable. By integrating the mathematical calculation method with the reconstructed neural network, the optimized algorithm is introduced into the neural network to improve the simulation calculation ability of the system. Display in the visualization window is to make the visualization effect more excellent and to improve the accuracy of recognition so as to better serve the function. By adding these functions, the visual simulation analysis software display module of fourth-order partial differential equations has been better expanded, which can provide users with better observation effects and better visual experience.

2. Related Work

The OpenGL array stack operation mode realizes the synchronous rotation of the boundary and small coordinates of two different geometric contour models at different origins and realizes the visual effects of asynchronous movement and asynchronous scaling of these two models [8]. The light source is associated with the color, and the function of setting the color of the particle is realized so that the simulated particle can display different colors according to its size, speed, and type so that multiple physical attributes can be displayed on the screen intuitively [9]; it enables OpenGL blending attributes to combine colors, realizes the function of border transparency after coloring, makes the display effect more beautiful and changeable enhances the virtual edge display effect through grid operation, makes the visualization effect more realistic, and uses the timer mechanism in MFC to perform the display of simulation time and playback time function [10]. The program reads and displays the STL file, adds a manual sphere filling method based on the original particle sphere automatic filling method, and manually enters the radius and position of the sphere used to fill the particle model through the dialog box, which is finally determined by the operator and the size and shape of the aspheric particle model [11]. The literature studies the Kohonen intrusion detection method based on the Kohonen network as the main algorithm and adds an output layer after the network concurrency layer, making the unsupervised Kohonen neural network a supervised Kohonen neural network, which is used to solve the problem that the classification category is larger than the actual category. The problem is as follows. In the face of a neural network, its initial weight is set, and the set number is often random, which will cause problems such as low classification accuracy and unstable network output [12]. In view of this problem, the determination of random weights has certain defects, so it is necessary to use a certain neural network optimization algorithm to make it clear. The system first uses packet capture software to capture packets, then analyzes and extracts the data, and finally uses MATLAB for system design. Data are detected through the designed intrusion detection system and the detection results are displayed on the page [13]. The relevant knowledge and existing problems of Kohonen neural network improves the neural network for this problem and then makes a brief analysis of the emerging metaheuristic algorithm of invading weeds algorithm [14, 15]. For the definite local values, the differential evolution algorithm should be used to optimize the initial weights [16]. First, introduce the data set used in the experiment and then digitize and normalize the data set. Then a brief description of several evaluation indicators used in the intrusion detection model is given. Finally, a comparative test is set up. Through the analysis of the experimental results, the superiority of the model proposed in this paper is proved.

3. Research on the Numerical Solution of Fourth-Order Partial Differential Equations

3.1. Design of the Dimensionality Reduction Scheme for Fourth-Order Partial Differential Equations. We will focus on the case where Ω is a spherical region, namely, $\Omega = \{(x, y, z) \in \mathrm{R3}: x2 + y2 + z2 < R3\}$. First, define the differential operator as

$$\mathscr{L}\mathrm{v} = \frac{1}{\mathrm{r}^2}\frac{\partial}{\partial \mathrm{r}}\left(\mathrm{r}^2\frac{\partial \mathrm{v}}{\partial \mathrm{r}}\right) + \frac{1}{\mathrm{r}^2}\Delta_s \mathrm{v}, \tag{1}$$

of which

$$\Delta_s \mathrm{v} = \frac{1}{\sin\theta}\frac{\partial}{\partial\theta}\left(\sin\ \theta\frac{\partial \mathrm{v}}{\partial\theta}\right) + \frac{1}{\sin^2\theta}\frac{\partial^2 \mathrm{v}}{\partial\phi^2}. \tag{2}$$

It can be clearly seen that the weak form of (1) and (2) find $u \in \mathrm{H20}(\Omega)$ such that

$$\begin{aligned} &\int_\Omega \Delta \mathrm{u}\Delta\bar{\mathrm{v}}\mathrm{dx}\,\mathrm{dy}\,\mathrm{dz} + \alpha\int_\Omega \nabla \mathrm{u}\nabla\bar{\mathrm{v}}\mathrm{dx}\,\mathrm{dy}\,\mathrm{dz}, \\ &+\beta\int_\Omega \mathrm{u}\bar{\mathrm{v}}\mathrm{dx}\,\mathrm{dy}\,\mathrm{dz} = \int_\Omega \mathrm{f}\bar{\mathrm{v}}\mathrm{dx}\,\mathrm{dy}\,\mathrm{dz}, \forall \mathrm{v} \in \mathrm{H}_0^2(\Omega). \end{aligned} \tag{3}$$

Applying the spherical coordinate transformation $x = r\sin\theta\cos\varphi$, $y = r\sin\theta\sin\varphi$, $z = r\cos\theta$ in (1) and (2), we can get

$$\mathscr{L}^2\psi - \alpha\mathscr{L}\psi + \beta\psi = g,\ (r,\theta,\phi) \in \mathscr{D} = (0,R)\times[0,\pi)\times[0,2\pi), \tag{4}$$

$$\psi(R,\theta,\phi) = \frac{\partial\psi}{\partial r}(R,\theta,\phi) = 0, \theta \in [0,\pi). \tag{5}$$

Of which:

$$\begin{cases} \psi(r,\theta,\phi) = u(r\sin\theta\cos\phi, r\sin\theta\sin\phi, r\cos\theta), \\ g(r,\theta,\phi) = f(r\sin\theta\cos\phi, r\sin\theta\sin\phi, r\cos\theta). \end{cases} \tag{6}$$

From equation (2), we know that the weak form of (3) and (4) is

$$a(\psi,\varphi) = (g,\varphi), \tag{7}$$

of which

$$\begin{aligned} a(\psi,\varphi) = \int_0^R\int_S r^2\mathscr{L}\psi\mathscr{L}\overline{\varphi}\,dr\,dS + \alpha\int_0^R\int_S r^2\mathscr{L}\psi\overline{\varphi}\,dr\,dS, \\ +\beta\int_0^R\int_S r^2\psi\overline{\varphi}\,dr\,dS, \\ (g,\varphi) = \int_0^R\int_S r^2 g\overline{\varphi}\,dr\,dS. \end{aligned} \tag{8}$$

Here, S is the unit sphere. Y_m^l is a characteristic function of the operator Δs, namely,

$$\Delta_s Y_m^l = -m(m+1)Y_m^l,\ (m \ge 0, |l| \le m), \tag{9}$$

and

$$\int_S Y_m^l Y_{m'}^{l'}\,dS = \delta_{mm'}\delta_{ll'}. \tag{10}$$

Make

$$\begin{cases} \psi(r,\theta,\phi) = \sum_{|m|=0}^{\infty}\sum_{|l|=0}^{m}\psi_m^l Y_m^l, \\ \varphi(r,\theta,\phi) = \sum_{|m|=0}^{\infty}\sum_{|l|=0}^{m}\varphi_m^l Y_m^l, \\ g(r,\theta,\phi) = \sum_{|m|=0}^{\infty}\sum_{|l|=0}^{m} g_m^l Y_m^l. \end{cases} \tag{11}$$

According to (1) and (11),

$$\mathscr{L}\psi = \sum_{|m|=0}^{\infty}\sum_{|l|=0}^{m}\frac{1}{r^2}\left[\partial_r\left(r^2\partial_r\psi_m^l\right) - \frac{m(m+1)}{r^2}\psi_m^l\right]Y_m^l. \tag{12}$$

Therefore, the essential conditions that make (12) more meaningful are

$$m(m+1)\psi_m^l(0) = 0. \tag{13}$$

Using extreme condition (10), a series of one-dimensional fourth-order problems equivalent to equations (3) and (4) can be obtained as follows:

$$l_m^2\psi_m^l - \alpha l_m\psi_m^l + \beta\psi_m^l = g_m^l(r), r \in (0,R), \tag{14}$$

$$(1)\psi_m^l(R) = \left(\psi_m^l\right)'(R) = 0,\ (m=0), \tag{15}$$

$$(2)\psi_m^l(0) = 0, \psi_m^l(R) = \left(\psi_m^l\right)'(R) = 0,\ (m \ge 1). \tag{16}$$

3.2. Discrete Format Design of Fourth-Order Partial Differential Equations. To derive the weak form of equations (14)–(16) and its discrete form, we first introduce appropriate-weighted Sobolev space as

$$L_\omega^2(I) \coloneqq \left\{f: \int_I \omega f^2 dx < \infty\right\}. \tag{17}$$

The corresponding inner product and norm can be given as

$$(f,g)_\omega = \int_I \omega f g\,dx, \|f\|_w = \left(\int_I \omega f^2 dx\right)^{1/2}, \tag{18}$$

where $I = (0,1)$ and $\omega = x2$ is the weight function. Then, we further introduce the nonuniform weighted Sobolev space as follows:

$$\begin{aligned} &\widetilde{H}_{0,\omega,m}^2(I): \\ &= \left\{u: \mathscr{L}_m f \in L_\omega^2(I), m(m+1)u_m^l(0) = u_m^l(1) = \left(u_m^l\right)'(1) = 0\right\}. \end{aligned} \tag{19}$$

The corresponding inner product and norm are

$$(f,g)_{2,\omega,m} = \left(\mathscr{L}_m f, \mathscr{L}_m g\right)_\omega, \|f\|_{2,\omega,m} = (f,tf)_{2,\omega,m}^{1/2}. \tag{20}$$

Therefore, the weak form of equations (14)–(16) is

$$a_m\left(u_m^l, v_m^l\right) = F_m\left(v_m^l\right), \forall v_m^l \in \widetilde{H}_{0,\omega,m}^2(I). \tag{21}$$

3.3. Error Estimation and Reasoning of Fourth-Order Partial Differential Equations. From the extreme conditions (15) and (16), we can get

$$\begin{aligned} \int_I 2x\left[\left(u_m^l\right)''v' + \left(u_m^l\right)'v''\right]dx = -2\int\left(u_m^l\right)'v'\,dx, \\ \int_I \frac{2m}{x}\left[\left(u_m^l\right)'v + u_m^l v'\right]dx = 2m\int_I \frac{1}{x^2}u_m^l v\,dx, \\ \int_I m\left[\left(u_m^l\right)''v + u_m^l v''\right]dx = -2m\int_I\left(u_m^l\right)'v'\,dx. \end{aligned} \tag{22}$$

For $\forall u_m^l \in \widetilde{H}_{0,\omega,m}^2(I)$, the following inequality holds true:

$$\begin{aligned} \int_I\left(xu_m^l\right)^2 dx \le \int_I\left[x\left(u_m^l\right)'\right]^2 + m(m+1)\left(u_m^l\right)^2 dx, \\ \int_I\left[x\left(u_m^l\right)'\right]^2 + m(m+1)\left(u_m^l\right)^2 dx \le \int_I\left(x\mathscr{L}_m u_m^l\right)^2 dx. \end{aligned} \tag{23}$$

3.4. Effective Implementation and Verification of the Numerical Solution. Using the algorithm proposed in this

Table 1: For different M and N, the error between the exact solution and the approximate solution.

N	$M = 2$	$M = 4$	$M = 6$	$M = 8$
10	5.9017 ± 07	5.9017 ± 07	5.9017 ± 07	5.9017 ± 07
15	1.1921 ± 07	1.1921 ± 07	1.1921 ± 07	1.1921 ± 07
20	3.8197 ± 08	3.8197 ± 08	3.8197 ± 08	3.8197 ± 08
25	1.5768 ± 08	1.5768 ± 08	1.5768 ± 08	1.5768 ± 08

Table 2: Different convergence rates for M and h.

h	$M = 2$	$M = 4$	$M = 6$	$M = 8$
1/4	0.0656	0.0655	0.0403	7.4179 ± 06
1/8	0.0641	0.0641	0.0641	0.0641
1/16	0.0634	0.0634	0.0634	0.0634
1/32	0.0633	0.0633	0.0633	0.0633

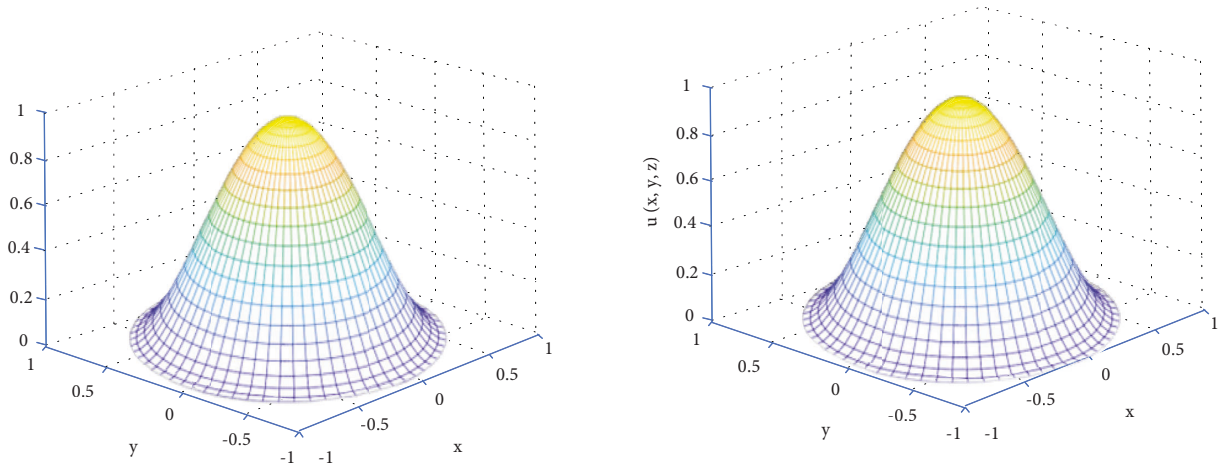

Figure 1: When $N = 20$, $M = 12$, the graph of the approximate solution (a) and the exact solution (b).

article for different M and different N, respectively, list the error (uM $h(x, y, z)$ and $u(x, y, z)$) in Tables 1 and 2, respectively.

The convergence rates for different M and h are shown in Table 2:

In this paper, the approximate solution and the exact solution image are shown in Figure 1.

To verify the effectiveness of the algorithm, it is necessary to clarify the error between the approximate solution and the exact solution, so the algorithm simulation shown in Figure 2 is designed and implemented.

4. Visualization Software Simulation and Result Analysis Based on the Improved Neural Network Algorithm

4.1. Improved Neural Network Algorithm Design. In order to facilitate calculation, the data set is divided into two parts: normal data set and abnormal data set. The abnormal data are divided into four major attack categories, namely, Dos, Probe, U2U, and R2L. Use the Kohonen neural network to select and classify part of the data set. The results are shown in Table 3.

As can be seen from Table 3, when classifying data sets, data sets correspond to nodes in the network. If the divided regions correspond to one category, the ranking result often exceeds five categories, which makes the classification result not good. Aiming at the above shortcomings, an improved method of adding an output layer converts the unsupervised Kohonen neural network into a supervised learning network (SKohonen network). The SKohonen network structure diagram is shown in Figure 3:

As can be seen from Figure 3, the difference between the two data networks is that SKohonen has one more output layer than unsupervised Kohonen, and the number of nodes in this output layer is related to the data type brought in. Therefore, when two data networks are converted, these two layers need to be converted.

4.2. Visualization Implementation Method Based on Software. Although OpenGL provides many efficient graphics rendering functions that can be independent of the operating system and window system, OpenGL does not include any event response mechanism or input or window management, which makes it impossible to carry out related messages between OpenGL and Windows. Therefore, if

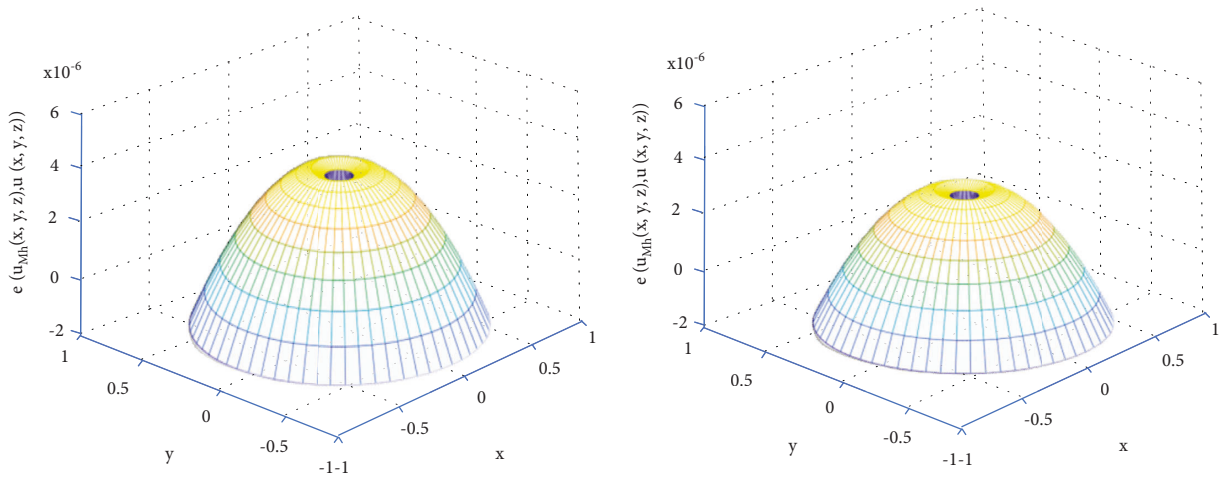

Figure 2: The error graph of the approximate solution and the exact solution when $N = 10$, $M = 6$, $N = 25$, and $M = 10$.

Table 3: Experimental results.

Category	Node number
1	1,6
2	15,20 ~ 7
3	7 ~ 9,15
4	4 ~ 4,11 ~ 12,17
5	14

people want to use OpenGL for 3D modeling and animation display in the Windows environment, people must use a window system, and MFC (Visual C++ Basic Class Library) has powerful events, window management, and control functions and is considered as 3D visualization software which develop more commonly used platforms. The 3D discrete element method simulation analysis software developed by the research group combines OpenGL and MFC to perform the related functions of its visual simulation system. OpenGL is used to create and draw complex 3D models of particles and boundaries.

In MFC, the CView explains that class is the base class of all view classes and is associated with the CDocument base class to implement the display function and interactive working mechanism of document data. Use App Wizard and Class Wizard in Visual C++ environment to generate the application framework. In this document view structure, the document class is mainly responsible for computing operations, and the visual class is responsible for displaying content in the window. In the visual class CView, the CDC device scene class can be directly used to draw simple two-dimensional graphics, but Visual C++ does not provide a ready-made class that can directly use OpenGL for drawing, so the program is derived from the CView class to create a TDEMView class, encapsulate the resources, device description table, and palette used for OpenGL drawing, and complete the association between the Windows window and OpenGL in the process. Graphics Device Interface (GDI) objects in Windows are drawn through a device handle (DC) device driver, while OpenGL drawing requires a Render Context (RC) drawing environment, and it must be the current drawing environment. Generating the current OpenGL drawing environment requires the following three steps: setting the window pixel format, generating RC, and setting it as the current RC. After allocating the drawing environment for OpenGL and completing the initialization operations such as clearing the cache and setting lighting, the OpenGL function library can be directly used to call OpenGL drawing commands to render 3D graphics.

The TDEMView class defines member functions for scene initialization and 3D drawing:

bool CTDEMView: Initialized OpenGL (CDC ∗pDC) function is used to generate drawing description table and set device description table and color palette; void CTDEMView: the SceneInit() function is used to initialize OpenGL parameters and set static scenes such as material and lighting information; bool CTDEMView: the RenderScene() function is used to draw graphics, and all drawing and rendering operations are implemented in this function. These functions are called by the corresponding message handle in CView of MFC. After a window is created, a message named WM_CREATE is sent to the operating system. The OnCreate() function in MFC is used to feedback the message. The function InitializeOpenGL(CDC ∗pDC) is called in OnCreate() to create a visual window and allocate device handles and the current drawing environment for the graphics device interfaces GDI and OpenGL. Since it takes a lot of processing time to generate an RC, in order to obtain a smoother and higher performance display effect, the RC is only generated once and used all the time. The drawing environment is not deleted until the OnDestroy() function is called at the end of the program. In MFC CView, the OnDraw (CDC ∗ pDC) function is used to complete most of the graphic design work. All codes for drawing operations in the client area of the application window must be written in this function. When the window changes, such as resizing the window, showing or hiding the window area, OnDraw(CDC∗ pDC) will be called to redraw the window to refresh and fill the view client area again. In addition, people can also call the visual class member function Invalidate () to

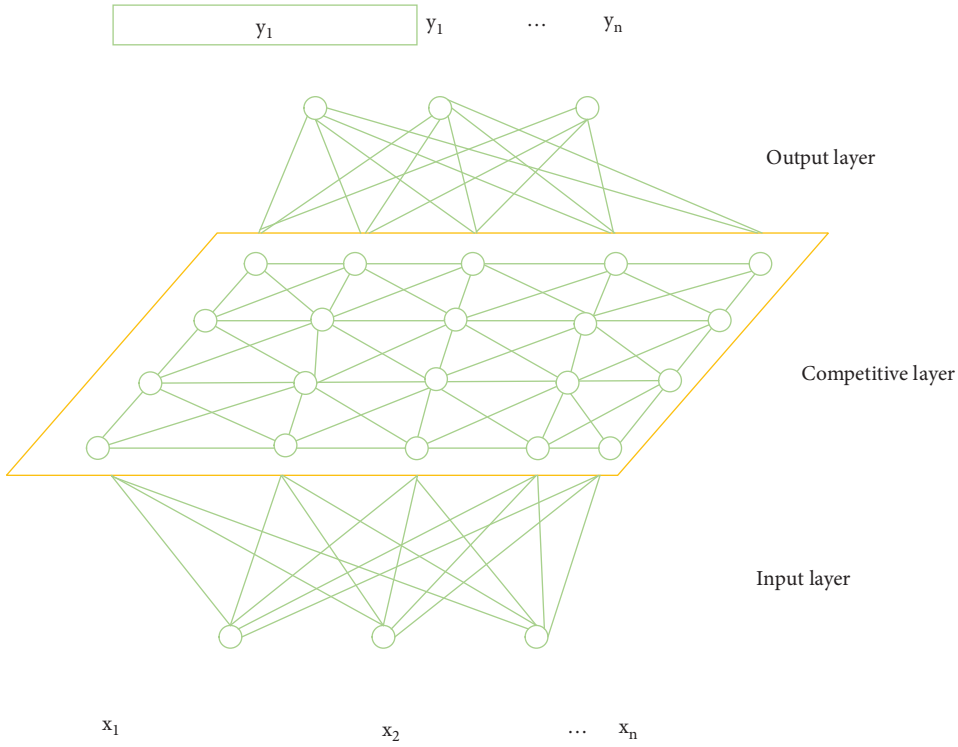

Figure 3: Improved neural network structure diagram.

Table 4: Correspondence table of file suffix and storage content.

File extension	Store content
tdeh	The relevant parameters and control information set by the user in the calculation module through the dialog box
tdep	Particle attribute information, number, geometric parameters (size and sphere center coordinates), physical information (force, velocity, and angular velocity), etc
tdec	Identify the parameters of the particle information selection and storage used to calculate the length of the relevant information of each particle in the tdep file
tdeb	Boundary attribute information, geometric parameters (shape and position), motion information (translation and rolling), etc
tdei	Attribute information, geometric information, movement information, etc. of the inlet

explicitly trigger the call to the OnDraw() function. In order to enable the mouse operation to act on the displayed image to change the display effect, the Invalidate() function is called in the function OnMouseMove() in response to the mouse sliding operation and the function OnMouseWheel() in response to the mouse scroll operation. The program calls the SceneInit() function and the RenderScene() function in the OnDraw() function to enable the 3D graphics drawn by OpenGL to be displayed in the client area and refresh the image when the client area changes. The visualization module of the 3D discrete element method simulation analysis software is carried out in this framework.

The postprocessing module of the 3D discrete element method simulation analysis software includes two parts: simulation display and performance analysis. Therefore, not only must all geometric information be written into the result file for display during the calculation process but also a large number of parameters, physics, and other information must be analyzed and stored for performance. The simulation process often involves tens of thousands of particles, and the calculation process involves the force, velocity, angular velocity, flow, and other information of the physical movement of each particle. In order to meet the user's calculation and simulation needs while saving computer storage space, TDEM implements a selective storage function to selectively store physical particle information. This information is written into multiple files with different suffixes. The suffixes of the files used for simulation visualization are tdeh, tdep, tdec, tdeb, and tdei. The correspondence between these file suffixes and file content is shown in Table 4.

In the simulation process, four files other than the tdeh file should be read multiple times in units of time steps. Whenever the simulation information is read in the current time step, it must be configured for each file. Mark the offset variable of the current reading position. The next time the

file is read, it will be read from this offset position. The tdeh file is only read when the program reads the file for the first time, that is, when the play() function is called for the first time. File parameters are quantitative during the simulation process, such as the parameters m_nPModeIndex and m_nInModeIndex representing the shape of the particles and the inlet shape, the m_nFModeIndex parameter representing the mechanical model, the m_dWholeTime parameter representing the simulation time, and the time step interval representing the m_dDeltaTime parameter interval of the model Wait. These parameters will not change with the simulation time step and are used to control the subsequent file reading and the operation of the entire drawing process. Since particle information can be selectively stored, the size of the memory occupied by each particle is uncertain. There are three marker parameters in the tdec file: li, sudu, and jiaosudu, which are used to determine whether the particle strength, velocity, and angular velocity information are stored in the tdep file. Only when these three parameters are known can you get the proportion of each particle in the file. The length is the particle offset, and the correct reading of the particle information is completed. Therefore, whenever the play() function is called, the tdec file must be read and the offset of the particle must be read, and then the tdep file of the particle must be read. When reading information from the tdep file, each time you read a particle, you need to reread the tdec file to determine what information is currently being read from the particle until all the particle information in a time step is read. Update the read position. Each time the play() function is called, the information in the tdeb file and the tdei file will also be read to obtain all relevant information about the inner boundary and the feed inlet of a time step.

4.3. Technical Analysis of Visual Modeling and Adjustment of the Sphere. To implement the manual sphere filling modeling function, we must first create a new dialog resource dedicated to manual modeling of the filling sphere with the help of MFC, and the number is IDD_NONAUTO, and the dialog title is "Manually Fill the Sphere." This resource creates a dialog box class CNonAuto and encapsulates all the functions that respond to the dialog box operation in this class. In the manual modeling process, even if the operation dialog box is opened, it is necessary to be able to use the main view window of the program. Therefore, the "Manually Fill the Sphere" dialog box should be created as a modeless dialog box. To create a modeless dialog box, first allocate memory for the dlg_NonAuto pointer through the new CNonAuto() operation, then use the dlg_NonAuto- > Create (IDD_NONAUTO) command, and finally use the dlg_NonAuto-command > -ShowWindow (SW_SHOWNORMAL) to manually complete the creation of the dialog box. Screen the dialog box for filling the sphere which appears on the top. In addition, in order to facilitate the user to perform manual filling operations correctly according to the content of the 3D scan file, the range of the center position of the sphere must be adjusted in the operation dialog box. The three directions of x, y, and z must be provided. These ranges are correct. People can determine them after scanning the document and reading it. In the dialog box "Manually Fill the Ball" dialog box at initialization, these range values are assigned to the corresponding static text control. Eight types of text captions are operated by SetWind owText() and range information can be displayed in the corresponding position of the displayed dialog box.

In order to facilitate the operation of the sphere data and ensure safety, the program defines a sphere class to encapsulate the attributes of the sphere. The double type member array is used to store the sphere center position attribute of the sphere, and the s_radius member variable is used to represent the radius of the sphere. Create a sphere type container Sp in the CParticle_fillView class. The effective filling balls set by the "Manually Fill the Sphere" dialog box are stored in the container for subsequent display and operation; the Sp1 sphere container type is also created in the CNonAuto dialog box, which is used to store relevant information during manual modeling. Fill the sphere with temporary information. The CNonAuto class adds four member functions: OnBnClickedADD(), OnBnClickedDEL(), OnOK(), and OnBnClickedCancel(), which are used to respond to the "application," "cancel application," "OK," and "cancel" operations in the dialog box.

When the "Apply" button is clicked, the OnBnClickedADD() response function is activated and called. If the geometric information of the input ball is legal, put the ball into the container Sp1 through the push_back() operation. The value of the variable sID representing the number of particles plus 1 is used to number the ball, and the value is specified as the corresponding static in the dialog box. The text title of the text control implements the effect of automatic numbering of filled balls. Next, call the Invalidate() function to initiate the refresh operation of the visualization window and redraw all the spheres saved in Sp1 in the RenderScene() function so that the currently set component spheres are displayed on the specified position of the visualization window. The method of implementing "cancel application" is similar to that of "application." After clicking the button to activate the OnBnClickedDEL() function, if the Sp1 container is not empty, use the Sp1.pop_back() operation to remove a ball element at the end of the Sp1 container, and then redraw all the constituent spheres in Sp1 to move from the visualization window in addition to the effect of the new configuration of the composition of the ball.

Finally, if you click the "OK" button, the On OK() function will put all the particle elements in the current Sp1 into the Sp container, determine the effective composition spheres in the filling model, and complete a manual sphere filling modeling operation; if you click "Cancel" button, the OnBnClickedCancel() function clears the temporary container through Sp1.clear() and triggers refreshing of the view window to cancel this modeling operation.

After completing the manual modeling of the particle model using the "Manually Fill the Sphere" dialog box, select the file import option in the manual modeling module to save the information about the filled model data to a file. In this operation, add the void CParticle_fillView:

Table 5: Simulation calculation parameter selection table.

Parameter	Granules and granules	Grain and boundary
Normal stiffness coefficient (N/Kg)	5200	10400
Tangential stiffness coefficient (N/Kg)	3468	6934
Normal damping coefficient (Ns/m)	0.35	0.58
Tangential damping coefficient (Ns/m)	0.29	0.49
Coefficient of static friction	0.28	0.36
Sliding friction coefficient	0.24	0.25
Rolling friction coefficient	0.00006	0.00006
Particle density (Kg/m^3)	1238	
Particle radius (mm)	6	
Actual movement time of simulated particles (s)	7	

OnNonAuto_Filesave() response function, define a CString type variable original name in the function, and specify the default file name of the saved file as the particle name set in the dialog box. The program uses the CFileDialog class constructor to create a file save dialog box and specify the default file name. The specific statement is as follows:

```
CFileDialog∗hFileDlg = newCFileDialog(FALSE,
“txt,“originalname, OFN_EXPLORER
|OFN_HIDEREADONLY|OFN_OVER-
WRITEPROMPT, szFileFilter, NULL)
```

After successfully creating a file using the Save File dialog box, use the C++ formatted write function fprintf() to write the position coordinates of the center of each ball and the radius of the ball in floating point format (% f) to the file. Using the fputs() function standardizes the save file format and saves the geometric information of the spheres in the file in units of lines, and each sphere information occupies a line in the file. After importing the model information into the file, you can view the contents of the saved file in the view window through the view calculation result file option under the view function bar. OpenGL provides a method glut-SolidSphere() that directly represents the sphere. In the RenderScene() function, the geometric information read from the result file is used to draw all the constituent spheres, which can complete the visual presentation of the entire particle model.

The results of manual modeling are saved in a file, and the filled particle model can also be written into a database table using the database import function. For the manually filled multisphere particle model, the program uses ODBC database connection when implementing database storage, which requires the CDatabase and CRecordSet of the database-related classes in the MFC base class library. The CDatabase database class is responsible for connecting and operating the data source; the CRecordSet record set class is responsible for binding the record set extracted from the data source. In the 3D aspheric particle modeling software, there are two tables used to store the manually filled multisphere particle model information, and the table names are lsy_combined_sphere and lsy_combined_particle.

When the manually filled particle model is written into the database table, you must first call the Open() function to open the lsy_combined_sphere table, and use the MoveLast() function to move the file pointer to the last record in the table. If the table allows adding data, then import data into the table. After completing data delivery, update the record set through Update(), and call the function Close() to close the table. In order to ensure the consistency of the database, use the previous method to write to the lsy_combined_particle table to ensure that the same primary key data in the two tables is consistent.

4.4. Analysis of the Visual Simulation Effect. Since the improved program changes the file reading and writing operations of the original program, it is necessary to perform simulation calculations in the two versions of the program before and after the improvement and to match the corresponding calculation result files for the two different versions of the program in order to separately and perform correct playback. In order to be able to compare the playback effects before and after the improvement, the simulation parameters selected in the two versions of the program must be exactly the same. However, due to the unreproducibility of engineering calculations, even if the simulation process is exactly the same, it is difficult to obtain exactly the same reproduction results. It can only ensure that the overall trend of particle movement is consistent. When playing a file, the current simulation time and actual playing time can be displayed at the upper left corner of the screen at the same time. In the case of the same simulation time, the shorter the actual playback time, the faster the rendered image, and the smoother the playback effect. Aiming at the complexity of the boundary and the number of particles, spherical particles with uniform radius, simple cylindrical barrel boundary, and complex spiral conveyor boundary are used as simulation objects, and experiments are carried out on the playing effects of the program before and after the improvement. The selection of relevant parameters in the simulation calculation process is shown in Table 5.

After opening the simulation result file and selecting the entity playback mode, we click the boundary effect setting button to open the boundary effect setting dialog box. We click the color setting button in the dialog box to specify a color for the boundary model. After setting the color for the boundary of the cylinder and the boundary of the screw conveyor, the display effect is shown in Figure 4. Through

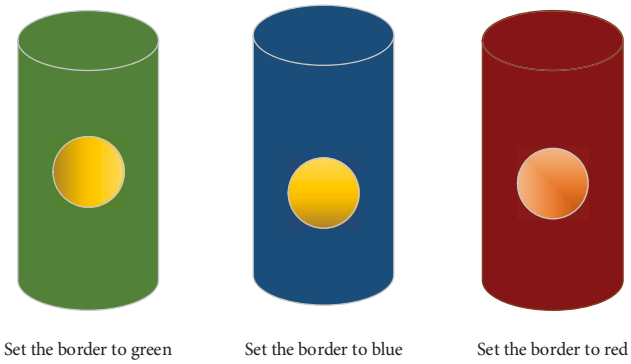

Figure 4: Simple border color setting display effect.

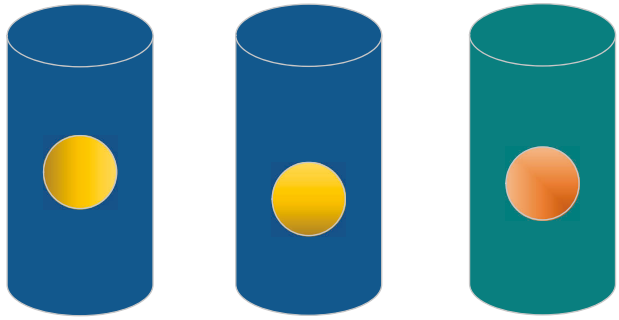

Figure 5: Simple border transparency setting display effect.

the test, the usability and correctness of the border color setting function are verified.

After selecting the entity playback mode, the border transparency can be set through the slider operation in the border effect setting dialog box. The display effects of adjusting the boundary of the cylinder and the transparency of the boundary of the screw conveyor are shown in Figure 5. Through the test, it can be found that the border transparency display effect meets the setting requirements so that the usability and correctness of the border transparency setting function are verified.

5. Conclusion

With the improvement of the fourth-order partial differential equations studied in this article, the continuous improvement and optimization of the fourth-order partial differential equation simulation analysis software, the continuous expansion of simulation analysis functions, more information is displayed on the screen in a visual manner, and more complex visual effects. After analyzing the research background, in this paper, the evaluation of the fourth-order partial differential equation as the basis algorithm with the help of improved neural network related technology and the construction of visual software simulation technology uses the basic class library MFC of OpenGL and Visual C++ to optimize the existing visualization module and improve its functions and to provide users with better observation and visual experience. In addition, on the basis of the existing 3D aspheric particle modeling software of the research group, related functions have been added to the software file reading module and the sphere filling module. Finally, in order to verify the correctness and usability of the work carried out, the visualization module of the fourth-order partial differential equation simulation analysis software was added to improve the existing visualization module of the software and was compared with the improved fourth-order partial differential equation simulation analysis software so as to simulate the effect and test the relevant new functions.

Data Availability

The data used to support the findings of this study are available from the corresponding author upon request.

Conflicts of Interest

The authors declare that they have no conflicts of interest.

References

[1] B. Pausader and S. Shao, "The mass-critical fourth-order Schrödinger equation in high dimensions," *Journal of Hyperbolic Differential Equations*, vol. 07, no. 04, pp. 651–705, 2010.

[2] M. Winkler, "Global solutions in higher dimensions to a fourth-order parabolic equation modeling epitaxial thin-film growth," *Zeitschrift für Angewandte Mathematik und Physik*, vol. 62, no. 4, pp. 575–608, 2011.

[3] W. Ma, R. Wang, X. Zhou, and X. Xie, "The finite element analysis–based simulation and artificial neural network–based prediction for milling processes of aluminum alloy 7050," *Proceedings of the Institution of Mechanical Engineers - Part B: Journal of Engineering Manufacture*, vol. 235, no. 1-2, pp. 265–277, 2021.

[4] B. Pausader, "The cubic fourth-order Schrödinger equation," *Journal of Functional Analysis*, vol. 256, no. 8, pp. 2473–2517, 2009.

[5] P. Loreti and R. March, "Propagation of fronts in a nonlinear fourth order equation," *European Journal of Applied Mathematics*, vol. 11, no. 2, pp. 203–213, 2000.

[6] K. Hochradel, T. Hacker, T. Hohler, A. Becher, S. Wildermann, and A. Sutor, "Three-dimensional localization of bats: visual and acoustical," *IEEE Sensors Journal*, vol. 19, no. 14, pp. 5825–5833, 2019.

[7] Y. L. Zhuang, "A research of the application of visual simulation technology in college English teaching," *Advanced Materials Research*, vol. 1044-1045, pp. 1565–1567, 2014.

[8] C. Zhao, M. Estep, and F. Moinian, "Teaching undergraduate computer graphics: game design and implementation utilizing the OpenGL library and the windows API," in *Proceedings of the 2017 International Conference on Computational Science and Computational Intelligence (CSCI)*, pp. 1195–1198, IEEE, Las Vegas, NV, USA, 2017.

[9] K. J. Kim and N. Baek, "Providing profiling information for OpenGL ES application programs," *Cluster Computing*, vol. 22, no. S1, pp. 937–941, 2019.

[10] Y. Wu, W. Cao, L. Tang, Y. Zhu, and H. Liu, "OpenGL-based visual technology for wheat morphology," *Transactions of the Chinese Society of Agricultural Engineering*, vol. 25, no. 1, pp. 121–126, 2009.

[11] A. Slobozhanyuk, S. H. Mousavi, X. Ni, D. Smirnova, Y. S. Kivshar, and A. B. Khanikaev, "Three-dimensional all-

dielectric photonic topological insulator," *Nature Photonics*, vol. 11, no. 2, pp. 130–136, 2017.

[12] L. Jin, M. Chen, Y. Jiang, and H. Xia, "Multi-traffic scene perception based on supervised learning," *IEEE Access*, vol. 6, pp. 4287–4296, 2018.

[13] W. Deng, R. Chen, B. He, Y. Liu, L. Yin, and J. Guo, "A novel two-stage hybrid swarm intelligence optimization algorithm and application," *Soft Computing*, vol. 16, no. 10, pp. 1707–1722, 2012.

[14] J. Huang, G. Zhang, and Y. Shen, "IWO Optimization SKohonen Network in the Application of Detecting Malicious Domain Name," in *Proceedings of the 2020 IEEE 11th International Conference on Software Engineering and Service Science (ICSESS)*, pp. 67–70, IEEE, Beijing, China, 2020.

[15] A. Kaveh and M. Khayatazad, "A new meta-heuristic method: ray optimization," *Computers & Structures*, vol. 112-113, pp. 283–294, 2012.

[16] M. Yaghini, M. M. Khoshraftar, and M. Fallahi, "A hybrid algorithm for artificial neural network training," *Engineering Applications of Artificial Intelligence*, vol. 26, no. 1, pp. 293–301, 2013.

Hindawi
Mobile Information Systems
Volume 2022, Article ID 7730157, 10 pages
https://doi.org/10.1155/2022/7730157

Research Article

Color Enhancement in Art Works Based on Image Processing Technology of Contourlet Domain

Fei Wang

School of Art and Design, Guangxi Science & Technology Normal University, Laibin, Guangxi 546199, China

Correspondence should be addressed to Fei Wang; 1501212210@zjbti.net.cn

Received 18 June 2022; Revised 17 July 2022; Accepted 29 August 2022; Published 14 September 2022

Academic Editor: Shadi Aljawarneh

With the rapid development of network technology and image processing technology, people can obtain data in a number of ways. Although the emergence of digital works has brought convenience to people's lives, it has also brought many hidden dangers in the field of copyrights, for example, illegal copying, dissemination, and disclosure of digital art works. Sensitive information contained in digital art works can easily be stolen or illegally tampered with through the Internet, thereby destroying the legitimate rights and interests of copyright owners. Therefore, the emergence of digital watermarks provides convenience and practicality for copyright protection. This paper proposes an image digital watermarking algorithm based on SVD and contourlet domain changes. Contourlet transforms the carrier image, divides the direction subbands with high energy values into blocks, performs SVD on each sub-block, and adds the watermark according to the parity quantization rule. The color information-based image enhancement discussed in this article uses the characteristics of multichannel color images to meet application requirements. It mainly involves three aspects: color image enhancement technology that dyes grayscale images into color images, image enhancement technology that uses the colorization algorithm to improve the accuracy of the reconstructed chromaticity image in the process of super-resolution reconstruction, and grayscale image color enhancement technology that preserves the characteristics of the color image during the conversion of the artwork image to the grayscale image. This paper studies the image processing technology based on the contourlet domain and applies it to the research of color enhancement of art works to promote the further development of art works.

1. Introduction

A digital image is usually a digital representation of a two-dimensional image, which is generally expressed as a binary system. According to whether the image can be of fixed resolution, it can be of vector or raster type. Raster images have a limited set of numerical values called pixels [1]. A digital image includes a fixed number of pixels in rows and columns. A pixel is the smallest single element in the image and represents a fixed value of the brightness of a specific color. Normally, pixels are stored in the computer's memory as raster images or raster maps, which are small integers in a two-dimensional array [2]. After the image is converted into binary digital information, there is a huge amount of information, which also puts forward huge requirements for the transmission source, transmission medium, transmission means, and storage medium, which has also become a bottleneck problem in the digital communication field [3]. Contourlet domain conversion can separate multiscale analysis and direction analysis at the same time. Images are the most important information carrier in human social activities. According to the statistical results, about 75% of the information obtained by a person comes from visual images [4].

In this article, we have conducted a detailed study on the contourlet domain transformation, decomposing the LP transform and decomposing the image to capture multiple points, while the directional filter bank decomposes the Laplacian pyramid at the same point to synthesize the coefficients [5]. Among them, image enhancement technology is an important field of image processing technology research, which is based on subjective needs. Or according to different application requirements, some image information is highlighted by processing existing images to obtain useful

images more suitable for specific applications. Or through image processing methods, irrelevant or unnecessary information is weakened or deleted, so that the original image is more suitable for human or machine analysis and processing [6]. The enhanced image mainly pursues subjective and objective effects and does not necessarily need to be close to the original image. Traditional image enhancement is mostly performed on art works, such as image smoothing and denoising, contrast stretching, edge sharpening, histogram alignment, and homomorphic filtering. Among them, multichannel color images are compared with single-channel grayscale images [7]. With richer information, based on the processing of color information, it will provide new research content and methods for traditional image color enhancement that only processes grayscale images. This article introduces the research background and importance of image enhancement based on color information [8].

2. Related Work

This paper introduces the details and color enhancement algorithm in image defogging and restoration, as well as the background and significance of its research. Based on whether to use physical model in image defogging algorithm for image restoration, this paper discusses the research status of the two algorithms [9]. Finally, the content composition of this article is introduced. The basic theories of dehazing algorithms based on image enhancement and physical models are outlined. First, we introduce the atmospheric model, dark channel prior theory, and dehazing algorithms. Then, we introduce an image quality evaluation method and give the theoretical basis for comparing algorithm analysis and evaluation indicators in the subsequent experimental part [10]. An improved guided filtering algorithm based on the gradient domain is proposed to increase the transmittance in the atmospheric scattering model and improve the details of the image in the process of dehazing. The effectiveness of the algorithm is proved through experiments with traditional guided filtering and weighted guided filtering [11]. Then, a detailed enhancement operator is proposed, the last step in the dehazing process is processing for detail enhancement, and the influence of different parameter conditions on the extraction of detail information is analyzed [12]. The image defogging color restoration algorithm is introduced, introducing three color factors into the pyramid fusion technology and applying the improved pyramid fusion technology to image defogging processing [13].

According to different fused image information, parameter weight analysis and detailed information are added. The more and the richer the image, the greater the weight, the foggier images can be merged, and a fog-free image with richer color information and higher definition can be obtained [14]. The literature summarizes the dehazing image details and color enhancement algorithms, improves the optimized transmittance details of the guided filter, introduces the color restoration of the fog image based on color factor and parameter fusion, and finally adds the detail enhancement operator to realize the foggy image [15]. The details and color enhancement algorithms in the restoration process are analyzed from both subjective and objective aspects through multiple sets of experiments [16].

3. Contourlet Domain and Image Processing Technology

3.1. Contourlet Transformation Theory. The contourlet base cover interval is a rectangular structure. This rectangular structure changes with the aspect ratio when the scale changes. It has directionality and anisotropy. The contourlet transformation is more conducive to the sparse expression of the curve. Its basic idea is similar to wavelet transform. The original image passes through a two-stage filter. The first stage image signal is decomposed into multiple subbands from the frequency band passing direction through a pyramid filter structure (LP) filter. The second stage directional filter (DFB) synthesizes singular points distributed in the same direction through contour wave coefficients by capturing the direction information of the image, as shown in Figure 1.

The Laplacian pyramid is very similar to the Gaussian pyramid. The difference is that it saves the difference image between the blurred versions of each level. At each layer of the Laplacian pyramid, a downsampled low-pass image is decomposed. The difference between the original image and the predicted image becomes the difference image (bandpass image). H is the analysis filter, G is the synthesis filter, M is the sampling matrix, and Mn is the integer matrix. The sampling matrix in the multidimensional filter is used to represent the sampling. This process is implemented in the downsampling of the low-pass signal, for example, by M. The downsampled signal $x[n]$ is expressed as $xd[n] = x[Mn]$. Based on the use of tight frames and oversampling filter banks, LP can draw $h[n] = g[-n]$. LP using orthogonal filters can provide a tightly supported frame with a boundary of 1. The dual-frame operator realizes the optimal linear reconstruction, and its advantage is that when the noise exists, the optimal linear reconstruction has a significant improvement and breakthrough in performance on the existing basis. The filter bank is an important analysis method in the field of digital signal processing. In signal processing, the filter bank is an array of bandpass filters that divides the input signal into multiple components, and each component carries a single-frequency subband of the original signal. An application of the filter group is a graphic equalizer, which decomposes multiple components to varying degrees and recombines them to form an improved version of the original signal. The process of decomposing the filter bank is called analysis. The number of filters in the output filter bank means that a subband signal includes the same number of subbands. The reconstruction process is called synthesis, which means that it is generated from the filtering process. The reconstruction process is called synthesis, which means that it is a signal generated by the filtering process to complete signal reconstruction.

3.2. Image Coding Processing Technology. The subband energy value obtained in step 1 is calculated by formula (1). The larger the energy value, the richer the texture.

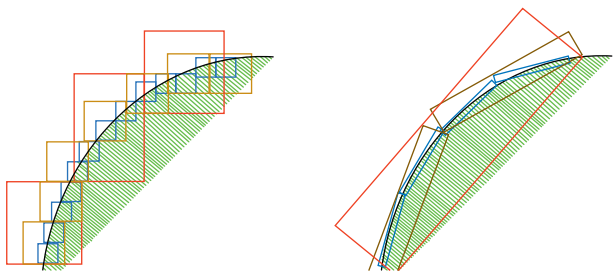

Figure 1: Curve representation of different base structures.

Therefore, the sub-block with the largest energy value is selected to add the watermark. The calculation formula is as follows:

$$E_k = \frac{1}{128 \times 128} \sum_{i=1}^{12s} \sum_{j=1}^{12S} \left(A_k(i, j)\right)^2. \tag{1}$$

Then, we use the above formula to quantify the first eigenvalue $S(1, 1)$ of S. The quantitative formula is

$$\lambda_{ij} = \text{round}\left(\frac{S(1,1)}{\delta}\right), \tag{2}$$

where round is the rounding function and δ is the quantized value which is calculated as follows:

$$\delta = \frac{\left(\log_2 \ 1000 * E\right)}{1000 + 10}. \tag{3}$$

According to the relationship between the watermark information, the reconstructed S component is

$$S'(1,1) = \begin{cases} S(1,1) - \frac{1}{2}\delta, \lambda_{ij} + w_{ij} = 1 \,(\text{mod}\, 2), \\ \\ S(1,1) + \frac{1}{2}\delta, \lambda_{ip} + w_{ij} = 0 \,(\text{mod}\, 2). \end{cases} \tag{4}$$

Decompose the sub-block A_{ij} as SVD and then use the formula to quantify the first eigenvalue $(1, 1)S'$ of S':

$$\lambda'_{ij} = \text{floor}\left(S'(1,1)\delta\right). \tag{5}$$

According to whether λ_{ij} can be divisible by 2, the watermark is obtained, and the specific formula is as follows:

$$w_{iv} = \begin{cases} 1, & \lambda'_{ij} = 1 \,(\text{mod}\, 2), \\ 0, & \lambda'_{ij} = 0 \,(\text{mod}\, 2). \end{cases} \tag{6}$$

4. The Color Information Image Enhancement Algorithm and Evaluation Application of Art Works

4.1. Color Detail Enhancement Algorithm. In the process of image defogging restoration, detailed information is easy to lose, especially the edge area, so the maintenance of edge information has a great influence on the defogging effect. The traditional guide filter has a weak edge information retention ability, and based on this, the introduction of weights is used to improve its edge information retention ability. To strengthen this ability, three aspects need to be considered: First, the improved guided filter is very sensitive to edge judgment, that is, to accurately find the edge of the image. Second, the detail enhancement edge part is given different weighted enhancement coefficients according to the content edge or color edge to avoid losing information in the process of defogging. Third, in the nonedge part, the noise is smoothed, and the noise elimination has an impact on the defogging restoration. First of all, in order to achieve the first part, the edge area of the image needs to be obtained. In digital image processing, the edge of the image can be obtained by gradient. The gradient can be represented by a vector, reflecting the rate and direction of the pixel point, and the gradient of the image is right derivation of the image, namely,

$$G_j = \left[\frac{\partial I_i}{\partial x}, \frac{\partial I_j}{\partial y}\right]. \tag{7}$$

Analyzing the numerical information of the image shows that if a point is in the edge part, its gradient value will be larger; otherwise, the gradient value will be smaller. Considering this part, it is necessary to define a threshold of 1 to filter and distinguish the edge area or the nonedge area. When $G < t$, it is considered that the pixel i is at a nonedge, and when $G \geq 1$, it is considered that the pixel i is on the edge. The specific definition of the threshold is

$$t = 0.15^* \text{DR}, \tag{8}$$

where DR is the dynamic range of the absolute value of the gradient of all pixels in the guide image and 0.15 is the experimental data. When the DR is set to a multiple of 0.15, the judgment of the threshold is closer to the real image. Then, the formula for judging the edge area is

$$\left|G_i - 1\right|. \tag{9}$$

Second, in order to determine the edge area of the image, we need to propose different weighted enhancement coefficients according to the edge area. When the image is located in the edge area, the edge information is enlarged for enhancement. When the image is not in the edge area, the image needs to be smoothed in order to suppress noise:

$$T(i) = \lambda + \left|G_i - t\right|^{a(t)}. \tag{10}$$

The weight is brought into the guided filter, and the formula is rewritten as

$$E' = \sum_{i \in w_k} \left(\left(a_k I_i + b_k - p_i\right)^2 + \frac{\varepsilon}{T(i)} \left(a_k - \psi_k\right)^2 \right), \tag{11}$$

in which

$$\psi_k = 1 - \frac{1}{1 + e^{-a^+ \text{mean}(i) + 0.5}}. \tag{12}$$

After calculation, the corresponding a_k and b_k become

$$a_k = \frac{\mid 1/\omega_1 \mid \sum_{i\in\omega_k} I_i p_i - \mu_k \overline{p_k}}{\left(\sigma_k - \psi_k\right)^2 + \varepsilon/\phi(i)},$$
$$b_k = \overline{p_k} - a_k \mu_k. \tag{13}$$

The final output image is

$$q_i = \frac{1}{|\omega|} \sum_{k\in\omega_i} a_k I_i + \frac{1}{|\omega|} \sum_{k\in\omega_i} b_k. \tag{14}$$

Through experiments, it can be seen that subjective evaluation means that, from a human perspective, the image processed by traditional guided filtering is too smooth and loses image information details; although weighted guided filtering is relatively improved, the colors are gorgeous and not suitable for people. The algorithm proposed in this paper maintains the image details while smoothing the image, and has a good sense. For example, the details of the central stamen are more consistent with the original photo, and the petal edges are more clear and distinct. This article not only looks at subjective evaluation but also focuses on objective evaluation. Table 1 shows its objective evaluation value.

4.2. Color Restoration Algorithm. The original image G is set as the bottom layer of the pyramid. The low-pass filter $w(m,n)$ uses this method to perform convolution calculation, and the transaction performs image downsampling to obtain the upper layer of the gold word. Each level of image is obtained by performing low-pass filter convolution calculation on the previous layer and then downsampling every other row and column, as follows:

$$G_L(i,j) = \sum_{m=-1}^{2} \sum_{n=-2}^{2} w(m,n) G_{L-1}(2i+m, 2j+n),$$
$$1 \le L \le N, 0 < i < C_L, 0 < j < R_L. \tag{15}$$

The downsampled image is subtracted from the interpolated and enlarged image to obtain a pyramid of detailed information. The mathematical expression is as follows:

$$LP_l = G_l - \text{Expand}\left(G_{L+1}\right), 0 \le L \le N,$$
$$LP_N = G_N L = N. \tag{16}$$

The fusion image is designed to be processed with 2 or more images. All fused images need to be pyramid constructed. After completion, they are fused, that is, the information is superimposed. Finally, the enhanced detail layer is added to the fused pyramid. The enhanced image G_j fused with different image color information is obtained, as follows:

$$G'_N = LP_N + \text{Fusion}\left(G_L\right) 0 \le L \le N. \tag{17}$$

In the process of watermark embedding, the choice of quantization step size is very important. The larger the quantization step size, the better the robustness of the algorithm, but the invisibility of the algorithm will decrease. In the adaptive quantization step size watermarking algorithm, the value of the initial quantization step size is fixed.

Table 1: Objective evaluation value.

—	Original image	Guided filtering	Weighted guided filtering	This article improves guided filtering
ssim	—	0.8834	0.9365	0.9411
psnr	—	33.4342	38.3511	38.7685

Therefore, how to choose an appropriate initial quantization step size is a key technology to balance the robustness and invisibility of the embedding algorithm. In this paper, through multiple experiments on three images of Lena, Baboon, and Peppers, it is found that the robustness of the algorithm is low when the initial quantization step size is 25. When the initial quantization step size is 55, a slight change is observed in the carrier image. When the initial quantization step size is 55, the invisibility of the algorithm is already poor. This article compares the robustness and invisibility effects and selects the initial quantization step size in the interval 25–55 to determine the final quantization step size. Figure 2 shows the NC value relationship diagram corresponding to the watermarked image when it is compressed by JPEG when different initial quantization steps are selected.

As shown in Figure 3, the NC value increases as the initial quantization step size increases. From the perspective of the correspondence between the initial quantization step size and the PSNR, the larger the initial quantization step size, the smaller the corresponding PSNR value and the invisible watermark. The performance decreases with the increase of the quantization step in a certain interval. However, the NC value changes significantly in the 40–45 interval, so the value between 40 and 45 is used as the candidate value, which is used as the initial quantization step for attack experiments.

4.3. Chroma Image Super-Resolution. The reason for the simple processing of chrominance images is that the human eye's tolerance for color distortion is higher than the tolerance for brightness information. When the application requirements are not high, this processing method can basically meet the requirements. However, when the image structure is more complex, the color information is rich, or the reconstruction multiple is large, and the chrominance image obtained by the interpolation algorithm by this method is prone to distortion such as edge blur and jagged, which affects the overall effect of color image super-resolution reconstruction. Because the structural properties of the luminance component and the chrominance component of an image are different, many super-resolution reconstruction techniques suitable for luminance images cannot be directly used for chrominance images. Therefore, it is necessary to find a technology suitable for reconstructing high-resolution chrominance images. In order that the colorization algorithm of color diffusion can be well adapted to this demand, first of all, the high-

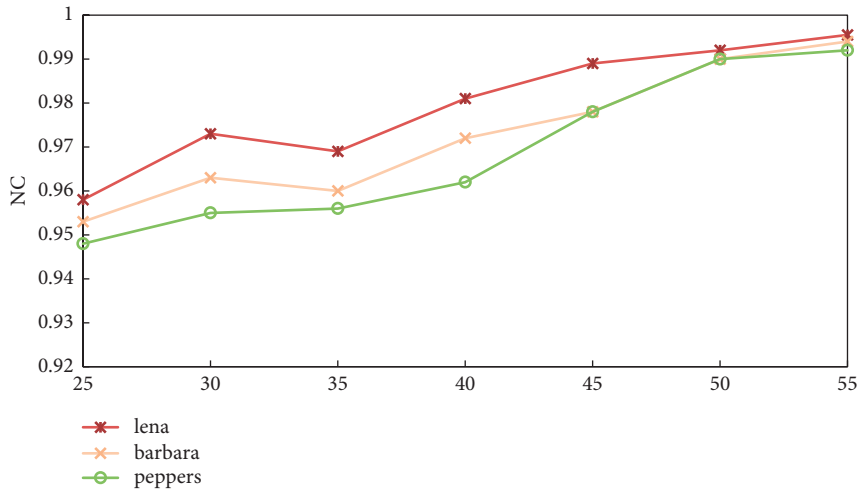

Figure 2: Correspondence between the initial quantization step size and the Gaussian noise (0.005) attack.

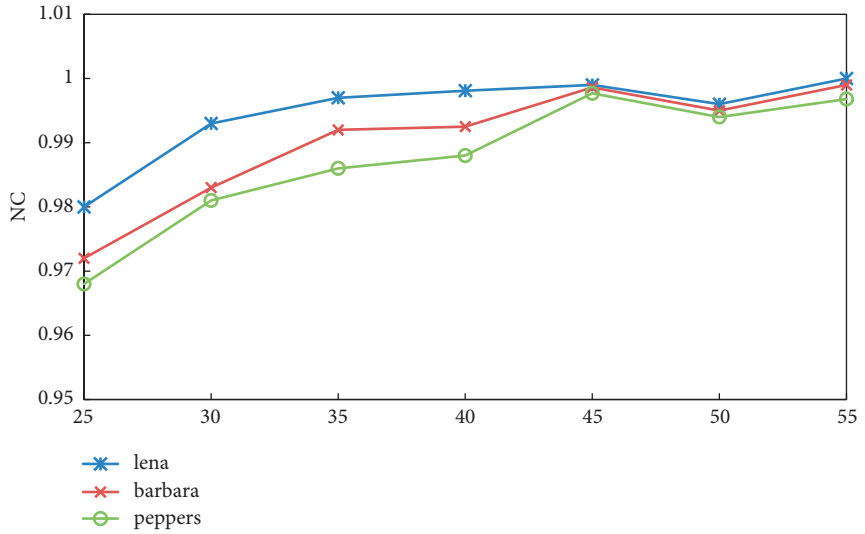

Figure 3: Correspondence between the initial quantization step size and the JPEG (20) attack.

resolution brightness image obtained by the grayscale image super-resolution reconstruction technology can be used as the grayscale image to be colorized. The color information is regarded as the points that have been dyed with the original color in the high-resolution image to be obtained, and the colors of other points can be obtained through the colorization algorithm based on color diffusion to complete the super-resolution reconstruction of the chromaticity image. Image super-resolution reconstruction technology simulates the image degradation process of the imaging system and reconstructs high-quality images. The image degradation process is expressed as a matrix as follows:

$$I_L = DLI_H + \eta. \tag{18}$$

The IBP algorithm is an image super-resolution reconstruction algorithm. Its core idea is that the reconstructed ideal image undergoes the same degradation process as the original degradation model and the same image as the original low-resolution image should be produced. Therefore, the reconstruction error $e(I_H)$ can be minimized through an iterative process, which is defined as

$$e(I_H) = \| I_L - DLI_H \|_2^2. \tag{19}$$

There are many colorization algorithms based on color diffusion. This paper selects a colorization algorithm that can effectively use the edge information of the image to improve the edge distortion that cannot be solved by the interpolation algorithm, which has a faster calculation speed. The starting point of the algorithm is that, in the YUV color space, if the brightness Y of adjacent pixels is similar, the chromaticity U should also be similar. If the chromaticity value of the current point r is set to $U(r)$, then it can be expressed by the weighted summation of the chromaticity values of the pixels in the pixel set $N(r)$ in its neighborhood, and the error energy is as follows:

$$\left[U(r) - \sum_{seN(r)} w_{rx} U(s)\right]^2, \tag{20}$$

where w_{rs} is the weighted value of each neighborhood pixel. Calculate the total error energy $J(U)$ for all the unknown color points and minimize $J(U)$:

$$\begin{aligned} U_H &= \arg\min_U J(U) \\ &= \arg\min_U \sum_r \left[U(r) - \sum_{seN(r)} w_{rs} U(s)\right]^2. \end{aligned} \tag{21}$$

According to the starting point of the algorithm, the weighted value w_{rs} is related to the brightness difference between the pixel and the neighborhood and satisfies that the smaller the brightness difference from the current point r, the greater the neighborhood pixel weight, and the sum of all weighted values is 1. The weighted value calculation formula is as follows:

$$w_{Js} = \frac{1}{W_r} e^{-(Y(r)-Y(s))^2/\alpha\sigma_r^2}. \tag{22}$$

For a more intuitive comparison, Figure 4 shows a partial enlargement of the result image of each algorithm to compare the algorithms subjectively. List the PSNR and SSIM values between these local blocks and the chrominance components of the original high-resolution color image blocks for objective comparison. The local block enlargement of the "butterfly" image reconstruction result is shown in Figure 4.

The partial block enlargement of the image reconstruction result is shown in Figure 5.

By comparing the numerical results listed in Tables 2 and 3, it can be seen that the proposed IBPCSR algorithm has obtained better subjective effects and higher PSNR and SSIM values, which shows that it is necessary to perform targeted processing on chrominance images. It can effectively reduce the color distortion of the reconstructed image and improve the display effect of the obtained high-resolution color image. In order to improve the efficiency and performance of the algorithm, based on the super-resolution reconstruction of chrominance image, this paper further proposes to use the high-resolution image as the guide image. Guided filtering has high computational efficiency and high performance of maintaining image edges to improve the quality of the reconstructed high-resolution chrominance image. The details are shown in Table 2.

The SSIM values for image component comparison are shown in Table 3.

Image guided filtering (GF) is an image edge-preserving filtering method. The processing process involves three images: input image p, filtered output image q, and guidance image G. The guided filter assumes that there is a locally linear relationship between G and q. In the window W_r centered on the pixel r, the linear function is expressed as follows:

$$q_s = a_r G_s + b_r, \forall s \in W_r, \tag{23}$$

where a_r and b_r are fixed values in a square window W_r, which are related to the input image and guide image in the window. This local linear assumption can ensure that the output q_s has similar features to the local G_s of the guiding image, and it also shows that the output image has the same edge information as the guiding image. Because the luminance image has similar but more prominent edges to the chrominance image, the reconstructed high-resolution luminance image YH is used as the guide image to improve the edge performance of the chrominance image, and the initial high-resolution chrominance image U_H^0 is used as the guide image. The input image is processed by guided filtering. The parameters a_r and b_r of the guidance filter can be directly calculated by the following formula after derivation:

$$\begin{aligned} a_r &= \frac{1}{\#\{W_r\}} \frac{\sum_{seW_t} G_s p_s - \overline{G}_r \overline{p}_r}{\sigma_r^2 + \zeta}, \\ b_r &= \overline{p}_r - a_r \overline{G}_r. \end{aligned} \tag{24}$$

Because in actual processing, in order to ensure data smoothness and accuracy, overlapping windows are used, there will be multiple windows containing pixels s, and the calculated q_s of different windows will be different, so the formula is updated to

$$q_s = \overline{a}_r G_s + \overline{b}_r, \tag{25}$$

in which

$$\begin{aligned} \overline{a}_r &= \frac{1}{\#\{W_r\}} \sum_{s|r\in W_x}, a_s = \frac{1}{\#\{W_r\}} \sum_{s\in W_r} a_s, \\ \overline{b}_r &= \frac{1}{\#\{W_r\}} \sum_{slr\in W_x}, b_s = \frac{1}{\#\{W_r\}} \sum_{s\in W} b_s. \end{aligned} \tag{26}$$

This paper presents the experimental results of three chromatic image super-resolution reconstruction algorithms (IBPCSR, GFCSR, and POCSCSR algorithms), bicubic interpolation algorithm, Liu algorithm, and Huang algorithm and conducts 4x super-resolution reconstruction experiments and low-resolution experiments The image is obtained by blurring and downsampling the original high-resolution color image. The blurring filter uses a Gaussian low-pass filter with a window size of 5×5 and a variance of 2. The grayscale image super-resolution reconstruction algorithm based on sparse representation is used to obtain the high-resolution luminance image YH as the luminance component of the results of all algorithms to be compared.

Compare the results of all algorithms with the original high-resolution chrominance image, calculate the average color difference $\triangle E$ of PSNR, SSIM, and CIEDE2000, and record them in Tables 4–6.

The SSIM values of the algorithm results compared with the U and V components of the original high-resolution chrominance image are shown in Table 5.

From the numerical comparison results in Tables 4–6, it can be seen that the three methods proposed in this paper have obtained better results than bicubic interpolation, Liu's algorithm, and Huang's algorithm, especially the combination of guided filtering. The performance of the latter two algorithms (GFCSR and POCSCSR) is significantly

(a) (b) (c) (d) (e)

Figure 4: Local block enlargement of the "butterfly" image reconstruction result. (a) Bicubic interpolation. (b) A. (c) B. (d) IBPCSR. (e) Original HR image block.

(a) (b) (c) (d) (e)

Figure 5: Partial block enlargement of the "butterfly" image reconstruction result. (a) Bicubic interpolation. (b) A. (c) B. (d) IBPCSR. (e) Original HR image block.

Table 2: PSNR (dB) values of the local block of each algorithm result compared with the U and V components of the original high-resolution chrominance image.

Experimental image block		Algorithm			
		Bicubic interpolation	Liu	Huang	IBPCSR
Butterfly	U	32.55	32.91	34.02	34.13
	V	29.00	29.86	31.24	31.40
Flower	U	27.31	27.53	29.30	29.69
	V	31.92	32.58	33.59	33.74
Boy	U	37.61	38.40	40.90	41.43
	V	43.02	43.31	46.18	46.46
Tsing yi	U	27.19	27.99	28.42	29.81
	V	24.44	24.56	26.04	26.71

Table 3: SSIM values of the comparison between the local block of each algorithm result and the U and V components of the original high-resolution chrominance image.

Experimental image block		Algorithm			
		Bicubic interpolation	Liu	Huang	IBPCSR
Butterfly	U	0.7936	0.8088	0.8550	0.8582
	V	0.7397	0.7531	0.8050	0.8154
Flower	U	0.7769	0.8109	0.8554	0.8658
	V	0.7900	0.8020	0.8433	0.8460
Boy	U	0.9393	0.9505	0.9705	0.9785
	V	0.9739	0.9812	0.9886	0.9911
Tsing yi	U	0.7034	0.7104	0.7306	0.7583
	V	0.6902	0.6948	0.7266	0.7687

improved compared to that of other algorithms. The results obtained by these two algorithms are very close under the measurement of PSNR, SSIM, and $\triangle$E standards, and the pros and cons of the two cannot be distinguished by these three metrics.

Color image super-resolution reconstruction is a research hotspot in the field of image processing, and the performance of various algorithms is constantly improving. However, in addition to learning-based algorithms that consider the three-channel information of color images as a whole, the process of color image super-resolution reconstruction processing usually converts the image into a color space where luminance and chrominance information are separated, studies the luminance image, and interpolates only the chrominance image in order to obtain an enlarged image. The process is usually performed to convert the image into a color space in which the luminance and chrominance information is separated and study the luminance image, and in order to obtain an enlarged image, only the chrominance image is interpolated. This simple processing of chrominance information is likely to affect the final reconstruction. Therefore, it is necessary to study the super-resolution reconstruction algorithm of image that meets the characteristics of chrominance image. The relationship between the color image super-resolution reconstruction framework and the colorization model based on color diffusion, the correspondence and difference between image brightness information and chroma information, and algorithm efficiency are analyzed, and three chroma values are progressively proposed.

First of all, according to the feature that the colorization algorithm based on color diffusion can improve the edge performance of chroma image super-resolution reconstruction, the IBPCSR algorithm based on optimized colorization and iterative backprojection is proposed. The initial value position is not adjusted, and the colorization algorithm incorporated into iterative backprojection, instead of the usual interpolation magnification for iterative solution, this algorithm can usually obtain better than bicubic interpolation, the Liu algorithm that also uses colorization for super-resolution reconstruction of

Table 4: PSNR (dB) values of the results of each algorithm compared with the U and V components of the original high-resolution chrominance image.

Experimental image block		Algorithm					
		Bicubic interpolation	Liu	Huang	IBPCSR	GFCSR	POCSCSR
Tiger	U	42.95	42.27	43.14	43.42	44.41	44.48
	V	39.40	38.37	39.49	39.67	40.89	41.01
Flower	U	27.16	27.62	28.52	28.70	28.98	28.94
	V	32.11	31.66	32.23	32.26	32.82	32.85
Boy	U	44.40	45.11	46.29	46.50	47.73	47.49
	V	48.24	48.88	49.02	49.11	50.52	50.39
Tsing yi	U	32.44	31.76	32.56	32.75	33.61	33.72
	V	31.21	30.57	31.42	31.64	32.58	32.71
Hat	U	44.70	44.81	45.33	45.55	46.54	46.60
	V	46.02	46.31	46.65	46.94	47.40	47.58
Butterfly	U	33.80	33.76	34.00	34.07	34.86	34.90
	V	37.10	37.15	37.22	37.40	38.28	38.45
Miss	U	36.55	36.27	37.12	36.80	37.50	37.55
	V	38.52	38.06	39.34	39.59	40.40	40.23
Peony	U	45.44	44.63	44.88	45.99	46.39	46.89
	V	47.87	47.48	47.76	47.92	48.39	48.61
Balloon	U	37.65	37.28	38.58	38.90	40.06	40.26
	V	37.32	37.35	37.51	37.45	40.22	40.48
Toy	U	35.15	34.14	35.63	35.76	37.71	37.70
	V	35.30	34.59	35.89	35.96	36.74	36.82
Plant	U	33.86	33.83	34.50	34.65	35.24	35.18
	V	37.13	36.94	37.37	37.83	38.53	38.50
Basin	U	39.81	38.98	40.02	39.99	41.05	41.07
	V	39.82	38.84	39.84	39.87	40.93	40.94

Table 5: SSIM values of the results of each algorithm compared with the U and V components of the original high-resolution chrominance image.

Experimental image block		Algorithm					
		Bicubic interpolation	Liu	Huang	IBPCSR	GFCSR	POCSCSR
Tiger	U	0.9682	0.9643	0.9688	0.9687	0.9744	0.9748
	V	0.9381	0.9362	0.9410	0.9412	0.9507	0.9517
Flower	U	0.7415	0.7696	0.8029	0.8098	0.8172	0.8150
	V	0.7766	0.7629	0.7861	0.7883	0.8074	0.8084
Boy	U	0.9858	0.9876	09883	0.9884	0.9914	0.9910
	V	0.9918	0.9921	0.9922	0.9928	0.9946	0.9944
Tsing yi	U	0.8751	0.8400	0.8749	0.8755	0.9008	0.9024
	V	0.8721	0.8541	0.8773	0.8783	0.9009	0.9030
Hat	U	0.9927	0.9925	0.9937	0.9941	0.9948	0.9949
	V	09937	0.9919	0 9945	0.9947	0.9950	0.9951
Butterfly	U	0.8513	0.8482	0.8557	0.8563	0.8804	0.8813
	V	0.9191	0.9002	0.9219	0.9228	0.9323	0.9348
Miss	U	0.9202	0.9148	0.9250	0.9264	0.9427	0.9431
	V	0.9460	0.9434	0.9517	0.9536	0.9621	0.9608
Peony	U	0.9884	0.9845	0.9867	0.9898	0.9908	0.9916
	V	0.9822	0.9814	0.9876	0.9887	0.9932	0.9935
Balloon	U	0.9548	0.9520	0.9554	0.9553	0.9657	0.9663
	V	0.9553	0.9538	09561	0.9567	0.9678	0.9694
Toy	U	0.9226	0.9148	0.9244	0.9258	0.9447	0.9442
	V	0.9086	0.9006	0.9107	0.9147	0.9267	0.9273
Plant	U	0.8908	0.8971	0.9052	0.9084	0.9177	0.9164
	V	0.9385	0.9382	0.9413	0.9445	0.9525	0.9520
Basin	U	0.9609	0.9523	0.9655	0.9681	0.9737	0.9738
	V	0.9604	0.9513	09648	0.9660	0.9714	0.9714

Table 6: The average value of the CIEDE2000 color difference between the results of each algorithm and the original high-resolution color image $\triangle E$.

Experimental image	Algorithm					
	Bicubic interpolation	Liu	Huang	IBPCSR	GFCSR	POCSCSR
Tiger	3.6457	3.6672	3.6402	3.6365	3.5689	3.5622
Flower	7.9195	7.7018	6.8537	6.8251	6.6494	6.6716
Boy	1.1340	1.1183	1.1132	1.0769	1.0352	1.0443
Tsing yi	5.7234	5.9239	5.6601	5.7142	5.4962	5.4724
Hat	1.2398	1.2634	1.2730	1.2274	1.2104	1.2086
Butterfly	5.3692	5.5605	5.3262	5.3674	5.1581	5.1495
Miss	2.4472	2.4600	2.3799	2.3788	2.2733	2.2743
Peony	1.2060	1.2621	1.2211	1.2010	1.0749	1.0545
Balloon	2.4218	2.5474	2.3634	2.3535	2.0358	2.0026
Toy	3.2938	3.3163	3.1371	3.1224	2.9079	2.9092
Plant	2.6441	2.6464	2.5058	2.4849	2.3839	2.3881
Basin	4.3562	4.4127	4.3542	4.3423	4.1798	4.1833

chrominance images and obtains the overall high resolution based on learning The Huang algorithm of high-resolution color image plus iterative backprojection results, but the running time is too long. Therefore, in order to maintain the high computational efficiency of the guided filtering algorithm for the edge of the image, the luminance image presentation can contain more edge and detailed information than the chrominance image. This paper further proposes to use the reconstructed luminance image as the guiding image. The guided filtering of the IBPCSR algorithm replaces the optimized colorization algorithm used in the iterative backprojection of the IBPCSR algorithm to perform the iterative processing of the GFCSR algorithm. This algorithm improves the image reconstruction effect and reduces the running time. However, due to the need to optimize the matrix equation for color processing, the running time of the GFCSR algorithm is much higher than that of the commonly used interpolation algorithm. In order to further improve the efficiency of the algorithm, considering that the kernel function of the steering filter with the luminance image as the guide image should meet the local constraints of the chromaticity value proposed by the optimized colorization algorithm, but the backprojection meets the overall constraints, according to the convex set projection framework, a POCSCSR algorithm is proposed, which analyzes the local neighborhood relationship between the navigation filter kernel function and the colorization algorithm and uses the highly computationally efficient navigation filter algorithm to complete the optimized colorization process with the GFCSR algorithm The same job. When measured by objective numerical values (PSNR, SSIM, $\triangle E$), the results of the POCSCSR algorithm are very close to those of the GFCSR algorithm, but because its running time is greatly shortened, it is no different from the time of the interpolation algorithm and the iterative backprojection algorithm.

5. Conclusion

In this paper, the similarities and differences between wavelet transform and contourlet transform and their respective properties are studied. The application and implementation methods of contourlet transform in the fields of image watermarking, image fusion, and image compression are studied. Based on the principle of contourlet, the pyramid and direction are studied. For the structure and principle of the filter, a watermark encoder with geometric transformation and robust image compression is also proposed. Based on the theory of contour transformation and principal component analysis, the contour transformation coefficient covering the image direction subband is selected as the embedding position. The main component of the contour coefficient is used to embed the watermark, and the noise recognition function is used to adaptively adjust the watermark embedding strength. The experimental results show that, after various possible distortions, the watermark can be detected with high accuracy. This paper also studies three aspects of art image enhancement based on color information, including colorization of grayscale images that enhances the display effect of grayscale images by dyeing grayscale images. In the framework of color image super-resolution reconstruction, it replaces the usual color matching. The processing method of chromaticity image interpolation and enlargement is used to improve the chromaticity image super-resolution reconstruction of the reconstructed chromaticity image quality. When the color image is displayed and researched in grayscale, the color image is grayscaled to enhance the contrast and perceptual consistency.

Data Availability

The data used to support the findings of this study can be obtained from the author upon request.

Conflicts of Interest

The author declares no conflicts of interest.

Acknowledgments

This work was supported by the "U-G-S" fund of art normal students from the perspective of "normal professional

certification," Construction and implementation of training mode 2021 education reform project of the Henan Provincial Department of Education, no. 2021-jsjyyb-058.

References

[1] M. Boroumand, M. Chen, and J. Fridrich, "Deep residual network for steganalysis of digital images," *IEEE Transactions on Information Forensics and Security*, vol. 14, no. 5, pp. 1181–1193, 2019.

[2] X. Zhang and S. Xu, "Research on image processing technology of computer vision algorithm," in *Proceedings of the 2020 International Conference on Computer Vision, Image and Deep Learning (CVIDL)*, Chongqing, China, July 2020.

[3] H. H. Lu and Z. X. Zhu, "Research and application of image retrieval improved algorithm based on BOF," *International Journal of Signal Processing, Image Processing and Pattern Recognition*, vol. 8, no. 3, pp. 155–168, 2015.

[4] W. Cai and Z. Wei, "Remote sensing image classification based on a cross-attention mechanism and graph convolution," *IEEE Geoscience and Remote Sensing Letters*, vol. 19, pp. 1–5, 2022.

[5] J. Zhang, Y. Liu, H. Liu, and J. Wang, "Learning local–global multiple correlation filters for robust visual tracking with Kalman filter redetection," *Sensors*, vol. 21, no. 4, p. 1129, 2021.

[6] M. Suthar, H. Asghari, and B. Jalali, "Feature enhancement in visually impaired images," *IEEE Access*, vol. 6, pp. 1407–1415, 2018.

[7] Z. Shi, Y. Li, M. Zhao, Y. Feng, and L. He, "Multi-stage filtering for single rainy image enhancement," *IET Image Processing*, vol. 12, no. 10, pp. 1866–1872, 2018.

[8] M. Adil, M. Attique, M. M. Jadoon, J. Ali, A. Farouk, and H. Song, "HOPCTP: a robust channel categorization data preservation scheme for industrial healthcare Internet of things," *IEEE Transactions on Industrial Informatics*, vol. 18, no. 10, pp. 7151–7161, 2022.

[9] H. Sadia, F. Azeem, H. Ullah, Z. Mahmood, S. Khattak, and G. Z. Khan, "Color image enhancement using multiscale retinex with guided filter," in *Proceedings of the 2018 International Conference on Frontiers of Information Technology (FIT)*, Islamabad, Pakistan, December 2018.

[10] T. Cui, L. Qu, J. Tian, and Y. Tang, "Single image haze removal based on luminance weight prior," in *Proceedings of the IEEE International Conference on Cyber Technology in Automation, Control, and Intelligent Systems (CYBER'16)*, pp. 332–336, Chengdu, China, June 2016.

[11] C. Science and M. Studies, "Image enhancement techniques for different atmospheric conditions," *International Journal of Advance Research in Computer Science and Management Studies*, vol. 3, no. 2, pp. 49–52, 2015.

[12] G. Meng, Y. Wang, J. Duan, S. Xiang, and C. Pan, "Efficient image dehazing with boundary constraint and contextual regularization," in *Proceedings of the 14th IEEE International Conference on Computer Vision (ICCV'13)*, pp. 617–624, Sydney, NSW, Australia, December 2013.

[13] M. Abdolmaleky, M. Naseri, J. Batle, A. Farouk, and L. H. Gong, "Red-Green-Blue multi-channel quantum representation of digital images," *Optik*, vol. 128, pp. 121–132, 2017.

[14] Y. Xu, J. Wen, L. Fei, and Z. Zhang, "Review of video and image defogging algorithms and related studies on image restoration and enhancement," *IEEE Access*, vol. 4, pp. 165–188, 2016.

[15] Y.-K. Wang and C.-T. Fan, "Single image defogging by multiscale depth fusion," *IEEE Transactions on Image Processing*, vol. 23, no. 11, pp. 4826–4837, 2014.

[16] S. Kwon, H. Lee, and S. Lee, "Image enhancement with Gaussian filtering in time-domain microwave imaging system for breast cancer detection," *Electronics Letters*, vol. 52, no. 5, pp. 342–344, 2016.

Hindawi
Mobile Information Systems
Volume 2022, Article ID 4162088, 11 pages
https://doi.org/10.1155/2022/4162088

Research Article

Design of Sports Training Data Monitoring System Based on Wireless Internet of Things

Wang Yao[1] **and Zhang Zhihai**[2]

[1]*Personnel Department of Cangzhou Normal University, Cangzhou, Hebei 061000, China*
[2]*Meishan Pharmaceutical Vocational College Public Teaching and Research Department, Meishan, Sichuan 620200, China*

Correspondence should be addressed to Zhang Zhihai; 196151201@mail.sit.edu.cn

Received 11 July 2022; Revised 30 July 2022; Accepted 17 August 2022; Published 13 September 2022

Academic Editor: Shadi Aljawarneh

With the development of the times and the continuous improvement of science and technology, people's living standards are getting better and better, living conditions are getting more and more abundant, the infrastructure of cities is becoming more and more perfect, the comprehensive strength of the country is constantly increasing, and the speed of development is also increasing fast. However, under conditions of continuous development, the physical health of adolescents and children has not improved, the physical fitness of adolescents has declined, and many problems have appeared. This survey will combine embedded software and Internet technology, focusing on testing the safety of the sports training system and collecting data. It is very necessary for us to investigate the safety of the sports training system. The system also has potential for development. Only when the safety of the sports training system is determined can we understand the most suitable exercise methods for contemporary youths and ensure that they are not right in order to make the relevant sports training methods more confidently when a second injury occurs to the body. The sports training system to be studied this time consists of three basic technologies, namely, data collection terminals, database stations, and web servers. We will install the relevant equipment of the data collection system in the campus, such as teaching buildings or campus buildings and roads on the open space next to it, and a chip with a wireless transmission system will be placed in the student's campus card. This chip is small in size, high in transmission efficiency, and easy to carry by students. Therefore, when each student holds the campus card, the related equipment in the campus card will be signal linked with the equipment installed in the school. This mode is wireless, which is very convenient and fast. In this way, we can collect the identity information and money storage status of the campus card through the web server. When the student ID is displayed on the computer screen, it proves that the student has swiped the card successfully.

1. Introduction

With the development of the times and the continuous improvement of science and technology, people's living standards are getting better and better, living conditions are getting more and more abundant, the infrastructure of cities is becoming more and more perfect, the comprehensive strength of the country is constantly increasing, and the speed of development is also increasing fast. However, under conditions of continuous development, the physical health of adolescents and children has not improved, the physical fitness of adolescents has declined, and many problems have appeared [1, 2]. According to the National Health Survey in recent years, we can see that the obesity rate of adolescents and adults has increased significantly, and more and more people are plagued by obesity [3]. At the same time, we can see from the data that the physical health problems of college students today are prominent, the physical fitness level of college students has dropped significantly, and the downward trend is more obvious. These problems deserve our attention [4]. College students are at the center of the youth group and account for a large proportion of the number of young people. The development of a country and the future are inseparable from the development of young people. Young people are a powerful driving force for the improvement of the country's comprehensive strength [5]. Therefore, a young person with

development potential should not only focus on cultivating good quality and achieving better results but also focus on cultivating a healthy body and a stable mental state. Only by combining these aspects will the future of young people be brighter, the development will be faster, and the strength will be stronger [6].

Through relevant data surveys, we can find that today's fitness system and health model have not received much attention. People use the Internet, high-tech digital systems, and intelligent related equipment to exercise and improve their own health [7]. The level of understanding of them is low, so sometimes you will encounter situations where you do not know how to train or what kind of exercise is suitable for you. Therefore, the effect of training is not very good, and the effect of physical exercise cannot be achieved. There are also people who suffer physical damage due to blind training and overtraining [8]. The sports training system is mainly composed of the central component of each equipment and the main part of each fitness method. The central component and related systems are connected using Internet technology, the central system is the main component, and the other fitness systems are supplemented [9]. Through the bottom-up data collection of each layer of the real situation, the final data collection can be achieved, and it can also be compared with historical data. The fitness system can also directly affect those who want to exercise [10].

2. Related Work

In the current era, people's physical health is getting less and less attention. The way people use the Internet, high-tech digital systems, and smart equipment to improve their health has not been popularized. There are also a series of problems, such as low level of understanding. In order to solve the above problems, literature successfully designed a green platform ITIHP that can exercise through the Internet and promote the health of the whole people through practical exploration [11]. This platform uses a Bluetooth system to connect fitness equipment and related systems through signal transmission so that while the machine is operating, it uploads the time and calories consumed by the person using it to the mobile phone or computer to achieve fitness, entertainment, and informationization, and there will be dedicated personnel to compare the information uploaded by people and the information of people's previous physical conditions [12]. Finally, according to each person's different physique and different situations, users will be provided with more personalized and accurate fitness plans and diet plans. Through further exploration, literature successfully designed a series of network intelligent digital collection systems, and this system is mainly used in gyms. It includes human body and mind perception system, network system capable of collecting data, data collection system, and comprehensive analysis application system [13]. The main function of the perception system is to measure the body-related conditions of the fitness person and the pressure that the body can bear [14]. The network system converts the obtained customer information into useful data, transmits it to the relevant computer server, and then transmits it to the staff after sorting. The application system is mainly for data storage and extraction functions [15]. Literature puts forward a problem that needs to be solved urgently. Nowadays, fitness equipment is relatively single, and users are not interested in using it. The newly designed fitness equipment combines modern high technology, which can first verify the user's identity and then provide a personalized mode. Since the new system combines the simulated reality technology, it can give users a better experience, so it is more attractive [16, 17]. The system can not only guide people's fitness methods but also record the data and results of people's exercise in real time, avoiding the disadvantage of poor communication with users and making fitness equipment more personalized and digitizing. We specifically use treadmills as an example. The treadmills under the new technology have added embedded technology, perception technology, and automatic collection technology, which can verify people's identities, collect statistics during and after exercise, make fitness distribution of functions between the equipment, fitness people, and fitness coaches more reasonable [18, 19], and increase the communication between the three to maximize advantages, diversify exercises, and make data more accurate.

3. Principle Analysis of Sports Training Safety System Based on Human Dynamics

3.1. Human Arm Motion Analysis. Bring the relevant position of the connecting rod into the formula established according to the coordinate system, and the transformation law can be obtained. The specific relation formula is as follows:

$$ {}_{i}^{i-1}T = Rot(z,\theta_i) \times \mathrm{Trans}(0,0,d_i) \times \mathrm{Trans}(a_i,0,0) \times Rot(x,a_i). \tag{1} $$

The specific explanation of the above formula is as follows:

$$ {}_{i}^{i-1}T = \begin{pmatrix} c\theta_i & -s\theta_i c\alpha_{i-1} & s\theta_i s\alpha_{i-1} & \alpha_{i-1}c\theta_i \\ s\theta_i & c\theta_i c\alpha_{i-1} & -c\theta_i\alpha_{i-1} & \alpha_{i-1}s\theta_i \\ 0 & s\alpha_{i-1} & c\alpha_{i-1} & d_i \\ 0 & 0 & 0 & 1 \end{pmatrix}. \tag{2} $$

In order to study the impact of the sports training system on people, we need to introduce the D-H model to calculate the transformation law between the human arm joints and the joints. We bring the relevant collected human arm joint change data into the following formula:

$$ {}^{R}TH = {}_{1}^{0}T \times {}_{2}^{1}T. \tag{3} $$

The specific calculation process of the above formula is as follows:

$$ \begin{cases} {}_{1}^{0}T = Rot(Z_1,\theta_1)\mathrm{Trans}(l_1,0,0) \\ {}_{2}^{1}T = Rot(Z_2,\theta_2)\mathrm{Trans}(l_2,0,0). \end{cases} \tag{4} $$

When we perform shoulder-related exercises, the most commonly used sports equipment is the shoulder press. When people use this type of exercise equipment to

exercise, their arm movements are carried out on a relatively inclined horizontal surface, including up and down or back and forth, two modes of exercise. Combining the above conditions, we need to fix the positions of the two rods. If in the coordinate system we have established, where people are located is the origin of the coordinate system, when the inclination of the arm and the ground is 30 degrees, we can bring relevant data into the formula to observe the result:

$$\text{basel} = \text{Trams}(0, 0.22, 1.1) * Rot\left(x, \frac{-65}{180\pi}\right)$$

$${}^{R}TH = \begin{bmatrix} c_1c_2 & -s_1s_2 & 0 & l_2c_1c_2 + l_1c_1 \\ 0.42s_1s_2 & 0.42c_1c_2 & 0.91 & 0.42l_2s_1s_2 + 0.42l_1s_1 + 0.22 \\ -0.91s_1s_2 & -0.91s_1s_2 & 0.42 & 1.1 - 0.91l_2s_1s_2 \\ 0 & 0 & 0 & 1 \end{bmatrix}. \tag{5}$$

The real data obtained in the coordinate system is

$$\begin{aligned} {}^{R}TH &= \text{base} \times {}_1^0T \times {}_2^1T = Rot(Z_1, \theta_1) \\ &\text{Trans}(l_1, 0, 0) Rot(Z_2, \theta_2) \text{Trans}(l_2, 0, 0). \end{aligned} \tag{6}$$

Bring the relevant data into the DH system to get smaller data:

$${}^{R}TH = \begin{bmatrix} c_{12} & -s_{12} & 0 & 0.24c_{12} + 0.31c_1 \\ 0.42s_{12} & 0.42c_{12} & 0.91 & 0.22 + 0.1s_{12} + 0.13s_1 \\ -0.91s_{12} & -0.91c_{12} & 0.42 & 1.1 - 0.28s_1 - 0.21s_{12} \\ 0 & 0 & 0 & 1 \end{bmatrix}$$

$$\text{among} \begin{cases} c_1 = \cos\theta_1, & s_1 = \sin\theta_1, \\ c_2 = \cos\theta_2, & s_2 = \sin\theta_2. \end{cases} \tag{7}$$

Since the shelf of the referral equipment can only be composed of one component, we can only build a change matrix. Of course, we still have to calculate on the basis of the DH system, so we can describe the motion formula of the relevant machinery as

$${}^{R}Th' = {}_1^0T = Rot(z_3, \theta_3) \text{Trans}(l_3, 0, 0). \tag{8}$$

Next, we need to bring in more specific relevant data to verify the hypothesis. First, we need to make a plan to specify the length of the mechanical lever and ensure that the human arm joints and the mechanical level are consistent so that they are in the same coordinate experiment under the department. At this time, we record the coordinates of the lever. But it is also worth noting that when people use shoulder presses to exercise, the direction of the arm force is not parallel to the plane, but in an inclined state, the angle of inclination is about 25 degrees, so we must also include the rotation angle, so we can combine the data in the shoulder pusher coordinate system with the original data and then convert the specific steps as follows:

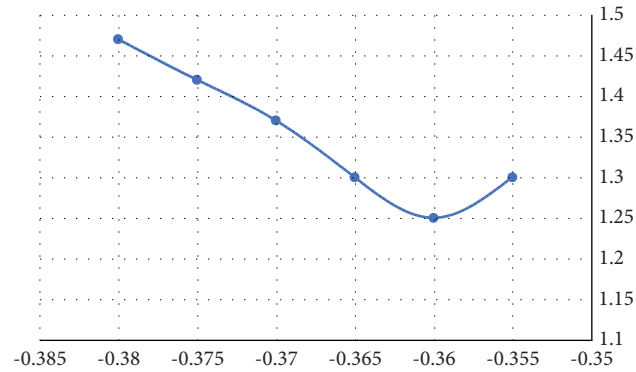

Figure 1: Recommended end space displacement curve.

$$\text{base} = \text{Trans}(-1.5, 0.168, 1.29) * Rot\left(x, \frac{-69}{180\pi}\right). \tag{9}$$

Next, get a more specific formula:

$${}^{R}Th' = \text{base} \cdot A_3 = \text{base} \cdot Rot(z_3, \theta_3) \text{Trans}(l_3, 0, 0),$$

$${}^{R}TH' = \begin{bmatrix} c_3 & -s_3 & 0 & l_3c_3 - 1.5 \\ 0.36s_3 & 0.36c_3 & 0.93 & 0.36l_3s_3 + 0.17 \\ -0.93s_3 & -0.93c_3 & 0.36 & 1.3 - 0.93l_3s_3 \\ 0 & 0 & 0 & 1 \end{bmatrix}. \tag{10}$$

Bring in

$${}^{R}TH' = \begin{bmatrix} c_3 & -s_3 & 0 & -1.5 + 1.1c_3 \\ 0.36s_3 & 0.36c_3 & 0.93 & 0.17 + 0.41s_3 \\ -0.93s_3 & -0.93c_3 & 0.36 & 1.3 - 1.1s_3 \\ 0 & 0 & 0 & 1 \end{bmatrix}. \tag{11}$$

We can make adjustments to relevant data, such as changing the angle at which the exercise equipment is placed or the angle when the human body moves, perform a more realistic measurement of the equipment, and finally get the end space displacement curve, as shown in Figure 1.

According to the angle that the human body and the machine can rotate when moving, we count the angle and the recording angle of each rotation of the machine lever device and input the relevant formula to obtain the rotation angle and the recording angle of the arm joint during the movement. Then, we calculate the difference between the two rotation angles and finally obtain the corresponding rotation speed of the human body joint. Then, we bring the data of the rotation angle of the human arm into the differential calculation so that we can get the specific situation of the change of the rotational acceleration of the arm joint. The specific data selection and experimental results change are shown in Figure 2. Figure 2(a) shows the angle of the joint, Figure 2(b) shows the angular velocity of the joint, and Figure 2(c) shows the angular acceleration of the joint.

3.2. Human Dynamics Analysis. If we decompose the weight of the human arm, the weight distribution of the front arm and the back arm of the human is the same, and we can record the relevant quality data as c_1 and c_2. The formula for calculating the mass of the forearm is as follows:

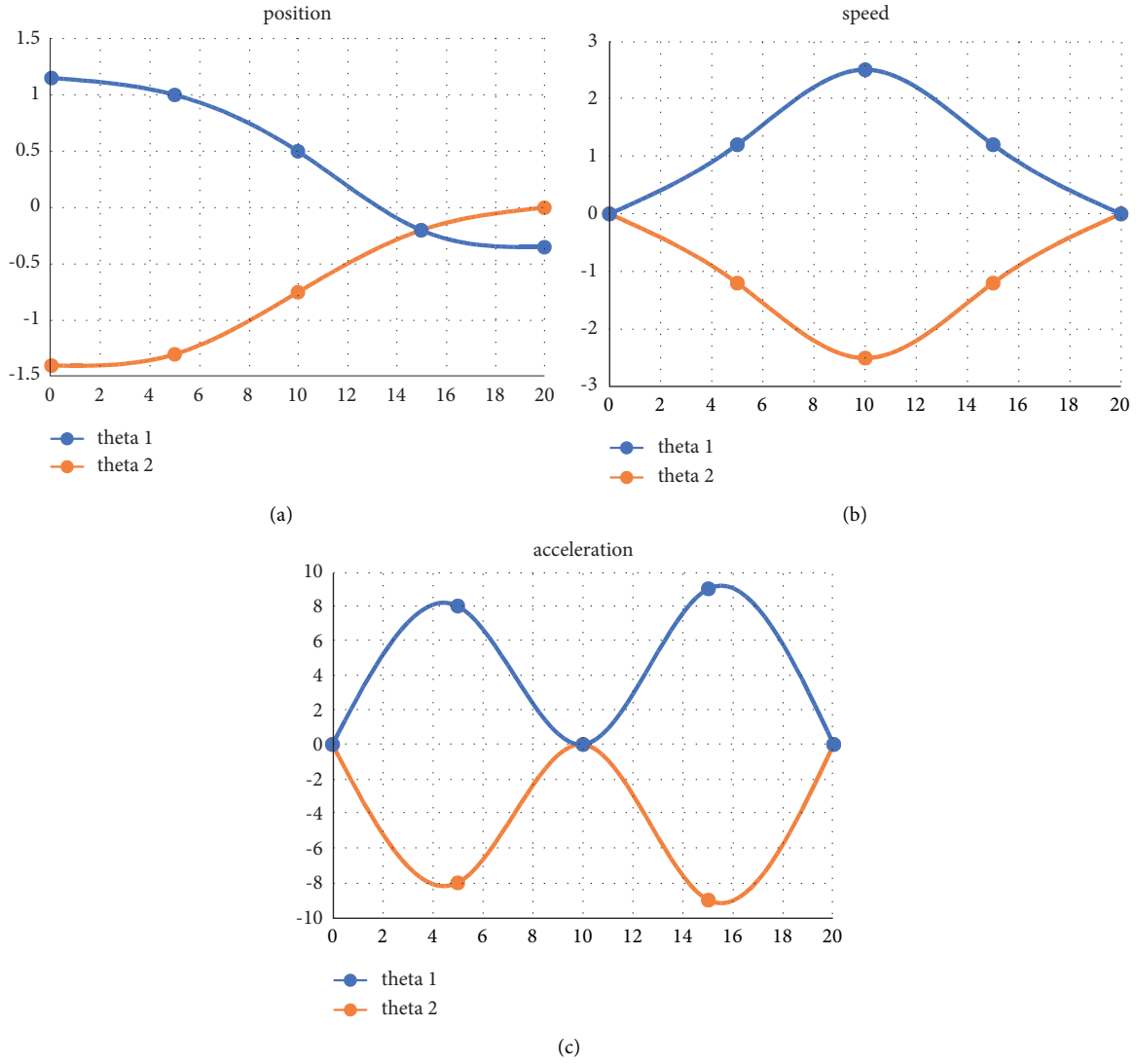

Figure 2: Arm joint motion curve.

$$c_1 = \begin{bmatrix} 0.5l_1 \cos\ \theta_1 \\ 0.5l_1 \sin\ \theta_1 \\ 0 \end{bmatrix}. \tag{12}$$

The mass calculation formula of the back arm is

$$c_2 = \begin{bmatrix} l_1 \cos\ \theta_1 + 0.5l_2 \cos(\theta_1 + \theta_2) \\ l_1 \sin\ \theta_1 + 0.5l_2 \sin(\theta_1 + \theta_2) \\ 0 \end{bmatrix}, \tag{13}$$

is calculated by

$$\dot{c}_1 = \begin{bmatrix} 0.5l_1\dot{\theta}_1 \sin\ \theta_1 \\ 0.5l_1\dot{\theta}_1\ \cos\ \theta_1 \\ 0 \end{bmatrix},$$

$$\dot{c}_2 = \begin{bmatrix} l_1\dot{\theta}_1\ \sin\ \theta_1 + 0.5l_2\left(\dot{\theta}_1 + \dot{\theta}_2\right)\sin(\theta_1 + \theta_2) \\ l_1\dot{\theta}_1\ \cos\ \theta_1 + 0.5l_2\left(\dot{\theta}_1 + \dot{\theta}_2\right)\cos(\theta_1 + \theta_2) \\ 0 \end{bmatrix}, \tag{14}$$

and followed by

$$\dot{c}_1 = \begin{bmatrix} -0.5l_1\left(\dot{\theta}_1 \sin\theta_1 + \dot{\theta}_1^2 \cos\theta_1\right) \\ -0.5l_1\left(\dot{\theta}_1 \cos\theta_1 + \dot{\theta}_1^2 \sin\theta_1\right) \\ 0 \end{bmatrix},$$

$$\ddot{c}_2 = \begin{bmatrix} -l_1\left(\ddot{\theta}_1 \sin\theta_1 + \dot{\theta}_1^{\,2} \cos\theta_1\right) - 0.5l_2\left\{\left(\ddot{\theta}_1 + \ddot{\theta}_2\right)\sin(\theta_1+\theta_2) + \left(\dot{\theta}_1 + \dot{\theta}_2\right)^2 \cos(\theta_1+\theta_2)\right\} \\ -l_1\left(\ddot{\theta}_1 \cos\theta_1 + \dot{\theta}_1^{\,2} \sin\theta_1\right) - 0.5l_2\left\{\left(\ddot{\theta}_1 + \ddot{\theta}_2\right)\cos(\theta_1+\theta_2) - \left(\dot{\theta}_1 + \dot{\theta}_2\right)^2 \sin(\theta_1+\theta_2)\right\} \\ 0 \end{bmatrix}. \tag{15}$$

The equation for calculating the force of the forearm is as follows:

$$\begin{aligned} f_{0.1} - f_{1,2} + f_1 &= m_1 \ddot{c}_1, \\ m_{0,1} + \frac{1}{2} f_{0,1} l_1 - m_{1,2} - \frac{1}{2} f_{1,2} l_1 &= I_{cI} e_I. \end{aligned} \tag{16}$$

The calculation equation about the force of the rear arm is as follows:

$$\begin{aligned} f_{1,2} - f + f_2 &= m_2 \ddot{c}_1, \\ m_{0,1} + \frac{1}{2} f_{0,1} l_1 - m_{1,2} - \frac{1}{2} f_{1,2} l_1 &= I_{cI} e_I. \end{aligned} \tag{17}$$

Among them,

$$\begin{cases} f_1 = \begin{bmatrix} 0 & m_1 g \cos\beta & 0 \end{bmatrix}^T \\ f_2 = \begin{bmatrix} 0 & m_2 g \cos\beta & 0 \end{bmatrix}^T \end{cases}, \quad \begin{cases} m_{0,1} = m_1 = \begin{bmatrix} 0 & 0 & m_{11} \end{bmatrix}^T \\ m_{1,2} = m_2 = \begin{bmatrix} 0 & 0 & m_{22} \end{bmatrix}^T \end{cases}, \tag{18}$$

which is substituted into

$$\begin{cases} m_2 = I_{c2}\varepsilon_2 - \frac{1}{2}\left(m_2 \ddot{c}_2 - m_2 g \cos\beta\right) l_2 + m, \\ m_1 = I_{c1}\varepsilon_1 - \frac{1}{2}\left(m_1 \ddot{c}_1 - m_1 g \cos\beta\right) l_1 + m_2. \end{cases} \tag{19}$$

Among them,

$$l_1 = \begin{bmatrix} l_1 \cos\theta_1 \\ l_1 \sin\theta_1 \\ 0 \end{bmatrix}, \quad l_2 = \begin{bmatrix} l_2 \cos(\theta_1+\theta_2) \\ l_2 \sin(\theta_1+\theta_2) \\ 0 \end{bmatrix}. \tag{20}$$

Combine the above formula to get

$$\begin{aligned} m_2 = \begin{bmatrix} 0 \\ 0 \\ m_{22} \end{bmatrix} &= \begin{bmatrix} I_{x2} & 0 & 0 \\ 0 & I_{y2} & 0 \\ 0 & 0 & I_{z2} \end{bmatrix} \begin{bmatrix} 0 \\ 0 \\ \ddot{\theta}_1 + \ddot{\theta}_2 \end{bmatrix} \\ &- \frac{1}{2} m_2 \begin{bmatrix} \ddot{c}_{2x} \\ \ddot{c}_{2y} - g\cos\beta \\ 0 \end{bmatrix} \times \begin{bmatrix} l_2 \cos(\theta_1+\theta_2) \\ l_2 \sin(\theta_1+\theta_2) \\ 0 \end{bmatrix} + \begin{bmatrix} 0 \\ 0 \\ m \end{bmatrix}, \\ m_1 = \begin{bmatrix} 0 \\ 0 \\ m_{11} \end{bmatrix} &= \begin{bmatrix} I_{x1} & 0 & 0 \\ 0 & I_{y1} & 0 \\ 0 & 0 & I_{z1} \end{bmatrix} \begin{bmatrix} 0 \\ 0 \\ \ddot{\theta}_1 \end{bmatrix} \\ &- \frac{1}{2} m_1 \begin{bmatrix} \ddot{c}_{1x} \\ \ddot{c}_{1y} - g\cos\beta \\ 0 \end{bmatrix} \times \begin{bmatrix} l_1 \cos\theta_1 \\ l_1 \sin\theta_1 \\ 0 \end{bmatrix} + \begin{bmatrix} 0 \\ 0 \\ m_{22} \end{bmatrix}. \end{aligned} \tag{21}$$

So the specific equation of Newton Euler about force is as follows:

$$
\begin{aligned}
m_{22} = {} & \ddot{\theta}_1 \left(l_{z2} + \frac{1}{4} m_2 l_2^2 + \frac{1}{2} m_2 l_1 l_2 \cos\ \theta_2 \right) \\
& + \ddot{\theta}_2 \left(l_{z2} + \frac{1}{4} m_2 l_2^2 \right) \\
& + \dot{\theta}_1^{\,2} \begin{bmatrix} \frac{1}{2} m_2 l_1 l_2 \sin\ \theta_2 + \\ \\ \frac{1}{2} m_2 l_2^2 \sin(\theta_1 + \theta_2) \cos(\theta_1 + \theta_2) \end{bmatrix} \\
& + \dot{\theta}_2^{\,2} \frac{1}{2} m_2 l_2^2 \sin(\theta_1 + \theta_2) \cos(\theta_1 + \theta_2) \\
& + \dot{\theta}_1 \dot{\theta}_2\ m_2 l_2^2 \sin(\theta_1 + \theta_2) \cos(\theta_1 + \theta_2) \\
& - \frac{1}{2} m_2 l_2 g\ \cos\ \beta\ \cos(\theta_1 + \theta_2) + m, \\
m_{11} = {} & \ddot{\theta}_1\ l_{z1} - \frac{1}{2} m_1 l_1 g\ \cos\ \beta\ \cos\ \theta_1 + m_{22}.
\end{aligned}
\tag{22}
$$

After we know the specific machine composition, machine state, machine rotation speed, and machine force, we will combine the data with the R system. The relationship between the specific machine angle and the machine force is shown in Figure 3.

3.3. Establish a Basic Exercise Prescription Generation Model. The relevant model designed in this experiment not only has the model foundation of the ordinary model but also makes relevant adjustments according to the development of the times. The main features are as follows.

The model used in this experiment is a model with a personalized design for people of different age groups and people with different physical conditions. According to the different characteristics of exercise intensity that children, youth, adults, and the elderly can withstand, the exercise methods we recommend for each type of people are also different, and the exercise effects that can be achieved are also different. For example, for younger children or older people, we should use a less-intensity mode to exercise their cardiorespiratory capacity, muscle endurance, or flexibility so as not to have a bad effect on their bodies; for people and adults, they can withstand greater intensity and can exercise for a longer time, so we can relatively increase their cardiorespiratory capacity, muscle endurance, or flexibility exercises so that their exercise can produce a good effect. In addition, we must pay more attention to the problems of the body itself; that is, for people with heart disease, asthma, and other diseases, their exercise style will be very different from the exercise style of ordinary people; otherwise, there will be very serious consequences, which may be life-threatening. Another point worthy of our attention is that although sports are good for people's bodies, we still have to consider people's subjective wishes and see where they want to perform specific exercises. For example, girls pay more attention to body shape adjustments, boys pay more attention

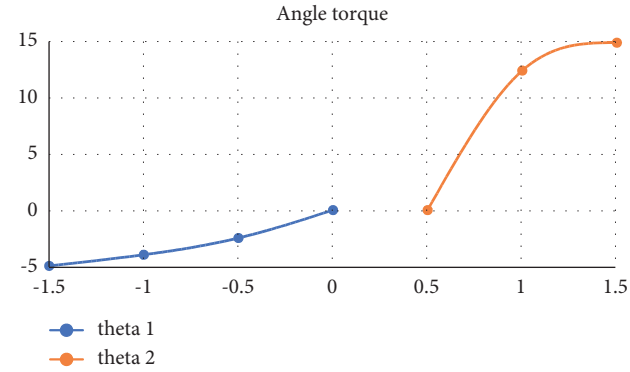

Figure 3: Joint angle-torque diagram.

to the strengthening of muscle strength, and some people exercise to increase lung capacity, so the exercise system must combine multiple aspects to plan the exercise mode.

The general exercise method has limitations. The exercise equipment is relatively single. During the exercise, we can only measure the amount that each person can do each time or each person per group, and the data collection is relatively incomplete. Under the new sports model design, we have added a new recording method to the original sports mode. We will check the speed of each exercise of each person, the highest point that the referral can reach, and the time between each referral or the exercise, monitor the heartbeat frequency and other aspects of the participants, and make relative adjustments to the planning of people of different ages, different physical conditions, and different exercise purposes.

During people's exercise, people's physical condition is not a static state but constantly changes with the time and frequency of the exercise and maintains a more continuous state during this exercise. Therefore, in the process of constant change, the new model can capture the changing process of people's bodies and make timely adjustments. The specific data to be referred to are as follows.

3.3.1. The Pressure on the Body during the Referral Process. In this experiment, we will use the most accurate RM system to represent the pressure that the body bears during the referral process. The pressure that each person's muscles can bear is different, and the maximum bearing capacity of each person's muscles is also different, so we have to collect the maximum number of times and the longest time that each person can exercise. For example, if the maximum weight recommended by a person is 30 kg, then the maximum strength recommended by him is 30 kg. These data correspond to each other. The specific data are shown in Table 1.

3.3.2. Maximum Referral Height. The measurement of the lifting height refers to a calculation method of how high people can lift equipment of different weights during the lifting exercise; that is, we need to focus on the movement process and distance of the equipment. We can divide the reference height into two categories: one is the height that can be reached each

Table 1: Different groups are suitable for exercise intensity.

Intensity selection	1-RM indicator	Suitable for the crowd	Effect
Larger-large	80%	Experienced exerciser	Power
Medium-large	60%–70%	Beginner	Power
Low-low	40%–50%	The elderly	Power
Low-medium	<50%		Endurance

time in the dynamic reference process, and the other is the maximum height that people can reach in the static time. Moreover, the arm length of people of different heights and genders is different, so the recommended height is also different. In the experiment, by analyzing the maximum value of the recommended height, we can get the relationship between it and the rotation angle of the motion machine, and finally, we can get the motion cycle data in real time.

3.3.3. Pushing Speed. In the process of exercise, we must pay attention to muscle stretching and contraction and pay attention to the time and frequency of exercise. When performing a press exercise, we should control the force used for the upward movement of the arm and the speed of the upward push, try to maintain a uniform speed with a relatively uniform time interval, and ensure smooth breathing. When exercising and pushing, every time we want to accelerate the exercise, we must first ensure a slow and uniform increase so that the muscles have a process of adaptation and also maintain a more stable state after acceleration. In the same way, every time we want to decelerate, we must first ensure that the speed is reduced slowly and uniformly so that the muscles have an adaptation process and also maintain a relatively stable state after deceleration so as to ensure that it will not be accelerated due to rapid acceleration or slow down and damage the muscle. For people who want to achieve different goals, the speed of the press is different. For those who pursue lung capacity exercise and muscular endurance exercise, we can reduce their press speed and then increase the number of presses, but for those who want to exercise muscle power of people, we can increase the speed of recommendation appropriately.

3.3.4. Recommended Interval. It is best to keep the interval within a few seconds.

3.3.5. Recommended Number. For those who want to improve muscle power, the number of recommendations can be increased to about 10 as a group. This type of data is suitable for young people and adults with better health, but for the elderly, it is too intense, and the referral is not suitable for them, so we can adopt a strengthening strength training program, control the number of each group to about 10, and increase the interval of referrals appropriately. If middle-aged and elderly people want to improve muscle endurance, you can increase the number of recommendations to no more than 20 and practice repeatedly on this basis. The number of suitable exercises for different groups is shown in Table 2.

3.3.6. Interval between Exercises. We can divide the interval of each group of exercises into two types: one is the longer rest time, which can control the rest time within 3–4 minutes, and the other is the shorter each group exercise interval mode. The rest time is controlled between 40 and 50 seconds. Choosing a suitable rest method and a more flexible rest time can strengthen muscle training and improve the effect of exercise.

3.3.7. Number of Recommended Groups. According to the relevant standards set by the country, we can strengthen training for adults and young people with better physical conditions. They can set the number of referrals to more than two groups, but it is best not to exceed four groups, and the intensity and speed of the referrals should not be too strong; for middle-aged and elderly people with relatively poor physical conditions and people who have just started to involve this exercise method, the number of referrals needs to be controlled within one group.

3.3.8. Training Frequency. In accordance with relevant national standards, we suggest that ordinary people should be able to set aside 1–3 days a week for physical exercise and at least one set of recommended exercises each time. If people need to do multiple press exercises in a day, the interval between two consecutive press exercises should not be less than 9 hours, and the muscles should be fully relaxed; otherwise, it will cause damage to the body. After several weeks of exercise, you can record your exercise results and compare with the previous data to see if there is a better and more suitable training method.

4. Sports Training Safety System Design Based on Embedded Software System and Internet of Things

4.1. System Overall Design. The method used in this experiment to collect data is mainly to use the monitoring system to collect exercise data in the gym. Different types of fitness equipment have different monitoring methods, which has changed the single type and relatively boring mode of the previous fitness equipment. Equipment is more carefully divided into two types: aerobic and anaerobic. Regarding aerobic equipment, its main function is to reduce fat, reduce weight, shape the body, and exercise lung capacity. Common equipment includes spinning and treadmills. As for anaerobic exercise, its main function is to increase muscle endurance, explosive power, and so on. The main types are barbells, dumbbells, and so on, which mainly exercise

Table 2: Number of suitable exercises for different groups.

Number of single group recommendations	People suitable	Effect
8–12	Adult	Strength and explosiveness
10–15	The elderly	Power
15–20		Endurance

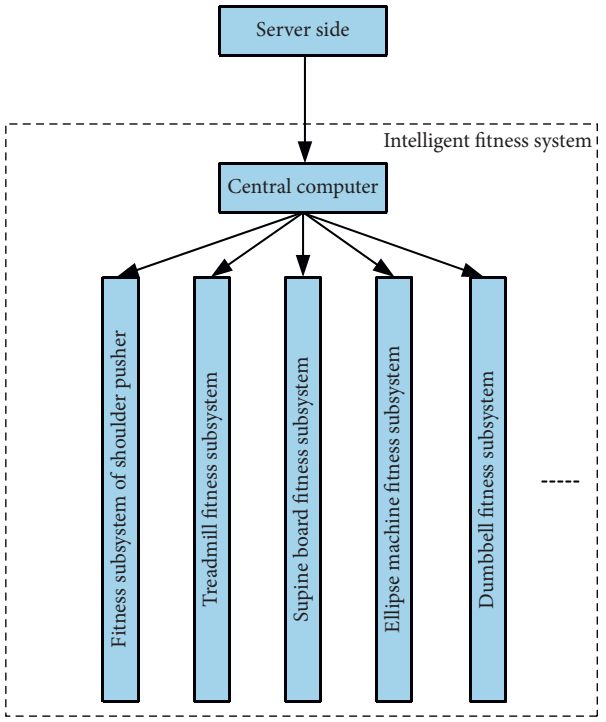

Figure 4: Overall system structure.

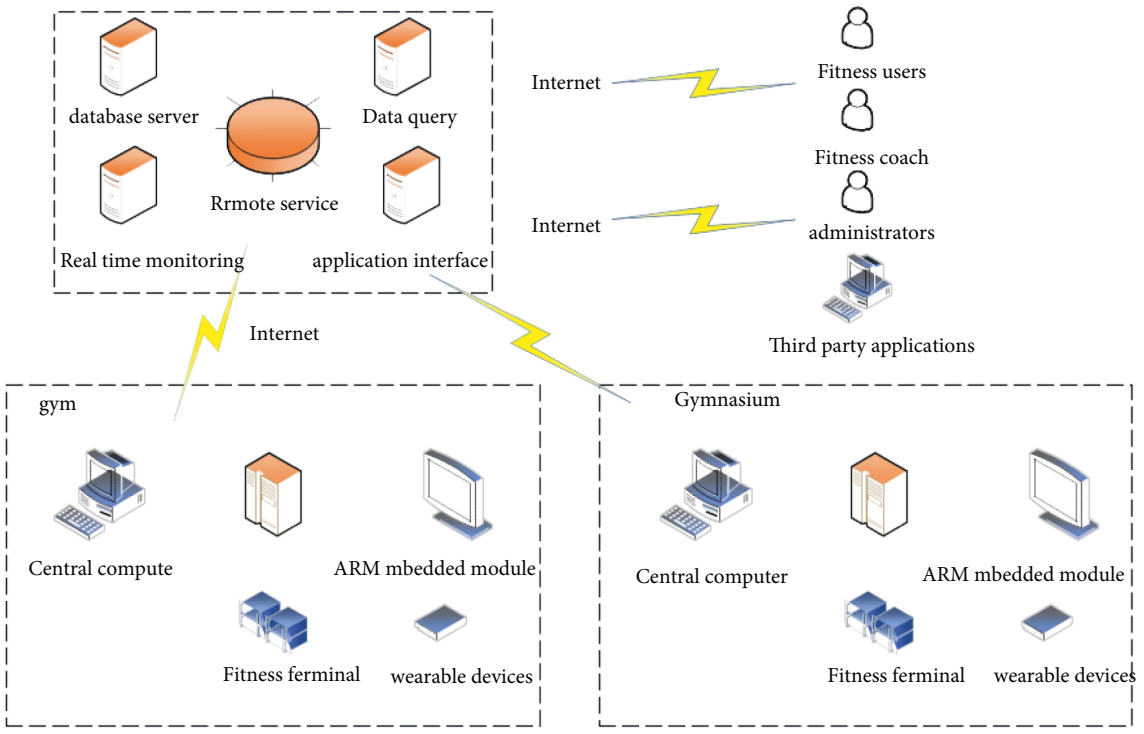

Figure 5: Network topology diagram.

Table 3: Main features of several communication methods.

Types	ZigBee	Bluetooth	WiFi	Z-wave
Distance	10∽100 m	10 cm∽10 m	50∽100 m	30∽100 m
Transfer speed	250 kbits	1 Mbps	1∽11 Mbps	9.6/40 kbits
Working frequency	2.4–2.483 GHz	2.4 GHZ	2.4 GHZ	908.42 MHZ
Network time	10–30 ms	3∽10 s	0∽3s	10–30 ms
Number of nodes	255/65535	7	32	255/65535
Power consumption	Lowest	Lower	High	Very low

various parts of the body such as thighs, buttocks, and biceps.

The sports training system used in this experiment is a system that combines a variety of smart devices, which is both personalized and targeted and can make people feel interesting; the specific components of the sports training system built through the server are as shown in Figure 4.

When we apply the above training system to our lives, we will use related intelligent tracking modes to monitor people's movement patterns and processes. The model connects the relevant equipment with the central processor through the network transmission system and then realizes the data transmission through the relevant website or platform. Use the Bluetooth system to connect the fitness equipment to the relevant system so that the machine can operate, and at the same time, it can also be used to upload people's exercise time, calories consumed, and other related data to the mobile phone or computer, and special personnel will conduct a comparative investigation on the information uploaded by people and finally provide users with more personalized and accurate fitness programs and diet programs according to each person's different physiques and different situations. The network topology is shown in Figure 5.

The main communication methods are shown in Table 3.

4.2. Functional Analysis of Embedded Software System and Internet of Things. The main function of the software is to combine the relevant data of the human body with the relevant data of the sports equipment and quickly process and calculate. The function of this mode can be related to the following aspects: the human body produces data during the exercise; data is constantly changing; especially after strenuous exercise, our body is actually in a relatively fragile state. When the body is relatively tired, the rate of change of human body data will be faster, so we have to beat the human heart. The changes in data such as speed and vital capacity are very concerned because these data can show people's physical condition. The most important data is the change in the heart rate. If the heart rate recovers faster after strenuous exercise, it means that the human body has better physical health and stronger cardiopulmonary function. On the contrary, if the recovery speed of the heart rate is slow after strenuous exercise, it means that the body's physical fitness is poor and the cardiopulmonary function is weak. Therefore, monitoring the data generated by the human body during people's exercise is very important to judge the performance of the human body.

4.3. System Hardware Design. After we have completed the design of various systems and functions, the ultimate goal is to apply them on the campus of the university to have a positive impact on the health of students. We install a chip with countless transmission systems in the student's campus card. This chip is small in size, high in transmission efficiency, and easy to carry by students. Therefore, when each student holds the campus card, the related equipment in the campus card will be signal linked with the equipment installed in the school. This mode is wireless, which is very convenient and fast. In this way, we can collect the identity information and money storage status of the campus card through the web server. When the student ID is displayed on the computer screen, it proves that the student has swiped the card successfully.

4.4. Database Design. The software of the lower computer uses wireless technology to transmit various data. The main function of the upper computer software is to integrate and analyze the data transmitted to each other and then upload the data to the relevant website, and students can check it by themselves.

The database includes the following information:.

(1) User-related information, such as name, gender, height, and weight. User information form is shown in Table 4.

(2) Related information generated when the user exercises, such as data generated by raising or lowering the arm. User exercise record is shown in Table 5.

(3) What is the effect produced by the user during the exercise, such as the force required to raise or lower the arm, and the overall effect after the completion of the press exercise. Exercise effect evaluation form is shown in Table 6.

5. Sports Training Safety System Test and Result Analysis

5.1. Lower Computer Installation and Performance Test. Design specific hardware facilities according to relevant data, and the bottom PCB design of the data acquisition terminal is shown in Figure 6. Top PCB design drawing of data acquisition terminal is shown in Figure 7.

We will take a school in a certain place as an example to practice the experimental model designed above and then see how effective it is. First, after the students have created their own accounts, they enter the correct user name and

Table 4: User information form.

UserTable		
Field name	Type of data	Length
Account ID	char	10
Name	char	10
Gender	char	1
Age	char	1
Height	char	1
Body weight	char	1
Boom size	char	1
Forearm size	char	1
Past medical history	mediumtext	

Table 5: User exercise record table.

Field name	Type of data	Length
Account ID	char	10
Store ID	Int	4
Date	timestamp	
Movement data of left arm up	mediumtext	
Left arm stay motion data	mediumtext	
Lower left arm movement data	mediumtext	
Right arm up exercise data	mediumtext	
Right arm stay motion data	mediumtext	
Lower right arm movement data	mediumtext	

Table 6: Exercise effect evaluation form.

EffectTable		
Field name	Type of data	Length
Account ID	char	10
Store ID	Int	4
Date	timestamp	10–30
Evaluation of the effect of raising the left arm	decimal	10–30
Evaluation of the effect of left arm stay	decimal	10–30
Evaluation of the effect of lowering the left arm	decimal	10–30
Evaluation of the effect of raising the right arm	decimal	10–30
Evaluation of the effect of right arm stay	decimal	10–30
Evaluation of the effect of lowering the right arm	decimal	10–30
Overall evaluation	decimal	10–30

password to enter the corresponding interface, where they can formulate their own sports mode and sports goals according to their own situation, and they can receive the administrator-related notices, some practical health recommendations, and so on; the system can monitor the students' exercise and avoid cheating. If students forget their account or password, they can log on to the relevant website to retrieve it, which is simple and convenient.

Secondly, after we let the teacher create his own account, they enter the correct user name and password to enter the corresponding interface and check the student's movement through related functions.

Finally, the students created their own accounts. After entering the correct user name and password to enter the corresponding interface, they can view the schedule of each sports course and choose the course they like.

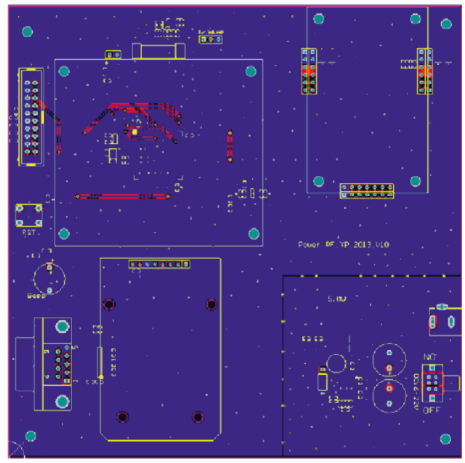

Figure 6: The bottom PCB design of the data acquisition terminal.

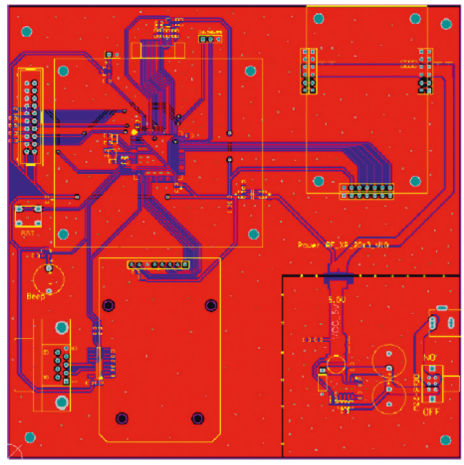

Figure 7: Top PCB design drawing of data acquisition terminal.

5.2. Analysis of Test Results. Through specific practice in a school in a certain area, we can know that the accuracy of the data is high, the network signal is better, the data transmission speed is faster, and the transmission distance is longer, which can cover the entire campus. After about 5 months of practical testing in a school in a certain area, no obvious problems were found. The information collection and network transmission functions are good, and the students' evaluation is high.

6. Conclusion

In the era of rapid development of the Internet, intelligent technology has become a part of our life and has been applied to many fields; now, there are more and more high-tech emerging and developing; this paper mainly uses the embedded software to model the sports training system and studies the development of its security performance. We use the Internet to collect a large number of data and then

compare them with the traditional sports equipment data; we found that the new system is more personalized and professional and has scientific outstanding advantages and found out the shortcomings of the traditional mechanical equipment to avoid a similar situation in the new model. We have also independently established a wireless network signal enhancement system to ensure the real-time data collection and transmission and ensure that, even in the case of bad weather, our signal remains in a relatively stable state, without information loss and signal interruption. We have also installed and tested the system. Before the system is installed, we need to plan the installation plan and carry out a series of tests at the set point to test the ideal distance between the two points and the packet loss rate. After finding a good point, the whole system is installed to simulate the normal operation state, and the students will test it, including the system pressure test. For the upper computer, it also needs a large amount of access data to test the pressure of the web page. Before the system is officially put into use, it has been running in the school for five days. According to the student visits and the running status of the website, it evaluates the whole background server and analyzes the reasons.

Data Availability

The data used to support the findings of this study can be obtained from the corresponding author upon request.

Conflicts of Interest

The authors declare that they have no conflicts of interest.

References

[1] P. Patalay and S. H. Gage, "Changes in millennial adolescent mental health and health-related behaviours over 10 years: a population cohort comparison study," *International Journal of Epidemiology*, vol. 48, no. 5, pp. 1650–1664, 2019.

[2] P. Patalay and E. Fitzsimons, "Development and predictors of mental ill-health and wellbeing from childhood to adolescence," *Social Psychiatry and Psychiatric Epidemiology*, vol. 53, no. 12, pp. 1311–1323, 2018.

[3] J. P. Sekhobo, L. S. Edmunds, D. K. Reynolds, K. Dalenius, and A. Sharma, "Trends in prevalence of obesity and overweight among children enrolled in the New York state WIC program, 2002–2007," *Public Health Reports*, vol. 125, no. 2, pp. 218–224, 2010.

[4] T. J. Cole, M. C. Bellizzi, K. M. Flegal, and W. H. Dietz, "Establishing a standard definition for child overweight and obesity worldwide: international survey," *British Medical Journal*, vol. 320, no. 7244, pp. 1240–1243, 2000.

[5] B. Balkau and M. A. Charles, "Comment on the provisional report from the WHO consultation. European group for the study of insulin resistance (EGIR)," *Diabetic Medicine: A Journal of the British Diabetic Association*, vol. 16, no. 5, pp. 442-443, 1999.

[6] H. Liu, Y. Zhang, K. Lian, O. Sanjuán, and R. G. Crespo, "Health Care Data Analysis and Visualization Using Interactive Data Exploration for Sports Person," *Sciece China. Information Sciences*, vol. 65, pp. 1–25, 2021.

[7] N. J. Simkiss, N. S. Gray, G. Malone, A. Kemp, and R. J. Snowden, "Improving mental health literacy in year 9 high school children across Wales: a protocol for a randomised control treatment trial (RCT) of a mental health literacy programme across an entire country," *BMC Public Health*, vol. 20, no. 1, pp. 727-728, 2020.

[8] V. Talasila, M. Mahadasyam, K. Madhubabu, N. Atchala, L. Kande, and L. Kande, "The prediction of diseases using rough set theory with recurrent neural network in big data analytics," *International Journal of Intelligent Engineering and Systems*, vol. 13, no. 5, pp. 10–18, 2020.

[9] H. Hu, Z. Liu, and J. An, "Mining mobile intelligence for wireless systems: a deep neural network approach," *IEEE Computational Intelligence Magazine*, vol. 15, no. 1, pp. 24–31, 2020.

[10] T. Wang, Y. Chen, M. Qiao, and H. Snoussi, "A fast and robust convolutional neural network-based defect detection model in product quality control," *International Journal of Advanced Manufacturing Technology*, vol. 94, no. 9-12, pp. 3465–3471, 2018.

[11] C. A. Emery, C. van den Berg, S. A. Richmond et al., "Implementing a junior high school-based programme to reduce sports injuries through neuromuscular training (iSPRINT): a cluster randomised controlled trial (RCT)," *British Journal of Sports Medicine*, vol. 54, no. 15, pp. 913–919, 2019.

[12] L. Shen, Q. Huang, Y. Zhai, Y. Qiu, and J. Liu, "Construction of data remote monitoring and auditing system for clinical trials, " Zhejiang Da Xue Xue Bao," *Journal of Zhejiang University Medical Sciences*, vol. 49, no. 4, pp. 531–536, 2020.

[13] S. J. McLaren, T. W. Macpherson, A. J. Coutts, C. Hurst, I. R. Spears, and M. Weston, "The relationships between internal and external measures of training load and intensity in team sports: a meta-analysis," *Sports Medicine*, vol. 48, no. 3, pp. 641–658, 2018.

[14] A. Nässi, A. Ferrauti, T. Meyer, M. Pfeiffer, and M. Kellmann, "Psychological tools used for monitoring training responses of athletes," *Performance Enhancement & Health*, vol. 5, no. 4, pp. 125–133, 2017.

[15] W. Xu, "Toward human-centered AI: centered AI: a perspective from human-computer interaction," *Interactions*, vol. 26, no. 4, pp. 42–46, 2019.

[16] T. Guzsvinecz, V. Szucs, and C. Sik-Lanyi, "Suitability of the Kinect sensor and leap motion controller-a literature review," *Sensors*, vol. 19, no. 5, Article ID 1072, 2019.

[17] K. H. Behr and P. L. Kuhn, "Key factors in career development and transitions in German elite combat sport athletes," *Martial Arts Studies*, vol. 8, pp. 19–35, 2019.

[18] Z. Wang, Z. Zhou, H. Zhang, G. Zhang, H. Ding, and A. Farouk, "AI-based cloud-edge-device collaboration in 6G space-air-ground integrated power IoT," *IEEE Wireless Communications*, vol. 29, no. 1, pp. 16–23, 2022.

[19] D. Li, C. Yi, and Y. Gu, "Research on college physical education and sports training based on virtual reality technology," *Mathematical Problems in Engineering*, vol. 2021, Article ID 6625529, 8 pages, 2021.

Hindawi
Mobile Information Systems
Volume 2022, Article ID 6177427, 13 pages
https://doi.org/10.1155/2022/6177427

Research Article

Sentiment Classification of Educational Tourism Reviews Based on Parallel CNN and LSTM with Attention Mechanism

Ying Wang,[1,2] **Chengxi Chu**,[3] **and Tian Lan**[4,5]

[1]*Tourism College, Sichuan University, Chengdu, Sichuan 610064, China*
[2]*The Engineering & Technical College of Chengdu University of Technology, Leshan, Sichuan 614000, China*
[3]*Faculty of Electrical Engineering and Computer Science, Ningbo University, Ningbo, Zhejiang 315201, China*
[4]*College of Art and Design, Changchun University of Technology, Changchun, Jilin 130000, China*
[5]*College of Management, Shih Chien University, Taibei 10462, Taiwan*

Correspondence should be addressed to Ying Wang; wy808212@163.com

Received 18 May 2022; Revised 13 July 2022; Accepted 4 August 2022; Published 9 September 2022

Academic Editor: Shadi Aljawarneh

With the rapid development of the Internet and tourism, the Internet has been widely used in the tourism industry. Tourism enterprises and tourists use the Internet to publish and obtain travel-related information. Educational tourism is a new type of tourism activity. As a combination of "tourism + education," it has gradually attracted the attention of tourists. With its convenience, fast speed, and low barrier, tourism text data provide great convenience for tourists' sentiment calculation and have become one of the main sources of big data for tourism. However, the reviews of educational tourism have a lot of redundant information and complex sentence patterns, leading to a relatively low classification accuracy of the existing sentiment analysis algorithms. In order to effectively obtain the implicit semantic information of short text reviews for sentiment orientation recognition, a sentiment classification model for educational tourism online reviews based on parallel CNN and LSTM with multichannel attention mechanism is proposed. Firstly, Word2Vec technique is used, and based on noise word filtering, the feature words of educational tourism reviews are extracted to preprocess the input data set. Then, parallel CNN and LSTM are used to extract text local information and contextual features, and a multichannel attention mechanism is used to extract the attention values from the LSTM output. Finally, the output information of the multichannel attention mechanism is fused to effectively extract text features and focus on important words. The experimental results show that compared with other advanced methods, the proposed algorithm achieves improvements in terms of precision, recall, and $F1$ value and improves the AUC performance. It will help the educational tourism bases to carry out targeted development and construction in response to tourists feedback, enhance the sense of gain and happiness of tourists in educational tourism activities, improve tourism experience, and promote the rapid development of high-quality educational tourism.

1. Introduction

"Big data" refers to massive amounts of information and data. Tourism big data are data generated by tourism practitioners and tourists, including data generated by tourist attractions, hotels, travel agencies, and tour operators as well as data in other fields related to tourism, such as economic data and traffic data [1]. Among them, the data generated by tourists have the greatest application value [2]. Tourism big data come from a wide range of sources. Through the mining of tourism big data, information with research value related to tourism flow, tourism economy, and tourism resources can be obtained. The wide application of big data creates opportunities for the development of experiential tourism [3]. Sentiments are the attitudes and experiences that people have about whether objective things meet their needs. Tourist sentiments refer to the pleasure, excitement, sadness, anger, regret, and other emotional experiences of tourists who are influenced by personal factors or external environment in tourism activities and whether the tourism activities meet the basic needs and social needs of individuals. Therefore, the sentiments of

tourists are diverse and volatile [4]. These sentiments not only constitute an important travel experience for tourists but also have an important impact on travel motivation, satisfaction, behavioral intentions, and interpersonal interactions [5]. During travel, tourists obtain information and share their travel experiences through online platforms and social media. The texts, images, audios, and videos uploaded by tourists have become the main data sources of tourism big data. Among them, the text content has the advantages of convenience, simplicity, intuitiveness, and fast speed with a low barrier for entry, which provides convenience for tourists to express their emotions and exchange information, and occupies an increasingly important position in tourism big data [6]. Through the mining of text data, it can provide decision support for tourism planning and marketing, making sentiment analysis in tourism big data a hot issue in the field of tourism research [7, 8].

As a combination of "tourism + education," educational tourism combines tourism resources with quality education and has become a new star in today's global tourism development. Educational tourism is a comprehensive tourism product developed based on certain tourism resources. Compared with general tourism products, it has the characteristics of rich connotation, wide-ranging category, and strong comprehensiveness. The development of educational tourism helps to integrate local tourism resources, promote the optimal combination of tourism products, the transformation and upgrading of tourism formats, and the comprehensive development of tourism destinations, which is bound to promote and deepen the development of all-for-one tourism [9].

The emotional tendency of educational tourism review information is an important basis for travel planning of tourists [10]. In recent years, the research on sentiment analysis in the field of tourism is not deep enough, and a lot of works focus on online product reviews, movie reviews, short texts on social media, etc., without considering the characteristics of educational tourism texts themselves. Educational tourism texts usually include multiple indicators such as scenery, ticket prices, accommodation quality, services, and interests. The complexity and diversity of texts lead to inefficiencies and misclassification of existing algorithms, making it difficult for tourists to obtain effective information [11].

Educational tourism base is the basis for carrying out educational tourism, and the Internet is an important medium for tourists to search for information [12]. In this paper, through the sentiment analysis of educational tourism reviews, it can be determined that whether the educational needs of tourists have been met. On the one hand, it is helpful to understand the changing laws of the tourist source market, and then, it can provide guidance and assistance for the development and construction, marketing management, and actual passenger flow forecasting of the educational tourism base. On the other hand, it is beneficial to grasp the supply and demand relationship between the actual development of the educational tourism base and the needs of tourists and lay the foundation for optimizing its spatial structure. By analyzing the characteristics of online reviews of educational tourism bases, the types of educational tourism bases that are popular with tourists can be concluded. In response to these analysis results, the educational tourism bases can make accurate and timely response measures to the actual passenger flow and provide tourists with high-quality tourism services. In addition, it can also enrich the types of educational tourism bases in the future base construction, in order to enhance people's sense of acquisition and happiness in tourism activities, improve tourism experience, and promote the rapid development of high-quality tourism [13].

In this paper, a large-scale data set of educational tourism reviews is constructed, and a sentiment classification model for educational tourism reviews based on the multichannel attention mechanism of convolutional neural network (CNN) and long short-term memory (LSTM) is proposed. In the proposed model, CNN can effectively extract local key information when extracting features. Compared with RNN, LSTM can process long text more effectively, alleviate the gradient problem, and can better extract contextual semantic information. The attention mechanism can focus on words that have a greater impact on the final result by setting different weights. As a result, the sentiment classification performance of educational tourism reviews can be further improved, and the most critical and valuable information in text information can be fully utilized. The main contributions of this paper are listed as follows:

(1) Using word embedding technique to train word embedding to represent text information as a low-dimensional dense matrix; a method for extracting feature words of educational tourism reviews based on noise word filtering using Word2Vec is proposed, which fully considers contextual semantic information, and can further improve the performance of feature word extraction. By classifying the sentiments of educational tourism reviews at the level of educational tourism characteristics, it is beneficial to analyze the sentiment tendencies of educational tourism.

(2) CNN and LSTM are used to extract text local information and contextual features, and the output information is used as the input of multichannel attention to extract attention scores.

(3) The output information of the multichannel attention model is fused to obtain the final text information vector representation, and then, the sentiment classification of educational tourism reviews is performed.

The proposed model makes full use of the advantages of CNN and LSTM to extract text features, and on this basis, a multichannel attention mechanism is introduced and different weights according to the impact of different words on the classification results are assigned so that words play different roles in classification tasks, thereby achieving the purpose of improving the classification performance of educational tourism reviews.

The rest of this paper is organized as follows. The related methods on the sentiment classification of educational tourism reviews are introduced in Section 2. The knowledge

background of educational tourism reviews is explained in Section 3. Section 4 describes in detail the proposed sentiment classification method for education tourism reviews based on CNN and LSTM-Attention. Section 5 presents the experimental results and discussions. Finally, Section 6 summarizes the full text.

2. Related Methods

Sentiment analysis aims to identify emotional tendencies through effective analysis and mining of information [14]. Medhat et al. [15] consider sentiment analysis as the focus of research in the field of text mining, that is, the computational processing of texts. The early sentiment analysis methods are mainly based on text data to perform sentiment calculation of word semantics and text sentiment calculation. With the deepening of research, sentiment analysis has become more refined, and researches such as sentiment calculator, sentiment summarization, and product attribute mining have appeared. In recent years, with the development of big data, researchers have proposed many sentiment analysis models and software, providing strong support for sentiment research [16].

Choi et al. [17] utilize text data to study the Macau tourism image and verified that text analysis methods can not only conduct qualitative research but also quantitative research. Govers et al. [18] adopt artificial neural network to analyze the text content related to the images of seven tourist destinations. Radojevic et al. [19] propose a sentiment analysis method based on more than 2 million online review data from more than 6,000 hotels in Europe and conclude that reviews are the most significant factor affecting hotel satisfaction.

Sentiment computing is the process of analyzing texts with emotions and classifying them into positive, negative, and other emotional types. If sentiment is divided into positive, neutral, and negative sentiment, then sentiment calculation is a classification problem; if sentiment is a specific numerical value or an ordered value in a given interval (such as 1–5 points), then sentiment values can be calculated by regression methods. Based on the granularity of text, sentiment computing can essentially be viewed as a multilevel hierarchy of words, phrases, sentences as well as articles. In the existing tourist sentiment research, high-frequency feature word statistics, content analysis software analysis, sentiment dictionary analysis, machine learning, and deep learning methods are mainly used to study the images of the destinations and the image differences of different destinations [20].

The methods based on content analysis software are based on the statistical method of high-frequency feature words and sentiment dictionary, and by writing logic codes, word segmentation, word frequency statistics, clustering, co-occurrence analysis, co-citation analysis, semantic network, co-occurrence analysis matrix, and other analysis methods are integrated into one software to realize the processing of texts. The commonly used software are CATPAC II, ICTCLAS, ROST, and so on. The sentiment lexicon analysis methods are mainly based on one or more dictionaries containing labeled sentiment words, sentiment phrases with corresponding intensities, combined with degree adverbs, negative words, conjunctions, and syntactic structures to construct sentiment computing models for sentiment analysis. Some researchers use machine learning to perform tourist sentiment calculations. A sentiment calculator is obtained by manually annotating a portion of texts that express positive or negative sentiments and training a machine learning algorithm with these texts. The sentiment calculator is used to perform positive and negative sentiment calculations on text data and finally gives a specific score of 0 or 1 or gives the positive and negative probabilities of the texts [21].

In machine learning research, methods such as logistic regression, decision tree, and support vector machine (SVM) are commonly used to perform sentiment analysis. The short text sentiment classification methods based on machine learning design features and use multiple classifiers for sentiment analysis. Based on the word collocation features of dependent syntax and the deep features of combined semantics, Li et al. [22] propose a semi-Markov conditional random field text sentiment analysis model with phrases as the main clue, which plays an important role in solving the problem of implicit sentiment analysis. Gurkhe et al. [23] propose a naive Bayesian sentiment classification algorithm based on the weight features of knowledge semantics, in which the features are fused into the Naive Bayes classifier based on the correlation between the dictionary polarity distribution information and document sentiment classification to improve the accuracy of document-level sentiment classification.

Kalaivani et al. [24] propose a generic algorithm that incorporates the information gain for feature selection and combined with KNN to improve sentiment classification performance. Li et al. [25] propose an SVM classifier based on multiple features and resources such as sentiment lexicon and word embedding. At the same time, an iterative method is used to assign different weights to the probability outputs, which improves the classification accuracy.

The above methods have achieved good sentiment classification results, but manual feature selection is a time-consuming and labor-intensive process. In recent years, with the rise and rapid development of deep learning techniques, these problems can be effectively solved. Deep learning methods use large-scale corpus to allow the model to actively learn the potential syntactic and semantic features in the text to achieve better understanding, effectively making up for the lack of artificial extraction features in information representation, thereby achieving better flexibility, robustness. Deep learning also has many applications in the field of short text processing. The convolution and pooling operations of CNN can be well applied to local feature extraction. Attardi et al. [26] use convolutional neural networks for sentiment classification and achieve good results on three-category data sets. Deriu et al. [27] exploit large amounts of data for remote supervision, train a convolutional neural network model, and combine it with a random forest classifier to optimize performance in polarity classification. Xu el al. [28] propose an LSTM neural network, by

introducing storage unit and gating mechanism to capture long-term dependencies in the sequence to decide how to use and update the information in the storage unit, and then obtain a more durable memory, expanding the advantages of deep computing. Tang et al. [29] adopt the LSTM model to combine target information, which significantly improves the accuracy of target-dependent sentiment analysis. Hao et al. [30] propose a novel sentiment-analysis model based on the parallel-CNN architecture which concatenates the representation of each segment to obtain the final representation of the text. Wang et al. [31] propose a regional CNN-LSTM model consisting of regional CNN and LSTM to predict the sentiments of texts. By combining the regional CNN and LSTM, both local information within sentences and long-distance dependency across sentences can be considered in the prediction process.

3. Research Background

3.1. Definition of Educational Tourism. Educational tourism originated in Japan after World War II and became popular in developed countries such as Europe and the United States in the 1970s. It is considered to be an important part of contemporary quality education. However, there is no unified concept at home and abroad, and scholars have three main views:

(1) Educational tourism refers to a tourism activity with students as the main body and education as the purpose. Prakapienė et al. [32] define educational tourism as a tourism product with students as the main body and the purpose of visiting educational institutions and learning knowledge. The development of educational tourism can not only broaden the horizons and increase skills but also strengthen the communication between teachers and students during the journey and increase the feelings of teachers and students.

(2) Educational tourism is a tourism activity characterized by "study as the mainstay and travel as the supplement." Tomasi et al. [33] describe educational tourism as tourists visiting and studying in historical sites, scientific research institutes, or well-known universities so as to improve cognition of the tourists.

(3) Educational tourism refers to the tourism activities in which tourists "promote their studies through travel and learn from each other." Hales et al. [34] take the meaning and purpose of tourism as the starting point and draw the conclusion that educational tourism relies on specific tourism resources, combining tourism products and education content to improve personal ability, learn knowledge, and achieve physical and mental cultivation.

According to the above different viewpoints, it can be seen that the concept of educational tourism can be divided into narrow and broad concepts. In a narrow sense, it specifically refers to tourism activities in which students are the main body of tourism, with the purpose of learning knowledge and cultivating skills. In a broad sense, educational tourism refers to tourism activities that rely on certain tourism resources to achieve the goal of education and study through tourism products; this study adopts the latter concept.

3.2. Educational Tourism Base. As a special tourism base, an educational tourism base must have certain tourism resources and at the same time provide a high level of comfort. As a learning place, it should have facilities to meet the teaching needs and be equipped with corresponding academic staff to complete the teaching tasks. According to the types of tourism resources that the educational tourism bases rely on, these bases can be divided into natural landscape educational tourism bases and human landscape educational tourism bases.

The former refers to understanding natural science and cultural knowledge while enjoying the natural scenery, such as Xishuangbanna Tropical Botanical Garden and Hexigten Global Geopark; the latter refers to understanding the history, culture, customs, literature, and art of the tourist destination during the tour, such as Xibaipo Memorial and Xuanzhi Culture Park.

3.3. Educational Tourism Review Data. In terms of data sources, this paper selects travel e-commerce websites and social platforms with abundant domestic travel reviews, including Baidu Travel.com, Qunar.com, Ctrip.com, and Sina Weibo. The web crawler tool is used to capture about 60,000 comments related to different educational tourism bases. For details, please refer to Section 5.2.

4. Sentiment Classification of Educational Tourism Reviews Based on CNN and LSTM-Attention

Both convolutional neural networks and long-short-term memory neural networks have their own advantages in sentiment classification tasks. CNN uses multiple convolution kernels to perform convolution operations on the word embedding of texts to effectively mine the potential semantic information of texts, while LSTM networks can better predict the semantics of text sequences. Combining these two types of neural networks, a neural network model based on CNN-LSTM-Attention is proposed. The structure is shown in Figure 1.

4.1. Word Embedding Layer Based on Word2Vec. Before the classification task, the text needs to be converted into a digital matrix that can be recognized by the computer and represented by a fixed-length real number. This representation is called word embedding. Early research mostly used one-hot encoding for conversion, representing each word as a digital matrix with corresponding dimensions according to the size of the vocabulary. Although this method can uniquely identify each word, it cannot reflect the correlation between words, and the dimension of the

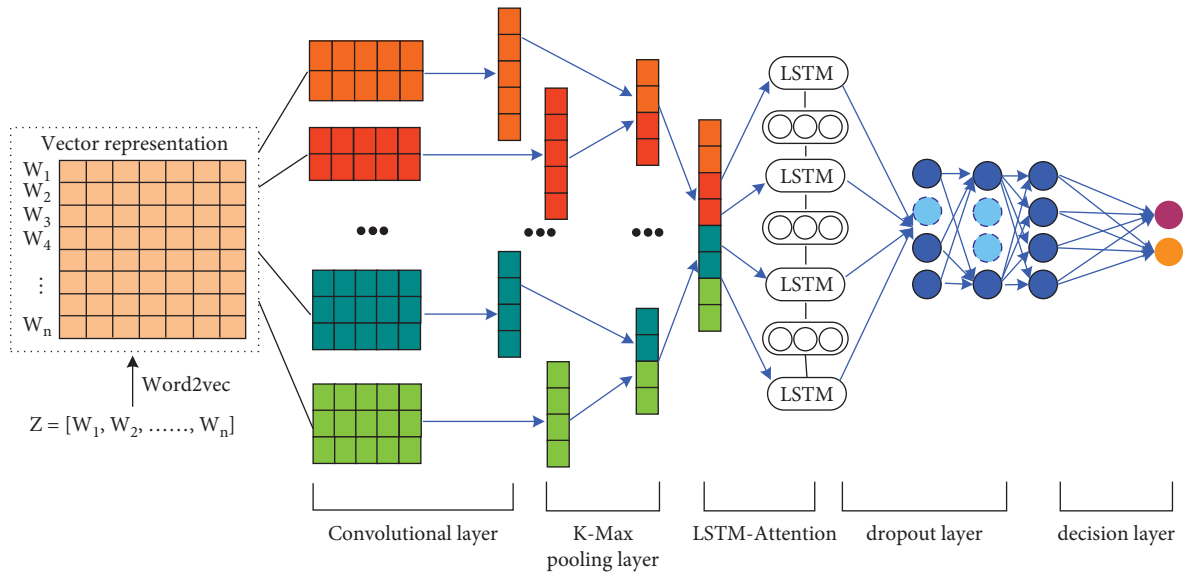

Figure 1: Sentiment classification model.

embedding is positively correlated with the size of the vocabulary, which can easily lead to the dimension disaster problem.

Word2Vec is a word semantic computing technique proposed by Google in 2013. Through Word2Vec training, the processing of text content can be simplified into vector operations in the K-dimensional vector space, and the similarity in the vector space can be used to represent the semantic similarity of the text. Word2Vec provides two classic language models for training: CBOW model and Skip-gram model. For these two models, Word2Vec gives two frameworks which are designed based on Hierarchical Softmax and Negative Sampling, respectively [35]. This paper adopts the Skip-gram model based on Hierarchical Softmax.

Hierarchical Softmax uses a Huffman tree structure to represent the words of the output layer, where the words of the output layer exist as leaf nodes, and each node represents the relative probability of its child nodes. In a Huffman tree, there is always an optimal path from the root node to each leaf node. The Skip-gram model consists of a three-layer network model, namely the input layer, the projection layer, and the output layer, as shown in Figure 2. The training goal of the Skip-gram model is to find word representations that help predict similar words in a sentence or document.

During the training process of Skip-gram, the conditional probability value of the intermediate word embedding W_t is used to solve the contextual word embedding, which can be calculated as

$$P(W_i|W_t) = \frac{P(W_t * W_i)}{P(W_t)}, \quad i = t-1, t-2, t+1, t+2. \tag{1}$$

Let the number of words in a sentence to be input into the model be N, and the two-dimensional matrix $\mathbf{Z} = [W_1, W_2, ..., W_n]$ is used to represent this text. After the

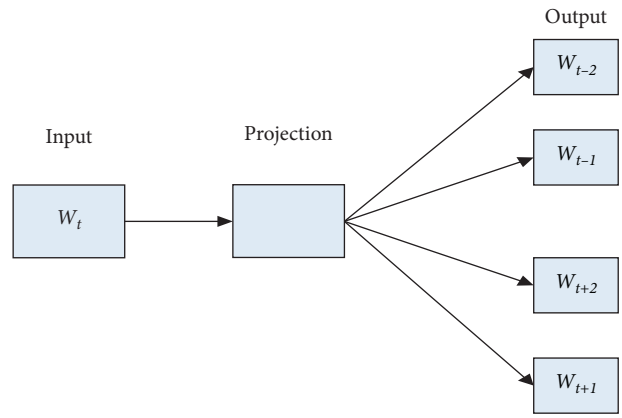

Figure 2: Skip-gram model structure.

word embedding layer, the text representation is converted into $\mathbf{X} = [x_1, x_2, ..., x_n]$, $x_i \in \mathbf{R}^d$, where d denotes the dimension of the word embedding.

4.2. CNN Layer. The CNN network consists of several convolutional layers, pooling layers, and fully connected layers, and it has strong feature extraction capabilities. By setting convolution kernels with different sizes, local key information can be effectively extracted, and then, the input feature map is compressed through the Pooling layer to make the feature map smaller and simplify the computational complexity of the network. Finally, all the features are connected by the fully connected layer, and the output values are sent to the classifier.

The main function of the convolution layer is to use the convolution kernels to perform convolution operations on the word embedding matrix from the input layer to obtain deeper text features. Each convolution kernel corresponds to the extraction of a certain part of the feature. In this paper, the number of convolution kernels is set to 128. The

following convolution operations are performed on each sentence matrix $\mathbf{X}$ output by the embedding layer:

$$\mathbf{S} = \zeta(\Omega\mathbf{X} + b), \tag{2}$$

where $\mathbf{S}$ represents the feature matrix extracted from the convolution operation; weight Ω and bias b are the learning parameters of the network. To facilitate computation, a nonlinear mapping of the convolution results of each convolution kernel is required:

$$\zeta = \text{relu} = \max(0, x), \tag{3}$$

where the relu function is one of the excitation functions commonly used in neural network models. In order to extract features more comprehensively, this paper simultaneously uses convolution windows of size 2 and 3 to extract binary features and triplet features of sentences, respectively.

The main function of the pooling layer is to perform feature selection and information filtering on the text embedding extracted by the convolutional layer, reduce the parameters and computation of the next layer while preserving the main features, and prevent overfitting. The K-Max pooling operation is used in this paper, which selects the Top-K maximal values of each filter to represent the semantic information of the corresponding filters. The expression for K value is

$$K = \lfloor \frac{l - \zeta_{\text{size}} + 1}{2} \rfloor, \tag{4}$$

where l is the length of the sentence vector, which is set to 50 in this paper. ζ_{size} is the convolution window size. After the pooling operation, the number of feature embedding extracted by each convolution kernel is significantly reduced, and the core semantic information of the sentence is retained.

Through the convolution operation and the pooling operation respectively, the convolutional layers and the pooling layers of CNN perform feature extraction on short text sentences and obtain the generalized binary and ternary feature vectors. After the fusion layer, the two types of feature vectors are merged together and used as the input matrix of LSTM-Attention.

4.3. LSTM-Attention Layer. LSTM is an improved version of RNN. By adding input gate i, forget gate f, output gate o, and internal memory unit c to neurons, it has more advantages in processing long sequences of text and alleviates the problems of gradient disappearance and explosion so that LSTM can extract textual context information more effectively than RNN. The input gate i controls how much of the input X_t of the network at the current moment is saved to the unit state C_t, the forget gate f determines how much of the unit state C_{t-1} at the previous moment is kept to the current moment C_t, and the output gate o controls how much of the unit state C_t is output to the current output value H_t of the LSTM. The model structure is shown in Figure 3.

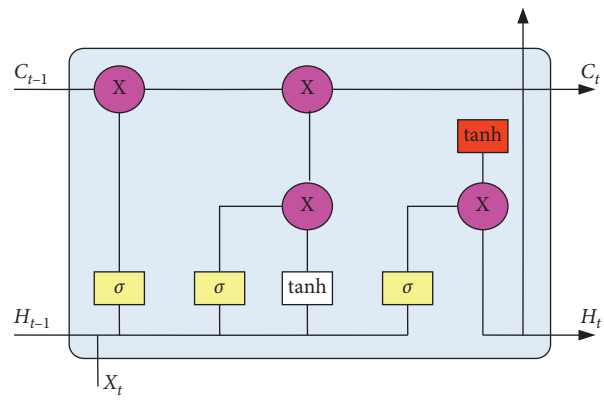

Figure 3: LSTM structure diagram.

When the input text word embedding matrix is $\mathbf{X} = [x_1, x_2, ..., x_k]$, the LSTM can be updated as

$$\begin{aligned} i_t &= \sigma(\Omega_i \cdot [H_{t-1}, x_t] + b_i), \\ o_t &= \sigma(\Omega_o \cdot [H_{t-1}, x_t] + b_o), \\ f_t &= \sigma(\Omega_f \cdot [H_{t-1}, x_f] + b_f), \\ C_t &= f_t \otimes C_{t-1} + i_i \otimes \tanh(\Omega_c \cdot [H_{t-1}, x_t] + b_c), \\ H_t &= o_t \otimes \tanh(C_t), \end{aligned} \tag{5}$$

where $\sigma(\cdot)$ denotes the Sigmoid activation function, $\tan h(\cdot)$ is the hyperbolic tangent function, Ω denotes the corresponding weight, b is the bias term, and H_t is the final output. The output H_t obtained by LSTM after extracting textual context information is used as the input of the multichannel attention mechanism, and the model structure is shown in Figure 4.

After H_t is processed by the LSTM-Attention model, the final vector $\mathbf{T}$ is obtained, which not only contains the textual context information but also focuses on important words, which better represents the semantic information. After that, the embedding matrix output by the LSTM-Attention model is input into the Dropout layer to prevent data overfitting. Then, the embedding matrix is input into the fully connected layer for dimensionality reduction. Finally, through the excitation function, the sentiment classification probability is obtained.

5. Experiments and Discussion

5.1. Experimental Environment. The experiments are performed on a computer running Windows 10 system with Intel i5-7400 CPU, the deep learning framework is TensorFlow 2.1.0, and Python 3.6.0 is used as the programming language. In order to better represent semantic information, Skip-gram is used to train word embedding, and CUDA10.1 is used for computational acceleration. The specific experimental environment is shown in Table 1.

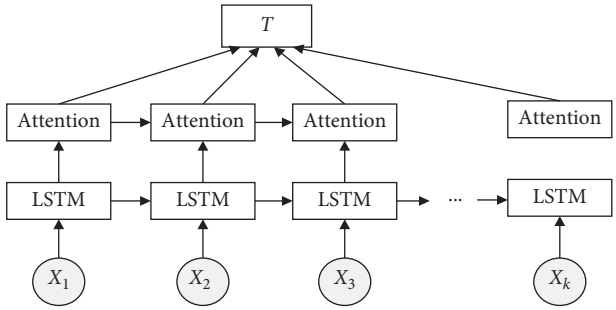

Figure 4: LSTM-Attention structure diagram.

Table 1: Experimental environment.

Parameters	Configuration
Operating system	Win 10
CPU	Intel (R) Core (TM) i5-7400 3.40 GHz
Memory	16 GB
Deep learning framework	TensorFlow 2.1.0
Word embedding training tool	Word2Vec (gensim 2.3.0)
Programming language	Python 3.6.0
CUDA version	10.1

5.2. Data Collection and Processing. In order to build a scientific tourist sentiment analysis model, it is necessary to have a data reference system that can be verified, and at the same time, an exclusive data set for educational tourism reviews should be established, and the factors of semantic logic and emotional expression tendencies should be considered. Eight educational tourism bases in China are selected as data collection points, namely Shanghai Science and Technology Museum, Chengdu Dujiangyan irrigation system, Shaanxi History Museum, Anyang Red flag canal, Chifeng Hexigten Global Geopark, Xuancheng City Chinese Xuanzhi Culture Park, Xishuangbanna Tropical Botanical Garden, and Shijiazhuang Xibaipo Memorial.

Details of data collection from several tourism bases in China are shown in Table 2. Firstly, some meaningless educational tourism reviews are cleaned, and finally, a total of 60,365 educational tourism reviews are obtained after filtering. Secondly, the jieba word segmentation package in the Python language is used to tokenize the review texts in the review set and label the parts of speech. Finally, based on the common stopword list, by performing word frequency statistics on the words in the educational tourism review set after word segmentation, and selecting words with high frequencies that have nothing to do with educational tourism characteristics and sentiments, a stopword list suitable for educational tourism reviews is constructed, and it is used to remove stopwords from the segmented data set. The educational tourism review data set collected in this paper can scientifically and comprehensively reflect the perceptions of tourists on tourism resources, products, and services. It contains objective reference data, with a certain scientific nature.

5.2.1. Feature Words of Educational Tourism Reviews. The preprocessed educational tourism review data set is used for the word embedding training corpus, and the build-in function in the Word2Vec library in the gensim package of the Python language is used to train the word embedding and build a word embedding model. The parameter settings of Word2Vec are shown in Table 3.

Firstly, the word frequency statistics analysis is performed on the nouns and noun phrases in the preprocessed educational tourism review data set, and the top 200 high-frequency nouns and noun phrases related to educational tourism features are extracted as initial feature words. Classify these feature words according to the categories of educational tourism features to form an initial feature word list. Secondly, the build-in function *most_similar*( ) of Word2Vec in the gensim package of the Python language is used to calculate the similarity between the nouns and noun phrases in the educational tourism review data set and the initial feature words. From the top 50 words with the highest similarities with the educational tourism feature words, the words that are truly related to the characteristics of educational tourism are selected to expand the initial feature word list; then, a noise word list is built on the basis of the feature word list.

With the help of the trained word embedding model, the feature words contained in each educational tourism review are extracted to form a list of feature words corresponding to the educational tourism review data set. Then, the noise word list is used to filter out the noise words in the educational tourism review feature word list to generate a noise-free feature word list.

In order to facilitate the comparative analysis with the existing feature word extraction methods, this paper adopts the precision (P_{extract}), the recall rate (R_{extract}), and the $F1$-score ($F1_{\text{extract}}$) as the evaluation metrics of the feature word extraction. P_{extract}, R_{extract}, and $F1_{\text{extract}}$ can be calculated as (6), where c_i denotes the feature word set extracted by the feature extraction method from the ith educational tourism review, d_i denotes the feature word set attached to the ith educational tourism review itself, and Q indicates the number of reviews in the educational tourism review set to be processed.

$$\begin{aligned} P_{\text{extract}} &= \frac{\sum_{i=1}^{M} |c_i \cap d_i| / |c_i|}{Q}, \\ R_{\text{extract}} &= \frac{\sum_{i=1}^{M} |c_i \cap d_i| / |d_i|}{Q}, \\ F1_{\text{extract}} &= \frac{2 \times P \times R}{P + R}. \end{aligned} \tag{6}$$

500 educational tourism reviews are selected from the data collection and are processed using the TF-IDF method [36], the TextRank method [37], and the proposed feature word extraction method, respectively, and the results are shown in Figures 5(a)–5(c). It can be seen from Figure 5 that when using the proposed extraction method for feature word extraction with settings, the precision (P_{extract}) and $F1$-score ($F1_{\text{extract}}$) are better than that of the TF-IDF method and Text Rank method. The recall rate (R_{extract}) is also on par with the TF-IDF method and the Text Rank method when the number of feature words is set to 8–10.

Table 2: Data collection from 8 educational tourism bases in China.

Educational tourism bases	Reviews	Positive words	Negative words
Shanghai science and technology museum	24,408	86,930	10,575
Dujiangyan irrigation system	6,889	25,340	4,019
Shaanxi history museum	2,638	9,654	1,379
Anyang red flag canal	918	3,491	475
Hexigten global geopark	6,567	24,078	3,192
Chinese Xuanzhi culture park	3,656	14,851	2,047
Xishuangbanna tropical botanical garden	6,284	23,606	3,850
Xibaipo memorial	9,005	39,832	6,298
Total	60,365	227,782	31,835

Table 3: Parameter setting in Word2Vec.

Parameters	Value
Algorithm	Skip-gram
Word embedding dimension	128
Minimum word frequency	3
Training window size	5
Parallel threads	4

Therefore, for short texts such as educational tourism reviews, the proposed feature extraction method based on noise vocabulary filtering is more effective than other methods.

5.3. Training Parameter Settings. Firstly, semantic segmentation is performed on each review in the educational tourism review set, then the segmented set is preprocessed and divided into three parts: training set, validation set, and test set according to the ratio of 6 : 2 : 2. The role of the training set is to fit the model and to train the classification model by setting the parameters of the classifier. The function of the validation set is to use the trained model to predict the validation set data, adjust the model parameters, and select the parameters corresponding to the model with the best performance. The role of the test set is to use the trained CNN-LSTM-Attention model to perform sentiment classification for educational tourism reviews.

In order to prevent the occurrence of overfitting, the Drop_out value is set to 0.5 in the CNN and LSTM network layers, and 50% of the neural units are randomly deactivated. Using the ReLu activation function can speed up the convergence speed and further prevent overfitting. The cross-entropy loss function commonly used in multiclassification tasks is adopted. The optimizer is Adam, the Batch_size is 256, and the Epoch is 10. The specific parameters are shown in Table 4.

5.4. Model Evaluation Metrics. Commonly used evaluation metrics for classification tasks including accuracy, precision, recall, and $F1$-score are used for the evaluation of the proposed model. Accuracy (Acc) represents the ratio of correctly predicted samples to the total samples, precision (Pre) represents the ratio of correctly predicted positive samples to all positive sample predictions, recall rate (Rec) represents the ratio of correctly predicted positive samples to all actual positive samples, FPR (False Positive rate) is the negative-positive rate, which represents the ratio of falsely predicted positive samples to all actual negative samples, and $F1$-score is the weighted harmonic mean of precision and recall rate. The confusion matrix is shown in Table 5, and the metrics can be calculated as

$$\begin{aligned} \text{Acc} &= \frac{\text{TP} + \text{FN}}{\text{TP} + \text{TN} + \text{FP} + \text{FN}}, \\ \text{Pre} &= \frac{\text{TP}}{\text{TP} + \text{FP}}, \\ \text{Rec} &= \frac{\text{TP}}{\text{TP} + \text{FN}}, \\ F1 &= \frac{2 \times \text{Pre} \times \text{Rec}}{\text{Pre} + \text{Rec}}, \\ \text{Fpr} &= \frac{\text{FP}}{\text{FP} + \text{TN}}, \end{aligned} \tag{7}$$

where TP is the number of positive samples correctly identified, TN is the number of negative samples correctly identified, FP is the number of positive samples incorrectly identified, and FN is the number of negative samples incorrectly identified.

The number of positive and negative samples in the experimental data set is unbalanced. The ROC curve is commonly used as the performance evaluation criterion to resolve the data imbalance problem, where Rec represents the vertical coordinates and Fpr represents the corresponding horizontal coordinates. By adjusting the threshold used in the classification of the classifier, a curve passing through points (0, 0) and (1, 1) will be obtained, that is, the ROC curve of this classifier. Usually, this curve should be above the line connecting (0, 0) and (1, 1). Because the ROC curve formed by the connection of (0, 0) and (1, 1) actually represents a random classifier, the area under the ROC curve is the AUC value, and the larger the AUC value, the better the classifier performance.

5.5. Sentiment Classification Results of Educational Tourism Reviews. In order to verify the prediction performance of the proposed model, the classical machine learning algorithms SVM [25], KNN [24], classical CNN algorithm [26], LSTM model [28], parallel CNN [30], and CNN + LSTM

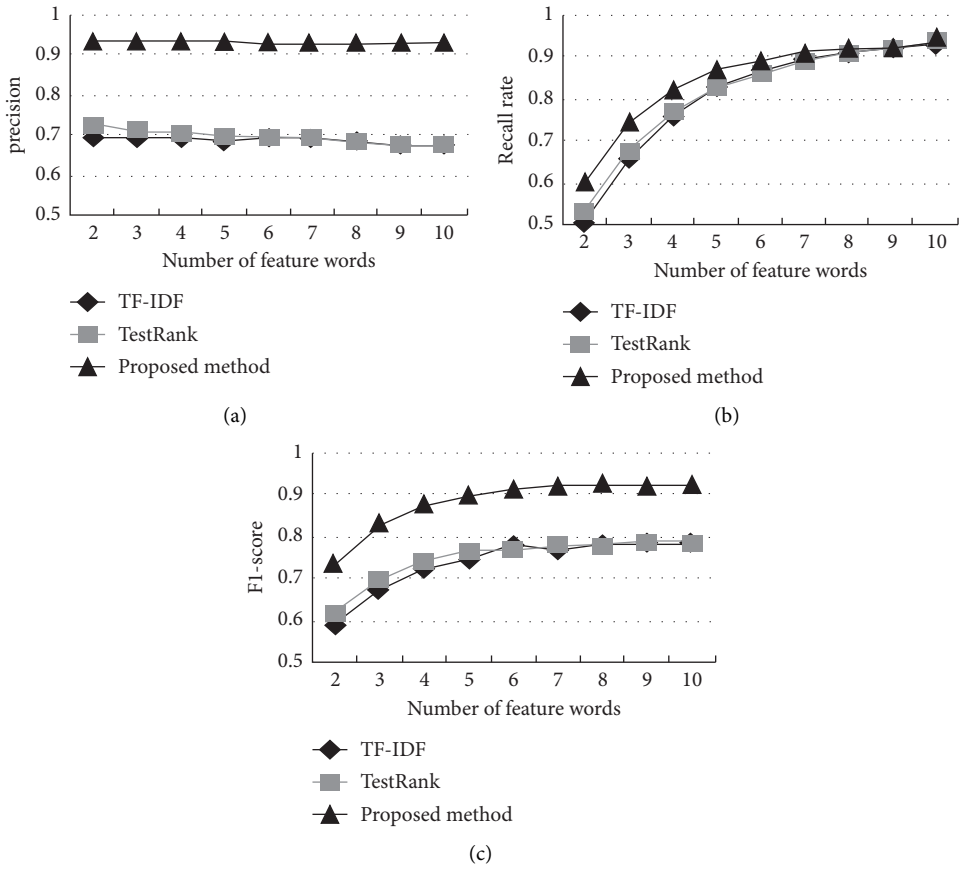

Figure 5: Comparison of feature word extraction. (a) Precision $P_{extract}$. (b) Recall rate $R_{extract}$. (c) $F1$-score $F1_{extract}$.

Table 4: Network parameters.

Network parameters	CNN	LSTM
Word embedding dimensions	256	256
Learning ratio	0.001	0.001
Kernel size	128	—
Convolution window size	2, 3	—
Hidden layers	—	256
Drop_out	0.5	0.5
Activation function	ReLU	ReLU

Table 5: Confusion matrix.

	Positive	Negative
True	True positive (TP)	True negative (TN)
False	False positive (FP)	False negative (FN)

Table 6: Comparison of sentiment classification results.

Model	Acc	Pre	Rec	$F1$
SVM [25]	55.88	55.14	55.92	55.60
KNN [24]	61.77	61.88	62.09	61.99
CNN [26]	81.77	81.01	81.62	81.11
LSTM [28]	83.95	83.97	84.12	83.36
Parallel CNN [30]	85.88	85.23	85.36	85.62
CNN + LSTM [31]	88.91	87.97	88.29	88.47
Proposed method	91.24	91.31	90.90	91.77

method [31] are compared with the proposed method under the same experimental environment. The results on the educational tourism reviews data set are provided in Table 6.

It can be seen from the table that the proposed model has the best performance on the experimental data set and greatly improves the performance of sentiment classification of educational tourism reviews. The conventional machine learning methods SVM and KNN have poor classification performance and are not suitable for the sentiment classification task of educational tourism reviews. CNN and LSTM methods achieve significantly better performance than machine learning methods. Compared with the CNN + LSTM model, the Acc, Pre, Rec, and $F1$ results of the proposed method are improved by 2.33%, 3.34%, 2.61%, and 3.3%, respectively. This is because the CNN-LSTM model uses a progressive structure. Although CNN can effectively extract local key information when extracting features, it will lead to the loss of some information. The semantic information extracted by CNN is incomplete when transmitted backwards. The proposed method not only extracts the local key information but also effectively extracts the context information. The information is complete when it is passed backwards, so the classification effect will be better. In addition, the proposed model introduces the Attention

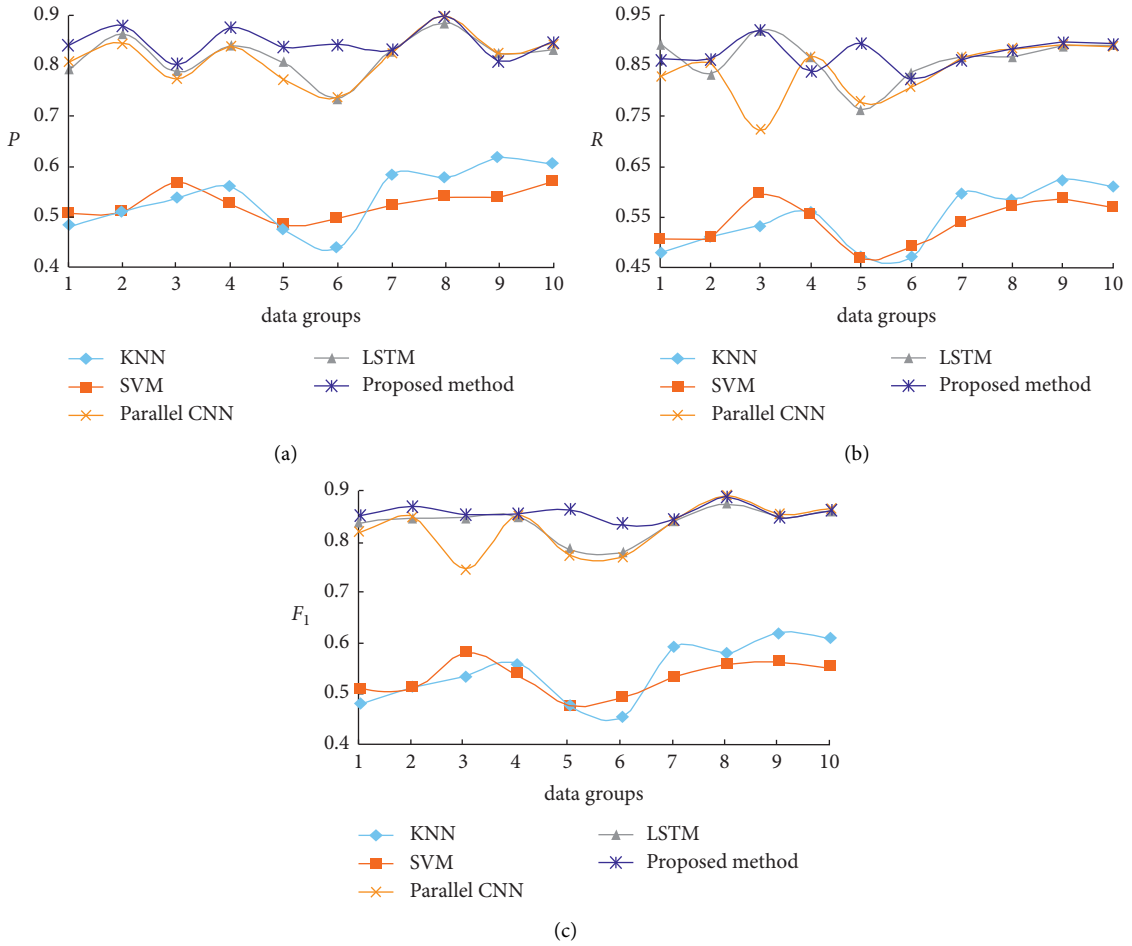

Figure 6: Performance comparison using different models. (a) Precision. (b) Recall rate. (c) $F1$-score.

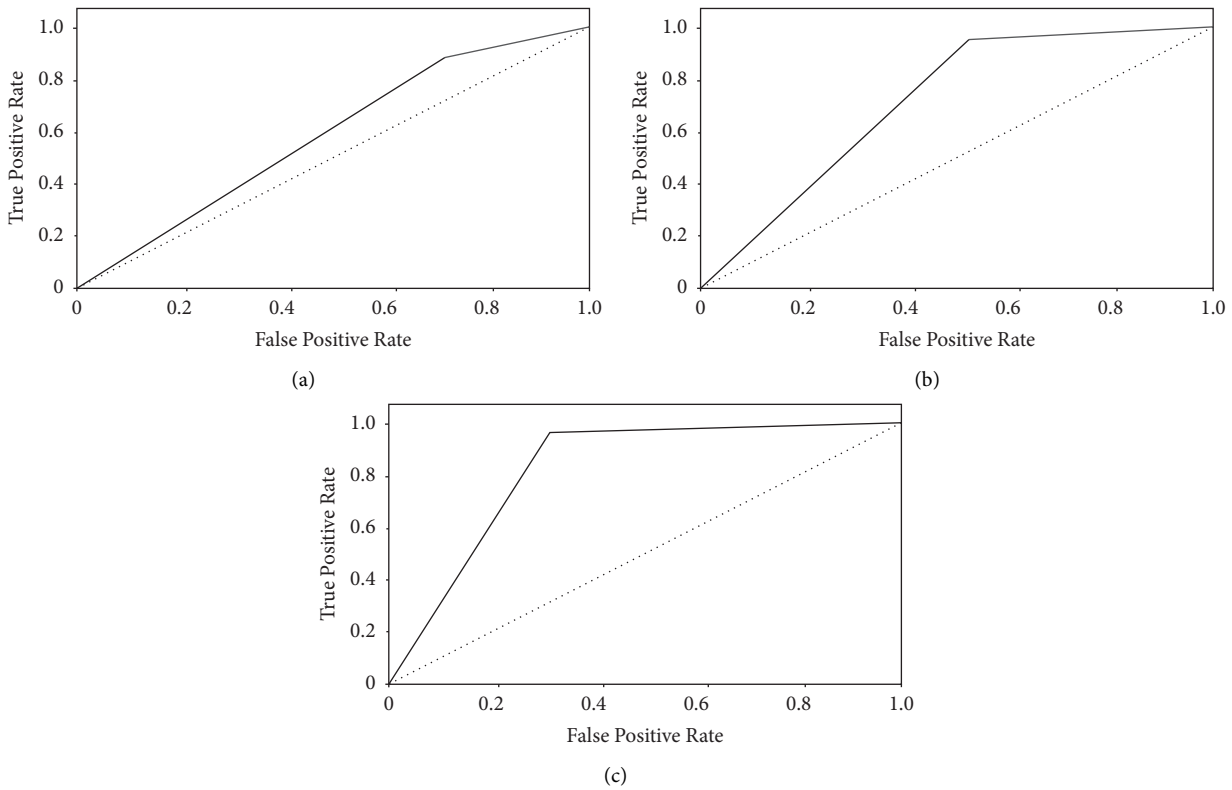

Figure 7: ROC results. (a) SVM, ROC curve (area = 0.61). (b) CNN, ROC curve (area = 0.72). (c) Proposed, ROC curve (area = 0.85).

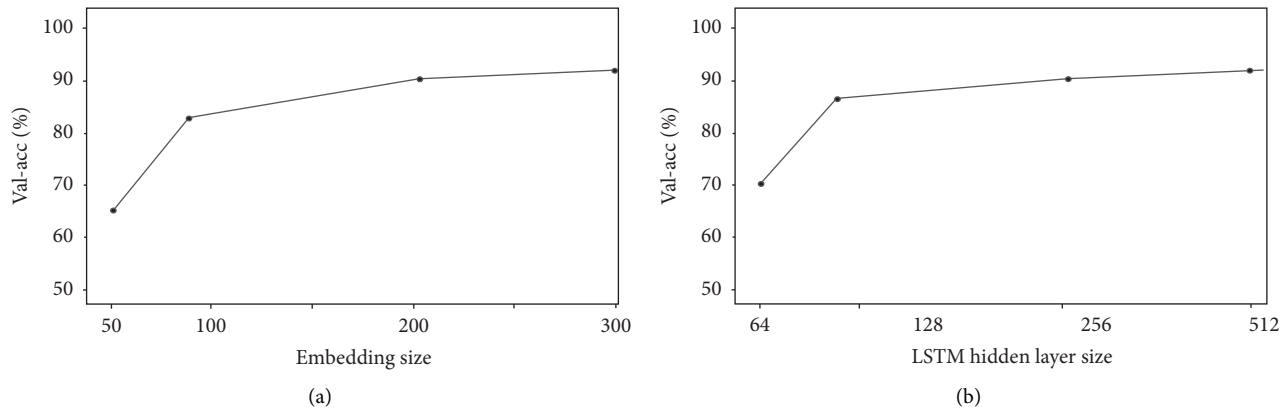

Figure 8: Hyperparameter analysis. (a) The experimental result when the embedding dimension is set to 50, 100, 200, and 300. (b) The experimental result when the number of LSTM hidden layers is set to 50, 100, 200, and 300.

mechanism on the basis of CNN + LSTM and assigns different weights to each word by calculating the attention score so that the words that have a greater impact on the classification result can be effectively identified, therefore obtaining significantly better classification performance than the CNN + LSTM model.

In order to further verify the effectiveness of the proposed model compared with common machine learning algorithms, basic neural network models LSTM, and parallel CNN models, a significance test experiment is designed. On the experimental data set, using word frequency as the feature, KNN classifier [24], SVM classifier [25], LSTM model [28], parallel CNN model [30], and the proposed model are used for 10-fold cross-validation, and the precision, recall rate, and $F1$-score are used for evaluation. The results are shown in Figure 6.

It can be seen from Figure 6 that for the experimental data set, when only word frequency is considered as features, the values of the three evaluation indicators obtained with the machine learning method KNN and SVM are mostly distributed between 0.5 and 0.7, and the performance is relatively low. The LSTM model and the parallel CNN model have better classification results, and the values of the three indicators are distributed between 0.7 and 0.9. The classification accuracy of the proposed model is better than the other four models, and the three evaluation index values are in the range of 0.8 to 0.9, which is significantly better than the classification results of KNN and SVM. The improvement in classification performance is also larger than that of the LSTM model and the parallel CNN model, and the proposed method achieves higher stability.

When using SVM [25], CNN [26], and the proposed method for sentiment classification of the educational tourism reviews, the ROC curves of each model are shown in Figure 7, where the corresponding AUC values are given.

As can be seen from Figure 7, the classification performance of the convolutional neural networks is better than the classical machine learning algorithm SVM. In deep learning, the quantity and quality of the data sets are the key factors for classification and discrimination. In the big data environment, the better the learning effect, the closer the classification results of the classifier will be to the ground truth.

In the proposed method, based on the convolutional neural network CNN, the features of the short comment text are extracted, and the convolution windows of different sizes are used to extract the binary features and triplet features of the sentences, respectively. The long- and short-term memory neural network LSTM combined with the attention mechanism is used to predict the sentimental tendency of the review texts, and finally, the outputs from CNN and LSTM are merged to realize the classification of positive and negative sentiments, thereby improving the classification performance. The experimental results verify the effectiveness of the proposed method.

5.6. Hyperparameter Analysis. The setting of hyperparameters has an important impact on the final experimental results. In order to further improve the performance of the proposed model, the embedding dimensions and the number of LSTM hidden layers are further explored. Keeping other hyperparameters unchanged, the embedding dimension is set to 50, 100, 200, and 300, and the experimental result is shown in Figure 8(a). In addition, set the number of LSTM hidden layers to 64, 128, 256, and 512 and keep other parameters unchanged. The result is shown in Figure 8(b).

It can be seen from Figure 8(a) that when the embedding dimension is 300, it is close to the optimal classification performance, but considering the model complexity and classification efficiency, this paper chooses to set the embedding dimensions to 256. It can be seen from Figure 8(b) that the classification performance of the proposed model on the experimental data set increases with the increase of the number of LSTM hidden layers. When the number of hidden layers is greater than 256, the growth rate slows down, and the classification performance when the number of hidden layers is 512 is close to that when the number of hidden layers is 256. This is because the number of words in the text of the experimental data set is large, and the increase in the number of hidden layers enables better extraction of semantic information. When the number of hidden layers is greater than the number of text words, the classification performance will decrease as the number of hidden layers increases. So, the number of LSTM hidden layers should be set to 256.

6. Conclusion

The educational tourism industry is gradually prospering. It is of great practical significance to provide accurate recommendations to tourists and to provide tourists' feedback to educational tourism bases. It is helpful to make full use of tourism resources, improve the protection of architectural facilities and relics, promote the development of scenic spots at different levels, enrich the types of educational tourism bases, and meet the diversified education and tourism needs of tourists. This paper proposes a text classification model with multichannel attention mechanism based on CNN and LSTM for the classification of educational tourism reviews. Firstly, the input text is represented as a low-dimensional dense word vector matrix with word embedding, then the local key information and contextual semantic information are extracted by CNN and LSTM, and the attention score of the output information of LSTM is extracted by the multichannel attention mechanism. Finally, the output information of the multichannel attention mechanism is fused, which realizes the effective extraction of text features and focuses on important words and improves the performance of text classification. Through comprehensive experiments, the advantages of the proposed model are further demonstrated by comparing with other models. Since most of the tourists gave positive reviews, there is an imbalance in the data set, resulting in a relatively low AUC value of the proposed model. In the future, we will focus on using an improved oversampling algorithm to improve the classification accuracy of minority samples.

Data Availability

The data used to support the findings of this study are included within the article.

Conflicts of Interest

The authors declare that there are no conflicts of interest regarding the publication of this paper.

References

[1] J. Li, L. Xu, L. Tang, S. Wang, and L. Li, "Big data in tourism research: a literature review," *Tourism Management*, vol. 68, pp. 301–323, 2018.

[2] Z. Xiang and D. R. Fesenmaier, "Big Data analytics, tourism design and smart tourism," in *Proceedings of the Analytics in Smart Tourism Design*, pp. 299–307, Springer, Cham, October 2017.

[3] M. Fuchs, W. Höpken, and M. Lexhagen, "Big data analytics for knowledge generation in tourism destinations – a case from Sweden," *Journal of Destination Marketing & Management*, vol. 3, no. 4, pp. 198–209, 2014.

[4] S. Hosany and G. Prayag, "Patterns of tourists' emotional responses, satisfaction, and intention to recommend," *Journal of Business Research*, vol. 66, no. 6, pp. 730–737, 2013.

[5] W. Chen, Z. Xu, X. Zheng, Q. Yu, and Y. Luo, "Research on sentiment classification of online travel review text," *Applied Sciences*, vol. 10, no. 15, p. 5275, 2020.

[6] A. R. Alaei, S. Becken, and B. Stantic, "Sentiment analysis in tourism: capitalizing on big data," *Journal of Travel Research*, vol. 58, no. 2, pp. 175–191, 2019.

[7] A. P. Kirilenko, S. O. Stepchenkova, H. Kim, and X. R. Li, "Automated sentiment analysis in tourism: comparison of approaches," *Journal of Travel Research*, vol. 57, no. 8, pp. 1012–1025, 2018.

[8] C. A. McGladdery and B. A. Lubbe, "Rethinking educational tourism: proposing a new model and future directions," *Tourism Review*, vol. 72, pp. 319–329, 2017.

[9] P. Williams, "Educational tourism: understanding the concept, recognising the value," *Tourism Insights*, 2010.

[10] N. L. Staus and J. H. Falk, "The role of emotion in ecotourism experiences," *International handbook on ecotourism*, p. 520, 2013.

[11] M. Afzaal, M. Usman, and A. Fong, "Tourism mobile app with aspect-based sentiment classification framework for tourist reviews," *IEEE Transactions on Consumer Electronics*, vol. 65, no. 2, pp. 233–242, 2019.

[12] A. M. Abubakar, B. H. T. Shneikat, and A. Oday, "Motivational factors for educational tourism: a case study in Northern Cyprus," *Tourism Management Perspectives*, vol. 11, pp. 58–62, 2014.

[13] A. Sharma, "Educational tourism: strategy for sustainable tourism development with reference of Hadauti and Shekhawati regions of Rajasthan, India," *Journal of Business Economics and Information Technology*, vol. 11, no. 4, pp. 1–12, 2015.

[14] G. Xu, Y. Meng, X. Qiu, Z. Yu, and X. Wu, "Sentiment analysis of comment texts based on BiLSTM," *IEEE Access*, vol. 7, pp. 51522–51532, 2019.

[15] W. Medhat, A. Hassan, and H. Korashy, "Sentiment analysis algorithms and applications: a survey," *Ain Shams Engineering Journal*, vol. 5, no. 4, pp. 1093–1113, 2014.

[16] M. V. Mäntylä, D. Graziotin, and M. Kuutila, "The evolution of sentiment analysis—a review of research topics, venues, and top cited papers," *Computer Science Review*, vol. 27, pp. 16–32, 2018.

[17] S. Choi, X. Y. Lehto, and A. M. Morrison, "Destination image representation on the web: content analysis of Macau travel related websites," *Tourism Management*, vol. 28, no. 1, pp. 118–129, 2007.

[18] R. Govers, F. M. Go, and K. Kumar, "Virtual destination image a new measurement approach," *Annals of Tourism Research*, vol. 34, no. 4, pp. 977–997, 2007.

[19] T. Radojevic, N. Stanisic, and N. Stanic, "Ensuring positive feedback: factors that influence customer satisfaction in the contemporary hospitality industry," *Tourism Management*, vol. 51, pp. 13–21, 2015.

[20] F. C. Manosso and T. C. Domareski Ruiz, "Using sentiment analysis in tourism research: a systematic, bibliometric, and integrative review," *Journal of Tourism Heritage & Services Marketing (JTHSM)*, vol. 7, no. 2, pp. 17–27, 2021.

[21] P. K. Jain, R. Pamula, and G. Srivastava, "A systematic literature review on machine learning applications for consumer sentiment analysis using online reviews," *Computer Science Review*, vol. 41, Article ID 100413, 2021.

[22] H. Li and W. Lu, "Learning latent sentiment scopes for entity-level sentiment analysis," *Thirty-First AAAI Conference on Artificial Intelligence*, vol. 31, 2017.

[23] D. Gurkhe, N. Pal, and R. Bhatia, "Effective sentiment analysis of social media datasets using Naive Bayesian classification," *International Journal of Computer Application*, vol. 975, no. 8887, p. 99, 2014.

[24] P. Kalaivani and K. L. Shunmuganathan, "An improved K-nearest-neighbor algorithm using genetic algorithm for sentiment classification," in *Proceedings of the 2014 International Conference on Circuits, Power and Computing Technologies [ICCPCT-2014]*, pp. 1647–1651, IEEE, Nagercoil, India, March 2014.

[25] P. Li, W. Xu, C. Ma, J. Sun, and Y. Yan, "Ioa: improving svm based sentiment classification through post processing," in *Proceedings of the 9th international workshop on semantic evaluation (SemEval 2015)*, pp. 545–550, Denver, Colorado, June 2015.

[26] A. Salinca, "Convolutional neural networks for sentiment classification on business reviews," 2017, https://arxiv.org/abs/1710.05978.

[27] J. Deriu, M. Gonzenbach, F. Uzdilli, A. Lucchi, V. D. Luca, and M. Jaggi, "Swisscheese at semeval-2016 task 4: sentiment classification using an ensemble of convolutional neural networks with distant supervision," in *Proceedings of the 10th international workshop on semantic evaluation*, pp. 1124–1128, San Diego, California, June 2016.

[28] J. Xu, D. Chen, and X. Qiu, "Cached long short-term memory neural networks for document-level sentiment classification," 2016, https://arxiv.org/abs/1610.04989.

[29] D. Tang, B. Qin, X. Feng, and T. Liu, "Effective LSTMs for target-dependent sentiment classification," 2015, https://arxiv.org/abs/1512.01100.

[30] Y. Hao, Q. Zheng, Y. Lan et al., "Improving Chinese Sentiment Analysis via Segmentation-Based Representation Using Parallel CNN," in *Proceedings of the International Conference on Advanced Data Mining and Applications*, pp. 668–680, Springer, Cham, October 2017.

[31] J. Wang, L. C. Yu, K. R. Lai, and X. Zhang, "Dimensional sentiment analysis using a regional CNN-LSTM model," in *Proceedings of the 54th annual meeting of the association for computational linguistics (volume 2: short papers)*, pp. 225–230, Berlin, Germany, August 2016.

[32] D. Prakapienė and L. Olberkytė, "Using educational tourism in geographical education," *Review of International Geographical Education Online*, vol. 3, no. 2, pp. 138–151, 2013.

[33] S. Tomasi, G. Paviotti, and A. Cavicchi, "Educational tourism and local development: the role of universities," *Sustainability*, vol. 12, no. 17, p. 6766, 2020.

[34] R. Hales and G. Jennings, "Transformation for sustainability: the role of complexity in tourism students' understanding of sustainable tourism," *Journal of Hospitality, Leisure, Sports and Tourism Education*, vol. 21, pp. 185–194, 2017.

[35] Y. Goldberg and O. Levy, "word2vec Explained: deriving Mikolov et al.'s negative-sampling word-embedding method," 2014, https://arxiv.org/abs/1402.3722.

[36] E. Haddi, X. Liu, and Y. Shi, "The role of text pre-processing in sentiment analysis," *Procedia Computer Science*, vol. 17, pp. 26–32, 2013.

[37] K. Ying, P. Jingchang, and W. Minglei, "Research on sentiment analysis of micro-blog's topic based on TextRank's abstract," in *Proceedings of the 2017 International Conference on Information Technology*, pp. 86–90, Singapore, December 2017.

Hindawi
Mobile Information Systems
Volume 2023, Article ID 9761629, 1 page
https://doi.org/10.1155/2023/9761629

Retraction

Retracted: Recommendation of Knowledge Graph Convolutional Networks Based on Multilayer BiLSTM and Self-Attention

Mobile Information Systems

Received 13 September 2023; Accepted 13 September 2023; Published 14 September 2023

This article has been retracted by Hindawi following an investigation undertaken by the publisher [1]. This investigation has uncovered evidence of one or more of the following indicators of systematic manipulation of the publication process:

(1) Discrepancies in scope

(2) Discrepancies in the description of the research reported

(3) Discrepancies between the availability of data and the research described

(4) Inappropriate citations

(5) Incoherent, meaningless and/or irrelevant content included in the article

(6) Peer-review manipulation

The presence of these indicators undermines our confidence in the integrity of the article's content and we cannot, therefore, vouch for its reliability. Please note that this notice is intended solely to alert readers that the content of this article is unreliable. We have not investigated whether authors were aware of or involved in the systematic manipulation of the publication process.

Wiley and Hindawi regrets that the usual quality checks did not identify these issues before publication and have since put additional measures in place to safeguard research integrity.

We wish to credit our own Research Integrity and Research Publishing teams and anonymous and named external researchers and research integrity experts for contributing to this investigation.

The corresponding author, as the representative of all authors, has been given the opportunity to register their agreement or disagreement to this retraction. We have kept a record of any response received.

References

[1] Y. Qiu, Y. Liu, Y. Tong, and X. Xiang, "Recommendation of Knowledge Graph Convolutional Networks Based on Multilayer BiLSTM and Self-Attention," *Mobile Information Systems*, vol. 2022, Article ID 8247846, 9 pages, 2022.

Hindawi
Mobile Information Systems
Volume 2022, Article ID 8247846, 9 pages
https://doi.org/10.1155/2022/8247846

Research Article

Recommendation of Knowledge Graph Convolutional Networks Based on Multilayer BiLSTM and Self-Attention

Yao Qiu, Yajie Liu, Ying Tong, and Xuyu Xiang

School of Computer and Information Engineering, Central South University of Forestry and Technology, Changsha, Hunan 410004, China

Correspondence should be addressed to Yao Qiu; 20191100317@csuft.edu.cn

Received 14 June 2022; Accepted 22 July 2022; Published 7 September 2022

Academic Editor: Shadi Aljawarneh

To solve the problems of cold start, sparse data, and poor recommendation performance in collaborative filtering recommendation, an end-to-end framework algorithm based on BiLSTM and BAGCN was proposed. In order to discover the higher-order structural information in the knowledge graph, stacked BiLSTM is used to extract the features of embedded entities and relationships, respectively, and the depth dependence features of user-item interaction matrix are mined. The neighborhood representation of each entity is then calculated by sampling adjacent entities of a fixed size. Then, the self-attention mechanism is used to learn the semantic association between entities and neighboring entities to obtain the final neighborhood information. Aggregators are used to combine neighborhood information and bias information when computing node representations. By extending the sampling of adjacent entities to multihop simulation of higher-order adjacent information, users' potential long-distance interests can be captured. Compared with the baseline model, the superiority of this method is verified.

1. Introduction

With the explosive growth of Internet information, users are faced with the problem of information overload [1], and traditional search engines have been unable to meet users' retrieval needs, so the recommendation system have emerged as the times require.

Traditional methods, such as collaborative filtering (CF) [2], exploit the entire user-item interaction matrix to mine users' interest, which suffer from cold start and data sparsity problems. The matrix factorization (MF) model [3] added the concept of latent vector to the existing matrix, strengthening the model's ability to deal with sparse data. Koren [4] put forward SVD, which transforms both items and users into the same hidden factor space. The space tries to explain the rating by describing the items and users by the factors that are automatically inferred from user feedback. He et al. [5] proposed the matrix factorization model NCF based on the neural network structure, which takes into account both the user's explicit rating and implicit feedback on the item. Followed by this, Guo et al. [6] proposed DeepFM to explicitly describe user preferences for different factors. The above methods model each pair of user-item interaction data as an independent data instance and do not consider the association between them, so attribute-based collaboration information cannot be extracted from user behavior.

The graph structure can well describe the degree of association between data, and knowledge graph (KG) is a natural graph data that contains a lot of heterogeneous information [7]. The essence of KG is a large-scale semantic network, which contains rich semantic features among items. It can help to discover users' potential interest as auxiliary information for recommender systems. At the same time, the data with semantic correlation can make the recommendation results interpretable while learning.

The current mainstream knowledge graph-based recommendation can roughly be divided into two categories: path-based methods and embedding-based and joint-based methods. Embedding-based methods all use the knowledge graph embedding (KGE) method [8] to map entity vectors or

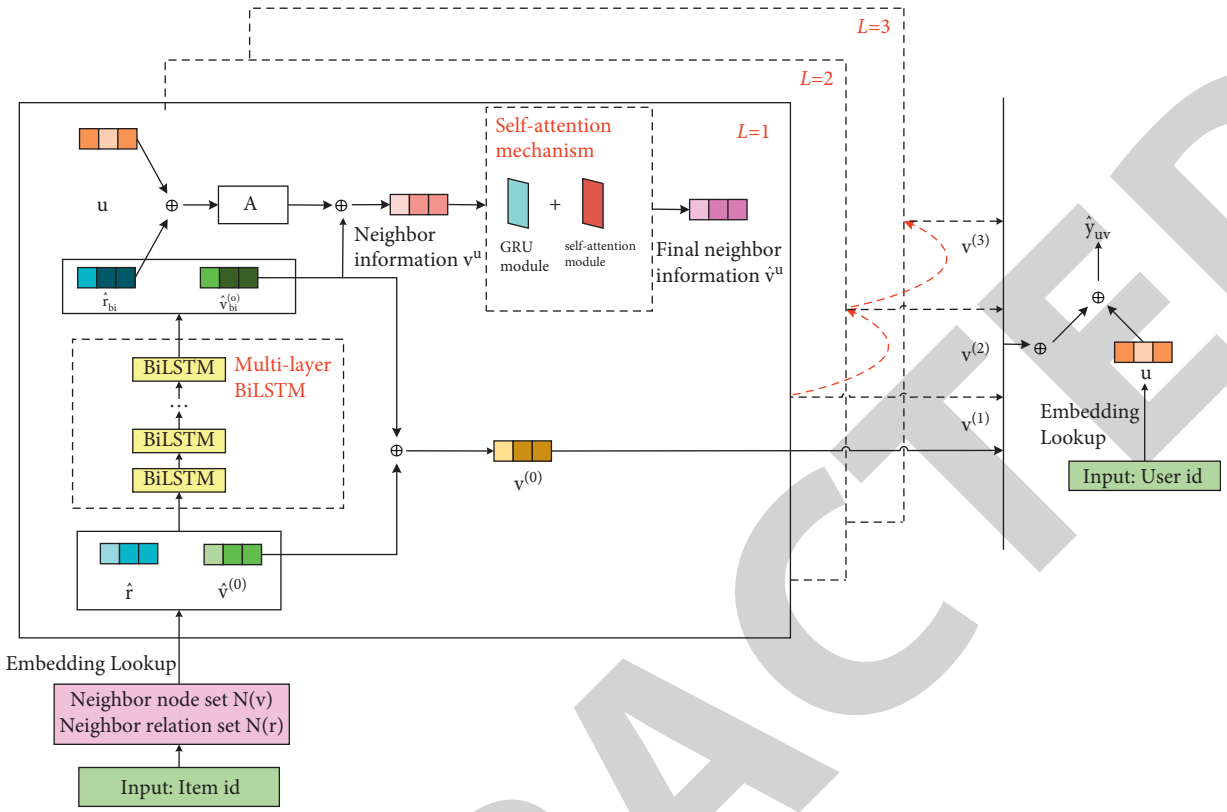

Figure 1: Overall framework of BAGCN.

relation vectors to a low-dimensional vector space, such as CKE proposed by Zhang et al. [9] and DKN proposed by Wang et al. [10]. However, this method ignores the connectivity of information in KG and lacks interpretability.

Path-based methods use the user-item graph to calculate the path similarity of users or items by predefining metapaths and use semantic connectivity in KG for recommendations. The Hete-MF, proposed by Yu et al. [11], utilized L different metapaths to find the similarity between items on each path. Luo et al. [12] proposed Hete-CF, which uses the similarity between users and items together as a regularization to find items of interest for users. The PER algorithm treats KG as a heterogeneous information network and extracts latent features from metapaths to represent the connectivity in different relational paths between users and items. However, the type and number of metapaths of such methods need to be manually defined, and the performance is easily affected [13].

The joint method combines the above two methods, which not only makes full use of the semantic information in KG but also inherits the interpretability of the path-based method. For example, RippleNet [14] used the embedding-based propagation idea to model users by analogizing the propagation process of user preferences to ripple diffusion. Subsequently, Wang et al. [15] proposed the KGCN model, which characterized nodes by mining the association attributes between entities on the KG, capturing the correlation between items and aggregating the information of neighbor nodes. However, this scheme is greatly affected by sparse data, and the representation of nodes is not accurate enough, so the performance of model prediction needs to be further improved.

Therefore, in order to solve the above problems, this paper proposes a recommendation algorithm for knowledge graph convolutional networks based on multilayer BiLSTM and self-attention mechanism. Long and short-term neural network is a kind of recurrent neural network, while bidirectional short and long-term memory network is divided into two independent long and short-term neural network. First, we apply the stacked multilayer BiLSTM to perform feature extraction on the initial entity and relationship vectors and then combine the learned entity feature vector with the initial vector to obtain the entity's own vector, that is, the 0-order representation. Finally, we realize high-order information representation through information transfer. The influence of data sparseness on the model is slowed down to a certain extent by adding its own information. Meanwhile, the self-attention mechanism can further learn the relationship between entities and adjacent entities, making the representation of nodes more accurate and effectively improving the performance of the recommendation system.

2. The Recommendation Algorithm Based on Multilayer BiLSTM and Self-Attention Mechanism

The overall framework of our method is shown in Figure 1, which is divided into a knowledge graph embedding layer, a neighborhood information calculation layer, and a

prediction layer. L indicates that the neighborhood information is extended to the first, second, third, or higher order.

2.1. Problem Description. In a recommendation scenario, a user set and an item set are given, which is denoted as $U = \{u_1, u_2, \ldots, u_m\}$ and $I = \{i_1, i_2, \ldots, i_n\}$. The interaction matrix of users and items is $Y \in R^{m \times n}$, interaction data is defined as (u, y_{ui}, i), and m and n are the number of users and items, respectively. $y_{ui} = 1$ indicates that there is interaction between the user and the item, which is regarded as a positive example of user-item interaction; otherwise, it indicates that no interaction has occurred, which is regarded as a negative example. Given a knowledge graph G and a user-item interaction matrix Y, we need to predict the probability that a user u will interact with an item i without interacting before. The learning objective function can be expressed as $\widetilde{y}_{ui} = F(u, i; \theta)$, where $\widetilde{y}_{ui}$ represents the probability that the user will interact with the item and θ represents all model parameters of the function.

2.2. BAGCN Layer. The BAGCN algorithm is widely used in accurately capturing the higher-order structural proximity between entities in knowledge graphs and the semantic association of relations between entities and adjacent entities. The self-attention mechanism is actually a kind of network attention mechanism that is actually a kind of network configuration [16, 17].

2.2.1. Knowledge Graph Embedding. Knowledge graph embedding is an effective way to convert entities and relations into vector representations, which can transfer high-dimensional sparse features into low-dimensional feature vectors, to obtain a more convenient form for model input. The user, $U = \{u_1, u_2, \ldots, u_m\}$, obtains the corresponding vector representation by querying the user embedding matrix $I \in R^{m \times T}$, where T is the dimension of the embedding vector. Given a candidate pair of user u and item (entity) v, the entity vector and the relation vector get the corresponding initial embeddings $\widehat{v}^{(0)}$ and $\widehat{r}$ in the entity embedding matrix and the relation embedding matrix through embedding lookup.

In this paper, we apply the multilayer BiLSTM to learn features for entity and relation embeddings. The single-layer BiLSTM has achieved good results in simple prediction tasks, but the potential interest of users are often deeply hidden in the user-item interaction matrix. Therefore, this paper proposes to use the stacked multilayer time series network BiLSTM to extract the deep dependency features in the user and item interaction matrix to mine the potential interest of users. A single-layer BiLSTM [18] is composed of a forward LSTM and a backward LSTM, the former calculates the hidden layer state $h(h_1, h_2, \ldots, h_t)$ and the latter calculates the hidden layer state $h(h_1, h_2, \ldots, h_t)$, which can be spliced to obtain the final hidden layer state. The multilayer BiLSTM network is composed of the forward multilayer LSTM and backward multilayer LSTM, and the input of the Nth layer is the output of the $N-1$th layer. The model structure can be seen in Figure 2.

First, take $\widehat{v}^{(0)}$ and $\widehat{r}$ as the input of the multilayer BiLSTM model for feature extraction and then splice the extracted entity embedding vector with the initial embedding vector $\widehat{v}^{(0)}$ to obtain the 0th-order information $v^{(0)}$ of the entity, that is, the representation vector of the entity itself. Its process can be formulated as

$$\begin{cases} X_n = B(X_{n-1}), \\ X_{n-1} \leftarrow \cup < X_{n-1}^{c_1}, X_{n-1}^{c_2}, \ldots, X_{n-1}^{c_m} >, \\ R_n = B(X_{n-1}) \cup B(X_{n-2}), \\ X_{n-1} \longleftarrow \cup < X_{n-1}^{c_1}, X_{n-1}^{c_2}, \ldots, X_{n-1}^{c_m} >, \\ v^{(0)} = \widehat{v}^{(0)} + X_n, \end{cases} \tag{1}$$

where X_n and R_n are the embedded representations of entities and relations obtained after feature extraction, respectively. $C_1, C_2, \ldots C_m$ represents hidden layer nodes, and the number of internal hidden layer nodes is determined by the dimensions of entities and relationships. $\cup$ indicates the feature stacking symbol.

Since the input of BiLSTM contains the output of forward and backward LSTM, we sum and average the forward and backward features to effectively utilize the forward and backward feature information, which can be formulated as

$$X_{n-1}^{c_1} = X_{n-1}^{\text{Forward}_1} + X_{n-1}^{\text{Backed-Output}_1}{}^{H}_{1 \le c \le N}, \tag{2}$$

where H is the number of hidden layer nodes and N is the total number of cells. $X_{n-1}^{\text{Forward}_1}$ represents the forward LSTM output vector and $X_{n-1}^{\text{Backed-Output}_1}$ represents the backward LSTM output vector.

2.2.2. Neighborhood Information Calculation. The aggregation calculation of neighborhood information needs to integrate the information of neighboring nodes. Specifically, $N(v)$ represents the set of neighbor nodes directly connected to entity v, $r_{x,y}$ indicates the relationship between e_x and e_y, and the neighborhood of entity v is represented as $\mathrm{v}_{\mathrm{P}(\mathrm{v})}^{\mathrm{u}}$. When calculating the information representation of the neighborhood, the inner product function z: $R^d \times R^d \longrightarrow R$ is used to calculate the weight matrix between the user vector and the adjacency vector.

$$A = z(u, r), \tag{3}$$

where d represents the dimension and A represents the impact of different relationships on users by adding user information. In order to characterize the neighborhood structure of entity v, first calculate the linear combination of neighborhood as

$$v_{N(v)}^{u} = \sum_{e \varepsilon P(V)} \widetilde{A} e, \tag{4}$$

where $\widetilde{A}$ is the normalized matrix of A.

$$\widetilde{A} = \frac{\exp(A)}{\sum e \varepsilon P(v) \exp(A)}, \tag{5}$$

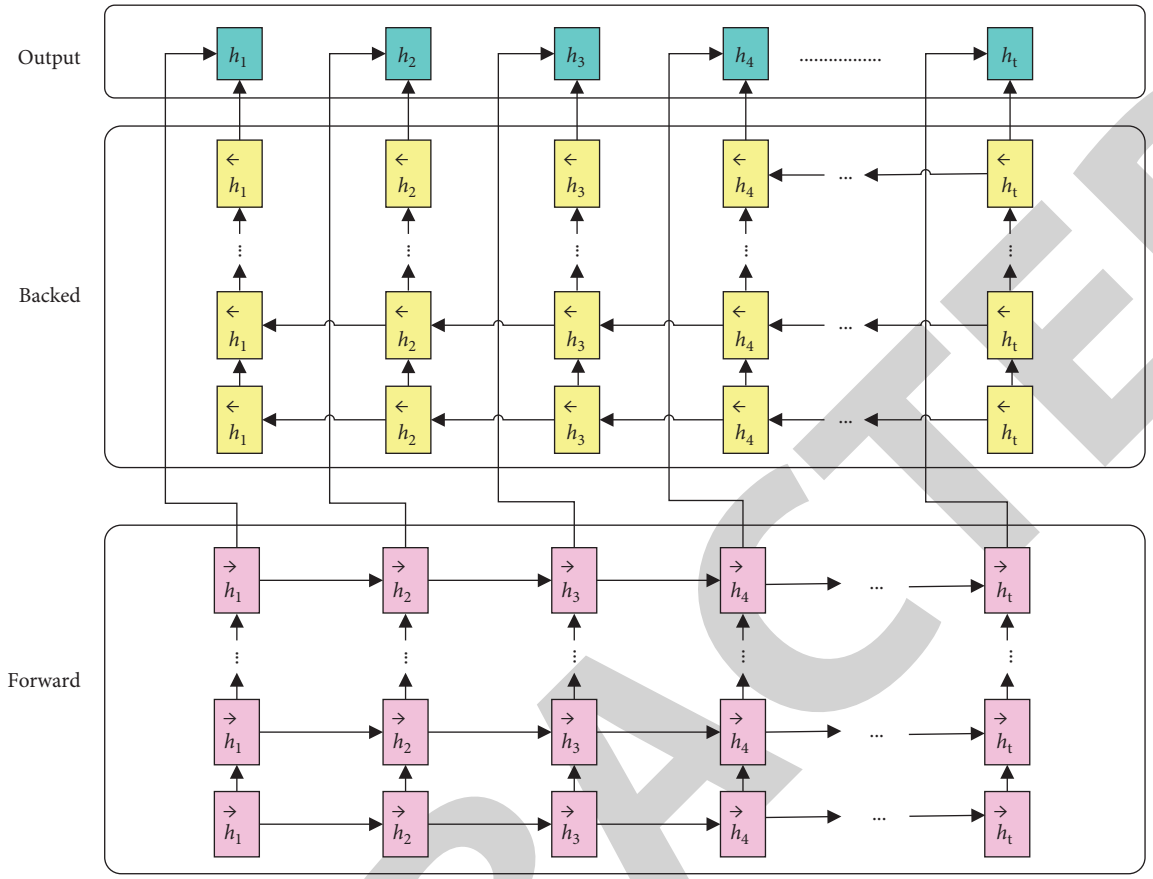

Figure 2: BiLSTM structure with multiple layers stacked.

where e is the vector representation of the neighbor entity.

2.2.3. Self-Attention. Attention mechanism [19, 20] was initially applied in the field of machine translation, and now, it has been widely applied in image processing, recommendation system, and other aspects. This method draws on the mechanism of human visual selective attention, and its core purpose is to screen out the important content of the current task from a large amount of information. The self-attention mechanism proposed in this paper consists of a gated recurrent unit (GRU) module and a self-attention module. The calculated neighborhood representation $\hat{v}^{u}_{P(v)}$ is taken as the input of self-attention, and the aggregation features of lower-dimensional neighborhood information are extracted through the GRU module. Input the obtained feature vector into the self-attention module to further learn the semantic association between entities and adjacent entities and more accurately calculate the representation of neighborhood information. The specific implementation process is as follows:

Firstly, $v^{u}_{P(v)}$ is sent to the GRU module as the input feature to extract the low-dimensional feature, and the output feature I is obtained through the learning of function h.

$$I = h\left(v^{u}_{P(v)} \mid u, r\right). \tag{6}$$

Then, the function body *Atten* is created, which is consistent with the implementation process of ordinary self-attention mechanism. The feature vector I processed by the GRU module is used as the input of the self-attention module, and the specific operation is shown in the following formula:

$$\begin{cases} v = \tanh\left(I \bullet \mathbf{W}^{\mathbf{a}} + \mathbf{b}\right), \\ v' = v \bullet \mathbf{u}, \\ a = \text{soft}\max\left(yI\right), \\ O = I * a, \end{cases} \tag{7}$$

where $\bullet$ is the tensor-dot operation, $\mathbf{w}^{\mathbf{a}}$ is the trainable transformation matrix, $\mathbf{b}$ and $\mathbf{u}$ are vectors for training, α is the normalized weight, and O is the final output feature of self-attention.

Finally, a full connection layer is used to obtain the final neighborhood information representation $\hat{v}^{u}_{P(v)}$, and the specific calculation process is as follows:

$$\hat{v}^{u}_{P(v)} = \text{FC}\left(O\right), \tag{8}$$

where **FC** is the operation function of the full connection layer.

2.2.4. Information Aggregation. The last step of the BAGCN layer is information aggregation. The model aggregates the node's own information $v^{(0)}$ and all its neighborhood information $\hat{v}^{u}_{J(v)}$ as the final representation of the node through the aggregator, takes the sum of the two vectors, and then performs nonlinear transformation on them. Here, $|J(v)| = K$, K is a configurable constant, representing the

Table 1: Basic data set information.

		Movielens-20M	Book-crossing	Last.FM
User-item' interactive information	Users	138159	19676	1872
	Items	16954	20003	3846
	Interactions	13501622	172576	42346
KG information	Entities	102569	25787	9366
	Relations	32	18	60
	KG triples	499474	60787	15516

Table 2: Hyperparameter settings.

Hyperparameter	Movielens-20M	Book-crossing	Last.FM
K	4	8	16
d	8	16	8
λ	10^{-7}	2×10^{-5}	10^{-4}
η	2×10^{-2}	2×10^{-4}	5×10^{-4}
H	1	1	1
Batch_size	65536	256	128

Table 3: Model performance on MovieLens-20M.

Model	ACC	AUC	$F1$	Pre@1	Recall@1
SVD [4]	—	0.9630	0.9190	—	—
CKE [9]	—	0.9240	0.8710	—	—
PER [13]	—	0.8320	0.7880	—	—
KGCN [15]	0.9235	0.9720	0.9242	0.9165	0.9321
BAGCN	0.9335	0.9780	0.9343	0.9228	0.9461

Table 4: Model performance on Book-Crossing.

Model	ACC	AUC	$F1$	Pre@1	Recall@1
SVD [4]	—	0.6720	0.6350	—	—
CKE [9]	—	0.6770	0.6110	—	—
PER [13]	—	0.6170	0.5620	—	—
KGCN [15]	0.6010	0.6471	0.6159	0.5975	0.6403
BAGCN	0.6268	0.6791	0.6425	0.6203	0.6682

Table 5: Model performance on Last.FM

Model	ACC	AUC	F1	Pre@1	Recall@1
SVD [4]	—	0.7690	0.6960	—	—
CKE [9]	—	0.7440	0.6730	—	—
PER [13]	—	0.6330	0.5960	—	—
KGCN [15]	0.7093	0.7848	0.7107	0.7089	0.7154
BAGCN	0.7196	0.7913	0.7188	0.7227	0.7175

number of neighbors sampled. Technically, if $|J(v)| < K$, this paper samples with a put back; otherwise, it randomly samples fixed K neighbor nodes. In the real knowledge graph, there are great differences in the number of neighbor nodes of different entities. In this paper, the complete set of neighbor nodes is not included in the calculation, but a fixed size neighborhood set is sampled for each entity to ensure the same calculation mode and calculation efficiency of each batch. Its calculation is as follows:

$$\text{agg} = \sigma\left(W \cdot \left(v^{(0)} + \widehat{v}^{u}_{J(v)}\right) + b\right), \tag{9}$$

where $\mathbf{W}$ and b are transformation weights and bias terms, respectively, and σ is a nonlinear function.

The initial embedding representation of an entity is zero-order, and it is propagated to its neighbors to obtain first-order representation. The process is repeated from first-order representation to higher-order representation. The high-order representation can tap deeper potential interest of users.

2.3. Prediction Layer. The prediction layer predicts the probability of interaction item i of user u by inputting a function $f: R^d \times R^d \longrightarrow R$, as shown in the following formula:

$$\widehat{y}_{u,i} = f(u, i). \tag{10}$$

2.4. Loss Function. The cross-entropy loss function is used to train the model in this paper, and the specific formula is as follows:

$$\text{loss} = \sum_{u\varepsilon U}\left(\sum_{i:\ y_{ui=1}} J\left(y_{ui}, \widehat{y}_{ui}\right) - \sum_{n=1}^{T^u} E_{i_n} \sim Q(v_n) J\left(y_{ui_n}, \widehat{y}_{ui_n}\right)\right) + \lambda \|F\|_2^2, \tag{11}$$

where J is the cross-entropy loss, Q is the negative sampling distribution, and T^u is the negative sample number of user u. In this paper, $T^u = |\{v:\ y_{uv} = 1\}|$, Q follows uniform distribution and the last term is $L2$ regularization.

3. Experimental Results and Analysis

3.1. Datasets. We evaluate the proposed BAGCN model by recommending movies, books, and music on three datasets, i.e., MovieLens-20M, Book-Crossing, and Last.FM, respectively. The triple information of constructing the knowledge graph of each dataset comes from Microsoft Satori, and a subset of triples is selected in the entire knowledge graph, whose confidence is greater than 0.9. Table 1 records the basic information of the three datasets.

These three datasets belong to explicit feedback. In order to mine user preference information, we convert explicit feedback into implicit feedback to learn model recommendation in this paper. In implicit feedback, the user with a positive interaction with an item can be counted as 1, and a sampled negative sample set for each user is counted as 0,

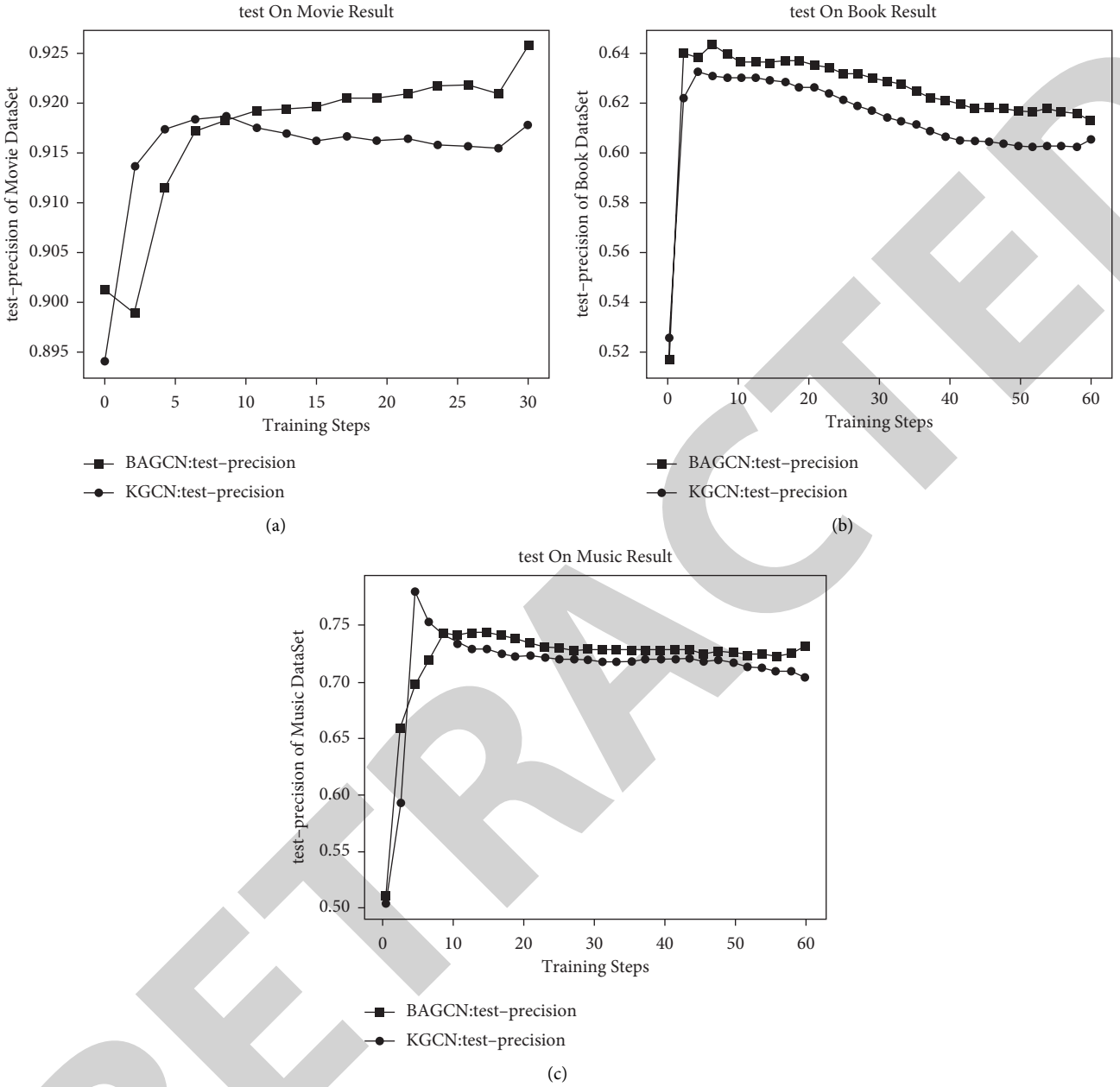

Figure 3: (a) The performance of pre on MovieLens-20M. (b) The performance of pre on Book-Crossing. (c) The performance of pre on Last.FM.

which means the sample set has not been observed. The rating range of the MovieLens-20M dataset is 1~5, and the rating range of Book-Crossing is 1~10. Meanwhile, the rating threshold of the MovieLens-20M dataset is set to 4, which means a rating greater than 4 is regarded as a positive interaction. The two datasets, Book-Crossing and Last.FM, are sparser than MovieLens-20M, so we do not set a threshold.

3.2. Comparative Models Introduction. SVD [4]: a classic CF-based model. It analyzes the user's liking of each factor and the degree to which the item contains each factor based on the existing data.

CKE [9]: integrate various auxiliary information such as structured, textual, and visual knowledge with CF in a unified recommendation framework for joint training.

PER [13]: viewing the knowledge graph as a heterogeneous information network, it represents the connectivity between users and items by extracting latent features of meta-paths.

KGCN [15]: a representative of a hybrid recommendation training model. It implements recommendation by integrating the characteristics of knowledge

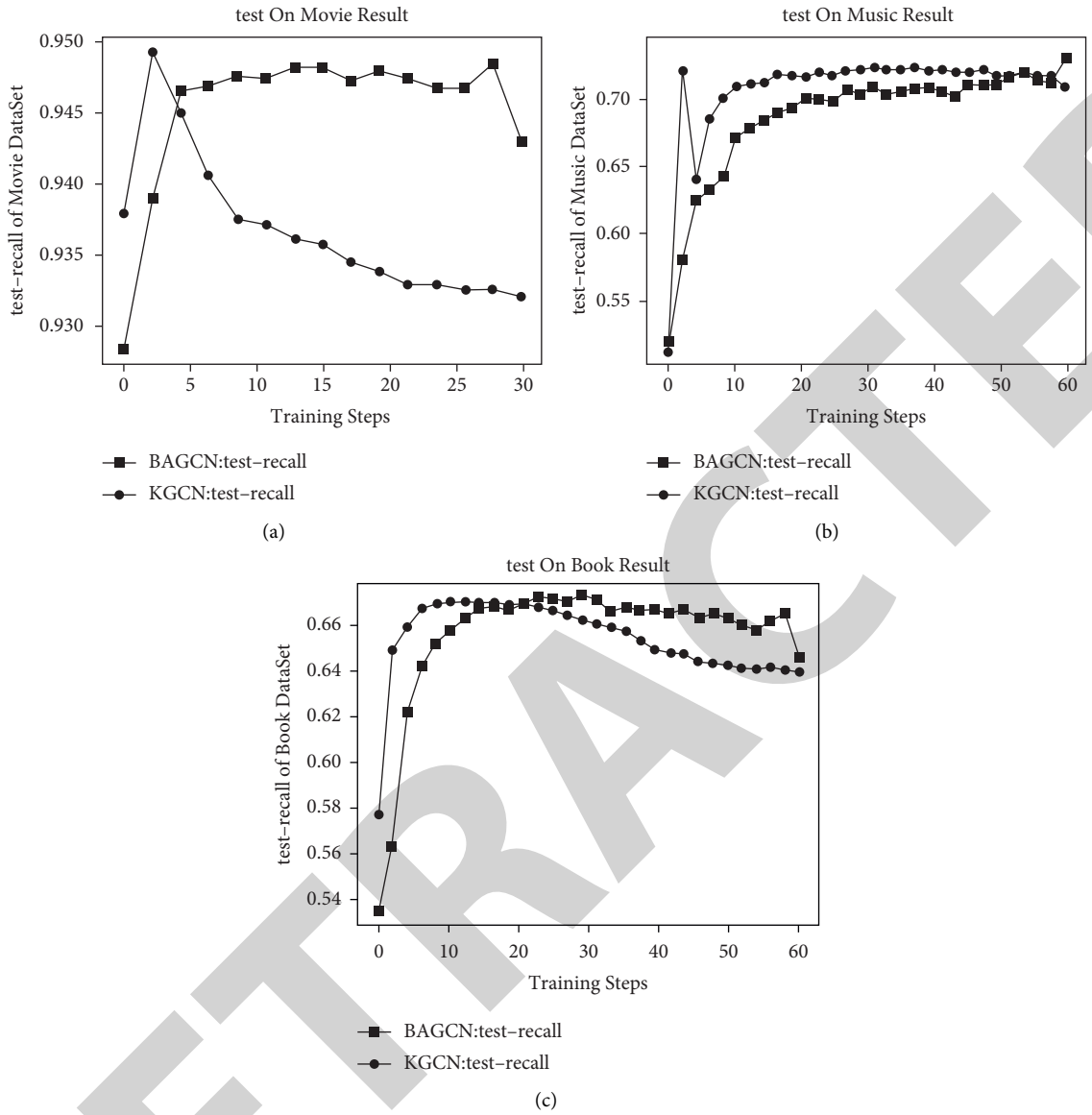

Figure 4: (a) The performance of recall on MovieLens-20M. (b) The performance of recall on Last.FM. (c) The performance of recall on Book-Crossing.

graphs and graph convolutional neural networks and aggregating neighbor information and bias to obtain item representations [21–24].

3.3. Experimental Setup. In BAGCN, we set the functions z and f that are the inner products, σ is the activation function ReLU of the nonlast layer aggregator, and tanh is the activation function of the last layer aggregator. Table 2 provides other hyperparameter settings of this model. K denotes the number of neighbors of each sampled entity, d denotes the dimension of the embedding, H denotes the number of iterations, η denotes the learning rate, and λ denotes the regularization term coefficient. The hyperparameters are sized by optimizing AUC on the validation set, and the ratio of training set, evaluation set, and test set is set to 6 : 2:2. We evaluate the BAGCN algorithm in two experimental scenarios: (1) in CTR prediction, the trained model is used to predict each interaction in the test set, and AUC, $F1$, and ACC are used to evaluate CTR prediction. (2) In top-N recommendation, the trained model is designed to select N items with the highest predicted click probability for each user in the test set for recommendation. By default, $N = 1$. All trainable parameters are optimized using the Adam algorithm.

PER uses artificially designed paths as features, SVD sets MovieLens-20M, and Book-Crossing $d = 8$, $\eta = 0.5$. For Last.FM, $d = 8$, $\eta = 0.1$. The dimension d of the three datasets of the CKE model is set to 64, 128, and 64, respectively, the training weight for the KG part is 0.1, and the learning rate is set the same as SVD. The KGCN model is set to $K = 4$, $d = 32$, $\eta = 0.02$, $H = 2$, and $\lambda = 10^{-7}$ in the MovieLens-20M dataset, and the parameters of Book-Crossing are set to $K = 8$, $d = 64$, $\eta = 0.0002$, $H = 1$, and $\lambda = 2 \times 10^{-5}$, respectively. In Last.FM,

$K = 8$, $d = 16$, $\eta = 0.0005$, $H = 1$, $\lambda = 10^{-4}$, and H represents the number of aggregation iterations. The number of training rounds is set to 60, and the number of training rounds for MovieLens-20M is set to 30 for the Last.FM and Book-Crossing datasets.

3.4. Experimental Results Analysis. The CTR prediction and top-N recommendation results in different datasets are displayed in Tables 3–5, Figures 3, and 4. Overall, the BAGCN model outperforms the baselines on all three datasets tested, including ACC, AUC, $F1$, precision, and recall. Comprehensively comparing the performance of various indicators in the three datasets, our method has improved the accuracy rate (ACC), while AUC has increased. The multilayer bidirectional recurrent neural network BiLSTM can effectively utilize the forward and backward feature information of entities and relationships. At the same time, adding an attention mechanism layer can perform biased aggregation of neighborhood information to make the representation of nodes more accurate. By observing the experimental results, the following conclusions can be drawn:

(1) The performance of BAGCN is better than that of all the compared baseline models. Compared with the KGCN model in the three datasets of movies, books, and music, ACC is improved by 1.00%, 2.58%, and 1.03%, and the pre is improved by 0.63%, 2.28%, and 1.38%.

(2) PER performs the worst due to its heavy reliance on manually designed meta-paths, and the optimal path is difficult to define in reality.

(3) In the three data sets, Book-Crossing and Last.FM are more sparse than MovieLens-20M data, but the improvement of each index is more obvious, indicating that the BAGCN model proposed in this paper can alleviate data sparsity to a certain extent sexual problems.

3.5. Hyperparameter Optimization. Different hyperparameters will affect the effect of the model. In order to find the best value of the model on the validation dataset, it is necessary to optimize the super parameters. This section optimizes the number of sampling neighbors K and the embedding dimension d.

3.5.1. The Influence of Different K on the Model. The use efficiency of the knowledge graph is studied by changing the number of sampling neighbors K. It can be observed from Table 6 that, for the datasets MovieLens-20M, Last.FM, and Book-Crossing, the model has the best performance when $K = 4$, 16, and 8, respectively. Because the dataset of MovieLens-20M is denser than the other two, only fewer neighbors need to be sampled. If K is too small, the model cannot include enough neighbor information to represent nodes; but if K is too large, noise will be introduced, which will affect the recommendation effect of the model.

Table 6: AUC result of BAGCN with different K

K	2	4	8	16	32
MovieLens-20M	0.9775	**0.9780**	0.9777	0.9778	0.9777
Last.FM	0.7900	0.7907	0.7890	**0.7913**	0.7905
Book-Crossing	0.6766	0.6745	**0.6791**	0.6754	0.6743

Table 7: AUC result of BAGCN with different d.

d	4	8	16	32	64
MovieLens-20M	0.9762	**0.9780**	0.9768	0.9726	0.9689
Last.FM	0.7876	**0.7913**	0.7811	0.7690	0.7546
Book-Crossing	0.6739	0.6708	**0.6791**	0.6691	0.6643

3.5.2. The Influence of Different d on the Model. In addition, the influence of different embedding dimensions d, which is also the number of hidden nodes of BiLSTM, on the model is studied. It can be observed from Table 7 that increasing the size of d at first can improve the recommendation effect of the model, but as the value of d continues to increase, the performance of the model becomes worse instead. This is because a larger d will cause the model to be overfitted, which will affect the effect of the model.

4. Conclusion

Aiming at the problems of cold start, data sparsity, and poor performance of existing recommendation algorithms, this paper proposed the BAGCN algorithm. The algorithm extracts the features of the embedding of entities and relationships in the knowledge map, learns the semantic information in the knowledge map through the self-attention mechanism, aggregates the neighborhood information in a biased way, and then extends to multihop simulation of high-order structure information to tap the potential interest of users. Through experiments on several datasets, the BAGCN model is proved to be superior to the baseline model in various performance evaluation indexes of film, book, and music recommendation. In this paper, negative samples are sampled in a uniform way, and high-quality negative samples are as important for model learning as positive samples. In addition, the user's demographic information and the recommendation model will be considered as auxiliary information to improve the performance of user integration.

Data Availability

The data used to support the findings of this study are available in the following URL: https://github.com/hwwang55/KGCN/tree/master/data.

Conflicts of Interest

The authors declare that they have no conflicts of interest regarding this work.

Hindawi
Mobile Information Systems
Volume 2022, Article ID 1544981, 10 pages
https://doi.org/10.1155/2022/1544981

Research Article

Research on Network Data Monitoring and Legal Evidence Integration Based on Cloud Computing

Li Ge[1] **and Peng YanLi**[2]

[1]*School of Law, Northwest Minzu University, Lanzhou, Gansu 730030, China*
[2]*Gansu University of Political Science and Law, Lanzhou, Gansu 730070, China*

Correspondence should be addressed to Li Ge; 20151011141@stu.qhnu.edu.cn

Received 12 July 2022; Revised 9 August 2022; Accepted 20 August 2022; Published 5 September 2022

Academic Editor: Shadi Aljawarneh

In today's society, technologies such as social network, mobile Internet, and Internet of things are developing by leaps and bounds, and data are growing at an unprecedented rate. How to manage and reasonably use such data sources has become the most popular research topic, and cloud computing technology can provide powerful computing and storage capabilities for data sources, further enhance the comprehensive processing capacity of big data, and realize the real value of data sources. Based on this point, this paper focuses on the nature of data network delivery and its requirements for real-time accuracy and performance monitoring, and studies the key computing flow technology for network data monitoring. The main achievement is to build a data processing and analysis platform based on computing flow, and design and implement the overall structure of the platform and data anomaly monitoring model. Finally, this paper uses big data technology to design and build an integrated auxiliary legal service system. The system can help judges and prosecutors fully understand the progress and research results of guiding cases, and provide them with a series of applicable laws and regulations, so as to maximize work efficiency. The system can also help implement the investment of legal education, so as to provide basic legal services for the public, integrate legal evidence, and timely implement public opinion guidance for some public opinion media on legal topics and cases, so as to minimize social risks. This paper combines cloud computing technology with network data detection and applies it to the research field of legal auxiliary services, which greatly promotes the development of legal evidence integration technology.

1. Introduction

Through the comprehensive application of big data and cloud computing processing technology, this paper analyzes and studies the data monitoring process, data processing process, and data diagnosis process of various devices. The results show that the necessary factors for building a powerful intelligent network are data integration and information interaction technology [1]. With the gradual development of the network transmission center to the integration of supervision, more and more various data will be transmitted to the data monitoring center for processing. Therefore, the monitoring and processing technology of historical data and real-time data will face great challenges. For a wide range of equipment data processing application scenarios, this paper plans a comprehensive cloud computing platform architecture [2]. The platform is based on a shared IT multi-structure computing framework. This design can not only help the computing platform save investment and maintenance costs, but also make data integration and information interaction more convenient [3]. The system can provide computing services in the optimal resource framework according to the user's network data detection and processing requirements. Based on this point, this paper proposes a centralized computing method for parallel series processing of massive digital signal components according to Hadoop MapReduce [4]. The adaptive discharge amplitude threshold and flow interval threshold are used to double filter the local excess points in the discharge signal phase, so as to improve the

computational efficiency of large data parallel processing [5]. With the progress of e-commerce and e-government, the application of electronic data is increasing, and electronic evidence has gradually attracted people's attention [6, 7]. At the same time, the phenomena of network information crime and e-commerce crime emerge one after another. Therefore, the integration of electronic legal data has become the best way to solve this kind of conflict [8]. However, the legal form definition of electronic evidence is controversial in the current era, which will hinder its practical application to a certain extent, so it is difficult to solve the dispute in time. This paper holds that electronic evidence can be divided into two types of legal forms [9]. One is whether electronic evidence has qualified evidence qualification, especially whether its manifestation is consistent with the legal category in China; the second is the specific use of electronic evidence, that is, whether the investigation and evidence collection law and court evidence collection procedures can be connected with electronic evidence [10, 11]. Based on the above two points, this paper discusses the practice and theoretical basis of the legal form of electronic evidence in judicial proceedings. Based on this, this paper designs a complete legal service assistant comprehensive system, which can effectively provide legal assistance to law enforcement personnel and the public, thus effectively reducing social risks [12].

2. Related Work

The literature has constructed a data analysis and processing platform based on stream computing technology, classified and explained its design and implementation process, and designed a data network abnormality monitoring model [13]. Spark Streaming based on the Apache Spark platform carries out an open-source computing framework design and introduces components such as Kafka message columns and Redis memory databases to provide efficient data sources and data service interfaces for the data analysis platform, enabling it to perform real-time analysis and processing of various data [14]. This completes the network monitoring application. The literature gives a data aggregation scheme that adapts to model changes, and achieves the aggregation of state data based on the CIM model described in the SCL model; because it is necessary to achieve efficient data integration and storage at the same time, the introduction of cloud computing technology solves the above technology difficulty [15]. The literature analyzes the connotation and nature of MCCA and its data sources, and uses the theory of evolution to explain the resource integration mechanism of MCCA data sources. On this basis, the overall structure of MCCA data aggregation mechanism is designed, including data recovery and storage mechanism, data source grouping, and merging mechanism [16]. The literature proposes a parallel empirical full modal decomposition (EEMD) algorithm compatible with Spark memory computing technology, which overcomes the deficiencies of Hadoop MapReduce in the case of complex data processing. At the same time, the parallelism of the EEMD algorithm in processing time series signals is analyzed, and two parallel EEMD algorithms with different structures based on the parallel EMD process in parallel segmentation bands are designed [17]. The proposed parallel algorithm is used to extract the components of the waveform emission signal, and the calculation performance of the serial EEMD algorithm and the parallel EEMD algorithm based on Hadoop MapReduce are compared [18]. The literature describes the focus of disputes over the legal form of electronic evidence in judicial practice and theory. It is believed that electronic evidence does not conform to China's closed evidence classification system, and supports the reconstruction of the national evidence classification system [19].

3. Design and Application of Network Data Monitoring Platform Based on Cloud Computing

3.1. Data Resource Clustering of the Mobile Cloud Computing Alliance. The cloud computing alliance data source clustering can effectively classify the alliance data source. In this process, an efficient and appropriate clustering method must be selected to share the resources in the alliance data. Using FCM clustering method in cloud computing to group alliance data sources can be described as follows: assume that the set $X = \{x_1, x_2, \ldots,$ is $Xi = \{xi_1, xi_2, \mathrm{L}, xi_p\}$, and xi_p is the pth attribute of the data resource xi. In the cloud computing alliance, the objective function of the FCM algorithm is as follows:

$$\min J_m(U, V) = \sum_{i=1}^{n} \sum_{j=1}^{c} u_{ij}^m d_{ij}{}^2. \tag{1}$$

Obtain the minimum value under the constraint of

$$\sum_{j=1}^{c} u_{ij} = 1. \tag{2}$$

Using Lagrangian multiplication and combining the constraints of equation (2) to derivate equation (1), we get

$$u_{ij} = \frac{1}{\sum_{k=1}^{n} \left[d_{ij}/d_{ik} \right]^{2/m-1}}, \qquad v_j = \frac{\sum_{i=1}^{n} u_{ij}^m x_i}{\sum_{i=1}^{n} u_{ij}^m}. \tag{3}$$

Breadth first search (BFS) is a method of traversing graphs. It is a type of hierarchical search process that can access all nodes in the graph and has global search capabilities. To this end, this paper adopts the breadth search first idea and proposes an improved clustering algorithm with breadth priority, which not only has the ability to search the whole world, but also has the ability to exclude noisy data, including

$$S_i = \min \left\{ S_i^{rk} \right\}, r \le n, k \le n. \tag{4}$$

The specific algorithm of the improved clustering algorithm in this paper is as follows: calculate the weight

between any two nodes in the weight network, that is, equivalence, record it as the equivalence degree of S_k^{ij} measured objects x_i and x_j with respect to the attribute factors in W_k, and then consider all attribute relationship factors. Then, the similarity of the measured object x_i and x_j is as follows:

$$s_{ij} = \frac{\sum_{k=1}^{d} \left(x_{ik}w_k\right)\left(x_{jk}w_k\right)}{\sqrt{\sum_{k=1}^{d} \left(x_{ik}w_k\right)^2 \sum_{k=1}^{d} \left(x_{jk}w_k\right)^2}}. \tag{5}$$

Among them, W_k is the weight of the K attribute factor; $i = 1,2, \ldots, n$; $j = 1,2, \ldots, n$; d represents the number of attribute factors; and x_{ik} is its corresponding attribute value. After constructing the undirected weight graph, the equivalent matrix is created. From equation (5), it can be seen that $S^{ij} = S^{ji}$ and $S^{ii} = 1$, so the equilateral matrix is symmetric about the diagonal backbone.

Based on the above, in order to obtain a more accurate cluster center and cluster number, this article aims to construct a relevant cluster analysis function and select the optimal threshold to determine the optimal cluster center and cluster number. The sample center formula is

$$x^{(i)} = \frac{\sum_{i=1}^{n_i} x_k^{(i)}}{n_i}. \tag{6}$$

The overall sample center formula is

$$x = \frac{\sum_{i=1}^{n} x_j}{n}. \tag{7}$$

Definition of firmness:

$$\text{Intra\_dis} = \frac{1}{n_i} \sum_{i=1}^{n_i} \| x_j^{(i)} - x^{(i)} \|^2. \tag{8}$$

Definition of separation:

$$\text{Inter}_{\text{dis}} = \| x^{(i)} - x \|^2. \tag{9}$$

The cluster validity evaluation model is

$$\text{F} = \frac{\sum_{\text{i=1}}^{\text{C}_x} \text{Inter} - \text{di s/C}_s - 1}{\sum_{\text{i=1}}^{\text{C}_x} \text{Intra\_di s/n} - \text{C}_s}. \tag{10}$$

The initial cluster centers can be expressed as

$$v_i = \left(x^{(1)}, x^{(2)} \ldots, x^{(i)}\right). \tag{11}$$

The greater the F value, the greater the distance between the class and the class; that is, the greater the difference between the class and the class, the better the classification effect. The threshold S is the optimal threshold corresponding to the F value. Relatively, its classification is the optimal classification result, where $1 < \text{Cs} < n$.

In order to improve the anti-noise ability of the FCM algorithm and minimize the influence of noise data on the grouping results, the change weighting method is used to determine the contribution rate of each attribute, and the attribute weight with strong separation is emphasized, while the noise attribute weight is reduced; assuming a data set $X = \{x_1, x_2, \ldots, x_n\}$, the formula for calculating the coefficient of variation v_x is as follows:

$$v_x = \frac{S_x}{|\overline{X}|}. \tag{12}$$

The weight formula of each attribute factor is

$$w_k = \frac{v_k}{\sum_{k=1}^{p} v_k}, \tag{13}$$

where w_k represents the weight of the kth attribute factor; p represents the number of sample attributes; and the objective function of the improved FCM algorithm is as follows:

$$\min J_m(U,V) = \sum_{i=1}^{n} \sum_{j=1}^{c} u_{ij}^m d_{ij}{}^2 w. \tag{14}$$

The objective function of the introduced Lagrange multiplier is

$$J(U,V,\lambda) = \sum_{i=1}^{n} \sum_{j=1}^{c} u_{ij}^m d_{ij}^m w - \sum_{i=1}^{n} \lambda_i \left(\sum_{k=1}^{c} u_{ik} - 1 \right). \tag{15}$$

The update formula based on the above membership degree is

$$u_{ij} = \frac{\left(1/d_{ij}^2\right)^{1/m-1}}{\sum_{k=1}^{c} \left(1/d_{ik}^2 w\right)^{1/m-1}}, \tag{16}$$

$$\cdots \text{among } d_{ij} = \| x_i - v_j \|.$$

The update formula based on the above cluster centers is

$$v_j = \frac{\sum_{i=1}^{n} u_{ij}^m x_i w}{\sum_{i=1}^{n} u_{ij}^m w}. \tag{17}$$

3.2. Design of Mobile Cloud Computing Network Data Integration Scheme. The data resource combination process of the mobile cloud computing alliance is roughly as follows:

(1) The user agent automatically executes the user agent request activity according to the application parameters input by the user and then asks whether the DR service request is registered in the ontology database service and whether there is a public data source service of the user agent, so as to screen the optimal DR service. We call the service to provide the agent interface, interact with the DR service agent, and then run specific user services.

(2) If the DR service request entered by the user cannot be found in the ontology database of the DR service, then it is determined whether the task belongs to the combined multi-task situation, and CDRSMA must decompose the required task. First, a combination plan is found that meets the needs of combined services in DR. If the matching is successful, the best combination plan will be screened out and returned to the DR combination service.

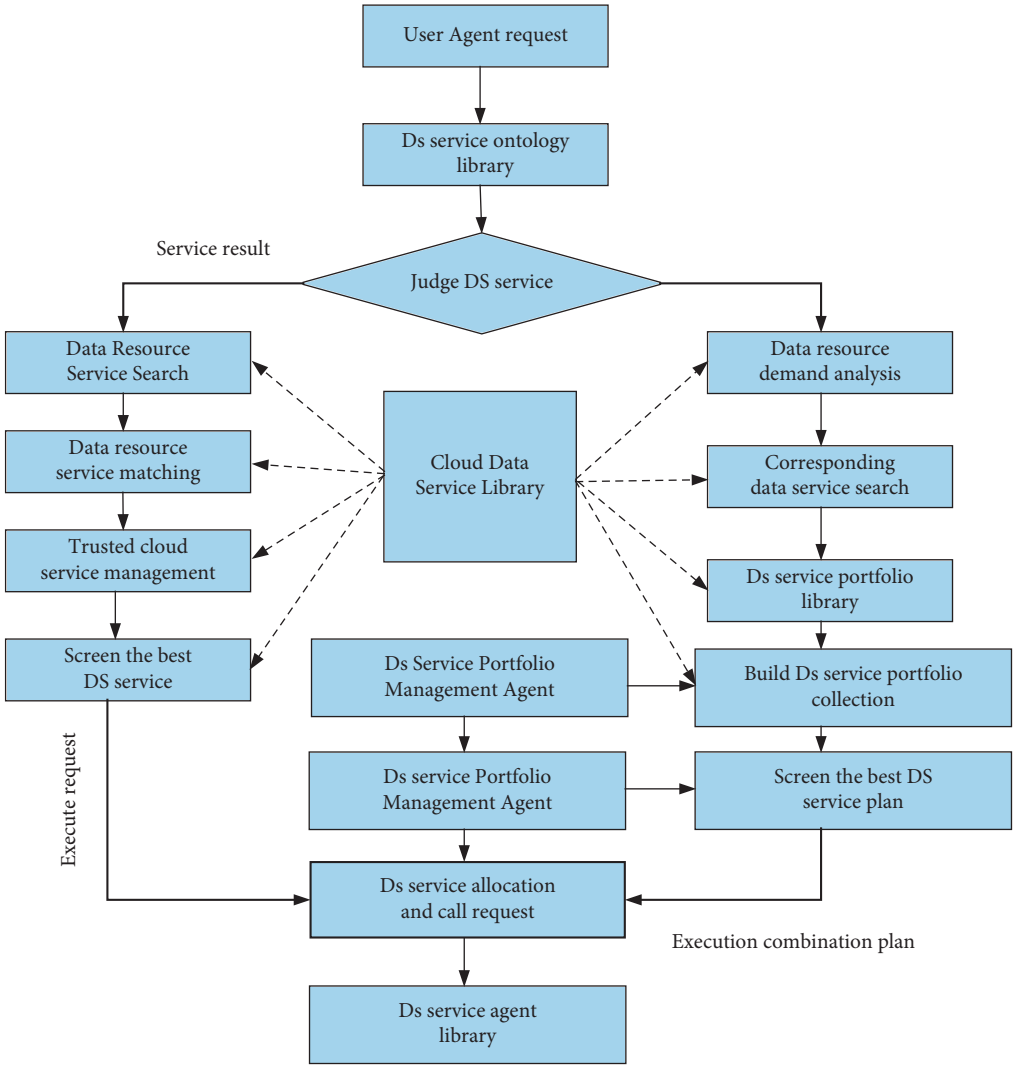

Figure 1: Flowchart of data resource combination of mobile cloud computing alliance.

(3) If the matching fails, the DR agent that provides the service will automatically provide the data resources that meet the requirements and return to the CDRSMA end, automatically personalize the DR service combination according to the user's needs, and then update the DR combination service library. When filtering the best service combination plan, the DR service agent provides a dial-up interface and executes user-specific service plans. The process is shown in Figure 1.

In the process of adjusting the threshold selection, the determination process of the vertical threshold T_1 and the horizontal threshold T_2 is very important, which can directly affect the detection result. However, like other methods in related literature, T_1 and T_2 values are usually set manually based on experience. Even though the same threshold can be used for signals from the same monitoring source, more accurate detection results can be obtained by manually setting the threshold. However, if there are multiple monitoring sources, it will inevitably lead to a large amount of manual work, so it is difficult to determine the automatic processing of the output signal components. Therefore, how to adaptively determine these two thresholds is a problem worthy of attention.

In the field of statistics, variance can measure the dispersion level of a data set. The higher the variance value, the higher the dispersion level. If a specific T threshold is used to split the original data, two clusters can be obtained, the difference between the two clusters is the largest, and their variance is the largest at this time. The theoretical basis of this method will be explained in detail below.

Suppose there is a set of discrete values of length N, $\{x_i | i = 1,2,\ldots,N\}$, where the maximum and minimum values are $x_{\max}$ and $x_{\min}$, respectively. First, the gray value of the discrete value needs to be changed; then

$$d_x = \frac{(x_{\max} - x_{\min})}{L}. \tag{18}$$

Secondly, count the number of each discrete value falling within the corresponding grayscale interval, where the

Table 1: Test data set information.

Data set number	Total number of files/piece	Number of monitoring sources	Total number of signals/cycle	Total size/MB
1	8	4	335/8	512
2	16	4	335/16	1024
3	24	4	335/24	1536
4	32	4	335/32	2048
5	40	4	335/40	2560
6	48	4	335/48	3072
7	56	4	335/56	3584
8	64	4	335/64	4096

grayscale interval with the grayscale value of l is converted according to

$$[(l-1)\cdot d_x, l\cdot d_x]. \tag{19}$$

If we consider the number of discrete values in the grayscale range $[(l-1)\cdot d_x, l\cdot d_x]$ and set it to $n1$, then $n1$ is called the number of pixels with a grayscale value of l, and then the total number of pixels must be equal to the total number of discrete values; there are

$$N = \sum_{l=1}^{L} n_i, l = 1, 2, \ldots, L. \tag{20}$$

Then, the probability of occurrence of the gray value l is denoted as P_1, which is obtained by

$$p_l = \frac{n_l}{N}. \tag{21}$$

First set the threshold to kd_x and apply this threshold to divide $\{x_i | i = 1,2, \ldots, N\}$ and divide it into C_0 and C_1 clusters; in the two groups, $C0$ represents the interval $[0, k_{dx}]$ discrete value, $C1$ represents the discrete value in the interval $[(k+1)\cdot d_x, L\cdot d_x]$, and then the probabilities of the two groups and their respective average gray values are

$$\begin{aligned}
\omega_0 &= P(C_0) = \sum_{l=1}^{k} p_l = \omega(k), \\
\omega_1 &= P(C_1) = \sum_{l=k+1}^{L} p_l = 1 - \omega(k), \\
\mu_0 &= \sum_{l=1}^{k} l \cdot P(l \mid C_0) = \sum_{l=1}^{k} l \frac{p_l}{\omega_0} = \frac{\mu(k)}{\omega(k)}, \\
\mu_1 &= \sum_{l=k+1}^{L} l \cdot P(l \mid C_1) = \sum_{l=k+1}^{L} l \frac{p_l}{\omega_1} = \frac{\mu - \mu(k)}{1 - \omega(k)}.
\end{aligned} \tag{22}$$

For any value of k, it is easy to verify the following equation.

$$\begin{aligned}
\mu &= \sum_{l=1}^{L} lp_l = \mu_0\omega_0 + \mu_1\omega_1, \\
\omega_0 &+ \omega_1 = 1.
\end{aligned} \tag{23}$$

So far, the threshold calculation is transformed into an optimization problem.

3.3. Network Data Monitoring Performance Test and Analysis. In this paper, according to cloud computing technology, a variety of signals are collected through simulated radiation models and experiments, including four types of corona discharge, suspension discharge, bubble discharge, and oil discharge. The sampling frequency is set to 5 MHz, and the data are stored in binary format. Each sampling point occupies 2 bytes, and each file continuously stores various forms of signals in units of power cycles. The information of the collective data used in the experiment is shown in Table 1. The size of the data set is gradually increased according to the number, and data sets 2 to 8 are integer multiples of number 1. The 4 monitoring sources are equivalent to 4 different discharge types, and the amount of data is the same. Each file stores 335 power frequency cycle partial discharge signals, and the size is about 64 MB. Test data set information is shown in Table 1.

Parallel granularity refers to the size of each small load after partition. Here, it can be considered as the size of files or blocks, which usually affects the creation and performance of parallel programs. The discharge signals with the same size as the No. 8 data set are reorganized according to different file sizes to obtain the data set shown in Table 2.

With the increase of the number of files, the program values that take the most time and the least time slowly approach. This is because the uniform granularity will become finer and finer, resulting in more and more balanced load. Therefore, the time-consuming difference when running multiple times is approaching. From the above analysis, it can be seen that the parallel granularity makes some idle computing nodes unable to be fully used in part of the time. Although the granularity is too small, it can balance the load, but the cost is to increase the general switching activity overhead. Therefore, the Hadoop size of parallel granularity should be selected according to the Hadoop cluster size.

In order to analyze the performance of data mode by combining data storage and query conditions, two kinds of experiments of data import and query are carried out on the established cluster platform, and they are compared with the integration scheme in single-machine mode. In stand-alone mode, SQL Server 2005 database management system is used to store the latest real-time detection data. The data import

Table 2: Test data sets with a different granularity.

Data set number	Total number of files/piece	Number of monitoring sources	Total number of signals/cycle	Total size/MB
8_1	8	4	2680/8	4096
8_2	16	4	1340/16	4096
8_3	24	4	893/24	4096
8_4	32	4	670/32	4096
8_5	40	4	536/40	4096
8_6	48	4	447/48	4096
8_7	56	4	383/56	4096
8_8	64	4	335/64	4096

mainly compares the creation of HBase-based database and traditional relational database, and the query experiment mainly compares the creation of access status data of stand-alone and spark cluster systems. The data import and query experiments were carried out three times, respectively, and the average value was taken. In order to display the experimental results more intuitively, we use a broken line graph. The ordinate represents the execution time in seconds, and the abscissa represents the amount of data.

Experiment 1. The amount of data imported into HBase and SQL Server 2005 is 50000, 100000, 200000, 500000, 1 million, 3 million, and 7 million. The experimental results are shown in Figure 2.

Experiment 2. The comparison of query time between stand-alone system and cluster platform when the amount of query data is 1000, 5000, 10000, 30000, 100000, 1 million, and 3 million, respectively. The results are shown in Figure 3.

From the analysis in Figures 3 and3, the following results can be obtained:

(1) If importing data, when the amount of data is less than or equal to about 300,000, the SQL Server import time is less than the import time of the HBase database. As the amount of data increases, the import time of HBase database will gradually increase, while the import time of SQL Server will increase sharply. When it reaches a certain node (7 million data), the import time of SQL Server will far exceed HBase database.

(2) If data query is performed, and the amount of data is small, that is, the number of data items in the experimental query is less than 30,000, the data query time of the single-machine system is shorter than that of the cluster system. As the amount of data increases, the time of the cluster system gradually increases, while the time of the stand-alone system increases significantly. Table 3 shows the results of cluster analysis of Spark combined with parallel DBSCAN data.

After grouping analysis, it can be seen from Table 3 that the data are divided into 5 categories, including normal states and 4 different types of data attack states. The calculation shows that P is the overall accuracy result of 92.48%, which is very accurate.

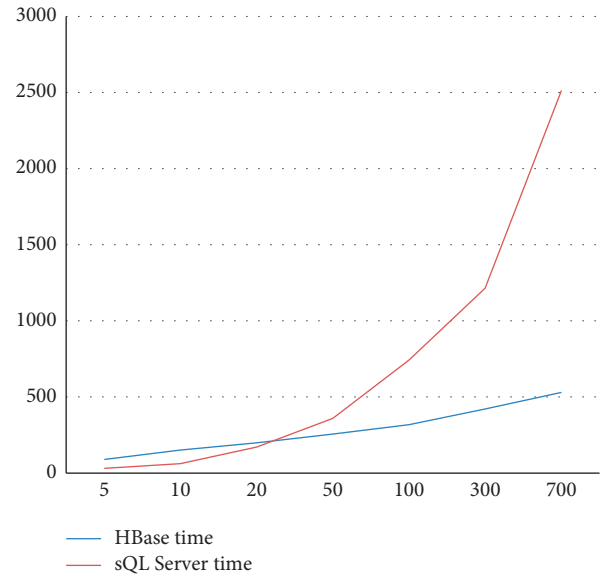

Figure 2: Performance comparison chart of data import test.

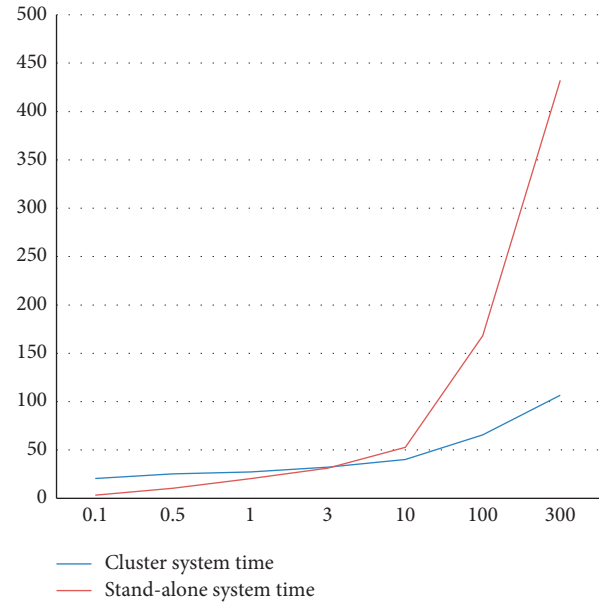

Figure 3: Comparison of data query experimental results.

Train 5 traffic monitoring states, and use the classifier for classification training to check the correct rate of the classes

Table 3: Detection results of abnormal flow division.

Cluster class number	0	1	2	3	4
Attack type	Normal	Neptune	Smurf	Teardrop	IP sweep
Number of records of this attack	93402	22527	5488	9705	11356
Number of other records	424	47	0	0	328
Total number of records	93824	22573	5486	9703	14621
Clustering accuracy	92.67%	99.83%	98.7%	98.7%	77.64%

Table 4: Accuracy of abnormal state identification.

Category number	0	1	2	3	4	5
Category	Normal	Neptune	Smurf	Teardrop	IP sweep	Outlier
Recognition accuracy	98.8%	89.8%	95.6%	97.7%	99.93%	97.35%

executed through the test set. The training set for each state is used to train the appropriate classification. The training results of the classifier and the accuracy of the corresponding test set are shown in Table 4.

The classification results of all different data points are statistically recorded. The results show that the classification accuracy of the classification combination of all different data points is accuracy = 96.93%. This shows that the combination of classifiers for multi-state recognition has high classification accuracy and good generalization ability.

4. Research on Legal Evidence Integration Strategy under Big Data Environment

4.1. Design of Legal Evidence Integration Service Data Platform. With the development of national politics, society, and economy, citizens' legal awareness is increasing, and the demand for all kinds of legal services is also rising. Generally, most legal services have the characteristics of repeatability, sharing, and versatility. In today's real life, legal service information system has important and unique social significance and complete technical possibilities. This paper uses big data technology to design and build an integrated auxiliary legal service system, which can provide basic legal services or auxiliary services for the people and legal workers. The purpose of designing the system is to provide a new way of access for ordinary people and legal professionals, so as to save time for relevant workers, improve the efficiency of legal services, and reduce the cost of litigation process. The main modules applicable to the whole system are shown in Figure 4.

Database conceptual model is the key link of conceptual design. It will provide technical support for database design and can be used for legal case retrieval. Based on the field of mathematics, the technical core of the system is data information modeling, and the most commonly used conceptual model is E-R model. As for program design, E-R diagram is designed in the requirement analysis stage. E-R diagram is entity relationship diagram, which includes entity, attribute, and relationship. The entity in E-R diagram refers to the data object in the data model; the property of Er graph is the property of data set object itself; the relationship in the E-R diagram refers to how the data are connected to each other. The structure of Er case retrieval diagram is shown in Figure 5.

The main task of designing logical database structure is to use ER diagram to create corresponding two-dimensional database tables. Generally, the logical structure of database has four basic structures: set structure, line structure, tree structure, and graphic structure. This article chooses to use MySQL database, which usually contains 6 columns of associated data tables. The name and function of the data are shown in Table 5.

4.2. Judicial Big Data Integration and Optimization Strategy under Big Data Environment

4.2.1. Pay Attention to the Cultivation of Judicial Personnel's Data Ability. In the process of training legal talents, we need to pay more attention to the improvement of their data ability. Due to the cognitive gap and prejudice of thought, the social masses are more willing to believe in irrational news than the so-called syllogism demonstration process. However, because the statistical data are intuitive and empirical, it can often produce better persuasion effect. In today's society, groups with active control algorithms have more power in the ethical direction, but the initial purpose of determining data learning ability is not to obtain power, but to bear more responsibility for judicial justice in the new era. If we want to make the argument more in line with the background and requirements of the times, it is necessary to improve the legal proceedings and make the evidence more convincing through the ability of finding data, analysis, sorting, and application.

4.2.2. Development Suggestions for Judicial Big Data Development. First, we should gradually improve the judicial data research model, develop and strengthen team cooperation, and improve the proportion of legal data research talents. The problems exposed by judicial big data at the technical level will greatly affect the accuracy and reliability of the technical services finally provided by the auxiliary system of judicial big data system. Therefore, the deficiencies based on big data technology in the judicial field can truly reflect the current social expectations for the development of compound talents and judicial data technology talents.

Second, we should establish a judicial database and merge it for development. Because the quality of the sample

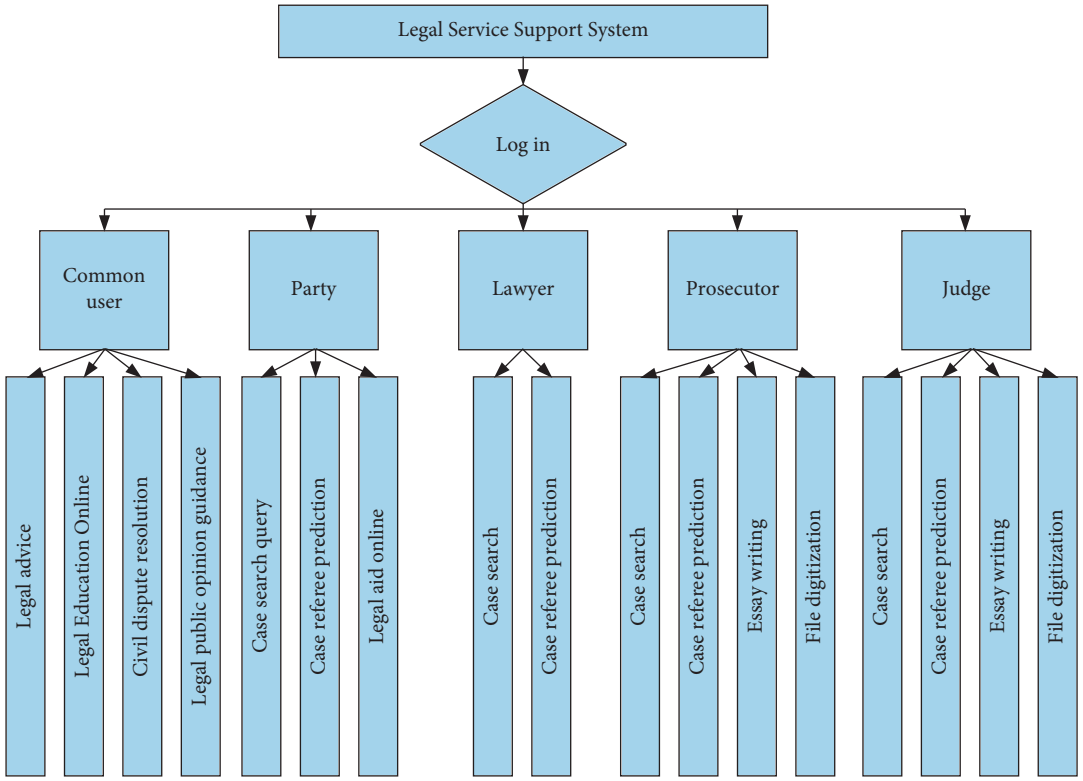

Figure 4: Main functional modules of legal aid system.

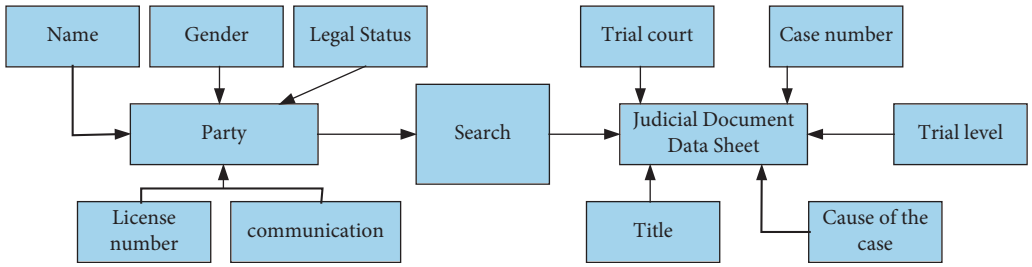

Figure 5: Case retrieval ER diagram.

Table 5: Database table structure.

Table name	Meaning	Effect
Litigant	Party information form	Used to store information about the parties
Data_laws	Laws and regulations data sheet	Used to store massive databases of laws and regulations
Trial_cases	Trial case table	Mainly store existing judicial precedents
Judicial_doc	Judicial document data sheet	Mainly store judicial documents
Case_info	Case information form	The main information of judicial trial cases
judicial_inter	Judicial interpretation form	Mainly store the judicial interpretations of the courts

determines the accuracy of the final prediction of the data model, the defects such as arbitrators' disputes and arbitrators' own shortcomings should be excluded. In reviewing the data, the number of appeals and nonrepresentative cases should be minimized.

Third, we should pay attention to cultivating compound talents. In the past, the research on judicial big data was mainly based on procedure researchers, but the obstacles found and encountered by researchers in the research process of legal theories and methods have also become the difficulties in promoting judicial big data technology. Therefore, it is necessary to cultivate more compound talents to improve the proportion of legal talents in the field of judicial big data.

The core of forensic data technology is the algorithm itself, and the core of the focus dispute of legal behavior is

also the algorithm. The judiciary has power because it has rules that cannot be ignored and despised, and carries out fair trials in accordance with existing rules. Even though the algorithm can extract some laws through a thorough understanding of judicial data, as the jurist Kirchmann said, "the change of legislators can turn all documents into waste paper," that is, the rule of law is the rule of rules rather than the rule of law. Therefore, different arbitrators may give completely different arbitration results.

Today, China's judicial big data technology exists only as an auxiliary technology, and the judicial judgment and sentencing suggestions made according to the above methods may directly affect the judge's subjective judgment. In addition, due to the discriminatory and opaque characteristics of the algorithm itself, it is particularly important to finalize the laws and regulations regulating the algorithm procedure as soon as possible. Therefore, it is particularly important to finalize the laws and regulations regulating the algorithm program as soon as possible. Therefore, the author suggests the following points:

(1) Improve the legal regulation system of judicial big data algorithm discrimination: in order to avoid the inevitable discrimination of judicial data sets, the principle of general legislature must be established first. The first is the principle of equality. All citizens are equal in law, including the principles of gender equality and ethnic equality, which are also the basic principles established in China's constitution. These principles must also apply fair judicial data rules to ensure their implementation. Secondly, we should adhere to the principle of openness. In order to avoid the opacity caused by the black box operation of judicial data and the unexplainability of the conclusion of judgment algorithm, the public procedure of justice must be observed to the greatest extent.

(2) Formulate the development restriction and accountability mechanism of judicial big data algorithm: both judicial data producers and judicial data users shall bear the same responsibility for the civil liability caused by algorithmic discrimination. If the infringer requires the algorithm producer or the judicial user of the data algorithm (including the court) to interpret the relevant algorithms, in order to protect the victims' rights of infringement relief, it is very important to explain the rules and responsibility mechanism of the corresponding algorithms.

(3) Establish a regulatory mechanism for judicial big data application before applying a large amount of judicial data to trial, and the algorithm should be tested. The test and prediction test of big data forensics algorithm should be carried out jointly by the court, citizens, and development companies. Through multi-dimensional monitoring, we can ensure that the forensics algorithm method can improve the accuracy of the test and ensure the fairness and openness of the trial to the greatest extent.

Although new technologies have brought about the improvement of production efficiency, they are accompanied by security challenges caused by new technologies. This phenomenon is inevitable in the era of big data. The urgent demand for judicial data in China's judicial field also confirms the importance of judicial big data. Today, in-depth research on judicial big data is imminent, and what is needed is the disclosure of a large number of judicial data. The disclosure of forensic data is the basis of forensic research and forensic data development—it provides data sources and research samples for forensic data research. The danger of using judicial data is that by exchanging a large number of judicial data, judicial data will interfere with state secrets, personal privacy, data sovereignty, and even the release of judicial information, affecting the fairness and credibility of the trial. Therefore, it is necessary to establish a self-disclosure management system of judicial data, limit private data, blur some judicial data, improve data anti-climbing countermeasures and protection mechanisms, and protect data.

5. Conclusion

This paper summarizes the research status of mobile cloud computing, cloud computing alliance, and big data at home and abroad. Through the analysis of the causes, connotation, and characteristics of the emergence and development of mobile cloud computing alliance, the organizational forms, characteristics, and differences of data sources, this paper reveals the relevant evolution theory of integrating mobile cloud computing alliance mechanism according to data sources. On this basis, the integration mechanism of data monitoring and analysis design of mobile cloud computing alliance is designed, including the acquisition and storage mechanism of mobile cloud computing alliance data resources in the cloud and parallel grouping mechanism. Then, taking a mobile cloud computing alliance as an example, this paper verifies the data integration mechanism. Today, China's judicial big data technology is still in the entry stage, and the development of legal artificial intelligence is also in the stage of weak artificial intelligence. However, it is very necessary to set up countermeasures in advance for the problems in the development of judicial data technology in the future. In the future, the judicial field and even the whole legal field will face more challenges brought by scientific and technological progress. The correct way is to meet the challenges and find strategies to actively deal with them. What the judiciary and academia need is to jointly introduce industry restrictions, maintain industry rules in the process of program design through the joint participation of academic and judicial personnel, and complete the industry self-discipline specification of judicial big data under this background, so as to improve the management and development of legal auxiliary service system.

Data Availability

The data used to support the findings of this study are available from the corresponding author upon request.

Conflicts of Interest

All the authors have no conflicts of interest.

References

[1] M. N. I. Sarker, M. Wu, and M. A. Hossin, "Smart Governance through Bigdata: Digital transformation of public agencies," in *Proceedings of the in 2018 international conference on artificial intelligence and big data (ICAIBD)*, May.2018.

[2] J. Fan, M. Zhang, A. Sharma, and A. Kukkar, "Data mining applications in university information management system development," *Journal of Intelligent Systems*, vol. 31, no. 1, pp. 207–220, 2022.

[3] M. Sarnovsky, P. Bednar, and M. Smatana, "Big Data and Cognitive Computing," *Big data processing and analytics platform architecture for process industry factories*, vol. 2, no. 1, 2018.

[4] B. M. Balachandran and S. Prasad, "Procedia Computer Science," *Challenges and benefits of deploying big data analytics in the cloud for business intelligence*, vol. 112, pp. 1112–1122, 2017.

[5] R. V. Mendonça, J. C. Silva, R. L. Rosa, M. Saadi, D. Z. Rodriguez, and A. Farouk, "A lightweight intelligent intrusion detection system for industrial internet of things using deep learning algorithm," *Expert Systems*, vol. 39, Article ID e12917, 2021.

[6] J. Dean and S. Ghemawat, "MapReduce: simplified data processing on large clusters," *OSDI*, vol. 51, pp. 107–113, 2008, https://dl.acm.org/toc/cacm/2008/51/1https://doi.org/10.1145/1327452.1327492.

[7] B. Luo, Y. Feng, J. Xu, X. Zhang, and D. Zhao, "Learning to Predict Charges for Criminal Cases with Legal Basis," in *Proceedings of the 2017 Conference on Empirical Methods in Natural Language Processing*, Copenhagen Denmark, September 2017.

[8] Y.-H. Liu, Y.-L. Chen, and W.-L. Ho, "Predicting associated statutes for legal problems," *Information Processing & Management*, vol. 51, pp. 194–211, 2015.

[9] C. Liu, C. Chang, and J. Ho, "Case instance generation and refinement for case-based criminal summary judgments in Chinese," *Journal of Information Science and Engineering*, vol. 20, no. 4, pp. 783–800, 2004.

[10] Y. Aoudni, C. Donald, A. Farouk et al., "Pattern Recognition Letters," *Cloud security based attack detection using transductive learning integrated with Hidden Markov Model*, vol. 157, pp. 16–26, 2022.

[11] H. Zhong, Z. Guo, C. Tu, C. Xiao, Z. Liu, and M. Sun, "Legal Judgment Prediction via Topological Learning," in *Proceedings of the 2018 Conference on Empirical Methods in Natural Language Processing*, Brussels Belgium, November 2018.

[12] H. Chen, D. Cai, W. Dai, Z. Dai, and Y. Ding, "Charge-based prison term prediction with deep gating network," in *Proceedings of the 2019 conference on empirical methods in natural language processing and the 9th international joint conference on natural language processing (EMNLP-IJCNLP*, Hong Kong China, November 2019.

[13] K. S. Warner and M. Wäger, "Building dynamic capabilities for digital transformation: an ongoing process of strategic renewal," *Long Range Planning*, vol. 52, pp. 326–349, 2019.

[14] M. Zaharia, M. Chowdhury, M. J. Franklin, S. Shenker, and I. Stoica, "Spark: cluster computing with working sets," in *in Proceedings of the 2nd USENIX conference on hot topics in cloud computing (HotCloud '10), USENIX Association*, Boston, MA, June 2010.

[15] Y. Li, R. K. Shyamasundar, and X. Wang, "Special issue on computational intelligence for social media data mining and knowledge discovery," *Computational Intelligence*, vol. 37, pp. 658-659, 2021.

[16] I. A. T. Hashem, I. Yaqoob, N. B. Anuar, S. Mokhtar, A. Gani, and S. Ullah Khan, "The rise of "big data" on cloud computing: review and open research issues," *Information Systems*, vol. 47, pp. 98–115, 2015.

[17] A. G. Frank, G. H. Mendes, N. F. Ayala, and A. Ghezzi, "Technological Forecasting and Social Change," *Servitization and Industry 4.0 convergence in the digital transformation of product firms: a business model innovation perspective*, vol. 141, pp. 341–351, 2019.

[18] B. Hindman, A. Konwinski, M. Zaharia et al., "Mesos: a platform for fine-grained resource sharing in the data center," in *Proceedings of the 8th USENIX conference on networked systems design and implementation*, Boston USA, April 2011.

[19] J. Dean and S. Ghemawat, "MapReduce: a flexible data processing tool," *Communications of the ACM*, vol. 53, pp. 72–77, 2010.

Hindawi
Mobile Information Systems
Volume 2022, Article ID 9943452, 10 pages
https://doi.org/10.1155/2022/9943452

Research Article

Application of Blockchain Based on Deep Learning Algorithm in Enterprise Internet of Things System

Liang Guo

Department of Mathematics and Information Engineering, Liaocheng University Dongchang College, Shandong, Liaocheng 252000, China

Correspondence should be addressed to Liang Guo; 20140131@nxmu.edu.cn

Received 7 July 2022; Revised 28 July 2022; Accepted 12 August 2022; Published 30 August 2022

Academic Editor: Shadi Aljawarneh

The purpose of an IoT enterprise business system is to form a global open network structure. The main task of this process is to build the Internet of Things system based on the internal enterprise, and link the upstream and downstream enterprises to interact with the Internet of Things system. However, existing blockchain systems often have limited performance and capacity, so they cannot be used in many scenarios, resulting in reduced scalability. The most common solution is to use the deep learning algorithm to find the optimal blockchain parameters. Based on deep learning and blockchain technology, this article proposes an enterprise Internet of Things system, which divides the whole Internet of Things into three layers—device layer, edge layer, and application layer, so as to build a reliable edge layer platform, so as to integrate the application network and blockchain network of the enterprise Internet of Things system and ensure the data security of the enterprise Internet of Things system. Finally, in order to verify the design proposed in this article, we build a distributed IoT business system, implement the deployment of experimental datasets on multiple hardware platforms, and design experiments to verify the security and effectiveness of the system designed in this work. By using blockchain technology based on the deep learning algorithm, the accuracy and time efficiency of the enterprise Internet of Things system are improved, and the burden of enterprise operators is greatly reduced. This article studies the deep learning algorithm and blockchain technology, and applies it to the design process of the enterprise Internet of Things system, thus promoting the development of the enterprise Internet of Things system.

1. Introduction

Scientific and technological progress is the power source of social and economic development, and it is also the main development goal. In recent years, with the continuous progress of Internet technology in China, the application of new technologies has brought new opportunities and challenges to all fields of economic development [1]. Artificial intelligence based on deep learning can quickly process a large amount of information, and even partially replace artificial intelligence for intelligent prediction and decision-making, so as to effectively improve the efficiency of transaction processing, so as to achieve economies of scale [2]. In recent decades, terminal intelligence, communication technology, cloud computing, and big data technology have developed rapidly. Affected by the above technologies, Internet of Things technology has developed rapidly in the fields of smart home, smart city, and autonomous driving [3, 4]. At present, the number of Internet of Things terminals entering the network continues to grow. Cloud computing is limited by network bandwidth, delay, and other factors, and there are still many deficiencies in the data processing of edge nodes. At the same time, the consumer-oriented Internet of Things is developing rapidly, and its demand for IoT terminals and applications is growing. Driven by internal and external factors, edge computing is developing rapidly [5]. Blockchain has the characteristics of distributed data storage, point-to-point transmission, consensus mechanism, encryption algorithm, and smart contract. It is a new kind of distributed infrastructure. The blockchain structure facilitates the storage and tracking of data. In order to ensure

the consistency of network data in a distributed environment, the blockchain uses a deep learning algorithm to generate block update registers [6]. Modern cryptographic technology ensures the security of blockchain data sending and storage. Using smart contracts to write automated scripts can build distributed applications. Blockchain adopts distributed consensus to maintain all system data at the same time, so as to effectively resist malicious attacks. Therefore, blockchain technology can help the enterprise Internet of Things system build a safe and reliable network environment [7]. The technical characteristics of blockchain technology, such as decentralization, data invariance, traceability, public-private key signature, and smart contract, naturally meet the needs of enterprise Internet of Things systems, and it is hoped to break through the reliance on third-party systems, so as to reduce transaction costs and improve operation efficiency [8]. The progress of Internet information technology such as blockchain has played an important role in promoting the innovation of enterprise Internet of Things system, providing new ideas for truly solving the pain points of the development of the real economy, and effectively optimizing the development and innovation methods of system applications [9].

2. Related Work

The literature believes that public chain is the original concept of blockchain technology, which means that everyone can participate in it. Compared with traditional trading systems, using public chain can save transaction costs and liberate productivity in data mining and data sharing. The literature believes that the smart contract designed based on blockchain technology has the characteristics of automatic execution [10]. If the smart contract is executed, the code hash value and digital signature will be copied into the smart contract at the same time, so the accuracy of contract execution can be improved. Blockchain is a technology that does not need to rely on intermediaries to reach a credit consensus [11]. Decentralization is the main feature of blockchain. Literature studies have found that the main reasons for the high cost of remittances in Africa are imperfect payment systems and poor market information. It is proposed to use blockchain technology to build a system without financial intermediary participation, such as bitcoin, to reduce costs and increase efficiency [12]. The literature combs the academic research on the consensus mechanism and compares the blockchain consensus mechanism with traditional technologies. The application of blockchain technology such as decentralization, tamper resistance, consensus mechanism, and smart contract seems to be a perfect solution, but this is not the case [13, 14]. The weakness of the pow algorithm and uncertain potential security limitations are pointed out in the literature. At present, the research on the application value of blockchain technology is more theoretical and lacks quantitative or empirical research and analysis, but these theories provide direction for the application of blockchain technology and lay the foundation for further research [15]. We need to seek the results of using blockchain technology in various disciplines, including computer, economic, and social research [16]. A multilevel secure Internet of Things model based on blockchain is proposed in the literature. According to the model description, the Internet of Things system is composed of two layers: the edge layer and the top layer above the edge layer. The definition of the edge layer is a local area network, which is composed of multiple devices under the control of a central node [17]. The edge layer node maintains a NoSQL database to store edge layer object information, including UUID, identity information, status dataset, function set, and format document. There is no central node at the top level, so each data node is independent and self-managed. The data exchange between nodes is recorded in the blockchain registers maintained by all nodes. Blockchain consensus algorithms have different choices. This mode ensures the security of the Internet of Things deployed in the wide area environment, but this scheme increases the cost of the whole network and requires a lot of time and resources to maintain the smart contract [18]. In order to solve the security problem of the industrial Internet of Things, the literature has designed an integrated identity management system based on blockchain and implemented the access control mechanism by using edge computing [19]. The system uses lightweight self-authentication password to detect the registration and authentication of network entities [20]. Each entity in the system has an identity, and each identity corresponds to a unique implicit certificate. Identity information and certificates are stored in the blockchain network to ensure that they are not deleted or tampered with. The literature uses convolutional neural network (CNN) technology to provide a wide range of video data storage and real-time monitoring [21]. Compared with the traditional video surveillance system, this system has many technical advantages, and there is still room for improvement in data access control and large-scale testing.

3. Analysis of Blockchain Technology Based on Deep Learning Algorithm

3.1. Principle and Model of Deep Learning Algorithm. Deep learning is one of the key technologies in the outbreak of artificial intelligence. It has made progress in the field of computer vision and natural language processing, which has brought AI technology into a new stage of explosive development. The wide and deep model consists of wide components and deep components. Its frame structure is shown in Figure 1.

It can be seen from Figure 1 that the wide component is a generalized linear model, and its shape is shown in the following formula:

$$y = w^T [x, \Phi(x)] + b, \tag{1}$$

where x is the original feature, Φ (x) is the cross-product feature, b is the default polarization value, and W is the weight parameter.

Deep neural network is a part of deep. The neural network first learns low dimensional dense embeddings for the feature vector and then uses the original dense feature as

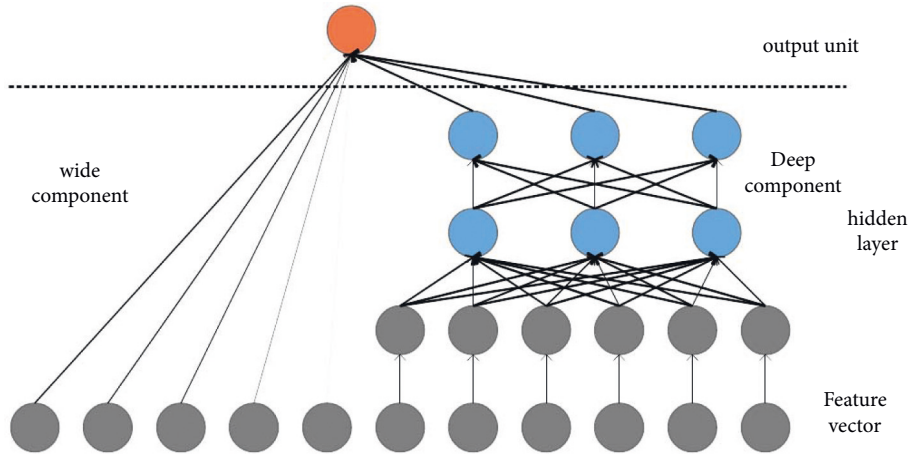

Figure 1: Wide and deep model architecture based on deep learning.

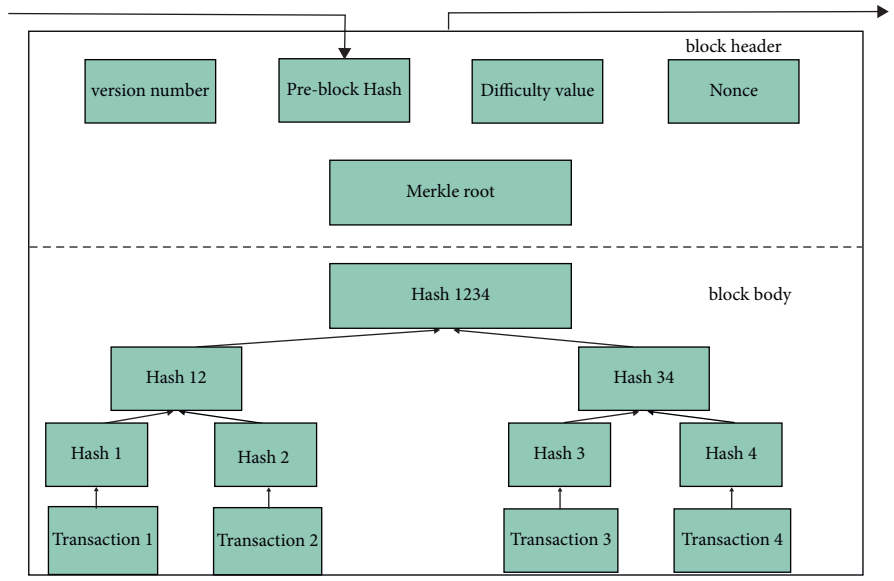

Figure 2: Basic structure of blockchain.

the input of the network. The calculation of each hidden layer is shown in the following formula:

$$a^{l+1} = f\left(W^l a^l + b^l\right), \tag{2}$$

where a^l, W^l, and b^l represent the activation, weight, and polarization values of the first layer of the hidden layer, respectively, and f represents the activation function. The loss function is logistic loss. At this time, the prediction result of the wide and deep model is shown in the following formula:

$$p(y = 1 \mid x) = \sigma\left(w_{\text{wide}}^T [x, \varphi(x)] + w_{\text{deep}}^T a^{lf} + b\right), \tag{3}$$

where σ represents sigmoid function, $\Phi(x)$ represents the cross-product function, and a^{lf} represents the activation value of the last layer.

Wide and deep is a common type of training, and joint training is different from integrated training. In integrated training, each model is trained separately, and the results are combined after training. Compared with joint training, integrated training requires that each part of the training be trained independently and summarized only when certain requirements are met, so the size of the model is larger. The wide component of joint training only uses a small part of the training sample set as the training set and uses its eigenvector to carry out product crossover to make up for the memory defects of deep components.

3.2. Blockchain Data Structure. Since its inception in 2008, blockchain technology has been regarded as a technology for sharing data between untrusted parties. A common form of blockchain is chain blockchain. This blockchain structure is the basis of different blockchain structures and the common feature of other blockchains. Blockchain is composed of interrelated block records. The order of blocks corresponds to the order of time stamps stored internally, as shown in Figure 2.

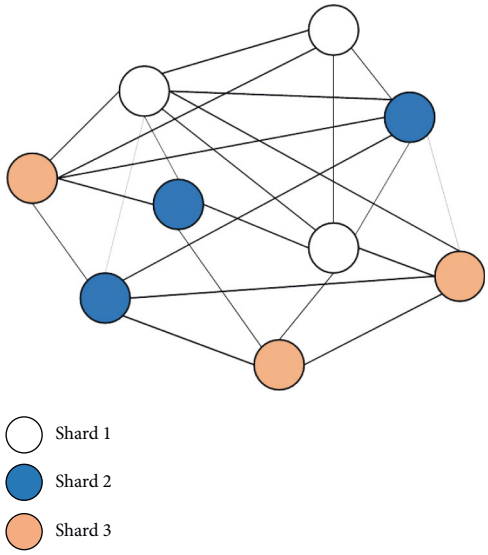

Figure 3: Spatial dimension of blockchain fragmentation.

Blocks are considered the basic unit of blockchain. Each block stores the hash value of the previous block. These blocks are closely connected in this way. If a block cannot obtain the hash value of the previous block, the block cannot be linked to the blockchain. This structure not only ensures the integrity of data, but also prevents malicious users from modifying blockchain data.

Using blockchain fragmentation, nodes are divided into different shards, and each shard only processes a small part of all data. In this way, transactions are processed equally and in parallel. The partitioned nodes reach an agreement on a set of transactions by running a consensus mechanism. For different application scenarios, information transmission between partitions may occur, so communication protocols between partitions must be designed to handle transactions between partitions.

As shown in Figure 3, the physical fragmentation process realizes grouping for real network nodes. For fragmented public chain nodes, their tasks are the same, and they all need to check the block consensus. Now, the tasks to be completed in the blockchain network are assigned to different partitions according to specific rules, so that different partitions can cope with different tasks. For such a partition structure, each partition is equivalent to an independent small blockchain operating system, and the nodes in each small system must continue to rely on consensus to ensure the consistency of internal data.

3.3. Hash Algorithm Design of Blockchain. Hash algorithm is an important technology in the field of information technology, which is widely used in blockchain. After binary data of any length is mapped to the hash function, it is converted to fixed-length output, and the output value is the hash value of the data. There are many hash functions, and the hash algorithm is the most widely used in blockchain technology. Using this algorithm, binary data of any length can be converted into hash values of 256 bits and 32 bytes. The hash algorithm has the advantages of unidirectional, random, timing, fixed length, and so on.

(1) Unidirectionality: the output data can be easily extracted from the input data, but the input data cannot be calculated from the output data.

(2) Randomness: even if the input data is only slightly modified, the output data may change greatly, so different input data will not produce the same hash value.

(3) Timing: any input data with different lengths will consume approximately the same time period through the same type of hash calculation.

(4) Fixed length: any input data with different lengths can generate output data with the same length after the hash calculation of the same type.

Hash function is usually defined according to the generated hash value. There are two main methods.

Hash based on addition and multiplication is achieved by returning data elements and then adding each initial value associated with the data elements. Usually, the value of an element is multiplied by a prime number.

The following formulas provide a hash calculation method based on addition and multiplication:

$$h(m) = h^{-1} \oplus (m \oplus p), \tag{4}$$

$$h(m) = \sum_{i=0}^{m} m_i \otimes p_i, \tag{5}$$

$$h(m) = h^{-1} \otimes (m \otimes p), \tag{6}$$

$$h(m) = \prod_{i=0}^{m} m_i \otimes p_i. \tag{7}$$

Like additive hashing, shift-based hashing also uses each element of the data string, but unlike additive hashing, shift-based hashing algorithms prefer to transmit data. It is usually a combination of left and right transfer operations, and the number of transfers is the quality. The result of each shift is only some additional aggregation operations, and the final result of shift calculation is the final result of change hash calculation. The formula of the shift hash algorithm is shown in the following formulas:

$$h(m) = h^{-1} \oplus (m \ll p) \otimes (m \gg q), \tag{8}$$

$$h(m) = \sum_{i=0}^{|m|} (m_i \ll p_i) \otimes (m_i \gg q_i), \tag{9}$$

$$h(m) = \prod_{i=0}^{|m|} (m_i \ll p_i) \otimes (m_i \gg q_i). \tag{10}$$

Merkel is a binary hash tree. In the Merkel tree, each leaf node is the hash value of a transaction. This article takes the Merkel tree with only four leaves as an example.

Table 1: Comparison of common consensus algorithms.

Feature	PoS	PoW	DPoS	PBFT
Transaction throughput	General	Low	High	High
Fault tolerance	<50%	<50%	<50%	<33%
Single transaction speed	min	10 min	s	ms
Number of supported nodes	Many	Many	Many	Less
Byzantine fault tolerance	Support	Support	Support	Support
Computing resource consumption	General	High	General	Low
Network resource consumption	General	Lower	General	High

(1) Use the sha256 hash algorithm twice to calculate the hash value of each transaction and calculate the hash value of each transaction. Here, four hash values of H_A, H_B, H_C, and H_D can be calculated, that is, the four-leaf nodes of the Merkel tree. article paper takes H_A calculation as an example:

$$H_A = SHA256(SHA256(\text{“otrade”}A)). \quad (11)$$

(2) Combine the hash values of two leaf nodes H_A and H_B. This article takes H_{AB} calculation as an example:

$$H_{AB} = SHA256(SHA256(H_A + H_B)). \quad (12)$$

(3) Perform the same combined hash calculation as in step (2) on the existing two hash values H_{AB} and H_{CD}, and finally, get a new hash value H_{ABCD}. The calculation of H_{ABCD} is as follows:

$$H_{ABC\,D} = SHA256(SHA256(H_{AB} + H_{C\,D})). \quad (13)$$

At present, the workload proof mechanism is considered to be the most efficient blockchain consensus algorithm, but it takes a long time to reach a consensus, which will consume a lot of computing power and resources, so it is not suitable for large-scale promotion and application. The characteristics of various consensus algorithms widely used in blockchain are shown in Table 1.

There are four private nodes in the experimental system chain. Each node needs real-time data sharing, with high data rate and low hardware computing power. Through comprehensive analysis, the PBFT consensus algorithm is the most suitable for this experimental system, so it is selected as the private chain consensus algorithm of this system to build the private chain of this system.

4. Architecture Design of Enterprise Internet of Things Based on Related Technologies

4.1. System Architecture. This article proposes a distributed Internet of Things system based on blockchain technology and edge computing, which is composed of a device layer, an edge layer, and an application layer. The device layer is composed of various intelligent and nonintelligent IoT terminals, forming a distributed IoT database. The edge layer is composed of multiple edge computing servers, and blockchain is used as the network infrastructure to connect each node of the edge computing server. After the data collected from the device is processed by the edge layer computing framework, part of the data is processed by the edge server and returned to the terminal device for local service closed-loop, and the other part of the data is uploaded to the application layer cloud computing center as the basic data of the top-level application. The application layer is equivalent to the cloud computing hub of the traditional Internet of things architecture, and responsible for the design of top-level business logic and application deployment. The overall architecture of the enterprise Internet of Things system based on blockchain and deep learning technology is shown in Figure 4.

4.2. Equipment Level Design. The IoT terminal at the device level is a bridge connecting the physical world and cyberspace. Terminal devices detect changes in the world's physical environment and digitally transmit analog data to higher-level IoT applications. According to the intelligent degree of terminal equipment, it can be divided into intelligent equipment and limited resource equipment. Intelligent devices have specific computing and storage capabilities, and can perform preprocessing, encryption, data transmission, and other functions independently. On the other hand, equipment with limited resources can only recognize and collect environmental data and convert analog signals into digital signals. In the distributed Internet of Things, we roughly divide IoT terminals into two types of devices: acquisition devices and execution devices. The collection equipment is the producer of data, and the execution equipment is the consumer of data. Therefore, the terminal device can be a collection device, an execution device, or have two identities at the same time. The terminal is connected to the adjacent edge computing server through NB-IoT, Lora, WiFi, NFC, and other communication protocols.

4.3. Edge Layer Design. Edge computing servers are all over the Internet of Things. To meet the requirements of internal data security processing, we have implemented Edge *X* Foundry computing framework, Hyperledger Fabric blockchain, and trusted platform deployment based on microservice architecture.

As an excellent open-source edge computing framework, Edge *X* Foundry provides device services for device-level terminals through a variety of communication protocols. Users can write Edge *X* Foundry control commands to manage their devices, and their devices send their production data through the restful API. Edge *X* Foundry publishes data to edge or cloud applications for further processing according to certain rules. Edge *X* Foundry is based on the microservice architecture. Each microservice is logically independent and functionally decoupled. The core service layer of Edge *X* Foundry is divided into an equipment service layer, a basic service layer, a support service layer, and an export service layer. To ensure the stability of Edge *X* Foundry during operation, it also provides security and

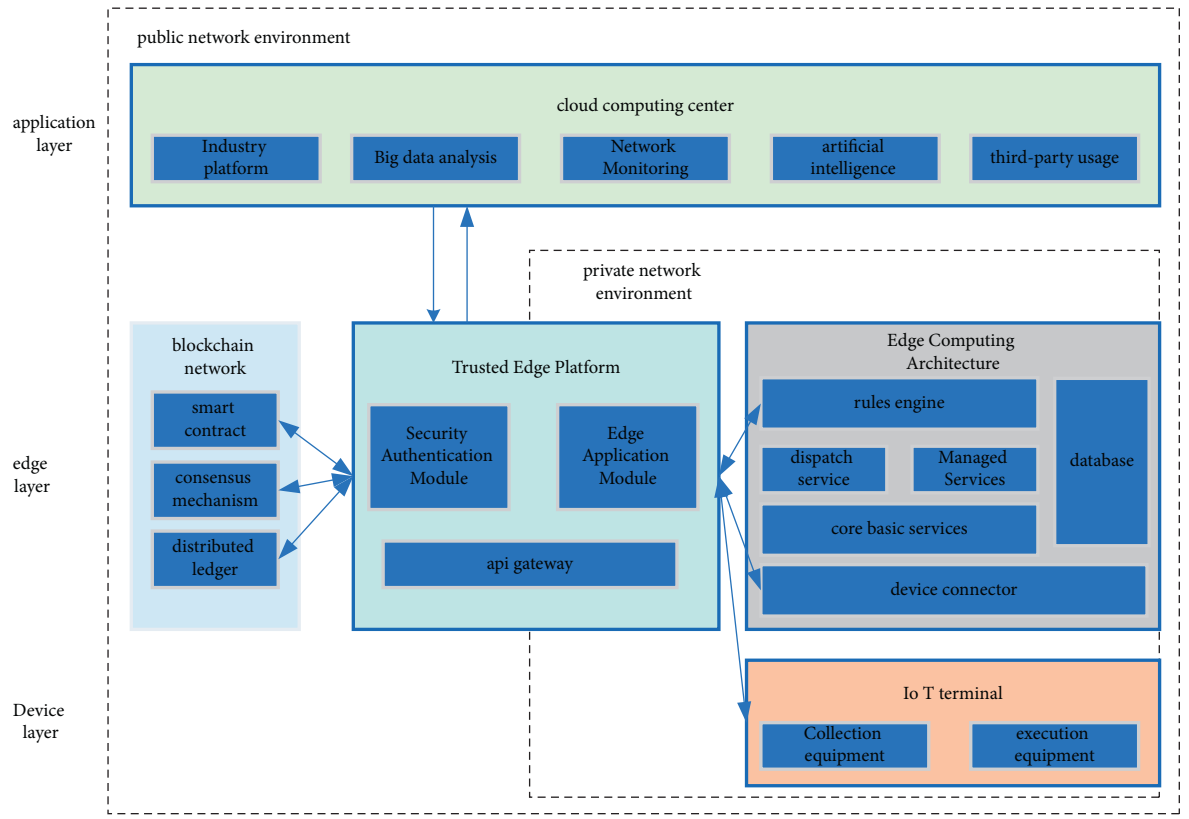

Figure 4: Architecture design of enterprise Internet of Things based on related technologies.

system management services. Each layer of Edge *X* Foundry has several components that communicate with each other through the restful API. In the edge computing environment, we adopt the key functions required to define the Edge *X* Foundry concept and integrate them into the design platform. From the perspective of users, the functions of the edge computing framework can be obtained as a collection of APIs. With excellent interface design, rich protocol support, and heterogeneous data processing capabilities, Edge *X* Foundry plays the role of edge-level data processing. Although Edge *X* Foundry provides security services, this service is only for single-point devices and is not applicable to the entire edge computing network, so we have introduced blockchain technology.

Blockchain network realizes a secure, reliable, and decentralized intelligent system in the edge environment, and solves the security and privacy problems in edge computing. A blockchain network is shared by multiple server edge nodes, and each node, as a network participant, can communicate with other nodes in the blockchain network. Due to the limited computing capacity of some terminal devices, they cannot participate in blockchain business. We use the edge server to provide blockchain services for terminal devices. The identity information of all these terminals is recorded and stored in the blockchain network through the edge server. Once the blockchain verifies the identity information, the authorized final entity can read the blockchain data, but the data can only be written to the edge server, which helps to avoid excessive data exposure. Users can access the edge server to edit smart contracts to create blockchain applications that meet the needs of terminal devices. In the edge computing environment, device identity information, access control information, and access control policies are stored in the decentralized blockchain network, which can effectively prevent data corruption.

4.4. Performance Parameter Index Design. For fragment content, in the process of verifying the consensus of new blocks, it is defined that the block manufacturer generates a local block with a maximum size of Bt (bytes) within each packaging interval T_n of the block. If the average transaction size is b_t, the block header size is B_{lk}, and the number of slices is k, the scalability within the slice can be obtained as follows:

$$\Phi\left(B_I, T_{II}\right) = \sum_{i=1}^{K} \frac{\left|\left(B_I - B_{\frac{I}{l_2}}\right)/b_I\right|}{T_{II_i}}. \tag{14}$$

If the transaction reaches a consensus within the shard, a local block will be formed. The shard will transfer the local block to the directory shard for final consensus and write it into the final blockchain. In the final consensus stage, check the blocks formed by K partitions, define the partition producer in the block directory, and generate a final block with a maximum size of B_F (bytes) within each block interval period T_F. If the average transaction size is b_F, the block

header size is B_{H}, and the scalability of directory fragmentation can be obtained as follows:

$$\Phi\left(B_F, T_F\right) = \frac{\left|\left(B_F - B_H\right)/b_F\right|}{T_F}. \tag{15}$$

Because the blockchain transaction consensus is divided into two processes—the number of transactions that each process can handle is represented by the scalability of internal partitions and directory partitions, and assuming that the scalability of internal partitions and directory partitions are the same, it is recorded as Tt′, and that the block header size is the same, it is recorded as $B_{\mathrm{H}}{}'$. Then, the scalability of the whole blockchain is recorded as

$$\begin{aligned}\Phi(B,T) &= \Phi\left(B_I, T_{II}\right) + \Phi\left(B_F, T_F\right) \\ &= \sum_{i=1}^{K} \frac{\left|\left(B_I - B_{Ih}\right)/b_I\right|}{T_{I_i}\,|} + \frac{\left|\left(B_F - B_h\right)/b_F\right|}{T_F} \\ &= \frac{\left|k\left(B_I - B_H'\right)/b_I + \left(B_F - B_H'\right)/b_F\right|}{T_I'}.\end{aligned} \tag{16}$$

The total propagation time of the internal consensus of the partition is

$$\begin{aligned}T_{\mathrm{in}\,p}^{k} &= \frac{1}{M}\left(T_{\mathrm{in\_preprepare}}^{k}+\right)T_{\mathrm{in\_prepare}}^{k} + T_{\mathrm{in\_commit}}^{k}\,) \\ &= \frac{1}{M}\max_{i\in[1,\ldots,k]}\left(\min\left(\max_{j\neq p}\left(\frac{MB}{R_{n_{i,p},n_{i,j}}}\right),\zeta\right) + \min\left(\max_{j\neq l}\left(\frac{MB}{R_{n_{i,l},n_{i,j}}}\right),\zeta\right) + \min\left(\max_{j\neq l}\left(\frac{MB}{R_{n_{i,l},n_{i,j}}}\right),\zeta\right)\right),\end{aligned} \tag{17}$$

Where, $n_{i,\,p}$ represents the master node p in the slice i, $n_{i,\,j}$ represents the node j in the slice i, and $R_{ni,\,p,\,ni,\,j}$ represents the transmission rate between the master node p and the replica node j in the slice i.

Assuming that the computing power of the replica node is $C_{\mathrm{i,j}}$, the processing time of the internal consensus verification fragment of the replica node is

$$T_{in\_re\_}^{i} = \frac{\left\{M\beta + \left[\left(MC + 4\left(N_i - 1\right)\right)\alpha\right]\right\}}{c_{i,r}}. \tag{18}$$

In addition, the process of checking the master node and the replica is the same. Therefore, the verification time of each message in the intraslice consensus request can be expressed as

$$T_{in\_v}^{k} = \frac{1}{M}\max_{i\in[1,\ldots,k]}\left(T_{\mathrm{in\_pri}i\_v}^{i}, T_{\mathrm{in\_ree\_}v}^{i}\right). \tag{19}$$

In the final consensus process, the node receives blocks from each partition. The master node of the shard directory can combine all local blocks in ascending order according to their shard numbers to generate the final consensus blocks and then create the final consensus according to the PBFT consensus algorithm. The information in the last block includes the block maker, timestamp, data size, and transaction hash. The last block of the directory is broadcast, and the consensus process is repeated. The time of final consensus is

$$\begin{aligned}T_{f_p}^{k} &= \frac{1}{M}\left(T_{f\_\mathrm{equest}}^{k} + T_{f\_\mathrm{preprepare}}^{k} + T_{f_{\mathrm{prepare}}}^{k} + T_{f\_\mathrm{comnit}}^{k} + T_{f\_\mathrm{epply}}^{k}\right) \\ &= \frac{1}{M}\left(\min\left(\max_{i\in[1,\ldots],j\in[1],\ldots,\ldots,l\in[1,\ldots C]}\left(\frac{MB}{R_{n_{l,j},n_{DS\,,,}}}\right),\zeta\right) + \min\left(\max_{l\neq p}\left(\frac{MB}{R_{n_{DS\,,p},n_{DS\,J}}}\right),\zeta\right)\right) \\ &\quad + \min\left(\max_{u\neq p,u,l\in[1,\ldots,C]}\left(\frac{MB}{R_{n_{DS\,,u},n_{DS\,,}}}\right),\zeta\right) + \min\left(\max_{u\neq l}\left(\frac{MB}{R_{n_{DS\,,u},n_{DS\,J}}}\right),\zeta\right) + \min\left(\max_{i\in[1,\ldots k]}\left(\frac{kMB}{R_{n_{DS\,,\psi},n_{i,j}}}\right),\zeta\right),\end{aligned} \tag{20}$$

where $n_{ds,p}$ represents the master node p in the directory partition, $\mathrm{n_{DS,j}}$ represents the node j in the directory partition, and $R_{DS,p,DS,j}$ represents the transmission rate between the master node p and the replica node j in the directory partition.

The final consensus must go through five steps: (1) the final stage of requesting consensus—fragmentation starts with requesting directory fragmentation; (2) the prestage of final consensus preparation; (3) the final preparation stage of requesting consensus; (4) the

Table 2: Transaction attributes of the training set.

Attribute name	Illustrate
fromAddrcss	Account address (sender)
toAddrcss	Account address (receiver)
gasPricc	Gas price
gasLimit	Gas limit
inputDatalf	Whether the inputData field contains data
cvcntDatalf	Whether the event field contains data
contractIf	Whether it is represented as a contract transaction

Table 3: Embedded capacity and success rate.

Embedded capacity	Embedding success rate	Extraction success rate
1 bytc/T	0.99	0.99
4 bytcs/T	0.98	0.98
8 bytcs/T	0.96	0.94
12 bytcs/T	0.87	0.74

submission stage of final consensus; and (5) the response stage of final consensus: directory fragmentation will respond to the final consensus result of fragmentation. Like the consensus within the partition, timeout is set for each stage.

The blocks after consensus through k partitions are transferred to the directory partition for final consensus. Directory fragmentation uses the PBFT algorithm to regain consensus. Before that, KM signatures and MAC are verified, and then, the merged blocks are passed to all other nodes. After the final consensus, the consensus results will be transmitted to N–C nodes outside the directory partition for N-C MAC generation operations. Therefore, similar to the internal consensus check time within the partition, the verification time of the master node and the replica node of the final consensus in the directory partition are, respectively,

$$T^k_{J\_m\_v} = \frac{\{kM\beta + [kM + 4(C-1) + (N-C)M]\alpha\}}{c_{DS\ ,p}}, \quad (21)$$

$$T^k_{J\_rp\_v} = \frac{\{kM\beta + [4(C-1) + (N-C)M]\alpha\}}{c_{DS\ \gamma}}, \quad (22)$$

where $C_{DS,p}$ and $C_{DS,j}$ represent the calculation speed of the master node and the replica node in the directory partition, respectively. Therefore, the final consensus verification time for each request is

$$T^k_{f\_v} = \frac{1}{M}\max\left(T^k_{f\_pri\_v}, T^k_{f\_re\_v}\right). \quad (23)$$

According to the blockchain fragmentation process based on PBFT consensus algorithm, we can clearly obtain that in order to achieve the results of network consensus, we must go through two main stages: one is the internal consensus process of fragmentation, and the other is the final consensus of directory fragmentation for the internal consensus process. The time required for each step includes message expansion time and message verification time. Then, the segmented blocks of the segmented blockchain based on the PBFT consensus algorithm can be expressed as

$$T_{\text{total}} = T_I + T^k_{\text{con}} = T_I + T^k_{\text{in}} + T^k_f = T_I + T^k_{\dot{m}\_p} + T^k_{\dot{m}\_v} + T^k_{f\_p} + T^k_{f\_1}. \quad (24)$$

The above formula calculates the blockchain delay based on PBFT consensus. The consensus delay of blockchain transactions must be completed within a limited number of consecutive block intervals (U is usually taken as 5~7) to make the blockchain consistent.

$$T_{\text{total}} \le uT^I. \quad (25)$$

5. System Security Design and Implementation

5.1. Data Source. First, 130000 Ethereum transactions were crawled from Etherscan, of which 100000 transactions were used as the training set, 15000 transactions as the verification set, and the remaining 15000 transactions as the test set. The web3.js tool is used to view and deploy transactions. The programming language used in the experiment is Python 3.7, and the deep learning framework is PyTorch-1.4.0, CUDA version 10.1, and CuDNN 7501. The transaction characteristics of the training set are shown in Table 2.

5.2. System Test. Since the automatic coding network is used to embed and retrieve information, the generated secret transactions may not be successfully sent to the blockchain. If the generated secret transaction cannot be deployed, Alice can reset the transaction attributes and merge again. In addition, the extracted secret information does not have to be the same as the original information, so it is necessary to calculate the success rate of embedding and extracting secret information. The average embedding capacity of 100000 transactions and the corresponding embedding success rate and extraction success rate are shown in Table 3.

The unit of embedded capacity in Table 3 is the embedded byte size of each transaction. The embedding success rate is the percentage of 100000 transactions successfully executed. The extraction success rate is the ratio of the number of retrieved correct information bytes to the number of embedded information bytes. It can be seen from Table 3 that with the increase in embedding amount, the success rate of embedding and extracting secret information decreases. Whether it is 4 bytes or 8 bytes of secret information, it has a higher embedding capacity, embedding success rate, and successful extraction rate. If the embedded capacity increases to 10 bytes/t, the success rate of extracting information decreases to 0.81. Therefore, it is best to embed 8 bytes of secret information in each transaction.

5.3. System Safety Analysis. Ethereum transactions are deployed directly on the blockchain, so the stability of this scheme is equivalent to the tamper resistance of the blockchain itself. After the training generator and extractor, Alice and Bob must save the trained network model parameter file (pt format). Before the two communicators disclose the stored model parameters, the attacker will not be able to crack the secret information. Therefore, deep learning based on blockchain steganography has high security.

6. Conclusion

As an application paradigm integrating distributed databases, P2P networks, consensus, and encryption algorithms, blockchain is characterized by good decentralization and openness, which can prevent tampering, complete anonymity, and trace data. In addition to the relevant characteristics of blockchain itself, fragmented blockchain is also more efficient than single chain blockchain, so it has better prospects in the application of value chain management. With the development of economy, enterprises have formed a value chain in the process of manufacturing products or completing services, thus improving the efficiency of enterprises. Using blockchain technology in the commercial Internet of Things system can improve the operation efficiency of the commercial Internet of Things and reduce the operation cost. In this context, after introducing the deep learning algorithm, this article expounds the efficiency of data collection and the reliability of data storage in the modern Internet of things system, and summarizes the basic business logic of the Internet of Things. A blockchain-based enterprise Internet of Things system model is proposed. Based on the in-depth study of the business development and business needs of modern Internet of Things, combined with the current blockchain hotspot technology, this article uses the deep learning algorithm to model and proposes a business development-oriented enterprise Internet of Things system model. It provides specific guidance for manufacturers on how to widely use technology to improve the functions of the Internet of Things system and reduce operating costs in the future.

Data Availability

The data used to support the findings of this study are available from the corresponding author upon request.

Conflicts of Interest

All the authors do not have any possible conflicts of interest.

Acknowledgments

The research was supported by the project Research on curriculum Reform of Industry University Cooperation for Software Engineering Major under New Engineering (Project no. 202002191027).

References

[1] S. Li, "Innovations in Chinese engineering education with digital technologies: a brief review of recent advances," *Computer Applications in Engineering Education*, vol. 26, no. 5, pp. 1081–1088, 2018.

[2] S. Makridakis, "The forthcoming artificial intelligence (AI) revolution: its impact on society and firms," *Futures*, vol. 90, pp. 46–60, 2017.

[3] Y. R. Lee and J. Lee, "Deep learning-based late fusion of Multimodal information for emotion classification of music video," *Multimedia Tools and Applications*, vol. 80, no. 2, pp. 2887–2905, 2021.

[4] D. Liu and Q. Hu, "Practice of China's new high-level university of science and engineering's international development: a case study of dongguan university of technology," *Region - Educational Research and Reviews*, vol. 1, no. 2, pp. 28–33, 2020.

[5] P. Mamoshina, L. Ojomoko, Y. Ostrovski et al., "Converging blockchain and next-generation artificial intelligence technologies to decentralize and accelerate biomedical research and healthcare," *Oncotarget*, vol. 9, no. 5, pp. 5665–5690, 2018.

[6] A. Farouk, A. Alahmadi, S. Ghose, and A. Mashatan, "Blockchain platform for industrial healthcare: vision and future opportunities," *Computer Communications*, vol. 154, no. 15, pp. 223–235, 2020.

[7] K. Fan, Y. Ren, Y. Wang, H. Li, and Y. Yang, "Blockchain-based efficient privacy preserving and data sharing scheme of content-centric network in 5G," *IET Communications*, vol. 12, no. 5, pp. 527–532, 2018.

[8] T. McGhin, K.-K. R. Choo, C. Z. Liu, and D. He, "Blockchain in healthcare applications: research challenges and opportunities," *Journal of Network and Computer Applications*, vol. 135, pp. 62–75, 2019.

[9] Y. Miao, X. Liu, K.-K. R. Choo, R. H. Deng, H. Wu, and H. Li, "Fair and dynamic data sharing framework in cloud-assisted internet of everything," *IEEE Internet of Things Journal*, vol. 6, no. 4, pp. 7201–7212, 2019.

[10] X. Yang, G. Chen, M. Wang, T. Li, and C. Wang, "Multi-keyword certificateless searchable public key authenticated encryption scheme based on blockchain," *IEEE Access*, vol. 8, pp. 158765–158777, 2020.

[11] Q. Shao, C. Jin, and Z. Zhang, "Blockchain: architecture and research progress," *Chinese Journal of Computers*, vol. 41, no. 5, pp. 969–988, 2018.

[12] J. Luo, "Analysis of an efficient traceability system for agricultural product quality and safety based on alliance blockchain," *Computer Knowledge and Technology*, vol. 16, no. 6, pp. 272-273, 2020.

[13] J. Long, "Design of blockchain system in BDCP using hyperledger fabric," in *Proceedings of the 2019 World Symposium on Software Engineering (WSSE 2019)*, pp. 79–83, Wuhan, China, September 2019.

[14] D. Wu, Y. Xiang, and C. Wang, "Data protection technology for information systems based on blockchain," *Journal of Command and Control*, vol. 4, no. 3, 2018.

[15] X. Weng, P. Zhang, and W. Wang, "Remote attestation mechanism for platform integrity based on unbalanced-hash tree," *Journal of Computer Applications*, vol. 2, pp. 433–437, 2014.

[16] H. Mir, A. H. Mir, A multi-biometric system based on multi-level hybrid feature fusion," *Herald of the Russian Academy of Sciences*, vol. 91, no. 2, pp. 176–196, 2021.

[17] I. Kotenko, I. Saenko, and A. Kushnerevich, "Parallel big data processing system for security monitoring in internet of things networks," *Journal of Wireless Mobile Networks, Ubiquitous Computing, and Dependable Applications*, vol. 8, no. 4, pp. 60–74, 2017.

[18] Z. Wang, Z. Zhou, H. Zhang, G. Zhang, H. Ding, and A. Farouk, "AI-based cloud-edge-device collaboration in 6G space-air-ground integrated power IoT," *IEEE Wireless Communications*, vol. 29, no. 1, pp. 16–23, 2022.

[19] J. Li, M. Wang, and J. Zhang, "Application of block chain technology in the construction of safety production informatization," *Quantum*, vol. 41, no. 2, pp. 88–93, 2020.

[20] R. Buyya, C. S. Yeo, S. Venugopal, J. Broberg, and I. Brandic, "Cloud computing and emerging it platforms: vision, hype, and reality for delivering computing as the 5th utility," *Future Generation Computer Systems*, vol. 25, no. 6, pp. 599–616, 2009.

[21] C. B. Tan, M. H. A. Hijazi, Y. Lim, and A. Gani, "A survey on proof of retrievability for cloud data integrity and availability: cloud storage state-of-the-art, issues, solutions and future trends," *Journal of Network and Computer Applications*, vol. 110, pp. 75–86, 2018.

Hindawi
Mobile Information Systems
Volume 2022, Article ID 4881321, 9 pages
https://doi.org/10.1155/2022/4881321

Research Article

Intelligent System Application in Clinical Management of Medical Teaching Based on Deep Reinforcement Learning

Min Zhu,[1] **Ju Zhou**,[2] **Liang Chen**,[3] **Xueping Zhao**,[4] **and Chunhui Li**[4]

[1]*College of Anhui City Management Vocational College, Hefei, Anhui, China*
[2]*Medical Skill Experiment Teaching Center, Suzhou Medical College of Soochow University, Suzhou, Jiangsu, China*
[3]*School of Mechanical and Electric Engineering, Soochow University, Suzhou, Jiangsu, China*
[4]*School of Nursing, Suzhou Medical College of Soochow University, Suzhou, Jiangsu, China*

Correspondence should be addressed to Chunhui Li; chunhuili2006@suda.edu.cn

Received 8 July 2022; Revised 29 July 2022; Accepted 11 August 2022; Published 30 August 2022

Academic Editor: Shadi Aljawarneh

When dealing with engineering projects, there are many kinds of planning schemes. There are many problems to be solved in the performance and economic conditions of these indicators and engineering contents we study. Recently, many researchers have made great achievements in optimizing various subject projects. One of its purposes is to optimize and improve intelligent multi-objectives to make it more effective. Therefore, it is of great significance to develop intelligent multi-objective projects in academia and more engineering fields. The purpose of this study is to make efforts to strengthen the learning and construction of rapidly developing multi-objective optimization programs, and closely link these programs with neural network, fuzzy technology, interactive technology, and give a lot of examples of multi-objective optimization improvement program methods, which can eliminate the uncertainty in the multi-objective project plan, The purpose is to solve some difficult problems of multi-objective optimization and give the best suggestions. In this study, the strengthening of learning construction is combined with the clinical experiment, and most of this teaching method is put in the clinical management experiment of medical teaching. At the end of this study, we compared the performance of deep reinforcement learning with its dual structure version and interleaved structure version in different medical teaching clinical management environments and make a detailed analysis. Deep reinforcement learning provides a new idea for the improvement of intelligent multi-objective optimization and clinical management of medical teaching.

1. Introduction

There are three model learning methods in machine learning: one is enhanced learning, the other is supervised learning, and the other is unsupervised learning. Enhanced learning and supervised learning are not the same as unsupervised learning [1]. The enhancement of learning construction is not a professional guidance label with intelligence like supervised learning, but is a stage in which learning and absorbing knowledge and nutrition to expand its own advantages in the environment [2]. Enhancing learning construction is a stage of constantly enhancing its own experience. Unsupervised learning construction is to find hidden structures in data without label. In this respect, it is different from enhancing learning construction [3]. The purpose of enhancing learning construction is to enlarge the reward. If a hidden structure of environment is found, it can not maximize reward, because unsupervised learning structure is not the same as enhancing learning construction. One of the important fields in machine learning is deep learning. In recent years, it has developed rapidly, and has been favored by many scholars at home and abroad [4]. With the rapid development of the computer age, deep learning has also been widely used in many realities. In recent years, researchers have put the reinforcement of learning construction and deep learning together. Deep enhancement learning combines the two closely related advantages, and has no shortcomings [5]. For example, it is good at analyzing

high-intensity data and the best way to contact the environment.

In this study, we use the advantage of deep enhancement learning to apply it to intelligent multi-objective optimization to gradually improve the medical teaching and clinical management experiment. In practice, in this paper, most neural network structures like structure types are designed [6]. The input mode is model parameters, and the output method is the value of the Pareto solution of model parameters. After several rounds of mutual absorption, the final result value Pareto solution is obtained [7]. Then, the data model that designers like is used as the optimization goal of the ANN model. It is better to find a new plan to improve the target and take the intelligent optimization objective as the improvement development guidance scheme [8]. The deep enhancement learning scheme is used to study the teaching improvement of medical clinical experiment in detail, which can enhance the overall ability and teaching level of the doctor team [9]. The knowledge system learned should be improved, the learned knowledge should be consolidated, the interest and hobby of learning should be cultivated, and the students' practical ability should be strengthened to adapt to the educational learning mode in modern medical field in line with the development of globalization [10].

2. Related Work

The important viewpoints about reinforcement learning: we study two aspects of bias and variance analysis, and compare the results of reinforcement learning structure stability. The bias variances are positive bias, negative bias, delusional bias, random variance, and importance sampling variance. These are derived from the examples of the formula and the calculation of the equation, which can directly get the specific causes of the deviation and variance and the impact on the stability, and provide effective evidence for future solutions [11]. There are positive and negative deviations in the deviation, and the method adopted in this study intuitively and clearly states the factors and influences to solve the deviation. A novel access method is interleaving method, which can solve the problem of positive and negative deviation quickly [7]. There are three kinds of interleaving access methods: coupling estimator, adaptive coupling rate device, and interleaving access method. These three methods together constitute the interleaved access method. The formula in this paper can prove the method of interleaving access. Literature interleaving methods can be applied to many fields, such as experiments in reinforcement learning and deep reinforcement learning [12]. In this study, we can see a new computing method. Finally, the experimental results show that the performance of the new algorithm is the best. The design scheme of intelligent multi-objective project interaction is proposed in the literature, which makes the optimization of many objectives solved and improved [13]. In the scheme of model optimization, the designer needs to provide the value of parameter vector. In real life, designers can design their own favorite model, and take the input as the parameter, and the Pareto solution as the output. These conclusions are obtained by several rounds of training. The double beam crane is proposed as the object of multi-objective project optimization [14]. Their weight and safety are taken as the optimization index. Designers add these two indicators to the trade-off of goals, and they can get more satisfactory answers within the allowed time [15].

3. Intelligent Multi-Objective Optimization Improvement of Deep Reinforcement Learning

3.1. Deep Reinforcement Learning. First of all, we need to understand the background knowledge and related symbols of enhancing learning stability, such as the calculation method and definition of Markov, and then we can judge the reasons for enhancing learning stability. Markov decision process can enhance learning. Markov decision-making process is based on mathematical model, which can simulate the decision-making in the intelligent environment of the system. It has nothing to do with any state previously arrived and any action performed. The strategy is the action probability distribution of performing a certain action in a certain state, and the expression formula is:

$$\pi(s \mid a) = P(A_t = a \mid S_t = s). \tag{1}$$

Expectation function of Markov decision process:

$$V^{\pi}(s) = E\left(\sum_{t=0}^{\infty} \gamma^t R_{t+1} \mid S_t = s\right). \tag{2}$$

The correlation function equation obtained by the Markov decision process under the condition of following the strategy:

$$Q^{\pi}(s,a) = E\left(\sum_{t=0}^{\infty} \gamma^t R_{t+1} \mid S_t = s, A_t = a\right). \tag{3}$$

The true value of the highest expected value in X is:

$$\mu_*(X) = \max_i \int_{-\infty}^{+\infty} f_i(x)\mathrm{d}x. \tag{4}$$

Bias is often different from real data. Based on the above, we estimate a definition of bias:

$$\mathrm{Bias}(\widehat{\mu}) = E(\widehat{\mu}) - \mu_*. \tag{5}$$

Use the largest estimated value to estimate the value of the random variable, the expression is:

$$\widehat{\mu}_*^{ME}(S) = \max \widehat{\mu}_i(S)_i. \tag{6}$$

Knowing that the maximization function is a convex function, for any set of samples and any unbiased estimator, we can get:

$$E\left(\widehat{\mu}_*^{ME}(S)\right) = E\left(\max \widehat{\mu}_i(S)_i\right). \tag{7}$$

Randomly select a sample, and then draw a random number of 100 as the mean. The statistical table is shown in Table 1:

Table 1: The maximum estimator's sampling estimation table for four random variables.

Variable name	X1	X2	X3	X4	Maximum estimator value
Sample 1 mean	1.54	1.90	2.12	2.15	2.15
Sample 2 mean	1.43	2.04	2.15	1.67	2.16
Sample 3 mean	0.76	1.73	2.16	1.36	2.14
Sample 4 mean	0.98	1.28	2.22	2.74	2.72
Sample 5 mean	1.26	2.33	2.17	1.93	2.33
Sample 6 mean	1.04	2.15	2.29	2.45	2.44
Sample 7 mean	1.07	1.57	2.15	2.61	2.66
Sample 8 mean	1.41	2.25	2.18	2.75	2.70
Sample 9 mean	1.18	2.01	2.23	1.84	2.27
Sample 10 mean	1.02	2.24	2.22	2.22	2.27
Final sample average	1.16	1.93	2.24	2.03	2.38

The upper bound of the estimated variance of the dual estimator and the lower bound of the estimated negative deviation are both proved in this study. The negative deviation is always less than 0, so its upper bound is 0, and its lower bound expression:

$$\mathrm{Bias}\left(\widehat{\mu}_*^{DE}(S)\right) = E\left(\widehat{\mu}_*^{DE}(S)\right) - \mu_*. \tag{8}$$

The upper bound expression of the estimated variance of the double estimator:

$$j = \arg\max \widehat{\mu}_j(S_1),\ \widehat{\mu}_*^{DE}(S) = \widehat{\mu}_j(S_2)_i. \tag{9}$$

The double estimator finds the subscript of the maximum sample mean variable in the estimator 1. This is because the samples used by the estimators 1 and 2 are independent of each other. The subscript of the maximum value in the estimator 1 is equivalent to a random Variables, as shown in Table 2.

As shown in Table 3, the largest subscript in estimator 1 may be the largest or the smallest if it is checked in estimator 2. Therefore, if the sampling mean selected by estimator 2 is divided into two categories, one is the sampling mean with the true value variable selected, and the other is the sampling mean without the true value variable selected, then the expectation of the first category is the maximum expectation. The second kind of expectation must be less than the maximum expectation, so the combination of the two must be less than the maximum expectation, and the double estimator will cause underestimation.

The learning methods of reinforcement learning can be roughly divided into two categories, one is the Monte Carlo method, and the other is the temporal difference method. The calculation formula of the expected value of all state action values:

$$\begin{aligned} E\left(\widehat{\mu}_*^{DE}(S)\right) &= E\left(\widehat{\mu}_j(S_2)\right), \\ E[Q(s',a')] &= \sum_{a' \in A} \pi(s'|a')Q(s',a'). \end{aligned} \tag{10}$$

This article introduces the n-step timing difference algorithm. After performing the n action steps, it is updated

Table 2: Estimator 1 sampling estimation table for four random variables.

Variable name	X1	X2	X3	X4	Estimator 1 takes the subscript
Sample 1 mean	0.84	2.03	2.54	1.28	3
Sample 2 mean	1.70	2.77	2.27	2.25	2
Sample 3 mean	1.14	2.14	2.15	2.45	2
Sample 4 mean	1.33	1.06	2.26	1.95	3
Sample 5 mean	1 25	1.86	2.17	2.23	3
Sample 6 mean	0.99	1.97	2.17	1 28	3
Sample 7 mean	1.27	1.86	2.20	2.23	3
Sample 8 mean	1 20	1.57	2.23	1.52	3
Sample 9 mean	1.78	1.49	2.21	1.56	4
Sample 10 mean	0.44.	2.44	2.15	2.26	2
Final sample average	1.19	1.93	2.18	1.97	—

Table 3: Estimator 2 sampling estimation table for four random variables.

Variable name	X1	X2	X3	X4	Estimator 2 takes the value
Sample 1 mean	1.12	2.24	2.23	2.54	2.24
Sample 2 mean	0.53	2.35	2.25	1.81	2.35
Sample 3 mean	0.25	2.43	2.25	2.06	2.05
Sample 4 mean	0.84	1.70	2.21	1 95	2.21
Sample 5 mean	1.16	2.25	2.15	1.77	1.76
Sample 6 mean	1.15	2.16	2.22	2.11	2.22
Sample 7 mean	0.64	2.04	2.23	1.83	1.87
Sample 8 mean	0.84	2.04	2.19	0.99	2.19
Sample 9 mean	1.06	1.69	2.16	1.97	2.18
Sample 10 mean	1.66	1.73	2.27	1.96	1.72
Final sample average	0.97	2.04	2.21	1.84	2.08

according to the return value obtained during this period and the estimated value of the previous round of value function. The n-step return formula is expressed as:

$$G_t\colon t+n = R_{t+1} + \gamma R_{t+2} + \cdots + \gamma^{n-1}R_{t+n} + \gamma^n R_{t+n-1}(S_{t+n}). \tag{11}$$

The return is a special case of the conforming return. It weights all possible n-step updates in proportion, and finally multiplies it by the regular term to guarantee the weight and the sum is 1. Its formula is expressed as:

$$G_t^\lambda = (1-\lambda)\sum_{n=1}^{\infty}\lambda^{n-1}G_t\colon t+n. \tag{12}$$

The calculation items after these terminal states can be separated from the main summation items:

$$G_t^\lambda = (1-\lambda)\sum_{n=1}^{T-t-1}\lambda^{n-1}G_t\colon t+n+\lambda^{T-t-1}G_t. \tag{13}$$

On the basis of Q-learning, through the calculation of convolution, multi-dimensional data can be processed well, and features can be extracted from high-latitude information such as pictures, which makes it possible to use continuous pictures as output. The calculation used by the Q′ network to predict the target:

$$Y_t^{\mathrm{DQN}} = R_t + \gamma \max_{a'} Q\prime\left(S_{t+1}, a'; \theta_t'\right). \tag{14}$$

The calculation of the update target of deep Q-learning is the same as that of Q-learning, which uses the maximum Q value in the next state as the target. The difference is that in deep Q-learning, the fixed past nerve is used to estimate the maximum Q value. The algorithm process diagram of deep Q-learning is shown in Figure 1:

Deep double Q-learning can effectively reduce the overestimation of deep Q-learning through such a simple small change. Its modification formula:

$$Y_t^{\mathrm{doubleDQN}} = R_t + \gamma Q'\left(S_{t+1} + \mathrm{argmax}_{a'} Q\left(S_{t+1}, a'; \theta_t'\right), \theta_t'\right). \tag{15}$$

The algorithm structure diagram of deep double Q-learning is shown in Figure 2:

Hasselt described the depth of this version in the study. In the deep double Q-learning paper experiment, we can see that the deep double Q-learning under this version does reduce the overestimation compared to the deep Q-learning. However, due to the high correlation between the two Q-value networks, deep double Q-learning still has a certain overestimation, as shown in Figure 3:

Figure 3 is from Hasselt's deep double Q-learning paper. It can be seen that in the performance of the four games given, deep double Q-learning greatly reduces the overestimation of deep Q-learning, but deep double Q -Studying in Space Invaders and Zaxxon games still has high overestimations, satisfying the principle of independent cross-estimation in the double Q-learning thought. The updated objective function is the formula:

$$Y_t^{\mathrm{doubleDQN}} = R_t + \gamma Q'\left(S_{t+1} + \mathrm{argmax}_{a'} Q\left(S_{t+1}, a'; \theta_1'\right), \theta_1'\right). \tag{16}$$

The specific update target is calculated as:

$$Y_t^{\mathrm{doubleDQN}} = R_t + \gamma Q'\left(S_{t+1} + \mathrm{argmax}_{a'} Q\left(S_{t+1}, a'; \theta_1'\right), \theta_2'\right). \tag{17}$$

The classical reinforcement learning algorithm Sarsa and Q-learning algorithm both use the ϵ-greedy algorithm in the action strategy, but in the update strategy, the Q-learning uses the greedy algorithm and the Sarsa uses the ϵ-greedy algorithm, the expression is:

$$Y_t^{\mathrm{interleaveDQN}} = R_t + \frac{1}{2}\gamma Q_1'\left(S_{t+1} + \mathrm{argmax}_{a'} Q_2'\left(S_{t+1}, a'; \theta_2'\right), \theta_2'\right). \tag{18}$$

3.2. Intelligent Multi-Objective Optimization and Improvement. In the case of solving multiple target projects, you can find a variable to optimize all project goals. Requirements for each small goal:

$$\mathrm{minimize} f(x) = \{f_1(x), f_2(x), \ldots, f_m(x)\} \mathrm{Subject}\, x \in X. \tag{19}$$

The general model of goal planning can be expressed as:

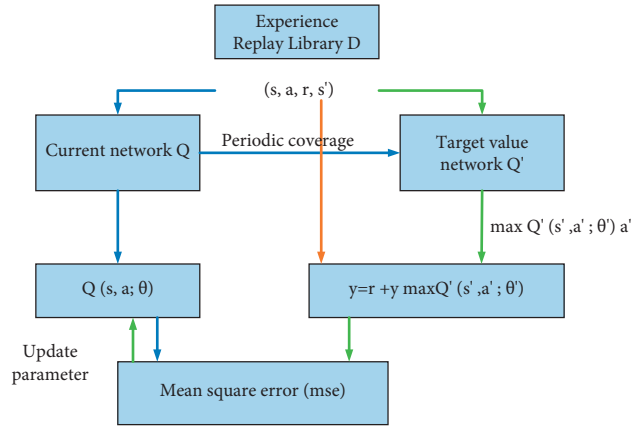

Figure 1: Algorithm structure diagram of deep Q-learning.

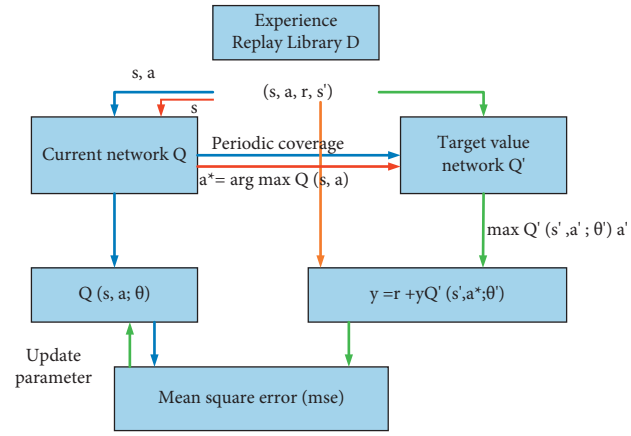

Figure 2: Structure diagram of deep double Q-learning algorithm.

$$\min \sum_{i=1}^{L} P_i \left\{ \sum_{k \in J_i} \left(w_k^+ d_k^+ + w_k^- d_k^-\right) \right\}. \tag{20}$$

The linear problem of the weight coefficient:

$$\min \sum_{i=1}^{m} \lambda_i f_i(x). \tag{21}$$

Commonly used functions to describe deviation are:
P modulus function:

$$h(f(x)) = \left[\sum_{k=1}^{m} \lambda_k \left| f_k(x) - \overline{f_k} \right|^p\right]^{1/p}. \tag{22}$$

Maximum deviation function:

$$h(f(x)) = \max_{1 \le k \le m} \left\{ \lambda_k f_k(x) - \overline{f_k} \right\}. \tag{23}$$

Geometric mean function:

$$h(f(x)) = \left[\prod_{k=1}^{m} \left| f_k(x) - \overline{f_k} \right|\right]^{1/m}. \tag{24}$$

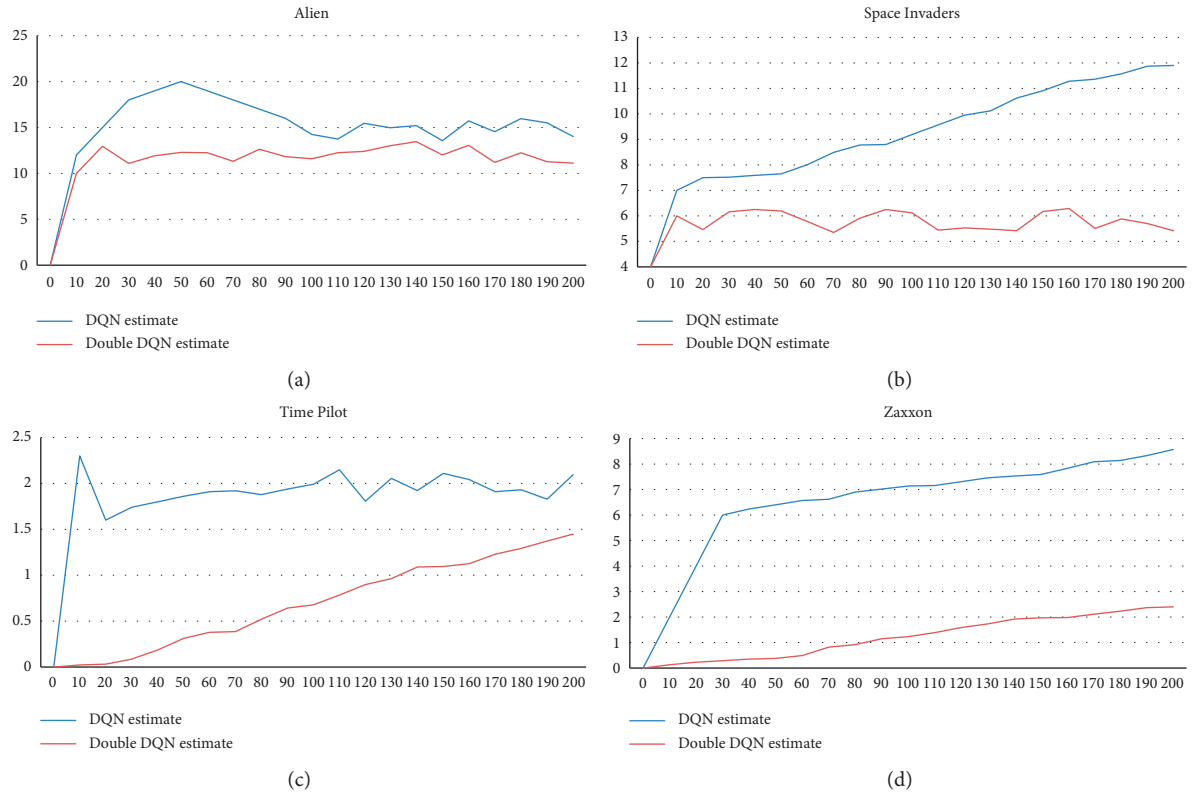

Figure 3: Graph of experimental results in Hasselt's study.

Because the extremely large deviation function cannot be calculated, the calculation is very difficult. Generally, it can be calculated with the same value as its properties:

$$\min t\ s.t\lambda_k\left(f_k(x) - \overline{f_k}\right) = t\,(k = 1, \ldots, m). \tag{25}$$

The interval value range of each objective function is shown in Table 4.

In the case of specific problems in the design of project goals in reality, every designer wants to add his own love and dislike to achieve the design criteria for each project under the premise of getting the latest version of the scheme. Improvements and optimizations will not be until the final stage of the project to design a pleasing design plan. Therefore, interlaced design methods have received widespread attention and application in today's society. And because every designer's favorites and preferences are not the same, and each structure has its own outline structure, the situation when meeting the optimization and improvement target schemes is also different from each other, including large-scale. The problem of how to optimize the optimization of multi-objective projects such as small and medium-sized projects can create a satisfactory, mature, effective, intelligent, and convenient method of optimizing project objectives that people can quickly accept. Pareto's curve function icon shows that the height of the surface is not a linear function, and the surface of the surface is not smooth enough. One possibility is that there is no continuity. The characteristic of the well-known neural network system is that there is no linear model function and there may be discontinuous curved surfaces. We put the Pareto surface to be designed in the range that we can see and show it to the designers in the form of graphs or charts. The purpose is to let the designer grasp the optimized scale in a certain situation, so as to improve the design efficiency more effectively and quickly, and obtain the improvement results faster after the design. The shape of Pareto is shown to us in the form of a histogram, and its form of existence is an environmental space with a high degree of satisfaction, as shown in Figure 4.

In dealing with the problem of neural network system, we use the interlaced processing methods to solve the complex problems existing in the calculation method and find the most suitable solution under the effective situation, so as to make the problems we encounter more practical, more common and more effective.

4. Establishment and Improvement of Clinical Management of Medical Teaching

4.1. Current Situation of Clinical Teaching Management System. Nowadays, in the field of medicine, the teaching method of clinical medicine is the embodiment of a medical student's basic medical literacy, and it is also one of the key points of innovation in the teaching characteristics of medical colleges. In recent years, with the continuous reform and innovation and development of higher education, the cheers of reform and education innovation in many medical colleges are increasing. In the environment of this reform,

Table 4: The interval boundary and parameter σ of each design objective preference function.

Design goals	Preference function type	G_{i5}	G_{i4}	G_{i3}	G_{i2}	G_{i1}		
Natural frequency (Hz)	2-S	100	110	120	150	200	$+\infty$	0.460
Expenses (¥/m^3)	1-S	16000	15600	15200	14400	8000	$-\infty$	22.23
Width (m)	2-S	0.34	0.45	0.43	0.45	0.54	$+\infty$	0.0027
Length(m)	2-S	3.0	3.3	3.5	4.0	6.1	$-\infty$	0.017
Mass (kg)	1-S	2900	2700	3000	2500	2700	$-\infty$	5.570
Height (m)	1-S	0.60	0.55	0.60	0.45	0.54	$+\infty$	0.0028
		Not feasible					Feasible	
Thickness of the first layer (m)	2-H	—	—	—	—	0.01	$+\infty$	—
Thickness of the second layer (m)	2-H	—	—	—	—	0.01	$+\infty$	—
Thickness of the third layer (m)	2-H	—	—	—	—	0.01	$+\infty$	—

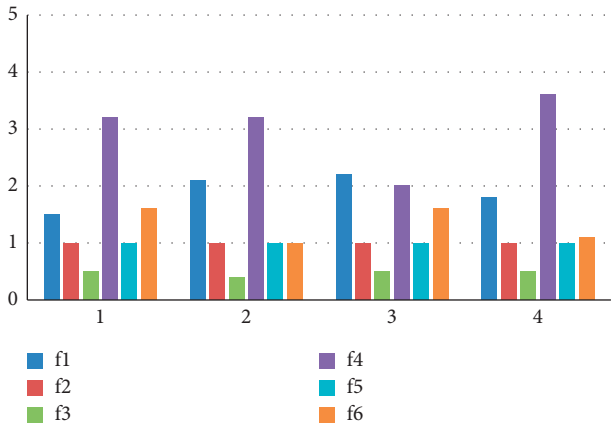

Figure 4: Visualization of pareto solution.

the education management center and core content of traditional Chinese medicine are the top priority and the focus of the reform. In this journey of reform and innovation, we have absorbed the development mode and operation system of higher education at home and abroad to supplement the educational problems and loopholes existing in China's educational background, which has a far-reaching impact on the future development of China's education, It plays an important role in the training of talents and the development of education, and also has a guiding role in the future development of young people.

There are many problems in the management system of Chinese higher medical education, such as whether the laboratory teaching management is centralized or decentralized. The centralized education management system is to establish the medical department with the University as the center. The management department is composed of all the research institutes, medical colleges, departments and laboratories related to the hospital in the University. And they are responsible for all the medical education management, research and development experiments, medical facilities, and so on. The Institute of medicine has an independent management organization, which can be established independently without being attached to the University. This characteristic is very similar to the Japanese education system. The characteristic requirement of the decentralized education management system is to be named as the second unit of the same school as the hospital directly under it. In addition, there is no direct relationship between the Affiliated Hospital and the Affiliated Hospital in China's Medical University. According to the above problems, they will appear in medical clinical experiments, and the Affiliated Hospital and the medical university often have differences on some matters.

In the hospital management system, the clinical medicine and Affiliated Hospital of medical university can be merged into one and two different institutions, but the nature is the same, which is of great significance in the situation of rescuing the wounded and rescuing the dying. There is also a situation where the clinical medicine of the Medical University and the affiliated hospital have no relationship and influence with each other. There is a legend that an American educator named Miller once drew a pyramid in medicine. It mainly tells about the basic literacy of a medical staff and his ability to solve clinical problems. As shown in Figure 5, Miller pyramid, which can be called classic, was also very famous at that time, Miller pyramid shows that a qualified medical staff should have their own learning and growth process at each stage, and constantly absorb and train their clinical medical ability at each stage to achieve their goals step by step.

There are some problems in the implementation of the system of "hospital integration", some medical teaching processes have many different places and differences, and we need to seriously deal with them: in the complex social relations, there are differences in the communication content, such as medical university, Medical University College, Affiliated Hospital, etc. In this pyramid system, there are many conflicts among different classes, the groups are different leadership classes, different employees in different posts, and the concept of teaching management level, which are the conflicts and contradictions existing in solving problems in three units. At the same time, there are also great differences in management teaching, but the leadership cannot organize and communicate in time to solve them. Thus, the conflicts between the three parties cannot be reduced and the contradictions can only be intensified constantly.

The hospital has no independence, which makes it impossible for the hospital to have its own management power, and others can intervene in any matter. Especially in financial accounting affairs, there are also personnel exchanges and personnel relationship handling relationships

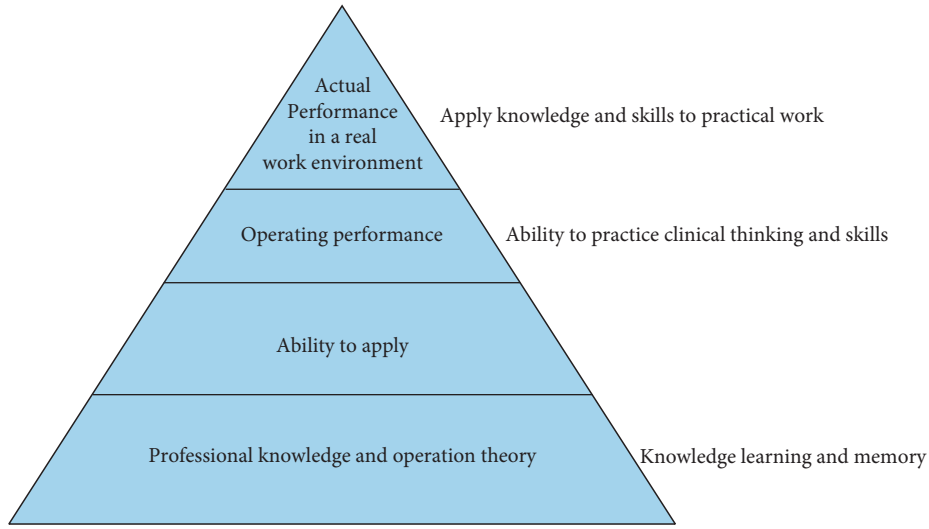

Figure 5: Miller pyramid model.

in hospitals. Hospitals cannot make decisions on their own. If they cannot say anything important, the development in the next stage has great limitations. They cannot realize their ideas and keep their hands tied. Even with good suggestions, they can not practice. These are all the consequences of the inability to meet the conditions of the external environment. Basically, it's all in vain.

There are also some common and serious problems in the teaching management of the supervision of the prosecution system is not complete. The purpose of the regulatory prosecution system is to improve the management level and measure system of teaching medicine. Even if there are many facilities and equipment in Medical University and relevant systems, these systems can not be completely convincing. There is also a situation where the implementation of the problems will be in a bad way.

In contrast, hospitals will pay attention to the cost of the economy, and it is difficult to invest too much in teaching. There are also some medical hospitals with formal but small sizes. They only pay attention to short-term profit and increase the utilization rate of cost, but ignore the medical teaching and scientific research innovation, especially not. At this time, the proportion of teaching management and research and development experiments is less and the status will fall. The number of teachers' tasks in clinical experimental Department of learning teaching management is increasing. After the hospital is integrated, doctors have multiple roles, that is, when doctors and teachers, of course, the tasks of doctors are also diverse. They should do not only clinical medical experiments but also teaching management. The contradiction is that the workload in both directions cannot be well arranged to continue, which will cause trouble to the work, and then delay the progress and slow down the efficiency.

4.2. Operation Mechanism of Higher Medical Education. The education management of colleges and universities is to deal with relevant matters according to the rules and regulations stipulated by the Education Bureau, which is also a standard that the education department must abide by. Among the types of education, the development of medical education is the most characteristic, and it is also a very special type of education. Therefore, its characteristics are similar to those of ordinary colleges and universities, but also different from those of colleges and universities. In the educational purpose of colleges and universities, their main responsibility is to train high-tech medical talents for the country, develop better medical products and service equipment, strengthen community construction and improve the medical and health security of urban people. The most fundamental characteristics are as follows: it has the social function of human beings, in essence, the complexity of the content is inconsistent with the facts, the practical activities related to medical clinical experiments, and the inconsistency of teaching management. All of these prove that the management of medical education is a combination of practice and theory. The proportion of practice is a little more than that of education. This requires educators to pay more attention to practical teaching than theoretical output while cultivating students. Affiliated hospitals can be a channel for students to practice, medical knowledge in education, and an important part of higher medical education. Interns can learn professional clinical experiment opportunities in class, and learn new knowledge that is not in textbooks through clinical experiments in practice. They need to explain clinical professional theoretical knowledge through classroom teaching. In addition, we must teach students clinical practice skills through the medical practice of outpatient and inpatient departments.

In today's society, with the arrival of the new era, it also brings many new challenges and opportunities. Along with it comes the doctor's moral standards and the complex relationship between doctors and patients' families, which are hot topics in today's society. All of them are what the society needs to face, so many solutions have been put forward according to these problems, that is, the requirements of the society are higher and higher on the professional quality of

Table 5: The basic elements of cognitive apprenticeship.

Content	Domain knowledge, strategic knowledge (heuristic strategy, control strategy, learning strategy)
Method	Demonstration, guidance, construction of scaffolding, dismantling of scaffolding (core technology), clear expression, reflection and exploration
Sequence	Increasing complexity and diversity of knowledge and skills, global skills ahead of local skills strategies
Sociality	Emotional learning, sociality, internal motivation, cooperation, and competition

doctors, and the patients and nurses in hospitals also need to know a lot of theoretical basis and rich social practice. Patients need more care and care from doctors and nurses when they are facing diseases, It is the commonwealth of all patients and even their families to have excellent psychological quality, experience from long-term surgical experiments, and a professional doctor with love and responsibility.

To build an institution different from the previous education system can not only improve the establishment and improvement of clinical teaching management system and mechanism, but also help to ensure and improve the quality of medical personnel training, as well as the self-development of medical colleges and affiliated hospitals, as shown in Table 5.

5. Conclusion

The performance of deep reinforcement learning and its dual structure version and interleaved structure version are compared in different medical teaching and clinical management environments and analyzed in detail. Deep reinforcement learning provides new ideas for the improvement of intelligent multi-objective optimization and clinical management of medical teaching, while retaining some of the problems they face, such as unstable factors in reinforcement learning, which will also be inherited in deep learning. Unstable algorithms will have adverse effects on the learned results and strategies. So this article has launched an in-depth study on this and proposed a series of stable reinforcement learning and deep reinforcement learning algorithms. This article applies deep reinforcement learning to intelligent multi-objective optimization and improvement and clinical management of medical teaching. In this article, we use the advantages of deep reinforcement learning and apply it to intelligent multi-objective optimization to gradually improve medical teaching and clinical management experiments. In practical applications, most neural network structures that like structure types are designed in this article. The input method is model parameters, and the output method is the value of the model parameters corresponding to the Pareto solution. After several rounds of mutual absorption of each other's advantages, the final result is a Pareto solution. Then, use the data model that the designer himself likes as the optimization target of the ANN model. It is best to find a new plan to improve the target and use the intelligent optimization target as the improvement guidance plan. The deep-enhanced learning program is used to meticulously study the teaching improvement of medical clinical experiments, which can enhance the overall ability and teaching level of the doctor team. Improve the knowledge system learned, consolidate the knowledge learned, cultivate the interest and hobby of learning, and strengthen the students' practical ability to adapt to the modern medical education and learning mode in line with the development of globalization. This article aims at the characteristics of clinical medical education in China, combined with the actual needs of medical education in medical schools, and systematically analyzes modern distance medical education, medical education models, and clinical skills training, and combs relevant pedagogy theories from different theoretical perspectives. Constructed a remote medical education clinical skills training model and developed a remote clinical skills training platform prototype based on the model design. It provides a set of effective clinical skills training methods for the vast number of medical workers in China, and also makes useful explorations on how to effectively use the Internet to carry out distance medical education.

Data Availability

The data used to support the findings of this study are available from the corresponding author upon request.

Conflicts of Interest

All the authors do not have any possible conflicts of interest.

References

[1] G. B. Huang, Q. Y. Zhu, and C. K. Siew, "Extreme learning machine: theory and applications," *Neurocomputing*, vol. 70, no. 1-3, pp. 489–501, 2006.

[2] G. E. Hinton, S. Osindero, and Y. W. Teh, "A fast learning algorithm for deep belief nets," *Neural Computation*, vol. 18, no. 7, pp. 1527–1554, 2006.

[3] Y. Bengio and Y. LeCun, "Scaling learning algorithms towards AI," in *Large-Scale Kernel Machines*, L. Bottou, O. Chapelle, D. DeCoste, and J. Weston, Eds., MIT Press, Cambridge, MA, USA, 2007.

[4] D. F. Wulsin, J. R. Gupta, R. Mani, J. A. Blanco, and B. Litt, "Modeling electroencephalography waveforms with semi-supervised deep belief nets: fast classification and anomaly measurement," *Journal of Neural Engineering*, vol. 8, no. 3, Article ID 036015, 2011.

[5] F. Agostinelli, S. Mcaleer, A. Shmakov, and P. Baldi, "Solving the Rubik's cube with deep reinforcement learning and search," *Nature Machine Intelligence*, vol. 1, no. 8, pp. 356–363, 2019.

[6] A. Flexer, G. Gruber, and G. Dorffner, "A reliable probabilistic sleep stager based on a single EEG signal," *Artificial Intelligence in Medicine*, vol. 33, no. 3, pp. 199–207, 2005.

[7] V. Mnih, K. Kavukcuoglu, D. Silver et al., "Human-level control through deep reinforcement learning," *Nature*, vol. 518, no. 7540, pp. 529–533, 2015.
[8] J. Bernal, K. Kushibar, D. S. Asfaw et al., "Deep convolutional neural networks for brain image analysis on magnetic resonance imaging: a review," *Artificial Intelligence in Medicine*, vol. 95, pp. 64–81, 2019.
[9] J. D. Williams, K. A. Atui, and G. Zweig, "Hybrid Code Networks: Practical and Efficient End-To-End Dialog Control with Supervised and Reinforcement Learning," 2017, https://arxiv.org/abs/1702.03274.
[10] J. Waring and C. Lindvall, "Review of the state-of-the-art and opportunities for healthcare," *Renato Umeton Automated machine learning*, vol. 16, no. 12, p. 104, 2020.
[11] H. Van Hasselt, A. Guez, and D. Silver, "Deep Reinforcement Learning with Double Q-Learning," 2016, https://arxiv.org/abs/1509.06461.
[12] S. Tim, J. Ho, X. Chen, S. Sidor, and I. Sutskever, "Evolution Policies as a Scalable Alternative to Reinforcement Learning," 2017, https://arxiv.org/abs/1703.03864.
[13] G.-G. Wang, M. Lu, Y.-Q. Dong, and X.-J. Zhao, "Self-adaptive extreme learning machine," *Neural Computing & Applications*, vol. 27, no. 2, pp. 291–303, 2016.
[14] H. Wang, Y. Gao, and X. G. Chen, "Transfer of reinforcement learning: the state of the art," *Acta Electronica Sinica*, vol. 36, no. S1, pp. 39–43, 2008.
[15] S. Khadka and K. Tumer, "Evolutionary Reinforcement Learning," 2018, https://arxiv.org/abs/1805.07917.

Hindawi
Mobile Information Systems
Volume 2022, Article ID 6372258, 10 pages
https://doi.org/10.1155/2022/6372258

Research Article

Financial System Design for High-Tech Enterprise Based on Cloud Service and Task Scheduling Algorithm

Yi Zhang, Zhiyong Fang, Yanling Xu, and Zhao Bao

School of Business, Wuchang University of Technology, Wuhan, Hubei 430223, China

Correspondence should be addressed to Yi Zhang; 201812210201008@zcmu.edu.cn

Received 17 July 2022; Revised 1 August 2022; Accepted 16 August 2022; Published 30 August 2022

Academic Editor: Shadi Aljawarneh

So far, with the development of the network, a new era of cloud computing is gradually advancing. Cloud services based on cloud computing technology have long become a new business model with broad application prospects. This paper studies the design of a high-tech enterprise financial system based on cloud service and task scheduling algorithm. The project can fully meet the following requirements: the establishment of a financial management system can improve the degree of automation and computerization of financial management and reduce the labor intensity of financial personnel. It is an analysis and decision-making program for the financial management of high-tech enterprises that can be shared using financial management software. Using a financial management system in actual work can achieve rapid financial data entry and improve the accuracy of data accounting. The high-tech enterprise financial management system is a very suitable and convenient management system, which substantially meets the daily business needs of high-tech financial management of enterprises.

1. Introduction

So far, with the development of the network, a new era of cloud computing is gradually advancing. Cloud services based on cloud computing technology have long become a new business model with broad application prospects. Cloud services provide customers with cloud computing servers such as hardware configuration equipment, software, and information content as services, thereby generating the core concept of IT services [1]. In recent years, with the rapid development of various electronic information technologies and the continuous increase and improvement of the basic theories of automatic control systems, we have become more aware of the practicability, stability, coordination, high frequency, and low cost of automatic control [2]. Until the emergence of the CAN network technology, this provides a good solution for many traditional automatic control systems and solves the problems that traditional integrated automatic control systems cannot solve [3]. We all know that the CAN bus is not like other simple system buses, and it is a field device level. In various fields, especially the industrial control system industry, the CAN bus has many advantages and characteristics that different types of field buses do not have compared with other types of field buses [4]. In addition, in the core technology of the entire process of data collection in the scientific research distributed system, a solution to increase data collection was obtained, a database query incremental recognition system was introduced in detail, and a special analysis tool for fully automatic acquisition of incremental data was developed and designed [5]. In view of the increase in the amount of data information, combined with the characteristics of the online financial system in the work, we added online financial audit early warning information and an online approval control module to improve the efficiency of the online financial system and reduce financial risks [6]. With the emergence of cloud computing technology and network big data, mobile network technology service platforms, financial accounting instant information management systems, network databases, online network platforms, and applications, the quiet penetration of cloud computing technology has made traditional financial auditing difficult [7]. The new cloud computing financial audit system software method is slowly becoming a research hotspot on the internet and will also

become a key application method in the next sales market [8]. At this stage, risk research under the cloud computing audit mode appears urgent and necessary. At the same time, with the continuous development of big data mining technology, a new audit procedure is provided for electronic computer financial audit [9]. Using big data mining technology to solve the massive amount of information in the financial audit industry can help financial auditors quickly grasp the overall status of the audited enterprise, gain insight into the relationships and standards in data information, and provide financial auditors with clues to financial audit cases.

In financial management, improving the efficiency and accuracy of information processing is the goal of high-tech business managers. Through continuous research and practice, domestic financial management software has become more mature and can carry out detailed system design, including system architecture design, database design, and detailed design of the core module dynamic model, showing some screenshots of the system and main modules and some code implementations. Finally, the operability and performance tests of the developed system are carried out. The test results show that the developed high-tech enterprise financial management system has complex functions, clear permissions, sufficient permissions, strict data planning, strong security, strong versatility, and good operational stability. It has high requirements for system software design. The ultimate goal of the project is to enable high-tech enterprises to use this system so that the financial staff of high-tech enterprises can understand what is happening in the financial business.

2. Related Work

The literature introduces the research results and main uses of clusters at the level of data and information parallel computing, integrates the current financial audit industry's regulations on massive information analysis, and proposes a technical route that combines database clusters and audit applications [10]. The literature introduces the technical aspects of building intelligent audit system software, including the application of big data mining technology in internal control auditing, text mining technology, basic elements of financial audit analysis methods, basic elements of entity models, data management systems, and classification status [11]. It mainly describes the expert diagnosis system. The literature introduces the reliability design of the power supply circuit of the acquisition control module, and analyzes the key links in the design scheme from the consideration of pulse signal interface, analog switch, and A/D acquisition power circuit. The literature describes the entire detection process of the CAN bus temperature acquisition system, and the role of the system has been certified [12]. Through a large number of tests and statistical analysis of data, it is proved that the design of the CAN bus acquisition system can meet the requirements of the task. The literature introduces the advantages and characteristics of the distributed system automatic control system, combined with the necessary functions of the handling robot and the modular design concept, derives the CAN-based distributed system handling robot control system structure diagram bus, and clarifies the program modules [13].

The literature shows that in recent years, with the rapid development of financial informatics and information technology, computers and education have become indispensable things in everyone's life. The world economy is gradually converging. The requirements for using computers in the financial management solutions of high-tech companies are getting higher and higher [14]. The competition among high-tech companies is becoming more and more fierce. The financial department plays a central role in the activities of high-tech companies. The financial department is an important functional department for the operation and development of high-tech enterprises, and its role in the operation of high-tech enterprises is irreplaceable [15, 16]. The task of the financial department is to strengthen financial supervision, control financial risks, and improve profitability. The finance department is responsible for the capital transactions of high-tech enterprises and provides funds for various departments of high-tech enterprises [17]. The literature points out that with the rapid development of China's economy and the deepening of financial system reforms, domestic high-tech companies are facing increasing competitive pressure in the developing market economy. In the new economic environment, the key to the sustainable development of high-tech enterprises lies in whether they can change their business philosophy, improve service methods, deepen service content, and increase their competitiveness in an increasingly competitive market [18]. These changes will inevitably lead to changes in the development of high-tech enterprises, and breakthroughs have been made. At present, most high-tech enterprises in China are implementing financial information system management to improve the quality and quality of customer service. This article studies the financial management information system of high-tech enterprises based on the actual work of the financial department of high-tech enterprises [19].

3. System Design

3.1. Task Assignment and Problem Research. The node periodically reports its heart rate to the node through the RPC protocol. Whenever the node receives a control signal, it determines whether the node has an idle time slot or an idle time slot. If there is a free slot, the corresponding task is assigned to the free node. When assigning slots to tasks, priority will be given to the location of the data, that is, to schedule tasks on the node where the data are located as much as possible. In addition to searching, it also considers unfinished tasks, the scheduling sequence of backup tasks, etc. For tasks, the tasks in the unfinished task list simply pass through the queue, regardless of the performance of its nodes, indicating that the task is running.

Table partition number is PartitionNum, a number represented by ReduceNum. In this case, the data restored each time will be evenly distributed. In a homogeneous environment, the processing power of each node is basically the same. Therefore, it is meaningful to use the standard hash function to evenly distribute the matching results in the

Table 1: Test results of Algorithm 1on the WebDocs database.

Support (%)	The total number of items in frequent 1-itemsets L	Total frequent itemsets	Running time (s)	
			FP growth algorithm	New algorithm
50	5	13	267	305
40	10	45	295	367
30	23	218	311	442
20	67	2,393	443	478
10	278	199,627	5,214	3,875
1	2,900	845,761,472	—	67,512

partition step to reduce the matching results, and better performance can also be obtained. However, in an unbalanced environment, due to mismatches in network bandwidth, processor frequency, memory size, hard disk read and write speed, etc., the performance of each node will greatly vary. In this case, if the standard hash function is used to allocate data, the data are recovered in the splitting phase to reduce the nodes with poor performance.

The WebDocs database is a comprehensive data mining database, which is created based on real-life web hypertext files. The experimental results are listed in Table 1.

Using the information indicated by the last element in the table, we construct the basis of the condition template of element A and then construct its FP-tree condition. Then, the frequent dies containing element A can be split in the FP-tree condition. Then, the header A in the DLC list is deleted. Another appropriate DRL is used to cover the transaction of deleting the header to form a new DLC list group based on the differences in its subsequent members.

3.2. Overview of ASP. The financial information system discussed in this article is based on ASP.net, and ASP software is a standard platform for developing distributed applications. An important function that distinguishes ASP from other job development platforms is that it provides a more flexible design and development method. It is a component design and development method. With the development of ASP, it greatly facilitates the financial management information system. The ASP server provides ready-made external services in the form of components, which components can be installed to achieve the required functions, and the ASP block diagram is shown in Figure 1.

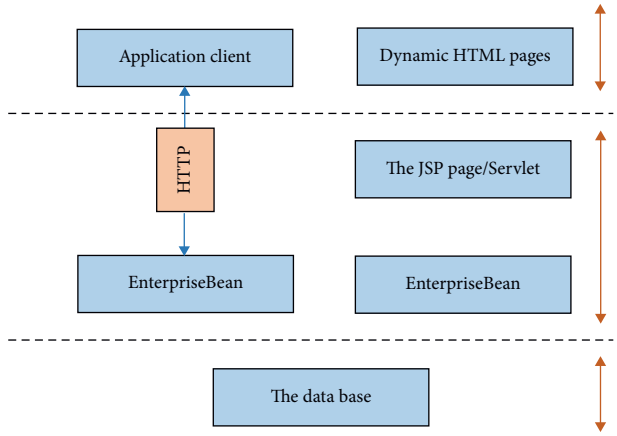

Figure 1: ASP structure diagram.

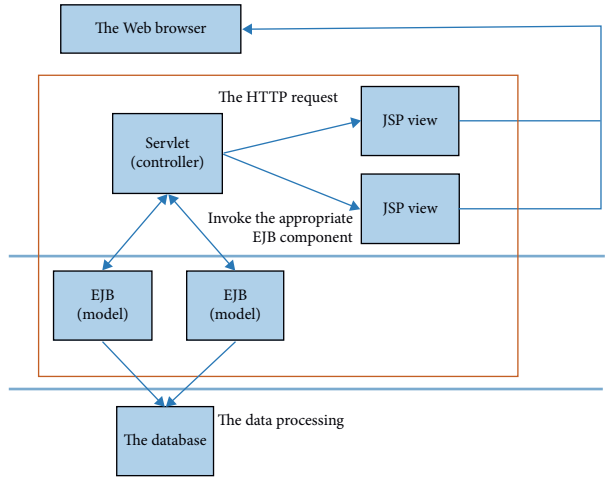

Figure 2: ASP platform built in MVC mode.

4. Design and Optimization of a Distributed Online Financial Audit System Based on Cloud Services

4.1. Design of Database System. In order to solve the shortcomings of the traditional C/S system structure, ASP was designed and constructed. Compared with other architectures, C/S architecture programs require many user roles, so information management is advanced. Every time the C/S architecture program is updated, it becomes very problematic, and the system continues to grow. At the same time, the support for other software systems and the scalability of C/S itself cannot meet the requirements. Its internal logical data relationship must also be handled by many different entities, which components can be installed to achieve the required functions.

With the rapid development of modern science and information technology, the traditional C/S architecture program can no longer meet the needs of today's high-tech enterprises for information management systems. The detailed design is shown in Figure 2.

It can be seen from the dataflow in Figure 2 that when developing an information system for high-tech enterprise financial management, the entire internal design process is that HTML first receives user operation requests on the

high-tech enterprise financial management client. Then, the user operation request is sent to the ASP server, and then, the server passes the user operation request to the logical processor. The processed data are sent to the client through the view and then displayed to the user.

The system requirement analysis reference introduces the user's business requirements for the system in detail. The requirement analysis is the basis of the system function design. When designing a high-tech information system for company financial management, a secure network environment must be created first, and the existing information system should be fully utilized as a development requirement. The basic design principles to be followed include the following:

The principle of system openness: in order to ensure that the system can easily connect to higher-level equipment and expand service functions, it must comply with industrial standards.

System compatibility principle: the realization of the system must have a good system operating platform, which can be effectively combined with the existing information system. System compatibility is very important. If the compatibility problem cannot be solved, this leads to severe system limitations.

System scalability principle: the scalability of a system determines its ability to adapt to future development, and the system must be scalable in many ways. Through effective expansion, the system can be continuously optimized to achieve higher cost performance.

There are many database tables in the financial management information system. Only a few are listed here. The system data tables are shown in Table 2:

The deployment methods of the online financial system include private cloud storage, public cloud, and hybrid cloud. Private cloud storage is a natural cloud environment built by an enterprise or other enterprises for its own applications. It uses an intranet to provide IT capabilities as a service to the internal employees of the company or organization within the server firewall. A cloud computing platform is a natural cloud environment created and shared by related companies or enterprises to create and share resource applications. According to the role of network IT and business processes, it is usually given to many external customers as a service item. Public clouds are generally constructed by a single third party (i.e., cloud service providers). Customers charge for applications without high-tech authoritative experts or mastering obscure technical expertise, and they can obtain cloud services after obtaining authorization. The cloud computing platform is a natural cloud environment formed by organic chemical integration of private cloud storage and the service items provided by the cloud computing platform. Customers consider business process requirements and limiting factors (including current IT equipment and security factors), and choose the appropriate integration methods: it is essential to formulate current policies or standards for cloud computing platform applications.

4.2. Optimization of Distributed Cloud Service Distributable Load Scheduling Problem. We consider a very simple situation, that is, the system software contains only one RCc and one RPv. The amount of input information and the estimated workload of the total computing task are denoted by S and F, respectively. The free resources of RCc and RPv are denoted as Cc and Cv, respectively. It is supposed $S = \gamma v$, where γ is the balance factor. If RC only uses its own resources to calculate the daily task, then the time of the daily task is $T1 = V/Cc$. Assuming that the wireless channel information content between c and v is known to each other, the wireless network transmission speed between RCc and RPv is as follows:

$$R_{c,v} = \log(1 + \mathrm{SNR}) = \log\left(1 + \frac{p_c |h_{c,v}|}{\sigma^2}\right). \tag{1}$$

Among them, pc is the push output power, and SNR represents the signal-to-noise ratio of the wireless channel. $H_{c,y} \sim \mathrm{CN}(0, 1)$ represents the attenuation index of the wireless network link, and σ^2 is the additional Gaussian white noise output power of the receiving wireless antenna.

If RCc and RPv perform the total estimated daily tasks together, we use $0 \le \beta \le 1$ to indicate the proportion of the subtasks assigned to RP in the total amount of calculation to better reduce the minimum task completion time, and β needs to reach the following:

$$\frac{(1-\beta)V}{C_c} = \frac{\beta S}{R_{c,v}} + \frac{\beta V}{C_v}. \tag{2}$$

The solution is as follows:

$$\beta^* = \frac{R_{c,v} C_v V}{S C_r C_c + R_{c,v} C_c V + R_{c,v} C_v V}. \tag{3}$$

In this case, the completion time of the total task can be expressed as follows:

$$T_c = T_t + T_p = \frac{\beta^* \gamma V}{R_{c,v}} + \frac{\beta^* V}{C_v}. \tag{4}$$

Among them, T_1 represents the wireless data transmission time, and T_p represents the daily task execution time. Therefore, the time saved based on the input calculation, that is, the time gain value of the system software, can be expressed as follows:

$$T_{sr} = \max(T_i - T_c, 0) = \max\left\{\frac{V}{C_c} - \frac{\beta^* \gamma V}{R_{c,v}} - \frac{\beta^* V}{C_p}, 0\right\}. \tag{5}$$

Obviously, T_{sv} increases the amount of free resource storage C_v. We introduce a remuneration system in the terminal cloud service. RP, as a resource service provider, hopes to obtain remuneration by providing idle cloud computing servers. The amount of resource storage given is related to the amount of remuneration paid by RC. Therefore, the key issue for improvement is how to allocate subtasks to measure the amount of idle resources and set a "price" so that RC and RP can reach an agreement and minimize the execution time of the overall task.

Table 2: List of system data sheets.

Data sheet name	Data sheet purpose
Chart of accounts	Save corporate financial accounting title setting information
Account balance sheet	Save the balance information of the financial account
Accounting entry form	Used for entry in voucher management
Voucher table	Used for credential input management
Entry history table	After the entry is confirmed, the data are put into the history
Voucher history table	After the voucher input is confirmed, the data are put into the history
Detailed ledger	Used for the input of enterprise financial details' account book
Project account comparison table	Compare specific items with accounting subjects
General ledger	Used for the input of the corporate financial general ledger book
This year's detailed account book	Summary of annual account books
General ledger book of the year	Summary of annual ledger books
Historical detailed ledger	Save detailed account book history
Historical ledger	Save the ledger history
Statement of changes in financial status	Save the financial status change table information of the enterprise
Internal voucher table	Voucher information sheet by internal number
Annual income statement	Save the annual income statement information of the company's finances
Annual balance sheet	Save the annual balance sheet information of the company's finances
List of fixed assets	Save the basic information of the company's fixed assets
Table of changes in fixed assets	Save information on changes in the company's fixed assets
Internal record	Debit and credit information by internal number
Change data history table	Save the history of changes in the company's fixed assets

Below, we will expand the single RP scenario to a multiple RP scenario. Assuming that there is a group of RPs stored in the terminal device cloud service system, and their combination is represented by A_c, the wireless network transmission speed between the client and the jth RP in this scenario is as follows:

$$R_{c,j} = \sum_{k=1}^{N_{Rg}} s_{k,j} \log\left(1 + \frac{p_c \left|h_{c,j}\right|}{\sigma_j^2}\right), j \in \mathscr{A}_c. \tag{6}$$

Among them, $h_{c,j}$ is the channel gain between the client and the jth RP, and σ_j^2 is the noise output power index of the receiving wireless antenna of the jth RP. NRB represents the total number of resource blocks transmitted by the system software. In a proxy-based system, the transmission resource block can refer to the frequency resource block (FDD system) or the time slot resource block (TDD system). In the self-organizing structure, the transmission resource block is the time slot resource Block, because FDMA is not suitable for the current D2D scene. $S_k j = 1$ ($S_k j = 0$) means that the kth transmission resource block is allocated for data transmission between the RC and the jth RP.

Obviously, in order to maximize the time gain of the system, β_j needs to meet the degree-like constraints as follows:

$$\frac{\beta_0 V}{C_c} = \frac{\beta_j S}{R_{c,j}} + \frac{\beta_j V}{C_j}, j \in \mathscr{A}_c, 0 \le C_j \le \overline{C}_j. \tag{7}$$

Among them, C_j is the idle resource that the jth RP is willing to provide to the client, and $\overline{C}_j$ is the larger amount of idle resources that the jth RP can give.

$$\begin{aligned} \beta_j &= \frac{\beta_0 V R_{c,j} C_j}{S C_c C_j + V C_c R_{c,j}}, \\ \beta_0 &= \frac{1}{1 + \sum_{j \in A_t} V R_{c,j} C_j / \left(S C_c C_j + V C_c R_{c,l}\right)}. \end{aligned} \tag{8}$$

Therefore, the time gain obtained by introducing parallel calculation in the multi-RP scenario can be expressed as follows:

$$T_{mv} = \max\left(T_l - T_c, 0\right) = \max\left(\frac{V}{C_c} - \frac{\beta_0 V}{C_c}, 0\right). \tag{9}$$

The SPG issue can be seen as the whole process of negotiation between the buyer and the seller. The buyer in this model is the RC that must perform daily tasks, and the seller is the RP. The seller expects to get the most profit, while the buyer expects to invest a smaller cost. In the terminal equipment cloud service system software, RC motivates each RP to allocate unused resources for calculation based on a certain reward. Therefore, a SPG problem with RC and RP as participants is clearly proposed, and the corresponding Stackelberg equilibrium can be regarded as a solution to the problem. This SPG problem can be described as a two-stage game process from two levels.

Buyer: RC expects to obtain the most resources at the lowest price, so there is an expected supply and demand relationship, which can be obtained according to the following formula:

$$\max U_c = T_{mv} - \sum_{j \in A_c} \lambda_j C_j, \text{s.t.} 0 \le C_j \le \overline{C}_j. \tag{10}$$

Seller: RP deducts a certain amount of remuneration to borrow its own idle resources and hopes to increase the resource price of each enterprise as much as possible. Therefore, the expected supply and demand relationship between the seller and the seller can be shown as follows:

$$\max U_j = \lambda_j C_j^{b_j} - \eta_j C_j^{b_j}. \tag{11}$$

Among them, $b_j \geq 1$ is a constant compromise factor.

In the whole process, the information that buyers and sellers must exchange includes the price of unit resources and the amount of resource storage used. In a typical SPG problem, participants are the core of the rules of the game, and management decisions are made based on the reflection of other participants. The entire game process will eventually converge to the Stackelberg equilibrium, which is defined as follows: the main parameters λ_j^{SE} and C_j^{SE} are SPG The clearly proposed Stackelberg balance needs to meet the following criteria. When it is fixed,

$$U_c\left(\left\{C_j^{SE}\right\}\right) = \sup_{0 \leq (:_j \leq \bar{Y}_j} U_c\left(\left\{C_j\right\}\right), j \in \mathscr{A}_c. \tag{12}$$

When C_j^{SE} is fixed,

$$U, \left(\left\{\lambda_t^{SE}\right\}\right) = \sup_{\lambda} U_j\left(\left\{\lambda_i\right\}\right), j \in \mathscr{A}_c. \tag{13}$$

The following analyzes the Stackelberg equilibrium in the proposed SPG problem from two aspects:

Buyer: as a resource consumer, RC can be aware of the seller, that is, RP will respond to its clearly proposed countermeasures. According to the previous analysis, RC drives sellers to respond based on the amount of resource storage that they decide to purchase from each RP, so as to maximize profits. According to the definition of the Stackelberg equilibrium, when λ_j^{SE} is fixed and U_c is derived from C_j, we can get the following:

$$\begin{aligned}\frac{\partial U_c}{\partial C_j} &= -\frac{V}{C_c}\frac{\partial \beta_0}{\partial C_j} - \lambda_j \\ &= \frac{V}{C_c\left\{1 + \sum_{j \in A_e} VR_{c,j}C_j / SC_cC_j + VC_cR_{c,j}\right)\}^2} \\ &\quad \cdot \frac{V^2 C_c R_{c,j}^2}{\left(SC_cC_j + VC_cR_{c,j}\right)^2} - \lambda_j \\ &= \frac{\beta_0^2 V^3 R_{c,j}^2}{\left(SC_cC_j + VC_cR_{c,j}\right)^2} - \lambda_j.\end{aligned} \tag{14}$$

With

$$\frac{\partial^2 U_c}{\partial C_j^2} = \frac{2\beta_0 \partial \beta_0 / \partial C_j V^3 R_{c,j}^2 \left(SC_cC_j + VC_cR_{c,j}\right) - 2\beta_0^2 V^3 R_{c,j}^2}{\left(SC_cC_j + VC_cR_{c,j}\right)^3} < 0. \tag{15}$$

The optimal solution to the problem can be derived as follows:

$$C_j^* = u_j \sqrt{\frac{1}{\lambda_j}} - v_i. \tag{16}$$

Among them,

$$\begin{aligned} u_i &= \frac{VR_{c,j}\sqrt{V}}{SC_c + VR_{c,j} + SC_c w_i}, \\ v_j &= \frac{VC_cR_{c,j}\left(1 + w_j\right)}{SC_c + VR_{c,j} + SC_c w_j}, \\ w_j &= \sum_{i \in \mathscr{A}_r, i \neq j} \frac{VR_{c,i}C_i}{SC_cC_i + VC_cR_{c,t}}. \end{aligned} \tag{17}$$

Finally, the optimal number of resources borrowed by the user from the jth RP can be expressed as follows:

$$C_j^* = \min\left(C_i^*, \overline{C}_j\right). \tag{18}$$

Seller: RP maximizes its profit by setting the best unit resource price. By deriving the utility function of RP with λ_j and setting its value to 0, we can get the following:

$$\frac{\partial U_j}{\partial \lambda_j} = \left(C_j^*\right)^{b_j} + \lambda_j b_j \left(C_j^*\right)^{h_1 - 1}\frac{\partial C_j^*}{\partial \lambda_j} - \eta_j b_j \left(C_j^*\right)^{b_1 - 1}\frac{\partial C_j^*}{\partial \lambda_j} = 0. \tag{19}$$

To derive the above formula, there are the following:

$$\left(C_j^*\right)^{b_j - 1}\left(C_j^* + b_1 \frac{\partial C_j^*}{\partial \lambda_j}\left(\lambda_j - \eta_j\right)\right) = 0. \tag{20}$$

From the above formula, $C_j = 0$, that is, the user will not purchase any resources from the Jth RP. Otherwise,

$$C_j^* + b_j \frac{\partial C_j^*}{\partial \lambda_j}\left(\lambda_j - \eta_j\right) = 0. \tag{21}$$

This formula has a unique solution as follows:

$$\lambda_j^* = \eta_j - \frac{C_j^*}{b_j \partial C_j^* / \lambda_j^*}. \tag{22}$$

In order to better obtain the optimal solution for this SPG, we chose an iterative algorithm to clarify the unit resource price of each RP and the amount of resource storage used by RC for each RP. We use $\lambda = \{\lambda_j\}$ to represent the price space vector, and $F(\lambda)$ represents the update function, then

$$\lambda_j = F_i(\lambda) = \eta_j - \frac{C_j^*}{b_j \partial C_j^* / \partial \lambda_j}. \tag{23}$$

Table 3: SPG problem-solving steps.

	SPG problem-solving steps
1	Reset: for each RP, we reset the price space vector $\lambda(0) = \{\lambda_j(0)\}$, $j \in A$ and tell the mobile grid customer to reset the resource storage used by each RP, namely, $C_j(0)$. Set t to 1
2	The whole process of RC iterative update: according to formula (16), we use $\lambda(t)$ to get the best use of each RP by the customer
3	Resource storage capacity, we get $C(t+1) = \{C_j(t+1)\}$, $j \in A$
4	The whole process of the iterative update of the RP party: according to the $C(t+1)$ obtained in the previous step, the optimal price λ_j of each RP unit resource is calculated according to formula (23), which is recorded as $\lambda(t+1)$. We upgrade load production scheduling management decision βj and iteration number t

The update equation can be written in the following vector form:

$$\lambda(t+1) = F[\lambda(t)]. \tag{24}$$

Among them, $F = \{F_j\} j \in A$, and t is the number of iteration updates. The SPG acquisition process can be divided into four steps, as shown in Table 3.

The following is based on system software simulation based on the SPG analysis of the characteristics of the load production scheduling optimization algorithm clearly proposed in this article. The simulation scenario is described as follows: a square indoor space is placed with a certain number of mobile terminals that can be used as RPs. There is a wireless repeater in the middle of the house. RC is a node in the wired domain. RC and RP can communicate with each other based on the wireless repeater. For simplicity, we assume that the average frequency stability of the wireless channel from the connection point to the remote RP (house edge) is OdB. Responsive number allocation technology and 16MCS are used in the simulation. The main parameters of other simulations are shown in Table 4:

For the first time, the convergence characteristics of the clearly proposed SPG optimization algorithm are evaluated. When there are 5 RPs in the system software, Figure 3 shows the change in the price of each RP enterprise cloud computing server with the iterative update frequency. Under the same initial value setting, the unit resource prices of five RPs converge to five different standard values, and the higher price setting results from higher resource quality, such as better channel quality.

In the simulation, we evaluated the time gain value obtained by introducing parallel processing. Two typical production scheduling optimization algorithms were used in the simulation: cyclic production scheduling and maximum weight production scheduling f8U to allocate wireless resources.

Figure 4 shows the correlation between the number of RPs available in the grid graph and the percentage of time saved. It can be seen that different wireless resource production scheduling optimization algorithms have a certain impact on the characteristics of the SPG optimization algorithm, so the SPG optimization algorithm is clearly proposed; it should be combined with advanced resource production scheduling optimization algorithms to improve system software characteristics.

Table 4: Simulation parameter table.

Parameter	Value
Room size	10 m ×10 m
Number of RP	3–12
Mobile device spacing	3–10 m
Path loss model	$P(d) = Pd^{-\alpha}$
α	4
Bandwidth	10 MHz
Frequency	2 GHz
Scheduling gap length	1 ms

4.3. Design of System Business Process. The online financial system uses virtual technology to centralize various hardware facilities and system software to form a virtualized resource sharing pool. The resources required by financial auditors to run the system software will be immediately obtained from the virtual resource pool. In addition, financial audit company data information, financial audit analysis results, and other audit information are integrated and stored on the financial audit cloud service platform, and the virtual resource pool realizes multiparty resource sharing and integration. It is a key factor for the centralized integration of various financial auditing system software and the construction of anti-heterogeneous infrastructure, which can be quickly deployed in accordance with the application software regulations.

The online financial system is the use of resource pool division and management methods to perform financial audits on all resources of the cloud platform under the support of virtual technology, assign and appoint the supervisory power of each cluster or server resource, and establish multiple resource pools, which are clusters or servers. which are the direct child nodes of the cluster or server. It solves the needs of financial audit business process transformation and is faster, more convenient, and more efficient than traditional financial audit. Therefore, when financial audit institutions carry out financial audit activities, online financial audits can dynamically expand and allocate financial audit resources according to customer needs, and use cloud collaboration systems to centralize storage, unified management, and centralized resources. The previously scattered and incomplete resources are integrated and upgraded to enrich and expand the existing financial audit resource management system. The website administrator resets the financial audit system software on the cloud

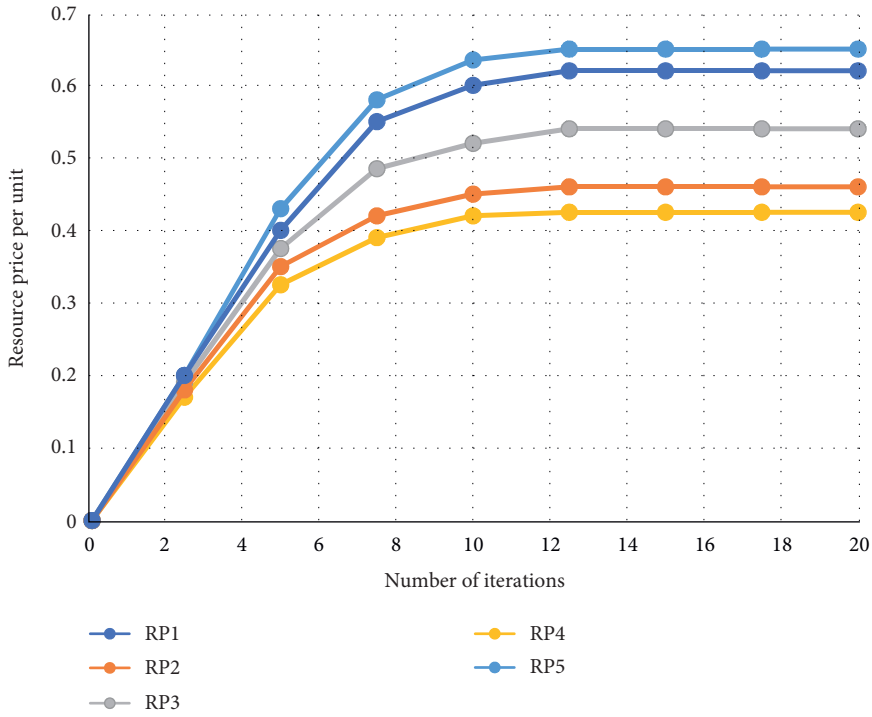

Figure 3: Convergence of the price per unit resource per RP in the iteration.

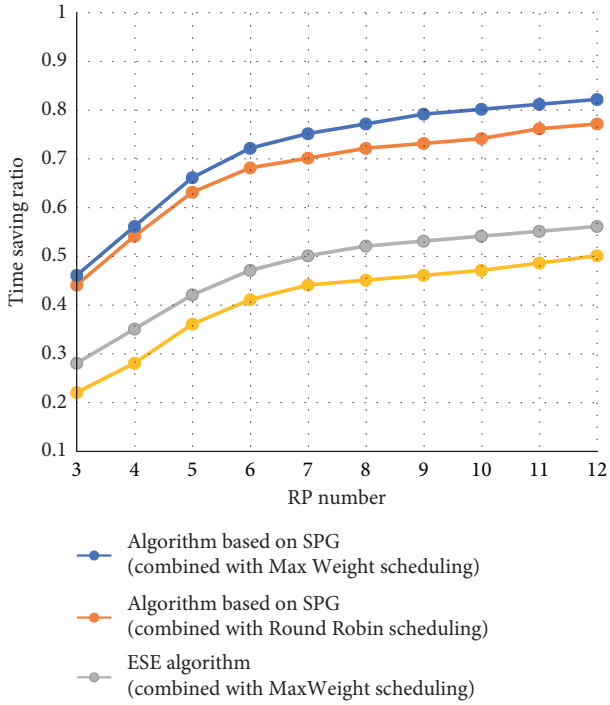

Figure 4: System time gain under different algorithms.

service platform in advance, generates environment variables, and expands the basic system software. The cloud platform administrator accurately and in detail applies for registration of the basic system software in the service project archive catalog, creates a clear system catalog, so that the financial auditors can enjoy the service process conveniently and quickly, and further executes the financial audit business process.

Taking into account the functions developed in the enterprise financial management high-tech information system, the process of the user management module is planned in detail. The following are some detailed designs. When users use the financial information system, they must log in first. The user login process is shown in Figure 5.

When a user needs to log in to the financial management information system of a high-tech enterprise, the system is sent to the scene for verification at the same time. Only in the financial management information of high-tech enterprises, the system background will check the correctness of the user's input data before the user successfully logs into the system. If there is a problem with the user's input, the system will remind the login personnel that there is a pop-up input error.

After a successful login, the user will perform system operations according to his authority. The financial staff must work according to the allocation of accounting positions, registration, and verification of accounts. This requires managing account information, including account number, name, type, etc.

High-tech enterprises are also the source of capital management. Since the working capital of high-tech enterprises must rely on credit, the credit management process can adapt to demand.

In addition to the above four aspects, the system has also developed a statistical office process, which can perform statistical analysis based on financial data in a timely manner, so that high-tech business managers can perform statistical analysis on financial data and extract management data.

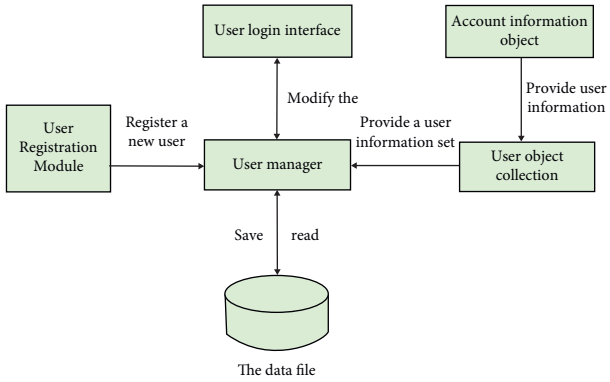

Figure 5: User login process design.

This article introduces the detailed design of the high-tech information management system for the company's financial management. First of all, it will describe in detail the principles and financial management information system of the high-tech information system for the company's financial management and the company's financial management. The financial management information system database mainly for high-tech enterprises was introduced in detail, and the financial management information system database tables for high-tech enterprises were developed. Finally, the financial management information system was tested in detail. The test results show that the high-tech enterprise financial management information system developed by this theme can meet the requirements before the project.

The cloud service platform creates corresponding financial audit entity models according to the operating steps, characteristics, and laws of each business process type, and quickly and accurately discovers the defects in the auditing enterprise. Financial auditors input standardized data information solved by massive informatization solution technology into corresponding financial audit entity models, purposefully analyze data, identify abnormal data information, and find clues to financial audit cases. During the new financial audit project, financial auditors will implement on-site audits, policy tracking or key tracking, extended audits, and continuous audits to reveal risks, fraud, and other violations of laws and regulations in the company's various businesses.

5. Conclusions

The B/S structure selected by the control system has excellent advantages. The project can fully meet the following requirements: the establishment of a financial management system can improve the degree of automation and computerization of financial management, and reduce the labor intensity of financial personnel. It is an analysis and decision-making program for the financial management of high-tech enterprises that can be shared using financial management software. Using a financial management system in actual work can achieve rapid financial data entry and improve the accuracy of data accounting. The high-tech enterprise financial management system is a very suitable and convenient management system, which substantially meets the daily business needs of high-tech financial management of enterprises, thus greatly reducing the time spent on tedious financial management work and improving the efficiency of financial management, and improving the correct plan and the use of information for the implemented financial management. The overall structure of the system is clear, the interface is very good, and the operation is very simple.

Data Availability

The data used to support the findings of this study are available from the corresponding author upon request.

Conflicts of Interest

The authors do not have any possible conflicts of interest.

References

[1] P. K. Senyo, E. Addae, and R. Boateng, "Cloud computing research: a review of research themes, frameworks, methods and future research directions," *International Journal of Information Management*, vol. 38, no. 1, pp. 128–139, 2018.

[2] T. Velmurugan and T. Santhanam, "Performance evaluation of K-means and fuzzy C-means clustering algorithms for statistical distributions of input data points," *European Journal of Scientific Research*, vol. 46, no. 3, pp. 320–330, 2010.

[3] P. P. Bonissone, F. Xue, and R. Subbu, "Fast meta-models for local fusion of multiple predictive models," *Applied Soft Computing*, vol. 11, no. 2, pp. 1529–1539, 2011.

[4] G. Shafiee, M. M. Arefi, M. R. Jahed-Motlagh, and A. A. Jalali, "Nonlinear predictive control of a polymerization reactor based on piecewise linear Wiener model," *Chemical Engineering Journal*, vol. 143, no. 1–3, pp. 282–292, 2008.

[5] F. Chen, X. Du, S. Lai, and M. L. Z. Ma, "Does the use of honorific appellations in audit reports connote higher financial misstatement risk? Evidence from China," *Asian Review of Accounting*, vol. 26, no. 2, pp. 154–181, 2018.

[6] J. Wonglimpiyarat, "What is it about strategic implications of using financial models in the process of technology management?" *The Journal of High Technology Management Research*, vol. 30, no. 1, pp. 82–90, 2019.

[7] G. Barta, "The increasing role of it auditors in financial audit: risks and intelligent answers," *Business, Management and Education*, vol. 16, no. 0, pp. 81–93, 2018.

[8] M. Lai, "Smart financial management system based on data ming and man-machine management," *Wireless Communications and Mobile Computing*, vol. 2022, pp. 1–10, Article ID 2717982, 2022.

[9] R. Yu, C. Wu, B. Yan et al., "Analysis of the impact of big data on E-commerce in cloud computing environment," *Complexity*, vol. 2021, no. 2, pp. 1–12, Article ID 5613599, 2021.

[10] J. Y. Yeh and C. H. Chen, "A machine learning approach to predict the success of crowdfunding fintech project," *Journal of Enterprise Information Management*, vol. 14, 2020.

[11] L. Ogiela, M. R. Ogiela, and H. Ko, "Intelligent data management and security in cloud computing," *Sensors*, vol. 20, no. 12, p. 3458, 2020.

[12] S. Kaffash and M. Marra, "Data envelopment analysis in financial services: a citations network analysis of banks,

insurance companies and money market funds," *Annals of Operations Research*, vol. 253, no. 1, pp. 307–344, 2017.

[13] Y. Zhao, "Decision support system for economic management of large enterprises based on artificial intelligence," *Wireless Communications and Mobile Computing*, vol. 2022, pp. 1–11, Article ID 9453580, 2022.

[14] F. Du, Y. Cai, Z. Guan, F. Tang, and D. Wu, "Optimization research on CAN bus transmission delay," *Automobile Technology*, vol. 1735, no. 1, pp. 1–6, 2021.

[15] H. Wang, F. Zuo, L. Yang, and Y. Zhang, "Design of battery performance monitoring system based on," *CAN Bus. Instrument Technique and Sensor*, vol. 2021, no. 6, pp. 77–81, Article ID 1786926, 2021.

[16] J. F. Sreih, R. N. Lussier, and M. C. Sonfield, "Differences in management styles, levels of profitability, and performance across generations, and the development of the family business success model," *Journal of Organizational Change Management*, vol. 32, no. 1, pp. 32–50, 2019.

[17] M. Adil, J. Ali, M. Attique et al., "Three byte-based mutual authentication scheme for autonomous Internet of vehicles," *IEEE Transactions on Intelligent Transportation Systems*, vol. 23, no. 7, pp. 9358–9369, 2022.

[18] L. Xu, R. Gao, Y. Xie, and P. du, "To be or not to be? Big data business investment decision-making in the supply chain," *Sustainability*, vol. 11, no. 8, p. 2298, 2019.

[19] P. Vandekerkhof, T. Steijvers, W. Hendriks, and W. Voordeckers, "Socio-emotional wealth separation and decision-making quality in family firm TMTs: the moderating role of psychological safety," *Journal of Management Studies*, vol. 55, no. 4, pp. 648–676, 2018.

Hindawi
Mobile Information Systems
Volume 2022, Article ID 5849422, 11 pages
https://doi.org/10.1155/2022/5849422

Research Article

Noncontact Defect Detection Method of Automobile Cylinder Block Based on SVM Algorithm

Juncen Yan

School of Optoelectronic Engineering, Changchun University of Science Technology, Changchun, Jilin 130000, China

Correspondence should be addressed to Juncen Yan; 20100040@nxmu.edu.cn

Received 22 June 2022; Revised 21 July 2022; Accepted 4 August 2022; Published 29 August 2022

Academic Editor: Shadi Aljawarneh

Based on the problems encountered in the gateway system, this article developed the SVM algorithm support vector machine auxiliary system based on the function of the hybrid network gateway to help the gateway dynamically adjust its operating status to ensure the stability of the gateway system and the real-time internal data. This paper studies the noncontact defect detection system of automobile cylinder block on the basis of the SVM algorithm. There are many thin holes in the wall of automobile engine cylinder block, the structure is complex, and the processing is easy to deform. In order to solve the problem of deformation of the automobile engine cylinder block during the milling process, this paper uses a combination of simulation and experiment to analyze the clamping deformation and milling deformation during the machining of the top surface of the automobile cylinder block and proposes the control of the milling deformation profile error measure. Aiming at the problems of backward detection technology, low detection efficiency, and low detection accuracy for the detection of defects on the inner surface of the master cylinder of automobile brakes, this paper uses the machine vision technology to choose the noncontact method of measurement. The use of laser nonultrasonic contact systems is not limited to workpieces having regular shapes, such as planes and cylinders. It is limited to workpieces with regular shapes such as planes and cylinders. In the automotive and other industrial fields, for various curved parts with free-form surfaces, nondestructive testing techniques of laser nonultrasonic contact systems are generally required to find defects. In the research of the noncontact defect detection method of the automobile cylinder block based on the SVM algorithm, this paper hopes that the detection efficiency and detection accuracy of the inner surface of the brake cylinder can be improved, and the defect location can be accurately found.

1. Introduction

With the development of automobiles, consumers have gradually increased their requirements for automobiles, and continuous breakthroughs in current technical barriers have become the core competitiveness of current auto companies. In this article, the gateway load prediction node is constructed to support the gateway system. Based on the SVM algorithm, the time attention mechanism, the space attention mechanism, and the recently strengthened network structure optimization model are designed to improve the prediction accuracy of the gateway load. In order to eliminate the influence of the fuzzy mode, the fuzzy samples are subdivided to further improve the prediction accuracy [1]. In the machining automation industry, affected by the characteristics of the workpiece material, mechanical vibration, and machining technology, various defects will appear on the surface of the parts. These defects not only destroy the appearance of the parts but also reduce the performance of the parts, mainly reflected in the loose sealing, easy wear, and fatigue strength reduction of the parts. These defects will not only affect the performance of the component but also affect the operation of the component's equipment, thereby shortening the service life of the equipment and ultimately bringing greater safety risks. In order to ensure the quality of products in the industrial production process, the surface inspection technology of mechanical parts is widely used [2]. The research content of this article includes the compensation hole of the master cylinder of the automobile brake. When inspecting the automobile cylinder, the nondestructive detection of defects using the noncontact method is to use some

scientific treatment without damaging the performance of the inspected object and its microstructure, such as the method and special equipment for detecting the change of the characteristics of the object to be measured [3]. The noncontact method of defect detection occupies an important position in industrial production, and it has an irreplaceable guarantee for the safety of production and the reliability of products. As a new generation of nondestructive testing methods, the laser ultrasonic defect nondestructive testing technology has played an important role in industrial production [4]. Laser ultrasonic defect detection technology uses laser pulses to irradiate the surface of the test sample to excite ultrasonic waves and uses contact or noncontact methods to detect the ultrasonic waves that carry effective information about the test object. Through postsignal processing and analysis, the test object is finally realized [5]. Compared with traditional ultrasonic defect detection methods, laser ultrasonic defect detection technology has the advantages of noncontact, broadband, high time, and space resolution. In addition, the technology can be applied to harsh environments such as high temperature, high pressure, and severe corrosion [6]. Laser ultrasonic technology also shows more and more obvious advantages in nondestructive inspection of test objects with complex curved surfaces. This method overcomes the shortcomings of manual visual inspection and ultrasonic inspection methods, such as low detection efficiency, complex detection process, low detection accuracy, and high false detection rate, and realizes the high-precision, noncontact, high-speed measurement, and intelligentization required for modern measurement [7]. The characteristics provide a certain effect for improving production efficiency, controlling product quality, and testing automated production.

2. Related Work

The application of the SVM algorithm based on the statistical learning theory in classification and prediction was introduced. The penalty factor and kernel function parameters directly affect its accuracy. Usually, it is necessary to optimize the SVM parameter settings. It is carried out by combining optimization techniques, including genetic algorithms and particle algorithms. These methods have a good effect on improving the classification accuracy [8]. The simulation analysis of the top surface deformation of the cylinder block caused by the combined action of the milling force and the clamping force in the milling of the engine block and establishes the relationship between the top surface of the cylinder block and the profile [9]. Orthogonal experiment was used to calibrate the coefficients of each parameter in the cutting force model, and the cutting force model during the milling process of the top surface of the cylinder block was established to provide the required cutting force value for the simulation process of the top surface of the cylinder block milling deformation [10]. Through the simulation of milling deformation, the deformation law of the top surface of the cylinder body was analyzed, and the relationship between the milling deformation of the top surface of the cylinder body and the profile was established. In actual industrial production, the equipment under test often does not have a known contour model. To detect such a complex surface object, it is first necessary to obtain the contour information of the surface object under test [11]. The three-dimensional reconstruction of the object shell based on the monocular camera multicontour occlusion technology used in this paper can obtain the three-dimensional information of the measured surface object, extract the normal displacement of each detection point, and finally realize the automatic nondestructive laser ultrasound in the complex surface component [12]. The application in testing provides key technical achievements. The manual sampling visual inspection method is not only difficult to observe but also very exhausting after working for a long time, which leads to an increase in the false detection rate, and the detection quality cannot be guaranteed, and there are certain hidden safety hazards [13]. In view of this, some companies have tried to use ultrasonic, electromagnetic wave, and other measurement techniques for the research of new detection methods, but the effect is not very satisfactory [14]. This type of detection method has low accuracy and slow detection speed, but it has high requirements for environmental factors and is not suitable for rapid and accurate detection of compensation hole surface defects [15, 16]. The more and more important role of automobile braking system in the safe driving of vehicles was introduced. As the main component of the braking system, the processing quality of the inner surface of the master cylinder is particularly important. Therefore, the demand for braking is constantly increasing [17]. There are more stringent requirements on the quality of brakes. The development of technology provides a solid backing for this emerging detection technology and promotes the wide application of this technology in modern industrial production, especially for quality inspection and processing control products [18].

3. Car Network-Related Theories Based on SVM Algorithm

3.1. Optimization Principle of Support Vector Machine. The Volterra series model can effectively meet the description requirements and achieve a more accurate description process through the description of the nonlinear system. After the analog circuit fails, the core of the Volterra series will change accordingly. It can be described as

$$y(k) = \sum_{n=1}^{\infty} \sum_{m_1=0}^{\infty} \cdots \sum_{m_n=0}^{\infty} h_n(m_1, m_2, \ldots, m_n) u(k - m_1), \ldots, u(k - m_n). \quad (1)$$

The specific expressions of the first three-order time-domain kernels are

$$\begin{cases} y_1(k) = \sum_{m_1=0}^{L_1-1} h_1(m_1)u(k-m_1), \\ y_2(k) = \sum_{m_1=}^{L_2-1}\sum_{m_2=}^{L_2-1} h_2(m_1,m_2)u(k-m_1)u(k-m_2), \\ y_3(k) = \sum_{m_1=0m_2=0}^{L_3-1}\sum_{m_3=0}^{2_3-1} h_3(m_1,m_2,m_3), \\ u(k-m_1)u(k-m_2)u(k-m_3). \end{cases} \tag{2}$$

Breeding: there is the lowest and highest fitness among all individuals in the population. When determining the number of seeds produced by each weed, in addition to these two fitness values, the fitness value of a single weed must also be considered when determining the seed. The expression for the calculation amount is

$$\omega_n = \frac{f - f_{\min}}{f_{\max} - f_{\min}}\left(s_{\max} - s_{\min}\right) + s_{\min}. \tag{3}$$

Spatial distribution: the average value of the individual weed seeds during the reproduction process is the location of the individual, and the calculation expression of the specific relationship is

$$\sigma_{\text{cur}} = \frac{\left(\text{iter}_{\max} - \text{iter}\right)^n}{\left(\text{iter}_{\max}\right)^n}\left(\sigma_{\text{init}} - \sigma_{\text{final}}\right) + \sigma_{\text{final}}. \tag{4}$$

Variation: this paper adopts the optimal difference strategy to produce the specific expression of the intermediate individual as

$$V_i^k = X_{\text{best}}^k + G \times \left(X_{r1}^k - X_{r2}^k\right). \tag{5}$$

The expression of the cross operation is

$$U_{i,j}^k = \begin{cases} V_{i,j}^k, & \text{if } \left(\text{rand}(1) \le CR \text{ or } j = j_{\text{rand}}\right) \\ X_{i,j}^k, & \text{otherwise.} \end{cases} \tag{6}$$

Choose to judge the superiority of the fitness value. The specific expression is

$$X_i^{k+1} = \begin{cases} U_i^k, & \text{if } \left(f\left(U_i^k\right) \le f\left(X_i^k\right)\right), \\ X_i^k, & \text{otherwise.} \end{cases} \tag{7}$$

Considering that the IWO algorithm lacks a diverse late-stage weed population, the global search ability is reduced, and it is easy to fall into the local optimum. To this end, this paper integrates the DE algorithm into the IWO algorithm to obtain the DEIWO algorithm. The specific operation steps are as follows: firstly, after each generation of individuals in the weed population completes the reproduction and elimination operations, the individuals with the optimal fitness value are processed by differential mutation. Realize the generation of intermediate individuals and then complete the generation of test individuals by cross-processing the original population and the intermediate population, complete the generation of the test population, and finally screen the test population. The expressions of these two functions are

$$f(x) = \sum_{i=1}^{n} x_i^2, \tag{8}$$

$$f(x) = \sum_{i=1}^{n}\left(x_i^2 - 10\cos\left(2\pi x_i\right) + 10\right). \tag{9}$$

The convergence process of the DEIWO algorithm under the Rastrigin function is faster and more accurate in higher dimensions and effectively solves the problem of the IWO algorithm that is easy to fall into the local optimum and can obtain the global optimum solution.

3.2. Simulation Training of SVM Model. Although the simple two-way LSTM network has a more accurate prediction of the 0 and 1 load, the prediction performance of the 2 load is extremely poor. Compared with the two-way LSTM network, although the optimized network greatly improves the shortcomings of the former, the classification of load levels 1 and 2 is still relatively rough. According to analysis, this situation is said to be unable to resolve the boundary of fuzzy samples. The problem caused the error in the prediction result. Therefore, this article will perform simulation tests on the basic SVM model and the fusion model to verify its feasibility.

After training the input training set of the established SVM model, the confusion matrix diagram shown in Figure 1 can be obtained.

The SVM model roughly predicts the gateway load 0, 1, and 2. At the same time, combined with the ROC (Figure 2) after training, it can be seen that the SVM model has relatively general convergence for the prediction of load levels 0, 1, and 2. The prediction result is not bad. Although the actual gateway load forecasting does not satisfy people, it is enough that the fusion model eliminates the problem of fuzzy sample boundary. People are satisfied, but it is enough that the fusion model eliminates the problem of fuzzy sample boundaries.

After completing the training of all SVMs and optimized network models, it is necessary to determine the final weight ratio of the fusion model to achieve the best prediction effect. During the experiment, during the simulation data input process of the two models, the weight ratio of different combinations was continuously verified, and the actual prediction results of different combinations were recorded. Some weight combinations obtained after repeated training are shown in Table 1:

As shown in Table 1, when the weight of W_r is low and the weight of W_s is high, the prediction success rate is significantly reduced; when the weight of W_r is relatively high and the weight of W_s is low, although the predicted gateway increases significantly, the forecast rate will remain at a fixed value without significant changes.

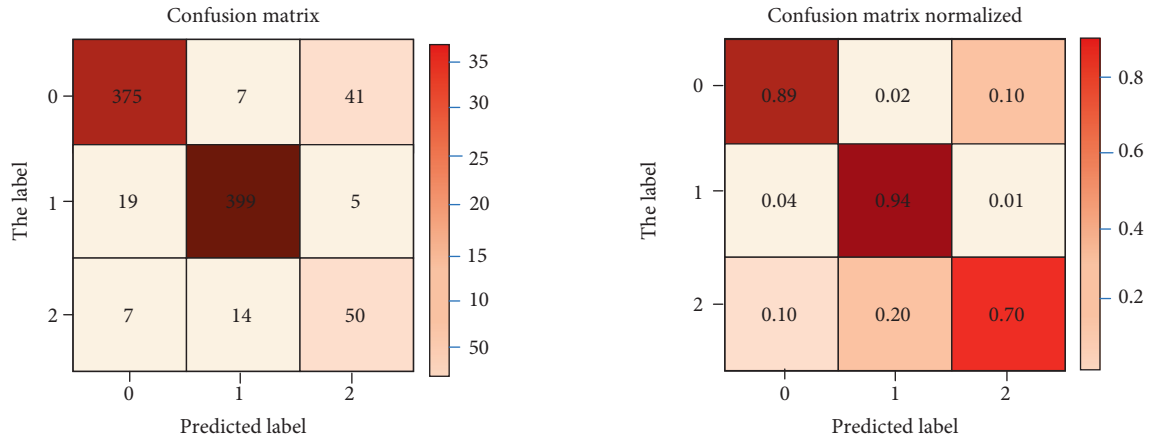

Figure 1: SVM model confusion matrix diagram: (a) confusion matrix diagram; (b) confusion matrix normalization diagram.

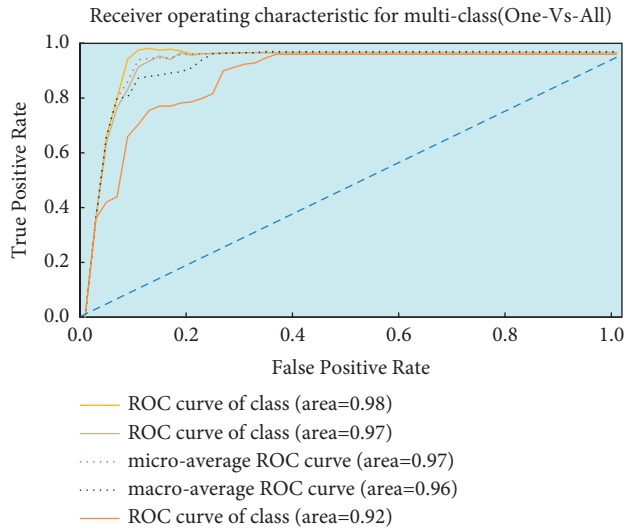

Figure 2: SVM model ROC curve.

Table 1: Fusion model weight test table.

W_r/W_s	0.68	0.55	0.48	0.37	0.25	0.11
0.32	0.76	—	—	—	—	—
0.45	—	0.82	—	—	—	—
0.52	—	—	0.88	—	—	—
0.63	—	—	—	0.97	—	—
0.75	—	—	—	—	0.96	—
0.89	—	—	—	—	—	0.94

4. Research on Noncontact Defect Detection Method of Automobile Cylinder Block

4.1. Correlation Analysis of Automobile Cylinder Profile. The basic parameters of the process system of the cylinder block production line of a company's production base are shown in Table 2.

Apply the correct contact pair in the finite element model by understanding the cylinder clamping process. This article will introduce in detail the OP190 station clamping layout and clamping force calculation and the establishment of the cylinder clamping deformation, which provides the corresponding clamping information and clamping force information for the finite element model.

"Profile" is used to evaluate the change between the actual measured profile and the ideal profile of the part. The contour tolerance zone is generally the upper and lower envelopes of a series of spheres with a diameter of t, the center of which is in the reference plane. The area defined by the surface is shown in Figure 3.

The evaluation object of N12 cylinder block top surface contour is the cylinder block top surface. The defined tolerance is 0.1 mm, taking the bottom surface of the cylinder block as a reference, and the distance value is related to the actual shape of the top surface itself. Since the theoretical contour of the cylinder top surface is a plane parallel to the reference plane, the contour value of the cylinder top surface is only related to the distance between the top surface of the cylinder block and the bottom surface of the cylinder block and the reference plane. If the distance L between the top surface of the cylinder block and the bottom surface is too large or too small, the tolerance zone will not surround the actually machined top surface, resulting in contour error. In the machining process, the milling deformation of the top surface of the cylinder block is the main reason for the fluctuation of the distance L value. Therefore, the deformation of the top surface of the cylinder block can be used to reflect the contour error of the workpiece. The deformation of the top surface of the cylinder block is equal to the contour error, and the symbol is opposite.

In order to check whether the deformation of the top surface of the cylinder block can reflect the contour error of the top surface of the cylinder block, the actual statistical data Q-DAS data of op190 station of M1 and M2 production lines of engine cylinder block in a base are shown in Table 3.

In order to make the new tool processing more intuitively reflect the data law of the top surface profile of the N12 cylinder, the above data are drawn into a chart, as shown in Figure 4.

It can be seen from Table 3 and Figure 4 that when the T22096 turning needle mills the top surface of the N12 cylinder, the average profile data of point 1 is 236.0031 mm,

Table 2: The basic parameters of the process system of the cylinder block production line.

Process system	Parameter
Artifact	N12 gray cast iron HT250 rough parts produced by a foundry
Machine tool	A five-axis CNC machining center produced by a German company, the CNC system is fanuc, the maximum speed is 10000r/min, the maximum power is 60kw, and the maximum feed speed is 60 m/min
Knives	The main models are guhring, ingesol, SADVIK, seco, etc. The detection method of the tool status is generally to detect 50 pieces at a time and determine the degree of wear of the tool according to the flatness, profile, and tool marks of the workpiece surface, so as to determine whether to change the tool.
Fixture	Designed by a German company and integrated with a five-axis CNC machining center

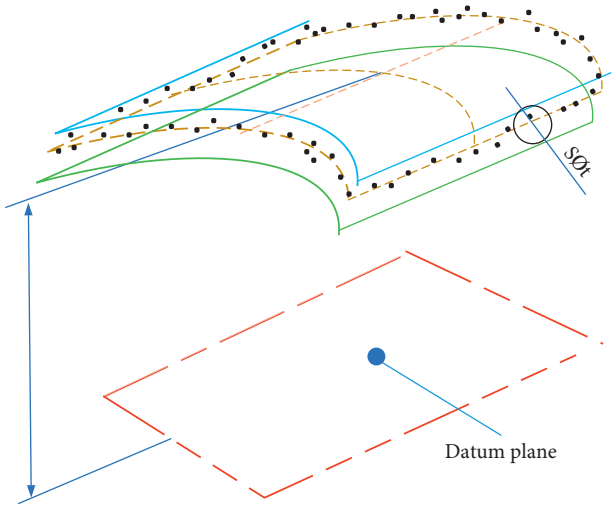

Figure 3: Contour tolerance zone chart.

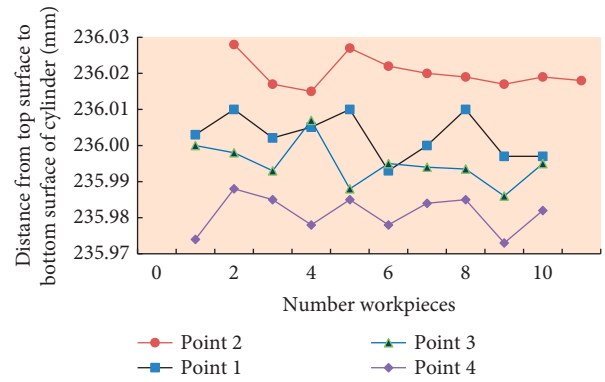

Figure 4: Data law of the cylinder top surface profile.

and the average profile error is 0.0031 mm; the average profile data of point 2 is 236.0209 mm, and the average profile error is 0.0209 mm; the average data of the point 3 profile is 235.9959 mm, and the average profile error is −0.0044 mm; the average data of the point 4 profile is 235.9818 mm, and the average profile error is −0.0190 mm.

4.2. Analysis of the Principle of Noncontact Defect Detection. The measurement method based on pulse echo and the time-of-flight analysis method based on diffraction are two traditional methods that use ultrasonic laser technology to detect material defects. Taking surface defects as an example, when the depth of the sample defect is less than the center wavelength of the ultrasonic wave, most of the ultrasonic energy will be diffracted from the bottom of the defect, resulting in small changes in the reflected echo signal and transmitted surface wave signal, and it is not easy to find. Therefore, these two methods are not suitable for detecting surface defects whose depth is less than the wavelength of sound waves. Aiming at the problem that the defect is too small to be accurately detected, the researchers based on the characteristics of the ultrasonic laser technology proposed a method of scanning the laser source. This technology makes full use of the ultrasonic advantages of laser excitation, transforms the original detection mechanism based on the interaction of surface acoustic waves with defects into a detection mechanism based on the interaction of the laser source with the defects and the use of shape changes, and then analyzes the defects. The focal size of the laser source is much smaller than the wavelength of ultrasound. Therefore, the laser source scanning method can greatly improve the ability of laser ultrasound to detect small defects. At the same time, this method has high signal-to-noise ratio and response sensitivity.

The scanning process of the laser source scanning method is shown in Figure 5.

During the scanning process of the laser beam along the sample surface from the far field to the near field and then to the defect area, the laser beam gradually approaches the defect until it passes over the defect. In this process, the interaction between the laser beam and the defect causes the detected surface wave signal to change significantly in terms of amplitude, peak value, and frequency components. Small defects with a depth less than the center wavelength of the ultrasound can also cause significant changes in the ultrasound signal. The study found that when the relative position of the laser beam and the defect changes, the amplitude of the received surface acoustic wave signal also changes significantly. By analyzing the change of the ultrasonic signal during the laser beam scanning process, information such as the position and size of the defect can be obtained.

The laser ultrasonic excitation system and the ultrasonic signal detection system are the main components of the laser ultrasonic noncontact nondestructive testing system. The detection principle is shown in Figure 6.

The excitation system is mainly composed of a laser and a scanning mirror. The pulsed laser is used to generate ultrasonic signals on the surface of the material to be measured, and then the scanning mirror is used to instruct

Table 3: Profile data of the cylinder top surface.

Experiment number	Contour of point 1		Contour of point 2		Contour of point 3		Contour of point 4	
	Actual value	Error value	Actual value	Error value	Actual value	Error value	Actual value	Error value
1	236.0034	0.0034	236.0284	0.0284	236.0005	0.0005	235.976	−0.026
2	236.0096	0.0096	236.0178	0.0178	235.9985	−0.0017	235.9878	−0.0122
3	236.0023	0.0023	236.0166	0.0166	235.995	−0.007	235.9847	−0.0155
4	236.0058	0.0058	236.0285	0.0285	236.0076	0.0076	235.9792	−0.0208
5	236.0108	0.0108	236.0217	0.0215	235.9886	−0.0116	235.9853	−0.0147
6	235.9937	−0.0065	236.0207	0.0207	235.9966	−0.0036	235.9787	−0.0213
7	236.0001	0.0001	236.0198	0.0198	235.9955	−0.0047	235.9835	−0.0167
8	236.0088	0.0088	236.0164	0.0164	235.9948	−0.0054	235.986	−0.016
9	235.9983	−0.0019	236.0205	0.0203	235.9875	−0.0127	235.974	−0.029
10	235.9983	−0.0019	236.0188	0.0188	235.9947	−0.0053	235.983	−0.018
Average value	236.0031	0.0031	236.0209	0.0209	235.9959	−0.0044	235.9818	−0.0190

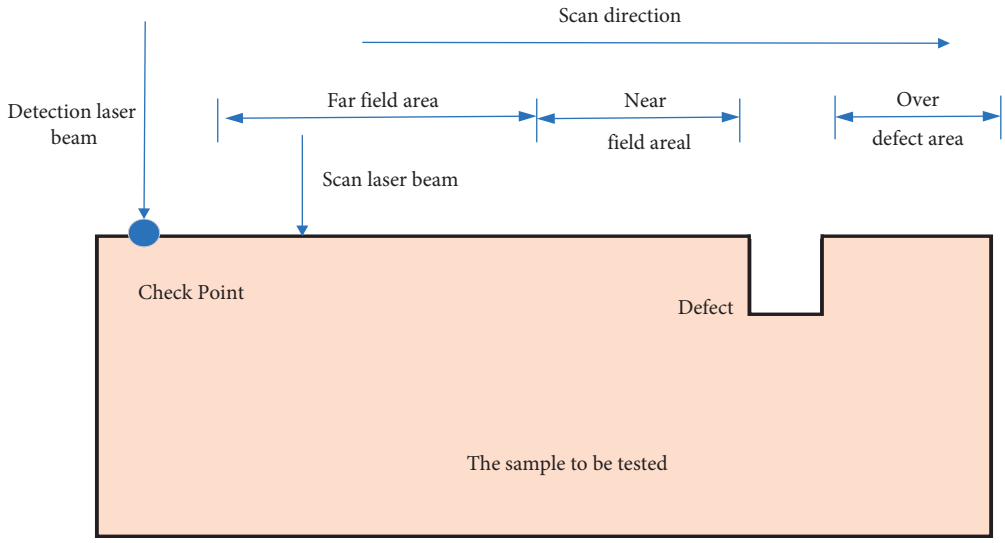

Figure 5: Scanning laser source method.

the laser beam to scan. Ultrasonic laser detection system mainly includes focal Fabry–Perot interferometer, signal amplifier circuit, and other parts. Detect the ultrasonic surface displacement signal generated by the optical interference detection method. The ultrasonic detection system realizes the advantages of noncontact excitation, noncontact reception of ultrasonic signals, and good detection reliability and is suitable for rapid detection in industrial sites.

4.3. Image Acquisition System Design. MER-500-7UM/UC series digital camera is a newly developed digital camera with USB 2.0 interface developed by Daheng Imaging. It adopts 1/2.5 line exposure CMOS sensor chip. The appearance is extremely small and compact, only $29 \times 29 \times 29$ mm, with built-in I/O interface. Cable locking device is provided, which can work stably in various harsh environments. The main performance parameters of the industrial digital camera with high reliability and cost performance are shown in Table 4. Its main performance parameters are shown in Table 4.

The lens uses a 5-megapixel low-distortion zoom lens, model MG3Z1228FC-MP. Its main performance parameters are shown in Table 5.

The automatic rotating table adopted by the system is a precision electric rotating table, and the model is ZT300-X. The turntable adopts a precisely developed worm gear structure, which is convenient to move and can be rotated back and forth in any direction. Its main performance parameters are shown in Table 6.

The internal parameter model of the camera reflects the conversion relationship between the pixel coordinate system and the camera coordinate system. From the above model analysis of the camera internal parameters, it can be seen that the camera internal parameters mainly include the focal length, the pixel spacing along the X-axis and Y-axis directions. The origin coordinates are transformed from the image coordinate system to the pixel coordinate system and the first-order radial distortion coefficient.

The position of the world coordinate system can be selected arbitrarily, so for the convenience of calculation, the world coordinate system is defined to match the camera

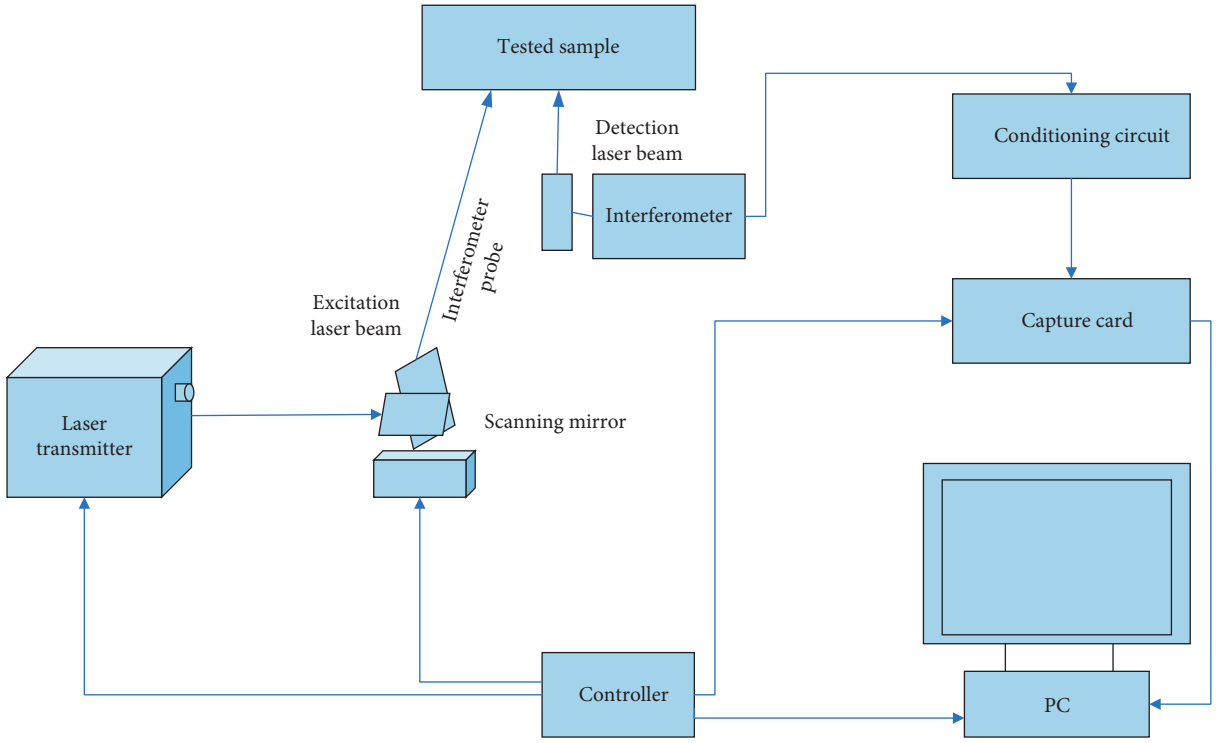

Figure 6: Schematic diagram of the laser ultrasonic noncontact detection system.

Table 4: Industrial camera performance parameter table.

Model	MER-500-7UM/UC
Resolution	2592 (H) × 1944 (V)
Frame rate	7 fps
Sensor type	1/2.5 "line exposure CMOS
Pixel size	2.2 μm × 2.2 μm
Spectrum	Black and white/color
Image data format	MONO8/RAW8 (Bayer)/MONO12/RAW12 (Bayer)
Data interface	Mini USB2.0
Power consumption	Rated < 1 W (@5V DC)
Lens interface	C
Mechanical dimensions	29 mm × 29 mm × 29 mm, without connectors
Weight	41 g

Table 5: Lens performance parameter table.

Model	MG3Z1228FC-MP
Target surface size	2/3"
Focal length	12~36 mm
Maximum imaging size	8.8 × 6.6 (Φ11) mm
Aperture range	F2.8~F360 C
Working distance	0.2~inf m
Aperture control	DC automatic aperture
Filter thread	M358 × P0.5 mm
Interface	C
Mechanical dimensions	Φ 41.6 × 52 × 53 mm

Table 6: Turntable performance parameter table.

Model	ZT300-X
Angle range	360° around *X*, Y, *Z* axes
Resolution	0.005°
Positioning accuracy	0.005°
Table size	150 × 150 mm
Transmission ratio	180:1
E body material	Aluminium alloy
Center bearer	10 kg
Weight	25 kg
Mechanical dimensions	Φ 41.6 × 52 × 53 mm

coordinate system, and the plane of the calibration board is on the Zw = 0 plane of the world coordinate system. Use p_i to represent each column vector of the rotation matrix R, and σ represents the scale factor (σ is a parameter introduced to facilitate matrix operations. For homogeneous coordinates, the existence of σ will not change the coordinate value). For any point on the plane, there are

$$\begin{aligned}\sigma\begin{bmatrix}u\\v\\1\end{bmatrix} &= M\begin{bmatrix}p_1 & p_2 & p_3 & t\end{bmatrix}\begin{bmatrix}x_w\\y_w\\0\\1\end{bmatrix} = M\begin{bmatrix}p_1 & p_2 & t\end{bmatrix}\begin{bmatrix}x_w\\y_w\\1\end{bmatrix}\\ &= A\begin{bmatrix}x_w\\y_w\\1\end{bmatrix},\end{aligned} \tag{10}$$

$$\begin{cases} M = \begin{bmatrix}\alpha & \gamma & u_0\\ 0 & \beta & v_0\\ 0 & 0 & 1\end{bmatrix}\\ A = \begin{bmatrix}a_{11} & a_{12} & a_{13}\\ a_{21} & a_{22} & a_{23}\\ a_{31} & a_{32} & 1\end{bmatrix}\end{cases}. \tag{11}$$

If the space coordinates and image coordinates of some characteristic points on the calibration plate are known, the unique mapping matrix A can be solved. Substituting formulas (11) into (12),

$$\begin{cases} \sigma u = a_{11}x_w + a_{12}y_w + a_{13}\\ \sigma v = a_{21}x_w + a_{22}y_w + a_{23}\\ \sigma = a_{31}x_w + a_{32}y_w + 1\end{cases}. \tag{12}$$

Let $a' = [a_{11}a_{12}a_{13}a_{21}a_{22}a_{23}a_{31}a_{32}]$, then

$$\begin{bmatrix}u\\v\end{bmatrix} = \begin{bmatrix}x_w & y_w & 1 & 0 & 0 & 0 & -ux_w & -uy_w\\ 0 & 0 & 0 & x_w & y_w & 1 & -vx_w & -vy_w\end{bmatrix}a'. \tag{13}$$

After obtaining the homography matrix A, the internal parameters of the camera need to be further analyzed. Use ai to represent the column vector of A, and then

$$A = [a_1, a_2, a_3] = \varepsilon M[p_1, p_2, t]. \tag{14}$$

Substitute p_1 and p_2 into the combination of $a1$, $a2$, and M as an expression, that is, $p_1 = a_1M-1$, $p_2 = a_2M-1$. Based on these two constraints, the following two constraint equations are obtained:

$$\begin{cases} a_1^T M^{-T} M^{-1} a_2 = 0,\\ a_1^T M^{-T} M^{-1} a_1 = a_2^T M^{-T} M^{-1} a_2.\end{cases} \tag{15}$$

Order:

$$\begin{aligned} G = M^{-T}M^{-1} &= \begin{bmatrix}G_{11} & G_{12} & G_{13}\\ G_{21} & G_{22} & G_{23}\\ G_{31} & G_{32} & G_{33}\end{bmatrix}\\ &= \begin{bmatrix}\frac{1}{\alpha^2} & \frac{-\gamma}{\alpha^2\beta} & \frac{\gamma v_0 - \beta u_0}{\alpha^2\beta}\\ \frac{-\gamma}{\alpha^2\beta} & \frac{\gamma}{\alpha^2\beta^2} + \frac{1}{\beta^2} & \frac{-\gamma(\gamma v_0 - \beta u_0)}{\alpha^2\beta^2} - \frac{v_0}{\beta^2}\\ \frac{\gamma v_0 - \beta u_0}{\alpha^2\beta} & \frac{-\gamma(\gamma v_0 - \beta u_0)}{\alpha^2\beta^2} - \frac{v_0}{\beta^2} & \frac{(\gamma v_0 - \beta u_0)^2}{\alpha^2\beta^2} + \frac{{v_0}^2}{\beta^2} + 1\end{bmatrix}.\end{aligned} \tag{16}$$

According to formula (16), G is a symmetric matrix. Let: $g = [G_{11}G_{12}G_{22}G_{13}G_{23}G_{33}]\ T$. Suppose the vector of A is $ai = [ai1, ai2, ai3]\ T$, then

$$a_i^T G a_j = V_{ij}^T g, \tag{17}$$

of which

$$V_{ij} = \begin{bmatrix} a_{i1}a_{j1}\\ a_{i1}a_{j2} + a_{i2}a_{j1}\\ a_{i2}a_{j2}\\ a_{i3}a_{j1} + a_{i1}a_{j3}\\ a_{i3}a_{j2} + a_{i2}a_{j3}\\ a_{i3}a_{j3}\end{bmatrix}. \tag{18}$$

Using constraint conditions, the following equations can be obtained:

$$\begin{bmatrix} V_{12}^T\\ V_{11}^T - V_{22}^T\end{bmatrix} g = 0. \tag{19}$$

Suppose the number of calibration images is N, and the equations corresponding to N images are superimposed, then:

$$V \times g = 0. \tag{20}$$

Among them, V is a $2N \times 6$ matrix.

Perform coordinate conversion calculations: assuming that the translation transformation matrix from the camera coordinate system to the rotating coordinate system is TCA, the rotation transformation matrix is RCA, and the coordinate transformation matrix is MCA, then

$$M_{CA} = R_{CA} \times T_{CA} = R_{CA}\begin{bmatrix} 1 & 0 & 0 & -X_A \\ 0 & 1 & 0 & -Y_A \\ 0 & 0 & 1 & -Z_A \\ 0 & 0 & 0 & 1 \end{bmatrix}. \tag{21}$$

Suppose the transformation matrix that rotates θ° counterclockwise around the O_AY_A axis of the rotation axis coordinate system is $R_{y\theta}$, then

$$R_{y\theta} = \begin{bmatrix} \cos\theta & 0 & -\sin\theta & 0 \\ 0 & 1 & 0 & 0 \\ \sin\theta & 0 & \cos\theta & 0 \\ 0 & 0 & 0 & 1 \end{bmatrix}. \tag{22}$$

Assuming that the translation transformation matrix from the rotating coordinate system to the initial camera coordinate system is T_{AC}, the rotation transformation matrix is R_{AC}, and the coordinate transformation matrix is M_{AC}, then

$$M_{AC} = T_{AC} \times R_{AC} = \begin{bmatrix} 1 & 0 & 0 & X_A \\ 0 & 1 & 0 & Y_A \\ 0 & 0 & 1 & Z_A \\ 0 & 0 & 0 & 1 \end{bmatrix} R_{AC}. \tag{23}$$

In this way, the point of the object P is rotated clockwise by θ from the coordinates P_0 (x_0, y_0, z_0) in the camera coordinate system around the rotation axis, thereby obtaining the three-dimensional coordinates P_θ (x_w, y_w, z_w) in the initial camera coordinate system. Assuming that the total conversion matrix is $R\theta$, then

$$\begin{aligned} P_\theta = R_\theta \times P_0 &= M_{AC}\left(R_{y\theta}\left(M_{CA} \times P_0\right)\right) \\ &= \left(M_{AC} \times R_{y\theta} \times M_{CA}\right)P_0, \end{aligned} \tag{24}$$

of which

$$R_\theta = T_{AC}\left(R_{AC} \times R_{y\theta} \times R_{CA}\right)T_{CA} = T_{AC} \times W \times T_{CA}. \tag{25}$$

And, the rotation transformation matrix R_{AC} and R_{CA} are orthogonal matrices; then, $R_{CA} = R_{AC}^{-1} = R_{AC}T$.

Make

$$\begin{aligned} R_{AC} &= \begin{bmatrix} a_1 & b_1 & c_1 & 0 \\ a_2 & b_2 & c_2 & 0 \\ a_3 & b_3 & c_3 & 0 \\ 0 & 0 & 0 & 1 \end{bmatrix}, \\ R_{CA} &= \begin{bmatrix} a_1 & a_2 & a_3 & 0 \\ b_1 & b_2 & b_3 & 0 \\ c_1 & c_2 & c_3 & 0 \\ 0 & 0 & 0 & 1 \end{bmatrix}. \end{aligned} \tag{26}$$

Among them, $[a^1a^2a^3]$ T, $[b^1b^2b^3]$ T, and $[c^1c^2c^3]$ T are the unit direction vectors of the coordinate axes O_AX_A, O_AY_A, and O_AZ_A of the rotating coordinate system, which are satisfied by the following formulae:

$$\begin{cases} a_1 = b_2c_3 - b_3c_2 \\ a_2 = b_3c_1 - b_1c_3 \\ a_3 = b_1c_2 - b_2c_1 \end{cases}$$
$$\begin{cases} b_1 = c_2a_3 - c_3a_2 \\ b_2 = c_3a_1 - c_1a_3 \\ b_3 = c_1a_2 - c_2a_1 \end{cases} \tag{27}$$
$$\begin{cases} c_1 = a_2b_3 - a_3b_2 \\ c_2 = a_3b_1 - a_1b_3 \\ c_3 = a_1b_2 - a_2b_1 \end{cases}$$

Organize the formula into

$$\begin{aligned} W &= R_{AC} \times R_{y\theta} \times R_{CA} \\ &= \begin{bmatrix} a_1 & b_1 & c_1 & 0 \\ a_2 & b_2 & c_2 & 0 \\ a_3 & b_3 & c_3 & 0 \\ 0 & 0 & 0 & 1 \end{bmatrix}\begin{bmatrix} \cos\theta & 0 & -\sin\theta & 0 \\ 0 & 1 & 0 & 0 \\ \sin\theta & 0 & \cos\theta & 0 \\ 0 & 0 & 0 & 1 \end{bmatrix}\begin{bmatrix} a_1 & a_2 & a_3 & 0 \\ b_1 & b_2 & b_3 & 0 \\ c_1 & c_2 & c_3 & 0 \\ 0 & 0 & 0 & 1 \end{bmatrix}. \end{aligned} \tag{28}$$

In the formula, $[b_1b_2b_3]$ T is the unit direction vector of the rotation axis L in the camera coordinate system. After finishing,

$$\begin{bmatrix} \left(b_1^2 + \left(1 - b_1^2\right)\cos\theta\right)(X_0 - X_A) + \left(b_1b_2(1 - \cos\theta) + b_3\sin\theta\right)(Y_0 - Y_A) \\ +\left(b_1b_3(1 - \cos\theta) - b_2\sin\theta\right)(Z_0 - Z_A) + X_A \\ \left(b_1b_2(1 - \cos\theta) - b_3\sin\theta\right)(X_0 - X_A) + \left(b_2^2 + \left(1 - b_2^2\right)\cos\theta\right)(Y_0 - Y_A) \\ +\left(b_2b_3(1 - \cos\theta) + b_1\sin\theta\right)(Z_0 - Z_A) + Y_A \\ \begin{bmatrix} \left(b_1b_3(1 - \cos\theta) + b_2\sin\theta\right)(X_0 - X_A) + \left(b_2b_3(1 - \cos\theta) - b_1\sin\theta\right)(Y_0 - Y_A) + \left(b_3^2 + \left(1 - b_3^2\right)\cos\theta\right)(Z_0 - Z_A) + Z_A \\ 1 \end{bmatrix} \end{bmatrix}. \tag{29}$$

It can be seen that given the unit direction vector $[b_1 b_2 b_3]\ T$ of the axis of rotation line L in the camera coordinate system and the three-dimensional coordinates of any point on the line, the three-dimensional coordinates of the object point in the camera coordinate system can be obtained by formulas. The three-dimensional coordinates in the initial camera coordinate system, which is the world coordinate system, after the rotating shaft rotates a certain angle, confirms the external parameter model of the image acquisition system.

4.4. Design of Noncontact Defect Detection Process for Automobile Cylinders. The detection system cannot be completely separated from manual participation, and the system must manually participate in the preparatory work before it works. First of all, the system cannot distinguish between different types of workpieces to be tested, or even if it can be automatically identified through programming, it is a complex and arduous task. Therefore, the system uses manual participation to change the positioning position and limit of the fixture according to different types of workpieces. Therefore, the system uses manual participation to change the positioning position of the fixture and the position of the baffle according to different types of workpieces. The system also needs to change the corresponding initial parameter settings in the system software. Secondly, the clamping work of the workpiece also requires manual participation. Compared with the use of motor control to achieve workpiece clamping, manual participation is more convenient and faster. Finally, the initialization of many hardware devices also requires manual participation, such as the power supply of the motor and the turning on of the light source.

After the preparatory work is completed, the detection method of the detection system will be introduced in detail. The system function has been visually presented on the main interface of the inspection system. The specific inspection steps are as follows: fix the fixture for the rainbow, and enter the workpiece number in the corresponding position on the main interface of the inspection system. According to the model of the part to be tested, set the step length and stop position of the endoscope moving motor in the main interface and set the step length and stop position of the endoscope rotating motor according to the angle of view of the selected endoscope. People click the forward button on the endoscope motion motor module on the main interface, send the endoscope into the brake iris body, and stop moving forward within the maximum coverage of the endoscope. At the same time, the system cooperates with the grating ruler to calculate the position of the endoscope at this time. At this time, select the "capture image" command to take the image at this time. Click the forward button on the endoscope rotating motor module to make the endoscope rotate clockwise, and stop when it reaches the next step to perform the operation. In this process, the system will run the image processing program in the background to detect the image in the image and save the results. The rotating motor continues to rotate the endoscope and stops when it reaches the next step length, and the system runs the image processing program in the background. Repeat the operation until the moving motor reaches the initial stop position and stops. The moving motor pushes the oscilloscope forward and stops when it reaches the next set step. During this process, the rotating motor returns to its initial position in a counterclockwise direction. Repeat four steps until the running motor reaches the stop position and stops. After checking the inner surface of the entire part, move the motor out of the brake cylinder and return to its initial position. At this point, the detection of defects on the inner surface of the entire part is completed, and finally the system saves the entire detection result for printing and reference. For defective parts, the system will also send out an audible and visual alarm, and the entire discovery process takes about two minutes.

There is a "measurement kit" command in the graphics menu of the main interface of the system. Clicking this command, the system will open a measurement suite dialog box; in this dialog box, you can directly manually manipulate the collected images. The picture has a small flaw. You can use the "ellipse" command in the "operation" menu to roughly wrap the fault area in an ellipse and then click the "measurement manager" command in the "measurement" menu to open the measurement manager dialog box and measure. The manager will list the measurement operations performed on the image, select the ellipse measurement operation, and click the "view" button, you can view the detailed information of the area, such as the center point coordinates, perimeter, and area. Of course, what operation is performed on a certain area of the defect in the image depends on the characteristic shape of the defect. The principle of selection is to ensure that the selected operation can be consistent with the shape of the defect, so as to minimize the error of the defect information of the detected defect. Through the measurement setting dialog box, you can intuitively and vividly obtain the general information of the defect, and at the same time, you can compare these data with the system measurement result to verify the feasibility of the system measurement.

5. Conclusion

This paper proposes a noncontact measurement scheme in view of the backward detection technology, low detection efficiency, and low detection accuracy of the surface defect detection of the automobile brake master cylinder. It is based on machine vision. It has done certain research on the clamping deformation, milling deformation, and contour error control of the top surface of the automobile engine cylinder, and has achieved some results. However, the machining process of the cylinder block of an automobile engine is very complicated, and the machining quality of the cylinder block is affected by many factors. The milling contour error of the top surface of the cylinder block is controlled; from the point of view of machining optimization, during the machining process, the contour error of the cylinder top surface can be controlled by optimizing the clamping force, multipass or variable path machining;

considering machining optimization and machining compensation comprehensively, through the joint optimization of clamping force and machining parameters, the contour error of the upper surface of the cylinder is controlled. Experimental results show that different optimization strategies have different error control effects. Among them, the upper surface contour error control effect based on the optimization of clamping force and processing parameters is the most ideal.

Data Availability

The data used to support the findings of this study are available from the corresponding author upon request.

Conflicts of Interest

The authors declare no conflicts of interest.

References

[1] G. Paul, T. Tanizawa, S. Havlin, and H. E. Stanley, "Optimization of robustness of complex networks," *The European Physical Journal B*, vol. 38, no. 2, pp. 187–191, 2004.

[2] I. Yamaguchi, J.-I. Kato, and S. Ohta, "Surface shape measurement by phase-shifting digital holography," *Optical Review*, vol. 8, no. 2, pp. 85–89, 2001.

[3] Z. Y. Feng, F. Jia, and J. H. Zhou, "Three-Dimensional surface shape measurement of big objects by image splicing in digital holography," *Chinese Journal of Lasers*, vol. 35, no. 12, pp. 2017–2021, 2008.

[4] P. Sun, L. Zhang, and C. X. Tao, "Measurement of 3D morphology of objects based on fourier transform method of LCD digital projection technology," *Acta Photonica Sinica*, vol. 34, no. 8, pp. 1250–1252, 2005.

[5] P. B. Nagy, "Fatigue damage assessment by nonlinear ultrasonic materials characterization," *Ultrasonics*, vol. 36, no. 1–5, pp. 375–381, 1998.

[6] N. Rtayli and N. Enneya, "Selection features and support vector machine for credit card risk identification," *Procedia Manufacturing*, vol. 46, pp. 941–948, 2020.

[7] D. J. Hughes, E. L. Heeley, and C. Curfs, "A non-destructive method for the measurement of residual strains in semi-crystalline polymer components," *Materials Letters*, vol. 65, no. 3, pp. 530–533, 2011.

[8] J. Li and Z. Peng, "Statistic optics discussion on the formula of digital holographic 3D surface profiling measurement," *Measurement*, vol. 43, no. 3, pp. 381–384, 2010.

[9] K. Bennett and O. Mangasarian, "Combining support vector and mathematical programming methods for induction," *Advances in Kernel Methods SV Learning*, pp. 307–326, 1999.

[10] S. Yin, G. Wang, and H. R. Karimi, "Data-driven design of robust fault detection system for wind turbines," *Mechatronics*, vol. 24, no. 4, pp. 298–306, 2014.

[11] H. Abulkasim, A. Farouk, S. Hamad, A. Mashatan, and S. Ghose, "Secure dynamic multiparty quantum private comparison," *Scientific Reports*, vol. 9, no. 1, pp. 1–16, 2019.

[12] S. Yin, X. Li, H. Gao, and O. Kaynak, "Data-based techniques focused on modern industry: an overview," *IEEE Transactions on Industrial Electronics*, vol. 99, 2014.

[13] W. M. Cheng, M. Y. Chen, and Z. Ding, "Measurement of three-dimensional shape by multi-aperture stitching in cylindrical coordinates," *Acta Optica Sinica*, vol. 19, no. 6, pp. 92–96, 1999.

[14] F. Jia, Z. Y. Feng, and L. B. Zhou, "Pre-imaging digital holography for measuring 3D morphology of large objects," *Acta Photonica Sinica*, vol. 37, no. 11, pp. 2239–2243, 2008.

[15] J. Cervantes, F. Garcia, L. Rodriguez, R. M. Lisbeth, and A. Lopez, "A comprehensive survey on support vector machine classification: applications, challenges and trends," *Neurocomputing*, vol. 408, pp. 189–215, 2020.

[16] J. C. Li, "Introduction of digital color holographic wavefront reconstruction algorithm," *Chinese Journal of Lasers*, vol. 38, no. 5, Article ID 0501001, 2011.

[17] X. M. Guo, C. Chen, and W. S. Wang, "Three-Dimensional shape test based on digital holography," *Natural Science*, vol. 1, no. 1, pp. 34–38, 2015.

[18] F. Chen, M. Cheng, B. Tang, B. Chen, and W. Xiao, "Pattern recognition of a sensitive feature set based on the orthogonal neighborhood preserving embedding and adaboost_SVM algorithm for rolling bearing early fault diagnosis," *Measurement Science and Technology*, vol. 31, no. 10, Article ID 105007, 2020.

Hindawi
Mobile Information Systems
Volume 2023, Article ID 9786865, 1 page
https://doi.org/10.1155/2023/9786865

Retraction

Retracted: Adaptive Feature Analysis in Target Detection and Image Forensics Based on the Dual-Flow Layer CNN Model

Mobile Information Systems

Received 1 August 2023; Accepted 1 August 2023; Published 2 August 2023

This article has been retracted by Hindawi following an investigation undertaken by the publisher [1]. This investigation has uncovered evidence of one or more of the following indicators of systematic manipulation of the publication process:

(1) Discrepancies in scope
(2) Discrepancies in the description of the research reported
(3) Discrepancies between the availability of data and the research described
(4) Inappropriate citations
(5) Incoherent, meaningless and/or irrelevant content included in the article
(6) Peer-review manipulation

The presence of these indicators undermines our confidence in the integrity of the article's content and we cannot, therefore, vouch for its reliability. Please note that this notice is intended solely to alert readers that the content of this article is unreliable. We have not investigated whether authors were aware of or involved in the systematic manipulation of the publication process.

Wiley and Hindawi regrets that the usual quality checks did not identify these issues before publication and have since put additional measures in place to safeguard research integrity.

We wish to credit our own Research Integrity and Research Publishing teams and anonymous and named external researchers and research integrity experts for contributing to this investigation.

The corresponding author, as the representative of all authors, has been given the opportunity to register their agreement or disagreement to this retraction. We have kept a record of any response received.

References

[1] N. Liang, H. Xu, W. Zhang, and L. Cui, "Adaptive Feature Analysis in Target Detection and Image Forensics Based on the Dual-Flow Layer CNN Model," *Mobile Information Systems*, vol. 2022, Article ID 7140594, 14 pages, 2022.

Hindawi
Mobile Information Systems
Volume 2022, Article ID 7140594, 14 pages
https://doi.org/10.1155/2022/7140594

Research Article

Adaptive Feature Analysis in Target Detection and Image Forensics Based on the Dual-Flow Layer CNN Model

Nannan Liang,[1,2] **Haifeng Xu**,[1] **WanLi Zhang**,[1] **and Lin Cui**[1]

[1]*School of Informatics and Engineering, Suzhou University, Suzhou 234000, China*
[2]*Key Laboratory of Mine Water Resource Utilization of Anhui Higher Education Institutes, Suzhou 234000, China*

Correspondence should be addressed to Nannan Liang; lnannan@ahszu.edu.cn

Received 31 May 2022; Revised 26 July 2022; Accepted 9 August 2022; Published 28 August 2022

Academic Editor: Shadi Aljawarneh

With the rapid development of artificial intelligence technology, image editing technology has evolved from relying on software such as Photoshop and GIMP for manual modification to using artificial intelligence technology to achieve intelligent and automated tampering of images. Editing, falsifying, and disseminating digital images have become simple and easy, leading to a crisis of confidence in digital images and reducing their reliability as judicial evidence. Therefore, how to identify falsified images, improve their trustworthiness, and avoid judicial injustice has become a problem that must be overcome in the information age. In this paper, we propose a target detection and adaptive feature analysis in image forensics based on a dual-flow layer CNN model, which can effectively perform image forensics. The results show that our algorithm has a clear theoretical basis, a small operational complexity, and a high detection accuracy.

1. Introduction

People's daily life is full of image information data. In the era of image information flooding, it becomes more and more difficult to get effective and valuable image information from it quickly when we are faced with so much image information. Computer vision plays an important role in medical, security, transportation, aerospace, automation, control, and other fields. Humans get 91% of their information in cognition of the world from vision, so computer vision is the basis of cognition of the world by machines and devices. As a major vehicle for information dissemination, humans generally focus on only part of the information in an image. In daily life, only certain people or objects are the focus of attention. For example, the license plate number of a moving vehicle, the seat belt wearing of a driver, a suspicious pedestrian in a crowded place, the helmet wearing of a worker in a factory, and so on. It has become a popular research direction to find out the main targets of people's attention in images quickly and effectively and to label them with the correct classification. Therefore, the research of target detection is important for robotics, video surveillance, automated inspection, road traffic, aerospace, and other fields.

Natural scenes have great complexity, and target detection is affected by scene changes, natural lighting, weather changes, object shapes, sizes, scales, and stacking methods, making detection more difficult. Therefore, how to quickly and effectively separate targets and attenuate the effects of target scale, shape, size variation, and background complexity has become a challenge in the direction of target detection. The equipment for obtaining photos has gradually diversified. Nowadays, professional cameras, ordinary cameras, and smartphones with high-definition photo functions are common in life, among which smartphones with high-definition photo functions are far more popular than other devices in the population with their low prices, portable size, and uncompromising photo functions.

However, everything has both positive and negative aspects, and while photo images are easy to access and edit, they also bring serious negative effects to life in the information age. Some people, for various purposes, maliciously tamper with and disseminate some carefully faked photo images, reversing black and white and confusing people's

minds, causing an uproar in society and subverting the basic common sense that seeing is believing.

Digital photo image tampering forensic technology is a kind of digital image forensic technology, which relies on computer technology to judge whether the original content is still maintained in the process of transmission and dissemination of photo images taken by digital cameras. If we want to forensically examine the authenticity of photo images, we should first understand the means of photo image tampering, and the more common tampering methods include copy-paste of the same image, splicing of different images, image retouching, and image enhancement.

1.1. Copy-and-Paste Tampering with the Same Image. Paste a part of the image to other parts of the image as in Figure 1. The original photo image is on the left, and the tampered image on the right is created by copying the lawn in the figure and covering the person.

Heterogeneous image stitching tampering: a part of one image is stitched into another image by two or more images. The stitching tampering between different images has the following characteristics: (1) the tampering trace is not visually noticeable; (2) some statistical characteristics of the image are changed by the tampering behavior. As shown in Figure 2, the yellow flowers in the original image 2(a) are stitched into the original image 2(b) to obtain the tampered image 2(c).

1.2. Image Retouching. It is an image restoration operation commonly used in artistic photos to make the people in the photos more beautiful; it is also commonly used after image copy-paste tampering or splicing tampering to eliminate the edge traces of tampering. In the original image of Figure 3(a), the human face has more obvious spots, while the face of the tampered Figure 3(b) becomes smooth and more beautiful after retouching.

1.3. Image Enhancement. An operation that blurs or highlights information somewhere in an image. This type of tampering technique is usually achieved by changing the hue or contrast of a certain part of the image. Figure 4(a) blurs a large amount of detailed information by adjusting the contrast and hue, so that the original image is tampered with, creating a tampered Figure 4(b).

Incidents of photo tampering such as the one mentioned above have emerged, seriously affecting the public's correct judgment of things. In the present case, the negative impact of photo tampering and the crisis of confidence caused by it are worrying. If doctored photos are used in news reports, they may distort the facts and mislead the public, which may intensify social conflicts; if doctored photos are used as evidence in court, they may lead to false cases, obstruct justice, and allow criminals who should be punished to escape from the net of justice; if doctored photos are used in insurance claims, they may cause unnecessary economic disputes; in international relations, the use of doctored photo images may lead to political turmoil, diplomatic discord and even military conflict, and other extremely serious consequences.

2. Related Work

The traditional target detection methods are Viola-Jones, HOG + SVM, and DPM. Among them, Viola-Jones uses integral graph features and AdaBoost method. HOG + SVM method detects pedestrians as targets. It first extracts HOG features from the candidate regions of the target and then uses SVM classifier for classification decision. DPM is a variant of HOG feature detection, and DPM adds additional strategies. DPM method is the most effective and best performing method among all traditional target detection methods. Its advantages are the intuitive and simple method, block computing speed, and adaptation to animal deformation. It has been verified by a large number of scholars that its detection accuracy, generalization ability, and detection speed are better than traditional methods.

The two-stage-based target detection model refers to the extraction of features using convolutional neural network (CNN) first, then the recommendation of candidate regions using region candidates, and finally marking the target box location and classifying the marked target boxes. The most typical representative is the RCNN series of networks. The one-stage target detection model is a regression model that directly regresses the position of the target frame without generating a candidate frame in the middle of the network and directly converts the target frame location problem into a regression problem. The most representative one is the yolo series network. The large number of prior frames increases the computation and memory usage. For targets with extremely large aspect ratios in the scene, the method of preset a priori frames is not only time-consuming but also prone to false detection problems. Different data sets require different target detection models, so different a priori frames need to be set, resulting in reduced model generalization capability.

Photo image tampering forensics is emerged in the last decade. Despite the short development time, photo image tampering forensic technology has gained great progress with the continuous development and improvement of image processing, pattern recognition and artificial intelligence and other related theories, and the continuous discovery of relevant experts and scholars' research. According to the current research theoretical results, the photo image tampering forensic process is briefly summarized, as shown in Figure 5.

Since the tampered part of the tampered photo image differs from the untampered real part in certain types of features, such features can be extracted from each part of the photo image to be tested during forensics, and then the extracted features can be classified to arrive at the verdict of authenticity of the photo image to be tested. According to the different features extracted, this paper divides the photo image tampering forensics into two categories: tampering forensics based on image content features and tampering

(a) (b)

Figure 1: Copy-paste forgery within same image. (a) Original image. (b) Tampered image.

(a) (b) (c)

Figure 2: Splice forgery between different images. (a) Original Figure 1. (b) Tampered figure. (c) Original figure.

(a) (b)

Figure 3: Image blur forgery. (a) Original image. (b) Tampered image.

forensics based on imaging features, which are briefly introduced below.

2.1. Tampering Forensic Techniques Based on Content Features of Photo Images. The consistency of the content features (such as natural statistical characteristics, key points, lighting direction, and texture) of tampered photo images will be destroyed, and the researcher can make a decision on the authenticity of the image by detecting the changes of these content features.

2.1.1. Forensic Techniques Based on Natural Statistical Features. The natural statistical properties such as mean, variance, histogram, and higher order statistics of images in

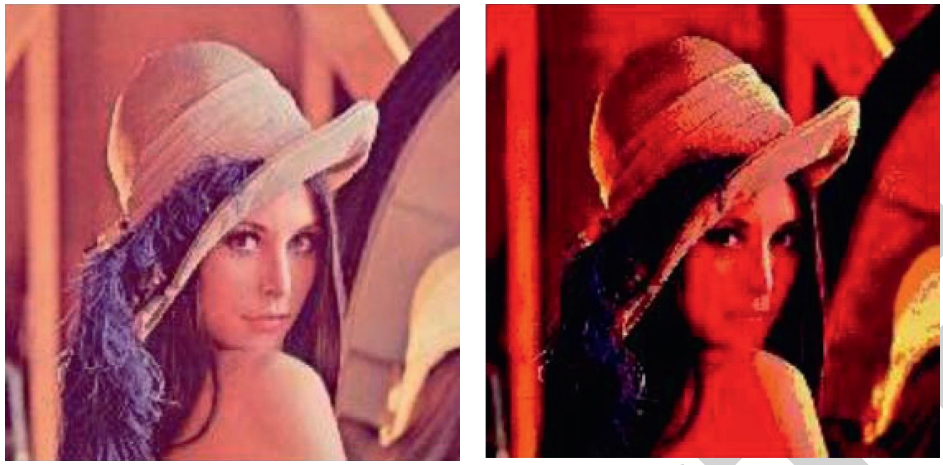

(a) (b)

Figure 4: Image enhancement tamper. (a) Original image. (b) Tampered image.

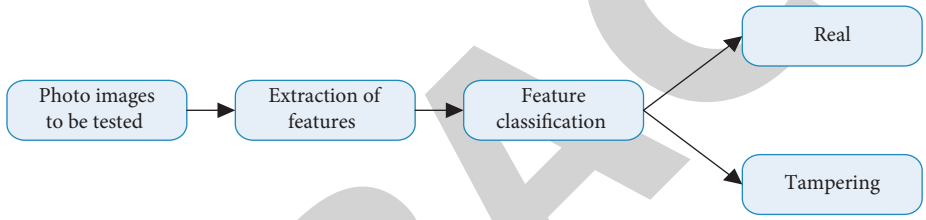

Figure 5: The process of photo image tamper forensics.

the null and transform domains are some basic features of images and an important means to study the essential properties of images.

The literature [1] proposes a copy-paste forensic algorithm based on DCT coefficients, which adopts a sliding window chunking strategy for the image to be tested, then calculates the DCT coefficients of each image block, quantifies the obtained DCT coefficients to construct feature vectors, and then performs dictionary sorting on all feature vectors. If there are similar or identical image blocks in the image to be tested, the positions of their corresponding feature vectors will be closer, and the similar blocks in the image can be identified by calculating the displacement vector to achieve the purpose of tampering detection. On this basis, the DCT quantization coefficients are dimensionalized in the literature [2]. [3] made an improvement on the chunking strategy by using a circular chunking method, followed by the construction of DCT coefficient feature vectors. The literature [4] proposed to construct feature vectors by calculating the difference matrix of the DCT coefficient matrix of an image and then detect them using SVM, and subsequently the improved method achieved an average recognition rate of 97.92% and 91.2% on the stitched image libraries of CASIAv1.0 and CASIAv2.0; however, such methods did not achieve tampering localization. The literature [5] argues that the tampered images are compressed and saved again causing changes in the DCT coefficients, whereby the histogram difference of the DCT coefficients and the double quantized mapping relationship are used to detect the stitched tampered images, respectively, to achieve the localization of the tampered regions. To further improve the forensic effect, [6] suggested extracting LBP features in the DCT domain for detection. Considering that the tampered images may be contaminated by Gaussian blur filtering and Gaussian white noise, the DCT algorithm is improved in the literature [7].

In [8], wavelet transform-based image forensic algorithms are proposed to extract features for matching detection of subband information of the wavelet transform of the image to be detected. For example, the wavelet decomposition has two subbands of low and high frequencies, and the copy-paste block is detected by comparing the correlation of the Zernike moments at the corresponding positions of the two subbands in blocks. The detection of the tampered region by comparing the similarity on the high-frequency subband after wavelet transform as proposed in literature [9]. [10] proposed to extract LBP features in the low-frequency subband to identify tampering.

2.1.2. Key Point-Based Forensic Techniques. For same-image tampering, there are two or more identical or similar regions in an image, and key points are extracted for the whole image. Since the key point characteristics of the identical or similar regions are closer, the tampered region can be located by correlation matching of all key points. Based on this principle, a detection method based on Harris point detection is proposed in the literature [11], which has better

robustness to posttampering compression. The literature [12] uses Harris points combined with the mean value of the circular neighborhood as feature points, which can solve the copy-and-paste operation of the visual structure plane region. The literature [13] extracts image feature points with Harris operator and uses a new forensic feature matching method to improve detection accuracy and efficiency.

The literature [14] proposed the SIFT feature points of the image to be tested are extracted, the feature points are matched using the G2NN matching criterion, and then the key points on the match are clustered to determine the copied and pasted regions, but the detection effect is more dependent on the clustering results. The literature [15] suggests J-linkage clustering, but the algorithm is not accurate in locating pasted blocks after rotating and scaling operations, and the detection efficiency is not ideal. To further improve the robustness of the algorithm, it is proposed to extract SIFT features using e measured after wavelet transform to reduce noise interference.

The SURF key points are proposed, and it is suggested that SURF is extracted, so the localization of the pasted blocks is not ideal; to overcome this drawback, a combination of SURF algorithm and SIFT algorithm is used to extract key points to achieve precise localization while improving the efficiency of the algorithm. The literature [16] combines both SURF and HOG features, and the experimental results are significant.

2.1.3. Forensic Techniques Based on Light Consistency Features. In photographs, there is generally a relatively fixed illumination environment (e.g., sun, interior lighting), which makes the illumination intensity and direction consistent in the photograph. For stitched blocks from other photographs, the illumination will not be consistent with the illumination of the real region in the tampered image. Farid's team proposes an image recognition model under 3D light sources, which uses a spherical harmonic model to estimate the direction of the light sources of objects in the photographs and then detects them based on the consistency of the direction. Using the detection of the consistency of the direction of the shadow region caused by the light with the direction of the light, it is robust to multiple tampered targets. Since the above method is subject to relatively strict assumptions that limit its practical applicability, it has been experimentally shown to improve the light direction estimation error and is more applicable [17].

2.1.4. Forensic Techniques Based on Texture Features. Texture is an important feature to describe and distinguish different objects. Given that it is difficult to keep the texture features of the tampered block consistent with the original image, which inevitably destroys the periodicity, directionality, and randomness of the original image texture, it provides another possible method for stitching tampering forensics. By dictionary sorting, the Tamura texture features of each image block and then calculating the feature similarity based on the Euclidean distance, the forged image regions can be detected and located. The literature [18] proposes an LBP-based texture feature description method with some robustness.

2.2. Tampering Forensic Techniques Based on Imaging Features. The general imaging model of a digital camera is shown in Figure 6. First, an optical filter to filter the color light other than red, blue, and green, after which the color information of each position is recorded by the color filter array, and then the light signal is converted into an electrical signal through the sensor, and then the CFA (Color Filter Array) interpolation algorithm is applied to each. At this time, the signal is then processed by a series of digital image processing techniques such as white balance and gamma correction, and then compressed according to certain rules to obtain the final digital photo image.

The analysis of the camera imaging model shows that in the process of digital photo image generation, after a series of hardware processing and software operations, some imaging features such as CFA interpolation noise, pattern noise, and compression noise are inevitably introduced. Due to the use of different hardware and software processing methods, it makes the photo images taken by different brands and models of cameras, only have the imaging features of that camera, so such features can be used for forensics to detect tampered and forged photo images.

2.2.1. Tampering Forensic Techniques Based on CFA Interpolation Noise. Current photo images usually use a single sensor in the generation process, and each pixel point can only record one color information, and the other two-color information are obtained by interpolating the surrounding pixels, which leads to the correlation between neighboring pixels will exist. Since different cameras may not use the interpolation method, the correlation between pixels will be different and can be used to detect tampering. The literature [19] locates splicing tampering by re-CFA interpolation of images to reconstruct their pixel neighborhood consistency, detects whether there is splicing tampering operation by analyzing the distribution of color difference images at high frequencies, extracts CFA features using Gaussian filtering based on posterior probability estimation of CFA interpolation noise, and achieves forensic purposes by classifying the features. The literature [20] considers the spectral correlation introduced by CFA interpolation and identifies the image authenticity based on this property.

2.2.2. Tampering Forensics Based on Camera Response Function. The process of generating photos of natural scenes through a series of hardware and software operations inside the camera can be called Camera Response Function (CRF). Each camera is an independent individual and its corresponding function is not the same, so the authenticity of the image can be identified by comparing the consistency of CRFs in each region of the image. The literature [21] estimated the CRF of each region by the geometric invariance of the pixels in each region of the image and then used crossover for statistical classification, achieving a

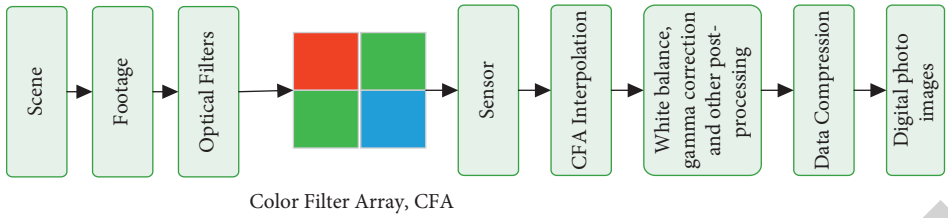

Figure 6: Digital camera imaging model.

detection rate of 87% for stitched images. Based on this, the differential invariants of the images were calculated to estimate the CRF. The literature [22] used a maximum posterior probability model to estimate the normality of the CFR to discriminate the authenticity of the photographs.

2.2.3. Tampering Forensic Techniques Based on Compression Characteristics. Photo images are usually saved in a certain compression format during the generation process, and images are usually compressed one or more times again after tampering, so the differences of individual image blocks after compression are detected to identify tampering. In the literature [23], an iterative method is proposed to estimate the original quantization table of an image to determine the approximate tampered region, and then the estimated original quantization table is used to perform another JPEG compression on the tampered region to precisely locate the tampering according to the difference in pixel values before and after compression. In the literature [24], the similarity of the synthetic images before and after compression is obtained by estimating the quantization factor to identify the location of tampering. Compressing the image again produces a double quantization effect on the DCT coefficients of the real region, whereby tampering is suggested to be identified based on the change in the DCT coefficients of different regions before and after compression. The literature [25] argues that images produce uniform quantization noise after JPEG compression, and tampered blocks corrupt this property and propose a quantization noise estimation model to detect the differences between image blocks. Considering that JPEG compression produces a grid effect, the presence of unaligned grids in the image can be detected to identify the tampered locations.

2.2.4. Pattern Noise-Based Tampering Forensic Technique. Pattern noise is caused by the imperfection of the camera sensor and the inconsistency of the materials used, resulting in the imperfect conversion of light signals into electrical signals, and is stable in every picture taken by the camera. Since the sensor of each camera is unique, its mode noise is also unique; in addition, each pixel point on the sensor is different, resulting in inconsistent performance of mode noise in each pixel point. Based on these two characteristics, the pattern noise can be regarded as a camera fingerprint and applied to photo image tampering forensics, which can be generalized to a variety of tampering operations such as copy-paste of the same image and stitching of different images.

In addition to the above features, Markov features, Fourier-Mellin transform features, image quality features, and color features are often used for photo image tampering detection。

3. Methods

Figure 7 presents a generalized framework for digital image source forensics under the CNN model theory. In the image preprocessing, the image to be detected is first cut into image blocks (P_k in Figure 8(a) indicates the kth image block), and then the image fingerprint characterizing the source of the shot is extracted using CNN, and the detection result Y_k of each image block is output (Y_k in Figure 8(c) indicates the feature extractor predicts the label for the k th image block), and the majority voting algorithm is used to fuse the detection results of the kth image block and output the image-level prediction results, i.e., device model multiclassification identification.

It was found that the FPN feature fusion algorithm improved the detection of small targets but did not improve the detection of large targets, and there was information redundancy after feature fusion. Since then, researchers have proposed some variants of FPN, such as PANet, Libra-RCNN, which are built on the assumption that the weights are the same when the features of two layers are fused, ignoring the feature that the contribution values of features in different layers are different. Therefore, this section proposes a new feature pyramid named dual-stream feature CNN (DS-CNN) using autonomous learning weights and jump connection method.

As shown in Figure 8, FPN is a simple top-down one-way information, while PANet adds bottom-up information flow to FPN to enhance higher-level semantic information for semantic segmentation, which is better than FPN but more computationally intensive. LibraRCNN collects feature information from each layer and then refines the output to the feature layer, with the idea of fusion before segmentation. NASFPN adopts the idea of AutoML and uses search for feature fusion; ASFF learns the weight contribution value of each layer, but it is a fully connected method with high computation and requires higher performance computing equipment, which is not convenient for practical applications.

As shown in Figure 9, BiFPN is a feature fusion algorithm proposed in the Efficient Det network, in which a jump connection approach and a weighted fusion approach are used for feature fusion, taking into account both efficiency and accuracy. Its calculation equations are shown in (1) and (2).

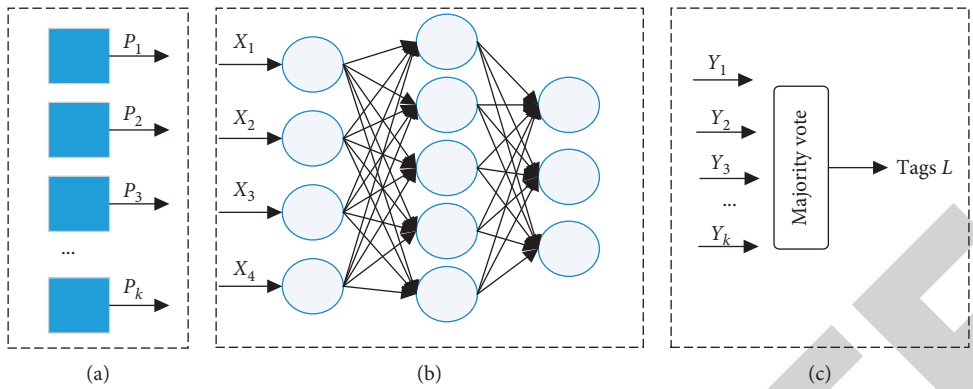

Figure 7: Digital image source framework based on CNN; (a) image preprocessing; (b) image feature extraction; (c) classification result voting.

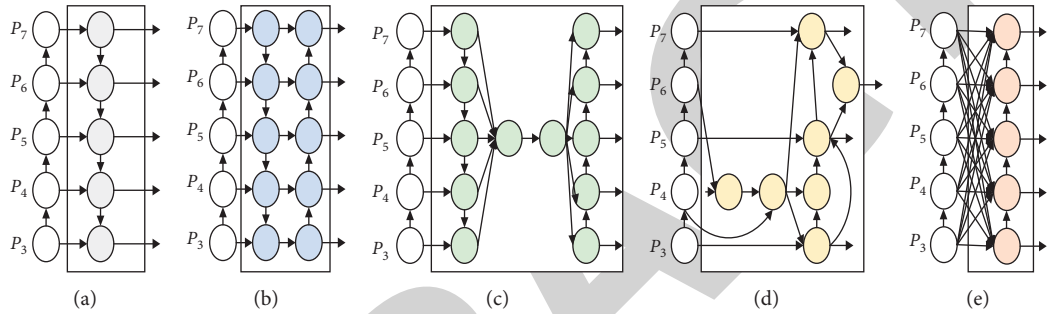

Figure 8: Feature network design diagram; (a) FPN; (b) PANet; (c) LibraRCNN; (d) NAS-FPN; (e) ASFF.

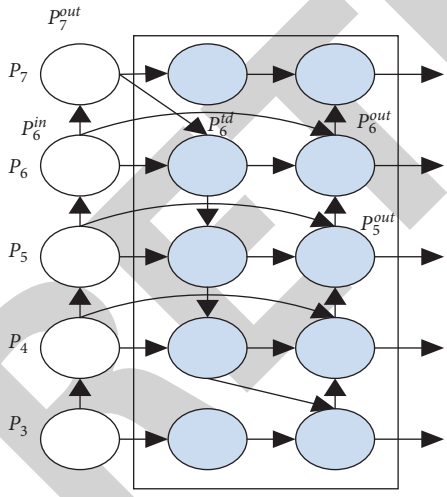

Figure 9: BiFPN basic structure.

$$P_6^{\text{td}} = \text{conv}\left(\frac{w_1 * P_6^{\text{in}} + w_2 * \text{Resize}\left(P_7^{\text{out}}\right)}{w_1 + w_2 + \varepsilon}\right), \quad (1)$$

$$P_6^{\text{out}} = conv\left(\frac{w_1' * P_6^{\text{in}} + w_2' * P_6^{\text{td}} + w_3' \text{Resize}\left(P_5^{\text{out}}\right)}{w_1' + w_2' + w_3' + \varepsilon}\right). \quad (2)$$

Resize denotes up sampling, and nearest neighbor interpolation is used here, and ε is set to 0.0001 to prevent division by zero.

Each feature layer in BiFPN has different weights, which are theoretically normalized to 1 when fused to the same layer, but how to normalize the weights?

(1) Unbounded strategy.

$$O = \sum_i w_i \cdot I_i. \quad (3)$$

(2) Based on softmax.

$$O = \sum_i \frac{e^{w_i}}{\sum_j e^{w_j}} \cdot I_i. \quad (4)$$

(3) Fast regularity

$$O = \sum_i \frac{w_i}{\varepsilon + \sum_j w_j} \cdot I_i. \quad (5)$$

It is found that the BiFPN algorithm with fast regularization can eliminate the exponential operation in the softmax method, reduce the computational overhead, and speed up the computation although the accuracy is slightly lower than the softmax method, but the performance is the best among the three strategies.

We propose a new dual-stream feature CNN (DS-CNN), for the FCOS structure of fused area-ness. It is mainly improved based on the BiFPN algorithm, following its jump connection and weighted fusion, while improving the FCOS model structure based on the fused area-ness in Chapter 3. The general structure is shown in Figure 10.

As shown in Figure 10, the network is obtained from ResNeXt101 to obtain C_3, C_4, C_5 layers, and then it is convolved by $1 * 1$ for dimensionality reduction to obtain a 256-dimensional P_3, P_4, P_5 feature map, which is convenient for feature fusion. P_6, P_7 is the feature map obtained after down sampling P_5, P_6 separately.

The dual-stream feature CNN (DS-CNN) can enhance the semantic information of each prediction layer though. However, the analysis of information inflow from each node shows that the information inflow and outflow at P_5 is unbalanced. From Figure 10, it can be seen that layer P_5 has only one information input in layer C_5, but three information outflows (the arrows can indicate the information inflow and outflow of P_5). Whether sufficient information can be obtained has an important impact on the subsequent feature fusion of node P_6, P_7. Therefore, in this thesis, the information of node P_5 is enhanced based on the dual-stream pyramid, and the information of layer C_3, C_4 is also fused directly to layer P_5. However, layer C_3, C_4, C_5 has different contribution values to P_5 feature layers, so it is necessary to learn different weights for layer C_3, C_4, C_5 first before feature fusion. In this paper, we name this feature fusion method as Adaptive Dual Streaming Feature CNN (A-DS-CNN), and the specific structure is shown in Figure 11.

As in Figure 11, layer C_3, C_4 will increase the information inflow in layer P_7 by means of adaptive feature fusion. The adaptive weights are calculated as in -) (6):

$$y_{ij} = conv\left(\alpha_{ij}^3 * x_{ij}^3 + \beta_{ij}^4 * x_{ij}^4 + \gamma_{ij}^5 * x_{ij}^5\right), \tag{6}$$

$$\begin{aligned} \alpha_{ij}^3 &= \frac{e^{\lambda_{\alpha_{ij}}^3}}{e^{\lambda_{\alpha_{ij}}^3} + e^{\lambda_{\beta_{ij}}^4} + e^{\lambda_{\gamma_{ij}}^5}}, \\ \beta_{ij}^4 &= \frac{e^{\lambda_{\beta_{ij}}^4}}{e^{\lambda_{\alpha_{ij}}^3} + e^{\lambda_{\beta_{ij}}^4} + e^{\lambda_{\gamma_{ij}}^5}}, \\ \gamma_{ij}^5 &= \frac{e^{\lambda_{\gamma_{ij}}^5}}{e^{\lambda_{\alpha_{ij}}^3} + e^{\lambda_{\beta_{ij}}^4} + e^{\lambda_{\gamma_{ij}}^5}}, \end{aligned} \tag{7}$$

where $\alpha_{ij}^3, \beta_{ij}^4, \gamma_{ij}^5$ denotes the weight of C_3, C_4, C_5, respectively, i, j denotes the location coordinates of the feature map, $x_{ij}^3, x_{ij}^4, x_{ij}^5$ denotes the value at location (i, j) in layer C_3, C_4, C_5, and y_{ij} denotes the final output to the value at location (i, j) in P_5.

The network structure of the final target detection algorithm in this thesis is shown in Figure 12.

To improve the basic convolutional network, the Backbone layer adopts the ResNeXt101 structure and uses 64 paths with each path width of 4 to reduce the computational effort. For better feature extraction, the Channel of C_3, C_4, C_5 layers is first converted to 256 dimensions and then input to A-DFN for feature fusion. The adaptive feature fusion is performed to P_5 for layer C_3, C_4, C_5, where the weights are normalized by Soft max, in order to provide more information for the subsequent feature fusion without sacrificing accuracy. And the subsequent weight normalization used for weighted feature fusion from layer P_3, P_4, P_5, P_6, P_7 is fast regular, which aims to make the network run better by slightly sacrificing accuracy while ensuring performance. Head layer is divided into a shared part and a branch part, and since area-ness is more closely related to location, it is divided into the same branch as regression to help the model perform better target box position regression.

4. Experiments

The COCO dataset, known as Microsoft Common Objects in Context, is a dataset acquired by the Microsoft team to perform target recognition, target segmentation, and target detection competitions. The schematic diagram of the COCO dataset is shown in Figure 13. COCO dataset is divided into 2014 version and 2017 version. The current version used in this thesis is the 2017 version, which contains 80 target categories, 118287 training sets, totaling 19.3 G, 5000 validation sets, totaling 1814.7 M, so the 2017 version COCO dataset has 123287 sheets.

From Figure 14, it can be seen that the COCO dataset has more categories than the PASCALVOC dataset, and the number of instances corresponding to each category is also higher. Therefore, the COCO dataset is more difficult to detect the target and can better represent the performance of the target detection model.

As shown in Figure 15, the area of most targets in the COCO dataset is only about 6% of the image size; 41.43% of all targets appearing in the COCO training dataset are small targets, 34.4% are medium targets, and 24.2% are large targets. By analyzing the COCO data, it is found that small and medium targets account for a larger proportion, so this dataset is more concerned with the detection of small and medium targets.

We mainly detect the coco dataset and divide it. During training, the image data are first preprocessed, resize the image to match the target detection model size, and then input to the target detection model, train the appropriate number of iterations, and get the final detection results. Finally, the test-test-dev data results are submitted to the coco Detection Challenge competition to obtain AP values and AR values.

In order to better compare the anchor-base and anchor-free methods, this thesis is based on a unified benchmark, i.e., the COCO dataset and uses a unified evaluation criterion: MAP values (MAP values are equivalent to AP values in coco data), and compares their MAP values for large, medium, small targets and different IOU thresholds. The MAP values are compared for large, medium, small targets and different IOU thresholds.

According to Table 1, CenterNet511 and CornerNet511 take longer to test one image under the same conditions,

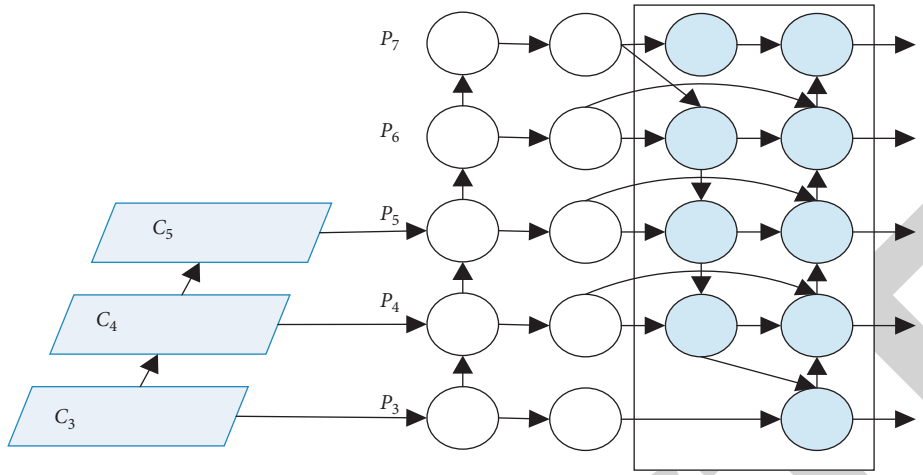

Figure 10: Dual-stream feature CNN.

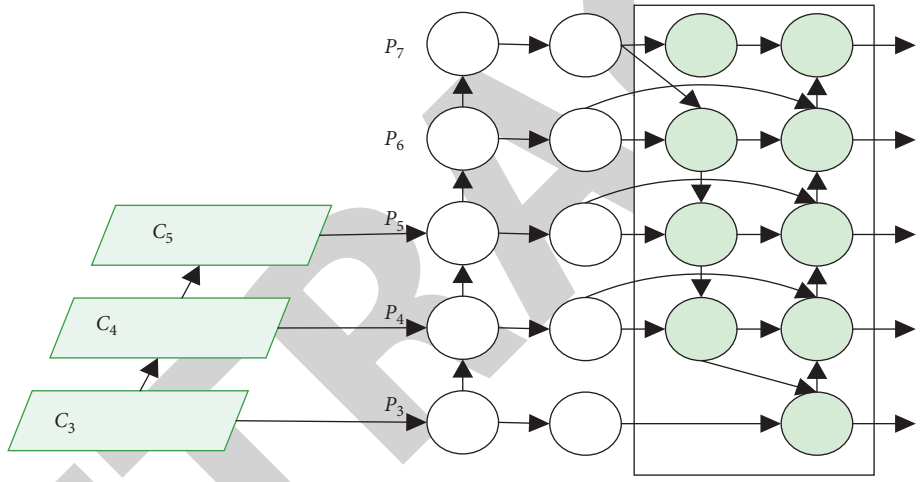

Figure 11: Adaptive dual-stream feature CNN.

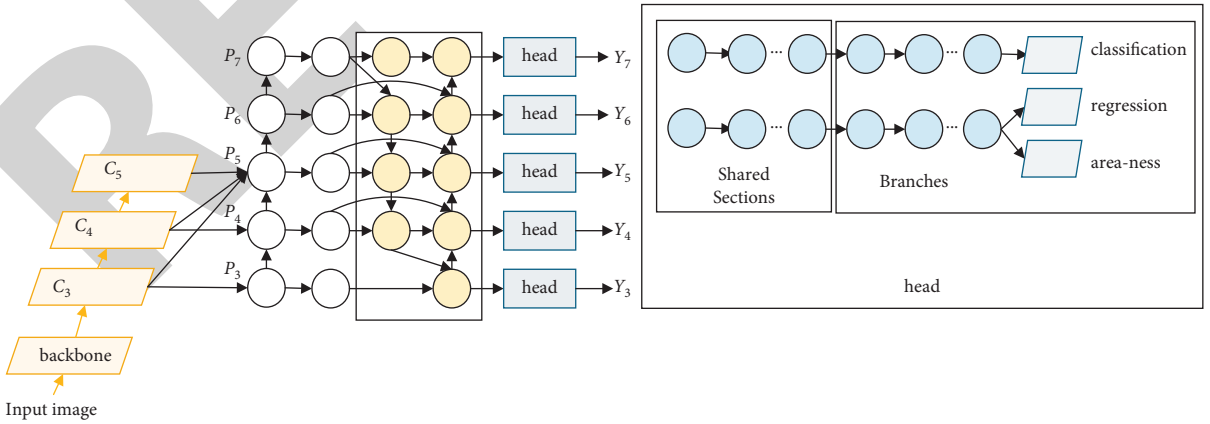

Figure 12: Schematic diagram of the overall network structure.

indicating that CenterNet511 predicts slower because CenterNet511 predicts one more centroid than CornerNet511, which brings more computation. Both CenterNet511 and CornerNet511 use the hourglass network as the backbone layer, which is computationally intensive and has a slow computing speed. In contrast, the ResNeXt-

Figure 13: Schematic diagram of coco target detection dataset.

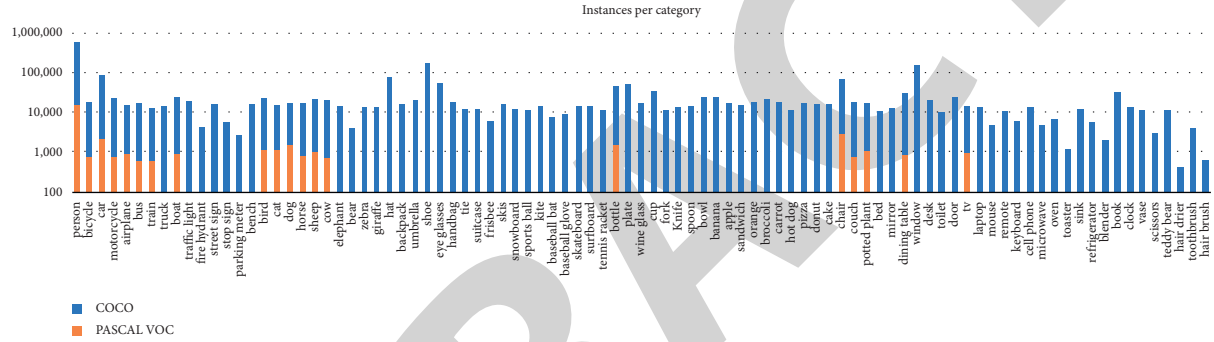

Figure 14: Comparison of the number of instances between the COCO dataset and the PASCAL VOC dataset.

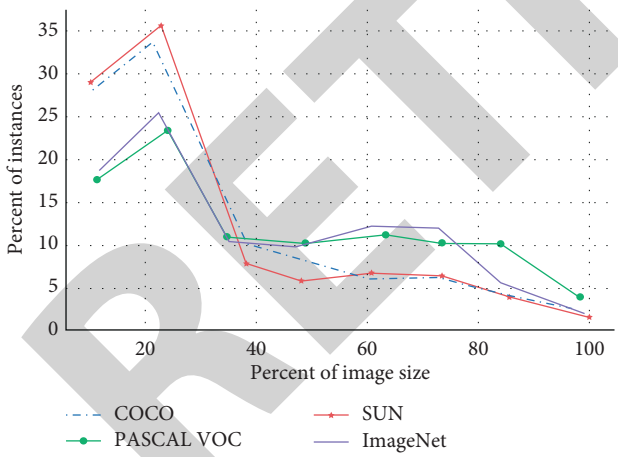

Figure 15: Example image size and percentage of the COCO, PASCAL VOC, ImageNet, and SUN datasets.

Table 1: Comparison of FCOS and CenterNet511, CornerNet511 prediction speed.

Method	Backbone	Testing time/image
CenterNet511	Hourglass52	270 ms
CenterNet511	Hourglass104	300 ms
CenterNet511	Hourglass104	340 ms
FCOS	ResNeXt-101	112 ms

(Note: 511 means the input image size is 511 ∗ 511).

Table 2: FCOS prediction accuracy values using different backbone.

Method	Backbone	AP	AP_{50}	AP_{75}	AP_s	AP_m	AP_l
FCOS w/ FPN	ResNet-101	41.6	60.6	45.1	24.3	44.9	51.5
FCOS w/ FPN	ResNeXt-32x8d-101	42.6	62.3	46.2	26.1	45.5	52.5
FCOS w/ FPN	ResNeXt-64x4d-101	44.8	64.1	48.5	27.5	47.4	55.7

(Note: 32 ∗ 8d means 32 paths, the width of each path is 8).

101 prediction used by FCOS is fast and has a better performance in terms of average accuracy mean, so this thesis uses the FCOS algorithm as the base algorithm for improvement.

According to Table 2, the MAP value can reach 44.8 when FCOS adopts ResNeXt-64x4d-101-FPN (i.e., 64 paths, each with a width of 4) as the backbone, which is 3 and 2 points higher than that of ResNet-101 and ResNeXt-32x8d-101, respectively. Therefore, ResNeXt-64x4d-101 is used as the backbone of the target detection model in this thesis.

According to Table 3, the mean accuracy of target detection using center-ness is 0.2 points lower than the area-ness designed in this paper when the feature fusion method is FPN. In the DS-CNN fusion method, the area-ness is 0.4 points higher than the MAP value of center ness. It means

Table 3: MAP values of area-ness and center-ness on FCOS algorithm.

Method	Centrality method	Feature fusion method	AP	AP_{50}	AP_{75}	AP_s	AP_m	AP_l
FCOS	Center-ness	FPN	44.8	64.0	48.5	27.5	47.6	55.7
FCOS	Area-ness	FPN	44.8	64.4	48.6	27.4	47.5	55.8
FCOS	Center-ness	DS-CNN	46.2	65.7	49.9	26.8	49.7	58.4
FCOS	Area-ness	DS-CNN	46.6	66.1	50.3	27.3	49.5	59.2

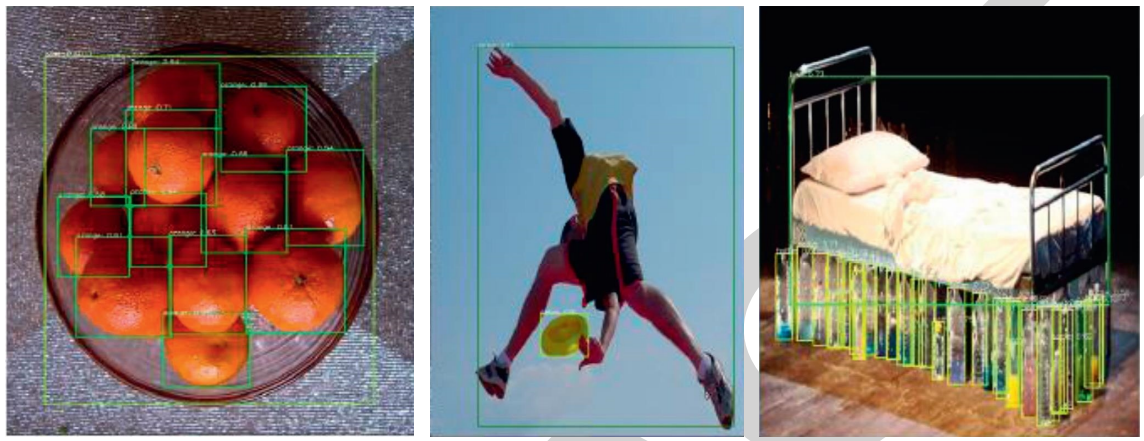

Figure 16: Visualization results of partial object detection by the algorithm proposed in this thesis.

Table 4: Comparison of detection results.

Algorithm		TPR/%	FAR/%	Average time to detect an image
Traditional pixel-by-pixel sliding window fixed threshold algorithm	$\tau = 0.006$	88.5	1.903	727.5 s
	$\tau = 0.001$	95.7	4.942	
	$\tau = 0.014$	97.7	9.029	
	$\tau = 0.03$	98.9	15.37	
The proposed algorithm		98.9	1.896	26.75 s

that the area-ness designed in this paper is better than the center-ness of the original FCOS.

As shown in Figure 16, the algorithm of this thesis is able to accurately detect even a compact orange placed in the fruit tray or an empty water bottle placed by the bed, indicating that the prediction layer is able to acquire a sufficient number of features. When the target frames of people and Frisbees overlap, the algorithm of this thesis is still able to predict them each.

The authenticity detection results for each test image can be divided into two categories: tampered and true. To evaluate the performance,

$$\begin{aligned} \mathrm{TPR} &= \frac{\mathrm{TN}}{\mathrm{FP} + \mathrm{TN}}, \\ \mathrm{FAR} &= \frac{\mathrm{FN}}{\mathrm{FN} + \mathrm{TN}}. \end{aligned} \tag{8}$$

Authenticity detection results: tampering detection experiments are performed on 500 real images and 500 tampered images from the image library given in Table 4 using the traditional fixed-threshold sliding window method based on correlation coefficients and the proposed SPCE-based adaptive threshold nonoverlapping chunk matching + ZNCC algorithm, respectively.

The methods based on fixed thresholds will have different detection results at different thresholds, and four more desirable thresholds of 0.006, 0.01, 0.014, and 0.03 were selected for comparison through experiments. In order to be able to evaluate the detection results objectively, the pattern noise in both types of algorithms is obtained by wavelet noise reduction and then processed with ZM + WF. In the calculation of TPR and FAR, if the number of pixels of a certain image tampering localization result is less than 20, it is judged to be a real image and vice versa; it is considered as tampering. The detection results of the two algorithms are shown in Table 4.

The proposed adaptive thresholding algorithm has a TPR of 98.9% and FAR of 1.896% for 1000 images to be tested, while the fixed thresholding algorithm has different detection results at different threshold values. It is 0.01, 0.014, and 0.03, and although the TPR is similar or equal to it, the FAR is much higher than this paper. At 0.006, the FAR is similar to the algorithm in this paper, but the TPR is much lower than that in this paper. Meanwhile, the average detection time of the two algorithms on 1000 images is given in Table 4, and the comparison results show that the proposed algorithm effectively reduces false alarms while maintaining a high detection rate and detection efficiency.

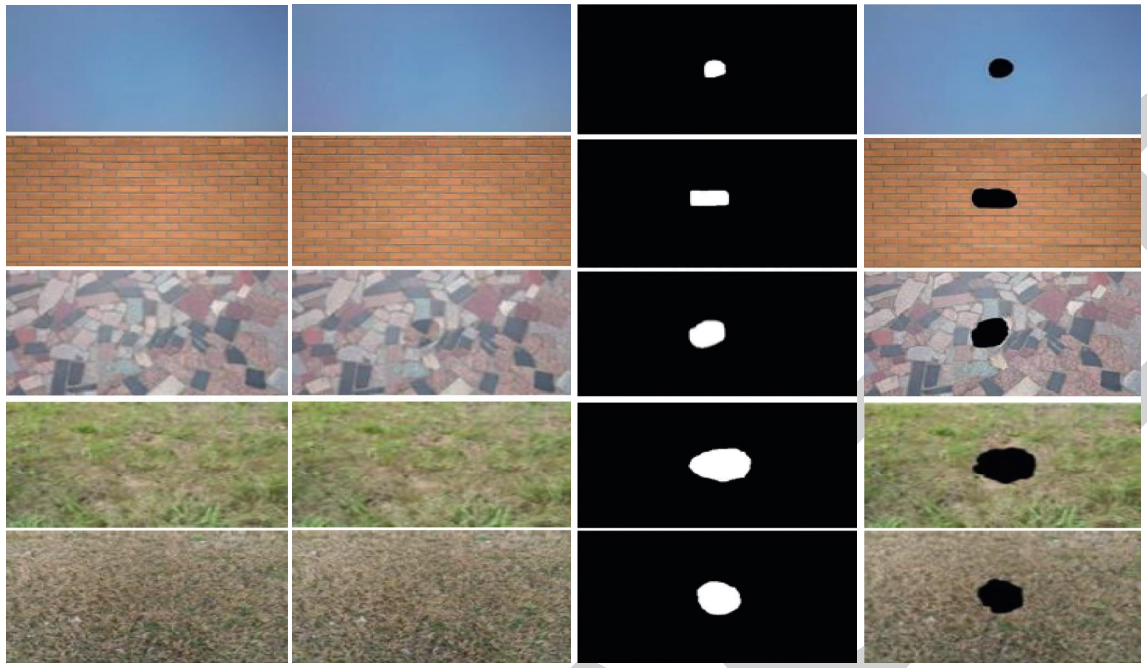

(d) (c) (b) (a)

Figure 17: The location results of tampered images with different texture. (a) Original image. (b) Tampered image. (c) Tampered position. (d) Positioning effect.

Table 5: The detection accuracy of Seam-carving tampering images.

P-value ratio selection	Tampering				
	Untampered image (%)	0.9 (%)	0.8 (%)	0.7 (%)	0.6 (%)
G.R. sheng	67.86	64.27	85.72	83.92	87.50
0.9	67.84	78.58	89.28	85.72	87.50
0.8	69.65	76.77	87.51	89.28	91.08
0.7	71.43	78.56	94.63	85.72	89.28

(Note: G.R. Sheng is the detection result based on the extended Markov feature, the rest are the detection results when different thresholds are selected by the adaptive detection feature extraction method, the results in the table are all correct results).

Table 6: The comparison between the proposed method and G.R. Sheng's method.

P-value ratio selection	Tampering				
	Untampered image (%)	0.9 (%)	0.8 (%)	0.7 (%)	0.6 (%)
G.R. sheng	67.86	64.27	85.72	83.92	87.49
Algorithm of this paper	69.25	77.98	90.488	86.89	89.31

(Note: The detection result of this algorithm is the average correct rate using three thresholds of 0.7, 0.8 and 0.9).

Compared with the traditional fixed threshold judgment method, the adaptive threshold judgment method, which is based on the texture complexity of the image block to be tested, selects a suitable threshold value, thus realizing "specific problem specific analysis."

In Figure 17, the first to fourth columns show the original image, the tampered image, and the tampered location, respectively. The second column gives five tampered images with simple to complex texture complexity, where the texture complexity of the first local block of blue sky image is $k \in [0.1857, 0.2886]$; the texture complexity of the second local block of wall image is $k \in [0.3288, 0.4372]$; the texture complexity of the third local block of floor image is $k \in [0.3511, 0.5296]$; the texture complexity of the fourth local block of green grass image is $k \in [0.6601, 0.8442]$; and the texture complexity of the fifth local block of dead grass image is $k \in [0.6927, 0.9463]$.

Observing the localization results of the proposed adaptive thresholding algorithm for five tampered inspection images shows that whether the texture of the tampered image is simple or complex, which effectively eliminates the influence of texture on forensics (see Tables 5, 6).

5. Conclusion

In the information age, photography is one of the most important means to ensure public access to information, but the continuous tampering of photos forces people to reexamine. As Professor Hani Farid of Dartmouth said, "we live in a place where we no longer believe what we hear. As an important information carrier, digital photos should have broad application space. Justice and safeguarding justice are indisputable. This paper proposes an adaptive characteristic analysis method based on two-layer CNN model, which effectively solves this problem and is of great significance to the research in this field.

Data Availability

The experimental data used to support the findings of this study are available from the corresponding author upon request.

Conflicts of Interest

The authors declared that they have no conflicts of interest regarding this work.

Acknowledgments

This work was supported in part by the Key Laboratory of Mine Water Resource Utilization of Anhui Higher Education Institutes, Suzhou University (Grant no. KMWRU202107), in part by the Outstanding Youth Talents in Anhui Provincial Education Department (Grant no.2019gxbjZD43), in part by the Open Research Fund of National Engineering Research Center for Agro-Ecological Big Data Analysis and Application, Anhui University (Grant no.AE202201) , in part by the Open Foundation of the Anhui Key Laboratory of Intelligent Building and Building Energy Conservation (Grant no.IBES2020KF03), in part by the Key Research and Development Project of Anhui Province in China (Grant no. 202004b11020023), in part by the Academic support project for top-notch talents in disciplines (majors) of Colleges and Universities at Anhui Province in China (Grant no. gxbjZD21081), and in part by the school-level key disciplines of computer science and technology at Suzhou University in China (Grant no. 2019xjzdxk1) and in part by the Collaborative Innovation Center—cloud. computing industry (Grant no. 4199106).

References

[1] A. M. Al-Azab, A. A. Zaituon, K. M. Al-Ghamdi, and F. M. A. Al-Galil, "Surveillance of dengue fever vector *Aedes aegypti* in different areas in Jeddah city Saudi Arabia," *Advances in Animal and Veterinary Sciences*, vol. 10, no. 2, pp. 348–353, 2022.

[2] L. Cai, Q. Sun, T. Xu, Y. Ma, and Z. Chen, "Multi-AUV collaborative target recognition based on transfer-reinforcement learning," *IEEE Access*, vol. 8, pp. 39273–39284, 2020.

[3] R. Tong, Y. Zhang, H. Chen, and H. Liu, "Learn the temporal-spatial feature of sEMG via dual-flow network," *International Journal of Humanoid Robotics*, vol. 16, no. 04, Article ID 1941004, 2019.

[4] A. R. Alqahtani, A. Badry, S. A. Amer, F. M. A. Al Galil, M. A. Ahmed, and Z. S Amr, "Intraspecific molecular variation among Androctonus crassicauda (Olivier, 1807) populations collected from different regions in Saudi Arabia," *Journal of King Saud University Science*, vol. 34, no. 4, Article ID 101998, 2022.

[5] Di Wu, Y. Lei, M. He, C. Zhang, and Li Ji, "Deep reinforcement learning-based path control and optimization for unmanned ships," *Wireless Communications and Mobile Computing*, vol. 2022, pp. 1–8, Article ID 7135043, 2022.

[6] R. Ali, M. H. Siddiqi, and S. Lee, "Rough set-based approaches for discretization: a compact review," *Artificial Intelligence Review*, vol. 44, no. 2, pp. 235–263, 2015.

[7] M. Afrasiabi, H. Khotanlou, and T. Gevers, "Spatial-temporal dual-actor CNN for human interaction prediction in video," *Multimedia Tools and Applications*, vol. 79, no. 27-28, pp. 20019–20038, 2020.

[8] G. Cai, Y. Fang, J. Wen, S. Mumtaz, Y. Song, and V. Frascolla, "Multi-carrier M-ary DCSK system with code index modulation: an efficient solution for chaotic communications," *IEEE Journal of Selected Topics in Signal Processing*, vol. 13, no. 6, pp. 1375–1386, Oct, 2019.

[9] I. Castillo Camacho and K. Wang, "A comprehensive review of deep-learning-based methods for image forensics," *Journal of Imaging*, vol. 7, no. 4, p. 69, 2021.

[10] K. Chandra, A. S. Marcano, S. Mumtaz, R. V. Prasad, and H. L. Christiansen, "Unveiling capacity gains in ultradense networks: using mm-wave NOMA," *IEEE Vehicular Technology Magazine*, vol. 13, no. 2, pp. 75–83, June 2018.

[11] X. Liao, K. Li, X. Zhu, and K. J. R. Liu, "Robust detection of image operator chain with two-stream convolutional neural network," *IEEE Journal of Selected Topics in Signal Processing*, vol. 14, no. 5, pp. 955–968, 2020.

[12] F. B. Saghezchi, A. Radwan, J. Rodriguez, and T. Dagiuklas, "Coalition formation game toward green mobile terminals in heterogeneous wireless networks," *IEEE Wireless Communications*, vol. 20, no. 5, pp. 85–91, 2013.

[13] B. Chen, W. Tan, G. Coatrieux, Y. Zheng, and Y. Q. Shi, "A serial image copy-move forgery localization scheme with source/target distinguishment," *IEEE Transactions on Multimedia*, vol. 23, pp. 3506–3517, 2021.

[14] S. Palanisamy, B. Thangaraju, O. I. Khalaf, Y. Alotaibi, S. Alghamdi, and F. Alassery, "A novel approach of design and analysis of a hexagonal fractal antenna array (HFAA) for next-generation wireless communication," *Energies*, vol. 14, no. 19, p. 6204, 2021.

[15] B. Bayar and M. C. Stamm, "Constrained convolutional neural networks: a new approach towards general purpose image manipulation detection," *IEEE Transactions on Information Forensics and Security*, vol. 13, no. 11, pp. 2691–2706, 2018.

[16] O. Mayer and M. C. Stamm, "Forensic similarity for digital images," *IEEE Transactions on Information Forensics and Security*, vol. 15, pp. 1331–1346, 2020.

[17] A. Abd, A. Fahd Mohammed, and S. P. Zambare, "New species of flesh fly (Diptera: sarcophagidae) Sarcophaga (Liosarcophaga) geetai in India," *J Entomol Zool Stud*, vol. 4, no. 3, pp. 314–318, 2016.

[18] S. Nagi Alsubari, S. N Deshmukh, A. Abdullah Alqarni et al., "Data analytics for the identification of fake reviews using supervised learning," *Computers, Materials & Continua*, vol. 70, no. 2, pp. 3189–3204, 2022.

Hindawi
Mobile Information Systems
Volume 2022, Article ID 5124707, 9 pages
https://doi.org/10.1155/2022/5124707

Research Article

Cloud Computing Database and Travel Smart Platform Design Based on LSTM Algorithm

Dongfeng Chen

Graduate School Hotel Tourism Department, Tongmyong University, Busan 48520, Republic of Korea

Correspondence should be addressed to Dongfeng Chen; 2007048@muc.edu.cn

Received 2 July 2022; Revised 27 July 2022; Accepted 8 August 2022; Published 26 August 2022

Academic Editor: Shadi Aljawarneh

Information technology has played a key role in the development of the tourism planning service industry and has now become an important foundation for the survival and rapid development of the industry. In this context, due to the fast updating and popularization of information technology, it has greatly promoted the development of the tourism industry. In order to meet the current public demand for tourism information, this paper integrates cloud computing, VR technology, and big data analysis technology to build a smart platform for intelligent perception tourism information services. The system can obtain tourism information through mobile Internet terminals. Among them, the database of the smart tourism planning platform is the most important module. Aiming at the many difficulties in adapting data encryption in cloud storage applications, this article designs an adaptive CloudCrypt data encryption system based on cloud computing technology and proposes dynamic JavaScript dynamic analysis and automatic identification of data technology, through adaptive different cloud applications to obtain data encryption protection. CloudCrypt is suitable for typical cloud applications, such as mail and storage. The entry cost of the system is extremely low; it can fully guarantee the security of the tourism information platform database and can integrate wireless sensor networks into the tourism information platform. The network system composed of sensor nodes activates detection, calculation, and communication modules through wireless communication and has the advantages of low cost, low power consumption, and fast networking speed. In this paper, through the construction of integrated wireless sensor technology and cloud computing database, it is applied to the construction of a tourism smart platform, thereby promoting the development of smart travel technology.

1. Introduction

Smart tourism concept has not yet had a clear unified view of the industry. Generally speaking, smart tourism is often regarded as a new type of information technology, such as cloud platforms and the Internet, which can connect to each other and exchange data through the Internet [1]. The use of Internet terminals can enable the public to quickly and conveniently obtain travel information, so as to realize the planning and modification of travel plans and conduct intelligent perception processing of travel information [2]. With the further development of the Internet, personalized tourism and multipolar tourism technology have been promoted as never before, enabling more and more tourists to learn about tourism information around the world in this relatively simple way [3].

At present, the development potential of China's tourism industry is based on the gradual expansion of the supply market, and the development of personalized tourism is more obvious. On the one hand, the number of tourists continues to increase; on the other hand, the proportion of tourists and individual tourists has also continued to increase [4]. Therefore, higher requirements are put forward for the design and practical application of the tourism planning service platform. This article first conducts a detailed investigation of the technical characteristics and theoretical knowledge of smart tourism construction and elaborates on the feasibility of cloud computing construction mode and cloud computing resource library design [5]. Subsequently, based on the actual situation of a certain scenic spot, the demand analysis is carried out from multiple perspectives of users, such as tourists, tourism targets in the scenic spot, service providers, and tourism management agencies, so as to clarify customer needs and examine their overall demand trends [6]. Subsequently, the article carried out general planning and detailed planning for the implementation of smart tourism construction, explained in detail

the construction content, construction plan, technical approach, and other details, and provided necessary data support and ideas for construction. Therefore, based on China's smart tourism service, the current construction status has created a tourism smart platform [7]. Among them, database security is the top priority of researchers. In view of its difficulty in balancing data encryption and storage functions, this paper designs a cloud ciphertext retrieval system EncBox for analysis and proposes a security gateway-based model [8].

In addition, the ciphertext retrieval method of cross-gateway data security sharing does not require the cooperation of cloud providers to achieve this solution and only needs to obtain data encryption protection to preserve the original search function of the cloud service to the maximum extent [9]. Experiments show that EncBox can not only transparently encrypt and protect data, but also retain the original search function, thereby minimizing the introduction of production costs and completely solving the database security problem [10]. Finally, this article investigates wireless sensor network technology, compares the advantages and disadvantages of a variety of commonly used wireless sensor technologies, and finally chooses ZigBee communication technology to create a type of wireless sensor network installation positioning system, so as to provide users with better scenic location positioning function.

2. Related Work

The research background and importance of the wireless sensor network positioning system compatible with the ZigBee protocol were introduced. By studying the status quo of various nonsatellite positioning technologies, comparing and evaluating their advantages and disadvantages, the sensor network based on the ZigBee protocol is finally selected [11]. CloudDLP, a cloud computing-oriented sensitive data recognition and desensitization system, was designed; an improved end-to-end CTPN-MASK text recognition model and a sensitive BERT-CRF data recognition model were proposed, which can effectively solve sensitive content recognition and insensitive scene recognition poor ability and other issues [12, 13]. Experiments show that the accuracy of intelligent desensitization recognition of photos and documents can reach 93.5% and 97.98%, respectively.

An adaptive data encryption system for cloud browser storage applications was proposed, which can automatically identify and adapt different cloud applications to ensure the encryption and protection of sensitive data in different cloud applications [14]. CloudCrypt uses dynamic JavaScript analysis technology to monitor the upload behavior of each client program in cloud applications and encrypts file content by identifying file operation requests. This technology can safely isolate sensitive data and fundamentally solve the problem of cloud application adaptation [15, 16].

A new cloud data platform login and identity verification system was proposed, which is equipped with a fingerprint authentication and identification module, which has the advantages of high information security and strong antiattack ability [17]. After testing, this technology improves the security and validity of the connection and access to the cloud data platform without affecting the user experience [18]. The security performance requirements of the cloud data platform application in the communication process authentication were analyzed. The article designs the platform access framework based on fingerprint authentication by realizing the security of the multidomain access identity authentication in the cloud data platform [19, 20]. And, for the fingerprint feature extraction of the platform fingerprint authentication module, it lays the foundation for connecting the cloud data platform and interdomain access, so as to realize the design of anonymous account encryption and decryption.

3. Database Security Design Based on Cloud Computing

3.1. Technical Principles of Database Security Based on Cloud Computing. LSTM. Long short-term memory (LSTM) networks are different from repetitive neural networks (RNN). The structure of the LSTM network can merge long and short memories by adding thresholds, thereby solving the problem of only short-term memory due to gradient loss in RNN. The calculation is as follows:

$$f_t = \sigma\left(W_f\left[h_{t-1}, x_t\right] + b_f\right). \tag{1}$$

The input gate first clarifies what information can be stored and then creates a new candidate vector value according to the tan$h$ function. The calculation is as follows:

$$\begin{aligned} i_t &= \sigma\left(W_i\left[h_{t-1}, x_t\right] + b_i\right), \\ \widehat{C}_t &= \tanh\left(W_C\left[h_{t-1,x_t} + b_C\right]\right). \end{aligned} \tag{2}$$

The output gate decides which part of the unit state is output according to the unit state information and then multiplies the output of the output layer with the tan$h$ layer to extract the specified part of the output. The calculation is as follows:

$$\begin{aligned} o_t &= \sigma\left(W_o\left[h_{t-1}, x_t\right] + b_o\right), \\ h_t &= o_t \tanh\left(C_t\right). \end{aligned} \tag{3}$$

Given the input x and the tag order, the sum of all probability paths that can be mapped to l in the mapping of relationship B is the probability of appearing in the tag sequence, and the final result is the most likely path annotation.

$$\begin{aligned} p(\pi|x) &= \prod_{t=1}^{T} y_{\pi_t}^t, \forall \pi \in L^T, \\ p(l|x) &= \sum_{\pi \in B^{-1}} p(\pi|x), h(x) = \operatorname{argmax}_{l \in L^{\leq T}} p(l|x). \end{aligned} \tag{4}$$

According to the threshold scheme of cryptography, the idea of "secret sharing" is adopted, which is a threshold scheme algorithm based on Lagrangian polynomial interpolation. The shared threshold scheme has the advantage of

risk sharing. The specific calculation of the threshold (t, k) is as follows:

$$f(x) = key + a_1 x + a_2 x^2 + \cdots + a_{t-1} x^{t-1}. \quad (5)$$

Set the identification ID and subkey of the known user t and use the Lagrangian difference formula to reconstruct the polynomial method, as shown in the following equation:

$$f(x) = \sum_{i=1}^{t} \left(f(x_i) \prod_{j=1 j \neq i}^{t} \frac{x - x_i}{x_i - x_j} \right). \quad (6)$$

Assuming that the scheme of Shamir threshold (t, k) divides the key into k parts, the division of information x is denoted by $\text{key}|_x$ key$x$ and the key of the distribution process is shown in the following equation:

$$\text{Shamir}(t,k)\{\text{key}\} = \text{key}|_x. \quad (7)$$

Then, the key recovery process is shown in the following formula:

$$\{\text{key}|_x\}\text{Shamir}(t,k) = \text{key}. \quad (8)$$

The purpose of digital signature is to prevent the signer from rejecting his signature. The digital signature is based on a password, and the digital signature information is generated based on the key that only the signer knows and the information waiting to be signed. The digital signature consists of a signature algorithm and a verification algorithm. The algorithm and signature key are private information of the signer, and the algorithm and verification key are public information, so that it is convenient for others to verify the result of the user's digital signature.

When the system is turned on, each user has unique identification information I. After the user identification information is changed through the hash function $H()$, the hash value $J = H(I)$ is obtained. Assuming that the user identity information in A is IA, and the corresponding hash value is JA, a third-party TTP trusted by all users can choose the RSA algorithm to generate secret SA parameters for user A. The specific process is as follows: select multiple secret prime numbers p and q, calculate $n = pxq$ accordingly, and then select e according to

$$\gcd(e, (p-1) \times (q-1)) = 1. \quad (9)$$

Generate the public key (e, n) and private key (d, n) of user A, where

$$d = e \bmod ((p-1) \times (q-1)). \quad (10)$$

Based on this, the secret parameter SA of A is generated:

$$S_A = J_A^d \bmod n. \quad (11)$$

Here,

$$\begin{aligned} &1 < J_A < n, \\ &\gcd(J_A, (p-1) \times (q-1) = 1). \end{aligned} \quad (12)$$

3.2. Analysis of Desensitization Effect of Cloud Computing Database. The text recognition experiment data is divided into two parts: the first part mainly comes from the ICDAR2017 Chinese text analysis competition data, of which the total data values of 20,000 pictures are used as training samples; the second part of the data uses artificially annotated sensitive data desensitization scene graphs. The total amount of data is about 1600 pieces, the total number of data in the image training set is 1000 pieces, and the total number of data entered in the test image data is 600 pieces.

The text recognition data is mainly composed of synthetic pictures. About 30 M Chinese and English texts were searched in the set corpus. Most of these libraries are computer-related, and there are 20 Chinese and English fonts in total, of which there are about 10,000 background images; one is randomly selected as the background wallpaper. A piece of randomly generated text and font, size, color, etc., is combined with the background image, and the text image thus generated can be used as a sample.

The text detection analysis index 110S is composed of the accuracy rate P (precision), the recall rate R (recall), and the average harmonic score F (F-score) of the two. Among them, the accuracy rate P is the ratio of the correct value of the text recognition box to the value of the number of all text recognition boxes; the recall rate R is the ratio of the value to the correct number when recognizing the text. F-score can be comprehensively evaluated by accuracy rate P and recall rate R. The calculation formula is as follows, where G represents the actual marked text recognition box, D represents the text recognition box to be predicted, and Best M is the best match (BestMatch) in text recognition. The actual mark in the box and Best Mp are the best match in the actual text recognition box:

$$\begin{aligned} R &= \frac{\sum_{i=1}^{|G|} Best\, M_G(G_i)}{|G|}, \\ P &= \frac{\sum_{j=1}^{|D|} Best\, M_D(D_j)}{|D|}, \\ F - score &= \frac{2^* P^* R}{P + R}. \end{aligned} \quad (13)$$

The character recognition evaluation index adopts the single character recognition accuracy rate Prec to measure the character recognition algorithm, among which

$$P_{rec} = \frac{N_{rec}}{N_{total}}. \quad (14)$$

The text analysis training data is composed of a text recognition competition data set and a manual labeling part of the data set. First, the first group of data is trained, and then the second group of data is used to improve and fine-tune the network foundation. Finally, 600 photos of data-sensitive desensitization scenes were tested, and the 600 pieces of test data were further divided into three groups of test data.

The text recognition test results of CTPN-MASK model and CTPN model are shown in Table 1. The measurement accuracy of the CTPN-MASK text detection model is 77.3%, the recall rate is 75.9%, and the F-score score is 76.6%. It can

Table 1: Comparison of CTPN-MASK and CTPN overall test results.

Model	Accuracy rate P	Recall rate R	F-score
CTPN	0.551	0.568	0.559
CTPN-MASK	0.773	0.759	0.766

Table 2: Test data set 1-CTPN-MASK and CTPN test results comparison.

Model	Accuracy rate P	Recall rate R	F-score
CTPN	0.628	0.624	0.627
CTPN-MASK	0.762	0.731	0.746

Table 3: Test data set 2-CTPN-MASK and CTPN test results comparison.

Model	Accuracy rate P	Recall rate R	F-score
CTPN	0.481	0.512	0.496
CTPN-MASK	0.768	0.758	0.763

Table 4: Test data set 3-CTPN-MASK and CTPN test results comparison.

Model	Accuracy rate P	Recall rate R	F-score
CTPN	0.484	0.518	0.502
CTPN-MASK	0.793	0.806	0.798

Table 5: CRNN-MASK and CRNN overall test results comparison.

Model	Accuracy
CRNN	0.905
CRNN-MASK	0.925

be seen that the three data items of this model are all higher than those of the CTPN model.

Tables 2–4 are the comparison of CTPN-MASK and CTPN text recognition test results in the three sets of test data. Experiments have confirmed that the CTPN-MASK model proposed in this section has certain advantages in the accuracy of text recognition.

The test data set 2-CTPN-MASK and CTPN test results are shown in Table 3.

The test data set 3-CTPN-MASK and CTPN test results are shown in Table 4.

The overall test results of CRNN-MASK and CRNN are shown in Table 5.

Table 6 shows the comparison of the test results of CRNN-MASK and CRNN on the three test data sets.

The comparison of the overall test results of CTPN-MASK + CRNN-MASK and CTPN + CRNN is shown in Table 7.

Table 8 shows the comparison of the test results of CTPN-MASK + CRNN-MASK and CTPN + CRNN on the three test data sets.

3.3. Test Method of Cloud Computing Database Security. The cloud service platform user enters the user name and password on the login page to complete the login. In order to avoid affecting the initial authentication process, you only need to edit the authentication page, add a fingerprint connection module and related registration modules, and add them to the authentication page to confirm cross-domain fingerprint recognition. In this way, the authentication system can be transformed on the basis of preserving the functions of the original connected website.

Table 6: Comparison of test results between CRNN-MASK and CRNN on three test data sets.

Model	Test data set 1	Test data set 2	Test data set 3
CRNN	0.885	0.942	0.829
CRNN-MASK	0.892	0.941	0.926

Table 7: Comparison of overall test results of CTPN-MASK + CRNN-MASK and CTPN + CRNN.

Model	Accuracy
CTPN + CRNN	0.807
CTPN-MASK + CRNN-MASK	0.917

The test platform provides two authentication interfaces, one for intradomain authentication and the other for cross-domain authentication. The platform verifies the identity verification information between internal users and domains through different interfaces accessed by users. If the verification is passed, it will automatically enter the homepage of the test platform. If the verification fails, go to the failed verification page. The home page of the test platform can display all verified user account records. Table 9 shows the main files related to the test platform.

This feature uses a temporary account registered on the cloud platform to enable intradomain and cross-domain authentication on the test platform and analyzes the authentication impact of the cross-domain authentication system based on the authentication results.

Create an anonymous account: enter the cloud platform login page, use the cloud user test to register a personal domain name, and retrieve 10 account information.

Identity verification test: the test platform continuously uses 10 temporary accounts for intradomain and cross-domain identity verification and calculates the result of each identity verification and the total identity verification time. After the authentication is successful, the page will display the login information of the successfully authenticated domain and display the previous authentication records, authentication parameters, and certificates used.

3.4. Test Results and Analysis of Cloud Computing Database Security. Figure 1 shows the statistical information of the test platform results after using 10 temporary accounts for intradomain authentication.

Figure 2 shows the use of 10 temporary accounts for intradomain authentication and the statistical information of the results of the test platform.

The results of intradomain authentication and cross-domain authentication are shown in Figure 2. In addition to modifying the intradomain authentication parameters of

Table 8: Comparison of the test results of CTPN-MASK + CRNN-MASK and CTPN + CRNN on three test data sets.

Model	Test data set 1	Test data set 2	Test data set 3
CTPN + CRNN	0.802	0.867	0.672
CTPN-MASK + CRNN-MASK	0.897	0.928	0.926

Table 9: Class files mainly included in the test platform.

Class file name	Class belonging to package	Class function description	Owned functional module
Action.java	Controller	Intradomain authentication	Intradomain authentication module
CrossAction.java	Controller	Cross-domain authentication	Cross-domain authentication module
ShowRecordList.java	Controller	Get data list	Data display module
RecordListDAO.java	DAO	Perform data list database operations	Database operation module
CertiRecordList.java	Model	Certification record list management	Register module

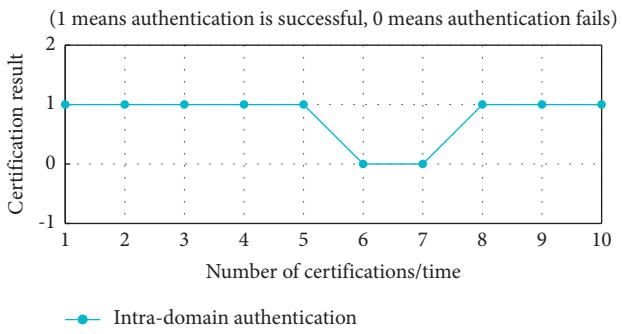

Figure 1: Intradomain authentication result statistics.

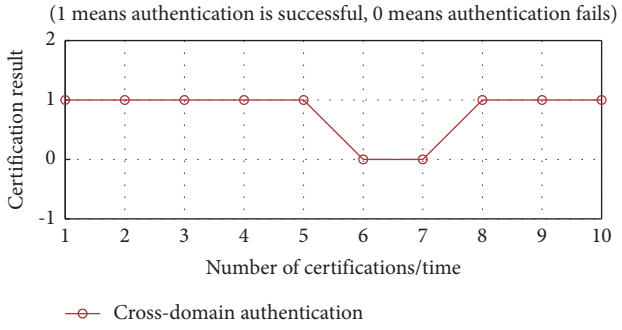

Figure 2: Statistics of cross-domain authentication results.

accounts 6 and 7, other temporary accounts can successfully verify their identity through participating in the test. The results show that the cross-domain authentication system can effectively identify the identity. Comparing the intradomain authentication time and the cross-domain authentication time, it can be concluded that the time spent in each cross-domain authentication exceeds the time spent in the intradomain authentication. This is because a large number of encryption operations are performed during the cross-domain authentication process, which makes the verification time longer. As the authentication time accumulates, the time difference between the two authentication processes will gradually increase, thereby reducing the time required for the interdomain authentication process. Therefore, it is necessary to improve encryption and decryption algorithms and improve the efficiency of identity

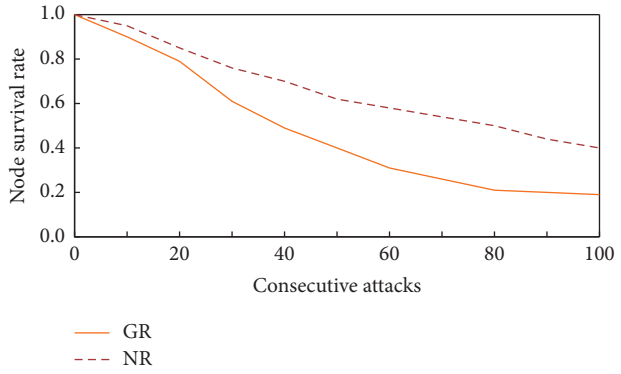

Figure 3: System vulnerability comparison.

verification. Such problems will become the focus of future research.

For information security under attack mode, test how to stably access the system. Robustness refers to the stability of the system. Whether the system can provide services normally under abnormal conditions depends more on the stability of the system itself.

According to statistics, 10,000 pieces of user registration data were sent to the user registration function in the system, and the number of abnormalities in the user registration function was 102 times. It can be seen that if the system is attacked, the abnormal rate of the system is 1.02%, which is generally kept at a low level.

In order to better measure the stability of the attacked system, a system vulnerability index is introduced here for analysis and measurement. System vulnerability refers to the degree to which system performance is impaired when the system is attacked. The vulnerability measurement formula is

$$R_n = \frac{M'}{M}. \tag{15}$$

Figure 3 shows the comparison of the vulnerability analysis of the general system (GR) and this system (NR) when they are attacked, which shows that the robustness of this system is better.

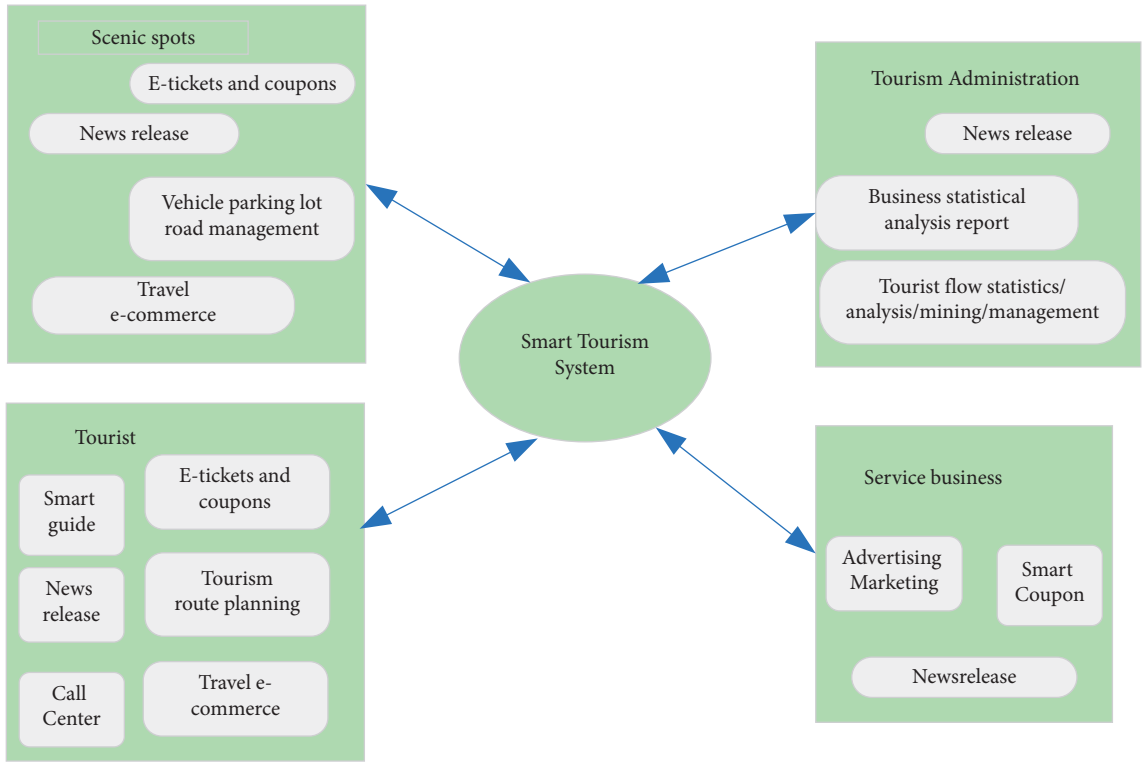

Figure 4: Smart tourism demand relationship.

4. Design and Application of the Sensor-Based Tourism Smart Platform

4.1. Demand Analysis of The Tourism Smart Platform. Smart tourism takes the integration of service resources as the core, focuses on user travel needs, and integrates data sources with the e-government tourism system as the basis. Through demand analysis, it adopts the analysis method facing the user. Smart tourism has four types of objects: tourists, scenic spots, service companies, and tourism management agencies, as shown in Figure 4.

To make a good product, we must not only fully meet the specific requirements of customers for system functions, but also continuously optimize the nonfunctional modules in the system, so that users have a better experience. According to the characteristics of SNS itself, combined with some specific requirements for the operation of mobile social systems, this article will discuss the nonfunctional requirements of the system from the aspects of compatibility, reliability, ease of use, ease of maintenance, and adaptability.

Because different tourists will use different Android client mobile phones, different mobile phones will be different in terms of brand, operating system version, screen resolution, etc. Therefore, the system that we created needs to ensure better compatibility, so that visitors from different Android customers can quickly get started using the system.

Maintainability focuses on a set of attributes related to the work required to make clear changes, including stability, ease of analysis, ease of testability, and ease of change. The application program created with this system should have the above characteristics to ensure that the subsequent maintenance work is simpler and the maintenance cost is lower.

Technological progress in the modern world is changing with each passing day, especially in the fast-updated software industry. Therefore, when designing the system, we need to ensure that it can meet the user's requirements for new technologies in a certain period of time in the future. In the process of designing the system, we need to introduce hierarchy and modularity in order to expand it in the future.

4.2. Model Design of the Sensor-Based Network Positioning System. The positioning system uses a mesh network topology to build a ZigBee wireless sensor network. The ZigBee wireless sensor network has a coordinator, router, and terminal equipment and connects the network to the computer through the coordinator. According to the received signal strength principle realized by RSSI, the router is designed as a fixed reference node, and the PC configures the coordinates of each recommended node through the coordinator; the terminal device is designed as an anonymous node, and the anonymous node uses the RSSI configuration algorithm to calculate the coordinates and transmits the ZigBee wireless network to the computer.

The wireless sensor network positioning system model based on ZigBee protocol designed in this paper is shown in Figure 5.

4.3. System Architecture Design. The Android client of this system adopts C/S structure. However, the Android client of this system first transmits the data to the Web side and then

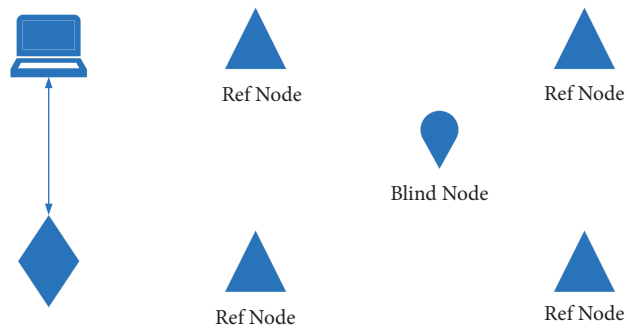

Figure 5: Wireless sensor network positioning system model based on the ZigBee protocol.

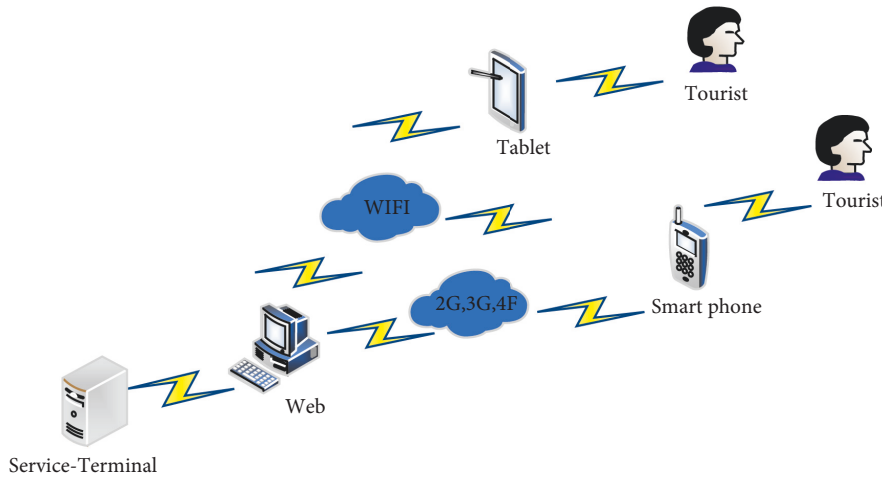

Figure 6: Physical architecture diagram of the Android client.

accesses the server side based on the Web side. The physical architecture diagram of the Android client of this system is shown in Figure 6.

Users, namely, tourists, communicate with the Web terminal through Android smart mobile terminal devices such as smart phones or tablet computers, and the Web terminal interacts with the server for data processing and operations. Finally, the results are delivered through a return form specific to the Android client user.

4.4. Realization of the Functions of the Tourism Smart Platform. Unregistered Android client users must register before they can continue to log in to access the Android client. Android users need to fill in some relevant registration information on the signup.xml page, including user name, password, nickname, e-mail, and birthday information. The user name and password are required information, and a unique password must be filled in during registration to ensure that the user does not enter wrong information when entering the password for the first time. After completing all the information, the user can click the registration button. After completing the registration information, the information will be taken to the background activity. In the background activity, people first obtain the relevant reference of the registration button and add a listener for the registration button, so as to ensure that the correct information jump is recorded. Then, they prepare the URL for receiving server-side information. The URL for receiving information in this application is Register.action. Open the connection website and send the relevant record information to the registered users on the server. Then, the RegisterAction server reads the corresponding parameter information from the HttpServletRequest. Then, call the corresponding UserDao method to manipulate the database data and verify whether the registration information has been registered. The log function is implemented using the POST method of the HTTP protocol.

In the realization of the travel service module, related functions are involved in searching for nearby locations. Searching for neighborhood locations obviously means searching for specific locations around the user based on the user's specific location. This method has many implementations. One of the most easily considered methods is to directly search the entire database on a certain scale; that is, we search the entire database according to specific requirements, and if the appropriate conditions are met, it will be regarded as a pair, but this method is the yield that is relatively poor, and the effectiveness is very low. Therefore, we made the following idea: whether we can divide the search area into several small areas first, that is, search the small areas first and then combine these results to get more

search results, in this case, the search efficiency will be higher. The answer is yes. R-tree two-dimensional search can solve such problems, but the structure of R-tree is very complicated. If the map is very large, many new ones will appear (complicated question). Moreover, the fragmentation and integration of R-tree are also an annoying problem. Therefore, the production cost of this method is not very high.

There are two formulas for calculating the distance between any two interior points according to the latitude and longitude coordinate information, namely, the Great-circle distance formula and the Haversine formula. There are obvious differences between the two formulas. The former is composed of several cosine formulas, while the latter has multiple sine formulas. If the distance between the two interior points that we want to calculate is too small, then the Great-circle distance formula will give a large error, while the Haversine formular formula will not produce this situation. This is the reason why the Haversine formular is used here in this article, which is defined as

$$\text{haver sin}\left(\frac{d}{R}\right) = \text{haver sin}\left(\phi_2 - \phi_1\right) + \cos\left(\phi_1\right)\cos\left(\phi_2\right) \text{haver sin}\left(\varnothing_2 - \varnothing_1\right). \tag{16}$$

Here,

$$\text{haver sin}\left(\theta\right) = \sin^2\left(\frac{\theta}{2}\right) = \frac{\left(1 - \cos\left(\theta\right)\right)}{2}. \tag{17}$$

Let us first calculate the range between the longitudes on the east and west sides. In the Haversine formula, letting $\varphi 1 = \varphi 2$, we can get

$$\Delta\varnothing = 2\arcsin\left(\frac{\sin\left(d/2R\right)}{\cos\left(\phi_1\right]}\right). \tag{18}$$

Then, we come to find the boundary of the range of latitudes on both sides of the north and south. In the Haversine formula, letting $\varphi 1 = \varphi 2$, we can get

$$\Delta\phi = \frac{d}{R}. \tag{19}$$

In this way, we can get the coordinates of the four points in the rectangular area according to the coordinates of the current point, thereby obtaining the search range. In addition, establishing proper indexes in the longitude and latitude columns can improve the order of queries for effective measurement.

The function of the information of the surrounding scenic spots is that, after obtaining and locating the specific location of the tourist, the status of the surrounding scenic area of the tourist can be displayed according to the specific location of the tourist, thereby facilitating the arrangement of the travel itinerary. In the process of realizing this function, you must first know the longitude and latitude coordinates of the user's location on the Android client, and then the system searches the surrounding locations through algorithms, finds relevant information about the surrounding scenic spots, and combines the information according to the longitude and latitude information of the tourist location and returns it to the Android client user. The details of the specific implementation process are as follows: first, the customer uses a certain map software to find the latitude and longitude coordinates of the current Android customer's location. Then, the latitude and longitude information is sent to the back-end server, and then the server calls the relevant redirection layer method to query the content of the database and finally returns the query result to the Android client to display to the relevant user.

5. Conclusion

In recent years, the tourism industry has received more and more attention from the national and local authorities. The Director of the China National Tourism Administration has repeatedly suggested that the construction of localized smart tourism in China should be realized as soon as possible. The National Tourism Administration has also implemented the determination of the "Smart Tourism Year." It can be seen that smart tourism is developing in an extremely rapid manner in China. Based on this, in the Internet, with the continuous advancement of information technology such as multiple data analysis, cloud computing, and mobile communications, the public's demand for tourism information services has become more vigorous, which has provided technical support and motivation for the flourishing development of the tourism industry. Smart tourism uses modern information technology to create a smart tourism service construction plan. By analyzing the status quo and customer needs, it gathers relevant elements of the tourism industry to promote the in-depth integration of modern information technology and the tourism industry. This article takes a certain scenic spot in China as an example, starts from the perspective of smart tourism, examines the correlation between smart tourism and the development of traditional tourism, considers the role of smart tourism in promoting the development and innovation of traditional tourism, and establishes the basis of this research. The smart tourism system was developed, and the construction plan, system operation mechanism, and technical realization were comprehensively analyzed and explained in depth.

Data Availability

The data used to support the findings of this study are available from the author upon request.

Conflicts of Interest

The author declares no conflicts of interest.

References

[1] C. Li, Y. Fang, and B. Sukoco, "Value proposition as a catalyst for innovative service experience: the case of smart-tourism destinations," *Service Business*, vol. 15, no. 2, pp. 281–308, 2021.

[2] Z. Ghaderi, P. Hatamifar, and L. Ghahramani, "How smartphones enhance local tourism experiences?" *Asia Pacific Journal of Tourism Research*, vol. 24, no. 8, pp. 778–788, 2019.
[3] A. Caldeira and E. Kastenholz, "Spatiotemporal tourist behaviour in urban destinations: a framework of analysis," *Tourism Geographies*, vol. 22, no. 1, pp. 22–50, 2020.
[4] S. Mandal, "Exploring the influence of big data analytics management capabilities on sustainable tourism supply chain performance: the moderating role of technology orientation," *Journal of Travel & Tourism Marketing*, vol. 35, no. 8, pp. 1104–1118, 2018.
[5] G Nikoli and A Lazakidou, "The impact of information and communication technology on the tourism sector," *Almatourism - Journal of Tourism, Culture and Territorial Development*, vol. 10, no. 19, pp. 45–68, 2019.
[6] F. Fusté-Forné and T. Jamal, "Co-creating new directions for service robots in hospitality and tourism," *Tourism and Hospitality*, vol. 2, no. 1, pp. 43–61, 2021.
[7] J. Lemley, S. Bazrafkan, and P. Corcoran, "Deep learning for consumer devices and services: pushing the limits for machine learning, artificial intelligence, and computer vision," *IEEE Consumer Electronics Magazine*, vol. 6, no. 2, pp. 48–56, 2017.
[8] Y. Zhang, J. Ren, J. Liu, C. Xu, H. Guo, and Y. Liu, "A survey on emerging computing paradigms for big data," *Chinese Journal of Electronics*, vol. 26, no. 1, pp. 1–12, 2017.
[9] S. Toapanta, O. Escalante Quimis, L. Gallegos, and M. Maciel Arellano, "Analysis for the evaluation and security management of a database in a public organization to mitigate cyber attacks," *IEEE Access*, vol. 8, pp. 169367–169384, 2020.
[10] P. Casas, F. Soro, J. Vanerio, G. Settanni, and A. D'Alconzo, "Network security and anomaly detection with Big-DAMA, a big data analytics framework," in *Proceedings of the 2017 IEEE 6th International Conference on Cloud Networking (CloudNet)*, pp. 1–7, Prague, Czech, September 2017.
[11] E. Nadimi, H. Søgaard, T. Bak, and F. Oudshoorn, "ZigBee-based wireless sensor networks for monitoring animal presence and pasture time in a strip of new grass," *Computers and Electronics in Agriculture*, vol. 61, no. 2, pp. 79–87, 2008.
[12] C. Yang, Y. Liu, and X. Tao, "Assure deletion supporting dynamic insertion for outsourced data in cloud computing," *International Journal of Distributed Sensor Networks*, vol. 16, no. 9, Article ID 1550147720958294, 2020.
[13] J. Zhao and S. Hu, "A new adaptive weighted fusion algorithm for multi-sensor tracking," in *Proceedings of the 1st International Conference on Machine Learning and Cybernetics*, pp. 285–287, Beijing, China, November 2002.
[14] G. Bian and J. Chang, "Certificateless provable data possession protocol for the multiple copies and clouds case," *IEEE Access*, vol. 8, pp. 102958–102970, 2020.
[15] C. Cervellera, D. Macciò, and M. Muselli, "Deterministic learning for maximum-likelihood estimation through neural networks," *IEEE Transactions on Neural Networks*, vol. 19, no. 8, pp. 1456–1467, 2008.
[16] S. Heidari, M. Abutalib, M. Alkhambashi, A. Farouk, and M. Naseri, "A new general model for quantum image histogram (QIH)," *Quantum Information Processing*, vol. 18, no. 6, pp. 175–220, 2019.
[17] L. Ruff, J. R. Kauffmann, R. A. Vandermeulen et al., "A unifying review of deep and shallow anomaly detection," *Proceedings of the IEEE*, vol. 109, no. 5, pp. 756–795, 2021.
[18] C. Wu, S. Shao, and C. Tunc, "An explainable and efficient deep learning framework for video anomaly detection," *Cluster Computing*, vol. 25, no. 4, 2021.
[19] M. Vadursi, A. Ceccarelli, E. Duarte, and A. Mahanti, "System and network security: anomaly detection and monitoring," *Journal of Electrical and Computer Engineering*, vol. 2016, pp. 1-2, Article ID 2093790, 2016.
[20] C. Chahla, H. Snoussi, L. Merghem, and M. Esseghir, "A deep learning approach for anomaly detection and prediction in power consumption data," *Energy Efficiency*, vol. 13, no. 8, pp. 1633–1651, 2020.

Hindawi
Mobile Information Systems
Volume 2022, Article ID 5830760, 10 pages
https://doi.org/10.1155/2022/5830760

Research Article

A Heuristic Task Scheduling Strategy for Intelligent Manufacturing in the Big Data-Driven Fog Computing Environment

Rong Zhou

The University of Hong Kong, Hong Kong 999077, China

Correspondence should be addressed to Rong Zhou; zhourong2020@gsm.pku.edu.cn

Received 14 June 2022; Revised 23 July 2022; Accepted 29 July 2022; Published 26 August 2022

Academic Editor: Shadi Aljawarneh

A heuristic task scheduling strategy for intelligent manufacturing in the big data-driven fog computing environment is proposed to address the problem that current resource scheduling and allocation methods in the fog computing environment cannot comprehensively consider the dynamics and uncertainty of resources, resulting in the prolonged delay and high energy consumption. First, a system model with three computing modes for intelligent manufacturing is constructed based on intelligent terminal devices, fog nodes, fog servers, fog gateways, and the cloud. Then, the objective function is optimized by jointly considering the delay matrix, the energy consumption matrix, and the reliability matrix, and corresponding constraints are given based on the selection of computing modes, the decision variables of fog nodes as well as the constraints about the delay. Finally, the intervals of crossover-mutation operators are divided according to the fitness value, and individuals of the population are updated by taking different operations based on the operators in different intervals, so as to achieve an improvement on the traditional genetic algorithms. Meanwhile, a fog resource scheduling algorithm is proposed based on the improved adaptive genetic algorithm. Simulation experiments are conducted to compare and analyze the delay, energy consumption, and reliability of the proposed method with three other methods under the same conditions. The results show that the proposed method has the lowest delay and energy consumption and the highest reliability, with values of 361.3 s, 352.4 J, and 94.6%, respectively, when the number of task requests is 500. The performance is better than the other three comparison methods.

1. Introduction

With advances in information technology such as the Internet of Things (IoT) and fog computing, the "smart factory" controlled by cyber-physical systems (CPS) is also developing rapidly [1, 2]. The Intellectualization of information and production methods has led to a higher level of interconnectivity, smarter devices, and more powerful data processing in intelligent manufacturing. Through the connected information, statistical data, and dynamic analysis, intelligent manufacturing makes the production smarter, leaner, more effective, and more energy-efficient [3–5]. The introduction of the IoT technology in intelligent manufacturing places new and higher demands on data sensing, collection, consolidation, transmission, and reverse control in smart factories. At the same time, the spread of intelligent devices and terminals and the use of various kinds of sensors will bring about ubiquitous sensing and connectivity, generating a constant flow of industrial data [6–8].

The efficient processing of large volumes of data in traditional manufacturing can be achieved using cloud computing. However, due to the complexity of networking in the IoT and the limited computing capacity of devices in the bottom layer, traditional data processing methods cannot be used for delay-sensitive applications of intelligent manufacturing services [9, 10]. Fog computing, as a highly virtualized platform that locates on the edge of the local network, can provide computing and storage services near the underlying network and the Internet. Therefore, it is a good solution to the problem of rapid response and bandwidth consumption for delay-sensitive applications [11, 12]. When terminal devices request services from the

cloud data center, fog computing can first perform data filtering, data pre-processing, and analysis before delivering it to the cloud computing system, thus reducing the burden on the cloud data center. Fog computing resources are therefore ideal for terminal users today [13]. Due to the dynamic and uncertainty of resources and the high variability and unpredictability of the fog computing environment, rational resource scheduling and allocation are particularly important, which have become a research hotspot in the industry [14, 15].

A heuristic task scheduling strategy for intelligent manufacturing in a big data-driven fog computing environment is proposed to address the problems of prolonged delay, high energy consumption, and low reliability of current resource scheduling and allocation methods in fog computing environment. The basic ideas are: (1) First, a system model for intelligent manufacturing that can be used for computing mode selection is constructed. (2) The corresponding objective function and constraints are given in the consideration of delay, energy consumption, and reliability. (3) The applicability of the genetic algorithm to the problem under study is improved by making appropriate refinements to it. Compared with traditional task scheduling strategies, the main contributions of the proposed method can be summarized as follows:

(1) Intelligent devices, fog nodes, fog servers, fog gateways, and the cloud are taken into account when constructing the system model, greatly improving the utilization of fog computing resources.

(2) The objective function is optimized in terms of three aspects of task scheduling: delay, energy consumption, and the success rate of task execution.

(3) The traditional genetic algorithm is improved by dividing the crossover-mutation operators into intervals to further enhance the reliability of task scheduling.

The remaining chapters of this paper are arranged as follows: the second chapter introduces the efficient resource allocation and task scheduling strategies for intelligent manufacturing in the fog computing environment, and some current research results. The third chapter establishes the system model. The fourth chapter introduces the proposed fog resource scheduling method based on a genetic algorithm. In Chapter 5, experiments are designed to verify the performance of the proposed algorithm. The sixth chapter is the conclusion, which summarizes this study and puts forward the further improvement direction.

2. Related Works

Some scholars have done relevant research and achieved certain results on resource allocation and task scheduling strategies for intelligent manufacturing in the fog computing environment. Li et al. standardized and normalized the attributes of resources, and combined the fuzzy clustering method with particle swarm optimization method to reduce the scale of resource search and divide the resources [16]. It proposed a new resource scheduling algorithm based on optimized fuzzy clustering for fog computing. However, the method only optimizes the processing time and cost of the tasks without considering the limited computational resources in the smart factory. In Yang et al., aiming at the multi-objective task scheduling problem in fog computing, a multi-objective task scheduling model was designed based on the Pareto optimal solution [17]. However, the method cannot reduce the overall reliance on large data centers and the Internet data are distant from the users. Ren et al. addressed the problem of limited resources in mobile devices and used fog computing to improve the WAN delay for delay-sensitive and resource-intensive applications [18]. It proposed an improved three-layer fog-to-cloud architecture and the schedule fit algorithm, which can provide computational resources and transmission delay according to the delay sensitivity of applications. The method fails to minimize the processing delay of the task and needs further improvement. Based on Lyapunov drift and the penalty function on the queue length, a scheduling strategy for tasks in the queues was proposed in Reference [19] to decide the number of tasks to be offloaded to the underloaded fog nodes to fully utilize the computational resources offered by all fog nodes in the network. However, this approach does not consider the service delay. By extending the architecture of fog computing, Tang et al. proposed a computational resource allocation scheme based on stable matching for open fog computing environment [20]. Based on the idea of stable matching, the allocation problem between tasks and computing service devices is solved by combining the priority list of subtasks and the preference lists of subtasks and computing service devices. However, the fog computing network is heavily used in this method. Alqahtani et al. classified requests to real-time, important, and time-tolerant, and proposed a scheduling method for allocating customers' requests to the resources of the cloud-fog environment by considering load balancing among resources while allocating requests to them [21]. But the algorithm does not take the cost and energy consumption of resource scheduling into account. In Reference [22], in order to solve the resource scheduling and load balancing problems in fog computing, an optimized fuzzy clustering-based resource scheduling and dynamic load balancing algorithm was proposed. On this basis, an enhanced fuzzy C-means and the crow search optimization algorithm in fog computing were used to solve the problem. However, the method does not combine the characteristics of smart factories as a whole to fully optimize them.

3. System Model

3.1. System Model Description. Different from the traditional computing mode selection strategies, the proposed computing mode selection strategy is applicable to fog computing platforms with the combination of heterogeneous computing modes. In the fog computing platform, if the traditional strategies are still used, not only will the resource utilization of fog computing be reduced, but also the tasks which are related to intelligent manufacturing will not be

guaranteed to be real-time, energy-efficient, or reliable. In order to improve the utilization of resources in fog computing, a system model of computing mode selection for intelligent manufacturing is established, which is shown in Figure 1.

As can be seen from Figure 1, the system model of computing mode selection for intelligent manufacturing consists mainly of intelligent terminal devices, fog nodes, fog servers, fog gateways, and the cloud. The intelligent terminal devices can either execute tasks locally or transmit the tasks that they cannot execute to other computing nodes. The fog node is the middleware that connects the intelligent terminal device to the cloud, and using the fog node as well as the cloud can enhance the computing capacity of the intelligent terminal devices. The fog node provides a real-time and distributed fog computing model for intelligent terminal devices in task execution. The cloud provides a remote and centralized cloud computing model for intelligent terminal devices in task execution. Different from the traditional strategies where all of the tasks are transmitted to the cloud to be executed, each task in the fog computing environment has a choice of three computing modes.

Intelligent terminal devices forward the tasks through the fog nodes. Task requests from intelligent terminal devices are transmitted to the fog nodes, and all information of task requests is gathered at the fog gateway and subsequently forwarded to the fog server. The fog server can sense the global information of the fog nodes, which provides a reference for the dynamic selection of the computing modes of the task. The fog server manages the tasks, calculates the priority of each task, and adjusts the task queue according to the priority of the task, and then it formulates the optimal selection scheme of computing modes for the task. The fog server sends the selection scheme of computing modes to the fog gateway, and the fog gateway then sends the set of allocated tasks to the corresponding intelligent terminal devices, thus implementing the function of computing mode selection for the intelligent terminal devices when executing tasks.

All devices in the system model are described below. The system model contains z intelligent terminal devices, n fog nodes and a cloud server. The set of intelligent terminal devices is represented by Z, where $Z = \{E_1, E_2, E_3, \ldots, E_z\}$ and the attributes of the intelligent device E_i can be modeled as a triple (C_i, P_{0i}, P_{1i}). C_i represents the computing capacity of the intelligent terminal device E_i. P_{0i} represents the transmission power of the intelligent terminal device E_i. P_{1i} denotes the computation power of the intelligent terminal device E_i. N denotes the set of fog nodes, where $N = \{F_1, F_2, F_3, \ldots, F_n\}$. And the computation power of the fog nodes is denoted as J_N. The computing capacity of the cloud server is denoted as J_C. T is a compound task and can be partitioned into n subtasks according to certain rules, which can be represented as $T = \{T_1, T_2, T_3, \ldots, T_n\}$. The attributes of the task T_i can be modeled as a triple $(D_i, \rho_i, t_{\max i})$. D_i represents the amount of data of the task T_i. ρ_i represents the computational density of the task T_i. $t_{\max i}$ denotes the maximum tolerance time of the task T_i. The system model of computing mode selection shows that each

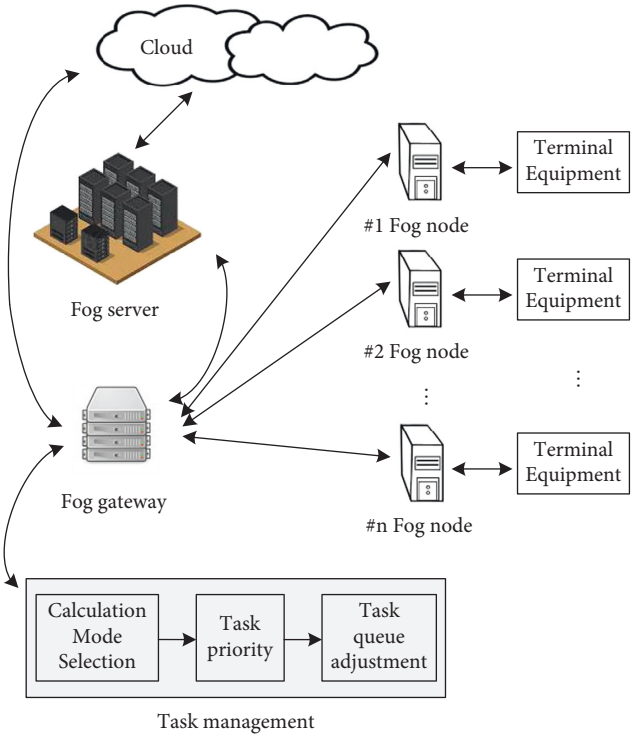

Figure 1: The system model of computing mode selection for intelligent manufacturing.

task can be executed through one of the three computing modes. The task can be either executed locally in the intelligent terminal device or transmitted to a fog node or a cloud server for execution. For the task T_i, the delay and energy consumption in the local execution mode are recorded as t_{i1} and e_{i1}, respectively. The delay and energy consumption in fog computing mode are recorded as t_{i2} and e_{i2}, respectively. And the delay and energy consumption in cloud computing mode are recorded as t_{i3} and e_{i3}, respectively.

3.2. Optimization Objectives. In order to facilitate the description of the computing mode selection problem and better formulate the computing mode selection algorithm proposed in this section, relevant definitions and optimization objective functions are given to provide a basis for implementing the selection of computing modes. Based on the above analysis, the delay of the task T_i can be expressed as follows:

$$t_i = \alpha_{i1} t_{i1} + \alpha_{i2} t_{i2} + \alpha_{i3} t_{i3}, \tag{1}$$

where $\{\alpha_{i1}, \alpha_{i2}, \alpha_{i3}\}$ represents the set of decision variables for the selection of the computing mode for the task T_i. When $\alpha_{i1} = 1$, it indicates that the task T_i selects the local execution mode, which means that the task T_i will be executed by the intelligent terminal device E_i. Otherwise, $\alpha_{i1} = 0$. When $\alpha_{i2} = 1$, it indicates that the task T_i selects the fog computing mode, which means that the task T_i will be executed by a fog node. Otherwise, $\alpha_{i2} = 0$. And when $\alpha_{i3} = 1$, it indicates that the task T_i selects the cloud

computing mode, which means that each T_i will be executed by a cloud server. Otherwise, $\alpha_{i3} = 0$. The task T_i can only selects one of the computing modes, i.e., $\alpha_{i1}, \alpha_{i2}, \alpha_{i3} \in \{0, 1\}$.

We define the computing mode selection decision matrix as A, where the number of tasks being executed based on (1) is taken as the row and the number of computing modes that can be selected are taken as columns, as follows:

$$A = \begin{Bmatrix} \alpha_{11} & \alpha_{12} & \dots & \alpha_{1J} \\ \alpha_{21} & \alpha_{22} & \dots & \alpha_{2J} \\ \dots & \dots & \dots & \dots \\ \alpha_{I1} & \alpha_{I2} & \dots & \alpha_{IJ} \end{Bmatrix}, \tag{2}$$

a_{ij} denotes the decision variables for the task T_i in the computing model j, where $i = 1, 2, 3, \dots, I$ and $j = 1, 2, 3, \dots, J$.

We define the delay matrix as T_t. According to the computing mode selection decision matrix A, the delay of each task in the task set T under three computing modes can be obtained. Thus, the delay matrix T_t for the task set T can be constructed as

$$T_t = \begin{Bmatrix} t_{11}, t_{12}, \dots, t_{1J} \\ t_{21}, t_{22}, \dots, t_{2J} \\ \dots, \dots, \dots, \dots \\ t_{I1}, t_{I2}, \dots, t_{IJ}, \end{Bmatrix}, \tag{3}$$

where t_{ij} indicates the delay of the task T_i in the computing mode j, $i = 1, 2, 3, \dots, I$, $j = 1, 2, 3, \dots, J$. For tasks that select the fog computing mode, they will be allocated to all of the fog nodes according to the polling algorithm. h_{in} denotes the selection decision of fog nodes for the task T_i, and $h_{\text{in}} = 1$ denotes that the task T_i selects to be executed by the fog node lF. Otherwise, $h_{\text{in}} = 0$. Hence, $h_{\text{in}} \in \{0, 1\}$ and $\sum_{n=1}^{N} h_{\text{in}} = 1$, $(i = 1, 2, \dots, I)$.

The energy consumption matrix is defined as E. Based on the computing mode selection decision matrix A, the energy consumption of each task in the task set T under three computing modes can be calculated. Hence, the energy consumption matrix E for the task T can be written as

$$E = \begin{Bmatrix} e_{11}, e_{12}, \dots, e_{1J} \\ e_{21}, e_{22}, \dots, e_{2J} \\ \dots, \dots, \dots, \dots \\ e_{I1}, e_{I2}, \dots, e_{IJ} \end{Bmatrix}, \tag{4}$$

where e_{ij} represents the energy consumption of the task T_i in the computing mode j, $i = 1, 2, 3, \dots, I$, $j = 1, 2, 3, \dots, J$.

The reliability matrix is defined as K, and it is used to evaluate the execution performance of each task in the task set T within its maximum tolerance time. The reliability matrix can be expressed as

$$K = \begin{Bmatrix} k_{11}, k_{12}, \dots, k_{1j} \\ k_{21}, k_{22}, \dots, k_{2j} \\ \dots, \dots, \dots, \dots \\ k_{i1}, k_{i2}, \dots, k_{ij} \end{Bmatrix}, \tag{5}$$

where k_{ij} represents the execution performance of the task T_i in the computing mode j, and it should meet the following constraints:

$$k_{ij} = \begin{cases} 0, & \alpha_{ij} t_{ij} \le t_{\max i}, \\ 1, & \alpha_{ij} t_{ij} > t_{\max i}. \end{cases} \tag{6}$$

If the task T_i can be completed within its maximum tolerance time, the task T_i will be executed successfully. Otherwise, the task T_i fails. The number of successfully executed tasks is counted as z_C and the higher the value of z_C, the better the reliability of the task. The success rate of a task is given by p, which can be calculated as

$$p = \frac{z_C}{z} \times 100\%. \tag{7}$$

The energy consumption of all tasks in the task set T can be described as

$$e_S = \sum_{i}^{I} \left(\alpha_{i1} e_{i1} + \alpha_{i2} e_{i2} + \alpha_{i3} e_{i3} \right). \tag{8}$$

The optimization objective of the computing mode selection strategy is to minimize the task delay and energy consumption, which can be formulated as

$$f_o = \min \begin{Bmatrix} \max\limits_{1<i<I} \left(\alpha_{i1} t_{i1} \right) \\ \max\limits_{1<n<N} \left(\sum\limits_{i=1}^{I} \alpha_{i2} h_{ni} t_{n2,i} \right) \\ \max \left(\sum\limits_{i=1}^{I} \alpha_{i3} t_{i3} \right), e_S \end{Bmatrix}. \tag{9}$$

The constraints are shown as

$$\begin{cases} \alpha_{i1}, \alpha_{i2}, \alpha_{i3} \in \{0, 1\}, & i = 1, 2, 3, \dots, I, \\ \alpha_{i1} + \alpha_{i2} + \alpha_{i3} = 1, & i = 1, 2, 3, \dots, I, \\ h_{i1}, h_{i2}, h_{i3}, \dots, h_{in} \in \{0, 1\}, & i = 1, 2, 3, \dots, I, \\ \sum\limits_{n=1}^{N} h_{in} = 1, \ (i = 1, 2, \dots, I), & i = 1, 2, 3, \dots, I, \\ t_i \le t_{\max i}, & i = 1, 2, 3, \dots, I, \end{cases} \tag{10}$$

where the first and second constraints are about the decision variables of the computing mode selection, ensuring that only one computing mode can be selected for each task. The third and fourth constraints are about the decision variables of the fog node selection, which guarantee that only one fog node can be selected for each task. The last inequality indicates the constraint about the delay for each task.

4. Fog Computing Task Scheduling Algorithm

4.1. Overview of the Algorithm. Based on the aforementioned analysis, a fog resource scheduling method is proposed based on an adaptive bi-adaptive genetic algorithm. Population optimization is carried out by drawing on biological phenomena such as heredity, mutation, natural selection, and hybridization in the theory of biological evolution to find the optimal individual. The algorithm takes the individual in the population as a solution and evaluates the performance of the individual by the dual fitness function. The genetic operations can be divided into three main operators, which are selection, crossover, and mutation. The roulette wheel method is used in the selection operation to maintain genetic diversity in the survival of the fittest. However, as the mutation of chromosomal genes is random, the chromosomal solutions generated may not be feasible solutions, which mean that they do not satisfy the constraint between tasks. Therefore, in the selection operation, a repair strategy is also required for the selected individuals, which allows maximizing the maintenance of genes while changing infeasible solutions into feasible ones. Traditional single-point crossover and partial mapping crossover are combined in the crossover operation. The partial mapping crossover is used for scheduling sequences, and the traditional single-point crossover is used for fog node allocation sequences.

4.2. Improved Genetic Algorithm

4.2.1. Encoding. Initialization of the adaptive genetic algorithm: set the termination conditions of the population iteration as the number of iterations reaching the maximum, the appearance of the optimal solution, or the iteration time reaching the constraint time. Set the optimization weights of delay and communication load as $c1$ and $c2$, respectively.

By encoding chromosomes, genetic algorithms make a chromosome correspond to a solution of the optimization problem. The general encoding methods are direct encoding and indirect encoding. In this paper, indirect encoding is used. Thus, the mapping relationship between task requests and fog nodes is represented by a set of sequences (S, A), where S represents the scheduling ordered sequence and A represents the fog node allocation sequence. Each task request is mapped into a fog resource. A single task request corresponds to a single fog resource, and a single fog resource can correspond to multiple task requests. Each bit in the sequence S and the sequence A represents the number of task requests and the fog resource, and all of them are positive integers. The length of the sequence S and the sequence A is equal to the total number of task requests, which is denoted as k. And the gene value represented in the sequence A corresponds to the number of fog resources allocated to the task. The total number of fog nodes in a fog cluster is l, the total number of task requests is k and a set of sequences (S, A) is called a chromosome.

Chromosome decoding strategy: The fog resource allocation strategy can be derived from the chromosome encoding rules. For example, a chromosome $\{(9, 5, 1, 7, 3, 8, 4, 6, 10, 2), (1, 2, 3, 3, 2, 1, 3, 2, 1, 2)\}$ means that 10 tasks will be allocated to 3 fog nodes for execution. First, the task T_9 will be allocated to the fog node F_1 for execution, then the task T_5 will be allocated to the fog node F_2 for execution, and so on. Finally, the allocation strategy can be obtained, where the task T_9, T_8, and T_{10} will be executed in the fog node F_1 in turn. Also, the task T_5, T_3, T_6, and T_2 will be executed in the fog node F_2 in turn, and the task T_1, T_7, and T_4 will be executed in the fog node F_3 in turn.

4.2.2. Populations Initialization. Population initialization is quite important for scheduling terminal user tasks in a fog computing architecture. The initial population is generated randomly and invalid solutions are excluded based on constraints. Let the size of the initial population be P, and the number of iterations is initialized as $i = 0$. The constraints ask that the time-critical requests from the terminal user must be scheduled to the fog that is close to the user for execution, while requests which are not so urgent should be allocated to the cloud for execution. Meanwhile, in order to avoid severe load disparity, all requests from users cannot be placed on the same resource simultaneously.

4.2.3. Fitness Function. The fitness function is the key to assessing the direction of population evolution when scheduling the terminal user tasks in a fog computing architecture. In order to make the fitness function remain meaningful when the total cost of the service provider is zero, it is defined as

$$f(W) = e^{-W}. \tag{11}$$

W represents the total cost of the service provider.

4.2.4. Genetic Manipulation. Once traditional genetic algorithms have selected suitable individuals using the roulette wheel operator, they take crossover and mutation operations to obtain the next generation of individuals. However, traditional genetic algorithms adopt a uniform crossover variation operator for the evolution of populations, which is not conducive to either the retention of good individuals or the generation of even better individuals. Therefore, in this paper, the interval division of crossover-mutation operators is adopted. After the fitness value of individuals in the population is calculated based on the fitness function, all individuals are divided into different intervals according to the fitness value, which are the mutation interval with low fitness value, the retention interval with high fitness value, and the asymptotic interval with moderate fitness value. The population is then updated by applying different crossover-

mutation operators to the individuals in the different intervals.

Individuals with high fitness values are retained directly, ensuring that the best individuals are preserved at each iteration. For individuals with low fitness values, mutation operation is taken to change their chromosomes. By doing this, it gives the opportunity to mutate individuals with low fitness values into individuals with high fitness values, allowing the population to jump out of the local optimum and avoid premature convergence during the iteration, so as to improve the performance of global searching. For individuals with moderate fitness values, the custom interval division operator is used to select the parent individuals and then retain the better individuals by crossover operations. The main idea of the interval division crossover-mutation operator is shown in Figure 2.

The crossover operator, which is a search operator in genetic algorithms, is mainly used when generating new individuals by crossing over the chromosomal genes of the current parent individuals. In this paper, a combination of traditional single-point crossover and partial mapping crossover is used. Specifically, the partial mapping crossover operation is used for the scheduling sequence S and the traditional single-point crossover operation is used for the fog node allocation sequence A. In addition, a mechanism of individual self-adaptation is introduced, which means that the crossover rate changes with the fitness value.

In the partial mapping crossover operation, a crossover selection position is set between any two adjacent genes in each chromosome subsequence S, where the indexes are 1, 2,. . ., $k+1$ from left to right. There are $k+1$ different crossover selection positions in total. A partial mapping crossover is a random selection of two positions from $k+1$ crossover selection positions, and the two parent chromosomes will produce a corresponding pair of genes between these two crossover selection positions. This pair is used to replace the genes of two parent chromosomes, respectively, resulting in two new children chromosomes. For example, if there are two parent sequences {8, 5, 9, 2, 7, 1, 3, 6, 4} and {1, 3, 7, 4, 6, 8, 2, 9, 5}, and the crossover selection positions are randomly generated to be 5 and 8, then the corresponding pair will be {7 : 6, 1 : 8, 3 : 2} and the two children chromosomes resulting from the partial mapping crossover operation will be {1, 5, 9, 3, 6, 8, 2, 7, 4} and {8, 2, 6, 4, 7, 1, 3, 9, 5}. In the single-point crossover operation, a crossover position is set between any two adjacent genes in each chromosome subsequence A, where the indexes are 1, 2,. . ., $k-1$ from left to right. There are $k-1$ different crossover positions in total. In the single-point crossover operation, a crossover position is randomly selected among $k-1$ crossover positions, and all genes in those two chromosomes are exchanged from the positions onwards. For example, if the parent sequences are {3, 1, 1, 2, 3, 2, 1, 3, 2} and {1, 2, 3, 2, 2, 3, 3, 1, 1}, and the randomly generated crossover position is 5, then the two children chromosomes resulting from the single-point crossover operation will be {3, 1, 1, 2, 3, 3, 3, 1, 1} and {1, 2, 3, 2, 2, 2, 1, 3, 2}.

The adaptive crossover rate can be obtained as

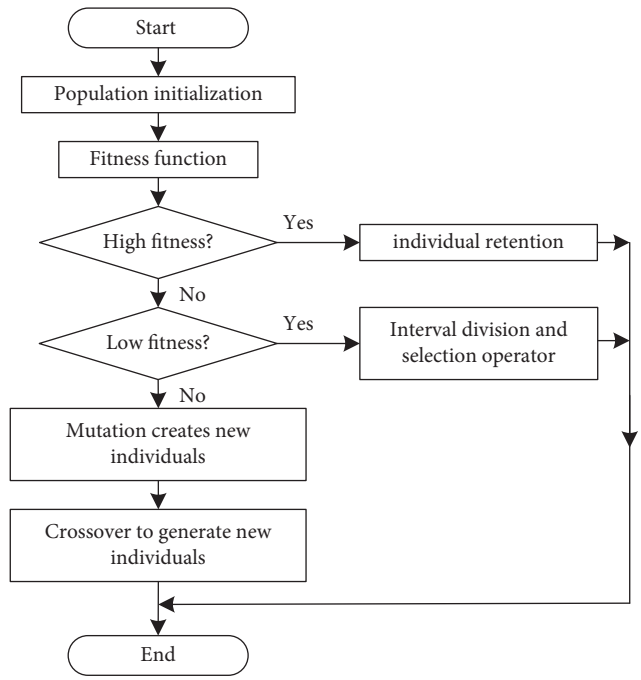

Figure 2: The process of interval division of crossover-mutation operators.

$$\begin{cases} f_t = \dfrac{\sum_{m=1}^{M} f_t(m)}{M}, \\ f_c = \dfrac{\sum_{m=1}^{M} f_c(m)}{M}, \end{cases} \tag{12}$$

$$P_I = \begin{cases} \beta_1 \dfrac{f_{\max} - f_0}{f_{\max} - f}, & f_0 \geq f, \\ \beta_2, & f_0 \geq f, \end{cases}$$

where f_t and f_c denote the average fitness values for the maximum time span and communication overhead, respectively. P_I is the crossover rate of the two individuals. β_1 and β_2 are constant coefficients of the crossover rate and satisfy the constraints of $0 < \beta_1 < 1$ and $0 < \beta_2 < 1$. Two crossed individuals will generate two fitness values each. The fitness function, which can generate the smallest fitness value among the four fitness values, is chosen as the criterion for crossover, i.e., one of $f_t(m)$ and $f_c(m)$ is chosen as the criterion $f(m)$, where $f(m) = [f_t(m) \mid f_c(m)]$ and $f = [f_t \mid f_c]$. f_0 is the larger fitness value of the two individuals $f(m)$ and $f_{\max}$ is the largest fitness value of the current population $f(m)$.

The mutation operator combines the methods of basic bit mutation and inversion mutation. Heuristic mutation is applied for the scheduling sequence S and basic bit mutation is applied for the fog node allocation sequence A. The inversion mutation is applied for the chromosome subsequence S. In the inversion mutation, two gene bits are randomly selected from the k gene bits and the values of genes at these two bits are exchanged. For example, there is

the parent sequence {3, 6, 1, 5, 2, 9, 7, 4, 8}, and if the two randomly generated gene bits are 2 and 6, a subsequence {3, 9, 1, 5, 2, 6, 7, 4, 8} will be generated after the inversion mutation. The basic bit mutation is applied for chromosome subsequence A. In the basic bit mutation, a gene bit is randomly selected from the k gene bits and a number from {1, 2, 3,...,n} is randomly selected to replace the gene at the current gene bit, which means that a new fog resource is randomly selected to replace the original fog resource. For example, if the parent sequence is {3, 1 ,1, 2, 3, 2, 1, 3, 2}, and the index of randomly generated gene bit for mutation is 3 and the random gene value selected for replacement is 2, then a child sequence {3, 1, 2, 2, 3, 2, 1, 3, 2} will be generated by the basic bit mutation. Mutation generates new genes and provides the diversity of the population. Like the crossover operator, the mutation operator introduces a mechanism of individual adaption, thus the mutation rate varies with the fitness value.

The adaptive mutation rate can be written as

$$P_V = \begin{cases} \lambda_1 \dfrac{f_{\max} - f_0}{f_{\max} - f}, & f_0 \geq f, \\ \lambda_2, & f_0 \geq f, \end{cases} \tag{13}$$

where P_V is the mutation rate for an individual. λ_1 and λ_2 are constant coefficients of the crossover rate and they satisfy the constraints of $0 < \lambda_1 < 1$ and $0 < \lambda_2 < 1$. The fitness function which can generate the smaller fitness value of the current individual is used as the criterion for mutation, which means that one of $f_t(m)$ and $f_c(m)$ is chosen as the criterion $f(m)$, where $f(m) = [f_t(m) \mid f_c(m)]$ and $f = [f_t \mid f_c]$. $f_{\max}$ is the largest fitness value in the current population $f(m)$.

Genes are constantly evolving in each generation by operations such as selection, crossover, and mutation. Therefore, in order to keep each generation of individuals as feasible solutions, gene repair is required for individuals after the mutation operation.

4.3. Steps for Scheduling Fog Computation Tasks. The flow of the task scheduling algorithm in the fog computing environment for intelligent manufacturing is shown in Figure 3.

The specific process of the algorithm is given as follows:

(1) Population initialization: the users submit the terminal request and the initial population is randomly set based on the request. A counter for the number of iterations is initialized as well.

(2) Fitness value calculation: the fitness values of individuals are calculated according to the fitness function.

(3) Judgment of termination conditions: when the number of evolutionary generations reaches the specified number of iterations, the result is output and a better solution for fog computing task scheduling should be obtained. Otherwise, go to step (4).

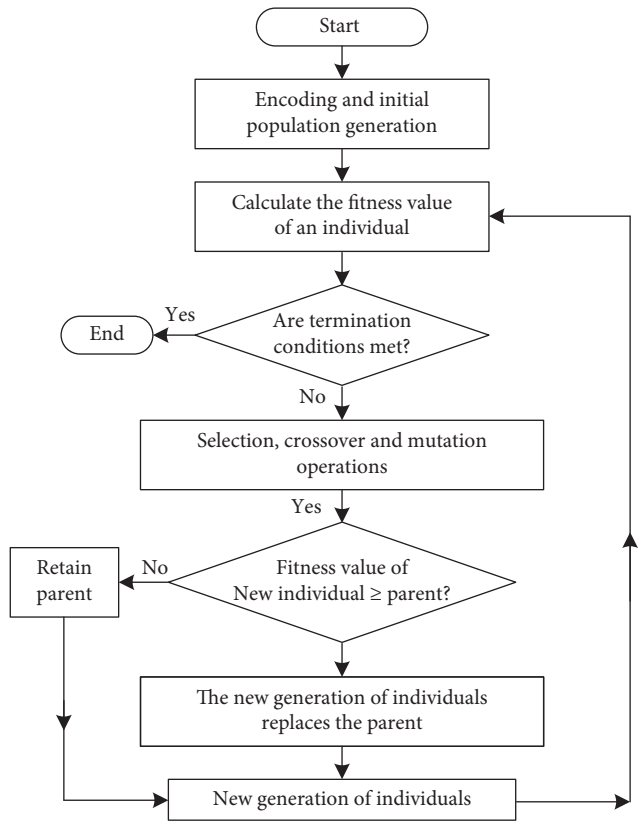

Figure 3: The flow of task scheduling algorithm in fog computing environment.

(4) Selection operation: a roulette wheel method is used to perform selection operations on the population.

(5) Crossover operation: according to the crossover method in the improved genetic algorithm, two individuals are randomly selected among those produced by the selection operation and then operated according to the crossover rate to generate new individuals.

(6) Mutation operation: according to the mutation method in the improved genetic algorithm, some individuals are selected from the new individuals generated by crossover operation and then operated according to the mutation rate to generate new individuals.

(7) Judgment of fitness value: the fitness value of the mutated individuals is judged, and if the fitness value is smaller than that of the parent, the parent is retained; if it is greater than or equal to that of the parent, the parent is replaced.

(8) Update the iteration counter: add 1 to the iteration counter and go to step (2).

5. Experiments and Analysis

5.1. Simulation Environment and Parameter Settings. The simulation platform is configured with an Intel i5 processor with a CPU of 3.3 GHz and 4 GB of memory. A simulation

environment for the selection of computing models for intelligent manufacturing is set up in MATLAB R2020a. A scenario of the intelligent production line is established in the simulation environment, the production object is the personalized candy packaging, and the production link, which is the manufacturing task, is the identification of multiple categories of candy. The size of task data is randomly selected between 1 and 10 Mb, and the number of tasks is taken as 10, 30, 40, 50, 90, 100, 300, 500, 700, and 900, respectively. The parameter set in the simulation is shown in Table 1.

5.2. Simulation Analysis. The delay and energy consumption of the method under the different number of task requests and the reliability of the method for task execution are important evaluation metrics for the performance of the task scheduling method. In the following, the heuristic task scheduling strategy for intelligent manufacturing in big data-driven fog computing environment proposed in this paper is compared and analyzed with the methods proposed in References [16, 17, 20] under the same conditions in terms of three evaluation metrics.

First, the comparative analysis for the delay of the methods is conducted under the different number of task requests. The performance of delay in different methods is simulated in two different cases with a small number of task requests and a large number of task requests. The results are shown in Figures 4 and 5, respectively.

As can be seen from Figures 4 and 5, the delay of all task scheduling strategies tends to rise as the number of tasks increases. However, compared to the other three methods, the heuristic task scheduling strategy proposed in this paper is more advantageous in terms of delay, as it has a smaller delay both in the case of a smaller number of task requests and in the case of a larger number of task requests. The delay is 123.4 s and 361.3 s, respectively when the number of task requests is 100 and 500. This is because the proposed method can better allocate the time-critical task requests to the fog computing resource nodes for execution. Compared with the traditional methods that all of the tasks are executed on the cloud, it can more effectively reduce the delay.

The energy consumption of the methods under the same conditions when there are different numbers of task requests is compared, and the results are shown in Figure 6.

It is shown in Figure 6 that the energy consumption of the system all shows an increasing trend with more task requests. However, the energy consumption of the proposed strategy is always the smallest and the most energy efficient compared to the other three comparison methods. When the number of task requests is 100 and 500, the energy consumption is 205.2 J and 352.4 J, respectively. The energy consumption of the task is determined by the delay of the task and the power of the computing node. In addition, the power of the computing node is a fixed value, and the delay of the task is the main factor that affects the performance of energy consumption of the task. As the delay of the proposed method is small, its energy consumption is also relatively small.

Table 1: Simulation experiment parameters.

Parameter	Value
Number of intelligent terminal devices	200
Number of fog nodes	15
The size of task data (Mb)	1–10
Maximum tolerance time for task	1–3 s
Computing capacity of cloud server (Gcycles/s)	10
Computing capacity of cloud server (W)	50
Computing capacity of fog nodes (Mcycles/s)	300–500
Computational density of tasks (cycles/bit)	300
Transmission power of smart device (M)	3–6
Computational power of smart device (M)	3–6
Network bandwidth of smart device (M)	150
Fog node network bandwidth (M)	120
Cloud server network bandwidth (M)	5
Real-time intensity weight for tasks	0.8
Complex intensity weight for tasks	0.3
Crossover rate	0.8
Mutation rate	0.1
The maximum number of iterations	150
Number of species	100

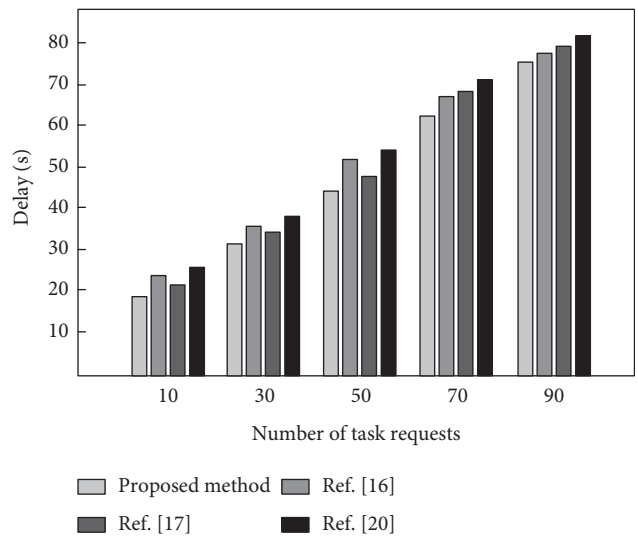

Figure 4: Delay of different methods in the case of a small number of task requests.

Then, the success rate of task execution is calculated for the different number of task requests under the same conditions to verify the reliability of the respective methods. The results of success rates of task execution are shown in Figure 7.

As shown in Figure 7, the reliability of all four methods decreases as the number of tasks increases, but the reliability of the proposed method decreases the least and it remains the highest as the number of task requests changes. The task execution success rates of 95.3% and 94.6% are achieved for 100 and 500 task requests, respectively. This is because the proposed method takes into account the delay matrix, the energy consumption matrix and the reliability matrix in the process of objective optimization. The traditional genetic algorithm is improved in the calculation process. In the proposed method, the fitness function is used to calculate the

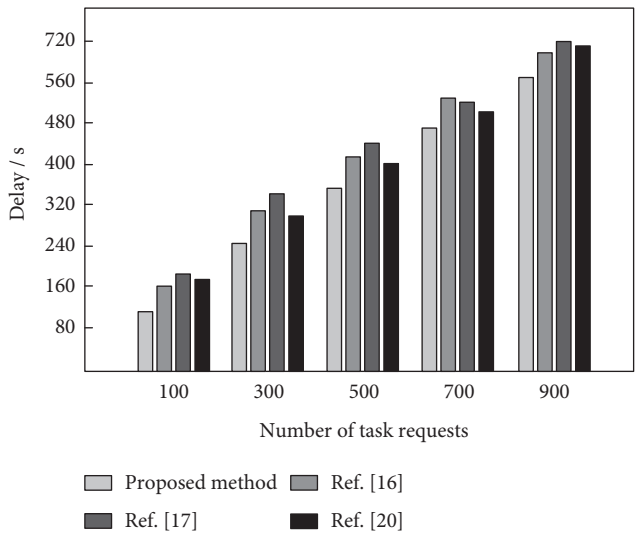

Figure 5: Delay of different methods in the case of a large number of task requests.

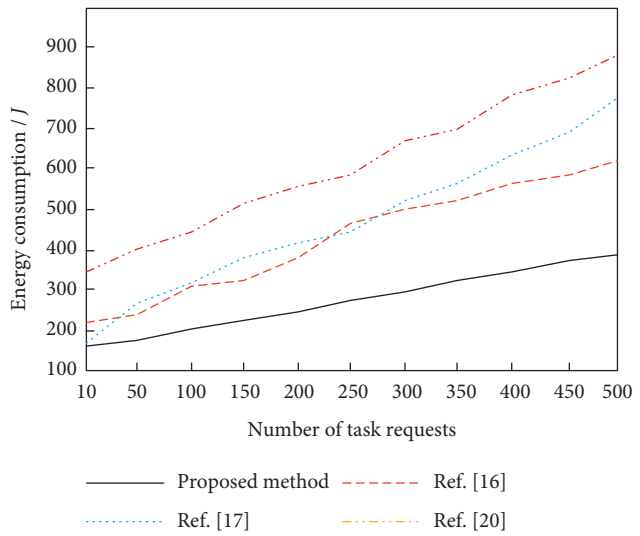

Figure 6: Energy consumption of different methods under different number of task requests.

fitness value of individuals in the population, and all individuals are divided into different intervals according to their fitness values. Also, the crossover-mutation operators are divided by intervals. Therefore, it can generate better individuals in the global scope, which improves the success rate and reliability of the proposed method in task execution.

6. Conclusion

A heuristic task scheduling strategy for intelligent manufacturing in the big data-driven fog computing environment is proposed to address the problems of prolonged delay, high energy consumption, and low reliability of resource scheduling and allocation methods in the fog computing environment. The proposed method and three other comparative methods are compared and analyzed through

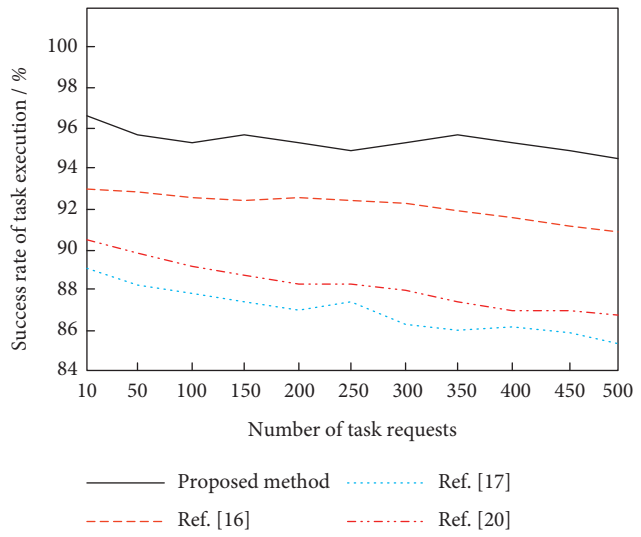

Figure 7: Success rate of task execution of different methods under the different number of task requests.

simulation experiments. The results show that the comprehensive consideration of fog nodes, fog servers, and fog gateways on the basis of intelligent terminal devices and the cloud can significantly improve the utilization of fog computing resources. Optimization of the objective function with the constraints of delay, energy consumption, and success rate can improve the overall performance of the algorithm. By dividing the crossover-mutation operators into intervals, the genetic algorithm can generate better individuals and thus improve the reliability of task scheduling. Future work will delve into the impact of the dynamic characteristics of network and storage resources on fog computing and the improvement method.

Data Availability

The data used to support the findings of this study are included within the article.

Conflicts of Interest

The author declares that there are no conflicts of interest regarding the publication of this paper.

References

[1] S. D. Wang, T. Y. Zhao, and S. C. Pang, "Task scheduling algorithm based on improved firework algorithm in fog computing," *IEEE Access*, vol. 8, no. 15, Article ID 32385, 2020.

[2] K. Matrouk and K. Alatoun, "Scheduling algorithms in fog computing: a survey," *International Journal Of Networked And Distributed Computing*, vol. 9, no. 1, pp. 59–74, 2021.

[3] M. Kazemi, S. Ghanbari, and M. Kazemi, "Divisible load framework and close form for scheduling in fog computing systems," in *Proceedings of the 4th International Conference on Soft Computing and Data Mining (SCDM)*, pp. 323–333, Melaka, Malaysia, January 2020.

[4] Z. N. Liu, X. M. Yang, Y. Yang, K. Wang, and G. Mao, "DATS: dispersive stable task scheduling in heterogeneous fog networks," *IEEE Internet of Things Journal*, vol. 6, no. 2, pp. 3423–3436, 2019.

[5] H. Rafique, M. A. Shah, S. U. Islam, T. Maqsood, S. Khan, and C. Maple, "A novel bio-inspired hybrid algorithm (NBIHA) for efficient resource management in fog computing," *IEEE Access*, vol. 7, no. 6, Article ID 115760, 2019.

[6] P. Varshney and Y. Simmhan, "Characterizing application scheduling on edge, fog, and cloud computing resources," *Software: Practice and Experience*, vol. 50, no. 5, pp. 558–595, 2020.

[7] H. E. Refaat and M. A. Mead, "DLBS: decentralize load-balance scheduling algorithm for real-time IoT services in mist computing," *International Journal of Advanced Computer Science and Applications*, vol. 10, no. 9, pp. 92–100, 2019.

[8] M. R. Hossain, M. Whaiduzzaman, A. Barros et al., "A scheduling-based dynamic fog computing framework for augmenting resource utilization," *Simulation Modelling Practice and Theory*, vol. 111, no. 37, pp. 201–209, 2021.

[9] B. Jamil, M. Shojafar, I. Ahmed, A. Ullah, and K. Munir, "A job scheduling algorithm for delay and performance optimization in fog computing," *Concurrency and Computation: Practice and Experience*, vol. 32, no. 7, pp. 323–330, 2019.

[10] S. Ghanavati, J. Abawajy, and D. Izadi, "Automata-based dynamic fault tolerant task scheduling approach in fog computing," *Ieee Transactions On Emerging Topics In Computing*, vol. 10, no. 1, pp. 488–499, 2022.

[11] R. M. Ding, X. J. Li, X. Liu, and J. Xu, "A cost-effective time-constrained multi-workflow scheduling strategy in fog computing," in *Proceedings of the 16th International Conference on Service-Oriented Computing (ICSOC)*, pp. 194–207, Hangzhou, China, November 2019.

[12] R. Vijayalakshmi, V. Vasudevan, S. Kadry, and L. K. Ramasamy, "Optimization of makespan and resource utilization in the fog computing environment through task scheduling algorithm," *International Journal of Wavelets, Multiresolution and Information Processing*, vol. 18, no. 1, pp. 37–35, 2020.

[13] J. H. Sun, S. Choudhury, and K. Salomaa, "An online fair resource allocation solution for fog computing," *International Journal of Parallel, Emergent and Distributed Systems*, vol. 3, no. 2, pp. 105–113, 2022.

[14] H. Y. Sun, H. Q. Yu, and G. S. Fan, "Towards energy and time efficient resource allocation in IoT-fog-cloud environment," in *Proceedings of the 16th International Conference on Service-Oriented Computing (ICSOC)*, pp. 387–393, Hangzhou, China, November 2019.

[15] O. H. Ahmed, J. Lu, A. M. Ahmed, A. M. Rahmani, M. Hosseinzadeh, and M. Masdari, "Scheduling of scientific workflows in multi-fog environments using markov models and a hybrid salp swarm algorithm," *IEEE Access*, vol. 8, no. 51, Article ID 189404, 2020.

[16] G. S. Li, Y. C. Liu, J. H. Wu, D. Lin, and S. Zhao, "Methods of resource scheduling based on optimized fuzzy clustering in fog computing," *Sensors*, vol. 19, no. 9, pp. 352–360, 2019.

[17] M. Yang, H. Ma, S. Wei, Y. Zeng, Y. Chen, and Y. Hu, "A multi-objective task scheduling method for fog computing in cyber-physical-social services," *IEEE Access*, vol. 8, no. 12, Article ID 65085, 2020.

[18] Z. B. Ren, T. Lu, X. Wang, W. Guo, G. Liu, and S. Chang, "Resource scheduling for delay-sensitive application in three-layer fog-to-cloud architecture," *Peer-To-Peer Networking And Applications*, vol. 13, no. 5, pp. 1474–1485, 2020.

[19] M. Mukherjee, M. Guo, J. Lloret, R. Iqbal, and Q. Zhang, "Deadline-aware fair scheduling for offloaded tasks in fog computing with inter-fog dependency," *IEEE Communications Letters*, vol. 24, no. 2, pp. 307–311, 2020.

[20] L. Tang, J. Jiang, and K. Gu, "Computing resource allocation scheme based on fog computing," *Computer Engineering and Application*, vol. 55, no. 19, pp. 96–104, 2019.

[21] F. Alqahtani, M. Amoon, and A. A. Nasr, "Reliable scheduling and load balancing for requests in cloud-fog computing," *Peer-To-Peer Networking And Applications*, vol. 14, no. 4, pp. 1905–1916, 2021.

[22] B. Sarma, R. Kumar, and T. Tuithung, "Optimised fuzzy clustering-based resource scheduling and dynamic load balancing algorithm for fog computing environment," *International Journal of Computational Science and Engineering*, vol. 24, no. 4, pp. 343–353, 2021.

Hindawi
Mobile Information Systems
Volume 2022, Article ID 2205362, 10 pages
https://doi.org/10.1155/2022/2205362

Research Article

Innovation of Visual Communication Design Based on Wireless Virtualization Network Architecture

Hua Zhu

Art College of Zhengzhou Business University, Zhengzhou 451200, China

Correspondence should be addressed to Hua Zhu; 1601412134@zjbti.net.cn

Received 25 June 2022; Revised 28 July 2022; Accepted 8 August 2022; Published 25 August 2022

Academic Editor: Shadi Aljawarneh

With the continuous development of the times and the continuous development of science and technology, embedded technology is constantly improving and more and more innovative methods have broken the situation of traditional multimedia use and combined visual language with design models, which has promoted the development of culture and the development of science and technology. The purpose of this experiment is to design a new structure by combining it with an image processing system based on embedded technology. In the experiment, we will use the QT graphics interface to connect with another same system interface, according to the characteristics of embedded technology data and image processing, design a new interface model, make the image binary, and then use calculations to prove the new feasibility of the way. In this report, we showed some of the programming steps and fully explained the design and results of the model, but it took a long time. The result of the test is that the embedded technology has a long-term experimental value and application value because the system can process images in real time and collect and store data faster; the resolution of the obtained images is also higher, and less energy is lost.

1. Introduction

With the continuous development of the times and the continuous development of science and technology, embedded technology is constantly improving, and the technology that people use to process images is also constantly developing, so more and more people are focusing on embedded technology [1]. Before wireless network systems and computer technology have been widely promoted, people often transmit collected pictures and data through analog circuits and then use other systems to organize the data. Since the world's first computer came out in the 1940s, the world's science and technology are developing faster and faster, and more and more people are focusing on the upgrading of intelligent technology [2]. The collection and analysis of image data are one of them. The collection and analysis of image data have an important position in many fields because this technology must be used in security monitoring or network teaching. Therefore, image data acquisition and analysis technology have become an important part of social development and research progress. Nowadays, the 4G era is gradually replaced by the rapid development of 5G. The rapid development of 5G has brought about major changes in Internet technology and has also produced major changes in people's lifestyles, but it has also produced many problems. Moreover, the research and update of the network system is too complex, so the development of embedded technology is not plain sailing. The network data processing time is too long, the amount of information is too large, the system is unstable, and other problems need to be solved [3, 4]. In the era of rapid development, visual technology has been combined with science and technology to become a comprehensive discipline, which can not only diversify the development of model design but also promote people's innovative thinking. Nowadays, people have abandoned traditional design models and have carried out new model designs in multimedia systems and other aspects. Electronic products have gradually replaced the original models, and the newly developed models have also brought huge benefits to the development of multimedia under the Internet. With changes, printed products such as newspapers and magazines have gradually become less popular.

2. Related Work

Some research pointed out that, with the continuous advancement of science and technology, the country's comprehensive capabilities have made significant progress, the society is constantly developing, people's quality of life has been significantly improved, and the improvement and development of new design technology has continuously made art [5]. The land is progressing, and we must seize the opportunity to create a better future. There are different design methods and design thinking in different periods, and the continuous development of science and technology has played a role in promoting visual design in various fields, and more and more methods can be applied to visual technology. Nowadays, people are not only entrepreneurs but also occupy a certain position in the embedded technology level. Each field needs to update and upgrade the new model according to the characteristics of its field, so as to achieve the development of technology. More and more types of multimedia technologies provide great convenience for us to conduct experiments, but they also face certain challenges. So, we have to extract the advantages of traditional culture and combine it with new designs to create the best modern civilization. We must seize the opportunity, open up our minds, and use high technology to achieve innovative development. Some research believes that if we want to innovate a certain system, it must be affected by science and technology and social culture, so when we carry out scientific and technological reforms and Internet technology updates, some new designs will appear. With the increase of new technologies and new multimedia, social civilization is constantly increasing, people's spiritual power is constantly accumulating, and society is constantly changing. Some research shows that, through data surveys, we can know that, in the last few decades, science and technology have penetrated into every part of the world, and we are now inseparable from science and technology. More and more people use the Internet, regardless of whether it is industry, agriculture, or handicraft, all rely on high-tech products to operate [6]. Today, more than 4.5 billion people worldwide are using the Internet, but there are also many problems. The Internet has higher and higher requirements for data storage systems and signal transmission systems. The internal procedures of the Internet system are becoming more and more complex. We no longer use traditional methods, and gradually increase service functions to improve network security. Some research proposes that today's image analysis technology is more modern, and the collection and analysis of image data are applied in various fields, including aviation, agriculture, and industry. The rapid transmission of data is the prerequisite for data analysis, so we must tell the importance of the rapid transmission of data. Some research proposed that the way of information transmission has undergone tremendous changes. Since the rapid development of multimedia technology, the traditional transmission method has become a thing of the past. Nowadays, most people use advanced multimedia for communication and the transmission method of the visual system, which has changed greatly compared with the past. For model builders, we need to have a long-term vision, use visual language in a flexible way, and combine visual information with the information conveyed by pictures to make data transmission more efficient and effective. Users were given better experience. Some research pointed out that the development of wireless network technology nowadays still needs a certain amount of time to complete because the number of Internet users has become more and more, and more and more functions are needed. At the same time, 5G technology needs to be more perfect. The existing network management model can no longer meet the needs of users, so the combination of virtualization technology and Internet technology is our best choice.

3. Wireless Network and Embedded Digital Image System Design

3.1. Related Research on Wireless Network Virtualization. The traditional Internet model framework has no way to promote the development of network virtualization technology. Therefore, if we want to carry out the original cellular data at night, we must introduce a wireless network system and build a new model based on wireless network technology. This is an important link in the development of virtualization technology.

We can combine the wireless network system with the virtualized structure and divide the virtualized structure into three levels: data collection plane, joint cooperation plane, and virtualized control plane [7]. The new frame structure in the wireless network system and the different manifestations and functions of each level are shown in Figure 1.

3.1.1. Data Collection Plane. The data collection plane refers to the connection of interfaces in different wireless network systems, and data collection stations in different regions can transmit data through similar contacts. We can combine advanced technologies such as 5G, WLAN, Wi Max, and their respective transmission equipment, so that the equipment can quickly transmit data and ensure the normal progress of the experiment [8]. The main function of the data collection plane is to store the information and data in the wireless network system in this plane. In the environment of the wireless network system, each plane is allowed to store wireless resources and use virtualization technology to realize resource allocation.

3.1.2. Joint Cooperation Plane. In the joint cooperation plane, we have carried out real-time monitoring of the information and data in the plane, which can not only make reasonable allocation of resources in wireless network technology but also analyze the specific situation more flexibly. For example, we can use the situation, information status, and geographic location that are monitored. The joint cooperation plane can more accurately detect the quality of the network signal [9]. Through the different ways everyone

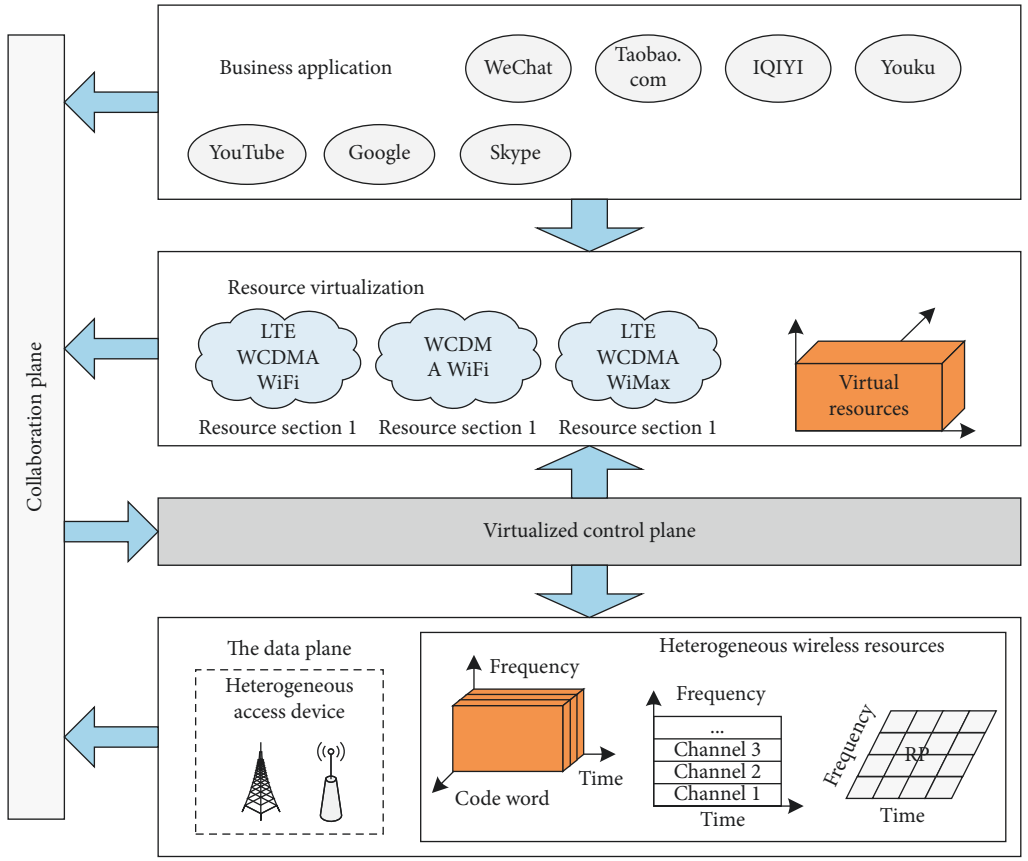

Figure 1: Wireless virtualized network architecture.

use, it can classify the virtualization technology information differently and can also simplify the information interface.

3.1.3. Virtualization Control Plane. The virtualized control plane combines the user's information with the network status. Through the division of wireless network technology functions, different network chips are obtained to form different data partitions. Network chips include the rapidly developing 5G system, which makes network services more complete and enables the use of wireless network technology.

Virtualization technology has many functional advantages and can be applied to various fields. Our main requirement in this network technology is to detect the classification of virtualization technology information. This is an important link in the rapid development of virtualized networks. We can divide this more complex task into multiple models for processing and then classify them and perform data analysis [10, 11]. In addition, for the embedded structure and virtualization technology under different models, the processing methods and required resources are also different, and the difficulty in the solution process is also different. In this case, we divide this technology into two aspects: satisfying node resources and link resource services, so as to minimize the resources consumed in the experiment process, minimizing the cost invested in the experiment process, and making the experiment process maximize the benefits gained from the system, making the system management procedures more perfect and balancing the two service systems.

When we study virtualization technology, we should focus on the links of nodes in the virtual technology system. Through the connection between each node and basic equipment, data can be transmitted and analyzed.

(1) Mathematical Model. The mathematical model is to allocate different resources according to different needs. The specific allocation model is shown. We use appropriate equipment to reasonably classify data and information and then enter it into different business layers. Users can choose different service systems according to their needs, and then the system will provide corresponding services according to users' choices [12, 13]. Because the digital model is a combination of network resources and virtualization technology, in order to achieve experimental results, we need to focus on the measurement of whether the data output is accurate and develop personalized services. Virtual network resource allocation is shown in Figure 2.

(2) Performance Evaluation Model. In the process of resource allocation of science and technology, our requirement is to reduce the use of energy as much as possible, shorten the time used in the experiment, and speed up the processing of information, while maintaining the maximum benefit. The specific benefit obtaining formula is shown as

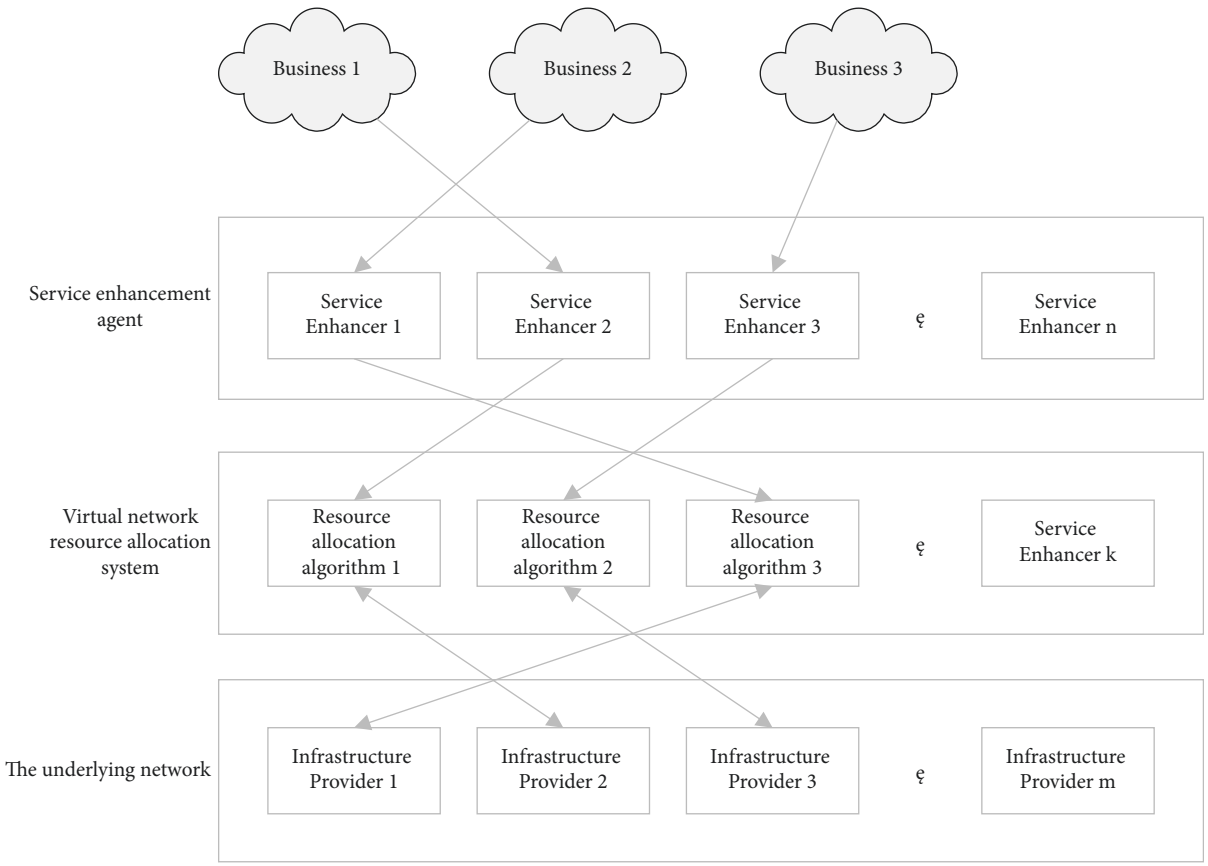

Figure 2: Virtual network resource allocation problem business model.

$$\text{Revenue}\left(G^v, t\right) = \alpha_R \sum_{n^v \in N^v} \text{CPU}\left(n^v\right) + \beta_R \sum_{l^v \in L^v} Bw\left(l^v\right). \quad (1)$$

In the above formula, R is the weight. The specific function is to connect the node with the basic device, and the obtained data can be used as a sample to be brought into the next formula. The specific calculation formula is as follows:

$$\lim_{r \longrightarrow \infty} \frac{\int_{t=0}^{T} \sum_{G^N \in G^N(t)} \text{Revenue}\left(G^v, t\right)}{T}. \quad (2)$$

If we want to ask for the amount of resource consumption required in the virtual technology, we have to reach the node output value and the time used. The specific formula is as follows:

$$\text{Cost}\left(G^v, t\right) = \alpha_R \sum_{n^v \in N^v} \text{CPU}\left(n^v\right) + \beta_C \sum_{l^v \in L^v} \text{hop}\left(l^v\right) \cdot Bw\left(l^v\right). \quad (3)$$

The VI shown in the formula refers to the amount of data successfully passed through the system, and C represents how much energy the node consumes, so the solution formula for the total consumption is as follows:

$$\lim_{r \longrightarrow \infty} \frac{\int_{t=0}^{T} \sum_{G^N \in G^N(t)} \text{Cost}\left(G^v, t\right)}{T}. \quad (4)$$

We compare the energy required during the experiment with the energy required for data classification, we can know the energy consumed by the average network system, and the specific formula is as follows:

$$\lim_{r \longrightarrow \infty} \frac{\int_{t=0}^{T} \sum_{G^N \in G^N(t)} \text{Revenue}\left(G^v, t\right)}{\int_{t=0}^{T} \sum_{G^N \in G^N(t)} \text{Cost}\left(G^v, t\right)}, \quad (5)$$

where T represents that, in the continuous operation mode, the energy required after the node is connected to the basic equipment is

$$\text{Load}\left(N^S, 1\right) = \frac{1}{\left|N^S\right|} \sum_{n^s \in N^S} \left(\frac{\sum_{R^v \uparrow R^E} R\left(n^v\right)}{c\left(n^s\right)} \right). \quad (6)$$

In the above expression, we can know that SN represents the total number of nodes in the system, and the pressure that each node can bear is as follows:

$$\text{Load}\left(L^S, 1\right) = \frac{1}{\left|L^S\right|} \sum_{l^s \in L^S} \left(\frac{\sum_{l^v \uparrow l^E} \text{BW}\left(l^v\right)}{\text{BW}\left(l^s\right)} \right). \quad (7)$$

After the experimental data is successfully transmitted, the proportion of the successfully transmitted data in the overall data is the data transmission success rate. The specific solution formula is as follows:

$$\text{acceptance ratio} = \lim_{r \longrightarrow \infty} \frac{\int_{t=0}^{T} G_B^V(t)}{\int_{t=0}^{T} G^V(t)}. \tag{8}$$

Nowadays, the wired network is developing well, and the wireless network technology needs to be strengthened. There are many problems waiting for us to solve. The specific problems are as follows:

(1) The transmission of wireless signal is poor, and there are often intermittent signals, which affect the transmission of information and uneven resource allocation

(2) The stability of the wireless network is poor, the signal is often interrupted, and the information and data are damaged or lost

(3) Difficulty in the allocation of lines, too long allocation time, and low efficiency

(4) The distribution of resources is unbalanced, and errors sometimes occur in the calculation process, leading to incorrect data results and the entire experiment failure

(5) In the case of poor environmental conditions, wireless networks are often affected, causing signal interruption and resource loss

3.2. Wireless Virtual Network Mapping Algorithm Based on Node Aggregation Centrality. The formula for calculating the energy required by each node is

$$\text{Avail}\left(n^S\right) - \text{CPU}\left(n^S\right) - \sum_{\forall R^V \uparrow R^E} \text{CPU}\left(n^v\right) + \sum_{\forall R^V \uparrow R^E} \text{Rel}\left(\text{CPU}\left(n^v\right)\right). \tag{9}$$

The energy of the remaining nodes in each resource is

$$\text{Avail}\left(l^S\right) - \text{CPU}\left(l^S\right) - \sum_{\forall t^V \uparrow r^E} \text{CPU}\left(l^v\right) + \sum_{\forall t^V \uparrow r^E} \text{Rel}\left(\text{CPU}\left(l^v\right)\right). \tag{10}$$

There are interference signals between each line, so the quality of service will be reduced. The specific interline interference index is

$$\text{LI}\left(l^s\right) = \frac{\gamma . d_i\left(l^S\right).\text{Avail}\left(n_i^S\right) + \omega d_j\left(l^S\right).\text{Avail}\left(n_j^S\right) + 1}{\left(d_i\left(l^S\right) + d_j\left(l^S\right)\right).\text{Avail}\left(l^S(i,j)\right)}. \tag{11}$$

If the energy consumption between the lines is too large, the energy given to other resources will be relatively reduced, so the energy required by the system will increase, and the required cost will increase relatively, so that the load between the lines will also be increased. We can use the following formula to calculate the cost of the line as

$$\text{price}\left(l^S\right) = \frac{\eta}{\text{Avail}\left(l^S\right)}. \tag{12}$$

In the virtual network, the newly constructed VG system can reduce the complexity of the VNC system, and we can calculate the result in two steps. In the first step, we need to select a node that meets the system. The second step is to connect the node and the device in the virtual system to meet its geographic constraints and bandwidth resource constraints. The specific constraint data are as follows:

$$\text{dis}\left(\text{loc}\left(n^v\right)\text{Joc}\left(n^s\right)\right) \le D\left(n^v\right). \tag{13}$$

Figure 3 reflects the mapping process and mapping results of virtual network technology.

In virtual network technology, we have to consider the importance of nodes. In order to enable each node to connect with its neighboring nodes, we need to upgrade the network system so that the database can store more resources so that the nodes can be linked. The signal is better, which is conducive to the experiment. The specific definition is as follows:

$$\text{DC}^v\left(n_1\right) = \sum_{t^N \longrightarrow \infty} l^v(i). \tag{14}$$

In virtual technology, we have to consider the overall development, so the stronger the connection between the node kernels, the more data can be processed. The kernel strength of the nodes in the virtual technology system is defined as

$$\text{BC}^v\left(n_1\right) = \frac{P_1}{p}. \tag{15}$$

The relationship between a node and its neighbors is close, and the evaluation formula for the importance of a node is

$$E^V = \begin{bmatrix} BC_1DC_1 & \frac{a_{12}BC_2DC_2DC_2}{2m} & \cdots & \frac{a_{1n}BC_nDC_1DC_n}{2m} \\ \frac{a_{21}BC_1DC_2DC_1}{2m} & BC_2DC_2 & \cdots & \frac{a_{2n}BC_nDC_2DC_n}{2m} \\ \vdots & \vdots & \cdots & \vdots \\ \frac{a_{n1}BC_1DC_nDC_1}{2m} & \frac{a_{n2}BC_2DC_nDC_2}{2m} & \cdots & BC_nDC_n \end{bmatrix}. \tag{16}$$

The specific experimental results are as follows:

$$\text{BAC}^v\left(n_1\right) = \sum_{j=1}^{n} E^v(i,j) = \text{DC}^v\left(n_1\right)\text{BC}^v\left(n_1\right) + \sum_{j=1, j \ne i}^{n} E^v(i,j). \tag{17}$$

In the physical network structure, we need to consider the problem comprehensively, so we combine the distance between the nodes and the tightness of the node kernel, and the formula is

$$\text{CC}^s\left(n_1\right) = \sum_{j=1}^{n} \text{CPU}^s\left(n_1\right) \times e^{-\left(d(i,j)LI^R(i,j)/\text{MwBw}^s(i,j)\right)}. \tag{18}$$

Through the above analysis, we used the distance between the nodes and the connection between the node kernels to measure the physical network structure, and the obtained node evaluation method is

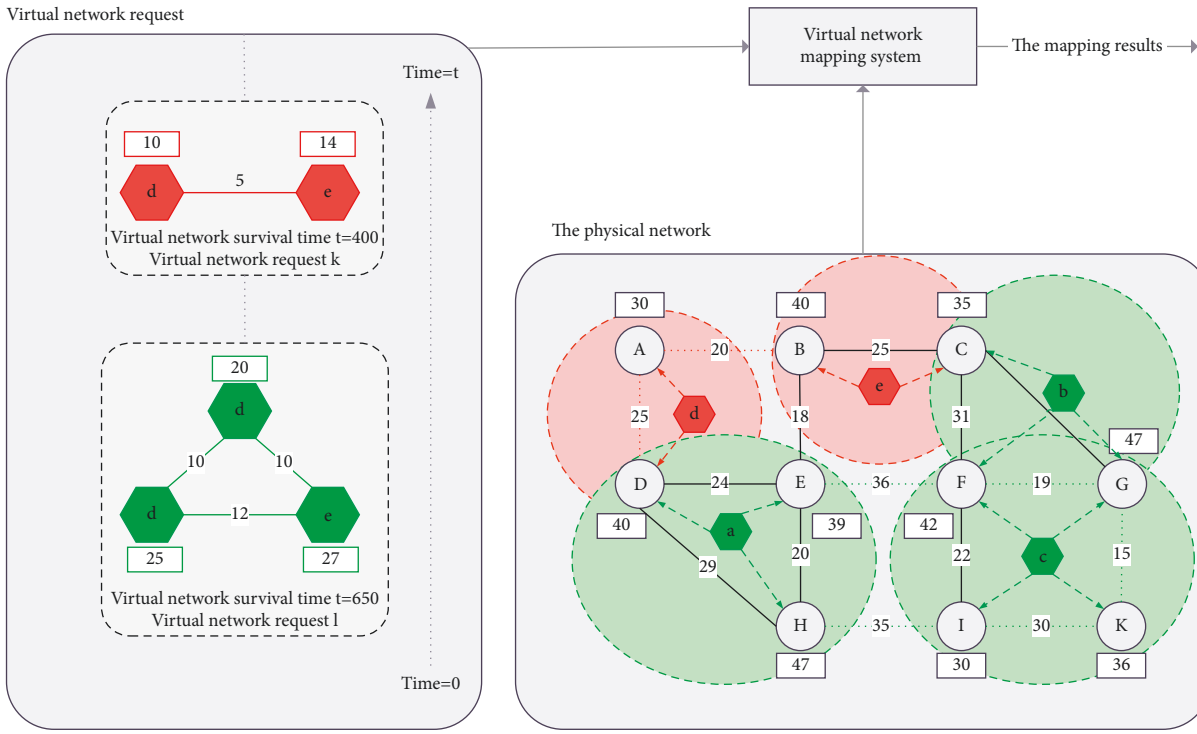

Figure 3: Virtual network request mapping scheme.

$$E^V = \begin{bmatrix} CC_1DC_1 & \frac{b_{12}CC_2DC_2DC_2}{2e} & \cdots & \frac{b_{1h}CC_hDC_1DC_h}{2e} \\ \frac{b_{21}CC_1DC_2DC_1}{2e} & CC_2DC_2 & \cdots & \frac{b_{2h}CC_hDC_2DC_h}{2e} \\ \vdots & \vdots & \cdots & \vdots \\ \frac{b_{h1}CC_1DC_hDC_1}{2e} & \frac{b_{h2}CC_2DC_hDC_2}{2e} & \cdots & CC_hDC_h \end{bmatrix}. \quad (19)$$

Through the interconnection between nodes, the kernel distribution density of physical nodes is obtained as

$$\mathrm{CAC}^v(n_1) = \sum_{k=1}^{h} E^S(k,g) = \mathrm{DC}^S(n_k)\mathrm{CC}^S(n_k) + \sum_{k=1,g\neq k}^{h} E^S(k,g). \quad (20)$$

In order to expand the bandwidth distance between nodes, we obtain the definition by the following formula:

$$\mathrm{Local}(n^v) = \mathrm{Avail}(n^v) \times \left(\frac{\sum_{t^v \in t(N^T)}^{t^v} \mathrm{Avail}(l^v)}{d(L(n^v))} \right). \quad (21)$$

Based on the data obtained, the virtual node mapping priority variable is solved:

$$\mathrm{EP}^v(n^v) = \mathrm{Local}(n^v) \times \mathrm{BAC}^v(n^v). \quad (22)$$

We sort these nodes and then operate according to the order and select different data according to different node characteristics. The formula for expanding the distance between nodes is as follows:

$$\mathrm{Local}(n^s) = \mathrm{Avail}(n^s) \times \left(\frac{\sum_{t^s \in t(N^s)}^{t^s} \mathrm{Avail}(l^s)}{d(L(n^s)\mathrm{LI}(I^s))} \right). \quad (23)$$

We can learn from the calculation formula of the node and process the mapping priority variable of the physical node according to the physical network. The specific formula is

$$\mathrm{EP}^s(n^s) = \mathrm{Local}(n^s) \times \mathrm{CAC}^s(n^s). \quad (24)$$

The acceptance rate calculated by different algorithm formulas is different. The NACA structure is obviously better than other calculation methods because the NACA structure comprehensively analyzes the connections and characteristics between nodes from a global perspective, which not only makes the experiment process more reasonable but also makes the results of the experiment more accurate [14]. Figure 4 shows the comparison of the load intensity of the underlying node structure of the physical network. It can be seen from Figure 4 that the load intensity of the NACA structure is smaller, which is conducive to resource conservation and utilization. Average mapping overhead is shown in Figure 5.

Figure 5 shown above compares the NACA structure with another model. The NACA structure mainly analyzes the resources used between nodes. In order to make the results of the experiment more in line with the requirements, we can choose a suitable location and enrich the data resources. At the same time, in order to reduce resource consumption and prevent signal interruption, we can calculate the load level through the cost of node connection.

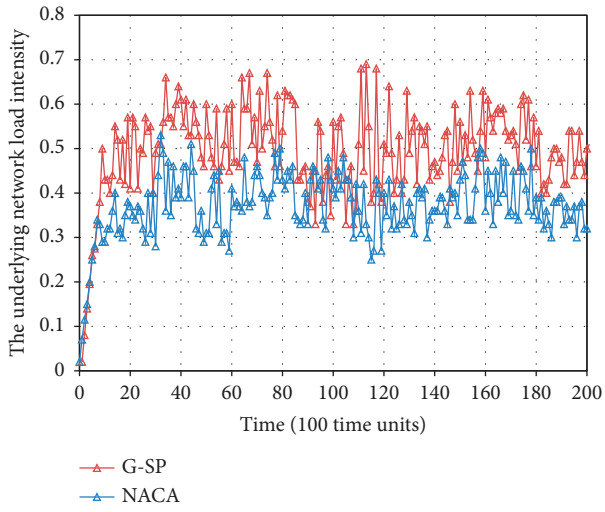

Figure 4: Underlying network load intensity.

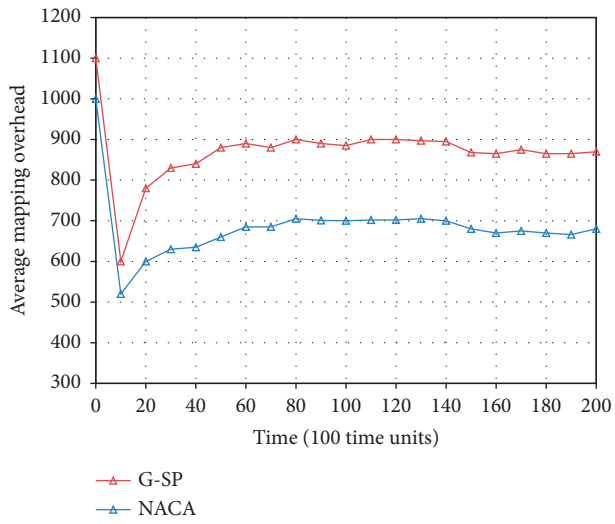

Figure 5: Average mapping overhead.

3.3. Zynq Embedded Platform and Key Technologies. The processor systems can be connected through different interfaces to make the signal of each link better, and the processor system can also analyze data faster [15]. We can divide the functions of the processor system into functional interfaces and hardware interfaces. The former can control signal transmission and the latter can program the processor system to realize data exchange. Various interface performance is shown in Table 1.

In order to make the signal more stable and reduce the dependence on the system during data transmission, we use the AIX interface as the main transmission tool. Classification of AXI protocol is shown in Table 2.

The summary of specific data transmission methods is shown in Table 3.

The specific signal changes are shown in Table 4.

4. Innovation and Development of Visual Communication Design

4.1. Practical Innovation of Visual Communication Design. With the development of multimedia technology, visual technology has also been greatly improved, and people have begun to use new methods to replace traditional methods for communication and interaction. The visual communication design in the new media era is a continuation of the traditional printing design, but it is not limited to pure beautification and information transmission, but more people are involved to interact and communicate with it.

The dynamic design under the multimedia technology has increased the frequency of people's interaction. The dynamic design is getting better and better at any time, and the user experience is getting better and better. In new media, the "dynamic" of dynamic design not only refers to the dynamic performance of visual elements but also the dynamics of information dissemination media. Broadly speaking, the process of new media dissemination of information is dynamic, which reflects the strong interaction of new media dissemination [16]. Through the visual dynamic design, the people's attention reception rate is significantly increased, so that visual information can be presented more accurately. The combined moving and changing graphics carry a richer amount of information, allowing people to stay focused on the changing images for a long time, so that visual information can be accurately and effectively delivered to the audience.

We can communicate not only with images but also with words, so the font design can stimulate people's eyeballs and be more artistic. Font design is the use of styling rules and expression skills for the connotation of fonts through in-depth creative thinking development, so that it has both innovative aesthetic vision and better semantic transmission. Image design is an analysis of text. Through media, dynamic design is more valuable and can also promote the development of commercialization [17, 18]. At present, the application of visual image design is more extensive, from books and magazines to the current digital media such as web pages and mobile apps. As the media changes, its artistic language and expression space have also changed, not only for traditional static but also for more infectious dynamics.

4.2. Thinking and Prospect of Visual Communication Design. Multimedia technology is a derivative of the development of science and technology and has a bright future and a research value. We must overcome difficulties and improve visual technology. The development of media technology has injected fresh blood into art design and brought new directions to the research of visual design in the new era. In terms of its nature, new media is a new thing born of scientific and technological innovation and development. It is full of vigor and vitality and has bright and unlimited development prospects.

With the continuous development of multimedia technology, intelligent systems and digital systems occupy a dominant position, and their forms are becoming more and

Table 1: Various interface performance of PS and PL.

Interface	Types	Interface bit width (bit)	Interface time type (MHz)	Read/write bandwidth (MB/S)	Number of interfaces	Total bandwidth (MB/S)
AXI_GP	Slave interface	32	150	600	2	2400
AX1_GP	Main interface	32	150	600	2	2400
AXI_HP	Slave interface	64	150	1200	4	9600
AXI_ACP	Slave interface	64	150	1200	1	2400
DDR	External storage	32	1066	4264	1	4264
OCM	Internal storage	64	222	1799	1	3557

Table 2: Classification of AXI protocol.

Interface	Characteristic	Similar agreement
AXI4	Address/burst data transmission	PLBv46, AHB
AXI4-stream	Only transfer data, burst transfer	Local link, FIFO
AXI4-lite	Address/single data transmission	PLBv46-single. APB

Table 3: Comparison table of PS and PL data transmission methods.

The way	Advantage	Disadvantage	Suggested use	Estimated throughput rate
CPU control I/O	Simple software, minimal logic resources, simple logic access	Lowest throughput rate	Control function	<25 MB/s
PS part controls DMAC	Minimal logic resources, medium throughput rate, multiple channels, simple logic interface	DMAC configuration is difficult	When PL's DMA is not enough	600 MB/S
DMA in AX1_HP and PL	Highest throughput rate, multiple interfaces with FIFO buffer	Can only access DDR/OCM. Complex logic design.	High-performance transmission of large blocks of data	1200 MB/S
AXI_ACP and DMA in PL	The highest throughput and lowest latency can be selected as cache consistency	Large block data transfer causes cache problem, shares CPU bandwidth, and more complex logic design	High-speed data transmission directly related to small blocks and cache	1200 MB/S
DMA in AXI_GP and PL	Moderate throughput rate	More complex logic design	The module used for PL to control the PS accesses the I/O peripherals of the PS part	600 MB/S

Table 4: VDMAIP core system signal.

Signal name	Input/output	Function description
m_axi_mm2s_aclk	Input	AX14 read clock
m_axi_s2mm_aclk	Input	AX14 write clock
m_axis_mm2s_aclk	Input	AXI4-stream read clock
m_axis_s2mm_aclk	Input	AXI4-stream and clock
axi_resetn	Input	VDMA reset

more diverse. They have brought tremendous impetus to the development of society, and more and more people are thinking about problems with innovative thinking. New ideas have been imported into the world. One thing we need to admit is that the continuous development of multimedia technology and the continuous digitization and informatization of the world are all important foundations for the dissemination of advanced cultures and also important factors for promoting cultural diversity. When we are immersed in the convenience brought by the continuous development of multimedia, some problems also arise, such as how to make the system more complete and more efficient. Science and technology are our means of survival and are our indispensable tools. Therefore, if we want to develop visual technology, we must combine visual technology with science and technology to better complete the experiment.

The development of science and technology is the guarantee of people's lives and the foundation of national development. Therefore, the emergence of new multimedia is the fundamental reason for promoting the development of visual technology, and it is an important embodiment of science and technology in the field of art. The development of visual technology is based on the development of science and technology. On this basis, innovative thinking and human aesthetic requirements are added to enable its functions to meet people's needs and provide convenient conditions for people's lives. With the continuous development of the times, there have been great changes in visual technology. People combine their innovative thinking with computer networks, multimedia functions, and various software and platforms to design more distinctive models. Making the connection between art and science and technology closer, not only promoted social changes but also changed the traditional communication methods, replacing traditional paper information exchange with multimedia technology and making the art field gradually become the main industry of social development.

5. Conclusion

With the continuous development of the times and the continuous development of science and technology, embedded technology is constantly improving, and the technology that people use to process images is also constantly evolving, so more and more people are focusing on embedded technology. In terms of image processing technology, these two technical methods have become very popular research projects at the moment and are used in many fields, including agriculture, industry, and medicine. In virtual systems, the development of wired networks is relatively mature, so more and more people are focusing on wireless network systems, but there are still many difficulties in developing wireless network systems. With the broadening of people's thinking, more and more innovative methods have broken the situation of traditional multimedia use and combined visual language with design models, which has promoted the development of culture and the development of science and technology. The purpose of this experiment is to design a new structure by combining it with an image processing system based on embedded technology. In the experiment, we will use the QT graphics interface to connect with another same system interface, according to the characteristics of embedded technology data and image processing, design a new interface model, make the image binary, and then use calculations to prove the new feasibility of the way. In this report, we showed some of the programming steps and fully explained the design and results of the model, but it took a long time. The result of the test is that the embedded technology has a long-term experimental value and application value because the system can process images in real time, collect and store data faster; the resolution of the obtained images is also higher, and less energy is lost. We will continue to work hard to make the embedded technology more perfect.

Data Availability

The data used to support the findings of this study are available from the author upon request.

Conflicts of Interest

The author declares no conflicts of interest.

Acknowledgments

This work was supported by the Research on the Innovation Path of Henan Intangible Cultural Heritage Promoting Rural Revitalization under the Background of Agricultural, Tourism, and Cultural Integration, Henan Soft Science Research Plan Project, under project no. 222400410416; ZhengzhouB usiness University , Cultural Tourism and Rural Revitalization Integration Innovation Research Team, under project no. 2021-cxtd-06; and Research on the Activation and Inheritance Path of Traditional Village Culture in Rural Revitalization under the Background of Cultural and Tourism Integration, A School Level Project of Zhengzhou Business University.

References

[1] N. Dutt, A. Jantsch, and S. Sarma, "Toward smart embedded systems," *ACM Transactions on Embedded Computing Systems*, vol. 15, pp. 1–27, 2016.

[2] J. U. Hou and H. K. Lee, "Layer thickness estimation of 3D printed model for digital multimedia forensics," *Electronics Letters*, vol. 55, pp. 86–88, 2019.

[3] W. Zheng, H. Wu, and C. Nie, "Integrating task scheduling and cache locking for multicore real-time embedded systems," *ACM SIGPLAN Notices*, vol. 52, no. 5, pp. 71–80, 2017.

[4] P. P. Nair, A. Sarkar, N. M. Harsha, M. Gandhi, P. P. Chakrabarti, and S. Ghose, "ERfair scheduler with processor suspension for real-time multiprocessor embedded systems," *ACM Transactions on Design Automation of Electronic Systems*, vol. 22, pp. 1–25, 2016.

[5] L. Zhang, *The visual elements in film poster design based on photoshop," Big Data Analytics for Cyber-Physical System in Smart City. BDCPS 2019*, Springer, Shenyang, China, pp. 1620–1625, 2020.

[6] J. Reyna, J. Hanham, and P. Meier, "A taxonomy of digital media types for Learner-Generated Digital Media assignments," *E-Learning and Digital Media*, vol. 14, pp. 309–322, 2017.

[7] S. S. S. Kruthiventi, K. Ayush, and R. V. Babu, "DeepFix: a fully convolutional neural network for predicting human eye fixations," *IEEE Transactions on Image Processing*, vol. 26, pp. 4446–4456, 2017.

[8] X. Chen, X. Hu, and J. Zhu, "Minimum Data Aggregation Time Problem in Wireless Sensor Networks," in *Mobile Ad-Hoc and Sensor Networks, vol. 3794 Of lecture notes in computer science*, pp. 133–142, Springer, Berlin, Germany, 2005.

[9] Q. Bramas and S. Tixeuil, "The complexity of data aggregation in static and dynamic wireless sensor networks," *Information and Computation*, vol. 255, no. 3, pp. 369–383, 2017.

[10] S. C.-H. Huang, P.-J. Wan, C. T. Vu, Y. Li, and F. Yao, "Nearly constant approximation for data aggregation scheduling in wireless sensor networks," in *Proceedings of the 26th IEEE*

International Conference on Computer Communications, pp. 366–372, IEEE, Anchorage, AK, USA, May 2007.

[11] J. Wolfartsberger, "Analyzing the potential of virtual reality for engineering design review," *Automation in Construction*, vol. 104, pp. 27–37, 2019.

[12] H. Abulkasim, H. N. Alsuqaih, W. F. Hamdan et al., "Improved dynamic multi-party quantum private comparison for next-generation mobile network," *IEEE Access*, vol. 7, pp. 17917–17926, 2019.

[13] A. Ghosh, Ö. D. Incel, V. S. A. Kumar, and B. Krishnamachari, "Multichannel scheduling and spanning trees: throughput–delay tradeoff for fast data collection in sensor networks," *IEEE/ACM Transactions on Networking*, vol. 19, pp. 1731–1744, 2011.

[14] J. Yang, C. Wang, B. Jiang, H. Song, and Q. Meng, "Visual perception enabled industry intelligence: state of the art, challenges and prospects," *IEEE Transactions on Industrial Informatics*, vol. 17, no. 3, pp. 2204–2219, 2020.

[15] S. Ji, R. Beyah, and Z. Cai, "Snapshot/continuous data collection capacity for large-scale probabilistic wireless sensor networks," in *Proceedings of the IEEE Conference on Computer Communications, INFOCOM*, pp. 1035–1043, Orlando, FL, USA, March 2012.

[16] F. Tian, "Immersive 5G virtual reality visualization display system based on big-data digital city technology," *Mathematical Problems in Engineering*, vol. 2021, 9 pages, Article ID 6627631, 2021.

[17] J. Grönkvist, "Assignment methods for spatial reuse TDMA," in *Proceedings of the 1st ACM international symposium on Mobile ad hoc networking & computing*, pp. 119–124, IEEE Press, Piscataway, NJ, USA, November 2000.

[18] F. G. Wu, C. Y. Tseng, and C. M. Cheng, "The composition of visual texture design on surface for color vision deficiency (CVD)," *Computers in Human Behavior*, vol. 91, no. 2, pp. 84–96, 2018.

Hindawi
Mobile Information Systems
Volume 2022, Article ID 4121907, 10 pages
https://doi.org/10.1155/2022/4121907

Research Article

Intelligent Development of Enterprise Management Innovation Based on Artificial Neural Network

Jintao Wu[1,2] **and Xinlong Ding**[3]

[1]*Department of Economic and Social Management, Maanshan Teacher's College, Maanshan, Anhui, China*
[2]*Graduate School, Lyceum of the Philippines University, Cavite, Philippines*
[3]*School of Electrical and Information Engineering, Anhui University of Technology, Maanshan, Anhui, China*

Correspondence should be addressed to Jintao Wu; jintao.wu@lpunetwork.edu.ph

Received 23 June 2022; Revised 12 July 2022; Accepted 22 July 2022; Published 25 August 2022

Academic Editor: Shadi Aljawarneh

Artificial intelligence technology is gradually entering all aspects of our lives while also promoting the development of various fields. Artificial intelligence can also solve problems that could not be solved by computing before. This paper combines artificial intelligence and network function virtualization, two very advanced and popular technologies in modern society, and uses neural networks to solve and develop the service chain problem in network function virtualization. The simulation shows that all algorithms almost decrease linearly with the change of VNR. This decrease means that there is no noise. The optimal mapping of each VNE problem can be achieved within the scope of the existing solutions, and the heuristic method is to try to find possible mappings. In terms of enterprise management innovation, this article points out the need to strengthen in-depth cooperation and exchanges between universities and enterprises. At the same time, the government, as a third party in cooperation, should play an active leadership role and an intermediary coordination role. In terms of innovation management cooperation, the establishment and improvement of government plans and policy support mechanisms are important external driving factors.

1. Introduction

China's economic and social leaps and progress are closely linked to the development of manufacturing. Regarding the improvement of the innovation capability of enterprises, the current theoretical research lags behind actual needs, which has a negative impact on the development of my country's manufacturing industry. On the one hand, advanced equipment and technology promote the progress of the manufacturing industry. In terms of introducing management methods and innovative management methods, many manufacturing companies in China are also facing management problems related to back management methods and rigid management methods. The research on innovation in the business sector is relatively mature, while business management innovation, especially the research on innovative methods of production methods, is still in its initial stage, and manufacturing companies lack the necessary theoretical support and guidance. The emergence of network function virtualization technology provides operators with new ideas [1]. In order to solve the above problems, this technology uses software to realize the functions originally performed by proprietary devices and converts network requests into an orderly arrangement of multiple virtual network functions. Compared with the existing system, the performance of this system is significantly improved [2, 3]. Artificial intelligence technology is gradually entering all aspects of our lives while also promoting the development of various fields. Artificial intelligence can also solve problems that could not be solved by computing before [4]. As a typical artificial intelligence method, an artificial neural network (ANN) constructs a set of nonlinear signal processing systems [5]. In order to solve some large and complex problems of the biological neural system, the simulation of the nonlinear system not only greatly improves the time cost but also has good parallel processing ability.

2. Related Work

The results of NFV system research include many indicators. The literature proposes to establish a hybrid linear model to determine the total energy consumption of a minimum server, router ports, repeaters, optical cable amplifiers, switches, etc. [6]. It constantly searches for the optimal solution and adds a taboo list to ensure that the resource results are working towards the best solution so as to achieve better resource utilization. A key feedback of a closed-loop algorithm is proposed, which uses the reflection of the main topology of the mapping to jointly improve the deployment of NFV and finally achieve the idea of saving bandwidth [7]. Similarly, some research also pointed out two protection measures to ensure the safety of the system. The creation of better scheduling plans to update the original transportation delay problem and points out the current research direction [8]. The virtualization of network functions is not limited to a single network but can also be used in large-scale data centers, optical networks, and other network environments, and related research continues. In the current popular neural network technology, this method is used to simulate the working principle of biological neurons, and a set of high-performance computer models is established [9]. In recent years, the neural network model has been continuously improved and used to deal with various complex problems. The current classic neural networks include the recurrent neural network (RNN), convolutional neural network (CNN), deep neural network (DNN), and others. Due to its response system, RNN is mainly used to solve timing or correlation problems [10]. It is recommended to use the time series characteristics of the recurrent neural network to judge the weather.

Virtual network technology can build multiple virtual networks on the basic physical network with the help of abstraction, isolation, and other mechanisms. In the software logical network topology, different needs of the service network can be met so that network resources can be configured and managed more flexibly without worrying about the physical topology of the basic network [11]. The creation of virtual networks can make the network richer and improve the efficiency of network utilization. At the same time, network management means will be well strengthened to provide operable methods for the intelligent information needs of Internet users [12]. In order to make the network more widely used, it is necessary to make necessary improvements and breakthroughs to the traditional network [13, 14]. Virtual network technology is a powerful method to strengthen the richness of the network, improve the use of network resources, and strengthen the network management and is one of the research focuses of researchers in the world in recent years [15]. The literature proposed that network technology can enable network operators to apply new network architectures, protocols, and procedures without affecting the normal operation of the network, thereby effectively supporting the improvement of network architecture and technology [16]. The literature proposes that virtual network technology can not only allow it to develop from the current network to the future network but is also one of the key features of the future Internet. Therefore, virtualization technology has attracted more and more attention from the research community and the business community. Become the center of network research. In the academic field in the future, science and technology research programs in western developed countries have begun to support network technology research, and China has also implemented many related research projects and content.

3. Analysis of the Virtualization of Network Functions Based on Artificial Intelligence

3.1. Analysis of Artificial Intelligence Related Content. In general, an artificial neural network usually consists of several layers, and different measures are taken for the information connected to different layers. After the system accesses the signal, each layer will process it in time and finally output the processing result. As mentioned above, commonly used neural network systems generally include an input layer, a hidden layer, and an output layer. Data are transmitted and processed in each layer. Finally, the system becomes more stable. The theoretical characteristics of artificial intelligence mainly include the following four aspects: calculation performance, convergence performance, and summary statistics performance. Convergence reflects the performance of the system for big data processing, inductive statistics reflect the learning performance of the system, the education process is the process of inductive statistics, and the output of the neural network can be expressed as follows:

$$y = f\left(\sum_{i=1}^{n} w_i x_i + b\right). \tag{1}$$

3.2. Overview of Network Virtualization. In a virtual network, there are three different parts: Infrastructure Provider (InP), Service Provider (SP), and End User (EU). The infrastructure provider is responsible for the construction and management of the basic physical network, providing such as physical network connection and routing to the service provider; the service provider is responsible for renting out physical network resources from the basic physical network facilities to establish a virtual network that provides end-user transmission services, reducing the cost of operating and maintaining the physical network, as shown in Figure 1.

The important role of virtual management of network resources is to meet the service requirements of end users in different aspects. By connecting the basic physical network, we can enhance our understanding of basic network resource information, connect the physical network and the virtual network, and allow users to configure and manage the necessary resources. Therefore, end users can use physical network resources through virtual networks and plan according to specific needs.

As shown in Figure 2, there are differences in resource management, and virtual management of network resources can be divided into three specific parts: first, virtual

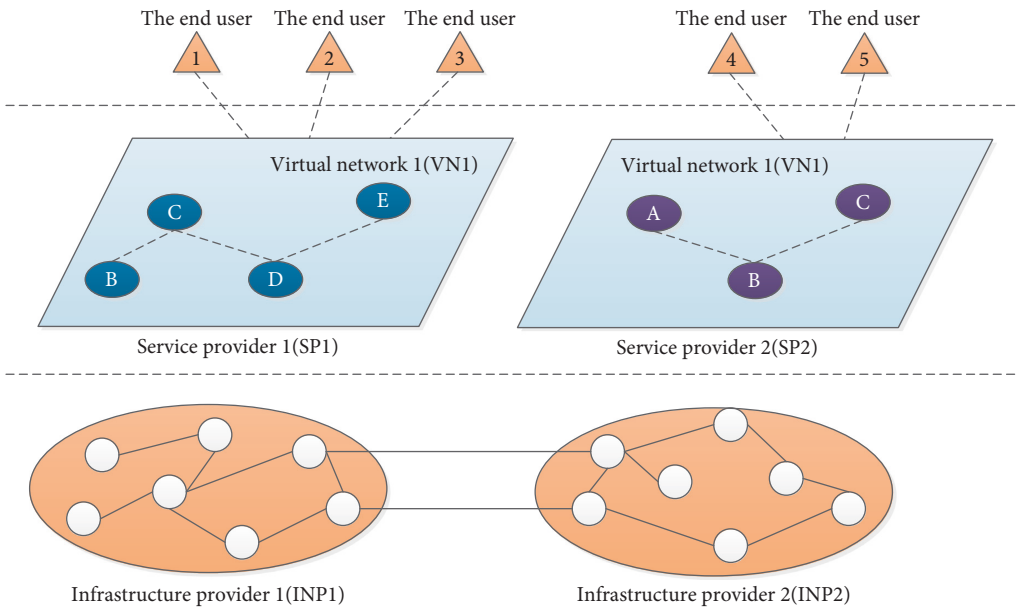

Figure 1: Network virtualization model.

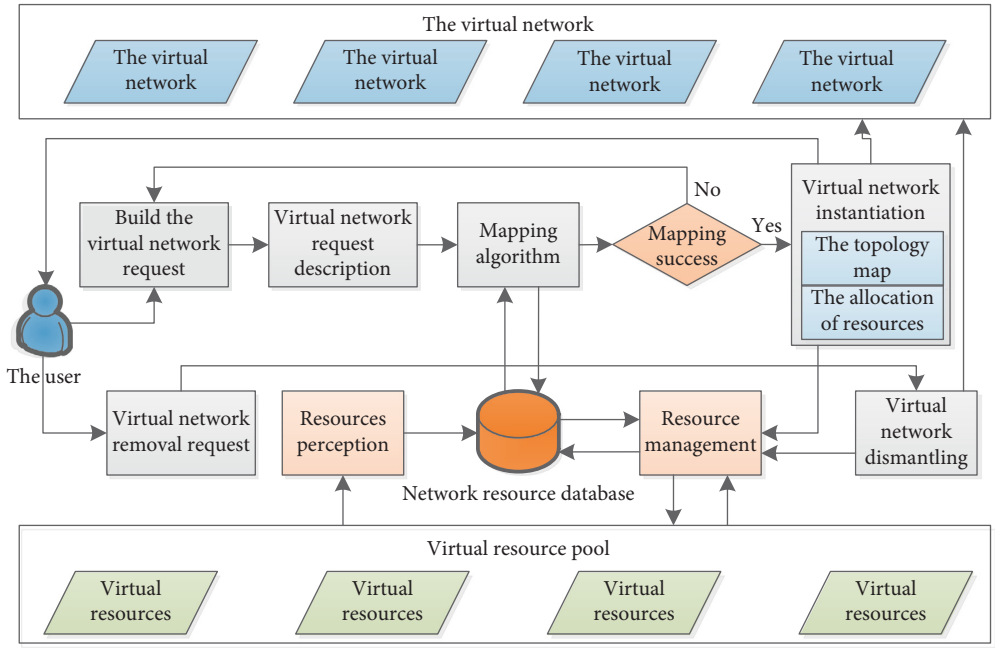

Figure 2: Virtual network resource management model.

management of network resources, that is, leasing network resources from the underlying network to establish virtual resources. Use the resource library to search and feel physical resources and categorize these resources to promote a unified narrative and application of virtual resources. Secondly, in virtual resource mapping, the module dynamically allocates and arranges the leased network resources according to the received service needs, maps the service requests required by the network, and coordinates the network resources. Thirdly, virtual network management is to meet the requirements of the virtual network by running the virtual network management part of all resource libraries, so as to reasonably allocate the virtual network and allocate the physical resources to the most appropriate area. Solve the physical needs of the virtual network through the resource library, provide a reasonable solution for optimizing resource allocation, and help to dynamically manage resources.

The most important deployment of network virtualization is to separate the underlying infrastructure and multiple service networks from traditional ISPs, which will greatly help the dexterity, clarity, and security of future networks. This article divides the role of the traditional ISP into several different parts and proposes a number of

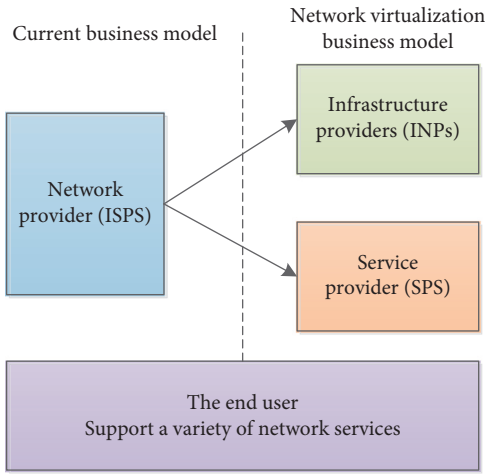

Figure 3: Current business model and NV business model.

different NV models. Figure 3 shows the difference between the current business model and the NV model.

How to successfully deploy the various nodes and connection resources of the virtual network to the physical network is the core and key of virtual network mapping. Virtual network mapping is not only an efficient and reasonable mapping of virtual networks to one or more basic physical networks. It is the core issue of virtual network mapping. Due to the virtual network folder, the efficient management and application of the underlying physical network are an NP problem, and the relevant solutions are mainly heuristic algorithms, as shown in Figure 4.

Virtual network mapping is mainly divided into two parts: node mapping and link mapping. When a user initiates a virtual network request, based on the physical network resources that the service provider has, the node mapping function is

$$M_N(M) = M_N(N). \tag{2}$$

The link mapping function is

$$M_N(\ ): N_V \longrightarrow N_s. \tag{3}$$

The reception rate formula of a virtual network is as follows:

$$ar = \frac{\text{VNRs}_{\text{accepted}}}{\text{VNRs}_{\text{total}}}. \tag{4}$$

Generally, the cost ratio R/C is the standard to judge the efficiency of mapping, which is as follows:

$$\frac{R}{C} = \frac{R\left(G^V\right)}{C\left(G^V\right)}. \tag{5}$$

The average transmission delay divided by the number of virtual links is

$$\text{Delay}_{av} = \frac{\sum_{MN \in \text{VNRs accepted}} \text{Delay}_{MN}}{\text{Num}_{MN}}. \tag{6}$$

The coordinates x and y are used to represent the position of the node:

$$\text{Dis}(\text{loc}(m), \text{loc}(M)) \le LR(M). \tag{7}$$

In VNE, the formula for the bottom remaining nodes is as follows:

Remaining bandwidth of link mn is

$$R^s(mn) = B^s_{mn} - \sum_{MN \uparrow m} B^V_{MN}. \tag{8}$$

The available bandwidth of path mn is

$$R^S\left(P_{mn}\right) = \min R^S(ab). \tag{9}$$

The virtual node in VNR should be reflected on the bottom node. It is subordinate to

$$\begin{aligned} C^V_M &\le R^S\left(M_N(M)\right), \\ \text{Dis}\left(\text{loc}\left(M_N(M)\right),\ \ \text{loc}(M)\right) &\le LR(M). \end{aligned} \tag{10}$$

Virtual link mapping in VNR is restricted by

$$\begin{aligned} B^V_{MN} &\le R^S\left(P_{M_N(M)M_N(N)}\right), \\ D_{M_N(M)M_N(N)} &\le D^V_{MN}. \end{aligned} \tag{11}$$

3.3. Network Function Virtualization Optimization Model and Its Algorithm Implementation. The position of the virtual node can be deviated as

$$\begin{aligned} &\text{Dis}\left(\text{loc}\left(M_N(M)\right), \text{loc}(M)\right) = \sqrt{\left(X_M - X_m\right)^2 + \left(Y_M - Y_m\right)^2}, \\ &\sqrt{\left(X_M - X_m\right)^2 + \left(Y_M - Y_m\right)^2} \le LR(M). \end{aligned} \tag{12}$$

The binary variable x is on the subbottom node m of the virtual node M. The virtual node variable values are

$$x^m_M = \begin{cases} 1, & M \longrightarrow m, \\ 0, & m. \end{cases} \tag{13}$$

The virtual link value is

$$x^{mn}_{MN} = \begin{cases} 1, & MN \longrightarrow mn, \\ 0, & \text{other}. \end{cases} \tag{14}$$

The virtual node is mapped to the underlying node and assigned to the virtual node M:

$$\forall M \in N^V, \sum_m x^m_M = 1. \tag{15}$$

The relationship between the virtual node M and the underlying node m is as follows:

$$\forall m \in N^S, \sum_M x^m_M = 1. \tag{16}$$

The node capacity mapped from the virtual node M to m is as follows:

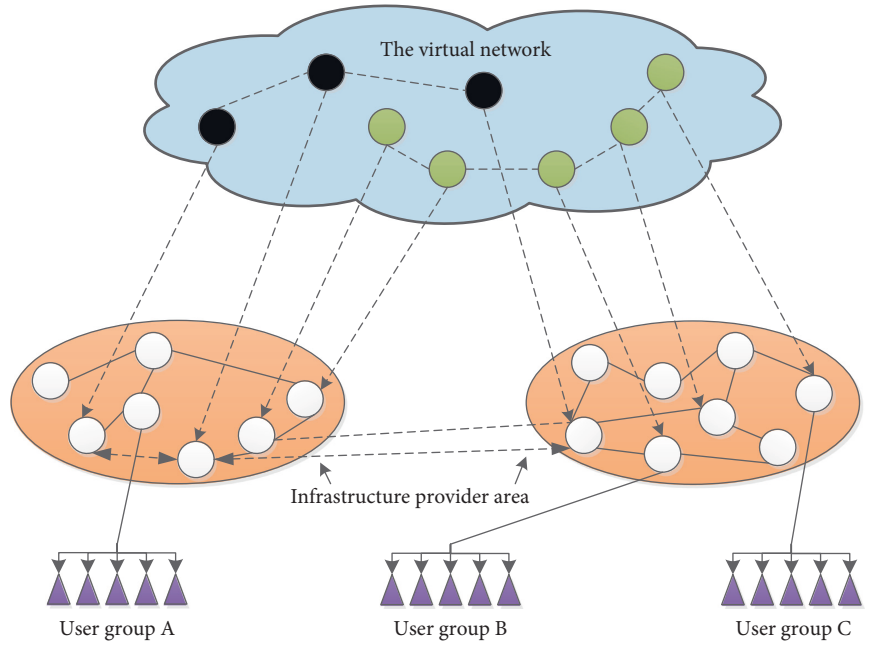

Figure 4: Virtual network mapping problem model.

$$\forall m \in N^S, \sum_M x_M^m \cdot C_M^V \le C_m^S. \tag{17}$$

Commodity flow will increase the delay propagation of virtual link as

$$\begin{aligned} &\forall mn \in P_{mn}^s, \\ &\exists MN \in L^V, \\ &\sum_{mn} B_{MN}^V \left(y_{MN}^{mn} + y_{NM}^{mn}\right) \le B_{mn}. \end{aligned} \tag{18}$$

The link bandwidth must protect the spare link bandwidth and meet the requirements of mapping bandwidth:

$$\begin{aligned} &\forall mn \in P_{mn}^s, \\ &\exists MN \in L^V, \\ &\sum_{mn} B_{MN}^V \left(x_{MN}^{mn} + x_{NM}^{mn}\right) \le B_{mn}. \end{aligned} \tag{19}$$

In the VNE algorithm, virtual link delay propagation is added:

$$\begin{aligned} &\forall MN \in L^V, \\ &\exists MN \in P_{mn}^s, \\ &\sum_{mn} D_{mn} \left(y_{MN}^{mn} + y_{NM}^{mn}\right) \le D_{MN}^V. \end{aligned} \tag{20}$$

According to the VNR revenue, the CF function is formulated to reduce the bottom node capacity and link bandwidth:

$$\min\left(\alpha \sum_M x_M^m C_M^V\right) + \beta \sum_{MN} \sum_{mn} \left(y_{MN}^{mn} + y_{NM}^{mn}\right) D_{MN}^V D_{mn}. \tag{21}$$

If the propagation of the underlying link is delayed, then

$$\min\left(\alpha \sum_{MN} \sum_{mn} \left(y_{MN}^{mn} + y_{NM}^{mn}\right) D_{mn}\right). \tag{22}$$

CF function optimizes the mapping of VN as

$$\min\left\{\alpha \sum_m \sum_M \frac{x_M^m C_M^V}{R^s(m)} + \beta \sum_{MN} \sum_{mn} \frac{\left(y_{MN}^{mn} + y_{NM}^{mn}\right) D_{MN}^V D_{mn}}{R^s(mn)}\right. \tag{23}$$

The other VNE algorithms are greedy mapping and shortest path mapping (g-sp), greedy mapping and multipath mapping (g-mcf), mapping of uncertain coordination nodes, and shortest path connection graph (r-vins-sp). The shortest path connection is nr-sp. Node mapping and several kinds of material flow mapping is nr-mcf. These are the typical VNE algorithms in VNE research.

3.4. Experimental Results and Analysis. Figure 5 shows the average VNR frequency, which is the main data for evaluating different VNE algorithms. It can be seen from the figure that the receiving speed of all algorithms almost decreases linearly with the change of VNR. This decrease means that there is no noise. Unlimited basic resources accept more VNRS. In addition, vne-cnpa is better than heuristics, and the gap between the optimal heuristic and vne-cnpa-cf is at least 20%. Therefore, the optimal mapping of each VNE problem can be achieved within the scope of the existing solutions, and the heuristic method is to try to find possible mappings. Another reason is that vne-cnpa will consider all possible solutions instead of some partial solutions.

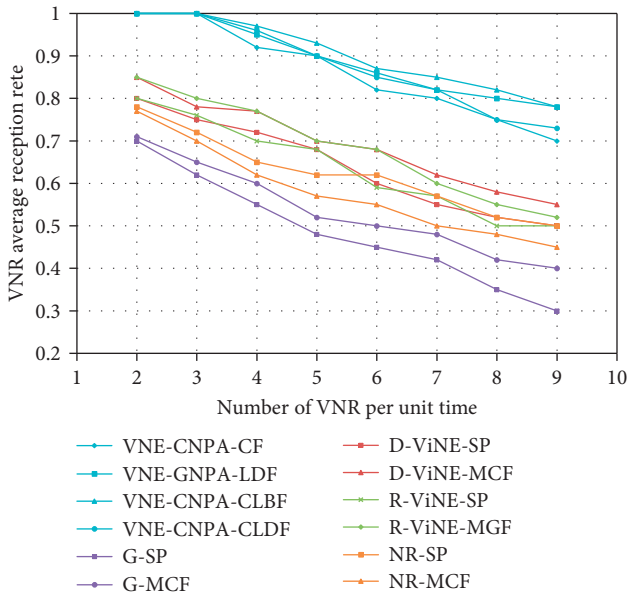

Figure 5: VNR average reception rate.

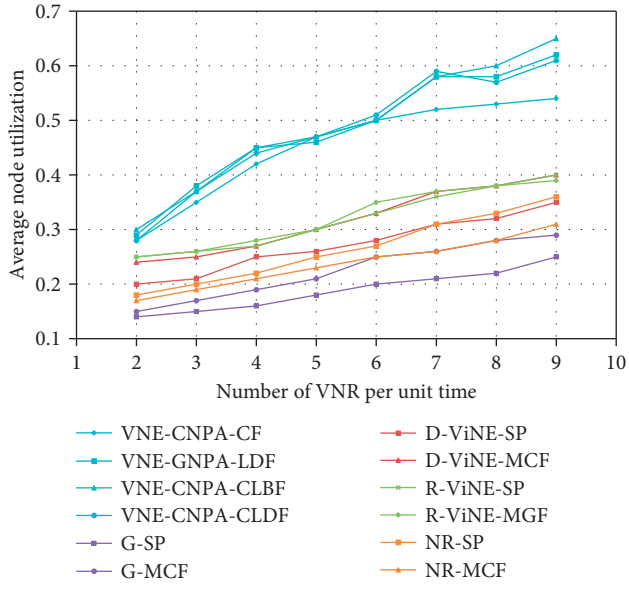

Figure 6: Average node utilization.

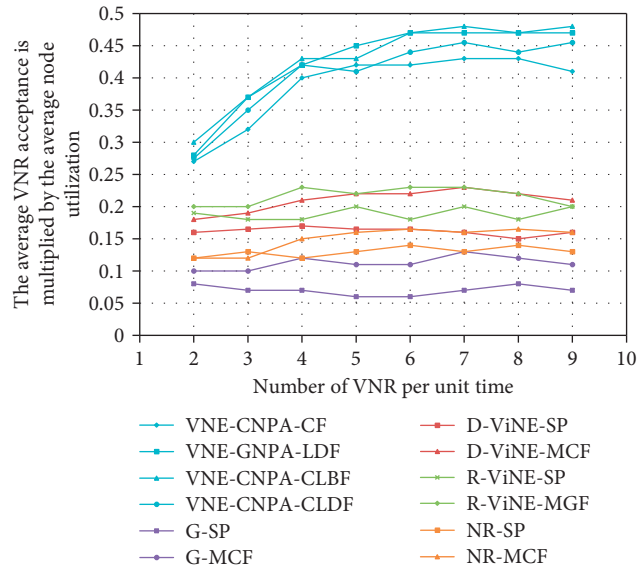

Figure 7: Average VNR reception rate multiplied by node utilization.

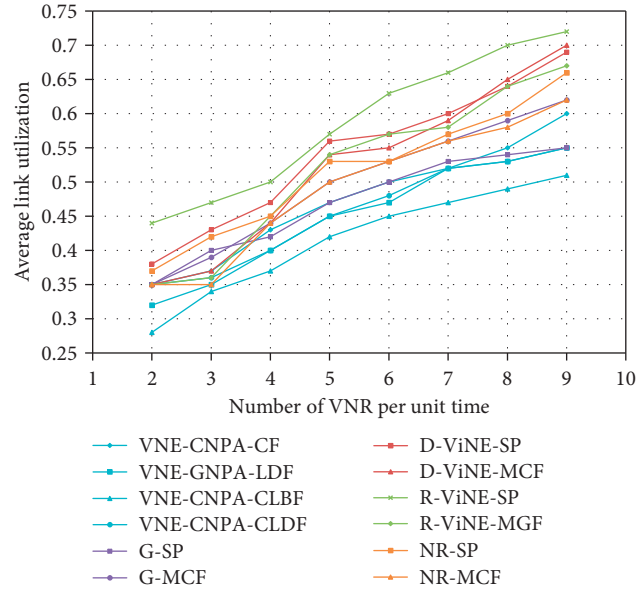

Figure 8: Average link utilization.

The average usage of nodes is shown in Figure 6. As the arrival speed increases, the node utilization of all selected algorithms also increases. In the two VNRS, the usage rates of heuristic and vne-cnpa are reduced by 29% and 35%. As shown in Figure 7, the node utilization rate of vne-cnpa is higher than the heuristic algorithm because vne-cnpa can absorb more VNRS than the heuristic algorithm. If the VNRS data value is huge, the vne-cnpa algorithm can clearly map the VNR and expand the underlying network node to the maximum capacity.

The connection utilization of all algorithms is shown in Figure 8. Obviously, the vne-cnpa algorithm is the low-level connection utilization of the vne-cnpa-clbf algorithm; in Figure 8, the connection utilization of the algorithm using the greedy directory graph (nr-sp, g-sp) is small. Although MCF is suitable for link mapping, it is important to map virtual nodes and synchronize links according to a mathematical programming model, so vne-cnpa is tightly coupled with the use of links.

As shown in Figure 8, the connection utilization also depends on the VNR reception rate, and Figure 9 shows the VNR reception multiplied by the connection utilization. The arrival rate rises to 5. Heuristics is selected, and the others are basically constant.

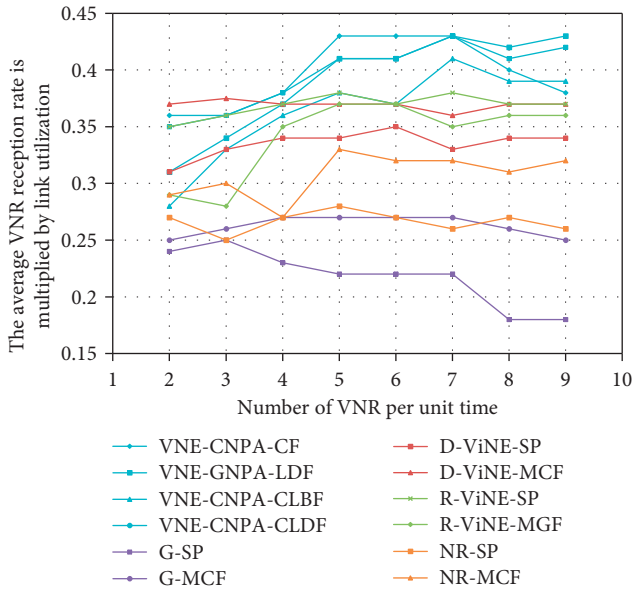

Figure 9: Average VNR reception rate multiplied by link utilization.

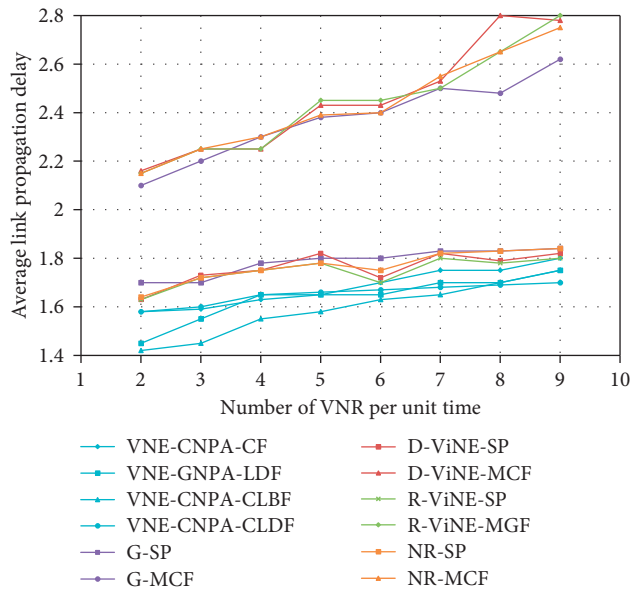

Figure 10: Average link propagation delay.

Figure 10 plots the average virtual link extension delay versus VNR arrival speed, and in contrast to the increase in the number of VNRSs, the average virtual link extension delay for all selected algorithms increases, which is the same as the nodes shown before.

4. Innovative Design and Application of Business Management Based on Digitalization

4.1. Data Collection and Collation. Table 1 is the case identification situation of CK company's production management innovation method, which is explained in 4 categories.

Based on the basic theory, through the public decoding, principal axis decoding, and selective decoding of the data of Chinese enterprises, the scope and categories that affect the way of management innovation of Chinese enterprises are extracted. Table 2 shows the relationship between 18 concepts and five categories. Finally, selective decoding is performed using the five categories mentioned above to connect to the complete story. The main category is the selection of enterprise management innovation. The efficiency of data collection and decoding is verified, and four subcategories are realized, namely the industrial sector, enterprise strategic management and team cooperation, and enterprise innovation.

4.2. Innovative Design Method of Enterprise Management Based on Digitalization. Modern information and communication technologies are becoming more and more popular among companies and always generate large amounts of data. The intelligent connection of everything enhances the fluidity of factors. The source of business is transformed from traditional production factors in the industrial economy to new production factors in the digital economy. On the one hand, the speed and scope of data technology have exploded, and collecting and transmitting at low cost becomes a reality; on the other hand, by analyzing and using a large amount of unstructured data, companies can find user needs and increase productivity through data analysis. With the rapid development of the digital economy, new business practices continue to emerge, and the industrial characteristics of cross-border integration are particularly prominent. Based on the intelligence of the network and cross-border integration, the number is the element, the business is the main factor, and the business management innovation theory that focuses on the analysis of complex organizations and system structures has become a powerful tool for managing cross-border integration.

Industry boundaries, organizational boundaries, and supply-demand boundaries are constantly being eliminated. The reconstruction of territory and the innovation of organizational forms have become the main content of enterprise management innovation. The integration of financial capital and intellectual capital is the company's new development momentum. Organizational forms are becoming more and more grid-like. The new organization has several characteristics of self-organization, infinity, decentralization, and teamwork. The business world is increasingly seeking professionals and composite personnel. Some traditional jobs in the company are gradually disappearing, and the demand for complex, professional, and technical personnel as well as high-quality personnel continues to grow.

4.3. Policy Recommendations to Promote the Development of Innovative Methods of Corporate Management. Enterprise management innovation cooperation is part of the cooperation between universities and enterprises. The government plays an important role in university research

Table 1: Open decoding of CK company production management innovation method cases.

Data	Concept	Category	Category nature	Property attribute
a1: the chairman believes that technology and management innovation are the dual cores of promoting enterprise development	Promote innovation	Team innovation	Team innovation form	Radical or conservative
a2: the chairman believes that the entrepreneurial team composed of three to four people has a close innovative spirit for development and exploration	Innovative spirit			
a3: in 2011, the company produced 160 million as output value through 82 people	Teamwork			
a4: after the company outsources, the company's mechanism is streamlined and efficient	Organizational flattening	Organizational culture innovation	Innovative atmosphere	Organizational culture innovation: high or low
a5: the company strengthens innovative training for employees	Human resources			
a6: from the outside, due to lack of competent authorities or industry associations, the standards cannot be updated	Industry instability	Industry environment	The complex and unstable environment of the company's industry	Industry environment: high or low instability
a7: the company faces fierce competition, and foreign-funded enterprises have also entered the Chinese market.	Fierce competition			
a8: at present, the company has cooperated with related professional research institutes and well-known universities in China.	Combining industry and research			
a9: in 2009, the company was focused on training by the government, and all aspects received government support.	State aid			
a10: the company has cooperated to develop a new system, but it does not have core technology and cannot meet customer requirements	Stable customer demand			
a11: the company adheres to the development concept and uses new ideas to promote the company's development	Strategic policy	Corporate strategic management	Company strategy orientation	Strategic orientation: cost leadership, differentiation, and focus strategy
a12: the chairman believes that the company has strong decision-making capabilities and resource acquisition capabilities	Strategic management system capabilities			
a13: the corporate label is used emphatically, and the corporate brand and development are greatly supported	Brand honors			
a14: the company sums up its experience in failure and obtains a national patent	Practice of innovative methods			

Table 1: Continued.

Data	Concept	Category	Category nature	Property attribute
a15: the company has changed the traditional model, and the company has achieved significant development	Progressive management innovation	Abrupt management method innovation	Innovation in management methods	Progressive management method innovation
a16: the chairman believes that the company's return rate is low, but the downtime is long, and production needs to be further improved.	Mature production method			
a17: participate in the study of government organizations many times to improve the management innovation ability	Learn and grow			
a18: all work must be performed in accordance with regulations and constantly updated and improved	System innovation			

Table 2: The corresponding relationship between categories and concepts of influencing factors of management innovation methods in Chinese manufacturing enterprises.

Category	Concept
Team innovation spirit	Promoting innovation and group collaboration
Organizational innovation culture	Solid organization and brand reputation
Industry environment	Industry instability, customer demand diversity, state aid, business combination
Corporate strategic management	Catastrophe management method, strategic management system capability
The choice of management innovation method	The innovation of the mutation management method and gradual management method

cooperation. It has been verified by other countries that the government often needs to play different roles in different periods of industrial development. Universities should conduct research based on their goals and actual conditions. First, the government should play a leading role. The government should formulate incentive measures and guidelines to promote cooperation in management innovation, especially in the following areas: financial support, property rights definition, and regulatory support. Secondly, the government should play the role of a regulator, and government service departments should support the cooperation between universities and the business world through relevant systems and departments and carry out intermediate coordination and adjustment.

The government must lead the overall situation more macroscopically and formulate long-term development plans and policies based on local conditions to guide the development of cooperation. It is necessary for the government to promote the retention of the cooperative intentions of individual subjects throughout the process. The government must formulate a development plan that combines the medium and long terms with the short term to ensure that companies, universities, intermediaries, and other institutions are profitable, thereby achieving the goal of improving the city's overall innovation capabilities. The first is to promote the development of university scientific research cooperation, encourage scientific research institutions and enterprises to cooperate, encourage cooperation from low-level to high-level collaborative development, and expand the aspects of collaboration. From simply investing in scientific research results, patented technology, and production process procurement, we should turn to the road of high-level collaboration, such as business collaboration in schools, development of information of R&D centers, and technology sharing; secondly, strengthen guidance in university scientific research cooperation.

5. Conclusion

This paper combines artificial intelligence and network function virtualization, two very advanced and popular technologies in modern society, and uses neural networks to solve and develop the service chain problem in network function virtualization. In terms of enterprise management innovation, this article points out the need to strengthen in-depth cooperation and exchanges between universities and enterprises. At the same time, the government, as a third party in cooperation, should play an active leadership role and an intermediary coordination role. In strengthening innovation management, the government should issue corresponding support for the policies and measures of the People's Republic of China and give some policy dividends to support. In terms of innovation management cooperation, the establishment and improvement of government plans and policy support mechanisms are an important external driving force for enterprise management innovation cooperation in the initial stage.

Data Availability

The data used to support the findings of this study are available from the corresponding author upon request.

Conflicts of Interest

The authors declare that they have no conflicts of interest.

References

[1] Etsi Industry Specification Group (Isg) Nfv, *ETSI GS NFV 002 V1.2.1: Network Functions Virtualization (NFV); Architectural Framework*, ETSI: European Telecommunications Standards Institute, Frankfurt, Germany, 2014.

[2] G. A. Gallardo, B. Baynat, and T. Begin, "Performance modeling of virtual switching systems," in *Proceedings of the IEEE 24th International Symposium on Modeling, Analysis and Simulation of Computer and Telecommunication Systems (MASCOTS)*, pp. 125–134, London, UK, September 2016.

[3] S. Azodolmolky, R. Nejabati, M. Pazouki, P. Wieder, R. Yahyapour, and D. Simeonidou, "An analytical model for software defined networking: a network calculus-based approach," in *Proceedings of the IEEE Global Communications Conference (GLOBECOM)*, pp. 1397–1402, Atlanta, GA, USA, December 2013.

[4] D. Watson, J. Womack, and S. Papadakos, "Rise of the robots," *Critical Care Nursing Quarterly*, vol. 43, no. 3, pp. 303–311, 2020.

[5] M. Chen, U. Challita, W. Saad, C. Yin, and M. Debbah, "Artificial neural networks-based machine learning for wireless networks: a tutorial," *IEEE Communications Surveys & Tutorials*, vol. 21, no. 4, pp. 3039–3071, 2019.

[6] R. Bolla and R. Bruschi, "Linux software router: data plane optimization and performance evaluation," *Journal of Networks*, vol. 2, no. 3, pp. 6–17, 2007.

[7] M. Dobrescu, N. Egi, K. Argyraki, B. C. Chun, K. Fall, and G. Lannaccone, "RouteBricks: exploiting parallelism to scale software routers," in *Proceedings of the ACM SIGOPS 22nd symposium on Operating systems principles*, pp. 15–28, Montana, USA, October 2009.

[8] Z. Su, B. Baynat, and T. Begin, "A new model for DPDK-based virtual switches," in *Proceedings of the IEEE Conference on Network Softwarization (NetSoft)*, pp. 1–5, Bologna, Italy, July 2017.

[9] H. Li, Z. Bian, P. Zhang et al., "Application-oblivious L7 parsing using recurrent neural networks," *IEEE/ACM Transactions on Networking*, vol. 28, no. 5, pp. 2009–2022, 2020.

[10] W. Lucas, C. Hartmann, M. Thiele, D. Habich, and W. Lehner, "Cardinality estimation with local deep learning models," in *Proceedings of the Second International Workshop on Exploiting Artificial Intelligence Techniques for Data Management (aiDM '19)*, New York, NY, USA, July 2019.

[11] M. Adil, J. Ali, M. Attique et al., "Three byte-based mutual authentication scheme for autonomous internet of vehicles," *IEEE Transactions on Intelligent Transportation Systems*, vol. 23, 2021.

[12] R. Kawashima, S. Muramatsu, H. Nakayama, T. Hayashi, and H. Matsuo, "A host-based performance comparison of 40G NFV environments focusing on packet processing architectures and virtual switches," in *Proceedings of the 5th European Workshop on Software-Defined Networks (EWSDN)*, pp. 19–24, The Hague, The Netherlands, October 2016.

[13] L. Rizzo and G. Lettieri, "VALE, a switched Ethernet for virtual machines," in *Proceedings of the 8th international conference on Emerging networking experiments and technologies*, pp. 61–72, Nice, France, December 2012.

[14] R. V. Mendonça, J. C. Silva, R. L. Rosa, M. Saadi, D. Z. Rodriguez, and A. Farouk, "A lightweight intelligent intrusion detection system for industrial internet of things using deep learning algorithm," *Expert Systems*, vol. 39, Article ID e12917, 2021.

[15] B. Zhang, X. Wnag, R. Lai, L. Yang, Z. Wang, and Y. Luo, "Evaluating and optimizing I/O virtualization in kernel-based virtual machine (KVM)," in *Proceedings of the IFIP International Conference on Network and Parallel Computing*, pp. 220–231, Zhengzhou, China, September, 2010.

[16] Q. Xiao, S. Chen, Y. Zhou et al., "Cardinality estimation for elephant flows: a Compact solution based on virtual register sharing," *IEEE/ACM Transactions on Networking*, vol. 25, no. 6, pp. 3738–3752, 2017.

Hindawi
Mobile Information Systems
Volume 2022, Article ID 1909312, 9 pages
https://doi.org/10.1155/2022/1909312

Research Article

Microblog Emotion Analysis Method Using Deep Learning in Spark Big Data Environment

Junya Yan and Xiaohui Ma

School of Information Engineering, Shanxi Vocational University of Engineering Science and Technology, Shanxi, Jinzhong 030619, China

Correspondence should be addressed to Junya Yan; yanjunya@sxgkd.edu.cn

Received 7 May 2022; Revised 13 June 2022; Accepted 19 July 2022; Published 24 August 2022

Academic Editor: Shadi Aljawarneh

Aiming at the problem that the existing methods in the big data environment cannot extract the emotional features of microblog sufficiently and the average accuracy of analysis results is low, a microblog emotion analysis method using deep learning in spark big data environment is proposed. First, the Jieba word segmentation method is used to process text comments, so as to reduce the interference of irregular grammar and nonstandard words on the emotion analysis task of microblog text. Then, features based on affective rules, unary word features, syntactic features, and dependent word collocation features are selected. In order to prevent the dimension disaster caused by excessive feature dimensions, the feature selection method of information gain is used to reduce the dimension of features. Finally, a microblog emotion analysis method based on deep belief network (DBN) is established, and the DBN is parallelized through spark cluster to shorten the training time. Experiments show that when the feature set is composed of TOP2000 features, the classification accuracy of the fusion of four features is 90.94%, which is higher than that of the comparison method. In addition, the training time of DBN algorithm parallelized by spark cluster is only 27.78% of that of single machine. Therefore, compared with the comparison method, the proposed method can significantly improve the performance of the microblog emotion analysis system.

1. Introduction

The development of network technology makes users communicate more and more frequently online, including blogs, forums, and e-commerce website comments [1]. Users express their feelings about certain events or things by publishing information. Analyzing the words in social networks can help the government and other management institutions understand the social mood fluctuations, conduct public opinion analysis, further judge the development of the situation, give reasonable guidance, and maintain social stability [2–5]. From a commercial perspective, with the rise and popularity of e-commerce platforms such as Taobao and Amazon, users can give product evaluation after purchase, making the information of purchasing products more transparent. The quality of product comments will greatly affect users' purchase desire. Therefore, businesses can analyze users' comments, improve goods or change sales strategies in time, further analyze users' consumption characteristics and hobbies, draw user portraits, and make decisions to maximize business profits. In addition, emotion analysis can also be used to predict the stock market, election support, and other fields [6–9]. It can be seen that emotional analysis has important value in the fields of society, business, politics, and management [10].

With the rapid development of domestic microblog, many netizens participate in the discussion of various events, from personal trivia to enterprise marketing, and then to global major events. Microblog has become a social platform for public opinion release. Through the analysis of user emotion in microblog, it is of far-reaching significance for the development of government, enterprises, and individuals [11–15].

According to the granularity of research, emotion analysis tasks can be divided into three categories: document level, sentence level, and aspect level [16]. Document level emotion analysis regards the whole document as a basic unit and believes that a document as a whole only expresses one polar emotion. However, the document contains multiple sentences, and different sentences may have different emotional polarity classifications [17–19]. Sentence level emotion analysis is more fine-grained than document level, which is used to classify the emotional polarity of a single sentence. Aspect level emotion analysis is different from document level and sentence level affective analysis. It will more finely consider the emotion polarity and the target of corresponding emotion. The target here is attribute words or aspects, which usually exist in the form of entity or entity characteristics [20].

Aiming at the problem that the existing methods in the big data environment cannot extract the emotional features of microblog sufficiently and the average accuracy of analysis results is low, a microblog emotion analysis method using deep learning in spark big data environment is proposed. The main innovations are as follows:

(1) Jieba word segmentation method is used to process text comments, which effectively reduces the interference of irregular grammar and nonstandard words on the emotion analysis task of microblog text

(2) The feature dimension reduction operation is carried out by using the feature selection method of information gain to prevent the dimension disaster caused by too large feature dimension

(3) A microblog emotion analysis method based on DBN is established, and the DBN is parallelized through spark cluster, which effectively shortens the training time of the model

The rest of the sections are arranged as follows: Section 1 is related work, which introduces the current research status of emotion analysis. In Section 2, the structure and principle of deep confidence network are described. Section 3 describes deep belief network. In Section 4, the proposed DBN microblog emotion classification model based on spark parallel optimization is introduced in detail. Section 5 is the experiment. Section 6 summarizes this study.

2. Related Works

Deep learning method can better capture the grammatical and semantic features of text, which is a research focus of emotion analysis. Jebbara et al. used the bidirectional gated recurrent unit (GRU) to extract attribute words and specific aspects of emotion and extract features from the text for prediction of sentence labels [21]. Considering the characteristics of part of speech and corpus, Liu et al. proposed a method to complete the task of attribute word extraction by using RNN, which achieved better performance than the traditional system based on conditional random field [22]. In order to overcome the limitation of fixed window size of convolutional neural network (CNN) model and better capture context information, Chen et al. combined with the named entity recognition (NER) task method, proposed a text emotion analysis method based on BiLSTM-CRF model to classify BIO labels of entities in sentences [23]. Yin et al. proposed a long short-term memory (LSTM) model for cross-domain attribute word extraction, which combined the rule-based method to generate the auxiliary label sequence of each sentence [24]. Li et al. incorporated attention into the task of attribute word extraction and aspect category recognition and constructed a truncated historical attention and selective conversion network on LSTM [25]. Wang et al. proposed a GRU-based coupled multilayer attention (CMLA) model to extract attribute words and opinion words [26]. In the learning process, it encoded and decoded the dual propagation of attribute words and opinion words, not just limited to syntactic relations. Zhang et al. proposed a text emotion classification model integrating content features and user features [27]. Jamal et al. proposed a Twitter emotion analysis framework based on the Internet of Things, which used the mixed model of term frequency inverse document frequency (TFIDF) and deep learning model for emotion analysis, filtered the original tweets with the tokenization method, so as to capture useful features without noise information, and used TFIDF statistical technology to estimate the importance of local and global features. The adaptive comprehensive class balance technology is used to solve the class balance problem between different emotions [28]. Jelodar et al. used the LSTM method to classify the comments of COVID-19. The research results have a certain impact on the guidance and decision-making of COVID-19-related issues [29]. Wei et al. proposed a BiLSTM model based on multipolarity orthogonal attention for implicit sentiment analysis. Compared with the traditional single attention mechanism model, this method can effectively identify the differences between words and emotional tendencies and has been verified in experiments [30].

3. Deep Belief Network

3.1. DBN Model Structure. DBN is a neural network model with multiple hidden layers. It is difficult to optimize the weight in deep structures such as deep confidence network, so a greedy unsupervised training method is proposed to solve this problem. Figure 1 shows a structure diagram of a deep confidence network with three hidden layers h_1, h_2, and h_3. x is the input data and y is the output label corresponding to the input data. In the first step, DBN pairs each two adjacent neural network layers, trains the parameters between the two layers with the parameters of the input layer, and constructs the output layer. Moreover, the propagation of input layer and hidden layer is bidirectional, which is divided into forward process and backward process to learn data distribution. This method of building networks between layers is realized by the restricted Boltzmann machine (RBM) model. RBM is a recurrent neural network with two layers. Each node in the same layer is not connected to each other, and the output and input layer nodes are connected symmetrically without direction, which is equivalent to the connection of an undirected graph. An

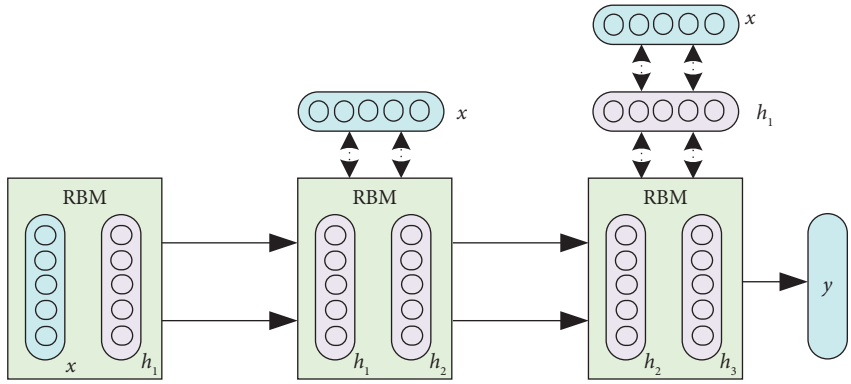

Figure 1: Deep belief network structure.

RBM consists of a hidden layer composed of random hidden units and a visible layer composed of random visible units.

Due to the special structure of RBM model, which has connection between layers and no connection within layers, it has the following important properties: when the visible unit state is given, the jth neuron in the hidden layer is calculated according to the neuron state of the visible layer, and the activation probability is as follows:

$$p\left(h_j = 1|\mathbf{v}\right) = \sigma\left(b_j + \sum_{i=1}^{m} w_{ij} v_i\right), \tag{1}$$

where σ is the sigmoid activation function, v_i represents the ith visible unit, h_j represents the jth hidden unit, w_{ij} is the weight between the ith visible unit and the jth hidden unit, and b_j is the offset threshold of the jth hidden unit.

Similarly, when the state of the hidden unit is given, the probability of the binary state v_i being 1 can be calculated, that is, the activation probability of the visible unit can be expressed as

$$p\left(v_i = 1|\mathbf{h}\right) = \sigma\left(a_i + \sum_{j=1}^{n} w_{ij} h_j\right), \tag{2}$$

where a_i is the offset threshold of the ith visible unit.

For the determination of the deep belief network model, the first thing is to know the number of nodes in the visible layer and the hidden layer. The number of nodes in the visible layer is the input data dimension. Second, the number of nodes in the hidden layer is related to the number of nodes in the visible layer in some research fields, such as processing image data with convolution restricted Boltzmann machine, which is not analyzed here. However, in most cases, the number of hidden layer nodes needs to be determined according to the use, or the number of hidden layer nodes that minimize the energy of the model under certain parameters.

3.2. DBN Model Training. The training of DBN model is divided into two parts: unsupervised pretraining process based on RBM and supervised parameter adjustment process.

The unsupervised pretraining process of DBN model adopts the layer-by-layer greedy learning strategy. The initial input layer is the visible layer, and the input data are the text feature vector. The data vector of the visible layer v combined with the weight w_1 is used to infer the data vector of the hidden layer h_1, which is the training process of RBM1. Then, the data vector of the hidden layer h_1 is combined with the weight w_2 to infer the data vector of the hidden layer h_2, which is the training process of RBM2, and so on. That is, multiple RBMs are stacked, the output of the previous RBM is the input of the next RBM, and the hidden layer of the previous RBM is the visible layer of the next RBM. By step-by-step training to the last layer, the pretraining process of DBN is completed. The specific steps are as follows:

Step 1. Randomly initialize the weight (W, a, b), in which W is the weight vector matrix, $a = [a_1, a_2, \ldots, a_n]$ is the offset coefficients of visible layer, and $b = [b_1, b_2, \ldots, b_n]$ is the offset coefficients of hidden layer. $v = [v_1, v_2, \ldots, v_n]$ is visible neurons, number is n; $h = [h_1, h_2, \ldots, h_n]$ is hidden neurons, number is m.

Step 2. Assign X value to the visible layer $v^{(0)}$ and calculate the probability that the hidden layer neurons can be activated:

$$p\left(h_j^{(0)} = 1|v^{(0)}\right) = \sigma\left(W_j * v^{(0)} + b_j\right). \tag{3}$$

Step 3. Perform a Gibbs sampling to obtain the value of each neuron in the hidden layer:

$$h^{(0)} \sim p\left(h^{(0)}|v^{(0)}\right). \tag{4}$$

Step 4. Reconstruct the visible layer v with the obtained $h^{(0)}$ in formula (4) and calculate the probability density:

$$p\left(v_i^{(0)} = 1|h^{(0)}\right) = \sigma\left(W_i * h^{(0)} + a_i\right). \tag{5}$$

Step 5. Perform Gibbs sampling again and reconstruct the value of each neuron in the visible layer. Let $r_i \in random[0, 1]$:

$$v_i = \begin{cases} 1, & p\left(v_i^{(0)} = 1|h^{(0)}\right) > r_i, \\ 0, & \text{otherwise.} \end{cases} \tag{6}$$

Step 6. Calculate the activation probability of hidden layer neurons again with the reconstructed visible layer neurons:

$$p\left(h_j^{(1)} = 1|v^{(1)}\right) = \sigma\left(W_j * v^{(1)} + b_j\right), \tag{7}$$

where $\sigma(\cdot)$ adopts sigmoid activation function, and its function image is shown in Figure 2. Sigmoid is used to activate the function because its definition field is R and its value field is (0, 1). Therefore, no matter what range the input data of neurons in the visible layer is, the activation probability of nodes can be obtained by sigmoid function.

Step 7. Obtain the new weight vector matrix W, visible layer offset coefficient a, and hidden layer offset coefficient b:

$$\begin{aligned} a &= a + \varepsilon\left[v^{(0)} - v^{(1)}\right], \\ b &= b + \varepsilon\left[p\left(h^{(0)} = 1|v^{(0)}\right) - p\left(h^{(1)} = 1|v^{(1)}\right)\right], \\ W &= W + \varepsilon\left[p\left(h^{(0)} = 1|v^{(0)}\right)v^{(0)T} - p\left(h^{(1)} = 1|v^{(1)}\right)v^{(1)T}\right], \end{aligned} \tag{8}$$

where ε is the learning rate.

To sum up, pretraining only needs to iteratively calculate RBM1, RBM2, and RBM3 parameters in turn and finally get the best weight (W, a, b).

The supervised parameter optimization training of DBN model first uses the forward propagation algorithm to determine whether the hidden layer neurons are activated by using the parameters W and b obtained in the pretraining. Let l be the number of layers of the neural network and calculate the excitation value of each hidden layer neuron:

$$h^{(l)} = W^{(l)} * v + b^{(l)}. \tag{9}$$

Then, we propagate upward layer by layer, calculate the excitation values of neurons in all hidden layers using formula (9), standardize them with activation function, and finally calculate the excitation value $h^{(l)}$ and output vector $\widehat{X}$ of output layer:

$$\begin{aligned} h^{(l)} &= W^{(l)} * h^{(l-1)} + b^{(l)}, \\ \widehat{X} &= f\left(h^{(l)}\right). \end{aligned} \tag{10}$$

Then, the back propagation algorithm is used to update the parameters of the whole DBN network. The back propagation algorithm adopts the reconstruction error criterion, and the cost function is as follows:

$$E = \frac{1}{N}\left(\widehat{X}_l\left(W^{(l)}, b^{(l)}\right) - X_i\right)^2, \tag{11}$$

where E is the reconstruction error, $\widehat{X}_l$ is the actual output of the output layer, X_i is the theoretical output of the output layer, and $(W^{(l)}, b^l)$ represents the weight and offset coefficient of the layer l. The reconstruction error can reflect the likelihood of the training data to a certain extent. Finally, the gradient descent (GD) algorithm is used to update the weight and offset coefficient of the whole DBN network:

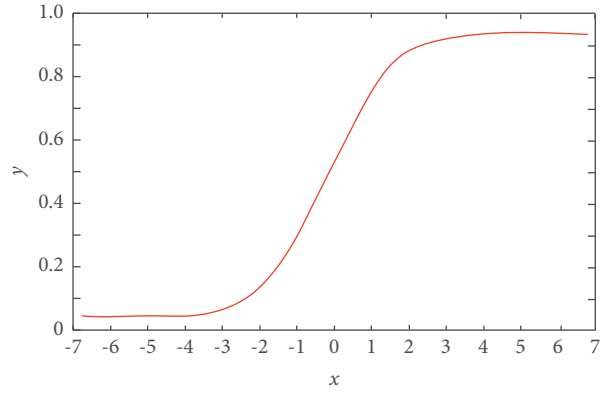

Figure 2: Sigmoid function image.

$$\left(W^{(l)}, b^{(l)}\right) = \left(W^{(l)}, b^{(l)}\right) - \varepsilon\frac{\partial E}{\partial\left(W^{(l)}, b^{(l)}\right)}. \tag{12}$$

To sum up, the training purpose of DBN model is to maximize the fitting of input data, and the output result is the reconstruction of training data. The visible layer neurons transfer their own features to the hidden layer neurons. The hidden layer neurons capture the higher-level features shown by the visible layer neurons through iterative training, so as to enhance the ability of feature extraction of the model.

4. DBN Microblog Emotion Classification Model Based on Spark Parallel Optimization

Figure 3 shows the work flowchart of microblog emotion analysis of the proposed method. Before classifying microblog emotion, it must be processed into a form that can be calculated by computer, that is, the representation model of data. Then, an emotional dictionary is built, the emotional features are extracted in the microblog text, the extracted features are taken as input, the whole spark parallel DBN model is trained, the classification results are obtained, and the emotional analysis of the microblog text is realized.

4.1. Microblog Preprocessing and Feature Vector Construction

4.1.1. Preprocessing. Text preprocessing is an indispensable part of the task of text emotion analysis. In text comments, due to the great differences in everyone's emotional thinking and speaking methods, it is often filled with strong personal emotional styles. All kinds of irregular grammar and nonstandard words will interfere with the task of text emotion analysis, so text preprocessing is very important. The text preprocessing part of this study includes as follows: filtering out repeated corpus, filtering out irregular words, removing stop words, emoticon processing, and Chinese word segmentation. The Chinese word segmentation part selects Jieba word segmentation. Jieba word segmentation can collect the dictionary established by users, and its Chinese word segmentation effect is good, which can well meet the needs of this study.

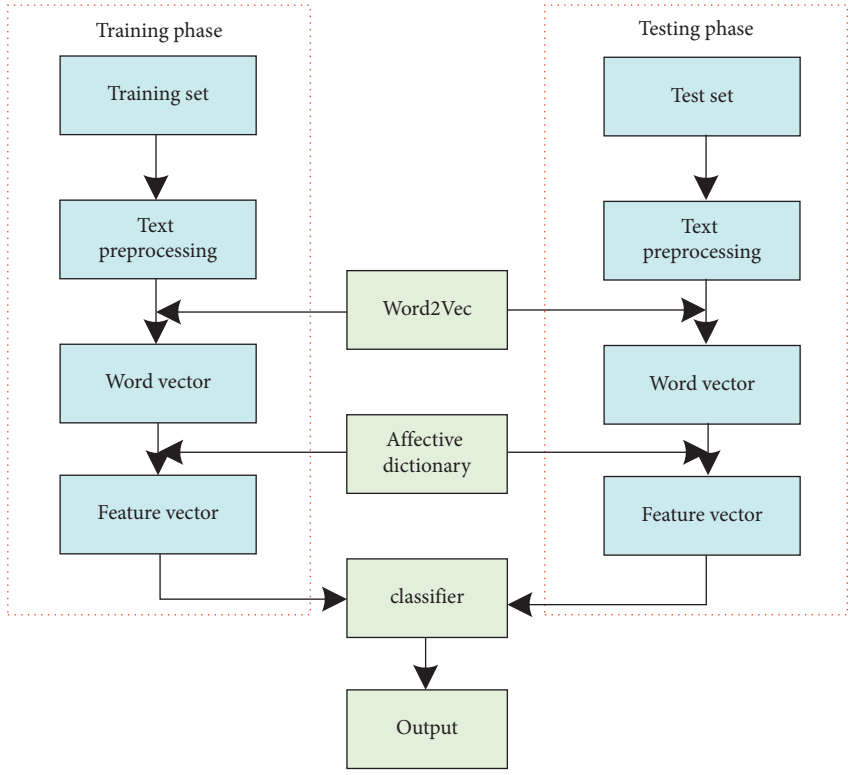

Figure 3: Flowchart of microblog emotion analysis.

4.1.2. Feature Construction. Text feature selection is a key step of machine learning, which determines the accuracy of emotion classification. This study selects four categories of features: features based on emotional rules, unigram features, syntactic features, and dependent word collocation features. The rule feature based on emotion is the feature obtained by extracting its effective information after improving the new rule method on the basis of predecessors. Considering that phrase structure can reduce sentence ambiguity, we add bigram and its combined part of speech tagging as features to the feature set. Dependency feature is the dependency identifier obtained from the dependency parsing tree. It plays an important role in the annotation of emotional category information and can save the information directly related to emotional words and other hidden information.

The method based on emotion dictionary plays an important role in the development history of text emotion analysis. Its core idea is to superimpose the polarity of emotion words and judge the emotional tendency of the text by numerical value. The formula of the classical method is as follows:

$$S = \sum_{i=1}^{n} Sw_i. \tag{13}$$

In the above formula, the parameter Sw_i represents the polarity of emotional word i. The parameter n represents the number of emotional words in the text. The method based on emotional dictionary can barely complete the task in some simple text tests, but considering the complex text grammar and the existence of various language structures in real use, the actual use is limited. Therefore, considering the defects of classical methods, a new emotion rule method is proposed. Considering that the length of the comment text is generally short and is basically a separated sentence, the method takes each clause as a meta unit. On the basis of considering the negative words, connectives, and other grammatical structures, the emotion calculation formula (equation (14)) is proposed to calculate the emotion tendency of each unit. The final text emotion tendency is judged by the value obtained by the superposition of the score values of each unit. If the score value is positive, the text emotion is classified as positive; if the score is negative, the text emotion is classified as negative:

$$S\,\text{unit} = \sum_{i=n}^{n} \left(K * Pw_i * \prod_{j=1}^{m} \text{mod}_j \right), \tag{14}$$

where the parameter n represents the number of emotional words in the text, the parameter Pw_i represents the emotional extremum of emotional word i, the parameter m represents the number of words modifying emotion word i, the parameter mod_j represents the weight of the corresponding modifier, and the parameter k represents the weakening or strengthening coefficient of rules. This parameter exists to solve a problem often ignored in emotion analysis tasks—the deviation of emotion analysis results caused by subject confusion.

Table 1 lists a brief description of the emotional rules designed by the proposed method. Generally speaking, the more complete the emotional rules are, the better the effect of the emotional rule method is. After combining the

Table 1: Brief emotion rules table.

Rule name	Rule content
Negative emotion rule	When negative affective words are detected, the affective polarity and intensity are reversed.
Expression emotion rule	When an expression word is detected, the corresponding score is given directly according to the expression dictionary.
Emotional rules of turning conjunctions	When the preinflection word is detected, it is weakened according to the strength value of the conjunction dictionary.
Borrowed emotion rules	Used to strengthen/weaken demonstrative pronouns.

emotional rules, the final score is calculated according to formula (14), and then, three parameters are extracted as emotional features: the score of emotional words, the number of positive/negative emotional words, and the ratio of strengthening/weakening times of rules.

For the other three emotional features, "the scenic spot service is really good, I like it very much!" is taken as an example sentence to show the feature extraction process and the corpus is input into Jieba word segmentation to get "scenic spot /*n* service /*n* really /ad good /*a* , /*wd* I /rr very /d like /*vi* ! /*wd*", where /*n* stands for noun, /ad stands for adverbial word, /*a* stands for adjective, /*wd* stands for punctuation mark, /rr stands for pronoun, /*d* stands for adverb, and /*vi* stands for verb.

Based on the above results of word segmentation and tagging, the syntactic features can be obtained: scenic spot service, service really, really good, good I, I very, like it very much, *n*, ad, *a*, rr, *d*, *vi*. The number of features is 12. After the result of word segmentation is obtained, the dependency and word collocation features of the input example sentences can be obtained by calling the StanfordNlp natural language processing toolkit. The specific relationship and collocation are listed in Table 2.

In practical use, in order to avoid various problems caused by excessive feature dimension, the feature selection method of information gain (IG) is adopted for feature dimension reduction. The formula is as follows:

$$IG(T) = -\sum_{i=1}^{n} P(C_i)\log_2 P(C_i) + P(t)\sum_{i=1}^{n} P(C_i|t)\log_2 P(C_i|t), + P(\bar{t})\sum_{i=1}^{n} P(C_i|\bar{t})\log_2 P(C_i|\bar{t}), \tag{15}$$

where the parameter $P(C_i)$ is the probability of category C_i, the parameter $P(t)$ is the probability of feature t, the parameter $P(C_i|t)$ is the probability of simultaneous occurrence of feature t and category C_i, and the parameter $PP(C_i|\bar{t})$ is the probability that the category C_i appears when the feature t does not appear. The score of the feature is calculated according to the formula, and the feature of TOP N is selected according to the score, so as to select and reduce the dimension of the feature.

4.2. Parallel Optimization of Emotion Classifier Based on Spark Platform. The master node provides initialization parameters $\theta = \{W, b, c\}$ for training and distributes them to each worker node. Each worker node uses the training data on all split slices for parameter learning and uses minibatch as the criterion for training parameter update. When the worker node completes the training data of a batch, the generated parameter change $\Delta\theta$ is sent to the master management node for parameter update until all training is completed, and the feature data processed in each training are converted into RDD form for storage. The specific algorithm is shown in Algorithm 1.

Table 2: Dependency of example sentences.

Dependency	
Assmod (service-2, scenic spot-1)	Advmod (good-4,-5)
Punct (good-4, service-2)	Advmod (like-8,I-6)
Nsubj (good-4, good-3)	Root (like-8, very-7)
Nsubj (root-0, good-4)	Conj (good-4, like-8)

The parallelization structure of DBN network based on spark platform is shown in Figure 4.

5. Experiment and Analysis

5.1. Experimental Data and Evaluation Indices. The dataset of this experiment comes from COAE2015 Task 3. There are 133201 microblog sentences, including a large number of interfering sentences. Datasets are divided into four different areas to evaluate, including books (BOO), audio products (DVD), electronic products (ELE), and kitchenware (Kit). Each dataset contains 2000 positive and 2000 negative comments.

In this study, the accuracy is used as the evaluation index of the experiment, and the calculation formula is as follows:

$$\text{accuracy} = \frac{\text{Num}(\text{correct})}{\text{Num}(\text{all})}, \tag{16}$$

where Num (correct) is the number of samples correctly predicted by emotion classification and Num (all) is the total number of samples in the test corpus.

5.2. Relationship between Iteration Times and Prediction Accuracy. The advantage of deep neural network over shallow neural network is that it can iteratively learn, extract features, and constantly modify the model, but too high or too low iteration times will affect the overall performance. In a task, if the number of iterations is lower than a certain value, it will lead to incomplete learning of features and imperfect release of performance. If the number of iterations is higher than a certain value, it will take a too long time and be inefficient. Therefore, the selection of iteration times is very important in the task. In the experiment, with Ft1 as the

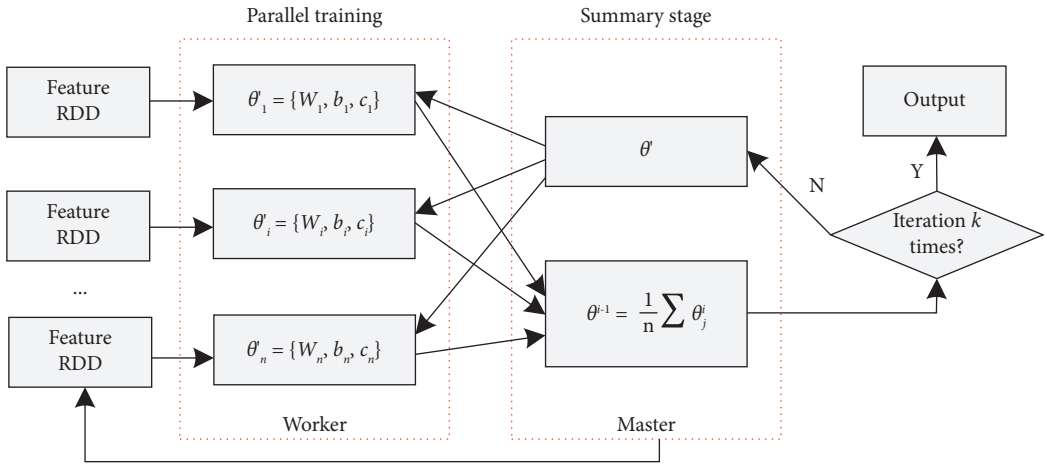

Figure 4: Parallelization structure of DBN network based on spark platform.

feature, the relationship between prediction accuracy and iteration times is shown in Figure 5. It can be seen from the figure that when the number of iterations is less than 60, the recognition rate increases significantly with the increase of the number of iterations. When the number of iterations is 65, the change range of accuracy is small and almost reaches a balanced state. Based on the above analysis, for the number of iterations, 65 iterations are selected to ensure the stability of the results.

5.3. Experimental Results and Analysis of Emotion Classification under Different Methods. Table 3 lists the experimental results of the text emotion classification method based on deep belief network designed in this study. In the network, the input is the vector composed of 1000-, 2000-, and 4000-dimensional features with the top information gain. The text abstract features are learned through hidden layer nonlinear mapping. The specific results are as follows: for the 1000-dimensional feature set, the training iteration of restricted Boltzmann machine is 100 times, and the node parameter corresponding to the network structure "input layer-hidden layer-output layer" is "1000-300-100." For the 2000-dimensional feature set, the training iteration of restricted Boltzmann machine is 100 times, and the node parameters corresponding to the network structure are "2000-600-300." For the 4000-dimensional feature set, the training iteration of restricted Boltzmann machine is 100 times per layer, and the node parameters corresponding to the network structure are "4000-600-300." It can be seen from Table 3 that the method based on depth belief network achieves the best classification accuracy of 90.94 when the structure is 2000-600-300 and the four features are combined.

In order to verify the learning and expression ability of the method in this study, the same features are used to compare the methods in reference [27], reference [28], and the proposed method. The recognition rates of reference [27] and reference [28] are 87.11% and 87.69%, respectively. When the structure of the proposed method is 2000-600-300,

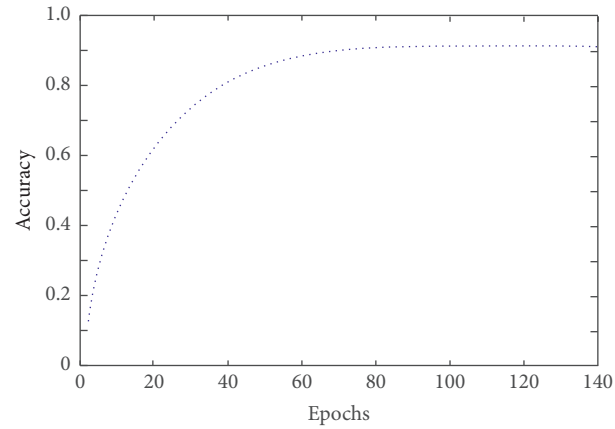

Figure 5: Relationship between iteration times and prediction accuracy.

the combination of four features achieves the best classification accuracy of 90.94%. Moreover, it can be found that the overall accuracy of the proposed method is higher than that of the methods in reference [27] and reference [28], because the proposed method will obtain more emotional knowledge than the comparison methods in the learning of features, so as to obtain better performance, as listed in Table 4.

5.4. Microblog Emotion Analysis Results under Spark Platform. The DBN network is optimized in parallel under the spark platform. The spark cluster used in the experiment is composed of 10 servers. One server is used as the management node of spark cluster, and the other nine servers are used as the computing nodes of spark cluster. The hardware configuration is CPUXeonE5520, 20 GB memory, and 1 TB hard disk. In Figure 6, the abscissa represents the size of the training data and the ordinate represents the time-consuming. It can be seen from the figure that when the amount of data increases to 60000, the spark training time is only 27.78% of the single machine training time. The Jieba word segmentation method is used to reduce the interference of irregular grammar and nonstandard words on the emotion

Input: Training data set S, set S as the feature vector set after microblog preprocessing
Output: Emotion classification result set
Determine the number of iterations K and the parameter θ^0 for initializing RBM
For $i = 0$ **to** K **do**
The Master node broadcasts θ^i to each Worker node;
The Worker node uses the data on Split to train the parameters of RBM network;
All Worker nodes send $\Delta\theta$ to the Master node;
The Master node calculates $\theta^{i+1} = 1/n \sum \theta^i_j$. The feedback mechanism of BP network is used to adjust and fine-tune the DBN network model.
End

Algorithm 1: Spark parallelized DBN network.

Table 3: Results based on the deep belief network method.

Method	Feature structure	Ft_1	$Ft_1 + Ft_2$	$Ft_1 + Ft_2 + Ft_3$	$Ft_1 + Ft_2 + Ft_3 + Ft_4$
Proposed method	1000-300-100	89.42	89.59	89.67	89.89
	2000-600-300	90.21	90.29	90.24	90.94
	4000-600-300	90.14	90.21	90.22	90.87

Table 4: Comparison of experimental results of different methods.

Method	Accuracy
Reference [27]	87.11
Reference [28]	87.69
Proposed method	90.94

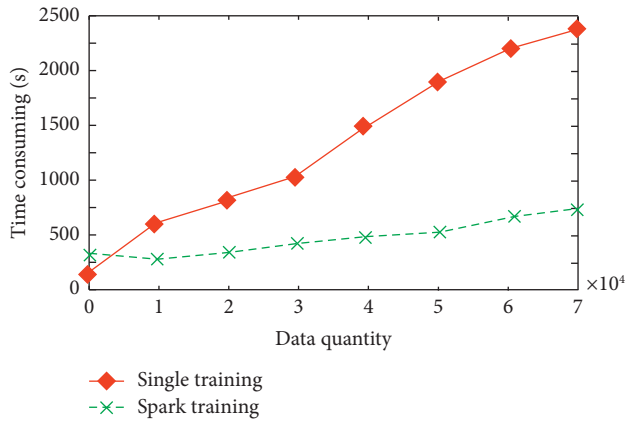

Figure 6: Comparison of training time changes when data increase between a single node and spark parallel computing.

analysis task of microblog text. The feature dimensionality reduction operation is carried out by using the feature selection method of information gain to avoid the problem of dimension disaster. It can be concluded that the parallel DBN algorithm based on spark platform can effectively improve the operation efficiency when processing massive data.

6. Conclusion

Aiming at the problem that the existing methods in the big data environment do not extract the emotional features of microblog sufficiently and the average accuracy of the results is low, a microblog emotion analysis method using deep learning in the spark big data environment is proposed. The DBN is parallelized through spark cluster, which greatly shortens the training time. Experimental results show that the proposed algorithm has good microblog emotion analysis ability.

In this study, the factors considered in the study of data parallel fragmentation strategy are not comprehensive enough. More data fragmentation strategies should be tried in the future. In the follow-up, other parallel optimization algorithms can be used for reference to improve the parallel speedup ratio of the algorithm. Moreover, in addition to word vector representation, researchers have developed new representation methods in recent years, such as Atlas and tree database, to represent text information. Therefore, the text emotion classification algorithm proposed in this study can be further improved. How to embed more and more effective text semantic information is still the focus of the next step.

Data Availability

The data used to support the findings of this study are included within the article.

Conflicts of Interest

The authors declare that they have no conflicts of interest.

Acknowledgments

This work was supported by the 2020 Horizontal Project (no. HX2020029).

References

[1] P. Gangamohan, S. R. Kadiri, and B. Yegnanarayana, "Analysis of emotional speech-A review," *Toward Robotic Socially Believable Behaving Systems-Volume I*, vol. 2, no. 14, pp. 205–238, 2016.

[2] A. M. Mohsen, A. M. Idrees, and H. A. Hassan, "Emotion analysis for opinion mining from text: a comparative study," *International Journal of e-Collaboration*, vol. 15, no. 1, pp. 38–58, 2019.

[3] D. Xu, Z. Tian, R. Lai, X. Kong, Z. Tan, and W Shi, "Deep learning based emotion analysis of microblog texts," *Information Fusion*, vol. 64, no. 7, pp. 1–11, 2020.

[4] A. Chatterjee, U. Gupta, M. K. Chinnakotla, R. Srikanth, M. Galley, and P. Agrawal, "Understanding emotions in text using deep learning and big data," *Computers in Human Behavior*, vol. 93, no. 3, pp. 309–317, 2019.

[5] F. Xia and Z. Zhang, "Study of text emotion analysis based on deep learning," in *Proceedings of the 2018 13th IEEE Conference on Industrial Electronics and Applications (ICIEA)*, pp. 2716–2720, IEEE, Wuhan, China, May 2018.

[6] L. Cao, S. Peng, and P. Yin, "A survey of emotion analysis in text based on deep learning," in *Proceedings of the 2020 IEEE 8th International Conference on Smart City and Informatization (iSCI)*, pp. 81–88, IEEE, Guangzhou, China, February2020.

[7] L. Ran, L. Zheng, and L. Hailun, "Text emotion analysis: a survey," *Journal of Computer Research and Development*, vol. 55, no. 1, pp. 30–39, 2018.

[8] S. Peng, L. Cao, Y. Zhou et al., "A survey on deep learning for textual emotion analysis in social networks," *Digital Communications and Networks*, vol. 23, no. 5, pp. 12–21, 2021.

[9] X. Wang, L. Kou, V. Sugumaran, X. Luo, and H Zhang, "Emotion correlation mining through deep learning models on natural language text," *IEEE Transactions on Cybernetics*, vol. 51, no. 9, pp. 4400–4413, 2021.

[10] L. Zhang, S. Wang, and B. Liu, "Deep learning for sentiment analysis: a survey," *Review: Data Mining and Knowledge Discovery*, Wiley Interdisciplinary, vol. 8, no. 4, pp. 1253–1260, 2018.

[11] J. Choudrie, S. Patil, K. Kotecha, N. Matta, and I Pappas, "Applying and understanding an advanced, novel deep learning approach: a covid 19, text based, emotions analysis study," *Information Systems Frontiers*, vol. 23, no. 6, pp. 1431–1465, 2021.

[12] B. Kratzwald, S. Ilić, M. Kraus, S. Feuerriegel, and H Prendinger, "Deep learning for affective computing: text-based emotion recognition in decision support," *Decision Support Systems*, vol. 115, no. 7, pp. 24–35, 2018.

[13] S. Ahmad, M. Z. Asghar, F. M. Alotaibi, and S Khan, "Classification of poetry text into the emotional states using deep learning technique," *IEEE Access*, vol. 8, no. 6, pp. 73865–73878, 2020.

[14] E. A. H. Khalil, E. M. F. E. Houby, and H. K. Mohamed, "Deep learning for emotion analysis in Arabic tweets," *Journal of Big Data*, vol. 8, no. 1, pp. 136–148, 2021.

[15] E. Batbaatar, M. Li, and K. H. Ryu, "Semantic-emotion neural network for emotion recognition from text," *IEEE Access*, vol. 7, no. 2, pp. 111866–111878, 2019.

[16] N. Majumder, S. Poria, A. Gelbukh, and E Cambria, "Deep learning-based document modeling for personality detection from text," *IEEE Intelligent Systems*, vol. 32, no. 2, pp. 74–79, 2017.

[17] U. Rashid, M. W. Iqbal, and M. A. Skiandar, "Emotion detection of contextual text using deep learning," *IEEE*, in *Proceedings of the 2020 4th International Symposium on Multidisciplinary Studies and Innovative Technologies (ISMSIT)*, pp. 1–5, Istanbul, Turkey, November 2020.

[18] F. A. Acheampong, C. Wenyu, and H. Nunoo-Mensah, "Text-based emotion detection: advances, challenges, and opportunities," *Engineering Reports*, vol. 2, no. 7, pp. 12189–12198, 2020.

[19] S. Tripathi, S. Tripathi, and H. Beigi, "Multi-modal emotion recognition on iemocap dataset using deep learning," vol. 1, no. 9, pp. 23–31, 2018, https://arxiv.org/abs/1804.05788.

[20] Y. Kumar, D. Mahata, and S. Aggarwal, "Bhaav-a text corpus for emotion analysis from Hindi stories," vol. 10, no. 4, pp. 1634–1642, 2019, https://arxiv.org/abs/1910.04073.

[21] S. Jebbara and P. Cimiano, "Aspect-based sentiment analysis using a two-step neural network architecture," *Semantic Web Evaluation Challenge*, pp. 153–167, Springer, Cham, 2016.

[22] P. Liu, S. Joty, and H. Meng, "Fine-grained opinion mining with recurrent neural networks and word embeddings," in *Proceedings of the 2015 conference on empirical methods in natural language processing*, pp. 1433–1443, Lisbon, Portugal, September 2015.

[23] T. Chen, R. Xu, Y. He, and X. Wang, "Improving sentiment analysis via sentence type classification using BiLSTM-CRF and CNN," *Expert Systems with Applications*, vol. 72, no. 3, pp. 221–230, 2017.

[24] W. Yin, K. Kann, and M. Yu, "Comparative study of CNN and RNN for natural language processing," vol. 6, no. 1, pp. 200–207, 2017, arXiv preprint arXiv.

[25] X. Li, L. Bing, and P. Li, "Aspect term extraction with history attention and selective transformation," *IJCAI*, vol. 3, no. 11, pp. 4194–4200, 2018.

[26] W. Wang, S. J. Pan, and D. Dahlmeier, "Coupled multi-layer attentions for co-extraction of aspect and opinion terms," in *Proceedings of the AAAI Conference on Artificial Intelligence*, pp. 3316–3322, CA, USA, February 2017.

[27] C. Zhang, L. Xie, Y. Aizezi, and X Gu, "User multi-modal emotional intelligence analysis method based on deep learning in social network big data environment," *IEEE Access*, vol. 7, no. 2, pp. 181758–181766, 2019.

[28] N. Jamal, C. Xianqiao, F. Al-Turjman, and F. Ullah, "A deep learning–based approach for emotions classification in big corpus of imbalanced tweets," *ACM Transactions on Asian and Low-Resource Language Information Processing*, vol. 20, no. 3, pp. 1–16, 2020.

[29] H. Jelodar, Y. Wang, R. Orji, and S. Huang, "Deep sentiment classification and topic discovery on novel coronavirus or COVID-19 online discussions: NLP using LSTM recurrent neural network approach," *IEEE Journal of Biomedical and Health Informatics*, vol. 24, no. 10, pp. 2733–2742, 2020.

[30] J. Wei, J. Liao, Z. Yang, S. Wang, and Q. Zhao, "BiLSTM with multi-polarity orthogonal attention for implicit sentiment analysis," *Neurocomputing*, vol. 383, pp. 165–173, 2020.

Hindawi
Mobile Information Systems
Volume 2022, Article ID 4947586, 12 pages
https://doi.org/10.1155/2022/4947586

Research Article

Resource Cache Sharing System of Education Information Center Network Based on Internet of Things

Wang Juan

School of Management, Anhui Vocational and Technical College, Hefei, Anhui 430074, China

Correspondence should be addressed to Wang Juan; 2007041@muc.edu.cn

Received 14 June 2022; Revised 6 July 2022; Accepted 5 August 2022; Published 24 August 2022

Academic Editor: Shadi Aljawarneh

The development of the internet of things has spawned new information concepts such as educational information sharing. Due to the openness of the internet of things, all kinds of mobile terminal devices can rely on the internet of things for data communication, information interaction, and resource sharing. Although the development of the internet of things has brought convenience to people's lives, the internet of things is facing severe challenges in the fields of internal data sharing and cache sharing of educational information. The existing resource sharing systems do not fully consider the problems of privacy, shared data security, and data access control. This paper mainly studies the network integrated resource cache sharing system of the education information center based on internet of things. The data management system of the network education information center is developed on the basis of the school teaching management system and lifelong education public service platform, combined with the actual situation of student information. This paper combines the enrollment and information workflow of the student information management website, analyzes the problems existing in the current workflow, and then uses computer technology to standardize and transform the workflow, realize the information of the built-in resources in the data management, and solve the problems of data cache sharing and data statistics in the management of the education information center. The simulation results show that with the increase in the number of concurrent threads, the average response time of the edge cloud system deployed with two servers is smaller than that of the edge cloud system deployed with a single server, and the cloud system has good scalability.

1. Introduction

The internet of things is an open network. Each terminal device can freely transmit data, exchange information, and share built-in resources between devices. Its emergence promotes the rapid development of data detection, wireless intelligent transmission, intelligent information processing, and other technologies [1]. At the same time, the development of these information technologies makes people's life more convenient and improves people's quality of life [2]. The rapid development of the internet of things and wireless communication technology has driven the rapid development of mobile terminals, giving birth to a series of computing-intensive and delay-sensitive related applications [3]. Nowadays, data information has become an important factor in today's social life. Through the analysis and processing of internet of things data, the quality of applications and services in the network can be improved, so as to promote the rapid development of society and life [4]. At the same time, the demand for massive terminal devices for data resources has high response time and security. Therefore, in the complex internet of things environment, how to effectively and safely exchange data information is a severe challenge. This paper studies the problem of the built-in resource cache sharing system of the education information center network based on the internet of things [5]. With the continuous promotion of the learning society and the continuous improvement of the school's modern distance education brand, more and more students choose to improve their academic qualifications through network education in order to improve their own quality. Therefore, the number of students managed by the off-campus education

information center is increasing, which makes the management of the education center more difficult [6]. At present, the student data management of the education information center is still in the stage of Excel table management, and there is no perfect student data management platform for unified management [7]. At the same time, in order to improve the service quality of students, the "one-stop" service mode has brought problems such as data dispersion and individual war. Through the construction of the student information data management system, we further organize and optimize the workflow of the education information center to solve the problems caused by the "one-stop" service [8]. In the construction of a student information and data management system, it is necessary to combine the quantitative evaluation indicators of employee work performance, dynamic statistical analysis of student sources, and return visit of student problem records, so as to realize the dynamic statistical analysis and return visit records of student sources, data fusion of student status information, automatic statistical calculation, and cache sharing of various pass rates, so as to help the education information center find student source growth sites in time, master students' overall learning process, fully understand students' information, reduce statistical accounting of duplicate data, and realize students' data sharing, dynamic statistical analysis of students' sources, tracking of students' files, and students' management level [9].

2. Related Work

This paper proposes an edge cloud collaboration method based on differentiated tasks, which realizes the collaborative utilization of computing resources [10]. The comprehensive priority of the task is defined according to the importance and response ratio of the request task, and the resources are scheduled according to the global priority of the task. This paper introduces the proposed technologies and methods and puts forward the design and implementation of an edge cloud collaborative internet of things platform for large-scale heterogeneous scenes [11]. The platform has the functions of flag mapping, resource description, node dynamic access, node discovery, permission management, and so on. In the current internet of things environment, there are more and more data resources interaction and sharing between mobile terminals, so it is necessary to store and process data more efficiently and safely. In order to ensure the safe storage and management of data resources, an efficient, secure, and lightweight storage mode is proposed [12]. The sharing and analysis of internet of things data resources is the driving force of the rapid development of information technology. In order to realize the secure sharing and utilization of data resources, secure and flexible access control policies are implemented for data access and exchange [13]. According to the existing student resources of the education information center, we summarize the student unit information, improve the information accumulation of surrounding units, improve the education needs of employees in each unit, implement corresponding incentive policies, improve the education level of each unit, and form a dynamic education demand information database [14]. By recording and summarizing the existing data and new data to provide the basis for enrollment publicity and timely discovery of potential students, the education information center has established a dynamic information database of existing data and new data, urged the head teacher to conduct telemarketing, promoted enrollment publicity, decomposed the indicators according to the enrollment tasks of the education information center, and provided data support for the work assessment and evaluation of head teachers.

3. Research on Resource Cache Sharing and Its Security Based on the Internet of Things

3.1. Design of Side Cloud Collaborative Task Scheduling Model Based on the Internet of Things. The resource types of the platform mainly include computing, network, and storage. Users who call platform services will obtain a corresponding number of resources in the edge cloud or cloud computing center.

The overall architecture of the edge cloud model is shown in Figure 1.

Platform resources mainly include computing resources, network resources, and storage resources. The service uses the resources provided by the platform to process client requests, and the sensing device itself also has certain computing, network, and storage resources. The resource model of the platform will be described in detail below.

The usage scenarios of the edge cloud determine that its storage resources are limited. For a single server deployment, the total storage resources of edge cloud N are as follows:

$$\text{AllStore edge } N = \text{Disk}_{\text{edge}N} - \text{Pro Disk}_{\text{edge } N} - \text{SysDiskedge } N. \tag{1}$$

The task processing request of the edge cloud collaborative architecture IoT platform first arrives at the edge cloud. The edge cloud allocates tasks based on its own resources and the resources needed to process tasks.

The overall architecture of the edge cloud task processing model is shown in Figure 2.

The edge cloud service interface forwards the received task to the task allocation module. The task allocation module uses the corresponding allocation strategy for task allocation. There are three allocation strategies: the first is to deal with it separately in the edge cloud; the second is to transfer the task to the cloud computing center for processing; and the third is task segmentation. Some are processed in the edge cloud and some in the cloud computing center. Finally, the edge cloud integrates the processing results and returns them to the task requestor.

Edge cloud computing resources are limited, and processing tasks in edge cloud requires waiting time. The time required to complete the task is

$$\text{Time Edge} = \text{Wait}_{\text{edge } N}(\text{Task}) + \text{CPU}_{\text{edge } N(\text{Task})}. \tag{2}$$

The edge cloud transfers the task to the cloud computing center for processing. Because the network bandwidth of the cloud computing center is much larger than that of the edge

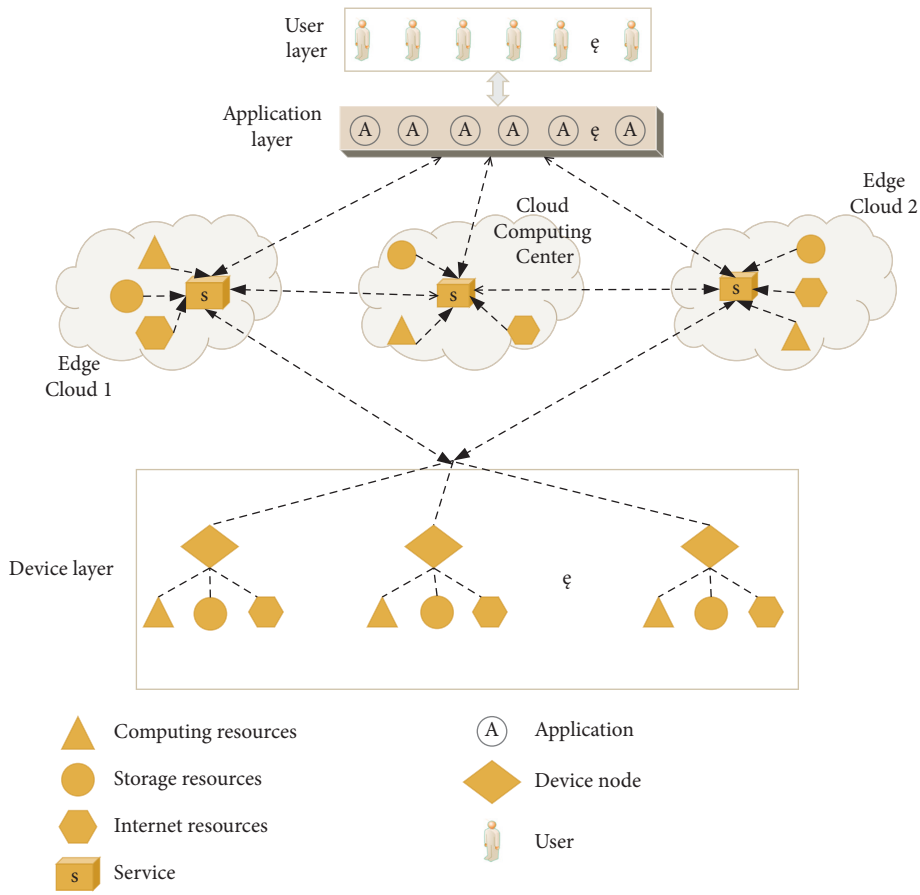

Figure 1: Overall architecture of the edge cloud resource model.

cloud, the network transmission time of the task depends on the available bandwidth of the edge cloud. The cloud computing center has a large number of computing resources, and the task processing of the cloud computing center does not need to wait. The time required to complete the task is

$$\text{Time Cloud} = \text{Net}_{\text{cdge}N}(\text{Task}) + \text{CPU}_{\text{cloud}(\text{Task})}. \quad (3)$$

Edge cloud segmentation task: tasks are processed in the edge cloud and transferred to the cloud computing center for processing. Finally, the edge cloud integrates the results of the two parts and returns them to the requester. The time required to complete the task is

$$\text{Time Mix} = \max\left\{\frac{\text{Wait}_{\text{edge}N}(\text{Task}) + \lambda * \text{CPU}_{\text{edge}N}(\text{Task})}{(1-\lambda) * \text{Net}_{\text{edge}N}(\text{Task}) + (1-\lambda) * \text{CPU}_{\text{cloud}}(\text{Task})}\right\}. \quad (4)$$

According to formulas (2)–(4), the response report of each task allocation strategy is as follows:

Edge cloud individual management response report:

$$\text{Res Ratio Edge} = \frac{\text{Time Edge} + \text{Queue}_{\text{wait}}(\text{Task})}{\text{CPU}_{\text{edge}N}(\text{Task})}. \quad (5)$$

Transfer to cloud computing center processing response ratio:

$$\text{Res Ratio Cloud} = \frac{\text{Time Cloud} + \text{Queue}_{\text{wait}}(\text{Task})}{\text{CPU}_{\text{cloud}}(\text{Task})}. \quad (6)$$

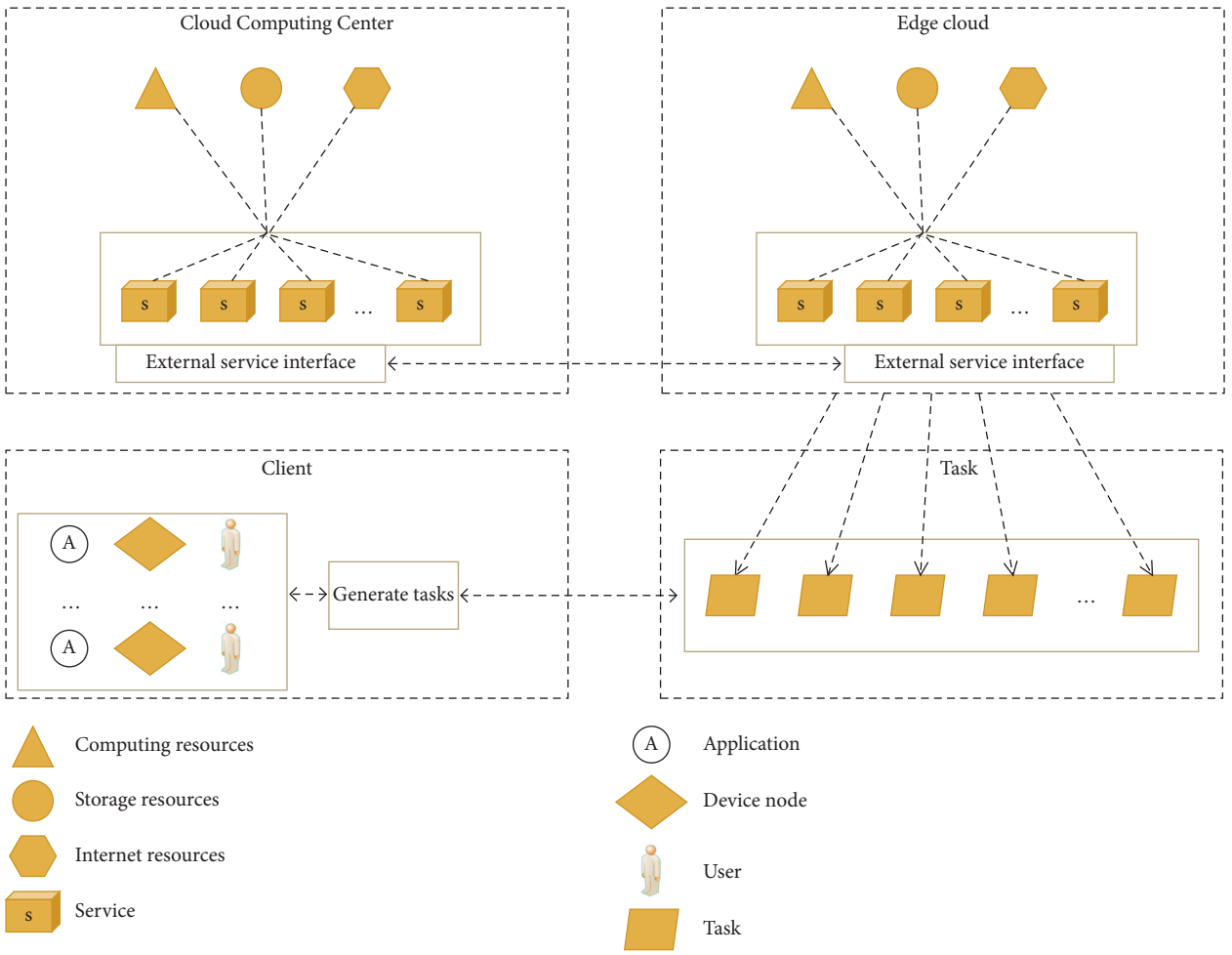

Figure 2: Overall architecture of the edge cloud task processing model.

Mixed processing response ratio:

$$\text{Res Ratio Mix} = \frac{\text{Time Mix} + \text{Queue}_{\text{wait}}(\text{Task})}{\max\left\{\lambda * \text{CPU}_{\text{edge}N}(\text{Task}), (1-\lambda) * \text{CPU}_{\text{cloud}}(\text{Task})\right\}}. \tag{7}$$

The global priority is set by task priority and processing response ratio to ensure that the tasks with high priority are executed first and avoid the hunger for low priority tasks. Task scheduling algorithm can achieve a balance between task priority and response ratio and meet the actual needs of the internet of things application scenarios. Based on the task priority definition method and task processing response ratio proposed above, the comprehensive priority is calculated as follows:

$$\text{Com Priority} = \gamma^* \text{Response Ratio} + (1-\gamma)^{*I\,\text{Priority}}. \tag{8}$$

The certification authority (CA) is equivalent to the system administrator. Set up the system for access control and distribute the key and authority level information to the terminal equipment. The data sharer encrypts the shared data and then uploads the encrypted data resources to the cloud server for other users to access. The data acquirer is interested in the data stored in the cloud server, and then the user can view and download the relevant data on the cloud server according to their access rights. The cloud server is a public storage platform where data sharers can store and share encrypted data. The data requester can freely access and download the data stored on the cloud server according to his own authority.

3.2. Security Resource Sharing Access Control Scheme Design. The certification authority (CA) uses the elements in the ordered network attribute set to construct an R-order polynomial according to the attribute order specified by the network system:

$$\begin{aligned} f(x) &= (x - A_R)(x - A_{R-1}) \cdots (x - A_1) \\ &= b_R x^R + b_{R-1} x^{R-1} + \cdots + b_0. \end{aligned} \tag{9}$$

The certification center (CA) receives the message sent by the user interface of the terminal member. The certification center (CA) calculates and verifies the user interface identifier of the terminal member u_i by verifying (9). If the verification is successful, the certification authority (CA) will calculate the following formula:

$$\begin{cases} b_0\lambda_i g_1 + b_1 a_{i,1}\lambda_i g_1 + \cdots + b_R a_{i,1}^R \lambda_i g_1 = f\left(a_{i,1}\right)\lambda_i g_1, \\ b_0\lambda_i g_1 + b_1 a_{i,2}\lambda_i g_1 + \cdots + b_R a_{i,2}^R \lambda_i g_1 = f\left(a_{i,2}\right)\lambda_i g_1, \\ \cdots, \\ b_0\lambda_i g_1 + b_1 a_{i,r}\lambda_i g_1 + \cdots + b_R a_{i,j}^R \lambda_i g_1 = f\left(a_{i,r}\right)\lambda_i g_1. \end{cases} \tag{10}$$

If the following formula passes verification

$$\begin{cases} f\left(a_{i,1}\right)\lambda_i g_1 = 0, \\ f\left(a_{i,2}\right)\lambda_i g_1 = 0, \\ \cdots, \\ f\left(a_{i,r}\right)\lambda_i g_1 = 0. \end{cases} \tag{11}$$

This means

$$\begin{cases} f\left(a_{i1}\right) = 0, \\ f\left(a_{i,2}\right) = 0, \\ \cdots, \\ f\left(a_{i,r}\right) = 0. \end{cases} \tag{12}$$

Any terminal member u_i obtains authorization parameters from the information of registered members and calculates the following formula:

$$\begin{aligned} T_{\text{pub},j} &= T_{j,0} = \lambda_j g_1, \\ T_{\text{pri}} &= \sum_{\tau=1}^{r} T_{j,\tau} = \sum_{\tau=1}^{r} t_{j,\tau}\lambda_j g_1 \\ &= \left(t_{j,1} + \ldots + t_{j,r}\right)\lambda_j g_1. \end{aligned} \tag{13}$$

The terminal member u_i selects a random number and calculates and constructs an R–1 order polynomial based on the previously saved attribute authority value:

$$f(x) = m_j K_{j,r-1} x^{r-1} + m_j K_{j,r-2} x^{r-2} + \cdots + m_j K_{j,1} x + M_j. \tag{14}$$

The terminal member u_i accesses the link, downloads the corresponding encrypted resource, and calculates the corresponding attribute authorization value according to the permission setting of the terminal member u_i shared resource and the corresponding threshold value. Then, the terminal member u_i constructs a polynomial according to the information and Lagrangian interpolation theorem:

$$f(x) = \sum_{x=1}^{r} \prod_{1 \le \omega \le r, \omega \ne x} \frac{x - w_{i,w}}{w_{i,x} - w_{i,\omega}} y_{j,x}. \tag{15}$$

And calculate the constant term:

$$\begin{aligned} M_i = f(0) &= \sum_{x=1}^{r} \left(\prod_{1 \le \sigma \le r, \omega \ne x} \frac{-w_{i,w}}{w_{i,x} - w_{i,\omega}} \right) y_{j,x} \\ &= M_j. \end{aligned} \tag{16}$$

3.3. Analysis of the Effect of the Security Sharing Scheme. Any legal terminal member in the system can download encrypted resources with corresponding access rights. CS opens the corresponding shared resource link. According to the characteristics of bilinear mapping, there are

$$\begin{aligned} &e\left(\eta_{i,h}, pk_{u_4}\right) \\ &= e\left(SK_A\left(t_{i,1} + t_{i,2} + \ldots + t_{i,r}\right)g_1, sk_u g_1\right) \\ &= e\left(\left(t_{i,1} + t_{i,2} + \ldots + t_{i,r}\right)g_1, g_1\right)^{SK_i sk_{n_i}}. \end{aligned} \tag{17}$$

The attribute permission setting is signed by the terminal member and the cloud service platform (CS), which means that the cloud service platform (CS) can determine that the terminal member has access rights, and then the cloud service platform (CS) opens the link to the corresponding encrypted resource for the terminal member. Member u_j can download the corresponding encrypted resource according to the link.

Here,

$$\begin{aligned} T_{\text{pub},j} &= T_{j,0} \\ T_{\text{pni}} &= \left(t_{j,1} + \ldots + t_{j,r}\right)\lambda_j g_1, \\ p_{u_j} &= m_j \lambda_j g_1, \\ M_j &= m_j T_{pn}, \\ \eta_{j,h} &= SK_A\left(t_{j,1} + t_{j,2} + \ldots + t_{j,r}\right)g_1. \end{aligned} \tag{18}$$

Then, the terminal member u_i uses the key it solved to do the following calculations:

$$
\begin{aligned}
&V_j \oplus H_3\left(e\left(v_j, M_i\right)\right) \\
&\quad = m \oplus H_3\left(e\left(p_{u_j}, \eta_{j,h}\right)^{\varsigma_j}\right) \oplus H_3\left(e\left(v_j, M_i\right)\right) \\
&\quad = m \oplus H_3\left(e\left(m_j\lambda_j g_1, SK_A\left(t_{j,1} + t_{j,2} + \cdots + t_{j,r}\right)g_1\right)^{\zeta_j}\right) \oplus H_3\left(e\left(\varsigma_j PK_A, m_j T_{pri}\right)\right) \\
&\quad = m \oplus H_3\left(e\left(m_j g_1, \left(t_{j,1} + t_{j,2} + \cdots + t_{j,r}\right)PK_A\right)^{\lambda_j\varsigma_j}\right) \oplus H_3\left(e\left(\varsigma_j PK_A, m_j T_{pri}\right)\right) \\
&\quad = m \oplus H_3\left(e\left(m_j g_1, \left(t_{j,1} + t_{j,2} + \cdots + t_{j,r}\right)PK_A\right)^{\lambda_j\varsigma_j}\right) \oplus H_3\left(e\left(PK_A, m_j T_{pni}\right)^{\varsigma j}\right) \\
&\quad = m \oplus H_3\left(e\left(m_j g_1, \left(t_{j,1} + t_{j,2} + \cdots + t_{j,r}\right)PK_A\right)^{\lambda_j\varsigma}\right) \oplus H_3\left(e\left(PK_A, m_j\left(t_{j,1} + \cdots + t_{j,r}\right)\lambda_j g_1\right)^{\zeta_j}\right) \\
&\quad = m \oplus H_3\left(e\left(m_j g_1, PK_A\right)^{\left(t_{j1}+t_{j,2}+\cdots+t_{j,r}\right)\lambda_j\varsigma_j}\right) \oplus H_3\left(e\left(PK_A, m_j g_1\right)^{\left(t_{j1}+\cdots+t_{j,r}\right)\lambda_j\varsigma_j}\right) = m.
\end{aligned}
\tag{19}
$$

If $w_{j,1}, w_{j,2}, \ldots, w_{j,r}$ are different numbers in the number field F, then $y_{j,1}, y_{j,2}, \ldots, y_{j,r}$ are any set of numbers in the field F. The following is a single polynomial of order not greater than $r-1$:

$$
f(x) = \sum_{x=1}^{r}\left(\prod_{1\le\varpi\le r,\omega\ne x}\frac{x - w_{j,w}}{w_{j,x} - w_{j,\varpi}}\right)y_{j,x}. \tag{20}
$$

Assumptions are as follows:

$$
\begin{cases}
c_0 + c_1 w_{j,1}^1 + c_2 w_{j,1}^2 + \cdots + c_{r-1} w_{j,1}^{r-1} = y_{j,1}, \\
c_0 + c_1 w_{j,2}^1 + c_2 w_{j,2}^2 + \cdots + c_{r-1} w_{j,2}^{r-1} = y_{j,2}, \\
\cdots, \\
c_0 + c_1 w_{j,r}^1 + c_2 w_{j,r}^2 + \cdots + c_{r-1} w_{j,r}^{r-1} = y_{j,r}.
\end{cases} \tag{21}
$$

This is an unknown system of linear equations, and the determinant of its coefficients is as follows:

$$
\begin{aligned}
|A| &= \begin{vmatrix}
1 & w_{j,1}^1 & w_{j,1}^2 & \ldots & w_{j,1}^{r-1} \\
1 & w_{j,2}^1 & w_{j,2}^2 & \ldots & w_{j,2}^{r-2} \\
\ldots & \ldots & \ldots & \ldots & \ldots \\
1 & w_{j,r}^1 & w_{j,r}^2 & \ldots & w_{j,r}^{r-1}
\end{vmatrix} \\
&= \begin{vmatrix}
1 & 1 & \ldots & 1 \\
w_{j,1}^1 & w_{j,2}^1 & \ldots & w_{j,r}^1 \\
w_{j,1}^2 & w_{j,2}^2 & \ldots & w_{j,r}^2 \\
\ldots & \ldots & \ldots & \ldots \\
w_{j,1}^{r-1} & w_{j,2}^{r-1} & \ldots & w_{j,r}^{r-1}
\end{vmatrix} = \prod_{r\ge i>\tau\ge 1}\left(w_{j,i} - w_{j,\tau}\right).
\end{aligned}
\tag{22}
$$

According to the user interface parameters of the corresponding terminal member u_i, the terminal member u_i cannot construct a polynomial but can only construct a system of linear equations with unknown numbers:

$$
\begin{cases}
c_0 + c_1 w_{j,1}^1 + c_2 w_{j,1}^2 + \cdots + c_{r-1} w_{j,1}^{r-1} = y_{j,1}, \\
c_0 + c_1 w_{j,2}^1 + c_2 w_{j,2}^2 + \cdots + c_{r-1} w_{j,2}^{r-1} = y_{j,2}, \\
\cdots, \\
c_0 + c_1 w_{j,r-1}^1 + c_2 w_{j,r-1}^2 + \cdots + c_{r-1} w_{j,r-1}^{r-1} = y_{j,r-1}.
\end{cases} \tag{23}
$$

3.4. Analysis of the Performance Test Results of the Resource Cache Sharing System. The edge-cloud collaborative IoT platform is designed for large-scale heterogeneous scenarios. When invoking highly concurrent services, the platform still needs to ensure that the service is stable and available. Use ApacheJMeter to simulate the throughput and response time of the test platform at different concurrency levels. The platform is mainly divided into two parts: cloud computing center and edge cloud system. The cloud computing center adopts high-performance service cluster deployment, which can dynamically expand system resources to provide services for each edge cloud and application layer; the edge cloud system has limited resources and is an important part of the external services provided by the platform. Therefore, we mainly measure the performance of edge cloud systems.

During the test, we used ApacheJMeter to simulate service requests from edge cloud clients and set up different numbers of threads to simulate concurrent service requests from different clients. Edge cloud systems are divided into single-server deployment and dual-server load balancing deployment. The number of simulated concurrent clients increased from 1 to 50 and then to 100 and then increased by 100 for each test to ensure the authenticity of customer request data and behavior in the simulated environment. Taking the actual requests in the system log as the data source, the test results of cloud edge systems deployed with single- and dual-server load balancing are shown in Tables 1 and 2, respectively. The task queue represents the proportion of the backlog of tasks in the task queue in the cloud edge system.

The test results of a single server are shown in Table 1.

The test results of the two servers are shown in Table 2.

Table 1: Single server test results.

Number of analog clients	Average response time (ms)	Error rate (%)	Task queue (%)	Throughput (TPS)
1	19	0	0	54.7
50	85.3	0	0	228.3
100	117.5	0	0	247.4
200	141.3	0	0	254.4
300	182.5	0	0.7	258.6
400	203.8	0	1.4	256.8
500	224.4	0	2.6	253.5
600	273.3	0	4.3	251.8
700	315.8	0	4.9	247.5
800	420.6	0.23	6.3	242.7
900	607.4	1.38	7.6	215.5

Table 2: Dual server test results.

Number of analog clients	Average response time (ms)	Error rate (%)	Task queue (%)	Throughput (TPS)
1	17.5	0	0	55.4
50	51.4	0	0	235.3
100	86.6	0	0	277.3
200	123	0	0	310.4
300	141.9	0	0	334.9
400	163.8	0	0	347.7
500	170.4	0	0	430.5
600	208.6	0	0	476.8
700	210.5	0	0.9	431.4
800	230.5	0	1.8	397.8
1,000	254.4	0	2.6	384.6
1,200	306.2	0	5.4	388.8
1,400	374.2	0.17	7.3	345.9
1,600	582.8	1.5	8.7	314.7

The relationship between the amount of edge cloud swallowing and the number of concurrent threads of a single server is shown in Figure 3.

With the increase in the number of concurrent threads, the average response time of the edge cloud system deployed by two servers is less than that of the edge cloud system deployed by a single server. When the number of concurrent threads is greater than the maximum number of threads supported by the edge cloud, the average response time will increase significantly. As shown in Figure 3, when the concurrency is 300, the throughput of the edge cloud system deployed by a single service reaches the maximum, which indicates that when the concurrency is less than 300, the number of tasks is not saturated; When the number of concurrent tasks is greater than 300, the number of tasks reaches saturation, but when the number of concurrent tasks is less than 800, the system throughput does not decrease significantly.

The relationship between the throughput of the dual server edge cloud and the number of concurrent threads is shown in Figure 4.

Similar to a single server, analyze the edge cloud swallowing volume of dual server deployment according to Figure 4. For a single-server deployed edge cloud system, when the number of concurrent tasks reaches 300, the task queue begins to accumulate, but the system can still process tasks in time, and the task processing error rate is 0. When the number of concurrent tasks reaches 800, request processing exceptions begin to occur; when dual server deployment is adopted, the number of concurrent tasks reaches 700, and the task queue begins to accumulate tasks. When the number of concurrent tasks reaches 1,400, request processing exceptions begin to appear. The deployment processing capacity of two servers is about twice that of one server, which proves that the edge cloud system has good horizontal scalability. The increase of servers can improve the concurrency of edge cloud support.

4. Design and Application of the Network Resource Management System in Education Information Center

4.1. Demand Analysis of the Education Information Center Network System. The source of students in the education information center mainly includes the following aspects: due to the influence of the school, students come to sign up, visit and guide enterprises through the education information center, and cooperate with enterprises to establish enterprise classes. The enrollment personnel of the education information center shall go out for publicity and distribute

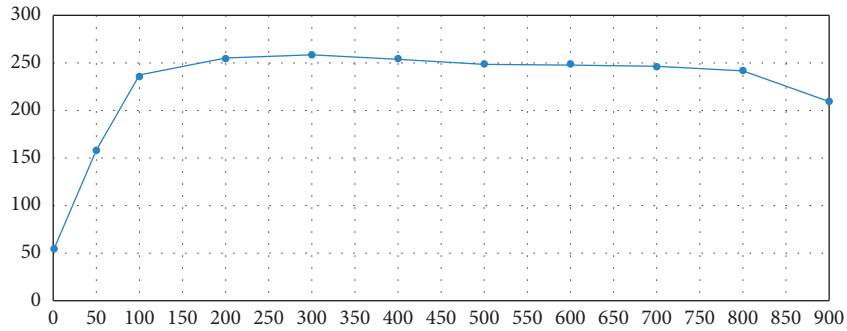

Figure 3: Single server throughput.

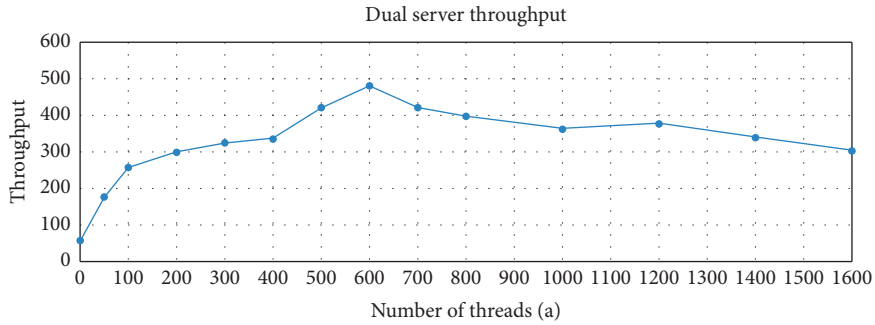

Figure 4: Dual server throughput.

brochures and other publicity materials or recommended by school students. In order to encourage the head teacher of the education information center to publicize the old and bring the new, the college has also formulated the corresponding objectives and tasks of the head teacher of the education information center as the basis for performance appraisal. The number of old and new students is generally recorded by the enrollment personnel and notified regularly in the education information center. Students usually do not know the student number of the recommender and only record the name. Sometimes, there are typos in the name, which may lead to inaccurate records and need to be rechecked in the future. The effect is not very ideal.

In the student support service of the education information center, in addition to solving various problems encountered by students in the learning process, it is also necessary to actively communicate with students at each key node of teaching activities. Understand student information, urge students to select courses, complete various learning activities organized by the school on time, and carry out graduation design and network unified examination according to the division of responsibilities of the education information center. Enrollment management and other business modules are part-time by the corresponding head teacher, so there is cross management. In order to avoid excessive service, it is necessary to share student return visit information with the head teacher.

The graduation certificate management of the education information center is different from that of the school. The education information center does not manage the number and processing time of student certificates, but the school distributes the student graduation file information to the education information center. The education information center arranges the students' graduation certificates, graduation records (transcripts, enrollment information forms), and tuition invoices and notifies the students. Because students receive more people, it is easy to cause confusion. At the same time, adult students are scattered, and the collection cycle is long. The education information center should also archive student cards and other documents at any time to facilitate students receiving them. The system can query whether the certificate storage location, number information, and data of the education information center are complete. It can quickly locate the graduation certificate number and storage location for students to receive.

The network unified examination is the national unified network education undergraduate examination. School students need to participate in College English B and computer culture basic examination. In order to do a good job in the general examination enrollment management, encourage students to practice and participate in guidance and pay a return visit to the students enrolled in this batch to understand the basic situation of students so as to provide guidance. At present, there are some problems in the online examination management of the education information center. First, the list obtained from the online examination office contains not only the data of the education information center but also the data of other education information centers. You must manually sort out and summarize the registration data of this education information center. During the registration period, we have to rearrange the calculation every day, which is very troublesome. Secondly,

after the students' scores are published, there are the same problems between the uploaded score data and the registration data. The corresponding accounting can only be carried out after filtering the data of other education information centers. Finally, after the online examination results are published, each head teacher needs to sort out the students' comprehensive examination results this year and sort out the list of failed students, so as to inform the students to sign up next time.

4.2. System Architecture Design. The data management system of the education information center will cover the record of enrollment publicity information and the maintenance of student enrollment information during the operation of the education information center (mainly maintaining student telephone, business unit, and enrollment change data), the unified examination data management of national network education, score processing and certificate issuing management, daily problem tracking, and record management, and the division of labor of the education information center (i.e., authority management) and enrollment management module mainly focus on the release of rules and regulations. The student basic information management module mainly maintains the management of students' telephone, unit, grade information, and grade head teacher information. The unified examination management module mainly realizes the batch, registration, counseling, and score management of network unified examination. The graduation management module mainly manages graduation information (including file management and distribution management), and the student return visit module mainly manages the return visit records of the education information center through telephone, QQ, WeChat, and so on.

The system functional architecture is shown in Figure 5.

4.3. Design of the Network Resource Database of Education Information Center. The grade table is designed by a separate table, which is actually relatively simple. In addition to grade ID and grade name, there is also a head teacher field to associate with the username in the user table. Therefore, head teachers and students are linked. The student basic information module adopts two forms, one is the enrollment information table and the other is the grade information table. The student information table contains all registration information because the student number is unique, while other tables are based on the student number, so the student information form takes the student number as the primary key. Use the grade table to associate the head teacher with the user table.

The enrollment module management module includes five forms: unit profile form, old with new form, unit enrollment specialist, enrollment publicity form, and part-time propagandist form. The form is designed as follows: the form of part-time propagandists records the name, identity, account number, telephone number, information recorder, registration time, and whether to continue to work part-time, and contains the basic information of propagandists. The external publicity and promotion form records the types of external publicity (including visits to enterprises, issuance of enrollment brochures, etc.). The company profile shall include name, address, contact number, contact person, company website, company nature, scale and number of people, and education policy information. The old band new record records the student ID number, the name of new student, the number of identity card, the person who records the information, the time of registration, and so on. The enrollment specialist form contains the student number, registrant, registration time, validity period, and other information of the enrollment specialist.

The network unified examination module consists of three tables: unified examination batch table, unified examination information table, and unified examination guidance table. The unified examination batch table contains examination batch information, unified examination information table, examination subjects, and student scores. The unified examination guidance form contains information such as the batch, time, and place of guidance participated by students.

The graduation management module is mainly composed of two tables. One is the graduation certificate information table, which is used to record the graduation certificate and file information organized by the education information center. You also need to represent data when issuing a certificate. The second is the graduation extension application form, which contains the materials for applying for an extension for special reasons, such as the graduation certificate information form, the graduation extension application form, including the issuance batch information, the materials attached to the graduation certificate (documents, invoices), and the certificate receiving status information etc. The application form for delayed graduation records the student number, reasons for applying for delayed graduation, application materials for delayed graduation, recorder of information, recording time, batch of student certificates, and so on.

The student return visit module is used to record telephone return visit data. Considering the uncertainty of the reason for this revisited data, this field is treated as a separate table for addition or modification. The student return visit module has two tables: one is the return visit reason management table, which is used to record the return visit reasons (including urging payment, unified examination registration, course learning, etc.), and the other is the return visit information record table. The system automatically obtains the username of the submitter in the return visit information record table, which can be associated with the head teacher's information for reference during the return visit of the head teacher of the education information center. The return visit type table mainly records the ID and name of the return visit type, and the return visit information table mainly records the student number, return visit method, date, and result information of the return visit student.

4.4. System Operation Test and Result Analysis. The main contents of the system login test include the username and password test when the system logs in and the test of directly entering the system function page when not logging in.

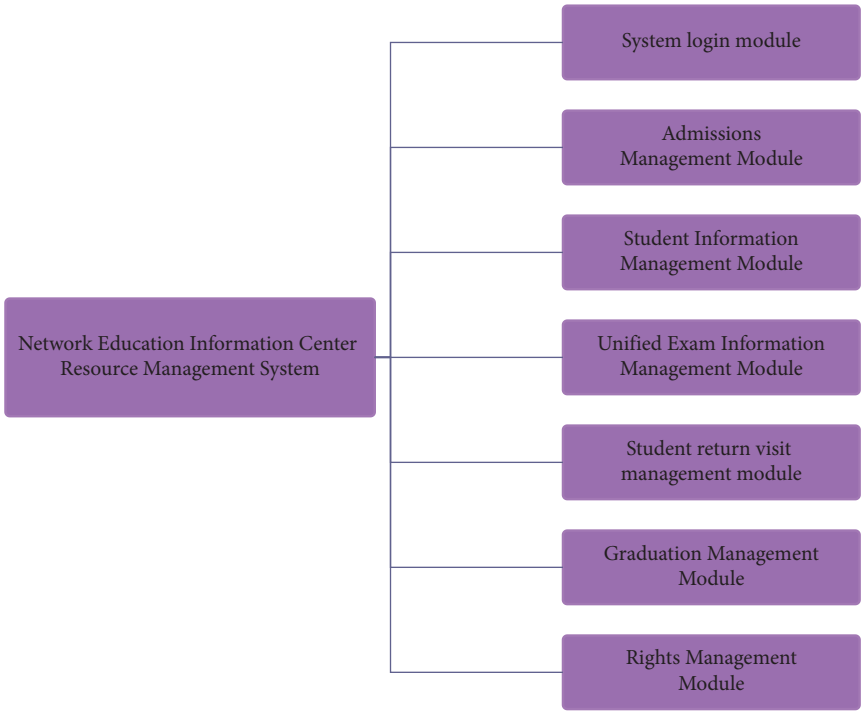

Figure 5: Overall architecture of the student data management system in education information center.

Table 3: User login function test record.

Test content	Step	Expected result	Test results
User login	Enter the correct username and password	Login successful	Passed the test
	Enter the correct username and wrong password	Cannot log in, prompting that the username and password are wrong	Passed the test
	Enter the wrong username and correct password	Cannot log in, prompting that the username or password is empty	Passed the test
	Do not enter username or password	Cannot log in, prompting that the username or password is empty	Passed the test
Login authentication	Direct access to the function menu page without logging in	Jump to the login page	Passed the test

Table 4: System authority module test record.

Test content	Test steps	Expected outcome	Test results
Directory permission test	Do not assign permissions to users	There is no menu directory after login	Passed the test
	Assign all permissions to users	Display all permission directories and form a directory tree	Passed the test
	Assign permissions to users by role	Display the corresponding directory	Passed the test
Button permission test	Click the function button without assigned permissions	Prompt no permission	Passed the test
	Assign permissions to click the function button	Perform corresponding data manipulation functions	Passed the test
Authorization verification	Access the function page without assigning permission	Jump to the prompt page, prompting that there is no permission	Passed the test

The test contents and results are shown in Table 3.

For the test of the system access permission module, the access test is divided into two categories: one is the permission to the test directory; only authorized users can view the menu directory, and the other is the button function permission; only authorized users can click this button to perform this operation.

The test results are shown in Table 4.

Table 5: System function module test record.

Test content	Test module	Test steps	Expected outcome	Test results
New data	Enrollment, unified examination, return visit, graduation, permission module	Fill in the corresponding data according to the system requirements	Data is added normally	Passed the test
		Duplicate data addition	Tips are repeated and cannot be added	Passed the test
		Enter data in the wrong format	Prompt data format error	Passed the test
		Null value of required field	Trigger nonempty verification	Passed the test
Data query	All modules	Do not set query conditions	Show all data	Passed the test
		Enter search criteria	Query the corresponding data	Passed the test
Data modification	All modules	Select data modification to view the modified page situation	Display the data information to be modified	Passed the test
		Modify the data to fill in as required	Prompt data format error	Passed the test
Data deletion	All modules	No data is selected and click Delete	Prompt to select at least one row of data	Passed the test
		After selecting the data, click Delete	Data is no longer displayed	Passed the test
Statistics	Old with new, unified exam module	Show all data statistics	Statistics data is consistent with the list data	Passed the test
		Query statistics by time period	The statistical results are consistent with the data in the same time period in the data list	Passed the test
Data output	All modules	Export data without setting query conditions	Export all valid data in the database	Passed the test
		Set query conditions to export data	Export valid data that meets the conditions	Passed the test
Data import	Unified examination, student information, graduation management	Import eligible data	Import the database normally	Passed the test
		Duplicate data import	The system prompts to repeat, do not import	Passed the test

Business function test includes general process test and special process test. The general process mainly includes data addition, editing, deletion, export, display, and query through the data addition page. The functions of each module are basically similar, and the system test is carried out uniformly. Through the whole process test of the system, the input and output results of the system are consistent with the expected results, indicating that the system logic is no problem and the system runs normally.

The system test results are shown in Table 5.

5. Conclusion

Based on the analysis of the daily business process and existing problems of the education information center, this paper uses the internet of things technology to gradually complete the system requirements analysis, functional structure design, and database design; the data management system uses the B/S structure to achieve coding, mainly to achieve the education information management of enrollment data in the center and real-time query and statistics of old and new data. It played a certain incentive role for the promotion of the original education information center, provided corresponding data for performance appraisal, realized the daily management of the education information center, and provided strong support for the development of the education information center. Providing references for the education information center to comprehensively understand students and provide targeted services will help improve the overall service level of the education information center, realize the automatic integration of student data on multiple platforms, effectively avoid a large number of duplicate data statistics, and improve work efficiency. The student management was changed from excel records to platform management, which improved the information management level of the education information center. The education information center data management system basically meets the work requirements of the education information center data management, but some functions have not yet been realized. With the opening of the education public service platform, the changes in

concepts and processes brought about by the conversion of the semester system to the credit system will also affect the current system functions. Therefore, the system functions need to be updated and improved continuously.

Data Availability

The data used to support the findings of this study are available from the author upon request.

Conflicts of Interest

The author declares that there are no conflicts of interest.

References

[1] Z. Xin-yong, "The realization of wisdom physical logistics based on the internet of things," *Journal of Changzhou Institute of Technology*, vol. 24, no. 5, pp. 46–48, 2011.

[2] L. Zheng, "Jiangsu smart logistics enhances logistics integration capability under "internet+" research on countermeasures," *Logistics Engineering and Management*, vol. 42, no. 8, pp. 21–24, 2020.

[3] X. Wang, J. Zhou, and Y. Gu, "Smart logistics deployment in the context of new retail model study: taking ali hema xiansheng as an example," *Logistics Engineering and Management Li*, vol. 42, no. 1, pp. 22–25, 2020.

[4] A. Oberoi, M. Arora, and V. K. Garg, "A novel approach for dynamic information integration," *International Journal of Reasoning-Based Intelligent Systems*, vol. 13, no. 2, pp. 76-77, 2021.

[5] S. Siekmann, "Which web course management system is right for me? acomparison of webct 3.1 and blackboard 5.0," *CALICO Journal*, vol. 18, no. 3, pp. 590–617, 2013.

[6] V. Fratto, M. G. Sava, and G. J. Krivacek, "The impact of an online homework management system on student performance and course satisfaction in introductory financial accounting," *International Journal of Information and Communication Technology Education*, vol. 12, no. 3, pp. 76–87, 2016.

[7] E. Coatanea, R. Roca, H. Mokhtarian, F. Mokammel, and K. Ikkala, "A conceptual modeling and simulation framework for system design," *Computing in Science & Engineering*, vol. 18, no. 4, pp. 42–52, 2016.

[8] U. Hüseyin, T. Murat, and P. Y. Ezgi, "The effects of the authentic learning approach with a course management system (moodle) on students mathematics success and online authentic learning self-efficacy," *Educational Research and Reviews*, vol. 15, no. 11, pp. 679–689, 2020.

[9] A. N. Alkhaldi and A. M. Abualkishik, "Predictive factors for the intention to adopt a mobile blackboard course management system: the case study of university of hail in Saudi Arabia," *Indian Journal of Science and Technology*, vol. 12, no. 19, pp. 1–12, 2019.

[10] V. S. Tabar, M. A. Jirdehi, and R. Hemmati, "Energy management in microgrid based on the multi objective stochastic programming incorporating portable renewable energy resource as demand response option," *Energy*, vol. 118, pp. 827–839, 2017.

[11] R. Xu, C. Wang, X. Luo, and J. Li, "Based on the background of "internet +" research on deep intelligence of logistics real estate," *Logistics Technology*, vol. 40, no. 3, pp. 7–11, 2017.

[12] W. U. Zhao-Hui, "Research on the application of internet of things technology to digital museum construction," *Acta Geoscientia Sinica*, vol. 38, no. 2, pp. 293–298, 2017.

[13] S. Zhao, S. Li, and Y. Yao, "Blockchain enabled industrial internet of things technology," *IEEE Transactions on Computational Social Systems*, vol. 6, no. 6, pp. 1442–1453, 2019.

[14] L. W. Wardana, "Paper airplane and talking stick learning methods to increase students understanding about management information system courses," *IOSR Journal of Business and Management*, vol. 18, no. 09, pp. 164–169, 2016.

Hindawi
Mobile Information Systems
Volume 2022, Article ID 8620277, 10 pages
https://doi.org/10.1155/2022/8620277

Research Article

Artificial Intelligence of Internet of Things Based on Machine Learning and College Student Management

Zhiqi Qiu [1] **and Jiwei Han** [2]

[1]*School of Artificial Intelligence, North China University of Science and Technology, Tangshan, Hebei 063000, China*
[2]*School of Management, North China University of Science and Technology, Tangshan, Hebei 063000, China*

Correspondence should be addressed to Jiwei Han; hjwyh01@ncst.edu.cn

Received 4 June 2022; Revised 2 July 2022; Accepted 5 August 2022; Published 23 August 2022

Academic Editor: Shadi Aljawarneh

Under the background of the development of higher education, according to the characteristics of college student management, after analyzing its background and practical significance, this study constructs an intelligent college student management system of Internet of things based on machine learning. The data volume of the Internet of things is huge, so ensuring the normal and efficient operation of the system is the primary goal. In this study, the data management model of the system is constructed with the help of cyclic neural network in machine learning algorithm to predict the data and optimize the computer program. At the same time, the system data are filled and classified by the k-nearest neighbor model, and the data are trained and simulated by constructing a safe bilstm neural network system. Because the information related to students in the university database involves personal privacy, in order to ensure the security of the system and avoid relevant data leakage, in the judgment standard of configuration error data flow, this study calculates the monitoring abnormal data and loss function through the dark network flow and ip2vec algorithm, so as to establish the system abnormal monitoring model and identify the system error data flow. Finally, it constructs the college student management system and expounds on the basic requirements of the system use cases. After a series of tests of system performance, capacity, and stability, the results meet the basic requirements of system operation, which provides a certain reference for the application of college student management in the future.

1. Introduction

The normal operation of students' work in colleges and universities is the basic to ensure the primary education and teaching work, so it is called "the second classroom." With the proposal of the goal of quality education, students' after-school activities in addition to basic teaching are increasing, including collective activities such as community activities, social practice, and practical training, as well as personal activities such as mental health and ideological and political education [1]. Therefore, student work needs to cover all work related to students in colleges and universities from enrollment to graduation. This is undoubtedly a huge task. The traditional student work management mode cannot adapt to the development of modern colleges and universities and cannot cope with the transformation of students' learning and life mode in the new era. Therefore, combined with the progress of science and technology, the reform and development of colleges and universities, and the actual needs of student work in the new era, it is urgent to build an intelligent, humanized, efficient, and safe college student management and service system [2]. The intelligent student management system can save the human and material resources of the school and change the time wasted in the process of hierarchical communication of traditional paper documents, save school resources, reduce the pressure of student work offices and confidential files, improve the overall operation efficiency of the school, and further maintain the operation of basic education and teaching [3].

With the advent of the information age, while information technology has brought great changes to society, all walks of life have also realized innovation and upgrading with the help of information technology [4]. The traditional working mode cannot adapt to modern society, and the

intelligent working mode in various fields has gradually become a social consensus. The traditional working mode depends on manual rules and knowledge base, so it is easy to have errors and safety problems. The intelligent working mode depends on the assistance of computer technology. All kinds of intelligent terminals are an important part to ensure work efficiency [5]. The research and development of the Internet of things include subthemes in many fields. Among them, machine learning algorithm, cloud computing, big data, and other technologies are the basic technologies to realize intelligent work [6]. In addition, with the expansion of the scale of the Internet of things and the continuous increase of equipment, the security detection technology of intelligent work system is also the basis to ensure the smooth implementation of the work [7]. The data classification algorithm based on machine learning can collect a variety of data generated in the operation of the equipment in real time, monitor the working state of the equipment in real time, submit abnormal data, and ensure the security of the data, which is used to detect the abnormal activities of network equipment [8]. This is not only the basic principle of intelligent work mode but also one of the objectives of this study.

2. Related Work

The Internet of things has great development potential, and the research on the Internet of things is also deepening. The definition of Internet of things in the literature is very broad; that is, it allows individuals to establish connections with other individuals through certain ways at any time, place, and other states [9]. The literature explains it from the perspective of technology. The Internet of things refers to the global network of uniquely addressable interconnected objects based on standard communication protocols [10]. According to the description of the Internet of things in the literature, the Internet of things should cover many functions, such as data exchange, data tracking, voice interaction, and privacy protection. At the same time, the system should also have certain class scalability and be suitable for emergencies in a variety of operating environments [11]. Due to the increasing number of Internet of things devices at this stage, more stringent requirements are put forward for the existing Internet of things system. For example, it is mentioned in the literature to reassess the expectation of the Internet of things, carry out large-scale expansion, reconstruct the architecture of the Internet of things, etc [12]. The literature emphasizes that the huge system of the Internet of things is a heavy task for any operating system. How to solve the storage and transmission of massive data is an important task to be considered in the research of Internet of things technology for a long time [13]. Therefore, these problems are explained in the literature, and it is pointed out that these problems can be solved by data mining technology and machine learning algorithms. The literature expounds on the advantages of machine algorithm [14]. Because machine learning involves a large number of data calculation, edge calculation is one of the important methods to solve the problem of large data volume. In addition, there are data training and reasoning methods of deep neural network. Agree, the literature also explains that the edge computing method is to save data transmission time and improve the performance of the system through preprocessing after storing the data in the edge node of the Internet of things [15].

The research on the intensive management of college students' work and computer system assistance began in the 1990s, especially after the gradual popularization of Internet application. The literature introduces the intensive management mode of college students, which ensures the efficient operation of the system and enables the school collective to play the overall function [16]. Especially with the help of computer technology, student information is shared, which is conducive to the connection between various parts, so as to improve the organizational efficiency and ensure the security and privacy of student information. In particular, the literature points out that the use of college student achievement management system can correctly examine the current learning situation for both teachers and students [17, 18]. It can not only reduce the workload of academic staff but also help students understand their real achievements as soon as possible and improve learning efficiency. The literature mentioned that the establishment of college student management system and the realization of artificial intelligence education need to integrate the knowledge of multiple disciplines, including computer technology, artificial intelligence, educational science, and other fields, expand talent training in the field of intelligent education, and cultivate comprehensive talents for AI-driven education and social and economic development. For the construction of intelligent university management system, the literature expounds that the university student management system used to be based on LAN and assisted in the form of web page access, which needs to be upgraded constantly. In the modern environment with the rapid development of 5g network, with the popularization and application of mobile devices, the university information management system is more mobile and can be used flexibly with a variety of mobile terminals. At the same time, the literature also points out that with the continuous development of the Internet of things system, the system security needs to be improved. The powerful function of computer not only brings convenience to the society but also produces problems such as privacy disclosure. Therefore, the problem of security is particularly important in the college student work management system. Similarly, this is also one of the research focuses of this study.

3. Research on Key Technologies of Internet of Things Based on Machine Learning

3.1. Cyclic Neural Network. Machine learning algorithm is mainly based on the previous data experience to predict some possible behaviors, so as to optimize the main computer programs. This is also the working method of artificial intelligence. This section mainly adopts the cyclic neural network algorithm. The calculation of forgetting gate, input gate, and output gate is shown as follows:

3.1.1. Forget the Door. F-LSTM formula is as follows:

$$\overrightarrow{f_t} = \sigma\left(\overrightarrow{W_f}, \left[\overrightarrow{h_{t-1}}, x_t\right] + \overrightarrow{b_f}\right). \tag{1}$$

B-LSTM formula is as follows:

$$\overleftarrow{f_t} = \sigma\left(\overleftarrow{W_f}, \left[\overleftarrow{h_{t-1}}, x_t\right] + \overleftarrow{b_f}\right). \tag{2}$$

3.1.2. Input Gate. F-LSTM formula is as follows:

$$\begin{aligned} \overrightarrow{i_t} &= \sigma\left(\overrightarrow{W_i}, \left[\overrightarrow{h_{t-1}}, x_t\right] + \overrightarrow{b_i}\right), \\ \overrightarrow{\tilde{c}_t} &= \sigma\left(\overrightarrow{W_c}, \left[\overrightarrow{h_{t-1}}, x_t\right] + \overrightarrow{b_c}\right), \\ \overrightarrow{c_t} &= \overrightarrow{f_t} \times \overrightarrow{c_{t-1}} + \overrightarrow{i_t} \times \overrightarrow{\tilde{c}_t}. \end{aligned} \tag{3}$$

B-LSTM formula is as follows:

$$\begin{aligned} \overleftarrow{i_t} &= \sigma\left(\overleftarrow{W_i}, \left[\overleftarrow{h_{t-1}}, x_t\right] + \overleftarrow{b_i}\right), \\ \overleftarrow{\tilde{c}_t} &= \sigma\left(\overleftarrow{W_c}, \left[\overleftarrow{h_{t-1}}, x_t\right] + \overleftarrow{b_c}\right), \\ \overleftarrow{c_t} &= \overleftarrow{f_t} \times \overleftarrow{c_{t-1}} + \overleftarrow{i_t} \times \overleftarrow{\tilde{c}_t}. \end{aligned} \tag{4}$$

3.1.3. Output Gate. F-LSTM formula is as follows:

$$\begin{aligned} \overrightarrow{o_t} &= \sigma\left(\overrightarrow{W_o}, \left[\overrightarrow{h_{t-1}}, x_t\right] + \overrightarrow{b_o}\right), \\ \overrightarrow{h_t} &= \overrightarrow{o_t} \times \tanh\left(\overrightarrow{c_t}\right). \end{aligned} \tag{5}$$

B-LSTM formula is as follows:

$$\begin{aligned} \overleftarrow{o_t} &= \sigma\left(\overleftarrow{W_o}, \left[\overleftarrow{h_{t-1}}, x_t\right] + \overleftarrow{b_o}\right), \\ \overleftarrow{h_t} &= \overleftarrow{o_t} \times \tanh\left(\overleftarrow{c_t}\right). \end{aligned} \tag{6}$$

3.2. Configuration Error Data Flow Determination. When configuring the judgment algorithm of wrong data traffic, this study obtains the correlation degree between the packet information in the dark network database and the actual data value of the Internet of things, so as to judge the wrong traffic. If we want to associate the two, we need to clear, filter, and select the data. After filtering out the wrong configuration data caused by system error, the remaining data are detected. Suppose D is the IP address list of the dark network, and the probability distribution is shown in the following formula:

$$\mathrm{P}_{\mathrm{misc}}(d_i) = \frac{n_{\mathrm{src}}(d_i)}{\sum_{\forall d_j \in D} n_{\mathrm{src}}(d_i)}. \tag{7}$$

There are two main ways to define the probability distribution of dark network data. One is to assume that the dark network source will be detected in a random and uniform distribution. At this time, the probability of malicious data source accessing the dark network is shown in the following formula:

$$\mathrm{P}_{\mathrm{mali}}(d_i) = \frac{1}{|D|}. \tag{8}$$

Another definition method is to assume that the dark network source is detected according to the normal distribution. At this time, the probability of malicious data source accessing the dark network is shown in the following formula:

$$\mathrm{P}_{\mathrm{mali}}(d_i) = \frac{1}{\sigma\sqrt{2\pi}} e^{-(x-\mu)^2/2\sigma^2}. \tag{9}$$

Then, suppose that the probability of the system capturing the data generation source is $P(Di)$, and $P(Di)$ is also used as the probability of S_i accessing a specific data combination, then

$$P(D_i) = P\left(D_i = \{d_{i1}, d_{i2}, \ldots, d_{im}\} D_i| = m\right) \times P\left(\left|D_i\right| = m\right). \tag{10}$$

Assuming that there is an incorrectly configured data source in the system, then the first item in formula (10) is obtained as follows:

$$P_{\mathrm{misc}}\left(D_i = \{d_{i1}, d_{i2}, \ldots, d_{im}\} D_i|\right) = \frac{1}{K} \prod_{\forall d_i \in D_i} P_{\mathrm{misc}}(d_i). \tag{11}$$

For malicious data sources in the system, the first item in formula (10) is obtained as follows:

$$P_{\mathrm{mali}}\left(D_i = \{d_{i1}, d_{i2}, \ldots, d_{im}\} D_i|\right) = \frac{1}{K} \prod_{\forall d_i \in D_i} P_{\mathrm{mali}}(d_i). \tag{12}$$

Then, the Bayesian probability normalization constant k is used to make the sum of probabilities 1, that is

$$K = \frac{|D|!}{m!(|D| - m)!} \times \frac{1}{|D|^m}. \tag{13}$$

According to the characteristics of abnormal data, the source with wrong configuration can only access one or several targets, while the malicious source can access relatively more target space, which poses a threat to the security of the system. Therefore, the probability of accessing the dark network address is also the main basis for judging whether a source is an error source or a malicious source.

The probability distribution modeling method of error data source is as follows:

$$P_{\mathrm{misc}}(D_i) = \frac{1}{K(e-1)\left|D_i\right|!} \prod_{\forall d_i \in D_i} P_{\mathrm{misc}}(d_i). \tag{14}$$

The probability distribution modeling method of malicious data source is as follows:

$$P_{\mathrm{mali}}(D_i) = \frac{1}{K\left|D_i\right|} \prod_{\forall d_i \in D_i} P_{\mathrm{mali}}(d_i). \tag{15}$$

3.3. Abnormal Network Traffic Monitoring Algorithm. This study calculates the abnormal data through the 2vec algorithm. Among them, ip2vec algorithm is an important

part of the system model in this study. The data source and target network can be embedded into the vector together and encoded with the help of encoder. The two automatic encoders jointly train the decoder to decode the message format characteristic information and finally identify whether it is abnormal network traffic. Because the network traffic with similar content usually has a certain similarity in coding characteristics, the method of decoding message format characteristics and attack model characteristics with the help of ip2vec algorithm has certain applicability, which can map the traffic of devices with similar functions to a wider space and improve the operation efficiency of the system. The loss function of the model is calculated as follows:

The loss function of the classifier is as follows:

$$L_{avd1}(\Theta_c) = -\sum \log\ p(l_i|\text{Encoder}(x_i;\Theta_e);\Theta_c). \tag{16}$$

The loss function of the encoder is as follows:

$$L_{avd2}(\Theta_e) = -\sum_{i=1}^{M}\sum_{j=1}^{N} \text{H}(p(j|\text{Encoder}(x_i;\Theta_e);\Theta_c)). \tag{17}$$

The loss function of the decoder is as follows:

$$L_{\text{decoder}}(\Theta_e,\Theta_d) = \sum_{i=1}^{L} L^i_{\text{seq 2 seq}}\left(\Theta_e,\Theta^i_d\right). \tag{18}$$

The total loss function of the model is as follows:

$$\begin{aligned} L_{\text{total}}(\Theta_e,\Theta_d,\Theta_c) = {} & L_{avd1}(\Theta_c) + L_{avd2}(\Theta_e) \\ & + L_{\text{decoder}}(\Theta_e,\Theta_d). \end{aligned} \tag{19}$$

4. Implementation of Intelligent College Student Management System of Internet of Things

4.1. System Use Case Requirements Analysis. College student management involves all aspects of students' school life, and due to the large number of students, it is easy to encounter a variety of problems in the process of work development. Therefore, the primary goal of this system design is to integrate the work contents at all levels of student affairs management, make the business operation flow, and simplify the whole student service process. Through the analysis of college student work business, it can be concluded that according to different business categories, it is mainly divided into user levels such as students, teachers, parents, administrative personnel, and school level leaders, as well as departments at all levels such as class, age, secondary college, student work office, and logistics office. The system needs the help of campus network to realize the work application, processing, and query of all user levels and departments at all levels. In addition, the use method of the system should be simplified as much as possible to meet the operation level of different users.

This section takes the student operation as an example to show the student behavior use cases of the university management system. Among them, student groups, including students and graduates, can query personal information in the system. The student behavior use case is shown in Figure 1.

In the college student management system designed in this study, student achievement query is the basic module of this system. In order to pursue the stability of the system, the system is designed by data flow modeling. The data flow of the basic layer is shown in Figure 2.

In the student achievement management module, first, the school system administrator adds the basic data of the system, establishes the data entry grid, maintains the system functions during the use of the system, and processes various transaction requests and results. At the beginning of the semester, the data management personnel of the Academic Affairs Office add student information in the units of departments, majors, and classes, and reasonably arrange corresponding teachers according to the course opening plan of each specialty and the syllabus and teaching plan of each course. After the basic information of the system is added, teachers can log in to the system to view their schedule-related information and enter and confirm their grades after the final examination. Once the result is confirmed, it is not allowed to modify it without application. After confirming the results, the data manager of the Academic Affairs Office informs the students to query. In addition to students and teachers, teaching related staff, educational administrators, teaching leaders, and counselors can also log in to the system to query students' scores.

4.2. Design of Database Table. In the construction of college student management system, this study uses Access2000 database system to convert the collected data into the actual data model supported by the computer system. The database table design of this study mainly includes student information structure table, teacher information structure table, student achievement information structure table, course information structure table, student discipline violation information registration table, and comprehensive evaluation list.

The student information table is mainly used to store the basic information of students, including student number, name, gender, and photo. The field description is listed in Table 1.

The teacher information table is mainly used to store the basic information of teachers, including teacher job number, major, class name, and teacher category. The field description is listed in Table 2.

The student grade information table is mainly used to store the student's grade information of various subjects, including class, student number, semester, and course. The field description is listed in Table 3.

The course information table is mainly used to store the extended information of each professional course, including semester, course name, teacher number, and classroom. The field description is listed in Table 4.

The student discipline violation information registration form is mainly used to store the student's performance

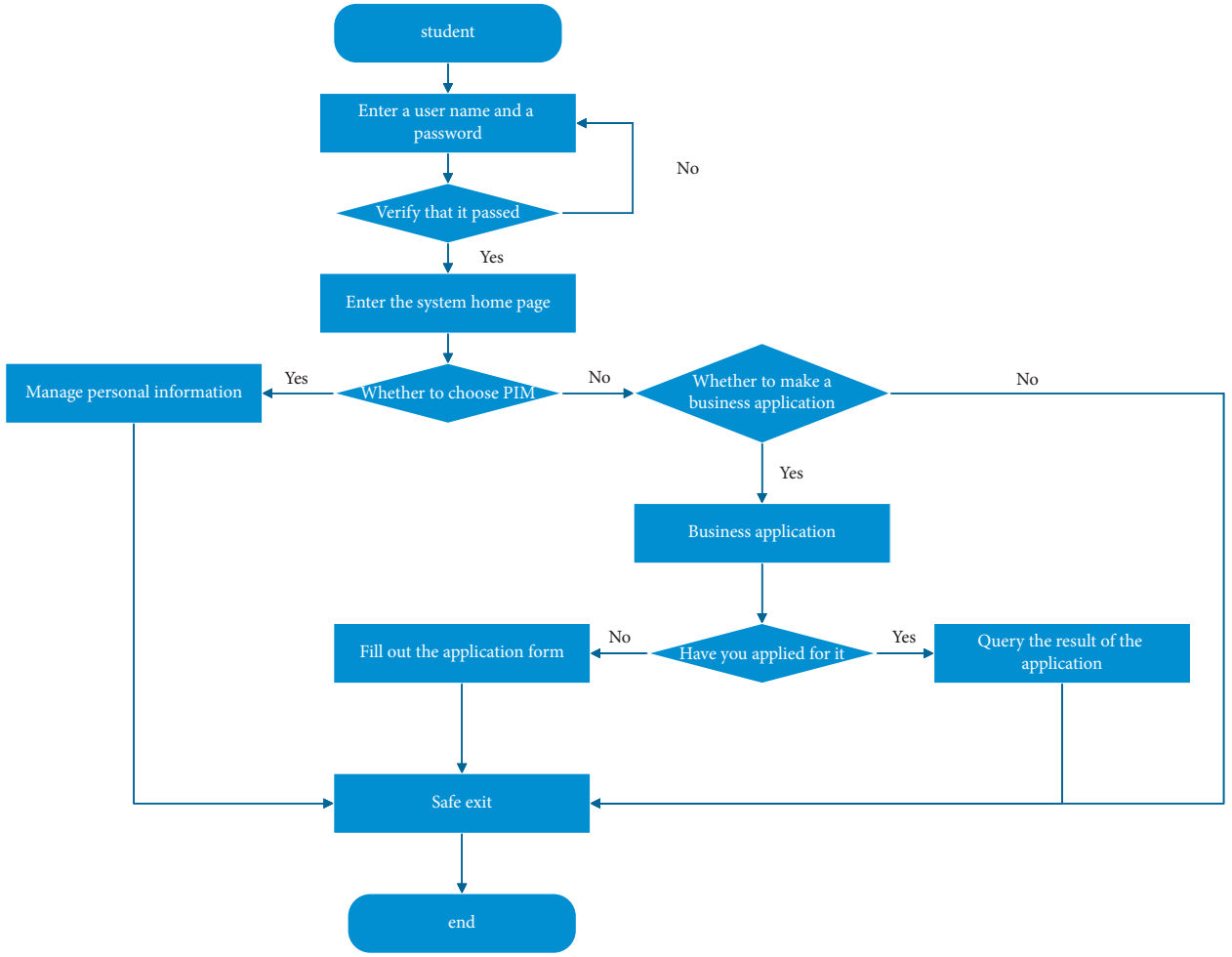

Figure 1: Student behavior process.

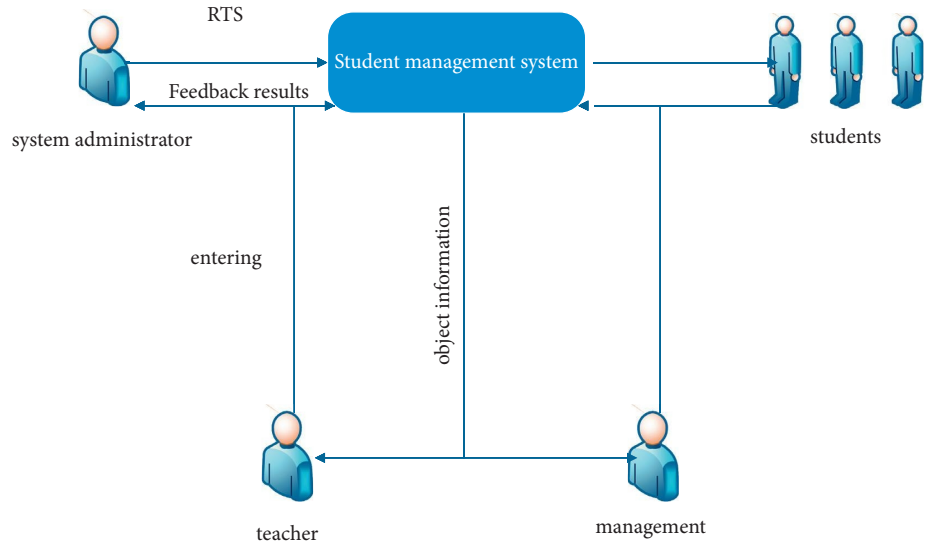

Figure 2: Data flow diagram of student achievement management module.

information of various subjects, including class, student number, semester, and course. The field description is listed in Table 5.

The comprehensive evaluation information table is mainly used to store students' comprehensive evaluation score information, including semester, grade ID, actual

Table 1: Student information structure.

Field description	Field identification	Field type	Width	Whether it is allowed to be empty	Primary key
Student ID	studno	Integer	—	N	Y
Name	studname	Varchar	20	Y	N
System	xino	Integer	—	N	Y
Professional number	zhuanyeno	Integer	—	N	Y
Class number	banno	Integer	—	N	Y
Age	age	Integer	—	Y	N
Gender	sex	Integer	—	Y	N
Nationality	minzuno	Integer	—	Y	N
Student category	ksno	Integer	—	N	Y
Address	address	Varchar	—	Y	N
Telephone	telph	Varchar	8	Y	N
Photo	ptotono	Varchar	8	Y	N

Table 2: Teacher information structure.

Field description	Field identification	Field Type	Width	Whether it is allowed to be empty	Primary key
Teacher number	teacherno	Integer	—	N	Y
Teacher name	teachername	Varchar	20	N	Y
System	xino	Integer	—	N	Y
Name	xiname	Integer	20	N	Y
Profession	subject	Integer	—	N	Y
Gender	sex	Integer	8	Y	N
Teacher category	leixin	Varchar	—	N	Y
Telephone	telph	Varchar	—	Y	N
Photo	ptotono	Varchar	—	Y	N
Classification	lessonname	Varchar	—	Y	N

Table 3: Student achievement information structure.

Field description	Field identification	Field Type	Width	Whether it is allowed to be empty	Primary key
Student ID	admin	Integer	--	N	Y
Classification	lessonname	Varchar	20	N	Y
Name	name	Varchar	20	Y	N
Semester	xueqi	Varchar	20	Y	N
Class	banno	Integer	—	Y	N
Professional number	zhuanyeno	Integer	—	N	Y
Professional name	zhuanyename	Varchar	20	Y	N
System	xmo	Integer	—	Y	N
Classification	lessonname	Varchar	—	Y	N
Fraction	fenshu	Integer	—	Y	N
Type	leixing	Varchar	8	Y	N

Table 4: Course information structure.

Field description	Field identification	Field Type	Width	Whether it is allowed to be empty	Primary key
Semester	xueqi	Varchar	20	N	Y
Curriculum	lessonno	Integer	--	N	Y
Classification	lessonname	Varchar	20	Y	N
System	xmo	Integer	--	Y	N
Professional number	zhuanyeno	Integer	--	Y	N
Grade number	Imo	Integer	--	Y	N
Class number	banno	Integer	--	Y	N
Teacher number	teacherno	Integer	--	Y	N
Student number	studnum	Integer	--	Y	N
Classroom	room	Varchar	8	Y	N
Week	week	Varchar	8	Y	N

Table 5: Student discipline violation information registration form.

Field description	Field identification	Field Type	Width	Whether it is allowed to be empty	Primary key
Semester	xueqi	Varchar	20	N	Y
System	xmo	Integer	—	Y	N
Professional number	zhuanyeno	Integer	—	Y	N
Grade number	Imo	Integer	—	Y	N
Class number	banno	Integer	—	Y	N
Student number	studnum	Integer	—	Y	N
Accommodation information	roominfo	Varchar	—	Y	N
Disciplinary date	wjrq	Varchar	—	Y	N
Disciplinary type	wjlx	Varchar	—	Y	N
Cause of discipline	wjyy	Varchar	—	Y	N
Remark	wjbz	Varchar	8	Y	N
Add a person	addman	Varchar	8	Y	N

Table 6: Comprehensive evaluation information.

Field description	Field identification	Field type	Width	Whether it is allowed to be empty	Primary key
Semester	xueqi	Varchar	20	N	Y
System	xmo	Integer	—	Y	N
Professional number	zhuanyeno	Integer	—	Y	N
Scholar logo	xh	Varchar	—	N	Y
Grade ID	degreeid	Varchar	—	N	Y
Actual score	score	Number	—	N	Y
Review status code	appshzt	Number	—	N	Y
Original score	ysfz	Number	—	N	Y
Score value remarks	fzydbz	Varchar	—	N	Y
Remark	wjbz	Varchar	8	Y	N

score, and approval status. The field description is listed in Table 6.

4.3. Analysis of Simulation Results. In order to further verify the stability of the system, the detection accuracy of abnormal traffic intrusion is analyzed. First, SVM and K-means classifiers are trained on the original target network traffic, and the auxiliary data set trained by the classifier is classified and trained to obtain the target recognition results. The experimental data are shown in Figure 3.

The blue part represents the classification results based on the original target network traffic, and the yellow part represents the classification results of the auxiliary data sets newly generated by training SVM, K-means, and other classifiers. It can be seen that the auxiliary data sets improve the monitoring accuracy to varying degrees, which proves the effectiveness of the machine algorithm in the field of data target recognition.

In addition to the test of target recognition accuracy, combined with the recognition accuracy, this study makes statistics on the number of hidden nodes in each data set, and the results are shown in Figure 4.

It can be seen from Figure 4 that when the number of hidden nodes is less than 100, the training accuracy and test accuracy gradually increase with the increase of nodes. The training accuracy continued to rise until the hidden nodes reached about 550 and began to decline gradually. The test accuracy gradually shows a steady state when the

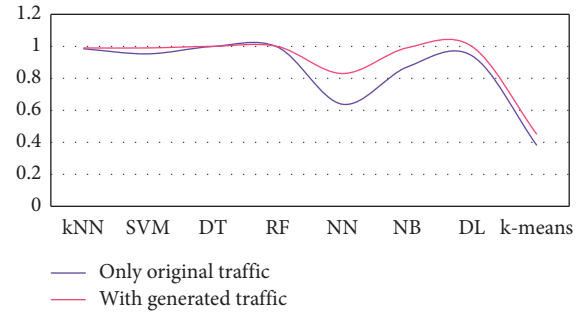

Figure 3: Classification performance of abnormal traffic in terms of accuracy.

hidden node is about 150 and begins to decline when the hidden node is about 550. Therefore, it can be concluded that the optimal number of hidden nodes of the system is about 550.

Finally, this study constructs a relatively complete intelligent college student work management system based on machine learning algorithm and carries out performance test. The test content mainly includes business function, data function, and system function, including student authentication management, large data test, stress test, and resolution test. During the system test, the maximum number of concurrent users is 500, the average processing success rate is greater than 99%, the average time is less than 1 second, and the maximum time is 2223 milliseconds. The system response time curve is shown in Figure 5, and the specific function test results are

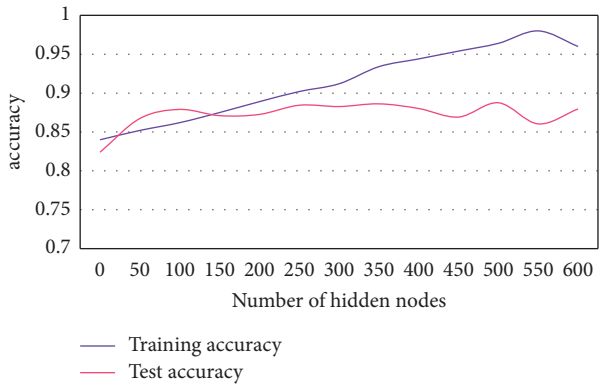

Figure 4: The accuracy increases with the number of nodes.

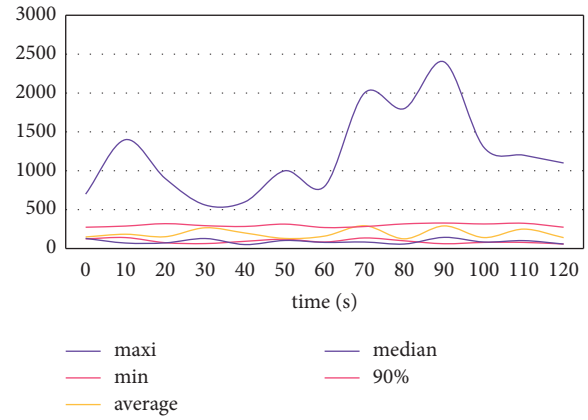

Figure 5: System response time curve.

listed in Table 7. It proves the effectiveness and enforceability of the college student management system designed in this study.

5. Development Strategy of College Student Management Based on Artificial Intelligence Application

5.1. Management Strategy of Intelligent College Student Work. From an economic point of view, the use of college student management system will greatly improve the efficiency of the overall work of the school and save a considerable part of the cost. First of all, the development of the system makes the computer replace the complex labor of manpower, which is very convenient for the collection, sorting, archiving, retrieval, and use of students' materials. Second, student information does not need to be transmitted in paper form. In addition to the necessary student status information, it can be digitized, which reduces the waste of resources in the school and saves the material storage pressure of confidential archives. In addition, this study designs a relatively simple and feasible student information management system, which occupies less resources. Generally, the campus network server can meet the operation requirements of the system, can bear the minimum 300 user load, and can still operate normally in the peak period.

Starting from the system development environment, the university student management system based on machine learning can support a variety of data types, provide comprehensive control instructions, and cooperate with the development of various work of the school. It can also ensure the modularity of the code, which is feasible for the later system maintenance and the expansion of the new system. At the same time, the monitoring scheme of abnormal flow data is added in the design process of the system, and the security of the system is also well guaranteed.

College student management system has a wide range of users, including students, teachers, administrative staff, school leaders, and logistics department, and other user groups with different roles and functions may have the right to log in to the system for data operation in their respective fields of responsibility. Different user roles have different use methods and permissions for the system, and the student information they can view is also different, which protects the privacy of students to a certain extent. At the same time, the use of computer student management system reduces the possibility of a large number of data contact. Therefore, compared with the traditional student data management mode, it can improve the security and confidentiality of student information. In order to further maintain the stability of the system, the designer needs to strictly follow the relevant standards in the overall architecture, software and hardware, database, report programming, input program, and other aspects of the student management system and set the viewing and modification permissions. In the system, the public information and personal information viewing authority are classified and designed to avoid data leakage caused by too complex data exchange process. In the functional modules such as system review and evaluation, we strictly follow the computer and assist manual inspection and confirmation to avoid too much human interference and ensure the fairness of the system.

The construction of college student management platform needs to start from the actual situation of the development of colleges and universities; combined with the school running philosophy and characteristics, the actual needs of school management are taken as the premise, and the cultivation of professional talents is taken as the goal. The design of student management system platform needs to follow the principle of integrity, organically combine the essential requirements of serving students with all links of student management, and integrate the coordination and cooperation of school level departments into the overall application of student management system. In addition, the data statistical content of the student information management platform should not only include performance management, mental health analysis, and other data but also provide enrollment data analysis, student learning analysis, and other aspects, with deeper data mining functions. This puts forward higher requirements for the design of college student management system. The construction of each functional module of the system should be gradually improved and continuously optimized to give better play to the overall advantages of the system.

Table 7: System function test results.

Test case	State	Result	Remarks
Business functions			
Certification management	It has been executed	Test passed	Functional testing
Selection management	It has been executed	Test passed	
Student work management	It has been executed	Test passed	
Student performance management	It has been executed	Test passed	
Student apartment management	It has been executed	Test passed	
Data function			
Big data volume test	It has been executed	Test passed	Performance testing
Load test	It has been executed	Test passed	
Pressure test	It has been executed	Test passed	
Unauthorized access	It has been executed	Test passed	
System function			
Resolution test	It has been executed	Test passed	Compatibility test
Browser test	It has been executed	Test passed	
Platform test	It has been executed	Test passed	

5.2. Intelligent College Education and Teaching Management Strategy. At this stage, with the support of artificial intelligence and other technologies, the intelligent teaching platform has preliminarily realized the real-time monitoring of the classroom and the analysis of students' learning situation, which is not only conducive to teachers' supervision of students' learning but also can dynamically manage the classroom according to students' actual classroom behavior, but also conducive to the interaction between students and teachers, and feedback their own problems to the learning platform in time. Interactive classroom depends on the realization of human-computer interaction technology but also requires teachers to master the intelligent teaching platform. In this context of intelligent education, to create an interactive classroom, teachers should timely change their traditional education and teaching mode and gradually adapt to the construction of online courses in the new era. First of all, in terms of teaching methods, teachers can use the intelligent teaching platform to create teaching situations, which is the same as the actual offline teaching methods. The intelligent teaching platform should also have complete classroom activities such as classroom guidance, teacher-student interaction, and Q&A, classroom practice, and chapter test. Second, in addition to basic teaching activities, the intelligent teaching platform also includes the integration of a variety of online resources and the construction of high-quality courses, as well as diversified and targeted teaching design case sharing, which is conducive to teaching mutual assistance between different teaching teams. Finally, with the help of new technologies such as multimedia, speech recognition, and virtual reality, the intelligent classroom platform can carry out a variety of teaching activities around students, increase the fun of the classroom, provide targeted teaching content, and further promote the improvement of students' comprehensive quality and personalized development.

In addition to the support of schools and the change of teachers' team teaching concept, the overall education management system based on Internet of things, artificial intelligence is inseparable from the efforts of all fields of society. First of all, we need to strengthen the research and development of the core technology of educational intelligence and constantly apply artificial intelligence and other technologies to the education industry. For example, the data training and prediction algorithm based on machine learning studied in this study can be used to predict students' learning behavior in the classroom management system and can also push appropriate educational resources based on students' learning interests. Another research direction of machine learning, deep learning algorithm can analyze data information such as text, image, and language, so as to identify the learning performance of students in the learning system and carry out intelligent evaluation and personalized push. In addition, various search engine technologies, data mining algorithms, language processing systems, and other computer technologies can improve technical support for the construction of intelligent classroom management system.

In a word, the management of college students in the context of artificial intelligence of the Internet of things is inseparable from the efforts of many parties. It not only needs the basic technical support of science and technology, society, and education system but also needs teachers to improve their students' management ability and the change of new educational ideas. Only with the joint efforts of the internal and external environments, we can promote the establishment of intelligent student management system faster.

6. Conclusion

With the continuous expansion of the scale of colleges and universities, the number of students also increases. In addition, the student-centered education goal requires that college education should cover many aspects, including education and teaching, community activities, mental health, ideological and political education, and comprehensive quality. Accompanied by not only educational pressure, but also makes the management of students' affairs in colleges and universities more complex. Therefore, it is

very important to change the traditional student management mode with the help of modern computer technology. It can save a lot of manpower and material resources for colleges and universities and ensure the smooth, efficient, and intelligent operation of students' education and teaching. Starting from the actual needs, this study designs an intelligent college student work management system based on machine learning. The computer program is optimized with the help of cyclic neural network, and the k-nearest neighbor model is used to fill and classify the system data. At the same time, considering the security of campus database, the system anomaly monitoring model is established through dark network traffic and ip2vec algorithm to identify the system error data traffic. Finally, the university student work management system is constructed. The intelligent student work management system is one of the strategies to adapt to the development of colleges and universities in the new era. It can improve the efficiency of student management and service, so as to assist the development of basic education and teaching. We hope this study can provide some reference for the application of college student management in the future.

Data Availability

The data used to support the findings of this study are available from the corresponding author upon request.

Conflicts of Interest

The authors declare that they have no conflicts of interest.

References

[1] K. Opstoel, L. Chapelle, F. J. Prins et al., "Personal and social development in physical education and sports: a review study," *European Physical Education Review*, vol. 26, no. 4, pp. 797–813, 2020.

[2] Y. Ding, Y. Li, and L. Cheng, "Application of Internet of Things and virtual reality technology in college physical education," *IEEE Access*, vol. 8, pp. 96065–96074, 2020.

[3] H. Huang and J. Chen, "Comprehensive evaluation of teaching quality of public physical education in colleges and universities," *Educational Sciences: Theory and Practice*, vol. 18, no. 6, 2018.

[4] X. Zhang, "Thoughts on large-scale long-distance web-based teaching in colleges and universities under novel coronavirus pneumonia epidemic: a case of Chengdu University," in *Proceedings of the International Conference on Culture, Education and Economic Development of Modern Society*, vol. 416, pp. 1222–1225, Moscow, Russia, March 2020.

[5] J. Pei, K. Zhong, J. Li, J. Xu, and X. Wang, "ECNN: ECNN: evaluating a cluster-neural network model for city innovation capabilityvaluating a Cluster-Neural Network Model for City Innovation Capability," *Neural Computing and Applications*, vol. 34, no. 15, pp. 12331–12343, 2021.

[6] A. Williams and W. Thies, "M. D. Ernst," *Computer Science and Artificial Intelligence Laboratory*, vol. 1, no. 1, pp. 113–126, 2008.

[7] Y. Zhu, H. Lu, P. Qiu, K. Shi, J. Chambua, and Z. Niu, "Heterogeneous teaching evaluation network based offline course recommendation with graph learning and tensor factorization," *Neurocomputing*, vol. 415, pp. 84–95, 2020.

[8] J. Canny, "A computational approach to edge detection," *IEEE Transactions on Pattern Analysis and Machine Intelligence*, vol. 8, no. 6, pp. 679–698, 1986.

[9] D. Giusto, A. Iera, G. Morabito, and L. Atzori, Eds., *The Internet of Things*, Springer, New York, NY, USA, 2010.

[10] Q. Mei, D. Cai, D. Zhang, and C. Zhai, "Topic modeling with network regularization," in *Proceedings of the 17th International Conference on World Wide Web WWW '08*, pp. 101–110, Urbana, IL, USA, April, 2008.

[11] S. Liu, S. Wang, X. Liu et al., "Human memory update strategy: a multi-layer template update mechanism for remote visual monitoring," *IEEE Transactions on Multimedia*, vol. 23, pp. 2188–2198, 2021.

[12] T. Minka and J. Lafferty, "Expectation-propagation for the generative aspect model," in *Proceedings of the 18th Conference on Uncertainty in Artificial Intelligence*, pp. 352–359, Pittsburgh, PA,USA, August, 2002.

[13] T. B. Trafalis and R. C. Gilbert, "Robust support vector machines for classification and computational issues," *Optimization Methods and Software*, vol. 22, no. 1, pp. 187–198, 2007.

[14] N. R. Zhou, X. R. Liang, Z. H. Zhou, and A. Farouk, "Relay selection scheme for amplify-and-forward cooperative communication system with artificial noise," *Security and Communication Networks*, vol. 9, no. 11, pp. 1398–1404, 2016.

[15] P. Drineas, A. Frieze, R. Kannan, S. Vempala, and V. Vinay, "Clustering large graphs via the singular value decomposition," *Machine Learning*, vol. 56, no. 1–3, pp. 9–33, 2004.

[16] S. Wang, T. Tuor, T. Salonidis et al., "When edge meets learning: adaptive control for resource-constrained distributed machine learning," in *Proceedings of the IEEE INFOCOM 2018 - IEEE Conference on Computer Communications*, pp. 63–71, Honolulu, HI, USA, April 2018.

[17] A. Abdelhadi and M. Nurunnabi, "Engineering student evaluation of teaching quality in Saudi Arabia," *International Journal of Engineering Education*, vol. 35, no. 1, pp. 262–272, 2019.

[18] P. Fan, "Application of deep learning and cloud data platform in college teaching quality evaluation," *Journal of Intelligent and Fuzzy Systems*, vol. 39, no. 4, pp. 5547–5558, 2020.

Hindawi
Mobile Information Systems
Volume 2022, Article ID 9990603, 11 pages
https://doi.org/10.1155/2022/9990603

Research Article

Evaluation of Water Resources Environment and Regional Agricultural Economic Development Based on SAR Imaging Algorithm

Ying Meng

College of Economics and Finance, Xi'an International Studies University, Xi'an, Shaanxi 710128, China

Correspondence should be addressed to Ying Meng; 20150125@nxmu.edu.cn

Received 30 June 2022; Revised 21 July 2022; Accepted 2 August 2022; Published 23 August 2022

Academic Editor: Shadi Aljawarneh

Synthetic aperture radar (SAR) is a new high-tech radar that uses SAR principles and pulse compression technology to perform high-resolution imaging of ground targets. Because it is not affected by various factors such as location, time, and climate, it is widely used in the civilian and military fields, bringing huge social and economic benefits. Moreover, the environment of agricultural water resources and the development of regional agricultural economy can be studied using the SAR imaging algorithm. With the serious shortage of water resources and the increase of the world's population, the use of water resources for agriculture must not only achieve the goal of saving water, but more importantly, achieve efficient production on the premise of saving water. However, the shortage of water resources in China has become a serious constraint on the development of agriculture and rural economy and has become an important factor restricting the sustainable development of agriculture and rural economy. Therefore, the development of efficient and sustainable use of water resources is very important to establish a water-saving society for the sustainable development of China's economy and society. For the spaceborne SAR system, an azimuth-based multi-channel range ambiguity suppression method is proposed in this chapter. The simulation results show that after adopting the azimuth phase encoding technology, the azimuth spectrum of the signal in the ambiguous area can be moved to suppress the distance ambiguity.

1. Introduction

The synthetic aperture radar (SAR) unit system uses pulse compression technology and SAR principles to achieve two-dimensional high-resolution imaging of the target. This is one of the main technologies developed by modern radars [1]. Compared with other remote sensing technologies such as optics and infrared, SAR microwave radiation has a wider range and is not affected by weather and light. In addition, within a specific frequency band, electromagnetic waves penetrate the surface of hidden objects such as vegetation and walls, and can also detect targets with a depth of tens of meters or the back of the wall [2]. Based on the above characteristics, SAR systems are widely used in military, geology, surveying, map making, rescue, and other fields. Water is an indispensable resource for human survival and development. Insufficient water is a problem on the scale of the Earth. China is one of the most water-scarce countries in the world. The shortage of water resources has brought serious impact on agricultural production and people's lives [3]. With the sustained and stable development of China's social economy and the continuous progress of urbanization, industrial and domestic water use should increase substantially [4]. With the total amount of water resources in China unchanged, agricultural water use will indeed decrease. Therefore, China's agricultural water resources will grow negatively, and the contradiction between water supply and demand will become more obvious [5]. Therefore, rational development and utilization of water resources, promotion of unified management of water resources, and strengthening of water resources protection are important content of water resources utilization. Agriculture provides a

very important material guarantee for China's economic development [6]. The steady and rapid development of the rural economy is also an important part of China's overall economic development, and it has very important significance and value for the stable and lasting development of China's future economy. Now, the importance of agriculture is becoming more and more significant. In today's society, the rural economy is one of the main factors that promote economic development [7]. With the changes in China's agricultural modernization assessment, the agricultural spatial model has also changed. Taking agricultural economic management as the starting point, we will further promote the development of the modernization level of China's rural economy and realize the sustainable development of agriculture. There are still problems in the development of China's rural economy [8]. It is necessary to analyze specific problems in detail and implement further measures to improve the agricultural economy. It is necessary to provide timely response measures related to cultural economic management, pay close attention to issues, implement them in accordance with scientific management requirements, and effectively improve the actual effects of rural economic development, avoid rural economic problems, and achieve sustainable agricultural economic development [9].

2. Materials and Methods

2.1. Overview of the Study Area. A certain county is a transition zone between the northern subtropical zone and the warm temperate zone. It belongs to the H river system and enters the H river from south to north. The H river enters a certain county from Fengtai Pass and flows through the northern end of a certain county. The length of the river in the prefecture is about 26 km. The maximum flow of rivers in this area is 12000 m^3/s, and the minimum flow is 57 m^3/s.

2.2. Theoretical Basis. In spaceborne SAR, a broad mapping zone can be used to complete global surveillance, and a specific area can be repeatedly monitored in a short period of time. According to the high resolution, more detailed features of the scene can be obtained. Therefore, high-resolution imaging with a wide mapping band is an important development direction for spaceborne SAR. In the previous single-channel spaceborne SAR system, due to the limitation of the minimum antenna area, a wide range of mapping bands and high azimuth resolution are mutually restricted [10]. Spaceborne SAR platforms are usually hundreds of kilometers high and have speeds of thousands of meters per second. The small-range directional beam can cover an inclination range of tens to hundreds of kilometers. On the other hand, in order to ensure high azimuth resolution, the azimuth antenna adopts a small effective aperture, and as a result, the range becomes blurred. Therefore, distance blur is an unavoidable problem of spaceborne SAR, which will reduce the image quality and seriously affect the observation performance of the spaceborne SAR system [11].

In order to suppress the ambiguity of distance, scholars at home and abroad have proposed several methods. The general method is to design an antenna pattern to reduce the antenna side lobe energy or antenna gain in the blurred area to reduce the energy of the echo signal in the blurred area. Using the alternating radiation of positive or negative linear frequency modulation signals, the fuzzy area of the echo signal distance of the point target cannot be effectively accumulated when pressing the artery and vein, the suppression range is blurred, and the signal energy of the blurred area will not be reduced, thus affecting the SAR image signal-noise ratio. Therefore, this method is only suitable for point target scenes, not for scattered target scenes [12]. Using azimuth phase coding (APC) technology, the azimuth spectrum of the signal in the blurred area is moved through modulation and demodulation, and then the azimuth band-pass filtering process is used to reduce the blur energy. This method can be implemented simply, but must completely suppress the echo in the lower fuzzy area. It can be seen from the following analysis. The PRF must be several times the azimuth bandwidth of the imaging area signal, but if the PRF is increased, the width of the mapping band of the imaging area will become narrower, so a single-channel spaceborne SAR system cannot meet the above conditions. Multiple channels are used to receive echo signals, and digital beamforming (DBF) technology is used to form an equivalent naro beam reception that is aligned with the useful echo through appropriate weighting of each receiving channel [13]. Zero adjustment in the direction where the echo reaches the blurred area can suppress the area ambiguity. However, this method forms a good antenna pattern, because it knows the surface curve function, and it cannot effectively deal with the scenes of undulating terrain. In the azimuth scanning method, related scholars have proposed a pulse beam, which converts the distance of the blurred signal into the same azimuth multi-directional channel ambiguity signal and uses the azimuth position of the multi-channel ambiguity information solution. The method of blurring distance depends on the pulse width [14]. The interval is limited to sub-pulses, which is naturally more extensive than the measurement and mapping requirements.

For satellite-borne SAR systems, this chapter proposes a multi-channel range ambiguity suppression method based on azimuth. The core method absorbs the concept of conventional azimuth phase encoding and uses direction-encoded signals to send and receive. At the same time, it uses the fuzzy equivalent performance of the down-sampled azimuth signal to transform the fuzzy signals at different distances. At this time, in order to filter and separate the desired signal and the azimuth spectrum of the signal in the imaging area, a spatial filter will be constructed through multiple channels to obtain a high-resolution SAR image of the unblurred area [15]. In short, this method converts the ambiguity of the echo signal range into the ambiguity of the azimuth angle and then uses the azimuth angle multi-channel to suppress the ambiguity of the range [16].

2.3. Research Methods. The radar platform moves uniformly in a straight line along the X-axis at a speed v. The action mode of the radar is that one unit signal can receive 3 unit signals, and X_q ($q = 1, 2, 3$) is the position of the phase center of three equivalent antennas. In a spaceborne SAR, due to the large width of the mapping band covered by the beam and different illumination scenarios, the echo signals generated by the transmit pulses of different distance units can reach the receiving antenna at the same time, and the range may become blurred. The nth echo in the imaging field and the $n+1$th echo in the negative first-order blurred area, R_g and $R_{amb}^{(k)}$, respectively, represent the shortest tilt from the center of the same phase to the center of the scene in the imaging area and the K-th blurred area distance.

The radar sends a linear frequency modulation signal, and the basic frequency echo signal of the target in the imaging area can be expressed as follows:

$$S_{\text{img}}(f_r, t_a) = A_g(f_r)a_a(t_a)\exp\left[-j\pi\frac{f_r^2}{\gamma}\right]\exp\left[-j\frac{4\pi}{c}R(t_a; R_b)(f_r + f_c)\right]. \tag{1}$$

If the APC technology is not used, the basic frequency echo signal of the k-order ambiguity point target in the range frequency domain can be expressed as follows:

$$S_{amb}^{(k)}(f_r, t_a) = A_{amb}^{(k)}(f_r)a_a(t_a)\exp\left[-j\pi\frac{f_r^2}{\gamma}\right]\exp\left[-j\frac{4\pi}{c}R\left(t_a; R_{amb}^{(k)}\right)(f_r + f_c)\right]. \tag{2}$$

In Equation (2), t_a represents the low-speed time, c represents the speed of light, γ represents the modulation frequency of the transmitted signal, and f_c represents the carrier frequency of the radar. In addition, A_g and $A_{amb}^{(k)}$ are determined by the echo response amplitude of the target in the imaging area, the k-th order blur area field, and the frequency domain window function of the linear frequency modulation signal, and a_a () represents the azimuth time domain window function. The azimuth spectrum of the echo signal of the imaging area and the echo signal of the k-th blurred area is represented by $S_{\text{img}}(f_r, f_a)$ and $S_{amb}^{(k)}(f_r, f_a)$, respectively.

$$\begin{aligned} S_{img}(f_r, f_a) &= FFT_{t_a}\left(S_{img}(f_r, t_a)\right), \\ S_{amb}^{(k)}(f_r, f_a) &= FFT_{t_a}\left(S_{amb}^{(k)}(f_r, t_a)\right). \end{aligned} \tag{3}$$

After adopting the azimuth phase encoding technology, the azimuth spectrum of the signal in the blurred area can be moved, and the energy of the blurred signal can be partially removed by the azimuth band-pass filter to suppress the distance blur. The realization of the azimuth phase encoding technology is divided into the following three steps:

(1) The azimuth angle and phase code modulation of the transmitted signal

(2) Demodulation of the received signal

(3) The echo signal in the fuzzy area is suppressed by band-pass filtering

The APC modulation phase can be expressed as follows:

$$\phi_{\text{mod}}(n) = -\frac{\pi}{M}n^2, \tag{4}$$

where n is the number of transmitted pulses and $M \geq 2$ is the azimuth frequency shift coefficient.

The APC demodulation stage can be expressed as follows:

$$\phi_{\text{dem}}(n) = \phi_{\text{mod}}(n - m). \tag{5}$$

Among them, m is the blur number, which is determined by the two-way distance delay between the sending signal and the scene area of the imaging field:

$$\frac{m}{PRF} \leq \frac{(m+1)}{PRF}. \tag{6}$$

For the image imaging scene area, the modulation item of the echo signal can be deleted after demodulation. In the k-th fuzzy region, after modulation and demodulation, the remaining modulation phase can be expressed as follows:

$$\phi_{res}(n, k) = \phi_{\text{mod}}(n - k) - \phi_{\text{mod}}\left(= \frac{2\pi}{M}kn - \frac{\pi}{M}k^2 = 2\pi\frac{k \times PRF}{M}t_n - \frac{\pi}{M}k^2\right). \tag{7}$$

In Equation (7), $t_n = n/PRF$. The frequency shift area of the signal in the k-th blur is

$$\Delta f(k) = \frac{k \times PRF}{M}. \quad (8)$$

3. Results

3.1. Analysis of the Status Quo of Agricultural Water Resources Environment. As shown in Table 1, the total area of a certain lake is 122.66 billion km^2, and the total storage capacity when the water level is 25 m is 4.12 billion m³. "The world's first pond" is the main source of irrigation water for the county's irrigation area. A pond is the main source of irrigation water for the county's irrigation area. Its area is 387.4 km^2, and the total storage capacity of the reservoir is 9.74 million m³ at 29.74 meters. The Dajing Reservoir covers an area of 33.7 square kilometers and has a water level of 42.77 meters, and its total storage capacity is 53 million m³. The H reservoir has an area of 6.21 km^2, a water level of 46.23 m, and a total storage capacity of 11 million m³.

By 2020, a county's total water resources will reach 870 million m³, annual precipitation of 2.246 million m³, surface water resources of 775 million m³, and groundwater resources of 232 million m³. There is no need to double groundwater and surface water. The calculated water production coefficient is 39 million m³. The production coefficient of water is 291500m³ per square kilometer. In 2014, the county's precipitation area was 2986 km^2, and the precipitation in 2020 was 939.6 mm, which is equivalent to 2.86 billion m³. Last year, the county's precipitation was 2.246 billion m³, and the average annual precipitation was 2.757 billion m³. The county's precipitation in 2020 has increased by 24.9% compared to last year. This is an increase of 1.8 percentage points over the annual average precipitation. From the analysis of annual precipitation frequency, the county's precipitation frequency is 43.8%, which is a normal year compared with the average annual precipitation frequency. In 2020, the county's surface water resources will be 775 million m³, with an average outflow depth of 259.4 mm, which is 60.9% more than last year's value and 2.3% less than the year's value. In 2020, the county's groundwater resources will be 232 million m³, mountainous areas 48 million m³, plain areas 178 million m³, and plains 404 million m³.

It can be seen from Table 2 that the total water resources of the county in 2020 will be 870 million m^3, and the total water supply will be 729 million m^3, of which surface water supply will be 721 million m^3 and groundwater supply will be 8 million m^3. In 2014, the county's total water supply was 83.79%. The county's water supply is mainly from surface water sources, but because it is difficult to conserve groundwater sources, the water supply is limited. The water supply of the reservoir is 583 million m^3, accounting for 80.83% of the surface water.

As shown in Table 3, the county's total water consumption in 2020 is 729 million m^3, of which irrigation water is 642 million m^3, accounting for 87.93% of the total water consumption. The water consumption of forest breeding, fishery, and livestock is 18 million m^3. Industrial water consumption is 21.07 million m^3; urban public water consumption is 8 million m^3. Household water consumption is 0.4 million m^3; water consumption for the ecological environment is 3 million m^3. By 2020, our county's total water consumption will be 465 million m^3, of which farmland irrigation consumption will be 418 million m^3. The water consumption of animal husbandry, fishery, and livestock is 14 million m^3. Industrial water consumption is 6.05 million m^3; urban public water consumption is 24 million m^3. The water consumption of the ecological environment is 1.7 million m^3. The water consumption of arable land irrigation accounts for 73.68% of the county's total water resources, making it the most important water consumption department in the county. With the development of the county's economy, water consumption in industry, urban public, residential, and ecological environments has increased, and irrigation water for farmland has been forced to decrease.

As shown in Table 4, in 2020, the total population of the county is 1,405,208, the agricultural population is 1,242,355, and the per capita water resources are 642 m^3. The county's total water supply is 729 million m^3, of which agricultural water supply is 696 million m^3, water consumption is 465 million m^3, water resource utilization rate is 63.79%, and per capita water supply is 518.78 m^3. The per capita agricultural water supply is 560.38 m^3, and the ecological environment water consumption is 140 million m^3. The county has a total planting area of 19,633,000 hectares, an effective irrigation area of 1,599,500 hectares, and water resources of 354.66 m^3. The water-saving irrigation area has increased from 809,200 hectares in 2014 to 835,000 hectares in 2020, but the growth is very slow. Each person in the county can get 642 m³ of water. According to the United Nations, 1700 m³ of water resources per person has exceeded the per capita water resource occupancy standard of 1700~1000 m³. It is not a water-deficient area that is moderately poor, and 1000–700 m³ is a moderately water-deficient area. According to this regulation, the whole county belongs to the area where the per capita water consumption is relatively small in the world. As a large agricultural county, in addition to household water, agricultural water resources will become a major obstacle to the county's sustainable development.

3.2. Analysis of Agricultural Water Resources and Environmental Issues. As shown in Figure 1, the county is affected by floods and droughts to varying degrees every year. As a result, crops have decreased to varying degrees. In recent years, disaster-affected areas have also tended to increase.

Figure 2 shows that in recent years, the investment of water conservancy funds has undergone tremendous changes, the regional investment is insufficient, and the central water conservancy investment has undergone tremendous changes. In 2017, a total of RMB 504.29 million was invested in water conservancy projects, including RMB 37.54 million from the central government and RMB 108.75 million from local governments. Local governments accounted for 34% of the total, 52.2% of the central government's input, and less than half of the central government's input. The total investment in

Table 1: Basic situation of main lakes and reservoirs in a county.

Name	Area (square thousand m)	Total storage capacity (100 million m^3) corresponding water level m
A lake	1026.6	41.2 25
A reservoir	387.4	0.933 29.74
B reservoir	33.7	0.53 42.77
C reservoir	6.21	0.11 46.23

Table 2: Water supply of a county.

Water supply from surface water sources (100 million m^3)					Groundwater source water supply (100 million m^3)	Total water supply (100 million m^3)
Water storage	Diversion	Lift water	Nonengineering water supply	Subtotal	—	—
5.83	0.61	0.54	0.02	7.21	0.08	7.28

Table 3: Statistics of water consumption in a county.

Unit: billion m^3	Farmland irrigation	Lin, mu, fishery, and livestock	Industry		Town public	Resident life	Ecosystem	Total
			Fire (nuclear) power industry	Nonfire (nuclear) power industry				
Water consumption	6.42	0.18	0.0007	0.21	0.08	0.35	0.03	7.2
Water consumption	4.18	0.14	0.0005	0.06	0.24	—	0.017	4.6

water conservancy in 2018 included 35,647,900 yuan for the central government and 5,085,200 yuan for local governments, which was close to 85.5 million yuan, which was higher than that of the central government. In 2019, including the central government's 64.8 million yuan and the local government's 175.2 million yuan, a total investment in water conservancy is 240 million yuan. Among them, the central government's input accounted for 27% of the total input, and the regional input accounted for 73% of the total input. The total investment in water conservancy in 2020 is 287.43 million yuan, including 167.54 million yuan for the central government and 127.38 million yuan for local governments. There is almost no difference in investment in water conservancy between the central government and local governments.

It can be seen from Figure 3 that the combination of water resources environment and agricultural economy is a deep two-way connection for the purpose of achieving sustainable use of agricultural water resources. In order to ensure that the water resources environment and agricultural economy play a better role in the integration process, they must be restricted by the water resources environment.

It can be seen from Figure 4 that the combined development mechanism of water resources environment and agricultural economy is a complicated process. From a system perspective, the coupling is divided into four subsystems: water resources for agriculture, agricultural economy, water treatment, and water environment. From the perspective of process, coupling can be divided into system input, production, output, and other processes. In addition, it is also restricted by the environmental capacity of water resources, ecological understanding, comprehensive water pollution management, and water environmental safety.

3.3. Analysis of the Status Quo of Regional Agricultural Economic Development. As shown in Figure 5, the *X*-axis represents the gradual increase in per capita wealth in economic development. The *Y*-axis represents the environment. The country's economic development level is low (natural economic period, before the industrial revolution), per capita wealth is relatively small, environmental pollution is relatively light, environmental damage is small, and environmental degradation is low; however, with the acceleration of economic development, it enters the industry. In the era of globalization and sustained economic growth, the rise of the large machinery industry, the active development of agriculture and other resources, the accumulation of per capita income and growth, and the exhaustion rate of resources are higher than the purification capacity and the regeneration rate of resources, which have brought serious problems to the environment.

Environmental pollution is deteriorating with economic growth, even exceeding the ecological limit. Directly transition to the transitional period, accelerate the process of industrialization, and reach a certain level of economic development. In this process, the degree of environmental degradation will increase for the first time after a downward trend. In other words, there is a critical point for the transition point. After the turning point, the economy continued to improve. With the accumulation of per capita wealth and the alleviation of environmental pollution, the quality of alleviation began to improve. In the postindustrial era, the economic structure has changed, and the clean industry has gradually begun to vigorously develop. People's awareness of environmental protection and environmental consumption has increased, and the government has paid more attention to the implementation and improvement of environmental quality and environmental laws and policies.

Table 4: Population and cultivated land in a county.

Years	2012	2013	2014	2015	2016	2017	2018	2019	2020
Population (10,000 people)	133.3	134.8	135.4	136.5	137.1	137.6	137.8	138.8	140.4
Cultivated land area at the end of the year (hectares)	117288	1178711	118159	121411	122343	122234	122253	123628	196301

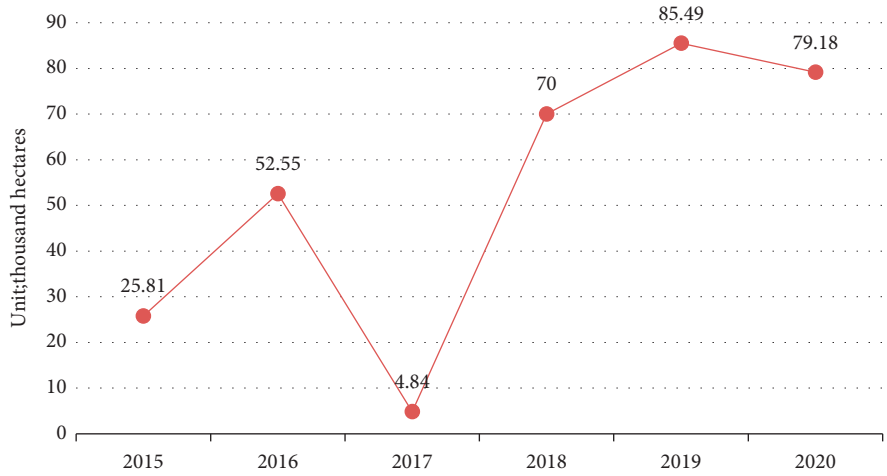

Figure 1: The affected area of crops in a county.

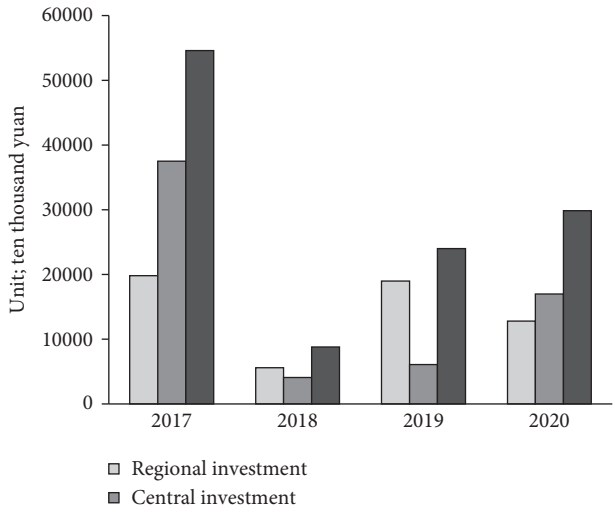

Figure 2: Water conservancy capital investment in a county.

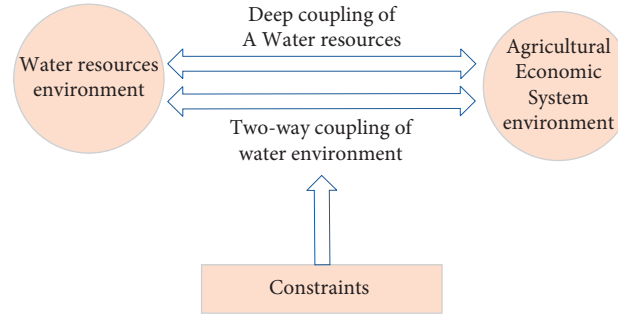

Figure 3: Coupling relationship between water resources environment and agricultural economy.

It has reached a certain critical point or "turning point" and achieved certain economic development. At the same time, it has accumulated in the progress of science and technology and innovation, the continuous increase of per capita income, and the continuous improvement of related laws. There is a clear understanding of the concept, the degree of environmental pollution, the improvement of environmental quality, and the tendency to change from high to low. This phenomenon is called the environmental Kuznets curve.

According to Figure 6, the two relationships can be represented by the regression equation $Y = b_0 + b_1X + \mu$ with one variable. Y represents the per capita net income of farmers in the survey area, and X represents COD. In other words, the formula $b0 = -8293$, $b1 = 1159$, and $\mu = 0$, and these two relations can be expressed by the regression equation $y = 1159x - 8293$ of one variable.

According to the return ceremony, COD will have a positive impact on the agricultural economic development of the surveyed area. On the other hand, from the point of view of the distribution of scattered points, the basic distribution is on both sides of the line, and the fitting results are also very good. From the perspective of the correlation index (coefficient of determination), the effectiveness is high. This article is based on the COD data of the livestock and poultry breeding industry in 2014. In an empirical study of the relationship between agricultural nonpoint source pollution and China's economic development, apart from Beijing, agricultural pollution emissions and economic growth in Shanghai, Tianjin, and other provinces and cities are also on the rise, and economic growth has a positive relationship with COD. Therefore, the process of economic growth in the survey area will still be accompanied by an increase in COD emissions. However, if the COD emission

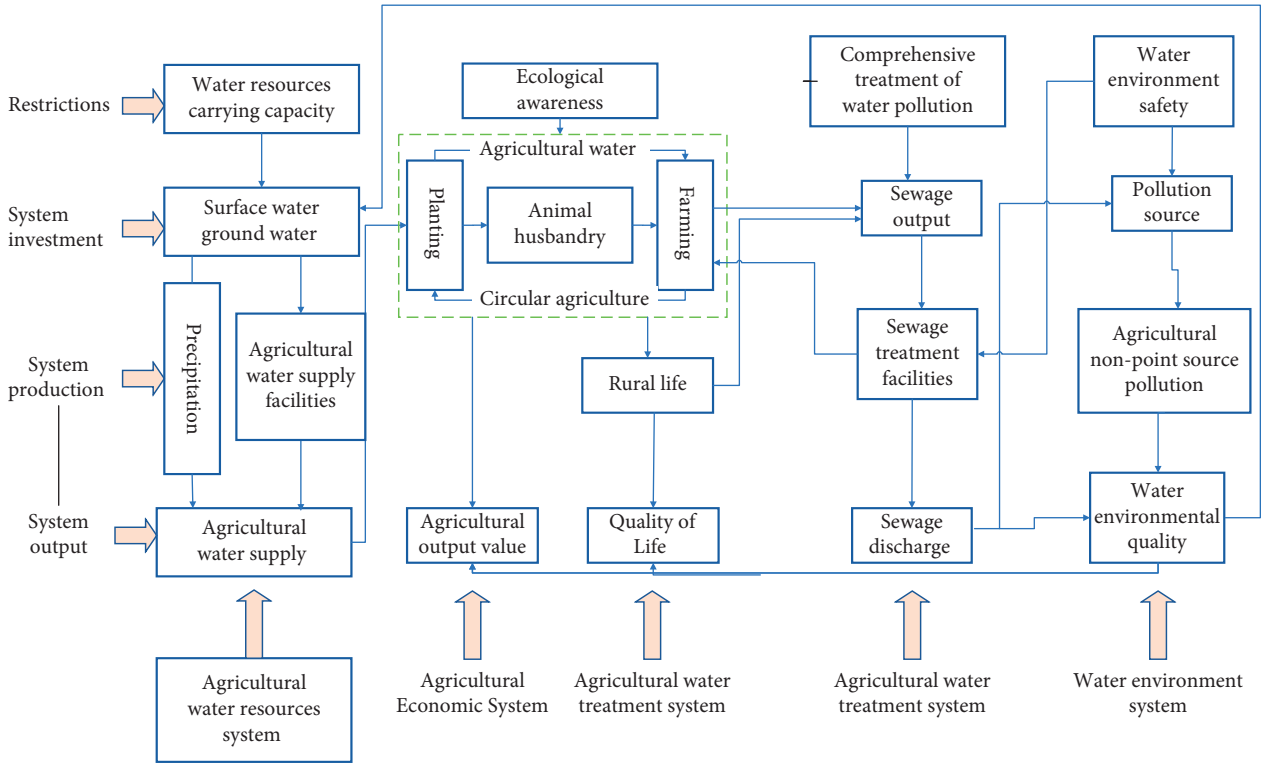

Figure 4: Coupling mechanism of water resources environment and agricultural economic system.

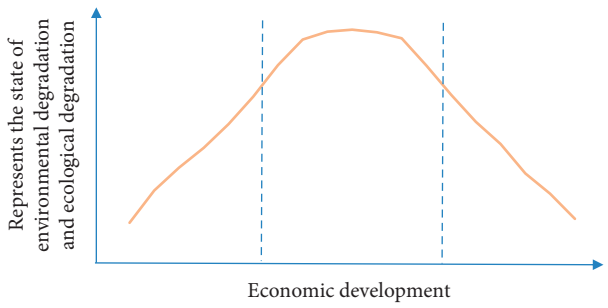

Figure 5: Environmental Kuznets curve.

reaches 14, the sharp increase in net income per capita is worthy of attention.

According to Figure 7, the two relationships can be represented by the regression equation $Y = b_0 + b_1X + \mu$ with one variable. Y represents the per capita net income of farmers in the survey area, and X represents TN. In other words, $b_0 = -26478$, $b_1 = 6463$, and $\mu = 0$, and the relationship between the formulas can be characterized by the regression equation $y = 6463x - 26478$ with one variable.

According to the regression formula, TN has a positive relationship with agricultural growth in the surveyed area. On the other hand, from the point of view of the distribution of scattered points, the basic distribution is on both sides of the line, and the fitting results are also very good. The correlation index shows high effectiveness.

According to Figure 8, the two relationships can be represented by the regression equation $Y = b_0 + b_1X + \mu$ with one variable. Y represents the per capita net income of farmers in the survey area, and X represents TP. In other words, $b0 = -24089$, $b1 = 59961$, and $\mu = 0$, and the relationship of the formula can be expressed by the regression formula $y = 59961x - 24089$.

According to the regression formula, TP will have a positive impact on the agricultural growth of the surveyed area. Judging from the distribution of the scattered points, the basic distribution is on both sides of the line, which also shows that the fitting results are good. From the perspective of related indexes, the effectiveness is high. TP is indeed estimated data for planting and breeding of livestock and poultry, because in the surveyed area is the main agricultural production; if TP emissions increase, it means that grain production and meat production will increase in the surveyed area. In the field of research on agricultural economic growth, positive relationships are reasonable.

3.4. Measurement Analysis of the Gap in Regional Agricultural Economic Development. Since 1978, the gap in agricultural economic development between southern and northern China has been significantly reduced, and the gap in agricultural economic development between eastern and western China has narrowed. However, the gap in agricultural economic development in China has become apparent at this stage and is an important obstacle to agricultural economic development. However, the above analysis can only explain the gap between regions and cannot reflect the development characteristics of the agricultural economy in the region. For example, the relatively small Theil coefficient between the north and the south only

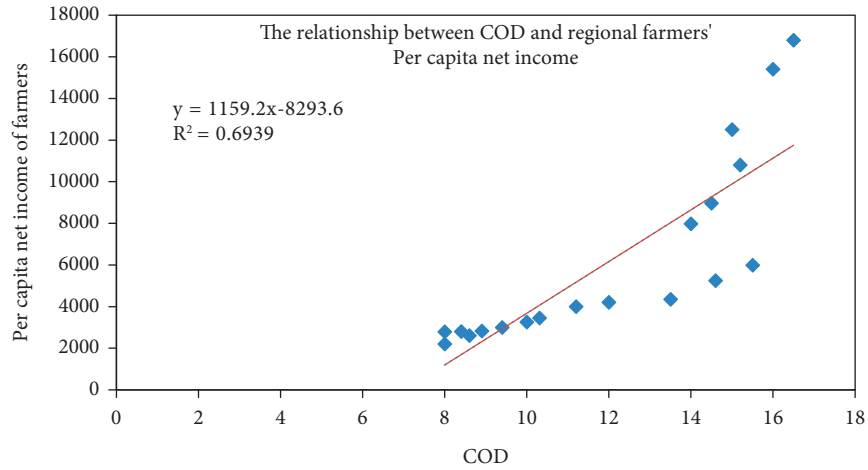

Figure 6: The relationship between the per capita net income of farmers and COD in the study area from 2001 to 2020.

indicates that the regional development has achieved a relative balance in the total amount and does not cover the possibility of regional differences between states. Therefore, it is necessary to further study the development model of agricultural economy in various regions. Generally speaking, the more the individuals, the higher the Theil index. From the perspective of the regional development gap, the north, south, east, central, and western regions include several administrative regions. The economic Theil index of the regional development gap is higher than the inter-regional Theil index calculated above. Therefore, the author believes that in the process of analyzing regional differences, more attention must be paid to the volatility tendency of the Theil index rather than the absolute value.

4. Discussion

4.1. Countermeasures to Improve the Agricultural Water Resources Environment. The governments should improve the organizational awareness of all levels of ecological agriculture and increase the citizens' sense of responsibility for participating in the prevention and control of water pollution. Efforts should be made to raise the ecological awareness of government departments and organizations in various fields of agriculture, and more importantly, to raise the ecological awareness of large-scale agricultural households and enterprises. Through various forms of propaganda, public opinion positions, multi-level, multi-form, comprehensive education, and propaganda, as well as relevant national policy documents, the publication and popularization of laws and regulations will make the people aware of water environmental protection and agricultural economic development. The quality of life of farmers is closely related. By formulating the compensation and punishment mechanism for water environment protection, the government should encourage rural residents to participate in agricultural water environment protection and governance, and enhance their sense of responsibility for water pollution protection and governance.

Reasonably develop and utilize water resources, strengthen effective management of water pollution, and improve the environmental containment capacity of agricultural water resources. At present, the widespread waste and shortage of water resources in agriculture have led to the contradiction between water pollution and water resources protection. It is necessary to develop water-saving agriculture, reduce the loss and waste of agricultural water resources in irrigation, transportation, and utilization, and improve the efficiency of water use. While innovating cultivation systems, rationally developing resources, and managing pollution sources, we also use pesticides and fertilizers rationally, strive to deal with livestock excrement and achieve safe production of agricultural products, and reduce water environmental pollution. Through a series of effective implementation of water resources, water pollution has been effectively suppressed, and the environmental capacity of agricultural water resources has been effectively improved.

Actively develop resource reuse agriculture and strengthen water resources and environmental protection mechanisms. Explore the construction of the ecological recycling agricultural industry system, accelerate the exchange and utilization of products and wastes in various agricultural industries, effectively combine planting and breeding, and change the extensive production mode of traditional agriculture. At the same time, it is necessary to strengthen the construction of agricultural water resources and environmental protection laws and regulations, and limit the methods and intensity of resource utilization. Establish and improve a resource protection mechanism system that combines planning guidance, red line protection, ecological compensation, capital investment, labor incentives, and long-term management of agricultural water resources and the environment.

Strengthen the main body consciousness of comprehensive treatment of agricultural water pollution, and innovate the multi-body treatment mode. In accordance with the new provisions of the Water Pollution Prevention and Management Law "Agricultural and Local Water Pollution

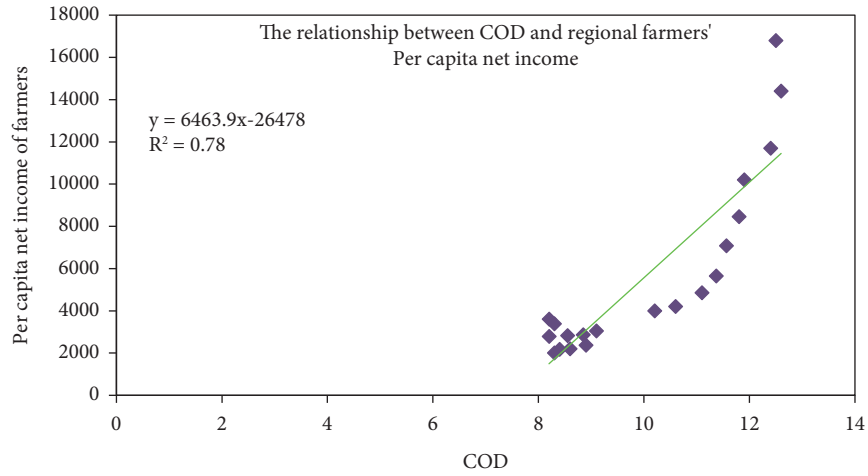

Figure 7: The relationship between TN and the per capita net income of farmers in the study area from 2001 to 2020.

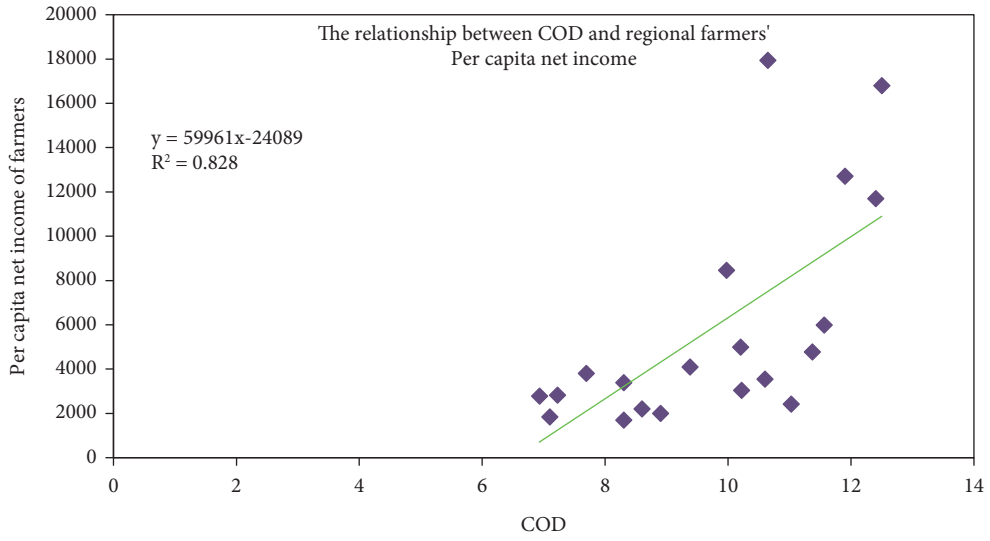

Figure 8: The relationship between TP and the per capita net income of farmers in the study area from 2001 to 2020.

Management and Treatment," the agricultural department under the jurisdiction undertakes to organize, guide, and supervise the prevention and management of agricultural water pollution. Use the pollution prevention mechanism that combines finance, village subsidies, family expenses, and social capital to continuously increase the construction of environmental protection facilities required for the treatment of rural sewage and garbage. Explore the mechanism of purchasing services from profit-making service organizations, and encourage major agricultural enterprises and large-scale breeding farms to become the third party in agricultural water pollution management through performance contract services. In order to achieve effective improvement of agricultural water pollution, financial support, tax preferential measures, credit support, and other measures will be used to support the establishment of agricultural water pollution prevention and management business service systems in which multiple relevant personnel participate, so as to integrate and coordinate the development of water resources and environment and agricultural economic system.

4.2. Measures to Promote the Development of Regional Agricultural Economy. People should pay attention to the complementary effects of regional agricultural production and improve the cooperative mechanism of regional agricultural cooperation. According to different regions, the structure of agricultural production also varies greatly. In order to realize the effective complementarity of agricultural production between regions, since the reform and opening up, the country has abolished the agricultural product procurement and transportation system, promoted the transformation of the agricultural product circulation system to the market, optimized the regional layout of agricultural production, and divided the main functional areas. However, the conclusion of this paper shows that there is still a big gap in the development of agricultural economy in some areas.

Therefore, when formulating regional agricultural policies, we should not ignore the interaction of agricultural production between different regions, but build a regional adjustment of agricultural division of labor and an effective agricultural production cooperation mechanism to improve spatial complementarity and spatial layout efficiency and ensure the effectiveness of agricultural labor productivity.

In order to optimize the input of agricultural factors, deepen agricultural capital investment, and improve the level of scientific and technological progress, more rapid action is required. The results show that although the agricultural economy in eastern China has the characteristics of a "small sector," agricultural labor productivity is very high, which is a major factor in the deepening of agricultural capital and technological progress. In China, especially in the northern, central, and western regions, as an important method to improve the quality of agricultural economic development, it is necessary to improve the industrial structure and raise the level of agricultural mechanization. With the continuous development of the regional economy, the added value of the primary industry and the scale of labor are gradually decreasing, and the proportion of the three industries is also gradually decreasing. In the future, it is necessary to reform and improve the agricultural technology extension system and promote agricultural remote sensing and advanced production technology in drought and water-saving agriculture, the national modern agricultural industry technology system, the technological innovation alliance, the industrial innovation center, the high-tech industry demonstration zone, and the construction of science and technology parks. Strengthen the leading effects of agricultural science and technology innovation, improve agricultural production conditions, and increase the rate of agricultural mechanization.

We must attach importance to the development experience accumulated in competitive regions and give full play to the backwardness advantages of backward regions. The coordinated development of the current agricultural economy between regions must start with the industrialization of agriculture and improve the industrial structure system. Regions with relatively backward agricultural economic development can learn from the effective development experience of other regions to realize the profit scale of agricultural economic production. For example, as a region with a strong Internet economy, Zhejiang Province has accelerated the expansion of network technology to agriculture and rural areas. By constructing an Internet + agriculture model, it has given full play to optimizing the role of the Internet in the distribution and integration of agricultural production factors. The same experience can be promoted nationwide to promote the development of agricultural economy based on regional conditions, and to promote the development of regional agricultural economy with experience.

5. Conclusion

As an active ground-based microwave remote sensing technology, synthetic aperture radar (SAR) has the characteristics of all-weather and long-distance, which greatly improves the radar's information acquisition capabilities. Obtaining focused broadband and high-resolution images is the development goal of SAR. SAR has experienced 60 years of development, and the image technology is slowly maturing. However, in the ultra-high resolution or static configuration, SAR imaging has several difficulties to solve problems, which are also hot topics in this field. Water is irreplaceable for human existence, but the state and use of water resources can be replaced. In the process of sustainable economic development, the environmental capacity of water resources and the sustainable development of agricultural water resources must be considered. It is impossible for water resources to solve the water shortage by looking for alternative means like other energy sources. The path of sustainable use of water resources has its own characteristics. The efficient and sustainable use of water resources, the safety of water engineering, the management and treatment technology of water pollution, the use and reasonable distribution of water resources, and the management and treatment technology of water pollution must always be in line with the sustainable development of water resources. Although agricultural development is the main national plan, if there is no agriculture, the country's economic development will be severely restricted, which is also very detrimental to the country's food security. Promoting the development of the rural economy and establishing a complete agricultural industry chain can consolidate the status of the country. Facing the demands of agricultural development for China's resources, talents, creativity, and system development, local governments combine the characteristics of agricultural development and the level of economic development to formulate specific economic management measures, construct an eco-agricultural economic development model, make it scientific and standardized, and enable farmers to share the fruits of national economic development and increase income.

Data Availability

The data used to support the findings of this study are available from the corresponding author upon request.

Conflicts of Interest

The author declares that there are no conflicts of interest.

References

[1] M. Martorella, E. Giusti, L. Demi et al., "Target recognition by means of polarimetric ISAR images," *IEEE Transactions on Aerospace and Electronic Systems*, vol. 47, no. 1, pp. 225–239, 2011.

[2] S.-H. Park, M.-G. Joo, and K.-T. Kim, "Construction of ISAR training database for automatic target recognition," *Journal of Electromagnetic Waves and Applications*, vol. 25, no. 11-12, pp. 1493–1503, 2011.

[3] D. P. Loucks, E. van Beek, and J. R. Stedinger, *Water Resources Systems Planning and Management: An Introduction to Methods, Models and Applications*, UNESCO, Paris, France, 2005.

[4] I. Fischhendler, "Institutional conditions for IWRM: the Israeli case," *Ground Water*, vol. 46, no. 1, pp. 91–102, 2008.
[5] L. Jin, G. H. Huang, Y. R. Fan, X. Nie, and G. Cheng, "A hybrid dynamic dual interval programming for irrigation water allocation under uncertainty," *Water Resources Management*, vol. 26, no. 5, pp. 1183–1200, 2012.
[6] A. K. Biswas, "Integrated water resources management: a reassessment," *Water International*, vol. 29, no. 2, pp. 248–256, 2004.
[7] M. Hammouda, J. Wery, T. Darbin, and H. Belhouchette, "Agricultural Activity concept for simulating strategic agricultural production decisions: case study of weed resistance to herbicide treatments in South-West France," *Computers and Electronics in Agriculture*, vol. 155, pp. 167–179, 2018.
[8] O. Kuzminov and I. Kuzminov, "Global challenges and trends in agriculture: impacts on Russia and possible strategies for adaptation," *Foresight*, vol. 19, no. 2, pp. 218–250, 2017.
[9] A. Farouk, M. Zakaria, A. Megahed, and F. A. Omara, "A generalized architecture of quantum secure direct communication for N disjointed users with authentication," *Scientific Reports*, vol. 5, no. 1, p. 16080, 2015.
[10] A. Coppola, S. Ianuario, G. Chinnici, G. Di Vita, G. Pappalardo, and M. D'Amico, "Endogenous and exogenous determinants of agricultural productivity: what is the most relevant for the competitiveness of the Italian agricultural systems?" *Agris On-Line Papers in Economics and Informatics*, vol. 10, no. 2, pp. 33–47, 2018.
[11] M. Gaffar, W. A. J. Nel, and M. R. Inggs, "Selecting suitable coherent processing time window lengths for ground-based ISAR imaging of cooperative sea vessels," *IEEE Transactions on Geoscience and Remote Sensing*, vol. 47, no. 9, pp. 3231–3240, 2009.
[12] Y. J. Huang, X. Wang, X. Li, and B. Moran, "Inverse synthetic aperture radar imaging using frame theory," *IEEE Transactions on Signal Processing*, vol. 60, no. 10, pp. 5191–5200, 2012.
[13] J. M. Hu, W. Zhou, Y. W. Fu, X. Li, and N. Jing, "Uniform rotational motion compensation for ISAR based on phase cancellation," *IEEE Geoscience and Remote Sensing Letters*, vol. 8, no. 4, pp. 636–640, 2011.
[14] C.-M. Yeh, J. Xu, Y.-N. Peng, X.-G. Xia, and X.-T. Wang, "Rotational motion estimation for ISAR via triangle pose difference on two range-Doppler images," *IET Radar, Sonar & Navigation*, vol. 4, no. 4, p. 528, 2010.
[15] M. Martorella, "Novel approach for ISAR image cross-range scaling," *IEEE Transactions on Aerospace and Electronic Systems*, vol. 44, no. 1, pp. 281–294, 2008.
[16] M. Berizzi and F. Berizzi, "Time windowing for highly focused ISAR image reconstruction," *IEEE Transactions on Aerospace and Electronic Systems*, vol. 41, no. 3, pp. 992–1007, 2005.

Hindawi
Mobile Information Systems
Volume 2023, Article ID 9785954, 1 page
https://doi.org/10.1155/2023/9785954

Retraction

Retracted: The Application of AI-Based Technology in Computer Network Operation and Maintenance

Mobile Information Systems

Received 1 August 2023; Accepted 1 August 2023; Published 2 August 2023

This article has been retracted by Hindawi following an investigation undertaken by the publisher [1]. This investigation has uncovered evidence of one or more of the following indicators of systematic manipulation of the publication process:

(1) Discrepancies in scope
(2) Discrepancies in the description of the research reported
(3) Discrepancies between the availability of data and the research described
(4) Inappropriate citations
(5) Incoherent, meaningless and/or irrelevant content included in the article
(6) Peer-review manipulation

The presence of these indicators undermines our confidence in the integrity of the article's content and we cannot, therefore, vouch for its reliability. Please note that this notice is intended solely to alert readers that the content of this article is unreliable. We have not investigated whether authors were aware of or involved in the systematic manipulation of the publication process.

Wiley and Hindawi regrets that the usual quality checks did not identify these issues before publication and have since put additional measures in place to safeguard research integrity.

We wish to credit our own Research Integrity and Research Publishing teams and anonymous and named external researchers and research integrity experts for contributing to this investigation.

The corresponding author, as the representative of all authors, has been given the opportunity to register their agreement or disagreement to this retraction. We have kept a record of any response received.

References

[1] L. Li, "The Application of AI-Based Technology in Computer Network Operation and Maintenance," *Mobile Information Systems*, vol. 2022, Article ID 2971393, 10 pages, 2022.

Hindawi
Mobile Information Systems
Volume 2022, Article ID 2971393, 10 pages
https://doi.org/10.1155/2022/2971393

Research Article

The Application of AI-Based Technology in Computer Network Operation and Maintenance

Li Li

Teacher's College, Xi'an University, Xi'an, Shaanxi 710065, China

Correspondence should be addressed to Li Li; lili@xawl.edu.cn

Received 7 June 2022; Revised 17 July 2022; Accepted 28 July 2022; Published 23 August 2022

Academic Editor: Shadi Aljawarneh

As an emerging IT technology, artificial intelligence has unique advantages in data extraction and data processing. In this paper, an artificial intelligence search method based on the K-means algorithm is proposed. According to the similarity between data samples, the samples are divided into many different categories. The ARIMA algorithm is used to perform regression analysis on the traffic data, and a Boosting model is established to improve the time series prediction accuracy. And, we use the relative distance between elements to represent the degree of dissimilarity of different types of variables. It can process massive data in a short time and obtain user behavior information. A large number of experiments show that the method proposed in this paper can complete information search more effectively and complete information classification quickly.

1. Introduction

The current network operation environment presents high speed, high flexibility, and high adaptability conditions. [1].

Traditionally, computer network management relies on managers using management software to regulate the condition of the network system. Due to the large workload, heavy tasks, and personnel load of network management, the application of artificial intelligence technology can eliminate many trivial manual operations and generally improve people's lives and the timeliness of network management. Due to the increasing amount of data generated in people's working life and the complexity of data sources, network monitoring is less effective and control is insufficient as far as traditional computer network technologies are concerned [2]. The number of web pages is even higher, reaching 315.5 billion [3]. These applications and websites handle a large amount of business every day, so IT (information technology) operations and maintenance play a very critical role in ensuring the healthy and stable operation of business systems in these industries.

Computer networks contain a large amount of unknown, cumbersome, and ambiguous data covering many domains, which would be very difficult to handle with traditional computer networks. The data used in the AI analysis process do not need to be completely accurate, and by simulating human thought patterns, it can flexibly analyze and handle fuzzy problems. The costs incurred in data center operations are increasing today in order to meet the growing demand in various fields. The main algorithm used in AI is the control algorithm, which has a higher computing speed and consumes fewer resources, which can effectively reduce the costs incurred during operations [4].

The early IT operation and maintenance method is relatively backward and is manually completed by the personnel. Enterprises urgently need an efficient, fast, accurate, and low-cost operation and maintenance to meet the growing demand for digital operations and maintenance, so the combination of Internet, AI, and operations and maintenance of AIOps (AI for IT Operations, intelligent operations, and maintenance) was born and the concept of intelligent operations and maintenance was first proposed by Gartner in 2016 [5].

In some enterprises, the task of network operation and maintenance may even go through layers of dispatch and the final work efficiency is very low. This iterative discrete operation and maintenance model seriously restricts the efficiency and timeliness of network operation and

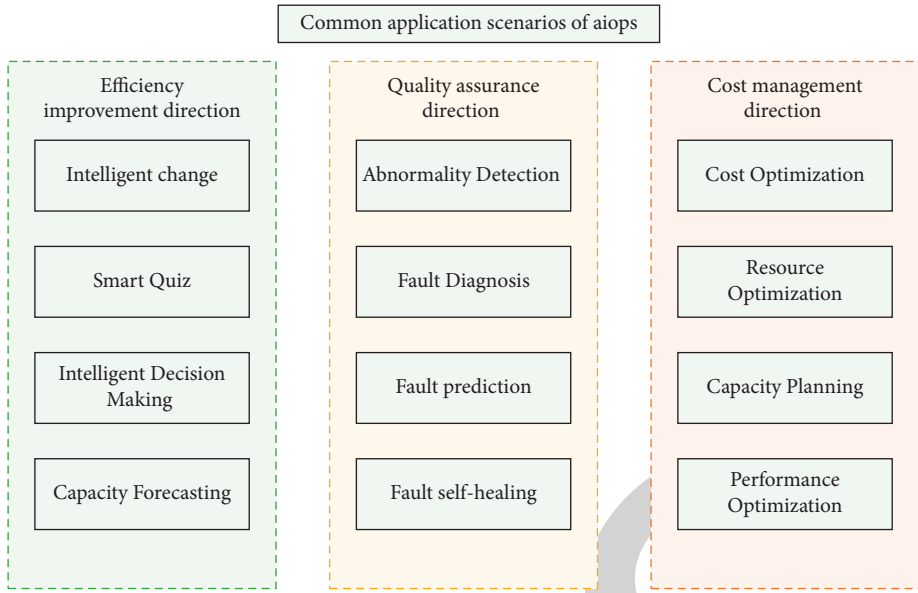

Figure 1: AIOps scenario.

maintenance, staff work more passively, enterprises focus only on the management of personnel, ignoring the impact of other factors on the network, and it is more difficult to start normal network operation and maintenance work [6, 7].

The current stage of network traffic contains a huge amount of information; how to extract and analyze the useful security information from it is the top priority to solve the network operation and maintenance problems. Only the timely and effective mining, analysis, and utilization of security data can sharply catch the abnormalities in data traffic and can effectively predict, analyze, and defend against security risks [8, 9].

This paper proposes an AI search method based on the K-means algorithm, which divides samples into many different categories according to the similarity between data samples. In the era of big data, the integration of artificial intelligence technology and computer network can greatly increase measurement time and improve information security. With the passage of time, the rapid development of computing network is also facing difficulties. The operation strategy of artificial intelligence in the network needs continuous exploration and research to improve the intelligence level of the network.

2. Related Work

Traditional operation and maintenance methods are time-consuming and labor-intensive, and the mode of relying on manual analysis can no longer cope with the performance monitoring requirements of complex networks and massive devices [10]. How to monitor massive network performance indicators in real time, reduce manual involvement, and achieve early fault detection with higher efficiency is a key issue that operators need to address in the process of industry competition and O&M transformation [11].

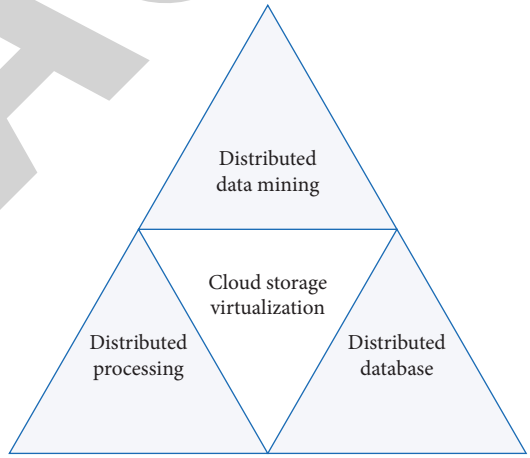

Figure 2: Relationship between big data and cloud computing.

In recent years, the theoretical foundation of machine learning algorithms has become more and more complete. Among them, time series prediction models have received attention from many researchers and have been widely used in many fields such as engineering technology, medical engineering, economics, and network communication with good results. The traditional modeling methods include linear regression, differential autoregressive moving average model (ARIMA), cubic exponential smoothing (Holt–Winters), Kalman filter, etc. [12]. These models have clear concepts and relatively advanced development, and there are many forecasting examples at home and abroad. With the development of AI technology, time series forecasting methods based on neural networks have been rapidly developed [13].

At present, domestic and foreign research in the field of operations and maintenance is not synchronized; foreign companies have been established for intelligent operations and maintenance of this piece of comprehensive research,

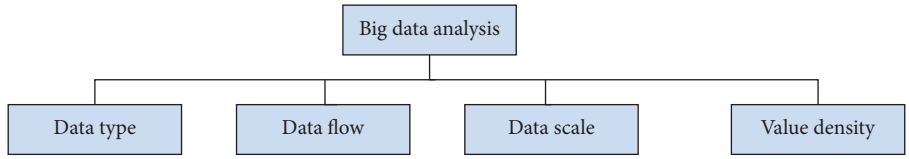

Figure 3: Characteristics of big data.

but only a small number of large enterprises in China, such as BAT and Huawei, begin to explore the field of intelligent operations and maintenance [14]. Therefore, intelligent operation and maintenance research must be on the agenda, and more experts and enterprises should pay attention to this, so that there is hope in the field of intelligent operation and maintenance to lead the world, or even like Huawei 5G as the industry leader to develop the corresponding standards [15, 16].

In 2018, the white paper "Enterprise AIOps Implementation Recommendations," jointly sponsored and developed by the Efficient Operations Community and the AIOps Standards Working Group (with members from BAT, 360, Jingdong, Huawei, and other well-known enterprises), provides an overall introduction to AIOps, and the book details common application scenarios for AIOps and key technologies for implementation. [17]. The main task of operation and maintenance engineers is to be able to extract intelligent demand analysis from the technical operation of the business, and according to the standard data format; the main task of operation and maintenance development engineers is to be responsible for the development of intelligent operation and maintenance platform-related functions and modules [18].

The common application scenarios of AIOps can be divided into three directions, as shown in Figure 1.

In the direction of efficiency improvement, it can be divided into intelligent change, intelligent Q&A, intelligent decision, and capacity prediction and in the direction of quality assurance, it can be divided into anomaly detection, fault diagnosis, fault prediction, and fault self-healing; in the direction of cost management, it can be divided into cost optimization, resource optimization, capacity planning, and performance optimization. In different directions, AIOps business is oriented to different focuses to respond to the differentiated needs of different enterprises, with the overall goal of maximizing the comprehensive benefits of quality, cost, and efficiency [19, 20].

2.1. Big Data Analytics Technology. Big data analytics is currently the key applicable area of AI, and this technology can greatly improve the scale of storing, managing, and analyzing data. As can be seen from Figure 2, big data analytics is mainly realized through the combination of distributed data mining, processing, and data storage with cloud storage and virtualization [21].

Big data and cloud computing, as the right and left arms of AI technology in the data field, can improve the decision-making power, insight, and process optimization ability of network operation and maintenance. As can be seen from Figure 3, big data analysis has four characteristics: multiple data types, fast data flow, large data scale, and low-value density.

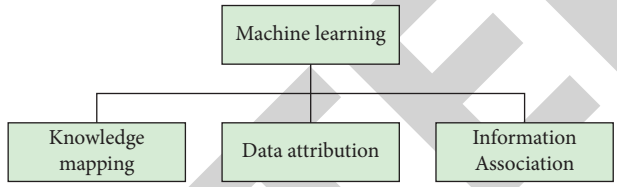

Figure 4: Application of ML.

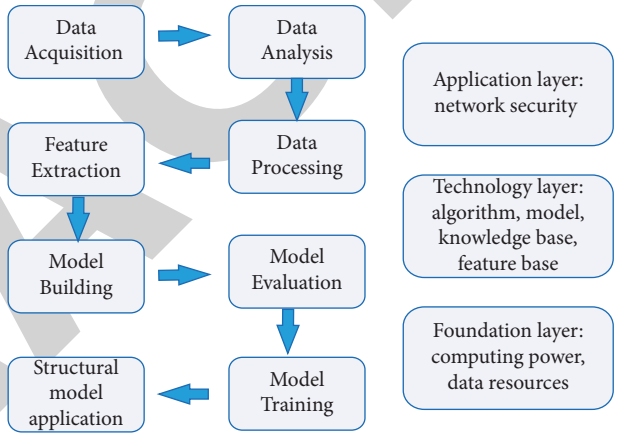

Figure 5: Architecture of AI.

2.2. Machine Learning (ML). ML is also another important area of AI, which gives the characteristics of computer intelligence and has application areas in all aspects of AI. From Figure 4, ML can be used for intelligent operation and maintenance to help dig deeper into the textual information of traffic, build a complete knowledge base system from six levels of knowledge acquisition, compilation, application, update, data utilization, and intelligence, and promote and unify the knowledge graph [22].

Then, the intelligent operation and maintenance system can refine the association and bearing relationship between data in the information system and use the real meaning and interrelationship of data presented in the knowledge graph to significantly improve the storage and retrieval ability of the computer [23–25].

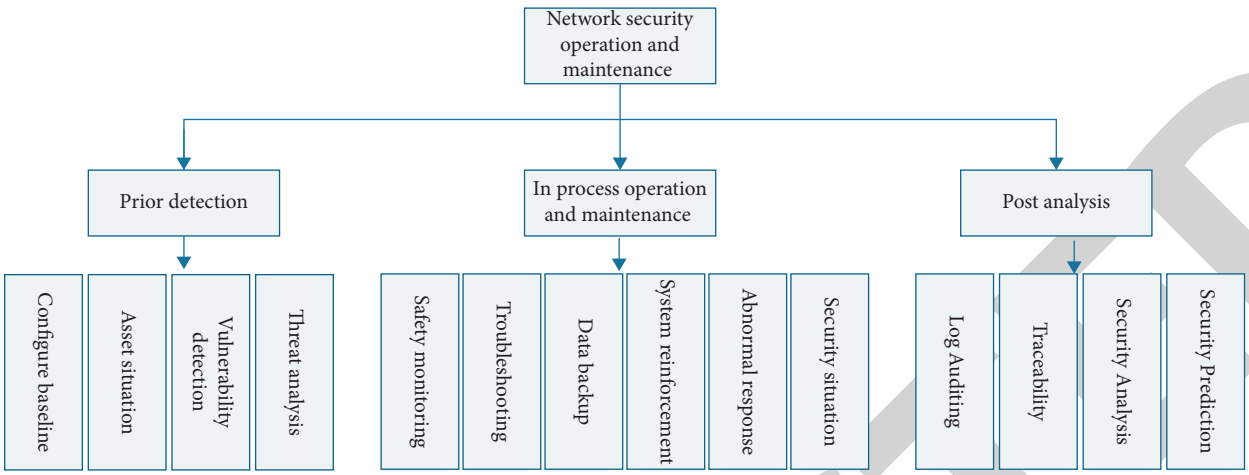

Figure 6: Network security operations and maintenance services architecture.

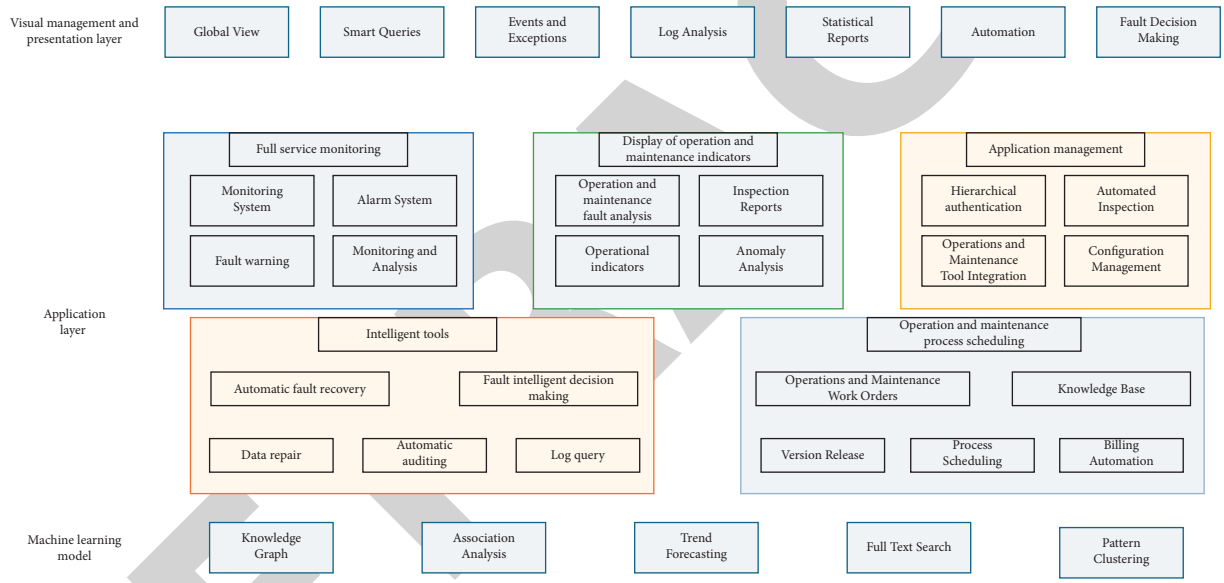

Figure 7: Functional framework of intelligent operation and maintenance platform.

3. Methodology

The architecture of AI technology is generally divided into three layers. As can be seen from Figure 5, the foundation layer is used for data acquisition, analysis, and processing, which contains the computing power and data resource acquisition capability; the technology layer includes algorithms, and models.

Large enterprises contain many divisional organizations and should adapt the concept of centralized operation and maintenance and adapt cloud-loaded computing units to realize reasonable network security operation and maintenance services. Network security O&M services can be divided into three stages: before, during, and after, and the advantages of AI technology can be played in the whole life cycle of network security O&M services to realize intelligent operation, as shown in Figure 6.

The functional framework of the intelligent operation and maintenance platform is shown in Figure 7. Traditional computer network maintenance has low efficiency, long cycle time, and difficulty in guarantee the quality, which cannot keep up with the needs of users. Among them, intelligent fault tracing technology can filter and filter classified alarm information, extract fault characteristics, and conduct AI learning based on KPI indicators and fault handling experience to form a fault diagnosis database and trace faults according to the relationship between alarm information.

The specific process is shown in Figure 8. AI, supported by massive data, can be used as a carrier for information distribution, establish an intelligent database, collect user behavior information for learning and feedback, and then perform expected analysis for different environments to provide users with intelligent decision specifications.

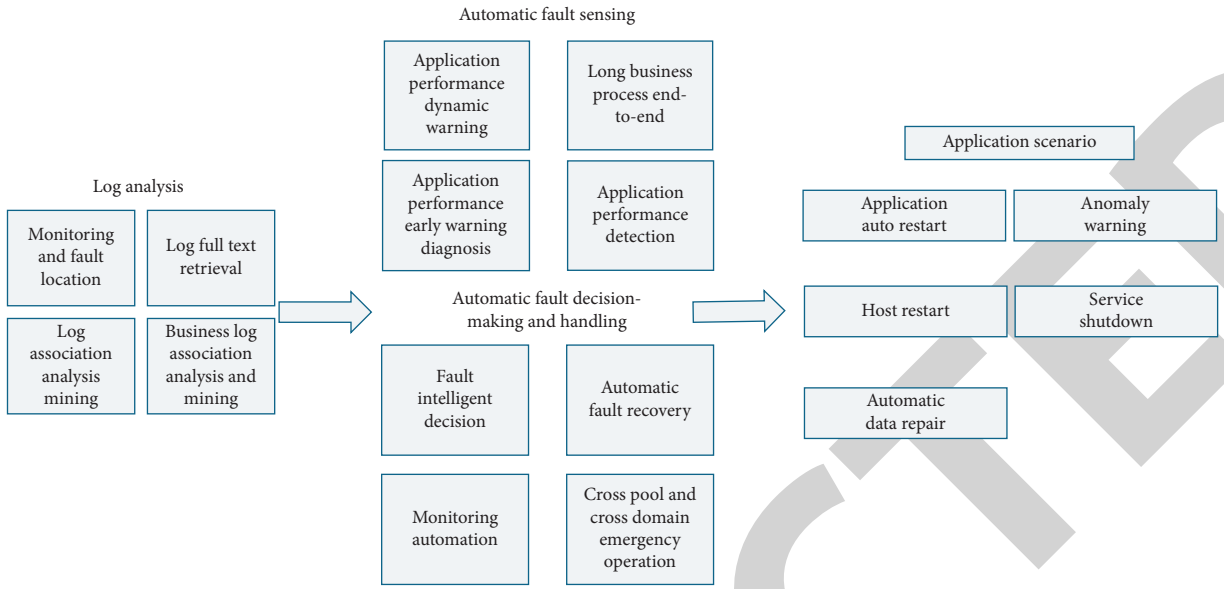

Figure 8: Flow chart of fault-aware processing.

3.1. Computer Network Management. In view of the popularity of intelligence and information technology, enterprises and various organizations and even people's lives rely more and more on computer technology. The high integration of computer networks and AI technology can improve the operation efficiency of databases, greatly improve the efficiency of network management, reduce management difficulties, and provide decision-making directions for enterprise work. Based on this, K-means algorithm can be used to process massive data in a short period of time, obtain user behavior information, analyze people's needs to provide reasonable optimization solutions, and improve computer network management. K-means algorithm is widely used in the direction of ML and data mining.

It is a typical unsupervised learning algorithm, which divides samples into many different categories according to the similarity between data samples. The flow of the K-means algorithm is shown in Figure 9.

In general, we use the relative distance between elements to express the dissimilarity of different types of variables, and several common distance calculation methods are described in the following.

3.1.1. Euclidean Distance. Euclidean distance is the geometric distance between the sample and the center of mass in Euclidean space, which has the characteristics of intuitive and interpretable; therefore, Euclidean distance is widely used in daily life.

3.1.2. Manhattan Distance. The Manhattan distance is the length of the projection of the line connecting two points on the coordinate axis in the right-angle coordinate system, and its distance is calculated.

The traditional K-means algorithm is tedious in steps and processes, and the K-means algorithm can be optimized. First, a sample is randomly selected from the data set as the initial center of mass μ_1, $d(q_i, \mu_1)$, and the farthest sample point is selected as another center of mass μ_2. Then, the distance between two centers of mass μ_1 and μ_2 is calculated $d(\mu_1, \mu_2)$, and the sample point q_j is selected according to the spatial three-dimensional geometry property; if $2\,d(q_j, \mu_1) \le d(\mu_1, \mu_2)$, then $d(q_j, \mu_1) \le d(q_j, \mu_2)$; that is, the sample point q_j is closer to the center of mass μ_1; otherwise, it is closer to the center of mass μ_2, and there is no need to

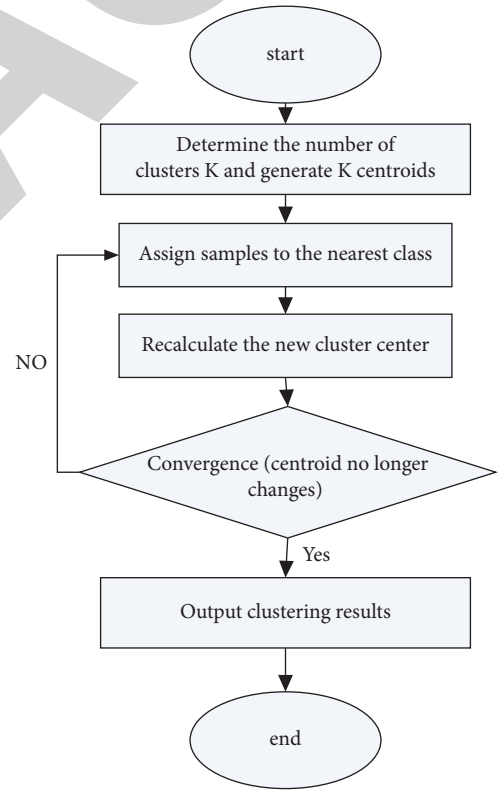

Figure 9: K-means algorithm flow.

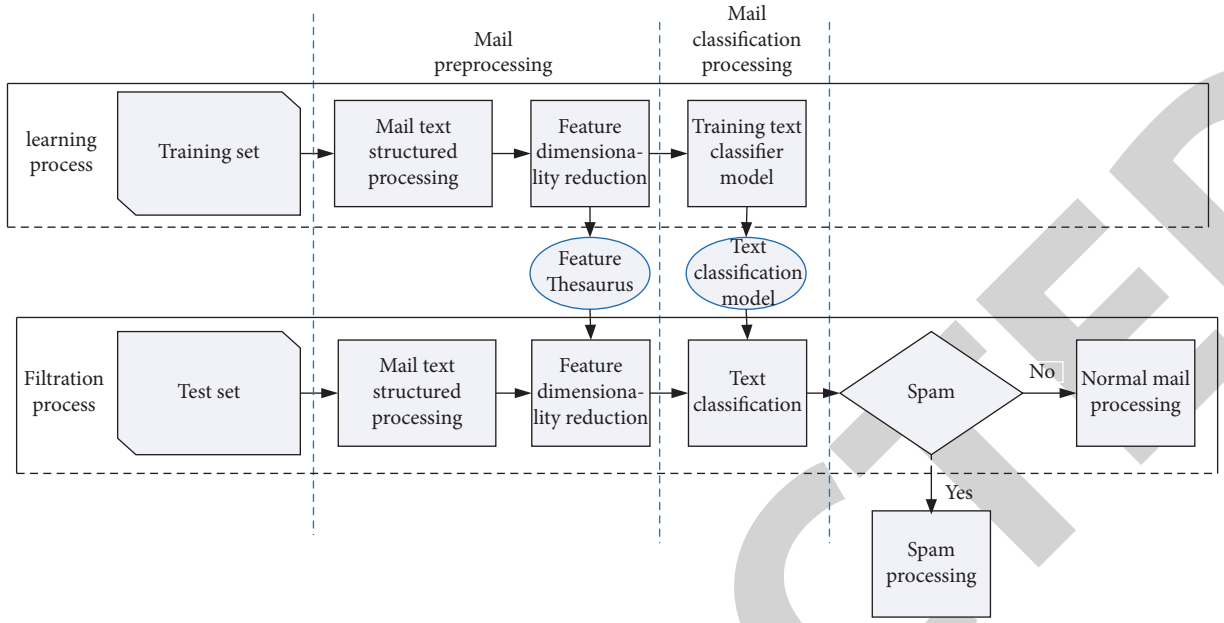

Figure 10: Spam classification process.

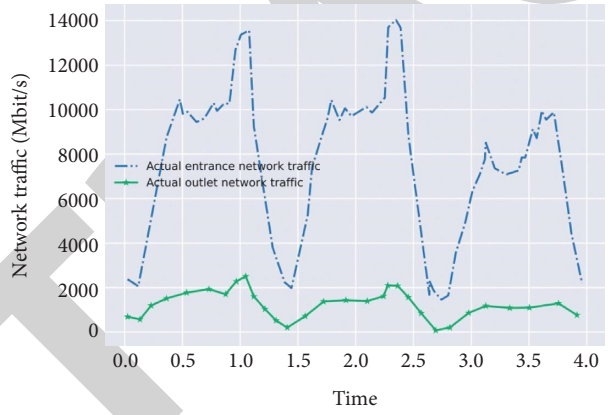

Figure 11: Service traffic prediction results based on linear regression.

Table 1: Comparison of prediction accuracy of ARIMA and ARIMA + boosting.

Prefecture (city)	Input rate accuracy/%		Output rate accuracy/%	
	ARIMA	ARIMA + Boosting	ARIMA	ARIMA + Boosting
A	72.21	92.37	71.52	97.23
B	70.85	93.5	80.8	98.97
C	87.6	96.43	77.79	89.92
D	81.5	96.19	73.62	94.43

calculate $d(q_j, \mu_2)$ again so that each sample can be assigned to the class with the closest interval. Then, the new center of mass of each class is found once again and the sample points are assigned, and the above process is continued until the center of mass does not change anymore.

3.2. Computer Network Security Management. In the context of gradually expanding the popularity of big data, various important information is stored in computer networks. In order to effectively guarantee the privacy of users' personal information and enhance the security of data, AI can be introduced into computer networks to strengthen computer security management capabilities. Based on the Naive Bayes algorithm, spam can be filtered. The specific process is shown in Figure 10. The k values of $P(a_j|b_i)$ are calculated, and if $P(a_j|b_i)$ is the maximum of these k values, mail b_i is classified into a_j classes.

Naive Bayes algorithm is a ML method for classifying sample data based on probability statistics, which assumes

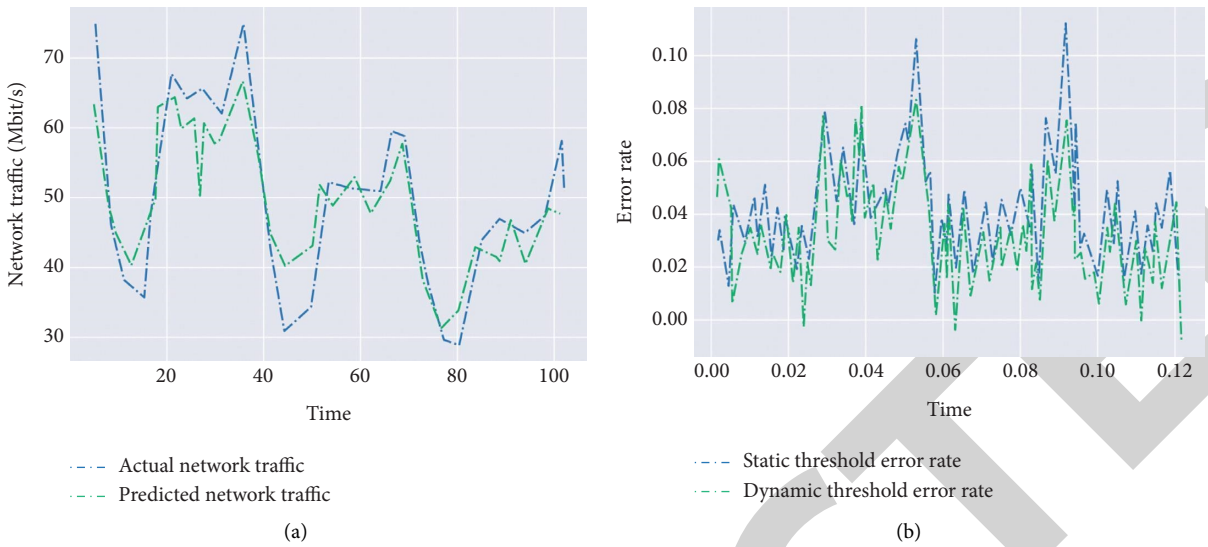

Figure 12: Flow forecasting based on ARIMA + boosting + dynamic threshold model. (a) Flow forecast results. (b) Error rate curve.

the prerequisite that the samples are independent of each other. Let the category set be $(a_1, a_2, a_3, ..., a_n,)$ and the mail document be b_i; then, the probability that the sample b_i belongs to a category a_j is calculated.

In order to improve the computing time efficiency, the traditional Naive Bayes algorithm can be optimized by fusing Naive Bayes algorithm with incremental learning, which improves the spam screening and correct rate. Since spam classification is a real-time updating process and new web languages are emerging all the time, the training set of a priori samples is not comprehensive enough.

4. Case Study

Network performance metrics (i.e., time series) have stability or regularity, and past trends will continue in the future. Based on this core idea, in order to achieve real-time monitoring of each metric, this paper takes into account data characteristics, modeling complexity, prediction accuracy, and application scenarios.

Company A used classical linear regression, ARIMA + Boosting model, and Holt–Winters algorithm in several AI innovation projects and chose dynamic threshold and static threshold methods, respectively, to achieve time series prediction and anomaly alert function for existing network indicators and achieved good application results. The following is a detailed description of the 3 sets of solutions.

Constructing a suitable algorithmic framework to mine the metric change patterns, accurately predicting the network performance metrics through feature learning of historical data, and selecting a suitable threshold setting method, we finally realize the alerting of abnormal events.

4.1. Application of Linear Regression in Performance Metrics Prediction. With the development of services in the direction of diversification and differentiation, network change (cutover) has become a daily operation for operators to cope with the demand of multiple scenarios such as relay expansion and equipment entry. A company has now developed and launched an AI network unmanned system to solve the problem of time consumption, high risk, and low efficiency of cutover tasks.

In the process of determining the flow anomaly, this program uses the dynamic threshold method of the base 3σ criterion to trigger the alarm. We define the error rate $\Delta = |\text{predicted value} - \text{actual value}|/\text{predicted value} \times 100\%$. By calculating the error rate of the historical flow data, the mean μ and variance σ of the error rate are obtained. If the error rate Δ of the current moment satisfies $|\Delta - \mu| \geq 3\sigma$, the flow is considered to be abnormal at this time and the cutover verification is triggered to fail.

Figure 11 shows the prediction results of a customer service traffic of IDC equipment using linear regression and the abnormal trigger based on the 3σ criterion, and the abnormal traffic is found at the arrow. The method can better fit the trend of indicator changes and can effectively detect anomalies to achieve postcutover healthiness decisions.

4.2. Application of ARIMA in Performance Metrics Prediction. A company uses Big Data + AI capabilities to perform traffic modeling to help network departments predict network and service traffic and guide network expansion with precision. In this paper, we use the ARIMA algorithm to implement traffic data regression analysis and build the Boosting model to improve the prediction accuracy of time series.

In this paper, the logic of using static thresholds to implement traffic anomaly alerts is to calculate the error rate and issue an alert when the error rate is greater than a set threshold. The error rate $\Delta = |\text{predicted value} - \text{actual value}|/\text{predicted value}$ is set when the error rate is greater than a fixed threshold value to issue an alarm. This alarm method has a major drawback.

The model is trained using the historical data of the past week, and the trend prediction of traffic rate for the next 24 h

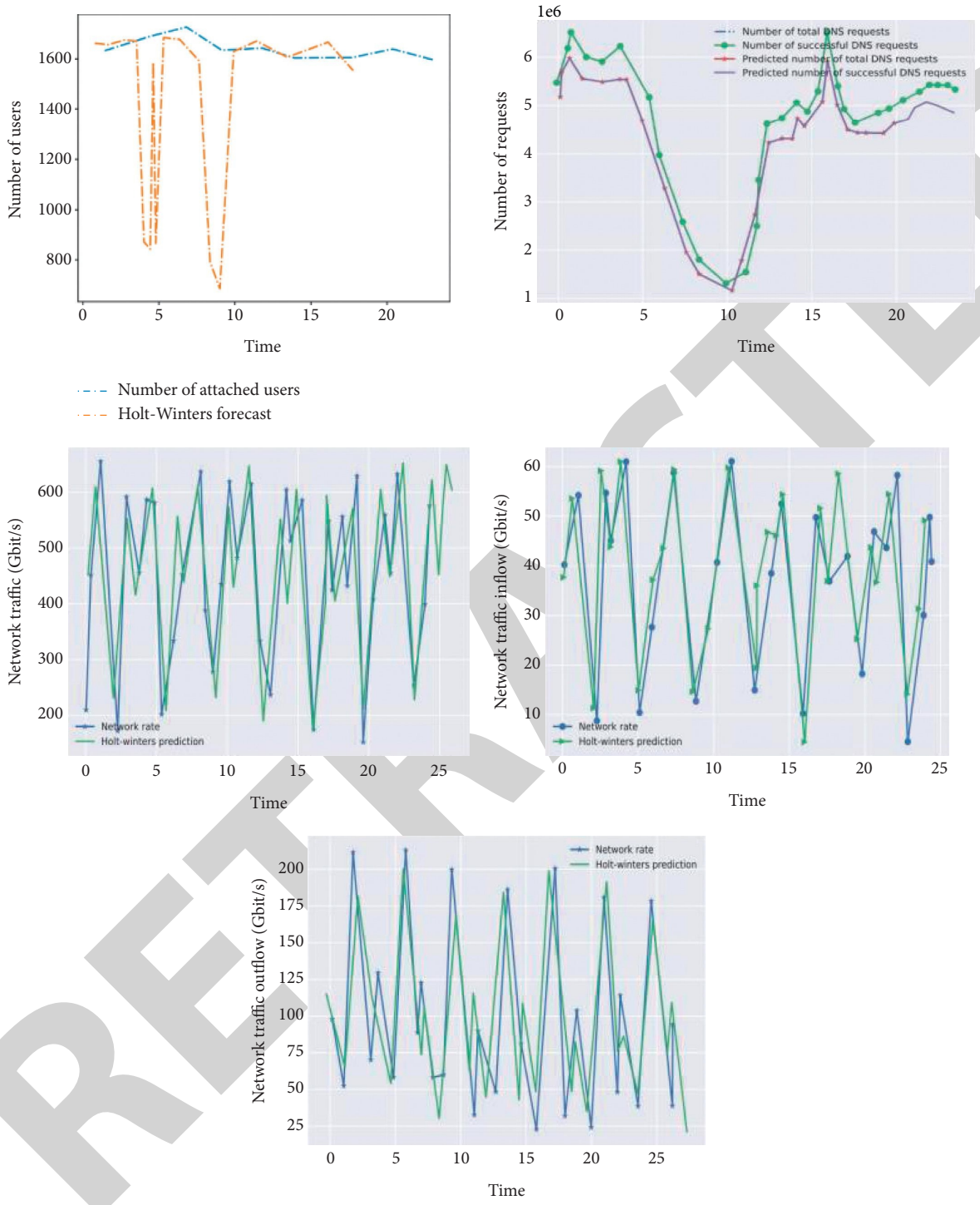

Figure 13: Graph of Holt–Winters prediction results across disciplines and multiple indicators.

is performed. The prediction value = 0.5 × ARIMA prediction value + 0.5 × Boosting prediction value. Table 1 compares the accuracy of the ARIMA and ARIMA + Boosting models, and the results show that Boosting greatly optimizes the prediction performance and improves the accuracy by nearly 20%.

To address the above issues, this solution uses a dynamic threshold method to implement anomaly alerts. When training the model using the historical data of the previous week, the value of the 85th percentile (P85) of the data set is calculated statistically, where the 85th percentile is the traffic rate value that falls at the 85% position of the length of the data set by

sorting the traffic data from smallest to largest. Traffic anomalies are determined based on the following: error rate $\Delta = |\text{predicted value} - \text{actual value}|/|H \geq \xi$, where $H = (P_{85} + \text{predicted value})/2$ and ξ is the set threshold value.

As shown in Figure 12(a), the ARIMA + Boosting model can achieve accurate prediction for periodically varying flows, but the fit needs to be improved for the detailed part of the random fluctuations of the data. As can be seen from Figure 12(b), the error rate value in the trough region of the prediction curve with the improved dynamic threshold method is smaller than that with the static threshold, which can reduce the false alarm rate in the trough region.

The prediction results of some performance indicators based on the Holt–Winters + static threshold method are shown in Figure 13, and the red part of the graph indicates that the indicator abnormality is detected at that time. From Figure 13, it can be seen that the framework can make accurate predictions for a variety of metrics, helping O&M staff to detect faults in advance.

4.3. Application in Performance Metrics Prediction. Specifically, the system collects historical data on several metrics such as MAN/carrier network/IoT traffic, number of packet network attached users and success rate, number of IoT/fixed-line broadband users, and DNS request volume. The solution uses the Holt–Winters algorithm to take the data of the past week for model training to achieve the data prediction of the future day. To ensure the accuracy and validity of the alarms, the system sets strong alarm rules and actual value and predicted value are greater than the corresponding threshold value. For different indicators, each profession sets different thresholds according to the alarm rules to achieve abnormal warnings.

5. Conclusion

The 5G era and the big data era have brought new challenges to network operations. The traditional network communication technology can no longer meet the actual needs. This paper proposes an artificial intelligence search method based on the K-means algorithm and uses the relative distance between elements to represent the degree of dissimilarity of different types of variables. As an emerging IT technology, artificial intelligence has unique advantages in data extraction and data processing. Compared with traditional measurement methods, artificial intelligence and measurement methods are more effective and flexible and can also adapt to different environments. Network security services have made great contributions to ensuring the safe operation of information infrastructure. It is necessary to actively apply AI technology, analyze its role in promoting network security, establish the concept of network security intelligent operation, and improve the intelligence and automation level of network security services.

Data Availability

The experimental data used to support the findings of this study are available from the author upon request.

Conflicts of Interest

The author declares no conflicts of interest regarding this work.

References

[1] Y. Y. Chen, Y. H. Lin, C. C. Kung, M. H. Chung, and I. H. Yen, "Design and implementation of cloud analytics-assisted smart power meters considering advanced artificial intelligence as edge analytics in demand-side management for smart homes," *Sensors*, vol. 19, no. 9, p. 2047, 2019.

[2] A. M. Al-Azab, A. A. Zaituon, K. M. Al-Ghamdi, and F. M. A. Al-Galil, "Surveillance of dengue fever vector *Aedes aegypti* in different areas in Jeddah city Saudi Arabia," *Advances in Animal and Veterinary Sciences*, vol. 10, no. 2, pp. 348–353, 2022.

[3] A. H. Sodhro, S. Pirbhulal, and V. H. C. De Albuquerque, "Artificial intelligence-driven mechanism for edge computing-based industrial applications," *IEEE Transactions on Industrial Informatics*, vol. 15, no. 7, pp. 4235–4243, 2019.

[4] F. A. Al-Mekhlafi, R. A. Alajmi, Z. Almusawi et al., "A study of insect succession of forensic importance: Dipteran flies (diptera) in two different habitats of small rodents in Riyadh City, Saudi Arabia," *Journal of King Saud University Science*, vol. 32, no. 7, pp. 3111–3118, 2020.

[5] S. S. Gill, S. Tuli, M. Xu et al., "Transformative effects of IoT, Blockchain and Artificial Intelligence on cloud computing: e," *Internet of Things*, vol. 8, Article ID 100118, 2019.

[6] A. Abd, A. Fahd Mohammed, and S. P. Zambare, "New species of flesh fly (Diptera: sarcophagidae) Sarcophaga (Liosarcophaga) geetai in India," *J Entomol Zool Stud*, vol. 4, no. 3, pp. 314–318, 2016.

[7] F. B. Saghezchi, A. Radwan, J. Rodriguez, and T. Dagiuklas, "Coalition formation game toward green mobile terminals in heterogeneous wireless networks," *IEEE Wireless Communications*, vol. 20, no. 5, pp. 85–91, 2013.

[8] N. Syam and A. Sharma, "Waiting for a sales renaissance in the fourth industrial revolution: machine learning and artificial intelligence in sales research and practice," *Industrial Marketing Management*, vol. 69, pp. 135–146, 2018.

[9] S. Nagi Alsubari, S. N Deshmukh, A. Abdullah Alqarni et al., "Data analytics for the identification of fake reviews using supervised learning," *Computers, Materials & Continua*, vol. 70, no. 2, pp. 3189–3204, 2022.

[10] B. H. Li, B. C. Hou, W. T. Yu, X. B. Lu, and C. W. Yang, "Applications of artificial intelligence in intelligent manufacturing: a review," *Frontiers of Information Technology & Electronic Engineering*, vol. 18, no. 1, pp. 86–96, 2017.

[11] Q. Liu, C. Liu, and Y. Wang, "etc. Integrating external dictionary knowledge in conference scenarios the field of personalized machine translation method [J]," *Journal of Chinese Informatics*, vol. 33, no. 10, pp. 31–37, 2019.

[12] Di Wu, Y. Lei, M. He, C. Zhang, and Li Ji, "Deep reinforcement learning-based path control and optimization for unmanned ships," *Wireless Communications and Mobile Computing*, vol. 2022, Article ID 7135043, 8 pages, 2022.

[13] M. Q. Raza and A. Khosravi, "A review on artificial intelligence based load demand forecasting techniques for smart grid and buildings," *Renewable and Sustainable Energy Reviews*, vol. 50, pp. 1352–1372, 2015.

[14] G. Cai, Y. Fang, J. Wen, S. Mumtaz, Y. Song, and V. Frascolla, "Multi-carrier M-ary DCSK system with code index modulation: an efficient solution for chaotic

Hindawi
Mobile Information Systems
Volume 2022, Article ID 9999056, 11 pages
https://doi.org/10.1155/2022/9999056

Research Article

Software Simulation in English Translation Platform Based on Gaussian Hybrid Model

Nan Peng,[1] **Yingying Wei**,[2] **Lu Liu**,[1] **and Junzhong Zou**[3]

[1]*Department of Basic Teaching and Research, East University of Heilongjiang, Heilongjiang, Harbin 150066, China*
[2]*Department of Management, East University of Heilongjiang, Heilongjiang, Harbin 150066, China*
[3]*Department of Human Resources, East University of Heilongjiang, Heilongjiang, Harbin 150066, China*

Correspondence should be addressed to Lu Liu; liulu@hljeu.edu.cn

Received 26 June 2022; Revised 22 July 2022; Accepted 4 August 2022; Published 21 August 2022

Academic Editor: Shadi Aljawarneh

In this article, we will first try to create a general development platform for embedded systems. The goal of this step is to establish an experimental platform that can support various peripheral modules and can be reused. The connection between the modules can be reconfigured to meet the different needs of embedded research and learning. On this basis, the system uses the audio frequency spectrum program as an input function to represent the dispersion pattern of signal energy, which can be tested with characteristic nodes simulated by convolutional neural network software. In addition, the auxiliary neural network software simulation core can continuously learn the detailed characteristics of the audio frequency spectrum, making it easy to recognize environmental sounds. In addition, the sound signal and the neural cycle are related in time. The neural network can study the relationship between different frames in the time domain to compensate for the defects caused by the complex neural network in modeling time series. Finally, this article focuses on the process of building an English translation platform based on the mobile cloud data model. The client is targeted at the Android platform, while the server is based on the laaS system. According to the model of mobile cloud data processing, the calculation of mobile phones in computer-intensive programs is studied. Through the hardware design and distribution of the system, we are able to use mobile cloud technology as a desktop-intensive program to solve the problem of effectiveness in the solution. The article promotes the development of an English translation platform by applying the research results of environmental sound recognition based on embedded system software simulation to the design of the English translation platform.

1. Introduction

This article first analyzes the actual application background of the embedded system and then develops and designs a general experimental platform composed of embedded processor core modules, custom connection modules, and external facility modules based on application requirements [1]. How to select, design, write, and test the hardware peripheral modules of the platform, and transplant basic drivers for each module is the focus of this article [2]. The common experimental platform is built with an embedded STM32 processor [3]. It has the advantages of high performance and low cost. It can be used as the core module of the experimental system. We have also developed a motherboard supporting circuit for this core module [4]. On this basis, it has deeply studied how to improve the data of environmental sound recognition and proposed an improvement plan for the problem of environmental sound recognition in the online mode [5]. At present, the amount of data contained in the public environmental sound data set is relatively small, and it is difficult for the model to obtain good generalization performance in limited training [6]. In this article, we describe the data expansion method of existing software simulation and then propose an online data expansion program based on this technology [7]. The improved scheme directly processes the spectrogram of the input sound in the training phase, which not only provides a wide range of

training samples, but also improves the flexibility of the system, and significantly improves the recognition performance of the proposed extension scheme on several public data sets [8]. Finally, due to the high development cost of traditional server-side equipment, there are cumbersome upgrades, maintenance, management, and expansion complexity, as well as other key issues that affect the performance of computing-intensive mobile device applications. Finally, this article introduces the English translation platform based on OpenNebula's open source platform in detail [9]. The author provides a mobile cloud computing environment for testing in combination with an online translation system [10]. Through basic research on the development model and system architecture of mobile-intensive applications, we can optimize the development, operation, deployment, and use of traditional mobile applications and effectively manage virtual resources. Finally, it provides network services with excellent scalability and realizes a dynamically scalable system model. On this basis, combined with the key technologies discussed in this article, we make full use of the advantages of mobile cloud computing and finally provide an English translation platform in the mobile cloud computing model [11]. In order to verify the effectiveness of the development model and system architecture proposed in this article, the platform will be tested by simulation testing [12].

2. Related Work

The literature introduces the overall framework of computing-intensive mobile application development based on the mobile cloud computing model. According to the analysis of system requirements, the key technologies involved in the mobile cloud computing model are integrated with OpenNebula, and the specific implementation methods and methods of the online translation system are given to process and verify its feasibility [13]. The literature introduces the theoretical basis of environmental sound recognition and deep learning [14]. First, the typical system framework, common feature extraction methods, and typical features, common classification algorithms, and evaluation indicators of environmental sound recognition tasks are analyzed and described in detail, and then the theoretical basis of deep learning is introduced [15]. The literature introduces the advantages and disadvantages of deep learning basic network structure applied to environmental sound recognition tasks, and it designs a convolutional recurrent neural network structure to learn from the characteristics of sound spectrograms [16]. The literature introduces existing sound data enhancement methods and proposes an online data enhancement scheme, including mask enhancement and hybrid enhancement, which directly act on each batch of data in the model training process. According to different parameter settings, we have designed several enhancement strategies and conducted an experimental analysis [17]. The literature introduces the hardware circuit design of the experimental platform's network connection module, audio signal receiving module, TFT liquid crystal display module, data storage card module, and the general layout of the embedded system's general experimental platform [18].

3. Embedded System Software Simulation and Environmental Sound Recognition

3.1. Embedded System. The processor of the embedded system is the central component of the entire system, and it is the key to check the operation of the entire system. At present, the main embedded processors on the market can be divided into the following categories:

Chip programming system: it is a hardware programming system in which the software core of the microcontroller can be loaded into the chip. The system will automatically call other required hardware IP modules.

DSP digital signal processor: this processor is designed to deal with the data transmission problem of digital signals. The DSP has a dedicated hardware multiplier, is capable of pipeline operation, and provides dedicated DSP instructions.

Embedded Microprocessor (MPU): it is a standard computer processor and is currently the most widely used processor. And the cost is low, and it has an excellent performance in temperature control and reliability.

Embedded microcontroller (MCU): it is also called a single-chip microcomputer, its structure and performance are not as good as MPU, and its utilization rate is low.

According to the different function types of each microprocessor, the choice of the peripheral circuit of the embedded system is also very different. The basic module of the peripheral circuit is usually mainly composed of the power management circuit, the data storage circuit, and the operating program module. The existence of all submodules is necessary for the normal operation of the microprocessor. The external hardware of the embedded system will change according to the needs of the system, and usually the input device will be changed according to the different external hardware that needs to be configured.

In some more complex embedded systems, an embedded operating system is usually required. Generally speaking, the operating system has two basic functions: to promote the correct use of system resources by applications and to manage hardware devices. In addition, multitasking is also an important function of embedded operating systems that can work in real time.

Under normal circumstances, embedded system development consists of two parts: program development and hardware development. The development process is mainly composed of 4 parts, which are

Overall structural design: it is the overall structural framework of the absolute system, including the division of system programs and hardware functions and

the assignment of target tasks, as well as the compatibility of other hardware.

Co-design of hardware and software: according to the requirements of the system structure, detailed design comparisons of the system hardware and software versions are carried out respectively.

Requirement analysis: after analyzing the characteristics of the system and the use environment, the goals and tasks are determined, and unified standards are used as the guidelines for system design.

System test: we will perform a complete machine test on the combined system after debugging to verify whether it meets the functional requirements in the setting.

3.2. Basic Principles of Environmental Sound Recognition. Environmental speech recognition is an important issue in speech recognition. The goal of many existing systems is to be able to accurately predict the characteristics of certain types of sounds. As shown in Figure 1, we input a speech signal that can express its classification characteristics into the environmental speech recognition system. In this way, regardless of the internal working environment of the environmental speech recognition system, the speech recognition system will issue a predetermined category, such as "dog barking."

Preprocessing the data is a preliminary process for extracting environmental acoustic characteristics. The data are imported into a unified specification by measuring the dimensionality of the original data to ensure its consistency. In the actual test, due to the fluctuation of the collection environment, the collected data are usually noisy. We can use the end marker to solve this problem.

Highlighting the particularity of environmental speech is a key step for the system to solve the problem of accuracy. In the actual test, the range of the noise configuration is very high, and the difference between different configurations has not been studied yet. Therefore, the important step is to use the signal processing source to extract more features of the sound configuration and to highlight the salient features of the entire signal with a lower dimension. The recognition performance of a system usually depends on the ability to highlight the sound features. In the work of environmental speech recognition, common features include short-range energy, sound vibration amplitude, zero-crossing level, mile spectrum, mile frequency interval coefficient, and so on.

The classification model is a necessary functional module of the environmental speech recognition system. The classification model is usually based on the existing labeled data, is trained and updated continuously in the repeated process, and finally integrated into the validation set. In addition, it requires a lot of calculations to classify the distance between different sounds and data in the sample features.

3.3. Algorithm Model. At present, most of the sound features are converted into data by the Fourier transform formula. But this article also refers to other frequency domain

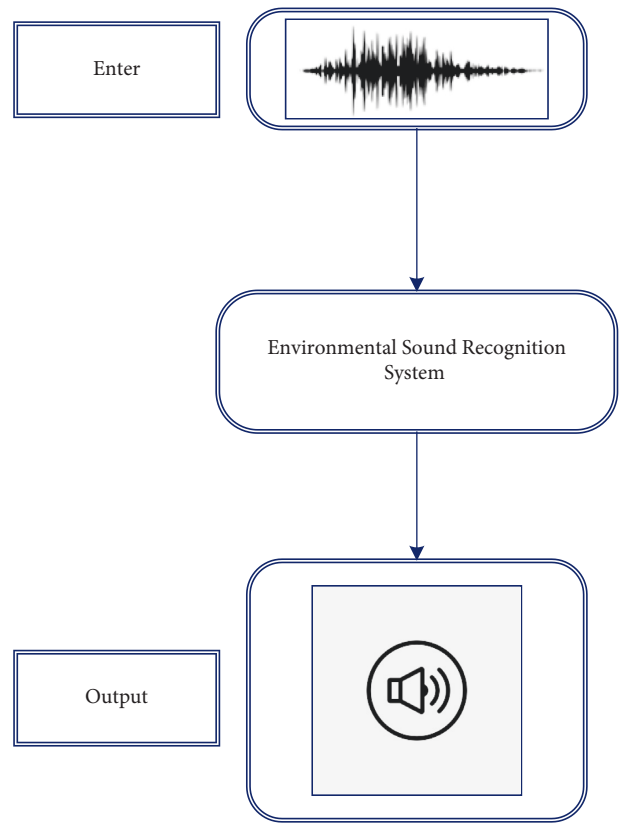

Figure 1: Overview of the environmental sound recognition system.

conversion methods, such as constant Q conversion (CQT) and continuous violet conversion (CWT).

Zero crossing rate (ZCR) is an important feature of instantaneous sounds (such as percussive sounds), and its calculation formula is as follows:

$$Z = \frac{1}{2(n-1)} \sum_{n=1}^{N-1} |\operatorname{sgn}(x(n+1)) - \operatorname{sgn}(x(n))|. \quad (1)$$

In the formula, (n) represents the signal, N is the sampling point, and $(\bullet)$ is the symbolic function, and we obtained

$$\operatorname{sgn}(x(n)) = \begin{cases} 1, & x(n) \geq 0, \\ -1, & x(n) < 0. \end{cases} \quad (2)$$

STE describes the distribution of the signal in the time domain and expressed as

$$E_n = \frac{1}{N} \sum_{m} x(m) w(n-m)^2, \quad (3)$$

where (n) is the window function and we obtained

$$w(n) = \begin{cases} 1, & 0 \leq n \leq N-1, \\ 0, & \text{others}. \end{cases} \quad (4)$$

The response of the triangle filter is

$$H_m(k) = \begin{cases} 0, & k < f(m-1), \\ \dfrac{2(k - f(m-1))}{(f(m+1) - f(m-1))(f(m) - f(m-1))}, & f(m-1) \le k \le f(m), \\ \dfrac{2(f(m+1) - k)}{(f(m+1) - f(m-1))(f(m) - f(m-1))}, & f(m) \le k \le f(m+1), \\ 0, & k \ge f(m+1). \end{cases} \tag{5}$$

The energy spectrum after frequency domain conversion is as follows:

$$S(m) = \sum_{k=0}^{N-1} |X(k)|^2 H_m(k). \tag{6}$$

Here, (k) is the amplitude spectrum after Fourier transform.

After applying a filter to the sound spectrum, a logarithmic transformation is usually required. The frequency spectrum of a sound signal is composed of high frequency and low frequency. The low frequency can reveal the spectrum network, and the high frequency shows the details of the spectrum. The sound signal spectrum includes important information for formants to distinguish different tones. Converting the high- and low-frequency parts of the spectrum from multiplication to addition makes it easy to perform calculations. It behaves as

$$\ln(X(k)) = \ln(H(k)E(k)) = \ln(H(k)) + \ln(E(k)). \tag{7}$$

Cepstrum is a coefficient characteristic obtained by filtering the sound signal using DCT (Discrete Cosine Transform). Among them, DCT is an important measure to make further processing on the basis of Fourier exchange to minimize the signal filter. The main feature after the change is in the lower part. The DCT transformation form is as follows:

$$C(n) = \sum_{m=0}^{N-1} \ln(S(m)) \cos\left(\frac{\pi n(m - 0.5)}{M}\right), \quad 0 \le n \le L. \tag{8}$$

Optimize as follows:

$$\begin{aligned} &\min_{\omega,b} \frac{1}{2}\omega^T\omega, \\ &s.t.\ y_i\left(\omega^T x_i + b\right) \ge 1, \quad i = 1, 2, \ldots, m. \end{aligned} \tag{9}$$

The training model is not necessarily a new line, but the current equation improvement cannot get a solution. For this particular problem, we introduced the Soft Margin concept and built an optimized system with a small number of models. So that you can write an improvement plan accordingly:

$$\begin{aligned} &\min_{\omega,b,\xi_i} \frac{1}{2}\omega^T\omega + C\sum_{i=1}^{m}\xi_i, \\ &s.t.\ y_i\left(\omega^T x_i + b\right) \ge 1 - \xi_i\xi_i \ge 0, \quad i = 1, 2, \ldots, m. \end{aligned} \tag{10}$$

The SVM method can introduce core functions under nonlinearity, drag samples into high-dimensional space, and separate them directly. Expressing the function vector of (in) in the high-dimensional space as $\phi(x)$, we obtained

$$f(x) = \omega^T\Phi(x) + b = \sum_{i=1}^{m} \alpha_i y_i \kappa(x, x_i) + b. \tag{11}$$

The Gaussian Hybrid Model (GMM) is a classic application model that solves the data collection problem by distributing samples. Therefore, the Gaussian Hybrid Model is also considered an extension of the K-means algorithm. This model assumes that data propagation is dominated by a large number of Gaussian components with independent parameters, which is defined as follows:

$$G(x, \mu, \sigma) = \frac{1}{\sqrt{2\pi}\sigma} \exp\left(-\frac{(x - \mu)^2}{2\sigma^2}\right). \tag{12}$$

We use σ to denote the variance and μ to denote the mean, and we obtained

$$P(x) = \sum_{i}^{K} w_i G(x, \mu, \Sigma_i). \tag{13}$$

The neuron output y is calculated as follows:

$$y = \sigma(w_1 \cdot x_1 + w_2 \cdot x_2 + b). \tag{14}$$

Accuracy is the most common weighted index for classification problems. Accuracy refers to the relative ratio between the number of samples that are correctly classified and the total. The following is the accuracy value of the classification model f in the data set D:

$$\text{accuracy}(f, D) = \frac{1}{N}\sum_{i=1}^{N} I(f(x_i) = y_i). \tag{15}$$

Among them, (xi, yi) represents the feature and category label of the ith sample, N is the total number of samples, and I is the indicator function, defined as follows:

$$I(x) = \begin{cases} 1, & x \text{ is true,} \\ 0, & x \text{ is false.} \end{cases} \tag{16}$$

Windowing: the number of frames is replaced with a window function to ensure continuity and attenuation on both sides of the frame. The most common ones are Hamming window and the Hanning window. After comparison, it is found that the Hamming window is controlled by different weighting coefficients, which can better avoid the problem of spectrum leakage after the Fourier transform. The expression of Hamming window is as follows:

$$W(n,a) = (1-a) - a \times \cos\left(\frac{2\pi n}{N-1}\right), \quad 0 \le n \le N-1. \tag{17}$$

FFT transformation: most of the characteristics of the sound signal are hidden in the frequency domain information, so it is necessary to convert the sound signal to the frequency domain to analyze its energy distribution pattern. Fast Fourier transform is one of the most common and effective methods. The transform form of Fast Fourier transform is as follows:

$$X(k) = \sum_{n=0}^{N-1} x_w(n) e^{-(j2\pi k/N)}, \quad 0 \le k \le N-1. \tag{18}$$

Gammatone filter: Gammatone filter is the result of multiplying the Gamma distribution function and the sine wave, and its calculation formula is defined as follows:

$$g(t) = Kt^{(n-1)} e^{-2\pi Bt} \cos(2\pi f_c t + \varphi), \quad t > 0. \tag{19}$$

The energy spectrum converted by the Gammatone filter is expressed as follows:

$$S(m) = \sum_{k=0}^{N-1} |X(k)|^2 H_m(k). \tag{20}$$

Calculate the logarithmic energy: do a log transformation of the energy spectrum obtained through the Gammatone filter to obtain the logarithmic energy spectrum, as follows:

$$LGS(m) = \ln(S(m)) = \ln\left(\sum_{k=0}^{N-1} |X(k)|^2 H_m(k)\right). \tag{21}$$

In the research conducted in this article, we need to find a function that can describe the relationship between the input set of the Ks component and the output target signal I, and listen to the normal P distribution (Ks, I). To this end, we define the missing function $\mathscr{L}$ to measure the difference between the model predictions $f(k)$, where $(k, i) \sim P$, the mean decreases. Minimizing the loss of data distribution caused by $\mathscr{L}$ is called expected risks:

$$R(f) = \int \mathscr{L}(f(x), y) \mathrm{d}P(x, y). \tag{22}$$

The approximate distribution obtained by using the training data set D is called empirical distribution.

$$P_\delta(x, y) = \frac{1}{n} \sum_{i=1}^{n} \delta(x = x_i, y = y_i). \tag{23}$$

The corresponding optimization method is called empirical risk minimization.

$$R_\delta(f) = \int \mathscr{L}(f(x), y) \mathrm{d}P_\delta(x, y) = \frac{1}{n} \sum_{i=1}^{n} \mathscr{L}(f(x_i), y_i). \tag{24}$$

Time Stretch refers to the scale transformation of the sound waveform in the time dimension. The goal is to control the sound signal to be accelerated or decelerated.

$$z = \text{time\_stretch}(y, \text{rate}). \tag{25}$$

Pitch Shift refers to the scale transformation of the sound waveform in the frequency dimension. The goal is to increase or decrease the pitch of the sound (Pitch).

$$z = \text{pitch\_shift}(y, n\text{steps}). \tag{26}$$

Adding Noise means to mix the sample with another signal containing a different acoustic scene or background noise to enhance the diversity of the sample, which is expressed as follows:

$$z = (1-w) \cdot x + w \cdot y. \tag{27}$$

Among them, y is the original sound signal, x is the background noise signal, z is the sample after mixing, and w is a weight parameter that represents the mixing ratio of the signal.

3.4. Simulation Analysis. In addition, because the hyperparameter α in the hybrid improvement method will change the mixing ratio of random samples, we conducted a differential test on different α values to test the effect of some α hyperparameters on the realization of the model. It can be seen from Figure 2 that when the abscissa $\alpha = 0.2$, the model satisfies the true reliability of the variables ESC-10, DCASE2016 Dev, and DCASE2016 Eval. According to ESC50 data collection, the average difference in the model is $\alpha = 0.3$, which is higher than expected, but the performance difference is no different from $\alpha = 0.2$. Therefore, it can be concluded that the change of the hyperparameter α has little effect on the performance of the test model, and is not the main influencing factor.

After the data are improved, the training samples are reprocessed, and the sample input text and the high-dimensional spatial distribution of the model research are modified to better study the impact of the previously proposed data enhancement scheme on the model. We can use key point calculation (PCA) to reduce the output size and data spread of the relevant link layer. Specifically, you can see the following figure. Figure 3(a) shows the data distribution without data improvement, and Figure 3(b) shows the data distribution after data improvement.

Figure 3 shows that there is a very significant degree of difference between the data distribution using the data

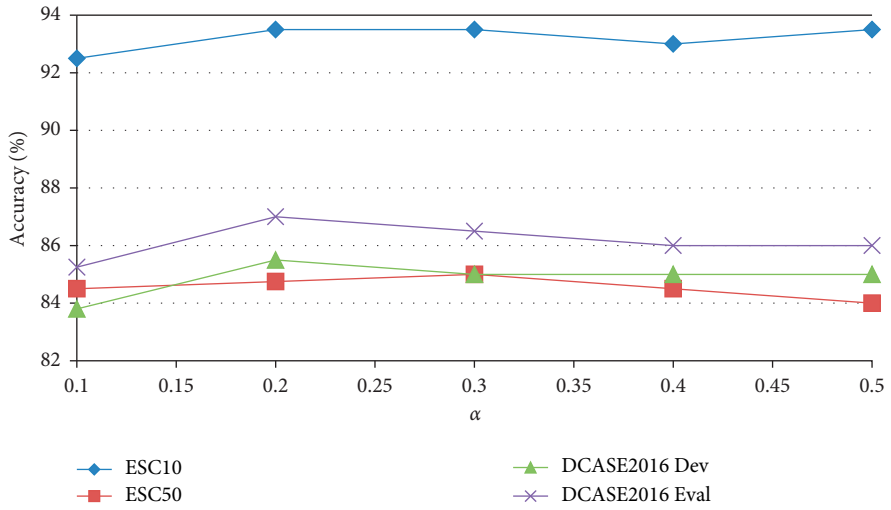

Figure 2: Comparison of recognition performance under different values of α in hybrid enhancement.

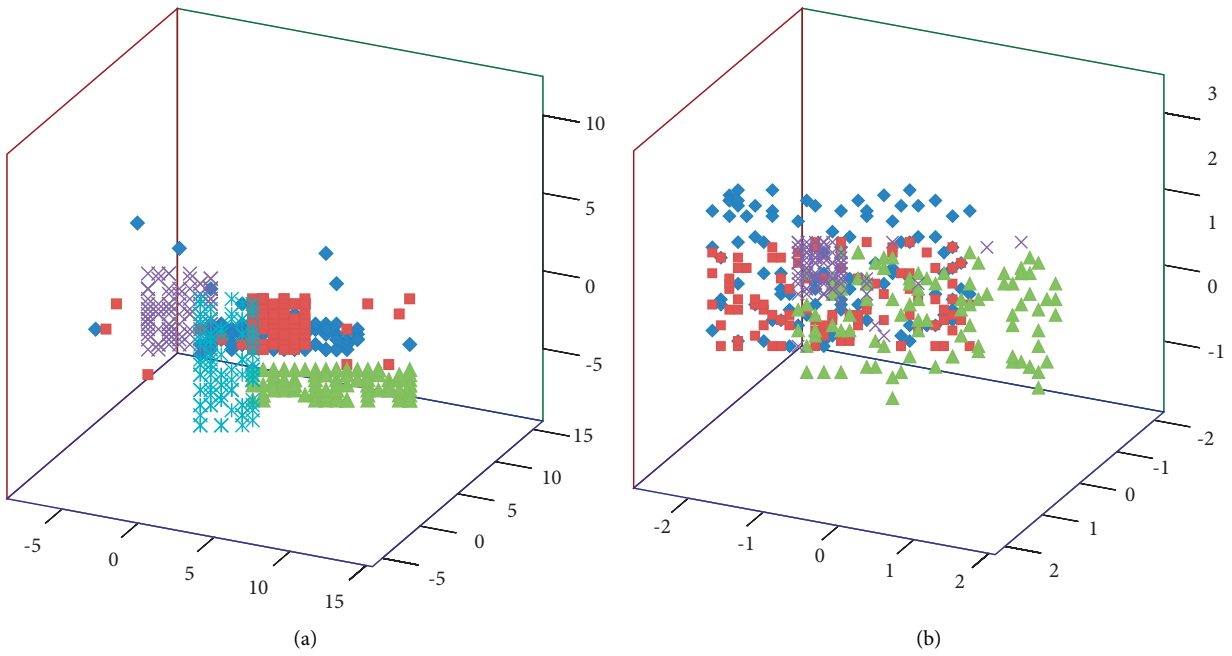

Figure 3: Visualization of the output data distribution of the fully connected layer after dimensionality reduction using PCA (a) unused data enhancement and (b) using data enhancement.

enhancement scheme and the data distribution without the enhancement scheme. For the data obtained without a data improvement program, some categories will have very large internal variances. Of course, there are also some internal variances with smaller types. The distance differences between them are also quite different. The model will be because of this phenomenon and improve the ability to recognize some special types of samples. The data-improved scheme has excellent robustness, and the within-class variance of each subgroup is easier to calculate.

4. Research on English Translation Platform Based on Related Technology

4.1. Translation Platform Demand Analysis. Vocabulary 16 to be used in this article is a relatively common application type. The advantage of local dictionary applications is that they can perform local translation functions without connecting to the World Wide Web. Therefore, electronic dictionaries usually implement online translation functions based on part of the functions of local dictionaries. Taking

smartphones as the representative, many smart devices have appropriate restrictions on the response speed, hardware allocation, power capacity, memory size, and other factors due to their portability and mobility requirements [19]. Therefore, users will have a better experience with online translation based on the local translation in the thesaurus. But this will also be limited by resources such as the type and capacity of the lexicon.

The other is an online dictionary based on the implementation of online translation, and the system architecture usually adopts the project C/S model. No matter what kind of client, the server will share part of the workload for the mobile client using this project mode. Usually, according to different operating conditions, such as network transmission conditions and mobile phone hardware configuration, software programs can use mobile computing models to make appropriate plans for task allocation between mobile devices and servers. However, traditional data centers often suffer from congestion during peak periods of application usage, resulting in users not getting corresponding feedback. However, if the number of servers is increased, when the utilization rate of mobile applications is low, most of the servers added by developers in the data center will be useless, which not only leads to a low average utilization rate of servers, but also damages the economic interests of developers. So there will be situations where software developers cannot predict when the next usage rate will reach the peak, nor can they switch on the server's task allocation, causing developers to often suffer losses when the number of visits increases.

The current translation function often requires the input of the target text in the translation box for translation. Many large-language users do not have a big problem with this method, but some small-language users do not have a language library that can be consulted, and do not know how to input the language at all, or their mobile phones do not directly support this language input, which causes a lot of problems and big trouble. For example, when a foreign tourist is interested in the traditional text of another country that is completely unknown to him and wants to know its true meaning, he will find that the traditional query method based on manual input cannot meet the needs of users at all.

Based on the above problems in practical applications, this article proposes a project model of an OCR-based network translation system in a mobile computing environment. The project goals of this system are as follows:

First of all, in order to avoid the inconvenience caused by large-scale manual input to users, the final input method of this system can accept images taken by mobile phone cameras. The user can take a photo of the disputed text with a mobile phone, and the data will be recorded in the form of a photo. The whole process does not require a text control basis. Of course, the user can also input the required query content in the system interface. In this way, you can not only query the photos taken on-site but also take the photos saved on your mobile phone as input content. The source language and target language can be set. The translation results and the text extracted by OCR can be saved in the form of text on the phone. For the content of interest in the translation result, you can directly call the built-in hyperlink to perform a Google search.

Second, integrate Google framework services on the server side, and implement online translation functions by calling Google Translate API. After all, Google Translate is the fastest and most accurate machine translation available today. Just set your source language and target language, enter the language text you need to translate, and Google will immediately perform a translation search [20]. The translation module currently used by Google combines United Nations documents as the source of the contents of this multilingual library. The translation result has very good accuracy and can support the real-time conversion of hundreds of languages, surpassing all local translation dictionaries.

Finally, considering the limited memory of most mobile phones now, the network translation system designed in this article will be based on the thin client model and try to migrate complex data processing to the backend server. Because the traditional C/S architecture server is inconvenient to maintain and difficult to expand. All the systems will realize the large-scale application of electronic dictionary translation programs through the OpenNebula cloud platform. Based on the OpenNebula cloud platform server, users can significantly improve use efficiency and reduce learning costs.

4.2. Translation Platform Structure Design. With the rapid development of information and digital technology, the application universality of smartphones has surpassed that of representative electronic computing devices such as desktop computers. But in the computing power of electronic devices, the role of mobile phones is still very limited. This is why we want to use clients as little as possible when creating customer mobile services. Most of the data processing is handed over to the server side, and the client side simply stores the edited photos, sends the request, and receives the result. After each translation process, the client will automatically disconnect from the server and will not reconnect until the translation is completed. Since the client does not need to connect to the server 24/7, the mobile phone can also have better battery life. The system structure is shown in Figure 4.

It can be seen from Figure 4 that this system works a lot on the server backend of the OpenNebula platform. In addition to the OCR test program, it also integrates Google's online translation. And because the Internet image engine adopts the OCR function, it may destroy other system tools during execution, so the OCR engine is often located on the server side. In addition, OCR is the starting point of all operations, so we need to have multiple OCRs together to form a processor, and reasonably control the distribution function through the equalizer. Therefore, the server component is divided into three parts: OCR engine, load balancer, and translation processor.

The user of the mobile device establishes a connection with the server through a wireless network. The wireless networking can support 3G, 4G signals or use WIFI. On the

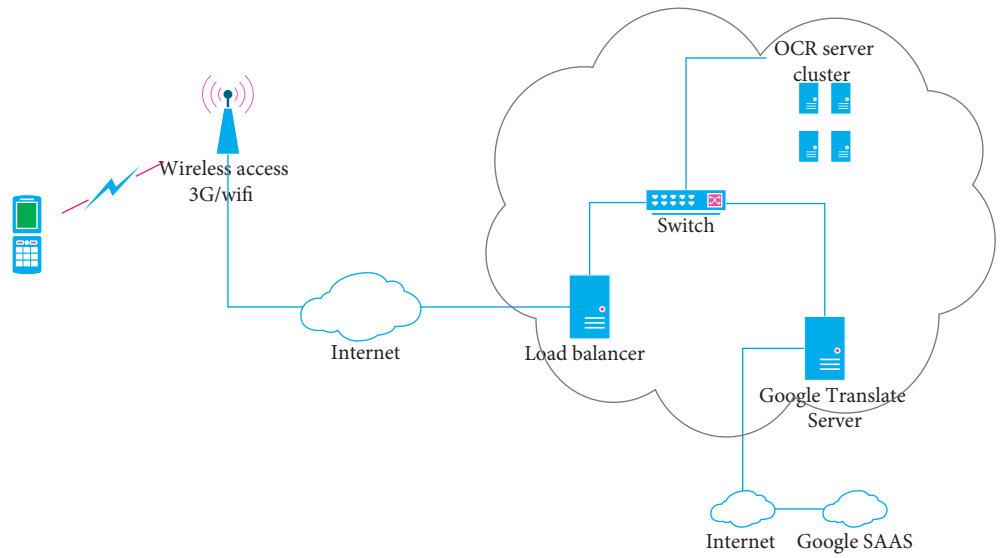

Figure 4: The whole system structure diagram.

server side of the OpenNebula cloud platform, there will be a web hosting server, OCR engine exchange server, and translator to form a small local area network for enabling and configuring various server resources. In addition, the server and the conversion server have an Ethernet interface that matches any Ethernet interface that intervenes in the Internet address. The shared server can receive client requests, and the World Wide Web connection can be used for Google translation services and retrieve client translation results. The number of OCR configuration servers will change according to the data fluctuations of their applications, so the configuration of translation servers and serial servers will also change according to the number of functions to be carried out.

The translation server integrates the Google application framework, that is, it can call the Google Translate API to translate the extracted words and sentences into the target language. Google Translate is not only an online translation function. Users can download the Google Translate plug-in and paste the document into the translation page, and the document to be translated will be sent to https://translate.google.com for processing. Google also provides a complete human translation team for the Translate API. Users can translate into the program using Google Translate API.

The translation server uses the Google Translate API in conjunction with the Google service framework to identify online translation services. The system puts the user's request in different threads through the Java multi-thread counting machine, and each link request is processed by a separate thread. In this way, when another user issues a request again, the processor can continue to receive other commands without affecting the previous work. The process is shown in Figure 5.

The whole system is based on the C/S architecture and is divided into two parts: server-side and client-side.

The server side is built using the OpenNebula cloud platform, which can provide various tools used in the server building process and ensure that at least one main network is used to connect the front end. The user end is rooted in the Android platform. Android was born from Google, and there is an Open Handset Alliance (OHA) that is stronger than ever. The design idea of the Android platform is more flexible than the previous platform, and it is more versatile and safer.

4.3. Database Design. This section will explain the names, types, concepts, and descriptions of each part of the translation system. The conversation message table stores conversations and conversation messages, and the specific structure is shown in Table 1.

Every message on the computer must be written in the original language. Although this system is currently only suitable for translation into Chinese and English, the possibility of translation into multiple languages has been considered here, and an interface has been reserved for this, and the translation template in the original language and the result in the target language are stored separately. MessageType is a message type. The receiver has the id information of the message sender, which is used to communicate with each other.

The language table stores the language types supported by the translation system, and the specific structure is shown in Table 2.

The LangName in the table is the key for storing the language name. Because the system can support multiple languages, the final text displayed on the screen layer should not be a fixed character, but can be customized according to the user's language. In iOS, the system provides related configuration files for multi-language conversion modules. By specifying the corresponding key in the code, you can read the corresponding text in the configuration file according to the computer language.

Table 3 shows a framework designed for system expansion.

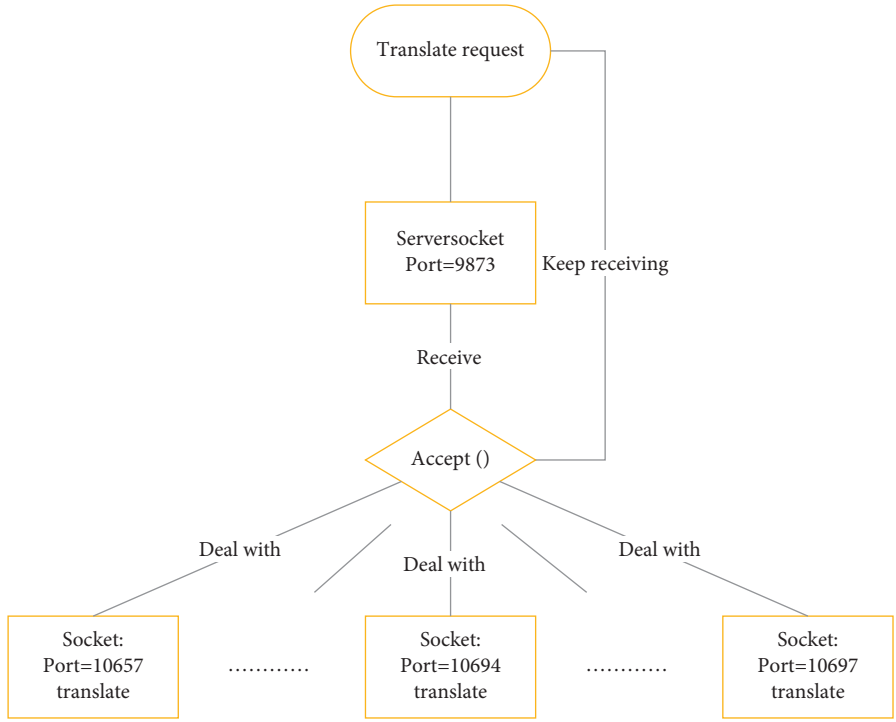

Figure 5: The processing flow of the translation server.

Table 1: Conversation message table.

Serial number	Field name	Types of	Attributes	Description
1	id	varchar(32)	PRIMARY KEY	Message id
2	sreLang	tinyint	FK, NOT NULL	Source language
3	destLang	tinyint	FK, NOT NULL	Target language
4	sreSentence	varchar(255)	NOT NULL	Source language sentence
5	destSentence	varchar(255)	—	Target language sentence
6	onversationType	tinyint	NOT NULL	Dialogue type
7	messageType	tinyint	NOT NULL	Message type
8	messageTime	varchar(32)	—	Message time
9	Sender	varchar(32)	FK	Message sender id
10	Receiver	varchar(32)	FK	Message recipient id
11	senderName	varchar(32)	-	The name of the message sender

Table 2: Language list.

Serial number	Field name	Types of	Attributes	Description
1	id	tinyint	PRIMARY KEY	Language type
2	langName	varchar(32)	—	Language name
3	Description	varcahr(255)	—	Language description

Table 3: Language translation table.

Serial number	Field name	Types of	Attributes	Description
1	sreLang	tinyint	PRIMARY KEY	Source language
2	destLang	tinyint	PRIMARY KEY	Target language
3	nterpretable	tinyint	—	Can it be translated

Table 4: User information table.

Serial number	Field name	Types of	Attributes	Description
1	id	varchar(32)	PRIMARY KEY	User id
2	Name	varchar(32)	—	User name
3	lang	tinyint	FK	User language
4	Sex	tinyint	—	User gender
5	Region	varchar(32)	—	User's area
6	Phone	varchar(32)	—	User phone
7	Birthday	varchar(32)	—	User birthday
8	AvatarUrl	varchar(255)	—	User avatar url

This framework preserves the relationship between translatable languages and provides support for future multilingual translation.

The user information table stores system user information and the specific structure can be seen in Table 4.

This table is used to store and manage user information, and it records many specific user information.

4.4. Realization of Functional Modules of Translation Platform. In the Android program, the user interface will be configured with View and ViewGroup, and there are multiple types of displays. All display interfaces are subparts of the system vision class. The display object is a data system processing unit used to store specific icon layouts and content attributes on the screen. Service plug-ins are a collection of subparts used to design interactive elements. The plug-ins used in this system are: Image Display, Editext, and Radio Button. The function of ViewGroup is to load and manage low-level views and other view groups, which can add some structure to the custom UI. When the Activity is activated, the system will instruct the Activity to use the root node to draw them based on the node distance measurement, and each ViewGroup node is responsible for drawing its direct child nodes.

HttpClient is an affiliate program of Apache Jakarta Commons. You can request updates of themes, parameters, and content structure through the HttpClient link. All background services of the system are operated and run based on the cloud virtual machine of the OpenNebula platform. The implementation process of the OCR processor has been shown above, using Tornado written in Python as an online container, through a simple and extensible barrier-free IO server, to achieve timely response communication. Compared with other web servers, Tornado can respond faster and better to the huge influx of traffic. At present, there are many real-time needs of websites that need to be built using Tornado. In the application of this article, an online translation system is established, so the real-time requirements are relatively high, so it is best to use Tornado as a web server.

Load balancing can be used to handle the process of Elastic Load Balancing on the cloud computing platform. In the OpenNebula operating system, we can use Sunstone to view the process and related data of the OCR processing server. If the existing OCR is already in a high load state, the response speed of the system will slow down. Therefore, we will use it as a virtual machine to help OCR perform data processing, and load balancing will effectively distribute system tasks on these multiple servers, thereby improving the robust performance of existing servers to a certain extent. The elastic load balancing function can observe the status of all current virtual machines and allocate tasks according to the number of idle virtual machines and the total number of tasks, ensuring that each OCR server has the same workload. At certain points in time, when user demand is low and OCR workload is low, a certain number of OCR processing servers can be shut down to ensure server utilization efficiency.

5. Conclusion

First of all, this article introduces the current development status and industry prospects of embedded systems at home and abroad. On this basis, it analyzes the function and feasibility of embedded computers as a test platform and proposes a configuration scheme for a general test platform. And use the platform designed in this paper to introduce deep learning algorithms into the recognition of environmental sounds as research materials, and conduct in-depth research and exploration on the basic construction of deep learning networks and data optimization schemes. At the end of the article, this article takes the popular mainstream OCR processor as an example, introduces the operating system based on OpenNebula and elaborates the process of creating an OCR-server virtual machine to assist the OCR server in data optimization processing, and then respectively introduces Load balancer LVS-reserve-server and Google Translate API. And give a key explanation on their technical background, implementation methods, impact on the client, and operation process. Finally, it describes in detail the two main functional modules that the mobile client based on the Android operating system relies on, and implements the language conversion operation of the English translation platform.

Data Availability

The data used to support the findings of this study are available from the corresponding author upon request.

Conflicts of Interest

The authors declare that they have no conflicts of interest.

Acknowledgments

This work was supported by A Study on the Reconstruction of College English Teaching Model in the "Internet+" era, a General Project of the National Social Science Foundation (No.: 17BYY102).

References

[1] A. Martini and J. Bosch, "Architectural technical debt in embedded systems," *Incose International Symposium*, vol. 26, no. 1, pp. 1029–1043, 2016.

[2] K. Wang, M. Du, D. Yang, C. Zhu, J. Shen, and Y. Zhang, "Game-theory-based active defense for intrusion detection in cyber-physical embedded systems," *ACM Transactions on Embedded Computing Systems*, vol. 16, no. 1, pp. 1–21, 2016.

[3] A. P. Rodrigues, B. Santos, P. F. Carvalho et al., "Taking advantage of the intercommunication features of IPMCs in ATCA CDAQ systems," *Fusion Engineering and Design*, vol. 128, pp. 138–142, 2018.

[4] J. Yang and R. K. Das, "Long-term high-frequency features for synthetic speech detection," *Digital Signal Processing*, vol. 97, Article ID 102622, 2020.

[5] Z. Wu, X. Xiao, E. S. Chng, and H. Li, "Synthetic speech detection using temporal modulation feature," in *Proceedings of the IEEE International Conference On Acoustics, Speech And Signal Processing*, pp. 7234–7238, IEEE, Canada, CA, USA, March 2013.

[6] Z. H. Wu, R. K. Das, J. Yang, and H. Li, "Light convolutional neural network with feature genuinization for detection of synthetic speech attacks," in *Proceedings of the Interspeech 2020*, Shanghai, China, October 2020.

[7] J. Sanchez, I. Saratxaga, I. Hernaez, E. Navas, and D. Erro, "A cross-vocoder study of speaker-independent synthetic speech detection using phase information," in *Proceedings of the Fifteenth Annual Conference of the International Speech Communication Association*, Singapore, September 2014.

[8] Y. Zhang, F. Jiang, and Z. Duan, "One-class learning towards synthetic voice spoofing detection," *IEEE Signal Processing Letters*, vol. 28, pp. 937–941, 2021.

[9] N. Chatterjee and S. Gupta, "Efficient phrase table pruning for Hindi to English machine translation through syntactic and marker-based filtering and hybrid similarity measurement," *Natural Language Engineering*, vol. 25, no. 1, pp. 171–210, 2019.

[10] S. Feng, "The acquisition of English definite noun phrases by Mandarin Chinese speakers," *Studies in Second Language Acquisition*, vol. 41, no. 04, pp. 881–896, 2019.

[11] G. F. Peng, H. T. Wu, J. Y. Xu, and J. S. Chang, "Mining and clustering phrases for English for special purpose: travel writing," in *Proceedings of the 2020 International Conference on Technologies and Applications of Artificial Intelligence (TAAI)*, pp. 97–101, IEEE, Taipei, Taiwan, December, 2020.

[12] M. Schoeberl, A. E. Dalsgaard, R. R. Hansen et al., "Safety-critical Java for embedded systems," *Concurrency and Computation: Practice and Experience*, vol. 29, no. 22, p. 3963, 2017.

[13] M. Adil, H. Alshahrani, A. Rajab, A. Shaikh, H. Song, and A. Farouk, "QoS review: smart sensing in wake of COVID-19, current trends and specifications with future research directions," *IEEE Sensors Journal*, vol. 2022, Article ID 3170055, 1 page, 2022.

[14] N. Fernando, S. W. Loke, and W. Rahayu, "Mobile cloud computing: a survey," *Future Generation Computer Systems*, vol. 29, no. 1, pp. 84–106, 2013.

[15] H.-q. Gao and Y.-j. Zhai, "System design of cloud computing based on mobile learning," in *Proceedings of the 2010 Third International Symposium on Knowledge Acquisition and Modeling*, pp. 239–242, IEEE, Wuhan, China, October 2010.

[16] N. Abbas, Y. Zhang, A. Taherkordi, and T. Skeie, "Mobile edge computing: a survey," *IEEE Internet of Things Journal*, vol. 5, no. 1, pp. 450–465, 2018.

[17] J. Yang, R. K. Das, and H. Li, "Significance of subband features for synthetic speech detection," *IEEE Transactions on Information Forensics and Security*, vol. 15, pp. 2160–2170, 2020.

[18] D. Paul, M. Pal, and G. Saha, "Spectral features for synthetic speech detection," *IEEE Journal of Selected Topics in Signal Processing*, vol. 11, no. 4, pp. 605–617, 2017.

[19] R. Joyce and N. Audsley, "Exploring storage bottlenecks in Linux-based embedded systems," *ACM SIGBED Review*, vol. 13, no. 1, pp. 54–59, 2016.

[20] Z. Wang, Z. Zhou, H. Zhang, G. Zhang, H. Ding, and A. Farouk, "AI-based cloud-edge-device collaboration in 6G space-air-ground integrated power IoT," *IEEE Wireless Communications*, vol. 29, no. 1, pp. 16–23, 2022.

Hindawi
Mobile Information Systems
Volume 2022, Article ID 3001697, 10 pages
https://doi.org/10.1155/2022/3001697

Research Article

Data Sharing and Online Political Education Based on Edge Computing Network Optimization

Yihua Zeng[1] **and Mingwan Luo**[2]

[1]*Loudi Vocational and Technical College, Loudi 417000, Hunan Province, China*
[2]*Yangjiang Polytechnic, Yangjiang 529500, Guangdong Province, China*

Correspondence should be addressed to Yihua Zeng; 20150161@nxmu.edu.cn

Received 14 June 2022; Revised 6 July 2022; Accepted 20 July 2022; Published 21 August 2022

Academic Editor: Shadi Aljawarneh

The rapid development of Internet of Things services and the rapid growth of new broadband services have promoted the ever-increasing computing demands of mobile devices. As an emerging mobile computing technology, mobile edge computing is an important key technology to improve computing services for mobile devices. Mobile edge computing technology provides an important way for users to provide computing services with low latency and high computing performance. At the same time, it also provides technical means to develop online education. Online education called E-learning is an education model that uses the Internet as a medium. Through the Internet, students can conduct educational activities thousands of miles away from the teacher. In addition, students can learn at any time by referring to and downloading network code resources, thereby breaking the space and time constraints. The development of informatization of university education is an important part of the development of informatization, and it is the adaptation and combination of the application of information technology in the education field. At present, the informatization of universities at home and abroad has ushered in the era of digital campus construction, and most of its focus is on the reorganization of functional departments and the integration of independent systems. By analyzing the needs of data sharing and exchange, this article plans to use existing mature technologies, such as data warehouse, data synchronization update, and data security, based on DataX to design the data sharing and exchange plan of the public data platform, including data standards, coding standards are designed to achieve uniform rules, formats, and codes to build an online political education platform.

1. Introduction

With the rapid development of Internet of Things services and the rapid growth of new broadband services, the intelligent Internet of Things that integrates communication, caching, and mobile computing technologies are an inevitable trend for the next generation of Internet of Things [1]. In recent years, the high user experience business has gradually risen, and it has continued to develop rapidly at a speed beyond expectations [2]. The remote computing task loading method based on cloud computing technology will face severe challenges due to long communication delays and high operating costs [3]. At the same time, the rapid growth of mobile terminals and the rapid development of sensor-based smart cities, smart homes, smart grids, intelligent transportation, health care, and other areas of the Internet of things urgently need to solve the problems of limited computing power and long-term sustainable enjoyment, and the contradiction between delay and high user experience service requirements [4]. As an emerging mobile computing technology, the mobile edge computing (MEC) network places edge computing servers close to users who need to perform computing tasks, shortening the computing task loading distance, reducing communication delays, and improving computing, the important key technology of efficiency has received extensive attention from academia and industry since its introduction [5, 6]. The continuous construction of digital campuses and "smart campuses", as well as the continuous increase of management platforms and all-in-one card service platforms for universities, and

the accumulation of data in the information environment of universities are gradually increasing, forming a more comprehensive big data environment [7]. How to effectively share and exchange management of big data in colleges and universities, improve the management model of teachers and students on campus through big data mining and analysis ideas and methods, and use the results of big data analysis to provide clearer and more detailed services for campus life, which is now a college service issue that cannot be ignored in system construction [8]. In order to adapt to the requirements of the development of the times and follow in the footsteps of the times, more and more universities have begun to pay more attention to the construction of information [9]. With the development of today's society, in the modern university education management, the level of informatization has maintained a trend of increasing year by year, the widespread use of the campus card and the accumulation of data from the office system of various business departments over the years have formed campus online political education [10]. The large amount of university data are mainly reflected in a variety of types and large-scale teacher and student data [11]. The rational and effective unified management of teacher and student data and the intercommunication with business departments are the key to the data management of universities. If a data sharing and exchange platform can be established within the university, various departments can share data safely and quickly, and this will not only improve the utilization rate of data but also provide the most effective assistance for the integration of campus online political education.

The literature points out that mobile edge computing can provide mobile devices with low-latency and high-performance computing services. Mobile edge computing has two working modes, namely partial computing loading mode and binary computing loading mode [12]. In part of the computing loading mode, computing tasks can be split, some are performed locally, and the other part is loaded to the mobile edge computing server to perform calculations; in the binary computing loading mode, computing tasks cannot be split, and mobile devices can only choose to execute local calculations or all load to the mobile edge computing server to perform calculations [13]. The literature shows that a multi-user MEC system considering wireless charging is proposed, and a wireless energy transmission MEC design is proposed, in which a multi-antenna access point (integrated with the MEC server) broadcasts wireless power to charge multiple users, and each user node depends on the collection energy to perform computational tasks [14]. The literature shows that the report "Promoting Teaching and Learning Through Educational Data Mining and Learning Analysis: Problem Introduction" issued by the Office of Educational Technology of the U.S. Department of Education clearly deploys the development path of educational big data, focusing on the prediction of data mining and learning analysis technologies [15]. It uses students' learning behavior to optimize teaching strategies and evaluate teaching effects. The literature shows that online education platforms can support teachers, students, and policy analysts to make better decisions, use data facts as the basis for their own decisions, and be more convincing and able to propose education in a more targeted manner [16]. The literature pointed out that the time delay optimization problem in the single-user MEC system was studied in the study of minimizing task delay optimization [17]. All unloading modes include the task unloading decision, that is, whether all tasks are executed locally or unloaded to the MEC server execution target [18, 19].

2. Research on Collaborative Optimization of Task Scheduling and Data Sharing in Edge Computing Networks

2.1. System Model and Problem Description. The goal is to design a joint coordination mechanism for online scheduling and allocation. The main idea is shown in Figure 1. Different colors represent different types of services or tasks, and the numbers on the squares represent the corresponding deadlines of users. The user arrives at the system at any moment, and submits a heterogeneous housing request through the associated access point; considering the difference in load and resource costs of different edge clouds, MEC provider determines whether to admit the newly arrived task, if it is admitted, then charge it for services and offload tasks to the appropriate edge cloud; due to limited storage capacity, each edge cloud must wisely decide which services to configure. The task urgency is modeled as a dynamic priority weight, and perform priority-based edge cloud processing and discard control. Here, "discard" only means that tasks are not processed at the edge of the network, and the lost tasks will be offloaded to resource-rich ones. Remote cloud processing will incur more painful costs.

In order to balance the system load, it is necessary to design effective resource allocation and pricing strategies. On the one hand, network resources have a greater impact on the quality of uninstallation. If more network resources (such as spectrum resources) are allocated, the offloading quality provided by the edge cloud will increase. Therefore, a reasonable configuration of network resources is essential to improve resource utilization and offloading efficiency. On the other hand, pricing can effectively increase users' willingness to participate. Generally, lower service prices can attract more users to access, while excessive prices will push users to other edge clouds.

(1) Offload quality: it is assumed that each edge cloud provides offload services for users with constant transmission power as

$$\Gamma_{i,n}[t] = \frac{P^r_{i,n}[t]}{\sum_{n \in N_i[t]/\{0,n\}} P^r_{i,n}[t] + P^{\text{noise}}_i[t]}. \quad (1)$$

Based on the current network conditions, MEC providers first need to configure resources. Obviously, an inefficient configuration strategy will further aggravate network congestion and reduce offloading efficiency. The uninstall quality obtained by user i from edge cloud n is

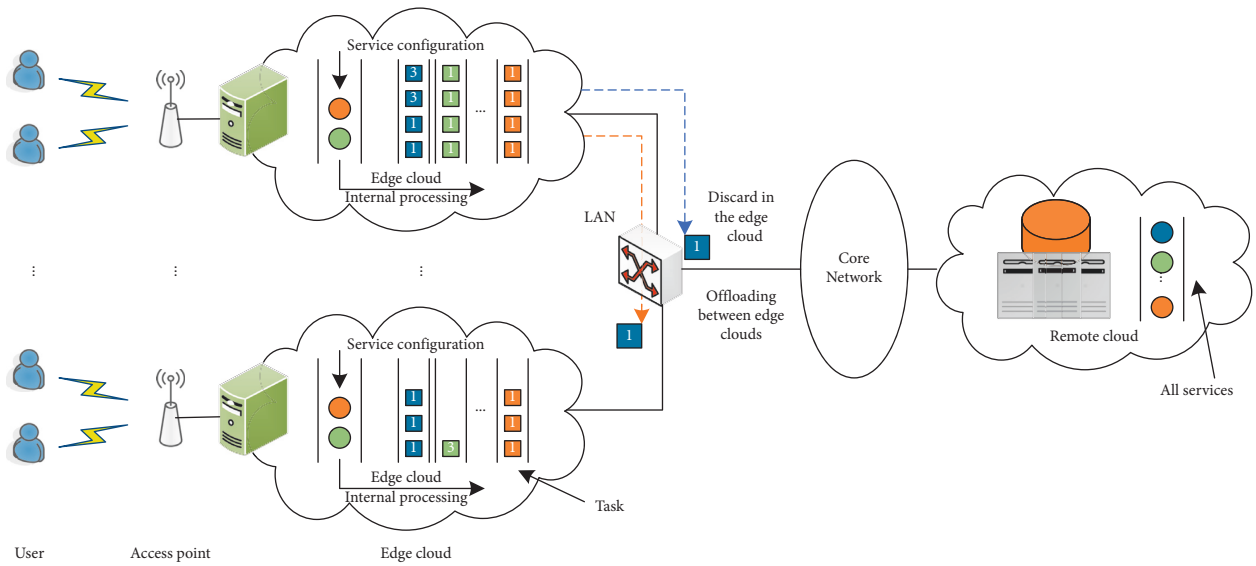

FIGURE 1: Schematic diagram of mobile edge computing network and service type based on peer-to-peer offloading.

$$r_{i,n}[t] = s_n[t]\log_2\left(1 + \Gamma_{i,n}[t]\right). \tag{2}$$

(2) Offloading and congestion constraints: due to user mobility, the edge cloud can only provide intermittent network connections. At any moment, each tasks can only be offloaded to one edge cloud or remote cloud at most, then the offloading constraint is

$$\sum_{n\in N} x_{i,n}[t] = \sum_{n\in N_i[t]} x_{i,n}[t] \le 1, \forall_i \in U. \tag{3}$$

Based on the task uninstall strategy, the uninstall quality obtained by the user is

$$r_i[t] = \sum_{n\in N} x_{i,n}[t] \cdot r_{i,n}[t], V_i \in U. \tag{4}$$

In the congestion-aware edge computing system, each resource-constrained edge cloud has a limited offload capacity. Edge cloud congestion constraints can be characterized as

$$\overline{X_n} \le a_n, \frac{\forall_n \in N}{\{0\}}. \tag{5}$$

(3) User satisfaction function: A satisfaction function is introduced to describe the degree of user satisfaction with uninstalled services.

$$V_i[t] = \ln\left(1 + \theta_i r_i[t]\right). \tag{6}$$

Queue dynamics plays a key role in characterizing the time-varying network environment and controlling decision-making. Use $Q[t]$ to represent the queue backlog, that is, the amount of unprocessed tasks waiting to be unloaded at the beginning of t. Assume that the task queue is initially empty, that is, $Q[0] = 0$. Therefore, the queue dynamics can be characterized as

$$Q[t+1] = \max\{Q[t] - r[t], 0\} + A[t], \forall_t \ge 0. \tag{7}$$

A queue is strongly stable if and only if its time average queue backlog is bounded, that is

$$\overline{Q} = \limsup_{t\longrightarrow\infty} \frac{1}{t}\sum_{\tau=0}^{t-1} E\{Q[\tau]\} < \infty. \tag{8}$$

For the obtained uninstallation quality $r_i[t]$, user i needs to pay the service fee $\pi_i[t]$ to the MEC provider. The value of uninstall service perceived by user i is defined as a user satisfaction function. Therefore, the utility function of i can be modeled as

$$U_i[t] = wV_i[t] - \pi_i[t]. \tag{9}$$

2.2. Maximization of User Collaborative Loading and Optimization of Computing Energy Efficiency and Resources. The mobile edge computing network based on OFDMA transmission studied in this chapter, the system model is shown in Figure 2.

During the time slot t1, the amount of data loaded by user U1 to the MEC server and user U2 are, respectively, expressed as

$$R_1^{t_1}(t,p) = t_1 B\log_2\left(1 + \frac{p_1 h_1}{\sigma^2}\right), \tag{10}$$

$$R_{co}^{t_1}(t,p) = t_1 B\log_2\left(1 + \frac{p_1 h_{co}}{\sigma^2}\right). \tag{11}$$

It represents the relevant time and power variables. During time slot t21, the amount of data that user U2 transmits the decoded loading task of user U1 to the MEC server is expressed as

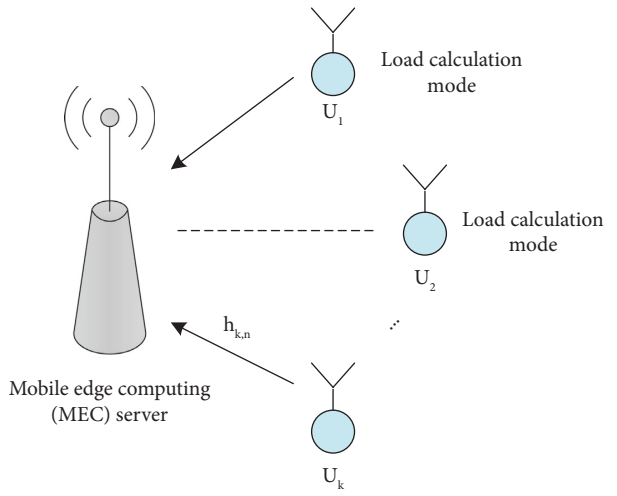

Figure 2: System model.

$$R_1^{t_{21}}(t,p) = t_{21}\text{Blog}_2\left(1+\frac{p_{21}h_2}{\sigma^2}\right). \tag{12}$$

According to the DF protocol, the size of the loaded data of the user U_1 performing remote calculations on the MEC server should be the smaller value between the size of the decoded data at the MEC server and the size of the decoded data at the user U_2, namely

$$R_1(t,p) = \min\left\{R_1^{t_1} + R_1^{t_{21}}, R_{co}^{t_1}\right\}. \tag{13}$$

The amount of data loaded by user U_2 is the amount of data transmitted by user U_2 to the MEC server during the time slot t_{22}, expressed as

$$\text{R}_2(\text{t},\text{p}) = \text{t}_{22}\text{Blog}_2\left(1+\frac{\text{p}_{22}\text{h}_2}{\sigma^2}\right). \tag{14}$$

In this mode, the energy consumption of user U_1 and user U_2 are, respectively,

$$E_{\text{off},1} = t_1(p_1 + p_c). \tag{15}$$

$$E_{\text{off},2} = (t_{21}p_{21} + t_{22}p_{22}) + (t_{21}+t_{22})p_c. \tag{16}$$

Thus, the total loading energy consumption of the system is

$$E_{\text{off}} = \overset{\zeta(p_1t_1+p_{21}t_{21}+p_{22}t_{22})}{\text{partial loading}} + \text{fixed} \overset{(t_1+t_{21}+t_{22})p_c}{\text{circuit consumption}}. \tag{17}$$

2.3. Implementation and Application of Data Sharing and Exchange. Storage capacity constraint: this chapter focuses on the finiteness of edge cloud storage capacity, and assumes that edge cloud $n \in N$ provides at most S_n types of services at the same time at any time, namely

$$\sum_{r\in R}\alpha_n^r[t] \le S_n, \forall_n \in N. \tag{18}$$

Conservation constraints: the total amount of offload tasks (including local reserved tasks) of each edge cloud must be equal to the amount of tasks allowed to enter the system at the current moment, namely

$$\sum_{i\in A_m^{r,t}}\sum_{n\in N}\beta_n^i[t] = O_m^r[t] + D_m^r[t], \forall_r \in R, m \in N. \tag{19}$$

Stability constraint: the number of r-type tasks offloaded to edge cloud n at each moment does not exceed the maximum service rate,

$$\sum_{m\in N}\sum_{\in A_m^{r,t}}\beta_n^i[t] \le f_n^r, \forall_r \in R, m \in N. \tag{20}$$

Incentive constraint: This constraint is mainly aimed at the resource consumption problem in providing shared offloading services.

$$\frac{1}{T}\sum_{t\in T}e_n^r[t] \le E_n^r, \forall_n \in N, r \in R. \tag{21}$$

Priority constraints:

$$R_n^r(i)\left\{\begin{array}{l} < R_n^r(j), \text{if} \text{d}_i < d_j \\ > R_n^r(j), \text{if} \text{d}_i \ge d_j \end{array}\right\}. \tag{22}$$

Under the assumption of best-effort, the online joint collaborative control problem can be modeled as

$$\min\frac{1}{T}\sum_{t\in T}C[t]. \tag{23}$$

Without considering the user deadline tolerance, users are promised that once they are admitted to the system, they can get services at the edge of the network, which means that there is no task discarding. In order to support the promised service, previous related work usually highlights service locality constraints:

$$\beta_n^i[t] \le \alpha_n^r[t], \forall_i \in A_m^{r,t}, r \in R, n, m \in N. \tag{24}$$

First, study the collaborative optimization problem of scheduling and configuration (sDO-JCPS) that does not consider the user deadline tolerance in a single slot, and model it as an integer linear programming (ILP).

$$\min\sum_{n,m}\sum_{r}\left(c_n^r[t]\alpha_n^r[t] + \sum_{i\in A_m^{r,t}}c_n^{i,o}[t]\beta_n^i[t]\right). \tag{25}$$

Under the constraints of stability, the limitation of service capacity makes the offloading decisions of different tasks coupled.

$$\min\sum_{n,m}\sum_{r}\left[(1-\sigma)c_n^r[t]\alpha_n^r[t] + \sum_{i\in A_m^{r,t}}\beta_n^i[t]\left(\frac{\sigma c_n^r[t]}{f_n^r} + c_n^{i,o}[t]\right)\right]. \tag{26}$$

Suppose the total configuration and the scheduling cost of the optimal solution of problem (26) are $C_{\text{place}}^{(9)}$, and $C_{\text{schedule}}^{(9)}$, we can get

$$\frac{\gamma_s}{\gamma_p}C_{\text{place}}^{(9),\mathscr{A}} + C_{\text{schedule}}^{(9),\mathscr{A}} \le \gamma_p \frac{\gamma_s}{\gamma_p}C_{\text{place}}^{(9)} + C_{\text{schedule}}^{(9)} \le \gamma_s \cdot \text{OPT}. \quad (27)$$

When extracting source data, due to years of storage of data, inconsistent standards, and no fixed maintenance personnel in various business systems, the source data may have problems such as incomplete data, data duplication, data errors, or data irregularities. At this time, data correction, duplicate elimination, and standardization need to be completed through data cleaning. The main types of data that need to be cleaned are as follows: input or input incorrect data (missing values, slack metadata definitions, inconsistent allocations, inappropriate definitions or application of consistency constraints, etc.). For example, the student basic information table may contain data that needs to be cleaned, such as the student's contact phone number, hometown, and transfer major, and there are irregular formats that need to be cleaned. The time format field is written as a string, whether in public data management or subsequent. All data mining and analysis needs to clean the data first, that is, complete data, remove duplication, standardize time, and unified format.

Data cleaning includes the following steps: data analysis, actual situation analysis, mastering the basic information, and constraints of metadata, mining data without matching constraints and manually input or input data. Define cleaning rules and mapping relationships, define cleaning rules based on analysis results, map contradictory metadata, deal with missing data based on actual conditions, and try to correct data or input incorrect data. Before and during data conversion, the data that needs to be converted will be cleared according to the defined cleaning rules.

First, establish a data type mapping table (Table 1), find out various data types and possible correspondences that are missing in the central database of different databases, and put the correspondences in the mapping table in advance. Then, in order to eliminate the inhomogeneity of the data type, the extracted data is compared with the preset standard of the data type mapping table for conversion and repair.

Then use the data naming rules (structure such as Table 2) to place the source data name and the converted execution data name, database name, table name, and other attributes. If the extracted data exists in the table, then change the source data name to a standard data name, and then compare the database name and table name given in the table to get the standard data value, if it does not exist, add a new record. The data name is established according to the standard. The structure of the source operation table is shown in Table 3.

2.4. Analysis of Simulation Results. Figure 3 shows the relationship between the user's safe computing energy efficiency and the user's maximum transmission power under the three scenarios. Three different schemes are proposed in this chapter, the partial loading scheme based on OMA and the global loading scheme only. Observing it, we can see that the scheme proposed in this chapter can achieve better energy efficiency of safe computing than the other two schemes. The reason is that compared with OMA technology, the user's loading efficiency is higher when using NOMA technology. In addition, in the safe calculation energy efficiency of all schemes, the safe calculation energy efficiency first increases as the user's maximum transmission power increases. When the user's maximum transmission power is large enough, the safe calculation energy efficiency will remain unchanged. And it can be clearly seen that under the same network mechanism, the partial loading scheme based on OMA achieves higher energy efficiency for safe computing than the OMA-based global loading scheme. Through analysis, it can be seen that the reason is that in the case of using partial computing loading mode, users can flexibly allocate resources to computing loading, local

Table 1: Data correspondence table.

Field name	Type of data	Allow empty	Description
ID	Integer	No	Mark a record
DB_Type	Character type	No	Type of database
DB_Ver	Character type	No	The version number of the database
Type	Character type	No	Type of data
Des_Type	Character type	No	Default mapped data type
Fun	Character type	No	The name of the conversion function to be called for type conversion

Table 2: Data correspondence table.

Field name	Type of data	Allow empty	Description
ID	Integer	No	Mark a record
Name_Src	Character type	No	Original data name
Name_Des	Character type	No	Data standard name
DB	Character type	No	The name of the database
Table	Character type	No	Table name

Table 3: The structure of the source operation table.

Field name	Type of data	Allow empty	Description
ID	Integer	No	Mark a record
Data_Key	Homologous table field type	No	The primary key value of the record
Name_column	Character type	No	Modified field name
Data_column	Homologous table field type	No	The modified field value of the field
Oper_Type	Character type	No	Type of operation
Update_time	Character type		Update time

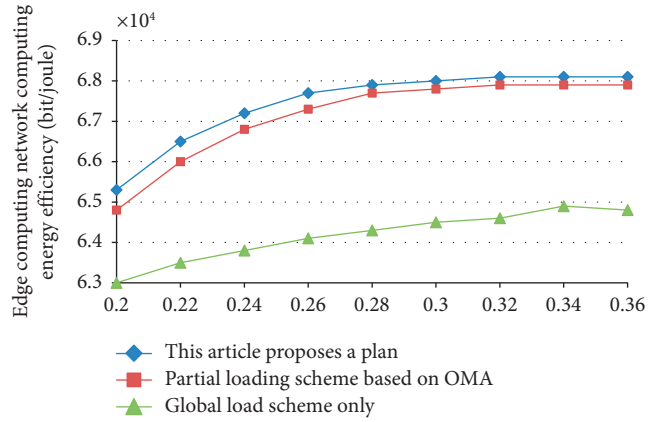

Figure 3: Safe calculation of energy efficiency and user's maximum transmission power under different schemes.

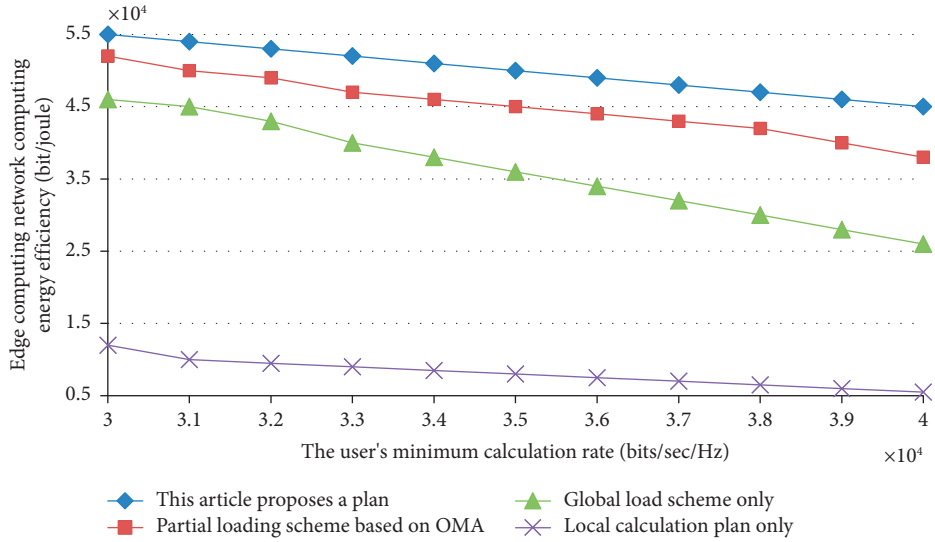

Figure 4: Safe computing energy efficiency and user's minimum computing rate under different schemes.

computing, and achieving good resource allocation. Figure 4 shows the comparison between the user's safe computing energy efficiency and the user's minimum computing rate under the four scenarios. The three schemes are the schemes proposed in this chapter, the partial loading scheme based on OMA, the global loading scheme only, and the local calculation scheme only. Observing it, we can see that the safe computing energy efficiency maximization scheme proposed in this chapter is better than other schemes. Moreover, it can be seen that the safe computing energy efficiency obtained by the scheme proposed in this chapter or the other three schemes decreases as the minimum calculation rate required by the user increases. This shows that the growth rate of the required computational energy is faster than the growth of the corresponding calculation rate; that is, the growth rate of the calculation rate is less than the growth rate of the energy consumption to achieve the calculation rate.

Figure 5 shows the relationship between the safe calculation energy efficiency and the user's maximum transmission power using the calculation energy efficiency maximization scheme and the calculation bit maximization scheme proposed in this chapter. As shown in Figure 5, when users have the same maximum transmission power, the traditional calculation of bit maximization to obtain safe calculation energy efficiency is lower than the safe calculation energy efficiency obtained in the scheme proposed in this chapter.

Figure 6 illustrates the convergence of computing edge, computing network security, and computing energy efficiency based on the iterative algorithm of SCA proposed in this chapter and compares it under different user maximum transmission powers. As shown in Figure 6, the safety calculation efficiency obtained by our proposed SCA-based iterative algorithm first increases rapidly as the number of iterations increases, and then reaches convergence after several iterations. Moreover, the safe calculated energy efficiency achieved by the maximum transmission power of three different users matches the trend of energy efficiency values in the figure.

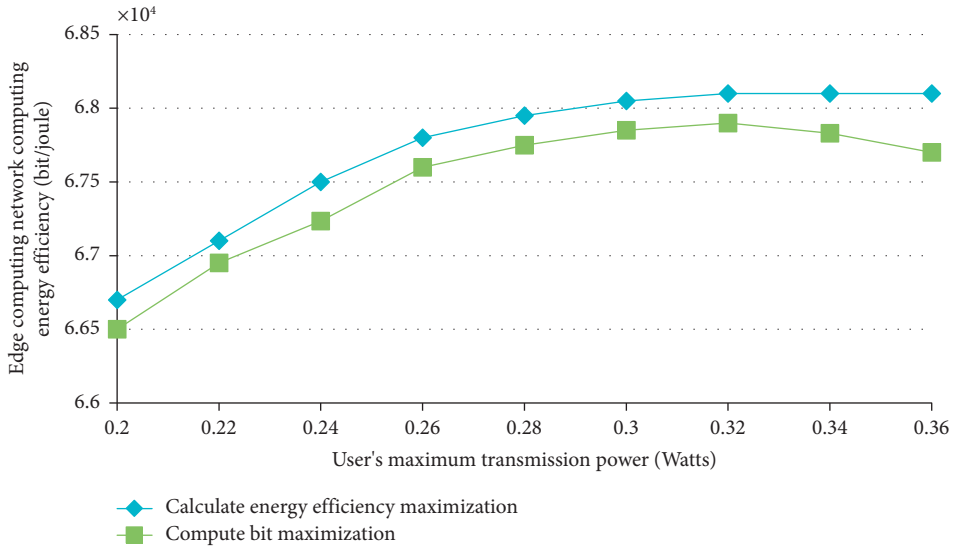

Figure 5: Safe calculation of energy efficiency and maximum transmission power under different optimization goals.

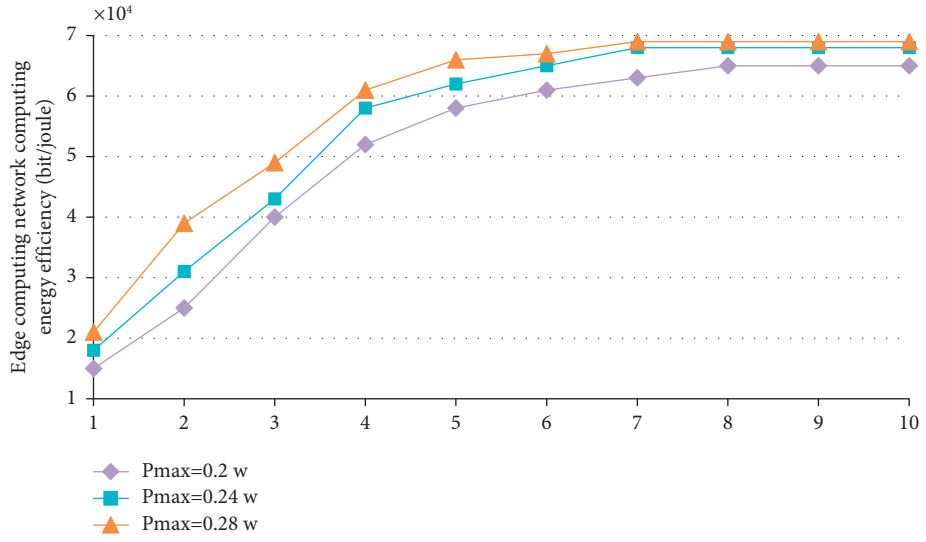

Figure 6: Safe calculation of energy efficiency and optimization algorithm iteration times under different maximum transmission powers.

3. Research and Implementation of the Online Political Education Platform Based on Resource Sharing

3.1. Technical Architecture of the Online Political Education Platform. The design of the educational resource sharing platform is also designed in accordance with a three-tier architecture. The interface of each functional module of the platform is responsible for the interaction with users and is the presentation layer. Some tasks and stored procedures that perform data preprocessing in the database of the business logic layer of the platform also belong to the scope of business logic. In the data layer, SQL Server 2008 is used for data storage and persistence. SQL Server can store various types of data such as XML files, text files, and binary files and provide efficient query and processing capabilities.

3.2. Database Logical Structure Design. Through the overall ER diagram of the system and the relationship between each entity, the database tables of the system can be designed mainly including student table, teacher information table, course information table, department information table, professional information table, course selection information table, grade information table, and credit information table. The teacher information table is shown in Table 4.

The student information table is shown in Table 5.

The teaching videos of teachers and the learning materials of students are stored in the material information table. The table structure of the data information table is shown in Table 6.

3.3. Strategies for the Development of Online Political Theory Teaching. First, people use big data thinking for teaching

Table 4: Teacher information table.

Column name	Description	Types of	Remarks
TeacherNum	Numbering	Char (10)	Primary key
DeptNum	Department number	Char (10)	Not null
TeacherName	Name	Varchar (20)	Not null
TeacherSex	Gender	Varchar (20)	Male or female
TeacherBirthday	Birthday	Varchar (20)	Not null
TeacherTitle	Job title	Varchar (20)	Not null

Table 5: Student information sheet.

Column name	Description	Types of	Remarks
StudentNum	Student ID	Char (10)	Primary key
MajorNum	Department number	Char (10)	Foreign key
StudentName	Student name	Varchar (40)	Not null
StudentSex	Student gender	Varchar (20)	Not null
StudentBirthday	Date of birth	Varchar (30)	Not null
StudentPassword	Login password	Varchar (20)	Md5 encryption

Table 6: Data information sheet.

Column name	Description	Types of	Remarks
ResourceNum	Resource number	char (10)	Self-incrementing primary key
TeacherNum	Upload teacher ID	char (10)	Available
FileType	File type	Varchar (30)	Not null
FilePath	File path	Varchar (30)	Not null
FileContent	File introduction	Varchar (30)	Not null
UploadTime	Upload time	Date and time	Not null

design. Teaching goals are scientifically formulated. Teaching design is based on the further development of teaching objectives. The teaching objectives of ideological and political theory courses have not changed from a large level. However, with the development of time, we have many different needs for many detailed content. How to scientifically and accurately determine the teaching target of each knowledge point after refining the teaching target is a key step to improve the teaching quality of ideological and political theory courses. The teaching goals determined through personal subjective consciousness, experience, and lessons are not supported by data, and to a certain extent are unconvincing. Analyze the complex big data information and use the results reflected by the data to formulate teaching goals based on the data, so that teaching is more scientific and accurate. Apply the principle of big data accuracy to the teaching of ideological and political theory courses. By tracking the teaching trajectory of the teacher, the learning trajectory of the student and the interactive data between the two, the teaching characteristics of the teacher, the learning characteristics of the students, and the psychology of the students are obtained. Features accurately present the characteristics of different objects, and then implement teaching decisions, scientifically determine the teaching goals of ideological and political theory courses, promote the formulation of teaching goals more scientifically, and better meet the needs of current student development, and better realize the ideological and political theory courses. Accurate teaching: The second science chooses teaching content. Big data technology is a product of the development trend of informatization. Its wide application promotes the transformation of the teaching thinking of ideological and political theory courses in colleges and universities from perceptual qualitative analysis to rational quantitative analysis. In traditional ideological and political theory courses, teachers often teach courses based on long-term teaching experience. Now the application of big data technology in ideological and political theory courses has greatly improved this situation. Using big data to transform teaching thinking, change the qualitative analysis teaching thinking based on teachers' perceptual cognition and form a rational quantitative analysis teaching thinking based on student needs, which is conducive to enhancing the effectiveness of ideological and political theory courses.

Secondly, in traditional ideological and political theory teaching, teachers' teaching judgments are basically based on their own years of teaching experience. However, students of different ages and different age groups are different in their mental thinking and knowledge reserves. Using previous teaching method to carry out teaching, the teaching effect achieved is not particularly significant. The wide application of big data in ideological and political theory courses in colleges and universities have changed the way teachers perceive students. It is no longer judged by experience but judged by accurate data analysis results, thus changing the way teachers choose teaching methods. Using big data to analyze students' dynamics in real time, grasp first-hand information, and promote the transformation of teachers' teaching situation; using big data to promote teachers' cognitive style from their own empiricism to rational data judgment that will be a new era of ideological and political lessons. Teachers better choose teaching methods to provide a basis for judgment. There are unified teaching standards and requirements for the teaching of ideological and political theory courses, and the teaching materials are used uniformly throughout the country, but the teaching resources and teaching methods of each school are full of flowers. The balanced development of big data technology in the ideological and political theory courses of Chinese universities will promote the transformation of the current scattered teaching status to the direction of teaching resource sharing. Through the establishment of university alliances or led by national government departments and

local education management departments, the integration of regional big data technology application resources, so that big data technology can be exchanged and shared, and jointly promote the transformation of the scattered state of ideological and political theory teaching to agglomeration and sharing, which is truly realized in order to promote the teaching reform and innovation of ideological and political theory courses in colleges and universities in the new era. Through online education, the best teachers can also be directly displayed in front of students. Excellent public teachers can often summarize the learning rules and application rules of the teaching objects, and can grasp the key points of subject learning and integrate with the classroom, and effectively help students acquire knowledge in order to achieve good teaching results. At the same time, the unique personality charm of outstanding public sports teachers can also be spread to more people through online education, attract more students to pay attention to ideological and political theories, and increase their interest in learning.

4. Conclusion

The advent of the Internet age has brought great convenience to online education. Now, many schools have begun to adopt the method of online education, and the learning of online education has also been accepted in various schools and has become an important part of the evaluation of students' university studies. Although there are already some universities that gradually carry out online education, they are basically fighting alone without forming a system. Nowadays, college students have a wide range of interests and hobbies, and different teaching methods may bring great differences in learning knowledge. Therefore, breaking the threshold of online education among universities, increasing the sharing of educational resources, and promoting information exchange and resource sharing between schools and students have become a development trend. This paper studies the weighted computing bit and maximized resource allocation strategy of the edge computing network of the online political education platform to improve computing performance and energy collection efficiency; and in the mobile edge computing network based on non-orthogonal multiple access, the resource optimization strategy is proposed to maximize the energy efficiency of safe computing improves the energy efficiency and security of computing.

Data Availability

The data used to support the findings of this study are available from the corresponding author upon request.

Conflicts of Interest

The authors declare that they have no conflicts of interest.

Acknowledgments

This paper was funded by the project: Research on Patriotism Education Innovation of College Students in "Internet plus" Era(No. 21C1449).

References

[1] V. Govindraj, M. Sathiyanarayanan, and B. Abubakar, "Customary homes to smart homes using internet of things (IoT) and mobile application," in *Proceedings of the International Conference on Smart Technologies for Smart Nation*, August 2017.

[2] R. Majeed, N. A. Abdullah, I. Ashraf, Y. B. Zikria, M. F. Mushtaq, and M. Umer, "An Intelligent, Secure, and Smart home Automation System," *Scientific Programming*, vol. 2020, Article ID 4579291, 14 pages, 2020.

[3] A. Bhagat, S. L. Satarkar, and P. M. Jawandhiya, "Secure data sharing on cloud using triple-DES algorithm," *International Journal of Advent Research in Computer and Electronics*, vol. 4, no. 4, pp. 28–32, 2020.

[4] L. M. Gladence, V. M. Anu, R. Rathna, and E. Brumancia, "Recommender system for home automation using IoT and artificial intelligence," *Journal of Ambient Intelligence and Humanized Computing*, vol. 11, pp. 1–9, 2020.

[5] F. Vhora and J. Gandhi, "A comprehensive survey on mobile edge computing: challenges, tools, applications," in *Proceedings of the 2020 Fourth International Conference on Computing Methodologies and Communication (ICCMC)*, pp. 49–55, Erode India, April 2020.

[6] M. McClellan, C. Cervelló-Pastor, and S. Sallent, "Deep learning at the mobile edge: opportunities for 5g networks," *Applied Sciences*, vol. 10, no. 14, p. 4735, 2020.

[7] M. Liu and J. Bu, "Deep integration of physical health education based on intelligent communication technology," *Journal of Healthcare Engineering*, vol. 2021, Article ID 4323043, 6 pages, 2021.

[8] W. Hu and L. Ye, "Impact of big data technology on the diversity of physical education teaching methods," *Journal of Physics: Conference Series*, vol. 1744, no. 4, Article ID 042205, 2021.

[9] X. Zhang and J. Sun, "Discussion on new media communication strategy of sports events based on large data technology," *Cluster Computing*, vol. 22, no. S2, pp. 3395–3403, 2019.

[10] E. Morgulev, O. H. Azar, and R. Lidor, "Sports analytics and the big-data era," *International Journal of Data Science and Analytics*, vol. 5, no. 4, pp. 213–222, 2018.

[11] T. Xiong, "Research on the practice of big data in college physical education," *Journal of Physics: Conference Series*, vol. 1992, Article ID 022131, 2021.

[12] F. Guo, L. Ma, H. Zhang, H. Ji, and X. Li, "Joint load management and resource allocation in the energy harvesting powered small cell networks with mobile edge computing," in *Proceedings of the IEEE INFOCOM 2018 - IEEE Conference on Computer Communications Workshops (INFOCOMWKSHPS)*, pp. 299–304, Piscataway, NJ, USA, April 2018.

[13] Q. Chen, X. Xu, H. Jiang, and X. Liu, "An energy-aware approach for industrial internet of things in 5g pervasive edge computing environment," *IEEE Transactions on Industrial Informatics*, vol. 17, no. 7, pp. 5087–5097, 2021.

[14] D. Wu, J. Wang, Y. Cai, and M. Guizani, "Millimeter-wave multimedia communications: challenges, methodology, and applications," *IEEE Communications Magazine*, vol. 53, no. 1, pp. 232–238, 2015.

[15] C. Yuan, Y. Yang, and Y. Liu, "Sports decision-making model based on data mining and neural network," *Neural Computing & Applications*, vol. 33, no. 9, pp. 3911–3924, 2021.

[16] L. Juchem and M. d. M. Nascimento, "Programa "DT-Tênis 60+": uma proposta de sistematização para o aprendizado do tênis e prevenção de quedas de idosos," *Caderno de Educação Física e Esporte*, vol. 18, no. 2, pp. 115–122, 2020.

[17] S. Barbarossa, E. Ceci, M. Merluzzi, and E. Calvanese-Strinati, "Enabling effective mobile edge computing using millimeter wave links," in *Proceedings of the 2017 IEEE International Conference on Communications Workshops (ICC Workshops)*, pp. 367–372, Paris, France, May 2017.

[18] M. Adil, M. A. Jan, S. Mastorakis et al., "Hash MAC DSDV Mutual Authentication for Intelligent IoT Based Cyber Physical Systems," *IEEE Internet of Things Journal*, vol. 9, 2021.

[19] C. Ben, "Application of image recognition based on wireless sensors in dance teaching system," *Computational Intelligence and Neuroscience*, Article ID 2440263, 12 pages, 2022.

Hindawi
Mobile Information Systems
Volume 2023, Article ID 9790269, 1 page
https://doi.org/10.1155/2023/9790269

Retraction

Retracted: The Impact of Rural Labor Force Feminizing Fluctuation on Grain Production and its Regional Differences: Evidence from China

Mobile Information Systems

Received 1 August 2023; Accepted 1 August 2023; Published 2 August 2023

This article has been retracted by Hindawi following an investigation undertaken by the publisher [1]. This investigation has uncovered evidence of one or more of the following indicators of systematic manipulation of the publication process:

(1) Discrepancies in scope

(2) Discrepancies in the description of the research reported

(3) Discrepancies between the availability of data and the research described

(4) Inappropriate citations

(5) Incoherent, meaningless and/or irrelevant content included in the article

(6) Peer-review manipulation

The presence of these indicators undermines our confidence in the integrity of the article's content and we cannot, therefore, vouch for its reliability. Please note that this notice is intended solely to alert readers that the content of this article is unreliable. We have not investigated whether authors were aware of or involved in the systematic manipulation of the publication process.

Wiley and Hindawi regrets that the usual quality checks did not identify these issues before publication and have since put additional measures in place to safeguard research integrity.

We wish to credit our own Research Integrity and Research Publishing teams and anonymous and named external researchers and research integrity experts for contributing to this investigation.

The corresponding author, as the representative of all authors, has been given the opportunity to register their agreement or disagreement to this retraction. We have kept a record of any response received.

References

[1] H. Wang, G. Li, and Y. Hu, "The Impact of Rural Labor Force Feminizing Fluctuation on Grain Production and its Regional Differences: Evidence from China," *Mobile Information Systems*, vol. 2022, Article ID 2004465, 9 pages, 2022.

Hindawi
Mobile Information Systems
Volume 2022, Article ID 2004465, 9 pages
https://doi.org/10.1155/2022/2004465

Research Article

The Impact of Rural Labor Force Feminizing Fluctuation on Grain Production and its Regional Differences: Evidence from China

Haifeng Wang, Guangsi Li, and Yunzhi Hu

Institute of Food and Strategic Reserves, Collaborative Innovation Center of Modern Grain Circulation and Safety, Nanjing University of Finance and Economics, Nanjing 210003, China

Correspondence should be addressed to Haifeng Wang; 22010013@nustti.edu.cn

Received 1 June 2022; Accepted 16 July 2022; Published 19 August 2022

Academic Editor: Shadi Aljawarneh

Based on panel data from 2002 to 2018, this study establishes a variable coefficient model of the interaction term between the proportion of rural female labor force and the ratio of mechanization. The influence of the increase in the rural female labor force ratio on grain production is discussed. The results show that the feminization of the rural labor force has a significant negative impact on grain-planting area and proportion, leading to an adverse impact on grain planting. Conversely, in the plain, which is relatively easy to mechanize with massive production, the adverse effects of feminization of labor on grain production will be weakened. The regional analysis found that feminization of the workforce reduces the area and proportion of food acreage planted in the eastern region, machinery use completely counteracts the negative impact of labor feminization in the eastern and western regions, with a positive effect, whereas in the central region, the impact of machinery use is not significant. Therefore, in the process of increasing the proportion of rural women, we should pay attention to its adverse effects on food cultivation and regional differences and take targeted measures to stabilize the food supply.

1. Introduction

With the rapid development of industrialization and urbanization in developing countries, a large number of rural laborers have moved to cities, resulting in significant changes in the structure of rural laborers. With economic development, the increase in employment opportunities and the improvement in income returns have attracted a growing number of male laborers to work in cities. Conversely, the left-behind female laborers are engaged in agricultural production, and a "male working and female farming" model has emerged [1, 2]. According to the sample survey data of 931 villages in China in 2011, the proportion of women engaged in agricultural production in rural areas was as high as 69.89% [3]. Men's opportunities and wages for working outside the home have been higher than those of women, whereas women traditionally perform housework and home care, which had led to more women engaging in agriculture. Therefore, how this condition has affected grain-planting warrants investigation. The agricultural production base in developing countries is weak, its land management is fragmented, and the level of technology application is not high. Therefore, the changes in the number or structure of the labor force will affect planting policy decisions. Questions such as whether the increase in the proportion of women engaging in agricultural labor would affect agricultural planting and whether this growth would have an impact on food supply security are issues that require attention and careful research.

The feminization of the agricultural labor force (some scholars call it agricultural feminization) is an unbalanced phenomenon of the gender structure of the agricultural labor force gradually formed with the transfer of the agricultural labor force to nonagricultural industries after the implementation of the contract responsibility system with joint output in rural China. The extent of this phenomenon and its substantive impact on agricultural production are very worthy of study. From the existing literature, the

research on this issue is mostly focused on the degree of feminization of agricultural labor, the causes, and the impact on the economy and society.

However, the existing research on the feminization of the agricultural labor force still has the following deficiencies: first, there is no consensus on the definition of the feminization of the agricultural labor force; second, the macrodata of its distribution and degree are lack of mining and analysis; third, due to the lack of the support of the above research, most of the existing research on the causes of feminization is based on the assumption that the agricultural labor force has been feminized, which is limited to the research on the reasons why the female labor force lags behind the men in the nonagricultural transfer of agricultural labor force and ignores the research on the characteristics of the gender allocation of the labor force in agricultural production; the fourth is the research on the impact of the feminization of agricultural labor force. Although there is no lack of empirical research, most of them are empirical studies on the data of regions and local villages, which are lack of representativeness. At the same time, the research on the impact of feminization of the agricultural labor force on agricultural production is relatively rare. This paper will be committed to making some breakthroughs in the above aspects. It will analyze the regional distribution and land scale distribution of the feminization of the agricultural labor force with macro statistical data, so as to accurately judge the actual degree of the feminization of the agricultural labor force in China, and on this basis, further analyze the reasons for the formation, and finally make an empirical analysis of the impact of the feminization of agricultural labor force on agricultural production.

This study has the following policy implications.

The key to stabilize food production and ensure food security lies in improving production efficiency, reducing labor costs, and realizing the scale effect. First, it is important to develop agricultural machinery suitable for different terrain, especially small machinery for mountainous and hilly areas, to improve agricultural machinery subsidies, and to reduce labor costs. Second, it is essential to guide the orderly transfer of rural land and to encourage the formation of large-scale business entities, thereby family farms and large planting households could become the backbone of food production and gradually could expand the scale of operation to form a scale effect. Third, it is vital to encourage the development of socialized service organizations for food production and to promote the diversified development of service organizations, involving all aspects of grain production, such as grain production, agricultural machinery services, and formula fertilization to realize the scale effect of all aspects of grain production. Through the replacement of labor by machinery, technology and services would further reduce labor costs, improve labor production efficiency, stabilize grain production, and ensure food security.

2. Literature Review

Many scholars have conducted fruitful research on the influence of the change of the rural labor structure on planting production. The influence of the feminization of the labor force on agriculture can be seen from the following two perspectives: (1) the female labor force is engaged in production as an agricultural producer; and (2) the female labor force manages production as agricultural managers.

2.1. The Influence of the Female Labor Force as Agricultural Producers. At present, a consensus has not been reached on the research of the feminization of the rural labor force. Some scholars believe that the feminization of the agricultural labor force has not had an adverse impact. When female laborers enjoyed equal rights to use key materials in production and were not more constrained compared with male laborers, the feminization of rural labor does not necessarily contribute to the reducing production efficiency [4]. After controlling the level of human capital [5], investment [6], irrigation intensity, and crop types [7], the efficiency of the rural female labor force in agricultural production was not significantly different from that of the male labor force. If the same levels of agricultural incentives were granted to the women as to their male counterparts, there would be an increase in the overall productivity of the entire farming populace [8]. The rural women in Sub-Sahara Africa, while providing the bulk of farm labor, were discriminated against with respect to the ownership of farm resources compared with the male farmers. Neither significant differences exist in crop productivity between male farmers and their female counterparts, nor were there any significant differences in the input production elasticities [9].

Other scholars hold different views, however. Kilic et al. [10] quantified the effect of the impact of gender differences on agricultural productivity and found that women are 22–37% less productive than men in agriculture and that this difference is due mostly to the innate gender difference, and this difference is magnified by child rearing, male off-farm employment, and agricultural fertilizer abuse. Owusu et al. [11] employed a met frontier approach to analyze the differences in the efficiency of male and female farmers. In China, scholars use both microdata and macrodata to conduct relevant research. In terms of microscopic data, Song et al. [12] found that the female labor force faces more difficulties in physical strength, technology, credit, and market information utilization, and their agricultural income was also low. Song and Vernooy [13] found that the female labor force is not dominant in terms of physical strength and capital acquisition, and the agricultural productivity of rural women is much lower than that of men. Cai et al. [14] used 2073 valid samples from Anhui Province to compare the gender differences of farmers' willingness through a logistics model. Their studies have shown that women farmers' willingness to farm is obviously lower than that of men, and their sensitivity to agricultural production costs and agricultural production methods also is considerably lower than that of men. Furthermore, in terms of macro data, Yang et al. [15] studied the influence of the female labor force on planting and found that areas with a higher proportion of female labor force would reduce food yield instead of planting cash crops with higher economic benefits.

2.2. The Influence of Female Labor Force as Agricultural Managers. Scholars also have paid attention to whether female-dominated families have the same agricultural production efficiency as male-dominated families. After men migrate to nonagricultural industries, women will dominate decision-making on farmland management [16]. Women cannot allocate too much time to agricultural land management because of the heavy family affairs and responsibilities [17]. Because of the unequal treatment of women in marriage, inheritance, and collective distribution, women usually do not have equal ownership of land rights and other means of production [18]. Women may be marginalized in the land leasing market [19]. A significant difference exists in agricultural efficiency between men and women when the manager of cultivated land is a woman [20]. In Niger, on average, plots managed by women produce 19 percent less per hectare than plots managed by men [12] The farmland run by women in rural China, however, is as efficient as that run by men, which mainly due to the highly competitive and efficient market and the wide application of modern agricultural technology and mechanization [21].

In summary, a wealth of literature has conducted the exploration of the impact of labor force shifts and structural changes on food production, but some deficiencies remain. First, some literature has studied the impact of the feminization of the rural labor force on food production, but the empirical analysis is limited and consistent conclusions are lacking. Second, the existing literature discusses the impact of the feminization of rural labor on grain production but has ignored topographic conditions, which cannot be generalized given China's vast territory and variable topography. Third, the existing literature has considered the impact of feminization of rural labor on grain production at the national level without taking into account of regional differences.

The contributions of this study are as follows: first, based on the provincial panel data, we analyze the influence of feminization of the labor force on food planting from a macro perspective and discuss the weakening effect of agricultural mechanization on gender differences of the labor force in combination with topographic conditions; and, second, we analyze whether regional differences exist between the influence of feminization of labor force on grain planting and the weakening effect of mechanization.

3. Theoretical Foundations

According to Lewis's dual economic structure theory, against the background of urbanization, the labor force shifts from agriculture to industry and from rural to urban. In terms of labor resource allocation, farmers are rational, and they maximize their own utility value through optimal allocation of resources, and labor factors will flow from sectors with low marginal productivity to sectors with high marginal productivity. The marginal productivity of the urban industrial sector is higher than that of agriculture, which will lead to the transfer of rural labor to the industrial sector until the wages of rural labor gradually align with those of urban labor.

According to the Todaro model, as shown in Figure 1, the abscissa represents the number of labors, and O_c and O_v denote the origin of urban and rural labors, respectively. The vertical coordinate represents regional wages, with the left side being urban wages and the right side being rural wages. Curves A and B are the demand curves of the urban and rural labor force, respectively. AA_0 is the demand curve of the urban formal sector labor, and AA_1 is the demand curve of the urban informal sector labor. The transfer of rural labor depends mainly on the expected wage difference between urban and rural areas. On the basis of this flow principle, the flow of rural labor is divided into two stages: the first stage is the transfer of rural surplus labor. A_0A_1 and curve B intersect at equilibrium point C, and the equilibrium wage level is $U_1 = R_1$, the number of the urban labor force is O_cL_1, and the number of the rural labor force is O_vL_1. Because of the technological progress and planting efficiency, there is a large surplus of rural labor, and the significant difference between urban and rural wages attracts rural laborers to work in cities. In addition, the migrant workers in cities mainly are men, whereas women stay in rural areas and take up planting tasks. Men work in leisure times, the farm in busy times, and maintain a status of half work and half farming; therefore, the proportion of women in the agricultural labor force has increased. The second stage is the migration of the effective rural labor force. With the rapid development of urbanization, the demand for urban labor has risen, and the demand curve of urban labor has risen from A_0A_1 to A_0A_2, intersecting with curve B at equilibrium point D, with a balanced wage level of $U_2 = R_2$. The amount of urban labor is O_cL_2, and the amount of rural labor is O_vL_2.

As shown in Figure 2, the abscissa indicates the grain-planting area, and the ordinate indicates the output and cost of agricultural production. Curve OC_1 represents the initial production function of the female labor force, and curve OP represents the cost function. When the marginal cost and the marginal benefit are equal, farmers have the maximum output. That is, the parallel line P_1 of the cost function OP and the initial production curve OC_1 are tangent to point A, and the planting area is S_1. In plain areas, machinery use instead of labor improves the food production efficiency of the female labor force, and the curve OC_1 rises to OC_2. Curve OC_2 is tangent to the parallel line P_2 of the cost function OP at points B, and the planting area is $S_2 > S_1$. In areas suitable for planting high value-added agricultural products, farmers choose cash crops that generate a higher income, require less physical demand, and take a longer time to replace food crops. Because of the variety of planting products, the food production efficiency of the female labor force decreased, and the curve OC_1 dropped to OC_3. Curve OC_3 is tangent to the parallel line P_3 of the cost function OP at points C, and the grain-planting area is $S_3 < S_1$.

In summary, the female labor force is engaged in agricultural planting and production, but compared with the male labor force, the female labor force is weaker in physical strength and more dispersed in energy. As a result, they may have more difficulties devoting themselves to the farming

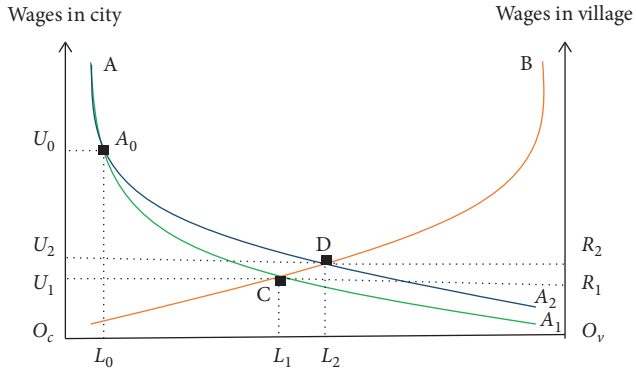

Figure 1: Rural labor migration and changes of agricultural planters.

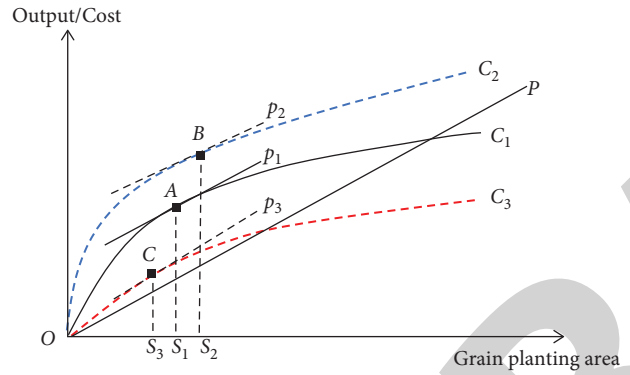

Figure 2: Production decision diagram of feminization of rural labor force.

process. The feminization of the agricultural labor force will result in two choices (Figure 3): first, the structural adjustment of factors and the adoption of machinery to replace the labor force to alleviate the shortage of labor force. Second, in the adjustment of product structure, cash crops that generate a higher income and require less physical demand but that are more time-consuming will be selected to replace food crops to reduce the grain-planting area and increase the planting of cash crops.

4. Empirical Model

4.1. Model Specification. In this section, we set up the following model:

$$Y_{it} = a_0 + a_1 X_{it} + a_2 P_{\text{it}} + a_3 W_{\text{it}} + a_4 F_{\text{it}} + a_5 PM_{\text{it}} + a_6 IND_{\text{it}} + a_7 IR_{\text{it}} + u_{it}, \quad (1)$$

with

$$u_{it} = v_i + \varepsilon_{it}, \quad (2)$$

where Y_{it} is the sown area of grain or the proportion of the sown area of grain to the total sown area of crops in province i during time period t; X_{it} is the ratio of the rural female labor force in province i during time period t; P_{it} denotes the price of grain, which is equal to the average price of rice, wheat, and corn; W_{it} denotes labor cost, which is the daily wage of the rural labor force; and F_{it} denotes food per capita, which directly reflects the status of grain production in each province. The higher the per capita grain possession, the more important the grain production in this area. PM_{it} denotes total power of agricultural machinery. In areas with a higher total power of agricultural machinery and richer cultivated land resources, grain production efficiency is also higher, and local farmers are more inclined to expand the grain-planting area. IND_{it} denotes the degree of industrialization, measured by the proportion of industry and service industry in the regional gross domestic product (GDP), and this index can reflect the differences of economic development in various regions to a certain extent. IR_{it} denotes an irrigated area, which measures the level of rural grassroots construction facilities; u_{it} is an error term, where the two components of this error term, the unobserved time-invariant heterogeneity $v_i \sim II\ D(0, \delta_v^2)$ and the idiosyncratic portion $\varepsilon_{it} \sim II\ D(0, \delta_\varepsilon^2)$, are assumed to be independent of one another and among themselves.

On the basis of this formula, the interaction term of the female proportion and the mechanized proportion is introduced, and the construction model is as follows:

$$Y_{it} = a_0 + a_1 X_{it} + a_2 X_{\text{it}} R_{it} + a_3 R_{\text{it}} + a_4 P_{\text{it}} + a_5 W_{\text{it}} + a_6 F_{\text{it}} + a_7 PM_{\text{it}} + a_8 IND_{\text{it}} + a_9 IR_{\text{it}} + u_{it}, \quad (3)$$

with

$$u_{it} = v_i + \varepsilon_{it}, \quad (4)$$

where R_{it} denotes mechanical convenience, which is measured by the ratio of the tractor-ploughed area to the total cultivated area and represents the topographic conditions [22]. In addition, to reduce the fluctuation range of variance and residuals, every real variable is in logarithmic form.

For panel-based models, either the fixed effects model (FE) or the random effects model (RE) can be selected for parameter estimation. These two methods each have advantages and disadvantages. In general, the fixed effects model is helpful to control endogenous problems. When the unobservable factors in the model are related to explanatory variables, the random effect estimator is biased, and the fixed effects estimator is more advantageous. When the unobservables in the model are independent of the explanatory variables, both fixed effects and random effects models yield consistent estimates, but the latter uses a combination of within-group dynamic information and between-group cross-sectional heterogeneity information in the parameter estimation, and thus its parameter estimation is more efficient.

4.2. Data Sources and Descriptive Statistics. The data used in this study are panel data consisting of relevant data from 26 provinces and cities in China for the calendar years 2002–2018. The data are obtained from the official statistical yearbooks, including the China Rural Statistical Yearbook, the China Statistical Yearbook, the National Agricultural Product Cost and Benefit Information Compilation, the

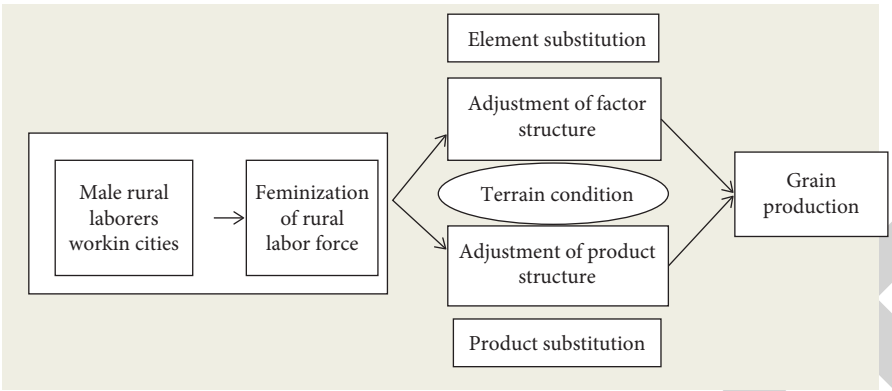

Figure 3: Theoretical analysis chart of the influence of feminization of labor force on grain production.

China Agricultural Machinery Industry Yearbook, and the China Population and Employment Statistical Yearbook. The results of the descriptive statistical analysis of each variable are shown in Table 1.

From 2002 to 2018, the female ratio of the rural labor force in China showed an upward trend. The proportion of women in rural labor increased from 49.41% in 2002 to 50.83% in 2018 (Figure 4). To reduce the fluctuations and observe the long-term trend, the data are processed and centralized in a three-year cycle. Clearly, the proportion of female rural laborers continues to increase, which is also consistent with the year-on-year growth of migrant workers in China.

The area under grain cultivation in China has increased steadily from 103,890,000 hectares in 2002 to 117,038,000 hectares in 2018 (Figure 5). According to the data of the China Statistical Yearbook of previous years, from 2002, this area decreased slightly to 99,410,000 hectares in 2003 and then increased to 119,230,000 hectares in 2016, which was an increase of 19.94%, with an average annual growth of 1.42%. In 2018, this area decreased slightly to 117,038,000 hectares. Overall, from 2002 to 2018, the grain planted area increased by 12.66%, with an annual growth rate of 0.74%.

5. Results and Discussion

5.1. Estimation of the Basic Model. As shown in Table 2, the feminization of the labor force has a significant negative impact on the grain-planting area, which indicates that the increase in the feminization of the labor force will lead to a decrease in the grain area. There are two reasons for this. First, compared with the male labor force, the female's physical strength tends to be weaker, and the energy women expend on planting is less than the energy men expend, which is not conducive to the grain-planting area. Second, female laborers may select less physically demanding and more profitable cash crops as food substitutes and thus increase cash crop cultivation for higher profits.

The price of food has a positive effect on the area of crop grown and its proportion. According to economist Schultz, farmers are rational and optimize the allocation of resources to obtain maximum benefits. The supply of food is an important manifestation of rational production, and farmers constantly adjust their decisions based on expected returns, which are based on the market price of food and the cost of cultivation. Food prices positively influence the area of plant cultivation and the proportion of cropland. The higher the food price is, the more farmers expand the area for grain cultivation to pursue more profits. Because of the limited land resources, the expansion of grain cultivation area inevitably will reduce the cultivation area of other crops, resulting in an increase in the proportion of grain cultivation area.

Labor costs have a negative effect on the area and its share of food cultivation, suggesting that as labor prices rise, the area and share of food cultivation in China will be reduced. A possible economic explanation lies in the fact that relative factor prices are the key determinant of product structure. To maximize profits, farmers can choose only factor substitution or product substitution. The former does not change the structure of agricultural cultivation, but rather optimizes the combination of production factors to reduce the cost of food production in accordance with the change of relative factor prices. The latter, however, will directly affect the structure of agricultural cultivation. To balance the increase of food production costs, farmers will invest in land, capital, and other agricultural products and also will increase the area planted with cash crops to obtain higher prices and income, which is not conducive to food production.

The influence of other variables on the grain-planting area and the proportion of the grain-planting area is basically in line with economic theory. The per capita grain output has a significant positive impact on the grain-planting area and its proportion. The more important the position of grain production is, for example, in the main grain-producing areas, the greater the grain-planting area and its proportion. In addition, the total mechanical power and mechanical convenience both have a positive impact on crop planting. The greater the total mechanical power, the easier it is to work in the area and the larger the grain-planting area. With economic development, it is possible that a large number of machines are developed and put into use. Therefore, it is easier for agricultural producers in the plain areas, where mechanization is relatively easy, to adjust the cropping

Table 1: Descriptive statistics for the total sample, 2002–2018, $N = 442$.

Variable	Symbol	Mean	SD	Minimum	Maximum
Grain sown area (1000 Ha)	Y_{it}	4220.52	2757.64	282.48	14283.1
Ratio female workforce (%)	X_{it}	49.65	0.99	46.57	52.86
Price of grain (RMB)	P_{it}	72.65	14.55	31.59	104.41
Labor cost (RMB)	W_{it}	51.20	27.89	7.5	126.82
Ratio of mechanization (%)	R_{it}	55.91	23.88	3.60	98.85
Food per capita (kg)	F_{it}	468.44	315.90	101.51	1992.36
Power of machinery (MW)	PM_{it}	32886.2	27300.0	2102.3	133530
Industrialization (%)	IND_{it}	87.41	5.42	65.4	96.6
Irrigated area (1000 Ha)	IR_{it}	2286.26	1445.81	168.3	6119.57
Ratio mechanization (%)	R_{it}	55.91	23.88	3.60	98.85

Sources: authors' calculations based on data provided by the official statistical yearbook.

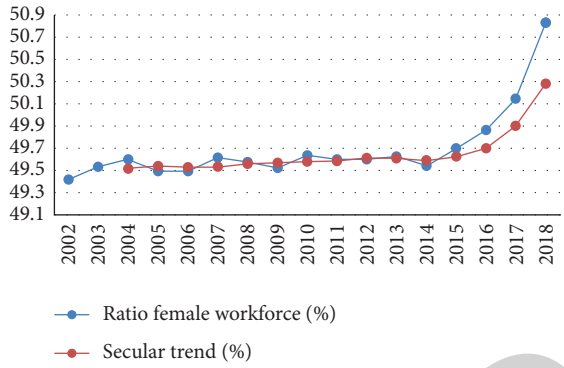

Figure 4: Trend chart of rural female labor force ratio in China from 2002 to 2018.

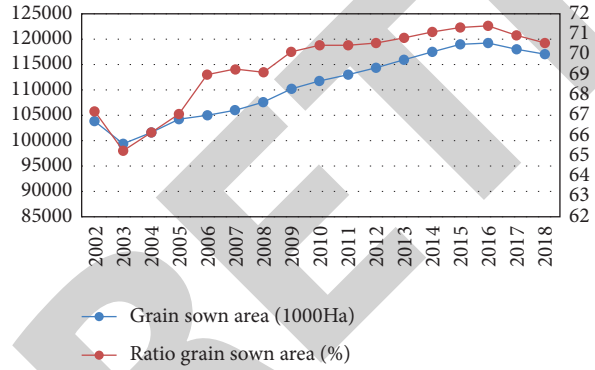

Figure 5: Trend chart of china's grain sown area and ratio from 2002 to 2018.

structure toward food crops and to reduce production costs through factor substitution and large-scale operation to obtain greater returns. Because of the scarcity of land resources, it also is possible that a large amount of land is used for industrial development, which definitely will reduce the grain-planting area and also reduce the cash crop-planting area. The general cash crops, such as vegetables, are planted near the suburbs of cities, so the land-crowding effect is more obvious than the planting and rural food. Thus, the proportion of food cultivation shows a positive effect.

5.2. Estimation of Model with Cross-Term. To study the superposition effect of the feminization of the labor force and the use of machinery, the cross-term of both is introduced. According to the regression results (Table 3), we found that the intersection of female proportion and mechanization convenience has a positive impact on grain-planting area and planting area proportion. This result shows that in areas where agricultural production mechanization is easier after the proportion of female rural labor force rises, agricultural producers will replace factors and adopt agricultural machinery to replace the labor force; in contrast, the family labor force will choose to maintain or even expand the area and proportion of grain sown to reduce production costs through a large-scale operation. This conclusion is basically in line with reality. In plain areas where mechanization is relatively easy, agricultural producers are more likely to adjust their planting structure toward food crops and to reduce production costs through factor substitution and scale operations to offset the negative impact of the feminization of the rural labor force on food production. In mountainous and hilly areas where mechanization is more difficult; however, it is challenging for machinery to replace labor to alleviate the impact of the labor shortage.

5.3. Robustness Checks. To check the robustness of the results, we removed about a quarter of the provinces and selected the top 20 provinces in China's plain area for regression analysis. The regression results are shown in Table 4, and both the significance and sign of the explanatory variables are relatively close to the results in Tables 2 and 3, indicating that the model regression results are relatively robust.

5.4. Regional Analysis. The main grain production areas in China are divided into three parts: first, Eastern China, which includes Liaoning, Jilin, Heilongjiang, Hebei, Shandong, Jiangsu, Zhejiang, Fujian, Guangdong, and Hainan provinces; second, the Central China, which includes Shanxi, Henan, Hubei, Hunan, Jiangxi, and Anhui provinces; and, third, Western China, which includes Chongqing, Sichuan, Guizhou, Yunnan, Guangxi, Shaanxi, Gansu, Ningxia, Inner Mongolia, and Xinjiang.

Table 2: Basic model estimation results.

	ln grain sown area		Ratio grain sown area	
	FE (1)	RE (1)	FE (2)	RE (2)
X_{it}	−0.016** (−2.14)	−0.016** (−2.16)	−0.449 (−0.96)	−0.390 (−0.80)
R_{it}	0.001 (1.26)	0.001* (1.81)	0.028 (0.90)	0.043* (1.52)
ln P_{it}	0.010 (0.26)	0.012 (0.30)	3.239* (1.59)	3.330* (1.79)
ln W_{it}	−0.044*** (−3.06)	−0.053*** (−3.75)	1.100 (1.13)	0.312 (0.35)
F_{it}	0.675*** (12.84)	0.665*** (11.63)	17.09*** (6.88)	16.62*** (7.05)
ln PM_{it}	0.037 (1.16)	0.049 (1.46)	−6.654*** (−2.84)	−5.635*** (−2.78)
IND_{it}	−0.002 (−0.45)	−0.001 (−0.20)	0.017 (0.09)	0.158 (1.02)
ln IR_{it}	−0.020 (−0.29)<	0.032 (0.56)	−2.301 (−0.72)	0.104 (0.04)
Constant	5.023*** (8.59)	4.547*** (8.78)	38.67 (1.50)	3.610 (0.16)
Observations	442	442	442	442
Number of province	26	26	26	26

Note. Numbers in parentheses are t statistics. Asterisks refer to p values: *** $p < 0.01$, ** $p < 0.05$, and * $p < 0.1$.

Table 3: Estimate result of a model with cross-term.

	ln grain sown area		Ratio grain sown area	
	FE (1)	RE (1)	FE (2)	RE (2)
X_{it}	−0.041*** (−3.35)	−0.041*** (−3.27)	−2.360*** (−2.79)	−2.343*** (−2.70)
$X_{it} \times R_{it}$	0.041** (2.09)	0.042** (2.02)	3.125*** (3.32)	3.191*** (3.16)
R_{it}	0.021** (2.20)	0.022** (2.13)	1.580*** (3.38)	1.625*** (3.25)
ln P_{it}	0.013 (0.35)	0.015 (0.40)	3.469* (1.70)	3.608* (1.95)
ln W_{it}	−0.046*** (−3.28)	−0.054*** (−3.87)	0.984 (1.01)	0.215 (0.23)
F_{it}	0.667*** (13.49)	0.657*** (12.47)	16.46*** (7.37)	16.15*** (7.85)
ln PM_{it}	0.041 (1.33)	0.052* (1.60)	−6.339*** (−2.76)	−5.469*** (−2.74)
IND_{it}	−0.002 (−0.42)	−0.001 (−0.15)	0.040 (0.24)	0.173 (1.25)
ln IR_{it}	−0.020 (−0.30)	0.029 (0.51)	−2.257 (−0.85)	0.082 (0.04)
Constant	6.235*** (7.29)	5.824*** (7.55)	131.8*** (3.45)	99.93*** (2.59)
Observations	442	442	442	442
Number of province	26	26	26	26

Note. Numbers in parentheses are t statistics. Asterisks refer to p-values: *** $p < 0.01$, ** $p < 0.05$, and * $p < 0.1$.

Table 4: Estimate result of the robustness test.

	ln grain sown area		Ratio grain sown area	
	FE (1)	RE (1)	FE (2)	RE (2)
X_{it}	−0.0413*** (−4.23)	−0.0418*** (−3.81)	−2.572*** (−4.33)	−2.448*** (−3.66)
$X_{it} \times R_{it}$	0.0474** (2.48)	0.0482** (2.34)	3.730*** (5.32)	3.843*** (4.01)
R_{it}	0.0239** (2.58)	0.0245** (2.44)	1.877*** (5.32)	1.949*** (4.10)
ln P_{it}	0.0345 (0.80)	0.0386 (0.90)	4.148* (1.74)	5.106*** (2.69)
ln W_{it}	−0.0419*** (−2.95)	−0.0510*** (−3.65)	1.709 (1.72)	−0.216 (−0.22)
F_{it}	0.647*** (12.57)	0.644*** (11.43)	14.81*** (6.76)	15.87*** (7.20)
ln PM_{it}	0.0247 (0.75)	0.0320 (0.95)	−5.355** (−2.51)	−4.229** (−2.11)
IND_{it}	0.001 (0.10)	0.002 (0.49)	−0.033 (−0.20)	0.330** (2.33)
ln IR_{it}	−0.003 (−0.04)	0.037 (0.63)	−4.070 (−1.71)	−1.232 (−0.45)
Constant	6.158*** (6.80)	5.739*** (7.88)	159.8*** (5.67)	89.17*** (2.97)
Observations	340	340	340	340
Number of provinces	20	20	20	20

Note. Numbers in parentheses are t statistics. Asterisks refer to p-values: *** $p < 0.01$, ** $p < 0.05$, and * $p < 0.1$.

According to the noted division, we further analyzed the influence of the increasing female ratio in Eastern China, Central China, and Western China on the sown area and its proportion of grain. In this part, we conducted a Hausman test on the model to select a relatively suitable estimation method for quantitative analysis.

As shown in Table 5, the substitution effect of machinery on the labor force varies across regions. In the eastern region, an increase in the proportion of females decreases the area and proportion of grain cultivation. When combined with the convenience of machinery, both the area and proportion of grain cultivation are significantly increased.

Table 5: Regional analysis results.

	ln grain sown area			Ratio grain sown area		
	Eastern China	Central China	Western China	Eastern China	Central China	Western China
X_{it}	−0.037* (−1.86)	−0.016 (−1.18)	−0.060** (−1.79)	−3.950***(−2.36)	−1.072 (−1.25)	−2.015 (−1.07)
$X_{\mathrm{it}} \times R_{it}$	0.039* (2.07)	0.020 (1.02)	0.0782* (1.69)	3.169* (1.89)	2.405* (1.54)	2.835 (1.00)
R_{it}	0.019* (1.93)	0.011 (1.13)	0.040* (1.77)	1.575* (1.89)	1.246* (1.58)	1.454 (1.06)
$\ln P_{\mathrm{it}}$	−0.015 (−0.36)	0.018 (0.36)	0.044 (0.75)	5.816* (1.53)	−4.980 (−1.79)	7.419* (1.85)
$\ln W_{\mathrm{it}}$	−0.018 (−1.24)	0.006 (0.25)	−0.064*** (−4.10)	−1.165 (−0.61)	3.553* (2.51)	−2.980** (−2.28)
F_{it}	0.710*** (14.60)	0.225* (2.13)	0.635*** (13.39)	18.230*** (12.99)	7.597 (0.95)	21.69*** (3.80)
$\ln PM_{\mathrm{it}}$	0.006 (0.09)	0.035 (1.25)	0.128* (1.79)	−5.104 (−1.57)<	0.767 (0.73)	−6.584 (−1.67)
IND_{it}	−0.008 * (−1.83)	0.009*** (5.52)	-0.013*** (−3.67)	0.662*** (2.73)	−0.113 (−0.53)	0.255 (0.85)
$\ln IR_{\mathrm{it}}$	−0.163** (−2.48)	0.161* (1.80)	0.205* (1.68)	4.687 (1.32)	12.910** (2.95)	−5.652 (−1.39)
Constant	5.591** (3.30)	−0.367 (−0.83)	5.885*** (5.32)	84.18 (1.38)	−12.23 (−0.18)	85.08 (0.91)
Observations	170	102	170	170	102	170
Number of province	10	6	10	10	6	10

Note. Numbers in parentheses are t statistics. Asterisks refer to p-values: $^{***}p < 0.01$, $^{**}p < 0.05$, and $^{*}p < 0.1$.

Moreover, in the eastern regions, because of the flat terrain and extensive use of machinery, the substitution effect of factors is greater than the debilitating nature of the female labor force, making the area and proportion of grain cultivation increase instead of decrease. For example, Heilongjiang, Jiangsu, and Shandong are located in the eastern regions, and the terrain is mainly plain with relatively flat arable land. Thus, when the rural labor force is feminized, the mechanical replacement of labor can be more smoothly realized, and agricultural producers may devote more resources to food production, thus weakening the negative impact of the rising proportion of female rural labor force. For example, during the period from 2001 to 2016, the sown areas of grain in the three provinces increased from 8,291,200 hectares, 4,822,600 hectares, and 6,912,600 hectares to 14,214,500 hectares, 5,475,900 hectares, and 8,404,800 hectares, respectively.

In the central regions, the feminization of the labor force and the cross-term of both do not significantly affect the grain-planting area, but the cross-term significantly and positively affects the proportion of the grain-planting area. This result indicates that the feminization of the labor force, including the superposition effect of the two factors will not lead to a decrease in the grain-planting area, but it will lead to a decrease in the cash crop-planting area and will make the proportion of area under grain cultivation higher. The possible reason for this may be that the central region belongs to the traditional grain-growing region, and its economy is not as developed as that of the eastern region. Thus, the demand for cash crops, such as vegetables, is not as high, and the planting takes longer. As a result, farmers prefer to grow grain. During the period from 2002 to 2018, the sown areas of peanuts, cotton, and melons in Shanxi Province decreased from 18,800 hectares, 72,300 hectares, and 46,300 hectares to 5,400 hectares, 2,300 hectares, and 16,200 hectares, respectively; and the sown areas of peanuts, cotton, and melons in Anhui Province decreased from 284,600 hectares, 321,200 hectares, and 211,400 hectares to 144,200 hectares, 86,300 hectares, and 8,000 hectares, respectively [22–24].

In the western region, the proportion of females has a significant and negative impact on the grain-planting area, whereas the cross-term has a positive impact on the grain-planting area, but both do not have a significant impact on the proportion of the grain-planting area. This result shows that after the proportion of the female labor force increased in the western region, the area planted with grain and cash crops decreased at the same time. Therefore, the proportion of planted area did not change significantly. After the use of machinery, however, the negative effect of the feminization of the labor force is weakened, increasing both the grain-planting area and the cash crop area. Because Sichuan and Guizhou are typical labor-exporting cities, a large number of male laborers go out to work, leaving women to engage in planting, and the loss of effective labor is unfavorable to agricultural cultivation. Because of the massive use of machinery, the originally barren land in the west was developed and planted, which increased the planting area. During 2002–2018, the sown areas of grain, cotton, vegetables, and fruits in Xinjiang increased from 1,514,600 hectares, 943,900 hectares, 164,200 hectares, and 83,000 hectares to 2,219,600 hectares, 2,491,300 hectares, 273,300 hectares, and 111,300 hectares, respectively [25].

The rising proportion of the rural labor force females mainly affects food production in eastern and western China. This effect may be due to the differences in socioeconomic conditions and natural geographic conditions of each province in China. In addition, the cultivation of food crops and cash crops in each region is bound to show different changes in accordance with economic development and income growth.

6. Conclusions

Based on the panel data of 26 provinces from 2002 to 2018, this study has analyzed the impact of the feminization of the rural labor force on grain planting and regional differences. Our results indicate the following: (1) the feminization of the rural labor force significantly negatively affects the grain-planting area and its ratio and has an adverse impact on grain planting. (2) The impact of the feminization of the labor force on grain planting is affected by topography. In flat areas where machinery is easier to operate, machinery will weaken the adverse impact of the feminization of the labor force on grain planting. (3) The influence of the

Hindawi
Mobile Information Systems
Volume 2022, Article ID 4207229, 10 pages
https://doi.org/10.1155/2022/4207229

Research Article

Platform Design of Psychological Teaching Classroom Evaluation Based on Mobile Edge Computing Resource Allocation

Yang Shen

Chifeng University, ChiFeng, Inner Mongolia 024000, China

Correspondence should be addressed to Yang Shen; 2013120@mail.tust.edu.cn

Received 23 June 2022; Revised 13 July 2022; Accepted 28 July 2022; Published 19 August 2022

Academic Editor: Shadi Aljawarneh

In recent years, with the rapid development of mobile communication and the increasing popularity of smart mobile devices, the number of mobile communication services has increased sharply, and mobile terminals have become resource-constrained devices. Traditional cloud computing methods have become increasingly unable to meet the needs of many mobile communications services. In order to improve the quality of user experience, mobile edge computing has become one of the key technologies of the fifth-generation mobile communication system. It provides an effective solution that can reduce the load on the basic network and improve the user experience and has received widespread attention from all over the world. In view of the important direction of big data research, how to obtain economically valuable information from audio information is the key; first, the basic technical characteristics of big data and the technology involved are analyzed, and then the basic technical relationship of speech recognition is analyzed and the data are merged, and finally the big information in speech recognition is analyzed. The processing architecture provides a combination of speech recognition technology and big data for the application development technology architecture and application process. The effect of classroom assessment will affect whether students' learning can be promoted and developed. For most psychology teachers, this is a topic worth exploring to determine what types of assessments can be used in the classroom to promote psychological teaching. The survey results show that in the current psychology classroom, the concept of teacher evaluation has changed, and student self-esteem and peer evaluation have appeared in the evaluation of teaching psychology. The content of the evaluation has gradually shifted to students' emotions, attitudes, and values, and the evaluation methods have also changed. The type of evaluation can be more praised and encouraged.

1. Introduction

The algorithm for replacing computers and communication resources is based on the pricing mechanism in the MEC system. The algorithm fully considers the network status and user interaction, and provides several methods to reduce the burden on computers. The limited computer and communication resources of the MEC server are used to allocate resources [1]. In the multicell scenario, the allocation model uses QoS-based resource allocation algorithms and effective pricing strategies to provide users with dynamically adapted traffic services and select the best computer. Disabling the offloading path that provides services to users, the macro base station and each LTE bring a small load to the base station, thereby balancing and maximizing the MEC operator's network revenue. The investigation of the MEC network solution is not thorough enough [2, 3]. For example, there are still many problems to be solved when sharing communication, computing, and storage resources. The MEC server has powerful and effective communication, storage, and computer functions, and is distributed at the edge of each access network. The MEC server is a resource-constrained device [4]. In recent years, computer offloading has become a research hotspot. In real life, different types of calculation problems have different requirements for network indicators. Therefore, in this article, the business priority will be divided according to the user's QoS indicators. With the improvement of computer computing and network skills, traditional large-scale word processing and data mining, complex systems, speech recognition, ontology, and other academic research have begun to lay a solid foundation for practical applications [5, 6]. Big data research

is gradually attracting the attention of scientists and operators. In terms of the development and application of new technologies, big data processing technologies are implemented into existing business systems. Converting academic research results into a real commercial value is a problem worthy of research [7]. Audio is one of the main ways to express information. Extracting commercial information from audio information is an important direction of big data research. In the classroom assessment, students' self-assessment and mutual assessment are considered. The content of the assessment gradually shifts to emotions, attitudes toward student values, and different assessment methods and levels are adopted. Classroom psychological teaching evaluation will also lead to some problems, such as the lack of opportunities for students to participate in the evaluation, the repeated evaluation of language, the evaluation effect needing to be improved, and the neglect of individual differences between students. Based on the investigation and analysis of the current situation, existing problems, and causes of psychological learning, we put forward corresponding countermeasures.

2. Related Work

If a user submits a computing task to the MEC server for execution, there are two transmission paths. The first is to let users outsource computing tasks to the SeNB, and then use the feedback between the SeNB and MeNB to transfer the tasks to the MEC server for execution [8]. If a load of a specific cell is too high, then the long delay required for users to upload tasks through the SeNB will cause a large delay. However, the current load of small base stations is too large, and the entire network is not conducive to the load of the base station. At this time, the second path can be used for load balancing, and delay-sensitive services can directly use the MeNB to offload computing tasks to the MEC server for execution [9, 10]. In the literature, computer offloading is an important feature and application of the MEC system. Since MEC was proposed, computer offloading research has always been a hot topic in MEC systems. Some computing tasks have been outsourced to MEC. If the computing tasks running locally consume computing resources for server execution, and reducing the burden of MEC execution requires additional communication overhead, MEC's powerful computing capabilities can be used to save equipment power and reduce access delays [11, 12]. In the traditional classroom assessment, the teacher's assessment is usually the standard, and the students are only the objects of the assessment and are not qualified for the assessment. In personal interviews with teachers in specific schools, it was found that the interviewed teachers had different levels of understanding and ideas about teaching assessment, but the understanding and application of teaching assessment concepts advocated by the new curriculum reform were not thorough enough, and the traditional classroom assessment concepts still have a certain impact [13]. The literature suggests that at the academic and social level, schools should create a favorable practice and research environment to evaluate psychology teachers in the classroom so that teachers can appropriately develop and improve their assessment skills while creating an environment that provides them with professional support [14]. To provide teachers with guidance, we conduct standardized assessment practices and research, and train teachers to improve classroom assessment methods and strategies [15]. However, it should be noted that when teaching psychology teachers in classroom assessment, in addition to teaching theoretical knowledge for teacher assessment, it is necessary to strengthen the training of teachers' practical ability to assess teachers. In addition, the survey results show that in the current psychology classroom, the concept of teacher assessment has changed [16, 17]. This article is suitable for the MEC system solution. Next, we mainly discuss the process and basic principles of uninstalling the computer, and the strategy of updating the latest content of the cache system. In the process of uninstalling the computer, various resources in the MEC system are virtualized and abstracted from computing and communication resources, and a price concept is proposed, an outsourcing strategy based on maximizing network revenue and improving traditional mobile resource allocation algorithms [18].

3. Mobile Edge Computing Resource Allocation and Voice Big Data

3.1. Mobile Edge Computing Resource Allocation. As shown in Figure 1, a scenario with multiple units and many users is considered. Each cell has a small base station. Each small base station is connected to the macro base station, and the user role can be a local role. Tasks can also be submitted to the MEC server for execution. In the future 5G system, these small base stations will form their own small base stations, which can each provide services to users.

In the system model, the M_eNB is connected to the MEC server, and each S_eNB is connected to the M_eNB. Corresponding to Shannon's theorem: between the user and S_eNB or between the user and S_eNB, as in the following formula:

$$C = B\log_2\left(1 + \frac{p_{k_n} G_{k_n,n}}{\sigma + \sum_{m=1,m\neq n}^{N} \sum_{i=1}^{K_m} p_{i_m} G_{i_m,n}}\right). \tag{1}$$

Use this option to show that p_{kn} is the percentage of the radio spectrum allocated by the small base station n to the user by k_n so that the data rate does not exceed the SeNB backhaul, as in the following formula:

$$\sum_{k_n \in K_n} R_{k_n} = L_n, \quad \forall n. \tag{2}$$

$s_{K_n} \in [0, 1]$, $\forall v$, k indicates that the total data rate of a user shall not exceed the throughput of the M_eNB backhaul, as in the following formula:

$$\sum_{n\in N} \sum_{k_n \in K_n} R_{k_n} = L. \tag{3}$$

In the case of backhaul between M_eNB and S_eNB, it is assumed that they are only connected by wired fiber, the bandwidth is limited, and the backhaul delay is proportional

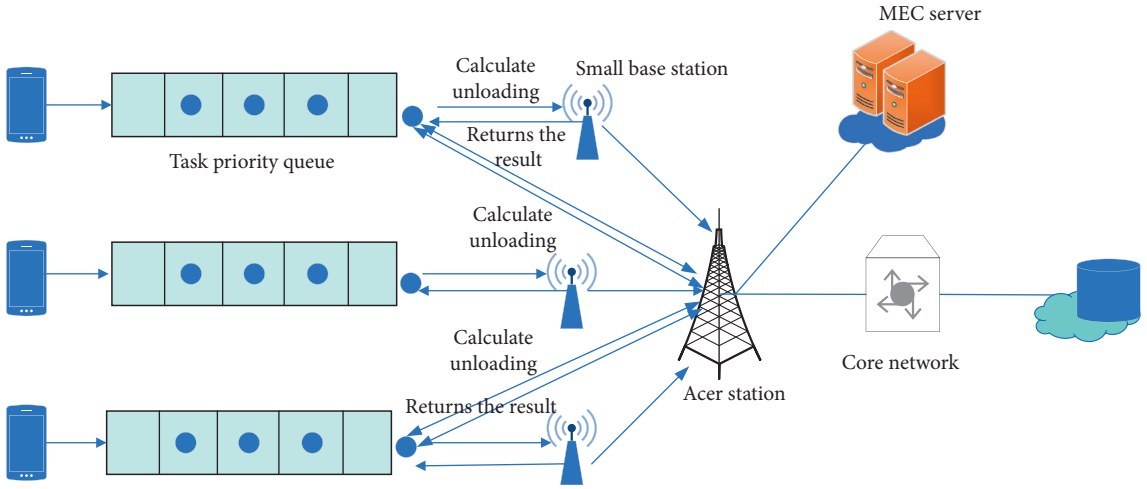

Figure 1: System model.

to the data length. According to the theorem, the uplink data rate at which users can access the MeNB can be expressed as in the following formula:

$$C_{i,k}^{M} = B\log_2\left(1+\frac{p_{k_n}^{M}G_{k_n,M}}{\sigma^2+\sum_{m=1,m\neq n}^{N}\sum_{i=1}^{K_m}p_{i_m}^{M}G_{i_m,M}}\right),\quad \forall n,\ k. \tag{4}$$

σ represents the power spectral density of the additive white Gaussian noise. Similarly, if the user accesses the S_eNB through channel h, we can get the k_n uplink data rate as in the following formula:

$$C_{i,k}^{S} = B\log_2\left(1+\frac{p_{k_n}^{S}G_{k_n,n}}{\sigma^2+\sum_{m=1,m\neq n}^{N}\sum_{i=1}^{K_m}p_{i_m}^{S}G_{i_m,n}}\right),\quad \forall n,\ k. \tag{5}$$

Different devices have different computing capabilities, and the local execution time can be expressed as in the following formula:

$$t_{k_n}^{L} = \frac{d_{k_n}}{f_{k_n}^{l}}. \tag{6}$$

This time includes the wireless uplink transmission time from the UE to the M_eNB and the time spent performing tasks on the MEC server, that is, the total elapsed time as in the following formula:

$$t_{k_n}^{M} = \frac{d_{k_n}}{r_{k_n}^{M}}+\frac{c_{k_n}}{f_0^{R}}. \tag{7}$$

f_0^R is the processing capacity of the MEC server. In order to pay attention to the impact of different computer offloading methods on the total system revenue, assuming the constants of various computer tasks f_0^R, $r_{k_n}^M$ represents the total uplink transmission rate from user k_n to M_eNB, that is, the following formula:

$$\begin{aligned} r_{k_n}^{M} &= \sum_{h=1}^{H}a_{k_n,2,k}r_{k_n,h}^{M} \\ &= \sum_{h=1}^{H}a_{k_n,2,k}B\log_2\left(1+p_{k_n}^{M}g_{k_n}^{M}/\sigma^2+\sum_{m=1,m\neq n}^{N}\sum_{i=1}^{K_m}a_{i_m,3,k}p_{i_m}^{S}g_{i_m}^{M}\right). \end{aligned} \tag{8}$$

The total energy consumption is as in the following formula:

$$e_{k_n}^{M} = \frac{b_{k_n}^{M}p_{k_n}^{M}d_{k_n}}{r_{k_n}^{M}}+c_{k_n}\delta^{R}. \tag{9}$$

δ^Rindicates that the MEC server has reached a certain power consumption per CPU cycle. Generally, the MEC server is more energy efficient than mobile devices. Therefore, $\delta^R\langle\delta^L, b_{k_n}^M$ indicates the number of channels used by the device to transmit data to M_eBS, as in the following formula:

$$b_{k_n}^{M} = \sum_{h=1}^{H}a_{k_n,2,h}. \tag{10}$$

The total time required for outsourcing tasks through the S_eNB includes the uplink transmission time from the user k_n to the S_eNB, the delay of the return flight, and the execution time of the MEC server. In other words, the total time spent is as in the following formula :

$$t_{k_n}^{S} = \frac{d_{k_n}}{r_{k_n}^{S}}+d_{k_n}\phi+\frac{c_{k_n}}{f_0^{R}}. \tag{11}$$

ϕ represents the single data backhaul delay rate and the uplink transmission rate, as in the following formula :

$$\begin{aligned} r_{k_n}^{S} &= \sum_{h=1}^{H}a_{k_n,3,h}r_{k_n,h}^{S} \\ &= \sum_{h=1}^{H}a_{k_n,3,h}B\log_2\left(1+p_{k_n}^{S}g_{k_n}^{S}/\sigma^2+\sum_{m=1,m\neq n}^{N}\sum_{i=1}^{K_m}a_{i_m,2,h}p_{i_m}^{M}g_{i_m}^{S}\right). \end{aligned} \tag{12}$$

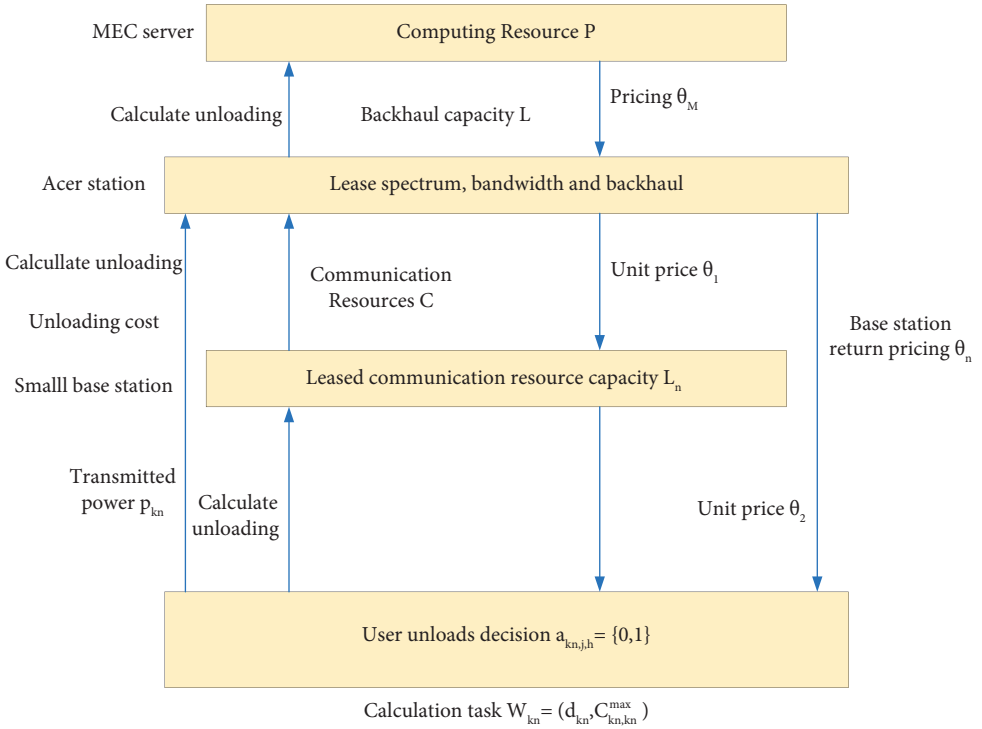

Figure 2: Schematic diagram of exchange of communication resources and computer resources.

The total energy consumption is as in the following formula :

$$e_{k_n}^S = \frac{b_{k_n}^S p_{k_n}^S d_{k_n}}{r_{k_n}^S + c_{k_n}\delta^R}. \tag{13}$$

This article discusses the problem of computer unloading. The main problem is to replace computer communication resources, fully consider the processing power and communication overhead of mobile devices and MEC servers, and use constraints based on meeting user QoS requirements to determine how many computer communication resources to allocate. Figure 2 shows a specific schematic diagram of the parameters used to replace communication and computing resources.

The simulation results are shown below. From the simulation result curve in Figure 3, it can be seen that when the number of users is less than 10, the calculation will be performed. The network profitability of this method is slightly lower than that of traditional algorithms. If the number of users exceeds 10, the network revenue of the algorithm proposed in this article will greatly exceed the usual revenue.

This paper effectively expands the MEC server by overlapping MBS and SBS and configuring each cache server. This hierarchical cache architecture can make full use of the advantages of MEC, improve the service functions of the MEC system, and improve user experience.

In the cache area of the MEC server, each data block stores an attribute representing the CRF weight. Since the cache exchange algorithm uses trade-off CRF to balance access time and access, calculations need to be performed.

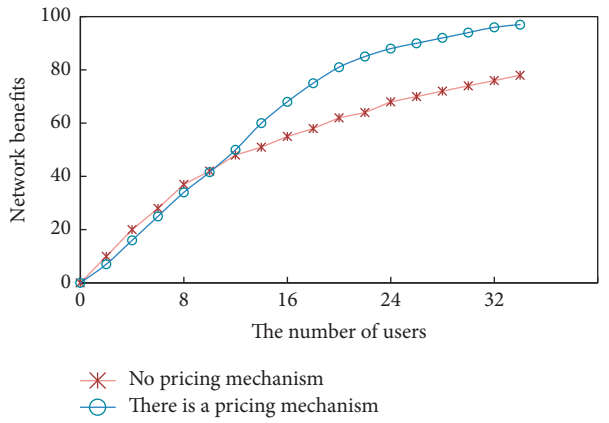

Figure 3: Network income comparison.

The formula for the CRF value of the resource file can be defined as in the following formula :

$$\mathrm{CRF}_{\mathrm{last}}(a) = f(0) + f\left(t_c - LA(a)^* \mathrm{CRF}_{\mathrm{last}}(a)\right). \tag{14}$$

In the above formula, such as in the following formula :

$$f(x) = \frac{1}{2}\lambda x. \tag{15}$$

$\mathrm{LA}(a)$ and $\mathrm{CRF}_{\mathrm{last}}(a)$ display the number of accesses to file a in the last time unit, and the CRF value and t_c of file a indicate the current number of times per unit of time.

The defined variable $c_j^{vl} \in \{0, 1\}$, $c_j^{vl} = 1$ indicates that the v_l video has been cached on server j, and the cache capacity of each server is limited, as in the following formula :

$$\sum_{v_l \in V} r_l c_j^{v_l} \le M, \quad \forall j \in K. \tag{16}$$

In order to express the possibility of passing the video request v_l to the server j, the vector is defined as in the following formula :

$$\left\{x_j^{vl}, y_{jk}^{vl}, z_j^{vl}, t_{jk}^{vl}\right\} \in \{0, 1\}. \tag{17}$$

As you can see from the above, one of the above situations occurred when the request was initiated, so constraints can be specified, as in formula :

$$\left(x_j^{vl} + z_j^{vl}\right) + \sum_{k \in K}\left(y_{jk}^{vl} + t_{jk}^{vl}\right) + z_{j0} = 1. \tag{18}$$

Therefore, the cost of receiving the video v_l from the j cache server on the return flight can be expressed by the following formula :

$$D_j(v_l) = r_l\left[d_{j0}x_{j0}^{vl} + \sum_{k \in K} d_{jk}\left(y_{jk}^{vl} + t_{jk}^{vl}\right)\right]. \tag{19}$$

The cost of the return flight reflects the business volume and the consumption of network resources in the return journey. Given the available resources, formulate the best objective function to minimize the return cost, as in the following formula :

$$\min \sum_{vi \in N} D_j(v_l). \tag{20}$$

As can be seen from the above formula, the number of videos that can be fully cached is as in the following formula :

$$C_f = \frac{tM}{b}. \tag{21}$$

The number of videos in which only the initial segment of the video is cached is in the following formula :

$$C_i = \frac{(1-t)M}{\mathrm{bn}}. \tag{22}$$

The total number of videos that each MEC server can cache is the following formula :

$$\begin{aligned} C_{\text{total}} &= \left(C_f + C_i\right) \\ &= \frac{(t(n-1)+1)M}{\mathrm{bn}}. \end{aligned} \tag{23}$$

Assuming that video popularity is evenly distributed, the cache hit rate can be expressed as the following formula :

$$H = \frac{(t(n-1)+1)M}{\mathrm{nbN}}. \tag{24}$$

The access delay of the cache error d_m and the access delay of the cache hit d_h ($d_m \rangle d_h$) are the average access delay, as shown in the following formula :

$$D = \mathrm{Hd}_h(1-H)\,d_m. \tag{25}$$

3.2. Voice Big Data. In the 1960s, dynamic programming and linear predictive analysis techniques implemented speech recognition for individual words of a specific person. In the 1970s, research on speech recognition was further developed. In the 1980s, HMM and artificial nerves have been successfully used in speech recognition. Since the 1990s, speech recognition has reached important milestones in the development of improved models, parameter extraction and optimization, and system adjustment. Speech recognition technology has begun to develop into real business applications.

This article has fully explored the technical architecture used to process large amounts of data in the industry, and there are many practical examples. The application system of this article uses data to perform business-oriented low-level operations, storage, combination, cleaning, and transformation of large data sets. At the same time, advanced technologies are used to determine the characteristic values of big data, which can be limited to the first level, or the data set generated from the first level can be processed. The business system can easily call, request, and display the processing results, or the analysis system can more effectively extract data features and perform appropriate analysis.

4. Psychological Teaching Classroom Evaluation

4.1. Status Quo of Classroom Evaluation of Psychological Teaching. Most of the content of classroom assessment includes three implementation forms: teacher assessment, student review, and student self-assessment. Table 1 shows the author's observations on teacher assessment.

It can be seen from the above table that in the teaching process of psychology class, teacher's assessment is the main factor, accounting for about 90% of the total assessment time. The forms of student mutual assessment and student self-assessment also appear in the education process. It accounts for approximately 10% of the total number of reviews, which shows that in the evaluation process of psychology classrooms, teachers try to get students to participate in the evaluation.

The new curriculum standards indicate that the content of student psychological learning assessment mainly includes the attention of students in the classroom, their learning attitude, the level of active participation, and the ability to use language. Table 2 shows the content of psychological education teaching assessment obtained from classroom observations case.

It can be seen from the results in the table that teachers' assessment of students' language skills accounts for approximately 86% of the total assessment time and approximately 14% of all other aspects. This shows that in addition to the knowledge of the students, the teacher's attention and evaluation of other aspects are the attitude, interest, and enthusiasm of some students to actively participate in the classroom.

Table 3 shows how primary school teachers use the classroom assessment methods discovered by the author through classroom observations and student questionnaires.

Table 1: Class evaluation.

Evaluation	Teacher	T1		T2		T3		T4	
	Total	Frequency 63	% 100	Frequency 62	% 100	Frequency 59	% 100	Frequency 61	% 100
Evaluation subject	Student self-evaluation	1	1.6	0	0	0	0	0	0
	Student mutual evaluation	4	6.3	7	11.3	3	5.1	5	8.2
	Teacher evaluation	58	92.1	55	88.7	56	94.9	56	91.8

Table 2: Evaluation content of psychology class.

Evaluation	Teacher	T1		T2		T3		T4	
	Total	Frequency 63	% 100	Frequency 62	% 100	Frequency 59	% 100	Frequency 61	% 100
Evaluation subject	Language knowledge	52	82.5	54	87.1	53	89.8	52	85.2
	Other	11	17.5	8	12.9	6	10.2	9	14.8

Table 3: The status of evaluation method in psychological teaching.

Evaluation	Teacher	T1		T2		T3		T4	
	Total	Frequency 63	% 100	Frequency 62	% 100	Frequency 59	% 100	Frequency 61	% 100
Evaluation subject	Spoken language	50	79.4	49	79	53	89.8	55	90.1
	Written	6	9.5	8	12.9	4	6.8	2	3.3
	Posture	5	7.9	3	4.8	2	3.4	4	6.6
	Material incentives	2	3.2	2	3.3	1	1.6	0	0

Table 4: Class type status.

Evaluation	Teacher	T1		T2		T3		T4	
	Total	Frequency 63	% 100	Frequency 62	% 100	Frequency 59	% 100	Frequency 61	% 100
Evaluation nature	No evaluation	7	11.1	62	14.5	6	10.2	7	11.5
	Positive comments	51	82	9	80.6	48	81.3	50	81.9
	Negative evaluation	5	7.9	50	4.9	5	8.5	4	6.6

It has been observed that psychology teachers usually require students to answer questions individually or collectively in the classroom throughout the class or group, and the teacher provides timely feedback on the evaluation. From the results in the table, this type of teacher oral assessment accounts for about 80% of the total assessment of psychology classes. Sometimes teachers often use body language, written grades, or grade rewards, such as smiling faces, red flags, postcards, and candy.

In the teacher's classroom, there are three types of evaluation: positive evaluation, negative evaluation, and nonevaluation. Positive evaluation refers to positive evaluation or praise, that is, motivational evaluation. Negative evaluation refers to the recommendation or ridicule of students or the incorrect handling of wrong answers given by students, usually refers to willingness to give correct answers, and etc. Insufficient grading means that the teacher did not evaluate the students' answers. Table 4 is an overview of the types of classroom assessment.

According to the results of classroom observations, psychology teachers can promote and reward students for most of the timetable in the classroom, accounting for about 82% of the total grades. The reactions of criticizing students, opposing students, or not evaluating students are few, accounting for about 18% of the total. From the analysis of the two charts above, it can be seen that after answering correctly or performing well, the teacher often asks, what will happen to the teacher if the answer is incorrect or poor consciousness; 72.8% and 85.3% of students tend to encourage and praise often. This shows that teachers can usually praise and reward students regardless of whether the student's answer is correct or not. Only when students do not observe discipline, such as talking to other students without being attentive, sitting casually, and waiting, will the teacher criticize and correct their assessments. Psychology courses are divided into two dimensions: language richness and observation of language ease of use, as shown in Table 5.

4.2. Strategies to Improve the Evaluation Effect of Psychological Teaching. The main function of all learning is to improve people's quality and to regard teaching as an integral part of overall learning. The main purpose of the evaluation should also be to promote the development of all aspects of the

Table 5: Classroom language assessment.

Evaluation	Teacher	T1		T2		T3		T4	
	Total	Frequency	%	Frequency	%	Frequency	%	Frequency	%
		50	100	49	100	53	100	55	100
Evaluation language	Simple	39	78	40	81.6	48	90.6	49	89.1
	Rich	11	22	9	18.4	5	9.4	6	10.9

quality of the subject. Classroom teacher evaluation should promote continuous and effective student learning and promote the healthy development of students in all aspects. This is the concept of transforming and supporting our teachers. Teachers should design an assessment framework to promote student development in three ways.

4.2.1. Fully Pay Attention to Student Development. Elementary school is the initial stage of psychological teaching. During this time, students' interest and enthusiasm for learning increase, which has a great impact on the future of psychological teaching. However, traditional assessment only considers the results of students' psychological learning and ignores the development of students in the process of psychological learning, such as learning style, learning attitude, learning strategy, interest, as well as screening and learning. Choosing the function of evaluation that is too prominent: the scores are different. Only a few students have passed the evaluation, established their confidence in learning, and gained the joy of success, while other students were ignored or even gave up, resulting in some students losing interest and confidence in learning. In order to avoid this situation, teachers need to follow the concept of the new curriculum reform. Combined with the new curriculum standards, we pointed out in the evaluation suggestions that when evaluating students, we should praise, encourage, and guide students' behavior and actual situation, attention, learning strategies, etc. according to each student's psychological level, protect students' confidence in learning psychology, and promote students' learning and self-development in all aspects.

4.2.2. Pay Attention to the Individual Differences between the Evaluation Objects. The implementation of classroom assessment concepts that help students develop is inseparable from understanding the individual differences of students. Traditional classroom assessment always uses the same external standards to evaluate students (e.g., tests) and classifies students based on test scores. This level was canceled, and the development opportunities of some students were destroyed. The constructivist theory believes that people have different views and interpretations of the outside world due to different experiences and backgrounds. When evaluating teachers in the classroom, differences in student knowledge and experience should also be considered. When evaluating different students, different evaluation standards and methods should be used. Under normal circumstances, teachers' choices of classroom assessment topics are very subjective, and they will discriminate against class teachers or students with good performance. These students usually provide more verification, as well as complete freedom of expression and thought. Because of the differences between them and the poor academic performance of other students, teachers often feel that this part of the students cannot learn and will not do well in other fields. Students become addicted and easily rely on the teacher, and the teacher's assessment directly affects their psychological learning. Therefore, psychology teachers must avoid subjective prejudice, respect differences in students' personalities and educational experiences, evaluate different content, and develop different standards for students of different levels and personalities. For some students with a high dropout rate or poor performance in school, teachers may evaluate their own characteristics or qualities beyond their knowledge level. For example, we may dare to speak, express opinions, and actively participate in classroom situational work as a standard for evaluation. Teachers should create opportunities and situations for these students so that they can practice the language as much as possible and encourage them to express themselves and communicate in appropriate statements. Teachers should praise and reward their small achievements, help them build confidence, and encourage their further development. We must encourage the best-performing students to maintain their standards, and at the same time, we must strongly encourage them to encourage their continuous improvement.

4.2.3. Encourage Students to Take Class Exams. Students' development cannot be separated from their own initiative. When studying psychology, they cannot give up the initiative to establish their own mental structure of knowledge. Students can participate in the assessment so that students can more clearly identify each other's shortcomings and areas for improvement while assessing each other. The new psychology curriculum standard stipulates in the evaluation recommendations that it should focus on combining teacher evaluation and student self-evaluation with student peer evaluation. Students are required to fully evaluate their own answers to questions, own weaknesses and strengths, other students' answers to questions, find out the reasons for their success or failure in learning, as well as nonintellectual aspects, such as language ability and student proficiency. Emotional attitudes play an important role in the development of education. It is an indispensable link in the process of scientific and meaningful learning for students. Teachers encourage students to participate in the evaluation of psychology classes. This is what should be done: First, to make students interested in the assessment, various situations related to the course content should be created. When

some teachers talk about the situation when they go to a restaurant to eat based on the content of the text, the students need to reproduce the content of the text after they are familiar with the text and understand the meaning of the text. Or let students practice this role and then let the students evaluate it after the performance to reproduce a problem that reveals the differences between Chinese and Western food cultures. Motivate learners to evaluate and mobilize their enthusiasm by setting up the context. Second, teachers should take time to give students the opportunity to participate in classroom assessments. Teachers should take time to participate in classroom assessments so that students can express themselves, prove themselves, and actively participate in the classroom. Finally, teachers must allow students to learn how to evaluate. When guiding students to participate in the evaluation, teachers should help students understand the content of the evaluation, take the evaluation methods and standards as the guide, and learn how to conduct the evaluation. For example, when students perform assessments, they must learn to "listen" and "see." This is the only way to find out what other students are saying and doing and what they have achieved. Finally, considering how they should evaluate and organize the evaluation language, and how they should be evaluated, students should also humbly listen to the feedback and opinions of others. Due to differences in students' language proficiency, vocabulary, sentence expression, etc., teachers need to understand and record students' differences in these aspects in psychology teaching, so that different students can participate in the assessment and give them opportunities to appear. It should be pointed out that when instructing students to conduct assessments, teachers should encourage students to cherish and learn from each other instead of focusing on each other's shortcomings, otherwise it can easily lead to student dissatisfaction, accusations, ridicule, and advice. Students will know how to cherish others, tolerate learning, create an atmosphere of solidarity and mutual assistance, and improve and develop together.

Advanced evaluation theory should be established. Combined with the evaluation concept of psychological courses and educational and teaching purposes, people should establish a reasonable and scientific psychological classroom evaluation system, carefully define the evaluation objectives of psychological classroom, clarify the evaluation contents and standards, and select appropriate evaluation methods and tools. The purpose of classroom psychological evaluation is to determine the premise of the content, standards, and methods of the evaluation. The evaluation goal should be based on the appropriate evaluation education theory, psychological education goals, and the concepts and evaluation requirements put forward in the new curriculum. As educational evaluation theory provides a theoretical foundation and support for classroom evaluation goals, the new curriculum proposes psychological education goals in order to provide specific evaluation content and evaluation standards for classroom evaluation to select specific evaluation methods and evaluations. The concepts and requirements of guidance should be provided for assessing classroom objectives. In order to scientifically and reasonably determine the purpose of assessment of psychology teaching, these two elements must be combined.

Students should appropriately develop knowledge skills, emotional attitudes, teaching strategies, and cultural awareness through some psychological teaching. Therefore, the selection of the evaluation content and the evaluation system definition criteria of the psychological office should also be multidimensional and adaptable.

(1) Extensive language knowledge and skills

The most basic assessment content of the psychological assessment is basic language ability. In the process of working in the classroom, in addition to questions, vocabulary dictation, classwork, reading texts, and exercises to obtain simple answers, teachers can also learn how students master language psychology. Create specific problem situations, for example, divide students into groups to perform, go shopping, to the doctor, and play, so that they can participate in actual problem-solving. In the process of problem-solving, students can be tested with language. The ability of expression, such as whether oral expression is clear, whether the pronunciation and intonation are standardized, whether they understand others, whether they can express their own thoughts, and the ability to act and innovate psychologically, are all reflected in the language. People should focus on the process of solving problems rather than copying the dialogue in the book.

(2) Emotions, relationships, and values

The evaluation system should assess learners' emotions, attitudes, and values, including learners' interest in learning when to participate in various classroom activities and encourage students to develop language skills. In addition to evaluating students' language proficiency, teachers should also evaluate whether students are listening carefully in the classroom, whether they are actively speaking, whether they can create new situations and use academic performance and learning ability to judge, whether they actively participate in group activities and perform joint tasks, etc.

The processing of psychological evaluation results in the classroom is mainly carried out after teachers quickly collect students' information, especially reasonable ranking, evaluation, and analysis. Teachers use language and methods that students can understand to explain so that psychological evaluation can be conducted in the classroom and students can understand. In this way, learners can immediately and directly understand their own progress or decline and make adjustments in time to better learn. The teacher's ability to provide timely feedback affects students' performance in the classroom. For example, a teacher reported that for a student or group, the best grade is the worst, and the teacher will reward individuals or groups. When the teacher with the worst academic performance is punished, the teacher must keep his promise in time to make the students feel that the teacher is trustworthy. The trust in the teacher will help the

students become positive in the future. At the same time, teachers should analyze the students' absorption of new knowledge so that they can adapt to their own activities.

In order to improve the knowledge framework of psychology teachers' self-assessment courses, they must continue to expand their knowledge of education and teaching assessment, pay attention to recent research on assessment teaching, and finally, assess the teaching of psychology. Teachers summarize these experiences, share assessment experience with colleagues and experts in schools and other places, gradually improve the knowledge structure of classroom psychological assessment, and constantly improve their assessment skills. This means that learning needs to reflect more than these practices. All aspects of assessment knowledge should also emphasize the background of the assessment, so that if teachers use different assessment standards, assessment methods, assessment language, etc., they should clearly understand the specific teaching environment of the assessment. Steadkins and Conklin said that teacher assessment training aims not only to teach teachers knowledge and survey techniques but also to teach teachers how to use practical tools and methods, and design and develop data collection procedures. Let teachers understand the common misunderstandings in assessment, such as assessment bias and abuse of assessment methods, so that teachers can avoid these misunderstandings by using correct attitudes and methods. At the same time, teaching knowledge should be closely related to the teacher's teaching experience: learning necessary and useful skills for assessment in the classroom.

5. Conclusion

This article summarizes the full text of the research and focuses on the resource allocation of mobile edge networks and optimization of computer, communication, and storage caching strategies. It focuses on offloading computers, pricing algorithms, and various cache refresh strategies. As a starting point for research, it is optimized together with communication resource allocation and cache allocation, and memory resource refresh algorithms. Finally, this article discusses the future application of general problems in the optimization of communication, memory, and computing resources in MEC systems. Combined with the current application direction, the focus is on the architecture of the key technology system voice big data, and provide the processing flow and direction of the big data voice application program. The future direction of research lies in algorithmic methods through which the variables and features at the end of language big data can be identified and analyzed, standardized, and semantic processing technology can be further integrated. It can help better understand and discover content to discover big data at the enterprise level. At the same time, the efficiency of the processing technology of the big data function for extracting and analyzing large amounts of data is being studied. Can a processing architecture be created for distributed computing? Large amount of data can be processed in parallel, and data attributes of business systems can be retrieved quickly. In enterprises, the rules for analyzing and invoking business systems need to be improved, and the design of reporting systems for business requirements and data mining also needs to be improved so that the value of big data can be fully reflected. Classroom assessment focuses on the learning process of the learner, not the learning outcome. It not only focuses on assessing learners' knowledge and skills but also on their participation in the classroom, learners' attitudes, emotions, and values, and the significance of promoting and improving the psychological evaluation of learners' learning environment. Therefore, classroom assessment research has important practical and theoretical functions.

Data Availability

The data used to support the findings of this study are available from the corresponding author upon request.

Conflicts of Interest

The author declares that there are no conflicts of interest.

References

[1] Standards Committee, *Wireless LAN Medium Access Control (MAC) and Physical Layer (PHY) Specifications: Amendment 8: Medium Access Control (MAC) Quality of Service Enhancements*, IEEE Computer Society, Washington, DC, USA, 2005.

[2] Q. He, G. Cui, X. Zhang et al., "A game-theoretical approach for user allocation in edge computing environment," *IEEE Transactions on Parallel and Distributed Systems*, vol. 31, no. 3, pp. 515–529, 2020.

[3] W. Shi, J. Cao, Q. Zhang, Y. Li, and L. Xu, "Edge computing: vision and challenges," *IEEE Internet of Things Journal*, vol. 3, no. 5, pp. 637–646, 2016.

[4] R. Cziva, S. Jouet, D. Stapleton, F. P. Tso, and D. P. Pezaros, "SDN-based virtual machine management for cloud data centers," *IEEE Transactions on Network and Service Management*, vol. 13, no. 2, pp. 212–225, 2016.

[5] R. Xie, Y. Wen, X. Jia, and H. Xie, "Supporting seamless virtual machine migration via named data networking in cloud data center," *IEEE Transactions on Parallel and Distributed Systems*, vol. 26, no. 12, pp. 3485–3497, 2015.

[6] N. K. Sharma and G. R. M. Reddy, "Multi-objective energy efficient virtual machines allocation at the cloud data center," *IEEE Transactions on Services Computing*, vol. 12, no. 1, pp. 158–171, 2019.

[7] Al-Jarrah, Z. Al-Zoubi, and Y. Jararweh, "Integrated network and hosts energy management for cloud data centers," *Transactions on Emerging Telecommunications Technologies*, vol. 30, no. 9, pp. 1–22, 2019.

[8] Y. Shen, R. Yin, H. Zhu, X. Chen, and C. Wu, "Resource management in MEC based muti-robot cooperation systems," in *Proceedings of the International Conference on Information and Communication Technologies for Disaster Management (ICT-DM)*, pp. 30–37, Hangzhou, China, December 2021.

[9] R. Yin, Y. Shen, H. Zhu, X. Chen, and C. Wu, "Time-critical tasks implementation in MEC based multi-robot cooperation systems," 2021, http://arxiv.org/abs/2111.11038.

[10] M. Adil, M. K. Khan, M. M. Jadoon, M. Attique, H. Song, and A. Farouk, "An AI-enabled hybrid lightweight Authentication scheme for intelligent IoMT based cyber-physical systems,"

IEEE Transactions on Network Science and Engineering, vol. 5, 2022.

[11] X. Lyu, W. Ni, H. Tian et al., "Optimal schedule of mobile edge computing for internet of things using partial information," *IEEE Journal on Selected Areas in Communications*, vol. 35, no. 11, pp. 2606–2615, 2017.

[12] L. Tong, Y. Li, and W. Gao, "A hierarchical edge cloud architecture for mobile computing," in *Proceedings of the 35th Annual IEEE International Conference on Computer Communications, INFOCOM 2016*, vol. 1–9, IEEE, San Francisco, CA, USA, April, 2016.

[13] Z. Wen, J. Cala, P. Watson, and A. Romanovsky, "Cost effective, reliable and secure workflow deployment over federated clouds," *IEEE Transactions on Services Computing*, vol. 10, no. 6, pp. 929–941, 2017.

[14] Q. Wang and S. Shaltiel, "Teacher evaluation model: contract plan method," *BMC Biochemistry*, vol. 4, pp. 5–8, 2003.

[15] Q. Li, "The comparative of two teacher evaluation systems research," *Journal of Teaching and Management*, vol. 8, pp. 23–25, 2002.

[16] W. Guo and D. Zhiming, "Exploration and research of the domestic teacher evaluation system," *Theory and Practice of Education*, vol. 9, pp. 39–41, 2007.

[17] A. Farouk, J. Batle, M. Elhoseny et al., "Robust general N user authentication scheme in a centralized quantum communication network via generalized GHZ states," *Frontiers of Physics*, vol. 13, no. 2, Article ID 130306, 2018.

[18] R. Wang, R. C. Purshouse, and P. J. Fleming, "Preference-inspired coevolutionary algorithms for many-objective optimization," *IEEE Transactions on Evolutionary Computation*, vol. 17, no. 4, pp. 474–494, 2013.

Hindawi
Mobile Information Systems
Volume 2023, Article ID 9803761, 1 page
https://doi.org/10.1155/2023/9803761

Retraction

Retracted: The Implementation Measures of Environmental Accounting in Heavy Pollution Industry in the Context of Sustainable Development

Mobile Information Systems

Received 1 August 2023; Accepted 1 August 2023; Published 2 August 2023

This article has been retracted by Hindawi following an investigation undertaken by the publisher [1]. This investigation has uncovered evidence of one or more of the following indicators of systematic manipulation of the publication process:

(1) Discrepancies in scope

(2) Discrepancies in the description of the research reported

(3) Discrepancies between the availability of data and the research described

(4) Inappropriate citations

(5) Incoherent, meaningless and/or irrelevant content included in the article

(6) Peer-review manipulation

The presence of these indicators undermines our confidence in the integrity of the article's content and we cannot, therefore, vouch for its reliability. Please note that this notice is intended solely to alert readers that the content of this article is unreliable. We have not investigated whether authors were aware of or involved in the systematic manipulation of the publication process.

Wiley and Hindawi regrets that the usual quality checks did not identify these issues before publication and have since put additional measures in place to safeguard research integrity.

We wish to credit our own Research Integrity and Research Publishing teams and anonymous and named external researchers and research integrity experts for contributing to this investigation.

The corresponding author, as the representative of all authors, has been given the opportunity to register their agreement or disagreement to this retraction. We have kept a record of any response received.

References

[1] C. Cui and D. Chen, "The Implementation Measures of Environmental Accounting in Heavy Pollution Industry in the Context of Sustainable Development," *Mobile Information Systems*, vol. 2022, Article ID 3614435, 11 pages, 2022.

Hindawi
Mobile Information Systems
Volume 2022, Article ID 3614435, 11 pages
https://doi.org/10.1155/2022/3614435

Research Article

The Implementation Measures of Environmental Accounting in Heavy Pollution Industry in the Context of Sustainable Development

Chun Cui [1] **and Dong Chen** [2]

[1]*School of Accounting, Capital University of Economics and Business, Feng Tai District 100070, Beijing, China*
[2]*Beijing Guojin Huide Engineering Management Co. Ltd, Xicheng District 100050, Beijing, China*

Correspondence should be addressed to Dong Chen; stephen_chen@sina.com

Received 2 June 2022; Accepted 14 July 2022; Published 18 August 2022

Academic Editor: Shadi Aljawarneh

Since the 21st century, China's science and technology and economy have been developing rapidly, but many enterprises are pursuing their economic interests at the expense of the environment. Therefore, research on the implementation of environmental accounting is not only of academic value but also of a practical significance to the implementation of the scientific concept of development and ecological environment. In this paper, we used literature analysis, case study, and fuzzy comprehensive evaluation to analyze the implementation of environmental accounting of "A" joint-stock company as an example and concluded that the problems of environmental information implementation in China are caused by imperfection of national macropolicies and laws and regulations, lack of concrete measures, and low management level, and lack of management concept of enterprises. Therefore, under China's current policy, further improving the implementation of the internal environmental accounting of enterprises is of constructive significance to promoting ecological civilization and sustainable development.

1. Introduction

In recent decades, China's economy has been in a stage of rapid development, and the ecological deterioration caused by industrial development has also followed, such as the persistent fog angle phenomenon, serious heavy metal pollution of land, industrial waste water pollution of rivers, and soil desertification. However, as China's economy has reached a new stage, people are more and more concerned about the ecological development, and the country has begun to implement environmental policies such as sustainable economic development and ecological civilization [1]. Environmental pollution mainly comes from production-based pollution, that is, manufacturing enterprises or agricultural production process of harmful substances emitted into environment: living pollution, transportation pollution, and other sources of pollution. According to the environmental protection department statistics, production-oriented pollutants accounted for 80% [2]. This requires enterprises to pay attention to the environmental protection issues and increase the environmental protection investment. Environmental protection departments should develop more stringent environmental protection policies. At the same time, enterprises are also obliged to implement environmental accounting to public in a timely and adequate manner, which serves as a bridge between internal information and external information of enterprises [3–5]. It plays a very important role for decision makers who use information to judge potential risks and competitive advantages of company based on environmental accounting [6].

The environmental accounting in China happened in recent years, and it is in the initial stage of influence of traditional financial accounting, whether in accounting theory system or mandatory laws and regulations [7]. Environmental accounting is an important part of accounting system, and many accounting scholars have made preliminary exploration on it in these years [8]. However, at present, there is still no mandatory regulation and system for implementation of environmental accounting, and enterprises usually consider

their own favorable factors when implementing information. There are selective behaviors. Implementation of environmental accounting is still very confusing in terms of content and form, and there is a lack of unified regulations, which leads to comparability of accounting information that cannot be fully reflected [9–12]. This is not conducive to users of accounting information to make reasonable guesses and evaluations of potential risks and future development of enterprises [13]. Therefore, it is necessary and essential to discuss current situation of information implementation in heavy pollution industry and analyze problems, to further improve implementation of environmental accounting.

This paper focuses on issues related to implementation of information in heavily polluting enterprises, that is, specific contents and methods of information implementation, as well as the status of contents and methods of information implementation and areas that should be improved. This paper further elaborates the concept of environmental accounting implementation in heavy polluting industries and characteristics of environmental accounting implementation in heavy polluting industries with case study of A JSC. This paper adopts a classification method to explain problems in implementation of environmental accounting of A JSC from perspective of internal and external causes and introduces experience of implementation of environmental accounting in heavily polluted industry in developed countries, such as US and Japan.

In this paper, we used literature analysis, case study, and fuzzy comprehensive evaluation to analyze implementation of environmental accounting of a joint-stock company as an example and concluded that the problems of environmental information implementation in China are caused by imperfection of national macro policies and laws and regulations, lack of concrete measures, and low management level and lack of management concept of enterprises. Therefore, under China's current policy, further improving the implementation of internal environmental accounting of enterprises is of constructive significance to promoting ecological civilization and sustainable development.

2. Related Studies

The study of environmental accounting began in the 1970s. Represented by two articles published by F. A. Beams in 1971, "The Transformation of the Social Cost of Controlling Pollution" and "The Accounting Problems of Pollution" published by J. T. Marlin in 1973," the prelude to environmental accounting research was unveiled. Due to prominent environmental problems, accounting theories generally pay attention to research on implementation of information, and a series of related laws and regulations by government agencies of various countries were also introduced. Private organizations also began to issue self-regulatory industry norms, and laws and regulations on implementation of information gradually became perfect [14]. We concluded that to improve the information implementation system and quality of information implementation, it is necessary to increase participation of public, widely publicize environmental protection laws and regulations among public, and report on pollution of environment by enterprises. The composition of the company's executives and information implemented by the company to the public will affect its own business situation to a greater or lesser extent and even affect survival and development of company. Reference [15] shows that the annual report is an effective way to implement environmental accounting, but the implementation of environmental accounting only in the annual financial report leads to a single implementation vehicle, and the implementation of separate environmental reports is a necessary development of theory and practice. It is considered that there are a series of problems in implementation of environmental accounting in enterprises, including incomplete implementation content, single mode of implementation, and low efficiency of implementation. Reference [16] analyzed social responsibility accounting information in annual reports of listed companies in heavy pollution industry and proposed a view that social responsibility information includes information, and financial reports should contain important information, such as introduction of laws and regulations closely related to environmental protection, introduction of environmental pollution control adopted by enterprises, and countermeasures against environmental risks, and they can be further subdivided [17]. After investigation and research, we believe that companies should mainly report the following information when implementing information: resource compensation fee, resource tax, greening fee, sewage fee, and environmental related certification related to environmental performance information, which is mainly in a monetary form when implementing, and also be annotated in notes to accounting statements [18, 19]. Analyzing a sample of 111 companies in A-share listed companies in heavy pollution industry and analyzing the external factors that affect implementation of environmental accounting, we concluded that the environmental protection department's financial investment in environmental management, national, and regional economic level can have a positive effect on implementation level of information, but the degree of public awareness of environmental protection has a little effect on implementation level of information. However, the level of public awareness of environmental protection has a little effect on the level of information implementation [20].

3. Environmental Accounting Framework

The environmental accounting standards should be established under auspices of Ministry of Finance, Securities and Futures Commission, and other relevant departments. Experts and scholars should be organized, successful experience of foreign countries should be considered, universal experience should be combined with special ones, principles of operability, foresight, and development should be followed, an environmental accounting standards system should be established (see Figure 1), and an environmental accounting guide should be added.

The governmental platform of environmental accounting (Figure 2) is built, and the information system of environmental performance evaluation of heavy polluting enterprises is established. The environmental performance of enterprises is publicly released and ranked on a regular

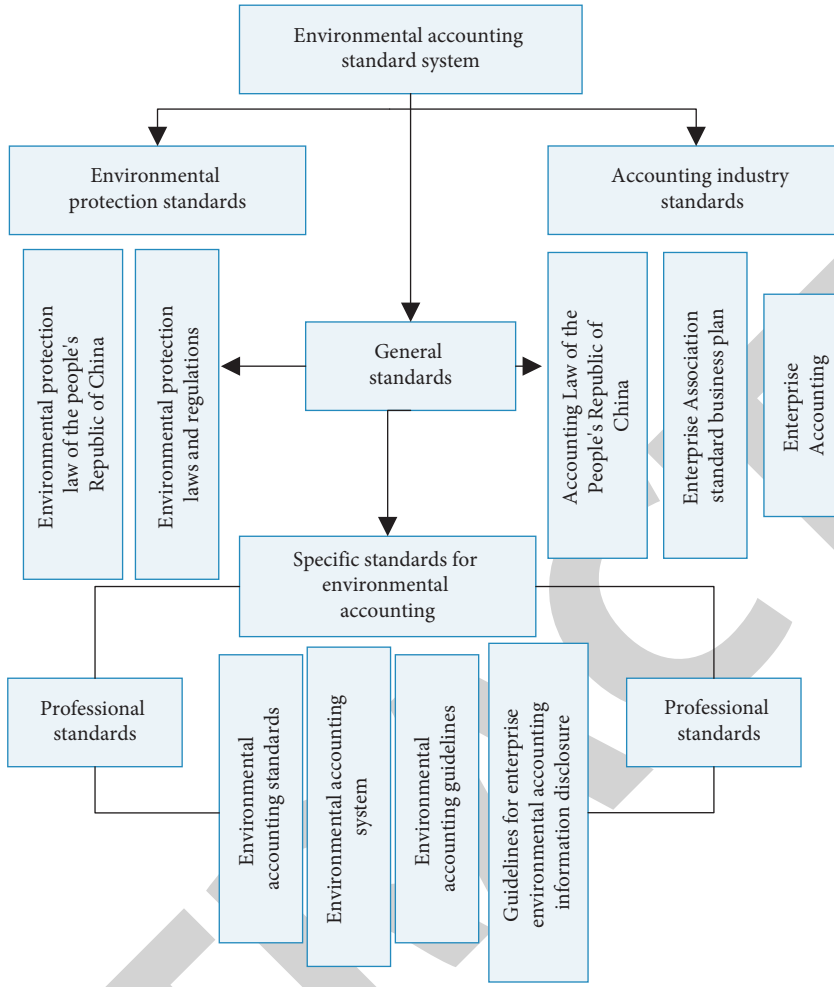

Figure 1: Construction ideas of environmental accounting standard system.

basis to accept supervision of public and various stakeholders. We will issue violation reports for all violations and accept supervision of supervisory and law enforcement departments and at same time set high fines and expose their violations through formal channels to increase cost of violations and pressure of public opinion.

"A" was incorporated in 1994 and was successfully listed on "XX" stock exchange in September 2001. It is a large paper company in "XX" province and has performed well in recent years in production of chemical products. The details are shown in Figure 3.

The main nonfinancial information currently involved in the implementation of environmental accounting in company A is environmental. The advantages of technology and implementation of policy and emission of pollutants are shown in Figure 4.

This paper is different from previous studies on implementation index of environmental accounting. In this paper, environmental accounting is divided into financial information and nonfinancial information, and different scores are assigned to government subsidies and construction in progress depending on the number of projects, and it is worth noting that, in Figure 5, the environmental protection and greening costs include environmental protection costs and environmental maintenance costs.

An overall goal of implementation of environmental accounting is to clarify future development direction of implementation of environmental accounting in China, and a specific goal is to make practical requirements for implementation of environmental accounting in enterprises. The goal of implementation of environmental accounting is to enhance the supervision of environmental protection of enterprises and promote the realization of sustainable development, which requires coordination of social, environmental, and economic benefits. If an enterprise ignores the environmental interests, this will have a serious impact on economic interests of the enterprise and the development of social community, which also depends on the environmental and economic benefits. These three benefits need to be reflected by monetary and nonmonetary information, as shown in Figure 6.

4. Fuzzy Integrated Evaluation Method

The main steps are as follows.

In the first step, the evaluation index system is established, and the weight of each index is calculated using hierarchical analysis to obtain the weight set.

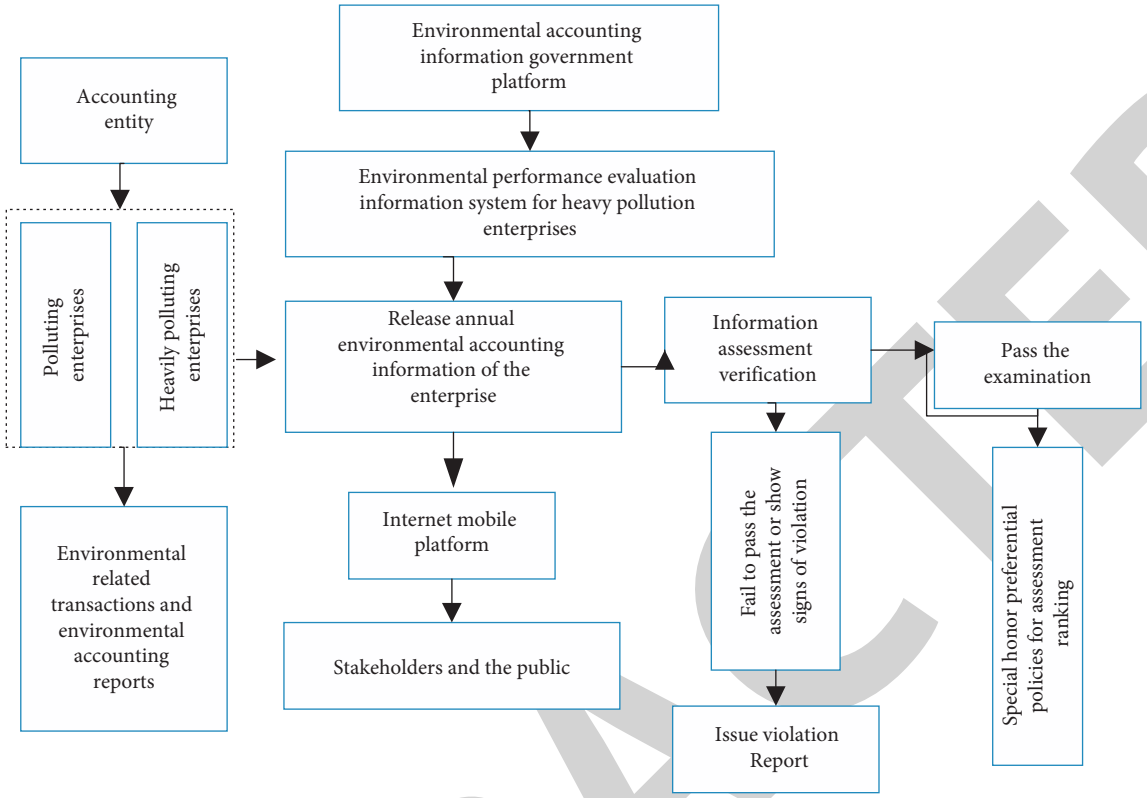

Figure 2: Government platform for environmental accounting information.

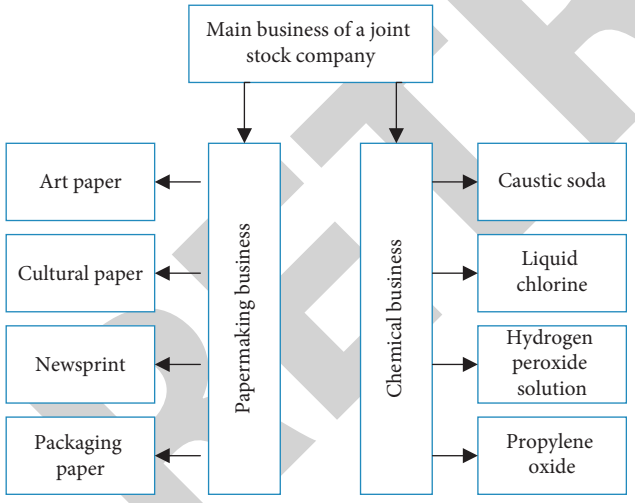

Figure 3: Production business relationship of a joint stock company.

In the second step, the evaluation set of comprehensive evaluation is established, and the evaluation level and corresponding score are clarified.

For example, if y valid questionnaires are returned, and x of them evaluate index $D1$ as "good," then the affiliation of index $D1$ corresponding to the evaluation level "good" is the degree of affiliation as follows:

$$r_{ij} = \frac{x}{y}. \tag{1}$$

Step 4: set weights through fuzzy operator "O" ω combined with membership matrix R; the evaluation result s is calculated.

$$s = \omega o R, \tag{2}$$

where "O" refers to the fuzzy operators. At present, there are four commonly used fuzzy operators.

(1) $M(\wedge, \vee)$

$$\begin{aligned} s_k &= V_{j=1}^{m}\left(\mu_j \wedge r_{jk}\right) \\ &= \max_{1\le j\le m}\left\{\min\left(\mu_j, r_k\right)\right\} \quad k = 1, \ldots, n. \end{aligned} \tag{3}$$

The evaluation result of this operator is determined by factors that play a major role in the evaluation process.

(2) $M(\cdot, \vee)$

$$\begin{aligned} s_k &= V_{j=1}^{m}\left(\mu_j, r_{jk}\right) \\ &= \max_{1\le j\le m}\left\{\left(\mu_j, r_{jk}\right)\right\},\ k = 1, \ldots, n. \end{aligned} \tag{4}$$

And $M(\wedge, \vee)$. There are certain similarities, but the calculation process is more comprehensive, and the results are more accurate. It not only highlights the

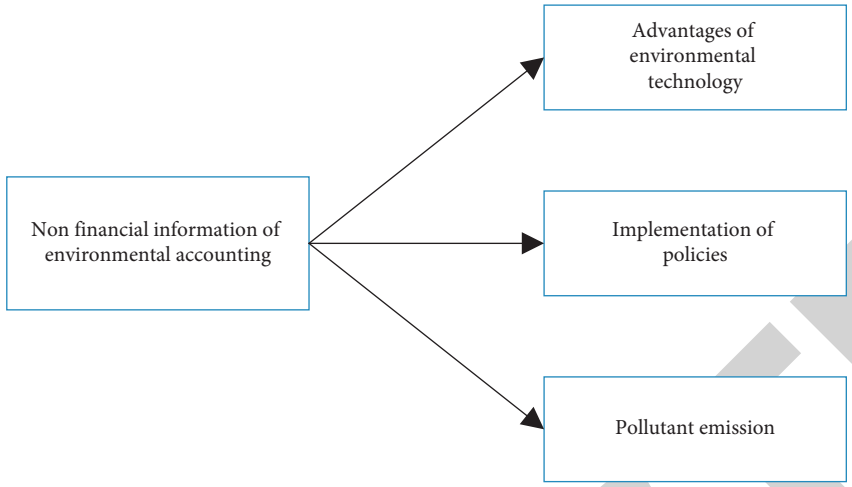

Figure 4: Current situation of environmental accounting nonfinancial information disclosure of a joint stock company.

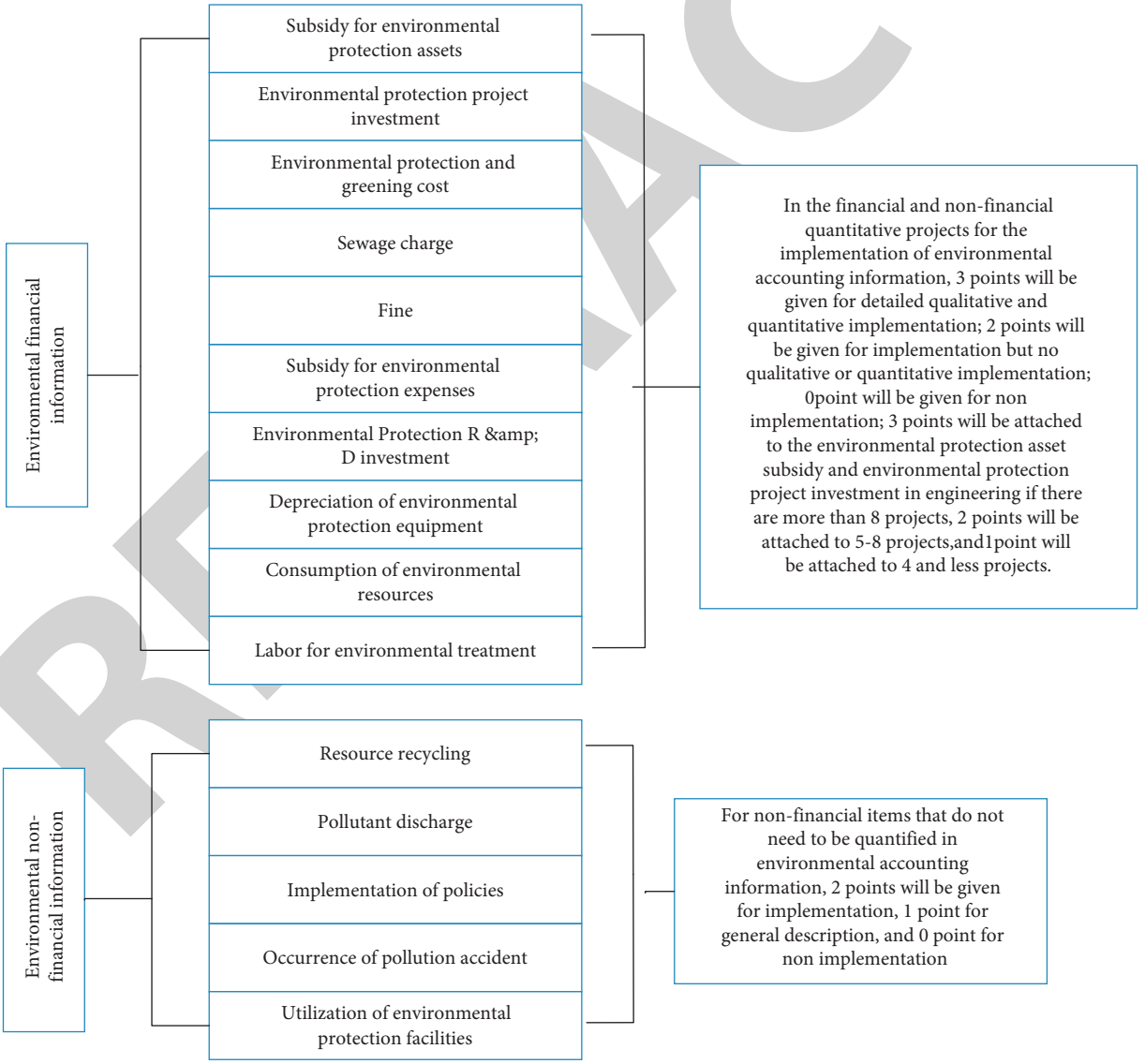

Figure 5: Scoring standards for environmental accounting information disclosure.

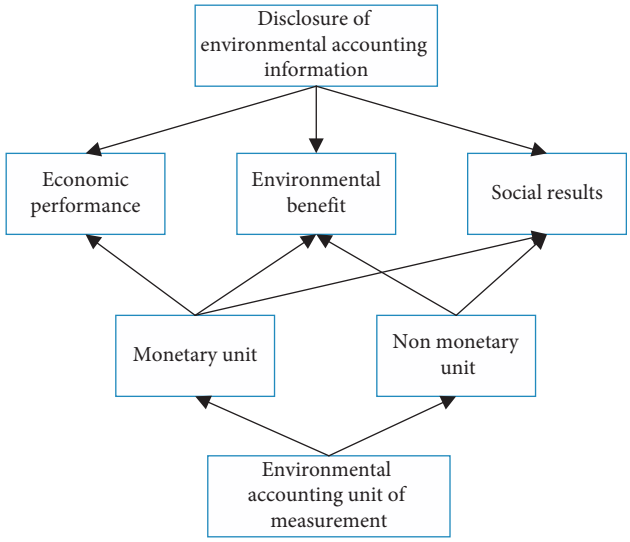

FIGURE 6: Relationship between environmental accounting information disclosure.

main factors but also considers the impact of other factors. This operator is applicable to $M(\wedge, \vee)$ situations that cannot be identified and require more accurate and comprehensive results.

(3) $M(\cdot, +)$

$$s_k = \min\left\{1, \sum_{j=1}^{m} \mu_j r_{jk}\right\}, \quad k = 1, \ldots, n. \tag{5}$$

The operator considers all the indicators and their weights comprehensively and can well meet the calculation needs of the maximum sum.

(4) $M(\cdot, \oplus)$

$$s_k = \min\left\{1, \sum_{j=1}^{m} \min\left(\mu_j, r_{jk}\right)\right\}, \quad k = 1, \ldots, n. \tag{6}$$

This operator has strict restrictions on the value of each factor. It can take neither a large nor small value. Otherwise, it is easy to make some factor evaluation information missing.

To improve calculation accuracy, evaluation results are calculated with four decimal places.

① Calculation of the evaluation results of the financial status ($C1$): membership of DL, $D2$, and $D3$:

$$R_{D1-3} = \begin{bmatrix} 0.0000 & 0.0000 & 0.3750 & 0.6250 & 0.0000 \\ 0.0000 & 0.5000 & 0.5000 & 0.0000 & 0.0000 \\ 0.0000 & 0.0000 & 0.6250 & 0.3750 & 0.0000 \end{bmatrix}. \tag{7}$$

DL, $D2$, and $D3$ index weights $\omega_{D1-3} = [0.1226, 0.3202 0.5571]^T$ perform a fuzzy operation according to a selected operator.

The fuzzy operation based on the selected operator is as follows:

$$R_{D1-3} \cdot \omega_{D1-3} = \begin{bmatrix} 0.0000 & 0.0000 & 0.0460 & 0.0766 & 0.0000 \\ 0.0000 & 0.1601 & 0.1601 & 0.0000 & 0.0000 \\ 0.0000 & 0.0000 & 0.3482 & 0.2089 & 0.0000 \end{bmatrix},$$
$$R_{D1-3}\omega_{D1-3} = [0.0000 \quad 0.1601 \quad 0.5543 \quad 0.2855 \quad 0.0000]. \tag{8}$$

According to the principle of maximum membership, the evaluation result of financial condition ($C1$) is general.

② Calculation of the evaluation results of the business results ($C2$): membership of $D4$, $D5$, $D6$, and $D7$:

$$R_{D4-7} = \begin{bmatrix} 0.0000 & 0.6250 & 0.3750 & 0.0000 & 0.0000 \\ 0.0000 & 0.2500 & 0.7500 & 0.0000 & 0.0000 \\ 0.0000 & 0.5000 & 0.5000 & 0.0000 & 0.0000 \\ 0.0000 & 0.0000 & 0.0000 & 0.2500 & 0.7500 \end{bmatrix}. \tag{9}$$

$D4$, $D5$, $D6$, and $D7$ indicator weights $\omega_{D4-7} = [0.0998, 0.3451, 0.3701, 0.1850]^T$ perform a fuzzy operation according to a selected operator:

$$R_{D4-7} \cdot \omega_{D4-7} = \begin{bmatrix} 0.0000 & 0.0624 & 0.0374 & 0.0000 & 0.0000 \\ 0.0000 & 0.0863 & 0.2588 & 0.0000 & 0.0000 \\ 0.0000 & 0.1851 & 0.1851 & 0.0000 & 0.0000 \\ 0.0000 & 0.0000 & 0.0000 & 0.0463 & 0.1388 \end{bmatrix},$$
$$R_{D4-7} \circ \omega_{D4-7} = [0.0000 \quad 0.3338 \quad 0.4813 \quad 0.0463 \quad 0.1388]^{\mathrm{T}}. \tag{10}$$

According to the principle of maximum subordination, the evaluation result of business results ($C2$) is general.

③ The evaluation result of the environmental protection attitude ($C3$): subordination degree of $d8$, $D9$, and $D10$:

$$R_{D8-10} = \begin{bmatrix} 0.0000 & 0.2500 & 0.7500 & 0.0000 & 0.0000 \\ 0.0000 & 0.1250 & 0.8750 & 0.0000 & 0.0000 \\ 0.0000 & 0.3750 & 0.6250 & 0.0000 & 0.0000 \end{bmatrix}. \tag{11}$$

$D8$, $D9$, and $D10$ indicator weight $\omega_{D8-10} = [0.1199, 0.2721 0.6080]^T$

The fuzzy operation based on the selected operator is as follows:

$$R_{D8-10} \cdot \omega_{D8-10} = \begin{bmatrix} 0.0000 & 0.0300 & 0.0899 & 0.0000 & 0.0000 \\ 0.0000 & 0.0340 & 0.2381 & 0.0000 & 0.0000 \\ 0.0000 & 0.2280 & 0.3800 & 0.0000 & 0.0000 \end{bmatrix},$$
$$R_{D8-10} \circ \omega_{D8-10} = [0.0000 \quad 0.2920 \quad 0.7080 \quad 0.0000 \quad 0.0000]. \tag{12}$$

The assessment result of the environmental protection attitude ($C3$) is general.

④ Calculation of the evaluation results of the environmental performance ($C4$): membership of DLL, $D12$, $D13$, $D4$, $D15$, and $DL6$:

$$R_{D11-16} = \begin{bmatrix} 0.2500 & 0.6250 & 0.1250 & 0.0000 & 0.0000 \\ 0.0000 & 0.0000 & 0.7500 & 0.2500 & 0.0000 \\ 0.0000 & 0.0000 & 0.1250 & 0.8750 & 0.0000 \\ 0.0000 & 0.0000 & 0.2500 & 0.7500 & 0.0000 \\ 0.0000 & 0.6250 & 0.3750 & 0.0000 & 0.0000 \\ 0.0000 & 0.5000 & 0.5000 & 0.0000 & 0.0000 \end{bmatrix}. \quad (13)$$

The weights of DLI, DL3, $D13$, $D14$, $D15$, and $D16$ indicators are as follows:

$$\omega_{D11-16} = [\,0.2426,\ 0.1726,\ 0.2426,\ 0.2426, 0.0591, 0.0405\,]^T. \quad (14)$$

The fuzzy operation based on the selected operator is as follows:

$$R_{D11-16} \cdot \omega_{D11-16} = \begin{bmatrix} 0.0607 & 0.1516 & 0.0303 & 0.0000 & 0.0000 \\ 0.0000 & 0.0000 & 0.1295 & 0.0432 & 0.0000 \\ 0.0000 & 0.0000 & 0.0303 & 0.2123 & 0.0000 \\ 0.0000 & 0.0000 & 0.0607 & 0.1820 & 0.0000 \\ 0.0000 & 0.0369 & 0.0222 & 0.0000 & 0.0000 \\ 0.0000 & 0.0203 & 0.0203 & 0.0000 & 0.0000 \end{bmatrix},$$
$$R_{D11-16} \circ \omega_{D11-16} = [\,0.0607\ 0.2088\ 0.2932\ 0.4374\ 0.0000\,]. \quad (15)$$

The evaluation result of the environmental performance ($C4$) is poor.

⑤ The membership degree of $D17$, $D18$, and $D19$ is calculated based on the evaluation result of information disclosure reliability ($C5$):

$$R_{D17-19} = \begin{bmatrix} 0.0000 & 0.0000 & 0.6250 & 0.3750 & 0.0000 \\ 0.0000 & 0.0000 & 0.5000 & 0.5000 & 0.0000 \\ 0.0000 & 0.2500 & 0.6250 & 0.1250 & 0.0000 \end{bmatrix}. \quad (16)$$

The weights of $D17$, $D18$, and $D19$ indicators are as follows:

$$\omega_{D17-19} = [0.6480, 0.1222, 0.2299]^T. \quad (17)$$

The fuzzy operation based on the selected operator is as follows:

$$R_{D17-19} \cdot \omega_{D17-19} = \begin{bmatrix} 0.0000 & 0.0000 & 0.4050 & 0.2543 & 0.0000 \\ 0.0000 & 0.0000 & 0.0611 & 0.0611 & 0.0000 \\ 0.0000 & 0.0574 & 0.1437 & 0.0287 & 0.0000 \end{bmatrix},$$
$$R_{D17-19} \circ \omega_{D17-19} = [\,0.0000\ \ 0.0574\ \ 0.6098\ \ 0.3441\ \ 0.0000\,]. \quad (18)$$

The evaluation result of information disclosure reliability ($C5$) is general.

⑥ Evaluation result calculation of information disclosure timeliness ($C6$): membership degree of $D20$ and $D21$:

$$R_{D20-21} = \begin{bmatrix} 0.0000 & 0.0000 & 0.0000 & 0.1250 & 0.8750 \\ 0.0000 & 0.6250 & 0.3750 & 0.0000 & 0.0000 \end{bmatrix}. \quad (19)$$

$D20$ and $D21$ indicator weight $\omega_{D20-21} = [0.3333, 0.6667]^T$.

Perform the fuzzy operation according to the selected operator:

$$R_{D20-21} \cdot \omega_{D20-21} = \begin{bmatrix} 0.0000 & 0.0000 & 0.0000 & 0.0208 & 0.1459 \\ 0.0000 & 0.4167 & 0.2500 & 0.0000 & 0.0000 \end{bmatrix},$$
$$R_{D20-21} \circ \omega_{D20-21} = [\,0.0000\ 0.4167\ 0.2500\ 0.0417\ 0.2916\,]. \quad (20)$$

Evaluation result of information disclosure timeliness ($C6$) is good.

5. Results

Take 2014–2018 as an example to see the basic situation of the main operating business of A JSC, as shown in Table 1. The trend of gross margin is shown in Figure 7.

As shown in Table 1, from 2014 to 2018, A AG's revenue is mainly based on sales of paper products, supplemented by sales of chemical products. Although the sales revenue of A AG's paper products is higher than that of chemical products, its production cost is also higher than that of chemical products. From the gross margin trend graph, we can conclude that the profit from the sales of chemical products of A JSC is better than the profit from the sales of paper products during 2014–2018. The paper industry is a heavily polluting industry, and chemical industry is resource-intensive and polluting to environment. Since the main industries of A are polluting to the environment and have a high demand for resources, implementation of environmental accounting should be more detailed and standardized than that of other companies. The environmental costs and potential benefits from environmental inputs and specific emissions should be reflected in annual report.

In Table 2, it can be seen that A JSC has been paying environmental protection fees and environmental maintenance fees for five years from 2014 to 2018, and since only data on these fees are mentioned in annual report, we conducted a field research on why these two fees were paid but did not receive a valid answer. We were informed that the resource tax was only listed in 2018 annual report, and that in previous years, resource tax was included in water fee, and water and salt are the main raw materials for the chemical production of A JSC. Meanwhile, we were informed that A JSC was in the transitional stage of fee to tax conversion in 2018, and fee to tax conversion would be completed in 2019; from then on, no more emission fees would be paid, and the environmental protection tax would be paid directly according to emission standard.

Table 3 shows that government subsidizes more environmental protection projects, which reflects importance of green production and high pollution level of production activities of "A." The field research and staff of finance

Table 1: Main business by industry (unit: 10000 yuan).

Category	Theme/year	2014	2015	2016	2017	2018
Business income	Paper products	7337547.87	702547.14	803571.41	1024851.23	1125728.39
	Chemical products	102587.58	136147.58	160748.74	212584.01	260024.23
Operating costs	Paper products	653571.2	524781.8	7028731.98	874124.23	9584476.35
	Chemical products	809578.56	1047005.14	139287.88	163574.87	2856471.35
Gross profit margin	Paper products	10.97%	11.25%	12.87%	15.56%	13.28%
	Chemical products	21.25%	23.02%	18.36%	25.34%	19.25%

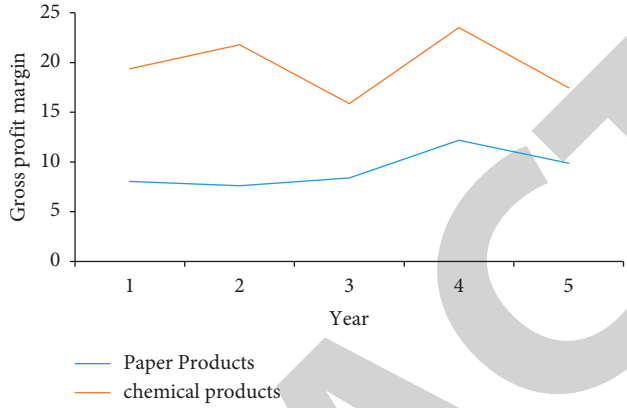

Figure 7: Trend of gross margin.

Table 2: A joint stock company's 2014–2018 expense income environmental accounting (unit: yuan).

Date	2018	2017	2016	2015	2014
Environmental protection fee	150547824.18	23547528.58	18324742.25	13258712.008	1874253254.41
Subsidy for environmental treatment	125942000	8524000	257420		
Sewage charge	3542145.15	174585435.12	12547562.74	8541225.62	9871248.12
Environmental maintenance fee	125483258.85	165147526.71	165871288.45	132557856.09	18475245.48
Resource tax	23365871.24				
Environmental protection tax	8258712.85				

Table 3: A" amortization items of government subsidies related to assets of joint stock company from 2014 to 2018 (unit: yuan).

Date	2018	2017	2016	2015	2014
Pollution control project	2351000.21	2350000	2350000	2395701	2350000
Ultra-low emission project	65827.12				
Special funds for recycling transformation	30000				
Advanced sewage treatment project	341254.5	4125873.6	4125684.5	4156552.8	4166687.2
Advanced wastewater treatment phase IV project	262030.25	402543.58	4032146.57	4932483.6	491666.65
Advanced wastewater treatment phase IV project	10165473.2	—	—	—	—
Dust control works	1000000	—	—	—	—
White water treatment technology transformation project	552000	552000	552000	552000	552000
Provincial environmental protection special treatment project	180000	180000	180000	180000	180000
Special water subsidy fund (phase II)	2708741.9	4166447.5	412655.85	222222.222	

department of "A" company were informed that key environmental management projects and environmental monitoring projects required by national and provincial authorities are usually subsidized with special funds for specified project expenses, which are based on financial expenditures, relevant construction contracts, and acceptance materials. After asking the staff of ultra-low emission project team, we learned that ultra-low emission project is based on original desulfurization, denitrification, and dust removal by adding equipment and transforming process to further treat sulfur dioxide, ammonia oxides, and soot in flue gas, so that index is reduced. The fourth phase of company's deep water treatment project was put into operation, which adopts world standard deep treatment process, and COD of drainage water was reduced to below 40 mg/l, and the color was less than 20 times, which became an advanced water treatment model project. However, after field research, it is found that this project will still produce waste gas,

Table 4: A list of projects under construction of joint stock company from 2014 to 2018 (unit: yuan).

Date	2018	2017	2016	2015	2014
Waste resource utilization (power plant)	54584726.51	—	—	—	—
Sewage upgrading and reconstruction	15478215.23	—	—	—	—
Soft drink bag recycling project	165871258.52	—	—	—	—
Thermoelectric energy saving transformation project	3325468.20	—	—	—	—
Ultra-low emission environmental protection project	4214582.21	5775249.45	199745843.73	—	—
Sewage treatment project	—	—	—	1685472.48	73248215.54
Boiler ultra-low emission project	—	27842624.15	11745260.9	—	—

Table 5: An environmental accounting information disclosure method of joint stock company.

Disclosure content	Annual report	Social responsibility report	Internal control report
Environmental asset information	Partial data information and text information of construction in progress	Undisclosed	Undisclosed
Environmental liability information	Undisclosed	Undisclosed	Undisclosed
Environmental cost information	Some data information	Undisclosed	Undisclosed
Environmental benefit information	Some data information (government subsidies)	Undisclosed	Undisclosed
Environmental R & D information	Text information	Undisclosed	Undisclosed
Environmental policy information	Text information	Text information	Undisclosed
Pollutant discharge	Quantitative information	Undisclosed	Undisclosed
Energy consumption	Text information	Text information	Undisclosed

wastewater, solid waste, and noise in the treatment of wastewater, so reasonable and effective measures should be taken during operation of project to ensure that pollutants meet discharge standards, such as chemical scrubbing + - photocatalytic oxidation equipment for treatment of waste gas, nitrobenzene, and aniline. For boiler flue gas denitrification transformation project, mainly to deal with exhaust gas, so as not to cause air pollution, the project in 2018 just amortized to nonoperating income. The wastewater treatment project and alkali recovery renovation project have not yet been put into operation. The dust control project was completed in 2017 and was fully amortized in 2017 and included in the nonoperating income. The white-water treatment project is to treat white water of papermaking, improve reuse rate of white water, reduce discharge of white water, and treat polluting substances contained in white water. The special subsidies for water are aimed at improving and reusing wastewater standards, increasing water availability, saving resources, and helping environmental protection.

Table 4 shows that there are several environmental projects under construction, and four new environmental projects are under construction in 2018, which shows that A JSC is making progress in environmental protection and constantly upgrading environmental projects. Among them, wastewater treatment project was completed and transferred to fixed assets in 2015. The boiler emission super low project was completed and transferred to fixed assets in 2017.

Table 5 shows that the implementation of environmental accounting of A JSC is not centralized. Although it has implemented some of the environmental accounting in its annual report, its data is included in the balance sheet, income statement, and cash flow statement of financial statements but not implemented directly. The information on construction in progress, government grants, and so on is obtained in notes to financial statements and is scattered, while social responsibility report of A JSC only briefly mentions environmental policy and energy consumption. However, the production of A JSC is both polluting and resource-intensive and should be implemented in social responsibility report. The implementation of environmental accounting in internal control report may be appropriate according to the company's actual situation and management's wishes [21, 22].

As can be seen from Table 6, in 2018, there are eight extra government grants amortized in the current period, and an additional three points are assigned. The government grants for assets are not only quantitative but also have detailed descriptions in notes for each of government grants related to environment, so three points should be assigned for government grants, and additional points should be assigned for a total of six points.

The Environmental are described in detail in statements. However, it is generally believed that the more the EDI is close to 1, the higher the quality of implementation of environmental accounting. Therefore, A AG still needs to further strengthen the implementation of environmental

Table 6: Current amortization amount of government subsidies (unit: yuan).

Project	Amount of money
Pollution control project	23500214.54
Ultra-low emission project	602547.25
Special funds for recycling transformation	30000
Advanced sewage treatment project	32451.07
Advanced wastewater treatment phase IV project	2620343.1
Used for boiler flue gas denitration transformation project	102543.35
60000 Nm^3/d biogas recovery resources comprehensive utilization project	492587.62
White water treatment technology transformation project	55254.04
Provincial environmental protection special treatment project	180000.0
Special water subsidy fund (phase II)	2785214.02

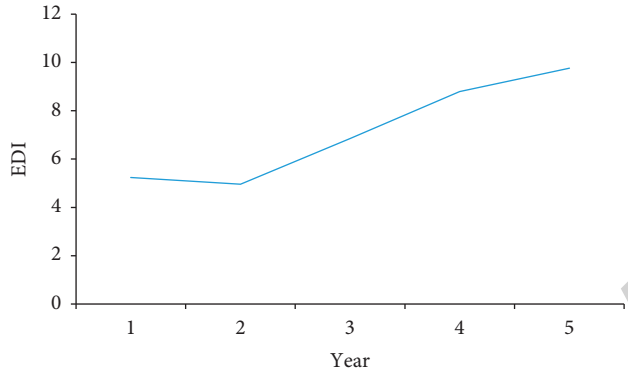

Figure 8: A line chart of share environmental accounting information index.

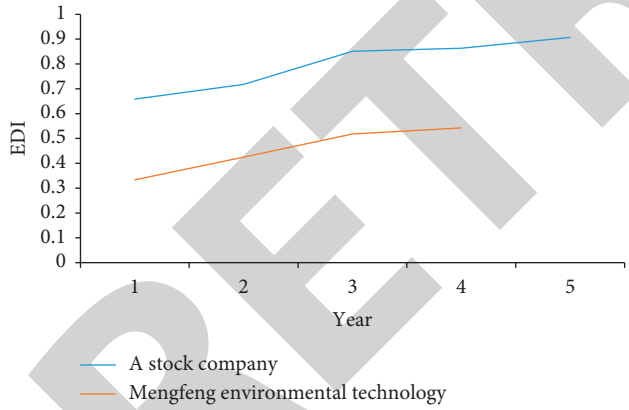

Figure 9: A line chart of comparison between "A" joint stock company and Meng Feng environmental technology.

accounting as shown in Figure 8. Accounting Information Implementation Index (EDI) is an assessment of the quality of implementation of environmental accounting. The line graph shows that EDI of A JSC is increasing from 2014 to 2018, which indicates that the quality of implementation of environmental accounting is gradually improving as more and more items

Meng Feng Environmental Technology is an environmentally friendly company, which is mainly engaged in environmental management, so it implements environmental accounting in more detail to highlight nature of its business. The comparison line graph in Figure 9 shows that the quality of environmental accounting implementation of Meng Feng Environmental Technology is better than that of "A." The implementation of information of "A" should be improved step by step, first to extent of Meng Feng's information implementation and then to further improve. In recent years, environmental accounting index of both companies has been on the rise, which should be related to the implementation of the strictest new Environmental Protection Law in history on January 1, 2015, and the subsequent introduction and release of programmatic documents such as "Water Ten" and "Notice on Construction Program of Ecological and Environmental Monitoring Network." The new law and regulations are closely related to the state's attention to environment, which has caused a high degree of concern among enterprises.

6. Conclusions

In this paper, we used A JSC as a case study of a heavily polluting company and found that its implementation level of environmental accounting from 2014 to 2018 is on an increasing trend, and the implementation level has improved significantly in recent years. However, there are still problems such as incomplete implementation, low value of implementation contents, and irregular implementation forms, which conceal some negative information. At present, the state is not strong enough to supervise the implementation of environmental information of enterprises, and relevant laws and regulations should be formulated to regulate it. To improve the level of implementation of environmental accounting, joint efforts of the "A" joint-stock company, third-party monitoring agencies, social groups, and government are needed.

Data Availability

The experimental data used to support the findings of this study are available from the corresponding author upon request.

Conflicts of Interest

The authors declare that they have no conflicts of interest regarding this work.

Hindawi
Mobile Information Systems
Volume 2022, Article ID 4139784, 9 pages
https://doi.org/10.1155/2022/4139784

Research Article

Sensor Vegetable Greenhouse and Agricultural Product Supply Chain Management Based on Improved Neural Network

Dandan Dou

Department of Management, Henan University of Technology, Zhengzhou, Henan 450001, China

Correspondence should be addressed to Dandan Dou; doudandan1956@stu.haut.edu.cn

Received 12 June 2022; Revised 10 July 2022; Accepted 18 July 2022; Published 18 August 2022

Academic Editor: Shadi Aljawarneh

In recent years, people have begun to collect environmental data in vegetable greenhouses. Therefore, this article studies the current internal control technology of vegetable greenhouses, and improves the sensor application in vegetable greenhouses, in a targeted manner by combining with the improved neural network algorithm. The model has more accurate prediction accuracy than traditional BP. By using the Android client and ZigBee artificial intelligence control technology it creates the most suitable living conditions for the vegetables, fruits, and other crops in the vegetable greenhouse by controlling the various valves, sun visors, and light supplementary switches inside the vegetable greenhouse. The simulation results show that the model proposed in this article has higher convergence accuracy. In addition, this article applies the improved neural network to the management of the agricultural product supply chain, starting from the agricultural product supply chain and agricultural product supply chain management. Based on this, the analytic hierarchy process is used to explore the influencing factors of agricultural product supply chain management, and the analysis shows that consumers are targeting different consumer demand raised by the agricultural product supply chain. The improved neural network provides new ideas for the research of sensor vegetable greenhouses and agricultural product supply chain management.

1. Introduction

With the continuous introduction of various high-tech science and technology into the vegetable greenhouses in today's society, the intelligent operation and management of vegetable greenhouses has been certified in many aspects [1]. Since the vegetable greenhouse is a closed environment constructed manually, it also makes it more convenient for managers to carry out arbitrary network construction and node maintenance and protection. Therefore, the actual application of the Internet to vegetable greenhouses makes them intelligent, which can improve agricultural production more efficiently, benefit farmers, and bring them more income [2]. With economic development, there are more and more vegetable greenhouses, and the area of the unit greenhouses is also getting larger. If we continue to use manual to manage the environmental changes in the greenhouses and still use cable wiring, there is no way to meet the needs of technicians for vegetable greenhouses, and high-speed and efficient work [3]. With the continuous development and application of remote intelligent system control technology and sensor networks, it provides practical technical support for intelligently managed vegetable greenhouses [4]. However, the existing sensor vegetable greenhouses still have some problems in the actual construction process, so this article will use the improved neural network to provide new ideas for the research of sensors in greenhouse vegetables [5]. The staff in charge of vegetable greenhouses can use the improved neural network sensor nodes to collect data, intuitively understand the environmental factors that contribute to the growth of crops in the greenhouse, and can also perform remote operations to artificially change the environment in the vegetable greenhouse [6].

Agricultural products are an indispensable thing in people's daily lives and occupy a high position in people's lives; this also makes people have more stringent requirements for the quality, type, and nutritional content of agricultural products, especially for the quality and safety of agricultural products [7]. However, due to the current small

production situation of agricultural products, it has brought huge difficulties to the production, processing, and sales of agricultural products in the face of huge market demand [8]. Supply chain management utilizes the coordination of supply, production, sales, and other links, which can bring high-speed, effective, and cost-reducing capabilities to enterprises [9]. Nowadays, Chinese enterprises are still in the period of exploration in the aspect of supply chain management [10]. How to use supply chain management to solve the problems that arise in each link of the agricultural product supply chain is particularly important for dealing with the problems of agriculture, rural areas, and farmers [11]. This article applies the improved neural network to the management of agricultural product supply chain and provides a reference for the management of China's agricultural product supply chain [12].

2. Related Work

A common neural network algorithm, back-propagation neural network algorithm, and heuristic algorithm optimization ideas for analysis were proposed. The seagull optimization algorithm is used to optimize the BP neural network model, and the performance of the proposed model is verified for specific water quality parameter prediction scenarios. Aiming at the shortcomings of the seagull optimization algorithm as an optimization aspect and then using the benchmark function, the performance test of the optimized algorithm is launched [13]. Using the new algorithm to optimize the neural network, we can get the model of the improved seagull optimization algorithm and the improved BP neural network system. After research and analysis, it can be seen that the optimized algorithm has greatly improved the prediction accuracy and can be better applied to actual problem-solving [14, 15]. The ACARS system cannot complete the relevant system model due to the data collected by it, but the data collected by the fast access recorder can make up for its shortcomings. Therefore, the model is built on the basis of intelligent algorithms [16]. During the process, this article can use the ACARS system and fast access recorder data to construct a sample. Due to the complexity of the engine system, a variety of diagnostic methods are needed to solve the engine system failure. For diagnostic decision-making, after summarizing the currently known methods, the final decision output is determined. Its advantage is that it can consider the problem more comprehensively than when only one method is used to diagnose the decision. The literature describes in detail an algorithm that can perform weighted fusion estimation of self-adapting environment. The core of this algorithm is based on the relevant characteristic attributes of the engine's own parameters, and by fusing the relevant characteristic attributes of existing parameters [17, 18]. After summarizing the currently known diagnostic knowledge methods, finally we determine what kind of decision-making fusion strategy method can be used and propose the multi-attribute characteristics of related diagnostic knowledge to integrate decision-making. Based on this method, the extension of decision knowledge is realized. People can build the engine fault diagnosis model that people need by using the strategy of intelligent systems so that they can break through some of the bottlenecks encountered in the traditional mathematical model and solve the problem [19]. An optimized artificial neural network system, which uses the ant colony algorithm to improve the initial weight vector of the algorithm, avoids a series of problems caused by people's subjective random selection of weights, and then uses its unique related characteristics to replace the related problems of BP algorithm gradient. By controlling the complexity of the training algorithm, it can improve the related convergence speed [20].

3. Sensor Vegetable Greenhouse Based on Improved Neural Network

3.1. Improve the Neural Network. Neural network algorithms have also been widely used in various specific scenarios. They establish a hierarchical model, and then continuously adjust the connection weights between each level according to the existing samples during the training process so that the final results are closer to reality. This article summarizes the characteristics of several common data fusion algorithms and their scope of application as shown in Table 1.

It can be seen from Table 1 that the neural network algorithm can not only be applied to low-level data fusion but also can be used for data fusion at a higher level. Although its structure is more complicated than general algorithms and has a higher computational load, it is used in practical applications. In general, it can usually exert better performance than general algorithms. There are many types of neural networks. Among them, the BP neural network, or back-propagation neural network, is the most widely used. It has a simple structure and can learn, organize, and adapt independently. It includes an input layer, a hidden layer, and an output layer. The hidden layer can include multiple layers, and it is widely used in prediction and other fields. The BP neural network belongs to a multi-layer feedforward network, which mainly includes forward-propagating signals and back-propagation errors. In the learning process, samples are passed through the input layer to the hidden layer, and the neurons in the hidden layer; the arithmetic processing is then passed to the output layer, and the actual data passed from the output layer are compared with the predicted data to obtain the error, and the error is propagated back. In the error propagation process, it is based on the gradient descent strategy to continuously adjust the connection weights between neurons in each layer until the final predicted value is the smallest compared to the actual value. The deviation of the hth neuron in the hidden layer is θ_{h}. Then its input formula is

$$A_h = \sum_{i=1}^{d} V_{ih} X_i. \tag{1}$$

The hidden layer transfer function is generally sigmoid function, namely:

Table 1: Comparison of data fusion algorithms.

Fusion method	Uncertainty	Fusion technology	Scope of application
Weighted average method	—	Weighted average	Convergence of low-level data
Bayesian estimation	Gaussian noise	Bayesian estimation	Convergence of high-level data
D-S evidence theory	—	Logical reasoning	Convergence of high-level data
Fuzzy logic reasoning	Membership	Logical reasoning	Convergence of high-level data
Neural networks	Learning error	Neural networks	Convergence of low-/high-level data

$$f(x) = \frac{1}{1+e^{-x}}. \tag{2}$$

The output formula of the hth neuron in the hidden layer is

$$B_h = f(A_h - \theta_h). \tag{3}$$

The input formula of the hth neuron in the hidden layer and the jth neuron in the output layer is

$$C_j = \sum_{h=1}^{g} W_{hj} B_h. \tag{4}$$

In this article, the transfer function of the output layer also selects the sigmoid function, and the output formula of the jth neuron in the output layer can be obtained as

$$Y_j = f\left(C_j - \theta_j\right). \tag{5}$$

If the actual value of the jth neuron in the output layer is set to R_j, then the error of the jth neuron is E_j, namely:

$$E_j = \frac{1}{2}\left(R_j - Y_j\right). \tag{6}$$

The total error of network output is

$$E = \frac{1}{2} \pm \sum_{j=1}^{l} \left(R_j - Y_j\right)^2. \tag{7}$$

The BP neural network needs to use the gradient descent method to obtain the optimal output and expand the error to the hidden layer. The formula is

$$E = \frac{1}{2} \sum_{j=1}^{l} \left(R_j - f\left(C_j - \theta_j\right)\right)^2. \tag{8}$$

The formula for the change in connection weights of the hth neuron in the hidden layer and the jth neuron in the output layer is

$$\Delta W_{hj} = -\eta \frac{\partial E}{\partial W_{hj}}. \tag{9}$$

According to the aforementioned formula, the formula is

$$\frac{\partial C_j}{\partial W_{hj}} = B_h. \tag{10}$$

According to the nature of the S function,

$$f'(x) = f(x).(1 - f(x)). \tag{11}$$

Then there is

$$g_j = \frac{\partial E}{\partial Y_j}.\frac{\partial Y_j}{\partial C_j} = -\left(Y_j - R_j\right).Y_j.\left(1 - Y_j\right). \tag{12}$$

Then the weight change amount is

$$\Delta W_{hj} = \eta g_j B_h. \tag{13}$$

The weight adjustment formula is

$$W_{hj}(n+1) = W_{hj}(n) + W_{hj}. \tag{14}$$

At the same time, the amount of change in the threshold can be expressed by a formula:

$$\Delta\theta_j = -\eta \frac{\partial E}{\partial \theta_j} = -\eta g_j. \tag{15}$$

The threshold adjustment formula is

$$\theta_j(n+1) = \theta_j(n) + \Delta\theta_j. \tag{16}$$

The weight adjustment formula is

$$V_{ih}(n+1) = V_{ih}(n) + \Delta V_{ih}. \tag{17}$$

The threshold change is

$$\Delta\theta_h = -\eta e_h. \tag{18}$$

The threshold is adjusted to

$$\theta_h(n+1) = \theta_h(n) + \Delta\theta_h. \tag{19}$$

Regarding many existing problems of neural networks, many researchers have proposed optimization methods. Among them, artificial intelligence-based heuristic algorithms are combined with them to improve the effect of neural network algorithms. This article mainly introduces the three most typical algorithms among which are the improved methods based on PSO, GA, and ACO.

PSO is a natural heuristic algorithm. It is a process of randomly initializing the solution and searching for the best solution through an iterative method. The obtained solution is judged by the fitness function to determine whether it is optimal. The PS0 algorithm is often used in the BP neural network because it can well solve the long time-consuming training of the BP neural network, causing the defect of local minimums. The speed and position update formulas are

$$\begin{aligned} V_{id}^{k+1} &= \omega V_{id}^{k} + c1r1\left(p_{id}^{k} - X_{id}^{k}\right) + c2r2\left(p_{gd}^{k} - X_{id}^{k}\right), \\ X_{\mathrm{id}}^{k+1} &= X_{\mathrm{id}}^{k} + rV_{\mathrm{id}}^{k+1}. \end{aligned} \tag{20}$$

GA is an algorithm that imitates the theory of biological evolution and finds the best solution by simulating the natural evolution process. GA sorts and combines the optimized parameters required using the BP neural network to form a chromosome. Multiple chromosomes form a population. The excellent genes in the population will be passed on to the next generation. New individuals can also be synthesized through crossover, mutation, and other methods. This is expressed as a formula:

$$P_c = \begin{cases} P_{\text{cmax}} & \left(f' < f_{\text{avg}}\right) \\ \dfrac{P_{\text{cmax}} - P_{\text{cmin}}}{1 + \exp\left[2A\left(f\prime - f_{\text{avg}}\right)/f_{\max} - f_{\text{avg}}\right]} & \left(f' \geq f_{\text{avg}}\right) \end{cases},$$
$$P_m = \begin{cases} P_{m\,\max} & \left(f < f_{\text{avg}}\right) \\ \dfrac{P_{m\max} - P_{m\min}}{1 + \exp\left[2A\left(f - f_{\text{avg}}\right)/f_{\max} - f_{\text{avg}} - 1\right]} + P_{m\min} & \left(f' \geq f_{\text{avg}}\right) \end{cases}. \tag{21}$$

ACO is an algorithm to find the optimal solution by imitating the ant foraging form, and it can also be used to find the global optimal path. It is expressed as a formula:

$$\tau_{ij}(t+1) = (1-\rho).\tau_{ij}(t) + .\tau_{ij}. \tag{22}$$

The increment of interest-bearing element is calculated as

$$\Delta\tau_{ij} = \sum_{k=1}^{K} \Delta\tau_{ij}^{k}. \tag{23}$$

The BP neural network in this article uses a three-layer structure. The prediction of ammonia nitrogen is of great significance to the accurate grasp of water quality. The following are input parameters of this article: water temperature, pH, dissolved oxygen, conductivity, turbidity, and permanganate index; the number of input layer nodes is 6, and the output selection is ammonia nitrogen (Cmg/L); the number of output layer nodes is 1, the number of hidden layer nodes is 6, the number of iterations is 100, and the training function is trainlm; the population of seagulls is 100, and the number of iterations is 100. Figure 1 shows the convergence comparison of the two model algorithms.

It can be observed from Figure 1 that the SOA-BP model converges faster than the BP model. In terms of convergence accuracy, the same is iterated 100 times, the convergence value of the BP model is $4.536\,e^{-7}$, and the convergence value of the proposed SOA-BP model is $2.029\,e^{-8}$; the convergence accuracy of the proposed model is higher. The simulation of 23 sets of verification data is shown in Figure 2.

3.2. Sensor Vegetable Greenhouse. In today's developed network environment, the wireless sensor network system has also become an emerging collection, transmission, and processing technology. According to the actual requirements of the collected environmental information in the vegetable greenhouse, this article studies the framework of the wireless sensor network and adjusts the important environmental factors that affect the vegetable greenhouse according to the collected data. Assuming that the technician who manages the vegetable greenhouse finds that the collected data and the parameter values that affect the environment set in advance have disagreements, then the ZigBee intelligent control technology can be used to implement remote operation of the on-off valves set in the vegetable greenhouse, human intervention, and control of the environment in the vegetable greenhouse. The schematic diagram of the experimental framework designed and studied in this article is shown in Figure 3.

The ZDO in the ZigB ee protocol stack is mainly responsible for the management plan of all sensor nodes. The application layer can use the ZDO service to obtain all the network information that it wants. In addition, ZDO provides binding services. The working mechanism of the protocol is shown in Table 2.

In this article, the SHT 10 sensors used in the vegetable greenhouse network are all calibrated in advance so that they can be directly linked with the CC2530 and used. The electrical characteristics of SHT 10 are shown in Table 3.

The functional characteristics are shown in Table 4.

The TSL2561 hardware in this article has a particularly precise and simple structure so that the clock and serial data lines can be directly connected to the CC25 30 through the 12 C bus and link. TSL2561 is suitable for various complex greenhouse environments because of its small size and low power consumption. The collected light intensity can also be converted into a digital signal for output so that the person who manages the vegetable greenhouse can obtain the change of the light intensity in the greenhouse through the system data.

The electrical characteristics of TSL2561 are shown in Table 5.

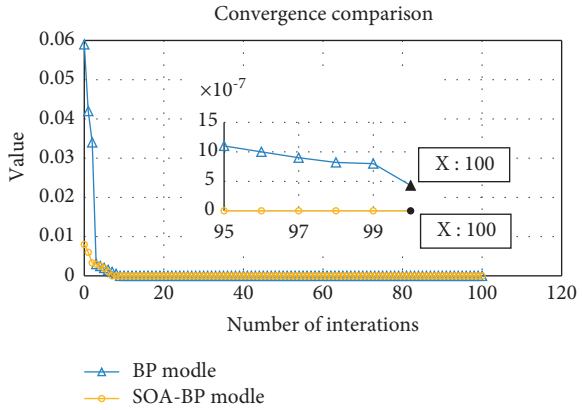

Figure 1: Comparison of SOA-BP and BP convergence.

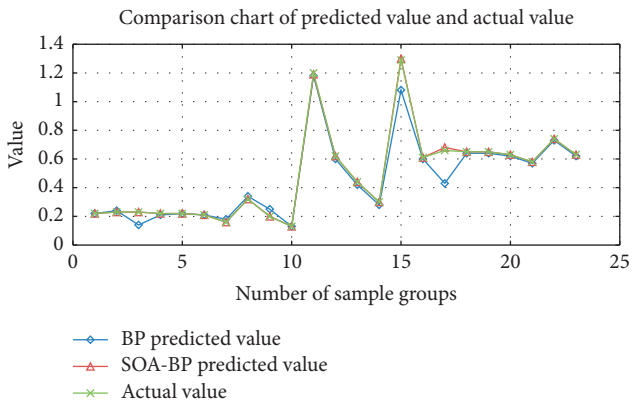

Figure 2: Comparison of SOA-BP and BP predicted and actual values.

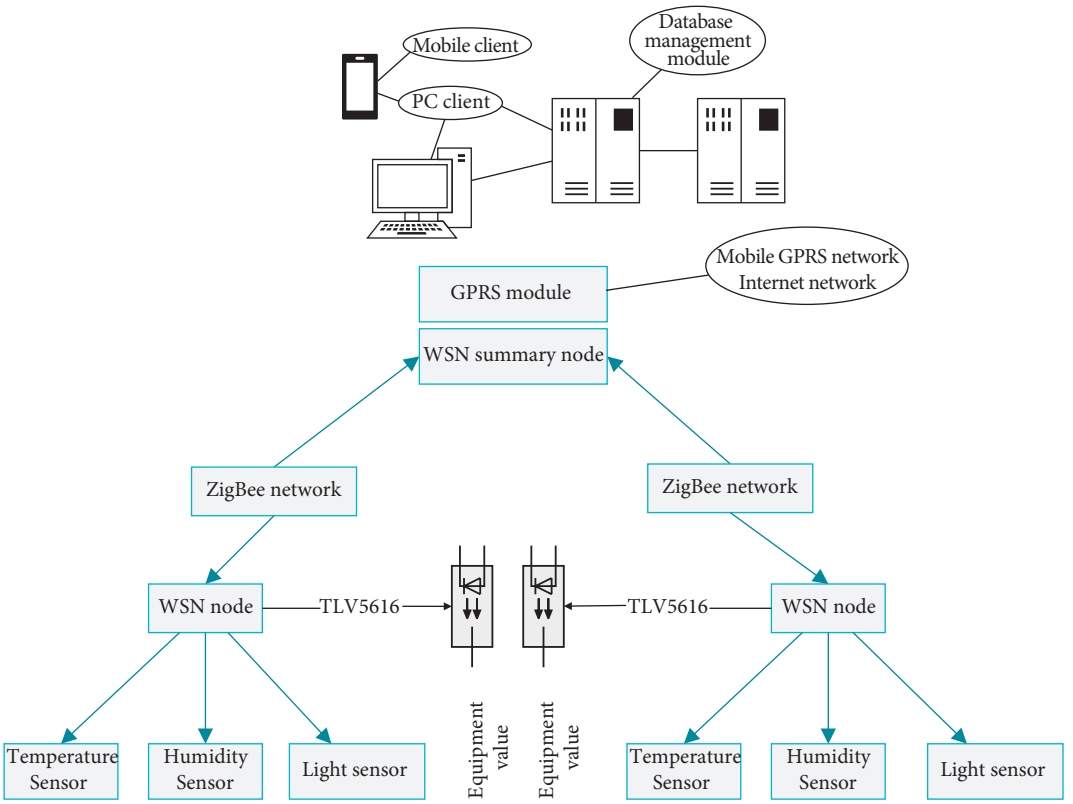

Figure 3: System overall architecture diagram.

Table 2: Protocol system and protocol code.

Layered protocol stack system	Protocol code file
Physical layer (PHY)	Hardware layer (HAL)
Control sublayer (MAC)	Link layer (Zmac)
Network layer (NWK)	Network layer (NWK)
Application support layer (APS)	Network layer (NWK)
Program framework (AF)	Profile and program
Zigbee device object ZDO	Device object directory ZDO

Table 3: SHT10 electrical characteristics.

Parameter	Condition	Min.	Typ.	Max.	Unit
Power supply DC	—	2.3	6	5.5	V
	Measuring		540	—	μA
Supply current	Average	2	27	—	μA
	Dormant	—	0.4	0.6	μA
Low-level output voltage	$l_{CL} < 4$ mA	0	—	260	mV
High-level output voltage	$R_p < 25$ kΩ	90%	—	100%	Vdd
Low-level input voltage	Falling edge	0	—	30%	Vdd
High-level input voltage	Rising edge	80%	—	100%	Vdd
Input current on the pad	—	—	—	1	μA

Table 4: SHT 10 functional characteristics.

Humidity		Temperature	
Parameter	Numerical value	Parameter	Numerical value
Measuring range	10~97% RH	Measuring range	−40~110°C
Resolution	0.03% RH	Resolution	0.02°C
Repeatability	0.02% RH	Repeatability	0.4°C
Measurement accuracy	−3.8% RH~3.9% RH	Measurement accuracy	−0.4°C~0.5°C
Hysteresis	−0.1% RH~0.1% RH	Drift	Less than 0.4°C

Table 5: Electrical characteristics of TSL2561.

Parameter	Switch	Lowest	Specification	Highest	Voltage
Supply voltage	—	2.8	3	3.5	V
SCL, SDA	—	−0.5	—	0.6	V
SCL, SDA	—	—	—	3.4	V
Power supply	Open	—	0.25	0.7	mA
Current	Turn off	—	3.3	16	μA

4. Agricultural Product Supply Chain Management and Model Construction

4.1. Current Status of Agricultural Product Supply Chain Management. The traditional agricultural product supply chain is basically a temporary one-off product trading market; that is, between the processing enterprises responsible for agricultural products and the farmers and sellers, they may all be one-time transactions or are particularly loose in a short time. The two parties or three parties rely on it. The current market prices of agricultural products carry out the trading of funds and agricultural products. The detailed structure diagram is shown in Figure 4:

It can be seen from Figure 4 that basically all transactions are temporary, which cannot ensure the stability between the three. The farmers and sellers of agricultural products are completely separated from each other, and they are unable to obtain timely and accurate information on the current market transactions, resulting in untargeted cultivation of agricultural products, and this also makes it impossible for agricultural product processing enterprises to obtain sustainable gains. The raw materials needed for agricultural products have led to higher production costs for enterprises. In addition, the quality of agricultural products cannot be uniformly planned and managed, which has also caused many problems. The structure diagram is shown in Figure 5, but the integrated structure model still has many drawbacks:

As many domestic enterprises are unable to move forward, it is difficult to determine the supply and demand relationship of agricultural products with farmers. The agricultural product processing enterprise was unable to determine whether to produce the product, which resulted in a breach of contract between the two parties, and the farmers also did not have the technical means of the agricultural product processing enterprise to help the quality of the agricultural products. This is also the reason that the enterprises responsible for agricultural products processing are too burdened. Agricultural products processing enterprises also need to increase the cost of organization and management to be able to coordinate the interests of each department, which also increases the difficulty of enterprise supervision. Doing so is also uncertain whether it can reduce production costs.

4.2. Main Issues of China's Agricultural Product Supply Chain Management. At present, the circulation of domestic agricultural products is still in the contradiction between small production scale and huge market scale. Small-scale production scale refers to the production model in which domestic agricultural products are grown and sold by scattered farmers. The farmers themselves cannot bring the products into the market for trading, and it is difficult for agricultural products to circulate in the market. This contradictory restraint has contributed to the current situation in China. A buying and selling market is dominated by a wholesale market. Today's agricultural product supply chain is divided into parts from production to circulation, which can be understood as moving from farmers to the wholesale market; there is another part from circulation to consumers, which is understood as the circulation from the wholesale market to the demanders, and from farmers to consumers. It is developed with the wholesale market as the center. Therefore, according to the existing wholesale market-centric form, the agricultural product supply chain is a small

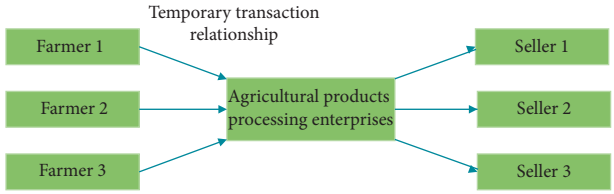

Figure 4: Traditional processing supply chain enterprise connection structure diagram.

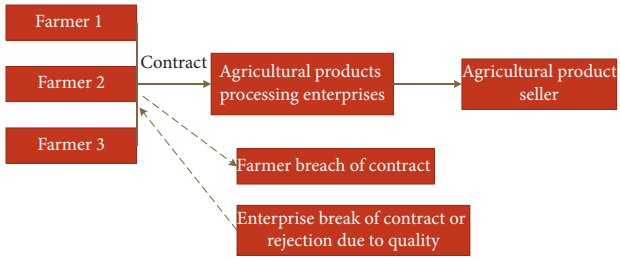

Figure 5: Vertical integration structure diagram.

short chain, and there is no way to apply the supply chain management model.

Since the members of the farm product supply chain are composed of different economic systems, there is a contradiction in economic interests between the two parties, and this contradiction will cause conflicts among the personnel, resulting in no way to target every step in the agricultural product supply chain. However, in the management process of the agricultural product supply chain, everyone needs to participate in the cooperation with each other to be better, to establish sufficient trust with each other, and to be able to make better use of the supply chain management model. When implementing supply chain management, in terms of enterprises, it is not necessary to use the original buying and selling thinking to consider issues in order to change their minds, and to share relevant responsibilities with partners and enjoy the benefits together.

The management model of important enterprises in the foreign agricultural product supply chain has evolved from internal cost and production management to external supply chain management. The points of competition among various enterprises have also changed from the original low-end price competition to the high-end long-term strategic choice and specific implementation aspects. The foreign agricultural product supply chain model is based on the unified and large-scale production of agricultural products. Each member of the agricultural product supply chain has relatively balanced rights in the demand market. Compared with other countries, there is a gap between China and other countries in terms of management ideas, cooperation methods, logistics systems, and information systems in agricultural supply chain management. Due to the existence of these problems, there is a gap between China and other countries in the production and operation model of agricultural products, and the composition of the industrial chain. Some important influencing factors are analyzed, as shown in Table 6.

4.3. Construction of China's Agricultural Product Supply Chain Management Model. Chinese consumers have a habit of eating fresh fruits and vegetables for a long time. This leads to two aspects in the form of purchase. One is direct consumption, that is, the purchase of agricultural products that do not need to be processed by factories or enterprises. Agricultural products that have only undergone simple processing are also known as non-processing and primary processing. Another is that agricultural products are purchased and consumed after processing by the enterprise, which is the use of fine processing or deep processing of agricultural products. Fine processing or deep processing refers to the secondary or more processing of agricultural products. It mainly refers to improving and reusing the protein components, plant fiber components, oil components, and new nutrients of agricultural products. Fine and deep processing will lead to the quality of agricultural products. The main objects of direct consumption are raw and fresh agricultural products, and the main objects of consumption after processing are processed agricultural products that can be used for food. Based on the aforementioned two key consumption methods, this article can divide the agricultural product supply chain into fresh agricultural product supply chain and agricultural product processing supply chain. The supply chain of fresh agricultural products can be understood as an economic activity in which fresh and live agricultural products go directly from the producers of agricultural products to consumers. Its focus is on how to ensure the freshness of agricultural products. The agricultural product processing supply chain can be understood as an economic activity in which processed products obtained after agricultural products are processed from enterprise processors to consumers, and its focus is to process agricultural products. Therefore, the management of the agricultural product supply chain must take into account the characteristics of the supply chain of various types of agricultural products.

The center of the agricultural product processing supply chain management is the enterprise responsible for agricultural product processing. The enterprise builds a good partnership with supply and demand companies, and then cooperates and manages agricultural product logistics, market information, and capital flow to complete agricultural product processing. The process of processing and value enhancement brings a variety of products to consumers. The premise of agricultural product processing supply chain management is the management of agricultural products, from the initial production of agricultural products to the process of processing, and finally to consumption. Then there is the management of the processing supply chain; the purpose is to average the benefits of each point in the supply chain, improve the economy of the entire supply chain, and also meet consumer needs. Through the processing of agricultural products, especially the deep processing of agricultural products, the original properties of agricultural products have been transformed and their value in the circulation process has been enhanced.

The ultimate goal of fresh agricultural product supply chain management is to meet the requirements of

Table 6: Comparison of Chinese and foreign agricultural product supply chains.

	China	Foreign
Supply chain management concept	Outdated concept, almost no supply chain management department	Adopt a supply chain management competition strategy
Cooperation mechanism	Small production leads to uneven market power, and it is difficult to establish a cooperative mechanism	Vertical integration or horizontal integration cooperation mechanism, contract system
Logistics system	Repeated construction, low response, low cold chain technology	Professional logistics, advanced technology and equipment, high level of cold chain
Information system	Insufficient application, low level of information technology, low sharing	Complete information center with openness, node applicability, and scalability

consumers. It centers on service companies, and builds good partnerships with supply and demand companies, and then through the logistics, market information, and funding of agricultural products. Cooperation and management of flow and other aspects to complete the increase in the value of fresh agricultural products provides consumers with fresh and live agricultural products. The premises of the management of the fresh produce supply chain and the management of the supply chain of produce processing are the same in this respect. They are both the process of transferring agricultural products from production to processing to the sales link, and then the management of the fresh produce supply chain. The ultimate goal of controlling the logistics and market information of agricultural products is to meet the needs of consumers. In addition, the increase in the service value of the fresh agricultural product supply chain can also be reflected in the operation and service management of service-oriented enterprises. For example, factors such as the shopping environment of consumers in retail supermarkets and the quality of employee services can also affect whether consumers buy or not.

5. Conclusion

In this article, the optimized neural network system sensors are added to the vegetable greenhouse. This article analyzes the environmental detection and control system in the vegetable greenhouse in detail, and summarizes the overall system separately. Among them, the sensor network using the ZigBee intelligent control technology collects environmental data in the vegetable greenhouse, and then builds the model based on the intelligent algorithm, uses the ACARS system and the fast access recorder data to construct the sample, and finally optimizes it. It not only improves the accuracy of the transmission process of the overall collected data but also balances the current network load capacity. In terms of collecting data sensors, this article also carried out a more detailed explanation of the system software and hardware of the sensors used in temperature, humidity, and light intensity, and explained their working principles and theoretical principles. We can also use the ZigBee intelligent control technology to remotely operate the switch valves set in the vegetable greenhouse to adjust the important environmental factors that affect the vegetable greenhouse. This method is used to artificially intervene and control the environment in the vegetable greenhouse. In addition, this article also applies the optimized and improved neural network system to agricultural product supply chain management. In view of the analysis of the current situation of China's agricultural product supply chain management, as well as the agricultural product processing supply chain management model and the fresh supply chain management model and the factors that affect them, the overall and comprehensive analyses of key enterprises and supply and demand enterprises in the supply chain, it can be concluded that the traditional agricultural product supply chain is basically a temporary one-off product trading market, that is, between the processing enterprises responsible for agricultural products, farmers, and sellers, they may all be one-off transactions or are particularly loose in a short period of time; the agricultural products are grown and sold by scattered farmers themselves. The farmers themselves cannot bring their products to the market for trading. It is difficult for agricultural products to be circulated in the market, resulting in a small short chain of agricultural product supply chain. Supply chain management mode application, which is the focus of the fresh agricultural product supply chain, is how to ensure the freshness of agricultural products. The ultimate goal of the fresh agricultural product supply chain management is to meet the requirements of consumers. The focus of the agricultural product processing supply chain is to process agricultural products. The center of agricultural product processing supply chain management is the enterprise responsible for agricultural product processing; therefore, the agricultural product supply chain management method must fully consider various types of supply chains.

Data Availability

The data used to support the findings of this study are available from the corresponding author upon request.

Conflicts of Interest

The author declares that there are no conflicts of interest.

References

[1] C. Sulmon, F. Ramel, G. Gouesbet, and I. Couée, "Improvement of environmental remediation by on-site phytoremediating greenhouses," *Environmental Science & Technology*, vol. 48, no. 11, pp. 6055-6056, 2014.

[2] T. Boulard and A. Baille, "A simple greenhouse climate control model incorporating effects of ventilation and

evaporative cooling," *Agricultural and Forest Meteorology*, vol. 65, no. 3-4, pp. 145–157, 1993.

[3] J. B. Cunha, "Greenhouse climate models: an overview," in *Proceedings of the 4th European Federation for Information Technologies in Agriculture, Food and the Environment Conference (EFITA '03)*, Debrecen, Hungary, October 2003.

[4] P. Salgado and J. B. Cunha, "Greenhouse climate hierarchical fuzzy modelling," *Control Engineering Practice*, vol. 13, no. 5, pp. 613–628, 2005.

[5] J. M. Herrero, X. Blasco, M. Martínez, C. Ramos, and J. Sanchis, "Robust identification of non-linear greenhouse model using evolutionary algorithms," *Control Engineering Practice*, vol. 16, no. 5, pp. 515–530, 2008.

[6] I. Seginer, "Some artificial neural network applications to greenhouse environmental control," *Computers and Electronics in Agriculture*, vol. 18, no. 2-3, pp. 167–186, 1997.

[7] M. Adil, H. Alshahrani, A. Rajab, A. Shaikh, H. Song, and A. Farouk, "QoS review: smart sensing in wake of COVID-19, current trends and specifications with future research directions," *IEEE Sensors Journal*, p. 1, 2022.

[8] J. W. Jones, E. Dayan, L. H. Allen, H. van Keulen, and H. Challa, "Dynamic tomato growth and yield model (TOMGRO)," *Transactions of the ASAE*, vol. 34, no. 2, pp. 663–672, 1991.

[9] E. Heuvelink and M. Dorais, "Crop growth and yield," in *Crop Production Science in Horticulture Series*, E. H. Tomatoes, Ed., pp. 85–144, CABI Publishing, Wallingford, UK, 2005.

[10] F. T. S. Chan, H. K. Chan, and H. J. Qi, "A review of performance measurement systems for supply chain management," *International Journal of Business Performance Management*, vol. 8, no. 2/3, p. 110, 2006.

[11] D. Estampe, S. Lamouri, J.-L. Paris, and S. Brahim-Djelloul, "A framework for analysing supply chain performance evaluation models," *International Journal of Production Economics*, vol. 142, no. 2, pp. 247–258, 2013.

[12] P. R. C. Gopal and J. Thakkar, "A review on supply chain performance measures and metrics: 2000-2011," *International Journal of Productivity and Performance Management*, vol. 61, no. 5, pp. 518–547, 2012.

[13] F. Zhu, C. Zhang, Z. Zheng, and A. Farouk, "Practical network coding technologies and softwarization in wireless networks," *IEEE Internet of Things Journal*, vol. 8, no. 7, pp. 5211–5218, 2021.

[14] N. Stefanovic and D. Stefanovic, "Supply chain business intelligence: technologies, issues and trends," in *Artificial Intelligence: International Perspectives*, M. Bramer, Ed., vol. 5640, pp. 217–245, Springer, New York, NY, USA, 2009.

[15] P. Allemar Jhone, A. M. Sison, and R. P. Medina, "Variable reduction-based prediction through modified genetic algorithm," *International Journal of Advanced Computer Science and Applications*, vol. 10, pp. 356–363, 2019.

[16] D. Karaboga and E. Kaya, "Adaptive network based fuzzy inference system (ANFIS) training approaches: a comprehensive survey," *Artificial Intelligence Review*, vol. 52, no. 4, pp. 2263–2293, 2019.

[17] Y. Liu, X. Zhu, and J. Yang, "Fault diagnosis of PV array based on optimised BP neural network by improved adaptive genetic algorithm," *Journal of Engineering*, vol. 2017, no. 13, pp. 1427–1431, 2017.

[18] L. Tang, S. Yuan, Y. Tang, and Z. Qiu, "Optimization of impulse water turbine based on GA-BP neural network arithmetic," *Journal of Mechanical Science and Technology*, vol. 33, no. 1, pp. 241–253, 2019.

[19] A. Mansouri, A. Nazari, and M. Ramazani, "A comparison of artificial neural network model and logistics regression in prediction of companies' bankruptcy (a case study of Tehran stock exchange)," *International Journal of Advanced Computer Research*, vol. 6, no. 24, pp. 81–92, 2016.

[20] Z. Lv, H. Song, P. Basanta-Val, A. Steed, and M. Jo, "Next-generation big data analytics: state of the art, challenges, and future research topics," *IEEE Transactions on Industrial Informatics*, vol. 13, no. 4, pp. 1891–1899, 2017.

Hindawi
Mobile Information Systems
Volume 2022, Article ID 8753660, 20 pages
https://doi.org/10.1155/2022/8753660

Research Article

Modeling and Simulation of Ultra-Wideband Communication Receiver Based on Balanced Sampling and Integrating Circuit

Zhiqi Wang, Zhonghua Huang, Shijun Hao, Zhe Guo, and Kaiwei Wu

School of Mechatronical Engineering, Beijing Institute of Technology, Beijing 100081, China

Correspondence should be addressed to Zhonghua Huang; huangzh@bit.edu.cn

Received 27 May 2022; Revised 11 July 2022; Accepted 25 July 2022; Published 18 August 2022

Academic Editor: Shadi Aljawarneh

In order to solve the problem of extracting signals from impulse radio ultra-wideband (IR-UWB) receivers in a low signal-to-noise ratio (SNR) environment, this paper uses circuit transient analysis to establish a mathematical model of an ultra-wideband wireless communication receiver based on a balanced sampling and integration circuit (BSIC). The effect of receiver circuit component parameters on the output signal is simulated and tested, and the optimization of circuit component parameters for UWB wireless communication receivers is achieved. The sampling capacitance in the receiver circuit ranges from 1 pF to 6 pF, depending on the 200 ps pulse width. The output signal amplitude increases as the sampling capacitance increases. The range of integral capacitance is from 2.5 pF to 25 pF, which is based on a 100 ns interval between two pulses. The output signal amplitude decreases as the integration capacitance increases and the signal waveform becomes better as the integration capacitance increases. The effect of SNR from 0 to −30 dB on the receiver output is simulated, and the results show that the Bit Error Ratio (BER) of the receiver is less than 10^{-3} when the SNR is greater than −15 dB. The simulation and test results show that the model developed in this paper is useful as a guide for optimizing the receiver parameters at low SNR.

1. Introduction

Impulse radio ultra-wideband (IR-UWB) has high application value in the Internet of Things (IoT) and wireless communications [1–3], and IR-UWB technology has been widely used in short-range communications, positioning, and radars [4, 5].

Receiver is the basis for the realization of IR-UWB technology. At present, there are many types of IR-UWB signal receiver. In [6–9], there are incoherent energy detection receivers for the additive Gaussian white noise channel environment and matched filter receivers for correlated reception. In [10, 11], there are RAKE receivers consisting of multiple parallel correlators for complex multipath channel environments and transmission reference (TR) receivers [12–15], which do not require complex channel estimation compared to RAKE receivers. In [16–21], the structure of the low-noise amplifier (LAN) is optimized to improve the gain of the LAN and reduce the noise so as to improve the data speed of the receiver and reduce the bit error rate (BER). In [22–25], the algorithm of analog-to-digital converter (ADC) is optimized to reduce the bit error rate of the receiver. These improvements can effectively reduce the BER of UWB receiver, and the data speed can reach 100 Mbps to 1 Gbps. And in [10, 12, 13, 20, 24], the effect of the environment on UWB receivers has been studied. However, most of these studies are carried out in high signal-to-noise ratio (SNR) environment, which has poor antinoise ability.

The balanced sampling and integration circuit (BSIC) [26] is a simple and low-complexity circuit for recovering rapidly changing weak signals that are drowning in noise. The difference between this receiver and other receivers is the different position of the amplifier. In other receivers, the received signal is first processed by LNA and then by energy detection or correlator. In contrast, sampling and integration receivers process the received signal before amplification by an amplifier, which reduces the amplifier requirements.

In order to enhance the anti-interference ability of UWB receiver, the circuit in [26] is improved by adding two resistors, so it is necessary to establish a new model of the receiving circuit. This article mainly adopts the circuit

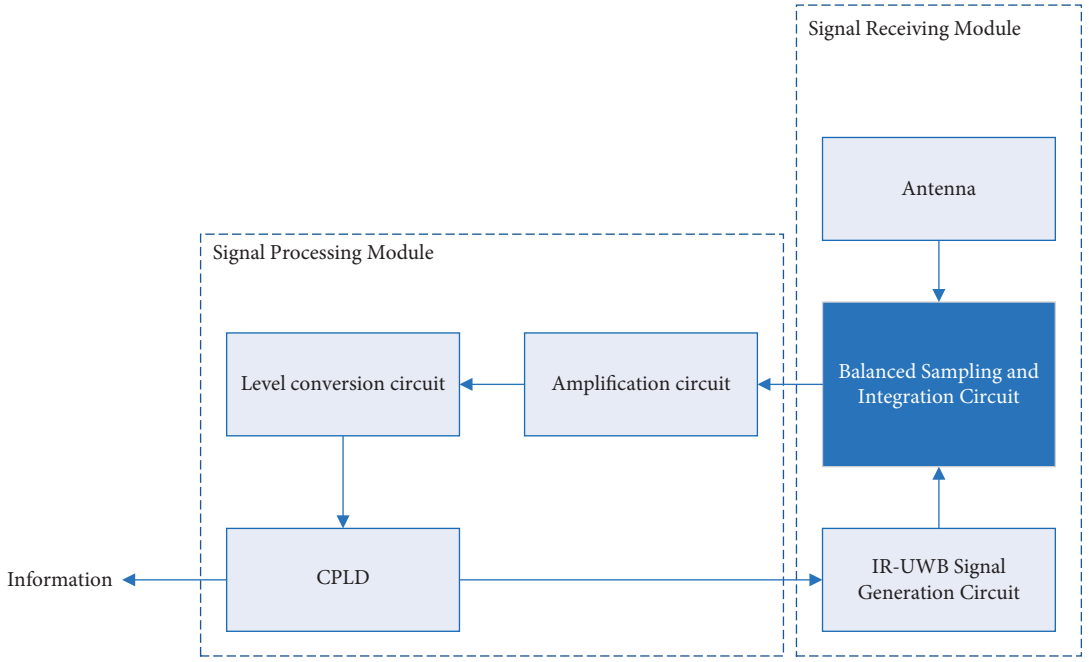

Figure 1: Block diagram of the IR-UWB receiver.

transient analysis method to establish the mathematical model of the UWB wireless communication receiver and obtain the receiver output signal expression through Laplace transform. The influence of receiver circuit component parameters on the output signal is studied, and the circuit component parameters of IR-UWB wireless communication receiver are optimized. The influence of different SNR on the output signal of receiver is studied by simulation.

The paper is structured in the following sections: Section 2 establishes the receiver model. Section 3 introduces simulation and measurement methods. Section 4 presents and discusses simulation and measured results. Section 5 describes the summary and future work of this article.

2. IR-UWB Receiver Modeling

In this section, an IR-UWB wireless communication receiver using a BSIC to achieve correlation calculations between sampling pulses and received signals is studied. The IR-UWB receiver block diagram is shown in Figure 1. The receiver consists of two parts, the signal receiving module and the signal processing module. The signal receiving module consists of an antenna, a BSIC, and an IR-UWB signal generation circuit. The signal processing module consists of an amplifier circuit, a level conversion circuit and a CPLD. Signal capture and decoding are performed on the CPLD.

The BSIC in IR-UWB wireless communication receiver is shown in Figure 2, which is composed of three parts: a sampling circuit, an integration circuit, and a high-pass filter circuit. The circuit in Figure 2 is an improvement on [26]. Resistors R_2 and R_3 in Figure 2 have been added to increase the anti-interference capability of the circuit.

The sampling circuit is composed of sampling capacitors C_1, C_2, diodes D_1, D_2, and resistance R_1, and the sampling pulse is U_p. The exponential integrating circuit is composed of integrating capacitors C_3, C_4 and resistors R_4, R_5. The high-pass filter circuit is composed of filter capacitors C_5, C_6 and resistors R_6, R_7. The input signal of the IR-UWB wireless communication receiver is the signal received by the antenna. Diode conduction is controlled by sampling pulse, and input signal is sampled by the sampling capacitor. The sampling values are integrated by capacitors C_3 and C_4 after the diodes are cut off. The low-frequency part of the integrated signal is filtered out by capacitors C_5 and C_6, and the signal is input to the differential amplifier. After multiple sampling periods, the output signal of the IR-UWB wireless communication receiver can be obtained.

2.1. Circuit Model of Sampling Process of IR-UWB Communication Receiver. According to the two different working states of IR-UWB communication receiver, the sampling process and the integration process, the mathematical models of the two working stages are established in one signal period.

The sampling process is the process in which IR-UWB wireless communication receiving circuit samples the input signal after the sampling pulse conducting the diodes D_1 and D_2. The resistors R_1, R_2, and R_3 are connected in parallel with an equivalent resistance of R_q when the diode is conducting. The circuit in the sampling process is shown in Figure 3. And ignore the effect of conduction diode resistors, because the resistors value of diode conduction is much smaller than R_1, R_2, and R_3.

R_q in the figure is

$$R_q = R_1//R_2//R_3 = \frac{R_1R_2R_3}{R_2R_3 + R_1R_3 + R_1R_2}. \quad (1)$$

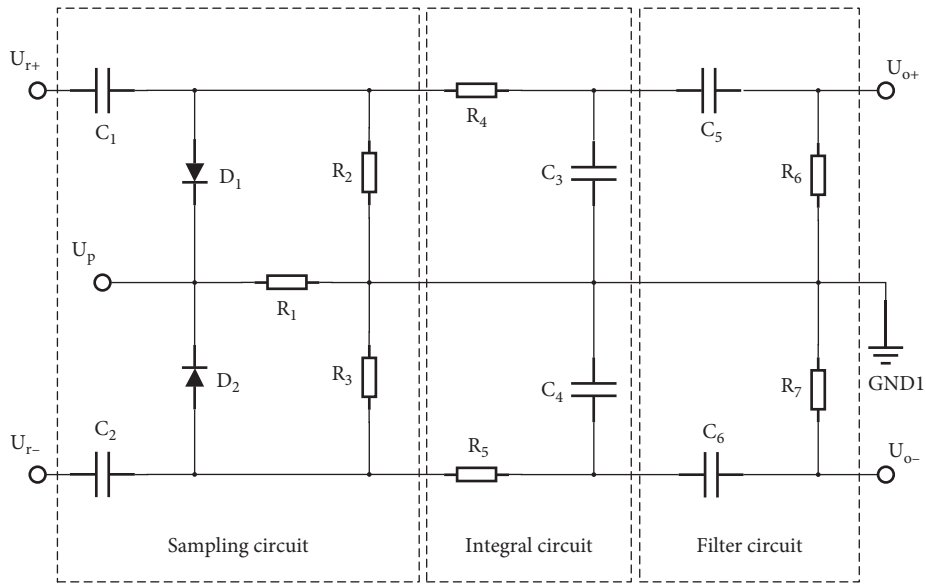

Figure 2: IR-UWB receiver circuit schematic diagram.

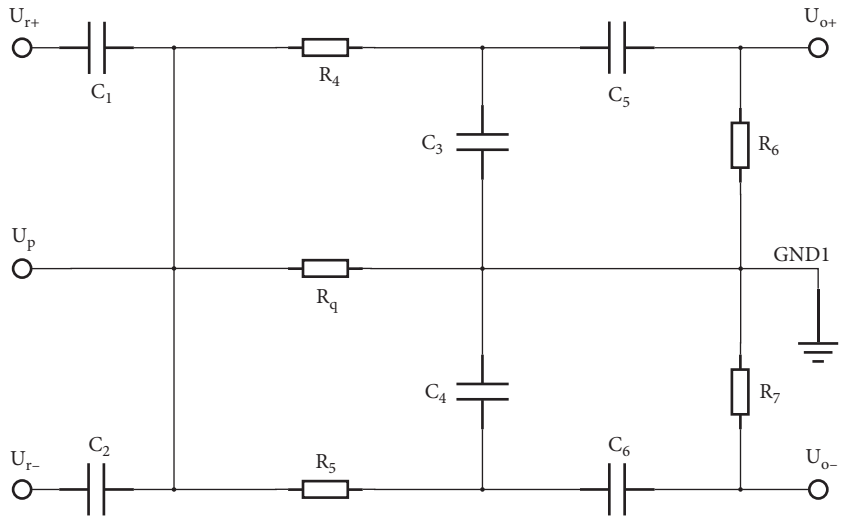

Figure 3: Equivalent circuit diagram of sampling process.

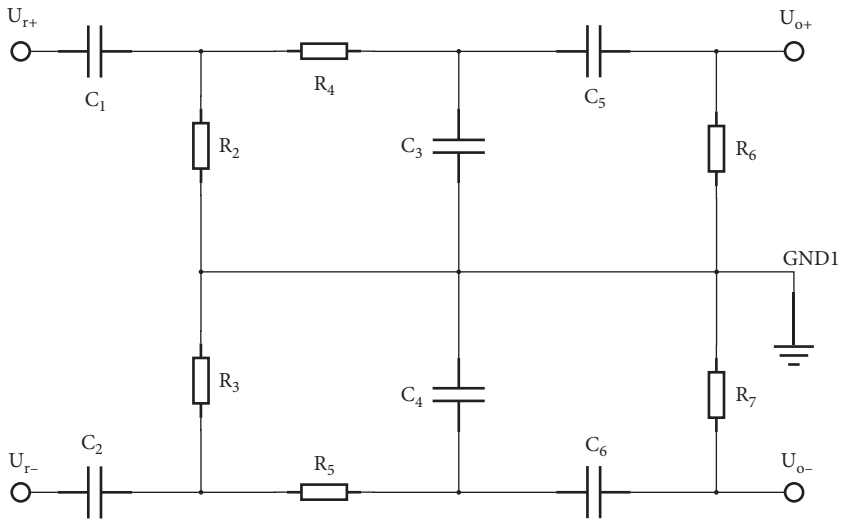

Figure 4: Equivalent circuit diagram of integration process.

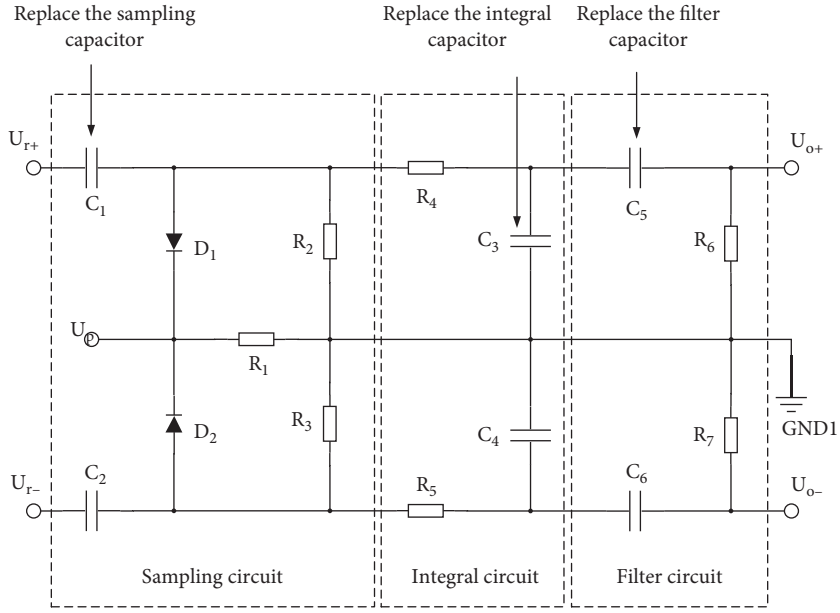

Figure 5: Circuit simulation and measurement principle block diagram.

Since the upper and lower parts of the BSIC have the same circuit principles, this article only elaborates on the derivation process of the upper part of the circuit model.

In the nth period, the initial states of C_1, C_3, and C_5 are assumed to be u_{n1}, u_{n3}, and u_{n5}, respectively, when the diode is conduction. According to Kirchhoff's voltage law, the simplified circuit model from Figure 3 is shown below.

$$\begin{cases} u_{r+} = u_1 + R_q\left(C_1\dfrac{du_1}{dt} - C_3\dfrac{du_3}{dt} - C_5\dfrac{du_5}{dt}\right) + u_p, \\ u_{r+} = u_1 + R_4\left(C_3\dfrac{du_3}{dt} + C_5\dfrac{du_5}{dt}\right) + u_3, \\ u_3 = u_5 + R_6C_5\dfrac{du_5}{dt}. \end{cases} \tag{2}$$

Because the frequency of the received UWB signal is on the order of GB, the parameters of the upper part of the circuit in Figure 3 satisfy $R_6 \gg R_4 \gg R_q$, $[R_4 + (R_6 + 1/j\omega C_5)//1/j\omega C_3] \gg R_q$, and $R_6 + 1/j\omega C_5 \gg 1/j\omega C_3$. So $i_{C_1} \gg i_{C_3} \gg i_{C_5}$; then, the system of equations (2) can be simplified to

$$\begin{cases} u_{r+} = u_1 + R_qC_1\dfrac{du_1}{dt} + u_p, \\ u_{r+} = u_1 + R_4C_3\dfrac{du_3}{dt} + u_3, \\ u_3 = u_5 + R_6C_5\dfrac{du_5}{dt}. \end{cases} \tag{3}$$

Perform Laplace transform on the system of equations (3), and perform inverse Laplace transform on the equations to get $u_1(t)$, $u_3(t)$, and $u_5(t)$ as follows:

$$\begin{aligned} u_1(t) &= \left(u_{n1} - u_{r+} + u_p\right)e^{-\left(t/R_qC_1\right)} + u_{r+} - u_p, \\ u_3(t) &= u_{n3}e^{-\left(t/R_4C_3\right)} + u_p\left(1 - e^{-\left(t/R_4C_3\right)}\right) \\ &\quad - \frac{R_qC_1}{R_qC_1 - R_4C_3}\left(u_{n1} - u_{r-} + u_p\right)\left(e^{-\left(t/R_qC_1\right)} - e^{-\left(t/R_4C_3\right)}\right), \\ u_5(t) &= u_{n5}e^{-\left(t/R_6C_5\right)} - \frac{u_{n3}R_4C_3}{R_4C_3 - R_6C_5}\left(e^{-\left(t/R_4C_3\right)} - e^{-\left(t/R_6C_5\right)}\right), \\ &\quad + u_p\left(1 - e^{-\left(t/R_6C_5\right)}\right) - \frac{u_pR_4C_3}{R_4C_3 - R_6C_5}\left(e^{-\left(t/R_4C_3\right)} - e^{-\left(t/R_6C_5\right)}\right), \\ &\quad - \frac{R_qC_1}{R_qC_1 - R_4C_3}\left(u_{n1} - u_{r+} + u_p\right) \\ &\quad \cdot \left[\frac{R_qC_1}{R_qC_1 - R_6C_5}\left(e^{-\left(t/R_qC_1\right)} - e^{-\left(t/R_6C_5\right)}\right)\right. \\ &\quad \left. - \frac{R_4C_3}{R_4C_3 - R_6C_5}\left(e^{-\left(t/R_4C_3\right)} - e^{-\left(t/R_6C_5\right)}\right)\right]. \end{aligned} \tag{4}$$

As shown in Figure 3, the upper part and the lower part of the BSIC are symmetrical. Assume that the initial states of the capacitors C_2, C_4, and C_6 during diode conduction are u_{n2}, u_{n4}, and u_{n6}, respectively. Similarly, the solutions of $u_2(t)$, $u_4(t)$, and $u_6(t)$ can be obtained as follows:

$$
\begin{aligned}
u_2(t) &= \left(u_{n2} - u_{r-} + u_p\right)e^{-\left(t/R_qC_2\right)} + u_{r-} - u_p,\\
u_4(t) &= u_{n4}e^{-\left(t/R_5C_4\right)} + u_p\left(1 - e^{-\left(t/R_5C_4\right)}\right),\\
&\quad - \frac{R_qC_2}{R_qC_2 - R_5C_4}\left(u_{n2} - u_{r-} + u_p\right)\left(e^{-\left(t/R_qC_2\right)} - e^{-\left(t/R_5C_4\right)}\right),\\
u_6(t) &= u_{n5}e^{-\left(t/R_7C_6\right)} - \frac{u_{n4}R_5C_4}{R_5C_4 - R_7C_6}\left(e^{-\left(t/R_5C_4\right)} - e^{-\left(t/R_7C_6\right)}\right)\\
&\quad + u_p\left(1 - e^{-\left(t/R_7C_6\right)}\right),\\
&\quad - \frac{u_pR_5C_4}{R_5C_4 - R_7C_6}\left(e^{-\left(t/R_5C_4\right)} - e^{-\left(t/R_7C_6\right)}\right)\\
&\quad - \frac{R_qC_2}{R_qC_2 - R_5C_4}\left(u_{n2} - u_{r-} + u_p\right),\\
&\quad \cdot \left[\frac{R_qC_2}{R_qC_2 - R_7C_6}\left(e^{-\left(t/R_qC_2\right)} - e^{-\left(t/R_7C_6\right)}\right)\right.\\
&\quad \left. - \frac{R_5C_4}{R_5C_4 - R_7C_6}\left(e^{-\left(t/R_5C_4\right)} - e^{-\left(t/R_7C_6\right)}\right)\right].
\end{aligned}
\tag{5}
$$

2.2. Circuit Model of Integration Process of IR-UWB Communication Receiver. At the interval between two sampling pulses, diodes D_1 and D_2 are cut off, and the input signal of the receiving circuit sampled by the sampling capacitors C_1 and C_2 is transferred to the integrating capacitors C_3 and C_4. After multiple sampling cycles, the integration process of the input signal of the receiving circuit is completed, and the low-frequency part of the signal is filtered out by the high-pass filter circuit. The equivalent circuit diagram is shown in Figure 4.

When the diode is cut off in the nth cycle, the initial states of the capacitors C_1, C_3, and C_5 in the upper half of the circuit are u_{n1}', u_{n3}', and u_{n5}', respectively. The equations can be obtained from the equivalent circuit diagram in Figure 4.

$$
\begin{cases}
u_{r+} = u_1 + R_2\left(C_1\dfrac{du_1}{dt} - C_3\dfrac{du_3}{dt} - C_5\dfrac{du_5}{dt}\right),\\
u_{r+} = u_1 + R_4\left(C_3\dfrac{du_3}{dt} + C_5\dfrac{du_5}{dt}\right) + u_3,\\
u_3 = u_5 + R_6C_5\dfrac{du_5}{dt}.
\end{cases}
\tag{6}
$$

For $i_{C_3} \gg i_{C_5}$, therefore, C_5du_5/dt in the first two equations can be ignored. So, the solution of the equation system can be simplified to

$$
\begin{aligned}
u_1(s) &= \frac{C_3R_4C_1R_2s^2u_{n1}' + C_3R_2\left(u_{r+} - u_{n3}'\right)s + u_{r+}}{\left(C_1R_4C_3R_2s^2 + C_3R_2s + 1\right)s},\\
u_3(s) &= \frac{C_3R_2u_{n3}'\left(R_4C_1s + 1\right) + C_1R_2u_{r+}}{C_3R_4R_2C_1s^2 + C_3R_2s + 1},\\
u_5(s) &= \frac{C_5R_6u_{n5}'\left(C_1R_2C_3R_4s^2 + C_3R_2s + 1\right)}{\left(C_5R_6s + 1\right)\left(C_3R_4C_1R_2s^2 + C_3R_2s + 1\right)}.
\end{aligned}
\tag{7}
$$

The result of the inverse Laplace transforms of the simplified $u_1(t)$, $u_3(t)$, and $u_5(t)$ can be obtained as follows:

$$
\begin{aligned}
u_1(t) &= u_{r+} + e^{-\left(t/2R_4C_1\right)}\left[\left(u_{n1}' - u_{r+}\right)\cosh\left(\frac{\alpha}{R_4C_1}t\right)\right.\\
&\quad \left. - \frac{2}{\alpha}\left(u_{n3}' + u_{n1}' - u_{r+}\right)\sinh\left(\frac{\alpha}{R_4C_1}t\right)\right],\\
u_3(t) &= u_{r+} + \left(u_{n3}' - u_{r+}\right)e^{-\left(t/2R_4C_1\right)}\\
&\quad \cdot \left[\cosh\left(\frac{\alpha}{R_4C_1}t\right) + \frac{1}{2\alpha}\sinh\left(\frac{\alpha}{R_4C_1}t\right)\right],\\
u_5(t) &= u_{n5}'e^{-\left(t/R_6C_5\right)}.
\end{aligned}
\tag{8}
$$

where $\alpha = \sqrt{(R_2C_3 - 4R_4C_1)/4R_2C_3}$.

As shown in the equivalent circuit diagram of the integration process of the receiving circuit in Figure 3, the upper and lower parts of the circuit are symmetrical during the integration process of the BSIC. In the same way, suppose the initial states of the capacitors C_2, C_4, and C_6 are u_{n2}', u_{n4}', and u_{n6}', respectively, and the results of $u_2(t)$, $u_4(t)$, and $u_6(t)$ can be obtained as

$$
\begin{aligned}
u_2(t) &= u_{r-} + e^{-\left(t/2R_5C_2\right)}\left[\left(u_{n2}' - u_{r-}\right)\cosh\left(\frac{\beta}{R_5C_2}t\right)\right.\\
&\quad \left. - \frac{2}{\beta}\left(u_{n4}' + u_{n2}' - u_{r-}\right)\sinh\left(\frac{\beta}{R_5C_2}t\right)\right],\\
u_4(t) &= u_{r-} + \left(u_{n4}' - u_{r-}\right)e^{-\left(t/2R_5C_2\right)}\left[\cosh\left(\frac{\beta}{R_5C_2}t\right)\right.\\
&\quad \left. + \frac{1}{2\beta}\sinh\left(\frac{\beta}{R_5C_2}t\right)\right],\\
u_6(t) &= u_{n6}'e^{-\left(t/2R_7C_6\right)}.
\end{aligned}
\tag{9}
$$

where $\beta = \sqrt{(R_3C_4 - 4R_5C_2)/4R_3C_4}$.

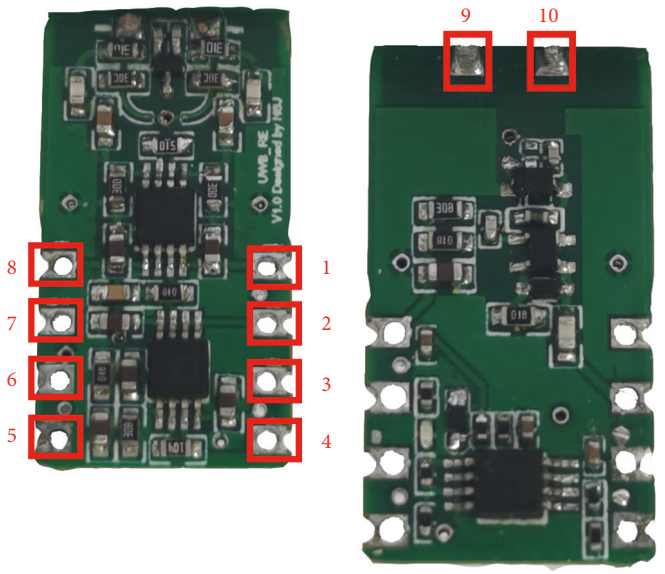

(a) (b)

Figure 6: The measured receiver. (a) Front of the receiver. (b) Back of the receiver.

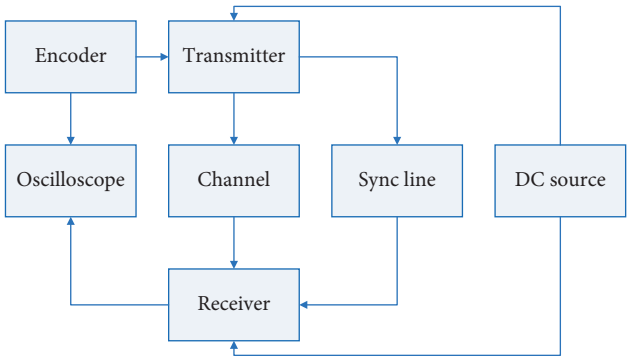

(a)

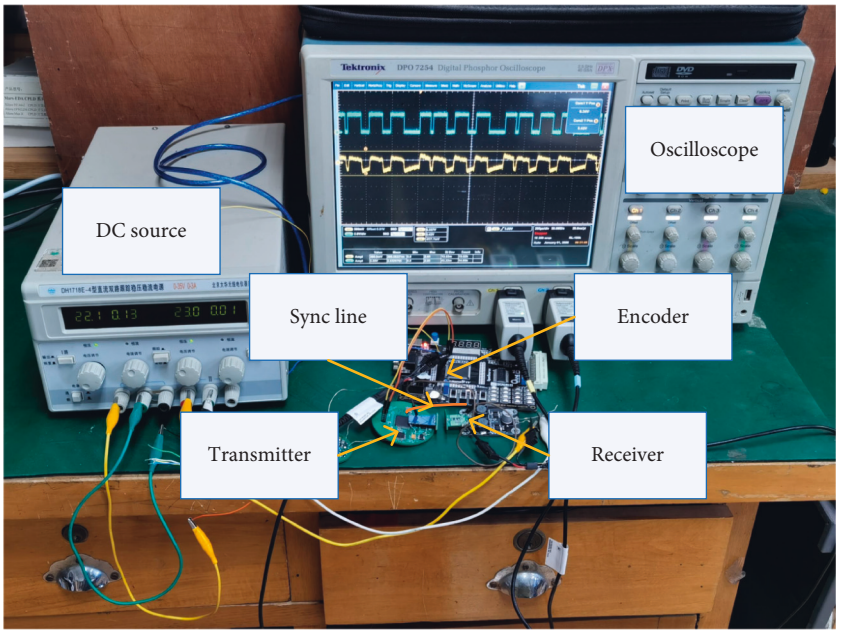

(b)

Figure 7: Block diagram and measurement photo. (a) Block diagram of the measurement receiver. (b) Photo of measurement receiver.

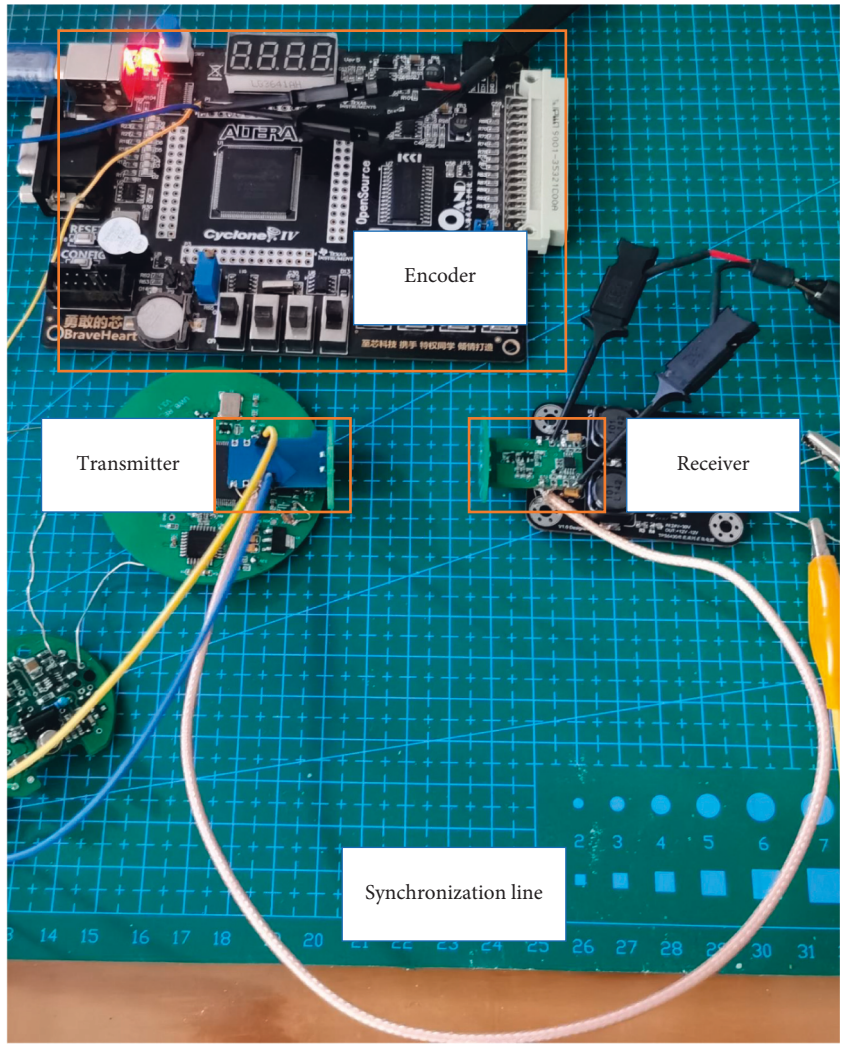

Figure 8: Photo of encoder, transmitter, receiver, and synchronization line.

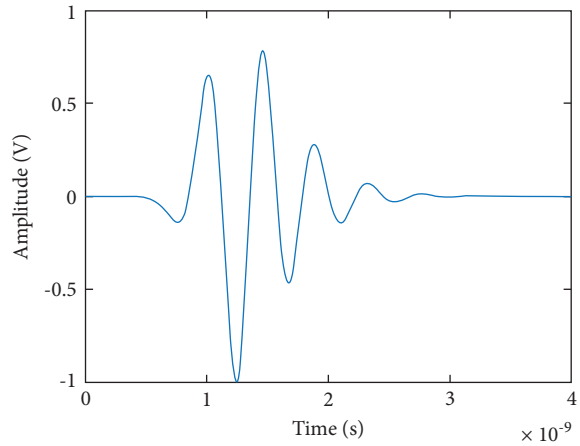

Figure 9: Single narrow pulse signal received by the receiving circuit.

In the process of circuit model calculation, the received UWB signal is iterated through equations (8) and (9), according to the initial states u_{n1}, u_{n3}, and u_{n5} of the three capacitors in the upper part of the circuit during diode conduction, and the final state values of u_{n1}', u_{n3}', and u_{n5}' of the capacitors C_1, C_3, and C_5 in the circuit sampling process

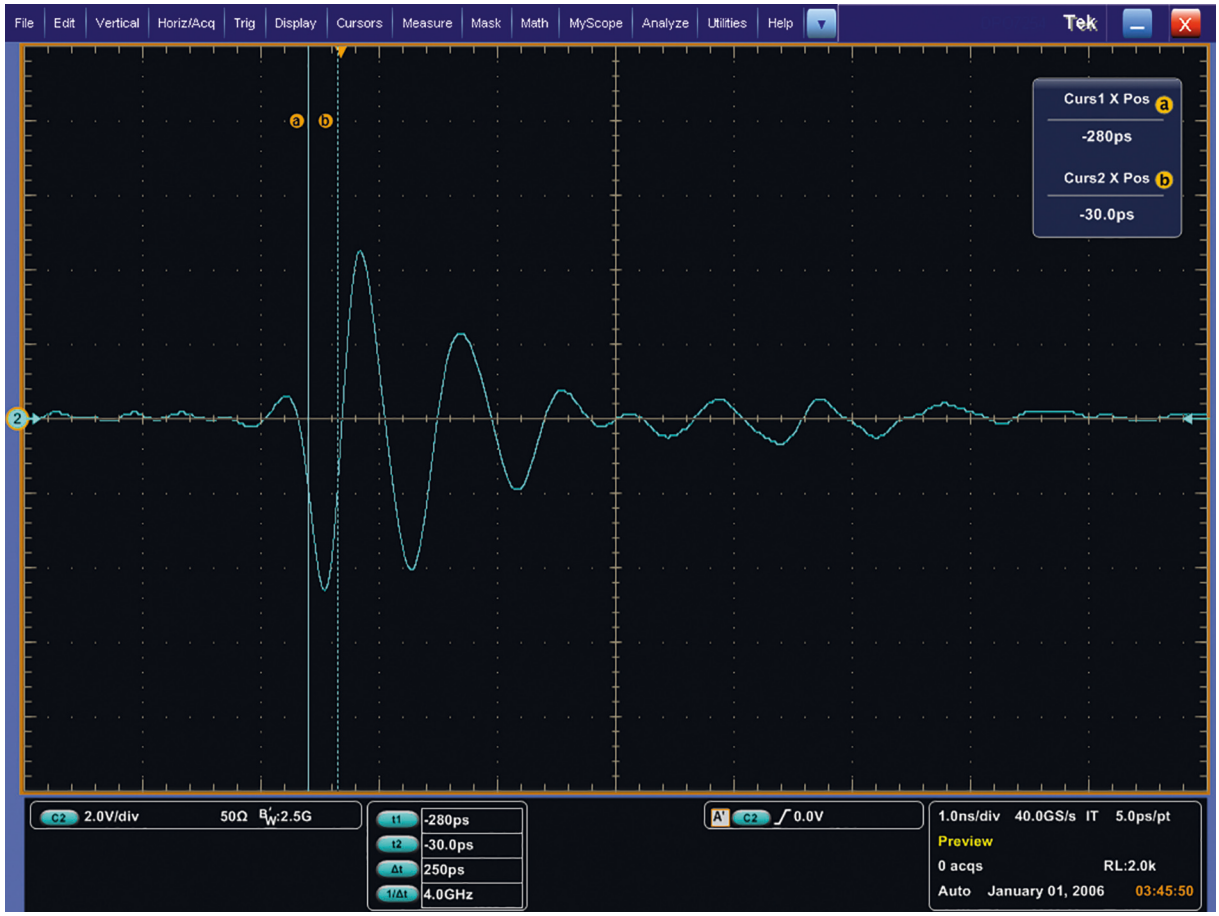

Figure 10: Single narrow pulse signal transmitted by the transmitter.

are obtained. u_{n1}', u_{n3}', and u_{n5}' are the initial state values of capacitors C_1, C_3, and C_5 in the circuit integration process at diode cutoff. Through the iterative operation of equations (8), the final state values of the three capacitors in the upper half of the nth cycle circuit can be obtained. $u_{(n+1)1}$, $u_{(n+1)3}$, and $u_{(n+1)5}$ are the initial states of the three capacitors during diode conduction in the next period.

The output signal of the upper part of the BSIC can be obtained by iterative calculation with the above method. In the same way, the output signal of the lower half of the BSIC can be obtained. The BSIC is connected to the differential amplifier, and $u_2 - u_3 - u_5 + u_6$ is taken as the output result of the whole circuit.

$$\begin{aligned} u_{\mathrm{OUT}} = {} & u_{r+} + (u_{n3}' - u_{r+}) e^{-(t/2R_4C_1)} \left[\cosh\left(\frac{\alpha}{R_4C_1}t\right) \right. \\ & \left. + \frac{1}{2\alpha}\sinh\left(\frac{\alpha}{R_4C_1}t\right) \right] - u_{n5}' e^{-(t/R_6C_5)}, \\ & - u_{r-} - (u_{n4}' - u_{r-}) e^{-(t/2R_5C_2)} \left[\cosh\left(\frac{\beta}{R_5C_2}t\right) \right. \\ & \left. + \frac{1}{2\beta}\sinh\left(\frac{\beta}{R_5C_2}t\right) \right] + u_{n6}' e^{-(t/R_7C_6)}, \end{aligned} \tag{10}$$

where $\alpha = \sqrt{(R_2C_3 - 4R_4C_1)/4R_2C_3}$, $\beta = \sqrt{(R_3C_4 - 4R_5C_2)/4R_3C_4}$.

3. Simulation and Test

3.1. Simulation and Test Methods. In this paper, the mathematical model of equation (10) BSIC is simulated, and the output signal of the actual circuit is measured to study the influence of circuit element parameters on the output signal so as to determine the parameters. The schematic block diagram of circuit parameter simulation and measurement is shown in Figure 5.

As shown in Figure 5, a modulated received signal is generated, and the received signal is input into a receiving circuit that has replaced different capacitance values. The capacitance values of the sampling capacitor, the integrating capacitor, and the high-pass filter capacitor in the circuit have been replaced, respectively. The influence of sampling capacitance, integrating capacitance and high-pass filter capacitance on the output signal of receiver, is studied through the waveform of output signal of receiving circuit.

The measured receiving circuit is shown in Figure 6.

In Figure 6, on the front side of the receiver (Figure 6(a)) are the BSIC and the amplification circuit. On the back of the receiver (Figure 6(b)) is the IR-UWB signal generation circuit. The BSIC, shown in Figure 5, is above the first black

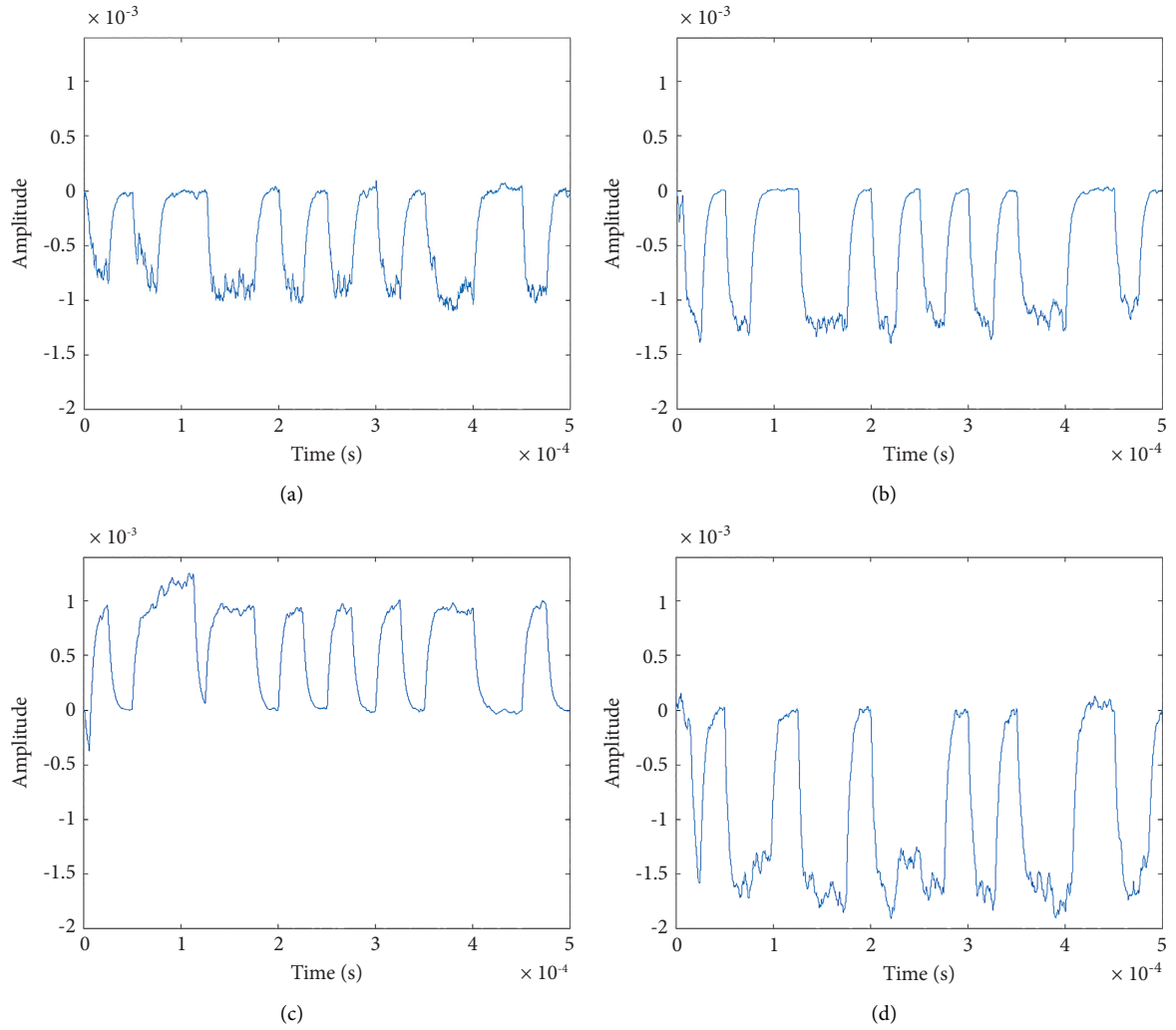

Figure 11: Simulation output waveforms of receiving circuit models with different sampling capacitors. (a) Sampling capacitance is 1 pF, (b) sampling capacitance is 2 pF, (c) sampling capacitance is 4 pF, and (d) sampling capacitance is 6 pF.

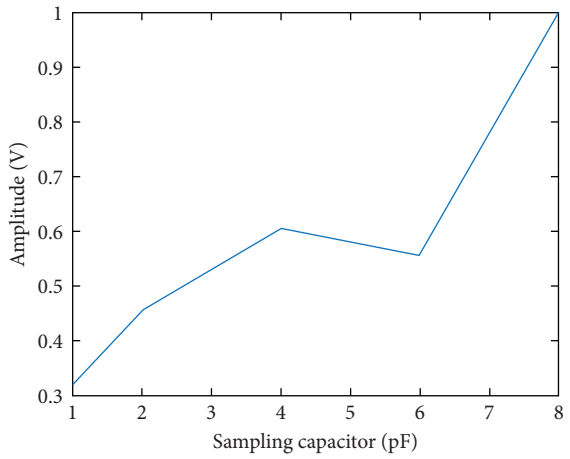

Figure 12: The relationship between the sampling capacitor and the normalized amplitude of the output signal of the receiving circuit simulated by equation (10).

Table 1: Output signal amplitude of BSIC with different sampling capacitors.

Sampling capacitance value (pF)	Circuit output signal amplitude (mV)
1	80
2	160
4	380

package amplifier in Figure 6(a). And ports 1 and 8 are 12 V and −12 V power supply. Port 2 is the output of differential amplifier. Port 3 is the output of comparator. Port 4 is the output of amplifier. Ports 5 and 6 connected to ground. Port 7 is the input signal, which controls the sampling switch. Ports 9 and 10 are connected to IR-UWB symmetrical dipole antennas.

The measured principle block diagram of the output signal of IR-UWB wireless communication receiver is shown in Figure 7, which is mainly composed of a transmitter, a

(a)

(b)

Figure 13: Continued.

(c)

Figure 13: The influence of different sampling capacitors on the output signal of the BSIC. (a) Sampling capacitance is 1 pF. (b) Sampling capacitance is 2 pF. (c) Sampling capacitance is 4 pF.

receiver, an encoder, a DC stabilized power supply, an oscilloscope, and a synchronization line.

Equipment models are as follows. Encoder: ALTERA Cyclone IV EP4CE6E22C8N. DC stabilized power supply: DH1718E-4. Oscilloscope: Tektronix DPO 7254 2.5 GHz 40 GS/s. Synchronization line: Coaxial line. The transmitter and receiver are made by ourselves.

As shown in Figures 7 and 8, the encoded signal generated by the encoder is modulated and then emitted by the transmitter, and the signal reaches the receiver through the wireless channel. At the same time, the transmitter sends the synchronous signal to the receiver through the synchronous line. Power supply for UWB wireless communication transmitter and receiver by DC stabilized power supply. The oscilloscope tests the output signal of receiver and the encoded signal of transmitter in different channels. The mathematical model of the receiver proposed in this paper is verified by measuring the output signal of the receiver, which has replaced the values of sampling capacitance, integrating capacitance and high-pass filter capacitance in the receiver.

When the parameters of the receiver are determined, a channel simulation module is added between the modulation signal and the receiver to simulate the channel noise, and the noise category is Gaussian white noise. The SNR is changed during simulation to test the receiver's antinoise ability.

3.2. Simulation and Test Setup. The single narrow pulse signal received by the receiver in the simulation is an ultra-wideband signal with a narrow pulse width of 200 ps. The normalized waveform is shown in Figure 9.

The signal in Figure 9 is obtained from a Gaussian second-order derivative by simulation of the antenna model in the CST software.

The OOK modulated binary code is used in the simulation, the narrow pulse repetition period is 50 ns, and the unit code length is 25 μs. The resistance R_1 is 51 Ω, R_2 and R_3 are 1 MΩ, R_4 and R_5 are 10 kΩ, R_6 R6 and R_7 are 200 kΩ, the capacitors C_1 and C_2 are 4 pF, C_3 and C_4 are 25 nF, and C_5, C_6 are 19.5 nF.

The narrow pulse signal transmitted by the transmitter during the test is shown in Figure 10, and the pulse width is about 250 ps.

The OOK modulated binary code is used in the simulation, the narrow pulse repetition period is about 52 ns, and the unit code length is 25 μs. The resistance R_1 is 51 Ω, R_2 and

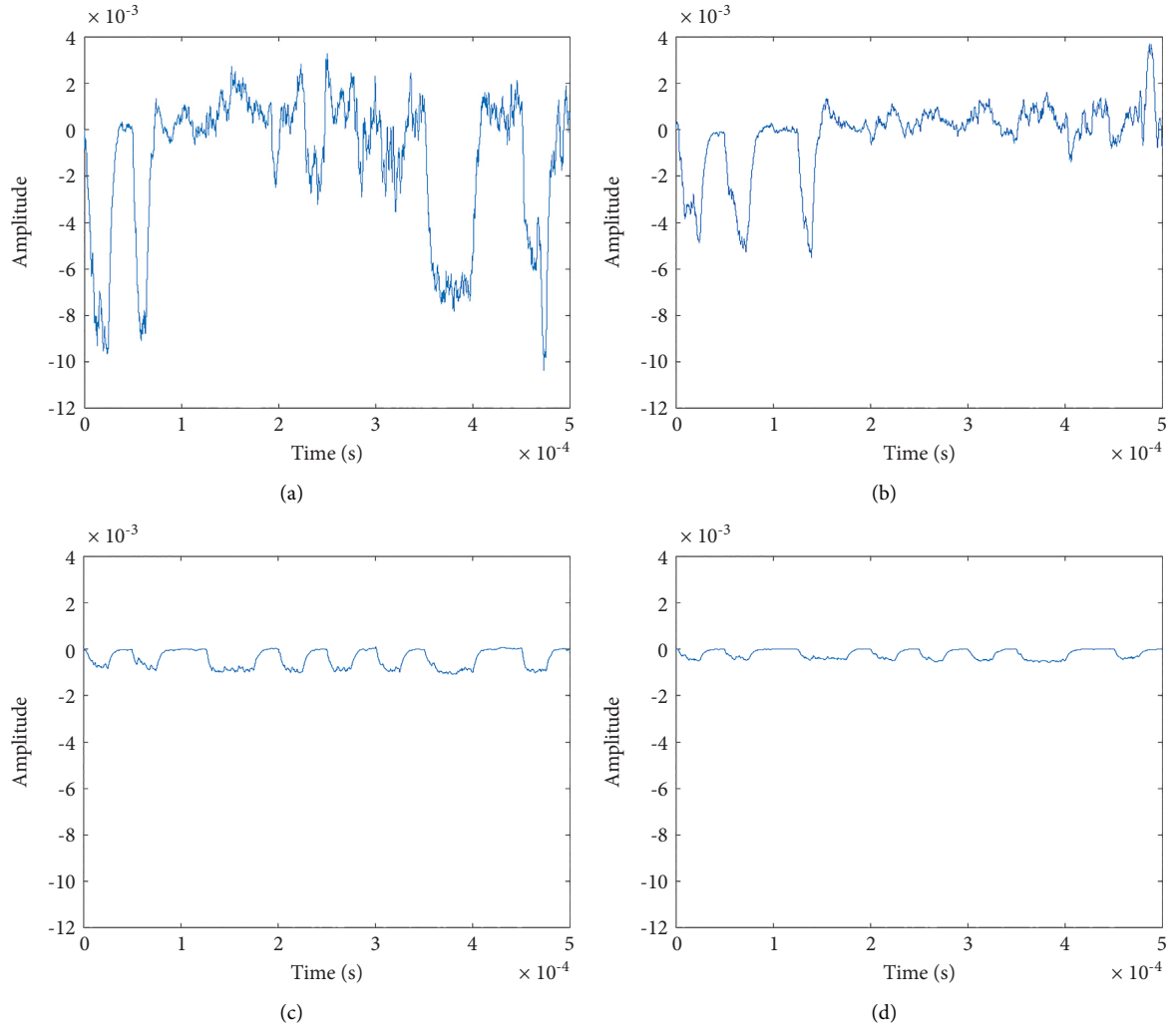

Figure 14: The simulation output waveform of the mathematical model of the receiving circuit with different integrating capacitors. (a) Integral capacitance is 2.5 nF. (b) Integral capacitance is 5 nF. (c) Integral capacitance is 25 nF. (d) Integral capacitance is 50 nF.

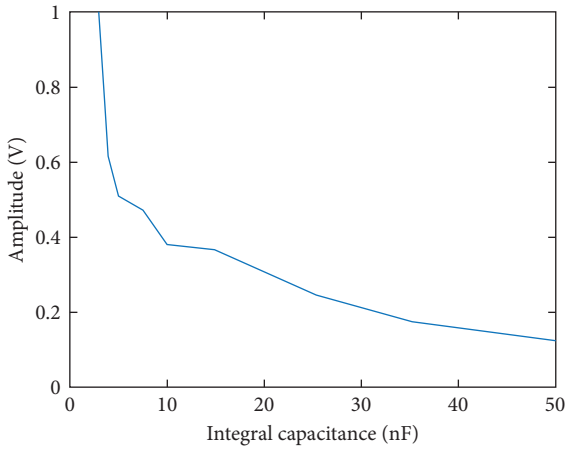

Figure 15: The relationship between the integrating capacitance and the output signal amplitude simulated by equation (10).

R_3 are 1 MΩ, R_4 and R_5 are 10 kΩ, R_6 and R_7 are 200 kΩ, the capacitors C_1 and C_2 are 4 pF, C_3 and C_4 are 22 nF, and C_5, C_6 are 18 nF.

4. Results and Discussion

4.1. Receiver Output Signal with Different Sampling Capacitors. The value of the sampling capacitor depends on the pulse width of the received UWB signal. The approximate value range of the sampling capacitor can be calculated by the principle of capacitor charging.

$$u_{C_1}(t) = u_{r_+}\left(1 - e^{-\left(t/R_qC_1\right)}\right), \tag{11}$$

where u_{r_+} is the receive voltage, u_{C_1} is the voltage of sampling capacitor, and R_qC_1 is the time constant τ.

For the UWB signal pulse width is 200 ps, τ can be 50 ps, 100 ps, 200 ps, and 300 ps. The corresponding sampling capacitors C_1 and C_2 are, respectively, 1 pF, 2 pF, 4 pF, and 6 pF; the output signal of the receiving circuit can be obtained through the simulation of (10) as shown in Figure 11.

The relationship between the value of sampling capacitance C_1, C_2 and the output waveform amplitude obtained by simulation of the receiving circuit through equation (10) is shown in Figure 12.

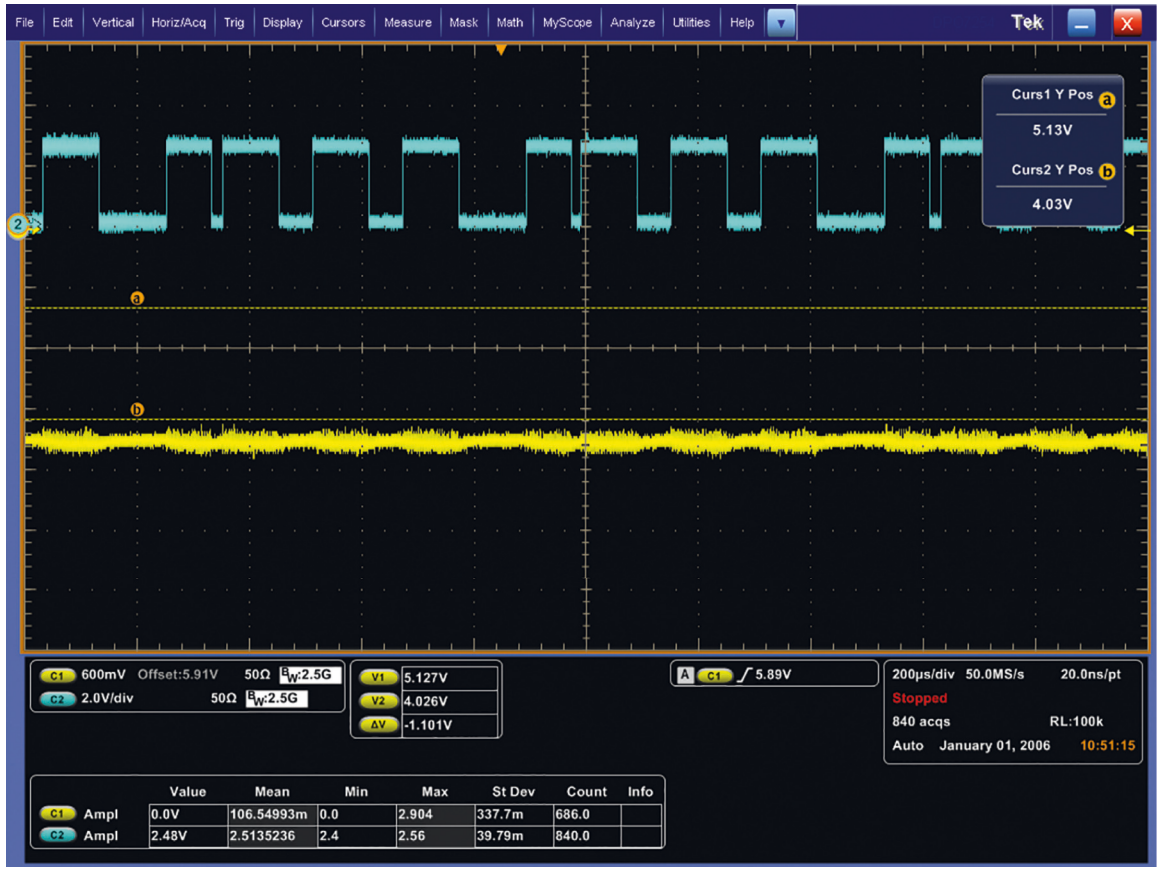

(a)

(b)

Figure 16: Continued.

(c)

Figure 16: The influence of different integral capacitance on the output signal of the balanced sampling integral receiver circuit. (a) Integrating capacitance is 22 pF. (b) Integrating capacitance is 4.7 nF. (c) Integrating capacitance is 22 nF.

It can be clearly seen from Figures 11 and 12 that when the sampling capacitance C_1 and C_2 is changed, the output waveform amplitude of the BSIC changes significantly. The output signal of the receiving circuit increases with the increase of the sampling capacitance. When the sampling capacitance is 6 pF, the output signal amplitude of the receiving circuit decreases slightly.

When the sampling capacitors C_1 and C_2 are, respectively, 1 pF, 2 pF, and 4 pF, the output signal waveform of the BSIC is shown in Figure 13.

The influence of different sampling capacitors on the output signal amplitude of the BSIC is shown in Table 1.

As shown in Figure 13 and Table 1, the amplitude of the output signal of the BSIC increases with the increase of the sampling capacitance, and the trend is the same as the simulation result, when the sampling capacitance does not exceed 8 pF.

4.2. Receiver Output Signal with Different Integral Capacitance. The value of the integrating capacitor is determined by the interval between two narrow pulses. The charging process of the integrating capacitor C_3 is the same as the discharge process of the sampling capacitor C_1. The discharge time constant for the sampling capacitor is as follows:

$$\tau = \frac{C_1 C_3}{C_1 + C_3} R_4. \tag{12}$$

Table 2: Output signal amplitude of different integral capacitor BSIC.

Integrating capacitance value (pF)	Circuit output signal amplitude (mV)
22	—
4700	648
22000	640

Because the interval between two narrow pulses is 100 ns, the integrating capacitors C_3 and C_4 are 2.5 nF, 5 nF, 25 nF, and 50 nF, respectively, the output signal of the receiving circuit can be obtained through the simulation of (10), as shown in Figure 14.

Figure 15 shows the relationship between the integrating capacitors C_3, C_4 and the receiving circuit through the simulation of equation (10).

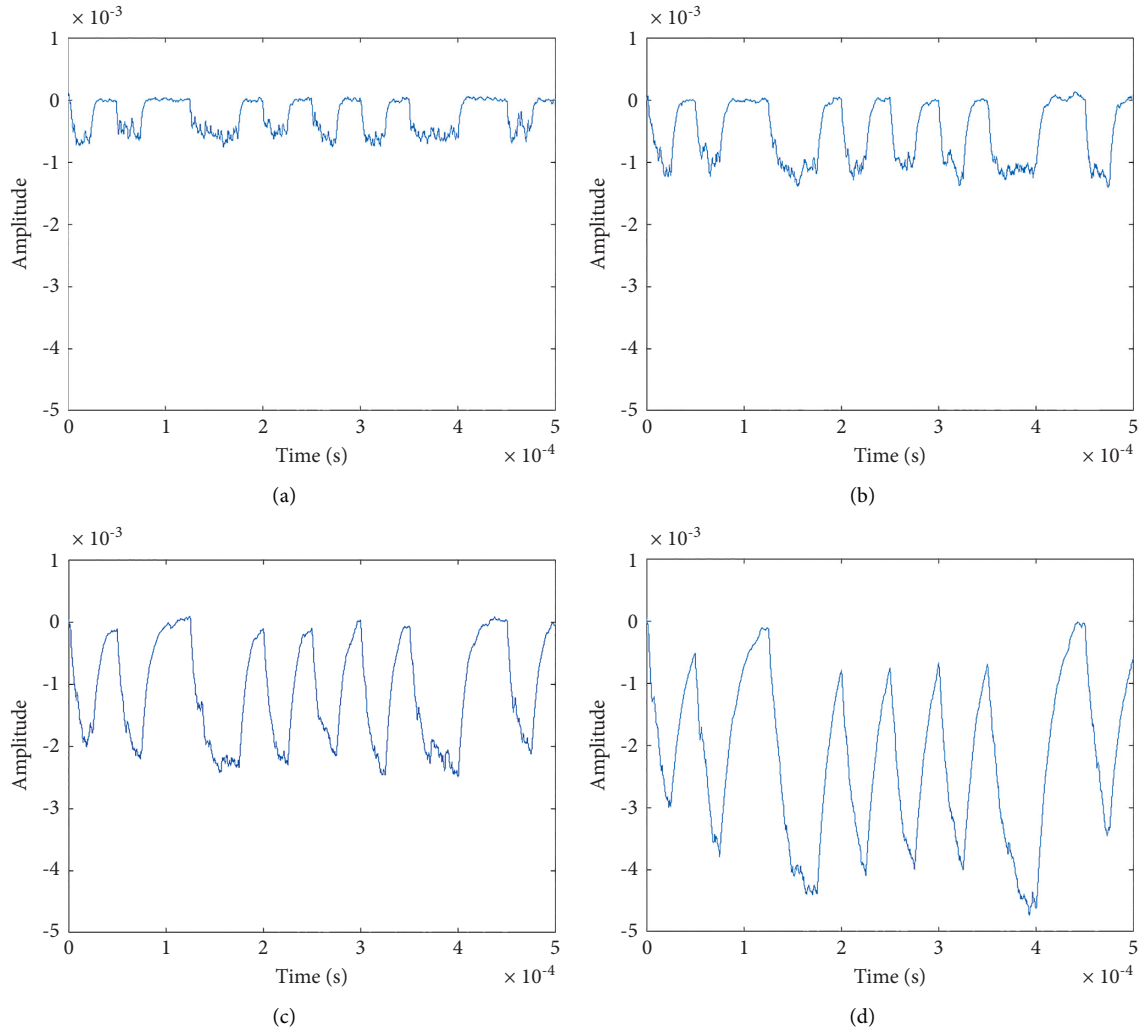

Figure 17: The simulation output waveform of the mathematical model of the receiving circuit with different filter capacitors. (a) Filter capacitance is 9.75 nF. (b) Filter capacitance is 19.5 nF. (c) Filter capacitance is 39 nF. (d) Filter capacitance is 78 nF.

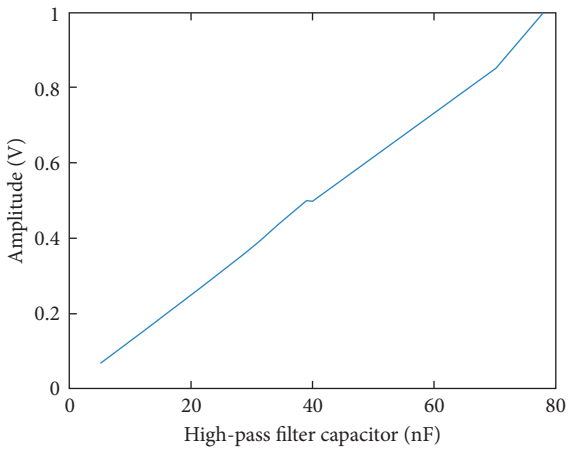

Figure 18: The relationship between the high-pass filter capacitance and the output signal amplitude simulated by equation (10).

As shown in Figures 14 and 15, the amplitude of the output signal of the receiving circuit decreases as the integral capacitance C_3 and C_4 increase. When the integrating capacitance increases to 5 nF, the output signal amplitude of the receiving circuit decreases rapidly. When the integrating capacitance increases from 5 nF to 50 nF, the output signal amplitude of the receiving circuit decreases gradually.

When the integrating capacitors C_3 and C_4 are, respectively, 22pF, 4.7 nF, and 22 nF, the output signal waveform of the BSIC is shown in Figure 16.

The influence of different integrating capacitors on the output signal amplitude of the BSIC is shown in Table 2.

As shown in Figure 16 and Table 2, when the integrating capacitor is 22 pF, there is no obvious waveform amplitude as a DC voltage. When the integrating capacitor is 4.7 nF, part of the waveform amplitude can be seen to be 648 mV. When the integrating capacitor is 22 nF, obvious waveforms can be seen, with an amplitude of 640 mV.

The simulated and measured results are the same in that the output waveform becomes better when the integrating capacitor is around 22 nF. The difference is in the output waveform when the integration capacitance is less than 22 nF.

(a)

(b)

Figure 19: Continued.

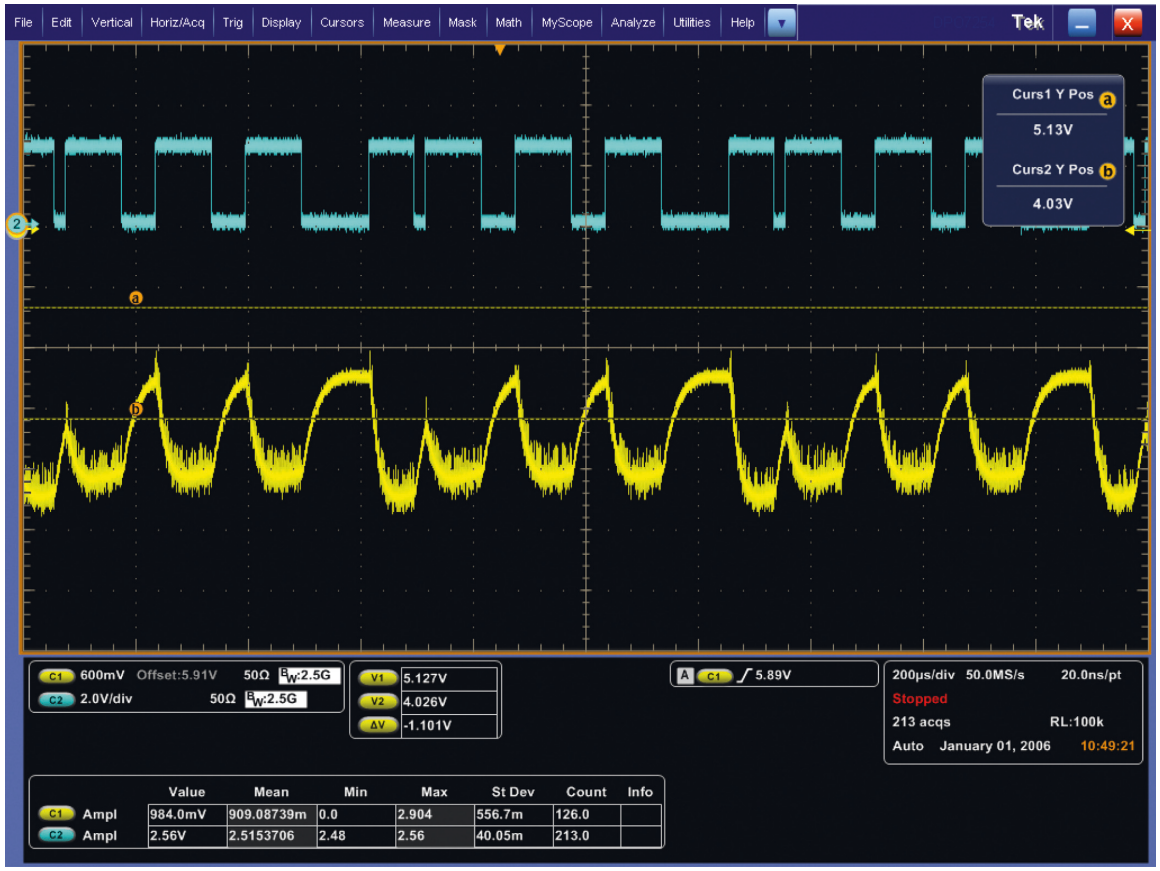

(c)

Figure 19: The influence of different high-pass filter capacitors on the output signal of the balanced sampling and integrating receiver circuit. (a) Filter capacitance is 10 nF. (b) Filter capacitance is 18 nF. (c) Filter capacitance is 39 nF.

4.3. Receiver Output Signal with Different Filter Capacitance. When the filter capacitors C_5 and C_6 are, respectively, 9.75 nF, 19.5 nF, 39 nF, and 78 nF, the output signal of the receiving circuit obtained by the simulation based on equation (10) is shown in Figure 17.

The amplitude relationship between different filter capacitors C_5, C_6 and the output signal of the receiving circuit simulated through equation (10) is shown in Figure 18.

It can be seen from Figures 17 and 18 that the amplitude of the output signal of the receiving circuit increases with the increase of the filter capacitors C_5 and C_6.

When the filter capacitors C_5 and C_6 are 10 nF, 18 nF, and 39 nF, respectively, the output signal waveform of the BSIC is shown in Figure 19.

The influence of different high-pass filter capacitors on the output signal amplitude of the BSIC is shown in Table 3.

As shown in Figure 19 and Table 3, the output signal amplitude of the BSIC increases with the increase of the high-pass filter capacitor value, but the waveform is obviously distorted when the waveform reaches 39 nF. The measured result trend is the same as the model simulation result.

Table 3: Output signal amplitude of different filter capacitor BSIC.

Filter capacitance value (nF)	Circuit output signal amplitude (mV)
10	300
18	920
39	984

4.4. Simulation Results of Received Signals under Different SNR. When SNR is −30 dB, the time-domain waveform diagram of the received signal and the receiver output signal is shown in Figure 20.

To show the differences between all receiver output signals, the receiver output SNR and BER of receiver output signal is provided in Figure 21. The input SNR is the ratio of signal to noise in the channel. The output SNR is the ratio of the receiver output signal to the output noise. The BER is obtained by dividing the number of error bits by the total number of bits transmitted. The number of erroneous bits is obtained by statistical method.

The receiver output SNR decreases as the SNR decreases in Figure 21, and the BER also increases as the SNR decreases. Figure 21 shows that the BER of the receiver output signal is less than 10–3 when the input SNR is greater than −15 dB.

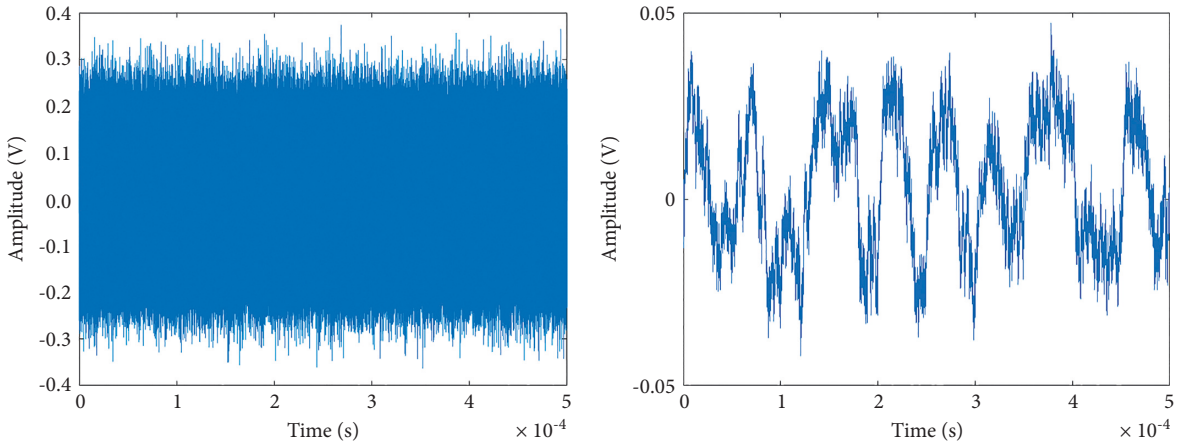

Figure 20: The time-domain waveform of the received signal and output signal of the receiver when SNR is −30 dB. (a) Receive signal. (b) Receiver output signal.

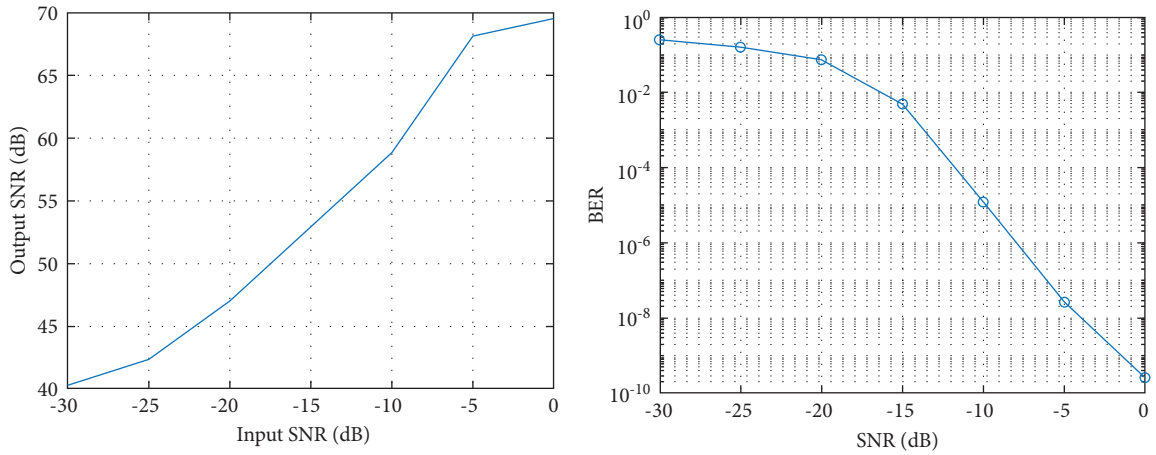

Figure 21: Receiver performance in low SNR environments. (a) Receiver output SNR. (b) BER of receiver output signal.

Table 4: Comparing with other published works.

	This work	Ref. [10]	Ref. [12]	Ref. [13]	Ref. [22]	Ref. [20]
Pulse width (ns)	0.20	—	Less 33	0.85	0.80	0.22
SNR of max. BER (dB)	−30	0	8	0	9	1
Maximum BER	10–1	10–1	10–1	10–1	10–1	10–1
SNR of min. BER (dB)	0	20	18	20	30	14
Minimum BER	10–9	10–8	10–4	10–5	10–5	10–5

The antinoise performance of the receivers in this paper is compared with other receivers in Table 4. The operating environment, BER, and pulse width of the receivers are compared in Table 4. It can be seen from the table that the UWB signal pulse width used in this paper is the narrowest. When BER is the highest, it is in the same order of magnitude as other receivers, but its corresponding SNR is the lowest, which is −30 dB. The receiver proposed in this paper is 1 to 4 orders of magnitude lower than other receivers at the minimum BER, and its corresponding SNR is also the lowest. This indicates that the receiver's antinoise ability is stronger than other receivers operating in high SNR environments.

5. Discussion

Through the simulation and measured results in Sections 4.1 to 4.3, it can be seen that the BSIC model established in this paper is consistent with the real circuit. However, in order to simplify the calculation, some parameters in the model are

ignored, which leads to a little difference between the calculated results using the model and the measured results.

In Section 4.4, the simulation results of the model in different SNR environments are compared with the results of some articles. The comparison results show that the anti-interference ability of BSIC receiver is stronger than other compared receivers. However, due to the characteristics of capacitor charging and discharging, the upper limit of data rate of BSIC receiver is lower than receivers with other structures. Therefore, the BSIC receiver can be mainly used in areas with relatively bad channel environment.

6. Conclusions

The IR-UWB receiver based on BSIC is improved to enhance its anti-interference ability. The mathematical model of the improved BSIC is established by using the circuit transient analysis method, and the expression of the output signal of the UWB wireless communication receiver is obtained by Laplace transform. The receiver parameters are studied and optimized based on BSIC model. The results of the study show that the integration capacitance in the receiver circuit has the greatest impact on the received signal waveform at an interval of 100 ns with a width of 200 ps; the smaller the integration capacitance, the worse the received signal waveform, in the range of 2.5 pF to 25 pF. This is basically the same as the test results. Simulation and test results show that the receiver model developed in this paper can serve as a guide for optimizing the receiver circuit parameters. The effect of noise on the output signal of the receiver was investigated and compared, and the results showed that the BER of the receiver is less than 0.005 when the SNR is greater than −15 dB. The comparison results show that the anti-interference ability of the improved BSIC receiver is stronger than that of other receivers. This improvement is effective. The next step is to increase the data transmission rate of this receiver.

Data Availability

The data used to support the findings of this study are included within the article.

Conflicts of Interest

The authors declare that there are no conflicts of interest regarding the publication of this paper.

References

[1] S. Sharma and Y. Hong, "UWB receiver via deep learning in MUI and ISI scenarios," *IEEE Transactions on Vehicular Technology*, vol. 69, no. 3, pp. 3496–3499, 2020.

[2] S. Sharma, A. Gupta, and V. Bhatia, "IR-UWB sensor network using massive MIMO decision fusion: design and performance analysis," *IEEE Sensors Journal*, vol. 18, no. 15, pp. 6290–6302, 2018.

[3] J. Zhang, P. V. Orlik, Z. Sahinoglu, A. F. Molisch, and P. Kinney, "UWB systems for wireless sensor networks," *Proceedings of the IEEE*, vol. 97, no. 2, pp. 313–331, 2009.

[4] J. Ren, T. Zhang, J. Li, L. H. Nguyen, and P. Stoica, "RFI mitigation for UWB radar via hyperparameter-free sparse SPICE methods," *IEEE Transactions on Geoscience and Remote Sensing*, vol. 57, no. 6, pp. 3105–3118, 2019.

[5] T. Wan, K. Jiang, H. Ji, and B. Tang, "Deep Learning-Based LPI Radar Signals Analysis and Identification Using a Nyquist Folding Receiver Architecture," *Defence Technology*, 2021.

[6] M. Crepaldi, G. N. Angotzi, and L. Berdondini, "A 0.34 mm^2 1 Gb/s non-coherent UWB receiver architecture with pulse enhancement and double PLL clock/data packet recovery," *IEEE Transactions on Circuits and Systems I: Regular Papers*, vol. 66, no. 7, pp. 2735–2748, 2019.

[7] Xi Qin, Y. Huang, and Z. Hong, "A 6-7 GHz, 40 dB receiver RF front-end with 4.5 dB minimum noise figure in 0.13μm CMOS for IR-UWB applications," *Journal of Semiconductors*, vol. 34, no. 3, Article ID 035006, 2013.

[8] L. Cai, L. Huang, Z. Fu, J. Yang, and W. Wang, "An energy detection receiver for non-coherent IR-UWB," *Journal of Semiconductors*, vol. 32, no. 6, Article ID 065006, 2011.

[9] D. C. Daly, P. P. Mercier, M. Bhardwaj et al., "A pulsed UWB receiver SoC for insect motion control," *IEEE Journal of Solid-State Circuits*, vol. 45, pp. 153–166, 2010.

[10] M. A. Rahman, S. Sasaki, Z. Jie, S. Muramatsu, and H. Kikuchi, "Evaluation of selective RAKE receiver in direct sequence ultra wideband communications in the presence of interference," *Ieice T Fund Electr*, vol. E87-A7 pages, 2004.

[11] R. Price and P. Green, "A communication technique for multipath channels," *Proceedings of the Ire*, vol. 46, no. 3, pp. 555–570, 1958.

[12] H. Khani, "Iterative Algorithms to Compensate for Quantization Noise in Monobit Transmitted-Reference Receivers," in *Proceedings of the 2014 IEEE International Conference on Ultra-WideBand (ICUWB)*, September 2014.

[13] H. Gharaee and A. Nabavi, "Baseband implementation of OTR-UWB receiver using FPGA," *AEUE - International Journal of Electronics and Communications*, vol. 64, no. 3, 2010.

[14] D. D. Wentzloff, F. S. Lee, D. C. Da Ly, M. Bhardwaj, and A. P. Chandrakasan, "Energy Efficient Pulsed-UWB CMOS Circuits and Systems," in *Proceedings of the IEEE International Conference on Ultra-wideband*, Singapore, September 2007.

[15] T. Quek and M. Z. Win, "Analysis of UWB transmitted-reference communication systems in dense multipath channels," *IEEE Journal on Selected Areas in Communications*, vol. 23, no. 9, 2005.

[16] M. Javadi, H. Miar-Naimi, and S. M. Hosseini Andargoli, "A UWB receiver with modified CS-CG LNTA: noise and nonlinearity analysis," *International Journal of Circuit Theory and Applications*, vol. 47, no. 5, pp. 654–665, 2019.

[17] D. Elsheakh, H. Shawkey, and S. Saleh, "A 9 - 10.6 GHz microstrip antenna—UWB low noise amplifier with differential noise canceling technique for IoT applications," *International Journal of Communications, Network and System Sciences*, vol. 12, no. 11, pp. 189–197, 2019.

[18] S. Arshad, R. Ramzan, and Q. U. Wahab, "50-830 MHz noise and distortion canceling CMOS low noise amplifier," *Integration, the VLSI Journal*, vol. 60, 2017.

[19] P. Jamshidi, "An Ultra Wideband Low-Power Low-Noise Amplifier Using Coupled Inductors," in *Proceedings of the Iranian Conference on Electrical Engineering*, Tehran, Iran, May 2015.

[20] Y. Shim, C. W. Kim, J. Lee, and S. G. Lee, "Design of Full Band UWB Common-Gate LNA," *Ieee Microw Wirel Co*, vol. 17, no. 10, 2007.

[21] C. F. Liao and S. I. Liu, "A Broadband Noise-Canceling CMOS LNA for 3.1-10.6-GHz UWB Receiver," *Custom Integrated Circuits Conference*, vol. 42, no. 2, 2005.

[22] S. Sharma, V. Bhatia, K. Deka, and A. Gupta, "Sparsity-based monobit UWB receiver under impulse noise environments," *IEEE Wireless Communications Letters*, vol. 8, no. 3, pp. 849–852, 2019.

[23] F. Sun, H. Yin, and W. Wang, "Finite-Resolution digital receiver for UWB TOA estimation," *IEEE Communications Letters*, vol. 16, no. 1, pp. 76–79, 2012.

[24] H. Yin, Z. Wang, L. Ke, and J. Wang, "Monobit digital receivers: design, performance, and application to impulse radio," *IEEE Transactions on Communications*, vol. 58, no. 6, pp. 1695–1704, 2010.

[25] L. Ke, H. Yin, W. Gong, and Z. Wang, "Finite-resolution digital receiver design for impulse radio ultra-wideband communication," *IEEE Transactions on Wireless Communications*, vol. 7, no. 12, pp. 5108–5117, 2008.

[26] Y. Yan, H. Zhonghua, and C. Zhanzhong, "Influence of sampling pulse on balanced sampling integral differential circuit performance," *Journal of Data Acquisition & Processing*, vol. 26, no. 2, 2011.

Hindawi
Mobile Information Systems
Volume 2022, Article ID 3744523, 12 pages
https://doi.org/10.1155/2022/3744523

Research Article

Mobile Edge Computing Application in English Teaching Classroom Evaluation System Based on BPSO Algorithm

Junling Yu

College of Foreign Languages, University of Shanghai for Science and Technology, Shanghai 200093, China

Correspondence should be addressed to Junling Yu; wendysunwater@usst.edu.cn

Received 24 June 2022; Revised 21 July 2022; Accepted 30 July 2022; Published 17 August 2022

Academic Editor: Shadi Aljawarneh

This paper proposes a multi-user and multi-MEC scenario based on mobile edge computing to maximize the overall revenue to complete the task and proposes business guarantee and resource constraints as conditions to form the optimal task offloading resource allocation problem based on the Lyapunov mobile edge computing theory. Because this problem is NP-hard problem, decoupling is proposed as a solution to the channel resource allocation problem, which is solved by the KKT task allocation condition and the 0-1 integer programming problem. Aiming at the high-speed mobile terminal scene, a high-speed unloading algorithm is proposed, which explains the task unloading system model in the high-speed mobile terminal scene. The task offloading algorithm first allocates several subtasks according to the number of MEC servers and the remaining available resources of the MEC servers. At the same time, taking campus as an example, the English teaching classroom evaluation application uses the big data evaluation scale to complete the evaluation and uses statistical software to test the reliability of the evaluation results. Based on the analysis results, it summarizes and reflects on the education evaluation index system and puts forward suggestions for improving the evaluation system and implementing the English education guarantee mechanism. This paper uses the research of mobile edge computing resources to allocate big data and applies it to the application of English teaching classroom evaluation, thereby promoting the rapid development of classroom teaching.

1. Introduction

With the advent of the big data era, many computationally intensive and latency-sensitive applications need to achieve low latency and low power consumption. However, the allocation of mobile edge computing resources of mobile devices is limited, which makes computing data have the disadvantages of high latency and high-power consumption of the device. Mobile edge computing is proposed to meet users' high-quality service requirements for the network. It uses servers located at the edge of the network to provide users with computing resources, resource allocation, and IT services, which will greatly improve the quality of service. At present, the problems of computing offloading and resource allocation are still unresolved, which has great research value. In order to minimize task execution delay and energy consumption, this paper mainly studies the cooperative mobile edge computing and resource allocation strategies in the MEC system [1]. Since the release of the experimental draft of the curriculum standards, the demand for art education in English teaching has continued to increase, and the pursuit of English teaching by front-line teachers, professionals, and scholars has kept pace with the times [2]. In recent years, with the continuous improvement of the application of English teaching classroom evaluation and educational practice, English culture education has also developed [3]. However, on the other hand, although English cultural education has attracted the attention of many scholars and teachers, it also has its drawbacks. In other words, the evaluation research of English art education has not kept up with the development of art education [4]. The big data questionnaire survey has enabled art education to be widely disseminated [5]. When I checked the literature, I found that the meaning, methods, and content of English art education have been deeply explored, and satisfactory results have been obtained. However, there are few studies on English classroom assessment [6]. There is a serious lack of art education

evaluation theory, and there is no operable index system for art education evaluation, which will affect the overall development of English art education [7]. From the perspective of English classroom teaching, this article has carried out an extended exploration of the application of current English teaching classroom evaluation, aiming to provide reference materials for the development and improvement of cultural education evaluation theory [8]. After determining the subject of constructing constructive and meaningful English teaching evaluation application system, this research focuses on relevant literature and big data, as well as the relationship between culture and language [9]. Based on the analysis of cultural education, we have carried out cultural education surveys and evaluations [10]. On the basis of research and analysis, this research conducted a preliminary assessment of art education and tried to analyze examples.

2. Related Work

The literature introduces the theory of multi-user and multi-MEC scenarios based on Lyapunov and proposes a collaborative optimization algorithm for task offloading resource scheduling [11]. Computing and channel resources are allocated according to factors such as user task load, MEC server processing capacity, mobile device processing capacity, and channel resource usage, so as to maximize the benefits of completing tasks for all users [12]. The literature introduces the research of Q learning on end-side cloud collaborative task offloading and resource allocation management. A computing offloading framework for end-to-side cloud collaboration is proposed, the two factors of time delay and energy consumption are considered to define the terminal benefit reflecting QoS guarantee, and the optimization goal is to maximize the terminal benefit [13]. Then, the problem is further formulated as a semi-Marco in the decision-making process, and Q learning is used to optimize the optimization target to obtain the best task offloading decision and resource allocation strategy [14, 15]. The literature introduces a distributed and cooperative joint computing offloading and resource allocation strategy. If there are frequent requests for computing tasks, the local MEC server with limited resources cannot meet the needs of users. Therefore, the calculation task is forwarded to the nearby MEC server to complete the calculation, and additional calculation is provided for the task in the local area that cannot meet the requirements, so that the load of the local MEC server is effectively reduced [16]. The literature introduces collaborative computing offloading and resource allocation strategies. This article first created a network model, a communication model, and a task calculation model [17]. The task execution cost was defined as the weighted sum of execution delay and energy consumption, and the task execution cost was minimized under the constraints of communication resources and computing resources [18]. The literature introduces the mathematical modeling of delay and energy cost in the process of task offloading and formulates an objective function to minimize task execution cost [19]. Then, the optimization problem is split, the resource allocation sub-problem is solved by the Lagrangian multiplier method, the computational unloading sub-problem is solved by the proposed computational unloading algorithm based on the greedy algorithm, and finally the experimental simulation and performance evaluation are carried out.

3. Mobile Edge Computing Resource Allocation and Big Data Evaluation System

3.1. System Model and Problem Description. In this section, we first introduce the multi-user multi-cell MEC network scenario, then formulate the system communication model and calculation model, and finally describe the established optimization problem.

Figure 1 shows a multi-user multi-cell MEC network scenario. In this network scenario, the MEC server is deployed in the macro base station (MacroBS, referred to as MBS) of each cell, and the calculation task is sent to other execution modules through the task offloading strategy, including the local device CPU, the local area MEC server, and the nearby area MEC server. Each user accesses the MEC server through a wireless channel in the mobile network, and the MBS of two adjacent cells is connected to each other through a high-speed backhaul link (backhaul). This chapter mainly optimizes the computing tasks of users in cell 1 and does not consider the optimization of computing tasks in other cells for the time being. When the computing resources of the MEC server in the local area cannot meet the offloading requirements of internal users, and the MEC server in nearby cell 2 still has remaining computing resources, the local computing task can be transferred to the nearby MEC server. At this time, the MEC server in cell 2 acts as an auxiliary calculation function.

Due to the variability of the number of users, the MEC server in cell 1 may be overloaded. In order to solve this problem, three execution methods for users to complete their computing tasks are considered:

(1) Local device execution: when the local and nearby MEC servers are overloaded, computing tasks can only be executed on the local device CPU.

(2) Offload to the local MEC server: the computing resources of the local MEC server can meet the task offloading requirements, and the user offloads the task to the local MEC server through the wireless uplink.

(3) Offload to nearby MEC server: when the local MEC server is overloaded and cannot meet the user task offloading requirements in the area, the computing task will be forwarded by the local MBS to the nearby MBS MEC server through the backhaul link.

Therefore, the binary variable of the uninstallation decision on the mobile device side is defined as x_i, namely,

$$x_i = \begin{cases} 0, & \text{Task } i, \\ 1, & \text{Task } i \text{ MEC server.} \end{cases} \tag{1}$$

The local MEC server needs to make further uninstall decisions based on its own computing resources. Whether the task is to be uninstalled on the local

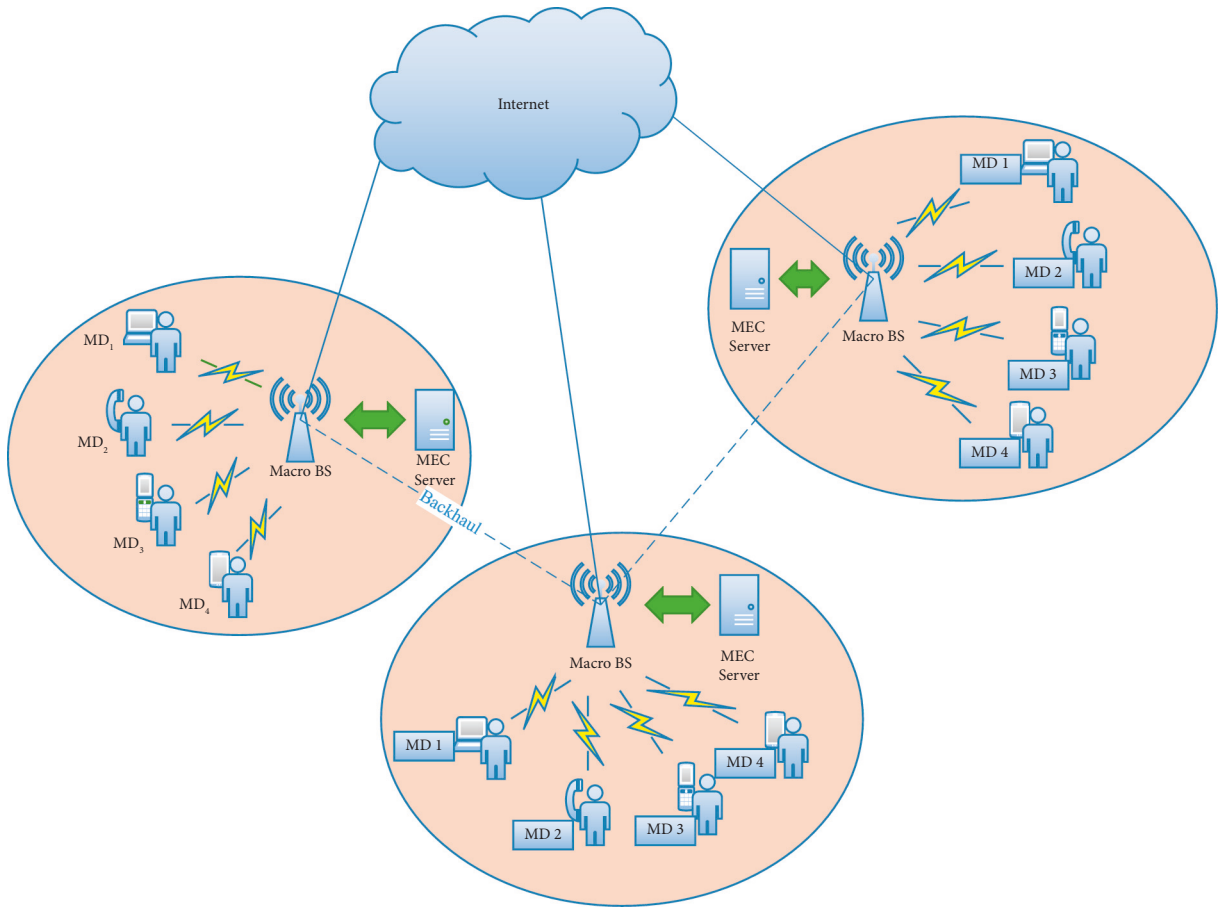

Figure 1: Multi-user and multi-cell MEC network scenario.

MEC server or the nearby MEC server, the server-side uninstall decision binary variable is defined as y_i, namely,

$$y_i = \begin{cases} 0, & \text{Task } i, \\ 1, & \text{Task } i \text{ Never MAC.} \end{cases} \tag{2}$$

If $y_i = 1$, the task i is first uploaded to the local MEC server via the wireless uplink and then forwarded between base stations via the backhaul link, and finally the task calculation results in the nearby MEC server are returned via the backhaul link again, and then via the wireless downlink road down to the user equipment.

This section introduces the communication model in the network scenario, including communication between users in a cell and base stations, and communication between base stations between cells. Since the result data volume of the computing task processed by the MEC server is very small and much smaller than the upload data volume, the delay and energy consumption of the task return phase (the task is transmitted to the user equipment via the downlink) are compared to the task upload and the execution stage is very small and generally ignored. The communication model in this chapter only considers the upload phase and does not consider the return phase for the time being.

In this cell, users upload tasks to the MEC server through the wireless uplink transmission channel. The user channel bandwidth is defined as w_i, and then the uplink transmission rate is

$$r_i = w_i \log_2\left(1 + \frac{p_i g_i}{\sigma^2}\right). \tag{3}$$

The time delay required for user equipment to transmit via the uplink is

$$T_i^t = \frac{B_i}{r_i}. \tag{4}$$

The data forwarding between the local area MEC server and the nearby area MEC server is transmitted through the high-speed backhaul link between the two base stations. In fact, the backhaul link is bidirectional transmission, but this article only considers the task forwarding from the local area MEC server to nearby regional MEC server. Assuming that the transmission rate between the two base stations is v, the delay required for forwarding calculation tasks between the base stations through the backhaul link is

$$T_i^r = \frac{B_i}{v}. \tag{5}$$

The CPU computing power of the mobile device is defined as f_i^l, and then the delay required for the execution of the computing task on the local device is

$$T_i^l = \frac{C_i}{f_i^l}. \tag{6}$$

Correspondingly, the energy consumption required for the execution of the computing task on the local device is

$$E_i^l = \varepsilon_i C_i = k\left(f_i^l\right)^r C_i. \tag{7}$$

Considering the cost of delay and energy consumption required for computing task execution, define γ as the preference parameter for task execution delay and δ as the preference parameter for task execution energy consumption, and satisfy $\gamma + \delta = 1$, specific preference parameter settings. It can be adjusted according to the task type or user needs. Define the calculation task execution cost as the weighted sum of delay and energy consumption, and then the total cost of task execution on the local device can be calculated as

$$C_i^l = \gamma T_i^l + \delta E_i^l. \tag{8}$$

Offload to the MEC server in the local area in this network scenario, the user first offloads the task to the MEC server deployed in the macro base station of the local cell, and the MEC server processes the task and then transmits the task result back to the mobile device. Define the computing resources of the local MEC server allocated to the task as *sic*, and the sum of the computing resources allocated to all tasks must meet the condition $\sum siNci = 1 \le S_{\max}^c$, where $S_{\max}^c$ is the maximum amount of computing resources available for the local MEC server. The time delay required to process the task is

$$T_i^{c,\text{exe}} = \frac{C_i}{s_i^c}. \tag{9}$$

The total delay of task offloading to the MEC server in the local area is the sum of upload delay, processing delay, and download delay. The download delay is too small to be ignored. Therefore, according to formula (4), the total delay required for task offloading is

$$T_i^c = T_i^t + T_i^{c,\text{exe}}. \tag{10}$$

When the task is offloaded, the energy consumption of the device in the idle state is very small, and it is ignored for simple calculations. The energy consumption during task offloading mainly considers the energy consumption of tasks uploaded from the device to the local MEC server. Therefore, the energy consumption required for task offloading is

$$E_i^c = p_i T_i^t = p_i \frac{B_i}{r_i}. \tag{11}$$

The total cost of offloading tasks to the MEC server in the local area is

$$C_i^c = \gamma T_i^c + \delta E_i^c. \tag{12}$$

According to formulas (8) and (12), it can be evaluated whether offloading tasks to the local MEC server can improve task offloading performance. If the system cost of offloading the task to the local MEC server is less than the cost of completing the calculation task in the local device, the decision to offload the task to the local MEC server to complete the calculation task is beneficial. Due to the limited resources of the local MEC server, if too many users simultaneously offload tasks to the local server to obtain computing resources, the computing resources of the MEC server in the area will be exhausted. Therefore, when the number of offloading tasks exceeds the maximum load of the MEC server in the local area, you can choose to forward the computing tasks to the MEC server in the nearby area to make full use of the remaining computing resources in the server.

Then, the delay required by the MEC server in the nearby area to process the task is

$$T_i^{n,\text{exe}} = \frac{C_i}{s_i^n}. \tag{13}$$

If the user decides to offload the computing task to a nearby MEC server, the task data transmission between the two base stations will cause additional delay. At this time, the total delay of task offloading to the nearby MEC server is the sum of upload delay, transmission delay, and processing delay. Therefore, according to formulas (4), (5), and (13), the total delay required for task offloading is

$$T_i^n = T_i^t + T_i^r + T_i^{n,\text{exe}}. \tag{14}$$

Similarly, the energy consumption required for task uninstallation is still the task upload energy consumption, that is, $E_{i^n} = E_{i^c}$. Therefore, the total cost of offloading tasks to nearby MEC servers is

$$C_i^n = \gamma T_i^n + \delta E_i^n. \tag{15}$$

Time delay and energy consumption are important indicators to measure system performance. We consider defining the total execution cost of the system as the weighted sum of the execution delay and energy consumption of all tasks in the unit, and jointly allocate unloading decisions, bandwidth allocation, and computing resources. The optimization problem is modeled as follows:

$$\begin{aligned}
&\min_{X,Y,W,S^c,S^n} \sum_{i=1}^{N} C_i^l(1-x_i) + C_i^c x_i(1-y_i) + C_i^n x_i y,\\
&\text{s.t.}C1:\ \sum_{i=1}^{N} s_i^c \le S_{\max_i}^c,\\
&C2:\ 0 \le s_i^c \le S_{\max}^c,\\
&C3:\ \sum_{i=1}^{N} s_i^n \le S_{\max}^n,\\
&C4:\ 0 \le s_i^n \le S_{\max}^n,\\
&C5:\ \sum_{i=1}^{N} w_i \le W_{\max},\\
&C6:\ 0 \le w_i \le W_{\max},\\
&C7:\ x_i, y_i \in \{0,1\},\\
&\forall i \in N.
\end{aligned} \tag{16}$$

3.2. Problem Solving and Algorithm Design. Uninstall to nearby area MEC server user set satisfies $N_0 + N_1 + N_2 = N$. The optimization problem can be transformed into

$$\begin{aligned}
&\min_{W,S^c,S^n} \sum_{i\in N_0} C_i^l + \sum_{i\in N_1}\left[\gamma\left(\frac{B_i}{w_i\log_2\left(1+\left(p_ig_i/\sigma^2\right)\right)}+\frac{C_i}{s_i^c}\right)+\delta\frac{p_iB_i}{w_i\log_2\left(1+p_ig_i/\sigma^2\right)}\right]\\
&\quad+\sum_{i\in N_2}\left[\gamma\left(\frac{B_i}{w_i\log_2\left(1+p_ig_i/\sigma^2\right)}+T_i^r+\frac{C_i}{s_i^n}\right)+\delta\frac{p_iB_i}{w_i\log_2\left(1+p_ig_i/\sigma^2\right)}\right],\\
&\text{s.t.}\sum_{i\in N_1} s_i^c \le S_{\max}^c, \forall i\in N_1,\\
&\quad\sum_{i\in N_2} s_i^n \le S_{\max}^n, \forall i\varepsilon N_2,\\
&\quad\sum_{i\in N_1\cup N_2} w_i \le W_{\max}, \forall i\varepsilon N_1\cup N_2.
\end{aligned} \tag{17}$$

The optimization problem is further transformed into

$$\begin{aligned}
&\min_{W,S^c,S^n} \sum_{i\in N_0} C_i^l + \sum_{i\in N_2}\frac{1}{\xi_i}\le 1, \forall i\varepsilon N_2\\
&\quad\sum_{i\in N_1}\left[\gamma\left(\frac{\lambda_i\vartheta_i}{W_{\max}}+\frac{C_i}{S_{\max}^c}\mu_i\right)+\delta\frac{p_i\lambda_i\vartheta_i}{W_{\max}}\right]\\
&\quad+\sum_{i\in N_2}\left[\gamma\left(\frac{\lambda_i\vartheta_i}{W_{\max}}+T_i^r+\frac{C_i}{S_{\max}^n}\xi_i\right)+\delta\frac{p_i\lambda_i\vartheta_i}{W_{\max}}\right],\\
&\text{s.t.}\sum_{i\in N_1}\frac{1}{\mu_i}\le 1, \forall i\varepsilon N_1,\\
&\quad\sum_{i\in N_1\cup N_2}\frac{1}{\lambda_i}\le 1, \forall i\varepsilon N_1\cup N_2.
\end{aligned} \tag{18}$$

Due to the large scale of calculation of this problem, the CVX toolkit is needed to solve it. Due to the discreteness of the unloading decision variables X, Y, this chapter designs a heuristic algorithm based on binary particle swarm to solve the optimization problem to obtain the unloading decision variables X, Y. Combined with the optimization problem, the fitness function is defined as

$$\text{Fitness} = \sum_{i=1}^{N} C_i^l\left(1-x_i\right)+C_i^cx_i\left(1-y_i\right)+C_i^nx_iy_i. \tag{19}$$

The fitness function can be used to measure the total cost of delay and energy consumption caused by the unloading scheme. The larger the fitness function, the higher the computational cost, indicating that the program has poor performance and is not suitable for execution. On the contrary, the smaller the fitness function, the more suitable the scheme as shown in Figure 2.

Create a N-dimensional particle search space, map $\{X, Y\}$ to the particle position according to the unloading decision variables X, Y, and define $Z = \{X, Y\}$ as the unloading decision set of all tasks. In the search space, consider a particle swarm containing K particles, and define the position vector of the ($\forall\ k \in K$) particle as

$$X_k = \left(x_{k1}, x_{k2}, \ldots, x_{kN}\right). \tag{20}$$

The velocity vector is

$$V_k = \left(v_{k1}, v_{k2}, \ldots, v_{kN}\right). \tag{21}$$

The optimal position of individual particles is

$$p_{\text{best}} = \left(p_{k1}, p_{k2}, \ldots, p_{kN}\right). \tag{22}$$

The optimal position of the particle swarm is

$$g_{\text{best}} = \left(g_1, g_2, \ldots, g_N\right). \tag{23}$$

The particle velocity update formula is

$$v_{kl}^{t+1} = \omega\cdot v_{kl}^t + c_1\cdot r_1\cdot\left(p_{kl}^t - x_{kl}^t\right)+c_2\cdot r_2\cdot\left(p_{gl}^t - x_{kl}^t\right). \tag{24}$$

In the traditional BPSO algorithm, the particle position value is limited to 0 or 1, and the velocity v_{kl} represents the probability of the position x_{kl} taking 1. Therefore, by defining a logistic regression activation function (v_{kl^t}) to achieve the particle position update, the position update formula is as follows:

$$\text{Sig}\left(v_{kl}^{t+1}\right) = \frac{1}{1+\exp\left(-v_{kl}^{t+1}\right)}, \tag{25}$$

$$x_{kl}^{t+1} = \begin{cases} 1, R_{kl} < \text{Sig}\left(v_{kl}^{t+1}\right), \\ 0, \text{other}. \end{cases} \tag{26}$$

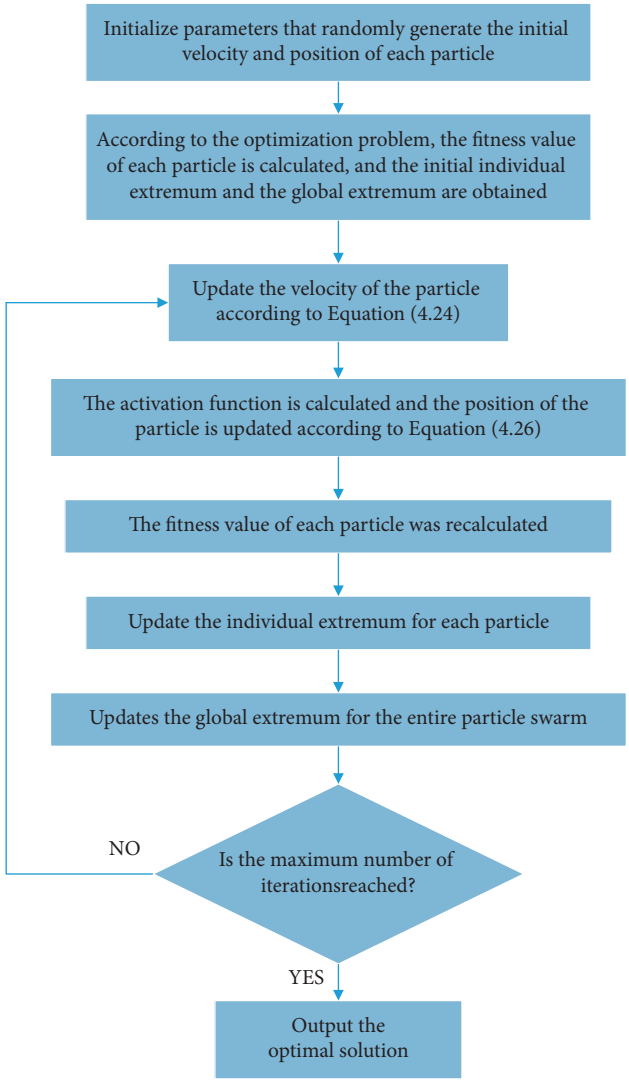

Figure 2: Flowchart.

Among them, *Rkl* is randomly generated from a 0-1 uniform distribution. In order to prevent the particles from prematurely converging in the search process and falling into the local optimal state, a new transfer function is used to replace formula (25) to update the particle position, and the formula is as follows:

$$\mathrm{Sig}\left(v_{kl}^{t+1}\right) = \left|\tanh\left(v_{kl}^{t+1}\right)\right|. \tag{27}$$

3.3. Experimental Simulation and Performance Evaluation. In the simulation scenario of a multi-user and multi-cell MEC system, the macro base station is located in the center of cell 1, the MEC server is deployed, and the coverage radius of the macro base station is 1000 m. The macro base stations in the two regions are connected through the backhaul link, and the data forwarding rate on the backhaul link is 10 MB/s. We set the number of mobile devices randomly distributed in the cell to 20~100, and the system communication bandwidth to 40 MHz. The experimental simulation parameters in this chapter are summarized as shown in Table 1.

Table 1: Simulation parameter table.

Parameter	Value
Number of mobile devices N	20, 40, 60, 80, 100
System communication bandwidth $W_{\max}$	40 MHz
Mobile device transmission power pi	0.5 W
Wireless channel gain g_i	$127 + 30 \times \log_{10}$d
Gaussian channel noise σ^2	2×10^{-13} W
Maximum calculation of local area MEC server Resources $S_{\max^c}$	20 GHz
	100 GHz
Maximum calculation of MEC server in nearby area	0.1 GHz
Resources $S_{\max^c}$	~U(500, 100) kB
Mobile device computing power f_{1i}	~U(1000, 100) megacycles
Task data size B_i	0.5
Task computing resources C_i	10 MB/s

First, the convergence of the algorithm proposed in this chapter is evaluated. Figure 3 shows a graph of the system cost varying with the number of iterations. The number of mobile devices is set to 40, 60, and 80, respectively. It can be seen from the figure that the system cost of the algorithm proposed in this chapter gradually decreases in the iterative process, and after a finite number of iterations, it can converge to a stable solution. At the beginning of the iteration of the algorithm, the fitness curve will appear flat. That is because the algorithm falls into the local optimum, but the algorithm can continue to generate new feasible solutions and jump out of the local optimum, which can further reduce the system cost. In addition, the convergence of the proposed algorithm is approximately linear with the number of devices.

Figure 4 shows the impact of the number of mobile devices on the system cost. It can be seen from the figure that the algorithm proposed in this chapter can achieve the lowest system cost compared with other schemes in the case of a small number of mobile devices (low cell load) and a large number of mobile devices (high cell load). For the random unloading algorithm, due to the randomness of unloading decision, the system cost also has great randomness. While only the local MEC server offloading algorithm is close to the cost of the algorithm mentioned in this chapter when the number of mobile devices is low, but as the number of mobile devices increases, the local MEC server will be overloaded, so the cost gradually increases.

Figure 5 shows the number of offloading tasks of different offloading algorithms in the local device, the MEC server in the local area, and the MEC server in the nearby area. The number of mobile devices in the system is set to 60. In the random offloading scheme, the number of tasks offloaded to the MEC server is random, so the delay and energy consumption costs are also random. In the local MEC server-only offloading solution, more computing tasks are executed on the local device, and the local MEC server has a relatively large load, which will cause a large delay and energy consumption. However, the algorithm proposed in this chapter offloads more computing tasks to nearby MEC

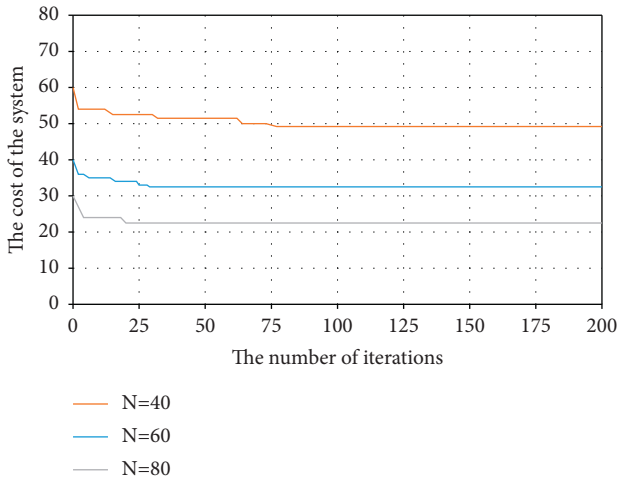

Figure 3: System cost under different iteration times.

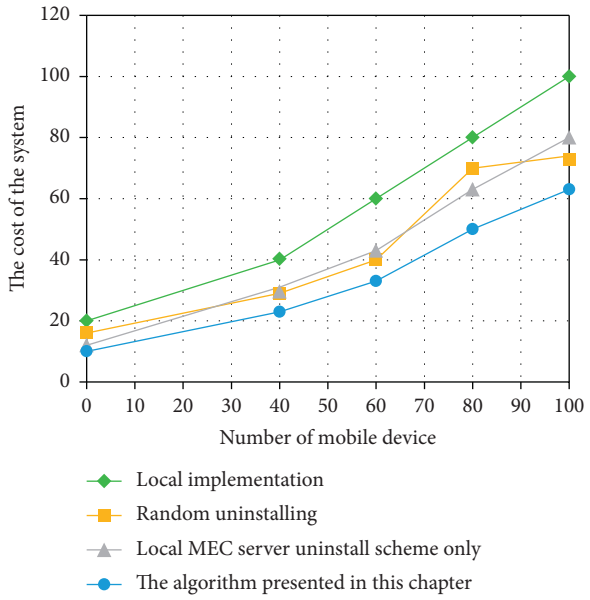

Figure 4: The impact of the number of mobile devices on the system cost.

servers, thereby reducing latency and saving energy consumption. Therefore, the distributed cooperative MEC system in this chapter can achieve better offloading performance than the single-server MEC system.

In order to evaluate the resource allocation strategy, the system costs when using average resource allocation and optimal resource allocation in different offloading algorithms were compared. In the average resource allocation, the user communication bandwidth is equal to the system communication bandwidth divided by the number of offloading tasks, and the computing resources allocated to each offloading task are equal to the maximum computing resources of the MEC server divided by the number of offloading tasks on the server. In the optimal resource allocation, the CVX toolkit is used to solve the problem and obtain the optimal communication bandwidth and computing resource allocation result.

Figure 6 evaluates the system cost under the average and optimal resource allocation, and compares the random offloading, only the local MEC server offloading scheme, and the algorithm proposed in this chapter. From the perspective of the three sub-graphs, the average resource allocation is relatively close to the system cost under the optimal resource allocation, but the system cost of the average resource allocation is slightly higher. This is because the task calculation scales in this experiment simulation are similar, resulting in the same amount of resource allocation. The system cost is relatively close. Therefore, in cells with little difference in calculation amount, the use of average resource allocation can simplify the algorithm and reduce the computational complexity.

There are three execution methods for the user's computing tasks. The calculation models are established for these three execution methods, respectively, and the optimization problem is designed with the goal of minimizing the system delay and the total cost of energy consumption. This section proposes a heuristic algorithm based on binary particle swarm to obtain the best offloading decision, bandwidth allocation, and computing resource allocation. Finally, experiments show that the algorithm can achieve convergence in a few times and can effectively reduce the overall execution cost of the system to ensure user QoE.

4. Application of Classroom Evaluation in English Teaching

4.1. Construction of the First-Level Index Evaluation System. From the perspective of cultural education, this research uses theoretical analysis to construct a school education evaluation index system with cultural and educational characteristics, and seeks expert opinions to continuously adjust and optimize the constructed index system. The theoretical analysis method is based on the theoretical analysis of the evaluation problem, dividing the measurement objects of the evaluation index system into several different components or different aspects, collectively called subsystems. Each part is described by specific statistical indicators and gradually decomposed into subsystems and functional modules at all levels until it is realized. Based on the analysis of the basic elements of the formation of English classroom culture, the evaluation indicators for students in grades 1–3 are formed, and finally an evaluation indicator system for the formation of English classroom culture is formed.

Like any other educational process, the education in English classroom includes three stages: the preparation stage of classroom education, the process stage of classroom education, and the stage of classroom education effect. In order to make the evaluation indicators formed by English teaching culture more reasonable, this paper makes a rational analysis of various educational evaluation works, referring to a large number of documents and master and doctoral dissertations, combined with expert suggestions. On the basis of research, the differences in cultural and educational stages have been determined, and a series of indicators for the first level have been formulated.

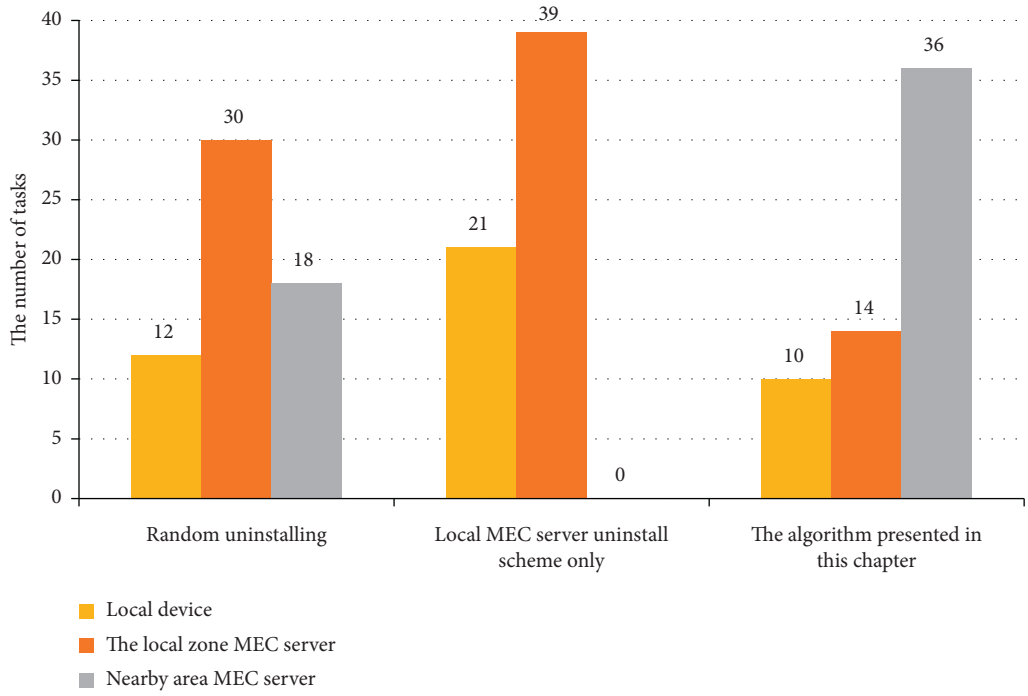

Figure 5: The number of tasks uninstalled by different algorithms in each execution mode.

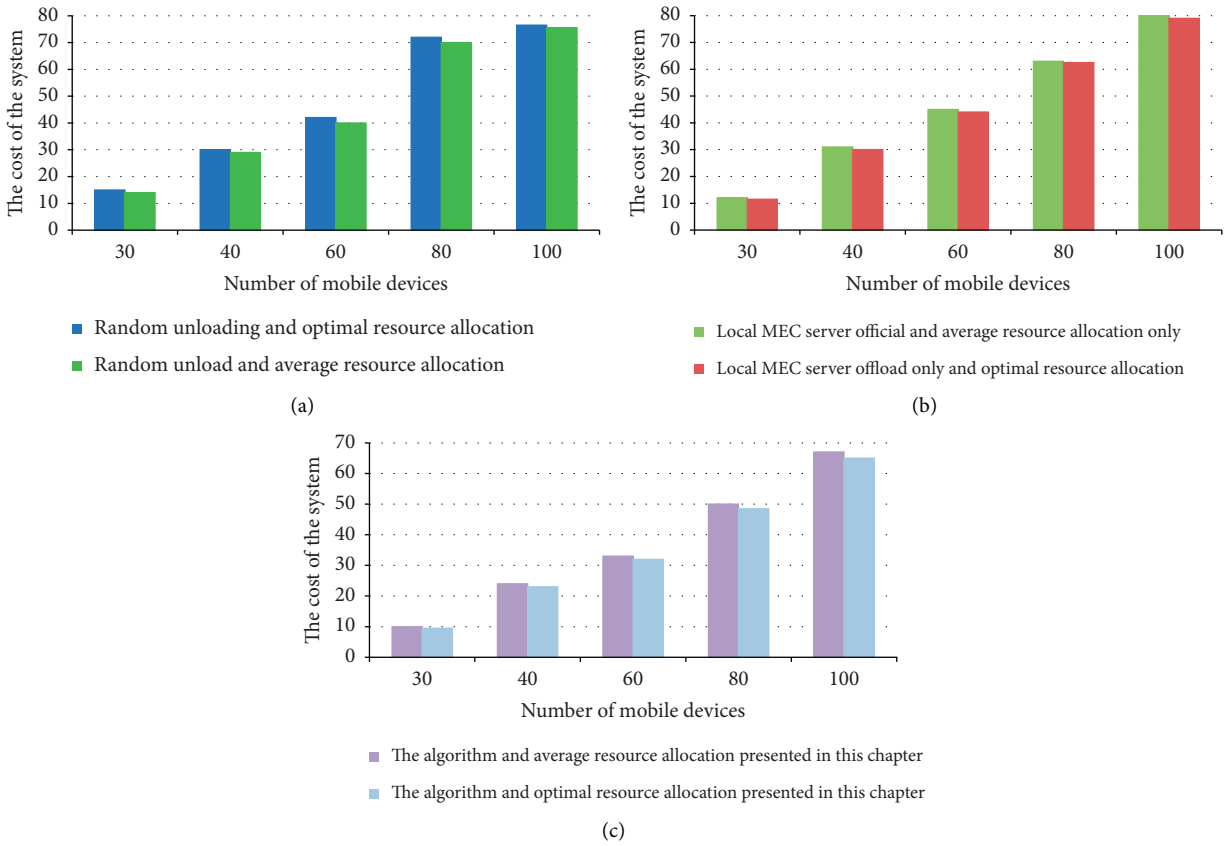

Figure 6: Comparison of system cost under average and optimal resource allocation. (a) System costs for random offloading. (b) System costs for local MEC server offloading. (c) The system cost of the algorithm presented in this chapter.

The main function of the classroom art education grading system constructed in this article is not to provide its tool value, but to provide an accurate reference for English art education grading.

In the following article, we will compile secondary and tertiary art education indicators for English teaching from three perspectives: classroom education preparation, classroom education process, and classroom education effect.

4.2. Construction of Secondary Index Evaluation System. For the construction of the secondary rating index system, this study mainly adopted methods such as theoretical analysis and expert advice. The theoretical analysis method has been explained before, so I will not elaborate too much here. The expert consultation method is a method by which auditors describe several evaluation indicators in a questionnaire based on the characteristics of evaluation objectives. Experts are required to make decisions based on their own knowledge and experience. The investigators finally summarize their opinions and then analyze and process the results of the consultation, and fed it back to the experts. If the experts reach a unified opinion after several consultations, a specific rating indicator system will be established in the final consultation. Although the methods of expert consultation are subjective, these indicators reflect the knowledge and experience accumulated by experts over the years. By absorbing the opinions of most experts, subjectivity can be transformed into objectivity to a certain extent. In the method suggested by experts, anonymous suggestions are usually adopted, and the reliability risk of the evaluation index system is eliminated through the mutual influence of experts.

Based on the evaluation indexes of the first stage, the evaluation indexes of the second stage shown in Table 2 are established through literature search, consulting faculty, experts, etc. Then, the applicability of each indicator is investigated through a questionnaire. A total of 60 questionnaires were distributed this time, including 30 English teachers of all grades in high school, 30 English majors, and 57 effective public opinion surveys. We use software to analyze the results and use the applicability of the inspection index as the secondary evaluation index. The results are as shown in Table 2.

According to the KMO indicator, it is found that it is less than 0.5 that the correlation is very weak, and it is not a qualified secondary indicator. From the statistical results in the above table, it can be seen that the relevant evaluation factors in the table, including teaching background, process, style, management, and attitude, have not passed the correlation test, and the abovementioned scoring factors cannot be included in the scoring system of English class art education.

The nine evaluation indicators determined by this research are shown in Table 3.

The main purpose of materiality testing is to eliminate nonessential indicators and retain indicators that may reflect key information. The importance test mainly uses the Delphi method, which is a statistical method developed by the American RAND Corporation. The process of using this method to determine indicators is as follows: by issuing questionnaires and talking to appropriate experts; after the first survey, immediately after statistical processing, report to the experts the overall response such as the average value and the frequency of each weight range; and then based on the feedback, the expert decides whether to change his mind and gives a second answer. Here, you can weigh and choose the indicators widely until the final result is consistent. The specific steps are as follows. First, you need to create a "Weight Distribution Consultation Form." Importance is usually divided into five levels: unimportant, general, important, very important, or extremely important, represented by 1, 2, 3, 4, and 5, respectively. The table format is shown in Table 4.

Later, a "Weight Allocation Consultation Form" was issued to valuation experts. In the first round, the weights of each index were independently allocated to experts, and the reasons were required to be fully explained. To recover the consultation form, the data need to be statistically sorted, and the average value and deviation value of each index are calculated.

4.3. Standards and Evaluation Points of the Secondary Rating Index System. The evaluation standard is the standard by which individuals make value judgments when performing evaluation activities. Therefore, the formulation and application of evaluation standards directly affect the quality and effect of evaluation. At present, there is no unified requirement for the formulation of evaluation standards. Generally speaking, standards should follow certain specifications and strive to ensure that the standards are simple, clear, and easy to use in order to achieve the goals of evaluation. In this study, the definition of the secondary evaluation index evaluation standard mainly includes two steps. The first is to subdivide each sub-indicator, and the scoring points are determined according to the main content and characteristics of each sub-indicator; the second is to determine the degree of satisfaction of each secondary index according to the degree of completion of each evaluation point. At present, there is no unified rule for determining the rating level, which can be determined according to needs. The higher the number of levels, the more accurate the classification.

The evaluation of teachers' classroom education preparation stage is mainly to prepare teachers for the next classroom education. The secondary evaluation indicators include teachers' classroom education philosophy, classroom education goals, and classroom education design.

The concept of classroom education is an important factor affecting the implementation of classroom skills education. The concept of classroom education involves two main aspects: on the one hand, whether teachers fully understand the necessity of classroom education, and on the other hand, whether teachers correctly understand the relationship between language education and classroom education inner relationship.

Table 2: Correlation analysis of secondary indicators.

Factor	Factor1	Factor2	Factor3	Factor4	Factor5
Cultural teaching philosophy	0.669	—	—	—	—
Cultural teaching goals	0.874	—	—	—	—
Cultural teaching background	0.423	—	—	—	—
Cultural teaching design	0.614	—	—	—	—
Cultural teaching content	—	0.725	—	—	—
Cultural teaching process	—	0.373	—	—	—
Cultural teaching style	—	0.336	—	—	—
Cultural teaching management	—	0.427	—	—	—
Cultural teaching attitude	—	0.314	—	—	—
Cultural teaching methods	—	0.778	—	—	—
Cultural teaching atmosphere	—	0.664	—	—	—
Class response	—	—	0.642	—	—
Teaching feedback	—	—	0.619	—	—
Teaching reflection	—	—	0.342	—	—
Compliance status	—	—	0.672	—	—

Table 3: Cultural teaching evaluation index system.

Teaching stage	First-level indicator	Secondary indicators
Teaching preparation stage	(A) Cultural teaching preparation	(A-1) Cultural teaching philosophy (A-2) Cultural teaching objectives (A-3) Cultural teaching design
Teaching process stage	(B) Cultural teaching process	(B-1) Cultural teaching content (B-2) Cultural teaching methods (B-3) Cultural teaching atmosphere
Teaching effect stage	(C) Cultural teaching effect	(C-1) Teaching feedback (C-2) Class response (C-3) Compliance status

Table 4: Consultation form for weight configuration.

Index number	A	B	C	D	…..
Weights	—	—	—	—	…..

The goal of classroom education is the expected result that students hope to achieve through classroom education activities of teachers in cultural learning. The goal of classroom education is not the one-sided goal of teachers and students. This includes not only the cultural teaching goals of teachers, but also the cultural learning goals of students. From the perspective of classroom education, the evaluation of classroom education goals should take into account the following two points. First, the description of art education goals should be clear and concrete, reflecting the integration of three-dimensional goals; second is whether the goals of classroom education focus on student culture and the development of awareness and understanding.

The classroom education process is the center of classroom education, so classroom education process evaluation is also the center of overall classroom education evaluation. The classroom education process refers to the classroom education activities organized and implemented by teachers in order to achieve the goal of English classroom education and guide students to develop cultural cognition. The first indicator of this stage is the process of cultural education. The second indicator mainly includes the content of teacher's classroom education, the methods of classroom education, and the cultural atmosphere of the classroom.

The classroom education content of high school English class is mainly textbooks and related classroom teaching materials. For the English teaching of high school English teachers, the assessment points of classroom teaching content mainly include two aspects. The first is the teacher's perception of cultural content. This is the requirement for English teachers to provide classroom education. If they do not have a comprehensive understanding of cultural content, there is no classroom education; the second is the teacher's exploration of cultural content, the cultural content that the teacher chooses, what kind of cultural content the teacher chooses to teach, and what kind of cultural content the teacher does not teach, which affect the quality of classroom education; the third is how teachers arrange cultural content, which cultural content is transmitted first, and which is transmitted later, which has a great influence on the effect of cultural education.

4.4. Determination of Index Evaluation System. Traditional educational effect evaluation usually uses testing methods. Educational effect evaluation methods commonly used in schools include formative evaluation, comprehensive evaluation, and diagnostic evaluation. These evaluation

methods have specific usage scenarios and advantages. However, in terms of classroom education, due to cultural complexity and abstract curriculum education, we believe that it is appropriate to adopt and shape the evaluation of the effectiveness of English classroom education, as well as evaluation and diagnostic evaluation or a combination of three evaluation methods. The main points of classroom education effect evaluation are as follows: firstly, in terms of students' classroom response and evaluation, whether the teacher's classroom education philosophy has stimulated students' interest in cultural learning, whether students actively participate in cultural learning, and whether the teacher's culture is in harmony with education.

Secondly, feedback is given. Classroom education should not ignore every student. It needs to be good at listening to every student's idea and suggestion and responding positively. There is no end to cultural education, and reflection on classroom education is essential to further improve the effectiveness of classroom education. Therefore, when evaluating the effectiveness of classroom education, we must also consider students' feedback on cultural teaching and teachers' thinking about classroom education. Third is the degree of achievement of cultural education goals, including the achievement of students' cultural learning, knowledge, skills, and emotional attitudes.

5. Conclusion

In this article, we will split and solve the optimization problem. First, the solution of the resource allocation subproblem is obtained based on the Lagrangian multiplier method, and then a computational offloading algorithm based on the greedy algorithm is proposed to solve the computational offloading sub-problem. Finally, the final solution of the problem is obtained through the joint algorithm, and the computational complexity is lower than the optimization algorithm and the traditional branch algorithm that proves the algorithm at the same time. Simulation experiments show that the proposed algorithm can achieve lower system cost compared with the benchmark scheme with local execution, complete offloading, and DPH offloading. We provide a platform to understand cultural education through evaluation. It can not only examine the cultural knowledge of students, but also consider the preparation and process of cultural education, and also consider the evaluation of education and the effect of cultural education, so as to evaluate the daily teaching of teachers. Through this construction and practice, it can provide reference for the further development of cultural evaluation theory.

Data Availability

The data used to support the findings of this study are available from the corresponding author upon request.

Conflicts of Interest

The author declares that there are no conflicts of interest.

Acknowledgments

This paper was supported by fund from Shanghai Municipal Education Commission: English taught Model Course Practical Business for International Students in Shanghai University, 2018–2020 International Exchange Office 301-31.

References

[1] Y. Dong, S. Guo, J. Liu, and Y. Yang, "Energy-efficient fair cooperation fog computing in mobile edge networks for smart city," *IEEE Internet of Things Journal*, vol. 6, no. 5, pp. 7543–7554, 2019.

[2] J. C. Richards, "Teaching English through English: proficiency, pedagogy and performance," *RELC Journal*, vol. 48, no. 1, pp. 7–30, 2017.

[3] B. Ayçiçek and T. Yanpar Yelken, "The effect of flipped classroom model on students' classroom engagement in teaching English," *International Journal of Instruction*, vol. 11, no. 2, pp. 385–398, 2018.

[4] H. Sundari, "Classroom interaction in teaching English as foreign language at lower secondary schools in Indonesia," *Advances in Language and Literary Studies*, vol. 8, no. 6, pp. 147–154, 2017.

[5] M. A. Saydaliyeva, E. B. Atamirzayeva, and F. X. Dadaboyeva, "Modern methods of teaching English in Namangan state university," *International Journal on Integrated Education*, vol. 3, no. 1, pp. 8-9, 2020.

[6] A. Coşkun, "The application of lesson study in teaching English as a foreign language," *İnönü Üniversitesi Eğitim Fakültesi Dergisi*, vol. 18, no. 1, p. 151, 2017.

[7] L. Susanty, Z. Hartati, R. Sholihin, A. Syahid, and F. Y. Liriwati, "Why English teaching truth on digital trends as an effort for effective learning and evaluation: opportunities and challenges: analysis of teaching English," *Linguistics and Culture Review*, vol. 5, no. S1, pp. 303–316, 2021.

[8] X. Wang, "Discussion on application of multimedia teaching in college English vocabulary teaching," *Open Journal of Modern Linguistics*, vol. 06, no. 03, pp. 177–181, 2016.

[9] L. Su, J. N. Liu, L. F. Ren, and F. Zhang, "An object classification approach based on randomized visual vocabulary and clustering aggregation," in *Proceedings of the 2nd International Conference on Mechatronics and Control Engineering*, pp. 778–782, Amsterdam, The Netherlands, October 2013.

[10] M. Naseri, M. A. Raji, M. R. Hantehzadeh, A. Farouk, A. Boochani, and S. Solaymani, "A scheme for secure quantum communication network with authentication using GHZ-like states and cluster states controlled teleportation," *Quantum Information Processing*, vol. 14, no. 11, pp. 4279–4295, 2015.

[11] M. Lamb and F. E. Arisandy, "The impact of online use of English on motivation to learn," *Computer Assisted Language Learning*, vol. 33, no. 1-2, pp. 85–108, 2020.

[12] Y. Du, K. Wang, K. Yang, and G. Zhang, "Energy-efficient resource allocation in UAV based MEC system for IoT devices," in *Proceedings of the IEEE Global Communications Conference (GLOBECOM)*, pp. 1–6, Abu Dhabi, UAE, December 2018.

[13] Z. Hu, F. Zeng, Z. Xiao, B. Fu, H. Jiang, and H. Chen, "Computation efficiency maximization and QoE-provisioning in UAV-enabled MEC communication systems," *IEEE Transactions on Network Science and Engineering*, vol. 8, no. 2, pp. 1630–1645, 2021.

[14] S. Wan, J. Lu, P. Fan, and K. B. Letaief, "Toward big data processing in IoT: path planning and resource management of UAV base stations in mobile-edge computing system," *IEEE Internet of Things Journal*, vol. 7, no. 7, pp. 5995–6009, 2020.

[15] Y. Mao, C. You, J. Zhang, K. Huang, and K. B. Letaief, "A survey on mobile edge computing: the communication perspective," *IEEE Communications Surveys & Tutorials*, vol. 19, no. 4, pp. 2322–2358, 2017.

[16] A. F. Metwaly, M. Z. Rashad, F. A. Omara, and A. A. Megahed, "Architecture of multicast centralized key management scheme using quantum key distribution and classical symmetric encryption," *The European Physical Journal-Special Topics*, vol. 223, no. 8, pp. 1711–1728, 2014.

[17] L. Yang, H. Yao, J. Wang, C. Jiang, A. Benslimane, and Y. Liu, "Multi-UAV-enabled load-balance mobile-edge computing for IoT networks," *IEEE Internet of Things Journal*, vol. 7, no. 8, pp. 6898–6908, 2020.

[18] F. Wang, J. Xu, X. Wang, and S. Cui, "Joint offloading and computing optimization in wireless powered mobile-edge computing systems," *IEEE Transactions on Wireless Communications*, vol. 17, no. 3, pp. 1784–1797, 2018.

[19] S. Bi and Y. J. Zhang, "Computation rate maximization for wireless powered mobile-edge computing with binary computation offloading," *IEEE Transactions on Wireless Communications*, vol. 17, no. 6, pp. 4177–4190, 2018.

Hindawi
Mobile Information Systems
Volume 2022, Article ID 1581274, 10 pages
https://doi.org/10.1155/2022/1581274

Research Article

Mobile Edge Computing Application in Enterprise Human Resource Management Platform Based on Task Scheduling Algorithm

Li Liu, Baoguo Sun, and Qingyun Xu

Jiangxi University of Engineering, Xinyu, Jiangxi 338000, China

Correspondence should be addressed to Qingyun Xu; 1732261178@xzyz.edu.cn

Received 6 July 2022; Revised 17 July 2022; Accepted 23 July 2022; Published 17 August 2022

Academic Editor: Shadi Aljawarneh

With the development of the social economy and the acceleration of economic globalization, human resources of enterprises have become an important factor restricting the development of enterprises. This paper creates an enterprise human resource management platform application based on twin network and mobile edge computing. By allocating computing and storage resources to the network edge close to users or data sources, mobile edge computing supports mobile to complete the computing offload of wireless access network applications. This process significantly reduces the end-to-end delay of the network and effectively reduces the processing load of the core network and data center. The simulation results can see that the average user benefit of all algorithms increases with the increase of network transmission speed and VCPU processing power. In addition to the introduction and popularization of information technology, the construction of enterprise human resources informatization also requires continuous and comprehensive monitoring and analysis of existing internal data, information, and data. The use of network communication technology to build a management information system, through information management, can significantly optimize and improve the efficiency of enterprise human resource management.

1. Introduction

The research object of this paper is a relatively large enterprise group. In recent years, the number and scale of enterprise subsidiaries have increased year by year; enterprise personnel have gradually increased; and there are more daily management work, which makes the management more difficult, and the problems have increased. The first is the poor interoperability of personnel information and data between the head office and its subsidiaries. The second is the high personnel cost, large investment in personnel departments, and low efficiency. Combined with the above aspects, the enterprise human resource management platform investigated in this paper is based on the enterprise human resource management needs and the design ideas and application conditions of the application of the existing domestic human resource management platform [1]. In this paper, we will consider the structure of an enterprise human resource management platform based on a twin network, which is system engineering with a large project investment. Moving edge computing, a relatively mature computing technology at home and abroad, is also used to ensure the progress and integrity of the design. Task scheduling and resource management are two key factors to be considered in the decision-making process of MEC unloading. On the one hand, the MEC environment is essentially a decentralized heterogeneous parallel computing environment. Only by properly planning tasks can we make full use of the performance advantages of the computing environment. When considering the dynamic changes in the network environment, you should also make planning decisions about when to uninstall tasks. On the other hand, the resources at the edge of the network are limited, so we should appropriately allocate the full potential of these resources so that they can give full play to their greatest advantages and improve their efficiency as much as possible. When there are a large number of users, you should also decide whether to allow them to uninstall (i.e., make permission decisions) to avoid

excessive resource contention. In this context, this paper focuses on graph-oriented task unloading planning, dynamic task unloading planning for complex task queues, and access decision and resource allocation considering user mobility from the perspective of users; considers the impact of various application unloading models in static and dynamic environments; and considers optimizing MEC computing unloading planning and resource management strategy to ensure the stable and continuous operation of the group management platform, so as to protect the existing investment. This design also considers the development trend of existing technology so that the enterprise's human resources platform can adapt to future technological development and changes and better solve the technical problems caused by the upgrading of the enterprise's human resources platform. In the process of realizing the enterprise human resources management platform to meet the relevant business needs of the enterprise human resources department to the greatest extent, the main principle of the platform is practicality, and the main goal of the platform construction is to find and timely deal with the problems related to personnel and human resources management.

Some research introduces an algorithm for predicting the appearance characteristics of moving targets. The algorithm uses memory-enhanced convolution long- and short-term memory networks to predict the changes in the appearance characteristics of targets and estimate the appearance characteristics of future targets. The tracker uses occlusion simulation to improve training and manage historical information to model the long sequence of dynamically changing targets and reliably predict the characteristics of the next frame [2]. This paper introduces the combination of kernel density feature map and edge detection algorithm, automatically generates ternary map to extract target contour information, and regenerates the tracking results according to the contour boundary. The literature introduces the use and application of personnel management platforms. The robust twin network tracking algorithm is introduced in the literature, which solves the problems of target scaling in the tracking process and makes the tracking algorithm more robust [3]. The literature introduces the generated image kernel density response diagram, which displays the weight of each pixel in the image.

2. Research on Target Tracking and Mobile Edge Computing Resource Management Optimization in Twin Networks

2.1. Target Tracking Algorithm Based on Twin Network

2.1.1. Target Relocation Algorithm. In this paper, we will use the target color function to represent the target model. In order to reduce the amount of calculation, only m color intervals need to be selected from the histogram of the target image. The target model can be derived using the following equation:

$$Q = \{q_k, k = 1, 2 \ldots m\}. \tag{1}$$

Calculate the probability density of the color interval as follows:

$$q_k = C \sum_{i=1}^{n} K_E(x_i), \tag{2}$$

where K_E is the kernel function of Epanechnikov. Since q_k needs to be normalized, C is expressed as follows:

$$C = \frac{1}{\max\limits_{0 \le i \le n} K_E(x_i)}. \tag{3}$$

The foreground area is close to the center of the target; the background pixels are few; the background area contains the entire target; and most of the background area is not in the target area. Definitions x_f and x_b represent pixels in the foreground area F and background area B, respectively, and their distribution probabilities in the histogram of the area are defined as p^f and p^b. The probability that a pixel belongs to the foreground area can be estimated as follows:

$$p(F \mid x) = \frac{p^f(x)}{p^b(x)}. \tag{4}$$

Now, we need to find the probability that pixels above q_k belong to the foreground area. Define the probability density of each interval in the foreground target histogram as q^f, and q^b as the background target interval model. The foreground probability model can be calculated using equation (4):

$$Q^* = \left\{ \frac{q_k^f}{q_k^b}, \quad k = 1, 2 \ldots m \right\}. \tag{5}$$

According to equation (5), Q^* intuitively shows that if q_k^f is greater than q_k^b, the calculation result is greater than 1. If q_k^f is less than or equal to q_k^b, the calculation result is also less than or equal to 1. Finally, Q^* must be normalized as follows:

$$Q_{\text{norm}}^* = \text{Normalize}\left(Q^*\right). \tag{6}$$

w is defined to represent the weight of each pixel obtained from Q_{norm}^*. The sum of the weights of all pixels in the image is calculated as follows:

$$m = \sum_{i=1}^{n} \frac{w_i}{-\ln(w_i)}. \tag{7}$$

In order to reduce the influence of images of different scales on the weights, we need to calculate the average weight of m. The record is as follows:

$$\overline{m} = \frac{1}{n} \sum_{i=1}^{n} \frac{w_i}{-\ln(w_i)}. \tag{8}$$

For two photos a and b, their average weights are represented by the average of m_a and the average of m_b, respectively, and the similarity between the two is calculated using the Bhattacharyya distance as follows:

$$d_{ab} = \sqrt{\overline{m}_a \cdot \overline{m}_b}. \tag{9}$$

2.1.2. Target Positioning Realization Framework. In most cases, the target will not be deformed in actual tracking, so the process of combining the tracking algorithm with the target appearance prediction can sufficiently reduce the appearance prediction part of the target. This section proposes a dual neural network tracking algorithm that will determine the deformation of the target and predict the appearance of the target. The specific framework is shown in Figure 1.

Among them, the tracking part is based on the algorithm structure of SiamRPN++; the input is the original target template and $t+1$ image; and the output of the tracking part is the detection frame information and the pattern similarity value [4]. The decision-making module must be based on the detection at $t+1$, The similarity score between the target and the original template is used to determine the state of the target If the target has a deformation problem, the ConvLSTM network is used to predict the appearance change of the target during the deformation process. At the same time, an external memory is needed to store the target images captured from $t-n$ to t, and input them into ConvLSTM as the preorder sequence for predicting the appearance of the target [5]. Finally, the predicted target feature is retrieved as an auxiliary template and re-entered into the twin network to calculate the new tracking result.

2.1.3. Research on Robust Optimization of Target Tracking Algorithm. Taking into account the various environmental interference factors encountered in the process of target positioning, this section combines the tracking displacement, target feature prediction, and tracking frame generation optimization methods proposed in this section to propose a robust tracking algorithm based on dual neural networks [6]. The algorithm shown in Figure 2 is divided into three main parts: the tracking part, the mixed decision part, and the tracking frame optimization part. This algorithm solves the inaccurate tracking performance of the traditional twin network tracking algorithm due to video jitter, blur, occlusion, fast movement, deformation, overscaling, and so on. from various angles and improves the robustness of the twin network tracking algorithm.

2.2. Key Technologies of Task Scheduling in Mobile Edge Computing

2.2.1. Task Scheduling Model. Assuming that the uplink rate from MD to MS is R^{ul} (bit/s), the time T_i^{u1} required for v_i to upload data can be expressed as follows:

$$T_i^{u1} = \frac{D_i^{in}}{R^{ul}}. \tag{10}$$

In the edge execution stage, C_i CPU cycles run on the VM of the MS. The total clock frequency of the virtual CPU (VCPU) allocated by the MS to the user is denoted by F^s. Multiple physical CPUs on the MS can provide the total clock frequency. The next step is the time required by v_i at this stage.

$$T_i^s = \frac{C_i}{F^s}. \tag{11}$$

The revolving phase of the result is similar to the task sending phase, and the revolving time can be expressed as follows:

$$T_i^{dl} = \frac{D_i^{\text{out}}}{R^{d1}}. \tag{12}$$

The energy consumption for unloading required by v_i is

$$E_i^s = P^{Tx} T_i^{ul} + P^{Rx} T_i^{dl}. \tag{13}$$

The local execution time T_i^1 can be expressed as follows:

$$T_i^1 = \frac{C_i}{F^1}. \tag{14}$$

F^1 is the clock frequency of the CPU on the MD, allowing P^1 to specify the CPU performance on the MD, which is widely used as a superlinear function of the CPU frequency F^1, namely

$$P^1 = \xi \cdot \left(F^1\right)^{\nu}. \tag{15}$$

The energy consumption of scheduling v_i for local execution is

$$E_i^1 = P^1 T_i^1 = \xi \cdot \left(F^1\right)^{\nu-1} C_i. \tag{16}$$

Assuming that v_i is to be executed locally, the preparation time for local execution of the task (i.e., the earliest time that the local CPU can execute the task) is defined as follows:

$$\mathrm{RT}_i^1 = \max_{v_j \in \mathrm{pred}(v_i)} \max\left\{\mathrm{FT}_j^1, \mathrm{FT}_j^{dl}\right\}. \tag{17}$$

The completion time of its local execution is

$$\mathrm{FT}_i^1 = \mathrm{ST}_i^1 + T_i^1. \tag{18}$$

Assuming that v_i is scheduled to run remotely, define the standby and startup time of v_i in these three stages, corresponding to the three stages of remote execution tasks. The waiting time for sending task v_i is defined as follows:

$$\mathrm{RT}_i^{ul} = \max_{v_j \in \mathrm{pred}(v_i)} \max\left\{\mathrm{FT}_j^1, \mathrm{FT}_j^{ul}\right\}, \tag{19}$$

where v_i is the sending end time:

$$\mathrm{FT}_i^{ul} = \mathrm{ST}_i^{ul} + T_i^{ul}. \tag{20}$$

The preparation time RT_i^s for executing task v_i on the VM can be expressed as follows:

$$\begin{aligned} \mathrm{RT}_i^s &= \max\left\{\mathrm{FT}_i^{ul}, \max_{v_j \in \mathrm{pred}(v_i)} \mathrm{FT}_j^s\right\}, \\ \mathrm{FT}_i^s &= \mathrm{ST}_i^s + T_i^s. \end{aligned} \tag{21}$$

When task v_i finishes execution (at time FT_i^s), v_i enters the ready state for return, namely

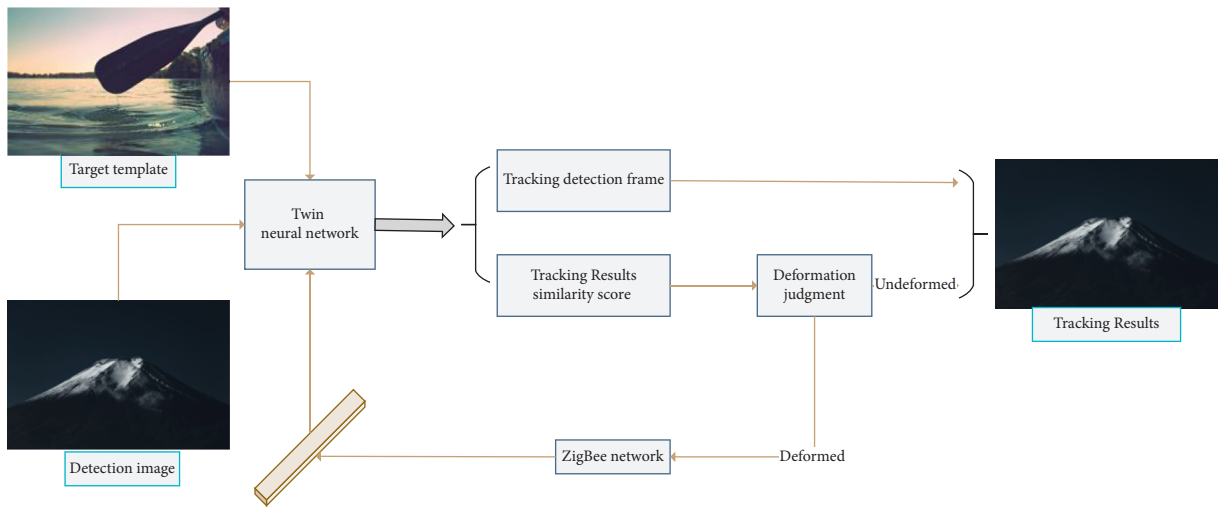

Figure 1: Algorithm implementation framework diagram.

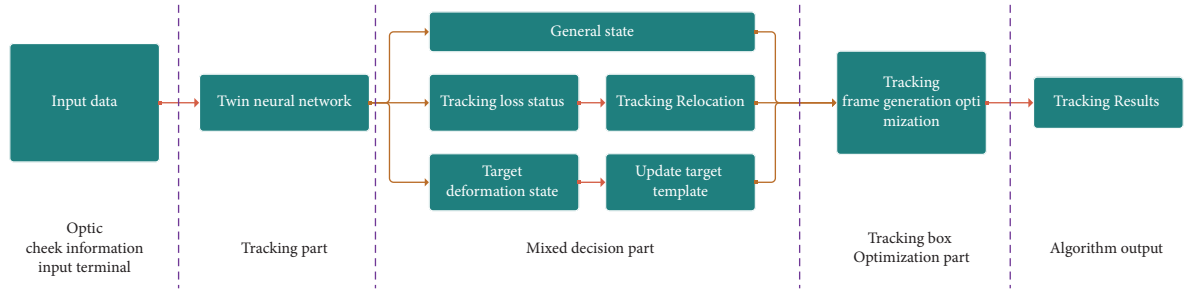

Figure 2: The basic structure of the proposed algorithm.

$$\begin{aligned} \mathrm{RT}_i^{dl} &= \mathrm{FT}_i^s, \\ \mathrm{FT}_i^{dl} &= \mathrm{ST}_i^{dl} + T_i^{dl}. \end{aligned} \tag{22}$$

2.2.2. Task Unloading Scheduling Scheme. The DAG task uses the execution mode to determine whether the task is executed locally or in a remote location. The scheduling priority determines the order in which tasks scheduled on the same processor should follow. The priority relationship between tasks in DAG application G is represented by the task sequence, called priority sequence, which is described as follows:

$$Q^G = \left(k_1, k_2, \ldots, k_{V|}\right). \tag{23}$$

If Topology (G) is the set of all topology types of G, then Q^G must satisfy

$$\begin{aligned} Q^G &\in \mathrm{Topology}\,(G), \\ A^G &= \left(a_1, a_2, \ldots, a_{|V|}\right). \end{aligned} \tag{24}$$

2.3. Network Performance Simulation Experiment Results and Analysis. Based on the purpose of MLO offloading scheduling, in a standard simulation environment, for different task sizes (i.e., N), the average DAG offloading planning delay of each offloading algorithm is compared. The experimental results are shown in Table 1. The result corresponding to ES is the optimal solution.

In addition, based on the purpose of MLO, the next step is to retrain the offload scheduling strategy of DRLOSM in different environments and evaluate the impact of different environments on the performance of all algorithms. To obtain the best reference solution for the experiment, the size of the DAG node is limited to 15 (too complicated for the time required by the exhaustive method) [7]. Figures 3 and 4, respectively, show the average DAG offload scheduling delay of each algorithm in the test set at different network transmission rates and different overall VCPU clock frequencies (allocated by MS; the rest of the parameters are default values). It can be seen that with the increase in network transmission speed and VCPU processing capacity, the offload scheduling delay of all algorithms is decreasing, except for LE, which does not perform task offload at all. For the purpose of MLO, the HEFT algorithm developed specifically for DAG scheduling delay works well. In most cases, its performance is better than some other basic algorithms. It is worth noting that if the network environment is very good and the VCPU is powerful enough, then offloading all tasks is also a good choice.

Figure 4 shows the average offload scheduling delay at various total VCPU frequencies based on MLO purposes.

Then, based on the goal of MUO, the offloading scheduling strategy of DRLOSM is retrained in a standard

Table 1: Average DAG offload scheduling delay of each algorithm under MLO purpose (milliseconds).

Number of nodes	ES	LE	OE	RS	RR	HEFT	DRLOSM
10	476.4	723.0	610.6	612.6	605.2	514.5	489.7
15	643.6	1,053.5	870.1	862.1	832.5	719.6	660.6
20	826.1	1,394.5	1,160.1	1,080.1	1,068.1	925.4	852.4
25	N/A	1,796.0	1,428.8	1,370.1	1,313.3	1,145.5	1,017.5
30	N/A	2,154.6	1,736.4	1,648.7	1,591.8	1,399.1	1,236.4
35	N/A	2,463.6	1,973.5	1,958.1	1,907.7	1,665.4	1,468.5
40	N/A	2,910.4	2,414.7	2,192.0	2,114.1	1,864.4	1,679.7
45	N/A	3,182.0	2,480.5	2,271.9	2,187.5	1,955.5	1,678.6
50	N/A	3,663.1	3,118.0	2,725.2	2,572.7	2,287.6	2,082.5

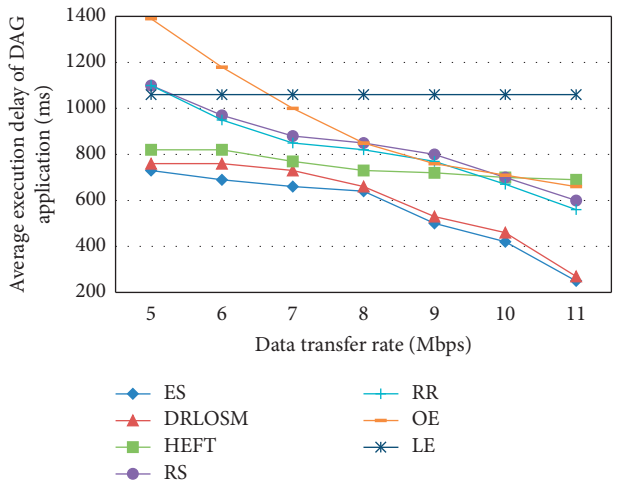

Figure 3: Average offload scheduling delay under different network rates based on MLO purposes.

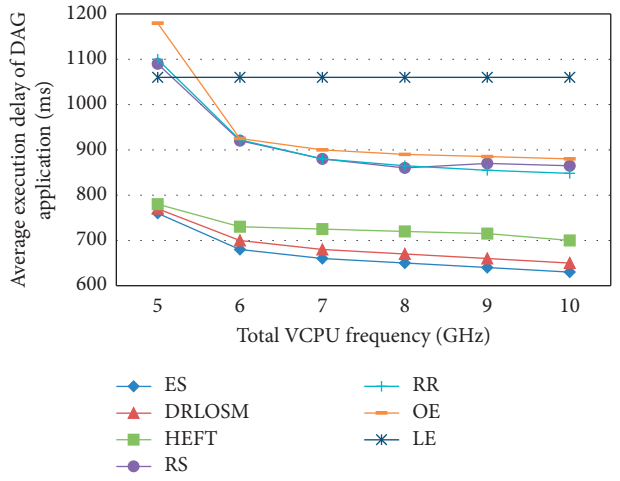

Figure 4: Average offload scheduling delay under different total frequencies of VCPU based on MLO purpose.

simulation environment and re-compared with the above-mentioned six basic algorithms. The experimental results are shown in Table 2.

Figure 5 shows the average user effect of each algorithm in the test set under different network transmission rates and different overall VCPU clock frequencies (other parameters are default values). It can be seen that the

Table 2: The average user utility of each algorithm under the purpose of MUO.

Number of nodes	ES	LE	OE	RS	RR	HEFT	DRLOSM
10	0.4565	0	0.4389	0.2414	0.2627	0.2455	0.4511
15	0.4691	0	0.4450	0.2571	0.2891	0.2693	0.4535
20	0.4809	0	0.4505	0.2884	0.3004	0.2905	0.4625
25	N/A	0	0.4660	0.2966	0.3243	0.3160	0.4786
30	N/A	0	0.4638	0.2936	0.3148	0.3044	0.4746
35	N/A	0	0.4665	0.2944	0.3006	0.2851	0.4760
40	N/A	0	0.4514	0.3051	0.3232	0.3168	0.4645
45	N/A	0	0.4735	0.3218	0.3391	0.3320	0.4865
50	N/A	0	0.4425	0.3034	0.3330	0.3260	0.4580

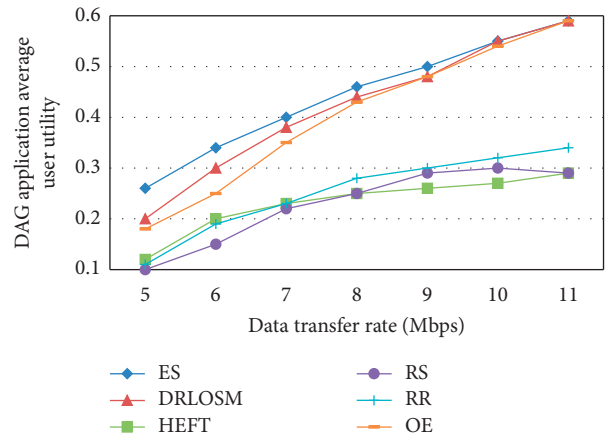

Figure 5: Average user utility under different network rates based on MUO purposes.

average user benefits of all algorithms increase with the increase in network transmission speed and VCPU processing power.

3. Design and Implementation of Enterprise Human Resource Management Platform under the Background of the Internet

3.1. System Architecture Design of Enterprise Human Resource Management Platform

3.1.1. System Infrastructure. Figure 6 shows the logical structure of the enterprise human resource management platform.

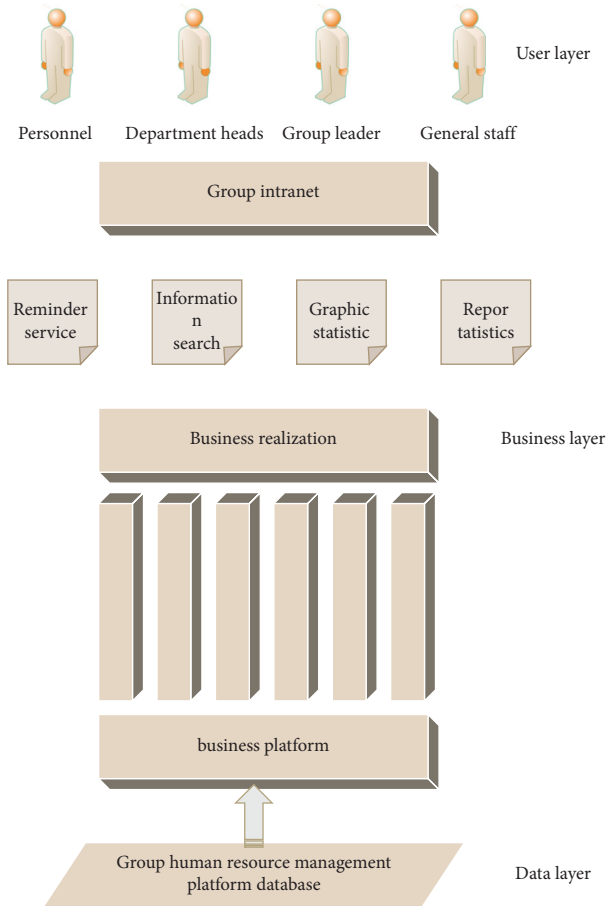

Figure 6: Logical frame diagram.

3.1.2. Platform Safety Management System. The security system of the human resource management platform includes a variety of security protection methods. However, in the actual implementation of security protection, it is not that the more advanced the technical means, the more reasonable and safer the enterprise human resource management system will be. As with any system construction, the economic capacity, rationality, and feasibility of the system need to be considered. When implementing a security protection system, it is necessary to find a balance between investment and profit and implement system security protection in stages.

Figure 7 is the security system diagram of the enterprise human resource management platform.

(1) System security

(a) Access management: According to the enterprise's access control requirements for application characteristics and data resources, the system must provide access management based on visitor role access control.

(b) Identity authentication: Ensure that the identity authentication of system users is safe and effective and carefully consider the security authentication mechanism in the enterprise. Combined with this, the security requirements of identity authentication are guaranteed.

(c) Session security: Web applications are based on the HTTP protocol. Due to its unique stateless and connectionless characteristics, the application must maintain the state of all user sessions. The session processing mechanism for securely tracking and managing authenticated users is the same as the security authentication process, which is very important for the overall security of web applications.

(d) Encryption processing: Encryption processing is an important means and method to control application security. The encryption method used by the system to store, send, and process data needs to be clear.

(2) Data security

(a) User account encryption: Encrypt the user account password so that the plaintext of the password does not appear anywhere. The system encrypts the user password with MD5 to prevent the password from appearing in clear text.

(b) Roles and permissions: Strictly control the permissions of ordinary users and do not grant permissions that should not be granted to the user. Depending on how the client is used, role permissions must be assigned accordingly. Appropriate permissions are granted according to different operations of users on data; the database audit mechanism provides monitoring of data access and system resource utilization in the database. These role and permission control strategies can effectively prevent illegal users from interacting with the database, prevent legal users from interacting with the database, and maximize the security of data.

(3) Storage backup and recovery

If necessary, Oracle logical or physical backups can be used to protect data as much as possible.

(a) Logical backup: The logical backup of the database is divided into two parts, reading database entries and writing files

(b) Physical backup: Physical backup is only the file information allocated to the database, and the parameter setting information and logical information in the database are not included in the scope.

Oracle supports two different types of physical file backups, offline backups and online backups.

(c) Offline backup: Offline backup is used to back up each data file after successfully shutting down the database.

(d) Online backup: Online backup can be used to back up databases running in archivelog mode. In this way, the online log is archived and a complete record of all operations in the database is created.

The online backup process requires specific steps. First, it provides a full point in time recovery and then keeps the database open when backing up the file system.

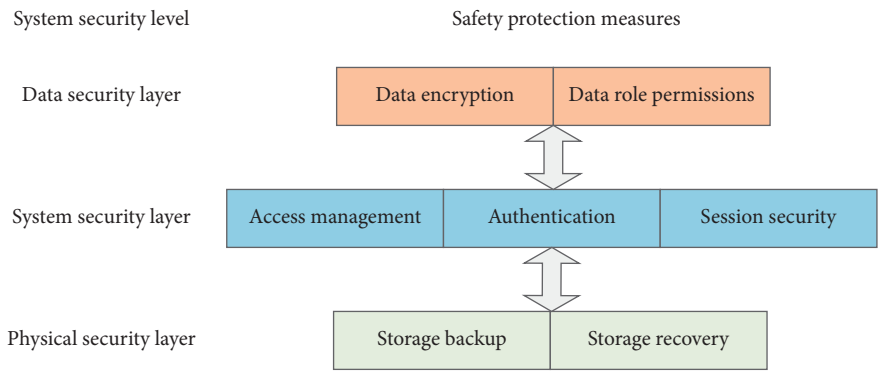

Figure 7: Safety system diagram.

The implementation strategies include the following.

Multiple server policies can be used to back up data on another server. The backup data file must match the parameter settings of the database, such as table structure and other information. If you need to recover data unexpectedly, the data recovery process can be completed with only a few changes.

Data files, log information, and control file information are backed up online regularly, and the database server exports them regularly once a week.

3.2. Database Design of Enterprise Human Resource Management Platform. Database design is a very important work in system development, which is directly related to the efficiency, performance, and security of system operation [8]. The enterprise human resource management platform includes different types of data, massive data, complex data description, and data processing. Providing a database that can meet the system objectives and effectively store and manage data is the key to building the system.

The main database tables and contents of the Oracle 10 g database used in this system are as follows.

The summary of the enterprise HR management platform is shown in Table 3.

The name of the employee work stage evaluation table is T_OA_JOBEVALUATION, and the fields in the table are shown in Table 4.

The name of the vacation record table is TOA LEAVE, and some fields are listed in Table 5.

3.3. Guarantee Measures for the Implementation of Enterprise Human Resource Management Strategy. Based on the description of the weak human base and framework conditions of enterprises in the current new era, we first pay attention to the internal talent development and incentive mechanism, especially the technology implementation and training [9]. We need to observe and create a good supporting and auxiliary environment for relevant external talents and career development and eliminate all bottlenecks and restrictive factors that hinder talents from entering the company, deeply implement the spirit of the Central Committee's opinions on deepening the reform of talent development system and other documents, build and establish a modern personnel system in line with the spirit of the times with market and competitiveness, and improve the recruitment, training, evaluation, flow, and incentive mechanism of talents.

Secondly, the times are advancing. At present, a company has room for improvement in some business or service innovations [10, 11]. For the establishment and development of innovative enterprises, based on innovation systems, equipment and facilities, talents, and relevant incentive mechanisms, it is necessary to formulate long-term plans to provide a good foundation for innovation and growth. Through regular training courses, we will promote and innovate an innovative corporate governance culture that meets the needs of the development of the market economy. In essence, promoting such an invisible code of conduct not only can actively promote the growth of the company but also can promote the long-term development of the company [12]. When discussing the maintenance and construction of corporate culture, enterprise leaders need to pay attention to the following basic requirements: first, corporate culture must deeply reflect the correct core values [13]. Corporate culture plays an important role in the orderly development of various production and operation activities and the establishment of market rules. Secondly, corporate culture should deeply reflect the unique temperament of the enterprise. Corporate culture is unique and intangible, but it is a very valuable asset [14].

Finally, corporate culture must be able to reflect a specific cultural vitality and vitality. Enterprise is the matrix of the corporate culture. They grow together, influence, and promote each other.

The survival and development of an enterprise depend directly on the comprehensive quality of its managers to a great extent. For enterprises, it is necessary to establish a good management team for large talent companies to implement all talent management and implementation [15]. Therefore, through the enterprise development strategy and the actual work of the enterprise, the enterprise needs to actively cooperate with the implementation of the quality improvement plan of human resources managers and establish and support the enterprise to form a professional large-scale human resources management department, which can be divided into two methods. One of them is the company's direct recruitment [16]. Through the selection of

Table 3: Summary of enterprise HR management platform.

Table name	Function description
T_PERSONNEL_CONFIG	Personnel information query configuration table
T_PERSONNEL_DEAD	Death
T_PERSONNEL_INVITE	Recruitment
T_PERSONNEL_MEMBERS	Personnel information
T_PERSONNEL_MOVE	Manpower shuffling
T_PERONNEL_APPROVEDPEOPLE	City planning office approved the number of people
TJPERSONEL_MEMBERS_RATIO	Personnel information comparison table
T_PERSONNEL_APPOINTD (_PROC)	Personnel appointment and dismissal solicitation form
T_PERSONNEL_ATTRITION (_PROC)	Attrition review form
T_PERSONNEL_ATTRITIONPROC	Attrition information table
T_PERSONNEL_GOABROADOB (_PROC)	Examination form for going abroad on business

Table 4: Periodic work assessment form for employees.

Listing	Data type	Length	Decimal places	Identification	Primary key	Allow empty	Defaults	Instruction
RECORDID	VARCHAR2	9	—	—	Yes	No	—	Employee work appraisal ID
CREATEUSERID	VARCHAR2	9	—	—	—	Yes	—	Creator ID
CREATEMEMBERNAME	VARCHAR2	21	—	—	—	Yes	—	Creator name
CREATEDEPTID	VARCHAR2	9	—	—	—	Yes	—	Creator department ID
CREATEDEPTNAME	ARCHAR2	21	—	—	—	Yes	—	Creator department name
CREATETIME	DATE	8	—	—	—	Yes	—	Creation time
UPDATETIME	DATE	8	—	—	—	Yes	—	Last update time
OFFICESOPINION	VARCHAR2	501	—	—	—	Yes	—	Personnel department review

Table 5: Leave record form.

Listing	Data type	Length	Decimal places	Identification	Primary key	Allow empty	Defaults	Instruction
RECORDID	VARCHAR2	9	—	—	Yes	No	—	Record ID
CREATEUSERID	VARCHAR2	9	—	—	—	Yes	—	Creator ID
CREATEMEMBERNAME	VARCHAR2	21	—	—	—	Yes	—	Create name
CREATEDEPTID	VARCHAR2	9	—	—	—	Yes	—	Create department ID
CREATEDEPTNAME	VARCHAR2	21	—	—	—	Yes	—	Create department name
APPLYREASON	VARCHAR2	101	—	—	—	Yes	—	Reason for leave
STARTTIME	DATE	8	—	—	—	Yes	—	Leave start time
ENDTIME	DATE	8	—	—	—	Yes	—	Leave end time
LEAVEDAYS	NUMBER	—	—	—	—	Yes	—	Days off

enterprise recruiters, headhunting recruitment, and recommendation, the management team talents of excellent large-scale human resources companies can directly join the company's management team from the department [17]. This is the most direct process and the most effective management method. Another method is to tap the potential internally. The selection and training within the enterprise improve the skills and quality of the existing employees of the company, so as to achieve the goal of further developing the employee structure. Although this type of management cost is low, the speed is slow, and there may be a significant delay, which requires enterprise decision-makers to make strategic decisions [18, 19].

In addition, entrepreneurs need to change their way of thinking and concepts, more recognize the special importance of human resources department management, strengthen the organizational leadership of relevant human resources departments, and coordinate various functions so that all aspects of organizations and plans can get the support of the whole society. At the same time, promoting the construction of a sound human resources management system to the enterprise strategic level and improving the

overall quality level of human resources are two of the strategic objectives of building a high-quality human resources department, so as to lay the foundation for building a high-quality human resources management department.

In order to support the company's personnel development, an internal coordination and cooperation mechanism has been established to further strengthen the publicity and promotion of the company's human resources strategic plan within the company so that all functional departments and all employees understand, recognize, and understand the importance of the company's human resources strategic plan and strategic plan. At the same time, establish a reasonable working system and mechanism to provide an institutional guarantee for the smooth implementation of strategic labor planning. In all the processes of human resources strategic planning and implementation, it enables unlimited cooperation between all departments and industries. At the same time, it is necessary to establish a reasonable resource allocation and mechanism to realize the sharing of resources and information between different functional departments and ensure the smooth and effective implementation of strategic planning.

Strengthen management participation. During the implementation of the strategy, the support and recognition of the company's internal management provide a good foundation and guarantee for the implementation of the talent strategic plan at the management, resource, and system levels. When implementing the company's human resources strategy, the cooperation between departments will inevitably bring problems. Relevant executives need to clarify the core content of personnel strategy implementation and effectively promote the sustainability of the strategy through participation in management. Some human resource management, such as detailed incentives and training, clearly require human and other resources. Some companies and management need to pay attention to resource investment and have a solid foundation for implementing a human resource management strategy.

In addition to the introduction and popularization of information technology, the construction of enterprise human informatization also needs to continuously and comprehensively monitor and analyze the existing internal data, information, and data. For example, establish performance systems for employees in different departments of the company, use performance indicators to form employee performance information management, establish personnel cost information system, and monitor specific cost indicators such as recruitment cost and labor cost of the company. Use the information system to enable the relevant data in the process of enterprise talent management to continuously and comprehensively analyze and apply the indicators.

Considering the current overall development of the company and the scale of employees, it is difficult to rely on the internal personnel department as the overall responsibility of the personnel strategy in terms of the number and professional scope of the management department It is very limited, which inevitably affects the efficiency of the company's overall human resource management. Therefore, we can give priority to making full use of external third-party specialized agencies to provide support and services for business personnel management and promote the improvement of resource utilization efficiency with the help of outsourcing of large-scale business enterprises.

Important work contents that do not include corporate culture or confidentiality, such as service delivery, can be regarded as part of the company's existing human resource management contents and strategy implementation. Institutions in various business areas are required to fully improve their professional level, retain sufficient practice and energy in the design and implementation of internal management strategy, and ensure the scientificity and coordination of enterprise personnel management strategy. Before cooperating with external service institutions, the company conducted scientific and complete preliminary research and investigation on the scope, organizational structure, and current overall operation and development of external service institutions through objective analysis. Therefore, the selection of appropriate institutions can be determined according to the evaluation and comparison of institutional performance. In addition, firstly, according to the internal workload and work content of the company, the hierarchical structure of the company's personnel outsourcing services should be carried out, then the work allocation and outsourcing agreement should be clarified, and the service outsourcing plan should be formulated, which can reasonably improve the efficiency of resource utilization.

4. Conclusion

The task of designing and implementing an enterprise human resource management platform in this paper is huge. The human resource department plays a very important role in this development. The human resource management platform of an enterprise makes use of today's relatively mature computer technology and the needs of human resource management to create a business system that can be integrated with the business field of the enterprise. This paper mainly focuses on the relatively low level of data interaction between the enterprise headquarters and its subsidiaries and the low efficiency of traditional human resource management and describes the design and implementation of the enterprise human resource management platform, which combines the existing hardware and software with the existing human resource management platform; based on the actual situation of twin network and mobile edge computing, we build an enterprise human resource management platform.

Data Availability

The data used to support the findings of this study are available from the corresponding author upon request.

Conflicts of Interest

The authors declare that they have no conflicts of interest.

Acknowledgments

This paper was supported by Jiangxi Educational Reform Project: Research on the Incentive Mechanism of University Teachers' Temporary Training in Enterprises, no. JXJG-20-28-4.

References

[1] L. Xiao, "Optimal allocation model of enterprise human resources based on particle swarm optimization," in *Proceedings of the 2020 International Conference on Computer Information and Big Data Applications (CIBDA)*, pp. 249–253, IEEE, Guiyang, China, April 2020.

[2] Y. Wu, J. Lim, and M.-H. Yang, "Online object tracking: a benchmark," in *Proceedings of the 26th IEEE Conference on Computer Vision and Pattern Recognition (CVPR '13)*, pp. 2411–2418, Portland, Ore, USA, June 2013.

[3] J. Zhang, X. B. Mao, and T. J. Chen, "Survey of moving object tracking algorithm," *Application Research of Computers*, vol. 26, no. 12, pp. 4407–4410, 2009.

[4] W. Zhong, H. Lu, and M.-H. Yang, "Robust object tracking via sparsity-based collaborative model," in *Proceedings of the IEEE Conference on Computer Vision and Pattern Recognition (CVPR '12)*, pp. 1838–1845, IEEE, Providence, RI, USA, June 2012.

[5] J. C. SanMiguel, A. Cavallaro, and J. M. Martinez, "Adaptive online performance evaluation of video trackers," *IEEE Transactions on Image Processing*, vol. 21, no. 5, pp. 2812–2823, 2012.

[6] X. Ling and H. Ling, "Robust visual tracking and vehicle classification via sparse representation," *IEEE Transactions on Pattern Analysis and Machine Intelligence*, vol. 33, no. 11, pp. 2259–2272, 2011.

[7] E. J. Wakin and M. B. Wakin, "An introduction to compressive sampling," *IEEE Signal Processing Magazine*, vol. 25, no. 2, pp. 21–30, 2008.

[8] Z. Sun, K. Strang, and S. Firmin, "Business analytics-based enterprise information systems," *Journal of Computer Information Systems*, vol. 57, no. 2, pp. 169–178, 2017.

[9] M. Adil, M. K. Khan, M. Jamjoom, and A. Farouk, "MHADBOR: AI-enabled administrative distance based opportunistic load balancing scheme for an agriculture internet of things network," *IEEE Micro*, vol. 42, no. 1, pp. 41–50, 2021.

[10] H. Ma, "Enterprise human resource management based on big data mining technology of internet of things," *Journal of Intelligent and Fuzzy Systems*, vol. 1, pp. 1–7, 2021.

[11] S. Ozcan, C. O. Sakar, and M. Suloglu, "Human resources mining for examination of R&D progress and requirements," *IEEE Transactions on Engineering Management*, vol. 99, pp. 1–16, 2020.

[12] P. Li, "On the application of big data technology in human resource management in the new era," *Journal of Physics*, vol. 1915, no. 4, p. 042038, 2020.

[13] X. Qi, "Countermeasures for enterprise human resource management reform in the era of big data," *Investment and Entrepreneurship*, vol. 7, pp. 136-137, 2020.

[14] J. He and L. Jin, "Research on human resource quality structure identification model based on BP neural network," *Science and Management*, vol. 39, no. 6, pp. 50–57, 2019.

[15] M. Naseri, S. Heidari, M. Baghfalaki et al., "A new secure quantum watermarking scheme," *Optik*, vol. 139, pp. 77–86, 2017.

[16] Z. Jin, L. Zhen, and J. Shen, "Prediction model of employee flow based on semi-Markov chain and its application analysis," in *Proceedings of the 2020 IEEE 5th Information Technology and Mechatronics Engineering Conference (ITOEC)*, pp. 1829–1833, IEEE, Chongqing, China, 2020.

[17] H. Boudlaie, H. Amoozad Mahdiraji, S. Amoozad Mahdiraji, V. Shamsi, A. Jafari-Sadeghi, and A. Garcia-Pereze, "Designing a human resource scorecard: an empirical stakeholder-based study with a company culture perspective," *Journal of Entrepreneurship, Management and Innovation*, vol. 16, no. 4, pp. 113–147, 2020.

[18] A. De Mauro, M. Greco, M. Grimaldi, and P. Ritala, "Human resources for Big Data professions: a systematic classification of job roles and required skill sets," *Information Processing & Management*, vol. 54, no. 5, pp. 807–817, 2018.

[19] B. Zhao, Y. Cheng, and J. Cheng, "Evaluation and image analysis of enterprise human resource management based on the simulated annealing-optimized BP neural network," *Computational Intelligence and Neuroscience*, vol. 2021, Article ID 3133065, 2021.

Hindawi
Mobile Information Systems
Volume 2022, Article ID 5367813, 9 pages
https://doi.org/10.1155/2022/5367813

Research Article

Remote Monitoring Application in Treatment of Gynecological Inflammation Based on Association Rule Algorithm

Qian Manjuan

Department of Obstetrics and Gynaecology of the Second People's Hospital of Nantong, Nantong, Jiangsu 226002, China

Correspondence should be addressed to Qian Manjuan; 2007032@muc.edu.cn

Received 12 June 2022; Revised 7 July 2022; Accepted 22 July 2022; Published 16 August 2022

Academic Editor: Shadi Aljawarneh

The storage center of the main data of the information system is called the database, and the database is often attacked. The traditional database security mechanism based on identity authentication and access control is a passive security mechanism that focuses on prevention, which cannot ensure the security of modern databases. This study analyzes the remote monitoring application in the treatment of gynecological inflammation based on the association rule algorithm. Medical remote monitoring can be realized through 5G technology, smart wearable devices, etc., and online HD consultation and medical image data synchronization can be realized through wired video. Based on the analysis of the unique query structure of the database, this study makes a comprehensive discussion on the theory and method of database anomaly detection technology and focuses on how to integrate data mining methods such as association rules and clustering into the database anomaly detection. The results show that the medical examination system in this study can effectively improve the medical level of gynecology, and has practical significance in the clinical practice of gynecological inflammation. With the development of 5G technology, there will be more remote monitoring medical equipment connected to the Internet, health information can be transmitted to professional health institutions, real-time monitoring of users' physical health through big data, and timely provision of health guidance and early warning.

1. Introduction

Due to the gradual development of information technology in various fields of society, people not only benefit from the wide range of opportunities given by information reform but also face the baptism of information security [1]. Because of the objective existence of system security vulnerabilities, it is difficult for operating systems, application software, and hardware devices to guarantee that there will not be many security problems. According to past experience, safety problems are unavoidable [2]. As intrusion methods continue to be enriched and more difficult to predict, it is difficult to follow the intruder and prevent the intrusion in advance. Traditional passive security such as access control technology based on identity authentication, multi-level security mechanism for controlling information flow, data encryption and firewalls, etc [3]. The mechanism can no longer meet the needs of the security situation. As an active security prevention mechanism, an intrusion detection system is the ultimate line of defense for security detection and has received more and more attention [4]. The main concept of the future 5G network architecture design is user-centric, which requires the 5G network to be capable of on-demand networking and flexible deployment for various business scenarios [5]. The 5 G network can meet the diverse needs of users and its traffic has grown on a large scale and the number of user terminals has increased sharply. However, the traditional packet core network is incapable of facing the diversification of the service industry, which makes it difficult to meet the needs of diversified services. With the diversified development of service objects and business scenarios, a dedicated plan is designed for each business or service, but the high cost and extremely low resource utilization make the plan extremely unrealistic [6]. Gynecological inflammation is a disease that often occurs in female genitalia. It has a great impact on girls' bodies and

minds, and the situation is not optimistic. Therefore, it is necessary to conduct research on gynecological inflammation [7]. This article discusses the symptoms, causes, diagnosis, and treatment of this disease, and provides a reference for the treatment of gynecological inflammation with integrated Chinese and Western medicine. The so-called gynecological diseases are the diseases of female reproductive organs we often say, including uterine diseases and vulvar diseases [8]. Through investigation and research on relevant medical materials, it can be found that more than 85% of women will have symptoms of gynecological inflammation, but the degree of disease is different, and most gynecological inflammations may have repeated attacks when they actually occur. If women themselves suffer from gynecological inflammation but fail to find out and carry out the targeted treatment the first time, it will not only have a huge impact on women's bodies, but also increase their chances of suffering from cervical cancer and pathological changes [9]. Therefore, we must solve our own problems through medical means in time for our physical discomfort, adopt some effective methods for treatment, and strengthen the prevention of diseases. This is of great significance for protecting women's health.

2. Related Work

The literature puts forward the concept of a multi-dimensional set, mathematical model, and its measurement space. It also talks about using multi-dimensional association rules to change the algorithm APMA-MSSD. Using its unique algorithm APMA-MSSD, the performance of running together is more perfect than running directly [10]. The concept of multi-dimensional collections and the semantics of the association rules of multi-dimensional collections is to change data from a single value to multiple values, so that it can be used by multi-valued data mining. The literature talks about the irregularity detection algorithm AD_Density based on the metric space. AD_Density uses density clustering data design to standardize the appearance and combine it into a metric index tree, so that searching with a fast speed is its detection process. In addition, density clustering is not sensitive to external structures and noisy sounds [11]. Therefore, this algorithm is used to make up for the problem of Lenoid and other anomaly detection algorithms based on cluster analysis, such as the detection rate of the impact of performance degradation in the metric space and the data distribution algorithm of the training set. This method can be regarded as irregularity checking of the database, and its core algorithm will be used for irregular checking of the database. This is because the database understands the characteristics of the metric space, and it is recommended that the APMA-MSSD algorithm be used in irregular checking of the database [12]. The nature and variants of the application. According to the literature, on the basis of a system with a high degree of trust, the hidden channels are eliminated by rolling back the confidentiality level of the transaction manager that works well in confidentiality, while maintaining the modularity and minimization of the trusted computing foundation [13, 14]. The security lock protocol is a highly reliable security database. The problem that must be solved is the realization of the hidden channel in the two-phase lock protocol and the need to maintain regionalization, which enriches the existing transaction protocols [15]. The literature introduces the research direction, existing technology, and existing problems of database anomaly detection technology, discusses the research and consideration of database anomaly detection systems in implementation technology and implementation mode, and also answers the benefits and methods of various technologies and methods for this purpose [16]. Finally, the data development technology is explained, especially the development of association law and the application of cluster analysis in irregular inspection, and the research on its benefits and problems that should be eliminated. The literature first talked about the concept of multi-dimensional sets, and then answered its similarity calculation method [17]. In addition, the mining algorithm for association rules of multi-dimensional sets is discussed, and examples are analyzed. Finally, the application of multi-dimensional sets in database irregularity checking is introduced. It explained its multi-level relationship simulation, and then, the classification strategy was discussed. In order to better observe the effects of treatment and preventive health care for common gynecological diseases, we select some patients with gynecological diseases and divide them into two groups arbitrarily.

3. Abnormal Database Access Detection and Medical 5G Network Application

3.1. Database Abnormal Access Detection. There are multiple well-ordered sequences in the same group because the inclusion relationship is a partial order relationship, as shown in Figure 1.

Calculating the similarity between sets and sets can be used to find suitable sets for matching or clustering, etc. These applications are set in similarity. Its measurement usually increases with the increase of the set and its value. Experience shows that past research has found a large number of set similarity measurement methods, in which up to five coefficients such as formulas (1)–(5) are used.

$$\mathrm{sim}(X,Y) = |X \cap Y|, \tag{1}$$

$$\mathrm{sim}(X,Y) = \frac{2^{*}|X \cap Y|}{|X| + |Y|}, \tag{2}$$

$$\mathrm{sim}(X,Y) = \frac{|X \cap Y|}{\left|X \bigcup Y\right|}, \tag{3}$$

$$\mathrm{sim}(X,Y) = \frac{|X \cap Y|}{\sqrt{|X|} * \sqrt{|Y|}}, \tag{4}$$

$$\mathrm{sim}(X,Y) = \frac{|X \cap Y|}{\min(|x|, |y|)}. \tag{5}$$

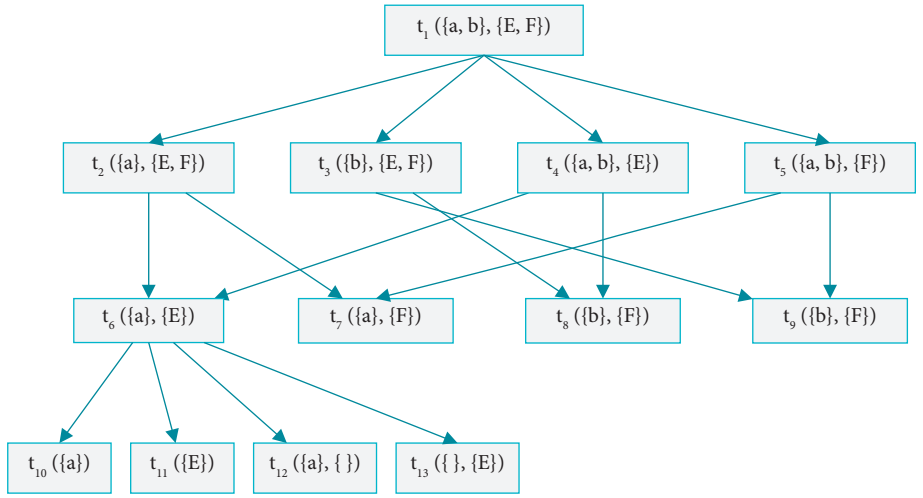

Figure 1: Example of cube containment relationship.

The given attribute set conforms to the total order relationship, and the formula of its average method similarity is shown in the following formula:

$$\mathrm{sim}_{\mathrm{avg}}(t_1, t_2) = \frac{\sum_{i=1}^{n} \mathrm{sim}(S_i, R_i)}{n}. \tag{6}$$

The distance formula is as the following formula:

$$\mathrm{dist}_{\mathrm{avg}}(t_1, t_2) = 1 - \mathrm{sim}_{\mathrm{avg}}(t_1, t_2). \tag{7}$$

The given attribute set conforms to the total order relationship, and its multiplicative similarity formula is as shown in the following formula:

$$\mathrm{sim}_{\mathrm{mul}}(t_1, t_2) = \prod_{i=1}^{n} \mathrm{sim}(S_i, R_i). \tag{8}$$

The distance formula is as the following formula:

$$\mathrm{dist}_{\mathrm{mul}}(t_1, t_2) = 1 - \mathrm{sim}_{\mathrm{mul}}(t_1, t_2). \tag{9}$$

The similarity formula is shown in the following formula:

$$E\mathrm{sim}_{\mathrm{avg}}(t_1, t_2) = \frac{\sum_{c \in A \cap B} \mathrm{sim}(S_c, R_c)}{\left|A \bigcup B\right|}. \tag{10}$$

The distance formula is as the following formula:

$$E\mathrm{dist}_{\mathrm{avg}}(t_1, t_2) = 1 - E\mathrm{sim}_{\mathrm{avg}}(t_1, t_2). \tag{11}$$

For any $d \in D$, the number of elements whose support degree of d in package s is equal to d is defined as the following formula:

$$\sup(\mathrm{d}, s) = |\{v | v \in s \wedge v = \mathrm{d}\}|. \tag{12}$$

The similarity formula between s and t is as in the following formula:

$$\mathrm{sim}_{\mathrm{bag}}(s, t) = \frac{\sum_{\mathrm{d} \in s \cap t} (\sup(\mathrm{d}, s) + \sup(\mathrm{d}, t))}{|s| + |t|}. \tag{13}$$

The formula for similarity between t_1 and t_2 is shown in the following formula:

$$E\mathrm{sim}_{\mathrm{mix}}(t_1, t_2) = \frac{\sum_{c \in A \cap B} \mathrm{sim}_{\mathrm{bag}}(S_c, R_c)}{\left|A \bigcup B\right|}. \tag{14}$$

The distance formula is as the following formula:

$$E\mathrm{dist}_{\mathrm{mix}}(t_1, t_2) = 1 - E\mathrm{sim}_{\mathrm{mix}}(t_1, t_2). \tag{15}$$

The dimensionality subsets of 2000 transaction action characteristics A1 and A3 with an average frequent item length of 3 are each obtained as 0.75 support and 0.25 reliability. This example uses 2000 transaction action characteristics with an average frequent item length of 4 as A2 The subset of dimensions. The most important thing is to let the dimensional subset get 2000 three-dimensional data sets according to the characteristics A1, A2, and A3 as the experimental data. If the pruning effect is compared by selecting the total number of elements, the results are shown in Table 1.

If the Apriori algorithm is used to obtain the support of the selection set without other algorithms, then all the data sets should be used when performing this operation, and the APMA-MS algorithm does not need to be other as long as the attribute column can be added.

Therefore, the transaction read subset (d) of Figure 2 is the amount of data read by the unit. Figure 2 shows the method of increasing the value of the minimum support. The reduction is easier to see, and the value of adjusting the support of the cube reaches the minimum. The algorithm is the longest known frequent item, and the number remains the same.

The multi-dimensional model is longer. Figure 3 compares with the FP-Growth algorithm and finds that the FP-Growth algorithm has better performance in the long-mode processing. Hardware environment: based on Intel structured microcomputer, CPUPentium 2.80 GHz, memory 512M; software environment: Windows2000 server,

Table 1: Comparison of pruning effects for mining frequent 3-dimensional sets.

Support threshold results and algorithms	Generate frequent 3-dimensional sets	APMA-MS algorithm	APMA-MSSD algorithm	Direct apriori algorithm
0.01	2856	8032	6744	8630
0.03	346	3864	2788	4146
0.05	244	3375	2185	3459
0.07	182	2062	2034	3283
0.09	105	1830	1824	3031
0.11	37	1613	1598	2801
0.13	15	1506	1456	2675
0.15	No	1341	1354	2625

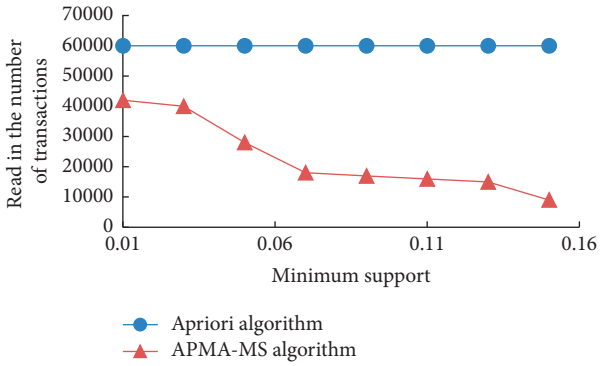

Figure 2: Mining frequent 3-dimensional set data read-in volume comparison.

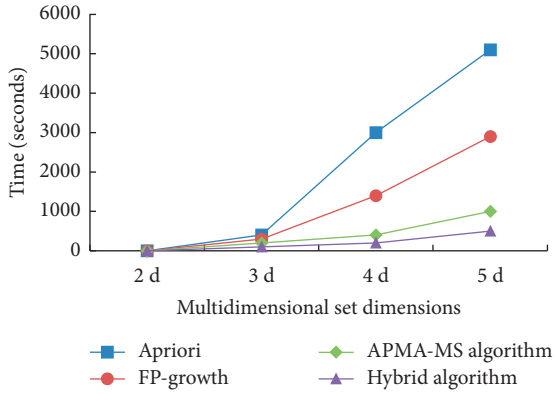

Figure 3: Comparison of algorithm execution time in different dimensions (min_sup = 0.09).

SolServer2000, using Netframework for programming. As long as the data set is scanned, it is regarded as a search and read of the database, and the test results in different dimensions are shown in Figure 3.

Under different threshold δ, the clustering results are shown in Table 2. The larger the δ, the greater the similarity between the internal members of the cluster, and the more compact the internal structure of the cluster.

Therefore, the clustering algorithm generates more clusters, especially small clusters. as shown in Table 3.

Table 4 shows the results of executing three read queries A, B, and C on an account relationship. If the value of the

Table 2: Number of clusters under different thresholds (δ).

Cluster size threshold	0.1	0.2	0.3	0.4	0.5	0.6
1	267	399	423	496	718	1241
2	46	7	16	45	170	332
3	15	3	9	47	105	193
(3, 10)	1	12	59	145	287	430
(10, 100)	17	46	124	201	234	207
>100	18	25	24	15	7	3
Total number of clusters	364	492	655	969	1521	2406

attribute in the execution result set is regarded as a one-dimensional set or wrapped in each attribute, and the order relationship with the attribute is regarded as a fully-ordered relationship, the query result can be regarded as a set of true multi-dimensional hybrids.

3.2. Medical 5G Network. The spectrum efficiency at each user base station is as shown in:

$$\eta_{i,j} = \log_2\left(1 + \mathrm{SINR}_{i,j}\right). \tag{16}$$

The signal-to-interference-to-noise ratio is shown in formula:

$$\mathrm{SINR}_{i,j} = \frac{P_j \cdot h_{i,j}}{\sum_{l \in J, l \neq j} p_l \cdot h_{i,l} + \sigma^2}. \tag{17}$$

Assuming that a user can only request one service at a certain time, a user can only connect to one base station as in:

$$\sum_{j \in J} x_{i,j} = 1, \forall i \in I^e \bigcup I^u. \tag{18}$$

There is no doubt that the base station will not enter without restraint. The maximum number of objects that can be entered by any base station j is as in:

$$\sum_{i \in I^e U I''} x_{i,j} \leq u_j, \forall j \in J. \tag{19}$$

For user I, the maximum data transmission rate of user I can use Shannon's formula as:

$$R_i = \sum_{j \in J} x_{i,j} y_{i,j} B_j \eta_{i,j}, \forall i \in I^e \bigcup I^u. \tag{20}$$

Table 3: Clustering results of DBSCAN under different Eps (MinPts = 10).

Eps	Number of clusters	Cluster size (the number in brackets is the number of clusters of that size)	Voice number
0.2	50	9(6), 10(3), 11(2)12(3), 13, 14(2), 15(3), 16(3), 19, 20, 21, 23, 28, 29(2), 33(3), 38, 40(2), 53, 54, 57(2), 60, 63(2), 64, 83, 107, 110, 285, 2544	5738
0.3	17	11(2), 12, 13, 14, 15, 16(2), 17, 21, 23(2), 40, 57, 65, 1911, 4930	2805
0.4	2	23, 8852	1125
0.5	2	17, 9412	571
0.6	1	9565	435

Table 4: An example of an account relationship and its read query results.

ID	Account	Password	Gender	System	Age
1	Zyq830	A123	Male	Mathematics	27
2	TianBel	H459	Male	Add up	36
3	Jimmy	H459	Female	Mathematics	48
4	Ljr3000	GC37	Female	Mathematics	45
5	Liu6021	NN14	Male	Computer	36
6	Rodger117	A563	Male	Chemistry	27

The range of all bandwidth resources allocated by I is less than or equal to the bandwidth resources of the j base station is shown in:

$$\sum_{i \in I^e \bigcup I^u} x_{i,j} y_{i,j} \leq 1, \forall j \in J. \tag{21}$$

MBBe film is to ensure the transmission rate and throughput of mobile broadband services. It not only ensures that all users on the MBBe chip meet the lowest throughput and latency performance but also improves the user's lowest throughput as much as possible. Therefore, the performance evaluation index of MBBe is defined as the minimum throughput as:

$$a \triangleq \min_{i \in E^e} R_i. \tag{22}$$

Compared with other services, the obvious feature of the RLLCu chip is that it needs ultra-low time delay as in the formula.

$$b \triangleq \max_{i \in I'} \frac{L_i}{R_i}. \tag{23}$$

Part of the mathematical model of the optimization problem is shown in:

$$\max_{x_{i,j}, y_{i,j}} \{wa - (1-w)b\}, \left(\frac{e}{\&u} - \mathrm{BOP}\right). \tag{24}$$

The slack variable can be understood as the probability that user i connects to base station j, so the connection plan between base station j and user i is as shown in:

$$\max_{y_{i,j}} \{wa^* - (1-w)b^*\}, \text{(BAP)}. \tag{25}$$

Four base stations are designed in the experiment. The distance between each base station is 250 m. The radius of any base station is 200 m. The types and positions of users under any base station are arbitrarily placed. The placement of users and base stations is shown in Figure 4.

The rule in this study is that the maximum number of user connections for each base station is 20, and the specific simulation parameters are shown in Table 5.

Figure 5 shows the performance analysis with the weight value w.

3.3. Application of 5G Network in the Medical Field. China has a vast territory and uneven allocation of medical resources. In order to make it easier for patients to see a doctor and make it more convenient for patients to receive diagnosis and treatment by authoritative experts, remote consultation technology has emerged. In the past, the general online consultation production and maintenance process required a lot of effort, and it was not convenient to move. It will be realized through wired video. The 5 G network can use 4 K/8 K online high-definition consultation and medical image data to synchronize in time. This is all because of the high speed of the 5G network. This performance allows experts to make timely and efficient judgments and treatments. Improve the efficiency of diagnosis and treatment and on-site guidance. Teaching is of great significance to surgery teaching. Traditional medical surgery observation and teaching are mainly performed on-site in the operating room or through video recording. The number of participants in on-site teaching is small, and the teaching and research efficiency is low. For some minimally invasive surgery, it is unable to connect to medical equipment and does not have the conditions for observation and teaching. Surgical video recording methods have problems such as the camera being electromagnetically interfered with by the surgical equipment, and the image effect is poor or cannot be recorded at all. The application of 5G network and 4 K medical equipment can display the operation screen in high-definition, the operating room and the conference center can communicate with audio and video, and the whole process of the operation can be broadcast live through audio and video communication, 5G network performance is good, smooth live broadcast and communication screen , no lag, clear details of the picture, and smooth sound transmission. At present, the application of 5G remote surgery teaching has been carried out in many provinces and cities and has achieved good results.

For example, the Gansu Provincial Health and Family Planning Commission relied on the provincial telemedicine information platform and used telecom 5G network

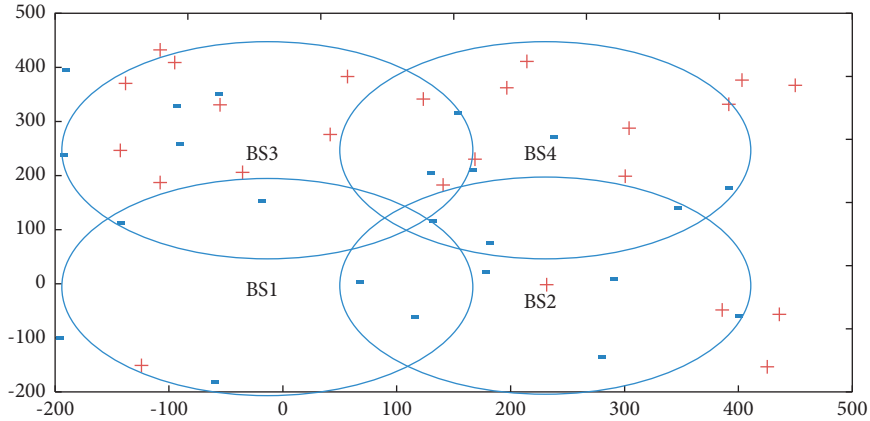

Figure 4: User base station distribution ($u = 60$).

Table 5: Simulation parameters.

Parameter	Numerical value	Parameter	Numerical value
Base station	4	Noise power	10 −13 w
User	0–80	Base station transmission power	46 dBm
Channel model	3D-uma	Base station bandwidth	20 MHz
Base station spacing	250 m	Carrier frame rate	2 GHz

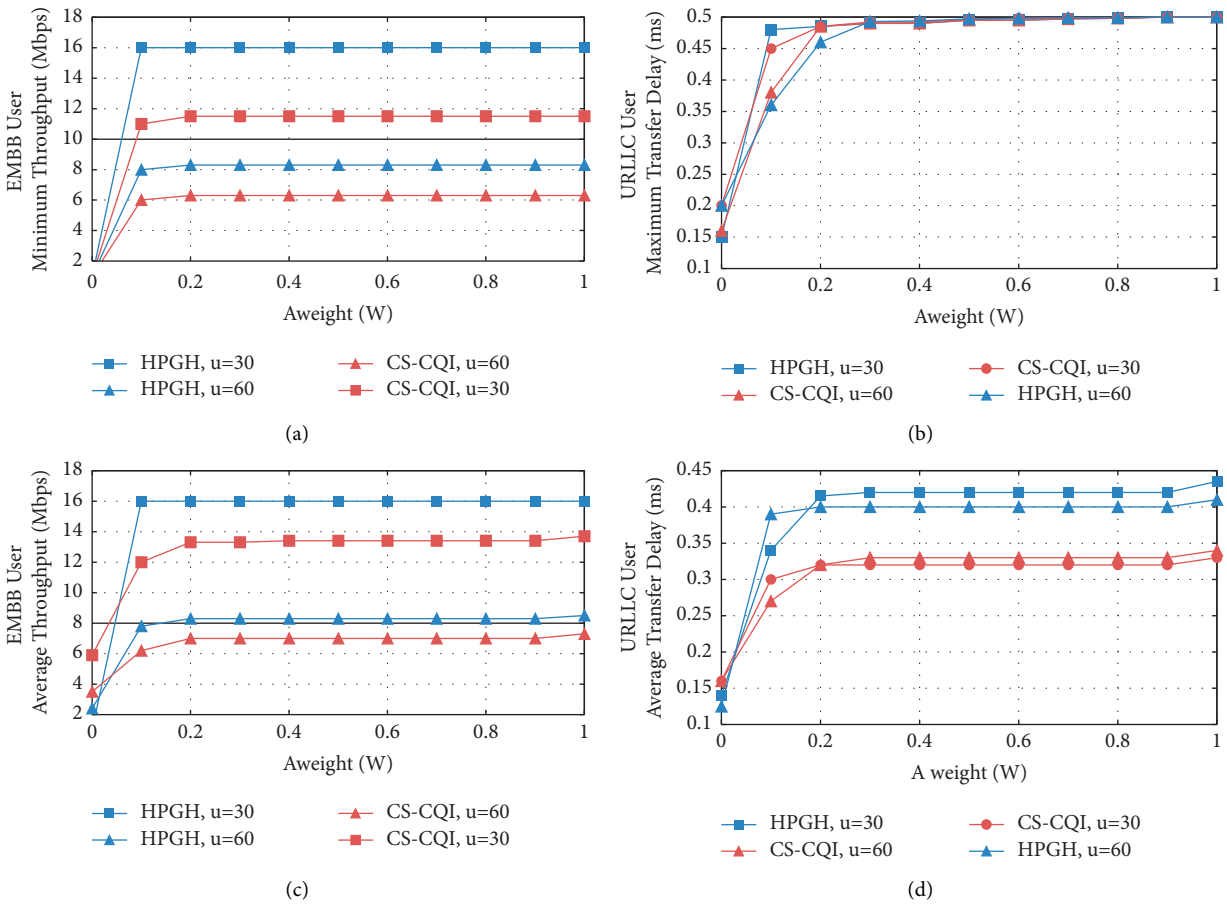

Figure 5: System performance changes with weight w. (a) Minimum throughput of the EMBB service, (b) maximum transmission delay for URLLC services, (c) average throughput of the EMBB business, and (d) average transmission delay of URLLC service.

technology to carry out the first surgical tele-teaching activities, and simultaneously promoted multiple provincial-level medical institutions to access the telemedicine platform. Experts from the Gansu Provincial Hospital of Traditional Chinese Medicine demonstrated the entire process of the decompression operation of the lumbar 5/sacral 1 nucleus pulposus through the laminar approach under local anesthesia through the provincial telemedicine information platform in the operating room. And the team's analysis in the process is very complete. Gansu Provincial Department of Health, Gansu Provincial Hospital of Traditional Chinese Medicine Online Consultation Center, Gansu Provincial Health Commission used 5G networks to interact with the online medical platform dispatch center. The 5 G network can enable the rapid spread of medical technology to the grassroots level and has a profound impact on the improvement of China's medical standards.

Remote monitoring can be achieved through 5G technology, smart wearable devices, etc. Medical monitoring and data transmission devices are worn or implanted in the human body using computer technology, the Internet, and the Internet of Things, such as glasses, watches, bracelets, anklets, jewelry, rings, necklaces, etc., in real-time, accurately and efficiently. It records human vital signs information and pathophysiology, and quickly displays it to patients and doctors through cloud transmission and analysis technology, making medical treatment, prevention, diagnosis and treatment, follow-up and other processes comfortable, convenient, and accurate. Health functions have become one of the core concerns of smart wearable devices. For example, smartwatches can provide functions such as ECG, atrial fibrillation monitoring, and real-time synchronization of health data to the cloud. With the development of 5G technology, there will be more remote monitoring medical equipment connected to the Internet, health information can be transmitted to professional health institutions, real-time monitoring of user health through big data, and timely health guidance and early warning.

4. Discussion on Treatment and Prevention of Gynecological Inflammation

4.1. Understanding of Gynecological Inflammation and Causes. Gynecological inflammation is characterized by recurring episodes and most women lack an accurate understanding of this. Many female friends have abnormal leucorrhea, genital itching, waist, and abdomen pain. They do not pay attention. They do not get treatment as soon as possible. Delays and missing the most suitable treatment time will cause them to evolve into other more serious chronic diseases. Chronic inflammation takes a long time. There are many disadvantages, and it is easy to get sick again after knowing it, which has a serious impact on the girls' bodies and minds, and makes the patients even more uncomfortable. If it is not treated quickly, it will easily develop into a serious infection of the reproductive system, which can easily lead to female infertility and ectopic pregnancy. Data show that about 15% of gynecological tumors in the world each year are caused by inflammatory infections.

Gynecological inflammation is a common gynecological disease for Chinese women. It has a great impact on women's physical and psychological quality. The location and types of gynecological inflammation are different, so it will cause a variety of symptoms, such as bad smell, abnormal leucorrhea, irregular physiological cycle, etc. Gynecological inflammation is divided into acute and chronic, acute gynecological inflammation may also be complicated with peritonitis, so that its stomach reaction is severe; Chronic pain usually makes girls feel bloating and pain in their stomachs and discomfort in their back. Leucorrhea is not normal, generally thin serous and abnormal color may also be accompanied by cervical erosion.

Since the female's vulva is not protected and the urethra and anus are close to each other, urination and defecation may lead to vulva pollution, which makes the vulva in a humid environment for a long time and is the breeding ground of various bacteria. Therefore, this physiological structure makes the growth and reproduction of bacteria more convenient. In addition, the monthly menstrual period of girls will be more likely to make genital infection inflammation. The female genitalia, such as the damage caused by tight vulva, frequent and violent sexual intercourse during underwear activities, as well as unsanitary underwear, unsanitary sexual intercourse, and poor immunity, are often infected by different bacteria, resulting in the outbreak of inflammation. Improper artificial medicine and the destruction of the balance of vaginal flora can also cause gynecological inflammation. Western medicine treatment of gynecological inflammation is mainly used to treat patients with inflammation and treat them with antibiotics. In addition, because of the popularity and promotion of antibiotics, antibiotic-resistant strains are increasing, drug resistance is strengthened, and the effect is more and more unsatisfactory and easy to relapse. The disease can not be effectively controlled, often get sick again, and greatly reduce the quality of life of patients.

4.2. Investigation Process and Results of Gynecological Inflammation Treatment. A total of 100 patients with gynecological inflammation in our hospital from May 2019 to April 2020 were studied. All patients were in the range of common gynecological diseases, and they were randomly divided into two groups. In the control group, they were treated in the usual way, but they were not given preventive health education. In the other group, they were given preventive health education while they were treated as usual. For the experimental group with preventive health care treatment, both the treatment results and the patients' liking degree are far higher than those in the normal treatment group. The difference between the two groups is significant, as shown in Table 6.

The basic symptoms of patients in the experimental group were significantly improved when the preventive health care treatment was implemented, and the degree of liking was significantly improved. Among them, 37 cases liked it, 11 cases were OK, and 2 cases didn't. The total liking degree was 96%. In the other group, 11 cases liked it, 23 cases

Table 6: The treatment results of the two groups were compared.

Group	Remarkable effect	Effective	Invalid	Total effective rate
Experimental group ($n = 50$)	33	14	3	94
Control group ($n = 50$)	11	24	15	70

Table 7: Comparison of satisfaction between the two groups after treatment.

Group	Satisfied	Commonly	Dissatisfied	Total satisfaction
Experimental group ($n = 50$)	37	11	2	96
Control group ($n = 50$)	11	23	16	68

were OK, and 16 cases didn't. The total liking degree was 68%. See Table 7 for details.

4.3. Discussion on Treatment and Prevention of Gynecological Inflammation. Women's body immunity will gradually weaken with age. If an unreasonable diet is standardized and lacks good hygiene habits, the incidence rate of gynecological diseases will increase. Gynecological common inflammation and symptoms: (1) Vulvar inflammation is the inflammation of the vulva or mucous membrane, mainly by a variety of bacterial infections or vaginal genital secretion of liquid infection caused by the disease. Symptoms are genital pruritus, discomfort, burning, even swelling, rash, erosion, ulceration. The disease for a long time will make the skin thickness increase, rough, dry crack, and more serious is the hair growth moss. (2) Vaginitis is the genital mucous membrane's outer wall and the connective tissue under the outer wall of the disease. It is basically when the self-defense function of the genitals is damaged, the virus enters and causes infection. Symptoms: genitalia produce more liquid, the odor has been difficult to accept, and severe pain after sexual intercourse. (3) Cervicitis caused by persistent infection of pathogens. Symptoms are the clinical effect of vaginal discharge is significant, which can improve the therapeutic effect of surgery, accelerate the recovery of patients after surgery, and make it easier for patients to recover, so it is necessary to apply it in clinical practice.

All in all, women with gynecological problems should attach great importance to and actively treat gynecological inflammation, learn relevant knowledge completely and skillfully, and learn how to prevent gynecological inflammation. Gynecological inflammation belongs to lumbago, stomachache, and other areas in TCM. The syndrome differentiation can be divided into damp heat injection type, spleen deficiency and dampness supplement type, kidney yin deficiency type, cold coagulation, and blood stasis type. The combination of topical and systemic medicine has a strong effect on repairing uterine tissue and promoting the healing of gynecological inflammation.

5. Conclusion

The key problem of database security is whether it is comprehensive and valuable. In the past, the main work of normal database security law is prevention, which should focus on the investigation of external users, so that the behavior of users is legal and avoid user behavior violations. However, the database security mechanism has great limitations, which can not prevent the abuse of legitimate users' rights and some identity spoofing network attacks, such as password sniffing, session hijacking, and so on. Therefore, it is a reliable method to make up for the deficiency of traditional database security mechanisms by intrusion detection. The existing research on intrusion detection mainly focuses on the host or network intrusion detection, while the research on the database as the core supporting software of information processing is less. The data in the database has its own structure and semantics, and the database users have their own unique behaviors. Through database intrusion detection, we can make up for the shortcomings of operating system and network intrusion detection, and improve the accuracy and effectiveness of detection. Based on the analysis of the unique query structure of database, this study makes a comprehensive discussion on the theory and method of database anomaly detection technology and focuses on how to integrate the data mining methods such as association rules and clustering into the database anomaly detection algorithm, On this basis, some other key technologies of the secure database are also discussed. The research work of this study puts forward some new ideas and directions for the research of secure database technology. In this study, the current clinical treatment process of gynecological treatment of common diseases and treatment of specific programs are studied, and according to the actual situation to develop the corresponding preventive measures.

Data Availability

The data used to support the findings of this study are available from the corresponding author upon request.

Conflicts of Interest

The authors declare that they have no conflicts of interest.

References

[1] A. Mukherjee, S. A. A. Fakoorian, J. Huang, and A. L. Swindlehurst, "Principles of physical layer security in multiuser wireless networks: a survey," *IEEE Communications Surveys & Tutorials*, vol. 16, no. 3, pp. 1550–1573, 2014.

[2] T. Jiang, T. Li, and J. Ren, "Toward secure cognitive communications in wireless networks," *IEEE Wireless Communications*, vol. 19, no. 4, pp. 82–88, 2012.
[3] S. Sicari, A. Rizzardi, L. A. Grieco, and A. Coen-Porisini, "Security, privacy and trust in internet of things: the road ahead," *Computer Networks*, vol. 76, pp. 146–164, 2015.
[4] A. Mpitziopoulos, D. Gavalas, C. Konstantopoulos, and G. Pantziou, "A survey on jamming attacks and countermeasures in WSNs," *IEEE Communications Surveys & Tutorials*, vol. 11, no. 4, pp. 42–56, 2009.
[5] F. Yu, C.-C. Chang, J. Shu, I. Ahmad, J. Zhang, and J. M. de Fuentes, "Recent advances in security and privacy for wireless sensor networks," *Journal of Sensors*, vol. 2015, no. 1, Article ID 169305, 2015.
[6] Z. Wang, Z. Zhou, H. Zhang, G. Zhang, H. Ding, and A. Farouk, "AI-based cloud-edge-device collaboration in 6G space-air-ground integrated power IoT," *IEEE Wireless Communications*, vol. 29, no. 1, pp. 16–23, 2022.
[7] F. Ishmanov, A. S. Malik, S. W. Kim, and B. Begalov, "Trust management system in wireless sensor networks: design considerations and research challenges," *Transactions on Emerging Telecommunications Technologies*, vol. 26, no. 2, pp. 107–130, 2015.
[8] J. I. Shim, A. K. W. Han, H. J. Jeon et al., "Clinical experience of uterine smooth muscle tumor of uncertain malignant potential in two gynecological centers: oncological and obstetrical aspects," *European Journal of Obstetrics & Gynecology and Reproductive Biology*, vol. 246, pp. 7–13, 2020.
[9] M. Virarkar, D. Ganeshan, C. Devine, R. Bassett, V. Kuchana, and P. Bhosale, "Diagnostic value of PET/CT versus PET/MRI in gynecological malignancies of the pelvis: a meta-analysis," *Clinical Imaging*, vol. 60, no. 1, pp. 53–61, 2020.
[10] H. Kameyama, Y. Shimada, K. Abe et al., "Digestive surgery intervention for gynecological malignant tumor," *Gan To Kagaku Ryoho Cancer & Chemotherapy*, vol. 46, no. 13, pp. 2176–2178, 2019.
[11] M. I. Ali, F. Feng, X. Liu, W. K. Min, and M. Shabir, "On some new operations in soft set theory," *Computers & Mathematics with Applications*, vol. 57, no. 9, pp. 1547–1553, 2009.
[12] C.-C. Hsu, C.-L. Chen, and Y.-W. Su, "Hierarchical clustering of mixed data based on distance hierarchy," *Information Sciences*, vol. 177, no. 20, pp. 4474–4492, 2007.
[13] T. Zhang, R. Ramakrishnan, and M. Livny, "BIRCH: an efficient data clustering method for very large databases," in *Proceedings of the ACM SIGMOD International Conference on Management of Data*, pp. 103–114, ACM, Montreal, Canada, June 1996.
[14] U. Azad, B. K. Behera, E. A. Ahmed, P. K. Panigrahi, and A. Farouk, "Solving Vehicle Routing Problem Using Quantum Approximate Optimization Algorithm," *IEEE Transactions on Intelligent Transportation Systems*, 2022.
[15] A. Yener and S. Ulukus, "Wireless physical-layer security: lessons learned from information theory," *Proceedings of the IEEE*, vol. 103, no. 10, pp. 1814–1825, 2015.
[16] W. Xu, W. Trapper, Y. Zhang, and T. Wood, "The feasibility of launching and detecting jamming attacks in wireless networks," in *Proceedings of the 6th ACM International Symposium on Mobile Ad Hoc Networking and Computing (MobiHoc '05)*, pp. 46–57, ACM, Chicago, Ill, USA, May 2005.
[17] S. Zahra, M. A. Ghazanfar, A. Khalid, M. A. Azam, U. Naeem, and A. Prugel-Bennett, "Novel centroid selection approaches for KMeans-clustering based recommender systems," *Information Sciences*, vol. 320, pp. 156–189, 2015.

Hindawi
Mobile Information Systems
Volume 2022, Article ID 3582899, 11 pages
https://doi.org/10.1155/2022/3582899

Research Article

Traffic Optimization Model Based on Regional Road Network Traffic Diversion Technology and Internet of Things

Fang Ma

School of Transportation Management, Zhengzhou Railway Vocational and Technical College, Zhengzhou, Henan 451460, China

Correspondence should be addressed to Fang Ma; 1180892070@zust.edu.cn

Received 14 June 2022; Revised 6 July 2022; Accepted 28 July 2022; Published 16 August 2022

Academic Editor: Shadi Aljawarneh

Today's traffic control system is developing in a more intelligent direction. The progress of electronic technology has created a traffic control and management system using a variety of control methods. The development of computers creates a more intelligent traffic optimization model for optimizing network traffic. In the limited road space, traffic control research will focus on maximizing the use of existing traffic management equipment to improve vehicle circulation efficiency and avoid congestion. In this context, combined with the temporal and spatial characteristics of traffic congestion, this study investigates the storage capacity of existing road space and seeks the optimal control method for local regional road network congestion. For the technical problems of traffic diversion in the existing two-phase control method and the queuing order in the adjacent lanes in the four-phase control method, the optimal control method is proposed, which solves the technical problems of traffic control and the phenomenon of "queuing injustice" in the adjacent lanes in one direction. The safety degree and traffic efficiency of vehicle operation are improved. The traffic flow from the same entrance to the main intersection forms a signal phase while slowing down or blocking these traffic flows can effectively improve traffic safety and traffic efficiency. Combined with the development of traditional traffic control system, this study introduces the development status of Internet of things technology and puts forward an intelligent traffic control system based on Internet of things technology. Real-time vehicle traffic information is sent to the Lora gateway through Lora wireless network, which is responsible for data transmission and protocol conversion.

1. Introduction

Urban congestion not only brings inconvenience to residents, prolongs travel time, increases fuel consumption and other negative effects, but also causes road traffic accidents, pollution and other problems, which often brings huge losses to urban life, road safety, and the national economy. According to the data released by the Ministry of transport, China's direct economic losses caused by traffic congestion amount to hundreds of billions of yuan every year. It can be seen that many inconveniences caused by congestion can not be ignored. The mitigation and management of regional road network have been highly valued by the government and relevant departments as an important issue related to the national economy and people's life. Excess vehicle traffic refers to the total number of vehicles passing through the intersection or road network in a certain period of time. During peak hours, more vehicles must "flow" to quickly evacuate the stagnant traffic flow, so as to avoid overcrowding due to waiting for vehicles in the road section, quickly get rid of the crowded traffic situation, and reduce the traffic pressure on the road section and prevent traffic congestion caused by overcrowding. Therefore, in the study of traffic diversion technology, many control methods have been optimized to maximize the traffic flow of intersections or road network. In the study of preventing supersaturation at major intersections, we also introduce a control model to optimize the peak traffic at intersections [1]. The search in the literature shows that the current oversaturated traffic optimization control has achieved successful results. However, due to the complexity of road traffic problems and their importance in daily life, people's interest in road congestion research has not weakened. Today's traffic control system is developing in a more intelligent direction. The progress of

electronic technology has spawned different methods to control traffic control and management systems. The progress of computers makes the network traffic control and management system more intelligent. The progress of artificial intelligence, big data, and Internet of things algorithms makes traffic management possible. The control system has higher efficiency and more functions. Traffic congestion usually occurs at a specific time and place, and has the characteristics of time zone and geographical constraints. Determine the congestion period according to the characteristics of the traffic optimization model, and formulate and implement appropriate optimization methods during this period, which can improve congestion, traffic pressure, and traffic performance indicators; Considering the regional characteristics of road congestion, the congested regional road network is selected as the research object to optimize the main intersections of the local road network, prevent congestion and form a comprehensive operation mode of the road network.

2. Related Work

Some research introduces the traditional congestion evaluation and detection methods, which depend on the evaluation of micro traffic mode or the calculation of traffic indicators at a single intersection or road section. Then, the weighted average network method is used to determine the traffic condition of the road network. However, it is impossible to consider the overall efficiency of the road network, such as the average saturation and average speed of the road network, and it is difficult to describe the operation of the road network from a macro perspective. The literature introduces the existing comprehensive urban traffic congestion indexes, such as RCI and TTI indexes proposed by a provincial transportation association and road network traffic use index proposed by a city, which can only simply express the absolute amount of congestion [2]. However, the traffic characteristics in different regions are different, so it is necessary to study the congestion change in the target region. The literature introduces that most of the research on the factors affecting traffic use is from the perspective of the traditional balance of supply and demand, but it is relatively weak in the specific practical trend, and less introduces the relevant relationship of road network in terms of traffic structure. The literature introduces the differences in land characteristics, time dimension, road network structure, and other factors [3]. Different regions have different congestion characteristics. However, it can not be generalized. In order to understand many factors causing traffic congestion, it is necessary to study the characteristics of all kinds of traffic congestion. In order to find an effective and simple way to express the impact, we should explore the relationship between urban congestion and various factors [4]. Compared with the statistical model, the algorithm technology based on Computational Intelligence (CI) has shown a strong ability to analyze highly nonlinear and complex data. If fewer conditions are assumed, more detailed regression results can usually be obtained. At present, domestic researchers have begun to use machine learning, deep learning and other algorithms in motion research, but there are still some deficiencies compared with foreign research or other fields [5]. They should try to study and implement better motion effect algorithms, so as to speed up the search progress and improve the accuracy.

3. Regional Road Network Traffic Diversion Technology

3.1. Regional Road Network Division. At present, the urban traffic index is released to monitor the status of the urban road network and overall traffic changes. However, the macro research and evaluation of the overall operation health of the city play a very limited guiding role in improving traffic congestion, mainly because it is impossible to determine the key areas, and it is not clear which areas should be monitored first to play a greater role in improving the overall operation effect of the city [6]. Therefore, it is necessary to further limit the assessment scope, divide the city into several different units, and then analyze the characteristics of each unit in the area from the aspects of traffic activity status and mutual relationship, which is called road network area. The purpose of road network area classification is to distinguish various characteristics of changes and link information such as changed local road conditions and terrain, so as to accurately identify the congested areas of major cities and analyze the conversion of these types, which lays a foundation for establishing the impact model of local activities and formulating relevant remedial measures.

The traffic condition data of the regional highway network can directly determine the feasibility of traffic diversion. The following indicators are analyzed.

Traffic volume refers to the number of traffic units passing through a given location, section, or lane at a given time. Among them, the average annual traffic volume (SADT) is the index of road design and management control [7]. Traffic management shall fully analyze the current situation and annual average daily traffic volume of each road in the network, and support sound traffic management by analyzing statistical data, regional distribution of road characteristics, and local road traffic volume. The research on the traffic condition of the regional road network is helpful to statistically calculate and extend the regional distribution and annual growth rate of current traffic volume, and provide a basis for predicting traffic volume and the construction of traffic control endpoints; By calculating the traffic distribution map of the road network in relevant areas, identify the distribution of congestion points and the remaining capacity of each road, so as to provide the basis for selecting traffic control routes and changing congestion points [8]. Predicting the traffic distribution of local road network is helpful to determine the indicators such as vehicle flow, traffic diversion mode, and diversion path. The traffic volume forecast in this study includes three parts: trend traffic volume forecast, induced traffic volume and restrained traffic volume forecast, and transfer traffic volume of off-road transportation. Induced traffic volume refers to new traffic generated by road construction or

reconstruction, which contributes to economic development [9]. Restraining traffic volume refers to the traffic volume loss caused by the deterioration of the driving environment or the decline of traffic capacity caused by the construction of commercial roads in the process of expressway expansion. The trend traffic prediction adopts a four-step prediction model composed of four steps: trip generation, trip distribution, mode split, and trip assignment. For specific road sections, the total traffic volume of each traffic area is allocated to each road section in the traffic network. According to the traffic distribution prediction, space data OD (OD traffic volume survey, "O" refers to "ORIGIN," "D" refers to "DESTINATION") is reserved for specific road network for distribution [10]. This project introduces the static multipath allocation method, and adjusts the road network by comparing the distribution results with the actual traffic flow of each section at the end of the year. By adjusting the occurrence and attraction of the road network and travel, the distribution result is close to the actual traffic volume, so as to predict the annual traffic of the road network.

3.2. Traffic Diversion Method. The importance of node Z is a measure of the socio-economic activities of the city where the node is located. It is a measure of the relative importance of these cities in the region in the network. The calculation model of node importance is calculated according to the following formula:

$$Z_i = \sum_{k=1}^{n} \alpha_k \frac{z_k}{z_a}. \tag{1}$$

The tolerance shall be calculated according to the following formula:

$$T_i = \sum_{k=1}^{n} (C_k - Q_k). \tag{2}$$

The calculation model of detour (average detour) is calculated according to the following formula:

$$R_i = \frac{\left(\sum_{k=1}^{n-1} (OD_k \times t_k)\right) / \left(\sum_{k=1}^{n-1} OD_k\right)}{\sum_{k=1}^{n-1} T_k / n}. \tag{3}$$

The collinearity (average collinearity) calculation model is calculated according to the following formula:

$$G_i = \frac{\sum_{k=1}^{n} \left(t_k / T_k\right)}{n}. \tag{4}$$

Benefit type indicators include node importance, tolerance, and saturation of project road sections, and cost type indicators include destination proximity and detour. The normalized index value of the utility index is equal to the index value of each node divided by the maximum value of the index, and the normalized cost index value is the reciprocal of the quotient of the index value of each node divided by the maximum value of the index, as shown in Table 1.

The weight of each indicator is determined by the analytic hierarchy process, as shown in Table 2.

Traffic control and management technology includes traffic monitoring and sensing technology, control strategy, traffic control data selection and sharing technology, mainline control mode, ramp entrance and exit control mode, road network control mode, etc., which requires a number of technologies to coordinate with each other. The control planning procedure is shown in Figure 1. Therefore, traffic diversion technology is a technical means to ensure the smooth and rapid implementation of daily management and production plan. This provides practical significance for improving management efficiency and effectively ensuring smooth and safe road transportation.

Trunk line control mode refers to the regulation, early warning, and control of traffic participants on the extended highway trunk line. Trunk line control adjusts highway traffic parameters based on traffic engineering theory to reduce the impact of trunk line congestion. Trunk line control can effectively coordinate the traffic flow at main intersections and key times [11]. Variable speed control uses various speed limit signs and variable information signs on the main roads to limit the speed between vehicles, so as to change the traffic congestion and lane utilization, maintain the stability of traffic flow, and finally increase the road width in terms of traffic capacity. The basic principle of speed control is to determine the optimal speed and optimal density under the maximum allowable traffic volume according to the relationship between climatic conditions, road and traffic volume and density, and according to the limit of extending the smooth and reliable operation of mainstream traffic on the highway. The relationship between the three parameters of traffic flow is shown in Figure 2.

4. Research and Application of the Traffic Optimization Model Based on Regional Road Network Traffic Diversion Technology

4.1. Application of Internet of Things Technology. At present, the Internet of things is a rapidly developing electronic technology. The core of the Internet of things is to electronically connect people's various life objects to the Internet by creating an intelligent network that can optimize them by retrieving, searching and requesting information. English is "Internet of things," also known as "Internet of everything" [12]. Simply put, "the Internet of things is the Internet connected with things." The Internet of things is known as the second billion-dollar technological revolution after the Internet. In the early stage of the Internet of things, many Internet applications of the Internet of things have been created. More and more Internet of things devices are connected to the network through wireless communication. Representative wireless technologies include Bluetooth, WiFi, rfid1, and ZigBee. The main task of this phase is to build network infrastructure and manage connected devices and endpoint intelligence at the same time [13]. In the second stage, the proliferation of networking terminals created massive data sources for the Internet of things and produced big data. At this time, sensors, instruments, and other devices

Table 1: Weight coefficient of each index.

Definition	Equally important	Slightly important	Light and strong are important	Strongly important
Scaling	2	4	6	8

Table 2: Judgment matrix.

Index	Node importance	Relative tolerance	Saturation of project section	Destination proximity	Detour	Weight
Node importance	2	1/6	1/8	1/4	1/4	0.04
Relative tolerance	6	2	1/4	4	4	0.26
Project section saturation	8	4	1	6	5	0.51
Destination proximity	3	1/4	1/6	2	2	0.11
Detour	4	1/4	1/6	2	2	0.11

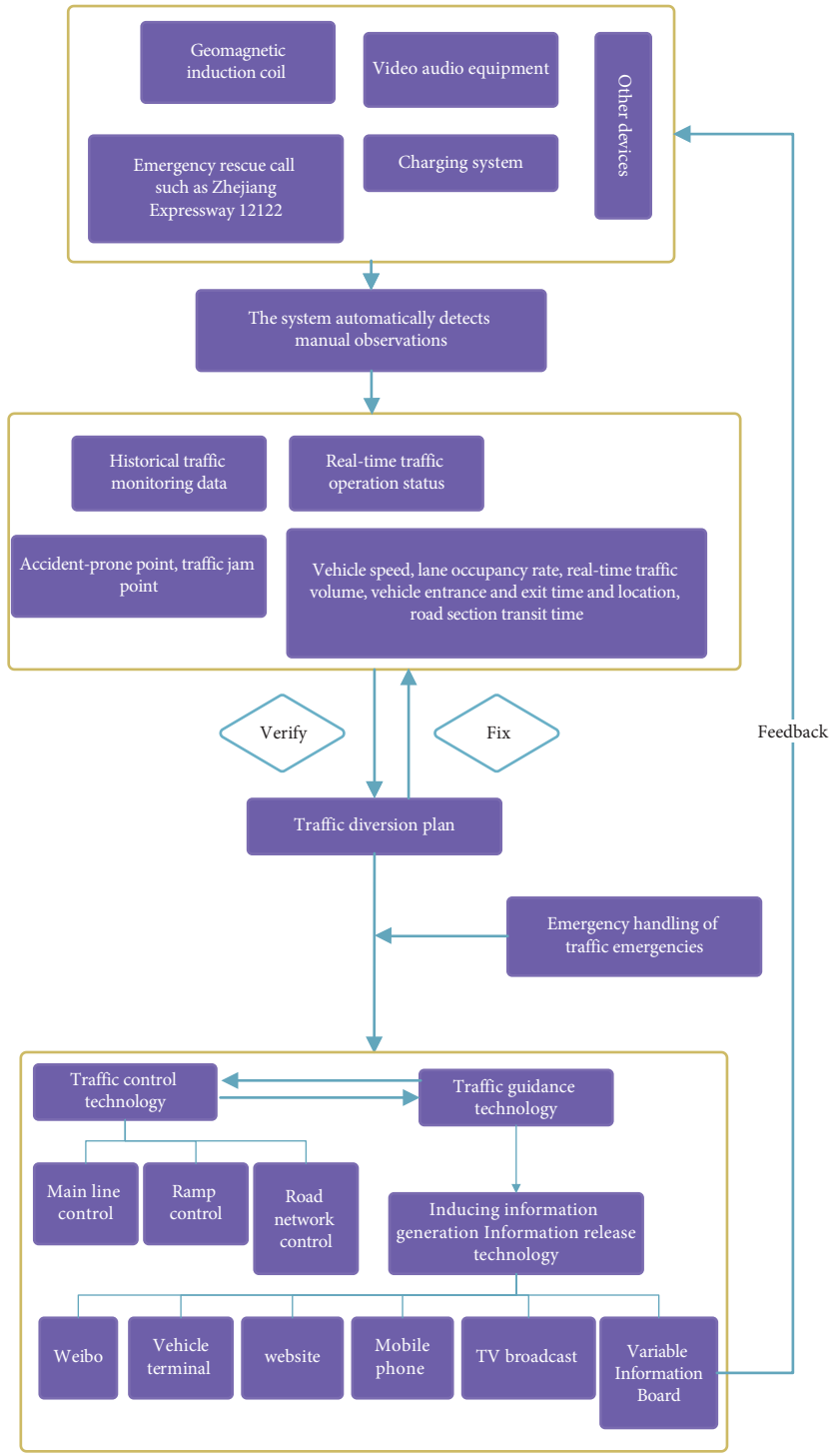

Figure 1: Design procedure diagram of traffic diversion control.

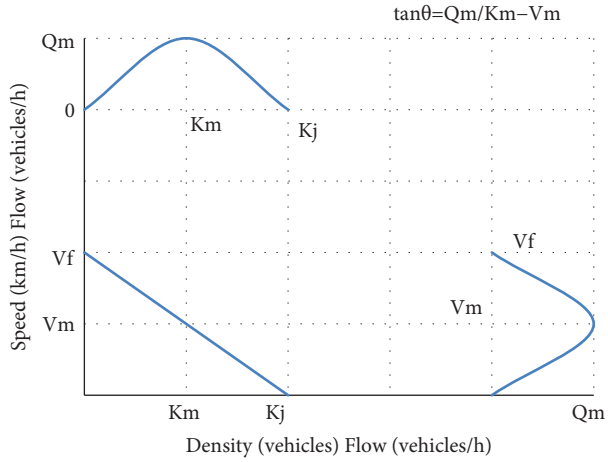

Figure 2: Relationship diagram of three parameters of traffic flow.

become more and more intelligent, and massive data sources create a computing platform. The platform organizes and stores data and provides users with various data services [14]. At present, the development of the Internet of things has reached a new stage, artificial intelligence has been realized, and data service and data analysis have included its basic value. At this time, Internet of things data has the greatest value. Enterprises analyze user behavior and carry out relevant marketing based on Internet of things technology.

4.2. Traffic Period Optimization Algorithm. Effective management of traffic lights at intersections can ensure safe and efficient traffic at intersections and improve various traffic indicators. At present, the commonly used signal control methods include clock control, adaptive control, and induction control. Among them, the control effect of adaptive control and induction controller depends on the operation state of media detection equipment and the accuracy of real-time traffic flow information [15]. In order to avoid the problem of control failure caused by sensor error or sensor error, the sequential control system usually needs to be defined when implementing adaptive induction control and control system. In the timing control system, the signal cycle length, green signal ratio, and phase deceleration sequence are constant. Because the traffic flow of urban road networks changes periodically, the one-time management system can not meet the changing traffic demand and various monitoring methods in different time periods of a day. Time of day (TOD) came into being. At a historic moment, multi-cycle control usually divides the 24 hours of a day into multiple traffic cycles according to the changes of traffic flow, and then formulates the traffic light control scheme most suitable for traffic demand according to the characteristics of traffic volume [16]. Accurate time allocation is a prerequisite for TOD to obtain all the benefits of control and improve control performance [17]. Therefore, how to achieve objective and accurate traffic time allocation results through scientific and reasonable allocation methods has become a research topic in the field of multitime monitoring [18]. People have subjective factors that interfere with the division of motion cycles. In this study, we propose a traffic cycle allocation method based on an image segmentation algorithm [19]. The first mock exam is to improve the segmentation accuracy. According to the coverage of daily traffic flow, the traffic flow is divided into three states, and the traffic data of the same mode are combined into the traffic data matrix to get the corresponding traffic volume. MATLAB image generation is used to convert each traffic flow data matrix into the corresponding traffic flow data image, and then the advanced FR FCM (fast robust fuzzy c-means clustering algorithm) mean clustering algorithm is used to segment the image to remove the fuzzy boundary, and the final result of traffic period distribution is obtained by comprehensively considering the change degree of traffic volume in each period [20, 21].

When determining the signal control level of the intersection, the traffic flow data shall be fully considered. The traffic volume at different times may reflect the change in the number of vehicles directly entering and leaving the intersection, which is an important standard for allocating traffic time. When the detector collects and transmits the traffic flow at each entrance of the intersection within a 1-hour sampling period, 24 values composed of daily traffic flow vectors are obtained, as shown in

$$x_d = [x_d(1)x_d(2)\cdots x_d(24)], \quad d = 1, 2, \ldots, 7. \tag{5}$$

Collect the daily traffic flow in the specified time period, and compile all daily traffic flow vectors on Monday from the traffic flow X_1 matrix on Monday according to

$$X_1 = \begin{bmatrix} x_1^1(1) & x_1^1(2) & \cdots & x_1^1(24) \\ x_1^2(1) & x_1^2(2) & \cdots & x_1^2(24) \\ \vdots & \vdots & \cdots & \vdots \\ x_1^N(1) & x_1^N(2) & \cdots & x_1^N(24) \end{bmatrix}. \tag{6}$$

The average traffic flow at any time of the day is not only an important index for evaluating traffic conditions, but also a key basis for planning signal synchronization. However, extreme conditions in the data set can easily affect the average value and can not reflect the range, so they usually can

not fully reflect the changes in traffic volume similar to specific days of the week. In this study, we propose a new concept of traffic flow distribution considering the change in daily traffic flow.

$$X_i(m) = \begin{bmatrix} x_i^1(m) \\ x_i^2(m) \\ \vdots \\ x_i^P(m) \end{bmatrix},$$

$$X_j(m) = \begin{bmatrix} x_j^1(m) \\ x_j^2(m) \\ \vdots \\ x_j^Q(m) \end{bmatrix},$$

$$R_{ij}(m) = \begin{cases} \dfrac{b-c}{d-a}, & a \le c < b \le d, \\ \dfrac{d-a}{b-c}, & c \le a < b \le d, \end{cases} \tag{7}$$

$$R_{ij}(m) = \begin{cases} \dfrac{d-c}{b-a}, & a \le c < d \le b \\ \dfrac{b-a}{d-c}, & c \le a < b \le d \end{cases}$$

$$R_{ij}(m) = 0, \begin{cases} c < d = a < b, \\ a < b = c < d, \\ c < d < a < b, \\ a < b < c < d. \end{cases}$$

Based on the above situation, calculate the coverage rate of the daily traffic distribution of i and j days according to the formula, that is, the total coverage rate of 24 days.

$$R_{ij} = \sum_{m=1}^{24} R_{ij}(m). \tag{8}$$

Using this formula, calculate the average traffic flow for each time period on a certain day of the week, and then perform cluster analysis on the 7-day average traffic flow vector.

$$\overline{X}_d = \frac{1}{N_d}\left[\sum_{i=1}^{i=N_d} x_d^i(1) \sum_{i=1}^{i=N_d} x_d^i(2) \ldots \sum_{i=1}^{i=N_d} x_d^i(24)\right], \quad d = 1, 2, \ldots, 7. \tag{9}$$

Looking at the data in Table 3, it can be seen that $R_{16} = 1.45$ is the minimum value in the table, that is, the "overlapping area" of traffic volume on Thursday and Saturday is the smallest. In other words, the difference between the traffic flow data on Thursday and Saturday is the biggest and is broken down into different categories. According to the traffic flow distribution values shown in Table 3, the traffic modes are divided into three categories: Monday, Tuesday, Wednesday, and Thursday belong to the same category, Saturday and Sunday are one category, and Friday is a separate category.

Table 3: Calculation result of traffic flow distribution coverage rate.

Week	1	2	3	4	5	6	7
1	—	7.67	8.68	4.82	7.45	1.45	4.53
2	7.67	—	7.12	10.16	5.72	1.84	3.3
3	8.68	7.12	—	8.95	5.4	2.71	4.32
4	4.82	10.16	8.95	—	4.25	2.97	1.84
5	7.45	5.72	5.4	4.25	—	3.06	4.61
6	1.45	1.82	2.71	2.97	3.06	—	7.48
7	4.53	3.3	4.32	1.84	4.62	7.48	—

Combine all traffic flow data from Monday to Thursday from the first matrix, all Friday traffic data from the second matrix, and all Saturday and Sunday traffic data from the third matrix. Use Matlab's "imagesc" command to convert the data matrix corresponding to the three traffic model models into traffic flow data images, as shown in Figure 3. The figure shows the corresponding ratio of each pixel to the traffic volume. The higher the traffic volume value, the more similar the colors. If you look at the drawing image of each data set, you can see that the color block depth and color transition color gamut boundary are different, but the color block distribution is similar to the changing trend in the same traffic flow image.

4.3. Traffic Optimization Model Parameter Settings. The weighted reward formula is as follows:

$$r_{t+1}^i = \left[\eta_1 \times \left(r_{t+1}^{i,j,1} + r_{t+1}^{i,j,2}\right)\right] + \left[(1-\eta_1) \times \left(r_{t+1}^{i,k,1} + r_{t+1}^{i,k,2}\right)\right]. \tag{10}$$

The weighted rewards with multiple weights are as follows:

$$r_{t+1}^i = \left[\eta_1 \times \left[\left(\eta_2 \times r_{t+1,1}^{i,j}\right) + \left((1-\eta_2) \times r_{t+1,1}^{i,k}\right)\right]\right] + \left[(1-\eta_1) \times \left[\left(\eta_2 \times r_{t+1,2}^{i,j}\right) + \left((1-\eta_2) \times r_{t+1,2}^{i,k}\right)\right]\right]. \tag{11}$$

Agent i chooses action a with probability P in state s_t^i as follows:

$$P_t^i\left(s_t^i, a\right) = \frac{e^{Qi/t\left(s_t^i, a\right)/\tau}}{\sum_{b \in A^i} e^{Qi/t\left(s_t^i, b\right)/\tau}}. \tag{12}$$

Action selection based on the UCB index is as follows:

$$a_t^{i,*} = \arg\max_{a \in A}\left\{-Q_t^i\left(s_t^i, a\right) + \sqrt{\frac{\ln N_t\left(s^i\right)}{N_t\left(s^i, a\right)}}\right\}. \tag{13}$$

The corresponding a of the largest Q value is as follows:

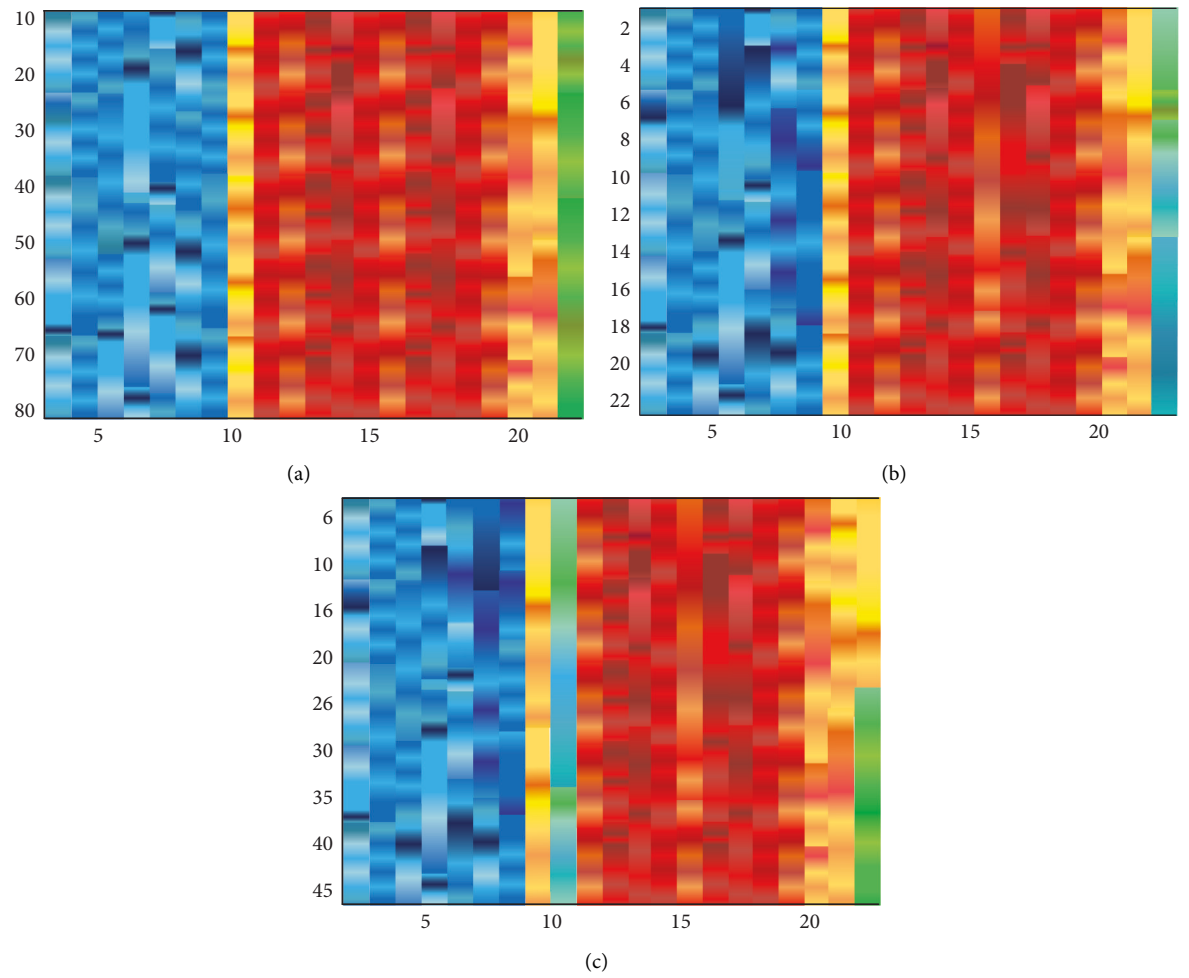

Figure 3: Corresponding image of traffic flow matrix. (a) The first set of data images. (b) The second set of data images. (c) The third set of data images.

$$a_t^{i,*} = \arg\max_{a \in A} \left\{ Q_t^i\left(s_t^i, a\right) \right\}. \tag{14}$$

Reward: calculate the reward r (s, a) according to the cooling time after the action:

$$r(s,a) = \begin{cases} 0, & wt > 2wt', \\ 1, & wt' < wt < 2wt', \\ 2, & wt < wt'. \end{cases} \tag{15}$$

Update of the Q table: update the Q value according to the following formula, a scalable game learning algorithm based on Q learning, and consider the overall node characteristics:

$$\begin{aligned} Q_{t+1}^i\left(s_t^i, a_t^i\right) \longleftarrow & (1-\alpha) Q_t^i\left(s_t^i, a_t^i\right) \\ & + \alpha\left[r_{t+1}^i\left(s_{t+1}^i\right)\right] + \gamma \max_{a^j \in A} Q_t^j\left(s_t^j, a^j + \sum_j \eta Q_t^{i,j}\left(s_t^j, a_t^j\right)\right). \end{aligned} \tag{16}$$

According to the actual transmission network, the detailed and complex information of the transmission network is required to be simplified, and the transmission network topology model is defined. When creating a parallel game network, each individual has only two states: betrayal (D) or cooperation (C). The description is as follows:

$$\begin{aligned} z_x &= \begin{pmatrix} 1 \\ 0 \end{pmatrix} \text{may be } z_x = \begin{pmatrix} 0 \\ 1 \end{pmatrix}, \\ A &= \begin{bmatrix} 1 & 0 \\ b & 0 \end{bmatrix}. \end{aligned} \tag{17}$$

The sum of individual income is expressed as follows:

$$R_x = \sum_{y \in \Omega x} Z_X^T A z_y. \tag{18}$$

The process of updating the Q table is as follows. If the state and behavior of node i is s and τ, then the update of element Q_{sa} is

$$Q_{sa}(\tau+1) = (1-\alpha)Q_{sa}(\tau) + \alpha\left[w(\tau) + \gamma Q^{\max}_{s'a'}(\tau)\right]. \quad (19)$$

Here (τ) represents the individual reward for this round given by

$$w(\tau) = \left(\frac{R_x}{n}\right)^{\theta}. \quad (20)$$

When individual i is in state s in the third shift, it chooses the optimal function according to table Q as follows:

$$a(\tau) = \text{argmax}_{a'}\{Q_{sa'}(\tau)\}. \quad (21)$$

4.4. Module Design of Traffic Optimization Platform. As shown in Figure 4, in this chapter, we design a Q-learning game model, which adds a parallel game network control module and the existing gain-based signal control system and the use of the game network node function When the transmission network signal optimization platform establishes connection control, the traffic network agent signal optimization process.

All the tracks in Figure 5 are divided into cells with 100 m as the unit, and the length of the track division is 200 m, and each cell can have multiple vehicles at the same time. Lane guidance is defined as two straight tracks and a right straight track. Vehicles follow the principle of keeping to the right on the road.

Traffic flow control: the traffic flow control in the road network accepts certain entry thresholds. The total number of vehicles entered during the simulation is 1501. The flow setting table is shown in Table 4.

In the experiment, the path configuration file is used to determine the behavior of the vehicle. Some behaviors are shown in Table 5.

4.5. Analysis of the Traffic Optimization Control Method. The intersection is not only a node for centralized evacuation of traffic in the road network but also a congestion point to promote vehicle aggregation and parking. Some intersections in the road network are located in the main sections with dense and complex traffic. It is an important task to transfer the traffic pressure to these sections. When traffic congestion occurs at these intersections due to poor traffic control, it is easy to wait on the roadside, resulting in traffic congestion or even paralysis, which affects people's travel and living environment. This has a great negative impact, so preventing major node congestion of the local road network is very likely to prevent major congestion of the local road network, so as to effectively ensure the normal operation of the whole regional road network. The so-called important intersection of the regional road network is an important intersection of the regional road network. They are usually located in the city center, connecting the east-west and North-South directions of major urban lines with heavy traffic. In this paper, we define these intersections as the key intersections of urban road network, and propose a new method to optimize the management of these intersections. The traffic flow from the same entrance to the main intersection forms a signal phase, and slows down or stops these traffic flows at the same time, so as to improve driving safety and efficiency. At the same time, it effectively prevents the "queuing injustice" phenomenon of traditional two-phase control method and four-phase control method from a traffic collision in adjacent frequency bands. Based on the analysis of the characteristics of traffic flow between main intersection and adjacent intersection, a synchronous control method of related three-turn traffic flow is proposed and applied to adjacent intersections to make adjacent intersections "serve" key intersections. As required, vehicles will arrive at the main intersection to avoid congestion at the entrance of the main intersection. Based on the road wave theory, a control system for adjusting the signal phase difference at adjacent intersections is being developed, which can increase the traffic volume at major intersections and reduce significant vehicle delays and parking times. The comprehensive control scheme of adjacent intersections with "incomplete" closure control method effectively prevents the saturation of key intersections and lays a foundation for the study of optimizing local road network traffic control. In the existing two-phase control mode, the turning lanes of the left and right opposite entrances (such as two north-south or two east-west) are released at the same time, and the traffic flow of the other two opposite entrances (two East-West entrances or two north-south entrances) is prohibited. The opposing traffic flow released at the same time meets at the conflict point of the intersection. During peak hours, there are fewer vehicles in each lane, so we can safely avoid the intersection by controlling the speed at the conflict point. When multiple slow flows meet at an intersection during peak traffic hours, the distance between vehicles in each traffic flow is very short. When the first vehicle in one traffic flow wins the right of release, other vehicles in the fleet will follow and release continuously. The other traffic flow blocked will queue up at the conflict point and wait for the traffic flow to pass before releasing. This not only losses the deceleration time, but also is prone to excessive collision due to road congestion. With the introduction of traditional four-phase steering, vehicles that hinder hitting or getting stuck at intersections will slow down at different times. Vehicles in different turning lanes at the same entrance are released on time, and the time of vehicles in adjacent lanes is not synchronized.

If drivers waiting for backup in a prohibited Lane see a convoy in an adjacent lane, they are more likely to change lanes and jump into lanes or join trailing vehicles. This will not only affect the continuity of free driving, waste the green light time, but also cause vehicle collision during lane change, disrupt the normal driving of subsequent vehicles, cause road congestion, and even transition to a large-scale power supply. In order to shorten the waiting time of vehicles and improve the work of intersections, the freedom rights need to be divided according to the waiting conditions of vehicles in different lanes, combined, and released arbitrarily as needed. A group of vehicles whose queue length meets the release target without temporary collision form a long queue and release at the same time. The combination of steps is flexible, which can be applicable to the

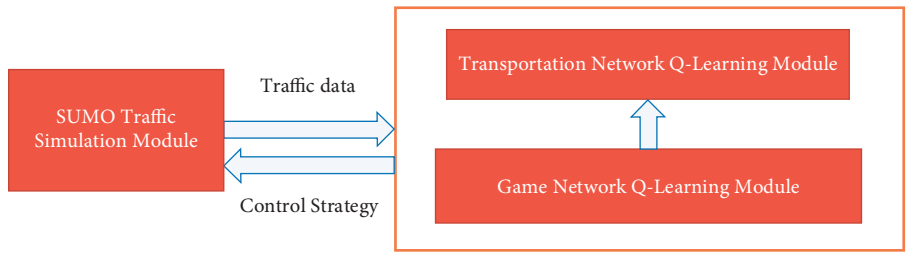

Figure 4: The framework of the traffic network signal optimization platform.

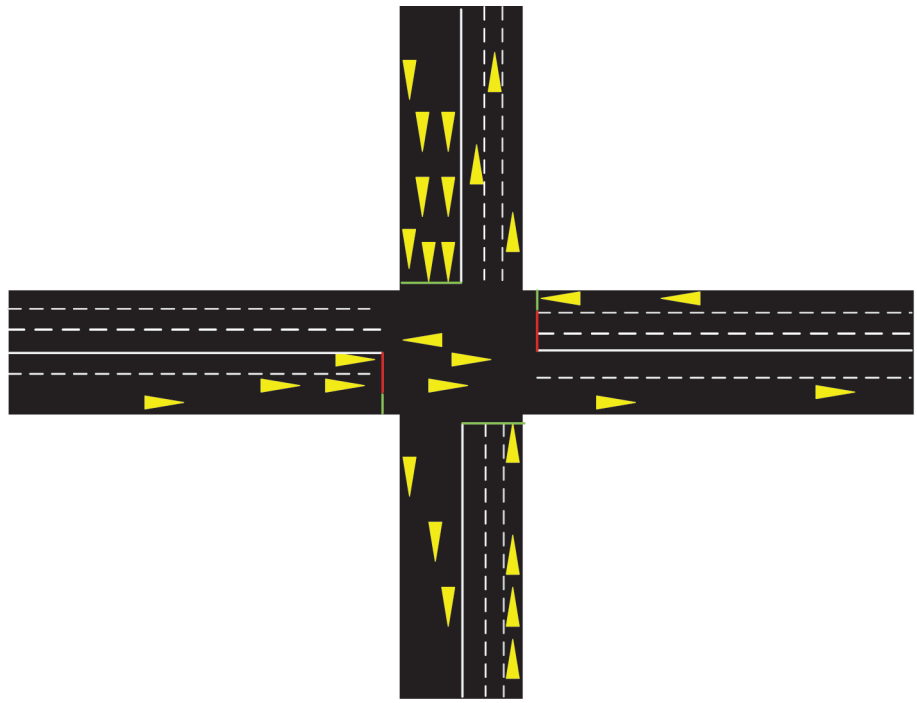

Figure 5: Schematic diagram of a single intersection.

Table 4: Flow setting schematic table.

Id	Lane entered by the vehicle	Start time	End time	Number of vehicles
0	eDJ7J2	0	1201	1501
1	eDJ1J3	0	1201	1501
2	eDJ2J1	0	1201	1501
3	eDJ3J3	0	1201	1501
4	eDJ8J4	0	1201	1501
5	eDJ10J7	0	1201	1501
6	gneE17	0	1201	1501
7	gneE15	0	1201	1501
8	GneE7	0	1201	1501
9	gneE2	0	1201	1501
10	eDJ9J5	0	1201	1501

implementation of release according to the emergency degree of vehicle departure. During travel time, the speed of vehicles entering the track is usually very high at each intersection, and the vehicle line reaches a deceleration rate, resulting in the same emergency situation for vehicles to leave each lane. The current free combination release state has actually changed to the release state of fixed duration and solid state, which has lost its original flexibility and adaptability. The phased binding release mode is only applicable to the peak period. Due to the small traffic flow, the

Table 5: Schematic diagram of route setting of some vehicles.

Vehicle id	Departure time	Vehicle path
0	0	eDJ7J1-eJ1J2-eJ2J3-eJ3J6-eJ6J5-eJ5J4-eJ4J1-eJ1DJ1eDJ1J1-eJ1DJ7
1	0	eDJ1J1-eJ1DJ7
2	0	eDJ2J2-eJ2J5-eJ5J4-eJ4J1-eJ1DJ1
3	0	eDJ3J3-eJ3J2-eJ2DJ2
4	0	eDJ8J3-eJ3J2-eJ2DJ2
5	0	eDJ10J6-eJ6J5-eJ5J2-eJ2J3-eJ3J6-eJ6DJ6-gneE21
6	0	gneE18-gneE15
7	0	gneE16-gneE14-gneE10-eDJ5J5-eJ5J6-eJ6DJ6-gneE15
8	0	gneE6-gneE19-gneE2-eDJ5J5-eJ5J6-eJ6DJ10-eDJ10J6eJ6J3-eJ3DJ8
9	0	gneE1-gneE2-eDJ535-eJ5J6-eJ6DJ6-gneE14-gneE12-gneE19-gneE0
10	0	eDJ9J4-eJ4DJ4-gneE20-gneE5

arrival time of each imported vehicle is slow and cannot be used during the peak period. The advantages, disadvantages, and relevant environment of the above common intersection segmentation methods shall be carefully analyzed and summarized, and suggestions shall be made for all one-way routes and congestion time of main intersections in the local road network, and the segmentation reduction method shall be used reasonably. SEFP (one-way all traffic) combines all turning traffic flows at an entrance of an intersection into one phase, and releases or prohibits traffic at the same time. And according to the sequence of stages, the queuing vehicles at the entrance of each intersection are released in turn.

5. Conclusion

Regional road network function evaluation is not only an important content of urban road network function research but also an important support for improving traffic management levels and road design improvement. By evaluating the function of the regional road network, the traffic situation of regional road networks can be predicted, which can help drivers choose better travel routes and save time. It can also reduce the occurrence of urban congestion, improve the coordination of urban traffic, and reduce the negative impact of traffic congestion. Aiming at the performance level of regional road networks, this paper proposes a traffic performance quality evaluation system based on the traffic volume of road networks in a city. Based on the comprehensive summary of traffic signal control methods in urban areas at home and abroad, when selecting the intersection strategy, the traffic conditions of adjacent intersections should be considered, and the combination of intersection game constructed by traffic optimization model and micro signal optimization is realized. The results show that the proposed scheme can improve the coordination of road traffic to a certain extent and provide convenience for people's life. However, it can be found in practical application that the model designed in this paper cannot be applied in all cases due to the uncertainty of road traffic. Therefore, in the follow-up research work, the model database should be constantly supplemented according to reality, so as to cope with the occurrence of various situations and improve the applicability of the model.

Data Availability

The data used to support the findings of this study are available from the author upon request.

Conflicts of Interest

The author declares no conflicts of interest.

References

[1] N. Jing, "Application of wireless sensor network in urban intelligent traffic information acquisition," *Automatic Control and Computer Sciences*, vol. 52, no. 5, pp. 431–438, 2018.

[2] B. Dadashova, X. Li, S. Turner, and P. Koeneman, "Multivariate time series analysis of traffic congestion measures in urban areas as they relate to socioeconomic indicators," *Socio-Economic Planning Sciences*, vol. 75, Article ID 100877, 2021.

[3] Fu-Yu Wang, C.-M. Ye, and Y. Li, "Study on reasons and countermeasures of traffic congestion of urban road based on the queuing models," in *Proceedings of the 2013 International Conference on Computational and Information Sciences*, June 2013.

[4] T. Nagatani, G. Ichinose, and K.-i. Tainaka, "Traffic jams induce dynamical phase transition in spatial rock-paper-scissors game," *Physica A: Statistical Mechanics and its Applications*, vol. 492, pp. 1081–1087, 2018.

[5] J. Song, C. Zhao, S. Zhong, T. A. S. Nielsen, and A. V. Prishchepov, "Mapping spatio-temporal patterns and detecting the factors of traffic congestion with multi-source data fusion and mining techniques," *Computers, Environment and Urban Systems*, vol. 77, Article ID 101364, 2019.

[6] R. Cervero, "Road expansion, urban growth, and induced travel:A path analysis," *Journal of the American Planning Association*, vol. 69, no. 2, pp. 145–163, 2003.

[7] L. J. Basso, F. Feres, and H. E. Silva, "The efficiency of bus rapid transit (BRT) systems: a dynamic congestion approach," *Transportation Research Part B: Methodological*, vol. 127, pp. 47–71, 2019.

[8] M. Adil, H. Song, J. Ali et al., "EAODV: a robust three phase priority-based traffic load balancing scheme for internet of things," *IEEE Internet of Things Journal*, vol. 9, p. 1, 2021.

[9] L. A. Guzman, J. Arellana, and V. Alvarez, "Confronting congestion in urban areas: developing Sustainable Mobility Plans for public and private organizations in Bogotá," *Transportation Research Part A: Policy and Practice*, vol. 134, pp. 321–335, 2020.

[10] X. Li and J.-Q. Sun, "Intersection multi-objective optimization on signal setting and lane assignment," *Physica A: Statistical Mechanics and its Applications*, vol. 525, pp. 1233–1246, 2019.

[11] M. Kohan and J. M. Ale, "Discovering traffic congestion through traffic flow patterns generated by moving object trajectories," *Computers, Environment and Urban Systems*, vol. 80, p. 101426, Article ID 101426, 2020.

[12] A. Aboudina and B. Abdulhai, "A bi-level distributed approach for optimizing time-dependent congestion pricing in large networks: a simulation-based case study in the Greater

Toronto Area," *Transportation Research Part C: Emerging Technologies*, vol. 85, pp. 684–710, 2017.

[13] Z. Kan, L. Tang, M.-P. Kwan, C. Ren, D. Liu, and Q. Li, "Traffic congestion analysis at the turn level using Taxis' GPS trajectory data," *Computers, Environment and Urban Systems*, vol. 74, pp. 229–243, 2019.

[14] E. Angelelli, I. Arsik, V. Morandi, M. Savelsbergh, and M. G. Speranza, "Proactive route guidance to avoid congestion," *Transportation Research Part B: Methodological*, vol. 94, pp. 1–21, 2016.

[15] Y. Aoudni, C. Donald, A. Farouk et al., "Cloud security based attack detection using transductive learning integrated with Hidden Markov Model," *Pattern Recognition Letters*, vol. 157, pp. 16–26, 2022.

[16] A. Zedgenizov and D. Burkov, "Methods for the traffic demand assessment based on the quantitative characteristics of urban areas functioning," *Transportation Research Procedia*, vol. 20, pp. 724–730, 2017.

[17] R. Li and M. Guo, "Effects of odd-even traffic restriction on travel speed and traffic volume: evidence from Beijing Olympic Games," *Journal of Traffic and Transportation Engineering*, vol. 3, no. 1, pp. 71–81, 2016.

[18] Z. He, G. Qi, L. Lu, and Y. Chen, "Network-wide identification of turn-level intersection congestion using only low-frequency probe vehicle data," *Transportation Research Part C: Emerging Technologies*, vol. 108, pp. 320–339, 2019.

[19] C. An, X. Guo, R. Hong, Z. Lu, and J. Xia, "Lane-based Traffic Arrival Pattern Estimation Using License Plate Recognition Data," *IEEE Intelligent Transportation Systems Magazine*, vol. 14, no. 4, pp. 133–144, 2021.

[20] M. L. Tam and W. H. K. Lam, "Application of automatic vehicle identification technology for real-time journey time estimation," *Information Fusion*, vol. 12, no. 1, pp. 11–19, 2011.

[21] M. Cai, Z. Lan, Z. Zhang, and H. Wang, "Evaluation of road traffic noise exposure based on high-resolution population distribution and grid-level noise data," *Building and Environment*, vol. 147, pp. 211–220, 2019.

Hindawi
Mobile Information Systems
Volume 2022, Article ID 6168361, 10 pages
https://doi.org/10.1155/2022/6168361

Research Article

Design of Multipoint Temperature and Humidity Silverware Forging for Engraving Process Measurement System Based on ZigBee Technology

Jinye Wei[1,2] **and Jiaqian Leng**[1,2]

[1]*King Mongkut's Institute of Technology Ladkrabang, Ladkrabang District, Bangkok 10520, Thailand*
[2]*Nanning University, Nanning, Guangxi 530200, China*

Correspondence should be addressed to Jiaqian Leng; lengjiaqian@nnxy.edu.cn

Received 12 June 2022; Accepted 20 July 2022; Published 13 August 2022

Academic Editor: Shadi Aljawarneh

This paper studies an embedded monitoring system centered on ZigBee technology to realize real-time temperature and humidity monitoring, and to ensure low power consumption, high reliability, low cost, and collection of environmental information. The communication is designed using the star topology, and the whole network structure is composed of a master node and three sensor receiving nodes to realize the unlimited transmission of network data. The main control point is to determine the coordination of the scope of the ZigBee network configuration system. The ZigBee network can communicate with the host through the data port to realize the acceptance of temperature and humidity data and the sending of commands. Based on this research, this paper determines the impact of non-target parameters on the actual measurement data of the multipoint temperature and humidity sensor, and at the same time determines the key influencing factors. For HMP-45D multipoint temperature and humidity, an improved genetic algorithm (GA) combined with a support vector machine (SVM) is used to compensate humidity and temperature data, which is designed to affect the actual measurement error of the multipoint temperature and humidity sensor. This paper studies the silver forging process, compares the environmental factors of silver carving, further puts forward the control strategy of Hagoun product forging and carving environment control from the perspective of temperature and humidity, and designs the environmental temperature and humidity measurement and control system from the perspective of temperature and humidity control. The system design proposed in this paper is mainly to construct and apply the silverware forging and engraving environment temperature and humidity measurement and control system on the basis of integration and maintenance-free and verify the effectiveness and feasibility of the system in the protection of cultural relics.

1. Introduction

ZigBee technology is widely understood as an energy-efficient network operation and a large-scale wireless communication protocol. We can also use routing methods to establish a theoretically unlimited communication network. ZigBee network technology is more complex and powerful than infrared, Bluetooth, and other network structures. ZigBee is widely used in various production and life fields, such as industrial production, environmental monitoring, commercial automation management, and automotive automation production. The world's leading manufacturers generally pay attention to the development of ZigBee technology and have great confidence in the future of the ZigBee market. At the same time, the ZigBee Technology Alliance is also expanding, cooperating with a number of chip manufacturers and software developers to establish a standardized organization. ZigBee technology is expected to have broader development prospects worldwide.

In this article, we designed a multipoint temperature and humidity measurement terminal, which is the core unit, uses ZigBee technology to implement unlimited communication, and collects multi-channel sensor data from the base station wireless network. The wireless base station control center is

equipped with an AT91SAM9263 microprocessor and combined with CC2530. This is a chip-based system that supports ZigBee applications and large SD card memory devices for multi-processor operation. The measurement result is controlled by the low power consumption of MSP430F2618. The core downloads the multifunctional humidity measurement dimension through the CC2530 wireless network module with field measurement, network connection, stability temperature sensor, and HHC2-S humidity sensor. This article introduces a network application program that supports multitasking with the Layer operating system, and the research and development of the ZigBee network based on the Z protocol stack of FA Enterprise.

Finally, through the detailed study of the silver forging process, this paper further expounds its processing technology and characteristics, analyzes the development status of the silver forging process and its application in modern metal technology, and applies ZigBee technology to silver forging and carving environment. The precise control and environmental humidity of the system are designed, and the hardware and software designs of the entire system are introduced in detail. It can be seen that +0.3°C means that the system temperature measurement accuracy can reach the level, and ±1.5% means the humidity measurement accuracy can reach the level. The humidity control accuracy can reach 3%. In addition, the maintenance-free automatic water replenishment function facilitates the temperature and humidity environment of silverware forging and engraving its own products. After experimental testing and field application, the system runs stably and reliably, and the measurement accuracy meets the design requirements.

2. Related Work

The literature introduces the traditional Gumgang handicrafts and modern hand-painted forgings applied to the craftsmanship and technology restoration and retains the craftsmanship and artistic characteristics of sculptures in some ethnic minority areas in southwest China. As a process of accumulation of cultural origin and experience of hand forging, it supports and promotes the development of hand forging technology. The literature introduces a wireless temperature and humidity monitoring system based on ZigBee technology, which allows temperature and humidity sensor modules to monitor temperature and humidity in real time within the network of the monitoring center; some literature describes the hardware design of the system [1, 2]. First, this paper introduced the technical advantages of ZigBee wireless sensors in the network. Based on the advantages of ZigBee, we will explain in detail the overall design of the farm's wireless temperature and humidity monitoring system, including the basic hardware configuration, software flow, and hardware based on ZigBee radio temperature and humidity monitoring [3]. And we create software according to the hardware structure, apply it to the temperature and humidity monitoring of the breeding field, realize the temperature and humidity monitoring of the breeding field, and analyze the experimental results. The literature introduces the star topology network structure and creates a method to improve the accuracy and reliability of the equipment in the software and hardware [4]. Experiments show that the key indicators of the equipment have reached the level of domestic and foreign products [5]. The literature introduces the main design of the single-chip microcomputer, using multiple sensors to collect data of temperature and humidity parameters under the control of the single-chip microcomputer. The system is mainly composed of temperature measurement theory, analog circuit, digital circuit, digital filtering algorithm, and single-chip microcomputer [6].

3. Model Design of Multipoint Temperature Based on ZigBee Technology

3.1. ZigBee Technology and Protocol. With the rapid development of semiconductor technology and communication technology in the world today, new short-range wireless communication devices have appeared one after another, and gradually replaced wired devices, occupying most of the market share [7]. In the 21st century, various non-technologies have been quite mature. Mid-infrared technologies such as Bluetooth technology and radio frequency technology have been widely used in production and life.

This technology is a new type of wireless touch network, which is becoming more and more common in low-speed wireless networks. It mainly utilizes the advantages of short distance, low data rate, low power consumption, and low cost, and is used for intelligent control and short distance wireless communication, and can be integrated into general equipment to develop a small and economical wireless sensor network [8]. The traditional ZigBee protocol structure is uniformly regulated by the ZigBee Technology Alliance. Figure 1 shows a block diagram of each layer structure.

The functions of data transmission and management tasks in the higher layer of the ZigBee protocol are provided and supported by the lower layer. After years of innovation and years of user practice by the ZigBee Alliance, the topology of the ZigBee network changes every day. Today, the most widely used network topologies in the world include star, mesh, and tree structures.

(1) Type topology: The star topology is the core of the entire network and is generally located in the center of the network. It can establish and maintain the star network in real time. The RFD node is responsible for implementing specific development functions [9]. This device can not only receive the signals obtained from the sensors, but also directly communicate with the coordinator. It is the connection channel between the outside world and the central controller. Of course, the coordinator can also be used on the terminal device, and all data must pass through the coordinator.

The star topology is structurally flexible and has poor portability. Each node must be connected to the coordinator, reducing the overall structure of the

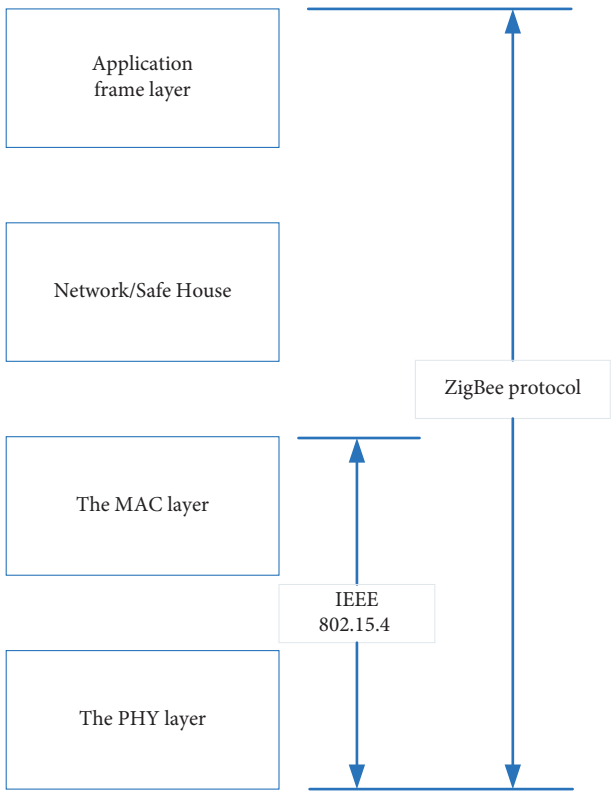

Figure 1: ZigBee protocol structure.

network [10]. Many endpoint devices are susceptible to network data expectations and other phenomena, leading to serious data loss. Due to structural commonality, if the ZigBee coordinator is abnormal, the entire network cannot continue to operate.

(2) Mesh topology: In contrast, the mesh topology is safer and more reliable. The entire network is usually coordinated by multiple coordinators to form the framework of the network. They are the same as each other and can transmit data between each node and the coordinator within the range. Each RFD can be used to tune the entire system, but it can only be tuned once [11]. The ownership of the coordinator is regulated by the upper network. Once the coordinator is confirmed, it can manage the functions of the entire network and bind the connection of each device without simply sending other data.

The mesh topology provides highly reliable performance and can be automatically created, organized, and self-repaired, so that it can quickly adapt in harsh environments. The path of data transmission is selectable in the network structure, rather than a single one, thus avoiding the possibility of network paralysis [12]. The variable coordinator will increase the time in the data transmission process, and at the same time will increase the network complexity and power consumption.

(3) Tree topology: A group of tree structures can be formed by connecting multiple groups of star combinations. Like the grid structure, the tree nodes are all composed of FFD, and the ownership of the coordinator is determined by the upper network. The end nodes of the network usually use RFD for operation and will also provide FFD under any circumstances [13].

3.2. Multipoint Temperature and Humidity Measurement Technology. The HMP-45D Pt100 Platinum resistance temperature sensor is manufactured by photolithography technology. The metal has high purity, good stability, and good reproducibility, is very sensitive to changes in ambient temperature, and has accurate reproducibility. Its value is 10^{-4}. Because of these characteristics, platinum resistors are often used to create laboratory standard equipment for instrument measurement and calibration [14]. The platinum resistance temperature measurement is based on the linear relationship between the platinum resistance conversion amount and the ambient temperature value. The relationship between resistance value and temperature value is reflected in formulas (1) and (2).

$$R_t = R_0 + \left[1 + At + Bt^2 + C(t-100)t^3\right] \quad -50 < t < 0^{\circ}C, \tag{1}$$

$$R_t = R_0 * \left[1 + At + Bt^2\right] \quad 0 < t < 80^{\circ}C. \tag{2}$$

The most important parameters of a moderately sensitive capacitive sensor are the capacitance value and quality factor. Among them, the production level is directly determined by the quality of the capacitor. The capacitance value C is obtained by measuring the circuit. In fact, the capacitance change is very small (usually less than 50pF), so the small capacitance value is converted to a voltage value between 0 V and 1 V by a high-frequency conversion circuit. The relationship between the last measured capacitance value and humidity value is corrected.

The corresponding relationship between the capacitance value of the humidity-sensitive capacitor and the relative humidity is described in formula (3).

$$C = \varepsilon_0 \varepsilon_r \frac{S}{D}. \tag{3}$$

Through the analysis of formula (3), it can be known that the dielectric constant, the effective relative area of the electrode plate, and the film thickness directly determine the capacitance value of the humidity-sensitive capacitor. Similarly, according to the characteristics of the material, temperature changes have little effect on the effective mating area of the storage substrate but have a greater effect on the humidity-sensitive film thickness [15, 16]. As the ambient temperature increases, heat will cause the humidity-sensitive film to expand and reduce its capacitance value, but there is a positive correlation between the effective area S and the capacitance value C [17]. In other words, the capacitors that are sensitive to humidity due to temperature changes have different effects, and the inevitable mathematical connection between the two cannot be expressed in the functional relationship [18, 19].

The humidity sensor is susceptible to interference from the ambient temperature when measuring relative humidity, and the actual humidity data observed will be displayed in a nonlinear manner. To correct the temperature nonlinear error interference in the observed data value of the humidity sensor, the mathematical model of the humidity sensor is:

$$y = f(x,t). \tag{4}$$

The inverse function of formula (5) is:

$$x = f^{-1}(y,t). \tag{5}$$

Formula (5) shows that relative humidity and ambient temperature are used as model input data to finally eliminate the measurement error caused by temperature t.

Start with limited sample data to obtain the best generalization ability to find the best balance between the complexity of the SVM algorithm and the learning ability. Compared with the empirical risk minimization model, the support vector machine can effectively prevent the local extreme and the "over-learning" state from showing certain advantages [20–22].

At the same time, in order to improve the fault tolerance of the support vector machine regression algorithm model, the relaxation factor F_i, ξ_i^* and the penalty factor C are introduced to perform the nonlinear conversion. Equation (6) provides an optimal solution to the problem:

$$\left\{\frac{1}{2}\|w\|^2 + C\sum_{i=1}^{l}(\xi_i + \xi_i^*)\right\},$$

$$\text{s.t.} \quad \left\{\begin{array}{l} [(w\cdot x_i + b)] - y_i \le \varepsilon + \xi_i \\ y_i - [(w\cdot x_i + b)] \le \varepsilon + \xi_i^* \\ \xi_i, \xi_i^* \ge 0, \quad i = 1,2,\cdots,l \end{array}\right\}. \tag{6}$$

Use the Lagrange multiplier to transform it into a dual problem:

$$\max\left\{\sum_{i=1}^{l}\alpha_i - \frac{1}{2}\sum_{i=1}^{l}\sum_{j=1}^{l}\alpha_i\alpha_j y_i y_j K(x_i, y_j)\right\},$$

$$\text{s.t.} \quad 0 \le \alpha_i \le C, \frac{1}{2}\sum_{i=1}^{l}\alpha_i y_i = 0. \tag{7}$$

Solving (7), we get:

$$w = \sum_{i=1}^{l}\alpha_i y_i x_i,$$

$$b = y_i - \sum_{i=1}^{l} y_i\alpha_i(x_i \cdot x_j). \tag{8}$$

Finally, the discriminant function is obtained:

$$f(x) = \operatorname{sgn}\left(\sum_{i=1}^{l}\alpha_i y_i K(x\cdot x_i) + b\right). \tag{9}$$

It can be seen from the above that SVM processes the data in the original sample space and uses the kernel to map it to a higher-dimensional space. The establishment of the classification plane can effectively avoid the disaster of dimensionality. Use the RBF kernel function that obeys the Gaussian distribution, that is

$$K(x_i, y_j) = \exp\left(\frac{-\|x_i - x_j\|^2}{(2*\alpha^2)}\right). \tag{10}$$

When establishing the SVM algorithm compensation model, it is necessary to accurately select the SVM algorithm parameters, but nowadays, the parameters are mainly selected through empirical methods, grid parameter optimization methods, etc. These parameters cannot guarantee the performance of further optimization. The SVM algorithm compensation model requires in-depth research on the solution of selecting SVM parameters.

In the process of genetic algorithm, the genetic information of each parent tends to be the same, which slows down the speed of genetic evolution or even interrupts the evolution, so that the genetic evolution reaches the local optimal solution. Therefore, it is necessary to select the best fitness function, optimize the genetic operator and parameter optimization, and improve the selection of genetic selection, crossover operator, adaptive crossover probability pc, and mutation probability pm. The specific improvements are as follows

The fitness function explains the prediction accuracy of the SVM algorithm and determines the direction of the algorithm's development. The specific situation is shown in formula (11):

$$MSE = \frac{1}{l}\sum_{i=1}^{l}(y_o - y_i)^2. \tag{11}$$

The objective function is:

$$\text{fitness}(i) = \frac{1}{MSE}. \tag{12}$$

The first is to optimize the genetic operator. At the same time, the operation of the operator is relatively simple, which can better ensure the diversity of population information, so it has been widely used. However, due to the random selection function, the algorithm has selection errors or unnecessary deterioration. Therefore, this article introduces the elite storage system and the classified working set into the traditional roulette selection algorithm. First, calculate the physical fitness values of all individuals, classify them from small to large according to their sizes, and then select and save the best individuals with the largest physical fitness values from the previous generation of 5%×n population; perform for the remaining individual's Roulette selection, ensuring individual safety (95% × n − 1), crossover and

mutation, to ensure the safety of all individuals in the next generation.

In addition to improving and optimizing genetic operators, it is also necessary to adjust the crossover probability and mutation probability according to the similarity of the parental genetic information. If the personal differences between parents are large, a larger probability of crossover and a smaller probability of change are needed to store good parental information. If the personalized information tends to be consistent, a smaller crossover probability and a higher mutation probability are required to maintain the diversity of demographic information and avoid falling into the regional optimal solution. Based on the individual similarity, crossover, and change probability, when $r > r_0$ is adjusted, as shown in formulas (13) and (14).

$$p_c = \begin{cases} p_{c1} * \left[\dfrac{r - r_0}{r} + \dfrac{f_{\max} - f}{f_{\max} - f_{\text{avg}}} \right], & f_{\text{ong}} \le f, \\ p_{c2} * \dfrac{(r - r_0)}{r}, & f_{\text{ang}} > f, \end{cases} \tag{13}$$

$$p_m = \left\{ p_{ml} * \left[\frac{r - r_0}{r} + \frac{f_{\max} - f'}{f_{\max} - f_{\partial v_o}} \right], f_{mg} \le f'. \right. \tag{14}$$

3.3. System Energy Consumption Control. The wireless measurement terminal designed in this paper adopts a specific energy consumption control strategy, which can make the system reduce power consumption. In order to ensure the stable operation of the system, reducing the use of auxiliary power is the basic method to solve the problem of system energy consumption. From the perspective of theoretical analysis, this article discusses how the system effectively uses battery power, balances the overall energy consumption of the control network, and maximizes the system's stable running time.

Based on the modular design of the wireless measurement terminal, the main part of the additional energy consumption in the wireless measurement terminal is the microprocessor module as the wireless communication module and the user interface module. The current running statistics of each module is shown in Figure 2.

Modules with high energy consumption are the main goal of controlling energy consumption. For liquid crystal displays, the steps taken are relatively simple, and program control can save money and make the most of them. After the mechanical interface stops working, by turning off the LCD power supply, the energy consumption of personnel can be reduced. When an operation on the mechanical interface is triggered, a new man-machine interface will be displayed on the LCD display. In order to realize the network communication of the system, energy consumption must be controlled under the premise of ensuring the quality of network communication. We will study and analyze the power consumption of wireless ZigBee networks.

This article uses a simple model to illustrate the energy consumption of wireless communication processing. Wireless communication includes wireless transmission and wireless reception. Transmission energy consumption includes transmitter energy consumption and drives circuit energy consumption. The transmission distance is the energy loss of the wireless communication module to transmit data between the next two nodes:

$$\begin{aligned} E_{Tx}(k,d) &= E_{Tx-\text{elec}}(k) + E_{Tx-\text{amp}}(k,d) \\ &= \begin{cases} kE_{\text{elec}} + k\varepsilon_{\text{friss-amp}} d^2 & d < d_{\text{crossover}}, \\ kE_{\text{elec}} + k\varepsilon_{\text{two-ray-amp}} d^4 & d > d_{\text{crossover}}, \end{cases} \\ E_{Rx}(k,d) &= E_{Rx-\text{elec}}(k) = kE_{\text{elec}}. \end{aligned} \tag{15}$$

Generally, the power consumption of the circuit is considered to be the same during transmission and reception. Because the energy consumption coefficients of the radio frequency amplifier are $\mathscr{E}_{\text{friss-amp}}$ and $\mathscr{E}_{\text{two-ray-amp}}$ respectively. Then, the coefficients of the model are:

$$\begin{aligned} E_{\text{elec}} &= \frac{50nJ}{\text{bit}}, \\ \varepsilon_{\text{friss-amp}} &= \frac{10pJ}{\text{bit}/m^2}, \\ \varepsilon_{\text{two-ray-amp}} &= \frac{0.0013pJ}{\text{bit}/m^4}. \end{aligned} \tag{16}$$

Because the main source of consumption is the transmission and reception of data. Therefore, active energy consumption control is performed during data transmission. Through wireless, reducing power and reducing energy consumption is the most direct and effective control method.

Assuming that the distance between nodes on the communication link of the router is the same as that of the coordinator, and k-bit data is sent to the coordinator at a fixed time interval, the node n farthest from the coordinator is forwarded to the node $n-1$ The energy consumption is as follows:

$$E_n = kE_{\text{elec}} + k\varepsilon d^2. \tag{17}$$

In addition to sending k-bit data from node $n-1$ to node $n-2$, it is also necessary to forward the k-bit data of node n. The energy consumption of node $n-1$ is as follows:

$$E_{n-1} = 3kE_{elec} + 2k\varepsilon d^2. \tag{18}$$

The energy consumption of the nth node and the mth node in the communication link can be estimated:

$$\begin{aligned} E_m &= (2n - 2m + 1)kE_{\text{elec}} + (n - m + 1)k\varepsilon d^2, \\ E_1 &= (2n - 1)kE_{\text{elec}} + nk\varepsilon d^2. \end{aligned} \tag{19}$$

By comparison, we can see that the energy consumption of the nth node is less than the energy consumption of the first node, and as the depth gradually increases, the difference is more obvious.

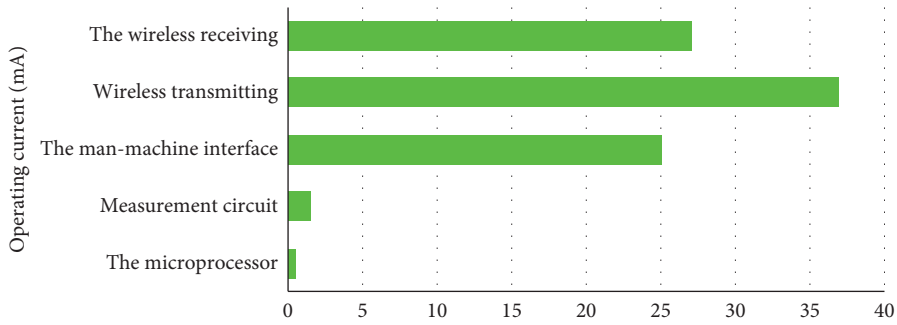

Figure 2: Energy consumption of each module of the wireless measurement terminal.

Based on the questions in the previous section, researchers have proposed various measures and methods to improve the life cycle of the network without supplementing energy. This section analyzes, compares, and proposes solutions to control the energy consumption of a single node and the difference in energy consumption between network nodes, and how to optimize energy consumption control strategies. The node residual energy model can be embodied in formula (20):

$$\begin{aligned} E_{\text{left}} &= E_0 - E_{Tx} - E_{Rx} \\ &= E_0 - \left(E_{\text{elec}} + \varepsilon_{\text{friss-amp}} d^2 E_{\text{elec}} + \varepsilon_{\text{friss-amp}} d^2\right) k_T - E_{\text{elec}} k_R. \end{aligned} \tag{20}$$

Considering the application of the system, during the measurement process, the nodes will not move their positions after placement, and in most cases, each node will transmit data to the coordinator along a fixed routing path. Each node transmits data at a fixed sampling interval, then:

$$\begin{aligned} k_T &= n_T \cdot t, \\ k_R &= n_R \cdot t. \end{aligned} \tag{21}$$

Equation (20) is further changed to

$$E_{\text{left}} = E_0 - \left(E_{\text{elec}} + \varepsilon_{\text{friss-amp}} d^2\right) \cdot n_T \cdot t - E_{\text{elec}} \cdot n_R \cdot t. \tag{22}$$

3.4. Energy Consumption Simulation. The simulation result is shown in Figure 3. In the left figure, we can see the simulation results that do not control the energy consumption, the nodes close to the coordination transfer a large amount of data, and the energy consumption is very fast, becoming the first dead node. The picture on the right uses a control strategy based on dynamic coordination. Due to node load distribution, most nodes will consume energy and leave the network until the first dead node appears in about 45,000 seconds. In a relatively short period of time, if the number of remaining nodes is the total number of nodes, the simulation time used by the two methods is similar. The last remaining node is the eccentric end node, because it does not need to transmit data from other nodes and consumes the least energy.

The node residual energy analysis calculates the residual energy of all nodes when the network is disconnected. The simulation result is shown in Figure 4. The left picture does not use the energy balance method, so when the first node is displayed, the remaining nodes have more energy and the energy distribution range is larger. The right figure uses a dynamic coordinated control strategy. From the results in the figure, the dynamic adjustment strategy has achieved a better energy balance effect.

Through the above simulation analysis, we can see that the area around the coordinator node in the wireless ZigBee network is the area with the highest energy consumption in the entire network. Nodes in this area need to transmit data from remote nodes. Therefore, it consumes the fastest energy. The main function of energy optimization control is to coordinate multipath from energy-intensive domain data to reduce the excessive energy consumption of certain nodes and balance the energy load of the entire network, thereby improving energy efficiency. The simulation results show that the energy optimization control has a positive influence on the nodes in the energy-intensive area.

4. Practical Application of Multipoint Temperature and Engraving Process

4.1. Overall Design of Multipoint Temperature and Humidity Measurement System. The system is mainly used for temperature and humidity measurement and control research. The system uses Palm certified Codewarrior 5.0 development platform. Compared with assembly language, C language has readability, flexibility, efficiency, module design and development, and rich library functions. This system is suitable for project management and multiple management.

System software design mainly includes the following parts: design temperature and humidity acquisition program, design humidity control program, design system communication software, and design human–computer interaction. The whole system of the system software is shown in Figure 5.

4.2. System Data Collection and Communication. Table 1 lists the communication protocol between the single-chip computer and the sensor module.

Serial communication is the basic method for the microprocessor to exchange data with the outside world. Few transmission lines are used for communication connection lines, and binary data sets are transmitted in bit order to share time in the software. MC9S12XS128 has two full-

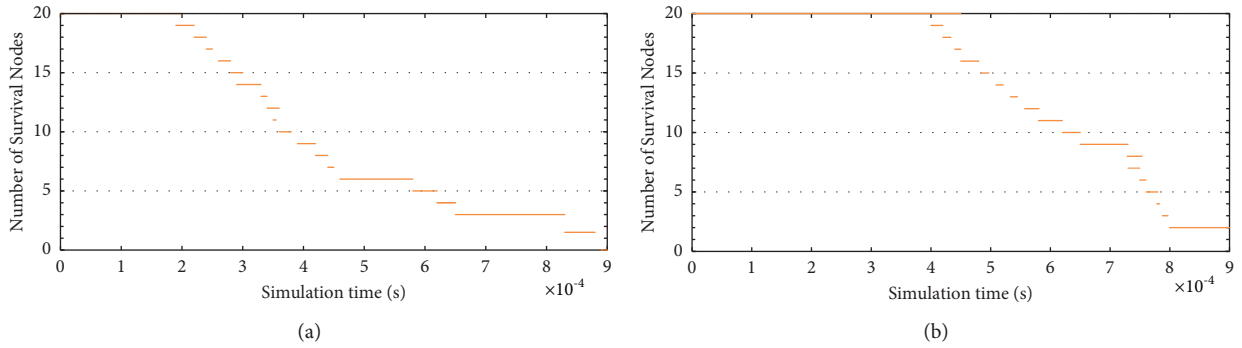

Figure 3: Network life cycle simulation without energy consumption control (a) and dynamic adjustment energy consumption control (b).

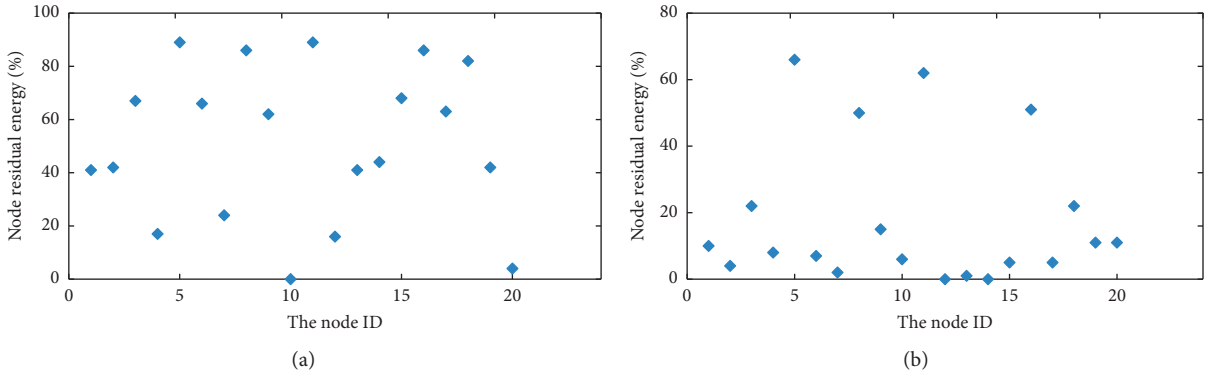

Figure 4: Node residual energy simulation without energy consumption control (a) and dynamic adjustment energy consumption control (b).

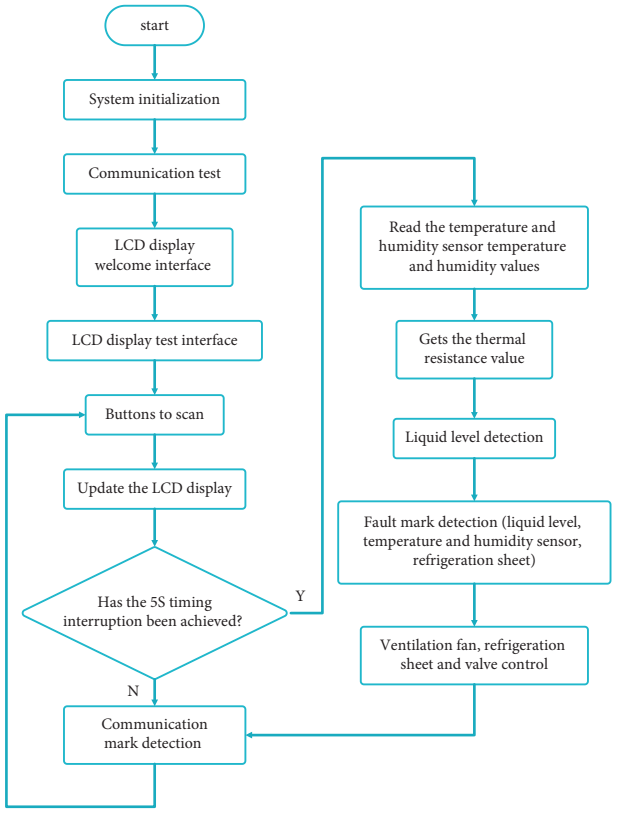

Figure 5: Overall block diagram of system software.

duplex serial communication interfaces SCI. The design uses query mode to enable data transmission and interrupt mode to enable data reception.

In order to ensure the integrity and reliability of the communication information, a more stringent communication protocol has been set up for data analysis communication. The specific content is shown in Table 2.

The communication protocol format is shown in Table 3.

In the second agreement, the sequence of data content is shown in Table 4.

In Article 4 of the agreement, the sequence of data content is shown in Table 5.

All numerical data are represented by high and low bytes.

In the 5th agreement, the data sequence of the temperature and humidity parameters to be set is shown in Table 6.

4.3. System Interface Design. After powering on the system, the "Welcome" interface will be displayed. After about 1 second, it will enter the inspection interface of the system itself to display the operating status of the device, the humidity setting target value, and the upper and lower limits of humidity. After 2S, go to the main data display interface, which displays the latest temperature and humidity data and the current time.

Table 1: Communication protocol between temperature and humidity monitor and sensor.

Serial number	Content	Number of bytes	Data flow direction	Remarks
1	52 18 3F 0A	4	Controller-sensor	Get temperature
2	48 16 temperature value corresponds to ASCII code 0A	7	Controller-sensor	Send temperature
3	52 20 3F 0A	4	Controller-sensor	Get humidity
4	48 16 humidity value corresponds to ASCII code 0A	7	Controller-sensor	Send humidity

Table 2: Communication protocol between temperature and humidity monitoring system and data analyzer.

Serial number	Character (data packet)	Content	Direction
1	A (0x41) + instrument address (0x01) + D (0x44) + instruction length (0x03) + data reserved byte (OxAA OxBB) + CRC (IB) 7 bytes in total	Intelligent data analysis loads temperature and humidity sensors and device status data into temperature and humidity monitors	Intelligent data analyzer-temperature and humidity monitor
2	a (0x61) + instrument address (0x01) + d (0x64) + instruction length (OxOB) + data content (10B) + CRC (1B) total 15 bytes	The temperature and humidity monitor sends temperature and humidity sensors and device status data to intelligent data analysis	Temperature and humidity monitor an intelligent data analyzer
3	A (0x41) + instrument address (0x01) + G (0x47) + instruction length (0x03) + data reserved byte (OxCC OxDD) + CRC (IB) 7 bytes in total	Intelligent data analysis can read the current temperature and humidity settings on the temperature and humidity monitor	Intelligent data analyzer-temperature and humidity monitor
4	a(0x61) + instrument address (0x01) + g (0x67) + instruction length (0x24) + data content (35B) + CRC (1B) 40 bytes in total	The temperature and humidity monitor feeds back the current temperature and humidity settings to intelligent data analysis	Temperature and humidity monitor-intelligent data analyzer
5	A (0x41) + instrument address (0x01) + S (0x53) + instruction length (OxOF) + temperature and humidity parameters to be set (14B) + CRC (IB) 19 bytes	Intelligent data analysis sends the set temperature and humidity parameters to the intelligent temperature and humidity monitor	Intelligent data analyzer-intelligent temperature and humidity monitor
6	a (0x61) + instrument address (0x01) + s (0x73) + instruction length (0x03) + data content (2B) + CRC (1B) 7 bytes in total	The intelligent temperature and humidity monitor can respond to the intelligent data analysis of the successfully set temperature and humidity parameters	Intelligent temperature and humidity monitor intelligent data analyzer

Table 3: Basic format of communication protocol.

Packet header (byte)	Instrument address (byte)	Function type (byte)	Data length (byte)	Data content	Check digit (byte)
1	1	1	1	*N* bytes	1

Table 4: Protocol 2 data content sequence.

Serial number	1	2	3	4	5
Name	Temperature value	Humidity value	Operation/fault	Humidification/dehumidification	Reserved byte
Number of bytes	2	2	1	1	4

Table 5: Protocol 4 data content sequence.

Serial number	1	2	3	4
Name	Humidity target value	Upper limit of humidity	Lower limit of humidity	Reserved byte
Number of bytes	2	2	2	8

Table 6: Protocol 5 data content sequence.

Serial number	1	2	3	4
Name	Humidity target value	Upper limit of humidity	Lower limit of humidity	Reserved byte
Number of bytes	2	2	2	8

Table 7: Button name and function description table.

Name	Function description
SET	(1) On the monitoring interface, press this key to enter the function setting (2) It is used to jump to the next configuration item in the configuration interface of the function
OK	Return to the status display interface in the function configuration interface, and complete the confirmation for confirming certain selections
LEFT	(1) Function configuration interface 1 is used to adjust the position of the selected item (2) The function configuration interface 2 is used to move the position of the selected number to the left
RIGNT	(1) Function configuration interface 1 is used to adjust the position of the selected item (2) The function configuration interface 2 is used to move the position of the selected number to the right
UP	The function configuration is used to increase the value of a specific number in interface 2
DOWN	The function configuration is used to increase the value of a specific number in interface 2

When the setting key is pressed from the main LCD display interface, it enters the setting state, initializes the setting data, and then determines the value of the next key. When entering this interface for the first time, the cursor will highlight the first position of the configuration, otherwise the cursor will remain at the last position when exiting the configuration interface last time. The left and right keys are used to change the cursor position, the up and down keys are used to increase or decrease the number, the set key is used to decrease the position bar, and the enter key is used to set the current value. The OK key is used to save the current values, exit the status and position setting interface, and return to the main display interface. Button name and function description are shown in Table 7.

4.4. Status Quo of Silver Forging and Engraving Process. China's Miao, Bai, Tibetan, and other ethnic minorities still use forging and carving techniques. This minority still maintains traditional handicrafts such as hammering and engraving ,and maintains certain traditional lifestyles and customs of its national culture. Due to the difference in development, we mainly study the hammering and engraving techniques of the Bai and Tibetans.

In addition to preserving and retaining the hammering and engraving techniques of some ethnic minorities, modern folk literature and art are also used for the restoration of handmade jewelry artifacts. The restoration of cultural relics is a very important task of the Archaeological Museum. The metal restoration techniques in the restoration of cultural relics include gold restoration, bronze restoration, and tin restoration. The original production process of cultural relics is mainly used after restoration to ensure the unity and integrity of cultural relics. It is a targeted crafting technique. For traditional Gumgwaung restoration techniques, hammering and engraving techniques are used in museums and archaeological projects. The restoration of cultural relics is diverse, complex, and targeted. Therefore, the restoration of cultural relics usually requires the comprehensive use of several technical tools. Cultural relic restoration workers inherit the traditional hammering and engraving techniques so that traditional techniques can reproduce the historical truth.

The theme of the development of modern metal craftsmen is to discuss the inheritance of traditional handicrafts and reflect the spirit of the times under contemporary art concepts. Hand forging includes the tradition and history of forging and engraving technology. The origin and development of forging and engraving technology continue to absorb production experience and use manual methods to express the author's creative ideas in the context of the new era. With the development of productivity, technology is constantly updated and improved. It is based on the experience of the predecessors and continues to innovate on this basis. As a new kind of handicraft, hand forging by modern metal craftsmen has special aesthetic importance. Traditional metal crafts often emphasize the beauty of the material itself and the value of the material, especially the artificial products with the greatest function made of the material. As a new kind of artwork, handicrafts may be eliminated, abandon the concept of utilitarianism, focus on pure artistic expression, and have a clearer aesthetic tendency. In the process of constantly seeking modern design, we are committed to expanding the expressive power and charm of metal materials, transcending the functional scope of materials, and giving them more spiritual and cultural meanings.

5. Conclusion

Since the advent of ZigBee wireless communication technology, it has been receiving extensive attention for its unique features such as simple protocol, low cost, powerful functions, and strong interference capabilities. At the same time, we will gradually expand to other areas, such as automation control. The system uses ZigBee technology to monitor the temperature and humidity of the environment. This article focuses on the hardware design for the collection and coordination of temperature and humidity data. Then, we will use ZigBee technology to develop and implement a star structure topology network with functions such as automatic network, environmental information collection, wireless data transmission, real-time LCD display, and serial data upload. Finally, the demand for network technology is measured based on forging and engraving tests. In addition, based on the rapid development of integrated sensors and wireless sensor technology, a high-precision, networked, on-site, and intelligent wireless temperature, and humidity measurement program was designed.

Data Availability

The data used to support the findings of this study are available from the corresponding author upon request.

Conflicts of Interest

The authors declare that they have no conflicts of interest.

References

[1] B. Aneja, S. Singh, U. Chandna, and V. Maheshwari, "Review of temperature measurement and control," *Ijarse Com*, vol. 3, no. 1, pp. 33–40, 2014.

[2] L. Yu, W. Wang, X. Zhang, and W. Zheng, *A Review on Leaf Temperature Sensor: Measurement Methods and Application. Computer and Computing Technologies in Agriculture IX*, Springer International Publishing, New York, NY, USA, 2015.

[3] L. L. Josephson, W. J. Galush, and E. M. Furst, "Parallel temperature-dependent microrheological measurements in a microfluidic chip," *Biomicrofluidics*, vol. 10, no. 4, Article ID 043503, 2016.

[4] G. Bonciolini, A. Demello, D. Vigolo, and E. Sciubba, "Microfluidic in-chip temperature control via the heat of mixing release," in *Proceedings of the ECOS 2016, International Conference on Efficiency, Cost, Optimisation, Simulation and Environmental Impact of Energy Systems*, Portorož, Slovenia, June 2016.

[5] X. Y. Chen, T. Y. Li, S. Zhang et al., "Research on optimizing parameters of thermal bonding technique for pmma microfluidic chip," *International Polymer Processing*, vol. 32, no. 3, pp. 394–398, 2017.

[6] L. Wang, Y. Yan, and K. Reda, "Comparison of single and double electrostatic sensors for rotational speed measurement," *Sensors and Actuators A: Physical*, vol. 266, pp. 46–55, 2017.

[7] D. M. Wan, K. Yang, Y. Y. Zhang, and K. N. Leung, "Design of temperature measurement system based on negative temperature coefficient," *China Medical Devices*, vol. 3, no. 11, pp. 98–103, 2017.

[8] C. Giebeler, D. Adelerhof, A. Kuiper, J. B. A. van Zon, D. Oelgeschläger, and G. Schulz, "Robust GMR sensors for angle detection and rotation speed sensing," *Sensors and Actuators A: Physical*, vol. 91, no. 1-2, pp. 16–20, 2001.

[9] L. Wang, Y. Yan, Y. Hu, and X. Qian, "Rotational speed measurement through electrostatic sensing and correlation signal processing," *IEEE Transactions on Instrumentation and Measurement*, vol. 63, no. 5, pp. 1190–1199, 2014.

[10] C. Li, Q. Tan, P. Jia et al., "Review of research status and development trends of wireless passive LC resonant sensors for harsh environments," *Sensors*, vol. 15, no. 6, pp. 13097–13109, 2015.

[11] B. Wang, M.-K. Law, J. Yi, C.-Y. Tsui, and A. Bermak, "A -12.3 DBm UHF passive RFID sense tag for grid thermal monitoring," *IEEE Transactions on Industrial Electronics*, vol. 66, no. 11, pp. 8811–8820, 2019.

[12] C. Li, Q. Tan, C. Xue, W. Zhang, Y. Li, and J. Xiong, "A high-performance LC wireless passive pressure sensor fabricated using low-temperature co-fired ceramic (LTCC) technology," *Sensors*, vol. 14, no. 12, pp. 23337–23347, 2014.

[13] C. Deng, W. Hu, S. X. Diao, F. Lin, and D. Qian, "Measurement error analysis and calibration technique of NTC-based body temperature sensor," *Chinese Journal of Medical Instrumentation*, vol. 39, no. 6, pp. 395–399, 2015.

[14] A. Farouk, A. Alahmadi, S. Ghose, and A. Mashatan, "Blockchain platform for industrial healthcare: vision and future opportunities," *Computer Communications*, vol. 154, pp. 223–235, 2020.

[15] P. Zhang, F. Wang, S. Yang, G. Wang, M. Yu, and X. Feng, "Flexible in-plane micro-supercapacitors: progresses and challenges in fabrication and applications," *Energy Storage Materials*, vol. 28, pp. 160–187, 2020.

[16] Y. T. Wu and Z. J. Pan, "The research status and development tendency of flexible wearable electronic sensors," *Modern Silk Science & Technology*, vol. 34, no. 5, pp. 22–25, 2019.

[17] M. D. Dankoco, G. Y. Tesfay, E. Benevent, and M. Bendahan, "Temperature sensor realized by inkjet printing process on flexible substrate," *Materials Science and Engineering: B*, vol. 205, no. 3, pp. 1–5, 2016.

[18] K. S. Karimov, F. A. Khalid, and T. M. S. Chani, "Carbon nanotubes based flexible temperature sensors," *Optoelectronics and Advanced Materials*, vol. 6, no. 1-2, pp. 194–196, 2012.

[19] S. Heidari, M. M. Abutalib, M. Alkhambashi, A. Farouk, and M. Naseri, "A new general model for quantum image histogram (QIH)," *Quantum Information Processing*, vol. 18, no. 6, pp. 175–220, 2019.

[20] K. Bennett and O. Mangasarian, "Combining support vector and mathematical programming methods for induction," *Advances in Kernel Methods—SV Learning*, vol. 1, pp. 307–326, 1999.

[21] C. Domeniconi and D. Gunopulos, "Incremental support vector machine construction," in *Proceedings of the IEEE International Conference on Data Mining (ICDM'01)*, pp. 589–592, San Jose, CA, USA, December 2001.

[22] J. Zhang, Z. Li, and J. Yang, "A divisional incremental training algorithm of support vector machine," in *Proceedings of the IEEE International Conference on Mechatronics and Automation (ICMA'05)*, pp. 853–856, Niagara Falls, ON, Canada, August 2005.

Hindawi
Mobile Information Systems
Volume 2023, Article ID 9842536, 1 page
https://doi.org/10.1155/2023/9842536

Retraction

Retracted: Data Mining and Video Target Detection-Based Analysis of Martial Arts Cultural Communication and Martial Arts Athletes' Posture

Mobile Information Systems

Received 1 August 2023; Accepted 1 August 2023; Published 2 August 2023

This article has been retracted by Hindawi following an investigation undertaken by the publisher [1]. This investigation has uncovered evidence of one or more of the following indicators of systematic manipulation of the publication process:

(1) Discrepancies in scope
(2) Discrepancies in the description of the research reported
(3) Discrepancies between the availability of data and the research described
(4) Inappropriate citations
(5) Incoherent, meaningless and/or irrelevant content included in the article
(6) Peer-review manipulation

The presence of these indicators undermines our confidence in the integrity of the article's content and we cannot, therefore, vouch for its reliability. Please note that this notice is intended solely to alert readers that the content of this article is unreliable. We have not investigated whether authors were aware of or involved in the systematic manipulation of the publication process.

Wiley and Hindawi regrets that the usual quality checks did not identify these issues before publication and have since put additional measures in place to safeguard research integrity.

We wish to credit our own Research Integrity and Research Publishing teams and anonymous and named external researchers and research integrity experts for contributing to this investigation.

The corresponding author, as the representative of all authors, has been given the opportunity to register their agreement or disagreement to this retraction. We have kept a record of any response received.

References

[1] Z. Ma and Y. Ma, "Data Mining and Video Target Detection-Based Analysis of Martial Arts Cultural Communication and Martial Arts Athletes' Posture," *Mobile Information Systems*, vol. 2022, Article ID 2214724, 8 pages, 2022.

Hindawi
Mobile Information Systems
Volume 2022, Article ID 2214724, 8 pages
https://doi.org/10.1155/2022/2214724

Research Article

Data Mining and Video Target Detection-Based Analysis of Martial Arts Cultural Communication and Martial Arts Athletes' Posture

Zhen Ma[1] and Yanping Ma[2]

[1]*Anhui Technical College of Mechanical and Electrical Engineering, Wuhu 241000, Anhui, China*
[2]*Anhui College of Traditional Chinese Medicine, Wuhu 241000, Anhui, China*

Correspondence should be addressed to Yanping Ma; 0127000112@ahcme.edu.cn

Received 13 June 2022; Accepted 20 July 2022; Published 11 August 2022

Academic Editor: Shadi Aljawarneh

With the continuous deepening of economic globalization and the continuous development of Internet big data, the spread of martial arts culture has attracted people's attention. The advent of the Internet big data era has brought new opportunities and media for the dissemination of martial arts culture but also brought certain risks and challenges. This paper firstly uses the literature method, logical analysis method, and related theories of communication, with the help of the SWOT strategic analysis method, to analyze the internal advantages and disadvantages faced by martial arts culture communication itself, as well as the external opportunities in the context of the Internet big data era and challenges. In order to realize the target detection and tracking task of Martial athletes, this paper proposes a target detection and tracking algorithm for Martial athletes. First, the algorithm constructs and trains a fully CNN-based athlete target detection model, which can detect the first frame of athlete targets in martial arts competitions or martial arts training videos. Experiments show that the athlete positioning information output by the detection model and the video frame sequence are jointly input into the athlete target tracking module based on neighborhood similarity, so as to realize the target tracking of martial arts athletes.

1. Introduction

As a unique sport of the Chinese nation, martial arts is loved by the Chinese people and the world because of its practicality, fitness, viewing, and cultural characteristics [1]. Wushu is an inherited technology of ancient military war. Practicing martial arts can not only strengthen the body but also defend the enemy's attack. Martial arts practitioners take "stopping invasion" as the technical guidance and lead practitioners into the traditional way of Enlightenment (martial arts) to understand the objective laws of man, nature, and society. It is the guidance and guarantee of human material civilization and a display of contemporary traditional martial arts. At the same time, martial arts culture has been integrated into the strong sense of responsibility and mission of the Chinese nation in the long history of development [2]. The spread of martial arts culture is limited and there is a lack of corresponding talents [3]. The transmission method of Martial mainly relies on the inheritance of masters and the education of Martial in schools [4]. Although the two transmission methods have their own advantages and disadvantages, they cannot complement each other [5]. At the same time, although there are many martial arts talents in our country, there are very few talents who have a comprehensive understanding of martial arts knowledge and can make full use of Internet big data to spread martial arts culture [6]. These disadvantages will increase the risk of faults in the spread of martial arts culture to a certain extent. With the change of modern people's way of life and production, philosophical concepts are constantly missing in the teaching and dissemination of martial arts [7].

Internet big data has predictive accuracy and intelligent services that can be accurately pushed according to people's needs [8]. Social media has become an integral part of modern life, and its low threshold allows people from all walks of life to participate. In this process, the public is both

a recipient of the information and a mass communicator. The external challenge to the spread of martial arts culture is the influence of foreign cultures on Chinese martial arts culture. Western sports culture accompanies economic and political activities and uses the Olympic Games as a medium to continuously export Western sports and humanistic concepts to China, which has led to the loss of traditional Chinese martial arts culture [9]. Foreign cultures have some reference value for us, but there is a threat of replacement of the culture of our martial arts in the exchange with foreign cultures, and we need to face the challenge [10, 11].

Martial arts culture is faced with impetuousness and utilitarianism in the process of dissemination, and it cannot be carried forward and inherited [12]. Chinese martial arts culture should use Internet big data to achieve mass communication and point-to-point communication, and officials should also actively lead the values of martial arts culture and enrich the connotation of martial arts philosophy [13]. Cultural and sports departments and martial arts associations should play a leading role, strengthen supervision and management, and sort out the content of dissemination. By entering new media, it will lead the cultural communication again and reshape the image of martial arts culture. At the same time, the main body of foreign communication should also play an important role. On the basis of fully understanding the education level and cultural background of foreign people, the Internet big data can be used to achieve point-to-point communication [14]. In the context of big data, martial arts culture needs to use the offline and online linkage effect to change its asymmetric status in international communication.

The lack of analysis talents in the martial arts culture industry limits the spread of martial arts culture, while strengthening the training of martial arts talents' ability to analyze big data, it is also necessary to strengthen the training of martial arts knowledge structure and ability, and finally achieve the purpose of precise service [15, 16].

According to the subjective visual analysis, the moving target area detected and located by the algorithm in this paper has a very high degree of coincidence with the area where the athlete can be distinguished by the human eye, and the number of background image pixels of the non-athlete target within the circumscribed rectangle is relatively small [17]. Therefore, through subjective visual analysis, it can be seen that the accuracy of target detection and tracking of the algorithm in this paper is high [18]. In the experiment part, some mainstream athlete target detection and tracking algorithms are objectively evaluated through the two objective evaluation indicators of average overlap rate and average pixel error [19]. Through data analysis, it can be seen that the average overlap rate and average pixel error of the proposed algorithm are better than other athlete target detection and tracking algorithms [20]. Therefore, the accuracy of target detection and tracking of martial arts athletes based on the algorithm in this paper is better than that of similar algorithms [21].

This paper proposes a video target detection and tracking algorithm for detecting and tracking targets of martial arts athletes [22]. The algorithm consists of an athlete detection model based on a fully CNN and an athlete target tracking algorithm based on neighborhood similarity [23]. This paper builds and trains a fully CNN to detect where martial arts athletes appear in static images [24]. In order to track the target of martial arts athletes, this paper calculates the Euclidean distance of the gray value of the neighborhood pixels centered on different pixels, this value is used to measure the similarity between each pixel in the target area of the current frame and each pixel in the possible target area of the next frame, so as to realize the target tracking task of martial arts athletes [25].

2. Pose Estimation Open Pose

Open Pose, an open source library based on deep learning proposed by Carnegie University in the USA, can realize the recognition and capture of human movements, finger movements, facial expressions, etc., perform a more accurate estimation of the human pose in the image, and extract multiple key points of the body, hand, or facial bones. It is suitable for single and multiplayer situations with excellent robustness.

This paper uses the feature of this algorithm to extract the key frames or pictures in the exerciser and the standard motion video and use it as the material for subsequent comparison, the key points of the human body are identified as shown in Figure 1.

3. Hybrid CNN-HMM

The hybrid CNN-HMM scheme in this paper is shown in Figure 2, this method embeds the output probability matrix of CNN into the observation probability matrix of HMM for modeling.

The input data stream is denoted as $X = X_1, X_2, \ldots, X_T$, the maximum posterior probability $P(S|X)$ of the CNN output is selected, and the best fitting sequence $\widetilde{S}$ of the model is obtained according to the Bayesian decision rule.

$$\begin{aligned}\widetilde{S} &= \arg\max_{S} P(S|X) \\ &= \arg\max_{S} \frac{P(X|S)P(S)}{P(X)}.\end{aligned} \tag{1}$$

Here, $P(S|X)$ is expressed as the product of the class prior probability $P(S)$, we can get the following equation:

$$\widetilde{S} = \arg\max_{S} P(X|S)P(S). \tag{2}$$

According to the time change of the input, using HMM modeling, using the first-order Markov assumption to maximize $P(X|S)$, we can get the following equation:

$$P(X|S) \approx \max_{S_1 \cdots S_T} \prod_{t=1}^{T} P(s_t|s_{t-1})P(x_t|s_t). \tag{3}$$

Converting $P(x_t|s_t)$ to likelihood according to Bayes' rule, we get the following equation:

Figure 1: The key points of the human body.

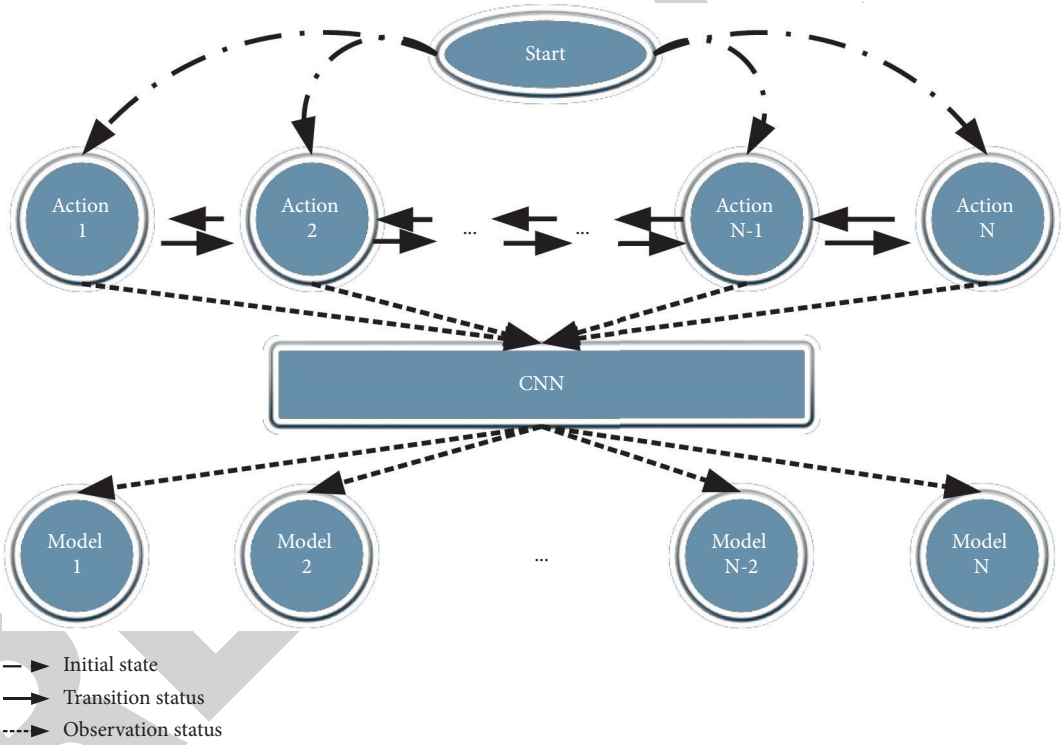

Figure 2: Hybrid CNN-HMM structure diagram.

$$P(x_t|s_t) = \frac{P(s_t|x_t)P(x_t)}{P(s_t)}. \quad (4)$$

Deleting the constant $P(x_t)$, the final action prediction sequence of the hybrid CNN-HMM method can be obtained according to equations (1) to (4):

$$\widetilde{S} = \arg\max_{S} \left\{ \left\{ \max_{s_1 \cdots s_T} \prod_{t=1}^{T} P(s_t|s_{t-1}) \frac{P(s_t|x_t)}{P(s_t)} \right\} P(S). \quad (5)$$

4. System Overview

The hybrid CNN-HMM human action recognition method is divided into two parts: training phase and testing phase; the purpose is to build a model on the training data set and evaluate the performance on the test data set, so as to obtain a human action recognition algorithm model with generalization ability.

The general idea of the Open Pose algorithm is as follows: the input image is processed by a 10-layer VCG19 network, the image feature F is extracted, and then the

feature F is put into two convolutional networks for calculation; that is, the key point confidence network S and the key point pro and the degree vector field network L and then predict the confidence and affinity vectors of each key point. Then, the key points are clustered through binary matching, the skeleton nodes of the same person are spliced, and finally the skeleton information of each person is obtained. Traditional pose estimation algorithms need to rely on depth camera calculations, while Open Pose can achieve excellent real-time performance using only a monocular camera.

4.1. Training Phase. In order to learn how to predict the output from the input, in the training phase, the best parameters are found using the labeled training dataset to build the best training model and predict the output, the process is shown in Figure 3 in the following steps.

In the preprocessing process, the training dataset is first cleaned up, then scaled in a certain proportion in a certain area, and the training dataset is divided into continuous data segments according to the experimental actions.

CNN is selected as the baseline classification algorithm, and the segmented data segments are introduced into the CNN-HMM hybrid algorithm for training.

To ensure the smoothness of the time series, the CNN classification results are combined with the hidden Markov model, and the initial and transfer probabilities of the hidden Markov model are generated in this step [26, 27].

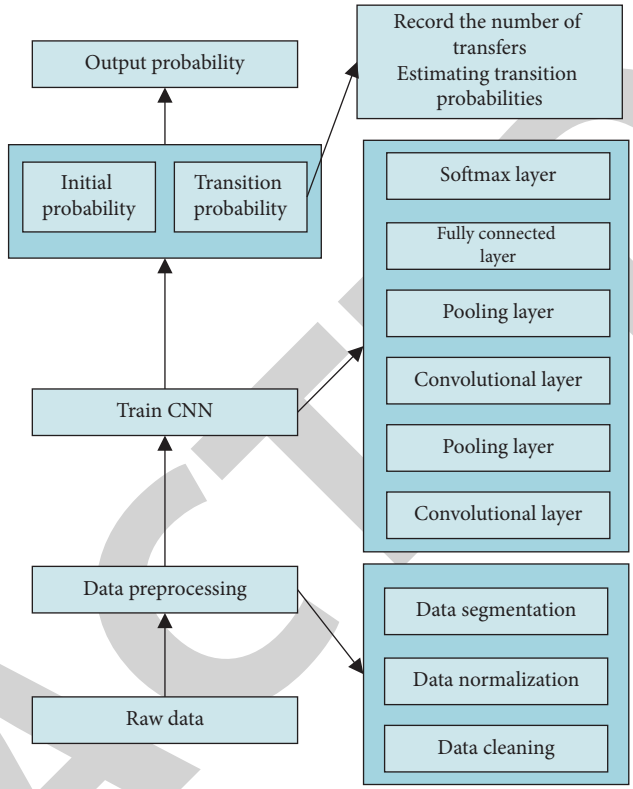

Figure 3: Hybrid CNN-HMM training.

4.2. Test Phase. In order to evaluate the performance of the model and test the final generalization ability, in the testing phase of the system, the never-used test data set is applied to the prediction model established in the training phase to complete the prediction of the action sequence, the process is shown in Figure 4, and the specific steps are as follows.

The experimental data is divided into data segments, called data windows, and these data are marked as test data.

the CNN model is used to classify the preprocessed data, and a posterior probability distribution is output whose sum is 1, that is, the probability corresponding to each action pattern.

In order to make full use of the time information in the experiment, the posterior probability distribution result output by CNN is embedded in the observation probability matrix of HMM, and the Viterbi algorithm is used to reclassify it to obtain the best action sequence.

The algorithm performance is tested according to different evaluation indicators.

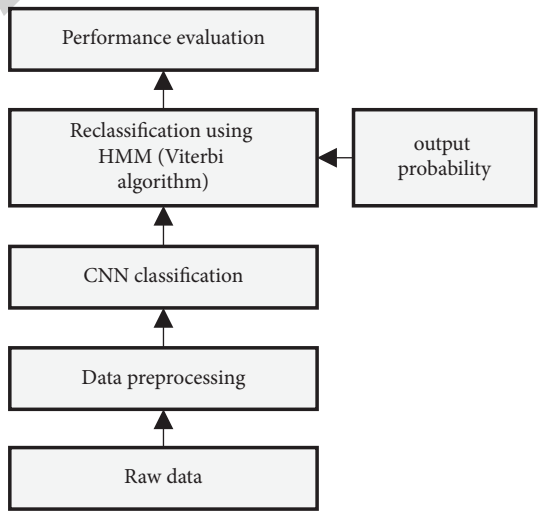

Figure 4: Hybrid CNN-HMM testing phase.

The front end of the fully CNN constructed in this paper contains 6 convolutional layers and 5 pooling layers. The backend of the fully CNN consists of 6 deconvolutional layers and 5 upsampling layers. If an image containing 224×224 pixels is fed into a fully CNN, the size of the image is changed to 1/2, 1/4, 1/8, 1/16, and 1/32 of the original input image size through five pooling layers, respectively. The size of the convolution kernel of the last convolutional layer is $7 \times 7 \times 32$, so the front end of the fully CNN outputs a $1 \times 1 \times 32$ feature map. The backend of the fully CNN performs 6 deconvolutions and 5 upsampling on the feature maps output by the frontend. Finally, a feature map with the same size as the original image is obtained, and then the detection task of the target of martial arts athletes is completed.

After completing the target detection of martial arts athletes, it is also necessary to track other frames in the video, so as to record the trajectory of the athlete's target. Aiming at this problem, this paper proposes an athlete target tracking algorithm based on neighborhood similarity.

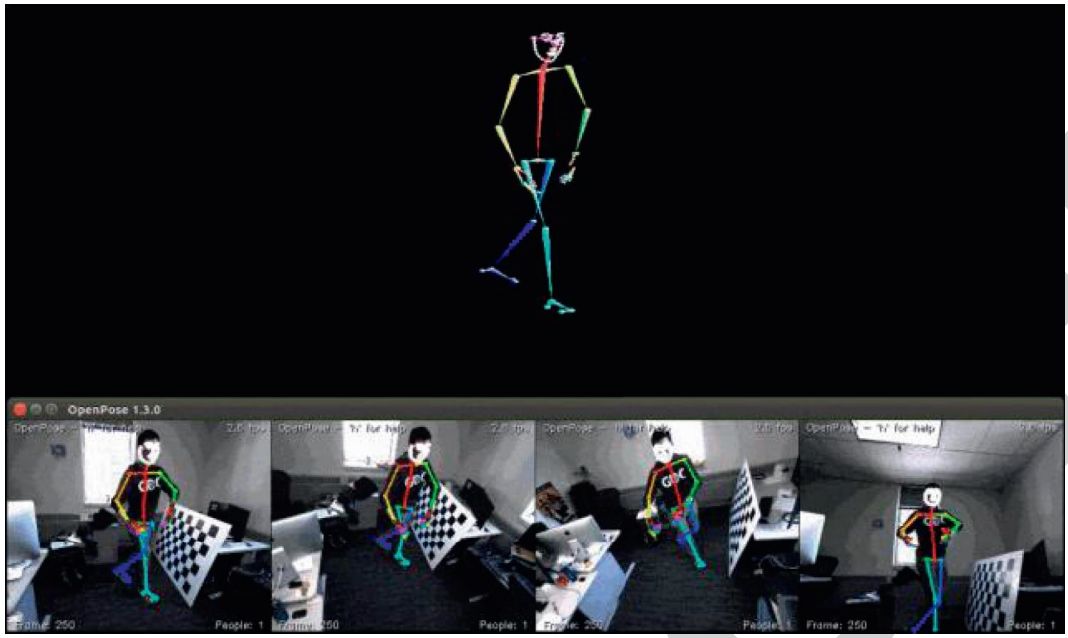

Figure 5: Human skeleton restored by openpose.

Figure 6: The input picture of the practitioner's actions.

Figure 7: Skeleton structure of practitioners.

Firstly, on the premise that the position of the athlete is detected in the first frame image, the circumscribed rectangle marking the position of the athlete is enlarged by 20% in the horizontal and vertical directions, respectively, so as to cover the possible position of the athlete in the next frame of the image. Secondly, the neighborhood similarity between the detected athlete target pixel in the current frame and all the pixels in the possible appearance area of the athlete target in the next frame image is calculated. The pixel with the highest similarity is selected as the position where the target pixel of the current frame appears in the next frame. Finally, repeat the above-given two steps to complete the athlete target tracking task in the martial arts competition video.

5. Test Effect

In the experimental part, the algorithm of target detection and tracking of Wushu athletes proposed in this paper is simulated and verified by a computer. The central processing unit of the computer is i7-11700 K, the memory frequency is 3200 Mhz, the capacity is 32 G, and the graphics card is RTX3070. The computer's operating system is Windows 10. In the experimental part, the algorithm is simulated and verified by Matlab 2016b. The input and output of the program are standard video images in AVI format. The experiment part verifies that the proposed algorithm can effectively detect and track the target of martial arts athletes through subjective visual analysis and objective evaluation indicators.

Different feature parts of the human body can be abstracted into 18 feature points, and the human skeleton composed of these feature points can reflect the posture of the human body at the moment. The angle value between specific joints can provide a reference for judging the accuracy of a person's actions, without being affected by different body types, skin color, clothing, and other characteristics. This paper will use this feature for action comparison.

After the image is processed by Open Pose, the coordinates of 18 feature points of the human body can be obtained, as shown in Figure 5. In some cases, the part of the human body in the plane picture cannot be completely

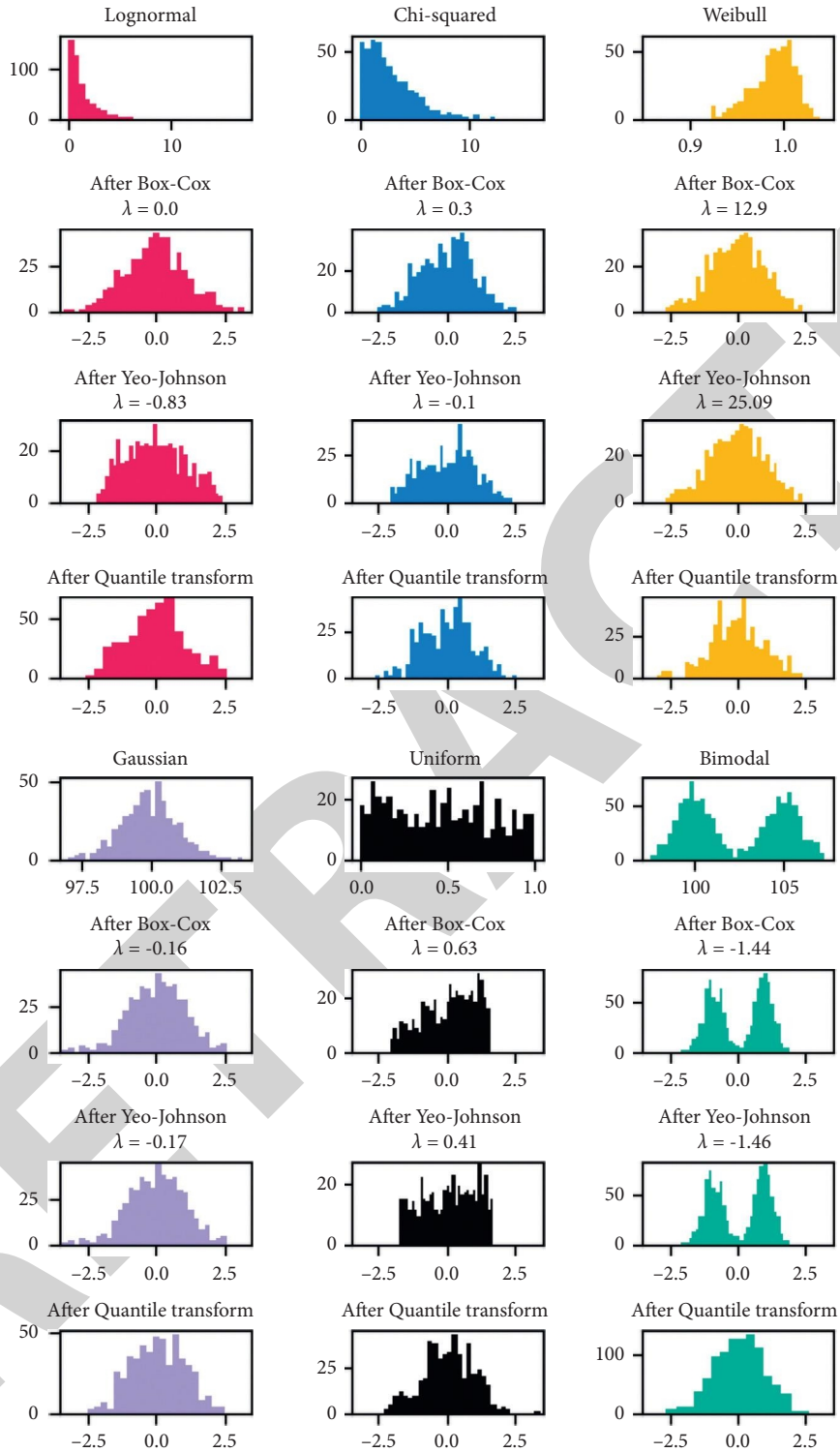

Figure 8: Recognition probability distribution of different poses.

presented, which will cause the corresponding coordinate of the feature point to be "None," which is the case in Figure 4. However, this experiment mainly focuses on the human torso skeleton, and the unrecognized eye feature points have little effect on the comparison of actions, so the facial data can be ignored.

The obtained human skeleton picture is shown in Figure 5. The length between two points can be obtained by calculating the Euclidean distance and then using the law of cosines to calculate the angle value of the angle between the specific joints that reflect the movement of the human body. This paper uses this method to process the standard action

pictures, respectively and obtains the joint angle value of the human skeleton in the picture, which is used as a comparison template. Then, the action picture of the trainer is input that needs to be judged and also gets the joint angle value.

The preintercepted key frames of the practitioner's actions are processed, and the human skeleton data containing multiple joint angles is obtained in this picture, as shown in Figure 6. At the same time, the human body in the picture will be marked with a skeleton structure containing key points, as shown in Figure 7. After that, the output data are compared with the standard motion data that has been processed in the same way in advance, and it can be roughly judged whether the trainer's motion is standardized.

However, in individual cases, there is a problem with the restoration of the human skeleton by Open Pose. For example, when the trainer's hand is raised vertically above the head, the algorithm will fail to restore the skeleton of the arm part. This is because Open Pose relies on two known skeleton points to generate a PAF connection during pose estimation. If one of the two skeleton points does not exist or the recognition fails, the PAF label will not be generated. Therefore, it is speculated that when the trainer's hand is raised above the head, only the wrist joint is identified, and the elbow joint fails to be identified, so the PAF connection is not generated, but this connection actually exists and should be generated, as shown in Figure 8.

6. Conclusion

In this paper, aiming at the recognition and comparison of traditional martial arts movements, the Open Pose algorithm is used to process the key frames of trainers and standard movements, restore the human skeleton, and obtain the human joint angle values; the comparison of the two has verified the feasibility of Open Pose and the comparison algorithm in the teaching of martial arts movements and has good practical significance and practical value for promoting martial arts teaching, inheritance, and promotion. This paper also has the following shortcomings: the samples used in this experiment are too single, and only a few specified human actions are identified and compared; in the future, the scope of the sample should be expanded to cover more martial arts varieties, moves, and movements, in order to explore the applicability of this method in the field of traditional martial arts movement identification and comparison.

Data Availability

The experimental data used to support the findings of this study are available from the corresponding author upon request.

Conflicts of Interest

The authors declare that they have no conflicts of interest regarding this work.

Acknowledgments

This study was funded by the 2016 Provincial Quality Engineering Teaching Research General Project of Anhui Colleges and Universities "Physical Education Research of Health Qigong in Physically Vulnerable Groups in Colleges and Universities" (Grant no. 2016jyxm0608).

References

[1] Y. Zhang, Q. Chen, and Y. Zhang, "Reflection on the inheritance and development of martial arts and national traditional sports visual measurement analysis based on Citespacev," *Jurnal Sains Sukan & Pendidikan Jasmani*, vol. 10, no. 1, pp. 45–54, 2021.

[2] X. Liu, "Comparative study on the development of shaolin zen martial medicine and zheng huaixian's martial medicine," *Tobacco Regulatory Science*, vol. 7, no. 5, pp. 2073–2081, 2021.

[3] D. Wu, Y. Lei, M. He, C. Zhang, and L. Ji, "Deep reinforcement learning-based path control and optimization for unmanned ships," *Wireless Communications and Mobile Computing*, vol. 2022, Article ID 7135043, 8 pages, 2022.

[4] M. J. Meyer, A. Molle, B. N. Judkins, and P. Bowman, "Martial arts in the pandemic," *Martial Arts Studies*, vol. 11, pp. 7–31, 2021.

[5] G. Cai, Y. Fang, J. Wen, S. Mumtaz, Y. Song, and V. Frascolla, "Multi-carrier M-ary DCSK system with code index modulation: an efficient solution for chaotic communications," *IEEE Journal of Selected Topics in Signal Processing*, vol. 13, no. 6, pp. 1375–1386, 2019.

[6] K. Lee, I. Song, and H. Choi, "On the origin of baekje MILITARY MARTIAL ARTS and the path and inflow of Japanese military martial arts," *International Journal of Military Affairs*, vol. 6, no. 2, pp. 1–10, 2021.

[7] K. Chandra, A. S. Marcano, S. Mumtaz, R. V. Prasad, and H. L. Christiansen, "Unveiling capacity gains in ultradense networks: using mm-wave NOMA," *IEEE Vehicular Technology Magazine*, vol. 13, no. 2, pp. 75–83, June 2018.

[8] F. B. Saghezchi, A. Radwan, J. Rodriguez, and T. Dagiuklas, "Coalition formation game toward green mobile terminals in heterogeneous wireless networks," *IEEE Wireless Communications*, vol. 20, no. 5, pp. 85–91, 2013.

[9] S. Palanisamy, B. Thangaraju, O. I. Khalaf, Y. Alotaibi, S. Alghamdi, and F. Alassery, "A novel approach of design and analysis of a hexagonal fractal antenna array (HFAA) for next-generation wireless communication," *Energies*, vol. 14, no. 19, p. 6204, 2021.

[10] S. N. Alsubari, S. N. Deshmukh, A. A. Alqarni et al., "Data analytics for the identification of fake reviews using supervised learning," *Computers, Materials & Continua*, vol. 70, no. 2, pp. 3189–3204, 2022.

[11] Q. Liu, C. Liu, and Y. Wang, "etc. Integrating external dictionary knowledge in conference scenarios the field of personalized machine translation method," *Journal of Chinese Informatics*, vol. 33, no. 10, pp. 31–37, 2019.

[12] S. A. Bansode, V. R. More, S. P. Zambare, and M. Fahd, "Effect of constant temperature (20 0C, 25 0C, 30 0C, 35 0C, 40 0C) on the development of the Calliphorid fly of forensic importance, *Chrysomya megacephala* (Fabricus, 1794)," *Journal of Entomology and Zoology Studies*, vol. 4, no. 3, pp. 193–197, 2016.

[13] F. A. A. Mekhlafi, R. A. Alajmi, Z. Almusawi et al., "A study of insect succession of forensic importance: Dipteran flies (diptera) in two different habitats of small rodents in Riyadh

Hindawi
Mobile Information Systems
Volume 2023, Article ID 9840459, 1 page
https://doi.org/10.1155/2023/9840459

Retraction

Retracted: Case Study on Berthing and Disembarking of Ships and Traffic Organization in Rugao Port of Nantong

Mobile Information Systems

Received 1 August 2023; Accepted 1 August 2023; Published 2 August 2023

This article has been retracted by Hindawi following an investigation undertaken by the publisher [1]. This investigation has uncovered evidence of one or more of the following indicators of systematic manipulation of the publication process:

(1) Discrepancies in scope
(2) Discrepancies in the description of the research reported
(3) Discrepancies between the availability of data and the research described
(4) Inappropriate citations
(5) Incoherent, meaningless and/or irrelevant content included in the article
(6) Peer-review manipulation

The presence of these indicators undermines our confidence in the integrity of the article's content and we cannot, therefore, vouch for its reliability. Please note that this notice is intended solely to alert readers that the content of this article is unreliable. We have not investigated whether authors were aware of or involved in the systematic manipulation of the publication process.

Wiley and Hindawi regrets that the usual quality checks did not identify these issues before publication and have since put additional measures in place to safeguard research integrity.

We wish to credit our own Research Integrity and Research Publishing teams and anonymous and named external researchers and research integrity experts for contributing to this investigation.

The corresponding author, as the representative of all authors, has been given the opportunity to register their agreement or disagreement to this retraction. We have kept a record of any response received.

References

[1] P. Lu, "Case Study on Berthing and Disembarking of Ships and Traffic Organization in Rugao Port of Nantong," *Mobile Information Systems*, vol. 2022, Article ID 4261240, 9 pages, 2022.

Hindawi
Mobile Information Systems
Volume 2022, Article ID 4261240, 9 pages
https://doi.org/10.1155/2022/4261240

Research Article

Case Study on Berthing and Disembarking of Ships and Traffic Organization in Rugao Port of Nantong

Ping Lu [1,2]

[1]*Merchant Marine College, Shanghai Maritime University, Shanghai 201306, China*
[2]*Changjiang Pilot Center, Jiangyin 214431, China*

Correspondence should be addressed to Ping Lu; 201640111003@stu.shmtu.edu.cn

Received 29 May 2022; Accepted 9 July 2022; Published 9 August 2022

Academic Editor: Shadi Aljawarneh

In order to meet the needs of a 12.5 m deep-water channel, Rugao port of Nantong plans to normally berth ship with a draft of 12.0 m. Based on the study of the current situation and development trend of restricted ships entering and leaving Rugao port in Nantong, taking the navigation environment as the boundary condition, and based on the case study of berthing and disembarking of real ships, this paper objectively analyzes and deals with various risks in the process of docking and berthing of restricted ships. The results show that under the smooth and orderly traffic organization, Rugao port in Nantong has the ability to normally berth ships with a draft of 12.0 meters.

1. Introduction

At present, the world's maritime vessels are increasingly large, standardized trend, the main maritime standard ship type have been in more than 50,000 tons, and the world's international seaports in the channel depth of 12.5 meters or more..

Jiangsu section of the Yangtze River waterway has been dredged for 8.5 m, 10.5 m, 12.5 m, and other times, which has a significant impact on the ports along the river. After the completion of 12.5 m deep water channel in the Jiangsu section of Yangtze River, it is upgraded from 10.5 m to 12.5 m (where the starting base below Jiangyin is the local theoretical lowest tide surface, and the starting base above Jiangyin is the navigational reference surface of Yangtze River mainline channel), which can meet the two-way navigation of 50,000-ton container ships (actual draft ≤11.5 m) and the two-way navigation of 50,000-ton other sea vessels with reduced load, taking into account the reduced load navigation of 100,000-ton bulk carriers. According to the statistics, the following 12,000 tons of Yangtze River vessels below Nanjing have been opened for navigation.

Severe cold cities are located at the highest latitudes, with the lowest winter temperatures, and are under the control of polar continental air masses throughout the winter. This natural geoclimatic feature adds many difficulties to the creation of urban landscapes. The main problems are that the urban landscape can barely serve people in winter, the outdoor ambient temperature is too low to be tolerated for a long time, the type of outdoor activities becomes monotonous, the capacity of snow-covered traffic space decreases or even prevents the disadvantaged from traveling, and public services are virtually nonexistent, resulting in too few users or too short a stay in the landscape, i.e., low vitality [1, 2].

With the rapid development of the shipping industry and the gradual enlargement of sea vessels entering the river, Nantong Rugao Port has gradually docked 12.0 m draft vessels after load shedding based on the previous docking of restricted vessels and adapting to the needs of 12.5 m deep water channel.

During the period from June 2, 2019 to March 25, 2022, berth 1# of Zhonglin Rugao Port has successfully docked 153 vessels with a draft ≥11.8 meters.

According to statistics, the construction of the 12.5 m deep water channel below Nanjing of the Yangtze River has effectively improved the navigation conditions below

Nanjing of the Yangtze River and enhanced the navigation capacity, with significant economic and social benefits. In 2018, the number of vessels of 50,000 tons, 100,000 tons, and 200,000 tons and above arrived in Hong Kong was 2.9, 3.4, and 4.9 times of 2011 respectively, and the actual carrying capacity was 4.0, 7.6, and 7.7 times of 2011 respectively. The number of ships of 100,000 tons and 200,000 tons and above arriving at the port was 2.9, 3.4, and 4.9 times that of 2011, respectively, and the actual carrying capacity was 4.0, 7.6, and 7.4 times that of 2011, respectively.

Based on the study of the current situation and development trend of restricted ships entering and leaving Rugao port in Nantong, taking the navigation environment as the boundary condition, and based on the case study of berthing and disembarking of real ships, this paper objectively analyzes and deals with various risks in the process of docking and berthing of restricted ships. The results show that under the smooth and orderly traffic organization, Rugao port in Nantong has the ability to normally berth ships with a draft of 12.0 meters.

2. Analysis of Ship Berthing and Unberthing Elements

2.1. Docks. Nantong Rugao Port (i.e., Zhonglin Rugao Port, commonly known as Rugao Port Service) belongs to Nantong Rugao Port Group Co. Ltd. The location of the terminal is located in the Yangtze River channel mileage of about 120 kilometers, under the mouth of Fujiang Sha North Waterway [3], the north bank of the Yangtze River, coordinates: 032°01.807′N 120°35.042′E, for bulk cargo terminal, berth numbers 1, 2, 3, and 4 (bottom-up).

As shown by the completion and acceptance certificate of the port project, berths 1# and.

The quay is shown in Figure 1, 2# of Zhonglin Rugao Port are 50,000-ton bulk berths, and the hydraulic structure of the terminal is reinforced and modified according to the berthing of 150,000-ton bulk vessels at reduced load. According to the scale of waterway, gyratory waters and harbor pond waters, and the actual draught of ships to be berthing, 150,000-ton bulk cargo ships can be berthing at a reduced load [4] (the draught of ships in the near future is controlled within 11.0 meters, and the draught of ships in the long term is controlled within 12.7 meters). The length of the berth is 557.32 meters, and the bottom elevation of the berth front is −14.4 meters (the local theoretical lowest tide surface is the reference surface).

2.2. Boat Type Selection. The standard ship type of the restricted vessels to be connected on a regular basis according to the design ship scale of bulk carriers in the Harbour Master Plan Design Code (JTS165-2013) is as followsin Table 1.

In this paper, a vessel with a draft ≥11.8 m is selected for a reference study of a 150,000-ton bulk carrier [5] berthing at berth 1# in Rugao Port, Zhonglin.

2.3. Choice of Berthing Time

2.3.1. Tidal Flood. The date of berthing is uncertain, and there is a distribution of both large and small tidal floods. See Table 2.

Due to the existence of tidal time difference, assuming that the tide between Wusong and Jiangyin is basically uniform, the tidal propulsion speed of the section from Tiansheng to Rugao can be deduced, as shown in Table 3. It is very important to master the tidal (high tide) propulsion speed in practice.

According to the records of 153 piloted ships in the past, 95.4% of the ships berth between high tide and low tide [6], 4.6% of the ships berth between low tide and high tide, of which no ships berth before and after 1 h of high tide. This result is consistent with the "common practice of the pilotage community to berth restricted ships in the Yangtze River is to rely on the first drop of water." The best berthing time is between 1 h after high tide and low tide, the berthing time is between low tide and 1 h before high tide, and the avoiding berthing time is 1 h before and after high tide. See Table 4.

2.3.2. Berthing Time Selection. In view of the restricted water conditions at the front of the terminal and the complex navigational environment, restricted vessels are berthing and unberthing operations in good daylight at a visibility distance of more than 1500 meters. See Table 5.

2.3.3. Choice of Anchorage. Restricted ships entering the port should try to choose direct berthing during the daytime to avoid or reduce restricted ships anchoring in the Jiangsu section of the Yangtze River [7] for berthing. As the time period into the Yangtze River is restricted by the time of importing vessels at the mouth of the Yangtze River, restricted vessels can choose anchor 1, Liu anchor, stop 1 at Taicang port, and anchor 5 at Nantong port if they need to anchor, and be assisted by navigation tug to anchor. See Table 6.

In accordance with the "Standards for the Equipping of Pilotage Tugboats for the Jiangsu Section of the Yangtze River Main Line," tugboats are prepared. See Table 7.

3. Examples of Ship Berthing and Unberthing

The 153 ships berthing in the first period show that the ships of 292 meters in length are loaded to 11.8 meters in draught, and the ships of 254 meters in length and below have 11.98 meters in draught or 12 meters in draught, which shows that the draught has more influence on berth 1# in Rugao Port of Zhonglin than the ship length, so the ships of 12 meters in draught are selected for the reference study of 150,000 tons bulk carrier load reduction berthing. Therefore, a vessel with a 12 m draft is selected for the reference study of 150 kt bulk carrier load shedding berthing.

Take the successful berthing of "Honest 19" with 12 m draught at berth 1# in Rugao Port of Zhonglin as an example, and analyze the berthing maneuvering of ships in Rugao Port of Nantong [8].

Figure 1: Zhonglin terminal in Rugao.

Table 1: Design dimensions of bulk carriers.

Ship tonnage DWT (t)	Design ship scale (m)			
	Total length L	Type width B	Type deep H	Full load draft T
150000 (135001 ~ 175000)	289	45.0	24.3	17.9

Table 2: Selection of berthing date.

Berthing date	Vessel (ship)	Percentage (%)
Large tidal flood (the first or fifteenth day of the lunar calendar)	9	5.9
Small tide flood (the eighth or twenty-third of the lunar calendar)	12	7.8
The rest of the time	132	86.3

Table 3: Reference table of tide (high tide) advancing speed from Tiansheng to Rugao.

Segment name	Mileage (km/nmile)	High tide time difference (h)	Tidal (high tide) advancement speed (Average value, km)
Tensho port ~ Rugao port	15/8.1	0.5	16.4

Table 4: Selection of berthing tide.

Berthing tides	Vessel (ship)	Percentage (%)
Pre-low tide 0 ~ 4 h	55	35.9
After the low tide 0.5 h	3	2.0
Pre-climax 2 h	4	2.6
After the orgasm 1 ~ 3.5 h	91	59.5

Table 5: Selection of berthing time.

Berthing time	Vessel (ship)	Percentage (%)
0600 ~ 1159 times	63	41.2
1200 ~ 1759 times	70	45.7
1800 ~ 2359 times	20	13.1
0000 ~ 0559 times	0	0

Table 6: Selection of navigation route.

Sailing path	Vessel (ship)	Percentage (%)
Wusong ~ Zhonglin Rugao port 1# berth	76	49.7
Taicang (anchor 1, Liu anchor, stop 1) ~ Zhonglin Rugao port berth 1#	30	19.6
Anchor 5 ~ Zhonglin Rugao port berth 1#	47	30.7

Table 7: Standard of auxiliary tug.

Region	Navigational aid situation		Number of tugboats equipped (ship) tugboat power (horsepower)	Number of tugboats equipped (ship) tugboat power (horsepower)
Taicang port	Access to the anchorage	Ship length ≥230 m or draft ≥11.5 m in and out of Taicang No. 1A, No. 1B, No. 1 anchorage need to turn around the operation of the ship	1	Not less than 3000
Nantong port	Access to the anchorage	Vessel length >220 meters or draft >11.0 meters in and out of No. 4, No. 5 anchorage need to turn around operation	1	Not less than 3000

3.1. Overview of "Integrity 19" Vessel. Overview of "Integrity 19" vessel is shown in Table 8.

3.2. The Voyage of "Integrity 19". We fully grasp the operation [9] characteristics of "Honest 19" and assess the channel conditions, complex traffic flow, bad hydro-meteorology and other influences; under the premise of leaving sufficient safety margin and coordination of multiple parties, we take avoidance actions cautiously [1]; when passing through shallow areas, bridge areas and other restricted areas, we make full use of tides, ship ballast and other means; when passing through restricted areas, such as shallow areas and bridge areas, we make full use of tides, ship ballast and other means to adjust the underwater and above-water scales scientifically and reasonably to choose the right time to pass under the premise of ensuring safety; during navigation, we give full play to the role of escort boats, keep the contact open, intervene and prevent potential risks in advance; the restricted ships [2] and the accompanying tugs cooperate closely to ensure that the accompanying tugs [10] can play their proper role in the first time under emergency situations. The specific navigation records are shown in Table 9.

3.3. The Amount of Sinking of the Hull of "Integrity 19". Hull sinking volume [11] is related to water depth, ship scale, and ship speed, and in the case of ships, the speed of the ship is a direct factor. Under certain conditions (water conditions, loading conditions and draught, square coefficient, etc. Are not very different), only the ship speed is changeable, the ship speed is fast, and the sinking volume is large; the ship speed is slow and the sinking volume is relatively small.

The maximum draught control standard for ships in the 12.5 m deep water channel of the Jiangsu section of Yangtze River announced on May 7, 2018 is: the maximum draught of ships in 12.5 m deep water channel below Jiangyin is controlled at 12.0 m and below. Understanding the amount of hull sinking when the ship navigates in shallow water is beneficial to leave enough surplus water depth. According to the "Regulations on Surplus Water Depth for Vessel Navigation on Yangtze River Main Line," sea vessels entering the river (subject to light draught) leave sufficient surplus water depth, according to the requirement that the actual draught is 10.5 meters and above, not less than 10% of the ship's draught.

The following is the sinking volume of the vessel "Honest 19" in restricted waters led on August 28, 2019. See Figure 2.

The surplus water depth of "Honest 19" is 1.2 meters; in order to reduce the sinking volume of the ship, the ship speed should be controlled within 10 knots before passing through the restricted shallow point waters [12] during navigation, so as to ensure that the ship has enough surplus water depth to pass through the shallow shoal and shallow point waters smoothly.

3.4. "Honest 19" Inbound Operation. The vessel "Honest 19," with a draft of 12.0 meters, entered the river from the mouth of the Yangtze River and sailed to berth 1# in Rugao Port of Zhonglin, which required passing through a narrow and complicated section of water [13]. When the vessel arrived at the berth, four high horsepower tugboats were arranged to assist [14–17] in berthing and other safety measures.

3.4.1. Full Tugboat Escort. In accordance with the requirements of the pilotage vessel accompanying tug in the Jiangsu section of the Yangtze River Main Line, see Table 10.

The requirements of the accompanying tug are shown in Figure 3.

(1) When "Honest 19" enters the river, arrange Changgang tug 6 maintenance from Yangtze River #3 floating to Suqiao #5 floating, and arrange Zhonggang tug 1001 maintenance from Suqiao #5 floating to Zhonglin Rugao port 1# berth, with 4000 horsepower of Zhonggang tug 1001.

(2) During the navigation, the accompanying tug adjusts its position according to the actual situation to make itself in the most favorable position to deal with water emergencies.

(3) During the voyage in the Jiangsu section of Yangtze River, "Honest 19" used light diesel fuel, prepared anchor head throughout the voyage, and prepared emergency towing cable on the port and starboard side of the bow.

3.4.2. Fugansha North Waterway Entrance to the Wharf front Waters. When "Honest 19" arrived at the entrance of Yangtze River Fugansha North Waterway, there were escort boats in the lower entrance of Fugansha North Waterway for maintenance. Three tugboats were arranged to assist in the main channel. The tugboats were located on both sides of "Honest 19" to assist "Honest 19" in controlling the heading

Table 8: Ship's particular.

Ship name	Integrity 19	Nationality	Hong Kong, China	Wail	VRJY9
Captain	254 m	Boat width	43 m	Draught	12 m
Total tons	64769	Clarity	36935	Deadweight tons	115396 ton
Ship type	Bulk carrier	Name of goods	Iron ore	Cargo capacity	85000 ton
Construction	2012	Port of origin and destination	Baoshan ~ Zhonglin Rugao port 1# berth	Previous port	Ningbo
Boarding and departure time			August 28, 2019 1200 to 2000 hours		

Table 9: Logbook.

Time	Ship position	Voyage records
1316time	Yangtze river #1 float	
1317time		Changgang towing 6 in Yangtze river #5 floating launch
1332time	Yangtze river #3 float	Changgang tug 6 floated down in Yangtze river #4 and started escorting
1509time	Yangtze river #1 float	
1518time	Yangtze river #3 float	
1532time	Yangtze river #5 float	Changgang tow 6 end maintenance, Zhonggang tow 1001 (horsepower 4000 horsepower) maintenance

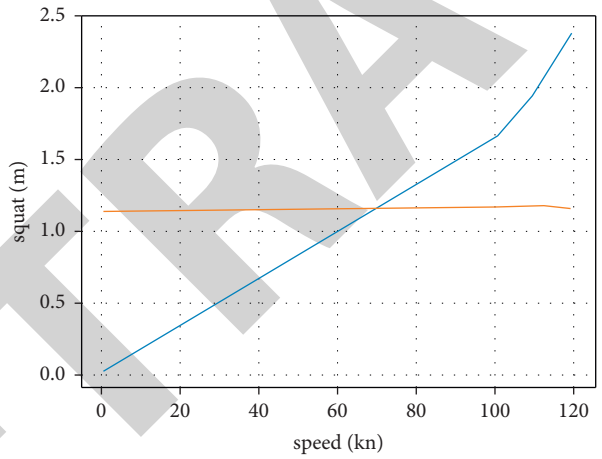

Figure 2: Case study on squat of "Chengxin 19" in restricted waters.

and decelerating.FB#2 black floating surplus water depth is small, need to deviate from the middle of the channel to choose 12.5 meters isobath navigation. If 3 tugboats are brought in the port side at the mouth of the north channel of Fujiang Sha, they cannot control the bow direction and position of the ship very well. The asymmetry of the towing force of the port tug produces a left deflection moment, and the rear tug produces a left deflection moment in order to control the hull top transom (the ship was turning the center amidships to the front), which causes the ship's bow to reverse to the left [17–20]. At this time, the advantages of tugboats placed on both sides of the ship respectively are manifested, and it is found that the bow is deflected to the left, so that the right full rudder can be used to enter at full speed, or the right rear tugboat can be used to top the stern or the right front tugboat can be used to pull the bow so that the ship can turn to the right and the bow can be reversed at full speed after the black float of FB#3. After passing the shallow point FB#2 black float safely, then put the 3 tugboats on the port side. See Figure 4.

3.4.3. Berthing and Handling Program. We choose slow flow to berth, allocate tugs reasonably, avoid berthing at a large angle, and stabilize the ship when approaching the quay to keep it parallel to the quay. During berthing, we use rudder step by step and use a tugboat to effectively reduce the kinetic energy of the ship and reduce the impact on the quay. Before leaving the berth, we fully consider the risk and difficulty of entering the channel after leaving the berth, give full play to the role of the escort boat, and choose the right time to leave the berth. As far as possible, the three processes of leaving the berth, turning around and entering the channel should be operated in steps to minimize the operational risks. See Table 11.

Table 10: Standard of accompanying tug.

Region	Accompanying navigation scenario	Number of tugs equipped (ship)	Companion segment
Yangtze river 12.5 m deep water channel below Nanjing	260 < length ≤ 300 meters of the ship	1	Full range
	Ships with draft >11.5 m below Jiangyin bridge	1	Full range

Note. 1. The tugboats in this table are full-swing tugboats with power >2000 HP, speed >12 knots, and good maneuvering performance. 2. The number of tugboats accompanying each section and situation in this table is not cumulative.

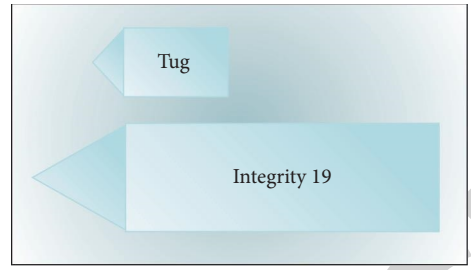

Figure 3: Tug following in whole voyage.

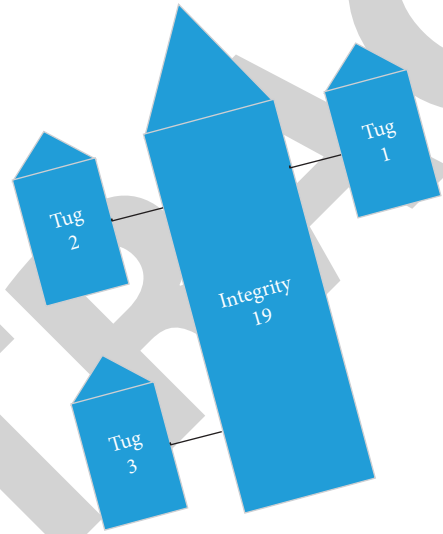

Figure 4: "Chengxin 19" approaching the entrance of Fujiangsha north channel in Yangtze River.

Table 11: Standard for tugs on berthing and disembarking in Yangtze River.

Length of boat (m)	Draught (m)	Number of tugs equipped (ship)	Tug power (hp)
260 < Captain ≤ 300	Draught > 11.0	4	Are not less than 3000, of which at least 2 not less than 4000

(1) Because "Honest 19" was the first time to berth at berth 1# in Rugao Port of Zhonglin with 12 m draft, 4 tugboats were used to assist in berthing. Four high-powered tugboats (at least 2 of them not less than 4,000 hp) assisted in berthing in advance to prepare for the berthing before "Honest 19" reached the front waters of the quay. "Tug 1" moved from the starboard side of the bow of "Honest 19" to the port side of the bow and worked with "Tug 2" to control "Honest 19." "Tug 1" moved from the starboard side of the bow of "Honest 19" to the port side of the bow, and worked with "Tug 2" to control the operation of "Honest 19." "Tug 3" and "Tug 4" were on the port side of the stern of "Honest 19".

According to the requirements of the "Standard for Equipping Tugboats for Berthing and Pilotage or Mooring Auxiliary Operations of Yangtze River Main Line Vessels," the standard for equipping tugboats for berthing and mooring auxiliary operations of Yangtze River main line vessels is as follows.

(2) Berthing principle. "Under normal circumstances, it is not recommended to berth on port side after turning operation of loaded and restricted vessels.

(3) Berthing principles. The ship "Honest 19" should control the remaining speed of berthing (in general, the lower end of the bow berth should not exceed 2 knots), adjust the angle of berthing, and keep enough distance across. Four tugboats controlled the forward and backward direction of "Honest 19" and the left and right direction of the bow and stern of the ship so that the ship slowly (normal speed not more than 0.05 m/s ≈ 0.1 km) and as far as possible parallel to the berth. See Figure 5.

(4) Sub-pile tethering each cable against the dock. The cableway is "422," that is, 4 bow (stern) cables, 2 horizontal cables, and 2 inverted cables. The bow cable and stern cable are each brought on two bollards. The ship's cable is shown in Figure 6.

Since the vessels departing from berth 1# at Zhonglin Rugao Port are 150,000-ton unladen vessels currently operating on a regular basis, they are not discussed further in this article. Our company should carry out regular mapping of the quay front, and accurately grasp the time of berthing of restricted vessels under the condition of ensuring the surplus water depth of vessels, and do a good job of unloading, and strengthen the inspection during berthing. Implement safety measures such as the stationing of high-powered tugboats to prevent the occurrence of dangerous situations such as broken cables and collisions.

It should strengthen coordination and contact, implement safety measures, ensure smooth communication channels, and effectively implement safety measures in order to timely respond to and prevent possible dangerous situations and accidents in the process of receiving and docking restricted vessels.

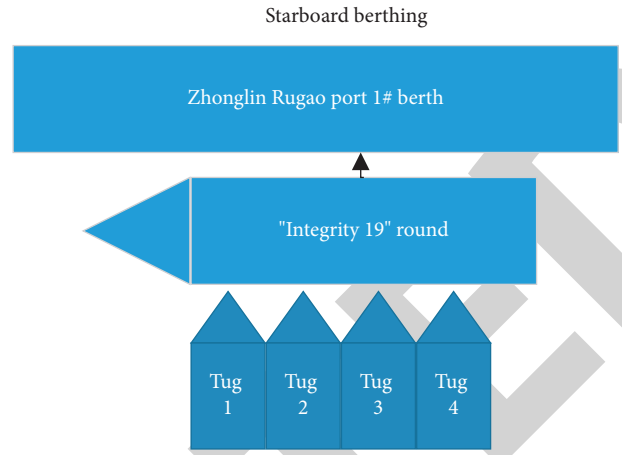

Figure 5: Before berthing of "Chengxin 19."

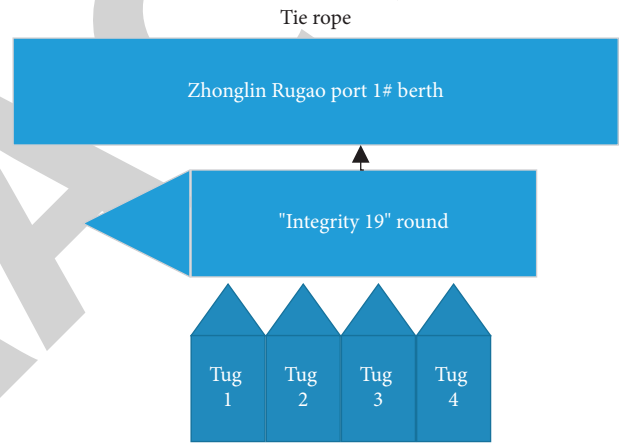

Figure 6: Mooring line of "Chengxin 19."

4. Traffic Organization

Develop the maintenance plan and traffic organization for restricted vessels [16] to ensure the safety of restricted vessel navigation and berthing.

After receiving the maintenance application, the VTS center will notify the information to the escort vessel in time, and the escort vessel will rush to the lower entrance of Fubei in advance to carry out on-site maintenance and traffic organization.

The escort boat issued the dynamic, standardized the navigation order of upstream and downstream vessels, reminded the upstream vessels to pay attention to the restricted vessels' dynamic, adjusted the heading and speed in time, passed through the restricted vessels' transom as far as possible, and did not rush the head navigation.

If there is a shallow point in FB#2 black floating waters, implement emergency measures such as tugboats in advance, and the channel department should organize dredging vessels for channel maintenance in time.

When berthing, the escort boat will release the restricted ship dynamic through high frequency without interruption to remind the nearby ships to drive carefully and cooperate with the restricted ship to berth; the restricted ship will strengthen the lookout and communicate with the ship in advance to eliminate the adverse effect brought by the blind area of the ship as far as possible. The traffic organization of the escorting vessel will continue until the restricted vessel safely berths.

Departure from berth, restricted vessels leave berth, turn around, and enter the channel according to the requirements of the implementation of tugboat assistance and other safety measures, if necessary, the scene of the sea patrol boat to do a good job in advance traffic organization.

Figure 7 shows the path diagrams during training; (a) to (d) are the results of the 423rd, 1,566th, 3,532nd, and 4,879th training sessions, respectively. Because of the high random probability in the early stage of training, our algorithm in Figure 4(a) does not converge and the unmanned boat collides with the obstacle [21].

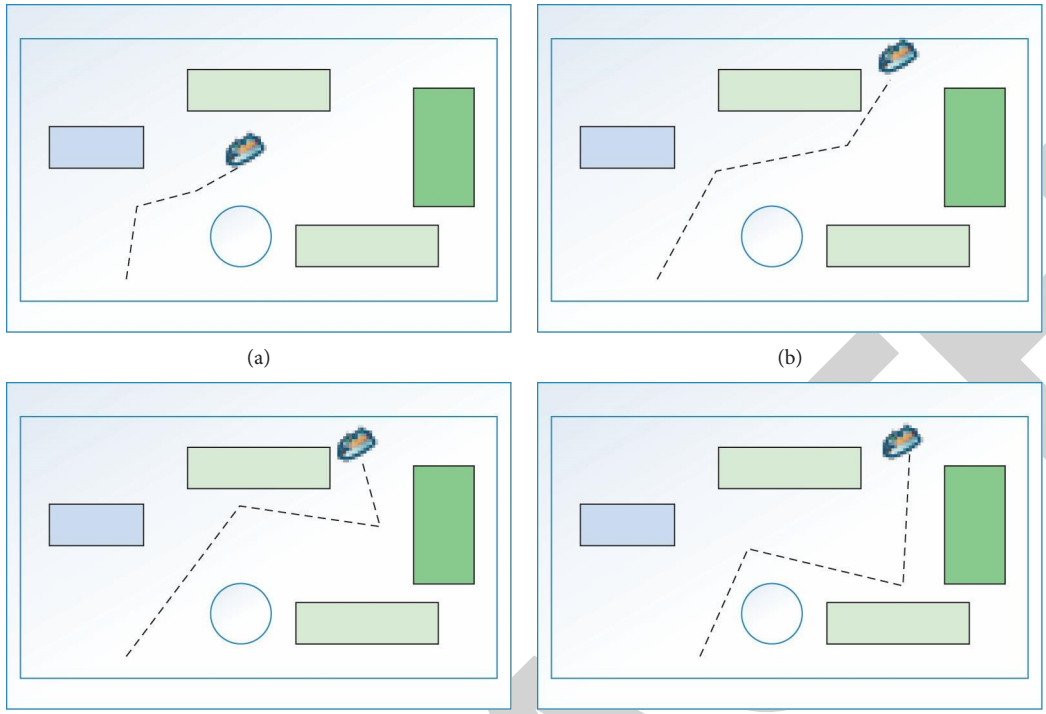

Figure 7: Path diagram of the training process.

5. Conclusion

Avoiding the 1 h before and after high tide, daytime, visibility distance greater than 1500 m, wind less than or equal to 6, implementing a high horsepower tug to escort the whole process, adding 2 more tugboats to assist in entering the waterway under the mouth of Fujiang Sha North Waterway, and an escort boat to escort the ship, 4 high horsepower tugboats to assist in berthing when it arrives at the port, and applying for VTS key monitoring and implementation of traffic organization and other safety measures. To prevent poor visibility and waiting for berthing, emergency anchorage should be implemented along the way [17]; anchor 1 and anchor 5 can be selected. Nantong Rugao Port is located in the lower section of the northern waterway of the Yangtze River Fujiang Sha, close to the Gaoxiang steam ferry line and Rongsheng shipyard wharf, where the water is crowded with ship traffic flow, frequent ship crossings, and an unusually complex navigational environment. In order to ensure the safety of berthing and loading/unloading operations of restricted vessels, it is necessary to implement various safety measures.

Data Availability

The raw data supporting the conclusions of this article can be obtained from the author upon request.

Conflicts of Interest

The author declared that there are no conflicts of interest regarding this work.

References

[1] Q. Liu, C. Liu, and Y. Wang, "Integrating external dictionary knowledge in conference scenarios the field of personalized machine translation method," *Journal of Chinese Informatics*, vol. 33, no. 10, pp. 31–37, 2019.

[2] P. An, Z. Wang, and C. Zhang, "Ensemble unsupervised autoencoders and Gaussian mixture model for cyberattack detection," *Information Processing & Management*, vol. 59, no. 2, p. 102844, 2022.

[3] P. Lois, J. Wang, A. Wall, and T. Ruxton, "Formal safety assessment of cruise ships," *Tourism Management*, vol. 25, no. 1, pp. 93–109, 2004.

[4] G. Cai, Y. Fang, J. Wen, S. Mumtaz, Y. Song, and V. Frascolla, "Multi-carrier M-ary DCSK system with Code index modulation: an efficient solution for chaotic communications," *IEEE Journal of Selected Topics in Signal Processing*, vol. 13, no. 6, pp. 1375–1386, 2019.

[5] K. Chandra, A. S. Marcano, S. Mumtaz, R. V. Prasad, and H. L. Christiansen, "Unveiling capacity gains in ultradense networks: using mm-wave NOMA," *IEEE Vehicular Technology Magazine*, vol. 13, no. 2, pp. 75–83, 2018.

[6] A. Radwan, M. F. Domingues, and J. Rodriguez, "Mobile caching-enabled small-cells for delay-tolerant e-Health apps,"

Hindawi
Mobile Information Systems
Volume 2022, Article ID 8571477, 10 pages
https://doi.org/10.1155/2022/8571477

Research Article

Effectiveness of Network Classroom Teaching Based on Genetic Algorithm

Chunjie Zou, Weijuan Wang, and Libo Zhu

Zibo Normal College, Department of Information, Zibo, Shandong 255130, China

Correspondence should be addressed to Weijuan Wang; 9049001008@zbnc.edu.cn

Received 3 June 2022; Revised 30 June 2022; Accepted 12 July 2022; Published 9 August 2022

Academic Editor: Shadi Aljawarneh

In online classroom teaching, the function of teaching system can play an important role in the effectiveness of classroom teaching. How to use genetic algorithm to optimize online classroom teaching system has become a research hotspot. Based on genetic algorithm, this paper proposes an adaptive genetic algorithm model based on the traditional algorithm. After setting the appropriate mutation probability, the model can improve the convergence speed. Moreover, based on adaptive genetic algorithm, combined with the direct value method and BT neural network theory, this paper constructs the online classroom teaching quality evaluation model and the teaching system test paper data model, and optimizes adaptive mutation genetic algorithm and BP neural network to evaluate the teaching effectiveness. Simulation experiments are carried out based on the algorithm model, and the visual parameter values are obtained. After experimental comparison, the initial value of the mutation rate is set between 0.002 and 0.004. For the network classroom teaching system, this paper introduces the system demand analysis, function module design, and database design in detail. Finally, through the questionnaire survey, this paper understands the network situation of students in class and the use of online classroom teaching platform in detail, analyzes the problems and influencing factors of online teaching, and finally puts forward the strategies to improve the effectiveness of online classroom teaching.

1. Introduction

With the continuous development of Internet technology, educational informatization is becoming more and more mature [1]. The mode of online classroom teaching has been well known. Due to the impact of the COVID-19, most of the teaching has changed from traditional classroom to online classroom, and people have fully realized the importance of online teaching [2]. Online classroom teaching has changed the traditional teaching mode, method, and management means of teachers. At the same time, it has also played an important role in students' learning style, motivation, and learning effect [3]. This teaching mode subverts the teaching and learning relationship between teachers and students in the traditional classroom, and breaks through the limitations of teaching time and teaching space. At the same time, the effectiveness of online classroom teaching is also affected due to the differences between online classroom and traditional classroom in teaching subjects, objectives, environmental carriers, and organizational forms [4]. At present, most online classroom teaching systems can only meet the needs of students' course selection and cannot cover the needs of all students for learning knowledge, training, examination, and comprehensive education [5]. Especially in the test paper generation system, because the algorithm model is too backward, there is no way to meet the current teaching requirements, and the scientificity, rationality, and comprehensiveness of the test paper cannot match the current teaching content [6]. The limitations of online classroom teaching platform have hindered students' learning motivation and cannot help students learn knowledge better. At the same time, because the online teaching platform cannot meet the teaching needs of teachers, the teaching quality has also decreased to a certain extent [7]. Therefore, how to improve the teaching quality is a problem that educational activities must face. How to evaluate the teaching quality scientifically and reasonably has become the focus of research [8]. The traditional teaching effectiveness evaluation

method is not suitable for online classroom teaching, so it is necessary to build a scientific and reasonable teaching effectiveness evaluation model to evaluate online teaching. Aiming at online classroom teaching, this paper applies the genetic algorithm model to the teaching evaluation and test paper design system, analyzes the influencing factors of the effectiveness of online classroom teaching, and puts forward the development strategy [9].

2. Related Work

The computational model of genetic algorithm is a method model to simulate biological evolution to obtain the optimal solution. At present, it has been widely used in various fields. The literature puts forward the complete structure and theory of genetic algorithm [10]. Later, more and more researchers carried out in-depth research on the promotion of genetic algorithm and the parameter control of coding mode, and obtained various genetic algorithms for deformation optimization. A crossover operator based on domain crossover is proposed in the literature. This algorithm model is applied to the crossover of individuals with genes represented by sequence numbers and can solve the TSP problem [11]. It has been verified by experiments. The random iterative genetic mountain climbing method proposed in the literature has also been verified. In addition, many experts and scholars have optimized and improved the crossover operator. The literature proposes that multipopulation genetic parallel evolution can solve the local convergence problem of genetic algorithm [12]. A parallel genetic algorithm based on gene block coding is proposed in the literature. This algorithm can effectively solve the problem that simple genetic algorithm cannot search large-scale combinations efficiently. The literature proposes that the application of genetic algorithm in intelligent test paper generation can simulate the process of biological evolution, initialize the test questions in the test question bank through coding population and iterative operation, and finally get the optimal result [13, 14]. The literature summarizes four operation modes of online teaching platform, namely, asynchronous distance teaching, synchronous distance teaching, interactive real-time distance teaching, and comprehensive distance teaching [15]. In addition, it also describes in detail the operation mode and task purpose of each operation mode of teaching platform [16]. The literature proposes that the operation mode of interactive real-time distance teaching adopts high-speed network and video conference technology [17, 18]. According to the literature, the ultimate purpose of online classroom teaching is to break through the limitations of teaching space and extend teaching activities to different regions, hoping to educate students [19]. This method is quite different from the teaching organization form of traditional teaching and does not gather students scattered in various regions in one space for teaching. The literature puts forward a new definition of distance interactive teaching. In terms of teaching space and teaching practice, teachers and students have been in a semipermanent separation state. In terms of teaching effect, the evaluation mainly includes the design of teachers' teaching content, the learning services provided for students, and the thinking ability that students can obtain through teaching. In the construction of teaching platform, we should meet the interactive requirements between teachers and students and ensure the emotional connection between teachers and students. The literature studies and analyzes the effectiveness of distance teaching, and puts forward that academic knowledge such as mathematics and science is suitable for traditional teaching mode, and computer business and military knowledge are more suitable for distance teaching mode. The researcher's view is that the purpose of distance teaching is not due to the development of teaching platform technology, but determined by the teaching methods of academic knowledge. This view can help the continuous improvement and development of distance teaching. According to the research on the construction of distance interactive teaching platform, the literature puts forward new design ideas and technical viewpoints. The literature holds that online classroom teaching should fully consider students' learning level, language level, input ability, and self-control ability. The literature suggests that the convenience of teachers and students should be considered in the system design of online teaching platform, as well as whether it can provide high-quality voice and video services.

3. Genetic Algorithm

3.1. Basic Principles. The basic theory of genetic algorithm is to simulate the mechanism of biological evolution and natural selection. After the survival of the fittest, the result of the problem will evolve in the continuous competition and finally get the optimal solution. The flowchart of standard genetic algorithm is shown in Figure 1.

3.2. Establishment of Teaching Quality Evaluation Model. The occurrence probability of mutation operation in traditional genetic algorithm is determined and unchanged. During the operation of the algorithm model, the mutation probability is determined and set according to the empirical value. However, in the actual natural environment, the variation probability is not invariable, and the variation probability will change with the change of the environment. This feature can help the continuous development of the population. Therefore, based on the traditional genetic algorithm, this paper proposes an adaptive mutation genetic algorithm (AGA), whose mutation probability is obtained through continuous experiments. In this paper, the calculation of adaptive mutation probability p is shown in the following formula:

$$P = \frac{(P_1 + P_2)}{2} = \frac{\left(P_0 - (P_0 - P_{\min}) * (m/M) + P_0 * \max_{X_K \int \Omega} F(X_K)/\overline{F}\right)}{2}. \quad (1)$$

In this paper, BP neural network is optimized by genetic algorithm through adaptive lesions, and an adaptive mutation genetic algorithm optimized BP neural network

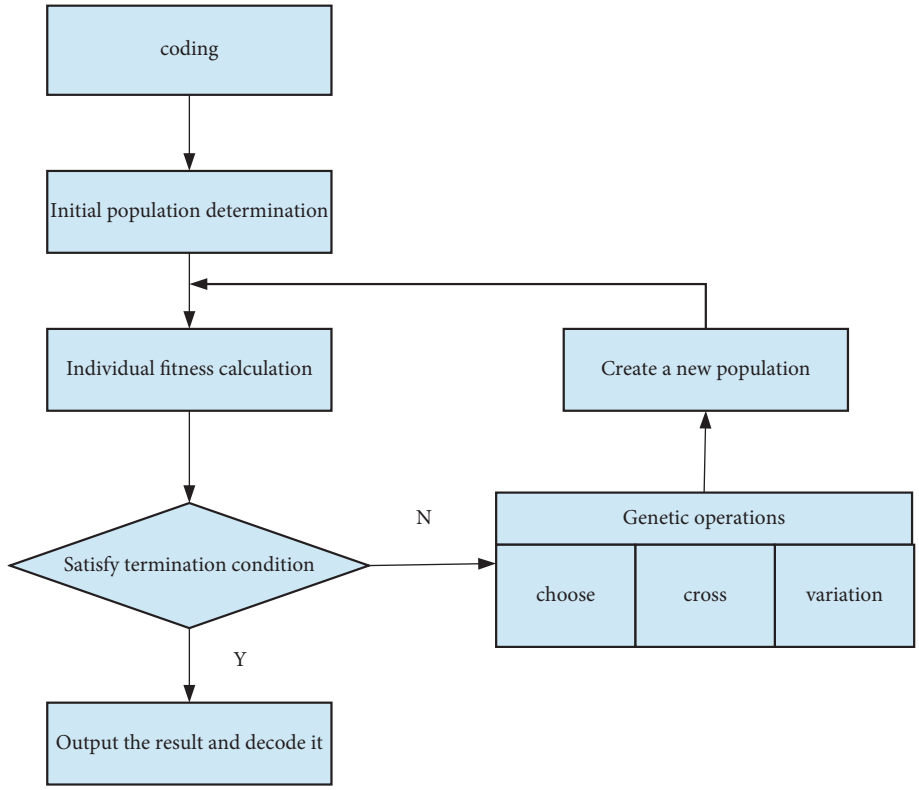

Figure 1: Flowchart of standard genetic algorithm.

model (AGA-BP model for short) is proposed. The model can optimize the weight and threshold of neural network, and solve the shortcomings of local minimum and slow search convergence. The trial-and-error method is one of the methods to determine the number of hidden layer nodes. Its initial value can be determined in three forms, as shown in the following formula:

$$m = \sqrt{n + l} + a, \tag{2}$$

$$m = \log 2^n, \tag{3}$$

$$m = \sqrt{nl}. \tag{4}$$

The number of nodes in the output layer depends on the dimension of the target variable in the actual problem. The nonlinear transfer function is used. The more commonly used nonlinear transfer function is hyperbolic function, which is shown in formula (4):

$$f(x) = \frac{1}{1 + e^x}. \tag{5}$$

The neural network vector model with single hidden layer is adopted in this paper. The input vector is shown in formula (5):

$$p = [p_1, p_2, \ldots, p_R]. \tag{6}$$

The threshold vector is shown in formula (6):

$$b_1 = \left[b_{1,1}, p_{2,1}, \ldots, p_{S_1,1}\right]. \tag{7}$$

The intermediate calculation result, that is, the weighted sum formula connecting the weight vector and the threshold vector (8), is shown in the following formula:

$$n1 = IW_1 p + b_1. \tag{8}$$

Output vector is shown in the formula (8):

$$n1 = IW_1 p + b_1. \tag{9}$$

In this paper, the initial weight of the model is $18 * 5 + 5 * 1 = 95$, the threshold is $5 + 1 = 6$, the coding length is $95 + 6 = 101$, and the initial population is set to 20. The fitness function is shown in formula (9):

$$\text{fitness} = \frac{1}{E}. \tag{10}$$

After calculating the probability of each individual being selected, it is necessary to determine whether the selected individual can continue to be inherited into the next generation of individuals according to the cumulative probability. The calculation formula is shown in formula (10):

$$q(a_k) = \sum_{j=1}^{k} z(a_j). \tag{11}$$

The normalized data are calculated by the direct value method, and the initial evaluation results are obtained. The calculation steps of the direct value method are as follows.

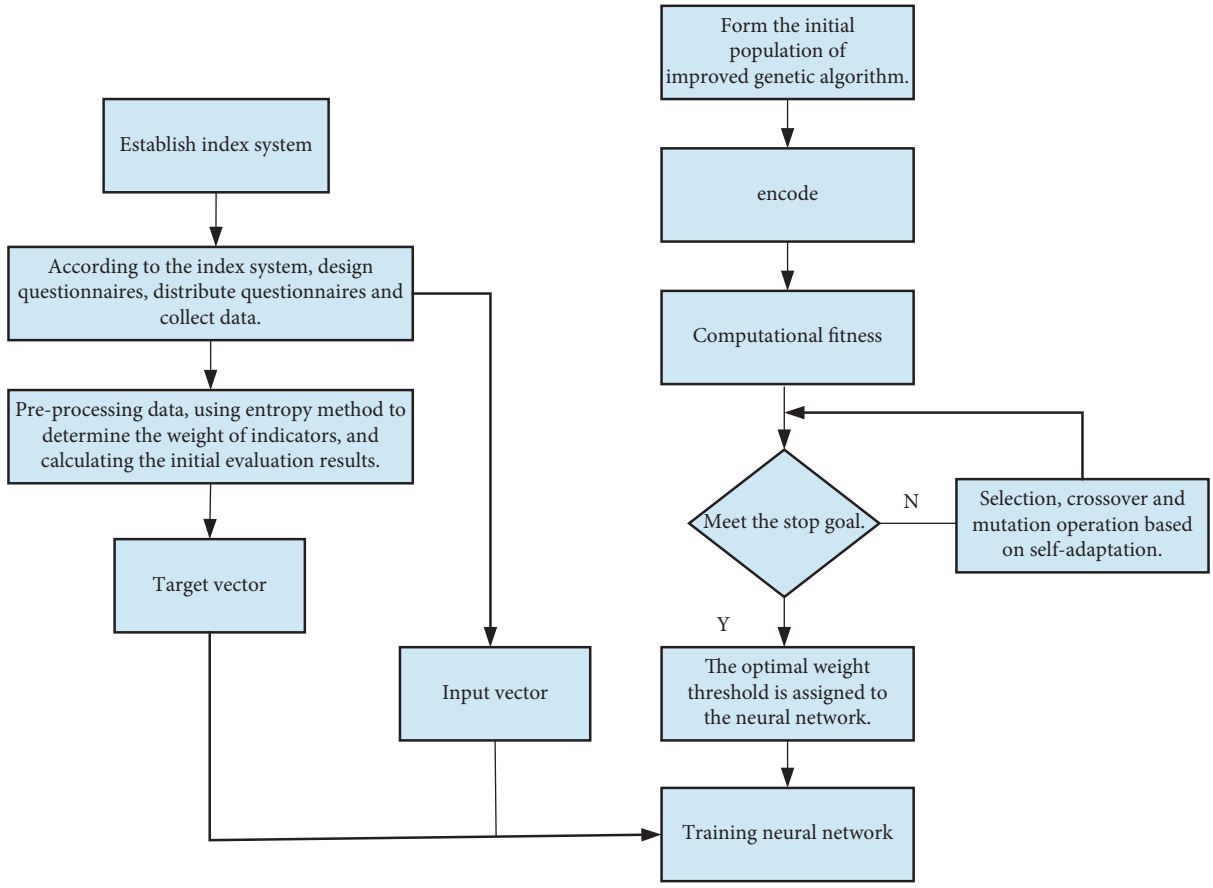

Figure 2: Establishment steps of teaching quality evaluation model.

(1) Standardization of original teaching quality evaluation data is as shown in equation (11):

$$x_{ij}' = \frac{\left(x_{ij} - \overline{x}\right)}{S_j}. \tag{12}$$

In order to meet the requirements of logarithm in entropy method, the standardized value shall be translated, as shown in formula (12):

$$Z_{ij} = x_{ij}' + A. \tag{13}$$

The evaluation indexes of teaching quality are quantified in the same degree, as shown in formula (13):

$$p_{ij} = \frac{Z_{ij}}{\sum_{i=1}^{m} Z_{ij} (i = 1, 2, \ldots, m;\ j = 1, 2, \ldots, n)}. \tag{14}$$

Entropy value of index J was calculated, as shown in formula (14):

$$E_j = -k \sum_{i=1}^{m} p_{ij} \ln\left(p_{ij}\right). \tag{15}$$

The difference coefficient of index J is calculated as shown in formula (15):

$$G_j = 1 - E_j. \tag{16}$$

The weight of the j-th index was calculated as shown in formula (16):

$$w_j = \frac{G_j}{\sum_{j=1}^{n} G_j}. \tag{17}$$

The teaching quality of the i-th sample was calculated as shown in formula (17):

$$F_j = \sum_{j=1}^{n} w_j p_{ij}. \tag{18}$$

The establishment steps of teaching quality evaluation model are shown in Figure 2.

The model constructed in this paper shows the advantages of direct value method and AGA-BP algorithm:

(1) AGA-BP algorithm model can realize nonlinear mapping within any accuracy. This model solves the problem of lack of horizontal comparison of direct value method.

(2) The direct value method can reduce the error caused by human factors and provide powerful help for the design of neural network. The a priori guidance samples of the AGA-BP algorithm model can get the determined results through the initial evaluation of this method.

3.3. Self-Adaptive Test Paper Model. Genetic algorithm is used in generating test paper. Due to many constraints of traditional test paper methods, such as slow running speed due to long gene coding, it loses the significance of coding. Therefore, this paper adopts the grouping real number coding method of genetic algorithm, which mainly takes the question type as the unit to randomly generate the initial population, so as to simplify the genetic operation process and form test paper faster. The fitness function is shown in the following formula:

$$\min(f(x)) = \max(-f(x)). \tag{19}$$

If the objective function is always positive, the fitness function problem is directly the objective function problem:

$$F(x) = f(x). \tag{20}$$

In order to avoid falling into the local optimal solution, the basic fitness function is adjusted

Linear transformation is as follows:

$$F(x) = \alpha f(x) + \beta. \tag{21}$$

Formula for determining coefficient is as follows:

$$\alpha = \frac{(C_{\text{mult}} - 1) f_{\text{avg}}}{f_{\max} - f_{\text{avg}}},$$
$$\beta = \frac{\left(f_{\max} - C_{\text{mult}} f_{\text{avg}}\right) f_{\text{avg}}}{f_{\max} - f_{\text{avg}}}, \tag{22}$$

or

$$\alpha = \frac{f_{avg}}{f_{avg} - f_{\min}},$$
$$\beta = \frac{-f_{\min} f_{avg}}{f_{avg} - f_{\min}}. \tag{23}$$

3.4. Algorithm Analysis. This paper uses MATLAB to simulate the algorithm, modifies the corresponding parameters, obtains different parameter values, and determines the initial value of the parameters through experimental comparison. When other parameters remain unchanged, the variation rate is 0.003. The influence of crossover rate on the convergence of genetic algorithm is shown in Figure 3.

As can be seen from Figure 3, the value of crossover rate can be preliminarily limited to 0.4–0.7.

Under the condition that other parameters remain unchanged, the crossover rate that can obtain the optimal solution in the above experiment is taken as 0.6. The schematic diagram of the influence of mutation rate on the convergence of the algorithm is shown in Figure 4.

Through the comparison between the two groups of experiments, the initial value of the variation rate is limited to 0.002–0.004.

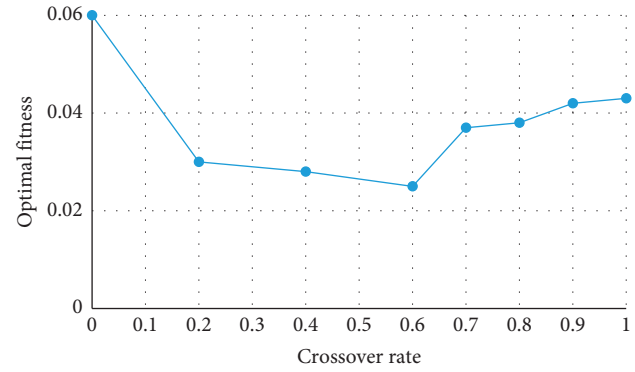

Figure 3: Effect of crossover rate on convergence of genetic algorithm.

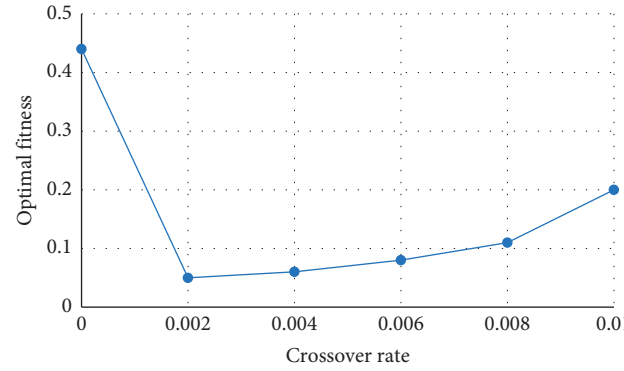

Figure 4: Effect of mutation rate on algorithm convergence.

4. Design of Network Classroom Teaching System Based on Genetic Algorithm

4.1. Teaching System Design

4.1.1. Teaching Management Module. The function of this module is composed of four modules: teacher management, teaching resource management, student management, and administrator module. The teacher management function needs to meet the needs of managing the role of teachers, the student management function needs to meet the needs of managing the role of students, and the administrator module function needs to meet the needs of managing teachers, students, and teaching resources. The teaching resource management module can design the attributes of labels to realize personalized teaching, such as labeling and classifying different teaching materials and contents. You can also use hierarchical settings for labels, set several primary labels through general direction classification, and then subdivide several secondary labels under the primary labels. After teachers label and classify different teaching resources, students can accurately obtain learning resources, so as to make rational use of teaching resources and realize personalized teaching.

4.1.2. Teaching Evaluation Module. The function of this module is composed of intelligent test paper generation and background monitoring. The intelligent test paper

Table 1: System course information.

Title	Data type	Whether it is empty	Primary key	Annotation
Id	int(10)	No	Yes	Curriculum
Name	varchar(255)	Yes		name
Video_url	varchar(255)	Yes		Video
Kejian_url	varchar(255)	Yes		Courseware
Zhuti	varchar(255)	Yes		Theme
Yingyong	varchar(255)	Yes		Application
Difficulty	varchar(255)	Yes		Difficulty
Specially	varchar(255)	Yes		Profession
Teacher	varchar(255)	Yes		Teacher
Popularity	varchar(255)	Yes		Degree of welcome
Image_url	varchar(255)	Yes		Curriculum picture
Create_time	datetime(0)	Yes		Creation time

generation of the system is realized through the improved genetic algorithm. After combining the genetic algorithm with the actual optimization, it can break through the problem of multicondition constraints, realize the intelligent test paper generation, and obtain the practical test paper with reasonable question type, rich knowledge points, moderate difficulty coefficient, and matching the expected teaching objectives. Background monitoring can help teachers master students' learning, examination, and classroom attendance, and feed back the data results to students themselves to help teachers teach better and students learn better.

4.1.3. Other Functional Modules. The function of this module is composed of discussion management, classroom Q&A, experimental practice, and sign-in management to cooperate with the use of online classroom teaching system.

The main user roles are system administrator, teacher, and student, which realize the functions of student management, teacher management, teaching resource management, and course announcement management. After teachers and students create accounts and log in to the system, they can view and modify their own information. At the same time, teachers and administrators can add, modify, view, and delete student information after logging in to the system. The main user roles are administrator, teacher, and student, which realize the function of intelligent test paper generation and background monitoring of learning. Intelligent test paper can realize the operation that teachers can manually change the test paper parameters. Students can modify the test difficulty, knowledge point range, and other parameters. Moreover, it can display students' learning, test results, and classroom performance. After the examination, the system can automatically mark the paper and summarize the results, which can be fed back to teachers and students.

MySQL database is used in this paper. The specific database table is as follows:

(1) Curriculum. It consists of course ID, primary key, course name, instructor, video materials, courseware materials, theme, application, difficulty coefficient, and other information. Specific information is shown in Table 1.

(2) System User Table. It can store the user's relevant information, which is composed of the user's ID primary key, role information, gender, telephone, and other information. In addition, it includes the user's knowledge, the user's learning expectation, teaching objectives, and the user's expectation difficulty. The specific information is shown in Table 2.

(3) Examination Information Table of the System. It is composed of test paper ID primary key, test question ID, test name, student name, student answer, test question answer, test question type, total score, and other information. Specific information is shown in Table 3.

4.2. Design of Test Paper Generation System

4.2.1. Teachers' Demand for Questions. The test question bank needs to meet the requirements of content sharing, efficient question generation, and meeting the standards and can realize effective management and maintenance. The test questions and answers in the test question bank can meet the query needs of teachers at the same time, and users can obtain specific topic content through certain query conditions. In addition, the system also needs to build a reasonable comprehensive evaluation system, which can correctly judge the rationality of the test paper and the comprehensive ability of students, and change the previous single evaluation standard of teachers relying on personal experience. The test paper generation system needs to meet the above functional requirements, achieve objective, fair and reasonable test paper evaluation, and obtain reasonable analysis results.

4.2.2. Student Training and Examination Function. The student training function refers to helping students train various knowledge points before the examination. The training module can not only label and classify different knowledge points but also help students review better through the examination outline. Therefore, the student training module needs to be interactive and operational, and can meet the learning and operation of students of different majors and ages at the same time. In addition to the final examination, phased examination training can also be

Table 2: System user information.

Title	Data type	Whether it is empty	Annotation
User_id	int(11)	No	User ID
Username	varchar(100)	No	Account
Password	varchar(200)	No	Password
Nick_name	varchar(200)	No	Character name
Avatar	varchar(200)	Yes	Avatar
Sex	int(11)	Yes	Gender
Phone	varchar(200)	Yes	Telephone
E-mail	varchar(200)	Yes	Mail
E-mail_verified	int(1)	No	E-mail verification
true_name	varchar(200)	Yes	Actual name
Id_card	varchar(200)	Yes	ID card
Birthday	Date	Yes	Birthday
Introduction	varchar(200)	Yes	Brief introduction
Organization_id	int(11)	Yes	Work ID
State	int(11)	No	State
Deleted	int(11)	No	Delete or not
Knowledge	int(11)	Yes	Only
Degree	int(11)	Yes	degree of difficulty
Target	int(11)	Yes	Expected goal
Create_time	timestamp(0)	No	Registration time
Update_time	timestamp(0)	No	Change the time

Table 3: System examination information.

Title	Data type	Whether it is empty	Annotation
Id	int(10)	No	Test papers ID
Ques_id	varchar(10)	Yes	Test ID
Stu_answer	varchar(255)	Yes	Student answer
Type	varchar(255)	Yes	Test type
Stu_name	varchar(255)	Yes	Student name
Kaoshi_name	varchar(255)	Yes	Test name
Count	int(10)	Yes	Total score

added. This intensive training can help students consolidate the learning content of the stage and carry out targeted review and training. The simulated examination is also an essential function of student training. Before the final examination, the simulated examination helps students better master the knowledge points of the examination outline. The simulated examination questions should be similar to the real questions. They should meet the examination needs of students in terms of knowledge point coverage, topic type, and examination difficulty, so as to simulate the real examination situation to the greatest extent. The examination function refers to that the background personnel can directly monitor the examination status of students, prohibit any cheating, and achieve the goal of invigilating the examination.

4.2.3. Background Monitoring and Marking Function. Background monitoring function, on the one hand, refers to that the teacher can monitor the students' examination status in real time during the examination process, and can also track the students' examination status after the examination. Through the operation, we can obtain whether the students are taking the examination or have taken the examination operation. Students' login information, such as login time and login IP address, can be obtained. In addition, if a student is found cheating in the examination, the teacher can force the student to end the examination. On the other hand, it means that teachers can master the learning situation of students in the background system. The system needs to accurately record the learning content and learning time of students every time and summarize them automatically. Students' learning efficiency and learning time can directly affect students' learning situation.

The marking function refers to that when the students finish the examination, the system can mark the examination papers automatically and generate the examination results. Students' test scores can be automatically fed back to students and teachers, and both students and teachers can view the test answer records. The system can also realize the analysis of students' scores and help students and teachers accurately judge the examination results and learning quality.

The test paper generation system consists of 12 modules, including collective management, project management, marking module, test question management, role management, and system maintenance module. The student side modules include training module, operation training

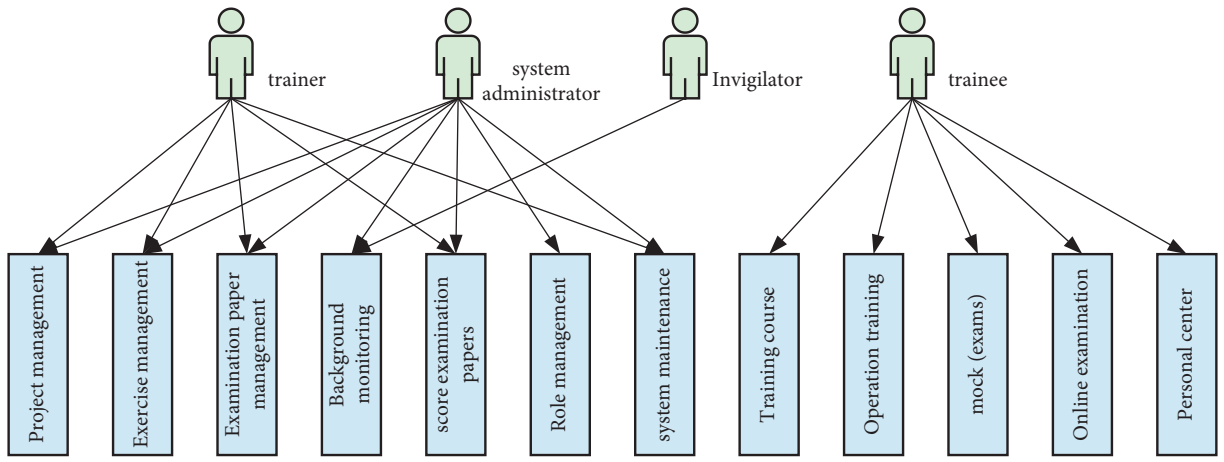

Figure 5: System function module diagram.

Table 4: Statistics of students' online classroom teaching network.

Option	Option content	No.	Proportion (%)
A	The network is very process, very satisfied	31	31
B	The Internet occasionally kattop, more satisfied	39	39
C	The network condition is average, general	25	25
D	The Internet is often stuck, and I am not satisfied with	5	5
E	The network card is serious, very dissatisfied	0	0

module, simulated examination module, online examination module, and personal center management. Each module has a clear division of labor and smooth operation. The system function module diagram is shown in Figure 5.

5. Strategies for Improving the Effectiveness of Online Classroom Teaching

5.1. Problems in Online Classroom Teaching. The most widely used operation mode of online classroom teaching is live teaching, which has particularly high requirements for network conditions. The network condition of teachers and students is the premise of live teaching and plays a key role in the effectiveness of teaching. Online teaching classroom can guarantee normal teaching only under good network conditions, and teachers and students can carry out teaching activities. Therefore, this paper understands the network situation of students' network classroom teaching in detail through questionnaire survey. The specific situation is shown in Table 4.

It can be seen from Table 4 that the network condition is not the main factor affecting students' learning. Most students have good network condition and can smoothly participate in online classroom teaching. Online classroom teaching platform is the basis of effective teaching. This paper conducts a student satisfaction survey on the six basic functions of online classroom teaching platform, as shown in Table 5.

It can be seen from Table 5 that most students are satisfied with the "course playback" function of the online teaching platform. The functions of "uploading and downloading learning resources," "examination and Q & A," and "online listening" basically achieve students' learning objectives. The two functions with the lowest satisfaction are "online interaction" and "after-school homework submission."

5.2. Influencing Factors of Online Classroom Teaching. Students' autonomous learning ability is one of the factors affecting the effectiveness of online classroom teaching. This ability is analyzed from four dimensions: basic ability, comprehensive ability, sincere ability, and aggressive ability, mainly cognitive ability, self-organization ability, independent thinking, and learning ability and self-control ability. Changing from traditional classroom to online classroom teaching has brought great challenges to teachers' professional quality and information literacy. Teachers' professional quality is mainly reflected in teaching philosophy, professional knowledge literacy, teaching ability level, professional ethics level, and information literacy. Among them, teachers' information literacy is the basic ability that contemporary teachers must have. With the continuous development of global informatization, teachers must master certain information technology, which is reflected in the cultural level of knowledge, information skills of ability, and positive consciousness of spirit.

The teaching environment of online classroom teaching and offline teaching has changed greatly. Therefore, the organizational form and teaching mode of online teaching are not suitable for the traditional supervision and management system, which poses a great challenge to the daily teaching management and supervision of the school. In different learning environments, students interact with

Table 5: Online classroom teaching platform satisfaction questionnaire.

Topic/option	Very satisfied (%)	Quite satisfied (%)	Commonly (%)	Quite dissatisfied (%)	Very dissatisfied (%)
Learning resources upload and download	25	60	9	3	3
Online listening	37	45	9	6	3
Online interaction	12	36	30	16	6
Courses	57	30	7	3	3
Postclass homework submission	27	33	33	4	3
Examinations and questions	33	51	9	3	4

teachers through the screen to complete their learning. Teachers and school management cannot maintain classroom order in real time. Therefore, management supervision has become an important part of teaching.

5.3. Strategies to Improve the Effectiveness of Online Classroom Teaching. Students need to improve their autonomous learning ability. They can continuously improve their autonomous learning ability and self-control ability by formulating appropriate learning objectives and learning plans. Teachers and parents should increase the number of interactions and help students form a good habit of self-discipline. Through the method of home school linkage, we help students make reasonable learning plans, guide students to study consciously, and improve their self-control ability. The interaction between teachers and students is the influencing factor for the improvement of students' learning quality; especially, after the emotional connection between teachers and students is established, it can promote students' learning enthusiasm. Therefore, teachers can strengthen the communication between teachers and students through online classroom teaching. In addition to the communication of learning content, there should also be emotional practice to establish a stable and solid relationship between teachers and students, which can help teachers create a positive classroom atmosphere and improve the effectiveness of online classroom teaching. In addition, students should also improve their ability to obtain information and data analysis, and improve the level of information retrieval and identification through certain learning, or students can independently obtain learning information and learning resources through the Internet platform.

To improve the effectiveness of online classroom teaching, teachers' qualification is a crucial factor. We should strengthen the operation skills and knowledge training of teachers' online classroom teaching platform, constantly improve teaching efficiency, improve teaching ability, and master various functional modules of online teaching software. Teachers should adhere to the good concept of continuous learning, actively improve their knowledge, and be able to help students better complete their studies through the online teaching platform. At the same time, they should strengthen the communication and interaction with students' parents, establish emotional ties with students, and create a positive, harmonious, and stable online parent classroom atmosphere. In addition, teachers must have the ability to deal with emergencies on the online teaching platform and can quickly solve the problems of jam, paralysis, inability to video, and so on. Through continuous learning, we can improve the informatization level of teachers and the utilization efficiency of online teaching platform, which is conducive to improving the effectiveness of online classroom teaching.

The management department should improve the construction level of online classroom teaching platform, constantly improve the function of teaching platform, ban online teaching platforms that do not comply with laws and regulations or affect normal teaching, integrate and optimize online platforms that comply with educational laws, and constantly improve the quality and effectiveness of online classroom teaching. We should strengthen the research of online classroom teaching, constantly improve the online teaching mode and teaching methods, put forward the theoretical guidance of online classroom teaching based on theoretical and practical experimental research, and reasonably design online classroom teaching activities. We should constantly strengthen the development and utilization of online classroom teaching resources, change the traditional utilization mode of teaching resources, constantly improve the utilization efficiency of online classroom teaching, and give full play to the advantages of online classroom teaching resources. We should establish a scientific teaching management mechanism, constantly improve the management level, and strengthen the supervision and management of online teaching. At the same time, we should timely adjust the online teaching plan and rhythm in combination with the actual teaching situation and the needs of teachers and students.

6. Conclusion

In this paper, the BP neural network is optimized by genetic algorithm, the BP neural network model optimized by adaptive mutation genetic algorithm is proposed, the teaching quality evaluation model is established, the grouping real number coding method of genetic algorithm is adopted, and the mathematical model of test paper generation is constructed. According to the characteristics of network classroom teaching, this paper analyzes the system design requirements of teaching system and test paper system, and designs the teaching management module, teaching evaluation module, and other functional modules of teaching system, as well as the teacher side and student

side functional modules of test paper system. Through a questionnaire survey, the students' network status and six functions of the teaching platform of online classroom teaching are investigated. Most students have good network status, and there are no problems affecting teaching. The "course playback," "learning resource upload and download," "examination and Q & A," and "online listening" of the teaching platform basically meet the needs of students, and only the "online interaction" and "after class homework submission" have the lowest satisfaction. Finally, this paper analyzes the main influencing factors of the effectiveness of online classroom teaching, mainly including students' autonomous learning ability, teachers' professional development level, and school supervision and management. Based on the three dimensions of students, teachers, and management departments, this paper puts forward strategies to improve the effectiveness of online classroom teaching, which lays a theoretical foundation for the improvement of the effectiveness of online classroom teaching.

Data Availability

The data used to support the findings of this study are available from the corresponding author upon request.

Conflicts of Interest

The authors declare that they have no conflicts of interest.

References

[1] A. Ciuffoletti, "Teaching networks to digital humanists," *IEEE Transactions on Education*, vol. 64, no. 3, pp. 253–260, 2021.

[2] M. Stoytcheva, "Collaborative distance learning: developing an online learning community," *AIP Conference Proceedings*, vol. 1910, no. 1, pp. 1–8, 2017.

[3] J. Fleck, "Blended learning and learning communities: opportunities and challenges," *The Journal of Management Development*, vol. 31, no. 4, pp. 398–411, 2012.

[4] C.-H. Lai, H.-W. Lin, R. M. Lin, and P. D. Tho, "Effect of peer interaction among online learning community on learning engagement and achievement," *International Journal of Distance Education Technologies*, vol. 17, no. 1, pp. 66–77, 2019.

[5] S. Molano and A. Polo, "Social network analysis in a learning community," *Procedia - Social and Behavioral Sciences*, vol. 185, pp. 339–345, 2015.

[6] J. Pei and P. Shan, "A micro-expression recognition algorithm for students in classroom learning based on convolutional neural network," *Traitement du Signal*, vol. 36, no. 6, pp. 557–563, 2019.

[7] F. L. Winanti, F. L. Gaol, H. Prabowo, and H. Prabowo, "A survey positive engagement of learning community for informal education to support community," *IOP Conference Series: Materials Science and Engineering*, vol. 662, no. 2, Article ID 022024, 2019.

[8] B. Hudson, "Developing an open and flexible networked learning community at doctoral level across Europe: national Teaching Fellowship update," *MSOR Connections*, vol. 5, no. 1, pp. 1–4, 2021.

[9] H. Abulkasim, A. Farouk, S. Hamad, A. Mashatan, and S. Ghose, "Secure dynamic multiparty quantum private comparison," *Scientific Reports*, vol. 9, no. 1, pp. 17818–17916, 2019.

[10] L. Zhou, F. Li, S. Wu, M. Zhou, and M. Zhou, ""School's out, but class's on", the largest online education in the world today: taking China's practical exploration during the COVID-19 epidemic prevention and control as an example," *Best Evidence of Chinese Education*, vol. 4, no. 2, pp. 501–519, 2020.

[11] Y. Sun, J. Xu, and G. Lin, *Adaptive Neural Network Control for Maglev Vehicle Systems with Time-Varying Mass and External Disturbance*, Neural Comput & Applic, Berlin/Heidelberg, Germany, 2021.

[12] J. Chen, Z. Wang, J. Chen, Z. Chen, and H. Zhen, "Design and research on intelligent teaching system based on deep learning," *Computer Science*, vol. 46, no. 6A, pp. 550–554, 2019.

[13] H.-E. Tseng, "Guided genetic algorithms for solving a larger constraint assembly problem," *International Journal of Production Research*, vol. 44, no. 3, pp. 601–625, 2006.

[14] M. Adil, H. Alshahrani, A. Rajab, A. Shaikh, H. Song, and A. Farouk, "QoS review: smart sensing in wake of COVID-19, current trends and specifications with future research directions," *IEEE Sensors Journal*, vol. 1, 2022.

[15] H. S. Wang, Z. H. Che, and C. J. Chiang, "A hybrid genetic algorithm for multi-objective product plan selection problem with ASP and ALB," *Expert Systems with Applications*, vol. 39, no. 5, pp. 5440–5450, 2012.

[16] G. Dini, F. Failli, B. Lazzerini, and F. Marcelloni, "Generation of optimized assembly sequences using genetic algorithms," *CIRP Annals*, vol. 48, no. 1, pp. 17–20, 1999.

[17] R. M. Marian, L. H. S. Luong, and K. Abhary, "A genetic algorithm for the optimisation of assembly sequences," *Computers & Industrial Engineering*, vol. 50, no. 4, pp. 503–527, 2006.

[18] X. Tao and Q. Niu, "Instructional feedback strategy generation algorithm based on an emotion learning ontology," *Computer Engineering and Science*, vol. 37, no. 2, pp. 320–328, 2015.

[19] B. Allan and D. Lewis, "The impact of membership of a virtual learning community on individual learning careers and professional identity," *British Journal of Educational Technology*, vol. 37, no. 6, pp. 841–852, 2006.

Hindawi
Mobile Information Systems
Volume 2022, Article ID 1260923, 12 pages
https://doi.org/10.1155/2022/1260923

Research Article

Architecture, Integrated Gateway Design, And Performance Evaluation for High Concurrency Access of Power Internet of Things

Fei Yu,[1] Wei Rao,[2] Chang Liu,[2] Jin Wang,[2] and Liang Zhou[2]

[1]*State Grid Hubei Electric Power Co. Ltd, Hubei, China*
[2]*State Grid Hubei Electric Power Research Institute, Hubei, China*

Correspondence should be addressed to Chang Liu; liuchang.sgcc@foxmail.com

Received 25 May 2022; Accepted 10 July 2022; Published 8 August 2022

Academic Editor: Shadi Aljawarneh

Power Internet of things (IoT) is deemed as a promising network platform with widely deployed infrastructure to boost efficient information delivery in the power grid. Due to the long history of the mature power grid and increased requirements from various industries, the architecture of power IoT should be carefully investigated. Specifically, a large number of end devices in the power grid are required to simultaneously report their sensed information to the management side. However, there are few works related to the uniform communication mechanism to support various devices made by different manufacturers. In this paper, we study the architecture of power IoT for high concurrency access. For each layer of power IoT, we study its fundamental structure and functionality. Moreover, according to the architecture of power IoT, we propose an integrated gateway to support multiple end device simultaneous access. The simulation results verify that the proposed gateway can work well in different network traffic and communication protocols.

1. Introduction

The Internet of things (IoT) is an intelligent service platform that can exchange information in the physical and virtual world by connecting objects, people, and systems based on various protocols through sensors [1–4]. The characteristics of IoT can be categorized in five folds: (1) various communication models and generalized terminal interconnection; (2) automatic intelligent and efficient access; (3) large data throughput and low latency; (4) fast, flexible, and convenient data acquisition; (5) high-security requirement for internal and external network data. On the other hand, with the various construction requirement of the new type of a power system, a large number of distributed power and energy storage equipment have been introduced into the power grid. The advanced smart grid is believed to present similar characteristics by taking advantage of distributed computing systems, communication networks, and information networks. As a widely deployed infrastructure, power IoT can connect different entities in the power grid, such as power users and their equipment, power grid enterprises and their equipment, power generation enterprises, and corresponding equipment, electrical equipment enterprises and their equipment, by means of extensive information interaction and collaborative control. The energy production, energy consumption, and enterprise operation can be greatly improved by digital management in the power grid and the corresponding facilities.

As a significant issue of power IoT, simultaneous access of a large number of end devices has to be well solved to enhance the communication and data exchange in the large area of the power grid. Low-power communications, such as WiFi, ZigBee, and Bluetooth, can support multiple access in a certain area of the network [5–7]. The fourth and fifth-generation communications can be used to transmit data from the local area network to the public networks at a long-range distance. In the application of power IoT, there are quite a large number of end devices in the power grid with a

long history [8]. These power devices employ different communication modules in terms of transmitting range, power, and network protocols due to different manufacturers. Thus, it is difficult to directly connect these devices to a public network without a uniform gateway or some similar mechanisms [9]. Moreover, how to process the different types of data from different devices in the uniform gateway should be carefully addressed to ensure data exchange and display. Currently, the state grid corporation of China boosts informatization in the power grid, which put IoT, mobile Internet, and the facilities of the power grid together to enhance the efficiency of data exchange [10–12]. Moreover, an integrated gateway with a high capacity of information perception, comprehensive information process, and control and management in the power grid is believed to realize real-time detection, high-accuracy localization, and construction supervision in power grid [13].

In this paper, we discuss the architecture of power IoT. Moreover, we analyze each layer of power IoT by taking the requirement of the power industry and current infrastructure into consideration. Then, we propose an integrated gateway for simultaneous access to various devices in power IoT. The performance evaluation shows that the proposed integrated gateway can work well to process multiple requirements from various end devices. The main contributions are summarized as follows:

(1) Compared with traditional power networks, we study the main framework of power IoT, including different layers of power IoT associated with various functions.

(2) Based on the framework of power IoT, we propose a novel integrated gateway for power IoT to support multiple power devices to simultaneously access.

The remaining of this paper is organized as follows. Section 2 presents the development of power IoT and the hierarchical design of power IoT. We also analyze each layer for power IoT in detail in Section 2. In Section 3, we present the design of an integrated gateway for power IoT and evaluate its performance in Section 4. The paper is concluded in Section 5.

2. Hierarchical Design of Power IoT

2.1. History of Power IoT. The development of power IoT evolves within three stages. In the first stage, a large number of sensing devices are deployed to enhance on-site digitization. The power grid is characterized by digital substation, dispatching automation, electricity information collection, distribution automation, intelligent station area, online monitoring of the status of power transmission, and transformation equipment. Within several years of digitization, the power grid side has basically met the requirements of the interconnection of things. The whole power grid is at the level of "observable". That is, the abstract process from the "physical grid" to the "logical grid" has been realized on the computer. Furthermore, the "digital twin" [14, 15] foundation of industry 4.0 has been realized based on the infrastructure of power IoT. From a comprehensive energy aspect, the power IoT is still in a preliminary stage because there is a huge digital bottleneck in the automation of industrial parks and the digitization of electricity using management. The second stage is referred as to interaction among things. More specifically, on the premise that the full digitization of power IoT and digital twin realization, how to use this digital information to improve the efficiency of management is an important issue. In a nutshell, things in power IoT can efficiently communicate with each other. On the power grid side, management information has been basically realized through several rounds of information technology investment, such as the informatization progress of production, marketing, scheduling, finance, and safety supervision. Specifically, the problem that needs to be solved is data interaction. The most typical data is marketing information and production information. Due to the division of departments, complete information and data systems are not easy to establish. As a result, it is difficult to put these two large systems together with efficient and unlimited interaction. Therefore, the power of IoT takes "data unification, operation, and distribution" as an important role. On the service side of comprehensive energy, the basic informatization of management is quite low. There are many small management systems existing in power grid companies. Due to the lack of full business standards and information models, these management systems form information isolated islands [16]. Artificial intelligence (AI) is involved in the third stage. In power system, for example, intelligent data analysis and intelligent unmanned aerial vehicle (UAV) applications can be utilized for the reduction of labor cost and decision-making [17, 18]. These artificial intelligence applications can enhance the perception and interaction in the power grid and self-healing capability. Furthermore, various data from different resources can be analyzed by artificially intelligent algorithms to improve the collaboration among the source power, network, charge, and storage in the power grid system. On the service side of comprehensive energy, within the establishment of the spot market, power grid companies can generate more services. For instance, allowing virtual power plants to participate in the spot and ancillary services trade, using price signals and service demands in each subject, link, and platform and finally forming the intelligent energy network ecosystem.

2.2. Hierarchical Design of Power IoT. Based on the application requirements of collaborative interaction between the source network and storage, we design a four-layer architecture, namely, the perception layer, network layer, platform layer, and application layer, which also follows the main business requirements of power IoT and various commercial network framework. The detailed structure is shown in Figure 1.

2.2.1. Perception Layer. The perception layer includes end-side devices and side-side devices. The end-side devices are responsible for providing basic data of the distribution network such as the operation status, equipment status,

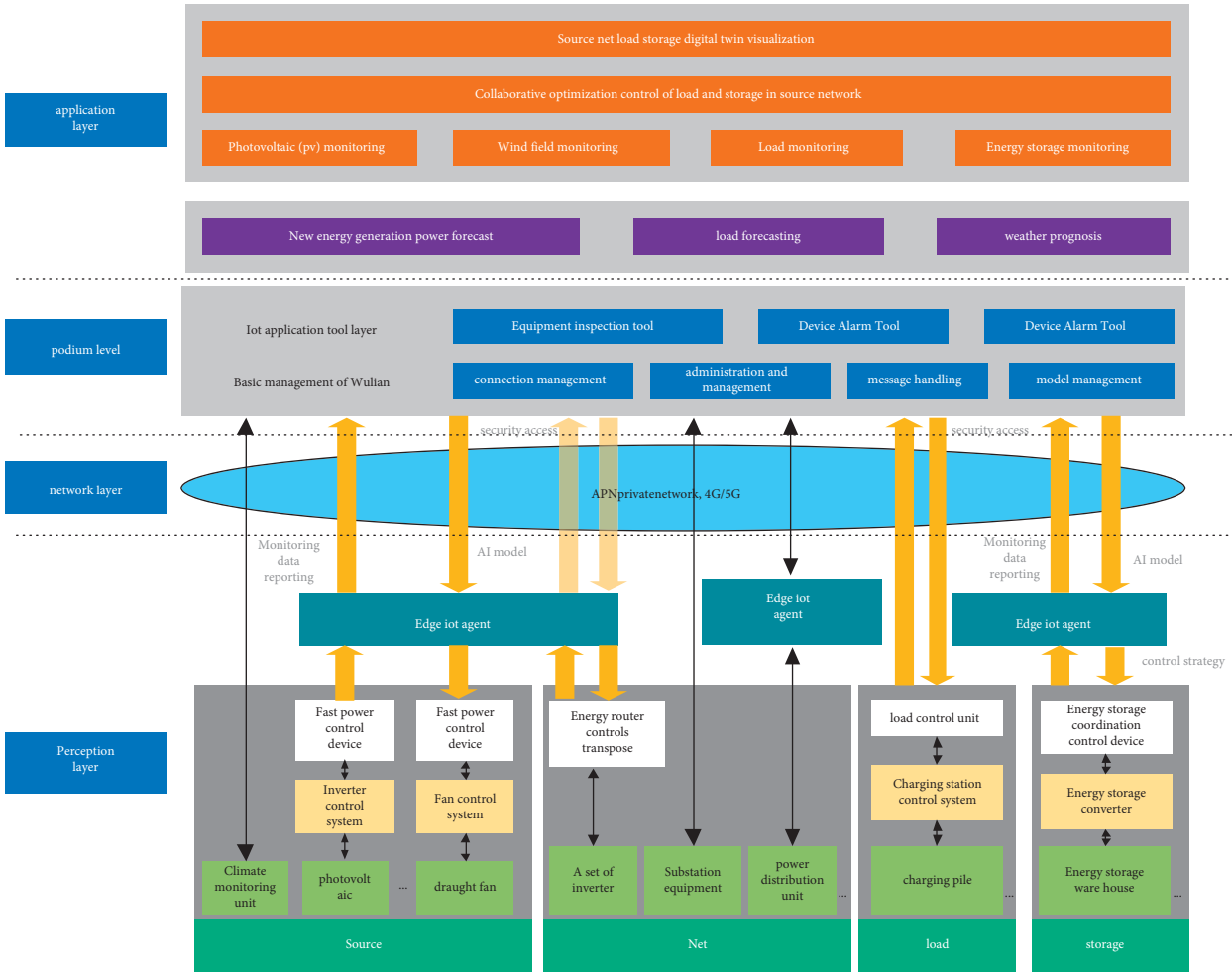

Figure 1: The architecture of power IoT.

environment status, and other auxiliary information to the platform. End-side equipment includes source nodes, network, load, and storage structured data collection of each link of the intelligent device. Based on the principle of on-demand deployment, side-side devices realize local data aggregation of all kinds of perception information in the region, which form open platforms to support multi-container, multi-channel, and multi-protocol modes. End-to-end collaboration is completed through data exchange to realize full data collection, full perception, and full control. Standardized processing and uploading of collected data are realized based on the object model. The real-time full-duplex interaction of key operation data was completed to achieve edge-cloud collaboration by taking the advantages of cloud computing and edge computing.

2.2.2. Network Layer. The network layer serves as an up-down data transmission channel, see Figure 2. It can be divided into remote communication networks and local communication networks. The remote communication network provides the data communication channel between the source, network, load, and storage interactive application and the edge computing node. The local communication network provides the data communication channel between the edge computing nodes and the terminal units. The communication technology 5 G/6 G and the visual private network (VPN) constructed by the power grid system are utilized to transmit perception data to the platform.

2.2.3. Platform Layer. The platform layer adopts big data, micro-service, container management, artificial intelligence, and other technologies to realize the comprehensive cloud and micro-service of the master station. This can meet the business requirements of plug and play of massive terminal devices, rapid online application, and effective data fusion of multiple platforms. The platform also can realize unified online management and remote operation and maintenance of all kinds of sensing layer devices and IoT applications.

2.2.4. Application Layer. The application layer contains advanced applications that are suitable for collaborative control of the source network load and storage. Advanced applications should be developed based on collaborative interaction strategies. The detailed application requirement is described as follows: (1) The Collaborative and interactive application. The core business of the application layer is

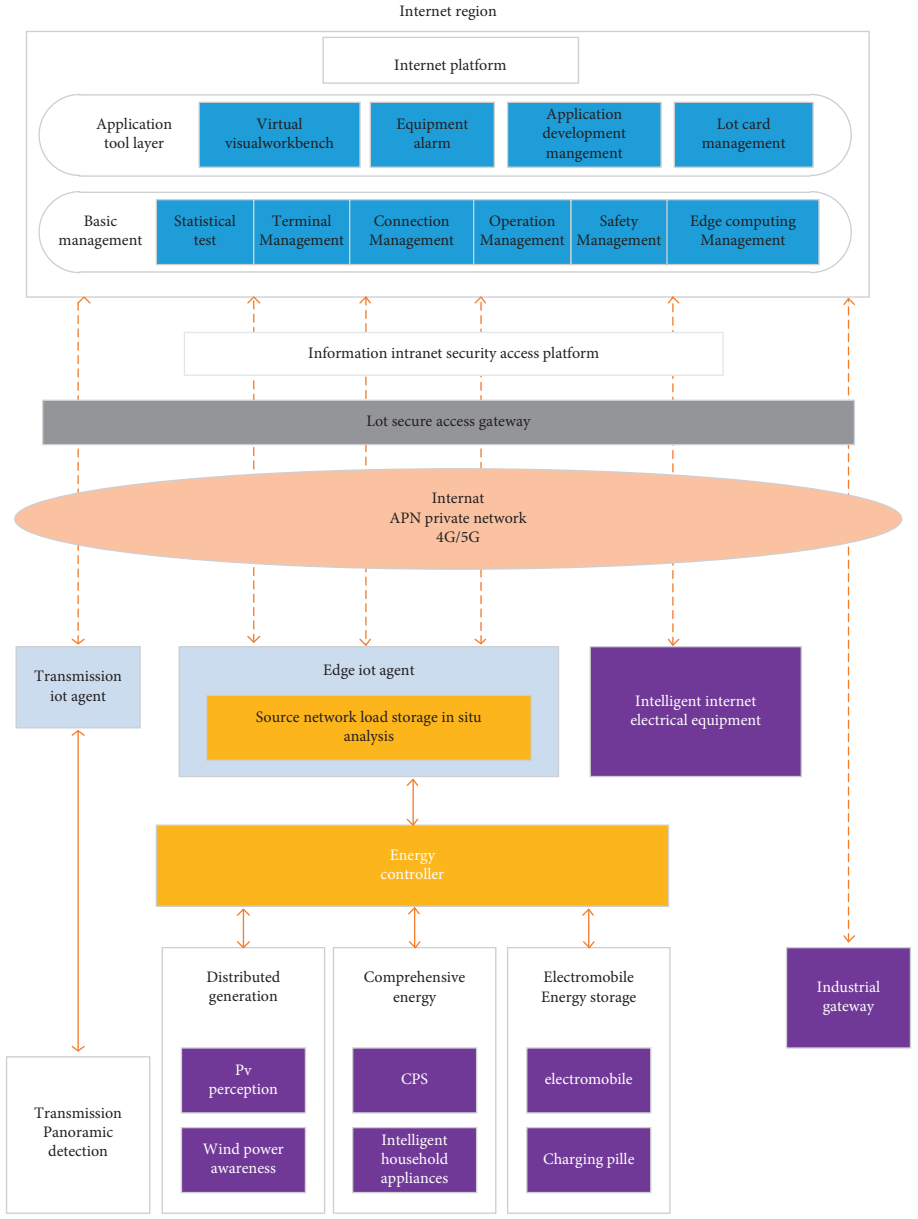

Figure 2: Logic and network data flow of the network layer in power IoT.

collaboration and interaction for power source, network, charge, and storage. Real-time coordination and optimization of the collaborative and interactive application of source, network, charge, and storage are based on massive information, such as state of charge (SOC), power generation output of new energy, and power grid operation. Based on the recognition of power grid operation mode in a stable power grid, the real-time closed-loop control of the power of common connection points, controllable power supply, charge and discharge of energy storage, and the flexible load is realized to ensure the coordinated optimal operation of the power grid. (2) Energy storage optimization. According to the spatial-temporal coupling correlation and complimentary matching characteristics of layered energy storage, the dynamic autonomous control strategy and distributed collaborative control strategy of energy storage are formulated to optimize the charging and discharging mode of energy storage and improve the power supply. (3) Optimization of electric vehicles. According to the current operating status of the system, the coordination control system in the charging station is adopted to control the charging of power electric vehicles. The system is also required to optimize the charging behavior of electric vehicles, which can enable electric vehicles actively participate in the power balance regulation of the system. (4) Management of demand side. Load demand response management mainly manages and evaluates users who participate in the demand response. The system stores user names, user addresses, contacts, contact information,

Table 1: Various potential devices accessing power IoT.

Device	Communication protocol	Data content	Area
Distributed wind-mill generator	Message queuing telemetry transport (MQTT) constrained application protocol (CoAP)	Blade angle and rotate speed, temperatures of battery box, axle box, and motor	Source
Distributed wind-mill inverter	MQTT, CoAP	Inverter status	Source
Distributed photovoltaic generator	MQTT, CoAP	DC and AC power, component temperature, daily power output, radiation value, dispersion rate, bus voltage etc.	Source
Bus converter	MQTT, CoAP	Forward active power, backward active power, forward reactive power, backward reactive power, and power factor	Source
User energy gateway	Power IoT, MQTT, CoAP	Messages of coordination command and date exchange among devices	Load
User energy gateway	Power IoT, MQTT, CoAP	Messages of coordination command and date exchange among devices	Load
Power collection terminal	Power IoT, MQTT, CoAP	Voltage, current, electric power, frequency, and power quality data	Load
Power monitoring terminal	Power IoT, MQTT, CoAP	Switch status	Load
Low voltage phasing device	Power IoT, MQTT, CoAP	Phase sequence	Load
Co-control device of charging station	Power IoT, MQTT, CoAP	Voltage, current, electric power, frequency, temperature, and operating status	Load
Energy storage centralized monitoring device	Optical fiber, industrial network protocol	Voltage, current, electric power, frequency, temperature, and state of charge	Storage
Distributed energy storage	Power IoT, MQTT, CoAP	Voltage, current, electric power, frequency, temperature, and state of charge	Storage

and maximum power response capacity. After the demand response control is delivered, the system releases the execution process of users participating in the demand response and then optimizes the implementation process of the demand response in real-time based on the actual situation.

3. Access Solution of Multiple Power Devices in Power IoT

In this section, we propose an integrated gateway to receive and process signals from various devices in power IoT. At first, we identify the requirement of multiple device simultaneous access in power IoT. Then, we present the framework of the integrated gateway, including central processing and peripheral modules. Furthermore, we specify the data format to support simultaneous accessing of multiple devices. In addition, we discuss the process of data parsing and protocol conversion.

3.1. Requirement of Multiple Devices Access in Power IoT. As discussed in Section 1, the state grid boosts the infrastructure establishment of power IoT in the past several years and there are a large number of end devices required to access the public networks. According to the suggestion and requirement from the state grid, we summarize different access requirements from source-grid-load-storage of the power grid in terms of device type, communication protocol, data content, and area as shown in Table 1.

3.2. Integrated Gateway Design for Multiple Protocols. As discussed in Section 3.1, there are various devices from source-grid-load-storage in power IoT. Therefore, the power IoT can be considered as a heterogeneous network to support different devices simultaneous accessing and data exchange. The proposed integrated gateway includes central processing and peripheral modules. As shown in Figure 3, the central processing module consists of data identification, buffer, data processing, and signal transmitting modules. The peripheral module contains ZigBee, WIFI, Bluetooth, LoRa, NB-IoT, Ethernet, and USB modules. Furthermore, power, reset, and display modules are designed. The peripheral module is connected to the central processing module by a two-way misconnection that is used for the whole system reset and running states display. The communication modules, such as ZigBee, WIFI, Bluetooth, LoRa, NB-IoT, Ethernet, and USB modules, are connected with central processing modules by a one-way link for data transmission. The central processing module also conducts the protocol conversion and cache data.

3.3. Data Preprocess and the Buffer Module Design. The data identification module is used to distinguish received signals from different end devices. In the proposed framework, ZigBee, WIFI, Bluetooth, LoRa, and NB-IoT are supported to report data to the central process modules through multiple communication ports. The received signals (i.e.,

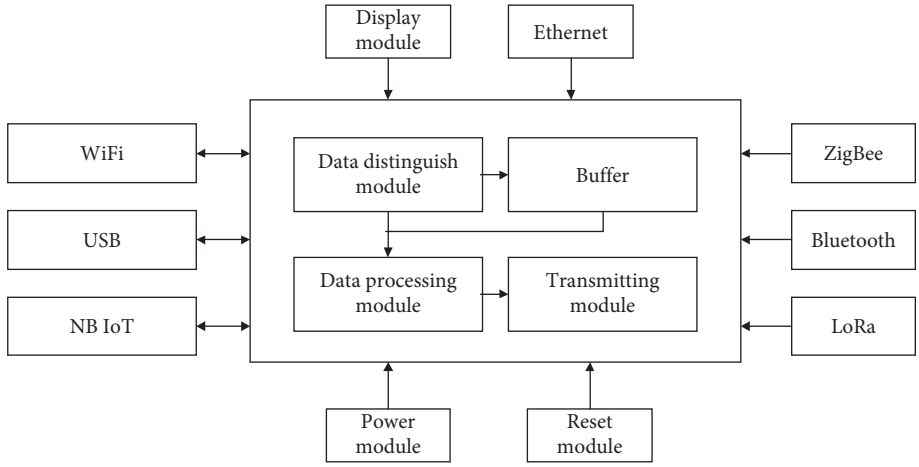

Figure 3: The framework of the proposed integrated gateway.

data frame) can be in the buffer to mitigate data congestion. As shown in Figure 4, if the data processing module is idle, the received data are sent to the data processing module. Otherwise, the received data are stored in the buffer.

We also design a buffer module to avoid data congestion in high data traffic. More specifically, the proposed buffer module provides a variable table, device type, protocol conversion, port number, IP address, and timer to store the received data, which can be used when the received data is requested by the corresponding modules. The processing flow is presented in Figure 5.

3.4. Data Processing and the Transmitting Module. The proposed data processing module is used for parsing and recombining data packets according to different protocols. For example, we can encapsulate received LoRa data after analyzing and storing data frames. Furthermore, the data processing module can reply to and coordinate different requests from other modules. We present the main flow of the data process in Figure 6. In Figure 6, the number of threads presents the performance of concurrent processing. When the volume of received data is larger than a certain threshold, the rest of the data is stored in the buffer. The new thread is called for data processing if the volume of data in the buffer is larger than the threshold. We also configure the maximum number of thresholds. If the data traffic is reduced, the threshold of data processing is also reduced when the volume of data in the buffer is small. In addition, the data transmitting module is utilized for communication between the proposed integrated gateway of power IoT and the base station. The data transmitting module can send data according to different communication types.

3.5. Peripheral Module Design. The peripheral module contains ZigBee, WiFi, LoRa, NB-IoT, and Ethernet modules, where ZigBee, WiFi, and Bluetooth can be used for short-range communications. LoRa and NB-IoT are employed for long-range communications. We observe that NB-IoT can realize large network coverage with a large number of connections and low costs. LoRa is an alternative

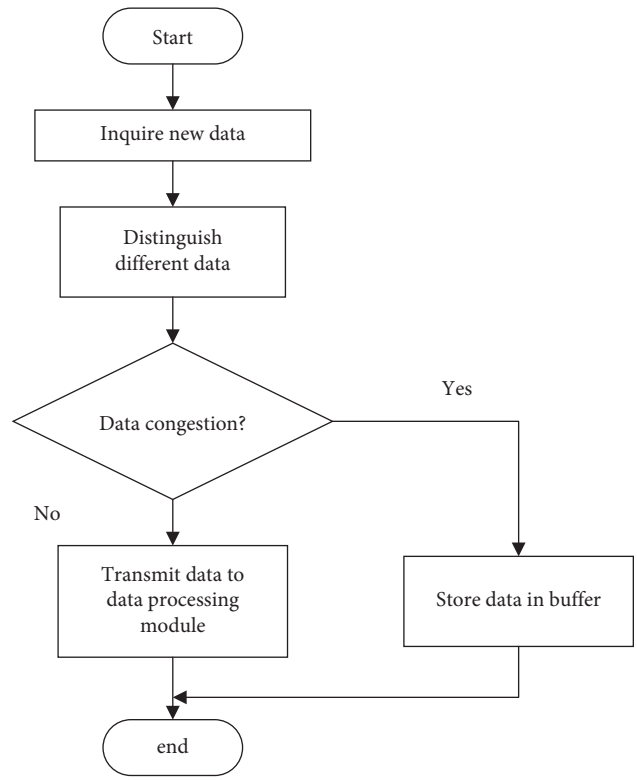

Figure 4: Data preprocessing flow.

for long-range communications with unlicensed frequency bands. We present the peripheral module in Figure 7.

We also design a power module to support the central processing, display, and peripheral modules. We adopt 3.3 V/4.2 V as working voltages for different scenarios. The reset module is used to reset the integrated gateway. The main resetting flow is shown in Figure 8.

3.6. Data Parse and Protocol Conversion. As we discussed in Sections 3.1 and 3.2, there are various end devices tended to access power IoT to report various data. However, it is worth noting that different end devices and the corresponding data format are specified by manufacturers or institutionalized.

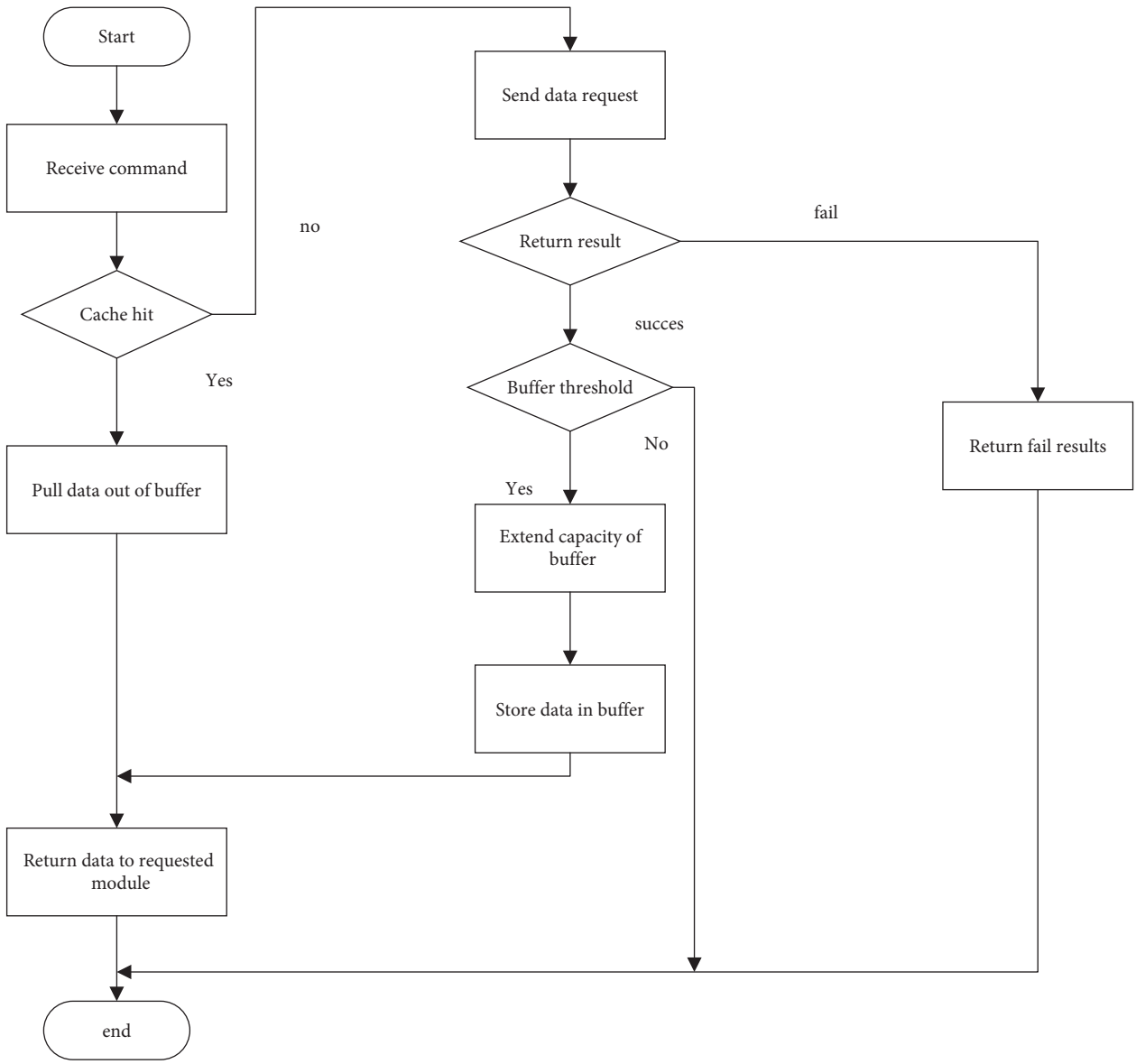

Figure 5: Buffer module design and corresponding processing flow.

Thus, we design the process of data conversion in Figure 9. We first identify the validation of the received data. If the received data is valid, we conduct the data extraction and parsing. Otherwise, we discard the invalid data packets. Then, we convert data according to the proposed uniform data format and deliver data according to different communication protocols.

In the proposed framework of the integrated gateway, we focus on data parsing and protocol conversion to process different types of data in a uniform data format. Table 2 presents the proposed data frame to uniformly process data packets.

The start field is the version number of the self-defined protocol format, which provides global authentication during version update and iteration of node data format. The authentication results are submitted to the management layer for processing. The communication parties must use the same protocol version for data exchange. The gateway system discard message with invalid format. In general, the amount of data transmitted in the Internet of Things application network is generally small. In order to make the gateway high compatibility, it is still necessary to consider the problems that occur when transmitting long data frames. To this end, a message sequence number is added into the protocol format to represent the sequence of network data transmission. The sending terminal sets the serial numbers according to its own data volume, and the receiving terminal integrates and splices data according to the defined format when receiving different serial numbers. During the network terminal equipment operation, distinguishing different each kind of data sources is required to distinguish. The unique information of each kind of data source is reflected in the control field. The control field is used to specify the message frame of specific types of control. In the concrete

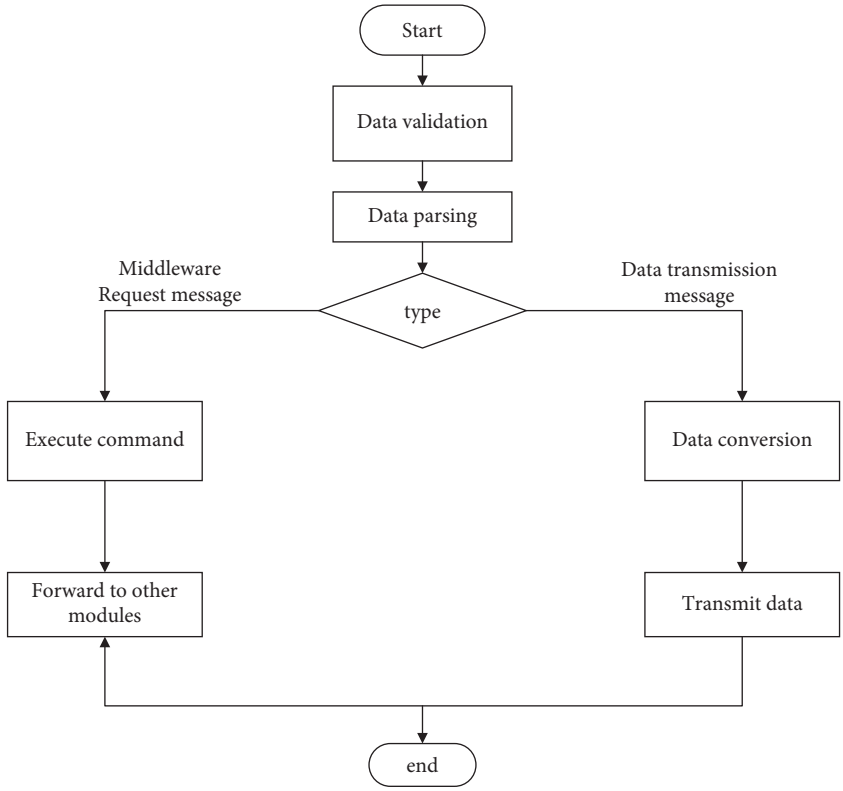

Figure 6: Data processing flow.

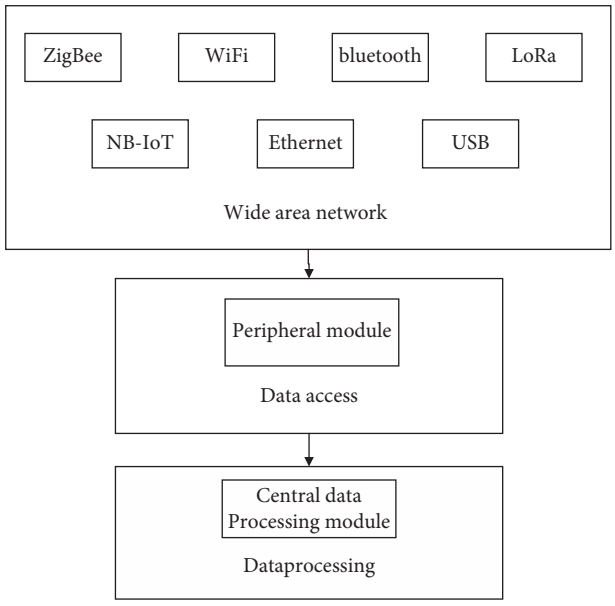

Figure 7: The framework of the peripheral module.

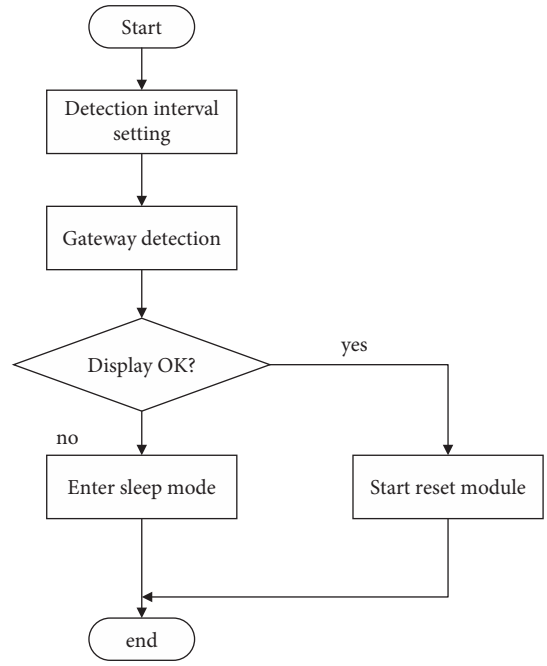

Figure 8: Display module with reset detecting flow.

implementation, the basic types include the data frame and the command frame, such as the start frame and the end frame type.

4. Performance Evaluation

We verify the dynamic loading access protocol modules for multiple end devices and corresponding middleware access based on the simulation framework with heterogeneous gateway protocols. The end devices adopt a shared library and a thread pool of Linux to enhance the reliability of simultaneous access. Specifically, we exploit the generalized object factory with the Linux shared library for a

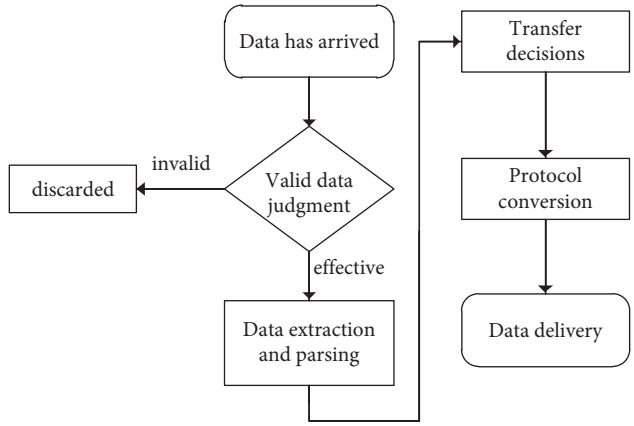

Figure 9: Data conversion process.

Table 2: Uniform data frame format in the integrate gateway.

Protocol version 1byte	Message sequence number 2 bytes	Control field 1 byte	Source address field 2 bytes	Destination address field 2 bytes	data load

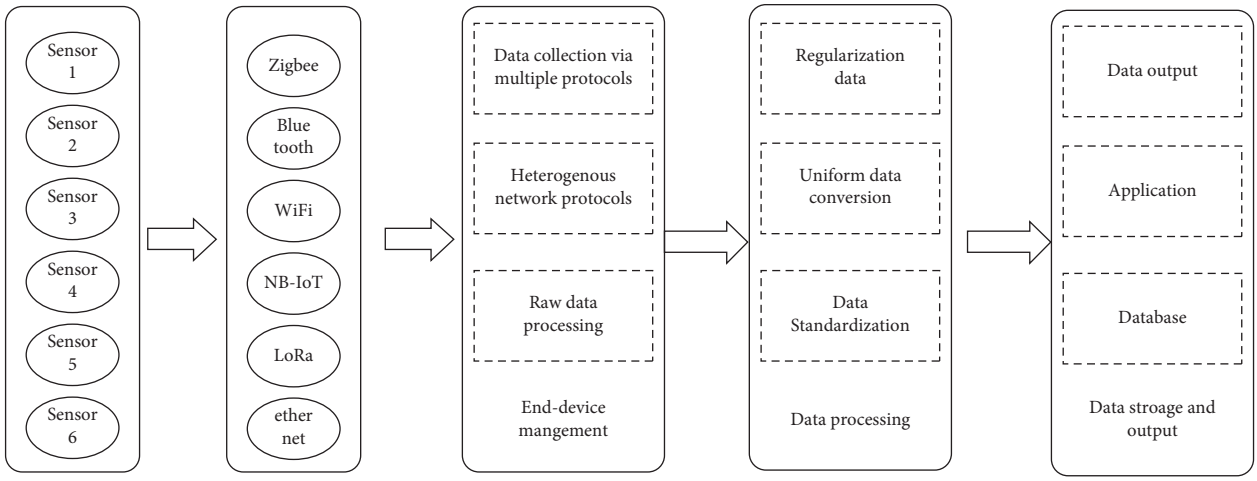

Figure 10: The simulation framework of the integration gateway for power IoT.

standardized data process, which can achieve the parse of heterogeneous application protocols with a low development cost. The simulation results show that the middleware gateway of power IoT can support access to multiple end devices simultaneously and avoid the heterogeneity of communication and application protocols. Furthermore, the gateway of power IoT can work well when a large number of new end devices are accessed, which can be utilized in different applications. We conduct the simulation and evaluate performance in terms of dropped packet ratio and system communication delay.

4.1. Simulation Configuration. We use Visual Studio as the main IDE (integrated development environment). "makefile" is used to define, compile, and link rules of the entire system and "CMake" is used to parse the commands in the makefile and to achieve automatic compile. We also run the system in Linux with C language due to the high requirement of computational and spatial complexity of protocol conversion. The simulation framework is shown in Figure 10. In Figure 10, according to the design objective, there are three modules in the framework, including end devices management, data processing, data output, and saving module.

The end device management module is for heterogeneous communication protocols, which is consisted of concurrent data collection with multiple protocols, the shared library of the heterogeneous communication protocols, and original data processing and analysis. To be more specific, data generated by heterogeneous sensor networks and sensors are collected by the end device management

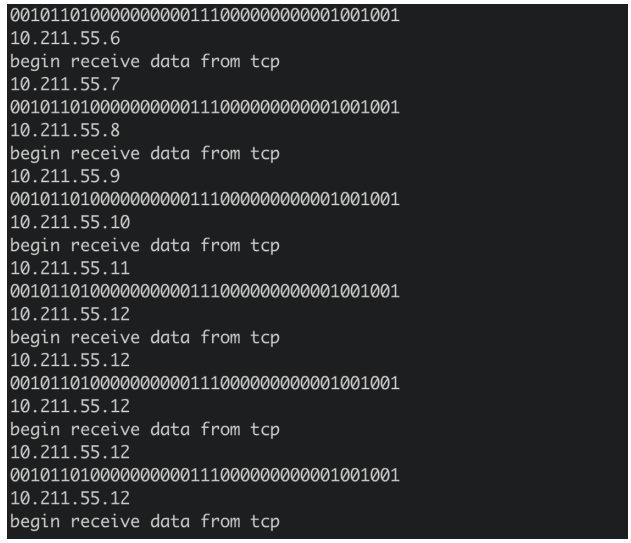

Figure 11: Average dropped packet ratio vs. number of sensors.

Table 3: Average delay.

Experiment number		1 (ms)	2 (ms)	3 (ms)	4 (ms)	5 (ms)	6 (ms)	7 (ms)
Number of sensors	6	58.08	61.00	55.80	62.41	50.23	66.15	62.29
	12	68.24	85.10	74.35	76.95	80.14	73.56	69.17
	18	85.36	92.68	87.44	91.40	88.46	93.54	83.39
	24	94.08	99.00	95.13	102.16	96.39	98.86	100.57

module, which is transmitted to the data processing module for parse. This end device management module is able to collect concurrent data from the perceived layer in different power IoT. Meanwhile, the integration gateway enhances access to new networks, such as sensor networks and IoT.

The standardized data processing module consists of rules of data processing, data conversion, and standardized data processing, which is used for heterogeneous application protocols. The collected data from the end device management module are extracted, compressed, and mapped for the required standardized data format. The standardized data processing module can immediately identify the data source with which sensors when receiving different data from different sensors. The data is also mapped to meet the application requirements. The data output and storage module has two parts, such as data output and database, which store the standardized data in the database and output the standardized data to applications.

4.2. Performance Evaluation. We verify the functionality of the integrated gateway for power IoT by simulating delivery data to the middleware of the gateway with multiple protocols. We generate data by running simulations on windows. The middleware gateway is working on the virtual machine that runs Ubuntu. The virtual serial port software is connected to COM1 and COM3. COM1 is on a PC and COM3 is on a virtual machine. Moreover, multiple protocol data generators can achieve data delivery between PC and gateway using TCP and UDP. The data generator can simulate six different sensor data. These different data can be parsed by functions implemented in the middleware gateway.

As shown in Figure 11, the proposed integrated gateway can achieve multiple sensors simultaneous access. The communication delay of the middleware gateway is defined as the time duration from receiving one frame at serial ports to storing this frame in the database. We deploy 6, 12, 24, and 30 sensors in the end device management module, respectively. Each sensor transmits 100 copies. There are six communication approaches in these sensors and the transmitting period is 5s. We conduct 7 experiments in 5 groups. The simulation results are reported in Table 3.

It is obvious that the average delay is caused by protocol conversion, data processing, and queuing delay. With the increase in the number of sensor nodes, the average delay increases. The average delay is less than 100 ms defined as IPTD in CCSA. We also observe that the protocol conversion and data processing results in the average delay, whereas the queuing delay is not the main factor of average delay. In practice, we should consider the propagation delay of the signal (which can be ignored when the transmission delay is short).

Figure 12 shows that the average dropped packet ratio increases when the number of communication protocols is larger. Moreover, the average dropped packet ratio also increases when the number of sensors increases. Time-out caused by data processing and queuing are the main factors in discarding packets.

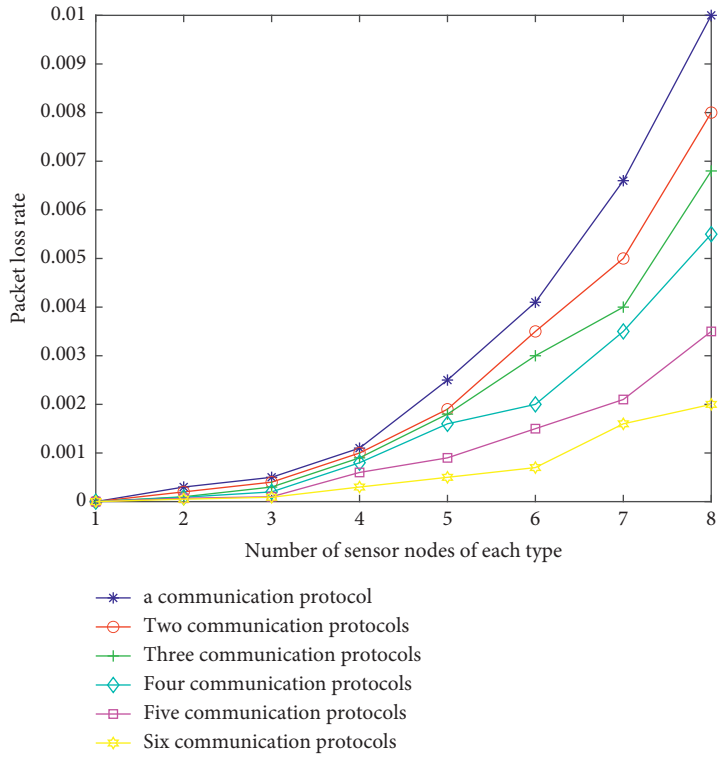

Figure 12: Average dropped packet ratio vs. number of sensors.

5. Conclusion

In this paper, we study the typical architecture of power IoT and the corresponding layer in terms of functionality and characteristics. Based on the comprehensive understanding of power IoT, we propose an integrated gateway for power IoT. The simulation result shows that the proposed gateway can support multiple protocols and multiple end devices for simultaneous access. In the future, we will implement the prototype of different layers of power IoT and conduct field experiments.

Conflicts of Interest

The authors declare that they have no conflicts of interest.

Authors' Contributions

Conceptualization was done by Fei Yu; methodology was done by Fei Yu, Wei Rao, Chang Liu, Jin Wang, and Liang Zhou; software was done by Li Tian and Jie Wang; formal analysis was conducted by Jiangpei Xu and Chang Liu; resources were carried out by Chang Liu; data curation was done by Chang Liu; writing-original draft preparation was written by Fei Yu and Wei Rao; visualization was done by Jin Wang and Liang Zhou; supervision was supervised by Rao Wei. All authors have read and agreed to the published version of the manuscript.

References

[1] B. Mazon-Olivo and A. Pan, "Internet of things: state-of-the-art, computing paradigms and reference architectures," *IEEE Latin America Transactions*, vol. 20, no. 1, pp. 49–63, 2022.

[2] Y. Liu, K. Wang, K. Qian, M. Du, and S. T. Guo, "Tornado: enabling blockchain in heterogeneous internet of things through a space-structured approach," *IEEE Internet of Things Journal*, vol. 7, no. 2, pp. 1273–1286, 2020.

[3] J. A. Ansere, G. Han, L. Liu, Y. Peng, and M. Kamal, "Optimal resource allocation in energy-efficient Internet-of-Things networks with imperfect CSI," *IEEE Internet of Things Journal*, vol. 7, no. 6, pp. 5401–5411, 2020.

[4] H. Tran-Dang, N. Krommenacker, P. Charpentier, and D. S. Kim, "Toward the internet of things for physical internet: perspectives and challenges," *IEEE Internet of Things Journal*, vol. 7, no. 6, pp. 4711–4736, 2020.

[5] H. Rao, W. Wu, T. Mao et al., "Frequency control at the power sending side for HVDC asynchronous interconnections between Yunnan power grid and the rest of CSG," *CSEE Journal of Power and Energy Systems*, vol. 7, pp. 105–113, 2020.

[6] X. Zhang, Y. Chen, Y. Wang et al., "Reactive voltage partitioning method for the power grid with comprehensive consideration of wind power fluctuation and uncertainty," *IEEE Access*, vol. 8, pp. 124514–124525, 2020.

[7] J. Li, W. Chen, Y. Chen et al., "A survey on investment demand assessment models for power grid infrastructure," *IEEE Access*, vol. 9, pp. 9048–9054, 2021.

[8] P. Mayer, M. Magno, and L. Benini, "Smart power unit-mW-to-nW power management and control for self-sustainable IoT devices," *IEEE Transactions on Power Electronics*, vol. 36, no. 5, pp. 5700–5710, 2021.

[9] G. Bedi, G. K. Venayagamoorthy, R. Singh, R. R. Brooks, and K. C. Wang, "Review of Internet of things (IoT) in electric power and energy systems," *IEEE Internet of Things Journal*, vol. 5, no. 2, pp. 847–870, 2018.

[10] A. Shiyun, L. Jianning, L. Wenjie, T. Ye, J. Peibo, and W. Yinzhong, "Data analysis and cloud computing of power grid infrastructure projects under the background of informatization," in *Proceedings of the IEEE 4th International Conference on Automation, Electronics and Electrical Engineering*, pp. 524–527, IEEE, Shenyang, China, November 2021.

[11] Z. Jiangfeng, L. Chunxiao, S. Shuzhe et al., "Research on decision-making optimization for operation system of power grid framework under smart grid and dijkstra algorithm," in *Proceedings of the IEEE International Conference on Data Science and Computer Application*, pp. 378–382, IEEE, Dalian, China, October 2021.

[12] X. Han, G. Zheng, D. Qin, Q. Chen, and Z. Xu, "Research on informatization planning and control design of power grid enterprises based on enterprise architecture," in *Proceedings of the IEEE Conference on Telecommunications, Optics, and Computer Science*, Shenyang, China, December 2020.

[13] R. Al-Syouf, M. M. Shurman, A. Alma'Aitah, and S. H. Alnabelsi, "A novel gateway selection protocol for three-layers integrated wireless networks," in *Proceedings of the IEEE-7th International Conference on Internet of Things: Systems, Management and Security*, December 2020.

[14] C. Shuo, W. Xinyun, Q. Jun, L. Qingyu, and Z. Rongkun, "Research on the logical relationship between multi-level resources in the operation mode of electric power communication," in *Proceedings of the 2020 International Conference on Wireless Communications and Smart Grid*, ICWCSG, Qingdao, China, June 2020.

[15] D. An and Y. Chen, "Digital twin enabled methane emission abatement using networked mobile sensing and mobile actuation," in *Proceedings of the 2021 IEEE 1st International Conference on Digital Twins and Parallel Intelligence*, DTPI, Beijing, China, August 2021.

[16] B. W. Yudha, S. Sasmono, W. Priharti, F. N. Nursalam, and Y. T. Asidda, "Spatial approach on the isolated island variable renewable energy based electricity planning," in *Proceedings of the International Electrical Engineering Congress*, pp. 1–4, iEECON, Khon Kaen, Thailand, March 2022.

[17] S. Stock, D. Babazadeh, and C. Becker, "Applications of artificial intelligence in distribution power system operation," *IEEE Access*, vol. 9, pp. 150098–150119, 2021.

[18] M. H. Lipu, M. S. Miah, M. Hannan et al., "Artificial intelligence based hybrid forecasting approaches for wind power generation: progress, challenges, and prospects," in *IEEE Access*vol. 9, pp. 102460–102489, IEEE Access, 2021.

Hindawi
Mobile Information Systems
Volume 2022, Article ID 2456151, 11 pages
https://doi.org/10.1155/2022/2456151

Research Article

Mobile Platform for MOCC Music Hybrid Teaching Based on Convolutional Neural Network

Xin Li

Daqing Normal University, Daqing, Heilongjiang, China

Correspondence should be addressed to Xin Li; li-xin@dqnu.edu.cn

Received 3 June 2022; Revised 29 June 2022; Accepted 13 July 2022; Published 3 August 2022

Academic Editor: Shadi Aljawarneh

With the wide application of Internet mobile devices in many industries, the hybrid teaching mode of online and offline has also become a research hotspot in the field of education. In the process of constructing the music online teaching platform based on mobile platform MOOC, the distribution of samples will affect the data recognition results of the system. Therefore, this paper uses convolutional neural network as the backbone network to extract data features and improve the resolution. At the same time, in the process of data compression, this paper realizes the global average pool and unified parameters by improving the attention mechanism, so that all parameters interact with their K adjacent parameter characteristics, so as to reduce the overdependence between channels and reduce the complexity of the overall calculation. For the analysis of complexity, this paper detects the time required for serial training and parallel training, intercepts the average value of the parameters of all nodes, and obtains the optimal number of nodes of this model. Finally, combined with the characteristics of music teaching, this paper designs a mobile MOOC music teaching platform based on convolutional neural network. The platform includes modules such as basic information management and music course resource construction and applies it to the actual music course teaching process. The performance of the algorithm and the feasibility of the system are verified by classroom activity test, hoping to provide some reference for the research in the field of music mixed education.

1. Introduction

Since the popularization of Internet and mobile communication technology, it has been more and more widely used in many fields, including the education industry [1]. Affected by the COVID-19, the pace of reform in the education industry has gradually accelerated. One of the innovations is MOOC online teaching with the help of Internet and mobile platform technology [2]. The traditional teaching mode can not meet the requirements of home-based learning during the epidemic. At the same time, there are some defects, such as single teaching mode and fixed teaching methods. With the development and application of intelligent teaching software based on mobile terminals, the emergence of online teaching system has added new learning means for students, which truly realized the acquisition of new knowledge at home and anywhere [3]. Students can also freely choose appropriate educational resources according to their preferences, which is conducive to the cultivation of personality [4]. However, there are still many deficiencies in the current online teaching system. Due to the lack of face-to-face communication between teachers and students, they cannot detect the actual learning situation of students in time and can not explain students' questions in detail. Therefore, relying solely on the online teaching system can not achieve better teaching results. The mixed teaching mode of "Online + offline" has solved these problems to a certain extent and has gradually attracted extensive attention in the field of education [5].

MOOC not only makes it convenient for students to carry mobile devices to the classroom, but also ensures the actual learning effect with the help of mobile devices [6]. The online teaching platform represented by MOOC also has the teaching activities of offline classroom, including new course teaching, classroom tasks, teacher-student interaction, after-school homework, and learning notice. At the same time, it

also has the functions that offline classroom cannot realize in class, such as learning record, real-time test, and teaching feedback [7]. In addition, combined with the practicality and professionalism of music teaching, the online teaching system needs to realize stronger functions such as voice interaction, voice recognition, audio and video production and recording, and multimedia playback, which requires the online teaching system to realize these functions with the help of a variety of computer technologies [8]. The application of convolutional neural network can improve the recognition accuracy of massive training data, solve the problem of difficult model training, and realize the recognition task of large-scale samples [9]. The application in the design of online music teaching system on mobile platform can improve the operation efficiency of the system and improve the speed of model training [10]. Therefore, after analyzing the background of music mixed teaching, this paper puts forward the application and design of mobile platform MOCC teaching system based on convolutional neural network.

2. Related Work

The concept of mixed teaching is defined in the literature as follows: combining the advantages of traditional learning methods with the advantages of network learning, we should give full play to the guiding role of teachers as knowledge instructors and control the whole teaching process. We should also take students as the center and give full play to students' subjective initiative as the main body of the classroom. Mixed teaching realizes the characteristics of the two teaching methods. The literature interprets MOOC as "online large-scale open courses," that is, a new teaching method with the characteristics of openness, large-scale, and online [11]. The literature mentioned that MOOC not only is a simple online video course, but also covers a variety of teaching resources, learning communities, student management systems, comprehensive evaluation systems, and other teaching means [12]. It is a digital form of offline courses. The literature emphasizes that MOOC is different from the general teaching method and adopts the form of networking and informatization [13]. Therefore, in the course design, we need to consider the characteristics of the network platform, and the user's computer operation ability is also one of its influencing factors. According to the literature, in addition to providing free online teaching resources, MOOC also has the function of managing large-scale learning users [14]. It can realize thousands of people's online learning, examination, test, and interactive communication at the same time, which can not be realized in the traditional classroom. At the same time, it is also the biggest feature that MOOC is different from the general classroom. The importance of MOOC is explained in the literature. It is believed that the online teaching platform with MOOC as the main form has realized remote teaching, created a new teaching mode, and truly promoted the dissemination of knowledge. Many scholars have questioned this teaching method. For example, the literature believes that online teaching systems should be carefully selected and used, especially for the courses of primary and secondary school students. The literature suggests that we should rationally treat online teaching methods such as MOOC, not blindly follow, let alone try to replace offline teaching methods [15]. We should combine the two and carry out mixed teaching. Through the research on MOOC and microcourses in the literature, it is considered that, at this stage, online teaching can only be used as an auxiliary way of professional teaching, and offline teaching should still be the main teaching method. Especially with regard to the practical application of online teaching platform, the literature believes that the development of computer and Internet technology at this stage can not meet the needs of large-scale online teaching, so the hybrid teaching mode of online and offline combination is particularly important [16].

In order to further improve the reliability of online teaching platform, the literature studies the effectiveness of students' evaluation function of online teaching platform by collecting the data of multiple MOOC platforms and using data analysis software. Experiments show that the online teaching platform can effectively grasp students' learning situation, and the function of students' mutual evaluation can also reflect students' learning achievements to a certain extent [17]. The operation of online teaching platform is inseparable from the development of computer technology. For example, the literature introduces the advantages of convolutional neural network and other algorithms in system target recognition, especially with the continuous improvement of the accuracy and real-time of convolutional neural network target detection algorithm, which greatly promotes its application in many fields [18]. Combined with the characteristics of music teaching, there are high requirements for the recognition of voice and video resources. It is mentioned in the literature that, compared with other computer algorithms, the speech recognition technology based on deep learning can extract features through the training of a large amount of data. In contrast, this method can improve the accuracy and accuracy of recognition. At the same time, it is also relatively simple and feasible in model construction. The literature shows that the convolutional neural network under the deep learning framework has strong network weight sharing characteristics, which can reduce the weight parameters required by the network in the system, so as to improve the performance of the whole network system and improve the accuracy of speech and image recognition. This is very important for music teaching system. In addition, in the research of music teaching, the literature mentioned that the existing music education in colleges and universities has different degrees of disadvantages, such as insufficient informatization, relatively closed teaching environment, and single teaching equipment. These problems can be solved through the Internet and computer technology, especially the application of online teaching methods such as MOOC. This is also one of the research focuses of this paper.

3. Research on Convolutional Neural Target Recognition for Mobile Terminals

3.1. Basis of Convolutional Neural Network. Compared with the traditional recognition methods, convolution neural network algorithm can distinguish the target faster in many training data and extract the data features of the image, mainly including convolution layer, pooling layer, activation layer, full connection layer, and batch normalization layer.

3.1.1. Convolution Layer. Suppose that the coordinates of the recognition target channel are (I, J), the size of the convolution kernel is $m * n$, and the weight of the convolution kernel is ω. Image brightness is v. The forward propagation process of the image through the convolution layer is shown in

$$Out\,put_{x,y} = \sum_{i}^{m*n} \omega_i v_i. \tag{1}$$

3.1.2. Pool Layer. In order to ensure that the edge information of the sample can be fully utilized, the filling operation will be used to roll up the layer. The output result is shown in

$$\text{Output} = \frac{\left(\text{map}_{\text{size}} - \text{kenerl}_{\text{size}} + 2 * \text{padding}\right)}{\text{stride}} + 1. \tag{2}$$

3.1.3. Active Layer. The activation layer is to activate the function to ensure the nonlinearity of the network and make the detection target more accurate and specific. Among them, the neural network can use sigmoid as the activation function, and the output expression is as shown in

$$\sigma(x) = \frac{1}{1 + e^{-x}}. \tag{3}$$

Meanwhile, the output expression of tanh is

$$\tanh(x) = \frac{1 - e^{-2x}}{1 + e^{-2x}}. \tag{4}$$

The common feature of sigmoid and tanh is that when the input is large or small, the gradient is almost 0. In order to avoid this situation and improve the network speed, this paper adopts the commonly used activation function relu, and its output expression is

$$\text{Re}LU(x) = \max(0, x). \tag{5}$$

3.1.4. Full Connection Layer. The full connection layer is mainly to provide different detailed feature recognition results for the convolution layer and reduce the error caused by feature position offset to feature classification. In fact, the full connection layer can also be said to be a data classifier.

3.1.5. Batch Normalization Layer. The batch normalization layer is usually used after the convolution layer. Firstly, learnable parameters are introduced γ and β. Define the batch input data and calculate its mean value, as shown in

$$\mu_B = \frac{1}{m} \sum_{i=1}^{m} x_i. \tag{6}$$

The variance of the data is

$$\sigma_B^2 = \frac{1}{m} \sum_{i=1}^{m} (x_i - m_B)^2. \tag{7}$$

Then standardize this part of data, and the result is shown in

$$\widehat{x}_i = \frac{(x_i - \mu_B)}{\sqrt{\sigma_B^2 + \varepsilon}}. \tag{8}$$

With learnable parameters γ, β, and normalized output, the final result is

$$y_i = \gamma \widehat{x}_i + \beta. \tag{9}$$

3.2. Improved Attention Mechanism. As mentioned earlier, in order to ensure that the edge information of the sample can be fully utilized, the filling operation will be used to roll up the layer. At the same time, the method of global average pooling will be adopted in the process of data compression; that is, the global spatial information compresses the nonlocal information. Its expression is as follows:

$$Z_C = F_{sq}(u_c) \frac{1}{H * W} \sum_{i=1}^{H} \sum_{j=1}^{W} u_c(i, j). \tag{10}$$

Next, in order to obtain the correlation between different channels, the method of expanding channels is adopted, as shown in

$$S = F_{ex}(z, W) = S(g(z, W)) = S\left(W_2 d\left(W_1 z\right)\right). \tag{11}$$

In the local communication module, the expression method of channel weight is shown in

$$\omega = s\left(f_{\{w\}} g(c)\right). \tag{12}$$

Let W be the width of the model feature, H be the height, and the channel parameter set $G(x)$ be

$$g(x) = \frac{1}{wh} \sum_{i=1,j=1}^{w,h} x_{i,j}. \tag{13}$$

The features after regularization are

$$f_{\{w\}} = \text{Re}LU(wy). \tag{14}$$

Formula (14) shows that this linear model is predictable. Therefore, the characteristic information of a parameter Y_i and K adjacent parameters are interacted, and the result is shown in

$$w_i = s\left(\sum_{i=1,j=1}^{k} w_i^j y_i^j\right). \tag{15}$$

In order to unify the parameters, all parameters are interacted with the characteristic information of K adjacent parameters:

$$\omega_i = \sigma\left(\sum_{j=1}^{k} \omega^j j^j\right). \tag{16}$$

Although the improved attention mechanism increases the complexity of part of the time, on the whole, the spatial complexity is greatly reduced because of the interaction of K channel feature information, which improves the overall performance of the system.

3.3. Time Complexity Analysis of Serial Training and Parallel Training. For the analysis of complexity, this paper detects the time required for serial training and parallel training and intercepts the average value of local parameters of all nodes, that is,

$$\left(W^{\text{out}}, b^{\text{out}}\right) = \frac{\left(W_2^{\text{out}}, b_2^{\text{out}}\right) + \cdots + \left(W_{m-1}^{\text{out}}, b_{m-1}^{\text{out}}\right)}{N-2}. \tag{17}$$

BP neural algorithm is divided into three stages: forward propagation, backpropagation, and parameter update. Suppose the total number of training samples is a, the number of training is B, and the hidden layer 1 contains three layers of neural networks, n_1, n_2, and n_3, respectively. The time used for point multiplication is T_m, the time used for addition is Ta, and the time used for activation value is T_{ac}. The forward propagation time of a sample is

$$\begin{aligned} t_1 &= \left(n_1 n_2 t_m + n_2 t_a + n_2 t_{ac}\right) + \left(n_2 n_3 t_m + n_2 t_a + n_3 t_{ac}\right) \\ &\approx n_2\left(n_1 + n_3\right) T_a + t_{ac}\left(n_2 + n_3\right). \end{aligned} \tag{18}$$

Of that,

$$T_a = \left(t_m + t_a\right). \tag{19}$$

The time required for backpropagation is about

$$t_a = n_2 n_3 T_a. \tag{20}$$

The time required to update the parameter matrix between the three-layer neural networks is about

$$t_3 = n_2\left(n_1 + n_3\right) T_a. \tag{21}$$

The duration of serial training is

$$T_{ser} = AB\left(t_1 + t_{2+} t_3\right) = AB\left[\left(2n_1 + 3n_3\right) n_2 T_a + \left(n_2 + n_3\right) t_{ac}\right]. \tag{22}$$

Set

$$\beta = 2n_1 + 3n_3 + \alpha. \tag{23}$$

Then,

$$T_{ser} = AB\left(\beta n_2 + \alpha n_3\right) T_a. \tag{24}$$

Assuming that there are n data nodes and each node is equally divided into N/A samples, the training duration of each single node is

$$t_{par\_d} = \frac{A}{n}\left(t_1 + t_2 + t_3\right) = \frac{A}{n}\left(\beta n_2 + \alpha n_3\right) T_a. \tag{25}$$

The algebraic sum of training time is

$$T_{par\_d} = \frac{A}{n} B\left(t_1 + t_2 + t_3\right) = \frac{AB}{n}\left(\beta n_2 + \alpha n_3\right) T_a. \tag{26}$$

Finally, the time result of parallel training batch BP algorithm is as follows:

$$T_{par} = T_{par\_d} + nT_{\text{com}} = \frac{AB}{n}\left(\beta n_2 + \alpha n_3\right) T_a + nT_{\text{com}}. \tag{27}$$

4. Design and Implementation of the Music Teaching System Based on Mobile Platform MOCC

4.1. Overall System Architecture. This system adopts Java EE framework structure and Android client. The system is divided into three layers, including function presentation layer, business logic layer, and data layer. The system architecture is shown in Figure 1.

The functional expression layer of the system covers the core functions, mainly including basic information management, online classroom management, and so on. The business logic layer includes the basic permission setting, query setting, and system configuration of the system. The data layer is mainly the database management of the system, which is an important part of the system. The functions of each server are independent and interconnected to jointly maintain the integrity and scalability of the system.

Combined with the characteristics of music teaching, the online intelligent teaching system designed in this paper focuses on the mobile platform technology, covers all links of offline teaching, and adds intelligent lesson preparation and teaching reflection links. The overall function of music teaching platform is shown in Figure 2.

The music teaching mode of mobile platform is the same as offline teaching, including three links before, during, and after class. Among them, teachers are assisted in intelligent lesson preparation by means of intelligent push of teaching resources before class. The links in the course include using the online teaching platform for real-time interaction, monitoring the teaching process, recording students' learning data, and timely learning situation analysis. The after-school link mainly aims at students' learning situation, provides personalized guidance for students, and carries out intelligent reflection teaching. The realization of the whole teaching process needs the technical support of mobile platform and the provision of adaptive resources to ensure the stable operation environment of the system.

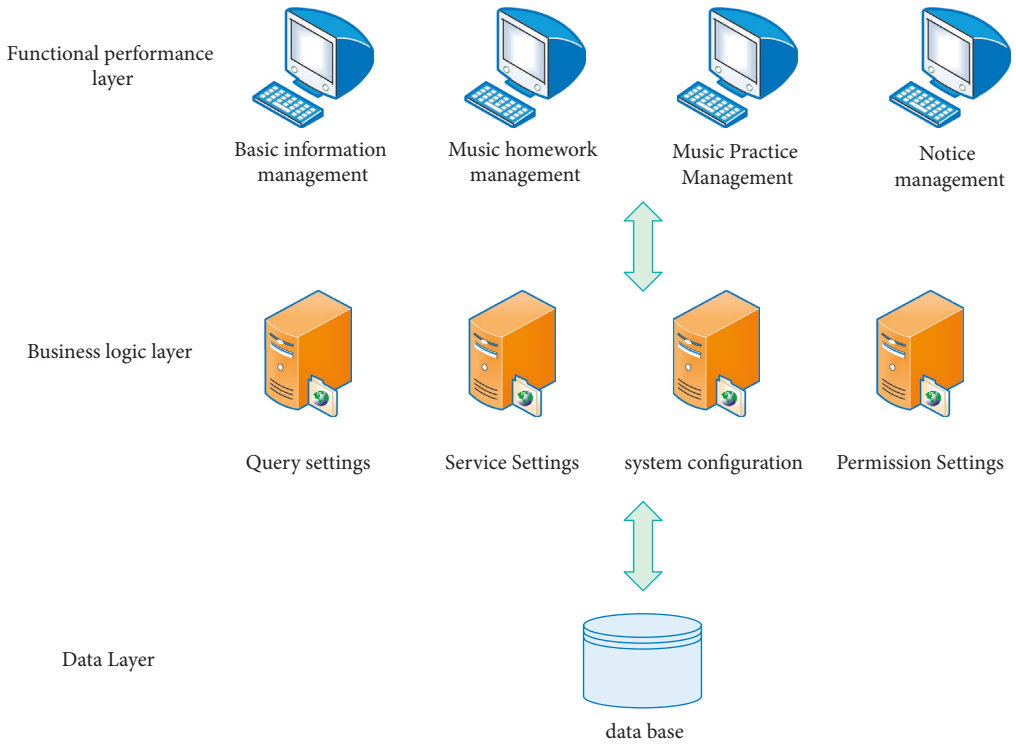

Figure 1: System architecture.

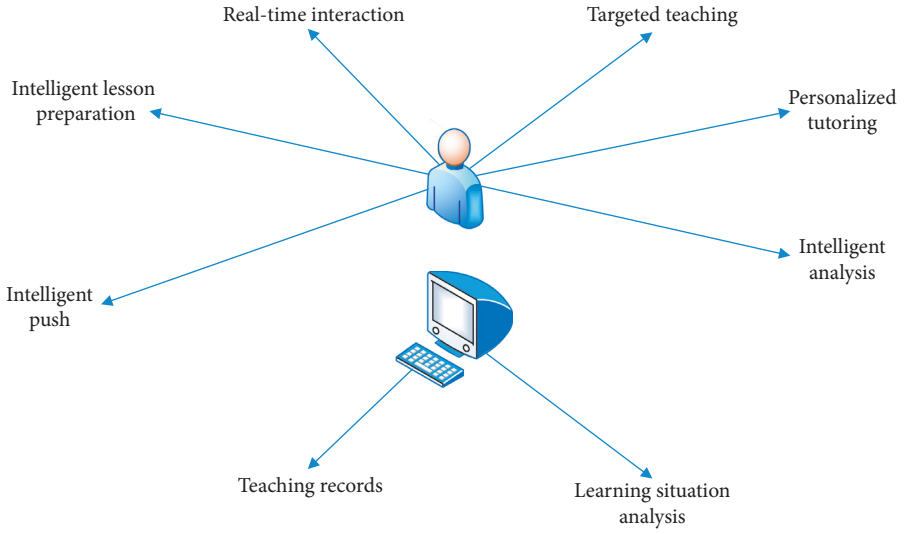

Figure 2: Mobile platform music teaching mode.

4.2. Design of the System Database Table. The design of database table is an important part of system physical design. In the construction of mobile platform music teaching system, the database table design of this paper mainly includes student information table, course information table, music resource information table, consultation information table, daily notice information table, and attachment information table. This chapter selects some tables to describe the main fields.

4.2.1. Student Information Form. The student information table is mainly used to store the basic information of students, such as name, student number, gender, and other information. The specific field description is shown in Table 1.

4.2.2. Course Information Sheet. The course information table is mainly used for students' course related information, such as semester, course name, major, teacher, and other information. The specific field description is shown in Table 2.

4.2.3. Music Resource Information Table. Music resource information table is mainly used to store the information of music video, audio, and other resources on the course

Table 1: Student information table.

Field name	Field identification	Type	Size	Allow to be empty	Remarks
Name	Studname	Varchar	20	N	Primary key
Student ID	Studno	Integer	20	N	—
Gender	Sex	Integer	10	N	—
Age	Age	Number	20	Y	—
Nationality	Nation	Integer		Y	—
Profession	Major	Integer	20	N	—
Student category	Leixing	Integer	20	N	Foreign key
Address	Address	Varchar	20	Y	—
Telephone	Telph	Varchar		Y	—
Photo	Ptoto	Varchar		Y	—
Remark	Bz	Varchar	50	Y	—

Table 2: Course information.

Field description	Field identification	Field type	Size	Allow to be empty	Remarks
School name	Schname	Varchar	20	N	Primary key
Semester	Term	Varchar	20	N	—
Classification	Lesson	Varchar	20	Y	—
Profession	Major	Integer	20	Y	—
Teacher number	Teacher	Integer		Y	—
Student number	Studnum	Integer	20	Y	—
Classroom	Room	Varchar		Y	—
Week	week	Varchar		Y	—
Review time	Shsj	Datetime	32	N	—
Reviewer	Checkman	Varchar	32	N	—
Uploader	Addman	Varchar	32	N	Foreign key
Remark	BZ	Varchar	50	Y	—

system, such as the name, type, upload time, uploader, and other information of music. The specific field description is shown in Table 3.

4.2.4. Music Information Table. The information table is mainly used to store the music related information released in the teaching system and assist teachers in teaching, such as information category, release time, specific content, number of visitors, and other information. The specific field description is shown in Table 4.

4.2.5. Daily Notice Information Form. The daily notice information table is mainly used to store the relevant notice information released by teachers in music online courses, including the arrangement of various teaching links. The database table mainly describes the notice title, notice content, release time, publisher, and other information. The specific field description is shown in Table 5.

4.2.6. Annex Information Sheet. The attachment information table is used to store the attachment information of documents related to students' works, including course assignments and works. The database table mainly describes the name, style, upload time, and other information of works. The specific field description is shown in Table 6.

4.3. Analysis of Simulation Experiment Results. In this paper, the training time of a single node is calculated by BP neural algorithm, and the data complexity of the system is analyzed. In order to further obtain the optimal number of nodes of the system model, the training efficiency under different number of nodes is calculated, and the results are shown in Figure 3.

As can be seen from Figure 3, there is little difference in the recognition rate when the number of nodes is 4, 6, and 8, and the stable recognition rate can be reached faster than serial training. At the same time, when the number of nodes is 4 and 8, the training time is more than when the number of nodes is 6, which verifies that the optimal number of nodes of the system model is 6. According to the analysis of the actual situation of the system, this result is mainly because the training efficiency of the system can reach the optimal saturation state when the number of nodes is 6. Therefore, in this case, the increase or decrease of the number of nodes will only increase the identification time of the system and reduce the operation efficiency. The optimal number of nodes is determined according to the characteristics of the system model, the amount of data, and the performance of hardware facilities. Therefore, the optimal number of nodes of different systems will also vary greatly.

In addition to the basic system performance, this paper also tests the basic performance of the login and discussion function module of the online music teaching system. The results are shown in Figures 4 and 5.

Table 3: Music resource information.

Field description	Field identification	Field type	Size	Allow to be empty	Remarks
Music resource ID	Id	Long		N	Primary key
Music name	Music	Varchar	32	N	—
Music	Type	Int	2	N	—
Belong to the country	Country	Varchar	16	Y	—
Profile	Introduction	Varchar	32	Y	—
Upload time	Upload	Datetime		Y	—
Uploader	Addman	Varchar	32	Y	—
Storage path	Storage	Varchar	32	Y	—
Music list ID	List	Long		Y	External key
Whether to pass the review	Audit	Int		N	0-Unparalleled; 1-pass
Music classification description	Classification	Varchar	32	N	—
Music comment	Review	Varchar	128	Y	—
Actor actress	Performer	Varchar	32	N	—
Creative time	Time	Datetime		Y	—
Remark	BZ	Varchar	50	Y	—

Table 4: Information table.

Field description	Field identification	Field type	Size	Allow to be empty	Remark
Music information number	YYZXBH	Integer	20	N	Primary key
Information title	ZXBT	Varchar	50	N	—
Information category	ZXLB	Varchar	10	N	—
Release time	FBSJ	Datetime		N	—
Publisher	FBR	Varchar	20	N	External key
Information content	ZXNR	Varchar	2000	N	—
Number of viewers	ZLRS	Integer		N	—
Browse class	LLBJ	Integer	100	N	—
Number of downloaders	XZRS	Integer			—
Remark	BZ	Varchar	50	Y	—

Table 5: Daily notification information.

Field description	Field identification	Field type	Size	Allow to be empty	Remark
Notice number	TZBH	Integer	20	N	Primary key
Notification title	TZBT	Varchar	50	N	—
Notification category	TZLB	Varchar	10	N	—
Release time	FBSJ	Datetime		N	—
Publisher	FBR	Varchar	20	N	External key
Notification content	TZNR	Varchar	2000	N	—
Number of viewers	ZLRS	Integer		N	—
Remark	BZ	Varchar	50	Y	—

Table 6: Attachment information table.

Field description	Field identification	Field type	Size	Allow to be empty	Remark
Record number	JLBH	Integer	20	N	Primary key
Document number	WDBH	Integer	20	N	—
Title	ZPMC	Varchar	50	N	—
Description	ZPMS	Varchar	100	Y	—
Style classification	FGFL	Varchar	50	Y	—
Style description	FGMS	Varchar	100	Y	—
File address	WJDZ	Varchar		N	—
Upload time	SCSJ	Datetime	20	N	—
Uploader	SCR	Varchar		N	External key
Number of viewers	ZLRS	Integer		Y	—
Review time	SHSJ	Datetime		N	—
Whether to pass	SFTG	Int	20	N	0-Unparalleled; 1-pass
Remark	BZ	Varchar	50	Y	—

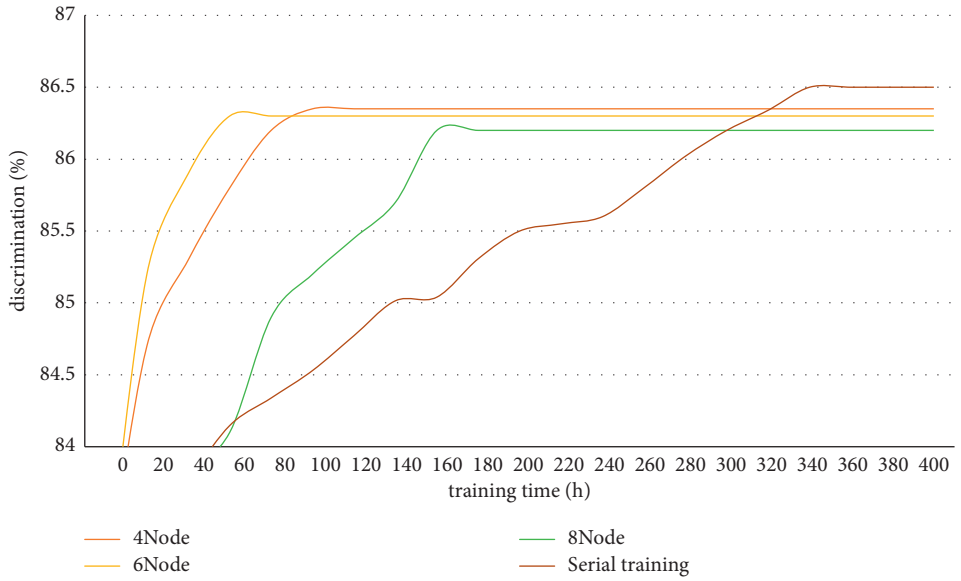

Figure 3: Training efficiency under different number of nodes.

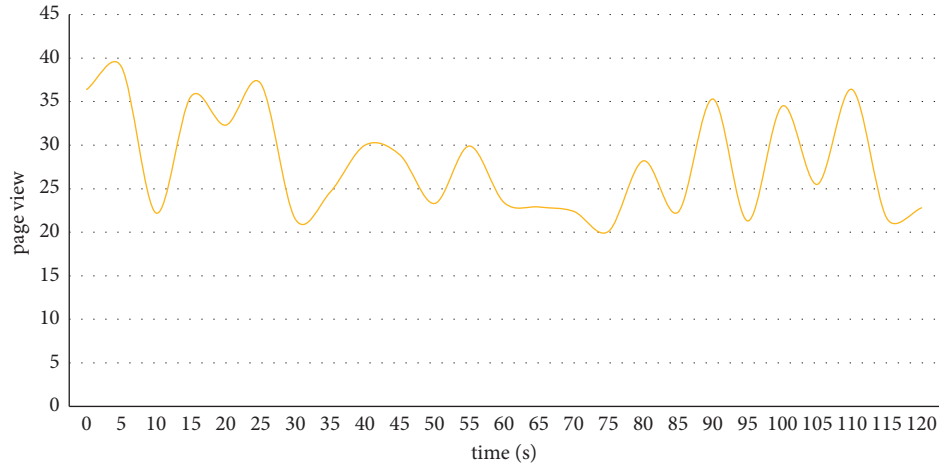

Figure 4: Visits.

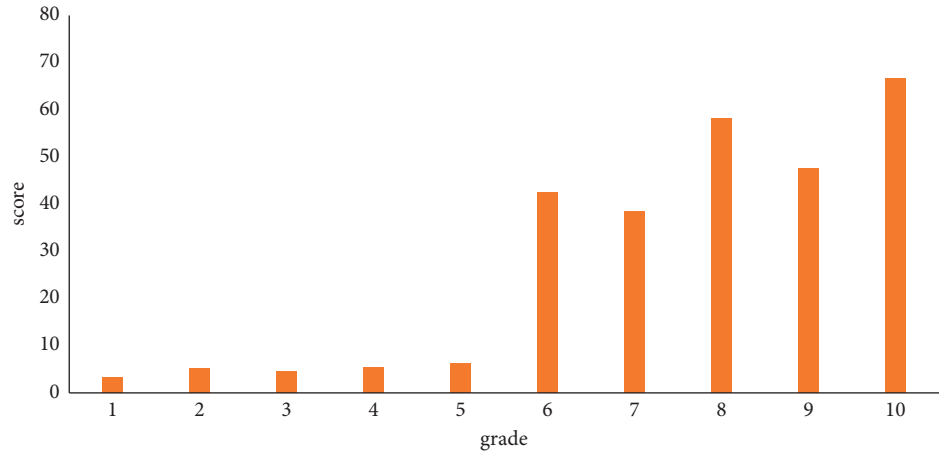

Figure 5: Score statistics.

4.3.1. Visits. During the test, the total number of visits to the system was 947, and the overall login success rate could reach 87.8%. Combined with the actual music online course arrangement, the system achieved the expected effect. Figure 4 extracts the statistics of platform visits within 1 minute.

4.3.2. Discussion Activities. In order to further test the effectiveness of the music teaching system, this paper launched a discussion activity on the platform according to the learned knowledge and made statistics on the classroom discussion results. A total of 266 discussion results were submitted by students. Taking 10 points as the statistical standard, it is qualified if it is higher than 6 points. The results are shown in Figure 5. The overall qualified rate reaches 92%, which can prove the learning effect of students' online classroom and the effectiveness of music teaching system to a certain extent.

5. Research on the Application Strategy of the Music Mixed Teaching Mode under Mobile Platform

5.1. Main Forms of the Mixed Teaching Mode. In the traditional music classroom, the teaching method of "teachers sing and students learn" and "teachers talk and students listen" ignores the subjective initiative of students as the main body of the classroom. In the process of online MOOC teaching, teachers and students have an equal dialogue relationship. Students can raise their own questions in time. Teachers can timely understand students' learning through the data collected by the online learning system. Therefore, mixed teaching combines the advantages of online and offline teaching methods and makes up for the shortcomings of single teaching mode. For music teaching, the advantage of offline teaching mode is that students can directly follow the rhythm of teachers in class to connect pronunciation and singing. The disadvantage is that they can not give feedback about the learning results to teachers in time. The advantages and disadvantages of online teaching are just the opposite. Students can submit their own learning results, but they can not communicate face-to-face with teachers for voice practice, etc. Mixed teaching combines the advantages of the two teaching modes. Therefore, it also requires teachers to change their teaching ideas in time, give full play to the advantages of online and offline teaching, and build three teaching stages of organic connection between preclass guidance, in class promotion, and after-school supervision, so as to design a mixed teaching mode that is more conducive to the development of students.

The mixed teaching mode is a combination of online and offline teaching modes, but online teaching is not a rigid copy of the traditional offline teaching mode. There are some commonalities and differences between them. The specific differences are shown in Table 7. Hybrid teaching organically integrates the places, knowledge transfer forms, educational approaches, advantages, evaluation methods, and teaching resources of online and offline teaching methods, realizes the way of face-to-face interaction, and can also timely grasp the students' learning after class with the help of the data of MOOC system. The online system can still be realized with the help of whiteboard, multiscreen interactive software, multimedia, and other information-based teaching tools. Students can conduct cooperative exploration in the online discussion area of the course and can watch the previous learning resources repeatedly after class.

5.2. Design of the Mixed Teaching Mode in the Mobile Platform Environment. In the context of the normalization of the epidemic, major universities have accelerated the construction of online courses, so many high-quality online course resources have been born. Under the mixed teaching mode, these teaching resources are required to be organically integrated. For example, schools can compile high-quality mixed teaching cases and establish a teaching material library. Teachers can also be organized to develop school-based resources and develop school question bank and teaching resource package according to the requirements of standardization and digitization. At the same time, with the help of the construction of online teaching platform, promote teachers' microcourse recording and online course construction, and form a school level professional course system with intellectual property rights. In the mixed teaching environment based on MOOC, network curriculum resources are one of the basic guarantees for its smooth implementation. Teaching materials are not the only teaching reference for teachers. The large number and variety of network resources can provide diversified support for the mixed teaching model. It is more conducive to the personalized cultivation of students.

In the process of mixed teaching, the data related to learning can be collected, monitored, and analyzed with the help of computer platform, and a relatively objective and fair evaluation can be obtained. At the same time, the cumulative learning results of students can be continuously recorded with the help of big data platform, including the participation degree of teaching activities, check-in times, test results, and homework completion and finally generate a relatively complete evaluation system according to different proportions. At the same time, teachers and students can become the main body of evaluation and being evaluated. The number of visits to the learning platform, the repeated viewing rate of teaching videos by learners, and the frequency of course interaction can reflect the level of teachers' curriculum design to a certain extent and can be used as one of the indicators of teachers' online curriculum evaluation. In addition, the online teaching platform also has the function of students' mutual evaluation, which can also reflect the learners' mastery of the knowledge.

5.3. Building an Integrated Intelligent Campus Platform. With the help of Internet and mobile communication technology, we can not only realize the mixed teaching mode, but also build an integrated intelligent campus management platform to realize intelligent management of the whole campus and student groups. The learning results of students' online courses can be used as one of the

Table 7: Comparison between MOCC music class and traditional music class.

	Face	Web lesson	Hybrid teaching
Place	Offline	Online	Online + offline
Intellectual	Relatively static	Relative flowing	Flow + integration
Way	Teacher teaching	Autonomous learning, online discussion	Teacher Teaching + Autonomous learning
Advantage	Systematic guidance	Abundant resources	Personalized teaching + team collaboration
Evaluation method	Cognitive evaluation	Process evaluation	Cognitive + emotion + practice
Interactive	Face-to-face	Online dialogue	Face-to-face + network tool
Education resources	Multimedia	Resource library, the Internet	Multimedia + resource library, Internet

indicators of students' comprehensive evaluation. Data collection can use a variety of computer technologies, especially big data, cloud computing, and other technologies to achieve more efficient and accurate statistics. At the same time, through the collection of intelligent teaching platform data, we can also understand the teaching situation of teachers and the evaluation results of students, which can assist the school in education and teaching management. The integrated intelligent campus platform is conducive to the organic integration of the whole school resources and can provide convenient and comprehensive campus services for teachers and students.

6. Conclusion

In the context of the Internet, the traditional classroom is gradually undergoing great changes. Especially in recent years, affected by the COVID-19, the reform speed of the education industry is gradually accelerating. The existing teaching model can no longer meet the diverse needs of students. Mixed teaching combines the advantages of the two teaching models. Therefore, the emergence of mixed teaching model has quickly become a research hotspot in the education industry. Based on the existing research on mixed teaching mode, aiming at the problems of low interactivity in traditional music teaching classroom, students' learning results after class can not be monitored in time, and traditional teaching mode can not meet the requirements of home learning during the epidemic; with single teaching mode and fixed teaching methods, combined with the development background of mobile platform MOOC, this paper constructs a music online teaching platform based on convolutional neural network. It mainly includes modules such as basic information management and music curriculum resource construction, which are applied to the actual music curriculum teaching process. The performance and feasibility of the system algorithm in this paper are verified by auxiliary classroom assessment and other links. Through this research, this paper puts forward the design of mixed teaching mode under the environment of mobile platform, hoping to provide some new ideas and methods for the research in the field of music mixed education.

Data Availability

The data used to support the findings of this study are available from the author upon request.

Conflicts of Interest

The author declares no conflicts of interest.

References

[1] M. Kan and J. Zhou, "How do colleges and universities respond to covid-19: the experience of chengdu sport university," *Asia-Pacific Journal of Public Health*, vol. 32, no. 4, pp. 170-171, 2020.

[2] Y. Zhu and L. Zheng, "Ideological and political teaching information management based on artificial intelligence and data security model," *Journal of Intelligent and Fuzzy Systems*, vol. 2021, no. 99, 11 pages, 2021.

[3] P. Paudel, "Online education: benefits, challenges and strategies during and after COVID-19 in higher education," *International Journal on Studies in Education*, vol. 3, no. 2, pp. 70–85, 2020.

[4] J. Jia and J. Zhang, "The analysis of online learning behavior of the students with poor academic performance in mathematics and individual help strategies," in *Proceedings of the International Conference on Blended Learning*, Springer, Hradec Kralove, Czech Republic, July 2019.

[5] Y. Tu and Y. J. Zhang, "An empirical study on the supervision model of knowledge construetion efect in online classroom," *Education Modemization*, vol. 41, no. 3, pp. 64–73, 2018.

[6] R. Garg, R. Kumar, and S. Garg, "MADM-based parametric selection and ranking of E-learning websites using fuzzy COPRAS," *IEEE Transactions on Education*, vol. 62, no. 1, pp. 11–18, 2019.

[7] H. Abulkasim, H. N. Alsuqaih, W. F. Hamdan et al., "Improved dynamic multi-party quantum private comparison for next-generation mobile network," *IEEE Access*, vol. 7, Article ID 17917, 2019.

[8] X. Tian and W. Jia, "Improved clustering and resource allocation for ultra-dense networks," *China Communications*, vol. 17, no. 2, pp. 220–231, 2020.

[9] B. V. Tucker, M. C. Kelley, and C. Redmon, "A place to share teaching resources: speech and language resource bank," *Journal of the Acoustical Society of America*, vol. 149, no. 4, p. A147, 2021 A147–A147.

[10] G. Chen, H. Meng, Y. Liang, and K. Huang, "GPU-accelerated real-time stereo estimation with binary neural network," *IEEE Transactions on Parallel and Distributed Systems*, vol. 31, no. 12, pp. 2896–2907, 2020.

[11] X. Dang and H. Zhu, "A feature-based data association method for multiple acoustic source localization in a distributed microphone array," *Journal of the Acoustical Society of America*, vol. 149, no. 1, pp. 612–628, 2021.

[12] L. Wang, G. Hu, and T. Zhou, "Semantic analysis of learners' emotional tendencies on online mooc education," *Sustainability*, vol. 10, no. 6, p. 1921, 2018.

[13] Z. Shao, "Examining the impact mechanism of social psychological motivations on individuals' continuance intention of MOOCs," *Internet Research*, vol. 28, no. 1, pp. 232–250, 2018.

[14] J. A. Ruipérez-Valiente, S. Martin, J. Reich, and M. Castro, "The unmoocing process: extending the impact of mooc educational resources as oers," *Sustainability*, vol. 12, no. 18, p. 7346, 2020.

[15] R. Pellerin and N. Perrier, "A review of methods, techniques and tools for project planning and control," *International Journal of Production Research*, vol. 57, no. 7, pp. 2160–2178, 2019.

[16] M. Naseri, M. Abdolmaleky, F. Parandin, N. Fatahi, A. Farouk, and R. Nazari, "A new quantum gray-scale image encoding scheme," *Communications in Theoretical Physics*, vol. 69, no. 2, p. 215, 2018.

[17] L. Q. Wu, "A comparative study on the effect of online classroom teaching and traditional classroom teaching," *Education Modernization*, vol. 6, no. 9, pp. 276-277, 2019.

[18] M. Gong, J. Liu, H. Li, Q. Cai, and L. Su, "A multiobjective sparse feature learning model for deep neural networks," *IEEE Transactions on Neural Networks and Learning Systems*, vol. 26, no. 12, pp. 3263–3277, 2015.

Hindawi
Mobile Information Systems
Volume 2022, Article ID 4816516, 10 pages
https://doi.org/10.1155/2022/4816516

Research Article

Application of Voice Database in Enterprise Human Resources Optimization Based on Improved Algorithm

Minmin Dong

Henan Light Industry Vocational College, Zhengzhou, Henan 450000, China

Correspondence should be addressed to Minmin Dong; niuxm@cscec.com

Received 1 June 2022; Revised 2 July 2022; Accepted 13 July 2022; Published 2 August 2022

Academic Editor: Shadi Aljawarneh

With the continuous development of IP network technology, VoIP technology has become more mature. However, due to the characteristics of the packet network itself, the voice quality of VoIP service is caused by delay and packet loss. This paper analyzes the application of the speech quality system in the optimization of human resources in enterprises. With the emergence and development of database systems, data sharing has been significantly improved, data integrity has been guaranteed, data security has been improved, and the development difficulty of embedded applications has been greatly reduced. Through system simulation, it can be seen that with the increase of the packet loss rate, the voice quality is obviously degraded, and the decline rate becomes slower with the increase of jitter. After designing and implementing a company's human resource allocation, achieving the most efficient allocation of resources requires continuous testing, evaluation, and improvement. Therefore, after completing the company's human resource allocation, it is necessary to establish a set of testing and evaluation mechanisms.

1. Introduction

In recent years, Internet technology and multimedia technology have developed rapidly, it has become a trend to provide multimedia services through the Internet, and it is also a hot research topic today [1]. With the rapid development of communication technology, VoIP has become a typical Internet multimedia service. Because VoIP is a data exchange process in the form of packets, VoIP phones provide more than just voice services [2]. The openness of the IP protocol allows developers to provide various other value-added services through VoIP services. Voice, as the most important and basic technology in the process of human communication, has made a huge leap in the human communication experience. Therefore, voice communication is one of the most important technologies in the communication system [3]. In the development of voice communication technology, the development of voice quality assessment technology provides an important basis for assessment [4]. The call quality directly affects the user's overall reputation for the service provided by the operator. With the development of science and technology and the progress of society, embedded systems are application-centric and computer-based, and embedded systems are achieving more and more extensive and detailed applications. Now, it has been widely used in analog systems, medical instruments, computer equipment, communication equipment, aerospace, and many other fields [5]. There are data management issues in many embedded system applications. When the amount of data that the system must process is not large, data management is still relatively simple. However, when the amount of data in the system increases to a certain scale, the conventional system will use the file system to organize and manage the data [6]. In addition, the development of many companies in many countries and regions in the world has almost one thing in common; that is, human resources are the point of dependence and support of society for economic and technological development [7]. In today's society, human resources have become the main resource for scientific and technological progress and business development. In order to adapt to the fierce international competition today and in the future, China will revitalize enterprises with Chinese characteristics and establish first-class human resources at

home and abroad [8]. The company team has become the primary factor. For this reason, it is necessary to make a fundamental change in human resources. The focus of human resource development has shifted to improving the quality and efficiency of human resources. How to focus on human resources strategy, retaining and attracting talents, and how to do a good job in the development and management of human resources have become the top priority of their work after China's entry into WTO [9].

2. Related Work

The subjective speech quality evaluation method is to evaluate the level of speech quality through the human subjective perception of speech [10]. ITUP.800 and P.830 define the subjective evaluation method of average opinion score, and the test method used is the absolute classification score test. It gives an average opinion score. The literature introduces that an accurate voice quality evaluation model is to find the relationship between various factors that affect voice quality and MOS scores [11]. The regression algorithm is an efficient algorithm based on statistical methods. It uses a mathematical-statistical method to study what we are concerned about [12]. We have uncertain dependencies and constraints between variables. The purpose is to use the obtained mathematical expressions to analyze unknown variables through known variables and display the law of change. The literature proposes and introduces some commonly used VoIP voice quality assessment methods and focuses on the two most commonly used methods, namely PESQ and E-Model [13]. The advantages and disadvantages of these two methods are theoretically analyzed to further verify the simulation data. In order to overcome the shortcomings of these two algorithms, Professor Sun proposed a hybrid *E* model/PESQ algorithm [14]. Data integrity is guaranteed, data security is improved, and the difficulty of developing embedded applications is greatly reduced. In theory, using it alone can make up for the first two shortcomings. In this article, we optimized the algorithm, added network jitter to the input parameters, improved the delay calculation, and proposed an improved hybrid *E* model/PESQ algorithm [15]. The literature puts forward that the purpose of optimizing the human resource allocation structure is to use certain methods to measure the reasonable structure, personnel deployment, and recruitment of the entire enterprise and various departments according to the company's current work structure and strategic goals, guided by the idea of sustainable development [16]. Work provides a strong human resource guarantee for being able to reach the level of enterprise management in medium-developed countries and realize the goal of modernizing enterprise management systems. Based on an organizational structure that can quickly respond to market changes, determining a reasonable structure of employee skills, number, age, cultural quality, and gender is a key issue for optimizing the allocation of human resources. With the intensification of the international competition environment of modern enterprises, the human resource problems faced by Chinese enterprises have become more and more prominent. The competition for human resources is also becoming increasingly fierce [17]. Enterprises undertake the dual tasks of enterprise and society, and performance is of greater significance to enterprises [18]. Due to the socialization of companies under China's planned economy, in order to ensure the number of jobs in society, companies usually assign more jobs than reasonable standards. When faced with nonenterprise in the same industry, this will lead to a decline in company performance and insufficient product prices. Therefore, a reasonable minimum number of employees in a company are of greater significance to the company [19].

3. Voice Quality System and Embedded Database

3.1. Voice Quality System. Testers must assess the overall quality of the audio without training. It can be seen from Table 1 that the tester finally gives the listening score according to Table 1 and finally uses the average score of all testers as the final average score.

The advantages of the MOS subevaluation method are obvious, and the results are closest to people's subjective feelings. Our ultimate goal is to understand how people think about voice quality. Therefore, this method can be considered as the most accurate. Figure 1 shows a schematic diagram of PESQ.

The premise of the E-model is to assume that voice quality impairment factors are always added physically. In short, if you can flexibly add network disruption factors, such as noise, echo, delay, encoder performance, and jitter, you can estimate the integrated network. Figure 2 shows the structure of the *E* model in G.107.

All influencing factors of F-model are attributed to the parameter *R*, which includes the effects of delay, packet loss, echo, and other factors.

The calculation formula of transmission performance *R* is shown in the following formula:

$$R = Ro - Is - Id - Ie - eff + A, \tag{1}$$

where *Ro* is the basic signal-to-noise ratio, which represents the damage caused by noise, such as background noise in a call environment or circuit noise generated by a circuit.

The expression of Ro is shown in the following formula:

$$Ro = 15 - 1.5(SLR + No), \tag{2}$$

$$\mathrm{No} = 10\log\left[10^{Nc/10} + 10^{Nos/10} + 10^{Nor/10} + 10^{Nfo/10}\right], \tag{3}$$

$$\mathrm{Nos} = Ps - SLR - Ds - 100 + 0.004(Ps - OLR - Ds - 14)^2, \tag{4}$$

where OLR = SLR + RLR, as shown in the following formula:

$$\mathrm{Nos} = RLR - 121 + \mathrm{Pre} + 0.008(\mathrm{Pre} - 35)^2. \tag{5}$$

Among them, the preexpression is as shown in the following formula:

Table 1: MOS score evaluation standard.

MOS score	Quality level	Distortion level
5	Excellent	Not aware of
4	Good	Just noticed
3	General	Noticeable and slightly disgusting
2	Difference	Obviously aware, acceptable
1	Very bad	Unacceptable

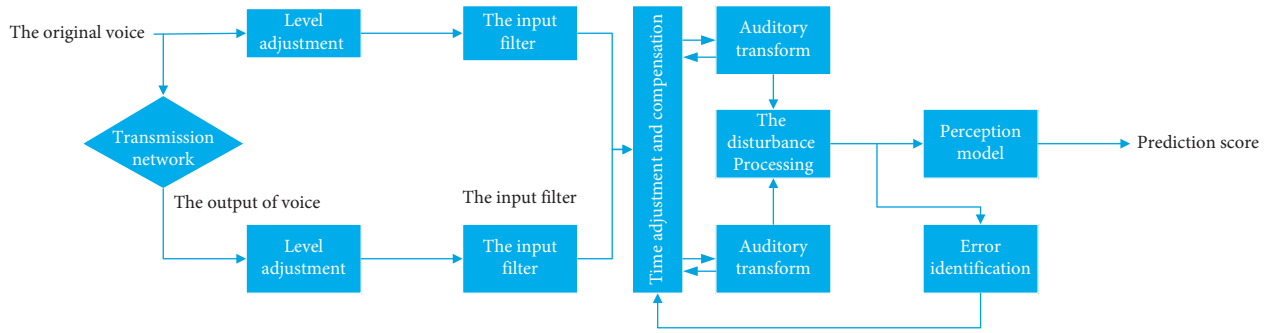

Figure 1: PESQ algorithm flow chart.

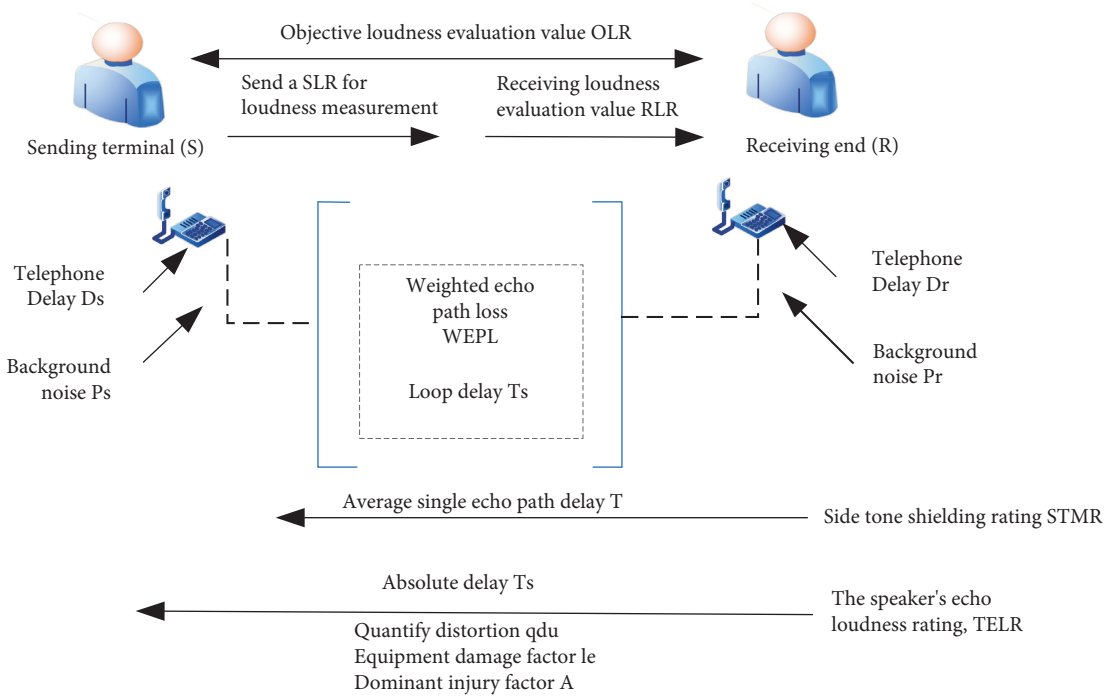

Figure 2: E-Model structure diagram.

$$\text{Pre} = \text{Pr} + 10\log\left[1 + 10^{\frac{(10 - LSTR)}{10}}\right]. \tag{6}$$

Nfo represents the noise at the receiving end, as shown in the following formula:

$$Nfo = Nfor + RLR. \tag{7}$$

Nfor is usually set to −64 dBmp, and the damage coefficient is calculated as follows:

$$\text{Is} = Iolr + \text{Ist} + Iq. \tag{8}$$

Iolr indicates that the voice quality is degraded because the loudness level OLR is too low, as shown in the following formula:

$$Iolr = 20\left[\left\{1 + \left(\frac{Xolr}{8}\right)^8\right\}^{1/8} - \frac{Xolr}{8}\right]. \tag{9}$$

Among them, the *Xolr* expression is as shown in the following formula:

$$Xolr = OLR = 0.2\,(64 + \mathrm{No} - PLR). \tag{10}$$

Among them, the expression of STMRo is as shown in the following formula:

$$\mathrm{STMRo} = -10\,\log\left[10^{-(\mathrm{STMR}/10)} + e^{-(T/4)}10^{-(\mathrm{TELR}/10)}\right]. \tag{11}$$

Iq is the impairment caused by the distortion produced by the speech during quantization, as shown in the following formulas:

$$Iq = 151\,\log\left[1 + 10^{Y} + 10^{Z}\right]. \tag{12}$$

Among them,

$$Y = \frac{R_o - 100}{15} + \frac{46}{8.4} - \frac{G}{9}, \tag{13}$$

$$Z = \frac{46}{30} - \frac{G}{40}, \tag{14}$$

$$G = 1.07 + 0.258Q + 0.0602Q^2, \tag{15}$$

$$Q = 37 - 15\,\log(q\ du). \tag{16}$$

The benefit coefficient A is shown in Table 2.

After considering that in the actual VoIP system, the main factors that affect the VoIP voice quality are the network quality and the encoder. Therefore, for Ro, Is, and the gain coefficient A, we can use the default values, which not only simplifies the calculation process but also saves a lot of input. The working of the parameters, such as the default parameters, is provided in Table 3.

Figure 3 shows the relationship between the transmission performance level R and the average opinion score MOS score.

In order to make the experiment process more convenient, we set the maximum value of the client jitter buffer to 100MS and, on this basis, simulate the data shown in Table 4. In order to eliminate the contingency of the data and make it universal, we set the maximum value of the client jitter buffer to 100MS. This combination of data simulates 50 voice calls.

Individual simulation data are shown in Table 5.

Draw the relationship between packet loss, jitter, and voice quality through simulated data, as shown in Figures 4 and 5.

In Figure 4, as the jitter increases, the voice quality decreases significantly, and the rate of decrease slows down as the packet loss rate increases.

In Figure 5, as the packet loss rate increases, the voice quality decreases significantly, and the rate of decrease slows down as the jitter increases.

The sample data used in the regression model come from the simulation in this article, and these data are obtained through simulation in a specific environment.

Coding: AMR-WB jitter buffer maximum: 100 ms.

When the above-mentioned environment changes, the parameters of the regression model will also change accordingly as shown in the simulation data in Figure 6.

3.2. Embedded Database. The step of searching for a keyword of 79 is shown in Figure 7. The node sequence to be searched in the search process is $A->C->F->I$, and the search is successful.

Next, we analyze and compare the storage usage of T-trees, unbalanced B-trees, and unbalanced T-trees to describe the nominal data load (denoted by w) or the maximum number of data items that can be accommodated. In order to facilitate performance analysis and comparison, unbalanced B-tree and unbalanced T-tree nodes can completely occupy the entire storage block, and their size is set to K.

Each node in the T-tree has three link pointers to the root node and parent node of the left and right subtrees, and two fields, namely the balance factor and the number of data elements, so the rated data load can be determined in the following way:

$$\begin{aligned} W_t &= \frac{(K - 3 * L - 2^{*} I)}{E} \\ &= \frac{(K - 14 * I)}{E}. \end{aligned} \tag{17}$$

Each node of the unbalanced B-tree has only one link pointer, which points to the root node of the rightmost terminal tree, plus a field for indicating the number of data elements, so the rated data load can be calculated by the following formula:

$$\begin{aligned} W_{ub} &= \frac{(K - L - I)}{E} \\ &= \frac{(K - 5 * I)}{E}. \end{aligned} \tag{18}$$

Each node of the unbalanced T-tree has two link pointers, which point to the root nodes of the left and right subtrees, respectively, plus a field for indicating the number of data elements, so the rated data load can be calculated by the following formula:

$$\begin{aligned} W_{ut} &= \frac{(K - 2 * L - I)}{E} \\ &= \frac{(K - 9 * I)}{E}. \end{aligned} \tag{19}$$

Therefore, in terms of nominal data load, unbalanced tree storage usage is not as good as unbalanced B-tree storage usage, but worse than T-tree storage usage.

Now, suppose that N_h represents the minimum number of nodes contained in a T-tree with a height of h. Obviously, $N_0 = 0, N_1 = 1, N_2 = 2$. From the definition of T tree, we can see, as shown in the following formula:

$$N_h = N_{h-1} + N_{h-2} + 1. \tag{20}$$

The solved formula is as follows:

$$Nh = \frac{\theta^{h+2}}{\sqrt{5} - 1\,(\theta = (\sqrt{5}\ + 1/2))}. \tag{21}$$

Table 2: Part A value specified by G.107.

Communication system example	The value of A (maximum value)
Traditional communication environment	0
Cellular mobile system inside a building	5
Vehicles driving inside the area	10
Remote areas, such as connecting via multiple relay satellites	20

Table 3: Default value and range of E model parameters.

Parameter	Abbreviation	Unit	Defaults	Allowable range	Note
Loudness level	SLR	dB	+8	0...+18	(Note 1)
Receive loudness level	RLR	dB	+2	−5...+14	(Note 1)
Side tone masking level	STMR	dB	15	10...20	(Note 2)
Side tone level	LSTR	dB	18	12...23	(Note 2)
D value of the phone on the sending side	Ds	—	3	−3...+3	(Note 2)
D value of the receiving side phone	Dr	—	3	−3...+3	(Note 2)
Speaker echo intensity level	TELR	dB	65	5...56	
Weighted echo channel loss	WEPL	dB	110	5...110	
The average word delay of the echo channel	T	ms	0	0...500	
4-wire loop round trip delay	Tr	ms	0	0...1000	
Absolute delay in echoless connection	Ta	ms	0	0...500	
Number of quantization distortion units	Qdu	—	1	1...14	
Equipment damage factor	Ie	—	0	0...40	
Packet loss intensity factor	Bpl	—	1	1...40	(Note 3)
Random packet loss probability	Bpl	%	0	0...20	(Note 3)
Burst ratio	Burs:R	—	1	1...2	(Note 3)
Circuit noise referenced to 0dBr point	Ne	dBm0p	−70	−80... −40	
Receive side noise floor	Nfor	dBmp	−64	—	(Note 3)
Indoor noise on the transmitting side	Ps	dB(A)	35	35...85	
Indoor noise on the receiving side	P	dB(A)	35	35...85	
Benefit factor	A	—	0	0...20	

Note 1: the total value of 0dBr points between the transmitter and the receiver. *Note* 2: fixed relationship: LSTR = STMR + D. *Note* 3: currently under study.

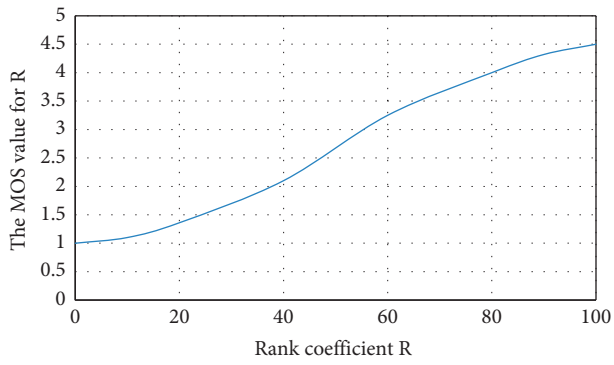

Figure 3: Function relationship between transmission grade coefficient R and MOS.

Table 4: Parameter setting table.

Network parameters	Setting situation
Coding	AMR-WB
Time delay	0–100 ms interval 10 ms
Jitter	0–100 ms interval 10 ms
Packet loss	0–10% interval 1%
Maximum jitter buffer	100 ms

In contrast, the maximum height of the n-node T-tree is $\log_\theta(\sqrt{5}\,(n+1)) - 2$. Therefore, the time complexity of searching in the T-tree is $O(\log n)$.

The nodes of the unbalanced B-tree form a singly linked list. When searching for boundary nodes, it is necessary to compare the minimum key value and the maximum key value of each node. Therefore, when the search is successful, the unbalanced B-tree will find the average search length ASL_{ub} of the boundary node as follows:

$$ASL_{ub} = \sum_{i=1}^{n} P(i) * 2n, \tag{22}$$

where $P(i)\,(i = 1, 2, \ldots, n)$ is the probability of finding the i-th node.

According to the previous assumption, the probability of finding each node is $1/n$, which is $P(i) = 1/n$. Therefore, the average search length of an unbalanced B-tree is

$$\begin{aligned} ASL_{ub} &= \frac{2}{n}(1 + 2 + \cdots + n) \\ &= n + 1. \end{aligned} \tag{23}$$

That is to say, when the search is successful, the time complexity of the search operation of the unbalanced B-tree is $O(n)$.

In the case of a successful search, an unbalanced T-tree with $n\,(n \geq 1)$ nodes, and one node in the left subtree, the average search length ASL_{node} for finding the bounding node is as follows:

Table 5: Part of the simulation data sheet.

Time delay (ms)	Packet loss (%)	Jitter (ms)	Jitter buffer (ms)	MOS-P	R	MOS
100	1	10	100	3.61	65.4	3.39
100	1	30	100	2.63	45.6	2.34
100	1	50	100	2.70	42.7	2.10
100	1	70	100	2.53	39.8	2.04
100	3	10	100	2.99	53.5	2.77
100	3	30	100	2.32	40.1	2.05
100	3	50	100	2.30	35.8	1.96
100	3	70	100	2.18	33.1	1.75
100	5	10	100	2.56	46.4	2.38
100	5	30	100	2.18	37.5	1.94
100	5	50	100	2.10	31.6	1.68
100	5	70	100	19.5	28.6	1.56
100	7	10	100	2.20	39.9	2.07
100	7	30	100	1.95	32.3	1.71
100	7	50	100	1.85	25.8	1.46
100	7	70	100	1.77	24.18	1.38
100	9	10	100	19.4	34.4	1.81
100	9	30	100	1.78	28.6	1.56
100	9	50	100	1.75	23.1	1.35
100	9	70	100	1.62	20.3	1.24

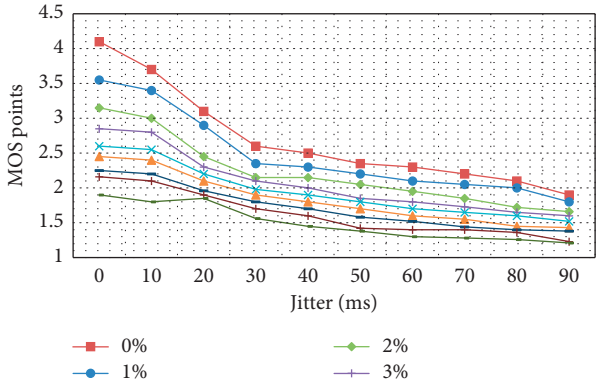

Figure 4: The relationship between jitter and voice quality.

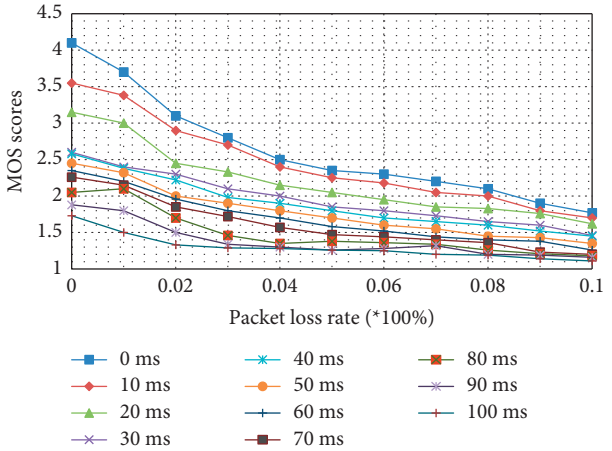

Figure 5: The relationship between packet loss rate and voice quality.

$$P(n,i) = \frac{1}{n}[2 + i * (P(i) + 1) + (n - i - 1) * (P(n - i - 1) + 2)], \quad n \geq 1, \tag{24}$$

where $P(i)$ is the average search length of an unbalanced tree containing one node, then $P(i) + 1$ is the average of the number of comparisons used to find each node in the left subtree, and $P(n - i - 1) + 2$ is to find each node in the right subtree, so the equation i in 25 can be averaged from 0 to n-to get the following formula:

$$P(n) = \frac{1}{n}\sum_{i=0}^{n-1}\left[\frac{1}{n}[2 + i * (P(i) + 1) + (n - i - 1) * (P(n - i - 1) + 2)]\right]$$

$$2 + \frac{2}{n^2}\sum_{n=1}^{n-1} iP(i), \quad n \geq 2. \tag{25}$$

Obviously, $P(0) = 0, P(1) = 2$.
The solved formula is as follows:

$$P(n) = 2\frac{n+1}{n}1mn + C, \text{Where Cisaconstan } t. \tag{26}$$

It can be seen that under random conditions, the average search length of an unbalanced T-tree is the same order of magnitude as LOGN; that is, the time complexity of the search operation is OLOGN.

4. Enterprise Human Resources Optimization Processing and Realization

4.1. Research on Optimization of Enterprise Human Resource Allocation Structure. The human resource structure is the composition and common positioning of all employees in

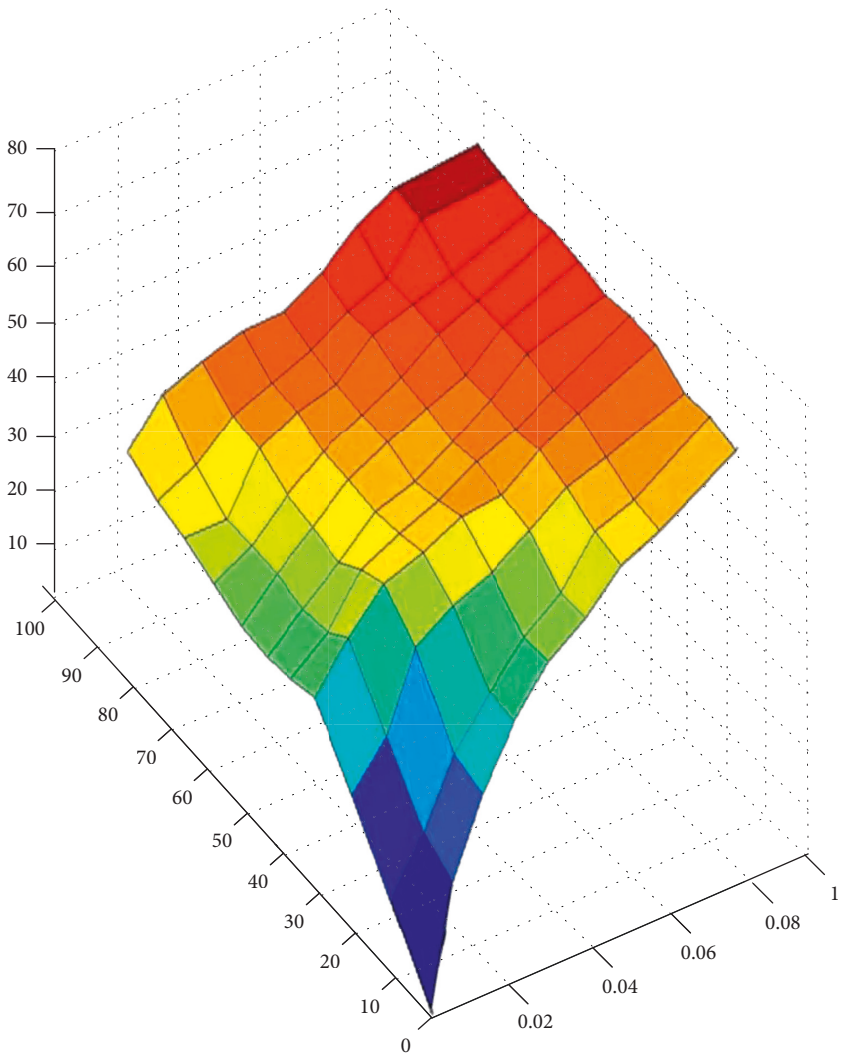

Figure 6: Packet loss rate, jitter, and Ier.

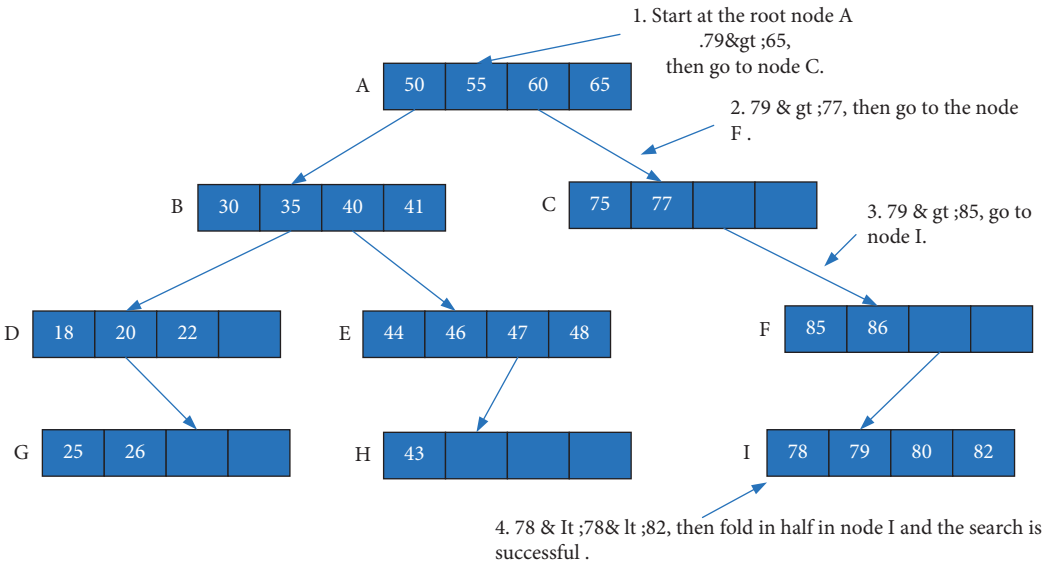

Figure 7: Steps to find the data element with the key of 79 in the unbalanced T-tree.

the operation of a company, and it can fundamentally reflect the actual situation of the company's human resource allocation. The company should optimize all aspects of the organization's internal departments and even the company's internal human resource structure, such as the personalized trend of team human resources. In any organization, there is the work organized by the manager and the managed, which often involves many different aspects, and each aspect requires different personnel and abilities to achieve it. Organization is the basic feature of society, so it must have a structure, that is, "organizational structure". As a specific organization, there are also problems with the organizational structure of the enterprise. There is a high degree of correlation between "organizational structure" and "corporate human resources allocation" because the optimal allocation of human resources is statically reflected in the staffing of the organizational structure; that is, a certain unit in the organizational structure corresponds to the people of this unit. Therefore, when the management organization and system are sound, the management effect is not necessarily the best. If the benefits of the management system cannot offset its costs, there is no need to establish such a management organization and formulation system. This requires reasonable and flexible arrangements for the organizational structure, focusing on the adjustment and innovation of the core business of the enterprise, and continuously optimizing and adjusting the structure of human resources.

A reasonable academic structure requires that the proportion of people with different academic qualifications in the organization is reasonable, and talents should not be wasted or lack of talents. Through in-depth investigation and research on some state-owned enterprises in China, it is found that the problem with enterprises with higher general education level is that the educational structure of various departments is unreasonable and the educational structure of all age groups is unreasonable. The educational structure of all age groups is unreasonable. Some measures to solve the problem of academic structure imbalance can be solved by the exchange or deployment of personnel in different departments, or a good education and training system can be established, with emphasis on the training of middle-aged and grass-roots employees. It has not yet been determined whether people with higher education are more beneficial to the development of Chinese companies. The key is to predict the demand and supply of human resources based on the different strategic goals and tasks of Chinese companies. It is not only a quantitative forecast but also a short-term, mid-term, and long-term academic qualification. It is not only a quantitative prediction but also a short-term, medium-term, and long-term academic qualifications, skills, and age structure, as well as human resource allocation plan. While performing these basic tasks, it is necessary to adapt to the educational structure of each department.

4.2. Research on the Realization of Optimal Allocation of Enterprise Human Resources. Production efficiency is the main factor for the company to maintain a reasonable gross profit margin, and ensuring reasonable jobs for the company is an important factor in improving the company's production efficiency. The minimum number of employees for a unit position refers to the minimum number of employees for appropriate positions adopted by the company to ensure job efficiency. In this problem, too many numbers will cause fluctuations between labor and internal consumption, and the waste of company resources will result in insufficient corporate resources. The number of people who complete the scheduled activities will affect the completion of the company's performance. Therefore, the principle of the lowest employment rate is the principle of the highest efficiency of the enterprise. First of all, it is necessary to conduct a reasonable analysis of the position. According to organizational performance, we calculate the upstream and downstream working methods of production positions and departments, comprehensively analyze the production workload that upstream and downstream positions can undertake, and then calculate the average workload of workers. The best way to get the number of workers required to complete 10% of the extra workload and the number of workers that can reach the average daily workload is to conduct actual production line tests and make continuous adjustments based on the data obtained in the production line. Throughout the process, we must avoid nondata-driven workload calculations, and everything is data-driven, which is a product of practice to determine the company's position. In this cycle, everything revolves around the product. To produce products, it is necessary to purchase raw materials. After the raw materials are purchased, they must be produced, and many links are involved in the production, which creates multiple positions in the production.

Human resource strategic planning belongs to the overall strategic category of an enterprise and is the support and basic role of organizational strategy. Human resource planning should consider the company's current discovery status and future development potential and make plans accordingly. Define and verbally describe the number of positions and human resources needed now and in the future. On the basis of maximizing corporate performance, attention should be paid to the improvement of quality and quantity. We must pay attention to the analysis of existing human resources and make plans. The training of corporate human resources is a very important part. At present, Chinese companies have done a lot of work in human resource training, but the effect is not good. Human resource training is very poorly targeted. It does not provide training for company needs nor does it design appropriate company training for successful operation and management experience. At present, the training of enterprises only pays attention to the form and ignores the effect. There is no certain evaluation and acceptance of the training effect, and an evaluation mechanism has been formed. As a result, the vacancy rate of company employee training is relatively high, employees are less motivated to participate in training, and their learning and growth are poor, so they cannot use the knowledge they have learned. Finally, the turnover rate of employees is relatively high.

After designing and implementing the company's resource allocation, to achieve the most effective resource allocation, continuous testing, evaluation, and improvement are required. Therefore, after completing the company's resource allocation, it is necessary to establish a set of resource allocation detection and evaluation mechanisms to continuously discover and optimize the company's current resource allocation problems, and it is necessary to establish a regular inspection and control system. Adjust management and coordination to ensure that the staffing can meet the company's strategic and development needs in a timely manner. The company's human resource allocation is closely integrated with the company's current business strategy, dynamically optimizing the human resource structure, promoting the company's sustainable development and innovation, as well as various intermediate businesses, start-ups, industries, and commerce. After testing the HR configuration, the current HR configuration needs to be adjusted and improved according to the test situation. Adjust the human resources allocation according to the existing management foundation and situation of the Chinese company, report to the company's senior management, strengthen communication with middle management and corresponding management, solve current problems, and understand and ensure employee safety. It is on the same step. This can effectively promote improved human resource allocation.

5. Conclusion

With the continuous development of IP network technology, VoIP technology has become more mature. However, due to the characteristics of the packet network itself, the voice quality of VoIP services is caused by delay and packet loss. The voice quality is not as good as the traditional PSTN telephone network, which limits the development of VoIP technology. With the emergence and development of embedded database systems, data sharing in the embedded environment has been significantly improved, data integrity has been guaranteed, data security has been improved, and the difficulty of developing embedded applications has been greatly reduced. By introducing and analyzing the basic principles of optimizing the human resource allocation structure of Chinese companies, we pointed out the dynamic optimization of hard structure age, educational background, profession, professional knowledge and soft structure knowledge, and ability and quality. The key to the internal talents of Chinese companies lies in the analysis of talents, which is an important issue related to the optimal allocation. The success of the optimization and coordination strategy for educational background, age, professional knowledge, and ability structure directly affects the realization of the strategic goals of state-owned enterprises. The basic principle of optimizing the allocation of human resources in state-owned enterprises is to ensure the effective operation of the organization and sufficient workload and to achieve true rationalization and high efficiency. It is necessary to optimize the specific content with the best configuration to achieve the best integration state of all the resources of the organization. Safeguard measures provide employees with talents, create development opportunities, allow employees to surpass themselves, develop their potential, and ultimately realize the company's human resource structure. It is to establish a fair, just, and open employment mechanism to achieve optimization.

Data Availability

The data used to support the findings of this study are available from the corresponding author upon request.

Conflicts of Interest

The authors declare that they have no conflicts of interest.

References

[1] E. Ardizzonep, L. Gatani, M. La Cascia, G. Lo Re, and M. Ortolani, "Enhanced P2P services providing multimedia content," *Advances in Multimedia*, vol. 2007, p. 12, Article ID 026070, 2007.

[2] J. M. Cortés-Mendoza, A. Tchernykh, and A.-M. Simionovici, "VoIP service model for multi-objective scheduling in cloud infrastructure," *International Journal of Metaheuristics*, vol. 4, no. 2, pp. 185–203, 2015.

[3] B. S. Atal, "Linear Predictive Coding of Speech," *Computer Speech Processing*, vol. 7, pp. 81–124, 1985.

[4] J. J. Jiang, Y. Zhang, and C. McGilligan, "Chaos in voice, from modeling to measurement," *Journal of Voice*, vol. 20, no. 1, pp. 2–17, 2006.

[5] B. Schatz, A. Pretschner, F. Huber, and J. Philipps, "Model-based development of embedded systems," in *Advances in Object-Oriented Information Systems*, pp. 298–311, Springer, Cham, Switzerland, 2002.

[6] D. Gay, P. Levis, R. von Behren, M. Welsh, E. Brewer, and D. Culler, "The nesC language: a holistic approach to networked embedded systems," *ACM Sigplan Notices*, vol. 49, no. 4S, pp. 41–51, 2014.

[7] X. Liu, X. Yang, and X. Wu, "Human resource management work allocation algorithm based on fuzzy relationship," *Soft Science*, vol. 17, no. 4, pp. 62–64, 2003.

[8] H. Zhu, "Research on Human Resource Recommendation Algorithm Based on Machine Learning," *Scientific Programming*, vol. 2021, Article ID 8387277, 10 pages, 2021.

[9] Y. Xu, "How to build a strategic human resource management system for state-owned enterprises," *People's Forum*, vol. 4, no. 5, pp. 96-97, 2021.

[10] I. Iriondo, S. Planet, J.-C. Socoró, E. Martínez, F. Alías, and C. Monzo, "Automatic refinement of an expressive speech corpus assembling subjective perception and automatic classification," *Speech Communication*, vol. 51, no. 9, pp. 744–758, 2009.

[11] C. Gobl and A. Ní Chasaide, "The role of voice quality in communicating emotion, mood and attitude," *Speech Communication*, vol. 40, no. 1-2, pp. 189–212, 2003.

[12] Q. Zhang, A. Zhou, and Y. Jin, "RM-MEDA: a regularity model-based multiobjective estimation of distribution algorithm," *IEEE Transactions on Evolutionary Computation*, vol. 12, no. 1, pp. 41–63, 2008.

[13] M. Naseri, M. Abdolmaleky, A. Laref et al., "A new cryptography algorithm for quantum images," *Optik*, vol. 171, pp. 947–959, 2018.

[14] J. Packer and W. Reuschel, "VoIP accessibility: a usability study of voice over internet protocol (VoIP) systems and a survey of VoIP users with vision loss," *Journal of Visual Impairment & Blindness*, vol. 112, no. 1, pp. 47–60, 2018.
[15] S. Karapantazis and F.-N. Pavlidou, "VoIP: a comprehensive survey on a promising technology," *Computer Networks*, vol. 53, no. 12, pp. 2050–2090, 2009.
[16] C. K. Gohel and K. I. Lakhtaria, "Implement VoIP based IP telephony with open source asterisk architecture," *International Journal of Interdisciplinary Telecommunications and Networking*, vol. 2, no. 1, pp. 1–11, 2010.
[17] P. Liu, W. Qingqing, and W. Liu, "Enterprise human resource management platform based on FPGA and data mining," *Microprocessors and Microsystems*, vol. 80, Article ID 103330, 2021.
[18] J. Delery and N. Gupta, "Human resource management practices and organizational effectiveness: internal fit matters," *Journal of Organizational Effectiveness: People and Performance*, vol. 3, no. 2, pp. 139–163, 2016.
[19] L. Cania, "The impact of strategic human resource management on organizational performance," *Serial Management*, vol. 17, no. 2, 2014.

Hindawi
Mobile Information Systems
Volume 2022, Article ID 3682194, 11 pages
https://doi.org/10.1155/2022/3682194

Research Article

Optimization of Entrepreneurship Education for College Students Based on Improved Random Forest Algorithm

Dongfeng Jia[1,2] **and Hui Zhao**[1,2]

[1]*Hunan Institute of Technology, Hunan 421002, Hengyang, China*
[2]*Adamson University, Manila 900, Philippines*

Correspondence should be addressed to Hui Zhao; 2020001067@hnit.edu.cn

Received 12 May 2022; Revised 17 June 2022; Accepted 27 June 2022; Published 31 July 2022

Academic Editor: Shadi Aljawarneh

As we all know, the random forest algorithm has the advantages of high classification intensity and wide application range. Nevertheless, it still has a lot of room for improvement. This paper introduces the basic idea and working principle of classification algorithm and random forest algorithm, so this paper proposes some improved algorithms on the basis of all current research studies. College students, as the most innovative and adaptable group, have gradually become a development direction of China's education reform to cultivate their innovative employment ability and develop innovative employment education. By constructing a model of the relationship between innovation and entrepreneurship education and college students' employability, this paper examines the impact of innovation and entrepreneurship education mode on college students' employment and entrepreneurship. At the same time, the model is tested by improving the random forest algorithm. The process of talent quality evaluation is to select talents with the best comprehensive quality based on various indicators of students' performance in school, which can be regarded as a classification problem of unbalanced data sets. The improved random forest algorithm proposed in this paper has little difference in precision and recall rate when it is used for talent training evaluation but has a certain degree of improvement in accuracy rate, which meets the design requirements.

1. Introduction

Because the random forest algorithm has many excellent features, when the random forest is used in biological prediction, fault detection, network attacks, and other fields, good results are achieved, but it is worth mentioning that there are relatively few improvement studies on the random forest algorithm itself [1]. It can be seen that the random forest has many advantages, but the random forest algorithm has some disadvantages that cannot be changed [2]. For example, the random forest cannot balance the data well, control or detect the specific conditions in the model, but simply try through parameter adjustment and random data [3]. Therefore, this article needs to optimize and improve the random forest algorithm and explain some situations about random forest. If we want to improve the random forest, we generally need to consider two aspects. The first aspect is to improve the classification strength of each classifier and each tree, which is determined by the overall characteristics of the entire random forest decision, which can show the strength of the classification of the random forest [4]. The other is to reduce the correlation between the various departments of the classifiers, so that each classifier becomes an "expert" in its own field [5]. Because trees exist independently of each other and determine the final result together, they become experts in their respective fields. The stronger the correlation between the trees, the worse the classification performance of RF [6]. The essence of innovation and entrepreneurship education is to improve the comprehensive education and employability of college students and enhance the employment and entrepreneurial capital of college students [7]. This article constructs a model of the relationship between innovation and entrepreneurship education and college students' employability and conducts related research on

college students' innovation and entrepreneurship against the background of the "Internet+." After several years of development in China, it can be seen that its innovation and entrepreneurship education has made great progress, and many experts and scholars have conducted research on the training effects of innovation and entrepreneurship education in colleges and universities [8]. Through combining the existing literature, it is found that the current research focus is mainly on the impact of innovation and entrepreneurship education on innovation and entrepreneurship ability and entrepreneurial willingness. From these studies, it can be seen that such educational activities as innovation and entrepreneurship courses, entrepreneurship competitions, innovation and entrepreneurship lectures, and entrepreneurial clubs can significantly improve the innovation and entrepreneurship ability and willingness of college students [9]. Entrepreneurship education and ideological education for college students are based on the theory of the all-round development of people, so that the combination of entrepreneurship education and ideological education for college students can play the guiding role of ideological education in entrepreneurship education and make entrepreneurship education the ideological education [10].

2. Related Work

The literature random forest is mainly applied to two types of related problems, classification and regression, and at the same time it also has the ability to reduce data and is suitable for dealing with data problems such as fault values, missing values, noise, and outliers. Random forest algorithm can also solve some problems that traditional algorithms cannot solve [11, 12]. For example, random forest algorithm can avoid problems caused by data imbalance. Due to the combination of models, the random forest algorithm reduces some of the bad effects caused by overfitting, finally having a better effect than that of the decision tree, and it has improved a lot [13]. According to the literature, under a large data set, oversampling is not as good as undersampling. The literature proposes an essential feature of the random forest algorithm-stratified sampling, and the use of a vector machine as a base classifier at the node splitting makes it a huge advantage and makes it better than traditional classification on text imbalanced data [14]. The literature shows that the radial basis function neural network of the random forest algorithm is based on the basis classifier, and it is suitable for the classification of work balance and unbalanced data. The definition of the essential neural network of the radial basis function neural network as the basis classifier of the random forest algorithm is also proposed; it can be applied to the classification problems of medium and high imbalance and balanced data that appear in the work [15]. In the literature, since the weighted weights of decision trees in the random forest algorithm have the same value, the idea of scientists wanting to modify the weighted weights has become popular and widespread [16]. This led to the emergence of weighted random forest algorithm. The weight setting is based on the similarity size and proportion between each tree. The weighted random forest algorithm has some better characteristics, which makes the effect and display better than the traditional random forest algorithm [17]. The literature combines the essential idea algorithm of k-nearest neighbor with the random forest algorithm, makes improvements, and then proposes the algorithm of k-PNNs, which has a huge impact and enlightenment on the algorithm circle [18].

3. Research on Improved Random Forest Algorithm

3.1. Overview of Random Forest Algorithms. For supervised learning, the steps are as follows: obtain several training samples, input X into each sample obtained, get one and only one output result Y, and then train a specific model (mapping $f : X \longrightarrow Y$); at the same time, this unknown sample X' can make predictions about the result Y'. If Y' is a discrete variable, such as whether smoking is harmful to your health and whether a robot can replace all human work, such a problem is a classification problem; but if it is a continuous variable, such a problem is a regression problem.

The combination of the two algorithms of bagging and random subspace is called the random forest algorithm. Decision trees are the most basic neural network unit and thus play an important role. By this way, the important role played by the combination of multiple decision trees can be improved. Through the classification accuracy such as $h_1(x)$, $h_2(x)$, . . ., $\mathrm{h}_n\mathrm{Tr}(x)$, we can get the random forest classifier we want (Figure 1). If we want to solve the problem caused by regression disorder, the result of the weighted average of the common results of all decision trees is required.

Randomly generating training set: Use the famous bootstrapping method to randomly sample the data of each tree. As shown in Figure 1, the data set of each tree is randomly composed of the original data set, and may contain some data repeatedly or may not contain some data.

Random selection of feature subsets: When the tree nodes of each tree start to split, we need to randomly select a subset of the overall data attributes without replacement, and the size of the subset K is required to satisfy the number of features less than the total attribute M. Then, we can randomly extract the selected data K from M, then calculate the various indicators of the continuous data changes under K splits, select the best split feature index, continue to divide, and at this time make the selection field MK.

According to the definition of entropy value we know, the entropy value of sample data T can be obtained:

$$\mathrm{Entropy}\,(T) = -\sum_{i=1}^{c} P_i \log_2 P_i. \tag{1}$$

Among them, P_i indicates how much of the sample of category i accounts for the total number of samples. When the obtained data feature A comes into play, the sample T will be divided into k parts. At this time, we can know that the obtained information entropy and information gain are as follows:

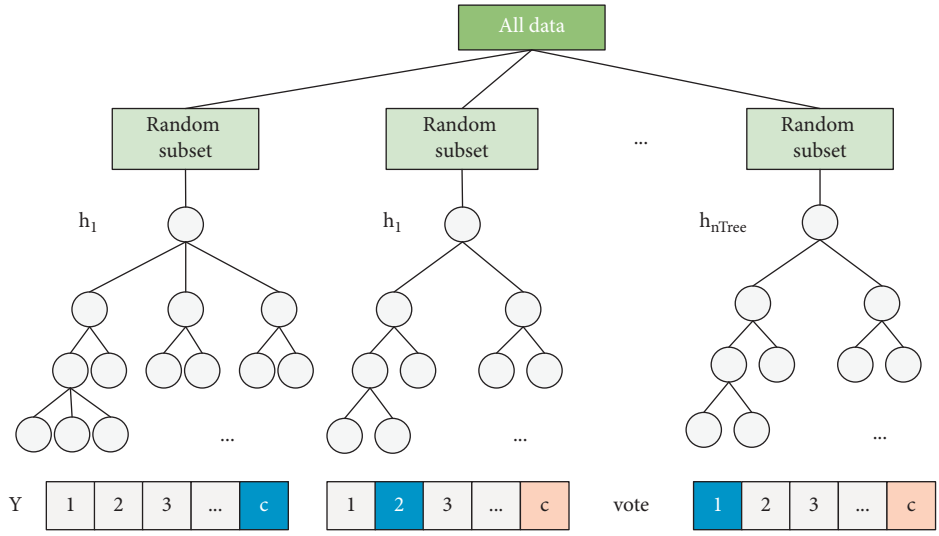

Figure 1: Schematic diagram of random forest.

$$\text{Entropy}(T_A) = -\sum_{j=1}^{k} \frac{|T_j|}{|T|} \cdot \text{Entropy}(T_j),$$
$$\text{Gain}(T, A) = \text{Entropy}(T) - \text{Entropy}(T_A). \tag{2}$$

And according to the definition of entropy in information theory, the gain efficiency of information is proportional to the effect of classification:

$$\text{GainRation}(T, A) = \frac{\text{Gain}(T, A)}{\text{SplitEntropy}(T, A)},$$
$$\text{SplitEntropy}(T, A) = -\sum_{i=1}^{c} \frac{|T_i|}{|T|} \log_2 \frac{|T_i|}{|T|}. \tag{3}$$

And according to the definition of entropy in information theory, the negative ratio between Gini coefficient and classification effect is

$$\text{Gini}(T) = 1 - \sum_{i}^{c} P_i^2,$$
$$\text{Gini}(T, A) = \sum_{j=1}^{k} \frac{|T_i|}{|T|} \text{Gini}(T_j). \tag{4}$$

Through the comparison of the above three attribute selection rules, it is found that the Gini coefficient measurement has less impact, so this article studies the Gini coefficient measurement.

The accuracy of classification can be defined as the accuracy of classification representing the total sample size:

$$\text{Accurcacy} = \frac{\text{TP} + \text{TN}}{\text{TP} + \text{TN} + \text{FP} + \text{FN}} = \frac{\text{TP} + \text{TN}}{N}. \tag{5}$$

The current F value, is an important indicator for evaluating unbalanced data sets. The size of β can indicate that the recall rate and the precision rate are more important and more prominent. When $\beta > 1$, the recall rate is more important, and when $\beta < 1$, the recall rate is less important. Take the value according to the actual situation; generally, $\beta = 1$ means that the recall rate and the precision rate are of the same importance. Only when both are high, the F value is larger, which means a better classifier effect.

$$F = \frac{\left(1 + \beta^2\right) g\text{RecallgPrecision}}{\beta^2 g\text{Recall} + \text{Precision}}, \quad \beta \in (0, 1],$$
$$F = \frac{2}{(1/\text{Precision}) + (1/\text{Recall})}. \tag{6}$$

G-mean, because in order to judge the fairness of the standard, we need to have the F value and the geometric mean, so we need the following formula:

$$G - \text{mean} = \sqrt{\text{Sensitivity} g\, \text{Specificity}}. \tag{7}$$

The contrast classifier is the purpose and theme of the simulation experiment in this section. First, we need to test some data to select the UCI data set; then, we divide these data into two categories, need to make their imbalance ratio gradually lower, and also make the agreed subcategory data not a negative category (Table 1).

Normalization processing: through Table 1, it can be found that due to the large difference in the attribute characteristics of the above data, they are not of the same order of magnitude, so before we build the data model, first, we need to normalize the input attribute characteristic matrix and carry out chemical treatment at the same time, and place it in [−1,1].

3.2. Optimization of Random Forest Algorithm. When the data obtained in the training set is unbalanced, the random forest algorithm will not balance the training data of each tree randomly selected in its self "random" process.

The small-class sample synthesis resampling technology is a relatively mature-SMOTE algorithm. Its specific thought

Table 1: Data set description.

Serial number	Data set	N	M	Positive	Negative class	IR	Category
1	Iris	100	4	50	50	1 : 1	Versicolor : virginica
2	Pokertrain	23092	10	10559	12493	0.8484 : 1	1 : 0
3	Wine	130	13	59	71	0.8310 : 1	1 : 2
4	Magic	19020	10	6688	12332	0.5423 : 1	g : h
5	Breast Cancer Wisconsin	702	10	243	459	0.5249 : 1	1 : 0
6	Haberman's survival	306	3	81	225	03600 : 1	2 : 1
7	Blood transfusion	748	4	178	570	0.3123 : 1	4 : 2

characteristics are as follows: firstly give a small-class sample X, obtain k adjacent samples for it, then randomly select n among these K samples, denote it as X_i, and add a new sample X_{new} by interpolation:

$$X_{\text{new}} = X_{\text{origin}} + \text{rand} \times \left(X_i - X_{\text{origin}}\right), \quad i = 1, 2, \ldots, n. \tag{8}$$

Although the SMOTE algorithm has some advantages, it also has many problems. For example, when selecting neighbors, you need to manually set the value of k by yourself, which is false and self-deceptive. Therefore, great scholars have made improvements and optimizations day and night and finally proposed the Borderline-SMOTE algorithm. The definition of the algorithm is shown in Table 2.

The traditional classification algorithm aims to maximize the classification accuracy of all data when the hypothesis is classified into the wrong class. Cost-sensitive learning is also based on traditional algorithms; however, it does not change the algorithm but assigns weights based on the cost caused by the wrong classification. Finally, the cost-sensitive classification algorithm is designed, but this design will classify small-class samples. The cost is not low.

Due to the imbalance of sample size data, the distribution of features also appears imbalanced. For example, some situations that appear in this article may only appear in some major categories. Therefore, we need to select the classification with the most discriminative ability based on the problems caused by the imbalance of the data classification, which will help improve the discrimination rate of the subcategories.

The CURE algorithm is a clustering algorithm for large databases developed by scientists:

Step 1. We need to normalize the data set, which has been mentioned above; then extract the data subsample X; and then calculate the mutual distance dist of the data subsamples. For a cluster class U that we obtain, Ur and Uc represent the collection point and center point of the data class U. Assuming that p and q are data items, we can get the formula for the distance between two clusters U and V:

$$\text{dist}(U, V) = \min_{p \in Ur, q \in V_r} dist(p, q). \tag{9}$$

Step 2. Set the number of clusters c, then cluster them, then merge the two clusters with the closest interval, and finally update the center point and the representative point.

Table 2: Definitions in Borderline-SMOTE.

Point	Definition
Noise point	$m = k$
Boundary points/dangerous points, easy to make mistakes	$m/2 \le k < m$
Safe point	$0 \le k < m/2$

$$Uc = \frac{|U| \cdot Uc + |V| \cdot Vc}{|U| + |V|},$$
$$Ur = \{p + \alpha \cdot (Uc - p) | p \in Ur\}. \tag{10}$$

Step 3. According to the newly revised SMOTE interpolation algorithm formula by the scientists, new data samples are generated. $X\overline{X}$represents the data sample points obtained after the CURE algorithm clustering. It is worth mentioning that the results we obtained will move randomly to representative points.

$$X_{\text{new}}^{n} = \overline{X} + \text{rand}(0, 1) \times (Ur - \overline{X}). \tag{11}$$

Step 4. We need to calculate the imbalance IR obtained by the data set. If the data set we obtain does not reach the lowest IR0, then return to Step 3.

Step 5. We need to use the convenience of the random forest algorithm to point out the new processed data set $X_{\text{new}} = \overline{X} \cup \left\{X_{new}^{p}\right\}$ and large class samples, and then start classification and a series of other operations.

So we can get the algorithm design flow chart as shown in Figure 2.

When performing data set selection and artificially generating data circle and unbalanced data set class in UCI, it can be seen that the training set and test set are divided into 3 : 1 stratified random sampling, and SPECT uses training and test files.

In this section, the random oversampling algorithm is used as an example to study the rules of each evaluation index of F, D-mean, AIC, and OOB error.

Objective function is as follows: $f(\text{nTree}*, K^*, \{\text{Attribute}_i | i = 1, 2, \ldots, M\}) = \text{argmin}(\text{avg OOB error})$.

Optimization variables are as follows: nTree, K, $\{\text{Attribute}_i | i = 1, 2, \ldots, M\}$.

Binary encoding: We can see that Figure 3 contains two tangent points and three fragments. nTree and K are the embodiment of binary data, 0 of $\{\text{Attribute}_i \mid i = 1, 2, \ldots, M\}$

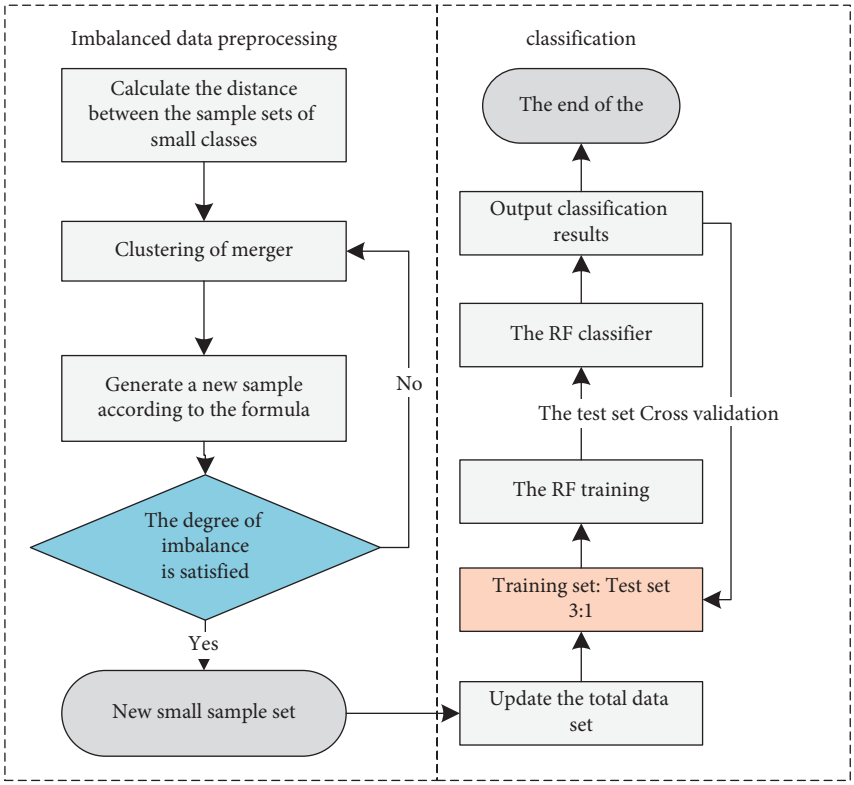

Figure 2: Schematic diagram of CURE-SMOTE algorithm.

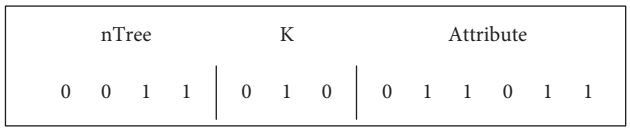

Figure 3: Schematic diagram of binary encoding.

means this part is not selected, and 1 means this part is selected. And the constraint condition is $K \leq \text{sum}(\text{Attribute}_i = 1)$.

Step 1. Combine the RF classification calculator to calculate $F = \max(1/f) =$, gen = 1.

Step 2. Selection operation: decide whether to select the individual according to the proportion of fitness value.

$$p_i = \frac{F_i}{\sum_{i=1}^{\text{popsize}} F_i}. \tag{12}$$

Step 3. Intersection operation: according to the single-point crossover method, we randomly select two individuals, make a random change of 0-1, and then judge whether the solution is correct.

Step 4. Change operation: we randomly select an individual, randomly select the changed position *j*, make the 0-1 switch, then judge whether the solution is correct, calculate the fitness value, and update the optimal solution.

Step 5. When the result of gen > maxgen appears, it means the end; otherwise, it returns to the third step.

Hybrid PSO-RF process design is as follows:

Step 1. Population initialization: the number of population popsize, the number of changes maxgen; the binary data position of the particle $X_K = \{Z_{K,1}, Z_{K,2}, \ldots\}$, $K = 1, 2, \ldots$ popsize; the required data speed V; the learned data factors c_1, c_2; and the false weight number w.

Step 2. We combine the RF classifier to start calculating the fitness $F = \text{mcax}(1/f)$, and input the parameter combination into the RF algorithm, gen = 1.

Step 3. The velocity $V^{(K+1)}$ and position $X^{(K+1)}$ of the particles to be used, and *kP PK* is expressed as part of the best position, and *Pĝk* is the best overall, where rand represents a random number.

$$V^{k+1} = wV^k + c_1 r_1\left(P^k - X^k\right) + c_2 r_2\left(Pg^k - X^k\right), \quad r_1, r_2 \in [0,1],$$
$$\text{sigmoid}\left(V^{k+1}\right) = \frac{1}{1+e^{-V^{k+1}}},$$
$$Z_{k+1,j} = \begin{cases} 0, & \text{rand} > \text{sigmoid}\left(V^{k+1}\right), \\ 1, & \text{rand} \le \text{sigmoid}\left(V^{k+1}\right), \end{cases} \quad \text{rand} \sim U(0,1). \tag{13}$$

Step 4. When the result of gen > maxgen appears, it means the end.

Hybrid AFSA-RF process design is as follows:

Step 1. Population initialization: the number of population is popsize, the number of changes is mxgen, the place where the fish school is $X\_K = \{Z_{K,1}, Z_{K,2}, \ldots\}$, $K = 1,2, \ldots$ popsize; the range visual that the artificial fish can see is popsie, the crowding factor is delta; the maximum number of attempts of the fish trynumber.

Step 2. We need to combine the RF classifier to calculate the concentration of fish food max$(1/f)$.

Step 3. At the same time, we need to carry out experiments on the grouping behavior and rear-end collision behavior of fish:

(a) Group behavior of fish: the current state of artificial fish is X_i, the number of fish partners in the viewing range is nf, and the center position of the lake is X_c. When $F_C/f >$ delta·Fitness, we change the position of the fish according to the following formula, and we start foraging behavior if it does not match.

$$Z_{k+1,i} = \begin{cases} Z_{k,i}, Z_{k,i} = Z_{c,i} \\ 0, Z_{k,i} \ne Z_{c,i}, rand > 0.5 \\ 1, Z_{k,i} \ne Z_{c,i}, rand \le 0.5 \end{cases}. \tag{14}$$

(b) Tail-catch behavior of fish: we find the fish $X_{\max}$ with the maximum food concentration $F_{\max}$ in the fish school. If $F_{\max}/nf >$ delta F, change the place of the fish with the following formula, calculate the concentration of fish food, and update the food concentration; if not, perform other foraging behaviors.

$$Z_{k+1,i} = \begin{cases} Z_{k,i}, Z_{k,i} = Z_{\max,i} \\ 0, Z_{k,i} \ne Z_{\max,i}, rand > 0.5 \\ 1, Z_{k,i} \ne Z_{\max,i}, rand \le 0.5 \end{cases} \tag{15}$$

(c) Foraging behavior of fish: the existing fish state is $X_K = \{Z_K\}$, and the random behavior performed by $d_{ij} \le$ visual within the visible range starts to select the state of the data $X_J = \{Z_{ij}\}$.

If $F > F_j$, you need to randomly regenerate their state $X_{(k+1)}$ for the fish and then finally perform the experiment of calculating the food concentration.

$$Z_{k+1,i} = \begin{cases} Z_{k,i}, & Z_{k,i} = Z_{j,i}, \\ 0, & Z_{k,i} \ne Z_{j,i}, \text{rand} > 0.5, \\ 1, & Z_{k,i} \ne Z_{j,i}, \text{rand} \le 0.5. \end{cases} \tag{16}$$

Step 4. Continuously update the latest living conditions of the optimal artificial fish. When gen > maxgen, the experiment ends; otherwise, return to Step 3.

3.3. Application of Random Forest Algorithm in the Evaluation of College Students' Talent. The process of talent quality evaluation is to select talents with the best comprehensive quality based on the various indicators of student performance in school, which can be regarded as a classification problem of unbalanced data sets. If you do not consider the balance of the indicators to directly model the original data, it is difficult to get an ideal model. You may need to use training data to improve the imbalance rate. The main way to achieve this is to measure the importance of data indicators through feature importance metrics. Using this as the index weighting standard, this paper chooses the Ranking method to measure the importance of the index points; on the other hand, because the random forest algorithm uses an average voting mechanism for the classifier, this voting mechanism makes the weak classifier to the final The results of the evaluation have an impact. In this paper, the F-measure algorithm is used to weight the classifiers to reduce the impact of weak classifiers on the results.

In order to solve the above problems, this paper uses the importance of each sample feature as the basis and selects the sample features with higher importance to reduce the possibility of weak classifier generation. There are many ways to measure the importance of features. This article uses a random forest sorting algorithm to calculate the importance of features. The following are the main steps of the method:

Step 1. Select a sample feature X, randomly introduce noise data, and calculate OOB again. The result is recorded as errOOB2, and the initial OOB calculation result is recorded as errOOB1. When there are N decision trees in the random forest, the formula for feature X is as follows:

$$I_X = \frac{\sum_j^N \left(\text{errOOB2}_j - \text{errOOB1}_j\right)}{N}. \tag{17}$$

Step 2. Follow the ordered features obtained in Step 1, select 75% of the features, and remove the next 20% of the features from the feature set.

Step 3. Repeat the above two steps until the number of features drops to M, a value set in advance. Finally, m final feature sets are obtained.

The traditional random forest method uses the average majority voting method when making classification decisions. Each decision tree outputs its own classification label, and the final result is the class with the most output. But in the classification process, the classification effect of the decision tree is different, and the poorly effective classifier has a negative impact on the result.

$$\begin{aligned} \text{Recall} &= \frac{\text{TP}}{\text{TP} + \text{FN}}, \\ \text{ACC} &= \frac{(\text{TP} + \text{TN})}{\text{TP} + \text{FP} + \text{FN} + \text{TN}}. \end{aligned} \tag{18}$$

Among them, TP represents the actual number of high-quality graduates predicted to be high-quality graduates, and TN represents the actual number of low-quality graduates predicted to be low-quality graduates. FP represents the actual low-quality graduates predicted to be high-quality graduates, and FN represents the actual high-quality graduates predicted to be low-quality graduates.

According to the F-measure calculation formula, the F-measure value of each decision tree that forms the random forest classifier is calculated.

$$F - \text{measure} = \frac{2 \times \text{recall} \times \text{precision}}{\text{recall} + \text{precision}}. \tag{19}$$

In the above formula, recall represents the recall rate, and precision represents the accuracy rate. First, input the data of the verification set into each decision tree; then, each decision tree will have a category prediction for each record in the verification set; and compare the prediction results of the decision tree with the real results.

The improved random forest algorithm reduces the impact of the average voting mechanism, reduces the impact of weak classifiers on the results, and improves the overall performance of the algorithm. It can be applied in talent quality evaluation or in other applications.

It can be seen that although the convergence speed, accuracy, and local optimization ability of the ASSABC algorithm on some test functions have been improved, the results on complex multimodal functions are not very satisfactory, and this is likely to be due to insufficient mining capacity and step length variables. The sensitivity is not enough to fall into the local optimum. The test results are shown in Figures 4 and 5.

The data source of this article is mainly the student data collected by a university's information college during the national engineering professional certification process. The data is composed of college archives, questionnaire surveys, comprehensive evaluation results, etc., including detailed data of more than 2000 graduates from 2011 to 2020, each of which contains about 35 fields, a total of 80,000 data.

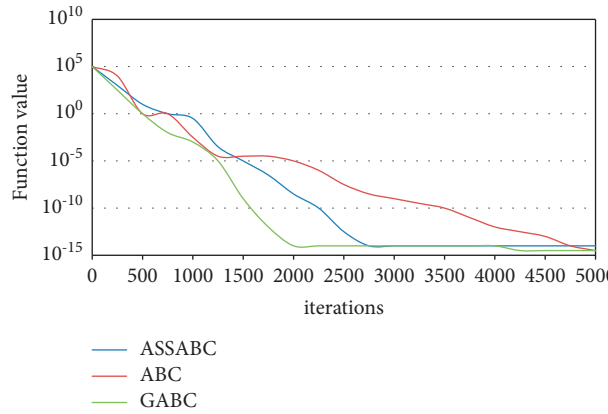

Figure 4: Convergence graph of F1.

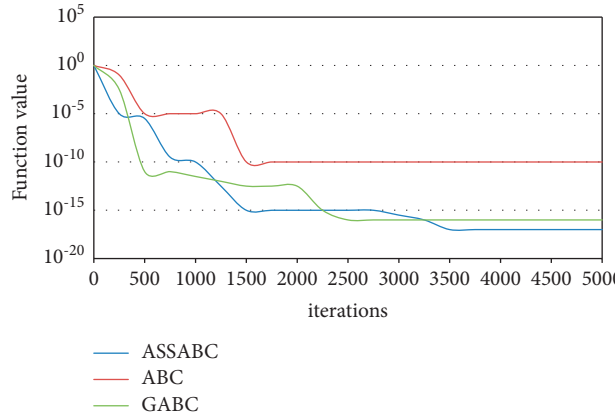

Figure 5: Convergence graph of F2.

According to the needs of talent training quality evaluation, we only need to select data closely related to the evaluation content to establish a database. In the end, only the fields shown in Table 3 are retained.

Among them, the sample data for a total of 8 years from 2011 to 2018 is used as the original training set, accounting for 80% of the total number of samples, and the sample data of two years from 2019 to 2020 are used as the test set.

This article has made two improvements to the RF algorithm. In order to verify that both improvements can have a positive impact on the evaluation results, this article verifies the two improvements separately to prove their effectiveness. In order to verify the enhancement of algorithm performance by feature selection, this paper compares the RF algorithm without feature importance weighting to the feature importance weighting algorithm. The results are shown in Table 4.

In order to verify the influence of the F-measure weighting algorithm on the performance of the algorithm, the RF algorithm of the ordinary voting mechanism is compared to the RF algorithm with the F-measure weighted voting mechanism. The results are shown in Table 5.

It can be seen from Table 6 that the random forest algorithm model based on the F-measure weighted voting mechanism has higher performance than the traditional one.

Table 3: Field information contained in the processed data.

Student ID	Name	Gender	Profession	Professional technical ability
Innovation and entrepreneurship	Knowledge learning ability	Management practice ability	Comprehensive development ability	Sustainability
Employment service satisfaction	Job satisfaction	Teaching satisfaction	Job relevance	Job satisfaction

Table 4: The impact of the feature importance method on the performance of the RF algorithm.

Algorithms	ACC (%)	Recall	F-measure	ROC area
RF	91.78	0.635	0.694	0.846
WRF	92.81	0.647	0.684	0.836

Table 5: The influence of F-measure weighting algorithm on algorithm performance.

Algorithms	JCC (%)	Recall	F-measure	ROC area
RF	91.78	0.635	0.694	0.846
WRF	92.2	0.642	0.711	0.850

Table 6: Data set description.

Serial number	Data set	N	M	Positive	Negative class	IR	Category
1	Circle	1362	2	229	1133	0.2021 : 1	1 : 0
2	Blood transfusion	748	4	178	570	0.3123 : 1	4 : 2
3	Haberman's survival	306	3	81	225	0.36 : 1	2 : 1
4	Breast Cancer Wisconsin	702	10	243	459	0.5249 : 1	1 : 0
5	SPECT.train	80	23	26	54	0.4815	1 : 0

In order to prove the role of FWRF algorithm in the evaluation of college students' graduation quality, this paper makes a horizontal comparison between several classical improved RF algorithms and FWRF algorithm. The experimental data is all categories in the data set. After the final screening, this paper selects the hybrid particle swarm random forest algorithm, hybrid genetic random forest algorithm, hybrid fish school random forest algorithm, and original random forest algorithm as the comparison algorithms. The performance evaluation index is mainly accuracy. The Python language is used in PyCharm. The above 4 algorithms are implemented using the scikit-learn library on the development platform. The experiment uses a tenfold cross-validation method to analyze the sample set and evaluates the classification results based on accuracy, recall, and F1 value. Table 7 shows the experimental results of the five methods.

It can be seen from Table 7 that compared with several classical modified random forest algorithms, the improved random forest algorithm proposed in this paper has little difference in accuracy and recall rate when used in the evaluation of talent training, but it is accurate. The rate has been improved to a certain extent, which meets the design requirements.

Table 7: Comparison of 5 experimental methods.

Algorithms	ACC (%)	Recall	F-measure	ROC area
RF	91.78	0.635	0.694	0.846
Mixed ion	92.46	0.656	0.717	0.866
Mixed inheritance	92.66	0.676	0.722	0.872
Mixed school	92.55	0.676	0.722	0.872
FWRF	93.45	0.697	0.723	0.897

4. Optimization of College Students' Entrepreneurship Education in the Era of Artificial Intelligence

4.1. Research Content of the Employment Ability Training Model of College Students in the Era of Artificial Intelligence. The education of traditional colleges and universities is mostly limited to the theoretical level, which leads to the fact that college graduates cannot keep up with the practical needs of the workplace after graduation. Many companies may need to spend a long time to cultivate talents that meet their own business practice requirements. Therefore, theoretical teaching in Colleges and universities needs to be combined with practical teaching. For example, innovative colleges and universities such as cash apprenticeship and

order classes are combined with enterprise teaching to officially try to solve the above problems and innovative attempts. When students are in school, they can be given company-based teaching or go to a company for practical learning, which can not only meet the requirements of improving the ability of college students in the artificial intelligence era, but also improve the learning efficiency of students.

Generally, college students have limited awareness and have less exposure to new artificial intelligence technologies. In particular, many vocational and technical college students are limited to employment in traditional industries. Therefore, schools should stimulate students' innovative potential. Every year, campus culture and art festivals and science and technology festivals are held to encourage students to participate in professional skill competitions, to study and ponder on their counterparts, and to cultivate the spirit and perseverance of learning, loving, and working hard. Innovation leads ideas; technology revolutionizes the world.

4.2. Innovativeness of the Employment Ability Training Model for College Students in the Era of Artificial Intelligence. After college students acquire entrepreneurial knowledge, companies can also sign some contracts with the colleges and universities the students belong to, to provide more outstanding graduates with more job opportunities. It is possible to further consolidate and apply knowledge in the practice base of undergraduate entrepreneurship education. And college students can also make full use of the school's equipment and facilities to make a judgment on their own abilities and then gradually enhance their own comprehensive quality.

Pay attention to the combination of theory and practice. At present, many colleges and universities still use the past teaching materials, so they will face the problem of gaps between the teaching content and materials and the cutting-edge technology of the society. Many college teachers have a single teaching method. Therefore, colleges and universities should increase the ability of masters, promote the reform of teaching courses, establish professional counterpart training rooms, and focus on the combination of professional practical operation and extracurricular research.

The current national employment and entrepreneurship policies run through it. By publicizing the deeds of party members in the new era and the deeds of outstanding students close to students' lives in the school, postgraduate entrance examination policies, college students' entrepreneurship, etc., college students can understand the current policies related to graduates and make their own college career and career planning.

4.3. Research on Innovation and Entrepreneurship Education and University Students' Employability. Employability is the embodiment of college students' comprehensive ability, and its level directly determines the employment quality and work performance of college students. Therefore, this article constructs a model to examine the influence of innovation and entrepreneurship education model on college students' employability and entrepreneurship. Through analysis, it is found that the current level of employability of college students is average. The level of teamwork, communication, and coordination skills is relatively high, while the level of professional innovation ability is relatively low. On the other hand, it reflects innovation and entrepreneurship courses, innovation and entrepreneurship simulation training. The education model is closely related to the employability and various dimensions of college students. Therefore, in order for innovation and entrepreneurship education to better play its role in promoting the employability of college students, the following suggestions are put forward:

(1) In order to improve the educational effect of innovation and entrepreneurship courses, colleges and universities can design innovation and entrepreneurship curriculum systems hierarchically and categorically according to the different stages of student learning and individual differences. Sophomore and junior students mainly study professional courses. At this stage, it is necessary to solve the problem of the integration of innovation and entrepreneurship courses and professional courses. Students should be instructed in how to apply the entrepreneurial awareness, skills, and spirit acquired in entrepreneurship education courses to their professional studies so as to obtain good professional knowledge understanding and absorption ability. The senior year is often a period when students are preparing to start a business or get a job. Therefore, special entrepreneurial intensification courses can be provided for students with entrepreneurial inclination and a clear career direction.

(2) Give full play to the leading role of entrepreneurship lectures. Colleges and universities can also invite entrepreneurs, especially successful alumni, to come to the school to conduct innovation, entrepreneurship, and employment seminars; combine their own professional experience and professional vision; and share innovation and entrepreneurship experience and employment status in the professional field, so that students can understand the development of society and enterprises. The requirements for the quality and ability of college students provide a direction for the development of high-quality employment for students.

(3) Colleges and universities should establish complete competition guarantees and incentive measures to organically integrate the participation in entrepreneurial competitions, evaluation, employment recommendation, and other matters closely related to college students' academic and employment, so as to increase students' enthusiasm for participation and improve project quality. For outstanding entrepreneurial competition project results, school incubators or cooperation with off-campus enterprises and

investment institutions can be used to promote the market transfer of projects.

(4) For students who intend to start a business or entrepreneurial projects with development potential, the school can assist in the formation of a cross-disciplinary and cross-professional entrepreneurial team and the establishment of the innovation and entrepreneurship practice base.

(5) Universities should strengthen laboratory construction, such as business simulation laboratory, consumer cognition laboratory, and business negotiation laboratory, and ensure the class hours of experimental courses. Through playing a role in the simulation experiment operation, students can experience the business process of the enterprise, feel the nature of different jobs, and perceive the correct management mode. At the same time, the school also needs to strengthen school-enterprise cooperation. Students can regularly go to the off-campus training base to receive entrepreneurship training and directly participate in the production and operation activities of the enterprise.

5. Conclusion

Nowadays, data mining algorithms are widely used. After studying several classification algorithms (LR, NB, SVM, GRNN, and RF), this paper focuses on the RF algorithm. For unbalanced data processing, we propose the CURE-SMOTE algorithm, which selects representative data points to prevent noise data, and artificially generated samples follow the original distribution. Under this influence and under the leadership of innovation driven in the era of artificial intelligence, college students have been integrated with career planning through education and services, and each region combines local economic characteristics, industrial upgrading, and integration, changing the traditional cheap labor model and optimizing the local economy. Against the background of the new era, college students need to give full play to their value as knowledge-based talents to give their country their strength and contribute their value. In the new era, college students also need to innovate themselves, strengthen their comprehensive quality capabilities, adapt to the changing times, and realize the reform and innovation of political, economic, and social talents in the era of artificial intelligence. At the same time, colleges and universities need to optimize education in terms of undergraduate entrepreneurship. Undergraduate entrepreneurship education and ideological and political education are based on the theory of human all-round development and actively develop the entrepreneurial education resources among them. Secondly, colleges and universities should vigorously support entrepreneurial associations, entrepreneurial centers, and entrepreneurial associations; provide support for their events and funds; and at the same time guide students to actively participate in teachers' scientific research and invention projects and effectively combine their own majors with scientific research and invention projects, so as to create a very strong sense of entrepreneurial atmosphere. In addition, schools should build a practice base for innovation and entrepreneurship and improve the incubation mechanism for entrepreneurial projects. After students gain entrepreneurship knowledge, they can further consolidate and apply knowledge in the college student entrepreneurship education practice base. And college students can also make full use of the school's equipment and facilities to make a judgment about their own abilities and then gradually enhance their own comprehensive quality. In addition, college students can give full play to the professional knowledge they have learned and gradually apply it to work areas closely related to their professions, and then they can constantly improve themselves, find out their own shortcomings, and improve them, without taking today's mistakes. Innovation and entrepreneurship should be realized not only in response to the call of the country, but also for the sake of college students. Through innovation and entrepreneurship, we can become stronger, better contact the society, and adapt to society in advance.

Data Availability

The data used to support the findings of this study are available from the corresponding author upon request.

Conflicts of Interest

The authors declare that they have no conflicts of interest.

Acknowledgments

This work was supported by the Teaching Reform fund XJT [2019] No. 291: Research Projects of Teaching Reform in Colleges and Universities of Hunan Province in 2019, "Design and Practice of the Flipped Classroom for Guidance of Career Development, Innovation and Entrepreneurship for College Students' Based on MOOC" (Fund Project No. 1024).

References

[1] T.-H. Lee, A. Ullah, and R. Wang, *Bootstrap Aggregating and Random Forest*, Springer, New York, NY, USA, 2020.

[2] J. L. Speiser, B. J. Wolf, D. Chung, C. J. Karvellas, D. G. Koch, and V. L. Durkalski, "BiMM forest: a random forest method for modeling clustered and longitudinal binary outcomes," *Chemometrics and Intelligent Laboratory Systems*, vol. 185, pp. 122–134, 2019.

[3] V. Jain, J. Sharma, K. Singhal, and A. Phophalia, *Exponentially Weighted Random forest," Pattern Recognition and Machine Intelligence*, pp. 170–178, Springer, Cham, Switzerland, 2019.

[4] N. Mohapatra, K. Shreya, and A. Chinmay, "Optimization of the random forest algorithm," in *Advances in Data Science and Management*, pp. 201–208, Springer, New York, NY, USA, 2020.

[5] R. Genuer, J. M. Poggi, C. Tuleau-Malot, and N. Villa-Vialaneix, "Random forests for big data," *Big Data Research*, vol. 9, pp. 28–46, 2017.

[6] J. Abellán, C. J. Mantas, J. G. Castellano, and S. Moral-García, "Increasing diversity in random forest learning algorithm via

imprecise probabilities," *Expert Systems with Applications*, vol. 97, pp. 228–243, 2018.

[7] European Commission, *Entrepreneurship in Higher Education, Especially with in Non-business Studies," Final Report of the Expert Group*, European Commission, Enterprise and Industry Directorate-general, Brussels, Belgium, 2008, http://ec.europa.eu/enterprise/policies/sme/files/support_measures/training_education/entr_highed_en.pdf.

[8] European Commission, *Implementing the Community Lisbon Programme: Fostering Entrepreneneurial Mindsets through Education and Learning, COM 33 Final*, Commission of the European Communities, Brussels, Belgium, 2006.

[9] J. Heinonen, "An entrepreneurial-directed approach to teaching corporate entrepreneurship at university level," *Education + Training*, vol. 49, no. 4, pp. 310–324, 2007.

[10] Y. Xu, "Design of human resource allocation algorithm based on improved random forest," in *Proceedings of the ICASIT 2021: 2021 International Conference on Aviation Safety and Information Technology*, pp. 656–661, New York, NY, USA, December 2021.

[11] P. Blenker, P. Dreisler, and J. Kjeldsen, "Entrepreneurship education—the new challenge facing the universities," *A framework or understanding and development of entrepreneurial university communities*, vol. 2, 2006.

[12] H. M. Gomes, A. Bifet, J. Read et al., "Adaptive random forests for evolving data stream classification," *Machine Learning*, vol. 106, no. 9-10, pp. 1469–1495, 2017.

[13] L. Breiman, "Random forests," *Machine Learning*, vol. 45, no. 1, pp. 5–32, 2001.

[14] P. Cremonesi, R. Turrin, and F. Airoldi, "Hybrid algorithms for recommending new items," in *Proceedings of the 2nd International Workshop on Information Heterogeneity and Fusion in Recomm ender Systems*, pp. 33–40, New York, NY, USA, October 2011.

[15] B. Xu, J. Z. Huang, G. Williams, Q. Wang, and Y. Ye, "Classifying very high-dimensional data with random forests built from small subspaces," *International Journal of Data Warehousing and Mining*, vol. 8, no. 2, pp. 44–63, 2012.

[16] R. Díaz-Uriarte and S. Alvarez de Andrés, "Gene selection and classification of microarray data using random forest," *BMC Bioinformatics*, vol. 7, no. 1, p. 3, 2006 article.

[17] T.-T. Nguyen, J. Z. Huang, K. Imran, M. J. Li, and G. Williams, "Extensions to quantile regression forests for very high-dimensional data," in *Advances in Knowledge Discovery and Data Mining*, pp. 247–258, Springer, Berlin, Germany, 2014.

[18] X. Sun, "Financial management system for undergraduate innovation and entrepreneurship education based on grid algorithm," in *Innovative Computing*, J. C. Hung, JW. Chang, Y. Pei, and WC. Wu, Eds., Springer, Singapore, 2022.

Hindawi
Mobile Information Systems
Volume 2022, Article ID 7600848, 7 pages
https://doi.org/10.1155/2022/7600848

Research Article

Civil Engineering Simulation and Safety Detection of High-Rise Buildings Based on BIM

Yinchen You, Yi Zheng, and Xiaohui Chen

Jinshan College of Fujian Agriculture and Forestry University, Fujian, Fuzhou 350000, China

Correspondence should be addressed to Yinchen You; 2004059@muc.edu.cn

Received 25 May 2022; Revised 26 June 2022; Accepted 8 July 2022; Published 31 July 2022

Academic Editor: Shadi Aljawarneh

In the process of vigorously promoting the development of China's smart city construction site engineering, the wide application of BIM technology and its advantages have been widely reflected in various places such as remote video site monitoring, visual chemical field technical data disclosure, and statistical engineering volume. BIM technology can effectively help enterprises manage the whole construction site, and can significantly and effectively improve the safety management level and work efficiency of the whole construction site. In this paper, a numerical simulation processing system for civil engineering is designed. This system can not only effectively predict and evaluate the design results of civil engineering but also help guide enterprises to obtain various earthquake-resistant and beautiful building structure designs, and various this kind of economical and reasonable engineering project construction decision-making. This paper uses simulation models to study the civil engineering of high-rise buildings, and conducts an in-depth study on the efficiency of simulation processing results and the analysis of visualization methods, which mainly include the efficient visualization of simulation time-varying vector fields and the efficient visualization after OpenSEES simulation processing.

1. Introduction

BIM 3D technology is mainly based on various building-related design materials and related data models of architectural engineering design projects. It uses a large number of digital information technologies to perform automatic simulation to simulate the real situation of 3D buildings [1]. Design-related management software automatically builds a model of a three-dimensional building to realize various functions such as the overall design, construction, and management of the three-dimensional building [2, 3]. With the continuous progress of China's characteristic well-off socialist industrial market economy and national scientific production technology, the structural complexity of high-rise buildings continues to increase, and the steel structure design of high-rise buildings also puts forward higher requirements [4]. The requirements of structural scale and function are also constantly changing, which greatly increases the complexity of high-rise building design [5]. At the same time, the level of civil simulation of high-rise buildings should also be continuously improved to adapt to the changes in the architectural scale and functional requirements of high-rise buildings. The traditional two-dimensional drawing CAD architectural design and construction methods are prone to construction drawing design differences, collaborative work design problems are difficult to complete, collision design problems are difficult to discover in time, information communication between all parties is difficult to coordinate, and engineering quantity data statistics are difficult. Problems have brought a lot of inconvenience to the management of a large number of construction projects. BIM design technology can solve these complex problems efficiently [6–8].

2. High-Rise Building Design Based on BIM Technology

2.1. High-Rise Building Design Based on BIM Technology

2.1.1. BIM Architectural Model. The architectural model of the project is the modeling software Revit Architecture, with BIM technology as the core, which can be designed

according to the thinking and ideas of expert designers in various architectural disciplines, and designed and produced by these software applications. The products are of good quality and high precision.

2.1.2. BIM Structural Model. The project's structural model adopts the BIM core modeling software Revit Architecture, which provides professional designers related to building structure with a set of specialized design methods and tools, which can effectively help architectural designers design high-efficiency building structures more accurately [9]. Revit Architecture is an intelligent building model built on the basis of advanced building model information technology. Through simulation and data analysis of architectural design documents, it accurately realizes the prediction and analysis functions, and uses the information contained in these intelligent building models [10, 11]. Geographic location coordinates and all other information greatly improves the quality and accuracy of architectural design documents.

In the construction project of a building A1# in a science and technology park, the structural model design was designed by a professional architectural structure design engineer. They used the Revit Architecture method to design and arrange the layout of the overall building structure.

2.1.3. BIM Electromechanical Model. The project electromechanical equipment model design adopts the construction modeling design software Revit MEP, with BIM as the design core. It designs various types of electromechanical equipment for professional buildings, such as heating, electrical, and land drainage [12, 13]. Design managers and architectural designers provide specialized building design management tools. Through advanced intelligent building professional information system model design technology, they can quickly design and develop extremely complex professional building information systems, and help derive professional building information systems with higher performance and efficiency [14, 15].

In the A1# project of a high-tech park area, the electromechanical system model was designed and used by professional electromechanical model engineers. Revit MEP completed the overall design of electromechanical water supply and drainage, HVAC, electrical, and other models, and established various plumbing. The design view and model template of the electrical system, respectively, clearly give basic parameter information such as the raw material and equipment component model of each electromechanical subsystem, and provide a complete statistical table of electrical wiring and electrical equipment model information.

2.2. BIM Collaborative Design. Project collaborative design uses BIM collaborative software Vault, which itself is a source control tool. Vault is not only powerful but helps all the data of the library stored in a SQL database.

In the development project of A1# office building in a Hangzhou high-tech park, this paper makes full use of the data resource management system platform in Vault and develops it into a data platform for BIM collaborative development and design. The specific process of BIM collaborative design can be roughly divided into the following five basic aspects:

(1) The BIM collaboration method has been innovated, and the BIM collaboration model has been established using Vault's database and information management platform.

(2) Combined with the national standardized quality supervision and management system, it avoids the damage of management efficiency and fully improves the implementation of management functions. Management documents and archives must be filed through the Internet in time.

(3) Vault + cloud technology realizes the design of Internet+, and realizes the submission of the overall architectural model of BIM.

(4) Use parallel review of relevant data stored on Revit. At the same time, the staff can quickly carry out a work flow of level-by-level assessment through the classification of the assessment documents-real-time change management of the status.

(5) Parallel file review on Vault. The software workflow of Vault review not only requires us to make full use of the technical advantages of various review software but also a set of continuous software review processes must be reasonably organized and designed in multiple software such as Revit and Navisworks, in order to truly achieve this parallelism.

2.3. BIM Pipeline Synthesis. Using BIM, the original two-dimensional graphic design drawings can be intuitively converted into a visual three-dimensional model for display on the Internet, which can directly optimize the comprehensive design and optimization of the structure of the electromechanical pipeline. In addition, the BIM technology used in this article also is able to realize the comprehensive design of the pipeline. This change directly provides the specific location and size of the space and holes reserved in the design of the electromechanical pipeline.

As shown in Figure 1, BIM technology can be used to analyze the clear height of the comprehensive arrangement of pipelines, and accurately calculate the vertical clear height of the building, so as to fully meet the functional requirements of the building.

Through BIM technology, we have carried out in-depth design for various types of building structural steel bars. By identifying and defining the characteristics and attributes of various types of steel bars, including data information such as types, diameters, and spacing of steel bars, various types of steel bars are identified in the building structure model. Carrying out three-dimensional positioning and shape display, so as to realize the three-dimensional visualization of the layout of the steel bars in the building structure, the collision detection between the steel bars of complex nodes,

Figure 1: Pipeline net height analysis.

and the accurate calculation of the blanking length of various types of steel bars were performed.

The in-depth analysis and design plan of the main reinforcement base of the project is to use a set of BIM design technology as the core reinforcement modeling design software Revit Structure, and use a BIM base reinforcement main structure design model drawing as the reinforcement design data carrier, and according to all, the steel bar design plan drawings provided by the author are designed for the deep analysis and design of the steel bar according to the longitudinal arrangement and distribution of the basic steel bar.

2.4. BIM Construction Drawing Output. By directly drawing the architectural drawings of various related disciplines through BIM technology, the information of the building can also be directly reflected in this model. BIM technology uses three-dimensional simulation modeling technology and parametric information technology to build a large database, and converts traditional drawings into data storage and extraction. In the whole process from the scheme design to the construction drawing design, the information of the building model will be continuously optimized and perfected. Through the output of these models to the construction drawing, it can save a lot of people's time to draw the drawing.

In a high-tech park A1# building project, the three-dimensional model of the first floor building is shown in Figure 2.

3. High-Rise Building Structure Based on BIM Technology

3.1. Establish a Finite Element Model

3.1.1. Definition of Material and Section Properties. In this design project, there are detailed definitions for the material and section properties of the main body and its components of the steel structure, see Table 1 for details.

3.1.2. Import Revit Steel Structure Model into Midas Gen. First, the main model of steel structure needs to be built by using Revit in BIM, the structural modeling and design software as the design core. Two Revit and Midas Gen interface plug-ins need to be installed in the computer, respectively. After all the plug-ins

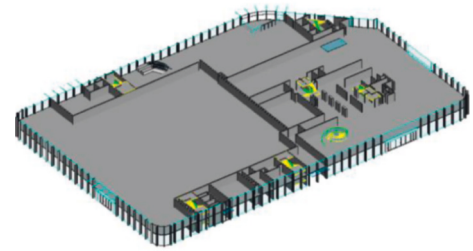

Figure 2: Three-dimensional model of the first-floor building.

Table 1: Steel structure materials and section characteristics.

Member number	Steel strength	Size
1	Q345B	83 * 6
2	Q345B	95 * 6
3	Q345B	102 * 6
4	Q345B	114 * 8
5	Q345B	152 * 8
6	Q345B	180 * 8
7	Q345B	203 * 10
8	Q345B	219 * 10
9	Q345B	245 * 10
10	Q345B	299 * 8

are installed, open a Revit steel matrix structure model that has been automatically created, click the title menu in the structural modeling design software Revit, find send model to Midas Gen and click. Then, you can make some simple plug-in settings in the pop-up settings dialog box. Finally, Revit models of these steel structures can be smoothly imported into Midas gen, so this paper can carry out some finite element analysis on the models of these steel structures.

3.2. Load Type

3.2.1. Load Conditions. The stress load to be borne by the steel structure at the same time can be divided into four categories in detail, mainly including dead load, rain load, and wind load. The classification and structure size are introduced in detail as follows:

Basic snow pressure s: 0.60 kn/;

Basic wind pressure L: 0.35 kn/m^2.

3.2.2. Combination Condition of Static Load. The combination condition of static load is shown in Table 2.

3.3. Boundary Conditions. According to the structural requirements of the steel frame column foot in the design process of the steel structure, one part of the steel structure is regarded as rigid connection, and the other part adopts the articulated node algorithm, and each welded part is released and restrained one by one, thereby simulating the scene as the actual situation.

3.4. Response Spectrum Analysis. The algorithm of mode decomposition response spectrum is actually through the seismic acceleration design of the single-degree-of-freedom

Table 2: Static load combination conditions.

Serial number	Load effect combination
1	$1.35 * D + 1.4 * (0.7) * (\mathrm{L})$
2	$1.2 * D + 1.4 * (\mathrm{L})$
3	$1.0 * D + 1.4 * (\mathrm{L})$
4	$1.35 * D + 1.4 * (0.7) * (L + S)$
5	$1.2 * D + 1.4 * (L + S)$
6	$1.0 * D + 1.4 * (L + S)$

system, the seismic response spectrum and the principle of each order mode decomposition, according to the appropriate analysis combination calculation method to match the different modes of the different orders with each other, and carry out with the combination of seismic action effect analysis, the maximum seismic response value can be accurately predicted, and finally more seismic actions of the single-degree-of-freedom effect system can be calculated.

Usually, only the first several different modes have their main functions. Generally speaking, only the function combinations of 3 different modes need to be considered. The seismic class of the building construction site is Class II, and the seismic damping ratio of the structure is 0.02.

4. Numerical Simulation of Civil Engineering

4.1. Topological Distribution of Particles in Stable Vector Field. In this paper, a topological layout method mainly used for streamlines has made some minor modifications to particle characteristics, and uses OpenCL to perform a parallelized layout acceleration. Compared with the implementation of a graphics card using a CPU, it has been greatly improved. The acceleration performance is dozens of times. The following briefly introduces the workflow of this algorithm and the implementation of parallelization in it.

After we find an eigenvalue and an eigenvector, we can redo a template topological layout based on the topological layout model, as shown in Figure 3.

4.2. Topological Importance Analysis of Particle Multiframe Data. The topological structure of the particle is analyzed above, and the seed point of the particle is correctly set by referring to the topological structure model. For all time-varying topological data, each frame must have an experimental result of time-varying topology analysis to analyze the importance of the time-varying topology of different frames, whether it is a topological analysis of the entire time-varying field, or it is of vital strategic significance to guide the topological placement strategy of the entire time-varying field.

This paper extends the critical importance analysis technology of the article to the critical measurement of data topology information under the time-varying vector field. If a topological particle system is also counted according to this statistical model, however the joint probability of obtaining mutual information cannot be counted.

4.3. Feature Points of Topological Distribution of Particles in an Unstable Vector Field. For the three-dimensional unstable vector field, only similar calculation processing methods are used, and the calculation process is too complex. However, if you directly consider using particles with high convection occlusion and high quality tolerance, this complex problem can be quickly get an effective solution, as shown in Figure 4.

4.4. Interactive Placement. In addition to using automated calculations to ensure optimal placement and to ensure that the main features of the vector field are not missed as much as possible, this article also allows users to interactively add dots to their most interesting areas. The following is a detailed introduction to the interactive layout of several networks.

4.4.1. Body Layout Point. Body layout point refers to a point layout space that is like a cube. When realizing, pick the two-dimensional position P_{2d} of a mouse, and then use the mouse wheel to adjust the depth desired by each user, and combine P_{2d} with the depth reversely mapped to the three-dimensional coordinate P_{3D}, and the keyboard is used to control the influence on the dotted cube. Finally, according to the coordinate area of this cube, a random point is generated according to the number of particles required.

4.4.2. Surface Layout Points. Sometimes users may need more detailed layout points, and surface layout points provide good distribution options. The specific operation is realized: the decision of the projection three-dimensional plane is a way of user interaction, using the control mouse and keyboard operations to determine the projection plane.

4.5. Analysis of Experimental Results of Interactive Placement. The following article shows a simple experimental result on the design of interactive dots. The experimental results will be introduced from two aspects: volume interactive dots and multipoint surface interactive dots.

Figure 5 shows the drawing effect comparison between the interactive method of body dot placement and the random dot placement method that does not use the method in this paper.

Source data: wind field data, specification: $66 \times 66 \times 66$.

The main parameters of the algorithm: number of particles: 8000, depth: 0.6, integration method: fourth-order Runge Kuta, integration step: 0.05. Result analysis: for a global random arrangement method as shown in Figure 5, the overall trend of the field can be grasped very well and accurately, but because of the occlusion problem, the details of the internal spiral structure cannot be seen well; using the volumetric interaction model in this article, it is possible for the user to arbitrarily select an area that one cares most about. Other places do not need to be placed, which clearly shows the spiral structure inside the field.

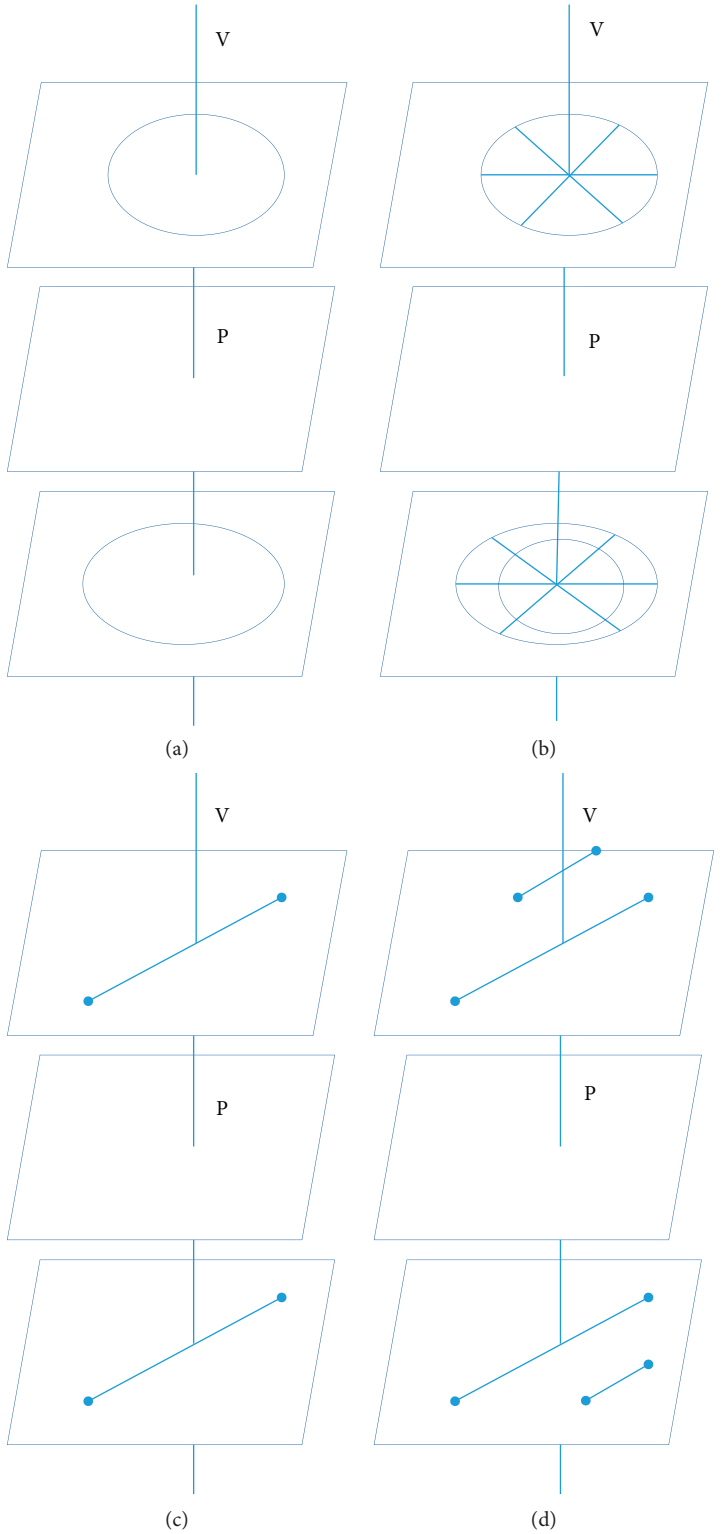

Figure 3: The layout template corresponding to different critical point types, improved by the streamline layout method.

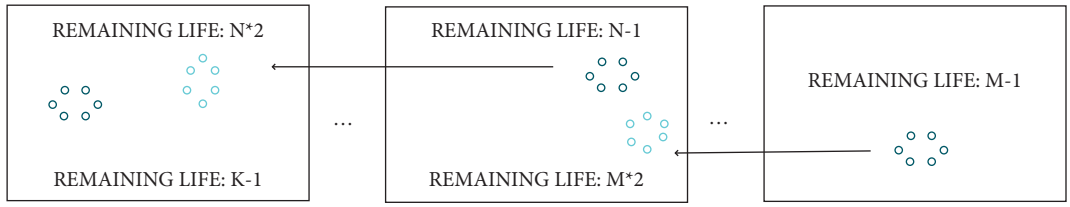

Figure 4: Schematic diagram of multiframe topology guided by importance.

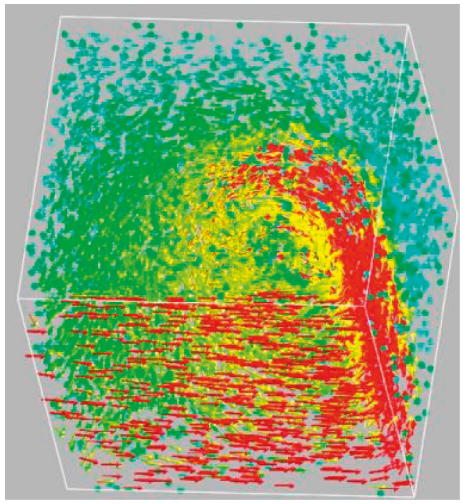

Figure 5: Body interactive placement.

5. Conclusion

The main research goal of this paper is to conduct a finite element analysis on the safety of high-rise buildings based on BIM. First, the basic definition of the raw materials and cross-section attribute models of the steel structure of high-rise buildings is carried out, and the attribute interface of the software design model is used to introduce this type of Revit steel structure model into the finite element analysis and calculation software Midas Gen to illustrate the main load measurement varieties and related load calculation and analysis methods and measurement standards. Then, through the finite element numerical calculation, the civil engineering simulation analysis of the internal member characteristics of the steel structure of the high-rise building was performed, and respectively, output the stress and deformation of the internal member of the steel structure of the high-rise building were analyzed. Then, the response spectrum analysis method is used to obtain the internal stress and displacement of the high-rise building steel structure under the action of strong seismic force. Finally, the results obtained by the above calculation methods are numerically analyzed according to the relevant international technical codes.

Data Availability

The data used to support the findings of this study are available from the corresponding author upon request.

Conflicts of Interest

The authors declare that they have no conflicts of interest.

References

[1] T. Fischer and M. Fischer, "Supporting the constructability review with 3D/4D models," *Building Research & Information*, vol. 35, no. 1, pp. 70–80, 2007.

[2] S. Zhang, J. Teizer, J. K. Lee, C. M. Eastman, and M. Venugopal, "Building Information Modeling (BIM) and Safety: automatic safety checking of construction models and schedules," *Automation in Construction*, vol. 29, pp. 183–195, 2013.

[3] B. Succar, W. Sher, and A. Williams, "Measuring BIM performance: five metrics," *Architectural Engineering and Design Management*, vol. 8, no. 2, pp. 120–142, 2012.

[4] R. van Berlo and L. Van Berlo, "Tool for benchmarking BIM performance of design, engineering and construction firms in The Netherlands," *Architectural Engineering and Design Management*, vol. 6, no. 4, pp. 254–263, 2010.

[5] V. Vignali, E. M. Acerra, C. Lantieri, F. Di Vincenzo, G. Piacentini, and S. Pancaldi, "Building information Modelling (BIM) application for an existing road infrastructure," *Automation in Construction*, vol. 128, Article ID 103752, 2021.

[6] X. Wang, K. Zhang, and X. Yin, "4D simulation based on BIM real-time construction model," *Journal of Guangxi University (Natural Science Edition)*, vol. 37, no. 4, pp. 814–819, 2012.

[7] F. Ji, D. Qu, and F. Shang, "Research on visual project schedule management under BIM scenario," *Construction economy*, vol. 35, no. 10, pp. 40–43, 2014.

[8] J. Zhang, M. Cao, and Y. Zhang, "Building construction 4D management system based on IFC Standard and engineering information model," *Engineering Mechanics*, vol. 2005, no. S1, pp. 220–227, 2005.

[9] F. Wang, X. He, and H. Gao, "Research on visual management technology of construction process of high-speed railway continuous beam bridge based on BIM," *Journal of building science and Engineering*, vol. 2021, Article ID 9738820, 9 pages, 2021.

[10] R. Harty and C. Harty, "Implementing "Site BIM": a case study of ICT innovation on a large hospital project," *Automation in Construction*, vol. 30, pp. 15–24, 2013.

[11] D. Bryde, M. Broquetas, and J. M. Volm, "The project benefits of building information modelling (BIM)," *International Journal of Project Management*, vol. 31, no. 7, pp. 971–980, 2013.

[12] K. Hong, "Development and Prospect of tunnel and underground engineering in China in recent two years," *Tunnel construction*, vol. 37, no. 2, pp. 123–134, 2017.

[13] P. Huang, X. Deng, W. Huang, and Q. Lin, "Research on safety of operation and maintenance of utility tunnel based on BIM and computer technology," *Journal of Physics: Conference Series*, vol. 1815, no. 1, Article ID 012009, 2021.

[14] H. C. J. Linderoth, "Understanding adoption and use of BIM as the creation of actor networks," *Automation in Construction*, vol. 19, no. 1, pp. 66–72, 2010.

[15] Q. Bai, "Establishment of construction party's BIM knowledge system based on the needs of project operation and maintenance," *China Construction Informatization*, vol. 22, pp. 18–21, 2016.

Hindawi
Mobile Information Systems
Volume 2022, Article ID 2320198, 13 pages
https://doi.org/10.1155/2022/2320198

Research Article

Application of Artificial Intelligence Algorithm and VR Technology in Vocal Music Teaching

Liu Jing

School of Art, Chongqing College of Humanities Science & Technology, Chongqing 401524, China

Correspondence should be addressed to Liu Jing; 18404043@masu.edu.cn

Received 1 June 2022; Revised 3 July 2022; Accepted 14 July 2022; Published 31 July 2022

Academic Editor: Shadi Aljawarneh

Traditional intelligent algorithms mainly artificially preselect the geometric features of the image and then classify and recognize the image based on these features. The geometric features of the manually selected working images are often interfered by human factors, resulting in inaccurate feature extraction and reduced classification accuracy. Aiming at the above problems, an intelligent recognition method based on artificial intelligence algorithm is proposed. We will deeply analyze the application of the core technology of the system and introduce the virtual education function of the application through relevant content. The application of this technology can effectively improve the efficiency of vocal music teaching and enable students to obtain a richer educational experience. Then, this paper finishes the other parts of the system again, realizes the functional modules of the system one by one, and elaborates the corresponding interface diagrams. Finally, a suitable testing method can be used to test the performance modules and performance conditions of the system to ensure that the system has good reliability and availability and put it into production. The voice teaching system based on virtual reality technology is more advanced and superior than other teaching systems on the market today and can provide users with a more realistic experience. In addition, users can have more choices in the process of virtual education, thereby improving the efficiency and quality of education.

1. Introduction

In recent years, with the development of information technology, computer technology has been widely used in many fields and can be used to improve the quality of information technology. The main academic systems are academic and engineering management systems, academic affairs management systems, library management systems, etc. [1]. The conversion experiment of the virtualization model is carried out in a virtual environment. Through this alternate deployment environment design and simulation, the experimental results are simulated and the virtuality of Tadashi is emphasized. The effect of the experiment is usually equivalent and more effective in the real world. Every university needs to use its network infrastructure to simulate daily situations and problems in order to improve students' ability to find and solve problems. Internet + education has become popular, and many colleges and universities have applied VR technology [2, 3]. In actual classrooms, typical applications are mainly VR innovation technology education, such as construction engineering, aerospace, etc. In fact, exhibition photos and videos of certain environments can only be displayed using traditional educational models, and relevant professional training is necessary. The application of virtual reality technology can combine all educational processes with actual practical projects. Students can brainstorm and create freely in the virtual environment, which helps to improve their innovative ability.

2. Related Work

By applying virtual reality technology to academic management, some studies can not only design various virtual situations for students, but also communicate with students in real time, so that students and teachers can learn from each other through the Internet [4]. Some research believes that the educational application of virtual technology is an innovation, which has solved some problems existing in the

traditional education model. In the actual teaching process, the choice of teaching methods and learning methods is very important, but the development of Internet technology has increased the difficulty and flexibility of choice, and the teaching methods have undergone great changes [5, 6]. Virtual education breaks the traditional education model. This innovative application can lead the development of education across the country and provide professional and technical personnel support for the progress and development of society. Some research proposed the concept of virtual reality technology and confirmed the world leader in this technology. In this era, the use of VR technology has entered many fields, especially in advanced technologies such as aerospace satellite technology and virtual reality technology. It is used for related training and high-end technology simulation exercises. In the military field, virtual battlefield environments and various forms of simulation training will be conducted to improve military operations capabilities and levels [7]. Some research takes into account the computer method; the existing map recognition efficiency and accuracy are very strong, so it is used for artificial intelligence calculation. By using intelligent recognition, we learned automatic features as input and achieved it through automatic failure and intelligent failure. Some research introduces the working graph recognition process of the deep learning model. In order to enter the deep learning model, the collected data must be preprocessed, including the normalization of the work graph data and the binarization and optimization of the work graph. Next, a working map label is created to finally display the details of CNN network and SSAENN network. Some research mainly introduces artificial intelligence and deep learning. Here, we will explain in detail the development process and application of artificial intelligence, the drawbacks of shallow learning to deep learning, and the advantages of using deep learning neural networks and then classify the model structures of deep learning and ordinary deep learning. This paper focuses on the model structure, algorithm principle and training process of convolution, and stacked sparse autoencoding neural networks in deep learning [8]. Some research believes that music teaching is mainly composed of classroom teaching and practical teaching. Classroom teaching is the foundation, and practical teaching is the assessment of class teaching. By discovering and solving the problems in the course, the efficiency of the course can be improved and the practical experience and expression ability can be improved. Through stage practice, students can discover and solve their own problems in time, enhance their psychological quality, and accumulate stage experience. This can enhance professional skills and increase students' stage experience [9].

3. Artificial Intelligence Algorithms and Virtual Reality Technology

3.1. Artificial Intelligence Algorithm. Deep learning is an algorithm model of deep neural networks. It is an extension of conventional neural networks and a branch of machine learning. Deep learning uses multiple nonlinear transformations to process data. It is an algorithm model with various characteristics. They initially proposed the application of deep learning to solve the complex problems of training data, and these complex data are in the shallow network of the neural network, which can not be effectively reflected. Deep learning can imitate the cognitive principles of the powerful nervous system of the human brain. When the characteristic information input to the neuron structure is extracted hierarchically, the neurons in each level can extract the target information more deeply and decompose the extracted feature information. The characteristic information is decomposed. Assuming that the input targets of the neuron are $1x$ and $2x$, the linear transformation has the following form:

$$Z = w^T x + b. \tag{1}$$

The output expression is

$$h_{w,h}(Z) = f(Z) = f\left(w^T x + b\right). \tag{2}$$

In a deep learning network, there are many structures of such neurons, and each neuron transfers the abstract features of the data to the next layer through the nonlinear mapping of the activation function. The final function will appear as the level deepens. Finally, the learned abstract features of the deep data can be sent to the classifier to classify and recognize the data.

Since the deep learning network has multiple hidden layers, it realizes the mapping conversion from low-dimensional to high-dimensional through multilayer nonlinear transformation. Now, these data have complex structure, image rotation, translation, scale conversion, and other characteristics [10]. As shown in Figure 1, to create a 3log (cos (exp (sin (x)))) with complex structure function, it is difficult to express this expression succinctly in a traditional shallow network, but by using a deep learning network, it can use a small number of parameters for layered expression, and the content to be expressed on each layer is simple.

In the process of shallow learning and deep learning, the input information will be nonlinearly transformed to create a mapping relationship from input to output, but when shallow learning is used to learn features, only features can be extracted manually and input into the model. Deep learning can use its own network structure to learn data features hierarchically and autonomously, but because the features it learns are too abstract, scientists are often confused and need further research.

3.1.1. Neural Network Infrastructure. Neural network is a new information processing mechanism extracted based on the basic understanding of the brain's organizational structure and activity mechanism. The neural network shows the characteristics of the human brain and has the basic functions of the human brain by simulating the activity mechanism and thinking principle of the human brain and nervous system [11]. In this network, the first-level detector processes the input data to make decisions and obtain simple results, and the second-level sensors process the first-level

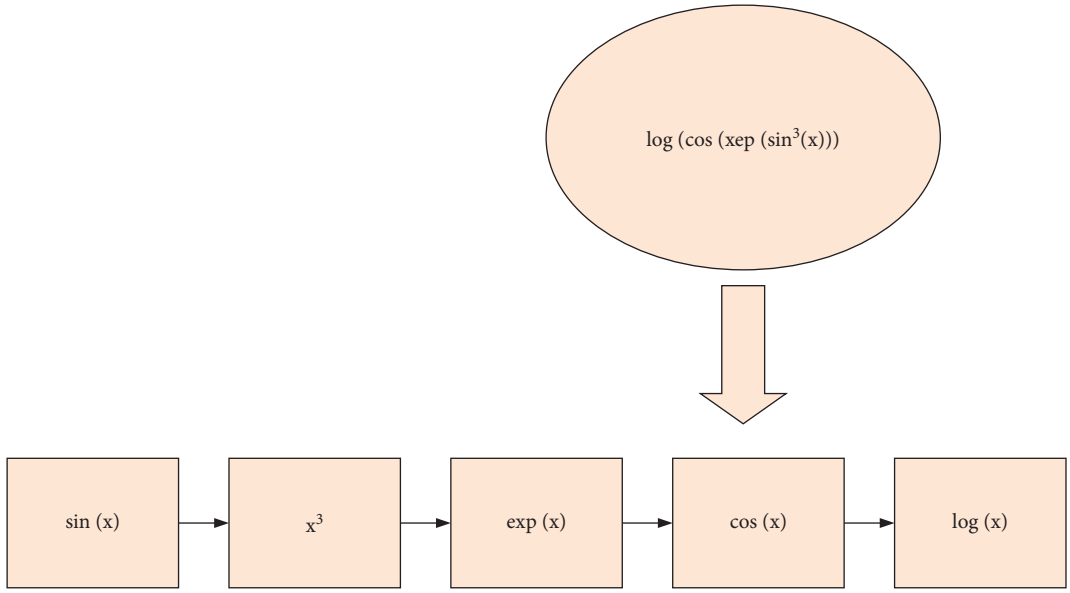

Figure 1: Multilayer network structure expresses complex functions.

data to obtain the decision results. In this way, the second-layer perceptron can make more complex and abstract decisions than the first layer. Similarly, the third layer of the neural network can perform more complex data processing. In this way, a deep model of the distributed neural network is constructed recursively, and the input signal value and the corresponding weight are added to obtain the output. This is the most basic way for nerve cells to process signals, and it is also the basis for building neural network models. Let us use a function as the activation function of the neural network (here, the threshold function) to filter the results. The content so far can be abstracted and summarized with a formula:

$$\text{out} = f\left\{\left|\sum_{i=1}^{n} w_{ij}x_i\left(t - t_{ij}\right)\right| - T_j\right\}. \tag{3}$$

3.1.2. Types of Neural Networks. The input data of the neural network is input from the input layer, and when passing through the interlayer neurons, the activation function will produce direct output data. The feedforward neural network has no feedback, so if you look at the topology of the neural network, you will find that the neural network is an undirected graph network. The output result of the feedforward neural network is the result of the interaction of each layer and the topology of the neural network, which describes the complexity of the activation function. Input data, weights, and offsets are input to the second layer after the activation function, and they eventually become the most commonly used chain structure in neural networks. The length of this chain is called the depth of the model, which is the origin of the term "deep learning" [12]. When using neural networks for training, the training samples will not directly specify the activity of neurons in other layers, but the learning algorithm will determine how to use these layers to produce the desired output. All neuron nodes can receive input from the outside world and output it to the outside world and have the function of processing information. This loss function is an important reason for neural networks to generate parameter feedback and is the key to distinguish feedforward networks. The neural network dynamically adjusts parameters by comparing whether the loss function is minimized.

$$C = \frac{1}{2n}\sum_{x}\left\|y(x) - a^{L}(x)\right\|^{2}. \tag{4}$$

3.1.3. Overfitting Problem and Normalization. In practice, machine learning models are usually trained on well-trained data sets and the parameters in the model are constantly adjusted. We usually test the trained model on different test data sets after training and evaluate the quality of the model based on the test results. The error displayed by the machine learning model in the training data set is called the training error, and the expected value of the error that appears in any test data sample is called the generalized error. In order to calculate the training error and the generalization error, the aforementioned loss function can be used, for example, the square error used in linear regression and the cross-entropy loss function used in multiple logistic regression [13]. Overfitting is the main problem of neural networks, which is especially common in modern networks due to the huge network weights. In order to conduct effective training, relevant techniques are needed to detect whether overfitting occurs to avoid overtraining. If the accuracy of the test data is not improved, the training will stop. Increasing the number of training samples is one way to reduce overfitting and another way to reduce the size of the network. However, large networks have greater potential than small networks, so you can choose to apply redundancy. Here, we show the most commonly used normalization method, sometimes called weight decay or L2 normalization. The idea of L2

normalization is to add an extra term to the price function, which is called a normalization term. The normalized cross-entropy is

$$\text{loss} = -\frac{1}{n}\sum_{xj}\left[y_j \ln^{a_j^L} + 1 - y_j \ln^{\left(1-a_j^L\right)}\right] + \frac{\gamma}{2n}\sum_{w} w^2. \quad (5)$$

The first term is the conventional cross-entropy equation. The second item added now is the sum of the squares of the ownership weight, if we can use the quantized and adjusted factor to prohibit the parameters in the factor. Of course, other price functions, such as quadratic price functions, can be standardized. A similar standardization is as follows:

$$\text{loss} = -\frac{1}{2n}\sum_{x}\left\|y - a^L\right\|^2 + \frac{\gamma}{2n}\sum_{w} w^2. \quad (6)$$

Intuitively, the effect of normalization is that the network tends to learn smaller weights. Only when the first term of the price function can be increased sufficiently is a larger weight allowed. In other words, normalization can be seen as a manifestation between finding small weights and minimizing the original price function. These two parts are controlled by values: the smaller the value, the smaller the original price function with the smallest deviation; on the contrary, the larger the value, the larger the original price function with the largest deviation. The weight learning rules are as follows:

$$w \leftarrow w - \eta - \frac{\eta\lambda}{n} w = \left(1 - \frac{\eta\lambda}{n}\right) w - \eta\frac{(\partial C_0)}{\partial w}. \quad (7)$$

Except for adjusting the weight w by a factor, this is the same as the normal gradient descent learning rule. This adjustment reduces weight and is sometimes called weight attenuation. As a result, the weight continues to drop to zero. But this is not the case, because if the original price function falls, other terms will increase the weight. This is the principle of gradient descent. Therefore, the normalized learning rules of stochastic gradient descent are as follows:

$$w \longrightarrow \left(1 - \frac{\eta\lambda}{n}\right) w - \frac{\eta}{m}\sum_{x}\frac{(\partial C_x)}{\partial w}. \quad (8)$$

As an effective recognition model, convolutional neural network has received widespread attention. The predecessor of CNN was invented in 1980 and has since evolved into the current convolutional neural network. Convolutional neural network is mainly composed of convolutional layer (c layer), pooling layer (s layer), and fully connected layer (fc layer) [14]. There are many feature maps in each layer, and each feature map has multiple neurons arranged as shown in the figure. The main principle of CNN is to fold the partial two-dimensional image of the input layer with multiple different folding cores to generate a folded feature extraction layer c1 and then merge the folded layer c1. Obtain the converted feature mapping layer s2. The s2 layer is folded again to produce a folded layer c3 and the c3 layer is assembled again in the same manner as the s2 layer to produce a pooled layer s4. Finally, the feature map of the s4 layer is input to the fully connected fc layer, and then the recognition and classification images are output, as shown in Figure 2.

Convolution operation fully reflects the two main attributes of CNN. Generally speaking, a local receptor area is a device in which each neuron in a hidden layer is only connected to neurons in a specific area of the layer, and the input data is window data in a local area of the image. Sharing weight means that each window data on the feature map shares a convolution kernel parameter set, that is, the same weight matrix [15]. By moving the window data around the image in fixed steps, the sum of the product of the window data and the convolution kernel is performed at each fixed step. Since it can be considered that the convolution process of the convolution kernel has been filtered by a filter, noise interference can be reduced and image characteristics can be emphasized. The selected window data is represented by JM, l jx represents the input of the j-th neuron in the feature map of the l-th convolutional layer, and $l1ix$ represents the output of the i-th neuron in the feature map of the l-th layer. f is the activation function, b is the bias parameter, $l\,jb$ is the bias parameter of the jth neuron of the lth convolutional layer feature map, k is the convolution kernel parameter, and $lijk$ is the lth convolutional layer feature map. Assuming it is the element of the convolution kernel parameter corresponding to the neuron, the convolution output equation is as follows:

$$x_j^l = f\left(\sum_{i\in M_j} x_i^{l-1} * k_{ij}^l + b_j^l\right). \quad (9)$$

The sigmoid function and the Tanh function are nonlinear, the saturation function has a saturation period, and the neural network training process will cause gradient diffusion. This is a diffusion problem, which has the characteristic of attaching most neurons directly to zero through a neural network, as shown in Figure 3.

After performing the convolution operation, the local features of the image can be extracted, but since the features of the image after the convolution are still many, it takes too much time to calculate when input to the classifier, and overfitting may occur. PCA must perform a merge operation, such as size reduction, to further reduce the image size. The pooling operation uses the overall characteristics of the adjacent output of the image area, rather than the network output at this location, and mainly includes the maximum pooling operation and the average pooling operation [16]. The maximum merging operation is an operation that selects the maximum value of the image area as the feature value in which the area is merged and can better extract the edge features of the image. The average pooling operation calculates the average value of the pooled image area as a feature value and better maintains the image background. Since the subject of this research is the working graph, it is necessary to extract and distinguish the edge features of the working graph, so the largest merging operation is selected. After the merge operation, the size of the feature map output to the merge layer will be reduced to the original $21/k$, and the useful features of the image will be extracted. The

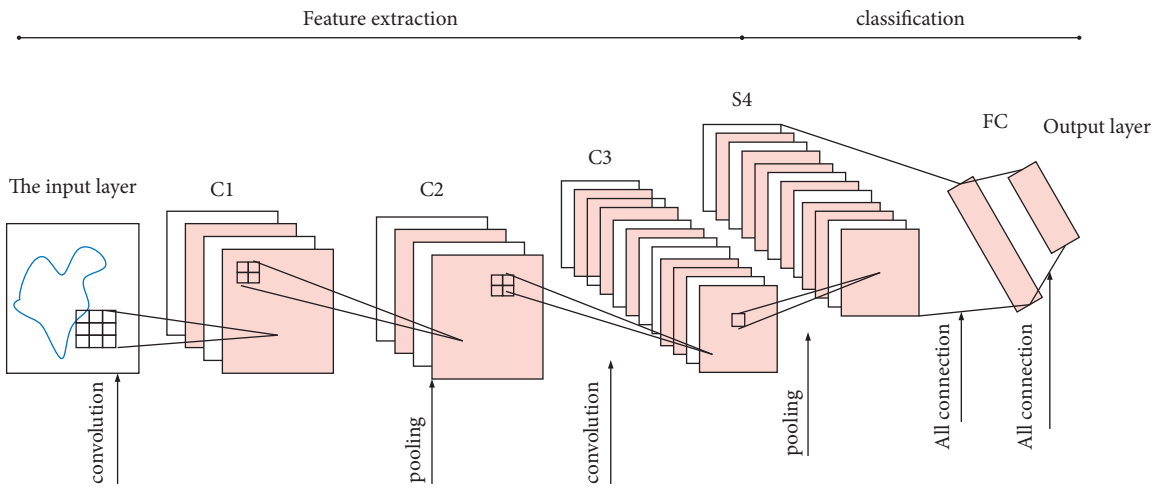

Figure 2: CNN network structure diagram.

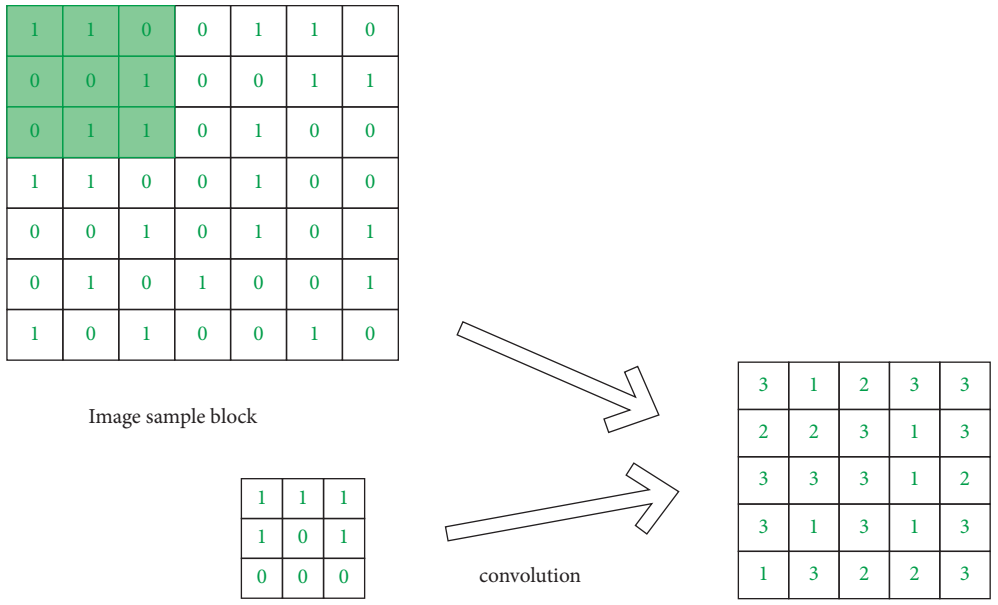

Figure 3: Convolution operation.

expression of the pooling feature output of the pooling layer is expressed as follows:

$$x_j^l = f\left(\max\left(x_i^{l-1}\right) * w_j^l + b_j^l\right). \tag{10}$$

By arranging in a one-dimensional feature vector, data is output from all connected layers and then classified. The formula for all connection outputs is expressed as follows:

$$x^l = f\left(w^l x^{l-1} + b^l\right). \tag{11}$$

A set of test data is input into the neural network, and the convolutional neural network may not provide very good recognition accuracy. In other words, the network model will overfit the training set data and therefore cannot be well generalized to the test set. To avoid overfitting the network model, a dropout method is added to the network model to optimize the model. It is essentially a regularization method applied to all connection layers of the CNN network. That is, the process of restoring the neurons in the next training to the original state by using only a part of the weight parameters and randomly selecting and operating until the end of the training. The test process embodies the idea of model averaging, which is equivalent to a network of different structures that has been activated and can operate all nodes. Each training will change the network structure. The adaptability to functions will be enhanced, and the network will have more generalization capabilities. Figure 4 shows the failure mechanism of some missing nodes in the network.

The user-based collaborative filtering algorithm finds products that users like from the relationship between different users' attitudes and preferences for the same products and content, calculates gender, and recommends users with the same taste. User-based collaborative filtering algorithm mainly includes two steps.

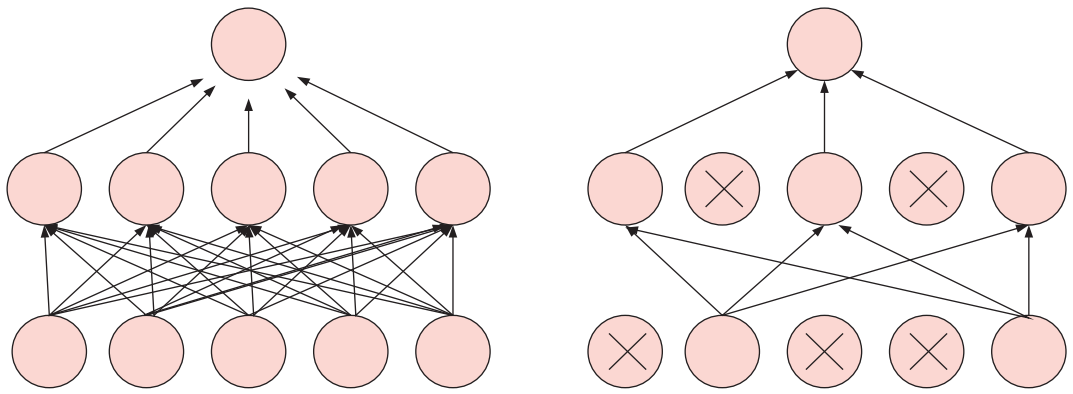

Figure 4: Dropout node failure mechanism.

(1) Calculate the similarity between users to obtain a similarity list.

(2) Search the similarity set, and find and recommend products that the user does not have among the users with the highest similarity.

The main point of step (1) is to calculate the similarity of interest of two users. Collaborative filtering algorithms mainly use the similarity of behavior. The interest similarity is calculated in the case of a given user u and user v, $n(u)$ represents a group of articles for which user u has positive feedback, and $n(v)$ user v represents an article for which positive feedback has been collected. Then, the interest similarity between u and v can be calculated by the following formula:

$$w_{uv} = \frac{|N(u) \cap N(v)|}{|N(u) \cup N(v)|}. \tag{12}$$

Or it can be calculated by cosine similarity:

$$w_{uv} = \frac{|N(u) \cap N(v)|}{\sqrt{N(u)}\sqrt{N(v)}}. \tag{13}$$

Assuming that the interest list of user a is $\{b, c\}$ and the interest list of user c is $\{a, b, d\}$, the similarity between user a and user c can be calculated.

$$w_{AC} = \frac{|(b,c) \cap (a,b,d)|}{\sqrt{(b,c)}\sqrt{(a,b,d)}} = \frac{1}{\sqrt{6}}. \tag{14}$$

The user cf algorithm recommends products that users did not intend to buy in the past. For example, step (3) measures the user's interest in the product.

$$P(u,i) = \sum_{v \in S(u,k) \cap N(i)} w_{uv} r_{vi}. \tag{15}$$

The similarity between the collaborative recommendation algorithm and the calculation will cause errors, and this error will be applied in practice. For example, listing popular products of common interest of users will affect the calculation of similarity.

When designing a recommendation system, there is usually more than one recommendation algorithm. In order to choose a suitable recommendation algorithm, it is necessary to analyze the data and solve the problem of information overload according to user needs.

As shown in the figure, the autoencoder uses unsupervised learning to perform network pretraining, encodes and reconstructs the input data, minimizes reconstruction errors, and characterizes the hidden layer of the input data. The data encoding process is from the input layer to the hidden layer, and the reconstruction process is from the hidden layer to the output layer. Here, the +1 in the circle is called the offset coefficient. w and b are autoencoders, including the following: (1) w and (1) b connect the input layer and the hidden layer, and (2) w and (2) b connect the hidden layer and the output layer. It is the weight matrix and the deviation matrix. It can be seen that the number of input layer nodes is the same as the number of output layer nodes. In other words, the autoencoder tries to learn the features in the hidden layer, optimizes the output Servlet x to make it as close to x as possible, and minimizes the reconstruction error. Finally, the feature extracted by the hidden layer is the input layer, as shown in Figure 5.

The hidden layer elements extracted by the autoencoder cannot effectively represent the data in the input layer. The sparse limit means that the output is activated when the value of the output function of the value neuron is as close to 1 as possible, and when the value of the output function of the value neuron is as close to 0 as possible, most of the output is suppressed. The completed operation is called the sparse limit.

$$\widehat{\rho}_j = \frac{1}{m} \sum_{i=1}^{m} \left[a_j(x') \right]. \tag{16}$$

Such dilution constraint is realized by adding a constraint factor to the autoencoder loss function by the neuron. The disciplinary factors are expressed as follows:

$$KL\left(\rho \| \widehat{\rho}_j\right) = \rho \log \frac{\rho}{\widehat{\rho}_j} + (1-\rho) \text{loglog} \frac{1-\rho}{1-\widehat{\rho}_j}. \tag{17}$$

The loss function of the model is expressed as

$$J(W,b) = \frac{1}{m} \sum_{i=1}^{m} \frac{1}{2} \left\| h_{W,b}\left(x^i\right) - x^i \right\|^2. \tag{18}$$

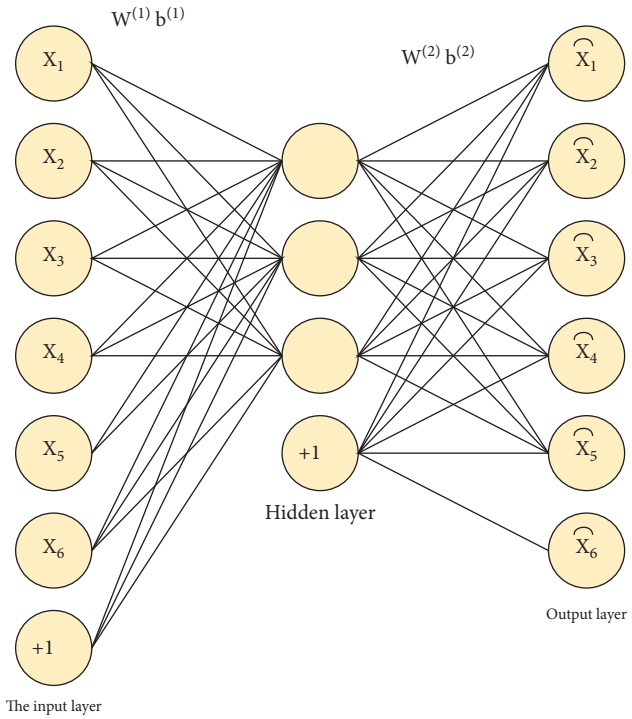

Figure 5: Autoencoder structure.

The loss function of the sparse autoencoder increases the discipline factor and limits the sparsity, which is expressed as follows:

$$J_{\text{square}}(W,b) = J(W,b) + \beta \sum_{i=1}^{n} KL\left(\rho \| \widehat{\rho}_j\right). \tag{19}$$

The size of the reconstruction error indirectly indicates the effectiveness of the encoding process used to extract sparse features. Since the size of the reconstruction error is evaluated by the loss function of the sparse autoencoder, the optimal weight matrix w offset matrix b can be obtained by using the backpropagation algorithm to minimize the equation, and finally is the sparse representation of the hidden layer of the input data characteristics.

Soft max is used as the input of the classifier in the hidden layer of the stacked sparse autoencoder, so that the samples can be finally classified. Multiclassification problems usually use the Soft max classifier to classify the features learned by the stacked sparse autoencoder. The Soft max classifier is a generalization of the logistic regression classifier for multiclassification problems. Its hypothesis function is expressed as follows:

$$h_\theta[x(i)] = \begin{bmatrix} p(y(i)) = 1|x(i);\theta \\ p(y(i)) = 2|x(i);\theta \\ \vdots \\ p(y(i)) = k|x(i);\theta \end{bmatrix} = \frac{1}{\sum_{i=1}^{k} e^{\theta_j^T x(j)}} \begin{bmatrix} e^{\theta_1^T x(i)} \\ e^{\theta_2^T x(i)} \\ \vdots \\ e^{\theta_k^T x(i)} \end{bmatrix}. \tag{20}$$

Using the maximum entropy model, the loss function is expressed as follows:

$$J(\theta) = -\frac{1}{m}\left[\sum_{i=1}^{m}\sum_{j=1}^{k} 1\{y(i) = j\} \log \frac{e^{\theta_j^T x(i)}}{\sum_{i==1}^{k} e^{\theta_j^T}\, x(i)}\right]. \tag{21}$$

The weight attenuation term is added to the loss function to reduce overfitting. This attenuation term has too many parameter values. At this time, the loss function is as follows:

$$\begin{aligned} J(\theta) = &-\frac{1}{m}\left[\sum_{i=1}^{m}\sum_{j=1}^{k} 1\{y(i) = j\} \log \frac{e^{\theta_j^T x(i)}}{\sum_{i==1}^{k} e^{\theta_j^T} x(i)}\right] \\ &+ \frac{\lambda}{2}\sum_{i=1}^{k}\sum_{j=0}^{n} \theta_{ij}^2. \end{aligned} \tag{22}$$

In the decentralized process, that is, the data processing process, the goal is to extract and process information about the accuracy of system design, which is characterized by the data that determines the user's purchase of products and the information in the user's own context. The information data system obtains the ideal information by reducing the interference to the data information. We aggregate the purchase status of customers for each product and obtain information about customers' purchase intentions. The accuracy and efficiency of neural network training are generally low, and as a result of classification, severe deviation is essential. In addition to data cleaning, data preprocessing must also consider the differences between data units and quantities. Therefore, a series of processes should be performed, such as data integration, conversion, and standardization. Data preprocessing aims to improve data quality while making it more suitable for specific mining techniques or tools. Before training a neural network, it is usually necessary to preprocess the input data. Due to the different units of the input data, some of the data is very large and some of the data is very small, which may cause the training time of the neural network to be too long and the convergence speed to be too slow. For a data set with a large input data distribution, the effect of the neural network classification algorithm may be too large, and the input effect at a point with a small data range may be small. Since the value range of the activation function of the output layer of the neural network is limited, it is necessary to map the target data of the network training to the value range of the activation function. The usual processing method is the normalization method of mapping the data to [0, 1] or [–1, 1]. The normalization algorithm is as follows:

$$x' = \frac{x - x_{\min}}{x_{\max} - x_{\min}}. \tag{23}$$

So far, the source code is carried out from the source site where the product exists through the crawling algorithm. Therefore, the analysis module needs to crawl the source code according to the analysis rules. The data obtained has various defects such as omissions and ambiguities. The neural network processes it first. The collected data is shown in Table 1.

Table 1: Neural network data.

User number	Product code	Property 1	Property 2	...	Property n	Category
19127	1	0.81472	0.16218		0.059619	1
19127	2	0.90579	0.79428		0.68197	1
19127	3	0.12699			0.042431	1
19127	4	0.91338	0.16565		0.071445	1

When dealing with missing data in a table, we show two ways to delete or insert data with columns. Since we are using a search engine to obtain n-dimensional product attribute data, the amount of data is very small. In order to ensure the integrity of product information, we interpolate missing data. The interpolation methods often used in data preprocessing include Lagrange interpolation, Newton interpolation, and average calculation. Substitute the coordinates of n points into the polymorphic function:

$$L(x) = \sum_{i=0}^{n} y_i \prod_{j=0.j\neq i}^{n} \frac{x - x_j}{x_i - x_j}. \tag{24}$$

Lagrange's interpolation formula is very useful for theoretical analysis and is widely used in data processing, but the following formula changes as the number of missing values increases or decreases. However, Newton interpolation is rarely used in practice. Newton interpolation is a formula of n known points (x_1, y_1), (x_2, y_2)...(x_n, y_n).

$$\begin{aligned} &f\left[x_{rv}x_{n-1}, \ldots, x_1, x\right] \\ &= \frac{f\left[x_{n-1}, \ldots, x_1, x\right] - f\left[x_n, x_{n-1}, \ldots, x_1\right]}{x - x_n}. \end{aligned} \tag{25}$$

Due to too much product feature data, it is necessary to reduce the data size. The commonly used data is replaced by a small number of new variables to reflect as much of the original variable data information as possible. In addition, since the new variables are orthogonal to each other, information that duplicates the original variables can be removed. The Lagrangian function is constructed as follows:

$$L = t_1' V t - \lambda_1 \left(t_1' t_1 - 1\right). \tag{26}$$

Its λ is the Lagrangian coefficient. Calculate the partial derivative of L with respect to λ, and set it to zero; then:

$$\begin{cases} \dfrac{\partial L}{\partial t_1} = 2Vt_1 - 2\lambda_1 t_1 = 0 \\ \qquad\qquad\qquad\qquad , \quad Vt_1 = \lambda_1 t_1. \\ \dfrac{\partial L}{\partial \lambda_1} = -\left(t_1' t_1 - 1\right) = 0 \end{cases} \tag{27}$$

It can be seen that λ is its corresponding eigenvalue. At this time

$$Var\left(P1\right) = t_1' V t = t_1' \lambda_1 t_1 = \lambda_1 t_1 t_1' = \lambda_1. \tag{28}$$

Principal component regression analysis = principal component analysis + multiple linear regression analysis. The product attribute data selected here is 100*400. Through analyzing the formula, it is found that the quasi-component of the data is determined, and appropriate neural network input data can be obtained. Principal component analysis mainly includes the following two steps:

(1) Standardize the data in all product attributes. In standardization, the average value of each attribute is set to 0, and the standard deviation is set to 1, to eliminate the quantitative difference between attributes. The sample standardized input variable matrix is

$$X = \left\{x_{i,j} | i = 1, \ldots, N, j = 1, \ldots, M\right\}. \tag{29}$$

(2) Obtain the correlation matrix between product attributes. The correlation matrix allows highly correlated indicators, and the covariance between these indicators can be referred to as another variable of the first component. After removing the first component, the residual correlation matrix is calculated. This residual correlation matrix gives the second set of related variables. These codispersions can be replaced by a second component, where the second component and the first component are orthogonal. In this way, it continues until all the distributions of the original product attribute data are extracted.

$$P_1 = X * t_1, \left\|t_1\right\| = 1. \tag{30}$$

Similarly, by inputting the information of the variable matrix, it can be seen from the perspective of probability statistics that the greater the variance of the variable, the more information the variable contains. Therefore, the above problem requires the variance of the variable p to be the largest. The dispersion of p is expressed by the following formula:

$$\mathrm{Var}\left(P_1\right) = \frac{1}{n}\left\|P_1\right\|^2 = \frac{1}{n} t_1 X' X t_1 = t_1' V t_1, \quad V = \frac{1}{n} X' X. \tag{31}$$

Usually the amount of data information in the first principal component is very large, and it is inferred in descending order. After obtaining the result graph of the component, the data dimension of the component is projected into the original space, which is the process of expanding the data sample.

3.2. Design of Vocal Music Teaching System Based on Virtual Reality Technology. Virtual reality education system is not only software development technology, network, and

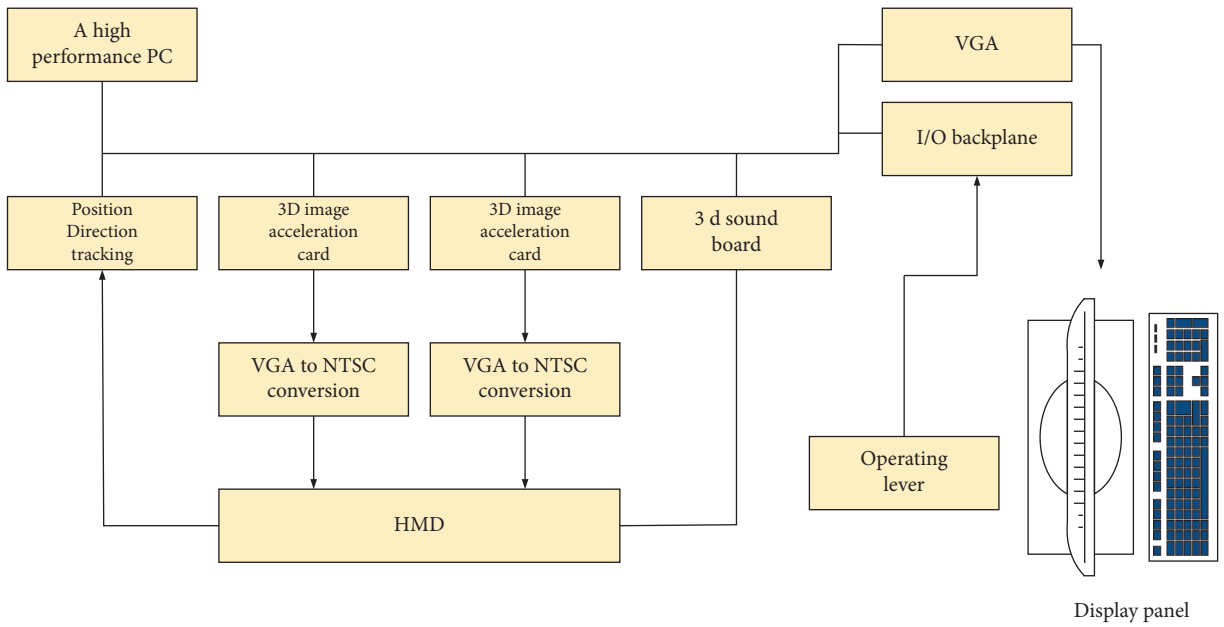

Figure 6: System architecture design diagram.

Table 2: Student information form.

Numbering	Field name	Field type	/F	Is null	Field depict
1	jx_zhbh	Int	Primary key	No	Account number
2	jx_yhc	Varchar (20)		No	User's nickname
3	jx_xb	Varchar (20)		No	Gender
4	jx_nl	Varchar (20)		No	Age
5	jx_txdz	Varchar (20)		No	Contact address
6	jx_jtzz	Varchar (20)		No	Home address
7	jx_yx	Varchar (20)		No	Mailbox
8	jx_sjhm	Int		No	Mobile phone number
9	jx_xh	Int		No	Student id
10	jx_sxzy	Varchar (20)		No	Major
11	jx_tcah	Varchar (20)		No	Special hobby

communication technology, but also many technologies. It is related to the hardware infrastructure of the profession. The virtual reality education system not only has basic education functions, but also needs to realize real-time interaction between humans and machines, which requires high system performance. With the development of science and technology, the cost performance of personal computers has been improved, and many application systems use high-performance PCs to support the system. The figure below intuitively illustrates the design of deploying a virtual reality system on a high-performance PC and the principle of use.

As can be seen from Figure 6, a complete virtual education system requires not only basic equipment, but also special hardware configuration, such as location tracking equipment, 3D image acceleration card, 3D sound board, etc.

When designing a database, information table design is the foundation. The information table consists of an information table and multiple pieces of information in the information table and is usually field type, field name, primary key information, etc. Because there are many functional modules in the system, each functional module displays only one information table, especially student information table, homework information table, scene information table, educational resource information table, examination question information table, and interactive information table.

Table 2 mainly contains information such as account number, nickname, gender, age, communication destination, major, special skills, hobbies, and majors.

(1) Job information table: The job information table mainly includes job number, subject, faculty, placement time, deadline, class, job details, and other information. For detailed information about job information, please refer to Table 3.

(2) Scene information is the main component of the 3D model. It is necessary to design a larger scene based on a larger teaching plan and teaching content and systematically record relevant information about the scene in detail. For details of the scene information table, please refer to Table 4.

Table 3: Work information sheet.

Numbering	Field name	Field type	/F	Is null	Field depict
1	jx_zhbh	Int	Primary key	No	Job number
2	jx_km	Varchar (20)		No	Subject
3	jx_krls	Varchar (20)		No	Subject teacher
4	jx_bzsj	Datetime		No	Set up time
5	jx_jssj	Datetime		No	Deadline
6	jx_bi	Varchar (20)		No	Class
7	jx_yx	Varchar (20)		No	Job details

Table 4: Scene information table.

Numbering	Fie Id name	Field type	P/F	Is null	Field depict
1	jx-tjbh	Int	Primary key	No	Field number
2		Datetime		No	Build time
3	jx_yssl	Int		No	Number of elements
4	jx_mrs	Varchar (20)		No	Capacity
5	jx_cjlx	Varchar (20)		No	Scene type
6	jx_sysj	Dttetime		No	Usage time
7	jx_sbsl	Int		No	Equipment quantity
8	jx_sykm	Varchar (20)		No	Use subjects

Table 5: Educational resource information form.

Numbering	Field name	Field type	/F	Is null	Field depict
1	jx_zybh	Int	Primary key	No	Resource number
2	jx_zykx	Varchar (20)		No	Resource type
3	jx_scsj	Datetime		No	Upload time
4	jx_xscs	Int		No	Download times
5	jx_scry	Varchar (20)		No	Uploader
6	jx_sskm	Varchar (20)		No	Subject

Table 6: An interactive information sheet.

Numbering	Field name	Field type	/F	Is null	Field depict
1	jx_zybh	Int	Primary key	No	Message number
2	jx_zykx	Varchar (20)		No	Publisher
3	jx_scsj	Varchar (20)		No	Interactive staff
4	jx_xscs	Varchar (20)		No	Type of interaction
5	jx_scry	Datetime		No	Interaction time
6	jx_sskm	Datetime		No	Release time
7	jx_fbdd	Varchar (20)		No	Release location

(3) The teacher resource information table mainly contains information such as resource number, resource type, download time, download times, uploader, and affiliation, as shown in Table 5.

(4) The interactive information table mainly includes information number, caller, distributor, delivery type, delivery time, delivery location, etc. For more information, see Table 6.

This article is based on the voice teaching system of virtual reality technology to carry out related elaboration. There are relatively many types of voice music involved, and the design only for teaching is introduced in detail. It involves modeling and final realization of people. The complexity of 3D modeling may affect the realization effect of VR technology to some extent. Improving the efficiency and level of 3D modeling is an important part of virtual reality. In a specific implementation, it is first necessary to clearly analyze the environment of the scene. The BNF-based paradigm rules provide a modeling language for the scene, create a dance model, and make it possible. They can demonstrate works on the stage and finally meet the students' independent learning needs, so that the entire system has good interactivity, including three main structures of the 3D model, one is the shape of the human body, the second is the action, and the third is the facial action. The basic principle of the model's behavior in this process is based on the changes in human bones and muscles. Therefore, based on biological principles, these expressions are expressed by a computer system that builds the surface model of the actor

by modeling using 3D modeling technology and finally realizes the work of ballet. It is lively and can stimulate students' interest in learning sounds. The complexity of the 3D model is inversely proportional to the speed of the system. That is, the larger the data of the constructed model, the more complex the model, and the longer the drawing time, but the more realistic the display effect, and vice versa. Creating models requires dedicated 3D modeling software, but the most popular software today is the 2013 version of 3Dmax, which has been used in various design fields and has a very good user experience. The software is also used for the formation of surface models.

In order to model the details, polygon modeling technology must be used to fine-tune the head and body of the model, and the details can be processed and adjusted by manipulating the surface of points and lines. The human face has a natural three-dimensional shape, and recognition based on the 3D data of the human face is a common method to solve the pose problem. Therefore, it is necessary to start with the smallest details. In particular, eye treatment is an important part of a person's vitality and has a major impact on the postrendering effect. At the same time, you need to pay attention to the beginning of the eye pupil. As you can see, hard-edging is not always possible. Otherwise, the actual effect in the later stage will seriously affect the effect. Body processing is also very important, especially in the processing of each joint, to control the number of model faces to prevent the model from stretching due to changes in future work.

The optimization and improvement of 3D deformation has also become one of the hottest issues in this field, especially by building a complete head model to improve modeling efficiency and further improve angles such as facial elements. Here, the model formed by the UV editor is used so that the visual effects of the actors can be reflected, and the texture, color, and texture effects of the points corresponding to the actual actors can be presented. After rendering the 3D model, choose the characteristics of a real person.

In order for an actor to perform a movement, he must have a skeletal system. The key to this process is to build a bone model and use the movement of the bone to represent the movement of the person. After running the program, execute skeleton processing through "Biped" in the "Create Panel" function menu. This process is the detailed processing part of the design. If each joint is not connected properly, it will have an adverse effect on the performer's subsequent movement. After completing this process, go through 3D max to check whether bone changes and muscle stretching will affect the model composition. At the same time, it is necessary to set the weight value for the model, which is a masking task, and the processing of the model joints is very important. The arrangement status of the weight parameters is displayed in the weight value on the left. If you want to adjust these parameters, you can adjust the value on the right. On the other hand, when managing the intensity of the model and the hue of heating and cooling, the heating and cooling can be adjusted through the overcolor adjustment of the model surface to express the real effect of the actors.

Since the design of the 3D model is based on different scenes, it is necessary to construct the scene before obtaining the basic motion data. In order to collect the movement data of each level, 10 shots of Eagle-4 were placed, and the complete movement was collected in Eagle, two of which were placed on both ends of the Eagle-4 lens. Divide into four groups, each group of eight, one of which stays in the corner of the triangle guard, and then capture the route from the angle of the hand. The other group can be placed at a higher position, that is, at the four corners above the stage, and the stage can be used in all directions. After deploying all the lenses, power them up uniformly and connect them to the PC desktop in the interface format, and complete the integration process of the basic work data of each Eagle lens through the PC. In order to easily manage the basic data, each shot needs to be numbered, and when searching for motion data, only the shot number is required to search for motions in a specific direction, which is very convenient. One is to put a "field"-shaped label on the ground to identify each area of the field. Secondly, in order to facilitate the later synthesis process and enhance the capture effect, it is necessary to identify obstacles in the field and capture data from all angles. There are always 30 dancing models, wearing special dance costumes, and marking points at their designated locations. In this way, the operating data can be reflected on the collector. In order to facilitate the rule management of these markers, the parameter setting part of ModelEdit will rename each marker according to scientific rules.

The performance on stage can objectively express students' understanding of knowledge. Performers will process and reorganize all life experiences expressed on stage based on their own real life experiences and emotions, combined with the professional knowledge gained in the learning process. After creation, it will appear in front of the audience in the form of voice. When singing onstage, pay attention to the matching of work. It is not suitable for clumsy singing and complicated work. We are looking for "Kamigata combination." On the stage, the actors and singing are integrated, the works come from the heart, and the pursuit of its beauty cannot be ignored. For this, we must develop regular practice, habits, and professional performance skills.

The speech course with stage practice is incomplete. Without the speech course, the stage practice will not be able to play its original role. In addition to regular courses, practice is also very important. Practice can be used as an effective method to verify the quality of education and can verify whether the quality of education affects the results of practice. Performers need to spread professional theoretical knowledge and advanced music skills to a larger audience. Voice exercises are a form of classroom knowledge. Students can quickly discover their own shortcomings in the practice process, so as to make effective corrections and improve the level of theoretical knowledge in the correction process. It not only effectively improves the professional level of vocal music, but also further expands the practice circle. The experience continuously summed up in practice will benefit the sound development of vocal music education in the future.

Good psychological quality is the foundation of student stage performance. Students must not only learn the skills of voice music, but also fully demonstrate their talents on the stage, enhance their expressiveness on the stage, and fully demonstrate their strengths.

(1) To cultivate stage expression ability in the classroom, teachers are required to actively cultivate students' performance ability and improve their stage expression ability. For the works familiar to students, let them create their own feelings and behaviors, and let them express better with words and gestures. In class, invite other students to practice singing and acting. Of course, it is best to record the performance of students, let them observe for themselves, find out what is good or bad for them, and let them correct immediately. Only in this way can we train the stage adaptability and psychological background.

(2) Training for overcoming stage phobia, the position, lighting, audience, etc. are different from those during practice, so it will deepen tension and fear. The desire to get high scores intensifies the psychological pressure and makes students feel emotionally nervous both physically and mentally. In order to solve this psychological problem, students must have a good mental state and the ability to overcome stage fear. However, this kind of courage and attitude cannot be strengthened through regular practice, only through practice. Students need self-confidence to succeed, and they need basic skills to gain self-confidence. Therefore, students should be prepared before performing, walk onto the stage with a good attitude, be familiar with the venue, and suggest that they can succeed.

(3) According to the actual situation of the students, choose songs suitable for stage practice and master the ability and psychological state of the songs to choose the more difficult songs. According to actual problems, according to the differences of the students' tone, singing voice, and intonation, choose appropriate and reasonable songs. At the beginner stage, the choice of songs should generally be slightly lower than the actual level of the students, which not only achieves the purpose of adequate practice in this way, but also helps to enhance students' self-confidence.

4. Conclusion

In this article, we compare deep learning and its improved model with other demonstration images of shallow network recognition, showing that deep learning and its improved model perform better in the recognition of demonstration images. After in-depth update and perfect neural network, the model can avoid the difficulty of extracting geometric features of some images and the phenomenon that the extracted features are unreasonable. The application of virtual reality technology in the education field can break the traditional education model and provide students with special virtual scenes, so that students can deal with specific scenes through their own knowledge. It can improve students' practical ability. The traditional education model cannot stimulate students' interest in learning, but more importantly, they cannot use the professional knowledge they have learned. In this article, we have developed and designed an art education system based on virtual reality technology to make up for these shortcomings. Aesthetic education occupies a very important position in phonetic education in colleges and universities, and it is particularly important to inculcate aesthetic education into phonetic education. To instill aesthetic education into high school phonetics courses, it can be mainly manifested as follows: first, improve teachers' professional skills and enrich teachers' teaching methods; second, improve students' understanding of musical instruments; third, carry out some music performance activities and enhance students' practical ability. Finally, the integration of emotional experience into speech can enhance the beauty of students and promote their healthy development.

Data Availability

The data used to support the findings of this study are available from the corresponding author upon request.

Conflicts of Interest

The author declares that there are no conflicts of interest.

References

[1] A. O. Ojo, M. Raman, and A. G. Downe, "Toward green computing practices: a Malaysian study of green belief and attitude among Information Technology professionals," *Journal of Cleaner Production*, vol. 224, no. 7, pp. 246–255, 2019.

[2] V. Fratto, M. G. Sava, and G. J. Krivacek, "The impact of an online homework management system on student performance and course satisfaction in introductory financial accounting," *International Journal of Information and Communication Technology Education*, vol. 12, no. 3, pp. 76–87, 2016.

[3] U. Hüseyin, T. Murat, and P. Y. Ezgi, "The effects of the authentic learning approach with a course management system (moodle) on students mathematics success and online authentic learning self-efficacy," *Educational Research and Reviews*, vol. 15, no. 11, pp. 679–689, 2020.

[4] Z. Lv, "Virtual reality in the context of internet of things," *Neural Computing & Applications*, vol. 32, no. 13, pp. 9593–9602, 2019.

[5] K. Ibraheem Arif, "Building an online course management system for Iraqi education colleges," *Indian Journal of Science and Technology*, vol. 11, no. 7, pp. 1–6, 2018.

[6] L. W. Wardana, "Paper airplane and talking stick learning methods to increase students understanding about management information system courses," *IOSR Journal of Business and Management*, vol. 18, no. 09, pp. 164–169, 2016.

[7] D. Zhou, "The development status of VR technology and its application field research practice," *Electronic Technology and Software Engineering*, vol. 25, no. 17, pp. 147-148, 2018.

[8] Z. Lv, X. Li, and W. Li, "Virtual reality geographical interactive scene semantics research for immersive geography learning," *Neurocomputing*, vol. 254, pp. 71–78, 2017.

[9] A. N. Alkhaldi and A. M. Abualkishik, "Predictive factors for the intention to adopt a mobile blackboard course management system: the case study of university of hail in Saudi Arabia," *Indian Journal of Science and Technology*, vol. 12, no. 19, pp. 1–12, 2019.

[10] A. S. Musleh, G. Chen, and Z. Y. Dong, "A survey on the detection algorithms for false data injection attacks in smart grids," *IEEE Transactions on Smart Grid*, vol. 11, no. 3, pp. 2218–2234, 2020.

[11] Y. Gao, L. Gao, X. Li, and X. Yan, "A semi-supervised convolutional neural network-based method for steel surface defect recognition," *Robotics and Computer-Integrated Manufacturing*, vol. 61, Article ID 101825, 2020.

[12] H. Zhao, H. Liu, W. Hu, and X. Yan, "Anomaly detection and fault analysis of wind turbine components based on deep learning network," *Renewable Energy*, vol. 127, pp. 825–834, 2018.

[13] A. Caggiano, J. Zhang, V. Alfieri, F. Caiazzo, R. Gao, and R. Teti, "Machine learning-based image processing for on-line defect recognition in additive manufacturing," *CIRP Annals*, vol. 68, no. 1, pp. 451–454, 2019.

[14] X. Li and S. Wang, "Object detection using convolutional neural networks in a coarse-to-fine manner," *IEEE Geoscience and Remote Sensing Letters*, vol. 14, no. 11, pp. 2037–2041, 2017.

[15] T. Chen, S. Lu, and J. Fan, "S-CNN: subcategory-Aware convolutional networks for Object detection," *IEEE Transactions on Pattern Analysis and Machine Intelligence*, vol. 40, no. 10, pp. 2522–2528, 2018.

[16] G. Huang, Z. Liu, L. Van Der Maaten, and K. Q. Weinberger, "Densely connected convolutional networks," in *Proceedings of the IEEE Conference on Computer Vision and Pattern Recognition (CVPR)*, pp. 2261–2269, IEEE, Honolulu, HI, USA, July 2017.

Hindawi
Mobile Information Systems
Volume 2022, Article ID 9226647, 10 pages
https://doi.org/10.1155/2022/9226647

Research Article

Cloud Computing Resource Prediction Model Based on Time Convolutional Network

Xin Feng, Haibo Gao, and Cheng Zhang

College of Information and Electrical Engineering, Hunan International Economics University, ChangSha, Hunan, China

Correspondence should be addressed to Xin Feng; 321195@whut.edu.cn

Received 30 May 2022; Revised 4 July 2022; Accepted 13 July 2022; Published 31 July 2022

Academic Editor: Shadi Aljawarneh

With the continuous progress and development of modern science and technology, the research on cloud computing-related fields is constantly conducting more in-depth exploration. During the real-life use of cloud computing operations, as the number of tenants continues to increase, the resource usage load capacity of the relevant platform has also undergone tremendous changes. In order to enable the tenants to complete higher-level optimization of the relevant performance and indicators during the actual work of the platform, this article explains how to perform related network resource models on the premise of cloud computing operation management. The researchers used this cloud computing network operation forecasting system as the basic point of view for experimental research and explained and summarized all relevant research results and specific instructions on multivariable load sequences in detail. The multivariable load sequence is embedded in the dimension of the phase space in the calculation process, and the generalization operation from single variable to multivariable can be carried out. However, every time the expansion calculation is performed, the selection criteria available for the researcher to calculate will be reduced, making the result a reconstructed phase space with uncertainty. Therefore, in order to ensure the accuracy of the data of the research experiment results, the researchers must simplify the model, focus on further discussing the correlation between multivariable load sequences in the mechanism, and reduce the number of data calculations in the process. The redundant information generated can select more reasonable data information as input variables in the research process.

1. Introduction

With the continuous development of modern technology, the scale of many enterprises has also expanded rapidly. Many traditional enterprises have adopted a decentralized enterprise computing operation model, but as the scale of the enterprise continues to expand, the burden on servers has also continued to increase, reaching a considerable number [1, 2]. As a result, it also brings a series of difficult problems for enterprises, such as more complicated and difficult-to-operate operation management models, control of computing operating costs, and application of key functions [3]. These problems are forcing researchers to improve the existing systems and re-centralize the servers in large-scale use machines [4]. The processing method of cloud computing is the solution proposed by the researchers for enterprises. First, compared with the previous resource management, cloud computing has significantly reduced the initial construction cost of resources, as well as the cost of resource operation and maintenance during use [5, 6]. This includes the server, platform storage equipment, network management tools provided by the platform, and a series of infrastructure required in the operation process; secondly, the main users of cloud computing are developers of application technologies in the Internet. The system platform simplifies and upgrades the system through operations such as the development of shielded software, such as the research and development of new distributed software systems, the testing of platform application systems, and the deployment of the system in use. Researchers doing system development can use cloud computing to improve the performance of the platform, the availability during actual operation, and the scalability of other related functions in the shortest time; the last point is the scalability and scalability of cloud computing

during use. The advantages of multi-tenant accommodation and platform configurability provide employees with a new and convenient way of thinking at work, as well as software operators, software developers and researchers, and the actual use of software. This brings more convenience and benefits.

2. Related Work

Some research mainly put forward the research results of researchers in the management of resource prediction models in the field of cloud computing. The ideas and viewpoints described in this article mainly come from the project "Cloud Computing and Its Supporting Network" [7]. This project is working to build a network communication service platform supported by a cloud computing system [8]. On this platform, the system can provide a series of related functions for operators using telecommunications, such as computing integration, storage aggregation, network protection, and other related functions to help enterprises carry out data management, and perform scientific and reasonable dynamic allocation of enterprise resources [9]. In addition, the platform can also provide related service management system equipment for telecom service providers. In order to better solve the problem of how to improve the efficiency and accuracy of the use of virtual machines in the cloud computing-related infrastructure, the researchers re-optimize the storage management methods of resources in the platform, and to better study this subject, the researchers also introduced an analysis and prediction system in the experiment [10]. Researchers have proposed a new type of prediction model in order to better model and predict the multi-variable load sequence generated during the study of the resource load sequence in the cloud computing platform [11]. This kind of forecasting model is still based on the multivariate load sequence as the main research foundation, and is mainly applied and suitable for cloud computing platform resource load sequence forecasting. The researchers summarized the data results obtained from the experiment, and comprehensively considered the multiple influence relationships of resources in the cloud computing platform. The researchers reasoned and deduced the data in the female experiment based on the principal component analysis method, and combined regarding the related theories of local forecasting method; a forecasting model of multi-variable load series is established. In the process of testing the effect of cloud platform use by researchers, the experimental results show that the multi-variable load sequence forecasting model proposed in this article is indeed currently predicting the direction of resources used by enterprises on cloud platforms as an effective method. And the prediction accuracy of this multivariate load sequence forecasting model is obviously different from that of the univariate load sequence forecasting model, and it has higher accuracy. Some research mainly studies the data and related processing and statistical methods of the resource load sequence in the cloud computing platform during use [12]. On the one hand, this new algorithm improves to a certain extent the identification of dirty data in the use of cloud computing platform resource load sequences, as well as the research, improvement, and optimization of dirty data computing algorithms [13]. On the other hand, this new algorithm also realizes the wavelet denoising data preprocessing algorithm in the use of cloud computing resource platform. In the process of researching the cloud computing platform, the relevant experimental data showed the researchers that the related identification of dirty data and the correction and optimization of dirty data algorithms mentioned in this article can realize and search the relevant data and information in the computing process to a certain extent [14, 15].

3. Analysis of the Theoretical Basis of Cloud Computing and Time Convolutional Networks

3.1. Time Data Concept and Related Theories. Time data is usually called time series by scholars, which refers to the data series formed by a certain phenomenon occurring in different time environments. In our real life world, changes in data are often closely related to time. Researchers call the data observations obtained by the research object in the order of time as time series data. Among them, the most common ones are changes in weather and temperature, changes in stock and bond prices, and so on. At present, researchers have summarized many scientifically mature time series mining algorithms so that people can more conveniently capture the deeper information contained in time series data. Spatial data refers to data information with a definable spatial coordinate position. Spatial data can be described quantitatively by people, which is very useful for some things with positioning significance and can better explain this phenomenon. In the real life world, people often use spatial data to describe and express the relative geographic location of actual objects in some space, the distribution characteristics of surrounding objects and the environment, which clearly shows that due to the geographic location. The difference in location leads to the standardization process of the entity to be observed and studied or the target time under the influence of such different spatial conditions. Spatiotemporal data refers to data that includes the temporal attributes of time data and the spatial attributes of spatial data. For example, we often use the Internet to book data sheets for vehicles in our daily lives. The creation of this order contains not only time attributes, but also spatial attributes. Another example is the GPS positioning data frequently used on mobile phones and vehicles. The accurate positioning coordinates of the target location reflect the spatial attributes of this data, and the time value of the sample target to be studied when the position changes. The phenomenon of change is the time attribute embodied by this phenomenon. We can think that there are many pieces of time series data in our lives, and each of these pieces of data is generated by different spatial position coordinates.

With the continuous development of current information technology-related technologies, mining related to the field of spatiotemporal data has become a hot topic discussed by researchers in the current data mining research field, and

this topic has been awarded in academic fields at home and abroad. Regarding the new project of spatiotemporal data mining, researchers are focusing on information computing technology with practical applications. And through this technology, those high-dimensional, massive, and complex data are analyzed in detail to better find and use the part of the data that can create the value. In the modern society of human life, people's complex behaviors in life and work often bring about the accumulation of temporal and spatial data. Researchers have carried out a deeper digging of this spatiotemporal data to find some phenomena in human social life. For example: Researchers analyze and mine the research target and the route and trajectory and travel rules of the research target by studying the movement behavior of the target location, and provide the researcher with relevant predictions and location recommendations of the location of the tracking target services; through people's social behaviors, the cloud computing system platform will analyze and study the spatiotemporal information data of the research samples based on the social activities that people generate in life and work. At the same time, the platform can also make inferences and judgments based on the identity information of the tested sample and the relationship between people during social activities; the cloud computing system platform will use the cloud computing system platform through the migration behavior of the research target's population in and out, transfer, etc. Perform statistical calculations on the population flow in the city, and scientifically interpret and predict the cluster behavior generated by the research goal through the systematic scientific analysis of the cluster behavior. The relationship attributes between time and space in spatiotemporal data usually have more complex relationships, especially many of them that can be quantified, and some time attributes and space attributes that cannot be quantified are included in these data. According to the analysis of the spatiotemporal data attributes, whether the temporal and spatial attributes of the data will change under different circumstances. According to this, the researchers analyze and mine the spatiotemporal data and classify them into the following three categories: (1) Some data is in progress, in the process of research, the time and space attributes of the data will not change and remain at a relatively stable value. This kind of data is called static data by researchers. For example, an airport and a shopping mall can be used as static data for observation of interest. Such data has fixed coordinates, fixed addresses, and fixed names. Once established, its spatial position will not change. The data information of time and space has static properties and is a kind of point data. (2) During the research process of some data, the spatial attributes of the data will not change, but the temporal attributes will change. For example: electronic sensors and surveillance camera probes installed on the road, their spatial position will not change during the research process, but the information that can be collected will change over time. This kind of data information has the characteristics of unchanged spatial attributes and changing temporal attributes. (3) There is a kind of data that both the temporal and spatial attributes studied during the research process will change. For example, simple and environmentally friendly shared bicycles, and currently popular online ride-hailing platforms, the user's data is scattered data in terms of time effect. For example, at a certain moment, a user is about to start from A and sends a request to the platform. After a period of time, a user sends a request again in place B. At this time, these two kinds of data belong to changes in both temporal attributes and spatial attributes. Spatiotemporal data are shown in Figure 1.

3.2. Theoretical Basis of Convolutional Neural Networks. Convolutional Neural Network (CNN) refers to a feedforward neural network that contains both convolutional computing power and deep learning structure characteristics. It is developed by researchers specifically for neural networks containing data similar to a grid structure. In recent years, as researchers continue to explore and improve the theoretical basis of deep learning, and the data computing equipment for research has also been improved and perfected to a certain extent, convolutional neural networks have been able to develop so quickly. And it is currently widely used in the fields of visual processing and natural language processing in the related use of computers. Convolution operation on a two-dimensional tensor is shown in Figure 2.

3.3. Cloud Computing Resource Prediction Model Foundation. The project based on the prototype of the cloud computing platform mentioned in this article is the project "Cloud Computing and Its Supporting Network", a collaboration between Northwest University and Huawei. The infrastructure facilities of this type of cloud computing platform are composed of two system structures. The two structures are the service management system and the operation monitoring system in the platform management as shown in Figure 3.

The analysis and prediction system used in the cloud computing platform mainly implements functions such as mining and analyzing data in the current state, analyzing the current operating state and future development trends, and providing alerts on user behavior. The data analysis performed in the cloud computing platform is mainly to predict and process the raw data that has not been processed in the platform; the trend prediction is mainly for the data after analysis and processing, and the platform will analyze and process the data according to the specific algorithm summarized by the researcher. The prediction model and prediction algorithm are improved and perfected, and the future development direction is scientifically predicted based on the results of data analysis. The prediction alarm in the cloud computing platform is mainly managed in the form of network communication. When the system is abnormal, the service system will reflect the abnormal state data of trend prediction by sending communication to the user, so that the user can make a response.

The cloud computing platform architecture diagram is shown in Figure 4.

The cloud computing platform prediction system architecture of this paper is shown in Figure 5.

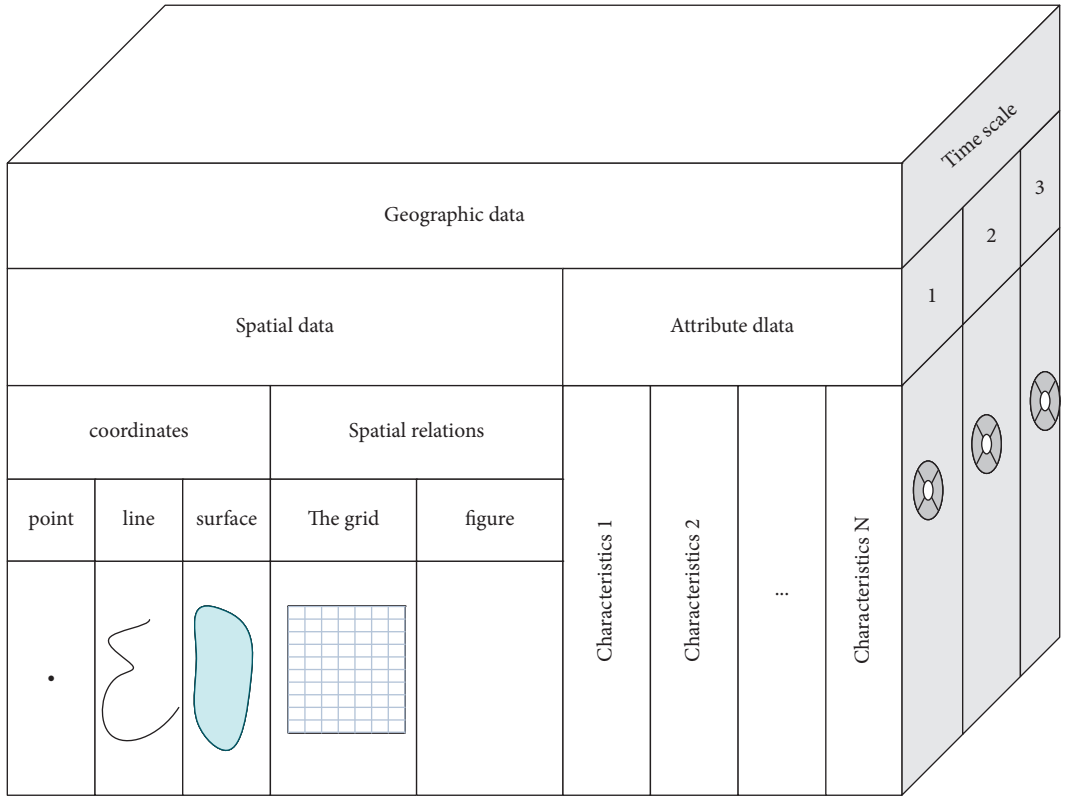

Figure 1: Spatiotemporal data.

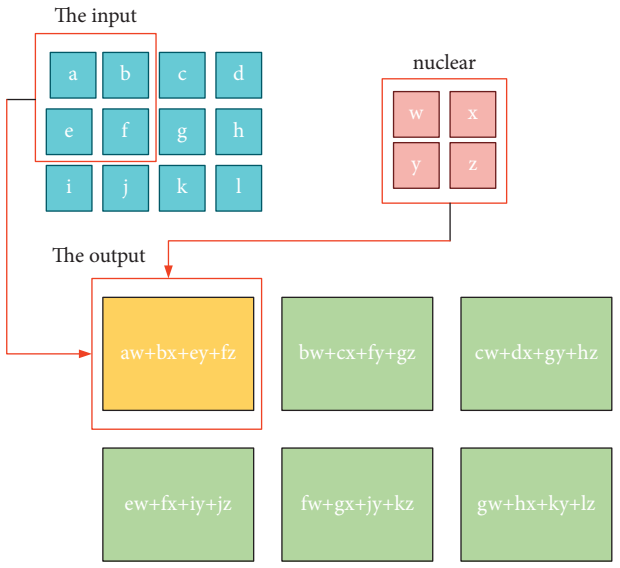

Figure 2: Convolution operation on a two-dimensional tensor.

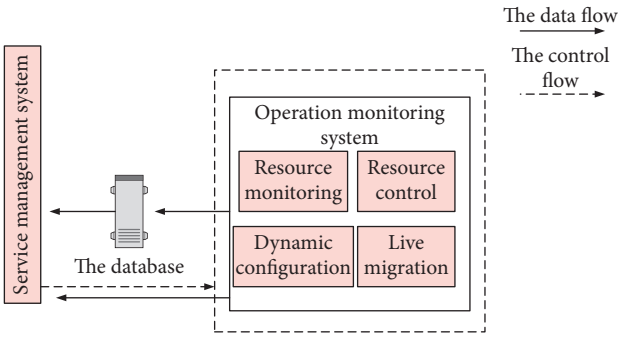

Figure 3: Cloud computing infrastructure architecture diagram.

3.3.1. Data Preprocessing Algorithm. Researchers consider that the cloud computing platform prediction system is likely to encounter data missing, data integrity problems, noise during the collection process, or inconsistencies in the data collection process during the process of research data collection. These factors often cause the cloud computing platform prediction system to produce great errors when calculating data, which will have a serious impact on the accuracy of the cloud computing platform prediction system platform. In order for researchers to better solve the above problems, this article will be divided into two parts to perform data preprocessing on the resource load sequence of the cloud computing platform prediction system.

3.3.2. Single Prediction Model. In order to better understand the resource load sequence in the cloud computing platform forecasting system, the author chose three single forecasting models in this article. The main reasons for choosing these three prediction models are as follows: Researchers can analyze and propose the relevant laws of holidays hidden in the resource load of the cloud computing platform prediction system through the phase space reconstruction prediction model, making the cloud computing platform

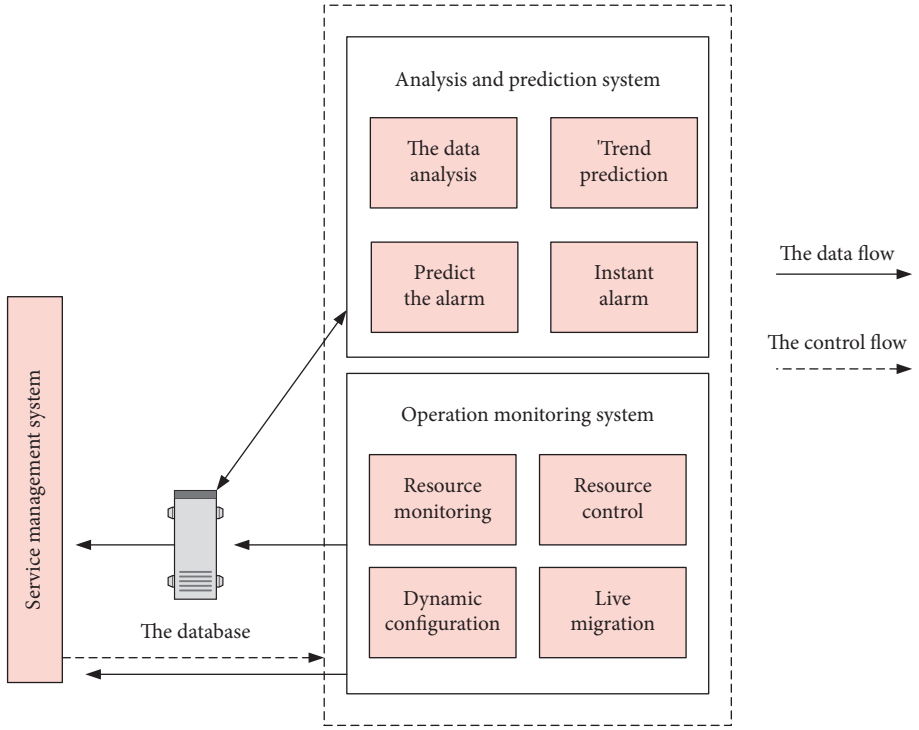

Figure 4: Cloud computing platform architecture diagram.

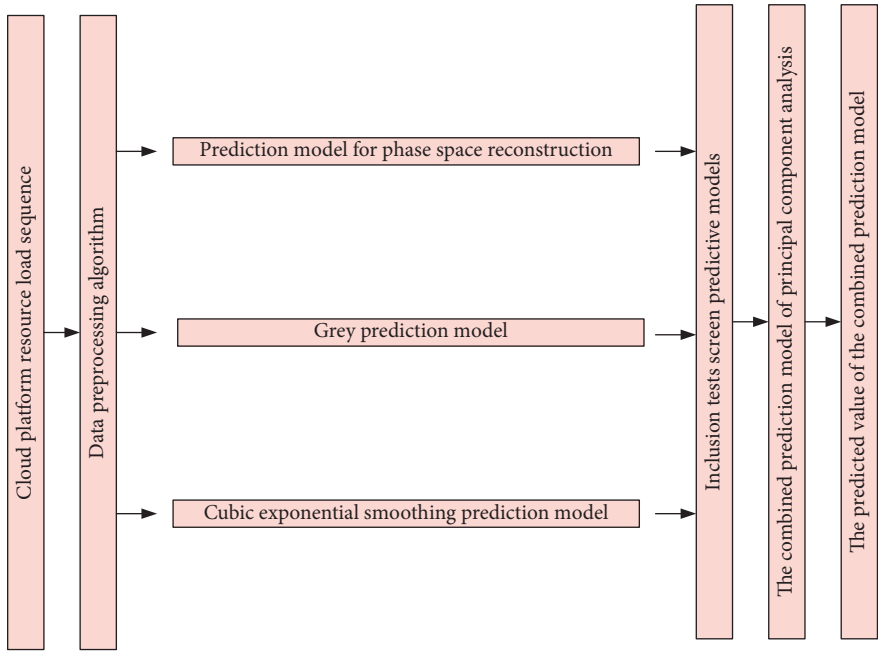

Figure 5: Cloud computing platform prediction system architecture.

prediction system the original characteristic state is analyzed and restored.

3.3.3. Inclusive Test. The existing combined forecasting model of the cloud computing platform forecasting system is just a relatively simple single forecasting model used by researchers to assign weights to the data obtained by the analysis of the cloud computing platform forecasting system. Because this type of prediction model is relatively simple, the operation process does not consider whether there will be some data effects that are not conducive to the experiment if the data of a single prediction model is only used in the process of combined prediction. On the one hand, the combined forecasting model in the cloud computing platform forecasting system will not necessarily improve when it

is used. Therefore, researchers have adopted the means of increasing the number of single forecasting models; on the other hand, there are likely to be some interrelated characteristics between each single prediction model in the cloud computing platform prediction system. This phenomenon will cause the phenomenon of information overlap in the combined prediction model when the input information is studied in the experiment, leading to the accuracy of the prediction reduce.

3.3.4. Combined Forecasting Model. When researchers conduct computational research on the cloud computing platform forecasting system, they use a single forecasting model, which to a certain extent cannot integrate the characteristics of the cloud computing platform resource load sequence, and the cloud calculated from the data results the prediction error of computing platform resource load is extremely large. Therefore, the combined forecasting model will become a key research area in the field of scientific research for the development of cloud computing platform resource load forecasting. Compared with a single prediction model, the combined prediction model in the cloud computing platform takes into account the various factors that may occur in reality. This model has more comprehensive information and more accurate calculation data. Compared with a single prediction model, it has obvious superiority.

4. Data Preprocessing Method and Prediction Model Design

4.1. Data Preprocessing Method and Correction Algorithm

4.1.1. Laida Criterion. The expression is as follows:

$$\left|x_i - \overline{x}\right| > 3\sigma. \tag{1}$$

Among them,

$$\overline{x} = \frac{1}{n}\sum_{i=1}^{n} x_i, \qquad \sigma = \sqrt{\frac{\sum_{i=1}^{n} x_i^2 - (1/n)\left(\sum_{i=1}^{n} x_i\right)^2}{n-1}}. \tag{2}$$

4.1.2. Shawville Criterion. The expression is as follows:

$$\left|x_i - \overline{x}\right| > Z_c\sigma. \tag{3}$$

4.1.3. Gadabus Criterion. The expression is as follows:

$$g_i \geq g(a, n). \tag{4}$$

Among them,

$$g_i = \frac{\left|x_i - \overline{x}\right|}{\sigma}. \tag{5}$$

4.1.4. T-Test Criteria. The expression is as follows:

$$\left|x_i - \overline{x}\right| > K\sigma. \tag{6}$$

In the process of data research and processing in this article, the researchers found that some data was not recorded under this processing method, and it is necessary to supplement and retrieve these unrecorded values.

In order to retrieve the lost data, the researchers studied the following methods:

(1) Retrieve the lost value manually: The advantage of this retrieval method is that it is simple to operate and easy to learn. However, the shortcomings of this approach are also very obvious. This method is not suitable for data sets that do have a higher ratio. If manual filling is used in this kind of data, the resulting data will be distorted easily. Among them, the mode imputation method and the mean imputation rule are the most commonly used methods when manually filling in missing values in the data.

(2) Fill in the missing values with constants: this method is to replace all missing positions in the whole article with a fixed constant when the researchers find that the missing data is found in the data consolidation process. This mode of operation is very simple and can be easily achieved. But the disadvantage is that the accuracy rate is very low. If the operator replaces all the missing values in the data with "Constant", the prediction model is likely to make judgment errors. Therefore, this method is not reliable.

(3) Replace the missing values in the data with the average value of the remaining data: When there is a data loss phenomenon in a set of samples, the researcher can add the remaining data and average again, using the average value in the data as a standard value is used to supplement the missing part of the data.

(4) Fill the most probable value with the most data based on scientific inference: Researchers can make inference predictions on the required data information based on the mathematical model derived from inference. For example: linear regression model, decision tree induction and other methods, the missing values of the sample data will be supplemented by the calculated prediction results.

The most common strategy used by researchers in academia is method (4), because in method (4) the missing data values in the sample are not obtained out of thin air, but researchers use scientific algorithms to analyze and calculate the remaining information inferred. This article analyzes and contrasts various methods for supplementing missing values of sample data in the current academic community, and finally chooses method (4) as the supplement of missing values of resource load sequence in the cloud computing platform.

What needs to be emphasized in this article is that in some specific cases, just as certain words and paragraphs in

the data information database must be allowed to be afraid, the occasional missing value in the data does not necessarily mean that the data is in progress. An error occurred during the collection process. Researchers use to determine the elimination method of numerical noise. This article conducts a more in-depth study on the following methods.

(1) Binning: researchers smoothly process the ordered value data by "neighboring" (that is, the values around the missing data). First, the researcher will put some "buckets" in the sample data, or ordered values in "bins". Based on this, the neighboring value of missing data was investigated and researched, so the smoothing strategy was chosen. The main smoothing strategies currently used by researchers are: box mean smoothing method, box median smoothing method, box boundary value smoothing method, and so on.

(2) Regression: the researcher eliminates the method of using the noise fitting function to give a certain value. The main method of this fitting function elimination can be divided into linear regression elimination method and multiple linear regression elimination method. Linear regression elimination method refers to the accurate value of an attribute in the known sample data, and on this basis, the fitting curve between two different attributes is known. And bring the known attribute value into the calculated fitting curve to predict the value of another attribute. The multiple linear regression forecasting method often involves multiple attributes in the sample data when data forecasting, and the other steps are generally the same as the linear regression forecasting method.

(3) Clustering: researchers classify data objects with similar properties and characteristics in the sample data information, and arrange them into groups. Then group these classified data information into a specific set, which is defined as a cluster. The researchers then perform information detection based on the similar characteristics of these information clusters. If the data is not in the form set, the researchers define it as an outlier.

In this article, based on the analysis information proposed above, the researchers will divide the data information into two major groups to discuss the closed value: If the value of i selected by the researcher is too large and exceeds a certain range, then the noise will be removed. The range is wider, and a lot of useful information will be eliminated and eliminated by the system; if the researcher selects a threshold smaller than a certain range when conducting the experiment, the noise removal will not have a particularly obvious effect, and there will be a lot of noise in the load sequence. It will continue to survive and cannot be eliminated.

Select the closed value as

$$n_i = M(j + 2 - i)^{\beta}. \tag{7}$$

The action mode of the hard threshold is

$$a_i = \begin{cases} d_i |d_i| \geq \lambda, \\ 0_i |d_i| < \lambda. \end{cases} \tag{8}$$

The soft threshold function is as follows:

$$\alpha_i = \begin{cases} \operatorname{sign}(d_i)(|d_i| - \lambda) |d_i| \geq \lambda, \\ 0_i |d_i| < \lambda. \end{cases} \tag{9}$$

Among them,

$$\operatorname{sign}(t) = \begin{cases} 1, \ t \geq 0, \\ -1, \ t < 0. \end{cases} \tag{10}$$

4.2. Forecasting Model Design of Multivariate Load Series. This article draws on the method of univariate reconstruction phase space to determine delay time τ and embedding dimension m.

Reconstruct the phase space as follows:

$$\begin{aligned} X(n) &= [x(n), \ldots, x(n - (m-1)\tau)]^T \in R \\ &(n = N, \ldots (m-1)\tau + 1). \end{aligned} \tag{11}$$

Reconstruct the multivariate phase space as follows:

$$\begin{aligned} Y(n) = {} & [x_1(n), x_1(n - \tau_1), \ldots, x_1(n - (m_1 - 1)\tau_1)] \\ & x_2(n), x_2(n - \tau_2), \ldots, x_2(n - (m_2 - 1)\tau_2) \\ & \cdots\cdots \\ & x_k(n), x_k(n - \tau_k), \ldots, x_k(n - (m_k - 1)\tau_k)^T \in R^{m_1 + \ldots + m_k} \\ & n = N, N-1, \ldots, \max_{1 \leq i \leq k} (m_i - 1)\tau_i + 1. \end{aligned} \tag{12}$$

Suppose there are currently K resource load sequence types, which are included by the cloud computing platform $Y_1, Y_2, \ldots, Y_k$ are the first vectors of the K underlying resource phase spaces, and the first vector $Y_q = [x_{q1}, x_{q2}, \ldots, x_{qm}]^T$ of the phase space is used as a variable Exist in different underlying resources, there are $q = 1, \ldots, K; m = \min_{1 \leq h \leq K} (m_h)$, which represents the variable $y_{i,i} (i = 1, 2, \ldots, m; j = 1, 2, \ldots, K)$ at the corresponding position in the matrix, and the matrix is obtained:

$$R = (r_{ij}), i = 1, 2, \ldots, m, j = 1, 2, \ldots, K. \tag{13}$$

Among them,

$$\begin{aligned} \overline{y_j} &= \frac{1}{n} \sum_{i=1}^{n} y_{ij}, \\ r_{ij} &= \frac{S_{ij}}{\sqrt{S_{ii} S_{jj}}}, \\ S_{ij} &= \frac{1}{n-1} \sum_{k=1}^{n} (y_{ki} - \overline{y_i})(y_{kj} - \overline{y_j}). \end{aligned} \tag{14}$$

Description of the number of neighborhood points in the phase space reconstruction process is as follows:

$$H = X\left(X^T X\right)^{-1} X^T,$$

$$D(K) = tr(H),$$

$$\sigma^2(K) = \frac{\left[y - yX^T\left(XX^T\right)^{-1}X\right]\left[y - yX^T\left(XX^T\right)^{-1}X\right]^T}{K - D(K)}. \tag{15}$$

The weight of point X_{mi} is defined as follows:

$$P_i = \frac{\exp\left(-c\left(d_i - d_m\right)\right)}{\sum_{i=1}^{q} \exp\left(-c\left(d_i - d_m\right)\right)}. \tag{16}$$

The first-order local linear prediction model is constructed as follows:

$$X_{Mi+k} = a_k e + b_k X_{Mi},\ i = 1, 2, \ldots, q. \tag{17}$$

Apply the weighted least squares theory, then

$$\min \sum_{i=1}^{q} P_i \left[\sum_{j=1}^{m} \left(x_{Mi+k}^j - a_k - b_k x_{Mi}^j\right)^2\right], \tag{18}$$

where x_{Mi}^j (18) is the jth element in the reference vector X Mi. After simplification, we can get

$$\begin{cases} a_k \sum_{i=1}^{q} P_i \sum_{j=1}^{m} x_{Mi}^j + b_k \sum_{i=1}^{q} P_i \sum_{j=1}^{m} \left(x_{Mi}^j\right)^2 = \sum_{i=1}^{q} P_i \sum_{j=1}^{m} x_{Mi+k}^j x_{Mi}^j, \\ a_k m + b_k \sum_{i=1}^{q} P_i \sum_{n=1}^{m} x_{Mi}^j = \sum_{i=1}^{q} P_i \sum_{n=1}^{m} x_{Mi+k}^j. \end{cases} \tag{19}$$

The matrix form is written as

$$\begin{pmatrix} \alpha & \beta \\ m & \alpha \end{pmatrix} \begin{pmatrix} a_k \\ b_k \end{pmatrix} = \begin{pmatrix} e_k \\ f_k \end{pmatrix}. \tag{20}$$

Among them,

$$\begin{aligned} \alpha &= \sum_{i=1}^{q} P_i \sum_{j=1}^{m} x_{Mi}^j, \\ \beta &= \sum_{i=1}^{q} P_i \sum_{j=1}^{m} \left(x_{Mi}^j\right)^2, \\ e_k &= \sum_{i=1}^{q} P_i \sum_{j=1}^{m} x_{Mi+k}^j x_{Mi}^j, \\ f_k &= \sum_{i=1}^{q} P_i \sum_{n=1}^{m} x_{Mi+k}^j, \\ \begin{pmatrix} a_k \\ b_k \end{pmatrix} &= \begin{pmatrix} \alpha & \beta \\ m & \alpha \end{pmatrix}^{-1} \begin{pmatrix} e_k \\ f_k \end{pmatrix}. \end{aligned} \tag{21}$$

Substitute the obtained ak and bk into the prediction formula as follows:

$$X_{M+K} = a_k e + b_k X_M. \tag{22}$$

The predicted value after k-step evolution is X_{M+K} is as follows:

$$X_{M+k} = \left(x_{M+k}, x_{M+k+r}, \ldots, x_{M+k+(m-1)r}\right). \tag{23}$$

In $X_{M+k} = (x_{M+k}, x_{M+k+r}, \ldots, x_{M+k+(m-1)r})$, the m-th element $x_{M+k+(m-1)r}$ is the k-step predicted value of the original load sequence.

4.3. System Analysis and Implementation. The prototype of the cloud computing platform mentioned in this article is actually a project "cloud computing and its supporting network" that Northwest University cooperates with Huawei. The main purpose of this project is to better test and evaluate the effect of the prediction model of the cloud computing platform resource load sequence. Denoising effects under different wavelet bases and different decomposition layers are shown in Table 1.

This article establishes a predictive model based on the CPU utilization load sequence of a cloud computing platform as an example. Among them, the load sequence of CPU utilization uses wavelet denoising theory to denoise these four types of resource load sequences. Denoising processing is shown in Figure 6. Main component characteristic root and contribution rate are as shown in Table 2. Principal component feature vector is shown in Table 3.

The main component table is

$$\begin{aligned} Z_1 &= 0.4753Y_1 + 0.4031Y_2 + 0.1216Y_3, \\ Z_2 &= 0.0058Y_1 + 0.1722Y_2 + 0.8219Y_3. \end{aligned} \tag{24}$$

The weight is the contribution rate of each principal component:

$$\begin{aligned} Y &= \frac{1.8394}{1.8394 + 0.9285} \times Z_1 + \frac{0.9285}{1.8394 + 0.9285} \times Z_2 \\ &= 0.6645 \times Z_1 + 0.3355 \times Z_2 \\ &= 0.3178Y_1 + 0.3256Y_2 + 0.3566Y_3. \end{aligned} \tag{25}$$

The multi-variable phase space embedding dimension of the virtual machine utilization rate is a multi-variable prediction model. Comparison of test results of the grey prediction model is shown in Table 4. The prediction results and accuracy comparison of the CPU utilization load sequence of the cloud computing platform are as shown in Table 5.

$$m = m_1 + m_2 + m_3 + m_4 = 8 + 2 + 2 + 2 = 14. \tag{26}$$

4.4. Combined Forecasting Model. MAPS is defined as follows:

$$\text{MAPE} = \frac{1}{N} \sum_{i=1}^{N} \left|\frac{f_i - y_i}{y_i}\right| \times 100\%. \tag{27}$$

Table 1: Denoising effects under different wavelet bases and different decomposition layers.

Wavelet base	Decomposition layer	Root mean square error (RMSE)	Signal to noise ratio (SNR)
db4	3	0.1993	32.2564
db4	4	0.2163	30.6250
db4	5	0.2335	29.0929

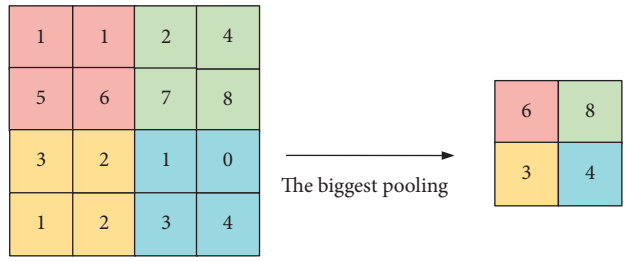

Figure 6: Denoising processing.

Table 2: Main component characteristic root and contribution rate.

Main ingredient	Eigenvalues	Contribution rate (%)	Cumulative contribution rate (%)
Z1	1.8394	61.31	61.31
Z2	0.9285	30.95	92.26
Z3	0.2320	7.74	100.00

Table 3: Principal component feature vector.

Resource category	Z1	Z2
Memory utilization	−0.6894	0.0764
Disk utilization	−0.6349	0.4150
Network load utilization	0.3487	0.9066

Table 4: Comparison of test results of grey prediction model.

Grey prediction model	Without denoising	Wavelet denoising processing
Posterior variance ratio C	0.2332	0.1476
Probability of small error	85.66%	92.38%

Table 5: The prediction results and accuracy comparison of the CPU utilization load sequence of the cloud computing platform.

Time series/day	CPU utilization actual value/%	Predicted value of phase space prediction model	Grey prediction model predicted value	Three times exponential smoothing model prediction value	Combination forecast model forecast value
1091	38.520	38.917	38.733	39.728	39.323
1092	38.760	38.945	38.735	39.763	39.354
1093	39.380	38.993	38.737	39.799	39.396
1094	39.636	38.956	38.739	39.836	39.396
1095	39.720	38.955	38.741	39.872	39.414
MAPE (%)		1.23	1.39	1.54	1.01

5. Conclusion

This article mainly carried out specific research on the resource prediction model in the cloud computing platform. Researchers realized the resource prediction function of the cloud computing platform through continuous in-depth research on the original system. Although the cloud computing platform has been greatly developed, there is still a lot of work that needs to be further studied on the system platform. Researchers will continue to conduct in-depth research and mining on the existing data and will summarize the algorithm applied to cloud computing resource load sequence. In this article, the researchers analyzed and studied the algorithms in the data processing function of data prediction, and have obtained considerable results of data prediction processing on the cloud computing platform. However, these methods are relatively simple and basic. In real life, in order to better remove the noise in the

data, researchers often use different methods of data generation, different sources of data, etc., and these collected data often contain some additional information. How to eliminate the redundant additional information contained in these data and the impact of this information on the prediction results requires researchers to conduct further research on the prediction processing methods of system data and combining various types of combined prediction models.

Data Availability

The data used to support the findings of this study are available from the corresponding author upon request.

Conflicts of Interest

The author(s) declare that they have no conflicts of interest.

Acknowledgments

This work was supported by (1) Hunan Provincial Department of Education Scientific Research Outstanding Youth Project (Nos.18B524 and 19C1069) and (2) Hunan Provincial Department of Education Educational reform project (No. HNKCSZ-2020-0633), Notice of Hunan Provincial Department of Education [2020] No.233.

References

[1] Y. Yu, "Research on the Evaluation Algorithm of Social Capital Influence of enterprise Network Marketing," *Security and Communication Networks*, vol. 2021, Article ID 7711322, 8 pages, 2021.

[2] H. Hwangbo, Y. S. Kim, and K. J. Cha, "Use of the smart store for persuasive marketing and immersive customer experiences: a case study of Korean Apparel Enterprise," *Mobile Information Systems*, vol. 2017, Article ID 4738340, 17 pages, 2017.

[3] B. Huang, J. Wei, Y. Tang, and C. Liu, "Enterprise risk assessment based on machine learning," *Computational Intelligence and Neuroscience*, vol. 2021, Article ID 6049195, 6 pages, 2021.

[4] Y. Zhao, "Sports enterprise marketing and financial risk management based on decision tree and data mining," *Journal of Healthcare Engineering*, vol. 2021, Article ID 7632110, 8 pages, 2021.

[5] A. F. S. Devaraj, M. Elhoseny, S. Dhanasekaran, E. L. Lydia, and K. Shankar, "Hybridization of firefly and Improved multi-objective particle swarm optimization algorithm for energy efficient load balancing in cloud computing environments," *Journal of Parallel and Distributed Computing*, vol. 142, pp. 36–45, 2020.

[6] X. Li, H. Jianmin, B. Hou, and P. Zhang, "Exploring the innovation modes and evolution of the cloud-based service using the activity theory on the basis of big data," *Cluster Computing*, vol. 21, no. 1, pp. 907–922, 2018.

[7] R. Buyya, C. S. Yeo, and S. Venugopal, "Market-oriented cloud computing: vision, hype, and reality for delivering it services as computing utilities," in *Proceedings of the 2008 10th IEEE International Conference on High Performance Computing and Communications*, Dalian, China, September 2008.

[8] P. K. Senyo, E. Addae, and R. Boateng, "Cloud computing research: a review of research themes, frameworks, methods and future research directions," *International Journal of Information Management*, vol. 38, no. 1, pp. 128–139, 2018.

[9] B. Liao and Y. M. Liao, "Research on enterprise risk knowledge graph based on multi-source data fusion," *Neural Computing & Applications*, vol. 34, no. 4, pp. 2569–2582, 2022.

[10] D.-W. Sun, G.-R. Chang, S. Gao, L.-Z. Jin, and X.-W. Wang, "Modeling a dynamic data replication strategy to increase system availability in cloud computing environments," *Journal of Computer Science and Technology*, vol. 27, no. 2, pp. 256–272, 2012.

[11] H. Liu and G. Liu, "An efficient and trustworthy resource sharing platform for collaborative cloud computing," *IEEE Transactions on Parallel and Distributed Systems*, vol. 25, no. 4, pp. 862–875, 2014.

[12] A. Comi, L. Fotia, and F. Messina, "A reputation-based approach to improve qos in cloud service composition," in *Proceedings of the 2015 IEEE 24th International Conference on Enabling Technologies: Infrastructure for Collaborative Enterprises*, pp. 108–113, Larnaca, Cyprus, June 2015.

[13] N. Alkhater, R. Walters, and G. Wills, "An empirical study of factors influencing cloud adoption among private sector organisations," *Telematics and Informatics*, vol. 35, no. 1, pp. 38–54, 2018.

[14] R. Arora, "A. Parashar, and Cloud Computing Is Transforming, "Secure user data in cloud computing using encryption algorithms," *International Journal of Engineering Research in Africa*, vol. 3, no. 4, pp. 1922–1926, 2017.

[15] G. Zhang, L. Liu, and H. Guo, "Investigating the impact of cloud computing vendor on the adoption of cloud computing," *Mobile Information Systems*, vol. 2021, Article ID 6557937, 18 pages, 2021.

Hindawi
Mobile Information Systems
Volume 2022, Article ID 2670241, 9 pages
https://doi.org/10.1155/2022/2670241

Research Article

Heterogeneous Group Risk Decision Behavior Simulation Based on Particle Swarm Optimization Algorithm

Na Lu

School of Economics and Management, Xi'an Aeronautical University, Xi'an 710077, Shaanxi, China

Correspondence should be addressed to Na Lu; luna@xaau.edu.cn

Received 26 May 2022; Revised 27 June 2022; Accepted 8 July 2022; Published 29 July 2022

Academic Editor: Shadi Aljawarneh

This paper studies the general SoC design AMBA bus and proposes an automatic generation method of software structure test data based on adaptive data optimization algorithm. By simplifying the basic particle expansion equation and eliminating the particle velocity term, an adaptive scheme based on inertia weight is proposed. In the research process, this article fully considers heterogeneous groups. Investment companies are divided into three types of decision-makers: reciprocal, intelligent, and leveraged, and their investment behavior is modeled. Given that factors such as technical level will affect the future of the project, and swarm simulation software is used to simulate and analyze the impact of the profitability of smart community microgrid construction projects on decision-making and to conduct dynamic research on market modeling risks. This article first outlines the construction of the renewable energy macro- and micro-market risk decision-making behavior model and clarifies the logic process of the market to promote the consumption of renewable energy. Then, it analyzes the causes of market risks based on dynamic models, first examines the relationship between key risks and risk factors, forms risks that affect returns (bilateral random risks and market efficiency risks), and then an analysis framework for the impact of renewable energy. This paper applies it to the analysis of data-based algorithms, thereby promoting the development of data-based algorithms.

1. Introduction

This article briefly summarizes the basis and importance of personal research, the status quo of CNC systems and multi-core processors, and the real-time analysis, real-time research, and modification of Linux operating system failures. It also studied the planning and real-time maintenance principles of the Linux operating system, and transplanted the patch to the multi-core ARM platform [1]. On this basis, this paper analyzes the characteristics of the data optimization algorithm and the correlation scheme between real-time tasks and specific CPU cores, and uses the delay monotonic rate to schedule the real-time tasks of the data optimization algorithm system [2]. Using the integrated version of Qt, Qt Embedded has developed a graphical user interface for CNC systems. A point-to-point linear interpolation algorithm is written to perform basic interpolation functions. The experimental test results show that the system constructed in this paper can effectively improve the real-time performance of the task scheduling of the data optimization algorithm system, which creates conditions for further shortening the cycle and improving processing efficiency [3]. This paper deeply analyzes the impact of different project incomes on the group's free use behavior and overall contribution level, and then establishes an overall project income distribution model under a certain project income, and changes the income distribution index as a reward. This paper mainly studies the impact of income heterogeneity groups on major investment behavior [4]. Finally, in response to the actual collective action problem of the self-financing construction of the smart community microgrid residents, it actually provides a scientific and feasible theoretical basis for city managers and project designers, and proposes countermeasures [5]. Build a bilateral random risk decision-making behavior control model to realize effective prediction of key risk factors. Based on the most important risk factors, different attributes of time series, and forecasting needs, this article also proposes a

variety of different forecasts and corrections: AdaBoost ELM regression model is designed for REC prices, ARIMA model is used for forecasting, and then learning methods are used for error correction, and it is recommended to make predictions based on LSTM. A deep LSMNet network with convolution, loop, loop jump, and autoregressive components is designed to predict load and line loss. A market risk management and decision simulation system are designed to transform and apply the theoretical results of this work [6]. Considering the subject of quota obligation, design enterprise-level cloud applications and distributed application integration schemes; for enterprise-level cloud applications, design the architecture of risk decision behavior management module, and examine the application of cloud service mode; for light distributed applications, the Tangle distributed ledger is used to simulate P2P energy transactions to verify the application value of blockchain technology in the energy market [7].

2. Related Work

The literature introduces one of the methods of Linux system; real-time conversion is to add real-time boot patches and discusses in detail the main real-time preference patch conversion technology, focusing on interrupt threads, high-precision clocks, key part preferences, and protocol priority inheritance [8]. The literature introduces the inspection and analysis of system performance, and tests the modified real-time Linux system, which usually interrupts the response time, context change time and clock accuracy, as well as the operating effectiveness of the graphical user interface and the operating efficiency of the interpolation program [9]. The literature introduces multi-source risks. The existing four benchmark simulation models examine the impact of various combinations of risk levels on system performance in order to provide effective guidance for the controlling society to make wise decisions about carbon resource allocation. It mainly introduces the experimental design, theory, risk-level modeling, and result statistical analysis to effectively evaluate the impact of risk factors on system performance. Related risk factors are composed of main characteristics, mechanisms, and multiple factors [10]. The literature introduces the decision-making simulation of the risk management of the renewable energy consumption market. Aiming at the risks arising from economic risks, energy risks, power quality risks, etc., a multi-objective risk decision model is constructed [11]. The key parameters of the model are obtained by simulating advanced energy markets at home and abroad to obtain decision-making solutions. It designs a risk management and decision-making simulation system, converts and implements theoretical research results, and simulates P2P energy transactions and risk decisions [12]. The literature introduces the experimental methods of using search technology to solve various software testing problems, especially through the automatic generation of structural test data, and many results have been achieved [13]. Research on automatic routing test data generation method is very important to improve software testing efficiency, ensure software quality, reduce the workload of testers, automate software testing process, and reduce software cost [14]. In the field of software testing, the research on automatic test data generation has developed into a hot spot for research and discussion by scientists at home and abroad.

3. Multi-Core ARM Data Optimization Algorithm and Heterogeneous Population Model

3.1. Multi-Core ARM Processor. The processor is an important part of the SoC system circuit. In the first stage of SoC design, the appropriate processor needs to be selected according to SoC functional requirements and actual application options. Make the performance of the processor meet the design requirements and, at the same time, will not waste too many resources on the chip, and achieve the purpose of optimizing the design. The processor mainly considers the processor type and the number of processor cores according to the requirements of the application scenario.

After data processing, the data are transmitted to the chip between chips, between boards, and between remote controllers through various high-speed peripheral interfaces; compressed, encoded, and decoded internally; and then sent to external advertisements of various specifications for display. Make the selected renderer compatible with optimized video rendering. On the other hand, the designed SoC circuit must meet the requirements that it can be used as an independent application processor, so that the selected processor can support the operation of different operating systems. Through the above analysis and summary, finally select the industry's most classic ARM Cortex-A9 as the processor core of the chip.

Reset mode: The reset signal designed by Cortex-A9 can be divided into independent reset processor. The reset mode of each reset signal is shown in Table 1.

The processor soft reset will initialize most of the logic circuits of the Cortex-A9 processor, except for the debug logic. Breakpoints and watch points are retained when the processor is restarted, and processor reset is usually used to restart a system that has been running for a period of time. Using nCPURESET and nNEONRESET to perform a soft reset corresponds to the reset sequence described in power-on reset. The only difference is that nDBGRESET must remain high during the restart sequence to ensure that all values in the debug log will not change.

3.2. Research on Heterogeneous Groups. A heterogeneous group refers to a group that is not completely homogenous, because in real life, individuals within a group show differences in public goods donations due to different income levels, input contributions, returns, and preferences for the final result. Heterogeneous social preferences in turn have a direct impact on the behavioral decisions of individual donations, showing varying degrees of cooperation. In the real system, there is almost no completely homogenous group, because the differences in factors such as age, wealth,

Table 1: Reset signal mode list.

Mode	nCPURESET	nNEONRESET	nDBGRESET
Power-on reset/cold reset	0	0	0
Processor reset/soft or warm reset	0	0	1
SIMDMPE power-on reset	1	0	1
Debug logic reset	1	1	0
Normal working mode	1	1	1

gender, knowledge, and experience have a certain impact on the behavior of participants. In addition, some studies have examined the heterogeneity of individuals in terms of social class, work industry, and religious beliefs.

By establishing a heterogeneity evaluation index system, this paper studies the relationship between heterogeneity and cooperation stability. The results of the study showed that the level of information determines the number of donations from heterogeneous groups. The investigation of the influence of the heterogeneity of individual social preferences on the supply effect of public goods shows that its contribution level is significantly higher than that of the general population. The demonstration effect of the first mover will also significantly improve the supply of public goods. Szolnoki et al. studied the evolution of cooperation in the space public product game where unconditional collaborators and various conditional collaborators coexist. Frean et al. suggested that there should be reasonable scheduling between cooperation and non-cooperation, and found that this strategy is very different from complete cooperation or complete betrayal.

3.3. Data Optimization Algorithm Model. The DRM algorithm is used for repetitive tasks, and the priority is determined based on the duty cycle. The shorter the time, the higher the priority. When a high-priority task arrives, it will overtake the low-priority CPU. RM is analyzed based on the following assumptions:

(a) All task requests are periodic.

(b) The request period of the b task is a constant.

(c) Tasks exist independently, the execution or end of a task will not depend on other task processes, and there is no communication between each other.

(d) Tasks can be advanced, and high-priority tasks can precede tasks with low CPU priority. For multiple independent periodic tasks, the lower limit of the system processor load rate programmed by the RM algorithm is

$$U = n\left(\sqrt[n]{2} - 1\right)(n > 1). \tag{1}$$

Schedule a set of tasks to meet this condition. Processor load is the sum of the load speed of all tasks:

$$U = \sum_{i=1}^{n} e_i / \mathbf{r}_i. \tag{2}$$

The monotonic rate planning algorithm does not consider the time required for context switching. When there are multiple short-term tasks in the system, because short-term tasks are prioritized, it tends to constantly change the context and involve developers of less important tasks. In this case, frequently switching tasks is time-consuming and even causes low-priority tasks to time out, thereby reducing real-time system performance.

The request with the lowest period and the longest period can directly enter the ready state, and requests for other tasks must be suspended first. The priority of the preparation task is higher than the delayed state. If the task delay time in the delayed state is 0, it will change from the delayed state to the ready state, and the task that has entered the ready state can no longer switch to the delayed state. If no task is in the ready state and the task currently being executed voluntarily exits the CPU, select the delayed state task scheduling execution.

The DRM algorithm defines the processor utilization of some tasks τ_i, τ_{i+1}, ..., τ_j, $1 \le i \le j \le n$, and the calculation formula is

$$U_{i\ldots j} = \sum_{k=i}^{j} e_k / \mathbf{r}_k. \tag{3}$$

The delay time of task τ_1 is

$$\Delta_1 = r_1 - e_1. \tag{4}$$

The time of the task τ_i, $i = 2, 3, \ldots, n-1$ in the delayed state is

$$\Delta_i = \alpha^* *_{r_l} * U_{i+1\ldots n}. \tag{5}$$

The DRM algorithm simulation test results confirm that the DRM algorithm not only reduces the frequent changes of the RM algorithm context, but also improves the processor utilization. When the system is overloaded, low-priority tasks can be delayed because high-priority tasks are processed first. The DRM algorithm is used as a criterion for evaluating time priority. But in CNC, there are not only real-time periodic tasks, but also sudden real-time tasks.

For each real-time task, calculate its slack time laxity. The current time is t, D_i is the absolute deadline of task τ_i, w_i is the remaining execution time of task τ_i, and then the relaxation time of task τ_i is

$$\text{Laxity}_i = D_i - (t + w_i). \tag{6}$$

If the downtime of the task is zero and the task cannot be scheduled, the task will exceed the deadline. In order to prevent unplanned tasks from running, tasks that have no

free time for scheduling are migrated to other CPU cores, and the CPU is replaced by tasks running on that core.

Next, use the RM algorithm and the extended DRM algorithm to compare the programming results. There are two real-time tasks τ_a and τ_b in the system. The unit time is t. The task parameters are shown in Table 2. The task τ_a has a period of 4 t, the worst-case execution time is 2 t, and the task τ_b has a period of 16 t. The time is 6 t.

The results of scheduling using two algorithms are shown in Figure 1. It can be seen from the figure that these two real-time tasks can be executed under the two scheduling strategies.

Particle swarm optimization is a population-based search technology proposed by Kennedy and Eberhart. With its simple concept, easy parameter setting, and simple implementation, it immediately attracted the attention of scientists in the field of evolutionary computing. For more than ten years, it has achieved rapid development. Theoretical research is becoming more and more perfect, and at the same time it has been applied to many practical engineering fields, and its scale has been continuously expanded, becoming a new entry point for academic research. Each particle updates its position and speed according to four pieces of information: current position and speed, individual guidance, and group world guidance. In the $t+1$ generation, the velocity and position of the particle i are updated as follows:

$$\begin{aligned} v_{id}(t+1) = {} & w \cdot v_{id} + c_1 \cdot r_1 \cdot \left(p_{id}(t) - x_{id}(t)\right) \\ & + c_2 \cdot r_2 \cdot \left(p_{\mathrm{ed}}(t) - x_{id}(t)\right), \end{aligned} \tag{7}$$

$$x_{id}(t+1) = x_{id}(t) + v_{id}(t+1), i = 1, 2, \cdots, n, d = 1, 2, \cdots, N. \tag{8}$$

In BPSO, the position of the particle is binary coded, and its value is only 0 or 1, but there is no such speed limit. Specifically, its location update formula is as follows:

$$x_{\mathrm{id}} = \begin{cases} 0 & \text{if} S\left(v_{\mathrm{id}}\right) < r_3 \\ 1 & \text{Other} \end{cases} \tag{9}$$

Among them, r_3 is a random vector in [0,1], and the velocity iv of the particle is still updated by formula (7); S(•) is the sigmoid function, and the formula is as follows:

$$S(v) = \frac{1}{1 + \mathrm{e}^{-v}}. \tag{10}$$

Generally speaking, particle swarm optimization is to set the neighboring particle swarm of specific particles in advance. At the same time, the size and number of these adjacent parts have a certain impact on the integration speed of the algorithm. There is evidence that the larger the adjacent nucleus, the faster the algorithm. If the adjacent particle is small, it can prevent the nucleus from approaching prematurely. Although Kennedy has studied the different topological structures between particles and their influence on particle swarm optimization methods, they still have not got a clear conclusion.

Table 2: Real-time task parameter table.

Task	Period()	Exe time(t)
Ta	4	2
Tb	16	6

Inertial weight: Inertial weight was originally proposed by Shi and Eberhart to balance the relationship between global optimization ability and local optimization ability. They can use the inertial weight to control the impact of the previous generation on the current speed. In general, choosing a smaller inertia weight can make the particles maintain a slower speed in the original direction, so that the particle swarm has better developability (local search ability); choosing a larger inertia weight will lead to particle movement and no good development in the original direction. It has a higher speed, so that the particle swarm has a better scanning ability (global search ability). Therefore, adjusting the size of w can effectively balance the exploration and development capabilities of the particle swarm. The following is the time-varying linear fitting method:

$$w(t) = w_{max} - \frac{\left(w_{max} - w_{min}\right) \cdot t}{T_{max}}, \tag{11}$$

In other words, it is impossible to optimize all performance indicators at the same time, but to achieve a balanced result between the various goals, as shown in the following formula:

$$\begin{aligned} & \max y = F(x) = \left(f_1(x), f_2(x), \ldots, f_M(x)\right), \\ & \text{s.t.} \begin{cases} g_i(x) \geq 0, & i = 1, 2, \ldots, p, \\ h_j(x) = 0, & j = 1, 2, \ldots, q. \end{cases} \end{aligned} \tag{12}$$

The C measure of the solution set A and B, denoted as C(A, B), represents the ratio of the number of elements in B that are dominated by the elements in A to the total number of elements in B, namely,

$$\mathrm{C}(A, B) = \frac{\left|\{b \mid b \in B, \exists a \in A, \ni : a \prec b\}\right|}{|B|}. \tag{13}$$

The SP measure is defined as follows:

$$\begin{aligned} & SP(S_1) = \sqrt{\frac{1}{n-1} \sum_{j=1}^{n} \left(d^*(S_1) - d\left(x_j\right)\right)^2}, \\ & \text{s.t.} \, d\left(x_j\right) = \min_{k \in (1,2,\ldots,n)} \left(\sum_{i=1}^{2} \left| f_i\left(x_j\right) - f_i\left(x_k\right) \right| \right), \\ & d^*(S_1) = \frac{1}{n} \sum_{j=1}^{n} d\left(x_j\right), \\ & j = 1, 2, \ldots, n. \end{aligned} \tag{14}$$

Figure 2 shows the principle diagram of particles moving in the solution space.

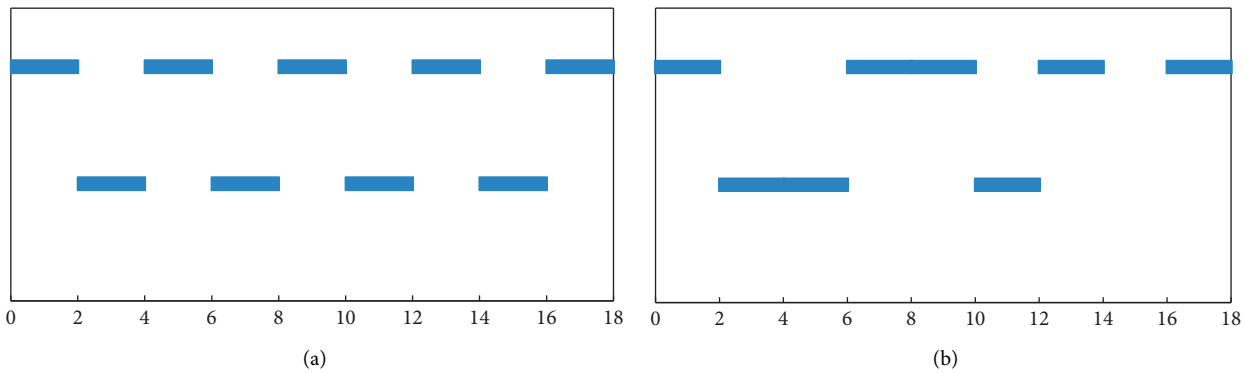

Figure 1: Example of scheduling using two algorithms. (a) An example of scheduling using RM. (b) An example of scheduling using DRM.

4. Simulation Research on Heterogeneous Group Risk Decision-Making Behavior

4.1. Risk Decision. Under C&T conditions, manufacturing companies face four decisions when allocating carbon resources: self-purification, carbon acquisition, quota consumption, and fines. Due to many uncertain factors, such as price fluctuations, construction time, and cost wait. Decisions regarding the allocation of carbon dioxide resources are also related to risks from multiple sources. On the basis of the research, combined with the specific circumstances of various decision-making, the research focuses on two types of decision-making risks, "self-cleaning risk" and "carbon purchase risk," and four types of marginal risks, that is, the marginal risks associated with related decisions. Due to the complexity of the model, there is no risk of temporarily controlling the use of quotas. The description and explanation of the related risks are shown in Table 3.

This research evaluates the risk level from the probability of occurrence of risk events and the severity of risk loss. The probability of occurrence of risk events is divided into five levels: low, low, high, high, and extremely high (see Table 4).

For details, see the master's thesis "Design of Multi-Source Risk Decision System for Enterprise Carbon Resource Allocation under Conditions of Total Control and Trading" as shown in Table 5.

The calculation formula is as follows:

$$I_i = L_i/PBT \times 100\%$$
$$PBT(t) = p(t) \times P\ d(t) \times (1 - SCR). \quad (15)$$

4.2. Risk-Level Control Model. The criteria for judging the risk loss level of carbon price fluctuations are as follows: tPre-tax profit = tperiod sales revenue ∗ (1-income cost rate) = tperiod product unit price ∗ tperiod sales volume ∗ (1-income cost rate).

$$PBT(t) = p(t) \times P\ d(t) \times (1 - SCR). \quad (16)$$

Among them, $P(t)$ is profit before tax in period t (without considering income tax); (t) is unit price of the product in period t; (t) is monthly output in period t; and SCR is cost of income ratio.

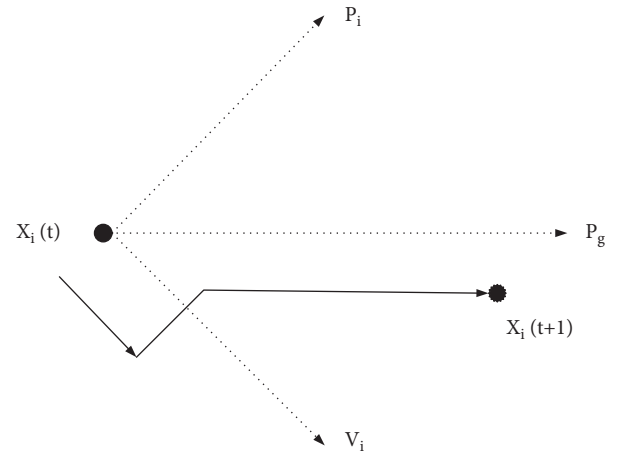

Figure 2: Schematic diagram of particle movement.

Actual risk loss due to carbon price fluctuations is

$$L_{21}' = \left(P_{e\,d}'(t) - P_{e\,d}(t)\right) \times q(t) = \left(P_{e\,d}'(t) - P_{e\,d}(t)\right) \times p(t) \times P\ d(t) \times \alpha_1 \times \alpha_2. \quad (17)$$

When the market carbon price risk loss index range is [0, 2],

$$\frac{L_{21}'}{PBT} = \frac{\left(P_{ed}'(t) - P_{ed}(t)\right) \times p(t) \times Pd(t) \times \alpha_1 \times \alpha_2}{p(t) \times Pd(t) \times (1 - SCR)}. \quad (18)$$

Calculate

$$P_{ed}(t) < P_{ed}'(t) \le P_{ed}(t) + \frac{\delta_m \times (1 - SCR)}{\alpha_1 \times \alpha_2}. \quad (19)$$

When the market carbon price risk loss index range is [3, 5],

$$\frac{L_{21}'}{PBT} = \frac{\left(P_{ed}'(t) - P_{ed}(t)\right) \times p(t) \times Pd(t) \times \alpha_1 \times \alpha_2}{p(t) \times Pd(t) \times (1 - SCR)} = \frac{\left(P_{ed}'(t) - P_{ed}(t)\right) \times \alpha_1 \times \alpha_2}{(1 - SCR)}. \quad (20)$$

Calculate

Table 3: Related risks involved in the decision-making process.

Decision type	Risk definition	Explain
Buy carbon	"Carbon price fluctuation risk"	The fluctuation of carbon price brings uncertainty to the expected cost of carbon procurement, which makes the cost of carbon procurement too high.
	"Failure to complete the self-purification target risk"	Failure to purify yourself or extend the time of self-purification increases the risk of not reaching the goal of self-purification.
Self-purification	"Excessive construction period risk"	The uncertainty of the construction period of the self-cleaning project will lead to costs and losses after the construction period is extended.

Table 4: P guidelines.

Probability of risk	Probability of a risk event	Remarks
(85%,100%]	Extremely high	Risk events are almost certain to happen
(60%,85%]	High	Risk events occur in more cases
(15%,60%]	Higher	Risk events occur under certain circumstances
(5%, 15%]	Lower	Risk events rarely occur
(0,5%]	Low	Risk events hardly happen

Table 5: C guidelines.

Risk loss index (severity of consequences)	Severity of loss of risk event (risk loss level)	Remarks (loss/exceeding pretax profit)
4~5	The essential	20% or more
3~4	Serious	1 0%~20%
2~3	Moderate	5%~1 0%
1~2	Small	1%~5%
0~1	Ignorable	1% or less

$$P_{e\,d}'(t) > P_{e\,d}(t) + \frac{\delta_s \times (1 - SCR)}{\alpha_1 \times \alpha_2}. \tag{21}$$

Assuming that the risk loss L22′ of failing to complete the self-purification target has the following nonlinear relationship with the time required for the risk factors to complete the remaining emission reduction target,

$$L_{22}' = max\left\{0, \frac{T_g - (T - t)}{T_g}\beta_1 \times q(t)\right\}. \tag{22}$$

Bring in the L_{22}' and PBT formula to get

$$\mathrm{T} - \mathrm{t} < T_g < (T - t)/\left(1 - \frac{\delta_m \times (1 - SCR)}{\beta_{1\times\alpha_1\times\alpha_2}}\right). \tag{23}$$

Bring in the L_{22}' and PBT formula to get

$$(T-t)/\left(1-\frac{\delta_c\times(1-SCR)}{\beta_{1\times\alpha_1\times\alpha_2}}\right) < T_g < (T-t)/\left(1-\frac{\delta_s\times(1-SCR)}{\beta_{1\times\alpha_1\times\alpha_2}}\right). \tag{24}$$

Finally, the following formula is obtained:

$$L_{31}' = max\left\{0, \frac{T_{sp}(t) - (T - t)}{T_{sp}(t)}\beta_1 \times q(t)\right\}. \tag{25}$$

4.3. Model Test Results. In order to test the model, we use the following 8 SPSS line software to check the suitability of the system performance.

The standardized residual of the actual annual carbon purchase cost is shown in Figure 3.

The standardized residual of the actual annual self-purification cost is shown in Figure 4.

The standardized residual of annual self-net risk loss is shown in Figure 5.

The results show that the actual cost of carbon purchases each year determines the total cost of carbon resource allocation, and the income from carbon sales determines the net cost of carbon resources. The carbon resources are distributed obliquely, and the difference meets the normality assumption. Therefore, the performance of the two systems has passed the applicability test of the model.

4.4. Risk Decision-Making Behavior Management Model. The theoretical innovations such as the risk management model established in this paper and the data analysis method system designed in this paper mainly provide knowledge base support for the risk management and decision-making simulation system. Especially enterprise-level cloud applications and distributed applications require big data support from multiple sources and advanced expert systems. The research results of this paper expand and enrich the knowledge base of the expert system, and provide a powerful theoretical tool for users to make use of the system for knowledge mining and buying and selling decisions based on big data. With the development of advanced information technologies such as the "big cloud mobile smart chain," the data sources of risk management and decision-making simulation systems have been further expanded. Distributed energy, smart energy equipment, etc., provide more and

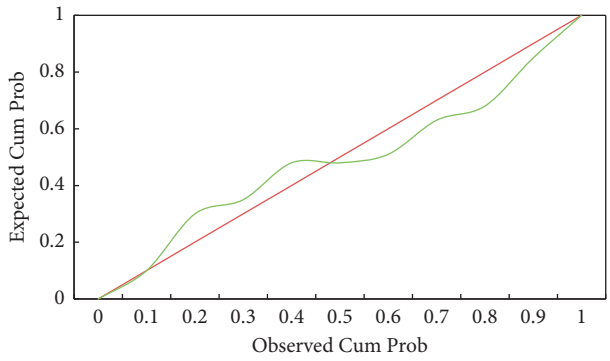

Figure 3: P-P plot of standardized residuals of the actual cost of carbon purchases in years.

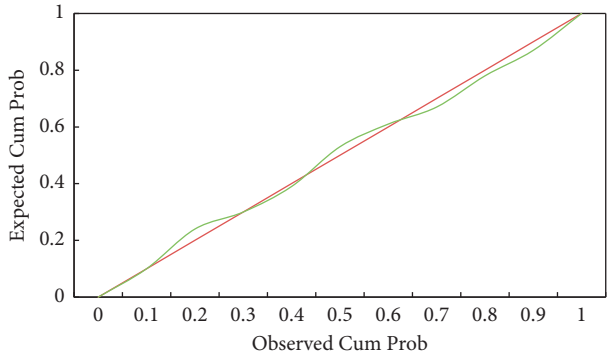

Figure 4: P-P graph of standardized residuals of carbon purchase risk loss in years.

more detailed multi-source data sources for the system. Multi-source data must not only be preprocessed and stored in the enterprise data center, but also distributed to distributed applications. These data also provide support for building a more powerful expert system. This paper is studying mining methods and models based on these data to improve the management and decision-making skills of the expert system.

The system considers the design of enterprise-level cloud applications and distributed applications from the perspective of different types of users. Both types of applications and distributed applications need to be tightly integrated. Especially for distributed applications, the situation of potential users is very complicated, and users can switch between the roles of energy producer and energy consumer repeatedly, which makes the design of system integration solutions more difficult from the user's point of view. Whether it is an enterprise-level cloud application or a distributed application, the objects of its management are the generation, consumption, and behavior of electricity transactions. Therefore, the system designs a system integration scheme from the perspective of the process meeting of both parties.

Renewable energy consumption market risk management and decision-making simulation system integration scheme mainly include the following elements:

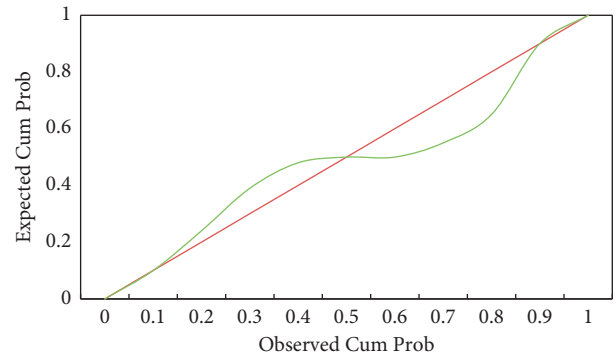

Figure 5: P-P chart of standardized residuals of self-net risk loss.

(1) Under the guidance of the integrated management strategy, combined with the characteristics of the development language and framework, the system structure and functions are designed by analyzing the business needs focusing on power generation, consumption, and commercialization.

(2) According to the application integration process, integration method, and integration rules on the power generation side, an integrated power generation side trend and information flow are formed according to business needs; an integrated energy flow and information flow on the energy side are also formed on the sales side.

(3) Based on market rules, design a two-way matching strategy on the power generation side and the power sales side, and design an integrated service application model based on two-way matching to further form a system operation mechanism.

(4) In the application, through the effectiveness feedback and process monitoring procedures, the comprehensive advantages of the system are evaluated, the integration mode is continuously optimized, the integration is deepened, and the application integration is guaranteed.

Enterprise-level cloud applications are mainly for business users such as e-commerce. The design of this section focuses on risk management modules. Enterprise-level cloud applications can also include visual statistical query and energy trading modules, but they have little to do with the research content of this article. The risk management module of enterprise-level cloud applications is similar to traditional information management systems. This section first designs the system architecture and then discusses the application of cloud models in enterprise-level applications.

Different hierarchical structures complete different functions:

(1) Infrastructure layer provides hardware and software foundation for system implementation. Important infrastructure for enterprise users includes data

centers and virtualized cloud facilities. Considering the interaction between enterprise-level cloud applications and distributed applications, the infrastructure layer also includes distributed infrastructure.

(2) The resource layer is a hierarchical structure built on the infrastructure layer, which mainly integrates the resources of enterprise-level cloud applications and distributed applications. These resources include not only the hardware and software installation provided by the infrastructure layer, but also the various power resources, information resources, and knowledge base resources of the research results of this article.

(3) Service layer management and use of resource layer to provide services for the realization of various applications. The design and implementation of the service layer are essential for business applications to go to the cloud. Generally speaking, providing distributed database services, file services, web services, cluster management, and parallel computing can effectively support cloud applications.

(4) The application layer mainly considers business requirements and implements system functions based on the services provided by the service layer. The enterprise-level cloud application risk management module developed in this section should implement functions such as market risk assessment, multi-objective risk decision-making, random risk management, and effective risk management.

The e-top architecture can build a cloud application risk management module at the enterprise level and further integrate it with the energy information system and energy market operation system to expand the functions of the system. In addition, the cloud application risk management module is subject to company-level guidelines, regulations, market rules, and technical standards, and it shares operation and maintenance management with the portal system.

The structure of each level is interrelated, and its application layer realizes the central function of the module, which is also the key to the transformation of the research results of this article into practical applications.

5. Conclusion

The background of this document is the design of a highly integrated SoC application processing chip based on the ARMA9 core. Through analysis and research on the application scenarios of the multi-core ARM processor architecture, AMBA bus protocol, and project requirements, SoC was designed on the basis of the multi-core ARM processor system architecture, and the simulation verification of the front-end system and FPGA prototype verification were completed. This article uses a simulation of the carbon resource allocation decision-making process of a carbon emission control company to describe the convenience of carbon procurement and the risks faced by carbon emissions. The clean decision-making and analysis of different systems, the output of the system under the combination of structure, and different risk levels are mainly control and emission.

Data Availability

The data used to support the findings of this study are available from the corresponding author upon request.

Conflicts of Interest

The author declares that there are no conflicts of interest.

Acknowledgments

This study was supported by Soft science research project of Science and Technology Department of Shaanxi Province: Research on the Interaction Mechanism and Evolution of Consistent Group Risk Decision Behavior Based on Computational Experiments in the Digital Era (Project no. 2019KRM093).

References

[1] L. Zheng, Y. Lu, M. Guo, S. Guo, and C.-Z. Xu, "Architecture-based design and optimization of genetic algorithms on multi- and many-core systems," *Future Generation Computer Systems*, vol. 38, pp. 75–91, 2014.

[2] S. Gao and G. D. Peterson, "GASPRNG: GPU accelerated scalable parallel random number generator library," *Computer Physics Communications*, vol. 184, no. 4, pp. 1241–1249, 2013.

[3] Q. Y. Duan, V. K. Gupta, and S. Sorooshian, "Shuffled complex evolution approach for effective and efficient global minimization," *Journal of Optimization Theory and Applications*, vol. 76, no. 3, pp. 501–521, 1993.

[4] L. Zhu and Y. Fan, "A real options-based CCS investment evaluation model: case study of China's power generation sector," *Applied Energy*, vol. 88, no. 12, pp. 4320–4333, 2011.

[5] X. Wang and L. Du, "Study on carbon capture and storage (CCS) investment decision-making based on real options for China's coal-fired power plants," *Journal of Cleaner Production*, vol. 112, no. 5, pp. 4123–4131, 2016.

[6] B. Suárez-Eiroa, E. Fernández, G. Méndez-Martínez, and D. Soto-Oñate, "Operational principles of circular economy for sustainable development: linking theory and practice," *Journal of Cleaner Production*, vol. 214, pp. 952–961, 2019.

[7] A. Fujihara, "Proposing distributed traffic information system using blockchain technology," *IEICE Technical Report*, vol. 117, p. 223, 2018.

[8] K. G. Savvidy, "The MIXMAX random number generator," *Computer Physics Communications*, vol. 196, pp. 161–165, 2015.

[9] J. Li, J. A. Besada, A. M. Bernardos, P. Tarrío, and J. R. Casar, "A novel system for object pose estimation using fused vision and inertial data," *Information Fusion*, vol. 33, pp. 15–28, 2017.

[10] A. S. M. S. Azad, V. Fang, and C.-H. Hung, "Linking the interest rate swap markets to the macroeconomic risk: the UK and US evidence," *International Review of Financial Analysis*, vol. 22, pp. 38–47, 2012.

[11] B. Yalabik and R. J. Fairchild, "Customer, regulatory, and competitive pressure as drivers of environmental innovation," *International Journal of Production Economics*, vol. 131, no. 2, pp. 519–527, 2011.

[12] S. Markose, S. Giansante, and A. R. Shaghaghi, "'Too interconnected to fail' financial network of us CDS market: topological fragility and systemic risk," *Journal of Economic Behavior & Organization*, vol. 83, no. 3, pp. 627–646, 2012.
[13] J. Wu, Y. Feng, and P. Sun, "Sensor fusion for recognition of activities of daily living," *Sensors*, vol. 18, no. 11, p. 4029, 2018.
[14] C. Melendez-Pastor, R. Ruiz-Gonzalez, and J. Gomez-Gil, "A data fusion system of GNSS data and on-vehicle sensors data for improving car positioning precision in urban environments," *Expert Systems with Applications*, vol. 80, pp. 28–38, 2017.

Hindawi
Mobile Information Systems
Volume 2022, Article ID 5411119, 11 pages
https://doi.org/10.1155/2022/5411119

Research Article

Experimental Research on Span Direction Effect of Vortex-Induced Vibration of Bridge Main Girder Based on Symmetric Algorithm

Xiaochuan Cao and Yuhu Luo

School of Civil Engineering, Chongqing Jiaotong University, Chongqing 400074, China

Correspondence should be addressed to Xiaochuan Cao; cxiaoch@cqjtu.edu.cn

Received 23 May 2022; Revised 18 June 2022; Accepted 5 July 2022; Published 22 July 2022

Academic Editor: Shadi Aljawarneh

Nowadays, the research of digital geometry is gradually shifting from low-level geometric attributes to high-level semantic attributes. The symmetry of the 3D geometric model is an important bridge between the underlying geometric information of the related model and the high-level semantic information. Symmetry analysis is an important issue in geometric processing. Bridge safety is a major issue related to the national economy and people's livelihood. Therefore, the bridge structure health monitoring system is becoming a research focus in academic and technical circles. Wireless sensor network has been widely used in bridge health monitoring system due to its convenient installation, low maintenance cost, and flexible deployment. This article summarizes the existing bridge health monitoring system based on wireless sensor network. In the bridge control system of wireless sensor network, the basic principles and typical methods are introduced in turn, and the key technologies in the system are analyzed in combination with several specific examples. Finally, the existing problems and future research directions of the existing system are summarized. During the operation stage, vortex-induced resonance often occurs below the wind speed. The vortex excitation force of the main actuator along the axis of the bridge is related to the actual wind field and its own structural vibration. This article briefly introduces typical cases and control measures of vortex-induced vibration of long-span bridges, and summarizes the current research status of vortex-induced vibration of bridge main girder structures. At the same time, the vortex-induced vibration of bridge girder is experimentally studied by using symmetrical algorithm.

1. Introduction

Since the 1970s in modern times, with the further rapid development and wide application of various sensors and 3D model system builders and other technologies, based on the symmetric semantic algorithm, we can analyze the basic structure of the model semantically, and symmetrically apply it to 3D solid geometric model, morphological view description, mode view segmentation, simulation, and view editing [1]. This paper analyzes the symmetry vector detection of the important research topic of the three-dimensional geometric model in the data analysis application field [2]. Based on the highest-level three-dimensional geometric model attributes under the three-dimensional geometric model, this paper analyzes the inherent symmetry of the three-dimensional model [3]. The most important thing is analyze the local symmetry of the local bottom layer of the model with higher complexity, and the local intrinsic symmetry of many different aspects, such as large noise and lack of complex data processing [4]. With the continuous advancement of 3D geometric model batch acquisition and model modeling processing technology, 3D geometric models have gradually received more and more international attention and attention [5]. The structural analysis and modeling processing of 3D geometric models, especially in the high-level 3D Geometric model processing has gradually become a hot topic, among which symmetry algorithm is widely regarded as a very critical basic structure processing information in 3D geometric models, and it is an important basis for how to perform high-level 3D geometric model

processing and modeling work [6]. This article will introduce the main research and development background of the subject in detail from two main perspectives: the semantic synthesis analysis of the three-dimensional geometric model and the important application significance of the symmetry inspection algorithm in the research of the semantic synthesis analysis of the geometric model [7]. The wireless sensor center network node is a new type of sensor node network, which is integrated by a large-scale wireless sensor network node with strong visual information perception realization ability, calculation and analysis ability, and Internet data communication processing ability [8]. With the rapid progress and continuous development of national modern detection and monitoring equipment and wireless sensor node network communication technology, some large-scale bridges have been prepared to deploy wired sensor networks during their normal construction and wiring process, which will be able to target the operation of each bridge in the future. Real-time monitoring is carried out, but the monitoring system has a high cost in the process of wiring installation and maintenance [9]. Special construction sites are difficult to wire and are vulnerable to harsh construction environmental conditions, and the distance of the data transmitted will also be affected by the traditional wiring process [10]. Due to the large length constraint, the wireless sensor node network can have several major advantages such as easy wiring installation of monitoring equipment, low maintenance cost and low cost, and flexible equipment deployment [11]. It can well solve the problems that the monitoring system may encounter in actual engineering applications. The large amount of data collected through real-time monitoring and collection of various wireless sensor node networks can be used for real-time comprehensive information processing and data analysis, and timely and accurately grasp the normal monitoring operation and operation status of each bridge in the safe production, use and engineering operation management of modern large-scale bridges provide basic guarantees [12]. With some revolutionary innovations in bridge science and engineering technology, people's technical level in the construction of various bridges has also been greatly improved. The main girder structure of modern bridges has many structural shapes. Some of them directly adopt streamlined auxiliary sections with good aerodynamic separation properties and are relatively stable. The main girder structures involved in these main girders are likely to directly cause a large amount of flow through the main girder subsidiary sections, resulting in tension adhesion and vibration separation. Its working principle can be roughly divided into structural measures and aerodynamic measures.

2. Related Work

The literature mainly introduces the symmetry point pair reflecting the potential symmetry in the model, which is to accurately define the two vertices corresponding to them to have similar symmetric geometric point pair properties according to the basic concept of symmetry, in order to quickly and effectively remove inappropriate corresponding point pairs to reduce the computational complexity of the model [13]. First of all, it is necessary to analyze and judge the relative point pair attributes according to the symmetric point pair attributes near the two corresponding vertices, construct, and give a basic symmetry constraint. And to prescribe conditions, and quickly exclude pairs of points that do not meet any basic constraint conditions at the same time [14]. The monitoring and analysis system mentioned in the literature mainly uses various types of sensor equipment to perform real-time monitoring and analysis, to obtain some relevant information about the internal environmental stress stimulus of the bridge and the stress response of the bridge structure, and then fully adopt wireless signal processing and analysis in the bridge design stage [15]. Some indexes related to the bridge state are analyzed and extracted by using data processor and other technologies. In the bridge design stage, the stress damage data in the bridge structure are fully used for dynamic identification, and the technology is used to comprehensively evaluate the health management state of relevant bridges. In order to effectively ensure the safe and normal operation of the bridge and provide a more scientific evaluation basis for its future maintenance work, the literature mainly introduces in detail the application modules that some sensor communication nodes need to consume information energy [16]. With the continuous improvement of the current communication integrated circuit design and manufacturing process, the energy consumption of multiple functional modules such as sensor node modules and signal processors has gradually become very small, and nearly 80% of communication nodes are concentrated on the energy consumption of multiple functional modules such as wireless communication. Therefore, in order to effectively reduce the energy data sent and received by each communication node, the wireless communication sensor adopts a duty-cycling processing mechanism in the field of international network communication and real-time processing of the related information energy in the network [17]. The wireless monitoring system introduced in the literature uses various types of sensors for real-time monitoring to obtain various bridge environmental stimuli and structural responses, and then uses signal analysis and data processing techniques to automatically extract the operating status indicators of the bridge [18]. The spontaneous excitation force directly determines the convergent vector value of the motion spanwise correlation coefficient of the spanwise vortex excitation force of the main beam section, while the forced excitation force directly affects the spanwise vortex excitation force of the main beam section. The greater the compulsive force, the greater the correlation length of the spanwise-related effects, and the slower the attenuation speed of the spanwise coefficient of the aerodynamic vortex [19]. Through design and in-depth analysis, the literature studies the main girder node segment structure model of the bridge model, and carries out the main girder wind tunnel test of the bridge synchronization main girder vibration measurement and the wind pressure test of the main bridge node segment structure model, and obtains the bridge main girder segment structure in the locked response interval of the main beam vortex vibration under different angles of

wind tunnel attack; the correlation coefficient of the vortex excitation force on the section of the main beam section is much larger than that of the main beam static state.

3. Symmetrical Algorithms and Research on Key Technologies of Sensors

3.1. Symmetry Analysis Based on Symmetric Point Pairs. Symmetrical point pair refers to two symmetrical vertices on a model. The spatial distance relationship formula (1) of the symmetrical shape symmetrical radial function between the two symmetrical vertices X and X' is shown as follows:

$$d_{SDDE}(X, X\prime) = \left\| E_{SDE}(X) - E_{SDE}(X\prime)_{L_2} \right\|, \tag{1}$$

where d is the vertex distance of a vertex shape radial function, E is the length description definition expression of a vertex distance X of the shape radial function.

When two pairs of points meet the condition of a certain distance constraint, or when the degree of asymmetry is much smaller than the threshold of a certain distance, it can collectively reflect a kind of intrinsic symmetry in the model, due to the degree of this asymmetry. And the distance between the two points where the point pair is located is related to each other, so we use a relative threshold, where max is the highest value of the geodetic distance between all vertices, and the condition of the distance constraint can also be written by (2).

$$\begin{aligned} &RD((X, X\prime), (Y, Y\prime)): d((X, X\prime), (Y, Y\prime)) \\ &= \max \left\| d_G(X, Y) - d_G(X\prime, Y\prime) \right\|. \end{aligned} \tag{2}$$

For the point pair $\{X, X'\}$ on the model M, the support point pair is not unique, but there may be many support point pairs. The set of all the support point pairs of the point pair $\{X, X'\}$ is

$$\Pi_{(X,X\prime)} = \{(X_i, X_i') | X_i \in M. \tag{3}$$

In this model, a set of support point pairs is often not exactly symmetrical, and the degree of asymmetry can be measured by an average relationship between the degree of asymmetry between two support point pairs.

$$d_{\text{symmetry}}\left(\Pi_{(X,X\prime)}\right) = \frac{\sum_{(X_i,X_i')\in\Pi_{(X,X')}} d(X, X\prime), (X_i, X_i'))}{\left|\Pi_{(X,X\prime)}\right|}. \tag{4}$$

where $d_{\text{Symmetry}}(\Pi_{(X,X\prime)})$ is the asymmetry degree of the point pair $\{X, X'\}$ supported by the point pair set.

$$\begin{aligned} S_{ij} &= S\left(X_i, X_j\right) \\ &= \inf_{f\in F:\ f(X_i)=X_j} D_f(X, f(X)), \end{aligned} \tag{5}$$

where f is an intrinsic combination transformation on the vertex model, and X is a vertex in the neighborhood of the combined vertex model X_i on the vertex model, where

$$D_f\left(X_i, X_j\right) = d_{\text{symmetry}}\left(\Pi_{\left(X_i, x_j\right)}\right). \tag{6}$$

Get the matrix $\widetilde{C}$:

$$\widetilde{C}_i = e^{-\left(S_{ij}/\sigma \text{SCM} \times d_{max}\right)^2}. \tag{7}$$

The symmetric unit number simplified matrix algorithm used in this article is mainly

$$C = D^{-1/2}\widetilde{C}D^{-1/2}. \tag{8}$$

In the distance between symmetric vertices, it is pointed out that under the precise symmetric physical conditions, the corresponding analysis matrix of symmetric solution is shown in Figure 1. In order to fully facilitate our real-time observation, the relationship system matrix of symmetric solution correspondence has been rearranged to rearrange all the symmetric vertices in the same track and their corresponding track rows and columns. By solving symmetrically, the values of nonzero characteristic points and symmetric eigenvectors of the relation matrix can be obtained directly, and the precise connotation and symmetry of the whole model can be obtained.

After the linear relationship vertex matrix decomposition corresponding to the symmetrical vertices is embedded in the spectrum curve diffusion space, the diffusion distance of the symmetrical vertex decomposition can also be simply regarded as a symmetry of a symmetrically diffused spectrum model on an overall model structure. The diffusion distance, the entire diffusion model can also be simply regarded as the overall structure of a diffusion graph.

According to this design feature, it can be used to design and construct the distance between the symmetrical decompositions between different vertices. The higher the symmetric gradient optimization degree, the smaller the distance between the symmetrical decompositions between the vertices. First, embed the vector relational expression corresponding to the symmetry into the spectral space in matrix form:

$$E^t(X_i) = \left(\lambda_1^t \Psi_1(X_i), \ldots, \lambda_n^t \Psi_n(X_i)\right). \tag{9}$$

The Euclidean distance is used to measure the degree of symmetry of the vertex, and the symmetry decomposition distance of the vertex is

$$\begin{aligned} d_{SER}'\left(X_i, X_j\right) &= ||E^t(X_i) - E^t\left(X_j\right)||^2 \\ &= \sum_{k=1}^{n} \lambda_k^t |\Psi_k(X_i) - \Psi_k\left(X_j\right)|^2. \end{aligned} \tag{10}$$

Since the feature distance values of the first few items are significantly larger than the feature distance values of the other models, when t is used to take a larger feature value, the later feature distance values of the symmetric model can be directly ignored, and the decomposition distance of the symmetric model is only the same as the previous one. The feature distance values of several items are related, and the feature distance values of the first few items directly correspond to the symmetry of the model, so the symmetric

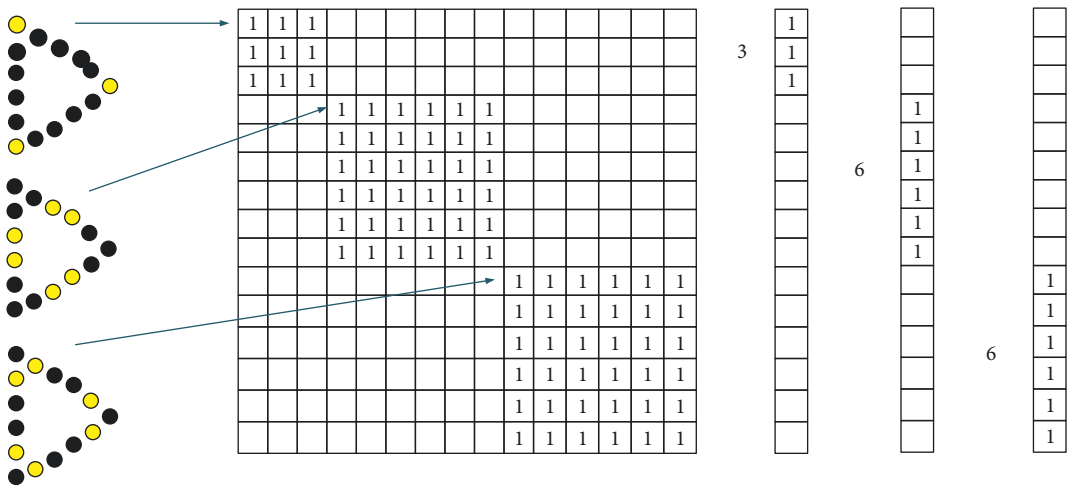

Figure 1: Schematic diagram of symmetric correspondence matrix and eigenvalue eigenvectors.

model decomposition distance value can be used to measure the model symmetry between the feature vertices of the same model.

Based on the above discussion, the thermocore descriptor itself has geometric vertex properties that are invariant to equidistant symmetric transformations. Therefore, we can even apply it to calculate and analyze the degree of symmetry transformation between the geometric vertices. The difference between the two geometric vertices x and y on the same mathematical model, and the difference between the geometric vertex attributes within a certain range can be used in a certain time area and the calculation integral of the thermal core description operator attribute difference is applied to measure it numerically.

$$\left(\int_{t_1}^{t_2}\left|S_{HKS}(x,t)-S_{HKS}(y,t)\right|^2 \mathrm{d}t\right)^{1/2} = \left(\int_{t_1}^{t_2}\left|k_t(x,x)-k_t(y,y)\right|^2 \mathrm{d}t\right)^{1/2}. \tag{11}$$

Then, the size of the gap between the two geometric vertices x and y in a certain adjacent domain can be expressed by the transformation of formula (12):

$$d_{HKS_{[t_1,t_2]}}(x,y)=\left(\int_{t_1}^{t_2}\left|\frac{k_t(x,x)}{\int_M k_t(x,\mathrm{x})}-\frac{k_t(y,\mathrm{y})}{\int_M k_t(y,y)}\right|^2 \mathrm{d}t\right)^{1/2}. \tag{12}$$

Calculate the thermocore descriptor:

$$d_{HKS_{[t_1,t_2]}}(x,y)=\left(\sum_{t_0=t_1}^{n}\left|\frac{k_t(x,x)}{k_t(x,\mathrm{x})}-\frac{k_t(y,\mathrm{y})}{\int_M k_t(y,y)}\right|^2\right)^{1/2}. \tag{13}$$

Since the thermocore descriptor only contains the information of the local vertex geometric model data set near a vertex, it does not contain the geometric displacement spatial relationship between the geometric part of the vertex model and the vertex as a whole.

$$d_{SYM_{[t_1,t_2]}}(x,y)=d_{HKS_{[t_1,t_2]}}(x,y)\times d_G(x,y). \tag{14}$$

An asymmetry degree matrix can be established at different times, each item of which is relative to the degree of asymmetry between each vertex on the model.

$$S_{[t_1,t_2]_{ij}}=d_{SYM_{[t_1,t_2]}}\left(x_i,x_j\right). \tag{15}$$

The model covered by the asymmetric matrix is a descriptor.

3.2. Key Technologies of Sensor Networks. As shown in Figure 2, the SPEM management module and CS optimization management module are added to the framework of the system structure health detection and monitoring system proposed in this article. These two optimization modules are configured between the finite element management model and the node management deployment type module. It is used to correctly select the reasonable health check points and data addresses. The SPEM optimization module mainly relies on the position information of the two analog quantities of the network structure, the data write set of the position information of the target node to be measured, and the number of positions of the target node that needs to be measured on-site to filter and calculate the most optimized measurement in a detection project. The specific location of the target node and the FIM simulation value of the location of each measurement node; the CS optimization detection module mainly relies on the original SPEM optimization module to write and output the position data, combined with the structural characteristics of the wireless measurement sensor detection network and the needs of specific practical applications, Recombinate and design a set of target detection point position data to be selected and a set of candidate detection points and node magnitudes required by the application. Multiple iterations between the detection modules can directly obtain a final target detection point.

The various node deployment methods mentioned above all have certain technical limitations: SPEM is mainly suitable for finite element analysis methods, mainly from the broad

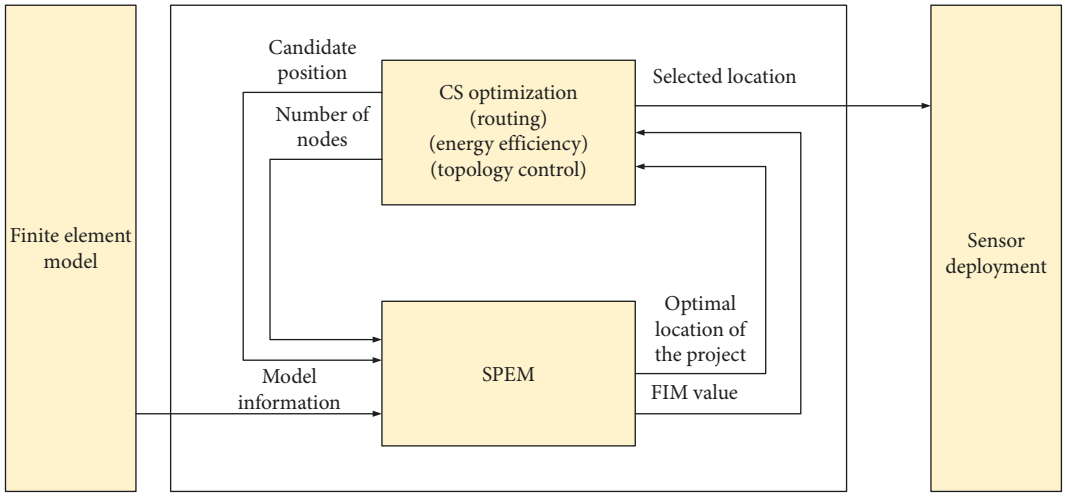

Figure 2: Node deployment method using EFI.

technical direction of structural health monitoring, taking into account the deployment of nodes, and passing experiments are performed on tower bridges and other buildings to obtain and verify their effects, but there are still certain differences between these bridges and their structures.

The sensor processing node first performs a subliminal numerical quantification judgment on the vibration radio frequency signal compression data threshold obtained by each sampler through collection and analysis, and saves and processes the vibration signal compression data whose data reaches a certain frequency threshold value. The data undergoes threshold quantization, subthreshold value judgment segmentation, run-length signal encoding, and encapsulation, and finally sends it to the base station node. When the network data collection manager located at the base station node needs to retrieve and review the original compressed data or when deleting the remaining data details, the compression information is sent by the base station node for secondary compression according to the original data compression sequence stored in the flash.

After each node receives the data packet of the previous node, it merges its own information and data, and then uses the same method to send it to the next node, and finally all the data reaches the node at the other end, in order to effectively balance the energy of each node, each time the data is transmitted according to the last transmission direction of a different node.

4. Experimental Study on the Spanwise Effect of Vortex-Induced Vibration of the Main Girder of a 4 Long-Span Bridge

4.1. Test Model and Working Conditions. In order to conduct in-depth discussion on the correlation between the spanwise directions of different main beam vortex excitation force models, 5 rows of pressure tapping holes are designed and arranged at different positions of the vortex excitation force spanning directions. The schematic design of the pressure tapping whole layout is shown in Figure 3. The new electromechanical pressure transmission scanning solenoid valve detection system of PSI Corporation of the United States is used, and the stability performance of the electronic pressure transmission is tested. When the model is undergoing pressure test, an electronic automatic pressure test scanning valve is directly placed inside the test model. The test hydraulic scanning valve is connected to each other with a hole equipped with a pressure measuring tube on the main surface of the model. The scanning valve and the computer are connected to each other again. It is connected through the use of the computer's pressure controller operation to directly and automatically complete the pressure test. The vibration frequency of each sampling of the electronic pressure scanning valve can be directly set to 331 Hz, and the duration of sampling at each wind speed can be directly set to 20 s.

The results of this experiment failed to propose in-depth the torsional vortex motion effect, but only considering the observation of a vertical vortex motion effect that the structure may produce, the motion equation is actually defined as (16):

$$m\frac{\partial^2 z}{\partial t^2} + C_z\frac{\partial z}{\partial t} + EI\frac{\partial^4 z}{\partial x^4} - H\frac{\partial^2 z}{\partial x^2} = -L(z, \varnothing, \mathrm{t}). \tag{16}$$

The vertical bending frequency of the brace model is expressed as:

$$f_z = \frac{1}{2L}\sqrt{\frac{H}{m} + \left(\frac{\pi}{L}\right)^2\frac{EI}{m}}. \tag{17}$$

The main advantage of the brace model is that the use of the steel wire rope's transverse bending tensile stiffness can effectively provide the brace model's own lateral motion stiffness, and for the brace forming model itself, the lateral bending tensile stiffness of the outer garment is relative to the brace model itself The contribution is very small and can be ignored. Then, (17) can be simplified as shown in (18):

$$f_z = \frac{1}{2L}\sqrt{\frac{H}{m}}. \tag{18}$$

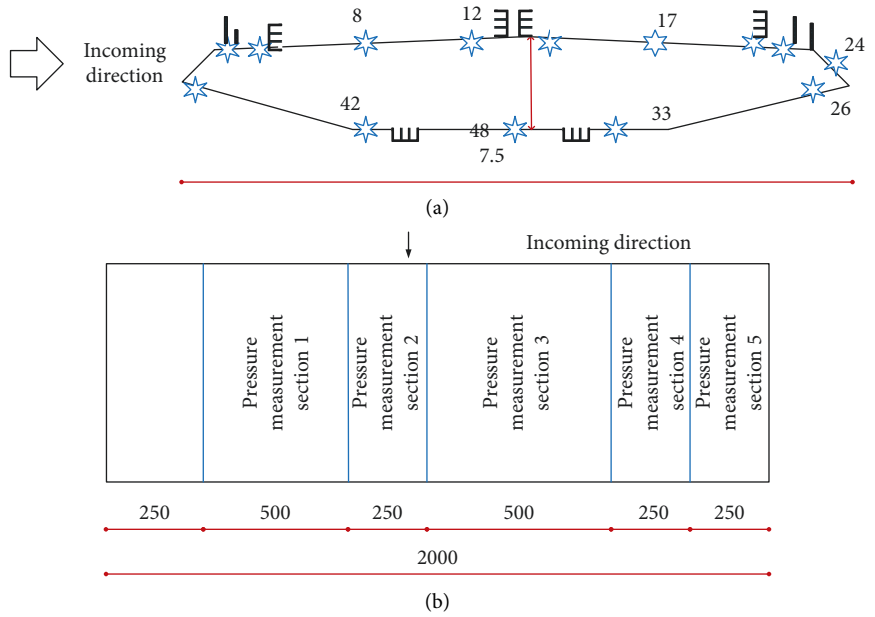

FIGURE 3: Schematic diagram of pressure measuring hole layout. (a) Layout of pressure measuring holes on each pressure measuring section. (b) Layout plan of the pressure measurement section along the span.

The brace model needs to follow the following similar principles during the design process, such as geometry, inertial parameters, elasticity, and damping parameters. Due to the limitation of the size and dimensions of the wind tunnel, the viscosity parameters failed to meet the requirements. Unlike the full-bridge aeroelastic model, the brace model can be designed without considering the influence on the gravity parameters.

The correlation coefficient is a unified measurement standard used to measure the complexity of the relationship between linear variables. The absolute value ranges of the variables that need to be used are [−1, 1], and the absolute value range of the correlation coefficient is the larger the value, the higher the complexity of this linear correlation may become. When its absolute value is 0, it is called irrelevant, and when its absolute value is 1, it is called complete correlation. The correlation coefficient of the two function variables of X and Y can be expressed clearly by the (19):

$$R_{XY} = \frac{\sum (X - \overline{X})(Y - \overline{Y})}{\sqrt{\sum (X - \overline{X})^2 \sum (Y - \overline{Y})^2}}. \tag{19}$$

Replace the two variables of X and Y in the above formula with different aerodynamic parameter variables of different pressure aerodynamic detection system sections, that is, we can directly analyze and obtain the spanwise-related aerodynamics of different aerodynamic forces between various pressure sections. Coefficient, namely,

$$R_{c_i}(\delta/D) = \frac{\cot[C_i(\delta/D)]}{\mathrm{Var}[C_i]}. \tag{20}$$

Existing experimental studies have provided an approximate formula for the correlation coefficient of the aerodynamic span of the bluff body section:

$$R_{C_i}(\delta/D) = \exp\left[-C_i \frac{\delta}{D}\right]. \tag{21}$$

The correlation size of the aerodynamic parameter c_i can also be defined by the span length:

$$\frac{L_i}{D} = \int_0^{\infty} R_{C_i}\left(\frac{\delta}{D}\right) \mathrm{d}\left(\frac{\delta}{D}\right) = \frac{1}{C_i}. \tag{22}$$

The spanwise correlation of the vibration of the structure is often greater than that of its static state, so when the structure vibrates, the (21) becomes the (23):

$$R_{C_i}\left(s_j, \frac{\delta}{D}\right) = \exp\left[-C_i(s_j)\frac{\delta}{D}\right]. \tag{23}$$

where s is a component statistical parameter related to the displacement of the location. That is to say, (23) also considers the spanwise correlation along with the change between spanwise spacing and vibration amplitude.

$$R_{C_i}\left(s_j, \frac{\delta}{D}\right) = \exp\left[-C_i(s_j)\left(\frac{\delta}{D}\right)^p\right]. \tag{24}$$

Regardless of whether it is for the vertical or torsional vortex state, the researchers have proposed a method. The ratios of the corresponding lift parameter-related system index and the attenuation fitting parameter between the vertical state and the torsional vortex state are expressed as:

$$C_i = \frac{0.01578}{0.02694 + (h/D)}, \qquad C_i = \frac{0.00551}{0.01058 + \alpha}. \tag{25}$$

Table 1: Comparison table of design parameters between the brace model and the segment model.

Parameter name	Symbol	Unit	Real bridge value	Design scale value	Segment model value		Stretch model value	
					Design value	Realized value	Design value	Realized value
Length of main beam	L	m	—	1/80	2	2	6	6
Width of main beam	B	m	39	1/80	0.5125	0.3251	0.3254	0.2415
Height of main beam	H	m	3.425	1/80	0.120	0.201	0.130	0.022
Equivalent mass	m_{eq}	Kg/m	28047	$1/80^2$	4.4521	4.2762	4.2145	4.2153
Vertical bending fundamental frequency	f_v	Hz	0.1425	20	5.685	4.52	5.654	3.210
Vertical bending damping ratio	ξ_v	%	0.2	1	0.6	0.215	0.4	0.526
Wind speed ratio	—	—	—	—	4	4.85	4	7.51

Table 2: Dynamic parameters of the first 3 modes of the brace model.

Mode shape	Frequency (Hz)			Damping (%)
	Theoretical value	Measured value	Error (%)	Measured value
First order vertical frequency	2.152	3.120	1.52	0.532
Second order vertical frequency	5.845	5.652	−1.35	0.854
Third order vertical frequency	8.685	8.669	−0.62	1.263

In this regard, it is proposed to use equation (26) to fit the spanwise correlation coefficient of the vortex excitation force during structural vortex vibration:

$$R_{c_i}\left(\frac{\delta}{D}\right) = (1 - d_i)\exp\left[-C_i\frac{\delta}{D}\right] + d_i. \tag{26}$$

Performing a pressure integration on the pressure of different materials in each row of sections can obtain the three-component force measurement coefficients on the sections of different pressure measurement materials, the comprehensive calculation of the lift coefficient, and the torque pressure coefficient. The integral processing formula is shown in (27) and (28).

$$C_L(t) = \frac{\sum_{i=1}^{n} p_i(t)\cdot L_i\cdot\cos(\alpha_i)}{0.5pU^2B}, \tag{27}$$

$$C_M(t) = \frac{\sum_{i=1}^{n} p_i(t)\cdot L\cdot\mathrm{Sin}(\alpha_i)d_{iy} + \sum_{i=1}^{n} p_i(t)\cdot L_i\cdot\cos(\alpha_i)d_{ix}}{0.5pU^2B^2}. \tag{28}$$

4.2. Model Parameters and Test Conditions. The test section wind tunnel has a length of 15 m, a width of 8.5 m, and a height of 2 m. The wind speed control range of the test section is generally 0 ~ 14 m/s. It is an open large-scale test section. The tail wind tunnel can be directly used to simulate large-scale rainfall phenomena. The main design is suitable for large-span highway bridges, large-scale high-rise buildings, power transmission model simulation wind tunnel test, large-scale pollution diffusion process simulation, and large-scale wind and rain combined effect simulation wind tunnel test. In this paper, the main design application parameters of a bridge brace design model corresponding to the main design application parameters of the segment model are shown in Table 1.

The comparison results of the theoretical value and the actual measured value of the vertical bending dynamic characteristics of the brace model are shown in Table 2. The range of wind speed in the test section of the brace model is 0 ~ 6 m/s, and the range of Reynolds number is 0 ~ 3.0122 × 104.

In Table 3, the spanwise correlation of the vortex lift coefficient and the selected important representative wind speed in the vortex vibration interval are shown. The vortex vibration interval is set to +3 without the underlined angle of attack value in Table 3, and when the vortex vibration interval is underlined the angle of attack value is set to +5°.

According to the coefficient value of the aerodynamic spanwise correlation between discrete force breakpoints, the system model design is fitted to a different wind attack angle as shown in Figure 4, and different spanwise wind speed discrete points when vortex vibration occurs; the lift curve in which the spanwise lift coefficient changes with the spanwise spacing. Therefore, as shown in Figure 4, each lift curve is continuously improving. The necessary time course and performance of the nonzero lift measurement coefficient show a huge correlation of the spanwise movement distance, which will continue to increase with the spanwise movement distance. And gradually it is shown that it can gradually decay exponentially. The spanwise correlation of the space curve spacing of the same spanwise node in the first locking part is smaller than that of the other two wind speed control nodes; the amplitude lift coefficient of the second locking part at the end of the rising section is much larger than the maximum point of the amplitude in the first lock interval.

Table 4 shows a parameter value that is fitted by the numerical method of calculating the system using the correlation of the angle of attack between the discrete points.

In other words, the gradual increase in the motion threshold of the wind angle of attack is the main decisive

Table 3: Wind speed selection table for spanwise correlation analysis of lift coefficient during vortex vibration.

Vibration state	First lock	First lock	First lock	First lock	First lock	Second lock	Second lock
Description	Zone starting point	Area ascending section	Area maximum point	Descent section	Zone end point	Area ascending section	Area maximum point
Wind speed (m/s)	1.52	2.52	2.42	2.52	2.95	5.10	5.75
Vertical immeasurable	8.2451	11.2541	12.6253	12.7541	13.5423	24.2235	28.1542
Gang wind speed	9.1557	11.1524	12.1320	12.2512	12.7541	23.1142	28.1532
Vertical immeasurable	0.0101	0.0320	0.1202	0.2152	0.0001	0.0323	0.0215
Amplitude	0.1020	0.3320	0.1200	0.4155	0.0011	0.0521	0.1362

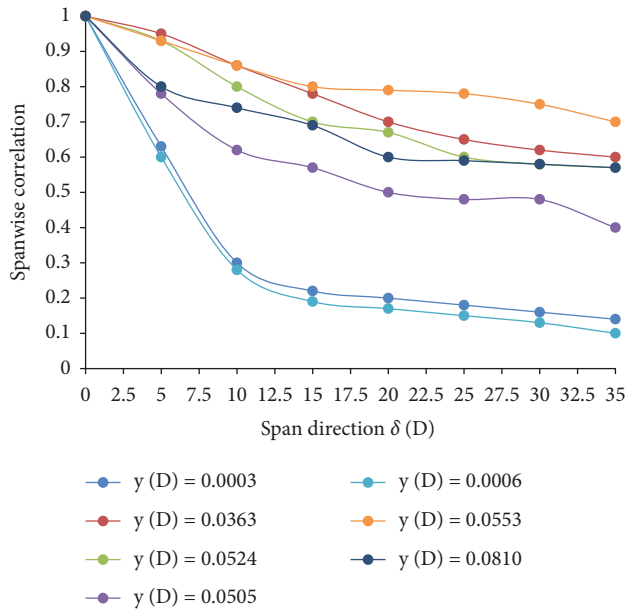

Figure 4: The spanwise correlation of lift coefficient varies with spanwise spacing during vortex vibration.

factor that directly leads to the spanwise motion correlation of the angle of attack.

4.3. Test Results and Analysis of Spanwise Effect of Vortex-Induced Vibration of Bridge Main Girder. Figure 5 shows the vertical dimensionless amplitude of the measurement points at the four positions of the +3° angle of attack as a function of the converted wind speed.

It can be seen from Figure 5 that the maximum amplitude of the first locking interval is much larger than that of the second locking interval.

Figure 6 shows the corresponding curves between the spanwise torque correlation coefficients and the time span spanwise correlation coefficients during the torsional wind vortex vibration between different spanwise wind speed points at different wind attack angles.

It can be clearly seen from Figure 6 that, generally speaking, the lifting torque coefficient corresponding to different wind speeds at various wind attack angles and the coefficient related to the spanwise direction change due to the increase of the spanwise spacing. With the acceleration of the wind attack angle, the final convergence value corresponding to the lift torque coefficient and the correlation coefficient will also increase overall, indicating that the wind attack angle is accelerated, which will lead to the acceleration of the self-excited force and the spread of the lift torque. The correlation coefficient has been greatly affected.

After the maximum detection value of the vortex vibration amplitude involved in various vertical vortex bending modes is converted through a normalized vibration model function calculation, the vortex amplitude of other selected detection points at their location can be directly obtained. The amplitude can be compared with the results in the actual vortex vibration test. Table 5 shows the actual estimated value of the vertical bending vortex amplitude value in the first stage and the measurement comparison of other test values. It can be clearly seen from Table 5 that the amplitude of the response of the vortex vibrator placed near the detection point at different detection positions should be roughly distributed according to the mode function.

Table 6 shows the comparison between the estimated value of the second-order vertical bending vortex amplitude value and the measured value. From Table 6, it can be seen that the different positions are roughly distributed according to the mode shape.

Table 7 shows the actual estimated value of the vertical bending vortex amplitude value in the third stage and the measurement comparison of the other test values. It can be seen from Table 7 that in the third test stage, the actual measurement error margin of the conversion test itself is relatively small, resulting in a large relative error between the converted value and the actual test value.

4.4. Application of Wireless Sensor Network in Bridge Health Monitoring. The application of wireless sensor network in bridge health monitoring can be seen: in actual engineering applications, it can be summarized as the following points.

(1) Selection and deployment of sensors

When selecting this type of sensor, it is necessary to determine its specific type and corresponding quantity according to the actual measurement situation and needs, and combined with the country's economic budget decision. Specifically, technical indicators such as measurement accuracy and measurement area range must be considered. Therefore, the deployment

Table 4: Fitting table of aerodynamic spanwise correlation parameters during vortex vibration.

Vibration state	First lock	First lock	First lock	First lock	First lock	Second lock	Second lock
Description	Zone starting point	Area ascending section	Area maximum point	Descent section	Zone end point	Area ascending section	Area maximum point
Fitting parameters	0.215	0.125	0.325	0.021	0.125	0.001	0.042
C_i	0.210	0.120	0.415	0.326	0.442	0.120	0.001
Fitting parameters	0.125	0.177	0.045	0.065	0.262	0.115	0.105
D_i	0.325	0.125	0.541	0.623	0.142	0.091	0.483
Obsessive-compulsive	5.262	21.142	21.324	12.023	4.523	8.521	9.241
Length $1/C_i$	5.021	36.102	36.132	18.524	5.865	6.652	7.021

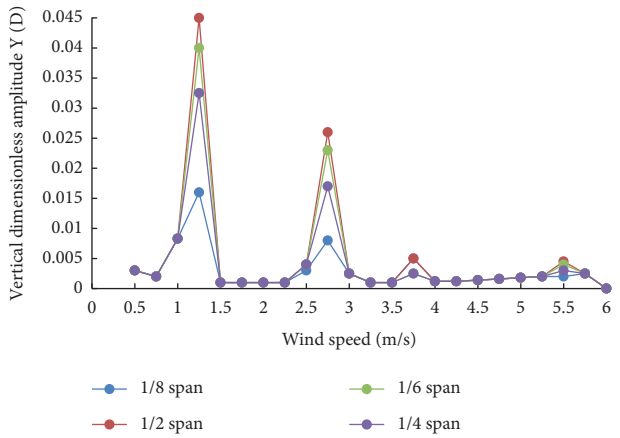

Figure 5: The vertical dimensionless amplitude of each measuring point varies with wind speed.

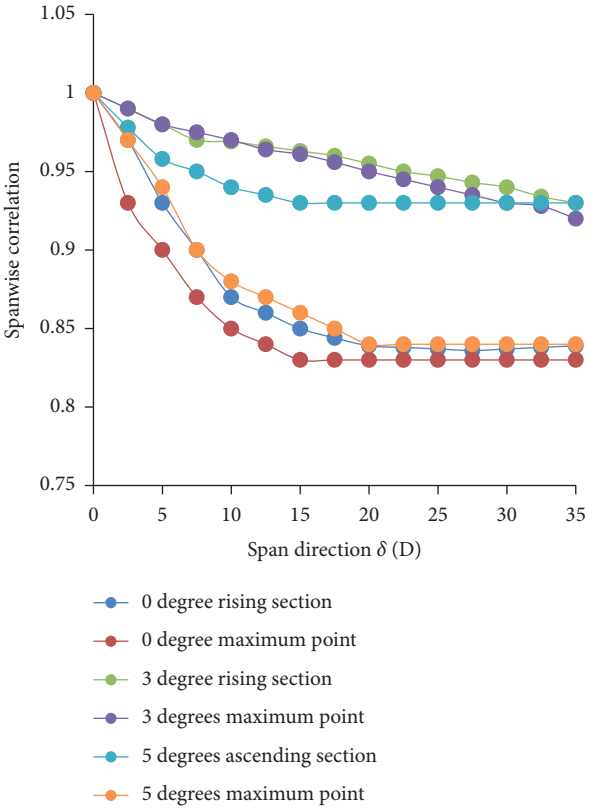

Figure 6: The spanwise correlation of torque coefficient varies with spanwise spacing during vortex vibration.

solution of sensor nodes is still a topic worthy of our in-depth exploration and research.

(2) Life of the health monitoring system

The service life of the health monitoring system mainly depends on the remaining energy of each node. Therefore, the energy efficiency of the node is also the first issue that we must fully consider in the process of designing the health monitoring system. Therefore, how to do this is for the bridge under the condition of normal operation of the health monitoring system, the energy of each node is used in a reasonable and targeted manner, and reliable energy signal collection and wireless charging technologies are used to compensate for the energy of the node in time. These technologies are worthy of our research and experimentation.

(3) Data storage and processing

The bridge health monitoring system generates a large amount of data on the network every day. If the information cannot be processed in a timely and effective manner, it will inevitably bring data disasters to the network. Therefore, on the one hand, for real-time collection and collection through sensors, data requires us to select appropriate algorithms for timely analysis and processing; on the other hand, we need to formulate reasonable data protection and storage strategies, and regularly and effectively remove excess resources from the entire database.

(4) The effect of structural damage recognition

Due to the incomplete and inaccurate measurement data and the limitations of the existing damage identification methods currently used, the practical application effect of structural damage identification is restricted, which directly affects the accuracy of the system evaluation results. Therefore, how to improve and increase the integrity of the detected data information database and the accuracy of the detection

Table 5: Comparison of the estimated and experimental values of the first-order vertical bending vortex amplitude.

Measuring point	Normalized coordinates	Normalized mode shape function	Test	Convert	Relatively error
	x/l	$\sin(n\pi x/l)$	Dimensionless vertical amplitude	Dimensionless vertical amplitude	
1/8	0.021	0.251	0.02415	0.01542	−5.65%
1/2	1.120	0.320	0.01253	—	—
1/6	0.524	0.452	0.12032	0.04512	0.35%
1/4	0.588	0.620	0.21530	0.12532	2.21%

Table 6: Comparison of estimated value and test value of second-order vertical bending vortex amplitude.

Measuring point	Normalized coordinates	Normalized mode shape function	Test	Convert	Relatively error
	x/l	$\sin(n\pi x/l)$	Vertical dimensionless amplitude	Vertical dimensionless amplitude	
1/8	0.214	0.532	0.01445	0.01622	4.55%
1/2	0.412	0.000	0.02135	0	—
1/6	0.523	−0.765	0.01523	0.12032	−8.35%
1/4	0.652	−1.010	0.12365	—	—

Table 7: Comparison of estimated value and experimental value of third-order vertical bending vortex amplitude.

Measuring point	Normalized coordinates	Normalized mode shape function	Test	Convert	Relatively error
	x/l	$\sin(n\pi x/l)$	Dimensionless vertical amplitude	Dimensionless vertical amplitude	
1/8	0.231	0.845	0.01021	0.02325	−11.14%
1/2	0.412	−1.021	0.02153	—	—
1/6	0.563	0.023	0.01532	0	—
1/4	0.625	0.652	0.02365	0.02032	35.65%

is the focus and direction that we need to further explore and research. On the other hand, we also need to actively explore and use new detected high sensitivity index technology to improve and enhance the effect of damage recognition.

5. Conclusion

This paper mainly researches and proposes a detection algorithm based on the local intrinsic symmetry of the model. This detection algorithm is not limited to the reflection symmetry of the local vertex of the symmetry detection. It is based on the three-dimensional geometric attributes near the local vertex of the model and the local symmetry decomposition between the local vertex of the distance relationship. Compared with the traditional manual detection and monitoring methods and modern wired network monitoring methods, wireless sensor networks are widely used in the field of bridge health monitoring and have certain advantages due to their simple installation, low maintenance cost, and flexible system deployment., The bridge structure health monitoring system based on wireless sensor network has become the focus of wide attention of academic circles and engineers at home and abroad. This article sorts out the wide application of wireless sensor network in bridge health monitoring system, and analyzes some of them in combination with some specific cases. Generally speaking, wireless sensor networks are currently widely used to monitor the bridges. There are still many difficulties. These problems are related to each other and hinder each other, which constitute the rich content of future research topics, but we can still be accurate. It is predicted that in the future, the bridge structure health monitoring system will play an increasingly important role in the management of bridges. The era of bridge digitalization is also quietly coming. In view of the problems of the vortex-induced vibration of the main shaft of long-span bridges, the use of two methods of synchronous vibration test and pressure test are adopted. The span-direction effect correlation test is carried out on the main beam segment model and the brace model under different wind attack angles. The response curve of the vortex-induced vibration lift response coefficient of the main bridge structure varying with the wind speed of the main girder was obtained. The bridge node wave band response model and the main girder tie section model were compared and analyzed. In the lift response to the vortex-induced vibration and the main girder, there is still a close correlation between the change of lift response coefficient and the spread direction for research. A dynamic identification method based on the system calculation model, a method for analyzing and identifying the excitation response of a rectangular vibration section of

the main beam, and an identification method for a streamlined main beam vortex-induced aerodynamic system were established. For the section, the response parameter calculation of the main beam vortex-induced vibration system and the comprehensive identification of the streamlined main beam vortex-induced aerodynamic system parameters were carried out, and the numerical comprehensive simulation of the method, the identification results, and the actual measurement results were combined for numerical comprehensive analysis and comparison. The application accuracy of the identification method in the actual calculation process is verified.

Data Availability

The data used to support the findings of this study are available from the corresponding author upon request.

Conflicts of Interest

The authors declare that they have no conflicts of interest.

References

[1] X. Fan, B. Zhou, and H. H. Wang, "Urban landscape ecological design and stereo vision based on 3D mesh simplification algorithm and artificial intelligence," *Neural Processing Letters*, vol. 53, no. 4, pp. 2421–2437, 2021.

[2] H. Santosa, F. Nur, and W. Adrian, "Management and enhancement of livable urban streetscape through the development of the 3D spatial multimedia system," *International Review for Spatial Planning and Sustainable Development*, vol. 9, no. 4, pp. 10–30, 2021.

[3] S. M. Cho, "Effects of digital elevation model in water quality modeling using geogrpahic information system," *International Journal of Internet, Broadcasting and Communication*, vol. 13, no. 2, pp. 14–19, 2021.

[4] M. Adil, M. Attique, M. M. Khan, J. Ali, A. Farouk, and H. Song, "Hopctp: a robust channel categorization data preservation scheme for industrial healthcare Internet of things," *IEEE Transactions on Industrial Informatics*, vol. 9, no. 3, p. 1, 2022.

[5] N. Tosa, P. Yunian, R. Nakatsu, A. Yamada, T. Suzuki, and K. Yamamoto, "3D modeling and 3D materialization of fluid art that occurs in very short time," in *Lecture Notes in Computer Science*, vol. 12523, pp. 409–421, Springer, Cham, Switzerland, 2020.

[6] D. A. Loaiza Carvajal, M. M. Morita, and G. M. Bilmes, "Virtual museums. captured reality and 3D modeling," *Journal of Cultural Heritage*, vol. 45, pp. 234–239, 2020.

[7] V. Di Pietra, E. Donadio, D. Picchi, L. Sambuelli, and A. Spanò, "Multi-source 3D models supporting ultrasonic test to investigate an Egyptian sculpture of the archaeological museum in b," *The International Archives of the Photogrammetry, Remote Sensing and Spatial Information Sciences*, vol. XLII-2/W3/W3, pp. 259–266, 2017.

[8] H. Abulkasim, A. Farouk, H. Alsuqaih, W. Hamdan, S. Hamad, and S. Ghose, "Improving the security of quantum key agreement protocols with single photon in both polarization and spatial-mode degrees of freedom," *Quantum Information Processing*, vol. 17, no. 11, p. 316, 2018.

[9] D. Shi, Y. Zhao, and J. Li, "Reconstructing part-level 3D models from a single image," in *Proceedings of the 2020 IEEE International Conference on Multimedia and Expo (ICME)*, vol. 42, pp. 65–79, IEEE, London, UK, July 2020.

[10] M. H. Anisi, A. H. Abdullah, S. A. Razak, and M. A. Ngadi, "Overview of data routing approaches for wireless sensor networks," *Sensors*, vol. 12, no. 4, pp. 3964–3996, 2012.

[11] F. Bajaber and I. Awan, "An efficient cluster-based communication protocol for wireless sensor networks," *Telecommunication Systems*, vol. 55, no. 3, pp. 387–401, 2014.

[12] F Ahmed, J. Batle, M. Elhoseny et al., "Robust general N user authentication scheme in a centralized quantum communication network via generalized GHZ states," *Frontiers of Physics*, vol. 13, no. 2, Article ID 130306, 2018.

[13] Y. Li, N. Yu, W. Zhang, W Zhao, X You, and M Daneshmand, "Enhancing the performance of LEACH protocol in wireless sensor networks," in *Proceedings of the*, pp. 16–21, Shanghai, April 2011.

[14] J. Yick, A. Bharathidasan, G. Pasternack, B. Mukherjee, and D. Ghosal, "Optimizing placement of beacons and data loggers in a sensor network - a case study," in *Proceedings of the 2004 IEEE Wireless Communications and Networking Conference, WCNC*, pp. 2486–2491, Atlanta, GA, USA, March 2004.

[15] K. S. Ahn, D. G. Kim, and B. S. Sim, "Balanced chain-based routing protocol(BCBRP) for energy efficient wireless sensor networks," in *Proceedings of the 9th IEEE International Symposium on Parallel and Distributed Processing with Applications Workshops*, pp. 12–21, Busan, Korea (South), May 2011.

[16] J. Yang, Y. Zhao, J. Liu et al., "No reference quality assessment for screen content images using stacked autoencoders in pictorial and textual regions," *IEEE Transactions on Cybernetics*, vol. 6, pp. 3–12, 2020.

[17] N. Zhaoyang, R. Yongxin, R. Chengao, and W. Xuehong, "ANSYS application in design of the main beam of crane," *Machinery for Lifting and Transportation*, vol. 5, pp. 31–33, 2008.

[18] G. P. Gupta, M. Misra, and K. Garg, "Towards scalable and load-balanced mobile agents-based data aggregation for wireless sensor networks," *Computers & Electrical Engineering*, vol. 64, no. 10, pp. 262–276, 2017.

[19] A. F. Metwaly, M. Z. Rashad, F. A. Omara, and A. A. Megahed, "Architecture of multicast centralized key management scheme using quantum key distribution and classical symmetric encryption," *The European Physical Journal - Special Topics*, vol. 223, no. 8, pp. 1711–1728, 2014.

Hindawi
Mobile Information Systems
Volume 2022, Article ID 8317138, 10 pages
https://doi.org/10.1155/2022/8317138

Research Article

Visual UI Design Image Sharing Scheme Based on Improved FEMD Algorithm

Danni Shen and Yu Dong

College of Art, Zhejiang Shuren University, Hangzhou 310015, China

Correspondence should be addressed to Yu Dong; 601239@zjsru.edu.cn

Received 23 May 2022; Revised 20 June 2022; Accepted 5 July 2022; Published 22 July 2022

Academic Editor: Shadi Aljawarneh

Based on the improvement of the FEMD algorithm, this article assumes a reversible sharing scheme that can encrypt images. UI design is the most important part of Internet applications, including three parts, namely, interaction design, interface design, and user research. Therefore, the UI directly affects the user experience. It is precisely based on the criticality and importance of the UI algorithm that we intend to further explore the most critical expression language in the product and to innovate the most important visual factors by further digging into the user's demands for the product. The three most important colors in the UI design process are colors, pictures, and text. And interaction design is the most important and critical part of UI design. We need to explore the dynamic relationship among applications, humans, and machines. For visual design, we not only need to deal with the relationship between application, human, and machine, but also better deal with the relationship between plane, time, and space on the basis of these three relationships. Our innovative interface for the UI algorithm is mainly to innovate the first interface that the user obtains, so that the user can get a better reading experience and browse, and the designer can beautify and collect the user interface to achieve the user the purpose of obtaining a better browsing sensory experience. This requires us to get rid of the old copy model, in order to innovate in thinking; innovate a better visual communication interface, and better integrate the user's research interface design and interaction, which is also the pursuit of this article.

1. Introduction

With the further popularization of the Internet in the twenty-first century and the arrival of the information age, the development of the big data era has been born to accelerate the further improvement of data transmission [1]. However, in the process of data transmission, how to encrypt data has become the most important and urgent problem to be solved in the process of image sharing application [2]. Among them, we need to classify different images according to their different characteristic attributes and characteristics. And from this to different people to manage. Suppose that the image we need to save privately is divided into N images, and only when a user has t $(2 < t < n)$ divided images at the same time can the original image that needs to be saved privately be restored [3]. This is used to prevent the private images from being too concentrated, so that a certain degree of security can be achieved. It is precisely based on the criticality and importance of the UI algorithm that we intend to further explore the most critical expression language in the product and to innovate the most important visual factors by further digging into the user's demands for the product [4]. The three most important colors in the UI design process are colors, pictures, and text. And interaction design is the most important and critical part of UI design [5]. We need to explore the dynamic relationship among applications, humans, and machines. For visual design, we not only need to deal with the relationship between application, human, and machine, but also better deal with the relationship between plane, time, and space on the basis of these three relationships [6]. From another perspective, if the user loses a certain part of the image, the user only needs to have the remaining images greater than or equal to t to recover the lost and damaged

secret images. Steganography is often used a technique used for information hiding. People use this technology to realize the safe storage of digital content and safe transportation in the network [7]. Based on steganography, designers deposit different images uploaded by users in different image carriers to achieve the privacy of sharing. Thus, N different dense images are generated. Then, by transporting the secret image, the purpose of safe transport of the secret image is completed [8].

2. Related Work

For the purpose of securely transmitting private images, literature first proposed a secret sharing technology based on the principle of Lagrangian polynomial interpolation, also known as (t, n) threshold secret sharing technology [9]. Literature on this basis, we also proposed a technology for the secret sharing of secret images. At the same time, this private image is not single; it is a connection between the users and cloud storage [10]. Only when the first user and the second user input the password correctly at the same time, this kind of picture can be transported. Literature proposes applying Huffman coding to differential image coding of secret images to reduce the number of divided images [11]. Literature proposed a secret image sharing scheme based on steganography, which hides the generated noise in multiple carrier images, and ensures that all the other people who do not know the password cannot obtain this kind of image, no matter what no means by any means [12]. Based on the algorithm framework, subsequent researchers have proposed many secret image sharing schemes based on steganography. Due to the relatively high value of the two images mentioned above, in order to further ensure the safety of medical images and military images, we need to break the original image transportation mode and adopt a more advanced one that can be private. Image sharing scheme for image sharing. Among them, literature uses OAEP and IDA to further improve the security of the shared secret image key, and uses the FEMD steganography algorithm to improve the quality of the steganographic image [13]. While adopting this technology, we can replace the technology mentioned above by further improving the algorithm and adopting new cell automation technology to improve the quality of the image and optimize the image carrier. Although this method improves the image quality of the data to a certain extent, it also has certain drawbacks and problems. For example, certain carrier images cannot be restored, including some special military images and some images related to medicine. Literature proposed a reversibility sharing mechanism for secret images [14]. For this problem, we have proposed a new improvement plan; this new improvement plan can solve the overflow problem well. The purpose of safe transmission of private images is to better save the images uploaded by users, so that the images uploaded by users will not be stolen by people with ulterior motives and used for other commercial purposes. Literature proposed a reversible bow and arrow workshop for secret images based on (t, n), and this shared development is active, but the quality of the private images generated in this atmosphere needs further improvement [15]. Literature proposed a reversible data sharing scheme, which embeds secret information in the spatial domain, but the amount of embedded data is small. We understand that this technology can meet the transportability of private images [16]. The image is saved through encryption during sharing, so as to further complete the protection of the images uploaded by the users.

3. Research on Image Sharing Background Knowledge of Visual UI Design with Improved FEMD Algorithm

3.1. Secret Sharing Technology. Secret sharing technology is based on the principle of Lagrangian polynomial interpolation. If the user needs to save his own secret, then the saved secret device S will be shared by a secret method. The specific time steps are as follows

$$\begin{aligned} F(x) &= \left(a_0 + a_1 x^1 + \cdots + a_{t-1} x^{t-1}\right) \mathrm{mod} GF(p) \\ y_i &= F(x_i), 1 \le i \le n, \end{aligned} \tag{1}$$

$$F(x) = \left[\sum_{i=1}^{t} y_i \prod_{\substack{j=1 \\ j \neq i}}^{t} \left(x_i - x_j\right)^{-1} \left(x - x_j\right)\right]. \tag{2}$$

3.2. FEMD Algorithm. In this design scheme, we extract specific methods and specific algorithms to achieve the transportation of dense images, and the quality of our extraction methods and algorithms directly determines and affects the quality of the image, which is related to an important and critical factor for the quality of dense images. In order to better enable the transportation of private images to meet the user experience needs, we further upgrade and improve this algorithm, and in the process of continuous practice and application, we will test whether this algorithm can meet the needs of the current design market.

$$\frac{Ibs^2}{2} \frac{\text{bit}}{\text{pixel}}. \tag{3}$$

So, in this square, the larger the X value we bring, the larger the corresponding S value, and the larger the amount of embedding, but at the same time, the corresponding embedding distortion will become more and more in this case. Based on the FEM calculation method, we embed a d in the S binary system into a pixel pair (a_i, $a_i + 1$) to obtain a dense pixel pair (b_i, $b_i + 1$). The specific steps are as follows.

Step 1 defines the extraction function $F(x_i, x_i + 1)$ as shown in the following equation.

$$F\left(x_i, x_{i+1}\right) = \left((s-1)x_i + s x_{i+1}\right) \mathrm{mod}\ s^2. \tag{4}$$

Step 2 establishes a corresponding 256×256 mapping matrix M, as shown in formula.

$$M[x_i][x_{i+1}] = F(x_i, x_{i+1}), x_i, x_{i+1} = 0, 1, 2, \ldots, 255. \quad (5)$$

Step 3 calculates the extraction function value $F(a_i, a_i + 1)$ of $(a_i, a_i + 1)$ according to formula (2).

Step 4 If $F(a_i, a_i + 1) = d$, $(b_i, b_i + 1) = (a_i, a_i + 1)$, the embedding is finished, otherwise, go to step 5.

Step 5: In the corresponding mapping matrix M, a square search box W centered on $(a_i, a_i + 1)$ that can be matched is designed, as shown in formula.

$$W(s, (a_1, a_{i+1}), r) = \{M[a_i - r + u][a_{i+1} - r + v]\}, \quad (6)$$

$$0 \le u \le 2r, 0 \le v \le 2r\}. \quad (7)$$

Step 6 Scan each element in the search box, and when the element meets the calculation conditions, it is brought to the next calculation.

$$D = |p - a_i| + |q - a_{i+1}|. \quad (8)$$

The mapping matrix M constructed in the FEMD algorithm when $s = 4$, as shown in Figure 1.

In this article, the FEMD algorithm we often mentioned is a steganography algorithm that is often used in the design process. This algorithm can complete higher embedding amount and better quality dense images. After that, scientists have improved and further upgraded this algorithm, and based on this, wrote a new algorithm. That is, in the process of data calculation, mathematical calculations can overcome a series of problems caused by the difference of the algorithm and the difference of the pixels, so as to better complete the privacy sharing.

4. The Layout of Visual Elements in UI Design

UI design contains many elements. In the process of UI design, we have applied many elements, such as abstract elements such as points, lines, and surfaces, as well as more specific elements such as pictures, text, and colors. Including the thinking and time that exist in reality, we have combined this series of elements effectively and scientifically, so that the designer can start from different horizontal and vertical planes and more three-dimensional thinking and time. Directions and ideas are explained and analyzed. At the same time, we vividly compare this method of problem-solving to a moving cubic nine-square grid. Just like the Rubik's Cube we often see in our lives, each corresponding grid is composed of three elements, namely, X, Y, and Z, which represent the abscissa, ordinate, and time and space coordinates of thinking. In the abscissa, we explained the distribution of points, lines, and planes in the longitudinal coordinates. We also focused on the psychological sequence of pictures, colors, and text when users read them, and unified the elements on this image into four dimensions. In terms of time, the unity of time, space, horizontal, and vertical is realized. Moving Cube Jiugongge as shown in Figure 2.

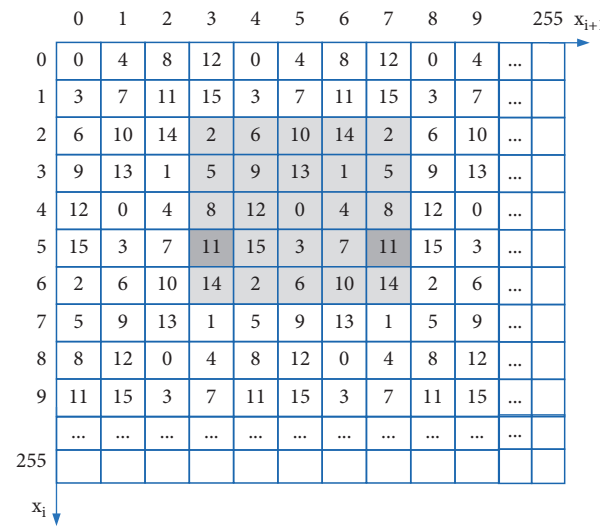

Figure 1: The mapping matrix M constructed in the FEMD algorithm when $s = 4$.

4.1. Horizontal Layout. In designing the image layout of the UI, we not only list the original points, lines, and surfaces, but also improve the two-dimensional design to the three-dimensional design, and change the original points, lines, and surfaces. Expressed in a better and more artistic way, so that the users can get better senses. Experience the horizontal plane structure not only to make the entire design interface look neater and more beautiful, but also to express more complete information, so that the readers can get more information and learn more about the limited pages.

The actual application of an algorithm to the market is often divided into two parts, one is the relationship between the designer and the page design company, and the other is the relationship between the company and the user. Among the companies and designers that commission the design, we need to clearly state which functions the company has commissioned the designers to design. These functions are specific and clear and should be accepted by both parties, because the design company is better than the users. A clearer understanding of a series of structures and procedures is required in the UI design. At the same time, designers have higher requirements to produce higher-quality and more efficient products, which can solve users to a certain extent. The lack of understanding of the series of problems caused by this product has enabled the market share and market CI degree of this product to be improved more broadly, and at the same time, it has also avoided direct contact between the designers and users. The role of a bridge can effectively complete the communication between designers and users. It not only provides a guarantee for designers, but also a guarantee for users, so that users can get more perfect users. With experience, designers can also improve the level and quality of service.

In the process of designing pages, designers should not only consider the use of design functions, but also the beauty of the design interface. In order to make the design interface better provide users with a better experience, designers often the interface is beautified and upgraded to make the

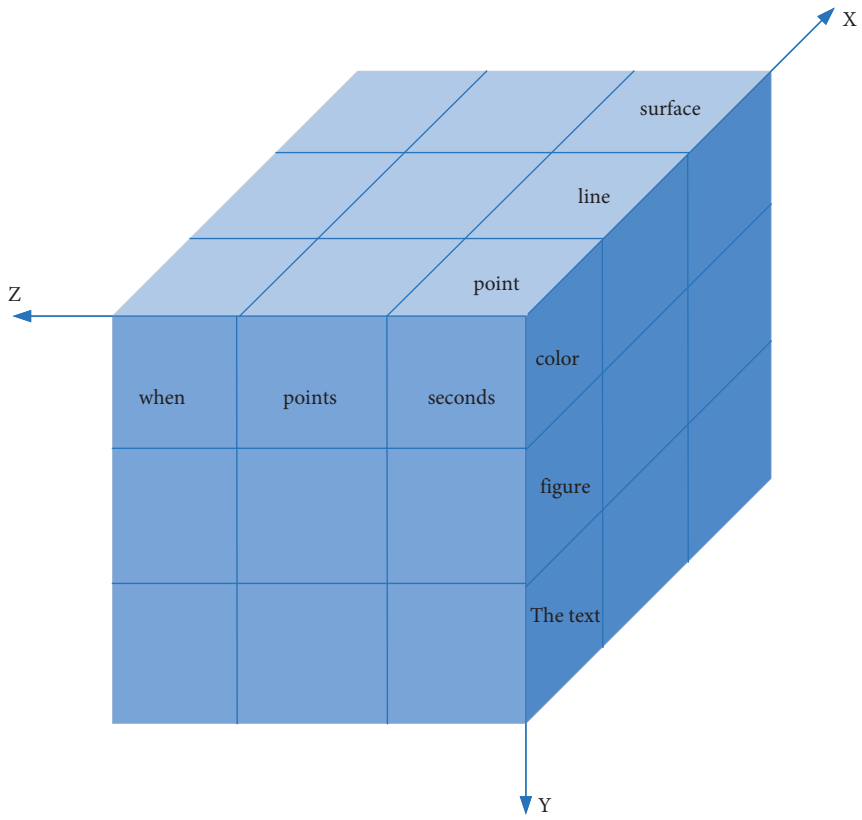

Figure 2: Moving cube jiugongge.

designed page more beautiful. Similarly, among products with the same functions, users tend to choose products with more beautiful user interfaces, simpler practical functions, and easier browsing and reading. In order to better meet the needs of the market, this also requires designers to design a more beautiful, more convenient, and more efficient browsing interface.

In the design process of the vertical space layout, designers regard this UI design as a specific textual expression. The designers use different carriers, such as colors, images, graphics, text, and other different elements to express. Enables the information between people and the information between humans and computers to complete the interaction, and on this interaction-based condition, this foundation is collectively referred to as referents, which not only affects the reading order of users, but also it affects the user's reading experience. From the color to the layer and finally to the text, it realizes the user's acquisition of information and the understanding of the information step by step, and can complete the reception of information in the horizontal and vertical directions, so that people can understand the color of the picture text from static to dynamic; the understanding of time, space, and four-dimensional plane completes the information reception and enhances the user's understanding of the product. Vertical spatial hierarchical structure is shown in Figure 3.

The first level is the color element. This is the first most critical element in this. It is an intuitive and powerful expression language. Color can complete the expression of the

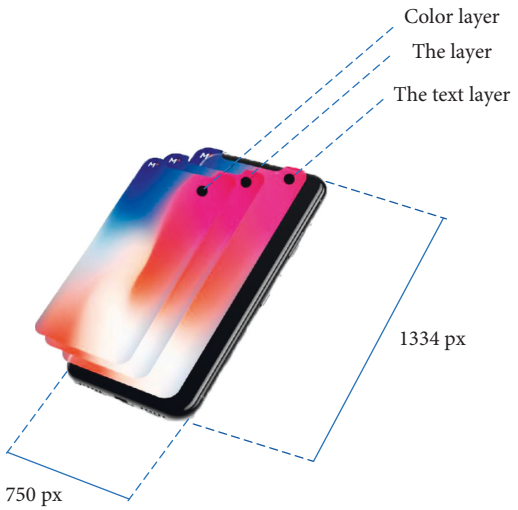

Figure 3: Vertical spatial hierarchical structure.

interface, improve the expressive charm of the interface, and display the attributes of the product. The more experienced designers are, the better they can use expressive colors to achieve the purpose of improving product expression elements. We can understand the role of color more vividly, just as color is like a person's face in this face-seeing era. It is very important for knowing a person and can effectively attract and grab the user's attention and attention. Color can have an impact on people's vision, as well as people's thinking. We can use a situation that appears most often in

Table 1: Summary of mobile device screen resolution.

Size	Resolution	Remarks
10 inches	$800 \times 600(5:4)\backslash l024 \times 768(4:3)$	
12 inches	$1280 \times 800(16:10)$	
13 inch	$1280 \times 800(16:10)$	
14 inches	$1024 \times 768(4:3)\backslash 1280 \times 800(16:10)\backslash 1280 \times 720(16:9)$	
15 inches	$1280 \times 800(16:10)\backslash 1440 \times 810(16:10)\backslash 1680 \times 945(16:9)$	Most used
17 inches	$1440 \times 900(16:10)\backslash 1440 \times 810(16:10)\backslash 1680 \times 945(16:9)$	
19 inches	$1440 \times 900(16:10)\backslash 1680 \times 945(1\ 6:10)\backslash 1\ 680 \times 945(1\ 6:9)$	
22 inches	$1680 \times 1050(16:10)\backslash 1680 \times 945(16:9)$	
24 inches	$1920 \times l200(16:10)\backslash l680 \times 945(16:9)$	

UI design to illustrate, for example, for designers, the simplest and most common prototype black and white. The draft is to avoid the impact of the difference in the color interaction design on the user's experience, so that the user's judgment standard is affected by the color. On the other hand, color can also strengthen the visual focus and refer to information. For example, the user can enter text in the search box, and different cursors and different colors will be displayed during the text input process.

Image transportation can break through the limitations of time and space, effectively convey information, and become a mode of transportation that users love very much. The expression of pictures is not only the expression of symbols, but also includes the understanding of the designers' thoughts and feelings. This relationship requires a certain logical perception of time and space. However, in the process of directly filling in by users, the color is usually obtained first, and then the picture is obtained, which leads to people's recognition of the picture later than the feeling of a color But the amount of information contained in pictures is often huge. People can use pictures to describe a lot of details. Pictures themselves are an expression of symbols and information. At the same time, designers can use this expression of symbols to attract users' attention, thereby achieving emotional resonance between designers and users.

The third level is text. Compared with pictures and colors, text can express more information. However, when users obtain information, they usually get text at the end. At the same time, text has forms of expression that pictures and colors do not have. Text is an important part of human culture. Compared with pictures and colors, text is static, while pictures and colors are dynamic. Therefore, in the user's intuitive experience of the interface, text is often the last thing the user gets, this determines to a certain extent that the text requires the user to read patiently. Although the text takes a long time, the effect of the text is also huge, and it can affect the user's direct experience. People can accurately and effectively obtain product information and product design elements through text, so when we are designing elements in the UI, in order to enable users to get a better experience and increase the frequency of reader users' use of the interface, it is often necessary that we put words on the third layer of visual expression.

However, due to the rapid development of the current information age, people are in an era of receiving a large amount of information. The further development of data technology enables people to obtain more information through different means. On the one hand, it increases the amount of people receiving information, and on the other hand, it also reduces people's patience for information reading. It is believed that the method of reading text is boring and takes a long time, which makes users visually fatigued. So, this requires us to increase the interest in text reading in the process of designing the interface, so that users can get happiness from text reading.

4.2. The Impact of Display Equipment on Visual Performance in UI Design. In the last century, the rapid development of Internet technology further gave birth to the era of big data. In the past few years, the rapid development of information technology in my country has made the Internet widely used, which has also given birth to different electronic products on the market, and the speed of updating among different electronic products is very fast. Some electronic products can be universally loved by users, but at the same time, most of the products were quickly eliminated and did not gain a high market share. Through this phenomenon, in order to enable our products to gain more users' love and be chosen by more users, which requires our designers to understand the needs of the market and the needs of users, so as to design a product that meets the needs of users and meets the needs of the market, as shown in Table 1.

In the process of an interface design, we have to consider many factors, including the size of the element, the shape of the element, and the volume of the element. If the element we select takes up too much of the entire interface, then this is not the case. Reasonable, it is also unreasonable if the proportion of the selected element in a design interface is too small, so we need to carefully consider the volume of the element we choose to better match the user. For the required size, in such a design process, we also abandoned the unnecessary and cumbersome procedures that existed before, and instead used a simple, convenient, and efficient method to enrich and perfect the user's sensory experience.

5. Design of Reversible Secret Image Sharing Algorithm

5.1. Improved FEMD Algorithm. Aiming at the problem pixel pairs encountered in the process of FEMD algorithm processing, this paper solves the problem of pixel pair

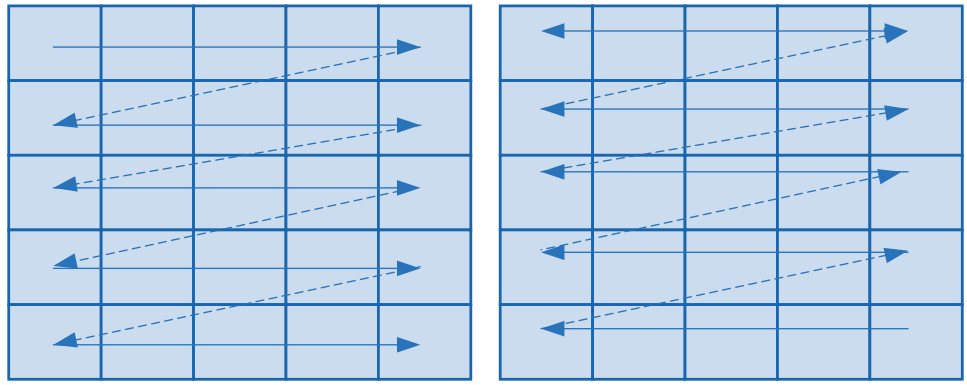

(a) (b)

Figure 4: Scanning direction. (a) Embedding process. (b) Recovery process.

reversibility recovery from two aspects: embedding process and overflow pixel pair processing. Scanning direction as shown in Figure 4.

For the data element that we first received, that is, the original data, we give a mark to record it, and then replace the pixels corresponding to this element with other elements, so that users need to get private pictures. This requires proofreading of the original pixel values and distinguishing between correct and incorrect conditions.

$$sf = \left(a_i \bmod (255 - r)\right)(r + 1) + \left(a_{i+1} \bmod (255 - r)\right). \tag{9}$$

Among them, only one certain element can be matched with it.

$$sf = \min\left(a_i \bmod (255 - r), a_{i+1} \bmod (255 - r)\right). \tag{10}$$

After an overflow pixel is processed by the above method, the following formula can be obtained

$$\begin{aligned} R_j &= \frac{R_j'}{255 - r}(255 - r) + \frac{sf}{r + 1} \\ R_{j+1} &= \frac{R_{j+1}'}{255 - r}(255 - r) + (sf \bmod (r + 1)) \\ X &= \frac{X'}{255 - r}(255 - r) + sf. \end{aligned} \tag{11}$$

Through the above-mentioned processing method of the overflow pixel pair, the value of the original overflow pixel pair can be restored based on the improved FEMD algorithm, and the lossless restoration of the carrier image can be realized.

5.2. Secret Image Sharing and Embedding. In the method proposed in this article, the algorithm we have mentioned and has been applied uses grayscale images as its carrier. This secret sharing technology is used to complete the division of the user interface, and finally FEMD based on the algorithm, a single image becomes N different dense images. When the user needs to obtain the final image, the user needs to provide different elements corresponding to it. In the process of constructing multiple images of $T-1$, we use the algorithm mentioned before. The specific process of the specific algorithm mentioned above is shown in Figure 5.

(1) Rearrange the data in I into a one-dimensional vector.

$$S = \left\{s_1, s_2, \ldots, s_{(h_i \times w_i)}\right\}. \tag{12}$$

(2) Express each pixel in S with a hexadecimal number method to form a vector

$$S' = \left\{d_1, d_2, \ldots, d_l, \ldots, d_{(h_i \times w_i \times 8/a)}\right\}. \tag{13}$$

Among them,

$$0 \le d_t \le 2^{\alpha}, l = 1, 2, \ldots, h_s \times w_s \times \frac{8}{\alpha}. \tag{14}$$

Otherwise, construct equation (14):

$$\begin{aligned} F_j(x) &= \left(f + sfx^1 + ds_1^j x^2 + \cdots + ds_{t-2}^j x^{t-1}\right) GF(2^{\alpha}). \\ F_j(x) &= \left(f + ds_1^j x^1 + \cdots + ds_{t-2}^j x^{t-1}\right) GF(2^{\alpha}). \end{aligned} \tag{15}$$

In this era of rapid development of information technology, the widespread application of big data makes it more convenient to share data, no matter how far apart two users are, whether it is altitude difference, cultural difference, or ethnic difference. They can all realize the sharing of data. This is the benefit that the development of science and technology brings to people. Technology is not superior. On the contrary, the advancement of science and technology can promote the progress of everyone's life. The emergence of technological inventions can be applied in different fields, such as industrial life. The advancement of science and technology can greatly increase the labor productivity of the society, shorten the necessary labor time, and maximize the output of the society within a certain period of time, thereby realizing the operations and further increasing the production profit of the enterprise. For schedule life, the further development of technology can enrich people's further needs for life. New products created by technology can be

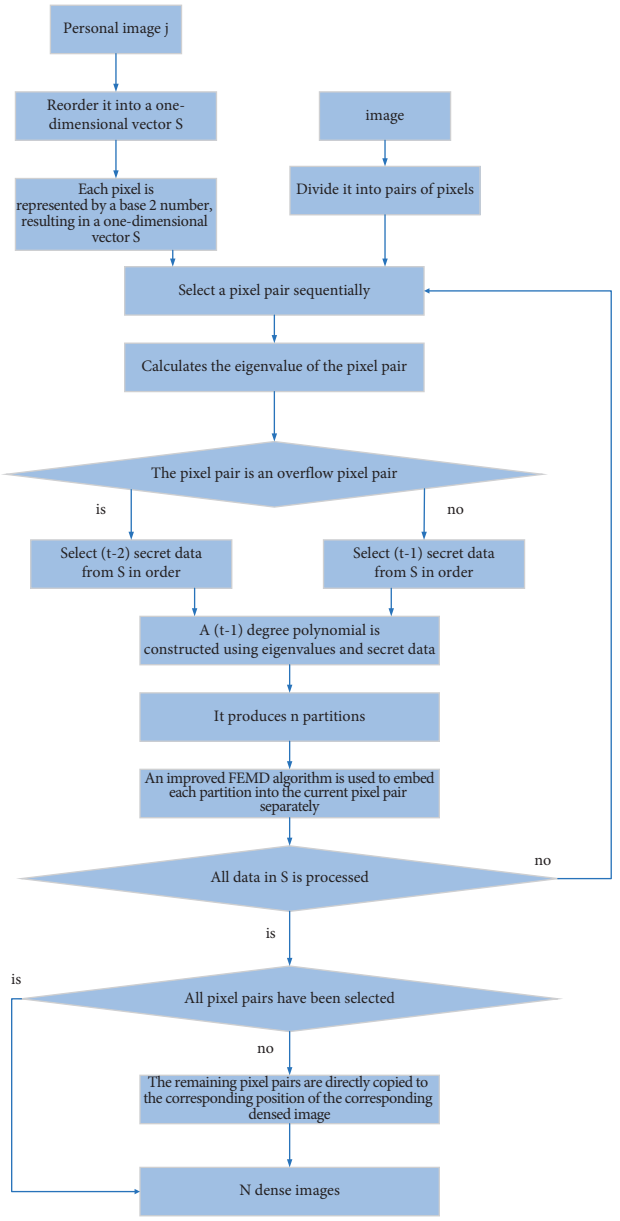

Figure 5: Reversible secret image sharing and embedding process.

applied to different people's lives. For example, light bulbs bring light to people in the dark. The advancement of medical technology makes cross-regional treatment possible. Technology is using its own unique mission to promote world changes step by step, improve people's quality of life and standard of living, and provide people with a higher level and higher quality and a more efficient life. At the same time, people's different needs in life promote the progress of science and technology. It is precisely because people have a variety of different needs, so in order to meet these different needs, scientists and designers will spur their own designs creating a better and more convenient technology for people to apply.

5.3. Secret Image Extraction and Carrier Image Restoration. According to the principle of (t, n)-threshold secret sharing technology, it takes at least t different secret images to recover the shared secret image. It is assumed that the provided secret images are $SI_1, SI_2, \ldots, SI_t$, and the corresponding participants. The keys possessed are $x_1, x_2, \ldots, x_t$, the process of extracting the secret image and restoring the original carrier image is as follows. For each dense image SI_i, $i = 1, 2, \ldots, t$, two adjacent pixels are selected in sequence as a pixel pair (SI, SI), and the extraction function value fi is calculated according to the formula. According to the previously obtained t sets of data (x_i, f_i), $i = 1, 2, \ldots, t$, the polynomial $F(x)$ is reconstructed, as shown in the following equation , where $\alpha = s$.

$$F(x) = \left[\sum_{\substack{i=1 \\ j \neq i}}^{t} \prod_{j=1}^{t} \left(x_i - x_j\right)^{-1} \left(x - x_j\right)\right]_{\mathrm{mod} GF(2^{\alpha})} = \left(a_0 + a_1 x^1 + \cdots + a_{i-1} x^{i-1}\right)_{\mathrm{mod} GF(2^{\alpha})}. \tag{16}$$

In the prediction process based on this algorithm, we can know that if a user wants to obtain a privately stored image, at least t different secret images are required. If the number of images provided by the user is insufficient, then the user will not be able to obtain the encrypted and saved images. Only when the number of encrypted images provided by the user is greater than the number specified by us, can the encrypted and saved images be obtained, which can be better based on this to ensure the privacy of user information, ensure the quality of use of users, and improve the user experience. When other people want to obtain images, but the number of secret images they hold is insufficient, they cannot obtain information about the secret images. At the same time, we will also tell this situation to the user who should have the secret image, usually in this case the user's password or image is threatened. After we inform the user of this situation, the user will think about and further adjust the number of images on the opponent or the password corresponding to it, thereby increasing the protection of this private information and making others the theft of private images by people has become impossible.

Figure 6: Secret image (300 pixels × 300 pixels).

Table 2: Contained image quality.

Carrier image	PSNR of stcgo-l (dB)	PSNR of stcgo-2 dB	PSNR of stcgo-3 dB	Average PSNR (dB)
1-cna	48.4334	48.3989	48.4819	48.4381
Baboon	48.4392	48.3905	48.5022	48.4439
Pepper	48.4293	48.3897	48.4482	48.4224
Boat	48.4547	48.3918	48.4903	48 4456
Bridge	48.4080	48.3437	48.4334	48.3950
Man	48.0157	47.9897	48.0132	48.0062
Tiffany	48.4128	48.3385	48.4199	48.3904
Zelda	48.4270	48.3583	48.3753	48.3869
Alainc	48.4387	48.3894	48.4911	48.4397
Barbara	48.4520	48.3971	48.4917	48.4469
Average	48.3910	48.3387	48.4147	48.3815

(a) (b) (c) (d)

Figure 7: Quality evaluation of dense image. (a) Carrier image. (b) Stego-1 (48.434 dB). (c) Stego-2 (48.3989 dB). (d) Stego-3 (48.4819 dB).

5.4. Experimental Results and Analysis. First of all, through the experimental results, we can know that the quality of the image obtained by this algorithm for different images matching different processing is different. Taking the image used in the simulation experiment we conducted before, we get the maximum size of the matching secret image that is different from the size obtained by the previous algorithm. In this experiment, the image we selected is shown in the figure. Based on this algorithm, we have made improvements and upgrades. We have ensured the application of this algorithm to a greater extent. By ensuring and improving the security of the algorithm to improve the privacy of users' images, the higher the security of the corresponding result, the higher the degree of protection of the

Table 3: Algorithm performance comparison.

Carrier image	Average PSNR (dB with density image)			
	Algorithm A	Algorithm B	Algorithm C	Algorithm
1-cna	42.0387	45.625	647.8035	48.4381
Baboon	42.0487	45.6208	47.8012	48.4439
Pepper	42.0551	45.6321	47.8101	48.4224
Boat	42.0378	45.6029	47.7915	48.4456
Bridge	42.1002	46 7146	47.8436	48.3950
Man	41.9939	45.6981	47.7859	48.0062
Tiffany	42.0353	45.6204	47.8252	48.3904
Zelda	42.0377	45.6236	47.7954	48.3869
Alainc	42.0452	45 6043	47.8068	48.4397
Barbara	42.0498	45.6173	47.8342	48.4469
Average	42.0387	45.7359	647.8035	48.4381

user's image by this algorithm, and the better the user experience.

$$h_s \times w_s = \frac{h_c \times w_c \times (t-1)}{2 \times 8/\alpha}. \tag{17}$$

The secret image selected in the experiment is an image of 300 pixels × 300 pixels, as shown in Figure 6, so the experimental parameters to be set are $t = 3$ and $n = 3$. For algorithms that implement the secret image sharing based on steganography, the less distortion of the generated secret image, the less likely it is to be detected by attackers during transmission on the network, and the better the security. This article uses PSNR index to measure the quality of the dense image.

In the chart shown below, we can see that the improved algorithm using the Md algorithm can get the required Hami image. In addition, Figure 6 also shows the image with the image as the carrier, so we have obtained three corresponding dense images. From the tables and pictures, we can get the results calculated by the improved F1FD algorithm under the conditions of the experiment and the results of the original images. There is not much difference between the calculated results, so we also confirm from another angle that this algorithm improves user privacy protection, and also proves from another angle that this algorithm does have its advantages and specialties, as shown in Table 2.

Quality evaluation of dense image is s shown in Figure 7. For the algorithm in this paper, when $t = 3$ and $s = 4$, using the algorithm in this paper to share and embed a piece of data, the error introduced on a pixel can be calculated as 1.375. When realizing the sharing and embedding of this data, the error introduced on a pixel of the carrier image can be obtained by calculation. When $t = 3$, $m = 3$, $\alpha = 2$, the introduced errors are 5 and 2.5, respectively. Therefore, the quality of the dense image obtained by this algorithm is better, as shown in Table 3.

$$E = \frac{\log_{16} 255}{3-1} \times \left(4 \times \frac{1}{16} + 4 \times \frac{2}{16} + 3 \times \frac{4}{16} + 4 \times \frac{5}{16}\right) \times \frac{1}{2} = \frac{44}{32} = 1.375$$

$$E_{15} = \frac{\log_m 255}{t-1} \times \left(\frac{1}{m} \times 1 + \frac{1}{m} \times 2^2 + \cdots + \frac{1}{m} \times (m-1)^2\right) \tag{18}$$

$$E_{16} = \frac{8/\alpha}{t-1} \times \left(\frac{1}{2^\alpha} \times 1 + \frac{1}{2^\alpha} \times 2^2 + \cdots + \frac{1}{2^\alpha} \times (2^\alpha - 1)^2\right).$$

6. Conclusion

This article focuses on the analysis of the reversible secret image sharing scheme based on steganography. In this article, we focus on discussing and analyzing the reversible privacy image sharing scheme based on the FEMD algorithm. On this basis, an improvement to the FEMD algorithm is proposed as a steganographic algorithm that can be implemented, because in the embedding process, our non-uniqueness of the overflow pixel processing has made the FEMB algorithm unable to complete the reversible image sharing scheme. In this article, we focus on whether the elements in the UI design can be effectively and efficiently used in actual applications. We have conducted an analysis of the feasibility of this, breaking the old concept, and being a UI designer we provide design categories that can be referred to. In this article, the most important and key research result we got is the ability to analyze four-dimensional time from the perspective of space and plane, and on this basis, we conducted a detailed analysis. We also use X, Y, Z, multi-dimensional coordinate axes, just like the Rubik's Cube that we commonly use in our lives, we compare it to a cubic nine-square grid. This requires us to get rid of the old copy model, in order to innovate in thinking, innovate a better visual communication interface, and better integrate the user's research interface design and interaction, which is also the pursuit of this article. To put it simply, we use the principle of Rubik's Cube in this. Each unit in the web page is formed by four spatial coordinates, and the pictures, texts, and colors in these spatial coordinates are expressed in what we mentioned earlier. In the artistic layout of and, in the vertical layout, we mainly express the reading level of colors, pictures, and text when users are reading. In the horizontal and vertical spatial layout, we use the original points, lines, and planes expressed in a better and more artistic way, so that users can get better senses. On this basis, we designed a new language using the improved FEMD algorithm, and proposed a reversible private image sharing scheme based on steganography. Through the experimental results, we can conclude that after improving the algorithm, we can obtain high-quality, high-privacy, and dense images. Applying this image to network transmission can greatly improve the security of the image in network transmission, higher

application value and market demand value, and higher practicability.

Data Availability

The data used to support the findings of this study are available from the corresponding author upon request.

Conflicts of Interest

The authors declare that they have no conflicts of interest.

References

[1] Y. Liu and Y. Liu, "Heterogeneous network multi ecological big data fusion method based on rotation forest," *Algorithms*, vol. 7, no. 3, pp. 978–981, 2021.

[2] A. Safi, "Improving the security of Internet of Things using encryption algorithms," *International Journal of Computer and Information Engineering*, vol. 11, no. 5, pp. 558–561, 2017.

[3] Y. Min, *Digital Image Processing*, China Machine Press, Beijing, China, 2006.

[4] C. Baur, "Ars Electronica and the media art economy," *Journal of Visual Art Practice*, vol. 19, no. 3, pp. 241–253, 2020.

[5] K. M. Dong and L. N. Dong, "Research on the application of environmental art design based on digital media technology," *Journal of Physics: Conference Series*, vol. 1915, no. 2, Article ID 22072, 2021.

[6] W. Latham, S. Todd, P. Todd, and L. Putnam, "Exhibiting mutator VR: procedural art evolves to virtual reality," *Leonardo*, vol. 54, no. 3, pp. 274–281, 2021.

[7] S. Jiang, D. Ye, J. Huang, Y. Shang, and Z. Zheng, "Smart-Steganogaphy: light-weight generative audio steganography model for smart embedding application," *Journal of Network and Computer Applications*, vol. 165, Article ID 102689, 2020.

[8] B. Jana, D. Giri, S. K. Mondal, and P. Pal, "Image steganography based on cellular automata," *International Journal of Pure and Apllied Mathematics*, vol. 83, no. 5, pp. 701–715, 2013.

[9] B. Li, M. Wang, J. Huang, and X. Li, "A new cost function forspatial image steganography," in *Proceedings of the Image Processing (ICIP) 2014 IEEE International Conference on*, pp. 4206–4210, IEEE, Paris, France, Octobar,2014.

[10] Z. Wang, Z. Qian, X. Zhang, M. Yang, and D. Ye, "On improving distortion functions for JPEG steganography," *IEEE Access*, vol. 6, Article ID 74917, 2018.

[11] B. Polaczyk, P. Chołda, and A. Jajszczyk, "Huffman coding inspired peer-to-peer multicasting," in *Proceedings of the 10th International Symposium on Electronics and Telecommunications (ISETC '12)*, Timisoara, Romania, November 2012.

[12] L. B. W. Ming Wang, L. Xiaolong Li, T. Shunquan Tan, and H. Jiwu Huang, "A strategy of clustering modification directions in spatial image steganography," *IEEE Transactions on Information Forensics and Security*, vol. 10, no. 9, pp. 1905–1917, 2015.

[13] Y. Yu and N. Yu, "Motion vector modification distortion analysis-based payload allocation for video steganography," *Journal of Visual Communication and Image Representation*, vol. 74, Article ID 102986, 2021.

[14] S. Wu, S. Zhong, and Y. Liu, "Deep residual learning for image steganalysis," *Multimedia Tools and Applications*, vol. 77, no. 9, Article ID 10437, 2018.

[15] H. Pan, Y. Lei, and C. Jian, "Research on digital image encryption algorithm based on double logistic chaotic map," *EURASIP Journal on Image and Video Processing*, vol. 2018, no. 1, Article ID 142, 2018.

[16] F. Tajeripour, M. Saberi, M. Rezaei, and Sh. Fekri-Ershad, "Texture Classification approach based on combination of random threshold vector technique and co-occurrence matrixes," in *Proceedings of the IEEE International Conference on Computer Science and Network Technology (ICCSNT)*, pp. 2303–2306, IEEE, Harbin, China, December 2011.

Hindawi
Mobile Information Systems
Volume 2022, Article ID 3340999, 10 pages
https://doi.org/10.1155/2022/3340999

Research Article

Voice Detection and Deep Learning Algorithms Application in Remote English Translation Classroom Monitoring

Zhenyu Niu

College of Foreign Languages, Anyang Normal University, Anyang, Henan, China

Correspondence should be addressed to Zhenyu Niu; 01355@aynu.edu.cn

Received 25 May 2022; Revised 20 June 2022; Accepted 7 July 2022; Published 21 July 2022

Academic Editor: Shadi Aljawarneh

With the continuous development of cellular networks, the traffic from voice services increases gradually. The wireless sensor network (WSN) is a distributed network consisting of a large number of peripheral nodes distributed in the surveillance area. The nodes in the network complete it in a self-organizing form, and the sink node collects the data from each sensor node. When sending data, the nodes near the receiver will quickly run out of energy and cannot perform further transmission tasks. The resulting "power supply emptiness" problem has a great impact on network performance. Therefore, the power consumption of the network must be considered when designing the WSN routing algorithm. In order to effectively improve students' academic performance and monitor students' teaching conditions, the classroom remote monitoring system places two cameras in the university's English translation classroom and uses technology to merge the information to execute the entire process. By recording the course, we can save the teacher's classroom content and the student's classroom performance and upload the recorded video in real time. In addition, the classroom remote monitoring system is a multiclient system, divided into teacher and student terminals. The user can log in, watch the video, and perform other necessary operations.

1. Introduction

The voice quality detection algorithm used in this article is a combination of the PESQ algorithm and the sine detection algorithm, which can help identify voice quality problems in different types of voice networks in more detail. By studying PESQ and sine analysis algorithms, a feasible mobile communication system optimization scheme is proposed. Study the algorithm principles and test plans for evaluating voice quality [1]. By analyzing the recommendations of the ITU-T algorithm for evaluating voice quality, it is possible to understand the scope and accuracy of common objective evaluation algorithms and choose an appropriate evaluation method [2]. Due to the heavy burden of subjective assessment, it is not suitable for daily work. Therefore, the voice quality assessment system uses the PESQ method to simulate the hearing process of the human ear to measure the perceptible voice quality and transmit the corresponding MOS value [3]. Wireless sensor network technology has been widely used in military, medical, and environmental monitoring fields, and is one of the most important technologies today. The wireless sensor network consists of a large number of small sensor nodes, which are randomly distributed in certain areas for data collection [4]. They have specific energy, storage capacity, communication capacity, and computing power. However, resources are limited, and traditional network protocols cannot be directly applied to wireless sensor networks. Therefore, it is very meaningful and valuable to study energy-efficient and efficient wireless sensor network routing protocols, and it is also one of the current research hotspots [5]. This article mainly starts from the energy-saving aspect and studies the routing protocol of wireless sensor networks. First, for the problems of poor convergence and uneven energy consumption of the HEED routing protocol, an OPFH routing protocol based on the OPTICS clustering algorithm is proposed [6]. The protocol first uses the OPTICS clustering algorithm to divide the network into multiple first-level clusters, and then simultaneously conducts cluster head elections in each first-level cluster; in the process of candidate cluster heads competing

to produce the final cluster head, the current energy and the distance to the base station are used as input parameters, and the competing cluster radius is used as the output parameter. Fuzzy logic control is used to obtain the optimal cluster radius. According to the obtained optimal cluster radius, the final cluster head is generated by competition, and finally, the cluster head nodes are established. Multihop routing mechanism to send data to the base station. Simulation experiments show that the energy consumption between clusters and within clusters is more balanced [7]. This effectively extends the life of the network. The remote monitoring system of English translation classroom usually consists of two parts. The top layer is the link layer, which is used to support application layer data requirements and related control of link-layer devices [8]. The main functions are video recording, video transmission, and camera control. The video collected on the link layer is sent to the host via Ethernet and the host can receive instructions on how to run the template matching algorithm. In addition, the host can control the camera through the processor. The bottom layer is the application layer that uses C# for programming and rents Alibaba Cloud servers to store data and videos. At the same time, we use CDN's complete site acceleration function to enable users to understand and watch videos in time and improve the round-trip speed of video data packets [9].

2. Related Work

The literature introduces the characteristics of WSN routing algorithms for mobile convergence and classifies and describes mobile strategies and data acquisition methods [10]. It describes some typical routing protocols based on mobile synchronization, distinguishes them from several aspects such as location detection, path planning, and data collection methods, and compares the performance of different typical routing protocols [11]. The literature introduces the problem of unreasonable cluster head selection and high-energy consumption of the LEACH algorithm in long-distance transmission and proposes an improvement plan [12]. In the improved algorithm, the role of the node is determined by two screenings, thus providing the preferred cluster head for high-energy nodes, while controlling the number and distribution of cluster heads [13]. Sink nodes calculate the shortest transmission path between clusters, compare the energy consumption of communication, and create routes between clusters based on the results. The literature describes the nature of the mobile WSN routing algorithm used for convergence. We propose an energy balance routing algorithm based on mobile receivers [14]. The algorithm starts with cluster split mode, data collection mode, and routing [15]. The cluster head is given by the receiver node, and the cluster is split according to the K-means algorithm. At the same time, according to different data delay requirements, combined with different data collection methods, the routing of the sink node is planned. The literature introduces various factors that affect voice quality in network operations and provides a corresponding test plan for each element of various voice quality defects [16]. The literature introduces the sine analysis algorithm, which can analyze the discrete sine sequence received by the receiver to determine whether it contains the transmitted sine wave, silent or intermittent [17]. By combining sine recognition algorithms and algorithms, it is possible to identify voice quality problems in different types of voice networks in more detail.

3. Voice Quality Detection and Wireless Sensor Network Model

3.1. Voice Quality Detection. Because the speech has the characteristics of short-term stability, it is divided into multiple small segments. This process is called framing. After framing, the endpoint detection problem is transformed into a frame-level speech/nonspeech (0/1) decision. The whole system is divided into training and testing phases, as shown in Figure 1.

In the training phase, training data and corresponding training targets need to be generated. Assuming that the interference noise is additive noise, the mixed speech can be directly obtained by adding the pure speech and the noise. We have the following:

$$x_t = s_t + n_t. \tag{1}$$

Average loss:

$$\mathscr{L}(\Theta) = \frac{1}{T}\sum_{t=1}^{T} L\left(f\left(X_{t,f};\Theta\right), y_t\right). \tag{2}$$

Fitting of the model to the data:

$$\widehat{\Theta} = \arg\min_{\theta} \frac{1}{T}\sum_{t=1}^{T} L\left(f\left(X_{t,f};\Theta\right), y_t\right). \tag{3}$$

For the binary classification problem of speech endpoint detection, cross-entropy is usually used as the loss function:

$$L = y_t \log \widehat{y}_t + (1 - y_t)\log\left(1 - \widehat{y}_t\right). \tag{4}$$

At present, the expressive ability of deep learning models has been continuously enhanced, gradually replacing the role of feature design and combination in the modeling process. The logarithmic amplitude spectrum is one of the simplest, most straightforward, and most commonly used features. Because the amplitude spectrum only transforms the speech in the time domain to the frequency domain, the method of using the amplitude spectrum as input can also be called an end-to-end method. The formula for calculating the amplitude spectrum is

$$\left|X_{t,f}\right| = \sqrt{X_{t,f}^2(\text{real}) + X_{t,f}^2(\text{imag})}. \tag{5}$$

The voice endpoint detection method based on deep learning regards VAD as a binary classification problem, and its calculation formula is

$$\text{ACC} = \frac{T}{T + F}. \tag{6}$$

In practical applications, the ratio of the voice part to the nonvoice part is usually not 1:1. In order to better evaluate

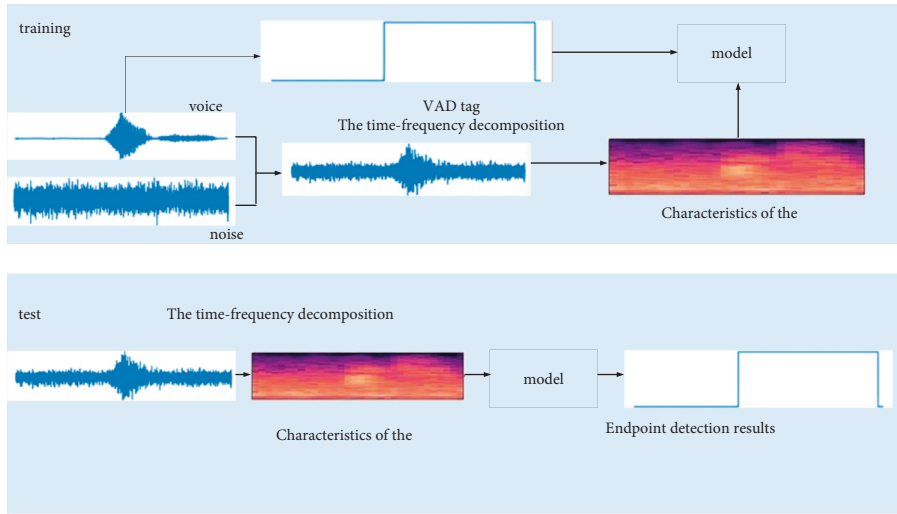

Figure 1: Flow chart of the deep learning voice endpoint detection system.

the performance of the model, usually refer to the voice hit rate (HIT) and false alarm rate (FA), shown as follows:

$$\text{HIT} = \frac{TP}{TP + FN}, \tag{7}$$

$$FA = \frac{FP}{FP + TN}. \tag{8}$$

Calculation formula for AUC is as follows:

$$\text{AUC} = \frac{\sum_{i=1}^{s} \text{rank}_i - M(M+1)/2}{M * N}. \tag{9}$$

All experiments in this article are performed on the TIMIT data set. TIMIT is a manually labeled data set, and it is easy to obtain training targets from the labeled word transcription files. In the label file of TIMIT, each sentence of speech has a corresponding word transcription file, and the file contains the time boundary of all words. Table 1 shows an example of a word transcription file, where the start time and the end time both represent the sampling points at the 16 kHz sampling rate. For example, the word "she" starts at the 9640th sample point and ends at the 12783rd sample point. We convert the time boundary into a label corresponding to the frame to get the training target.

Randomly select 2000 pure speech generation training sets from the TIMIT training set, and use the TIMIT core test set to generate the test set. The TIMIT core test set was recorded by 24 people, each with 8 sentences and a total of 192 sentences. These voices usually contain fewer silent segments. In order to balance the proportion of speech and nonspeech, in all experiments in this article, the selected speech is connected with a random length of the silent segment, so that the proportion of speech frames accounts for about 60%.

There are five types of noise for generating training speech: speech shape noise (SSN), noisy human voice (babble), factory noise (factory 1), destroyer power room noise (destroy engine), and destroyer operations room noise (destroyer operations room), the latter four noises are all

Table 1: Word transcription file.

Start time	Stop time	Word
9640	12783	She
12783	17103	Had
17103	18760	Your
18760	24104	Dark
24104	29179	Suit
29179	31880	In
31880	38568	Greasy
38568	45119	Wash
45624	51033	Water
52378	55461	All

from the NOISEX-92 data set. This combination has been proven to have a certain complementarity and can cover more noise scenes. In order to examine the performance of the model in various environments, in addition to the types of noise used in training, we also tested two types of noise that belong to the NOISEX-92 data set: another type of factory noise (factory 2) and pirate noise (buccaneer) and Two types of noise from the CHiME-4 data set: bus noise (bus) and street noise (street).

In order to ensure the independence of training noise and test noise, each noise is divided into two nonoverlapping parts to generate a training set and a test set. In order to maintain the diversity of samples, noise fragments are randomly cut from long noise before mixing. The signal-to-noise ratios of the generated training set are −5 dB and 0 dB, and the signal-to-noise ratios of the generated test set are −5 dB, 0 dB, and 5 dB. A total of 2000 (pure speech) × 5 (noise types) × 2 (signal-to-noise ratio) = 20000 pieces in the training set, and 10% in the verification set. In the end, the speech of the training set is about 30 hours. The trained and untrained noise is used to generate the test set. There are five types of training noise. The corresponding test voices are $192 \times 5 \times 3 = 2880$ pieces; there are four kinds of untrained noises, and the corresponding test voices are $192 \times 4 \times 3 = 2304$ pieces. Since the sampling rate of the

TIMIT data set is 16 kHz, all signals are resampled to 16 kHz before mixing, as shown in Table 2.

We compare the two-stage training CLDNN with four baseline systems, including one of the most commonly used statistical methods and three methods based on deep learning. The parameters of the model are shown in Table 2. Among them, SohnVAD represents the statistical method proposed by Sohn et al. In the table, T represents the number of frames, F represents the number of frequency bands, and T is 100 in the experiment. The input of all models is the characteristics of the current frame and the two frames before and after. This form of frame expansion provides the model with the most relevant context information for the current frame.

Since the two-stage training method can be regarded as an augmentation of the data, the better expression of the underlying convolution is due to the richer data patterns received, so we have verified all the methods on two scales of data. First, we conducted experiments on about 3 hours of training data. Table 3 lists the experimental results. The data shown in the table are the best results that the model can obtain under the same conditions using the same test set.

It can be seen from Table 3 that the statistical method SohnVAD performs worse than the deep learning method. LSTM shows better performance than CNN in all noise scenarios and a relative average increase of 2.02% and 7.44% in trained and untrained noise scenarios. Combining the advantages of CNN and LSTM, CLDNN is 10.49% higher than CNN in trained noise scenes, 8.29% higher than LSTM, and 11.99% and 4.22% higher in untrained noise scenes. Compared with the CLDNN baseline, the training method proposed in this article has a relative improvement of 3.08% in the trained noise scene and 1.48% in the untrained noise scene.

Figure 2 shows the ROC curve of each model tested in the trained noise scene and the untrained noise scene when the signal-to-noise ratio is 0 dB. The lower the false alarm rate (the smaller the abscissa), the better and the higher the hit rate (the larger the ordinate). Therefore, the more the ROC overall curve is to the upper left corner, the better the overall hit rate and false alarm rate of the system. The solid line in the curve represents the method proposed in this article, which has the best performance among the four methods.

Figure 3 shows the comparison between training data of different sizes. Compared with the model trained on 3 hours of data, when the training data is increased by 10 times, the improvement of CLDNN by the two-stage training method is reduced. It is foreseeable that when the amount of training data continues to increase, the gap between the two methods will be further reduced. The experiment proves that the two-stage training method has more advantages in small sample tasks.

3.2. Wireless Sensor Network. The trilateral positioning method is the most basic source node positioning algorithm. The basic idea is that when the distance from an unknown node to at least three anchor nodes is known, the geometric characteristics of the intersection of three circles at one point can be used to calculate its coordinates.

Then, there are the following equations:

$$\begin{cases} \sqrt{(x-x_a)^2+(x-x_a)^2} = l_a, \\ \sqrt{(x-x_b)^2+(x-x_b)^2} = l_b, \\ \sqrt{(x-x_c)^2+(x-x_c)^2} = l_c. \end{cases} \tag{10}$$

Calculating formula (10) shows that the coordinates of the unknown node O are

$$\begin{bmatrix} x \\ y \end{bmatrix} = \begin{bmatrix} 2(x_a-x_c) & 2(y_a-y_c) \\ 2(x_b-x_c) & 2(y_b-y_c) \end{bmatrix}^{-1} \begin{bmatrix} x_a^2-x_c^2+y_a^2-y_c^2+d_c^2-d_a^2 \\ x_b^2-x_c^2+y_b^2-y_c^2+d_c^2-d_b^2 \end{bmatrix}. \tag{11}$$

These variables should satisfy the following formula:

$$\begin{cases} (x-x_1)^2+(y-y_1)^2 = l_1^2 \\ \vdots \\ (x-x_n)^2+(y-y_n)^2 = l_n^2 \end{cases}. \tag{12}$$

Starting from the second line, each line is subtracted from the previous line to obtain

$$\begin{cases} x_1^2-x_n^2+2(x_1-x_n)x+y_1^2-y_n^2 \\ \quad -2(y_1-y_n)y = l_1^2-l_n^2, \\ x_{n-1}^2-x_n^2+2(x_{n-1}-x_n)x+y_{n-1}^2 \\ \quad -y_n^2-2(y_{n-1}-y_n)y = l_{n-1}^2-l_n^2. \end{cases} \tag{13}$$

Remember

$$B = \begin{bmatrix} x_1^2-x_n^2+y_1^2-y_n^2+l_n^2-l_1^2 \\ \vdots \\ x_{n-1}^2-x_n^2+y_{n-1}^2-y_n^2+l_n^2-l_{n-1}^2 \end{bmatrix}. \tag{14}$$

Then, the equation $AX = B$ can be obtained, so

$$X = \left(A^T A\right)^{-1} A^T B. \tag{15}$$

Then, the coordinates of node O can be estimated by the following formula:

$$(x_m, y_m) = \left(\frac{\sum_{m=1}^{M} x_m}{M}, \frac{\sum_{m=1}^{M} x_y}{M}\right). \tag{16}$$

The original LRMD model can be expressed as

$$\min_{U,V} \left\| M - UV^T \right\|_{\ell_p}. \tag{17}$$

The original LRMD can be transformed into a matrix reconstruction model by adding an orthogonal projection operator, which can be expressed as

$$\min_{U,V} \left\| P_\Omega\left(M - UV^T\right) \right\|_{\ell_p}. \tag{18}$$

Table 2: Detailed model parameters.

Model	Floor	Enter	Hyperparameter	Output
SohnVAD	—	$T \times F$	—	$T \times l$
CNN	Convolutional layer 1	40×5	Number of units 32; convolution kernel 3	38×32
	Convolutional layer 2	$38 * 32$	Number of units 64; convolution kernel 3	36×64
	Fully connected layer 1	2304	Number of units 64	64
	Fully connected layer 2	64	Number of units 1	1
LSTM	Long and short-term memory layer 1	$T \times 200$	Number of units 128	$T \times l.28$
	Long and short-term memory layer 2	$T \times l28$	Number of units 64	$T \times 64$
	Long and short-term memory layer 3	$T \times 64$	Number of units 1	$T \times l$
CLDNN	Convolutional layer 1	$T \times 40 \times 5$	Number of units 32; convolution kernel 3	$T \times 38 \times 32$
	Convolutional layer 2	$T \times 38 \times 32$	Number of units 64; convolution kernel 3	$T \times 36 \times 64$
	Long- and short-term memory layer	$T \times 2304$	Number of units 128;	$T \times 64$
	Fully connected layer	$T \times 64$	Number of units 1	$T \times l$
Proposed method	Same as CLDNN	Same as CLDNN	Same as CLDNN	Same as CLDNN

Table 3: Comparison of AUC indicators of voice endpoint detection models based on deep learning.

Signal-to-noise ratio	Types of trained noise				Untrained noise types			
	−5 dB	0 dB	5 dB	Average	−5 dB	0 dB	5 dB	Average
SohnVAD	56.13	62.83	68.51	62.49	65.14	70.97	76.77	70.96
CNN	75.71	82.84	87.04	81.86	71.12	77.62	83.71	77.48
LSTM	78.92	84.32	87.34	83.52	76.89	84.97	87.90	83.25
CLDNN	87.43	91.13	92.80	90.45	79.69	87.91	92.71	86.77
Proposed method	89.88	94.17	95.67	93.24	80.30	88.78	95.10	88.06

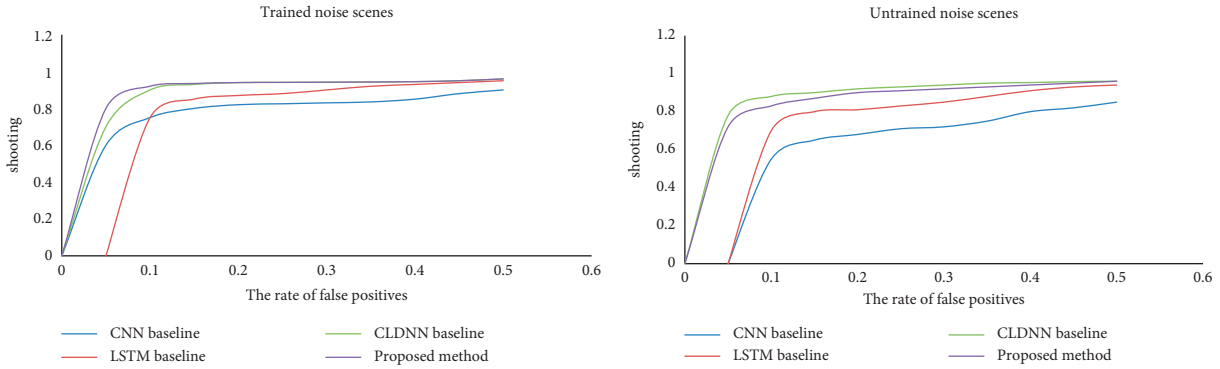

Figure 2: Comparison of ROC curves of various models.

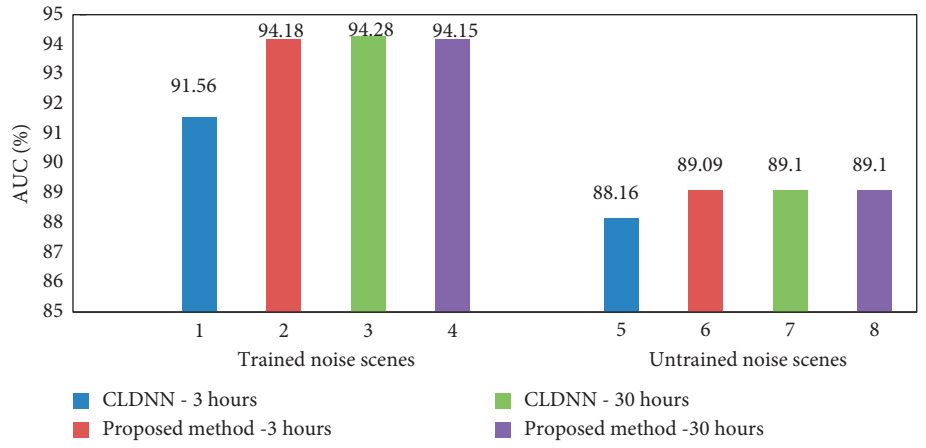

Figure 3: Comparison of model performance on training data of different scales.

We have the following:

$$\left[P_{\Omega}(M)\right]_{ij} = \begin{cases} M_{ij}, & (i,j) \in \Omega \\ 0, & \text{otherwise} \end{cases}. \tag{19}$$

It can be described as

$$\min_{U,V} \left\| P_{\Omega}\left(M - UV^{T}\right) \right\|_{MOG}. \tag{20}$$

The matrix X can be defined as

$$\|X\|_{2,1} = \sum_{i=1}^{m} \left(\sum_{j=1}^{n} X_{ij}^{2} \right)^{1/2}. \tag{21}$$

$$\|X\|_{p} = \left(\sum_{i=1}^{m} \sum_{j=1}^{n} \left| X_{ij} \right|^{p} \right)^{1/p}. \tag{22}$$

$$\|X\|_{F} = \left(\sum_{i=1}^{m} \sum_{j=1}^{n} X_{ij}^{2} \right)^{1/2}. \tag{23}$$

The nearest neighbor operator can be defined as

$$\text{prox}_{\tau F(X)}(M) = \arg\min_{X} \tau F(X) + \frac{\mu}{2}\|X - M\|_{F}^{2}. \tag{24}$$

The structural threshold operator is defined as

$$\text{prox}_{\tau \|X\|_{2,1}}(M) = \mathcal{J}_{\tau/\mu}(M). \tag{25}$$

4. Design and Application of the Remote English Translation Classroom Monitoring System

4.1. Demand Analysis of the Remote English Translation Classroom Monitoring System. Traditional classroom video surveillance only collects, transmits, and stores video data, and the video information can only be obtained through later viewing by relevant personnel. However, because the amount of video data is huge and contains a lot of irrelevant information, it takes a lot of manpower. In addition, manual viewing of video information is prone to misjudgment, so the classroom monitoring system needs to be further intelligent. Therefore, a video surveillance system that relies on artificial intelligence technology to identify abnormal behaviors in the classroom in real-time should be designed. In this article, the student's abnormal behavior recognition system is mainly divided into three parts, which are the embedded video data acquisition module, server intelligent processing module, and mobile phone APP alarm module. The server intelligent processing module mainly includes two parts: student and mobile phone target detection, and students' abnormal behavior recognition. This chapter puts forward the functional requirements of the system by analyzing the characteristics of the three abnormal behaviors of students in the classroom and then gives the overall design of the system.

Compared with an open environment or an indoor environment with a large flow of people, the video surveillance system in the classroom environment has unique environmental characteristics, that is, the flow of people is small, so the surveillance video can be obtained by video capture at a fixed position and a fixed angle. No need to consider tracking requirements. Through the analysis of the classroom environment, it is found that the first classroom is divided into regular classrooms and lecture rooms. The camera can be placed in the two corners of the classroom or in the middle of the classroom. After actual experiments, the latter was chosen for this design (taking into account the distortion of the side camera image), but under any of the abovementioned conditions, the camera position will not change. It should be noted that the camera's angle of view is best to look down at the students so that the camera can more clearly capture the movement information of each student. But despite this, some students will still be occluded, and when the length of the classroom exceeds 5 m, it has a smaller resolution for the student targets relatively close to the back of the classroom. In order to compensate the influence of classroom scene characteristics on behavior recognition, a higher resolution camera should be used in the system design. The resolution of the Logitech C270 camera can reach 1920×1080, which can compensate for the problems of occlusion and low resolution of the students behind. In the classroom scene, the fixed background target detection method is not suitable for this system, because the student's range of motion is narrow, and the placement of the object may change. Therefore, the images suitable for this design are selected from the COCO data set as the training data set.

In the classroom scenario, when students have abnormal behaviors of playing with mobile phones, there will be obvious mobile phone objects appearing in the image, and the mobile phone object is the closest to a certain student object. The student object's face is generally downward and part of the mobile phone object. The coincidence of the behavior and the duration of the behavior are generally more than 10 seconds. As for the behavior of sleeping in class, through image analysis, it is found that students' sitting posture has changed significantly. The most fundamental feature is that they can hardly see any facial features, and this state will last for a long time. Student communication is an abnormal behavior of multiple people at the same time. Generally, there are two or more students participating, one after the other, or one on the left and the other on the right. When this behavior occurs, the student's head will continue to rotate forward, backward, left, and right. The position of the student's entire body has undergone a major change, which exceeds the area of activity during normal lectures. The fundamental purpose of this system is to realize the recognition of abnormal behaviors of students in the classroom, but the recognition of abnormal behaviors is based on target detection. In order to achieve a more accurate recognition of abnormal behaviors, both the recall and accuracy of student target detection should reach more than 90%, and the recall and precision of small target mobile phones should both reach more than 85%.

The intelligent monitoring system designed in this article is mainly aimed at indoor collective activities such as meeting rooms, classrooms, and other places, and is mainly used to monitor the behavior of members under the situation of teachers teaching or leaders meeting. Because this type of scene is relatively small, the cost of its development must be low, so that the video surveillance system can be widely used. Based on the abovementioned reasons, this topic adopts a cost-effective embedded method for development. In addition, the use of wired network transmission makes networking easier in this type of scenario. The system should also have the performance of intelligent analysis, which can intelligently detect the relevant characters in the collected video. According to the characteristics and requirements of the classroom intelligent monitoring system, the system needs to meet the following requirements:

(1) The embedded camera must be able to realize a real-time collection of video data, video encoding, and transmission so that the terminal device can display video images without jams. Therefore, the embedded camera is required to collect video data at a higher sampling frequency.

(2) The embedded camera adopts digital, which is convenient for information transmission, storage, and processing, easy to connect with other communication equipment, and has strong compression potential, which can provide clearer video images. Due to its strong anti-interference ability, the image is less distorted.

(3) Data transmission is carried out through the wired network. Since the video data collected by the built-in camera must be transmitted through the network, the camera is connected to the router through a network cable in order to transmit the video data.

(4) With image analysis and processing capabilities, the collected video data is processed by behavior recognition algorithms, such as playing with mobile phones, sleeping, and communicating with each other. The behavior recognition algorithm detects the abovementioned behaviors and immediately transmits them to the teacher's mobile APP terminal, and the APP receives messages and realizes the alarm in the form of sound effects, vibration, and a pop-up message box.

(5) The server-side and mobile APPs have permission restrictions. When the teacher watches the monitoring screen received by the server and APP, he needs to enter the password when registering the server and APP. Only when the password is consistent with the registration password can he access the server and APP. In addition, when the administrator logs in to the server to process the received video data, it also needs to be consistent with the password during registration.

4.2. System Overall Framework Design. In order to enable the system to have the scalability of the number of users and the flexibility of the layout of the hardware facilities, the system chose to access the local area network, transplant the camera application on the ARM9 development board, and send the collected data to the server, and the server performs intelligence on the video data. The mobile APP can receive the identified abnormal behavior video data after communicating with each other by accessing the server, as shown in Figure 4.

According to the block diagram of the system, the system is mainly composed of an equipment terminal, router, internet, server intelligent detection module, and teacher's mobile APP terminal. This system uses the ARM-LINUX platform to collect video images using the video data collection module, sends the collected data to the server discovery module, and transmits the identification results of abnormal behavior to the teacher's mobile APP terminal.

Embedded camera module: under the ARM-LINUX platform, the video data is obtained through the V4L2 driver framework. Use the x264 video encoding library to implement H.264 encoding. Router: the main function is to connect the embedded camera to the network. Server intelligent detection module: it mainly uses FFmpeg and H.264 to decode the video data transmitted from the device terminal, YOLOv3 intelligent detection, and stores the video data for administrators and teachers to view after logging in.

Teachers' mobile phone APP terminal: receive the detection results of the server, such as detecting abnormal behavior of students, transmitting the image data to the APP, generating sound effects, vibrations, and pop-up message boxes at the same time. After seeing the alarm information, the teacher will check the image data received by the APP so you can locate a specific student.

4.3. System Development Environment Design. The following are the specific steps to build the environment:

(1) Install the virtual machine on the PC and then install the Ubuntu 12.04 version of the LINUX operating system on the virtual machine

(2) After entering the LINUX system, copy the compressed package to the LINUX system

(3) Decompress the cross-compiler compressed package through commands on the terminal of the LINUX system

(4) Configure the environment variables of the cross-compiler and check whether the cross-compiler is installed successfully

As we all know, for the LINUX system, there are very strict regulations and requirements on power consumption, functions, and costs. At the same time, it has a variety of different hardware interfaces to achieve strict management of the file system. In addition, it also has a series of different advantages, for example, easy to transplant, so the system has been generally welcomed by the industry.

Bootloader is the first program executed after the embedded device is powered on, and can read and write flash, initialize SDRAM, initialize clock, initialize serial port, etc.,

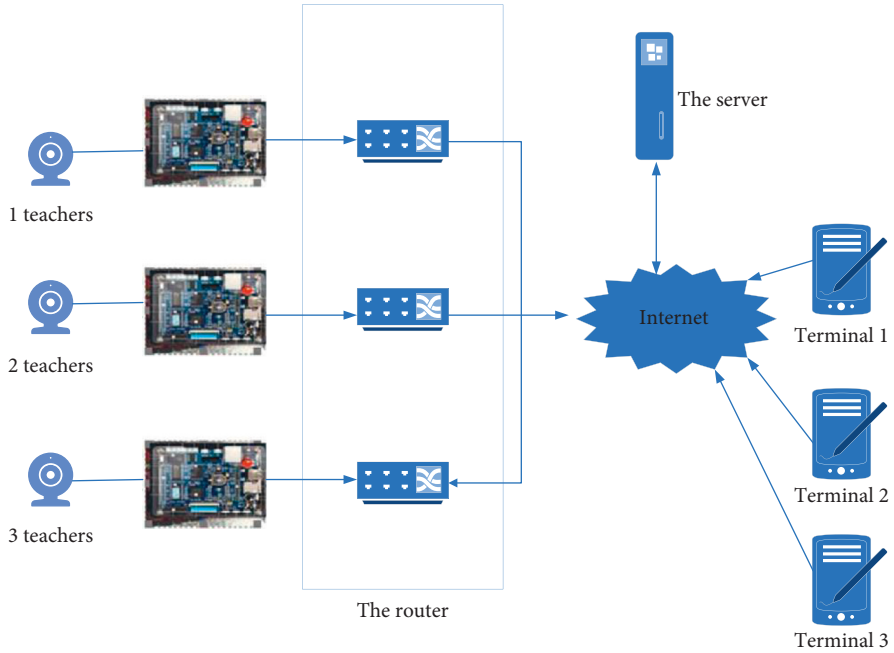

Figure 4: System frame diagram.

to achieve the function of starting the kernel. This article uses U-Boot 1.1.6, the specific operations are as follows:

(1) Download the U-Boot 1.1.6 version from a website, transfer it to the LINUX system, enter the directory, and decompress it through commands

(2) Download the patch file that matches U-Boot 1.1.6, transfers it to the LINUX system, and open the U-Boot patch by command

(3) Configure and compile U-Boot is configured through commands, and then make compiles

(4) Use the programming tool to program the compiled u-boot.bin file into the ARM development board

4.4. Video Capture Module Design. In order to make full use of LINUX system resources, the camera application originally designed uses the V4L2 interface to realize the collection of image data. The collection of image data is mainly divided into three steps, the first is the initialization operation of the image data collection, the second is the application for the operating space memory, and the last is the collection operation of the image data.

In the process of information transmission, the TCP/IP protocol is in a basic position, and it has a very common practical application in the internet field. For TCP/IP, it includes different levels, such as the hardware interface layer and transport layer. Through induction and summary, it can be concluded that TCP/IP has many advantages, and its basic structure is not complicated. This is because the protocol integrates the physical layer and data link layer of IOS to form a hardware interface layer and a session layer. And the presentation layer is included in the application layer.

In the design, the communication protocol between the embedded development card and the server uses the connection-oriented TCP protocol. The TCP protocol is used because the TCP protocol has the following characteristics:

(1) TCP is a connection-oriented protocol. Before data exchange is realized between the development board and the application program of the server, the connection must be established through three handshakes, and the link is always occupied during the communication again. Until the data exchange is completed, the two parties will dismantle the link through four waves of hands.

(2) TCP has the characteristics of high reliability of data transmission. After the connection between the development board and the server is established, the development board will send new data to the server only after the server receives the correct data. If the development board does not receive the confirmation message from the server, the development board will retransmit the data until the server sends back the confirmation message or the message is sent over time.

(3) TCP is a full-duplex communication protocol. The development board and the server can send information to each other at the same time.

(4) TCP has the characteristics of sliding window control. TCP can determine the transmitted data traffic according to specific network conditions.

Table 4: Embedded core board configuration parameters.

Configuration	Parameter
CPU processor	S3C2440, stable maximum frequency 400 MH
SDRAM	64 MB
NANDFLASH	256 MB
NORFLASH	2 MB
Core power	1.25 V
USB camera	Logitech C270
Embedded operating system	LINUX2.6.22.6 kernel version

Table 5: Behavior detection server configuration parameters.

Configuration	Parameter
CPU	i79700k
GPU	GTX1080
System memory	16G DDR4
GPU memory	8 G
Power	2 kW
Storage	500 G

4.5. System Test. The peripheral equipment and embedded system of the core board, as well as the video data acquisition application program run on TQ2440. The specific configuration parameters of the core board are shown in Table 4.

Behavior detection server: considering real-time requirements, the classroom behavior detection and recognition part cannot be directly run on the mobile platform, so this article uses the upper computer-side server to implement the main algorithm part of the classroom behavior detection and recognition. The server uses i79700CPU and GTX1080GPU as the core computing unit and uses SSH to communicate with the mobile phone APP. The specific parameters are shown in Table 5.

5. Conclusion

In recent years, considerable progress has been made in the objective evaluation of voice quality testing, but there are still many problems to be resolved in the objective evaluation of voice quality, such as valuation principles and valuation methods. With the support of the VQIT (mobile internet voice quality test rating system)project, this article first introduces the needs analysis of remote English translation courses, focusing on the study of language quality assessment systems and measures to ensure language quality. When implementing requirements analysis, start with two parts: functional requirements analysis and nonfunctional requirements analysis, and then decompose each functional module. In the analysis of functional requirements, the main function points are divided into nine parts: video recording, video transmission, camera control, registration, video search, teacher query, student information, course query, and personal management. The analysis of nonfunctional requirements is described from four aspects: scalability, performance requirements, maintainability, and security.

Data Availability

The data used to support the findings of this study is available from the author upon request.

Conflicts of Interest

The author declares no conflicts of interest.

References

[1] C. Drioli, G. Tisato, P. Cosi, and F. Tesser, "Emotions and voice quality: experiments with sinusoidal modeling," in *Proceedings of the ISCA Tutorial and Research Workshop on Voice Quality: Functions, Analysis and Synthesis (VOQUAL '03)*, pp. 127–132, ISCA, Geneva, Switzerland, August 2003.

[2] C. Gobl, E. Bennett, and A. Ní Chasaide, "Expressive synthesis: how crucial is voice quality?" *Proceedings of the IEEE Workshop on Speech Synthesis*, vol. 11-13, pp. 91–94, 2002.

[3] Y. Stylianou, J. Laroche, and E. Moulines, "High-quality speech modification based on a harmonic + noise model," in *Proceedings of the European Conference on Speech Communication and Technology*, pp. 451–454, Eurospeech '95, Minneapolis, MN, USA, 1995.

[4] M. H. Anisi, A. H. Abdullah, S. A. Razak, and M. A. Ngadi, "Overview of Data routing approaches for wireless sensor networks," *Sensors*, vol. 12, no. 4, pp. 3964–3996, 2012.

[5] T. Çevik and A. H. Zaim, "EETBR: energy efficient token-based routing for wireless sensor networks," *Turkish Journal of Electrical Engineering and Computer Sciences*, vol. 21, no. 2, pp. 513–526, 2013.

[6] O. Zytoune, Y. Fakhri, and D. Aboutajdine, "A fairly balanced clustering algorithm for routing in wireless sensor networks," *Sensor Review*, vol. 30, no. 3, pp. 242–249, 2010.

[7] A. Farouk, M. Zakaria, A. Megahed, and F. A. Omara, "A generalized architecture of quantum secure direct communication for N disjointed users with authentication," *Scientific Reports*, vol. 5, no. 1, p. 16080, 2015.

[8] G. Ferrari, M. Martalò, and R. Pagliari, "Decentralized detection in clustered sensor networks," *IEEE Transactions on Aerospace and Electronic Systems*, vol. 47, no. 2, pp. 959–973, 2011.

[9] G. J. Pottie and W. J. Kaiser, "Wireless integrated network sensors," *Communications of the ACM*, vol. 43, no. 5, pp. 51–58, 2000.

[10] G. Ferrari, M. Martalò, and A. Abrardo, "Information fusion in wireless sensor networks with source correlation," *Information Fusion*, vol. 15, no. 1, pp. 80–89, 2014.

[11] A. Pranali, N. Girigosavi, and G. Palan, "A mac protocol with interference avoidance mechanism for wireless sensor network," in *Proceedings of the SARC-IRAJ International Conference*, pp. 62–67, IJIEEE, Pune, India, June 2013.

[12] L. Tan, F. Ge, J. Li, and J. Kato, "HCEP: a hybrid cluster-based energy-efficient protocol for wireless sensor networks," *International Journal of Sensor Networks*, vol. 5, no. 2, p. 67, 2009.

[13] M. Naseri, M. A. Raji, M. R. Hantehzadeh, A. Farouk, A. Boochani, and S. Solaymani, "A scheme for secure quantum communication network with authentication using GHZ-like states and cluster states controlled teleportation," *Quantum Information Processing*, vol. 14, no. 11, pp. 4279–4295, 2015.

[14] S. Brienza, D. de Guglielmo, G. Anastasi, M. Conti, and V. Neri, "Strategies for optimal MAC parameter setting in

IEEE 802.15.4 wireless sensor networks: a performance comparison," in *Proceedings of the 18th IEEE Symposium on Computers and Communications (ISCC '13)*, pp. 898–903, IEEE, Split, Croatia, July 2013.

[15] S. Pollin, M. Ergen, S. C. Ergen et al., "Performance analysis of slotted carrier sense IEEE 802.15.4 medium access layer," *IEEE Transactions on Wireless Communications*, vol. 7, no. 9, pp. 3359–3371, 2008.

[16] P. Boersma, "Praat, a system for doing phonetics by computer," *Glot International*, vol. 5, no. 9-10, pp. 341–345, 2001.

[17] O. Turk, M. Schröder, B. Bozkurt, and L. M. Arslan, "Voice quality interpolation for emotional text-to-speech synthesis," in *Proceedings of the 9th European Conference on Speech Communication and Technology*, pp. 797–800, INTERSPEECH, Lisbon, Portugal, September 2005.

Hindawi
Mobile Information Systems
Volume 2022, Article ID 9050406, 7 pages
https://doi.org/10.1155/2022/9050406

Research Article

Surrounding Environment and Civil Airport Fire Emergency Management Based on Big Data Simulation

Jingyun Jia, Xiantao Chen, and Qiang Sun

Civil Aviation Flight University of China, Guanghan 618300, Sichuan, China

Correspondence should be addressed to Jingyun Jia; jiajingyun@cafuc.edu.cn

Received 21 May 2022; Revised 24 June 2022; Accepted 5 July 2022; Published 20 July 2022

Academic Editor: Shadi Aljawarneh

The new generation of information and communication technologies represented by the Internet of Things, big data, and cloud computing are developing rapidly. Through continuous integration with other emerging technologies, the Internet of Things technology accelerates its penetration into the fields of smart medicine, new energy, and materials. In this article, we will explore the airport peripheral environment and civil airport fire emergency management. In airport emergency management, bird strike and fire management are the most frequent problems. Bird strikes most often occur in aircraft take-off, taxi, and landing areas. Therefore, the study of airport environmental characteristics is particularly important. In order to improve the emergency support capability of the civil airport fire department and the level of airport operation support, it is necessary to clarify the factors that affect the emergency support capability of the airport fire department. This article is based on the research of the airport surrounding environment of Big Data Internet of Things and applies it to the research of civil airport fire emergency management, which improves the emergency ability of airport firefighters.

1. Introduction

"Big data" has become a buzzword in today's production and people's lives. Everywhere, such as mobile communication, website access, microblog news, video uploading, product generation, and scientific experiments, social and commercial activities will continue to generate various types of data [1]. The research value of big data is huge, especially when big data is integrated into today's Internet of Things, the integration of big data and the Internet of Things will surely elevate the intelligence of human society to a new level, and its development prospects are unlimited [2]. Nowadays, the Internet of Things is widely popularized, and the amount of big data has increased sharply. The integration of the Internet of Things and big data has become an inevitable trend in the development of various disciplines [3]. In this article, we will explore how big data affects the Internet of Things and how it integrates with daily production and life applications [4]. "Bird strike" is the abbreviation for safety accidents caused by planes colliding with birds during take-off, landing, or flight. It is also called "bird strike." Today, there are more than 10,000 bird strikes in the world every year, and the International Aviation Federation has upgraded bird strike disasters to category "A" aviation disasters. This article examines more than 30 existing flights in large civil airports [5]. First, it studies the environmental characteristics of the airport. The climate in the airport is suitable and the bird resources are relatively abundant [6]. Therefore, the bird community structure and environmental structure of the airport and its surrounding areas are studied. It is very necessary to conduct research. It is necessary to analyze the factors that may cause bird strikes in the airport and its nearby areas through the research results, find out corresponding preventive measures, and improve the flight safety factor of the airport [7]. According to the statistics of the International Civil Aviation Organization, the number of aircraft accidents during the take-off, taxiing, and landing phases accounted for more than 60% of the total number of aviation accidents [8]. In the above stages, the emergency response task of aircraft emergencies is mainly undertaken by the airport fire rescue department, and the emergency protection ability of airport firefighters is the key to ensuring

the smooth implementation of rescue activities [9, 10]. The results show that the most important impact on civil airport fire emergency management capabilities is the basic quality, followed by the professional quality, professional skills, and professional knowledge of firefighters. By attaching importance to these factors, our fire management capabilities will be improved [11, 12].

2. Materials and Methods

2.1. Overview of the Study Area. The research airport is 45 km away from the city. The traffic around the airport is developed. There is National Highway 2513 on the north side, connecting neighboring provinces and surrounding areas; on the east side, there is Provincial Highway 324, connecting the surrounding districts and cities; in front of the gate is 104 National Road, connecting the urban area and certain areas. As a large-scale civil airport, the airport is also the central airport of the economic zone. It can radiate air travel for the surrounding population of 100 km, including 20 prefecture-level cities, with a radiating population of 120 million. The research airport has an important influence on the economic development of the surrounding area. The airport covers an area of about 3800 mu, and it can transport up to 1 million passengers every year.

Most of the east side of the airport is a residential area. There are no farms in the village. The farmland is mainly planted with seasonal crops. There are several small forests scattered around the village. There is a lotus pond in the northeast corner with sufficient water resources and less vegetation. Close to the airport is the provincial highway and the abandoned Yellow River. The abandoned Yellow River is located in the east of the airport. The flow direction of the river section within the observation range is a U-shaped turning from northwest to southeast to southwest to northeast. The closest distance to the easternmost part of the airport is about 300 m, within the observation range. The widest part of the river is about 100 m. The riverbank is flat and the vegetation is lush, mainly cherry trees, willow trees, neem trees, and various weeds. There are no duck and goose farms in the observation area of the river.

Most of the airport fence is farmland and woods during the week, and most of the farmland is planted with seasonal crops. There is a forest close to the north and west of the airport fence, with an area of about 0.027 km^2, and the main tree species is poplar. There is a small river running north-south beside the forest, with a width of about 20 m. There is an airport drain in the middle of the north side of the fence. The sanitary conditions are poor and there is no cover. It is easy to breed mosquitoes and attract birds to forage. There is a nursery near the middle on the north side of the fence, which is roughly east-west and covers an area of about 0.253 km^2. The nursery mainly contains many kinds and numbers of plants, which provides a place for birds to forage and hide. There is a vegetable greenhouse on the east side of the nursery, which is enclosed. To the east of the north side of the fence is an orchard, covering an area of about 0.027 km^2. It is mainly planted with pear trees. Due to manual management, there are fewer weeds in the orchard. The expansion and construction in the southeast and southwest affected bird activities and brought some impact to the investigation.

The airport consists of a passenger waiting hall, an internal flight area, and an office area. The concrete pavement in the flight area of the airport has runways, taxiways, connection roads, patrol roads, etc., and the rest are lawns. The flight area is east-west, with a total length of 3600 m, and the light belts on the east and west sides are local dominant grass species. The flight area is dominated by lawns. The lawn vegetation composition is basically the local dominant grass species. Two rows of east-west bird blocking nets are arranged on the north side of the lawn near the fence. The bird blocking nets are parallel to the fence and perpendicular to the ground. The bird blocking nets are 3000 m in length, the height is 5 m, and the mesh size is 40 cm^2. The grass species in the lawn are mainly local dominant grass species with many species, and more insects in summer. The grass height in the lawn is basically kept below 20 cm, and the airport regularly organizes the spraying of pesticides on the lawn, including pesticides and herbicides. There are exposed drainage ditches near the fence in the north of the lawn, and the internal drainage ditches are all dark water ditches, which facilitate the drainage of the accumulated water in the flight area to the airport, and are covered by a linear drainage cover. The office area in the airport has a large green area and rich vegetation.

2.2. Research Methods. The Internet of Things is known as the third wave of development in the global information industry after computers and the Internet [13]. The International Telecommunication Union formally expounded the concept of the Internet of Things in its report. Any object in the Internet of Things exchanges information and communication anytime and anywhere to truly create a network of precise positioning, precise identification, and intelligent monitoring and management [14, 15].

The development of the Internet of Things is based on the expansion and extension of the Internet, and the ultimate development goal is comprehensive perception, reliable transmission, and intelligent processing [16]. Among them, the network layer is the link of information exchange between the perception layer and the application layer. Through the processing and exchange of sensor information, the application layer provides powerful resource support for the processing of different enterprises and truly realizes the intelligence and informatization of different industries. From July 2019 to June 2020, the transect method was used to collect statistics on birds and environmental changes in different seasons within an average of 5 km around Guanyin airport and its surrounding areas. The survey frequency was twice a month. The observed environmental factors include seasonal environmental factors, such as the types and growth status of crops in farmland, the area occupied, the vegetation composition, and change patterns of grassland and woodland; there are also factors that do not change with the seasons, such as rivers, ponds, and residential areas. Environmental factors are mainly measured and recorded, combined with interview methods.

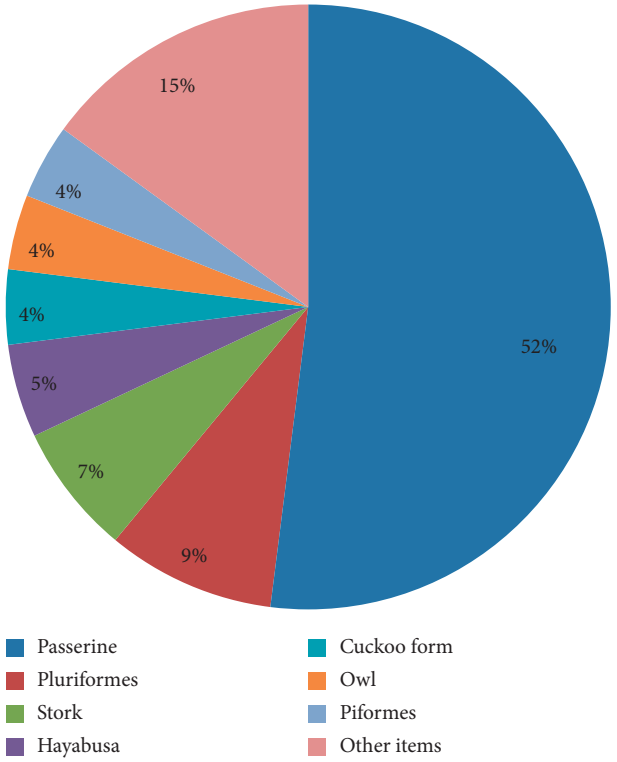

Figure 1: The species of birds in each order at the airport and surrounding areas.

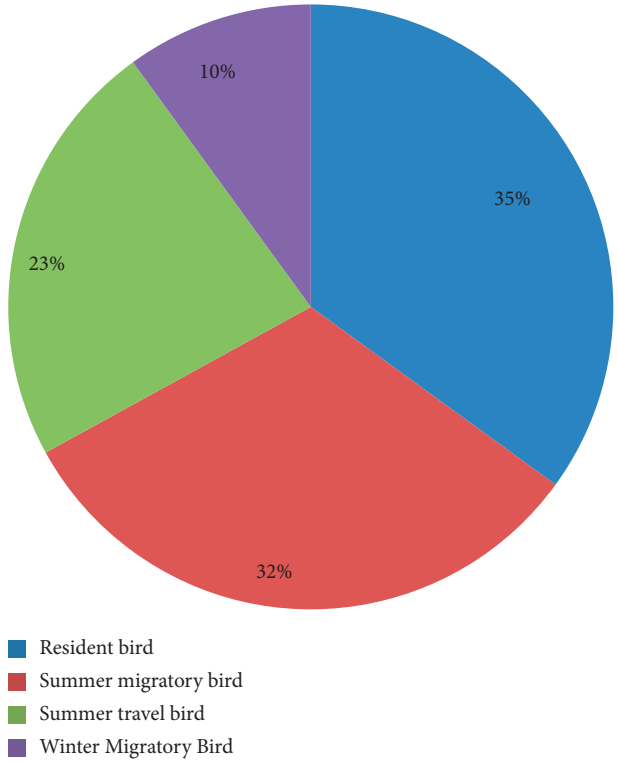

Figure 2: Airport and surrounding bird residence types.

3. Results

A total of 75 species of birds in 14 orders, 35 families, and 14 orders were found in the first anniversary of the airport from July 2019 to June 2020. There are 39 species in 19 families of Passeriformes, 52% of the total number of species, ranking first in the number of species; 3 families and 7 species of Platymoides, accounting for about 9.33% of the total number of species, ranking second in number of species; Gruciformes: there are 5 species in 1 family, and the number of species accounts for about 6.67% of the total, ranking third; the number of species of the remaining 11 orders is less than 5 species. See Figure 1 for the ratio of the number of different mesh types.

The airport is located in the southeastern part of the North China Plain. The number of resident birds is the largest, with 26 species, accounting for about 35% of the total; summer migratory birds are second, with 24 species, accounting for 32% of the total; and the third, 17 species of migratory birds, accounting for about 23% of the total; winter migratory birds are the least, 8 species, accounting for about 10% of the total. Resident birds and summer migratory birds are an important part of the birds around Guanyin Airport. Breeding birds accounted for 67% of the total number of species, and nonbreeding birds accounted for 33% of the total number of species (see Figure 2).

The types and proportions of 75 species of birds around the airport are shown in Figure 3.

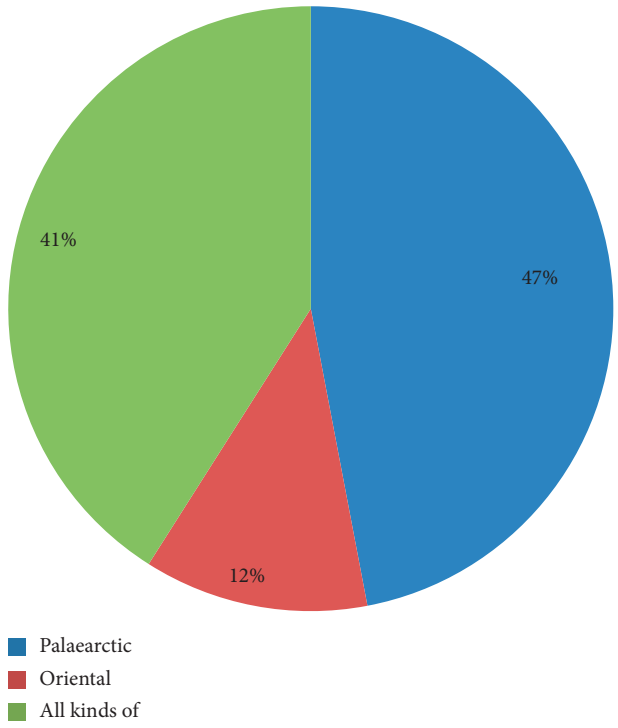

Figure 3: The airport and surrounding bird fauna map.

According to the relative importance value, there are 11 species of most important birds, accounting for 15% of the total number of species; 10 species of important birds, accounting for 13% of the total number of species; 22 species of less important birds, accounting for the 29% of the total number of species; 32 species of least important birds,

accounting for 43% of the total number of species. The details are shown in Figure 4:

Calculating the comprehensive risk of bird strikes for the birds in the airport fence shows that there are as many as 6 species of birds with $R > 0.7$. In this survey of the airport and its surrounding areas, a total of 75 species of birds were recorded. Through calculations, the relevant indices of bird community structure in each season were calculated and analyzed. See Table 1 for details.

The diversity index of the bird community in spring and autumn is high, the homogeneity index is high, and the degree of dominance is low. The community structure in spring and autumn is relatively stable, and the individual distribution among species is relatively even. Because it is an airport, the status of dominant species cannot be determined. The scale of bird migration in this area is not large, and the impact on the local bird community structure is small. Comparing spring and autumn, the community diversity index in spring was higher than that in autumn, and the community structure in spring was more stable than that in autumn. It is speculated that part of the reason is that there are more migratory birds in autumn than in spring. According to statistics, 8 species of migratory birds can be observed in spring, accounting for 2.5% of the total in spring. There are 14 species of migratory birds observed in autumn, accounting for 3.6% of autumn. The number of migratory birds observed in spring is lower than that in autumn. Among migratory birds, this is consistent with the observed results. In summer and winter, the diversity index is low, the homogeneity index is low, and the dominance index is high, indicating that the social structure is relatively unstable in summer and winter, and the dominant species are obvious. If we compare the diversity index of summer and winter communities, we can see that the diversity index in winter is higher than that in summer, and the community structure in winter is more stable than in summer; in winter, the number of species and birds decreases, and the distribution of individuals among different species is more even.

In the seven habitats divided by the airport, the diversity index is arranged from largest to smallest: nursery, water area, farmland, woodland, grassland, breeding area, and residential area. See Table 2 for the relevant indices of the community structure of each habitat.

The nursery structure is more complex, including trees and low shrubs. Most birds build nests on trees. Trees provide a habitat for birds, low shrubs provide a shelter for birds, and there are also seed-bearing weeds, which provide a food source for birds. The main plants in the nursery are ginkgo, eucommia, rose, cocklebur, bermudagrass, *Imperata cylindrica*, and other vines. In addition, there is sufficient water in the nursery to provide a water source for the survival of birds. The structural levels of this area are relatively rich, and the vegetation at different heights meets the habitat and survival requirements of different birds. Therefore, the nursery habitat is the most stable habitat type among the 7 habitats in Guanyin Airport and its surrounding areas.

The dominant species of birds in each plot are shown in Table 3.

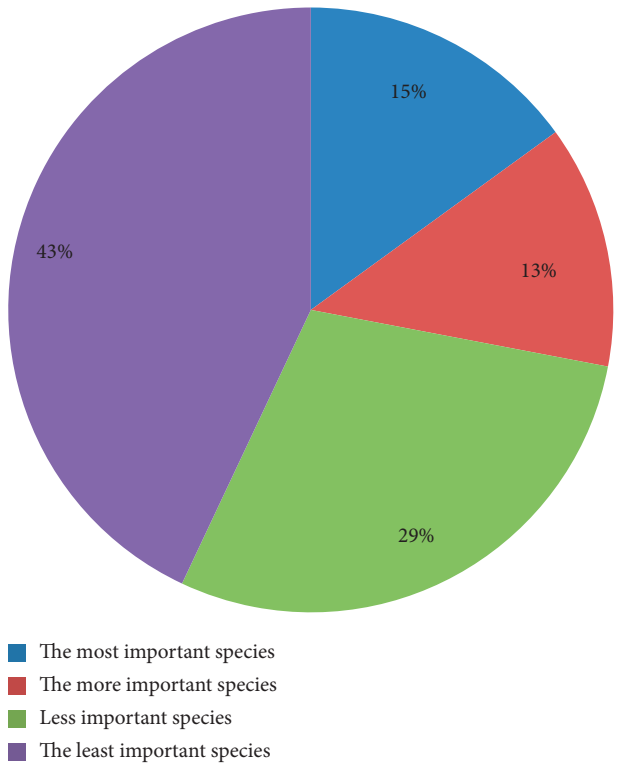

Figure 4: The relative importance of the airport and surrounding birds.

The composition of birds in different areas has a certain similarity. Among them, the similarity coefficient of plot 1 and plot 4 is the highest, and there are 34 common species; the similarity coefficient of plot 1 and plot 5 is the lowest, with 19 common species, as shown in Table 4.

Airport birds have different daily activity rhythms in different seasons, as shown in Figure 5.

There are significant differences in the daily activity frequency of birds in summer, as shown in Figure 6.

4. Discussion

4.1. Analysis of Influencing Factors of Civil Airport Fire Emergency. According to the basic rules of the airport fire department, the competency requirements of some airport firefighters were analyzed in detail. In the case of emergency aircraft rescue, firefighters must not only extinguish the affected aircraft but also provide basic medical assistance to the wounded, and use the knowledge of the fire brigade's emergency response capabilities in other areas. The multiple interactions between the commander and the airport firefighter finally determine the main factors that affect the firefighter's airport emergency response capability.

In recent years, the incidence and losses of fires in China have been increasing year by year, and the problem of a small number of firefighters and insufficient firefighters skills in China has gradually emerged. Overall, there is still a big gap between the number of firefighters in China and industrialized countries. Due to the lack of active firefighters, it is very necessary to organize full-time firefighters in areas far

Table 1: Bird community structure in different seasons in and around the airport.

Season	Diversity index	Evenness index	Dominance index	Average density (only/ha)
Spring	2.3594	0.6952	0.1384	1.2624
Summer	2.1352	0.3544	0.1646	3.1586
Autumn	2.3351	0.9575	0.1573	3.1358
Winter	2.4853	0.6843	0.1694	1.2568

Table 2: Bird community structure in different habitats at the airport and surrounding areas.

Habitat type	Diversity index	Evenness index	Dominance index
Nursery	2.6957	0.6584	0.1598
Farmland	2.3648	0.9755	0.1574
Grassland	1.9546	0.6824	0.6553
Woodland	1.3955	0.4687	0.2494
Breeding area	1.6844	0.4983	0.3614
Waters	2.1976	0.4586	0.1558
Residential area	1.5863	0.2392	0.3466

Table 3: The distribution of birds.

Plot	Number of species/species	Density/(only/hm^2)	Activity frequency (%)	Diversity index	Uniformity index	Advantage types
Plot 1	16.42 ± 1.45a	37.46 ± 10.45b	2.02 ± 0.34ab	1.33 ± 0.74b	0.14 ± 0.36b	Sparrow, goldfinch
Plot 2	9.51 ± 0.35b	9.35 ± 3.47b	1.12 ± 0.41ab	1.76 ± 0.36b	0.99 ± 0.05a	House swallow, sparrow, skylark, goldfinch, and magpie
Plot 3	9.64 ± 0.46b	7.95 ± 2.46b	0.42 ± 0.78ab	1.37 ± 0.18b	0.34 ± 0.06ac	House swallows, sparrows, bald crows, skylarks, and magpies
Plot 4	16.43 ± 1.35a	19.53 ± 3.45b	2.61 ± 0.47a	1.45 ± 0.26b	0.35 ± 0.45bc	House swallow, sparrow, and gray magpie
Plot 5	7.94 ± 0.17b	8.34 ± 1.54b	0.63 ± 0.07b	1.27 ± 0.17b	0.58 ± 0.64a	Sparrow, skylark, goldfinch, house swallow, and magpie
Plot 6	14.02 ± 1.65a	77.48 ± 11.58a	1.63 ± 0.23a	1.85 ± 0.07a	0.68 ± 0.01a	Sparrows, gray magpies, magpies, bead-necked turtledoves, goldfinches, and house swallows

Table 4: Similarity of bird spatial composition.

	Plot 1	Plot 2	Plot 3	Plot 4	Plot 5	Plot 6
Plot 1	—	0.652	0.644	0.796	0.578	0.794
Plot 2	22	—	0.734	0.675	0.764	0.646
Plot 3	28	22	—	0.657	0.684	0.643
Plot 4	37	22	25	—	0.622	0.752
Plot 5	19	17	18	19	—	0.651
Plot 6	33	20	23	29	18	—

away from many professional companies and the Chinese fire department, especially in key locations such as airports. Full-time firefighters not only have the opportunity to extinguish the first fire of the unit, but can also provide super-regional support and excellent protection for fire rescue. The same full-time firefighter also has many shortcomings, such as the vitality and combat effectiveness of the team is severely limited, unable to meet the requirements of large-scale fire rescue.

With the continuous development of China's economy and the issuance of national policies, China's trade exchanges with other countries have become more and more frequent. Civil aviation has also developed rapidly due to its large transportation volume and fast transportation speed. The importance of the fire brigade, which is an important part of the airport's safe operation, has gradually become prominent, and it has received more and more attention from the Civil Aviation Administration, airlines, and

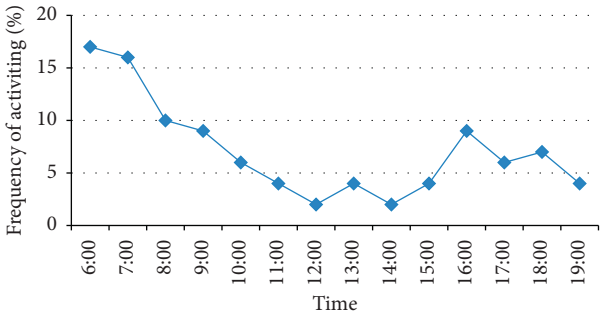

Figure 5: The daily activity rhythm of birds in spring.

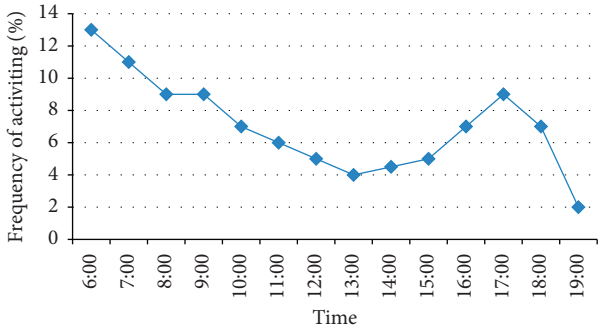

Figure 6: Daily activity rhythm of birds in summer.

airports. Therefore, the ability of airport firefighters is also a great challenge, and how to improve the emergency support ability of airport firefighters is also the focus of all aspects.

4.2. Fire Emergency Management Strategy for Civil Airports. The improper allocation of emergency resources in small and medium airports is not caused by unilateral dereliction of duty by the airport management department. This includes improper government regulations and improper airport resettlement. Therefore, to solve the problem of insufficient allocation of emergency resources in small and medium airports, the joint efforts of civil aviation management departments, local governments, and airports are still required.

Regulations and standards must conform to China's national conditions. If the highest-level aircraft at the airport has less than 700 take-offs and landings in the busiest three months, the fire and emergency protection level of the highest-level aircraft can be reduced by up to one level. No matter how big the airport is, whether it is crowded or not, aviation accidents will happen, but the possibility of occurrence is very small or unlikely; aircraft accidents happen on the same type of aircraft, regardless of the size of the airport, whether it is congested or not, in terms of emergency response time and handling methods no difference. Therefore, it is not appropriate to use airport congestion as compensation for fire safety and emergency rescue protection levels but to consider the response time and protection capabilities of airport fire protection and emergency rescue services as compensation.

Utilize the resources of the airport premises. For small and medium airports in operation, it is recommended to sign an airport rescue contract or local emergency rescue plan, and clarify the responsibilities and obligations of local government agencies, companies, and unit camps in accordance with relevant regulations. Utilize emergency resources from ministries, enterprises, and local government camps to reduce or exempt emergency resource allocation that can be provided by local government agreements and emergency rescue plans, reduce insufficient small-scale resource allocation, reduce resource allocation pressure, avoid resource duplication, and eliminate energy waste. Improve the airport rescue system. The airport undertakes the main task of emergency rescue, improves the emergency rescue plan, clarifies the responsibilities and obligations of all parties, and actively allocates emergency resources to various local government agencies, enterprises, and institutions. In terms of emergency resource allocation, emergency training and education, local government departments, and enterprise troops should provide maximum support to comprehensively improve the comprehensive emergency rescue level of airport rescue personnel and minimize property losses.

5. Conclusion

The current era is an information era, and big data is the key word of this era. Through the integration of big data and the Internet of Things, human society has reached an unprecedented level of intelligence, which has brought unprecedented convenience to people's production and lives. At the same time, it briefly introduces the integration, management, and technical framework in data processing. China is rich in bird resources and poses a great threat to flight safety. With the emphasis on the ecological environment in recent years, we must pay attention to the impact on the ecological environment while carrying out bird strikes. How to balance bird strike prevention and protection of the ecological environment has become an important difficulty. After sorting out the data from the airport, this paper uses various analysis methods to effectively analyze the community structure in each season and habitat. China has not yet established target standards for the training and skill assessment of airport firefighters, and cannot effectively control some aircraft emergencies in a timely and effective manner. Therefore, analyzing the factors that affect the emergency response capability of the airport fire brigade and determining the degree of influence of each factor is of great significance for improving the airport's operational security level.

Data Availability

The data used to support the findings of this study are available from the corresponding author upon request.

Conflicts of Interest

The authors declare that they have no conflicts of interest.

Acknowledgments

This paper was supported by the General Program of Civil Aviation Flight University of China (Grant no. J2019-029).

References

[1] T. Xiong, "Research on the practice of big data in college physical education," *Journal of Physics: Conference Series*, vol. 1992, Article ID 022131, 2021.

[2] E. Morgulev, O. H. Azar, and R. Lidor, "Sports analytics and the big-data era," *International Journal of Data Science and Analytics*, vol. 5, no. 4, pp. 213–222, 2018.

[3] X. Hong and R. Hu, "Evaluating connection in internet of things using big data fusion pattern," *Journal of Software Engineering*, vol. 26, no. 14, pp. 329–378, 2012.

[4] Y. J. Lin, C.-B. Lan, and C.-Y. Huang, "A realization of cyber-physical manufacturing control system through industrial internet of things," *Procedia Manufacturing*, vol. 39, pp. 287–293, 2019.

[5] S. Heimbs, "Computational methods for bird strike simulations: a review," *Computers & Structures*, vol. 89, no. 23-24, pp. 2093–2112, 2011.

[6] C. J. Welsh and V. Centonze, *Aircraft transparency testing-artificial birds, Report AEDC-TR-86-2*, US Air Force, Washington, DC, USA, 1986.

[7] C. Katie, "A strategy for bird strike simulations using abaqus/explicit. simulia online support document," *Best Practices for Birdstrike Analysis*, 2011.

[8] Y. G. Wang and X. M. Lu, "Grey relation analysis and grey model for civil aviation accidents forecasting," *Journal of Safety and Environment*, vol. 6, no. 6, pp. 127–130, 2006.

[9] Q. Cui and Y. Li, "The change trend and influencing factors of civil aviation safety efficiency: the case of Chinese airline companies," *Safety Science*, vol. 75, pp. 56–63, 2015.

[10] F. Zhu, C. Zhang, Z. Zheng, and A. Farouk, "Practical network coding technologies and softwarization in wireless networks," *IEEE Internet of Things Journal*, vol. 8, no. 7, pp. 5211–5218, 2021.

[11] J. Y. Ye, "Risk assessment of human factors in aviation safety using hazard regression model," *Environmental Earth Sciences*, vol. 65, no. 7, pp. 2063–2077, 2012.

[12] G. Tamasi and M. Demichela, "Risk assessment techniques for civil aviation security," *Reliability Engineering & System Safety*, vol. 96, no. 8, pp. 892–899, 2011.

[13] M. Adil, H. Song, J. Ali et al., "EnhancedAODV: a robust three phase priority-based traffic load balancing scheme for internet of things," *IEEE Internet of Things Journal*, vol. 99, p. 1, 2021.

[14] A. Kumari, S. Tanwar, S. Tyagi, N. Kumar, M. Maasberg, and K.-K. R. Choo, "Multimedia big data computing and internet of things applications: a taxonomy and process model," *Journal of Network and Computer Applications*, vol. 124, pp. 169–195, 2018.

[15] K. Alexopoulos, S. Koukas, N. Boli, and D. Mourtzis, "Architecture and development of an industrial internet of things framework for realizing services in industrial product service systems," *Procedia CIRP*, vol. 72, pp. 880–885, 2018.

[16] S. K. Sood, R. Sandhu, K. Singla, and V. Chang, "IoT, big data and HPC based smart flood management framework," *Sustainable Computing: Informatics and Systems*, vol. 20, pp. 102–117, 2018.

Hindawi
Mobile Information Systems
Volume 2022, Article ID 2106876, 10 pages
https://doi.org/10.1155/2022/2106876

Research Article

Performance Simulation of Identification System Based on Improved Neural Network Algorithm

Zhaolong Zhao, Minghui Huang, and Yibo Li

School of Mechanical and Electrical Engineering, Central South University, Changsha, Hunan 410083, China

Correspondence should be addressed to Zhaolong Zhao; 213712102@csu.edu.cn

Received 6 May 2022; Revised 21 June 2022; Accepted 5 July 2022; Published 20 July 2022

Academic Editor: Shadi Aljawarneh

After decades of development, neural network theory has made considerable progress in many research fields such as pattern recognition, automatic control, signal processing, decision support, and artificial intelligence. This article discusses the application of neural networks in pattern recognition and system recognition and proposes several new methods for recognizing system models and recognizing model parameters. In order to achieve high-precision control of smart structure actuators, a robust model must first be created. For various modeling tasks, many scientists have done a good job and proposed different modeling methods. There are three main ways to create a system model: one is a physical model based on the mechanism of the material itself, the other is an operator model based on experimental phenomena, and the third is an intelligent model based on computer intelligence. The problem of the recognition system stems from the fact that with the development of science and technology, the research methods of various disciplines have been further quantified. In industrial practice and scientific experiments, the purpose of observing and calculating the quantitative identification of complex objects that need to be studied is usual. According to its inherent laws, it is necessary to establish a mathematical model of the research object in order to make decisions such as analysis, design, prediction, and control. This article uses the neural network model to study the best improvement method of the dynamic process. The research results of this article represent the theoretical basis of future scientific research to a certain extent and have important research value.

1. Introduction

Neural network is a kind of abstraction, simplification, and modeling of the human brain. It reflects several basic characteristics of human brain function. Information processing in the network is carried out through the interaction between processors, which has the characteristics of parallel processing [1]. The knowledge and storage of information is manifested as a distributed physical connection between processing units. The training and recognition of the network is determined by the dynamic evolution process of the connection authority of the processing unit, which has the characteristics of associative memory [2]. The information processing function of the artificial neural network is realized by the powerful computing power of the computer, but it is different from the general computer system in that it has no predefined sequential arithmetic operations and serial operations. It is composed of many interconnected simple processing blocks [3]. After the learning is balanced, the distribution state of the entire network composed of the weights of each neuron is the desired result. This paper creates a random system whose input and output are disturbed by noise as the goal [4]. The system recognition problem is transformed into a pattern recognition problem by dividing the system error space [5]. This paper proposes a method to describe the system model and creates a corresponding neural network to identify the model. This model makes full use of known interference probability information, can quickly simulate the probability distribution information output by the system, and make the recognition results more intuitive and practical [6]. At the same time, the establishment of the rapid identification model also provides

a practical solution for the online identification of stochastic systems. This paper uses D-FNN and ANFIS in the fuzzy neural network, RBF, BP in the feedforward neural network and five advanced algorithms to simulate three sets of measured traffic flow data and the chaotic time series of McKee Glass [7]. This article first introduces the D-FNN and ANFIS. D-FNN method is applied to the principle of prediction. Second, it introduces the data sample, pre-processing method, prediction performance scoring index used in this paper, as well as the definition of D-FNN network structure and membership function [8]. Finally, when preprocessing the data, the input and output of the neural network are determined by using the above related theoretical methods. Based on the chaotic time series of Mackey-Glass, two sets of short-term traffic flow data and a set of video network flow data, this paper adopts appropriate methods to establish various prediction models and conduct comparative studies [9, 10]. A variety of methods are used to predict and test the chaotic McKee-Glass time series and traffic time series, and the experimental results of different methods are compared and analyzed to test the effectiveness of this method in traffic forecasting [11].

2. Related Work

The literature mentions that well-known scientists in the field of artificial intelligence wrote a very influential book "Perceptron," which had a negative impact on the research and development of perceptrons at that time [12]. Some scientists have turned their research interests to artificial intelligence or theories related to digital computers. This application has stimulated the development of artificial intelligence and made it dominate. The United States never funded neural network research in the next 15 years, which slowed down the development of neural network research. The literature shows that backpropagation neural network can be used for function approximation, pattern classification, statistical analysis, and data compression [13]. Then, this paper proposes a cellular neural network model, which is a large-scale nonlinear computer simulation system with dynamic characteristics of cellular automata. The literature points out that the perceptron is the simplest feedforward network in the traditional neural network. It is mainly used to classify images [14]. The RBF network is a radial basis function neural network with good local approximation ability and is often used for system identification. BP network is used for emergency processing, evaluation function, image recognition, model recognition, system management, and so on, due to its good approximation to nonlinear mapping [15]. Hopfield network is the main feedback network, mainly used for associative storage and calculation optimization. CMAC network is a typical local approximation network. It has the advantage of fast learning speed [16]. It is suitable for robot control, pattern recognition, signal processing, and adaptive control. It is especially suitable for adaptive modeling and control. Fuzzy neural network is similar to human this way of thinking, as well as the self-learning and adaptability of neural networks. In addition, there are many neural networks with special structures, such as adaptive resonance neural networks, stochastic neural networks, and HMM neural networks. It is mentioned in the literature that some researchers have established RBF neural network-based electrocutaneous actuator models to eliminate the multivalue display of hysteresis characteristics and write hysteresis coefficients based on the PI model. The Hammerstein model is constructed by combining the ARX function model to characterize the speed-dependent nonlinear hysteresis characteristics of the system. In this paper, the FIR filter algorithm is used to optimize the input data of the simulation, which improves the accuracy of the model and reduces the difficulty of calculation. Experimental results show that the constructed model can effectively adjust the hysteresis characteristics of piezoelectric actuators and adapt to changes in signal frequency. Based on the MPI model, this paper establishes the piezoelectric actuator model and the BP neural network model to establish the piezoelectric actuator model, compares the effects of the H model modeling, and analyzes the results. The literature introduces the working principle of the *d* SPACE hardware simulation platform and explains the entire experimental development process. Combined with the closed-loop PID compound control strategy, the forward compensation control based on the inverse model of RBF neural network is designed, and the control experiment of tracking signals of different frequencies is designed. At the same time, comparing the compound control strategy based on the MPI inverse model and the compensation control strategy based on the RBF inverse neural network model, the advantages and disadvantages of the three control strategies are analyzed.

3. Improved Experiment of Dynamic Process Neural Network

3.1. Mackey-Glass Chaotic Time Series Prediction Simulation. In order to create a chaotic McKee-Glass time series, this paper uses the BP algorithm and its five improved algorithms in the feedforward neural network method, RBF method, to optimize the differential evolution algorithm of the BP neural network. They are the network method and ANFIS used for prediction and benchmarking. Five improved BP algorithms include improved extra pulse algorithm, improved adaptive parameter tuning algorithm, elastic BP algorithm, improved conjugate gradient algorithm, and improved LM algorithm. BP algorithm has the advantages of nonlinear mapping, strong generalization, and so on, and is widely used in the field of prediction. BP algorithm and its five improved algorithms are RBF method, DE optimized BP neural network, ANFIS method, and D-FNN method. The error results are shown in Table 1.

It can be seen from Table 1 that the prediction accuracy of the BP neural network optimized for DE is higher than that of the feedforward neural network method. The prediction effect of ANFIS and D-FNN is better, but the performance of generalized D-FNN is better, slightly worse than ANFIS, but it does not affect the overall prediction effect of D-FNN.

Table 1: Comparison of six-step prediction of Mackey-Glass chaotic time series by different methods.

Method of prediction	Root mean square error
Standard BP network algorithm	0.0978
Improved algorithm for additional momentum	0.0972
Improved algorithm for adaptive adjustment of parameters	0.0970
Elastic BP algorithm	0.0956
Improved algorithm of conjugate gradient	0.0953
LM improved algorithm	0.0486
RBF network algorithm	0.0194
DE optimized BP neural network	0.0265
ANFIS	0.0032
D-FNN	0.0078

3.2. Example Prediction of Short-Term Traffic Flow at a Certain Inspection Station

3.2.1. Comparison Experiment of Short-Term Traffic Flow Prediction Based on Different Methods. Table 2 shows the prediction errors of all methods in the short-term traffic flow at a specific detection station in Beijing.

3.2.2. Prediction Performance Analysis of Different Embedding Dimensions and Time Delays. It can be seen from Table 2 that the LM algorithm of the feedforward neural network has a better prediction effect, but the prediction ability of the fuzzy neural network method is better than that of the feedforward neural network method.

The difference in network structure also leads to different prediction results. The embedding size and delay determine the input and output of the network structure. Various embedding sizes and delays are selected for further prediction experiments.

When $m = 3$ and $\tau = 1$, the data are normalized first, and the normalized data are divided into two groups. In order to reflect the forecasting effect of each forecasting model, the forecasting results of all forecasting models are summarized in Table 3.

If $m = 4\tau = 2$, divide these data into two groups and create a prediction model based on multiple neural network methods and a fuzzy neural network for experiments. The prediction results of all prediction models are shown in Table 4.

Table 4 shows that for $m = 4\tau = 2$, the prediction effect of each method is better, and the prediction effect of the D-FNN method is better than that of BP and RBF.

Table 5 shows that the usual root mean square error is used as a metric to evaluate the prediction results.

From Table 5, this paper can conclude that Table 5 reflects the prediction results of different methods of predicting models under different embedding sizes and time delays. The D-FNN method and the ANFIS method show higher prediction effects regardless of the time delay of the optimal embedding measurement or the time delay of the suboptimal embedding measurement. Therefore, the D-FNN technology is effective for predicting the time series of the transmission stream.

4. Identification Method of Neural Network Model

4.1. Dynamic Recognition of Neural Network Patterns. In the real world, most real-world patterns are created by objects with time-varying characteristics. The characteristic of this pattern is that its amplitude fluctuates repeatedly. The closed-loop neural network mentioned earlier in this article can be used to identify this type of system. Here is another model of the identification network: a time-delay neural network.

4.1.1. Deterministic Time Delay Neural Network. Deterministic neural networks with delay are usually divided into sequential and parallel structures as shown in Figure 1:

The serial delay neural network classifier has a network layer structure. The output layer and hidden layer of the network are exactly the same as the double-layer perceptron, except that the input port is composed of a tapped delay block formed by a serial delay line, and the input block is sent for processing. The number of delay units in the delay line is determined by the characteristics of the time-varying mode, and the parallel structure only provides interlayer delay operations. Depending on the circumstances, this may be a structure with multiple hidden layers. The transfer function of the hidden layer neuron can be a sigmoid function or a radial basis function, and the network algorithm can be a general BP algorithm. The working principle of the delay deterministic neural network is still similar to the approximation of the model display scale, and its application has mature theories. The random delay neural network mainly refers to the network model based on the Markov model.

Random time model mainly refers to Markov model or hidden Markov model. MM is a single random process with unknown state, and HMM is a double random process with unknown state and acting in the state.

The basic definition of Markov chain is given by:

$$P(X_0 = q_0, X_1 = q_1, \ldots, X_n = q_n) > 0. \tag{1}$$

And there is formula (2):

$$P\left(X_{n+1} = \frac{q_{n+1}}{X_0}, X_1 = q_1, \ldots, X_n = q_n\right) = P\left(\frac{X_{n+1} = q_{n+1}}{X_0 = q_0}\right). \tag{2}$$

Table 2: Forecast errors based on different methods.

Method of prediction	Regularized root mean square error	Equalization coefficient
Standard BP network algorithm	0.2790	0.9413
Improved algorithm for additional momentum	0.2706	0.9415
Improved algorithm for adaptive adjustment of parameters	0.2694	0.9436
Elastic BP algorithm	0.2685	0.9365
Improved algorithm of conjugate gradient	0.2720	0.9350
LM improved algorithm	0.2609	0.9253
RBF network algorithm	0.2678	0.9250
ANFIS	0.2667	0.9275
D-FNN	0.2683	0.9456

Table 3: $m = 3\tau = 1$ prediction performance comparison.

Method of prediction	Regularized root mean square error	Equalization coefficient
Standard BP network algorithm	0.4013	0.9013
Improved algorithm for additional momentum	0.3496	0.9154
Improved algorithm for adaptive adjustment of parameters	0.3765	0.9389
Elastic BP algorithm	0.3763	0.9345
Improved algorithm of conjugate gradient	0.3798	0.9311
LM improved algorithm	0.3391	0.9238
RBF network algorithm	0.3215	0.9261
ANFIS	0.2898	0.9276
D-FNN	0.2885	0.9336

Table 4: $m = 4\tau = 2$ prediction performance comparison.

Method of prediction	Regularized root mean square error	Equalization coefficient
Standard BP network algorithm	0.3510	0.9104
Improved algorithm for additional momentum	0.3346	0.9159
Improved algorithm for adaptive adjustment of parameters	0.2856	0.9165
Elastic BP algorithm	0.2895	0.9337
Improved algorithm of conjugate gradient	0.2783	0.9284
LM improved algorithm	0.2750	0.9219
RBF network algorithm	0.2890	0.9211
ANFIS	0.2763	0.9427
D-FNN	0.2798	0.9184

Table 5: Prediction errors under different embedding dimensions and time delays.

Method of prediction	$m = 3\tau = 1$	$m = 4\tau = 2$	$m = 4\tau = 1$
Steepest gradient descent	0.4012	0.3513	0.2890
Improved algorithm for additional momentum	0.3846	0.3046	0.2806
Improved algorithm for adaptive adjustment of parameters	0.3561	0.2348	0.2781
Elastic BP algorithm	0.3745	0.2798	0.2790
Improved algorithm of conjugate gradient	0.3764	0.2648	0.2716
LM improved algorithm	0.3135	0.2684	0.2749
RBF network algorithm	0.3546	0.2489	0.2887
ANFIS	0.2458	0.2478	0.2659
D-FNN	0.2168	0.2757	0.2680

This is called a discrete Markov chain. HMM is a double random process in which the state is implicit and the observed characteristics are related to probability. That is, the corresponding final Markov state is implicit. In addition, this article usually studies the first-order HMM, which implies two assumptions. The first is the Markov condition. The probability of a state at time $t + 1$ is only related to the state at time t and has nothing to do with the previous state. The second is the assumption of independence of conclusions. The probability of the conclusions of d and a is only observed in specific observations. At time t refers to the current state and has nothing in common with the past state.

From the perspective of training a multilayer perceptron network, HMM is seen as a repetitive neural network.

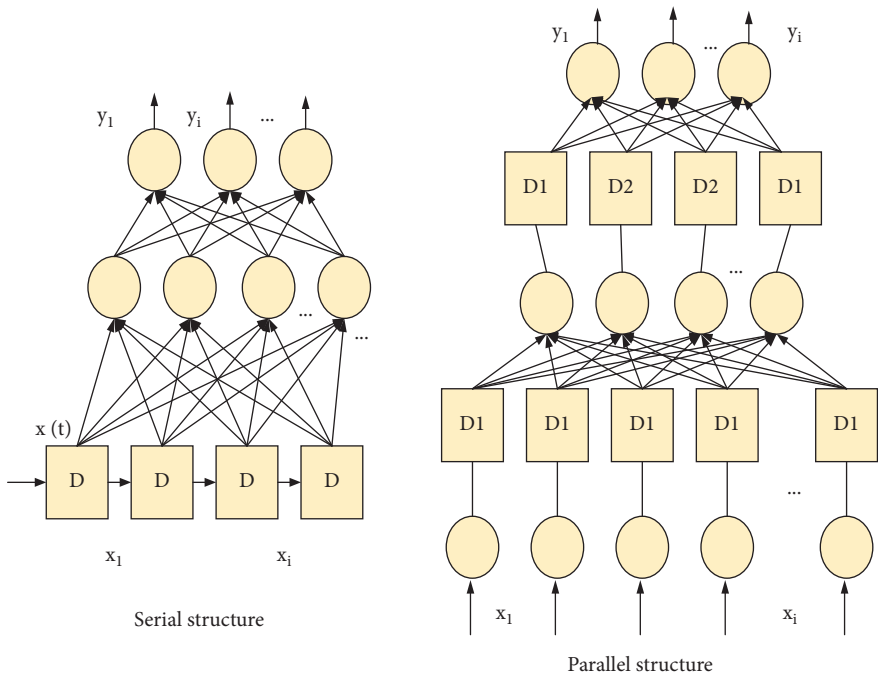

Figure 1: Two structures of time-delayed neural network.

Suppose that the N states of the HMM are counted as N neurons, and these N neurons expand over time to form a feedforward network. In fact, this network structure corresponds to the process of constantly updating the states of N neurons. It is actually a recursive network. The following objective function can be defined at the exit of the network as shown in the following formula:

$$E = \sum_{k=1}^{K} \Pr\left(\frac{O^k}{\Lambda}\right). \tag{3}$$

Baum-Welch iterative algorithm

① Given observation sequence C, as formula (4):

$$\begin{cases} a_{ij}^{o} = \dfrac{1}{N}, & j = 1, 2, \ldots, N, \\ b_{ij}^{o} = \dfrac{1}{M}, & j = 1, 2, \ldots, M, \forall i, j = 1, 2, \ldots, N, \\ \pi_{j}^{o} = \dfrac{1}{N}, & j = 1, 2, \ldots, N. \end{cases} \tag{4}$$

② Calculate the parameters from $t = 1$ to $t = T$ and from $k = 1$ to $k = N$, such as formulas (5)–(8):

$$a_i^{k(m)}(t+1) = b_i\left(O^k(t+1)\right) \sum_{j=1}^{N} a_{ij} a_j^{k(m)}(t), \tag{5}$$

$$\beta_i^{k(m)}(t) = \sum_{j=1}^{N} \beta_j^{k(m)}(t+1) b_j^m\left(O^k(t+1)\right) a_j^{k(m)}(t), \tag{6}$$

$$\xi_{ij}^{k(m)}(t) = a_{ij} \beta_i^{k(m)}(t+1) b_i^{(m)}\left(O^k(t+1)\right) a_i^{k(m)}(t), \tag{7}$$

$$\gamma_j^{k(m)}(t) = a_j^{k(m)}(t) \beta_j^{k(m)}(t). \tag{8}$$

③ Calculate according to the following formulas:

$$a_{ij}^{(m+1)} = \frac{\sum_{k=1}^{k} \sum_{r=1}^{r-1} \xi_{ij}^{k(m)}(t)}{\sum_{k=1}^{k} \sum_{r=1}^{r-1} \gamma_{ij}^{k(m)}(t)}, \tag{9}$$

$$b_i^{(m+1)} = \frac{\sum_{k=1}^{k} \sum_{r=1}^{r-1} \gamma_{ij}^{k(m)}(t)}{\frac{\Omega^{(k)}(t) = v_1}{\sum_{k=1}^{k} \sum_{r=1}^{r-1} \gamma_{ij}^{k(m)}(t)}}, \tag{10}$$

$$\begin{aligned} \pi_i^{(m+1)} &= \sum_{k=1}^{k} \frac{\gamma_j^{k(m)}(t)}{\Pr\left\{O^k/\Lambda\right\}}, \\ \Pr\left\{\frac{O^k}{\Lambda}\right\} &= \sum_{j=1}^{N} a_j^{k(m)}(T). \end{aligned} \tag{11}$$

④ The iteration ends.

Network test: Calculate any observation sequence, as in formula (12):

$$\Pr\left\{\frac{O}{\Lambda_c}\right\} = \sum_{j=1}^{N} a_j^k(T). \tag{12}$$

Use the following formula to select the category attribute of the specified sequence:

$$c_j = \arg\max\left\{\Pr\left(\frac{O}{\Lambda_c}\right)\right\}, \quad c = 1, 2, \ldots, C. \tag{13}$$

Then, ci is the category of the corresponding observation sequence.

The test is over, continue to test.

4.1.2. Model Checking. The detection model essentially calculates the probability that the output will be in different failure modes at the next moment based on current and historical inputs, as shown in Figure 2. The ideal signal and the actual output signal are combined into one, partially amplified. Figure 2 is a schematic diagram of the recognition results of $k = 377$ points; the local small coordinate system shows the failure mode probability value, and the system output of $k = 378$ points.

Figure 2 shows that if the two end points of the error subinterval correspond to the most probable system failure mode output, the system output has the highest probability of belonging to the third failure mode at the next moment.

4.1.3. Establishment of Recognition Neural Network for HMM System. Before configuring the HMM network, the system must convert the error output state and then construct a corresponding HMM network model for each mode. Similar to the RBPNN configuration process mentioned above, preprocessing and postprocessing modules need to be added as needed. The errors mentioned below, unless otherwise specified, refer to the difference between the observed value of the system and the ideal value.

Assuming that it is divided into N subslots, N failure modes are as shown in the following formula:

$$E = \{e_1, e_2, \ldots\}. \tag{14}$$

At the same time, assume that this set of failure modes can be applied at any time, that is, E is not a function of time and assume that the system input error mode set is given by:

$$E_I = \{e_{11}, e_{12}, \ldots, e_{\mathrm{IN}}\}. \tag{15}$$

Assuming that the setting error mode output by the system isgiven by:

$$E_O = \{e_{O1}, e_{O2}, \ldots, e_{\mathrm{ON}}\}. \tag{16}$$

When the system is running, the real-time system output error keeps jumping between different error modes. If the system outputs a failure mode at time k, as shown in the following formula:

$$e_{Oi},\ i = 1, 2, \ldots, M. \tag{17}$$

Defined as formula (18):

$$U^k = \{u(k), u(k-1), \ldots, u(k-n_b)\}. \tag{18}$$

This is the effective input of time k and can also be used as a generalized effective input.

If the system is still in a specific operating state, record its fault sequence and establish the corresponding HMM network model. A similar method can be used to compare a group of HMM models to determine the location of the system.

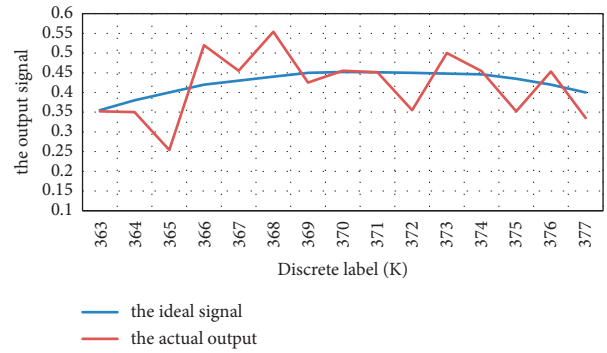

Figure 2: Schematic diagram of Markov neural network identification process.

4.2. Parameter Identification of Neural Network Mode. In fact, many systems not only require this article to evaluate its type but also require this article to understand some important parameters of the system. However, due to the constraints of objective or man-made conditions, this article cannot obtain accurate and complete system information, such as the chemical properties of unknown materials, and a certain evaluation of its physical parameters used to evaluate the type and extent of failure of a complex system and used to evaluate the type and characteristics of remote targets.

4.2.1. Problem Description and Related Concepts. The identification of the target system usually requires two aspects of information: the evaluation of the type or operation mode of the system, which is called quality evaluation. Obtaining the corresponding parameters or parameters of the current state of the system is called quantitative evaluation here.

For the sake of simplicity, now take the target recognition of a long-range ship as an example. First, we must selectively collect and process the target (current information such as radar image characteristics, trajectory, magnetic field emission, or hull vibration information), hereinafter referred to as all requirements. The collection of target information collected and processed is a measurement space. This article concludes that the target is the head aircraft carrier, not the small fishing boat. This is often based on the distribution of each piece of information in the target measurement space and the relationship between different types of information. This relationship is consistent with the information distribution and relationship in the aircraft carrier measurement room known in this article under the same conditions or closer, which is qualitative.

In practice, the system types are nested layers, qualitative and quantitative processes can be transformed into each other, and smaller types of assessments can be carried out. For larger category judgments, this is also a quantitative

process, and the values of target-related parameters are restricted to a smaller range.

This article makes the following assumptions or definitions: the motion state of the system can be described by a set of coupled differential equations, and the parameters in the equations are the key quantities that affect the spatial distribution of information during measurement.

If any $n-1$ dimensional state parameter in the extended state space takes a certain value, the remaining one-dimensional state parameters exist and only a finite number of values satisfy the corresponding equation, then the center of the state space is called the complete state point, hereinafter referred to as the state point. The subset obtained by dividing the state space of the equation in a certain way is called the sampling range corresponding to the equation. In practice, this article can only get a limited number of points in the sample area, that is, the sample set. Assuming that the known and measurable state parameters of a state point form known data, it is expressed as follows:

$$X_k = \{x_{k1}, x_{k2}, \ldots, x_{ki}\}. \tag{19}$$

Other unknown parameters are expressed as follows:

$$X_u = \{x_{u1}, x_{u2}, \ldots, x_{uj}\}. \tag{20}$$

Therefore, the combination of known and unknown parameters forms the state point of the equation, as shown in the following equation:

$$X = \{X_k, X_n\} = \{x_1, x_2, \ldots, x_n\}. \tag{21}$$

4.2.2. Neural Network Integration of Parameter Identification. An ideal set of samples should reflect the distribution characteristics of the parameters in the sample area. All neural networks involved in the following are trained from a set of samples.

(1) Selection of state parameters: assuming that the accuracy of the comparison of each parameter is guaranteed by the corresponding equation (function), secondary factors should be ignored as much as possible to reduce the size of the state point and save uptime. Second, the selection of state parameters should be as close as possible to the characteristic information of the system that this article is most interested in. The response characteristic parameters must effectively distinguish different types of systems, but they can still remain stable when the operating conditions of the same type of system change.

The mapping realized by the closed network group is $Y = F(X)$. Due to the certainty of the mapping, each individual network can have better approximation accuracy. According to the neural network approximation theory, it can be known that if the ideal state point X is inserted into a network group, it should be $Y = X$. There is a one-to-one correspondence between such a set of networks and the differential equations in a specific sample ranges. The process of calculating the closed network combination is given by:

$$\begin{cases} X^o = \{X_k, X_u^o\}, \\ X^i = \{X_k^i, X_u^i\} = F(X^i), \\ X^{i+1} = \{X_k, X_u^i\}, \end{cases} \tag{22}$$

where $i = 1, 2, \ldots$. That is to say, in each iteration, only X_a is updated.

Definition 1. The iteration error is as shown in the following formula:

$$E_x = \text{dist}(X^i, X^{(i+1)\gamma}). \tag{23}$$

The recognition error is given by:

$$E_R = \text{dist}(X^i, X^i). \tag{24}$$

The initial recognition error is given by:

$$E_o = \text{dist}(X_u^o, X_u). \tag{25}$$

In the above formula, X_u^* is the true value of the target, and dist(•) is the ranging function. When the balance index and ER are close to zero, the model is considered to be asymptotically to the equilibrium point. If the starting point of the iteration meets certain conditions, the network integration model approaches the equilibrium point asymptotically, and the recognition accuracy of the equilibrium point is approximately equal to the approximate accuracy of a single subnet.

Since each parameter of the state point is independent only in a mathematical sense, and there may be objective constraints between each other in practice, the sample area is neither a continuous multidimensional area in real space nor a possible subset of columns. Its spatial shape depends on the constraints between the parameters.

4.2.3. Stability Analysis of the Integrated Network Model. In addition, if it only comes from the sample area, rather than the corresponding point from the initial state of the sample set, it will cause the model to approach the equilibrium point asymptotically, and the corresponding memory will increase the capacity of the network. From the perspective of the entire integrated macrostructure model, it is similar to a Hop field neural network, except that each neuron of the Hop field neural network is replaced with an independent neural network as shown in Figure 3.

Figure 4 shows the error convergence curve of 100 times network training, and the minimum value of its Y coordinate is 10–1 and 10–8. Therefore, the state of the model represents information about the target category in probability, and it is necessary to try to replace models that match other domain examples. If a balance point is found in multiple recognition models at the same time, it can be interpreted as follows: if the target belongs to a certain sample area, the recognition result is the corresponding balance point.

The size of the initial detection network is [5 10 3], and all six individual networks are [5 10 1]. After 1000 times of training, the approximate error percentages of the sample set are [10–1,10–1] and [10–12,10-9, and], which means that the

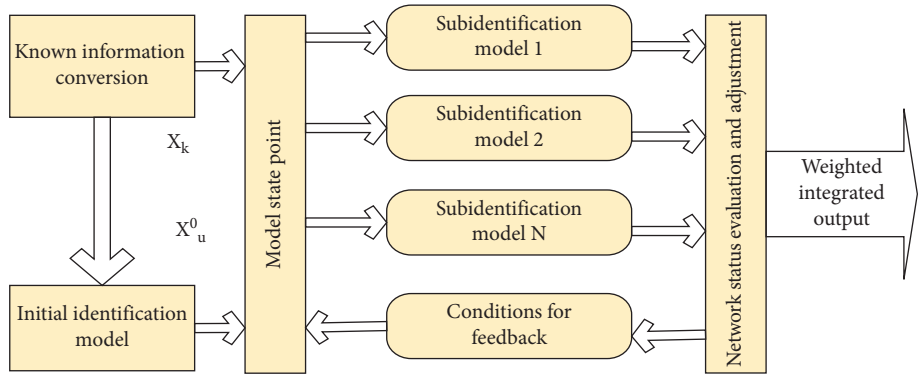

Figure 3: Network integration model of parameter identification.

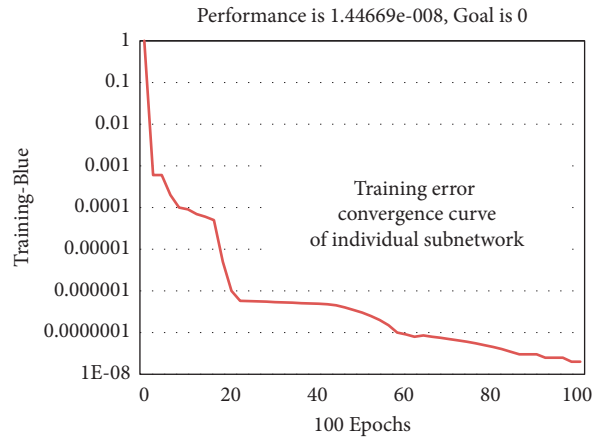

Figure 4: Individual network training error convergence curve.

accuracy output of an approximate five input and one subnet is at least three The initial detection network with one input and three outputs is several orders of magnitude higher. From the perspective of network training, this difference in accuracy is necessary and easy to implement. Aiming at the problem of right distribution in the current financial management of modern enterprises, this article believes that improvements and optimizations should be made from two aspects, based on the above-mentioned basic ideas and principles: first, modern enterprise financial management maximizes the value of stakeholders. As a guide, a power distribution model based on a static configuration structure should be established to allow all stakeholders to share the company's financial management authority, while balancing the configuration parameters of corporate financial management authority, and enhancing the interactive configuration of financial management authority between objects to make a certain Financial management achieves a balanced state of mutual restraint and mutual restraint among all configuration levels and objects. The second is to improve the distribution of modern financial management power by improving the company's internal management structure and stabilizing the company's external market mechanism. All parties can have equal opportunities to participate in the distribution of corporate financial management power to own their property rights.

This digital simulation experiment is based on the MATLAB/SIMULINK platform and neural network toolkit. In any case, the time is 5 seconds. Figure 5 shows the convergence process of a sample point in the corresponding recognition model, and the ordinate of the convergence trajectory graph is a logarithmic coordinate.

If the test sample points are inserted into a suitable integration model, the model can still converge to a (pseudo) equilibrium point, which reflects the generalizability of neural network integration. At this point, these diagrams are similar to Figure 6, except that if the final state is not close to zero and the initial state points from different scan sets are inserted into the recognition model, the state will diverge, and the program will automatically terminate with similar results.

It can be seen from the above simulation experiments that the model as a whole is close to the convergence state in the third iteration, that is, the overall recognition accuracy has reached the approximation accuracy of a single network. However, the process of model creation requires the identity modeler to have certain experience and relevant knowledge.

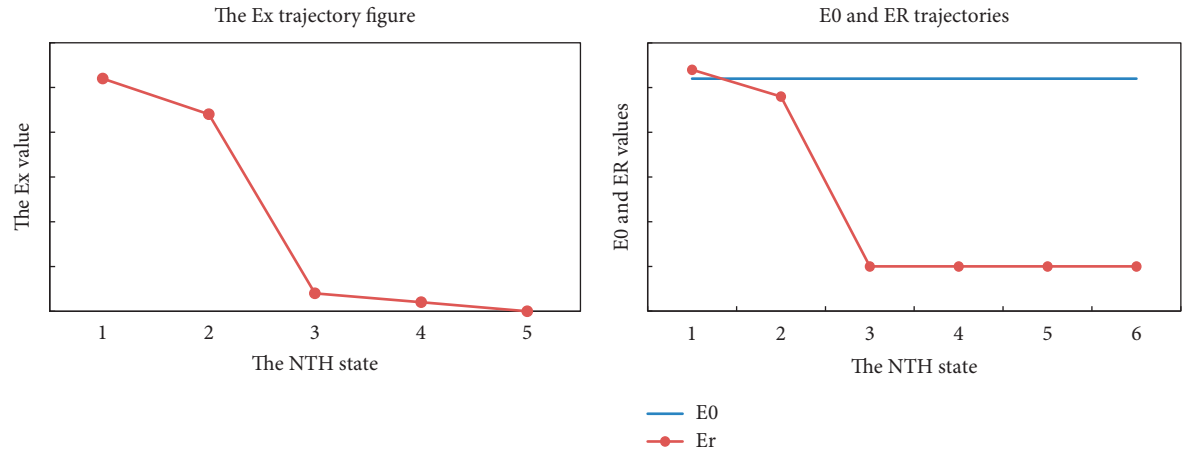

Figure 5: Convergence process of parameter identification accuracy E_x, E_r.

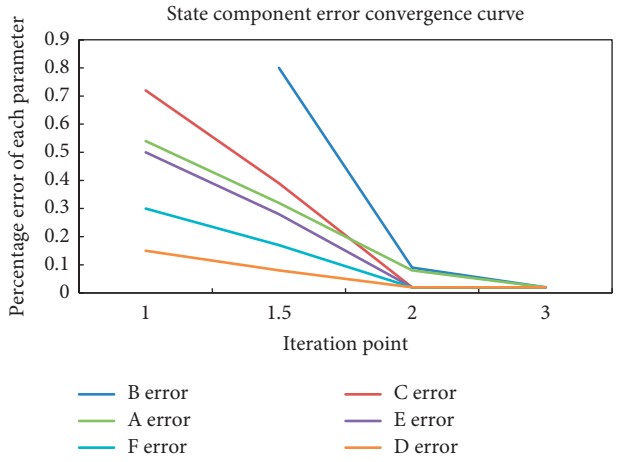

Figure 6: Convergence process of each component of the state point.

5. Conclusion

In terms of identifying system parameters, this paper proposes a new method of neural network integration based on the concept of complete state points. The method combines system type recognition and parameter recognition to ensure the accuracy and versatility of neural network integrated recognition, thereby reducing the requirement of the recognition system for test information knowledge. Neural network is an effective tool to identify the system. It does not need the internal mechanism of the system but only needs the input and output data of the system to simulate the NN model, which characterizes the input and output characteristics of the system and surpasses the traditional identification methods. Therefore, the system recognition based on neural network has a wide range of technical foundation, theoretical significance, and academic value. After systematically studying the wide application of neural networks in system identification and remaining problems, this paper proposes a separate method to build neural network models for various types of more complex systems. Before creating a predictive model, we must first define the input and output of the network structure. This article introduces chaos theory and uses chaotic phase space reconstruction technology to determine the input and output of the predictive model. This method solves the problem of determining the input and output definitions of the network structure based on intuitive experience. First, by calculating the maximum Lyapunov exponent, determine whether the three traffic flow data sets used in this paper are chaotic time series and then use the chaotic time series processing method to deal with these three time series are processed, and methods and methods of mutual information are used. This paper determines the embedding size and delay, based on the BP algorithm in the neural network method and its five improved algorithms, the ANFIS method in the RBF method, the fuzzy neural network method and the D-FNN method to construct nine prediction models, and combine these nine, the prediction model is applied to three sets of measurement data to test the prediction performance of D-FNN in the transmission basin. Choose different embedding sizes and time delays to create different prediction models for prediction experiments. Experiments show that the prediction model effect of the three sets of measurement data is the best in the optimal embedding measurement and time delay, indicating that the combination of chaos theory and D-FNN is useful for improving the prediction performance. At the same time, in terms of identifying system parameters, this paper proposes a new neural network integration method, which combines the identification of system types and parameters. On the basis of maintaining the accuracy and generalization of recognition, the neural network reduces the requirements for the recognition system, that is, it can deal with fuzzy, incomplete, or even uncertain system test information.

Data Availability

The data used to support the findings of this study are available from the corresponding author upon request.

Conflicts of Interest

The authors declare that they have no conflicts of interest.

References

[1] A. Savitzky and M. Golay, "Smoothing and differentiation of data by simplified least squares procedures," *Analytical Chemistry*, vol. 36, no. 8, pp. 1627–1639, 1964.

[2] Y. Xue, Y. C. Guo, H. Zhang, T. Xu, S. H. Zhang, and X. Huang, "Deep image synthesis from intuitive user input: a review and perspectives," *Computational Visual Media*, vol. 8, no. 1, pp. 3–31, 2022.

[3] L. Zhao, S. J. Pan, and Q. Yang, "A unified framework of active transfer learning for cross-system recommendation," *Artificial Intelligence*, vol. 245, pp. 38–55, 2017.

[4] A. Geiger, P. Lenz, C. Stiller, and R. Urtasun, "Vision meets robotics: the Kitti dataset," *The International Journal of Robotics Research*, vol. 32, no. 11, pp. 1231–1237, 2013.

[5] R. Zhang, P. Isola, A. A. Efros, E. Shechtman, and O. Wang, "The unreasonable effectiveness of deep features as a perceptual metric," in *Proceedings of the IEEE/CVF Conference on Computer Vision and Pattern Recognition*, pp. 586–595, Salt Lake City, UT, USA, June 2018.

[6] D. Toublanc, "Henyey-Greenstein and Mie phase functions in Monte Carlo radiative transfer computations," *Applied Optics*, vol. 35, no. 18, p. 3270, 1996.

[7] B. L. Zhou, H. Zhao, X. Puig, S. Fidler, A. Barriuso, and A. Torralba, "Scene parsing through ADE20K dataset," in *Proceedings of the IEEE Conference on Computer Vision and Pattern Recognition*, pp. 5122–5130, Honolulu, HI, USA, July 2017.

[8] T. Meng, Q. K. Pan, and H. Y. Sang, "A hybrid artificial bee colony algorithm for a flexible job shop scheduling problem with overlapping in operations," *International Journal of Production Research*, vol. 56, no. 16, pp. 5278–5292, 2018.

[9] P. Anand and S. Arora, "A novel chaotic selfish herd optimizer for global optimization and feature selection," *Artificial Intelligence Review*, vol. 53, no. 2, pp. 1441–1486, 2020.

[10] G. M. Lang, D. Q. Miao, and M. J. Cai, "Three-way decision approaches to conflict analysis using decision-theoretic rough set theory," *Information Sciences*, vol. 406, pp. 185–207, 2017.

[11] K. Cho, B. van Merriënboer, D. Bahdanau, and Y. Bengio, "On the properties of neural machine translation: encoder–decoder approaches," in *Proceedings of the SSST-8, Eighth Workshop on Syntax, Semantics and Structure in Statistical Translation*, pp. 103–111, Doha, Qatar, September2014.

[12] S. M. Bowles, "Is Congruence Dead? an Examination of the Correlation between Holland's Congruence and Job Satisfaction Using Improved Methodology," Ph.D. Thesis, West Virginia University, Morgantown, WV .USA, 2008.

[13] A. Krizhevsky, S. Ilya, and E. H. Geoffrey, "Imagenet classification with deep convolutional neural networks," *Advances in Neural Information Processing Systems*, vol. 25, 2012.

[14] G. Navarro and Y. Nekrich, "Top-k document retrieval in optimal time and linear space," in *Proceedings of the Twenty-Third Annual ACM-SIAM Symposium on Discrete Algorithms*, January 2012.

[15] M. Simon-Galvez and F. M. Fazi, "Room compensation for binaural reproduction with loudspeaker arrays," in *Proceedings of the European Acoustics Association (Euroregio). Porto*, Portugal, June 2016.

[16] M. Tornow, J. Kaszubiak, R. W. Kuhn, B. Michaelis, and T. Schindler, "Hardware approach for real time machine stereo vision," in *Proceedings of the 9th World Multi-Conference on Systemics. Cybernetics and Informatics*, pp. 111–116, Orlando, FL, USA, July 2005.

Hindawi
Mobile Information Systems
Volume 2022, Article ID 7795836, 10 pages
https://doi.org/10.1155/2022/7795836

Research Article

Development of Automatic English Translation System Based on Fuzzy Matching and Software Simulation

Qian Tan

Southwest Jiaotong University Hope College, Chengdu, Jintang, China

Correspondence should be addressed to Qian Tan; tanqian@swjtu.edu.cn

Received 14 May 2022; Revised 18 June 2022; Accepted 2 July 2022; Published 19 July 2022

Academic Editor: Shadi Aljawarneh

Software requirements are changeable, and the changes in requirements have led to many technical, economic, and management problems in the software development process, which are also considered to be the main source of software development risks. Based on the relationship between software requirements and design, this article analyzes the propagation process of requirement changes and the two dimensions of requirement change risk, opportunity and impact, and discusses software architecture customization that combines requirements, software architecture, and risk. On the basis of QFD and DSM, a composite relationship matrix is created according to requirements and software architecture, and two aspects of software architecture adaptability are analyzed from the perspective of the risk of changes in requirements. With the advent of the 5G era, this issue has gradually been paid attention to in its evolution. In order to further improve the intelligence level of the English translation system and improve the accuracy of English translation, this paper designs a translation algorithm that takes the changes in software requirements as the basis. On this basis, cross-compilation and multithreaded phrase translation loading methods are used to automate the translation system. System test results show that the system has high translation accuracy and good intelligence. Overall, the development of an automatic English translation system based on software change management and 5G networks will further enhance the intelligence and automation of English translation.

1. Introduction

Software requirements are an important part of software development and the basis of software design. As the source of software development, requirements define and constrain the requirements of the final software product. However, compared with conventional products, the abstraction and high complexity of software products make our demand for software products more uncertain, more unstable, more subjective, and more vague [1]. In the software development process, there will be many problems related to software requirements. Statistics about the practice of creating software projects show that most of the reasons for the failure of software projects are not technical problems in software development, but management problems; the most common of which is demand management problems [2]. Studies have shown that more than 50% of software requirements will change before the software product is officially released. In addition, more than 70% of large-scale software systems (for example, the total number of function points exceeds 1,000) will be subject to huge changes in demand during the development process. The widespread use of China's fourth-generation mobile network has further improved the quality of communication network applications and has also provided more convenience for current social development [3]. In this context, a large number of new mobile communication services continue to emerge, and people's demand for using mobile service networks has also been significantly improved [4]. By analyzing the status quo of China Mobile's technology development and its future development prospects, it can be concluded that in the future social development, 5G radio networks will gradually transform into mobile communication systems occupying a certain position [5]. Compared with the mobile networks used in the past, the advantages of 5G are

mainly reflected in the transmission speed and transmission quality [6]. In addition, the stability of information transmission is higher than that of other mobile networks. In general, the 5G wireless network has broad prospects for the future, and its unique high-frequency characteristics can enable users to better understand the network bandwidth. For 5G wireless networks in the medium and low frequency range, efficient and extensive network coverage can be achieved through mergers and connections [7]. With the development of information technology, the development of English translation systems based on changes in software requirements and 5G network management has greatly improved the intelligence and accuracy of English translation [8]. The systematic use of automatic translation is the most important software medium for performing English translation. Therefore, the design of automatic English translation system has important practical significance [8]. The automatic English translation system analyzes the characteristics of English vocabulary in detail through semantic analysis and effectively combines the methods of semantic fuzzy matching and automatic phrase analysis to perform large-scale automatic translation of vocabulary, ensuring the accuracy and reliability of translation [9].

2. Related Work

The literature shows that changes in demand have led to various technical, economic, and management problems in software development and are considered to be an important source of risk in software project development. The literature shows that changes to software requirements are not limited to the collection and analysis of requirements. It will affect the entire software development life cycle and most directly affect the design of the software architecture [10]. It is clearly pointed out in the literature that it is generally believed that the key influence of analyzing changing requirements on software development is usually the software architecture. Software architecture describes the components, connections, system properties, and behaviors of a software system, and is the core of software design [11]. Traditional software development models tend to separate requirements and carry out static and mechanical design. The literature shows that with the rapid development of China's network technology and the emergence of 5G networks, the future network will gradually develop in the direction of intelligent development, diversification, and integration [12]. The literature shows that when building a 5G wireless communication system, a suitable location for installing the antenna structure should be selected according to the actual requirements of the network structure to further increase the capacity of the dimensional space [13]. The literature suggests that attention should be paid to the use of culture and language skills in translation work, only in this way can the translation truly convey the cultural connotation of the original language [14]. Through the development of an automatic English translation system based on software demand change management and 5G networks, the literature has improved the intelligence and automation of English translation [15].

3. Relevant Research on Software Requirement Change Management and 5G Network

3.1. Software Requirements Change Management. According to the reasons and possible consequences of demand changes, demand can be divided into the following four categories: (1) variable requirements closely related to the application field of software products, for example, changes in user needs, advances in software technology, adjustments to organizational strategies or guidelines, etc. (2) Sudden demand: certain demands cannot be completely or accurately defined in the demand analysis stage. In the software development life cycle, software developers and users will have a deeper understanding of software requirements and application areas as the development progresses, and feedback information will be integrated into the requirements analysis. Changes in requirements caused by such feedback information are called sudden changes. Make a request (3): indirect demand: this kind of demand is driven by the software development activity itself. When the demand is unstable or suddenly arises, the software development activity must make appropriate adjustments to adapt to these changes, leading to many new demands called indirect demand.

The traditional software development model regards requirements analysis and software architecture design as two independent steps. However, there is no significant difference between software requirements specifications and software. For example, during development and execution, there are no structured software requirements and software architecture. Significant differences: by comparing and summarizing the relevant research on the "demand and design gap" from an empirical point of view, it can be assumed that the traditional software development method that separates software requirements and design will have a serious adverse effect on the entire software development process. In addition, this article points out that the process from requirements to software architecture is still an informal model, which lacks necessary guidelines and good practices, which to a large extent leads to the fact that software products cannot ultimately satisfy users. Requirements: this article analyzes the impact of software architecture on requirements confirmation from two perspectives: (1) how does the software architecture affect the confirmation of claims; (2) what aspects of the software architecture will affect the confirmation of claims? Research shows that nearly 60% of software requirements verification depends on the existing software architecture. Various aspects of the nine software architectures will affect the verification of software requirements, but different aspects have varying degrees of impact, of which the nonfunctional aspects account for 29% of the total exposure. The analysis results provide software developers with reference values for the requirements and processes of software architecture, software architecture design, software development plans, and risk management.

The initiator of software architecture must prove the impact of software requirements changes on software development. To evaluate the impact of requirements changes on software architecture design, it is necessary to start with the relationship between software requirements and software design. Software requirements are based on the knowledge and understanding of the real world by users or other relevant parties. The inconsistency between knowledge and information usually exists in the objective world, and there may be some contradictions in the requirements. These requirements are derived from information that may conflict with each other. Summary: Since requirements need to be expressed in spoken language, users often ignore some implicit requirements, functional requirements, and nonfunctional requirements. Different types of requirements (such as external interface requirements and requirements) and the methods to focus on and capture these requirements are different. Due to the excessively detailed requirements, the development schedule of the software project is delayed, and the cost is exceeded. Requirements depend on the software development process and are related to it. When requirements change, it is difficult to effectively analyze and evaluate the magnitude of its impact.

The software design process is based on the specification of software requirements (the description of the information, function, and behavior of the software system) to complete the software architecture design, data structure design, and software process design or architecture. This clear component dependency is the basis for analyzing change propagation. DSM separation also provides the convenience of disassembling and reorganizing the software architecture. The use of DSM to assess the risk of change propagation can be divided into three main steps:

(1) Create the component DSM of the target software architecture and describe the software design with dependencies between components;

(2) Use relevant data to analyze the influence relationship between components to obtain a risk model for spreading changes;

(3) Based on the propagation risk model, evaluate the propagation risk of changes in software components and architecture.

The risk of change propagation r is the product of the probability of change propagation and the probability of change impact, which is given by:

$$r = cpp \times im. \tag{1}$$

The possibility that the component C_i will be directly changed when the component is changed, and the possibility of the influence of the change means that the component is directly passed to the C_i component. Therefore, the risk propagated from the component to C_i is the product, as in the following formula:

$$r_{ij} = r\left(C_j, C_i\right) = cpp_{ij} \times im_{ij}. \tag{2}$$

Change propagation risk defines the single-layer risk of change propagation (direct risk). For two components C_i and C_j that cannot be directly accessed, the risk of a step change of m from component C_j to component C_i (indirect risk) means that the component changes the influence is passed m times through other m−1, and the component C_i is as in formula (3).

The cumulative risk of change propagation cr is the sum of the risk of direct change propagation and the risk of all indirect change propagation, which is given by:

$$cri_j = \begin{cases} \sum_{m=1}^{\infty} r_{ij}^{(m)}, & i = 1, 2, \ldots, n, j = 1, 2, \ldots, n, i \neq j, \\ 0, & i = 1, 2, \ldots, n, j = 1, 2, \ldots, n, i = j. \end{cases} \tag{3}$$

The degree of influence f is the sum of the direct risk of a specific component propagating changes to all other components and the indirect risk of the change propagating, which is given by:

$$f_j = \sum_{i=1}^{n} cr_{ij}, \quad j = 1, 2, \ldots, n. \tag{4}$$

The degree of influence e is the sum of the direct risk of a specific component C_i propagating changes through all other components and the indirect risk of propagating changes, which is given by:

$$e_i = \sum_{j=1}^{n} cr_{ij}, \quad i = 1, 2, \ldots, n. \tag{5}$$

Among them is formula (6)is the following formula:

$$\mathrm{TR} = \sum_{i} \sum_{j} cr_{ij}, \quad i = 1, 2, \ldots, n, j = 1, 2, \ldots, n. \tag{6}$$

According to formulas (2)–(4), the DSM model of the spread risk of software architecture changes, and cumulative changes is obtained.

The DSM diffusion risk model is shown in Figure 1.

Using formulas (4) and (5), calculate the value of the influence f of each component, the influence e and fe+, as shown in Table 1.

Using influence f as the horizontal axis and influence e as the vertical axis, draw a scatter chart to understand the risk of component change propagation in the target software architecture, as shown in Figure 2. The more other components it involves, or the greater the impact of the change activities they involve, the greater the risk of software development.

Take the change trend of the influence degree e of the component C as an example, the change is based on the number of propagation iterations of the change. As shown in Figure 3, in the four iterations of the propagation of the change, the influence degree of the component C increases significantly and then tends to decrease, minimizing the feedback information design module or reducing the occurrence of multiple propagation iterations between components.

Based on the risk assessment algorithm for software development costs and duration, this article imitates the

	A	B	C	D	E	F	G	H	I	J	K	L
A		0.23										
B					0.27	0.23						
C				0.58			0.22	0.11		0.05		
D			0.22				0.02	0.14				
E		0.27				0.18						
F			0.04				0.09		0.50	0.11		
G			0.05					0.07			0.50	0.11
H			0.05				0.08					
I										0.06		
J												
K										0.04		0.38
L												

(a)

	A	B	C	D	E	F	G	H	I	J	K	L
A		0.25	0.00	0.00	0.07	0.08	0.01	0.00	0.04	0.01	0.01	0.00
B			0.02	0.01	0.30	0.31	0.04	0.01	0.17	0.05	0.02	0.01
C				0.71			0.30	0.27		0.07	0.17	0.11
D			0.28				0.11	0.21		0.02	0.06	0.04
E		0.30	0.02	0.01		0.27	0.03	0.01	0.15	0.04	0.02	0.01
F			0.05	0.03			0.10	0.02	0.50	0.14	0.06	0.04
G			0.07	0.05				0.09		0.03	0.51	0.33
H			0.07	0.05			0.10			0.01	0.06	0.04
I										0.05		
J												
K										0.04		0.38
L												

(b)

Figure 1: DSM model of spreading risk and cumulative spreading risk. (a) Risk of change propagation. (b) Accumulated change propagation risk.

Table 1: The *f*, *e* and *fe*+ values of each component.

	A	B	C	D	E	F	G	H	I	J	K	L
f	D	0.604	0.568	0.951	0.413	0.728	0.771	0.678	0.967	0.513	1.008	1.059
e	0.53	1.031	1.812	0.797	0.951	1.059	1.201	0.356	0.06	0	0.46	0
fe+	0.53	1.635	2.38	1.748	1.363	1.786	1.971	1.032	1.026	0.513	1.468	1.059

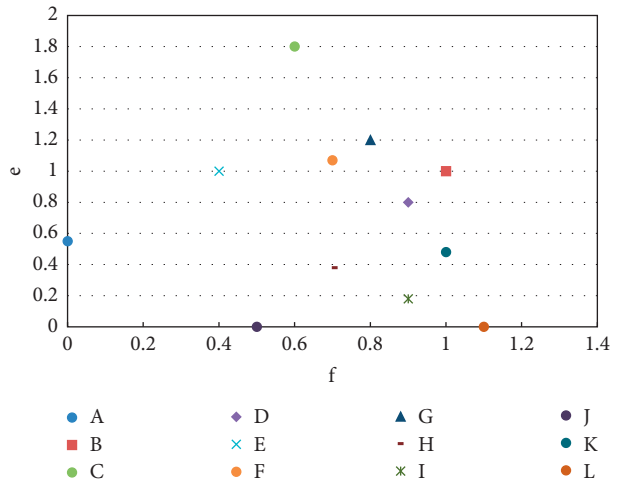

Figure 2: Scatter plot of change propagation risk.

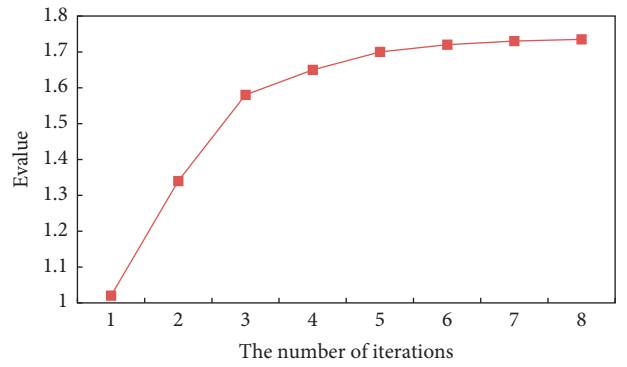

Figure 3: The degree of influence of the C component changes as the number of iterations increases.

DSM risk model to propagate changes. The cost and duration of software development are in thousands of yuan and days. Table 2 shows the input data used for simulation calculations.

The DSM model after modeling split, the probability distribution function and cumulative distribution function of the software development cost, and the simulation result of the construction time are shown in Figure 4.

To illustrate the impact of different design iterations on the cost and time required to develop software, this article also simulates DSM to assess the risk of change propagation. On the basis of the original software architecture, the order of the components was adjusted to obtain the new software architecture order {A, B, E, F, I, K, G, H, C, D, J, L} and the duration simulation in order to compare the impact of software architectures in different orders on the cost and duration of software development. Table 3 shows the simulation results of three groups of software architectures with different component layouts.

Table 2: Analog input data.

Time (days)		Cost (thousand yuan)					
2HTF minimum		Possible value	Max	Minimum	Possible value	Max	LP
A	5	8	10	7	8	12	0.8
B	9	10	12	8	9	13	0.6
C	2	4	6	4	6	8	0.2
D	7	8	10	10	11	13	0.7
E	12	15	18	41	45	50	1
F	5	8	10	8	9	10	0.9
G	8	10	12	5	8	10	0.5
H	14	16	19	14	20	28	0.4
I	3	5	6	3	5	6	0.6
J	9	10	11	11	14	15	0.7
K	13	15	18	24	28	30	0.5
L	6	8	10	7	9	11	1

Changing the parameter requirements is the source of the risk of changing the software requirements. If the requirements change, this will directly affect the components related to the changed requirements. By mapping the relationship between requirements and software architecture in this article, the QFD requirements model and software architecture can be obtained. Due to the changes in software requirements, the changes in component design in the T period are as follows:

$$re(t) = [xq(t) \times \mathrm{QFD}]^T. \tag{7}$$

When a component changes, in addition to its own changes, it will also cause the risk of changes to other components. Therefore, the parameter A in the dynamic model must contain these two attributes, which is given by:

$$A = \mathrm{CR} + E. \tag{8}$$

In the t-th stage, the correction coefficient of the state Sit of the component C_i is given by:

$$S_i^t = \frac{1}{5}\sum_{m=1}^{5} s_{im}^t. \tag{9}$$

Determine the state adaptation matrix $B(t)$ of the target software architecture at stage t using the following formula:

$$B(t) = \left[b_1^t, b_2^t, \ldots, b_n^t\right] = \left[S_1^t \times a_1, S_2^t \times a_2, \ldots, S_n^t \times a_n\right]. \tag{10}$$

Select l samples $X_i(t)$ multiple times and use Monte Carlo simulation to obtain a set of independent outputs from $Y_i(t)$. Therefore, we can obtain the distribution of this set of output values using the following formula:

$$\begin{aligned} f_{5i}^t(y_i) &= E[Y_i] = E[y_i(X_i(t))] \\ &= \lim_{I \longrightarrow \infty} \frac{y_{i1} + y_{i2} + \cdots + y_{iI}}{I}. \end{aligned} \tag{11}$$

The average value of all items in the set is the expectation that exceeds a certain risk level β, which is consistent with the definition of conditional expectation, which is given by:

$$\begin{aligned} f_{4i}^t(y_i) &= E[y_i(X_i(t))|y_i(X_i(t)) > \beta] \\ &= E\left[Y_\beta\right] \cong \frac{Y_\beta^{(1)} + Y_\beta^{(2)} + \cdots + Y_\beta^{(k)}}{k}. \end{aligned} \tag{12}$$

In addition, it mainly analyzes the differences, advantages, and disadvantages of different change management strategies compared with the "cost risk" weighing factor "λ." Formula (13) determines the trade-off factors of the strategy implementation cost and the value change risk between strategy a and strategy b in stage t under extreme change conditions. It represents the management cost required to reduce the risk of unit change costs when faced with extreme changes between different strategies.

$$\lambda_{f4|ab}^t = -\frac{\Delta f_1^t}{\Delta y(t)} = -\frac{f_1^t|_{a,f4} - f_1^t|_{b,f4}}{y(t)|_{a,f4} - y(t)|_{b,f4}}. \tag{13}$$

Determine the cost/risk ratio between the various strategies below the unconditional expected value. The cost–risk trade-off can be applied to a single component or a single component, which can also be applied to the entire software architecture. In the fourth step of the decision-making process, Tables 4 and 5 list the trade-off factors of the overall software architecture between the four groups of change management strategies and conditional expectations.

3.2. Network System. When establishing a 5G wireless communication system, it is necessary to select a suitable location for installing the antenna structure according to the actual needs of the network structure to further increase the space capacity. If the technology can be applied to the actual construction of 5G wireless networks in the future, it will help improve the broader functions of 5G networks. The application status of MIMO technology is being gradually introduced nationwide. However, theoretically speaking, the more antenna structures installed, the better the quality of information transmission can be guaranteed, and certain guarantees are also provided in terms of security. At present, manufacturers such as Huawei and ZTE have developed 16 (T/R), 32 (T/R), 64 (T/R), and 128 (T/R) AAU equipment. More than 20 provinces have gradually launched pilot projects, and the project has completed the construction of 5G radio networks using AAU equipment. In this context, the continuous introduction of MIMO technology into 5G construction has also brought many new challenges: First, if 5G construction is carried out based on the currently available location addresses, how to maximize economic benefits and what measures should be taken? The vision to solve existing problems is not satisfactory. Second, compared to the low frequency range currently used in China, it is 3.5 GHz. Frequency resources may not meet the requirements of large-scale operations, and the operational requirements of operators also pose challenges to network connections. In addition, before the development of the 5G

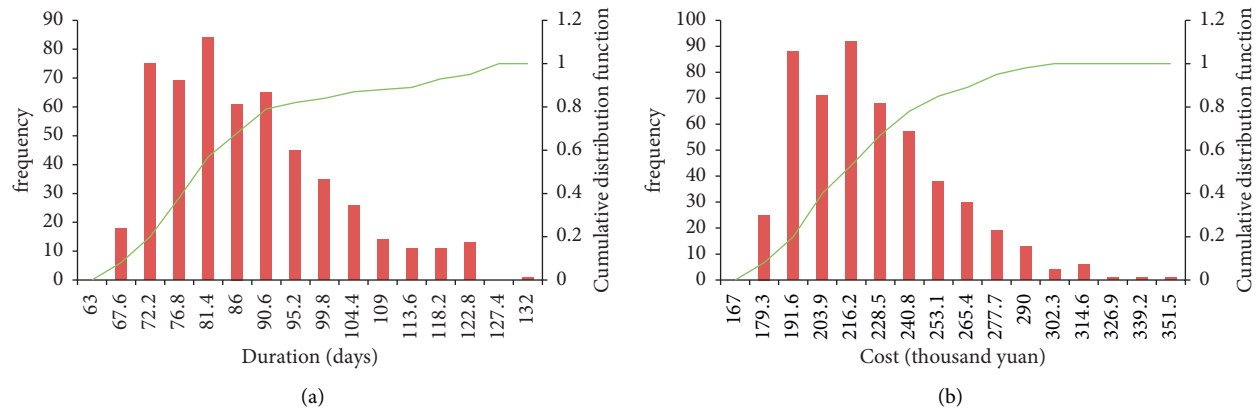

Figure 4: DSM's development cost and construction time modeling results have the risk of spreading changes.

Table 3: The results of modeling the cost and duration of the software architecture for different layouts of components.

	Cost (thousand yuan)		Duration (days)	
	Average value	Standard deviation	Average value	Standard deviation
Initial architecture	227.2	30	92	18
Partitioned architecture	217.5	30	84	12
New permutation architecture	240.3	45	104	13

Table 4: Factors for the compromise of conditional expectations among the four groups of strategies at level 4.

	Strategy one	Strategy two	Strategy three	Strategy four
Strategy one	—	0.5183	0.0925	0.1796
Strategy two	0.5122	—	−0.2804	−0.0222
Strategy three	0.0944	−0.2803	—	0.5002
Strategy four	0.1797	−0.0282	0.5705	—

network, the 4G network has been in a dominant position in the communication field for a long time, and this situation cannot fully occupy the existing 4G frequency resources. Third, the 5G downlink must be based on multiple antennas, and the transmission power must be increased to achieve wide coverage. However, in this case, it has a corresponding effect on the number of terminal antennas and transmit power of the uplink device. In this case, in order to increase the coverage of the downlink to achieve the construction goal, it is necessary to appropriately manage the coverage area. However, due to the current structure of the 4G website, the distance between the more concentrated regional stations has changed and is mainly controlled within 300 m. How to take effective measures? This measure further enhances the effect of information transmission by reducing the coverage area and reducing the space and at the same time increasing the number of wireless nodes to be established according to the demand of the network, which has certain difficulties.

4. Research on the Design of English Translation System

4.1. Technical Research on English Translation. Domestication translation technology is a method of transforming certain cultural elements into content familiar to the target language audience. The domestication translation method takes the target language as the target and interprets the same information and the same meaning from different perspectives of the source language. This translation method can help readers feel the similarities and differences in cross-cultural language communication, appreciate the charm of different languages and cultures, and make the translation better adapted to readers' reading, expression, and appreciation habits. For example, if there are major differences in translation practice in order to better convey the meaning of the source language while respecting the reading habits of readers in the target language, then the translation and the original text can achieve the same effect, certain components, or product templates After a special conversion, it can also be naturalized into the source language.

Different languages have developed in their cultural environment for a long time, gradually forming unique cultural expressions. If only one word is translated, not only the target effect of the translation cannot be achieved but there may even be contradictory expressions, which affects cultural transmission. Using different languages as carriers can express different meanings of the same psychological content. This way of expression does not mean that they have the same meaning in terms of form, connotation, and context. It is also a way of conveying the same information in the original language. Languages that are not smoothly translated from the front can be translated from the opposite perspective and vice versa. By analyzing the benefits, acceptability, and readability of the target language, and not using reserved forms, effective translation results can be achieved. The voice of foreigners is based on the cultural background of the source language, divided into

Table 5: Total cost, total risk, and total cost of strategy implementation of software architecture changes.

Strategy		Change cost risk > 0 (unit: yuan)				Strategy execution cost person (unit: yuan)			
		$Z = 1$	I = 2	I = 3	I = 4	I = 1	I = 2	I = 3	I = 4
One	F1	1781	1155.3	42068	13669.8	279.4	559.8	839.4	1119.6
	F2	297.0	1766.1	6437.0	20500.1	333.7	667.2	1001.6	1335.1
Two	F3	168.2	984.8	3312.3	9743.7	306.1	788.1	1545.3	3042.6
	F4	2814	1540.7	5254.9	15431.8	366.4	970.1	1988.6	39624
Three	F5	61.8	457.4	1652.1	5516.0	438.8	907.1	1435.5	1849.5
	F6	132.9	849.0	2999.6	9613.6	532.6	1129.5	1820.0	2331.0
Four	F7	62.0	347.7	10492	30665	4384	10023	1714.6	26749
	F8	133.0	690.0	2242.2	7164.0	533.0	1269.4	2262.3	3728.5

approximate forms, and then converted into the target language. This foreign language translation method can effectively convey the meaning and image of the original text, realize direct language and cultural exchanges, and reflect the appearance of the original text. It not only retains the meaning of the source language but also reflects the characteristics of the source text in the target language.

4.2. Design of English Translation System Based on 5G Background. This paper uses semantics to preprocess the English translation function based on semantic information to form an English phrase tree. The specific stages of the technical route are as follows: selection of word attributes, syntactic and semantic functions, training functions for forming decoded sentences, testing of decoded sentences, and output testing. Results: the words and grammar are aligned, the functions of the language part are marked according to the alignment, and the output becomes the attributes of the English phrase tree node. The technical route is shown in Figure 5.

During the operation of the system, the Linu platform was selected as the operating environment, and an English translation system was developed through MoseS. When phrases are used in the *G*. Der-side word corpus, the phrase length is explicitly set to 7.

The English automatic translation system is mainly composed of two parts: algorithm and software. The system software design is based on an embedded environment, which includes vocabulary collection, information processing, vocabulary planning, automatic control, and other modules. In order to extract the information that can reflect the characteristics of the distribution rules of the system, a method of combining information and intelligent planning is selected to realize the intelligent control and planning of the system. Design and develop automated translation system software based on embedded ARM environment, use Ti-ny0S to design the interface of system network components, and use Linux kernel to manage the cross-compilation of information management system software to enhance system management intelligence. The main function of the information management system of the automated translation system is to collect, merge, transmit information, plan integration, and so on. The FIFORAM buffer comprehensively analyzes the nature of fuzzy matching and the information about the translation status. The upper computer module is the carrier for remote transmission of the control information of the control system as shown in Figure 6.

(1) The realization of the semantic ontology modeling of the automatic English translation system is mainly through the organic combination of English translation and semantic feature analysis to develop related algorithms to realize the semantic ontology modeling of the system. Use the semantic feature extraction method to appropriately map and design the concept grid presented in translation and obtain the fuzzy inference related parameters of the system parametersusing the following formula:

$$\Delta((\beta) = \begin{cases} s_k, & K = \text{round}(\beta), \\ a_k = \beta - k, & a_k \in [-0.5, 0.5]. \end{cases} \tag{14}$$

Establish a robust semantic scoring index, use the method of logical fuzzy argumentation to construct the semantic tree of the concept, and obtain the model of the semantic ontology of the system. According to this model, a decision is made on the cross and complex assessment of English intelligence and automatic translation, and the following formulas are obtained:

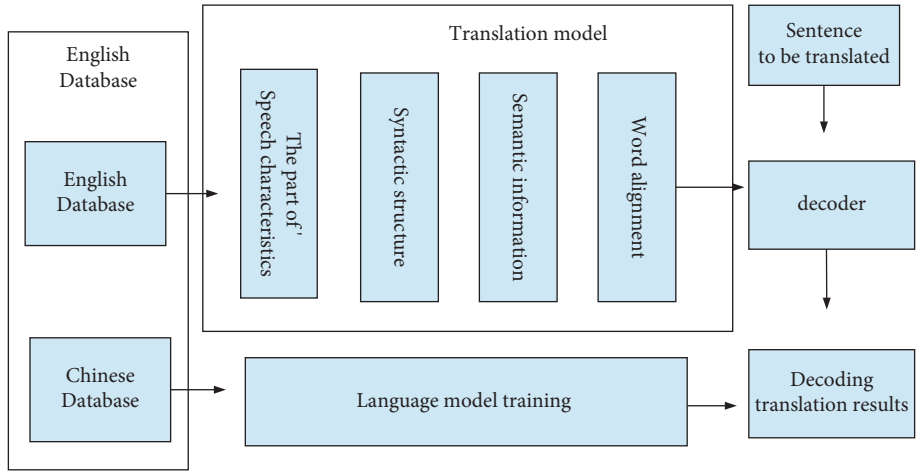

Figure 5: The technical route of the translation system.

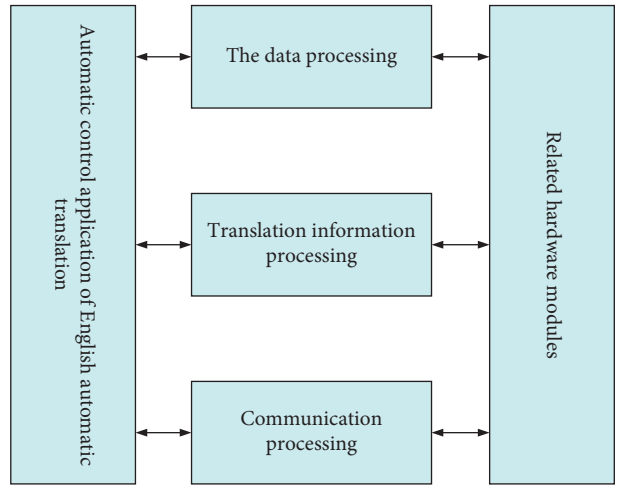

Figure 6: Information transmission model with three-tier architecture.

$$\left(\xi_{ij}^{+}, \eta_{ij}^{+}\right) = \Delta\left(\frac{\min_i \min_j \Delta^{-1} d\left(t, f^{+}\right)}{\Delta^{-1} d\left(t, f^{+}\right) + \rho \max_i \max_j \Delta^{-1} d\left(t, f^{+}\right)} + \frac{\rho \max_i \max_j \Delta^{-1} d\left(t, f^{+}\right)}{\Delta^{-1} d\left(t, f^{+}\right) + \rho \max_i \max_j \Delta^{-1} d\left(t, f^{+}\right)}\right), \tag{15}$$

$$\left(\xi_{ij}^{-}, \eta_{ij}^{-}\right) = \Delta\left(\frac{\min_i \min_j \Delta^{-1} d\left(t, f^{-}\right)}{\Delta^{-1} d\left(t, f^{-}\right) + \rho \max_i \max_j \Delta^{-1} d\left(t, f^{-}\right)} + \frac{\rho \max_i \max_j \Delta^{-1} d\left(t, f^{-}\right)}{\Delta^{-1} d\left(t, f^{-}\right) + \rho \max_i \max_j \Delta^{-1} d\left(t, f^{-}\right)}\right). \tag{16}$$

(2) The design of the translation algorithm optimizes the design of the translation algorithm through the combination of feature semantic analysis and phrase translation and develops and plans the combination of phrase translation. The specific matrix expressions are given by:

$$X_1 = \begin{bmatrix} M.G.P.P \\ P.VP.M.P \\ G.M.G.EP \\ VG.P.P.G \\ EG.EP.VP.M \end{bmatrix}, \quad (17)$$

$$X_2 = \begin{bmatrix} P.M.VP.VP \\ VP.EP.G.G \\ M.G.P.VP \\ EG.VP.VP.M \\ P.VP.M.VP \end{bmatrix}, \quad (18)$$

$$X_3 = \begin{bmatrix} G.P.VP.VG \\ VP.G.P.G \\ VG.VP.G.P \\ G.VG.EG.VP \\ P.VP.M.VP \end{bmatrix}, \quad (19)$$

$$\omega = \begin{pmatrix} \omega_1 \\ \omega_2 \\ \omega_3 \end{pmatrix} = \begin{bmatrix} M.G.VP.P \\ VP, VG, P, G \\ G.P.M.G \end{bmatrix}. \quad (20)$$

Realize predictive and automatic translation based on the relevance between phrases and obtain the dual semantic relevance of phrase translation combination as shown in the following formulas:

$$d_i^+ = \sqrt{\sum_{j=i}^{m} \Delta^- \left(\omega_j', \beta'\right) \Delta^{-1} \left(d\left(\left(x_{ij}, a_{ij}'\right), \left(x_i^{+\prime} + a_i^{+\prime}\right)\right)\right)} 2, \quad (21)$$

$$d_i^- = \sqrt{\sum_{j=i}^{m} \Delta^- \left(\omega_j', \beta'\right) \Delta^{-1} \left(d\left(\left(x_{ij}, a_{ij}'\right), \left(x_i^{-\prime} + a_i^{-\prime}\right)\right)\right)} 2. \quad (22)$$

The dimensionless processing of translated phrases is a specific process, which is given by:

$$D_i^+ = \frac{d_i^+}{\max_i d_i^+}, D_i^- = \frac{d_i^-}{\max_i d_i^-}, \quad i = 1, 2, \ldots, n, \quad (23)$$

$$R_i^+ = \frac{g_i^+}{\max_i g_i^+}, R_i^- = \frac{g_i^-}{\max_i g_i^-}, \quad i = 1, 2, \ldots, n. \quad (24)$$

According to the draft algorithm, combined with English translation, the optimization of the English automatic translation algorithm is realized. Cross-compilation and program loading methods are used to improve the algorithms to be loaded into the system information processing module. Based on software development, it further promotes the combination of machine intelligent translation and phrase translation.

This paper conducts a simulation experiment to further test the performance of the automatic English translation system based on the combination of machine intelligent translation and phrase translation. The accuracy of translation output and the memory speed of semantic information in English are selected as the test results. System tests show that the accuracy and recall speed of the system translation are high, and the degree of intelligence and automation is also high.

5. Conclusion

This article is mainly based on the early stage of software project development (including demand analysis and software architecture design). In the context of demand change, starting from the meaning of demand change, it discusses the adaptability of software architecture and the risk of software demand change. As we all know, in the past, network architecture systems based on traditional models could not effectively meet current social development and people's diverse needs for communication network services. We can also see that accelerated promotion and research and development of mobile networks are the inevitable trend of future social development. However, it is believed that with the advancement of current technology, the above-mentioned problems can be well solved through more active research and development. In general, the development of an automatic English translation system based on software change management and 5G networks will further enhance the intelligence and automation of English translation. In addition, due to the differences in professional experience and knowledge structure between users and software developers, it is often difficult to obtain complete and accurate requirements. The system design is mainly composed of two parts, namely the development of the software system and the development of the English translation algorithm. The automatic translation algorithm optimization project is based on the combination of semantic feature analysis and phrase translation, and the software design of the automatic translation system is based on an embedded environment.

Data Availability

The data used to support the findings of this study are available from the author upon request.

Conflicts of Interest

The author declares that there are no conflicts of interest.

References

[1] V. Szalvay, "An introduction to agile software development," *Danube Technologies*, vol. 3, 2004.

[2] T. E. Fægri and N. B. Moe, "Re-conceptualizing requirements engineering: findings from a large-scale, agile project," in *Proceedings of the Scientific Workshop Proceedings of the XP2015*, pp. 1–5, Helsinki, Finland, May 2015.

[3] J. G. Andrews, S. Buzzi, W. Choi et al., "What will 5G be?" *IEEE Journal on Selected Areas in Communications*, vol. 32, no. 6, pp. 1065–1082, 2014.

[4] A. Gupta and R. K. Jha, "A survey of 5G network: architecture and emerging technologies," *IEEE Access*, vol. 3, pp. 1206–1232, 2015.

[5] M. Agiwal, A. Roy, and N. Saxena, "Next generation 5G wireless networks: a comprehensive survey," *IEEE Communications Surveys & Tutorials*, vol. 18, no. 3, pp. 1617–1655, 2016.

[6] N. Shahriar, S. Taeb, S. R. Chowdhury et al., "Reliable slicing of 5G transport networks with bandwidth squeezing and multipath provisioning," *IEEE Transactions on Network and Service Management*, vol. 17, no. 3, pp. 1418–1431, 2020.

[7] P. Wang, Y. Li, L. Song, and B. Vucetic, "Multi-gigabit millimeter wave wireless communications for 5G: from fixed access to cellular networks," *IEEE Communications Magazine*, vol. 53, no. 1, pp. 168–178, 2015.

[8] J. Sangeetha and S. Jothilakshmi, "Speech translation system for English to dravidian languages," *Applied Intelligence*, vol. 46, no. 3, pp. 534–550, 2017.

[9] D. Xiong, F. Meng, and Q. Liu, "Topic-based term translation models for statistical machine translation," *Artificial Intelligence*, vol. 232, pp. 54–75, 2016.

[10] S. McGee and D. Greer, "Towards an understanding of the causes and effects of software requirements change: two case studies," *Requirements Engineering*, vol. 17, no. 2, pp. 133–155, 2012.

[11] E.-M. Schön, D. Winter, M. J. Escalona, and J. Thomaschewski, "Key challenges in agile requirements engineering," in *Lecture Notes in Business Information Processing*, pp. 37–51, Springer, Berlin, Germany, 2017.

[12] Y. Wang, Q. X. Chen, N. Zhang, C. Feng, F. Teng, and M. Y. Sun, "Fusion of the 5G communication and the ubiquitous electric Internet of Things: application analysis and research prospects," *Power System Technology*, vol. 43, no. 5, pp. 1575–1585, 2019.

[13] N. K. Kiem, H. N. B. Phuong, Q. N. Hieu, and D. N. Chien, "A novel metamaterial MIMO antenna with high isolation for WLAN applications," *International Journal of Antennas and Propagation*, vol. 2015, 9 pages, Article ID 851904, 2015.

[14] H. Zhu, L. Jing, and Y. Wang, "Knowledge representation and semantic inference of process based on ontology and semantic web rule language," *Transactions of Nan Jing University of Aeronautics & Astronautics*, vol. 34, no. 1, pp. 72–80, 2017.

[15] S. Ye and W. Guo, "Semi-supervised neural machine translation based on sentence-level BLEU metric data selection," *Pattern Recognition and Artificial Intelligence*, vol. 30, no. 10, pp. 937–942, 2017.

Hindawi
Mobile Information Systems
Volume 2022, Article ID 4284734, 8 pages
https://doi.org/10.1155/2022/4284734

Research Article

Application of Robust Data Link Optimization in Medical Protein Nutrition Intervention Based on Ensemble Learning Algorithms

Xiaowen Hou

School of Economics and Management, Beijing Information Technology College, Beijing, China

Correspondence should be addressed to Xiaowen Hou; houxw@bitc.edu.cn

Received 24 May 2022; Revised 21 June 2022; Accepted 5 July 2022; Published 20 July 2022

Academic Editor: Shadi Aljawarneh

Research on 6G-related technologies based on the Internet of Things (IoT) has attracted widespread attention from research units, universities, and industry, and there are still some important issues that need to be resolved urgently. How to ensure robust data link optimization for data transmission in a band-limited nonstationary environment at a lower cost is a very important issue. Based on the current research status of specific medical protein POCT products at home and abroad, this paper has designed and developed a specific medical protein detection system with simple operation, rapid detection, and small volume: according to the Lambert Beer's law, we adopt the transmission colorimetry method (transmittance Turbidity method), with the optical part, electronic part, and mechanical part as the structure, carry out the design work of optoelectronics and software. It also evaluates the serum nutritional indicators and gastrointestinal function of abdominal surgery patients after nutritional intervention combined with emotional nursing and expands the reference basis for intervention methods for abdominal surgery patients. Using this experimental method, after the samples are selected by the CART algorithm, the accuracy of the running results is higher.

1. Introduction

By collecting large amounts of mobile data and analyzing voice data mining, the wireless network can be optimized and the quality of the mobile communication network can be improved. Wireless network optimization refers to the reasonable allocation of the production network and formal investment of resources mainly through the collection of parameters and analysis of data, and reasonable optimization of the network operation status [1]. It is to find out the quality problems in the network operation process and use parameter settings to solve network quality problems. And, put forward reasonable network maintenance and find out various optimization methods for planning and construction plans. Based on the research of related theories about the application of voice data mining technology in mobile communication networks, find out a suitable data analysis method for mobile communication networks. This article introduces a low-complexity, low-power modulation, and demodulation transmission technology, namely, differential chaotic keying (DCSK) modulation [2]. And, this paper, respectively, describes and analyzes the robust data link optimization, advantages, and improvement methods of the system in standard and nonstandard transmission environments. At the same time, some new coding and modulation schemes based on multiple DCSK (MDCSK) will be provided to improve the transmission quality of the system in a band-limited environment, which will help in low-power, low-cost networks, especially on nonstationary channels. the robust data link optimization of the system is improved [3]. The results show that these optimization works have significantly improved the system performance. Afterwards, the optimization of system parameters for nonstationary channel characteristics and the adaptive transmission mechanism will become the focus of future research. The specific medical protein analyzer is a device that checks the level of specific immune proteins in serum, plasma, or urine to determine their content accurately and effectively to assist doctors in clinical diagnosis [4]. During the operation of the instrument, professional medical

personnel first collect, identify, process, and store the samples, separate the active ingredients from the samples to be tested obtained from the test objects, and mark all samples corresponding to their test objects [5]. At present, the most common test items of specific medical protein analyzers mainly include the detection of myocardial protein markers (myoglobin, etc.) and the detection of nephropathy protein markers [6]. The combination of nutritional intervention and emotional care can improve the nutritional status of diabetic patients. Patients undergoing abdominal surgery can enhance immune function, promote the recovery of gastrointestinal function, and reduce postoperative complications. In addition, the control group received routine nutrition interventions, such as health education, psychological care, primary care, and prevention of complications, and the observation group received a combination of early nutrition intervention and emotional care to realize the application of medical protein nutrition intervention [7].

2. Related Work

The literature introduces a large-scale automatic protein detection instrument with high throughput, automation, and high speed, which requires professional operation training and is operated by professional medical personnel [8]. The reagents and samples are processed before use and the detection can be performed automatically. Multichannel multisample detection can be processed at one time. Hospitals above Grade A and large testing institutions have a large number of people to test each day, and the testing needs are large. The automatic analyzer can automatically perform testing, and perform result judgment, and report printing, which reduces time and human resources, and satisfies the testing well [9]. The literature introduces the rapid and convenient POCT rapid detection. The outpatient volume of grassroots hospitals is small, and the samples are correspondingly small. The use and maintenance cost of high-throughput specific immune protein detection equipment is high, which is bound to cause waste. Therefore, a POCT type rapid tester should be selected in such facilities [10]. This type of product is also suitable for outpatient laboratories, emergency rooms, rapid test centers, municipal hospitals, etc. The literature introduces the importance of theoretical research on the classification of differentiated image data with several samples and the classification of speech data with one sample and emphasizes their application in high-throughput light screening and language-independent speech recognition, it depends on the angle of the speaker application [11]. By analyzing the problems in the existing image and audio data classification methods, the most important research content in this article can be determined. The literature describes the classification of cytoplasmic images [12]. Taking the information distance theory as a reference, the MPEG compression algorithm is used to rewrite the information distance equation, and according to the application characteristics of MPEG, the similarity between cytoplasmic images is evaluated [13]. Experimental results show that this method is similar to the results of traditional analysis methods. Because the cost of biological experiments is high, the data set used does not need to be verified for the second time by biological experiments, so it is impossible to compare the profit indicators of this method. The literature introduces a dynamic time warping algorithm for combining weights [14]. The attributes of speech data are analyzed, combined with the dynamic time warping algorithm, the reliability index is defined, and a new weighted dynamic time warping algorithm is proposed, which can be used for speech recognition in silent environments [15]. It can be seen from the results that this method can improve the recognition speed without affecting the accuracy of speech recognition.

3. Theoretical Basis of Voice Data Mining and Robust Data Link Optimization

3.1. Speech Data Mining Algorithm Design. The PD audio data samples contain 26 samples, which correspond to audio segments of 26 individuals. Due to the difference in the range and tone of each person's voice, some samples cannot describe the essential difference between PD patients and healthy people. Finding the most valuable samples in the right way is of great benefit to research. This article recommends using the CART algorithm to select samples.

Through the prior knowledge of the pathologist, the features in the PD data are extracted, which contains a total of 26 features. There is a big gap between feature values because different features have different physical meanings and calculation methods. Many machine learning algorithms are sensitive to the number of feature values. To solve this problem, this article uses a normalization method to normalize all functions to actual values between 0 and 1. Assuming that the training set is represented by X, the test set is represented by T, $x\_\max$ represents the largest vector of features, and x_min represents the smallest vector of features, then

$$X\prime = \frac{(X - x\_\min)}{x\_\max - x\_\min}, \tag{1}$$

$$T'\frac{(T - x\_\min)}{x\_\max - x\_\min}. \tag{2}$$

M classification task, P_m is the probability that the sample belongs to the m-th category, then the Gini coefficient of this probability distribution is defined as follows:

$$\mathrm{Gini}(p) = \sum_{m=1}^{M} p_m(1 - p_m) = 1 - \sum_{m=1}^{M} p_m^2. \tag{3}$$

For the binary classification problem, assuming that the probability of the first sample type is p, then the Gini coefficient of the probability distribution is

$$\mathrm{Gini}(p) = 2p(1 - p). \tag{4}$$

Given two types of sample sets D Gini index is defined as follows:

$$\text{Gini}(D) = 1 - \sum_{m=1}^{2}\left(\frac{|C_m|}{|D|}\right)^2. \tag{5}$$

$$\text{Gini}(D,T) = \frac{|D_1|}{|D|}\text{Gini}(D_1) + \frac{|D_2|}{|D|}\text{Gini}(D_2). \tag{6}$$

If CART is "too deep," overfitting will occur. In other words, the performance on the training set is very good, but the performance on the test set is very poor. Currently, pruning is a good way to do this. The cleaning algorithm is divided into two steps: first, get many subtrees, starting from the bottom of the entire spanning tree, and then continue cutting to the CART root node. The second is to choose the best subtree and use a different set of validations to cross-validate all subtrees and obtain the best structure. This operation can be performed when the amount of data is sufficient, but it is difficult to process medical data due to the small amount of medical data and the high cost of obtaining new samples. Therefore, this article uses another method to control the overfitting of CART. When generating CART, the minimum number of leaf node samples will be specified. This can effectively control the depth of the tree, so as to obtain the best effect on the model.

The Pearson correlation coefficient is usually used to measure the linear correlation between feature f and category C, as shown in the following equation:

$$R(i) = \frac{\text{cov}(X_i, Y)}{\sqrt{\text{var}(X_i)\text{var}(Y)}}. \tag{7}$$

The intraclass distance is the square of the distance between each sample in the same class. The distribution of the sample points around the mean is reflected by the within-class variance, and the formula is as follows:

$$d^2(w_i) = \frac{1}{N_i}\sum_{k=1}^{N_i}\left(\mathrm{x}_{i,k} - \mathrm{m}_i\right)^T\left(\mathrm{x}_{i,k} - \mathrm{m}_i\right), \tag{8}$$

$$S_{w_i} = \frac{1}{N_i}\sum_{k=1}^{N_i}\left(x_{i,k} - m_i\right)\left(x_{i,k} - m_i\right)^T. \tag{9}$$

The intraclass distance and intraclass scatter matrix are transformed into rank relations,

$$d^2(w_i) = Trr\left[S_{w_i}\right]. \tag{10}$$

The relationship between the intraclass, interclass, and total allocation matrix in multiclass situations,

$$S_w = \sum_{i=1}^{c} P_i S_{w_i} = \sum_{i=1}^{c} P_i \frac{1}{N_i}\sum_{k=1}^{N_i}\left(x_{i,k} - m_i\right)\left(x_{i,k} - m_i\right)^T. \tag{11}$$

The total between-class deviation matrix,

$$S_B = \sum_{i=1}^{c} P_i\left(m_i - m\right)\left(m_i - m\right)^T. \tag{12}$$

Overall scatter matrix,

$$S_T = \frac{1}{N}\sum_{l=1}^{N}\left(x_l - m\right)\left(x_l - m\right)^T = S_W + S_B, \tag{13}$$

$$d^2(\vec{x}) = Tr\left[S_w + S_B\right] = Tr\left[S_T\right]. \tag{14}$$

When deriving and actually applying certain relationships, the following statistics can replace them.

$$P_i = \frac{N_i}{N}, m_i = \frac{1}{N_i}\sum_{k=1}^{N_i}\vec{x}_k^{(i)}, m = \frac{1}{N}\sum_{l=1}^{N}\vec{x}_l. \tag{15}$$

Assuming that there are m neurons in the visual layer of RBM and n neurons in the hidden layer, the energy function of the neurons in the i-th visual layer is shown as follows:

$$E(V,H|\theta) = -\sum_{i=1}^{m} a_i v_i - \sum_{j=1}^{n} b_j h_j - \sum_{i=1}^{m}\sum_{j=1}^{n}\omega_{ij} v_i h_j. \tag{16}$$

The joint probability distribution of (V,H) is

$$P(V,H|\theta) = \frac{e^{-E(v,H\theta)}}{A(\theta)}, A(\theta) = \sum_{v,H} e^{-E(v,HH)}. \tag{17}$$

The observation of the data distribution V is the key point. It is the probability function of the common probability distribution $P(V, H|\theta)$ of the input data.

$$P(V|\theta) = \frac{1}{A(\theta)}\sum_{y} e^{-E(V,H|\theta)}. \tag{18}$$

RBM is an asymmetric structure. The activation probability of each neuron is conditionally independent of each other. The activation probabilities of the i-th unit in the visible layer and the j-th unit in the hidden layer are calculated separately.

$$P\left(v_i = 1|H,\theta\right) = \sigma\left(a_i + \sum_j \omega_{ij} h_j\right). \tag{19}$$

$$P\left(h_j = 1H,\theta\right) = \sigma\left(b_j + \sum_i v_i \omega_{ij}\right). \tag{20}$$

The integrated learning algorithm consists of two parts optimized based on the CART example. The first is to use the CART algorithm to select the best sample. The second is to combine the results of the RF, SVM, and ELM classifiers to perform joint decisions. In this section, LOO and LOSO will be used to organize experiments. It can be seen from the experimental results that LOSO can effectively overcome the differences in audio samples, is usually more effective than LOO, and mainly involves the final prediction of the object. We do not make requirements for the actual prediction of a single sample, so this section mainly uses experimental LOSO results to test performance.

Integrate three algorithms RF, SVM, and ELM to predict the test set. Using the Gini coefficient of the spanning tree model, RF contains 500 CARTs. After CART optimization, samples and features are randomly selected from the sample

Table 1: Integrated learning classification results under LOO.

Classification algorithm		LOO (%)		
		Correct rate	Sensitivity	Specificity
RF_with CART	Mean	70.80	72.20	69.50
	Best value	71.40	72.90	70.40
SVM(linear)_with CART	Mean	65.10	64.40	65.80
	Best value	65.10	64.40	65.80
SVM(rbf)_with CART	Mean	70.19	72.31	68.08
	Best value	70.19	72.31	68.08
ELM_with CART	Mean	60.13	62.44	57.83
	Best value	61.50	63.70	60.40
PD-EL_with CART	Mean	74.50	76.90	72.00
	Best value	75.50	78.30	73.30

set to ensure the diversity of the tree model and improve the stability of the model. For SVM, we use a linear kernel function and a radial basis kernel function. The radial core function solves the problem of linear separability in the source sample space by mapping the data set from the source space to the feature space and mapping the low-dimensional to the high-dimensional. The parameter g is used to control the degree of mapping. These two parameters control the generalization ability of the model. The smaller the parameter value, the higher the accuracy. In the algorithm of this work, the values of C and g are between 1 and 20. In the experiments in this chapter, setting C to 10 and g to 2 is the most effective. ELM is a single hidden layer feedforward neural network with powerful custom functions, but it is more sensitive to parameter selection. ELM training does not require backpropagation, so the calculation is faster and more common, but the results may vary greatly. By integrating multiple classifier models suggested in this chapter, we can effectively reduce variance and increase model stability.

3.2. Analysis of Results. After optimizing the CART example, use the new example set to train RF, SVM, and ELM models. A total of 4 result sets will be obtained. RF_withCART refers to an RF model trained with a new set of samples. SVM (linear)_withCART refers to the new linear kernel SVM training sample set. SVM(rbf)_withCART refers to the radial basis kernel SVM that has been trained using new example sentences. ELM_withCART refers to the ELM model trained with new example sentences. Table 1 lists the classification results of each model.

Compare the PD-EL_withCART algorithm to illustrate the effectiveness and superiority of the algorithm. So far, only four studies of Sakar et al.'s data have been tested, two of which show the classification accuracy of the validation set. It can be seen from the results that no matter how LOO or LOSO changes, the PD-EL_withCART algorithm achieves

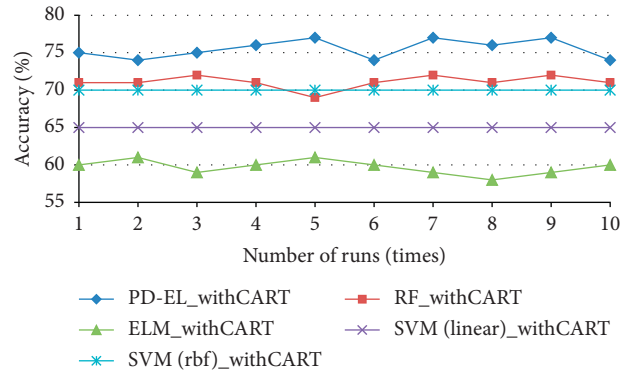

Figure 1: Correction rate curve under LOO.

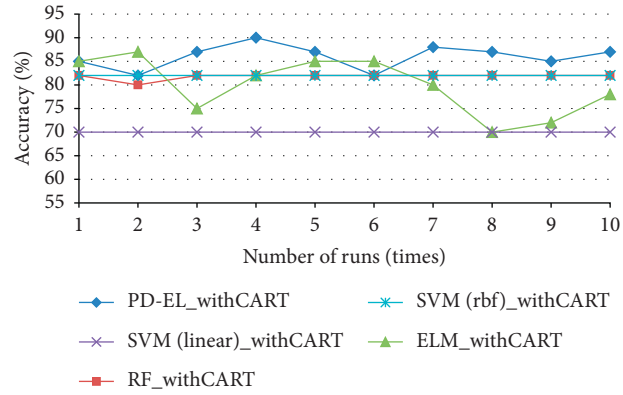

Figure 2: Correction rate curve under LOSO.

Table 2: Classification results of unoptimized samples under LOO.

Classification algorithm		LOO (%)		
		Correct rate	Sensitivity	Specificity
SVM no CART	Average	64.50	65.80	63.30
	The best	64.50	65.80	63.30
RF no CART	Average	67.39	71.65	62.36
	The best	68.46	76.92	60.00
ELM_no CART	Average	61.60	64.00	59.10
	The best	63.30	66.00	62.10
PD-EL_no CART	Average	72.40	74.80	70.00
	The best	73.80	76.20	71.50

the best classification performance in terms of classification accuracy, sensitivity, and specificity. At the same time, because LOSO effectively reduces the differences between volunteer samples, LOSO has better classification performance than LOO.

In order to conduct in-depth research on the classification performance and stability of the ensemble learning algorithm, we ran each algorithm ten times and calculated the correct rate curves for these five algorithms, as shown in Figure 1. The experimental results show that the PD-EL_withCART algorithm has the highest classification accuracy and sensitivity. However, the best stability is the RF_withCART algorithm.

Table 3: Compares the results of the integrated classification algorithm before and after sample selection.

Difference		L00 (%)			LOSO (%)		
		Accuracy	Flexibility	Specificity	Accuracy	Flexibility	Specificity
PD- EL_noCART	Average	72.40	74.80	70.00	83.50	90.00	77.00
	The best	73.80	76.20	71.50	87.50	95.00	80.00
PD-EL_with CART	Average	74.40	76.90	72.00	86.50	95.00	78.00
	The best	75.50	78.30	73.30	90.00	100.00	80.00

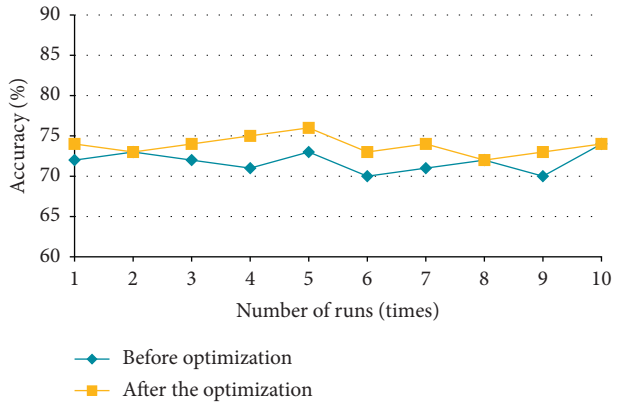

Figure 3: The accuracy curve of the integrated algorithm before and after sample optimization under LOO.

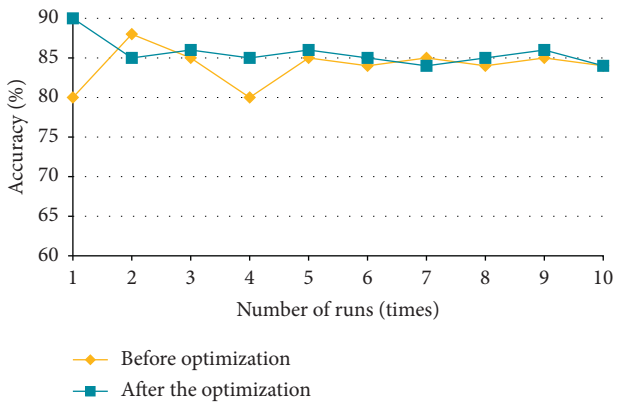

Figure 4: Accuracy curve of the integrated algorithm before and after sample optimization under LOSO.

As shown in Figure 2, the effectiveness of the integrated algorithm is proved by comparing the classification of each classification algorithm in the original data set with the situation after optimizing the CART sample.

As shown in Table 2, without optimizing the CART samples, the overall performance of PD-EL_noCART in this article is the best, with an average accuracy of 83.5%, which is higher than all single classifiers. It can be seen that the ELM algorithm is very sensitive to the initial parameters, and the results of each cycle are very different. Therefore, the ensemble model is suitable for classifying PD samples.

As shown in Table 3, the average accuracy of PD-EL_withCART in LOSO is increased by 3%, the average flexibility is increased by 5%, and the average specificity is increased by 1%, which is the same as the result of the LOO method.

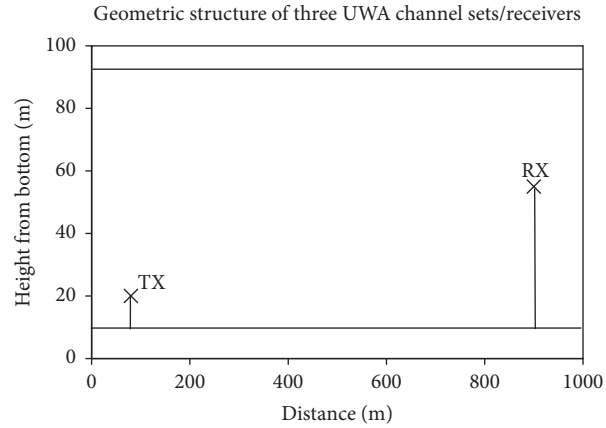

Figure 5: Geometric structure of three UWA channel sets/receivers.

Figure 3 shows the accuracy of the results of 10 executions of LOO and LOSO. Using these two experimental methods, after selecting samples through the CART algorithm, the accuracy of the results of 10 runs is usually the accuracy of the unoptimized sample set.

After optimizing the sample in LOSO, the variance of the accuracy of the 10 results is 0.016, and the variance without optimization is 0.024. After optimizing the sample, you can see that the results are clustered near the mean as shown in Figure 4.

3.3. System Robust Data Link Optimization Design Analysis. Mainly introduces several MDCSK (circular square) signal designs and corresponding coding and modulation systems based on low-cost and low-power consumption under nonstandard channel environment in 6G, respectively, which are optimized for specific nonstationary channel environments. And, the future development direction is given. First, the MDCSK system model used in this system is introduced. Secondly, the optimization of the system itself and the related research work of coding and modulation based on MDCSK are introduced. Then, through examples to demonstrate the constellation based on the MDCSK system and the related modulation and coding structure, code pattern, and related algorithm design and optimization, it can significantly improve the system performance without expanding the bandwidth and achieve low-power consumption. This provides some ideas for the optimal design of the MDCSK data link under nonstationary channels and provides examples of application solutions in specific nonstationary environments, providing the possibility of

Table 4: Comparison of turbidimetric method and turbidimetric method.

Detection method	Scope of test	Detection accuracy	Stability requirements	Reagent price	Calculation method
Turbidimetry	Larger	General	High	General	Simple
Nephelometry	Low concentration	Low concentration and higher	General	High	Complex

Table 5: The protein and calories contained in various foods are as follows.

Category	Weight per serving (g)	Calories (kcal)	Protein (g)
Cereals	25	90	2.0
Vegetables	500	90	5.0
Fruits	200	90	1.0
Soy	25	90	9.0
Milk	160	90	5.0
Meat and eggs	50	90	9.0
Hard fruit	15	90	4.0
Grease	10	90	—

low-cost and low-power implementation in other existing environments. The receiving end obtains the transmission information by directly correlating the signals in the t1 and t2 time periods without channel estimation. The specific positive and negative signals can be expressed as follows:

$$s_1(t) = \begin{cases} +c(t), & 0 \le t < \left(\frac{T}{2}\right), \\ +c\left(t - \left(\frac{T}{2}\right)\right), & \left(\frac{T}{2}\right) \le t < T, \end{cases} \tag{21}$$

$$s_2(t) = \begin{cases} +c(t), & 0 \le t < \left(\frac{T}{2}\right), \\ -c\left(t - \left(\frac{T}{2}\right)\right), & \left(\frac{T}{2}\right) \le t < T. \end{cases} \tag{22}$$

This modulation method has the characteristics of simple equipment and robustness under multipath fading channels, and the corresponding transmission rate decreases accordingly. In order to make the simulation more convincing, the simulation results of 1500 time-varying channel impulse response convolutions are obtained, among which there are channel scenes shown in Figure 5.

Through the performance analysis and research of DCSK in the PLC and UWA environment, it can be seen that because this modulation method does not require the advantages of channel estimation and equalization, it has excellent robustness under nonstationary channels, which is undoubtedly difficult to track and estimate at present.

4. Nutritional Intervention and Application of Medical Protein

4.1. Medical Protein Detection Algorithm Design. In the detection of specific immune proteins, some types of antigens and antibodies specifically bind to form a turbid solution. For example, the NGAL and Cystatin C items detected by this system are not applicable to Lambert Beer's law. It is necessary to select an analytical method for the determination of the concentration of turbidity solution-photoelectric turbidimetry. The photoelectric turbidimetric method is a method of qualitative and quantitative analysis by measuring the degree of turbidity of the solution. It is one of the commonly used medical methods in the detection of specific immune proteins. It has a history of more than 100 years and has played a very important role in many fields. Important role. It has advantages such as cost reduction, ease of use, and high sensitivity. The principle is that as long as the intensity of the incident light is constant, the change of the beam energy conforms to the law of conservation of energy. Because it is difficult to directly measure the intensity of light absorbed in the solution, the intensity of transmitted or scattered light is usually measured to achieve the purpose of quantitative analysis of protein content. The propagation path of light when passing through the turbidity solution can be divided into the transmittance turbidity method.

The calculation formula of the transmittance turbidity method is

$$I_t = I_0 e^{-(\alpha+s)l}. \tag{23}$$

The absorbance value of the suspension to be tested is defined as A, and the absorbance value can also indicate the concentration of the suspension to be tested.

$$A = \lg\left(\frac{I_0}{I_t}\right) = \ln(\alpha + s)l. \tag{24}$$

During the detection process, a beam of incident light with a specific wavelength of Io emitted by the light source passes through the reaction cup containing the suspension to be tested. At this time, equation (24) is derived as follows:

$$A = \lg\left(\frac{V_0}{V_t}\right). \tag{25}$$

Since the relationship between the ratio of incident light to transmitted light and the absorptance is a numerical relationship, the light source, photodetector, and photoelectric processing module in actual sample detection are more stable. When the concentration of the suspension to be tested is low, its absorbance value is correspondingly smaller. If the light source and photovoltaic cell are unstable and the voltage value fluctuates, the absorbance value will fluctuate exponentially. Therefore, this method puts forward higher requirements on the design of the constant current source of the light source and the effect of the photoelectric processing module.

The two turbidimetric detection methods are briefly introduced previosly. Table 4 compares the advantages and disadvantages of the two turbidimetric methods.

Table 6: Comparison of nutritional status between the two groups before and after intervention ($x \pm s$).

Group	n	BM I(kg/m^2)	Hb (g/L)	TP (g/L)	ALB (g/L)	TC (mmol/L)	TG (mmol/L)
Intervention group							
Before intervention	40	17.87 ± 3.32	89.32 ± 8.13	65.19 ± 8.12	36.86 ± 7.30	3.18 ± 0.54	1.25 ± 0.49
After the intervention	40	20.10 ± 4.08 *	97.56 ± 9.45*	70.07 ± 9.87*	41.84 ± 6.43*	4.14 ± 0.43 #	1.68 ± 0.51*
Control group							
Before intervention	40	18.08 ± 3.76	87.89 ± 8.07	67.21 ± 8.43	35.05 ± 5.98	3.21 ± 0.64	1.23 ± 0.46
After the intervention	40	18.57 ± 3.95	90.11 ± 9.85	67.42 ± 9.13	36.13 ± 7.09	3.25 ± 0.49	1.27 ± 0.45

The test method for the NGAL and Cystatin C items detected by the turbidimetric method adopts the two-point endpoint method, and the absorbance calculation refers to the equations (23) and (24) in the calculation of the colorimetric method, which can be obtained by the following equation:

$$\Delta A = A_{R2} - A_{R1}. \tag{26}$$

And, combined with formula (25) for derivation, the final calculation formula of the photoelectric turbidity method of this system is shown in the following equation:

$$A = \frac{5\left(\lg\left(V_0/V_{R2}\right) - \lg\left(V_0/V_{R1}\right)\right)}{3}. \tag{27}$$

4.2. Research Methods of Nutrition Intervention. This group consisted of 80 hemodialysis patients, who were randomly divided into intervention group and control group, with 40 cases in each group. Provide regular health education, and the nurse on duty explains to the patient how to enter the room and the dietary precautions to be taken. When the health education information is updated, the nurse will contact the patient in time and notify the request.

The specific content is sufficient protein and calorie intake: choose high-quality animal protein and instruct patients to perform hemodialysis twice a week. Protein intake should be 1.0–1.2 g per day; limit the intake of egg yolk 3 times a week; eat less seafood and offal. Need to consume a certain amount of calories, maintain a healthy body condition, and determine the daily protein and calorie intake according to the ideal body weight. Ideal weight: standard weight (kg) = [height (cm) − 100] × 0.9, protein intake: total protein (g) = protein intake per kilogram of standard weight × standard weight (kg); total calories (kcal) = Calorie intake per kilogram of standard body weight × standard body weight (kg), to understand the protein and calories required. Drinking water management: daily total fluid intake is limited to 1000 ml. If the urine output is 500 ml/d or more, then the daily water intake (ml) = daily urine output + 500 ml of water, and drink with a solid scale water cup. Daily weight gain should be kept within 1 kg. Sodium salt management: the intake of sodium salt is 3–4 g/day, and the water content is 1000 ml/day. The other is to add 1–2 g/d of salt. You can use vinegar, shallots, garlic, sugar, chili, mustard, etc., instead of salt to increase appetite. Potassium intake management: instruct people who have dialysis twice a week to control their potassium intake to 1.3 g/d. Boil the vegetables in boiling water or cook for 3 minutes before frying. Bibimbap in broth, low-salt, and unsalted soy sauce are prohibited. Frozen food at extremely low temperatures contains 1/3 less potassium than fresh food.

Based on the control group, a nutritional intervention model was established. As the person in charge of health education, nurses regularly and specifically explain how to improve diet and provide adequate nutrition for patients and their families. At the same time, the "24-Hour Diet Review Questionnaire" describes the purpose and method of filling in the form and regularly collects the form to promote patients to strictly abide by the nutritional intervention standards, and timely feedback and diet changes provide information about the nutritional composition. According to Table 5, arrange the required food.

4.3. Research Results of Nutrition Intervention. Generally, the BMI index is a comprehensive index used to assess a person's nutritional status. The BMI index decreases with weight loss, indicating that the body is malnourished. The mild malnutrition of hemodialysis patients reaches 33%, and the severe malnutrition reaches 6%–8%. Among the biochemical indicators, HP, ALB, and blood lipids are important indicators for evaluating nutritional status. The results are shown in Table 6 for a comparison of nutritional status between the two groups before and after the intervention.

4.4. Discussion and Analysis of Medical Protein Nutrition Intervention. The nutritional status of hemodialysis patients is closely related to the occurrence of clinical complications. Although dialysis is widely used, diet management plays an important role in improving the quality of life of patients with chronic renal failure. The incidence of malnutrition in hemodialysis patients is high. Research clearly shows that an insufficient protein energy diet is an important indicator of predicting patient mortality. In this study, the patient's dietary protein, water, potassium, sodium, phosphorus, and other indicators were extensively adjusted to improve the patient's nutritional status.

Drink water from a water cup with identifiable capacity, and every measurement plays a role in strict weight control. Through written teaching methods, patients and their families are taught to effectively manage potassium intake. By repeatedly explaining the diet, chewing calcium and phosphorus adsorbents and taking calcium and phosphorus adsorbents and phosphorus-containing foods at the same time can reduce blood phosphorus and increase blood calcium, supervise the intervention group of patients to learn a scientific and reasonable lifestyle.

5. Conclusion

Generally, the BMI index is a comprehensive index used to assess a person's nutritional status. The BMI index decreases with weight loss, indicating that the body is malnourished. Among the biochemical indicators, HP, ALB, and blood lipids are important indicators for evaluating nutritional status. The accumulation of various toxins in patients with end-stage renal disease can cause gastrointestinal symptoms, loss of appetite, and insufficient protein and calorie intake. A small amount of amino acids and protein are lost during hemodialysis. Some studies believe that ALB is the most valuable indicator for predicting the long-term survival of patients. Anemia in dialysis patients is a relatively common phenomenon. Therefore, evaluating anemia status is the basis for improving the nutritional status of patients. Studies have shown that effective nutritional interventions for hemodialysis patients can significantly increase their energy requirements. Properly regulating the nutritional status by combining the patient's diet and nutrition is very important for the improvement of the patient's survival rate and quality of life.

Data Availability

The data used to support the findings of this study are available from the author upon request.

Conflicts of Interest

The author declares that there are no conflicts of interest.

References

[1] D. Mohammed, M. Omar, and V. Nguyen, "Wireless sensor network security: approaches to detecting and avoiding wormhole attacks," *Journal of Research in Business, Economics and Management*, vol. 10, no. 2, pp. 1860–1864, 2018.

[2] W. M. Tam, F. C. M. Lau, and C. K. Tse, *Digital Communication with Chaos Multiple Access Techniques and Performance*, Elsevier Science, Amsterdam, The Netherlands, 2006.

[3] D. M. Rocke, "Robust control charts," *Technometrics*, vol. 31, no. 2, pp. 173–184, 1989.

[4] T. Nepusz, H. Yu, and A. Paccanaro, "Detecting overlapping protein complexes in protein-protein interaction networks," *Nature Methods*, vol. 9, no. 5, pp. 471-472, 2012.

[5] H. N. Chua, K. Ning, W. K. Sung, H. W. Leong, and L. Wong, "Using indirect protein-protein interactions for protein complex prediction," *Journal of Bioinformatics and Computational Biology*, vol. 06, no. 03, pp. 435–466, 2008.

[6] B. Xu, H. Lin, and Z. Yang, "Ontology integration to identify protein complex in protein interaction networks," *Proteome Science*, vol. 9, no. 1, p. S7, 2011.

[7] X. Tang, J. Wang, and Y. Pan, "Predicting protein complexes via the integration of multiple biological information," in *Proceedings of the 2012 IEEE 6th International Conference on Systems Biology*, pp. 174–179, IEEE, Xi'an, China, August 2012.

[8] X. Lei, F. Wang, F.-X. Wu, A. Zhang, and W. Pedrycz, "Protein complex identification through Markov clustering with firefly algorithm on dynamic protein-protein interaction networks," *Information Sciences*, vol. 329, pp. 303–316, 2016.

[9] Y. J. Zhang, H. F. Lin, Z. Yang, and J. Wang, "Construction of dynamic probabilistic protein interaction networks for protein complex identification," *BMC Bioinformatics*, vol. 17, no. 1, p. 186, 2016.

[10] L. Ou-Yang, D. Q. Dai, X. L. Li, M. Wu, X. F. Zhang, and P. Yang, "Detecting temporal protein complexes from dynamic protein-protein interaction networks," *BMC Bioinformatics*, vol. 15, no. 1, p. 335, 2014.

[11] B. Futcher, G. I. Latter, P. Monardo, C. S. McLaughlin, and J. I. Garrels, "A sampling of the yeast proteome," *Molecular and Cellular Biology*, vol. 19, no. 11, pp. 7357–7368, 1999.

[12] L. Salwinski, C. S. Miller, A. J. Smith, F. K. Pettit, J. U. Bowie, and D. Eisenberg, "The database of interacting proteins: 2004 update," *Nucleic Acids Research*, vol. 32, no. 90001, pp. 449D–451D, 2004.

[13] S. Brohée and J. van Helden, "Evaluation of clustering algorithms for protein-protein interaction networks," *BMC Bioinformatics*, vol. 7, no. 1, p. 488, 2006.

[14] M. He, Y. Wang, and W. Li, "PPI finder: a mining tool for human protein-protein interactions," *PLoS One*, vol. 4, no. 2, Article ID e4554, 2009.

[15] R. McDonald and F. Pereira, "Identifying gene and protein mentions in text using conditional random fields," *BMC Bioinformatics*, vol. 6, no. S1, 2005.

Hindawi
Mobile Information Systems
Volume 2022, Article ID 4362870, 12 pages
https://doi.org/10.1155/2022/4362870

Research Article

Design of Computer Economic Audit System and Intelligent Language Implementation Based on SURF Algorithm

Ding Ding

Audit Department, Anhui Audit College, Hefei, Anhui, China

Correspondence should be addressed to Ding Ding; 2012017@ahsjxy.edu.cn

Received 24 May 2022; Revised 19 June 2022; Accepted 2 July 2022; Published 19 July 2022

Academic Editor: Shadi Aljawarneh

Based on the SURF algorithm, the PROSAC (Progressive Sample Consensus) algorithm is first used to delete a large number of matching points to improve the accuracy of remote sensing image registration and to improve the speed of the SURF algorithm. Finally, PROSAC geometric verification is used in the study area to achieve accurate image stitching. In the field of computer economic auditing, there is a serious disconnect between theory and practice. As the company's electronic data becomes more and more abundant, the method of determining its authenticity has become an important issue that auditors need to solve immediately, and special research on the theory of data reliability is needed in the field of computer economic auditing. In this article, we will first introduce the background and practical significance of project development, explain system-related development technology, conduct system analysis and system design of the project, and discuss the effectiveness and economic benefits of project development technology. Detailed analysis and description of system design include system function module processing and system database design. The innovation of this paper is that the system can meet the actual financial and auditing needs of very professional enterprises. In addition, the work documents required for the audit are automatically generated according to the work requirements, which can completely clarify the responsibilities of each department and comprehensively improve the audit efficiency. At the same time, the entire system is safe and orderly, which can ensure the normal operation of the operation. The purpose of this article is to explore database-based natural language query technology. First, after introducing the database intelligent language, we will study the Chinese word segmentation and part-of-speech tagging algorithm based on HMM to explain the details of the continuous field matching algorithm.

1. Introduction

This paper proposes an effective SURF algorithm for image matching on a mobile platform. The algorithm uses images from other data sources and other scenes to evaluate its performance. Commonly used methods are used for comparative analysis, and the test results show that, based on a similar number of matches, the CC-SURF algorithm has a higher matching rate and matching accuracy than the SURF algorithm [1]. In order to obtain a good match and a good distribution, some homography matrices between the match and the image need to be obtained in the initial match [2]. In this paper, the selected homography or basic matrix is used for geometric matching, and the geometric relationship between image pairs is used to process part of the image information. This process can limit the corresponding points to a smaller search area to find more accurate matches [3, 4]. These coincident points are evenly distributed, highly reliable, and robust to weak texture and motion-blurred images [5]. The computer economic audit information system uses computers as the main tool to collect, record, store, process, and output various financial accounting data of the company, complete financial accounting information analysis and users' required financial affairs, and provide accounting information [6]. Improve company management and economic efficiency through management, forecasting, decision-making, and auditing. Computer economic auditing has been applied to manual accounting information system and is gradually replacing manual accounting information system [7]. Company financial information is important data that directly reflects the company's business environment, so it is necessary to comprehensively manage this data

and provide a data infrastructure for company decision-making [8]. The design of the company's financial audit information system uses various resources to convert the organization's economic business and transactions into audit information, which provides decision makers with an integrated information system to support various decisions [9]. After improving the system function, you can implement the system function many times, and after performing these multiple tasks, you can understand the problems that still exist in the system design. The design of selecting examples in the test should be very clear about the purpose of the test [10]. Only in this case can the test design a use case or plan suitable for the system. Based on the background of application requirements, how to reduce the distance between people and computers so that ordinary users can effectively use computer information resources has become an important topic in the field of computer research [11]. The intelligent language query interface is a research field with great theoretical and practical value [12]. It allows users to directly request and use intelligent language in daily life to obtain the information they need. Natural language query will be applied to the database, so that users can only use a specific application to access the database without having to understand the logic and storage structure of the database [13].

2. Related Work

The literature introduces how to construct and design a vocabulary. The vocabulary is the "brain" of the system. The system includes a general vocabulary, a database-specific related vocabulary, and a user-defined vocabulary, which plays a big role in word segmentation and syntactic analysis [14, 15]. The literature introduces lexical analysis and details the analysis process based on lexical analysis, such as determining query targets, determining query conditions, and generating final results for nested queries [16]. The literature describes the implementation process of the Adaboost algorithm [17]. Aiming at the poor adaptation of intelligent scoring samples in practice, the algorithm is improved to maximize the advantages of the original algorithm, and a single value of the algorithm is effectively produced to avoid this situation, thereby improving the accuracy of intelligent paper screening sex [18]. The literature introduces the introduction of a scoring model and a comment model into the review. The scoring model finally determines a three-tier evaluation index system. Based on this theme, an improved adaptive improvement algorithm and experimental results are proposed [19]. To this end, it was also verified through experiments [20]. The comment model in this article is also innovative. It not only provides natural language prompt feedback, but also provides learning suggestions for individuals, so that the goal of promoting learning through real evaluation can be achieved [21]. The literature describes the overall design and implementation of the system [22]. We will explain the preparation and implementation process of the improved Adaboost/CT algorithm proposed in this course, explain the basic framework of the system in detail, and introduce and display the modules of each subsystem.

3. Intelligent Language Implementation Based on SURF Algorithm

3.1. Design of SURF Algorithm. SURF uses the Hesse determinant to approximate the image. The Hessian matrix of a specific pixel P (x, y) in an image with a ratio of Yγ is defined as

$$H(X,\sigma) = \begin{bmatrix} L_{xx}(X,\sigma) & L_{xy}(X,\sigma) \\ L_{yx}(X,\sigma) & L_{yy}(X,\sigma) \end{bmatrix}. \tag{1}$$

After being represented by the box filter, the Hessian matrix determinant is

$$\det(H) = D_{xx}D_{yy} - \left(0.9D_{xy}\right)^2. \tag{2}$$

In order to obtain the corresponding feature points of the two rotated images, the unmatched points must be removed by the RANSAC algorithm. The RANSAC repetition time is determined based on the ratio between the inline point and the original data volume. Reducing the ratio between the two images will significantly increase the number of iterations, which will have a major impact on the overall efficiency of the algorithm. Therefore, geometric constraints are set according to the geometric relationship between the two images. If the detected matching feature points meet the geometric constraints, they are maintained or deleted, and other matching items are deleted using the RANSAC algorithm.

Assume that the initial matching feature point sets of the two images I1(x, y) and I2(x, y) to be spliced are

$$P1 = \{\mathrm{P1}[i] | i = 1, 2, \ldots, \mathrm{n}\} \text{and } \mathrm{P2} = \{P2[j] | j = 1, 2, \ldots, \mathrm{n}\}. \tag{3}$$

For i = j, P1[i] and P2[j] are a pair of corresponding points. The geometric constraints of these two images are as follows:

(1) The inclination of the matching point pairs corresponding to the two images to be spliced is relatively or almost the same.

(2) The Euclidean distance between the corresponding matching point pairs of the two images to be spliced is relatively or almost the same.

Euclidean distance is expressed as

$$d_i = \sqrt{\left(y_j - y_i\right)^2 + \left(x_j - x_i\right)^2}. \tag{4}$$

Because we use the calculated data to determine the median distance from the slope, considering that the feature points can be odd or even, the calculated values must first be sorted in ascending order. Then, the specific expression is as follows:

$$k = \begin{cases} k_n, n \\ \\ \dfrac{k_{n-1}}{2}, n \end{cases} \tag{5}$$

The two images are stitched together based on the acquired feature points, but the differences in illumination and geometric correction between the images may cause obvious seams. The merged image is not clear and looks too natural at the boundary of the merged image. In this article, we have adopted a fade-in and fade-out fusion algorithm, which can eliminate stitching seams and switch images better. Comparing the traditional weight fusion algorithm with the existing weight fusion algorithm, the weight d of the fusion algorithm has a linear relationship with the change of pixel position, and the relationship of the weight d is as follows:

$$d = 1 - \frac{j - L}{R - L}. \tag{6}$$

The fusion image is $f(x, y)$ and expressed as

$$f(x, y) = \begin{cases} f_1(x, y), (x, y) \in f_1 \\ d_1 f_1(x, y) + d_2 f_2(x, y), (x, y) \in f_1 \cap f_2 \\ f_2(x, y), (x, y) \in f_2. \end{cases} \tag{7}$$

The computer's CPU frequency is 2.2 GHz, memory is 4G, WIN10 operating system is used, and the experimental software is Matlab R2015b. Choose a group of 100 images taken with a mobile phone, the image size is 600×450 pixels, and use the original algorithm to calculate the exact ratio of the 100 image groups, which is an improved algorithm. We selected five statistical sets to calculate the number of feature points before and after the two algorithms enter the RANSAC algorithm, thereby eliminating the RANSAC execution time before and after nonmatching feature points. The stitched image is shown in Figure 1.

It is different from the traditional method of directly specifying the number of clusters to bring a functional dictionary. In this article, we dynamically increase the number of cluster centers, and if the number of cluster centers increases due to noise, we will calculate the probability distribution of clusters, and the coding matrix will pass through the cluster centers. As the center of each cluster coding matrix element, the following relationship can be used and represented by the B matrix.

$$\min_{w_i} \left\| X_i - B_w w_i \right\| s.t. 1^{\mathrm{T}} w_i = 1. \tag{8}$$

As shown in Figure 2, in different poses, the BoW feature distribution of the same type of feature target is similar. The target BoW feature distributions of other types of features are completely different. This shows that the BoW model used for job target recognition has excellent discrimination and robustness in feature representation.

The SVM model is a linear optimization statistical classifier based on structural risk minimization and high-dimensional theory. The core of the algorithm is to construct the best classification hyperplane of the sample feature space, so that the attributes of the classification samples have the largest geometric distance.

The hyperplane that can be classified as feature samples after sparse coding can be processed by the kernel function:

$$\omega^{\mathrm{T}} Y + b = 0. \tag{9}$$

It can be seen from the derivation that the constraints of the SVM model are

$$\min \Phi(\omega) = \frac{\|\boldsymbol{\omega}\|^2}{2}. \tag{10}$$

The equivalent equation is

$$s.t\, y_i \left[\left(\boldsymbol{\omega}^{\mathrm{T}} \mathbf{w}_i + b \right) \right] \geqslant 1 (i = 1, 2, \ldots, n). \tag{11}$$

The model can be obtained by introducing the Lagrangian multiplier, constructing the optimal objective function and obtaining the training parameters of the model.

$$\begin{cases} \max \sum_{i=1}^{n} \alpha_i - \frac{1}{2} \sum_{i,j=1}^{n} \alpha_i \alpha_j y_i y_j \left(w_i, w_j \right) \\ s.t \sum_{i=1}^{n} \alpha_i y_i \\ \alpha_i \geqslant 0 (i = 1, 2, \ldots, n). \end{cases} \tag{12}$$

The linear kernel function is introduced in the SVM model to create an inseparable linear feature vector in a low-dimensional space, convert it into a high-dimensional linear separability, and use a linear algorithm to process the high-dimensional feature space. The slack variable C can be introduced to further improve the fault tolerance of the target SVM model to quantify the impact of error samples on the classification surface in training. The following objective functions can be used:

$$f(\omega, b, \varepsilon) = \frac{1}{2} \|\boldsymbol{\omega}\|^2 + C \sum_{i=1}^{n} \varepsilon_i. \tag{13}$$

Since the SVM model is only used as a two-level classifier, it is necessary to use multiple SVM models (1-M) to configure a training model that classifies the target into multiple categories.

3.2. Intelligent Language Processing Technology. First, based on the feature word library, divide the sequence of Chinese character strings to be divided into multiple substrings. The substrings can be words or word groups containing multiple words, and use the actual word database and rules to subdivide word groups. When cutting words, we use specific grammatical knowledge to establish relevant and reverse tracking mechanisms. The relevant mechanism is associated with the relevant network and is composed of reasoning. The related network describes the word formation ability of each functional word. Correlation inferences determine that the functional words described using related networks are different words or components of another word. The backtracking mechanism is mainly used to process ambiguous sentences. This method increases the time and space complexity of the algorithm. However, this method is a faster and more effective word splitting method.

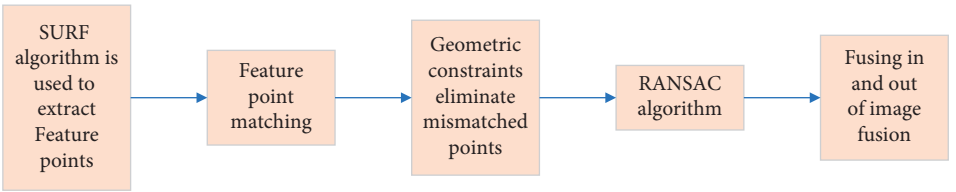

Figure 1: Block diagram of algorithm flow.

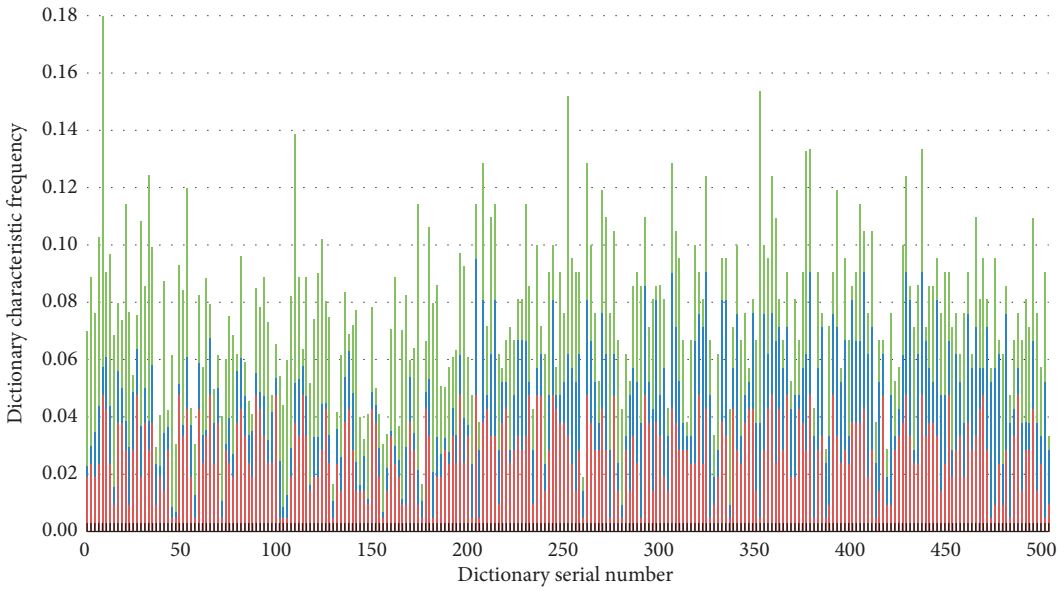

(a)

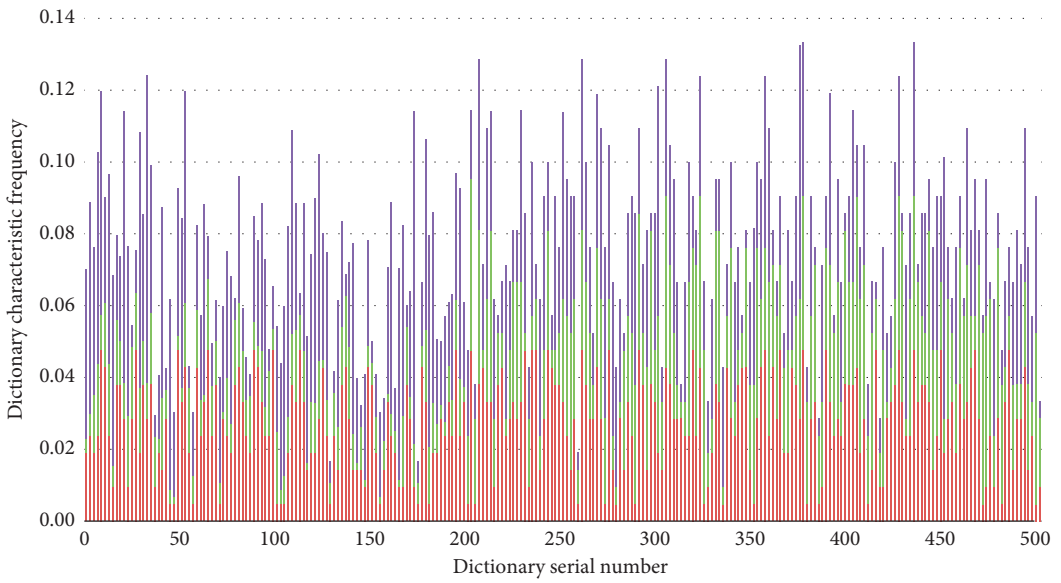

(b)

Figure 2: Continued.

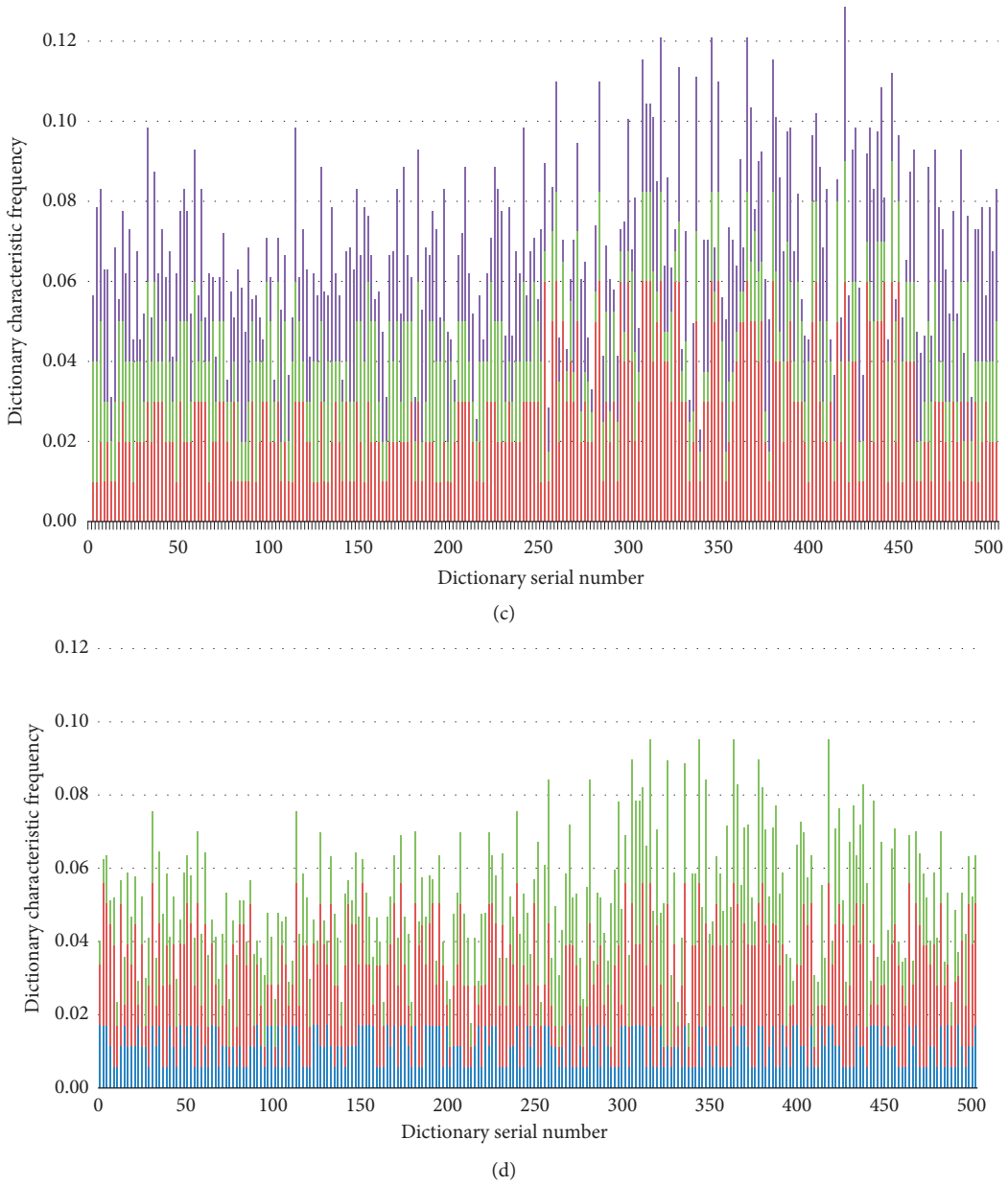

Figure 2: BoW feature effects of four workpiece targets in different poses. (a) Workpiece 1. (b) Workpiece 2. (c) Workpiece 3. (d) Workpiece 4.

This method uses the results of word frequency statistics to help deal with the ambiguous segmentation field in the process of word segmentation.

$$\widehat{W} = \arg\max_{w} P(W|S) = \arg\max_{w} \frac{P(W)P(S|W)}{P(S)}$$
$$\Rightarrow \arg\max_{W} P(W) = \prod_{i=1}^{k} P(w_i|w_1, \ldots, w_{i-1}). \tag{14}$$

Use hidden Markov chains to explain some changes in speech. The state here represents the part-of-speech tag of the word to be marked, and the state transition probability represents the relationship between parts of speech. The probability is obtained through a fixed word sequence. The largest part of the speech sequence T is the speech sequence part of the word sequence W, namely,

$$\underset{T}{arg}\,\mathrm{m}R(xT|W). \tag{15}$$

The binary model established by the HMM model to calculate the probability of each part-of-speech sequence of the multicategory sequence is as follows:

$$P_{\text{list}}(\text{list}_k) \approx P\left(t_{k,i}\right)P\left(w_i|t_{k,i}\right)\prod_{i=2}^{n} P\left(t_{k,i}|t_{k,i-1}\right)P\left(w_i|t_{k,i}\right). \tag{16}$$

The core idea of the algorithm Adaboost has been very clear, by selecting multiple weak classifiers that are more

accurate than random guessing and collecting them to finally form a powerful classifier. If there are enough weak classifiers, the error rate of strong classifiers will eventually tend to zero. The framework provided by the algorithm shows its advantages. There is no need to design a weak classifier, and various methods can be used to configure the weak classifier. On this basis, we do not need to understand the knowledge. Since the performance requirements of weak classifiers are not high, this algorithm is relatively easy to apply and is not used for feature selection. The most important point is that it has high accuracy and can be easily applied to classifiers that solve practical problems.

This article uses a simple example to demonstrate the classification process of the Adaboost algorithm. In the process of weak classifier classification, a horizontal or vertical straight line is used to classify the two categories. The sample with the displayed classification symbol indicates the sample that is misclassified and can be classified into other categories, and the sample distribution is updated when the weight of the misclassified sample is changed. The specific process is shown in Figure 3.

3.3. Natural Language Model Design. The development of natural language has gone through a period of initiation, development, and prosperity and has gradually developed from the early stage of natural language production. Nowadays, it can be combined with context to express and convey information. We want to realize how to understand natural language. The solution is to build a statistical language model for the contextual characteristics of natural language. According to the Bayesian algorithm, natural language is sometimes regarded as a random sequence, and the order model of words and sentences in the corpus is actually a probability model. The simplest solution is to assume that all words can follow this sequence, and the total probability of each word is N; then the probability of the word after any sequence is 1/N.

The method of calculating the probability of a string of words in a complete sentence is the main content of our research, and $P(S)$ considers that the display position of each word is independent, so $P(S)$ is extended to formula

$$P(S) = P(w_1, w_2, w_3 \ldots w_n). \tag{17}$$

We can use the chain rule of conditional probability to decompose probability. Since the probability of the sequence S is the product of the conditional probabilities of each word, this formula can be extended to formula (18), as shown below:

$$\begin{aligned} P(w_1, w_2, w_3 \ldots w_n) = {} & P(w_1) \cdot P(w_2|w_1) \\ & \cdot P(w_3|w_1 w_2) \cdots \\ & \cdot P(w_n|w_1 w_2 w_3 \ldots w_{n-1}). \end{aligned} \tag{18}$$

The conditional probability is calculated by moving the word backward. This will prevent many words from appearing in the learning sample. So, we only need to calculate the previous word; it has nothing to do with the previous word. Equation (18) can be simplified to equation

$$\begin{aligned} P(S) = {} & P(w_1) \cdot P(w_2|w_1) \\ & \cdot P(w_3|w_2) \cdots P(w_k|w_{k-1}) \cdots P(w_n|w_{n-1}). \end{aligned} \tag{19}$$

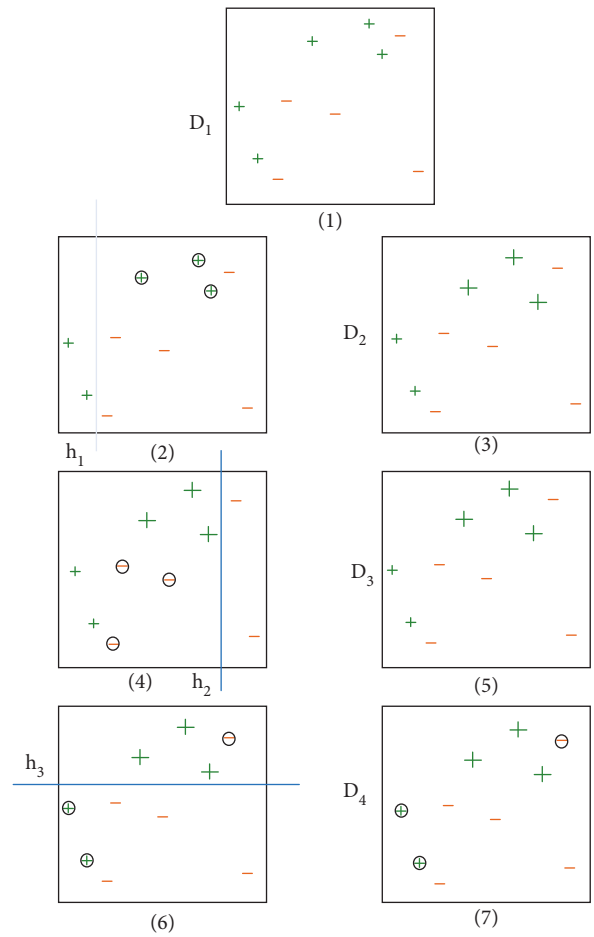

Figure 3: Adaboost classification implementation process diagram.

Equation (19) is the calculation formula of the binary grammar model. If you want to use the formula of the binary grammar model to calculate the probability of a meaningful sentence, you only need to calculate the product of the binary grammar probability of two adjacent words. The probability of the sentence model is expressed as

$$\begin{aligned} P(\text{Today is } a \text{ nice day}) = {} & P(\text{Today kb} >) \cdot P(\text{is} I \text{Today}) \\ & \cdot P(al\text{is}) \cdot P(\text{nice Ia}) \cdot P(\text{day} I \text{nice}). \end{aligned} \tag{20}$$

According to the corpus, it can obtain the number of occurrences of a specific binary grammar. Then formula (21) is obtained.

$$P(w_n|w_{n-1}) = \frac{C(w_{n-1} w_n)}{\sum_w C(w_{n-1} w)}. \tag{21}$$

The words in the trinomial grammar model depend on the first two words. Then the parameter estimation is expressed by formula

$$P\left(w_n | w_{n-N+1}^{n-1}\right) = \frac{C\left(w_{n-N+1}^{n-1} w_n\right)}{C\left(w_{n-N+1}^{n-1}\right)}. \quad (22)$$

Everything is closely connected. Some connections are clearer and more reliable, while others are not. It only depends on the single relationship of multiple things, so the linear equation of a variable is determined by a factor. Use the correlation in statistics to analyze and study the relationship between multiple variables (two or more variables), and determine the correlation between two or more variables according to the correlation coefficient.

Correlation analysis is widely used in practical analysis problems. For example, in the research of the intelligent scoring algorithm on the subject, several factors are extracted by searching for factors that affect the composition score, and the correlation with the composition is analyzed to determine the effect of predicting the composition score. Certain extracted feature indicators may have an impact on the composition score, and correlation analysis can be used to discover these influencing factors. According to the research theme of this article, we will mainly introduce the Pearson correlation coefficient.

The Pearson correlation coefficient is a correlation coefficient representing a linear correlation diagram between variables, and its calculation formula is shown in formula

$$r = \frac{\sum (x_i - \overline{x})(y_i - \overline{y})}{\sqrt{\sum (x_i - \overline{x})^2 \sum (y_i - \overline{y})^2}}. \quad (23)$$

Variables decrease with the increase of other variables and increase with the decrease of other variables. The two variables are not related to each other, and the changes of independent variables do not affect each other. Table 1 lists the magnitude and correlation of r values.

Hidden Markov Model (HMM) is a probability model proposed in the late 1960s. It evolved from the Markov model and is expressed as a parameter to explain the statistical characteristics of random processes.

The state of the hidden Markov model cannot be directly observed, but it can be observed using a series of vectors. Each vector is represented by several probability density distributions in various states, and each vector contains a response and generates a probability density distribution.

HMM (Hidden Markov Model) is used to describe random statistical characteristics. The state of the model can explain some global characteristics of the data, and this property is usually relatively stable. The statistical feature changes of the feature vector can be observed from a statistical point of view. The HMM is described below.

$$N = \{q_1, q_2, \ldots q_N\}. \quad (24)$$

A limited set of observations:

$$M = \{v_1, v_2, \ldots v_M\}. \quad (25)$$

Initial state probability vector:

$$\pi = (\pi_1 \sim \pi_N), \pi_i = P(q_1 = i), 1 \le i \le N. \quad (26)$$

State transition probability matrix:

Table 1: $|r|$ value and correlation.

$\|r\|$ range of values	The meaning of $\|r\|$
0.00–0.19	Very low correlation
0.20–0.39	Low correlation
0.40–0.69	Moderately related
0.70–0.89	Highly correlated
0.90–1.00	Very high correlation

$$A = \left(\alpha_{ij}\right)_{N \times N}, \alpha_{ij} = P\left(q_{t+1} = j | q_t = i\right), 1 \le i, j \le N. \quad (27)$$

4. Design and Practical Application of Computer Economic Audit System

4.1. Computer Economic Audit System. The state-regulated company financial audit refers to the relevant procedures and methods of the organization. We prepare audit reports objectively and fairly in accordance with the law and form audit opinions. The company's financial audit truly reflects the company's financial problems. In this chapter, we will take the relevant situation of a specific company's financial audit information system as an example to analyze the importance of the financial audit information system to the company and provide a template for future system construction.

The company's financial audit information system, as the most representative system in the information management system, audits and manages the company's various financial information in order to achieve the purpose of paperless management. Using the audit management system can accurately manage the overall financial status of the enterprise, conduct an objective and fair assessment, show the actual financial status, and make the financial status of state-owned enterprises macro. Therefore, finance and auditing have the following requirements:

(1) It is necessary to ensure the reliability of relevant data.

The data retained in the system is the financial data of the enterprise, and these data are the basis of all reports, so these data must be authenticated to prevent falsification of data.

(2) Ensure data integrity.

In order to ensure data integrity, we need to prevent data from being illegally modified, deleted, forged, or destroyed, and all data must retain relevant information.

(3) Guarantee the legality of the data.

The system operates in accordance with relevant regulations and is subject to company constraints and relevant regulations during the system life cycle.

(4) Ensure the security of system data.

Ensuring data security is an important function of the system. It is necessary not only to prevent data from damaging internal systems, but also to prevent external attacks and prevent data links from being monitored.

(5) Ensure the reliability of system data.

Reliable data means that, in the process of retransmitting data, it will not be retransmitted or verified through a certain mechanism, thereby ensuring reliable data transmission and preventing data damage in the database. In addition to backup data redundancy operations, more operations can be performed.

The content of the audit is relevant in many ways. Verification and audit items are particularly important in the company's financial evaluation. Through the analysis of the audit content, we can know that the company's financial audit information system must have the following functions: Audit project management is about managing projects. Relevant departments and employees formulate audit standards based on established work objectives, complete scientific planning and deployment of specific audit projects, and conduct digital management of audit projects. Accounting books are a very important part of the entire company's financial management process. It is set up based on corporate vouchers, and by recording every payment made by the company, sustainable and complete financial accounting can be carried out. Then, you can use the income and expenditure status of the entire fund at a specific moment to understand whether the company's production and operating conditions are favorable or suffer losses. The company's financial data is usually stored in the existing financial management system, then exported, and then imported into the audit information system.

For the above-mentioned specific business needs, we can understand the importance of the audit management system in the enterprise. Therefore, Figure 4 shows the complete functional structure of the system.

In addition to the principle of system function design, the financial audit information system starts from the entire system, decomposes the design of nonfunctional requirements into several small steps, designs according to each stage, and must expand its capacity to a certain extent to prevent future A system problem has occurred.

(1) Overall system performance.

The response time of the interface is less than 2 seconds, and the query time of the complex business database is less than 3 seconds.

(2) The system has high reliability.

System reliability also has certain requirements. There is no intermittent situation in the company's financial activities, so the financial management system needs to be able to run continuously and be stable for a long time without any actual failures. As far as system service hours are concerned, the system should operate without barriers during 7×24 working days.

(3) Security and confidentiality mechanism.

Financial audit information directly reflects the company's overall income and expenditure, and its data is the most important part of the company. How to prevent these data from being stolen is very important. Measures taken include site hosting, logging system, and automatic backup.

(4) Fault tolerance and disaster tolerance

In the course of operation, the financial management system often encounters sudden errors or other unexpected events. When solving these relatively common errors, the system provides good fault tolerance. Compared with relatively serious system failures and some abnormal external events, it can also withstand a certain degree of disaster; no matter what the situation is, the important data in the financial management system will not be lost or leaked.

4.2. Architecture Design of Computer Economic Audit System. The system is designed for the company's internal financial audit based on the C/S model. This is a client-server model, which is relatively easy to develop, easy to operate, and relatively safe and has a high response speed.

The system development is based on the software development of the MVC model, which realizes the hierarchical system-friendly maintenance and development. The abstract form of the object data is the information called the model layer. The main data model of the system is mainly the company's financial audit data. The interface is used as a display layer for users to view and interact, and the interface is connected to the data through the controller layer. The overall frame design of the system is shown in Figure 5.

The system mainly places some logic and processing display on the client and reads data from the company's internal database. The network topology structure diagram of the system is shown as in Figure 6.

4.3. System Database Design. The main information of the audit project needs to reflect the basic information of the project. The database table design of the audit project management module is shown in Table 2.

There are many sample forms of audit documents introduced using the fixed asset cycle. Fixed assets refer to the correlation between fixed assets and the financial statements of the audit department and the relationship of asset circulation. Control the distribution of fixed assets, pay attention to business activities, and check the change information of related accounts. Table 3 shows the design of the database table.

The design of the audit summary data table is shown in Table 4.

The system uses VB framework. Usually, according to the different new projects, the interface designed according to the needs uses standard EXE to add extended content. The database can use ADO to complete the connection. The implementation code of the database link code is as follows:

```
Sub Main()
On Error GoTo On_error'frmWelcome.Show
Set con = New ADODB.Connection
```

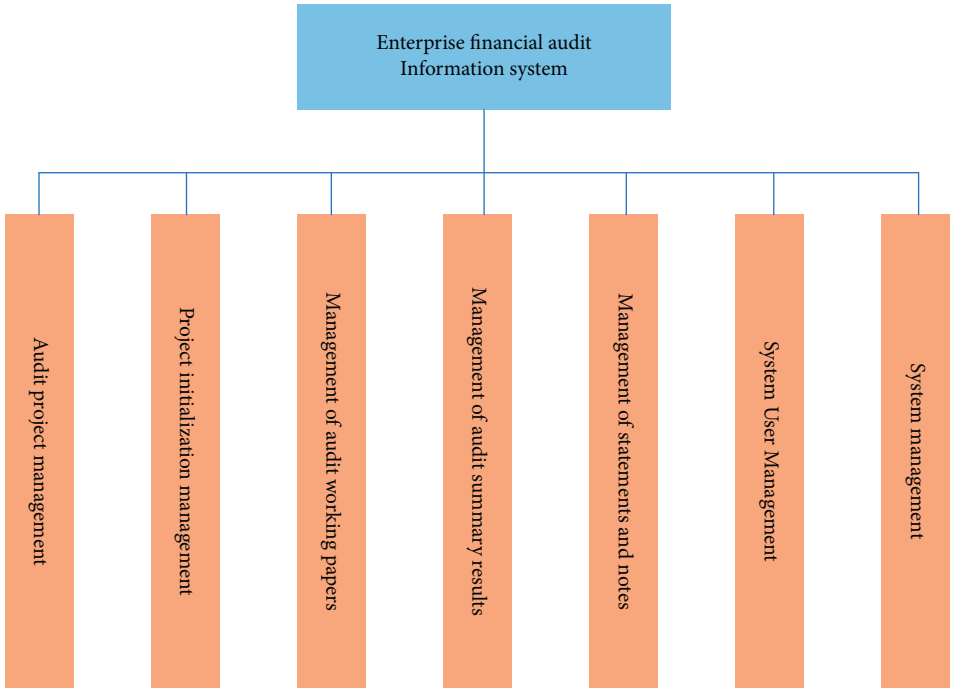

Figure 4: The overall functional structure of the system.

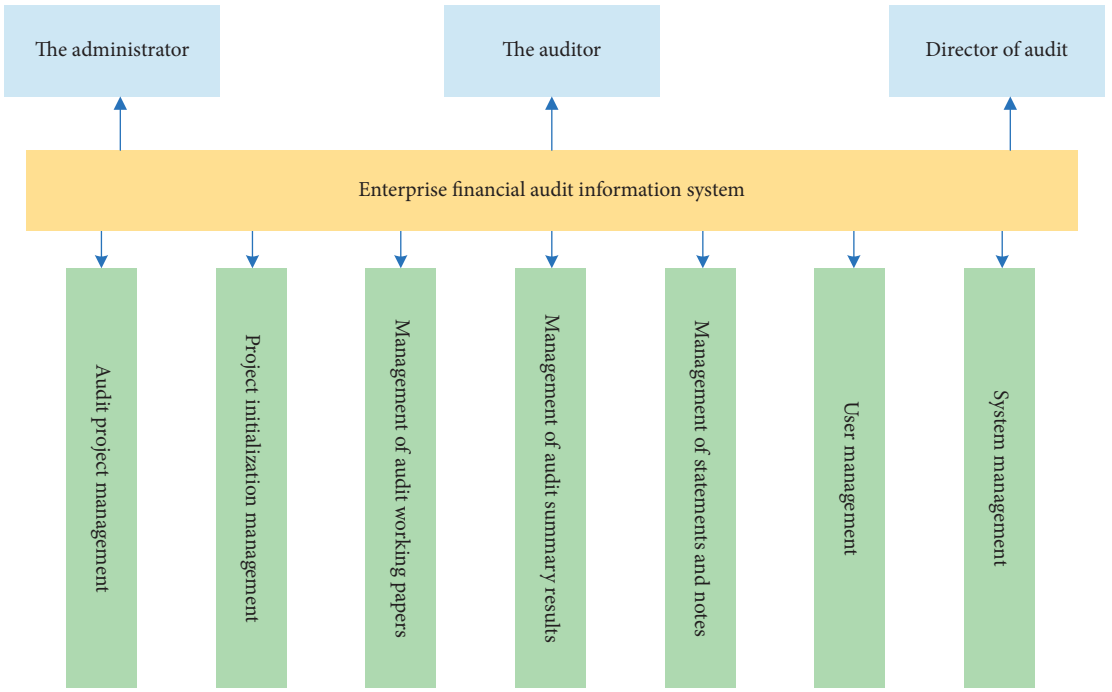

Figure 5: System overall framework design.

con.ConnectionString = ("Provider = SQLOLEDB; User ID = sa; PWD = ; InitialCatalog = human; Data Source = .")

con.Open.

con.CommandTimeout = 20Load frmLogin

frmLogin.Show vbModalExit Sub

On_error:

If Err.Number = -2147467259 Or Err.Number = -2147217900 ThenUnload frmWelcome

MsgBox "Check that SQL is not installed or the database required by the software is not installed..."&vbCrLf&" is further checking the installation of

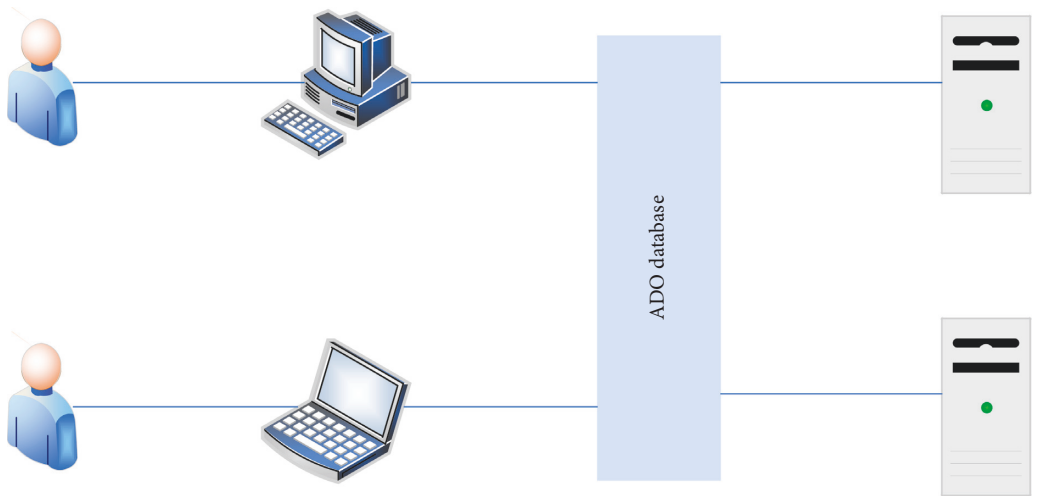

Figure 6: Network topology structure diagram.

Table 2: Audit project management database table.

Field name	Type of data	Primary key	Description
SJXM_SJ_ID	Plastic surgery	Primary key	Audit project ID
SJXM_SJ_KMID	Plastic surgery	Foreign key	Account number
SJXM_SJ_KMMC	Text	No	Subject name
SJXM_SJ_XJ	Floating point	No	Cash
SJXM_SJ_YHCK	Floating point	No	Bank savings
SJXM_SJ_QTHBZJ	Floating point	No	Other monetary fund
SJXM_SJ_YSPJ	—	No	Bill receivable
SJXM_SJ_FPJ	—	No	Attached documents
SJXM_SJ_DQTZ	Floating point	No	Short-term investments
SJXM_SJ_HZZB	Floating point	No	Bad debt provision
SJXM_SJ_YSZK	Floating point	No	Accounts receivable
SJXM_SJ_YFZK	Floating point	No	Prepayments
SJXM_SJ_YSBTK	Floating point	No	Subsidy receivable
SJXM_SJ_QTYSK	Floating point	No	Other receivables
SJXM_SJ_ZYMC	Text	No	Abstract name

SQL, if it has been started, the database will be installed...,"vbInformation + vbOKOnly,"System prompt"

Shell (App.Path and "Installdb.exe")End

Else

MsgBox Err.Number and Err.Description, vbInformation + vbOKOnly,"System Prompt"End

End IfEnd Sub

Table 3: Fixed assets cycle management database table.

Field name	Type of data	Primary key	Description
SJGL_GDZCJD	Plastic surgery	Primary key	Fixed asset management ID
SJGL_GDZC_MZ	Text	No	Fixed asset name
SJGL_GDZC_GG	Text	No	Specifications of fixed assets
SJGL_GDZC_SSBM	Text	No	Department of fixed assets
SJGL_GDZC_YZ	Floating point	No	Original value of fixed assets
SJGL_GDZC_DJRQ	Date	No	Registration date
SJGL_GDZC_SFBF	Boolean	No	Whether it is scrapped
SJGL_GDZC_ZCCZ	Floating point	No	Salvage value of assets
SJGL_GDZC_BSRQ	Date	No	Asset loss date
SJGL_GDZC_ZJRQ	Date	No	Depreciation date of the asset

Table 4: Audit summary data table.

Field name	Type of data	Primary key	Description
SJGL_HZ_ID	Plastic surgery	Primary key	Audit summary number ID
SJGL_HZ_SJHZBGLX	Plastic surgery	No	Audit summary report type
SJGL_HZ_SJHZMC	Text	No	Audit summary name
SJGL_HZ_ZS	Text	No	Main delivery
SJGL_HZ_BS	Text	No	Submit
SJGL_HZ_CS	Text	No	CC
SJGL_HZ_MJ	Text	No	Secret level
SJGL_HZ_QT	—	No	Other

4.4. Testing of Computer Economic Audit System. After the functions in the system are improved, the functions of the system can be implemented multiple times. After such multiple operations, check whether there are any other

Table 5: Test cases.

Numbering	Owning module	Action/event	Triggering conditions	Expected outcome	Actual observation result	Correct or not
1	Sign in	1. Enter the login interface 2. Enter the user name and password	Click the button	1. Enter the correct user name and password verification passed 2. Enter the wrong user name and password verification failed	Satisfy	Correct
2	Audit project management-entry catalog entry	1. Enter the audit project management entry interface	Click to enter	1. Can enter audit project information 2. Can be saved successfully	Satisfy	Correct
3	Audit project management-project modification	1. Enter the audit project management interface 2. Select the item to be modified II	Click the button	1. The audit item can be modified. When modifying the audit item, pay attention to the key information	Satisfy	Correct
4	Audit project management-view general ledger	1. Go to account book management 2. Select view general ledger	Click the button	View general ledger	Satisfy	Correct
5	Project initialization management-import balance sheet	1. Enter the project initialization management 2. Import balance sheet	Click the button	Importable balance sheet	Satisfy	Correct
6	Project initialization management-import profit table	1. Enter the project initialization management 2. Import the income statement	Click the button	Importable income statement	Satisfy	Correct
7	Audit work paper management-generating papers	1. Enter audit work paper 2. Generate paper	Click the button	Can generate audit work papers	Satisfy	Correct
8	Audit summary and fruit management-	1. View summary results	Click the button	View summary results	Satisfy	Correct
9	Statements and notes management-view the balance sheet	1. Click to view the balance sheet	Click the button	Show the company's assets and liabilities	Satisfy	Correct
10	Reports and notes management-view profit statement	1. Click to view income statement	Click the button	Show the company's income statement	Satisfy	Correct
11	Reports and notes management-view balance sheet	1. View the balance sheet	Click the button	Show balance sheet	Satisfy	Correct

problems in the system. In our tests, we choose to use examples for design. We must be very clear about what our test goals are. We should consider the problems more comprehensively during the test process. Only in this way can we ensure that the results obtained by the test are valid.

This article has many functional businesses. The following introduces some key function tests, and the specific conditions are shown in Table 5.

This chapter mainly introduces the system test technology and test cases and strictly verifies the system functions according to the software test requirements. The test results show that the financial management system can meet the implementation requirements and can guarantee the actual operation of the financial management business.

5. Conclusion

This article provides that GC-SURF is a multilevel matching method for visual images. The method includes feature extraction, initial matching, transformation matrix evaluation, and geometric matching. Geometric matching is to use the geometric transformation information between image pairs to find a match that satisfies the geometric transformation. Comprehensive experiments on optical images with different viewing angles, ambiguities, and texture complexity have been carried out. The experimental results show that the method provides accurate matching rate and matching accuracy while maintaining real-time performance. This research is

based on the background analysis of the current company's financial and auditing, as well as the current company's actual audit requirements and the company's development status. Clarify the importance and value of the financial audit information system in the Chinese economy and society. In the specific chapters of the system, requirements analysis, design implementation, and testing were carried out to complete the required system construction.

Data Availability

The data used to support the findings of this study are available from the corresponding author upon request.

Conflicts of Interest

The authors declare that they have no conflicts of interest.

References

[1] J. Zeng, M. Liu, X. Fu, R. Gu, and L. Leng, "Curvature bag of words model for shape recognition," *IEEE Access*, vol. 7, no. 11, pp. 57163–57171, 2019.

[2] B. Wang, D. Brown, Y. Gao, and J. L. Salle, "March: multi-scale-arch-height description for mobile retrieval of leaf images," *Information Sciences*, vol. 302, pp. 132–148, 2015.

[3] Y. Chengzhuan and W. Hui, "Plant species recognition using triangle-distance representation," *IEEE Access*, vol. 7, pp. 178108–178120, 2019.

[4] C. Yang and Q. Yu, "Multiscale fourier descriptor based on triangular features for shape retrieval," *Signal Processing: Image Communication*, vol. 71, pp. 110–119, 2019.

[5] Y. Zheng, B. Yan, and W. He, "O2o method for fast shape retrieval," *IEEE Trans. Image Process. Publ. IEEE Signal Process. Soc*, vol. 28, no. 11, pp. 5366–5378, 2019.

[6] G. E. Krokhicheva, V. V. Lesnyak, E. M. Selezneva, and E. S. Arakelyants, "Adaptive engineering management tools of enterprise economic security," *Management Science Letters*, vol. 8, no. 6, pp. 605–618, 2018.

[7] Y. Li, "Research on enterprise economic management mechanism based on decision process," in *Proceedings of the 2019 4th International Symposium on Management, Economics, E-Business and Marketing (ISMEEM 2019)*, pp. 511–519, Francis Academic Press, Hanoi, Vietnam, October 2019.

[8] W. Ding, "Research on enterprise economic management innovation under the new situation of value management," in *Proceedings of the 2019 5th International Conference on Education Technology, Management and Humanities Science ETMHS 2019*, Francis Academic Press, Xi'an, China, October 2019.

[9] G. Yuping, "Research on effective innovation measures of enterprise economic management based on innovation ability training," in *Proceedings of the 2019 5th International Conference on Economics, Business, Finance, and Management (ICEBFM 2019)*, Francis Academic Press, Shenzhen, China, June 2019.

[10] J. S. Busby, B. Green, and D. Hutchison, "Analysis of affordance, time, and adaptation in the assessment of industrial control system cybersecurity risk," *Risk Analysis*, vol. 37, no. 7, pp. 1298–1314, 2017.

[11] C. O. Learning and A. D. Bank, "Open and distance learning," *Dfid*, vol. 4, no. 3, pp. 297–305, 2017.

[12] P. Cui, *Research on the Intelligent Recognition Method of Academic Document Content Based on Text Mining*, Beijing Jiaotong University, Beijing, China, 2019.

[13] Y. Hao, Y. Huang, and Y. Feng, "Research on the application of big data technology in information statistics research system," *Journal of Physics: Conference Series*, vol. 1865, no. 4, Article ID 042112, 2021.

[14] W. Xue and Y. Lu, "Research on text mining technology," *Journal of Beijing Union University*, vol. 19, no. 4, pp. 59–63, 2005.

[15] F. Jiang, G. Li, and X. Yue, "Research method of document feature extraction based on semantics," *Computer Science*, vol. 43, no. 2, pp. 254–258, 2016.

[16] X. Xie, Y. Fu, H. Jin, Y. L. Zhao, W. Z. Cao, and H. Jin, "A novel text mining approach for scholar information extraction from web content in Chinese," *Future Generation Computer Systems*, vol. 111, pp. 859–872, 2020.

[17] B. B. Bogomolov, V. S. Boldyrev, A. M. Zubarev, V. P. Meshalkin, and V. V. Men'shikov, "Intelligent logical information algorithm for choosing energy- and resource-efficient chemical technologies," *Theoretical Foundations of Chemical Engineering*, vol. 53, no. 5, pp. 709–718, 2019.

[18] E. Y. Puspaningrum, B. Nugroho, A. Setiawan, and N. Hariyanti, "Detection of text similarity for indication plagiarism using winnowing algorithm based K-gram and jaccard coefficient," *Journal of Physics: Conference Series*, vol. 1569, no. 2, Article ID 022044, 2020.

[19] X. Li and M. Zhuang, "Free text information extraction technology," *Information Science*, vol. 7, pp. 48–54, 2004.

[20] M. Liu, X. Wang, and Y. Huang, "Data preprocessing in data mining," *Computer Science*, vol. 4, pp. 56–59, 2000.

[21] H. Azarbonyad, M. Dehghani, M. Marx, and J. Kamps, "Learning to rank for multi-label text classification: combining different sources of information," *Natural Language Engineering*, vol. 27, no. 1, pp. 89–111, 2020.

[22] A. Khan and S. S. Khan, "initKmix-A novel initial partition generation algorithm for clustering mixed data using k-means-based clustering," *Expert Systems with Applications*, vol. 167, no. 2, Article ID 114149, 2021.

Hindawi
Mobile Information Systems
Volume 2022, Article ID 8915889, 9 pages
https://doi.org/10.1155/2022/8915889

Research Article

Application of Internet of Things in Online Teaching of Adult Education Based on Android Voice Assistant

Yingjie Shen

Qianjuntao Art Musuem, Haining, Zhejiang 314400, China

Correspondence should be addressed to Yingjie Shen; 161841396@masu.edu.cn

Received 17 May 2022; Revised 18 June 2022; Accepted 5 July 2022; Published 19 July 2022

Academic Editor: Shadi Aljawarneh

Adult education is an important part of lifelong learning; with the rapid development of economy in recent years, the society has put forward many new requirements for lifelong education; and many new problems have emerged in adult higher education. Online education is the medium of distance learning. Due to the continuous development of Internet+ and the continuous growth and rapid development of online education, it provides unprecedented opportunities for the development and utilization of high-quality education resources. Based on the research on the recommendation method of online courses in adult higher education, this paper designs and develops an online education platform for Adult Higher Education. The intelligence of mobile devices has made mobile phones an indispensable device in people's lives, excellent human-computer interaction design, and open-source kernel code that make Android the best choice for developing mobile applications. Therefore, in this paper, we will build an adult online education framework based on Android voice for Internet of things technology, design a monitoring node for Internet of things, design and implement an online education monitoring system for adult NB people, and research, collect, and send the learning status information of Internet of things technology. The results show that the function of the system can be effectively realized, the operation efficiency is high, and the personalized course design can be provided.

1. Introduction

This paper analyzes the actual needs of adult education and studies and designs a relatively perfect online education network platform [1]. The subjects selected by students mainly include the integrated management subsystem of adult higher education, the network education subsystem of adult higher education, and the personal process suggestions and mobile education app. According to the needs and analysis, the detailed design is carried out, the scoring process of the subject is analyzed, and the recommended methods for the personality chemistry subject are put forward according to the relevant rules and cooperation [2]. According to the data selected by students in the past and the existing course information, the method can meet the basic requirements of recommended courses. Based on the B/S model of adult higher education, using the aspnet technology that is designed in detail based on the above needs analysis, to achieve student payment, system role setting and permissions, student online learning, and personal process. At the same time, we have developed an online education platform, which has key functions such as recommendation and mobile learning [3]. Android voice assistant has important theoretical value and broad application prospects and has made continuous development in recent years and has aroused great interest [4]. The research of artificial neural network greatly improves the accuracy and speed of speech recognition. In addition, Android language assistant technology has been moved to the commercial system of the laboratory, gradually affecting and improving people's work and life. BP network represents the most important idea of artificial neural network. Now, BP network or its variants have been basically used in the practical application of neural network. Nowadays, mobile phones can directly understand people's language and complete people's ideas without manual operation. It is the main development trend of intelligent device application. Android voice assistant realizes input, query, and control functions for some mobile phone users through voice interaction [5]. General applications such as voice input method can not only improve the

input efficiency but also leave space in some special environments to meet people's input needs. In this paper, we will first explain the background of the theme, such as the development of adult education, the Internet of things, Android speech recognition technology, the development status at home and abroad, the research content, and purpose [6]. This paper designs an online adult education system based on the voice support of Internet of things database, which solves the problem of adult education to a certain extent [7].

2. Related Work

This paper introduces the application program of computer web end to design system database. These application programs realize the functions of real-time system monitoring, real-time query, history query, route maintenance, and user management [8]. The database of attribute graph and system table related to entity is introduced. This paper introduces the basic structure and algorithm principle of artificial neural network, designs it according to the characteristics and learning rules of BP neural network, and realizes the algorithm of limited command recognition [9]. Then, according to the concept of software engineering, it determines the storage of mobile phones and recording files, Android Bluetooth communication, interaction between client and server, query and change of database, software requirements, and functions of mobile phones and SMS. Finally, it is based on Android platform, combined with speech recognition algorithm, and realizes all functions of supporting speech software [10]. This paper introduces the construction and development status of online education platform at home and abroad, analyzes the actual needs of industry lifelong education and online education, and designs the overall design of online education platform based on the current network platform, establishes the infrastructure, application foundation, and needs analysis [11]. Among them, the design of information portal system is complete and specific, including learning resource management, cloud course management, course learning preparation, online learning management, and academic performance evaluation. This paper deals with learning, learning resource management module related to the evaluation of education quality, in response to the actual needs of education management, departments, courses suitable for positions, learning placement module, and so on [12]. The management module of system classified examination question bank is designed in order. This paper introduces the user organization management using hierarchical tree structure, the task management suitable for enterprise employee mobility, the role management of various personnel permissions, the correlation with examination practice and pre education, and introduces the actual needs of education management in continuing education [13]. The systematic knowledge of conditional learning resource management, department and professional title course arrangement, examination question bank management, and examination preparation. In order to carry out the classification of curriculum set and the issue and management of Graduation Certificate in a sustainable way, it provide flexible, convenient, and fully functional online education and training services for all types of professionals. Through design and testing, the education network provides effective plans for education and training, improves the traditional face-to-face education and training with excellent technical ability and rich scientific knowledge, and provides us with all kinds of technology and scientific knowledge [14]. The service is provided by excellent management technicians and managers in the industry. The literature introduces the convenience of lifelong learning brought by the establishment of network education platform, but the network education platform also faces some problems [15]. First of all, the operating cost of the platform is relatively high, and it needs continuous investment to upgrade and improve to meet the continuous education needs of online education (including purchase), including hardware cost. On the other hand, the cost of high-performance server, the use of high network bandwidth, and human resources, including a large number of teaching material production, development, software system maintenance, and troubleshooting. Second, some functions of the platform are incomplete. For example, it can only be used on Windows system on PC and does not support Android system, IOS system, tablet computer, and mobile phone client. Moreover, the resources of teaching materials are still very limited. Participate in more training and educational institutions in the operation and management of the platform and make the best use of the functions of the cloud platform for resource sharing [16].

3. Research on Android Voice Assistant

3.1. Process Design. The application must run in the background to use all the functions of the software. If we open the software for the first time or close it carelessly when using it, we can search among multiple applications in the list without operating the mobile phone. Just double click the volume up button on the Bluetooth ear to start using it, and the voice will prompt the user. At the same time, according to the setting information, start the phone and SMS monitoring service to ensure the various permissions required by the offline table, and the application program completes its functions. The flow chart of software startup process is shown in Figure 1.

3.2. Algorithm Principle. Artificial neural network is a large parallel distributed processing system with receiving experience and available functions, making artificial sound detection system an important choice.

Neuron k:

$$\begin{aligned} u_k &= \sum_{j=1}^{m} w_{jk} x_j, \\ v_k &= u_k + b_k, \\ y_k &= f(v_k). \end{aligned} \tag{1}$$

Linear activation function:

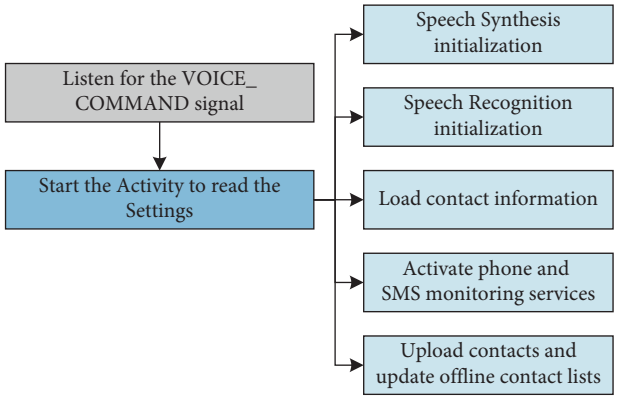

Figure 1: Process of software startup.

$$y_k = f(v_k) = Kv_k. \tag{2}$$

Threshold logic activation function:

$$y_k = f(v_k) = \begin{cases} 1, & v_k \geq \theta_k, \\ 0, & v_k < \theta_k. \end{cases} \tag{3}$$

Type logic activation function (Sigmoid function):

$$y_k = f(v_k) = \frac{1}{1 + \exp(-v_k)}. \tag{4}$$

Hyperbolic tangent activation function:

$$y_k = f(v_k) = th(u_k). \tag{5}$$

The output of the hidden layer neuron is

$$z_k = f_1\left(\sum_{i=1}^{n} v_{ki}x_i\right) k = 1, 2, \ldots, q. \tag{6}$$

The output of the output layer neuron is

$$y_j = f_2\left(\sum_{k=1}^{q} w_{jk}z_k\right) j = 1, 2, \ldots, m. \tag{7}$$

The error E_p of the p-th sample is

$$E_p = \frac{1}{2}\sum_{j=1}^{m}\left(t_{pj} - y_{pj}\right)^2. \tag{8}$$

For all samples, the global error is

$$E = \frac{1}{2}\sum_{p=1}^{p}\sum_{j=1}^{m}\left(t_{pj} - y_{pj}\right) = \sum_{p=1}^{p} E_p. \tag{9}$$

The BP algorithm is used to adjust the weight of the output layer in order to reduce the global error E. The amount of change is as follows:

$$\Delta w_{jk} = -\eta\frac{\partial E}{\partial w_{jk}} = -\eta\frac{\partial}{\partial w_{jk}}\left(\sum_{p=1}^{p} E_p\right) = \sum_{p=1}^{p}\left(-\eta\frac{\partial E_p}{\partial w_{jk}}\right). \tag{10}$$

Define the error signal as follows:

$$\delta_{xj} = -\frac{\partial E_p}{\partial S_j} = -\frac{\partial E_p}{\partial y_j}\cdot\frac{\partial y_j}{\partial S_j}. \tag{11}$$

For the first item,

$$\frac{\partial E_p}{\partial y_j} = \frac{\partial}{\partial y_j}\left[\frac{1}{2}\sum_{j=1}^{m}\left(t_{pj} - y_{pj}\right)^2\right] = \sum_{j=1}^{m}\left(t_{pj} - y_{pj}\right). \tag{12}$$

Partial differential of the transfer function of the output layer is as follows:

$$\frac{\partial y_j}{\partial S_j} = f_2'(S_j). \tag{13}$$

Then,

$$\delta xj = \sum_{j=1}^{m}\left(t_{pj} - y_{pj}\right)f_2'(S_j). \tag{14}$$

It can be calculated from the chain theorem that

$$\begin{aligned} \frac{\partial E_p}{\partial w_{jk}} &= \frac{\partial E_p}{\partial S_j}\cdot\frac{\partial S_j}{\partial w_{jk}} = -\delta_{xj}\cdot z_k \\ &= -\sum_{j=1}^{m}\left(t_{pj} - y_{pj}\right)f'_2(S_j)\cdot z_k. \end{aligned} \tag{15}$$

Therefore, the formula for adjusting the weight of each node in the output layer is

$$\Delta w_{jk} = \sum_{p=1}^{p}\sum_{j=1}^{m}\eta\left(t_{pj} - y_{pj}\right)f'_2(S_j)z_k \tag{16}$$

Finally, it is necessary to request the change of the hidden layer weight as follows:

$$\Delta v_{ki} = -\eta\frac{\partial E}{\partial v_{ki}} = -\eta\frac{\partial}{\partial v_{ki}}\left(\sum_{p=1}^{p} E_p\right) = \sum_{p=1}^{p}\left(-\eta\frac{\partial E_p}{\partial v_{ki}}\right). \tag{17}$$

The formula for adjusting the weight of each node in the hidden layer is as follows, which is similar to the method of calculating the weight change of the output layer:

$$\Delta v_{ki} = \sum_{p=1}^{p}\sum_{j=1}^{m}\eta\left(t_{pj} - y_{pj}\right)f'_2(S_j)w_{jk}f_1'(S_k)x_i. \tag{18}$$

3.3. Speech Recognition. It is a tedious task to directly use the programming language of neural network model to perform simulation-aided design. First of all, compilers are very complex. More importantly, only certain programs can be compiled to solve various specific problems. In this case, MATLAB software package brings a lot of convenience to people, which makes it more and more popular. Because data preprocessing is the premise and foundation of neural network model. Therefore, speech signal preprocessing plays a very important role in the process of speech recognition, the most important of which is the detection and feature extraction of audio signal endpoint. After obtaining the features of the audio signal, we can set up the neural network to match the work with the sample training.

The basic process of dual threshold endpoint detection algorithm is as follows: first, set a lower threshold to make the signal pass through with weak intensity, and then set a higher threshold for the signal whose short-term average energy reaches a certain intensity. If either of the two indicators exceeds the low threshold, the starting position shall be displayed to continuously detect the average energy and zero cross rate of the subsequent frame signals. If the values of the two indicators to be tested are lower than the lower threshold, it can be determined that the effective audio signal has not started and the current display start point has been cancelled, and the two indicators to be tested are higher than the upper limit, which means that the signal begins to belong to a valid voice segment. When the current state is the effective audio interval, the signal of the next frame will continue to be calculated. When the average energy and zero crossing rate return below the low threshold, the end position will be displayed, and the energy and zero crossing rate will be continuously detected in the subsequent frame signal. If the values of both parameters rise and exceed the upper threshold, it can be determined that the valid audio signal has not ended and the currently displayed endpoint has been cancelled. However, if there are not more than two indicators to be tested, the high threshold indicates that the audio signal is in the "start" state. A command can contain multiple characters, so the audio signal will go through the start, end, restart, and end process.

Figure 2 shows the results of a "confirm" instruction sample and a "cancel" instruction sample after double threshold endpoint detection.

The result of dual-threshold endpoint detection after MATLAB work is shown in Figure 3.

The specific relationship between Mel frequency and actual audio frequency is as follows:

$$f_{\text{mel}}(f) = 2595 \cdot \log\left(1 + \frac{f}{700\,\text{Hz}}\right). \tag{19}$$

The functional form of the maximum and minimum methods is as follows:

$$x_k = \frac{(x_k - x_{\min})}{(x_{\max} - x_{\min})}. \tag{20}$$

The functional form of the mean variance method is as follows:

$$x_k = \frac{(x_k - x_{\text{mean}})}{x_{\text{var}}}. \tag{21}$$

The number of unnatural neurons can be calculated by the following equation:

$$\begin{cases} l < n - 1 \\ l < \sqrt{m + n} + a. \\ l = \log_2 n \end{cases} \tag{22}$$

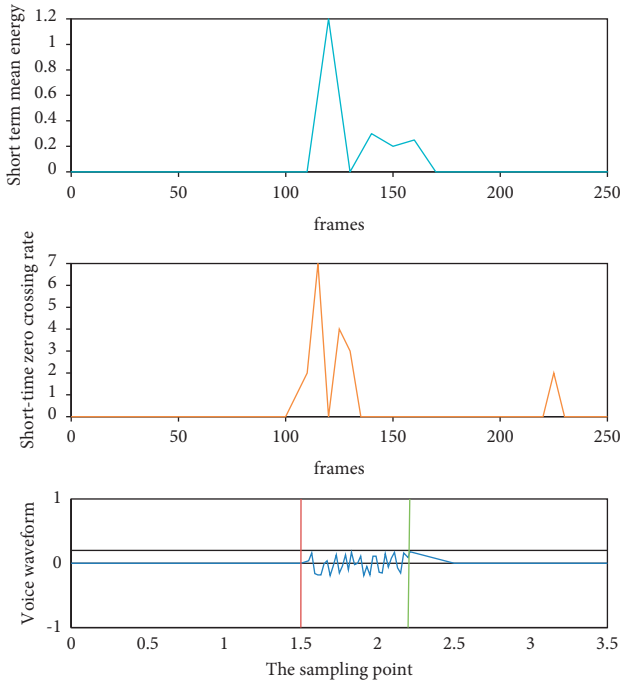

Figure 2: A sample "ok" instruction and a sample "cancel" instruction.

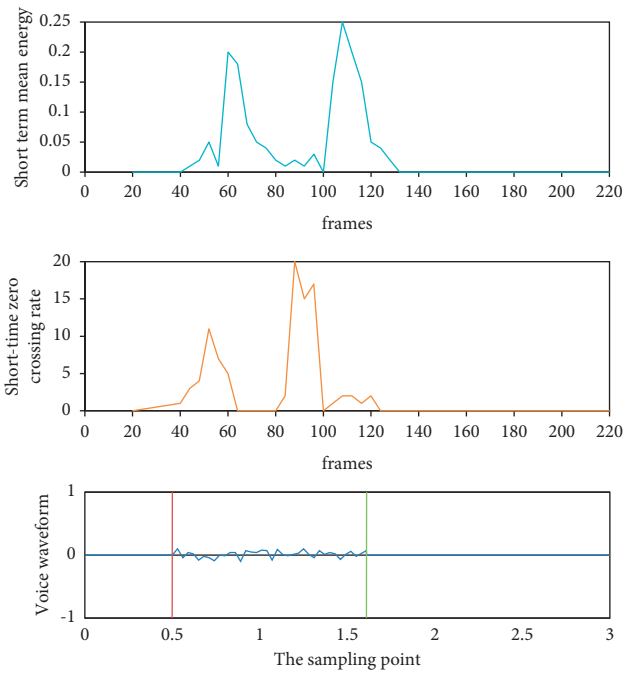

Figure 3: The result obtained after the dual-threshold endpoint detection MATLAB operation.

4. The Design and Practical Application of the Online Teaching System for Adult Education of the Internet of Things

4.1. Key Technologies of Online Teaching System. Under the B/S development model, the user interface is realized through the browser. The user implementation is only a small part of the three-tier data, which greatly simplifies the load on the client system and reduces system upgrade and maintenance costs. Therefore, we can use the B/S model to effectively manage permissions and protect our data platform and server database.

NET Framework is a widely used development platform that can be used to build applications such as Windows, Windows Server, and Windows Azure. At the top of the .NET Framework, the class library is ADO.NET and XML data, the higher layer of XML is ASP.NET, and the higher layer of Windows Forms is CLS and programming language (VB). Compared with the previous development model, ASP.NET has the following advantages: ASP.NET has a three-tier architecture model, the relationship between the hierarchical structure is independent, only need to make relevant changes to modify and maintain the system, and can be to a certain extent, the readability and scalability of the code are improved, and a lot of resources are saved for subsequent project system upgrades and maintenance, which is convenient for maintenance and management.

The ASP.NET 3-tier architecture is PL, BLL, and DAL. (1) Data access layer (DAL): this layer mainly performs data processing. (2) Business logic layer (BLL): the main task of this level is to combine the data authority level and the presentation level and provide all database-related functions. (3) Presentation layer (PL): located in the outermost layer of the third layer, it provides interactive functions with users. The presentation layer transmits parameters to the intermediate business logic layer to accept the parameters of the business logic layer.

Android is an open source operating system based on the Linux system, which is mainly used in mobile smart phones. For Android, it has the following characteristics: (1) reusable framework and components, (2) optimized for mobile phones, Dalvik virtual machine, (3) kit engine is a mobile browser, (4) embedded database SqLite storage Structured data, (5) the multimedia function library can support multiple formats, (6) we provide GSM mobile phone communication, (7) support Bluetooth communication and 3G and WiFi networks, and (8) have a rich development environment.

Collaborative filtering algorithm is a widely used algorithm, and its main feature is that it is not restricted by the characteristics and content of specific products. However, the collaborative filtering algorithm has the problem of sparse data. The principle of the collaborative filtering algorithm: allows users to recommend relevant interests and pass them to other users. As an information transmission process, recommending users can save time searching for other product information to choose whether to use, and it is recommended that collaborative filtering is a simulation of these processes. Different people usually have similar interests and hobbies, which are usually related to the similarity of growth experience. Therefore, we can make predictions and suggestions based on the similarity of interests. Based on this idea, collaborative filtering recommendation algorithm is applied to commercial recommendation. Collaborative filtering algorithms can be divided into two categories: model-based collaborative filtering algorithms and hybrid collaborative filtering algorithms. The process is shown in Figure 4.

Collaborative filtering algorithm has the advantages of original recommendation and has been studied and applied in various fields. Although collaborative filtering

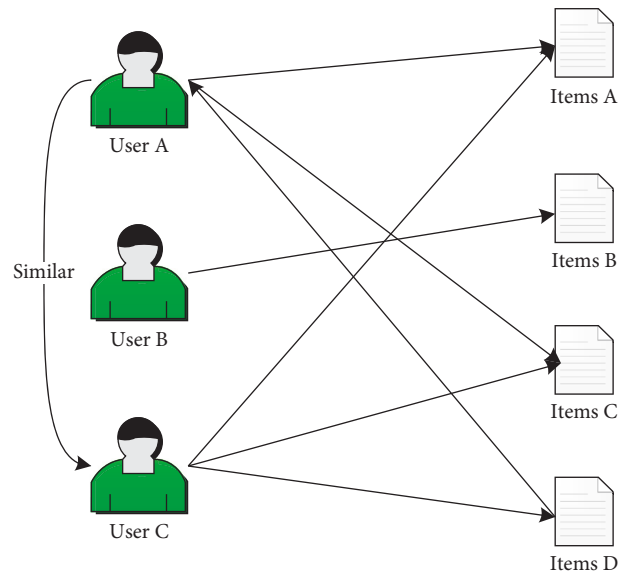

Figure 4: Collaborative filtering algorithm based on user similarity.

recommendation algorithm has become the most widely used recommendation algorithm, with the rapid development of Internet and the improvement of site structure complexity, collaborative filtering recommendation algorithm still faces some problems, as shown in Table 1.

As shown in formula (23), it can be explained that the recommendation based on the collaborative filtering algorithm is recommended to the user.

$$\forall c \in C, i'_c = \arg\max_{i \in I} f(c, s), \tag{23}$$

$$P_{u,i} = \frac{\sum_{\text{allsimilaritem}\varepsilon,N}\left(S_{i,N} * R_{u,N}\right)}{\sum_{\text{allsimilariten}\varepsilon,N}\left|S_{i,N}\right|}. \tag{24}$$

The correlation algorithm is a data mining algorithm suitable for recommended fields. The main idea of the correlation algorithm is to find a strong correlation rule based on the threshold setting, which is used to display the probability of two or more items at the same time. Find the user's general rules and use them to predict the outcome of each choice.

An item set is a collection of items. A group of items containing K items is called a K item group, such as a collection of two items (eg eggs, flour). The item set frequency is the number of all transactions, including the item set obtained by filtering the transaction set. The minimum support refers to the threshold defined by the user to identify whether the support is within a reasonable range. The minimum trust level is a user-defined threshold, used to identify whether the trust level is within a reasonable range and used to define relevance. The rule that has the lowest reliability and satisfies the minimum support threshold and the minimum trust threshold at the same time is called a strong rule.

Frequent item set: a process of looping through all items that meet the minimum support threshold. A group of items that meet these requirements is called a frequent item group.

Table 1: Project and user.

User	Item 1	Item 2
User 1	5	3
User 2	4	3
User 3	4	—

Create rules: carefully check the common things in the above steps to find all reliable rules, and these rules are called powerful rules.

4.2. System Requirement Analysis. Because traditional adult education cannot use intensive education, there are problems such as scattered educational resources, lack of resources in educational institutions, and complex educational administration. The purpose of adult higher education and online education system is to concentrate educational resources, promote student learning, and centralize educational management. Therefore, the system as a whole is divided into four parts: the first part is a comprehensive management system for adult higher education, and the goal is to centrally manage educational resources and the team of teachers and students. The second part is the online education system for adult higher education. The purpose of learning is to solve the problems of the inability to achieve the unity of learning time and learning location and the inability to use intensive education. The third part recommends a personalized course and selection system. The main feature of the system is to provide students with course selection services, and students can create a timetable. The fourth part is the mobile education application for adult higher education, which aims to provide a more convenient learning method and make full use of scattered time and "relieve contradictions."

System requirements must be considered when designing the system, and the requirements of the system scope should be based on the following characteristics: (1) feasibility and ease of use. The system should be based on actual requirements and easy to operate. (2) Reliability and robustness. The system is fault tolerant and must handle all emergency situations. (3) Scalability and possibility of change, the system should be easy to maintain and upgrade. (4) Security, the system must ensure the security of user information. (5) Completeness, the system needs complete functions.

The role of the system mainly includes the headquarters and the correspondence station, as shown in Table 2.

4.3. System Framework Design. The abovementioned system can help schools to centrally manage educational resources in adult education, while ensuring that "contradictions between work and study" are alleviated and providing convenient learning services for students. At the same time, we designed a mobile learning application to further increase student learning time and maximize the time allocated. APP is software for education platforms. It uses smart phones and an integrated management system based on personalized recommendations and uses online education systems and courses to select system connections. The main purpose of mobile education APP is to promote student learning, so the function of APP is mainly to provide online learning services. The functions are divided into four directions according to needs. The function settings are mainly used for basic knowledge, student functions, and other functions to facilitate students' use.

With reference to the actual functional requirements of system development, the system adopts a Web-based B/S structure model and uses development tools. We use a three-tier development model for system design and development. The system is divided into three stages, and this model has the effect of scalability. The specific situation is shown in Figure 5.

The "push" model is a new type of service based on the network environment, that is, information service providers use "push" technology to provide information services for specific users of the Internet. With this technology, network information services can not only directly push information about a specific user to him but also can effectively use idle network resources to obtain the information required by the user in time, thereby improving overall performance and system operating efficiency. Supporting multiple terminals means that we can learn information through multiple receiving channels such as computers, Web terminals, and mobile APP terminals. From a technical point of view, the "push" model is a network information service system with a certain level of intelligence that can automatically provide information services. Its characteristics are as follows.

(1) Appropriateness: push technology can search, process, and push to users' specific information needs. For example, when submitting scores, teachers must submit scores in time. If some teachers do not submit scores on time, they will automatically screen those who need to be notified in advance to push the system's SMS and e-mail notifications.

(2) High efficiency: the application of push technology is usually started when the network is idle, so that the network bandwidth can be effectively used. For example, the information push notification sent to teachers is usually set at around 7 am, and now most users will find it easier to push information when they are not using the Internet, and send wonderful course content to students. The system has set up multiple push perspectives, before pushing, if the network traffic is lower than the traffic limit. If the push continues to exceed the access limit, content push will be performed, and only a small amount of content will be pushed to the students, such as educational notifications, exchanges and discussion content.

(3) Flexibility: the "push" mode also allows us to customize the information that needs to be pushed according to user needs. The system contains various information. Usually, the platform will wait after the user publishes the information until it actively enters the platform to open the page, but the user must first

Table 2: List of management roles.

Serial number	Management level	Role							
		College leaders	Leaders in charge	Headmaster	System administrator	School administrator	Teaching administrator	Teacher	Student
1	College headquarters	*v*	✓	*v*	*v*	*v*	✓	*v*	*v*
2	Correspondence station		✓	✓	✓	✓		✓	*V*

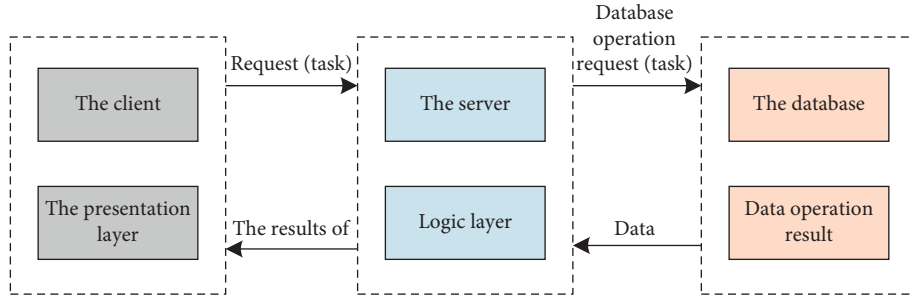

Figure 5: System framework design.

enter the platform to receive some important information. With this in mind, the system combines "complete mode" and "push mode" in the development process and designed a general information disclosure module. After successfully logging in to the platform, most users will be able to receive information in a timely manner. Students can confirm information and add important information at the same time, such as the teacher's class time notification "PUSH push notification" function, through which information is released and pushed, watching time videos, doing homework, and constantly reminding students of test questions.

4.4. System Implementation and Testing. The system grants privileges to users based on their roles, thereby facilitating integrated management of user privileges. Roles are divided into two levels: headquarters and communication station. The system can dynamically add roles and specify the privileges and operating function modules belonging to the user, so as to better realize the flexible and dynamic management of privileges.

The important data tables to realize this function such as communication station information table, user table, role table, role authority table, function module table, and communication station information table mainly contain the important information of the station: station number, communication station number. and name. The user table contains basic user information (user ID, number of users, and basic user identification information.). In the role table, the table mainly has three fields: F_jsbm (role code) type is a character string, and F_jsmc (role name) type is a character String and F_jsjb (role level). The display range varies depending on the role level. If it is a supported workstation, you can only view information about the supported workstation. The department can view the information of all supported sites, but can only change the information of the supported site. The role permission table has two fields: role code and module code. The role of the module code is a specific example of the module table, the function module table is the table of the abovementioned modules, and the role permissions and function permissions are listed in Table 3.

The T_XT_gnmk function module table is as shown in Table 4:

The main function of the network teaching system is to provide test practice and feedback, so background support requires a strong test question bank and flexible test paper technology. When designing the question bank, the system should be adapted to different disciplines. Different question types in the discipline design can be determined by selecting "test question types," single selections, etc., and distinguish between common question types and special question types. It is common for judging the type of short answer to be displayed in the blank. Basically, the question type is only the explanation of each topic. Special question types can only be displayed in specific fields. Other areas use the stored test question library. The general structure will be automatically applied to other question types. At the same time, they are grouped by the type of question displayed on the interface. Subjective questions appear in independent controls. Taking into account the particularity and diversity of examination questions in each subject, the system uses multimedia to store examination questions, options, answers, attachments, analysis, and so on and plain text as well as video, graphics, audio, video, hyperlinks, and other media elements. The system uses CKEditer (rich text html editor) to simplify the editing and saving of multimedia exam questions.

The core data table involved in the realization of this module function is shown in Table 5.

Table 3: T_XT_js_gnmk role authorization form.

Attribute	Chinese name	Data type and length	Is it empty	Primary/foreign key	Remarks
F _jsbm	Role coding	Varchar (2)	*N*	*P*	
F mkbm	Module code	Varchar (10)	*N*		
F_ czqx	Operation authority	Varchar (50)	*N*		The content of this field is a subset of the "operation function" in the module table

Table 4: T_XT_gnmk function module table.

Attribute	Chinese name	Data type and length	Is it empty	Primary/ foreign key	Remarks
F_mkbm	Module code	Varchar (l0)	*N*	*P*	Use codes to identify the menu level, 01 means the first-level menu, 0101 means the second-level menu, 010101 means the third-level menu
F_mkmc	Module name	Varchar (50)	*N*		
FJjdz	Link address	Varchar (l00)	*N*		
F_xssx	Display order	Int	*N*		
F_czgn.	Operation function	Varchar (50)			Operation functions include add, delete, modify, query, etc., separated by
F_sjcd	Module level	Int	*N*		Divided into 1, 2, 3 levels

Table 5: Question bank.

Field name	Chinese name	Data-type length	Constraint scope	Can it be empty	Remarks
F ID	ID	Int		*N*	Self-increasing 1
F wlkcID	Online course id	Int		*N*	
F zjID	Course chapter ID	Int		*N*	
F_stlxID	Question type id	Char (2)		*N*	Related question type table id
F_cslbID	Test category	Varchar (20)		*N*	Correlation test category table id, can store multiple id, separated by comma
F sttm	Question title	Text		*N*	
F stdaan	Answers to test questions	Text			
F_stfjmc	Accessory name	Nvarchar (l00)			
F_stfjdz	Question attachment address	Varchar (l00)			
F_daanjx	Answer analysis	Text			

5. Conclusion

This article details the development and key technologies of the adult education network online education platform and the status quo of adult higher education. It can be understood that online education is a way to solve the problems faced by adult higher education. Analyze the problem of information overload and point out that adult higher education requires individual course recommendations. In this article, we first analyze the functional requirements of the online education platform for adult higher education and design four systems: (1) an adult higher education comprehensive management system used to manage the education of students and teachers; (2) used to manage education and learning the online education system for adult higher education services; (3) the student course selection system based on personalized course recommendation provides students with personalized course preparations to realize the personalized development of adult education; and (4) mobile education applications are used for providing students with more convenient learning conditions. According to the demand analysis, we will design a network learning model based on the "push" mode and the basic functions of multiple terminals and the above four systems. Second, we will recommend related algorithms for existing courses and analyze the shortcomings of these algorithms. Then, according to relevant algorithms and collaborative filtering ideas, use course selection and scoring to design and recommend relevant algorithms for personalized courses. Taking into account the double standards of scores, the algorithm can choose a course to meet the real-time requirements of the recommendation algorithm and finally realize the functions of the designed system.

Data Availability

The data used to support the findings of this study are available from the corresponding author upon request.

Conflicts of Interest

The author declares that she has no conflicts of interest.

References

[1] X. J. Chen and C. J. Song, "Research and design of online learning platform based on mobile Internet," *Microcomputer Applications*, vol. 35, no. 1, pp. 35–38, 2019.

[2] A. Onan, "Sentiment analysis on massive open online course evaluations: a text mining and deep learning approach," *Computer Applications in Engineering Education*, vol. 29, no. 3, pp. 572–589, 2021.

[3] H. Zhang, "Research on the improvement of English autonomous learning ability of students in higher vocational college by network platform," *Value Engineering*, vol. 17, no. 22, pp. 94–100, 2017.

[4] J. Wang and H. H. Wang, "Application intelligent search and recommendation system based on speech recognition technology," *International Journal of Speech Technology*, vol. 24, no. 1, pp. 23–30, 2021.

[5] R. Masumura, T. Asami, T. Oba, S. Sakauchi, and A. Ito, "Latent words recurrent neural network language models for automatic speech recognition," *IEICE - Transactions on Info and Systems*, vol. E102.D, no. 12, pp. 2557–2567, 2019.

[6] A. Hannun, C. Case, J. Casper et al., "Deep Speech: Scaling up End-To-End Speech Recognition," 2020, https://arxiv.org/abs/1412.5567.

[7] P. Zhang, W. Wang, and C. Z. Zeng, "Construction of a learning behaviour tracking analysis model for a MOOC online education platform," *International Journal of Continuing Engineering Education and Life Long Learning*, vol. 30, no. 2, p. 89, 2020.

[8] C.-F. Lin, R.-K. Sheu, Y.-S. Chang, and S.-M. Yuan, "A relaxable service selection algorithm for QoS-based web service composition," *Information and Software Technology*, vol. 53, no. 12, pp. 1370–1381, 2011.

[9] L. I. Ru-Ping, L. Zhu, W. U. Fang-Shen, and X. U. Zhen-Yu, "BP neural network algorithm improvement and application research," *Journal of Heze University*, vol. 6, 2016.

[10] J. Jo, H. G. Kim, I. C. Park, B. C. Jung, and H. Yoo, "Modified Viterbi scoring for HMM-based speech recognition," *Intelligent Automation & Soft Computing*, vol. 25, no. 2, pp. 351–358, 2019.

[11] E. Heyden, J. Küchenhof, E. Greve, and D. Krause, "Development of a design education platform for an interdisciplinary teaching concept," *Procedia CIRP*, vol. 91, no. 3, pp. 553–558, 2020.

[12] Y. Xin, X. Zuo, and Q. Huang, "Research on the construction of seamless learning platform based on open education," *Asian Association of Open Universities Journal*, vol. 13, no. 1, pp. 88–99, 2018.

[13] X. Liu, K. Sun, D. Yang, J. Pan, and Z. Zhang, "A novel teaching platform design with CAI for EM education," *Computer Applications in Engineering Education*, vol. 26, no. 5, pp. 1318–1323, 2018.

[14] X. R. Wu, B. Q. Liu, and T. T. Yuan, "A new generation of smart class: concept, platform and system architecture," *China Educational Technology*, vol. 6, no. 3, pp. 81–88, 2019.

[15] Q. H. Zheng, B. Dong, B. Y. Qian, W. Bifan, Z. Weizhan, and L. jun, "The state of the art and future tendency of smart education," *Journal of Computer Research and Development*, vol. 56, no. 1, pp. 213–228, 2019.

[16] W. L. Shi and Y. H. Zhang, "Intelligent education platform design based on big data analysis technology," *Modern Electronics Technique*, vol. 43, no. 9, pp. 158–161, 2020.

Hindawi
Mobile Information Systems
Volume 2022, Article ID 4399243, 9 pages
https://doi.org/10.1155/2022/4399243

Research Article

Research on Real-Time Information Storage and Remote Piano Teaching Based on Bayesian Algorithm

Bo Pang

School of Music and Dance, Jiaying University, Meizhou, Guangdong 514015, China

Correspondence should be addressed to Bo Pang; 200801024@jyu.edu.cn

Received 20 April 2022; Revised 8 June 2022; Accepted 20 June 2022; Published 18 July 2022

Academic Editor: Shadi Aljawarneh

In recent years, big data has developed rapidly, but there are still some problems. In order to solve these problems, this article has carried out research on big data and integrated it into industrial equipment inspection, and designed a function for data processing. This function is based on the XML system and studies the relationship between the XML system and the database in order to switch between different types of data. At the same time, because of the error of the data processed by the sensor, we decided to improve the Bayesian prediction calculation method in order to improve the accuracy of the data and reduce the error of the data. In the process of extracting key data, the key data collected by the sensor will be transmitted to the cloud platform. This is to realize the free transmission of data on different devices without other forms of interference and hindrance. The processed data will be stored in the monitor or computer for further processing. In order to ensure that the data will not be disturbed or destroyed during the process of saving data, we have designed a data security system, which consists of encryption modules and key cracking modules, and has tested the performance of these modules through a large number of experiments. In order to improve the operating efficiency of the system and to extend the service life, online piano teaching is a part of online education. This article uses music education apps and piano online education to study new ways of piano education in the information age and expounds the combination of intelligent systems and piano education. This has a major impact on future education.

1. Introduction

In recent years, computers and the Internet have become popular and have been involved in all areas of life. This has also promoted the rise of emerging technologies such as the Internet of Things and big data [1]. Although human life has become more and more intelligent, it has also brought many problems. For many problems, such as the leakage or destruction of user information, the original information encryption system has no way to adapt to the development of the times, so we cannot just use the original system to encrypt the information in the cloud computing system. We need other auxiliary equipment [2, 3] and optimize and upgrade the original system. In the process of research, we found that trusted computing can be introduced to solve the problem of information leakage. The principle is to combine trusted computing technology with a data security system, and then design a data model, which is beneficial to increase the confidentiality and security of the information storage system. Reliability is also conducive to simplifying the calculation process, improving calculation efficiency, and reducing costs. Trusted computing technology can solve the information leakage and signal interference that may occur in the calculation process of big data, and can make the entire system run more efficiently and extend the service life of the system.

In recent years, with the development of online teaching, some problems have also appeared. For example, the quality level of platforms is too wide, and the teaching quality of some platforms is not up to the standard. Some platforms focus on grade examination and speed-up, instead of focusing on improving the ability and level of students. Most of the fast-learning courses are organized for adult students or senior students [4]. This is not just a platform issue but also has a lot to do with students. Many adult students have a certain purpose in learning piano, and they have relatively high learning and acceptance capabilities. At present, China online education platform is developing rapidly, but there is

still a gap compared with Western countries. We need not only to develop emerging technologies such as the Internet and big data, but also to standardize online teaching platforms, integrate the Internet and teaching deeply, make up for the shortcomings of traditional teaching models, and gradually establish a perfect and efficient online piano music teaching platform.

2. Related Work

Some research believes that domestic technologies such as big data and cloud computing have just risen. Although the research process is relatively short, great achievements have been made, and they have been widely combined with other fields to play a greater role [5]. Today, information projects such as integration and data collection have attracted more and more researchers and scholars and have become hot issues. Some research states that the current research focuses on transforming different types of information in order to improve the efficiency of system calculations, and realizes the integration and storage of different types of information. Some research designed an information integration system, which mainly uses big data to perform calculations and processing. On the basis of the Internet, the function of big data information integration is played. At the same time, the storage system is upgraded to improve the confidentiality of information. The processor classifies and stores different information, but in the actual application process, the efficiency is still relatively low. To solve this problem, researchers found that other information storage systems can be used, and data models can also be used in the process of information processing to improve the efficiency of information storage. In addition, you can also use the data integration model of middleware, use the three-tier architecture model, and innovatively introduce virtual databases in data processing to improve data query efficiency. The semistructured VII technology and cross-platform Java technology constitute the processing center [6, 7]. Between the underlying database and the upper application, some research studies describe an efficient information storage technology to realize the storage of all different types of data. However, the structure of this system is relatively simple, data cannot be extracted and transmitted, and other factors may be affected during the storage process. Interference: the information integration method proposed the functions of both computers and sensors, and uses data processing systems and encrypted storage technology to build an inseparable information integration system, which makes different types of data in different environments. It is possible to switch between them. However, using multiple information processing technologies at the same time and introducing them into the same system may consume a lot of energy without using environmental protection and ecological construction. Some research believes that using XMLSchema technology, this technology can realize the transmission of information between multiple devices such as databases, computers, and cloud platforms, and can improve the speed and efficiency of information processing, reduce costs, and provide users with greater convenience. However, the problem of how to store information for a long time under different environments has not been solved. The method is still very traditional, and the confidentiality of information needs to be improved.

3. Multisource Heterogeneous Data Processing Related Information

3.1. Multisource Heterogeneous Data Integration Technology. In the process of industrial inspection, if too many sensors are used, then it will cause data errors. Therefore, we need to classify the collected information and integrate different types of information according to certain standards. Make the data clearer and help improve the calculation efficiency of the whole process. However, the data and information collected from different computer equipment and different cloud computing platforms are very different, and the amount and variety are huge, which may reduce the speed of data integration. In response to this issue, we are still conducting more research.

3.2. Analysis of Data Integration Mode. Nowadays, the research on integrating different sources of information is mainly divided into three aspects: cloud platform computing system, computer transmission system, and big data storage system.

Cloud platform computing system: process and integrate different information databases, introduce cloud computing platforms into separate information databases, allow cloud computing systems to store data by themselves, and can realize mutual transmission between different devices. However, this system also has some problems, that is, when different types of information and data are transmitted, information leakage may occur and may be affected by other factors, such as the environment, and the operating efficiency of the system may decrease.

Computer transmission system: The computer transmission system is a system for information transmission. This system integrates different types of data into a file through sensors, then the sensors are transmitted to different devices through different interfaces, and the sensors information and data will be encrypted to improve the confidentiality of data.

Big data storage system: The big data storage system integrates all kinds of data on one platform. Although the form of information may change, the storage time is relatively long. This platform can extract key information and data and perform processing, which helps improve the efficiency of the system to process information and reduce costs. Data warehouse architecture is shown in Figure 1.

The information on the big data platform is collected on different devices, and key information is processed and processed to reduce the interference of unnecessary information. After collecting information from different platforms, the information is stored in a computer or other equipment. The use of ETL technology in the storage process can improve efficiency.

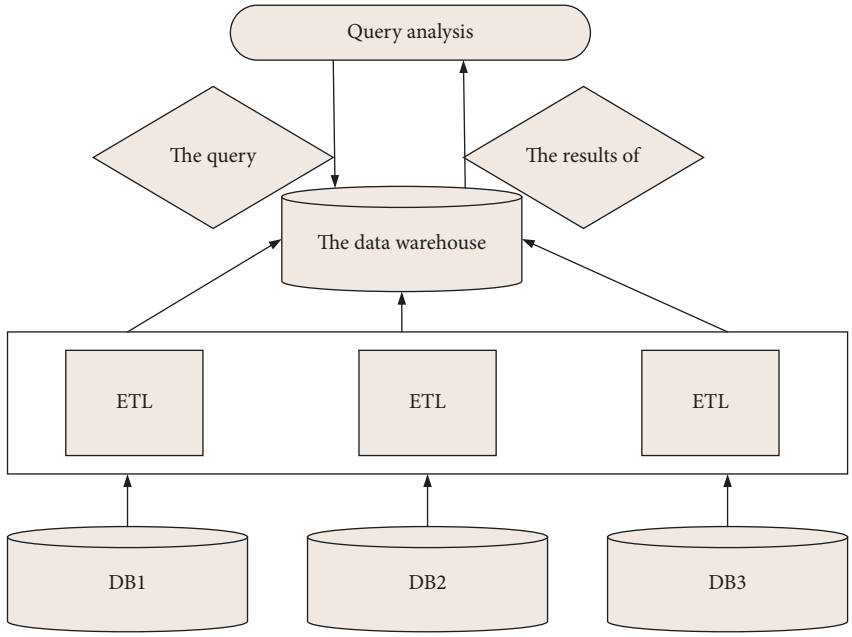

Figure 1: Data warehouse architecture.

3.3. Overview of Real-Time Processing Technology. The information real-time processing system requires shorter reaction time and higher calculation efficiency of other equipment, because the information in the real-time processing may reduce the efficiency of the current system operation. Therefore, when one of the data is processed for a long time, there is likely to be data leakage or interference with the processing of other information, and even damage the data processed by the system. There may be data leakage or interference with the processing of other information, or even damage to the data processed by the system. To study the integration and processing of different types of information, we must first use the real-time processing system of the real-time storage cloud platform.

The real-time information storage cloud platform mainly stores data in the form of files, but we still need to update and upgrade the encryption processing of key data. On the basis of the initial storage system, the real-time information storage cloud platform uses the encrypted form of the index to first collect the source and content of key data, and then uses the model to perform a series of encryption processing [8]. Because there is no interface connection between the device and the device, the free transmission of data cannot be carried out. We use the index to classify these different sources of information according to the standard and file size. Although this will increase the operating burden of the system, it can be classified after classification. Simplify the subsequent calculation process, so as to achieve a better data encryption effect. In this process, we use B+ index and Hash index. B+ tree index: this index method is optimized and upgraded on the basis of the trigeminal tree index, because each part of the trigeminal tree index can only store one information set. If it is introduced to the real-time information storage cloud platform, these different information sets may be stored in different systems, which may greatly reduce the operating efficiency of the system and even cause confusion and loss of information [9]. Each part of the B+ tree can store key information, and each part is connected and interoperable, which can realize the free transmission of data and information, which greatly improves the operating efficiency of the system.

Hash index: Hash index mainly categorizes data in cloud computing. Therefore, we need to use a hash algorithm to correspond different data to their respective hash values. The effect of this index method is better than the previous index method, because it will also takes a long time for data to be stored in different modules. Therefore, we use the hash value of the data to realize real-time storage of more data through the hash index, which is less time-consuming and low-cost. Hash index structure is shown in Figure 2.

Because we collect data on platforms that are not used, the amount of information is large and complex, not stable enough, and even interfered by other factors such as the environment. These are problems that we need to consider and solve, and sensors are processing information. There will also be many problems in the process, such as too much information and unstable sensors. The stability of the sensor plays a vital role in the whole process, because there may be errors in the processed information, so we need to integrate different information to reduce errors in the results.

The integration of different types of information is to classify and integrate information and data collected from different devices to obtain clearer and more critical information. We use the upgraded Bayes algorithm to process the collected data, which can reduce the instability of the data, improve the efficiency of data processing, and can effectively filter out unnecessary data [10]. The basic principle of the Bayesian algorithm is to fix the parameters of the data model within a range, and randomly select some variables, and obtain the prior distribution of the parameters in the data model through a large number of experiments. Through these

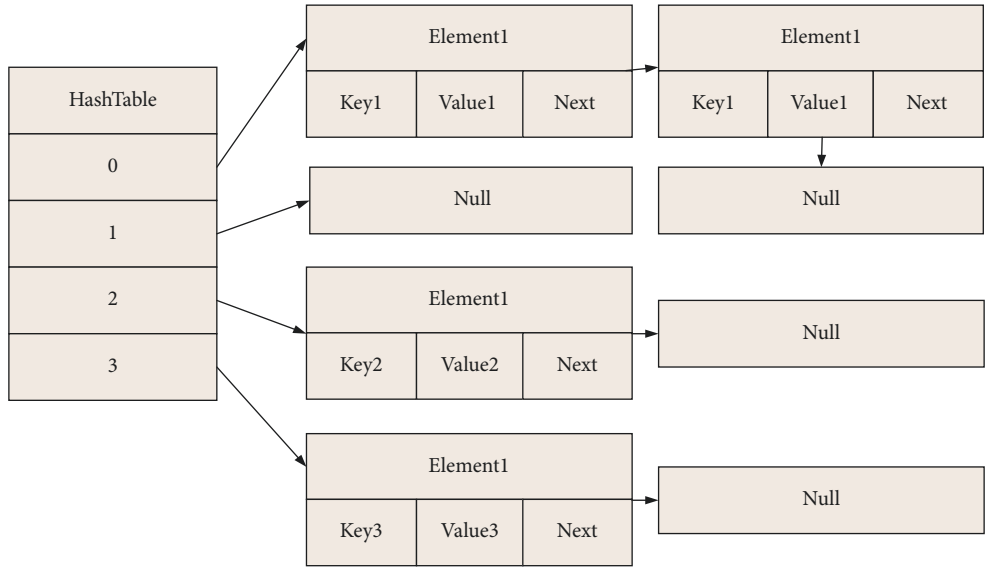

Figure 2: Hash index structure.

prior distribution information and variable information, for comparison, the posterior information is obtained by Bayesian algorithm, and then the function is used to calculate the range of the posterior distribution. In short, it is to use the distribution information of the parameters and the variable information to calculate the posterior distribution information through the Bayesian algorithm, and then use the posterior information to predict the index. The Bayesian estimation process is shown in Figure 3.

According to the Bayesian algorithm, it is assumed that the linear function $F(x, \theta)$ of the data set X, θ is the sampled sample, and $p(\theta)$ is the distribution value of θ. If there is a judgment function $d^*(X)$ in the judgment function image D, then we can consider that $d^*(X)$ is the Bayesian value range of θ. $R(d)$ is the maximum value of the judgment function $d*(X)$. The Bayesian value range is inversely proportional to $p(\theta)$, that is, if $p(\theta)$ is different, then the Bayesian value range of θ is the same. $p(\theta)$ and the square loss function are

$$d(x) = E(\theta|X = x)x\int_{\theta}\theta p(\theta|x)d\theta. \tag{1}$$

In this function, px is the posterior range of θ. The optimized Bayes algorithm is different from the original method because the Bayes algorithm combines posterior information and variable information. The Bayesian algorithm can set the parameters in the data model within the reasonable value range of the prior information. The value range of the prior information predicts the variables during the process corresponding to the value range of the posterior information [11]. That is to use variables to correct the previously set parameters. If the information in the X variable concentration is scattered before the prediction, then the value range of X a priori information is $P(X)$. After the Bayesian algorithm calculates the value range of the posterior information of X, Z is obtained, and the Bayesian algorithm calculates the value range of the prior information $P(X)$, $P(Z)$ and the value range of the posterior information. $P(ZX)$, the specific method is as follows:

$$p(X|Z) = \frac{p(Z|X)p(X)}{p(Z)}, \tag{2}$$

$p(Z|X)$ is proportional to the two functions $P(X)$ and $P(Z|X)$, and Z is inversely proportional to X. There is a certain relationship between the maximum value of the posterior information and the minimum value of the prior information and the sum of the judgment function, which can be obtained by the following calculation method:

$$x_{\mathrm{MAP}} = \mathrm{argmax}p(X|Z) \propto p(Z|X)P(X). \tag{3}$$

However, because the processed information of the sensor will finally calculate an average value, the sensor data model can make the collected information clearer. By substituting the sample set X, this data model can calculate the value range of Z. This value range is relative to the sensor and can be verified by a large number of experiments. The experiment shows that $P(Z|X)$ conforms to the negative-state distribution. The negative distribution means the distribution of the stability of the inductor:

$$p(Z = z_s|X) = \frac{1}{\sigma_s\sqrt{2\pi}}\exp\left\{-\frac{(x-z)^2}{2\sigma_s^2}\right\}. \tag{4}$$

The image of the variance can indicate whether the information processed by the sensor is valid. S represents the Sth sensor. Assuming that two sensor models are introduced into the above judgment function, it can be calculated by Bayesian function. The posterior distribution of the maximum value is

$$x_{\mathrm{MAP}} = \mathrm{argmax}\left[p(Z = z_1|X = x)p(Z = z_2|X = x)\right]. \tag{5}$$

$$x_{MAP} = \mathrm{argmax}\left[\frac{1}{\sigma_1\sigma_2 2\pi}\exp-\left\{\frac{(x-z_1)^2}{2\sigma_1^2} + \frac{(x-z_2)^2}{2\sigma_2^2}\right\}\right]. \tag{6}$$

It is concluded that

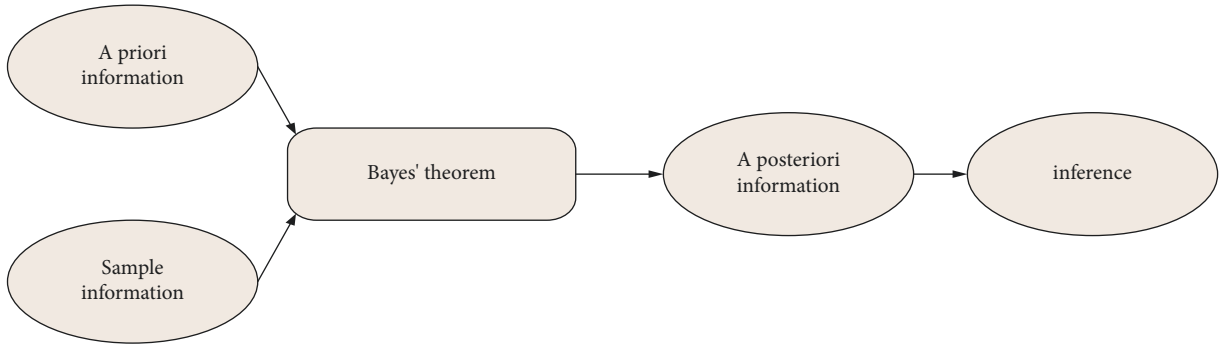

Figure 3: Bayesian estimation inference process.

$$x_{MAP} = \frac{\sigma_2^2}{\sigma_1^2+\sigma_2^2}z_1 + \frac{\sigma_1^2}{\sigma_1^2+\sigma_2^2}z_2 = \frac{1}{r^2+1}z_1 + \frac{1}{1/r^2+1}z_2. \quad (7)$$

Two functions are converted to calculate the probability value:

$$\sigma_v^2 = \frac{\sigma_1^2 \bullet \sigma_2^2}{\sigma_1^2+\sigma_2^2} = \frac{1}{\sigma_1+\sigma_2-4}. \quad (8)$$

In the actual application process, if the sensor has some problems or is affected by other factors such as the surrounding environment, the sensor may get unstable or error information. In order to solve this problem, we have optimized and upgraded the above methods:

$$p(X|Z=z_1,z_2) \propto \frac{1}{\sigma_1\sqrt{2\pi}}\exp -\frac{(x-z_1)^2}{2\sigma_1 Fac} \times \frac{1}{\sigma_2\sqrt{2\pi}}\exp -\frac{(x-z_1)^2}{2\sigma_2^2 Fac}. \quad (9)$$

The value of Fac is

$$Fac = \left\{\frac{m^2}{m^2-(z_1-z_2)^2}\right\}. \quad (10)$$

It can be seen that after the optimization and upgrade of the above method, we took into account the influencing factors in the environment and called it Fac, where m is the calculated maximum residual value and the optimized algorithm is mainly to solve the information in the sensor, Instability may be able to identify and filter out some unnecessary factors, and then get more accurate and clear calculation results [12]. This article will systematically explain the industrial equipment monitoring technology based on the data model and verify the calculation results of the function.

3.4. Missing Data Estimation Method

3.4.1. Optimize the Parameter Estimation Model. The information set of the cloud computing platform is Y, which includes k subsets. After calculation, we get the average and variance of Y. In order to determine the data model parameters, we built the following function to predict the value of the parameter:

$$f(\varphi) = -\frac{n}{2}\ln(2\pi) - -\frac{n}{2}\ln|\Sigma| - \frac{1}{2}\sum_{i=1}^{n}(x_i-\mu)^T \bullet \sum_{i}^{-1}(x_i-\mu). \quad (11)$$

When predicting the parameters of the data model, the smaller the function value, the greater the parameter error. It can be seen that we can turn the problem into a problem of selecting the optimal solution under certain constraints and conditions, and the function can be changed to

$$\max_{\varphi} f(\varphi). \quad (12)$$

It can be seen that when the function value is larger, the parameter value error is smaller, and the speed of the optimal solution is faster. The specific calculation process is as follows:

$$P_x(\varphi_i) = \frac{f(\varphi_i)}{\sum_{j=1}^{m} f(\varphi_j)}. \quad (13)$$

According to the calculation result of the above formula, we can get ia and ib, which are the maximum and minimum values of the ith data set. According to these two values, we can calculate the value range of the parameter as

$$\text{s.t.}\begin{cases} a_1 \le \mu_1 \le b_1, \\ a_2 \le \mu_2 \le b_2, \\ \cdots\cdots, \\ a_k \le \mu_k \le b_k, \end{cases} \quad (14)$$

The above formula calculates the value range of the parameter. This value range can be used as a standard to judge whether the calculation result is correct. If the calculation result is no longer in this interval, it means that the calculation result is wrong and further calculations are needed. Then, we need to find the most suitable parameter value. First, calculate the average value of jX according to formulas (3)–(5), denoted as jx:

$$\overline{x}_j = \frac{1}{\sum_{i=1}^{n}\text{Count}_{ij}}\sum_{i=1}^{n} x_{ij}. \quad (15)$$

In the formula, if the data is wrong, there is

$$\text{Count}_{ij} = \begin{cases} 1, & x_{ij} \text{is not lost,} \\ 0, & x_{ij} \text{is lost.} \end{cases} \tag{16}$$

If X_{ij} is missing, perform the following operations:

$$y_{1j} = \frac{\overline{x_j} - a_j}{b_j - a_j}, j = 1, 2 \ldots, k. \tag{17}$$

In order to find the most suitable parameters, we then filter the parameter values according to the logistic mapping in formulas (3)–(8):

$$y_{(i+1)j} = \xi \bullet y_{ij} \bullet \left(1 - y_{ij}\right) i = 1, 2, \ldots, m-1; \quad j = 1, 2, \ldots, k, \tag{18}$$

In the formula, i represents the change speed, K is the predictive index, and its interval is (1), (3). The sequence corresponding to the parameter interval is obtained by formulas (3)–(8). In order to make the sequence correspond to the parameter image, it is necessary to follow the formulas (3)–(9). Perform mapping to calculate the average interval. Then, average the interval to estimate the missing data. From this, the parameter values can be obtained. The specific calculation process is as follows:

$$x_{ij} = a_j + \left(b_j - a_j\right) y_{ij}; \quad i = 1, 2, \ldots, m; \quad j = 1, 2, \ldots, k. \tag{19}$$

3.4.2. Genetic Optimization Process. After obtaining the parameter set, we need to use the predictive function to identify the good and bad parameters. This process consists of three stages: parameter selection, parameter merging, and parameter change. Let cP be the parameter merging speed, select P parameters from the parameter set of size M, and merge them, and then perform the following operations:

$$\begin{cases} \varphi_i' = e\varphi_i + (1 - e)\varphi_j, \\ \varphi_j' = (1 - r)\varphi_i + e\varphi_j. \end{cases} \tag{20}$$

In the formula, e is a value in the range of (1) and (2).

$$x_{ij}' = \begin{cases} x_{ij} + \Delta\left(g, b_i - x_{ij}\right), \text{random}(\bullet) > 0, \\ x_{ij} - \Delta\left(g, x_{ij} - a_i\right), \text{random}(\bullet) < 0, \end{cases} \tag{21}$$

$$\Delta(g, x) = x\left[1 - \rho^{(1 - \delta/G)^{\varphi}}\right].$$

In the formula, j is a value in the (1,2,....,k) set, after the function operation, a variable value is obtained, G is the kangaroo after the parameter changes, and the value is taken in the range of (1), (2).

3.4.3. Chaos Disturbance of Excellent Parameters. Genetic algorithm is easy to cause errors in function calculation and the speed of function selection is too fast. Therefore, we decided to use the predictive function to interfere with the inferior parameters in the parameter set, so that the genetic algorithm can find the optimal solution and reduce the change speed. Interfere with M inferior parameters to avoid generating new parameters. Assuming that the function value of the current inferior parameter is mf, then there is the following formula:

$$\mu_1^* = \left\{x_{i1}^*, \ldots, x_{ij}^*, \ldots, x_{ik}^*\right\}, \quad x_{ij}^{**} = x_{ij}^* + \alpha \cdot \phi_j, \quad j = 1, 2, \ldots, k. \tag{22}$$

Through the above algorithm, continue to interfere with the retained inferior function, which can speed up the determination of the optimal function value and reduce the replacement efficiency. Assuming that it is changed i times, f_i^* is the function value of the excellent parameter. When equations (3)–(14) appear, the calculation ends, and the parameter of the function value f_i^* is the optimal parameter.

$$\left|f_i^* - f_{i-1}^*\right| < \varepsilon. \tag{23}$$

4. Design of Data and Information Security Storage Method under Cloud Computing Environment

In the era of big data, because the problem of information leakage occurs from time to time, information encryption is particularly important. Information encryption is to carry out confidential measures for key information, which is mainly composed of multiple steps such as key generation, key use, and key cracking. It is worth noting that information is the inverse of the encryption operation when the key is cracked. Operation, which means that this process requires the same key to crack the information, and the information can be stored in the file after being encrypted [13–15]. The information security encryption system designed in this paper introduces the principle of block cipher. Generally, the block cipher encrypts the unencrypted information with an algorithm, and then puts it in the folder in order. This sequence is the encrypted information collection. Data encryption module operation process is shown in Figure 4.

4.1. System Performance Test Analysis. The system performance test analysis can compare the ECC algorithm used in the big data information encryption system of this article with other encryption algorithms in order to get the advantages and disadvantages of different algorithms. We have simulated in MATLAB to compare the ECC algorithm and the RSA encryption algorithm and the DSA encryption algorithm is used to test the encryption effect. The standard is mainly composed of data stability, encryption efficiency, and file size.

4.2. Security Test Analysis. The stability of information storage can be shown by the anti-interference of the algorithm. Therefore, we compared the anti-interference effects

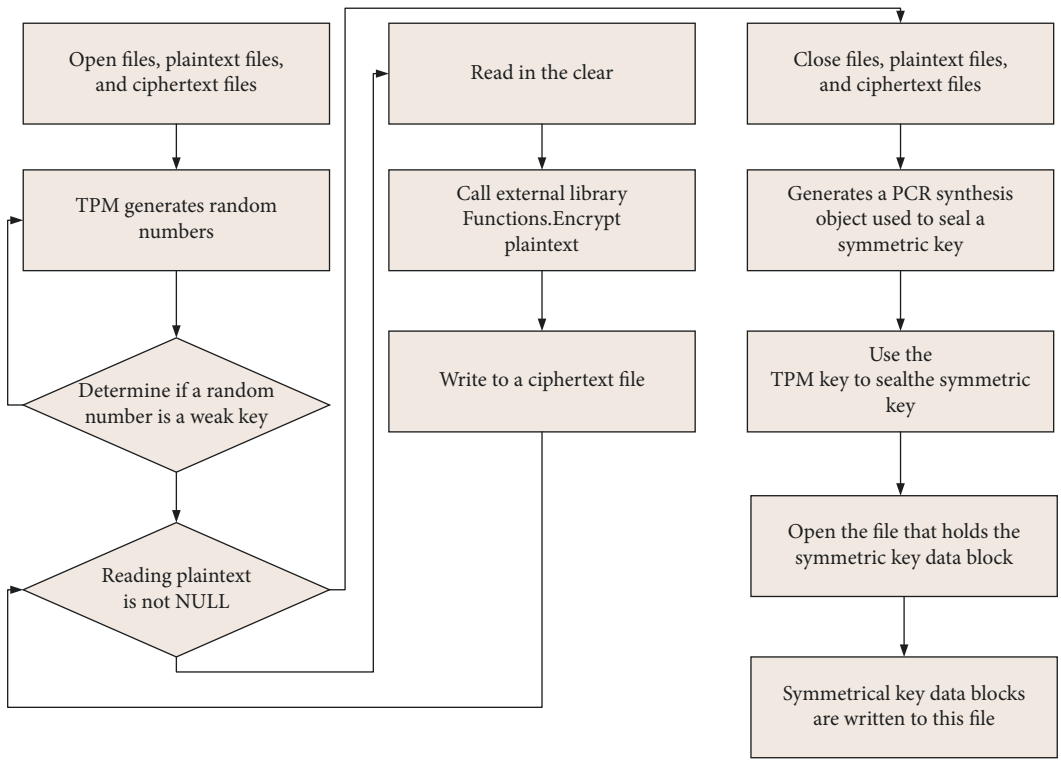

Figure 4: Data encryption module operation process.

of the ECC algorithm, the RSA encryption algorithm, and the DSA encryption algorithm, and the anti-interference performance is also related to the size of the key. There are relationships, and so we compared the key size of the encryption algorithm in MATLAB. Due to the large amount of calculation of the elliptic curve encryption algorithm, the calculation amount of the ECC algorithm changes with the change of the key, and the change is relatively large, but the calculation amount of the RSA algorithm and DSA algorithm is basically not affected by the change of key. Safety comparative analysis results are shown in Table 1.

Table 1: Safety comparative analysis results.

ECC algorithm (bii)	RSA algorithm (bit)	DSA algorithm (bit)
116	533	533
129	776	776
162	1019	1019
209	2103	2103

Studies have shown that when the key size of the RSA encryption algorithm is 173G, its encryption effect is the same as that of the EEC and DSA encryption algorithms with a size of 1231G; when the key size of the DSA encryption algorithm is 134G, the key size is RSA with 1091G. The encryption effect of EEC algorithm is the same.

4.3. Storage Space Test Analysis. Studies have shown that when the key size of the RSA encryption algorithm is 173G, its encryption effect is the same as that of the EEC and DSA encryption algorithms with a size of 1231G; when the key size of the DSA encryption algorithm is 134G, the key size is RSA with 1091G. The encryption effect of EEC algorithm is the same. Therefore, we can see that the DSA encryption algorithm has the smallest key size and the highest efficiency under the same encryption effect.

5. Remote Piano Music Teaching

5.1. Network—New Education Model. According to CNNIC's 30th Internet Report, before May 2014, there were already 481 million Internet users in China, an increase of 25.45 million in half a year. The Internet penetration rate is 45.2%. ②The average daily online time of the Chinese people is about 10 hours. The Internet is an emerging media that has developed after the traditional media such as magazines, TV, and radio. In recent years, mobile phones have also been continuously developed. Basically, one mobile phone is in hand. According to big data, statistics show that there are about 135 million teenagers with mobile phones. The mobile phone usage rate of Chinese people exceeds 65%, most of which are concentrated in young adults aged 12–45. From the perspective of academic qualifications, they are mainly concentrated in middle and high schools. The Internet has multiple purposes such as real-time calls, survey data, news newspapers, and online teaching. This shows that the Internet has become the most important way for us to live, study, work, and play. Nowadays, the Internet is also integrated into the teaching field. With the enhancement of young people's learning awareness, the role of the Internet in teaching has exceeded the role of entertainment and recreation, and this has enabled teaching to break through the limitations of time and space. The CEO of Microsoft said that the Internet will be mainly used for teaching in the next six years to meet the needs of

the knowledge economy era. Online education has been developing for decades, from correspondence education, broadcasting education, etc., to the use of Internet, big data, and other methods for teaching, increasing the way of education. As of 2007, mainly Ivy League schools, about 15 colleges have started online open courses.

Although China's online education started relatively late, it has made considerable achievements. Hongcheng Education is the largest online education platform in China with the longest existence. This platform was established in 1998. The service targets were only for adults, and later began to cooperate with various universities. By 2006, 102 online education platforms were merged to improve the higher education system. It was listed on the New York Stock Exchange in 2008 and was the first online education platform to be listed in China. Currently, there are more than 98 million users.

5.2. Overview of Online Piano Music Education. In recent years, online piano music teaching platforms have sprung up. The characteristics of these platforms are that they can provide some effective information with the changes of the times. Users can know the music resources in China and around the world and will hold regular music academic discussions. Meetings, various trainings, and competitions are conducted in order to show the style of music talents. The purpose of the online music teaching platform is to unite piano teachers, conduct piano music seminars, and reform the form of music education. Pianists exchange experience and research results, compile piano teaching materials, and conduct joint creations. On the basis of cultural inheritance, promote exchanges and cooperation with other countries, absorb the essence, and pave the way for the development and education of China's piano industry.

6. Conclusion

The principle of different information processing systems is to integrate and classify data extracted from different platforms through algorithms and other methods, and then save these data on the cloud computing platform. We have conducted research on information preservation in the context of big data, combined with trusted cloud computing to develop information security preservation technology, focusing on information encryption processing, key cracking, and other modules, and verified the results through a large number of experiments. The key has been optimized and upgraded to realize the efficient operation of the system. With the popularization and development of the Internet, this has brought a huge impact to traditional offline education forms. Schools are no longer the only way of teaching. Online teaching breaks the limitations of time and space. In order to meet the needs of the knowledge economy era, China has gradually established a perfect and efficient online piano teaching platform. Develop personalized teaching plans for students of different ages, different occupations, different educational backgrounds, and different identities, and use the rich teaching resources at home and abroad to train students, which has promoted the development of piano education in China, and even changed the Chinese teaching model.

Data Availability

The data used to support the findings of this study are available from the author upon request.

Conflicts of Interest

The author declares that there are no conflicts of interest.

References

[1] J. Park, H. Kim, Y. W. Tai, M. S. Brown, and I. S. Kweon, "High-quality depth map upsampling and completion for rgb-d cameras," *IEEE Transactions on Image Processing*, vol. 23, no. 12, pp. 5559–5572, 2014.

[2] A. F. M. Shahen Shah, H. Ilhan, and U. Tureli, "RECV-MAC: a novel reliable and efficient cooperative MAC protocol for VANETs," *IET Communications*, vol. 13, no. 16, pp. 2541–2549, 2019.

[3] N. Ta, G. Li, Y. Xie, C. Li, S. Hao, and J. Feng, "Signature-based trajectory similarity join," *IEEE Transactions on Knowledge and Data Engineering*, vol. 29, no. 4, pp. 870–883, 2017.

[4] C. C. Huang, J. H. Li, C. L. Mei, and W. Z. Wu, "Three-way concept learning based on cognitive operators: an information fusion viewpoint," *International Journal of Approximate Reasoning*, vol. 83, pp. 218–242, 2017.

[5] K. Do, T. Tran, and S. Venkatesh, "Graph transformation policy network for chemical reaction prediction," in *Proceedings of the 25th ACM SIGKDD international conference on knowledge discovery & data mining*, pp. 750–760, Association for Computing Machinery, Anchorage, AK, USA, August 2019.

[6] A. W. Astin and J. L. Holland, "The environmental assessment technique: a way to measure college environments," *Journal of Educational Psychology*, vol. 52, no. 6, pp. 308–316, 1961.

[7] B. C. Oliveira, A. A. Seibert, V. K. Borges, A. Albertazzi, and R. H. Schmitt, "Employing a U-net convolutional neural network for segmenting impact damages in optical lock-in thermography images of CFRP plates," *Nondestructive Testing and Evaluation*, vol. 36, no. 4, pp. 440–58, 2021.

[8] F. Claude, G. Navarro, and A. Ordóñez, "The wavelet matrix: an efficient wavelet tree for large alphabets," *Information Systems*, vol. 47, pp. 15–32, 2015.

[9] A. R. Kosiorek, A. Bewley, and I. Posner, "Hierarchical attentive recurrent tracking," in *Proceedings of the NIPS 2017*, pp. 2354–2451, Curran Associates Inc, Long Beach, CA, USA, December 2017.

[10] D. Mould and P. L. Rosin, "Developing and applying a benchmark for evaluating image stylization," *Computers & Graphics*, vol. 67, pp. 58–76, 2017.

[11] I. Sadeghi, A. Munoz, P. Laven et al., "Physically-based simulation of rainbows," *ACM Transactions on Graphics*, vol. 31, no. 1, pp. 1–12, 2012.

[12] H. I. Abbasi, R. C. Voicu, J. A. Copeland, and Y. Chang, "Towards fast and reliable multihop routing in VANETs," *IEEE Transactions on Mobile Computing*, vol. 19, no. 10, pp. 2461–2474, 2020.

[13] F. Kossentini, W. C. Chung, and M. J. T. Smith, "Conditional entropy-constrained residual VQ with application to image

coding," *IEEE Transactions on Image Processing*, vol. 5, no. 2, pp. 311–320, 1996.

[14] M. Guo, E. Chou, D. A. Huang, S. Song, S. Yeung, and L. Fei-Fei, "Neural graph matching networks for fewshot 3d action recognition," in *Proceedings of the European conference on computer vision (ECCV)*, pp. 653–669, Springer, Munich, Germany, Sempetber 2018.

[15] S. Kiranyaz, O. Avci, O. Abdeljaber, T. Ince, M. Gabbouj, and D. J. Inman, "1D convolutional neural networks and applications: a survey," *Mechanical Systems and Signal Processing*, vol. 151, Article ID 107398, 2021.

Hindawi
Mobile Information Systems
Volume 2022, Article ID 3773469, 10 pages
https://doi.org/10.1155/2022/3773469

Research Article

IOT-Oriented Visual Target Tracking and Supply Chain Art Product Design

Hua Song

Wuhan Polytechnic University, School of Art and Design, Wuhan 430048, Hubei, China

Correspondence should be addressed to Hua Song; huasong@whpu.edu.cn

Received 20 May 2022; Revised 19 June 2022; Accepted 29 June 2022; Published 15 July 2022

Academic Editor: Shadi Aljawarneh

Visual target tracking technology has always been one of the hotspots in the field of computer vision. After analyzing the above two problems and introducing real-time tracking, this article makes corresponding improvements to the visual target tracking structure of the Internet of Things. Based on this point, this article finally brings together related theories such as the Internet of Things and supply chain, starting from practical problems, inspecting the current situation of the supply chain of Chinese art product design companies, and proposing the necessity of establishing a systemic risk indicator system to use in the product supply chain; this article uses the HHM method to identify the risk factors of the artwork in the Internet of Things environment and promotes a multiangle risk analysis tailored to its own characteristics in the product supply chain. According to controllable risks and uncontrollable risks, combined with the structural level of the Internet of Things system, risks are divided into detection risk layer, network layer (information layer), application layer risk, and other risks. This article combines the above-mentioned visual target tracking technology with the relationship between the Internet of Things supply chains, uses the G1 method and the entropy weight method to determine the risk indicators for the subject and purpose of the risk weight, and classifies the risk indicators to propose risk control measures.

1. Introduction

Traditional visual target tracking algorithms cannot track part of the scene well due to insufficient functions, such as light changes and target deformations. In response to the above problems, this paper, based on the visual target tracking algorithm, conducts an in-depth analysis and improvement on image acquisition methods, target size estimation, occlusion, and missing target analysis and proposes a stable real-time visual target tracking algorithm [1]. It solves the problem of insufficient formal capture and description capabilities of the visual target tracking algorithm. The target tracking strategy is based on the weight fusion of multiple components in the response layer and introduces a method of estimating multiple dimensions [2]. Given the real performance of the algorithm, focus on the scale change of the target during the tracking process. According to the target position determined in this framework, the target set samples of different scales are constructed, and this set of sample input is used to drive the variable scale filter. The best real-time target proportion should be determined, so as to improve the tracking accuracy of the algorithm when the target proportion changes [3]. Next, based on the literature review, this research integrates and summarizes the Internet of Things, the supply chain of artworks, and other related content. In view of the current investigation situation, a company has relatively mature technology in the supply chain of art products, but on the surface, the company's early warning methods and early warning strategies are not ideal for new problems caused by the use of the Internet of Things technology. Based on the technical characteristics of the Internet of Things, this research combines the design characteristics of art products with the supply chain itself according to the hierarchical structure of the Internet of Things (psychological layer risk, network layer (information layer) risk, and application layer risk) and analyzes the product supply chain IoT applications at all levels of the chain. Finally, this article introduces the concept of artistic

product design around the supply chain through product experience and proposes specific methods of organization and management and its implementation measures. First of all, we should pay attention to the needs of consumer experience (from supply chain to product experience), the overall structure of the designated catalyst unit, and the large number of experiences generated by the overall structure of the catalyst when the product contacts customers. Second, use the most advanced technology to expand the scope of product expertise, create a value matrix in empathy design, and create a fusion mechanism for organizational management to provide more diversity and sustainability.

2. Related Work

The literature introduces related issues such as the Internet, the art supply chain, and the product supply chain. Through the system dynamics model, the risk perception layer, risk layer (information layer), and system risk application layer of the product supply chain under the Internet of Things environment are established [4]. This dynamic model is based on a system dynamic model that visualizes the risk layer, information layer risk (information layer), and application layer risk and builds a risk model for the entire art product supply chain. The object's network environment and model dynamic system are used to supplement the supply chain risk model for the product [5]. It can simulate a real and dynamic operating system and test the extremeness and sensitivity of the model through scientific means. The literature introduces the technology of the RFID anti-counterfeiting system [6]. The system focuses on label operations and can be divided into four subsystems, namely label storage system, label issuance system, label and seal system, and authentication system. The business logic of the four subsystems is designed in detail, the AES encryption algorithm and the MD5 algorithm are used to design the RFID data encryption method, and the AES encryption algorithm and the RSA encryption algorithm are used to design the data communication encryption algorithm [7]. The literature introduces manufacturing maturity evaluation indicators and prioritizes the algorithmic analysis of manufacturing factors based on the analytic hierarchy process, the representation method of manufacturing maturity based on fuzzy sets, and the content of the manufacturing maturity analysis method based on the estimated ideal value arrangement to obtain maturity [8]. A comprehensive analysis model is created for the product design solution. Taking an electronic pump produced by an automobile energy company as an example, the product design scheme was verified according to the maturity of the production, and the feasibility of the inspection method was proved [9]. The literature introduces a trend binding filter, which targets a tracking algorithm based on spatio-temporal regularization [10]. The target tracking algorithm based on correlation filtering uses cyclic shift operation for dense sampling, which indirectly improves the discriminative ability of the tracking model but also introduces the problem of boundary effects. In addition, this method is used to update the model, which is updated every frame to quickly cause model degradation. The literature describes the linear correlation of target tracking algorithms, which combines the statistical characteristics of colors [11]. Related filtering barriers can prevent forms used to identify target information from becoming template features, including manual template forms (HOG, CN) and CNN forms.

3. Visual Target Tracking Method Design

3.1. Learning Correlation Filters. Consistent with MOSSE, when multiple shape paths are found, we will independently learn a specific correlation filter for each shape segment. Assuming that the sample used to start the correlation filter x and the shape extraction operation is labeled f, then $f(x)$ represents the shape obtained from the sample x. L is the label part of the channel, $l \in \{l | l = 1, \ldots, \mathrm{d}\}$, any form of discharge flow in channel l is marked as fl. The correlation filter is marked as h, so the correlation filter of any channel in this format is marked as h^l. The relevant response of each channel is marked as $S_h(x, l)$, which is defined as follows:

$$S_h(x, l) = h^{l*} f^l(x), l = 1, \ldots, \mathrm{d}. \tag{1}$$

In order to solve the above-mentioned insufficient learning problem, we independently create a knowledge-specific filter to consider each function of the model and optimize learning to minimize the difference in response between each channel and label, without slowing down. In this case, all occurrence paths will be processed individually, and the associated filters can also be fully identified. Therefore, the shape channel is called a separate independent channel. In order to obtain the filter hl in each independent part of the component, the following target expression must be defined:

$$E(h, l) = \left\| S_h(x, l) - y \right\|^2 + \lambda \left\| h' \right\|^2, l = 1, \ldots, \mathrm{d}. \tag{2}$$

After solving the equation using the strategy provided by the reference, we obtained the correlation filter of the independent channel based on the shape of the Fourier domain.

$$H^l = \frac{\overline{Y} F^l(x)}{\overline{F^l(x)} F^l(x) + \lambda}, l = 1, \ldots, \mathrm{d}. \tag{3}$$

After obtaining the correlation filter, we use the correlation filter to estimate the new target state. Assuming that the current frame is t, we can obtain the response spectrum used by R_t^l to estimate the state of the natural channel l:

$$R_t^l = \mathfrak{g}^{-1}\left(\overline{H_{t-1}^l} F^l(z_t) \right), l = 1, \ldots, \mathrm{d}. \tag{4}$$

If it is the t-th frame, we denote the response spectrum in the current frame as R^l, then the final response spectrum can be obtained.

$$R = \sum_{l=1}^{\mathrm{d}} w^l R^l. \tag{5}$$

3.2. Confidence Combination Based on the Optimal Distribution of Time and Space. We introduce a synthesis operator to describe the spatial dependence of the response spectrum. Since some of the following indicators cannot fully measure the spatial distribution of the response spectrum, this operator uses multiplication to combine them. For any response spectrum R, we define the reliability of its spatial distribution as

$$J(R) = \prod_k J_k(R). \tag{6}$$

FMAX is the maximum value of the color response, which can be obtained in the following ways:

$$J^{\mathrm{FMAX}}(R) = \max(R). \tag{7}$$

PSOC is a measure between the highest peak and the second highest peak of the color response. We use PSOC to measure the significance of the most common peaks in the color response, which is defined as

$$\begin{aligned} J^{\mathrm{PSOC}}(R) &= \frac{\mathrm{peak1}(R) - \mathrm{peak2}(R)}{\mathrm{peak}(R)}, \\ &= 1 - \frac{\mathrm{peak2}(R)}{\mathrm{peak}(R)}. \end{aligned} \tag{8}$$

The definitions of peak 1 (R) and peak 2 (R) are as follows:

$$\mathrm{peak1}(R) = J^{\mathrm{FMAX}}(R). \tag{9}$$

Here, for the calculation of peak 2 (R), all peaks must be in the response spectrum R. The meaning is as follows:

$$\mathrm{peaks} = \{R(i,j)\, I\, R(i,j) > R(m,n),\ (m,n) \in U(i,j,q)\}. \tag{10}$$

Obtain peak 2 (R):

$$\mathrm{peak2}(R) = \left\{v \mid v = max\left(\left\{u | u \in \mathrm{peaks}, u \neq S^{\mathrm{FMAX}}(R)\right\}\right)\right\}. \tag{11}$$

PSR reflects the credibility of the estimated value of the target state. We use PSR to enhance the credibility of the spatial distribution of the response spectrum. The meaning of PSR is as follows:

$$J^{\mathrm{PSR}}(R) = \frac{J^{\mathrm{FMAX}}(R) - \mu(R)}{\sigma(R)}. \tag{12}$$

APCE measures the level of color response changes and then displays the confidence level by detecting shape-independent channels. The meaning of APCE is as follows:

$$J^{\mathrm{APCE}}(R) = \frac{|\max(R) - \min(R)|^2}{\mu\left(\sum_{i,j}(R(i,j) - \min(R))^2\right)}. \tag{13}$$

The optimal spatial distribution of the response spectrum is defined as follows:

$$\begin{aligned} &\underset{w_l}{\operatorname{argmax}}\, J(R), \\ &\text{where } J(R) = J\left(\sum_{l=1}^{\mathrm{d}} w^l R^l\right), \\ &\qquad = \prod_k J_k\left(\sum_{l=1}^{\mathrm{d}} w^l R^l\right), \\ &s.t. \sum_{l=1}^{\mathrm{d}} w^l = 1, \\ &w\prime > 0, l = 1, \ldots, \mathrm{d}. \end{aligned} \tag{14}$$

In order to obtain the weight w^l that satisfies the best time distribution, the goal is described as follows:

$$\begin{aligned} &\underset{w'}{\operatorname{argmax}} \sum_{i=2}^{t} J(R_i), \\ &\text{where } \sum_{i=2}^{t} J(R_i) = \sum_{i=2}^{t} J\left(\sum_{l=1}^{\mathrm{d}} w^l R_i^l\right), \\ &\qquad = \sum_{i=2}^{t} \prod_{i=2} J_k\left(\sum_{l=1}^{\mathrm{d}} w^l R_i^l\right), \\ &\qquad s.t. \sum_{l=1}^{\mathrm{d}} w^l = 1, \\ &\qquad w' > 0, l = 1, \ldots, \mathrm{d}. \end{aligned} \tag{15}$$

$$w\prime > 0, l = 1, \ldots, \mathrm{d}. \tag{16}$$

In order to easily adapt to changes in the target shape, we have updated the weights obtained online. In this case, the optimization problem (15) can be simplified to

$$\begin{aligned} w_{t+1}{}' &= (1-\varphi) w_t^l + \varphi w_{t+1}{}', l = 1, \ldots, \mathrm{d}, \\ w_{t+1}{}' &= \frac{w_{t+1}{}'}{\sum_{k=1}^{\mathrm{d}} w_{t+1}^k}, l = 1, \ldots, \mathrm{d}. \end{aligned} \tag{17}$$

After obtaining the corresponding natural channel weights according to the best spatial distribution and the best time distribution of the response spectrum, the final response spectrum of formula (5) can be effectively generated, and a new target state can be found.

3.3. Online Update of Relevant Filters in Independent Feature Channels. We provide VAF, which is the change rate of appearance characteristics. It can measure the degree of change in visual appearance patterns in different visual paths to track visual targets. Assuming that the current frame is t, the sample used for online update is tx. For each environmental channel, VAF is defined as follows:

$$r_t^l = \frac{N_t^l}{\mathrm{D}_t^l}, l = 1, \ldots, \mathrm{d}. \tag{18}$$

Table 1: Experimental performance comparison results of IFCT and fD SST on OTB-2015.

	AUC	DPt	OP	FPS f
IFCT	59.9	77.7	73.3	69.8
fDSST	55.4	72.5	67.2	100.9

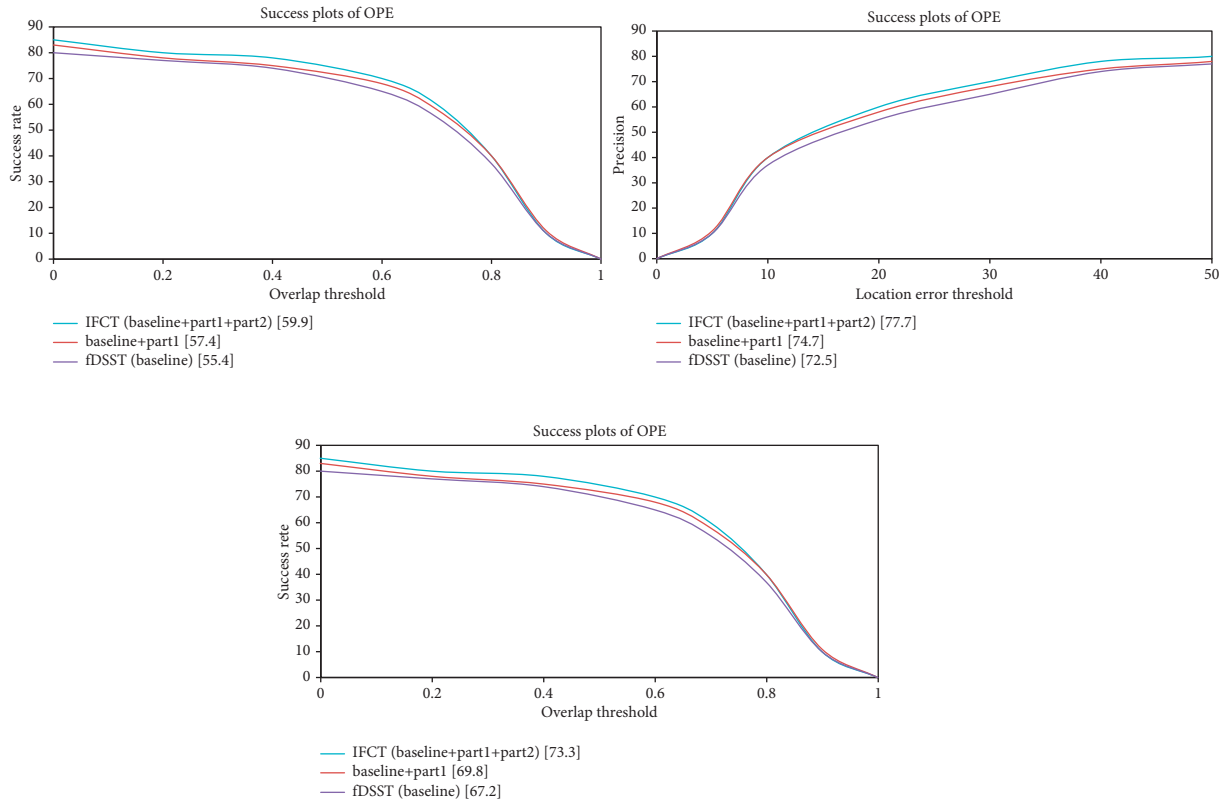

Figure 1: Showcase of experimental results for the validation of key parts on OTB-2015.

N_t^l is

$$N_t^l = \sqrt{\left|f^l(x_t) - f^l(x_{t-1})\right|^2}, l = 1, \ldots, \mathrm{d}. \tag{19}$$

D_t^l ensures that $r_t^l \in (0, 1)$ is

$$D_t' = \max\left(\left\{N_k^l | k = 2, \ldots, t\right\}\right), l = 1, \ldots, \mathrm{d}. \tag{20}$$

After obtaining the r_t^l feature change feature, you can independently update the relevant filters online in the feature channel. Unlike the improved and similar learning rate between channels, the learning rate we provide can reflect the feature changes between independent feature path frameworks, shown as follows:

$$a_t^l = r_t^l a_{\text{thres}}, l = 1, \ldots, \mathrm{d}. \tag{21}$$

For frame $t+1$, we obtain H_{t+1}^l by updating the A_t^l numerator and denominator B_t^l of H_t^l with the sample x_{t+1}.

$$\begin{aligned} H_t^l &= \frac{A_t^l}{B_t^l + \lambda}, \\ A_{t+1}^l &= (1 - \mathrm{d}_{t+1}')A_t^l + \mathrm{d}_{t+1}'\overline{Y}F^l(x_{t+1}), l = 1, \ldots, \mathrm{d}., \\ B_{t+1}^l &= (1 - a_{t+1}')B_t^l + a_{t+1}^l\overline{F^l(x_{t+1})}F^l(x_{t+1}), l = 1, \ldots, \mathrm{d}. \end{aligned} \tag{22}$$

3.4. Experimental Results. To estimate the position, we use a two-dimensional correlation filter. We use the shape with gray part and HOG-PCA. For the integrated part of the channel grayscale, we use the 4×4 size to combine the distribution of the grayscale image. For the HOG-PCA part of the channel, we reduced the size of the obtained part by 4 times. In order to measure the scale, we use a one-dimensional correlation filter, use HOG-PCA to obtain the shape, and finally set the λ parameter in regularization to 0.01.

It is known from the experimental results that our method has a significant improvement in tracking accuracy

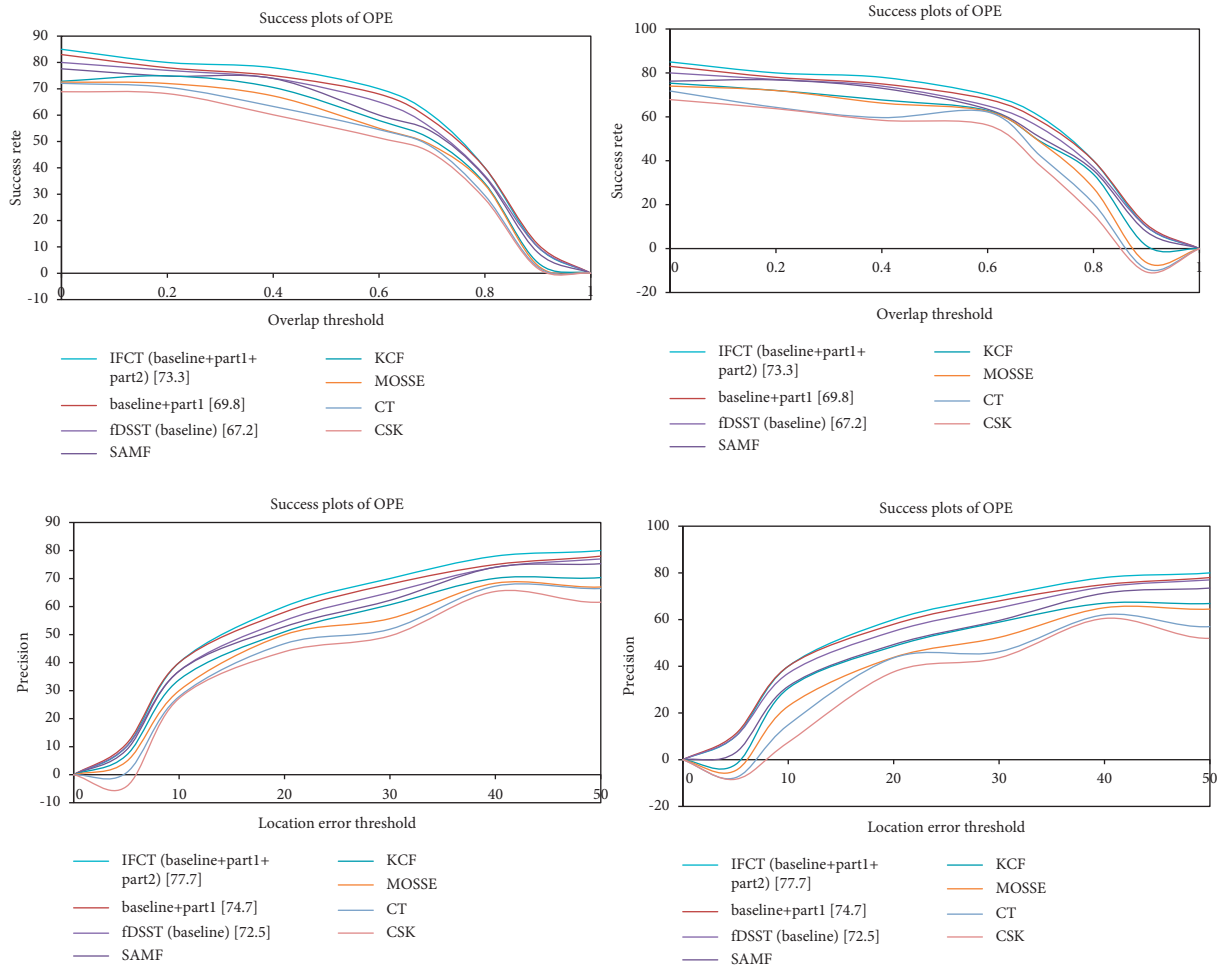

Figure 2: Comparison results of IFCT and many advanced algorithms on OTB-2013 and OTB-2015.

Table 2: Further comparison between many advanced visual target tracking algorithms and IFCT on OTB-2013 and OTB-2015.

	OTB-2013				OTB-2015			
	AUC	DP	OP	FPS	AUC	DP	OP	FPS
IFCT (ours)	63.7	83.5	79.9	72.0	59.9	77.7	73.3	69.8
SRDCF (ICCV2015)	62.6	83.8	78.1	4.9	59.7	78.8	72.6	4.7
CSR-DCF (CVPR2017)	59.3	80.3	73.8	8.6	58.6	80.2	69.8	8.4
LMCF (CVPR2017)	62.8	84.2	80.0	77.6	58.0	78.9	71.9	65.6
Staple (CVPR2016)	59.3	78.2	73.8	59.3	57.8	78.4	69.9	57.6
fDSST (TPAM2017)	60.0	80.3	74.7	107.6	55.4	72.5	67.2	100.9

compared with the initial value. For real-time execution, even if our method reduces the calculation speed to some extent due to many aspects of the tracking process, it can still guarantee the real-time execution of the process and keep the calculation speed tracking 70 FPS. The comparison results are listed in Table 1.

We independently verified the effectiveness of the main components of the OTB-2015 algorithm, and the experimental results are shown in Figure 1.

It can be seen that, according to the experimental method, fDSST control has been added to the first part of IFCT (i.e., including filters about independent form paths and subsequent color generation based on the contribution of the shape channel). In comparison, DP and OP increased by 2.0%, 2.2%, and 2.6%, respectively. After adding the second part of IFCT (the filter related to the online understanding of independent table channels), our method increases AUC, DP, and OP by 4.5%, 5.2%, and 6.1%, respectively, compared with fDSST. Therefore, compared with the experimental fDSST control method, each component of IFCT has a significant effect on its improvement, and the efficacy of the main component of IFCT is also confirmed.

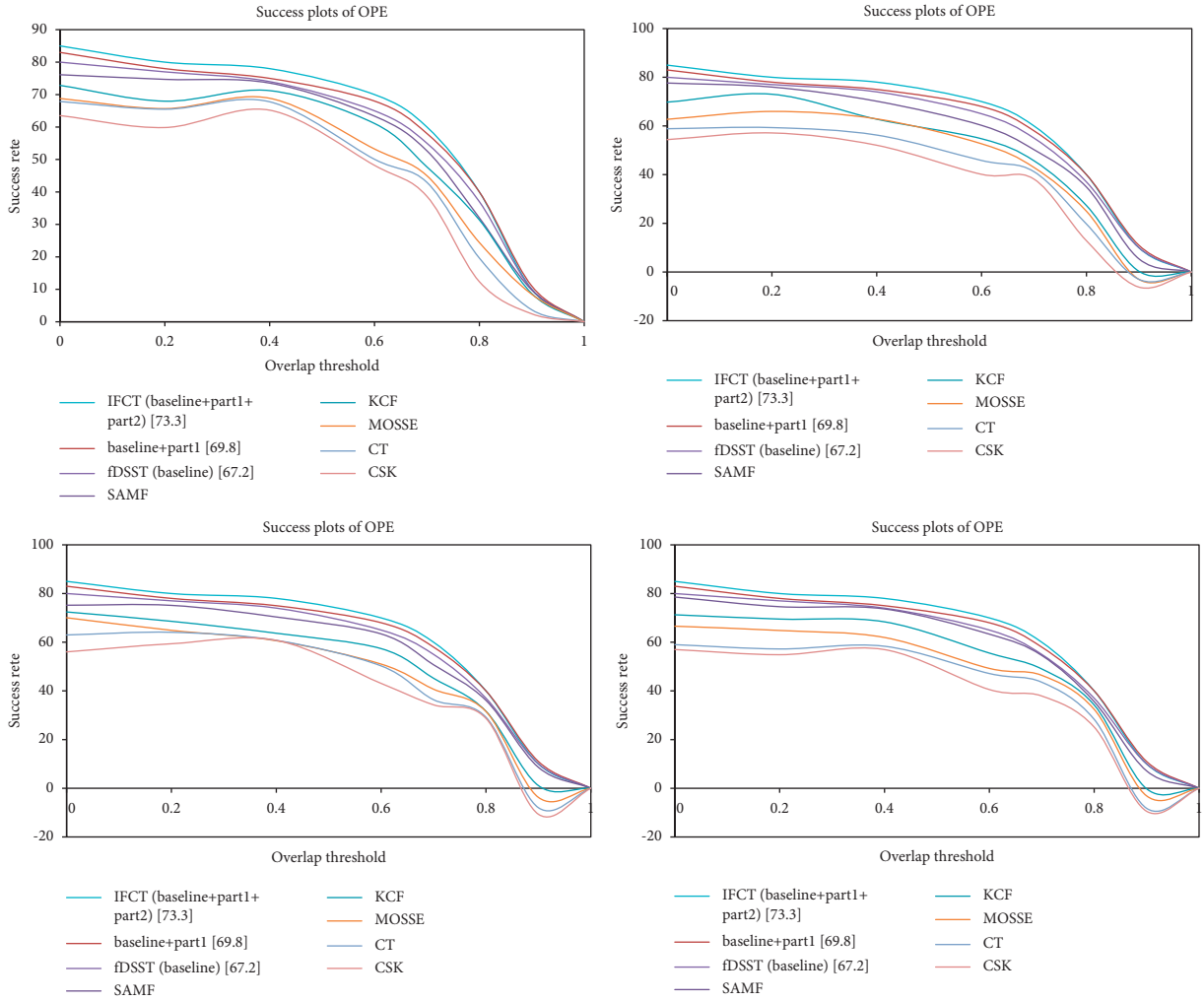

Figure 3: IFCT and many advanced methods compare results based on attributes of OTB-2013.

After starting the IFCT experiment and the fDSST control method, we compare the performance of other advanced algorithms in this chapter to track the visual targets of OTB-2013 and OTB-2015.

As shown in Figure 2, in OTB-2013, our IFCT method ranked first with an AUC score of 63.7%, which was 0.9% higher than LMCF, which ranked second with a score of 62.8%.

In order to better compare performance, we chose a typical comparison method to better compare and analyze our IFCT. The detailed information of the experimental results is shown in Table 2.

It is worth mentioning that between the two databases, IFCT not only has a good competitive advantage in tracking accuracy but also has some real-time performance advantages. Especially compared with SRDCF and CSR-DCF, our method is 15 times faster than SRDCF in calculation speed and 9 times faster than CSR-DCF. Figure 3 shows the results of the IFCT comparison and several advanced methods based on OTB-2013 features.

4. Supply Chain Art Product Design in the Context of the Internet of Things

4.1. IoT Architecture Design. With the support of Internet technology, the Internet of Things has become more intelligent and has become a mediator and link that connects everything. When studying the architecture of the Internet of Things, researchers further constructed their system structure in a layered manner, and many architectures rely on ISO/OSI as a reference model. Consistent with the nature of the Internet of Things, scientists divide it into three levels. These three levels correspond to the three components of the Internet of Things. These three layers not only overlap each other but are also connected to each other. Each level is supported by related technologies.

The perception layer is the key to identifying appropriate objects and collecting relevant information; the network layer processes relevant information and transmits the information from the perception layer to the application layer, as shown in Figure 4.

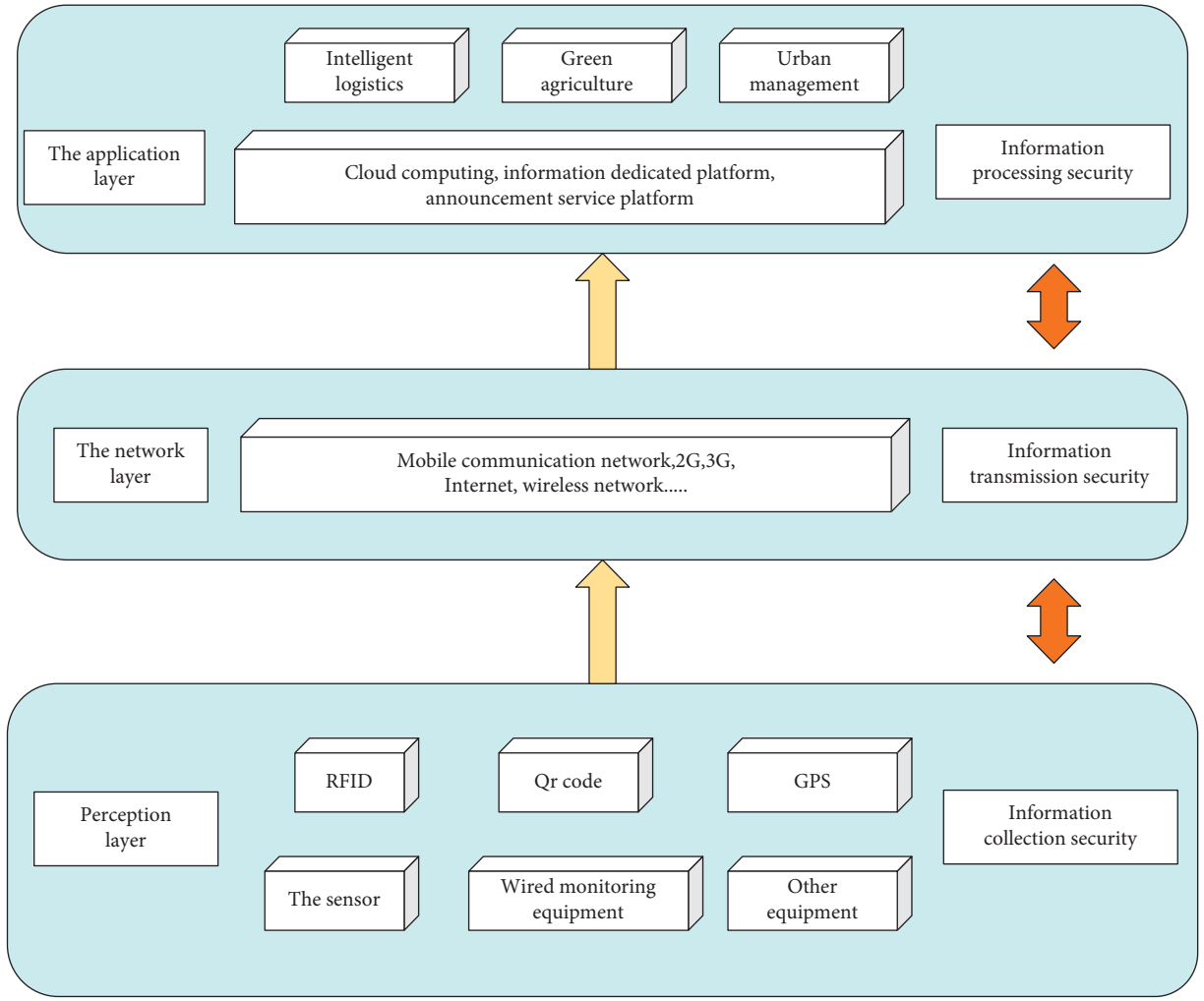

Figure 4: Three-tier architecture system of the Internet of Things.

It can be seen from Figure 4 that the functions of its three levels are different, and different levels are supported by different technologies.

4.2. The Basic Aspects of Artistic Design Based on the Product Experience Supply Chain. Design is undergoing a transition from "innovative style" to rapid "innovation." The plan has expanded from the link between the industrial chain and the innovation chain in the past to contribute to the system and the entire process. In the manufacturing process itself, traditional design is usually only seen as a specific and well-defined link in the production chain, which is connected to the "pipe" of the production chain in the form of "screws" and is located at the end of the chain. The supply chain with a product experience is based on sustainability thinking, and the nodes of product experience are connected to each other to form a general delivery chain of experience. From the perspective of consumer use, the artistic design of the supply chain around the product experience is generally defined as the "catalyst" and internal "catalyst" in contact with the customer's products.

According to traditional economic logic, people always weigh the value of products in terms of technology cost and

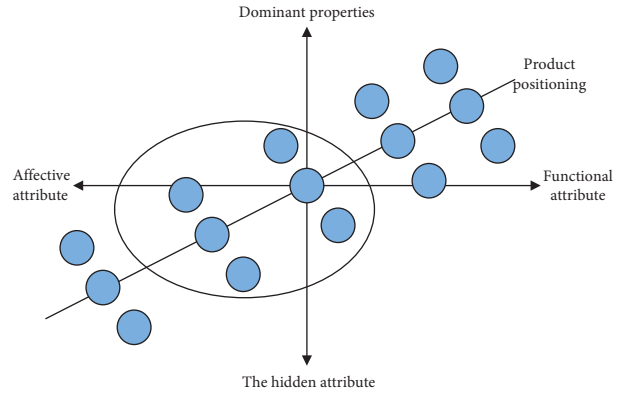

Figure 5: Extended design of product attribute dimension.

cost value, in order to increase the technical value of the product and increase the additional technical value of the product, or to improve the product by improving the manufacturing technology and reducing the cost of production. Nowadays, the aesthetic quality of products is no longer like decorative samples, but an organism that has been integrated into the product manufacturing process,

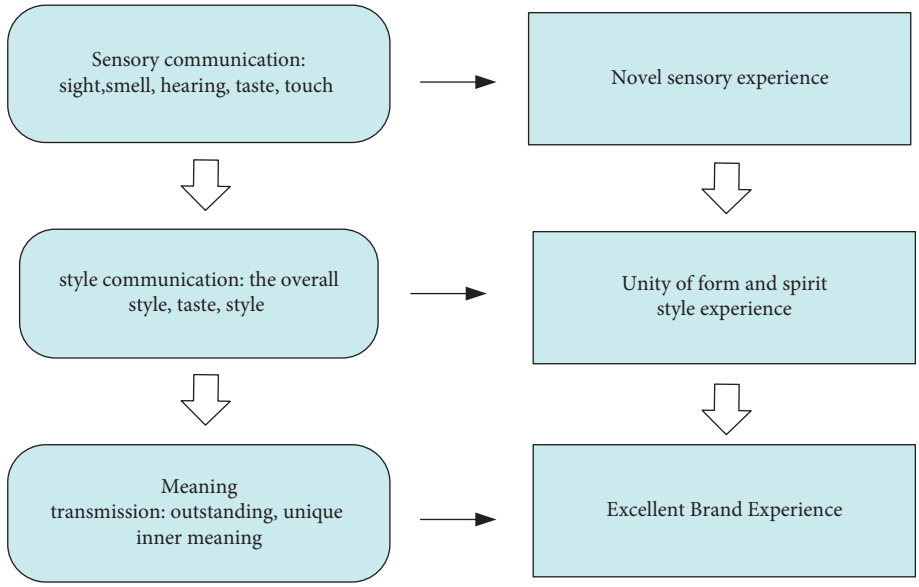

Figure 6: The value matrix of art design of product experience supply chain.

which is very important for consumption. In the continuous use of products by consumers, the manufacturer creates an aesthetic taste and brings an extraordinary experience to the product.

Consistent with this, the design concept of product experience supply chain art brings experience links, which can be included in products as chain units to maintain separate components and experience design [12]. The experienced supply chain art design not only expands the value channels of products but also makes the value chain of products become "organic expansion," that is, mutual connection and common value orientation. In this way, the geometric value of the product experience can be expanded, that is, the "$1 + 1 > 2$" effect. Different from traditional products with short added value, the quantity created by artistic design based on product experience in the supply chain is high-end cost and high-end capital, which is difficult to imitate and copy by competitors.

The production method available in art design is the latest supply chain, or it can be said to be a production system based on an intelligent network [13]. The experience of the product value chain covers the entire process of product development, manufacturing, marketing, and service and has a radiant impact on the entire product production chain and life cycle [14]. Nowadays, the testing and manufacturing of raw materials at the end of the industrial chain have begun to pay more and more attention to the transfer of aesthetic quality and aesthetic experience. At the same time, with the advancement of microcomputer technology, many aesthetic considerations can gradually be fully reflected in computer simulation and realized in the production process [15].

In addition, unlike the "pipeline" production chain where traditional design exists, the art design is no longer just a link in the industrial chain but becomes an "energy harvesting ring" in the industrial chain [16, 17]. These companies are mainly committed to combining the four basic resources of technology, production, brand, and market through art design. From exploring the concept connotation to ergonomic design, and then to manufacturers and users (setting production plans according to users' real-time response), creating brand image and management experience, the artistic design of users and services has gradually become the center of the whole product production value chain. The artistic design of users and services has gradually become the center of the entire product production value chain [18].

In the process of creating products, art design can be regarded as a method of creating beauty, emphasizing the paradigm method of observing specific aesthetic laws and specific product design techniques. The successful use of technology to create aesthetics is inseparable from the designer's abstract thinking and rational reasoning, as well as design thinking and intelligence. The designer must also have the ability to open up the product space and see it from the consumer's point of view. In addition, the emergence of new environments and new technologies has led to the continuous emergence of advanced methods of aesthetic creation. For example, an application program can automatically beautify photos or the shooting process according to the goal of the beautification law in product development and practice.

According to different dimensions, product experience attributes can be divided into four quadrants. From the perspective of explicit and implicit proof of product experience quality, detailed quality is made by consumers themselves and can be clearly expressed. There is a specific need to acquire or satisfy the inherent needs of an object. The requirements provided by hidden attributes have not yet been understood by people, and there is no explicit abstraction to meet them. Because these requirements are unconscious, consumers do not express them clearly. From the perspective of function and the sense of the quality of product experience, functional characteristics mainly refer to the usable value of the product, while emotion mainly refers to the intrinsic emotional value of the given

Table 3: Server side file description.

File name	Description
GetWorksId	Workslд generation and related processing modules
PerpaymentAction	Label authentication, settlement, and payment module
TagCommandAction	Label command control module
TaglnfoAction	Label information processing module
TagVisitRecordAction	Label operation record module
UploadTaglnfoAction	Tag data upload processing module
WorksInfoQueryAction	Work information acquisition module
WrtSendBlogAction	Social sharing module for signed works information
WrtUserlnfoAction	User information acquisition module

Table 4: Cloud platform continuous certification time-consuming test data.

Anticounterfeiting authentication times	Total time (ms)
10	353
20	1082
30	1208

characteristics of the product. Using aesthetic manufacturing technology to expand the scope of high-quality product experience is mainly to meet the basic needs of consumers, better meet the emotional needs, and pay attention to detect the invisible quality of the product itself in the unique position (process) in the market (see the oval in Figure 5), which is more attractive to consumers.

The core and key of the art design of product experience in the supply chain are to create aesthetic value systematically. The aesthetic value retention system mainly includes three value matrixes: sense transfer, style transfer, and definition transfer. The essence of experience is to explain the value matrix, and the effect of experience is the necessary purpose to reveal the basic aesthetic value of different matrices.

Product sensory communication is based on the visual image of the product itself, which usually brings people intuitive aesthetic feeling. Art design around product appearance is a kind of image design, which is based on appearance elements (such as product shape, pattern, color, and their combination), aesthetically beautiful and suitable for industrial application. The visual image of the product itself is no longer limited to the sensory characteristics of the product logo but extends to the multidimensional sensory experience and the taper aesthetic feeling of the image, such as emotional response and internal interaction. Under the joint action of multidimensional sensing, the product image brings people a comprehensive aesthetic experience. The value matrix of art design of product experience supply chain is shown in Figure 6.

Changing the inner meaning of products not only leads to new life concepts but also actively expands the significance of human existence. Therefore, the subversive change of the internal meaning of products is the mixture of art and design: art and design is the constant change of stereotypes and common "features" of products, as well as the continuous expansion of the existing lifestyle. By subversively aligning aesthetics and design with the concept, cost, shape, function, and service of the product, it provides an excellent brand experience. Classic art design conveys the inherent meaning of the product and provides consumers with a new way of life and the meaning of life experience.

4.3. Design and Implementation of Anticounterfeiting of Art Products. The web server program is created using MyEclipse, hibernate, Struts2, and spring framework. The source package operation file in wrt package is particularly related to label operation. A description of each file is provided in Table 3.

The main module of the system is the brand anti-counterfeiting authentication algorithm running on the server. This module is mainly composed of a physical verification algorithm and a label data processing algorithm corresponding to the label signature system. The system tested the time from the authentication request sent to the completion of the ongoing cloud platform forged authentication tags. Among them, there are 150 verifiable database tag records. The test data are shown in Table 4.

5. Conclusion

In order to simultaneously solve the model drift caused by the algorithm during the tracking process and the model drift caused by the scene, this article provides detailed information about RCF (regression of channel-independent part). Based on fix filters, the transferable correlation filter is independent of the flow based on the shape. Specifically, for the drift factor algorithm model, we have improved the algorithm based on the IFCT model. At the same time, for the derived model caused by the scene, we have studied the transmission mechanism based on the IFCT model to find the relevant filters. In addition, we are updating the RCF, taking into account the confidence when detecting different channels and changing levels. Finally, by introducing digital media into product design, this article enhances the function of product information in a variety of ways at the beginning of the design. In the design process, multimedia technology is used to communicate with enterprises and consumers through a network that is not limited by time and space. In the design process, multimedia technology is used to communicate with enterprises and consumers through the network that is not limited by time and space, and to connect and exchange information with designers in real time. In the design stage, designers can use digital multimedia to directly publish information between professional design platforms or network platforms, so as to improve the design ability and speed up the design process.

Data Availability

The data used to support the findings of this study are available from the corresponding author upon request.

Conflicts of Interest

The authors declare that they have no conflicts of interest.

References

[1] C. Sun, D. Wang, C. L. Hu, and M. H. Yang, "Learning spatial aware regressions for visual tracking," in *Proceedings of the IEEE Conference on Computer Vision and Pattern*, pp. 8962–8970, IEEE, Salt Lake City, UT, USA, June 2018.

[2] K. H. Galoogahi, A. Fagg, and S. Lucey, "Learning background-aware correlation filters for visual tracking," in *Proceedings of the IEEE International Conference on Computer Vision*, pp. 1135–1143, IEEE, Venice, Italy, October 2017.

[3] L. Yong-Hwan, A. Hyochang, A. Hyo-Beom, and L. Sun-Yuong, "Visual object detection and tracking using analytical learning approach of validity level," *Intelligent Automation and Soft Computing*, vol. 25, no. 1, pp. 205–215, 2019.

[4] J. T. Mentzer, W. DeWitt, J. S. Min et al., "Defining supply chain management," *Journal of Business Logistics*, vol. 22, no. 2, pp. 1–25, 2001.

[5] Y. Xia, S. Qu, S. Goudos, Y. Bai, and S. Wan, "multi-object tracking by mutual supervision of CNN and particle filter," *Personal and Ubiquitous Computing*, vol. 25, no. 6, pp. 979–988, 2021.

[6] B. Fahimnia, C. S. Tang, H. Davarzani, and J. Sarkis, "Quantitative models for managing supply chain risks: a review," *European Journal of Operational Research*, vol. 247, no. 1, pp. 1–15, 2015.

[7] F. L. Chung, "Privacy protection and mutual authentication scheme for RFID systems," *Journal of E-Business*, vol. 10, no. 3, pp. 715–726, 2008.

[8] N. Raza, V. Bradshaw, and M. Hague, "Applications of RFID technology," in *Proceedings of the IEE Colloquium on RFID Technology*, pp. 1–1–1/5, IEEE, London, UK, October 1999.

[9] B. Zhao, N. Guo, and X. Yu, *White Paper on the Maturity Model of Intelligent Manufacturing Capability*, China Institute of Electronic Technology Standardization, vol. 11, no. 4, Beijing, China, 2016.

[10] J. Gao and S. Gao, "Research and application of capability maturity model for Chinese intelligent manufacturing," *Procedia CIRP*, vol. 83, pp. 794–799, 2019.

[11] P. Radoglou-Grammatikis, K. Rompolos, P. Sarigiannidis et al., "Modeling, detecting, and Mitigating Threats against industrial Healthcare systems: a combined Software defined networking and Reinforcement learning approach," *IEEE Transactions on Industrial Informatics*, vol. 18, no. 3, pp. 2041–2052, 2022.

[12] R. Khan, S. U. Khan, S. Khan, and M. U. A. Khan, "Localization performance evaluation of extended Kalman filter in wireless sensors network," *Procedia Computer Science*, vol. 32, pp. 117–124, 2014.

[13] A. He, C. Luo, and X. Tian, "A twofold siamese network for real–time object tracking," in *Proceedings of the IEEE Conference on Computer Vision and Pattern Recognition*, pp. 4834–4843, IEEE, Long Beach, CA, USA, June 2018.

[14] X. Zhou, "Influencing factors and optimization measures of supply chain overall performance," *Journal of South-Central University for Nationalities (Humanities and Social Sciences)*, vol. S1, pp. 41-42, 2004.

[15] A. D. Papadopoulou, M. S. Gotsis, A. Wan et al., "Smart Irrigation system for Precision agriculture-the AREThOU5A IoT platform," *IEEE Sensors Journal*, vol. 21, no. 16, pp. 17539–17547, 2021.

[16] N. Tynan and J. Tynan, "Fashioning contemporary art: a new interdisciplinary aesthetics in art-design collaborations," *Journal of Visual Art Practice*, vol. 20, no. 1-2, pp. 143–162, 2021.

[17] S. Li, "The trend and characteristic of AI in art design," *Journal of Physics: Conference Series*, vol. 1624, no. 5, Article ID 052028, 2020.

[18] H. Liu, X. T. Zhang, X. M. Fu, Z. C. Dong, and L. Liu, "Computational peeling art design," *ACM Transactions on Graphics*, vol. 38, no. 4, pp. 1–12, 2019.

Hindawi
Mobile Information Systems
Volume 2022, Article ID 1076268, 10 pages
https://doi.org/10.1155/2022/1076268

Research Article

Simulation of Piano Teaching System Based on Virtual Data Space System and Neural Network

Liuqing Yang

School of Art, Hubei University of Education, Wuhan 430205, China

Correspondence should be addressed to Liuqing Yang; yangliuqing@hue.edu.cn

Received 20 May 2022; Revised 20 June 2022; Accepted 2 July 2022; Published 14 July 2022

Academic Editor: Shadi Aljawarneh

Cloud computing takes the analysis and digital processing technology based on virtual data space as the foundation and core of cloud computing technology development and research, and the significance and importance of data is self-evident. This paper designs a piano teaching system based on the virtual data space system and neural network, which can help users to master and use piano teaching information through the extensive application of this system. The functional test results show that the system fully realizes the automatic allocation of all virtual data spaces in the cloud computing environment and has the function of real-time synchronization with user terminals and applications in the virtual data space. Teachers can directly give lectures to students or give students detailed answers through live webcasting and other methods. Only by using this simple operation mode can they be able to solve the problems of piano teaching very conveniently. For the on-demand video, this paper manages the piano teaching videos by classification, that is, displays this type of video in an interface or table. The improved network recognition performance based on the loss function also achieves better improvement and improvement than the original network. The model has also achieved good performance in training and recognition on datasets in a strong noise environment.

1. Introduction

The distribution of network information resources based on virtual data space is a form of virtual network service for public release to the user's website. The service integrates many existing virtual data spaces to store network information management resources and other virtual network data services closely and directly [1]. Together, it is a concrete manifestation of the cross-integration of the virtual network data storage module and other network virtual data services. The data storage module is effectively used to manage and share the existing information and virtual data storage resources of each user [2]. Audio data recorded in real life scenes is usually accompanied by a certain strong noise environment, and sometimes the strong noise environment even drowns the speaker's voice, causing great interference to the complete extraction of the voice signal [3]. At present, the main solutions to such problems are speech noise reduction and speech enhancement. These algorithms are mainly to improve the audio-visual signal-to-noise ratio of the speech signal in the audio, but often cause the speaker's speech information to be lost, so that in many cases the audio recognition rate processed by these methods is not significantly improved [4]. In recent years, related research on improving the robustness of speaker recognition models to noise has become another major research direction [5]. In training, you can filter out clipped audio through voice clip detection to improve the quality of model training data; in practical application scenarios, audio quality classification and voice noise reduction are used to improve the input audio quality through audio signal-to-noise ratio calculations, thereby improving the performance of the speaker recognition system [6].

The modernization of information technology is becoming more and more in-depth and perfect, so that more and more young people can use this teaching method to master relevant professional knowledge, improve their own business ability and level, and can truly realize this method and there are more and more majors and disciplines in teaching, but there are still certain shortcomings and

incomplete adaptations to the work of piano music teaching [7]. The piano teaching process is an important part of music teaching. This type of piano teaching mode is different from the previous piano teaching, the teacher must give lessons, and the teacher will give a demonstration, pointing out the common problems of the students [8]. With the active organization and coordination of the piano teacher, the students can carry out meaningful and targeted training. Rapidly improving one's piano playing ability and quality means that one can gain more knowledge from it. The main purpose of the design and research and development of the piano teaching management system is to assist the smooth development of piano teaching, and classroom piano teaching is still in charge of teaching the main body that can give students good support and guidance of off-class resources [9]. The research, development, and design of the entire system are based on the modern music teaching curriculum as the main line of research. All the curriculum resources of each chapter and link are uploaded to the system, and then, the instructor can directly manage the curriculum resources he is responsible.

2. Related Work

Some research describes the rational allocation of user virtual data space and the management of the virtual user data space by the Cloudsync data synchronization system, and then, the specific implementation of the data classification and correlation mechanism of the terminal application and the system needs to be involved [10]. At the end of the data management, it describes the design of the synchronization mechanism of the two data transmissions and the correlation and acquisition of virtual incremental resource information [11]. Data allocation in the virtual incremental resource space is completed by the agent of the virtual space. The address of the virtual data space that needs to be allocated is specified, so that the administrator can choose the appropriate storage resource by himself, and realize the automatic allocation of the user's virtual storage resource [12]. The literature introduces in detail the allocation and management of virtualized data space for cloud computing users. The user's data resources are synchronized with the virtual space in the cloud computing environment on cloud computing applications and networks, which improves the density and security of user data. It supports users to manage various applications in their virtualized space and data on the network by using some traditional desktop software and other methods [13]. The literature uses voice clip detection to filter out clipped and strong noise ambient audio to improve the quality of model training data; in practical application scenarios, audio quality classification and voice noise reduction are used to improve input by calculating the audio signal-to-noise ratio of the strong noise environment. Audio quality, which in turn improves the performance of the speaker recognition system. The literature points out that the training of a high-precision and strong-noise environment model in the speech field often means that the amount of training data is large, and the model training may take a lot of time [14]. Therefore, if it can ensure that the recognition performance of the model is not reduced, i.e., the strong noisy environment model training parameters, then the training time of the strong noisy environment model will be effectively shortened. After a detailed investigation of a certain vocational and technical college, the literature has a clear understanding and understanding of the piano teaching management of this college, and is familiar with the entire teaching process [15]. Then, according to the analysis results to realize the structure and framework of each function, and finally use the object-oriented design method to complete the work. The literature has researched, designed, and developed based on the characteristics of the piano teaching management system. The piano teaching management system adopts the UML modeling method in the software development and design process, combined with the advantages of the three-level development framework, and completed the piano video on demand and music editing [16, 17]. The B/S mode is used to develop track editing, theme on demand, direct music on demand, teaching materials, user management, interactive teaching, and other services. For the storage of the database, the functions such as score editing are explained in detail. The literature shows that with the further development and deepening of China's piano physical education reform, in the past, our students were required to make urgent changes to the actual situation of piano learning based on the guidance of teachers. Students are more actively participating in piano teaching classes [18]. In the coming years, teachers should cultivate and improve students' piano learning and practical skills, so that they can rely solely on the teacher's thinking model for piano learning and gradually develop towards the students' self-growth.

3. Virtual Data Space System and Strong Noise Environment Recognition Technology

3.1. Principles of Virtual Data Space. Figure 1 is a schematic diagram of the structure of the Cloudsync block diagram of the data synchronization system. The data synchronization system mainly includes the service client for virtual data space access, user data space management, virtual data space service agent, data center, and other parts.

The functions of each part of data synchronization are described as follows:

(1) *Data Synchronization Client*. The client system can simultaneously realize multiple functions such as data synchronization and downloading of all application information, as well as real-time information synchronization and periodic data synchronization operations for all application data.

(2) *User Space Management*. Realizes the management of user virtual space information, including the user's operation interface and registration information management for virtual space information on the network.

(3) *Virtual Space Agency*. The virtual space agent provides users with the service of logging in to the virtual space, and is responsible for collecting and sorting

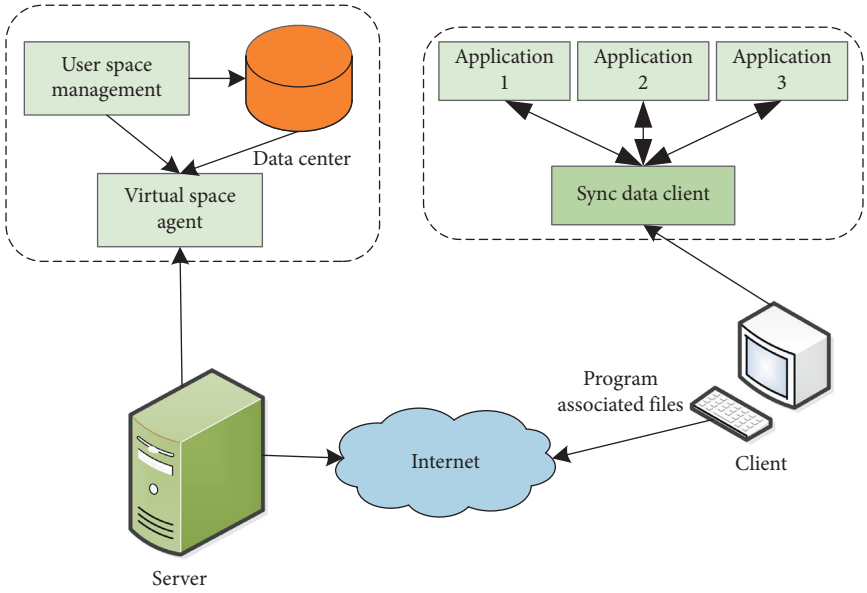

Figure 1: Data synchronization system architecture.

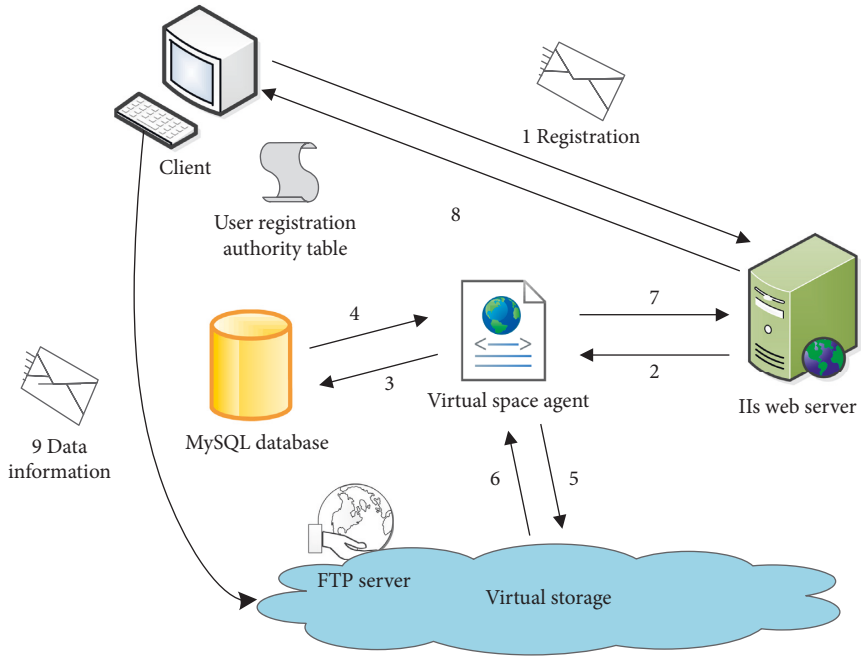

Figure 2: User virtual space allocation process.

information on the status of storage resources. At the same time, Cloudsync administrators can choose appropriate storage resources for themselves and create the required virtual space for users to use.

(4) *Data Center*. The Cloudsync data center built on a server side provides a virtual space, which is responsible for automatically realizing real-time data exchange between a client and the entire virtual data space. The current network data center is mainly running FTP network server and the main data information storage resources of two different operating systems of Linux at the same time. Therefore, more network protocols currently used for data information transmission network protocols are also completely adopted a relatively standardized FTP network protocol, a typical basic workflow of the FTP network protocol is that: first, a client initiates a network connection between the service network and the two parties will automatically establish a new FTP network to connect; then to the client, send a request to the server; then request data processing from the server; and eventually the server will automatically close the connection.

3.2. Distribution Process. Cloudsync website system administrators must first establish a related form in the MySQL website of the web server, and include all registered users' personal information, including their names, ID numbers, and original universal passwords, so that users can verify their real names. Figure 2 shows the specific operation process of a user applying for a virtual space in the Cloudsync system.

The specific process is described as follows: (1) The user fills in the login information related to the website and submits it to the web server. (2) The web server passes the information to the agent of the virtual space; (3) the service agent of the virtual storage space may automatically access the MySQL database. A list of virtual user names and authority information automatically is created by the service administrator of a local virtual storage space. (4) Automatically return the automatic authentication login information of the current user to a service agent of the local virtual storage space, if the information after user authentication is displayed if it is invalid, a corresponding verification prompt is given to the user. (5) A service agent and business personnel of a virtual storage space adopt a related management strategy method to automatically help the current user to correctly select the virtual storage resources needed for use. (6) Automatically return a virtual storage resource's permission list and send it to a virtual storage space service agent. (7) Automatically select the appropriate virtual storage application space according to user needs and automatically allocate resources and send them to the current user, and automatically determine that a current user has automatically registered a virtual user name that is a logical virtual storage application space name of a local virtual storage space. (8) Automatically send the current successful registration password information of the local client and the current virtual storage of the registered user space registration address information to your local client. (9) The current local client can also send login information to a local virtual storage space through automatic verification of the user name and login password, and synchronize all application logins on the current local mobile terminal data.

During the user's use, if the system administrator directly deletes one of the virtual users, the list between the virtual user name in the user database list and the registered user information will immediately delete the virtual user's registration information and assign it to the virtual user's virtual user. The user space is also accepted by the corresponding virtual user space service agent of the system and taken back for use by the next virtual user for space allocation.

3.3. Identification of Strong Noise Environment. Under normal circumstances, preemphasis around speech needs to be implemented with the help of a high-pass filter. In general, the transfer function that needs to be followed is shown in the following equation:

$$H(z) = 1 - ks^{-1}. \tag{1}$$

Here, k represents the preemphasis coefficient, and the value of k in this research experiment is all taken as 0.98. The voice signal structure of the sample point after windowing is shown in the following equation:

$$S(n) = V(n) \times W(n), \quad n = 0, 1, 2, 3, \ldots N. \tag{2}$$

Here, the i-th frame involves a speech signal, which follows the short-term energy formula, as shown in the following formula:

$$E_i = \sum_{n=0}^{L-1} y_i^2(n), \quad 1 \le i \le f_n. \tag{3}$$

The probability of false rejection refers to a classification problem, if two samples are the same person, but because of the system and mistakenly believes that they are not the same person, it is called a false rejection case. The false rejection rate can be calculated from the number of rejected legal speakers and the total number of legal speakers. Its definition is shown in the following equation:

$$\text{FRR} = \frac{\text{number of people refused to speak legally}}{\text{total number of legal speakers}} \times 100\%. \tag{4}$$

The false acceptance rate refers to a classification problem, if two samples are heterogeneous, but are mistaken as similar by the system, it is called a case of false acceptance. The false acceptance rate is calculated from the number of illegal speakers admitted and the total number of illegal speakers, and its definition is shown in the following equation:

$$\text{FAR} = \frac{\text{number of accepted illegally speakers}}{\text{total number of illegally speakers}} \times 100\%. \tag{5}$$

If it is a very large positive number, the output is 1, otherwise, the output is 0, which easily causes the gradient to disappear, and its function is asymmetric with the origin center.

$$\sigma(x) = \frac{1}{1 + e^{-x}}. \tag{6}$$

Compared with the activation convergence function in Sigmoid, Relu is not only simpler and easier to design and implement, but also more practical and effective to solve the fundamental design problem of the network due to the disappearance of gradient convergence so that large-scale network computing accelerates gradient convergence.

$$f(x) = \max(0, x). \tag{7}$$

Its function expression is shown in formula (6), assuming that the input of the residual block is x, the output is equal to

$$y = F(x, \{W_i\}) + x. \tag{8}$$

Here, $F(x, \{W_i\})$ is the goal to be learned, that is, the residual x-y of the output and input, and the residual part is a

double-layer weight with a Relu activation in the middle, namely,

$$F = W_2\sigma(W_1 x). \tag{9}$$

Here, σ refers to Relu, and W_1 and W_2 refer to two layers of weights.

Secondly, we expand the fast Fourier transform for $x(n)$ and obtain $|X_i(k)|$, phase spectrum $\theta_i(k)$, and power spectrum $P_y(k, i)$ in sequence.

$$P_y(k,i) = \left|X_i(k)\right|^2. \tag{10}$$

Then, we calculate the average amplitude spectrum and average power spectrum contained in the noise.

Again, after solving to obtain the talked frame and the nonspoken frame, the transfer function $H_i(k)$ that the Wiener filter needs to maintain is calculated.

Then, we calculate its actual output $W_i(k)$, and the specific formula is as follows:

$$W_i(k) = H_i(k)Y_i(k). \tag{11}$$

Noisy speech mainly includes speech signal and noise signal, and the main indicator to measure the energy strength of the two is the audio signal-to-noise ratio, which is defined as

$$\mathrm{SNR} = \frac{P_s}{P_n} = \frac{A_{\mathrm{signal}^2}}{A_{\mathrm{moise}^2}}. \tag{12}$$

When the unit of signal-to-noise ratio is db, its value is 10 times the ratio between logarithmic signal power and noise output power, which is defined as

$$\begin{aligned}\mathrm{SNR}(db) &= 10\log_{10}\left(\frac{P_s}{P_n}\right)\\ &= 20\log_{10}\left(\frac{A_{\mathrm{signd}}}{A_{\mathrm{notse}}}\right).\end{aligned} \tag{13}$$

According to our analysis of the FFT principle of high-frequency mathematics, it can be seen that any high-frequency signal may be directly converted into a fundamental wave and countless frequency harmonics through an FFT, so we can get

$$A^2_{\mathrm{signal}} = \sum_{n=0}^{N-1} A^2(n). \tag{14}$$

According to A_0 as the effective value of the fundamental wave voltage, A_n is the effective value of each harmonic voltage, combining the above formula can deduce a calculation method of SNR such as

$$\mathrm{SNR} = 10\log_{10}\frac{\sum_{n=0}^{N-1} A^2(n)}{A^2_{\mathrm{noise}}}. \tag{15}$$

We calculate the ratio of total of the number of windows, where k is the window size, nSample is the number of audio-sampling points, and the calculation formula is as follows:

$$\lambda = \frac{\mathrm{total}}{(n\,\mathrm{sample}/k)}. \tag{16}$$

Assuming that there are m neurons in the $l-1$th layer of the network, the output a_i^l of the jth neuron in the lth layer is

$$a_i^l = f\left(z_j^l\right) = f\left(\sum_{k=1}^{m} W_k^l a_k^{l-1} + b_j^l\right). \tag{17}$$

Obviously, using a basic form of matrix algebra to directly express the process of forward signal propagation for neural networks may become very complicated, and it can be directly transformed into a form of expression as a matrix.

$$a^l = f\left(z^l\right) = f\left(W^l a^{l-1} + b^l\right). \tag{18}$$

With formula (15), the input of each layer and the output of the last layer can be obtained. The output of the last layer of an L-layer network is as shown in (16):

$$a^L = f\left(z^L\right) = f\left(W^L a^{L-1} + b^L\right). \tag{19}$$

There are also many types of loss functions; here, we use the common mean-square-error notation to measure the loss. For a single sample, the loss function is defined as

$$J(W,b,x,y) = \frac{1}{2}\left\|a^L - y\right\|_2^2. \tag{20}$$

Then the gradients of W and b can be obtained, respectively,

$$\begin{aligned}\frac{\partial J(W,b,x,y)}{\partial W^L} &= \frac{\partial J(W,b,x,y)}{\partial z^L} - \frac{\partial z^L}{\partial W^L}\\ &= \left(a^L - y\right)\left(a^{L-1}\right)^T \odot f'\left(z^L\right)\frac{\partial J(W,b,x,y)}{\partial b^L}\\ &= \frac{\partial J(W,b,x,y)}{\partial z^L}\frac{\partial z^L}{\partial b^L} = \left(a^L - y\right)\odot f'\left(z^L\right).\end{aligned} \tag{21}$$

If there is a common part in formula (21), it can be directly extracted from it to the public location, and the mark form is

$$\delta^L = \frac{\partial(W,b,x,y)}{\partial z^L} = \left(a^L - y\right)\odot f'\left(z^L\right). \tag{22}$$

The gradient calculation formula of the Z-th layer has been calculated here. The problem is how to obtain $L-1$ and the gradient lower than the backward layer. For the inactive input of the L-th layer, its gradient formula can be used:

$$\delta^L = \frac{\partial J(W,b,x,y)}{\partial z^l} = \frac{\partial J(W,b,x,y)}{\partial z^L}\frac{\partial z^L}{\partial z^{L-1}}\frac{\partial z^L}{\partial z^{L-2}}\cdot\frac{\partial z^{l+1}}{\partial z^l}. \tag{23}$$

The gradient of W^l and b^l of the l layer is expressed as

$$\frac{\partial J(W,b,x,y)}{\partial w^l} = \delta^l \left(a^{l-1}\right)^T,$$
$$\frac{\partial J(W,b,x,y)}{\partial b^l} = \delta^l. \tag{24}$$

The key here is to obtain the value of δ^l. Assuming that the δ^{l+1} of the $l+1$th layer has been calculated, then there are

$$\delta^l = \frac{\partial I(W,b,x,y)}{\partial z^l} = \frac{\partial I(W,b,x,y)}{\partial z^l + 1}\frac{\partial z^{l+1}}{\partial z^l} = \delta^{l+1}\frac{\partial z^{l+1}}{\partial z^l}. \tag{25}$$

And $z^{l+1} = W^{l+1} f(z^l) + b^{l+1}$, so formula (25) can be written as

$$\delta^l = \delta^{l+1}\frac{\partial z^{l+1}}{\partial z^l} = \left(w^{l+1}\right)^T \delta^{l+1} \odot f'(t)^l. \tag{26}$$

In the first stage of error reverse transmission, an intermediate variable is defined. Through this intermediate variable, we can calculate the error gradient of each layer sum, and then update the minimum sum formula, the following formula is as

$$W^l = W^l - \alpha \sum_{t=1}^{m} \delta^{i,l}\left(a^{i,l}\right)^T,$$
$$b^l = b^l - \alpha \sum_{i=1}^{m} \delta^{i,l}. \tag{27}$$

In formula (27), α represents the learning rate and m represents the total number of training samples $\{(x_1, y_1), (x_2, y_2), \ldots, (x_m, y_m)\}$.

3.4. Simulation Analysis. According to the analysis of the test results in Figure 3, in the current test environment, when a small and large-data-volume information file is uploaded to all users, the average transmission speed to the network has been maintained at about 4.2 MB/s.

Compared with the test directory uploading multiple smaller files in Figure 4, in the case of test cases of different sizes, the more test files contained in the directory, the longer the upload time of test cases.

In the process of transferring a directory with a relatively large amount of data, the upload speed of the directory is determined by the total amount of data and the number of individual files contained.

4. Research on the Piano Teaching System Based on Related Technology

4.1. System Performance Analysis. After the system has determined all the performance indicators that need to be completed, it can determine all the content that needs to be completed in various performance aspects. For the non-performance demand analysis of the entire system, the main factors affecting the system are its response speed, the number of concurrent accesses, and other aspects; after fully considering these perspectives, and incorporating these factors into the scope of performance design, this kind of

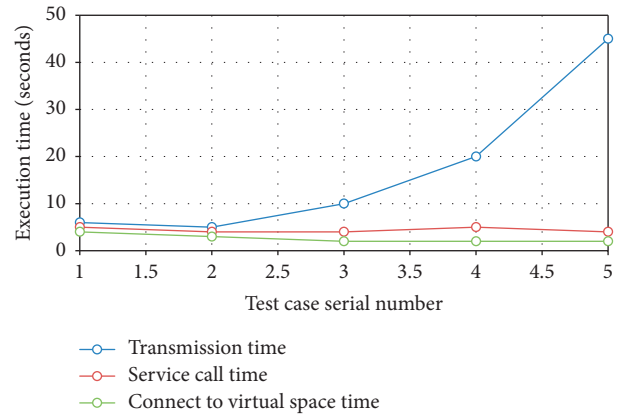

Figure 3: Cloudsync system single-file upload speed test.

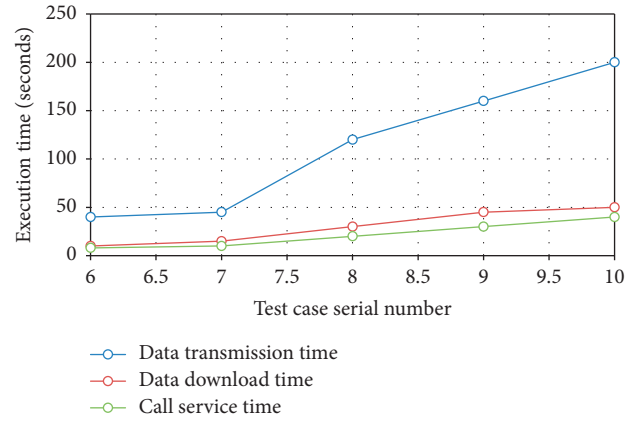

Figure 4: Cloudsync system upload and download directory speed test.

operation can play a relatively large role. Moreover, after the performance index of the system is determined, the requirements of the system can be different in different situations. Therefore, the system designed and developed should be able to meet the needs of users under various conditions:

(1) *System Response Speed.* For this system, it needs to be deployed and used in a Windows environment, which can satisfy multiple user operations after use. In order to ensure stable operation under the environment with the maximum number of users, the system needs to reduce the overall algorithm complexity, so as to improve the response speed of the system and also meet the computing needs of users. In addition, bandwidth needs to be increased as much as possible to meet the actual operation and needs of the users.

(2) *Processing Time of System Failure.* After the system is deployed and used, there will be abnormal situations and occurrences. After the system fails, certain means and methods need to be used to supplement and repair the failure. In addition, the system has a certain degree of fault tolerance, and other functional

modules should not be affected when an exception occurs, and processing operations need to be completed within 30 minutes.

(3) *System Throughput*. After conducting a demand survey on the system, it was found that there were not many people using it. After a comprehensive analysis, it was determined that the throughput should be above 2000000 b/s.

(4) *Continuous Working Time*. The system should be able to run continuously for a long time, and it is also necessary to determine whether the system can work continuously to meet the needs of users. After comprehensive analysis, the system should satisfy all-weather operation.

(5) *Safety Performance Requirements*. For the system, security is also a key consideration. This is because after the security is guaranteed, the system will be more stable and reliable in use. This article mainly needs to establish a complete protection mechanism so that a series of security technologies can be used to strengthen network access control.

In addition, the database of the system also needs to be strictly controlled to use permissions. A large number of staff's materials and information are stored in the database of the system. Therefore, the system needs to improve the security of the database. For a database, it needs to consider the use of encryption methods and technologies, which can greatly improve the security of access.

According to the market research and analysis results of the Chinese piano teaching management system, it can be accurately judged that the system files include the video playback on-demand for piano management teaching and the course audio for piano management teaching, the playback live broadcast of piano teaching courses, and the use of course resources. It can be accurately judged that the system files include the video on demand of piano management teaching, the course audio of piano management teaching, the playback and live broadcast of piano teaching courses, the use and management of course resources, the authority level management, music editing and comparison functions, and other modules. The function of piano teaching video on demand software mainly refers to allowing users to directly carry out video on demand of piano basic course courseware on the system operation interface of course software. At the same time, it also refers to some videos for piano basic courses. The on-demand function does some corresponding course control and management operations, and has the following functions. (1) The user can support the transmission and function of a single video when using it and the resumable transmission of video files exceeding 1G. (2) At the same time, it can support the automatic transcoding of various popular video formats; at the same time, it can also realize the all-round automatic switch codec for the more popular various video formats. (3) It supports automatic and manual rotation rate and code stream automatic setting and automatic setting of video resolution, which can easily realize low-video bandwidth, high-resolution video playback and high-definition, and automatic setting of video format switching. Automatic playback of high-resolution high-definition videos and mobile phone users can even easily set up multiple functions such as transcoding watermarks for mobile videos and video watermarks for mobile players.

Teachers can directly give lectures to students or give students detailed answers through live webcasts and other methods. Only by using this simple operation mode, can they solve the problems of piano teaching very conveniently. According to the analysis, its live broadcast functions are as follows: (1) Video users can usually directly use software encoder systems or video encoders to broadcast various types of video cameras, mirror heads, and other equipment, especially video programs such as on-demand TV, for live video broadcasting. (2) The video can be recorded during the live broadcast and will be available to users for on-demand use after the live broadcast. (3) You can choose to set the live video to a master mode or free live broadcast, but when it is set to a master mode, the teacher will perform a shared document operation at the same time during the live broadcast, and the user end will follow it. When the system is set to free mode, users can browse all shared files freely. (4) You can choose to set the live broadcast time, whether to open, and the charging pricing of the live program course, upload the live data and video files closely related to the course in the live room, etc. Users can also choose to set some more personalized live broadcast schedules and names after directly entering the live broadcast room for the first time. (5) The system can upload picture data to the system server, and then users can view these data, pictures, and information. (6) The administrator or other teachers in the entire live broadcast room also allow the following operations to be performed on all chats in the entire live broadcast room: delete, empty, prohibit entry, end, stop the video chat, automatically close, open the video scrolling screen, and view all live broadcasts video.

Music editing is a new function. The music score editing function is mainly to select the music score in the interface, and then use the editing method to pull the music score information into the editing interface. You can use this function to create a variety of music scores, which is convenient for users to operate and use. The music editing function can give the user a very clear feeling, and the editing function design is simple, but the application is complete; most of the score data can be easily edited into the operation interface, and the user can listen to the edited music after editing the music and modify the score. The user's operation is mainly done by pulling and tapping. After the music is played, the user can record it and compare it with the audio data of the system. After the comparison, it can be determined whether the user is playing well or not.

4.2. Overall System Design. In the design process, it is necessary to determine the logical structure and mode. After comprehensive analysis, this article uses the B/S design

mode. The specific structure is shown in Figure 5. This architecture mainly includes the presentation layer and the logic layer. The architecture belongs to the classic software development model. This development model is currently easy to use, can meet the actual needs of users, and has better scalability:

(1) *User Interface Layer*. At the top level of the entire logical structure, users need to use the interface to realize the control of human-computer interaction. This interface contains the main controls and operations, and each control and operation has a corresponding function. Users need to use functions to complete the corresponding processing and the entire system interface includes the verification part and the use part. The verification part is the content that the user needs to go through before entering the system, and the user's identity must be verified. The content of the use part is that the user completes the corresponding operation and processing with the help of various functional interfaces after entering the system.

(2) *Business Logic Layer*. In this level, the key parts of the system are included, which can operate and process various types of business, and can be transformed into various functional modules. Through this logical operation method, to assist in the design of various tasks of the system, and through the user interface layer after the completion of the operation, the user can obtain the corresponding result.

(3) *Data Access Layer*. The main work of the data access layer is to complete the operation of data storage. The main operation is to store the data that appears in the operation of the system, and at the same time to complete the processing of the data. After the processing is completed, the future data can be controlled, especially when the user sends the data. After the request, a lot of data information can be obtained from the database. In this way, the system can obtain data and content from the database even when it is running.

In the three-level development architecture, the presentation layer is a key part, and users use the presentation layer to complete the operation and processing of human-computer interaction. For the three-level development architecture, the simplicity of interface processing needs to be considered. The business logic layer needs the user to issue the corresponding command to be able to process it, analyze the user's data, and confirm that the command can be issued to the data layer. The data layer is to manage and maintain the data generated by the system, which is done with the help of database tools, as shown in Figure 5.

4.3. System Function Module Design. For video-on-demand, this article will classify the management of piano teaching videos, that is, display this type of video in an interface or table. The realization of this function is completed by the way of database query. When querying, the select statement is used to obtain, so that all the information and data can be displayed in the data table, and the user can determine the specific time to use and operate the content contained in the video. In addition, if users want to watch the video, they can click on the video to view the specific content. After viewing the video data, you can also record these data. After the user watches the video, the system interface can be restored to the original playback state, and the user can watch the instructional video repeatedly. All data needs to be obtained from the system database and can be saved to the database server.

For the audio function, it is similar to the video-on-demand function. In this paper, piano teaching audio is classified and managed, that is, this type of audio is displayed in an interface or table. The realization of this function is done by the way of database query. When querying, the select statement is used to get it, so that all the information and data can be displayed in the data table, and the user can see the teaching audio data in the data table. In addition, if the user is very interested in audio, click on the audio, and the system will be able to open the MediaPlayer control at this time to start the audio to play. The user can view the detailed data information of the audio when listening to the audio, which is convenient for recording these data. After the audio playback is completed, the system interface can be restored to the original playback state, and the user can listen to the audio data repeatedly. The audio information is obtained from the database of the system and can be stored in the database server.

For the function of live teaching, it is similar to the operation of answering questions. In the past, the operation was that the teacher and the student had face-to-face communication. In order to realize this function, it is necessary to use the data transmission protocol to complete the dialogue between the teacher and the student, and the student does not need to go to the teaching building. Moreover, the current computers have external video equipment, which can realize video dialogue interaction during operations such as answering questions, and use the provided functions to complete operations and process services. The face function is used to realize specific information dialogue and processing, and teachers can complete the operation more conveniently.

4.4. System Database Design. This article needs to determine the main data tables before designing and use these data tables to complete data storage and management:

(1) The user's basic data information is the management and maintenance of personal information. The content involved includes the user's code, name, and other related data. According to the analysis, its structure is shown in Table 1.

(2) The login information table is mainly used to record and store the basic information login of all registered users. It mainly contains the registered user code and other closely related data materials. The login table format is shown in Table 2.

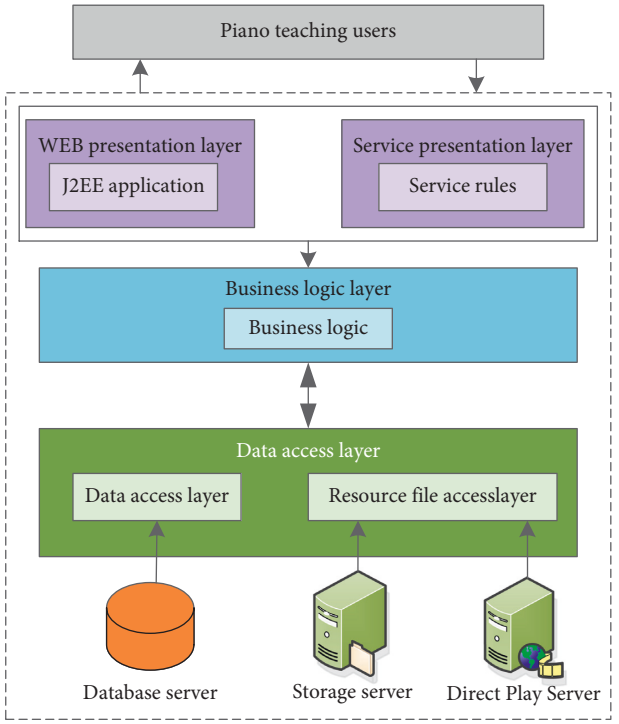

Figure 5: System logical structure design.

Table 1: Basic user information table.

Field name	Types of	Length	Description
User_ID	Int	10	ID number
Stu_name	Varchar	20	Name
Stu_name	Varchar	20	Gender
Stu_jg	Varchar	30	Hometown
Pol_sta	Varchar	10	Political status
Stu_bir	Datatime	12	Date of birth
Stu_nat	Varchar	10	Nationality
Stu_dep	Varchar	12	Department
Stu—spe	Varchar	10	Profession

Table 2: User login form.

Field name	Types of	Length	Description
U_ID	Int	10	ID number
Use_name	Varchar	20	Username
Use_pass	Varchar	20	Password
Ue_type	Varchar	20	User type

(3) This data table mainly automatically manages, saves, and maintains the content of network video image information and other network data in real time. The specific content of this main data table is shown in Table 3, and the main data content is also included and contains data content closely related to network video image information.

(4) The audio information list is mainly to save the data and information in the audio. Its table structure is shown in Table 4. The content of this data table contains a large amount of data information about audio.

(5) The course data sheet is mainly to save the video data and related information. The structure diagram of this course schedule is shown in Table 5. The content of the specific teaching computer course list includes the coding and data materials in the computer course.

(6) The system management list is mainly used to save the data and information of the system. The structure diagram of the table is shown in Table 6. The main attributes in the table are operation number, backup selection, recovery option, authority management, etc.

Table 3: Video information table.

Field name	Types of	Length	Description
s_ID	Int	10	Video ID number
s_name	Varchar	20	Video name
s_type	Varchar	20	Video type
s_size	Varchar	20	Video size
s_Time	Varchar	10	Video duration
S_FB	Varchar	10	Video publisher

Table 4: Audio information table.

Field name	Types of	Length	Description
Y_ID	Int	10	Audio ID number
Y_name	Varchar	20	Audio name
Y_type	Varchar	20	Audio type
Y_size	Varchar	20	Audio size
Y_Time	Varchar	10	Audio duration
Y_FB	Varchar	10	Audio publisher

Table 5: Course information table.

Field name	Types of	Length	Description
K_ID	Int	10	Course ID number
K_name	Varchar	20	Course title
K_type	Varchar	20	Course type
K_size	Varchar	20	Course size
K_FB	Varchar	10	Course publisher

Table 6: System management table.

Field name	Types of	Length	Description
G_ID	Int	10	Operation number
G_Back	Varchar	20	Backup selection
G_Restore	Varchar	20	Recovery options
G_Guan	Varchar	20	Authority management

5. Conclusion

This paper mainly studies the data synchronization process of virtual data space applications for cloud computing in depth, and promotes the effective development of data

synchronization services. The function test and performance evaluation of the Cloudsync data synchronization system for cloud computing have been done. The functional test results show that the system fully realizes the automatic allocation of all virtual data spaces in the cloud computing environment, and has the function of real-time synchronization with user terminals and virtual data space applications. Users can freely choose to use real-time in various situations. Users can freely choose to use the real-time synchronization mechanism and periodic synchronization mechanism in various situations so that devices connected to the Internet through the Internet can access the virtual data space and download all applications and data used in the virtual data space.

Experiments show that the model recognition method that uses deeper ResNet to extract the features of the spectrogram can better identify and characterize the characteristics of the speaker than the CNN network. The improved network recognition performance based on the loss function is also better than the original. The network has achieved better improvement and promotion results, and the model has also achieved better performance when data sets are trained and identified in a strong noise environment. The piano teaching management system up to now is actually a complex system. This piano teaching management system needs to be designed and developed with a variety of technologies. The wide application of this system can help users master and use piano teaching information. Therefore, this is a very huge project for us. This paper uses the technical advantages of the existing piano teaching information system to design and develop a set of piano teaching management system. The research, development, and design of this system use domestic and foreign masters. The operating system uses the database to manage and maintain the data when implementing the software, and conducts a comprehensive inspection of the database to implement important algorithms.

Data Availability

The data used to support the findings of this study are available from the author upon request.

Conflicts of Interest

The author declares no conflicts of interest.

References

[1] H. Y. Kan, V. G. Duffy, and C. J. Su, "An Internet virtual reality collaborative environment for effective product design," *Computers in Industry*, vol. 45, no. 2, pp. 197–213, 2001.

[2] D. Jianguang, Z. Yuelong, and Y. Huaqiang, "Dynamic data replication management strategy in cloud computing environment," *Journal of Huazhong University of Science and Technology (Natural Science Edition)*, vol. 43, no. 10, pp. 53–57, 2015.

[3] R. Gnanajeyaraman, K. Prasadh, and Ramar, "Audio encryption using higher dimensional chaotic map," *International Journal of Recent Trends in Engineering*, vol. 1, pp. 103–107, 2009.

[4] A. G. Acevedo, "Audio watermarking: properties, techniques and evaluation," *Information Security and Ethics: Concepts, Methodologies, Tools, and Applications*, vol. 6, pp. 23–61, 2007.

[5] A. Peinado and J. Segura, *Speech Recognition over Digital Channels: Robustness and Standards*, John Wiley & Sons, West Sussex, UK, 2006.

[6] D. Yu, L. Deng, J. Wu, Y. Gong, and A. Acero, "Improvements on Mel-frequency cepstrum minimum-mean-square-error noise suppressor for robust speech recognition," in *Proceedings of the 6th International Symposium on Chinese Spoken Language Processing (ISCSLP '08)*, pp. 69–72, December 2008.

[7] Z. Lian, "Research on aesthetic education in instrumental music teaching," *Journal of Literature and Art Studies*, vol. 10, no. 5, pp. 435–439, 2020.

[8] M. Adil, M. K. Khan, M. Jamjoom, and A. Farouk, "MHADBOR: AI-enabled administrative distance based opportunistic load balancing scheme for an agriculture Internet of things network," *IEEE Micro*, vol. 42, no. 1, pp. 41–50, 2021.

[9] D. B. Cevik Kilic, "Pre-service music teachers' metaphorical perceptions of the concept of a music teaching program," *Journal of Education and Learning*, vol. 6, no. 3, p. 273, 2017.

[10] X. Shengmin, "Analysis on the innovative strategy of national music teaching in colleges from the perspective of visual communication," *Studies in Sociology of Science*, vol. 7, no. 6, pp. 52–55, 2017.

[11] C. Joslin, T. Di Giacomo, and N. Magnenat-Thalmann, "Collaborative virtual environments: from birth to standardization," *IEEE Communications Magazine*, vol. 42, no. 4, pp. 28–33, 2004.

[12] T. Yongcai, B. Yang, S. Lei et al., "Management mechanism of dynamic cloud data replica based on availability," *Journal of Chinese Computer Systems*, vol. 39, no. 3, pp. 490–495, 2018.

[13] W. A. Xiuguo, "Replica strategy considering cost and storage space in cloud environment," *Computer Engineering*, vol. 44, no. 3, pp. 19–26, 2018.

[14] M. Naseri, S. Heidari, M. Baghfalaki et al., "A new secure quantum watermarking scheme," *Optik*, vol. 139, pp. 77–86, 2017.

[15] M. Barshan, H. Moens, S. Latre, B. Volckaert, and F. D. Turck, "Algorithms for network-aware application component placement for cloud resource allocation," *Journal of Communications and Networks*, vol. 19, no. 5, pp. 493–508, 2017.

[16] G. Cagirgan, "The opinions of the preservice music teachers regarding the teaching of orchestra and chamber music courses during distance education process," *Cypriot Journal of Educational Sciences*, vol. 16, no. 3, pp. 1088–1096, 2021.

[17] A. Chamberlain, M. Bødker, A. McGookin et al., "Audio technology and mobile human computer interaction," *International Journal of Mobile Human Computer Interaction*, vol. 9, no. 4, pp. 25–40, 2017.

[18] J. Waldron, R. Mantie, H. Partti, and E. S. Tobias, "A brave new world: theory to practice in participatory culture and music learning and teaching," *Music Education Research*, vol. 20, no. 3, pp. 289–304, 2018.

Hindawi
Mobile Information Systems
Volume 2022, Article ID 1050264, 9 pages
https://doi.org/10.1155/2022/1050264

Research Article

Clinical Analysis of Medical IoT and Acute Cerebral Infarction Based on Image Recognition

Juncheng Li, Wei Cui, Aiping Zeng, Yiju Xie, and Shengxian Yang

Wuming Hospital of Guangxi Medical University, Nanning, Guangxi 530100, China

Correspondence should be addressed to Shengxian Yang; xliu@stu.gxmu.edu.cn

Received 19 May 2022; Revised 17 June 2022; Accepted 28 June 2022; Published 14 July 2022

Academic Editor: Shadi Aljawarneh

Due to the mutual penetration and development of clinical medicine and informatics, medical image recognition can avoid the influence of subjective factors, and can diagnose the types of benign and malignant tumors in a timely and accurate manner, which is especially important for formulating effective treatment plans. This work mainly discusses fuzzy clustering and segmentation and SVM detection algorithms application in clinical medicine. The Internet of Things technology is a high-tech from the branch of the Internet, which plays a huge role in promoting the development and innovation of modern healthcare companies. The application of the Internet of Things technology has greatly changed the traditional medical model and effectively improved the relatively independent model in each unit system, thereby effectively promoting the scientific and informatization of modern intelligent medical care. Acute cerebral infarction is one of the most common clinical diseases, the clinical manifestations usually include tinnitus, headache, nausea, and vomiting. Acute cerebral infarction usually occurs suddenly and develops rapidly, which may eventually lead to hemiplegia, sensory disturbance, and language disturbance. This article analyzes the role of image recognition based on the medical Internet of Things in the clinical analysis of acute cerebral infarction and illustrates the clinical treatment methods through case studies. Simulation results prove that advanced IoT technology can more accurately track and monitor relevant patient information and can also play an important role in patient monitoring.

1. Introduction

With the development of electronic information and computer technology, medical imaging and image recognition technologies have developed rapidly, and have increasingly become powerful tools and key technologies for modern clinical analysis and medical diagnosis and treatment [1]. Although the imaging technology and equipment of modern medicine have made significant progress and improvements in recent years, the medical imaging film collected by modern medical equipment is still limited, and there are still many aspects such as low efficiency of the imaging engine of the equipment and imperfect technical materials. This is disappointing. For example, some medical imaging films have low spatial resolution, some medical imaging films contain a lot of noise and the signal-to-noise ratio is not good enough, or some medical imaging films must be combined with multipeak information for better clinical diagnosis. As an important branch of digital imaging technology, medical imaging technology combines technology and expertise in medical imaging, image graphics, and computer technology [2]. It can improve the visual quality of medical images and has been widely used in the medical film. The segmentation, selection, extraction, and recognition of medical images, as well as the completion of multipeak information fusion of medical images, have important practical significance in technology [3]. The research and development of medical imaging still faces many practical challenges [4]. For example, image recognition speed cannot meet the real-time requirements of medical clinics, and the accuracy of image segmentation has not been improved, because medical imaging technology has important practical significance for the research of medical clinical analysis and the diagnosis and treatment of clinical analysis [5]. In practice, patients with cerebral infarction have different manifestations, different symptoms, and different disease severity [6]. Some patients have mild symptoms, while others are severe. Acute cerebral infarction

usually occurs suddenly and progresses rapidly, which may lead to hemiplegia, sensory disturbances, and language disturbances [7]. The disease usually peaks after 3–5 days. As the disease worsens, the damage caused by the disease becomes more serious, and the permanent damage to the nerves also becomes more serious [8]. Therefore, timely treatment is needed to effectively restore the blood supply and oxygen supply of the necrotic tissue and improve cerebral blood perfusion. Consistent with the current clinical drug situation, thrombolytic therapy with urokinase is effective and widely used, but some scientists still have doubts about drug treatment options [9]. Therefore, this article studies the clinical effect of urokinase thrombolysis in the treatment of acute cerebral infarction [10].

2. Related Work

The literature first introduces the background and importance of the subject research, then analyzes the current research status of brain image segmentation and recognition technology at home and abroad, and finally points out the main research content of this article [11]. The literature mainly provides general basic knowledge for brain image segmentation and recognition and introduces in detail the fuzzy sequence clustering c-means algorithm in the segmentation module, as well as the algorithm of support vector machine and recognition module related knowledge. At the same time, the advantages and disadvantages of the c-means fuzzy clustering algorithm are summarized, and the criteria for evaluating the effectiveness of the algorithm are given [12]. An improved FLICM algorithm based on neighborhood information is proposed in the literature. To accurately describe the influence of adjacent pixels on the central pixel in c-means fuzzy local clustering, it makes full use of the spatial information between local adjacent pixels and uses the gray information to improve the fuzzy control coefficient to change the value of the objective function [13]. And based on gradient descent, the iterative expressions of membership matrix and cluster centers are rederived. The simulation experiment proves that the algorithm improves the performance of the noise reduction algorithm under the premise of achieving the segmentation effect, and is suitable for the segmentation of medical images with high noise pollution [14]. The literature proposes an improved FLICM algorithm combined with SCoW. First, the image is presegmented using the SCoW method, and then it is split into many small superpixel blocks without destroying the edge details of the image. Then, the average feature of each small block is extracted as the input sample of the clustering, which reduces the computational complexity of the algorithm. Finally, the gray-scale correlation between the organizations is used to measure the similarity between the organizations and improve the segmentation accuracy [15]. Simulation experiments prove that the algorithm solves the problem of insufficient memory during operation and greatly improves the algorithm's segmentation efficiency. The literature analyzes and summarizes the advantages and disadvantages of several typical algorithms with FCM extensions in fuzzy clustering algorithms [16]. To correct the disadvantages of the more traditional FLICM segmentation algorithm, refer to the ideas about improving other algorithms improved by FCM [17]. In addition, the literature also carried out in-depth research on two aspects of antinoise performance and segmentation efficiency, and then proposed an improved FLICM algorithm based on neighboring information, and combined with SCoW to propose an improved FLICM algorithm. Then, to more accurately distinguish brain tumors on brain images, the improved FLICM algorithm is used in combination with SCoW, and the brain tumors are determined according to the morphological, shape, and edge characteristics of the brain tumors after segmentation. The literature shows that the establishment of the medical Internet of Things platform solves the chaotic situation of the hospital's original wireless network structure, the reuse of wireless network resources, the difficulties and increased costs caused by management and maintenance, and the frequent interference between wireless network systems [18]. The effect of hospital network coverage was improved.

3. Theoretical Basis of Image Recognition and Its Application in the Field of Brain Images

3.1. Overview of Related Algorithms for Brain Image Segmentation and Recognition. Assuming that X represents the gray-scale pixel value or characteristic pixel value of the image, the image is composed of area C, the center of the area cluster is the membership matrix, and the objective function is formula (1):

$$J(U,V) = \sum_{i=1}^{n}\sum_{k=1}^{c} u_{ik}^{m} d_{ik}^{2}(x_i, v_i). \tag{1}$$

The objective cost function (1) satisfies the following conditions, such as formula (2):

$$\sum_{k=1}^{c} u_{ik} = 1, u_{ik} \in [0,1]. \tag{2}$$

The membership matrix and the expressions used for the iterative update of the cluster center can be obtained, such as formulas (3) and (4):

$$u_{ik}^{(t+1)} = \left(1 + \sum_{j=1, j\neq i}^{c} \left(\frac{d_{ik}}{d_{ij}}\right)^{1/(m-1)}\right)^{-1}, \tag{3}$$

$$v_k^{(t+1)} = \frac{\sum_{i=1}^{n}\left(u_{ik}^{(t+1)}\right)^{m} x_i}{\sum_{i=1}^{n}\left(u_{ik}^{(t+1)}\right)^{m}}. \tag{4}$$

Considering the influence of neighboring pixels on the central pixel in the objective function, the objective function of FCMS algorithm is as formula (5):

$$J(U,V) = \sum_{i=1}^{n}\sum_{k=1}^{c} u_{ik}^{m} d_{i_k}^{2}(x_i, v_k) + \frac{\alpha}{N_R}\sum_{i=1}^{n}\sum_{k=1}^{c}\sum_{x_j\in N_i} u_{jk}^{m} d_{j_k}^{2}\left(x_j, v_k\right). \tag{5}$$

The iterative update expressions of membership degree and cluster center are shown in formulas (6) and (7):

$$u_{ik} = \frac{\left(d_{ik}^2 + \alpha/N_R \sum_{x_j \in N_i} d_{jk}^2\right)^{-1/m-1}}{\sum_{j=1}^{c} d_{jk}^2 + \alpha/N_R \sum_{x_j \in N_i} d_{rk}^{2\ -1/m-1}}. \tag{6}$$

$$v_k = \frac{\sum_{i=1}^{n} u_{ki}^m \left(x_i + \alpha/N_R \sum_{x_r \in N_i} x_r\right)}{(1+\alpha)\sum_{i=1}^{n} u_{ki}^m}. \tag{7}$$

In order to further improve the performance of the FCMS algorithm, Chen et al. filtering technology based on FCMS is used to preprocess the pixel neighborhood information. The objective function is shown in formula (8):

$$J(U,V) = \sum_{i=1}^{n}\sum_{k=1}^{c} u_{ik}^m d_{i_k}^2 (x_i, v_k) + \alpha \sum_{i=1}^{n}\sum_{k=1}^{c}\sum_{x_j \in N_i} u_{jk}^m d_{j_k}^2 \left(\overline{x}_j, v_k\right). \tag{8}$$

Among them, such as formulas (9) and (10):

$$u_{ik} = \frac{\left(d_{i_k}^2 + \alpha \sum_{x_j \in N_i} d_{j_k}^2 \left(\overline{x}_j, v_k\right)\right)^{-1/m-1}}{\sum_{j=1}^{c} \left(d_{j_k}^2 + \alpha \sum_{x_j \in N_i} d_{r_k}^2 \left(\overline{x}_r, v_k\right)\right)^{-1/m-1}}, \tag{9}$$

$$v_k = \frac{\sum_{i=1}^{n} u_{ki}^m \left(x_i + \alpha \overline{x}_i\right)}{(1+\alpha)\sum_{i=1}^{n} u_{ki}^m}. \tag{10}$$

The objective function of EnFCM algorithm is as formula (11):

$$J(U,V) = \sum_{i=1}^{M}\sum_{k=1}^{c} \gamma_i u_{ki}^m (\xi_i - v_k)^2. \tag{11}$$

Among them, there is formula (12):

$$\xi_i = \frac{1}{1+\alpha}\left(x_i + \frac{\alpha}{N_R}\sum_{j \in N_i} x_j\right). \tag{12}$$

The expressions of the membership degree and iterative upgrade of the cluster center are as formulas (13) and (14):

$$u_{ki} = \frac{(\xi_i - v_k)^{-1/m-1}}{\sum_{j=1}^{c} \left(\xi_i - v_j\right)^{-1/m-1}}, \tag{13}$$

$$v_k = \frac{\sum_{i=1}^{M} \gamma_i u_{ki}^m \xi_i}{\sum_{i=1}^{M} \gamma_i u_{ki}^m}. \tag{14}$$

The FGFCM algorithm measures the correlation between local pixels through the spatial and gray information between input pixels instead of α parameters, preprocesses the image, reduces noise while preserving image detail information, and effectively improves the performance of the image segmentation algorithm. Effect, the standard definition for measuring the similarity between local pixels, is as formula (15):

$$S_{ij} = \begin{cases} e^{-\max\left(\left|p_i - p_j\right|, \left|q_i - q_j\right|\right)/\lambda_s - \left\|x_i - x_j\right\|^2/\lambda_g \sigma_i^2}, & i \neq j, \\ 0, & i = j. \end{cases} \tag{15}$$

The gray-scale variance of adjacent pixels is defined as formula (16):

$$\sigma_i = \sqrt{\frac{\sum_{j \in N_i} \left\|x_i - x_j\right\|^2}{N_R}}. \tag{16}$$

Then use formula (17) to filter the original image and obtain a new image defined as follows:

$$\xi_i = \frac{\sum_{j \in N_i} S_{ij} x_j}{\sum_{j \in N_i} S_{ij}}. \tag{17}$$

The FLICM algorithm does not need to manually select parameters, the clustering result is stable, and the target expression is shown in formula (18):

$$J_m = \sum_{i=1}^{n}\sum_{k=1}^{c}\left[u_{ki}^m \left\|x_i - v_k\right\|^2 + G_{ki}\right]. \tag{18}$$

Among them, there is formula (19):

$$G_{ki} = \sum_{j \in N_i, j \neq i} \frac{1}{d_{ij}+1}\left(1 - u_{kj}\right)^m \left\|x_j - v_k\right\|^2. \tag{19}$$

The expression of membership degree and the iterative update of cluster centers are shown in formulas (20) and (21).

$$u_{ki} = \frac{1}{\sum_{j=1}^{c}\left(\left\|x_i - v_k\right\|^2 + G_{ki} / \left\|x_i - x_j\right\|^2 + G_{ji}\right)}, \tag{20}$$

$$v_k = \frac{\sum_{i=1}^{n} u_{ki}^m x_i}{\sum_{i=1}^{n} u_{ki}^m}. \tag{21}$$

According to the correlation between classes and between classes, this paper compares the division factor V_{pc}, which is defined as formulas (22) and (23):

$$V_{pc} = \frac{1}{n}\sum_{i=1}^{c}\sum_{j=1}^{n} u_{ij}^m. \tag{22}$$

$$V_{pe} = -\frac{1}{n}\sum_{i=1}^{c}\sum_{j=1}^{n} u_{ij} \log\left(u_{ij}\right). \tag{23}$$

For image segmentation, it is always hoped that pixels are located closer to the corresponding cluster center and far away from other cluster centers. Therefore, the V_{xb} scoring function based on the degree of association between classes is used to evaluate the segmentation performance of the algorithm. When the V_{xb} value is small, the clustering effect of the algorithm is better. Its definition is as formula (24):

$$V_{xb} = \frac{-\sum_{i=1}^{c}\sum_{j=1}^{n} u_{ij}\left\|x_j - v_i\right\|^2}{n\min_{i\neq k}\left\|v_k - v_i\right\|}. \quad (24)$$

Since most of the images collected in real life are mostly noise-contaminated images, this paper also uses the SA segmentation accuracy index as the index of the comparison algorithm, which is defined as the formula (25):

$$SA = \sum_{i=1}^{c}\frac{\left|A_i \cap C_i\right|}{\sum_{k=1}^{c} C_k}. \quad (25)$$

Support vector machine is a new pattern recognition technology developed based on years of statistical learning theory. It is usually used for machine learning problems, such as small samples, nonlinearity, high dimensionality, and feature fitting. The original main idea is to find the best classification area under the condition of linear separation. The basic description is shown in Figure 1. The green and purple dots in the figure represent the two training modes, and H is the interface that separates the two types.

If you continue to use the standard of the linear best classification area when the linearity is inseparable, it will inevitably lead to incorrect classification of a part of the data. At present, the quarantine zone in the strict sense no longer exists. Even in this case, we can still apply the maximum isolation band standard so that part of the data can fall into the isolation band or even the decision-making area of the other party, but the amount of this part of the data must be strictly controlled because the optimal classification corresponds to the area The schematic diagram is shown in Figure 2.

3.2. Improvement of Brain Image FLICM Segmentation Algorithm Based on Neighborhood Information. The so-called telemedicine is to monitor patients remotely through sensor technology and network technology to track all changes in the patient's health and physiological laws. They are connected through the Internet. When the patient is in crisis, the patient's family can quickly obtain the required information, so that it can be quickly transferred to remote monitoring. Experts and remote experts use the Internet to check the patient's condition and quickly treat it. Get treatment, which saves time and helps patients get rid of life-threatening conditions. With the help of sensor technology, the corresponding sensor is connected to the patient, and the sensor is connected to the medical test equipment, so the doctor can remotely monitor, diagnose and treat the patient throughout the day. Nowadays, with the development of science and technology, it is possible to monitor the patient's electrocardiogram, cardiopulmonary function, and breathing. At the same time, doctors can also determine the patient's physiological characteristics and environmental characteristics. Comparison of segmentation results of different noisy images as shown in Figure 3.

Comparing the experimental results in Figure 3, this article also objectively confirmed the original intention of the original improved algorithm, and the experimental results are shown in Figure 4.

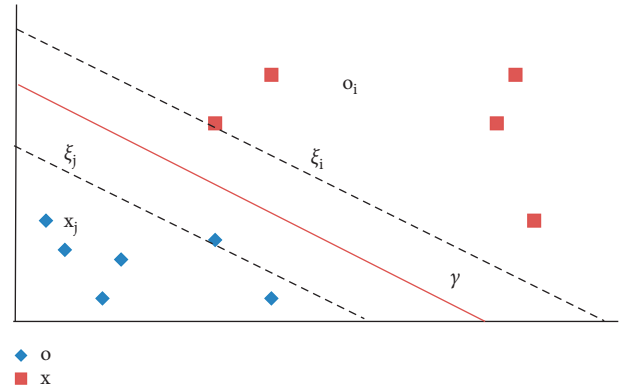

Figure 1: Find the best classification area under the condition of linear separation.

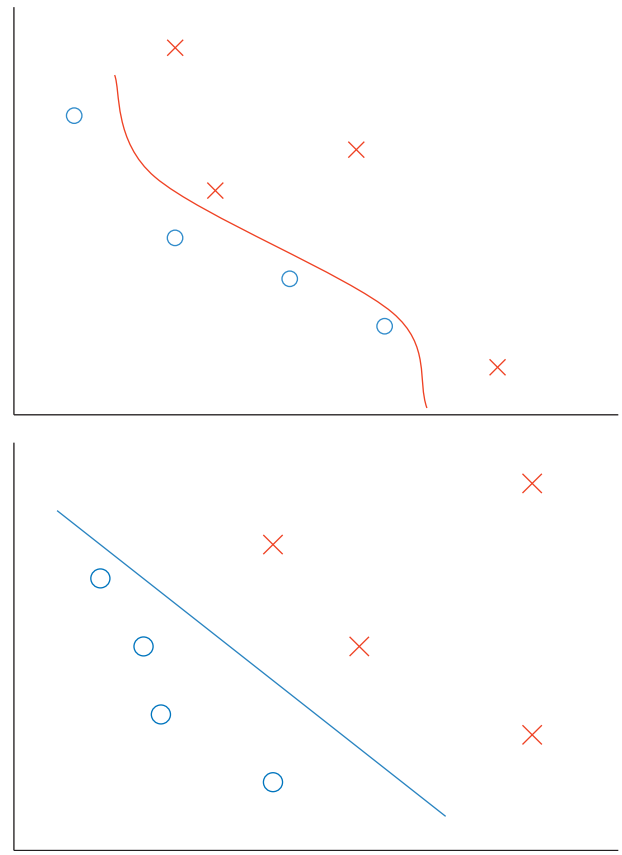

Figure 2: Schematic diagram of the linearly inseparable optimal classification surface.

The clustering results and segmentation accuracy of the algorithm proposed in Figure 5 are significantly better than other improved FCM algorithms, which further proves that the algorithm proposed in this paper is robust and feasible.

3.3. Medical Image Segmentation Results. To better understand the advantages and disadvantages of each algorithm, the experiment in this article compares the distribution coefficient V_{pc}, the distribution entropy V_{pe} and the estimator V_{xb} according to the correlation between the three

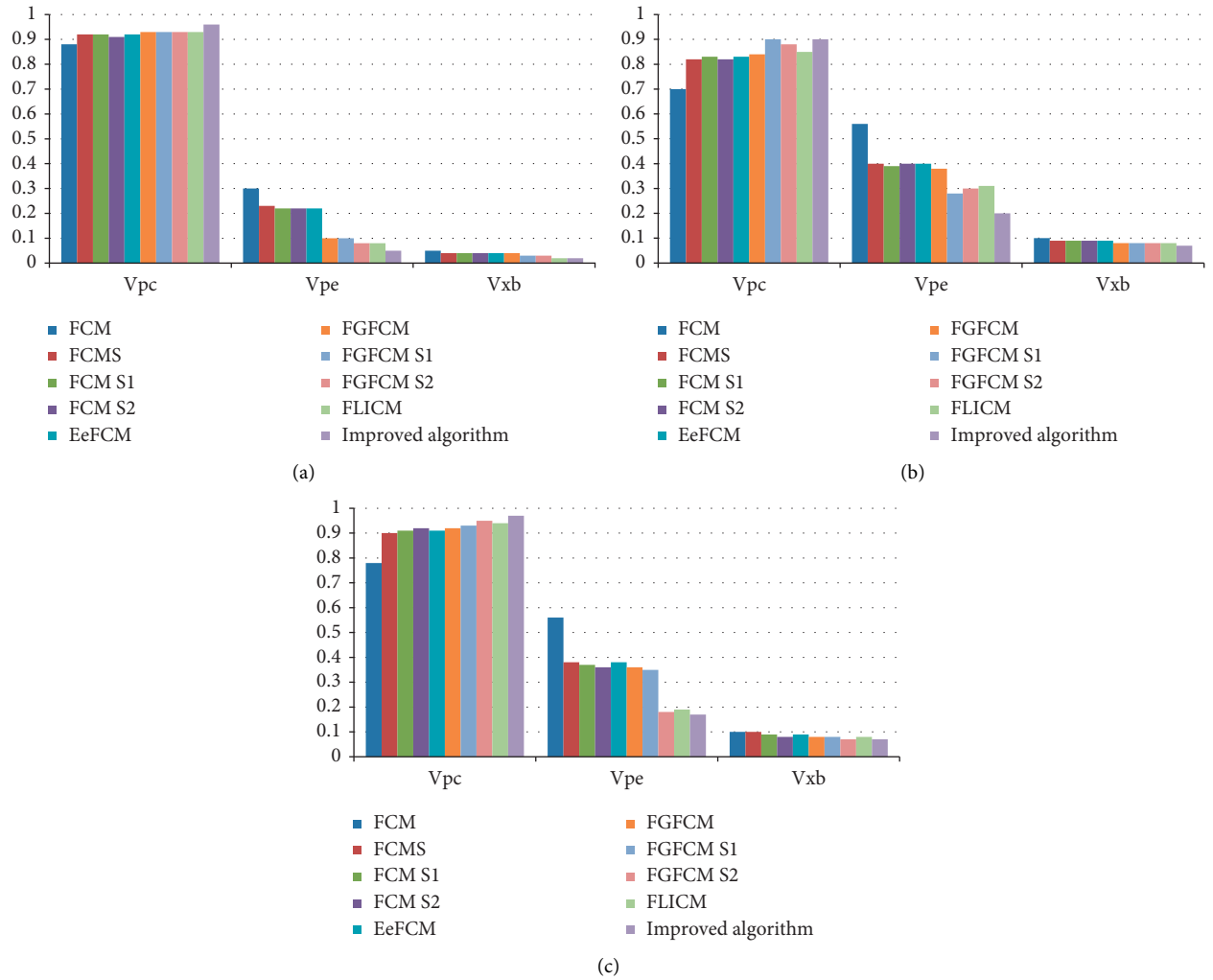

Figure 3: Comparison of segmentation results of different noisy images. (a) Containing 5% Gaussian noise. (b) Containing 20% Gaussian noise. (c) Contains 20% salt and pepper noise.

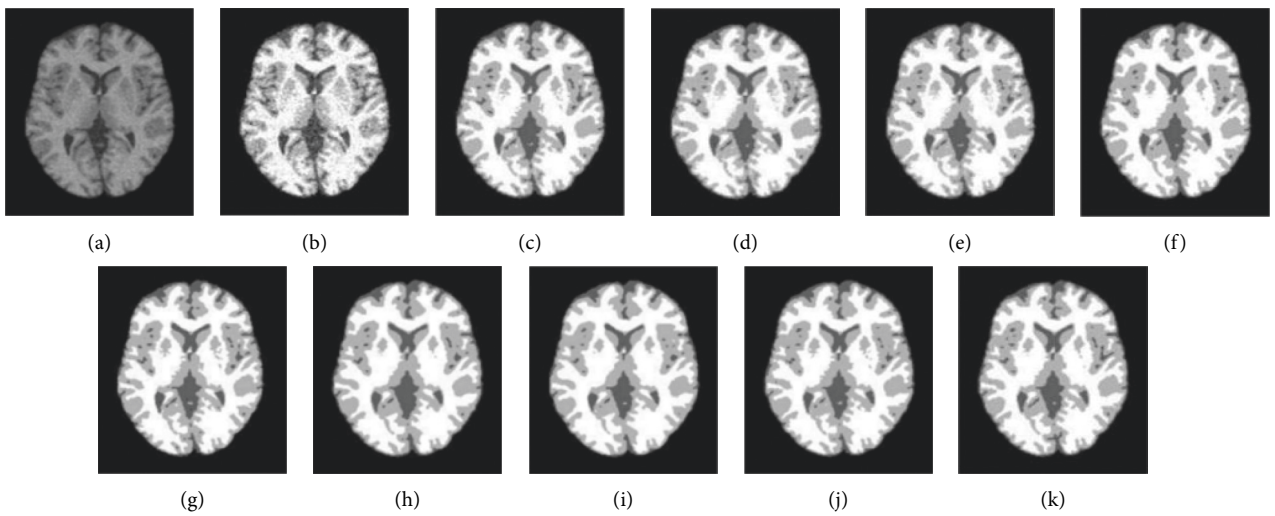

Figure 4: Comparison of brain image segmentation effects. (a) MRI brain images. (b) FCM segmentation results. (c) FCMS segmentation results. (d) FCM_S1 segmentation results. (e) FCM_S2 segmentation results. (f) EnFCM segmentation results. (g) FGFCM segmentation results. (h) FGFCM_S1 segmentation results. (i) FGFCM_S2 segmentation results. (j) FLICM segmentation results. (k) Improved algorithm MFLICM.

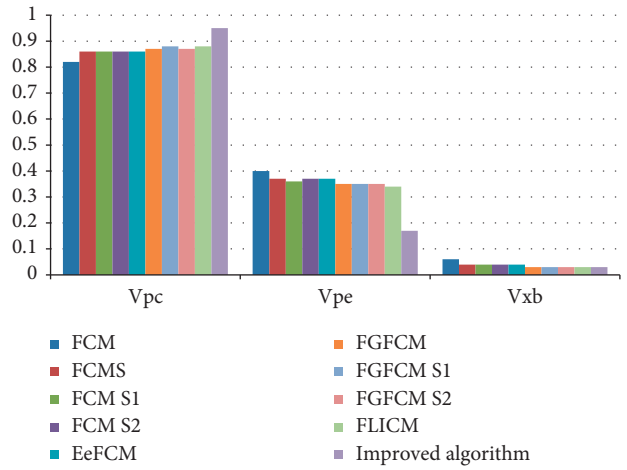

Figure 5: Comparison of brain image segmentation effects.

segmentation algorithms. The experimental results are listed in Table 1.

Table 2 also shows that the segmentation effect of the enhanced SCoW_FLICM algorithm in this paper is significantly better than that of the FLICM segmentation algorithm.

4. Clinical Analysis of Acute Cerebral Infarction under the Background of Intelligent Medical Treatment

4.1. Medical Internet of Things. At present, the development of smart medicine is rapid, but there are still some problems. For example, there are few talents with medical and Internet of Things technology, and the use of Internet of Things technology is full of certain security risks. Since doctors and patients are the main targets of smart medical services, the safety and privacy of both parties are very important, and the privacy of both parties must be respected. Despite the introduction of information management, the hospital information system still has some problems, such as the outpatient business process is still complicated, the information between departments is not smooth, and the information about patient diagnosis and treatment cannot be accessed and input. Moreover, detailed information about the circulation of purchased drugs cannot be obtained in time, and these problems severely limit the management of the hospital information system.

The main function of the electronic case is to record the identity of the patient, etc. The electronic medical record can collect information about the patient, process the collected information, and quickly and accurately understand the patient's diagnosis in the hospital when necessary, and save it in the personal electronic medical record in the record. The doctor can fully understand the patient's entire medical history, so that the existing problems can be solved effectively and accurately. Now all that is left is to use the Internet of Things to attach the corresponding RFID tag to the drug. Using this tag, you can fully understand all kinds of information about the drug, and it also has the corresponding anticounterfeiting function, so employees can quickly and accurately verify the drug. Drugs have greatly reduced the occurrence of health accidents.

The continuous updating and improvement of information technology has laid a solid foundation for smart medical care. The hospital information system can contribute to the normal operation of the hospital in the new century, and it is also an important technology to support the operation of the hospital. The main purpose of the hospital information system is the patient. The main purpose is to understand basic patient information, propose treatment plans and appropriately consider medical expenses, and integrate the healthcare, nursing and medical technology departments into the management information system, thus making us online Professionals-provide advice and telemedicine records.

4.2. Pathogenesis and Image Diagnosis Analysis in Patients with Acute Cerebral Infarction. In patients with acute cerebral infarction, within 6 hours after the onset, when the cerebral blood flow is reduced, the brain tissue remains ischemic and hypoxic. Therefore, in the hyperacute phase, it is difficult to accurately distinguish the infarcted brain tissue from the normal brain tissue, and the grayscale difference is the smallest. In patients with early cerebral infarction, changes in tissue function occur earlier than changes in morphology. DWI shows that the diffusion of water molecules is restricted, and the signal in the affected area is higher. Because CT is extremely sensitive to cerebral hemorrhage and calcification in patients with acute cerebral infarction, the main advantage of CT is that it can eliminate cerebral and thyroid hemorrhage.

Brain damage caused by decreased parathyroid function is of great significance for the further development of thrombolytic therapy with tissue plasminogen activator. However, for patients with acute and subacute diseases, the examination period starts from 6 to 24 hours, starting from 1 to 14 days, it gradually changes from the cytotoxic edema stage to the angioedema stage. At this time, the intracellular and extracellular water content increased significantly. CT and MRI images may show obvious abnormalities, including possible display of significant CT reduction, early shadow low density, unclear cortical and white matter boundaries, lenticular lens and pancreatic islet features, ventricles, and other changes, which were later visualized as a middle cerebral artery or high-density basement Signs of arteries. Among them, the early shadow of low density is a typical sign of cerebral infarction, and it is more common in the stage of cytotoxic brain edema. At this time, the boundary between the cortex and the white matter is fuzzy and uniform, the shadow is low-density, the boundary is fuzzy, and convolute, the groove of the ventricle and the change of the middle cerebral artery or the high-density area of the basilar artery occur relatively late. The first is caused by the expansion of brain tissue swelling, which only occurs when the brain sulcus, subarachnoid space, or even ventricular malformations and midline displacement are compressed. However, on CT, it is still difficult to detect brain stem and

Table 1: Comparison of segmentation effects.

Algorithm	V_{pc}			V_{pe}			V_{xb}		
	Brain	Liver	Red blood cells	Brain	Liver	Red blood cells	Brain	Liver	Red blood cells
FLICM	0.8860	0.8955	0.8469	0.8923	0.3114	0.4440	0.0342	0.0576	0.0394
MFLICM	0.9351	0.9218	0.8827	0.1793	0.2340	0.4065	0.0291	0.0483	0.0250
SCoW_FLICM	0.9210	0.9075	0.8923	0.2242	0.2790	0.4039	0.0299	0.0487	0.0245

Table 2: Comparison of segmentation effects.

Algorithm	V_{pc}			V_{pe}			V_{xb}		
	Aoyama	Flower bed	Lotus	Aoyama	Flower bed	Lotus	Aoyama	Flower bed	Lotus
FLICM	0.9424	0.9585	0.8601	0.1772	0.1188	0.1092	0.0287	0.0221	0.0257
MFLICM	0.9619	0.9678	0.9767	0.1293	0.0946	0.0683	0.0191	0.0187	0.0123
SCoW_FLICM	0.9616	0.9736	0.9760	0.1203	0.0783	0.0695	0.0193	0.0178	0.0126

cerebellar infarctions in the posterior fossa. At that time, the number of abnormalities detected by CT was still affected by factors such as imaging time, so 9.17% and 4.78% of the cases were still detected, respectively abnormal. Although studies have shown that DWI still shows limited diffusion and high signal. The results showed that during the 3d inspection period, the injury was related to angioedema, collateral vessel formation, and a large number of swollen cells. At this time, the DWI signal is relatively attenuated, and this study also shows that MRI is in a worsening stage. The incidence of first cerebral infarction was 97.92% and 100.00%, which were still higher than CT. 2.08% of patients underwent MRI examination within 6–24 hours after the onset of the disease, which showed that the lesion was in the brainstem. Therefore, patients with acute cerebral infarction need CT and MRI examinations, which can be used for clinical diagnosis and treatment of cerebral infarction.

4.3. Clinical Analysis of Urokinase Thrombolysis in the Treatment of Acute Cerebral Infarction. During the study period from February 2018 to January 2020, 120 patients with acute cerebral infarction were included in the database as experimental samples. The control group consisted of 36 men and 24 women with an average age of (66.8 ± 5.90) years old. The patients in the experimental group consisted of 29 men and 31 women (65.8 ± 6.10) years old from 53 to 75 years old. The experimental group adopted medical Internet of Things equipment to conduct more timely treatment interventions for patients, and update information in real time. Study patients, patients with poor physical tolerance who cannot be examined, pregnant women, and patients receiving appropriate treatment for three months. Enter the date of admission of the patient into the database, and the test result shows $P > 0.05$; the difference is not significant and can be compared.

The experimental results showed that the experimental group had shorter hospital stays in hospitals and intensive care units, and the difference was statistically significant ($P < 0.05$), see Table 3.

The experimental results show that after the treatment, the total effective treatment rate of the experimental group of patients is 85.00% (51/60), see Table 4.

Table 3: Comparison of the rehabilitation status of the two groups of patients.

Group	Number of cases	Hospital stay	Check-in time in ICU
Test group	60	33.4 ± 6.5	7.6 ± 1.6
Control group	60	26.7 ± 5.4	5.0 ± 1.0

The experimental results showed that after the treatment, the adverse reaction rate in the experimental group was 6.67% (4/60), while that in the control group was 26.67% (16/60) after treatment, see Table 5.

The older the patient, the greater the likelihood of an increase in the incidence of this disease. The disease has a significant impact on the specific functions of the patient and, in severe cases, the normal cognitive function of the patient. As far as the current situation is concerned, choosing a neurology treatment plan is the main theme of modern clinical practice when clinical treatment is started, and the use of urokinase to treat patients has also become a new focus of clinical research in recent years.

Urokinase is a direct plasmin activator, which can effectively remove a hematoma, dissolve embolism, and has a good therapeutic effect on acute cerebral infarction (onset within 6 hours), and the drug is relatively safe. When treating patients, choosing urokinase for treatment can ensure that the patient's infarction returns to normal and continue to obtain therapeutic effects. However, some studies have shown that urokinase can aggravate blood vessel damage and damage patients. When the patient receives urokinase treatment, the medication must be adjusted accordingly according to the patient's condition so that the patient can obtain adequate medical support during the treatment process. Therefore, clinical conservative treatment or surgical treatment drugs can be appropriately selected according to the situation of patients. In order to effectively control the mortality rate in patients to avoid recurrence or complications conditions to choose. In this study, patients with acute cerebral infarction received Xueshuantong therapy and urokinase thrombolytic therapy for a comparative study.

Table 4: Comparison of the total effective rate of treatment between the two groups of patients.

Group	Number of cases	Get well	Effective	Total effective rate
Test group	60	16 (26.67)	21 (35.00)	37 (61.67)
Control group	60	26 (43.33)	25 (41.67)	51 (85.00)
X^2	—	—	—	8.3523
P	—	—	—	0.0039

Table 5: Comparison of the incidence of adverse reactions between the two groups of patients.

Group	Number of cases	Delayed hydrocephalus	Intracranial infection	Bleeding again	Adverse reaction rate
Test group	60	1 (16.67)	1 (16.67)	2 (33.33)	4 (6.67)
Control group	60	2 (33.33)	5 (8.33)	9 (15.00)	16 (26.67)
X^2	—	—	—	—	8.6400
P	—	—	—	—	0.0032

Therefore, in the treatment of patients with acute cerebral infarction (onset within 6 hours), intravenous thrombolytic urokinase therapy may provide the best therapeutic effect, and in the case of actual use of urokinase, it should be taken as soon as possible to improve The overall condition of the patient. After the completion of the treatment, the effective treatment process for the patient and the reduction of the patient's recurrence rate.

5. Conclusion

Since the future development of the network is usually related to the networking and informatization of human life in the environment, the status of the hospital information structure related to the Internet of Things technology has become important. Advanced Internet of Things technology can not only be applied to related advanced equipment to track and monitor relevant patient information more accurately, but also can play an important role in patient monitoring. At the same time, it greatly reduces the possibility of health accidents and ensures the effective improvement of medical performance. Acute cerebral infarction is a type of cerebral infarction that lasts for 14 days. At this stage, cerebral ischemia and hypoxic injury are reversible, and the restoration of cerebral blood perfusion can save the traumatic brain injury to the greatest extent. How to detect a heart attack in time, effectively evaluate its size, location, etc., and respond as soon as possible within the effective thrombolytic time window to reduce the infarct size, restore ischemic penumbra infarction, and prevent long-term ischemia, so that The main problem we want to study. The effect on the function of the nerve nucleus is particularly important for restoring the normal function of nerve conduction. In this study, patients with acute cerebral infarction received Xueshuantong therapy and urokinase thrombolytic therapy for a comparative study. Therefore, in the treatment of patients with acute cerebral infarction (onset within 6 hours), intravenous thrombolytic urokinase therapy may provide the best therapeutic effect, and in the case of actual use of urokinase, it should be taken as soon as possible to improve The overall condition of the patient. After the completion of the treatment, the effective treatment process for the patient and the reduction of the patient's recurrence rate.

Data Availability

The data used to support the findings of this study are available from the corresponding author upon request.

Conflicts of Interest

The authors declare that they have no conflicts of interest.

Acknowledgments

This paper was supported by Research project funded by Health and Health Committee of Guangxi Zhuang Autonomous Region: Effect of urokinase intravenous thrombolysis on serum inflammatory factors and nerve function in patients with acute cerebral infarction (Z20190207).

References

[1] K. He, X. Zhang, S. Ren, and J. Sun, "Deep residual learning for image recognition," in *Proceedings of the 2016 IEEE Conference on Computer Vision and Pattern Recognition (CVPR)*, pp. 770–778, Las Vegas, NV, USA, June 2016.

[2] K. Suzuki, "Special issue on machine learning for medical imaging," *Algorithms*, vol. 2-3, 2010.

[3] C. Fortin, R. Kumaresan, W. Ohley, and S. Hoefer, "Fractal dimension in the analysis of medical images," *IEEE Engineering in Medicine and Biology Magazine*, vol. 11, no. 2, pp. 65–71, 1992.

[4] K. S. Fu and J. K. Mui, "A survey on image segmentation," *Pattern Recognition*, vol. 13, no. 1, pp. 3–16, 1981.

[5] K. Doi, "Current status and future potential of computer-aided diagnosis in medical imaging," *British Journal of Radiology*, vol. 78, no. 1, pp. S3–S19, 2005.

[6] M. Adil, M. K. Khan, M. M. Jadoon, M. Attique, H. Song, and A. Farouk, "An AI-Enabled Hybrid Lightweight Authentication Scheme for Intelligent IoMT Based Cyber-Physical Systems," *IEEE Transactions on Network Science and Engineering*, vol. 8, no. 4, pp. 125–136, 2022.

[7] S. Hallerstam, P. T. Larsson, E. Zuber, and S. Rosfors, "Carotid atherosclerosis is correlated with extent and severity of

coronary artery disease evaluated by myocardial perfusion scintigraphy," *Angiology*, vol. 55, no. 3, pp. 281–288, 2016.

[8] W. H. Chen, T. Yi, and Y. Chen, M. Zhang, Z. Wu, Y. Wu et al., Assessment of bilateral cerebral peduncular infarction: magnetic resonance imaging, clinical features, and prognosis," *Journal of the Neurological Sciences*, vol. 357, no. 1-2, pp. 131–135, 2015.

[9] K. Takamatsu, T. Takizawa, S. Sato, Y. Murakami, and T. Miyamoto, "Locked-in syndrome due to bilateral cerebral peduncular infarctions. A case report," *Nosotchu*, vol. 15, no. 3, pp. 225–231, 1993.

[10] A. Banerjee, Y. Chisti, and U. C. Banerjee, "Streptokinase-a clinically useful thrombolytic agent," *Biotechnology Advances*, vol. 22, no. 4, pp. 287–307, 2004.

[11] D. Collen and H. R. Lijnen, *Thrombolytic agents,Thrombosis and Haemostasis*, vol. 93, no. 4, pp. 627–630, 2005.

[12] T. L. Huang and X. Bai, "An improved algorithm for medical image segmentation," *WGEC*, in *Proceedings of the 2nd International Conference on Genetic and Evolutionary Computing*, pp. 289–292, Jinzhou, China, September 2008.

[13] P. D. Pantula, S. S. Miriyala, and K. Mitra, "An Evolutionary Neuro-Fuzzy C-means Clustering Technique," *Engineering Applications of Artificial Intelligence*, vol. 89, Article ID 103435, 2020.

[14] R. Krishnapuram and J. M. Keller, "The possibilistic C-means algorithm: insights and recommendations," *IEEE Transactions on Fuzzy Systems*, vol. 4, no. 3, pp. 385–393, 1996.

[15] M. Abdolmaleky, M. Naseri, J. Batle, A. Farouk, and L. H. Gong, "Red-Green-Blue multi-channel quantum representation of digital images," *Optik*, vol. 128, pp. 121–132, 2017.

[16] S. Wang, D. M. Yang, R. Rong, X. Zhan, and G. Xiao, "Pathology image analysis using segmentation deep learning algorithms," *American Journal Of Pathology*, vol. 189, no. 9, pp. 1686–1698, 2019.

[17] M. A. Balafar, A. R. Ramli, M. I. Saripan, R. Mahmud, S. Mashohor, and H. Balafar, "MRI segmentation of medical images using FCM with initialized class centers via genetic algorithm," *Proceedings of the International Symposium on Information Technology*, vol. 4, pp. 1–4, August 2008.

[18] S. M. Riazul Islam, D. Daehan Kwak, M. Humaun Kabir, M. Hossain, and K. S. Kwak, "The internet of things for health care: a comprehensive survey," *IEEE Access*, vol. 3, pp. 678–708, 2015.

Hindawi
Mobile Information Systems
Volume 2022, Article ID 9597429, 10 pages
https://doi.org/10.1155/2022/9597429

Research Article

Resource Allocation Strategy Using Deep Reinforcement Learning in Cloud-Edge Collaborative Computing Environment

Junjie Cen[1] **and Yongbo Li**[2]

[1]*College of Computer Science and Technology, Henan Institute of Technology, Xinxiang, Henan 453002, China*
[2]*College of Computer and Information Engineering, Henan Normal University, Xinxiang, Henan 453002, China*

Correspondence should be addressed to Junjie Cen; cen@hait.edu.cn

Received 26 April 2022; Revised 9 June 2022; Accepted 25 June 2022; Published 12 July 2022

Academic Editor: Shadi Aljawarneh

With the development of technologies such as IoT and 5G, the exponential explosion in the amount of new data has put more stringent requirements on ultrareliable and low-delay communication of services. To better meet these requirements, a resource allocation strategy using deep reinforcement learning in a cloud-edge collaborative computing environment is proposed. First, a collaborative mobile edge computing (MEC) system model, which combines the core cloud center with MEC to improve the network interaction ability, is constructed. The communication model and computation model of the system are considered at the same time. Then, the goal of minimizing system delay is modeled as a Markov decision process, and it is solved by using the deep Q network (DQN) which is improved by hindsight experience replay (HER), so as to realize the resource allocation with the minimum system delay. Finally, the proposed method is analyzed based on the simulation platform. The results show that when the number of user terminals is 80, the maximum user delay is 1150 ms, which is better than other comparison strategies and can effectively reduce the system delay in complex environment.

1. Introduction

In recent years, mobile devices have become essential tools in our daily life, such as communication, socializing, and entertainment. The demand for mobile computing continues to escalate, resulting in an explosion in the number of mobile devices [1]. However, battery capacity and computational resources are not sufficient to meet users' needs, so cloud computing, which allows the computation tasks to be transmitted to servers with more computing capacity from mobile devices, has been developed greatly to solve the challenge of limited resources for mobile devices [2]. Mobile cloud computing (MCC) combines the advantages of both mobile computing and cloud computing to further address this problem [3]. Meanwhile, [4] MCC enables the use of data from the Internet to extend the capabilities of mobile devices lacking in computing, communication, and caching and to extend effective working time within the limit of battery life.

Nowadays, the main implementation method is to offload tasks such as computing and storage to a remote public cloud platform [5]. However, the traditional architecture of MCC is also facing new challenges. On the one hand, users have to interact with data centers when using mobile applications, and network delay has a significant impact on some delay-sensitive applications depending on the relative distance between the user and the cloud data center. On the other hand, because all data interactions generated by applications must be carried out through the core network, there will be great pressure on the core network during network peak hours [6]. In order to solve the problem of high delay and alleviate the network pressure, mobile edge computing (MEC) technology came into being. The core idea of MEC is to decentralize part of the computing and storage capacity of the data center in MCC to the edge of the network, i.e., close to the user. Hence, the data-processing requirements generated by mobile applications can be executed by the MEC server which is located at the edge of

local network, and results can be returned without going through the core network and data center [7].

A resource allocation strategy using deep reinforcement learning in a cloud-edge collaborative computing environment is proposed to address the limitation of hardware resources such as server storage and computing as well as the nonuniformity of user distribution, which leads to problems such as higher network delay. Compared with traditional MEC system strategies, the main contributions of this paper are as follows:

(1) In order to make full use of the limited capacity of MEC servers while reducing the delay of user-service interaction, a collaborative MEC system model is proposed, which not only greatly relieves the pressure on the core network but also reduces the network delay of applications through the allocation of the cloud computing center and MEC.

(2) To address the reward sparse problem caused by complex environments, a special experience replay method, which is named as hindsight experience replay (HER), is introduced to give certain rewards to actions that do not reach the target state as well, so as to accelerate the learning efficiency of agents and guide them to the correct learning direction in order to achieve a global load-optimal strategy.

The remaining sections of this paper are arranged as follows: Section 2 introduces the related research in this field. Section 3 introduces the system model and optimization objectives. Section 4 introduces the resource allocation strategy based on deep reinforcement learning. In Section 5, experiments are designed to verify the performance of the proposed strategy. Section 6 is the conclusion.

2. Related Works

Computing offloading is an essential part in MEC, and the key point of offloading decisions is how they are designed. A flexible and effective network computational resource allocation strategy is an important guarantee for the efficient operation of MEC [8]. In this regard, scholars at home and abroad have already conducted some researches. In [9], a migration strategy of cloud collaborative computing was designed. Simulations verified the feasibility of selecting the optimal migration strategy based on task division. However, the overall computational efficiency still needs to be improved. Gao et al. proposed a hierarchical multi-agent optimization algorithm that combines the genetic algorithm (GA) and multi-agent optimization [10]. This algorithm implements an improved GA by maximizing resource utilization to find a set of service nodes for deploying the requested tasks so as to maximize resource utilization and bandwidth cost in cloud computing. The algorithm pays more attention to resource utilization of cloud computing, and cloud-edge collaboration is not fully considered. In [11], in order to realize effective edge learning on heterogeneous edges with constraints on resources, an online learning strategy was proposed based on the budget-constrained multiarmed slot machine model, which improves the computational efficiency in cloud computing environments. But the performance of bandwidth optimization should be enhanced during resource allocation. A resource allocation strategy for synchronous wireless information and power transmission relay systems under general interference was studied in [12]. A resource allocation coordinate system was established using the h_2 method to divide the energy harvesting area and DF area. The optimal value was obtained by applying the golden division method, but the overall communication delay still needs to be improved. A stochastic mixed integer nonlinear programming model was formulated in [13] to jointly optimize task offloading decisions, flexible computational resource scheduling, and radio resource allocation. The proposed problem was decomposed into four separate subproblems using Lyapunov's optimization theory and solved by convex decomposition method and matching game. A low probability of intercept based collaborative power and bandwidth allocation strategy for multi-target tracking was proposed in [14]. But the algorithm is biased toward the optimal allocation of bandwidth resources, and further improvement is required for computational resource allocation. By defining a reward function for each user with consideration of aggregation effects of the other users, Liu et al. developed a multi-agent reinforcement learning framework based on independent learners to solve the problem about resource allocation in the cloud computing environment [15]. However, this algorithm has yet to be further studied for collaborative resource optimization at the cloud edge in some complex situations.

3. System Model and Optimization Objective

3.1. System Scenario. Traditional cloud computing, whether the distributed storage computing is used or not, is still centralized at a macro level, and all service requests still need to be transmitted to the cloud for execution. However, the cloud data center will decide to execute tasks according to the optimization strategy, which makes it difficult for traditional cloud computing to adapt to the changes in users' requests over time, space, and other factors. And MEC can better deal with this problem.

The core idea of MEC is to offload part of computing and storage capacity of the data center in MCC to the edge of the network, i.e., close to the user. Data-processing requirements generated by mobile applications can be executed by the MEC server, and then results can be directly returned at the edge of their local network without going through the core network and data centers, which not only greatly relieves network pressure on the core network, but also significantly reduces network delay for applications [16]. In addition, [17] as MEC servers usually only serve the area for which they are responsible, they can be more integrated with local information. A typical collaborative MEC scenario is shown in Figure 1, consisting of a core cloud data center and M sub-MEC servers.

As shown in Figure 1, K services are running in the core cloud data center, while each MEC server is split into one area for task requests. The backhaul network connects each area to the core cloud data center, and users connect to the

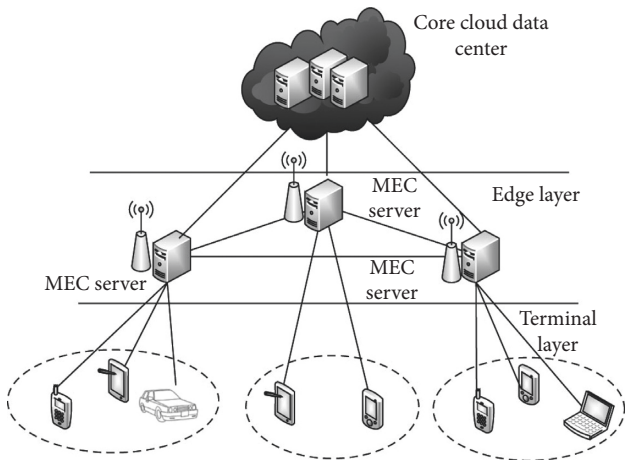

Figure 1: Typical collaborative MEC system.

core cloud data center to access services via the backhaul network. To better serve the users in each area and to reduce the interaction delay and the pressure on the backhaul network, services in the core cloud data center are offloaded to the MEC servers within their capacity, so that users in that area only need to connect to the MEC servers for services. In other words, if the requested service of a user in a certain area is in its local MEC server, the switching delay is produced by the device when connecting to the local MEC server [18]. Otherwise, besides communicating with the local MEC server, it also needs to connect to the MEC server that has recently been deployed with service to obtain it via the local MEC server. Therefore, the delay is correspondingly higher [19].

3.2. Communication Model. In the MEC system model, each user terminal can offload its computation tasks to the MEC server or execute them locally. Each user is associated with the nearest base station, and the MEC server which is connected to that base station can be referred to as the user's local MEC server. When a user terminal offloads a task to the MEC server, the user needs to transmit the task to the base station associated with it via a wireless link.

Define U_m as the set of user terminals associated with the base station m, and define B_m as the bandwidth of the base station m. Multiple user terminals choose to offload computation tasks at the same time, and then the wireless bandwidth is evenly allocated to the offloading user terminals to upload data. The uplink transmission rate $v_{n,m}$ of the wireless link of the user terminal n can be expressed as follows:

$$v_{n,m} = \frac{B_m}{|U_m|} \log\left(1 + \frac{p_n h_{n,m}}{(B_m/U_m)\delta_0}\right), \tag{1}$$

where p_n is the transmission power of the user terminal n to upload data through the wireless link, $h_{n,m}$ is the channel gain between the user terminal n and the base station m, and δ_0 is the power spectral density of white noise.

3.3. Computation Model. For each user terminal, there are three types of execution of computation tasks, which are local execution at the user terminal, execution at the user's local MEC server, and execution at the user's neighboring MEC server.

3.3.1. Local Execution Model. When a user terminal n chooses to execute a computation task φ_n locally, and f_n^L represents the local computing capacity of the user terminal n, which is the CPU frequency, then the time delay T_n^L for executing the computation task t_n locally can be calculated as follows:

$$T_n^L = \frac{C_n}{f_n^L}, \tag{2}$$

where C_n represents the number of CPU cycles required to execute the computation task φ_n.

3.3.2. Local MEC Server Computing Model. When a user terminal n chooses to execute a computation task φ_n at the local MEC server, the user n first needs to offload the computation task φ_n to its associated base station m via the wireless link, and the corresponding transmission delay is generated when uploading the computation task. According to the communication model, the uplink transmission delay $T_{n,m}^t$ of user n can be calculated as follows:

$$T_{n,m}^t = \frac{D_n}{v_{n,m}}, \tag{3}$$

where D_n represents the amount of the input data for the computation task φ_n.

Next, the MEC server in the base station allocates the computational resources to execute the task, which results in the processing delay of the computation task. Let $f_{n,m}$ denote the computational resources allocated by the base station m to the user terminal n; then, the processing delay $T_{n,m}^c$ for the MEC server to execute this task can be written as follows:

$$T_{n,m}^c = \frac{C_n}{f_{n,m}}. \tag{4}$$

Finally, the results are returned to the user terminal n from the MEC server. Generally, the amount of data returned by the computation task after processing is small, and the data rate of the downlink is high, so the delay due to returning the results can be ignored. From the above analysis, it can be inferred that the total delay when the computation task φ_n of user terminal n is executed at the local MEC server can be formulated as follows:

$$T_n^\Omega = T_{n,m}^t + T_{n,m}^c. \tag{5}$$

3.3.3. Neighborhood MEC Server Computing Model. When a user terminal n chooses to execute a computation task φ_n at a neighboring MEC server g, it first needs to offload the computation task φ_n to its associated base station

m via a wireless link. Next, the base station m transmits the task to the base station g via a wired link, and then the MEC server in the base station g allocates the corresponding computational resources to execute the task. Finally, the MEC server returns the results to the user terminal n.

Based on the above process, the total delay for executing the computation task at the neighboring MEC server g can be defined as $T_{n,g}^{\bar{O}}$, which mainly consists of the uplink transmission delay $T_{n,m}^{t}$, the transmission delay $T_{m,g}^{t}$ between base stations, and the processing delay $T_{n,g}^{c}$ in the MEC server. Like the local MEC server computing model, the delay incurred by the return of results to the user can be ignored. As the uplink transmission delay $T_{n,m}^{t}$ can be calculated in the same way as the local MEC server, it is not written in detail here. Let $f_{n,g}$ denote the computational resources allocated to the user terminal n by the base station g, and let $v_{m,g}$ denote the transmission rate between the base station m and the base station g; the processing delay $T_{n,g}^{c}$ in the MEC server can be formulated as follows:

$$T_{n,g}^{c} = \frac{C_n}{f_{n,g}}. \tag{6}$$

The transmission delay $T_{m,g}^{t}$ between base stations can be calculated as follows:

$$T_{m,g}^{t} = \frac{D_n}{v_{m,g}}. \tag{7}$$

Hence, the total delay $T_{n,g}^{\bar{O}}$ of the user terminal n when offloading the computation task to the neighboring MEC server g can be calculated as follows:

$$T_{n,g}^{\bar{O}} = T_{n,m}^{t} + T_{m,g}^{t} + T_{n,g}^{c}. \tag{8}$$

Further, the time delay of the user terminal n can be obtained as follows:

$$T_n = \alpha_n T_n^L + \beta_n T_n^{\Omega} + \sum_{g \in M} \gamma_{n,g} T_{n,g}^{\bar{O}}, \tag{9}$$

where α_n, β_n, and $\gamma_{n,g}$ are the weights of the local delay, the total delay when the task is executed at the local MEC server, and the total delay when the task is executed at the neighboring MEC server, respectively.

3.4. Optimization Objective. The objective of this work is to optimize the maximum task delay among all users of the system within the computational resource constraints of the MEC server, thus ensuring fairness among users. Therefore, it can be formulated as a joint optimization problem of offloading strategy $\prod = \{\alpha, \beta, \gamma\}$ and computational resource allocation $f = \{f_{n,m}, n \in N, m \in M\}$ for all user terminals, which can be shown as follows:

$$\prod, f, \min \max_{n \in N} T_n, s.t. \text{C1: } \alpha_n, \beta_n, \gamma_{n,g} \in \{0,1\}, \quad n \in N, g \in M_n, \text{C2: } \alpha_n + \beta_n + \sum_{g \in M_n} \gamma_{n,g} = 1, \quad n \in N, \text{C3: } \sum_{n \in N} f_{n,m} \le F_m, \quad m \in M, \text{C4: } f_{n,m} \ge 0, \quad n \in N, m \in M, \tag{10}$$

where $M_n = (M/m)$ represents the set of adjacent base stations of user terminal n. Constraints C1 and C2 are restrictions on the offloading strategy of each user terminal. Constraint C3 specifies that the sum of computational resources allocated to the user cannot exceed the computing capacity of the MEC server. Constraint C4 ensures that the computational resources allocated cannot be negative.

As there are both discrete and continuous variables in this optimization problem and the objective function is a min–max model, the optimization problem can be regarded as mixed integer nonlinear programming (MINLP) problem, which is NP-hard and non-convex. The solving complexity of such problems is very high, and they cannot be solved in polynomial time.

4. Resource Allocation Strategy Based on Deep Reinforcement Learning

4.1. Markov Decision Process. Markov Decision Progress (MDP) is a mathematical model of sequential decision making and is a combination of Markov process and deterministic dynamic programming, which can be used to model the policy and reward that the agent can achieve in a Markovian environment. The Markov property requires that the next state in the system is only related to the current state and has no relationship to all earlier states. Therefore, a state can be defined as having the Markov property when it does not have historical information and the current state can determine the next or future state. If each state in a random state sequence has the Markov property, then the random sequence can be regarded as a Markov process. And MDP is a Markov process that takes actions and returns into account [20, 21].

MDP is constructed according to the environment and the agent, which can be represented by a quadruplet (S, A, P, R). S is the state space, representing the set of states of the environment. A is the action space, representing the set of actions that can be performed by agents. P is the state transfer probability, representing the distribution probability of the current state becoming the next different state after selecting a different action. R is the reward function, which indicates the reward value obtained by the agent when selecting an action to transfer to next state, and the reward value indicates whether it is suitable to select this action

under the current state. Additionally, the discount factor λ ($\lambda \in [0, 1]$) is introduced, which is one of the parameters for calculating the cumulative reward. When λ tends to be 0, it means that the future reward is not important and only the current reward needs to be considered. When λ tends to be 1, it means that the future reward is very important, so it is necessary to take both future reward and current reward into consideration.

Mathematically, the interaction between agents with environment over a discrete time series T is usually described as a Markov process. At each moment t in T, the agent is in a state and needs to select an action, constituting the set of actions $A = \{a_0, a_1, \ldots\}$. And a reward value will be obtained when an action is selected, which constitutes the set of reward values $R = \{r_0, r_1, \ldots\}$.

In MDP, a policy is a mapping between the probabilities of selecting each action in the action space under the current state, indicating the action that the agent should perform based on the current state. There are two main types of policies. The first is the deterministic policy, which means that the agent can only select one action to perform in a certain state. The second is a stochastic policy, which indicates that the agent may perform one or more actions in a certain state. Hence, the policy π can be defined as the probability that the agent selects action a_t under state S_t at the moment t, which can be written as follows:

$$\pi(a_t|s_t) = \Pr\{A = a_t|S = s_t\}, \tag{11}$$

where $\pi(a_t|s_t) \geq 0$ and $\sum \pi(a_t|s_t) = 1$.

The state-value function is the expectation of the cumulative reward in the current state R_t, i.e., the expectation of the cumulative reward R_t after taking the policy π in the current state S_t. The state-value function is mainly used to evaluate each state of a given policy π. Therefore, the state-value function is associated with the policy and can be defined as $Q_\pi(s_t)$, which is the sum of the future reward values when all the actions selected according to policy π in current state S_t are multiplied by the discount factor λ. $Q_\pi(s_t)$ can be calculate as follows:

$$Q_\pi(s_t) = E_\pi\left[\sum_{i=0}^{T} \lambda^i r_{t+i+1}|S = s_t\right]. \tag{12}$$

Corresponding to the state-value function, the state-action value function represents the expectation of the cumulative reward R_t when the action a_t is selected based on policy π under the current state S_t. $Q_\pi(s_t, a_t)$ represents the sum of future reward values when the action a_t is selected with the discount factor λ based on policy π in current state S_t, which can be formulated as follows:

$$Q_\pi(s_t, a_t) = E_\pi\left[\sum_{i=0}^{T} \lambda^i r_{t+i+1}|S = s_t A = a_t\right]. \tag{13}$$

Therefore, MDP can be used in the scenario of finding the optimal policy. By means of random sampling and dynamic programming, MDP can be used to solve the problem of maximizing the cumulative reward value. And the proposed method applies deep Q network (DQN) to find the optimal strategy.

4.2. DQN-Based Offloading Strategy. The DQN uses experience replay to disrupt the correlation between the sample data, as there is a link between successive action states. But the neural network is a nonlinear model that requires the samples to be independently and homogeneously distributed. Thus, by random uniform sampling in the experience replay buffer, the data distribution is averaged, and the training process is smoothed. Because the off policy learning method is adopted, the parameters of the network generating data samples are different from those of the trained network, which is the Fixed Q-targets network. The two networks have the same structure but different parameters. One of the networks is used to obtain the estimated Q value, and the other network is used to obtain the realistic Q value. The second network will periodically replicate the parameters of the first network, thus reducing the correlation between two Q values to a certain extent and improving the network stability. However, deep learning can only be adapted to a specific environment and model, and these adapted hyperparameters will not be effective due to the large number of training episodes needed to adapt to the new environment. Meanwhile, due to the excessive complexity of the problem and sparse rewards in real-life scenarios, the reward function is required to obtain valid rewards from invalid actions to guide the agent to make better [22] decisions [23].

To deal with the problems mentioned above, HER is introduced, which is a good solution to the problem of sparse rewards and dichotomous rewards, as it allows rewards even if the final goal is not achieved and accelerates the learning process of the agent. It is assumed that the learning trajectory of the agent starts from the initial state s_0 and actually reaches the state $\hat{s}$ while the final goal is state s_∞. Then, the real learning process of the agent can be written as follows:

$$\{(s_0, s_\infty, a_0, r_0, s_1), (s_1, s_\infty, a_1, r_1, s_2), \ldots, (s_n, s_\infty, a_n, r_n, \hat{s})\}, \tag{14}$$

where s_0 represents the state at time 0 and a_0 represents the action taken by the agent at time 0. Similarly, a_1 is the action at time 1. And r_0 represents the reward received at time 0. If the target state s_∞ is replaced by $\hat{s}$, then even though the agent does not reach the target state s_∞, it will still have feedback when it arrives at $\hat{s}$. Hence, the learning process can be written as follows:

$$\{(s_0, \hat{s}, a_0, r_0, s_1), (s_1, \hat{s}, a_1, r_1, s_2), \ldots, (s_n, \hat{s}, a_n, r_n, \hat{s})\}. \tag{15}$$

The action taken by an agent at time t is determined by the current state s_t jointly with the target state s_∞, which can be written as follows:

$$a_t = \pi(\hat{s}, s_t). \tag{16}$$

The corresponding rewards can be shown as follows:

$$r_t = R(s_t, a_t, s_\infty). \tag{17}$$

Then, each experience from the learning process is placed into HER, including the current state s_t, the action taken a, the immediate reward obtained r_t, the next state s_t', and the final goal s_∞. A hypothetical goal $\hat{s}$ is generated by taking a policy, and the experience r' is calculated jointly with the current state and action and deposited into HER. Here, r' can be calculated as follows:

$$r' = R(s_t, a_t, \hat{s}). \tag{18}$$

The policy used to generate the hypothetical goal is "future." Specifically, there are l number of states which can be observed in the randomly selected episode. These states are used as target states to compute new experience values that will guide the agent in further learning. HER offers a new direction in solving the problem of sparse reward; that is, it is not necessary to achieve specific goals to learn useful experience [24]. It should be noted that the goal which is selected or achieved in the so-called "failed experience" should be related to the final goal in some way. And the learning performance will be very poor if the similarity between two goals is very low [25, 26]. The pseudocode for a deep reinforcement learning algorithm based on multiple objectives and experience replay is shown in Algorithm 1.

The proposed DQN structure is shown in Figure 2.

The structure of the proposed DQN is the same as a normal DQN, where the agent first reaches the state s_t, then inputs data into the neural network to calculate the estimated Q value and select the action with the largest Q value, executes this action to get the reward with the new state, puts the experience into the replay pool, randomly selects the minibatch when there is enough experience in the replay pool, and finally calculates the loss function between the Q value of the main network and $\widehat{Q}$ which is calculated based on the target network.

$$\begin{cases} L(\theta) = E\left[\left(Q - \widehat{Q}(s_t, a_t; \theta)\right)^2\right], \\ Q = r_{t+1} + \lambda \max_{a'} \widehat{Q}(s_{t+1}, a_t'; \theta^-). \end{cases} \tag{19}$$

The parameters in the network are updated by gradient descent, and the target network is periodically updated with parameters [27]. However, it should be noted that the replay pool here uses HER that randomly samples the target as a new hypothetical target in the same episode and then computes a new experience, overcoming the problem of sparse rewards and making the agent learn faster.

5. Experiments and Analysis

Consider a 520 m × 520 m area with 5 uniformly deployed base stations and N number of users, where each base station is equipped with a MEC server with 8 CPU cores and the path loss model is $h = 127 + 30\log(d[\text{km}])$ (operating system: Windows 10, CPU: Intel® Core™ 3.2 GHz, memory: 8 GB DDR3, 1600 MHz). Define the average rate at which users offload tasks to the MEC server at moment t of task as $\overline{v}_{n,m} = (1/t)\sum_{\tau=0}^{t-1} v_{n,m}(\tau)$. Considering that the number of tasks arriving in each time slot differs in magnitude from the power consumed by the users and the MEC, the parameters are set as follows. The revenue per task is set to be 1×10^{-3} units/bits, and the power cost per unit is set to be 0.2 units/W. Other simulation parameters are set as shown in Table 1.

5.1. Convergence of Markov Decision Algorithm. The convergence of Markov decision algorithm in different environments is first investigated, and the convergence performance of Markov decision algorithm is shown in Figure 3 when the number of tasks is 20.

As can be seen in Figure 3, the Markov decision algorithm converges quickly to the optimal value after 100 iterations, with a total system utility of approximately 0.2. Its computational complexity is much lower than the number of enumerations in an exhaustive search.

5.2. Comparison with Other Algorithms

5.2.1. Comparison of the Average End-to-End Delay of Different Algorithms. According to Little's law, the average waiting delay is proportional to the average queuing time, so the average waiting delay can be defined as the sum of the waiting time in the task queues of users and MEC servers. Then, the relationship between task arrival rate and end-to-end delay in the four algorithms is shown in Figure 4.

As illustrated in Figure 4, the algorithm proposed in [15] has the highest average end-to-end delay compared to the other algorithms due to its excessive reliance on cloud computing, while the other three algorithms consider local execution, which reduces the delay to some extent. For the algorithm developed in [12], the average end-to-end delay is higher because it does not consider the queuing threshold, which results in the increase of waiting delay in the queue, and the golden partition method causes more transmission delay. In addition, it can also be found in Figure 4 that when the task arrival rate is small, the performance of [9] is close to that of the proposed algorithm and the difference between these two algorithms broadens gradually when the arrival rate increases. This is due to the fact that the proposed algorithm optimizes the bandwidth resources while considering the power resource allocation, thus reducing the transmission delay of the task to a certain extent. And when the task arrival rate is 4 kbits/slot, the average end-to-end delay is about 450 ms.

5.2.2. Effect of Different Numbers of MEC Servers on Average Delay. As the main optimization objective of the proposed algorithm, the average network delay has an intuitive effect on the performance of the algorithm, and the average network delay indicates the time required for each service request to access the required service. The average network delay for different algorithms is illustrated in Figure 5 when the number of MEC servers is 10, 55, and 100.

It is indicated in Figure 5 that the average communication delay is decreasing as the number of MEC servers

Initialization:
Initialize experience playback memory;
Initialize behavior value function Q with random weight θ;
Initialize the target behavior value function $\widehat{Q}$ with weight $\widehat{\theta} = \theta$.
Begin
(1) **For** *episode* $i = 1, 2, \ldots, I$
(2) **do** The initial observation s_1 is received and the preprocessing s_1 is taken as the start state x_1
(3) **For** $t = 1, 2, \ldots, T$
(4) **do** Select behavior a_t randomly with random probability ε;
(5) Otherwise, select behavior: $a_t = \arg\max Q(x, a; \theta)$;
(6) Execute actions a_t in the system to obtain reward r_t and observe s_{t+1} at the next moment, and update s_{t+1} to x_{t+1};
(7) Store experience to experience playback memory;
(8) Obtain samples in random small batches from playback memory;
(9) Calculate the target Q value of the target DQN;
(10) Update the main DQN by minimizing the loss function $L(\theta)$;
(11) For network parameter θ, gradient descent is performed on $L(\theta)$;
(12) Update target network Q value.
(13) **End For**
(14) **End For**
(15) End

Algorithm 1: Pseudocode of DQN algorithm based on multi-objective and experience replay.

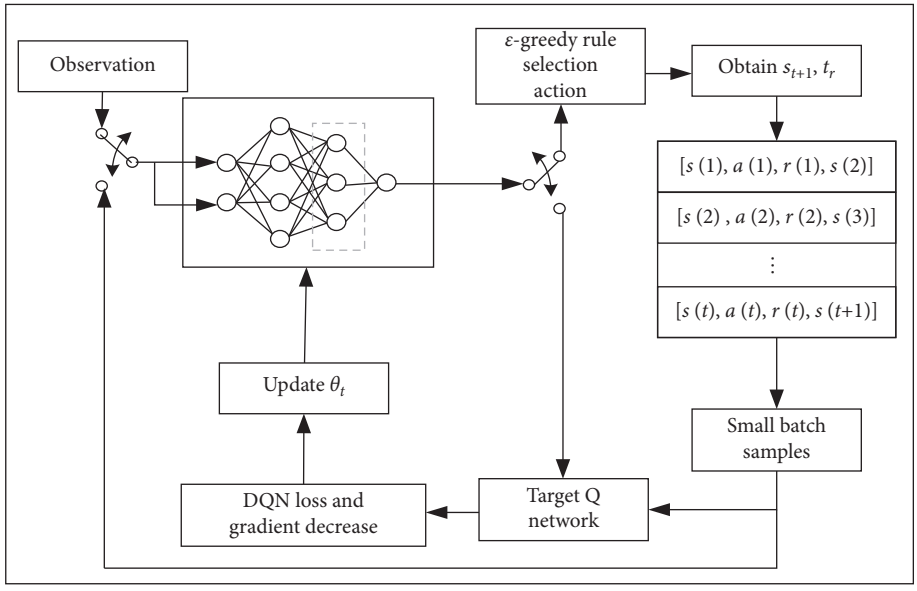

Figure 2: DQN structure.

increases, due to the fact that the increase of MEC speeds up the communication. Meanwhile, the proposed algorithm has the shortest average communication delay, which is below 300 m when the number of MEC servers is 100. Due to its cloud-edge collaboration approach, users do not need to offload tasks to a remote cloud computing center when the number of MEC servers is high, and the DQN strategy can get the best resource allocation scheme to reduce the communication delay. In contrast, [15] focuses on cloud computing environment, so the increase of MEC servers is not significant for the improvement of performance. The communication delay decreases a lot in [9]. Reference [12] has a higher overall delay which exceeds 600 ms due to the lack of a collaborative cloud-edge allocation model and a high-performance optimization algorithm.

5.2.3. Relationship between the Number of Terminals and the Maximum User Delay. The proposed algorithm is evaluated by the performance metric of maximum user delay, and the relationship between the number of user terminals and maximum user delay for different algorithms is shown in Figure 6.

It can be seen from Figure 6 that the maximum user delay increases with the number of user terminals, and the proposed algorithm has a smaller maximum user delay. The

Table 1: Simulation parameters.

Simulation parameters	Value
Bandwidth (MHz)	15
Noise power spectral density (dBm·Hz^{-1})	−174
Maximum transmission power (mW)	600
Local maximum computing power (cycle·s^{-1})	1×10^8
Maximum computing power of MEC single core (cycle·s^{-1})	3×10^8
Slot length (ms)	1
CPU cycles required for task calculation (cycle·bit^{-1})	1760
Task arrival rate (kbit·slot^{-1})	{1, 2, 3, 4}

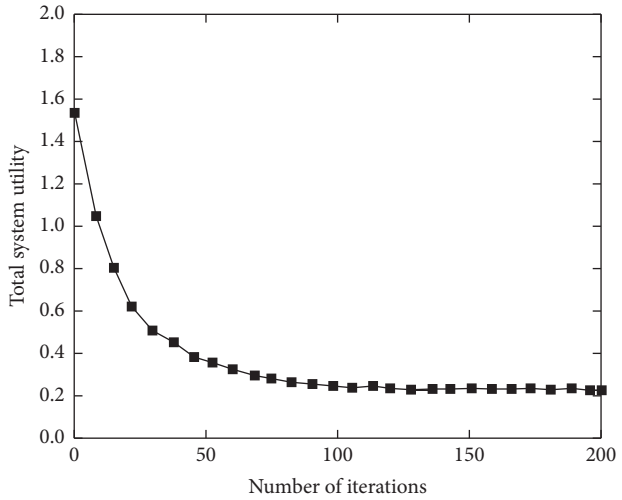

Figure 3: Convergence of Markov decision algorithm under low load.

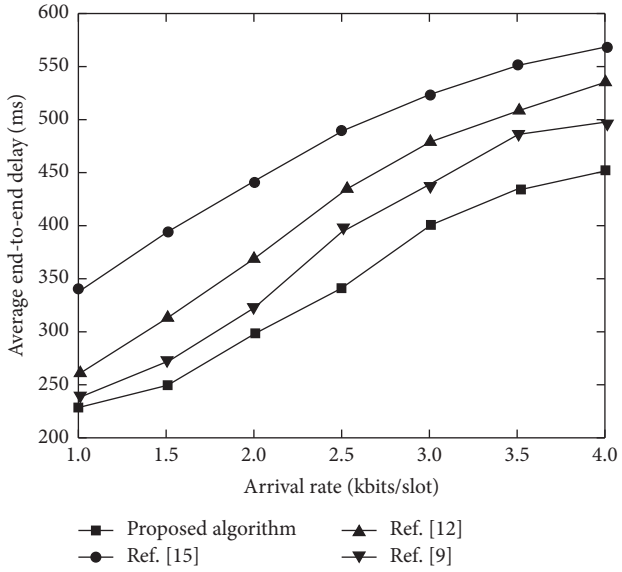

Figure 4: Comparison of average end-to-end delay of different algorithms.

proposed strategy maximizes the processing efficiency of computation tasks and reduces system delay by combining the advantages of cloud computing and MEC and

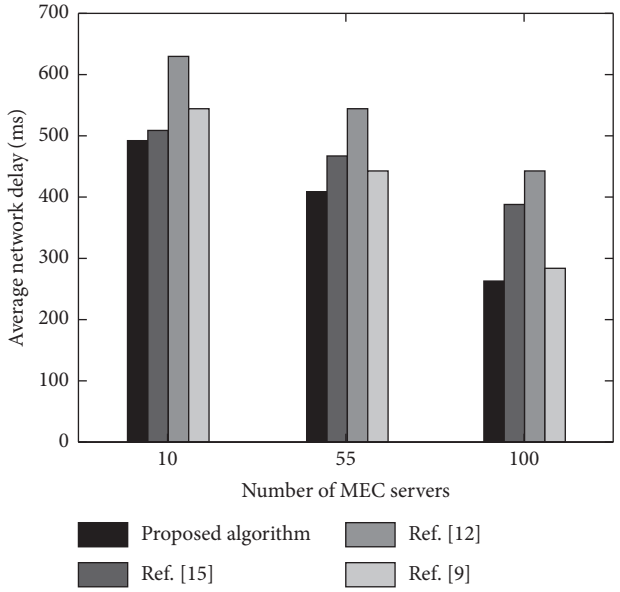

Figure 5: Effect of different numbers of MEC servers on average communication delay.

introducing DQN to design an offloading strategy. When the number of user terminals is 80, the maximum user delay is 1150 ms, which is better than other comparison strategies. On the other hand, although there are abundant resources in the cloud nodes, they are remote from the users and the transmission delay of the tasks is larger. Hence, the maximum user delay in [15] is more than 1240 ms. Therefore, when the number of computational tasks or users is within a certain range, the edge collaboration has better performance than the edge-cloud collaboration.

5.2.4. Relationship between User Terminal Computing Capacity and Maximum User Delay. The effect of user terminal computing capacity on the maximum user delay under different algorithms is depicted in Figure 7.

As shown in Figure 7, the maximum user delay in [15] decreases much more slowly, while the delay of the other three algorithms decreases with the increase of computing capacity. This is because the algorithm proposed in [15] does not consider local execution for users and mainly relies on cloud computing platforms; hence, changes in terminal computing capacity do not have a great effect on user delay. Additionally, it is also illustrated in Figure 7 that the difference between the collaborative scheme of [9] and the proposed algorithm and the non-collaborative scheme of [12] gradually becomes smaller, which is due to the fact that the advantage of the resource allocation algorithm will be less significant as the tasks tend to be executed locally at the terminal and fewer tasks are offloaded to the MEC servers when the terminal computing capacity improves.

Meanwhile, the proposed algorithm uses the multi-objective and HER-based DQN algorithm to find the optimal resource allocation strategy. And the maximum user delay is about 1300 ms when the user terminal computing capacity is

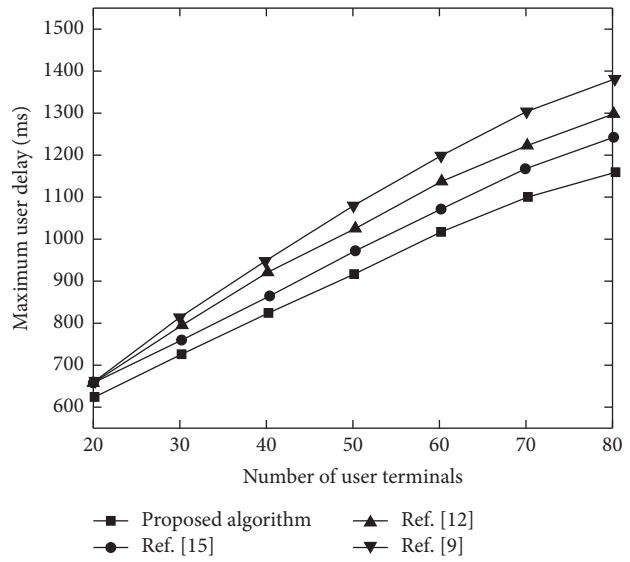

Figure 6: Relationship between the number of terminals and the maximum user delay.

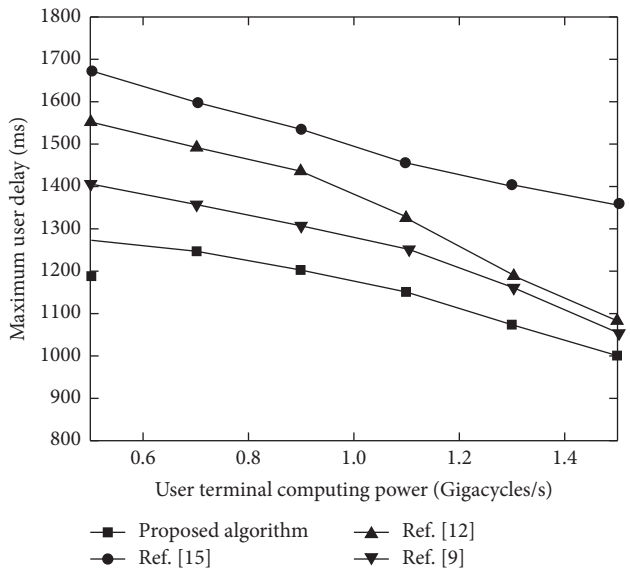

Figure 7: Relationship between user terminal computing capacity and maximum user delay under different algorithms.

0.6 Gigacycles/s, which can show better performance even when the terminal computing capacity is low.

6. Conclusion

To address the high application delay caused by the limitation of hardware resources such as storage and computing capacity of servers, a resource allocation strategy using deep reinforcement learning in cloud-edge collaborative computing environment is proposed. Based on the collaborative MEC system model, the optimization objective of minimizing system delay is designed, which is solved using HER-improved DQN to obtain the optimal resource allocation scheme. The results based on the simulation platform show that improving DQN by HER can accelerate the learning efficiency of the agents. It converges rapidly to the optimal value after 100 iterations, so the total system utility is about 0.2.

Data Availability

The data used to support the findings of this study are included within the article.

Conflicts of Interest

The authors declare that there are no conflicts of interest regarding the publication of this paper.

References

[1] C. Tang, C. Zhu, X. Wei, H. Wu, Q. Li, and J. Rodrigues, "Intelligent resource allocation for utility optimization in RSU-empowered vehicular network," *IEEE Access*, vol. 8, no. 1, pp. 94453–94462, 2020.

[2] H. Sun and H. Xi, "Resource optimization technology using genetic algorithm in UAV-assisted edge computing environment," *Journal of Robotics*, vol. 2022, Article ID 3664663, 8 pages, 2022.

[3] C. Li, Y. Zhang, and Y. Luo, "Adaptive handover based on traffic balancing and multi-dimensional collaborative resource management in MEC environment," *The Journal of Supercomputing*, vol. 78, no. 5, pp. 6752–6787, 2022.

[4] S. Zhou, W. Jadoon, and J. Shuja, "Machine learning-based offloading strategy for lightweight user mobile edge computing tasks," *Complexity*, vol. 2021, no. 3, pp. 1–11, 2021.

[5] S. K. U. Zaman, A. I. Jehangiri, T. Maqsood et al., "LiMPO: Lightweight Mobility Prediction and Offloading Framework Using Machine Learning for mobile Edge computing," *Cluster Computing*, 2022.

[6] W. Xia and L. Shen, "Joint resource allocation at edge cloud based on ant colony optimization and genetic algorithm," *Wireless Personal Communications*, vol. 117, no. 2, pp. 355–386, 2021.

[7] S. Janakiraman and M. D. Priya, "Improved artificial bee colony using monarchy butterfly optimization algorithm for load balancing (IABC-MBOA-LB) in cloud environments," *Journal of Network and Systems Management*, vol. 29, no. 4, pp. 1–38, 2021.

[8] T. Reis, M. Teixeira, J. Almeida, and A. C. D. Paiva, "A recommender for resource allocation in compute clouds using genetic algorithms and SVR," *IEEE Lat Am T*, vol. 18, no. 6, pp. 1049–1056, 2020.

[9] K. Wang, "Migration strategy of cloud collaborative computing for delay-sensitive industrial IoT applications in the context of intelligent manufacturing," *Computer Communications*, vol. 150, pp. 413–420, 2020.

[10] X. Gao, R. Liu, and A. Kaushik, "Hierarchical multi-agent optimization for resource allocation in cloud computing," *IEEE Transactions on Parallel and Distributed Systems*, vol. 32, no. 3, pp. 692–707, 2021.

[11] Q. Han, S. Yang, X. Ren, C. Zhao, X. Zhang, and X. Yang, "OL4EL: online learning for edge-cloud collaborative learning on heterogeneous edges with resource constraints," *IEEE Communications Magazine*, vol. 58, no. 5, pp. 49–55, 2020.

[12] J. Li, K. Zhao, X. Ding, and W. G. Shi, "Resource allocation strategy of SWIPT relay under general interference," *Wireless Personal Communications*, vol. 112, no. 3, pp. 1–15, 2020.

[13] Q. Zhang, L. Gui, F. Hou, J. Chen, F. Zhu, and F. Tian, "Dynamic task offloading and resource allocation for mobile-edge computing in dense cloud RAN," *IEEE Internet of Things Journal*, vol. 7, no. 4, pp. 3282–3299, 2020.

[14] C. Shi, L. Ding, F. Wang, S. Salous, and J. Zhou, "Low probability of intercept-based collaborative power and bandwidth allocation strategy for multi-target tracking in distributed radar network system," *IEEE Sensors Journal*, vol. 20, no. 12, pp. 6367–6377, 2020.

[15] X. Liu, J. Yu, Z. Feng, and Y. Gao, "Multi-agent reinforcement learning for resource allocation in IoT networks with edge computing," *China Communications*, vol. 17, no. 9, pp. 220–236, 2020.

[16] T. Pham and T. Nguyen, "Optimization of resource management for NFV-enabled IoT systems in edge cloud computing," *IEEE Access*, vol. 8, no. 4, pp. 178217–178229, 2020.

[17] J. Lin, D. Cui, Z. Peng, Q. Li, and J. He, "A two-stage framework for the multi-user multi-data center job scheduling and resource allocation," *IEEE Access*, vol. 8, no. 9, pp. 197863–197874, 2020.

[18] A. Montazerolghaem, M. H. Yaghmaee, and A. Leon-Garcia, "Green cloud multimedia networking: NFV/SDN based energy-efficient resource allocation," *IEEE Transactions on Green Communications and Networking*, vol. 4, no. 3, pp. 873–889, 2020.

[19] N. C. Luong, Y. Jiao, P. Wang, D. Niyato, D. I. Kim, and Z. Han, "A machine-learning-based auction for resource trading in fog computing," *IEEE Communications Magazine*, vol. 58, no. 3, pp. 82–88, 2020.

[20] M. Kolhar, F. Al-Turjman, J. Alameen, and A. A. Lameen, "Unified dynamic bandwidth allocation scheme for ethernet passive optical network," *IEEE Access*, vol. 8, no. 3, pp. 216176–216184, 2020.

[21] Y. Liao, L. Shou, Q. Yu, Q. Ai, and Q. Liu, "Joint offloading decision and resource allocation for mobile edge computing enabled networks," *Computer Communications*, vol. 154, no. 8, pp. 361–369, 2020.

[22] X. C. Chen, Y. C. Zhou, Y. Yang, and L. Lv, "Hybrid fog/cloud computing resource allocation: joint consideration of limited communication resources and user credibility," *Computer Communications*, vol. 169, no. 6, pp. 48–58, 2021.

[23] A. Mahdi, Y. Mina, R. Milad, J. Alireza, and R. K. Mohammad, "Efficient resource management and workload allocation in fog–cloud computing paradigm in IoT using learning classifier systems," *Computer and Communications*, vol. 153, no. 4, pp. 217–228, 2020.

[24] W. Zhang, Z. Zhang, S. Zeadally, H. C. Chao, and V. C. M. Leung, "Energy-efficient workload allocation and computation resource configuration in distributed cloud/edge computing systems with stochastic workloads," *IEEE Journal on Selected Areas in Communications*, vol. 38, no. 6, pp. 1118–1132, 2020.

[25] F. Shokri Habashi, S. Yousefi, and B. G. Ghalebsaz Jeddi, "Resource allocation mechanisms for maximizing provider's revenue in infrastructure as a service (IaaS) cloud," *Cluster Computing*, vol. 24, no. 3, pp. 2407–2423, 2021.

[26] M. Mukherjee, S. Kumar, C. X. Mavromoustakis et al., "Latency-driven parallel task data offloading in fog computing networks for industrial applications," *IEEE Transactions on Industrial Informatics*, vol. 16, no. 9, pp. 6050–6058, 2020.

[27] W. Hussain, O. Sohaib, M. Naderpour, and H. H. Gao, "Cloud marginal resource allocation: a decision support model," *Mobile Networks and Applications*, vol. 25, no. 4, pp. 1418–1433, 2020.

Hindawi
Mobile Information Systems
Volume 2022, Article ID 3455014, 10 pages
https://doi.org/10.1155/2022/3455014

Research Article

Emotion Monitoring of Hotel Staff Based on Mobile Network and Resource Allocation Algorithm

Minghua Lei

School of Qiandaohu International Hospitality Management, Tourism College of Zhejiang, Hangzhou 311700, China

Correspondence should be addressed to Minghua Lei; 201624551104@stu.yznu.edu.cn

Received 4 May 2022; Revised 16 June 2022; Accepted 29 June 2022; Published 12 July 2022

Academic Editor: Shadi Aljawarneh

With the continuous growth of the number of mobile devices and the continuous development of the mobile internet, people's demand for mobile communication services is also increasing. However, the wireless spectrum resources of cellular mobile communication networks are limited and are becoming increasingly scarce and tense. In order to improve the utilization of wireless spectrum resources, people have proposed the concept of device-to-device communication. In order to improve the robustness of the system and transmission delay tolerance service, which allows users to interrupt the probability method has certain tolerance, the maximum transmission power is greater than that of the traditional robust algorithm. By monitoring the emotions of hotel employees, it can be seen that the performance accuracy of the robust algorithm in this paper is high. Low job burnout will have a negative impact on hurt job satisfaction, while emotional fatigue and depersonalization will not directly affect job satisfaction. Among the two outcome variables of job burnout and job satisfaction, surface behavior positively affects emotional exhaustion and depersonalization but has no significant effect on job satisfaction. Deep behavior negatively affects depersonalization and low sense of accomplishment and positively affects work satisfaction.

1. Introduction

With the gradual maturity of the domestic hotel industry market, the focus of competition in the industry has changed from providing high-configuration hardware facilities to providing high-level customer service [1]. This means that the emotional expression of the hotel staff will affect the quality of service customers feel, as well as customer satisfaction [2]. Customer assets are important intangible assets of hotels. Therefore, the emotional management of hotel employees has always been the focus of hotel managers [3]. Among them, job burnout caused a lot of discussions. In addition to physical and mental work, hotel employees in a high-contact service industry, regardless of their emotional state, need to perform a large number of emotional displays required by the organization, which can lead to job burnout, affect job satisfaction and job performance, and even resign tendency [4]. A large number of other outcome variables can also be mediated or partially mediated through job burnout. Currently, relevant research focuses on emotional labor strategies [5]. Another aspect of emotional labor that belongs to the category of emotional labor is that emotional labor pays less attention, and the results of related research on emotional labor strategies often appear contradictory. Therefore, an in-depth and systematic study of emotional labor and job burnout can help clarify the mechanism of emotional labor and is a useful exploration for deepening the existing framework [6].

2. Related Work

Emotional labor has two meanings: one is the requirement of emotional labor and the other is the strategy of emotional labor. This research divides emotional work into emotional labor strategy and emotional labor demand [7]. From the perspective of labeling rules and interactive expectations, labeling rules and interactive expectations integrate the relevant content of emotional labor needs. When it comes to emotional labor, the literature integrates the two viewpoints of display rules and interaction expectations [8]. It analyzes

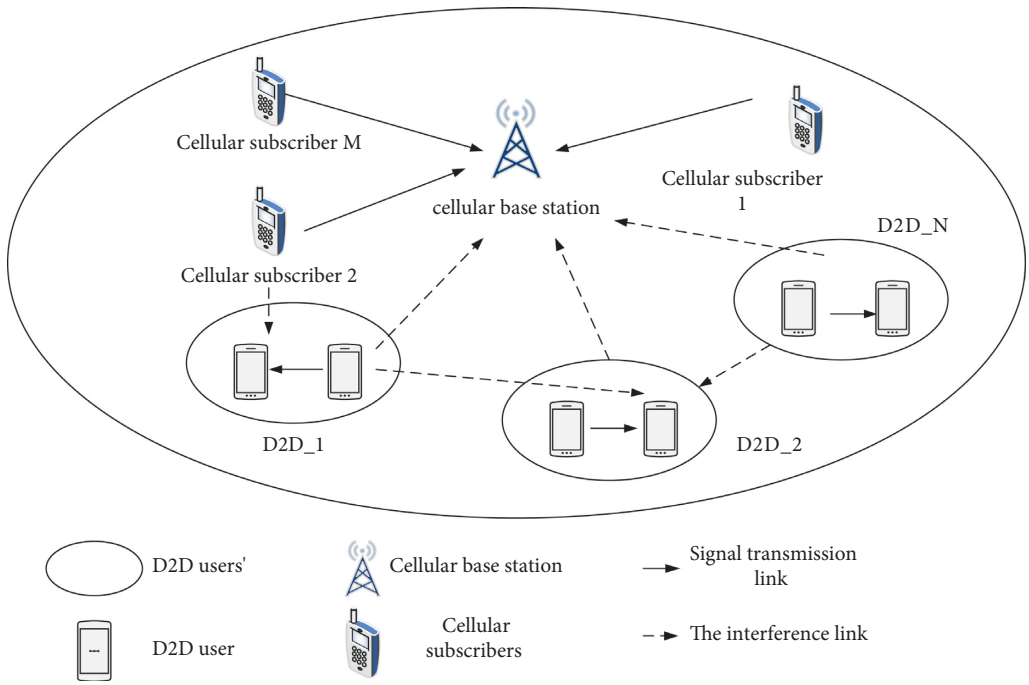

Figure 1: Multiuser underlying cognitive D2D communication network.

the role of identity theory on individuals, connects emotional labor requirements with emotional labor strategies, and proposes that identity can be used as an intermediary mechanism for the relationship between parameters. The importance of emotional management is recognized. The literature proposes that people believe that emotional labor includes the workload of emotional labor, and other aspect of emotional labor that belongs to the category of emotional labor is emotional labor [9]. Therefore, in-depth and systematic research on emotional labor and job burnout can help clarify the mechanism of emotional labor and have a direct impact on job burnout syndrome. The literature pointed out that emotional labor demand has a positive impact on job burnout syndrome, and other dimensions have received less attention [10]. Relevant research results on emotional labor strategies often appear contradictory. Therefore, an in-depth and systematic study of emotional labor and job burnout can help clarify the mechanism of emotional labor and is a useful exploration for deepening the existing framework [11]. We are discussing the impact of emotional labor on job burnout, and emotional labor requirements have a positive effect on job burnout [12]. Both deep acting and superficial acting play a complete mediating role in emotional labor demand and job burnout. The direct impact of emotional labor demand on job burnout is only in natural regulation, but it inhibits the second half of the coordination path. The literature proposes to integrate emotional labor demand into the emotional labor framework [13]. Finally, five dimensions of emotional labor workload, emotional labor routine, emotional expression diversity, positive emotional display rules, and negative emotional display rules are determined [14]. This division method will meet the organizational regulations of emotional labor and the actual needs of employees in emotional labor. The needs are divided in a unified way, which actively regulates the relationship between the employees' emotional work needs and the employees' superficial and deep roles [15, 16]. This is the basis for the dimensional division of emotional labor needs in this study.

3. D2D Network-Based Dynamic Quota Resource Allocation Algorithm Design

3.1. System Model. As shown in Figure 1, this article uses a multiuser mat cognitive D2D communication system in a spectrum sharing model. This system has n cellular base stations, m cellular ND2 users, and the user sets are defined as m and n, respectively. The spectrum resource of the cellular system is divided into multiple subchannels, and each cellular user uses an orthogonal subchannel for uplink data transmission, thus avoiding the influence of the same-layer interference between cellular users. Assuming that each pair of the D2D users has spectrum awareness capabilities, flexibly implements mode selection, and resource scheduling, since it is based on the underlying spectrum sharing mode, D2D users need to control their interference power to not to exceed a certain level when multiplexing cellular user frequency and it is assumed that all wireless channels obey this distribution.

Considering the interference of cellular users to D2D users and the interference of other D2D users to the current D2D users, the signal-to-interference-to-noise ratio of the nth D2D user receiver is as the following formula:

$$\gamma_n^m = \frac{p_n^m h_n^m}{p_c^m h_{c,n}^m + \sum_{i=1,i\neq n}^{N} p_i^m h_{i,n}^m + N_0}. \quad (1)$$

Therefore, the total rate of all D2D users can be described as the following formula:

$$R = \sum_{n=1}^{N}\sum_{m=1}^{N}\log_2\left(1+\gamma_n^m\right). \tag{2}$$

Define the circuit power consumption of each pair of D2D users as pc, and then the total power consumption of D2D users is as the following formula:

$$E = \sum_{n=1}^{N}\sum_{m=1}^{N} p_n^m + Np_c. \tag{3}$$

Further considering the need to protect the communication quality of each cellular user, there are the following interference power constraints:

$$\sum_{n=1}^{N} p_n^m g_n^m \le I_m^{th}. \tag{4}$$

where I_m^{th} is the tolerable peak interference power on each subchannel. Considering the limitation of the battery capacity of D2D users, the transmission power cannot be infinite, so the transmission power satisfies the following constraints:

$$\sum_{m=1}^{M} p_n^m \le p_n^{\max}. \tag{5}$$

where p_n^m is the maximum transmit power that can be provided by the nth D2D user. To maximize the energy efficiency of the D2D network and meet the communication quality of each cellular user, considering the above analysis results, the resource allocation problem based on the most energy-efficient is the following formula:

$$\begin{aligned} &\max_{p_n^m} \frac{\sum_{n=1}^{N}\sum_{m=1}^{M}\log_2\left(1+\gamma_n^m\right)}{\sum_{n=1}^{N}\sum_{m=1}^{M} p_n^m + Np_c} s.t.C_1: \\ &\sum_{n=1}^{N} p_n^m g_n^m \le I_m^{th} C_2: \sum_{m=1}^{M} p_n^m \le p_n^{\max}. \end{aligned} \tag{6}$$

The above problem does not consider the estimation error of the channel gain; that is, it is assumed that the channel gain g_n^m is accurately known. However, in actual cognitive D2D networks, with the presence of spectrum estimation errors and dynamic perception uncertainty, it is difficult to accurately obtain channel gain information. The optimal resource allocation algorithm based on traditional feedback channel information can no longer meet the needs of the actual system design. Therefore, it is necessary to take the channel estimation error into account in the algorithm design in advance, and it is particularly important to propose a robust resource allocation algorithm that can resist parameter perturbation.

3.2. Robust Resource Allocation Algorithm. Considering the influence of channel estimation error, the actual channel gain can be described by the following additive uncertainty model:

$$g_n^m = \widehat{g}_n^m + \Delta g_n^m. \tag{7}$$

However, Δg_n^m is a random quantity, which is the channel gain estimation error. Obviously, the direct assumption of $\Delta g_n^m = 0$ is an ideal situation. However, it is not satisfactory in the actual situation. Due to the influence of the estimation error, the C1 constraint condition of the optimization problem (6) will be interrupted. Therefore, the energy efficiency optimization problem based on the interference power interruption constraint can be described as follows:

$$\begin{aligned} &\max_{p_n^m} \frac{\sum_{n=1}^{N}\sum_{m=1}^{M}\log_2\left(1+\gamma_n^m\right)}{\sum_{n=1}^{N}\sum_{m=1}^{M} p_n^m + Np_c} s.t.\overline{C}_1: \\ &\Pr\left\{\sum_{n=1}^{N} p_n^m g_n^n \ge I_m^{th}\right\} \le \zeta_m C_2: \sum_{m=1}^{M} p_n^m \le p_n^{\max}, \end{aligned} \tag{8}$$

where ζ_m is the outage probability threshold of cellular user m. This problem is complex, and it is difficult to directly obtain an analysis of the resource allocation problem.

For outage probability constraints, there have been many commonly used methods to deal with, such as the relaxation probability integration method. However, in the actual cognitive D2D network, since there is no cooperation between users, it is difficult to obtain the statistical distribution information. In addition, due to the randomness of the wireless channel, the assumption of a certain probability distribution model in advance is invalid. Therefore, a new mechanism needs to be introduced to solve this problem. The minimum-maximum probability can solve the above problems well. Based on the minimum-maximum probability machine method, any interruption constraint can be described as the following form:

$$\inf_{x\sim(\overline{x},e)} \Pr\left\{a^T X \le b\right\} \ge 1-a, \tag{9}$$

where x is the parameter vector with uncertainty; a is the parameter vector; and α is the outage probability threshold. Based on the principle of the minimum-maximum probability machine, formula (9) can be equivalent to

$$\sup_{x\sim(\overline{x},te)} \Pr\left\{a^T X \ge b\right\} = \frac{1}{1+d^2}. \tag{10}$$

Among them,

$$\begin{aligned} d^2 &= \inf_{a^T X \ge b} (x-\overline{x})^T e^{-1} (x-\overline{x}) \\ &= \frac{\max\left\{\left(b-a^T x\right),0\right\}^2}{a^T e a}. \end{aligned} \tag{11}$$

Since formula (9) can be equal to $\sup_{x\sim(\overline{x},te)}\Pr\{a^T X \ge b\} \le \alpha$, formula (10) can be added to it to obtain the following:

$$a \ge = \frac{1}{1+d^2}. \tag{12}$$

Combined with formula (11), formula (12) can be obtained:

$$\frac{\max\left\{\left(b-a^T x\right),0\right\}^2}{a^T e a} \geq f(a). \tag{13}$$

In the formula $f(a)=\sqrt{(1-a)/a}$, after finishing formula (13), we can get

$$a^T \overline{x} + f(a)\sqrt{a^T e a} \leq b. \tag{14}$$

Equation (14) is the equivalent closed form of constraint (9), which defines the mean and variance of channel gain g_n^m as $\widehat{g}_n^m$ and ζ_n^m, respectively. Based on the form of (14) and combined with the minimum and maximum probability machine method, the outage probability constraint $\overline{c_1}$ can be converted as follows:

$$\sum_{n=1}^{N} p_n^m \widehat{g_n^m} + f(\varepsilon_m)\sqrt{\sum_{n=1}^{N}\left(p_n^m\right)^2 \delta_n^m} \leq I_m^{th}. \tag{15}$$

In the formula $f(\zeta_m)=\sqrt{\zeta_m/(1-\zeta_m)}$, therefore, the interruption interference interruption probability is converted into a closed form as shown in (15). However, due to the horizontal direction, the problem still cannot be solved. Therefore, based on Cauchy's inequality, we can convert (15) into the following form:

$$\sum_{n=1}^{N} p_n^m \overline{g}_n^m \leq I_m^{th}, \tag{16}$$

where $\overline{g}_n^m = \widehat{g}_n^m + f(\zeta_m)\sqrt{\sum_{n=1}^{N}\zeta_n^m}$ is a convex constraint.

The objective function is in fractional form. The problem is a nonconvex optimization problem under convex constraints. The objective function can be equivalent to

$$F\left(p_n^m\right) = \sum_{n=1}^{N}\sum_{m=1}^{M}\log_2\left(1+\gamma_n^m\right) - \eta\left(\sum_{n=1}^{N}\sum_{m=1}^{M} p_n^m + N p_c\right), \tag{17}$$

where η is the total energy efficiency of D2D users and $\eta \geq 0$. Due to the coupling relationship of the transmit power in the rate function, based on the continuous convex approximation method, the transmission rate can be approximated to the following equivalent convex form:

$$\log_2\left(1+\gamma_n^m\right) \geq a_n^m \log_2\left(\gamma_n^m\right) + b_n^m. \tag{18}$$

In the formula, $a_n^m = \overline{\gamma}$ and $b_n^m = \log_2\left(1+\overline{\gamma}_n^m\right) - a_n^m \log_2\left(\gamma_n^m\right)$ are auxiliary variables, the initial value can be set to $a_n^m = 1$ and $b_n^m = 0$, $\overline{\gamma}_{\mathrm{n}}^m$ represents the last iteration value of γ_n^m.

Therefore, the objective function (17) can be equivalent to

$$F\left(\mathrm{p}_n^m\right) = \sum_{n=1}^{N}\sum_{m=1}^{M} a_n^m \log_2\left(1+\gamma_n^m\right) - \eta\left(\sum_{n=1}^{N}\sum_{m=1}^{M} p_n^m + N p_c\right). \tag{19}$$

Therefore, combining formulas (16), (19), and (8), we can get the following optimization problem:

$$\begin{aligned} \max_{p_n^m} & \sum_{n=1}^{N}\sum_{m=1}^{M} a_n^m \log_2\left(\gamma_n^m\right) + \sum_{n=1}^{N}\sum_{m=1}^{M} b_n^m \\ & - \eta\left(\sum_{n=1}^{N}\sum_{m=1}^{M} p_n^m + N p_c\right) s.t. \widehat{C_1}: \\ & \sum_{n=1}^{N} p_n^m \overline{g}_n^m \leq I_m^{th} C_2: \sum_{m=1}^{M} p_n^m \leq p_n^{\max}. \end{aligned} \tag{20}$$

Equation (20) is an optimization problem, and optimization theory can be used to obtain an analytical solution for resource allocation.

The Lagrangian principle can be used to solve problem (20), and the Lagrangian function to construct the optimization problem (20) is as follows:

$$\begin{aligned} L\left(p_n^m, \lambda_m, \beta_n\right) = & \sum_{n=1}^{N}\sum_{m=1}^{M} a_n^m \log_2\left(\gamma_n^m\right) - \eta\left(\sum_{n=1}^{N}\sum_{m=1}^{M} p_n^m + N p_c\right) \\ & + \sum_{n=1}^{N}\sum_{m=1}^{M} b_n^m, \\ & + \sum_{m=1}^{M} \lambda_m \cdot \left(I_m^{th} - \sum_{n=1}^{N} p_n^m \overline{g}_n^m\right) + \sum_{n=1}^{N} \beta_n \cdot \left(p_n^{\max} - \sum_{m=1}^{M} p_n^m\right). \end{aligned} \tag{21}$$

In the formula, $\lambda_m \geq 0$ and $\beta_n \geq 0$ are Lagrangian dual variables. Equation (21) can be equivalently described as follows:

$$\begin{aligned} L\left(p_n^m, \lambda_m, \beta_n\right) = & \sum_{n=1}^{N}\sum_{m=1}^{M} L_{n,m}\left(p_n^m, \lambda_m, \beta_n\right) - \eta N p_c \\ & + \sum_{n=1}^{N}\sum_{m=1}^{M} b_n^m + \sum_{m=1}^{M} \lambda_m I_m^{th} + \sum_{n=1}^{N} \beta_n p_n^{\max}. \end{aligned} \tag{22}$$

Therefore, for every D2D user,

$$L_{n,m}\left(p_n^m, \lambda_m, \beta_n\right) = a_n^m \log_2\left(\gamma_n^m\right) - \eta p_n^m - \lambda_m p_n^m \overline{g}_n^m - \beta_n p_n^m. \tag{23}$$

According to the Lagrangian duality principle and formula (21), the dual problem is as follows:

$$\min_{\lambda_m, \beta_n} D\left(\lambda_m, \beta_n\right) s.t. \lambda_m \geq 0, \beta_n \geq 0. \tag{24}$$

The expression of the dual function is as follows:

$$D\left(\lambda_m, \beta_n\right) = \max L\left(p_n^m, \lambda_m, \beta_n\right). \tag{25}$$

According to the KKT condition and the subgradient update method, the analytical solution of the resource allocation algorithm can be obtained as follows:

$$p_n^{m,*} = \frac{a_n^m}{\ln 2\left(\eta + \lambda_m \overline{g}_n^m + \beta_n\right)},$$

$$\lambda_m(t+1) = \left[\lambda_m(t) - s_1 \times \left(I_m^{th} - \sum_{n=1}^{N} p_n^m \overline{g}_n^m\right)\right]^+, \quad (26)$$

$$\beta_n(t+1) = \left[\beta_n(t) - s_2 \times \left(p_n^{\max} - \sum_{m=1}^{M} p_n^m\right)\right]^+,$$

$$\eta = \frac{\sum_{n=1}^{N}\sum_{m=1}^{M} \log_2\left(1+\gamma_n^m\left(p_n^m\right)\right)}{\sum_{n=1}^{N}\sum_{m=1}^{M} p_n^m + N p_c}.$$

In the formula, s 1 and s 2 are the iteration steps and $[x]^+$ is the number of iterations. When an appropriate step factor is set, the algorithm can converge quickly.

3.3. Analysis of Simulation Results. The path loss index is 4, the shadow fading coefficient is 8 dB, the maximum transmit power threshold for D2D users is $p_n^{\max} = = 23$ dBm, the circuit power consumption is $p_c = 12$ dBm, the noise power is $N_0 = -114$ dBm, the number of D2D users and cellular users is [2, 50], and the interference power threshold value is $I_m^{th} = -30$ dBm, respectively. Without loss of generality, each of the subchannel is considered as a unit bandwidth in the simulation.

Figure 2 shows the relationship between the energy efficiency of cognitive D2D network users under different numbers of users. It can be seen from the figure that the total energy efficiency of the system increases as the number of D2D users increases. However, when D2D users increase exponentially, the energy efficiency of the system does not increase exponentially. The reason is that the cochannel interference between multiple D2D users will increase the interference of the currently active users, thereby reducing the signal-to-interference and noise ratio of the users in the existing network. In addition, the robust algorithm in this paper is more energy-efficient than the traditional nonrobust algorithm. As the outage probability threshold increases, the energy efficiency of the algorithm in this paper gradually increases. A large interruption probability threshold means that the effective transmission power in the interference power constraint is reduced, thereby providing better protection performance for cellular users.

Figure 3 shows the relationship between the total energy efficiency of D2D users and the outage probability threshold. It can be seen from the figure that as the variance of the channel gain error increases, the total energy efficiency of D2D users increases, because it can be seen from the interference power constraint that as the channel gain estimate increases, ζ_n^m increases, and the effective transmission power decreases to avoid harmful interference to cellular users. Therefore, power consumption is reduced and system energy efficiency is increased. In addition, the energy efficiency of the traditional nonrobust algorithm remains constant, because the outage probability of zero will make the second term of the robust interference constraint independent of the

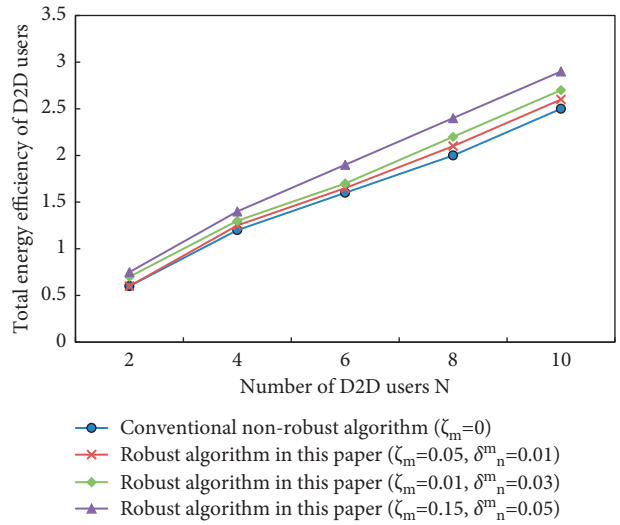

Figure 2: The relationship between user energy efficiency and the number of D2D users.

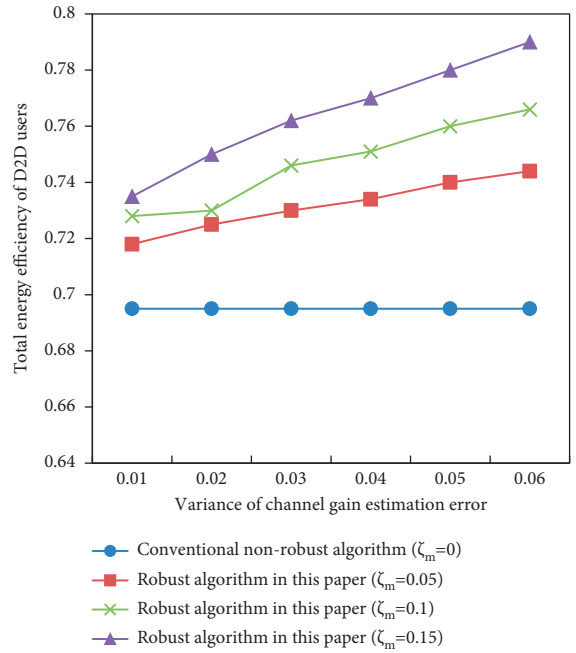

Figure 3: D2D user total energy efficiency and outage probability threshold.

variance of the channel gain estimation error, so it remains constant. From the figure, it can be found that as the interruption probability threshold allowed by cellular users increases, the total energy efficiency of D2D users also increases. As the probability of interruption is increased, the value of the second term is increased, thereby reducing the effective transmission power and reducing the total energy consumption.

Figure 4 shows the energy efficiency performance comparison of different algorithms under different transmit powers, where the number of D2D user pairs is 2. It can be seen from the figure that as the maximum transmit power

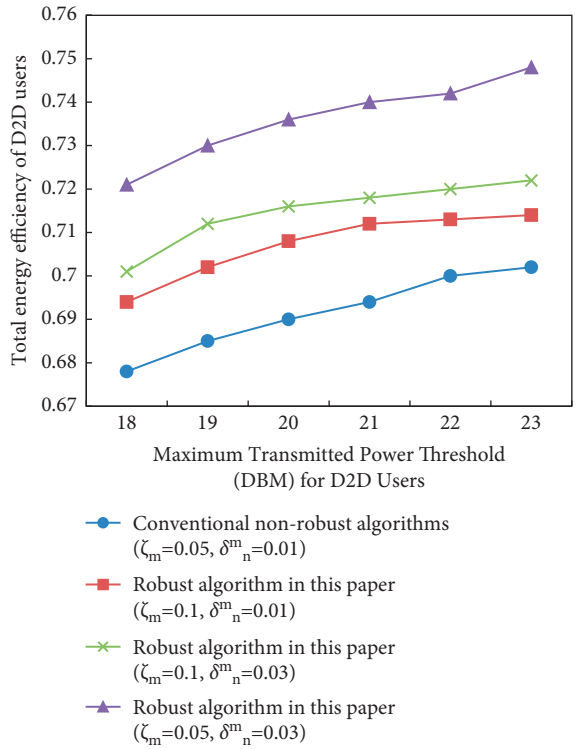

Figure 4: Comparison of energy efficiency performance of different algorithms under different transmission powers.

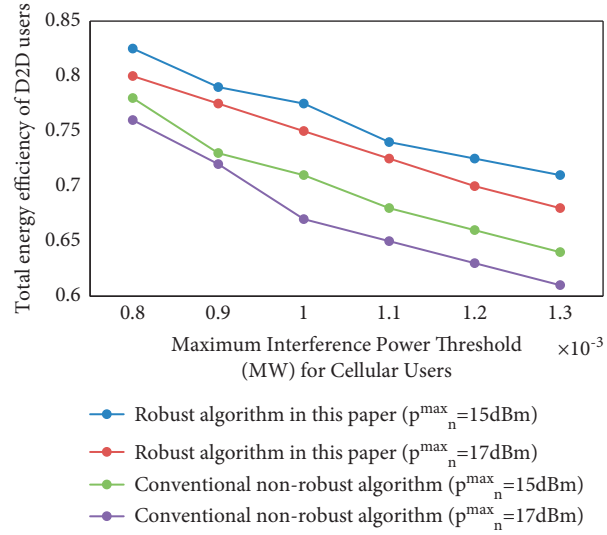

Figure 5: The relationship between D2D user energy efficiency and maximum interference power threshold.

threshold of D2D users increases, the total energy efficiency of D2D users gradually increases, because increasing the user threshold can allocate more power to each subchannel to improve user rate and energy efficiency. In addition, the energy efficiency of the robust algorithm in this paper is higher than that of the traditional nonrobust algorithm. Therefore, to improve the robustness of the system and the transmission of delay-tolerant services, the algorithm in this paper allows users to have a certain tolerance to the probability of interruption, and its maximum transmission power is greater than that of traditional nonrobust algorithms. From the perspective of different outage probability thresholds ξ m and estimated error variance, as the outage threshold increases, its energy efficiency gradually increases; as the estimated error variance increases, the total energy efficiency of D2D users increases. As the estimation error increases, the estimated channel gain value will deviate from its true value more and more, so it is necessary to increase the transmission power to overcome the influence of this part of the channel uncertainty on cellular users, thereby increasing the energy efficiency.

Figure 5 shows the total energy efficiency of D2D users under the maximum interference power of different algorithms. The outage probability and the estimated error variance are set to 0.05 and 0.01. It can be seen from the figure that the algorithm in this paper has a higher energy efficiency performance than the traditional nonrobust algorithm. As the maximum interference power allowed by cellular users in each subcarrier increases, the total energy efficiency of D2D users decreases. As the increased interference power can allow D2D users to transmit more power on the shared subchannels, thereby increasing power consumption and reducing overall energy efficiency, it is necessary to balance the relationship between transmission rate and energy consumption. To more intuitively reflect the advantages of the algorithm in this paper, the following analysis is shown in Table 1. It can be seen from the table that the robust algorithm in this paper has a performance improvement of close to 2% to 3% in energy efficiency performance, indicating that the algorithm in this paper has better energy efficiency performance, and as the feasible range of the transmittable rate increases, that is, the maximum transmits it power threshold of D2D users, the magnitude of this energy-efficiency performance improvement will further increase.

4. Job Burnout in the Process of Hotel Emotional Management and Improvement Strategies

4.1. Research Object Selection. The distribution and collection of the questionnaire were completed in November 2019. A total number of 220 questionnaires were distributed in this survey, and a total number of 215 questionnaires were returned, including 200 valid questionnaires. Based on the data obtained from the survey, the relationship between hotel employees' emotional labor, job burnout, and job satisfaction is studied. The effective response rate was 93. The following is a descriptive analysis of the sample (see Table 2).

Judging from the available data, women accounted for the majority of the respondents, 108, accounting for 58.4% of the total; in terms of age, the population aged 21–30 years old was the largest, 138, accounting for 49.7%. In terms of marital status, the majority of unmarried people are 135, accounting for 73%. In terms of academic qualifications, the subjects with a high school and college degree or above are the most, and the samples are unevenly distributed among

Table 1: Comparison of algorithm performance differences.

Algorithm type	Maximum transmit power threshold for cellular users		
	1 mW	1.1 mW	1.2 mW
Robust algorithm	0.7619 mW	0.736 mW	0.7123 mW
(15 dbm)	0.7415 mW	0.717 mW	0.6946 mW
Nonrobust algorithm	0.0204(2.75%)	0.019(2.65%)	0.0177(2.54%)
(15 dbm)	0.6965 mW	0.673 mW	0.6514 mW
Energy-efficiency difference (bits/Hz/J)	0.6701 mW	0.6481 mW	0.6281 mW
Robust algorithm	0.0264(3.93%)	0.0249(3.84%)	0.233(3.71%)

Table 2: The basic situation of the respondents.

Demographic characteristics		Frequency	Percentage (%)
Gender	Male	77	41.6
	Female	108	58.4
Age	20 years old and below	17	9.2
	21–30 years old	138	74.6
	31–40 years old	20	10.8
	41–50 years old	10	5.4
Education	Junior high school and below	26	14.1
	High school (vocational)	53	28.6
	Specialist	101	54.6
	Undergraduate	5	2.7
Marital status	Unmarried	135	73
	Married	50	27
Department	Lobby	15	8.1
	Food	132	71.4
	Room	33	17.8
	Recreation	2	1.1
	Other	3	1.6

Table 3: Factor loading values of job satisfaction scale.

Factor term	Minimum	Maximum	Mean	Standard deviation
Surface behavior	1.00	6.00	2.8724	1.15333
Deep behavior	1.00	6.00	4.5135	1.00300
Emotional exhaustion	.00	6.00	2.7103	1.43873
Depersonalize	.00	6.00	2.5880	1.41717
Low sense of accomplishment	1.00	4.00	1.5306	.85442
Job satisfaction	1.40	6.00	3.7503	.98539

various departments. Among them, the catering department has the most subjects, with 132 people, accounting for 71.4%.

4.2. Descriptive Statistical Analysis. To grasp the overall distribution of the sample, this study conducted a descriptive statistical analysis of the emotional labor, job burnout, and job satisfaction of the sample. The results are shown in Table 3.

4.3. Correlation Analysis of Emotional Labor, Job Burnout, and Job Satisfaction. The frontline employees of the hotel will adjust their inner emotions to meet the requirements of the workplace as much as possible. The results show that the standard deviation is small, indicating that the difference between the variables is not large. In this article, we analyzed the relationship between emotional work, job burnout syndrome, and job satisfaction.

This section explains whether there is a clear relationship between emotional labor, superficial behavior, deep behavior, and job satisfaction. The results are shown in Table 4.

Table 4 shows that emotional job depth behavior is significantly positively correlated with job satisfaction, while the correlation coefficient is significantly negatively correlated with surface behavior and job satisfaction. Therefore, there is no clear correlation.

In this part, we will analyze two aspects of emotional labor as follows: superficial behavior and deep behavior, and job burnout in three aspects as follows: emotional fatigue, depersonalization, and sense of accomplishment to test the correlation. The results are shown in Table 5.

Table 4: The correlation between emotional labor and job satisfaction.

		Surface behavior	Deep behavior	Job satisfaction
Surface behavior	Pearson correlation	1	0.076	0.166
	Significance (bilateral)		0.037	0.177
	N	185	185	185
Deep behavior	Pearson correlation	0.076	1	0.342
	Significance (bilateral)	0.307		0.000
	N	185	185	185
Job satisfaction	Pearson correlation	0.116	0.342	1
	Significance (bilateral)	0.117	0.000	
	N	185	185	185

Table 5: Correlation matrix between emotional labor and job burnout.

		Surface behavior	Deep behavior	Emotional exhaustion	Depersonalize	Low sense of accomplishment
Surface behavior	Pearson correlation	1	0.076	0.364	0.542	−0.080
	Significance (bilateral)		0.307	0.000	0.000	0.279
	N	185	185	185	185	185
Deep behavior	Pearson correlation	0.076	1	−0.064	−0.197	−374
	Significance (bilateral)	0.307		0.384	0.007	0.000
	N	185	185	185	185	185
Emotional exhaustion	Pearson correlation	0.364	−0.064	1	0.603	−0.201
	Significance (bilateral)	0.000	0.384		0.000	0.006
	N	185	185	185	185	185
Depersonalize	Pearson correlation	0.542	−0.197	0.603	1	0.078
	Significance (bilateral)	0.000	0.007	0.000		0.293
	N	185	185	185	185	185
Low sense of accomplishment	Pearson correlation	−0.080	−0.374	−0.201	0.078	1
	Significance (bilateral)	0.279	0.000	0.006	0.0.293	
	N	185	185	185	185	185

This part will be discussed from five aspects: job burnout, emotional exhaustion, depersonalization, low sense of achievement, and job satisfaction.

Correlation analysis was performed to test whether there is a significant correlation, and the results are shown in Table 6.

4.4. Measures to Improve the Effect of Emotional Management in the Hotel Industry. Regression analysis shows that the superficial behavior of hotel employees has a positive effect on emotional exhaustion and depersonalization but has no obvious effect on job satisfaction. Low job burnout will hurt job satisfaction, while emotional fatigue and depersonalization will not directly affect job satisfaction. Hotel managers cannot ignore this, seeing that it makes employees' emotional labor behavior smooth and tends to deepen performance strategies to prevent job burnout and improve job satisfaction. Combining the above research conclusions, we propose the following countermeasures: as an employer of hotel employees, hotel managers should pay attention for raising awareness of emotional management. Managers should pay close attention to the emotional labor of employees and combine the improvement of service quality with the mental health and emotional state of hotel employees. Timely communication and encouragement between hotel managers and service staff, especially during busy customer service hours, play an important role in encouraging the emotional initiative of the hotel staff. For hotel employees, especially for positions with high emotional labor, hotels facing daily emotional labor problems should use the emotional awareness and control ability of employees as an important selection indicator when hiring employees. Clarify emotional labor content in job responsibilities.

The job responsibilities list all the work tasks to be completed in a certain position, the equipment and materials

Table 6: Correlation matrix between emotional labor and job burnout.

		Emotional exhaustion	Depersonalize	Low sense of accomplishment	Job satisfaction
Emotional exhaustion	Pearson correlation	1	0.603	−0.201	−0.202
	Significance (bilateral)		0.000	0.006	0.006
	N	185	185	185	185
Depersonalize	Pearson correlation	0.603	1	0.078	−0.273
	Significance (bilateral)	0.000		0.293	0.000
	N	185	185	185	185
Low sense of accomplishment	Pearson correlation	−0.201	0.078	1	−0.255
	Significance (bilateral)	0.006	0.293		0.000
	N	185	185	185	185
Job satisfaction	Pearson correlation	−0.202	−0.273	−0.255	1
	Significance (bilateral)	0.006	0.000	0.000	
	N	185	185	185	185

needed for the working environment, and important information related to the job. Traditional job responsibilities focus more on formal standardization and detailed job descriptions while ignoring the needs of employee development. To reflect the personal values of employees, it is necessary to appropriately adopt a "role-based" game method to reflect employees' emotional issues in the work, enrich the work content, and change the strict work standards. Hotel performance evaluation should not only focus on the daily workload of employees but also consider the emotional contribution of service personnel in the service process. Based on the traditional wage system, hotels can establish an emotional labor standard system that conforms to the characteristics of the hotel industry and quantify various indicators.

5. Conclusion

This research divides emotional work into emotional labor strategies and emotional labor needs. From the perspectives of labeling rules and interactive expectations, the related content of emotional labor needs is integrated. The maturity scale is established from two perspectives. This division method separates the system rules of emotional work from the actual needs that employees must meet in the process of emotional work. This is the basis for dividing emotional labor demand in this research. It analyzes the role of identity theory on individuals, connects emotional labor requirements with emotional labor strategies, and proposes that identity can be used as an intermediary mechanism for the relationship between parameters. Studies have shown that emotional labor demand has a positive effect on job burnout syndrome. Deep and superficial behavior is a complete mediator of emotional labor demand and job burnout syndrome. Natural adaptability cannot be mediated, but this is the end of the mediation path, and it has an inhibitory effect. The direct impact of emotional labor requirements on job burnout syndrome is meaningful only in natural coordination. Actively regulate the relationship between employees' emotional work needs and employees' superficial and deep roles, which can better regulate interpersonal relationships.

Data Availability

The data used to support the findings of this study are available from the corresponding author upon request.

Conflicts of Interest

The author declares that there are no conflicts of interest.

Acknowledgments

The study was supported by "the Science and Technology Project of China Railway Corporation, China (Grant no. 1341324011)".

References

[1] S. A. M. Abdulla, G. S. Khalifa, A. E. Abuelhassan, B. B. Nordin, A. Ghosh, and A. Bhaumik, "Advancement of destination service quality management technology in tourism industry," *Journal of Critical Reviews*, vol. 7, no. 11, pp. 2317–2324, 2020.

[2] Y. N. Myo, G. S. Khalifa, and T. T. Aye, "The impact of service quality on customer loyalty of Myanmar hospitality industry: the mediating role of customer satisfaction," *International Journal of Management and Human Science (IJMHS)*, vol. 3, no. 3, pp. 1–11, 2019.

[3] E. Anasori, S. W. Bayighomog, and C. Tanova, "Workplace bullying, psychological distress, resilience, mindfulness, and emotional exhaustion," *Service Industries Journal*, vol. 40, no. 1-2, pp. 65–89, 2020.

[4] L. F. Hsieh, L. H. Lin, and Y. Y. Lin, "A service quality measurement architecture for hot spring hotels in Taiwan," *Tourism Management*, vol. 29, no. 3, pp. 429–438, 2008.

[5] U. Azad, B. K. Behera, E. A. Ahmed, P. K. Panigrahi, and A. Farouk, "Solving vehicle routing problem using quantum

approximate optimization algorithm," *IEEE Transactions on Intelligent Transportation Systems*, 2022.

[6] A. R. Alaei, S. Becken, and B. Stantic, "Sentiment analysis in tourism: capitalizing on big data," *Journal of Travel Research*, vol. 58, no. 2, pp. 175–191, 2019.

[7] S. Briggs, J. Sutherland, and S. Drummond, "Are hotels serving quality? An exploratory study of service quality in the Scottish hotel sector," *Tourism Management*, vol. 28, no. 4, pp. 1006–1019, 2007.

[8] J. M. Diefendorff, M. H. Croyle, and R. H. Gosserand, "The dimensionality and antecedents of emotional labor strategies," *Journal of Vocational Behavior*, vol. 66, no. 2, pp. 339–357, 2005.

[9] U. R. Schewe and A. F. Schewe, "On the costs and benefits of emotional labor: a meta-analysis of three decades of research," *Journal of Occupational Health Psychology*, vol. 16, no. 3, pp. 361–389, 2011.

[10] C. M. Grandey and A. A. Grandey, "Emotional labor and burnout: comparing two perspectives of "people work"," *Journal of Vocational Behavior*, vol. 60, no. 1, pp. 17–39, 2002.

[11] E. Demerouti, A. B. Bakker, F. Nachreiner, and W. B. Schaufeli, "The job demands-resources model of burnout," *Journal of Applied Psychology*, vol. 86, no. 3, pp. 499–512, 2001.

[12] R. H. Diefendorff and J. M. Diefendorff, "Emotional display rules and emotional labor: the moderating role of commitment," *Journal of Applied Psychology*, vol. 90, no. 6, pp. 1256–1264, 2005.

[13] K. Markman and K. M. Markman, "Online customer service and emotional labor: an exploratory study," *Computers in Human Behavior*, vol. 62, pp. 658–665, 2016.

[14] M. Adil, H. Alshahrani, A. Rajab, A. Shaikh, H. Song, and A. Farouk, "QoS review: smart sensing in wake of COVID-19, current trends and specifications with future research directions," *IEEE Sensors Journal*, vol. 7, no. 4, pp. 125–136, 2022.

[15] J. S. Kim, "Emotional labor strategies, stress, and burnout among hospital nurses: a path analysis," *Journal of Nursing Scholarship*, vol. 52, no. 1, pp. 105–112, 2020.

[16] A. A. Grandey, G. M. Fisk, and D. D. Steiner, "Must "service with a smile" be stressful? The moderating role of personal control for American and French employees," *Journal of Applied Psychology*, vol. 90, no. 5, pp. 893–904, 2005.

Hindawi
Mobile Information Systems
Volume 2022, Article ID 6215736, 8 pages
https://doi.org/10.1155/2022/6215736

Research Article

Human-Computer Interaction System Application in Hotel Management Teaching Practice

Xueyan Ding[1] **and Yi Zhang**[2]

[1]*Wuhan Polytechnic, Wuhan, Hubei 430074, China*
[2]*School of Electronic Commerce, Jiujiang University, Jiujiang, Jiangxi 332005, China*

Correspondence should be addressed to Xueyan Ding; 30963100@wtc.edu.cn

Received 13 May 2022; Revised 17 June 2022; Accepted 29 June 2022; Published 12 July 2022

Academic Editor: Shadi Aljawarneh

With the increasing demand for the performance and security of communication networks, the fifth-generation mobile technology has developed rapidly and has attracted unprecedented attention. At the same time, this article analyzes the current research status of visual gesture recognition and human-computer interaction based on the Internet of Things. In view of the current shortcomings of gesture recognition, this article proposes a solution that involves using Biaonect somatosensory sensors to recognize gestures and explore human-computer interaction. Then, we analyze how the Kinea somatosensory sensor works to obtain depth images, study the method of obtaining gesture positions and joint points based on the depth information, and combine the depth information and the skin color model to create a three-dimensional image of the gesture simulation. With the rapid development of China's tourism industry, China's hotel industry has entered an era, in which domestic and foreign competitors coexist in the hotel industry. The development of hotels urgently needs high-quality hotel professionals who have received professional training and are familiar with hotel management. In hotel management teaching, human-computer interactive learning can effectively improve learning interest. In this paper, the structure of the human-computer interaction system based on gesture recognition is established, which can effectively improve the recognition accuracy and is of great significance in the hotel management teaching system.

1. Introduction

This article mainly introduces the background of 5G security certification network technology research, outlines the security threats and security requirements of 5G networks, and analyzes the current status of security certification technology research at home and abroad [1]. At the same time, we introduced the main research content of this article and the structure of this article. 5G wireless networks are flexible, open, and highly heterogeneous. It can not only provide traditional voice and data transmission but can also be applied to scenarios such as the Internet of vehicles, smart grids, smart cities, and smart healthcare [2]. Although the 5G network is convenient for people to use, it also faces various security and performance issues, such as protecting user privacy, safe data transmission, restricted access, and limited resources [3]. Since the data sent by the sender contain a large amount of confidential information, when data are lost during data transmission, it will cause immeasurable losses to the user. Therefore, safe data transmission is very important [4]. In recent years, people have put forward higher and higher requirements for the performance and security of communication networks, and the fifth-generation mobile technology is developing rapidly. The 5 G network is a new generation communication system designed to meet the mobile communication needs after 2020 [5]. It comes from the 4G network. 5G provides faster connectivity, more bandwidth, better connection services, and better business experience. The 5G network structure is characterized by flexibility, openness, and high heterogeneity [6]. At present, the rapid development of 5G network systems is also conducive to the development of China's hotel tourism industry, which is an emerging industry. In recent years, with China's accession to the WTO, China's tourism industry has

developed rapidly and has entered an era of global competition. With the development of tourism, China's hotel industry has also become a promising point of economic growth [7]. According to hotel management practice (usually referred to as school education), it is organized and managed by the school according to the rules and objectives of the talent education plan through two methods of on-campus simulation learning and off-campus internship to adapt to the professional development of students, so as to adapt to the professional development of students and the application process of on-site education in practical training [8]. This major has been highly applied, and hands-on learning has become an important means and link for students to combine theory with practical work. Students will hone their professional skills in practical classes and improve their professionalism [9]. Through hands-on learning, the school continuously discusses the impact of educational methods on talent development, improves the quality of teaching, and then improves the practical training of hotel management to improve professional development [10].

2. Related Work

The literature pointed out that as IoT technology has been integrated into people's lives, more and more IoT terminals need to be connected to the network to meet the diverse needs of users [11, 12]. Today, there are more than 20 billion connected devices worldwide. Ericsson predicts that by 2021, the number of connected devices will grow to nearly 28 billion. In the future, 5G networks will support simultaneous access of a large number of users and devices and provide security guarantees for the realization of the "Internet of Everything". Therefore, 5G networks must not only continue to face the challenges of mobile Internet services [13]but alsoimprove spectrum efficiency and user data rate, reduce latency and increase mobility, and meet the various needs of IoT services. In the "Internet of Everything" scenario, the 5G security mechanism must not only protect a large number of access devices but also ensure that users will not lose information when the access devices exchange messages with the network [14]. The literature knows from the theory of pedagogy that there are three factors that determine education: one is the teacher, the other is education, and the third is the means of education. Education is the bridge between them [15]. Appropriate educational measures can not only educate educated people so that they can learn and benefit from it, but they can seamlessly and perfectly achieve their educational goals and contribute to society. According to the alternative education model of "study-work-study", the school avoids the vicious circle of high investment and low efficiency. It can not only use the technical characteristics, atmosphere, and environment of high-end hotels to achieve educational goals but also improve the quality of learning. Internships in international brand hotels not only improved their language skills and professional knowledge but also opened up the world, broadened their horizons, strengthened their self-confidence, and laid a good foundation for their future careers [16].

3. Human-Computer Interaction Systems

3.1. Sensor-Based Human-Computer Interaction System. 5G network is a new generation of communication system designed to meet the needs of mobile communication after 2020. It comes from 4G network. It can be seen from the network structure analysis that the 5G network is mainly composed of two parts: the access network and the core network, as shown in Figure 1.

In a visual gesture interaction system, it is very important to accurately track and recognize gestures. Formulas (1) and (2) show the conversion between YCbCr color space and RGB color space, which proves

$$\begin{bmatrix} Y \\ Cb \\ Cr \end{bmatrix} = \begin{bmatrix} 0.2290, 0.5870, 0.1140 \\ -0.1687, -0.3313, 0.5000 \\ 0.5000, -0.4187, -0.0813 \end{bmatrix} \begin{bmatrix} R \\ G \\ B \end{bmatrix}, \tag{1}$$

$$\begin{bmatrix} R \\ G \\ B \end{bmatrix} = \begin{bmatrix} 1, 1.40200, 0 \\ 1, -0.34414, -0.71414 \\ 1, -1.77200, 0 \end{bmatrix} \begin{bmatrix} Y \\ Cb - 128 \\ Cr - 128 \end{bmatrix}. \tag{2}$$

Use human skin color samples of different races to train the Gaussian model, the average vector $m = (\overline{C}b, \overline{C}r)$ in the YCbCr space, such as the following formulas:

$$\overline{C}b = \frac{1}{N} \sum_{i=1}^{N} Cb_i, \tag{3}$$

$$\overline{C}r = \frac{1}{N} \sum_{i=1}^{N} Cr_i. \tag{4}$$

The covariance matrix C is shown as the following formula:

$$C = \begin{bmatrix} \sigma_{CbCb}, \sigma_{CbCr} \\ \sigma_{CrCb}, \sigma_{CrCr} \end{bmatrix}. \tag{5}$$

Using the hue vector value of the input pixel $x = [Cb, Cr]^T$, the probability that it is the skin color is shown as the following formula:

$$p\left(\frac{x}{\text{skin}}\right) = \exp\left[-\frac{1}{2}(x-m)^T C^{-1}(x-m)\right]. \tag{6}$$

When using the Gaussian mixture model to create a skin color model, the formula is as follows:

$$\begin{aligned} x &= [Cb, Cr]^T, \\ x &= [Cb, Cr]^T. \end{aligned} \tag{7}$$

Among them, $P(j)$ represents the weight of the jth element, and M represents the number of elements in the Gaussian distribution, so the jth Gaussian distribution can be expressed as the following formula:

$$p\left(\frac{x}{j}\right) = \frac{\exp\left[-(1/2)(x-m)^T C^{-1}(x-m)\right]}{2\pi\sqrt{\left|C_j\right|}}. \tag{8}$$

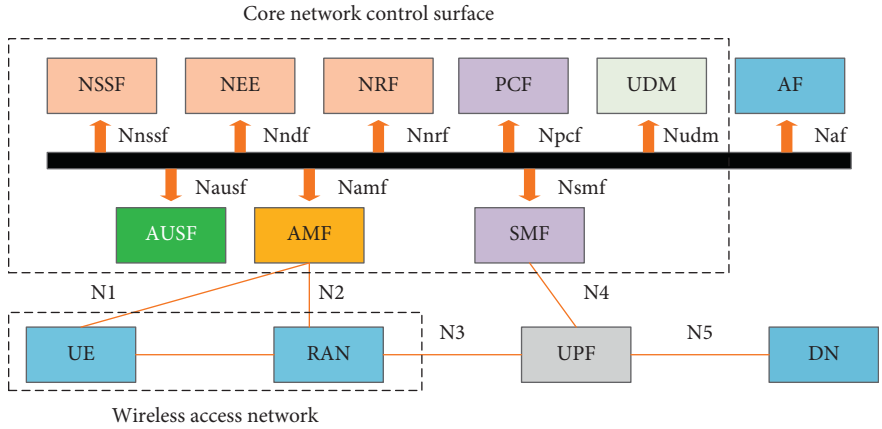

Figure 1: 5G network architecture diagram.

Among them, m_j and C_j, respectively, represent the mean vector and covariance matrix of the jth Gaussian distribution, and $P(j)$ satisfies the following formula:

$$\sum_{j=1}^{M} P(j) = 1, \quad 0 \le P(j) \le 1. \tag{9}$$

The ellipse limit model is defined as the following formula:

$$\varphi(c) = (c-\varphi)^T \Lambda^{-1} (c-\varphi), \tag{10}$$

where c is the color vector, and the model training process includes two stages: first, exclude more than 5% of low-frequency training color samples to eliminate noise and trivial data. Second, estimate the model parameters (Φ and Λ) as the following formula:

$$\begin{aligned} \varphi &= \frac{1}{n}\sum_{i=1}^{n} c_i, \\ \Lambda &= \frac{1}{N}\sum_{i=1}^{m} f_i \cdot (c_i-\mu)(c_i-\mu)^T. \end{aligned} \tag{11}$$

Each Haar-Like element is composed of two or three interconnected "black" and "white" rectangles. The $f(x)$ value of the hairy element is the difference between the sums of pixel values in the black and white rectangles, as shown in the following formula:

$$f(x) = \sum_{\text{black}} (\text{pixelvalue}) - \sum_{\text{white}} (\text{pixelvalue}). \tag{12}$$

The "integrated image" at the pixel position (x, y) contains the sum of the above-mentioned pixel value and the pixel value on the left side of the pixel, that is, as shown in the following formula:

$$P(x,y) = \sum_{x' \le x, y' \le y} p(x', y'). \tag{13}$$

According to the definition of "integral image", the sum of pixel values BIII can be calculated as the following formula:

$$P_{\text{SUM}} = P_1 + P_4 - P_2 - P_3. \tag{14}$$

Among them, there are $P_1 = A, P_2 = A + B, P_3 = A + C$, $P_4 = A + B + C + D$.

The corresponding weak classifier corresponds to the Haar-like feature fj is defined as the following formula:

$$h_j(x) = \begin{cases} 1, & p_j f_j < p_j \theta_j, \\ 0, & \text{other}. \end{cases} \tag{15}$$

They are mainly used in robotics research, interactive games, and other fields. The principle of 3D laser scanning is to use laser beams to obtain PointCloud data from spatial coordinates through rapid scanning technology. This technology can quickly create complex nonstandard scenes. The principle of structured light is to first emit structured light, and then the device directs a controlled light spot, light strip, or smooth surface structure to the target surface to be measured. Then, the camera captures the image and uses the principle of triangulation to calculate the 3D coordinates of the target from the image.

If the target is near the infrared camera, the reflected light spot from the target is captured again. At this time, the light spot should move a distance d in the image plane. According to the type of such triangles, formulas (16) and (17) are applied:

$$\frac{D}{b} = \frac{Z_0 - Z_k}{Z_0}, \tag{16}$$

$$\frac{d}{f} = \frac{D}{Z_k}. \tag{17}$$

The following formula is obtained:

$$Z_k = \frac{Z_0}{1 + (Z_0/fb)d}. \tag{18}$$

According to formula (18), the target depth can be calculated from the displacement image, and the parameters Z_o, f, and b are known. In addition, the plane coordinates of each target point can be obtained by replacing the coordinates of the image, such as the following formulas:

$$X_k = -\frac{Z_k}{f}(x_k - x_0 + \delta_x), \tag{19}$$

$$Y_k = -\frac{Z_k}{f}(y_k - y_0 + \delta_y). \tag{20}$$

Among them, x_k and y_k are the coordinates of the point image, x_0 and y_0 are the original coordinates, which are the lens distortion coefficients.

According to the received information about the depth of a given pixel x, the feature is calculated according to the following formula:

$$f_\theta(I, x) = d_I\left(x + \frac{u}{d_I(x)}\right) - d_I\left(x + \frac{v}{d_I(x)}\right), \tag{21}$$

where dl (x) is the depth of image I in pixel x, and the parameter $\theta = (u, v)$ describes the displacement of u and v.

In the distribution probability PI $(c \mid I, x)$ after training, the following formula can be obtained:

$$P(c|I, x) = \frac{1}{T}\sum_{i=1}^{T} P_i(c|I, x). \tag{22}$$

Train each tree on a different set of random synthetic images, the learning algorithm is as follows.

Divide φ sample $Q = \{(I, x)\}$ into two parts, such as the following formulas:

$$Q_I(\varphi) = \{(I, x)|f_\theta(I, x) < \tau\}, \tag{23}$$

$$Q_r(\varphi) = \frac{Q}{Q_I(\varphi)}. \tag{24}$$

The maximum amount of information acquisition can be calculated, namely, the following formulas:

$$\varphi^* = \arg\max_{\varphi} G(\varphi), \tag{25}$$

$$G(\varphi) = H(Q) - \sum_{s\in(I,r)} \frac{|Q_s(\varphi)|}{Q} H(Q_s(\varphi)). \tag{26}$$

If the maximum gain $G(\varphi^*)$ is still very high and the depth of the tree has not reached the maximum, the recursive operation continues on the left $Q_l(\varphi^*)$ and right subset $Q_r(\varphi^*)$ of the sum.

Determine the estimated density of each body part, as shown in the following formula:

$$f_e(\hat{x}) \cdot \sum_{i=1}^{N} w_k \exp\left(\left\|\frac{\hat{x} - \hat{x}_i}{b_c}\right\|^2\right), \tag{27}$$

where $\hat{x}$ is the coordinate in the space, w_{ic} is the number of pixels in the image, $\hat{x}_i$ is the weight of the pixel, $d_l(x_i)$ represents the coordinate of the projected pixel x_i according to the spatial depth, and b_c represents the width of the formed component.

3.2. Human-Computer Interaction System. Gestures can indicate a person's intention to operate a robot. Therefore, this article creates a human-computer interaction system structure based on gesture recognition for the platform. As shown in Figure 2, the structure of the human-computer interaction system based on gesture recognition includes two main processes: learning and recognition. Feature extraction module: extract important and unique features of the hand.

4. Construction of Hotel Management Teaching Practice System

4.1. Analysis of the Status Quo of Hotel Management Practice Teaching. According to industry feedback, there are two main drawbacks. First, it cannot ensure the sustainable development of practical skills and student innovation capabilities. Second, there are many traditional practice projects that are usually all-encompassing. Students cannot choose projects that are not beneficial to their personal needs and self-development. Practical training is a relatively independent learning system and does not contribute to the development of students' comprehensive qualities and skills, so it has not been strengthened or researched. General education colleges and universities have relatively clear educational goals for students who specialize in hotel management, but a common problem is that the practical learning goals of various tourism schools are not accurately set. It is mainly manifested in the following: firstly, there is no independent practical training plan; secondly, the content of practice does not completely correspond to the theoretical teaching, which is not conducive to improving the students' ability to use knowledge; secondly, the lack of practice, and greatly reduced the impact of the internship, and finally there was no improvement in the actual realization of the dungeon goal.

Most of the reception internships are based on knowledge, almost all of them are completed by one person, and most of them are based on the mastery of operational skills. In the past, practice courses in hotel management have taken cognitive exercises as their main goals. From the actual training of graduates, the lack of training in the field of hospitality and management, and the lack of information content, trying to use them is a shortcoming in current practice. Due to the school environment, the relationship between the actual hotel management classrooms is very weak, and the actual classrooms in the simulated classrooms are seriously lacking in equipment and related audio-visual materials, resulting in unstable learning outcomes.

By creating a talent learning model that combines hands-on learning with work and learning, a unique and dynamic teaching team must be created. In addition to teaching, teachers must be able to work. Teachers of this major should also go to the company to guide interns during the six-month internship provided by the company for students, so that teachers not only gain relevant theoretical knowledge

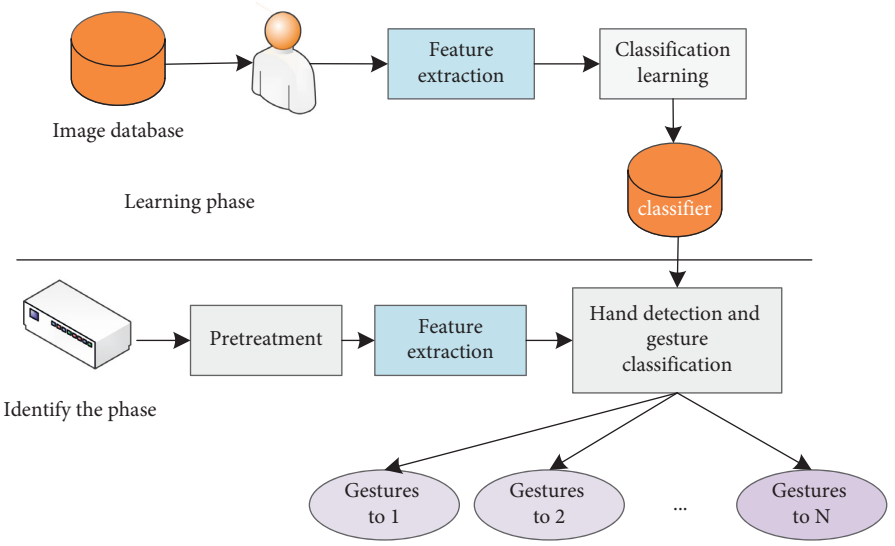

Figure 2: Gesture recognition framework.

Table 1: Internship courses for major subjects of hotel management in tourism vocational school.

Order	Time	Detailed arrangement	Plan implementation	Target setting	Internship period
1	First semester	Enterprise probation for one week; professional introduction	Participate in major hotels in a certain city to introduce the spirit of enterprise and industry characteristics	Preliminarily set a role to lay a foundation for the theory and form a preliminary understanding of the hotel management major	Short-term internship
2	Second semester	Four weeks of in-school training	Department leaders, professional teachers, etc., introduce the professional situation	Experience the working status of the hotel; take the vocational skills qualification test	Short-term internship
3	Third semester	Graduation internship	Submarine training; guest room training; etiquette training; catering training	Experience real work, accumulate experience, and exercise ability; be able to deal with and deal with problems at work alone	Long-term internship
4	Fourth semester	Internships around companies	The team is led by the internship instructor and enters all hotels for on-the-job internship work; the company will officially take up the job after one week of training, and the training will be led by the "mentor and apprentice" of old employees	Can be fully qualified for the grassroots work and various management tasks of various departments of the hotel	Long-term internship

but also gain practical experience and continuously improve their level. As the size of the university continues to expand, a large number of young teachers have taken up teaching positions. However, most teachers are scholars and have no practical experience. In hotel management courses, teachers not only master all technical skills but also have appropriate positions to practice, otherwise they will not be able to lead students well. The learning connection between internship and work/study combination not only puts forward new requirements for students but also puts forward new challenges for teachers. On the basis of mastering the practical skills of literacy, teachers should pay attention to the communication and interaction with the hotel in order to respond to the various problems of the practical class students in a timely manner. Teachers are accustomed to the learning environment of the school, and they urgently need to improve their ability to solve the professional and ideological problems of students during the internship.

Most hotel management majors in higher education management majors adopt another mode of talent training. The course stipulates that the proportion of practical training should not be less than 40%, and it focuses on cultivating students' practical skills. Most of the hands-on learning is carried out in off-campus internships in Hong Kong, such as hotels, and only a small part of them are taught on campus. In order to understand the possibilities and methods of strengthening the hotel management professional practice training in higher professional colleges, the author provides a detailed description in Table 1 based on the hotel management professional (two-year) practice training method.

According to market demand, schools and companies will form a professional steering committee to adjust the

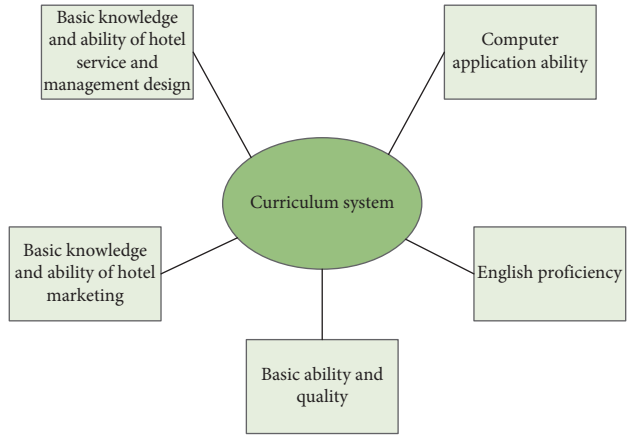

Figure 3: Professional hotel management course system scheme of tourism vocational school.

curriculum system and revise the curriculum in time, taking into account, the changes in professional skills requirements, that is, adjusting the parameters of the curriculum and the content of the curriculum. The application-based curriculum system is used in the main professional courses. On this basis, the subject of the course is determined, the content of the training is selected, training modules are developed, and the skill modules required for professional positions are determined in advance. Create a set of application systems that emphasize hands-on learning, professional knowledge, and professional skills. The course system is shown in Figure 3.

In the practical training system, there is only one theoretical course in each specific academic year, that is, there is no sub-target system for student skills, no specific goals and plans for various skills, no courses for practice, and no ability to improve students' skills. The specific annual target curriculum also does not include norms for cultivating students' practical and management skills.

We use questionnaires and interviews to track the internship status of hotel management students, as shown in Table 2:

Table 2: Satisfaction survey of hotel management trainees in the internship program.

Project	Evaluation grade	Percentage of people (%)
Internship	Satisfaction	2.0
	Basically satisfied	9.1
	Dissatisfied	7.0
Internship treatment	Poor	1.6
	General	95.9
	Better	1.6
	Great	0
Did the internship achieve the goal	Can achieve the goal	7
	Partially achieved the goal	81
	Cannot achieve the goal	12
Recognition of the profession after the internship	Know it better	61
	Relatively vague	31
	Cannot understand	8
Interns' views on the rationality of the internship plan	Reasonable	27
	Basically reasonable	38
	Unreasonable	30
	Still to be reformed	5

4.2. Construction and Implementation Countermeasures of Hotel Management Practice Teaching System. At present, postgraduate professional education is the most practical level of talent training for hotel management majors, and it is most suitable for industry needs. As far as the type of industry is concerned, the hotel industry is a capital-intensive and labor-intensive industry that requires a large number of highly skilled and high-quality personnel to serve and manage front-line personnel rather than high-precision machines. From the perspective of the education level of talents, the development of society, and their gradual integration into the international level, the demand for talents in the hotel industry is becoming more and more professional and better quality. It was replaced by highly educated employees, especially famous international hotel management groups. The requirements for talents and selection are higher, and the requirements for language skills are higher.

Quality and image are indispensable. Regrettably, the tension between industry development and talent shortage has become more and more obvious. On the one hand, the hotel pursues high-quality talents. On the other hand, some college and university hotel graduates are used as theories to introduce the "two skins" phenomenon. Without contact with practice, they cannot meet the needs of hotels. Moreover, many graduates are unable to meet the professional characteristics of the hotel industry from basic to professional transition, and in vain to upgrade the hospitality industry talent management major. Considering the hotel industry's thirst for talents, what kind of training model should be adopted to ensure that hotel graduates can not only meet industry requirements but also firmly

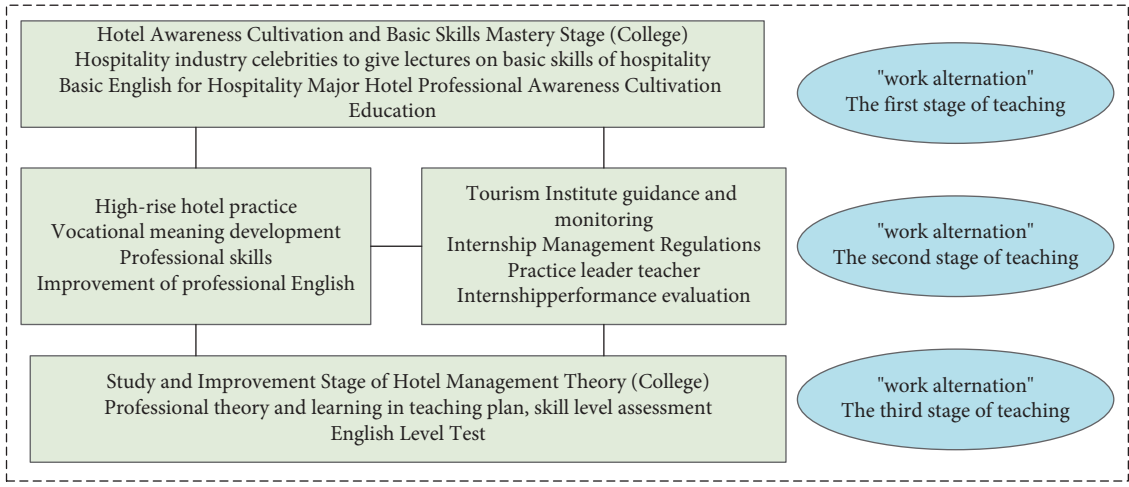

Figure 4: Three-step progressive diagram of the work-learning change learning process.

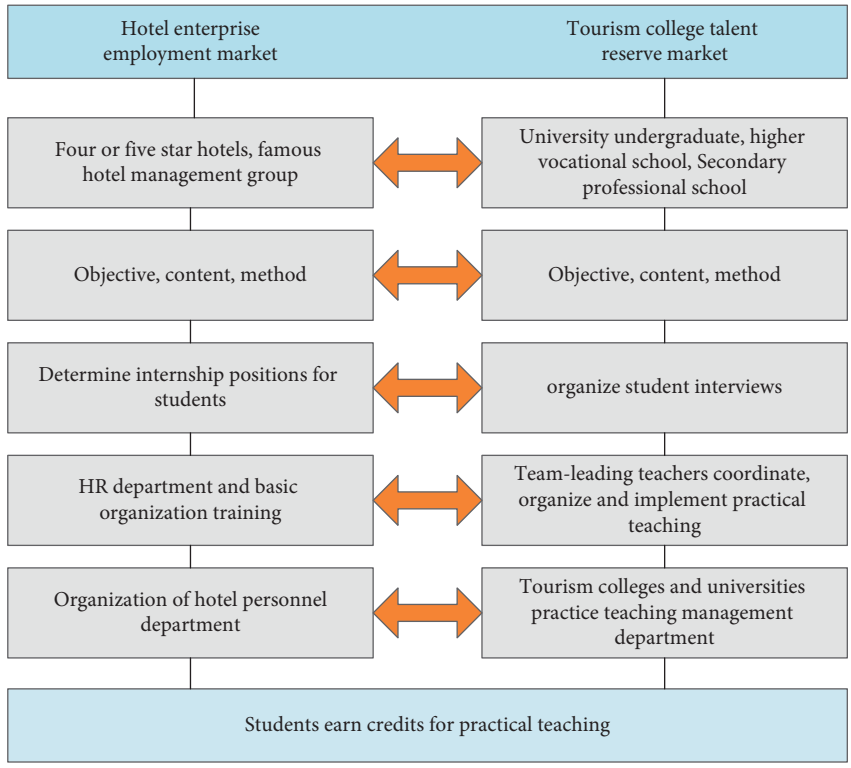

Figure 5: The organization and coordination plan of the company and school internship process.

establish a position at the forefront of hotel companies and gradually become the backbone of hotel services and management? This is a practical problem that the hands-on learning model is trying to solve. Since 2020, we have been trying to implement the "work-study" training model for the hotel management profession. In the implementation process, we usually divide the learning process of "changing jobs and learning" into three stages, as shown in Figure 4.

Figure 5 shows the process of organizing and coordinating the collaboration between the school and the company in the work-learn-alternate learning model.

5. Conclusion

With the continuous development and innovation of communication technology, 5G is a new generation of mobile communication technology, and its research value is obvious. On the one hand, the deep integration of vertical industries and cellular networks in the 5G era has led to more application scenarios, including simultaneous access to large IoT devices with limited resources, such as unattended sensors, sensors, and connected car components. On the other hand, the security model of the traditional network

architecture is no longer applicable, and the terminal faces greater security challenges. It is expected that the 5G security mechanism will ensure the security of communication in several application scenarios. Privacy and security authentication are the main issues facing 5G networks. This article analyzes the security threats faced by IoT endpoints and 5G networks during the communication process, including eavesdropping, replay attacks, forgery attacks, and DOS attacks, as well as the shortcomings of IoT scenarios (large scale), and defines the security requirements to meet the communication process. What needs to be done. Then, the hair-like function is used to extract the features of the gesture, which provides a good foundation for recognizing the gesture. Under the guidance of system theory, this article is based on the reform of hotel management professional practice teaching, and on the basis of the collected survey data, the current situation and existing problems of the hotel management system are obtained, referring to the professional staff of our hotel industry. On the basis of in-depth reading, the practical education system will be reformed. The purpose is to define and improve the core, content system, management system, and evaluation system needs around the target system.

Data Availability

The data used to support the findings of this study are available from the corresponding author upon request.

Conflicts of Interest

The authors declare that they have no conflicts of interest.

References

[1] M. Shafi, A. F. Molisch, P. J. Haustein, T. Haustein, and P. Zhu, "5G: a tutorial overview of standards, trials, challenges, deployment, and practice," *IEEE Journal on Selected Areas in Communications*, vol. 35, no. 6, pp. 1201–1221, 2017.

[2] P. Schulz, M. Matthe, H. Fettweis et al., "Latency critical IoT applications in 5G: perspective on the design of radio interface and network architecture," *IEEE Communications Magazine*, vol. 55, no. 2, pp. 70–78, 2017.

[3] S. Zhang, Q. Wu, S. Xu, and G. Y. Li, "Fundamental green tradeoffs: progresses, challenges, and impacts on 5G networks," *IEEE Communications Surveys & Tutorials*, vol. 19, no. 1, pp. 33–56, 2017.

[4] T. A. Zerihun, M. Garau, and B. E. Helvik, "Effect of communication failures on state estimation of 5G-enabled smart grid," *IEEE Access*, vol. 8, pp. 112642–112658, 2020.

[5] L. Lin, B. Qi, B. Li, X. Ye, and W. Mei, "Requirements and developing trends of electric power communication network for new services in electric Internet of Things," *Power System Technology*, vol. 44, no. 8, pp. 3114–3130, 2020.

[6] J. Tao, M. Umair, M. Ali, and J. Zhou, "The impact of Internet of Things supported by emerging 5G in power systems: a review," *CSEE Journal of Power and Energy Systems*, vol. 6, no. 2, pp. 344–352, 2019.

[7] T. C. Canada, "Tourism, that's your business," *A programme of financial management for the Canadian hotel industry, " Study Guide*, vol. 52, no. 12, pp. 22–36, 1983.

[8] M. Adil, J. Ali, M. Attique et al., "Three Byte-Based Mutual Authentication Scheme for Autonomous Internet of Vehicles," *IEEE Transactions on Intelligent Transportation Systems*, vol. 12, 2021.

[9] C. Burgess, "The hotel financial manager - challenges for the future," *International Journal of Contemporary Hospitality Management*, vol. 12, no. 1, pp. 6–12, 2000.

[10] C. L. Burgess, "The hotel financial controller: a member of the management team," in *Accounting and Finance for the International Hospitality Industry*Butterworth-Heinemann, Oxford, 1998.

[11] Z. Jia, "Problems and countermeasures in financial management of a star hotel in Shenzhen," *Research on Communication Power*, vol. 3, no. 6, pp. 185–187, 2019.

[12] S. Borkar and H. Pande, "Application of 5G next generation network to Internet of Things," in *Proceedings of the 2016 International Conference on Internet of Things and Applications (IOTA)*, pp. 443–447, Pune, October 2016.

[13] N. Zhang, J. Yang, Y. Wang, Q. Chen, and C. Kang, "5G communication for the ubiquitous Internet of Things in electricity: technical principles and typical applications," *Proceedings of the Chinese Society for Electrical Engineering*, vol. 39, no. 14, pp. 4015–4025, 2019.

[14] L. I. Lin, "Innovation and development of financial management in modern hotel industry," *Management & Technology of SME*, vol. 27, no. 1, p. 6, 2019.

[15] Y. Aoudni, C. Donald, A. Farouk et al., "Cloud security based attack detection using transductive learning integrated with Hidden Markov Model," *Pattern Recognition Letters*, vol. 157, pp. 16–26, 2022.

[16] K. L. Xie, K. K. F. So, and W. Wang, "Joint effects of management responses and online reviews on hotel financial performance: a data-analytics approach," *International Journal of Hospitality Management*, vol. 62, no. 62, pp. 101–110, 2017.

Hindawi
Mobile Information Systems
Volume 2022, Article ID 6922615, 11 pages
https://doi.org/10.1155/2022/6922615

Research Article

Social Media Information Credibility Based on User Perception and Cloud Computing System

Zhen Dai[1] **and Hongxiao Fei**[2]

[1]*School of Software, Hunan Vocational College of Science and Technology, Changsha, Hunan 10004, China*
[2]*School of Computer Science and Engineering, Central South University, Changsha, Hunan 410012, China*

Correspondence should be addressed to Hongxiao Fei; hxfei@csu.edu.cn

Received 13 May 2022; Revised 8 June 2022; Accepted 24 June 2022; Published 11 July 2022

Academic Editor: Shadi Aljawarneh

While people enjoy the convenience brought by more and more technological developments, its importance is also more widely known. Big data and cloud computing are the two most typical representatives of many new information technologies, and their combination is also the general trend. But big data will also have privacy and security issues in cloud computing. Displayed security mechanisms and implicit security mechanisms are the two main directions for discussion, so that user privacy and security can be in the big data that it is well guaranteed when processing the calculations and storage. The rapid development of social media has been widely used, but it has also brought new social problems, such as the increasing difficulty of verifying the authenticity of information. This article will discuss the influence of the credibility of social media on the credibility of social media from the perspectives of the credibility of the communicator and the information media, the quality of the information, the reason for the transmission, and the form of expression. The influence on information credibility and information quality is the relationship between information credibility and other influencing factors when trust tendency and information involvement have become moderating variables.

1. Introduction

The ways of obtaining information on the Internet are becoming more and more diversified under the promotion of Internet technology. Compared with the situation in which users passively receive information in traditional media, online media provides a relatively free expression space for a broad audience [1]. Users can not only receive network information, but also publish information and become information producers. This breaks the situation of passive information dissemination in the past. At the same time, information exchange and sharing are also completed in this process [2]. According to an article titled "Statistical Report on China's Internet Development Status" published by the China Network Technology Information Center on August 2019, in June 2019, China's Internet users had exceeded 800 million people, and the Internet penetration rate had exceeded 60%. With the improvement of network construction and the improvement of living standards, more and more individuals have joined the Internet application team. People communicate, entertain, and work through the Internet, making Internet applications gradually become an integral part of people's lives [3]. There are many types of products in the current network application market, and there are many communication and comprehensive social media [4]. The communication application software is mainly based on Tencent's QQ and WeChat, which can meet the basic social needs of the public and has a high usage rate. The integrated social application tools are mainly represented by Weibo and WeChat Moments, allowing users to enjoy, express yourself, and make new friends, and some social software provides users with social information consultation in certain areas, such as information and live video through the user's social circle, so that the information spread faster and promote to drive the rapid development of vertical social applications, further enrich the content of

social platforms, and enhance the user stickiness [5]. Mary Meeker emphasized in the "2019 Internet Trend Report" that short videos have promoted the growth of Internet traffic and usage time in China. The widespread use of new media systems such as short videos has changed the way people communicate and broke the pattern of traditional media and the law of information dissemination [6].

With the rapid advancement of information technology, human life has undergone earth-shaking changes. The benefits of this innovation are being enjoyed by more and more people, and its importance is gradually being recognized by more and more industries. Big data and cloud computing are undoubtedly the two most prominent examples of all new technologies, and the combination of the two has become an inevitable trend [7]. Like all network information technologies, user information security problems often appear with the network, and this problem also exists widely in cloud computing platforms [8]. This article will focus on solving this problem, starting from a safe mechanism, to make users trust the big data platform more.

2. Related Work

The literature found through combining the previous research results that the research on the credibility of social media information continues the research methods in traditional media, starting from the perspectives of information sources, information quality, information dissemination media, and user characteristics. We have researched and explored the influence mechanism of relevant factors [9]. The literature takes the Facebook platform as the research object, uses the detailed as much as possible model (ELM model) to determine the research factors of information credibility from the two aspects of information media and content, and establishes a research model to predict the individual's socialization perception of the credibility of information in the media platform. The results show that media dependence, content interaction, and the intensity of argumentation are important factors in judging the credibility of information [10]. Literature studied the influencing factors of the credibility of Weibo information, and pointed out that the internal characteristics of the information such as the number of repetitions, reposting, and the number of related hashtags in social media platforms and the number of fans of the author, authentication level, and other users' basic characteristics are the main factors affecting the credibility [11]. The Literature mainly conducts research from multiple aspects such as information source and content, information evaluation, and user's feelings and characteristics in order to build a model, and study the relationship between various elements through the ANP and DEMATEL systems [12]. The Literature pointed out that the objectivity, completeness of the content, the professionalism of the information source, the authority, and the motivation for publishing are important factors influencing the credibility of the virtual Q&A community, providing a reliable basis for relevant communities to enhance the credibility of the knowledge content [13]. Through a large amount of data analysis, the literature found that whether the information content is useful, objective, and whether it is related to reality will affect users' judgments on the credibility of social media information [14].

3. Construction of Cloud Computing Security Privacy System Based on User Perception

3.1. Cloud Computing System Framework. SaaS, PaaS, and IaaS are the three operating modes of cloud computing platforms. SaaS software is the service mode, and it can provide external services with the support of suppliers. This software does not require users to store and maintain their own data. But through the purchase of services to complete their tasks, and only need customers to purchase this service to obtain results. The PaaS platform is a form of service. This model of cloud service providers provides users with a computing platform. Users use the platform to create and develop applications. Users use the computing functions of the platform to design and develop software, which can also reduce costs. The IaaS platform is a service method, which reduces the cost of user monitoring infrastructure, and only needs to control and detect the operation process to maximize the benefits. Flow chart of cloud computing is shown in Figure 1.

The key to cloud big data lies in the storage and use of data. Therefore, it will inevitably encounter the problem of security and privacy protection. Compared with general data, big data has a longer storage time and can be accessed and used more frequently, but the privacy of customers is safe. The index is greatly reduced in the environment of big data, and there is a risk of data tampering. The information contained in big data is extremely valuable. Once leaked, it will cause huge losses to the company, country, department, or individual. The privacy and security issues caused by big data platforms are mainly concentrated in the following areas: the staff of big data companies may maliciously leak or use user information. Users of big data do not know where their information is stored, and there is no way to control their information. In the process of data uploading, user information is more likely to be stolen. At the same time, the big data environment is very complicated. The limitation of basic facilities and the intrusion of outside criminals make it easier for users to expose their personal privacy. Not only in the upload process, but also in the processing process, there are also high risks. When the data is processed by the platform, many technologies and encryption methods are not very reliable. These factors increase the security risk. Secondly, big data has the characteristics of liquidity and sharing, which undoubtedly caused great difficulties for management. Many problems such as account tampering, intrusion, identity theft, authentication errors, and password errors may bring many abuses and even cause privacy issues to users in the problem of leakage. However, the protection of user privacy and security is the basis for the widespread use of big data technology and an inevitable condition for its long-term development. Nowadays, the rapid development of network technology, network security, privacy security, and user information security are closely related, and the lack of any link cannot enable the long-term development of

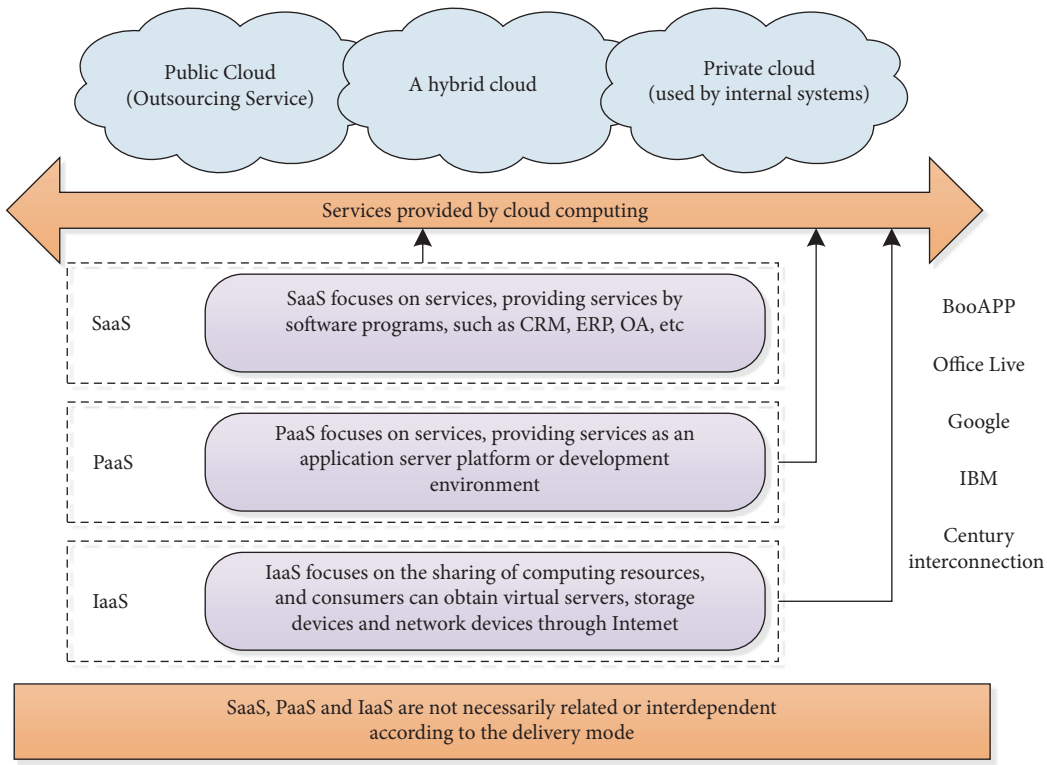

Figure 1: Flow chart of cloud computing.

big data cloud computing. The importance of user privacy and security is undoubtedly to gain the trust of users and improve the credibility of this technology, so as to attract more and more users and supporters in exchange for the long-term development of this technology. If a big data company wants to achieve results in privacy protection, it must devote itself to the research and development of technical directions, isolate hackers, and network viruses from the security barrier, so that the users of the information have the sole right to use the information. At the same time, in terms of law, enacting laws related to big data can effectively prevent some criminals from destroying the big data environment. Therefore, perfecting the law and speeding up the legislative process can fundamentally safeguard customer information privacy. Technical R&D personnel must continuously improve algorithms, strengthen the development of information protection technology, and improve related systems in experiments. When users use the big data platform, the protection of their personal information has aroused great attention from the society. If the big data platform wants to achieve long-term development, it is essential to improve privacy and security. Cloud computing big data platform is shown in Figure 2.

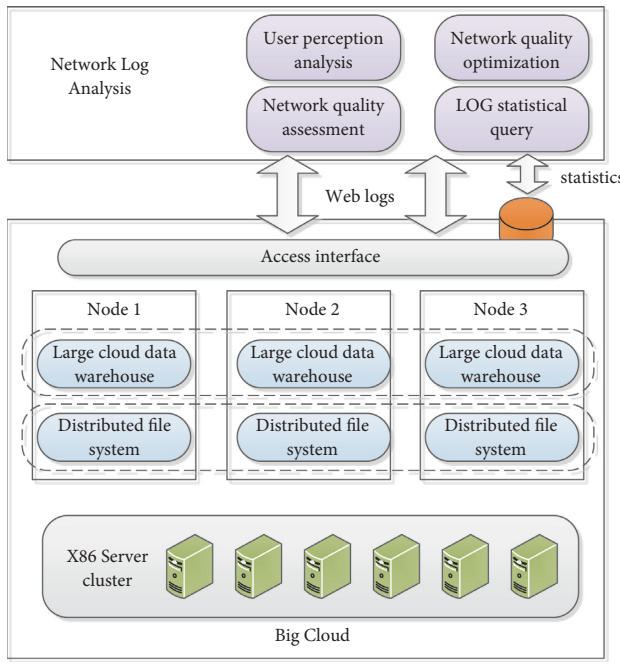

Figure 2: A cloud computing big data platform.

3.2. Design and Optimization of Security and Privacy Protection Schemes Using Implicit Mechanisms. Comparing the implicit mechanism with the encryption mechanism, its most prominent feature is that it solves the problem of passwords. This article will mainly discuss the use of invisible mechanisms to protect the privacy of customers. After the system is optimized, if thieves want to steal information and data, they must understand the encrypted information in the system. In real life, this is impossible to achieve, which adds a powerful barrier to information security. At the same time, the method of information calculation has also been optimized. After optimization, multiple cloud servers are used

simultaneously, and addition and multiplication are performed at the same time. According to this principle:

$$x^k + a_{k-1}x^{k-1} + \cdots + a_1 x + a_0 = 0. \tag{1}$$

Another way of writing it:

$$(x - r_1)(x - r_2)\cdots(x - r_k) = 0. \tag{2}$$

According to the nature of the univariate polynomial, we substitute data to obtain the following formula:

$$x^k + \sum_{i=1}^{k-1} a_{k-1}x^{k-1} \overline{=} 0 \bmod p. \tag{3}$$

The above formula can be converted to:

$$\prod_{i=1}^{k} \overline{(x - r_i)} = 0 \bmod p. \tag{4}$$

And so:

$$\prod_{i=1}^{k} \overline{(x - r_i)} = 0 \bmod p. \tag{5}$$

When data is stored in chunks on one or more servers, they cannot be transferred to each other through the network, so the users need to recreate the data through the available data chunks. In this solution, the user expands the data subblock from part to the whole, where this part needs to be integrated to rebuild the data, as shown in Figure 3 for the data partition storage model.

Construct a linear equation:

$$\begin{aligned} &a_{11}r_1 + a_{12}r_2 + \cdots + a_{1k}r_k = c_1 \\ &a_{21}r_1 + a_{22}r_2 + \cdots + a_{2k}r_k = c_2 \\ &\cdots\cdots \\ &a_{n1}r_1 + a_{n2}r_2 + \cdots + a_{nk}r_k = c_n. \end{aligned} \tag{6}$$

The above linear equations can also be written in the form of a matrix as follows:

$$\begin{bmatrix} a_{11} & a_{12} & \cdots & a_{1k} \\ a_{21} & a_{22} & \cdots & a_{2k} \\ \vdots & \vdots & \ddots & \vdots \\ a_{n1} & a_{n2} & \cdots & a_{nk} \end{bmatrix} \begin{bmatrix} r_1 \\ r_2 \\ \vdots \\ r_k \end{bmatrix} = \begin{bmatrix} c_1 \\ c_2 \\ \vdots \\ c_n \end{bmatrix}. \tag{7}$$

We need to group together any of the newly generated subblocks.

$$\begin{bmatrix} r_1 \\ r_2 \\ \vdots \\ r_k \end{bmatrix} = \begin{bmatrix} a_{m1} & a_{m2} & \cdots & a_{mk} \\ a_{n1} & a_{n2} & \cdots & a_{nk} \\ \vdots & \vdots & \ddots & \vdots \\ a_{i1} & a_{i2} & \cdots & a_{ik} \end{bmatrix}_{k\times k}^{-1} \begin{bmatrix} c_1 \\ c_2 \\ \vdots \\ c_k \end{bmatrix}. \tag{8}$$

Launch another root

$$r_k = d \cdot \left(r_1 \cdot r_2 \cdot \cdots \cdot r_{k-1}\right)^{-1} \bmod p. \tag{9}$$

For the r_ith subblock in a random subblock, it is easy to get

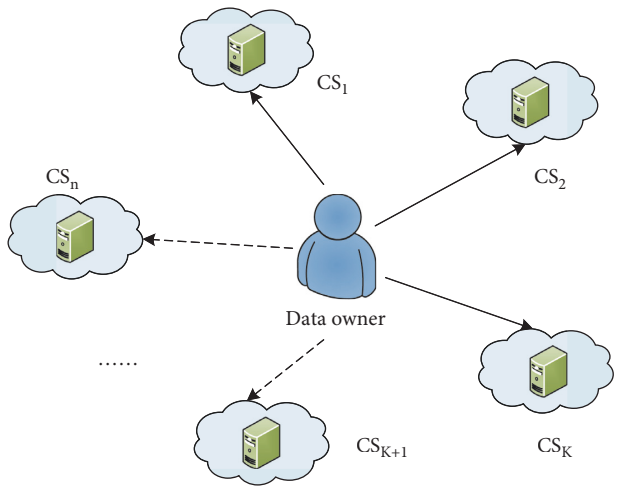

Figure 3: Information plate storage template.

$$r_{i,k} = r_i \cdot \left(r_{i,1} \cdot r_{i,2} \cdot \cdots \cdot r_{i,k-1}\right)^{-1} \bmod p. \tag{10}$$

Because it is the result obtained by the sum calculation, we will construct a new linear correlation that can be used to represent a new linear equation system:

$$\begin{aligned} &a_{11}r_{1,1} + a_{12}r_{1,2} + \cdots + a_{1k}r_{1,k} = c_{1,1} \\ &a_{11}r_{2,1} + a_{12}r_{2,2} + \cdots + a_{1k}r_{2,k} = c_{1,2} \\ &\cdots\cdots \\ &a_{11}r_{n,1} + a_{12}r_{n,2} + \cdots + a_{1k}r_{n,k} = c_{1,n}. \end{aligned} \tag{11}$$

Similarly, we have

$$\begin{aligned} &a_{i1}r_{1,1} + a_{i2}r_{1,2} + \cdots + a_{ik}r_{1,k} = c_{i,1} \\ &a_{i1}r_{2,1} + a_{i2}r_{2,2} + \cdots + a_{ik}r_{2,k} = c_{i,2} \\ &\cdots\cdots \\ &a_{i1}r_{n,1} + a_{i2}r_{n,2} + \cdots + a_{ik}r_{n,k} = c_{i,n}. \end{aligned} \tag{12}$$

In the same way, and so on, its related relationship is also displayed in the form of a matrix after simple calculation, namely,

$$\begin{bmatrix} a_{11} & a_{12} & \cdots & a_{1k} \\ a_{21} & a_{22} & \cdots & a_{2k} \\ \vdots & \vdots & \ddots & \vdots \\ a_{n1} & a_{n2} & \cdots & a_{nk} \end{bmatrix} \cdot \begin{bmatrix} r_{1,1} & r_{2,1} & \cdots & r_{n,1} \\ r_{1,2} & r_{2,2} & \cdots & r_{n,2} \\ \vdots & \vdots & \ddots & \vdots \\ r_{1,k} & r_{2,k} & \cdots & r_{n,k} \end{bmatrix} = \begin{bmatrix} c_{1,1} & c_{1,2} & \cdots & c_{1,n} \\ c_{2,1} & c_{2,2} & \cdots & c_{2,n} \\ \vdots & \vdots & \ddots & \vdots \\ c_{k,1} & c_{k,2} & \cdots & c_{k,n} \end{bmatrix}. \tag{13}$$

In order to facilitate the calculation later, let us define:

$$A=\begin{bmatrix} a_{11} & a_{12} & \cdots & a_{1k} \\ a_{21} & a_{22} & \cdots & a_{2k} \\ \vdots & \vdots & \ddots & \vdots \\ a_{n1} & a_{n2} & \cdots & a_{nk} \end{bmatrix}$$

$$C=\begin{bmatrix} c_{1,1} & c_{1,2} & \cdots & c_{1,n} \\ c_{2,1} & c_{2,2} & \cdots & c_{2,n} \\ \vdots & \vdots & \ddots & \vdots \\ c_{k,1} & c_{k,2} & \cdots & c_{k,n} \end{bmatrix} \tag{14}$$

$$R=\begin{bmatrix} r_{1,1} & r_{2,1} & \cdots & r_{n,1} \\ r_{1,2} & r_{2,2} & \cdots & r_{n,2} \\ \vdots & \vdots & \ddots & \vdots \\ r_{1,k} & r_{2,k} & \cdots & r_{n,k} \end{bmatrix}.$$

At this moment

$$A\cdot R\cdot A=C'=\begin{bmatrix} c_{1,1}' & c_{1,2}' & \cdots & c_{1,n}' \\ c_{2,1}' & c_{2,2}' & \cdots & c_{2,n}' \\ \vdots & \vdots & \ddots & \vdots \\ c_{k,1}' & c_{k,2}' & \cdots & c_{k,n}' \end{bmatrix}. \tag{15}$$

Because the matrix is an invertible matrix, there are:

$$R=A^{-1}C'A^{-1}. \tag{16}$$

If this correlation and data classification are determined, we can start storing the information, if we need to restore the data:

$$R=A^{-1}C'A^{-1}. \tag{17}$$

If the data owner wants to obtain the information of the data, he must have the detailed information of the calculation result in order to recover all the information. Similarly, the information that the stealer wants to obtain must also know the detailed information of the calculation result. Which is

$$\begin{aligned} R&=A^{-1}C'A^{-1} \\ &=\begin{bmatrix} a_{11} & a_{12} & \cdots & a_{1k} \\ a_{21} & a_{22} & \cdots & a_{2k} \\ \vdots & \vdots & \ddots & \vdots \\ a_{n1} & a_{n2} & \cdots & a_{nk} \end{bmatrix}^{-1}\begin{bmatrix} c_{1,1}' & c_{1,2}' & \cdots & c_{1,n}' \\ c_{2,1}' & c_{2,2}' & \cdots & c_{2,n}' \\ \vdots & \vdots & \ddots & \vdots \\ c_{k,1}' & c_{k,2}' & \cdots & c_{k,n}' \end{bmatrix}\begin{bmatrix} a_{11} & a_{12} & \cdots & a_{1k} \\ a_{21} & a_{22} & \cdots & a_{2k} \\ \vdots & \vdots & \ddots & \vdots \\ a_{n1} & a_{n2} & \cdots & a_{nk} \end{bmatrix}^{-1} \\ &=\begin{bmatrix} r_{1,1} & r_{2,1} & \cdots & r_{n,1} \\ r_{1,2} & r_{2,2} & \cdots & r_{n,2} \\ \vdots & \vdots & \ddots & \vdots \\ r_{1,k} & r_{2,k} & \cdots & r_{n,k} \end{bmatrix}. \end{aligned} \tag{18}$$

Calculate the stored data subblock information separately:

$$\begin{aligned} j&=x\times y\times z \\ &=x_1\times x_2\times x_3\times y_1\times y_2\times y_3\times z_1\times z_2\times z_3 \\ &=x_1\times y_1\times\times z_1\times x_2\times y_2\times z_2\times x_3\times y_3\times z_3 \\ &=j_1\times j_2\times j_3. \end{aligned} \tag{19}$$

The cloud server performs the following calculations:

$$\begin{aligned} u\times v\times w&=n_1(x_1+y_1+z_1)\times n_2(x_2+y_2+z_2)\times n_3(x_3+y_3+z_3) \\ &=n_1n_2n_3\times\begin{pmatrix} x_1x_2x_3+x_1x_2y_3+x_1x_2z_3+x_1y_2x_3+ \\ x_1y_2y_3+x_1y_2z_3+x_1z_2x_3+x_1z_2y_3+x_1z_2z_3+y_1x_2x_3+y_1x_2y_3+x_1x_2z_3+ \\ y_1y_2x_3+y_1y_2y_3+y_1y_2z_3+y_1z_2x_3+y_1z_2y_3+y_1z_2z_3+z_1x_2x_3+z_1x_2y_3+ \\ z_1x_2z_3+z_1y_2x_3+z_1y_2y_3+z_1y_2z_3+z_1z_2x_3+z_1z_2y_3+z_1z_2z_3 \end{pmatrix}. \end{aligned} \tag{20}$$

The cloud server performs the following processing:

$$\begin{aligned} s'&=u\times v\times w-(n_1n_2n_3x_1x_2y_3+n_1n_2n_3x_1x_2z_3 \\ &\quad+n_1n_2n_3x_1y_2x_3+\cdots+n_1n_2n_3z_1z_2y_3) \\ &=n_1n_2n_3(x_1x_2x_3+y_1y_2y_3+z_1z_2z_3). \end{aligned} \tag{21}$$

Calculate the required calculation result:

$$s_1=\frac{s_1'}{n_1},s_2=\frac{s_2'}{n_2},s_3=\frac{s_3'}{n_3}. \tag{22}$$

The calculation formula and model diagram are as follows:

$$s_1\times s_2\times s_3=\frac{s_1'}{n_1}\times\frac{s_2'}{n_2}\times\frac{s_3'}{n_3}=\frac{s'}{n_1n_2n_3}=x+y+z. \tag{23}$$

Calculation mode diagram is shown in Figure 4.

This kind of multiparty operation of big data requires the simultaneous use of several networks, as shown in Figure 5:

There are two users of this program, one is the data owner, and the other is the user of the data calculation results. In this respect, the cost of calculation mainly has three points: the data is checked by the response value obtained. This process is very simple and only involves the comparison operation of numbers, which cannot be considered. Decrypt the encrypted data again. In this process, only the encryption algorithm needs to be used reasonably, but it is not related to its own design and does not need to be

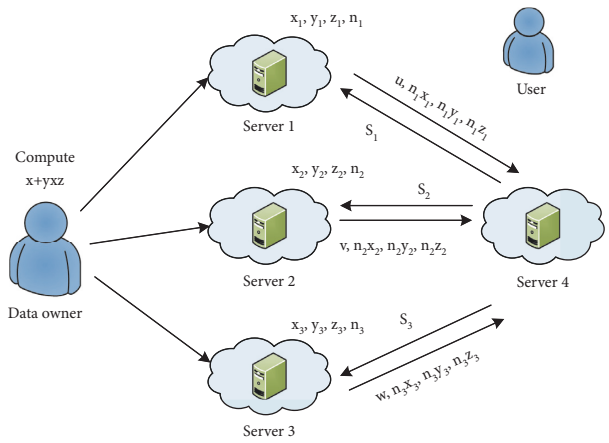

Figure 4: Calculation mode diagram.

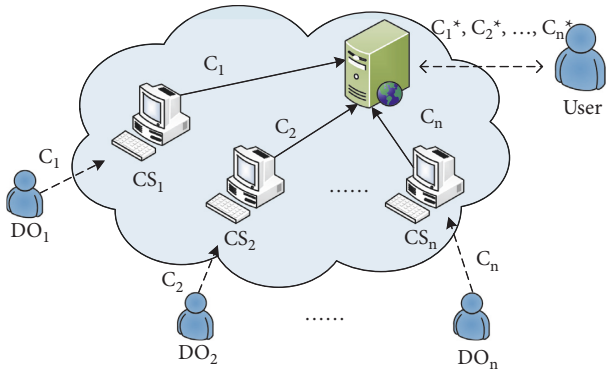

Figure 5: Cloud multiparty secure computing system diagram.

considered. Changes in precalculation time data are shown in Table 1.

Obviously, when the peak value of the number of information items does not change, as the maximum number of inspections x for each item combination increases, the precalculation time for DO increases linearly.

4. Analysis of the Credibility of Social Media Information Based on User Perception and Policy Recommendations

4.1. Empirical Analysis of the Credibility of Social Media Information Based on User Perception

4.1.1. Reliability Test. We use SPSS24.0 software to analyze the reliability of the 30 questions in the first part of the questionnaire, and use the Cronbach coefficient value as the analysis ruler to test the stability and internal consistency of each question in the pre-survey questionnaire. When the value of Cronbach's coefficient is greater than 0.7, it indicates that the reliability and internal consistency of the question item is better, and the reliability is higher. When the value of Cronbach's coefficient is less than 0.6, it indicates that the reliability of the question item is lower and the internal stability is higher. And the problem item needs to be modified. The value of each question item in the pre-investigation is shown in Table 2.

Table 1: Changes in precalculation time.

x	2	4	6	8	10
$t-s$	2000	4000	6000	8100	11000

4.1.2. Validity Test. Table 3 is the output result of the validity analysis of the first part of the 30 questions in the pre-survey questionnaire using SPSS24.0 software. By referring to the KMO value and the Bartlett sphere test result, it is judged whether the sample data can be factored, the size of the KMO value and the degree to which a sample is suitable for factor analysis is directly proportional. The KMO is greater than 0.9, which means it is suitable for analysis. If it is between 0.7 and 0.9, it can be analyzed. However, if the KMO is less than 0.5, whether the factor analysis can be performed, it needs to pass specific tests determined by inspection results.

4.1.3. Validity Analysis of Factors Affecting the Credibility of Social Media Information. KMO statistics and verification and Bartlett sphere test are also widely used in factor tests to verify the correctness of this chart. KMO statistical inspection and Bartlett sphere test are also important scales for judging whether there is a correlation between all the question items. KMO statistical inspection uses correlation coefficients to indicate the correlation between different variables. The KMO value can determine that the higher the validity, the stronger the correlation, and different variables are more suitable for factor analysis. When KMO is equal to 1, the criterion for determining the correlation is reached, and the closer it is to 1, the stronger the correlation. The Bartlett sphere test is mainly used to verify whether the various variables are independent. When the value is less than 0.05, it means that the factor analysis can be performed. Generally speaking, if the KMO statistical inspection data are greater than 0.7 and Bartlett's test coefficient is less than 0.01, this situation is most suitable for factor analysis, as shown in Table 4.

The results of the analysis of the validity of the modifier variables in this study are shown in Table 5. We can find that the statistical coefficient of KMO is 0.853, and 0.853 is greater than 0.7. At the same time, the result of Bartlett's spherical test is significant. The relevant data is more suitable for factor analysis. Using the above method for factor analysis, a total of 2 factors were extracted, and the overall variance contribution rate of these 2 factors was 63.650%, indicating that they represent variable information well. In addition, in the rotating component matrix, the two variables of information involvement and trust tendency become one component, respectively, so it can be explained that the structural validity of the moderating variable is better.

It can be seen from Table 6 that in this regression model, the regression coefficients of information quality, communication motivation, information presentation form, and information medium credibility are 0.210, 0.198, 0.174, and 0.210, respectively. This result indicates information quality and communication motivation. The form of information presentation and the credibility of the information medium

Table 2: Pre-investigation reliability analysis.

Variable	Cronbach's alpha value	Measurement question	Cranbach's α value after deleting the question	CITC
Information quality (IQ)	0.857	IQ1	0.795	0.753
		IQ2	0.823	0.688
		IQ3	0.792	0.763
		IQ4	0.859	0.611
Communicator reliability (TR)	0.916	TR1	0.910	0.754
		TR2	0.870	0.864
		TR3	0.876	0.853
		TR4	0.905	0.763
Communicator motivation (CM)	0.764	CMl	0.765	0.501
		CM2	0.634	0.64O
		CM3	0.610	0.661
Information presentation (PI)	0.710	PI1	0.708	0.608
		PI2	0.604	0.553
		PI3	0.517	0.621
Faith media reliability (IMR)	0.700	IMR1	0.607	0.567
		IMR2	0.666	0.518
		IMR3	0.621	0.540
		IHR4	0.620	0.605
		IMR5	0.712	0.502
Information involvement (INV)	0.710	INV1	0.643	0.523
		INV2	0.707	0.504
		INV3	0.583	0.528
		INV4	0.649	0.511
Propensity to trust (PT)	0.787	PT1	0.741	0.587
		PT2	0.737	0.588
		PT3	0.665	0.749
		PT4	0.789	0.523
Perceived information credibility (PCC)	0.842	PCC1	0.888	0.592
		PCC2	0.675	0.819
		PCC3	0.764	0.723

Table 3: Analysis of the validity of each variable in the pre-investigation.

Variable	KMO	Approximate chi-square detection	Probability of bartlett cucumber test significance	Degree of freedom
Information quality	0.805	82.672	0.000	6
Communicator credibility	0.804	135.478	0.000	6
Communicator motivation	0.639	38.374	0.000	3
Information presentation form	0.640	31.041	0.000	3
Credibility of information media	0.676	57.640	0.000	10
Information involvement	0.714	33.391	0.000	6
Trust tendency	0.712	59.471	0.000	6
Perceptual information credibility	0.652	66.881	0.000	3

will have a significant positive impact on the credibility of the perceived information, while the credibility of the disseminator will not have any significant effect on the credibility of the perceived information.

4.2. Suggestions for Improving the Credibility of Social Media Information. This paper conducts an in-depth analysis of the influencing factors of social media information credibility and verifies the effect of each influencing factor on perceived credibility. Based on the current status of social media development, and based on the experimental results obtained in this article, constructive opinions are put forward for the improvement of information credibility, which will further improve the network environment, which is of great significance.

4.2.1. Pay Attention to Information Quality, Build a Content Review Mechanism, And Realize Diversity of Information Forms. In the analysis results of this research, information quality significantly affects the perception of credibility of social media information, and its mediating effect as an intermediary variable on other credibility factors is also

Table 4: Validity test results.

Measurement question	Ingredient					
	1	2	3	4	5	6
IQ1			0.686			
IQ2			0.507			
IQ3			0.755			
IQ4			0.667			
TR1	0.704					
TR2	0.770					
TR3	0.788					
TR4	0.803					
CM1		0.825				
CM2		0.868				
CM3		0.779				
PI1						0.641
PI2						0.753
PI3						0.657
INR1						
INR2				0.608		
INR3				0.777		
INR4				0.734		
INR5				0.575		
PCC1						0.637
PCC2						0.805
PCC3						0.816
Variance contribution rate (%)	12.466	11.783	11.292	11.211	9.947	9.363
Cumulative variance contribution rate (%)	12.466	24.249	35.541	46.752	56.699	66.062

Table 5: Validity test results of modulating variables.

KNO statistical inspection volume	0.853	
Bartlett sphere test significance	0.00	
Coding	Factor loading factor	
	1	2
INV1	0.842	—
INV2	0.792	—
INV3	0.773	—
INV4	0.632	—
PTl	0.802	—
PT2	0.756	—
PT3	0.844	—
PT4	0.658	—
Variance contribution rate (%)	32.564	32.564
Cumulative variance contribution rate (%)	31.087	63.650

Table 6: Analysis of dependent variable regression model.

Model		Unstandardized coefficient		Standardization coefficient	T	Significance	Collinearity statistics	
		B	Standard error	Beta			Tolerance	VIF
M-PCC	Constant	0.331	0.264	—	1.251	0.212	—	—
	IQ	0.210	0.061	0.202	3.434	0.001	0.529	1.854
	TR	0.075	0.060	0.064	1.247	0.213	0.716	1.297
	CM	0.198	0.048	0.217	4.106	0.000	0.667	1.500
	PI	0.174	0.064	0.147	2.715	0 007	0.637	1.569
	IMR	0.210	0.068	0.169	3.071	0.003	0.616	1.623

significant. In the real environment, if the information expressed by the content is more objective, the more likely it is to be considered true information. Therefore, we have the right to determine that the objectivity, completeness, accuracy, and timeliness of network data information has an effect on the perception of individual information credibility while affecting the user's reading experience. Therefore, during the operation of social media, attention should be

paid to controlling the quality of information posted by platform users, analyzing the authenticity of the information, and deleting false and untrue information in a timely manner to improve the usefulness of the information content. In order to improve the quality of platform information, each social application media can establish a corresponding platform content review mechanism, increase the level of review and verification of platform information, conduct multilayer rigorous review of its content, and at the same time verify its provenance to form a benign information public opinion orientation, take the provision of accurate, objective, and reliable information content as the development goal, and enhance the trust of individuals in the media platform. This study not only clarifies that the form of information presentation has a direct impact on the credibility of perceived information, but also concludes that factors such as information quality and release time also affect the credibility of information, which has certain guiding significance for the content operation of social platforms. Therefore, on the basis of controlling the quality of information, each social platform can provide users with a variety of information editing forms, optimize the structural characteristics of information, and enrich the presentation forms of information. Authors are encouraged to combine plain text content with data, pictures, audio and video, and links and other forms of information display, which can make the content of the information richer and more diverse, make it more interesting and attract more people to read, stimulating the information. The receiver's visual experience enhances the information perception of "seeing is believing".

4.2.2. Cultivate the Media Literacy of Social Media Users. The characteristics of user-generated content make individuals not only receivers of information on social media platforms, but also publishers of information. The user's information recognition ability will affect their judgment on the credibility of social media information. Therefore, it is particularly important to cultivate the media literacy of the audience. Media literacy is an open, thinking, and questioning attitude that an individual holds towards media information. Information explosion is a very accurate vocabulary to describe the amount of current information and the speed of change. People are surrounded by a large amount of information every day and will inevitably be exposed to false information. At this time, information receivers are required to have high sensitivity and recognition ability, can effectively judge the authenticity and reliability of the information. At the same time, when users act as information publishers, they must also enhance their sense of responsibility. Before the information is released, whether it is original information or forwarded information, first make a simple judgment on the content of the information, check whether the content expression conforms to objective logic, whether there is official or professional argumentation support, whether it contains obvious semantic errors, etc., through preliminary inspection to reduce the spread of problems or false information. In addition, each social platform has its own user authentication method to distinguish the professional level and level of different users. Certified users should play the role of opinion leaders in social platforms and use their professional capabilities and influence to spread information in a good way and guide public opinion in the right direction. Finally, in addition to the improvement of users' own information level, the platform should also strengthen the serious review of the qualifications of social media users. The level certification of the communicator is the information point that individuals pay more attention to when searching for information. The higher the level of certification, the more professional and influence it is considered to have. However, the various roles on social media platforms are currently mixed, the platform's level certification standards are not perfect, and the certification process is not strict. This has caused some malicious propagators to transmit untrue information in online media and undermine the Internet atmosphere. Therefore, social media platforms must improve the user level certification audit standards, strictly control all aspects of level certification, and conduct periodic reviews of certified individuals to prevent information disseminators with bad motives from destroying the good subject information environment.

4.2.3. Improve Platform Functions and Establish Trust Levels. People's perception of the reliability of media platforms will affect their judgments on the credibility of social media information. To reflect the positive role of social platforms in information dissemination, some functional optimizations can also be made. For example, the platform can reduce user information acquisition costs by adding content tags. Mark the importance of the information content and attach official information links to reduce the time for users to search and select information and improve users' perception of ease of use. Multilevel information exchange channels can also be established to promote the trust among users at all levels. Current social media is mostly information exchanges between the people. In order to promote the dissemination of positive information and form a sensible network environment, it is also necessary to strengthen the communication between different departments, different organizations, celebrities, opinion leaders, etc., and the public. In the process of dialogue and communication, convey your own understanding and opinions on a certain phenomenon to users, and create a good network environment to enhance the customer trust and experience. In addition, the trust level of the social media platform can be constructed and the reliability of the platform can be improved. This study clarifies that the attributes of information media will also affect the public's perception of the credibility of social media information. Therefore, the trust level of each media platform can be quantified. Relevant departments have issued corresponding quantitative standards for the trust levels of social platforms, classifying each network platform, and urging each social platform to self-improve through periodic review and rating. This can not only provide media users with a reference basis, help users to perceive the credibility of their information through the trust level of the platform, but also improve the service level of the platform, promote the development of the platform itself, and improve the reliability of the social media platform.

4.2.4. Create a Good Social Trust Environment. With the rapid development of social media, various types of information are large in quantity and updated quickly, and the authenticity of information is difficult to guarantee. This has caused people to be skeptical about social media information and the surrounding environment. To improve the credibility of social media information, from a macro perspective, we need to start with the social environment, strengthen network management, purify the network environment, create a good social trust atmosphere, and enhance the trust between people and citizens in the entire society.

(1) Realizing the timely elimination of rumors is one of the reasons for social panic, especially the content of information closely related to public life. Some people will follow the direction of the rumors further and farther with the mentality that they prefer to be trusted. Therefore, it is necessary to promptly clarify the false information disseminated in social media, not only to delete the false information in time, but also to give an official or authoritative statement to correct the rumors, so that the audience can understand the truth of the matter and give the public correct guide, reduce the harm of rumors to the entire society, in order to build the audience's sense of trust in social media information.

(2) Make information open and transparent. Networks have gradually become the first means for the public to obtain information. People use various social media to learn about major issues in society and protect users' right to know. Only then can they gain the trust of users. Sharing transparency is essential. In response to some emergencies and threats to the public, all platforms must release official information in a timely manner, show the truth and the ins and outs of the facts to users, reduce social panic, avoid the growth of rumors and false information, create a pure information environment, and enhance people providing a sense of trust in the heart.

(3) The social media platform to protect the equal rights and interests of individuals has now developed into a window for people to convey their emotions and express their wishes. While supporting and praising, there will also be voices of criticism and accusation. In order to enhance the user's recognition and trust of the platform, each platform must form an inclusive emotional expression system to protect the public's freedom of speech and allow people to claim reasonable interests. If the legal speeches made by users of social platforms are restricted, it will affect people's views on the fairness and justice of the entire social media environment, and reduce the public's trust in social media platforms and the entire society.

5. Conclusion

With the rapid development of many new technological fields, big data and cloud computing are undoubtedly the two most prominent products. Their appearance has subverted people's traditional cognition of data processing, processing and storage methods, and brought tremendous changes to people's social production and life. The benefits of this technology have gradually covered people's lives. In more fields, more and more people have a deeper understanding of the importance of big data and cloud computing. The relationship between these two technologies is interdependent. If big data is the Daqing oil field, then cloud computing is the equipment to obtain these oils. The reason why big data is called big data is that the data is very large and exponentially growing. Therefore, a cloud computing platform is needed for analysis and storage, in order to maximize the information stored in these data. Cloud computing has strong scalability, its ability to allocate resources at will and high-strength processing capabilities are not available in traditional computer and Internet technology: if big data does not have cloud computing, it is like there is no edge. If cloud computing does not have big data, it will have nowhere to play its role. Therefore, the combination of the two is the general trend of the times.

In the new network environment, the rapid development of social media has been widely used. Although the expansion of social media can speed up the exposing, dissemination, and response speed of incidents, it has created new social problems. The authenticity of information is becoming more and more difficult to verify. A large number of untrue and untrustworthy content floods various platforms. In this context, based on the theory of user perception and information processing, this article analyzes the potential for perceiving social media information in terms of information quality, communicator credibility, communication motivation, information presentation form, and information media credibility. The mediating effect of information quality is the mediating variable between heuristic variables and perceived information credibility. When information involvement and trust tendency are used as adjustment factors, it will affect information credibility.

Data Availability

The data used to support the findings of this study are available from the corresponding author upon request.

Conflicts of Interest

The authors declare that they have no conflicts of interest.

Acknowledgments

This paper was supported by Natural Science Foundation of Hunan Province, Study on the Sentiment Analysis of Online-course Teaching Reviews in the Background of Post-epidemic, under Grant no. 2021JJ60048.

References

[1] C. B. Moon, J. Y. Lee, D. S. Kim, and B. M. Kim, "Multimedia content recommendation in social networks using mood tags and synonyms," *Multimedia Systems*, vol. 55, pp. 1–18, 2019.

[2] V. Roto, E. Law, A. Vermeeren, and J. Hoonhout, "User experience white paper: bringing clarity to the concept of user experience," in *Dagstuhl Seminar on Demarcating User Experience*vol. 12, 2011.

[3] M. E. David, J. A. Roberts, and B. Christenson, "Too much of a good thing: investigating the association between actual smartphone use and individual well-being," *International Journal of Human-Computer Interaction*, vol. 34, no. 3, pp. 265–275, 2018.

[4] A. Negahban, "Social networking on smartphones: when mobile phones become addictive," *Computers in Human Behavior*, vol. 29, no. 6, pp. 2632–2639, 2013.

[5] M. Röösli, "A latent class analysis on adolescents media use and associations with health related quality of life," *Computers in Human Behavior*, vol. 71, pp. 266–274, 2017.

[6] J. Davidson, B. Liebald, and J. Liu, "The Youtube video recommendation system," in *Proceedings of the fourth ACM conference on Recommender systems*, pp. 293–296, ACM, Barcelona, Spain, September 26-30, 2010.

[7] J. Park, S. J. Sang-Jin Lee, and S. Sung-Jun Lee, "Online video recommendation through tag-cloud aggregation," *IEEE Multimedia*, vol. 18, no. 1, pp. 78–87, 2011.

[8] A. Avizienis, J.-C. Laprie, B. Randell, and C. Landwehr, "Basic concepts and taxonomy of dependable and secure computing," *IEEE Transactions on Dependable and Secure Computing*, vol. 1, no. 1, pp. 11–33, 2004.

[9] X. Zhao, J. Yuan, and R. Hong, "On video recommendation over social network," *Advances in Multimedia Modeling*, Springer Berlin Heidelberg, Berlin, Germany, 2012.

[10] S. Aladhadh, X. Zhang, and M. Sanderson, "Location impact on source and linguistic features for information credibility of social media," *Online Information Review*, vol. 43, no. 1, pp. 89–112, 2019.

[11] E. K. Szczepaniuk, H. Szczepaniuk, T. Rokicki, and B. Klepacki, "Information security assessment in public administration," *Computers & Security*, vol. 90, no. 4, p. 101709, 2020.

[12] S. J. Cao and J. W. Chang, "Research on the influencing factors of information credibility of public health emergencies in social media take wechat as an example," *Modern Information*, vol. 351, no. 9, pp. 5–16, 2020.

[13] X.-L. Jin, M. Yin, Z. Zhou, and X. Yu, "The differential effects of trusting beliefs on social media users' willingness to adopt and share health knowledge," *Information Processing & Management*, vol. 58, no. 1, p. 102413, 2021.

[14] T. K. Sell, D. Hosangadi, and M. Trotochaud, "Misinformation and the US Ebola communication crisis: analyzing the veracity and content of social media messages related to a fear-inducing infectious disease outbreak," *BMC Public Health*, vol. 20, no. 1, p. 550, 2020.

Hindawi
Mobile Information Systems
Volume 2022, Article ID 9723817, 9 pages
https://doi.org/10.1155/2022/9723817

Research Article

Ultrasonic Image Monitoring of High-Risk Pregnant Women Based on Image Deblurring Method

Weihua Zhong[1] **and Dan Liu**[2]

[1]*Affiliated Hospital of Jinggangshan University, Ji'an, Jiangxi 343000, China*
[2]*Jinggangshan University, Ji'an, Jiangxi 343009, China*

Correspondence should be addressed to Dan Liu; 9920040078@jgsu.edu.cn

Received 17 May 2022; Revised 16 June 2022; Accepted 28 June 2022; Published 9 July 2022

Academic Editor: Shadi Aljawarneh

The method of image deblurring is one of the research hotspots in the field of image restoration, and its purpose is to restore the damaged blurred image to a clear image. Under normal circumstances, the image deblurring process is the key to accurately recovering unknown images, and it is crucial that the image recovery model can be used fully and effectively when configuring the image recovery model. The main task of this paper is to use an effective optimization model to obtain a more accurate core and restore a clear image. High-risk parturients refer to high-risk parturients in pregnancy and pregnant women with high-risk pregnancy factors, and other three-dimensional ultrasound images TUI dynamic monitoring technology provides timely clues to the fetus's kidney length, width, and abnormal development of the fetal kidney during pregnancy and tracks the fetus Renal pelvis has different outcomes beyond the normal range. In this paper, three-dimensional ultrasound is used to examine the kidneys. At the same time, 3D ultrasound image TUI technology is used to measure the long diameter, transverse diameter, and anteroposterior diameter of the fetal kidney, and the monitoring processing system is used to measure the volume of the fetal kidney. 30 fetuses with unilateral renal pelvis anterior and posterior diameter ≥10 mm were randomly examined during the case using two-dimensional ultrasound. Using three-dimensional ultrasound TUI and VOCA technology to measure the front and back of the renal pelvis, the thickness of the kidney, the resistance index of the renal hilar renal artery, and the resistance index of the renal pelvis content, this can reduce the risk of high-risk mothers and even reduce the risk to zero.

1. Introduction

As an important carrier of information, images are more and more widely used in many fields. However, during the acquisition process, transfer, and storage, some factors may affect the overall quality of the image, and the overall quality of the image being processed may be affected by the imaging device and external factors, making the image unclear. In order to enable image applications and image vision to meet the needs of high-definition images, we are studying methods to restore clear images based on decomposed images [1]. The image deblurring method is an important branch of image restoration, which has important significance and great research value [2]. Image Dutivem refers to a technology that maximizes the restoration of the original image based on the image's previous degradation information and image prior information [3]. It plays an important role for high-risk women. The common clinical situations of high-risk women are as follows: (1) adult pregnancy over 35 years old belongs to high-risk women. (2) Hypertension syndrome during pregnancy and gestational diabetes during pregnancy. (3) Patients with a history of pregnant liver and kidney function. (4) Patients with a history of cesarean delivery during pregnancy, these risks belong to high-risk women [4]. High-risk pregnant women should undergo regular check-ups during pregnancy. High-risk pregnant patients will have fetal abnormalities or pregnant women have abnormal conditions during pregnancy, which will lead to fetal death in the uterus, intrauterine growth retardation, and congenital malformations

[5]. At the same time, it will also lead to various chronic diseases in the mother. And, abnormal conditions will also appear in the perinatal period. Ultrasound imaging technology is a technology for related inspections of high-risk mothers so that abnormalities can be avoided as much as possible [6]. Ultrasound images can obtain information provided by X-rays and Y-rays. At the same time, it can reflect the difference in acoustic parameters in the medium. Ultrasound has a good resolution in human soft tissues, which allows the microscopic parts of biological tissues to be identified by simple methods [7]. At the same time, it can also obtain useful signal information within a dynamic range of up to 120 dB. Ultrasound images can obtain the required images without staining. Morphological diagnosis, ultrasound, and ultrasound diagnosis can be based on long-term tomography of morphological performance. This makes the connection between histology and anatomy changed, which can make a qualitative and quantitative diagnosis of the disease. And, the monitoring and processing system can be used to study the images produced by certain organs in the physiological tissues, or the changes in the ultrasound spectrum Doppler can be used to study [8].

2. Related Work

The literature describes how to estimate the blur kernel under the RGB channel and use it for deblurring in a robust image model [9]. Its main advantage is that it takes into account the different conditions of natural color images that are subject to blur kernels under RGB channels. On this basis, this article is different from the restoration method of only estimating the fuzzy kernel in the gray domain and the subchannel processing and proposes to use the edge information of the image as a priori constraint of the regularization and conducts it under a variety of conditions. In an iterative way, a more accurate blur kernel can be obtained. The literature introduces the accuracy of the blur kernel that provides us with the RGB channel and compares the image blur effect from the RGB channel with the blur kernel obtained in the gray field [10, 11]. Through comparison, we can know that the accuracy of the blur kernel from the RGB channel is more accurate. The literature introduces the use of the RGB channels obtained in the sparse representation model with the structural block as the reference block and the blur kernel obtained in the gray domain to blur the image and compares it with the restoration method with a better deblurring effect at this stage [12]. The literature describes conventional methods and traditional blurred images [13]. The application and feasibility analysis of the used images are carried out, in which the improved method of the blurred image can be obtained through detailed data, and the method can be used to improve the operation [14]. The literature introduces that as a factor of punishment, it affects the restoration of the image, and the value of the punishment factor is adjusted to a similar nature before and after the image restoration [15, 16]. An improved method for blurring the image using the ADMM-OGS-TVFN adaptive method is proposed [17]. It can be understood through experiments that the proposed algorithm for solving the model has been greatly improved both subjectively and objectively.

3. Image Deblurring and Ultrasound Image Monitoring Model

3.1. Image Deblurring. Due to the urgent needs of various industries for image clarity, in recent years, image deblurring methods have sprung up, and these methods have been widely used in engineering. When dealing with scientific research and practical problems, according to the cognition of the spread function, the image deblurring technology can be divided into blind deblurring and nonblind deblurring. Nonblind deblurring is performed on the premise of accurately obtaining the spread function; blind deblurring is performed on the spread function for which no information is obtained as shown in Figure 1.

Unblind image blur can be regarded as an independent branch, or applied to blind image deblurring, which can be used as the second stage of image deblurring operation. The nature of unblind image blur or blind image blur research will make the deblurring process very complicated. Using noise information to blur an image makes it difficult to achieve deblurring. Nonblind images provide an indispensable support for deblurring images and are also the basis for deblurring images. Due to the indispensable nature of nonblind images and the complexity of research, this paper only studies some models and algorithms of nonblind image blur.

Image deblurring is to deblur the image whose prior information has been damaged. Therefore, it is important to understand the process of image materialization to build a model. Generally, the image destruction process is considered to be spatially constant, and the mathematical model has degraded accordingly, as shown infd1.

$$g(x, y) = h(x, y) \otimes f(x, y) + n(x, y). \tag{1}$$

The process of image degradation is generally considered to be the influence of a spatial motion invariant function (denaturing function) and additional noise, and the process of image degradation can be expressed by the following formula:

$$g(x, y) = H[f(x, y)] + n(x, y). \tag{2}$$

In the formula, if the function H satisfies,

$$H[af_1(x, y) + bf_2(x, y)] = aH[f_1(x, y)] + bH[f_2(x, y)]. \tag{3}$$

In the formula, a and b are arbitrary constants; $f_1(x, y)$, $f_2(x, y)$ are arbitrary images of the same size, then the function H represents a linear system.

$$H[f(x - \alpha, y - \beta)] = g(x - \alpha, y - \beta). \tag{4}$$

Then, it is usually said that the system has space shift invariance. It shows that the output of any point in the system is only affected by the input of this point, but not by the spatial position of this point.

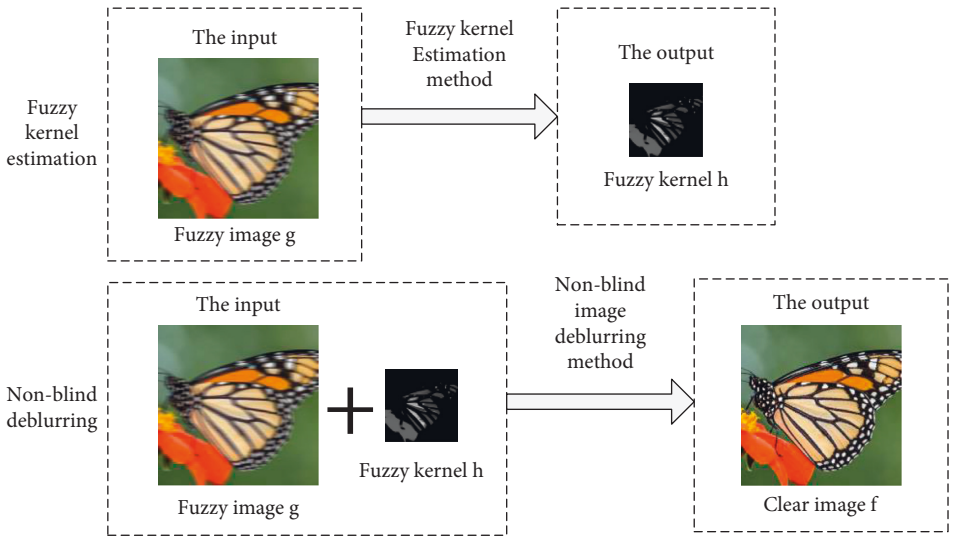

Figure 1: Image blind deblurring process.

The unit collision function in the digital signal processing system has the following definitions:

$$\begin{cases} \int_{-\infty}^{+\infty} \delta(t)dt = 1, & t = 0, \\ \delta(t) = 0, & t \neq 0. \end{cases} \tag{5}$$

The unit shock function has a function value only when $t = 0$, all output values except the Gajimyoi point are 0, and the unit shock function can be defined by the pulse with an integral of 1. If the time delay of the unit influence function (t) is $0t$, the following information is obtained:

$$\begin{cases} \int_{-\infty}^{+\infty} \delta(t - t_0)dt = 1, & t = t_0, \\ \delta(t - t_0) = 0, & t \neq t_0. \end{cases} \tag{6}$$

Then, for the one-dimensional time-domain signal $f(x)$,

$$f(x) = \int_{-\infty}^{+\infty} f(t)\delta(x - t)dt\ . \tag{7}$$

According to formula (7), the two-dimensional time domain signal (x, y) can be replaced by the following formula accordingly:

$$f(x, y) = \int_{-\infty}^{+\infty}\int_{-\infty}^{+\infty} f(\alpha, \beta)\delta(x - \alpha, y - \beta)d\alpha d\beta. \tag{8}$$

Substituting formula (8) into (2), we can obtain the following equation:

$$\begin{aligned} g(x, y) &= H[f(x, y)] \\ &= H\left[\int_{-\infty}^{+\infty}\int_{-\infty}^{+\infty} f(\alpha, \beta)\delta(x - \alpha, y - \beta)d\alpha d\beta\right]. \end{aligned} \tag{9}$$

Since the function H is a linear operator with spatial motion invariance, the formula (9) can be changed as follows:

$$\begin{aligned} g(x, y) &= \int_{-\infty}^{+\infty}\int_{-\infty}^{+\infty} H[f(\alpha, \beta)\delta(x - \alpha, y - \beta)]d\alpha d\beta \\ &= \int_{-\infty}^{+\infty}\int_{-\infty}^{+\infty} f(\alpha, \beta)H[\delta(x - \alpha, y - \beta)]d\alpha d\beta. \end{aligned} \tag{10}$$

Formula (10) can be converted to the following equation:

$$g(x, y) = \int_{-\infty}^{+\infty}\int_{-\infty}^{+\infty} f(\alpha, \beta)h(x, \alpha, y, \beta)d\alpha d\beta. \tag{11}$$

Due to the invariant characteristics of the space shift of the system H, we can obtain the following equation:

$$H[\delta(x - \alpha, y - \beta)] = h(x - \alpha, y - \beta). \tag{12}$$

So formula (11) can be converted to the following equation:

$$g(x, y) = \int_{-\infty}^{+\infty}\int_{-\infty}^{+\infty} f(\alpha, \beta)h(x - \alpha, y - \beta)d\alpha d\beta. \tag{13}$$

In this way, formula (11) can be converted as follows to generate additional noise:

$$g(x, y) = \int_{-\infty}^{+\infty}\int_{-\infty}^{+\infty} f(\alpha, \beta)h(x, \alpha, y, \beta)d\alpha d\beta + n(x, y). \tag{14}$$

Due to the invariance of the spatial motion of the system H, formula (14) can be transformed as follows:

$$g(x, y) = \int_{-\infty}^{+\infty}\int_{-\infty}^{+\infty} f(\alpha, \beta)h(x - \alpha, y - \beta)d\alpha d\beta + n(x, y). \tag{15}$$

Therefore, the convolution integral formula (15) can be expressed as follows:

$$g(x, y) = h(x, y) \otimes f(x, y) + n(x, y). \tag{16}$$

Then, the following formula is used to simplify and replace in the deblurring process:

$$g = h \otimes f + n. \tag{17}$$

According to the convolution summary, formula (16) can be converted into frequency domain representation.

$$G(u, v) = H(u, v)F(u, v) + N(u, v). \tag{18}$$

The subsequent image deblurring process is simplified and modified using the following formula:

$$G = HF + N. \tag{19}$$

The subjective evaluation method may also be a visual evaluation method that evaluates the test image through the subjective visual recognition of the tester. The most commonly used method for image deblurring is the absolute evaluation method, which is directly classified based on vision and distinguished by five evaluation scales according to international standards. The specific conditions are shown in Table 1. This method can best reflect the effect of restoring image quality, but due to the influence of other testers and other environments on image quality evaluation, different evaluation results will be produced.

It is important to choose the number of iterations in the MM algorithm because the MM algorithm has a greater impact on the time required to solve the subproblem. To see the influence of the number of repetitions of subquestions v_x and v_y on the results of the experiment, please select 1, 3, 5, 12, and 25 as the experiment objects. When the two-dimensional images overlap and when K is an odd number, it is a complete overlap centered on the overlap point. Theoretically, the experimental effect is better. Therefore, first, select the overlap degree of 3 for testing. After determining the parameters, you need to select a test image for testing. Here, the cleaned images "Cameraman" and "Goldhill" that are polluted by Gaussian blur and Gaussian noise can be used as test images. Among them, the fuzzy (Gaussian) kernel size is 7×7, the standard deviation is 2, and the noise uses Gaussian noise with BSNR = 40. At the same time, the same image (kernel size blur 7×7) polluted by average blur and Gaussian noise (BSNR = 40) is selected as the experimental supplement. The experimental results are shown in Table 2.

It can be seen from Table 2 that the number of repetitions of the subproblem is 3 times, and the deblurring method mentioned in the article achieves the best results in restoring the image. In this case, compared with the case where the number of repetitions is 5 and the PSNR value is 0.02 dB (the maximum difference is 0.04 dB), the calculation time is shortened to 0.5 seconds within 0.2 seconds. In addition, if the number of repetitions is 3 or more, the PSNR value of the restored image is basically unchanged, and it can be confirmed in the table that it only increases at runtime.

In this article, the choice of the degree of overlap of the image gradient K has a great impact on the image quality restored by the image deblurring algorithm, but the impact on the calculation time is basically negligible, so the parameters are determined at the end. The value chosen in the experiment is 1–10. The choice of the test image is the same as the choice of the MM algorithm, and the final experimental result is shown in Figure 2.

Figure 2 shows that other overlapping degrees of K will have a great impact on the image restoration results. Through the experimental data, we conclude that when the gradient of different blur types of images overlap K value of 3, different images have the best recovery effect. According to the results shown in the figure, we can understand that the setting of parameters in the image deblurring process is very important.

In order to compare the PSNR values of the restored images of different models more conveniently, please average the PSNR values of the restored images of different blur types in Table 2, and draw the obtained values with histograms. It can be seen more intuitively in Figure 3 that the model proposed in this paper can obtain a higher PSNR value.

3.2. Ultrasound Image Monitoring. According to the principle of ultrasound imaging technology, the reflected ultrasound will be attenuated or interfered during the recovery process, and the generated B-ultrasound image will show different brightness, that is, speckle noise. In the process of ultrasound imaging, because the reflected wave is generated by overlapping scattered wave signals from many scattered particles in space, the position where the reflected wave interferes is random, which leads to random noise in the entire image distributed. The following is the overlapping process and calculation method of the scattered wave signals emitted by the scattering particles.

Assuming that the scattered wave signal emitted by each scattering particle is X and the displacement is X, the overlapping result of the scattering signals of many particles is fd20.

$$X = Xe^{j\theta} = \sum_{i=0}^{N-1} X_i e^{j\theta_i}. \tag{20}$$

Among them,

$$\xi_i = \frac{X_i}{\sqrt{N}}. \tag{21}$$

Assuming that the number of scatterers in the resolution unit of the reflected wave signal is large enough, and its phase is uniformly distributed, the joint probability density is

$$P(X_r, X_i) = \frac{1}{2\pi\sigma^2} \exp\left(-\frac{X_r^2 + X_i^2}{2\sigma^2}\right). \tag{22}$$

The formula (23) can be obtained by formula (22).

$$X = \sqrt{X_r^2 + X_i^2}. \tag{23}$$

The probability density function of formula (24) is obtained from formula (23).

$$P(X) = \begin{cases} \dfrac{X}{\sigma^2} \exp\left(-\dfrac{X^2}{2\sigma^2}\right), & X \geq 0, \\ 0, & \text{other.} \end{cases} \tag{24}$$

Table 1: Subjective (absolute) evaluation methods.

Points	Hinder the scale	Quality scale
5 points	That's good	I cannot see that the image quality has deteriorated at all
4 points	It is good	We can see the image quality, but it will not affect the effect
3 points	General	The quality of the image is changing and it is clearly an obstacle to viewing
2 minutes	Difference	Hinder viewing
1 point	Very bad	Very serious obstruction to viewing

Table 2: The number of iterations of MM algorithm subproblems.

Image	Fuzzy kernel	Number of iterations	PSNR (dB)	time (s)
Cameraman	Gauss	l	28.4472	0.4472
		3	28.7454	0.5672
		5	28.7751	0.7328
		12	28.781	1.1 636
		25	28.7856	2.0611
		100	28.7856	9.4939
Goldhill	Gauss	l	30.01 69	l. 8244
		3	32.3056	2.5738
		5	32.3283	3.0667
		10	32.3348	4.8439
		20	32.3352	8.4673
		l00	32.3352	36.4351
Cameraman	Aver	l	29.1374	0.4489
		3	29.3999	0.5626
		5	29.4273	0.71 63
		10	29.4355	1.1 479
		20	29.4369	2.0214
		l00	29.4359	8.7783

Ja (Jain) proposed a classic model, which contains two types of noise: multiplicative and additive, as in

$$f(i,j) = g(i,j)n_m(i,j) + n_a(i,j). \tag{25}$$

The model of (23) can be simplified in (24), and the speckle noise model can use a model that only contains the unit conversion noise passed through,

$$f(i,j) = g(i,j)n_m(i,j), \tag{26}$$

$$\log[f(i,j)] = \log[g(i,j)] + \log[n_m(i,j)]. \tag{27}$$

In order to see the effect of the algorithm, this article uses the PM model Catte-PM, Lin Shi operator, and Wang Changhong for each kidney detection image and fetal head image and uses two ultrasound image algorithms. Compare filtering and provide a filtering effect diagram for each algorithm (as shown in Figure 4).

The comparison of the filtering effects of various algorithms for fetal images is shown in Figure 5.

According to the point noise in the kidney image, the noise density compares the PSNR and FOM of other images in Table 3.

According to the point noise in the kidney image, when comparing PSNR and FOM in other images, the noise density is shown in Table 4.

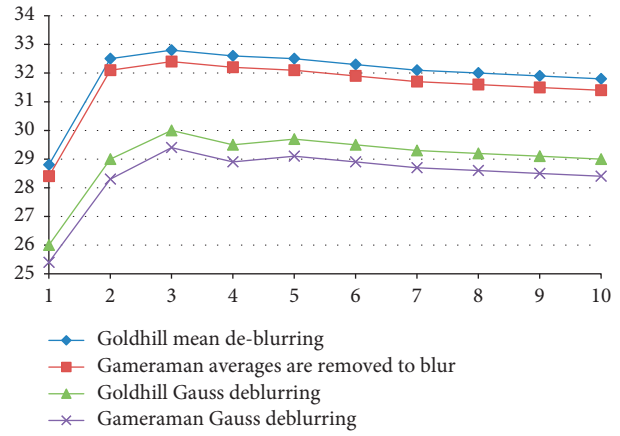

Figure 2: Test results of different K values.

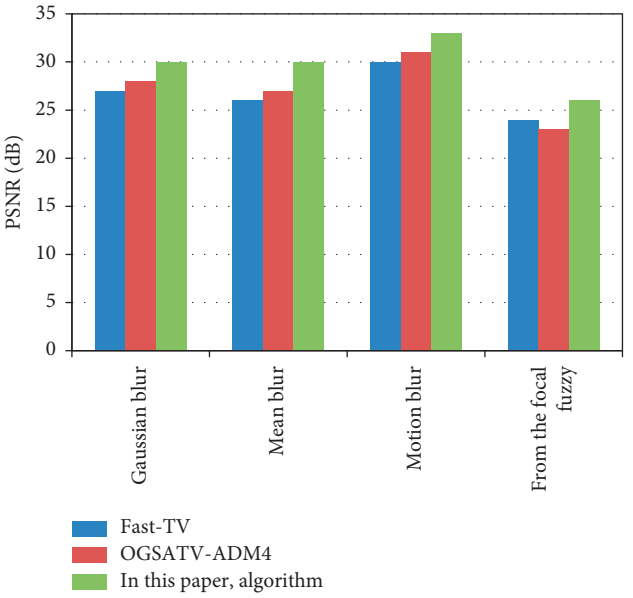

Figure 3: Average PSNR values of various restoration models of different blur types.

4. Design and Application of Ultrasound Image Monitoring and Processing System for High-Risk Parturients

4.1. System Requirement Analysis. The system mainly includes ultrasonic RAW image data collection, communication, and image data processing system. The main functions realized and provided by the data communication

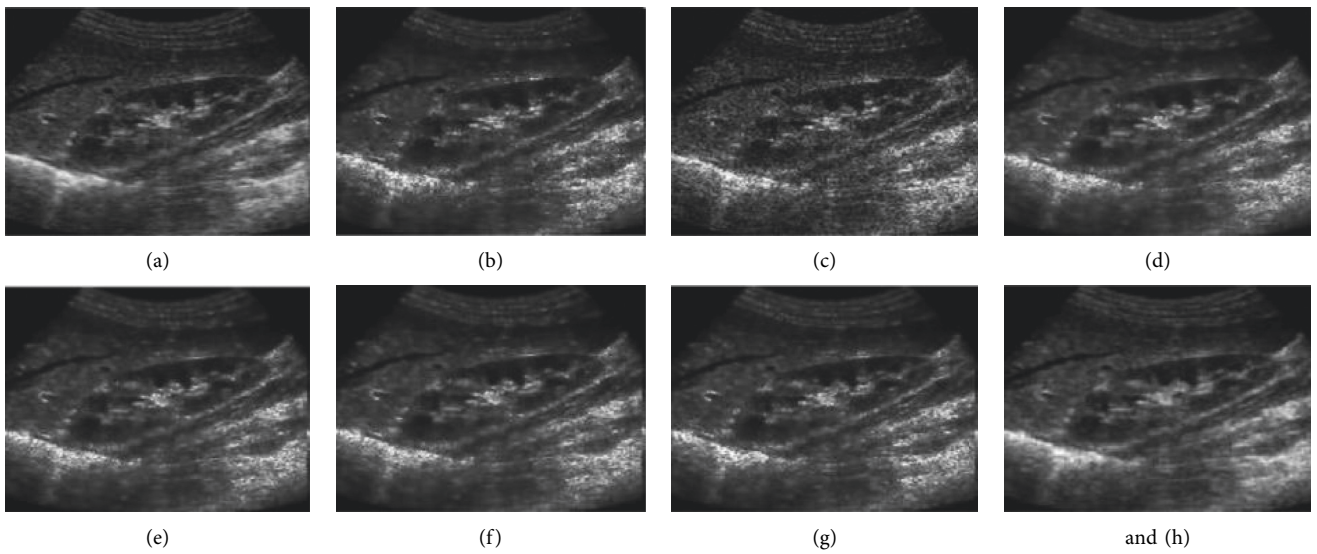

Figure 4: Comparison of filtering effects of various algorithms on kidney images. (a) Pollution-free map, (b) add noise graph, (c) P-M algorithm, (d) CATTE-PM algorithm, (e) forest stone operator, (f) Wang Changhong algorithm, (g) SRAD algorithm, and (h) algorithm in this paper.

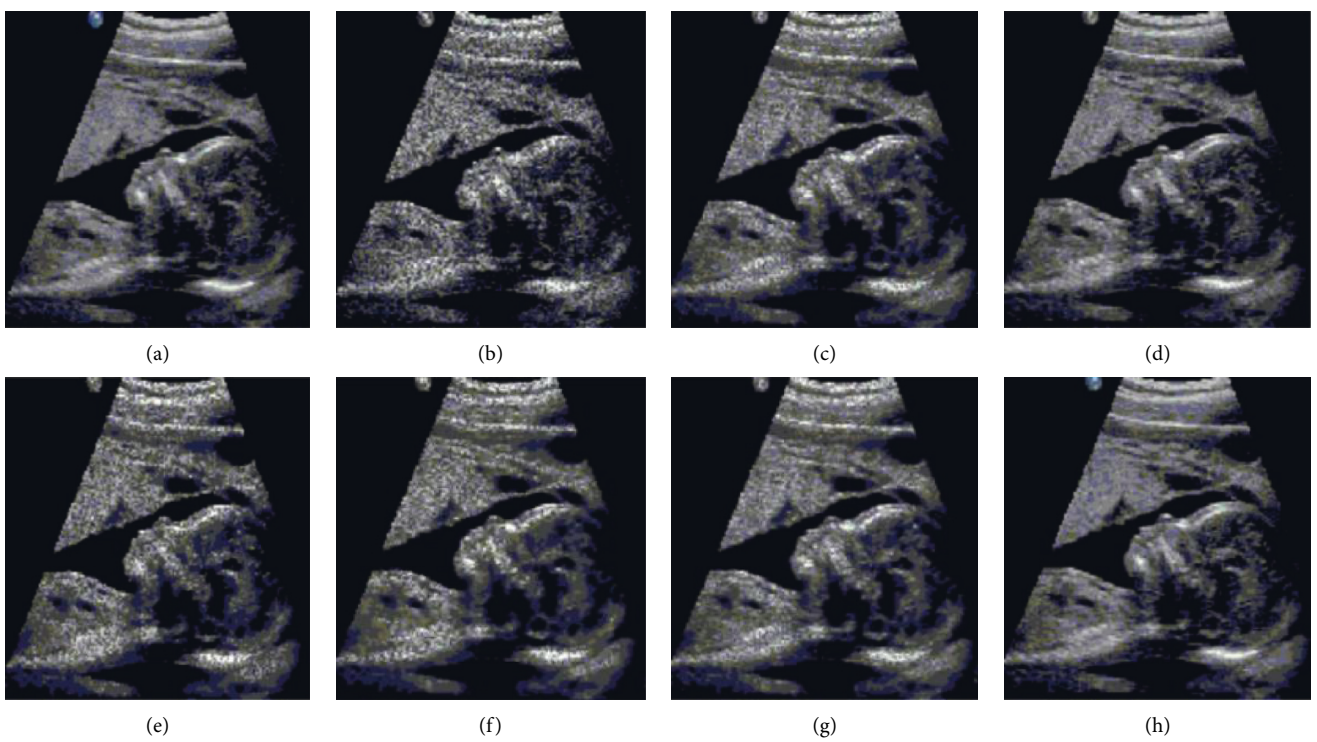

Figure 5: Comparison of filtering effects of various algorithms on fetal images. (a) Pollution-free map. (b) Add noise graph. (c) P-M algorithm. (d) CATTE-PM algorithm. (e) Forest stone operator. (f) Wang Changhong algorithm. (g) SRAD algorithm. (h) Algorithm in this paper.

subsystem to realize the normal interaction with each subsystem include the following parameters:

(1) Reception of ultrasound raw image data

(2) Analysis of ultrasound raw image data

(3) Preprocessing of ultrasonic RAW image data

(4) Transmission and execution of control commands

The super image processing system first supports the image processing algorithms that need to be implemented and delivered by the subsystem. The main points are as follows:

Table 3: Comparison of PSNR and FOM of various algorithms for kidney image.

Noise	P-M model		Catte-PM algorithm		Linshi algorithm		SRAD algorithm		Wang Changhong algorithm		Algorithm	
Density (%)	PSNR	FOM	PSNR	FOM	PSNR	FOM	PSNR	FOM	PSNR	FOM	PSNR	FOM
5	26.7791	0.8233	28.0415	0.611	28.8434	0.8215	29.1491	0.8545	27.9905	0.8241	31.2592	0.8727
10	22.9093	0.7974	26.0173	0.7744	26.8104	0.8007	27.6341	0.8053	25.5646	0.7922	29.3481	0.8587
30	17.4742	0.7474	22.3283	0.7312	23.3921	0.7512	22.9293	0.7889	20.9978	0.7711	24.9332	0.7921

Table 4: Comparison of PSNR and FOM of fetal image algorithms.

Noise	P-M model		Catte-PM algorithm		Linshi algorithm		SRAD algorithm		Wang Changhong algorithm		Algorithm	
Density (%)	PSNR	FOM	PSNR	FOM	PSNR	FOM	PSNR	FOM	PSNR	FOM	PSNR	FOM
5	25.9035	0.8434	29.0611	0.7959	28.0877	0.8057	29.5951	0.8907	27.6754	0.8297	31.7982	0.8869
10	22.2959	0.7977	26.8479	0.7576	26.7905	0.7978	27.3369	0.8678	25.0827	0.7995	29.1053	0.8412
30	17.7694	0.7798	24.4317	0.7318	22.1456	0.7413	22.9675	0.7992	21.4562	0.7694	24.2527	0.8031

(1) Adjust the brightness and contrast of ultrasound images

(2) False color of an ultrasound image

(3) Flip and transform the ultrasound image

(4) Ultrasound image zoom

(5) Correlation processing of ultrasound image frames

(6) Noise reduction processing after the ultrasound image is frozen

The main purpose of this course is to design and implement the original ultrasound image data by collecting it and using the image processing system to study and improve the method of ultrasound noise reduction. The data scanned by the ultrasonic front-end hardware (probe) are mainly transmitted to the data acquisition communication system via USB, and the data acquisition system receives and preprocesses the transmitted data (DSC, gray conversion, and noise reduction). The B-ultrasound image is processed at a frequency of 40 Hz in the image display area of the ultrasound interface to form a real-time dynamic ultrasound detection image that can be analyzed and diagnosed by a doctor. The system can also perform various basic processing and conversion on the active image in the display area, including image brightness, contrast, image scaling, image inversion, and image coloring. When the active image is fixed, the current image frame is processed to reduce noise and displayed. The system preprocesses the original ultrasound data so that doctors can adjust the brightness, color, proportion, etc., of the image according to their needs, so as to observe and improve the condition more clearly, and to further diagnose it. This topic is mainly divided into two subsystems of ultrasound data acquisition communication system and ultrasound image data processing system. The interface system is dedicated to auxiliary display.

4.2. System Module Design. The main function of the ultrasonic readout module is to read and analyze the frame of the original ultrasonic data of the image transmitted via USB, encapsulate the frame, send the hardware, and return the software that reads the status data. Applicable ultrasonic reading functions include: retrieving and analyzing the original ultrasonic frame of the data sent by the main device, the ultrasonic frame of encapsulating the data, sending a command to the device, reading the result, and transmitting it to the main trunk.

This article provides a block diagram of a module. The module mainly uses ProbeFactory to read ultrasound image data to create probes. A probe is a type of probe. OriginalImageBFrameReader is an ultrasound image reading class, which encapsulates an algorithm for reading a single ultrasound image inherited from ImageFrameReader. SCTRL_CMD is the data structure transmitted to the subcomputer. DbfHardware is a class that interacts with the subcomputer, and DbfFrameReader is the DbfHardware class. FrameReadThread is a thread class that can read data from the subcomputer.

For the original ultrasound image data, column headers are added to the data in 155 columns and 521 rows for reliable transmission. Due to the requirements of hardware equipment, the amount of data read each time must be an integer multiple of the minimum amount of data read.

In the process of collecting and storing ultrasound image data in the system, multiple data buffers are used. The following briefly introduces multiple data buffers. The data must be an integer multiple of the minimum read data volume. Original ultrasound data temporary storage buffer: each column of data analyzed by the original ultrasound data analysis buffer reads the first column number, and when 155 columns of data are read, the original ultrasound data temporary storage buffer will be temporarily stored in it. Therefore, these buffers are allocated globally and need to be reused and are not suitable for storage.

The ultrasound image data processing module mainly preprocesses the frames of the original ultrasound image data and manages the frame display buffer of the generated ultrasound image data. Its data processing thread functions

Table 5: Interface response time test.

Total number of tests	Maximum response time (ms)	Minimal response time (ms)	Average time consumption (ms)	Average drawing time (ms)
500	2.765	0.765	1.480	55

Table 6: Operational reliability test.

Test method	Frequency	Stuttering times	Normal times
No operation within 24 hours	100	0	100
Occasional small operations	100	0	100
Frequent large number of operations	100	1	99

include: additional processing of original frame data, generating a frame of ultrasound image data, and generating results; the transmission room is mainly used to process frames of ultrasound image data. After collecting the raw ultrasound data, it is preprocessed (in this Jean–Wiey section, only the preprocessed noise reduction algorithm is introduced, and the DSC algorithm and frame-related algorithms are introduced into the image processing system). The collected raw ultrasound data must be preprocessed because the ultrasound imaging mechanism will generate scale noise in the image, which will reduce the image quality and seriously affect the resolution of subtle features. As an image preprocessing noise elimination technology, it mainly filters noise interference.

Considering the real-time filtering performance requirements in the preprocessing process based on the ultrasonic speckle noise model, this paper uses an improved fast median filter to reduce the preprocessing noise. Through many practices, it has been found that the median filter can remove pink noise very well and has an excellent suppression effect on impulse interference and isolated point and line noise. With the excellent edge protection effect, we can obtain the collection effect in real time. However, the median filter does not have a good Gaussian noise suppression effect, and the noise reduction effect still cannot meet the requirements. In recent years, continuous progress has been made in the noise reduction of ultrasound images, and good results have been achieved in noise reduction and edge protection. However, due to the time limitation of the algorithm, it cannot be well applied to real-time processing.

The system uses a fast median filter algorithm for preprocessing, can better complete the work according to the system's real-time noise reduction requirements, and is more effective than other types of algorithms. Once the image in the active area is fixed, this article will implement an improved noise reduction algorithm, so that the doctor can make clearer calculations and more accurate diagnosis after the image is fixed, so that deeper effect processing can be performed.

The system has been improved in two main aspects by adopting a fast median filtering algorithm that has been improved for noise reduction preprocessing. You can consider sorting adjacent fields and use the sorted rows or columns directly in subsequent programs. Second, binary sort storage is used, and the time interval method is used to get the effect of removing the median O(1).

4.3. System Performance Test. The system sets the image refresh rate to 25 Hz so that the system can perform user interface operations normally and timely meets the system's requirements for digital image processing and has a better response rate. The test results are shown in Table 5.

Test method: first, turn on the power and run for 24 hours to check whether the whole machine is operating normally, sometimes after turning on the power and running for 24 hours, perform some functional test tasks continuously to ensure that it has stopped. Due to various operating systems, hardware, and software reasons, the specific response of a single operation is meaningless when testing the response time of the entire system. The test results are listed in Table 6.

5. Conclusion

The hot image deblurring technology in the field of image restoration has broad application potential and strong technical requirements, leading to the rapid development of today's multimedia communications. In general, we have a clear understanding of the process of deblurring images. Therefore, image restoration has also become a blind restoration problem. Accurate estimation of the fuzzy kernel function is very important for the restoration of clear images. In the process of establishing image restoration and effective prior knowledge, making full use of the signal itself to obtain the model also plays an important role. Then, relying on the digital B-ultrasound terminal software system to realize the collection and processing of digital B-ultrasound terminal medical image data, select the B-ultrasound image data as the research content, mainly design and realize the ultrasound image acquisition, communication, and processing system.

Data Availability

The data used to support the findings of this study are available from the corresponding author upon request.

Conflicts of Interest

The authors declare that they have no conflicts of interest.

References

[1] M. A. T. Figueiredo and R. D. Nowak, "An EM algorithm for wavelet-based image restoration," *IEEE Transactions on Image Processing*, vol. 12, no. 8, pp. 906–916, 2003.

[2] T. Chan, S. Esedoglu, F. Park, and A. Yip, "Recent developments in total variation image restoration," *Mathematical Models of Computer Vision*, vol. 17, 2005.

[3] L. Xu, S. Zheng, and J. Jia, "Unnatural L0 sparse representation for natural image deblurring," in *Proceedings of the 2013 IEEE Conference on Computer Vision & Pattern Recognition*, Portland, OR, USA, June 2013.

[4] I. Y. Järvelä, J. Juutinen, and P. Hartikainen, "Gestational diabetes identifies women at risk for permanent type 1 and type 2 diabetes in fertile age: predictive role of autoantibodies," *Diabetes Care*, vol. 29, no. 3, pp. 607–612, 2006.

[5] S. Surayapalem, V. Cooly, and B. Salicheemala, "A study on maternal and perinatal outcome in premature rupture of membranes at term," *International Journal of Reproduction, Contraception, Obstetrics and Gynecology*, vol. 6, no. 12, 2017.

[6] M. Adil, M. A. Jan, S. Mastorakis et al., "Hash-MAC-DSDV: mutual authentication for intelligent IoT-based cyber-physical systems," *IEEE Internet of Things Journal*, 2021.

[7] K. R. Leonard and M. K. Hinders, "Guided wave helical ultrasonic tomography of pipes," *Journal of the Acoustical Society of America*, vol. 114, no. 2, pp. 767–774, 2003.

[8] K. E. Thomenius, "Evolution of ultrasound beamformers," in *Proceedings of the IEEE Ultrasonics Symposium*, pp. 1615–1622, San Antonio, TX, USA, November 1996.

[9] M. Balík, "Importance of ultrasound examination in diagnosing acute conditions," *Vnitrní Lékarství*, vol. 65, no. 3, pp. 177–186, 2019.

[10] J. Pan and Z. Su, "Fast L0-regularized kernel estimation for robust motion deblurring," *IEEE Signal Processing Letters*, vol. 20, no. 9, pp. 841–844, 2013.

[11] R. V. Mendonça, J. C. Silva, R. L. Rosa, M. Saadi, D. Z. Rodriguez, and A. Farouk, "A lightweight intelligent intrusion detection system for industrial internet of things using deep learning algorithm," *Expert Systems*, vol. 39, Article ID e12917, 2021.

[12] W. Dong, L. Zhang, G. Shi, and X. Wu, "Image deblurring and super-resolution by adaptive sparse domain selection and adaptive regularization," *IEEE Transactions on Image Processing*, vol. 20, no. 7, pp. 1838–1857, 2011.

[13] T. Goto, Y. Kawamoto, Y. Sakuta, A. Tsutsui, and M. Sakurai, "Learning-based super-resolution image reconstruction on multi-core processor," *IEEE Transactions on Consumer Electronics*, vol. 58, no. 3, pp. 941–946, 2012.

[14] J. Yang, J. Wright, T. S. Huang, and Y. Ma, "Image super-resolution via sparse representation," *IEEE Transactions on Image Processing*, vol. 19, no. 11, pp. 2861–2873, 2010.

[15] A. H. Yousef, J. Li, and M. Karim, "On the visual quality enhancement of super-resolution images," *Proceedings of SPIE - The International Society for Optical Engineering*, vol. 8135, 2011.

[16] X. Chen, X. He, J. Yang, and Q. Wu, "An effective document image deblurring algorithm," in *Proceedings of the IEEE Conference on Computer Vision and Pattern Recognition (CVPR '11)*, pp. 369–376, Providence, RI, USA, June 2011.

[17] H. Cho, J. Wang, and S. Lee, "Text image deblurring using text-specific properties," in *Proceedings of the European Conference on Computer Vision (ECCV '12)*, Firenze, Italy, 2012.

Hindawi
Mobile Information Systems
Volume 2022, Article ID 7218277, 8 pages
https://doi.org/10.1155/2022/7218277

Research Article

Application of SVM-KNN Network Detection and Virtual Reality in the Visual Design of Artistic Images

Liang Wu [1] **and Lin Chen** [2]

[1]*College of Fashion and Design, Donghua University, Shanghai, China*
[2]*College of Fine Art, Shanghai Normal University, Shanghai, China*

Correspondence should be addressed to Liang Wu; 18403082@masu.edu.cn

Received 19 April 2022; Revised 7 June 2022; Accepted 18 June 2022; Published 9 July 2022

Academic Editor: Shadi Aljawarneh

The birth of computers has brought us unexpected progress and development in many ways. In this very real world of our human existence, the beginning of human perception of the world. It is a sensory organ that collects sensory information, and the same goes for people's artistic creation and design. This paper discusses the classification effect of the combined model of support vector machine and SVM-KNN on the problem of virtual reality art images, analyzes the parameters of the optimized combined model, and then conducts a series of simulation analyses on the optimized model. So using this method can make the collected data more real and reliable, and it will be very convenient for us to process. Use the SVM algorithm to train the classifier when performing data classification and compare different training sample sizes and different kernel functions for empirical analysis and in-depth analysis of the accuracy of the two and the impact of the model. Through the data comparative analysis of SVM-KNN, the obtained results are more real and effective.

1. Introduction

In this very real world in which we humans exist, the beginning of human perception of the world is the collection of sensory information by sensory organs, and the same goes for people's artistic creation and design [1]. The multidimensional information obtained from various sensory organs is vivid and specific, which is conducive to people's understanding and acceptance, is more in line with people's living habits, and stimulates people's creative thinking. Therefore, for thousands of years, human beings have made great efforts and spent a lot of effort to produce a multidimensional environment simulation that fits their own feelings. People have also made progress during this arduous exploration [2]. From ancient times to the present, in human art. In the history of development, while creating art, he has been using and exploring various senses, creating and receiving multidimensional information. However, restricted by technological factors, the underdevelopment of technology makes this goal never come true [3, 4]. Virtual reality art design opens up new methods for achieving goals. By using this technology, designers can truly experience human emotions through various physiological activities such as vision, smell, and touch and this give designers richer inspiration and imagination to immerse themselves or It is empathy, which combines the thoughts in the human brain with environmental factors and transforms the thoughts in the mind into things that are visible to the naked eye [5]. We use SVM-KNN classification to investigate and use real and reliable data based on actual conditions, and use what we have learned plus our innovation to propose more optimized calculation and verification methods. It will not only make the results more accurate but also make it more convenient and faster for us to collect data and provide good technical support for the visual design of information art technology.

2. Related Work

Some research describes the meaning and purpose of virtual reality when conducting art design research. "Virtual reality

art design" is a cutting-edge topic in modern art design [6]. It has found a new point of convergence between art and science and, at the same time, straddles art and science. Some research clarifies the basic content of virtual reality, immersiveness, and the unity of nature and man, expounds and explains the origin and history of design art. While discussing the art of design which is very virtual but realistic, it also explains the research object, research purpose, research method, and research reason of this article. Some research mainly explained the visual effects and research methods that are usually applied in virtual reality art design from three aspects [7]. Some research discusses that in virtual reality art design, we can give new characteristics to the produced works through this technology, give people a bright feeling, let people feel unheard of things, and even travel through time and space situation [8]. Some research discusses that after the use of virtual reality art design, people's lives have undergone a series of earth-shaking changes, which have had a huge impact on people's production and lives. Some research discusses that after the emergence and development of virtual reality art design, contemporary art has made an obvious development. It can be seen that virtual reality art has a far-reaching influence and helps in the prospect of modern art water design. Some research mainly reveals the unique and innovative aspects of virtual reality art design in life production, scientific development, entertainment, environmental protection, technical research, etc. Compared with the previous art design, this technology is now more complete, It is in a separate line and has higher compatibility [9, 10]. Some research uses examples to illustrate that from the birth of modern design to today, in the process of its development and growth, the chemical reaction of art and technology has occurred all the time, and the two have been combined with each other to develop until now, the two interlaced each other to appear as virtual reality art. Some research uses data as a direct entry point for comparative analysis and gives detailed introductions one by one of the types, characteristics, attributes, and sources of the data, which provides great convenience for later data processing and application [11] and saving processing time and processing costs. Some research uses the SVM model to train a SVM classifier in terms of the accuracy of data processing and then adds preprocessing and classification and grouping steps on this basis to make the data obtained by the calculation more accurate. Some research introduces the nearest proximity method and proposes the advantages of this method, and then improves the SVM model on this basis, and at the same time applies the SVM-KNN method to combine and compare artistic design with reality empirical analysis [12].

3. The Theoretical Basis of SVM-KNN Network Detection and Virtual Reality Technology

3.1. Principle of Linearly Separable SVM. It has been nearly a century since the birth of support vector machines. In these years, the technology of support vector machines has also been developed rapidly. In order to make this technology easier to learn and to be widely promoted, scientists have found several excellent methods. In SVM research, the most basic and most important problem is the problem of two classifications. We assume that the training sample is (x_i, y_i), where $i = 1, 2, \ldots, n$, category C_1, the category C_2 is originally on both sides of the constructed classification function. From the above figure, as long as a straight line that satisfies the linear division of the sample on both sides of the plane is obtained, no matter how many there are, it is the optimal classification hyperplane.

Assumption function: $g(x) = wx + b$, where w is the normal vector of the hyperplane, which determines its vector direction, b is the displacement vector, which determines the distance from the origin, and x is the observed value vector of the sample. At this time, the sample x_k to be classified needs to be judged which category it belongs to, only the value of $g(x_k)$ needs to be looked at. If $g(x_k) > 0$, it is judged that the sample x_k belongs to the category C_1: on the contrary, it is judged that the sample x_k belongs to the category C_2.

Then we get the following equation:

$$f(x) = \operatorname{sgn}[g(x)]. \tag{1}$$

In the second classification, the classification is marked with "+1" and "−1," which respectively indicate the two classification categories of the sample and define the interval from the sample point x_i to the hyperplane:

$$\delta_i = y_i(wx_i + b). \tag{2}$$

If the sample x_i belongs to the category as follows:

$$|g(x_i)| = |wx_i + b|, \tag{3}$$

normalizing w and b, we get the following equation:

$$\delta_i^* = \frac{1}{\|w\|}|g(x_i)|. \tag{4}$$

Obtain a hyperplane, so that the original sample points reach the farthest position from the classification hyperplane to obtain the following objective function at this time:

$$\operatorname{Max}\frac{1}{\|w\|}|g(x_i)|. \tag{5}$$

The distance between H_1 and H_2 can be expressed as:

$$\delta = \frac{1}{\|w\|}. \tag{6}$$

At this time H_1 is as follows :

$$wx_i + b = -1. \tag{7}$$

H_2 is as follows:

$$wx_i + b = +1. \tag{8}$$

H_3 is as follows:

$$wx_i + b = 0. \tag{9}$$

When $|g(x_i)| = 1$, the distances from other sample points to the classification hyperplane are not less than 1, then we get the following equation:

$$y_i(wx_i + b) \geq 1, \quad i = 1, 2, \ldots, n. \tag{10}$$

Use linear programming to find the hyperplane at this time as follows:

$$\begin{aligned} &\min \frac{1}{2}\|w\|^2 \\ &\text{s.t.} \quad y_i(wx_i + b) \geq 1 \\ &i = 1, 2, \ldots, n. \end{aligned} \tag{11}$$

Construct the Lagrange function as following:

$$L(w, b, \alpha) = \frac{1}{2}\|w\|^2 - \sum_{i=1}^{n} \alpha_i [y_i(wx_i + b) - 1]. \tag{12}$$

Among them, α_i is the constrained Lagrange multiplier. Since it is an inequality constraint condition, $\alpha_i \geq 0$. The optimization objective function is transformed as follows:

$$\min_{w,b} \max_{\alpha_i \geq 0} L(w, b, \alpha). \tag{13}$$

The objective function satisfies the KKT condition. According to the Lagrange duality, the optimization problem is transformed into an equivalent dual problem for the following solution:

$$\max_{\alpha_i \geq 0} \min_{w,b} L(w, b, \alpha). \tag{14}$$

First find the minimum value of $L(w, b, \alpha)$ under w and b, and then find the partial derivatives of w and b , respectively, as follows:

$$\begin{aligned} &\frac{\partial}{\partial w} L(w, b, \alpha) = w - \sum_{i=1}^{n} \alpha_i y_i x_i = 0, \\ &\frac{\partial}{\partial b} L(w, b, \alpha) = \sum_{i=1}^{n} \alpha_i y_i = 0. \end{aligned} \tag{15}$$

The normal vector corresponding to the optimal hyperplane can be obtained as follows:

$$w = \sum_{i=1}^{n} \alpha_i y_i x_i. \tag{16}$$

And the Lagrange multiplier corresponding to the most hyperplane satisfies the following condition:

$$\sum_{i=1}^{n} \alpha_i y_i = 0. \tag{17}$$

Eliminating w from the above formula gives the following equation:

$$\begin{aligned} \varphi(\alpha) &= \frac{1}{2}\|w\|^2 - \sum_{i=1}^{n} \alpha_i [y_i(wx_i + b) - 1] \\ &= \sum_{i=1}^{n} \alpha_i - \frac{1}{2} \sum_{i=1,j=1}^{n} \alpha_i \alpha_j y_i y_j {x_i}^T x_j. \end{aligned} \tag{18}$$

Maximize the above formula as follows:

$$\begin{aligned} &\max_{\alpha} \sum_{i=1}^{n} \alpha_i - \frac{1}{2} \sum_{i=1,j=1}^{n} \alpha_i \alpha_j y_i y_j x_i^T x_j \\ &\text{s.t.} \sum_{i=1}^{n} \alpha_i y_i = 0 \\ &\alpha_i \geq 0 \\ &i = 1, 2, \ldots, n. \end{aligned} \tag{19}$$

The above formula is equivalently exchanged as follows:

$$\begin{aligned} &\min_{\alpha} \sum_{i=1}^{n} \alpha_i - \frac{1}{2} \sum_{i=1,j=1}^{n} \alpha_i \alpha_j y_i y_j x_i^T x_j \\ &\text{s.t.} \sum_{i=1}^{n} \alpha_i y_i = 0 \\ &\alpha_i \geq 0 \\ &i = 1, 2, \ldots, n. \end{aligned} \tag{20}$$

Find the corresponding value of $w$as follows:

$$w^* = \sum_{i=1}^{n} \alpha_i^* y_i x_i. \tag{21}$$

After calculating w^*, the value of b is solved, then for any support vector we get the following equation The following inference can be drawn:

$$y_s(wx_s + b) = y_s\left(\sum_{i=1,j=1}^{n} \alpha_i y_i x_i^T x_j + b\right) = 1. \tag{22}$$

$$b_s^* = y_s - \sum_{i=1,j=1}^{n} \alpha_i y_i x_i x_s. \tag{23}$$

Finally we get the classification function:

$$f(x) = \text{sign}(w^* x + b^*) = \text{sign}\left(\sum_{i=1,j=1}^{n} \alpha^* y_i x_i x + b^*\right). \tag{24}$$

3.2. Improved SVM-KNN Method. In this paper, based on the literature research, we innovate and upgrade the calculation formula, adding the calculation of feature weights to better improve SVM-KNN. Using this method in the face of the general SVM-KNN algorithm, it can be used in the case of parameters. Next, find the optimal solution to the problem in time to improve the efficiency and accuracy of classification and detection.

Table 1: Table of common dangerous permission characteristics in Android.

Authority group name	Authority name	Permission description	Permission type
INTERNET	INTERNET	Access network	System authority
	CHANGE_NETWORK_STATE	Change network status	Paid
SMS	SEND_SMS	Send messages	Paid
	RECEIVE_SMS	Receive SMS	Privacy authority
	WRITE_SMS	Read SMS	Privacy authority
	READ_SMS	Edit SMS or MMS	Privacy authority
CONTACTS	READ_CONTACTS	Access contact information	Privacy authority
	WRITE_SMS	Write contact information	Privacy authority
PHONE	CALL_PHONE	Dial number	Paid
	READ_PHONE_STATE	Access phone status	Privacy authority
	READ_CALL_LOG	Read call log	Privacy authority
	PROCESS_OUTGOING_CALLS	Monitor and modify broadcast calls	Privacy authority

Table 2: Table of characteristics of common risk mechanisms in Android.

Risk mechanism characteristics	Confusion mechanism class	CRYPTO, ASCII OBFUSCATION
	Program mechanism class	NATIVE, DYNAMIC, PEFLECTION

Table 3: Common sensitive call API feature table A in Android.

Sensitive call API characteristics	Network class	GetNetworkInfo, getActiveNetworkInfo, openConnection, connect, GetInputStream, getOutputStream, openStream, isWifiEnabled, getScanResults, getConnectionInfo
	Privacy	getSubscriberId, getDeviceId,getSimSerialNumber, getLine1Number, invalidateAuthToken, openInputStream, getDefault, getAccounts, getlastKnownLocation, requestLocationUpdates, isProviderEnabled, sendData, setAudioSource, getPhoneContacts, getCellLocation
	Paid	sendMultipartTextMessage, sendTextMessage
	System class	setComponentEnabledSetting, new Wakelock, notify, addNotificaction, setAudioSource, setDefaults, execute, setAudioSource, getRingerMode, vibrate, reboot

We first need to process the vector of the data, using the support vector machine-based under-sampling balanced training set method to find a set of support vectors from the type of set with more original training sets and then extract them to form the balanced set [13]. In actual operation, if the differences between samples are directly ignored in the calculation, the evaluation results will be unstable and the classification accuracy will also be inaccurate. Therefore, we consider the use of an analytic hierarchy process to calculate the influence proportion of feature indicators, and then calculate the weight of different features. The classification accuracy rate is greatly improved.

3.3. Experimental Simulation Analysis of SVM-KNN Network Detection. In the experiment, a total of 200 training software samples were used. Among them, there were 100 normal software and 100 malicious software. The category labels were 1 (positive class) and −1 (negative class).

This article combines fine-grained permission declaration and risk mechanism, intent priority, sensitive API and other grammatical features, extracts the flowDroid-based privacy data taint propagation path set as semantic features, and uses a variety of effectively mixed static features to improve detection coverage and accuracy, etc. Among them, the common dangerous permissions in Android are shown in Table 1:

Some common risk mechanisms and sensitive API calls with threats are shown in Tables 2 and 3:

In addition, we also consider that a series of security risks may arise during the experiment or hackers may deliberately do it, so we have stepped up prevention to monitor the network input and output numbers from time to time. In addition, considering the difference between explicit and invisible hidden dangers, the general network request is rejected. Intent in Android usually refers to the transmission of information. Confidentiality is very important [14]. A little carelessness will bring huge losses. This will not only consume huge resources and money for maintenance but also cause some confidentiality violations. If it is not kept properly, there will be endless troubles. The protection technology can be used as an important feature to distinguish normal software from malicious software in the implementation process. This article proposes to use dynamic analysis technology and tools to monitor and extract the following features of Android applications, as shown in Table 4.

If only one method is used to judge whether the software is running normally, this judgment standard is not enough, because many software seem to be running normally but have lost their basic data processing and comprehensive analysis capabilities, and some software is even judged as Malware, but it works well in the process of running. So we should also collect a series of data for analysis based on the effect of the software at runtime and construct a suitable space vector model and function model to vectorize and store it [15]. If the feature does not appear in the Android application, it is recorded as 0, otherwise the frequency or

Table 4: Collect a list of behavior characteristics.

Category	Feature name
The Internet	TxBytes, RxBytes, TPacket, RxPacket
SMS	Send verification/delete SMS
Cell phone	Dial number
Address book	Send/delete address book
Media	Open the camera and record in the background
Position	Obtain precise positioning information
File	Open/read/copy/rename/delete files
CPU	CPU usage (including load distribution and usage rate.)
Process	Process ID, process name, running process
Battery	Temperature, cleaning consumption, level
RAM	Internal vss remaining memory, shared memory, virtual consumption
APP	Close the application in the background, check the information of the sen application

number of times it appears in the specified time is counted as 1 or n ($n > 1$). For example, if a software goes online or sends a message privately without receiving instructions, it is recorded as 1. If it appears multiple times, it is recorded as n, otherwise it is 0. Finally, the recorded values are counted to construct a function model, and then the multiple recorded data is used as the sample set of the improved SVM-KNN algorithm, as a method of this combination, to provide a line of defense for software security detection. This leads to the third "fuse" besides static and dynamic, as shown in Table 5.

Table 5: Table of classifier accuracy when taking different values of u and K.

K	u			
	0.1 (%)	0.2 (%)	0.3 (%)	0.4 (%)
1	75.000	85.000	86.667	85.000
3	78.333	88.333	93.333	91.667
5	83.333	91.667	88.333	81.667
7	81.667	90.000	80.000	76.667

3.4. Features of Virtual Reality Art Design. Virtual reality art has many characteristics, the most important of which can be summarized in the word "real." Let users really be able to achieve immersive goals with the help of this technology. Using virtual reality art, we can apply it to many aspects of life. For example, the special effects of movies and TV series that we are familiar with are simulated using this technology, and when actors perform some illusory scenes, they are usually given to actors. The feel of it facilitates its performance. Not only in these, but also in terms of network art, this technology is also very useful. Compared with traditional technology, this technology has great innovations and has caused rapid changes in many fields.

Immersiveness: immersive means that you are not in that environment but that you feel as if you are in that environment. Whether it is from sight, smell, or hearing, the requirements for being on the spot are very high. However, traditional art forms and artistic effects generally cannot meet this need. The traditional art forms we face are generally books. For example, through the description of the author and the reader's personal imagination, we can achieve a kind of empathy effect. However, with virtual reality technology, you can directly and accurately receive a series of information that the operator wants to convey without your own creation and imagination.

Interactivity: interactivity is whether people feel smooth and natural when they feel and receive information through virtual reality art. At the same time, it is also whether the creator of the work feels handy, easy to produce and express, rather than unable to convey the desire to express. If the person who conveys the information feels comfortable using this technology and the person who receives the information also feels connected, then it is highly manipulable and interactive.

Intuition: the so-called intuitiveness is whether the designer can intuitively see the problems in the design through the simulated scenes, and then quickly correct them. At present, this feature of this technology has also been widely used. Most of the construction of squares and platforms uses this technology, thinking that once the construction of these projects is started, most of them are irreversible, so the preliminary work must be done well In place.

Virtual reality: virtual reality has also been widely used at present. This technology mainly uses virtual reality technology to portray existing things with more realistic images or images, so that some blurred and unclear objects are clear and intuitive. Show in front of people. After repairing some very precious ancient paintings and ancient books, designers often use this technique to repair them. In addition to repairing some precious murals and restoring the colors of the murals, this technique is also used. The Dunhuang Mogao Grottoes as we know them are realized by using the virtual reality of VR art design.

Collaboration: collaboration mainly emphasizes that virtual reality art design can be transmitted and shared through the network, just like a document or a form, which is very convenient to transmit. As the name suggests, this convenience can allow more designers to participate into the design of the same work. Even if they are far away, as long as there is a network, they can

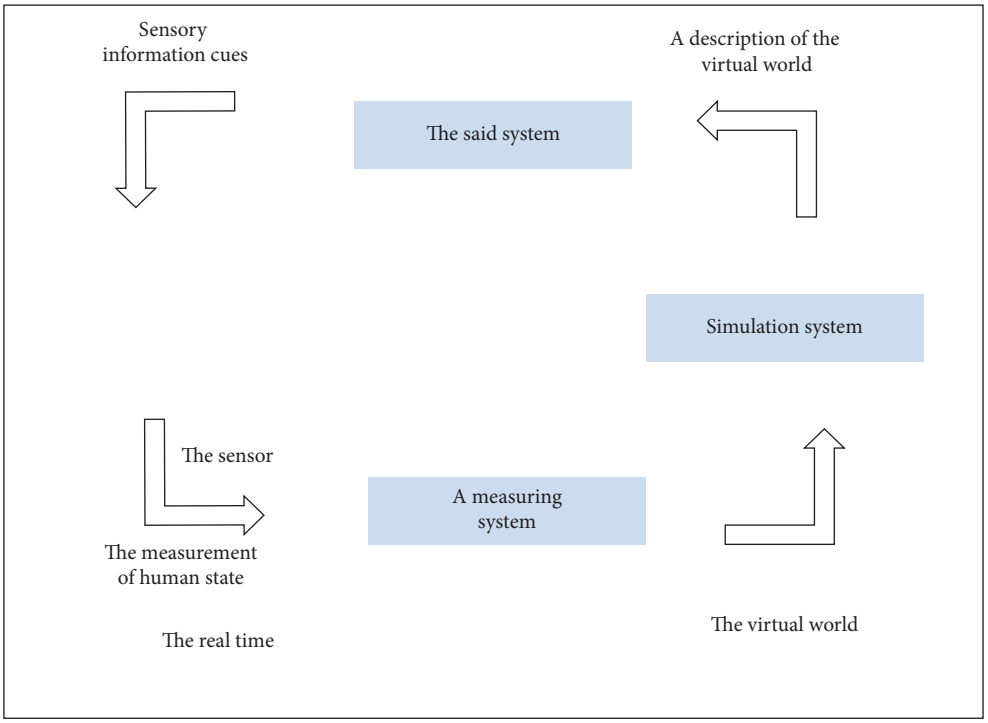

Figure 1: Realize the structure of virtual reality.

share and create in real time. Its collaboration is also an important feature that attracts resources.

First, a virtual object is simulated by the simulation system and also has other sensory characteristics, and then the record of this virtual world is transmitted to the presentation system. After the presentation system is processed, the sensory information prompts are transmitted from the sensor to the measurement system, and then feedback is given to the simulation system. This completes the process from the virtual world to the real world and then back to the virtual world. The structure of virtual reality is shown in Figure 1.

In virtual reality systems and their applications, technology has three outstanding characteristics: immersion, interaction, and imagination. Three characteristics of virtual reality are shown in Figure 2.

What are the modules of this system? I know that scholars from all over the world are arguing today, but the models proposed by each scholar are similar, so we believe that it is mainly composed of five parts. It is believed that this model will continue to improve and finally reach a consensus. Five typical components of the system are shown in Figure 3.

In fact, in addition to the conventional five typical components, scientists have also developed many new components because the sensor module is the core and the control module is also indispensable. The combination of these two modules is the most important part of this model. For the most part, the task is very heavy, so a detection module and a feedback module should be added to ensure smoother information transmission and higher accuracy. Composition of the VR system is shown in Figure 4.

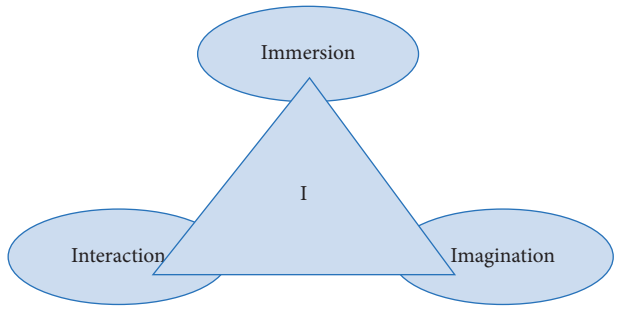

Figure 2: Three characteristics of virtual reality.

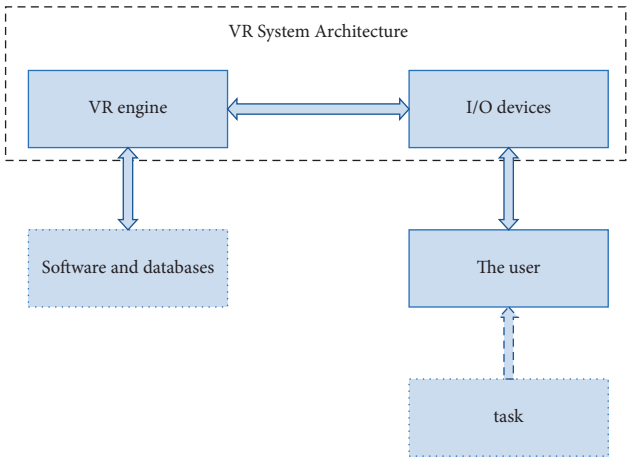

Figure 3: Five typical components of the system.

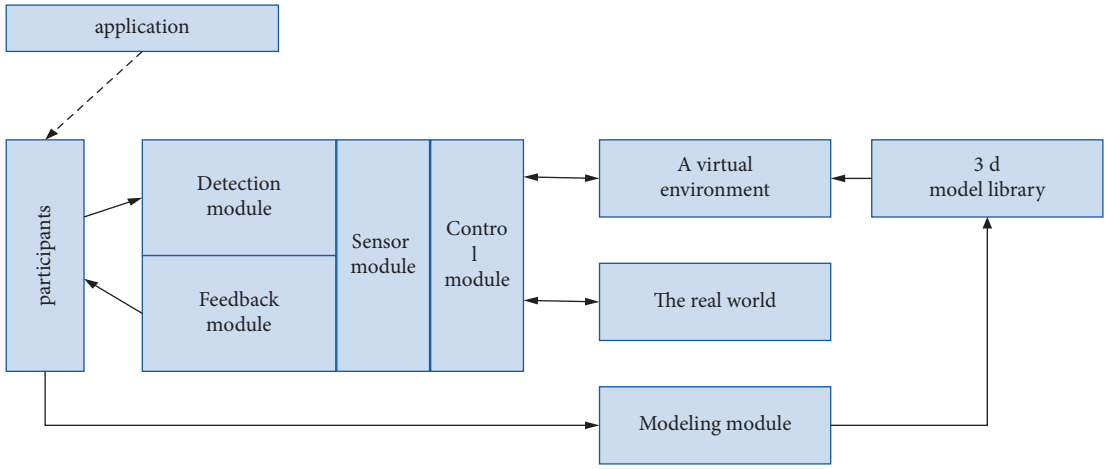

Figure 4: Composition of the VR system.

As shown in the figure, the application gives participants a message, and then the participant controls the sensor module to communicate with the virtual environment through the detection module. The feedback module provides real-time feedback to the participant. On the one hand, the sensor module accepts the participant's instructions to act on the virtual environment. On the other hand, feedback the results of the operation to the participants.

4. Art Image Visualization Design Strategy and Result Analysis

4.1. Realization of the Visual Design of Virtual Reality Art Images. Desktop virtual reality art is mainly divided into two aspects: hardware and software. The hardware uses computers and other equipment to input and output the simulated images. In simple terms, it uses computer keyboards, mice, monitors, and other hardware devices to show the designed work and let the designer modify it intuitively. The software aspect uses some computer software and APP for independent modification and design, first classifying the designed works and then replan the design according to each part. At present, this technology has been applied to daily life, leisure, and entertainment.

The development of this technology also makes people want a more realistic experience. People are no longer just satisfied with being visually realistic, but more concerned with the realistic effects of smell, touch, taste, hearing, and so on. This technology is also different in terms of hardware and software. These two aspects have different focuses. Virtual reality technology distinguishes these two technologies through hardware and software. In terms of visual effects, hardware has more visual impact than software. And software is more innovative and complex in terms of simulation and beyond reality. For virtual reality art, innovation is often more important, so the development of software is also more important, especially for the new, simpler, and more effective software design that can further enhance the development space of Internet computers and virtual reality art.

4.2. Visual Effects of Visual Design of Virtual Reality Art Images. This technology is a simulation technology. It is based on the characteristics of actual things and uses appropriate materials to construct an identical thing that expands and shrinks in the same proportion. For example, if we want to visit many places of interest but are far away or unable to go for some other reason, we can use this technology to construct a model for visit. Owning many famous cars is a dream of many people, but not everyone can afford all the cars they like, so you can buy a simulation model of the car to satisfy your desire.

To achieve "likeness" is to visually resemble the objects we see every day, so that people will know that they are such objects at first impression after seeing them. Not only that but also in terms of hearing, touch, and sensation, and the ability to be imitated things are very similar, just like watching a 5D movie, making people feel like they are in it.

Transcendental virtualization mostly virtualizes the environment that humans cannot personally experience and see with their own eyes in daily life. For example, when launching artificial rockets, we cannot really observe people's orbital changes in space. However, we can use virtual reality art to make animations to simulate this process, or when man-made satellites reach the Moon and Mars for landing, some semivacuum environments can also be simulated, which brings a lot of convenience to designers, but also reduces the failure rate.

4.3. The Influence of Virtual Reality Art on Image Visualization Design. The impact of virtual reality art is very far-reaching. For example, in terms of production, it is necessary to use this kind of virtual reality art to produce some simulated machines. And this production process is to first use this technology to outline and describe the precise shape of the product you want to design on the computer and then use 3D printing and other technologies to copy and print the product shape described. Products manufactured by this method are often simpler and easier to operate than traditional methods. Using this technology, it is often possible to manufacture some very precious and difficult items,

because this technology can depict the required scene very realistically, which enables the manufacturer to repeatedly adjust during manufacturing. This process is completely mechanical and accuracy rate is also very high, making it not easy to make mistakes and errors.

In daily teaching, virtual reality art is also used everywhere. At the same time, this technology is often used when researching big power weapons, such as airplanes, aircraft carriers, and tanks, when designing. In many schools, teachers use this technology in PPT to demonstrate and simulate unheard or unimaginable things to students. In addition, when studying the atomic bomb and hydrogen bomb, some of the more harmful explosion tests could not be carried out in real tests. They all used virtual reality art design and simulated experiments to obtain valid data for research. It not only saves a lot of expenses and reduces the cost of testing, but also makes the process safer and easier in the aftermath.

5. Conclusion

In the past many years, many things were very close and inseparable. Among them, technology and design are typical examples. If the industrial revolution is the source of design, today's virtual reality art design will bring new vitality to art design. Many characteristics of virtual reality art have laid a solid foundation for it to become a popular "candidate" in many industries. For example, it has been widely used in real-life CS games because it allows people to be in a virtual environment. People indulge in it and cannot extricate themselves from the situation in the wilderness battle. Another example is its organic combination with computer technology and 3D printing technology, which also makes many impossible possible by making many tedious tasks simple and efficient. Therefore, it is only a very forward-looking and developmental project. At the same time, this technology needs to be better developed. There are still many gaps that give it a lot of room for development. If this technology is further developed in the near future, it will bring huge changes to people's production and lifestyles. Moreover, it is inseparable from various fields, and it is a highly intersecting discipline. Its development will also drive the development of various fields, and the economic impact will be countless.

Data Availability

The data used to support the findings of this study are available from the corresponding author upon request.

Conflicts of Interest

The authors declare that there are no conflicts of interest.

References

[1] J. J. Zhou and X. F. Yao, "Advanced manufacturing technology and new industrial revolution," *Computer Integrated Manufacturing Systems*, vol. 21, p. 1963, 2015 –1978.

[2] S. Shang, L. Chen, C. S. Jensen, J.-R. Wen, and P. Kalnis, "Searching trajectories by regions of interest," *IEEE Transactions on Knowledge and Data Engineering*, vol. 29, no. 7, pp. 1549–1562, 2017.

[3] M. Abd Elaziz and I. Attiya, "An improved Henry gas solubility optimization algorithm for task scheduling in cloud computing," *Artificial Intelligence Review*, vol. 54, no. 5, pp. 3599–3637, 2021.

[4] P. Anderson, X. He, C. Buehler et al., "Bottom-up and top-down attention for image captioning and visual question answering," in *Proceedings of the IEEE Conference on Computer Vision and Pattern Recognition*, pp. 6077–6086, Salt Lake City, UT, USA, June 2018.

[5] P. A. Gore and S. D. Brown, "Simpler may still be better: a reply to eggerth and andrew," *Journal of Career Assessment*, vol. 14, no. 2, pp. 276–282, 2006.

[6] N. Saeed, H. Al Zarkani, and M. A. Omar, "Sensitivity and robustness of neural networks for defect-depth estimation in CFRP composites," *Journal of Nondestructive Evaluation*, vol. 38, no. 3, pp. 1–10, 2019.

[7] N. R. Brisaboa, Y. Cillero, A. Farina, S. Ladra, and O. Pedreira, "A new approach for document indexing usingwavelet trees," in *Proceedings of the 18th International Workshop on Database and Expert Systems Applications (DEXA 2007)*, pp. 69–73, Regensburg, Germany, September 2007.

[8] A. F. M. Shahen Shah, H. Ilhan, and U. Tureli, "RECV MAC: a novel reliable and efficient cooperative MAC protocol for VANETs," *IET Communications*, vol. 13, no. 16, pp. 2541–2549, 2019.

[9] N. Ta, G. Li, Y. Xie, C. Li, S. Hao, and J. Feng, "Signature-based trajectory similarity join," *IEEE Transactions on Knowledge and Data Engineering*, vol. 29, no. 4, pp. 870–883, 2017.

[10] C. C. Huang, J. H. Li, C. L. Mei, and W. Z. Wu, "Three-way concept learning based on cognitive operators: an information fusion viewpoint," *International Journal of Approximate Reasoning*, vol. 83, pp. 218–242, 2017.

[11] K. Do, T. Tran, and S. Venkatesh, "Graph transformation policy network for chemical reaction prediction," in *Proceedings of the 25th ACM SIGKDD International Conference on Knowledge Discovery & Data Mining*, pp. 750–760, Anchorage, AK, USA, July 2019.

[12] A. W. Astin and J. L. Holland, "The environmental assessment technique: a way to measure college environments," *Journal of Educational Psychology*, vol. 52, no. 6, pp. 308–316, 1961.

[13] G. M. Lang, D. Q. Miao, and M. J. Cai, "Three-way decision approaches to conflict analysis using decision-theoretic rough set theory," *Information Sciences*, vol. 406-407, pp. 185–207, 2017.

[14] K. Cho, B. van Merriënboer, D. Bahdanau, and Y. Bengio, "On the properties of neural machine translation: encoder–decoder approaches," in *Proceedings of the SSST-8, Eighth Workshop on Syntax, Semantics and Structure in Statistical Translation*, pp. 103–111, Doha, Qatar, October 2014.

[15] S. M. Bowles, *Is Congruence Dead? an Examination of the Correlation between Holland's Congruence and Job Satisfaction Using Improved Methodology*, Ph.D. Thesis, West Virginia University, 2008.

Hindawi
Mobile Information Systems
Volume 2022, Article ID 4336840, 11 pages
https://doi.org/10.1155/2022/4336840

Research Article

Facial Expression Recognition and Beauty Health Management Based on Image Feature Analysis

Shanshan Fu and Binbin Xu

Department of Medical Cosmetology, Department of Public Health and Medical Technology, Xiamen Medical College, Xiamen, Fujian 361000, China

Correspondence should be addressed to Binbin Xu; 200800010207@xmmc.edu.cn

Received 18 May 2022; Revised 16 June 2022; Accepted 25 June 2022; Published 8 July 2022

Academic Editor: Shadi Aljawarneh

Face recognition can convey a kind of intuitive and rich information to people. With the current Internet security problems becoming more and more prominent today, in order to better effectively guarantee the security of such digital images during Internet transmission, one of the most direct and effective solutions is to recognize the characteristics of such digital information on facial expressions. However, the customer service system of the beauty and health club itself is a customer service software system based on customer experience and marketing management as its core functions. This article discusses the main software design and system realization of the management platform of the beauty and health club customer information service system in the entire operation process from the application development trend of information software. Based on the theoretical research and application development of the current corporate customer business service management system of the beauty and health club, the basic concepts and operating methods of current corporate customers, business service information management, and business service customer management, as well as the corresponding corporate information customer management. The management technology and other issues are first briefly summarized in theory, and then based on the specific business development characteristics of the current beauty and health clubs, the main application functions and specific market requirements of the service company's corporate customer service management system are analyzed in detail and introduced the related functions of using the software.

1. Introduction

The development of mobile Internet information technology has made people's information work and daily life more convenient, happier, and more colorful [1]. However, in this convenient and colorful mobile Internet era, there are still many hidden network security risks and health in life threatened. Internet technology is an open information network with many insecure factors [2]. When recognizing user faces or expressions or transmitting user signal information, there may still be many opportunities for malicious tampering, sneak attacks, and other illegal copying in violation of regulations. The traditional standard algorithm for group data encryption of facial expressions is not suitable for the facial expression recognition data encryption. The main reason is that these encryption algorithms do not use grouping algorithms that are specifically used for data encryption for the recognition of the internal information of the expression text. The characteristics of large amount of data, high redundancy, uneven distribution of energy information, and high correlation with multiple adjacent encrypted pixels are main encryption features of digital image encryption information [3]. The special nature of these characteristics also leads to the difference between traditional digital grouped image encryption algorithms have extremely different encryption efficiency for the application of grouped encryption of digital images [4]. In the current information security application field, many technical methods have emerged, but the gray value of the image has not changed in any way. The attacker can even use some

statistical characteristics such as the gray histogram distribution of facial expressions or exhaustive method to crack these cipher-text images. Therefore, traditional network image information encryption algorithms may be more vulnerable when facing multiple different network attacks at the same time [5]. China Beauty Club, which uses facial expression information recognition, is also a leading enterprise that has developed rapidly in the application field of this technology and is constantly growing. In recent years, with the further expansion of its main business and asset scale, information management has developed into an important system construction content for future enterprise development [6]. This paper will discuss the application software design and hardware realization of the customer service information security management system of beauty and health clubs from the perspective of application software development [7]. The customer service management system of the beauty and health center is a comprehensive software system whose main core function is to provide customer management services. The main purpose is to support enterprise managers to efficiently, comprehensively, and accurately control their company's various businesses through network technology and to help the company achieve effective management and operation of data [8]. According to the business characteristics of the beauty and health club, the functional requirements of the club's customer service information management software system are analyzed [9].

2. Related Work

In the early twenty-first century, the literature proposed a multiscale image analysis CT transform based on facial expression recognition. This transform refers to the design and improvement of the traditional existing transform module by adopting the structure of the dual filter module group [10]. It can effectively reflect various geometric changes in facial expressions. CT transformation is composed of two components. The first component is the Laplacian Pyramid, which is mainly responsible for the multiscale decomposition and processing of image signals [11]. The second component refers to the image analysis of the subspace bandwidth after the decomposition of the DLP function in the first part, which can directly select the value of the image directionality through the image directional reflection filter [12]. The literature mainly expresses that the displayed facial recognition image data usually has two-dimensional and distributed characteristics. Generally, we encrypt its image source in the form of scrambling and diffusion [13]. However, this type of facial expression image using encryption diffusion algorithm not only has a relatively low-diffusion efficiency, but it also has many problems due to the complex calculation of diffusion efficiency and low security. Researchers and others proposed the SPCME digital image block encryption algorithm based on the chaotic code replacement structure based on the encryption technology and research of the chaotic program replacement structure of image block cipher [14]. The literature describes in detail that the library management information system is a new type of comprehensive general-purpose software designed, developed, and used specifically for the management, storage, protection, data access, management access, and statistical data processing of the data system [15]. In the design of the library management system, it is widely regarded as an important type of database transaction processing information system used in different data-intensive applications [16]. A database system is an entity that relies on its so-called "relational data simulation" to represent information internally. A relationship is expressed by a set of attribute data. An instance of a relationship is a set of unit tuples with specific attribute values, which become the corresponding relationship scale. As the market operation of contemporary, Chinese enterprises has gradually shifted from the traditional model with product service as the core to the modern model with customer service as the core. Enterprises need to further create a system that can effectively support and cultivate the discovery of customers' [6] potential and actual needs and their anticipated capabilities, tools, and methods. Taking customers as the service center is to enable companies to accurately identify their expectations and actual needs for customers and to respond quickly to the rapidly evolving customers. Therefore, various industries must transform their marketing management business models from the perspective of customers as the main service body, and the goal is to continuously meet the unique and differentiated needs of each type of customer [17]. The literature shows that the main business object in the customer service management system of the beauty and health club is the customers of the beauty and health club [18]. Therefore, the customer service and management system is an important technical basis for the information management of the beauty and health club [19, 20]. As a software system with unique customer relationship management information system functions and features, the information processing system must store all customer information.

3. Improvement of Facial Expression Recognition Method Based on Image Encryption Algorithm

3.1. Image Encryption Algorithm. Cryptography generally refers to the study of how to conceal or effectively preserve information. There is a close and indivisible relationship between many majors and fields such as cryptography and computer science. This is a discipline with comprehensive value. The generation of ciphers was mainly developed to adapt to the needs of human warfare in the early stage. It consists of two parts: cryptanalysis and cryptography.

With the rapid development of modern information technology, security issues in the field of digitalization and multimedia applications have become increasingly prominent. Video, images, etc., are all important parts of the multimedia application field. It is an image as one of the important ways and means of various multimedia dissemination of information, which can vividly convey the information it wants to display and express to people. In

today's environment with global Internet security problems, in order to effectively ensure the security of digital images, it must be strictly encrypted.

At present, the main types of image encryption technology used in the field of network information encryption technology are the following: first, network information encryption technology based on secret information sharing; second, digital image encryption technology based on matrix transfer transformation; third, based on chaos theory digital image encryption technology. In the encryption processing technology of these images, most of them use scrambling processing technology. Different image encryption technologies have different characteristics of image encryption technology, and the complexity, security, and speed of encryption and decryption of these image encryption technologies are also different.

The definition of Henon mapping is shown in formula (1):.

$$\begin{cases} x_{n+1} = 1 + y_n - ax_n^2, \\ y_{n+1} = bx_n. \end{cases} \tag{1}$$

Henon mapping has a single-valued inverse, and its inverse mapping is shown in formula (2):

$$\begin{cases} x_n = \dfrac{1}{b} y_{n+1}, \\ \\ y_n = ax_n^2 + x_{n+1} - 1. \end{cases} \tag{2}$$

Figure 1 shows the phase diagram of Henon mapping.

The security performance of the image encryption algorithm can be detected by the analysis technology of network security. The security requirements are the following: a guaranteed image encryption system must have the characteristics of small correlation between adjacent pixels and balanced distribution of the number of histograms, so as to effectively prevent and control various attacks.

After the pixel value of a certain pixel is cracked, input any number of data information on the neighboring pixels around the pixel:

$$\begin{aligned} r_{xy} &= \frac{\operatorname{cov}(x, y)}{\sqrt{D(x)} \cdot \sqrt{D(y)}}, \\ \operatorname{cov}(x, y) &= \frac{1}{N} \sum_{i=1}^{N} \left(\left(x_i - E(x) \right) - \left(y_i - E(y) \right) \right), \\ E(x) &= \frac{1}{N} \sum_{i=1}^{N} x_i, \\ D(x) &= \frac{1}{N} \sum_{i=1}^{N} \left(x_i - E(x) \right)^2. \end{aligned} \tag{3}$$

In formula (3), x and y, respectively, represent the average gray value of each element in an image. Co(x, y) is an organic correlation function representing the threshold of each pixel, $E(x)$ is the average value, and $D(x)$ is the average variance.

$P(\mathbf{r}_k)$ represents the probability of the gray level. The formula is shown in equation (4):

$$P(r_k) = \frac{n_k}{N}. \tag{4}$$

For analyzing images, the gray-scale and histogram analysis of the image is a convenient and quick analysis tool. The formula for finding the positive value of the histogram is shown in formula (5), and the formula for finding the variance of the histogram is shown in formula (6).

$$U = \sum_{i=0}^{255} i * P_i, \tag{5}$$

$$\partial^2 = \sum_{i=0}^{255} (i-)^2 * P_i. \tag{6}$$

The calculation of NPCR and UACI can be realized by formulas (7) and formula (8), where M and N represent the height and width of the $\mathbf{I}_1$ and $\mathbf{I}_2$ images.

$$\text{NPCR} = \frac{\sum_{i,j} E(i,)}{M \times N} \times 100\%, \tag{7}$$

$$\text{UACI} = \frac{1}{M \times N} \left[\sum_{i,j} \frac{\left| M_1(i, j) - N_2(i, j) \right|}{255} \right] \times 100\%. \tag{8}$$

In digital image encryption technology, image-scrambling technology is an important part of it. The image scrambling technology can realize the re-encoding and arrangement of each element and pixel matrix in the image, reduce the correlation of each element in the image, and then achieve the goal of image encryption and secure data transmission. In modern mathematics, the number sequence formula in Fibonacci takes a recursive function form for definition, such as formula (9):

$$\begin{aligned} &F(0) = 0, \\ &F(1) = 1, \\ &F(n) = F(n-1) + F(n-2) \left(n \geq 2, n \in N^* \right). \end{aligned} \tag{9}$$

Definition of two-dimensional isometric image scrambling transformation:

$$\begin{bmatrix} x' \\ y' \end{bmatrix} = \left[\begin{bmatrix} a & b \\ c & d \end{bmatrix} \begin{bmatrix} x \\ y \end{bmatrix} \right] (\text{mod} M). \tag{10}$$

According to the encryption formula (10), the encryption parameters are set as follows: $a = 1$, $b = 1$, $c = 1$, $d = 0$. The encryption method obtained is to encrypt the two-dimensional isometric image Fibonacci in the image scrambling after the transformation. As shown in the calculation formula (11):

$$\begin{bmatrix} x' \\ y' \end{bmatrix} = \left[\begin{bmatrix} 1 & 1 \\ 1 & 0 \end{bmatrix} \begin{bmatrix} x \\ y \end{bmatrix} \right] (M). \tag{11}$$

According to the encryption formula (10), the encryption method obtained by setting the encryption parameters

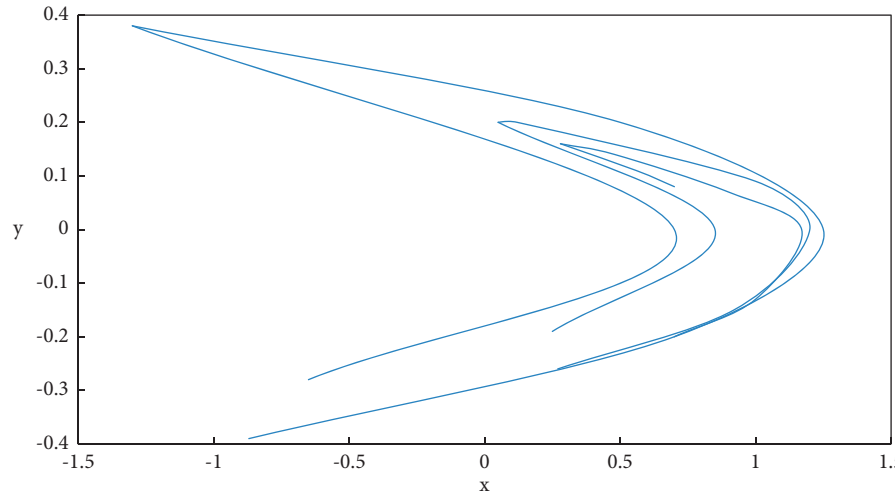

Figure 1: Henon mapping phase diagram.

as $a = 1$, $b = 1$, $c = 1$, $d = 2$ is actually an encryption function transformation of Arnold through the image input scrambler. As shown in the calculation formula (12):

$$\begin{bmatrix} x' \\ y' \end{bmatrix} = \left(\begin{bmatrix} 1 & 1 \\ 1 & 2 \end{bmatrix} \begin{bmatrix} x \\ y \end{bmatrix} \right) (M). \tag{12}$$

Specific steps of image encryption algorithm based on DNA encoding:

The first step: the use of image encoding encryption file mapping needs to choose the logistic mapping processing system. Consider a key mapping as the initial function value of a function as logistic and its mapping. Among them, the method of initially obtaining the key is to select an integer of 16 points from any point between 0 and 255. Such a smart key lock requires large enough space performance and can achieve relatively high security and efficiency in actual operation and use.

Step 2: differentiate or calculate each pixel value of the original plaintext image through the initial key.

Step 3: take the above two key codes as a key parameter and initialized value of logistic key mapping, respectively, and then replace it with codes again and use it to re-encode to generate a key sequence.

Step 4: encode the DNA sequence generated in Step 3 and the value of each element in the original plaintext image separately according to the coding schedule. This sequence is to convert the data information of each sequence and other images into DNA sequences.

Step 5: Perform alternative encryption operations on the image through calculation, as shown in Figure 2.

3.2. Improvement of Facial Expression Recognition Method. According to the different regional characteristics of the current facial expression local information feature distribution, this paper mainly proposes a new facial expression information feature recognition and analysis algorithm based on the widened local nearest Gabor neighbor feature and the broadened nearest local neighbor feature classifier. The practice of the model adopted on the JAFFE model database has proved that this method has achieved good results.

The core idea of facial expression recognition based on linear methods is to find a suitable transformation matrix W, and map the original sample x to the feature space y, as shown in formula (13):

$$y = W^T x. \tag{13}$$

The obtained feature vector is classified by the nearest neighbor classifier NN. The sample y category in the test set is the same as the training set sample x_λ category in the test set, which satisfies the formula (14):

$$\lambda = \arg\min_k \left\| x_k - y \right\|_2 \quad k = 1, 2, \ldots, n, \tag{14}$$

where $\|x_k - y\|_2$ is the Euclidean distance between the two-dimensional feature vectors X_k and y.

$$y_k = W^T x_k, \quad k = 1, 2, \ldots, N. \tag{15}$$

The total divergence matrix A is defined as follows:

$$S_T = \sum_{i=1}^{N} (x_i - \mu)(x_i - \mu)^T, \tag{16}$$

where $\mu \in R^n$ is the mean value of the input sample image. The divergence of the feature vector $y_1, y_2, \ldots, y_n$ obtained after the transformation of formula (15) is $W^T S_T W$. In PCA, the selection criterion of the transformation matrix W is to maximize the determinant of the total divergence matrix after projection, as shown in formula (16).

$$W_m = \arg\max_W \left| W^T S_T W \right| = [w_1 w_2 \ldots w_m]. \tag{17}$$

Equation (18) can be used to reconstruct the image:

$$\mathbf{x} = \mathbf{W}_m \mathbf{y}. \tag{18}$$

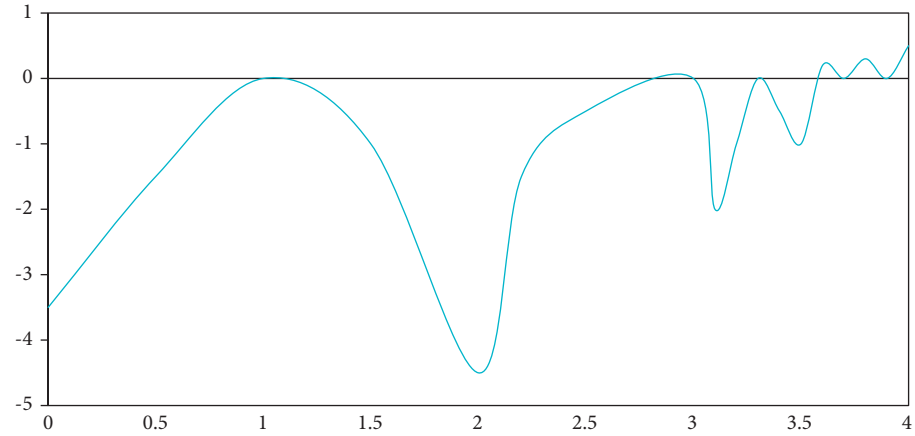

Figure 2: The change of Lyapunov exponent of logistic mapping.

According to the number of principal components m selected, the reconstructable image is shown in Figure 3. The first image on the left is the original image, and the following images are the images reconstructed when 3, 5, 10, 20, and 40 are selected in turn.

The original expression image A usually needs to be converted into a one-dimensional vector B. Some information may be lost in the conversion process, and calculating the total divergence matrix field C is a relatively large workload. 2D-PCA is the expansion of PCA in two-dimensional space, and it can directly map the input image matrix to the feature space.

Assuming that x is an n-dimensional vector and A is a matrix of, which represents the input image, then the projection of A on x can get the feature y:

$$y = x. \tag{19}$$

The quality of the projection vector x can be measured by using the total divergence matrix of the sample after projection. It is easy to know that the total divergence matrix after projection is shown in formula (20):

$$S(T) = \operatorname{tr}(\mathbf{S}_x) = \mathbf{x}^T \left[(\mathbf{A} - E\mathbf{A})^r (-E\mathbf{A}) \right] \mathbf{x}. \tag{20}$$

Define the image divergence matrix G_t as shown in the following formula:

$$\mathbf{G}_t = E(\mathbf{A} - E\mathbf{A})^T (\mathbf{A} - E\mathbf{A}) = \frac{1}{M} \sum_{j=1}^{M} \left(\mathbf{A}_j - \overline{A} \right)^T \left(\mathbf{A}_j - \overline{A} \right). \tag{21}$$

Then formula (21) can be expressed by formula (22):

$$J(\mathbf{x}) = \max_{\mathbf{x}} \mathbf{x}^T \mathbf{G}_t \mathbf{x}. \tag{22}$$

Figure 4 shows the effect of FLD and PCA on the mapping of two-dimensional samples to the feature space. It can be seen from the figure that the samples after FLD mapping are more separable than PCA.

The main data set used in the experiment is JAFFE, a famous Japanese female expression library. This article will be divided into two types of experiments: "human-dependent facial expression recognition" and "human-independent facial expression recognition." In "person-independent facial expression recognition," the strategy of "dropping a sample" is adopted, that is, each female's facial expressions are taken out as a training sample, and these residual samples are used as test samples. The training set contains 70 samples, and the test set contains 143 samples.

Table 1 shows the highest recognition rate of seven expressions based on the PCA method, and each row represents the probability of a certain expression finally classified into these seven expressions.

Table 2 shows the highest recognition rate of seven expressions based on the 2D-PCA method.

Figure 5 shows the results of facial expression recognition experiments with four linear methods of PCA, 2D-PCA, FLD, and 2D-FLD. The figure shows the variation of recognition rate with feature dimensions.

This step is mainly to cut and segment the expression image, as shown in Figure 6. The expression features are mainly concentrated in the facial area. First, the expression image is cut into a size of 144×127. In order to obtain local expression features, the expression image is then divided into areas that overlap each other by 50%. Assuming that the length (width) of the original image is n times the length (width) of the cropped image, then an image can be divided into $(2n-1) \times (2n-1)$ blocks of local regions. The selection of n will affect the performance and recognition rate. In this paper, n is equal to 4, which means that the original image is divided into 49 local regions.

4. Design and Implementation of Beauty and Health Management System

4.1. Design of Beauty Health Management System

4.1.1. Database ER Model. The beauty and health management system is currently mainly running in the clubhouse, using the client-server model. The background of the local system is used as a general database platform to centralize and manage the business, and it also allows users to access the internal database. Obtain authorized and

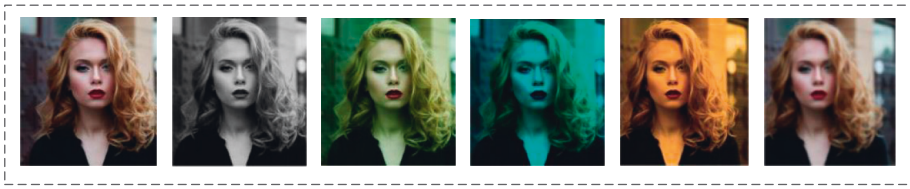

Figure 3: PCA reconstruction image.

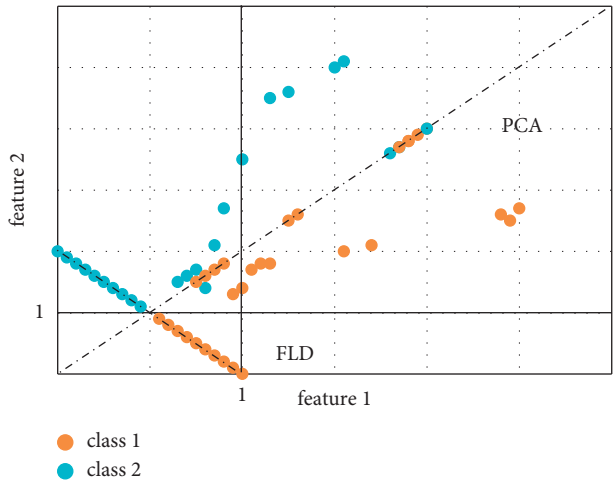

Figure 4: Comparison of PCA and FLD.

globally shared information. The attributes and data types of the main entity data of the database are described in Tables 3 and 4.

4.1.2. Rear Terminal Module. An important basic function of the customer service management information system is to achieve quantitative statistics and management for the comprehensive business information and data of customer service. To use this software, we must first obtain the data from the comprehensive business database of our company's customer service operations. Customer service-related data and complete data processing, and then saving these processing results in the enterprise's customer service management information system integrated business database to facilitate the account manager to perform statistics and analysis on subsequent customer service data [21]. The main internal structure of the database subsystem is used to perform access and statistical analysis of the integrity of customer data and service information and comprehensive business data and realize the internal data storage process as a database server. These processes are based on the original business comprehensive data records for the various responsibilities of the company and the account manager. The statistical data that need to be collected for query and calculation of business indicators need to be automatically extracted, and all the statistical results are integrated into a complete report for output at the same time, in the case of certain failures or abnormalities in the enterprise, and the information missing due to the failure has been reliably modified and restored. These warehousing procedures are also to realize the statistics and analysis of comprehensive business indicators, backup, dump, and database performance adjustment management of customer information and business data.

4.1.3. Front Terminal Module. The database publishes all the information in the background to the frontend through the Web server and spreads to the backend of users. The system's role configuration mechanism based on the database platform can complete the allocation of functional roles and access authorization for all legal users. The software in the system regulates the functions and data of which modules are allowed to be accessed based on its configured permissions.

Health care products, because health care products themselves are not only a subsidiary component of various health care and medical beauty services but also one of the main ways for the health club to obtain profit; therefore, we need to effectively target this category in this module. Information is used to achieve a set of professional management responsibilities. The information objects that need to be managed mainly include the names, current quantities, and suppliers of various types of health-care medical products currently in use.

The service item information records the development status of the beauty and health product items for each customer in detail. At the same time, the customer manager also records in detail the physical and mental health of each customer's feedback or return visit according to his actual situation. The purpose of the key recommendations is to enable the system to accumulate detailed dynamic data that occurred during the process of receiving services from customers within the company, so as to facilitate a comprehensive analysis of specific customers and overall customer satisfaction, potential demand signals, and market trends. At the same time, for all customer managers, it can constitute the most valuable enterprise operation management knowledge within the company.

The service function of the service information record management clubhouse is mainly through the above direct service data analysis and record management methods to indirectly statistics and export the clubhouse business service information related to its project. These business information are the basis for the system to be in the above service project data database, direct calculation and analysis on the above.

4.1.4. Customer Service Information Management. Customer service information management and its statistical analysis subsystem on the one hand provides more in-

Table 1: PCA's highest recognition rate.

	Happy	Sad	Surprised	Disgust	Anger	Scared	Neutral
Happy	80	0	7	3	0	0	10
Sad	3	85	0	0	3.67	3.33	5
Surprised	1.67	0	85	1.12	0	2.21	10
Disgust	0	6.9	0	86	3.7	3.4	0
Anger	0	0	0	6.67	83.33	0	10
Scared	0	9.5	6	4.5	0	75.00	5
Neutral face	0	3.33	0	3.33	7.67	0	85.67

Table 2: The highest recognition rate of 2D-PCA.

	Happy	Sad	Surprised	Disgust	Anger	Scared	Neutral
Happy	82	0	5	3	0	0	10
Sad	3	88	0	0	1	3	5
Surprised	2	0	90	1	0	2	5
Disgust	0	9	0	88	3	0	0
Anger	0	0	0	4	86	0	10
Scared	0	1.5	3.5	6	0	84	5
Neutral face	0	3.33	3.33	0	6.67	0	86.67

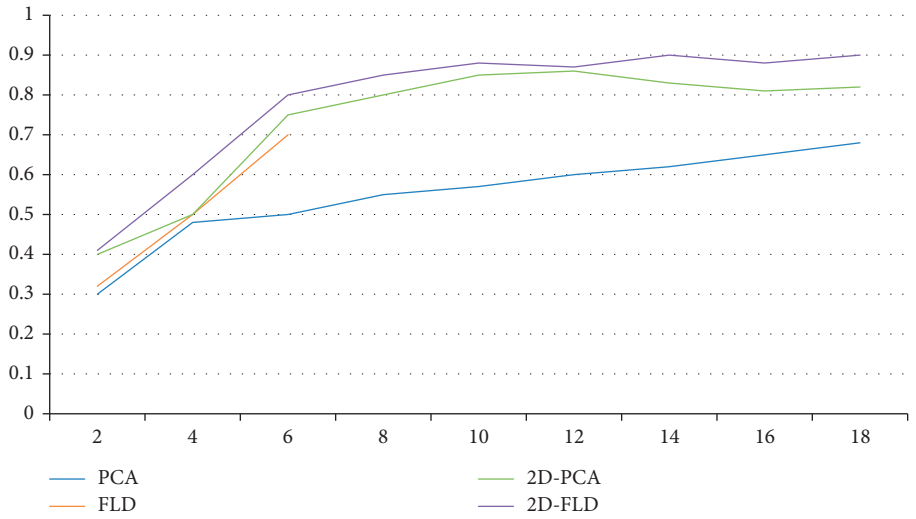

Figure 5: Comparison of linear method expression recognition.

depth multidimensional statistical data analysis and global business operation data analysis for the customers and service personnel of the club; on the other hand, it provides the company's group companies with a global operation data and business analysis basis.

4.1.5. Module Composition. According to the analysis of customer service needs, in the company's customer service information management software, relatively complex large-scale data processing functions require statistical calculations based on various marketing and customer needs analysis. To some extent, these indicators reflect customer satisfaction with actual services.

This system not only calculates the above statistical indicators within the specified time but also calculates the proportions related to the growth and change of various

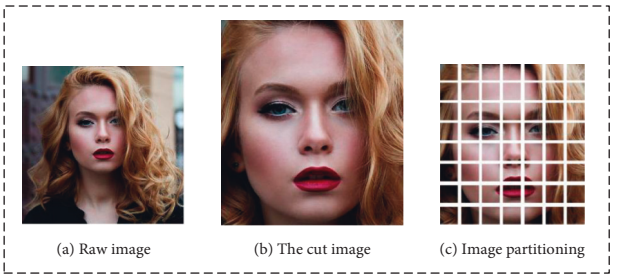

Figure 6: LF + ExtNN expression image preprocessing. (a) Raw image. (b) The cut image. (c) Image partitioning.

similar indicators in the corresponding year, so as to show the market trend that is valuable to the business manager of the enterprise information. For the management and decision-making level, the information provided by this

Table 3: Health product information table.

Property description	Attribute identification	Attribute data type
Health product label	HtCdld	Char (20)
Item type	HtCdType	Int
Full name	HtCdNm	Varchar (60)
Product standards	HtCdPrtld	Varchar (80)
Time to first market	HtCdFsTm	Datetime
Supplier legal person's full name	HtCdPrdvNm	Varchar (256)
Supplier's industrial and commercial registration location (domestic manufacturer)	HtCdAdr	Varchar (256)
Purchase contract number	HtCdDocSt	Varchar (40)
Purchase agreement price	HtCdPrice	Decimal (6,2)
Purchase agreement batch	HtCdBtc	Int
Agreement discount low volume	HtCdBtcMin	Int
Agreement minimum discount rate (nullable)	HtCdDstMin	Decimal (4,2)
Agreement discount highest discount rate batch (batch)	HtCdDstMax	Int
Agreement discount maximum discount rate	HtCdDstMax	Decimal (4,2)
Shelf life (months)	HtCdKmt	Int
Full name of the supplier's legal person	HtCdBkpPrdvNm	Varchar (256)
Alternate supplier's industrial and commercial registration location (domestic manufacturer)	HtCdBkpAdr	Varchar (256)
Alternative supply price	HtCdBkpPrice	Decimal (6,2)
Alternative supply lot	HtCdsBkpBtc	Int

Table 4: Health products purchase information table.

Property description	Attribute identification	Attribute data type
Purchase plan number	CpsId	Int
Plan name	CpsNm	Varchar(60)
Plan summary	CpsNptes	Varchar(1024)
Procurement responsible person number	CpsMgr	Int
Plan start time	CpsPSTm	Datetime
Actual start time	CpsRSTm	Datetime
Planned completion time	CpsPFTm	Datetime
The actual completion time	CpsRFTm	Datetime
Approval of opinions	CpsCfNt	Int
Approver ID	CpVfrld	Int
Total plan amount	CpsTlCpt	Int
Prepayment amount	CpsVfprePymt	Decima(8,2)
Prepaid time	CpsVfrprePyTm	Datetime
Supplier number	CpsVfProvld	Int
Settlement amount (record after settlement)	CpsVfRdPymt	Decima(8,2)
Settlement time	CpsVfRdPymtm	Datetime
Property description	Attribute identification	Attribute data type
Purchase plan number	CpsId	Int

module directly helps the company to effectively improve the company's internal operation and management.

This module is based on the cost data information calculated and calculated, and pays special attention to the realization of the internal cost of service projects, which can promote the management and decision-making level to grasp the actual profit space and an important direction for cost risk control.

By analyzing the operating value of a project, this module enables the management to know more clearly which service projects should be profitable and attractive to customers, and what are the main factors that lead to their profitability, which makes the technical personnel in the market more targeted development oriented of products and services with higher profitability.

This module is based on statistics and analysis of customer satisfaction indicators so that account managers and their marketing directors can accurately grasp the actual attractiveness of different types of service items to customers, all factors that attract customer needs, and other influences trends in customer needs.

The function of statistical analysis of operating costs is also realized through a separate set of procedures and links for hierarchical operations. As a service company, the club's operating cost composition and its measurement and accounting processing intermediate costs are quite large. The refinement and measurement of the company's operating costs also need to rely to a limited extent on more accurate and complete indirect cost data recording and reasonable cost allocation and calculation rules. The collection and

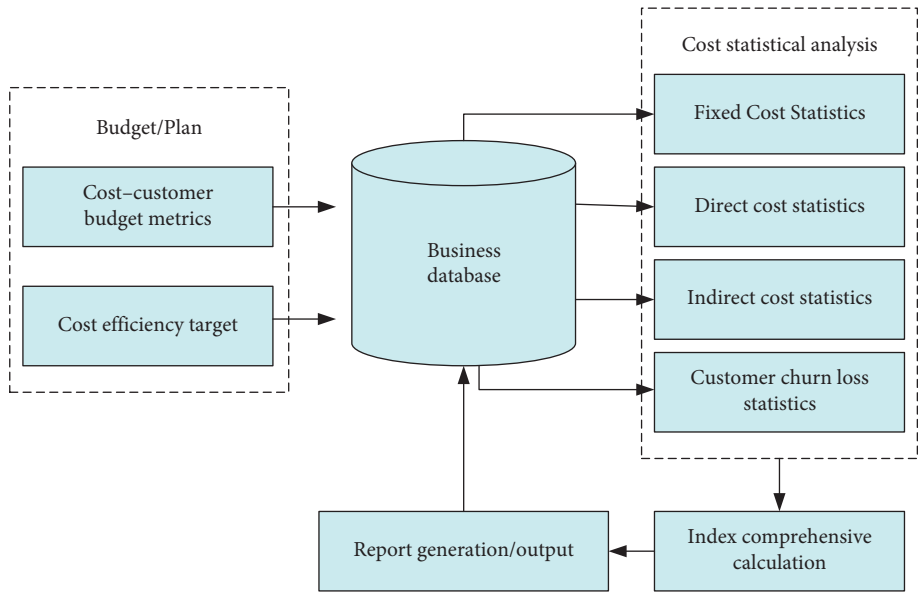

Figure 7: Business cost information processing flow.

processing of daily cost accounting data are mainly realized by the functions of the respective modules of the system. The processing principle of cost accounting is mainly carried out by the system on the basis of all cost data records within the scope of the system management module. The processing flow is shown in Figure 7.

4.2. Realization of Beauty and Health Management System

4.2.1. Program Development Project Organization. The goal of verification in program technology development, project development, and product testing is that all work organizations must be closely integrated in the first stage of project program development. The basic tasks of unit testing of programming software development and testing application modules are mainly based on the detailed test design plan of the entire enterprise software development system, such as the detailed design plan of some data structures and analysis algorithms, etc., which are used to directly complete the software source code serial programming of a certain new type of application programming language can directly carry out the serial test of each unit after the serial programming based on each unit. At this stage of development, the technology development based on the software inspection system is related to other specific algorithm programming languages, and is implemented through a new class of technical tools including software programming, translation, application debugging, and software inspection system testing.

4.2.2. Operating Environment. The operating environment of the application software system is based on Windows. The main functional unit is implemented by the database server on the SQLServer2008 relational network and is formed by the combination of page information processing functions on a built-in Web network of SQLServer. The user-side interactive processing and transaction request and analysis processing functions use the back-end database server and can use the application program written by T.SQL to directly realize the access and analysis and calculation of all business information of the management system.

4.2.3. Program Composition. One of the main core responsibilities of the company's customer service management information system is to quantify and manage the overall business and data of customer service. For this reason, the software first needs to be extracted from the company's customer service management integrated business database relevant information and data, and then save the results of its processing, and then store these information and data in the enterprise's customer service information integrated business database, so that the account manager can do statistics on the later customer service information, analysis, and other processing.

In the information system management layer based on the client and server, the corresponding application management function is to automatically access and preprocess the massive customer data stored by all customers in the customer database in real time. The basic data prediction and processing of the function call layer of each module are in the calling system, and the main function is embodied by a set of call functions applied to data processing, according to the function modules that need to be called by the upper layer and the function characteristics of the call objects of each function unit. Data-demand configuration and design have realized a set of corresponding call cases, so that other modules of the function call layer do not have to rely too much on accessing unnecessary basic analysis data, which greatly improves the efficiency of data access. It also saves a lot of time for repeated data processing for other basic analysis data processing call modules and increases the rapid accuracy of basic data processing for the entire system itself.

Table 5: System test examples.

Test content	Normal response
Use wrong username and password	Cannot log in to the system
Use the correct username and password	Jump to the function navigation table
Enter and business window through the menu bar of the system homepage	Pop up the corresponding module page
Enter data according to the required conditions in the query item window, and click the query button	Generate data that meets the conditions
Change related information in the edit window	Data updated successfully
Delete information in the edit window	Data deleted successfully
Change the progress information in the modify service item window	Information updated successfully
Delete task information in the service log window	Information deleted successfully
To view the inventory list, click the view button	Successfully display related inventory details
Enter relevant information on the add service or customer page	Information inserted successfully
Enter multiple query conditions on the base query page	Information query is successful
Enter information on the add new service item page	Information inserted successfully
View customer information	Read only under normal permissions

The main core data processing architecture of this management module is a function library interface for real-time access to the database and preprocessing for warehouse management. In the comprehensive statistical data analysis that needs to be realized in SQL-based programming, we need to continue to use more complex comprehensive statistical methods for data retrieval and analysis calculations in order to effectively ensure that the statistical performance of the entire program will not be affected by the computing system. The amount of existing data in the system is largely lost, the actual program time that needs to be executed is relatively compact, and the code execution form is less.

The testing of the software is one of the key contents of the software research in this article. Different types of testing methods are used to check and verify whether the software has clear programming logic and whether the actual operation can fully meet the functional specifications expressed in the analysis, and its performance requirements and reliability. As a large-scale enterprise application software, the system's software testing needs to be carried out in a planned way according to several stages and different levels. At the same time, it also needs to make full use of current software testing in its specific methods. Effective calculation tools in the technology and field to ensure the reliability and efficiency of its testing.

To sum up, the white box testing of the project is basically carried out on program units and operating system modules, while a dedicated testing team mainly carried out black box testing on the overall level. The testing work of the testing team focuses on verifying the various unit tests within the researcher's development team, and at the same time, it is tested and evaluated based on independent design and prepared test use cases and data, which are a core basis for testing. It is the confirmed and effective requirements analysis document. The software has been fully considered to meet various functional requirements as a whole, and the performance inspection and accuracy evaluation of the item by item have been carried out. The testing team graded and evaluated the faults found after the test according to the degree of impact on the software delivery—Table 5 In order to understand the test distance of the software, the test team listed the test content and the details of the response to the correctness of the program according to the characteristics and requirements of the system, compared with the test results and found out the cause of the failure.

5. Conclusion

With the popularization of mobile Internet and multimedia technologies, network security issues have become increasingly prominent. Image is an important signal transmission medium in the field of multimedia applications. People's daily study, life, and work are inseparable from a large number of digital images, but these large numbers of digital images are automatically transmitted through the Internet, and they are vulnerable to malicious tampering, theft, and other threats, especially some confidential military images. Information, medical image information involving citizens' privacy, etc., put forward stricter requirements for the protection and security of images; therefore, the most direct and effective way is to encrypt digital images. In modern cryptographic security science, two classifications are given: the basic structure of a general modern cryptographic security system and malicious attacks on new cryptographic systems. Among them, it introduces in detail all the unknown plaintext password attacks and known selected plaintext password attacks that can be selected in the plaintext password selection attack. In the assessment of the security of related technical standards for image gray-scale encryption, the technical analysis of image gray-scale histogram, differential image technology analysis, and gray-scale correlation analysis of two adjacent pixels in the image are introduced in detail. Technical criteria for evaluation in view of the company's main business and customer management characteristics, are the information system and has two core functions: the first type of function is the core function of the system as the main service item of customer dynamic service information analysis and management, which is mainly responsible for managing the company's beauty club. The planned and launched beauty and health care project activities and content project details, including

the specific names of the project activities, content project outlines, fee payment standards and relevant preferential policies, project marketing plans, current actual project operation progress are the major data, etc. The second category is the static information of health products, because health products are not only a subsidiary unit of medical and health and beauty projects, but also one of the main ways for clubs to make profits. Therefore, it is necessary to implement a set of independent management functions for this type of information. The detailed dynamic data during the period when customers receive the service facilitates a comprehensive analysis of the satisfaction of special customers and all customers, potential demand signals and market trends, and at the same time forms a valuable operating theory for all customer managers of the company.

Data Availability

The data used to support the findings of this study are available from the corresponding author upon request.

Conflicts of Interest

The authors declare that they have no conflicts of interest.

Acknowledgments

This paper was supported by (1) School Level: Exploration and Practice of Dual-System Talent Training Mode (no. J2017-06) and (2) Provincial Level: The Construction of Quality Evaluation System for Interdisciplinary Training of Cosmetic Technology and Engineering Talents (no. Fjjzx19-140).

References

[1] S. A. Alvi, B. Afzal, G. A. Shah, L. Atzori, and W. Mahmood, "Internet of multimedia things: vision and challenges," *Ad Hoc Networks*, vol. 33, pp. 87–111, 2015.

[2] W. Zhong, X. Yin, X. Zhang et al., "Multi-dimensional quality-driven service recommendation with privacy-preservation in mobile edge environment," *Computer Communications*, vol. 157, pp. 116–123, 2020.

[3] Y. Liu, X. Tong, and S. Hu, "A family of new complex number chaotic maps based image encryption algorithm," *Signal Processing: Image Communication*, vol. 28, no. 10, pp. 1548–1559, 2013.

[4] Z.-H. Guan, F. Huang, and W. Guan, "Chaos-based image encryption algorithm," *Physics Letters, Section A: General, Atomic and Solid State Physics*, vol. 346, no. 1–3, pp. 153–157, 2005.

[5] F. Y. Sun, S. T. Liu, and Z. W. Lü, "Image encryption using high-dimension chaotic system," *Chinese Physics*, vol. 16, no. 12, pp. 3616–3623, 2007.

[6] B. Chenglin, "The design and implementation on the network environment of the multimedia information processing system," *Computer Engineering & Software*, vol. 4, pp. 90–94, 2016.

[7] C. Iamsumang, A. Mosleh, and M. Modarres, "Monitoring and learning algorithms for dynamic hybrid Bayesian network in on-line system health management applications," *Reliability Engineering & System Safety*, vol. 178, pp. 118–129, 2018.

[8] F. B. Naini, J. P. Moss, and D. S. Gill, "The enigma of facial beauty: esthetics, proportions, deformity, and controversy," *American Journal of Orthodontics and Dentofacial Orthopedics*, vol. 130, no. 3, pp. 277–282, 2006.

[9] G. Perseo, "The "Beauty" of homo sapiens: standard canons, ethnical, geometrical and morphological facial biotypes. An explained collection of frontal north-Europide contemporary beauty facial canons. Part I," *Virtual Journal of Orthodontics*, vol. 30, pp. 150–162, 2002.

[10] A. Farouk, A. Alahmadi, S. Ghose, and A. Mashatan, "Blockchain platform for industrial healthcare: vision and future opportunities," *Computer Communications*, vol. 154, pp. 223–235, 2020.

[11] T. Zhuang, *CT Principle and Algorithm*, Shanghai Jiaotong University Press, Shanghai, China, 1992.

[12] T. P. Szczykutowicz, "Protocol optimization considerations for implementing deep learning CT reconstruction," *American Journal of Roentgenology*, vol. 216, no. 6, pp. 1–10, 2021.

[13] D. Liu, L. F. Wang, and H. F. Zhang, "Design of statistical analysis model based on big data," *Software Guide*, vol. 15, no. 7, pp. 28–30, 2016.

[14] X. Y. Xu, "Survey of face recognition technology," *Electronics Test*, vol. 2015, no. 5, pp. 885–894, 2015.

[15] X. Chai, X. Zheng, Z. Gan, D. Han, and Y. Chen, "An image encryption algorithm based on chaotic system and compressive sensing," *Signal Processing*, vol. 148, pp. 124–144, 2018.

[16] G. Donati and C. Woolston, "Information management: data domination," *Nature*, vol. 548, no. 7669, pp. 613-614, 2017.

[17] J. Zhang, "Trustworthy web services: actions for now," *IT Professional*, vol. 7, no. 1, pp. 32–36, 2005.

[18] S.-G. Deng, L.-T. Huang, J. Wu, and Z.-H. Wu, "Trust-based personalized service recommendation: a network perspective," *Journal of Computer Science and Technology*, vol. 29, no. 1, pp. 69–80, 2014.

[19] Z. Wang, Z. Zhou, H. Zhang, G. Zhang, H. Ding, and A. Farouk, "AI-based cloud-edge-device collaboration in 6G space-air-ground integrated power IoT," *IEEE Wireless Communications*, vol. 29, no. 1, pp. 16–23, 2022.

[20] S. Simoff and M. L. Maher, "Ontology-based multimedia data mining for design information retrieval," in *Proceedings of the ASCE Computing Congress*, Cambridge, UK, 1998.

[21] S. G. Lee, "Metadata-library Based Document Management Prototype System for Urban Renewal Promotion Plan," M.S. thesisThesis, University of Seoul, Seoul, Republic of Korea, 2009.